

AUTOMATIC AND REMOTE CONTROL

AUTOMATISME ET TÉLÉCOMMANDE

*Compte-Rendus du
Deuxième Congrès de la
Fédération Internationale de la Commande Automatique
(I.F.A.C.)*

Bâle, Suisse, 1963

REGELUNG UND FERNSTEUERUNG

*Bericht
über den zweiten Kongress
des Internationalen Verbandes für Automatische Regelung
(I.F.A.C.)*

Basel, Schweiz, 1963

AUTOMATIC AND REMOTE CONTROL

*Proceedings of
the Second Congress of the
International Federation of Automatic Control
(I.F.A.C.)*

Basle, Switzerland, 1963

Editor

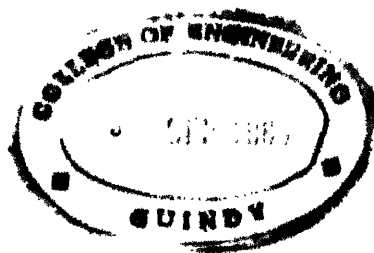
Prof. Dr. Ing. Victor Broïda
(France)

Co-editors

Derek H. Barlow
(United Kingdom)

Prof. Dr. Ing. Otto Schäfer
(Germany)

APPLICATIONS AND COMPONENTS



BUTTERWORTHS
LONDON

OLDENBOURG
MUNICH

1964

BUTTERWORTH & CO. (PUBLISHERS) LTD.

88 Kingsway, London, W.C. 2

- Australia: BUTTERWORTH & Co. (AUSTRALIA) LTD.
SYDNEY: 6-8 O'Connell Street
MELBOURNE: 473 Bourke Street
BRISBANE: 240 Queen Street
- Canada: BUTTERWORTH & Co. (CANADA) LTD.
TORONTO: 1367 Danforth Avenue, 6
- New Zealand: BUTTERWORTH & Co. (NEW ZEALAND) LTD.
WELLINGTON: 49-51 Ballance Street
AUCKLAND: 35 High Street
- Africa: BUTTERWORTH & Co. (SOUTH AFRICA) LTD.
DURBAN: 33/35 Beach Grove
- U. S. A. BUTTERWORTH INC.
WASHINGTON, D. C.: 7235 Wisconsin Avenue, 14

R. OLDENBOURG VERLAG

Germany: 8 München, Rosenheimer Strasse 145

Austria: Wien III, Neulinggasse 26

©

The several contributors named within
1964

PGE / N-15 .

EDITORIAL NOTE

To surpass success is difficult, but through teamwork and co-operative effort it can be done, as in the case of the Second Congress of the International Federation of Automatic Control.

The first I.F.A.C. Congress was held in Moscow in June-July 1960 and attracted some 1500 participants, and 286 papers which were published in four volumes of some 2000 pages only 15 months later; this First Congress set a high standard for subsequent ones to match.

Yet as judged by its participants, the Second I.F.A.C. Congress held at Basle in August-September 1963 did indeed match these standards. Although the number of papers was only 159, around 1500 participants accompanied by 200 ladies came from 32 different countries to attend these presentations.

Editing these papers into their present form also presented difficulties if the high standard attained with the Proceedings of the First Congress was to be maintained. A lot of these difficulties are, of course, common to all international congresses, but these become aggravated when several languages are used for the original manuscripts of the papers. In the Second Congress, 36 papers were originally submitted in Russian for publication in English, while nine papers were written and published in French. To make the operation truly international, an English Publisher was chosen working in conjunction with a German Printer.

Other difficulties that plague Editors of Congress Proceedings are delays in receiving the manuscripts, rapid translation requirements, and the lack of translators sufficiently expert in the intricacies and detailed knowledge of the field involved. All these problems were present when preparing the preprints of the papers for the Basle Congress. As a result, translations in the preprints were often not of the standard that one would have desired, since the inflexible publication date for the preprints prevented execution of revisions and changes that should have been made.

Even with all the goodwill and co-operation that the Printers and Publishers gave to the project, the 600 mile separation and language difference took their toll. Many typographical errors resulted in the preprints as there was no time for authors to receive and return proofs before the Congress. In spite of conscientious work by both Publisher and Printer after the Congress to check the 1.5 million words in the Proceedings, to improve the translations and to correct the typographical errors, it could be that some traces of these pre-Congress difficulties are still visible. If so, the Editors express their sincerest apologies for any errors that may still be found in these volumes.

Editing of the discussion remarks was greatly eased by the outstanding organization of the Congress by the Swiss Federation of Automatic Control, Professor Ed. Gerecke, Third I.F.A.C. President (1961-1963) and by the Congress Secretary Dr. A. von Schult-hess and the I.F.A.C. Honorary Secretary Dr. G. Ruppel. The main burden in preparing the edited discussion remarks was shouldered by Dipl.-Ing. E. Ruosch of Zurich. Leading an efficient team of scientific secretaries from the Eidgenössische Technische Hochschule of Zurich, the Technische Hochschule of Darmstadt and the University of Cambridge, Dipl.-Ing. Ruosch succeeded in supplying, often less than 48 hours after the presentation of each session, typewritten documents in English of all the discussion remarks on each paper in the session.

In the tedious and painstaking work of editing these volumes, the work of the Co-editors, Otto Schäfer of Aachen and Derek Barlow of London, has been invaluable, especially that of Mr. Barlow. Located in London and hence closest to the Publisher, Mr. Barlow bore the brunt of the detailed editing work, in particular the editing of the discussions on the applications and components papers. Editing of the final form of the Theory papers was done through the co-operation of the U.S.S.R. National Committee on Automatic Control.

Thanks are due also to the Publisher, particularly for the large amount of detailed sub-editing carried out by his co-operative staff, and also the Printer in overcoming the problems of printing scientific works in languages that were not of his own country.

EDITORIAL NOTE

It is hoped that, despite these problems and their effect on the Proceedings, the latter will become a long-living valued contribution in the development of the science of Automatic Control. The excellence of the Congress and the quality of the contributions certainly deserve this recognition.

It has been especially gratifying to the Editor and his colleagues to participate in what has been for them, as well as for all who attended the Congress, one of the most rewarding of human experiences—a fruitful international co-operative effort.

Boulogne sur Seine, France

VICTOR BRODA

June 1964

CONTENTS

EDITORIAL NOTE	V
LIST OF CONTRIBUTORS	XXXI

INTRODUCTORY SPEECHES

ADDRESS OF WELCOME	PROFESSOR ED. GERECKE (<i>President International Federation of Automatic Control</i>)	XXXV
HOW I.F.A.C. WAS FOUNDED	H. CHESTNUT (<i>First President, International Federation of Automatic Control, 1957-59</i>)	XXXVI
THE FIRST I.F.A.C. CONGRESS	PROFESSOR A. M. LETOV (<i>Second President, International Federation of Automatic Control, 1959-61</i>)	XXXVII
THE INFORMATION EVOLUTION AND ITS IMPACT ON AUTOMATIC CONTROL	J. L. AUERBACH (<i>President of the International Federation of Information Processing</i>)	XXXVIII

APPLICATIONS

THE ELECTRICAL UTILITY FIELD

Applications of Automatic Control in Electrical Utility Systems—A survey	B. Favez	5
Electric Utility		
Working Out a Method for the Cybernetic Control of Integrated Electric Power Systems	V. A. Venikov and L. V. Tsukernik	20
Some Recent Results in the Computer Control of Energy Systems	T. Vámos, S. Benedikt and M. Uzsoki	33
Optimal Control of Thermal-hydro System Operation	L. K. Kirchmayer and R. J. Ringlee	41
Automatic Systems with Learning Elements	G. K. Krug and A. V. Netushil	51
Principes et réalisations des automatismes liés à la manutention de combustible d'un réacteur nucléaire	P. Turpin and J. Thilliez	59
A Study of the Dynamics of Steam Voids in Boiling Water Nuclear Reactors	P. K. M'Pherson and M. Muscettola	70
Hydro-system Control		
On the Optimal Control of Hydro-electric Power Systems	H. Ruge	82
Exposé d'une méthode d'élaboration de graphiques exprimant les conditions de stabilité du réglage d'un groupe hydro-électrique	A. Tschumy	87
Digital Investigation of Multi-machine Power Systems	H. Glavitsch	98
Electric Utility-Machine Control		
Optimizing Control of Water Turbine Governors Considering the Non-linearity of Servomotor Speed	Th. Stein	104
Control Equations of a Hydro-electric Plant with Fixed Reference Values	L. Borel	110

CONTENTS

THE STEEL INDUSTRY

Applications of Automation and Automatic Techniques to Metal Rolling and Processing—A survey	<i>W. E. Miller</i>	117
Achievements in Automation of the Steel Industry—A survey	<i>A. Ya. Lerner</i>	126
Steel Industry		
Control for the Sintering Mixture Preparation	<i>G. DeGregorio, G. Litigio and G. Sironi</i>	132
Dynamic Planning for an Open-hearth Steel-making Plant	<i>M. Korobko and Yu. Samoilenko</i>	149
Automation of Heavy Forging	<i>J. G. Wistreich and A. Tomlinson</i>	157
Automation in a Steel Works with Special Reference to the Use of Digital Computers for Production Scheduling and Information Transmission	<i>S. E. Hersom and R. G. Massey</i>	167
On-line Computer Control of a Hot Strip Finishing Mill for Steel	<i>R. G. Beadle</i>	179
Optimum Control for Continuous Processes	<i>A. Ya. Lerner</i>	191
A Digital Optimal System of Programmed Control and Its Application to the Screw-down Mechanism of a Blooming Mill	<i>S. M. Domanitsky, V. V. Imedadze and Sh. A. Tsintsadze</i>	200
Computer Control of the Continuous Annealing Process	<i>J. T. Bradford, Jr.</i>	214

THE CHEMICAL AND OIL INDUSTRIES

A Survey of Application in the Chemical and Petroleum Industries	<i>H. W. Slotboom, J. de Jong and I. E. Rijnsdorp</i>	222
Chemical and Oil Industries		
Dynamic Characteristics of Binary Distillation Column	<i>K. Izawa and T. Morinaga</i>	229
Approximation Models for the Dynamic Response of Large Distillation Columns	<i>J. S. Moczek, R. E. Otto and T. J. Williams</i>	238
A Study on the Dynamic Behaviour of a Catalytic Cracker Power-recovery System by Means of an Analogue Computer	<i>C. A. J. M. van der Heyden and A. G. van Nes</i>	249
Statistical Analysis of a Novel Fluid Flow Control System	<i>R. C. Booton, Jr. and W. E. Sollecito</i>	261
Effects of Fluid Mixing and Its Expressions on Dynamics of Mass Transfer Process	<i>T. Takamatsu and E. Nakanishi</i>	269
Experimental Study of the Dynamic Behaviour of a Heat Exchanger and of a Mixing Process	<i>L. Delvaux</i>	275
Study of Industrial Production of Polyethelene Under High Pressures, and of the Automatic Control of the Process	<i>B. V. Volter</i>	290
A Study of the Dynamic and Static Characteristics of the Process of Fractional Distillation	<i>I. V. Anisimov</i>	300
Controllability and Allowable Compressor Capacity of a Flare Gas Recovery System	<i>F. J. Kylstra</i>	309
Analysis and Design of a Parameter-perturbation Adaptive System for Application to Process Control	<i>T. Isobe and T. Totani</i>	317
The Dynamic Properties of Rectification Stations with Plate Columns	<i>T. Závorka</i>	326
Une réalisation originale dans une raffinerie de pétrole: le chargement automatique des wagons citernes	<i>F. X. Montjean</i>	335

AUTOMATION IN INDUSTRIAL PROCESSES

Computer On- and Off-line		
Le traitement du problème d'optimalisation par A. 110	<i>E. Honoré</i>	341
Automation of a Portland Cement Plant Using a Digital Control Computer	<i>R. A. Phillips</i>	347
On the Stability and Design of Dither Adaptive Systems	<i>R. K. Smyth and N. E. Nahi</i>	358
Steam-system Control		
Predetermination of Control Results for Reheaters in Steam Generators	<i>W. Kindermann</i>	369
An Optimizing Control of Boiler Efficiency	<i>S. Fujii and N. Kanda</i>	380
Simulator for Steam Turbines with Reheat or Automatically Controlled Extraction	<i>H.-J. Ehling</i>	390
An Electro-hydraulic Control System for Reheat Turbines	<i>M. A. Eggenberger and P. H. Troutman</i>	398
Automotive Industry		
Une application industrielle d'un calculateur intérieur à un circuit de commande: l'équipement électronique de commande d'une machine à équilibrer les vilebrequins	<i>J. Csech</i>	408
Design Analysis of an Automotive Speed Control System	<i>W. H. Holl</i>	415

CONTENTS

COMBINED MAN-MACHINE SYSTEMS

Man and Machine

Modèles continus et échantillonnés de l'opérateur humain placé dans une boucle de commande	<i>P. Naslin and J.-C. Raoult</i>	421
Discrete Models of the Human Operator in a Control System	<i>G. E. Bekey</i>	430
Dynamic Analysis and Simulation of Management Control Functions	<i>R. B. Wilcox</i>	439
Outline of a Control Theory of Prosthetics	<i>R. Tomovic</i>	449
A Sampled-data Model for Eye Tracking Movements	<i>L. R. Young</i>	454

APPLICATION TECHNIQUES

Methods

Self-adaptive Method for Accommodating Large Variations of Plant Gain in Control Systems	<i>R. J. Kochenburger</i>	464
Hydraulic Line Dynamics	<i>R. Oldenburger and R. E. Goodson</i>	472
The Optimization of Computer-controlled Systems Using Partial Knowledge of the Output State	<i>B. G. Anderson</i>	480

AUTOMATIC CONTROL OF AEROSPACE SYSTEMS

Aerospace Systems

The Design Study of a Pressure Control System for a 5 ft. by 5 ft. Blowdown Wind Tunnel	<i>J. A. Tanner and W. Dietiker</i>	487
Missile Environment Simulation for Rocket Engine Test Facility	<i>G. J. Fiedler and J. J. Landy</i>	496
A Longitudinal Guidance System for Aircraft Landing During Flare-out	<i>F. J. Ellert and C. W. Merriam III</i>	504
Automatic Control of a Large Steerable Aerial for Satellite Communications	<i>F. J. D. Taylor</i>	512
Design Study of a Control System for a 210 ft. Radio Telescope	<i>R. G. Wheeler</i>	519
Dynamical Model for Fine Pointing Attitude Control of the Orbiting Astronomical Observatory	<i>R. E. Roberson</i>	529
Basic Response Relations for Satellite Attitude Control Using Gyros	<i>R. H. Cannon, Jr.</i>	535

REPORT

<i>W. E. Miller</i> (Chairman of the I.F.A.C. Technical Committee on Applications)		545
--	--	-----

COMPONENTS

New Design Principles and Control Devices—A survey	<i>J. L. Shearer and 16 co-authors</i>	549
--	--	-----

MECHANICAL, HYDRAULIC AND PNEUMATIC DEVICES

Mechanical, Hydraulic and Pneumatic Devices

A Hydraulic Torque Amplifier	<i>Y. Oshima and K. Araki</i>	572
A Rotary-drive Vibratory-output Gyroscopic Instrument	<i>G. C. Newton</i>	581
Some Problems of the Dynamics of a Hydraulic Throttle-control Servo-mechanism with an Inertial Load	<i>V. Khokhlov</i>	587
Realization of Sequential Machines by Means of Pneumatic Automation	<i>A. A. Tal</i>	593

ELECTROMECHANICAL DEVICES AND MAGNETIC AMPLIFIERS

Electromechanical Devices and Magnetic Amplifiers

Two-positional Functional Frequency Device for Automatic Regulation	<i>I. A. Maslaroff</i>	603
The Problems, Operation and Calculation of a New Component to be Applied in Certain Control Circuits	<i>O. Benedikt</i>	607
The Control of a Linear Electromagnetic Oscillating Mechanism	<i>J. C. West and B. V. Jayawant</i>	615
Step Motors with an Active Rotor	<i>Yu. K. Vasilev, Yu. A. Prokofiev and G. Ya. Wainberger</i>	622

ELECTRONIC COMPONENTS

Electronic Components

Some New Control Circuits Using Four-layer <i>p-n-p-n</i> Semiconductor Triodes	<i>J. Š. Haškovec and A. Klímek</i>	631
Turn-off Silicon Controlled Rectifiers	<i>H. F. Storm</i>	637
Ceramic Memories in Extreme Environments	<i>A. B. Kaufman</i>	646

DIGITAL DEVICES

Digital Devices

The Application of Digital Differential Analysers in Control Loops	<i>H. Rechberger</i>	652
Advantages and Possibilities of Digital Speed Control	<i>W. Fritzsche</i>	657
Digital Controllers	<i>T. M. Aleksandridi, S. N. Diligensky and H. K. Krug</i>	669

PROCESS INSTRUMENTATION

Various Components

A Universal Statistical Analyser	<i>J. Kryže</i>	676
The Behaviour of Adaptive Controllers	<i>J. L. Douce</i>	687
The Design Principles and Circuit of a Multi-channel Correlator—a Specialized Analogue Computer for the Statistical Treatment of Random Time Series in Industrial Control Systems	<i>A. S. Uskov and Yu. M. Orlov</i>	694

COMPONENT RELIABILITY

The Reliability of Components—A survey	<i>G. Glinski, B. S. Sotskov and H. Weissmann</i>	701
--	---	-----

Reliability

New Servovalves for Redundant Electrohydraulic Control	<i>K. D. Garnjost and W. J. Thayer</i>	709
The Reliability of Electronic Components	<i>G. W. A. Dummer</i>	715
Reliability Problems of Electromechanical Elements	<i>B. S. Sotskov, I. E. Dekabrun and L. S. Krivorotova</i>	728
A Study of Servomechanism Reliability in Nuclear Reactor and Plant Control Systems	<i>L. A. J. Lawrence and R. J. Scotcher</i>	736

REPORTS

<i>Gy. Boromisza</i> (Chairman of the I.F.A.C. Technical Committee On Components)	748
<i>Y. Oshima</i> (Vice-Chairman of the I.F.A.C. Technical Committee On Components)	749

List of contents of the volume on Theory

THEORY

Describing Function Technique

A New Method to Derive the Describing Function of Certain Non-linear Transfer Systems	<i>R. Lauber</i>
The Describing Function Method Applied for the Investigation of Parametric Excited Oscillations	<i>A. Leonhard</i>
On the Inverse Describing Function Problem	<i>J. E. Gibson and E. S. di Tada</i>
Relative Stability of Oscillations in Non-linear Control Systems	<i>Z. Bonenn</i>

Prediction Systems

Predictive Control of an On-Off System with Two Control Variables	<i>A. J. Adey, J. F. Coales and J. A. Stiles</i>
A Method of Prediction for Non-stationary Processes and Its Application to the Problem of Load Estimation	<i>E. D. Farmer</i>
On the Design of Predictor Control Systems	<i>S. Horing</i>
Method of Optimal Control Prediction	<i>F. B. Gul'ko and B. Ya. Kogan</i>

Non-linear Systems with Random Parameters

Optimalization of Non-linear Random Control Processes	<i>R. Kulikowski</i>
Non-linear Programming in the Investigation of Optimal Automatic Control Systems	<i>N. Y. Andreev</i>
Numerical Analysis of Non-linear Control Systems Using the Fokker-Planck-Kolmogorov Equation	<i>K. J. Merklinger</i>
Volterra Series Representation of Time-varying Non-linear Systems	<i>R. Flake</i>

Non-linear Stochastic Systems

The Application of Quasi-linear Methods to Non-linear Feedback Systems with Random Inputs	<i>H. W. Smith</i>
A Digital Procedure for the Study of Non-linear Systems for Random Processes	<i>T. Prasad and V. P. Sinha</i>
Time-optimal Systems with Random Noise Disturbances	<i>V. N. Novoseltsev</i>

DISCRETE SYSTEMS

Discrete Systems

Quasi-invariant Hybrid Multi-parameter Control Loops	<i>V. Strejc</i>
Optimum Control of Discrete-time Dynamic Processes	<i>B. Friedland</i>
Theory of Minimum Time Discrete Regulators	<i>C. A. Desoer, E. Polak and J. Wing</i>

Sampled-data Systems

On the Roots of a Real Polynomial Inside the Unit Circle and a Stability Criterion for Linear Discrete Systems	<i>E. I. Jury</i>
Analytical Approaches to Non-linear Sampled-data Control Systems	<i>B. Kondo and S. Iwai</i>
Continuous Compensation of Feedback Sampled-data Linear Control Systems	<i>B. M. Brown</i>
Fundamentals of the Theory of Non-linear Sampled-data Control Systems	<i>Ya. Z. Tsyppkin</i>
Synthesis of Optimum Sampled-data Systems	<i>L. N. Volgin</i>
Integral Pulse Frequency Modulated Control Systems	<i>C. C. Li and R. W. Jones</i>
Combination of Finite Settling Time and Minimum Integral of Squared Error in Digital Control Systems	<i>V. Peterka</i>

CONTENTS

Relay Systems

- Oscillations sous-harmoniques dans un asservissement par plus-ou-moins *J. C. Gille, S. Węgrzyn and J.-G. Paquet*
 Synthesis of Control Systems Operating Linearly for Small Signals and Approximately 'Bang-Bang' for Large Signals
 *E. V. Persson*
 Dual Input Systems with a Saturation Constraint *R. S. Gaylord*

Theory of Finite Automata

- Signalling and Prediction of Failures in Discrete Control Devices with Structural Redundancy *M. A. Gavrilov*
 Axiomatization of the Theory of Simplification of Combinational Automata *Gr. C. Moisil*
 Adaptive Control for a System with a Finite Number of States *S. Pashkovski*

OPTIMAL SYSTEMS

- Synthesis of Optimal Regulators—A survey *A. M. Letov*

Optimal Systems

- Approximation Methods in Optimal and Adaptive Control *J. H. Westcott and J. J. Florentin*
 An Optimal Guidance Approximation for Quasi-circular Orbital Rendezvous *J. D. Pearson, H. J. Kelly and J. C. Dunn*
 On Synthesizing Optimal Controls *L. W. Neustadt and B. Paiewonsky*
 An Application of Optimal Control to Midcourse Guidance *J. S. Meditch and L. W. Neustadt*
 On Necessary and Sufficient Conditions for Time-optimal Control of Second-order Non-linear Systems *E. B. Lee and L. Markus*
 On Optimal Control of Systems with Multi-norm Constraints *P. E. Sarachik and G. M. Kranc*
 The Approximate Calculation of a Class of Automatic Systems with Forced Parameter Optimization *Yu. I. Alimov*

Optimal Systems with Distributed Parameters

- Some Considerations on Optimized Integrated Control *R. Marcacci*
 Optimal Processes in Systems with Time Lag *N. N. Krasovskiy*
 Optimal Control of Systems with Distributed Parameters *A. G. Butkovskiy*

Synthesis of Optimum Systems

- Solution of Optimum Control Problems by Using Pontryagin's Maximum Principle *Y. Sakawa and Ch. Hayashi*
 Analysis and Synthesis of Time-optimal Control Systems *Sun Jian and Hang King-ching*
 Development of Dynamic Programming Techniques and Their Application to Optimal Systems Design *R. L. Stratonovich*
 A Modified Maximum Principle for Optimum Control of a System with Bounded Phase Space Coordinates *S. S. L. Chang*
 Optimum and Quasi-optimum Control of Third and Fourth Order Systems *I. Flügge-Lotz and H. A. Titus, Jr.*

Optimal Programming

- Programme Control and the Theory of Optimal Systems *Ye. A. Barbashin*
 The Realization of Optimal Programmes in Control Systems *G. S. Pospelov*
 Some Bounds on Quantization Errors in Dynamic Programming Computations *J. J. G. Guignabodet*

CONTENTS

THEORY OF SELF-ADJUSTING SYSTEMS

Adaptive and Self Optimizing Systems—A survey	<i>J. Truxal</i>
Learning Systems—A survey	<i>G. Pask</i>

Invariancy Problems

Invariance of Sampled Data and Adaptive Sampled-data Systems	<i>V. M. Kuntsevich and Yu. V. Krementulo</i>
Optimization and Invariance in Control Systems with Constant and Variable Structure	<i>B. N. Petrov, G. M. Ulanov and S. V. Emelyanov</i>
Synthesis of Systems with Fixed Characteristics of Equivalent Self-adjusting Systems	<i>M. V. Meyerov</i>

Self-adapting Systems

A Comparison of the Measuring Time in Self-adjusting Control Systems	<i>F. Mesch</i>
Adaptive Control Systems without Trial Input Signals	<i>E. P. Popov, G. M. Loskutov and R. M. Yusupov</i>
A Contribution to the Use of Self-adjusting Systems for the Mechanical Synthesis of Control Systems	<i>V. K. Chichinadze and O. A. Charkviani</i>
On the Searching of Extrema of Functions in Automatic Control Systems	<i>A. A. Voronov and M. B. Ignatjev</i>
Dominant Operators' Approach to the Theory of Adaptive Control Systems	<i>A. Straszak</i>
General Stability Analysis of Sinusoidal Perturbation Extrema Searching Adaptive Systems	<i>V. W. Eveleigh</i>
The Realization of a Self-adapting Control Programme in a System with a Digital Calculating Machine	<i>P. F. Klubnikin</i>

Learning Systems

A Pattern Recognizing Adaptive Controller	<i>W. K. Taylor</i>
STELLA: A Scheme for a Learning Machine	<i>J. H. Andreae</i>
Automatic Control Learning Systems (in the Light of Experiments on Teaching the Systems to Pattern Recognition)	<i>M. A. Aizerman</i>

Hill-climbing Technique

On the Theory of Self-tuning Systems with a Search for Gradient by the Method of Auxiliary Operator	<i>I. E. Kasakov and L. G. Evlanov</i>
Problems of Continuous Systems Theory of Extreme Control of Industrial Processes	<i>A. A. Krasovskii</i>
Principle and Application of an Extremal Computer	<i>R. Perret and R. Rouxel</i>
Dual Control Theory Problems	<i>A. A. Feldbaum</i>
The Application of Random Test Signals in Process Optimization	<i>P. M. E. M. van der Grinten</i>

TECHNIQUES FOR SYSTEM STABILITY ASSESSMENT

Liapunov's Stability Problem

A New Concept of Stability	<i>J. P. LaSalle and R. J. Rath</i>
Non-linear Stability Analysis for Restricted Non-linearities Using the Second Method of Liapunov	<i>H. Nour-Eldin</i>
The Use of the Technique of Linear Bounds for Applying the Direct Method of Liapunov to a Class of Non-linear and Time-varying Systems	<i>R. A. Nesbit</i>
On the Estimation of the Decaying Time	<i>L. Hwang</i>
New Methods for Constructing Liapunov Functions for Time-invariant Control Systems	<i>G. P. Szegö</i>
A Method of Investigating Stability	<i>H. H. Rosenbrock</i>

CONTENTS

SYSTEM DYNAMICS AND OTHER PROBLEMS

Process Dynamics and its Application to Industrial Process Design and Process Control—A survey *T. J. Williams*

System Dynamics

Determination of System Dynamics by Use of Adjustable Models *E. Blandhol and J. G. Balchen*

Les erreurs systématiques et aléatoires dans la détermination expérimentale des fonctions de transfert *J. Loeb*

The Applicability of the Relay Correlator and the Polarity Coincidence Correlator in Automatic Control
B. P. Th. Veltman and A. van den Bos

Notes sur une Fonction Aléatoire d'Aspect Physique *M. Pélégryn*

An Uncertainty Relation for Linear Mathematical Models *B. Qvarnström*

General Problems

Axiomatic Foundation of the Theory of Control Systems *E. Roxin*

The Inverse Problem of Integral Square Estimation of Transient Responses *W. Jaromínek*

On Systems with Automatic Control of Configuration *J. Beneš*

Approximation of Industrial Control Systems for Optimized Non-linear Control with Restricted Rate of Correction Using Conventional Controllers *E. Pavlik*

Nouvelle procédure d'optimisation statistique fondée sur la transformation $V = (Z - 1)/(Z + 1)$ *P. M. Lefevre*

The Control of Two Output-dependant Processes *C. N. Kerr and G. D. S. MacLellan*

REPORTS

Academician B. N. Petrov (Chairman of the I.F.A.C. Technical Committee on Theory)

Professor J. H. Westcott (Vice-Chairman of the I.F.A.C. Technical Committee on Theory)

TABLE DES MATIÈRES

LISTE DES AUTEURS	V
AVANT-PROPOS	XXXI

EXPOSÉS INTRODUCTIFS

ALLOCUTION DE BIENVENUE	PROFESSEUR ED. GERECKE (Président de l'I.F.A.C.)	XXXV
COMMENT L'I.F.A.C. A-T-ELLE ÉTÉ FONDÉE	H. CHESTNUT (Premier Président de l'I.F.A.C. 1957-1959)	XXXVI
LE PREMIER CONGRÈS DE L'I.F.A.C.	PROFESSEUR A. M. LETOV (Deuxième Président de l'I.F.A.C. 1959-1961)	XXXVII
L'ÉVOLUTION DE MÉTHODES D'INFORMATION ET SA RÉPERCUSSION SUR LES MÉTHODES DE COMMANDE AUTOMATIQUE	J. L. AUERBACH (Président de l'I.F.I.P.)	XXXVIII

APPLICATIONS

PRODUCTION, TRANSPORT ET DISTRIBUTION DE L'ÉNERGIE ÉLECTRIQUE

Les applications de la commande automatique dans les systèmes de production, de transport et de distribution de l'énergie électrique— Une synthèse	B. Favez	5
Production, transport et distribution de l'énergie électrique		
Mise au point d'une méthode pour la commande cybernétique de systèmes énergétiques électriques intégrés V. A. Venikov et L. V. Tsukernik		20
Quelques résultats récents dans la commande de systèmes énergétiques au moyen de calculateurs T. Vámos, S. Benedikt et M. Uzsoki		33
Commande optimale du fonctionnement de systèmes thermohydrauliques	L. K. Kirchmayer et R. J. Ringlee	41
Systèmes automatiques avec éléments à apprentissage	G. K. Krug et A. V. Netushil	51
Principes et réalisations des automatismes liés à la manutention de combustible d'un réacteur nucléaire	P. Turpin et J. Thilliez	59
Une étude de la dynamique de formation des bulles de vapeur dans les réacteurs nucléaires à eau bouillante P. K. M'Pherson et M. Muscettola		70
Le réglage des systèmes hydrauliques		
Le réglage optimal de systèmes de production hydro-électriques	H. Ruge	82
Exposé d'une méthode d'élaboration de graphiques exprimant les conditions de stabilité du réglage d'un groupe hydro-électrique	A. Tschumy	87
Étude au moyen de calculateurs numériques de systèmes de production d'énergie à machines multiples	H. Glavitsch	98
Commande des machines de production d'énergie électrique		
Commande optimale de turbines hydrauliques compte tenu des non-linéarités de la vitesse du servo-moteur	Th. Stein	104
Equations de commande d'une centrale hydro-électrique avec des valeurs de référence fixes	L. Borel	110

TABLE DES MATIÈRES

INDUSTRIE SIDERURGIQUE

Applications de l'automatisation et des techniques au laminage et au traitement des métaux — Une synthèse	<i>W. E. Miller</i>	117
Résultats obtenus par l'automatisation et la sidérurgie — Une synthèse	<i>A. Ya. Lerner</i>	126
Commande de la préparation de mélanges à agglomérer	<i>G. DeGregorio, G. Litigio et G. Sironi</i>	132
Planification dynamique d'une aciérie avec fours à sole	<i>M. Korobko et Yu. Samoilenko</i>	149
L'automatisation du forgeage de grosses pièces	<i>J. G. Wistreich et A. Tomlinson</i>	157
L'automatisation d'une aciérie avec référence particulière à l'emploi de calculateurs numériques pour la préparation de la production et la transmission des informations	<i>S. E. Hersom et R. G. Massey</i>	167
Commande d'un laminoir de finissage de bandes d'acier à chaud au moyen de calculateurs en ligne	<i>R. G. Beadle</i>	179
Commande optimale de processus continus	<i>A. Ya. Lerner</i>	191
Un système optimal numérique de commande programmée et son application au mécanisme de serrage d'un laminoir de blooming	<i>S. M. Domanitsky, V. V. Imedadze et Sh. A. Tsintsadze</i>	200
Système de commande du processus de recuit continu au moyen d'un calculateur	<i>J. T. Bradford, Jr.</i>	214

LES INDUSTRIES DE LA CHIMIE ET DU PÉTROLE

Une synthèse de l'application aux industries de la chimie et du pétrole	<i>H. W. Slotboom, J. de Jong, I. E. Rijnsdorp</i>	222
Caractéristiques dynamiques d'une colonne de distillation binaire	<i>K. Izawa et T. Morinaga</i>	229
Modèles approximatifs de la réponse dynamique de grandes colonnes de distillation	<i>J. S. Moczek, R. E. Otto et T. J. Williams</i>	238
Une étude du comportement dynamique d'un système de récupération d'énergie de cracking catalytique au moyen d'un calculateur analogique	<i>C. A. J. M. van der Heyden et A. G. van Nes</i>	249
Analyse statistique d'un nouveau système de réglage de débits de fluides	<i>R. C. Booton, Jr. et W. E. Sollecito</i>	261
Effets du mélange de fluides et de ses expressions sur la dynamique du processus de transfert des masses	<i>T. Takamatsu et E. Nakanishi</i>	269
Etude expérimentale du comportement dynamique d'un échangeur de chaleur et d'un processus de mélange	<i>L. Delvaux</i>	275
Etude de la production industrielle du polyéthylène sous des hautes pressions et du réglage automatique de ce processus	<i>B. V. Volter</i>	290
Etude des caractéristiques statiques et dynamiques de processus de distillation fractionnée	<i>I. V. Anisimov</i>	300
Adaptabilité au réglage et capacité admissible du compresseur d'un système de récupération d'un gaz inflammable	<i>F. J. Kylstra</i>	309
Analyse et étude d'un système adaptatif à perturbation de paramètres pour son application au réglage de processus	<i>T. Isobe et T. Totani</i>	317
Propriétés dynamiques de stations de rectification avec des colonnes à plateaux	<i>T. Závorka</i>	326
Une réalisation originale dans une raffinerie de pétrole: le chargement automatique des wagons citernes	<i>F. X. Montjean</i>	335

AUTOMATISATION DES PROCESSUS INDUSTRIELS

Le traitement du problème d'optimisation par A 110	<i>E. Honoré</i>	341
Automatisation d'une usine de ciment Portland au moyen d'un calculateur numérique de commande	<i>R. A. Phillips</i>	347
Sur la stabilité et l'étude de systèmes adaptatifs à oscillations exploratrices	<i>R. K. Smyth et N. Nahi</i>	358
Réglages des systèmes à vapeur		
Predétermination des résultats du réglage des résurchauffeurs de générateur de vapeur	<i>W. Kindermann</i>	369
Une optimisation du rendement de chaudières	<i>S. Fujii et N. Kanda</i>	380
Un simulateur de turbines à vapeur avec résurchauffe ou extraction réglée automatiquement	<i>H.-J. Ehling</i>	390
Un système de réglage électro-hydraulique de turbines à résurchauffe	<i>M. A. Eggenberger et P. H. Troutman</i>	398
Industries des moteurs		
Une application industrielle d'un calculateur intérieur à un circuit de commande: l'équipement électronique de commande d'une machine à équilibrer les vilebrequins	<i>J. Csech</i>	408
Analyse d'un système de réglage automatique de la vitesse d'un moteur	<i>W. H. Holl</i>	415

TABLE DES MATIÈRES

SYSTÈMES COMBINES HOMME-MACHINE

Modèles continus et échantillonnés de l'opérateur humain placé dans une boucle de commande	<i>P. Naslin et J.-C. Raoult</i>	421
Modèles discrets de l'opérateur humain dans un système de commande	<i>G. E. Bekey</i>	430
Analyse dynamique et simulation des fonctions de commande d'une direction d'entreprise	<i>R. B. Wilcox</i>	439
Esquisse d'une théorie de commande automatique de prothèses	<i>R. Tomovic</i>	449
Un modèle échantillonné des mouvements de poursuite de l'oeil	<i>L. R. Young</i>	454

TECHNIQUES D'APPLICATION

Méthodes

Méthode auto-adaptative permettant de tenir compte de grandes variations du gain du système réglé dans les systèmes de commande	<i>R. J. Kochenburger</i>	464
Dynamique des lignes de transmission hydrauliques	<i>R. Oldenburger et R. E. Goodson</i>	472
L'optimisation des systèmes de commande par ordinateur utilisant une connaissance partielle de l'état de la grandeur de sortie	<i>B. G. Anderson</i>	480

AUTOMATIQUE DES SYSTÈMES AERO-SPATIAUX

Systèmes aéro-spatiaux

Etude d'un système de réglage de la pression pour une soufflante de 1,50 m sur 1,50 m	<i>J. A. Tanner et W. Dietiker</i>	487
Simulation de l'ambiance de l'engin spatial pour une installation d'essais de moteurs de fusées	<i>G. J. Fiedler et J. J. Landy</i>	496
Système de pilotage automatique longitudinal d'atterrissage d'avion sans visibilité	<i>F. J. Ellert et C. W. Merriam III</i>	504
Commande automatique d'une grande antenne mobile de télécommunication avec des satellites	<i>F. J. D. Taylor</i>	512
Etude d'un système de commande automatique d'un radio-télescope de 63 m.	<i>R. G. Wheeler</i>	519
Modèle dynamique pour la commande d'altitude à visée fine de l'observatoire astronomique placé sur une orbite	<i>R. E. Roberson</i>	529
Relations fondamentales de réponse pour la commande d'altitude de satellites utilisant des gyroscopes	<i>R. H. Cannon, Jr.</i>	535

RAPPORT

<i>W. Miller</i> (Président du Comité Technique des Applications)	545
---	-----

LES COMPOSANTS

Nouveaux principes d'étude et dispositifs de commande — Une synthèse réalisée	<i>J. L. Shearer et 16 autres auteurs</i>	549
---	---	-----

DISPOSITIFS MECANIKES, HYDRAULIQUE DE COUPLE

Un amplificateur hydraulique de couple	<i>Y. Oshima et K. Araki</i>	572
Un instrument gyroscopique à entraînement rotatif et à signal de sortie vibratoire	<i>G. C. Newton</i>	581
Quelques problèmes de la dynamique d'un servo-mécanisme hydraulique à commande par laminage et charge inertielle	<i>V. Khokhlov</i>	587
Réalisation de machines séquentielles avec des moyens pneumatiques	<i>A. A. Tal</i>	593

DISPOSITIFS ÉLECTRO-MÉCANIQUES ET AMPLIFICATEURS MAGNÉTIQUES

Dispositif fréquentiel fonctionnel à deux positions pour le réglage automatique	<i>I. A. Maslaroff</i>	603
Les problèmes, le fonctionnement et le calcul d'un nouveau composant destiné à être appliqué dans certains circuits de commande	<i>O. Benedikt</i>	607
Le commande d'un mécanisme oscillant électro-magnétique linéaire	<i>J. C. West et B. V. Jayawant</i>	615
Moteurs pas-à-pas à rotor actif	<i>Yu. K. Vasilev, Yu. A. Prokofiev et G. Ya. Vainberger</i>	622

TABLE DES MATIÈRES

COMPOSANTS ÉLECTRONIQUES

Quelques nouveaux circuits de commande utilisant des triodes semiconductrices à quatre couches du type $p-n-p-n$	<i>J. Š. Haškovec et A. Klímek</i>	631
Redresseurs commandés au silicium à commutation	<i>H. F. Storm</i>	637
Mémoires céramiques dans les ambiances extrêmes	<i>A. B. Kaufman</i>	646

DISPOSITIFS NUMÉRIQUES

L'utilisation des analyseurs différentiels numériques dans les boucles de réglage	<i>H. Rechberger</i>	652
Avantages et possibilités du réglage numérique des vitesses	<i>W. Fritzsche</i>	657
Les régulateurs numériques	<i>T. M. Aleksandridi, K. S. N. Diligensky et H. K. Krug</i>	669

INSTRUMENTATION DE PROCESSUS

Composants divers

Un analyseur statistique universel	<i>J. Krýže</i>	676
Le comportement des régulateurs adaptatifs	<i>J. L. Douce</i>	687
Les principes d'étude et le circuit d'un corrélateur à canaux multiples — un calculateur analogique spécialisé pour le traitement statistique des séries temporelles aléatoires dans les systèmes de commande industrielle	<i>A. S. Uskov et Yu. M. Orlov</i>	694

FIABILITÉ DES COMPOSANTS

La fiabilité des composants — Une synthèse	<i>G. S. Glinski, B. S. Sotskov et H. Weissmann</i>	701
--	---	-----

La fiabilité

Nouvelles servo-valves pour la commande électro-hydraulique surabondante	<i>K. D. Garnjost et W. J. Theyer</i>	709
La fiabilité des composants électroniques	<i>G. W. A. Dummer</i>	715
Problèmes de la fiabilité d'éléments électro-mécaniques	<i>B. S. Sotskov, I. E. Dekabrun et L. S. Krivorotova</i>	728
Une étude de la fiabilité des servomécanismes dans les systèmes de commande des réacteurs et des centrales nucléaires	<i>L. A. J. Lawrence et R. J. Scotcher</i>	736

RAPPORTS

<i>Gy. Boromisza</i> (Président du Comité Technique des Composants)	748
<i>Y. Oshima</i> (Vice-Président du Comité Technique des Composants)	749

Table des matières du volume Théorie

THÉORIE

La théorie des systèmes non-linéaires

Les méthodes statistiques dans la commande automatique — Une synthèse *V. S. Pugachev*

Technique de la fonction descriptive

Une nouvelle méthode de détermination de la fonction descriptive de certains systèmes de transfert non-linéaires *R. Lauber*

Application de la méthode de la fonction descriptive à l'étude d'oscillations forcées paramétriques *A. Leonhard*

Sur le problème de la fonction descriptive inverse *J. E. Gibson et E. S. di Tada*

La stabilité relative d'oscillations de systèmes non-linéaires *Z. Bonenn*

Systèmes d'anticipation

La commande anticipante d'un système à deux variables par tout ou rien *A. J. Adey, J. F. Coales et J. A. Stiles*

Une méthode d'anticipation de processus non-stationnaires et son application au problème de l'analyse des variations de charge
E. D. Farmer

Sur le calcul des systèmes de commande à anticipation *S. Horing*

Méthode d'optimisation avec anticipation *F. B. Gul'ko et B. Ya. Kogan*

Systèmes non-linéaires à paramètres aléatoires

Optimisation de processus de commande non-linéaires aléatoires *R. Kulikowski*

La programmation non-linéaire dans l'étude des systèmes de commande optimaux *N. Y. Andreev*

Analyse numérique des systèmes de commande non-linéaires par l'emploi de l'équation de Fokker-Planck-Kolmogorov
K. J. Merklinger

La représentation au moyen de séries de Volterra de systèmes non-linéaires variant avec le temps *R. Flake*

Systèmes aléatoires non-linéaires

L'application de méthodes quasi-linéaires aux systèmes asservis non-linéaires à grandeurs d'entrée aléatoires *H. W. Smith*

Une méthode numérique d'étude de systèmes non-linéaires pour processus aléatoires *T. Prasad et V. P. Sinha*

Systèmes d'optimisation selon le temps avec perturbations de bruits aléatoire *V. N. Novoseltsev*

SYSTÈMES DISCRETS

Systèmes d'asservissement hybrides quasi-invariants à paramètres multiples *V. Strejc*

Optimisation de processus dynamiques à temps discret *B. Friedland*

Théorie des régulateurs discrets à minimum de temps *C. A. Desoer, E. Polak et J. Wing*

Systèmes échantillonnés

Sur les racines d'un polynôme réel à l'intérieur du cercle unitaire et un critère de stabilité pour systèmes discrets linéaires *E. I. Jury*

Manières analytiques d'envisager les systèmes de commande échantillonnés non-linéaires *B. Kondo et S. Iwai*

Compensation continue des systèmes de réglage échantillonnés linéaires *B. M. Brown*

Les fondements de la théorie des systèmes de commande échantillonnés non-linéaires *Ya. Z. Tsyarkin*

La synthèse des systèmes échantillonnés optimaux *L. N. Volgin*

Systèmes de commande à modulation par la fréquence d'impulsions intégrale *C. C. Li et R. W. Jones*

Combinaison du temps d'établissement fini et du minimum du carré moyen de l'erreur de réglage dans les systèmes de commande numériques *V. Peterka*

TABLE DES MATIÈRES

Systèmes à relais

Oscillations sous-harmoniques des asservissements par plus-ou-moins	<i>J. C. Gille, S. Wegrzyn et J.-G. Paquet</i>
Synthèse des systèmes de commande fonctionnant d'une manière linéaire pour les faibles signaux et d'une manière discontinue pour les signaux importants	<i>E. V. Persson</i>
Systèmes à deux entrées avec une contrainte de saturation	<i>R. S. Gaylord</i>

Théorie des automates à positions multiples

Signalisation et prévision de pannes dans les dispositifs de commande discrète à surabondance de moyens inhérente	<i>M. A. Gavrilov</i>
Axiomatisation de la théorie de simplification des automates combinatoires	<i>Gr. C. Moisil</i>
Commande adaptative d'un système présentant un nombre fini d'états	<i>S. Pashkovski</i>

THÉORIE DES SYSTÈMES OPTIMAUX

Synthèse des régulateurs optimaux — Une synthèse	<i>A. M. Letov</i>
--	--------------------

Systèmes optimaux

Méthodes d'approximation dans la commande optimale et adaptative	<i>J. H. Westcott, J. J. Florentin et J. D. Pearson</i>
Une approximation optimale de guidage pour le rendez-vous de deux satellites sur une orbite quasi-circulaire	<i>H. J. Kelly et J. C. Dunn</i>
Sur la synthèse des commandes optimales	<i>L. W. Neustadt et B. H. Paiewonsky</i>
Une application de la commande optimale au guidage d'engins à mi-course	<i>J. S. Meditch et L. W. Neustadt</i>
Sur les conditions nécessaires et suffisantes pour l'optimalisation selon le temps de systèmes non-linéaires du second ordre	<i>E. B. Lee et L. Markus</i>
L'optimalisation des systèmes de commande avec contraintes à normes multiples	<i>P. E. Sarachik et G. M. Kranc</i>
Le calcul approximatif d'une catégorie de systèmes automatiques avec optimalisation forcée des paramètres	<i>Yu. I. Alimov</i>

Systèmes optimaux à paramètres repartis

Quelques considérations sur la commande optimisée intégrée	<i>R. Marcacci</i>
Processus optimaux dans les systèmes avec constantes de temps	<i>N. N. Krasovskiy</i>
Commande optimale des systèmes à paramètres repartis	<i>A. G. Butkovskiy</i>

Synthèse des systèmes optimaux

Solution des problèmes d'optimalisation en utilisant le principe du maximum de Pontryagin	<i>Y. Sakawa et Ch. Hayashi</i>
Analyse et synthèse des systèmes d'optimalisation selon le temps	<i>Sun Jian et Hang King-ching</i>
Développement des techniques de programmation dynamique et leurs applications à l'étude des systèmes optimaux	<i>R. L. Stratonovich</i>
Un principe du maximum modifié pour l'optimalisation d'un système dont les cordonnées dans l'espace de phase sont limitées	<i>S. S. L. Chang</i>
Commande optimale et quasi-optimale de systèmes du troisième et du quatrième ordres	<i>I. Flügge-Lotz et H. A. Titus, Jr.</i>

Programmation optimale

Commande programmée et théorie des systèmes optimaux	<i>Ye. A. Barbashin</i>
La réalisation de programmes optimaux dans les systèmes de commande	<i>G. S. Pospelov</i>
Quelques limites des erreurs de quantification dans les calculs numériques de la programmation dynamique	<i>J. J. Guignabodet</i>

THÉORIE DES SYSTÈMES A AUTO-RÉGLAGE

Systèmes adaptatifs et à auto-optimalisation — Une synthèse	<i>J. Truxal</i>
Systèmes à apprentissage — Une synthèse	<i>G. Pask</i>

Problèmes d'invariance

L'invariance des systèmes échantillonnés et des systèmes adaptatifs échantillonnés	<i>V. M. Kuntsevich et Yu. V. Krementulo</i>
L'optimalisation et l'invariance des systèmes de commande à structures constante et variable	<i>B. N. Petrov, G. M. Ulanov et S. V. Emelyanov</i>
Synthèse de systèmes avec les caractéristiques fixes des systèmes à auto-réglage équivalents	<i>M. V. Meyerov</i>

TABLE DES MATIÈRES

Systèmes auto-adaptatifs

- Une comparaison du temps de mesure dans les systèmes de commande à auto-réglage *F. Mesch*
 Systèmes de commande adaptative sans signaux d'entrée explorateurs *E. P. Popov, G. M. Loskutov et R. M. Yusupov*
 Une contribution à l'utilisation des systèmes à auto-réglage pour la synthèse mécanique des systèmes de commande
 *V. K. Chichinadze et O. A. Charkviani*
 Sur la recherche des valeurs extrémales de fonctions dans les systèmes de commande automatique *A. A. Voronov et M. B. Ignatjev*
 Méthode de la théorie des systèmes de commande adaptative utilisant les opérateurs dominants *A. Straszak*
 Analyse générale de la stabilité des systèmes adaptatifs avec recherche des valeurs extrémales au moyen de perturbations sinusoïdales
 *V. W. Eveleigh*
 La réalisation d'un programme de commande auto-adaptatif dans un système au moyen d'un calculateur numérique *P. F. Klubnikin*

Systèmes à apprentissage

- Un régulateur adaptatif identifiant les espèces *W. K. Taylor*
 STELLA: le schéma d'une machine à apprentissage *J. H. Andreae*
 Systèmes de commande automatique à apprentissage (à la lumière des expériences rendant les systèmes aptes à identifier les espèces)
 *M. A. Aizerman*

Techniques de recherche de valeurs extrémales successives

- Sur la théorie des systèmes à accord automatique avec une recherche du gradient par la méthode de l'opérateur auxiliaire
 *L. E. Kasakov et L. G. Evlanov*
 Problèmes de la théorie des systèmes continus de commande extrême de processus industriels *A. A. Krasovski*
 Principe et application d'un calculateur extrême *R. Perret et R. Rouxel*
 Problèmes de la théorie de la commande double *A. A. Feldbaum*
 Application des signaux explorateurs aléatoires à l'optimalisation de processus *P. M. E. M. van der Grinten*

TECHNIQUES D'ÉVALUATION DE LA STABILITÉ DE SYSTÈMES

Problème de stabilité de Liapunov

- Un nouveau concept de stabilité *J. P. LaSalle et R. J. Rath*
 Analyse non-linéaire de la stabilité des non-linéarités restreintes en utilisant la seconde méthode de Liapunov *H. Nour-Eldin*
 L'utilisation de la technique des contraintes linéaires pour l'application de la méthode directe de Liapunov à une catégorie de systèmes
 non-linéaires et de systèmes variant en fonction du temps *R. A. Nesbit*
 Estimation du temps d'amortissement *L. Hwang*
 Nouvelles méthodes pour la détermination des fonctions de Liapunov pour des systèmes de commande invariants dans le temps
 *G. P. Szegö*
 Une méthode d'investigation de la stabilité *H. H. Rosenbrock*

DYNAMIQUE DES SYSTÈMES ET AUTRES PROBLÈMES

- Dynamique des processus et son application à l'étude et à la commande des processus industriels — Une synthèse *T. J. Williams*

Dynamique des systèmes

- Détermination de la dynamique des systèmes en utilisant des modèles réglables *E. Blandhol et J. G. Balchen*
 Les erreurs systématiques et aléatoires dans la détermination expérimentale des fonctions de transfert *J. Loeb*
 L'applicabilité du corrélateur à relais et du corrélateur à coïncidence de polarités dans la commande automatique
 *B. P. Th. Veltman et A. van den Bos*
 Notes sur une fonction aléatoire d'aspect physique *M. Pélégryn*
 Une relation d'incertitude pour les modèles mathématiques linéaires *B. Qvarnström*

Problèmes généraux

- Les fondements axiomatiques de la théorie des systèmes de commande *E. Roxin*
 Le problème inverse de l'estimation quadratique moyenne des réponses transitoires *W. Jarominek*
 Sur les systèmes à commande automatique de la configuration *J. Beneš*

TABLE DES MATIÈRES

Approximation des systèmes de commande automatique industrielle pour l'optimalisation non-linéaire à vitesse de correction limitée utilisant des régulateurs conventionnels	<i>E. Pavlik</i>
Nouvelle procédure d'optimisation statistique fondée sur la transformation $V = (Z - 1)/(Z + 1)$	<i>P. M. Lefevre</i>
La commande de processus dépendant de deux grandeurs de sortie	<i>C. N. Kerr et G. D. S. MacLellan</i>

RAPPORTS

<i>Académicien B. N. Petrov</i> (Président du Comité de Théorie)	
<i>Professeur J. H. Westcott</i> (Vice-Président du Comité de Théorie)	

INHALT

VERZEICHNIS DER VERFASSEN	V
MITTEILUNG DER HERAUSGEBER	XXXI

ANSPRACHEN

BEGRÜSSUNG	PROFESSOR ED. GERECKE (Präsident der International Federation of Automatic Control)	XXXV
WIE ES ZUR GRÜNDUNG DES IFAC KAM	H. CHESTNUT (1. Präsident des IFAC, 1957-1959)	XXXVI
DER 1. IFAC-KONGRESS	PROFESSOR A. M. LETOV (2. Präsident des IFAC, 1959-1961)	XXXVII
DIE ENTWICKLUNG DER NACHRICHTENÜBERTRAGUNG UND IHR EINFLUSS AUF DIE REGELUNG	J. L. AUERBACH (Präsident der International Federation of Information Processing Societies)	XXXVIII

ANWENDUNGEN

AUF DEM GEBIET DER ELEKTRISCHEN ENERGIEVERSORGUNG

Die Regelung in elektrischen Netzen — Übersichtsvortrag	B. Favez	5
Elektrizitätswerke und Lastverteilung		
Entwicklung eines Verfahrens zur Regelung großer Verbundnetze nach kybernetischen Gesichtspunkten	V. A. Venikow und L. V. Tsukernik	20
Einige neuere Ergebnisse in der Steuerung der Lastverteilung durch Rechner	T. Vámos, S. Benedikt und M. Uzsoki	33
Optimalregelung eines Verbundnetzes von Wärme- und Wasserkraftwerken	L. K. Kirchmayer und R. J. Ringlee	41
Energieerzeugung		
Über Regelsysteme mit lernfähigen Elementen	G. K. Krug und A. V. Netushil	51
Prinzip und Konstruktion von Mechanismen zur Steuerung der Brennelemente in einem Kernreaktor	P. Turpin und J. Thilliez	59
Eine Untersuchung der Dynamik der Blasenverteilung in Siedewasserreaktoren	P. K. M'Pherson und M. Muscettola	70
Regelung im Wasserkraftwerk		
Über die optimale Regelung von Wasserkraftwerken	H. Ruge	82
Vorschlag für ein Verfahren zur Ermittlung der Stabilitätsbedingungen der Regelung eines Wasserkraftwerks	A. Tschumy	87
Die Untersuchung des Verhaltens von Generatorgruppen mittels eines Digitalrechners	H. Glavitsch	98
Regelung der Kraftmaschinen im Elektrizitätswerk		
Optimale Auslegung der Regler für Wasserturbinen unter Berücksichtigung der Nichtlinearität im Stellmotor	Th. Stein	104
Die Regelgleichungen eines Wasserkraftwerkes bei festen Bezugswerten	L. Borel	110

INHALT

STAHLINDUSTRIE

Anwendung der Automatisierung auf den Walzwerksbetrieb — Übersichtsvortrag	<i>W. E. Miller</i>	117
Fortschritte in der Automatisierung der Stahlindustrie — Übersichtsvortrag	<i>A. Ya. Lerner</i>	126
Stahlindustrie		
Regelung beim Aufbereiten einer Sintermischung	<i>G. DeGregorio, G. Litigio und G. Sironi</i>	132
Dynamisches Programmieren im Siemens-Martin-Ofen	<i>M. Korobko und Yu. Samoilenko</i>	149
Automatisierung von Schmiedepressen	<i>J. G. Wistreich und A. Tomlinson</i>	157
Die Automatisierung in einem Hüttenwerk mit dem Einsatz eines Digitalrechners zur Steuerung des Produktionsablaufs und der Datenübertragung	<i>S. E. Hersom und R. G. Massey</i>	167
Über den Einsatz eines „On-line“-Prozeßrechners in einer Warmband-Fertigungsstraße.	<i>R. G. Beadle</i>	179
Optimalwertregelung von Bandprozessen	<i>A. Ya. Lerner</i>	191
Eine digitale Programmsteuerung und ihre Anwendung auf die Regelung der Walzenanstellung in einer Block-Brammenstraße <i>S. M. Domanitsky, V. V. Imedadze und Sh. A. Tsintsadze</i>		200
Die Steuerung einer kontinuierlichen Glühstraße durch einen Prozeßrechner	<i>J. T. Bradford, Jr.</i>	214

CHEMISCHE UND ERDÖL-INDUSTRIE

Eine Übersicht über die Anwendung der Regelung in der chemischen Großindustrie und Erdölaufbereitung <i>H. W. Slotboom, J. de Jong und I. E. Rijnsdorp</i>		222
Chemische und Erdöl-Industrie		
Dynamische Kenngrößen der Zweistoff-Trennkolonnen	<i>K. Izawa und T. Morinaga</i>	229
Näherungsmodelle für das dynamische Verhalten großer Trennkolonnen	<i>J. S. Moczek, R. E. Otto und T. J. Williams</i>	238
Über das dynamische Verhalten des Systems zur Energierückgewinnung einer Krackanlage mit Hilfe eines Analogrechners <i>C. A. J. M. van der Heyden und A. G. van Nes</i>		249
Entwicklung eines neuartigen Verfahrens zur Messung des Durchflusses von Flüssigkeiten	<i>R. C. Booton, Jr., und W. E. Sollecito</i>	261
Über Effekte, die bei der Mischung von Flüssigkeiten auftreten, und ihre Auswirkung auf das dynamische Verhalten von Anlagen mit Stofftransport	<i>T. Takamatsu und E. Nakanishi</i>	269
Experimentelle Untersuchungen zum dynamischen Verhalten eines Wärmetauschers und eines Misch-Prozesses	<i>L. Delvaux</i>	275
Untersuchung einer Anlage zur Polymerisation von Äthylen unter hohem Druck und die zugeordneten Regelprobleme	<i>B. V. Volter</i>	290
Eine Berechnung der dynamischen und statischen Kenngrößen von Anlagen zur fraktionierten Destillation	<i>I. V. Anisimow</i>	300
Über die Regelfähigkeit und zulässige Kompressorleistung einer Anlage zur Abgas-Wiedergewinnung	<i>F. J. Kylstra</i>	309
Analyse und Entwurf eines für die Verfahrensregelung geeigneten, selbsteinstellenden Systems mit Parametersteuerung <i>T. Isobe und T. Totani</i>		317
Die dynamischen Eigenschaften von Rektifizierkolonnen	<i>T. Závorka</i>	326
Über eine Verbesserung im Betrieb einer Erdöl-Raffinerie: Die automatische Beladung von Kesselwagen	<i>F. X. Montjean</i>	335

AUTOMATISIERUNG IN DER VERFAHRENSTECHNIK

Prozeßrechner

Die Lösung eines Optimierungsproblems mit Hilfe des Digitalrechners A. 110	<i>E. Honoré und Ste. Analae</i>	341
Die Automatisierung einer Portland-Zementfabrik mittels eines Prozeßrechners	<i>R. A. Phillips</i>	347
Über die Stabilität und Auslegung von selbsteinstellenden Systemen mit selbsterregter Suchschwingung	<i>R. K. Smyth und N. Nahi</i>	358

Regelung im Dampfkraftwerk

Vorausberechnung des Regelverhaltens von Zwischenüberhitzern im Dampfkessel	<i>W. Kindermann</i>	369
Eine Optimalwertregelung des Kesselwirkungsgrades	<i>S. Fujii und N. Kanda</i>	380
Ein Simulator für Dampfturbinen mit regelbarer Entnahme	<i>H.-J. Ehling</i>	390
Ein elektro-hydraulisches Regelsystem für Turbinen mit Zwischenüberhitzern	<i>M. A. Eggenberger und P. H. Troutman</i>	398

INHALT

Kraftfahrzeug-Industrie

Industrielle Anwendung eines Prozeßrechners auf eine Fertigungseinrichtung: Elektronisches Steuersystem für eine Maschine zum Auswuchten von Kurbelwellen	<i>J. Csech</i>	408
Entwurf eines Gerätes zur Regelung der Geschwindigkeit eines Kraftwagens	<i>W. H. Holl</i>	415

SYSTEME MIT REGELUNG UNTER MITWIRKUNG DES MENSCHEN

Der Mensch als Regelkreisglied

Kontinuierliche und Abtastmodelle für das Verhalten des Menschen im Gefüge eines Regelsystems . . .	<i>P. Naslin und J.-C. Raoult</i>	421
Zeitdiskrete Modelle für den Menschen als Regelkreisglied	<i>G. E. Bekey</i>	430
Analyse der Dynamik und Nachbildung der Steuerungsfunktionen in der Betriebsführung	<i>R. B. Wilcox</i>	439

Physiologische und medizinische Probleme

Grundzüge einer Theorie steuerbarer Prothesen	<i>R. Tomović</i>	449
Ein Abtastmodell zur Beschreibung der Zielbewegung des Auges	<i>L. R. Young</i>	454

WEITERE REGELVERFAHREN UND GERÄTE

Verfahren

Ein adaptierendes Verfahren zum Ausgleich großer Änderungen des Übertragungsfaktors einer Regelstrecke . . .	<i>R. J. Kochenburger</i>	464
Das dynamische Verhalten von Hydraulik-Leitungen	<i>R. Oldenburger und R. E. Goodman</i>	472
Die Optimierung eines durch einen Prozeßrechner gesteuerten Systems bei lückenhafter Information über die inneren funktionellen Zusammenhänge	<i>B. G. Anderson</i>	480

REGELUNG IN DER LUFT- UND RAUMFAHRT

Prüf- und Meßeinrichtungen

Entwurf eines Druckregelsystems für einen Windkanal von $1,5 \cdot 1,5 \text{ m}^2$ Strömungsquerschnitt . . .	<i>J. A. Tanner und W. Dietiker</i>	487
Ein Prüfstand für Raketenmotoren mit Nachbildung der realen Umweltbedingungen	<i>G. J. Fiedler und J. J. Landy</i>	496
Ein Leitsystem für die Längsbewegung eines Flugzeugs in der Landephase	<i>F. J. Ellert und C. W. Merriam III</i>	504

Hilfseinrichtungen zur Steuerung von Satelliten

Lageregelung einer großen Richtantenne für Fernmelde-Satelliten	<i>F. J. D. Taylor</i>	512
Untersuchung der Nachführeinrichtung eines 64-m Radioteleskops	<i>R. G. Wheeler</i>	519
Ein dynamisches Modell der Feineinstellung eines astronomischen Beobachtungssatelliten	<i>R. E. Roberson</i>	529
Probleme der Lageregelung von Raumfahrzeugen mit Hilfe von Kreiselssystemen	<i>R. H. Cannon, Jr.</i>	535

SCHLUSSBEMERKUNGEN

<i>W. E. Miller</i> (Vorsitzender des Technischen Ausschusses im IFAC über Anwendungsfragen)		545
--	--	-----

GERÄTE

Neue Konstruktionsgedanken und Regelgeräte — Übersichtsreferat *J. L. Shearer und 16 weiteren Autor*

MECHANISCHE, HYDRAULISCHE UND PNEUMATISCHE GERÄTE

Ein hydraulischer Drehmomentverstärker *Y. Oshima und K. Ara*
 Ein Kreiselgerät mit Spezialrotor und periodischem Ausgangssignal *G. C. Newt.*
 Über dynamische Probleme einer hydraulischen Steuereinrichtung bei Belastung mit schweren Massen *V. Khokhl*
 Der Aufbau von Sequenzsteuerungen mit Hilfe pneumatischer Schaltelemente *A. A. 1*

ELEKTROMECHANISCHE GERÄTE UND MAGNETVERSTÄRKER

Zweipunktregelung mit gesteuerter Frequenz der Arbeitsbewegung *I. A. Maslar*
 Probleme, Wirkungsweise und Berechnung eines neuen Maschinenverstärkers und seine Anwendung auf bestimmte Regelaufgab
O. Benedi
 Die Regelung der Bewegung eines translatorischen elektromagnetischen Schwingantriebs *J. C. West und B. V. Jayawa*
 Schrittmotoren mit aktivem Läufer *Yu. K. Vasilev, Yu. A. Prokofiev und G. Ya. Wainberg*

ELEKTRONISCHE BAUELEMENTE

Einige neuartige Steuerschaltungen mit Vierschicht-*p-n-p-n*-Halbleitertrioden *J. Š. Haškovec und A. Klím*
 Ein- und ausschaltbare Silizium-Gleichrichter *H. F. Stoi*
 Keramische Speicherzellen für außergewöhnliche Umweltbedingungen. *A. B. Kaufm*

DIGITALE ELEMENTE

Die Anwendung digitaler Integrieranlagen in der Prozeßführung *H. Rechberg*
 Vorteile und Aussichten der digitalen Drehzahlregelung *W. Fritzsc*
 Regler mit digitalen Rechenoperationen *T. M. Aleksandridi, S. N. Diligensky und H. Kr*

MESSEINRICHTUNGEN FÜR ANLAGEN

Ein universelles Analysiergerät für stochastische Vorgänge *J. Kry*
 Das Verhalten selbststellender Regler *J. L. Dou*
 Grundlagen und Schaltung eines Vielkanal-Korrelators — Ein Spezialanalogrechner zur statistischen Erfassung regelloser Vorgänge
 industriellen Anlagen *A. S. Uskov und Yu. M. Ori*

ZUVERLÄSSIGKEITSPROBLEME

Die Zuverlässigkeit von Bauelementen — Übersichtsvortrag *G. Glinski, B. S. Sotskov und H. Weissma*
 Neuartige Steuerventile für redundante elektrohydraulische Systeme *K. D. Garnjost und W. J. They*
 Die Zuverlässigkeit elektrischer Schaltelemente *G. W. A. Dunn*
 Fragen der Betriebssicherheit elektro-mechanischer Übertragungsglieder *B. S. Sotskov, I. E. Dekabrun und L. S. Krivorot*
 Eine Untersuchung der Zuverlässigkeit von Regeleinrichtungen für Kernreaktoren und Verfahrensregelstrecken
L. A. J. Lawrence und R. J. Scotel

SCHLUSSBEMERKUNGEN

Gy. Boromisza (Vorsitzender des Technischen Ausschusses im IFAC für Gerätefragen)
Y. Oshima (Stellvertretender Vorsitzender des Ausschusses im IFAC für Gerätefragen)

Inhalt des Bandes Theorie

THEORIE

THEORIE NICHTLINEARER SYSTEME

Statistische Verfahren zur Behandlung von Regelvorgängen — Übersichtsvortrag *V. S. Pugachev*

Technik der Beschreibungsfunktion

Eine neue Methode zur Ableitung der Beschreibungsfunktion bestimmter nichtlinearer Übertragungssysteme *R. Lauber*
 Anwendung des Verfahrens der Beschreibungsfunktion auf die Untersuchung von Schwingungen in Systemen mit veränderlichen Parametern *A. Leonhard*
 Über das Problem der inversen Beschreibungsfunktion *J. E. Gibson und E. S. di Tada*
 Die relative Stabilität von Schwingungen in nichtlinearen Regelsystemen *Z. Bonenn*

Prädiktionssysteme

Prädiktionsregelung eines Zweipunktsystems mit zwei Stellgrößen *A. J. Adey, J. F. Coales und J. A. Styles*
 Ein Prädiktionsverfahren für nichtstationäre Prozesse und seine Anwendung auf das Problem der Vorhersage der Lastverteilung im Verbundnetz *E. D. Farmer*
 Über den Entwurf von Prädiktions-Regelsystemen *S. Horing*
 Ein Verfahren zur zeitoptimalen Regelung mit Vorhersage *F. B. Gul'ko und B. Y. Kogan*

Nichtlineare Systeme mit zufallsbedingten Parametern

Optimierung nichtlinearer stochastischer Regelvorgänge *R. Kulikowski*
 Nichtlineares Programmieren bei der Untersuchung optimaler Regelsysteme *N. Y. Andreev*
 Numerische Analyse nichtlinearer Regelsysteme mit Hilfe der Gleichung von Fokker, Planck und Kolmogorow *K. J. Merklinger*
 Eine Darstellung zeitveränderlicher nichtlinearer Systeme mit Hilfe einer Volterra'schen Reihe *R. Flake*

Nichtlineare stochastische Systeme

Die Anwendung quasi-linearer Methoden auf nichtlineare Regelsysteme mit zufallsbedingten Eingangsgrößen *H. W. Smith*
 Ein Digital-Rechenverfahren zur Untersuchung nichtlinearer Systeme mit Anwendung auf zufallsbedingte Prozesse *T. Prasad und V. P. Sinha*
 Zeitoptimale Systeme mit stochastischen Störgrößen *V. N. Novoseltsev*

Stückweise kontinuierliche Systeme

Mehrfach-Regelkreise mit gemischt analog-digitaler Signalverarbeitung und beschränkten Störgrößeneinflüssen *V. Strejc*
 Optimalregelung eines nichtlinearen Prozesses mit Vorschriften über diskrete Zeitabschnitte *B. Friedland*
 Theorie der schnelligkeitsoptimalen Regler *C. A. Desoer, E. Polak und J. Wing*

Abtastsysteme

Über die Wurzeln eines reellen Polynoms innerhalb des Einheitskreises und ein Stabilitätskriterium für in diskreten Zeitabschnitten lineare Systeme *E. I. Jury*
 Analytische Verfahren zur Berechnung nichtlinearer Abtastsysteme *B. Kondo und S. Iwai*
 Ein stetigwirkendes Kompensationsfilter für lineare Abtastsysteme *B. M. Brown*

INHALT

Grundlagen der Theorie nichtlinearer Regelsysteme mit Abtastung	Ya. Z. Zypkin
Synthese optimaler Abtastsysteme	L. N. Volgin
Regelkreise mit Integral-Pulsfrequenz-Modulator	C. C. Li und R. W. Jones
Die Kombination endlicher Beruhigungszeit und minimalen quadratischen Fehlers in digitalen Regelsystemen	V. Peterka

Relais-Systeme

Subharmonische Schwingungen in einem Zweipunkt-Regelsystem	J. C. Gille, S. Wegrzyn und J. C. Paquet
Die Synthese von Regelkreisen mit linearem Verhalten bei kleinen, mit Zweipunkt-Verhalten bei großen Signalen	E. V. Persson
Systeme mit zwei Eingängen und Beschränkung in Gestalt einer Sättigung	R. S. Gaylord

Theorie der Logik-Schaltungen

Warnung und Vorhersage von Versagern in Steuerungssystemen mit Struktur-Redundanz	M. A. Gavrilov
Axiomatik der Theorie der Vereinfachung von Schaltkreisen	Gr. C. Moisil
Adaptierende Regelung eines Systems mit einer endlichen Anzahl von Zuständen	S. Paszhkovskij

OPTIMALE REGLER

Synthese optimaler Regler — Übersichtsvortrag	A. M. Letov
---	-------------

Theorie optimaler Systeme

Näherungsverfahren für Optimalwert- und Adaptiv-Regelung	J. H. Westcott, J. J. Florentin und J. D. Pearson
Eine optimale Leitbahnnäherung für fast kreisförmige Begegnungsbahnen von Flugkörpern	H. J. Kelly und J. C. Dunn
Zur Synthese optimaler Regelsysteme	L. W. Neustadt und B. H. Paiewonsky
Eine Anwendung der Optimalwertregelung auf die mittlere Flugphase von Flugkörpern	J. S. Meditch und L. W. Neustadt

Optimale Systeme

Über notwendige und hinreichende Bedingungen für geschwindigkeitsoptimale Regelung nichtlinearer Systeme mit Verzögerung 2. Ordnung	E. B. Lee und L. Markus
Über die zeitoptimale Regelung von Systemen mit mehreren Eingangsgrößen und unterschiedlichen Beschränkungen	P. E. Sarachik und G. M. Kranc
Die Näherungsberechnung einer Klasse von Regelsystemen mit selbsteinstellendem Netzwerk	Y. I. Alimov

Optimalsysteme mit verteilten Parametern

Einige Betrachtungen zur optimalen Regelung eines vermaschten Systems	R. Marcelli
Optimale Abläufe in Systemen mit Signalverzögerungen	N. N. Krasovskij
Die Optimalwertregelung von Systemen mit verteilten Parametern	A. G. Butkovskij

Synthese optimaler Systeme

Die Lösung eines Problems der geschwindigkeitsoptimalen Regelung mit Hilfe des Maximumprinzips von Pontryagin	Y. Sakawa und Ch. Hayashi
Analyse und Synthese zeitoptimaler Regelsysteme	Sun Jian und Hang King-ching
Entwicklung von Verfahren der dynamischen Programmierung und ihre Anwendung auf den Entwurf optimaler Systeme	R. L. Stratonovich
Ein abgewandeltes Maximumprinzip zur optimalen Regelung eines Systems mit begrenzten Phasenraum-Koordinaten	S. S. L. Chang
Optimale und fast-optimale Regelung von Systemen 3. und 4. Ordnung	I. Flügge-Lotz und H. A. Titus, Jr.

Optimales Programmieren

Programmsteuerung und Theorie von Optimalsystemen	Ye. A. Barbashin
Die Verwirklichung von Optimalprogrammen für Regelsysteme	G. S. Pospelov
Über die Grenzen von Quantisierungsfehlern bei Berechnungen zur dynamischen Programmierung	J. J. G. Guignabodet

THEORIE DER SELBSTEINSTELLENDEN SYSTEME

Adaptierende und selbstoptimierende Systeme — Übersichtsvortrag	J. Truxal
Lernende Systeme — Übersichtsvortrag	G. Pask

Invarianzprobleme

Über die Invarianzbedingungen bei gewöhnlichen und adaptierenden Abtastsystemen	V. M. Kunzewitsch und Yu. V. Krementulo
Optimierung aufgrund von Invarianzbedingungen in Regelsystemen mit fester und veränderlicher Struktur	B. N. Petrow, G. M. Ulanov und S. V. Emelyanov
Synthese von Systemen, bei denen das entsprechende selbsteinstellende Ersatzmodell feste Kennwerte besitzt	M. V. Mejerow

Adaptierende Systeme

Ein Vergleich der Auswertezeit in selbsteinstellenden Regelkreisen	F. Mesch
Selbsteinstellende Regelsysteme ohne Eingangs-Testsignale	E. P. Popov, G. M. Loskutov und R. M. Yusupov
Ein Beitrag zur Anwendung selbsteinstellender Systeme auf die automatisierte Synthese von Lernsystemen	V. K. Chichinadze und O. A. Charkviani
Das Auffinden von Extrema bei Funktionen, die in Regelkreisen auftreten	A. A. Woronow und M. B. Ignatjev
Versuch der Anwendung eines dynamischen Leitmodelles auf die Theorie adaptierender Systeme	A. Straszak
Verallgemeinerte Analyse selbsteinstellender Systeme, die auf einem Suchverfahren mit sinusförmigen Testsignalen beruhen	V. W. Eveleigh
Über die Durchführung eines Programmes der Adaptivregelung in einem System mit Digitalrechner	P. F. Klubnikin

Lernende Systeme

Ein adaptierendes Regelsystem mit „Formempfindung“	W. K. Taylor
STELLA: Ein Konzept für einen lernenden Automaten	J. H. Andreae
Lernfähige Systeme für technische Anwendungen — unter Berücksichtigung von Versuchen über die Möglichkeit, die Geräte ein Erkennen von Mustern zu lehren	M. A. Aizerman

Suchverfahren

Über die Theorie selbsteinstellender Systeme mit Gradientenbestimmung, nach dem Verfahren des Hilfsoperators	I. E. Kasakow und L. G. Eylanow
Über die Anwendung der Theorie kontinuierlicher Systeme auf die Extremwert-Regelung in industriellen Anlagen	A. A. Krasowski
Prinzip und Anwendung eines Optimalwert-Rechners	R. Perret und R. Rouxel
Probleme der „dualistischen“ Theorie der Optimalwert-Regelung	A. A. Feldbaum
Die Anwendung stochastischer Testsignale bei der Optimierung von Prozessen	P. M. E. M. van der Grinten

METHODEN ZUR ABSCHÄTZUNG DER STABILITÄT

Das Stabilitätsproblem nach Ljapunow

Über eine neuartige Erweiterung des Stabilitätsbegriffes	J. P. La Salle und R. J. Rath
Stabilitätsuntersuchung, mittels der 2. Methode von Ljapunow, an Systemen mit beschränkten Nichtlinearitäten	H. Nour-Eldin
Die Anwendung der Technik der linearen Bereichsgrenzen zur Übertragung der direkten Ljapunow'schen Methode auf eine Gruppe von nichtlinearen und zeitveränderlichen Systemen	R. A. Nesbit
Über die Abschätzung der Abklingzeit	L. Hwang
Neue Verfahren zur Ermittlung Ljapunow'scher Funktionen für zeit-invariante Regelsysteme	G. P. Szegö
Ein Verfahren zur Stabilitätsprüfung	H. H. Rosenbrock

INHALT

DYNAMIK DER SYSTEME UND VERWANDTE PROBLEME

Prozeßdynamische Studien und ihre Anwendung auf Entwurf und Regelung industrieller Anlagen — Übersichtsvortrag
T. J. Williams

Dynamische Probleme

Ermittlung des dynamischen Verhaltens von Regelkreisen mit Hilfe einstellbarer Modelle *E. Blandhol und J. G. Balchen*
Die systematischen und zufallsbedingten Fehler bei der experimentellen Bestimmung von Übertragungsfunktionen . . . *J. Loeb*
Die Anwendung des Relais-Korrelators und des Polaritäts-Korrelators auf Messungen an Regelkreisen
B. P. Th. Veltman und A. van den Bos
Bemerkungen zu einer Zufallsfunktion mit physikalischer Bedeutung *M. Pélérin*
Eine Unschärfe-Beziehung für lineare mathematische Modelle *B. Qvarnström*

Allgemeine Probleme

Axiomatische Begründung der Theorie geregelter Systeme *E. Roxin*
Das Umkehrproblem zur Bestimmung des quadratischen Integral-Kriteriums *W. Jarominek*
Über Systeme mit Regelung der Konfiguration *J. Beneš*
Annäherung industrieller Regelsysteme an optimale nichtlineare Regelungen mit begrenzter Stellgeschwindigkeit mittels konventioneller Regler *E. Pavlik*
Neues Verfahren zur Optimierung bei stochastischen Eingangsgrößen mittels der Transformation $V = (Z - 1)/(Z + 1)$
P. M. Lefèvre
Die Regelung von Anlagen über zwei Bereiche der Störampplituden *C. N. Kerr und G. D. S. MacLellan*

SCHLUSSBEMERKUNGEN

B. N. Petrow (Vorsitzender des Technischen Ausschusses im IFAC für Theorie)
J. H. Westcott (Stellvertretender Vorsitzender des Ausschusses im IFAC für Theorie)

Authors' Names and Addresses

APPLICATIONS AND COMPONENTS

AUSTRIA

RECHBERGER, H., Elektrotechnisches Institut, Gusshausstrasse 25, Wien IV

BELGIUM

DELVAUX, L., Université de Liège, Institut de Mécanique, 75 rue de Val Benoît, Liège

BULGARIA

MASLAROFF, I. A., The Institute for Scientific Research of Electrical Industry, P.O. Box 67, Sofia 45

CANADA

TANNER, J. A., Division of Mechanical Engineering, National Research Council, Ottawa 2, Ontario

CZECHOSLOVAKIA

HAŠKOVEC, J. S., Institute for Information Theory and Automation, Vyšehradská 49, Praha 2

KLÍMEK, A., Institute for Information Theory and Automation, Vyšehradská 49, Praha 2

KRÝŽE, J., Institute for Information Theory and Automation, Vyšehradská 49, Praha 2

ZÁVORKA, J., Institute for Information Theory and Automation, Vyšehradská 49, Praha 2

FRANCE

CSECH, J., 26 rue de Lyon, Paris 12

HONORÉ, E., Société ANALAC, 101 Blvd. Murat, Paris 16

MONTJEAN, F., 109 rue de Ville d'Avray, Sevres (Seine et Oise)

NASLIN, P., 20 Avenue Pricue de la Côte d'Or, Arcueil (Seine)

RAOULT, J.-C., 16 Avenue de Verdun, Vanves (Seine)

THILLIEZ, J., 175 Blvd. Murat, Paris 16

TURPIN, P., 175 Blvd. Murat, Paris 16

GERMANY

EHILING, H. J., AEG-Institut für Automation, 1 Berlin N 65, Brunnenstr. 107a

FRITZSCHE, W., AEG-Institut für Automation, 1 Berlin N 65, Brunnenstr. 107a

KINDERMANN, W., Continental Elektroindustrie AG, Askania-Werke, VR-Ta, 1 Berlin-Mariendorf, Grossbeerenstr. 2-10

HUNGARY

BENEDIKT, O., Budapest Műszaki Egyetem Villamosgépek Tanszék, Budapest XI, Egri József — u. 18

BENEDIKT, S., Institute for Electrical Power Research, Budapest, VI. Rudas L. u. 27

UZZSOKI, M., Institute for Electrical Power Research, Budapest, VI. Rudas L. u. 27

VÁMOS, T., Institute for Electrical Power Research, Budapest, VI. Rudas L. u. 27

ITALY

DE GREGORIO, G., Compagnia Generale di Eletticità, C.G.E., Milano

LITIGIO, G., Istituto Siderurgico Finsider, Genova-Cornigliano

SIRONI, G., Istituto Siderurgico, Finsider, Genova-Cornigliano

STEIN, T., Viale X Giugno 44 B, Vicenza

JAPAN

ARAKI, K., Institute of Industrial Science, University of Tokyo, Azabu-shinryudocho, Tokyo

FUJII, S., Dept. of Mechanical Engineering, Nagoya University, Furo-cho Chikusa-ku, Nagoya

ISOBE, T., Faculty of Engineering, University of Tokyo, Tokyo

IZAWA, K., Tokyo Institute of Technology, Oh-okayama, Meguro-ku, Tokyo

KANDA, N., Dept. of Mechanical Engineering, Nagoya University, Furo-cho Chikusa-ku, Nagoya

MORINAGA, T., Tokyo Institute of Technology, Oh-okayama, Meguro-ku, Tokyo

NAKANISHI, E., Kyoto University, Kyoto

OSHIMA, Y., Institute of Industrial Science, University of Tokyo, Azabu-shinryudocho, Tokyo

TAKAMATSU, T., Kyoto University, Kyoto

TOTANI, T., Faculty of Engineering, University of Tokyo, Tokyo

NETHERLANDS

KYLSTRA, F. J., Koninklijke/Shell-Laboratorium, Amsterdam

VAN DER HEYDEN, C.A.J.M., Bataafse Internationale Petroleum Maatschappij N.V.

VAN NES, A. G., Bataafse Internationale Petroleum Maatschappij N.V.

NORWAY

RUGE, H., Central Institute for Industrial Research, Blindern, Oslo

SWITZERLAND

BOREL, L., Epul, Lausanne

GLAVITSCH, H., Hertensteinstr. 23, Nussbaumen bei Baden

TSCHUMY, A., 109 rue de Lyon, Geneva

UNITED KINGDOM

ANDERSON, B. G., Guided Weapons Division, English Electric Aviation Ltd., British Aircraft Corporation Ltd., Stevenage, Herts

DOUCE, J. L., Electrical Engineering Dept., Queen's University (David Keir Bldg.), Belfast

DUMMER, G. W. A., Applied Physics and Technical Services, Royal Radar Establishment, St. Andrews Road, Great Malvern, Worcs.

HERSOM, S. E., Planning and Computer Developments Dept., Richard Thomas & Baldwins Ltd., Spencer Works, Newport Section, Llanwern, Nr. Newport, Mon.

LAWRENCE, L. A. J., Control and Instrumentation Division, Building B.41, Atomic Energy Establishment, Winfrith, Dorchester, Dorset

MASSEY, R. G., Planning and Computer Developments Dept., Richard Thomas & Baldwins Ltd., Spencer Works, Newport Section, Llanwern, Nr. Newport, Mon.

AUTHORS' NAMES AND ADDRESSES

M'PHERSON, P. K., Control and Instrumentation Division, Atomic Energy establishment, Winfrith, Dorchester, Dorset

MUSCETTOLA, M., Control and Instrumentation Division, Atomic Energy Establishment, Winfrith, Dorchester, Dorset

SCOTCHER, R. J., Control and Instrumentation Div., Building B. 41, Atomic Energy Establishment, Winfrith, Dorchester, Dorset

TAYLOR, F. J. D., Engineering Dept., G.P.O. Research Station, Dollis Hill, London, N.W. 2.

TOMLINSON, A., The British Iron and Steel Research Association, 11 Park Lane, London, W. 1.

WEST, J. C., Electrical Engineering Dept., Queen's University, Belfast

WHEELER, R. G., 121 Westminster Road, Davyhulme, Urmston, Lancs.

WISTREICH, J. G., The British Iron and Steel Research Association, 11 Park Lane, London, W. 1.

U.S.A.

BEADLE, R. G., G.E.C., 1 River Road, Schenectady 5, New York

BEKEY, G. A., Electrical Engineering Dept., University of Southern California, Los Angeles 7, California

BOOTON, R. C., Jr., Space Technology Lab. Inc., Redonda Beach, California

BRADFORD, J. T., Jr., Jones & Laughlin Steel Corp., 3 Gateway Center, Pittsburgh 30, Penn.

CANNON, R. H., Jr., Stanford University, Stanford, California

EGGENBERGER, M. A., G.E.C., 1 River Road, Schenectady 5, New York

ELLERT, F. J., General Engineering Lab., G.E.C., 1 River Road, Schenectady 5, N.Y.

FIEDLER, G. J., Sverdrup & Parcel and Associates, 915 Olive Street, St. Louis 1, Missouri

GARNJOST, K. D., Moog Servocontrols Inc., East Aurora, New York

GOODSON, R. E., Purdue University, Lafayette, Indiana

HOLL, W. H., AC Spark Plug Division, General Motors Corporation, Flint 2, Michigan

KAUFMAN, A. B., Litton Systems, Woodland Hills, California

KIRCHMAYER, L. K., Electric Utility Analytical Engineering, G.E.C., 1 River Road, Schenectady 5, New York

KOCHENBURGER, R. J., University of Connecticut, Storrs, Connecticut

LANDY, J. J., Sverdrup & Parcel and Associates, 915 Olive Street, St. Louis 1, Missouri

MERRIAM, C. W., III, General Electric Research Laboratory, G.E.C., 1 River Road, Schenectady 5, New York

MOCZEK, J. S., Monsanto Chemical Company, 800 North Lindbergh Boulevard, St. Louis 66, Missouri

NAHI, N., Autonetics, 3311 East La Palma Road, Anaheim, California

NEWTON, G. C., Jr., Electronic Systems Laboratory, Building 32, M.I.T., Cambridge 39, Mass.

OLDENBURGER, R., Purdue University, Lafayette, Indiana

OTTO, R. E., Monsanto Chemical Company, 800 North Lindbergh Boulevard, St. Louis 66, Missouri

PHILLIPS, R. A., Analytical Engineering, A.P. & P., G.E.C., 1 River Road, Schenectady 5, New York

RINGLEE, R. J., Electric Utility Analytical Engineering, G.E.C., 1 River Road, Schenectady 5, New York

ROBERSON, R. E., 1100 No. Cerritos Drive, Fullerton, California

SMYTH, R. K., Autonetics, 3311 East La Palma Road, Anaheim, California

SOLLECITO, W. E., Electronics Park, G.E.C., Syracuse, New York

STORM, H. F., G.E.C., 1 River Road, Bldg. 37-575, Schenectady, New York

THAYER, W. J., Moog Servocontrols Inc., East Aurora, New York

TROUTMAN, P. H., G.E.C., 1 River Road, Schenectady 5, New York

WILCOX, R. B., R.C.A. Aerospace Division, Burlington, Mass.

WILLIAMS, T. J., Monsanto Chemical Company, 800 North Lindbergh Boulevard, St. Louis 66, Missouri

YOUNG, L. R., Room 32-101, Massachusetts Institute of Technology, Cambridge 39, Mass.

U.S.S.R.

At the Institute of Automation and Telemechanics, Moscow I-53, Kalachevskaya 15-A:

ALEKSANDRID, T. A.

DOMANITSKY, S. M.

KHOKHLOV, V.

LERNER, A. Ya.

SOTSKOV, B. S.

TAL, A. A.

At the U.S.S.R. National Committee on Automatic Control, Moscow I-53, Kalachevskaya 15-A:

ANISIMOV, I. V.

USKOV, A. S.

VASILYEV, Yu. K.

VOLTER, B. V.

KOROBKO, M. I., Kiev 52, Nagornaya 22, Institute of Automation, Gosplan Ukrainian S.S.R.

KRUG, G. K., Moscow E-250, Krasnokazarmennaya 14, Moscow Power Institute

VENIKOV, V. A., Moscow E-250, Krasnokazarmennaya 14, Moscow Power Institute

YUGOSLAVIA

TOMOVIĆ, R., Beograd, Dobračina 13

The following authors have contributed to the volume on THEORY

THEORY

ARGENTINE

ROXIN, E., Directorio 1304, Haedo (FNDFS), Prov. B. Aires

CANADA

SMITH, H. W., 74 Reid Avenue, Ottawa 3, Ontario

CHINA

HANG KING-CHING, Institute of Mathematics, Academia Sinica, Peking

HWANG LING, Peking University, Dept. of Mathematics, Peking

SUN JIAN, Institute of Mathematics, Academia Sinica, Peking

CZECHOSLOVAKIA

BENEŠ, J., Institute for Information Theory and Automation, Vyšehradská 49, Praha 2

PETERKA, V., Institute for Information Theory and Automation, Vyšehradská 49, Praha 2

STREJC, V., Institute for Information Theory and Automation, Vyšehradská 49, Praha 2

FRANCE

GILLE, J.-C., Ecole Nationale Supérieure de l'Aéronautique, 32 Blvd. Victor, Paris 15

GUIGNABODET, J., 55 rue Caulaincourt, Paris 18

LEFEVRE, P. M., 3 rue Claude Matrat, Issy les Moulineaux (Seine)

AUTHORS' NAMES AND ADDRESSES

LOEB, J., 14 rue Alphonse Moguez, St. Cloud (Seine et Oise)
PÉLÉGRIN, M. J., 11 bis rue de la Planche, Paris 7

GERMANY

LAUBER, R., AEG-Institut für Automation, 6 Frankfurt/M.-Hausen, Tilsiter Str. 5
LEONHARD, A., Lehrstuhl für elektrische Anlagen an der Technischen Hochschule Stuttgart, 7 Stuttgart N, Breitscheidstr. 3
MESCH, F., im Institut für Regelungstechnik der Technischen Hochschule Darmstadt, 61 Darmstadt, Schlossgraben 1
PAVLIK, E., 75 Karlsruhe, Lassallestr. 9

INDIA

PRASAD, T., Bihar Institute of Technology, P.O. Sindri Institute, Dhanbad (Bihar)
SINHA, V. P., Bihar Institute of Technology, P. O. Sindri Institute, Dhanbad (Bihar)

ISRAEL

BONENN, Z., Scientific Dept., Israel Ministry of Defence, P.O.B. 7063, Hakirya, Tel-Aviv

ITALY

MARCACCI, R., Montecatini SPEB/PROS, Largo Donegani 1, 2, Milano

JAPAN

HAYASHI, C., Dept. of Electrical Engineering, Kyoto University, Kyoto
IWAI, S., Dept. of Electronic Engineering, Kyoto University, Kyoto
KONDO, B., Dept. of Electronic Engineering, Kyoto University, Kyoto
SAKAWA, Y., Dept. of Electrical Engineering, Kyoto University, Kyoto

NETHERLANDS

VAN DEN BOS, A., Dept. for Technical Physics, Technological University of Delft, Delft
VAN DER GRINTEN, P.M.E.M., Staatsmijnen in Limburg, Central Laboratory, Geleen
VELTMAN, B.P.TH., Dept. for Technical Physics, Technological University of Delft, Delft

NORWAY

BALCHEN, J. G., Eidanger Salpeterfabriker, Herøya, pr. Porsgrunn
BLANDHOL, E., Eidanger Salpeterfabriker, Herøya, pr. Porsgrunn

POLAND

JAROMINEK, W., Warszawa ul Grójecka 40a m 34
KULIKOWSKI, R., Polski Komitet Pomiarow I Automatyki, Warszawa ul Czachiego 3/5
PASZKOWSKI, St., Polski Komitet Pomiarow I Automatyki, Warszawa ul Czachiego 3/5
STRASZAK, A., Polski Komitet Pomiarow I Automatyki, Warszawa ul Czachiego 3/5

ROUMANIA

MOISIL, Gr. C., Academia R.P.R. Institutul de Matematica, Str. M. Eminescu 47, Bucuresti 3

SWEDEN

PERSSON, E. V., Research Laboratory, A.S.E.A., Västerås
QVARNSTRÖM, B., Chalmers Institute of Technology, Gibraltargatan 5 R, Gothenburg

SWITZERLAND

ELDIN, H. NOUR, Swiss Institute of Technology, Gloriastr., Zurich 6
PERRET, R., Division Internationale, Battelle Memorial Institute, 7 route de Drize, Geneva
ROUXEL, R., Division Internationale, Battelle Memorial Institute, 7 rout de Drize, Geneva

UNITED KINGDOM

ADEY, A. J., Dept. of Engineering, University of Cambridge, Cambridge
ANDREAE, J. H., Senior Engineer, Standard Telecommunication Laboratories Ltd., London Road, Harlow, Essex
BROWN, B. M., Royal Naval College, Greenwich, London, S.E. 10.
COALES, J. F., Dept. of Engineering, University of Cambridge, Cambridge
FARMER, E. D., Central Electricity Research Laboratories, Cleve Road, Leatherhead, Surrey
KERR, C. N., Engineering Laboratories, The University, Glasgow, W. 2.
MACLELLAN, G. D. S., Engineering Laboratories, The University, Glasgow, W. 2.
MERKLINGER, K. J., Engineering Laboratory, University of Cambridge, Trumpington Street, Cambridge
ROSENBROCK, H. H., University of Cambridge, Dept. of Engineering, Engineering Lab., Trumpington Street, Cambridge
STILES, J. A., Dept. of Engineering, University of Cambridge, Cambridge

TAYLOR, W. K., Dept. of Electrical Engineering, University College, Gower St., London, W.C. 1.

WESTCOTT, J. H., Imperial College, Exhibition Road, London, S.W. 7.

U.S.A.

CHANG, S. S. L., Dept. of Electrical Engineering, New York University, University Heights, New York 53
DESOER, C. A., Dept. of Electrical Engineering, University of California, Berkeley 4, California.
EVELEIGH, V. W., Electronics Laboratory, G.E.C., Electronics Park, Syracuse, N.
FLAKE, R., Electrical Engineering Dept., Washington University, St. Louis 30, Missouri
FLÜGGE-LOTZ, I., Division of Engineering Mechanics, Stanford University, Stanford, California
FRIEDLAND, B., General Precision Inc., Aerospace Research Center, 1150 McBride Avenue, Little Falls, New Jersey
GAYLORD, R., Aerospace Corporation, P.O. Box 95085, Los Angeles 45, California
GIBSON, J. E., Control and Information Systems Laboratory, School of Electrical Engineering, Purdue University, Lafayette, Indiana
HORING, S., Bell Telephone Laboratories, Whippany, New Jersey
JURY, E. I., Dept. of Electrical Engineering, University of California, Berkeley 4, California
KELLEY, H. J., Grumman Aircraft Engineering, Corp., Bethpage, Long Island, New York
LASALLE, J. P., RIAS, 7212 Bellona Avenue, Baltimore 12, Maryland
LEE, E. B., Minneapolis Honeywell Regulator Co., 2600 Ridgway Road, Minneapolis, Minnesota
LI, C. C., Dept. of Electrical Engineering, University of Pittsburgh, Pittsburgh Pennsylvania
MEDITCH, J. S., Aerospace Corporation, P.O. Box 95085, Los Angeles 45, California
NESBIT, R. A., Aerospace Corporation, P.O. Box 95085, Los Angeles 45, California
NEUSTADT, L., Aerospace Corporation, P.O. Box 95085, Los Angeles 45, California
SARACHIK, P. E., Dept. of Electrical Engineering, Columbia University, New York 27.
SZEGÖ, G. P., Control and Information Systems Laboratory, School of Electrical Engineering, Purdue University, Lafayette, Indiana
TITUS, H. A., Jr., U.S. Naval Postgraduate School, Monterey, California

AUTHORS' NAMES AND ADDRESSES

U.S.S.R.

At the Institute of Automation and Telemechanics, Moscow I-53, Kalachevskaya 15-A:

AIZERMAN, M. A.
ALIMOV, Yu. I.
BUTKOVSKII, A. G.
FELDBAUM, A. A.
GAVRILOV, M. A.
GULKO, F. B.
KASAKOV, I. E.
KRASOVSKII, A. A.

KRAZOVSKII, N. N.
MEEROV, M. V.
NOVOSELTSEV, V. N.
PETROV, B. N.
POSPELOV, G. S.
TSYPKIN, Ya. Z.

At the U.S.S.R. National Committee on Automatic Control, Moscow I-53, Kalachevskaya 15-A:

ANDREEV, N. I.
BARBASHIN, Ye. A.
KLUBNIKIN, P. F.

POPOV, E. P.
STRATONOVICH, R. L.
VOLGIN, L. N.

CHICHINADZE, V. K., Tbilisi 42, Pekin 56, Institute of Electronics, Automation and Telemechanics, Academy of Sciences, Georgian S.S.R.

KUNTSEVICH, V. M., Kiev 54, Chkalova 55-6, Institute of Electromechanics, Academy of Sciences, Ukrainian, S.S.R.

VORONOV, A. A., Institute of Electromechanics, Leningrad D-41, Dvortsovaya Naberezhnaya 18

The Second International Congress of I.F.A.C. in Basle 1963

EDUARD GERECKE, Third President of I.F.A.C.

This, the second I.F.A.C. Congress, is being held in Basle from 27th August to 4th September. 1476 participants and 200 ladies are present from the following countries: Argentine (1), Austria (11), Belgium (37), Bulgaria (8), Canada (5), China (10), Congo (3), Czechoslovakia (11), Denmark (10), Finland (25), France (173), Germany (212), Hungary (30), India (1), Israel (4), Italy (47), Japan (19), Mexico (1), Netherlands (83), Norway (22), Poland (32), Portugal (3), Roumania (10), Spain (6), Sweden (44), Switzerland (237), Turkey (7), United Kingdom (160), United States of America (154), Union of Socialist Soviet Republics (80), Yugoslavia (30).

As Automatic Control today covers a very large field, the Executive Council of I.F.A.C. selected the following limited fields for the Congress.

1. *Theory*
2. *Applications*
3. *Components*

As an innovation, 11 Survey Papers dealing with the actual state of automatic control in most fields of theory, applications and components will be read. All Congress delegates can attend these lectures, and will, I am sure, certainly appreciate the opportunity of getting a competent survey from outstanding specialists of today's position and of future developments in the different fields of Automatic Control.

Two hundred and sixty Discussion Papers were submitted to

I.F.A.C. in September 1962, and the I.F.A.C. Selection Committee accepted 159 of these, namely 82 on Theory, 57 on Applications, and 20 on Components. Fifty half-day sessions are planned for the discussion of these papers, 25 of them on Theory, 19 on Applications and 6 on Components. Undoubtedly the I.F.A.C. Basle Meeting will contribute to the promulgation of the new and more advanced chapters of Automatic Control.

The organization of such a large meeting requires the co-operation of a large number of individuals. The I.F.A.C. officials and many members of the Technical Committee did a great deal of preparatory work, all on a voluntary basis, and their help is very much appreciated. Our sincere thanks also go to the Honorary Secretary, Dr. G. Ruppel, Düsseldorf, for his indefatigable secretarial work and to the Honorary Editor, Professor V. Broïda, who prepares the Discussion Papers and the Proceedings with the aid of the Co-editors, D. H. Barlow, London, and Professor O. Schäfer, Aachen. I should like also to thank the Scientific Secretary, E. Ruosch, Zurich, for his most valuable assistance.

The expenses of the Congress, including the Preprints and the Survey Papers, amount to U.S. \$ 97,000 for which the Council members of the Swiss Society of Automatic Control are personally responsible. As third President of I.F.A.C. I should like to thank most heartily the Swiss Federation of Automatic Control and all those who contribute financially, especially the Authorities of the Canton of Basle Town, the Swiss Industries Fair and the Swiss Industry.

How I.F.A.C. was Founded

H. CHESTNUT, First President of I.F.A.C.

It is appropriate as we start this Second Congress of I.F.A.C. on Automatic Control that we look back at some earlier international meetings on automatic control and see what we may learn from the past that will give us some ideas that will be useful for the future. Within the past twenty-five years the science and art of automatic control has grown rapidly and interest has developed in such subjects as regulation, automation, and automatic control on the part of engineers, politicians, and laymen. We who are developing and using the techniques of automatic control are, in a way, charged with the responsibility of making automatic control most effective. It is important that the place of international activities, including meetings and congresses, be considered as a part of the process of helping us to accomplish our job of making automatic control better.

Although the first General Assembly of I.F.A.C. was held in Paris in September 1957, a number of meetings that were international in character if not in name had been held prior to that time. In 1951 at Cranfield, England, was held an outstanding meeting on 'Automatic and Manual Control' sponsored by the Department of Scientific and Industrial Research, the Proceedings of which were edited by Professor Arnold Tustin. In 1953 in New York under A.S.M.E. sponsorship was held a 'Frequency Response Symposium' that was international in its list of authors; its Proceedings were edited by Dr. Rufus Oldenburger.

By 1956 the heightened interest in automatic control caused a number of meetings to be held in Europe on or related to this subject. Outstanding among these was 'Regelungstechnik' in Heidelberg, Germany, in September 1956.

An earnest effort was made to obtain broad international participation on the part of authors from many countries serving to bring together many leading men in automatic control. This had the effect of increasing their interests in the possibilities of more regular and more internationally organized meetings on automatic control theory and practice that would be more broadly publicized and attended.

It was appreciated that similar progress in automatic control was being made in many parts of the world, in many cases with each group of people largely oblivious of the works of the others or without even knowing who these other people were. Furthermore, it was apparent that a great amount of time and effort would be required to push forward our understanding of automatic control and our ability to use it. Hence the help and benefit to be obtained by the sharing of ideas and information on an international basis would be valuable in making for more rapid progress.

Fortunately, a group of dedicated men, including Dr. Victor Broïda, Chairman; Dr. Otto Grebe, Professor A. M. Letov,

Professor P. J. Nowacki, Dr. Rufus Oldenburger, Dr. G. Ruppel, and Mr. D. B. Welbourn, were willing to devote their energies during the period September 1956 to August 1957 to helping in bringing about the formation of the International Federation of Automatic Control at the first General Assembly of I.F.A.C. in Paris, September 1957.

At this initial meeting a Constitution was adopted built around the principle of national rather than personal representation, and particular emphasis was placed on the holding of periodic international congresses. Another important objective was 'to promote the science of automatic control by the interchange and circulation of information on automatic control activities in co-operation with national and other international organizations'. Plans were laid for the first I.F.A.C. Congress to be held in Moscow, U.S.S.R., in 1960 about which you will hear shortly from Professor A. M. Letov who was President of I.F.A.C. at that time. The first I.F.A.C. Congress was a very successful one from which was obtained a fine, four volume set of Proceedings edited by John F. Coales.

The International Federation of Automatic Control is indeed fortunate that the Swiss Federation of Automatic Control was willing to serve as host for this second I.F.A.C. Congress here at Basle. The preparation and labour involved by members of the Swiss Federation of Automatic Control for this Congress are outstanding. On behalf of all those present here, I want to thank Professor Gerecke in his dual role as President of I.F.A.C. and as President of the Swiss Federation of Automatic Control for his help and for the efforts and skill of the members of the two groups which he represents and directs.

As first President of I.F.A.C., I am very pleased with the way that I.F.A.C. has developed and with the interest which its Congresses have stimulated. The growth of I.F.A.C. symposia on special subjects has been of particular interest to me. I look forward with hope for additional symposia on suitable topics of concern to experts in the field of automatic control.

We all have reason to be pleased with the fine progress that has been made in our automatic control accomplishments to date. Lest we become complacent, however, I should like to point out two other fields for serious attention by control people. These are:

- (1) The need for 'optimizing the process of making automatic control', i.e. bridging the gap between theory and practice.
- (2) The need for working with qualified people in the social, economic, and political fields to help make the net effect of automatic control and automation a cause for hope rather than a reason for fear.

For the past 5 years and more, one of the most popular topics of automatic control investigation has been the subject of optimum control. With all this emphasis on optimum control, it would appear possible to apply some of these general principles to permit us to perform the process of designing and building automatic controls more quickly, more cheaply, more reliably, or more favourably in some other sense which allows the desired balance of a number of these objectives. Not only should concern be given to determining how to make a system which will be optimum, but also the process of design itself should be one which can be readily applied by the large number of designers who will be applying these ideas to the making of better controls. Attention must be given from the theory point of view to including the practical application of these new control concepts. Efforts must be made from both sides to bridge the gap between theory and application.

The second problem which deserves more of our attention is that of automation, the popular term by which much of automatic control is known. Throughout the centuries, Man has hoped to find a way of obtaining goods and services with a minimum of effort to himself. With the advent of more and more automation, we are approaching the condition where a signifi-

cant proportion of the necessary production and services can be achieved with a minimum amount of direct human effort.

To realize the opportunity that automation can afford will require more than just the technical attention that we, working in automatic control, can apply. The changes in production and services brought about by automation will also involve changes in the way people live and earn their livelihood. I believe it will be more effective if engineers and scientists skilled in automatic control systems work with people skilled in dealing with social, economic and political problems to help bring about the needed changes in a smooth and socially acceptable fashion.

Unfortunately, the human time constant is one of the longest we have to deal with. Although the problems associated with the introduction of more widespread automation are great. The opportunities for a better world at peace make the challenge of using automation for the betterment of man one that is certainly worth working for.

From what I have seen of the preprints of the papers for this Congress, I am looking forward to an interesting week of discussions here. I am hopeful that the creativity and vision that have characterized I.F.A.C. from its beginning will continue to grow and flourish as we move ahead with this second I.F.A.C. Congress and on to the future.

The First I.F.A.C. Congress

A. M. LETOV, Second President of I.F.A.C.

Three years have passed since the Moscow Congress—the first I.F.A.C. Congress, which brought together 2,000 specialists from 28 countries; and at which some 300 papers dealing with the solution of major scientific and engineering problems of automation, were read and discussed.

Although reports of the Congress were published in newspapers and magazines in many countries, and the Congress Proceedings were published in Russian and English, I now remember the Congress not merely because it brought great satisfaction to those who took part, or because the aims of I.F.A.C.—so well expressed in the speech of our President, Professor Gerecke—were realized so widely for the first time in Moscow.

I recall the Congress for another reason; because, as the poet said, 'pleasant recollections are the fount of good inspiration', from which we draw new strength to develop the future activity of our Federation. The conditions for developing this activity are becoming more and more favourable.

We have now assembled at our second Congress. It has been organized by the Swiss National Federation, headed by our respected President Professor Gerecke. But the activity of the Federation is not characterized by this alone. The activity of I.F.A.C. is characterized, in particular, by the willingness of many other countries to organize subsequent I.F.A.C. Congresses. Such Congresses will undoubtedly be held.

Although it may be in 90 years time, I still hope fervently

that I can live to the noteworthy day when the I.F.A.C. Congress will have gone round all the countries in our Federation and returned once again to Russia—perhaps to Moscow—involving not 2,000 but 20,000 participants. I also look forward to the day when the linguistic difficulties of communication will have been overcome by the creation of miniature 'radio-computers' which will translate into one's own language the speeches of representatives of all countries on the globe; and to the day when science and technology will make it both pleasant and inspiring to look forward to what is to come a century ahead.

You will say that it is a very remote dream. As yet it is a dream, I grant you. Let me just say this. First, you are all people who do creative work—dreamers—and all the plans you implement so wonderfully begun with a dream.

Secondly, let me, by speaking of my dreams, give those with a sense of humour a chance to say, what else can a man do who, after 6 years of helping to run the Federation, and for the moment still its Past President, but relinquish the authority in three days when he retires.

Thank you, Mr. President, for the opportunity given me here to dream aloud; to my audience I say thank you for your patronage.

With all my heart I say, 'I look forward to meeting you at a new Moscow Congress, dear colleagues'.

The Information Revolution and Its Impact on Automatic Control

I. L. AUERBACH, President of the IFIP

The invention of the electronic digital computer in 1946 marked the beginning of the information revolution. The ensuing seventeen years have seen a development very much like the industrial revolution that followed the advent of the steam engine in 1765. In both instances, the advancement of civilization had created a growing need for new ways of accomplishing vital tasks. The major technological breakthrough not only filled the need, and opened new avenues in many fields, but led to the discovery of new fields, where development would have been out of the question without the new tool. Thus it was that the electronic computer brought about a revolution in information processing, rather than just advanced normal development in the field.

The essential feature of the industrial revolution was man's amplification of his brawn by the use of engines. In the information revolution the emphasis has shifted to the amplification of brain through computers and information processing systems. Already there are as many different kinds of computers as there are kinds of engines. The applications of digital data processing are limited only by the ingenuity of scientists and technologists in their respective technical fields.

There is a basic and fundamental difference between brawn and brain—a difference that is exaggerated when these faculties are extended and amplified by mechanical engines or electronic processors. A muscle or an engine consumes energy to accomplish work. The fuel can never be recovered or re-used. In contrast, information handling is non-destructive. Information is used and applied without being consumed. It can be used over and over again, and many of the applications augment the original supply, but none can diminish it.

The words in a book, for example, remain intact, and can be read by any number of people without loss of information content. The responses the words elicit in different minds may even go beyond the original content. Each new edition of a great book may have more footnotes than the one before it—words growing on words as they strive to capture ideas. Similarly, a computer manipulates information in a scientific computation, and generates new information from it. The information is never consumed by being processed; it can be retrieved and used repeatedly in many different ways.

This difference perhaps explains why the information revolution has been faster and more widespread in its implications than the industrial revolution. Electronic data processing is so broad a subject that only an infinitesimal fraction of it can be explored in a short time. I would like to take a brief look at the field where the engine and the computer work together; the impact of the information revolution on automatic control. In addition, at the request of your President, I will review the background of the International Federation for Information Processing (IFIP) and discuss the areas of cooperation between that body and the International Federation for Automatic Control (IFAC).

Figure 1 shows the basic structure of an automatic control loop. In it the status of a physical system is detected through

sensors or transducers and transmitted to a device labeled 'Computer'. This device identifies any differences between the indicated status of the system and its desired status, and activates controls to modify the physical system. The changes in status resulting from this modification are in turn sensed and transmitted to the computer, and so the operation of the loop goes on. The computer not only can guide the system through a series of steps, but can modify any future step on the basis of the results of previous steps.

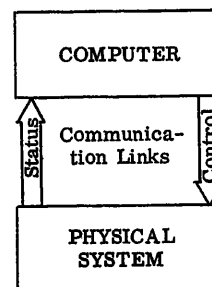


Figure 1. The automatic control loop

This simplified diagram illustrates how the computer performs the functions of a human operator. With its fantastic speed of reaction and calculation, its resistance to fatigue or distraction, and the great variety of inputs and outputs it can utilize, the computer can replace a human operator in many physical systems. More important, it can assume new tasks too taxing for human beings and thus make new physical systems feasible. The launching of a satellite, for example, simply could not be handled by anything short of an automatic computer system.

Still man's place in automatic control is a vital one. The loop shown in Figure 1 is usually part of a more complex loop as shown in Figure 2. The 'desired status' mentioned in the discussion of Figure 1 is determined by man. He observes the physical system, and applies his intelligence, his ability to judge situations rather than respond to them deterministically, and his set of values. He establishes the criteria and the end goals to be achieved by the system, and communicates his conclusions to the computer via programming. This is a critical input to the computer. It cannot be absent, as might be inferred from Figure 1, although it may precede in time the actual operation of the system.

This powerful combination of man, computer, and physical system multiplies the resources of all three. Automatic control combines the benefits of the industrial revolution and the information revolution, giving man an extension of his brain and his brawn, both applied to the same task. The digital computer makes this system quite distinct from the man-engine combination alone. It handles great quantities of data at tremendous speeds, extending the realm of operations that can be performed. Programming techniques also combine decision making with mathematical calculations, and this permits dis-

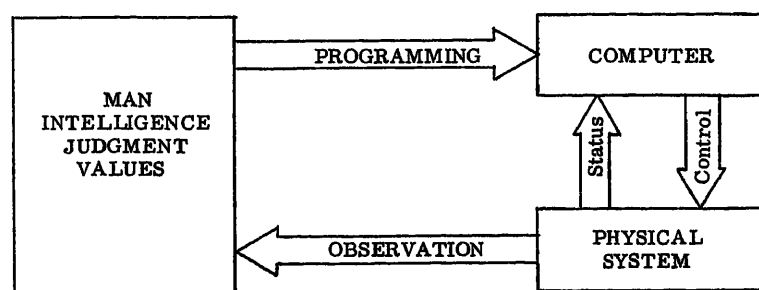


Figure 2. The man loop

continuous or discrete control to be intermixed with the various kinds of continuous or smooth control that are afforded by analogue devices.

It can be seen in *Figure 2* that man's portion of the loop, proceeding from the physical system to the computer, parallels the direct sensing of system status by the computer. Both connections are necessary, as each exploits the individual characteristics of its medium: man or machine. Some of the outstanding developments in recent computer history are directed toward man's turning over as many as possible of his own functions to the computer. Much of the programming process is being made automatic, and can be classified as computer reaction to a system status.

The computer may be multi-programmed, that is, may time-share or interleave a number of independent or interrelated programmes run at the same time. It is now feasible to have one computer run a programme that controls the physical system based on the results of an independent programme being run at the same time that derives economic and business criteria. For example, if the inventory and order control for a business were maintained by the same computer, then the output of the physical system would be based on the current requirements and permit very rapid response times. In addition, multi-computer systems are becoming more commonplace, and with appropriate communication links further broaden the variety of tasks that can be handled by computers in the automatic control loop.

The programming of the computer in the automatic control loop is far more complex than most people anticipated. The programme is actually interposed between the computer and the process or physical system it is to control. It is a necessary link in the computer controlled system. In this area, there is need for more work in automatic programming techniques and compilers specifically oriented toward process control. Multi-programme and multi-computer systems will add to the complexity and impose the need for far more sophisticated interrupt features and the techniques for their application. The skill required to formulate the computer programme is major and is far more difficult in complex interconnected computer systems. It should be clear that greater training for people capable of doing this work is essential.

It must be recognized that more and more is being done by computers that it was thought only human beings could do. Pattern recognition is one such extension of computer capabilities. There exist today devices for recognizing printed symbols in a number of different type fonts without human assistance. This enables the introduction of text from a printed page into a computer, where formerly translation into a digital form such as holes in paper was necessary. Similarly, it is possible for

computers to read maps and match them with the areas they represent.

Rather than belittle the activities of man's brain, these imitations of thought by computers show man's superior intelligence more clearly. The programming of artificial perception calls for not only the same perception on man's part, but a transcendent awareness of how that perception works. By reflecting on the way his own mind operates, man has been able to reduce many of its functions to the sort of simple instructions a computer can follow.

This has not been an easy process. In language translation, for example, great difficulties were encountered. Linguists were not immediately aware of how they translate. But linguists and computer engineers are consulting and coming to grips with the problem, and teaching both participants more about language than was ever known before. Completely new methods of linguistic analysis are opening up, which will be as useful to future language study itself as they are to computer applications.

Artificial learning is another field that has come into being as a result of mechanizing thought processes. The computer in the three-way loop can modify its own programme according to occurrences in the physical system. A man can programme a computer to play a game and then be beaten by the computer. Investigations in this area are shedding new light on the problems of educational psychology.

The area in which computer technology can be expected to make the most significant contribution to automatic control is in the optimization of continuous processes. This optimization will be achieved in two ways. The computer's computational capabilities will be utilized to make more effective use of data on the internal variables of the process. The computer also has the completely unique ability to help man to optimize a process on the basis of variables external, but related, to the process.

Process optimization on the basis of internal variables is coming about through the development of computer programmes that continually modify process parameters in the light of empirical experience. These are really automatic learning programmes in which the computer uses a model of the process to predict the response of a change in an operating variable. The computer then makes the change in the variable, observes the response (through sensory instrumentation), and modifies predictive methodology in the light of its empirical experience.

Process optimization on the basis of external variables is a concept that depends entirely upon the computer's unique capabilities. Going well beyond the concept of integrating the various loops in an individual process, work in this area is directed at integrating several individual but related processes,

plus such business variables as product orders, delivery, and inventory.

The benefits that can result from these two approaches to process optimization are obvious. However, the problems of realizing these benefits are extremely formidable. Success hinges upon how well we can integrate man, machine and the process into an effective closed loop. To do this requires an interdisciplinary effort on the part of the control, operating, and computer engineers.

Much work must be done on control theory and on formalizing the operating methods that are still largely intuitive. Before we can programme computers to effectively perform the process-control functions, we must deepen our understanding of the basics of continuous processes, and we must be able to establish explicit criteria for defining an 'optimum' condition. We must also learn how to translate the 'feel' human operators have for the process into computer programmes.

The effective application of the digital computer to process control is not only an analytical problem; it is also a software problem of major proportions. After the analyses, it is the computer systems engineers who must accept the final responsibility for developing and applying the proper software and programming skills, such as multi-programming and multi-computer programming, that will effectively relate the computer, the processes and the man to each other.

In a limited way, computers are reciprocating the effort to make them behave like men. They seem to be showing men how to behave like computers. The quantities of information handled in modern data processing systems have necessitated new approaches to the problems of indexing, storing, and retrieving information. The newly developed methods can be applied to situations not involving electronic computation at all. Even if all the electronic computers in the world ceased to exist, the effects of the information revolution would still be felt, and would exercise their influence on the future of civilization.

The potentialities of this revolution can best be realized with maximum communication within the field. This interchange of ideas should not be inhibited by national boundaries. It calls for international cooperation and international organizations such as IFIP and IFAC. Now I will turn to a discussion of the international Federation for Information Processing, the first international organization dedicated to all facets of the information processing sciences. As defined by IFIP, these information processing sciences include theory, mathematics, equipment, and application—all applied to the collection, transmission, computation, translation, storage, retrieval, reduction, and display of information.

As stated in its statutes, the aims of IFIP are threefold:

- (a) Sponsor international conferences and symposia on information processing, including mathematical and engineering aspects.
- (b) Establish international committees to undertake special tasks falling within the spheres of action of the member societies.
- (c) Advance the interests of member societies in international cooperation in the field of information processing.

One of the goals of IFIP is to expose the people of the world (those who will be affected by information technology as well as those directly associated with it) to some idea of the progress that can be made through the intelligent use of the electronic digital computer. We hope to make an increasingly greater

number of people aware of the information processing sciences and the benefits that can be derived from them.

In achieving the above aims, IFIP fulfills the need for better worldwide communication and increased understanding among scientists of all nations of the role information processing can play in accelerating technical and scientific progress. It is hoped that better dissemination and centralized control of information about computer technology and application techniques will result in greater scientific advances, which will achieve the two purposes of benefiting mankind and advancing the state of the art.

The first International Conference on Information Processing, sponsored by UNESCO, in June, 1959, provided a forum for the meeting of 1800 delegates from 37 countries. During the planning for this conference, it became apparent that future international meetings and other activities were essential to the development of the information sciences in many countries of the world.

On June 18, 1959, recognizing the importance and success of the UNESCO conference, representatives of the computer societies of 18 countries met in Paris to formulate the preliminary structure of IFIP. Statutes for the federation were drafted, and upon the agreement of 13 national technical societies (six more than the minimum required), IFIP came into official existence in January, 1960.

IFIP Congress 62

The IFIP Congress 62 was attended by more than 2800 scientists from 41 nations, who were exposed to a comprehensive survey of the technical achievements and goals that have been made possible and practical by the digital computer. This experience demonstrated to them the profound effect that the information revolution is having upon mankind.

In addition to the technical sessions at the Congress, the computer scientists and users attending had an opportunity to view an exhibition of the progress being made in hardware development. The INTERDATA exhibition included exhibits of 48 companies from eight nations. This exhibition, with its emphasis upon hardware, complemented the material presented in the technical sessions on the software and application aspects of information processing.

For the practical realization of its goals, IFIP has established three technical committees and one working group. The scope and accomplishments of these technical committees are summarized below.

IFIP TC-1 Terminology

The scope of this committee is the establishment of terminology of digital computers and data processing devices, equipments, media and systems. The objective is to promote the exchange of information, leading to the compilation of a multi-lingual glossary for information processing systems and related subjects.

The specific programme of work of this committee includes: select natural languages for which the terms shall be defined; collect documentation of pertinent glossaries; systematize a master list of terms and concepts requiring definition; create or adapt terms for missing concepts and assign these terms to one or more specific fields; choose, modify or originate accepted definitions.

To avoid duplication of effort, the IFIP Committee on Terminology was affiliated with a similar committee within the International Computation Centre of Rome to form 'IFIP/ICC TC-1 Terminology'.

This committee has met seven times to date, and by the end of 1963 will have defined and assigned words in the English language to approximately 1000 concepts. Then specific language area groups will translate these concepts into the major national languages so that the particular words may be chosen in whatever language describes each of the concepts most accurately. It is expected that a vocabulary of 1000 concepts will be published during 1964.

It is significant that the multilingual glossary being developed by IFIP/ICC TC-1 Terminology has been officially requested by the International Standards Organization through subcommittee 1 of its technical committee 97. ISO will use this glossary as the basic input in their effort to establish an international standard.

IFIP TC-2 Programming Languages

The scope of this committee is to promote the development, specification, and refinement of common programming languages with provisions for future revision, expansion and improvement. This specific programme of work includes: general questions on formal languages such as concepts, descriptions and classifications; the study of specific programming languages; and the study and, where appropriate, coordination of the task of developing new programming languages for which there appears to be a need.

Working Group 2.1 ALGOL

During the past year, a series of meetings was held between the original ALGOL authors and other experts who clarified and amplified certain aspects of ALGOL '60 language, removing ambiguities that existed. Through IFIP TC-2 the working group submitted the ALGOL '60 document to the council of IFIP which approved the document and made ALGOL '60 official IFIP language. Once again the International Standards Organization, through Subcommittee 5 of Technical Committee 97, has requested that certain specific additions to the ALGOL

language be considered and then submitted to ISO for consideration as an international standard.

IFIP TC-3 Education

At the August 1962 meeting of the Council of IFIP it was decided to form a new committee on education. The objective of this committee is to establish comprehensive training programmes and suggested curricula for the education of technical people from all over the world who are in fields in which the computer can make a significant contribution. Another function of the committee will be to generate material to acquaint the lay public with the computer and its impact on the various aspects of society. This committee will, in fact, serve as a central clearing house on all educational material pertaining to the information processing sciences. In this capacity, it will assist in preparing or providing translations, lists of available material, and other necessary information services.

The membership of each of the above IFIP committees is international, assuring each national group the opportunity to review and comment on all committee work before it reaches final, rigid form. This policy provides the committees with the additional advantage of having a consensus that includes the viewpoints of many diverse backgrounds.

The activities of IFIP require the time, effort and interest of many people from many parts of the world, all of whom are devoting their services willingly and without material reward. They are to be commended on their accomplishments, for through their endeavours they are demonstrating that people from diverse national backgrounds can work together and communicate effectively to achieve a worthwhile international goal.

There are many areas in which the work of IFIP and that of IFAC impinge upon each other. Cooperation can take place through the common membership of the same scientists in the national technical societies who are members of both our respective federations and by more direct cooperation of our technical committees. It is hoped that ways will be found in the coming years to increase the cooperation and coordination of the activities of these two international federations, and so to provide means for each of the federations to achieve its own goals more effectively and more quickly.

APPLICATIONS

IN THE ELECTRICAL UTILITY FIELD

Applications of Automatic Techniques in the Control and Operation of Electric Utility Systems

A Survey by B. FAVEZ

Introduction

Power transmission and production installations have always been open to the application of automatic techniques. Whilst turbine speed regulators may rightly be considered as the first large industrial regulators, automatic economic dispatching sets, which have been in service on certain networks for several years now, were the first large-scale realization of automatic optimization techniques. Furthermore, with regard to networks, automation, after having helped to overcome most of the technical difficulties, is being used more and more for reducing the cost of operation, which shows an advanced degree of technical development. Thus electric utility systems are considered by some to be the most automated groups in industry.

The very large variety of problems which face electrical utilities and the solutions developed by the latter are serious obstacles to the drawing-up of a clear and concise paper on the applications of automatic techniques in this field. The main object of automation development is, and always will be, the improvement of the quality of electrical supply, and, as this paper is mainly intended for consumers, these questions will be dealt with from the point of view of the different factors necessary to the quality of service, i.e. by successively examining the significance of utilities of improvements in the following basic characteristics: service continuity, minimization of voltage variations, minimization of frequency variations, and reduction of the cost of power supply.

Thus, after briefly stating the problems connected with each of the points, it will be shown how they have been satisfactorily solved by use of automatic techniques and the developments which can be expected in the more or less near future will be stated.

Use of Automatic Techniques for Improving Service Continuity

The permanence of supply can be affected by the appearance of a fault on one of the various elements of the network, i.e. transformation and production equipment, distribution and transmission lines.

Mechanical incidents, which may bring part of the production equipment to a halt, have no immediate electrical consequences, and, in order to prevent them having serious repercus-

sions, it is necessary, when the means of supply is cut off, to have sufficient generators on the network to supply the amount of power demanded by the customers. Though utilities take a certain safety margin in view of this kind of incident, its consequences cannot be directly avoided by use of special automatic techniques.

Therefore in this paper we shall examine only the automatic methods used for limiting the consequences of electric faults on transmission lines. The majority of such faults originate in the atmosphere (lightning) and there is no economic means of avoiding them. They can affect the permanence of supply either directly by reducing or even cancelling the voltage at the point of supply, or indirectly by provoking a loss of synchronism between network generators. We shall examine these points in turn.

Rapid and Selective Elimination of Faulty Lines

Electricity consumers are familiar with the use of protective relays which are safety automatic devices and we shall not dwell upon this point.

However, in the case of electrical networks, protection problems are rather different, due to the fact that generally the different transmission lines are meshed. Therefore a fault on one of these lines results in an over-intensity on all the lines terminating at the same sub-stations. The finding of the affected line by opening the circuit-breakers cannot be done by means of the classical maximum intensity relays frequently used in industry. Consequently more complicated protective techniques have been developed.

Some of these techniques are based on the comparison of the currents at the two terminals of a line. If the currents are the same, the line is intact; if they differ, the fault is detected and the circuit-breakers are brought into action. These methods meet with practical difficulties arising from the necessity of very rapidly transmitting signals from one end of the line to another. This is a common problem in the operation of networks which are industrial installations extending over very great distances and in which signal transmission is often a very important factor. This question will be returned to later.

Other protective devices, assuring good selectivity, have been perfected to the point of not needing telecommunication between the line terminals. These are 'distance protection devices' which, with only the local voltage and current values, measure the apparent impedance of the line. If this impedance becomes lower than the impedance which the line would have if it was short-circuited at the other end, it can be assumed that a fault has occurred on this line. Furthermore, measurement of the impedance enables the location of the fault to be evaluated, hence the name given to these automatic devices which in most cases provide excellent selectivity.

The development of such automatic protective devices over the last 40 years and of which we have obviously only given a superficial description, has enabled considerable reduction in the clearance time of faults; at present, a damaged line is detected in several hundredths of a second at the most, and in normal operation it is cleared in under 200 msec, sometimes even in 100 msec.

In addition to the expected technological changes which consist in replacing the electromechanical devices generally used at present by electronic equipment using semi-conductors, a marked evolution in the basic principles of protective equipment can be expected in the more or less near future.

At present, protective devices are directly associated with an element of the network (line or transformer), without any attempt at coordination between the information given by each of the different devices.

Such coordination, which would make network protective equipment more logical, could help to improve the situation in certain networks with very complex structures, and even with simple structures when an anomaly occurs in the working of one of the devices normally used for eliminating the defective element.

With present equipment, in very rare but not unpredictable cases, certain incidents can affect the permanence of supply. Such incidents call for action on the part of the operator, with all the inconvenience of slowness and risk of false moves that go with this unsatisfactory element of looped systems.

The development of 'logical' protective equipment, acting rapidly and surely according to strict instructions, should reduce even further the risk of interrupted supply.

Network Transient Stability and Automation

We cannot go into the details of the problem of network transient stability. We shall only mention the fact that synchronous generators, which form the major part of electrical supply, are, in normal operation, linked together by electromagnetic reactions. If we take a mechanical analogy, the rotors of the different alternators can be imagined as masses linked together by springs. As long as the springs resist the relative movements, the machines remain attached to one another and are in synchronism. If the masses separate too much, the springs are extended to breaking point and synchronous loss occurs, causing considerable fluctuation of the voltage and intense current circulations between the generators which may necessitate a service cut.

When a fault occurs on the network, the electromagnetic links between generators disappear and the rotors are free to separate from one another. If, when the fault is cleared, their position is such that it exceeds the separation corresponding to the breaking point of the springs in the mechanical analogy, then loss of synchronism occurs. The extent of the separation is pro-

portional to the time of application of the fault, hence the extra advantage of very rapid operating protective devices.

Having thus outlined the basic elements of network transient stability problems, we next consider the automatic devices which help to improve the situation.

If all the other factors are equal, the maximum angle between the rotors, in other words the separation between the masses which can cause the connecting spring to break, is directly dependent on the generator magnetic flux, i.e. on the alternator field current. This is why special systems of automatic control of alternator excitation have been developed. These improve the transient stability and are characterized by their very rapid and powerful action which takes into account various data on the voltage, its derivatives with respect to time, and even the angles between the rotors and their derivatives. These devices have in recent years been developed on an industrial scale, mainly in the U.S.S.R. where long-distance transmissions give rise to real transient stability problems, and are mentioned in the paper by Venikov and Tsukernik. Certain practical details on excitation automatic control equipment are given in the following paragraph.

Transient stability problems are very important on certain networks and it is necessary that such problems be taken into account in studies on network developments. Glavitsch's paper describes a method of studying the transient stability of multi-generator networks by means of digital computers. These very rapid automatic voltage control devices definitely improve the transient performances of networks, but are not the solution to all problems. In addition, the increase of generator power units, which is of undeniable economic interest, renders transient stability problems even more difficult and new automatic solutions are being considered.

Thus, generator set speed governors could be improved to prevent loss of synchronism by limiting their acceleration during the time the fault lasts. In the case of loss of synchronism, devices are being studied which would enable spontaneous resynchronization without having to separate the alternator from the network and to recommence the normal coupling procedure. At present, such procedures require human intervention and are very difficult when the network is perturbed after the incident.

Use of Automatic Techniques for Adapting Supply to Demand

Generalities

Apart from the always short-lived accidental and serious disturbances just mentioned, electrical networks are constantly being solicited by the variations in the power consumed at different points of the network. These power variations can be divided into two categories, according to whether they are approximately predictable, depending on variations in the weather, on human activities in the area supplied, or whether they are purely random, being caused by the overall load of a network resulting from the superimposing of a large number of single loads of relatively low unit power, of which the respective times of connection and disconnection are governed by random laws.

To give an idea of the possible extent of these load variations, the ratio of the maximum active power (generally late morning or late afternoon) and the minimum active power (generally in the middle of the night) demanded on the same day on one network can be over 2.

The random variations are much smaller. Their relative values depend on the size of the network and their absolute values are generally considered to vary approximately with the square root of the power of the network. For example, in a 10,000 MW network, these random load fluctuations remain for 95 per cent of the time under about 36 MW, i.e. 0.35 per cent of the total load.

At a given moment, the active power supplied by a generator set (the network frequency being equal to its reference value) is fixed by the position of the turbine admission valve. If a difference appears between the active power supplied and the active power demanded, then the generator rotation speed will tend to vary. Similarly, the reactive power supplied by a generator (the network voltage being equal to its reference value) is fixed by the alternator field voltage. If a difference appears between this reactive power and the reactive power demanded, the voltage of the network will tend to vary.

Thus, if there were no automatic control devices, the variations in demand would cause voltage and frequency variations. We would add that a difference between supply and demand, with voltage and frequency equal to their reference values, would not generally cause the total breakdown of a network, but that a new state would be established for different voltage and frequency values. In other words, network self-regulation, both of voltage and of frequency, is of some significance. However, if the demand-supply differences are of a certain magnitude, the resulting voltage and frequency differences could cause inconvenience to the customers, hence the need for devices adapting the reactive and active power supply to the respective demands. The control values of the voltage and frequency automatic control loops thus obtained are respectively the field voltages of generators and the positions of the turbine admission valves. The perturbing factors are respectively the active power variations and the reactive power variations.

Having thus outlined the problem, we have no intention of discussing questions of revolving electric set voltage and speed control, which are well known in the majority of industrial applications, and we merely give a few figures on the power levels of control devices used on power production equipment. On the contrary, we would draw attention to the special aspects of these questions on network speed and automatic voltage control. These special aspects are due either to the nature of certain equipment (for example steam and water turbines) or to the fact that, as a large number of generators operate in parallel onto one network, it is necessary for good technical and economical operation of the latter to maintain satisfactory distribution between these various sources of supply.

Minimizing Voltage Variations

The respective voltages at the different points of a network (voltage map) depend mainly on the transfers of reactive power between the generators. We must not forget that the reactive power at generator terminals can change its sign. In other words, contrary to what occurs in the case of active power, an alternator can either supply or absorb reactive power. Thus on networks, it is generally advisable to reduce reactive power transfers as much as possible in order to avoid the active losses caused by these reactive powers on transmission lines. Furthermore, these lines can either absorb for heavy loads or supply for low loads considerable quantities of reactive power, which

results in a marked variation of reactive power to be supplied or absorbed by the generators.

In the present state of network automation, generator sets are provided with voltage control equipment which has to maintain at a set value the voltage at the generator terminals, and if these reference values are well chosen, the flow of power between generators always remains low, whatever the load of the network. Thus the voltage map maintains a satisfactory appearance. The use of such local automatic control equipment

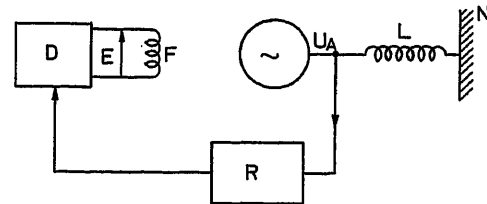


Figure 1. Example of a typical diagram used in studies on voltage automatic control of alternators on powerful networks

U_A Voltage at the alternator terminals; E Alternator field voltage; R Voltage regulator; D Alternator excitation system; F Alternator field winding; L HV-connecting line; N Very powerful network

does not generally present any difficulty with stabilization problems, except when it is used for increasing the flexibility of alternator operation from the point of view of reactive power absorption.

In order to outline the nature of this problem, of which the solution has been made easier by the use of classical methods of studying regulated systems, we shall take the general diagram in Figure 1, of an alternator connected by an HV line to a very powerful network. In this case, the transfer function relating the voltage variation at the alternator terminals to the variation of

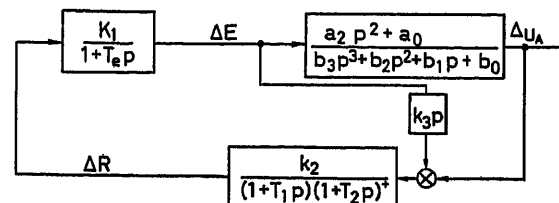


Figure 2. Block diagram corresponding to the typical diagram of Figure 1
 ΔE Relative variation of the alternator field voltage; ΔU_A Relative variation of the alternator output voltage; ΔR Relative variation of the control quantity of excitation system 'D'

its excitation voltage (which characterizes the controlled installation and is obtained by linearizing the performance of this installation around a balanced state) is given by the block diagram of Figure 2. The numerical values of the various coefficients depend on the balanced state under consideration, and calculation shows that from one of these states corresponding to absorption of a large amount of reactive power, the controlled installation becomes naturally unstable. In other words, this state corresponds to a relative position of the masses at which the springs are stretched to breaking point. Any disturbance, however small, in the wrong direction, will then cause alternator synchronous loss. Therefore such a state of operation cannot normally be accepted.

The use of an elaborate automatic system of voltage control enables the alternator to be stabilized again; a typical transfer function of one of the possible solutions is given in *Figure 2*. Under these conditions, it is possible for the alternator to operate in a previously prohibited zone and for it to absorb a far greater amount of reactive power than formerly possible.

As in the off-peak hours of large networks, HV transmission lines act as reactive power generators (main capacitive effect). This possibility is economically very advantageous, as it makes the installation of special equipment for absorbing this power (reactances) unnecessary.

To give an idea of the importance of this point, the use of a well adapted voltage regulator increases the reactive power that may be absorbed by a 125 MW alternator from 55 MVar to 110 MVar, these figures are obviously only approximations.

We now come to the characteristics of voltage automatic control equipment. Control devices have to supply the excitation windings of alternator rotors with electrical power of up to 400 kW for 125 MW machines, and 750 kW for 250 MW machines. Until recently these control devices were composed exclusively of d.c. revolving machines driven either directly by the main set or indirectly by an auxiliary motor. The time constants of such machines vary according to their design between 0.15 and 0.3 sec, and they can deliver for short periods voltages above the normal operation voltages in a ratio which, according to the case, varies between 1.4 and 4*. The recent development of the semi-conductor technique has enabled these factors to be considered for large synchronous generator excitation and, at present, various applications are already in use.

With regard to the actual voltage regulators, these have considerably progressed since they first appeared over 30 years ago. *Figure 3* gives the block diagrams of the different types on which

* Figures to be taken into consideration in studies on the influence of automatic voltage control in transient stability.

this progress can be observed. The first regulators were discontinuous acting instruments. Tirrill regulators are the most well known. Voltametrical scales used as vibrators regulate the average values of resistances placed in the excitation circuits of alternator exciters. We then got rheostatic regulators with driving motors commanded by voltametrical scales. The action of these regulators, by nature of the deviation detectors, is always discontinuous. Torque motor rheostatic regulators marked an important step in continuous acting regulators. The only discontinuity in this type of equipment comes from the definition of the excitation rheostat, which, on account of the powers involved, is a step rheostat.

However, this last solution does not easily carry out the more and more complicated transfer functions required by the increase in the transient steady-state stability limits and this last decade has seen the development of regulators of which the detection elements as well as the amplification elements are of the continuous acting electrical kind. Such regulators are now almost perfected and in general network utilities are satisfied with them.

Thus, at present, reactive power supplies are automatically adapted to the demands by the voltage regulators with which generator sets are equipped. The distribution of reactive power between generators and the reduction, to what is estimated as its optimum value, of the reactive power flowing between the generators is carried out by hand on the command points of these regulators. However, if no such action is taken, the network load variations do not provoke technically troublesome variations of these currents. Unlike developments in the field of supply and demand, automatic adaptation of active power, there are as yet no networks equipped with devices which automatically control the distribution of reactive power between the various machines according to a technical or economical criterion.

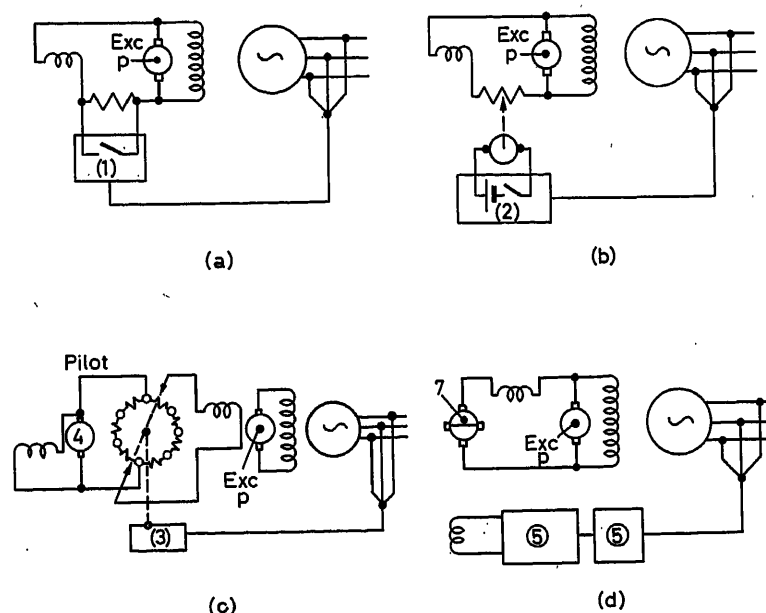


Figure 3. Basic diagrams of the various types of regulators used successively since 1930

(a) Tirrill vibrator; (1) voltametric scale; (b) Rheostatic system with voltametric scale (2) and without pilot exciter; (c) Rheostatic system with torque motor (3) and with pilot exciter (4); (d) Continuously acting system; (5) detector (6) static amplifier (7) rotating amplifier

Undoubtedly a marked development in methods of network operation can be expected in this field. Admittedly such centralized control would imply the existence of very developed systems of telecommunication. For this the substructure which often exists for active power control could be considered. If this has not already been done, it is mainly because the problem is in general not acute and because economical repercussions of approximative distribution are, *a priori*, not very important. The regulators used at present on generator sets could be used for possible extra control and a marked development cannot be expected in this field, except, obviously, in technological details. Thus voltage control automation is not, at present, essential to network utilities. This is confirmed by the fact that not one of the reports presented at this Congress deals directly with this question.

This is certainly not the case with regard to adaptation of supply to demand of active power, as it is this question which seems to have developed the most during the last few years as we shall now try to show.

Minimization of Frequency Variations

Speed Control of Hydro-electric Sets - Frequency control has always been an important subject to network utilities, as is shown by the fact that 6 of the 14 reports on network automation presented at this Congress deal with this subject. Stabilization of speed control of hydro-electric sets has up to now been the subject of a great deal of research, being a relatively difficult problem owing to the particular nature of controlled installations. The transfer function of the controlled installation presents a non-phase minimum element showing the hydraulic reactions and use of relatively complex regulators is necessary.

Since the beginning of the century, certain original solutions have been developed which have also been used later in other fields of application. The development of modern study methods of controlled systems has shown these solutions to be the best possible, and the principles of control have not noticeably altered in the last twenty years. However, such studies have resulted in a marked improvement in the choice of the optimum numerical values of the regulator characteristic parameters. The spectacular change in regulator conception, which occurred in 1953 on the introduction of electro-hydraulic control equipment, greatly benefited from these studies which had previously often

remained in the theoretical stage owing to the difficulties of adjustment of the characteristic parameters of mechanical control equipment.

Figure 4 is a typical block diagram of such a control set and includes the transfer functions of the hydro-electric installation, the overall set and network, and of a regulator of the accelerotachometric kind.

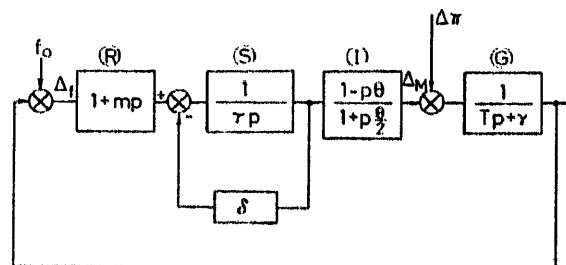


Figure 4. Typical block diagram of a speed control loop, for a hydro-electric set

R Speed regulator; *S* Valve control servomotor; *I* Hydraulic plant; *G* Turbo-alternator set; Δf Relative frequency variation (speed); ΔM Relative variation of the driving power (turbine); $\Delta \pi$ Relative variation of the load power (electric load)

In such plants the control devices are formed by hydraulic servomotors working the turbine input valve. These servomotors are among the most powerful of their kind used in industrial automation, as shown by Table 1.

The servomotors are governed by control valves worked by the detection, correction and amplification devices which form the 'brain' of the set. These devices were formerly based on hydraulic and mechanical techniques, but owing to the difficulty of adapting the characteristic parameters and to the lack of flexibility with regard to the introduction of outside signals into the regulators, which is becoming more and more important with the increase in network powers, electrical control governors have been developed in the last few years, the use of which is now tending to become general.

This problem is still being studied and is the subject of three reports presented at this Congress. They give very useful information on these studies which nowadays take into consideration as exactly as possible the real characteristics of the elements of this control set.

Table 1. Characteristics of a Few Servomotors of High Powered Turbine Admission Systems

Nature and power of the turbine	Servomotor size		Maximum oil pressure (kg/cm ²)	Maximum servomotor force (t)	Minimum servomotor manœuvre time		Cut-off frequency (linear process) (c/sec)
	Diameter (mm)	Stroke (mm)			0	F	
Hydraulic Kaplan 52 MW	Gate 550	700	28	65	20	5	0.16
	Blade 2,200	240	28	110	20	30	0.1
Hydraulic Francis 100 MW	Gate 500	450	20	39	15	4	0.2
Hydraulic Pelton 57 MW	Needle 345	170	30	28	20	23	0.25
	Deflector 210	450	30	10	20	3	0.25
Steam turbine 125 MW	Valve HP 260	200	13	6.8		0.6	1
Steam turbine 250 MW	Valve HP 270	249	22	12.5		0.40	1

The very complete formulation given by Borel provides the basic elements for optimization studies of regulator characteristics, by taking into account the real characteristics of the controlled installation, especially with regard to the turbine and hydraulic installation transient performances.

The paper by Stein shows the possible importance in these control systems of certain regulator non-linearities in view of the fact that the usual solution for certain installations leads to a conditional stability.

Finally, Tschumy's report gives an example of methods of determining the optimum characteristic parameters of regulators by means of digital computers.

We would also mention that very interesting studies have been made on the determination of the exact nature of the active load random fluctuations observed on networks. These studies have approximately fixed the disturbance statistic characteristics (frequency spectrum) to be taken into account for the determination of the regulator optimum adjustment.

Thus, we observe the importance attached to such questions, for which a certain development can still be expected. This could be mainly the perfecting of regulators which automatically adapt themselves to exact operating conditions, i.e. regulators having characteristics which vary in function of the generator loads and the hydraulic conditions of the moment (auto-adaptive systems). Electro-hydraulic regulators are well adapted to this possible development, and, in this field, no very spectacular changes can be expected.

Speed Control of Thermal Sets—Until recently, speed control of sets driven by steam turbines had not been studied to the extent of the problems just mentioned. In practice stabilization of the speed control of this kind of generator is less complicated than that of hydraulic sets, as the flow of steam lends itself better to sudden modifications than that of water. Hence the majority of studies on thermal sets have been on overspeed limitations after sudden unloadings, as these high speed rotation units do not tolerate overspeeds.

Development of reheating turbines and increase in unit powers which reduce set starting-up times have complicated both overspeed limitation and control stabilization. However, methods developed for hydraulic sets provide data and equipment adaptable to thermal set control equipment similar to that mentioned earlier, i.e. generalization of electro-hydraulic regulators. Two reports on this question are presented at this Congress.

Eggenberger describes an electro-hydraulic speed regulator for a reheating turbine, and shows its advantages compared with the mechanical regulators universally used until very recently. The flexibility of this type of equipment is very useful in this field, in which starting-up problems are very delicate. Furthermore, such devices enable easy linearization of the response curves of the overall control loop, which is most advantageous for operation. They also appear to be very satisfactory for overspeed limitation. This report mentions a possibility of overspeed limitation in the case of a sudden total unloading of 106 per cent of the rated speed by a set of only 5 sec starting-up time. Such a result could allow a reduction of the overspeed to be taken into account in studies on generator dimensioning, which could result in very obvious economic advantages.

The paper by Ehling studies the speed control of different types of steam turbines, and can be compared with Borel's report which gives the bases of such a study for a hydro-electric set. We expect to increase our knowledge of the transient behaviour

of controlled installations by more advanced physical and mathematical analyses of the processes and various experiments on existing sets. It will then be possible to improve the choice of turbine characteristic parameters and even their mode of action in the case of reheating turbines which have several control devices.

Thus, in this relatively recent field of study, there will certainly be a marked progress in regulator conception, their control function and their participation in the various very complex operations of thermal set stopping and starting up.

Heat Control—Command Automation of Thermal Power—If, in hydro-electric plants, only turbine regulators are used for automatic adaptation of the supply to the demand, in thermal power stations it is even more necessary to maintain steam pressure and temperature conditions at the turbine input by control of the fuel supply. This automatic system is referred to as a heat control system.

The problem of heat control is one of the most complicated problems in electrical power production, and up to date its solutions do not appear entirely satisfactory. Generally speaking, it amounts to the control of a multivariable system, as, among other things, it has the function of controlling the boiler thermal power, controlling the fuel, controlling the steam temperatures, and controlling the water level in the boiler tank (when it exists).

The difficulties of such control functions arise from the interaction between the different control loops. Thus the control quantity of one loop can be considered as the disturbance factor of another loop. This is due to the physical nature of the phenomena and cannot be avoided.

The importance of the quality of heat control is partly due to economic considerations. According to reductions in the differences between the effective values of the controlled quantities and their reference values, it is possible to choose the reference values near the technological limits of the equipment (for example, the maximum temperature of steam), which are beneficial both to the investment costs and to the theoretical operation of the plant. Thus the security margins usually allowed for dimensioning could be reduced. Furthermore, if the transient performance of the control loops is satisfactory, the plant could always be maintained almost at its optimum production, whatever the load variations imposed on the generator by variations in demand on the network.

To complete this rapid examination of problems on thermal power station operation, we would once again mention the importance of the starting-up and stopping processes in these plants. During these processes the boiler and turbine thermal states vary considerably, and great care has to be taken to avoid dangerous thermal and mechanical stresses on these different elements. Furthermore, on up-to-date sets, there can be almost a thousand points to supervise.

Having thus given the basic elements of the problem, we next briefly state the main steps in the development of automation in thermal power station operation. Formerly such stations were operated locally and by hand. A large staff were in local control of the various elements; and, in view of the natural interaction between the latter, this presented numerous difficulties.

The first automatic loops were introduced with fuel automatic control at the beginning of this century, but for a long time remained relatively rare. Only 30 years ago, thermal power stations, apart from a very few exceptions, were still operated locally and entirely by hand.

Operational difficulties first led to an attempt at control centralization, enabling a coordination in commands. However, the carrying out of these commands depended on network staff locally operating the various control equipment.

Little by little, local automatic control loops were developed, which led to the situation existing at present in most of the up-to-date thermal power stations, in which, from a central control room, a very reduced number of personnel can operate the various command elements of the boiler, the turbine and the alternator. These elements are equipped with local loops which automatically regulate the temperature, fuel, thermal power and level. The staff can alter the command points of the local control loops in the same way as they can take over purely manual control of the power station, which frequently occurs in the case of very large disturbances beyond the control of the automatic devices.

In view of this situation, attempts were made to perfect 'non-interacting' control systems, in other words systems which anticipate that necessary modifications of control quantities of local loops perturb the other loops and which provide against such perturbations by directly altering the control quantities of the other loops. These 'non-interacting' systems should prevent the oscillations around the reference values of the different controlled quantities which are observed with usual systems, and the gain in efficiency expected from suppression of these cycles is calculated at about 0.5 to 1 per cent, which is far from negligible.

These 'non-interacting' control devices are also expected to improve the control transient performance and enable it to overcome large-scale disturbances. However, in practice, such automatic equipment demands a good knowledge of the transient performance of the controlled installation; this fact has, over the last ten years at the most, given rise to numerous studies which at present are still not completed. Even if these non-interacting control loops are one day perfected, they will not answer the overall problems connected with thermal power station operation. Problems on the numerous important parameters, on starting-up and stopping and on efficiency optimization, remain essential and are further complicated by the increases in unit powers and the technical developments in the field of thermal generators. These reasons have led to a decisive development, i.e. the use of digital computers for the control and the command of these plants.

The use of computers was first studied in the United States about 1955 and was based on automatic collection of information on the state of the power station, on automatic supervision and efficiency calculations. Such equipment had no direct effect on the working of the plants, but considerably helped operators by taking over the supervising of about 1,200 quantities and providing them with very accurate information on what to do in order to improve the boiler performance.

Next command of the starting-up and stopping sequential operations by computers was examined, and put into practice. On receiving all the necessary data on the exact state of the different elements of the plant, the computer enabled acceleration of the starting-up time, without any detrimental stresses being applied to any part of the equipment. This form of computer sequential command has brought about a spectacular reduction of the starting-up time. An operation that formerly took between six and seven hours now takes only four hours and with no strain on the equipment.

Another step in computer use consists in using them directly in connection with the command points of local control loops, in order to continually improve the performance of the installation. Finally the suppression of these local loops can be considered. The computers would then be in direct command of the control instruments.

At present, there are about 50 thermal power stations in the world using digital computers for collection of data, automatic supervision and efficiency calculation. In about fifteen of these the computer is in direct permanent command of operations. The majority of these power stations are in the United States. The two most well known (the first to use computers for direct command of both the starting-up and the control) are those of Little Gipsy and Huntington Beach, which have been given a good deal of publicity lately in technical literature.

A few additional details give a clearer idea of the extent of the problem in question and of the interest to electrical utilities presented by the development of these techniques. The number of quantities dealt with by a computer (input elements) is about 1,200, of which approximately 600 are supplied in similar form (mainly temperature, 70 per cent) the others being 'all or nothing' signals. The speed of data is, at present, between 5 points and 150 points per second. The output quantities of a computer number about 400, of which approximately twenty are in analogue form, the remainder being 'all or nothing' signals. These computers must have considerable storage in order to inscribe the various programmes corresponding to all the situations considered, and the extent of storage capacity of present computers is between 50,000 and 100,000 words.

The main advantages to utilities of the generalized use of computers are as follows:

Improvement of the efficiency of the plant: a gain of 1 per cent being generally expected (to give a better idea, we could say that a 1 per cent efficiency improvement on a 250 MW thermal set means an economy in present values of about $3 \cdot 10^{11}$ kcal, which, for example, with the cost of the calorie in Western Europe provides an actualized economy of about 700,000 dollars).

Increase in operating flexibility, which is of marked interest for network operation. The inherent difficulty of heating control renders possibilities of computer adaptation of control loop characteristics (auto-adaptive system) very tempting.

Improvement of equipment reliability by better decisions on the occurrence of an incident. Consequently, the thermal sections will be more available, which will reduce the extra operating costs of replacing failing sections by older ones, accidental breakdowns will be decreased, hence a possible reduction of the revolving reserves and the risk of very serious accidents will also be cut down, which obviously is difficult to estimate.

Reduction of control staff. This is debatable, as certain utilities consider that they have already reduced their operating staff to a minimum.

Modification of the very conception of power station control equipment, which could result in marked investment economics. For example, the complete suppression of certain manual equipment can be anticipated. In present stations, this adapting of the main equipment to automatic command has not, for very good reasons, been fully accomplished. It is understandable to first want to make sure of the good operating performance of the new command techniques and the amount of confidence that can be placed in the new instruments for continuous industrial operation.

The economic interest of digital computers for thermal power stations will certainly be justified by present realizations, previous estimations having given favourable results. Cost of measurement and command equipment in classical power stations represents about 6 to 7 per cent of the total cost of the plant (i.e. about 25 to 30 dollars per installed kW). The additional costs of digital computer operation (including the adaptation of the detectors, of the control devices and the computer) are estimated at about 7.5 dollars per installed kW. Furthermore, we would point out that the increase in unit power economically justifies the use of computer control, the cost of these instruments being practically independent of the section to which they are attached.

In view of the importance of this question, it may seem surprising that no report on the subject has been presented at the present Congress. This could be explained by the amount of recent technical publications on it, but it is to be hoped that this aspect of network automation will be developed at future I.F.A.C. congresses.

Two papers only deal directly with heat control, one is by Kanda and the other by Kindermann. The former gives very interesting information on the perfecting and performances of an analogue optimization system of boiler combustion efficiency by automatic control of the arrival of air, and shows the practical difficulties of such control. These are mainly caused by the fluctuating character of various characteristic quantities of the equipment and of its fuel supply. This kind of problem generally exists in this type of industrial plant, and the same difficulties occur in connection with computer use.

Kindermann gives a good example of the kind of study methods to employ for determining the performances desirable for boiler control instruments; the particular case considered in this report is that of reheater control. Knowledge of the transient behaviour of the controlled plant is essential, and, though supported by physical and mathematical analyses, must always be based on results of experiments made on real plants.

A more thorough knowledge of transient behaviour is actually one of the main aims of those who plan for even more complete automation of thermal power stations. Studies are being carried out in various countries and we can expect to obtain, in the near future, complementary information which will enable another step to be taken in this direction.

Generalization of the use of digital computers in thermal power stations will certainly be, in the next few years, the most spectacular development in electrical power production. However, we must not underestimate the problem and numerous questions that will have to be answered before we obtain the ideal of an entirely automatic power station receiving from the network command instruments (automatic dispatching) only signals for stopping-starting-supply of active and reactive power, without the need of human intervention for it to accomplish its primary function of producing electrical power supply perfectly adapted to the need of the customers.

Automation of Nuclear Power Stations—Nuclear power stations came into being not long before the development of digital computers in plant control, and from the very first, this type of power station made use of the great possibilities of this technique.

In nuclear power stations the number of quantities to be supervised can be greater than in thermal power stations, and may attain over 2,000. However, the automation technique used

is not fundamentally different from that used for thermal power stations, though security has an even greater importance. Here again a knowledge of the transient behaviour of the controlled installation is a necessity, and M'Pherson and Muscettola deal with an aspect of the transient behaviour of a boiling water nuclear reactor, and this paper has a more general character. It shows the difficulties, which occur in all systems of this kind, of representing the performance of the mixture of steam and water.

Nuclear power stations have certain very special problems which necessitate special automatic solutions. This is the case, for example, of the charging of nuclear reactors which is rendered complicated by the number of necessary manipulations and the necessary accuracy for controlling in position the large mechanical instruments. One paper describes a solution using a hybrid technique of a perforated tape programme and analogue positioning systems.

Reactor transient control has also been the subject of numerous studies during recent years. The probable development of these kinds of automatic technique should render power stations entirely automatic, to enable its optimum use in the overall means of production of large interconnected networks.

Special Aspects of Frequency Control on Large Interconnected Networks. Power-frequency Control—Up to now we have described problems on speed control and load variations of hydro-electric and thermal generator sets resulting from the latter without making a distinction according to the kind of network under consideration. As for voltage control, when several generators supply one network, the problem of load distribution between them is added to that of the speed.

With regard to voltage control, the situation is the same today as it was at the beginning of network operation, i.e. sets equipped with static speed regulators supply active power, P_i , which, in theory, varies linearly with the frequency according to a steady state law:

$$P_i = P_{0i} - \frac{\Delta f}{f_0} \cdot \frac{P_{Ni}}{\delta_i}$$

(see Figure 4) an expression in which P_0 is a programme power set by hand on the speed regulator, Δf the frequency variation with respect to its reference value, δ the regulator statism, and P_{Ni} the rated power of the set in question. For the sake of simplification,

$$k_i = \frac{P_{Ni}}{\delta_i} \cdot \frac{1}{f_0}$$

As the frequency is the same at all the points of a network, the distribution of the total amount of consumed power is automatically carried out in proportion to the respective statisms of the different regulators on a basic distribution set by the respective values of the programme powers P_{0i} (see Figure 5 in the case of two generators).

Under these conditions, by neglecting the network auto-control, a deviation $\Delta\pi$ between the demand and the sum ΣP_{0i} of the programme powers provoke, in steady state, both a frequency variation

$$\Delta f = \frac{\Delta\pi}{\Sigma K_i}$$

and a variation

$$\Delta P_i = k_i \cdot \frac{\Delta\pi}{\Sigma k_i}$$

of the power supplied by each set with respect to its programme power.

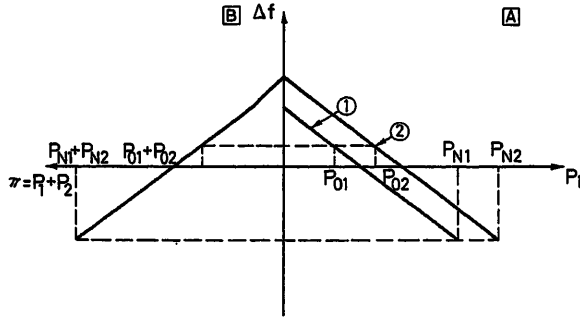


Figure 5. Principles of the automatic load distribution between two generators equipped with 'static' speed regulators

Δf Frequency variation; P_i Output power of generator i ; π Power demand; A Individual characteristics: frequency-generator power; B Overall characteristics: frequency-load power

Studies and tests carried out over the last ten years have shown that random fluctuations of network loads present a typical deviation σ_p , which is a function of the network total power and the nature of the load in accordance with the relationship $\sigma_p = \sqrt{mP}$, P being the network power and m a coefficient varying with the nature of the load, for example about 0.03 for Western European networks. Furthermore, with the statisms usually employed on set speed regulators, the overall statism of a network is about 10 per cent, i.e. $\sum k_i \approx 0.2 P$ for a 50 c/sec network.

Under these conditions, numerical calculation shows that, as soon as the network attains a certain power, the amplitude of frequency random variations remains low enough to refrain from seriously inconveniencing the customers. Thus for 2,500 MW networks, the typical deviation of the frequency fluctuations is 0.017 c/sec, and for 10,000 MW networks it is reduced to 0.0085 c/sec. As in practice these fluctuations are distributed according to a gaussian law, the amplitude of the frequency deviation is, in 95 per cent of cases, less than twice the typical deviation, which proves the excellence of the frequency control thus obtained.

In conclusion, the existence of load random fluctuations on large networks does not cause some frequency variations and does not call for the use of frequency automatic control devices other than those with which generator sets are normally equipped.

However, as we have always shown, the anticipated load variations are much greater, and it is necessary to modify the programme values P_0 , whatever the power of the network under consideration. Such automation calls for other control instruments.

Furthermore, the development of interconnected networks has raised the problem of load fluctuations on interconnecting lines. We can easily understand this problem by taking the typical diagram in Figure 6 which represents the connection of two networks A and B by an interconnecting line I .

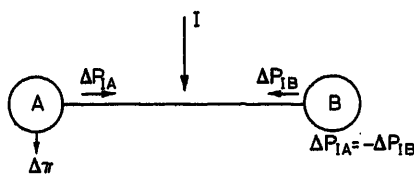


Figure 6. Basic diagram of the electrical interconnection between networks A and B

I Interconnecting line

If, during steady state operation, a load variation occurs, for example in network A , of amplitude $\Delta\pi$, the resulting frequency variation will be:

$$\Delta f = \frac{\Delta\pi}{\sum k_i + \sum k_i}$$

the power supplied by the generators of network B will vary by a quantity

$$\Delta P_B = \Delta f \cdot \sum k_i = \Delta P \cdot \frac{\sum k_i}{\sum k_i + \sum k_i}$$

As the demand on network B is assumed constant, the power variation is entirely on the tie-line and, if it persists too long, may cause the breaking of this line through overloading. Therefore it is necessary to control the exchange of power on the tie-lines. The first studies and applications of this kind of automatic control date back to about thirty years ago, and were used at about the same time on various United States and European networks. The problem took on additional importance when, in about 1950, the large Continental interconnections started to develop.

The solution almost generally adopted at present, in various forms, is that of the 'frequency-power' type of control. This consists in automatically varying the programme powers, P_0 , given to the regulators of the generator sets, as a function of the frequency variations and of the power variations of the interconnection, to cancel in a balanced state both the frequency deviation and the power deviation of the interconnection, hence the name given to this kind of control.

The method consists in working out at a point on the network a linear combination of the frequency deviation Δf and of the exchanged power deviation ΔP_I ,

$$\varepsilon = \Delta f + \frac{\Delta P_I}{\lambda}$$

and in varying the programme power of certain of the network generator sets at a speed proportional to this deviation. The sum of the programme powers of the network generators will be a linear function of the integral, with respect to the time of deviation ε . Thus, a network is balanced only when the sum

$$\left(\Delta f + \frac{\Delta P_I}{\lambda} \right)$$

equals zero, i.e. in Figure 7 at any point on the line of equation

$$\Delta f + \frac{\Delta P_I}{\lambda} = 0$$

If this control is applied simultaneously to two interconnected networks, the sign of the power deviation $|\Delta P_I|$ is obviously different for each of the networks, we can see that the only balanced point is the meeting point of the two balanced straight lines of the networks A and B . This balanced state corresponds to zero frequency and power deviations.

The use of the 'power frequency' control calls for a very important substructure of telecommunication means on the network, which transmit the power values of the interconnection lines both towards the network point where ε is calculated and from this point towards the various generators in charge of

control. It is advantageous for a considerable number of generating sets to participate in this control, which shows the indispensable development of telecommunication links.

Different 'power frequency' methods have been perfected and have contributed considerably towards the development of interconnections. At present the largest existing interconnection covers all the Eastern networks of North America and represents a power which must now attain and even exceed 112,000 MW.

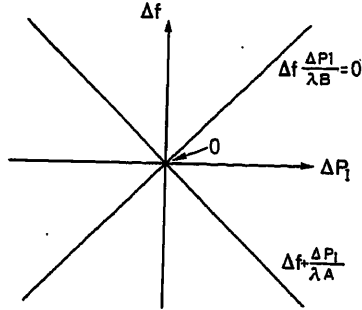


Figure 7. Static characteristic of the 'power-frequency' control equipment

Δf Frequency variation; ΔP_T Power variation (tie line); 0 Simultaneous balance point of the control equipments of networks A and B

The Western European networks form the second largest interconnection in the world, with a total power of over 50,000 MW. Not one report presented at this Congress deals directly with this question, yet had such a manifestation occurred several years ago it would probably have been the subject of the majority of the reports on the use of automation for electrical networks. As it is, this control technique is so perfected that interest has passed on to the economic aspect of network operation. Thus, whilst power frequency control enables the frequency variations to be overcome and very large interconnected groups to be technically operated, power distribution between generator sets follows a pre-established programme, as the load variations provoked by this control are distributed between the generators in proportion to influence coefficients set by hand. These coefficients are chosen according to certain rules, which do not necessarily operate the network at optimum conditions.

The telecommunication substructure demanded by power frequency control enables remote control of all the important machines on the network, and naturally led to the idea of using it for assuring economical distribution of supply. This brings us to the final aspect of use of automation on electrical networks, that of reducing the cost of power supply by optimization of the means of supply.

Minimization of the Cost of Power Supply

Basic Principles of Economical Dispatching

In order to simplify our explanation, we shall consider for the moment the case of a network entirely supplied by thermal sets. Therefore, we assume the network to have n generator sets and M points of power supply. The first problem consists of choosing the powers $P_1 \dots P_j \dots P_n$, supplied by each generator set in such a way as to obtain, once a balanced state has been established, the minimum cost of supply.

In order to obtain a normal state of operation, it is necessary that the power supplied to the network, i.e. $\sum P_j$ be equal to the power consumed, which is the sum of the power demanded by the consumers $\sum R_K$ and of the losses on the transmission network, i.e. p .

Whence the equation

$$\sum P_j - p - \sum R_K = 0 \quad (1)$$

The losses are a function of supply and demand, which depends on the structure of the network, and

$$p = p(P_1 \dots P_n, R_1 \dots R_K \dots R_M) \quad (2)$$

The total cost of power supplied by the thermal power stations in a unit of time depends entirely on the loads of all the power stations, and

$$F = F_1(P_1) + \dots + F_j(P_j) + \dots + F_n(P_n) \quad (3)$$

It is this function that has to be minimized, eqns (1) and (2) being respected.

In a first attempt at solving the problem, made before World War II, the losses on the transmission network were neglected, which gave:

$$\sum P_j - \sum R_K = 0$$

$$F = F_1(P_1) + \dots + F_j(P_j) + \dots + F_n(P_n)$$

Simple use of the calculation of variations leads to the solution of this problem, which consists in equalizing between themselves the partial derivatives with respect to the different powers produced by the cost function F , i.e.

$$\frac{dF_1}{dP_1} = \frac{dF_2}{dP_2} = \dots = \frac{dF_j}{dP_j} = \dots = \frac{dF_n}{dP_n} = \lambda$$

These various functions represent the marginal cost of production of the various power stations, quantities which depend only on the characteristics of these power stations. For a long time, this distribution method has been used for choosing the programme values P_0 to be given to the turbine speed regulators mentioned previously. This method of operation is still used in a large number of networks not having automatic dispatching.

However, on very extensive networks on which the transmission losses can reach up to 10 per cent of the power consumed, this simplified solution is not entirely satisfactory. Yet, consideration of the losses is very difficult, because of the complexity of eqn (2). If the form of this equation is known, then minimization of the cost is, in theory, quite simple; it is but a question of obtaining a supply distribution such that it makes no difference which of the power stations is used to compensate an elementary load variation dR_K occurring in one of the demand centres.

If power station j compensates this variation dR_K , its supply will vary by a quantity dP_j such that

$$dP_j - dp_{jK} - dR_K = 0$$

i.e.

$$dP_j = \frac{dR_K}{1 - \frac{dp_{jK}}{dP_j}}$$

Ratio dP_{jK}/dP_j is the network differential loss with respect to the power station j and demand centre K , which can be calculated if the form of function φ in eqn (2) is known.

The supply cost variation is then

$$dF_j = \frac{\partial F}{\partial P_j} \cdot dP_j = \frac{\frac{\partial F}{\partial P_j}}{1 - \frac{\partial P_j}{\partial P_j}} dR_K$$

We generally write

$$L_j = \frac{1}{1 - \frac{\partial P_j}{\partial P_j}}$$

this factor being termed 'penalty factor'.

The cost will be at its minimum if values dF_j are, under these conditions, all equal, i.e.

$$L_1 \frac{\partial F}{\partial P_1} = \dots = L_j \frac{\partial F}{\partial P_j} = \dots = L_n \frac{\partial F}{\partial P_n} = \lambda$$

λ being the marginal cost of supply.

This equation system is referred to as coordination equations and served as a basis for the first industrial realization of automatic economical dispatching.

In order to undertake such work, it was necessary to develop methods of calculating the differential losses, which has been the object of numerous studies over the last ten years. Several methods leading to more or less definite results have been suggested, and the discussions on the subject are still going on. The active losses on a network depend not only on active power transfers but also on those of reactive power, and supply optimization must apply not only to the active power distribution, but also to that of the reactive power.

Present Automatic Dispatching Realizations

The first economic dispatching outfit was used in the United States about 1955. In the form of an analogue computer, it did not directly operate on the generators, and enabled only the economical distributions of active power production programmes to be determined. It was based on approximative formulae of the differential losses. These programmes were set by hand onto the generators remaining under normal power-frequency control. Equipment of this kind, not connected to the plant, became known as dispatching computers. It also made possible the calculation of the marginal cost of power supply on the outskirts of the network, i.e. at the point of interconnection with the other interconnected networks, and proved very useful for fixing the tie-line power-exchange programmes according to economical considerations.

Later, about 1958, there also appeared in the United States the first automatic dispatching equipment directly connected to the plant. This economical step is superimposed onto the power frequency control by automatically changing the basic powers entering into this control. The economic effect is much slower than that of the power frequency control which thus retains its efficiency in the control of network transient behaviour. To give an idea of this type of equipment, Figures 8 and 9 give simplified block diagrams relating to both the dispatching computers and the automatic economical dispatching equipment. More recently digital equipment has appeared that has functions similar to those of the first analogue realizations.

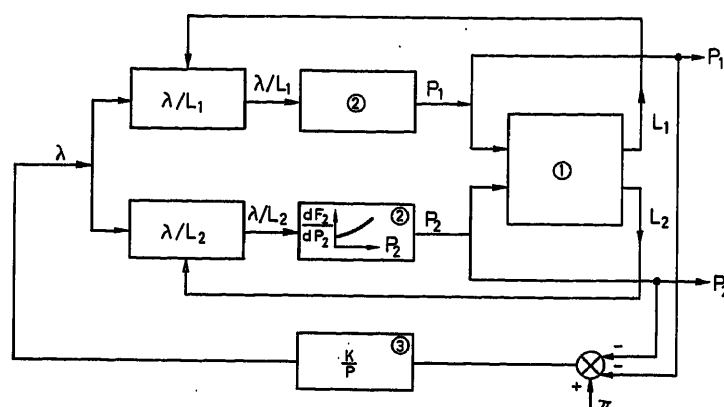


Figure 8. Basic diagram of a dispatching computer for the economical distribution between two power stations C_1 and C_2

Coordination equations $L_1 (dF/dP_1) = L_2 (dF/dP_2) = \lambda$, or
 $(dF/dP_1) = \lambda/L_1$, $(dF/dP_2) = \lambda/L_2$

Penalty factors L_1 and L_2 are assumed to depend only on active powers P_1 and P_2 and are calculated by the 'penalty factor computer'. Marginal production costs dF/dP_1 and dF/dP_2 depend only on the individual characteristics of each power station, and are represented by the 'cost' function generators. The usual form of these functions is shown on the loop corresponding to power station 2. For a given value of λ the computer delivers the respective optimum values P_1 and P_2 for both power stations. In order to supply a given power, the sum of $P_1 + P_2$ must be equal to power demand π hence the loop acting on λ in function of deviation $\pi - (P_1 + P_2)$. When the balance is reached, the computer delivers the optimum distribution.

At present both these types of equipment exist. Certain utilities are of the opinion that there is no point in using computers connected to the networks as long as this intermediate stage of automation cannot be surpassed, and prefer to use dispatching computers. They consider the differences between actual consumption and provision to be sufficiently small for economical distribution to be unnecessary, and that it is preferable to have dispatching computers, in order to anticipate further ahead the programme variations and uses of new production units, which is more difficult with directly connected automatic devices.

However, those who use these automatic devices seem satisfied with them and consider their use worthwhile. Obviously, it is difficult to assess their merit. On one hand, the marginal costs of production, or the marginal consumption, are very difficult to estimate, especially for power stations using coal. By exaggerating a little, we may wonder to what extent up to now the variation curves of this marginal cost, as a function of the power, have been chosen in view of facilitating the stabilization of economic distribution automatic equipment, rather than of representing the actual performance of thermal sets. The development of automatic thermal power stations can be expected to provide much more accurate information on this point.

On the other hand, present methods of differential loss calculation are based on simplifying the approximations, the repercussions of which are very difficult to evaluate and the validity of which certainly depends on the network in question. Even so, this step in the development of network automation is of considerable interest, as it is the first important industrial realization of automatic optimization of a system. It will, no doubt, be improved, but the basic principles are laid and will remain basically the same.

Present Development of Automatic Dispatching

Present studies in this field are mainly on two types of particularly delicate problems, the solving of which is likely to give rise to a spectacular generalization of network automatic command. These are:

The application of economic dispatching to networks partly supplied by hydro-electric power stations.

The choice of the means of production and the optimum structure of the network in view of the various existing requirements.

The difficulty of the first problem results from the random aspect of the available hydro-electric energy, which must be estimated as a function of future possibilities of utilization, the aim being, in a network with both thermal and hydro-electric sets, to attain the minimum fuel consumption possible in the thermal power stations. Thus it is exceptionally difficult for hydro-electric power stations to fix the marginal costs which would enable the use of the classical economical dispatching

directly connected with system control devices, and consequently it is a question of improving the dispatching computer equipment previously described.

Ruge's report deals with the problem in a more general way, as it aims at defining a long-term scale optimization criterion for a hydro-electric group. The author is of the opinion that whilst calculation by the variation method is well adapted for solving the problem at a given moment or for short-time planning, it does not provide a reliable solution to long-term investigations. Consequently, a new optimization criterion has to be found which takes into account, for a purely hydro-electric network, the utilization value of the supplied power which is a function of the power demand and of the time at which the power is demanded. The application of this method to the case of two reservoir power stations is described, but its extension to a large number of reservoirs of different characteristics meets with difficulties not yet overcome. Thus automatic dispatching is not yet entirely satisfactory for a network with an important proportion of hydro-electric supply.

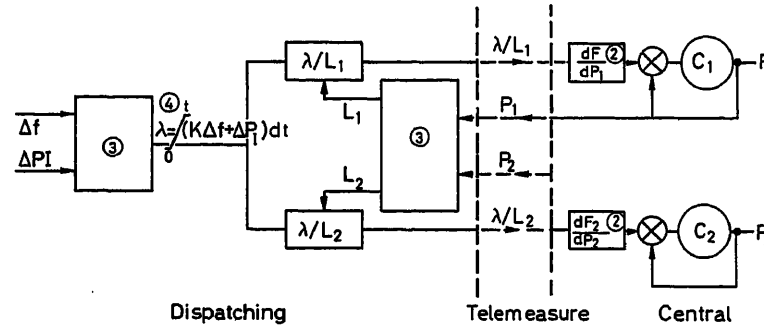


Figure 9. Basic diagram of economical dispatching automatic devices

The principles are the same as for dispatching computers. However, the power supplied by power stations (C_i) is directly dependent on the data delivered by their associated function generator (2). Penalty factor computers (3) deal with the powers actually supplied by the power stations. In a network, a deviation between the power demand and the power station programme power can be represented by the value of the binomial $(\Delta f + \Delta P/\lambda)$, not equal to zero. The integral of the binomial (4) is then used to bring the network to its balanced state. Conventional power-frequency control operates according to the same principles, but, since its action has to be primordial in case of fast variations, the action of the function generators is much slower than that of the power-frequency control which divides the load variations proportionally between the various machines; (5) Network regulator; Δf Frequency variation; ΔP_I Power variation (tie-line)

method. As long as we are dealing with the optimum operation of hydro-electric power stations, the studies cannot be made on an instantaneous basis.

Two papers presented at this Congress, one by Kirchmayer and Ringlee, the other by Ruge, are directly concerned with this problem and give an exact account of the actual state of studies on the subject.

The first report compares two methods of calculating the optimum distribution within a group of thermal and hydro-electric power stations on a short time scale, e.g. one day, in view of the various requirements which exist in reality.

In this case, the total quantity of water to be used during this period is taken as fixed for each of the hydro-electric power stations, and the authors give a few practical examples of the variation method and of the transient programming method. They conclude that the variation method seems best for this problem, in view of present means of computing. In this case, the aim of automation is to define a plan of operation and is not

In practice, the difficulties encountered for this type of network also exist for purely thermal networks, as even in the latter it is not possible to consider only a given instant. Whilst present methods make possible (in spite of their imperfections) the satisfactory approximate determination of distribution optimization between a certain number of thermal sets operating at a given time with a given network configuration, they only provide a sub-optimization corresponding to a particular case, which is not necessarily the most economical.

The choice of machines to be started up or stopped, the definition of the times at which they have to be started up or stopped, the closing or the switching off of certain meshes of the network appear to have economic repercussions at least as important as accounting for transmission network losses at the time of choosing the load distribution between generators. The cost of stopping or starting up a thermal set is far from negligible; equally so the increase in consumption per energy unit of this set, when its power output is reduced.

Vámos, Benedikt and Uzsoki partly deal with this problem and stress the importance of the requirements imposed on network structures by operation security. This report mentions various other aspects of dispatching and production automation, and shows all the difficulties met with in the application of these techniques.

System Development Studies

Thus, though network automation has been greatly developed, it cannot, as yet, be applied to all the problems facing utilities. Most technical problems can be considered as either completely solved or well on the way to being solved, and present studies are mainly on the economic aspect of operation. However, in connection with such problems it is not possible to consider only a state of the network, and due consideration must be given to the future. This is true not only for the operating of networks but also for their development. The increase rate of the power consumed on the various networks never slows down and maintains an average value varying, according to the case, from 6 to 12 per cent per year, which implies a rather rapid development (doubling of supply in 12 or 6 years). Therefore, it is normal to examine next the use of automatic techniques in network development studies.

The paper by Venikov and Tsukernik deals with this question and shows the advantage and even the necessity of cybernetics in this field of study. Not only has the examination of every aspect of network development to be coordinated, which, according to the authors, implies a change in conception and even in reasoning, but it has to be seen in a larger context, in other words, integrated into a general electrical plan. Present means of study, computers and simulators, allow audacious aims to be set. In the same way, the development of network statistical control could provide more accurate bases for network planning.

Such studies must be based on the new cybernetic theories, and should lead to truly optimum network structures and operation.

With regard to this subject, we would point out that network utilities have long been studying these questions, and that more or less empiric methods, adapted to existing material means of study, have been used and perfected; methods which still serve as a basis for decisions on network equipment. Whilst it is definitely of interest to develop the more efficient new methods rendered possible by present means of study, we must beware of erasing all previous methods and of neglecting results already obtained. The more complicated techniques need to be introduced gradually by the utilities most directly concerned, and experience gained gradually by the latter should certainly be taken into consideration. Thus, in particular, the development of water-tight terminology needs to be avoided, as it could discourage utilities and lose many of the advantages which can rightly be expected from the development of these new methods. Furthermore, this problem seems very general for everything connected with the application of automation in the electrical industry, and an effort is required from specialists on these questions towards simplifying the vocabulary and clarifying the analysis of the new techniques.

Synthesis of the Use of Automation on Electrical Power Systems and Conclusions

We have reviewed the different aspects of the use of automation on electrical systems and have been led to consider seem-

ingly very different problems. In conclusion, we consider it useful to try to show from the above analysis the general characteristics of the development of automation in this field.

Nature of the Problems

Improvement of the technical and economical quality of supply implies that the network elements are capable of rapid adaptation to the needs of the customers, shown by the active and reactive loads demanded. Therefore one of the essential qualities of electrical power production and transmission equipment is a maximum operation flexibility which allows it to stand up to demand variability. Automation of such equipment is essential, whether it be control automation (voltage, speed, network control) or sequential automation (rapid starting up and stopping of hydro-electric and thermal power stations). It has not always been easy for electrical utilities to get the constructors to accept this point of view. Obviously, it is natural for the latter to advocate suitable control systems for avoiding stresses on their material rather than to accept very rapid and large load variations; and utilities have to oppose this tendency in every way. Often a compromise is adopted, but for it to be satisfactory, it is necessary that the needs and the nature of the difficulties in question be clearly defined by both sides.

Another characteristic of large networks is the number of possible control quantities between which a coordinated action, the most economical possible, has to be made. Often these control quantities correspond to the different machines on the network, and safe and rapid telecommunication problems are of great importance.

Multivariable system control, which includes the automatic control of thermal power stations, can only be automated by digital computer methods.

Automation Study Methods

In general the development of automation has called for a better knowledge of the static and transient performance of the equipment in question, in particular of the alternators of hydraulic and steam turbines and of the boilers. In order to perfect this knowledge, studies need to be both theoretical and experimental. However, in the case of networks, the experimental part presents considerable difficulties in view of the amount of equipment concerned and its importance in daily operation. Consequently, the present tendency is to establish a mathematical model, the validity of which is checked during a limited number of tests on the actual installation before beginning the actual study of automatic techniques on the computer, simulator or small model which includes the future automatic equipment of the network.

Present State of Automation

We have shown that network automation applies to the following different fields:

Security automation (network protection, supervision of stresses on the equipment).

Control automation (voltage, speed, network control).

Sequential automation (starting up and stopping of power stations).

Automation of plant optimization (control of thermal power station economic dispatching).

This list corresponds to the chronological use of automatic techniques; the first applications of which date back almost sixty

years. At present we are justified in considering that the technical solutions for the first three classes of automation are generally satisfactory and enable the network to maintain a very high quality of service. The first applications of automatic optimization and the interest shown in such questions clearly show that the reduction of the cost of power supply is at present one of the main concerns of utilities.

From the point of view of the automatic techniques used, almost all present control methods are of the analogue type, with the obvious exception of the first applications of automatic optimization and plant logical command (thermal power stations). We do not consider it necessary to try to generalize the

of the installations (for example, reduction of the short-circuit ratio of alternators by the use of continuous and quick-acting voltage regulators; reduction of generator set inertia by use of perfected speed regulators; reduction of the surge chamber sections of hydro-electric installations by use of voltage and speed combined control, etc.).

In the same way, improvement of the quality of control can reduce the safety margins usually adopted for the choice of the plant characteristic parameters (for example in the case of the boilers of thermal power stations).

We would stress the improvements that may be expected from a coordinated study of the main equipment and of its auto-

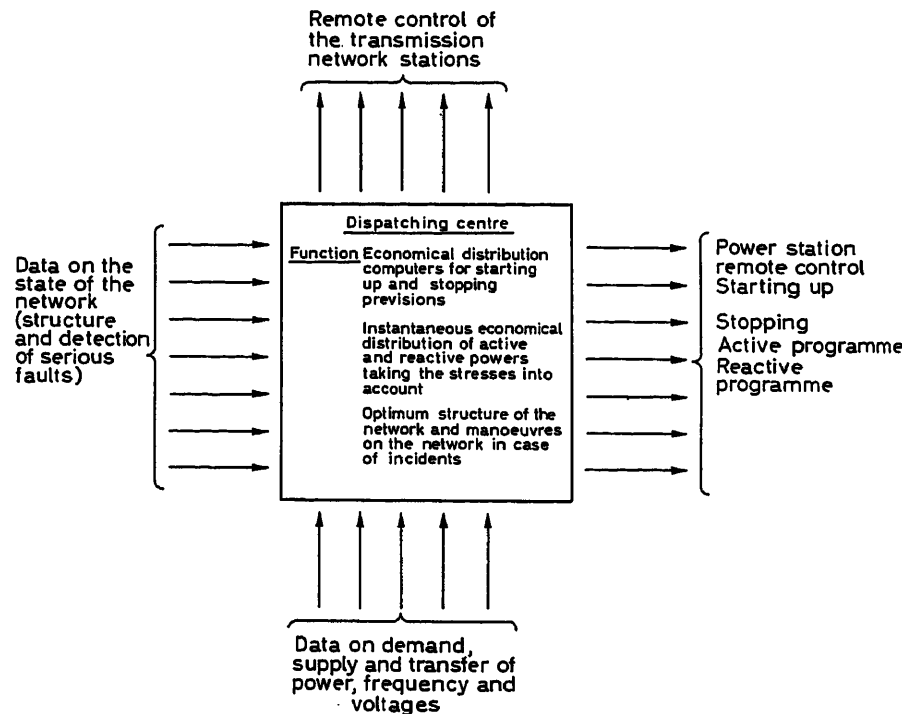


Figure 10. The functions attributed to a control device commanding an entirely automated network

uses of either analogue methods or numerical methods. There are often advantages to the simultaneous use of both these methods, which it would be ridiculous to neglect purposely.

Advantage of Automation

In addition to the possibilities of directly improving the quality of service by reducing the risk of service cuts and of voltage and frequency variations, use of automation has made possible the large-scale development of network interconnections which has considerable technical and economic advantages (regularization of the load curves, possible reduction of the revolving reserves). Furthermore, in many cases the investment cost of production and transmission installations can be reduced by the use of perfected automatic equipment.

It is often possible to obtain the same static and transient performance with a large size installation without a regulator, or equipped with very simple regulators, and with a much smaller installation fitted with complex regulators. As the economy resulting from a reduction in size far exceeds the extra cost of the regulator, automation sometimes greatly reduces the overall cost

at the time of planning the construction. Notable changes in equipment structure could result from the perfecting of optimum overall equipment and not from the juxtaposition of an optimum main equipment and an equally optimum control equipment.

We would also mention the interest of logical automatic techniques, which are being developed at present in connection with the reduction of the risk of serious incidents and faulty handling on very complex installations.

Possible Development and Conclusions

Use of automation on networks is thus already very much developed and appears to justify the opinion expressed at the beginning of this paper that the electrical industry is at present the most automated industry in the world. However, this automation is not complete. Apart from the generalization of the latest techniques on thermal power station control and economic dispatching in its present state, can further extension of network automatic command be anticipated? May we expect to see, one day, very large networks commanded from a central station

without any other human interference? Such a solution no longer seems to belong to a technical Utopia.

Already on certain networks the automatic adaptation of the active power production of the main generators depends on a central station. Already in certain power stations the stopping or starting up of a hydro-electric set or even of a thermal set is obtained by simply switching a contact. Already studies are being carried out which should perfect the practical methods of determining the best times of generator stopping and starting up, the best structure of networks, the optimum economic distribution, both of the active powers and of the reactive powers, and such studies take into account the various security requirements demanded at present, which appear necessary for operation control.

Theoretically, a logical computer which, on the occurrence of an incident, can take, according to strict pre-set rules, the decisions necessary to the power stations and to the networks, is not impossible.

Under these conditions we can seriously anticipate, for a not

too distant future, the generalized automatic operation of large electrical networks according to the principles summarized in *Figure 10*.

However, the economic advantage of such a solution would first have to be studied, and we are not certain that, in present economic conditions, this generalization of automation is justified. Already, with regard to thermal power stations, integral automation is not clearly economically profitable. The considerable development of telecommunication links required for the total automation of a network could be an extremely heavy expense.

Furthermore, security is so important in this industrial process that, before taking such a consequential decision, it would be necessary to be sure of the perfect quality of automation and telecommunication equipment and of the validity of the methods in question. Consequently, we may expect considerable time to elapse between the moment at which the total automation of a network is technically possible and the moment at which it is used for the first time.

Working Out a Method for the Cybernetic Control of Integrated Electric Power Systems

V. A. VENIKOV and L. V. TSUKERNIK

Summary

This paper gives a short description of the development of power engineering of the Soviet Union and shows the necessity of using cybernetic methods for the control and planning of power systems under development.

A review of the methods of application of cybernetic methods to specific problems of electric power engineering has made it possible to formulate the subject matter of a new study discipline, Cybernetics of Electrical Systems, and to outline directions of its development.

This discipline consists of a number of sectors that have been studied in detail, including problems of probability theory, physical and mathematical simulation of power engineering facilities and systems as a whole, the methodology of conducting experiments, and information theory specially adapted for electrical systems. The last sections reviews the overall approach to the creation of regulators and control devices of cybernetic types, and formulates the needs and conditions of work.

The paper not only provides a general posing of questions and contains the contents of the above-mentioned new discipline, but also gives concrete examples of tasks already solved, the technical contents of which are based on cybernetic methods, which give important results in practice.

Sommaire

Ce rapport donne une brève description du développement des réseaux d'énergie en Union Soviétique et montre la nécessité d'utiliser des méthodes cybernétiques pour le contrôle et la planification des réseaux d'énergie en cours de développement. L'examen des méthodes cybernétiques utilisées dans ce domaine permet de formuler les lignes directrices de cette nouvelle discipline que l'on peut appeler Cybernétique des Réseaux Electriques. Cette discipline comprend un certain nombre de secteurs qui ont été étudiés en détails: problèmes relatifs à la théorie de la probabilité, simulation physique et mathématique des réseaux et systèmes électriques, méthode d'organisation des expérimentations, et théorie de l'information appliquée aux systèmes électriques. La dernière section examine le problème général de création de régulateurs et d'éléments de commande du type cybernétique, et formule les besoins et conditions du travail.

En plus des aspects théoriques, ce rapport décrit également des exemples concrets rencontrés dans la pratique.

Zusammenfassung

Dieser Beitrag beschreibt kurz die Entwicklung der Kraftwerkstechnik in der Sowjetunion und zeigt die Notwendigkeit für die Verwendung cybernetischer Methoden bei Steuerung und Planung neu zu errichtender Kraftwerksnetze auf.

Betrachtet man die Anwendungen der Kybernetik auf besondere Probleme der elektrischen Kraftwerkstechnik, so kann man den Bereich einer neuen Fachrichtung „Kybernetik elektrischer Systeme“ abstecken und ihre Entwicklungsrichtung andeuten.

Diese Fachrichtung umfaßt eine Anzahl von schon vorhandenen Disziplinen, darunter Probleme der Wahrscheinlichkeitstheorie, physikalische und mathematische Nachbildung von Kraftwerkseinrichtungen und ganzen Systemen, die Versuchsplanung und die In-

formationstheorie elektrischer Systeme. Die letztgenannte Unterdisziplin befaßt sich allgemein mit dem Entwurf kybernetischer Regler und Steuerungsgeräte und formuliert deren Funktionsbedingungen.

Dieser Beitrag enthält daneben auch noch konkrete Beispiele bereits gelöster Aufgaben, deren technische Eigenarten auf kybernetischen Methoden beruhen und die bereits wichtige Ergebnisse erzielt haben.

The rapid development of power engineering in the Soviet Union, the planned expansion of electric power production to 2,700–3,000 billion kWh by 1980, the construction of electric power lines of various voltages several million km in length, and the creation of an integrated electric power system of the Soviet Union with a high degree of automation of its operations, all make it imperative to utilize new methods of analysis and synthesis and new methods and means of control, and to create cybernetics for electrical systems. Cybernetics is the science of purposeful control in complex systems irrespective of their physical natures. Cybernetics opens up vast possibilities for the scientific development and practical solution of problems of control in all highly complex electrical systems on the basis of overall rules and methods of research.

In an electrical system, the interaction of controlling and controlled elements should take place in conformance with a certain algorithm utilizing information received over various communication channels. This organized system interacts also with an external medium, which creates random or systematic interference. Feedback is used on a large scale in the control of an electrical system. All of this is characteristic for the problems handled with cybernetics.

In modern methods of studying electric power systems, one of the greatest deficiencies is the divergence of methodology for doing research on various aspects of functioning systems. This deficiency of the science of modern power engineering can in the future become a serious obstacle to its development. Cybernetics, which systematizes and absorbs approaches to the study of processes in various systems and finds common points among them, determines the direction of methodological and practical synthesis. For this reason, this is the right time to pose the question of applying specific methods of cybernetics to the solution of problems arising during the planning and operation of electrical systems¹.

The basic task of cybernetics of electrical systems is the observation of general principles of operation of an automated electric power system and its traits with realization of controlling algorithm which provides optimum indexes of operation quality, both from the aspect of economic feasibility and from that of quality of the power produced and the quality of supplying the consumer with it. In this regard, as shown in the dia-

gram in Figure 1, operating schedule reliability and the reliability of component elements of the system are figured in the scope of the term quality.

The development of machines, equipment, and regulators, the design of automatic control installations, and the transmission and processing of information, along with protective systems, are not included in the cybernetics of electrical systems, even though they have bearing on their overall circuitry and the analysis of their operations. Thus, irrespective of the apparent

all-embracing nature of the definition given above, the cybernetics of electrical systems has a rather sharply defined group of questions (Figure 2).

An important task of cybernetics is to develop the methods of analysis and synthesis of characteristics of the components of electrical systems and to obtain the kind of physical concepts and mathematical description of the function of the systems that can use information available in practice as a basis for finding the optimum conditions of system operation as a

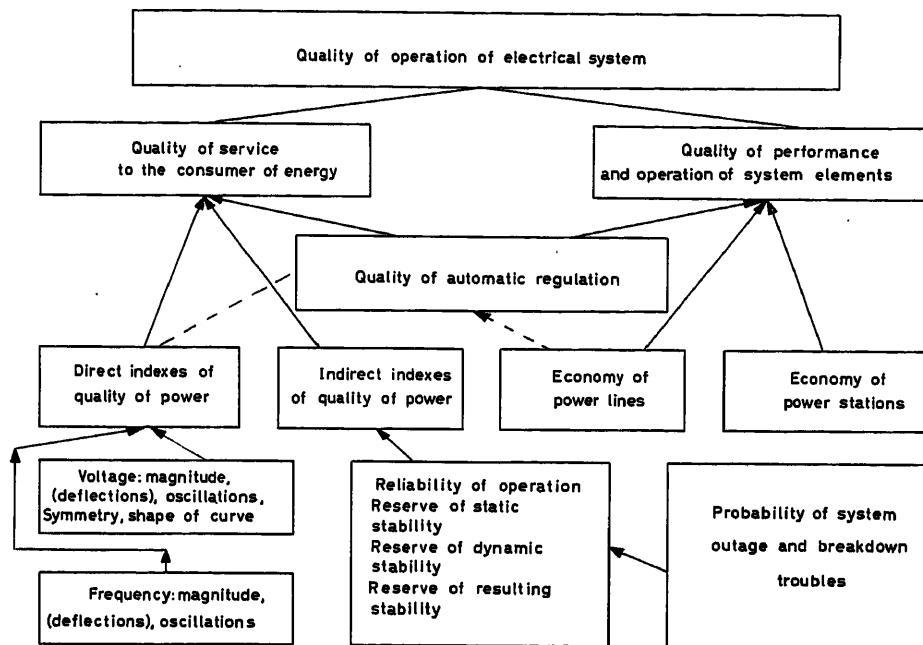


Figure 1. Interconnection of individual indices in the complex evaluation of the quality of operation of an electric power system and servicing of the electric power consumers

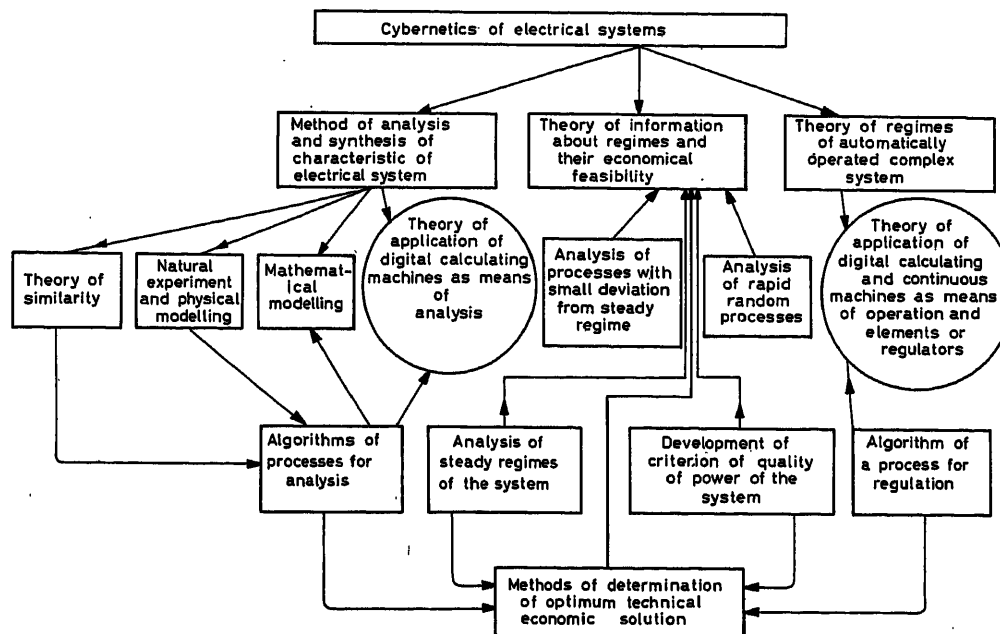


Figure 2. Constituent indices of the cybernetics of electric power systems and the interconnections among its basic sectors

whole, both with respect to determining the system's operating regimes and its transient performance. For this the specific definition of the physics of the phenomena is carried out in some cases with the use of the similarity theory and by simulation. Solution of the task is done with the application of algorithms.

The application of algorithms means, first, the mathematical description of the processes for the purpose of formulating their common rules, which are determined by complex study using the method of physical and mathematical simulation and natural research, and secondly, through the formulation of common methods of solving problems (on simulators and digital machines) for determining the desired structure, parameters, and regimes of the system.

It is difficult to over-estimate the role of the development of methods of applying algorithms carried out on a sufficiently broad scale. At present, the possibilities of computer technology of discrete operation and of methods of simulation should be utilized as more than a mere auxiliary supplementary means of research. These methods should be made the basis of the renovation of the methods of analysis themselves, which are used in the solution of engineering problems.

The use of modern computer and simulation equipment with old methods of analysis means not only a failure to use such equipment at full capacity, but also complete failure to find any way of applying it. This is why the application of algorithms, which covers the compilation of equations of physical phenomena in various processes, the determination of the order of computation, the indications of logical operation limitations, etc., for the purpose of obtaining the fullest possible solution of problems, is of primary importance in the development of any branch of modern natural and technical sciences.

The similarity theory and the simulation of electrical systems is linked to the work of creating principles of automation of production processes. The development of simulation travels in various directions. For electrical systems, the development of methods of incomplete physical simulation, which reproduces the occurrence of processes only in time or only in space, and of full physical simulation, which reproduces the processes under study both in time and in space, is of great importance³. It is also a good idea to utilize mathematical simulation, both analogous and structural, in which more attention should be given to problems of matching structural and analogous models; for example, the combination of simulating machines with the a.c. calculation panels.

The cybernetics of electrical systems stimulates the development of simulation with the aid of digital differential analysers, which should be regarded as simulation devices of a special type. This type of simulation, which combines elements of digital computers and characteristics of continuously operating machines (analogue computers) should justify themselves in a number of problems where no great accuracy of answers is required and where programming, and equipment used for universal digital computers, turns out to be exceedingly complex.

The problem of simulating electrical systems by means of the data of their normal operation is becoming of great importance³. In line with the creation of models of this type, a number of research projects are already under way, and must be guided along the proper directions with aid given to their development. This research should form the basis of methods of determining the dynamic characteristics of objects under normal operating conditions with normal natural interference, and with the

creation of special installations which give the system harmless test pulses. Research on simulating random processes in electrical systems is also necessary.

The determination of the dynamic characteristics of electric power systems by these methods of simulation must have an overall logical scheme, differing essentially by the algorithms of hunting the values of the parameters of the model: undetermined algorithms (random hunting), incompletely determined algorithms (determined hunting, but random preliminary values), and fully determined algorithms. The basis of the above-listed tasks of cybernetic simulation of electrical systems is composed of the following⁴:

(a) Similarity theory of electromagnetic and electromechanical phenomena, which makes it possible to acquire experimental data and to cut down the number of transient processes which are variable in their mathematical depiction. Similarity theory links mathematical and physical simulation of phenomena with experimentation and makes it possible to undertake the application of algorithms using the experimental data by the best means possible.

(b) Methodology of carrying out a natural and a simulated experiment is needed for greater knowledge of the nature of the phenomena occurring in electrical systems and for determining the interaction of individual elements and systems of these elements with various automatic control and regulation devices, in order to check the functioning of newly-developed instruments in the system and, what is most important, to define more precisely the mathematical depiction of their functions.

(c) Methodology of mathematical simulation makes possible the rapid reproduction of the variety of interaction of various elements of automatic regulation systems in conformity with the hypotheses found in the mathematical depiction of phenomena. Along with physical simulation, mathematical simulation makes possible a more effective reception of characteristics and descriptions of functioning of systems, which are adequate for the physics of the phenomena and suitable for practical problems already assigned.

It should be noted that the cybernetics of electrical systems should in no case be oriented merely toward high-speed discrete computation electronic computers.

Any systems of regulation, with uninterrupted or discrete devices, which solve the tasks of purposeful regulation and have automatic self-modification of their parameters in conformity to the type and magnitude of disturbance, should be considered akin to cybernetic systems.

Cybernetic regulation of an electrical system cannot occur without information on the system's functioning. Information theory should be used for specific problems of operation of electrical systems located within large areas and composed of a great number of elements, in which case, the operating regime of the systems requires a balance of generated, converted, and consumed electric power at desired qualitative levels each instant of time. Information in such systems should satisfy the most rigid conditions with regard to the capability of obtaining the quantity and quality of information transmitted.

The most important thing in this case is the question of the minimum amount of information necessary for the regulation of the system's operation, and the reliability of transmitting and coding this information for solving these and other concrete problems for the regulation of electrical systems. This concerns

the problems of assuring the necessary transmission capacity of the information transmission channels and for communicating a quantity of information with a probability of making contact and with a capability of withstanding interference. In this section, disturbances occurring as random with a basic effect on the system's operation, which are sometimes decisive, should be studied.

To illustrate the above-noted cases with concrete examples, certain specific problems already encountered in electrical systems are now reviewed:

(1) The obtaining of information on the regularity of disturbances and fluctuations of the operating regime which occur in electrical systems.

An electrical system constantly undergoes changes in load and other disturbances of a random nature, which cause fluctuation of voltage and frequency and changes in the power currents flowing in the interconnected lines, along with changes in the consumption of power by the load. These fluctuations of an electrical system have a decisive significance for the establishment of reserves of stability of automated systems and for setting up specifications for the devices used to regulate frequency, voltage, and power flows in the interconnected lines.

In reviewing the given group of problems, such as the role of the cybernetics of electrical systems, an engineer should mainly concern himself with determining the rules of the system's fluctuations. Information on these fluctuations should be broken down into characteristic groups; its minimum necessary quantity should be determined along with methods of converting and transmitting this information to cybernetic regulation and system control installations.

(2) Receiving information necessary for the economic distribution of produced power among the stations of a system (planned and operational information). This task is analogous to the preceding one with the difference that the reception of the minimum necessary information on the system's operating regime (loads, power stations and networks parameters) should be used for determining such active and reactive powers as may be produced by the stations of the system, and for selecting the design of the generating apparatus so as to have the minimum overall cost of all power supplied to the consumer and to supply him with the power of the quality he needs—in the first approximation of the evaluation of quality.

(3) The reception of information for providing the quality of electric power, in the second approximation of the evaluation of quality, and, in connection with the solution of this problem, the regulation of frequency and voltage in systems and power pools composed of interconnected systems. The automatic maintenance of frequency and power current flow should be done in such a way as to use existing equipment and operating regimes of systems to the optimum. For this purpose information must be used as shown in (2). This information is processed in cybernetic control and regulation installations which influence the proper servo-mechanisms, without which the task of cybernetic control of a system's regime could not be solved.

(4) The reception of the necessary information on the beginning and duration of breakdown processes. Regulating installations of the cybernetic type should not merely regulate one or another parameter of the operating regime in conformance with changes in the regime of the system that happened in the past, but

should evaluate the possible future change in regime and predict the nature of its passage. For all cybernetic installations, the problem of receiving the necessary information in a sufficient quantity is a decisive one.

It is noted that cybernetic traits are already present in a number of modern regulators, which are discussed in detail below. In particular, this concerns the high-power excitation regulators, which react to the speed and acceleration changes in regime parameters, but not to the changes themselves alone⁵. In using these regulators in a complex system, the question arises: What limitations of information should be kept in view in the designing of regulators. For example, the highly effective regulation of excitation of generators with the use of the first and second time derivatives of the angles of divergence of the electromotive forces of the transmitting stations and the receiving system, i.e., according to the slip and acceleration of machines. However, it is always possible to find this angle in a complex system. Furthermore, if the angle is found, the question arises of how to transmit it: what effect will mistakes in tele-transmission have; what effect will short or long disruptions in transmission have; what should the accuracy be?

It is understood that similar and even more complex questions arise also with other methods of regulation and control. For this reason, the establishment of a method of receiving and transmitting the necessary information plays a prominent role in the cybernetics of electrical systems.

Cybernetics of electrical systems must provide means for determining the optimum technical and economic solutions for the national economy, and for finding the minimum technical and economic information needed for the long-range planning of electric power systems, for calculating the plans for their development, and for operating them. In long-range planning, a large number of variants of electric power supply of regions, countries, and international power unions are calculated.

Information forming the basis which should be used for making such calculations is very extensive and multifaceted. In many cases this information is of a probabilistic nature and has substantial interrelations, which are true to the nature of a complex system. Even such a comparatively simple and apparently particular problem as the calculation of a city or industrial network requires the application of probability theory⁶. The summary load of such a network is a random value, and a change in its momentary values, maximum values and their coincidences, and average values is nothing more than a random process. In calculating a network, attention should also be given to competitive factors, which, for example, reflect the dynamics of change of resources of non-ferrous metals in the country during the period of time under study.

The calculation of electric power at the time it is supplied to the consumers, who are very numerous in the network, should take place on the basis of the limit theorem of Liapunov. Modern methods of calculation striving mainly for the 'engineering simplicity' of calculated formulae make grievous errors. A conversion to methods of analysis, which make allowance for the above-mentioned complex interrelations and for decreased error (i.e., approximation of the optimum value) for instance of 10 per cent in calculating the cross-section area of conductors, makes possible, as rough calculations have shown, to save on non-ferrous metals by 25 per cent, and to effect a cut of at least 15 per cent in the installed capacity of transformers.

These figures were obtained for industrial plant and city

networks. If high-voltage long-distance transmission lines and rural networks were added, these results would be even more striking. Of course the development of a cybernetic installation for giving the actual optimum solution of the problem of selecting the optimum arrangement of an electrical network, and the optimum cross-section of its wires, needs proved initial premises of the price or cost of metal and power and the possible limitations. The science of socialist economics is capable of giving truly objective indicators of the effectiveness of capital investment suitable for practical application. Only by this method can cybernetics produce a complete solution and indicate the actual national economic optimum. However, even the possibility of increasing the number of calculated factors and the acceleration of computation gives a definite effect.

A much more extensive problem is now touched upon, that of locating planned thermal electric and hydro-electric power stations on the territory of the U.S.S.R. Solutions being tackled at present will never cover the problem as a whole. They are usually based on the use of the concept of 'substituting' variants and assume that to find the optimum solution it is possible to compare the proposed variant with another, sometimes fictitious, variant used as a secondary variant. Of course from some of the 'substituting' solutions it is practically impossible to select the actual optimum solution. The selection usually is of a subjective 'volitional' nature and sometimes leads to gross errors. A way out of this situation is found in approaching the selection of truly optimum variants by starting with the determination of available and future resources of the country among the branches of the national economy and branches of power engineering connected with these.

Modern capabilities of cybernetics supplemented by the development of solutions of economic problems, with the use of high-speed computers, will make it possible in the near future to set up and solve such an overall problem, and in addition, individual tasks. Thus, for example, the problem of selecting such ways of developing electric power systems that money allotted for operation and construction would provide for the greatest possible increase in growth of electric power with the least possible consumer cost, could be solved with the aid of modern computers and cybernetic methods. An intensification of the utilization of these, plus the development of methods for obtaining the needed information for them is entirely necessary.

In planning electric power systems as a whole it is necessary to specify a number of indicators: power and load curve, distribution of power in an electrical system with consideration for the hypothesis of development by stages, etc. To select a locality for the construction of an electric power station, the possible variants of its position and hunting data should be indicated. On the basis of this and other supplementary information and the use of a computer, the optimum solution can be found, which will conform to those indicators which will be accepted for the evaluation of the selected variants. Research will make it possible to find the specific capital investment per installed kilowatt at the power station and per kilowatt transmitted over the lines. Specific expenditures for the production of 1 kWh of power, the number of hours of utilization of installed capacity, the cost of wasted power, etc. should be determined.

From a purely mathematical aspect, minimization of linear or non-linear functions of a number of independent variables in

the solution of the problem of finding the optimum development of an electric power system is wholly feasible; however, the development of the indicators themselves requires technical-economic research, which should concern not only power engineering questions alone, but the entire national economy as a whole, including research and study of the details of the development of the consumers of electric power. It would be possible to give an infinite number of examples showing the necessity for receiving information, and, to use such information on the basis of its cybernetic processing to find one or another rule in the power systems; however, this paper is deliberately limited to what is available.

The modern theory of regimes of automatically controlled electrical systems and the theory of interaction of elements of a complex automated power system should apply to the study of methods of such a use of information that would provide the optimum operating conditions of a self-adjusting cybernetically-controlled system. The cybernetics of electric power systems should provide for the optimization of the regime of an electrical system and for the creation of the means for realizing these optimum regimes.

In cybernetics practice, such as in the operation and planning of electrical systems, methods of the probability theory and dynamic programming should be utilized. The immediate task of this section of cybernetics of electrical systems is the development of a structural scheme of electrical systems as a whole based on a single approach and including all elements producing electric power, transmitting and distributing it; regulators acting on the excitation and on the prime mover, and installations for improving the regime. Here should also be included the development of schemes of regulators, which change their parameters and setting with respect to the present condition of a regime and what will happen in said regime in the future, as determined by the computer devices of these cybernetic installations.

The cybernetics of electrical systems solves this group of problems on the basis of analysis of the structural schemes of electrical systems and their regimes, and makes it possible to find methods of building regulating and control devices on the basis of continuous or discrete computers. These devices evaluate the changes in a regime and after finding the optimum conditions for its activity, produce self-adjusting parameters. Installations for controlling the distribution of loads among stations of electric power systems can serve as examples of cybernetic devices. These installations should receive the necessary information from the system, process it, and, in conformance with the established criteria of economic feasibility, at the same time counting other operational indices, for example, operational reliability, stability, etc., should produce the optimum figures and transmit them in the simplest case to the dispatcher of the system. In a more complex case (more highly developed) they should produce and send control commands to the proper devices controlling the machinery of the stations, and also the switching equipment of the network, the transformers, and the generators.

The final goal, the full optimum cybernetic control of the system, cannot be achieved very rapidly, however, since at first it has to undergo gradual stages of development. Such a development is shown in *Figure 3*, where in case (a) a person receives information on the condition of the system's elements (continuous line), feeds the programme and data into the com-

puter M , receives the results of the solution, and on the basis of the solution takes one or another action, feeding a command (broken line) to the system's elements, and in this way causing feedback. In case (b), the machine partially receives information directly from the system, and in case (c), it receives all information *in toto* and not only consults the engineer of the control system, but also does part of the operations itself. In case (d), all functions of obtaining information, processing it, and giving control commands are transferred to the machine; a human being merely has the functions of developing and feeding programmes and tending the machine. Control in this case becomes entirely cybernetic. One of the important tasks of cybernetics of electrical systems is the realization of the optimum combination of 'man and machine' on the above-mentioned stages of development of control. In this connection,

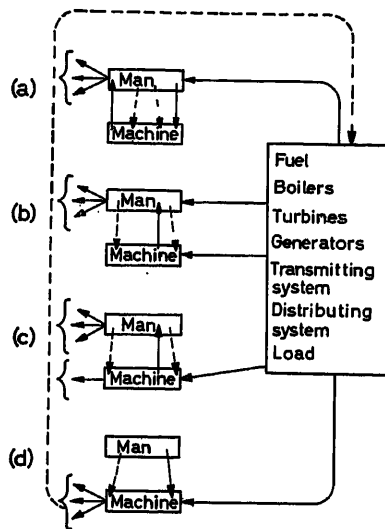


Figure 3. Stages of gradual transition to cybernetic control of an electric power system: (a) The machine is a consultant for man; (b) The same with the partial feeding of data directly into the machine; (c) the same with the feeding of all data into the machine and partial control of the system with the use of the machine; (d) complete cybernetic control

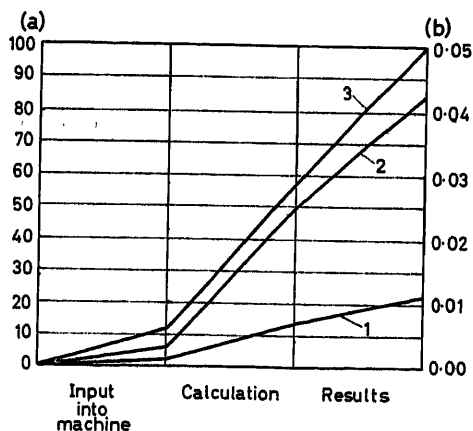


Figure 4. Time (in sec) needed for the operation of a computer for controlling an electric power system: (1) Load distribution in a simple system of three stations [scale (a)]; (2) Load distribution in a complex system of five to seven stations [scale (a)]; (3) Control of the operating regime of the system in a transient process [scale (b)]

research in the field of 'engineering psychology' has already started. In this research, much attention is given to conditions of work of the personnel of electric power systems⁷.

To solve the problems of distributing the load among the stations in a stable or slowly changing regime, successful use can be made of both high-speed digital computers and continuously operating types of machines. The use of digital computers for calculating stable or slowly changing regimes of power systems does not pose any difficulties with regard to the provision of high-speed work during control operations (Figure 4). However, it would be incorrect to think that cybernetic control and regulation in electrical systems can be achieved only with the very high speed of the computers which are utilized. It was noted previously that cybernetic regulators in their simplest form have already appeared in our systems. The appearance of such regulators, naturally, is the result of the gradual development of various types of regulation, a development during which the features of another more progressive type of regulation are gradually introduced into one type of regulation. In the table given in Figure 5, characteristic curves are given of the development of methods of regulating electrical systems. This primarily refers to regulating the excitation of synchronous machines; however, the same can be fully applied to other regulating devices, such as frequency regulators, speed regulators, etc. as examples.

The cybernetic features of an excitation regulator are dwelt upon in some more detail. Assume, that regulation takes place according to the displacement angle of the rotor δ . If the regulator reacts to a deviation of the displacement angle $\Delta\delta$ [Figure 6 (a)], then its effectiveness is comparatively small; however, if the time derivatives of angle δ are introduced into the regulation law [Figure 6 (b)], then the regulator will react to them and will receive in effect the ability to foresee the flow of the operating regime and to become a highly powerful acting regulator having the traits of a future cybernetic regulator. The addition of a high-speed computer [Figure 6 (b)] converts the regulator into a cybernetic device searching for the optimum conditions of operation, and makes it possible to have forecasts of the process not on a short-range, but on a long-range basis.

Interest is also shown in the solution of cybernetic control problems by automatic regulators with 'memory' devices, which make it possible to introduce the function of the derivative of angle δ (Figure 7) without tele-transmission. This is equivalent to the dependence on the slip and acceleration of machines, or on the vector of the network voltage at a fixed point relative to the axis of the reading, which rotates with a synchronous speed of the original uninterrupted regime, converting during the regulating process to the synchronous speed of the newly established regime. In Figure 7 (a) is shown the structural diagram of the measuring unit of this type for an automatic high-power excitation regulator⁸. Figure 7 (b) shows the structural diagram of a measuring block of this type for an automatic regulator of ion converters of highly power-consuming industries, and other consumer facilities⁹. This kind of regulator is designed for increasing stability and attenuating variations of power systems in long-distance electrical transmissions by means of proper changes in the dynamic load curve. This is a basically new type of cybernetic control in a power system in which not only the generating installations and transmission system are the objects of control, but the consumers of electric power as well.

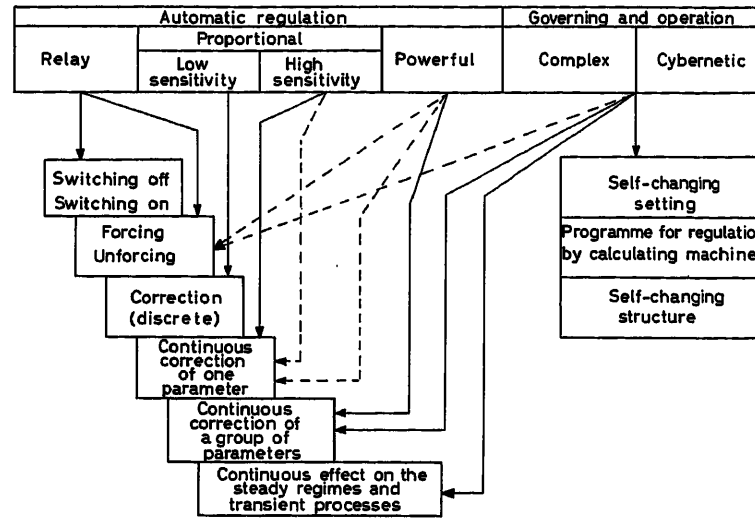


Figure 5. Past and impending development of types of automatic regulation in power systems

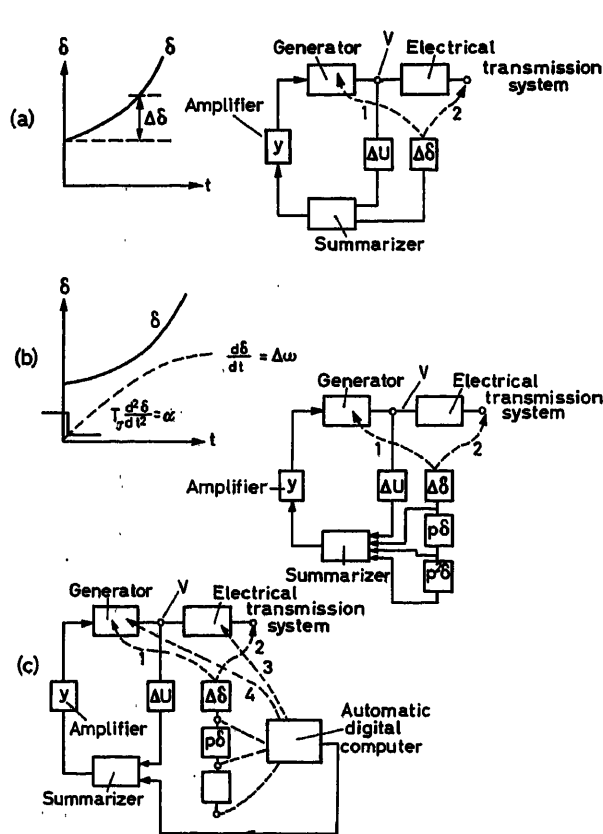


Figure 6. Juxtaposition of the principles of automatic regulation of excitation of a synchronous generator in an electric power system: (a) Regulation by deviation of voltage and angle (simple regulation); (b) Regulation by deviation of current, angle, and its derivatives (complex regulation); (c) Regulation with the aid of automatic digital computer (cybernetic regulation)

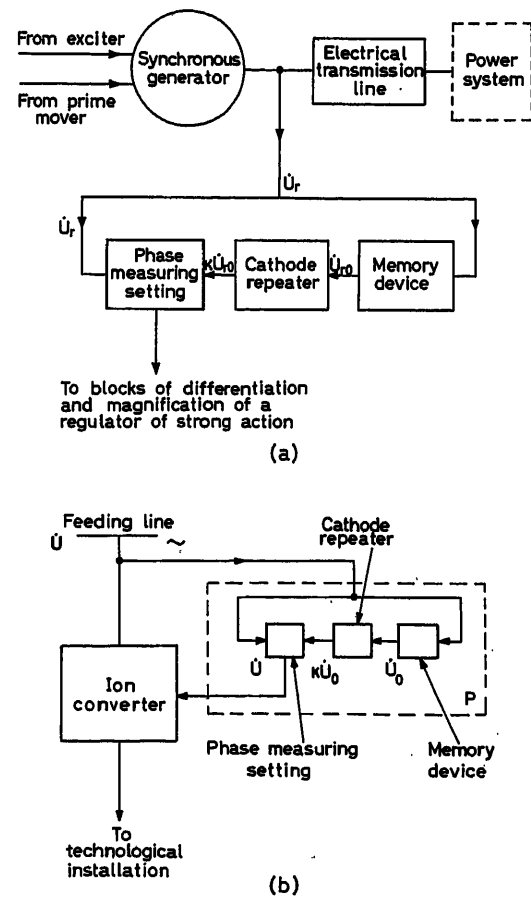


Figure 7. The structural diagrams of automatic regulation with 'memory' devices: (a) Regulation of excitation or speed of synchronous generators; (b) Regulation of ion converters for changing dynamic characteristics of the load of the power system

It should be noted that the long well-known successful utilization of 'memory' devices for automatic oscillographs for the purpose of recording pre-breakdown operating regimes is achieving a rebirth in the cybernetic control systems of electric power systems. Another example of a regulator with cybernetic traits which has been put into practical use is the excitation regulator of synchronous motors, which was made in the U.S.S.R. This regulator is a passive self-adjusting regulator without active hunting for its optimum setting¹⁰.

Under normal voltage level of the network, a regulator should maintain unchanged the power factor of a motor, which, for example, equals a unit, thus providing for the most economically feasible operating regime of the motor. When the voltage is lowered the regulator should increase the excitation of the machine in conformance with the desirability of maintaining a constant voltage of the feeder circuit, thereby increasing the reliability and quality of the electric power supply of other fellow consumers. When the maximum permissible value of rotor voltage or stator current is achieved, the regulator should automatically convert to the stabilization of these parameters for the purpose of averting overloads of the respective networks. Limitation of the stator current when needed can be carried out with a time delay so as not to obstruct the momentary boosting of the excitation, which is carried out by a regulator with decreasing of the voltage of the feeder circuit for increasing the stability of the system and the motor. When circuit voltage is raised higher than normal, the regulator should lower the excitation until the desired power factor is attained without permitting the kind of de-excitation of the motor that would cause the motor to desynchronize. This rule of regulation is a programme of self-adjustment of the regulator. The first basic part of this programme stabilization of the power factor of the motor with the calculation of the voltage level of the feeder circuit can be carried out by a system with a self-changing setting; the second part of this programme, the introduction of limitations, can be carried out by a system with a self-changing structure.

The system of control is composed of four main units, which correct the power factor, the circuit voltage, the rotor voltage, and the stator current (Figure 8). Operating experience has also shown that the regulator described above increases the operational stability of synchronous motors and facilitates their resynchronization when they become desynchronized. The short-

stated considerations concerning the necessary development of a mathematical description of a complex regulated or cybernetically-controlled electrical system should be extended. Two features are evident here. First is the great complexity of the system, which contains practically a limitless number of degrees of freedom, reflecting its complex internal connections. In developing methods of analysis, it is necessary while maintaining the basic properties of the system as a whole, to reject the superfluous stages of freedom and to simplify the computation system; otherwise, its analysis will be impossible even with the application of extremely suitable high productivity computer equipment. Second is the presence in the electrical system of probability processes which markedly influence the nature of the operating regimes and their technical-economic evaluation*.

The fact that control and regulating devices should be included in the circuitry of a system in the form of an integral part and as a single whole is essential in the mathematical description and compilation of a structural diagram of a system. In this connection, it is necessary to obtain new equations and to devise structural diagrams for representation of an automatically regulated machine and a regulated system. In these equations and diagrams, consideration should be given to the possibilities of modern computer technology; therefore, the fact is not excluded that in a number of cases they should be based on new principles. For example, it will be possibly feasible to reject the method of two reactions in the theory of synchronous machines in studying electrical systems and to convert to the forms of setting up equations which would have periodic coefficients.

The further development of the cybernetics of electrical systems requires a sharper definition of the mathematical depiction of the operating regime of a system from the aspect of technical-economic indices. Without this finer definition, and without the establishment of criteria of the technical-economic optimum the capability of digital computers and cybernetics cannot be used¹¹.

* At first, progress with regard to application of probability methods was very slow. The first criteria of reliability was the computed probability of the fact that power of switched-off generators would not exceed the reserve power during the period of peak load. The method of computation was developed and methods were found which connect the probability of emergency circuit breaking and the duration of the peak, and even began to determine the probability of insufficient output of electric power, etc. At present, the use of probability methods has reached such a state of development that they can be a genuine working tool. However, a large number of unsolved problems make a continuation of research urgently necessary, especially the setting up of studies on simulators.

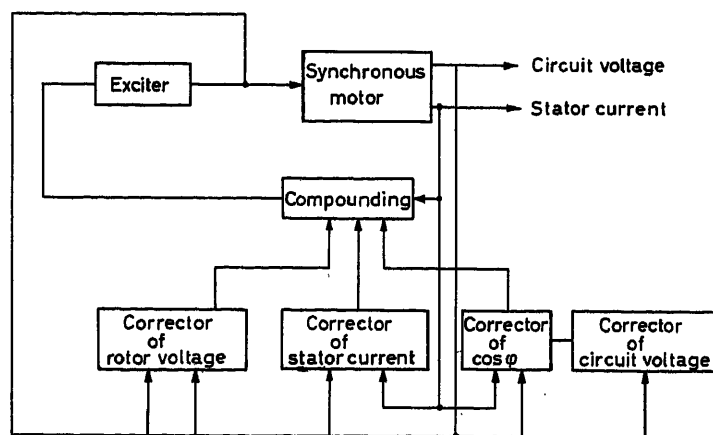


Figure 8. Structural diagram of an automatic regulator of the excitation of high-power synchronous motors

An overall analysis of the work of a system, and an analysis of the distribution of the load among the stations of the system, makes it possible to arrive at conditions under which costs of power supplied to the consumer would be the lowest possible. The development of such an analysis in the form of methods of incremental costs (specific savings) or methods of direct testing (Monte Carlo) or the 'gradient methods', for the purpose of determining the regime most economically feasible is a task that must be solved before any other. However, having equations of transient processes, which make it possible to determine how the process is going along from both a qualitative and quantitative aspect in case of any disturbance, and equations for determining the operating regime that is optimal according to economic indices, there would still not be enough information for the optimal control of a system.

In a system's operation, along with low cost, provisions should also be made for the quality of power and the operational reliability of the system as a whole, including the operational reliability of regulating and control devices. For this reason, an obligatory condition for the realization of cybernetic control should be the establishment of criteria of the operational quality of a system. The quality of the electric power is characterized by two indicators: maintenance of stable voltage for the consumer, and stable frequency in the system or in its individual unified sections. Of the criteria of quality of voltage, the most promising is the use of the integral criterion proposed by Ayre¹². This criterion evaluates the quality of maintaining steady voltage with the calculation of the amount, duration, and probability of its deviation. Instead of unproved 'permissible deviation limits', this integral criterion makes it possible to determine the probable time of operation of a network with various deviations.

The quality of network voltage can be approximately evaluated with the use of special integrating devices, which measure the above mentioned criterion. An analogous integral criterion can be proposed also for the evaluation of the maintenance of stable frequency. Thus, from direct measurements, which earlier had characterized the operating regime, one should now convert in an ever-greater degree to the measurement of indirect values, which characterize the work of the system with probability processes and interferences inherent in a cybernetic system.

The new criteria should be considered as indices to be used for the regulation of a system. The resulting conditions of optimum regulation should be found by calculating all indices of reliability and quality of the operating regime. A further important task of the cybernetics of power systems will be, as one can assume, the creation of automatic self-adjusting devices, which provide the criteria discussed above. The development of these devices should take place side by side with the utilization of regulation devices based on the techniques of continuous mathematical machines. As for the first, from the aspect of cybernetics, high-power excitation regulators, which in the future will be developed into self-adjusting regulation systems [see table (Figure 5)] have so far been very incompletely developed. As for the second, these are regulators and devices made with the use of digital computers. The optimum distribution of loads among the stations of a system or systems is done with the large-scale use of such machines. This kind of application of machines is still limited in most cases to the computation of optimum operation with the results of said computations being

given to a dispatcher. Further development should include the transmission of signals for the cybernetic control of a system.

Difficulties appearing during the conversion from manual or semi-manual control of a system to automatic, and later on, to cybernetic control, are at present linked to the insufficient development of technical-economic indices of optimum operating regime, the lack of transmitters for converting parameters of the operating regime for feeding into the machine, and an insufficient clarity with regard to which of these parameters should be measured for an exhaustive characteristic of the system's operation. There is no doubt that these tasks will be solved in the near future.

The following stage of research should be composed of the analysis of the possibility and feasibility of application, as noted previously, of extra high-speed machines for the optimum control of a system in the transient processes. Such control can be conceived: according to information received on the characteristic of disturbance according to changes in the parameters of the operating regime the machine computes the future nature of the procedure of the process, and carries out one or another operation to provide for the occurrence of the process reflecting the desired criteria of optimality. A regulator with hunting will make tests, and, in accordance with the reaction of the system to these tests, should correct the settings of the control and regulation devices. Another approach is possible: for example, comparison with earlier computed typical circumstances, etc.

The role of one or another type of machine for regulation will be determined by research and practical experience. A wide range of studies should be devoted to the analysis of the operations of an electrical system as a whole, having at the same time various means of cybernetic control: (a) with self-changing setting—adjustment, (b) with self-changing programme or algorithm of operation, (c) with self-changing parameters and self-changing non-linear characteristics or conversion algorithm, and (d) with self-changing structure.

A study of these tasks will lead to the creation of a general theory of automatically regulated electrical systems. It should be noted that the analysis of the above-mentioned systems should also include the determination of the necessary and sufficient conditions for assuring the stability of the regulated system, and if necessary, the conditions of non-variation of regulation in the face of various types of interference.

Conclusions

The problems which have been reviewed and certain particular problems, which cybernetics of electrical systems should concern itself with, do not, of course, fully exhaust the substance of such cybernetics, and in many cases, can be a subject for discussion.

The originality of the question makes it possible to regard what has been mentioned above as mere material for discussion. However, it is possible to insist that the branch of science of cybernetics of electrical systems should possess the characteristic features which have been noted in this paper. The concept of the continuity of methods of mathematical analysis and physical (natural and simulated) experiment outlined here is being proved by the entire development of practical application of regulation and automatic control of an electrical system. Having at hand only certain possibilities of setting up experiments, it is possible to put into use quickly new cybernetic-type

devices now under development. Attempts at the juxtaposition of experiments and mathematical analysis and the proposal to eliminate experiments and simulation should be studied, and, conversely, it should be noted that 'cybernetics of electrical systems' provides for a synthesis of these methods.

In the definition of the concept 'cybernetics of electrical systems' which is covered in this report, various well-known theoretical conditions are joined together, but this circumstance does not at all contradict the fact that with the use of overall ideas of cybernetics on the basis of these conditions, a single theory and a single scientific field are being created, and knowledge of electrical systems is being developed and being orientated toward its relationships with other branches of sciences, and toward a certain scientific synthesis.

References

- ¹ VENIKOV, V. A. Cybernetics of Electrical Systems. *Nauch. Dokl. Vysshey shkoly, 'Energetika'*, Scientific Report of Higher Educational Institutions, No. 1 (1958)
- ² VENIKOV, V. A. and IVANOV-SMOLENSKIY, A. V. *Physical Simulation of Electrical Systems*, 1956
- ³ WESTCOTT, J. H. Analysis of dynamic processes according to data of normal operation. *Proc. Conf.*, at Cambridge (April 1956). London (1957)
- ⁴ VENIKOV, V. A. Interaction of natural and simulated experiments. *Mathematical Modelling, and Computer Technology in Calculating the Regimes of Electrical Systems*, State Publishing House of Power Engineering Literature, 1968 (sic). To be published
- ⁵ GNEDENKO, B. V. Theoretical-probability principles of the statistical method for calculating the electrical loads of industrial enterprises. *Izv. Vuzov 'Elektromekh.'*, Information Bulletin of Higher Educational Institutions, No. 1 (1961)
- ⁶ OSHANIN, D. A. Psychological study of production operations. *Problems of Psychology*, No. 1 (1959)
- ⁷ TSUKERNIK, L. V., SHESTOPALOV, V. N. and KAMYNIN, S. M. *U.S.S.R. Invention Certificate* No. 138093 (1960)
- ⁸ TSUKERNIK, L. V. *U.S.S.R. Invention Certificate* No. 143126 (1961)
- ⁹ KOSTYUK, O. M., RYBINSKIY, V. Ye. and TSUKERNIK, L. V. Automatic self-adjusting regulator of excitation of synchronous motors. *Power and Electrical Engineering Industry*, Kiev, 1961, No. 2
- ¹⁰ VENIKOV, V. A., MARKOVICH, I. M., SOVALOV, S. A., TAFT, V. A. and TSUKERNIK, L. V. The current status of the utilization of computing equipment for the operation and planning of power systems; tasks in the field of utilization of computing equipment in the operation and planning of power systems. *Elektrichestvo*, No. 11 and 12 (1960)
- ¹¹ VENIKOV, V. A. and SOLDATKINA, L. A. The problem of the quality criteria for electric power and automatic control of the operating regime of electric power systems. *Elektrichestvo*, No. 12 (1959)

DISCUSSION

N. COHN, *Leeds and Northrup Company, 4901, Stenton Avenue, Philadelphia 44, Pa., U.S.A.*

The three papers presented at the session reflect the high interest in many nations in seeking and achieving optimum performance of energy conversion and distribution systems. Many questions have already been asked of the authors and I have but one—somewhat more sophisticated than specific—that I would like to address to authors Venikov and Tsukernik. A point that is not clear in their paper is their statement that 'design of automatic control installations is not included in the cybernetics of electrical systems'. Perhaps the authors intend this exclusion simply as a matter of terminology. One might say, however, that the analysis and studies that are undertaken to develop a method of cybernetic control of a power system gain force and meaning when control equipment is designed and installed and yields in operations the results obtained by the analytic studies.

I think it is proper to place great emphasis on achieving practical operating installations to match the best available analytic studies. I would imagine that authors Venikov and Tsukernik place such emphasis on linking successful applications to sound theory, and I am curious about their reasons for excluding the design of a control installation from the scope of their definition of cybernetics.

It may be of interest in this discussion to comment briefly on some recent aspects of the progress made in the U.S.A. in the control of generation and power flow on interconnected power systems. Interconnections in the United States have continued to grow in capacity and geographical extent. The country's largest interconnected system has been extended to include all of the eastern seaboard and eastern Canada. Its capacity is now well in excess of 115,000 MW. There has been corresponding extension of the automatic control system. The company with which I am associated has built, or is in the process of building, about 30 large centralized computer control installations for simultaneous interchange control and economic dispatch. They reflect increasingly the predominance of 'machine' and the minimizing or elimination of 'man' as exemplified by sketch (d) in Figure 3 of the Venikov-Tsukernik paper.

Until now most of these installations have been of the analogue type, but additional functions have become possible by utilization of digital computers. These additional functions are included in the following list of system functions:

- Economic dispatch and control
- Economy interchange evaluation
- Energy accounting
- Interchange billing
- Unit scheduling
- Area security checking
- Other system studies
 - (a) Hydro coordination
 - (b) loading curves
- Data logging

Very recently the Detroit Edison Company has brought into operation a 4,200 MW digital analogue system having seven stations and a number of ties with adjacent systems. The general arrangement of these digital analogue computers is shown in Figure A. The digital computer automatically directs the operation of the analogue control system. In addition the digital computer is programmed to calculate regulating margins, factors of system security advantages, interchanges with adjacent utilities, and interchange billing. Also, timing and sequence of generator scheduling and commitment to operation are calculated.

Finally, another interesting installation, a seven state 6,000 MW 16 station system, is being constructed for the American Electric Power Company. A centralized digital computer with direct centrally located analogue assembly which will regulate directly, on an individual generator basis over a 1,700 mile microwave communication system, the 40 generators of the American Electric Power Company's system.

These installations will incorporate many interesting features, including extensive digital telemetering, and communication of the digital dispatching computer to a large-scale tape-oriented IBM 7074 computer which will handle accounting, billing, and other data processing work.

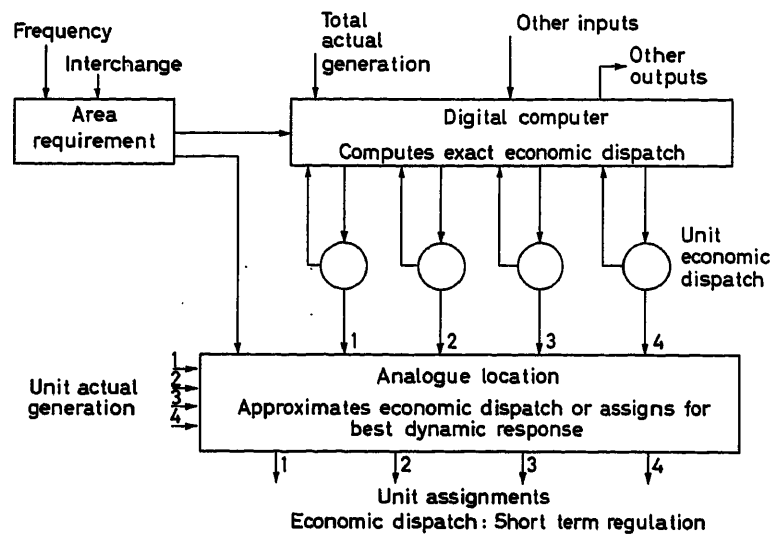


Figure A. Role of the digital computer for economic dispatch

D. ERNST, Siemens-Schuckertwerke A.G., Scharowskystrasse 2-4, Erlangen, Germany

The authors have given a remarkable analysis of the control problems in integrated power generation and distribution. There are indeed manifold correlations between the networks, the generators and prime movers and the consumers.

The application of digital computers in this control field therefore requires close attention. In general, a properly designed control system has to meet three requirements:

- (1) To improve the quality of the supply of energy (voltage, frequency etc.).
- (2) To improve the economy of generation and transmission.
- (3) To provide safe reaction in case of faults and to restrict the harmful effects of drastic faults to a minimum.

When a computer has to take over all these tasks, a number of problems arise, as follows.

The Time Schedule Problem During the Design Stage

Large plants are frequently built in steps over a number of years and there are always changes in the design and operational order from the first concept until commissioning. The computer programme has

to grow along with the building of the plant and is also subject to changes: in practice there will be a time delay because the computer is not ready to operate when the plant is.

The Priority Problem

The sequence of computer action as laid down in the programme is following a standard operational schedule. However, there can be varying schedules, especially during faults; therefore, the priority of actions has to be adapted to the many possible situations of the process. In practice, a multitude of priority lists have to be considered.

The Reliability Problem

In case of failures in the computer it is usually not justified to also shut the plant down. Operation, for example of a power station, must continue perhaps in a less automated mode.

We feel that these problems can be overcome, at least to some extent, when the automation and cybernetic control is based on independent sub-loops. These sub-loops should be very well standardized and technologically organized. The computer should then control the many parallel operating sub-loop controls. Then, the hardware and software for the automation of a plant can be organically designed.

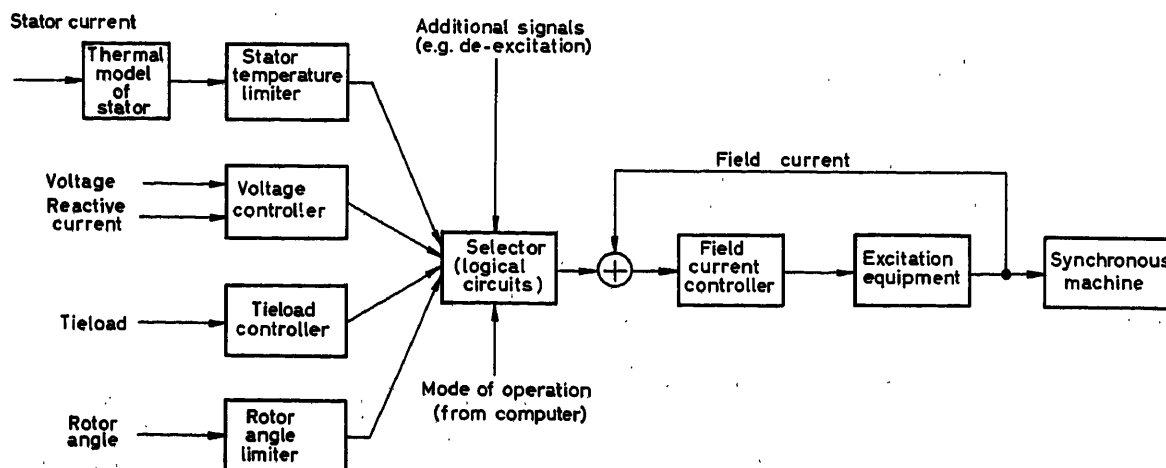


Figure A. Cascaded control system for synchronous machines

There will be horizontal layers which determine the degree of automation, as well as vertical ones which subdivide a plant and process into technological sections. Programming then becomes more logical and the flow diagrams are not so interacting with one another.

In the case of control of excitation of synchronous machines, which the authors have dealt with in their paper, an example for the approach described here is given in *Figure A*.

A cascaded control system here provides all means for the machine control. An inner loop is designed for field current control, the set point of which is given by a number of other loops for the control of voltage, rotor angle, reactive load, stator current limiting, etc. The computer would select the mode of operation of the sub-loop control system over the indicated selector device. In this way, the control system can be commissioned in steps and the computer programme is not burdened with all the information processing on the lower levels. Should the computer be out of service, operation continues with the sub-loops, less sophisticatedly, but the plant can still be kept in service.

L. K. KIRCHMAYER, *General Electric Company, Schenectady, N.Y., U.S.A.*

I wish to commend the authors for their vision in noting the needs for improved methods of analysis and synthesis in the control and planning of power systems. It is thought of interest to note some of the parallel activities of the General Electric Company on related problems.

(1) *Process Algorithms*

The increase in size of generating units and the demands for economy and reliability of operation are demanding more sophisticated control arrangements. The achievement of improved controllers requires the ability to model more accurately the dynamics of the process. In undertaking this task we have developed non-linear models of power plants whose solution is only feasible by means of high-speed digital computers. Our large-scale simulation studies of complex processes are now done almost exclusively on digital computers through means of a flexible set of subroutines portraying various system elements. These subroutines may be readily connected together by programme statements, thus readily allowing the solutions of complex problems with a minimum of effort.

(2) *Dispatching of Power Systems¹*

Work has progressed very rapidly in the application of digital computers to the problems of operations planning, control and accounting. Here a digital computer is used to automatically collect data across the system; make evaluations concerning future operations; execute instant-by-instant control action; and make accounting calculations after the fact. Such applications, it is believed, encompass some aspects of the cybernetic control of systems as visualized by the authors. In some of our digital computer dispatch applications, all of the conventional analogue sub-loops are being replaced by the digital computer.

Would the authors please comment on the present status within the U.S.S.R. of digital computers for on-line control of power systems.

(3) *Planning of Power Systems²*

Important progress has been made in the development of mathematical methods and techniques as well as digital computer programmes to achieve the optimum plan for a power system. Total System Planning is the name we have given to a philosophy of expansion planning that has as its objective the integrated design of an optimum total system, beginning with the sources of fuel and ending with the delivery of power to the customer. It considers, in the light of performance and cost, each sub-system individually and as it relates to other sub-systems; thus leading to an overall design which meets specified technical criteria at minimum present worth of total costs.

During the last five years, considerable progress has been made in realizing the goals set by the Total System Planning concept. A set of integrated digital computer programmes is available today to assist system planners in developing economic and reliable patterns of ex-

pansion in the generation-transmission area. A similar set of programmes is available to assist in the area of distribution system expansion planning.

The concept of generation-transmission planning by means of a set of integrated digital computer programmes may be visualized as a logical flow through three sequential stages:

Stage I. Determination of installation dates for new generation and the sizing of system interconnection.

Stage II. Specification of the internal transmission system required by the increasing load and generation capability.

Stage III. Evaluation of the present worth of total costs required to execute a specified expansion plan.

It would be of interest for the authors to comment on the status of digital computer programmes available to conduct such analysis in the Soviet Union. Several questions of general interest are:

(1) The author points out the need for simulating electrical systems by means of data of their normal operation. It would be of interest for the author to report upon their successes in this area of studies since the publication of the paper.

(2) I agree with the authors' views that the indicators of performance themselves require considerable technical economic research. We also concur with the idea that probability methods have reached a state of development that they are a genuine working tool. In the planning of power systems we can readily calculate a measure of system reliability and the cost of systems to meet various system reliabilities. However, the indicator which presents the value of reliability as a function of reliability has not been established. Have the authors established a value of reliability which they use in optimizing a power system design?

(3) The authors suggest that in cybernetics practice dynamic programming should be utilized. Our experience has been that dynamic programming is severely limited in practical problems because of the high dimensionality of real life problems. Have the authors used dynamic programming in the solution of problems of many dimensions?

(4) The author refers to the need for establishing equations of transient processes so as to determine optimal control according to economic indices. Have the authors developed such equations and controls for steam-electric generating plants?

In conclusion, I wish to encourage the authors to continue their fine efforts in this area of research.

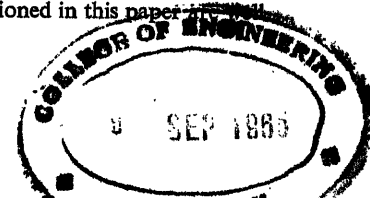
References

- ¹ BEYER, W.G., FIELDER, H. J. and KIRCHMAYER, L. K. Digital computer dispatching systems. *P.I.C.A. Conf.* Phoenix, Arizona. April 1963.
- ² GALLOWAY, C. D. and KIRCHMAYER, L. M. A progress report on total system planning. *Conference on Analytical Methods for Power System Design and Operation.* Queen Mary College, London. Sept. 1963.

Mr. TOPSETT, *English Electric Company, Ltd., London, England*

One general remark will perhaps assist those participants whose interest in power system problems may be only recent. There has existed for over 40 years an international conference at which are discussed all technical aspects of electric power systems and power plant. This is the conference internationale de Grands Reseaux Electriques (CIGRE) which meets every two years in Paris. At last year's conference, 45 different countries were represented. The next CIGRE will be in 1964 and presumably in 1966 meetings of both CIGRE and IFAC will take place. I suggest that while cross-fertilization in their respective fields will be excellent, it would be unfortunate if unnecessary duplication should result simply because knowledge of both conferences is limited to a rather small group of people.

Turning now to the paper by Venikov and Tsukernik I would mention that Professor Venikov is a distinguished participant at CIGRE conferences. Many of the problems mentioned in this paper are well



known to power-system engineers and have been the subject of CIGRE papers from many different countries. Some of these might have been mentioned in the list of references. This paper is, in effect, a sort of additional survey paper in this field, but it also attempts to look into the future. An electrical system exists to serve the ultimate consumers of electrical energy. These are frequently subdivided into: (1) Industries of all types. (2) Transportation and other services. (3) Commercial premises and activities. (4) Domestic consumers, in their homes. One of the most basically difficult and controversial aspects of the whole subject is the relative quality of the supply to be given to these four groups of consumers and the price they should pay for it. The authors touch on this matter in somewhat provocative tones, but offer no specific concrete opinions except to say that the aim is to provide the greatest possible increase in growth of electric power with the least possible consumer cost. I am sure that as users of electricity in our own homes none of us will quarrel with that objective. However, I myself work for a manufacturer of electrical generators and I am not prepared to accept a failure of continuity of my salary in return for improved continuity in my electricity supply. I invite the authors to comment further on this point and to mention the sort of criteria they have in mind about the quality of the service.

W. LEONHARD, *Siemens-Schuckertwerke A.G., Scharowskystrasse 2-4, Erlangen, Germany*

The authors have compiled an impressive list of problems to be solved for optimum design and operation of integrated power systems. The utilities and the electrical industries have surely been aware of some of these problems, for example when planning a new power plant, and have attempted to use all the technical and economical information available, and all the means to process this information including digital computers. It is an interesting proposal to coordinate all these activities under the heading of cybernetics.

It is not completely clear what the authors mean by cybernetic control and cybernetic regulators. First it appears that the authors have in mind the generalized approach, where not only narrow technical viewpoints are considered, but where reference is also made to other disciplines such as mathematics, economy etc.; the term cybernetic control is applied to fully automatic systems, to self-adapting systems using computers etc. Then some examples for regulators, exhibiting cybernetic features are given. These examples are not in line with this broad definition; also they are not convincing since the problems described can be, and are, solved with normal methods in com-

mon use, that is, a derivative influence of the feedback quantity in one case and an overriding or a cascaded control in the other.

In order to clarify these points, a brief definition of the terms 'cybernetic control' and 'cybernetic regulator' and the differences to conventional techniques would be helpful.

S.-C. YEN, *The Electrical Research Institute, Peking, China*

Have the excitation generators with the tele-transmission of δ , $p\delta$, $p^2\delta$ signals already been placed into operation in the electric power system of the U.S.S.R.? What are the conditions for obtaining optimal regulations when combining high-speed computers with this regulator?

In the automatic frequency regulation and economic dispatching of active power Mr. Mockareb of the U.S.S.R. has proposed a distributed method. Will you tell us how to unify his method with the method of cybernetic control mentioned in this paper?

How do you proceed to solve the problem of combined automatic control of voltage, frequency, active and reactive power? To what degree have the electric systems of the U.S.S.R. realized such control?

PROFESSOR LEBEDEV, *in reply*

I thank Mr. Kirchmayer for his very interesting remarks concerning the paper and will be glad to transmit them to Professors Venikov and Tsukernik. Following from these remarks, the methods of investigation used by G.E.C. in the field of electric power systems have no major divergencies from the methods presented in this paper. At the present time in the U.S.S.R. the use of learning machines is only in the first stages and it would be premature to give any recommendations, for there are not yet sufficient test results in practice.

Replies to certain questions can be found in the references given at the end of the paper.

The authors of the paper would like to receive more critical remarks concerning the methods of cybernetics applied to power systems which was the subject of this paper. Persons who were taking part in the discussion did not reject the principles presented as the basis of the methods developed by Professors Venikov and Tsukernik. These methods are taught at the Moscow Power Institute to students specializing in designing electric power stations. Concerning the several detailed questions presented in the discussion, I am unfortunately not able to give any detailed reply to them, but will, of course, be very glad to transmit them to the authors of the paper. I thank all who took part in the discussion and for the interest shown in the subject.

Some Recent Results in the Computer Control of Energy Systems

T. VAMOS, S. BENEDIKT and M. UZSOKI

Summary

In the paper the ideas of computer controlled power dispatching are summarized. A brief report is given about a new adaptive analogue computer solution of economic load distribution, some remarks are made on the power efficiency measuring techniques, especially devoted to continuous fuel analysis and on the problems of the best determination of estimation periods for efficiency optimization. The method of dynamic economic load dispatching is outlined, considering the transient costs, formulated as a multistage decision process. A more rigorous mathematical definition of power plant availability is suggested together with a way of building these data into the above programming method, thus approximating the logical decision making work of the power dispatcher. Some steps are reviewed especially for quick dispatching systems, and a few for the quick estimation of load flow change effects and the application of the theory of games for searching out the optimal network configuration switching operation. Some data are given for the required storage, computer time and telemetering capacity.

Sommaire

Ce rapport traite de la répartition optimale au moyen de calculateurs de la production d'un réseau électrique. Il donne quelques indications sur l'adaptation automatique de la répartition de la charge selon des critères économiques, au moyen d'un calculateur analogique. Il examine en particulier les techniques de mesure du rendement des différentes installations, en particulier des centrales thermiques à alimentation continue. Il traite du problème de la meilleure détermination des périodes d'estimation à prendre en considération pour cette optimisation. Il esquisse une méthode d'optimisation dynamique de la répartition de la charge prenant comme base les coûts des régimes transitoires. Une définition mathématique de l'aptitude des centrales à participer aux variations de charge est indiquée pour une programmation dynamique de cette optimisation. En prenant comme base les décisions logiques qu'un répartiteur de réseau est amené à prendre, le rapport indique certaines étapes conduisant à une optimisation automatique de la production d'un réseau électrique tenant compte très rapidement de la répercussion économique des modifications des échanges d'énergie dans ce réseau; il montre comment appliquer la théorie des jeux en vue de déterminer la structure optimale de ce réseau. Il donne certaines indications sur le temps de calcul, la capacité de mémoire et l'ampleur des télémesures que nécessite cette optimisation.

Zusammenfassung

In diesem Aufsatz sind die Gedanken über die rechner-gesteuerte Lastzuteilung zusammengefaßt. Es wird kurz über eine neue Lösung für die wirtschaftliche Lastverteilung mittels eines anpassungsfähigen Analogrechners berichtet; daran schließen sich einige Bemerkungen über Meßverfahren für den Gesamtwirkungsgrad. Hierbei stehen kontinuierliche Analysenverfahren für Brennstoffe im Vordergrund. Weiter enthält der Beitrag eine Bemerkung über die Bestimmung der Vorhersageperioden bei der Optimierung des Wirkungsgrades. Das Verfahren der dynamischen wirtschaftlichen Lastverteilung wird unter Berücksichtigung der Übergangskosten als mehrstufiger Entscheidungsprozeß formuliert. Der Beitrag enthält Vorschläge für eine strengere mathematische Definition der Anpassungsfähigkeit der Kraftwerke an Lastschwankungen und über ein Verfahren zur Berücksichtigung

dieser Daten bei der Programmierung. Bei der Nachahmung der logischen Entscheidungen eines Lastverteilers werden hauptsächlich Betrachtungen zur schnellen Lastverteilung angestellt. Einige Betrachtungen beziehen sich auch auf schnelle Entscheidungen über die wirtschaftlichen Folgen einer Umleitung des Energieflusses. Die Theorie der Spiele wird angewendet, um die optimale Struktur des Netzes zu suchen. Es werden Angaben über die benötigten Rechenzeiten, den Speicherumfang und die Fernmessungseinrichtungen gemacht.

The results of automation in the Hungarian energy system were reported in earlier papers^{1, 2}. The most important equipment realized is an automatic economic load dispatcher, based on new principles, calculating the effect of the network losses (differing from the usual solutions) from the actual network configuration. The special analogue computer of *Figures 1 and 2* calculates the matrix B using the well-known formula^{3, 4} $P_v = P B P$, according to the scheme of *Figure 3*. The potentiometers k^g in section G of the figure have the values

$$k_i^g = \left| \frac{1 - j \frac{Q_i}{P_i}}{\bar{U}_i} \right|$$

characterizing the generators, where Q_i/P_i is the active and reactive power rate, U_i the generator terminal voltage, while

$$k_i^l = \left| \frac{I_i^l}{\sum_{r=1}^m I_r^g} \right|$$

in section L characterizes the proportions of the loads on the total loss, where I_{il} is the load current at the i th node; I_{l0} is the

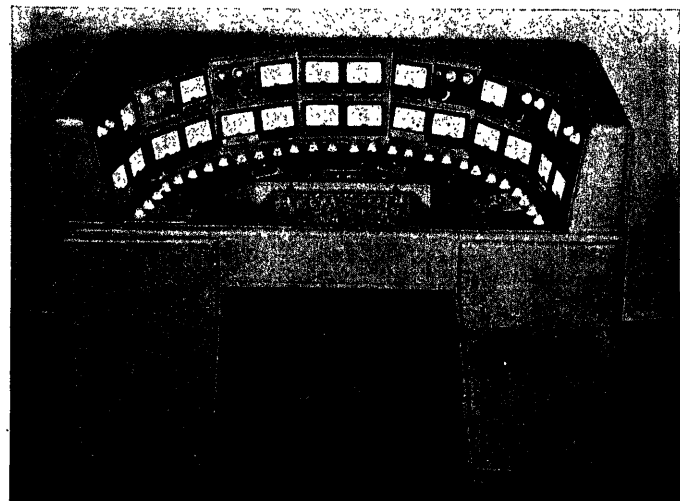


Figure 1

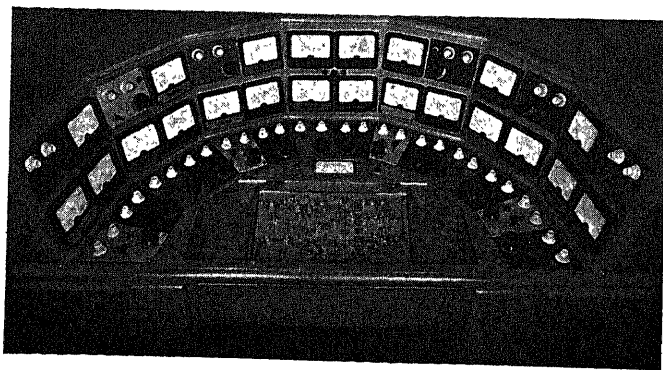


Figure 2

power station current at the i th node; and N is the direct current model of the actual network.

By a more detailed analysis it may be proved⁵ that if the voltages corresponding to the generator powers P_g^0 (without the network losses and formed similarly to the previous analogue computer solutions) are the driving voltages of the scheme's input, the voltages $\Sigma B_{ij} P_{ij}$, being proportional to the network incremental losses, are obtained at the output, which provide with a suitable feedback the optimum load distribution considering the network losses. The papers quoted prove that accuracy of the method (considering the omissions) exceeds the practically reasonable limits.

The analogue single-purpose machine for such a solution, installed in the system control, takes into account, as compared with the former solutions, the active-reactive power proportions of the generator bus-bars, as well as variations in the load proportions.

With the part simulating the actual network (matrix N), one obtains an adaptive system, resetting the economic load distribution by switching the elements of network H (that is, the actual lines, by hand, or automatically with remote control).

The experiences with the automatic load dispatcher have shown that the methods developed up to now for evaluating the economy (the incremental heat rate curves, plotted on statistical bases) are not satisfactory. In connection with this, the following problems have arisen:

(a) Continuous evaluation of the economy characteristics (efficiency, increment costs).

(b) Determination of the estimation periods for the data processing and economic load distribution, permitting filtering of the measurement uncertainties and other short cycle, transitory disturbances, but giving information about the effect of the system variations (e.g. fluctuations in connection with the frequency and power control).

(c) Measurement accuracy corresponding to better calculating and data processing possibilities and improvement of the sensing elements.

(d) Calculation of the transient phenomena effect (e.g. un-load, increase in load) in the automatic load distribution system.

(e) Problems of availability, probability of breakdown, objective judgement of the operation during partial disturbances, or unfavourable service conditions for an automatic dispatcher.

(f) The complex logical decision problems of the automatic energy system dispatcher control for searching the most favourable network connection manipulations.

Among the above problems (a) is generally solved, and a great number of power system data processors are operating. It is worth mentioning, that as regards development, these problems are not resolved. The endeavour for a practically perfect service safety, the complications of practice in connection with the electromechanical output equipment, the reasonable combination of the analogue and digital elements, and the development of a more reliable and cheaper annunciator system, rendering the whole apparatus less expensive, justify numerous new solutions.

Problem (b) must be regarded as the most open one. The digital instruments have generally a class accuracy of 0.1 per cent, while the digital computing technique is practically of absolute accuracy. At the same time the power system measuring and control instruments are of class 1–2 per cent, but in practice instruments and sensing devices for a higher accuracy can be reproduced, but these are accuracy limits under service conditions. Determination of the most important quantities, such as fluid and solid material flows, heat content, ash content, etc., leads to the greatest number of uncertainties, and here the measurement accuracy is 2–5 per cent. The error is increased with the data calculated from such uncertainly measured values, e.g. with the quotient formation necessary for the efficiency. This is the pivotal question and basic contradiction of the whole energetical optimization. We want to attain prospective efficiency improvements of 0.5–1 per cent, the sum of which may be in one

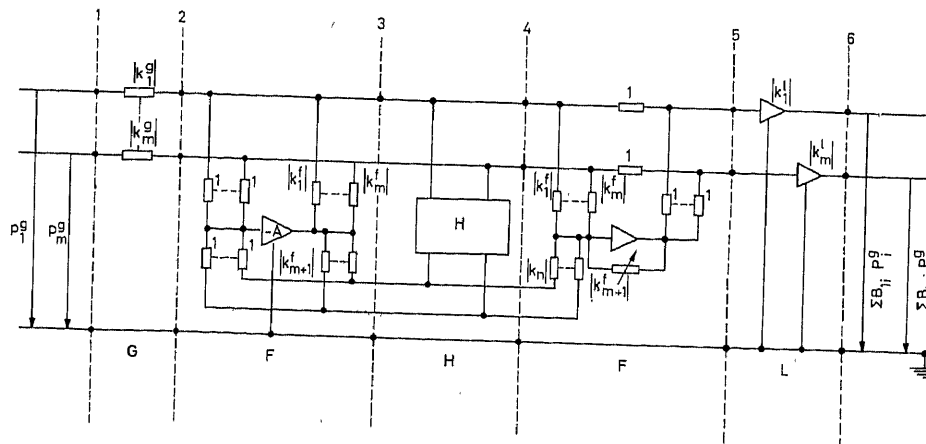


Figure 3

country in an integrated average many millions, perhaps many tens of millions, of dollars per year, based on a measurement uncertainty of 1-5 per cent.

Up to now attention has been concentrated on the problem that has not yet been completely solved, i.e. continuous and more accurate control of the coal heat content value, this being all the more justified in Hungary as the fuel quality varies considerably, and most of the power stations are thermal ones working with coal. Based on some former results^{6-8, 11}, a definite improvement has been attained in the field of coal analysis by radioisotopes^{9, 10}. We have succeeded in deriving a method permitting the continuous control of the heat content of the coal, at least within the accuracy of the laboratory calorimetric method, which is unacceptable from the statistical sampling point of view. The main experiences were as follows:

(a) In the case of thorough sample preparation a correlation of better than 0.9 may be reached with laboratory calorimetric control, which covers the uncertainty range of the laboratory method measurement accuracy.

(b) With mechanical sample preparation, the measurement accuracy is much influenced.

(c) In the case of considerably varying coal composition, a multi-ray method of different discrete energies can be advised, combined with a suitable, simple computer.

Generally it may be concluded that the next most important step in process automatization will not so much concern the automatic system itself, but rather the development of the quality analysing and quantity measuring devices and sensing elements.

In designing the process optimization a very important and insufficiently considered viewpoint is the determination of the estimation period of the characteristic to be optimized.

This view is especially clear when optimizing the efficiency, as efficiency samples taken for too short a time may lead, for example, to an efficiency value exceeding one after a former storage period, while sampling periods which are too long eliminate the possibilities of estimation of system variations that may be important for optimization. Determination of the ideal sampling period is complicated by the fact that in a boiler the transit and storage time constants of the single energy quantities are extremely different, changing even during the operation. The ideal accurate evaluation of the efficiency could be accepted only for a complete start-operation-stop period. The criterion of duration regarding the estimation period τ is that the deviation between the efficiency calculated from the efficiency taken for the total operation time and from that taken for the partial times should not exceed the error ε , caused by the measurement inaccuracy, i.e.

$$\eta = \frac{\int_{t_b}^{t_e} x_{out} dt}{\int_{t_k}^{t_e} x_{in} dt} = \frac{1}{n} \sum_{i=1}^n \eta_i \pm \varepsilon = \frac{1}{n} \sum_{i=0}^n \frac{\int_{t_i}^{t_{i+1}} x_{out} dt}{\int_{t_i}^{t_{i+1}} x_{in} dt} \pm \varepsilon$$

where x_{in} = power quantity supplied during the measurement; x_{out} = power quantity taken out during the measurement; t_b = initial time of measurement; t_e = final time of measurement; η = process efficiency; η_i = efficiency of the i th partial time, and n = number of samples taken during the whole process.

The estimation period must be chosen as the shortest one meeting this accuracy criterion.

There may be several practical solutions among which the most simple is the working with a time τ fixed by experience on the basis of the above criterion. With the boilers used in Hungary there is an interval of 10-15 min, taking values into consideration only if deviation between the output and input energy levels is less than 3-5 per cent from the beginning to the end of the estimation. The greater variations are, in any case, to be processed separately. The other system adjusts adaptively the evaluation interval on the basis of the auto and cross correlations of the output and input energy characteristic. The numerical results show also, in an apparently entirely identical mode of operation and circumstances, efficiency changes of 2-6 per cent. This is partly due to the considerable variations in the fuel quality. A test made in Czechoslovakia¹² shows variations of ± 10 per cent for coal quality fluctuations within a very short time. The experiences in Hungary gave similar, or even worse, results, and coal quality fluctuates sometimes by minutes. The effect of the system power and frequency control on the change of efficiency is also most interesting, the load fluctuations having relatively rapid frequencies resulted in an efficiency deterioration of 2-3 per cent in some cases, against the same level steady state operation. The experience in Czechoslovakia justifies the introduction of a corrective control working on the basis of quick coal analysis, while that in Hungary demonstrates the necessity of sensing the effect of the relatively faster changes upon the efficiency.

From the foregoing it follows that the former view of the static load distribution is not satisfactory for calculating the economic load distribution, and the costs of the necessary alterations (heating, unload, switchover, etc.) must be considered.

The problem is clarified by the following example. A power station is operating with four identical boilers, each being loaded to 90 per cent. If the demand increases so that loading of the boilers is to be raised to 100 per cent, the alternative may be considered, i.e. starting a fifth boiler of similar capacity, as a consequence of which the single boilers may operate with 80 per cent load, generally the optimum efficiency level. In this case the expenses of the transients (start, possible later stop, loss of life due to manifold start and stop) must be compared with the savings of the more economical steady-state operation for the expected interval. These circumstances are taken into account already, though in a more simple way, in the present load distribution practice.

The former static load distribution methods are to be generalized to an optimum energetical programming, taking into consideration also the presumable changes. These methods start, as a rule, from Lagrange's method of constrained extrema and are calculated on the basis of the equal incremental costs. The generalized task is the typical case of the multi-step decision problem. On the basis of the power demand given, the system must be programmed in an optimal way, considering afterwards the transition to the power demand expected for subsequent periods and the optimal mode of operation on the new levels. Considering the calculating difficulties and practical demands, the programme was realized for two steps, consequently, besides the system performance level given, the search for the optimum is realized for the next two levels. Consideration of the second change provides information about the first alteration

being justified. (In our example the heating up of the new boiler is made reasonable by the time elapsing until the next change and by the direction of the next variation.)

The optimum energetical programming must calculate the availability of the system and its units also, and therefore the probability factors must be considered not only when estimating the power demand, but also when calculating the available power system capacities and network interconnections. In the period to be planned, the system service conditions are characterized by the prospective capacity distributions of the individual units (power stations, machine units, etc.), that is, the probabilities of the available capacities as a function of time, and further, the probability cost values relative to these. These cost values are probability variables not only in the sense that they belong to probable power values, but they are also in themselves only probable values, e.g. the efficiency of the condensation machines is considerably dependent on the cooling water temperature, and consequently on the probable factors of the weather. The third important characteristic, from the optimization point of view, as mentioned earlier, is the excess cost of the transient states, this corresponding not to the expenses integral taken along the static time diagram of the given capacities, but generally exceeding it.

Consequently, for the predictive characterization of the availability, the following are needed. (1) Probability distribution of the capacities depending on the time and direction of transients, (2) the probability cost distributions belonging to these values, and (3) the time integrals of the expense distributions along time tables to be considered.

That is, the availability A is a set:

$$A = \{p_1 = f_1(P, t); p_2 = f_2(K, P, t); \dot{p}_3 = f_3(P, K, \int K dt)\}$$

where p_1, p_2, p_3 are the probabilities discussed above.

Accordingly, the availability A at instant t is the set of the possible power capacity values P , where to each value P belongs a value K (the costs of the service in steady state conditions) and to each curve $P_i = P_i(t)$ belongs an integral cost curve $\int K dt$.

The task of optimization is as follows. The lines of constraint of the possible power capacities $P_i = P_i(t)$ are given, that is, the boundary surfaces of a solution space of dimension n , the lower and upper power limits belonging to the individual units and changing in time. Given the probable system power $\sum P_i(t) = P_s(t)$. The trajectory of the vector P of n dimensions is to be determined (the vector characterizing the power output condition of the system units), the vector being, under the above conditions,

$$\min \sum_{i=1}^n \int_{t_0}^t K_i [P_{i, opt}(t)] dt$$

that is, providing the minimum of the cost integral taken along the trajectory. The line integral taken along the trajectory in the coordinate space P forms no conservative space, as the line integral is not independent of the path and the integral taken along the closed curves (the cost of returning to the same power distribution) is not zero.

The probability influence of the availability and of the costs have been derived according to the following considerations:

(a) One determines for all equipments the operation time permitted on an experimental basis, that may be considered—if there is no special fault indication—as a time of practically

perfect safety. During this time the service costs of operating the apparatus in steady-state conditions correspond to the value calculated in general till now.

(b) At the beginning of operation (primary disorders) and over the service time permitted, the probability of outage is greater. Here a penalty tariff is stated, depending on the time and calculating from the former outfall statistics and from the probable economic consequences of the outfall.

(c) Similar penalty tariff is stipulated in case of some error signals (fault indications).

(d) For all important units the transient costs (the expenses of the transient conditions) obtained by experience or calculation are stored, adding to this in some cases the penalty tariff calculated from the disturbance danger relative to the transition.

The above data can be elaborated by the individual power station data processors with a relatively small storage and time requisition to data necessary for the load distribution. These are the curves corresponding to the classical increment cost curves, corrected by the penalty tariffs considering the availability, the possible time functions of the transients and the integral cost curves of the transient conditions. For power stations a relatively slow processing of about 10–20,000 data is needed and the communication of about 300–400 data with the central load dispatcher, as a result of the above calculation. The latter must be dispatched only in case of and to the degree of change. The knowledge of these 300–400 data per power station accomplishes the two-step optimizing programme mentioned earlier.

In this manner, with the aid of suitable power station data processors, by the otherwise available telemetering channels and by a central, medium size computer, energetical automatic optimization may be realized, which takes into account the economic consequences of the power system transient conditions and of its availability, and also the changes in production costs and efficiencies during operation.

The optimum system control referring to the whole power system does not make superfluous the optimization of the individual control circuits, which may be considered partly to be autonomous. Reference is made here, for example, to the control of coal pulverizers, which may be controlled directly by a continuous analyser of ash, assuring the given fuel quantity as a primary condition. As against the non-interacting control systems suggested recently by many authors, installing fixed matrix connections into the control circuits considered previously autonomous, we think to be rather practicable such semi-autonomous adaptive circuits, as the rigid functional connections give suitable results only under perfectly steady-state conditions (e.g. time constants), this condition being chiefly realized with boilers.

In the course of the dispatcher control automatization, the question arose to what extent the dispatcher work may be mechanized in addition to chart preparation and beyond the tasks of the continuous economic load distribution. This idea is supported by the fact that the switching, manipulating and failure suppression activity of the dispatcher control is motivated by subjective factors; extremely hazardous decisions must be made in a short time, and the presence of mind, momentary mood and luck of the dispatcher influence considerably his activity in this field. Mechanization of the task is complicated by the fact that the methods of judgement of the situations were

partly subjective ones, based on the experiences and intuitive improvisation capabilities of the dispatcher, as there is no possibility for accurate analysis in the case of rapid decisions. Accordingly, mechanization of the dispatcher control permits the application in practice of cybernetics in a narrow sense, and the adoption of recognition and heuristic search.

In the course of elaborating the problem the method of approximating the tasks step by step has been chosen, selecting a single logical task of the dispatcher control. It is seen, taking into account the present machine capacities, that the question arises as to how this task can be elaborated and, after solving this, the kind of further tasks that remain for the dispatcher to solve. By this one can remove from the total dispatcher's activity the parts having not been exactly formulated up to now and examine their weight in the total work and how to handle them. In any case, as more tasks are mechanized and separated from the dispatcher's control, the more time and possibility remain for accomplishing the part demanding the most complicated intellectual activity.

As a first task, estimation of the possible circuit diagram was examined from the overloading point of view. Similar calculations (load flow programmes in the network) have been made regularly for more than a decade on digital machines, but this was the first digital computer application in the power systems. At the same time the methods complying with computer requirements are not fully practicable for automatic control purposes, due to their other demands. Here the analogy of differences between the measuring instruments and the sensing elements of automatic control must be referred to. In sensing systems, however, detecting identical quantities using identical physical principles as measuring instruments the difference in their field of application, demands different approaches. For automatic control we have confined ourselves to a load flow computing method of an accuracy of 5-8 per cent, but being most rapid, providing the results for a 40 node network on a medium size machine in less than 1 sec. The storage capacity demanded is about 1,000 words over the programme. Otherwise the method was a generalization of the well-known method of current distribution factors and imaginary loads, reducing the evaluation of a network of n nodes to the solution of a complex, linear equation system of about i unknowns, if the calculated network differs from a basic configuration with i lines.

The next step was the determination of the optimum connection configuration of the connection manipulations (maintenance, disturbance) tested from a safety point of view. When elaborating the programme, the theory of games has been adopted, interpreting the dispatcher's work as a two-step game of two persons, a game against nature. The pure strategies of one of the players, i.e. the dispatcher, are the available connection manipulations, while those of the other player, that is, the nature, are the disturbances imaginable in the system. The game is two-stepped, first a favourable main network connection diagram is selected by the dispatcher, not knowing yet what kind of disturbances may arise during the validity of this circuit diagram. After this the nature 'moves', a possible disturbance ensues, and as a last step, a changeover strategy is chosen by the dispatcher which reduces the power limitation produced by the disturbance to the minimum. To adopt the minimax principle, a suitable pay-off criterion had to be found by which the elements of the game matrix may be filled and the optimal strategy may be evaluated. This criterion is established on the basis of the

damage caused by the possible power outage and the weight functions formed by the outage probability. On the basis of several considerations, the outage probability p is not directly applied for weighting, but this is done, however, with the relation

$$k=f(p_i)=\frac{1}{1-\ln p_i}$$

so the criterion of the optimal game is:

$$\min_i \left(\max_j W_{ij} K_{ij} \frac{1}{1-\ln p_j} \right)$$

where W_{ij} is the power outage caused by the i th dispatcher's strategy and the j th disturbance possibility (kWh), K_{ij} is the specific damage due to the above disturbance (\$/kWh), and p_j is the probability of the j th disturbance.

The machine time for analysing a complete situation in the case of a medium size machine and of a starting position deviating not from the normal one but at most with the state of the four lines is about 4-5 min for a 40 node network, its storage demand being without programme about 800-1,000 words.

The availability of the network, and that of the power stations, may be considered along similar lines making use of the suggestions mentioned earlier, thus extending further the possibility of the objective evaluation of the network configuration. The programme evaluating the manipulations may include the data referring also to the stability. As examination of the stability conditions of a single situation demands considerable time even by a computer, the application of the pre-calculated, stored stability data, as well as the continuous processing of the data of the stability reserve indicators, are referred to here.

Control of the dispatcher by computers would not make superfluous the application of less complicated network automatics, such as protections, overswitch and backswitch automatics, etc.

It must be emphasized that in the field of the present summarizing report on the authors' developments and ideas, these are up to now mainly theoretical achievements calculated for a mathematical model, prepared for simulation on a digital computer. Their expediency and adaptability must be decided, however, by practice, for many technological and other realization difficulties must be overcome.

References

- 1 UZSOKI, M. and VAMOS, T. Some questions regarding control of power systems. *Automatic and Remote Control*. 1961. London; Butterworths
- 2 VAMOS, T., UZSOKI, M. and BOROVSKY, L. Novűj, nyeposredsztvennyj, masinnűj szposzob ekonomicsnova raszpregyellenyija nagruzki mezsdu elektrosztancijami i nyeszkojko voproszov szvjazannűch sz optimizaciej enyergoszisztym. *Symposium of Automation of Large Energetical Units*. 1961; Prague.
- 3 KRON, G. Tensorial analysis of integrated transmission systems. The six basic reference frames 1. *Trans. Amer. Inst. elect. Engrs*, 70 Pt II. (1951) 1239
- 4 KIRCHMAYER, L. K. *Economic Operation of Power Systems*. 1958. New York; Wiley
- 5 UZSOKI, M. Uj, gűpi műdszer a gazdasűgos teherelosztűs szűmítésűra. *Colloquium of Automatic Control*. 1962. Budapest

- ⁶ NAUMOV, A. A. O primenyenii obratno rasszejannovo β -izlucseniya dlja avtomaticheskovo kontrolja szosztava szloznich szred. *Avtomaticseszkoje upravlenije*, pp. 152-159. 1959. Moscow; Izdatyelsztvo Acad. Nauk SSSR
- ⁷ PRIVOVAROV, L. L. O primenyenii javleniya pogloscheniya γ -izlucseniya dlja avtomaticheskovo kontrolja szosztava mnogo-komponentnich szred.
- ⁸ DIJKSTRA, H. and SIESWERDA, B. S. Apparatus for continuous determination of the ash content of coal. *Int. Coal Prep. Conf.*, 1958; Liège
- ⁹ BISZTRAY-BALKU, S., Dr. LÉVAL, A., KAKAS, J., NAGY, M. and VARGA, K. Szenek fűtőértékének meghatározása radiológiai módszerrel. *Energia és Atomtechnika*, 6 (1960) 472
- ¹⁰ BISZTRAY-BALKU, S., KAKAS, J., NAGY, M., VARGA, K. and LÉVAL, A. Die Bestimmung des Heizwerts von Kohlen durch radioaktive Strahlung. *Isotopentechnik*, Nr. 5-6 (1960-61)
- ¹¹ BELUGOU, P. and CONJEANUD, P. The determination of the ash content of coals by means of x-rays. *1st Int. Coal Prep. Conf.*, 1950. Paris
- ¹² IBLER, J. Trebovaniya k regulirovaniyu energeticheskikh blokovo sz tocski zreniya upravleniya energeticheskoi szisztemy. *Symposium of Automation of Large Energetical Units*. 1961; Prague

DISCUSSION

L. K. KIRCHMAYER, *General Electric Company, Schenectady, N.Y., U.S.A.*

The authors have done an excellent job in outlining present dispatch practices on the Hungarian Power System as well as indicating future areas of profitable research. I have several comments and questions for their attention:

(1) Transmission Loss Formula

The authors' treatment of transmission losses is certainly unique and appears to allow ready modifications for different circuit arrangements.

Recent work conducted by G.E.C. has lead to significant improvements in the accuracy and ease of calculation of transmission loss formulas^{1, 2}. In references 1 and 2, the reactive power of each generator is treated as a function of the reactive output of that particular generator and the total system load. This reactive approximation leads to improved accuracy over the use of the ratio Q/P as indicated in eqn (1) of the authors' paper. The method described in references 1 and 2 has also provision for treating the loads as a complex linear function instead of just a complex linear fraction of the total load. Reference 2 also rigorously treats the effect of tappers in the network. As a question to the authors, I would like to ask how the effect of tappers would change Figure 3 of their paper.

(2) Analogue Versus Digital Dispatch Computers³

I thought it would be worth while to note that the current trend in the U.S.A. is to use digital computers as on-line computer controllers for the operation of power systems. These computers serve not only to take care of the instant-by-instant load frequency control and economic allocation of generation, but also serve as an important tool in solving the problem of operations planning and accounting.

We visualize, in the future, the possible interconnection of the power plant digital computer and the central dispatch computer in order to ensure that the instant-by-instant dispatch is accomplished using the current thermodynamic performance of the power plant.

(3) Effect of Transients on Thermodynamic Efficiency

There is, indeed, a need for determining more precisely the effect of transient phenomena upon the thermodynamic efficiency. The authors refer to a deterioration of efficiency of 2-3 per cent in the case of load fluctuations having rapid frequencies. Do the authors have sufficient data to present this efficiency deterioration as a function of frequency?

(4) Unit Start-up and Shut-down

In our applications, the dispatching computer is used to arrive at the optimum schedule of unit start-up and shut-down through use of a gradient method. This method to date does not, however, consider the probability of outage of the various elements, but does provide a stated minimum spinning reserve.

(5) Optimum Network Configurations

The authors discuss the use of the theory of games to determine the optimum network configuration. Have the authors evaluated the improvement in performance obtained by this method compared to solutions obtained by earlier methods?

Our applications to date involve the use of the dispatch computer to run load flows but not to search for the most favourable connection. Our philosophy of system design is that the transmission network is designed for all elements to be in service except for emergency conditions, which, are taken care of through a properly designed relaying system.

(6) Stability Reserve Indicators

The authors also refer to stability reserve indicators. Would the authors kindly describe the nature of the indicators which they have in mind?

(7) Computer Specifications

The authors state, through means of a central medium size computer, that energetic optimum may be realized which takes into account the automatic consequence of the power system transient conditions, and of its availability, and also the changes in production costs and efficiencies during operation. Would the authors please indicate the computer storage and operating times which they visualize for this computer?

In conclusion, let me compliment the authors in visualizing possible opportunities in improving the economic performance of power systems.

References

- ¹ KIRCHMAYER, L. K., HAPP, H. H., STAGG, G. W. and HOHENSTEIN, J. F. Direct calculation of transmission loss formula—I. *Trans. Amer. Inst. elect. Engrs.* 79, Pt. 3 (1960), 962-968
- ² KIRCHMAYER, L. K., HAPP, H. H., STAGG, G. W. and HOHENSTEIN, J. F. Direct calculation of transmission loss formula — II. *I.E.E.E. Summer Meeting*. Toronto, Canada. June, 1963
- ³ BEYER, W. G., FIEDLER, H. J. and KIRCHMAYER, L. K. Digital computer dispatching systems. *P.I.C.A. Conf.* Phoenix, Arizona. April, 1963

P. PROFOS, *Federal Institute of Technology, Zurich, Switzerland*

Mr. Vámos mentioned a rapid method of determination of heat content by radioisotopes. I have some questions in relation to this method.

(1) Have you already gained some field experience with these types of sensors, if so, is it satisfactory?

(2) It is well known that accuracy and dynamic response of measuring heat content depends to a great extent on the method of taking

representative fuel samples, this being particularly difficult with coal. Is the sampling technique used still the same, or are there also substantial improvements in this respect?

(3) Due to the fact of considerable and rapid fluctuations of the actual heat content it will be necessary to filter (to average, roughly speaking) the signal of the heat content sensor for the purpose of computation of the boiler efficiency. Is there a real need to improve the response of the heat content sensor or is this merely of academic interest?

(4) The goal of computer control is, I think, to realize an economically optimal load distribution: roughly speaking, to produce and distribute energy in such a way that the overall production cost per kilowatt hour is a minimum at any instant. An important part of this cost is, of course, the fuel, the latter depending on the specific coal consumption of the plants and the price of the fuel. As long as the fuel is purchased by weight and not on the basis of heat content, it seems to be sufficient to use as a basis of economic load distribution the incremental cost per kilowatt hour produced by a given power station. To determine this magnitude it is not necessary to compute the thermal efficiency of the plant and hence also the determination of heat content will not be necessary.

Does the price of the fuel in Hungary depend on the actual heat content of the coal burnt, or are there other special reasons for taking care of the heat content of the coal in relation to computer control of energy systems?

D. A. ABDULAEV, *National Committee U.S.S.R., Kalantschevskaja 15 a, Moscow, U.S.S.R.*

In the use of computers for optimal control of regimes of large electrical systems, various schemes are possible for the transmission and processing of signals resulting from disturbances appearing in the system. What structure of systems of transmission and processing of information does the author consider to be the most efficient?

Is there a connection of the type object-computer or are there any other types of connection possible?

In order to increase the efficiency of utilizing computers, a problem arises of improving the accuracy of primary measuring instruments. With existing errors of measuring instruments, what magnitude of error does the author consider admissible for an optimal and most efficient control of electric system?

J. CARPENTIER, *Electricité de France, 12 Place des États-Unis, Paris 16^e, France*

Which types of data processors are to be put in the thermal power plants? Are they simple data-loggers or digital computers? Are they likely to perform any other tasks, such as operation optimization, start-up and shut-down of the plant? Has an economic study been made of this subject?

Concerning the use of the theory of games to determine the best connection configuration of the network, by what considerations has the disturbance probability been replaced by functions of these probabilities?

Concerning the load flow computation made by the dispatcher, it is interesting to notice that a method of economic dispatch giving an account of limitations of loads of the lines has been realized in France. In these methods, called 'injections methods', economic dispatch and load flow are computed at the same time, and the dispatcher must not begin the economic dispatch computation again if a line is overloaded as it might well be.

Reference

CARPENTIER, J. *Bull. soc. franç. Elect.* Aug. 1962

D. ERNST, *Siemens-Schuckertwerke A.G., Scharowskystrasse 2-4, 852, Erlangen, Germany*

The authors have given a very interesting possible application of computers in the electric power field. Problem (b) on the first page of their paper deserves special attention and should be highly appreciated.

The use of computers for economic load dispatching is well under way and there is no doubt over the justification of this application. A question of the future, however, is how the computer can be adapted to the automatic operation of transmission systems and switch plants, on the on-line closed-loop mode. Some possible aspects would be:

- (1) Continuous determination of the redundancy of systems.
- (2) Switching of feeders, transmission lines, etc.
- (3) Activating the protective relay scheme by direct switching actions in case of faults.

Again, the problems of trying to realize an overall computer approach arise, as I have indicated in the discussion to the previous paper. Also a centralized computer control would require a larger number of very effective and—in some cases redundant—telemetering channels. The reliability problem and the priority problem are also of paramount importance. Therefore, it is felt that the question of using sub-loops on the lower levels of automation should be revised.

In the process of distributing electrical energy, the products are always the same. However, a vast amount of apparatus is engaged in the process and the information flow is tremendous. Therefore, a powerful data reduction system with computers would improve substantially the situation for the dispatching personnel.

It would be interesting to hear the authors' opinion on the question of centralized or decentralized control of large transmission and distribution systems.

T. VAMOS, *in reply*

Mr. Kirchmayer's first question concerning the effect of tappers can be solved in the scheme by d.c. transformers (i.e. by the use of d.c. amplifiers), or by an a.c. scheme based on the same idea, though in our network this is not needed.

We have no exact idea about the use of analogue on-line computers in the future. The analogue computer used by us costs \$ 50,000 approx., one magnitude less than a digital one, though the latter can be used for other purposes, too. Maybe the ultimate solution will be a hybrid computer.

Data on deterioration of thermodynamic efficiency by fluctuations are insufficient and unreliable. The 2-3 per cent mentioned is given by two power plants operated for a period by a frequency controller exciting fluctuations of a period of a few minutes. Average fluctuations of C.V. of about 7 per cent caused a deterioration of 0.5 per cent.

The consideration of probability values for unit start-stop is only an idea for the later calculations. This means the collecting of data for about a decade to reach results that can be adopted with confidence. The same remark is valid also for the application of gaming theory for the search of optimal network configuration.

The stability reserve indicators were developed by another group in our institute, led by Mr. Bókay. The main idea is the measurement of generator reactive, stator and exciting currents. Further details may be found in CIGRE Paper No. 308, 1960, and in a paper¹.

We use the Elliott 803/B computer for model purposes. Further development may require a larger device.

Professor Dr. Profos asked about the measurement of C.V. For two years we have had an experiment in two power stations, and the results are encouraging but not sufficient. The sampling technique may be a new one, using a continuously operating by-pass of coal-flow. The main possibility to be expected from the radioisotope method is continuous sampling and analysing. If the C.V. is changing, as in our case, with a standard deviation of 7 per cent, the efficiency deterioration can be improved by about 0.5 per cent with the continuous setting of air/fuel, or air/steam ratio and through regulating the coal prepara-

tion (e.g. mills). Referring to the question of coal prices, we try to use approximate production prices in our country, i.e. for every coal-mine the real production and transport costs².

Replying to Mr. Abdulaev's questions, we consider the use of an object-computer scheme, that is, an on-line computer in the power station operating in the first instance as data logger and processor. We do not consider the classical control sub-loops unnecessary. The required accuracy of the measuring instruments is dependent on the average effect of the parameter on overall efficiency of the process, calculated on the basis of statistical data. This value varies from 0.2 to 2 per cent.

Mr. Carpentier's questions regarding the type of computer used may be answered as follows: We develop a system with a step-by-step approach from data logging to automatic optimization of the whole process, including start, stop and other transients. The probability

estimation function of the gaming model is given on p. 37 of our paper. For further details see reference 3.

Further contributions to the question asked by James, Ernst and Gonzales are very interesting with regard to the exchange of practice and views.

References

- ¹ BÓKAY, B. Continuous control of the steady-state stability in a multi-synchronous machine system with cylindrical rotors. (*Dissertation in Hungarian*) Budapest, 1963
- ² VÁMOS, T. Some principal questions on energetic optimization. (*Dissertation in Hungarian*)
- ³ BENEDIKT, Sz. Some problems on the computer control of power systems. (*Dissertation in Hungarian*)

Optimal Control of Thermal-hydro System Operation

L. K. KIRCHMAYER and R. J. RINGLEE

Summary

Significant progress has been achieved in the application of dynamic optimization techniques to obtain the most economical operation of a combined thermal-plant and hydro-plant electric utility system. These methods have resulted in significant improvements in the operating economy of such electric utility systems. This paper presents the mathematical theories used in achieving optimization, discusses computer solution of these methods, as well as on-line computer control implementation.

One example concerns the application of variational methods to the hydro scheduling problem where head variations may be neglected. Over the stated period, it is desired to use specified volumes of water from the various reservoirs, observing the constraints on reservoir elevations and plant maximum and minimum outputs. This solution was achieved by application of variational methods and the use of Lagrangian multipliers to handle the constraints.

The rigorous treatment of the effect of head variations and particularly the constraints upon the allowable variation in reservoir level are difficult to consider by classical variational methods. The constraints that must be applied to the reservoir levels at each point in time may be designated as point or saturation constraints. A dynamic programming algorithm has been formulated which will properly account for the point type constraints and head effects and will yield the water schedule resulting in minimum production costs.

Sommaire

Un progrès appréciable a été réalisé dans l'application des techniques d'optimisation dynamique pour obtenir le fonctionnement le plus économique d'un système combiné de production d'énergie électrique à centrales thermiques et hydrauliques. La présente communication expose les théories mathématiques employées pour réaliser l'optimisation, discute la solution de ces méthodes utilisant des calculateurs de même que l'équipement avec des calculateurs dans la boucle de commande.

Un exemple concerne l'application de méthodes variationnelles au problème de programme hydraulique dans lequel les variations de la hauteur de charge peuvent être négligées. On desire utiliser, pendant la période envisagée, des volumes donnés d'eau en provenance des divers réservoirs tout en observant les limitations dans les élévations des réservoirs et les productions maximales et minimales de la centrale. Cette solution a été réalisée en appliquant des méthodes, variationnelles et en utilisant les multiplicateurs de Lagrange pour traiter les limitations.

Le traitement rigoureux de l'effet des variations de la hauteur de charge et, en particulier, les limitations dues à la variation admissible du niveau dans le réservoir sont difficilement réalisables par les méthodes variationnelles classiques. Les limitations qui doivent être appliquées aux niveaux dans les réservoirs à chaque instant peuvent être considérées comme des limitations ponctuelles ou de saturation. Un algorithme de programmation dynamique a été formulé; il tient compte des limitations du type ponctuel et des effets de hauteur de charge et fournit le programme hydraulique ayant pour résultat le prix de revient de production minimum.

Zusammenfassung

Bei der Anwendung dynamischer Optimierungsmethoden für die wirtschaftlichste Betriebsweise eines kombinierten elektrischen Verbund-

netzes mit thermischen und Wasserkraftwerken sind bemerkenswerte Fortschritte gemacht worden. Derartige Methoden haben in betriebswirtschaftlicher Hinsicht beachtliche Verbesserungen für solche Verbundnetze erbracht. Dieser Beitrag bringt die mathematischen Theorien, die zur Optimierung verwendet werden, bespricht Rechnerlösungen für diese Methoden und auch die Ausstattung für direkt regelnde Rechner.

Ein Beispiel beschäftigt sich mit der Anwendung von Variationsmethoden auf die Probleme der Wasserversorgung, wenn Änderungen der Standhöhe vernachlässigt werden können. Innerhalb der vorgegebenen Zeitspanne ist es erwünscht, ganz bestimmte Wassermengen aus verschiedenen Staubecken zu verwenden, um dabei die zwangsläufigen Bedingungen für die Höhenlage der Becken und für die Höchst- und Niedrigstleistungen der Werke im Auge zu behalten. Diese Lösung wurde durch Anwendung von Variationsmethoden und mit Benutzung des Lagrange-Multiplikators zur Berücksichtigung der Nebenbedingungen erzielt.

Eine ins einzelne gehende Behandlung der Auswirkungen von Standhöhenänderungen und im besonderen die Nebenbedingungen für die zulässige Änderung der Stauhöhen sind bei Benutzung der klassischen Variationsmethoden nur schwer in Betracht zu ziehen. Die Nebenbedingungen, die an jeder Stelle zu gegebener Zeit den Stauhöhen zugeordnet werden müssen, können als Punkt- oder Sättigungsbedingungen bezeichnet werden. Ein Algorithmus für das dynamische Programmieren wurde aufgestellt, der die punktförmigen Nebenbedingungen und die Standhöheinflüsse berücksichtigt und eine Wasserverteilung ergibt, die den niedrigsten Erzeugungskosten entspricht.

Introduction

Electric power generation by thermal and hydraulic means represents a significant factor in the economy of each nation. The decision processes utilized for the control of hydro-electric and thermal-electric power generation affect the expenditure of large amounts of natural resources. Further, effective utilization of these facilities and resources can reduce future capital commitments for additional equipment. Relatively small errors in the coordination of these resources can therefore cause significant monetary losses. Only by careful control or coordination of resource expenditures can the maximum value of the resources be realized.

The entire problem of thermal-hydro-electric power integration is one involving the determination of future power and energy demands as well as future resource availability and matching plant capability in such a way as to maximize the value received from the resources and capital invested. This is a broad problem involving both probabilistic and deterministic factors¹⁻³.

The problem of optimization to be treated here concerns the short range coordination of hydro-electric and thermal power generation with specified plant capability. Plant capital investment is assumed fixed; and, for the period of operation, it is assumed that the quantity of water available for electrical energy production is specified. The criterion for operation is thus to operate

the power production system in such a manner that the expected demand for power is met continuously with not more than the assigned quantity of water consumed and the expenditure of thermal fuel resource minimized. A number of physical constraints are imposed upon the power system. These include maximum and minimum limits upon the storage capacity of reservoirs, upon the discharge rates for hydraulic turbines, and upon the generating capability of the thermal plants.

This challenging problem has been under study for many years⁴. Because of its complexity, early contributions were based on many simplifying assumptions and approximate solutions were achieved by hand computational methods. Only within the era of the high-speed digital computer have careful analytical or numerical solutions been feasible. It is the purpose of this paper to discuss two of the mathematical techniques by which this problem may be solved, and the means by which the solution may be used to generate the information to control the power system.

First, the problem has been formulated in continuous time and solved by integration of the Euler-Lagrange equations resulting from the calculus of variations⁵⁻⁷. Second, the problem has been formulated in discrete time as a sampled data system and solved as a mathematical programming problem⁸⁻¹².

Implementation of the results of these two mathematical methods will be discussed in the paper and a digital control system described. Also a comparison will be offered of the relative advantages and disadvantages of the two methods based upon experience gained in producing digital computer programmes for the two methods.

The Variational Formulation

Development of Theory

Written as the minimization of an integral criterion, the problem is one of the general class of isoperimetrical problems. For illustrative purposes, the problem will be initially phrased in its simplest form as the optimization of the control for one hydro and one thermal-electric power generation plant. As formulated⁵⁻⁷, it is required to minimize the cost of fuel expended for thermal generation $F(P_S)$ over the period of time $0 \leq t \leq T$, subject to the constraint that the demand for power P_R must be met continuously by the thermal generation P_S and the hydro generation P_H .

The relationship between power generated and received is given as

$$P_R = P_S + P_H - P_L \quad (1)$$

P_L is the transmission loss and is a quadratic function of the power generated P_H, P_S ¹³.

The reservoir acts as an integrator; the rate of change of storage dV/dt is equal to the inflow r minus the sum of the outflow q discharged through the hydraulic turbines and the non-power generating release S . S may be a planned or controlled release, or may be a function of the forebay such as the spill that may occur when the forebay exceeds the crest of the reservoir.

The differential equation governing the state of the reservoir is given by

$$\frac{dV}{dt} = r - q - S \quad (2)$$

The short-range hydro-thermal scheduling problem is usually phrased as the search for the discharge function $q^*(t)$ that results in a stationary value for the integral of fuel costs over the optimizing period,

$$E = \min \int_0^T F(P_S) dt \quad (3)$$

subject to the algebraic constraint equation (1) and the differential constraint equation (2). These two constraining relations may be introduced directly in the integral (3) by the use of two time varying Lagrange multipliers λ and γ . The new functional to be minimized now appears as

$$J = \int_0^T \left\{ F(P_S) + \lambda(P_R + P_L - P_S - P_H) + \gamma \left(\frac{dV}{dt} - r + q + S \right) \right\} dt \quad (4)$$

From the first variation of (4) there develops the Euler-Lagrange equation set

$$\frac{\partial F}{\partial P_S} - \lambda \left(1 - \frac{\partial P_L}{\partial P_S} \right) = 0 \quad (5)$$

$$-\lambda \left(1 - \frac{\partial P_L}{\partial P_H} \right) \cdot \frac{\partial P_H}{\partial q} + \gamma = 0 \quad (6)$$

$$-\lambda \left(1 - \frac{\partial P_L}{\partial P_H} \right) \cdot \frac{\partial P_H}{\partial V} - \frac{d\gamma}{dt} + \frac{\partial S}{\partial V} \gamma = 0 \quad (7)$$

with the associated differential equation (2) and the algebraic equation (1).

The additional boundary condition imposed upon this problem is that the endpoints of the reservoir storage are specified. The problem is thus of the two-point boundary value type. The implication is, of course, that the value of the Lagrange multiplier γ at $t = T$ is non-zero.

There are, of course, certain operating constraints upon the ranges of the variables P_S, q, V , in practical problems. These can frequently be set in the form

$$P_{S_{\min}}(t) \leq P_S(t) \leq P_{S_{\max}}(t) \quad (8)$$

$$q_{\min}(t) \leq q(t) \leq q_{\max}(t)$$

$$V_{\min}(t) \leq V(t) \leq V_{\max}(t)$$

The Lagrange multiplier γ becomes a constant in time for the problem in which the hydro-electric output is only weakly dependent upon the reservoir storage and the variation of S with V is neglected.

Illustrative System Problem

Such a problem has been solved by digital computer for the Southern California Edison System¹⁴ involving seven hydro reservoirs and two equivalent steam plants. The hydro facilities treated included the portion of the Big Creek project shown in Figure 1, and the Hoover-Edison plant. The Euler-Lagrange equations for this case take the form of simultaneous non-linear equations:

$$\frac{dF_n}{dP_{Sn}} = \lambda \left(1 - \frac{\partial P_L}{\partial P_{Sn}} \right) \quad (9)$$

$$\gamma_j \frac{dq_j}{dP_{Hj}} = \lambda \left(1 - \frac{\partial P_L}{\partial P_{Hj}} \right) \quad (10)$$

where $\frac{dF_n}{dP_{Sn}}$ = incremental production cost for thermal plant n

$\frac{\partial P_L}{\partial P_{Sn}}$ = incremental transmission loss for thermal plant n

$\frac{dq_j}{dP_{Hj}}$ = incremental water rate for hydro plant j

$\frac{\partial P_L}{\partial P_{Hj}}$ = incremental transmission loss for hydro plant j

λ = incremental cost of received power

γ_j = water rate conversion coefficient for hydro plant j

A simplified logic flow diagram for solution of these equations is given in Figure 2. In the power loop, equations (9) and (10) are solved by a Gauss-Seidel iteration method for trial

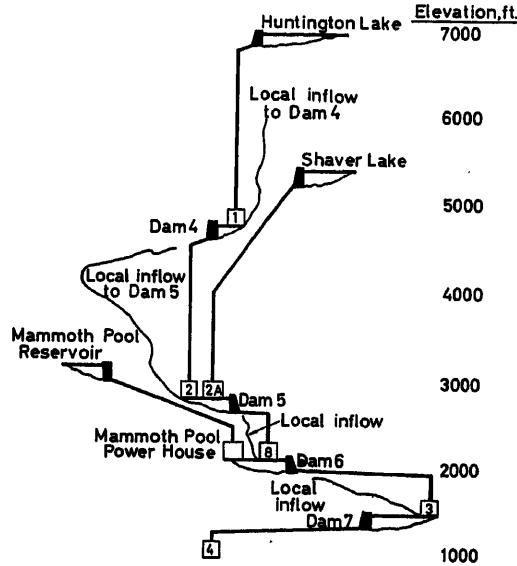


Figure 1. Schematic profile of part of Big Creek project (Southern California Edison Company)

values of λ and γ_j . The lambda loop ensures that the received load is served to a desired tolerance. The hour loop indexes the programme through the desired number of hours which for this case is twenty-four. Next, the withdrawals obtained are compared to the desired values. If satisfactory agreement is not achieved, new gamma values are simultaneously specified through solution of simultaneous equations relating changes in withdrawals to change in the gamma values.

This programme has been written in FORTRAN for use with the IBM 7090 Monitor System. Computing time for production runs varies from 2 to 3 min for a 24 h dispatch.

Treatment of Constraints

The constraining relations fall naturally into two classes. The first, or equality constraints, have been handled by the use

of the Lagrange multipliers λ and γ . The next class is the saturation type constraints represented by eqns (8). These constraints come about due to practical operating or physical characteristics of the plants. Constraints on generation P_S , P_H , or discharge q , do not pose a serious problem. These constraints may be handled by the method of Valentine¹⁵, which in effect sets limits on the permissible choice for the variable.

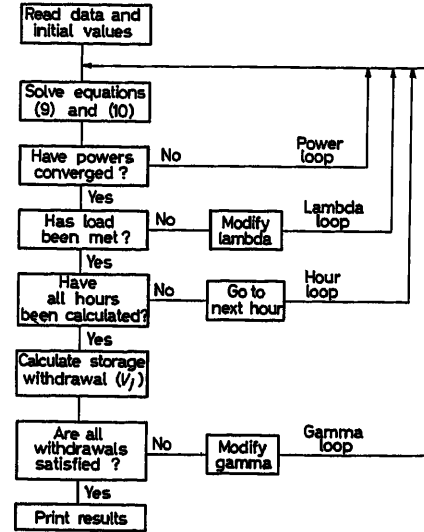


Figure 2. Logic flow diagram for variational solution

The last of constraints (8) on the storage, which in this case is the state variable, poses a difficult question on implementation of the solution of the Euler-Lagrange equations. For this class of point type or saturation type constraints, the Lagrange multiplier γ has a jump discontinuity as the trajectory of V traverses the boundary V_{min} or V_{max} ^{11, 16}.

In certain practical cases, such as pumped storage hydroelectric systems, the permissible discharges, q , are limited to certain discrete values rather than to a continuous bounded range. In this event, the problem must be reformulated either in the format of the maximum principle¹⁶ or Bellman's optimality principle¹⁷.

Dynamic Programming Formulation

Development of Theory

Dynamic programming¹⁷ presents a means for determining the optimum discharge schedule by treating the problem as a sequence of hourly water allocation problems. For purposes of discussion, we again return to the single thermal- and hydro-plant system.

In discrete form, the differential equation governing the state of the reservoir is given by

$$V_{n+1} = V_n + r_n - q_n - S(\bar{V}_n) \quad (11)$$

$$\bar{V}_n = 1/2(V_n + V_{n+1})$$

where V_n = reservoir storage of the beginning of the n th interval and r_n , q_n are the inflow and discharge during the n th interval.

The minimization is to be taken over the discrete sum:

$$E_j(V_j, V_{N+1}) = \min_{q_n \in Q} \left[\sum_{n=j}^N F(PS_n) \right] \quad (12)$$

subject to the process eqns (1) and (2) and the constraint eqns (8). Thus the admissible choices q_n must be in the region Q which satisfies the eqns (8). Since V_{N+1} is assigned as a fixed terminal value, the minimum of the expected fuel cost will be a function of the reservoir storage at the start of the interval.

By forming a sequence of problems of determining the optimal allocation of discharge for successively greater intervals of time, the optimal schedule for any desired interval is generated. By dynamic programming techniques, a recursive relation is developed between successive intervals:

$$E_j(V_j) = \min_{q_j \in Q} \left[F(PS_j) + \min_{q_n \in Q} \left(\sum_{n=j+1}^N F(PS_n) \right) \right] \\ = \min_{q_j \in Q} [F(PS_j) + E_{j+1}(V_{j+1})] \quad (13)$$

but by (11) V_{j+1} is dependent upon the choice q_j . Thus

$$E_j(V_j) = \min_{q_j \in Q} [F(PS_j) + E_{j+1}(V_j + r_j - q_j - S(\bar{V}_j))] \quad (14)$$

For E_N , of course, the choice is constrained to satisfy the boundary value V_{N+1} . A set of (V_j) values is assumed for each starting interval j and the optimal choice (q_j) for each of the V_j determined.

Straightforward extension of this method to greater numbers of reservoirs runs into computational and memory storage difficulty, as the expected fuel cost, E , becomes a function of the state of each reservoir. Thus, if K alternates are considered for each reservoir and there are R reservoirs, K^R optimal combinations must be determined for each interval. Except for very small K , systems of R equal to three or greater are unfeasible. An alternate approach¹⁰ is to use successive approximations in which the search is applied successively to the storages in one reservoir while the storage values in the other reservoirs are fixed. In this way, improved schedules are found for each reservoir in succession.

Illustrative System Problem

The dynamic programming method has been applied to two series connected reservoirs on the Susquehanna River. Flow and storage constraints as well as variable head effects and unit commitment effects are considered.

A simplified flow diagram of the computer logic is given in Figure 3. The programme starts from an initial feasible but not optimal schedule for plant discharges as functions of time and performs a search for improved schedules on each plant in succession.

The search starts at the last time period and moves backwards in time comparing alternative discharges that result in minimum fuel cost for the remainder of the optimizing period. At each time period, a set of reservoir storages is selected and the optimum discharge determined for each corresponding storage V plus the associated fuel cost, E , for the remainder of the optimizing period, T .

These values are then used to develop a similar set of data for

the next earlier time period. The search continues until the entire operating period is included. The new discharge schedule of lower fuel cost is then determined for the particular plant. The search then switches to the other plant and the process is repeated. The searching continues until the cost improvement is less than a pre-assigned value following the completion of an iteration.

The recognition of individual turbines causes the fuel cost function E to be multimodal. For such functions the successive approximations method runs the risk of converging to a relative minimum. Numerical results obtained for this study demonstrated that the error caused by convergence to a relative minimum was inconsequential.

Although the direct output of the dynamic programming method is the optimal schedule of discharges for particular

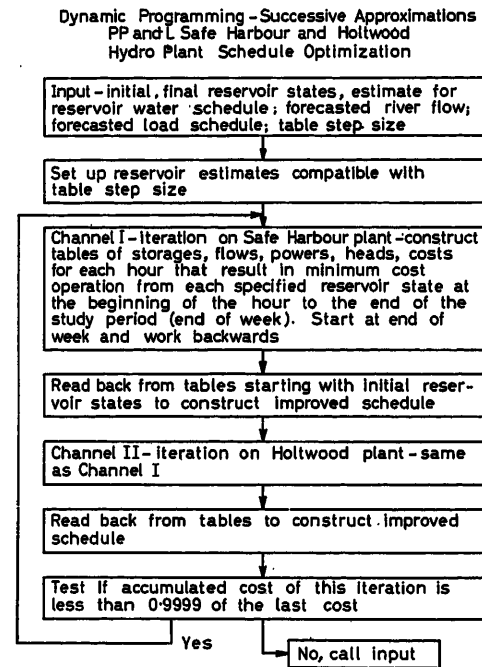


Figure 3. Logic flow diagram for the dynamic programming solution

initial and final conditions of reservoir state, additional information is available such as the direct determination of the incremental water value from the rate of change of expected fuel cost, E , with reservoir storage, V . As the time interval for each period is reduced, it is readily verified that in the limit the derivative— $dE(V)/dV$ is precisely the Lagrange multiplier γ of the Euler-Lagrange formulation. Typical performance schedules are presented in Tables 1 and 2 (see next pages). Tabulations of $\Delta E/\Delta V$ are listed for the two reservoirs in Table 2.

Table 1 presents the inflow, discharges, heads, forebays, and storages for the two reservoirs. Columns 2 through 7 are associated with the Safe Harbour or upstream reservoir. Columns 8 to 13 relate to the Holtwood Plant. The units of discharges, storages and inflows are in $\text{ft}^3/\text{sec} - \text{h} \times 10^{+3}$.

Table 2 presents the hydro-electric generation and the incremental water values— $\Delta E/\Delta V$ and thermal generation incremental cost. Other data available from the computer output

OPTIMAL CONTROL OF THERMAL-HYDRO SYSTEM OPERATION

Table 1. Hydro Study Results
GE Programme for Operation of Safe Harbour and Holtwood Hydro Plants

Study ident. No. 25162. Iteration No. 21. Date of this run on computer 32062

Day	Safe Harbour Forebay computations						Holtwood Forebay computations					
Hour code	Safe Harb. inflow	Elevatn of Forbay	Withdrn from storage	Maximum permiss. withdrn	Plant dischge	Plant head	Elevatn of Forbay	Withdrn from storage	Maximum permiss. withdrn	Plant dischge	Spill-over	Plant head
415	25-000	226-238	47-500	281-000	25-250	55-879	168-942	24-844	205-500	29-206	0-044	50-990
416	25-000	226-514	34-375	281-000	11-875	57-047	168-367	42-094	205-500	29-125	0-000	50-675
417	25-000	226-671	26-750	281-000	17-375	57-109	167-969	53-844	205-500	29-125	0-000	50-189
418	25-000	226-289	45-125	281-000	43-375	54-863	168-426	40-344	205-500	29-875	0-000	49-860
419	25-000	225-791	68-000	281-000	47-875	54-048	169-008	22-844	205-500	30-374	0-001	50-140
420	25-000	225-492	81-250	281-000	38-250	54-306	169-254	15-344	205-500	30-308	0-442	50-586
421	25-000	225-365	86-750	281-000	30-500	54-641	169-250	15-469	205-500	29-756	0-869	50-972
422	25-000	225-226	92-750	281-000	31-000	54-469	169-291	14-219	205-500	28-762	0-988	51-463
423	25-000	225-243	92-000	281-000	24-250	54-882	169-152	18-469	205-500	27-768	0-732	51-879
424	25-000	225-272	90-750	281-000	23-750	54-971	169-070	20-969	205-500	26-039	0-211	52-562
501	25-000	225-426	84-125	281-000	18-375	55-438	168-988	23-469	205-500	20-836	0-039	54-740
502	25-000	225-732	70-625	281-000	11-500	56-147	168-756	30-469	205-500	18-500	0-000	55-537
503	25-000	226-158	51-250	281-000	5-625	57-048	168-329	43-219	205-500	18-375	0-000	55-257
504	25-000	226-563	32-000	281-000	5-750	57-752	167-977	53-594	205-500	16-125	0-000	55-748
505	25-000	226-947	13-000	281-000	6-000	58-418	167-556	65-844	205-500	18-250	0-000	54-531
506	25-000	227-198	0-125	281-000	12-125	58-403	167-335	72-219	205-500	18-500	0-000	54-110
507	25-000	227-200	0-000	281-000	24-875	57-298	167-465	68-469	205-500	21-125	0-000	52-991
508	25-000	227-200	0-000	281-000	25-000	57-275	167-422	69-719	205-500	26-250	0-000	50-799
509	25-000	227-200	0-000	281-000	25-000	57-295	167-317	72-719	205-500	28-000	0-000	49-919
510	25-000	226-833	18-750	281-000	43-750	55-434	167-836	57-719	205-500	28-750	0-000	49-775
511	25-000	226-368	41-375	281-000	47-625	54-680	168-460	39-344	205-500	29-250	0-000	50-109
512	25-000	225-894	63-375	281-000	47-000	54-197	169-041	21-844	205-500	29-486	0-014	50-599
513	25-000	226-012	58-000	281-000	19-625	56-017	168-731	31-219	205-500	28-986	0-014	50-973
514	25-000	225-741	70-250	281-000	37-250	54-647	168-996	23-219	205-500	29-250	0-000	50-825

are the steam generation and the hydraulic turbine unit commitment.

One interesting side result of this investigation is the numerical corroboration in discrete form of the theorem¹⁶ of the time position of the discontinuity of the incremental water value $\Delta E/\Delta V$, due to the junction of the trajectory with a phase space boundary. The permissible range of the reservoir storage for the Safe Harbour reservoir was bounded in this study. Note that during hours 507 to 509 the trajectory for the storage was on the boundary. Note further the change in the incremental water values $\Delta E/\Delta V$ for the Safe Harbour plant.

The computer programme for the two reservoir study was written in FORTRAN and compiled for the IBM 7090 monitor system. Computing time was 1.3 min per iteration on both reservoirs for a 168 h optimizing period. The search range for this computing time was ten alternate storage withdrawals in addition to the initial value for each hour.

Comparison of Variational versus Dynamic Programming Formulations

The methods of computation employed in the two example problems led to two different philosophies of solution. With the variational method, the scheduling of water releases always followed the Euler-Lagrange equations and hence were always 'optimal' in this sense. The satisfaction of the desired reservoir storage endpoint was gained after successively correcting the initial values for the stored water. In this sense at each iteration

the variational method gave an 'optimal but not feasible' solution converging finally to the optimal and feasible solution. Conversely, the dynamic programming method scheduled the water releases such that at all times the endpoint values and physical constraints upon the system were satisfied. Thus the results of each iteration of the dynamic programming method gave a 'feasible but not optimal' solution converging finally to the feasible and optimal solution.

Computer requirements for the two methods differ as well. For comparable thermal-hydro problems, the stored programme requirements for the variational method are roughly twice those for the dynamic programming method. However, the data storage requirements for the dynamic programming method exceed the requirements for the variational method sufficiently to require greater total memory requirements.

The two methods differ appreciably as well on the treatment of physical constraints. Both methods handle point type constraints on control variables such as hydro-electric or thermal-electric generation with little difficulty. However, treatment of point type constraints upon state variables such as reservoir storages must be handled differently by the two methods. With dynamic programming, no complications arise in recognition of state space constraints. This type constraint merely limits the search range performed by the computer. With the variational method, however, the state space constraints may cause the incremental water values to change abruptly at times of junction of the state variables with the boundary. These discontinuities may lead to difficulties with computational stability.

Table 2. Hydro Study Results
GE Programme for Operation of Safe Harbour and Holtwood Hydro Plants

	Study ident. No. 25162. Iteration No. 21. Date of this run on computer 32062						
Day	Units		MW of hydro generation		Incremental water value		Thermal Incremental
Hour Code	Safe Harbour	Holtwood	Safe Harbour	Holtwood	Safe Harbour	Holtwood	
415	4-000	10-000	102-702	97-635	27-500	7-500	4-9589
416	2-000	10-000	49-357	96-791	27-250	7-625	4-7228
417	3-000	10-000	72-269	95-808	27-250	7-375	4-7157
418	7-000	10-000	173-097	96-879	27-250	6-500	5-6064
419	7-000	10-000	187-495	98-521	26-875	6-250	6-1148
420	6-000	10-000	150-973	99-346	26-125	5-875	5-5302
421	5-000	10-000	121-203	98-938	25-750	6-125	4-9340
422	5-000	10-000	122-782	97-412	24-375	7-125	4-3386
423	4-000	10-000	96-810	95-329	23-250	7-500	3-8003
424	4-000	10-000	94-954	90-805	23-000	8-875	3-4364
501	3-000	8-000	74-137	75-638	22-750	9-875	3-1521
502	2-000	7-000	46-980	68-156	22-625	9-875	3-0445
503	1-000	7-000	23-352	67-346	22-500	9-750	2-9893
504	1-000	6-000	24-195	59-641	22-375	9-625	2-9698
505	1-000	7-000	25-568	66-003	22-375	9-625	2-9684
506	2-000	7-000	51-658	66-414	22-125	9-500	3-0361
507	4-000	8-000	103-879	74-276	22-375	9-500	3-2120
508	4-000	10-000	104-353	88-506	23-625	9-375	3-5990
509	4-000	10-000	104-391	92-304	27-750	9-250	4-6999
510	7-000	10-000	176-488	94-035	29-125	9-125	5-3704
511	7-000	10-000	188-863	95-953	28-750	8-750	5-8171
512	7-000	10-000	184-794	97-526	28-250	8-375	5-8352
513	3-000	10-000	79-961	97-033	27-875	8-125	4-9645
514	6-000	10-000	148-042	97-409	27-625	8-125	5-2262

Implementation with Computer Control

Various analogue computer control arrangements have been used to obtain continuous economic allocation of thermal generation while simultaneously maintaining system frequency and the net tie line flow^{7, 18}. More recently, combined digital computer and analogue control arrangements have been conceived. The principal advantage of this combined arrangement over the straight analogue scheme is that, in addition to the problem of continuous economic allocation, many problems related to the planning decisions and accounting for system operation may be also encompassed¹⁹ on a time-shared basis. The combined arrangement also permits direct solution of the thermal-hydro problem.

In the operations planning function, the digital computer can determine by either the variational or dynamic programming methods the value of $\gamma(t)$, the incremental water value for the reservoir storage. With $\gamma(t)$ specified, the on-line dispatch is given from the solution of the non-linear algebraic equations (5) and (6) subject to the constraining relations given by equations (1) and (8).

Figure 4 presents a schematic of a digital computer and analogue control arrangement suitable for this application. An analogue system continuously monitors the system frequency and power transfer to neighbouring power systems. An area control error is generated proportional to frequency and interchange deviation. This error is combined with total unit requirement so as to determine the desired system generation. As

indicated in Figure 4 for Unit 1, analogue circuitry is used to determine the desired unit generation based upon a base point and participation adjustment. These adjustments are made as required by the digital computer. A comparison of the unit

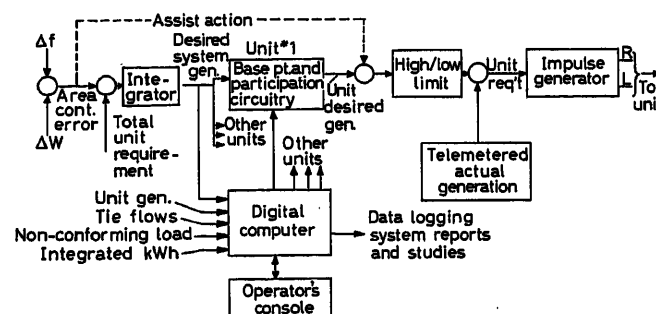


Figure 4. Computer controller for thermal-hydro system

desired generation and the unit actual generation determines the unit requirement. Impulses proportional to unit requirement are telemetered to the unit control equipment. If desired, proportional assist action may be obtained as indicated by the dotted line.

Conclusions

Significant improvements in the economic performance of thermal-hydro power systems have been achieved by application of optimization techniques. Practical solutions and computer

programmes have been developed based upon variational calculus and dynamic programming for systems of moderate size. Implementation by a combined digital computer and analogue control arrangement offers an economical and technically feasible solution to continuous application of such optimization techniques.

Based upon the work undertaken to date, it appears that the extension of optimization method to large-scale systems will best be realized by a form of the variational calculus method.

References

- ¹ KIRCHMAYER, L. K. and GALLOWAY, C. D. Computers aid system generation planning, *Proc. Amer. Power Conf.*, XXII (1960) 591-597
- ² LINDQUIST, J. Operation of a hydro-thermal electric system, *Amer. Inst. elect. Engrs, Power and Apparatus Systems*, No. 59, (April 1962) 1-7
- ³ GAUSSENS, P., PARDIGON, J., CALVERT, AUGES, MESTRES, Modern methods in the economic engineering study of networks, *C.I.G.R.E. Sess. Pap. No. 326* (1962)
- ⁴ NOAKES, F. and ARISMUNANDAR, A. Bibliography of optimum operation of power systems: 1919-1959. *Trans. Amer. Inst. elect. Engrs, Power and Apparatus* (1962)
- ⁵ CHANDLER, W. G., DANDENO, P. L., GLIMN, A. F. and KIRCHMAYER, L. K. Short-range economic operation of a combined thermal and hydro-electric power system. *Trans. Amer. Inst. elect. Engrs*, 72, Pt. III (1953) 1057-1065
- ⁶ CYPSEY, R. J. Computer search for economical operation of A Hydro-thermal electric system. *Trans. Amer. Inst. elect. Engrs*, 73, Pt. III-B (1954) 1260-1267
- ⁷ KIRCHMAYER, L. K. *Economic Control of Interconnected Systems*. 1959. New York; Wiley
- ⁸ BERNHOLTZ, B., SHELSON, W. and KESNER, O. A Method of scheduling optimum operation of Ontario Hydro's Sir Adam Beck-Niagara Generating Station. *Trans. Amer. Inst. elect. Engrs*, 77, Pt. III (1958) 981-991
- ⁹ BERNHOLTZ, B. and GRAHAM, L. J. Hydro-thermal economic scheduling, Pt. I. Solution by incremental dynamic programming. *Trans. Amer. Inst. elect. Engrs*, 79, Pt. III (1960) 921-932
- ¹⁰ BERNHOLTZ, B. and GRAHAM, L. J. Hydro-thermal economic scheduling, Pt. II, *Amer. Inst. elect. Engrs*, 81, Pt. III (1962) 1089-1096
- ¹¹ ANSTINE, L. T. and RINGLEE, R. J. Short-range hydro-thermal coordination for two hydro plants on the Susquehanna River. *Amer. Inst. elect. Engrs*, 1962, Chicago, Illinois, Oct. 1962
- ¹² FUKAO, T. and YAMAKAZI, T. A computational method of economic operation of hydro-thermal power systems including flow-interconnected hydro-power plants *E.T.J.*, Tokyo (Dec. 1959) 22-26
- ¹³ KIRCHMAYER, L. K. *Economic Operation of Power Systems*. 1958. New York; Wiley
- ¹⁴ DRAKE, J. H., MAYALL, R. B., KIRCHMAYER, L. K. and WOOD, H. Optimum operation of a hydro-thermal system. *Trans. Amer. Inst. elect. Engrs.*, Gen. Meet., New York, Pap. 62-100 (Jan.-Feb. 1962)
- ¹⁵ VALENTINE, F. *Contributions to the Calculus of Variations*. pp. 403-447, 1933-1937. University of Chicago Press
- ¹⁶ BOLTYANSKII, V. G., GAMKRELIDZE, R. V., MISHCHENKO, E. F. and PONTRYAGIN, L. S. The maximum principle in the theory of optimal processes of control. pp. 1004-1008, Vol. 2 *Automatic and Remote Control*. 1961. London; Butterworths
- ¹⁷ BELLMAN, R. *Introduction to Dynamic Programming*. 1957. Princeton University Press
- ¹⁸ KIRCHMAYER, L. K. Optimizing computer control in the electric utility industry. pp. 63-70, Vol. 4. *Automatic and Remote Control*. 1961. London; Butterworths
- ¹⁹ FIEDLER, H. J. and KIRCHMAYER, L. K. Automation of system operation. *Proc. Amer. Power Conf.*, XXIII (1961) 779-789

DISCUSSION

K. W. JAMES, *Central Electricity Research Laboratories, Cleve Road, Leatherhead, Surrey*

The three papers in this session, taken in order, are extremely interesting. The first covers the whole field of automatic control of a power generation system in a very general style and perhaps raises more questions than it answers. The second paper covers the problems raised by the installation of an automatic economic load dispatcher and we can see these problems as part of the more general problems discussed in the first paper. The third paper deals with a specific problem of control, namely that of the economic scheduling of a mixed hydro and thermal system. Thus the papers cover the whole aspect of automatic control of a power system in differing depths arriving at a specific solution to one problem.

The paper by Venikov and Tsukernik stresses, very rightly in my opinion, the probabilistic nature of the problems to be faced. Too much emphasis cannot be placed on this aspect and its effect on the correct formulation of the problems to be solved. Two items which have a statistical and probabilistic content concern load measurement and load prediction. Another paper which deals with load prediction is presented later and it would be interesting to know what other work is going on in this field.

The paper by Vámos *et al.* points out the difficulties which are encountered when one examines closely the problems which are thrown up as a result of the installation of an automatic economic load dispatcher. The difficulties mentioned in this paper emphasize the fact that when considering the application of automatic control to a system many aspects of system control are poorly defined and many measure-

ments are not what they seem to be. Automatic control will be the result of a better understanding of the system and possibly this latter point may be more important than the achievement of automatic control itself.

The paper by Kirchmayer and Ringlee deals with a specific problem and it is much easier to ask questions of the authors. I am not very clear as to how state constraints are dealt with. Perhaps the authors could give more details regarding this point.

At this stage it may be worth while mentioning briefly what we are doing in the C.E.G.B. in England with regard to the automatic control of our power system.

We have installed an on-line security assessor (*Figure A*) in the National Control. This is a mixed analogue digital machine receiving

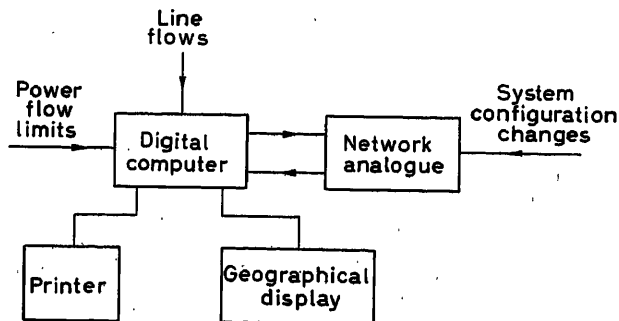


Figure A. On-line 275 kV security assessor

telemetered information about line flows and information about switch positions. Using a d.c. superposition method in conjunction with a small specially built computer, the security of the 275 kV system is investigated for the loss of single or double circuits. Information is presented to the operators via an illuminated semi-geographical display and typewriter output. The typewriter output has proved to be a success with the operators. The semi-geographical display has met with a luke-warm reception and is difficult to update. Experience with the device, so far, shows that updating of the analogue network and the semi-geographical display is a major task.

In our approach to the problem of the control of a power system we are taking a more practical path than would seem to be the case indicated by the papers presented in this session. We are tackling it in two stages. The first will be in the laboratory and the second in the field. In the first stage the generating, distribution and load absorbing system is represented by a model with a capacity of 40 generators, 100 lines and 30 loads. This system may be interconnected in any suitable manner. It is not intended to reproduce transient effects of machines, but it should represent system effects with period of 5 to 10 sec or greater. Automatic tripping of lines is not included. The system can be run in isolation or as a system with boundary effects. These boundary effects are obtained via a simulator which consists of loads/generators and lines. The simulator has been developed with the

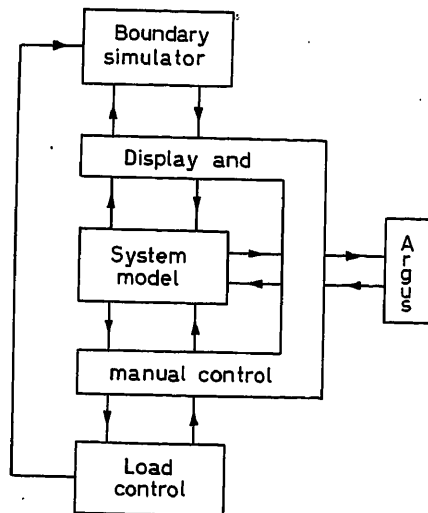


Figure B. Laboratory experiment

aid of load flow studies and should represent quantitatively the effect of the boundary flows and any sudden changes in them on the system under study. The loads in the system model and the loads/generators in the boundary condition simulator are controlled from a load replay unit which utilizes information which has been recorded directly on the power system. The whole system will be controlled from an Argus process controller in conjunction with a display console. This latter equipment is used for setting up the model manually, ready to be taken over by the process control computer. All the individual items of the system have worked satisfactorily and they are now being integrated as a system. The laboratory set-up is illustrated in Figure B. After working in the laboratory for approximately one year, we intend to transfer the process controller to the field where, in conjunction with telecommunications equipment and plant controllers, it will control part of the system during daily operation.

Some comments on the programmes which are being developed for the process controller may be useful. Our approach has been to develop special methods for the special problems which arise. These methods do not in all cases give the theoretical optima but are expected to give results close to these. We have studied the dynamic programming

approach but have not so far been able to produce a method which is practicable in respect of the amount of storage needed and the time required for calculation.

Typical of the programmes being developed for Argus are the following:

(1) Plant Loading Programmes

These calculate the generator outputs necessary to meet a predicted value of required total generation. Optimization is done by ranking the generators in order of incremental cost in a so-called 'order of merit' table. The result produced is consistent with various constraints, including rates of acceptance and rejection of load, on generator and station outputs and with the need to provide a specified total of 'spare capacity'. It is assumed that generator start-up and shut-down times have been calculated previously (manually or eventually on a rational basis by a control computer). In the existing programme no account is taken of network security except for a feature which allows the output of one or more generators at certain times to be manually specified so as to cope with expected 'local' insecurities. The programme in its present form takes no account of line losses but it has been written so that this feature can easily be incorporated using a 'penalty factor' method. The principle of this is to estimate the cost of meeting, from each generator in turn, a small increase in demand. This enables a revised order of merit table to be formed. An iteration loop is set up so that an initial schedule is used to calculate a new order of merit table, which in turn is used to calculate a new schedule and so on.

(2) Security Checking Programme

Given a schedule of generator outputs and the necessary network data, this programme checks the network 'security'. An upper limit is specified for the permissible real power flow in each line and the network is said to be secure if no line is overloaded as a result of any one of several specified occurrences. The programme uses a d.c. model of the a.c. supply network and will check for line overloading following the loss of a single generator or the loss of any number of lines. In practice, the programme will be used to check security following: (a) loss of a generator; (b) loss of certain specified single and double circuit lines; (c) busbar faults which result in several lines tripping out. The calculation of flows after line outages uses a method which although not developed from Kron's techniques, is in fact a simple application of the method of tearing.

(3) Network Updating Programme

The network data stored in the computer must be updated to correspond to: (a) actual configuration changes as indicated by telemetered information from the supply system (or as read from the system model input equipment in the laboratory experiment); (b) predicted configuration changes which are inserted manually.

In the d.c. approximation, the network is represented by a set of real linear simultaneous equations

$$I = YV$$

The basic problem is: Given I , find V

The programme actually calculates V from $V = Y^{-1}I$ the matrix Y^{-1} being permanently stored and updated as necessary to correspond to the networks for which calculations are required.

All network changes can be reduced to combinations of four basic operations, viz. (a) adding a node; (b) removing a node; (c) inserting a branch; (d) removing a branch.

The stored network data comprises

- (a) Y^{-1} ; (b) branch/node connection table; (c) table of line impedances; (d) various tables relating busbars to nodes etc.

The updating of Y^{-1} is done by a simple application of Kron's method. The updating programme is also used to calculate an initial matrix by building up the network from a network consisting of a single node.

H. RUGE, *Central Institute for Industrial Research, Forkingsueien 1, Blindern, Oslo, Norway*

I would like to compliment the authors for their clear and valuable comparison of variational methods and dynamic programming in optimal control of hydro-power systems. The work seems to strengthen the impression that optimization of larger systems in a more general sense, including long-term planning with stochastic inflow and consumption, must be based on some combination of the two methods.

Concerning the results in Table 2: Is there any obvious reason for the larger P -variations in Safe Harbor, as compared to Holtwood?

My second question concerns your conclusion that 'significant improvements in economic performance' have been achieved. Working in the same field I would like to know whether this statement on economic justification is based on systematic comparisons with experienced operators, or some assumptions concerning the errors in 'unoptimized' operations.

G. QUAZZA, *Via Giambellino 48, Milan, Italy*

My first question concerns on-line applications of computers to optimal control of hydrothermal systems including water reservoirs. The examples quoted by the authors in their paper refer to off-line computation of optimum schedules for power generation, while a schematic block diagram of possible arrangement for an on-line computer control system is indicated in Figure 4.

Have any on-line applications of computers been made for short-range optimum generation scheduling of hydrothermal systems, to the authors' knowledge? While the thermal system computer control has had already several years of operating experience, and it is well known how many outstanding contributions have been given by Dr. Kirchmayer himself also in the practical realization of such systems, we do not know of any on-line computer control of hydrothermal system now in operation. An obvious problem, posed by on-line computer control and not existing in off-line optimization, derives from the fact that power demand, not to speak of meteorological conditions, will never be exactly equal to the expected demand, on the basis of which the variational problem is solved with integral constraint on water withdrawals from reservoirs. The computer must be expected to revise its optimized schedule, as long as time goes on, say every hour, but this can of course be done in several ways. The authors' comments will be appreciated.

The second question is closely related with the first one. The authors state that, no matter whether variational calculus or dynamic programming (what about the newly announced variational gradient method?) is used, memory requirements on the digital computer become exceedingly large even for simple systems having only a few reservoirs. As they quote the use of an IBM 7090, the question arises whether today one can consider it feasible in technical economical sense to solve optimum scheduling problems for systems with tens or hundreds of reservoirs, such as one can frequently find in practice, for example in Italy. One may infer that one way or another of simplifying the system by equivalent sub-systems must be found: it would be very interesting to hear the authors' opinions on this matter. Further, do the authors think that analogue computers, using Euler-Lagrange equations, may perhaps come back again into the picture, especially for on-line applications, with closed loop searching of water equivalent costs? Or does the greater difficulty in setting constraints, lower flexibility especially as far as function generators and cost descriptions are concerned and lower reliability rule out any chance for analogue computers?

S. MITTER, *Department of Electrical Engineering, Imperial College of Science and Technology, London, S.W. 7., England*

The authors have rightly pointed out that state-variable constraints present no difficulty in the dynamic programming formulation, but one runs into the now well-known dimensionality difficulties. There

seems to be a certain amount of difficulty in handling state-variable inequality constraints in the framework of the classical calculus of variation. The authors have also pointed out that state-variable constraints may be handled by using a gradient technique and penalty functions.

If the constraining differential equation is linear and if the equality and inequality constraints and the cost function are convex, by considering a discrete approximation, the problem may be formulated as a problem in convex programming and solved by the gradient projection method due to Rosen. I would be interested to know the number of state variables and constraints the authors' gradient technique can handle and the number of points it was necessary to take in the period 0 to T , for the problems solved by the authors.

J. E. IBENSCHÜTZ, *International Atomic Energy Agency, Kärntnerring 11, Vienna 1, Austria*

Have nuclear power stations been considered to be one of the components in the system to be automatically controlled, and if so, how are they treated in comparison with conventional steam stations?

M. CUÉNOD, *Société générale pour l'industrie Geneva, 7 pl. Clapartè, Genève, Switzerland*

The energy produced by the new big thermal plants can be considered as very economic provided that production occurs without large and quick variations. The hydraulic power plants are very suitable, when the storage capacity of their reservoirs are sufficient, to cover important load variations without supplementary costs.

The optimal control criterion given in the paper by Kirchmayer and Ringlee takes into account steady-state conditions such as production costs and transmission losses. It would be possible to add to this steady-state optimal control a dynamic optimal control taking into account the cost of the production load variations and the ability of the different plants to cover these load variations. I would be very interested to have the opinion of the authors about this suggestion.

J. CARPENTIER, *Electricité de France, 12 Place des Etats-Unis, Paris 16^e, France*

The studies made at the Electricité de France have shown the same conclusions as the authors concerning the comparison between dynamic programming and variational methods.

In the example described with seven reservoirs by the variational method how many iterations were necessary? (i.e. how many different sets of values of γ .) Are the equations relating changes in withdrawals to change in the γ values full or empty? Does the resolution time of this system grow like the third power of the number of plane, or less quickly?

On a more general point, can the authors indicate how the computation time varies with the number of reservoirs? Is it easy to apply the method to a system of 60 reservoirs?

In the variational method, it does not seem possible to make an account of the time taken by water to go from one dam to the next one. Have any attempts been made to generalize the variational method in this case, or else is it necessary to use dynamic programming?

L. K. KIRCHMAYER and R. J. RINGLEE, *in reply*

The methods described have been applied to studies of several different power systems. In a number of these studies, comparisons were made of the operating economy achieved by prior methods with that achieved by application of the optimization techniques. Improvements of from 25 to 100 dollars per year per megawatt of installed hydro capacity have been indicated.

We believe that the variational method is preferable to the two methods discussed. More recently a variational gradient method has been devised which: (a) handles all constraints; (b) requires significantly

less memory than dynamic programming; (c) makes best use of current estimates; (d) is computationally very stable. This new method is described in a subsequent paper. We believe a system of up to 60 fixed-head hydro plants may be handled on a computer of the 7090 variety with a variational method.

The plants at Safe Harbor and Holtwood have low heads and the Holtwood tail water has an adverse elevation versus plant discharge. Hence we believe the P values should be compared on a per unit basis at each plant rather than on an absolute scale. Further, for dispatching purposes the variations in the difference of P for Safe Harbor and P for Holtwood are significant. On this basis the maximum and range for the Holtwood P values are 9.875 and 4.000, and for the difference in P values at Safe Harbor, the maximum is 20.000 and the range is 7.375. On a per unit basis the daily range for the Holtwood Reservoir is actually the larger.

Mr. Ruge's question concerning economic justification is partially answered in the reply to Mr. James.

Savings estimates were based upon comparisons of schedules determined by standard dispatching practices and by computer methods. In addition to the fuel savings resulting from instant-by-instant optimal control, savings in fuel costs and manpower are achieved by application of the computer on a time-shared basis to the problems of operation planning and accounting. A brief survey of these problems is given¹.

As Mr. Quazza has indicated, the digital process computer control installations to date have been for thermal systems. To our knowledge, the first hydro system application will be the system being supplied by General Electric for the Bureau of Reclamation to control the water releases for the hydro-electric projects of Region 4 of the Colorado Storage Project. This installation has visualized the need for providing corrections for deviations from forecast. A preplanning programme will determine the incremental water values and the reservoir schedules for a period of time in the future. Through means of a predictor programme, the computer will compare actual with forecasted water usage and make appropriate corrections to the incremental water value and unit incremental characteristics. This information will be used in the economic dispatch programme to provide an instant-by-instant optimum digital dispatch.

We believe it readily possible to handle tens of reservoirs with the GE-412 computer. For hundreds of reservoirs we recommend simplification of the system and the use of equipment sub-systems. We do not visualize that analogue computers would be as readily applied to this problem as digital process control computers such as the GE-412. Digital computers are inherently more versatile and can handle a number of related problems in operations planning and accounting. It is known, however, that one analogue computer system is planned for short-range thermal-hydro coordination for the Chubu Electric Power Company, Nagoya, Japan.

Mr. Mitter suggests that the thermal-hydro coordination problem can be solved as a problem in convex programming. One recent paper² reports the results of studies along this direction. Comparisons of the computational efficiency of the programming and the variational methods would be very useful. How many state variables and constraints the gradient method can handle is an open question. To partially answer Mr. Mitter, here is a summary of pertinent statistics of a variational gradient sub-routine that has been utilized to study pumped hydro-electric installations.

Max. No. of hydro plants	6
Thermal system representation	Incremental cost function
Max. No. of intervals	168
Max. and min. limits on plant outputs	Each interval
Max. and min. limited on reservoir storages	Each interval (by penalty function)
Max. and min. limits on thermal system output	Each interval
Memory requirements (programme plus data)	5,000 words

Running time (IBM 7090) 75 iterations in 4 min for runs of 168 intervals. To follow load patterns adequately it was felt necessary to choose time intervals in the range of 1–2 h.

To date, nuclear plants have been treated only by approximate methods. The fuel costs may be classified into two components: (a) fixed; (b) dependent upon output. The cost of item (b) influences the incremental cost of production which is used in comparing the thermal plants. It is anticipated that this incremental cost for future nuclear plants will be sufficiently less than the thermal plant incremental costs and that the nuclear plants will initially be base-loaded. Additional research effort is to be devoted to this problem.

Mr. Cuénod currently points out that the method of the paper may be readily extended to include the effect of the cost of imposing load changes upon the plant. This solution would require the development of data relating the cost in additional dollars per hour of fuel consumption as a function of the regulating burden placed upon the machine. Such data are not readily available. We believe Mr. Cuénod's suggestion is worthy of additional research.

We are pleased to have Mr. Carpentier's concurrence with our conclusions concerning the comparison between dynamic programming and the variational boundary iteration method.

The number of iterations required for the 7-reservoir problem solved by the variational boundary iteration method was greatly influenced by the starting values. For good starting values, convergence is obtained in several iterations. The equations relating changes in withdrawals to changes in values are full, but the diagonal elements tend to be larger than the off-diagonal.

We would estimate the calculation time exponent to be in the range 1.5 to 2.0 with the number of reservoirs, and believe large systems of 60 reservoirs may be handled if head variations are neglected and sub-grouping is used.

To date, we have not taken account of the time taken by the water to go from one dam to the next one. We believe that this problem may be treated by the variational method through the use of incremental reservoirs and that it will not be necessary to resort to dynamic programming.

References

- ¹ BEYER, W. G., FIEDLER, H. J. and KIRCHMAYER, L. K. Digital computer dispatching systems. *P.I.C.A. Conf.* Phoenix, Arizona, April, 1963.
- ² SOKKAPA, B. G. Optimum scheduling of hydrothermal systems—A generalized approach. *I.E.E.E. Trans.*, 81, Pt. III (1962), Paper No. 62-1366

Automatic Systems with Learning Elements

G. K. KRUG and A. V. NETUSHIL

Summary

This paper deals with the problem of control systems for industrial processes. These systems contain learning elements, which are being developed in the laboratory of the Faculty of Automatics and Telemechanics-Remote Control of the Moscow Power Institute (MEI). The systems are required to solve two problems—the study and the optimal control of the plant. Different solutions can be found for these problems, depending on the influence of uncontrolled factors.

If these influences are small it is possible, by means of a supplementary experiment, to draw up a programme for the regulator which will conduct the further process under the optimal conditions. If the influences are large, the different control situations are 'remembered', and control proceeds on the basis of acquired experience, in accordance with the criteria of quality and productivity.

Two main principles of information storage are used—the table principle and the formula principle. The paper gives the statistical theory of finding approximating polynomials; this is based on the use of the time weighting function of the quality. Also dealt with are possible fields of application of control systems with studying elements.

Sommaire

Ce rapport traite de la conduite automatique d'installations industrielles. Les systèmes envisagés comprennent des éléments d'apprentissage, et sont en cours de développement au Laboratoire d'Automatique et de Télécommande de l'Institut de l'Energie de Moscou (MEI). Ces systèmes doivent résoudre deux problèmes: l'étude et la commande optimale de l'installation. Selon les influences des facteurs incontrôlables, diverses solutions peuvent être envisagées.

Si ces influences sont faibles, un essai supplémentaire permettra de programmer le régulateur pour conduire l'installation à un fonctionnement optimal. Si ces influences sont grandes, les différentes structures de commande sont mémorisées; la conduite se fait alors sur la base de l'expérience acquise, et en accord avec les critères de qualité et de productivité.

La mémorisation de l'information utilise deux principes de base: tableau et formule. On décrit la théorie de l'approximation polynomiale statistique utilisant la fonction de pondération temporelle de la qualité. On montre également le champ d'application possible du système de conduite avec éléments d'étude.

Zusammenfassung

Dieser Beitrag befaßt sich mit Problemen der Regelung industrieller Prozesse. Die hier beschriebenen Systeme enthalten Lernelemente, die im Laboratorium der Fakultät für Automatik, Telemechanik und Steuerungstechnik am Moskauer Energieinstitut (MEI) entwickelt worden sind. Derartige Systeme werden benötigt, um zwei Probleme zu lösen: die Untersuchung und die Optimalregelung einer Anlage. Für diese Probleme sind verschiedene Lösungen möglich, die vom Einfluß ungeregelter Faktoren abhängen.

Sind derartige Einflüsse klein, so ist es möglich, mit Hilfe eines zusätzlichen Versuches ein Reglerprogramm vorzugeben, das den weiteren Verfahrensgang unter optimalen Bedingungen abwickelt. Sind die Einflüsse groß, so „erinnert“ sich das System der verschiedenen Regelungssituationen und die Regelung nimmt auf der Grundlage der gewonnenen Erfahrung ihren Fortlauf, wobei Kriterien für die Qualität und die Produktivität beachtet werden.

Für die Informationsspeicherung werden zwei Grundprinzipien verwendet: die Tabelle und die Formel. Der Beitrag enthält eine statistische Theorie für das Auffinden der Näherungspolynome, wobei die Zeit-Gewichtsfunktion der Qualität als Grundlage dient. Es werden des weiteren mögliche Anwendungsgebiete für Regelsysteme mit Lernelementen behandelt.

In the automation of continuous processes in the chemical industry (polymerization, fractional distillation, desiccation), in metallurgy (blast-furnace processing, rolling), in the paper, cement, food, and other industries, and also for the heat treatment of various materials, a number of difficulties are encountered which are due to incompleteness or lack of a mathematical description of the process.

Knowledge of the physicochemical laws determining the process gives only a qualitative idea of the principal relationships—insufficient for automatic control of the process.

Quantitative investigation of complex processes is carried out by experimental statistical methods¹⁻³. As a result of mathematical treatment of sufficient information on the process, some equations of the connections between the parameters of a plant can be obtained. However, the presence of uncontrolled disturbances not only determines the probability character of these equations, but at the same time leads to the necessity of constantly examining them. In controlling such processes, the operator is guided to a considerable degree by past experience and intuition.

The algorithm of the functioning of automatic devices, designed for the optimal control of a process, must formally resemble in many respects the algorithm of control by a man. The operator, on taking control of the plant, has only the most general information on the nature of the actions required in various cases. As work proceeds, control experience is accumulated, and using past experiences definite tactics are worked out for use in the various situations. By constant improvement in methods of working, control of the plant is learned. In so doing, the results of experimental observations on the plant are often used, without going into the physical or chemical nature of the processes taking place.

With the object of obtaining fuller information on the controlled plant, the operator sometimes carries out test variations of the parameters according to a specific programme, and, having analysed the results, carries out the appropriate alteration to the method of operation.

Thus the control process can be presented in the form of a combined solution of two problems: (a) the study of the controlled plant, and (b) the control of the plant with the aim of obtaining the optimal behaviour.

Depending on the nature of the process, study of the plant can precede the development of a control algorithm, be periodically repeated during the control process, or be organically

combined with the control process, providing continuous correction of the control algorithm.

Consider the set-up of the problem of control of the plant shown in Figure 1, classifying the parameters of the object of control as follows:

(1) *The set of primary controlled parameters of the process (the vector X)*—The magnitude of this set of parameters cannot be varied by the operator; for instance, the measurable characteristics of the input item or of incoming components, humidity,

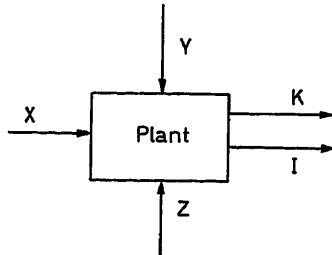


Figure 1. Plant

chemical composition, consistency, and certain indices characterizing the course of the process, such as change of the condition of the equipment, etc. Certain physical restrictions are laid upon the values of the primary parameters.

$$X \in \Gamma_X$$

where Γ_X is the region of possible values of X .

(2) *The set of secondary controlled parameters of the process (the vector K)*—This characterizes the state of the plant output, i.e., the quality of the end product (chemical composition, physical characteristics). There is a certain domain Γ_K where the values of K satisfy the prescribed requirements for the quality of the product.

(3) *The set of control parameters (the vector Z)*—The operator can influence this to vary the process, i.e. flow rate of water, fuel or raw material, conveyor speed, and pressure and temperature in different zones of the installation.

(4) *Index of the efficiency of the processes (I)*—In calculating I the cost price and productivity of the installation are taken into account. The productivity of the process alone can be taken as I .

(5) *The set of uncontrolled effects (the vector Y)*—This includes changes in characteristics of equipment owing to ageing, uncontrolled changes in quality of the input components, and uncontrolled variation of the process parameters, such as ageing of the catalyst.

In formal terms the process can be described as follows. At the plant input there occurs a variation of X . In the plant some alteration of the primary, control and uncontrolled parameters takes place, the results of which are felt at the plant output (K) after the expiration of the time of the technological cycle (τ_3) peculiar to the plant.

In the general case, the problem of controlling a process reduces to satisfying the following conditions:

$$K \in K_0 \quad I = I_{\max}$$

In discrete processes, for every cycle X and K , and also I , are constants. Each of the components of Z can be a time function

with the interval $0 < \tau < \tau_3$. Minimizing the departure of these functions from some prescribed mode often determines the quality of the product. The presence of uncontrolled factors and their nature are of the greatest importance in the choice of a control system.

The effect of uncontrolled factors can be partially reduced by the installation of a system of stabilizers of the various process parameters, which neutralize the effect of random disturbances in the control network, and by the implementation of control by acting upon the corresponding settings of local stabilizers. Complete elimination of the effect of random factors is, however, theoretically impossible. Depending on the value of the uncontrolled factors, the control principles can be divided into the following three groups.

(1) Investigation according to a particular algorithm with the aim of establishing an optimal law of control, with subsequent realization of this law.

(2) Optimizing the process by means of a continuous, automatic predetermined search for the extremal regime.

(3) Optimization based on automatic statistical processing of experience of control, and application of the learning principle.

The first control principle finds application when it is possible to minimize the effect of the uncontrolled factors.

When the influence of the uncontrolled factors is considerable and the necessary information concerning the plant is lacking, the second or third principle of automatic optimization may be applied, according to the degree of complexity of the process.

Work is in progress in the laboratory of the Faculty of Automation and Telemechanics of the Moscow Institute of Power on the development of all three principles of self-adaptation of automatic control systems. Some of the questions the laboratory is working on are set out below.

Combined System of Programmed Control

It often happens that a definite relationship can be established between the quality of the product and some index of the regime. In these cases it is expedient to implement programmed control according to this index, thus securing the required quality of the product. This system is feasible if the index in question can be related to the number of controlled parameters X . When, owing to the complexity of the mathematical description of the plant, it is difficult to establish the required law of control according to the controlled parameter, the law must be found experimentally. One method for finding this law is to find a parameter Y , which is uncontrolled under normal control conditions, and is such that the quality of the product uniquely depends on it.

If, during the adjustment time of the process, it is possible to control the process temporarily by this index, and if there is a definite relation between this index and another controlled index by which it is possible to carry out control in normal operating conditions, then the solution of the problem can be found by a combined system of programmed control.

Let there be two indices of the course of the process, M and N . To obtain the requisite product quality it is sufficient that

$$N(\tau) \in N_H(\tau)$$

where $N_H(\tau)$ is the mode prescribed by technological considerations.

If during the adjustment time of the process it is possible to control the process by N , given a programme $N_H(\tau)$, it is possible to carry out a series of trials, storing the resulting law $M(\tau)$. After statistical treatment of a series of such functions $M(\tau)$, a law of control can be chosen by M and the required law specified $M_H(\tau)$.

Continuation of the process reduces to conventional programmed control by $M_H(\tau)$.

Thus in the first part of the control process

$$\begin{aligned} Z(\tau) &= N(\tau) \\ X(\tau) &= M(\tau) \end{aligned} \quad (1)$$

In the second part of the process

$$Z(\tau) = M(\tau) \quad (2)$$

This control principle is employed in a combined programmed controller for the process of induction tempering, in which $N(\tau)$ is the surface temperature of the item, measured by means of a thermocouple soldered on to it, and $M(\tau)$ is the voltage on

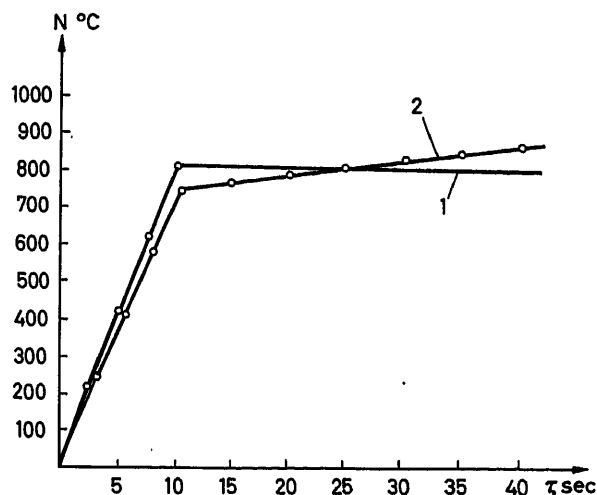


Figure 2. Heating characteristics of sample during tempering

the inductor. To obtain the required quality of tempering, heating must comply with a given law, for instance, rapid heating at constant speed followed by holding at constant temperature (curve 1 in Figure 2) or by slow heating at constant speed (curve 2 in Figure 2).

Exact calculation of the variation of the inductor voltage corresponding to the required temperature changes involves certain difficulties, since it is necessary to solve simultaneously three-dimensional Maxwell and Fourier equations for non-linear inhomogeneous media⁴.

Setting the programmed temperature controller according to a specified law and 'remembering' the variation of inductor voltage in the process of temperature control (full line in Figure 3) make possible the determination of this law experimentally, and a programme can be drawn up for control of the tempering process by the inductor voltage (broken line in Figure 3). Programmed control of the inductor voltage dictates the course of the tempering temperature, thus ensuring the required quality.

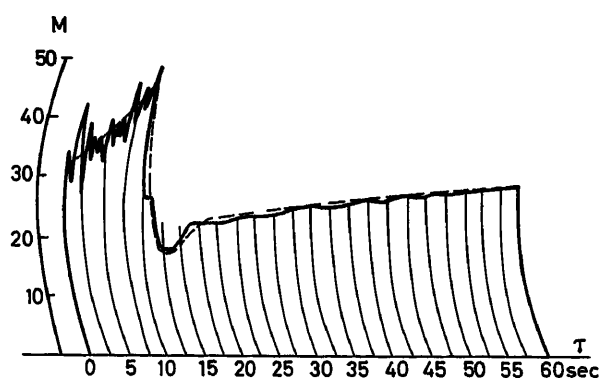


Figure 3. Variation of voltage on inductor

The accuracy with which the temperature process is carried out depends on the extent of the influence of the uncontrolled factors (variation in material of the billets, of the current frequency, parameters of the generator, etc.). When these factors are relatively stable, this system for controlling the process provides the required quality of production.⁵

Control Systems Based on the Learning Principle

If the uncontrolled disturbances vary continually with time, automatic optimizers can be used, which carry out a predetermined search of the extremal regime⁶⁻¹⁰.

The disadvantage of using optimizers is that often the algorithm realized by the system does not match the complexity of the problem of control of many processes simultaneously.

Consider a system of the learning type based on the principle of accumulation of positive control experience. It is assumed that from the dynamic point of view the plant is a non-linear element with pure time delay τ_3 for every pair of parameters affecting its input and output.

The block diagram of Figure 4 shows two interconnected blocks, one of which (Unit 1) supplies the control actions, in accordance with the method of operation of the process, in relation to the values of the primary parameters; that is, it realizes the principle of input control (by disturbance). To find the required law of control, feedback of the incentive type is introduced to signal the results of control, on the basis of the values of the secondary parameters (incentive feedback are shown in the figures as a broken line).

Unit 2 takes into account the values of the secondary parameters and trims Unit 1 in accordance with variation in characteristics of the plant. The functioning of Unit 2 is in some degree

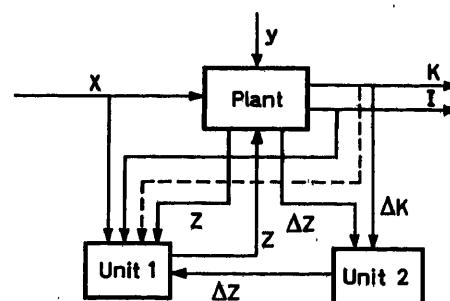


Figure 4. Block diagram of automatic device

similar to that of automatic control systems which realize the principle of control by error. Application of the combined principle of control is the most promising method for the design of an automatic control device.

The information stored in the memories of Units 1 and 2 must, in an integral manner, be a mathematical model of the process controlled in the best way in a predetermined manner. If the uncontrolled disturbances are of a varying nature, the mathematical model must constantly vary and adjust itself.

Two methods of information storage are possible—the table method and the formula method. With the former, the information is stored in the form of tables whose contents change in accordance with the algorithm governing writing and reading.

Table 1 shows a possible arrangement of the tables applicable to Unit 1 and Unit 2.

In the table for Unit 1 the values of Z are stored at the location of X . When coupled with the vector Z , the index I

Table 1. Information storage in automatic control device

Unit 1				Unit 2			
X_1	$Z_1'I_1'$	$Z_1''I_1''$		ΔK_1	$\Delta Z_1'$	$\Delta Z_1''$	
X_2	$Z_2'I_2'$	$Z_2''I_2''$		ΔK_2	$\Delta Z_2'$	$\Delta Z_2''$	

defines the efficiency of the process for the prescribed combination of controlled primary parameters and control parameters.

In the table for Unit 2 the values of the vector ΔZ , that is, those values of variation of the control parameters which have restored the quality of the product from the state ΔK to the required level Γ_k , are written in the location of the vector ΔK which characterizes the departure of the quality vector of the end product from the specific value.

With the formula method, the quantitative connection between the controlled parameters is fixed in the form of a set of equations, in a polynomial form, for instance.

For Unit 1, the equation for one of the components of the vector has, in the general case, the form (for standardized values of the variables²):

$$z_i = a_1 X_1 + \dots + a_m X_m + a_{m+1} X_1^2 + \dots + a_{2m} X_m^2 + \dots + a_H X_m^p \quad (3)$$

or in more compact form

$$Z_i = \sum_{j=1}^H a_j \prod_{k=1}^m X_k^{a_{jk}} \quad (4)$$

where

$$\sum_{k=1}^m \alpha_{jk} \leq p$$

For Unit 2 the equation for one of the components of the vector has the form:

$$\Delta Z_i = b_1 \Delta K_1 + \dots + b_n \Delta K_n + \dots + a_M \Delta K_n^S \quad (5)$$

or in more compact form:

$$\Delta Z_i = \sum_{j=1}^M b_j \prod_{k=1}^n \Delta K_k^{\alpha_{jk}} \quad (6)$$

where

$$\sum_{k=1}^n \alpha_{jk} \leq S$$

It may be presumed that, by means of a special algorithm for writing and reading the current information characterizing the controlled process, it can be said that the automatic devices incorporating either the formula or the table principle will be in some sense equivalent.

In whichever form the information may be stored, there must be an algorithm allowing processing of the incoming information in such a way that the contents of the memory express in the best way possible the current model of the controlled process. In the following an algorithm realizing the formula principle is considered.

Control Algorithm

The control algorithm is based on three coefficients: (a) prediction coefficient; (b) time weighting coefficient; and (c) quality weighting coefficient.

Prediction Coefficient

The higher the power of the approximating polynomial, the more precisely can the main connections in the plant be described. However, with increase in the power of the polynomial there is a considerable increase both in the complexity of the programme and in the time for calculating the coefficients. A criterion is needed which makes it possible to evaluate quantitatively the precision with which the polynomial obtained approximates the actual relationship. This criterion is called the prediction coefficient since with its aid the dependability of the polynomial when used in the domain of the variables which have not yet been encountered can be evaluated.

The coefficients of the polynomial are determined from the minimum of the mean square of the approximation.

Use is made of the method of bringing a multiple non-linear correlation to the linear form³.

The whole set of parameters X entering into each term of the polynomial eqn (4) is regarded as an independent parameter

$$c_j = \prod_{k=1}^m X_k^{a_{jk}} \quad (7)$$

then eqn (4) has the form

$$Z_i = \sum_{j=1}^H a_j c_j \quad (8)$$

The auto-correlation coefficient of eqn (8) is found and expressed in terms of the auto- and cross-correlation coefficients of the variables

$$K_{ZZ} = \frac{\sum_{j=1}^T Z_j^2}{T} = \sum_{i=1}^T \sum_{j=1}^T a_i a_j c_{i1} c_{j1} \quad (9)$$

where

$$k_{e_i e_j} = \frac{\sum_{i=1, j=1}^T e_i e_j}{T}$$

and T is the number of successive measurements of the variables. For convenience of analysis, eqn (9) is normalized, selecting as the norm the dispersion

$$D_{Z_0} = \frac{\sum_{j=1}^T Z_{0j}^2}{T} \quad (10)$$

where Z_{0j} is the observed value of the function.

Dividing eqn (9) by eqn (10) gives

$$\frac{K_{ZZ}}{D_{Z_0}} = \frac{\sum_{i=1, (j=1)}^T a_i a_j k_{e_i e_j}}{D_{Z_0}} \quad (11)$$

If $Z_i = Z_{i0}$, both sides of eqn (11) are identically equal to one.

In fact, the following inequality holds:

$$\theta = \frac{\sum_{i=1, j=1}^T a_i a_j k_{e_i e_j}}{D_{Z_0}} \leq 1 \quad (12)$$

since by determining the coefficients of the approximating polynomial by the method of least squares a 'smoothing' is produced, the magnitude of which depends on the power of the polynomial.

The quantity θ quantitatively expresses the degree of the probability prediction, i.e. the quality of the approximation.

Fixing a definite degree of prediction ($0 - 1$) and passing successively from $p = 1$ to $p = 2.3$ etc., the system will cyclically check the actual degree of prediction by eqn (12), and seek the correlation $\theta \geq \theta_0$.

It is also expedient to estimate the weight of each term of the polynomial. This can be done with the aid of the coefficient

$$\beta_j = \frac{a_j^2 k_{e_j e_j}}{D_{Z_0}} \ll 1 \quad (13)$$

Setting the minimal level β_0 for the coefficient β_j , it is arranged that after each operational cycle, β_i is calculated for all the terms. Terms with $\beta_i < \beta_0$ are eliminated from eqn (8), freeing the equation from weakly expressed connections of secondary importance.

The coefficients of the approximating polynomial are functions of the auto- and cross-correlation coefficients for the variables e_i and the approximated quantity Z_{0i} .

Coefficient of Time Weighting

Owing to the unstable nature of the vector Y , the coefficients of the approximating polynomial must continually vary. The object of time weighting is to calculate the new values of the paired products of the variables which determine the correlation coefficient with a greater weight than the previous one, and gradually to forget the past values. The simplest method of time weighting is that of the sliding interval. With this method the

correlation coefficient is calculated with respect to T previous values of the paired products

$$k_{e_i e_k} = \frac{\sum_{j=1}^T (e_i e_k)_{N-j}}{T} \quad (14)$$

where N is the serial number of the measurement.

The disadvantages of this method are the presence of a 'transient process' in the calculation of the correlation coefficient (for $N < T$), and the necessity for storing in the memory all the values of the paired products used for calculation.

A method of continuous weighting is possible, for which each paired product is multiplied by a weight function of the form

$$G_b = \alpha^{N-i} \quad (15)$$

where N is the serial number of the last cycle; i is the serial number of the information for which the weighting coefficient is being calculated; and $\alpha < 1$ is the coefficient of time weighting.

It can be shown that when the weighting function is introduced like this it is sufficient to store only the resulting value of the correlation coefficient for the $(N - 1)$ th cycle.

In fact:

$$(k_{e_i e_k})_N = \frac{\sum_{i=1}^N (e_i e_k)_i \alpha^{N-i}}{N f(G_b)} \quad (16)$$

where $f(G_b)$ is a coefficient taking into account the attenuation of the information summed up in the numerator of eqn (16). Putting $(e_i e_k)_1 = (e_i e_k)_2 + \dots = (e_i e_k)_N = e_i e_k$, the values of the coefficient

$$f(G_b) = \frac{\sum_{i=1}^N \alpha^{N-i}}{N} \quad (17)$$

Hence, substituting eqn (17) in eqn (16) gives

$$(k_{e_i e_k})_N = \frac{\sum_{i=1}^N (e_i e_k)_i \alpha^{N-i}}{\sum_{i=1}^N \alpha^{N-i}} = \frac{\alpha \sum_{i=1}^{N-1} (e_i e_k)_i \alpha^{N-i-1} + (e_i e_k)_N}{\sum_{i=1}^N \alpha^{N-i}} \quad (18)$$

Call the total coefficient of attenuation per cycle

$$L_N = \sum_{i=1}^N \alpha^{N-i}$$

Then

$$L_N = \alpha \sum_{i=1}^{N-1} \alpha^{N-i-1} + 1 = \alpha L_{N-1} + 1 \quad (19)$$

Bearing in mind that

$$(k_{e_i e_k})_{N-1} = \frac{\sum_{i=1}^{N-1} (e_i e_k)_i \alpha^{N-i-1}}{L_{N-1}}$$

write

$$(k_{e_i e_k})_N = \frac{\alpha L_{N-1} (k_{e_i e_k})_{N-1} + (e_i e_k)_N}{\alpha L_{N-1} + 1} \quad (20)$$

Thus to calculate the correlation coefficient in the N th cycle the value of the correlation coefficient in the $(N-1)$ th cycle must be stored, and also the total coefficient of attenuation in this cycle.

If N tends to infinity, the limit value $(K_{\varepsilon_i \varepsilon_k})$ is given by

$$(k_{\varepsilon_i \varepsilon_k})_N = \alpha (k_{\varepsilon_i \varepsilon_k})_{N-1} + (1-\alpha) (\varepsilon_i \varepsilon_k)_N \quad (21)$$

since

$$\lim_{N \rightarrow \infty} L_{N-1} = \frac{1}{1-\alpha}$$

It must be remembered that the calculated correlation coefficients are modified indices of the interconnection of two random functions. It is therefore more accurate to call these coefficients pseudocorrelation coefficients¹⁸.

Coefficient of Quality Weighting

Besides being weighted for time, the information arriving from the plant must be weighted for quality. In other words, evaluation of the information must depend on the magnitude of the technical and economic index to which it corresponds.

The introduction of quality weighting allows purposeful accumulation of information with deliberate 'reinforcement'. Although the polynomial so calculated approximates the interconnection between Z and ε in a distorted form, its value lies in the fact that it expresses the control problem.

In the general case, the quality index p is a function

$$p = \varphi(k, I)$$

Introducing the coefficient of quality weighting g , which depends on the value of the quality index p , $g = G_k(p)$

$$g=0 \quad \text{when} \quad p < p_0$$

$$0 < g \leq 1 \quad \text{when} \quad p \geq p_0$$

where p_0 is some specified level of the quality index.

Taking into account weighting with respect to time and quality, the correlation coefficient is written in the form

$$(k_{\varepsilon_i \varepsilon_k})_N = \frac{\alpha \sum_{i=1}^{N-1} (\varepsilon_i \varepsilon_k) \alpha^{N-i-1} g_i + (\varepsilon_i \varepsilon_k)_N g_N}{\sum_{i=1}^N \alpha^{N-i} g_i} \quad (22)$$

Using the notation

$$\sum_{i=1}^N \alpha^{N-i} g_i = R_N$$

as with eqn (20) gives

$$(k_{\varepsilon_i \varepsilon_k})_N = \frac{\alpha R_{N-1} (k_{\varepsilon_i \varepsilon_k})_{N-1} + (\varepsilon_i \varepsilon_k)_N g_N}{\alpha R_{N-1} + g_N} \quad (23)$$

Selection of the Control Coefficients

The introduction of the coefficients θ_0 , β_0 , α , g makes it possible to work out the current mathematical description securing the best control of the process. The success of the work depends to a considerable extent on the correct choice of numerical values of the coefficients. The system must be capable of automatically varying the values of these coefficients in

accordance with the variation of the statistical characteristics of the vector of the uncontrolled factors.

In fact, in the periods of time in which a variation of the vector Y takes place it is necessary to secure the quickest possible renewal of the memory (to decrease α), to reduce the power of the polynomial and simplify its form (to decrease θ_0 and β_0) and to increase the significance of a successful control trial (to increase g_0).

It appears that the difficulties of the problem are insuperable, since the vector itself does not enter into the polynomial in explicit form; however, some approaches to its solution may be noted.

As an indirect measurement of the variability of the vector, the mean square of the variation of all the correlation coefficients in one cycle of calculation can be taken

$$A^2 = \frac{\sum_{i=1}^{\theta} [(k_{\varepsilon_i \varepsilon_k})_N - (k_{\varepsilon_i \varepsilon_k})_{N-1}]^2}{\theta} \quad (24)$$

where θ is the number of correlation coefficients subject to calculation, and

$$\theta = \frac{H(H-1)}{2} \quad (25)$$

where m is the number of terms of the approximating polynomial.

To average this evaluation and to eliminate the effect of disturbances of short duration, a quantity A , calculated from a finite number of cycles in the sliding interval of the average, can be used.

The evaluation can also be continuously averaged with the aid of time weighting, as in eqns (20) and (21).

Using the evaluation of the non-stationary vector A , it can be connected with (in linear form, for instance) the coefficients θ_0 , β_0 , α , g which control the mathematical model of the controlled process.

Realization of the Algorithm of Control

As an illustration, Figure 5 shows a programme of the functioning of a learning system of the formula type (without automatic trimming of θ_0 , β_0 , α , g).

The programme is realized by means of a digital computer. The programme envisages random search for ΔZ in the case when application of the recommendations held in Unit 2 does not lead to the required result.

The memory device is divided into two blocks, independently dealing with only the primary or only the secondary parameters of the process, in contemplation of linear introduction of the control parameters into the general connection equation; that is, automatic devices of this design are best used with plants whose connection equations have the form

$$k_i = \sum_j Z_j [F_{1k}(X, Y) + F_{2i}(X, Y)] \quad (26)$$

where F_{1k} and F_{2i} are any functions of the primary parameters and uncontrolled factors Y .

Depending on the characteristics of the process, and in particular on the nature of the variation of the uncontrolled factors (vector Y), and also depending on technical and economic

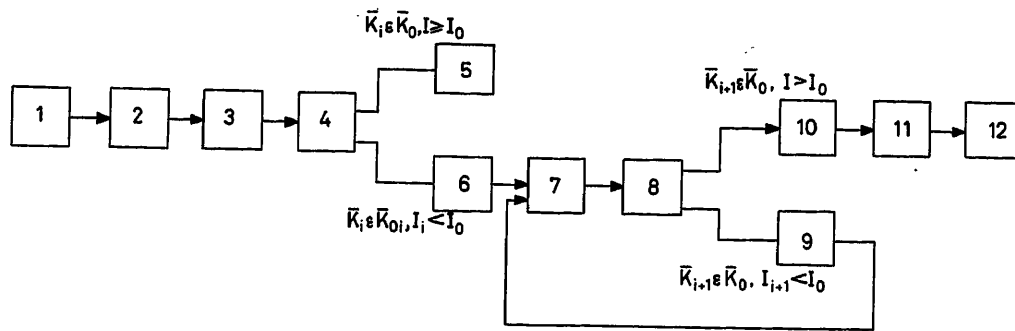


Figure 5. Programme of formula-type automatic device

1: Input of parameters X_i ; 2: calculation of parameters Z_i from eqn (3); 3: action upon plant; 4: input and analysis of K_i and I_i ; 5: stop; 6: calculation of correction ΔZ_i from eqn (5); 7: action upon plant; 8: input and analysis of K_{i+1} and I_{i+1} ; 9: random search for process input ΔZ_{i+1} ; 10: conversion of K_{s_i} and D_{z_0} ; 11: change of control coefficient [eqns (3) and (5)]; 12: stop

considerations, the mode of operation may be continuous, cyclic or one-time.

With continuous operation, the automatic device is connected with the process permanently, and learning is continuous. This mode of operation is suitable for processes in which the uncontrolled factors vary continuously and substantially.

The cycle mode of operation consists of periodic connection of the automatic device to the plant for correction of the law of control. The interval of time during which automatic control is carried out by a rigid programme worked out by the automatic device is determined by the periodicity of the variation of the uncontrolled factors. In this method of operation, the device can serve several processes at the same time.

The one-time mode of operation can be successfully applied during running-in tests of technological processes for which variation of the uncontrolled parameters is small. A final mathematical description of the process worked out by the device is used for further control of the process in the form of flow charts, for the simplest programmed control systems realizing the law of control obtained.

References

- ¹ BORODYUK, V. P., and KRUG, G. K. Finding connection equations in complex plants. *Automat. Telemekh., Moscow* 11 (1961)
- ² LUKOMSKII, YA. I. Correlation theory and its application to production analysis. GSI (1958)
- ³ HAL'D, A. Mathematical statistics with technical applications. IIL (1956)
- ⁴ NETUSHIL, A. V. The object of induction or radiation heating as an element in a control system. *Izv. OTN Energet. Automat.* 2 (1962)
- ⁵ KOLOMETSEVA, M. B. A combined programmed control for an induction heating process. *Tech. Cybernet.* 1 (1963)
- ⁶ FELDBAUM, A. A. *Computers in Automatic Systems*. 1959. Moscow; Fizmatgiz
- ⁷ KRASOVSKII, A. A. The principles of search and dynamics of continuous optimizing control systems. *Symp. on Automatic Control and Computer Technique* No. 4. 1961. Moscow; Mashgiz
- ⁸ KAZAKEVICH, V. V. Investigation of non-linear processes in an optimal regulator. Theory and application of discrete automatic systems. *Izd. AN SSSR* (1960)
- ⁹ NETUSHIL, A. V. Self-oscillation in discrete automatic systems. *Automat. Telemekh., Moscow* 3 (1962)
- ¹⁰ UIDROU, B. A self-adapting sampled-data system. *Automatic and Remote Control*. 1961. London; Butterworths
- ¹¹ NETUSHIL, A. V., KRUG, G. K., and LETSKII, E. K. Use of 'learning' systems for the automation of complex production processes. *Izv. VUZOV SSSR, Mashinostroyenie* 12 (1961)
- ¹² KRUG, G. K., and LETSKII, E. K. A learning automatic device of the table type. *Automat. Telemekh., Moscow* 10 (1961)
- ¹³ KALMAN, R. E. Design of a self-optimizing control system. *Amer. Soc. mech. Engrs Pap.* 57, RD 12 (1957)
- ¹⁴ IVANOV, A. Z., KRUG, G. K., KUSHELEV, YU. N., LETSKII, E. K., and SVECHINSKII, V. B. Learning-type control systems. *Proc. Moscow Power Inst.* 44

DISCUSSION

T. J. WILLIAMS and R. OTTO, *Monsanto Chemical Company, 800 North Lindbergh Boulevard, St. Louis 66, Missouri, U.S.A.*

I would like to make some comments on the paper. Perhaps it would be correct to state that the Unit 1 of the automatic device acted in a feedforward manner to control the process while the Unit 2 part acted in a feedback fashion to correct the operation of Unit 1.

It appears that Table 1 is incorrect in its list of the outputs of the units of the automatic control device. A more correct diagram might be:

Unit 1		Unit 2	
X_1	Z_1	ΔK_1	ΔZ_1
X_2	Z_2	ΔK_2	ΔZ_2

Eqn (3) indicates that the X 's are individual variables. There should thus be only one correction vector Z for each variable which might be out of desired limits. There is no reason to multiply Z by I since by definition I is already a measure of process efficiency.

The paper sets up some of the principles and potential methods of attack of problems in setting up automatic optimization and self-adaptation systems by the Faculty of Automation and Telemechanics of the Moscow Institute of Power. However, it does not present any results or statements of progress on any of the methods described. It would be very helpful if the authors would supply these.

This paper lists several methods of attack which are fairly well known in the automatic control literature. It would be much more of

a contribution if the authors would present a critical evaluation of the methods they propose with perhaps an actual example of the applications to which they could be applied.

A. V. NETUSHIL, *in reply*

I should like to thank Mr. Williams for these very helpful comments. As for the remarks related to memory units 1 and 2, I should only mention that while expelling a yield coefficient and series of z and ΔZ values for every given address of the memory there is no possibility to choose statistically the optimal mode of control and learning of a system. That is why the proposal of Mr. Williams cannot be accepted. As for a practical application the first device in question was used in industrial systems of high frequency heating. The results were published by Mrs. Kolomeitseva in *Technical Cybernetics*, No. 1 (1963).

The second more complicated control system with statistical method of selection of control signal value is a further development of the automation which simulates an optimal behaviour in an unknown environment. This automation was designed at our laboratory and was referred to in Mr. Pask's paper. Mr. Brainess and Mr. Walpalkov took part in the development. At the present time we are trying to find a practical solution to the problem and we hope that a special purpose device designed at Moscow Power Institute will help. It is possible to use these general purpose control systems, e.g. 'Dnipro', designed by Mr. Malinovsky, who is participating at this Congress. More detailed information on the basic automation principles can be found in the Moscow Power Institute Proceedings No. 44 (1962). I do not know any other paper where similar automatic devices are described; if Mr. Williams knows of such, I would be grateful for the references.

Principes et Réalisations des Automatismes liés à la Manutention de Combustible d'un Réacteur Nucléaire

P. TURPIN et J. THILLIEZ

Summary

The article describes the electric and electronic solutions adopted for solving, in a modern manner, the problems in handling fuel cartridges in a nuclear reactor of the graphite gas type.

The reactor comprises about 2,500 channels containing, in all, 30,000 cartridges of uranium. The moderating element is the graphite, and cooling is provided by CO_2 under 28 kg/cm² of pressure.

The main difficulties to be overcome are: the large number of elementary movements to be controlled (more than several thousands for one handling cycle for 34 cartridges); the great accuracy required by the latest improvements; and the fact that these handling operations must be carried out while the reactor is working, that is, at a temperature of 350° and under a CO_2 pressure of 28 kg/cm².

Automation had led to the use of a console desk comprising very few control levers by which the whole handling circuit is directed. The paper describes the different solutions based on digital programmers with punched tapes, with analogue and numerical servomechanisms which have made it possible to solve this problem.

Sommaire

La communication décrit les solutions électriques et électroniques adoptées pour résoudre de manière moderne les problèmes de manutention des cartouches de combustible dans un réacteur nucléaire du type graphite gaz.

Le réacteur comprend environ 2.500 canaux contenant au total 30.000 cartouches d'uranium. Le modérateur est le graphite et le refroidissement est assuré par du gaz carbonique à 28 kg/cm² de pression. Les principales difficultés à surmonter sont le grand nombre de mouvements élémentaires à provoquer et contrôler; la grande précision requise pour certains positionnements; le fait que ces opérations doivent être accomplies le réacteur étant en marche, c'est-à-dire à une température de 350° et sous une pression de 28 kg/cm².

L'automatisation conduit à la conception d'un seul pupitre comportant le minimum des commandes à partir desquelles toute la manutention doit être dirigée. La solution d'ensemble étudiée par la Compagnie Générale d'Automatisme comprend des programmeurs numériques à bandes perforées et des servomécanismes analogiques et numériques utilisant les informations distribuées par les programmeurs.

Zusammenfassung

Der Aufsatz beschreibt die mit Hilfe von elektrischen und elektronischen Mitteln eingeschlagenen Wege zur Lösung der Probleme bei der modernen Handhabung von Kern-Brennelementen in einem gasgekühlten Graphitreaktor.

Der Reaktor enthält etwa 2500 Kanäle mit zusammen 30000 Uranbrennelementen. Der Moderator ist Graphit und die Kühlung geschieht durch CO_2 mit einem Druck von 28 kp/cm².

Die zu überwindenden Hauptschwierigkeiten sind: die große Anzahl der zu regelnden elementaren Bewegungen, die Notwendigkeit großer Genauigkeit für bestimmte Stellungen und der Umstand, daß die Vorgänge während des Betriebs des Reaktors, d. h. bei Temperaturen von 350°C und einem Druck von 28 kp/cm² erfolgen müssen.

Die Automatisierung führte zu einem Steuerpult, das mit einem Minimum von Schalthebeln die gesamte Steuerung betätigt. Der von der Compagnie Générale d'Automatisme erprobte Steuer teil umfaßt

digitale Programmierereinheiten mit Lochstreifeneingabe sowie analoge und digitale Nachlaufregelgeräte, die die von der Programmierereinheit erhaltene Information weiterverarbeiten.

Introduction

Au cours des dix dernières années, nous avons pu assister à l'utilisation de plus en plus fréquente des techniques de l'automatisme pour résoudre des problèmes industriels délicats. Une utilisation judicieuse de programmeurs et de servomécanismes conduit à une centralisation des commandes et à une diminution notable du personnel nécessaire.

Nous allons décrire ci-dessous un exemple caractéristique d'application de l'automatisme. Le problème à résoudre est l'automatisation complète de la manutention des cartouches de combustible dans un réacteur nucléaire de puissance. Cette automatisation doit conduire à la conception d'un pupitre unique comportant le minimum de commandes, à partir desquelles toute la manutention doit pouvoir être dirigée.

Caractéristiques Générales du Réacteur Considéré

Le combustible utilisé est l'uranium naturel. Le graphite est utilisé comme modérateur. Le fluide de refroidissement est le gaz carbonique à 25 kg/cm². Le nombre des canaux est 2.479. Le combustible est constitué de cartouches d'uranium naturel gainées au magnésium et supportées par des chemises cylindriques en graphite. Chaque canal comporte 12 cartouches d'une hauteur de 60 cm.

Le modérateur est constitué par un empilement de briques en graphite ayant la forme de prismes droits. Le caisson d'acier a un diamètre de 18,3 m. Son épaisseur est de l'ordre de 95 mm et il pèse environ 1.300 tonnes. Le chargement-déchargement du réacteur se fait par la partie supérieure en marche et sous pression. L'appareil de chargement comporte quatre machines se déplaçant sur un système de pont tournant et de voies radiales. La première de ces machines appelée 'machine auxiliaire' permet la mise en place du bras articulé desservant chacun des canaux. Deux autres de ces machines appelées 'machines principales de chargement' se succèdent sur le bras ainsi placé. Elles retirent les cartouches usagées et les remplacent par des cartouches neuves. La quatrième machine est appelée 'machine de dépannage'.

Description Sommaire de la Manutention (voir Figures 1 et 2)

Puits et cellules — Les canaux du réacteur sont desservis par 85 puits de chargement-déchargement. La dalle supérieure du réacteur comporte donc 85 ouvertures. Chacun des 85 puits permet le chargement-déchargement de 34 canaux du réacteur.

L'association de 34 canaux desservis par un même puits s'appelle une cellule.

Machine Auxiliaire — La machine auxiliaire, dont il a été parlé précédemment, vient déposer le bras de chargement dans le puits qui a été choisi. Cette opération se fait évidemment sous pression et à chaud pendant le fonctionnement du réacteur. La machine auxiliaire comporte un magasin tournant appelé barillet dans lequel peuvent être stockés des bras de chargement ou des bouchons de protection, et un treuil de manutention permettant la dépose ou l'enlèvement des organes stockés. Quand la machine auxiliaire a déposé le bras, elle est évacuée sur une voie fixe appelée voie nord, et elle est remplacée sur le réacteur par une machine principale.

Machine Principale — Elle comporte un magasin fixe dans lequel peuvent être stockés des cartouches neuves, des cartouches irradiées, et des bouchons de protection. Elle comporte un treuil appelé treuil de manutention dont le câble se termine par le manipulateur de manutention. Le manipulateur est descendu à travers le conduit formé par le canal central du magasin de la machine, le bras de chargement placé dans le puits jusque dans le canal choisi où il va accrocher la cartouche irradiée supérieure; cette cartouche est remontée jusque dans la partie supérieure de la machine, et un organe mécanique appelé potence de distribution place cette cartouche dans un canal du magasin. Toutes les cartouches usagées du canal du réacteur sont ainsi retirées. Quand le canal a été vidé, le manipulateur prend les cartouches neuves dans le magasin de la machine et les dépose une à une dans le canal.

Toutes les opérations indiquées ci-dessus se font évidemment sous pression et en température. Un organe mécanique complexe appelé fourreau amovible permet l'accouplement de la partie inférieure de la machine au puits du réacteur considéré. Quand la machine de chargement a terminé le travail sur le réacteur, elle est évacuée par le pont tournant sur une voie fixe appelée voie est; elle se positionne en une position bien précise qui permet l'accouplement au système d'évacuation des cartouches en piscine. Ce système d'évacuation comporte un magasin intermédiaire desservi par un bras de manutention dans lequel les cartouches sont provisoirement stockées, de façon qu'elles se refroidissent.

Un système de sas appelé sas d'évacuation en piscine permet de faire passer ultérieurement les éléments irradiés refroidis de l'atmosphère de gaz carbonique à 25 kg/cm² à la pression atmosphérique. Tout cet ensemble s'appelle bâtiment de combustible irradié (BCI).

Un système de sas appelé sas d'introduction des éléments neuves permet de faire passer les cartouches neuves de la pression atmosphérique à la pression de gaz carbonique de 25 kg/cm². Le treuil de la machine principale prend un à un ces éléments neuves et les place dans le magasin; la machine principale est alors prête pour une deuxième opération sur le réacteur.

Quand la machine principale a quitté la voie fixe, un treuil appelé treuil auxiliaire est amené sur le BCI. Ce treuil auxiliaire prend les éléments irradiés se trouvant dans le réservoir de refroidissement intermédiaire et les évacue en piscine grâce aux sas d'évacuation en piscine.

Caractéristiques du Problème à Résoudre

La capacité du magasin de la machine principale permet de stocker 56 cartouches et fausses cartouches. Quand la machine

est sur le réacteur, elle retire 56 éléments irradiés et les remplace par 56 éléments neuves. Dans cette opération, les organes suivants interviennent: le treuil de manutention de la machine principale; la potence de distribution; le bras de manutention; le système électro-pneumatique du fourreau amovible, et les organes électriques de liaison avec la détection de rupture de gaine, etc.

Appelons par exemple, mouvement élémentaire la montée du manipulateur du niveau inférieur au niveau supérieur, ou le mouvement inverse, ou bien un déplacement de potence, ou bien un déplacement d'un organe quelconque. Le travail d'une machine principale sur le réacteur comporte plus de 1.000 mouvements élémentaires. Le travail d'une machine principale sur le BCI comporte environ 1.000 mouvements élémentaires. Le travail d'un treuil auxiliaire sur le BCI comporte environ 1.200 mouvements élémentaires.

Nous voyons donc, une caractéristique essentielle du problème posé: la grande quantité de mouvements élémentaires (presque 5.000) que nécessite un aller et retour de machine sur le réacteur. La deuxième caractéristique du problème est la grande précision exigée par certains positionnements:

pont tournant: $\pm \frac{2}{50.000}$ soit environ une minute d'angle

bras de manutention: $\pm \frac{0,7}{1.000}$ soit environ 30 minutes d'angle.

A titre de comparaison et de point de repère, nous rappellerons que l'antenne cornet de telstar est positionnée avec une précision de la minute d'angle.

Caractéristiques Générales de la Solution Adoptée

La solution adoptée fait appel aux techniques électriques les plus diverses:

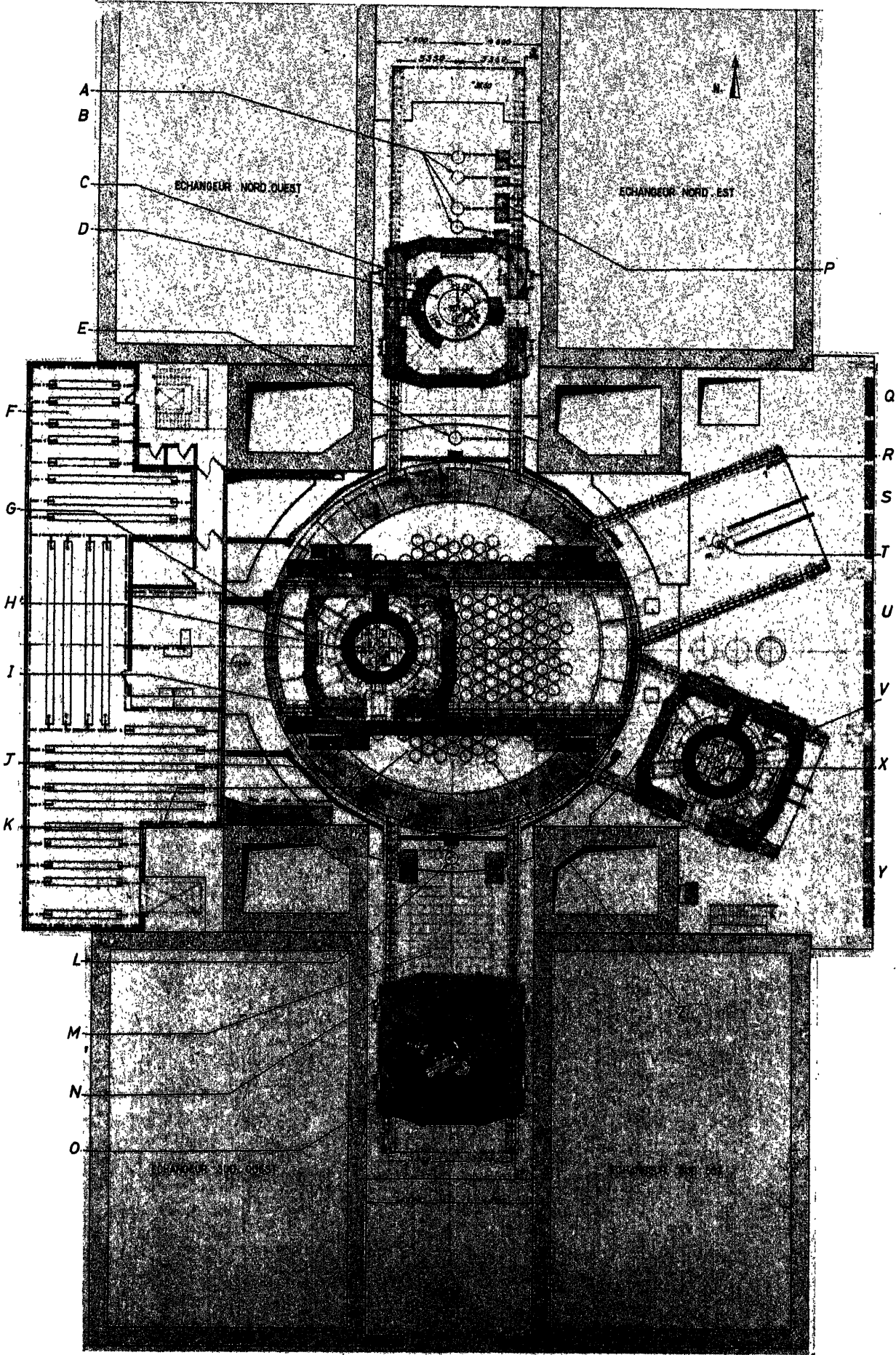
(a) techniques classiques: disjoncteurs, contacteurs, relais;
(b) techniques modernes expérimentées: servomécanismes industriels;

(c) techniques modernes moins souvent expérimentées: programmation digitale, programmeurs à bande, en général à base de semi-conducteurs;

(d) techniques de l'installation proprement dite: le choix des câbles et de certains éléments comme les contacteurs de fin de course ont posé beaucoup de problèmes. En effet, d'une part la place disponible est restreinte, d'autre part, il faut tenir compte des conditions de température, de radiations et de pression.

Figure 1. Vue en plan du réacteur →

A	Cimetière Zone Nord	N	Charlot Machine de dépannage
B	Bouchons des canaux de cimetière	O	Machine de dépannage
C	Chariot de machine auxiliaire	P	Stockage d'éléments neuves
D	Machine auxiliaire en position sur le poste d'essais des bras	Q	Monte charges B. C. I.
E	Cimetière de Treuils de barre de contrôle	R	Voie Nord-Est.
F	Salle de commande et de relayage	S	Salle des ventilateurs
G	Chariot de machine de chargement	T	Treuil auxiliaire en position sur un B. C. I.
H	Machine de chargement	U	Postes de chargement en éléments neuves
I	Pont tournant	V	Voie Sud-Est.
J	Plateau tournant	X	Machine de chargement en position sur un B.C.I.
K	Aire de chargement	Y	Salle des compresseurs
L	Cimetière de treuils de barre de contrôle	Z	Mise à la terre des puits de chargement
M	Salle de décontamination		



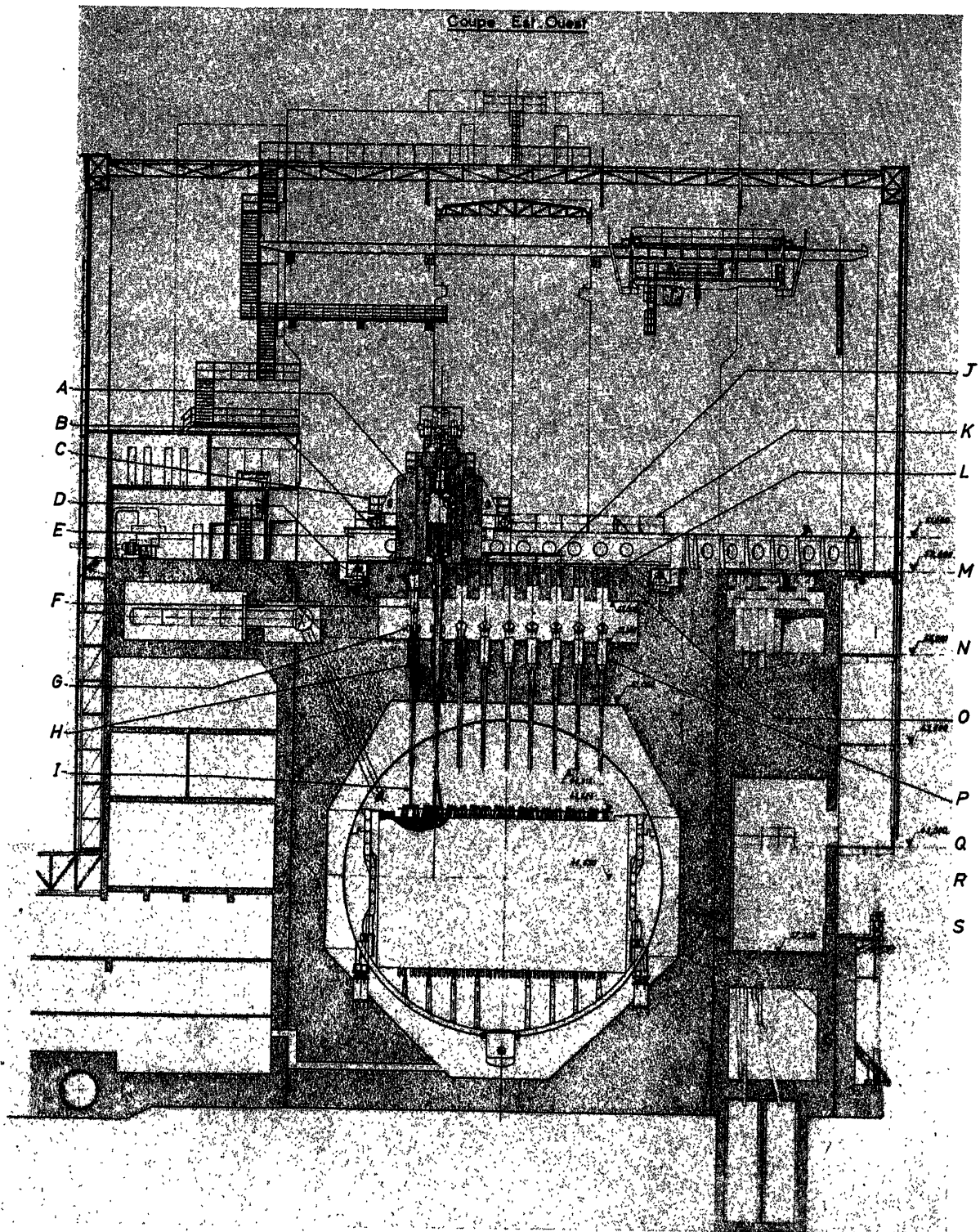


Figure 2. Coupe est-ouest du réacteur

- | | | | |
|--------------------------------------|---------------------------------|--------------------------------|---------------------------------------|
| A Machine de chargement | F Fourreau amovible | K Passerelles | P Plan guide de la dalle plan indatom |
| B Voir détail du patin | G Capot des puits de chargement | L Bouchon de la Fausse dalle | Q Réservoir de stockage |
| C Charlot de machine | H Puits de chargement | M Aire de chargement | R Salle des éléments irradiés plan |
| D Voir détail du passage de la fosse | I Bras de chargement | N Chargement en éléments neufs | S Vannes à passage intégral |
| E Pont tournant | J Trainard électrique | O Fausse dalle | |

Difficultés du Problème

Le problème de la manutention s'est révélé d'une grande complexité et par suite, toute solution donnée est inévitablement complexe. Nous avons choisi une solution raisonnablement moderne, respectant au maximum les principes de sécurité.

La quantité de matériel mise en œuvre est grande. Si nous plaçons côte à côte les baies d'électronique, de relais et de contacteurs, nous obtenons un tableau d'une longueur de 180 m et d'une hauteur de 2 m.

Par suite, à côté de problèmes relevant d'une technicité élevée nous avons eu à résoudre un certain nombre de problèmes concernant la réalisation du matériel et son installation de façon à éviter les parasites, les interférences de fonctionnement ou les mauvais contacts.

Techniques Utilisées

Comme dit précédemment, elles sont les suivantes :

Les techniques sensiblement classiques, c'est-à-dire, celles des disjoncteurs, des contacteurs et des relais. Elles ont été utilisées pour résoudre les problèmes suivants : la distribution des secteurs 380 V 50 périodes et 127 V continu ; l'automatisme local des 14 sas ; la commutation des trainards des machines, et la commande des circuits pneumatiques.

Mais la quantité de matériel mise en œuvre est à souligner. Par exemple, l'automatisme local des 14 sas nécessite environ 600 relais et contacteurs et 14 cycleurs mécaniques à 12 pas. Par suite, bien que ces techniques soient classiques, la crainte des mauvais contacts et des pannes nous a poussé à prendre des précautions un peu inhabituelles.

La technique des servomécanismes industriels. Un certain nombre d'organes sont positionnés au moyen de servomécanismes, parce que les mouvements doivent être exécutés avec une grande précision dans un délai relativement bref.

Les servomécanismes utilisés sont du type industriel. Ils sont différents des servomécanismes de calculateurs : ils sont plus robustes ; leurs performances dynamiques sont moins poussées, et les puissances mises en jeu sont plus élevées $\frac{1}{3}$ cv à 50 cv dans le cas présent.

Nous avons utilisé deux sortes de servomécanismes :

(a) *Les servomécanismes analogiques* : Ils ont été largement utilisés pour résoudre les problèmes suivants : positionnement du pont tournant ; positionnement des chariots, et positionnement des bras de manutention, etc.

La précision du positionnement peut être théoriquement très grande si l'on augmente le gain de la chaîne, et si la bande passante est satisfaisante. Elle est pratiquement limitée par les jeux mécaniques. La Figure 3 nous indique le principe de fonctionnement d'un tel servomécanisme.

(b) *Les servomécanismes digitaux*. Leur technique est plus récente que celle des servomécanismes et par suite moins connue. Ils présentent toutefois l'avantage d'utiliser sans transformation les informations données par un programmeur lui-même digital. Nous les avons utilisés pour résoudre le problème du positionnement de la potence de distribution ou du treuil de manutention. La Figure 4 montre le principe d'un asservissement de position digital.

La Technique de la Programmation et des Programmeurs — Le travail des machines principales ou de la machine auxiliaire sur le réacteur ou sur le BCI nécessite plusieurs milliers de déplacements élémentaires, comme nous l'avons vu précédemment.

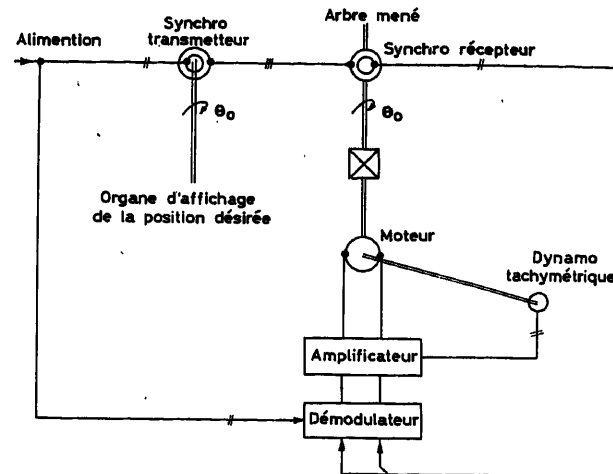


Figure 3. Principe d'un servomécanisme analogique

Tous ces mouvements élémentaires sont reproduits identiquement si une machine recommence un travail identique sur le même puits du réacteur ou sur un puits voisin. Une intervention humaine à chaque mouvement est inconcevable. Par suite, un très important problème de stockage et de distribution d'informations a dû être résolu. De plus l'utilisateur désire avoir la possibilité de modifier sans difficulté le mode de chargement-déchargement. Par suite, le programmeur à bande perforée a été choisi comme organe de distribution d'information. Il permet un changement de programme facile, et un fonctionnement pas à pas facile. En effet, il doit diriger une succession de mouvements dont la durée n'est pas négligeable, et le déplacement de la bande n'est donc pas continu.

Deux sortes d'informations sont distribuées sous forme de signaux électriques représentant un code binaire : (a) les informations d'adresse, et (b) les informations de niveau.

Toute la manutention est commandée par cinq programmeurs à bande perforée.

Découpage de l'équipement Electrique

De façon à faciliter la réalisation du matériel et son installation, l'équipement électrique a été divisé en un certain nombre

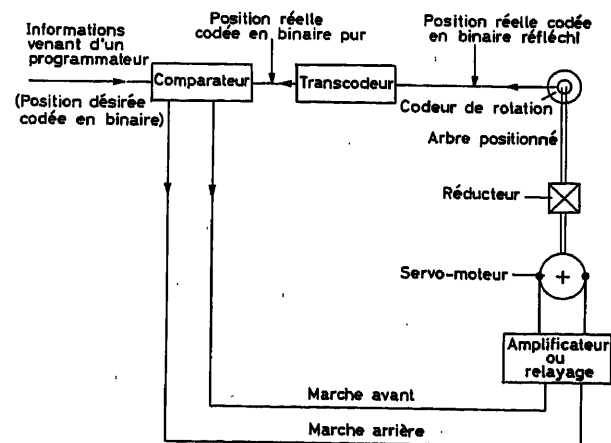


Figure 4. Principe d'un servomécanisme digital

d'ensembles appelés ensembles fonctionnels. Leur nombre est environ 80. Par exemple, l'équipement électrique recevant des instructions d'un programmeur et commandant les mouvements d'un bras de manutention est: l'ensemble fonctionnel du bras de manutention.

Les ensembles composant l'équipement électrique peuvent être divisés en quatre groupes:

(a) les ensembles non programmés par un programmeur digital, mais comportant des asservissements. C'est par exemple, le cas de l'ensemble de positionnement du pont-tournant (Figure 5) ou des ensembles de positionnement des chariots. Ces mouvements sont commandés par l'opérateur humain pour deux raisons: leur fréquence est relativement faible, et il a été jugé préférable de laisser à l'opérateur humain l'initiative de certains déplacements importants.

(b) Ensembles asservis et programmés par le programmeur digital, c'est par exemple, le cas de l'ensemble du bras de manutention, du treuil de manutention, etc. La succession des mouvements est relativement rapide et de plus, il est rare que deux mouvements consécutifs soient identiques. Une intervention humaine à chaque mouvement est inconcevable. La Figure 6 montre le principe de commande de plusieurs ensembles programmés par le programmeur associé à la machine principale no. 1.

(c) Ensembles sans asservissement et non programmés. C'est le cas d'un certain nombre d'installations auxiliaires comme l'équipement électrique de la salle de décontamination.

Description de la Solution Donnée au Positionnement du Pont Tournant

Définition du Problème

Le pont tournant a les caractéristiques suivantes:

- diamètre de roulement, 17,56 m
- diamètre de la crémaillère, 16,80 m
- poids sans machine de chargement, 200 tonnes
- poids avec une machine de chargement, 700 tonnes
- poids avec deux machines de chargement, 1.200 tonnes

Deux buts sont recherchés:

(a) Le positionnement d'une machine sur un puits du réacteur défini en coordonnées polaires. Dans ce cas, le positionnement du pont doit être obtenu avec une précision de 10 mm.

(b) Le positionnement du pont sur une voie fixe pour le débarquement ou l'embarquement d'une machine.

Pour que le verrouillage du pont sur une voie soit possible, il faut que la précision du positionnement soit de l'ordre de ± 2 mm.

Principe de la Solution Adoptée (Figure 5)

L'entraînement est fait par deux pignons à axe vertical attaquant la crémaillère périphérique. Chaque extrémité du pont comporte 1 pignon. Chaque pignon est entraîné par un moteur à courant continu à excitation constante et tension d'induit variable d'une puissance de 25 cv.

L'utilisation de deux moteurs sans liaison mécanique a permis de réduire au minimum la mécanique de mise en mouvement du pont en la concentrant au voisinage du pignon. De cette façon, la mécanique est de meilleure qualité et les jeux sont

réduits. Le pont tournant n'a pas d'axe de rotation réel. Il faut donc assurer électroniquement la synchronisation des deux pignons d'attaque. Pour que la rotation soit convenable la désynchronisation des pignons ne doit pas dépasser ± 2 mm, la mesure étant faite sur la crémaillère, soit environ $\pm 2/50.000$ de la circonférence, soit environ 1 minute d'angle.

L'opérateur dispose d'un clavier comportant 85 boutons-poussoirs. Chaque bouton-poussoir représente un puits; l'action sur l'un des boutons-poussoirs positionne le pont sur le puits correspondant. L'opérateur a également, à sa disposition un cadran d'affichage gradué en degrés et minutes sur lequel il peut afficher la position désirée au moyen d'une manivelle.

La servocommande comporte trois servomécanismes de position du type analogique. Les capteurs de position sont des synchro-machines classiques de taille 31 et 23.

Chaîne de Pilotage (Figure 5) — De façon à rendre l'accélération et la décélération du pont indépendantes des manœuvres de l'opérateur, il a été prévu une chaîne dite de 'pilotage'. La tension d'erreur qui apparaît au rotor du synchro-détecteur liée à l'affichage manuel sur cadran est une représentation électrique de la différence de l'angle de ce synchrodétecteur et de l'angle du synchro-transmetteur liée au moteur pilote. Cette tension d'erreur est amplifiée et démodulée et fait tourner le moteur pilote jusqu'à annulation, ce qui a lieu lorsque le moteur pilote a donné au transmetteur la même position angulaire que celle du synchro-détecteur.

Chaîne des Boggies — Les synchro-détecteurs fixés sur les boggies sont liés au pignon d'attaque de la crémaillère du pont. Ils sont alimentés en parallèle par le synchro-transmetteur de la chaîne pilote. La tension d'erreur issue de chaque synchro-détecteur attaque après amplification le moteur de chaque boggie, grâce à un groupe Ward-Léonard comportant deux génératrices de 25 kW. Pendant les déplacements ou à l'arrêt du pont, les synchro-récepteurs des boggies restent synchronisés au transmetteur de la chaîne de pilotage. Par suite, les deux boggies sont synchronisés entre eux et les lois de vitesses et d'accélération du pont s'identifient à celles de la chaîne de pilotage. Ces lois sont déterminées de façon à éviter au pont-tournant des efforts mécaniques nuisibles.

Détecteur d'erreur — Des systèmes « détecteurs d'erreurs » constatent l'absence de tension d'erreur entre la chaîne de pilotage et les boggies et provoquent un arrêt d'urgence en cas de désynchronisation.

Affichage de la Position des Puits — De façon à éviter à l'opérateur un affichage manuel fastidieux, le pupitre de commande général comporte 85 boutons-poussoirs, chaque bouton-poussoir correspondant à un puits. L'enfoncement d'un bouton-poussoir affiche une position du pont-tournant au moyen d'un système comportant des relais, des transformateurs, et des résistances de précision. Ce système remplace donc 85 groupes de synchro-récepteurs calés une fois pour toute sur la position des puits.

Réalisation des Chaînes d'asservissement

Les synchro-machines représentées sur la Figure 5 sont en réalité triplées de façon à augmenter la précision du positionnement. Les tensions d'erreur recueillies par les trois synchros d'une même chaîne sont envoyées à un dispositif commutateur gros-fin de façon à sélectionner l'erreur, grosse, moyenne ou

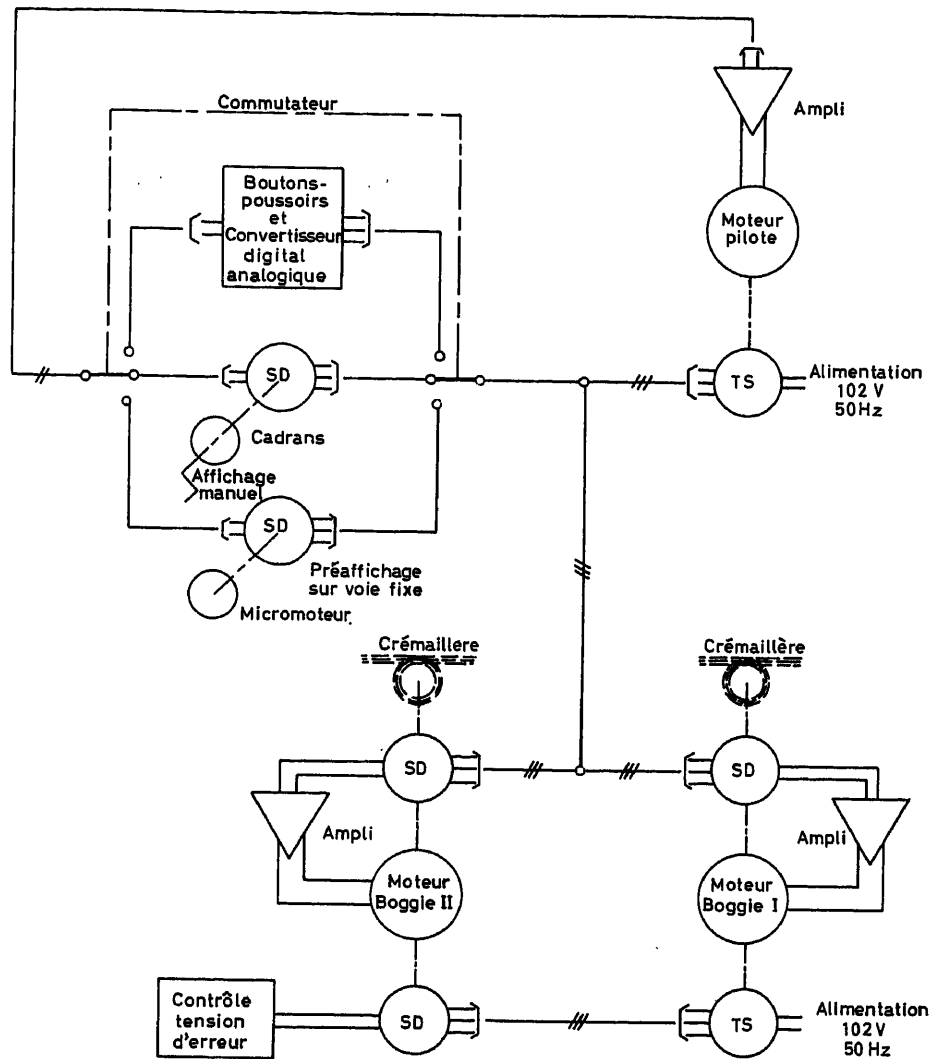


Figure 5. Pont tournant: principe de la solution

fine, selon que le servomécanisme est loin ou près de sa position d'équilibre.

Le démodulateur placé à la sortie du commutateur gros-fin transforme la tension d'erreur alternative en une tension continue, amplifiée, dont la polarité dépend de la phase. Cette tension continue est à son tour amplifiée par un amplificateur à lampes et par des amplificateurs magnétiques, de façon à pouvoir attaquer les enroulements d'excitation de la génératrice correspondante. Chaque moteur comporte une génératrice tachymétrique dont le rôle est de stabiliser les chaînes d'asservissement.

Description de la Solution Analogique Donnée au Positionnement des Chariots-machines

Définition du Problème

Les caractéristiques des chariots-machines sont les suivantes:

poids total, 500 tonnes

longueur hors-tout, 8,36 m

largeur de la voie, 6,70 m

longueur de la voie la plus longue, 22 m

Le but recherché est le positionnement des chariots-machines sur l'un des puits sélectionnés par l'opérateur, ou sur le puits d'accès au système d'évacuation des cartouches en piscine. La précision demandée est de l'ordre de 10 mm.

Principe de la Solution Adoptée

La solution adoptée comporte une triple chaîne de synchro-machines, un commutateur fin-grossier, un amplificateur démodulateur et des amplificateurs magnétiques attaquant un groupe Ward-Léonard comportant une génératrice de 20 kW et un moteur de 20 cv. L'opérateur désirant effectuer un positionnement, a, à sa disposition un cadran gradué, commandé par une manivelle ou bien les 85 boutons-poussoirs, dont nous avons déjà parlé. Dans ce cas, l'enfoncement d'un des 85 boutons-poussoirs provoque le positionnement simultané sur le puits sélectionné du pont tournant et de la machine se trouvant sur le pont.

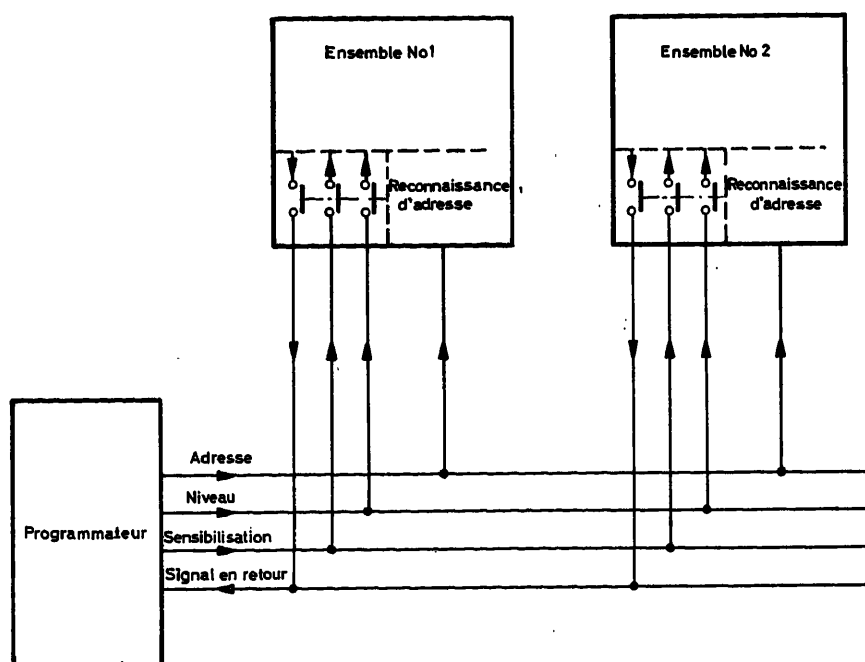


Figure 6. Principe de commande de plusieurs ensembles par un programmeur

Description de la Solution Donnée au Problème du Positionnement du Bras de Manutention

Définition du Problème

Une cellule du réacteur desservie par un puits comporte 34 canaux. Ces 34 canaux sont réparties selon 24 directions sur 6 cercles concentriques. Le bras de manutention doit pouvoir prendre 24 orientations différentes et 6 inclinaisons différentes appelées « brisures ». Ces orientations et ces brisures doivent être obtenues avec une grande précision, parce que les canaux d'une même cellule sont très voisins. Le bras de manutention comporte deux tubes concentriques. L'orientation est donnée par la rotation simultanée de ces deux tubes, et la brisure est donnée par la rotation d'un tube par rapport à l'autre. La rotation de ces tubes est limitée à deux tours. La précision demandée correspond à un écart angulaire absolu de 0,5 degré et à un écart angulaire relatif de :

$$\pm \frac{0,5}{2 \times 360} = \pm \frac{0,7}{1.000}$$

Principe de la Solution Adoptée

La solution adoptée comporte deux chaînes de servomécanismes analogiques dont les organes capteurs sont des synchro-machines. Un groupe Ward-Léonard à grande amplification commande les servomoteurs d'orientation et de brisure d'une puissance de 300 watts. Les 24 orientations et les 6 brisures sont préaffichées au moyen de transformateurs et de résistances. Le programmeur digital dirigeant présentement la manutention donne des directives codées à ces servomécanismes et le bras est alors positionné conformément aux ordres du programmeur. Dans le cas présent, l'opérateur humain n'intervient pas.

Principes Généraux de la Programmation

L'organisation de la programmation tient compte du fait que plusieurs machines sont connectées en parallèle aux bornes

de sortie d'une même programmeur. Le programmeur doit fournir d'une part, des informations d'adresse qui désignent l'organe à mettre en œuvre et d'autre part des informations de niveau qui spécifient l'ordre donné à l'organe. Le support d'informations est une bande perforée standard à sept canaux qui est explorée ligne par ligne par l'organe lecteur; un bloc d'informations, comprenant tous les éléments nécessaires à l'exécution d'un ordre, comprend sept lignes (Figure 7).

1° ligne: début de bloc d'informations

2° et 3° lignes: informations dites « d'adresse ».

4°, 5°, 6°, 7° lignes: informations dites « de niveau ».

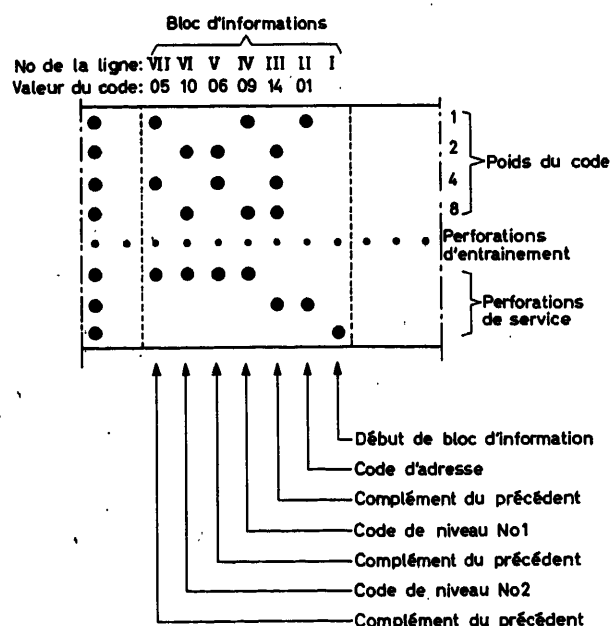


Figure 7. Bloc d'information d'une bande perforée

Le code utilisé est le code binaire pur.

Les informations contenues dans les sept lignes d'un bloc d'informations, déchiffrées ligne par ligne au moyen du lecteur de bande, sont mises en mémoire et distribuées en parallèle sur les bornes de sortie de l'appareil, où elles sont disponibles sous forme d'informations permanentes.

Les règles de sécurité de fonctionnement du matériel imposent une vérification de la transmission correcte des signaux

Le fonctionnement est alors le suivant (*Figure 8*): lorsqu'un organe reconnaît son adresse, elle ouvre les portes de ses circuits logiques aux informations de niveau représentant le mouvement qu'elle doit accomplir. Le signal de départ (sensibilisation) est fourni par le programmeur, avec un retard réglé par un circuit de temporisation à une valeur qui recouvre le temps de réponse de tous les circuits. La machine exécute alors l'ordre spécifié par les informations de niveau. Lorsque l'opération est

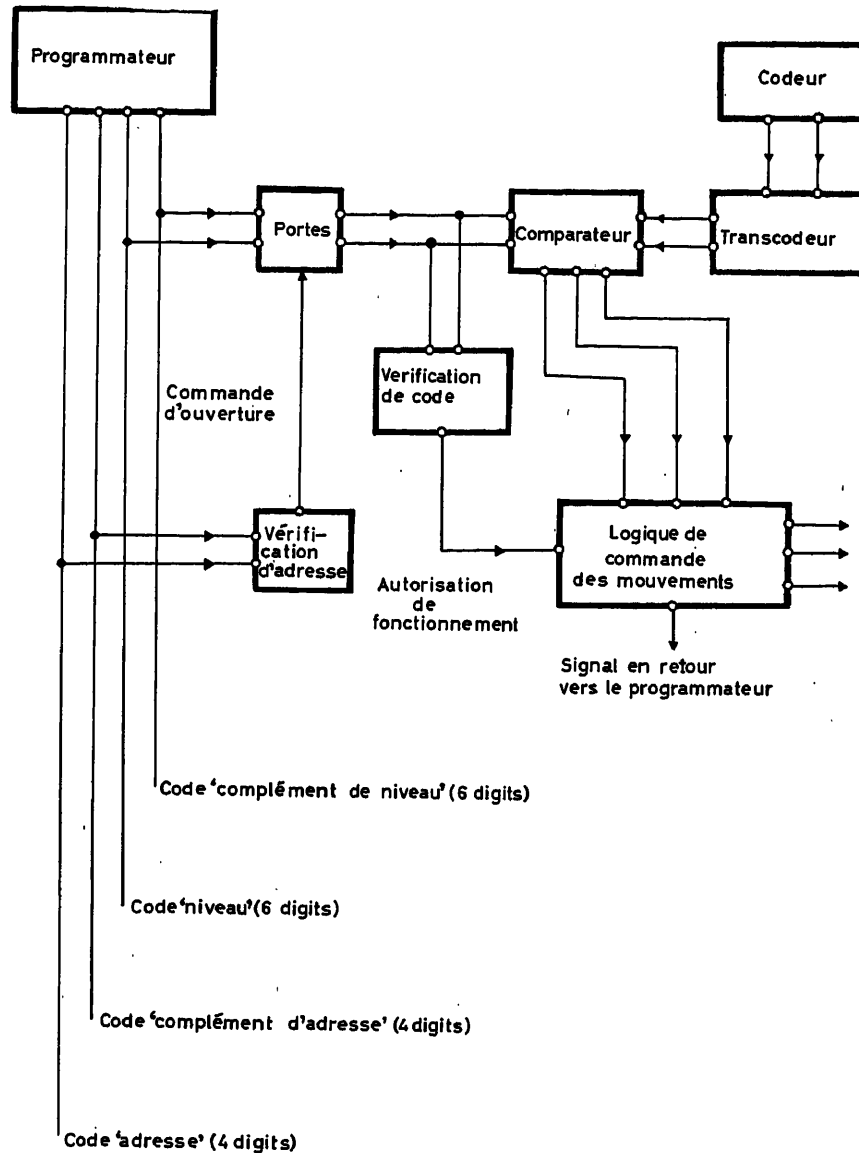


Figure 8. Bloc diagramme d'un ensemble programmé

à la machine. A cet effet, chaque combinaison d'adresse ou de niveau est accompagnée de la combinaison obtenue en remplaçant chaque digit par son complément binaire (la combinaison d'adresse de la ligne 3 est la combinaison complémentaire de la ligne 3, et les combinaisons de niveau des lignes 5 et 7 sont les compléments respectifs des lignes 4 et 6); des circuits de vérification, intégrés à la logique de la machine, vérifient la compatibilité de chaque digit et de son complément.

terminée, la machine produit un signal « signal en retour » qui fournit au programmeur l'ordre d'avancement.

L'articulation correcte de toutes ces fonctions est indispensable, et l'on peut dire que la sécurité du fonctionnement de tout l'ensemble de la manutention du combustible repose sur la sécurité du fonctionnement du programmeur.

Pour bien faire comprendre l'articulation du fonctionnement des organes du programmeur et des machines qui doivent

exécuter ses ordres, nous examinerons maintenant plus en détail, un programmeur et une machine « treuil de chargement » choisie parmi les autres à titre d'exemple.

Description d'un Programmeur (Figure 9)

La bande perforée est explorée ligne par ligne au moyen du lecteur de bande; un bloc d'informations complet représente sept lignes de la bande, le programmeur comporte un transformateur série-parallèle, qui rend disponibles en permanence les informations relevées aux cours d'une rafale de lecture de sept lignes de bande. Ce transformateur série-parallèle est un registre à glissement comprenant sept canaux parallèles à sept positions de transfert; les organes de lecture des sept canaux de la bande sont connectés respectivement aux circuits de la première position du registre à glissement. Les signaux de transfert du registre et les ordres d'avance du lecteur sont synchronisés de façon que le registre soit rempli progressivement par les informations lues successivement sur les sept lignes de la bande constituant de bloc d'informations.

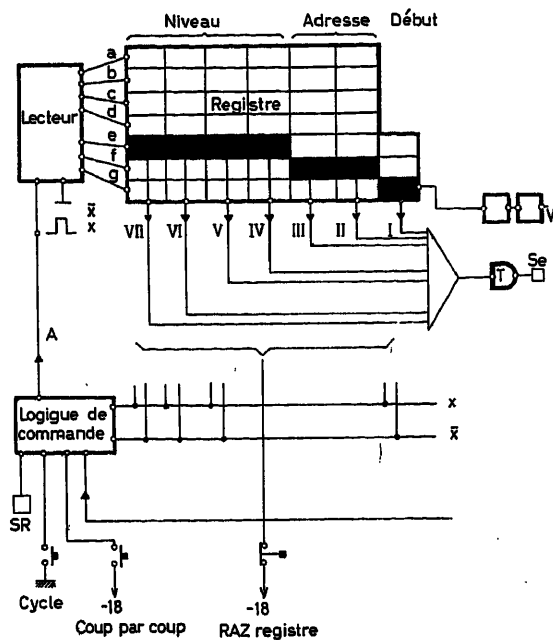


Figure 9. Principe de fonctionnement d'un programmeur

Ce fonctionnement à répétition automatique est interrompu lorsque les sept positions de transfert du registre sont garnies d'informations; cette fonction est réalisée par l'arrivée des informations perforées sur la première ligne du bloc d'informations (ligne « début de bloc d'informations ») dans la septième position de transfert du registre.

Une fonction de vérification de la présence des informations lues sur les six autres lignes de la bande (deux lignes d'« adresse » et quatre lignes de « niveau ») excite alors un circuit de temporisation qui fournit avec un temps de retard réglable l'ordre de départ à la machine (signal de « sensibilisation »).

Le « signal en retour » de la machine provoque la reprise du mouvement automatique de lecture et d'enregistrement des sept lignes de bande constituant le bloc d'informations suivant.

Description d'un Treuil de Chargement

Le treuil de chargement est une machine destinée à mettre en mouvement un manipulateur chargé de véhiculer les cartouches d'uranium, les bouchons de canaux, les culasses de récupération de débris, etc., dans les canaux du réacteur et dans les tubes du magasin de la machine de chargement. Il est constitué d'un cabestan entraîné par un moteur à courant continu de 2 cv, d'un câble supportant le manipulateur, et d'un pantin dont la position angulaire est fonction de la tension du câble (Figure 10).

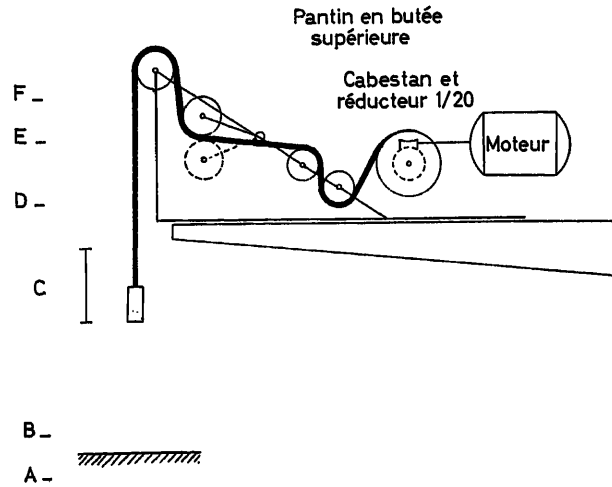


Figure 10. Principe de commande par pantin

Il a fallu prévoir des dispositifs particuliers de sécurité à l'égard d'un coincement accidentel du manipulateur dans un conduit; mais la principale difficulté consiste à réaliser la commande d'arrêt en fin de mouvement de montée ou de descente. En effet, la position du manipulateur échappe à tout contrôle direct; elle ne peut être déduite qu'approximativement de la position du cabestan, car la longueur du câble ne peut être considérée comme constante (allongement dû à la température, à l'usure du câble, etc.).

Des considérations de cadence obligent d'autre part à utiliser, en montée ou en descente, trois vitesses différentes: grande, moyenne et petite; la grande vitesse étant celle du déplacement normal du manipulateur dans les conduits, la moyenne vitesse est adoptée dans les passages coudés, et la petite vitesse est utilisée pour l'accostage en fin de montée ou de descente.

Pour réaliser le fonctionnement dans les conditions qui viennent d'être décrites, le moteur du cabestan travaille sous l'effet de deux dispositifs de commande indépendants (Figure 11):

Asservissement analogique: la vitesse de rotation du moteur est stabilisée, en montée ou en descente, aux trois valeurs spécifiées, et asservies en descente à la position du pantin qui est chargé de commander l'accostage en fin de descente.

L'accostage du manipulateur en fin de descente est détecté par le pantin qui se met en mouvement lorsque le câble a tendance à mollir. Le couple de rappel du pantin (grâce auquel le câble est maintenu tendu) est réglé de façon que le poids du manipulateur suspendu à l'extrémité du câble suffise pour maintenir le pantin sur sa butée supérieure. Le dépôt du mani-

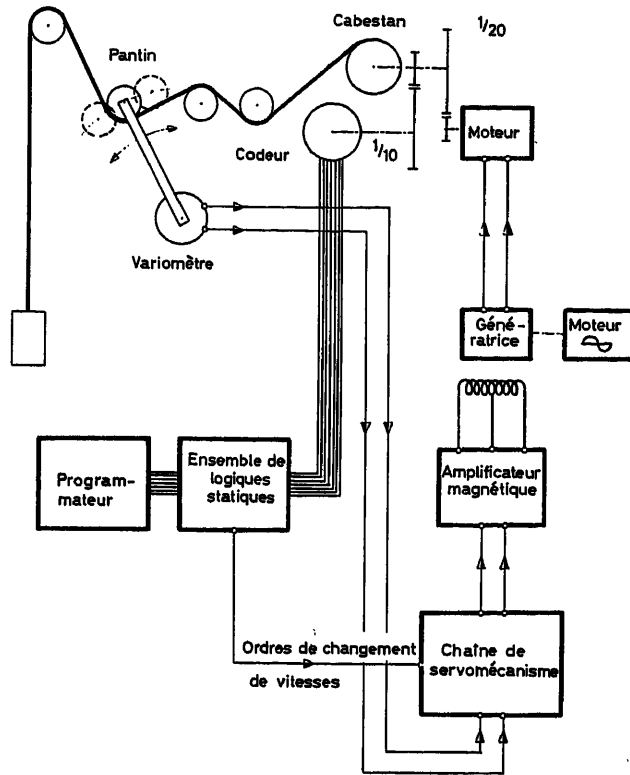


Figure 11. Principe d'un treuil de manutention

pulateur à la fin de la course de descente soulage le câble et provoque le mouvement du pantin qui quitte sa butée en maintenant le câble tendu. Un variomètre électrique entraîné par l'axe du pantin fournit une image électrique de sa position. La tension fournie par le variomètre est utilisée comme référence de vitesse de l'asservissement; cette tension (alternative 50 Hz) a sa valeur maximum lorsque le pantin est sur sa butée supérieure; elle décroît jusqu'à la valeur zéro lorsque le pantin arrive en position médiane, ce qui provoque le ralentissement et l'arrêt du moteur. Si le pantin dépasse la position médiane, la tension croît à nouveau, mais sa phase est inversée; il s'ensuit que le moteur tourne alors en sens inverse. Ceci veut dire que le cabestan déroule du câble jusqu'à ce que soit atteinte la position médiane du pantin, et qu'il rebobine l'excédent de câble déroulé si le pantin a dépassé

cette position; on voit que la position médiane du pantin est une position d'équilibre, et que le câble est maintenu tendu dans toutes les conditions.

L'accostage du manipulateur en fin de montée est détecté par un interrupteur «fin de course», qui provoque l'arrêt instantané du moteur par mise en court-circuit de son induit.

Asservissement digital (Figure 11): les changements de vitesse en cours de montée ou de descente sont commandés par un ensemble digital comportant essentiellement, en dehors du programmeur qui a été décrit plus haut, un codeur digital de position entraîné par le cabestan et un ensemble logique de commande.

Cet ensemble logique comporte un circuit de vérification d'adresse qui, reconnaissant l'adresse du treuil, ferme les portes qui permettent l'entrée des informations de niveau. Ces informations font l'objet d'une vérification de code, chaque digit devant être l'opposé de son complément respectif. Les informations de position issues du codeur, sous forme d'un code binaire réfléchi, sont traduites par un transcodeur en code binaire pur. Les informations de niveau et les informations de position sont comparées dans le circuit comparateur qui fournit un signal +, -, ou =. Le signal + commande la montée, le signal - la descente, et le signal = l'ordre de changement de vitesse qui précède l'accostage sous le contrôle de l'asservissement analogique.

Les circuits constituant la logique de commande des mouvements agissent directement sur le dispositif d'asservissement analogique de commande de vitesse et fournissent, lorsque l'ordre a été exécuté, le signal en retour qui est acheminé vers le programmeur; celui-ci progresse alors d'un pas, afin de commander la machine qui doit exécuter le mouvement suivant.

Conclusion

Le problème de la manutention des cartouches est donc caractérisé essentiellement par:

un problème de stockage et de distribution d'informations. Plusieurs milliers de séquences doivent être stockées.

des problèmes de positionnements. La précision demandée est parfois la minute d'angle.

La solution ci-dessus décrite fait appel aux techniques modernes de l'automatisme:

les programmations digitales à bandes perforées, les servomécanismes industriels.

A Study of the Dynamics of Steam Voids in Boiling Water Nuclear Reactors

P. K. M'PHERSON and M. MUSCETTOLA

Summary

The dynamics of boiling water nuclear reactors are an important consideration in their design since engineering and economic limits are set by the stability of the water recirculation loop and by the interaction between the steam voids and neutron production process (called void reactivity feedback effect). In the natural circulation type of boiling water reactor (BWR) considerations of recirculation loop stability are all important, while in a forced circulation pressure tube reactor (PTR) interesting problems in control and stability are posed by the freedom to design in a void reactivity coefficient that may provide positive or negative feedback.

The paper discusses in general terms the influence of the void reactivity coefficient on reactor stability and control, and demonstrates that sophisticated control systems might be feasible if intimate control of the void distribution in the reactor core were possible. A detailed dynamic model of two-phase flow in a boiling channel is required before study of such control systems can be made, as the dynamics of void production must be clearly expressed if the voids are to be controlled during transients. A simple model is used to demonstrate the stability of void-flow interaction in the water recirculation loop.

Sommaire

L'étude dynamique des réacteurs nucléaires à eau bouillante a acquis une grande importance pour l'établissement des projets d'installation, étant donné que la stabilité du circuit de recyclage de l'eau d'une part, l'interaction entre les vides résultant du dégagement de vapeur et le dispositif de production des neutrons d'autre part (appelé effet de réaction de réactivité des vides — «void reactivity feedback effect»), imposent des limitations technologiques et économiques. Dans un réacteur à eau bouillante du type à circulation naturelle (BWR), les considérations relatives à la stabilité du circuit de recyclage de l'eau ont toutes leur importance propre. Dans un réacteur du type à tube sous pression (PTR) où la circulation est forcée, d'intéressants problèmes de commande et de stabilité se posent par suite de la liberté du constructeur de choisir un coefficient des réactivité des vides donnant une réaction soit positive, soit négative.

La communication a pour objet une discussion en termes généraux du rôle joué par le coefficient de réactivité des vides sur la stabilité du réacteur et de son dispositif de commande. Elle démontre que des systèmes de commande fort complexes pourraient être conçus si l'on pouvait agir sur la répartition des vides dans le cœur du réacteur. L'étude de cette action requiert une analyse préalable sur un modèle dynamique détaillé de l'écoulement de deux phases dans un canal à ébullition: il faut en effet connaître à fond la dynamique de la création des vides si l'on veut maîtriser ces derniers en régime transitoire. A l'aide d'un modèle simple, on montrera la stabilité de l'interaction vides — écoulement dans le circuit de recyclage de l'eau.

Zusammenfassung

Beim Entwurf von Siedewasser-Kernreaktoren spielt die Reaktordynamik eine große Rolle, da die Stabilität des Wasserkreislaufes und die Wechselwirkung zwischen Dampfblasen und dem Prozeß der Neutronenerzeugung (Rückwirkung durch den Einfluß des Blasen-volumens auf die Reaktivität) technische und wirtschaftliche Grenzen setzen. In Siedewasser-Kernreaktoren mit natürlichem Umlauf (BWR)

sind Betrachtungen der Stabilität des geschlossenen Kreislaufes außerordentlich wichtig; in einem Druckröhrenreaktor mit Zwangsumlauf (PTR) ergeben sich dadurch interessante Regel- und Stabilitätsprobleme, daß man einen Blasenkoeffizienten der Reaktivität vorgeben kann, der eine negative oder eine positive Rückkopplung bewirkt.

Diese Arbeit befaßt sich ganz allgemein mit dem Einfluß des Blasen-koeffizienten der Reaktivität auf die Stabilität und Regelung eines Reaktors und zeigt, daß verbesserte Regelsysteme möglich sind, wenn die Blasenverteilung im Reaktorkern vollkommen regelbar wäre. Ein ausführliches dynamisches Modell einer Zweiphasenströmung in einem Siedekanal ist zur Untersuchung eines solchen Regelsystems erforderlich, da die Dynamik der Blasenerzeugung eingehend bekannt sein muß, wenn die Blasen während eines Übergangsvorganges des Reaktors geregelt werden sollen. Ein einfaches Modell wird benutzt, um die Stabilität der Wechselwirkung zwischen Strömung und Blasen in einem geschlossenen Wasserkreislauf zu zeigen.

Introduction

Considerable attention has been devoted to the boiling water nuclear reactor¹ during the last decade as a possible steam generator for an economically attractive power plant. In this type of nuclear reactor the circulating coolant—which can be light or heavy water—flows past the uranium fuel rods absorbing the heat of thermal fission and boils. The steam generated is collected and conveyed either directly to a turbine or to an intermediate heat exchanger. In either case the nuclear reactor is an integral part of a recirculating water boiler loop similar to the La Mont Process.

Dynamic stability has been a topic of concern since the inception of a boiling water reactor, as in addition to the hydrodynamics of the recirculating water loop the boiling and fission processes interact in a manner that provides a feedback path round the neutron production process. This is as if the boiling of water in a conventional boiler affected the rate of fuel flow to the burners. Consequently the literature is now relatively well supplied with studies of BWR dynamics²⁻⁶. The detailed physics of boiling heat transfer and two-phase flow is of particular concern in boiling water nuclear reactors because the accurate prediction of the volume and distribution of steam in the heated sections is needed in order to calculate both the distribution of fission power over the reactor and the details of the feedback interaction. These factors may also have an important influence on the margin against burn-out^{7, 8}.

The presentation of a dynamic model representing a boiling water nuclear reactor should thus be of interest to an audience outside nuclear reactor technology because of its attention to the detail of boiling water dynamics, and because of the interesting dynamic and control problems that are raised when considering the operation of the reactor in combination with a turbine.

The analytical portion of this paper will concentrate on the dynamics of two-phase flow in the boiling channel, as not only is this subject of wide interest, but it also represents an area in which a considerable amount of theoretical and experimental research is required before models can be derived which predict the fluctuations of the boiling process during short term transients.

Model of a Boiling Water Reactor

Representations of boiling water reactors are shown in Figure 1. The natural circulation boiling water reactor (BWR) is shown in Figure 1(a) where it is seen that the heavy water acts both as coolant and moderator and undergoes natural circulation in a large high pressure tank. Circulation is assisted by

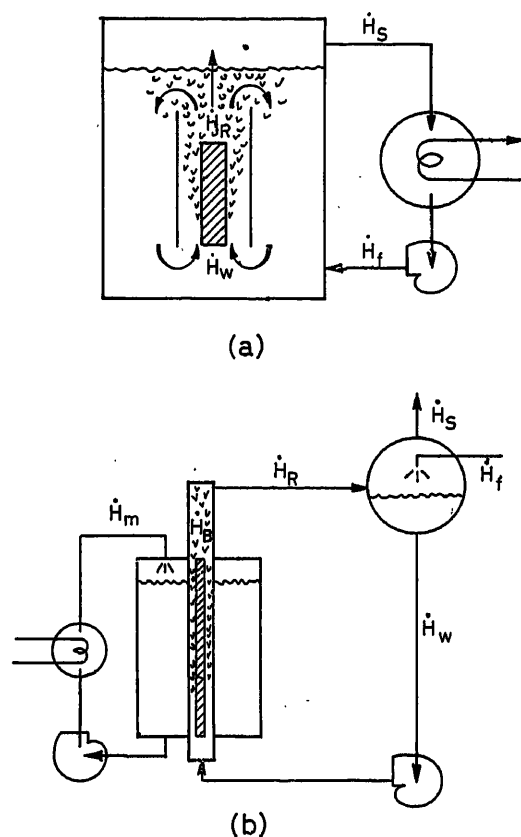


Figure 1. (a) Natural circulation boiling water reactor (BWR); (b) forced circulation pressure tube reactor (PTR). \dot{H} —enthalpy transport rate. Subscript: f —feedwater, w —recirculating water, R —boiling channel exit; R —riser; s —steam load; m —moderator

enclosing the fuel element clusters in shrouds, thereby dividing the vessel into downcomer and upcomer regions. The steam is collected at the top and passed to a heat exchanger.

Figure 1(b) illustrates a particular example of a forced circulation reactor of the pressure tube variety (PTR). Here light water is pumped past a fuel element enclosed in pressure tubes, the steam being separated from the water in a drum as in conventional practice. The heavy water moderator is outside the tubes in a low pressure tank, and is also circulated through a heat exchanger to remove the small amount of heat acquired while

in the reactor core—there is no intentional heat transfer between the pressure tubes and the moderator.

There are several variations on this theme, but considerations of neutron and engineering economy must be discussed when comparing their relative merits⁹. Such topics are outside the scope of this paper.

A block diagram of a BWR is shown in Figure 2 illustrating the main processes of the plant apart from the turbine, condenser, and feedwater systems which may be assumed to be conventional. The reactor plant may be divided into the following processes.

Neutron Kinetics and Fuel Element Heat Transfer

The neutron production process is characterized typically by the one forward path associated with neutron power (N) and thermal power (Q) production in response to the reactivity change (δk). The moderator is also heated by heat transfer from the fuel region and by a small amount of neutron thermalization and γ -ray heating. Three feedback paths are shown due to fuel element and coolant temperature and density changes. The consequent change in their physical properties modifies the neutron capture rate and influences the criticality of the reactor.

The heat transfer process is concerned with the description of the heating of the uranium fuel rods as a result of fission power. The resulting axial and radial temperature gradients in the fuel elements will then permit the heat available for transfer to the coolant to be known as a function of position and time.

The neutron production, fuel element heat transfer, and temperature reactivity feedbacks complete the model for neutron kinetics alone. Transfer function representations are now well established^{10, 11} for both lumped and distributed parameter models. In addition, the great majority of the quoted references on boiling water reactor dynamics contain transfer function treatment, though not necessarily based on point models. It is convenient to treat neutron kinetics with a one-point model for dynamic analysis, as this is amenable to transfer function methods. Axial or radial distribution of the neutron flux can be superimposed on the one-point model to define the power available at particular locations within the core. This assumes that the distortion of the spatial distribution has essentially only one mode, and that the power at any location varies in proportion to the change of the one-point model. Rigorous treatments of space-time core dynamics are also available.

Water Recirculation Loop

The dynamics of the water recirculation loop result from the interactions between power input to the heat channel, the resulting steam volume, circulation velocity, pressure, gravity head, and the steam load demands of the turbine. The two quantities of interest in the loop are the pressure drop Δp round the loop and the enthalpy transport rate \dot{H} . The pressure differentials provide the driving head which governs the circulation flow rate, the enthalpy defines the increase of energy in the system, and the rate at which it is changed in the loop.

The main difficulty in an analytical approach to the dynamics of the recirculation loop is the formulation of relationships between variables during the two-phase flow in the boiling channel and riser without recourse to experimental correlations which may not have been justified for the particular geometry

and conditions under examination. Transfer functions for neutron kinetics and fuel element heat transfer will not be presented. One point kinetic transfer functions are well known¹¹, and the dynamics of cylindrical fuel rods is also well documented^{12, 13}.

The Void-reactivity Feedback

A change in fission power will alter the volume of steam present in the core. For the usual designs of undermoderated reactor, the increase of voidage effectively reduces the rate at which neutrons become thermalized, and increase of void has therefore a negative feedback effect on reactivity. The influence of boiling on reactivity is shown in Figure 2 as a feedback path

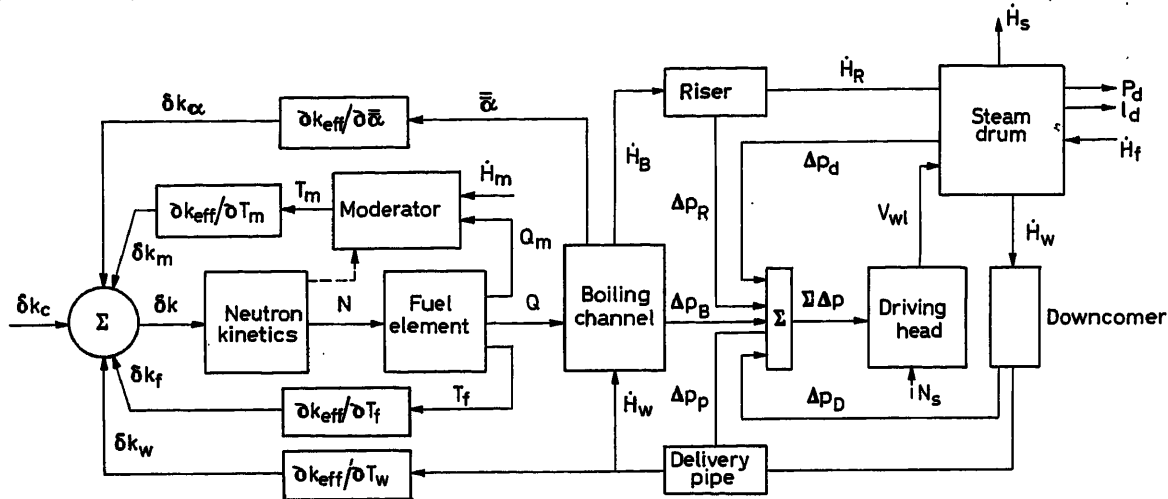


Figure 2. Block diagram of a boiling water reactor. N —fission power; Q —thermal power; p —pressure; Δp —pressure drop; l_d —drum water level; δk —reactivity change; k_{eff} —effective neutron multiplication; N_s —synchronous speed of pump; V_w —downcomer water velocity; T —temperature; \dot{H} —enthalpy transport rate; $\bar{\alpha}$ —weighted average void. Subscript: c —control; m —moderator; α —void; w —recirculating water; f —fuel or feedwater; B —boiling channel; R —riser; d —drum; D —downcomer, P —delivery pipe

from the boiling channels in which the void $\bar{\alpha}$ introduces a change of reactivity δk_α .

The magnitude and sense of the void coefficient of reactivity K_α is dependent on the physical characteristics of the core, in particular on the ratio of moderator to fuel volumes, the enrichment of the uranium fuel, and the geometrical arrangement of the fuel element lattices⁹. It is possible to vary the value of K_α from positive to negative by adjusting these parameters, thus—for a given fuel optimized for the reactor application— K_α may be increased or decreased by altering the pitch of the fuel elements (effectively altering the moderator to fuel ratio).

The void-reactivity effect introduces a variable in the design of boiling water reactors which makes them at once more difficult and more interesting than conventional fossil-fuelled boilers which have no interaction between steam volume and the energy release rate of the fuel (i.e. conventional boilers have zero void coefficients). There is not usually complete freedom to design in any desired void coefficient, but the range of variables leads to some interesting problems in stability and control.

* The void coefficient of reactivity is defined as $K_\alpha = \partial k_{eff} / \partial \bar{\alpha}$, where ∂k_{eff} is the change in effective neutron multiplication for a change $\partial \bar{\alpha}$ in the average void.

The Dynamics of Void Formation

The study of the dynamic characteristics of the void-reactivity interaction requires a realistic dynamic model of two-phase flow in a vertical heated channel with which the factors that influence the void distribution during transients can be investigated. The boiling channel model can then be inserted into standard kinetics and steam plant models for the study of the dynamics of the overall plant in general and of the reactor-void interaction in particular.

A simple model, however, can establish the general dynamic behaviour of the void in response to perturbation if axial distributions of the void can be ignored. Consider the representa-

tion of Figure 3(a) in which saturated water is entering a heated channel.

The volume of steam relative to that of the fluid is denoted by the void fraction $\alpha(z, t)$. A linear void gradient up the channel will be assumed for convenience. The actual gradient will depend on the axial distribution of the heat flux $Q(z, t)$ and the instantaneous distribution of steam bubbles in transport up the channel. The steam bubbles have an increased velocity relative to the water phase. The ratio of steam to water velocities is called slip S , defined by

$$S(z, t) = \frac{v_s(z, t)}{v_w(z, t)} = \frac{x(z, t)}{(1-x)(z, t)} \cdot \frac{(1-\alpha)(z, t)}{\alpha(z, t)} \cdot \frac{\rho_w^s(z, t)}{\rho_s^s(z, t)}$$

where x is the quality or ratio of steam to mixture by weight.

The starting point for analysis is always the three equations of mass, energy, and momentum conservation. These are stated for a two-phase mixture in Derivation I, [eqns (1), (2), (8)]. If one assumes homogeneous flow, $S = 1$, and the need to find a fourth equation to solve for the additional variable (steam velocity) is by-passed.

Two expressions are found in Derivation I relating void and exit velocity to the inputs to the simple channel of Figure 3(a), [eqns (14), (15)]. There are always involved expressions relating

pressure to the other variables in two-phase flow analysis, due to the dependence of local saturated conditions on the absolute pressure. These terms are comprised of two parts: (a) that due to the pressure drop in the channel due to friction and acceleration effects, and (b) that due to the change in absolute pressure due to external conditions in the plant (change of turbine load for example).

The time lag τ_α is associated with the transport of voids up

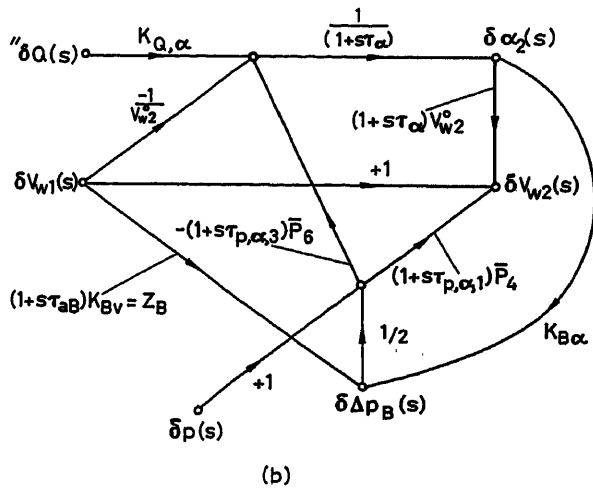
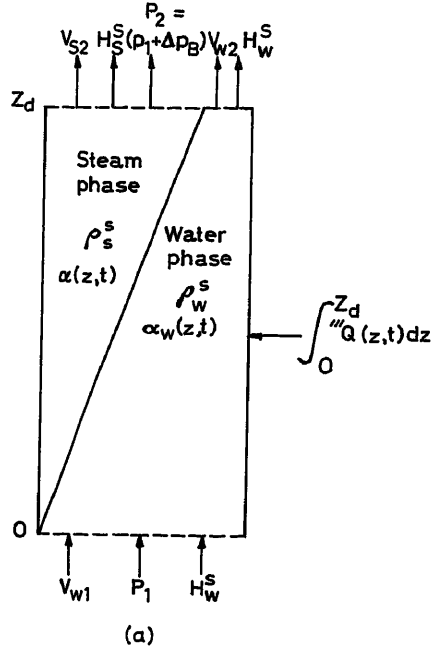


Figure 3. (a) Simple model of a heated channel; (b) signal flow-graph for the dynamics of a heated channel (see Derivation I for meaning of symbols)

the channel as the local bubbles are augmented by the bubbles already produced further upstream at a previous time.

Figure 3(b) shows a signal flow graph for the simple channel. The gain $K_{B\alpha}$ is dependent largely on the differential density head assisting circulation up the channel due to the mixture density being less at the exit—which provides the force for

driving natural circulation systems). $K_{B\alpha}$ is a function of α . The other pressure feedback arises from the resistance to flow and the acceleration of the mixture of the channel. In fact the gain $(1 + st_{\alpha B}) K_{B\alpha}$ can be regarded as an impedance Z_B since it describes the channel's resistance to flow.

The dynamics of the loop as a whole can be considered by fitting the above heated channel model into a loop model as shown in Figure 4(a).

Considering first a natural circulation loop and ignoring any effects introduced by a steam drum, the loop equation is found

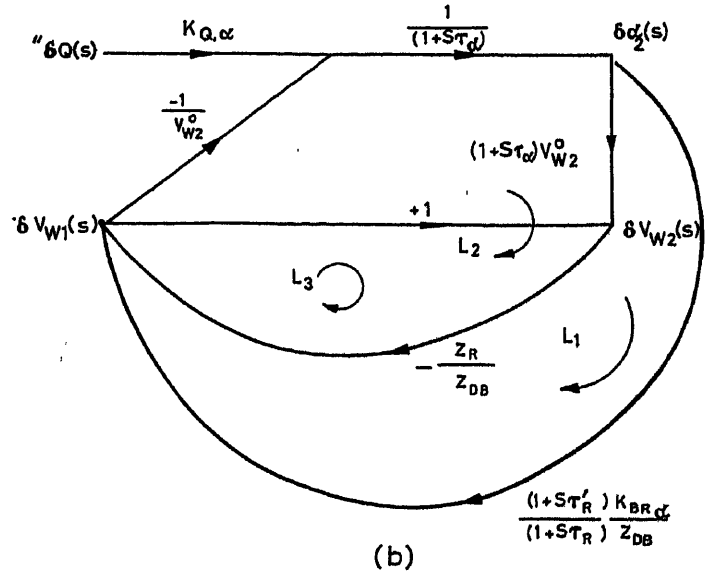
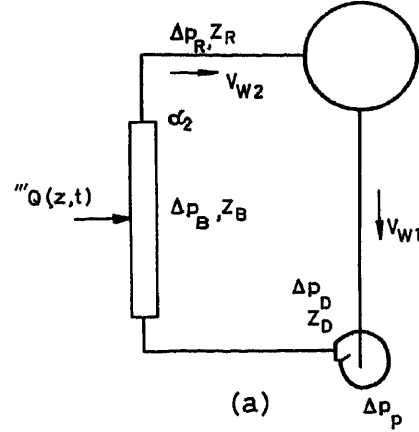


Figure 4. (a) Schematic of recirculating water loop; (b) Signal flow-graph of recirculating water loop (see Derivation II for meaning of symbols)

by equating the sum of the pressure drops to zero. From this it is shown that the channel inlet velocity is void dependent [eqn (27)]. The associated signal flow-graph [Figure 4(b)] shows three feedback loops of which loop L_3 is destabilizing. The increased resistances due to faster flow rates will tend to reduce the driving head so that flow rate at the channel inlet is actually reduced. Reduced flow rate (for constant heat input rate) increases the void still further.

Further reduction leads to Figure 5(a) (ignoring pressure effects) which has a void production transfer function [eqn (15)] in the forward path and a void-flow interaction transfer function [eqn (27)] in the feedback path. The criterion for stability is apparent from [eqn (28)] and is dependent on loop transport delays and impedances, particularly the riser impedance. This stability criterion is frequency dependent. One feels intuitively that the inertia of the loop as a whole would prevent high frequency oscillations building up, and that such oscillations (if they occur) would probably be bounded by the non-linearities. It is possible that the noisy flow velocity measurements obtained from rigs may contain amplitude limited high-frequency oscillations due to the void-flow interaction.

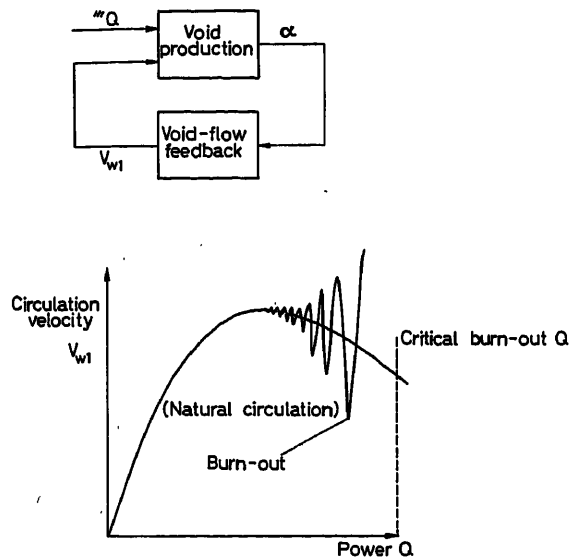


Figure 5. (a) Void-flow interaction feedback loop; (b) flow rate—power characteristic for natural circulation

This is a possible explanation of the burn-out of fuel elements reported for heat fluxes lower than critical. A typical flow rate—heat flux curve is shown for a natural circulation loop in Figure 5(b). Flow rate increases with void (\propto heat flux) until the frictional resistance has increased to such an extent that further heat flux increments produce a net reduction in flow rate. As a result there will be a critical heat flux at which all the water in contact with the channel walls is vaporized and burn-out occurs. However, if the stability criterion is not satisfied for some lower heat flux, noise may drive the loop into oscillations which build up and cause burn-out well before the critical heat flux has been reached.

The addition of a circulation pump can be allowed for in Derivation II by replacing the Z_{DB} terms by $(Z_{DB} - Z_p)$ where Z_p is the pump impedance found from the pump characteristics, Z_p is the change of pump head/change of flow rate. Z_p is often taken as infinite which eliminates void-flow feedback. However, there will be some interaction, and the stability criterion should still be checked, particularly with long risers.

Stability of a Hydraulic Loop

It is as well to define stability when considering the flow of a steam-water mixture. It is clear that a true steady state does

not exist during boiling in a recirculating loop, as a glance at a laboratory boiling rig with transparent pipes will quickly show. The process is essentially stochastic with the volumetric content of the bubble population at a point in the heated channel undergoing rapid fluctuations for a constant heat input rate and a nominally constant inlet water flow rate. In addition to the usual stochastic pattern of turbulent flow, there may be specific periodic oscillations. For example, with given external conditions, the flow can tend from bubbles in water (bubble flow) to alternate slugs of water and steam of considerable volume (slug flow) to a central steam core (annular) as the steam fraction increases up the channel. Stability therefore depends on the time scale adopted, and for the purposes of this study the short term fluctuations in bubble population will be classified as noise, although they represent the high-frequency oscillation of a non-linear system with bounded stability. The recirculation loop will be regarded as stable providing that the conditions of circulation and boiling averaged over the transit delay through the core are stationary.

The Complete Reactor-recirculation Loop Model

To study the general stability of the interactions between the (linearized) neutron production—void formation—and water circulation processes, further transfer functions are required for the steam drum (equivalent to the steam-water volume above the shrouds in natural circulation systems). Comparatively straightforward models for steam drum dynamics are available in the literature¹⁴. In Figure 6 the drum is represented by a general heat and mass balance block, with a dynamic term $K_d, p/(1 - L_d)$ representing the lags inherent in the mixing

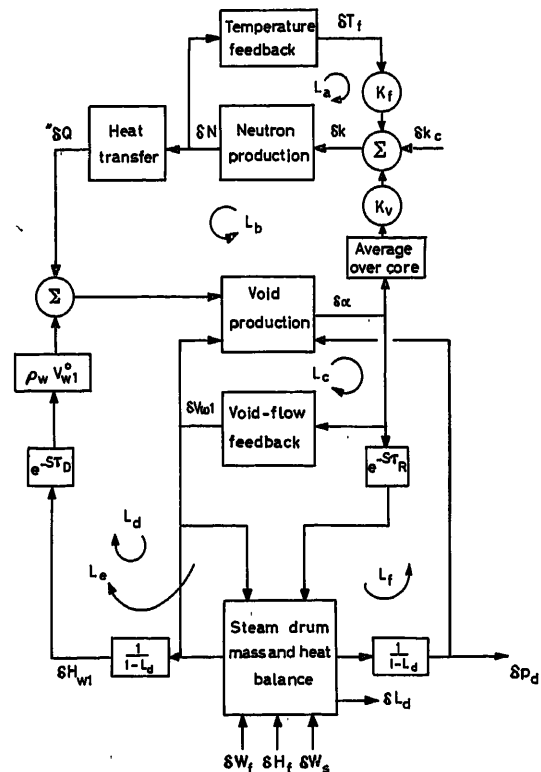


Figure 6. Schematic of complete reactor-recirculation loop model

process between the incoming saturated water from the riser and the sub-cooled feedwater.

A general block diagram representing the dynamic interactions of the units in Figure 2 can now be compiled as in Figure 6, where L_a is the fuel element (Doppler) reactivity feedback loop and is usually stabilizing. The fuel element time lag is in the feedback path, in most cases of a few seconds magnitude. L_b is the void-reactivity feedback loop. The fuel element time lag is in the heat transfer block, and the lag in the void formation block is associated with the water transit time up the channel. L_c is the void-flow interaction loop whose stability has already been discussed, and L_d is the recirculation rate-void interaction loop due to the changes of inlet water enthalpy as a result of the steam drum responses to circulation changes. The loop includes the term for drum dynamics $K_{d,p}/(1 - L_d)$ and a transport delay $e^{-s\tau_D}$ representing the water transit time between the

duced is fed directly to a turbo-alternator. The question to be decided is the appropriate value for K_v (the void coefficient) for the indicated control system which—in maintaining the plant steam pressure p_s constant—matches the reactor's power N to the demanded load $(D)L$.

Case I—Constant Electrical Load L . Reactivity Perturbation $+\delta k$

With negative K_v , the increase of neutron power and steam void will produce a reduction of δk_a , which is a stabilizing response. With positive K_v , the perturbation would result in a further increase of neutron power which is destabilizing.

Case II—Reactor in Equilibrium. Electrical Demand $+(D)L$

With negative K_v , the increased flow of steam resulting from the throttle opening in response to $(D)L$ will lower the steam

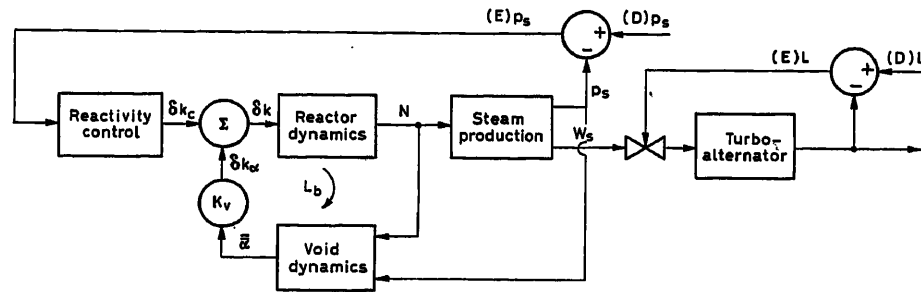


Figure 7. Boiling water reactor and plant control. N —neutron power; W_s —steam flow rate; p_s —steam pressure; L —electrical load; V —void; δk_a —void reactivity change; δk_c —control reactivity change; (D) —demand; (E) —error

drum and the boiling channel inlet. This can be of several seconds duration. L_c is the void-power interaction loop due to variations in the inlet water enthalpy as a result of changes in mixture quality entering the steam drum. It has an additional delay $e^{-s\tau_R}$, representing the mixture transit time up the riser. Finally, L_f is the pressure-void feedback loop representing the flashing of steam (or *vice versa*) in response to changes of absolute pressure. These changes will be induced by variations in the turbine steam rate demand W_s . There will also be changes in system pressure due to the recirculation rate as well.

The stability of the system as a whole depends on the interaction of these several loops and is clearly a matter for computer solution. However the stability criterion is simply stated:

$$1 - L_a - L_b - L_c - L_d - L_e - L_f + L_a L_c + L_a L_d + L_a L_e + L_a L_f > 0$$

where the L are the frequency dependent loop gains.

When considering stability of the plant as a whole, three matters have to be borne in mind: (a) the interaction between loops which may force oscillatory behaviour onto the plant, e.g. the delayed water enthalpy response in loop L_d as a result of increased heat flux in loop L_b ; (b) the stability of the loops themselves, and (c) the response of the plant to load changes.

The Influence of the Void Coefficient on the Stability and Control of Direct Cycle Boiling Water Reactor Plant

Consider a boiling water nuclear reactor with a direct cycle power plant as illustrated in Figure 7, in which the steam pro-

duced is fed directly to a turbo-alternator. This will cause the steam void to increase due to flashing, and the neutron power to reduce. The reactor will thus be opposing the control system which will be endeavouring to increase the power. With positive K_v , the reactor will tend to be load following.

For direct cycle plant therefore the choice lies between either an inherently stable or an inherently load-following reactor. It is understandable that the decision has always been made in favour of the inherently stable reactor on the grounds of safe operation, although an automatic safety control system is invariably fitted in addition to the operational automatic control system. The safety control system can override the latter and shut the reactor down should a possibly dangerous increase in reactor power occur.

There may, however, be an economic penalty to be paid if the decision is in favour of negative void coefficients, as the fuel enrichment must be increased to overcome the reactivity deficit held in the voids and to allow for the slight undermoderation usually necessary to provide a negative coefficient⁹. Capital cost considerations on the other hand operate in the opposite direction.

In addition the void coefficient is a function of power for a given core design. Figure 8 (taken from Campbell *et al.*⁹) illustrates variation of K_{eff} with coolant density, void fraction and power (assuming constant forced recirculation rate) for a given fuel enrichment and varying fuel lattice pitch for a reactor of the PTR type. A similar set of curves with the same general character can be drawn for varying enrichment on a given lattice pitch. The magnitude and sense of K_v depends on the slope of the

curves, and it is shown that closing the lattice pitch (decreasing moderator to fuel ratio) has the effect of providing large negative void coefficients for high void contents. For a large PTR there may be a limit below which the pitch cannot be closed, imposed by engineering considerations. On the other hand, there is a limit on the amount by which the void coefficient can be negative imposed by conventional considerations of feedback loop stability.

The Independent Control of Voids

It is worth considering for certain types of PTR design whether the control engineer can make a significant contribution to the economic feasibility of boiling water reactors by devising safe and reliable control systems which will allow the reactor to

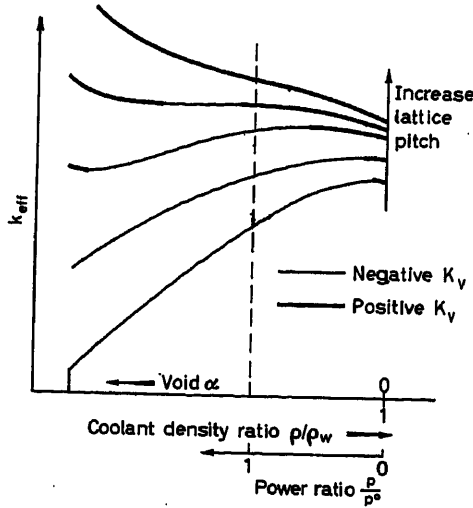


Figure 8. Influence of coolant density and lattice pitch on void coefficient K_v .

$$K_v = \frac{\delta k_{eff}}{\delta \alpha}; \quad \frac{Q}{Q_w} = (1-\alpha) + \alpha \frac{Q_s}{Q_w};$$

K_{eff} is effective neutron multiplication in core

operate over a wide range of void coefficients. This may increase the choices available to the designer who is attempting to achieve an economic optimum.

The destabilizing reactivity feedback effect can be effectively damped out if the voids are maintained independent of power and power transients. Thus an internal control loop is suggested which will match the flow of the coolant being recirculated to the power demand, as for example in conventional once-through or monotube boilers¹⁵. This is an expression of the ideal towards which the designer of the control system would aim. One method of controlling the voids might be to insert a control system within the recirculation loop that would trim the recirculation flow rate in response to changes in void. A controlling signal for the loop could be derived by using the pressure difference method of measuring quality, the pressure sensors in the risers giving an indication of the average quality (or sector quality if the neutron flux has spatial freedom).

Conclusion

The dynamics and engineering feasibility of such loops cannot be discussed until studies of the dynamics of void forma-

tion have been made in detail, and these must wait until the development of a transient boiling channel model from which the restriction to steady state empirical correlations has been removed. The basis for such a model requires the detailed study of the dynamics of the steam and water phases in two-phase flow. Momentum exchange, together with the analysis of the forces acting on the bubbles, is likely to lead to such a model¹⁶, but its validity cannot be established until experimental results from dynamic heat transfer rigs are available, with which the model's predictions of dynamic behaviour can be compared. Research into the dynamics of heat transfer and two-phase flow is a new departure and is as much an instrumental and analytical problem as it is one of engineering difficulty. Its purpose is to establish the behaviour of two-phase mixtures in space and time while undergoing transient motion from one equilibrium state to the next. The pioneering work of Zivi¹⁷ must be mentioned in this context.

It is to be hoped that this paper will have shown the absorbing problems that boiling water nuclear reactors (or even laboratory boiling heat transfer rigs) can present to the dynamist and control engineer. It is a rewarding field, as a rigorous analytic treatment of the boiling process is still not available. It is sometimes surprising to realize that an everyday process like the boiling of water in a kettle should lead to such theoretical difficulties.

Derivation I—Transfer Function Model for a Linearized Boiling Channel

Assume, for analytical convenience only, that (i) boiling starts at channel inlet, (ii) the pressure drop across the channel is small relative to absolute pressure, consequently the axial dependence of saturated densities and enthalpies can be neglected, and enthalpy can be used instead of internal energy for the time partial derivative in the conservation of energy equation, (iii) axial distribution of void and density along the channel is linear and (iv) uniform heat flux axial distribution is $'''Q(z, t)$.

Conservation of Mass

$$\frac{\partial}{\partial t} [\alpha_w \rho_w^s + \alpha \rho_s^s] + \frac{\partial}{\partial z} [\alpha_w \rho_w^s v_w + \alpha \rho_s^s v_s] = 0 \quad (1)$$

Conservation of Energy

$$\frac{\partial}{\partial t} [\alpha_w \rho_w^s H_w + \alpha \rho_s^s H_s] + \frac{\partial}{\partial z} [\alpha_w \rho_w^s H_w v_w + \alpha \rho_s^s H_s v_s] = '''Q(z, t) \quad (2)$$

(1) may be rearranged to give

$$\begin{aligned} & \frac{\partial}{\partial t} \alpha_w(z, t) + \frac{\partial}{\partial z} (\alpha_w v_w)(z, t) \\ &= -\frac{\rho_s^s(z)}{\rho_w^s} \left\{ \frac{\partial}{\partial t} \alpha(z, t) + \frac{\partial}{\partial z} (\alpha v_s)(z, t) \right\} \\ & - P_1(z, t) \frac{\partial}{\partial t} p(z, t) \end{aligned} \quad (3)$$

where

$$P_1(z, t) = \frac{\alpha(z, t)}{\rho_w^s} \left[\frac{\rho_s^s}{p} \right] \quad (4)$$

From (2) and (4)

$$\frac{\partial}{\partial t} \alpha_w(z, t) + \frac{\partial}{\partial z} (\alpha_w v_w)(z, t) = -\frac{'''Q(z, t)}{\rho_w^s H_{ws}(t)} + P_3(z, t) \frac{\partial}{\partial t} p(z, t) \quad (5)$$

where

$$P_3(z, t) = \frac{\alpha_w(z, t)}{H_{ws}(t)} \left[\frac{H_w^s}{p} \right] + \frac{\alpha(z, t) \rho_s^s(t)}{\rho_w^s H_{ws}(t)} \left[\frac{H_s^s}{p} \right] \quad (6)$$

$$H_{ws}(t) = H_s^s(t) - H_w^s(t) \quad (7)$$

Conservation of Momentum

$$\begin{aligned} \frac{\partial}{\partial z} p(z, t) &+ \frac{1}{g'} \left\{ \frac{\partial}{\partial t} [\alpha_w \rho_w^s v_w + \alpha_s \rho_s^s v_s] + \frac{\partial}{\partial z} [\alpha_w \rho_w^s v_w^2 + \alpha_s \rho_s^s v_s^2] \right\} \\ &+ F_{PT}(z, t) + \frac{g}{g'} [\alpha_w \rho_w^s + \alpha_s \rho_s^s] = 0 \end{aligned} \quad (8)$$

Eqns (3), (5) and (8) are general for two phase dynamics and have in fact only used assumption (ii).

The treatment will now be simplified, using the remaining assumptions—saturated conditions, axial and time dependence being understood. Note the initial condition $\alpha_w(0, t) = 1$, $\alpha(0, t) = 0$. Let the boiling length be z_b . Integrate (3) over z_b ; and write for small perturbations from the equilibrium in Laplace transform notation. Hence

$$\begin{aligned} \delta \alpha_2(s) &= \frac{1}{(1 - S_2^0 R)(1 + s\tau_{v,a})} \left\{ (\alpha_w^0 + S_2^0 R \alpha_2^0) \frac{\delta v_{w2}(s)}{v_{w2}^0} - \frac{\delta v_{w1}(s)}{v_{w1}^0} \right\} \\ &- \left(\frac{1 + s\tau_{p,a,1}}{1 + s\tau_{p,a}} \right) \frac{\bar{P}_4 \delta p(s)}{(1 - S_2^0 R) v_{w2}^0} \end{aligned} \quad (9)$$

where

$$\tau_{v,a} = z_b(1 - R)/2(1 - S_2^0 R) v_{w2}^0; \quad \tau_{p,a,1} = \bar{P}_2/\bar{P}_4 \quad (10)$$

$$\bar{P}_4 = \frac{\rho_s^0}{\rho_w^0} \alpha_2^0 v_{s2}^0 \left[\frac{\rho_s^s}{p} \right], \quad R = \frac{\rho_s^0}{\rho_w^0}, \quad \text{slip ratio } S = \frac{v_s}{v_w} \quad (11)$$

Similarly (5) becomes

$$\begin{aligned} \delta \alpha_{w2}(s) &= \frac{-1}{(1 + s\tau_{Q,a})} \left\{ \frac{'''Q(s)}{\rho_w^0 v_{w2}^0 H_{ws}^0} + \left(\alpha_w^0 \frac{\delta v_{w2}(s)}{v_{w2}^0} - \frac{\delta v_{w1}(s)}{v_{w1}^0} \right) \right\} \\ &+ \left(\frac{1 + s\tau_{p,a,2}}{1 + s\tau_{Q,a}} \right) \frac{\bar{P}_5 \delta p(s)}{v_{w2}^0} \end{aligned} \quad (12)$$

where

$$\bar{P}_5 = \frac{'''Q^0}{\rho_w^0 H_{ws}^0} \left[\frac{H_{ws}}{p} \right]; \quad \tau_{Q,a} = \frac{z_b}{2v_{w2}^0}; \quad \tau_{p,a,2} = \bar{P}_3/\bar{P}_5 \quad (13)$$

The R and SR terms will now be ignored since this is an approximate treatment only, and because R and S are small at high pressure. For example, at 68 atm $R = 0.048$ and $S \leq 2$. Thus $\tau_{v,a} = \tau_{Q,a} = \tau_a$ and $v_s \cong v_w$.

(9) now becomes

$$\delta v_{w2}(s) = (1 + s\tau_a) v_{w2}^0 \delta \alpha_2(s) + \delta v_{w1}(s) + (1 + s\tau_{p,a,1}) \bar{P}_4 \delta p(s) \quad (14)$$

and (12) becomes

$$\begin{aligned} \delta \alpha_2(s) &= \frac{1}{(1 + s\tau_a)} \left\{ \frac{'''Q(s)}{\alpha_w^0 \rho_w^0 v_{w2}^0 H_{ws}^0} - \frac{\delta v_{w1}(s)}{v_{w2}^0} \right\} \\ &- \left(\frac{1 + s\tau_{p,a,3}}{1 + s\tau_a} \right) \frac{\bar{P}_6 \delta p(s)}{\alpha_w^0 v_{w2}^0} \end{aligned} \quad (15)$$

where

$$\bar{P}_6 = \bar{P}_5 - \alpha_w^0 \bar{P}_4; \quad \tau_{p,a,3} = \frac{\alpha_w^0 \bar{P}_2 - \bar{P}_3}{\alpha_w^0 \bar{P}_4 - \bar{P}_5} \quad (16)$$

A conventional expression will be used for pressure drop across the channel instead of deriving one directly from the momentum eqn (8).

$$p_1 - p_2 = \frac{r \rho_w v_{w1}^2}{g'} + \frac{1}{g'} \left(\frac{\partial F_{TP}}{\partial v_w^2} \right) \rho_w v_{w1}^2 + \frac{g}{g'} \bar{p} z_d + \frac{1}{g'} \bar{\rho} v_{w1} \quad (17)$$

where r is the Martinelli-Nelson acceleration multiplier

$$r = \frac{(1 - x_2)^2}{(1 - \alpha_2)} \frac{1}{\rho_w} + \frac{x_2^2}{\alpha_2^2} \frac{1}{\rho_s} - \frac{1}{\rho_w} \approx \left(\frac{\alpha_2}{1 - \alpha_2} \right) \frac{1}{\rho_w} \quad (18)$$

for low qualities. The small perturbation drop is therefore

$$\begin{aligned} \delta \Delta p_B &= \delta(p_1 - p_2) = - \left\{ \frac{\rho_w v_{w1}^2}{g'(1 - \alpha_2^0)} - \frac{g}{g'} \frac{z_d}{2} (\rho_w^0 - \rho_s^0) \right\} \delta \alpha_2(s) \\ &+ \left\{ \frac{2\alpha_2^0 \rho_w v_{w1}^0}{g'(1 - \alpha_2^0)} + \frac{2}{g'} \left(\frac{\partial F_{TP}}{\partial v_w^2} \right) \rho_w v_{w1}^0 \right\} \delta v_{w1}(s) + \frac{z_b \bar{\rho}^0}{g'} s \delta \bar{v}_{w1}(s) \end{aligned} \quad (19)$$

Half this pressure drop will be considered as influencing the pressure dependent parts of eqns (14) and (15).

Write eqn (19) as

$$\delta \Delta p_B(s) = K_{B\alpha} \delta \alpha_2(s) + \mathcal{Z}_B \delta v_{w1}(s) \quad (20)$$

where \mathcal{Z}_B is an impedance,

$$\mathcal{Z}_B = (1 + s\tau_{aB}) K_{Bv} \quad (21)$$

K_{Bv} is the coefficient of δv_{w1} in eqn (19) and

$$\tau_{aB} = \frac{z_d \bar{\rho}^0}{g'} K_{Bv}^{-1} \quad (22)$$

Derivation II—Recirculation Loop Stability (Power to Void)

Consider first a natural circulation loop. For the pressure drops round the loop

$$\begin{aligned} \delta \Delta p_D + \delta \Delta p_B + \delta \Delta p_R &= \mathcal{Z}_D \delta v_{w1} + \mathcal{Z}_B \delta v_{w1} + K_{B\alpha} \delta \alpha_2 \\ &+ \mathcal{Z}_R \delta v_{w2} + K_{R\alpha} \delta \alpha_2 = 0 \end{aligned} \quad (23)$$

therefore

$$(\mathcal{Z}_D + \mathcal{Z}_B) \delta v_{w1} + \mathcal{Z}_R \delta v_{w2} = - \left\{ K_{B\alpha} + \frac{K_{R\alpha}}{1 + s\tau_R} \right\} \delta \alpha_2 \quad (24)$$

where $(1 + s\tau_R)^{-1}$ is introduced to allow for transport delays in the riser. Define

$$\mathcal{Z}_{DB} = \mathcal{Z}_D + \mathcal{Z}_B; \quad K_{BR\alpha} = K_{B\alpha} + K_{R\alpha}; \quad \tau_R' = \frac{K_{B\alpha}}{K_{BR\alpha}} \tau_R \quad (25)$$

Then eqn (24) becomes

$$\delta v_{w1}(s) = - \frac{\mathcal{Z}_R(s)}{\mathcal{Z}_{DB}(s)} \delta v_{w2}(s) - \frac{(1 + s\tau_R')}{(1 + s\tau_R)} \frac{K_{BR\alpha}}{\mathcal{Z}_{DB}(s)} \delta \alpha_2(s) \quad (26)$$

These additional feedbacks are shown added to the basic boiling channel in the signal flow-graph of Figure 5(b). From the figure the flow response to void can be expressed as

$$\delta v_{w1}(s) = \left\{ \frac{\left(\frac{1+s\tau_R}{1+s\tau} \right) K_{BR\alpha} - (1+s\tau_\alpha) \mathcal{Z}_R(s)}{\mathcal{Z}_{DB}(s) + \mathcal{Z}_R(s)} \right\} v_{w2}^0 \delta \alpha_2(s) \quad (27)$$

The closed-loop transfer function for the recirculation loop then becomes

$$\frac{\delta \alpha_2(s)}{\delta Q(s)} = \frac{1}{(1+s\tau_\alpha)} \times \frac{K_{Q,\alpha}}{\left\{ 1 + \frac{1}{\mathcal{Z}_{DB}(s) + \mathcal{Z}_R(s)} \left[\frac{(1+s\tau_R) K_{BR\alpha}}{(1+s\tau_R)(1+s\tau_\alpha)} - \mathcal{Z}_R(s) \right] \right\}} \quad (28)$$

where

$$K_{Q,\alpha} = \frac{1}{\alpha_2^0 \rho_w^0 v_{w2}^0 H_{ws}^0} \quad (29)$$

For the loop to be stable, the denominator of the second term must be positive.

Nomenclature

F	Frictional resistance/unit length, lb./ft. ³
g	Gravity acceleration, 32.2 ft./sec ²
g'	Acceleration factor, 32.2 ft. lb./lb. sec ²
H	Specific enthalpy, B.Th.U./lb.
K	A gain defined locally
$K_{B\alpha}$	DI. 19
K_{Bv}	DI. 22
$K_{BR\alpha}$	DII. 25
$K_{Q,\alpha}$	DII. 29
P	Pressure dependent gains (DI)
p	Pressure, lb./ft. ²
Q	Total heat flux, B.Th.U./sec
$''Q$	Total heat/unit area, B.Th.U./ft. ² sec
$'''Q$	Total heat/unit volume, B.Th.U./ft. ³ sec
R	Density ratio ρ_g/ρ_w
r	Acceleration multiplier (DI. 18)
S	Slip ratio v_g/v_w
s	Complex variable, sec ⁻¹
T	Temperature, °F
t	Time coordinate, sec
v	Velocity, ft./sec
x	Steam quality
z	Time coordinate, ft.
Z	Pipe impedance, defined locally, lb./ft. ² sec/ft.
\mathcal{Z}_B	DI. 21, lb./ft. ² sec/ft.
$\mathcal{Z}_{D,R}$	DII. 23, lb./ft. ² sec/ft.
\mathcal{Z}_{DB}	DII. 25, lb./ft. ² sec/ft.
α	Void fraction
ρ	Density, lb./ft. ³
τ	A time constant, defined locally, sec
$\tau_{v,\alpha}$	DI. 10, sec
$\tau_{Q,\alpha}$	DI. 13, sec
τ_α	DI. 14, sec
τ_{p,α_1}	DI. 10, sec
τ_{p,α_2}	DI. 13, sec
τ_{p,α_3}	DI. 16, sec
$\tau_{\alpha B}$	DI. 22, sec
τ_R	Riser transport delay, sec
τ'_R	DII. 25, sec

Subscripts

B	Boiling region	TP	Two phase
b	Boiling boundary	w	Water
D	Downcomer	ws	Evaporation
R	Riser	1	Inlet
s	Steam	2	Exit

Superscripts

s	Saturated value	-	mean
0	Steady state value	.	d/dt

Prefixes

δ	Difference	Δ	Small perturbation value
----------	------------	----------	--------------------------

Coefficients or polynomial fits from the steam tables are denoted:

$$\left[\frac{H_w}{T_w} \right], \left[\frac{\rho_s}{p} \right], \left[\frac{H_w}{p} \right], \left[\frac{H_s}{p} \right], \left[\frac{H_{ws}}{p} \right]$$

Gratitude is expressed to the United Kingdom Atomic Energy Authority for permission to publish this paper. The constructive criticism of Mr. R. J. Cox and Mr. J. Fell was much appreciated, and the help of the staff of Dynamics Group is gratefully acknowledged—in particular that of Dr. J. D. Cummins and Mr. C. B. Guppy. All these persons are at the Atomic Energy Establishment, Winfrith, Dorset.

References

- KRAMER, A. W. *Boiling Water Reactors*. 1958. Reading, Mass; Addison-Wesley
- BECKJORD, E. S. Dynamic analysis of natural circulation boiling water power reactors. *ANL-5799* (1958)
- DESHONG, J. A. and LIPINSKI, W. C. Analysis of experimental power reactivity feedback transfer function for a natural circulation boiling water reactor. *ANL-5850* (1958)
- THIE, J. A. Dynamic behaviour of boiling reactors. *ANL-5849* (1959)
- FLECK, J. A. The dynamic behaviour of boiling water reactors. *J. nucl. Engng.* 11 (1960)
- AKCASU, A. Z. Theoretical feedback analysis in boiling water reactors. *ANL-6221* (1960)
- Heat extraction from boiling water reactors. *Lecture notes, adv. course, Netherlands-Norwegian Reactor School*. 1959, Norway; Institutt for Atomenergi
- The dynamic behaviour of boiling water reactors. *Lecture notes, adv. course, Netherlands-Norwegian Reactor School*. 1962, Norway; Institutt for Atomenergi
- CAMPBELL, C. G., FELL, J., and HOLMES, J. E. R. Nuclear physics problems of water reactors. *BNES Symp. on Water Reactors for Power Generation*, Manchester (July 1962)
- GYFTOPOULOS, E. P. Transfer function representation of nuclear power plants. *ANL-6205* (1960)
- SCHULTZ, M. A. *Control of Nuclear Reactors and Power Plant*. 2nd ed. 1961. New York; McGraw-Hill
- SCHMIDL, H., AMBROSINI, G., RYDELL, N. and VAPAAVIO, O. A transfer function model of the HBWR plant. *HPR-5* 1960. Norway; Institutt for Atomenergi, Halden
- RANDLES, J. Heat diffusion in cylindrical fuel elements of water cooled reactors. *AEW-R96* (1961)
- CHIEN, K. L., ERGIN, E. I., LING, C., and LEE, A. Dynamic analysis of a boiler. *Trans. Amer. Soc. mech. Engrs*, Col. 80 (November 1958)
- DIETHELM, M. The control of Sulzer monotube steam generators with reheating. *Sulzer techn. Rev.* 41 (1959)
- BECKJORD, E. S., and HARKER, W. H. Hercules I—the steady state calculation of vertical two-phase flow. *GEAP-3261* (1959)
- ZIVI, S. and WRIGHT, R. W. Power-void transfer function measurements in a simulated SPERT 1A moderator coolant channel. *ANL-6205* (1960)

DISCUSSION

D. E. DOUGHERTY and C. N. SHEN, *Rensselaer Polytechnic Institute, Troy, N.Y., U.S.A.*

By combining the hydrodynamic aspects of two-phase flow with the neutron kinetics of a BWR, the authors have delineated an important and difficult study. The importance of a load-following capability for a BWR was clearly pointed out. With regard to this problem, would the authors care to expand upon the type of control system they envisage for a plant having a positive void coefficient, and how this would compare with the 'dual cycle'¹ approach? As suggested by the authors, an internal control loop for maintaining a constant power-to-flow ratio would be useful in minimizing the external control (rods, etc.), but this would be costly in pumping power, have a sluggish response, and present a safety problem in case of a pump failure.

An alternative to maintaining a constant power-to-flow rate would be to vary the feedwater enthalpy and or flow rate and thereby maintain a relatively constant net void reactivity. In essence, this is what is accomplished by the 'dual cycle BWR'.

It is our opinion that due to the strong non-linearities which are manifest in two-phase flow phenomena, the linearized analysis presented in this paper is a useful but limited first step in defining the design limits of a BWR. For example the inception point for oscillatory flow may be well removed from the conditions of core burn-out, or the steam drum carryover limit due to the existence of a stable flow limit cycle. Thus we concur with the authors' suggestion that improved boiling models be developed, especially if maximum performance is to be obtained from the BWR power plants.

In our minds, there are some minor points in the derivations that may be generalized or corrected.

(1) The assumption whereby enthalpy is substituted for internal energy in the energy equation can be mitigated without introducing any significant complexities by rewriting eqn (2) as²

$$\begin{aligned} \frac{\partial}{\partial t} [\alpha \omega \rho_w^s H_w + \alpha \rho_s H_s - p/\gamma] \\ + \frac{\partial}{\partial z} [\alpha \omega \rho_w^s H_w V_w + \alpha \rho_s H_s V_s] = {}^m Q(z, t) \end{aligned}$$

and thus eqn (6) becomes

$$P_3 = \frac{a_w}{H_{ws}} \left[\frac{H_w}{p} \right] + \frac{\alpha \rho_s}{H_{ws} \rho_w} \left[\frac{H_s}{p} \right] - \frac{1}{\gamma H_{ws} \rho_w}$$

(2) A more general result may be obtained again by assuming the vapour fraction and the channel heat input approximately separable in space and time³ so that $\alpha(z, t) = \bar{\alpha}(t)f(z)$ and ${}^m Q(z, t) = {}^m \bar{Q}(t)g(z)$ where $f(z)$ and $g(z)$ are respectively the normalized initial steady state vapour fraction and heat input distributions.

(3) Considering eqn (17) we have been unable to discern a time-dependent acceleration pressure drop. Probably the last term on the right-hand side of eqn (17)⁴ is

$$\frac{1}{g}, \bar{\rho} \bar{b}_{w1}.$$

References

- ¹ A design description of the Dresden nuclear power station, GER-1301, 1957, General Electric Co.
- ² KNUDSEN and KATZ. *Fluid Dynamics and Heat Transfer*. 1958. New York; McGraw-Hill, p. 39, eq 2-41
- ³ MEYER, J. E. Hydrodynamic models for the treatment of reactor thermal transients. *Nucl. Sci. & Engng* 10 (1961)
- ⁴ MEYER, J. E. and ROSE, R. P. Application of a momentum integral model to the study of parallel channel boiling flow oscillations. *ASME Heat Transfer*. Feb. 1963, p. 1

P. K. M'PHERSON, *in reply*

Shen and Dougherty have posed an interesting question. How does one control a BWR with positive void coefficients? To date most BWRs have significantly negative void coefficients so that this question has not arisen. But the need to reduce the costs of nuclear electricity is likely to make void coefficients less negative, even positive perhaps, as effort is made to reduce fuel enrichment. In replying I will confine my attention to a direct cycle BWR of the Pressure Tube type (PTR) with forced circulation. An example of one is shown in *Figure 1*. It can be seen that this is a conventional La Mont boiler cycle with nuclear heating instead of combustion heating. Everything else is standard.

The original study of means whereby a reactor with a positive void coefficient might be controlled looked for subsidiary fast control loops. Control of primary flow was an obvious choice and computer studies have shown that this would be an effective stabilizing loop. The recirculating pump would have (say) three fixed speeds corresponding to 100, 50 and 20 per cent power. A power reactor will normally be

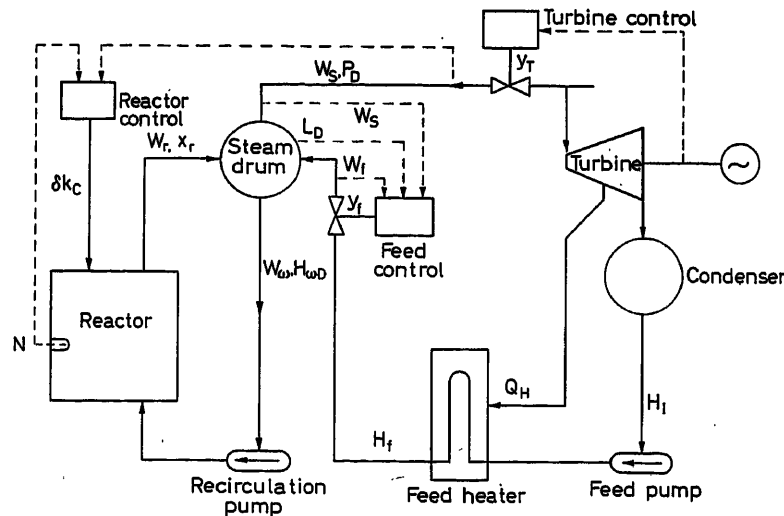


Figure 1

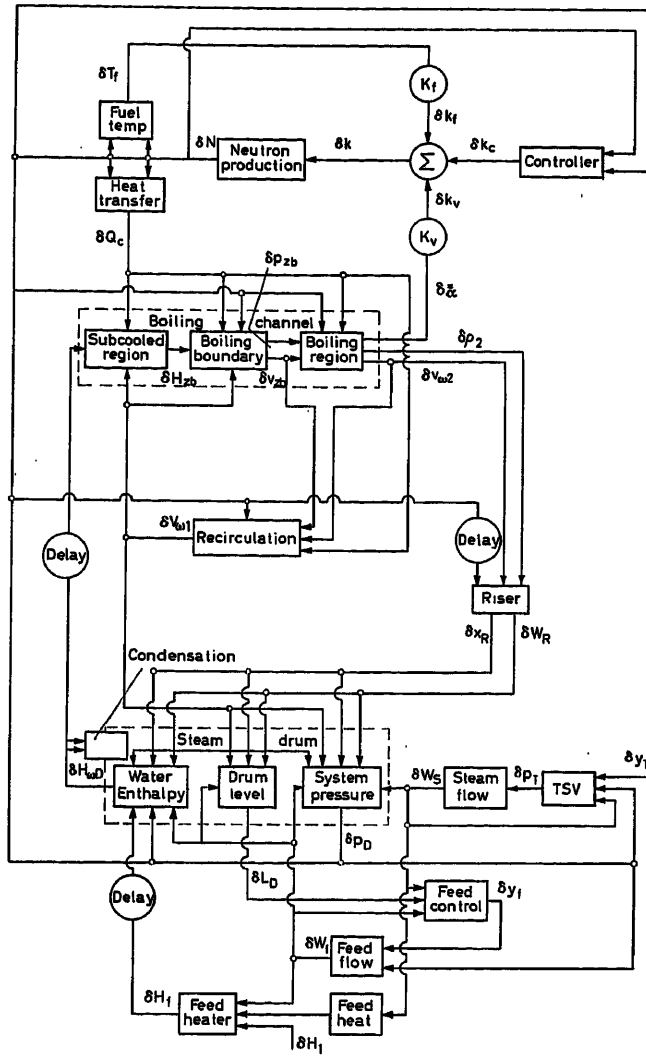


Figure B

at 100 per cent power, the other two powers represent short term power or set back states. A by-pass valve would be inserted to divert up to 5 or 10 per cent of pump discharge back to suction to provide fast trim control of flow. The by-pass valve might be actuated by a servo following (ideally) average void in the core. More realistically average exit steam quality would suffice if a dynamic sensor of steam quality were available. However, studies showed that actuation by perturbations in neutron flux provided good control. This sub-control loop is, of course, strongly dependent on the prevailing value of the void coefficient.

An alternative is to regulate the sub-cooling of the primary flow entering the core. This is similar to the dual cycle concept as shown by the discussors. A control method is not feasible with the type of plant being considered (Figure A) as there will be considerable delays before sub-cooling changes reach the core due to transportation lags of the water from the enthalpy change point to the core inlet.

In answer to the question how does one control a BWR with a positive void coefficient? I would suggest that a more profitable solution is the study of steam plant interactions with the boiling process in the core. This process is strongly dependent on pressure variations and our studies have shown that it is possible to adjust the design of the steam plant in such a way that the pressure feedback effects of the boiling process provide a stable plant overall even though the reactor

itself may have an inherent positive feedback due to the void-reactivity effect. I would like to illustrate this with an example. Figure B is an extension of Figure 6 in the paper, and represents a block diagram for a dynamic model of a realistic plant. More detailed boiling channel and steam drum representations have been added, feedwater heating and flow control are included and all the pressure feedbacks are represented. These are: (1) Pressure term to the controller for pressure regulation; (2) Heat transfer in the reactor is dependent on boiling temperature which is a function of pressure; (3) Pressure enters recirculation as the flow friction pressure drop in the two-phase region is pressure dependent; (4) Pressure enters the riser to provide flashing effects; (5) The heat balance in the drum is pressure dependent due to changes of saturation temperature with pressure; (6) Steam flow is, of course, dependent on steam pressure, and (7) Steam drum pressure is the back pressure against which the feedwater system operates.

The two dominant feedback effects are: (1) The direct pressure feedback to the channel adjusting the saturation temperature, and (2) The delayed change of sub-cooling at boiling channel inlet due to the change of saturation temperature in the steam drum.

Figure C shows the effect of these two feedbacks quite clearly. The model here is of the La Mont boiling loop only, all nuclear effects have been withdrawn. The input is a terminated ramp of heat flux δQ_c into the boiling channel which a constant setting of the turbine throttle

Input	1	2	3
δQ_c	✓	0	0
δp_d	✓	✓	0
δH_{wD}	✓	✓	✓

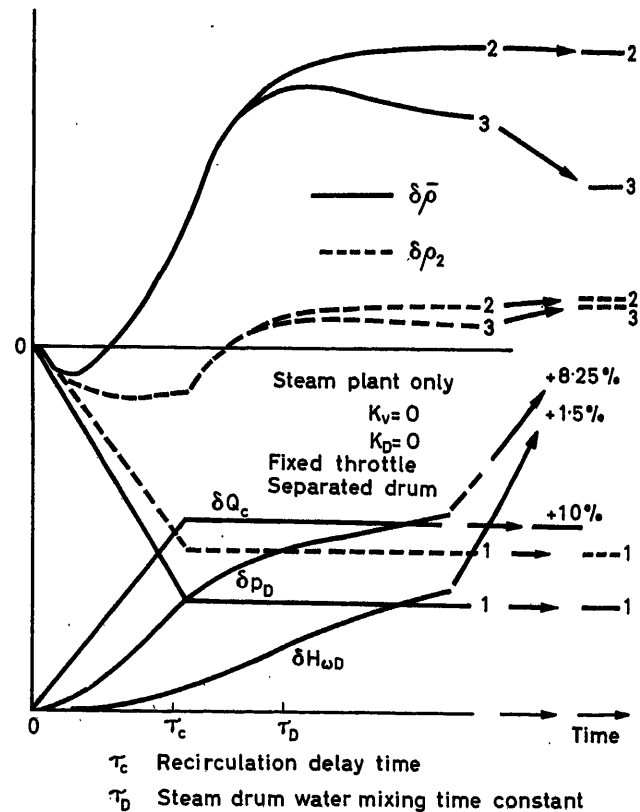


Figure C

assumed. The consequent rise of pressure drop δp_D and delayed rise of water enthalpy in the drum δH_{wD} are also shown. The curves 1, 2, 3 show the response of average coolant density $\bar{\rho}$ and exit coolant density ρ_2 as the feedback effects due to pressure and water enthalpy are added. The model of the steam drum assumes mechanical separation of the steam and water phases with mixing of relatively cool feed-

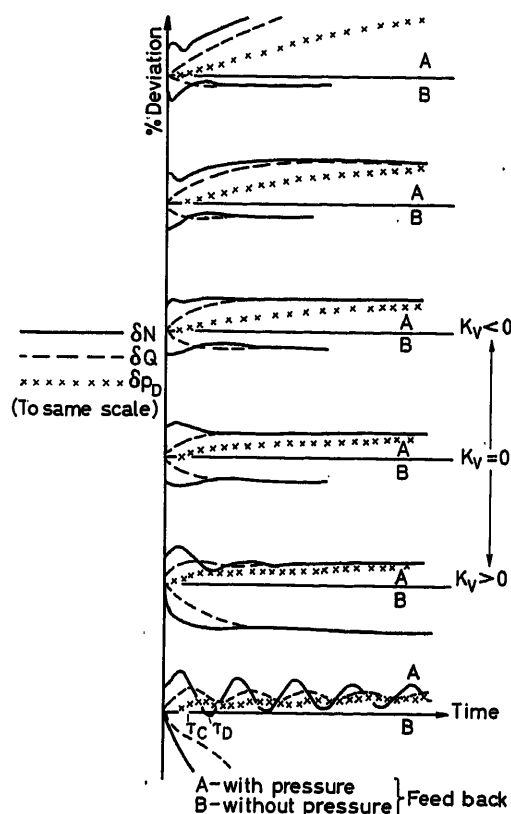


Figure D

water in the drum so that the water in the drum is significantly sub-cooled in the steady state. A cosine axial distribution of heat flux is also implied. The curves show clearly that with this model the net effect of the pressure feedbacks is to increase the average coolant density in response to an increase of heat flux although the exit density is reduced as would be expected. In other words the heat flux to steam void transfer function has a negative coefficient when pressure effects

are included (with this configuration of steam drum). This, combined with a positive void-reactivity coefficient, can then produce an overall stable plant.

The strong influence of the pressure feedback on overall plant dynamics is shown in Figure D, which represents the responses of the plant shown in Figure B. (Note that the responses of curves B have the same scheme as those of curves A; they are indicated with a negative sense solely for ease of illustration.) The reversal of plant dynamic behaviour, depending on whether the pressure feedback effects are allowed free rein or are suppressed, is clearly shown.

I thank the professors for their comments on the dynamic analysis of a boiling loop included in the paper, but I hasten to point out that the analysis was only included to provide some simple transfer functions and flow graphs for the introduction of the problems to an audience of control engineers. Our treatment of hydrodynamics in power reactor studies is, of course, as rigorous as knowledge and modern computing techniques will allow. Finally I echo their suggestion that we need a better knowledge of the dynamics of boiling and two-phase flow but I would suggest that we need experimental evidence rather than even more theoretical models. At the moment there is very little experimental data obtained with proper transient rigs with which the theoretical models can be evaluated.

R. QUACK, *Technische Hochschule, Stuttgart, Germany*

The problems studied by the authors are discussed in several publications by Dozent Dr. Kirchmayer, who came from the Tech. University in Beograd (Yugoslavia), stayed for some time at our institution in Stuttgart and is now connected to the research staff of AEG.

I emphasize that the authors for their further work should use the frequency-response equations of Kirchmayer, which have delivered us a very near theoretical approach to the real transient behaviour of the boiling-water reactor, as it is published in American papers. I will send the bibliographic dates of Kirchmayer's publications to the authors.

P. K. M'PHERSON, *in reply*

In answer to Professor Quack, I am familiar with Dr. Kirchmayer's work. He has provided the BWR literature with very complete transfer function models which are most interesting. However, his models tend to assume average spatial distribution for those quantities that are both time and space dependent. I would not recommend the use of these models in a BWR study until a detailed analysis has been made of the distributed parameters in the boiling channel, etc., using finite difference techniques on digital or analogue computers. One can then progress to a simplified lumped parameter model by fitting transfer functions to the results of the rigorous distributed parameter analysis.

On the Optimal Control of Hydro-electric Power Systems

H. RUGE

Summary

The purpose of optimizing a hydro-electric power system is to maximize the utility value of the available natural energy which exists in varying quantities. This makes in-line control considerably more complicated than in thermo systems, where the fuel cost may be minimized at any time.

The present paper defines an optimization criterion based on a utility function of the consumed power; the potential production of the system and its gradient, whose components appear as the probable value of the water in the reservoirs. Estimates of these values may be used in the coordination equations for on-line control.

Sommaire

L'exploitation optimale d'un ensemble des centrales hydrauliques est celle qui conduit à la valeur maximale de la production. Ceci est de son côté une fonction des conditions hydrologiques futures et inconnues. De ce fait un réglage automatique de la production devient un problème complexe par rapport au problème de la commande des centrales thermiques dont le but est de minimiser le coût instantané du combustible consommé.

Cet article définit d'abord un critère d'optimalité basé sur une fonction d'utilité dépendant de la puissance utilisée, ensuite la production potentielle du système et enfin le gradient du potentiel dont les composantes apparaissent comme la valeur de l'eau dans les réservoirs. On pourrait envisager l'utilisation de ces valeurs dans les «équations de coordination» pour une commande automatique et continue (on-line control).

Zusammenfassung

Die Aufgabe der Optimierung eines Wasserkraftwerkes ist es, einen maximalen Ausnutzungsgrad der in veränderlichen Mengen anfallenden natürlichen Energie zu erreichen. Dadurch wird die direkte Regelung schwieriger als in Wärmekraftwerken, wo die Brennstoffkosten jederzeit minimierbar sind.

Die vorliegende Arbeit definiert ein Optimalwertkriterium, das auf einer Ausnutzungsfunktion der verbrauchten Leistung beruht und betrachtet das Produktionspotential des Systems und seine Änderung, die vom wahrscheinlichen Wassergehalt in den Speichern abhängen. Die Abschätzungen dieser Werte können in den Gleichungen zur direkten Regelung verwendet werden.

Introduction

Automatic optimal control of the load distribution in electric power systems has received great interest in recent years. A large number of authors have dealt with the problem, especially in systems dominated by thermal power stations where the aim has been defined as minimizing the value of the fuel flow into the system for any given power consumption. This problem is elegantly solved by variational methods¹, which result in the so-called coordination equations:

$$\frac{dF_i}{dp_i} + \lambda \frac{\partial P_L}{\partial p_i} = \lambda \quad (1)$$

where p_i = generator output, F_i = value of fuel input, P_L = sum

of electric losses, dF_i/dp_i = incremental cost at power station, and λ = incremental cost at place of consumption.

These equations, which are necessary conditions for optimal load distributions, state the general economic principle that a given production should be distributed in such a way that incremental (or marginal) cost is the same for all units in operation. The equations form the theoretical basis for automatic dispatching systems like Early Bird² and others. Here the incremental costs are continuously computed on the basis of fuel prices and generator load. Hydro generators may be included by assigning a value to the water, based on the fuel it may substitute.

In a system dominantly driven by regulated rivers, this problem of water values requires considerably more attention. The available natural energy is a statistical variable with large fluctuations, and its cost does not exist on the budget. Its value must be judged in terms of its later use, which is dependent on the present and future state of the system. This means that the optimization cannot be performed simply by minimizing the instantaneous losses; one has to find an optimal path through a longer period of time. On the other hand, the coordination equations are fitted for on-line computation and control as opposed to dynamic programming. This makes it desirable to arrive at a scheme where the high frequency power changes are met by the coordination equations, while the slower changes in the hydrological states are handled by more complicated and infrequent off-line computations of water values. The present paper is a contribution to such a scheme.

Optimization Criterion

In a hydro-electric system there is no natural balance between natural energy and energy consumption, and the economic output may be improved considerably by stimulating the consumption according to the water conditions. This means that the power delivered to the consumers has a utility value, S , which is a non-linear function of power and time of delivery:

$$S = S(p, t)$$

This function is identical to what the consumer is willing to pay for the power in a long-term contract, and it depends on the individual consumers, especially on their facilities for the utilization of cheap, off-season energy and the need for a minimum, guaranteed delivery. On the basis of the individual S functions, one may estimate an average S function for the system as a whole, defining the consumption pattern of the area. This function is roughly specified by three properties:

- (1) The incremental utility value is always positive, making S a monotonically increasing function of p .
- (2) The S function must change with time (day/night, week-day/holiday, summer/winter), for instance, in the same way as the mean consumption.

(3) At p values below the normal, the function must reflect the consumers' losses due to a forced reduction in consumption.

As an example one may use the function

$$S = K_1 E[P(t)] \cdot \ln K_2 [P(t) - \varepsilon]$$

$E[P(t)]$ is here the estimated, unstimulated consumption at the time in question, K_1 and K_2 being constants (Figure 1).

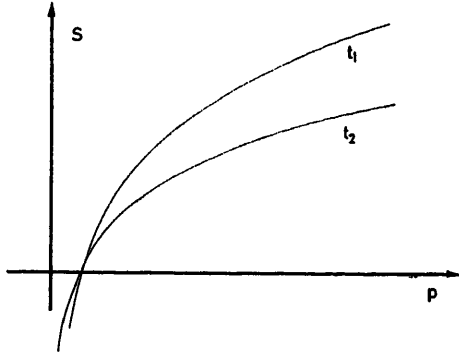


Figure 1

The purpose of the optimization will be to maximize the future capitalized production in terms of S :

$$\max \int_t^\infty e^{-a\tau} S(\tau) d\tau \quad (2)$$

subject to the constraints given by the system and the available water. \bar{p} , whose components are the load on the individual generators, is the control vector of the system. The S function, which also may be influenced by the management, is considered given, with a as the rate of interest.

Potential Production and Water Value

At any time, the outlook for the system production is dependent on the volume of water in the reservoirs, some significant flows, etc. These data may be concentrated in a state vector, \bar{q} , which consists of a number n of controllable components, the reservoir volumes; and a number r of other components which are independent of the control vector.

At any time, the value of the integral (2) may be estimated on the basis of the present state of the system and relevant statistical data. This estimate is denoted by G :

$$G(t, \bar{q}) = \max_{p(\tau)} E \int_t^\infty e^{a(t-\tau)} S(\tau) d\tau \quad (3)$$

This maximum value of the capitalized future production, averaged over the statistical variables involved, is a function of state and time

$$G = G(\bar{q}, t)$$

and is denoted by the potential production of the system. The components of its gradients

$$\frac{\partial G}{\partial q_i} = g_i \quad (4)$$

are called the g factors of the state variables, and the g factors of the reservoirs are defined as the value of the water. It is a

function of time, of the amount of water in this particular reservoir, and of all the other state variables.

Optimal Dispatch

The principle of optimality⁴ gives, for sufficiently small Δt :

$$\begin{aligned} G(t) &= \max_{p(t)} E[S(t) \Delta t + G(t + \Delta t)] \\ &= \max_{p(t)} E[S(t) \Delta t + G(t) + \Delta G] \\ &= \max_{p(t)} E[S(t) \Delta t + \Delta G] = 0 \end{aligned}$$

Hence, at any given time one has to compare the value of the production with the estimated change in G . This term is normally negative, and if the step is non-optimal, it will dominate. ΔG may be expressed by its partial derivatives

$$\Delta G = \left(\sum_{i=1}^{n+r} \frac{\partial G}{\partial q_i} \cdot \frac{dq_i}{dt} + \frac{\partial G}{\partial t} \right) \Delta t$$

and the dispatch problem will at any time be to maximize

$$\max_{p(t)} E \left[S(t) + \frac{\partial G}{\partial t} + \sum_{i=1}^{n+r} g_i \frac{dq_i}{dt} \right] \quad (5)$$

The problem in on-line control is mainly the distribution problem. S is known as the control instant, and the only terms influenced by the control are the last terms representing the reservoirs:

$$\max \sum_{i=1}^n g_i \frac{dq_i}{dt} \quad (6)$$

For all the production units known, the relation between water flow, w , and power:

$$w_i = f_i(p_i)$$

which usually may be approximated by a parabola, describing the energy losses in water tunnels, turbines and generators:

$$w = a + bp + cp^2$$

The power stations are generally hydraulically connected; an example is shown in Figure 2. For the simplicity of notation, it is assumed that only one turbine is connected to each reservoir.

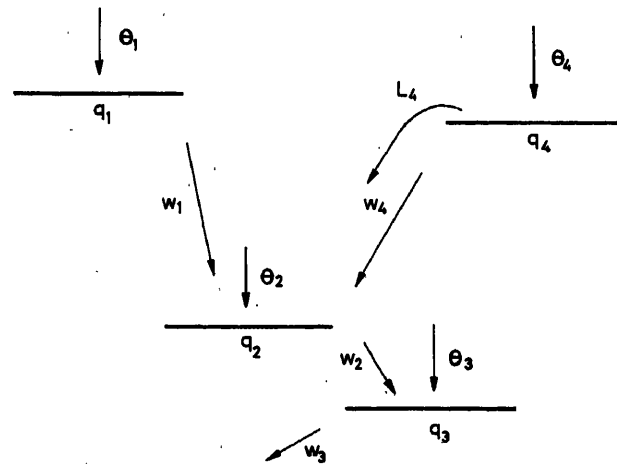


Figure 2

Ignoring the time delay between the outflow of one power station and inflow into the succeeding reservoir, the following relation is obtained.

$$\frac{dq_i}{dt} = \theta_i - w_i + w_{i+1} + L_{i+1}$$

L represents the overflow, θ the separate inflow.

Introducing the new variable

$$x_i = g_i - g_{i+1}$$

and setting this equal to zero for overflowing reservoirs, the sum (6) may be expressed as

$$\sum_{i=1}^n g_i \frac{dq_i}{dt} = \sum_{i=1}^n (\theta_i g_i - w_i \eta_i)$$

The last terms are defined as the production cost.

The inflows θ are not subject to control, and the load distribution is optimized for minimum value of:

$$\sum_{i=1}^n w_i \eta_i = F \quad (7)$$

which is defined as the operating cost. Formally the dispatching problem is now identical to the corresponding problems in thermal systems, and following Kirchmayer¹, the necessary conditions for optimum are the coordination equations in the form:

$$\eta_i \frac{dw_i}{dp_i} + \lambda \frac{\partial P_L}{\partial p_i} = \lambda \quad (8)$$

In addition one has to decide which turbines should be in operation. Theoretically this is a far more complicated question and is not handled here.

Distribution of the load according to the estimated g factors does not guarantee a permanent optimal programme, because these are based on estimates of the statistical variables θ and p . Errors in these estimates may accumulate and the g factors must therefore be periodically corrected to ensure maximum G .

Computation of g Factors

Only for trivial systems may the g factors be computed directly from their definitions as functions of state variables; generally they must be computed by other means. According to their interpretation as the probable utility value per volume unit of the water in the top layer, they are dependent on the probable incremental price dS/dE per energy unit; the probable efficiency, and the potential energy of the water.

Two properties will, however, contribute to the practical use of the formalism:

(1) To find the optimal distribution of a certain energy on the different reservoirs, one assumes a certain state and different production schemes resulting in the same production of electric energy dE . Interest is in the final state giving maximal G , and assuming two groups of reservoirs:

$$dE_1 + dE_2 = 0$$

$$\frac{\partial E_1}{\partial q_1} dq_1 + \frac{\partial E_2}{\partial q_2} dq_2 = 0$$

The corresponding change in G is

$$dG = g_1 dq_1 + g_2 dq_2$$

$$dG = dq_1 \left[g_1 - g_2 \cdot \left(\frac{\partial E}{\partial q} \right)_1 / \left(\frac{\partial E}{\partial q} \right)_2 \right]$$

In optimum this is zero, which gives

$$\left[\frac{g}{\frac{\partial E}{\partial q}} \right]_1 = \left[\frac{g}{\frac{\partial E}{\partial q}} \right]_2$$

The same operation may be performed on all couples of reservoirs, resulting in the following condition for optimum:

$$\frac{g_i}{\eta_i e_i} = k \text{ for all } i$$

where η is used for the expected efficiency of the unit, and e means the potential energy per unit volume of the water. Hence, the optimal state is characterized by all g factors being proportional to their electrical equivalence.

(2) A similar reasoning may be applied to the time variation of the g factors: the optimum policy implicit in G assumes a certain variation $g(t)$. If g at a certain instant should be smaller than at a later instant, this must imply that constraints, such as height of the dam, etc., make it impossible to store the water until the later instant, and *vice versa*. Hence, the ideal production schedule involves constant g factors.

This last property actually forms the basis for the methods developed by Lindquist, Stage and Larsson^{5, 6} for computing water values in a combined hydro-thermal system. Here one starts with an estimate of the water value as a function of time and total reservoir volume, and on the basis of a given relation between thermal production, secondary consumption and power price. This estimate is used in a Monte-Carlo simulation

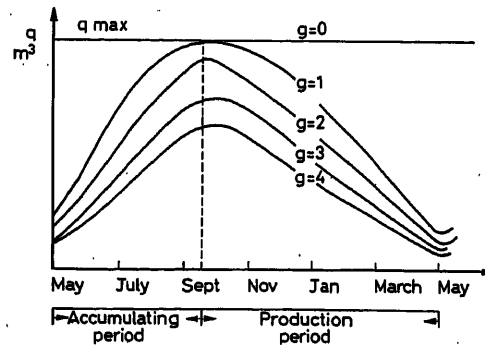


Figure 3

and improved iteratively until one gets a realistic production scheme following curves of equal water value. The method may also, with heavy computational work, be extended to systems with two reservoirs. For multidimensional systems there exist, to the author's knowledge, no satisfactory solution method.

Figure 3 shows a set of $g(q, t)$ curves for a reservoir with dominantly accumulation during spring and summer, and production mainly for electric heating during the winter.

Another approach to the problem is to find a set of differential difference equations relating the variables g , q and t , to

the statistical parameters describing the inflow and the total production p . These equations may then be solved more or less directly, generating the g curves.

A basic equation is, for instance,

$$\frac{dq}{dt} = E(\theta) - E[w(g)] \quad (9)$$

where the relation $w(g)$ is defined through $S(p, t)$ and $w(p)$. In addition, the absolute values of the g factors, which define the price level, must be adjusted to ensure balance between the time average of inflow and outflow.

If one assumes a system governed by the coordination equations and g factor of the simple form

$$g = g_0 - k(t) \Delta q \quad (10)$$

where Δq is the deviation from a certain water level curve, one will have a system negative feedback as shown for two variables in Figure 4.

One assumes that the system is run by: (i) g factors being periodically adjusted according to the relation (10) and the

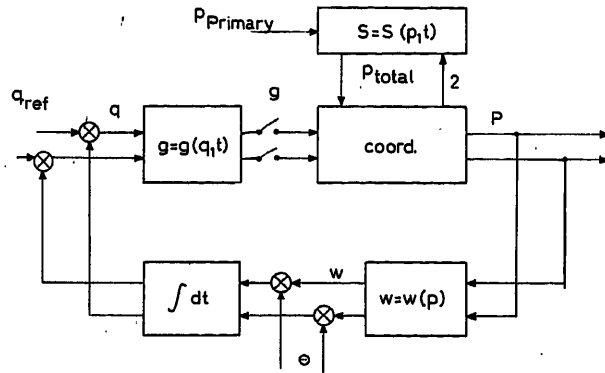


Figure 4

measured water levels; (ii) the total load is at any instant distributed according to coordination equations and supplementary conditions minimizing the instantaneous cost.

These computations also generate the incremental cost of the system, which may be used for control of variable load and power exchange with neighbour networks.

It is seen that the gradient $\partial g / \partial q = k$, when negative, acts to correct deviations from the predicted water level curve, because it will result in a corresponding change in g factors and hence a change in the water consumption from this particular reservoir.

If the load is unaffected by this change, it will also cause a corresponding change in the consumption from all other reservoirs, and later in their g factors. All g factors will, as a result, be dependent on each other through the action of the system itself, and tend to a stationary state where they are proportional in accordance with the requirement for optimality. This effect may be analysed theoretically using sampled system theory, and research is being performed along these lines, aiming at finding values of k_i which make optimal response to disturbances in power consumption and hydrological state.

Conclusion

There is developed a set of statistically defined concepts which forms a theoretical basis for an optimum control of hydro-electric power systems. By the Bellman Principle of Optimality these concepts are related to the Kirchmayer coordination equations, making possible an optimal dispatch on the basis of incremental production costs.

A main problem is the practical computation of the expected water values, the g factors, in systems with a large number of reservoirs. The most practical way of performing these computations seems to be through a number of difference differential equations describing the functional relations $g(q, t)$, and the research is performed along these lines.

This work is done in cooperation with Oslo Lysverker, whose production system in the near future will include some 30 aggregates and about 10 reservoirs.

References

- 1 KIRCHMAYER, L. *Economic Control of Interconnected Systems*. 1959. New York; Wiley
- 2 KOMPASS. The Early Bird goes automatic. *Control Engng*, N. Y. (1956)
- 3 PETERSON. *Statistical Analysis and Optimization of Systems*. 1961. New York; Wiley
- 4 BELLMAN. *Adaptive Control Processes*. 1961. Princeton; Princeton University Press
- 5 LINDQUIST. Operation of a hydro-thermal electric system, a multistage decision process. *Trans. Amer. Inst. elect. Engrs*, 80 (1961) Pt III
- 6 STAGE and LARSSON. Incremental cost of water power, *Trans. Amer. Inst. elect. Engrs* (August 1961) Pt III
- 7 DARIN, LIND, LARSSON, RYMAN and SJOLANDER. Principles of power balance calculations for economic planning and operation of integrated systems. *VAST*, Stockholm (1959)
- 8 LITTLE. The use of storage water in a hydroelectric system. *J. Op. Res. Soc. Balt.* (May 1955)
- 9 DEBREU. *Theory of Value, an Axiomatic Analysis of Economic Equilibrium*. 1959. New York; Wiley

DISCUSSION

L. K. KIRCHMAYER, *General Electric Company, Schenectady 5, N.Y., U.S.A.*

Mr. Ruge has presented a most interesting and thought-provoking paper related to the possible practical implementation of on-line optimal control of hydro-electric power systems. We have several comments and questions for his attention.

(1) Is it anticipated that the scheme of Figure 4 will be implemented in the near future on the Norwegian power system?

(2) Have they determined the g factors for a system of more than one storage reservoir?

(3) Has the author considered the effect of forebay constraints upon the determination of the g factors as suggested in his sub-section 'Computation of g factors'?

(4) Is not the intent of the second equation on page 84 relating the g factors to relate instead the gamma factors? That is, would not the expression appear as

$$\gamma_i \eta_i e_i?$$

(5) Would the author please comment on the method he proposes to use to determine the k factor, or feedback coefficient, listed in eqn (10) of his paper? Does he anticipate obtaining this from a graph

such as Figure 3, or does he have some shorter method in mind? It is not clear to us how the g factors would be periodically adjusted according to eqn (9). A further explanation of this would be helpful.

(6) On page 84 the author states that the ideal production schedule involves constant g factors. Does the author intend here to state that the initial and final values are the same for corresponding storage points?

Work is currently under way at the General Electric Company to provide an on-line digital dispatch computer to control the water releases for the hydro-electric projects of Region 4 of the Colorado River Storage Project, U.S. Bureau of Reclamation. The control com-

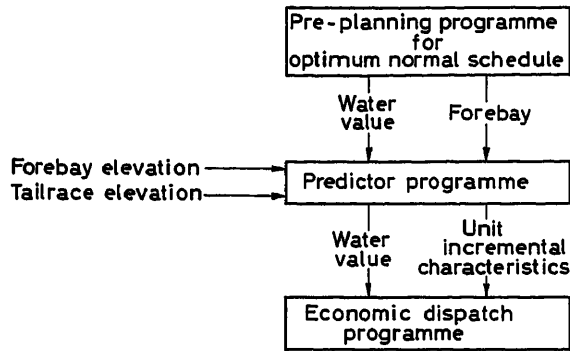


Figure A. Thermal-hydro optimizing

puter will optimize the releases of water from the hydro-electric plant by a control system shown in Figure A. The method bears strong resemblance to the techniques suggested by Mr. Ruge. The Preplanning Programme will determine the incremental water values and the reservoir schedules for a period of time in the future. Through means of the Predictor Programme the computer will compare actual with forecasted water usage and make appropriate corrections to the incremental water value and unit incremental characteristics.

This information is used in the Economic Dispatch Programme to provide an instant-by-instant on-line optimum digital dispatch.

H. RUGE, in reply

(1) No decisions have yet been taken concerning future computer control on the Norwegian power system, and I think extensive technical and economic studies must be completed first. Such studies are under way, and this paper represents an intermediate result of a study carried out in cooperation with Mr. Oslo Lysverker and the Research Institute for Electricity Supply. These studies also include geophysical research into relations between meteorological and hydrological observations, retarded water inflows etc., which have some bearing on the complete optimization scheme. Organizational changes of some form must also take place, which takes time, and for the moment I do not think the power companies feel any pressing need to update their control methods.

(2) We have computed water values for two-reservoir systems, using a modification of Lindquist's method. This is actually not dynamic programming, but an iterative trial method using historical hydrological records. To my knowledge Little⁶ is the only one who has used dynamic programming for systems with stochastic inflow and that was for the Colorado river.

(3) and (6) As mentioned in the paper, the amount and time constants of the water values represent ideal, unconstrained conditions, and every deviation from this, imposed by constraints such as finite dam heights, limited water release etc., involves a loss in economy. However, it should also be stated that the reasoning leading to the time constants is based on a negative $\partial g/\partial q$, which holds for ordinary background reservoirs. This condition is, however, not satisfied for reservoirs with a considerable head variation with q , and such reser-

voirs will also have a positive feedback coefficient, shown in Figure 4, with the result that disturbances cannot be taken care of adequately by the coordination equations alone. The rate of interest will also disturb the time constants of the water values.

(4) Yes, when there are downstream power stations.

(5) The function of this k is to adjust the production in accordance with deviations from the predicted conditions, and I can indicate one basis for computing it; for simplicity in a single reservoir system with stationary statistics, where the water values are independent of time. After a disturbance, q , this gradient k will be the one which maximizes the sum of the increased production value in the next period, and the remaining water at the end of the period, evaluated by means of the same k . Both terms will in this case be relatively simple functions of k . For multiple, time-varying systems, the problem is considerably more complicated, but the method may be a fruitful method of attack, resulting in some field equations for the g -functions.

I have a general feeling that the size of the problem could be reduced considerably by using more adequate physical descriptions of the set of reservoirs. Such as their time constants with respect to inflow and outflow, non-linearity of machinery, and perhaps also a more adequate description of the inflow statistics.

It was indeed interesting to see Mr. Kirchmayer's proposal for the Columbia river project, and I look forward to the disclosure of the technical and computational details involved.

J. CARPENTIER, *Electricité de France, 12 Place des États-Unis, Paris 16^e, France*

At Electricité de France, similar work to that described by Mr. Ruge has been done. Two problems of optimal operation of hydro-electric systems were solved using dynamic programming, one purely theoretical, the other studied the future operation and equipment of the power system for the town of Abidjan in Africa. This had the wonderful property that energy was supplied by only one big reservoir and thermal power plants.

The results obtained are quite similar to these of Mr. Ruge. In particular, dynamic programming is very difficult to apply to systems with more than two reservoirs; for such systems a solution based on simulation is easier to carry out, and research is being done in this direction.

I wish to ask Mr. Ruge the following questions:

(1) In the economic value of the delivered power, there is a term including a penalty due to a forced reduction in the consumption by the consumers. What value was taken for this penalty? (It is rather difficult to obtain the figure from the investigations by economists.) Were different values tried, and what was the sensitivity of the model to the changes in the value of this penalty? In France, we found that, when varying this penalty, the curves of the results changed, but the effective operation did not change very much over a rather wide band of variation in the penalty.

(2) Concerning the use of differential difference equations, how does the time involved in this resolution grow with the number of reservoirs?

H. RUGE, in reply

(1) In Norway we have experienced exactly the same difficulties over getting realistic values for the lower part of the S function, i.e. the penalties for delivery reductions. Except for certain power applications with clear economic alternatives, I think these values must be based on estimates from independent economists. It is important to have this curve non-linear, reflecting the fact that minor reductions may take place without any real inconveniences for the consumers. As to the sensitivity of the loading schedule to changes in the S curve, I have no exact data, but an increase in penalty will definitely result in a more careful storage policy.

(2) I would assume a quadratic relationship between the number of reservoirs and computation time.

Exposé d'une Méthode d'Elaboration de Graphiques Exprimant les Conditions de Stabilité du Réglage d'un Groupe Hydro-électrique

A. TSCHUMY

Summary

The stability characteristics (such as stability limit, damping factor, pulsation of the regulating oscillation, phase margin etc.) can be determined by the proposed method by graphs drawn for the various operation conditions of the hydro-electric set.

The paper describes the preliminary calculations and the programmes of the electronic calculating machines elaborated for obtaining the various curves of the graphs. It is worth noting that one has used the frequential behaviour methods applied to the various transfer functions of the elements forming the whole hydro-electric set.

Sommaire

La méthode proposée permet de connaître les conditions de stabilité (limite de stabilité, degré d'amortissement, pulsation de l'oscillation de réglage, marge de phase, etc. etc.) par des graphiques établis pour les différents régimes de fonctionnement du groupe hydro-électrique. Nous décrivons les calculs préalables et les programmes de la calculatrice numérique élaborés pour obtenir les différentes courbes de ces graphiques. Il a notamment été fait appel aux notions introduites par la considération du comportement fréquentiel des divers éléments constituant l'ensemble du circuit de réglage.

Zusammenfassung

Die vorgeschlagene Methode erlaubt die Stabilitätsbedingungen (Stabilitätsgrenze, Dämpfungsgrad, Kreisfrequenz der Regelschwingung, Phasenrand usw.) für die verschiedenen Betriebszustände eines Wasserkraftwerkes graphisch darzustellen.

Der Aufsatz beschreibt die Vorausberechnung und die Programme für die elektronischen Rechenmaschinen, die zur Ermittlung der verschiedenen Kurven dienen. Zur Bildung der Struktur des gesamten Wasserkraftwerkes wurde die Frequenzgangmethode auf die Übertragungsfunktionen der einzelnen Teile angewendet.

Introduction

Le nombre croissant des interconnexions entre réseaux peut faire penser que le problème de la stabilité du réglage de vitesse d'un groupe hydro-électrique perd de son importance. Il n'en reste pas moins vrai que chacun des groupes couplés à un grand réseau doit être stable par lui-même et que les cas de marche d'un groupe sur réseau séparé sont encore assez fréquents. Ce mode de fonctionnement se présente, lors de dérangements, parfois lorsque les groupes alimentent des industries particulières ou des petits réseaux.

La recherche de la plus stricte économie qui influe quelquefois sur les projets d'aménagements hydro-électriques, risque de rendre précaires les conditions de stabilité à tel ou tel régime de fonctionnement. La détermination de ces conditions sur la base de renseignements faisant appel à des notions statistiques ou à des caractéristiques globales, en assimilant par exemple la turbine à un orifice, n'est plus suffisante. Il est nécessaire de

contrôler avec soin le point de fonctionnement du groupe hydro-électrique (utilisation de la colline de fonctionnement de la turbine, connaissance des caractéristiques de la conduite forcée, du genre de réglage de tension), compte tenu de la nature de la charge du réseau.

Equations du Réglage, Hypothèses de Base et Conditions de Stabilité

Les équations fondamentales du réglage d'un groupe hydro-électrique sont les suivantes^{1, 3}.

Equation des masses tournantes:

$$\frac{d}{dt} \Delta \omega = \frac{1}{T} \left(\Delta p_0 + \frac{3-\beta}{2} \Delta h - \alpha \Delta \omega \right) \quad (1)$$

Equation du dispositif de réglage:

$$\frac{d}{dt} \Delta p_0 = -\frac{1}{\tau'} \left(\Delta \omega + m \frac{d}{dt} \Delta \omega \right) \quad (2a)$$

en réglage accélérotachymétrique

$$\frac{d}{dt} \Delta p_0 = -\frac{1}{\tau' e} \left(\Delta \omega + \tau'' \frac{d}{dt} \Delta \omega \right) \quad (2b)$$

en réglage avec asservissement temporaire.

Equation du coup de bélier:

$$\Delta h = -\theta \cdot f \left(\frac{1}{j} \frac{d}{dt} \Delta p_0 + \frac{1-\beta}{2} \frac{d}{dt} \Delta h + \beta \frac{d}{dt} \Delta \omega \right) \quad (3)$$

Les équations (1), (2a), (3) du système différentiel ci-dessus caractérisent le réglage dans les hypothèses suivantes:

- (a) Le groupe fonctionne seul sur un réseau séparé.
- (b) L'usage des relations linéaires auquel conduit, à des infiniment petits du deuxième ordre près, l'emploi de valeurs relatives, exige que les écarts des grandeurs par rapport à leurs valeurs de régime restent faibles.
- (c) Les courbes représentatives des diverses grandeurs sont assimilées à leurs tangentes, au point de fonctionnement, en régime stationnaire.
- (d) L'équation du coup de bélier tient compte de l'effet de sa période propre (conséquence de l'élasticité de l'eau et des parois de la conduite forcée).
- (e) L'influence de la perte de charge dans la conduite forcée est négligée.
- (f) Bien que nous ayons écrit l'équation du régulateur dans les deux cas du réglage accéloro-tachymétrique et du réglage avec asservissement temporaire, nous conduirons la suite du calcul en réglage accélorotachymétrique.
- (g) Le statisme permanent du dispositif de réglage est admis égal à zéro.

Si nous posons $\Delta\omega = \lambda_1 e^{rt}$, $\Delta p_0 = \lambda_2 e^{rt}$, $\Delta h = \lambda_3 e^{rt}$, l'équation caractéristique du système des 3 équations (1), (2a), (3) a la forme suivante:

$$a_0 r^3 + a_1 r^2 + a_2 r + a_3 = 0 \quad (4)$$

équation dans laquelle on peut toujours faire en sorte que $a_0 = 1$.

Le système d'équations (1), (2a), (3), peut être mis sous forme matricielle:

$$\boxed{\text{Eqn (5a)}}^*$$

correspondant à la forme générale:

$$\begin{bmatrix} \frac{d}{dt} \Delta\omega \\ \frac{d}{dt} \Delta p_0 \\ \frac{d}{dt} \Delta h \end{bmatrix} = \begin{bmatrix} a_{11} & a_{12} & a_{13} \\ a_{21} & a_{22} & a_{23} \\ a_{31} & a_{32} & a_{33} \end{bmatrix} \begin{bmatrix} \Delta\omega \\ \Delta p_0 \\ \Delta h \end{bmatrix} \quad (5b)$$

En appliquant le critère de stabilité d'Hurwitz, nous obtenons les conditions suivantes pour caractériser la stabilité du système.

$$a_1 > 0 \quad (6)$$

$$\begin{vmatrix} a_1 & a_0 \\ a_3 & a_2 \end{vmatrix} \geq 0 \text{ soit } a_1 a_2 - a_3 \geq 0 \quad (7)$$

Le signe = dans l'équation (7) définit la limite de la stabilité et le signe > dans la même relation signifie que l'oscillation de réglage est amortie. (Voir Pingoud².)

a_1, a_2, a_3 sont des polynômes composés des coefficients $a_{11}, a_{12}, \dots, a_{33}$ du système (5a), (5b), et ont les valeurs suivantes:

$$a_1 = \frac{A+\alpha}{T} + \frac{B}{\theta f} - \frac{Cm}{\tau' T} \quad (8)$$

$$a_2 = \frac{mB}{\tau' T \theta f} - \frac{C}{\tau' T} + \frac{\alpha B}{T \theta f} \quad (9)$$

$$a_3 = \frac{B}{\tau' T \theta f} \quad (10)$$

Représentation Graphique des Conditions de Stabilité

En posant $r = -x \pm i\bar{\omega}$, ce qui donne aux solutions de l'équation (5a) la forme d'une oscillation amortie, si $x > 0$, nous obtenons par l'équation (4) une relation qui permet de calculer le facteur d'amortissement x .

$$8x^3 - 8a_1 x^2 + 2(a_1^2 + a_2)x - a_1 a_2 + a_3 = 0 \quad (11)$$

La pulsation $\bar{\omega}$ (ou pseudo-pulsation) de l'oscillation de réglage est donnée par la relation suivante:

$$\bar{\omega}^2 = 3x^2 - 2a_1 x + a_2 \quad (12)$$

Le décrétement logarithmique, la pulsation et le coefficient d'amortissement sont liés par la relation suivante:

$$\delta^* = \frac{2\pi}{\bar{\omega}} x \quad (13)$$

En remplaçant les grandeurs a_1, a_2, a_3 par leurs expressions (8), (9), (10) dans les équations (11) et (12), nous obtenons les relations suivantes:

$$\begin{aligned} & 8x^3 - 8x^2 \left(\frac{A+\alpha}{T} \right) \\ & + \frac{B}{\theta} \frac{\bar{\omega}L}{a \cdot \text{tg} \frac{\bar{\omega}L}{a}} \left[-8x^2 + \left(\frac{A+\alpha}{T} \right) \left(4x - \frac{m}{\tau' T} - \frac{\alpha}{T} \right) \right. \\ & \left. + C \left(-4x \frac{m}{\tau' T} + \frac{1}{\tau' T} + \frac{m^2}{(\tau' T)^2} + \frac{m\alpha}{T^2 \tau'} \right) \right. \\ & \left. + 2x \left(\frac{m}{\tau' T} + \frac{\alpha}{T} \right) + \frac{1}{\tau' T} \right] + \left[\frac{B}{\theta} \frac{\bar{\omega}L}{a \cdot \text{tg} \frac{\bar{\omega}L}{a}} \right]^2 \left(2x - \frac{m}{\tau' T} - \frac{\alpha}{T} \right) \\ & + \frac{C}{\tau' T} \left[\left(\frac{A+\alpha}{T} \right) (1 - 4xm) + 8x^2 m - 2x \right] \\ & + \frac{C^2 m}{(\tau' T)^2} (2xm - 1) + 2x \left(\frac{A+\alpha}{T} \right)^2 = 0 \end{aligned} \quad (14)$$

$$\begin{aligned} \bar{\omega}^2 = & 3x^2 - 2x \left(\frac{A+\alpha}{T} \right) + \frac{B\bar{\omega}L}{\theta T a \text{tg} \frac{\bar{\omega}L}{a}} \left(\alpha - 2xT + \frac{m}{\tau'} \right) \\ & + \frac{C}{\tau' T} (2mx - 1) \end{aligned} \quad (15)$$

Nous établirons le graphique exprimant les conditions de stabilité en adoptant comme coordonnées m et τ' . Ces deux temps caractérisent le dispositif de réglage et peuvent être ajustés à volonté. Cet ajustement est particulièrement facile à effectuer sur des régulateurs électriques.

A chaque valeur constante du facteur d'amortissement x ou du décrétement δ^* ou de la pulsation $\bar{\omega}$ (période T'') correspond une série de paires de valeurs m et τ' , c'est-à-dire dans le graphique une courbe déterminée par les équations (14) et (15); les coefficients de ces équations sont déterminés par les données de l'installation et celles du régime considéré.

* Eqn (5a):

$$\begin{bmatrix} \frac{d}{dt} \Delta\omega \\ \frac{d}{dt} \Delta p_0 \\ \frac{d}{dt} \Delta h \end{bmatrix} = \begin{bmatrix} -\frac{\alpha}{T} & +\frac{1}{T} & +\frac{\varepsilon}{T} \\ +\frac{m}{\tau' T} \left(\alpha - \frac{T}{m} \right) & -\frac{m}{\tau' T} & -\frac{\varepsilon m}{\tau' T} \\ +\nu \left[\frac{\alpha\beta}{T} + \frac{m}{\tau' T j} \left(\frac{T}{m} - \alpha \right) \right] + \nu \left(\frac{m}{\tau' T j} - \frac{\beta}{T} \right) & -\nu \left(\frac{1}{\theta f} + \frac{\varepsilon\beta}{T} - \frac{\varepsilon m}{\tau' T j} \right) \end{bmatrix} \begin{bmatrix} \Delta\omega \\ \Delta p_0 \\ \Delta h \end{bmatrix} \quad (5a)$$

Elaboration du Graphique. Emploi d'une Calculatrice Electronique

On obtient la courbe « limite de stabilité » c'est-à-dire à facteur d'amortissement nul en introduisant $x = 0$ dans l'équation (14); la relation entre m et τ' qui en découle détermine la courbe cherchée.

Si nous posons en outre $f = \text{tg } z/z = 1$, ce qui peut être admis dans le cas de basses chutes (grandes valeurs de ρ) il en résulte une expression en m et τ' qui est celle d'une hyperbole.

Si l'on donne ensuite au facteur d'amortissement x des valeurs constantes successives x_1, x_2, x_3 , etc., chacune de ces valeurs définit l'équation représentative d'une courbe (également une hyperbole) qui peut être tracée de la même manière que la courbe « limite de stabilité ». L'équation (15) permet de déterminer les courbes à pulsation $\bar{\omega}$ de l'oscillation de réglage, de valeur constante.

Cette méthode approchée ne convient que dans le cas où l'on considère le phénomène du coup de bélier comme un phénomène de masse ($f = 1$). Il n'est souvent pas possible de faire cette hypothèse simplificatrice et les équations (14), (15) doivent être traitées dans leur ensemble avec une valeur de

$$f = \frac{\text{tg } z}{z} = \frac{\text{tg } \frac{\bar{\omega} L}{a}}{\frac{\bar{\omega} L}{a}} \neq 1$$

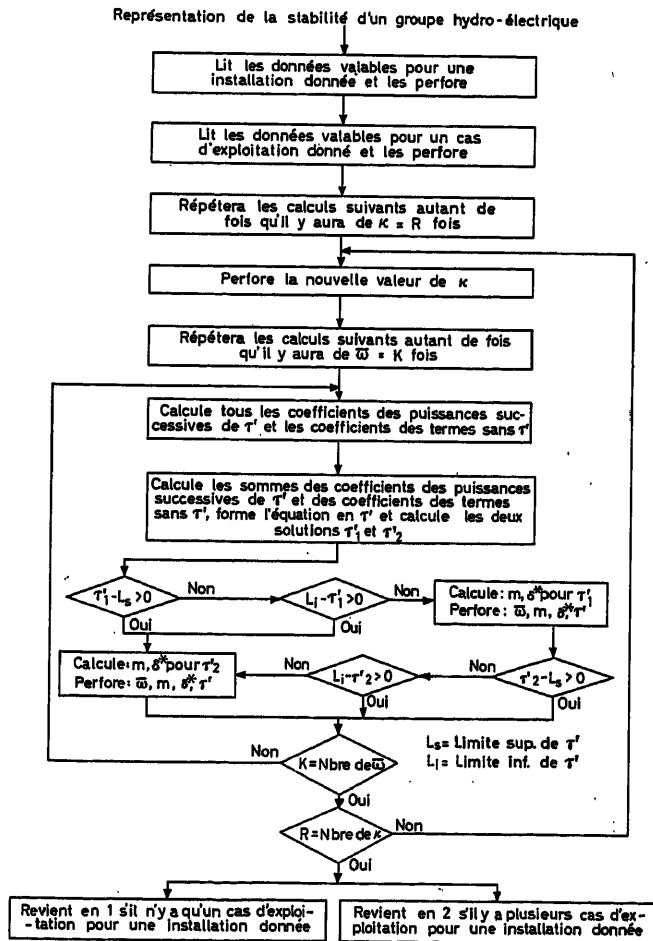


Figure 1. Organigramme simplifié du calcul de $m, \tau', \bar{\omega}$ et δ^*

Il est alors nécessaire de procéder par approximations successives, afin d'obtenir des points du plan m, τ' satisfaisant les équations précitées. L'emploi d'une calculatrice numérique permet de résoudre aisément le problème. Par la mise en œuvre d'un tel moyen, le temps de travail est considérablement réduit et il est ainsi possible de procéder à l'étude de plusieurs régimes de fonctionnement d'une même installation.

Le programme de calcul représenté par l'organigramme simplifié de la Figure 1, indique la suite des opérations à effectuer par la calculatrice, afin d'obtenir les courbes désirées.

Ce programme peut être suivi d'un sous-programme qui ordonne l'impression directe des résultats sous la forme du graphique m, τ' demandé. Dans ce cas le travail de l'opérateur se borne à relier par un trait continu les différents points du graphique (m, τ') sur lequel figure, en plus, la condition donnée par la relation (6): $a_1 > 0$. Ainsi la zone d'instabilité est clairement définie et les points du plan compris dans la zone de stabilité sont cotés en valeurs de la pulsation $\bar{\omega}$ de l'oscillation de réglage (ou de sa période T'') du facteur d'amortissement ou du décrement logarithmique.

Utilisation des Diagrammes Fréquentiels pour Exprimer les Conditions de Stabilité (Marge de Phase et Marge de Gain)

Les équations fondamentales du réglage (1), (2a), (3) permettent de calculer les fonctions de transfert du dispositif de réglage, du groupe hydro-électrique et par conséquent du circuit de réglage au complet.

Fonctions de Transfert

(a) Du dispositif de réglage:

$$G_1 = -\frac{1 + mp}{\tau' p} = \frac{\Delta p_0}{\Delta \omega} \quad (16)$$

(b) Du groupe hydro-électrique:

$$G_2 = \frac{\frac{1}{\varepsilon} + \left(\frac{\theta}{v\varepsilon} - \frac{\theta}{j} \right) p}{\frac{\alpha}{\varepsilon} + \left(\frac{T}{\varepsilon} + \frac{\theta\alpha}{v\varepsilon} + \theta\beta \right) p + \left(\frac{\theta}{v} \cdot \frac{T}{\varepsilon} \right) p^2} = \frac{\Delta \omega}{\Delta p_0} \quad (17)$$

(c) Du circuit de réglage:

$$G = (-G_1)$$

$$(G_2) = \frac{[1 + mp] \left[\frac{1}{\varepsilon} + \left(\frac{\theta}{v\varepsilon} - \frac{\theta}{j} \right) p \right]}{[\tau' p] \left[\frac{\alpha}{\varepsilon} + \left(\frac{T}{\varepsilon} + \frac{\theta\alpha}{v\varepsilon} + \theta\beta \right) p + \left(\frac{\theta}{v} \cdot \frac{T}{\varepsilon} \right) p^2 \right]} \quad (18)$$

p est l'opérateur complexe qui pour le cas de sollicitations sinusoïdales prend une valeur purement imaginaire $i\bar{\omega}$.

La fonction de transfert (18) permet d'examiner le comportement fréquentiel du circuit de réglage. Pour ce faire, il est nécessaire de déterminer le module $|G_G|$ et l'argument θ_G pour des valeurs de la pulsation $\bar{\omega}$ se répartissant sur une gamme suffisamment étendue.

La représentation graphique de $|G_G|$ et de θ_G peut se faire de diverses manières. Nous choisirons le diagramme amplitude-

phase, qui nous permettra de définir la marge de phase et la marge de gain dont dépend le degré de stabilité. Les échelles seront dès lors les suivantes:

Pulsation ou fréquence angulaire $\bar{\omega}$: échelle logarithmique en abscisse.

Module de $G_G(i\bar{\omega})$: en décibels sur une échelle linéaire, en ordonnée.

Argument de $G_G(i\bar{\omega})$: en degrés sur une échelle, en ordonnée.

La Figure 2 donne un diagramme amplitude-phase et la Figure 3 donne la représentation correspondante dans un diagramme polaire.

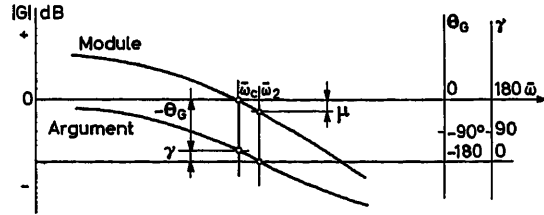


Figure 2. Diagramme amplitude-phase

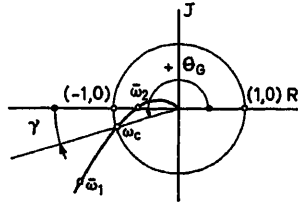


Figure 3. Représentation en diagramme polaire. μ : marge de gain; γ : marge de phase; θ_G : argument de G ; $\bar{\omega}_c$: pulsation de coupure

Module:

$$|G_g| = \frac{(1 + [m\bar{\omega}]^2)^{\frac{1}{2}} \left[\left(\frac{1}{\varepsilon} \right)^2 + \left[\left(\frac{\theta}{v\varepsilon} - \frac{\theta}{j} \right) \bar{\omega}^2 \right]^2 \right]^{\frac{1}{2}}}{\tau' \bar{\omega} \left[\left(\frac{\alpha}{\varepsilon} - \left(\frac{\theta}{v} \cdot \frac{T}{\varepsilon} \right) \bar{\omega}^2 \right)^2 + \left[\left(\frac{T}{\varepsilon} + \frac{\theta \cdot \alpha}{v \cdot \varepsilon} + \theta \beta \right) \bar{\omega} \right]^2 \right]^{\frac{1}{2}}} \quad (19)$$

Argument:

$$\theta_g = \arctg m\bar{\omega} + \arctg \varepsilon \left[\frac{\theta}{v\varepsilon} - \frac{\theta}{j} \right] - 90^\circ - \arctg \frac{\left[\left(\frac{T}{\varepsilon} + \frac{\theta \alpha}{v\varepsilon} + \theta \beta \right) \bar{\omega} \right]}{\left[\frac{\alpha}{\varepsilon} - \left(\frac{\theta}{v} \cdot \frac{T}{\varepsilon} \right) \bar{\omega}^2 \right]} \quad (20)$$

La marge de phase a l'expression suivante:

$$\gamma = 180^\circ + \theta_g \quad (\text{voir Figure 3}) \quad (21)$$

ainsi

$$\gamma = 90^\circ + \arctg m\bar{\omega} + \arctg \varepsilon \left[\frac{\theta}{v\varepsilon} - \frac{\theta}{j} \right] - \arctg \frac{\left[\left(\frac{T}{\varepsilon} + \frac{\theta \alpha}{v\varepsilon} + \theta \beta \right) \bar{\omega} \right]}{\left[\frac{\alpha}{\varepsilon} - \left(\frac{\theta}{v} \cdot \frac{T}{\varepsilon} \right) \bar{\omega}^2 \right]} \quad (22)$$

A chaque couple de valeurs m, τ' correspond pour une installation et un régime de fonctionnement donnés, une valeur $\bar{\omega}_c$ dite pulsation de coupure pour laquelle $|G_G| = 1$ ou ce qui revient au même $20 \log |G_G| = 0$ dB.

La valeur de $\bar{\omega}_c$ définit alors une marge de phase γ selon l'équation (22).

La marge de gain est la valeur μ du gain (module) lorsque la marge de phase est nulle. (Voir Figure 2 et 3.)

Détermination de la Marge de Phase et de la Marge de Gain. Utilisation d'une Calculatrice Electronique

L'élaboration du graphique amplitude-phase peut se faire aisément au moyen des diagrammes approximatifs d'amplitude. La courbe $|G_G| = f(\bar{\omega})$ est remplacée par les asymptotes à ses divers tronçons (voir Garsoux⁷). Toutefois, si ce travail ne présente pas de difficultés particulières, il est long et fastidieux pour un grand nombre de points.

Nous avons élaboré un programme de calcul destiné à une calculatrice numérique qui détermine pour chaque point du plan (m, τ') la valeur de la marge de phase γ , correspondant à un régime de fonctionnement déterminé d'une installation. L'organigramme simplifié de la Figure 4 montre la suite des opérations à effectuer par la calculatrice pour obtenir la valeur de la marge de phase.

Représentation de la stabilité d'un groupe hydro-électrique

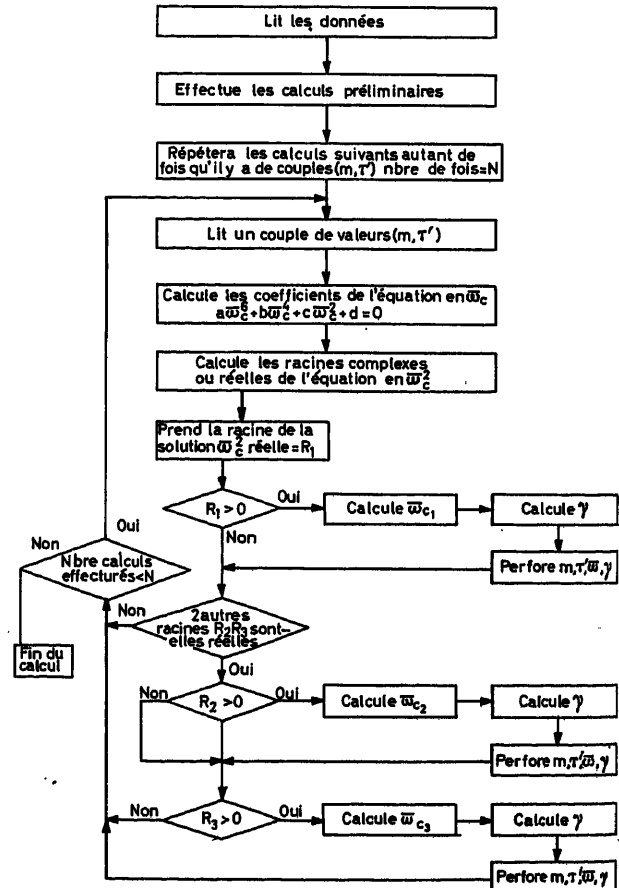


Figure 4. Organigramme simplifié du calcul de la marge de phase

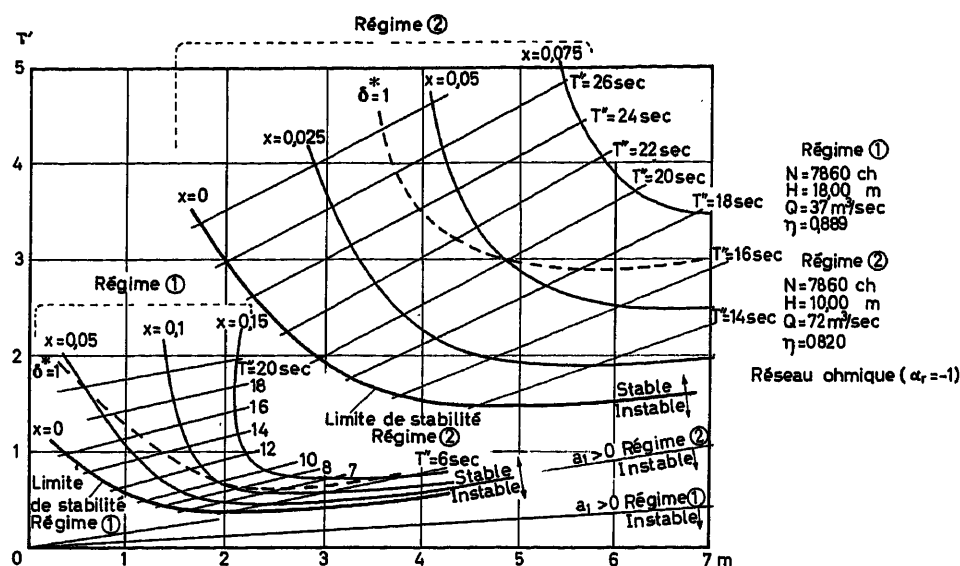


Figure 5. Exemple de calcul pour une turbine KAPLAN. x : coefficient d'amortissement; δ^* : décrement logarithmique; T'' : pseudo période de l'oscillation

La marge de gain peut être calculée de la même manière que la marge de phase.

Les courbes marge de phase nulle ($\gamma = 0$), marge de gain nulle ($\mu = 0$), coefficient d'amortissement nul ($x = 0$), décrement logarithmique nul ($\delta^* = 0$), se recouvrent toutes sur une unique courbe qui correspond à la limite de stabilité.

Dans le plan m, τ' de la Figure 6 sont tracées les courbes $\gamma = \text{Cte}$ et $\mu = \text{Cte}$ (voir le chapitre suivant).

Exemple d'un Calcul

Nous avons appliqué la méthode exposée ci-dessus à l'installation d'une turbine KAPLAN, dont l'alternateur fonctionne isolément sur un réseau séparé. Nous avons étudié deux cas, cherchant à montrer la différence entre les conditions de stabilité selon les régimes de fonctionnement considérés.

Cas A

Nous admettons que le groupe hydro-électrique fournit une puissance donnée à un réseau de caractéristique purement ohmique: $\alpha_r = -1$ dans un régime de chute maximum et dans

un régime de chute réduite. Les caractéristiques définissant ces deux régimes de fonctionnement figurent dans le Tableau 1.

Sur le graphique de la Figure 5 ont été tracées les courbes $x = \text{Cte}$, $\delta^* = \text{Cte}$ et $T'' = \text{Cte}$ correspondant aux deux régimes de fonctionnement.

Le graphique montre combien différentes peuvent être les conditions de stabilité pour un groupe débitant la même puissance sur un réseau de même nature, mais sous des chutes et avec des débits différents.

Tableau 2

		Régime 1	Régime 2
Puissance	ch	7 860	
Chute nette	m	10,00	
Débit	m³/sec	72,00	
Rendement		0,820	
PD^2	kgm²	465 000	
T	sec	7,7	
θ	sec	2,5	
Vitesse de rotation	t/min	187,5	
α		0,51	2,51

Cas B

Nous admettons que le groupe hydro-électrique fournit une puissance donnée à un réseau qui dans un premier régime est purement ohmique: $\alpha_r = -1$ et auquel dans un deuxième régime, le réglage de tension relève la pente de la courbe du couple résistant à $\alpha_r = +1$. Les caractéristiques définissant ces deux régimes de fonctionnement figurent dans le Tableau 2.

Sur le graphique de la Figure 6 ont été tracées les courbes $\gamma = \text{Cte}$, $\mu = \text{Cte}$. Ce graphique montre clairement l'influence de la valeur d' α (différence des pentes des courbes des couples moteur et résistant) sur les conditions de stabilité. Cette influence

Tableau 1

		Régime 1	Régime 2
Puissance	ch	7 860	7 860
Chute nette	m	18,00	10,00
Débit	m³/sec	37,00	72,00
Rendement		0,885	0,820
T	sec	7,7	7,7
θ	sec	0,67	2,5
α		1,26	0,51
PD^2	kgm²	465 000	
Vitesse de rotation	t/min	187,5	

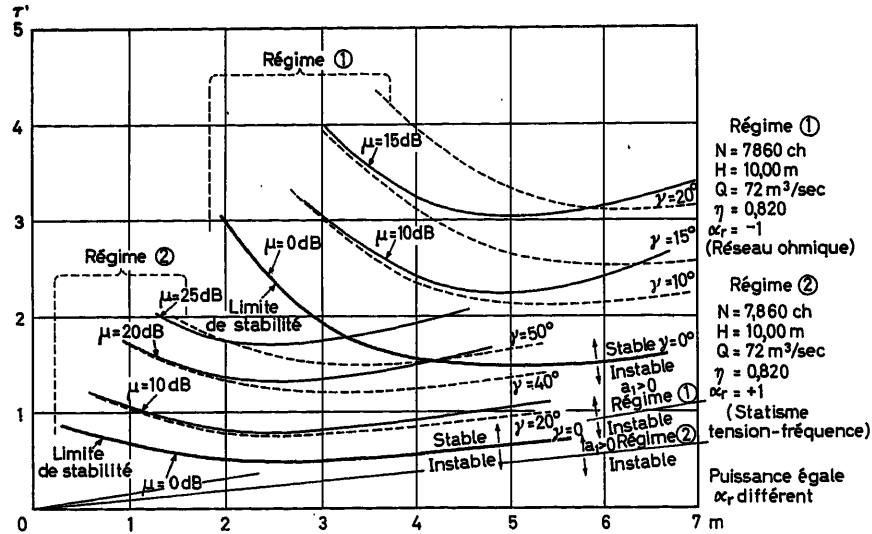


Figure 6. Exemple de calcul pour une turbine KAPLAN. μ : marge de gain; γ : marge de phase

est fort connue des praticiens, qui préconisent alors d'agencer le régulateur de tension de façon à permettre d'ajuster la valeur du statisme tension-fréquence.

Conclusions

La méthode proposée permet d'avoir une vue d'ensemble des conditions de stabilité du réglage d'un groupe hydro-électrique. Les exemples présentés montrent combien les conditions de stabilité varient avec les régimes de fonctionnement considérés. L'établissement de ces graphiques permet de déterminer par avance, lors des études, les conditions de stabilité. On en déduit les valeurs de m et τ' à réaliser par le régulateur lors de la mise en service. Dans la suite des données, il reste en général une imprécision: la valeur de α_r , caractérisant le couple résistant. L'emploi d'une calculatrice numérique permet d'étudier rapidement plusieurs cas possibles correspondant à différentes valeurs de α_r . Mais ces graphiques permettent surtout de se rendre compte des exigences des « Cahiers des Charges » des différents clients et d'apprécier ces exigences avec les conditions de l'installation et les nécessités de la construction.

Nomenclature

Le système de notation utilisé est basé principalement sur ceux employés dans les ouvrages^{1, 2}, ceci afin d'en faciliter le raccord.

Ce chapitre définit les symboles principaux. Certains sont définis dans le cours du travail.

L'indice $_0$ caractérise la valeur de régime.

Systèmes Hydraulique, Electrique et des Masses Tournantes

- H Chute nette à l'entrée de la turbine
- Q Débit variable de la turbine
- P Puissance variable de la turbine
- Δh Écart relatif de chute $H - H_0/H_0$
- Δq Écart relatif de débit $Q - Q_0/Q_0$
- Δp Écart relatif de puissance $P - P_0/P_0$
- Δp_0 Écart relatif de puissance sans l'effet de l'écart de vitesse du groupe, ni celui de l'écart de chute

- $\Delta \omega$ Écart relatif de la vitesse (fréquence) $= \omega - \omega_0/\omega_0$
- Δp_r Écart relatif de la puissance résistante de l'alternateur
- L Longueur totale des conduites d'amenée et de restitution entre le niveau de la chambre d'équilibre et le niveau de restitution
- T Inertie spécifique du groupe hydro-électrique
- a Célérité de l'onde du coup de bélier
- g Accélération terrestre
- θ Inertie spécifique de la conduite
- q Caractéristique de la conduite
- α_m Pente de la courbe de l'écart relatif Δc_m du couple moteur en fonction de l'écart relatif de vitesse $\Delta \omega$
- α_r Pente de la courbe de l'écart relatif Δc_r du couple résistant de l'alternateur en fonction de l'écart relatif de vitesse $\Delta \omega$
- $\alpha = \alpha_r - \alpha_m$
- η Rendement de la turbine
- β Pente de la courbe de l'écart relatif de débit Δq absorbé en fonction de l'écart relatif de vitesse $\Delta \omega$
- $\varepsilon = \frac{3-\beta}{2}$ $\nu = \frac{2}{1-\beta}$ $j = \frac{1}{1 - \frac{\partial \eta}{\partial \Delta p_0}}$ } Abréviations utilisées dans les calculs
- $A = \varepsilon \cdot \nu \cdot \beta$ $B = \nu$ $C = \frac{\varepsilon \cdot \nu}{j} - 1$

Système de Réglage

- m Temps caractéristique du dosage accélérométrique
- τ' Temps caractéristique de la rapidité de réponse du régulateur (promptitude)
- $\bar{\omega}$ Pulsation (pseudo-pulsation) de l'oscillation de réglage
- $z = \bar{\omega}L/a$ grandeur caractérisant l'influence de la conduite forcée
- $f = \text{tg } z/z$ abréviation introduite dans les calculs
- $T'' = 2\pi/\omega$ période (pseudo-période) de l'oscillation de réglage
- x Facteur d'amortissement
- δ^* Décroissement logarithmique relatif à une pseudo-période $\delta^* = (2 \cdot \pi/\bar{\omega}) \cdot x$
- τ_e Temps caractéristique effectif de la rapidité de réponse du régulateur dans le cas de l'asservissement temporaire
- τ'' Temps caractéristique de la rigidité de l'asservissement temporaire

References Bibliographiques

- ¹ GADEN, D. *Considérations sur le Problème de la Stabilité*. 1945. Lausanne; La Concorde
- ² PINGOUD, P. Calcul théorique et pratique de la condition de stabilité du réglage accéléro-tachymétrique d'un groupe hydro-électrique fonctionnant isolément. *Inform. Techn. Charmilles* 6 (1956)
- ³ GADEN, D. *Influence de Certaines Caractéristiques Intervenant dans la Condition de Stabilité*. Lausanne; La Concorde
- ⁴ BOREL, L. Essai de systématisation de l'étude du réglage d'un groupe hydro-électrique. *Bull. tech. Suisse Romande* 7 (1958)
- ⁵ BOREL, L. *Stabilité de Réglage des Installations Electriques*. 1960. Lausanne; Payot
- ⁶ RAEER, V. Stabilité de réglage d'un groupe hydro-électrique. *Bull. tech. Vevey* (1959)
- ⁷ GARSOUX, J. *Les Systèmes Linéaires. I. Analyse fréquentielle; II. Régimes transitoires*. 1961. Paris; Dunod
- ⁸ PUN, L. Régulation de vitesse de groupes hydro-électriques. Analyse et recherche d'une condition optimum. *Bull. Soc. franc. Elect.* 58 (1955)

DISCUSSION

Introduction par l'auteur

Le rapport qui vous a été soumis fait partie d'un travail plus vaste concernant la stabilité des groupes hydro-électriques. L'un des buts de ce travail est de pouvoir déterminer par avance les valeurs des paramètres d'ajustement du régulateur, afin de réaliser une mise en service aussi rapide que possible et sans aucun tâtonnement.

Le texte proposé explique les moyens permettant de déterminer facilement les graphiques exprimant les conditions de stabilité. Nous avons utilisé une calculatrice électronique qui rend le travail très rapide et précis.

Mais il existe des cas où il est nécessaire de pouvoir tracer ces graphiques avec des moyens plus simples, lorsqu'on est dans une centrale par exemple et que l'on ne dispose pas de moyens de calcul aussi efficace qu'une calculatrice. En admettant que le coup de béliet soit un phénomène de masse, ce qui est parfaitement valable pour les basses chutes (grande valeur de ρ), il est alors possible de déterminer assez rapidement le centre, les axes et les asymptotes de l'hyperbole représentant la limite de stabilité et les courbes à coefficient d'amortissement constant. Le calcul est à faire pour chaque valeur de κ . Le fait que l'équation des différentes hyperboles ne comprend pas de terme constant, signifie que la courbe passe par l'origine, ce qui facilite encore la construction.

Figure A. En complément du rapport, j'aimerais insister maintenant sur quelques points particuliers.

Si l'hypothèse du coup de béliet en qualité de phénomène de masse est parfaitement admissible pour des basses-chutes, ce n'est plus le cas pour des installations à moyenne et haute chute. Nous avons représenté sur la Figure B, deux calculs relatifs à une turbine PELTON fonction-

nant sous 480 m de chute et alimentée par une conduite de 2326 m de longueur.

Le réseau de courbes en trait plein correspond au calcul fait en considérant le coup de béliet sous forme d'onde.

Le réseau de courbes en trait interrompu correspond au calcul fait en considérant le coup de béliet comme un phénomène de masse.

La différence particulièrement grande est due aux caractéristiques de l'installation. Néanmoins, cela montre clairement que l'hypothèse du coup de béliet comme phénomène de masse n'est pas admissible dans certains cas.

Données concernant la Figure B

PD^2	40000	kgm ²
n	600	t/min
L	2326	m
S	0,8	m ²
a	1080	m/sec
N	9350	ch
Q	1,7	m ³ /sec
H_n	480	m
η	0,88	
T	5,5	sec
θ	1,08	sec
ρ	0,24	

La question principale que l'on se pose lorsqu'on établit une méthode de calcul est de savoir si les bases admises pour le calcul sont suffisamment proches de la réalité et si la méthode de calcul est suffisamment exacte. Pour répondre à cette question, nous avons procédé à une série d'essais sur des machines industrielles afin de déterminer pour

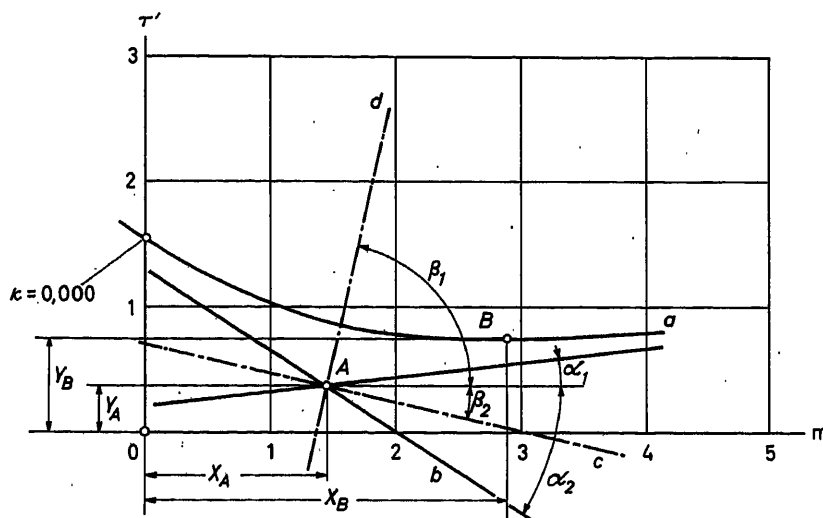


Figure A. Étude de la stabilité d'un groupe hydro-électrique construction par voie graphique de la courbe. $\kappa = 0,000$

un certain nombre de points de fonctionnement les conditions de stabilité, que nous comparons avec les résultats d'un calcul entrepris avec les mêmes bases. Je ne veux pas entrer dans le détail de la nature et du déroulement de ces essais, mais ne vous cacherai pas que l'exécution de telles mesures offre passablement de difficultés.

La Figure C est la reproduction d'un enregistrement d'une oscillation amortie. Il s'agit d'un groupe KAPLAN de 12950 ch débitant sur un réseau isolé.

Données concernant les Figures C et D

PD^3	465000	kgm ²
n	187,5	t/min
L	40,90	m
	12,00	m ²
a	1300	m/sec
N	7850	ch
Q	40	m ³ /sec
H_n	16,80	
η	0,89	
T	7,7	sec
θ	0,635	sec
ρ	10,7	

Le réseau résistant est constitué par une chaudière électrique et le régulateur de tension est en service. Statisme turbine 0 per cent ainsi que le statisme tension-fréquence.

$$\delta^* = 0,40$$

$$\kappa = 0,023$$

La Figure D est la reproduction d'un enregistrement d'une oscillation amplifiée. Nous nous trouvons ainsi dans la zone d'instabilité et sans qu'aucun ordre ou perturbation ne soit donné, dès que les paramètres m et τ' sont ajustés aux valeurs fixées pour l'essai, les organes de la turbine et la fréquence entrent en oscillations amplifiées.

Il s'agit dans cet essai de la même installation que celle au cliché précédent.

La Figure E est la reproduction d'un enregistrement d'une oscillation amortie. Il s'agit d'un groupe KAPLAN débitant sur une résistance hydraulique.

Données concernant la Figure E

PD^3	3410000	kgm ²
n	136,4	t/min
l	72	m
s	21,40	m ²
a	1300	m/sec
N	14200	ch
a	56,60	m ³ /sec
H_n	20,35	m
η	0,925	%
T	16,3	sec
θ	0,94	sec
η	8,5	
δ^*	0,75	
κ	0,42	

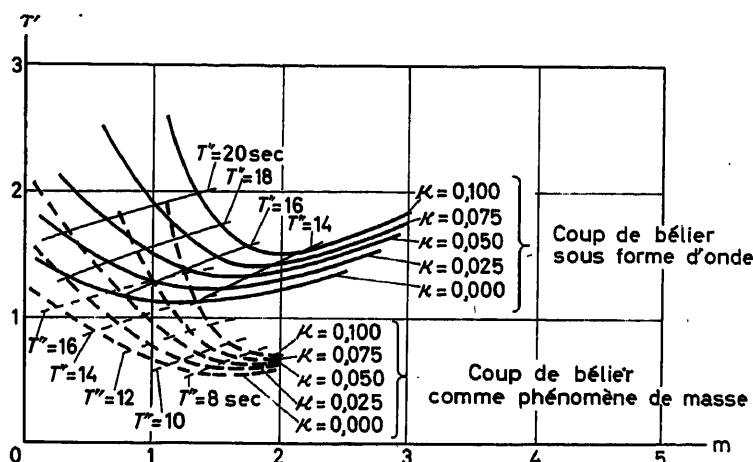


Figure B. Étude de la stabilité d'un groupe hydro-électrique turbine PELTON, 9350 ch. Comparaison entre les calculs: $f = 1$ coup de bélier de masse; $f \neq 1$ coup de bélier sous forme d'onde

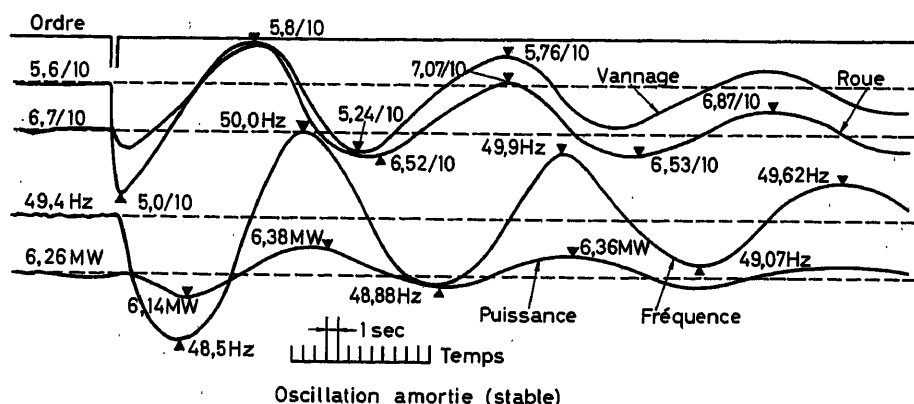


Figure C. Étude de la stabilité d'un groupe hydro-électrique turbine KAPLAN, 12950 ch. Pt de fonctionnement: $N = 6,26$ MW; $Q = 40$ m³/sec; $\tau' = 1,03$ sec; $H_n = 16,8$ m; $m = 1$ sec. Réseau séparé constitué par une chaudière électrique

EXPOSÉ D'UNE MÉTHODE D'ELABORATION DE GRAPHIQUES EXPRIMANT LES CONDITIONS DE STABILITÉ DU RÉGLAGE

Le régulateur de tension n'est pas en service ce qui donne une allure stabilisante à la loi du couple en fonction de la fréquence.

Ces quelques exemples vous montrent des résultats de mesure sur des machines industrielles. Il est nécessaire de comparer ces résultats avec le calcul effectué dans les mêmes conditions que pour les essais.

La Figure F représente la comparaison entre le calcul et les mesures dans le cas de la turbine KAPLAN de 12950 ch dont le réseau séparé sur lequel elle débite est une chaudière. Le réseau de courbe correspond au calcul effectué selon la méthode préconisée. Les points mesurés sont placés sur le réseau. Dans un certain nombre d'essais, nous avons pu

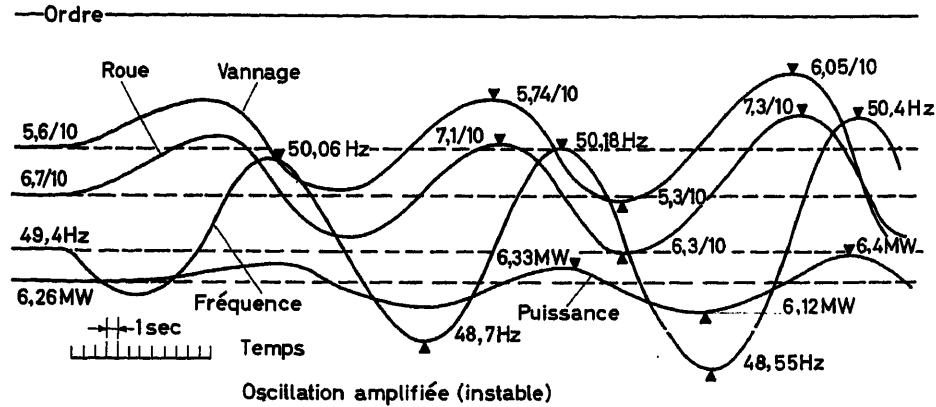


Figure D. Étude de la stabilité d'un groupe hydro-électrique turbine KAPLAN, 12950 ch. Pt de fonctionnement: $N = 6,2 \text{ MW}$; $Q = 39 \text{ m}^3/\text{sec}$; $\tau' = 1,26 \text{ sec}$; $H_n = 16,8 \text{ m}$; $m = 0,4 \text{ sec}$. Réseau séparé constitué par une chaudière électrique

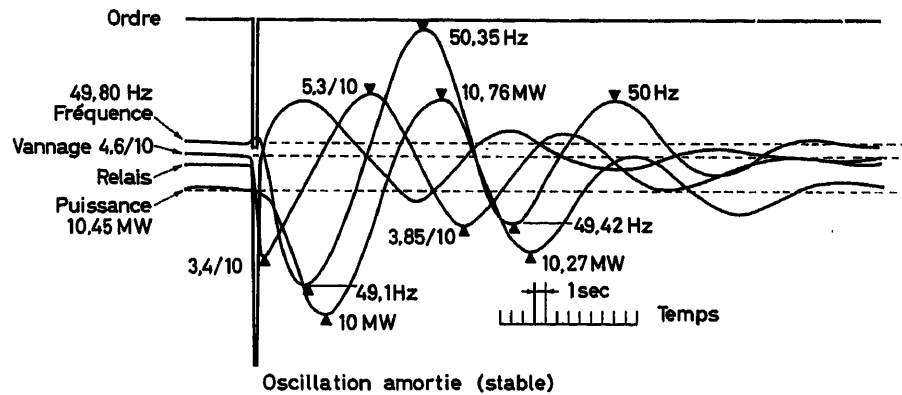


Figure E. Étude de la stabilité d'un groupe hydro-électrique turbine KAPLAN, 31 500 ch. Pt de fonctionnement: $N = 10,45 \text{ MW}$; $Q = 56,6 \text{ m}^3/\text{sec}$; $\tau' = 0,54 \text{ sec}$; $H_n = 21,20 \text{ m}$; $m = 0,66 \text{ sec}$. Réseau séparé constitué par une résistance hydraulique

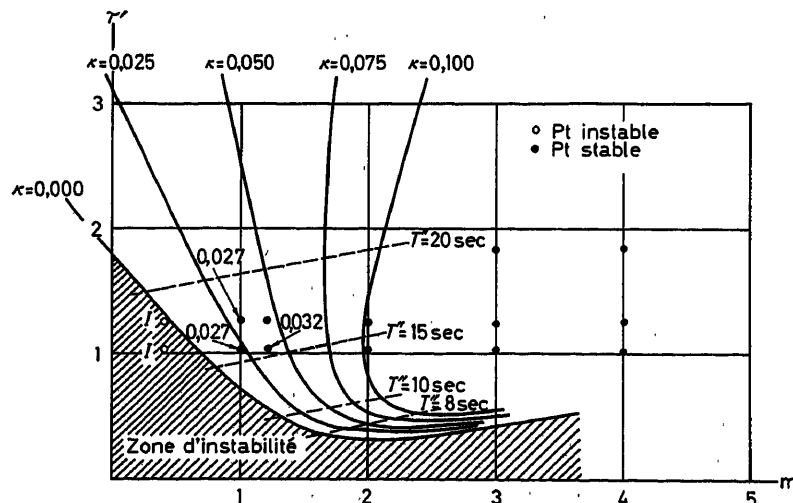


Figure F. Étude de la stabilité d'un groupe hydro-électrique turbine KAPLAN, 12950 ch. Comparaison entre le calcul et les mesures

Essai No.	Pt. fonctionnement		Valeurs calculées		Valeurs mesurées		Remarques
	m	τ'	δ^*	κ	δ^*	κ	
	sec	sec					
702	0,66	0,66	0,94	0,043	0,75	0,040	Turbine KAPLAN 31 500 ch
902	0,66	0,54	0,72	0,037	0,75	0,042	
1102	0,66	0,50	0,63	0,035	0,64	0,038	
S 5	1,0	1,03	0,40	0,023	0,41	0,027	Turbine KAPLAN 12950 ch
S 11	1,0	1,26	0,40	0,030	0,45	0,027	
S 17	1,4	1,03	0,54	0,035	0,50	0,032	
S 6	0,4	1,03	Instable		Instable		
S 12	0,4	1,26	Instable		Instable		

Figure G. Étude de la stabilité d'un groupe hydro-électrique comparaison entre résultats d'essais et mesures

déterminer les valeurs de κ (δ^* , T'') alors que pour d'autres l'oscillation est tellement amortie que la détermination de κ par mesure de plusieurs oscillations n'était pas possible.

La Figure G présente la comparaison entre le calcul et les résultats d'essais et ceci sous forme de tableau de chiffres. La comparaison est faite sur les 2 turbines déjà citées et nous constatons une bonne concordance. J'estime cette concordance bonne en connaissant les difficultés qu'il y a à effectuer des calculs et exécuter des essais dans des conditions exactement identiques.

En complément du rapport j'ai voulu par ces quelques exemples vous montrer combien les conditions de stabilité peuvent être différentes suivant les divers points de fonctionnement et qu'il est nécessaire de serrer le problème de près (abondance de la turbine-orifice, du coup de bélier de masse dans certains cas). Les mesures faites sur des machines industrielles, bien qu'encore en nombre relativement réduit, montrent une bonne concordance avec les calculs.

B. FAVEZ, *Electricité de France, 12 Place d'Etats-Unis, Paris 16, France*

(1) What is the author's opinion on the advisability of taking into account the random nature of load fluctuations when calculating the optimal values for the controller parameters?

(2) Does the author think that the two types of controller considered in his paper are the optimal ones for the control of hydraulic turbines supplying single alternator networks?

(3) In the author's example of a KAPLAN turbine, does he take into account the control of the turbine blades as well as that of the gate, or only the control of the gate?

A. TSCHUMY, *in reply*

(1) The small random load variations for the calculation of optimal values of the parameters have not been taken into consideration. Our tests on industrial machines have shown that these variations were, for the network used, quite small compared with the linear perturbations created. We believe that these small variations might be neglected.

(2) Our paper deals with the case of the accelero-tachometrical controller and mentions the case of the temporary automatic controller because of its practical development. The Society where I am working has designed and successfully developed the accelero-tachometrical controller, first the mechanical version, then the electrical type. The production of electrical controllers allows us to realize, also quite easily, a temporary automatic controller. These are the reasons of our choice. We do not think that they are types of an 'optimum' controller as our method is not connected with any controller type. It is sufficient to introduce the equation corresponding to the controller.

(3) We assume that in the case of a KAPLAN turbine there is a perfect relationship which allows us to operate on the envelope curve of the minor extremities. Our controllers are based on these principles.

I admit, however, that in practice the double regulation of KAPLAN turbines is a source of error and delay.

If you wonder why we have made comparative studies of KAPLAN turbines alone, the reason is that we have two customers who provided us with separate systems, and the controllers were fitted to turbines of that kind.

I hope to be able to experiment on turbines with simple regulation, such as Francis turbines.

D. RUMPEL, *Siemens-Schuckertwerke, Erlangen, Germany*

Mr. Tschumy gave an interesting paper on an investigation of turbine stability using a digital computer. Here I wish to present another method (Figure A) which has several advantages and some disadvantages over that of Mr. Tschumy.

We have compiled a programme which computes the stability region of any linear control system. Two of the parameters V_1 and V_2 of the control loop under investigation may be varied, e.g. the parameters τ' and m in Mr. Tschumy's paper. The coefficients of the characteristic polynomial equation of the system will be functions of the parameters V_1 and V_2 . Using Routh's stability criterion, the programme systematically searches the V_1 and V_2 plane for stable and unstable points. Each time the stability boundary is crossed with constant ordinate V_1 , the abscissa V_2 of the boundary is improved by successive interpolative approximations. For this interpolation, the step length is reduced by a factor of two after each step. Hence, after ten steps the accuracy is better than one thousandth of the probing step length. The coordinates of the stability boundary found by this method are then punched out.

If the characteristic equation is transformed by substituting p' for p where $p' = p + x$, this programme will compute curves of constant damping factor x , instead of the stability boundary. Figure B shows the stability boundary of a KAPLAN turbine. In this case the time constants of the two main servomotors for the runner blades and the guide vanes are the parameters V_1 and V_2 . The investigation determined the damping resulting from different values of these two parameters. The damping was measured here in terms of a damping time constant.

Figure C shows a second example, the stability boundary for a PELTON turbine. The parameters are the gain and reset time of the regulator. A third parameter is the inertia time constant. The transportation lag of the pipeline was represented by a third order Padé approximation. The pipeline in this plant is relatively long and inclined at a relatively small angle to the horizontal. The first resonant frequency of the pipeline is therefore nearly coincident with that of the whole system. I wish to stress this point, because I am not sure whether or not the iteration procedure in Mr. Tschumy's programme is convergent in this case.

The main advantages of this digital method are its broad scope and flexible application. Indeed, there are almost no restrictions on

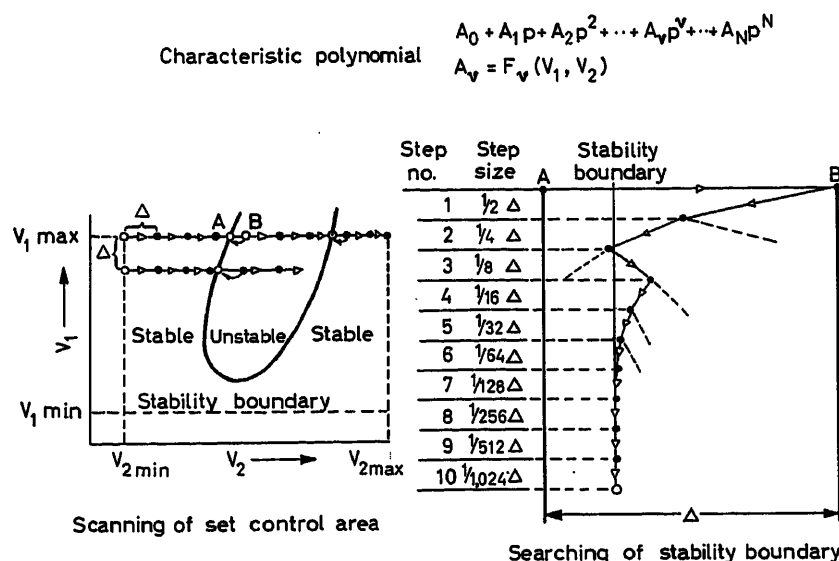


Figure A. Digital computer. Programme for calculation of stability limit

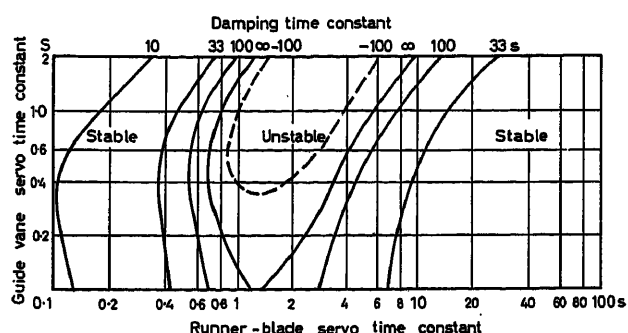


Figure B. Control of KAPLAN turbines. Influence of time constants of main servomotors on stability

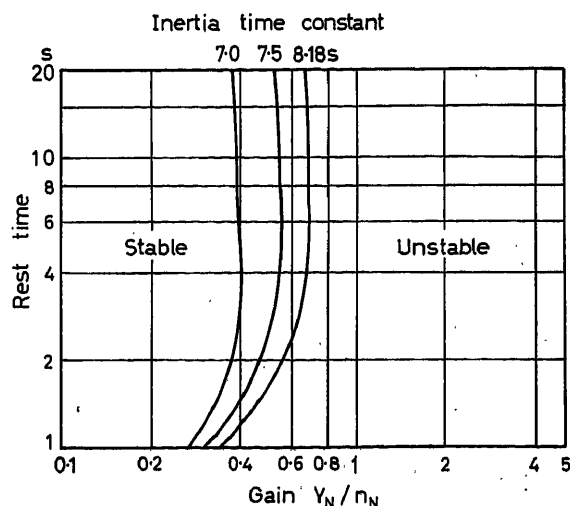


Figure C. PELTON turbine control. Stability limits with varying starting time constants

the structure and order of the system or on the choice of the parameters to be varied. The disadvantages are the need to calculate by hand the characteristic equation from the system data (this will be changed in the near future), the fact that the resonant frequency is not computed and the amount of computing time required, which is probably more than that with Mr. Tschumy's programme.

A. TSCHUMY, in reply

Dr. Rumpel establishes stability curves using parameters that differ from our own. This is perfectly feasible, but I would like to point out, however, that on our electric controllers we find that two commutators allow us to adjust m and τ' . During operation, stability is ensured by proper adjustment of these two parameters. The choice is therefore made for good practical reasons.

Dr. Rumpel emphasizes that his calculations are precise to the order of 0.1 per cent. It is quite unnecessary to work to this degree of accuracy and I am sure anyone who has experimented in this field will agree with me.

With regard to the effect of the pipe, I can say that we are taking account of this in the equation for ram pressure. If we introduce this into our calculations we have a complete picture of the conditions for stability or instability of the system.

L. BOREL, E.P.U.L., Epalinges, Switzerland

(1) The damping factor x of the two conjugate roots does not appear sufficient for judging the degree of stability of the installation. In fact a characteristic equation of the third order has three roots. It may be that the third root, which is real, gives rise to better damping than that of the two conjugate roots. This problem becomes even more important when the characteristic equation is higher than third order.

(2) The example of the KAPLAN turbine has been treated by taking into account the three hydraulic parameters α_m , β and j . In practice the hydraulic behaviour of a KAPLAN turbine is determined by six hydraulic parameters.

A. TSCHUMY, in reply

(1) The case of a root situated on the real axis of the complex plane did not escape us. This is the case of an aperiodic damping. This point has to be studied in the same way as in the general case.

(2) As to the KAPLAN turbine, we have considered this as an ideal KAPLAN, but we are quite aware of the difficulties which occur in practice.

Digital Investigation of Multi-machine Power Systems

H. GLAVITSCH

Summary

In order to satisfy the need for a scheme by which transients in multi-machine power systems could be calculated more accurately, a digital programme was developed which is based upon the two-reaction theory. The terms due to the time variation of the armature flux linkage are neglected and saturation is not taken into account. Damping due to the rotor windings of the synchronous machines is represented correctly according to the two-reaction theory. The representation of the synchronous machines includes speed governors and voltage regulators. Because of the required storage capacity and operating time the outlined digital method is not practical for systems with numerous machines. It should rather be applied to systems with a limited number of machines in order to make thorough studies. The digital programme here was set up for a three-machine problem. By the chosen integration method (Runge-Kutta-Gill) non-linear regulating devices can also be handled. To illustrate how this programme can be used the transient stability of a long-distance power transmission consisting of power station, synchronous condenser and infinite bus is investigated. Curves show the rotor angles as functions of time for various governor and regulator arrangements and the effect of the damper windings.

Sommaire

Un problème qui se pose actuellement est le traitement, d'une manière aussi exacte que possible, des phénomènes transitoires dans un système formé de machines synchrones reliées par un réseau. Il a été établi dans ce but un programme pour une calculatrice numérique basé sur la théorie de Park. Les effets de saturation et de la variation du flux statorique ont été négligés, par contre, l'amortissement provoqué par les enroulements rotoriques est calculé en suivant exactement la théorie. La représentation des machines synchrones comporte des régulateurs de vitesse et de tension. Les bases théoriques sont valables pour un nombre quelconque de machines; les difficultés proviennent du fait que les besoins en capacité de mémoire et en temps de calcul croissent rapidement avec le nombre de machines. Il est intéressant d'étudier d'une manière approfondie les systèmes comportant un petit nombre de machines; le programme actuel est limité au cas de trois machines. La méthode d'intégration (Runge-Kutta-Gill) permet d'examiner l'effet de régulateurs non linéaires. Comme exemple de calcul, on analysera la stabilité dynamique d'un système de transmission à grande distance, consistant en une usine électrique reliée à un réseau de puissance infinie par l'intermédiaire d'une longue ligne au milieu de laquelle se trouve un compensateur synchrone. On trouvera des représentations graphiques, donnant pour diverses valeurs des paramètres de réglage l'angle polaire en fonction du temps, et exprimant l'effet des enroulements amortisseurs.

Zusammenfassung

Um dem Bedürfnis einer möglichst exakten Behandlung der dynamischen Vorgänge in Synchronmaschinen, die über ein passives Netz miteinander verbunden sind, Rechnung zu tragen, wurde ein digitales Rechenprogramm erstellt, das sich auf die Zweiachsentheorie aufbaut. Der transformatorische Effekt des Statorflusses sowie die Sättigung werden außer acht gelassen. Entsprechend der Zweiachsentheorie wird die Dämpfung durch die Rotorwicklungen der Maschinen exakt berücksichtigt. Die Synchronmaschinen werden mit Drehzahl- und Spannungsregler dargestellt. Die dargelegten theoretischen

Grundlagen gelten ganz allgemein für ein Mehrmaschinensystem, jedoch ist die hier gewählte Darstellungsweise aus Gründen der Speicherkapazität und Rechenzeit nicht für ein System mit einer sehr großen Anzahl von Maschinen geeignet. Es ist vielmehr daran gedacht, Systeme mit wenigen Synchronmaschinen eingehend behandeln zu können. Das ausgeführte Rechenprogramm wurde für ein Dreimaschinenproblem aufgestellt. Das gewählte Integrationsverfahren (Runge-Kutta-Gill) erlaubt auch die Behandlung von nichtlinearen Reglern. Als Beispiel für das Rechenprogramm wird die dynamische Stabilität einer Übertragung über große Entfernungen untersucht, die aus Kraftwerk, Phasenschieber und starrem Netz besteht. Kurven zeigen den zeitlichen Verlauf der Polradwinkel für verschiedene Regelparameter und die Wirkung der Dämpferwicklungen.

Introduction

Modern control systems have found a wide field of application in the regulation of generators in power systems. There voltage regulators and speed governors have to be built according to the conditions of parallel operation and with the total system in view. Hence the necessity arises of predicting the effects of different characteristics of these devices on the dynamic behaviour of the system with the aim of securing transient stability which is of prime importance. In a thorough analysis of the dynamic behaviour of a network the knowledge of the internal characteristics of the synchronous machines interconnected by the network is essential. As investigations on digital and analogue computers have shown, damper windings are of prime importance for stability in critical cases. Hence the representation of the generators and the network should be as comprehensive as possible in order to get a true picture of how the system is affected by the different control elements. A method treating one generator only in connection with an infinite bus is not sufficient since mutual effects between the different synchronous machines may be important. It was these facts that caused the working out of a dynamic digital programme characterized by the following points:

- (1) Treatment of several synchronous machines interconnected by a network.
- (2) Comprehensive representation of the synchronous machines according to Park-Gorev's equations.
- (3) Inclusion of linear or non-linear voltage regulators and speed governors.
- (4) Discontinuous change of the characteristics of the network to represent disturbances and faults.
- (5) Integration of the system by the method of Runge-Kutta-Gill.

Saturation is not considered, neither, as in general practice, are the terms due to the time variation of armature flux linkage. The theory applied in the following is generally valid for a multi-machine system, but owing to the limited storage capacity

of digital computers and the operating time which increases rapidly with a growing number of generators, this method is practical only for systems of moderate size.

The digital programme described in this paper is laid out for a system of three synchronous machines in compliance with the points given above. The intention is to use it on problems showing the basic features of the parallel operation of synchronous machines and how the system is affected by the control devices.

Similar programmes have already been set up^{1, 3, 5}, either intended for a single machine connected to an infinite bus or designed for systems with numerous machines where certain characteristics of the system are represented in an approximate fashion only, e.g. damping.

Especially on analogue computers, various investigations^{4, 6, 7} of this kind have been carried out showing that the set-up becomes quite elaborate if the representation includes secondary effects as well.

Problem Delineation

Figure 1 shows a schematic diagram of a multi-machine system as it will be represented by the digital programme. The network is assumed to be linear and passive. Transmission lines and loads have impedances independent of frequency. Each of the synchronous machines has two control circuits, the driving and the excitation system. Assuming a balanced load a single phase

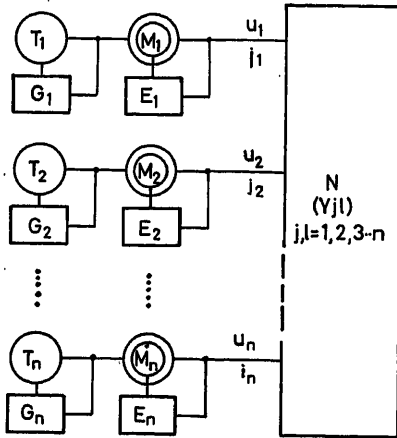


Figure 1. Schematic diagram of a multi-machine power system

- N Network characterized by the admittances Y_{ij}
 - i, u_i Current voltage at the terminals
 - M_i Synchronous machine
 - E_i Excitation system
 - T_i Prime mover
 - G_i Speed governor
- } driving system

representation of the network is sufficient, and by means of sequence networks an unbalanced case can be handled as well. All the characteristic data of the synchronous machines are known as well as the steady-state loadings. The driving and the excitation systems are described by equations or transfer functions.

In a problem of this kind simulation and observation of the dynamic behaviour are the only means of judging the stability of the system and the performance of the individual elements

since the application of stability criteria is impossible. Hence the various electrical and mechanical quantities in the system have to be computed as functions of time.

The Fundamentals of the Programme

All the following equations are written in per-unit.

The Network

As the network, all of the elements between the terminals of the synchronous machines are taken according to Figure 1. Since it is linear and passive the relationship between the variables at the terminals can be expressed by a matrix equation:

$$I = Y_{ji} \cdot U \quad (1)$$

$$I = \begin{bmatrix} i_1 \\ i_2 \\ \vdots \\ i_n \end{bmatrix}; \quad U = \begin{bmatrix} u_1 \\ u_2 \\ \vdots \\ u_n \end{bmatrix} \quad (2)$$

where i_j, u_j are current and voltage at the terminals, n is total number of machines, and Y_{ji} ($j, l = 1, 2, 3, \dots, n$) is the matrix of input and transfer admittances where $Y_{ji} = Y_{lj}$. The elements of these vectors and matrices are complex quantities.

The Synchronous Machines

Their dynamic behaviour will be described by means of the two-reaction theory (Park-Gorev's equations⁸) where the terms due to the time variation of the armature flux linkage are neglected. It is feasible to include saturation in the frame of the two-reaction theory, but owing to lack of storage capacity it could not be included in the present programme.

The equations of Frey and Althammer¹ for a single synchronous machine are employed here with some supplements with consideration of the above-mentioned simplifications.

The equation of the rotors

$$u_{ml} = i_{ml} + T_{ml} \frac{d\psi_{ml}}{dt} \quad (3)$$

The equation of the armatures

$$\begin{aligned} u_{dl} &= n_l \psi_{ql} \\ u_{ql} &= n_l \psi_{dl} \end{aligned} \quad (4)$$

The mechanical relationships

$$\frac{dn_l}{dt} = \frac{1}{2H_l} (\psi_{dl} \cdot i_{ql} - \psi_{ql} \cdot i_{dl} + m_{dl}) \quad (5)$$

$$\frac{d\beta_k}{dt} = \omega_n (n_l - n_k) \quad (6)$$

$$i_{l+1}\beta_k = i_l\beta_k + i_{l+1}\beta_l \quad (7)$$

where n_l is speed of the l th machine, m_{dl} the driving torques, ψ_{ml} the flux linkages of the rotors, ψ_{dl}, ψ_{ql} the flux linkages of the armatures, i_{dl}, i_{ql} the armature currents, i_{ml}, u_{ml} the rotor currents and voltages (field voltages). T_{ml} the time constants of the rotor windings, H_{ml} the inertia constants, k the subscript of the reference machine, ω_n is the nominal angular frequency, $m = 1, 2, 3; l = 1, 2, 3, \dots, n$, and m denotes the field winding, direct axis and quadrature axis damper winding.

It should be mentioned that the rotor angles β_k refer to a reference machine and not to an axis rotating with constant speed. Only these angular differences are meaningful in judging the stability. In other words, the relative position of the rotor is important no matter what the actual speed (frequency) of the system is.

In addition, the following linear relationships between currents and flux linkages for unsaturated synchronous machines hold:

$$\psi_{ml} = b_{dl}^{(m)} i_{dl} + b_{ql}^{(m)} i_{ql} + \sum_{i=1}^3 a_{mi}^{(m)} i_{mi} \quad (8)$$

$$\psi_{dl} = b_{dl}^{(d)} i_{dl} + \sum_{i=1}^3 a_{mi}^{(d)} i_{mi} \quad (9)$$

$$\psi_{ql} = b_{ql}^{(q)} i_{ql} + \sum_{i=1}^3 a_{mi}^{(q)} i_{mi}$$

where

$b_{dl}^{(m)}, b_{ql}^{(m)}, a_{mi}^{(m)}$ etc. are coefficients dependent upon the reactances and stray coefficients of the synchronous machines. The variables at the terminals of eqn (1) may be expressed by the variables in the two axes of eqns (8) and (9) using eqn (4) leaving a system of linear equations containing all the relationships between currents and flux linkages of the system. Thus, the mutual couplings of the machine are expressed by these equations which are given in matrix form:

$$\begin{aligned} \psi_R &= A I_S + B \psi_S \\ 0 &= C I_S + D \psi_S \end{aligned} \quad (10)$$

where ψ_R is the vector of flux linkages of the rotors, ψ_S the vector of flux linkages of the armatures, I_S the vector of all currents in both axes, and A, B, C, D are matrices.

By partitioning and inversion ψ_S and I_S may be expressed in terms of ψ_R . This system of finite and differential equations is now sufficient to describe completely the multi-machine power system under the above assumptions. In terms of control, the network with its synchronous machines could be denoted as plant, whereas driving torques and excitation voltages appear as controlling variables. The controlled variables, on the other hand, are the speeds of the rotors and the terminal voltages, in some cases the reactive current or reactive power at the terminals of the machines.

The Control Systems

In general, the plant of a power system having n generators will be controlled by $2n$ control circuits which frequently are not all necessary to guarantee stable operation. The behaviour of these control circuits is described either by differential equations or by their transfer functions from which, in most practical cases, a system of differential equations of the following form can be derived:

$$\frac{dx_i}{dt} = f(x_1, x_2, \dots, x_i, \dots, x_r) \quad (11)$$

where r is the number of variables of integration of the control system.

Quite often non-linear systems may be represented in this way too. The controlling variables, i.e. the output of these control systems, cannot exceed certain minimum and maximum values (limiting).

As a method of integration the one by Runge-Kutta-Gill is employed as already mentioned in the introduction. The variables of the synchronous machine to be integrated are as in¹ the rotor flux linkages, the speed and the rotor angle. For the control circuits the variables of integration are given in the form of eqn (11).

The Digital Programme

Based upon the fundamentals given above, a programme for the Siemens 2002* digital computer was set up, whose basic operations are illustrated by the flow diagram in Figure 2. Besides the characteristics of the network, of the synchronous machines and of the control circuits, the steady-state loadings of the machines have to be specified†. Starting from these loadings, which are characterized by active power and terminal voltage, the initial values of the network are calculated by an iterative process (Pos. 1). Having found the values at the terminals,

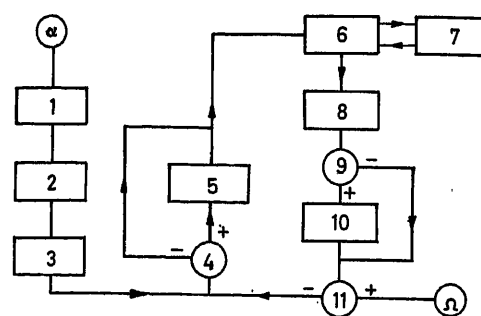


Figure 2. Flow diagram of the digital programme

- | | |
|------------------|---|
| α, Ω | Start, end of computation |
| 1 | Determination of initial conditions of the network by iteration |
| 2 | Initial condition of the synchronous machines |
| 3 | Selection of regulators and their initial conditions |
| 4 | Alteration of network yes (+) or no (-) |
| 5 | Alteration of network |
| 6 | Integration programme |
| 7 | Solution of the finite equations |
| 8 | Limiting of the controlling variables |
| 9 | Print yes (+) or no (-) |
| 10 | Print |
| 11 | End of computation yes (+) or no (-) |

the other initial quantities of the machines can be computed directly (Pos. 2). The programme already contains a series of sub-routines describing customary speed governors and voltage regulators which are called up by characteristic numbers built into the programme accordingly (Pos. 3). For every new control system not contained in the programme a sub-routine has to be set up. Before starting the integration process the network may be altered (Pos. 4 and 5). After a predetermined number of steps of integration (Pos. 6, 7, 8) the instantaneous values of the chosen quantities are printed (Pos. 10). On demand, a special print sub-routine can be added which prints the results in diagram form. The alteration of the network is achieved by substitution (Pos. 5) of another admittance matrix.

The operating time of 9 sec/step (4-6-7-8-9-4) is relatively high, but this is the price for the detailed representation.

* 2,000 word core, 10,000 word drum storage.

† For n machines only $n-1$ active loads have to be specified.

Special Cases of Application

One Synchronous Machine as Infinite Bus

By setting dn_s/dt of one machine equal to zero and substituting very small reactances, this machine will behave like an infinite bus. In this case the torque as well as the field voltage does not require any control.

Separation of One Synchronous Machine from the Network

In this case the machine is completely isolated and has to be operated with speed governor and voltage regulator for a satisfactory steady-state operation. The separation is achieved by inserting very small admittances between the machine and the network.

Synchronous Machine without Damper Windings

It is possible that a machine in the system is not equipped with a damper winding in one of the two axes, or may be in neither of them. Any of these cases will be treated correctly by the programme by setting the corresponding sub-transient time constants equal to zero.

Applications

Parallel Operation of Several Synchronous Machines of Finite Power

This mode of operation may occur in local networks which are separated from an infinite bus as in industry or in very large

systems where groups of generators can be replaced by equivalent machines. A typical example is the study of load-frequency control where the controlled variables of the driving systems are linear combinations of a power in one location of the system and the system frequency.

Parallel Operation of Several Synchronous Machines with an Infinite Bus

For this application one of the machines (see beginning of this subsection) will be converted into an infinite bus. The other machines may represent generators, power stations or groups of power stations.

By taking advantage of the possibility of altering the network (Pos. 5) disturbances caused by short circuits, line droppings etc. and their effects on the total system may be studied. Optimum adjustment of the control systems will be found by trial and error.

Results

As a sample calculation a power transmission over a distance of 600 km is investigated. On one end there is a power station the output of which—in this case it is the characteristic power of the transmission line—is transmitted to an infinite bus. Halfway between power station and infinite bus a synchronous condenser is installed in a substation.

In one of the two circuits of the line between the power station and the substation a short circuit occurs which is cleared after 0.1 sec by dropping this circuit; after another 0.1 sec the circuit

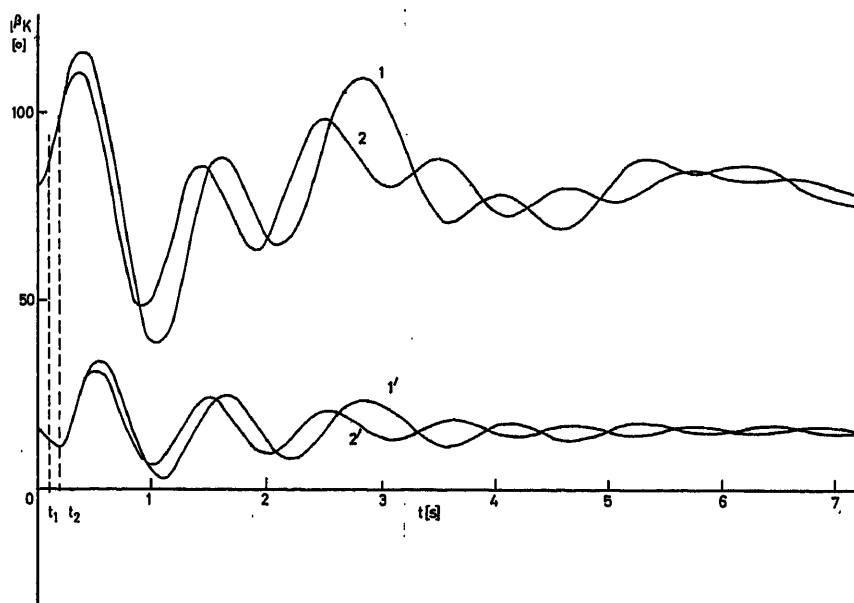


Figure 3. Angular swings in a multi-machine system
(Effect of speed governor)

0 Moment of short circuit
 t_1 Clearing of short circuit
 t_2 Reclosing of circuit
 K, K', K_r Amplification factors
 T_1, T_2, T_r etc. Time constants

Numbers with dashes refer to angles between network and synchronous condenser; numbers without dashes refer to angles between network and power station.

Curves 1. Transfer function of the voltage regulator in the power station

$$G(p) = \frac{K}{(1 + T_1 p)(1 + T_2 p)} = \frac{20}{(1 + p)(1 + 0.1 p)}$$

in the substation

$$G'(p) = \frac{K'}{1 + T_1 p} = \frac{20}{1 + p}$$

Transfer function of the speed governor in the power station

$$H(p) = \frac{K_r}{1 + T_r p} = \frac{25}{1 + p}$$

Curves 2. The amplification factor of the speed governor is raised to $K_r = 100$ against Curves 1

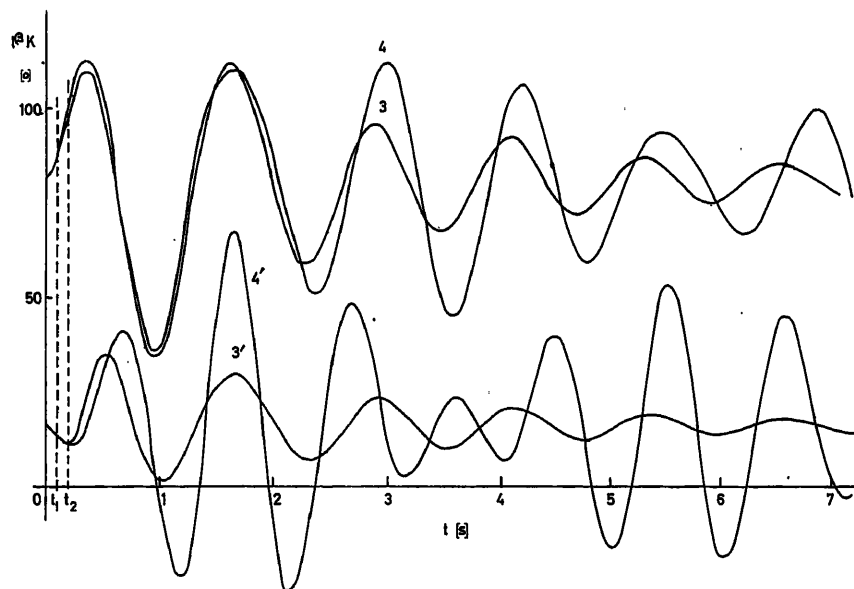


Figure 4. Angular swings in a multi-machine power system
(Effect of the damper windings)

The same denotation holds as for Figure 3

Curves 3. Transfer function of the voltage regulator in the power station

$$G(p) = \frac{K}{1 + T_1 p} = \frac{20}{1 + 0.5p}$$

The speed governor of the power station and the voltage regulator of the substation are left unchanged against Curves 1

Curves 4. Against Curves 3 the damper windings are completely omitted

is reclosed again. The effect of this sequence of switching operations on the total system, the transient stability and how it is affected by the control systems are of interest.

The power station and the substation are equipped with voltage regulators, and the generators have speed governors too. Figure 3 shows graphs of the rotor angles for two different adjustments of the speed governors of the power station: the favourable effect of a higher amplification (Curve 2) is quite obvious, but unfavourable mutual effects between speed governors and voltage regulators cannot be detected. A second pair of curves (3 and 4) illustrate the efficiency of the damper windings. In the system represented by Curve 4 all the damper windings are omitted, resulting in a considerably smaller margin of stability. Hence, in critical cases the damper windings must not be neglected. On the other hand, when systems represented without dampers are shown to be stable in a computer investigation they will certainly be stable in reality too, but the underlying assumptions are pessimistic.

Conclusions

The last-mentioned example shows that the application of this digital programme is justified for systems which cannot be studied on an a.c. network analyser and for those which would require a very elaborate set-up on the analogue computer. Primarily, the programme was set up to study the parallel operation of several synchronous machines in detail and to investigate such a system including all controls comprehensively.

In many cases it will be possible to reduce large systems by substituting equivalent machines, thus creating a configuration to which the programme may be applied. This will be even easier when the present programme is extended.

References

- 1 FREY, W. and ALTHAMMER, P. Investigating the transient stability of synchronous machines with the aid of a digital computer. *Brown Boveri Rev.* 48 (1961) 5/6 p. 356-366
- 2 LAIBLE, T. *Die Synchronmaschine im nichtstationären Betrieb.* (1952). Springer-Verlag
- 3 DYRKACZ, M. S., YOUNG, C. C. and MAGINNISS, F. J. A digital transient stability program including the effects of regulator, exciter and governor response. *Power Apparatus and Systems.* (Feb. 1961) 1245-1257
- 4 RICHARDSON, G. G. and WANG, T. C. Use of the A-C network analyzer and electronic differential analyzer in the study of load frequency control. *Power Apparatus and Systems.* (Feb. 1962) 1143-1148
- 5 GUPTA, P. P. and DAVIES, M. W. H. Digital computers in power system analysis. *Proc. Inst. elect. Engrs*, 108 A 41 (1961) 383-404
- 6 ALDRED, A. S. Electronic analogue computer simulation of multi-machine power system networks. *Proc. Inst. elect. Engrs* 109, A 45 (1962) 195-202
- 7 MILES, J. G. Analysis of overall stability of multi-machine power systems. *Proc. Inst. elect. Engrs*, 109 A 45 (1962) 203-217

DISCUSSION

L. K. KIRCHMAYER, *General Electric Company, Schenectady, N.Y., U.S.A.*

The simulation of the dynamics of a power system by means of a digital computer provides a powerful tool to the control system analyst for the study of the behaviour of the system during transients. We concur with Mr. Glavitsch's observation that time-domain synthesis is the only practical way of judging the performance of such complex systems.

The emphasis on fast control action during system disturbances places a premium on a complete and accurate analytical representation. The need for accuracy is further emphasized by the fact that the multi-machine power system inherently exhibits very poorly damped behaviour. The addition or subtraction of small amounts of damping by the voltage regulators or speed governors can be critical to system stability.

The digital computer programme described in this paper is an important forward step in the analysis of power system dynamics. Digital programmes for machine and small system simulations being used at the General Electric Company have proved of great value in determining the feasibility of new control schemes, particularly in the area of excitation systems. We were interested in the author's decision to neglect generator saturation in his representation. Our own studies have indicated that the simulation of generator saturation is important both from the effect it has on generator performance and because it loads the non-linear excitation system to the correct operating region. The latter reason is of significance primarily during large power system disturbances.

The use of sub-routines for providing programme flexibility in the definition of the characteristics of the speed governors and voltage regulators follows our own experience.

The operating time of 9 sec per time step is larger than we have experienced in running our programmes on a high speed, all-core computer. We find that problems such as those illustrated can be run in approximately real time including the automatic plotting of results.

Although the author does not indicate how the difference between machine rotor angles are treated in coupling the units through the external network, it must be assumed that this factor has been accounted for. This treatment is necessary because the generator equations have reference to their own direct and quadrature axes and not to an arbitrary set of axes. Would Mr. Glavitsch please comment on the manner in which this coupling is accomplished?

In conclusion, we wish to compliment the author for his excellent contributions in successfully applying a moderate-scale digital computer to this important area of power system analysis.

H. GLAVITSCH, *in reply*

In answering the questions raised by Mr. Ewart and Mr. Kirchmayer, I would like to start with the last one, namely, how the machines are coupled through the network and how the rotor angles are treated. For this purpose I will refer to the eqns (1-10) in the paper.

It has been stated that the rotor flux linkages ψ_{m1} , being the components of the vector ψ_R , have been chosen as variables for integration. In addition, the speeds n_i and the rotor angles β_k are integrated.

Assuming that a step of integration has just been completed, then ψ_R is known and one has to calculate the currents i_{a1} and i_{q1} (which are components of I_S and the flux linkages ψ_{a1} and ψ_{q1} , which are components of ψ_S), by inverting the matrix

$$\begin{vmatrix} A & B \\ C & D \end{vmatrix}$$

The elements of the matrices A and B can be taken from eqns (8) and (9) and those of C and D can be derived from eqns (1), (2) and (4).

It should be noted that in B and C many zeros will occur, hence, it is economical to partition the matrix and invert just D . Then this inversion supplies all the information to perform the next step of integration. The coupling of the machines is thus obtained by the matrix D , the exact rotor angle is obtained by eqns (5) and (6), which again will affect matrix D .

In order to be able to start the integration process the initial values at $t = 0$ have to be calculated by some other means, but this requires just a steady-state solution.

As far as the saturation of the armature flux is concerned I have to agree with Mr. Ewart and Mr. Kirchmayer, although there will be cases where it is not so important. We have been aware of the fact that an error is introduced by neglecting saturation, but within the present method it would have meant a considerable complication. Nevertheless, as a next step in completing the programme, we are planning to include it.

In replying to the comment on the computation time I would like to point out that the matrix inversion mentioned above has to be performed four times per step when using the Runge-Kutta-Gill method, and this takes time.

T. LAIBLE, *Oerlikon Engineering Works, Zürich, Switzerland*

The exact inclusion of damping effects in a multi-machine case is a real innovation. For the case of one machine connected to an infinite bus the inclusion of a damping torque proportional to slip is quite satisfactory. In special cases it is possible to extend this method to multi-machine systems. This can be done if it is possible to find somewhere in the system a point where the voltage remains at least approximately constant. Then one can reference all the load angles to this voltage vector and their time derivatives will be suitable slips from which to calculate the damping torques. But in the general case it is not possible to find such a voltage vector and then this simplified method is no longer applicable. The normal approach then is to neglect damping altogether, which is quite unsatisfactory as the author of the paper has shown.

I would comment on the statement that for synchronous machine stability problems only actual calculation and observation of the results can assure the existence of stability. For a single-machine case Professor Yanko-Trinitzki has applied the Liapunov method, using the sum of the kinetic energy, the energy equivalent to the system losses and the energy required for excitation as the Liapunov function. It seems possible that this way of attack might be extended to multi-machine problems, but to my knowledge it has not actually been done.

Reference

YANKO-TRINITZKI, A. A. A new method for analysing the performance of synchronous motors during short perturbations. Gosznergoizdat, 1958

H. GLAVITSCH, *in reply*

The simplified method which is widely used in the analysis of multi-machine power systems and which is referred to by Mr. Laible is often applicable when the system has numerous machines, as full detailed analysis is not always required for all systems.

It might be possible that the stability of a multi-machine system can be assessed by a similar analysis, as mentioned by Mr. Laible. But it is felt that in most cases the inspection methods as shown in the paper are most practical. In addition, the swing curves also reveal the degree of stability (damping).

Optimizing Control of Water Turbine Governors Considering the Non-linearity of Servomotor Speed

T. STEIN

Summary

A case of water-turbine hunting when the station was isolated from the grid, could only be explained and completely eliminated by calculations of transfer functions, introducing, contrary to the usual linearization, that zone of non-linearity, which is decisive for damping. Neglecting all transfer lags of the main servomotor, formerly, a short damping time was introduced as optimum criterion, which has been confirmed by analogue computers as being the only one valid for water turbines. Calculations prove that this optimum formula retains its complete validity in spite of the non-linearity. Means for improving the non-linear shift are explained.

For closed-loop tests, Moscow Power Institute uses real governors of steam turbines simulating all other elements. For water turbines the hydraulic shock must be simulated too. Furthermore, with a simulated servomotor, the hydraulic and friction reactions of the controlled water turbines may be considered. Thus already with workshop-tests optimizing control can safeguard the reliability in cases of disconnection disturbances without power station tests.

The avoidance—by calculation or simulation—of artificial disconnections for tests which are becoming less and less practicable with progressing interconnection, represents a particularly advantageous application of control theory.

Sommaire

L'instabilité d'une turbine hydraulique, fonctionnant sur un réseau isolé, pouvait seulement être expliquée et complètement éliminée par le calcul du comportement fréquentiel en introduisant, contrairement à la linéarisation usuelle, la zone de la non-linéarité, qui est décisive pour l'amortissement. En négligeant tous les retards du servomoteur principal, un temps d'amortissement bref fut autrefois introduit comme critère de réglage optimale qui a été confirmé par des calculateurs analogiques comme étant le seul utilisable pour les turbines hydrauliques. On déduit que, malgré la non-linéarité, cette formule d'optimum reste pleinement valable. On explique les moyens qui améliorent la caractéristique de la non-linéarité.

L'institut des centrales électriques de Moscou examine pour des essais en boucle fermée des régulateurs effectifs de turbines à vapeur en simulant les autres éléments du circuit de réglage. Pour les turbines hydrauliques, il faut aussi simuler le coup de bélier. En outre, un servomoteur simulé permet de prendre en considération les réactions des forces hydrauliques et du frottement de la turbine réglée. Ainsi, des essais en usine permettent déjà d'assurer le réglage optimal en cas d'interruptions, sans essais en service. Vu l'interconnexion progressive, les interruptions artificielles pour essais sont de moins en moins praticables. Leur abolition par calcul ou simulation représente une application particulièrement avantageuse de la théorie du réglage.

Zusammenfassung

Die aufgetretene Instabilität einer Wasserturbine im Inselbetrieb ließ sich durch Aufstellung der Ortskurven erst erklären und vollkommen beseitigen, indem man, entgegen der bisher üblichen Linearisierung, das für die Dämpfung maßgebende Gebiet der Nichtlinearität berücksichtigt. Unter Vernachlässigung aller Verzögerungen im Hauptservomotor wurde früher eine kleine Abklingzeit als Optimal-Kriterium

eingeführt, was nach Analogrechner-Versuchen für Wasserturbinen das einzig brauchbare Kriterium ergibt. Es wird abgeleitet, daß die so aufgestellte Beziehung für das Optimum trotz Nichtlinearität vollkommen gültig bleibt. Es werden Möglichkeiten erläutert, um den Verlauf der Nichtlinearität zu verbessern.

Das Moskauer Kraftwerksinstitut prüft ausgeführte Dampfturbinenregler, in dem es die übrigen Regelkreisglieder simuliert. Für Wasserturbinen muß man auch den Druckstoß nachbilden. Ein simulierter Servomotor kann ferner die veränderlichen hydraulischen Gegenkräfte und die Reibungskräfte der geregelten Wasserturbine berücksichtigen. So läßt sich ohne Betriebsversuch schon in der Werkstatt die Optimierung zur Sicherung für Störungsfälle erproben.

Die Berechnung oder die Simulation zur Vermeidung künstlicher Netztrennungen, die mit zunehmendem Verbundbetrieb immer schwieriger durchführbar sind, stellt eine besonders vorteilhafte Anwendung der Regelungstheorie dar.

Special Difficulties with Water Turbines

The optimizing control of water turbines is one of the most difficult practical problems of automatic control due to the following facts:

(1) A change of gate position causes at first a reaction of the turbine load in the wrong direction: when opening the gate the load does not increase but decreases for the first moment, due to the hydraulic shock. This strong disturbance of the control behaviour explains the failure of all usual optimum criteria such as the minimum area of the square of control deviations or the Nyquist plots with the prescriptions found for the best setting of servomechanisms. This has been tested by simulation with analogue computers⁶. At the same time, the disturbing influence of the hydraulic shock increases due to the continual trend to reduce rotating masses (WR^2) and adopt narrower conduits with higher water velocities, in order to reduce investment costs⁸.

(2) The amount of regulating work of the oil-hydraulic servomotor, namely up to more than 100,000 kpm, is the largest used in automatic control. Therefore, the pumping work for the oil-actuated servomotors must be reduced as much as possible. This is brought about by providing laps on the distributing edges of the valves, which reduce the increase of servomotor speed for small valve strokes. A zone of non-linearity thus results between valve stroke and servomotor speed, which, till now, was not considered.

(3) With the progressive interconnection of power stations stability is, in fact, facilitated⁷, but when stability is needed for the isolated power station (also at full load, where the hydraulic shock has the maximum effect) in order to maintain its reliability

if disconnected from the grid in case of disturbance, this problem becomes, on the contrary, extremely difficult with the continuous interconnected service: badly adjusted governors which are stable during interconnected service may hunt when the power station is disconnected; artificial disconnections for tests to find out the optimum setting prove to be more seldom practicable as the interconnection progresses.

Therefore, means must be found to secure optimizing control without power station tests. It will be reported on results of a governor hunting first when the power station was isolated from the grid, for which, based on calculations, a perfect optimizing control has been obtained. Then it is shown how to find the optimal control, by simulation already in the workshops, without the need for tests in the power station disconnected from the grid.

Optimization

With the simplified assumption, that the transfer lag of the main servomotor may be neglected, the optimizing coordination of proportional band x_p and the integral action time T_n was formerly⁴ calculated. The optimizing criterion was then based on a minimum damping time³ for the reduction of a disturbance to 1/10 of its initial value (Figure 1). Analogue computer tests⁶ have confirmed that in the special case of water turbines the optimum conditions can be found with no other criterion. With a larger product of proportional band x_p and integral action time T_n the reaction speed of the governor is reduced and the frequency deviations increase. In order to improve the frequency control a damping time $T_{1/10}$ was therefore recommended⁴, which is only ten times larger than the acceleration time T_a of the water column, instead of six times larger corresponding to the possible minimum value. Furthermore, for a given damping time the broken line optimum curve was indicated, for which the product of proportional band x_p and integral action time T_n is a minimum. This in order to have a further improvement of frequency control by a quicker reaction of the governor.

Optimum condition: minimum of $x_p T_n$ (1)

So it was found, neglecting the transfer lag of the main servomotor, according to Figure 1 for the optimum point (Opt):

Optimum setting: $x_p = 1,8 \frac{T_c}{T_a}$ $T_n = 4 \cdot T_c$ (2)

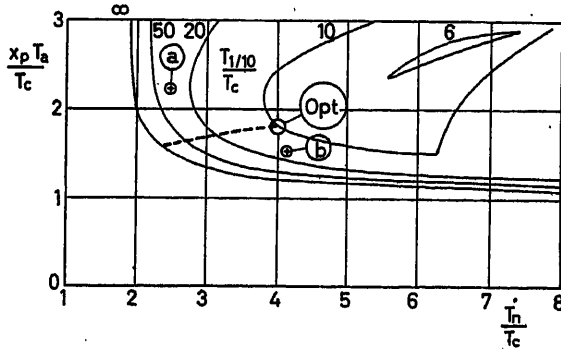


Figure 1. The point (Opt) indicates the optimizing control for water turbines in isolated service: minimum value of the product of proportional band x_p and integral action time T_n with short damping time $T_{1/10}$. This optimum criterion remains valid too, if the non-linearity of servomotor speed due to its control value is considered

Automatic Control System

Figure 2 shows the block diagram of the closed loop of a water turbine control system. If the transfer lags in the automatic controller including preliminary servomotors are neglected, the transfer function of a proportional and integral control is represented¹ by the first block element. The proportional band x_p is the sum of the transient proportional band x_{pt} and the permanent proportional band x_{p0} . Together with the following main servomotor the transfer function of the automatic controller is:

$$F(p) = \frac{1 + T_n p}{x_p \cdot T_n \cdot T_m p^2 + (x_p T_n + x_{p0} T_m) p + x_{p0}} \quad (3)$$

Non-linearity

Figure 3 shows that for large strokes, y , of its controlling valve, the speed of the servomotor dm/dt must be restricted to the values 1a and 1b in order to limit the pressure variations

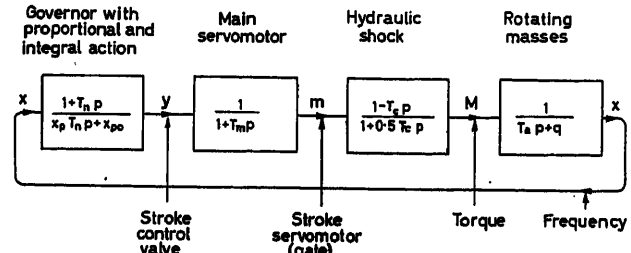


Figure 2. Block diagram for the frequency control of a water turbine

in the conduit caused by the hydraulic shock. It is well known that this non-linearity, which is realized by diaphragms, has no influence on the stability. In the case of linearization for calculations and simulation with analogue computers, a shift A-B of the servomotor speed was, until now, always presumed. This shift results with the assumption of a linear proportional increase of the servomotor speed up to its maximum value limited by the diaphragms. A certain shift presumed in such a manner is characterized by a time constant T_m^1 of the servomotor. This assumption, which practically corresponds to an average value 2 of the shifts 3 and 4 is practicable for the normal case of water turbines working in parallel with a grid.

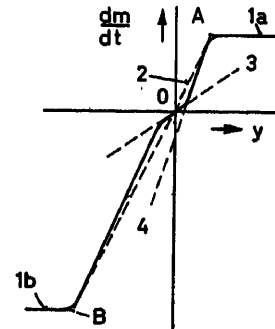


Figure 3. Non-linearity of the shift between the servomotor speed dm/dt and the stroke of its control valve. With the usual presumption of a shift 2 according to a linearization A-B, hunting in a case of disconnecting the power station from the grid remained inexplicable, because the lower shift 3 is decisive for control behaviour

However, in the difficult case of a test with the power station disconnected from the grid the governor hunted considerably. This fact could not be explained by the transfer locus plots calculated with formula (3), nor was it possible to find indications for an optimum setting under the conditions of the control station isolated from the grid. On the contrary, with the usual assumption of the average value 2 of Figure 3 according to the broken line curve of the transfer locus plot 2 in Figure 4, the governor should have been stable.

Elimination of Hunting

The instability of the governor really existing in the isolated power station can be explained, if instead of the average value 2 of the shift according to Figure 2, the shift 3 in the zone influenced by laps on the distributing edges of the valves is introduced. This zone is decisive for the automatic control behaviour. The result is the unstable transfer locus plot 2 in Figure 4. But that con-

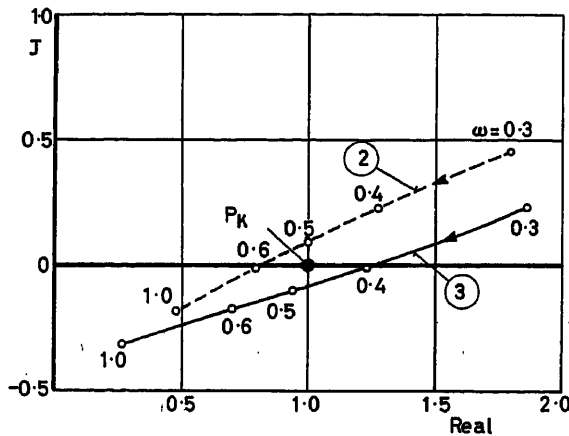


Figure 4. Calculated transfer locus plots. Contrasting with the effective hunting the transfer locus plot calculated as usual with the shift 2 in Figure 3 shows a stable behaviour; only the introduction of the shift 3 explains the real instability. — P_k = critical point for stability

formity with the real behaviour does not yet give indication how to eliminate the instability.

With formula (3) it can be investigated how to approach the conditions to the not exact assumption, that the servomotor following the governor works without transfer lag ($T_m = 0$). In the denominator there is, as factor of p , the term $x_{p0} T_m$, which is always so small that it may be neglected in comparison with $x_p T_n$. Therefore, the hunting must have origin in the factor of p^2 which is not zero. For an optimizing control, in spite of non-linearity, the factor of p^2 must be made as small as possible, so there is received as condition for optimizing control

$$\text{a minimum of } x_p T_n \cdot T_m \quad (4)$$

But according to formula (1) the condition that $x_p T_n$ must be a minimum is already introduced in the optimizing setting of Figure 1.

Therefore, by the non-linearity which was not considered, the optimum line, Figure 1, the optimum point (Opt) and the optimum formulae (2) do not lose their validity. On the contrary they safeguard the best coordination of proportional band and integral action time and according to formula (4), reduce herewith to a minimum the spoiling influence of non-linearity on the

stability. This optimizing control is valid, in spite of non-linearity, if the slow shift according to line 3 in Figure 3 is considered. So first the values 'a' have been introduced in Figure 1, for which the governor was hunting. It may be seen from the large deviation from the optimum point (Opt) that the proportional band x_p is too large and the integral action time T_n too short.

Whilst generally the increase of proportional band is considered as an always effective remedy, in this test rather the contrary has been observed. The non-linearity Figure 3 explains it according to formula (4). With the considerable time lag T_m caused by shift 3, the disturbing effect of the factor of p^2 predominates when x_p increases. But, on the other hand, a proportional band which is too small, point 'b' in Figure 1 gives also a deviation from the optimum point. The reason is that the stabilizing factor of p in the denominator of formula (3) decreases. In correspondence herewith the calculated transfer locus plots (broken lines) of Figure 5 show that the control is unstable with too large as well as too small proportional bands.

In order to eliminate the hunting which occurred in isolated service of the power station and basing on this calculation, the governor was set exactly to the optimum point (Opt) of Figure 1 and non-linearity slightly reduced by modifying the edges of the control valve. Thus from the calculated transfer locus plot (Opt) in Figure 5 there results a stable control behaviour. This already without considering the inherent regulation of the plant, which in this case existed, but was weak.

The immediate result of a new test with the power station isolated from the grid and the optimizing control of the governor based on these calculations, was perfect control behaviour, without any modification of the setting fixed beforehand. This in contradistinction to the preceding test.

Improvement of the Non-linear Shift

The maximum value 1b (Figure 3) of servomotor closing speed dm/dt , limited by diaphragms, is reached approximately, when the opening area $II DY$ on the circumference of the control valve (Figure 6) equals the area of the diaphragms³. Increasing by three times the stroke proportion of the preliminary

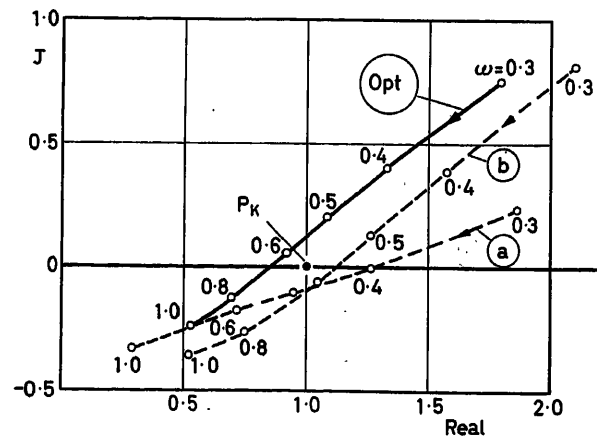


Figure 5. Calculated transfer locus plots. Realizing the optimizing control point (Opt) of Figure 1 the stability disappeared in conformity with the calculated plots; they show instability for too large values (a) as well as for too small values (b) of the proportional band, if non-linearity is considered. — P_k = critical point for stability

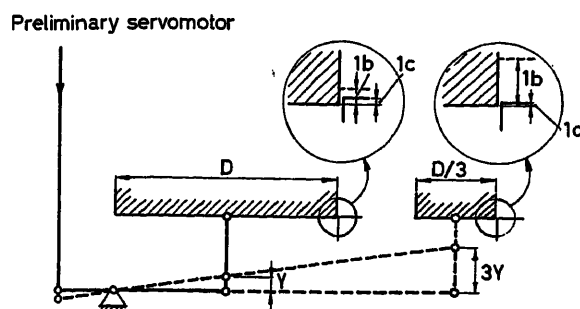


Figure 6. A substantial improvement of non-linear shift is obtained with increased proportion between the stroke of servomotor valve and that of the preliminary servomotor using smaller valve diameters. Y = valve stroke, $1b$ = stroke for maximum servomotor speed, $1c$ = overlapping

servomotor to that of the control valve, the maximum value $1b$ (Figure 3) is reached with a valve diameter three times smaller. Laps on the distributing valve edges are introduced, causing the non-linear zone, which reduces the oil flow for small valve strokes. These are represented in Figure 6 at increased scale and in a simplified manner.

If it is only requested that the control valve has practically no leakage in the steady-state position, this requirement can be realized three times easier with a valve diameter and circumference three times smaller. But if it is also specified that the oil flow will increase only slowly for small frequency deviations, a lap $1c$ three times smaller is sufficient to maintain the same increase (as shift 3 of Figure 3) having the same flow on the oil distributing edges. But considering that the stroke for reaching the maximum servomotor speed $1b$ in Figure 3 is three times larger with the smaller valve, the proportion between overlap $1c$ and stroke $1b$ corresponding to the maximum servomotor speed is reduced to $1/9$ th according to Figure 6. Therefore, the non-linear zone with a reduced increase 3 in Figure 3 is much narrower in the y direction.

Notwithstanding the fact that the calculated formula for optimum setting maintains its validity, it is not easy to calculate how much the control behaviour approaches to the conditions A-B without time lag in the servomotor (Figure 3) due to reduced width of the non-linear zone 3 in the y direction. Since the improvement by introducing smaller valves with larger strokes is chiefly interesting for new governors, simulation of closed loops in the workshops is the appropriate test method for optimizing control.

Simulation

In the Moscow Power Institute for testing the closed loops of automatic control systems, steam turbines are simulated by electric motors, which are automatically controlled by the real governors used for the steam turbines.

Workshop tests with real water turbine governors can include the effect of all shift zones of non-linearity of the servomotor speed due to its control valve (Figure 3). Practically, this cannot be realized by analogue computers, because the shift of the non-linearity, which changes substantially by any slight modification on the valve edges, cannot be exactly calculated with all non-linear transitions from one zone to the other. Furthermore, all imperfections of the real automatic controller and the detecting element are included in the test.

All other elements of the closed loops can be linearized for simulation, and without any test disturbing the service of the power station, the optimizing control for isolated service conditions can be tested by simulation. Also, modifications on the valve edges with the reducing effect on control oil quantity can be experienced in the workshops.

An optimizing test in the workshops is specially desirable, because it results from calculations, that already slight deviations of the optimum point (Figure 1) and slight reductions of non-linearity have a considerable influence on the quality of the control.

Contrary to control tests for steam turbines, however, the water shock must be simulated for water turbines according to the 3rd block element in Figure 2. Therefore, the following initial conditions must be considered:

- Due to the hydraulic shock a step function of the gate is followed for the first moment by a load change of 200 per cent in the wrong direction of the output M (torque) against the input m (gate position).
- The water flow remains constant for the first moment due to the inertia of the water masses.

It is advantageous to simulate also the rotating masses (4th block element Figure 2) with the inherent regulation factor q as a feedback. So it is unnecessary to destroy the energy of the generator driven by the motor controlled by the water turbine governor. It is advisable to go ahead, also simulating the servomotor, by a model (2nd block element Figure 2) with the strong reactions of friction and hydraulic forces on the gate. The shift of these forces is known by measurements of similar water turbines². These measurements are also the indispensable basis for calculating the regulation work. Even the insensitiveness of the main servomotor due to leakages of its piston⁶ can be simulated by an adjustable leakage.

The simulation here has particularly important practical advantages. Already in the workshops the optimizing control for isolated service can be tested, namely without power station tests with their disturbing artificial disconnection from the grid. With the continually progressing interconnection it is becoming increasingly difficult to isolate a local network from the grid simply for tests. Nevertheless, the workshop simulation tests give the guarantee, that in a real case of disturbance with disconnection, the safety in service is secured by the optimizing control of the water turbine.

Nomenclature

Values related to load-differences between full load and idle load:

x	Frequency	} relative deviations
y	Valve position of the main servomotor	
m	Position of main servomotor (proportional to gate opening)	
M	Torque	
x_{pi}	Transient proportional band	} for full load
x_{p0}	Permanent proportional band	
x_p	$x_{pi} + x_{p0}$ = proportional band	
T_n	Integral action time	
T_m	Transfer time lag of main servomotor	} for full load
q	Inherent regulation factor	
T_a	Acceleration time of rotating masses	
T_c	Acceleration time of conduit water column	
$T_{1/10}$	Damping time for reduction of a disturbance to 1/10 of its initial value	

References

- ¹ HUTAREW, G. *Regelungstechnik*. 2nd edn. 1961. Berlin/Göttingen/Heidelberg; Springer-Verlag
- ² GERBER, H. Investigations of the forces involved in regulating water-turbines. *Escher Wyss News* 1942/43, p. 151
- ³ STEIN, T. The influence of self-regulation and of the damping period on the WR^2 value of hydro-electric plants. *Engng. Dig.* (Brit. edn) May 1948: Extract from *Drehzahlregelung der Wasserturbinen*. *Schweiz. Bauzeitung* Nos. 39–41 (1947)
- ⁴ STEIN, T. Die optimale Regelung von Wasserturbinen. *Schweiz. Bauzeitung* No. 20 (1952), p. 287–292. Extract: *Regelungstechnik* No. 7 (1953) 158–160
- ⁵ STEIN, T. Wasserturbinenregler mit identischer Integral- und Differential-Wirkung. *Schweiz. Bauzeitung* Nos. 11, 12 (1954)
- ⁶ SCHIOTT, H. Optimum setting of water-turbine governors. *Trans. Soc. Instrum. Techn.* No. 1 (1960) 22–29
- ⁷ STEIN, T. Stabilitätsgrenzen und Optimalregelung der Wasserkraft in Verbundnetzen. *Regelungstechnik* No. 4 (1962)

DISCUSSION

D. RUMPEL and H.-V. ELLINGSEN, *Siemens-Schuckertwerke A.G., Erlangen, Stettiner Strasse 34, Germany*

We have met this same problem on non-linearity of servomotor speed in an investigation of Kaplan turbine control systems. This investigation was carried out together with Dr. Lein of the J. M. Voith GmbH machine factory.

In the stability map (Figure A) the time constants of the runner servo and the gate servo are used as coordinates. As shown, there are two stable regions: one for small runner time constant and one for large runner time constant. In between is a region of instability.

As Mr. Stein has shown, the medium overall slope of the servo speed characteristic is steeper than the slope in the range of overlap; therefore the servo time constant is smaller for large deviations than for small deviations. For Kaplan turbines especially the overlap of the runner-blade servo is material, because this servomotor with its large force and small stroke usually has the greater overlap and the

greater efficiency in regulating action. That is why, with decreasing amplitudes of deviation, the point of operation in the map moves to the right. If the original point lies left of the instable region, it may be that the point passes the stability limit and the oscillation will build up. This performance corresponds to the case discussed by Mr. Stein. On the other hand, if at small amplitudes the point of operation lies immediately right of the instable region it will move left at large disturbances and the turbine will become instable.

Such a case is shown in Figure B, derived from analogue computation. For small disturbances (load step of 5 per cent) the oscillation is damped to zero; for a load step of 7 per cent the oscillation increases up to an amplitude where the diaphragms become active and again reduce the medium slope. Oscillations originating from large disturbances (in the picture a load step of 22 per cent) are damped down to the very same amplitude, at which the turbine continues to hunt.

There is a marked influence of the diaphragms on stability, especially in the case with the operating point to the left of the instability region. Here one can find the opposite performance: instability in the low amplitude range, stability in the medium amplitude range and, again, instability in the high amplitude range.

T. STEIN, in reply

In the discussion remarks the influence of runner and gate servo is investigated. These time constants, which determine the increase of servo speed with the position of the valve, can have a great importance when the controller is not optimally adjusted.

Then there can be zones of instability (Figure A). For a non-optimally adjusted controller a stabilization can be obtained coordinating the time constants of runner and gate.

From our experience resulting from two practical power station tests with disconnection from the grid, we have tried such adaptations of these time constants; but it seems better to obtain the stability by the optimum setting of the controller. It is then advisable to reduce the time constants of runner and gate to a minimum.

B. FAVEZ, *Electricité de France, 12 place des États-Unis, Paris 16^e, France*

(1) Can the author give additional information about the failure of optimum criteria of minimum of the square of control deviation in the case of water turbine control?

(2) The paper deals with a case of conditional stability, where the gain of a direct loop has a large importance; the characteristics of a main servomotor, which we usually call 'promptitude', are fundamental for the stability and we know it is difficult to build such a large element with an absolutely known and linear parameter. In that case is it not better to use a normal valve and servomotor with a tachometer feedback, which give a good linearity independently of the quality of the servomotor, rather than to try to increase the quality of the main part of equipment? Such a feedback is easy to introduce with an electro-hydraulic controller and we ask the author if he thinks that this experience is another reason for the use of this kind of controller.

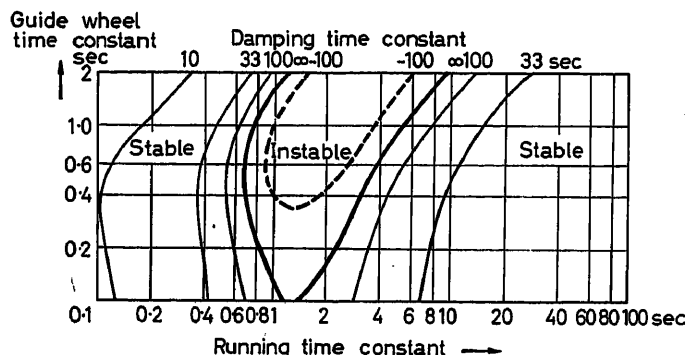


Figure A. Kaplan turbine control—influence of time constants of main servomotors on stability

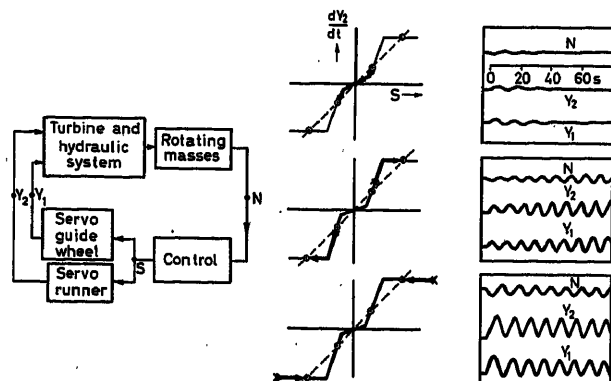


Figure B. Kaplan turbine—influence of non-linearity of runner servomotor on stability

T. STEIN, *in reply*

(1) As shown in the illustration in the paper by H. Schiott (Reference 6 of this paper) and in a more recent work¹, the optimum criteria of minimum of the square of control deviations is not very satisfactory regarding the actual number of oscillations occurring. It seems that hydraulic shocks give sharp changes of the deviation signals, so that for a minimum of the deviation area the number of oscillations is not so small as it could be.

(2) The origin of the paper was the preoccupation to know what to do with the great number of existing water turbines to safeguard stability without making power station tests. For turbines with new electrohydraulic governors it may be useful to linearize the servomotor speed by an electric feedback, if there are no disturbances of stability due to time lags in this internal feedback loop.

Reference

- ¹ EVANGELISTI, G. On the problem of frequency control in hydroelectric stations. *Automatic and Remote Control*, Vol. 4, p. 105. 1961. London; Butterworths

D. ERNST, 852 Erlangen, G.-Scharowskystrasse 2-4, Germany

The author has given a comprehensive description of the well-known difficulties encountered in the control of water turbines with special emphasis on the non-linearity of servomotor speed. I would like to put forward for discussion a method which was developed during research work on electrohydraulic regulation of water turbines and which might be helpful in overcoming the described difficulties. Figure A shows the control loop adapted for this method.

To overcome the difficulties of non-linearity a sub-loop control for gate opening has been introduced, which comprises an electric position-

ing controller, the electrohydraulic transducer, and the gate mechanism. Opening of the gate is measured and used as feedback. With the use of this loop, the static and dynamic compensation of servomotor characteristics can be achieved.

The speed controller with proportional and integral action provides the set point for the gate-opening control loop. Limitations can be entered at will.

Since the rate of change of gate opening is limited according to the characteristics of the turbine installation, it is very important now to adapt the speed controller to this limitation. Its input changes (either from *P* or *I* action) should never exceed the maximum rate of gate travel, otherwise the integrator output would overshoot, which may lead to hunting in the control loop. It seems that this property of a non-adapted integral controller has sometimes been the undetected cause of difficulties.

A circuit of an electric speed controller with such properties is also shown in Figure A.

T. STEIN, *in reply*

From two practical tests on power plants with disconnection of the local network from the grid, good behaviour of the control loop was obtained using mechanical governors, notwithstanding the non-linear zones. It is only necessary to adapt the control parameters according to the formula for optimizing control. Therefore there is no need to eliminate the non-linearity.

To apply the electrical feedback proposed for the elimination of non-linearity, practical tests in a power station would be necessary. In fact, with electrohydraulic governors the connection of two points of the loop with intermediate oil-hydraulic loop elements has led to hunting. This was due to the time lags in the intermediate oil-hydraulic loop elements.

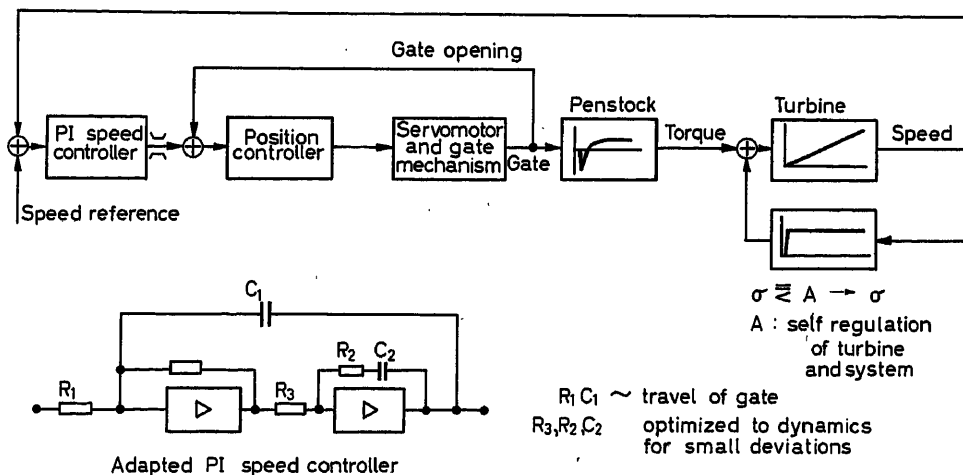


Figure A. Electrohydraulic control system for water turbines

Control Equations of a Hydroelectric Plant with Fixed Reference Values

L. BOREL

Summary

In the work entitled 'Stabilité de réglage des installations hydro-électriques' (Payot, Lausanne and Dunod, Paris 1960), the author presented a method of calculating the control stability of hydroelectric installations in which the relative values are defined as being the relation between the absolute instantaneous value and the absolute value of the permanent regime of the values considered. In this method of calculation, the reference values are different for each proposed permanent regime. This is the 'method with floating reference values'.

Unfortunately, this latter is impracticable when the absolute value of the permanent regime of one of the values is zero, since the corresponding relative value is infinity. The present work demonstrates a very general method of calculation which does not present the above fault. In this method of calculation, the reference values are invariable whatever the proposed permanent regime. This is the 'method with fixed reference values'.

First, the author indicates the manner in which the reference values are chosen, then defines the formation of the relative values. A definition of the control parameters and the relationships between the hydraulic parameters are given. Finally, the fundamental equations translating the dynamic behaviour into the control of the installation and the complete functional diagram and the principal transfer functions of the installation are presented.

Sommaire

Dans l'ouvrage intitulé « Stabilité de réglage des installations hydro-électriques » (Payot Lausanne - Dunod Paris - 1960) l'auteur a présenté une méthode de calcul de la stabilité de réglage des installations hydroélectriques dans laquelle les valeurs relatives sont définies comme étant le rapport de la valeur absolue instantanée à la valeur absolue de régime permanent des grandeurs considérées. Dans cette méthode de calcul, les valeurs de référence sont différentes chaque fois que le régime permanent envisagé est différent. C'est la « méthode avec valeurs de référence flottantes ».

Cette dernière est malheureusement en défaut quand la valeur absolue de régime permanent de l'une des grandeurs est nulle, car alors la valeur relative correspondante est infinie. Le présent travail expose une méthode de calcul très générale qui ne présente pas le défaut ci-dessus. Dans cette méthode de calcul, les valeurs de référence sont fixes quel que soit le régime permanent envisagé. C'est la « méthode avec valeurs de référence fixes ».

Tout d'abord, l'auteur indique la manière de choisir les valeurs de référence. Ensuite, il précise la formation des valeurs relatives. Puis, il indique la définition des paramètres de réglage. Il donne les relations entre les paramètres hydrauliques. Il présente les équations fondamentales traduisant le comportement dynamique en réglage de l'installation. Enfin, il montre le schéma fonctionnel complet et les fonctions de transfert principales de l'installation.

Zusammenfassung

In dem Buch: „Stabilität de réglage des installations hydroélectriques“ hat der Verfasser eine Berechnungsmethode für die Stabilität der Regelung von Wasserkraftwerken angegeben; die in der Berechnungsmethode definierten Relativwerte stellen das Verhältnis zwischen dem absoluten Augenblickswert und dem absoluten Wert des Beharrungs-

zustandes dar. Daher ändern sich bei dieser Berechnungsart die Bezugswerte mit jeder Änderung des vorgesehenen Beharrungszustandes. Dies ist die „Methode mit schwankenden Bezugswerten“.

Leider versagt diese Methode, wenn der absolute Wert des Beharrungszustandes einer Größe Null ist, da dann der betreffende Relativwert Unendlich wird. Die vorliegende Arbeit zeigt eine allgemein gültige Berechnungsart, welche diesen Mangel nicht aufweist. Bei dieser Berechnungsmethode ändern sich die Bezugswerte nicht, gleichgültig welcher Beharrungszustand vorgesehen ist. Dies ist die „Methode mit festen Bezugswerten“.

Die Arbeit erläutert zuerst die Art der Wahl der Bezugswerte und anschließend die Bildung der Relativwerte. Es folgen eine Definition der Regelgrößen und die Angabe der Beziehungen zwischen den hydraulischen Parametern. Sie führt außerdem die Grundgleichungen an, die das dynamische Verhalten der Anlage bei der Regelung erklären. Zum Schluß werden das Gesamtschaltbild und die Hauptübertragungsfunktionen der Anlage angegeben.

Introduction

In the author's previous work¹ on control stability, a method of calculation was presented in which the relative values were defined generally as the ratio between the absolute instantaneous value and the absolute steady-state value of the magnitudes considered.

With this method of calculation the reference values vary, that is to say, they are different for each steady state considered. In the general control terminology, it is convenient to call this method the 'Method with floating reference values'. Unfortunately this is not practicable when the absolute steady-state value of one of the quantities is zero, because then the corresponding relative value is infinity.

Example—When the installation is running without load:

$$\begin{array}{lll} \dot{E}_0 = 0 & \Delta \dot{E}^* = \infty & t_5 = t_6 = t_9 = \infty \\ \eta_0 = 0 & \Delta \eta^* = \infty & t_3 = t_4 = t_{11} = \infty \end{array}$$

The present paper gives a very general method of calculation which does not exhibit the above defect. In this method the reference values are invariable, whatever may be the steady state considered. In the general control terminology it is convenient to call this the 'Method with fixed reference values'.

For notational purposes, the following rules are used throughout the paper: (a) The fixed reference values are labelled by the index 0; (b) the steady state values by the index x, and (c) the relative values by an asterisk.

Reference Values

The reference values relating to a certain plant are fixed once and for all. They are chosen so as to correspond if possible

to some particular values of the plant. If no special difficulties exist, the following method will be adopted.

From the mechanical point of view, for the reference lengths of stroke, values corresponding to the maximum stroke of the elements will be taken.

From the hydraulic and electrical points of view, for the reference mass energies, rates of flow, powers, velocities and voltages, the *nominal values* of net mass energy, of kinetic and pressure drop mass energies, of the rate of flow, of driving power, of velocity and of voltage, will be taken.

It should be pointed out that, instead of choosing the nominal values as reference values, it may be of interest to choose the *optimal values*, i.e. those which correspond to the peak of the efficiency curve. It should be understood that the above recommendations are not compulsory and that, in principle, the reference values could be arbitrary. However, it would not be convenient to choose reference values which would be completely independent of each other.

The system leading to the simplest calculations is obtained by adhering to the following relationships:

$$e_{g0} = K_g \dot{V}_0^2 \quad (1)$$

where K_g is the coefficient of pressure drop of the feed chamber.

$$e_{h0} = K_h \dot{V}_0^2 \quad (2)$$

where K_h is the coefficient of pressure drop of the pipeline.

$$e_{w0} = K_w \dot{V}_0^2 \quad (3)$$

where K_w is the coefficient of the mass kinetic energy at the entrance to the chamber.

$$Y_0 = K_r N_0 \quad (4)$$

where K_r is the coefficient of displacement of the slide-valve.

$$N_{e0} = K_e N_0 \quad (5)$$

where K_e is the angular speed coefficient of any power-consuming machine on the network.

$$\eta_0 = \frac{\dot{E}_0}{\mu \dot{V}_0 k_0} \quad (6)$$

It should be noted that η_0 is a purely fictitious efficiency in the general case when \dot{E}_0 , \dot{V}_0 and k_0 are arbitrary, and it represents the real efficiency only in the particular case, when \dot{E}_0 , \dot{V}_0 and k_0 correspond simultaneously to a well-determined reference steady state, for instance, to the nominal or to the optimal value.

Following is the list of chosen reference values:

A_0	Maximum opening of the turbine gating
\dot{E}_0	Driving power of the turbine
N_0	Angular speed of the group
$N_{e0} = K_e N_0$	Angular speed of any power-consuming machine on the network (corresponding to N_0)
U_0	Voltage at the terminals of the alternator
\dot{V}_0	Volumetric rate of flow of the water in the turbine
X_0	Length of stroke of the servomotor piston
$Y_0 = K_r N_0$	Length of stroke of the slide-valve (corresponding to N_0)

$e_{g0} = K_g \dot{V}_0^2$	Pressure drop mass energy in the feed chamber (corresponding to \dot{V}_0)
$e_{h0} = K_h \dot{V}_0^2$	Pressure drop mass energy in the pipeline (corresponding to \dot{V}_0)
$e_{w0} = K_w \dot{V}_0^2$	Kinetic mass energy at the entrance to the chamber (corresponding to \dot{V}_0)
k_0	Net mass energy
$\eta_0 = \frac{\dot{E}_0}{\mu \dot{V}_0 k_0}$	Efficiency of the turbine (corresponding to \dot{E}_0 , \dot{V}_0 and k_0)

Relative Values

The reference values just defined lead to the following relative values:

$A^* = \frac{A}{A_0}$	Opening of the turbine gating
$\dot{E}^* = \frac{\dot{E}}{\dot{E}_0}$	Driving power produced by the turbine
$\dot{E}_r^* = \frac{\dot{E}_r}{\dot{E}_0}$	Resistive power demanded by the network
$\dot{E}_\lambda^* = \frac{\dot{E}_\lambda}{\dot{E}_0}$	Load of the network
$N^* = \frac{N}{N_0}$	Angular speed of the group
$N_m^* = \frac{N_m}{N_0}$	Stroke of the velocity range change device expressed in terms of velocity
$U^* = \frac{U}{U_0}$	Voltage at the terminals of the alternator
$U_m^* = \frac{U_m}{U_0}$	Stroke of the voltage range change device expressed in terms of voltage
$\dot{V}^* = \frac{\dot{V}}{\dot{V}_0}$	Volumetric rate of flow of water in the turbine
$\dot{V}_c^* = \frac{\dot{V}}{\dot{V}_0}$	Volumetric rate of flow of water in the chamber
$\dot{V}_g^* = \frac{\dot{V}_g}{\dot{V}_0}$	Volumetric rate of flow of water in the gallery
$\dot{V}_h^* = \frac{\dot{V}_h}{\dot{V}_0}$	Volumetric rate of flow of water in the pipeline
$X^* = \frac{X}{X_0}$	Length of stroke of the servomotor piston
$X_c^* = \frac{g X_c}{k_0}$	Level difference in the chamber
$Y^* = \frac{Y}{Y_0}$	Length of stroke of the distribution slide-valve
$e_a^* = \frac{e_a}{k_0}$	Mass energy at the entrance of the chamber (in the steady state: $e_{a0}^* = e_{b0}^* - e_{g0}^*$)
$e_b^* = \frac{e_b}{k_0}$	Gross mass energy, i.e. at the water intake

$e_g^* = \frac{e_g}{e_{g0}}$	Pressure drop mass energy in the gallery
$e_h^* = \frac{e_h}{e_{h0}}$	Pressure drop mass energy in the pipeline
$e_p^* = \frac{e_p}{k_0}$	Mass energy due to the hydraulic recoil
$e_w^* = \frac{e_w}{e_{w0}}$	Kinetic mass energy at the entrance of the chamber
$k^* = \frac{k}{k_0}$	Net mass energy, i.e. upstream of the turbine (in the steady state: $k_0 = e_{a0} - e_{h0}$)

Control Parameters

Given the relative values defined in the preceding section, it is convenient to write all the control equations under the relative form. It is then necessary to determine the control parameters by combining the reference values in the most logical way. Among all the combinations that can be considered, it is obviously convenient to choose the simplest and the most adequate.

A thorough study of this problem has allowed us to establish a series of combinations which lead to equations, in the method with fixed reference values, the form of which is strictly identical to that of the equations of the method with floating reference values.

Here is a list of control parameters which have been defined.

$A_{11} = \frac{J_a N_0 N_x}{\dot{E}_0}$	Characteristic time of mechanical inertia of the rotor of the alternator
$C_1 = \frac{\dot{V}_0}{k_0} \int_0^{L_g} \frac{dL_g}{S_g}$	Characteristic time of hydraulic inertia of the gallery
$C_3 = \frac{S_c k_0}{g \dot{V}_0}$	Characteristic time of the filling of the chamber
$E_{11} = \frac{\sum [J_e N_{e0} N_{ex}]}{\dot{E}_0}$	Characteristic time of the mechanical inertia of the rotors of the full set of power-using machines
$H_1 = \frac{\dot{V}_0}{k_0} \int_0^{L_h} \frac{dL_h}{S_h}$	Characteristic time of the hydraulic inertia of the pipeline
$M_1 = T_{11} + A_{11} + E_{11}$	Characteristic time of the total mechanical inertia of an installation, operating separately
$R_1 = -\frac{X_0}{N_0} \left[\frac{dN}{d\left(\frac{dX}{dt}\right)} \right]_{\substack{R_3=0 \\ R'_3=0 \\ r_4=0}}$	Characteristic time of the performance of a tachometer servomotor in an acceleration tachometer governor
$R'_1 = R_1 + (r_4 + r'_4) R'_3$	Characteristic time of the performance of a tachometer servomotor in a governor with transient feedback
R_3	Accelerometric proportioning
R'_3	Relaxation time (damping) of the dash-pot

$$T_{11} = \frac{J_t N_0 N_x}{\dot{E}_0}$$

$$a_1 = \frac{N_0}{U_0} \left(\frac{dU}{dN} \right)_{pt}$$

$$c_2 = \frac{e_{g0} \dot{V}_{gx}}{k_0 \dot{V}_0}$$

$$c_4 = \frac{e_{w0} \dot{V}_{wx}}{k_0 \dot{V}_0}$$

$$e_1 = \frac{N_0}{\dot{E}_0} \left(\frac{\partial \dot{E}_r}{\partial N} \right)_{\substack{U_x \\ \lambda_x}}$$

$$e_2 = \frac{U_0}{\dot{E}_0} \left(\frac{\partial \dot{E}_r}{\partial U} \right)_{\substack{N_x \\ \lambda_x}}$$

$$h_2 = \frac{e_{h0} \dot{V}_{hx}}{k_0 \dot{V}_0}$$

$$r_2 = \frac{X_0}{A_0} \left(\frac{dA}{dX} \right)_x$$

$$r_4 = -\frac{X_0}{N_0} \left(\frac{dN}{dX} \right)_{pt}$$

$$r'_4 = \frac{X_0}{N_0} \left(\frac{dN}{dX} \right)_{\substack{R'_3=0 \\ r_4=0}}$$

$$t_1 = \frac{k_0}{\dot{V}_0} \left(\frac{\partial \dot{V}}{\partial k} \right)_{\substack{N_x \\ A_x}}$$

$$t_2 = \frac{A_0}{\dot{V}_0} \left(\frac{\partial \dot{V}}{\partial A} \right)_{\substack{N_x \\ k_x}} = \frac{A_0 N_x}{\varphi_0 N_0} \left(\frac{\partial \varphi}{\partial A} \right)_{\psi_x} = \frac{A_0 k_x^{\frac{1}{2}}}{\tau_0 k_0^{\frac{1}{2}}} \left(\frac{\partial \tau}{\partial A} \right)_{\eta_x}$$

$$t_3 = \frac{k_0}{\eta_0} \left(\frac{\partial \eta}{\partial k} \right)_{\substack{N_x \\ A_x}} = \frac{\psi_0 N_0^2}{\eta_0 N_x^2} \left(\frac{\partial \eta}{\partial \psi} \right)_{\psi_x} = \frac{A_0 k_x^{\frac{1}{2}}}{\tau_0 k_0^{\frac{1}{2}}} \left(\frac{\partial \tau}{\partial A} \right)_{\eta_x}$$

$$t_4 = \frac{A_0}{\eta_0} \left(\frac{\partial \eta}{\partial A} \right)_{\substack{N_x \\ k_x}} = \frac{A_0}{\eta_0} \left(\frac{\partial \eta}{\partial A} \right)_{\psi_x} = \frac{A_0}{\eta_0} \left(\frac{\partial \eta}{\partial A} \right)_{\eta_x}$$

$$t_5 = \frac{k_0}{\dot{E}_0} \left(\frac{\partial \dot{E}}{\partial k} \right)_{\substack{N_x \\ A_x}}$$

$$t_6 = \frac{A_0}{\dot{E}_0} \left(\frac{\partial \dot{E}}{\partial A} \right)_{\substack{N_x \\ k_x}}$$

Characteristic time of the mechanical inertia of the turbine rotor

Angular coefficient of the voltage-frequency characteristic of the voltage controller (the subscript *pt* indicates a steady state)

Pressure drop in the gallery in steady state and of non-dimensional nature

Kinetic energy at the entrance of the chamber in steady state and of non-dimensional nature

Frequency sensitivity of the resistive power

Voltage sensitivity of the resistive power

Pressure drop in the pipeline in steady state and of non-dimensional nature

Non-linearity of the transmission servomotor-turbine gating

Steady-state angular coefficient of the servomotor stroke-speed characteristic

Transient angular coefficient of the servomotor stroke-speed characteristic

Sensitivity of the rate of flow of the turbine to the net mass energy

Sensitivity of the rate of flow of the turbine to the turbine opening

Sensitivity of the efficiency of the turbine to the net mass energy

Sensitivity of the efficiency of the turbine to the turbine opening

Sensitivity of the driving power to the net mass energy

Sensitivity of the driving power to the turbine opening

$$t_7 = \frac{N_0}{\dot{V}_0} \left(\frac{\partial \dot{V}}{\partial N} \right)_{k_x, A_x} = \frac{Q_0}{\tau_0} \left(\frac{\partial \tau}{\partial \rho} \right)_{A_x} \quad \text{Sensitivity of the rate of flow of the turbine to the speed}$$

$$t_8 = t_2 t_5 - t_1 t_6$$

$$t_9 = \frac{N_0}{\dot{E}_0} \left(\frac{\partial \dot{E}}{\partial N} \right)_{k_x, A_x} \quad \text{Sensitivity of the driving power to the speed}$$

$$t_{11} = \frac{N_0}{\eta_0} \left(\frac{\partial \eta}{\partial N} \right)_{k_x, A_x} = \frac{Q_0 k_0^{\frac{1}{2}}}{\eta_0 k_x^{\frac{1}{2}}} \left(\frac{\partial \eta}{\partial \rho} \right)_{A_x} \quad \text{Sensitivity of the efficiency of the turbine to the speed}$$

$$\alpha = \beta - t_9 \quad \text{Coefficient of the autoregulation of a separately operating plant (speed sensitivity of the difference between the driving and resistive powers)}$$

$$\beta = e_1 + a_1 e_2 \quad \text{Resulting sensitivity of the resistive power to the frequency}$$

$$\gamma = t_5 t_7 + \alpha t_1$$

Relations Between the Hydraulic Parameters

The relations between the hydraulic parameters of the turbine in the method with fixed reference values are not as simple as those which exist in the method with floating reference values. But it must not be forgotten that they are much more general.

These relations should be used to calculate all the hydraulic parameters of a turbine from the fundamental parameters related to a given mode of representation of its operating characteristics.

Mode of Representation ψ - φ - η - A :

From the fundamental parameters t_1, t_2, t_3 and t_4 it is possible to calculate the other parameters with the help of the following relations.

$$t_5 = \frac{\dot{V}_x \eta_x}{\dot{V}_0 \eta_0} + \frac{k_x \eta_x}{k_0 \eta_0} t_1 + \frac{k_x \dot{V}_x}{k_0 \dot{V}_0} t_3 \quad (7)$$

$$t_6 = \frac{k_x \eta_x}{k_0 \eta_0} t_2 + \frac{k_x \dot{V}_x}{k_0 \dot{V}_0} t_4 \quad (8)$$

$$t_7 = \frac{\dot{V}_x N_0}{\dot{V}_0 N_x} - 2 \frac{k_x N_0}{k_0 N_x} t_1 \quad (9)$$

$$t_9 = \frac{\dot{E}_x N_0}{\dot{E}_0 N_x} - 2 \frac{k_x^2 \eta_x N_0}{k_0^2 \eta_0 N_x} t_1 - 2 \frac{k_x^2 \dot{V}_x N_0}{k_0^2 \dot{V}_0 N_x} t_3 \quad (10)$$

$$t_{11} = -2 \frac{k_x N_0}{k_0 N_x} t_3 \quad (11)$$

Mode of Representation q - τ - η - A :

From the fundamental parameters t_2, t_4, t_7 and t_{11} it is possible to calculate the other parameters with the help of the following relations:

$$t_1 = \frac{1}{2} \left(\frac{k_0 \dot{V}_x}{k_x \dot{V}_0} - \frac{k_0 N_x}{k_x N_0} t_7 \right) \quad (12)$$

$$t_3 = -\frac{1}{2} \frac{k_0 N_x}{k_x N_0} t_{11} \quad (13)$$

$$t_5 = \frac{1}{2} \left(3 \frac{\dot{V}_x \eta_x}{\dot{V}_0 \eta_0} - \frac{\eta_x N_x}{\eta_0 N_0} t_7 - \frac{\dot{V}_x N_x}{\dot{V}_0 N_0} t_{11} \right) \quad (14)$$

$$t_6 = \frac{k_x \eta_x}{k_0 \eta_0} t_2 + \frac{k_x \dot{V}_x}{k_0 \dot{V}_0} t_4 \quad (15)$$

$$t_9 = \frac{k_x \eta_x}{k_0 \eta_0} t_7 + \frac{k_x \dot{V}_x}{k_0 \dot{V}_0} t_{11} \quad (16)$$

Fundamental Equations

The fundamental equations shown on page 60 of the author's previous work¹ are relative to the method with floating reference values. In order to pass to the fundamental relative equations of the method with fixed reference values, it is convenient to

Table 1

ΔA^*	$A^* \frac{A_0}{A_x}$	$\Delta \dot{V}_h^*$	$\Delta \dot{V}_h^* \frac{\dot{V}_0}{\dot{V}_{hx}}$	t	t
C_1	$C_1 \frac{k_0 \dot{V}_{gx}}{e_{ax} \dot{V}_0}$	ΔX^{**}	$\Delta X^* \frac{k_0}{e_{ax}}$	t_1	$t_1 \frac{k_x \dot{V}_0}{k_0 \dot{V}_x}$
C_3	$C_3 \frac{e_{ax} \dot{V}_0}{k_0 \dot{V}_{gx}}$	a_1	$a_1 \frac{N_x U_0}{N_0 U_x}$	t_2	$t_2 \frac{A_x \dot{V}_0}{A_0 \dot{V}_x}$
$\Delta \dot{E}^*$	$\Delta \dot{E}^* \frac{\dot{E}_0}{\dot{E}_x}$	c_2	$c_2 \frac{k_0 \dot{V}_{gx}}{e_{ax} \dot{V}_0}$	t_3	$t_3 \frac{k_x \eta_0}{k_0 \eta_x}$
H_1	$H_1 \frac{k_0 \dot{V}_{hx}}{k_x \dot{V}_0}$	c_4	$c_4 \frac{k_0 \dot{V}_{gx}}{e_{ax} \dot{V}_0}$	t_4	$t_4 \frac{A_x \eta_0}{A_0 \eta_x}$
M_1	$M_1 \frac{N_x \dot{E}_0}{N_0 \dot{E}_x}$	Δe_a^*	$\Delta e_a^* \frac{k_0}{e_{ax}}$	t_5	$t_5 \frac{k_x \dot{E}_0}{k_0 \dot{E}_x}$
ΔN^*	$\Delta N^* \frac{N_0}{N_x}$	Δe_b^*	$\Delta e_b^* \frac{k_0}{e_{bx}}$	t_6	$t_6 \frac{A_x \dot{E}_0}{A_0 \dot{E}_x}$
R_1	$R_1 \frac{N_0 X_{gx}}{N_x X_0}$	e_1	$e_1 \frac{N_x \dot{E}_0}{N_0 \dot{E}_x}$	t_7	$t_7 \frac{N_x \dot{V}_0}{N_0 \dot{V}_x}$
R'_1	$R'_1 \frac{N_0 X_{gx}}{N_x X_0}$	e_2	$e_2 \frac{U_x \dot{E}_0}{U_0 \dot{E}_x}$	t_8	t_8
R_3	R_3	h_2	$h_2 \frac{k_0 \dot{V}_{hx}}{k_x \dot{V}_0}$	t_9	$t_9 \frac{N_x \dot{E}_0}{N_0 \dot{E}_x}$
R'_3	R'_3	Δk^*	$\Delta k^* \frac{k_0}{k_x}$	t_{11}	$t_{11} \frac{N_x \eta_0}{N_0 \eta_x}$
ΔU^*	$\Delta U^* \frac{U_0}{U_x}$	r_2	$r_2 \frac{X_x A_0}{X_0 A_x}$	α	$\alpha \frac{N_x \dot{E}_0}{N_0 \dot{E}_x}$
$\Delta \dot{V}^*$	$\Delta \dot{V}^* \frac{\dot{V}_0}{\dot{V}_x}$	r_4	$r_4 \frac{N_0 X_{gx}}{N_x X_0}$	β	$\beta \frac{N_x \dot{E}_0}{N_0 \dot{E}_x}$
$\Delta \dot{V}_g^*$	$\Delta \dot{V}_g^* \frac{\dot{V}_0}{\dot{V}_{gx}}$	r'_4	$r'_4 \frac{N_0 X_{gx}}{N_x X_0}$	γ	γ

replace each magnitude by the expression which is equivalent to it.

By virtue of the definitions of the work and of those which are presented previously in this paper, the equivalent expressions are given in *Table 1*.

The substitution of the equivalent expressions shows that the fundamental equations obtained in the method with fixed reference values have a form strictly identical to that of the equations in the method with floating reference values. Obviously this is not just chance, but the result of a judicious choice of the new control parameters.

To summarize, the dynamic control behaviour of a hydroelectric plant provided with an equilibrium chamber, equipped with an accelero-tachometer controller and transient feedback, can be expressed when generating separately through six fundamental equations which, in operational form, are the following.

Equation of feed chamber:

$$\Delta \dot{e}_a^* = \Delta \dot{e}_b^* - (2c_2 + C_1 \dot{p}) \Delta \dot{V}_g^* \quad I$$

Equation of equilibrium chamber:

$$C_3 \dot{p} \Delta \dot{e}_a^* = (1 + 2c_4 C_3 \dot{p}) \Delta \dot{V}_g^* - \Delta \dot{V}_h^* \quad II$$

Equation of the pipeline:

$$\Delta \dot{k}^* = \Delta \dot{e}_a^* - (2h_2 + H_1 \dot{p}) \Delta \dot{V}_h^* \quad III$$

Equation of the rate of flow of the turbine:

$$\Delta \dot{V}^* = t_7 \Delta \dot{N}^* + t_1 \Delta \dot{k}^* + t_2 \Delta \dot{A}^* = \Delta \dot{V}_h^* \quad IV$$

Equation of revolving masses:

$$M_1 \dot{p} \Delta \dot{N}^* = -\alpha \Delta \dot{N}^* + t_5 \Delta \dot{k}^* + t_6 \Delta \dot{A}^* - e_2 \Delta \dot{U}_m^* - \Delta \dot{E}_\lambda^* \quad V$$

Equation of the accelero-tachometer speed controller with transient feedback:

$$(r_4 + R_1' \dot{p} + R_1 R_3' \dot{p}^2) \Delta \dot{A}^* = -r_2 [(1 + R_3 \dot{p})(1 + R_3' \dot{p}) \Delta \dot{N}^* - (1 + R_3' \dot{p}) \Delta \dot{N}_m^*] \quad VI$$

Let it be recalled that equation III, relative to the pipeline, was obtained by considering the mass hydraulic recoil. In the case where it is wished to consider the hydraulic recoil of the wave, it is necessary to follow the procedure which is shown below. It has been seen especially that in order to study the harmonic regimes, and in the case where the downstream part of the system is negligible it is sufficient to substitute H_1 by the expression:

$$\frac{tg \kappa}{\kappa} H_1 \quad (17)$$

with

$$\kappa = \frac{\omega H_3}{2} \quad (18)$$

and

$$H_3 = \frac{2L_h}{0} \quad (19)$$

where L_h is the length of the conduit and 0 the speed of diffusion of the waves.

Block Diagram and Transfer Functions of the Plant

Figure 1 shows the complete block diagram of the hydroelectric plant under consideration. The principal transfer functions of the elements of the installation are the following.

Speed controller:

$$\dot{G}_r = -\frac{r_2(1 + R_3 \dot{p})(1 + R_3' \dot{p})}{r_4 + R_1' \dot{p} + R_1 R_3' \dot{p}^2} = \frac{\Delta \dot{A}^*}{\Delta \dot{N}^*} \quad (20)$$

Equilibrium chamber:

$$\dot{G}_c = -\frac{2c_2 + C_1 \dot{p}}{1 + 2(c_2 + c_4)C_3 \dot{p} + C_1 C_3 \dot{p}^2} = \frac{\Delta \dot{e}_a^*}{\Delta \dot{V}_h^*} \quad (21)$$

Pipeline:

$$\dot{G}_h = -(2h_2 + H_1 \dot{p}) = \frac{\Delta \dot{k}^*}{\Delta \dot{V}_h^*} \quad (22)$$

I Equilibrium chamber pipeline system:

$$\dot{G}_{ch} = \dot{G}_c + \dot{G}_h = \frac{\Delta \dot{k}^*}{\Delta \dot{V}^*} \quad (23)$$

Complete electrical system:

$$\beta = e_1 + a_1 e_2 = \frac{\Delta \dot{E}_{re}^*}{\Delta \dot{N}^*} \quad (24)$$

Equilibrium chamber + pipeline + turbine + alternator + network system:

$$\dot{G}_a = \frac{t_6 + t_8 \dot{G}_{ch}}{\alpha - \gamma \dot{G}_{ch} + (1 - t_1 \dot{G}_{ch}) M_1 \dot{p}} = \frac{\Delta \dot{N}^*}{\Delta \dot{A}^*} \quad (25)$$

The overall transfer function of the installation is:

$$\dot{G} = \dot{G}_r \cdot \dot{G}_a \quad (26)$$

that is to say, by virtue of the above relations:

$$\dot{G} = -\frac{r_2(1 + R_3 \dot{p})(1 + R_3' \dot{p})(t_6 + t_8 \dot{G}_{ch})}{(r_4 + R_1' \dot{p} + R_1 R_3' \dot{p}^2)[\alpha - \gamma \dot{G}_{ch} + (1 - t_1 \dot{G}_{ch}) M_1 \dot{p}]} \quad (27)$$

Conclusion

In the present work the author has considered the dynamic control behaviour of a hydroelectric plant provided with an equilibrium chamber, equipped with an accelero-tachometer governor having a transient feedback and generating separately.

A very general method of calculation is given in which all the reference values are fixed. This last is called the 'Method with fixed reference values'.

First of all, the way of choosing the reference values is indicated and a list of these is given. Next, the way of forming relative values, and a definition of the control parameters are indicated. The relations between the hydraulic parameters are shown.

The six fundamental equations corresponding to the dynamic control behaviour of the plant have been presented in operational form. Thanks to a judicious choice of the new control parameters, these equations have a form strictly identical to that of the equations in the method with floating reference values.

CONTROL EQUATIONS OF A HYDROELECTRIC PLANT WITH FIXED REFERENCE VALUES

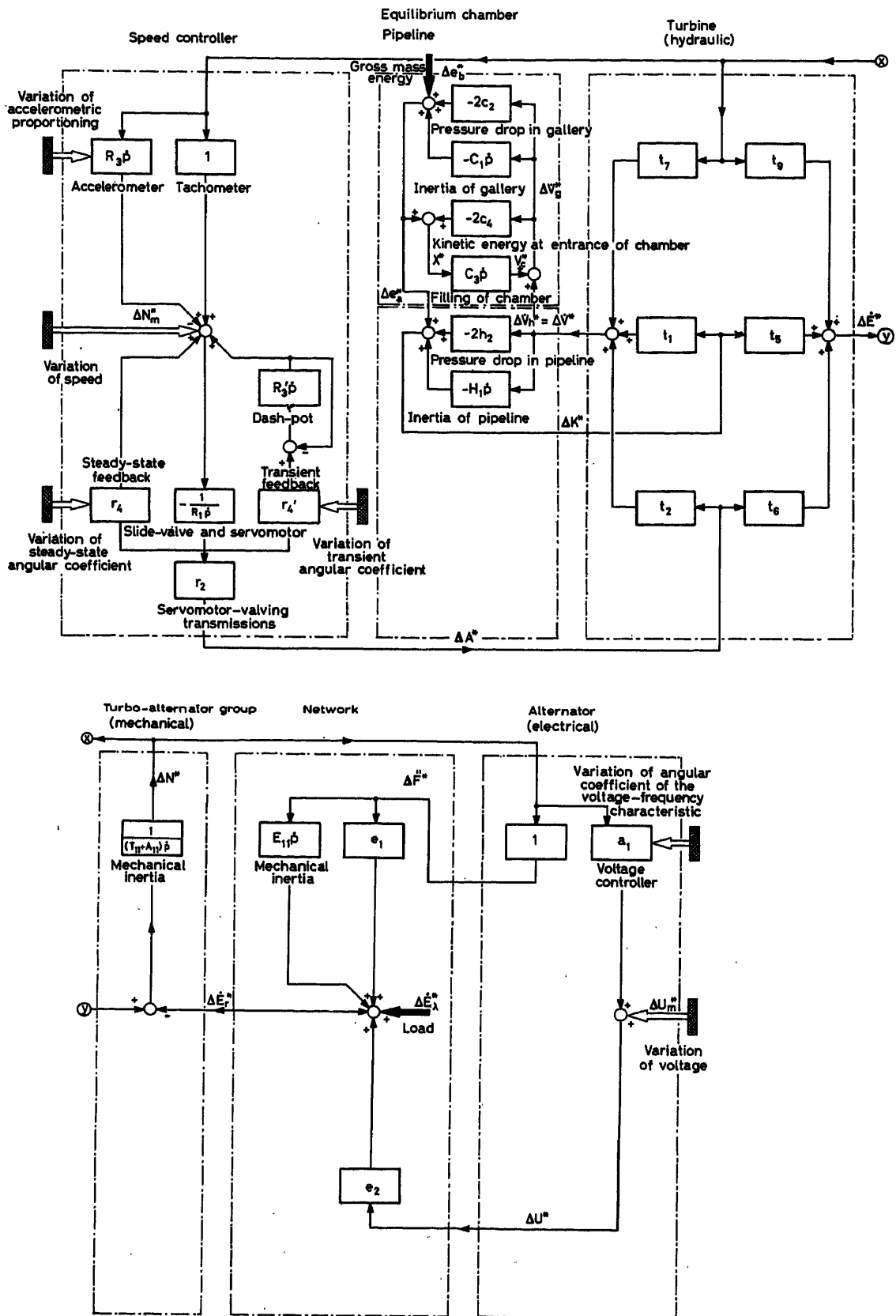


Figure 1. Block diagram of a hydroelectric plant provided with an equilibrium chamber, with accelero-tachometer controller, having a transient feedback and operating separately

Finally, the complete block diagram of the plant has been shown, and the transfer functions of the main elements are given as well as the total transfer function of the plant.

The method of calculation conserves its validity even when the absolute steady-state value of one of the magnitudes is zero. On the other hand, the method involves practically no complications from the mathematical point of view.

It may therefore be said that the method with fixed reference values, in addition to being as simple as the method with floating reference values, possesses the great advantage of being more general.

References

- ¹ BOREL, L. *Stabilité de réglage des installations hydroélectriques*. 1960. Lausanne; Payot. Paris; Dunod
- ² GADEN, D. *Considérations sur le problème de la stabilité*. 1945. Lausanne; La Concorde
- ³ DANIEL, J. Accélération du réglage de vitesse des turbines hydrauliques. *Houille blanche* 1, 2 (1948)
- ⁴ GARDEL, A. *Chambres d'équilibre*. 1956. Lausanne; F. Rouge et Cie
- ⁵ MEYER, R. Comportement et stabilité des régulateurs contenant des éléments à caractéristique non linéaire. *Houille blanche* 3-5 (1952)
- ⁶ CUENOD, M., GARDEL, A. et WAHL, J. Le réglage d'un groupe hydroélectrique en marche isolée, exprimé avec le langage et les symboles de l'automatique. *Bull. tech. Suisse Romande* 5 (1958)
- ⁷ RANSFORD, G. La détermination des caractéristiques optima d'un régulateur hydraulique, compte tenu de l'autorégulation et de la pente de la courbe de rendement. *Houille blanche* 3 (1958); 1, 6 (1959)

DISCUSSION

Author's Opening Remarks

The control equations which were the object of my communication in order to solve the problem of dynamic behaviour of the Kaplan turbine, have now been completed.

In order to explain the hydraulic behaviour of the turbine two supplementary parameters have been introduced which increases their number to six. In order to formulate the behaviour of the controller six supplementary parameters are now added which makes it possible to control the turbine gate and runner in an absolutely symmetrical way.

With these established equations, calculations were made on digital computers and, more recently, on analogue computers. The results showed that the hypothesis which had been made concerning the Kaplan turbine lead to conclusions which it is necessary to modify.

B. FAVEZ, *Electricité de France, 12 Place des États-Unis, Paris 16^e, France*

The purpose of the control system suggested is, as I understand it, to reduce to the minimum the deviations between the blades and the distributor during the transitory state. In this case I believe that an efficient behaviour of this control system should lead to an ideal turbine where the deviation is always perfect. Under conditions such as this, the differences between the stability diagrams b_3 and e_3 presented by Professor Borel are surprising to me.

L. BOREL, *in reply*

The system I have suggested is not equivalent to the realization of an ideal Kaplan turbine. Actually it is possible to determine the five new parameters introduced so as to obtain the best dynamic behaviour of the device. It seems to me, accurately, that this adjustment does not correspond with the case of the so-called ideal Kaplan turbine.

THE STEEL INDUSTRY

Application of Automation and Automatic Techniques to Metal Rolling and Processing

A survey by W. E. MILLER

Automation has captivated the interest of all groups of steel plant personnel: management, engineers and labour. All including the general public expect rapid acceptance, and look upon automation as the key to further improvements in steel plant operating efficiency and product quality. The steel industry occupies this position of unique attention because of its complex processes, large investment and high throughput.

In the steel industry automation is evolutionary; there always have been improvements and there always will be continuing improvements. The author does not know of any steel plant whose management considers their plant fully automated, or of any successful process automation where the management considers the job 100 per cent complete for ever.

The management that is awaiting 'cook book', 'patent medicine' or ultimate solutions to such complex processes, expensive providing practice and operational situations as exist in the steel industry will always be waiting. Direct copies of existing systems will probably be inadequate, disruptive to production and eventually more expensive because they are late and do not meet the then current competitive requirements. An OR & S (Operations Research & Synthesis) approach is a must for earlier operation, long term success and lowest overall cost.

The terms automation, process computer, computer control and automatic control are not precisely defined as engineers and scientists should like them defined for clear understanding and wide acceptance. We as engineers and managers must face these facts and live with them. Technical papers and proposal specifications must be read, understood and compared. Each author is sincere in his reporting of his achievements and contributions. His definitions fit his circumstances, his problems and his solution. A proposal specification may be entirely for the purpose of lowest price. The reader and purchaser must be sure that the solution truly is the correct solution for his needs.

The technology is here. Installations, both successful and unsuccessful, exist on almost all steel plant processes. Unfortunately, there have been failures. However, initiative, effort, ability, experience, true engineering understanding and unemotional evaluation will almost always guarantee success in installation, operation and pay-off. With this background will be presented

several examples of approaches considered and in use on rolling mills and processing lines. Professor Lerner will describe applications to material preparation, iron and steel making.

Applying Digital Computers

Digital computers are widely accepted and used by the steel industry for business and scientific purposes. Production is not directly delayed or disturbed by malfunction or lack of operation of such a computer. Production delays do not occur because the computers are off-line, that is, not connected to the process.

Of course, if pay cheques were delayed for weeks, or errors continually made, plant operations could come to a disturbing halt. Such things do not happen because such computers are generally used only 8 or 16 hours a day and plenty of time is available for maintenance.

Conditions on a hot strip mill are quite different. The mill operates 24 hours a day, usually a full week, possibly even longer without a scheduled shutdown. Every piece of equipment that is on-line must be designed and capable of such operation. Unscheduled delays are costly and will not be tolerated.

Digital process control computers are in on-line use on steel plant processes. The degree of success has varied widely for several basic reasons.

First in importance is technical approach. It is one thing to talk about a process, but it is quite another thing to write a comprehensive and exact explanation in logic diagram and mathematical form. While a technical approach may be modified, it is extremely expensive and time consuming to change to an entirely different concept of operation or control once equipment is installed and the process is in full production. A computer may even turn out to be completely inadequate in memory size or calculating speed. Interface equipment may be all wrong.

Some approaches attempted in the steel industry have been based entirely upon imitation of operators. While system operation was obtained, performance was significantly poorer than that of average operators. The author does not know of any case where a final decision has been made to stay with this initial technical approach.

Most steel plant management recognize that operators rarely understand the process phenomena. They control through reactions based upon training and experience. For most steel processes it will be less expensive and more productive to continue to use the operators than just attempt to imitate them. More installations have failed to become fully operational because of an incorrect or an inadequate initial technical approach than for any other cause.

Second in importance is reliability. The system should be capable of operating without delays or planned shutdown for weeks. Any failure must be fail-safe in so far as the steel in process, the mill and the basic drive equipment are concerned. There are such systems installed and operating—they are expensive, but one accident or one significant delay could more than offset the initial difference in cost.

System compatibility can be a difficult obstacle blocking the road to successful operation. Control computers must be connected to steel processes by sensors and actuators. They must operate that process through a multitude of feedback and open-loop control systems. There are large noise-producing obstacles of cranes, rectifiers, arcing breakers, contactors and relays. There are environmental conditions of dirt, water, steam, oil, acid, metallic scale, heat and vibration to contend with. Input-output devices may be scattered over half a mile.

To the uninitiated the formidable problems that develop can be a harrowing, expensive experience. All problems can be solved. Certainly, it is less expensive and less frustrating to face fully the problem at the time of initial budgeting and scheduling.

Integrated Automation—Total Systems Concept

Increasing attention is being given to plant scheduling and providing practice. Use of large-scale digital computers can provide significant savings over prevalent clerical methods.

Two approaches are being followed. One is strictly and permanently off-line and uses conventional business computers. The other is intended to become on-line as part of an integrated automation system. For system compatibility and reliability, present or future, a process type computer offers significant advantages. Such a computer might be provided with an input-output section for both business and process purposes.

Ultimately, steel plants will have integrated automation systems (Figure 1). Business, scheduling and process control

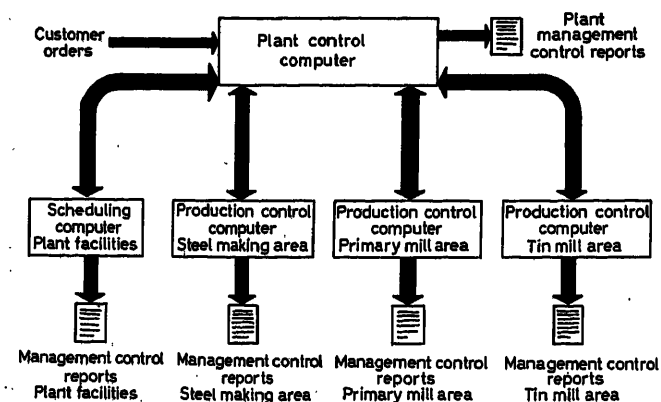


Figure 1. Ultimately, steel plants will have integrated automation systems. Business, production and process control computers will be linked

computers will be linked. Plant operations will be better scheduled and better coordinated. Yield should be higher and products significantly closer to specifications. There will be a total systems concept for the business.

Actually, the first step can be taken today. A long-range plan can be developed for step-by-step implementation. Each step should be as self-sufficient as possible, fit into the overall plan

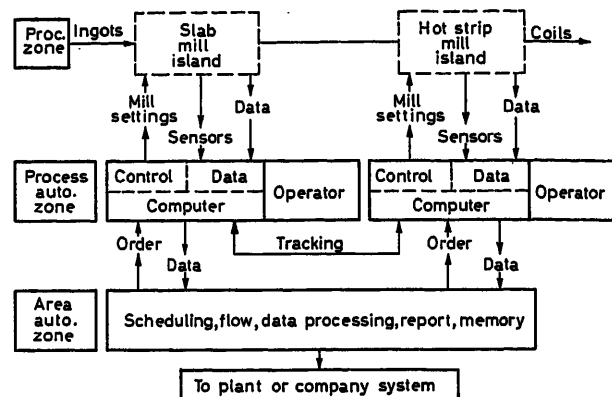


Figure 2. Communications with scheduling, accounting and process can be controlled from a control area

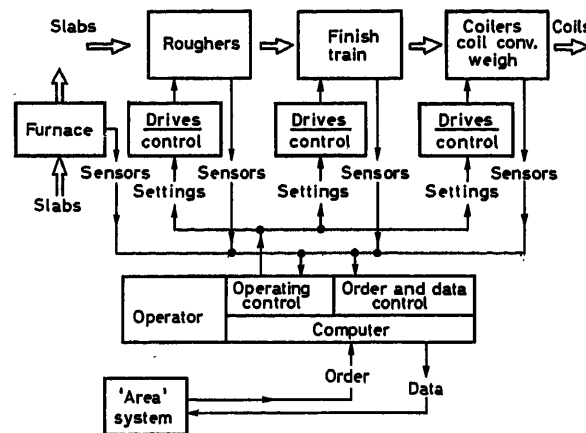


Figure 3. Each sector will be automated in a consistent pattern so that feedback relationships can be established

and meet the business needs of the particular plant and company (Figures 1 and 2). The first such system is now being placed in operation at Richard Thomas & Baldwins' Spencer Works, Great Britain, and is described in the paper by S. E. Hersom.

Predictive, Adaptive or Optimizing Techniques

Practically all steel plant process systems being installed today utilize combinations of predictive and adaptive control. A few systems might be said to optimize automatically a limited number of variables. This paper is intended to treat concepts of plant and process operation and automation. The discussion of concepts that follows is intended to apply to the total echelon of process operations and not, for example, to one particular process drive system such as roll screwdowns.

Large-scale digital process control computers are admirably suited to combine predictive, adaptive and optimizing techniques for steel plant process control. However, some processes such as reversing hot mills producing special shapes are not suited to achieve full advantage of this capability. Simpler, less expensive control techniques may be all that is necessary for process control. Even so, a computer may be 'a better buy' because of its ability

Second, rolling schedules must be calculated and cards must be punched, catalogued, stored, selected and transported to the process control card reader for use. Cards can become lost, inter-mixed, torn, late, or there just may be far too many of them.

An obvious alternate is to use a computer to calculate the rolling schedules 'on-line', storing the computation results in memory and thereby eliminating the intermediate punched cards.



Figure 4. On newer reversing hot mills operator monitors fully automatic operation with aid of closed circuit television and instruments

to provide also such non-control functions as information storage, production reporting, quality control reporting, crew incentive pay calculations, process cost data, productive maintenance advice, engineering data and analyses, and special 'on-demand reports'. Each process should be considered on the basis of a long-term strategy or plan before making a process automation decision.

Reversing Hot Mills

Automation systems at present in operation on reversing hot mills are predictive systems with programme input via computer calculation, punched card, punched tape, decade pushbutton or slide wire. Newer systems (Figure 4) provide for fully automatic operation of all functions associated with every pass of the ingot, slab, bloom or plate through the mill (Figure 5). Several are designed to provide automatic manipulation, or turning of ingots rolled either singly or in tandem. One punched card installation, which has been in operation for over two years, has rolled every single ingot since the second automatically, including manipulation.

While there are many punched card programmed mills in very successful operation, several limitations are recognized. First, pass reductions are based upon expected normal and uniform rolling temperatures and an average metallurgy. If significant variations occur, the operator must take over.

The computation may use one of a series of stored power curves representing the power requirements for rolling various alloys and stored rolling practice. This system remains strictly 'open loop' in that it does not correct for temperature or hardness variations. This approach is being used on one installation for approximately 75 per cent of the production. The remainder of the production is rolled manually. Manipulation of all ingots is performed manually.

A second approach is to utilize a process computer 'on-line' to calculate on a pass-by-pass basis. During each pass, mechanical and electrical data are fed back to the computer and used in

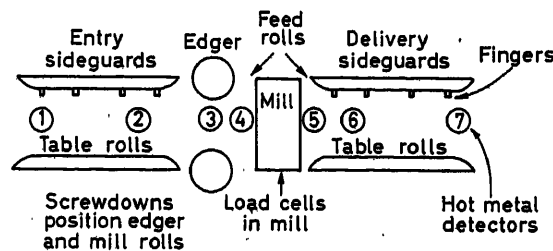


Figure 5. Slabbing mill main and auxiliary drives indicated operate automatically with every pass of ingot through mill. Fingers used to turn ingot operate when turning required. Punched card used for programming. Hot metal detectors and load cells used as basic sensors

calculating the next pass. Mill loading is optimized to give maximum production within thermal, mechanical and metallurgical limits of equipment and metal being rolled. Drafting may also be optimized, for such products as plate, to obtain proper width, shape and final thickness. Effects of roll separating force, mill housing stretch, roll bending, roll flattening, roll crown and product spread may all be evaluated in producing an on-line pass-by-pass rolling schedule.

Four digital computer systems intended for combined predictive-adaptive control are known to be installed on reversing hot mills producing flat products. One mentioned earlier is currently used for a pure predictive calculation which is stored and read pass-by-pass from memory. The other three are at present operated as conventional punched card programme input systems with information from each card being stored in a core memory.

The latter three systems are reported to depend upon accurate measurement of slab or plate temperature and difference in temperature from pass to pass along with roll separating force. Consistent and accurate measurements of differences in temperature are difficult to obtain because of scale, water, steam and changing top and bottom surface cooling. The mill environment has made it difficult to obtain adequate sensor accuracy and reliability.

Another technical approach that has been developed and tested utilizes a more sophisticated mathematical model and thus more extensive computer programming to calculate changes in temperature. Variations between the calculated and actual values of roll separating force are used to calculate the necessary constants for the mathematical model as the slab or plate is rolled. A modification of this model has been very successfully and continuously used since December 1962 in the computer set-up and operation of a hot strip finishing mill.

There are other similar instances in steel plant processes where either process environment or lack of a sensor of proper type, accuracy or reliability renders a laboratory or paper design

unworkable. In some cases ingenious analysis and design can utilize the capabilities of the process computer to achieve full adaptive control in spite of a sensor handicap.

The Hot Strip Mill

The hot strip mill area extends from the slab yard to the finish coilers. There may be from two to five slab reheating furnaces of as many different designs (*Figure 6*). There may be four or five continuous roughing mill stands driven by synchronous motors (*Figure 7*), or there may be a reversing rougher similar to the mill type just discussed.

A delay table precedes the finishing mill to permit the plate to reach a proper temperature before finishing rolling (*Figure 8*). There may be a crop shear automatically operated from scanning sensors that check plate width and rate of change of width to crop head and tail ends.

Following descaling the plate enters the finishing train. During most of the rolling period the plate is being reduced in thickness simultaneously by all stands. Reduction is effected not only by the preset roll openings, but also by tension or changes in tension between stands. Both front and tail ends are rolled without being in all stands simultaneously and may vary in thickness as the result.

The strip proceeds down the run-out table where it is sprayed with cooling water to cool for grain structure and desired coiling temperature (*Figure 9*). It reaches and enters one of several coilers while normally travelling at a speed of 1,000 to 2,200 ft./min. The same strip will probably be in the coiler, on the run-out table and in all finishing stands. At this time this group of drives may accelerate to 3,000 or 3,500 ft./min. As the tail end leaves each stand, that stand must be quickly reset to proper speed and roll opening for the front end of the next plate. The new plate may be of different width, thickness and metallurgy. The time interval between plates must be kept short to fully utilize productive capacity and to maintain uniform roll temperature.

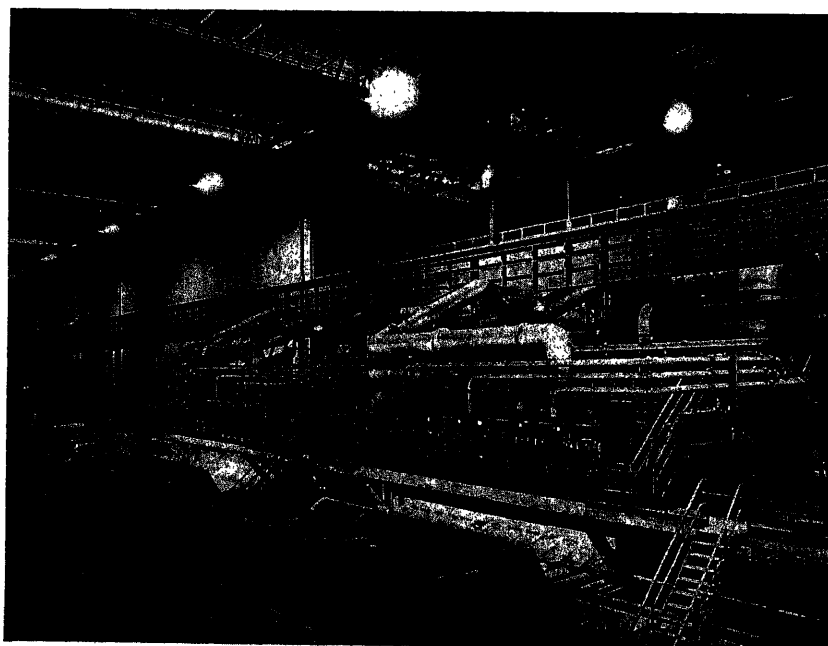


Figure 6. Slabs are heated in reheating furnaces and delivered to tables at entry end of hot strip mill

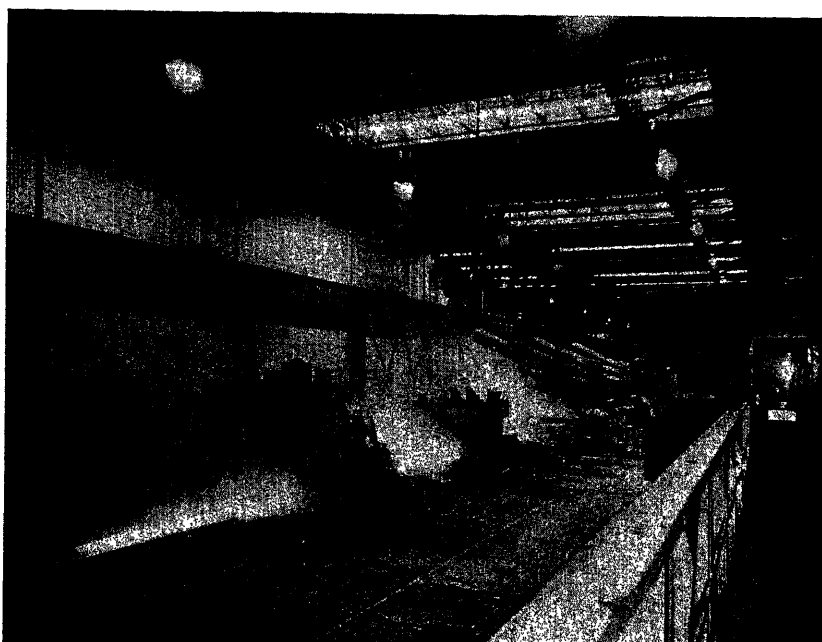


Figure 7. Slab proceeds right to left from reheating furnace through scale breaker and No. 1 Rougher

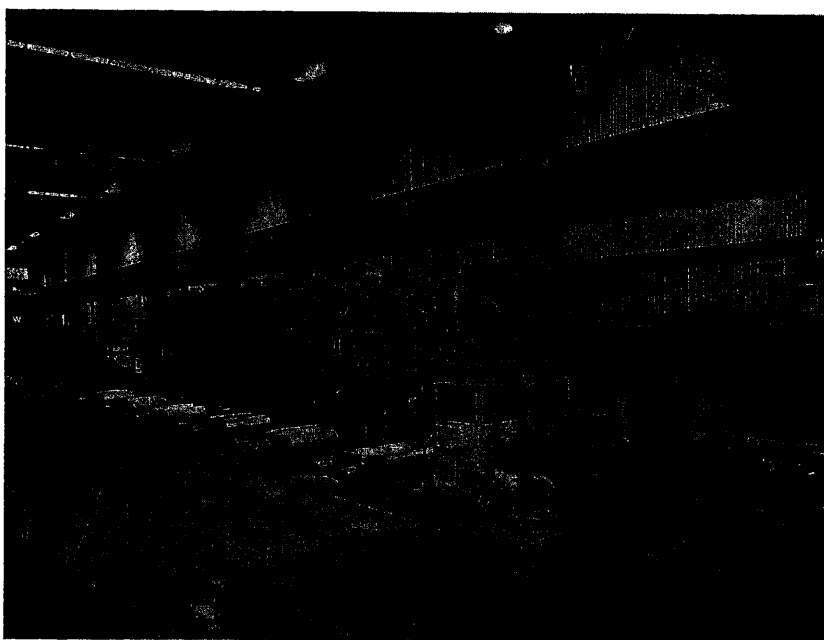


Figure 8. After being held on delay table for proper rolling temperature, front and tail ends of plate are cropped automatically by shear, descaled and entered into six stand finishing mill

Digital process control computers (*Figure 10*) are installed on two hot strip mills in the U.S.A. The first at McLouth Steel Corporation, Trenton, Michigan, was placed in partial operation early in 1962. On 1 December 1962 computer control on the McLouth mill was agreed to be complete. McLouth assumed responsibility and extended operation to full three shift, seven day week basis. The old monthly tonnage record was soon broken and new monthly production records continue to be made.

Computer availability as of 12 June 1963 has been in excess of 99 per cent. Availability would be practically 100 per cent except for one period when servicing was delayed. Improvements in plant yield, product quality and operating cost have been gratifying. Operators and management speak with enthusiasm about product quality, mill performance and the computer.

The McLouth system utilizes a comprehensive mathematical process model or simulation stored in the computer's memory

(Figure 11). In popular press terms it truly operates as a 'thinking machine' to determine an optimum finishing mill set-up based upon only three items of manual input data describing the product to be rolled, plus sensor inputs. This process computer system continuously demonstrates an as yet unequalled ability for mill set-up and rolling performance on schedule changes and initial start up after roll changes.

The second hot strip mill digital control computer is installed at National Steel's Great Lakes Steel Division, Ecorse, Michigan.

The system is reported to have been operated through a catalogue of stand set-up schedules stored in the computer memory. The *Wall Street Journal* reported on 19 February 1963 that the company says it is not yet in full operation.

A third digital process control computer is now being installed on the hot strip mill at the new Spencer Works, Richard Thomas & Baldwins, Great Britain (Figure 12). The system is patterned after the very successful McLouth system but is of significantly broader scope and utilizes a larger faster computer.

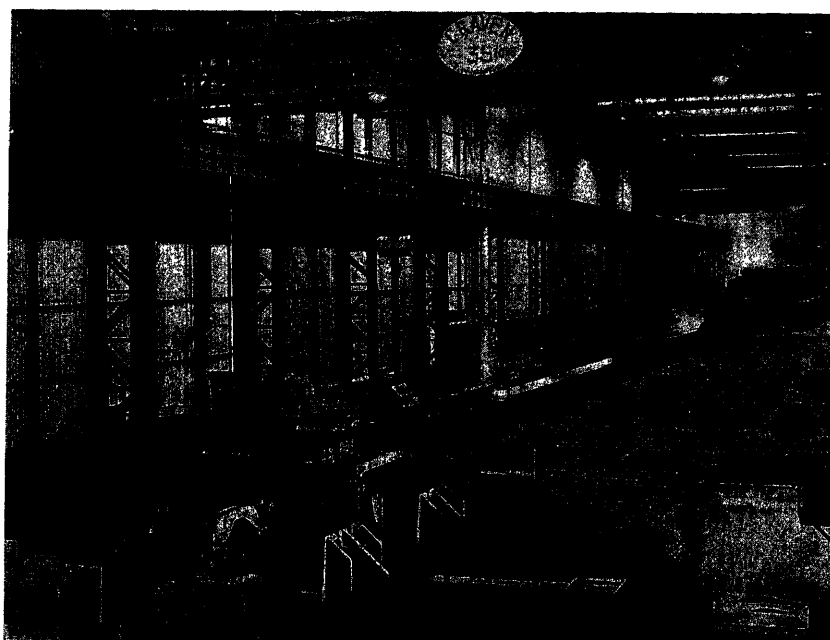


Figure 9. Strip is cooled by sprays on runout table and enters a coiler

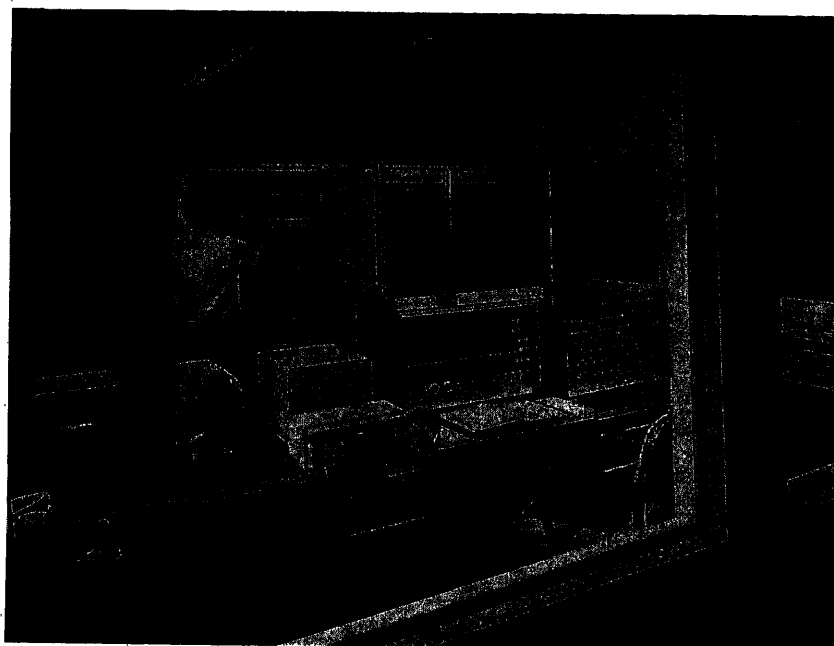


Figure 10. General Electric (USA) 412 process computer 'operates' hot strip mill from reheat furnaces through coilers



Figure 11. Finishing mill pulpit, McLouth Steel Corp. where General Electric (USA) 312 process computer 'operates' 6-stand finishing mill

Here the scope of operations is from reheat furnaces through coilers and includes all main and necessary auxiliary drives and systems between these limits.

The I.F.A.C. application paper by R. G. Beadle provides a comprehensive description of a complete computer automation system for a hot strip mill. However, for completeness and accuracy of this paper it is necessary to mention that the computer provides set points, and monitors several important sub-systems required prior to, or with the addition of, the computer. Principal sub-systems are the following:

- (1) Speed regulators for finishing mill stands.

- (2) Finishing mill automatic gauge control.
- (3) Finishing mill looper position regulators.
- (4) Positioning regulators for programming principally screw-downs, and sideguides on roughing and finishing mills.

The current world-wide count for automatic gauge control systems for steel and aluminium hot strip mills, either installed or purchased, is estimated at 30. These systems vary significantly in scope and performance. Approximately 80 per cent of these systems have been provided by one U.S. manufacturer.

Simple numerical data classifiers and loggers are installed and continuously used on several mills. Such loggers also have been used to test before and after performance for various levels of automation. Some data have been published.

Operating experience has proved that a digital process control computer can be used profitably to calculate automatically mill drafting, set up stand speeds and roll openings, monitor many feedback control systems and upgrade continuously process operation in spite of degrading influences such as roll wear, mill and steel temperature variations, varying metallurgy and frequent order changes—even every coil rolled. It is believed that the necessary high level of performance can be achieved only with an on-line computer which, by adaptive feedback, can keep its mathematical model current with a changing process.

Cold Reduction Mills

Today the majority of American cold reduction mills are equipped with some form of automatic gauge control. Even so, with or without AGC, all produce off-gauge strip at both ends of a coil. Today significant attention is being devoted on new high production tandem mills to reduce the amount of off-gauge strip at the ends, as well as in the main body of the coil, to the lowest practicable value. The ultimate objective is to produce no more than a few feet of off-gauge product.

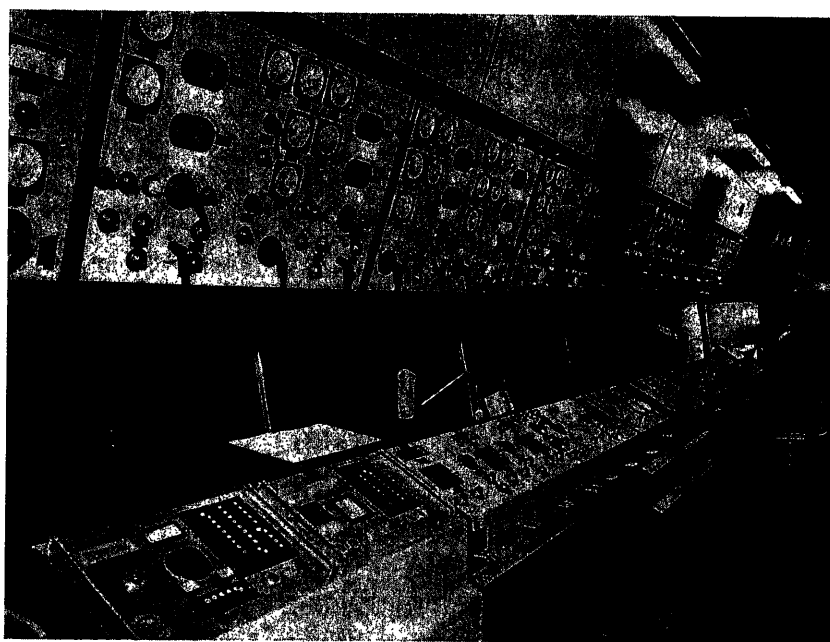


Figure 12. Finishing mill pulpit, Richard Thomas & Baldwins, Great Britain, where General Electric (USA) 412 process computer will 'operate' complete hot strip mill from reheat furnaces to coilers

Innovations being installed include improved broader scope forms of gauge control (*Figure 13*) systems for threading the mill automatically at higher roll speeds and digital process computer mill set-up calculations, control and monitoring.

Automatic threading at higher speeds reduce off-gauge strip caused by the higher coefficient of roll bite friction existing at low speeds. Better utilization of the facility is achieved also since threading time is reduced. An automatic threading system has been built and tested. It is now being placed in operation on a new U.S.A. tandem tinplate mill.

Computer control has been purchased for two tandem mills,

both processes. Various process set-up calculations, process control, process monitoring functions are properly provided by the process computer.

Three process computers have been applied to electrolytic tinning lines. Two will provide a broad range of process control, the third tracks and makes certain on-line calculations. It is planned to enlarge the latter computer scope to control.

A process computer is installed and in operation on a continuous annealing line at Jones & Laughlin's Aliquippa works. The system and operating experience are the subject of the paper by J. T. Bradford, Jr.

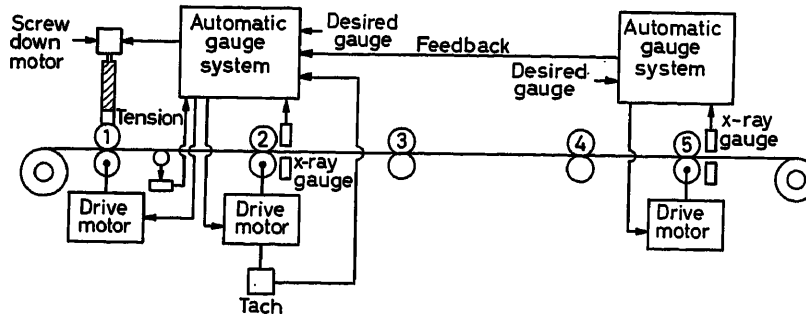


Figure 13. Improved, broader scope forms of tandem cold mill automatic gauge control will reduce off-gauge strip at ends and improve uniformity of gauge in the main body of the coil

one in the U.S.A. and one in the U.K. The process computer can provide the same basic set-up calculations, control and monitoring provided for the hot strip mill. However, there are significant differences in the technical approach, mathematical model and computer programme because of the significantly different process characteristics and roll bite phenomena.

In the U.S.A. the computer is to be installed this year on the mill equipped with automatic threading. The computer will permit faster set-up changes between coils. The digital computer applied with automatic threading, and expanded scope automatic gauge control promises a new concept of tandem mill operation that will be more completely described in planned technical papers.

Continuous Processes Lines

Large steel strip processing lines such as electrolytic tinning lines and continuous annealing lines more nearly approach the automotive concept of automation than most steel processes. Many operations previously handled separately have been combined into one coordinated process system that may extend over 600 feet and involve as many as 150-160 adjustable voltage d.c. strip propelling motors alone. Usually there are multiple storage loops so that entry and delivery zones may be started and stopped without disturbing strip speed in critical processing or treatment zones.

Product value becomes quite high (*Figure 14*); yield becomes ever more important. The electrolytic tinning line and annealing line are truly continuous processes with discrete segments of strip requiring specific treatment to meet order specifications.

Higher processing speeds and more competitive markets result in shorter operating periods per order. A process computer offers unique tracking and process programming capabilities on

Strip processing lines continue to grow in size and complexity. Process adjustments are many and varied. Product value is at its highest level. Data loggers for quality control are required for many processes. New computers are now available that are easily expandable from data logging and calculating to process control. For many plant situations the economics can favour such a computer over the conventional wired programme logger. It is expected that many future tinning, and annealing lines may be planned for a degree of computer control.

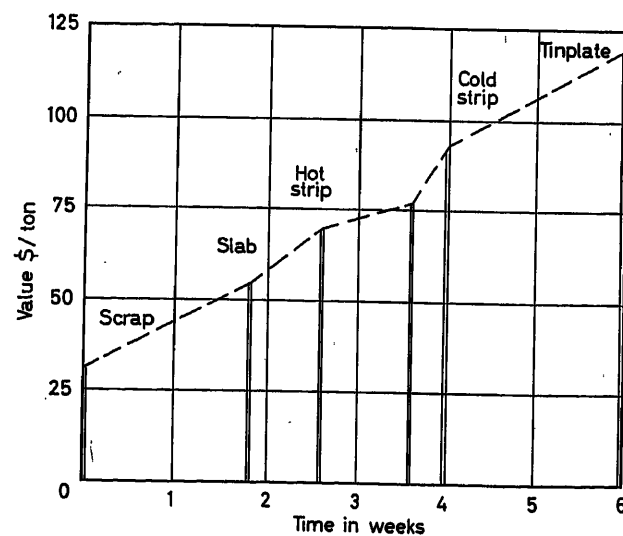


Figure 14. Electro tinplate value and production time are significant. Improvements in anneal line and tinning line yield represent potentially large savings

Conclusion

Highly reliable and accurate local regulators are in extensive use throughout the steel industry. The next logical step is to let a process computer direct these local regulators by supplying the regulator set points. In some cases the computer also may provide some local regulating functions. The digital process control computer is ideally suited for this task because of its nearly unlimited capacity for speed, memory and extreme consistency with lack of fatigue. Process computer control is not only desirable, it has become a reality and is rapidly developing into a necessity to maintain a steel company's competitive market position in the face of ever-increasing demands for improved product quality.

Since computers are incapable of originality, the degree of success achieved on any installation is dependent upon the correctness of the operating computer programme (the software) stored in the computer's memory. Experience with current applications has proved that hardware alone does not suffice to implement a working system of permanent significant value. A very considerable amount of process know-how and experience is required to prepare a successful computer programme.

Mathematical models of many orders of sophistication have been developed for various steel plant processes by a number of companies. It is the privilege of the purchaser to decide at which level of sophistication and first cost he is to take his step into process computer automation. Those who have made several applications, or who have thoroughly studied the history of current successes and failures have developed extreme caution towards proposals with broad future expectations or claims, long term on-line development programmes, and the lowest price.

Yet those who wait for a standard solution may always wait since those who were successful will continue to build additional success upon their initial success. Our exploding information and control technology is a challenge not only to engineers, but to all levels of management. The risks of management increase yearly. Decisions will become even more difficult since as the scope of the effects broaden survival of the enterprise may be affected by making the correct decision at the correct time. It is hoped that this Congress and the overall programme has provided information and knowledge to engineers and management on the broad basis necessary to use the available technology for continued growth of the world economy.

Bibliography

- A steel company's date with a data machine. *Business Wk*, May 4, 1962, 142
- Three interlinked computers to run new British steel works. *Control Engng*, June 1962, 128
- DQC in the steel industry. *Control Engng*, Sept. 1962, 139
- Integrated automation for steel plants. *Iron & Steel Engr*, Oct. 1961
- Automation in a steel works with special reference to the use of digital computers for production scheduling and information transmission. *Automatic and Remote Control*, 1963
- Application of digital control computers to steel industry process control. *Iron & Steel Engr*, Dec. 1960, 134
- Computers start to run the plants. *Business Wk*, Nov. 5, 1960, 50
- Considerations in applying digital computers in process control automation. March 1962, 56
- Electrical equipment for metal rolling mills. *Blast Furnace & Steel Plant*, Oct., Nov., Dec. 1962; Jan., Feb. 1963; 38 pages
- Programmed slabbing mill. *Blast Furnace & Steel Plant*, May 1963, 373
- Operating experience with the automated slabbing mill. *Iron & Steel Engr*, April 1963, 105
- An evaluation of automatic control performance in hot rolling. *Iron & Steel Engr*, January 1963
- On-line computer control of a hot strip finishing mill for steel. *Automatic and Remote Control*, 1963
- Use of computers in continuous strip mills, *J. Iron & Steel Inst.*, Nov. 1961, 262
- Modern process control. *International Science and Technology*. May 1963, 28
- Heard on the Street. *Wall Street Journal*, Feb. 19, 1963, 31
- L'Automazione del Laminatoi Continui a caldo per nastri. *Estratto dai Rendiconti dell'AEI 1961*
- Bringing hot strip mills under automatic control. *Control Engng*, Sept. 1960, 146
- A computer controlled hot strip mill. *J. Iron & Steel Inst.*, Jan. 1962, 31
- On-line gaging benefits hot strip mill. *Control Engng*, July 1961
- Automatic gage control on reversing cold strip mills. *Iron & Steel Engr*, August 1961, 77
- Developments in drive systems and gage control for reversing cold mills. *Iron & Steel Engr*, Nov. 1961, 151
- Digital computers for accounting and control of continuous processing lines. *Iron & Steel Engr*, April 1961

Achievements in the Automation of Ferrous Metallurgy*

A survey by A. YA. LERNER

Production processes in ferrous metallurgy are extremely diverse and complex. For the most part they are high-temperature physico-chemical processes taking place in expensive units into which numerous materials are fed to take part in the reactions¹. Each of these processes requires precise organization for operation and imposes a great number of constraints upon the initial materials and on the operating conditions.

A result of these properties particular to ferrous-metallurgy processes is the low efficiency of those control systems which do not take sufficient account of the specific features of the process—particularly its physico-chemical aspect†. Recent years have demonstrated the effectiveness of building control systems, on the basis of deep penetration of control into the physico-chemical specific aspect of the process, starting from a specific industrial or economic aim.

Nowadays progress in automation in process control has become inseparable from progress in the study of processes. New information about a process gives rise to ideas and means of control; conversely, the desire to make a process controllable and able to be monitored stimulates the study of processes and the development of the necessary means of control. There are now many examples of a process and a unit being changed to make them more convenient for control, and there are even examples of the creation of basically new processes and units created, and adapted for monitoring and control.

The complexity of processes means that control algorithms will be complex. The aim of control is no longer stabilization of some specified mode, but the optimization of processes. Control itself must not be merely just any permissible control made, but must be a precisely defined optimal control.

The complexity of control algorithms stimulates extensive use of modern computing equipment. Developing such systems of centralized control and monitoring makes it possible to put into controlling equipment an ever greater volume of information, which must serve to continuously improve the control algorithm. The extensive employment of adaptive and self-organizing systems makes it possible initially to use a computer for study of the process, from which the control algorithm will be formulated; then the computer serves as a model of the process in the adaptive system, attains a trained state, when it can be used as the operator's 'adviser' after which it may be included in a closed control loop, eliminating the operator from this function and providing better control in the sense that machine control is closer, on average, to optimal.

The most urgent problems today seem to be first the creation of control algorithms (in essence means of implementing algorithms are already available); secondly, the creation of new measurement and metering devices. The third pressing problem, to solve which the efforts of control specialists and technologists

are being combined, is the creation of continuous processes and continuous-action units, such as the direct reduction process, the continuous-action steel-smelting unit, etc.^{2, 3, 17}.

This paper goes on to consider, in the light of these processes, achievements in the control of specific ferrous-metallurgy production processes.

Sintering

The sintering process can be considered as a combination of four technological operations: preparation of the charge, roasting on the sinter strip, conveying operations and cooling of the finished sinter. The control problem can be formulated in the form of a requirement either to maximize output for a prescribed sinter quality, or to minimize production cost. From this general problem there follow problems for each technological operation.

Control of the charging process must ensure the required quantity of sinter of the specified composition. Here there arises the problem of optimizing the charge composition (e.g., according to the criterion of cost) by varying the ratio of its various components. Yet another optimization problem is posed: deviation from the specified chemical composition must be minimal.

Systems of weight batching of the charge components have been successfully introduced in a number of countries (U.S.A., Great Britain, West Germany, Japan). X-ray analysers are used to detect variations in the composition of the components (U.S.A.). The problems involved in sintering are extremely complex. Researches in the Soviet Union, the U.S.A. and West Germany have shown that the quantity of sinter is mainly determined by the content of carbon in the charge, whereas the productivity of a sintering machine (i.e. the yield of suitable sinter) is decisively influenced by the gas-permeability of the charge, which is determined by its moisture content. In a control system (Figure 1) which is being designed in the Soviet Union, it is proposed to maximize the output of the machine (the yield of suitable sinter) according to the moisture (i.e. by acting upon the supply of water to the charge) and to optimize sinter quality according to the content of fuel by consecutive search of the optimal contents of moisture and fuel on a computer which gives instructions to 'charge-fuel' and 'charge-water' ratio control systems. This system also controls the sinter-machine speed to match the horizontal speed of travel of the sinter strip to the vertical rate of sintering. The system also includes two computers: for determining the endpoint of the sintering process from the difference in the temperatures of the waste gases in three vacuum chambers, and for calculating the true output of suitable sinter from the difference in the weights of the charge and the return material.

A patent was granted in West Germany in 1958 for control of sintering on the basis of analysis of the waste gases for CO and CO₂, taking into account the quantity and moisture content of the waste gases. From this data the computer continuously calculates the content of C in the charge and its moisture content,

* Engineer S. A. Maly gave the author a great deal of help in compiling this review.

† This statement can also include human operators when they perform as the controlling element in the control system.

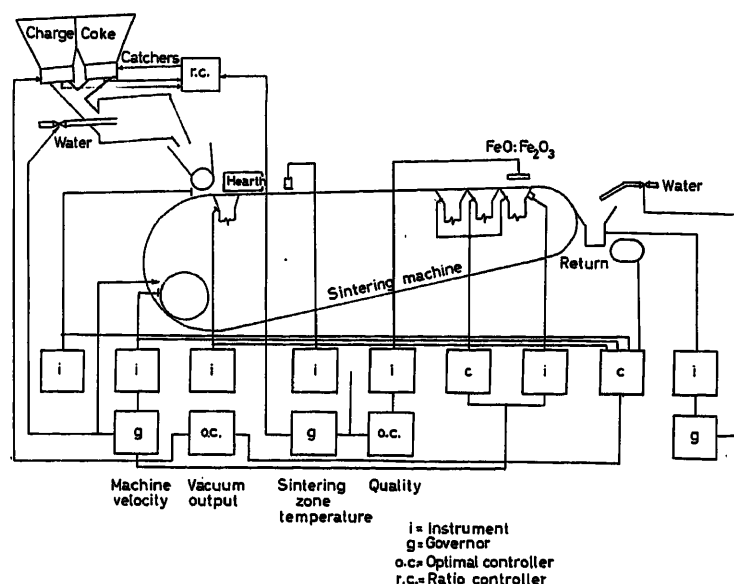


Figure 1. Sintering machine automation

thus making it possible to vary the supply of coke and water while the speed of the pallets is unchanged, thus increasing both quality and output.

As is known, the optimal moisture content value varies with changes in the grain size, mineralogical composition and burden base. It has been suggested in the Soviet Union that automatic control be effected with the aid of two autonomous control systems and an optimizer. The process is mainly conducted by analysis of the waste gases for carbon content (i.e. CO and CO_2) and moisture. When there is a variation in the quality of the charge, an additional control system is put into operation; this maintains the prescribed difference of temperatures of the waste gases in the last vacuum chambers by acting upon the speed of the strip. The optimizer acts upon the moisture content of the charge and finds the maximum gas-permeability of the charge, which is evaluated from the rarefaction in the vacuum chamber. The optimal moisture-content value for the given condition, having been found, is maintained henceforward by the main control systems.

As for measurements and metering devices, mention must be made, above all, of the success of the firm of Lurgi (West Germany) in developing the means necessary for charging; also worthy of mention are the development of an x-ray charge analyser (U.S.A.), instruments for moisture content control, developed by Elliott's (Great Britain), and an instrument for measuring the magnetic susceptibility of a charge, developed in the Soviet Union⁴⁻⁸.

Blast-Furnace Production

Very considerable progress has been made in automation of blast-furnace control. Research has been developing on a broad scale, primarily in the U.S.A. and the Soviet Union, into the use of computers for studying the blast-furnace process and operative control of it. A great deal of information on the process is being gathered. Analogue or digital computers, on the basis of the proposed mathematical descriptions of the blast-furnace pro-

cess, calculate the material and thermal balances, heat-transfer to the burden, the development of direct and indirect reduction; they determine the influence of the variation of different parameters of blast-furnace smelting, e.g., moisture-content, natural-gas additions, etc., upon the process indices.

The mathematical descriptions, however, do not as yet cover all the aspects of the process, so there is a parallel development of experimental methods of investigation of the process. Researches conducted in this direction in the Soviet Union have revealed the extremal relationships which exist between certain quantities, which suggests the possibility of the use of optimizers on blast furnaces.

Great progress has also been made in automation of elements and assemblies. Solid-state (using semiconductors and magnetic amplifiers) circuits for controlling furnace charging are being successfully developed and introduced. Such units are already in operation at some American plants and will soon be working in the Soviet Union. Research is being conducted in the Soviet Union into automation of car-scales with registration of the weight and composition of the burden.

Wide use is made in the United States, France, Italy, West Germany and the Soviet Union of automatic distribution of the blast around the furnace tuyères. For this purpose use is made of instruments forming part of composite and unified systems (Minneapolis-Honeywell, B.I.F. Industries, Hagan and Siemens, and in the Soviet Union TsLA and N.I.I. Teplopribor).

Already working successfully in the Soviet Union is a system for controlling a rotary burden distributor, which considerably evens out the temperature of the throat gas over the whole cross section of the furnace. One Soviet furnace employs a system for controlling the relation between the flow rate of the natural gas and the hot blast, taking into account the oxygen concentration of the blast. Wide use is made of a system for controlling the operation of the air heaters, which switches the heaters to control their thermal performance. Control of the ignition of the jet when transferring an air heater to gas is effected by a special light-sensitive relay, which reacts only to the pulsating flame of the jet.

Since blast temperatures are now increased to 1,200° C, the air-heater heating and crown-shielding control system required special attention. Units with a radiation pyrometer aimed at the upper portion of the burden are in successful operation.

The intensification of blast-furnace operation requires the sophistication of monitoring control, and this has led to the creation of centralized monitoring systems. Such systems have been designed, for example, in West Germany—Siemens Teleperm—and in the Soviet Union—TsLA system. Many new means of monitoring have been evolved. X-ray analysers and mass-spectrometric instruments have been developed in the U.S.A., Great Britain and the Soviet Union for analysis of the chemical composition of the raw material. The Siemens firm in West Germany has developed a reliable instrument for determining blast moisture content with the aid of a lithium-chloride absorber. Hygrometers with good metrological indices have also been designed in East Germany, Hungary, Czechoslovakia and Poland.

Siemens has built reliable and accurate CO and CO₂ gas analysers (2nd class of accuracy). An isotope level-meter has been developed, first in the Soviet Union and then in the United States. A pulsating probe has been designed in East Germany. Both these instruments are used to determine the charging level. Equipment has been designed and introduced in the Soviet Union for continuous measurement of the temperature of the iron on the outlet.

Of great interest is the research conducted in East Germany and Czechoslovakia, aimed at creating methods of taking representative samples for analysis of the composition of the ore part of the burden and the moisture content of the coke. Another interesting feature is the use which is now being made in the Soviet Union of computers for control of the ore area^{17, 18}.

Steel-making—Converter Production of Steel

According to available estimates, an experienced operator can maintain the required temperature conditions for only 60 to 65 per cent of working time in the U.S.A., as against 70–80 per cent in Japan. Present experience in the use of control systems indicates that their employment enables the steel-making time to be cut by 20–40 per cent. Studies of the process are being made in a number of countries (U.S.A., West Germany and the Soviet Union) to work out a mathematical description of the process. The problem of controlling converter smelting consists of determining the moment of tilting the converter with the attainment of the prescribed composition and prescribed temperature of the steel. Two methods of stopping the blowing at a prescribed carbon content are most promising. In the first place, it is a question of calculating the amount of O₂ required per heat to produce the specified content of carbon, and secondly, continuous determination of the content of carbon in the bath according to its balance. The second method is effective only with a sufficiently high carbon content. With a low content, to determine the moment of stopping blowing according to the appearance of the flame above the top of the converter, use is made of instruments of the bolometer type (TsLA in the Soviet Union). Thermocouples or optical pyrometers are mainly used to measure the temperature of the converter bath. These methods do not offer the necessary precision. Therefore, it is necessary to calculate the quantity of cooling agents (steel scrap, ore, sinter, etc.) per blowing, according to the equations of the thermal balance; the coefficients in these equations are established by

means of continuous statistical processing of the results of previous blowings.

Another important need in carrying out smelting is calculation of the quantity of oxidizers and alloying additives on the basis of information about the composition of the ferro-alloys, and also about the composition and temperature of the metal.

The approach described above is characteristic of most of the studies being made in many countries (in the U.S.A. Jones and Laughlin Co., Great Lake Steel Corp., Minneapolis-Honeywell; in Great Britain B.I.S.R.A.; in the Soviet Union the Central Ferrous Metallurgy Research Institute, the Automation Institute of the Ukrainian S.S.R., and others).

Figure 2 shows a layout¹⁵, for complex converter automation. This scheme envisages the use of a computer which, on the basis of the characteristics of furnaces and raw materials will guarantee the chemical composition and temperature of the steel produced by issuing instructions about the amount of the required additives. In the Soviet Union, a digital computer is used for controlling converters. It is used to calculate the amounts of oxygen and coolants per heat to obtain, at the moment blowing ceases, the specified content of carbon and temperature of the steel, the quantity of slag-formers for the production of slag of the specified basicity, the amounts of deoxidizers and alloying additions per heat, etc.

At the first stage the results of the calculations on the machine will be given out in the form of recommendations, but after proving the algorithms, the machine will be given the functions of control. The Cybernetics Institute of the Ukrainian Academy of Sciences has made some interesting experiments, in the course of which control of the tilting of converters operating in Dzerzhinsk was effected from Kiev^{11–15}.

Open-hearth Production

Production of steel in open-hearth furnaces predominates at the present time. The complex periodic process of making steel in an open-hearth furnace still cannot be satisfactorily monitored. Because of this, great efforts are being made all over the world, and vast sums are being spent, on the development of methods of measurement and instruments.

For measuring the temperature of the metal in the furnace pool, in addition to immersion thermocouples, use is made of small radiation pyrometers which are placed in blown-through tubes.

The temperature of the combustion products on the vertical channels of the furnace is measured by the intensity of the spectral bands characteristic of CO₂, with the aid of the optico-acoustic pyrometer.

The temperature of the air after heating in the regenerator is measured by the speed of passage of ultrasonic waves. A spark discharge is used as the noise source, while the receiver is a capacitor microphone. An unusual solution has been found in the Soviet Union to the problem of measuring the temperature of the inside surface of the crown. Telescopic units which 'inspect' the crown, are used.

The level of automation of elements and thermotechnical monitoring of open-hearth furnaces is the same in most industrial countries. An example is the structure of an open-hearth furnace control system, widely used in the Soviet Union (Figure 3).

The main peculiarity of this system is control of the thermal load by constraints. Since the efficiency of operation of open-

ACHIEVEMENTS IN THE AUTOMATION OF FERROUS METALLURGY

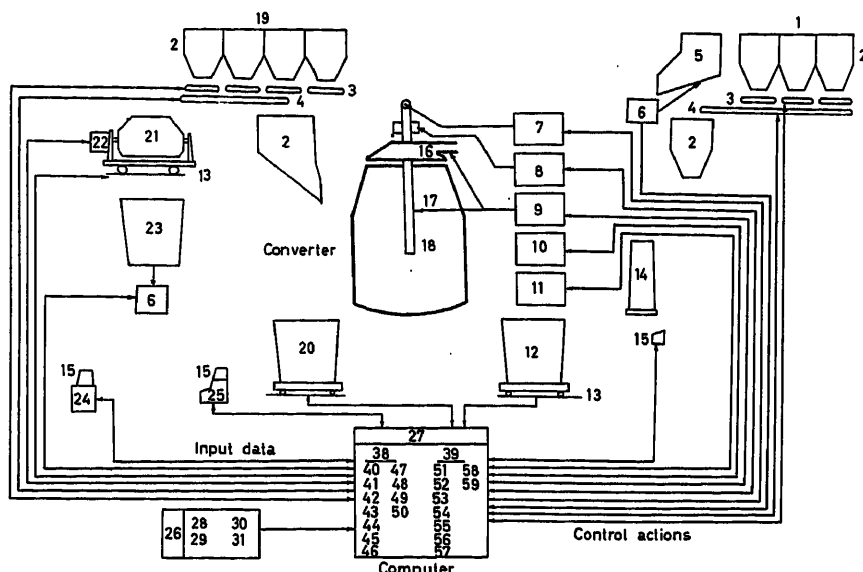


Figure 2. Converter automation

- | | | | |
|---|--|--|--|
| 1 Ladle addition agents bunkers | 16 Watercooled cap | 30 Iron from blast furnace, temperature and analysis | 46 Scrap consumption for cooling |
| 2 Feed bunkers | 17 Converter | 31 Fluxes | 47 Supplementary blowing conditions |
| 3 Conveyer scales | 18 Tuyère | 32 Adjusted limits | 48 Mould inventory data |
| 4 Conveyer | 19 Flux bunkers | 33 Scrap | 49 Blowing efficiency |
| 5 Scrap bunker | 20 Slag pot | 34 Sizes and quantity of the iron moulds | 50 Process data |
| 6 Balance | 21 Mixer-type ladle | 35 Moulds inventory data | 51 Choice of the blowings |
| 7 Pressure and quantity of O ₂ (measured and controlled) | 22 Electric drive | 36 Hot metal temperature | 52 Ladle turning |
| 8 Tuyère position control | 23 Hot metal pot | 37 Hot metal analysis | 53 Fluxes weighting and charging |
| 9 Cooling water control (pressure and amount) | 24 Record in the shop manager office | 38 Computations | 54 Tuyère position |
| 10 Bath temperature | 25 Operator desk, manual control | 39 Signalling and control | 55 O ₂ consumption |
| 11 Steel analysis | 26 Input data | 40 Hot metal weight | 56 Blowing time |
| 12 Teeming ladle | 27 Computer | 41 Scrap weight | 57 Scrap weighting and charging |
| 13 Rail platform scales | 28 Blowing temperature | 42 Flux weight | 58 Scrap charging for cooling |
| 14 Moulds | 29 Set analysis, temperature, and weight | 43 Tuyère position | 59 Addition agents weighting and charging into the ladle |
| 15 Typewriter unit of the teeming span | | 44 O ₂ consumption | |
| | | 45 Blowing time | |

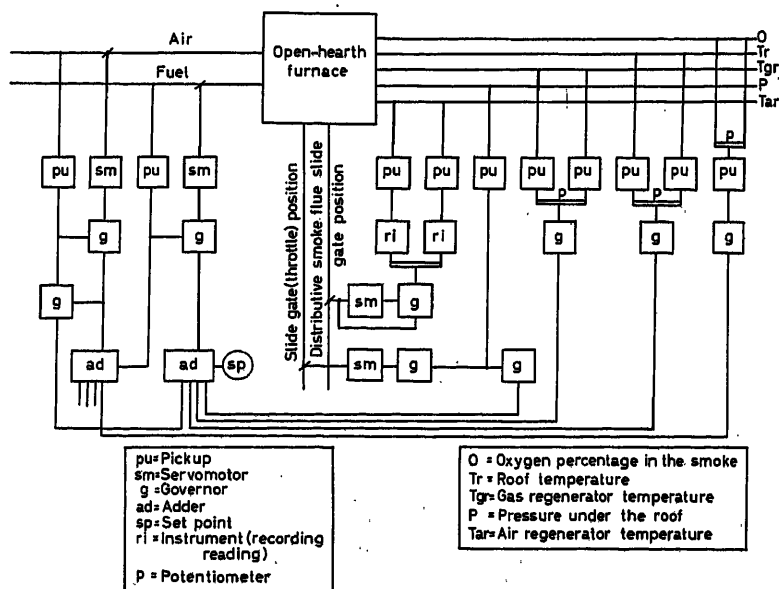


Figure 3. Open-hearth furnace

hearth furnaces in the domain of permissible conditions rises monotonically with an increase in the thermal load, the optimal mode is one in which the thermal load is always maintained at the maximum level compatible with the constraints peculiar to the given equipment. Such constraints for the thermal load of an open-hearth furnace are, for example, crown temperature, regenerator top temperature, pressure in the combustion space, etc.

In the layout shown, maximization of the thermal load within permissible limits is achieved by the fact that an increase in the load occurs only when this is permitted by all the constraining factors, and a reduction occurs when this is required by even one of the factors.

However, the control system described does not take sufficient account of the specific features of the technological process of each heat. In order to overcome this drawback, intensive research is being conducted into algorithmization of open-hearth furnace control and the use of computers for monitoring and control of thermal and technological modes.

The algorithms will be based on the relationships of the rate of burn-out of the carbon, the thermal assimilation of the pool and the coefficient of useful thermal utilization to the controlling parameters of the process. These relationships are realized in an analogue device now in use in the Soviet Union. A system of complex automatic control of the thermal mode, using the latest pneumatic equipment, is now in the test stage. This control scheme limits the thermal load in accordance with the temperature of the crown and the regenerators, the pressure in the combustion space in the furnace and the content of oxygen in the flue gases.

Another—still experimental—device, which is being introduced in the Soviet Union, will be used for producing a mathematical description of the process on the basis of: (a) automatic gas analysis for CO , CO_2 , O_2 and H_2 in the vertical channels, the space above the regenerator checkerwork and in the furnace flues; (b) measurement of the amount of flue gases with the aid of Venturi tubes installed in the flues; (c) the air preheat temperature, as measured by an ultrasonic pyrometer; (d) the temperature of the flue gases, measured by an optico-acoustic pyrometer, and also the weight of the slag, the temperature of the metal in the pool, and other measurements. A method has also been developed and checked in practice of monitoring the burn-out of carbon according to the oxygen balance of the furnace combustion space. The error in determination of the content of carbon in the pool does not exceed 0.3 per cent as a rule.

Great interest is being shown in problems of organizing running control of an open-hearth shop. For example, the layout envisages the collection and printing of information on the work of the furnaces for subsequent analysis, and also evaluation of the course of smelting in each furnace with display indication of deviations from the specified conditions.

Automatic flow control of open-hearth shop by regularization of production and handling operations is now being introduced in the Soviet Union. The automatic control system, with the aim of ensuring a smooth work flow of all sections of the shop forming part of the flow, carries out coordination of all the working schedules of the sections in such a way that both mechanism and materials advance at the proper time. This control is effected in accordance with the flows of materials. In addition to this, use is made of flow control for the sections of the shop (furnace span, charge area, teeming span, and also the stripper

section and the components preparation section). Here the operations of planning the preparation of the equipment in accordance with the schedule of heats are effected automatically: the issuing of instructions for the execution of production and handling operations, and also checking of the execution and true tempo of work of the sections¹⁸⁻²¹.

Electric Steel-making

At the present time many of the problems involved in mechanization of electric steel-making furnaces have been, and are being, solved successfully. This has created extensive opportunities for automatic control of the process of smelting in such furnaces. Great progress has been made in the study of electrical and physico-chemical processes, and this has provided a foundation for the solution of the control problem.

Adaptive mathematical analogues, designed to determine the coefficients and the differential equations characterizing the process of input of electrical energy into a furnace and for calculating the smelting process, have been developed in the Soviet Union. High-speed automatic power controllers have also been evolved. Several extremely sophisticated controllers have also been built in the U.S.A., West Germany and other countries.

Considerable progress in studying the thermal conditions of smelting and heat-exchange, and in the development of methods for measuring the fettling temperature, primarily in the Soviet Union and Great Britain, has led to the building of the first models of controllers of thermal conditions.

Researches have revealed the influence of arc currents and voltages upon the rate of heating of the metal and the fettling and upon the magnitude of the thermal efficiency factor. These relationships are of an extremal nature, and it may be expected that effective use will very soon be made of automatic optimizers in the arc control system.

There can be no doubt that the latest measurement methods and meters mentioned above, could also be used in electric steel-making, and that this would have a considerable effect. An example is the use of devices for measurement and automatic regulation of temperature. These control systems decrease by two to three times the temperature dispersion of the steel and considerably reduce the variation of its physico-chemical parameters²³⁻³⁰.

Continuous Teeming of Steel

Continuous teeming of steel is being used on an ever-increasing scale. The technological process of continuous teeming requires sophisticated monitoring and stabilization of many parameters.

The level of automation of these units for continuous teeming is roughly the same in all countries where such units exist. Soviet units will be considered.

The main elements of the control system are the controllers of the metal level in the intermediate ladle and the crystallizer.

The intermediate-ladle level controller consists of a tensometric weighing device with automatic compensation of the weight of the empty ladle, and a pneumatic controller which acts upon the stopper of the teeming ladle. The crystallizer metal level controller consists of a radioactive level-sensing element, a compensator to eliminate the influence of swinging of the crystallizer and a controller which acts on the intermediate-ladle

stopper drive. In addition to these two control systems, use is also made of control of the temperature of the fettling on the walls of the intermediate unit, the consumption of water on cooling, etc. The units are fitted with automatic outfits for autogenous cutting of strip into measured lengths.

Conclusion

In conclusion, I should like to underline some of the directions of control science, the use of which in ferrous metallurgy will have, in my opinion, a considerable effect. Systems-engineering, as the scientific basis of control of complex systems, makes it possible to optimize ferrous-metallurgy processes on branch and works scales, and also to formulate more clearly criteria and specifications for individual units and processes.

The use of operations-study methods will make it possible statistically to evaluate the effectiveness of control and to ensure the adoption of the most advantageous solutions in regard to the organization of production.

The physico-chemical processes which take place in the majority of ferrous-metallurgy plants are described, as a rule, by equations in partial derivatives.

The theory of optimal control of plants with distributed parameters is an apparatus which will make it possible to create systems of optimal control of such equipment as chamber and straight-through heating and thermal furnaces, blast and open-hearth furnaces, crystallizers, etc.

In such a brief communication it is not possible to deal in more detail with the most interesting problems which today demand the use of the latest achievements of the theory of means of control for their solution.

Neither is it possible to list all the problems which face us in this branch of industry. Furthermore, a short review cannot cover all the existing points of view on ways of further automating production, and of controlling this production.

However, I think that this communication can be concluded by stressing the enormous role of control science in the progress, not only of production automation, but also of production technology.

The time has already arrived, when automation of production control is one of the technical progress³²⁻³⁴.

References

- ¹ THRING, M. W. *The Science of Flames and Furnaces*. 1952. London; Chapman and Hall
- ² *Encyclopedia of Measurements Control and Automation*
- ³ *Encyclopedia of Production Automation and Industrial Electronics*
- ⁴ VEGMAN, E. R. *The Sintering Process*. 1963. Moscow; Metallurgizdat
- ⁵ SHALLOCK, E. W. *Blast Furnace*, No. 2 (1961) 145-147, 150
- ⁶ HAMILTON, D. E. and HONLTON, R. L. *Blast Furnace* (1960), 569-576
- ⁷ *International Seminar on Automatic Control in Iron and Steel Industry*. February 1962. Bruxelles
- ⁸ *First International Symposium on Agglomeration*. April 1961, Philadelphia, Pa., U.S.A.
- ⁹ LOSKUTOV, V. I. *Mathematical Control Machines*. 1962. Moscow; Mashgiz
- ¹⁰ BRAZHNIKOV, I. V. and BONDARENKO, V. I. *Automation of Blast-furnace Production*. 1962. Moscow; Metallurgizdat
- ¹¹ SLATOSKY, W. G. *J. Iron St. Inst.* 200, Pt. 1 (1962)
- ¹² SLATOSKY, W. G. *J. Metals*, N.Y. 12, No. 3 (1960)
- ¹³ VAN STEIN GALLENFELS, G. W. *J. Iron St. Inst.* (Feb. 1962), 132-135
- ¹⁴ Developments in the Iron and Steel Industry during 1961. *Iron Steel Engr* (Jan. 1962), 116-120
- ¹⁵ GALEY, J. et al. *Rev. Metall.*, VII, 56, No. 2 (1959), 69-78, 93
- ¹⁶ GORDON, M. M. *Automat. Telemekh.*, XXI, No. 6 (1960)
- ¹⁷ CHELYUSTKIN, A. B. *The Use of Computers for Control of Metallurgical Equipment*. 1960. Moscow; Metallurgizdat
- ¹⁸ STEELE, K. A. *Instrum. Pract.*, 14, No. 6 (1960), 647-652
- ¹⁹ LIESEGANG, W. Die Regelung von Siemens-Martin-Öfen. *Siemens-Z. Heft 10/11* (1957), 477-481
- ²⁰ TULUEVSKY, YU. N. et al. *Byull. TsNIChM*, No. 15 (1962)
- ²¹ ABROIMOV, E. V. et al. *Izv. VUZov, Chern. met.*, No. 11 (1962)
- ²² CHERNOGOLOV, A. I. *Izv. VUZov, Chern. met.*, No. 12 (1962)
- ²³ FRANCY, R. A. *J. Iron St. Inst.*, 9, No. 5 (1962), 32-34
- ²⁴ SHWABE, W. E. *Iron Steel Engr*. No. 6 (1957); Nos. 8, 12 (1958)
- ²⁵ BROSOVIC, J. A. *Iron Steel Engr*. No. 11 (1958); No. 6 (1960)
- ²⁶ GLAISHER, W. H., PRESTON, M. and RAVENSCROFT, J. *J. Iron St. Inst.* 183, No. 1 (1956)
- ²⁷ EFROIMOVICH, E. YU. *Elektrichestvo*, Nr. 3 (1954); No. 8 (1961)
- ²⁸ Complex Automation of the Process of Steel Smelting in Arc Furnaces, *Proc. 1st I.F.A.C. Conf.*, Moscow (1960)
- ²⁹ VOKAS, CH. *Iron St. Engr*. No. 2 (1955)
- ³⁰ RAVENSCROFT, J. *Iron Coal Tr. Rev.*, 180, No. 4 (1960), 789
- ³¹ RAVENSCROFT, J. *J. Iron St. Inst.*, 192, pt. (1959), 34
- ³² MORSE, PH. M. and KIMBALL, G. E. *Methods of Operations Research*. London; Chapman and Hall
- ³³ BUTKOVSKY, A. G. and LERNER, A. YU. *Automat. i telemekh.* No. 6 (1960) 682-691
- ³⁴ FINTSER, L. N. *Automat. i telemekh.*, XXII, No. 1, 7, 8 (1961); No. 2 (1962)

Control for the Sintering Mixture Preparation

G. DE GREGORIO, G. LITIGIO and G. SIRONI

Summary

The operations involved in the sintering process are performed on solid materials and described by mathematical equations.

The operations are in three separate cycles:

- (1) Sinter Mix: composition, transport, mixing and moistening, deposition of sinter mix on the machine.
- (2) Hearth Layer: separation of hearth layer by screening the sintered product, transport, hoisting, stocking in the hopper and deposition on the machine.
- (3) Return Fines: separation of return fines by screening the sintered product, transport, hoisting, stocking in the bin for the recycling (cycle 1).

The cycle of sinter mix preparation, in its component phases, raises the problem of some important controls. These controls cover the sinter chemical composition and technological properties and the fuel proportioning as a function of the mechanical properties of product and the output rate.

Control of sinter flow and composition has been examined in detail. The composition is continuously determined on the plant by an x-ray fluorescence analyser. This control has been studied in its various possibilities and is based on set base-indices as fuel-ore ratio, basicity ratio, slagging materials-iron ratio.

Consideration of such ratios, characterizing the sinter, refers to evaluation of sinter plant as an homogenizing filter of ferrous materials for the blast furnace charge. In this condition the above-mentioned ratios are fixed, or related to sinter with variable indices, and submitted directly to blast furnace requirements.

The study, which refers to the two most used indices, can be applied to other indices such as alumine index, and other particular ratios concerning sinter gangue, and to the control of limits set for such elements as Cu, P, As. Various applicable dispositions are described and their advantages and limits discussed. Compound systems structurally analogous to the control are considered more suitable to needs of the examined case. In certain typical diagrams, the equations, governing the static behaviour, are reported and discussed, assuming the use of zero error control systems.

The adhesion of the control loops gives the limits for the fields of permissible variations in the composition of additives, and conclusions suitable in most cases of application are also reported.

A dynamical analysis on a typical scheme has been performed after linearization of the system of equations representing the scheme.

The stability has been analysed by use of classic criteria (Routh-Hurwitz) and of a method introducing and analysing the fundamental ways for decomposition of the system under study. The last method can be used for the analysis of response. Absolute and relative errors are defined and the project relations are found, corresponding to a principle of equipartition of these errors on output (indices). It is shown that the introduction of these principles imposes the consideration of multiple interaction systems.

Sommaire

Les opérations effectuées sur les matières solides intervenant dans le processus d'agglomération sont décrites par des équations mathématiques se référant au temps.

Les opérations correspondent à trois cycles séparés:

- (1) Mélange à agglomérer: composition, transport, mélange et humidification, dépôt du mélange à agglomérer sur la machine.

- (2) Charge de foyer: Séparation de la charge de foyer par tamisage du produit aggloméré, transport, levage, stockage dans la trémie et dépôt sur la machine.

- (3) Fines de retour: séparation des fines de retour par tamisage du produit aggloméré, transport, levage, stockage dans la caisse pour le recyclage (cycle 1).

Le cycle de la préparation du mélange à agglomérer, dans ses phases composantes, soulève le problème de quelques réglages importants. Ces réglages concernent la composition chimique et les propriétés technologiques de l'aggloméré et le proportionnement de combustible en fonction des propriétés mécaniques du produit et de l'allure de production.

Le réglage du débit et de la composition de l'aggloméré a été examiné en détail. La composition est continuellement déterminée dans l'installation par un analyseur de fluorescence à rayons X. Ce réglage a été étudié dans ses diverses possibilités et se trouve basé sur des indices de base prédéterminés tels que le rapport combustible-minéral, le rapport de basicité, le rapport matières fluidisantes/fer.

La prise en considération de tels rapports caractérisant l'aggloméré se rapporte à l'évaluation de l'installation d'agglomération en tant que filtre d'homogénéisation de matières ferreuses pour la chargement du haut-fourneau. Dans ces conditions, ces rapports sont fixes ou, lorsqu'ils se rapportent à des agglomérés avec indices variables, sont directement soumis aux exigences du haut-fourneau.

L'étude, qui se rapporte aux deux indices les plus usuels, peut être appliquée à d'autres indices, tels l'index d'alumine, et à d'autres rapports particuliers intéressant la gangue d'aggloméré et au réglage des limites imposées à certains éléments, tels le cuivre, le phosphore, l'arsenic. Les diverses dispositions pouvant être appliquées sont décrites et leurs avantages et limites d'emploi sont discutés. Les systèmes mixtes, analogues par leur structure au réglage, sont considérés comme convenant davantage au cas examiné. Dans le cas de certains diagrammes typiques, les équations régissant le comportement statique sont exposées et discutées dans l'hypothèse d'emploi du système de réglage à annulation d'écart.

L'adhésion des boucles de commande donne les limites des champs de variation admissibles de la composition des matières d'addition. Les conclusions convenant à la plupart des cas d'applications sont également données.

Une analyse dynamique selon un schéma typique a été réalisée après linéarisation du système d'équations représentant le schéma.

La stabilité a été analysée par l'emploi de critères classiques (Routh-Hurwitz) et d'une méthode introduisant et analysant les manières fondamentales de décomposer le système étudié. Cette dernière méthode peut être employée pour l'analyse de la réponse. Les erreurs absolues et relatives sont définies et les relations de projet, correspondant à un principe d'équipartition de ces erreurs sur la production (indices), sont trouvées. Il est montré que l'introduction de ces principes impose la nécessité de considérer des systèmes à interactions multiples.

Zusammenfassung

Die bei Sinterprozessen ablaufenden Vorgänge werden durch mathematische Gleichungen im Zeitbereich beschrieben. Der Ablauf, geschieht in drei getrennten Arbeitsgängen:

- (1) Aufbereitung des Sinterproduktes: Zusammensetzung, Transport, Mischen und Anfeuchten, Einbringen der Mischung in die Maschine.
- (2) Sinterschicht: Trennung des Ofenbelages durch Sieben des gesinterten Produktes, Transport, Anheben, Speichern und Ablage auf der Maschine.
- (3) Rückstände: Trennung der Rückstände durch Absieben des Sinterproduktes, Transport und Speichern im Behälter zur Wiederholung des Arbeitszyklus.

Die Stufe zur Vorbereitung der Sintermischung führt in ihren Teilvorgängen auf einige wichtige Regelprobleme. Sie beziehen sich auf die chemische Zusammensetzung und die technologischen Eigenschaften der Ausgangsprodukte sowie auf die Zugabe von Brennstoff in Abhängigkeit von den mechanischen Eigenschaften und dem Durchsatz des Ausgangsproduktes.

Die Regelung des Mengenstromes und der Zusammensetzung der Sintermasse wurde eingehend untersucht. Die Zusammensetzung wird in der Anlage laufend durch ein Röntgenstrahl-Analysiergerät überwacht. Die verschiedenen Möglichkeiten der Regelung wurden untersucht; sie beruhen auf den vorgegebenen Kennwerten, wie dem Verhältnis Brennstoff: Erz, dem Basizitätsgrad und dem Verhältnis Schlacke: Eisen.

Bei Berücksichtigung solcher Verhältniszahlen, welche die Sintermasse kennzeichnen, faßt man die Sinteranlage als homogenisierendes Filter für eisenhaltige Stoffe zur Beschickung von Schachttöfen auf. Unter diesen Voraussetzungen sind die oben erwähnten Verhältniszahlen fest, in anderen Fällen werden sie — wenn sie sich auf eine Sintermasse mit wechselnden Eigenschaften beziehen — unmittelbar nach den Anforderungen des Schachtofens gewählt.

Die Untersuchung, welche sich auf die beiden gebräuchlichsten Eigenschaften stützt, kann auch auf andere, wie den Aluminiumgehalt und weitere spezielle Kennwerte, die sich auf den Gehalt des Sinters an Ganggestein beziehen, ausgedehnt werden, sowie auf die Grenzwertregelung für einige Elemente wie Cu, P, As. Verschiedene ausführbare Anordnungen werden beschrieben und hinsichtlich ihrer Vorteile und Grenzen betrachtet. Die Verbundsysteme, in ihrer Struktur dem Regelkreis analog, scheinen den Ansprüchen des untersuchten Problems besser zu entsprechen. Für einige typische Anordnungen werden die Gleichungen, die den Beharrungszustand bestimmen, angegeben und unter der Annahme diskutiert, daß Regler mit I-Verhalten Verwendung finden.

Die Auslegung der Regelkreise liefert die Grenzen der Bereiche, in denen die Zusammensetzung der Zuschläge variieren darf. Die für die Mehrzahl der Anwendungen gültigen Schlußfolgerungen werden angeführt.

Das dynamische Verhalten einer typischen Anlage wurde nach der Linearisierung der Systemgleichungen untersucht. Die Stabilitätsprüfung geschah mit Hilfe der klassischen Kriterien (Routh, Hurwitz) und mit Hilfe eines Verfahrens, das von der grundlegenden Möglichkeit der Zerlegung des betrachteten Systems ausgeht. Die letztere Methode ist auch zur Analyse der Übertragungseigenschaften brauchbar. Die absoluten und relativen Fehler werden definiert; daraus ergeben sich Beziehungen für die Planung, die einem Prinzip der gleichmäßigen Verteilung der Fehler auf die Ausgangsgrößen entsprechen. Es zeigt sich, daß die Einführung dieser Prinzipien auf die Behandlung von mehrfach gekoppelten Systemen führt.

Preliminary Considerations

The present paper is devoted to an analysis of the control of mix composition, flow rate and fuel proportioning in a modern sintering plant.

The chemical composition of the mix is a basic characteristic for achieving a satisfactory performance in the operation of a sintering plant. But the importance of a control on mix composition extends outside the sintering plant. Due to the trend in iron and steel works operation of using a high percentage of

self-fluxing sinter in the blast furnace charge, the possibility of controlling effectively the materials composition at the entry of the sintering plant allows the reduction of, or even the avoidance of, the blending practices in burdening the blast furnace.

This should give undoubted advantages; in fact the proportioning operation can be performed continuously if it is associated with a sintering plant, while when done at the blast furnace top it is affected by the discontinuous nature of the charging operation. As a consequence, complications are met with and a lower uniformity of results is obtained from the operation at the blast furnace. Also the layout of homogenizing yards can undergo substantial simplification.

The flow rate control is fundamental in order to assure the constancy of level and the uniformity of the sinter characteristics; for this purpose the flow rate control may be connected, for instance, to a measure of the burn-through point location¹.

It is not intended to deal in this paper with the interaction of the various sub-assemblies of a sintering plant and with the relationship between sintering plant and reduction furnaces or blast furnaces. The set points have been chosen from the many possible ones. A particular emphasis was put on flow rate (iron ores, charge materials or pig iron), fuel-ore ratio, basicity index, slagging materials/iron ratio, but the resulting considerations may immediately be applied to control of other less common reference parameters (alumina index or other ratios, affecting sinter gangue) or, alternatively, to the control of upper limits for such elements as Cu, P and As.

The considerations reported here allow a wide freedom about the particular structure of the control system inside the sintering plant or about the characteristics of the filtering action to be assigned to this sub-system in view of homogenizing the materials to be charged into the blast furnace. Also the diagrams considered have no limited significance for the particular case which is treated; they are chiefly used to describe the fundamental aspects of the problem. The terminology, used particularly for the dynamic analysis of the problem, refers to analogue solutions as far as the regulators are concerned, but from this point of view the results are still valid in the case of digital solutions.

To introduce and consider the fundamental aspects of the subject, reference is made to *Figure 1*, reproducing, with some minor change, a scheme already proposed in the past by Hamilton and Houlton¹. For the symbols one should refer to a list reported in the Appendix. This section deals only with a qualitative survey of the system; the quantitative analysis is considered in the following section.

For the sake of simplicity, the number of raw materials storage bins has been reduced to three—iron ore (acid gangue is supposed), an addition agent (therefore basic), and coal to bring the material to incipient melting.

Flow rate and chemical composition measurements are performed continuously at the exit of each bin. A continuous and reliable chemical composition determination, that is obviously essential for the automatic control of a proportioning system, represented for a long time an unsolved problem. Only in recent times have satisfactory results been obtained by x-ray fluorescence spectrometry. More detailed particulars on the subject may be found, for example, in a paper by Furbee².

Taking *Figure 1* again into consideration, the control on the ore bin feeder acts when the flow rate value of ore differs from reference value K_1 . The particular type of actuators for the feeder drive is not examined. A local control loop, having as a set point,

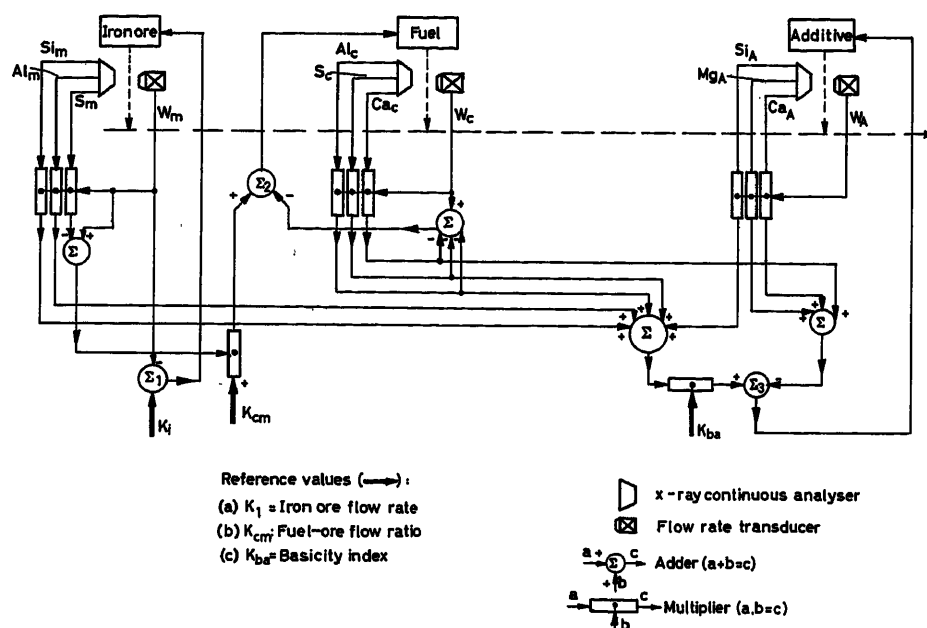


Figure 1. Cascade control

the flow rate, may be supposed in operation; afterwards it is seen that the presence of local loops on the actuators can be avoided. The control on the fuel bin feeder acts when the ratio between iron ore and carbon flow rate (with exclusion of sulphur if any) differs from reference value K_{cm} . The control on the additive bin feeder acts when the 'basicity index' differs from reference value K_{ba} .

The various schemes examined in this paper, a typical example of which is the above described Figure 1, have both the characteristics of feedback controls (therefore they present stability problems) and of forward (open loop) controls, chiefly from the point of view of their relations with the plant. They will be termed 'compound circuits' in this paper. Consideration of this concept affords an opportunity of mentioning other possible control classes besides the compound circuits; a fuller examination of the subject is therefore useful.

It must be stated that it is necessary, due to the nature of the values taken as reference, to use a computer of elementary type, calculating ratios of variables whether directly measured or given by a process simulator. The indices are indeed—as the efficiencies in power generation—values that are drawn for their nature from processing of variables directly measured.

In a closed loop system these variables must be measured, by definition, after the proportioning equipment. However, in the scheme of Figure 1, the output variable, i.e. the materials composition after the automatic proportioning equipment, is not directly measured. On the contrary, the materials composition and flow rate are determined at the bins outlet; in this way, the channels, through which all the disturbances are supposed to enter into the system, are directly monitored. It should be taken into account that from a general point of view other physical variables, for instance moisture variations, contribute to the determination of the process behaviour affecting the chemical and thermal balances; it will be assumed that moisture variations are slow if compared with the other noises affecting the process, and that it is possible to introduce them from outside as a com-

pensation in the continuous weighing systems, in order that the output from these systems may be considered as representative of dry mix weight.

With regard to the plant, all the regulators in the compound systems are in the condition of a forward control without any possibility of a direct comparison of set points with the output values. On the other hand, some of the set points are, for definition, indices, evaluated on output material, i.e. after mixing. Therefore it will be conceptually necessary to provide some plant simulation in order to give to the index computer the data to be processed. In the case of the proportioning systems, examined here, the problem is almost trivial because it is only necessary to calculate continuously weighted averages, where the weight is constituted by measured values of flow rates.

From the index computer output onwards, the signal processing is the same as in a closed system. The indices, and generally the controlled quantities, are compared with set points and the errors, usually through a multivariable controller, act on feeding actuators of the various bins.

Suppose that all the communication channels between external environment and the system, or at least those considered significant as far as results are concerned (in this case set points, flow rates and compositions), are measured and that process characteristics do not vary; the results will be satisfactory both in compound and closed loop systems. Actually, in the plants having such elementary characteristics as the proportioning systems, a lack of correspondence in the functional relationship between inlet and outlet variables would imply obviously abnormal operating conditions. For example, it should be assumed that a certain quantity of material fed at the entry would not be discharged at the exit (for instance, a secondary belt conveyor from additive storage bin to main belt conveyor not running or not able to discharge the feed material quantity) or that some material coming from the outlet does not correspond to the material delivered at the inlet (for instance the quantities due to air pollution that must be considered always negligible).

From a static point of view, it should be stated that for the plants under examination the results given by compound systems are comparable with those obtained by closed loop systems. On the other hand, from a dynamic point of view, the preference is given to compound systems. In fact in closed loop systems of this sort the problem of obtaining a steady and fast response regulation is a very difficult one, due to transport delays in the loop and the noise which is likely to be high enough due to the very nature of measured variables. The characteristics of noise are little known and are strongly dependent on the ore source; however, in any case, its presence limits the response band of the system and therefore increases the response time. Furthermore it should be added that, the system being non-linear, stability and quality of the response must be achieved by the designer over the whole operating range of the plant. The process, as seen later, can present different dynamical characteristics in the various working zones. It is very interesting to note that in compound systems the time constants of continuous analysers do not appear explicitly in stability discussions (while they affect the response quality); obviously it does not happen in this way in closed loop controls, and this introduces a source of further complication in the quantitative analysis of their dynamics.

After examination of the relationship between compound and closed loop systems, it is necessary to compare compound and open loop systems. For greater evidence, reference is made to Figure 2 where a comparison is made between these three limit cases considered here. For simplicity, the used representation method is the unipolar block diagram; in practice, many of the interconnections will be of a multipole type. In order to

maintain a useful connection with what is reported later, the authors have already used in this figure the set-point values of the simplified universal diagram reported in Figure 7; they have the same function of the reference values in Figure 1. This representation clarifies how the necessity of introducing measured flow rate values in indices computation leads to the build up of a set of closed loops in the regulation system itself (assume also that the feeders are included in it) and it raises stability problems. It may be possible to avoid these closed loops, if the actual flow rate values are not introduced into the calculation. As will be seen in more detail later on, it is always possible to write down the equations expressing mixing conditions in such a form as to obtain from calculation the flow rates, satisfying external reference values (indices, productivity, etc.), as functions of continuously measured compositions. These calculated flow rates are given as input values to the amplifiers of the actuators. Because the relationship between input to feeder mechanisms and output flow rate is not well known and varies with operating conditions, it is very likely that these amplifiers contain some negative feedback provisions through a flow rate measure. Therefore the control is of the cascade type.

With regard to the equipment, there is no difference from the compound type. In Figure 2(c) the controller has been simply decomposed into a computation section C2 (containing, for instance, the dynamic compensators to improve regulation quality) and an amplifying section A. In this way the W_{ic} (i.e. the calculated flow rates) are pointed out. For systems of few equations it is possible, even if it is not always easy, to write explicit expressions for flow rates. As soon as the number of equations increases, it is well known that digital techniques do not employ direct methods as subsequent elimination or matrix inversion and are using generally iterative methods on step by step approximation where flow rates of first approximation are again introduced into the algorithm in order to get a second approximation and so on. Therefore these methods also show the loop closure (this is the significance of dotted line in the scheme 2c) with consequent stability problems. The need appears explicitly, as is seen later, when analogue techniques would be used for the calculation.

It seems doubtless that the use of calculated flow rate values instead of measured data, gives a lower control quality. The possible stability problems that should raise for the presence of computational loop, are generally easy to solve because all the variables are at the disposal of the designer. On the contrary, in the case of compound systems the feeders, being elements from various points of view independent for the control designer, are included in the loop and therefore directly affect its stability.

However, the greater simplicity of investigation and the lower response time of open loop or compound systems is repaid with a greater number of detectors; on the contrary, the need of a process simulator is not of concern in the cases here examined, since it is reduced to quite elementary expressions.

Statics

Basic Diagrams and Relative Equations—Again examining the scheme of Figure 1, the equations representing the system equilibrium are three, in conformity with the related regulation subsets. The form of equations reported here, as with all those considered in the present work, is referred to as static zero error control systems.

$$W_m = K_1 \quad (1)$$

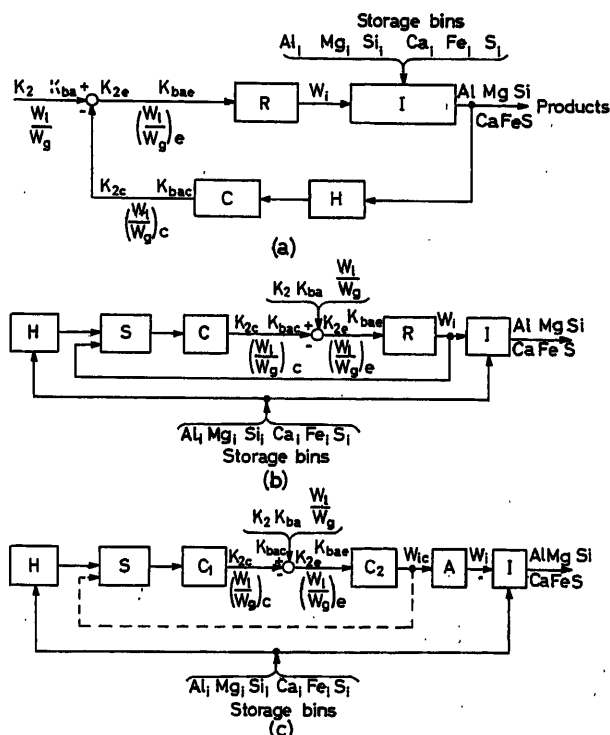


Figure 2. Comparison between possible control systems: (a) closed loop system; (b) compound system; (c) open loop system

R controller (multiple); A amplifier; I proportioning equipment; H transfer function of continuous analysers; S process simulator; C production indices computer; i: storage bin indices

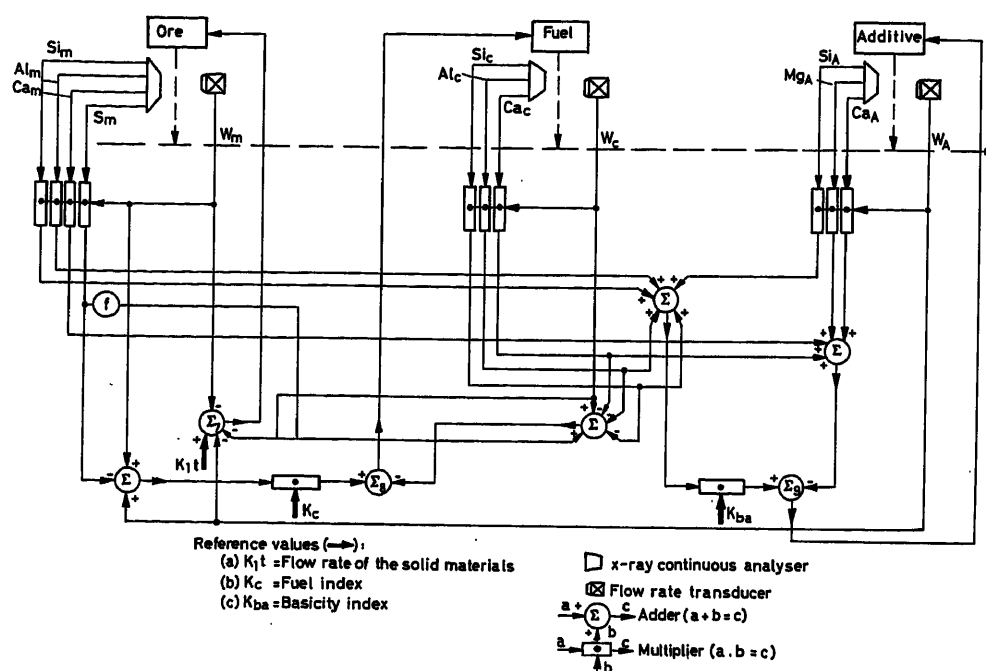


Figure 3. Interacting control.

$$K_{cm}W_m(1-S_m)=W_c(1-Al_c-Si_c-Ca_c) \quad (2)$$

$$K_{ba}(W_mSi_m+W_mAl_m+W_cAl_c+W_cSi_c+W_ASi_A) \\ =W_A(Mg_A+Ca_A)+W_cCa_c \quad (3)$$

In this scheme the use of ore with acid gangue is supposed. Successively, the addition of basic materials, that in some cases can be considerable, is taken into account. In eqn (2) it is assumed that all the sulphur takes part in the combustion. This is not exactly in accordance with practice. For a more detailed consideration of the subject, see Sironi⁶ and Giedroyc⁷.

To form the basicity index (B. A. ratio), magnesium oxide has simply been added to calcium oxide. A proportionality factor (56/40) will be adopted, when it should be preferable to assume molal units.

Since the above-mentioned equations are materialized with the establishment of reference nodes, equations and reference nodes of the system have been signed with the same numbers. The function of operators Σ and multipliers is to prepare the various component terms of the above-mentioned equations, i.e. the signals flowing together with the reference nodes.

For definition it follows that:

$$Si_m+Al_m+S_m+Fe_m=1 \quad (4)$$

$$Al_c+Si_c+Ca_c+C_c=1 \quad (5)$$

$$Si_A+Mg_A+Ca_A=1 \quad (6)$$

By this it is supposed that the elements are present in raw materials as oxides. If the case is different, left members will contain suitable coefficients that may be easily obtained by components stoichiometry. From the practical point of view of the applications it can be noted that x-ray emission analyser automatically performs an elementary analysis. Since the

equations are based on the existence, as reference values, of indices based by definition on oxides contents, it is supposed for these applications that the analyser output can be calibrated in oxide percentage. Therefore the above-mentioned stoichiometric coefficients may be included in instrument calibration.

The scheme of Figure 1 is suitable for operation with materials whose characteristics are assumed to vary in a rather narrow range. For example eqn (2) assures for the mixture an amount of heat sufficient to bring to incipient fusion the iron ore only. The system described in Figure 1 gives the remarkable advantage of avoiding any interaction among the sub-systems, since the three equations are in cascade. Therefore, if every one of the three control loops realizing the system is stable in itself, the whole control system will also be stable. It is obvious that transmission characteristic W_A/K_1 will be the product (loops in series) of the single characteristics. The designer is careful to avoid the superposition of the control subset resonances otherwise W_A final value will be reached only after an unacceptable hunting phenomenon. In other words, it is evident that it will be necessary to have the first loop faster than the second, and the second faster than the third.

A more general scheme is reported in Figure 3. It will be noted that:

(a) Basic components have been added to the ore.

(b) In defining the coal ratio all the materials to be treated (including the additive) are taken into account. For simplicity, the additive is just added to the ore; a further improvement would be the introduction of a multiplicative coefficient, weighing in a different way the two materials with regard to the thermic requirements of the sintering.

(c) The sulphur, removed from the ore, has been added to carbon by a fixed multiplicative constant. Assuming as complete the combustion of the sulphur, this constant corresponds to the

combustion heat ratio S/C. In practice it will be modified to take into account the experimental results considered by Sironi⁶ and Giedroyc⁷.

(d) The flow rate set point is referred to the whole quantity of sintered material instead of the ore only; since the additive and the coal rates are dependent on ore composition, the difference from the scheme of Figure 1 is substantial.

The equations are written as follows:

$$W_m + W_c + W_A = K_{1t} \quad (7)$$

$$K_c(W_m + W_A) = W_c(1 - Al_c - Si_c - Ca_c) + (f + K_c)W_m S_m \quad (8)$$

$$K_{ba}[W_m(Si_m + Al_m) + W_c(Al_c + Si_c) + W_A Si_A] = W_A(Mg_A + Ca_A) + W_m Ca_m + W_c Ca_c \quad (9)$$

The subset coupling of Figure 1 is reported schematically in Figure 4 (a). The coupling, corresponding to Figure 3, is reported

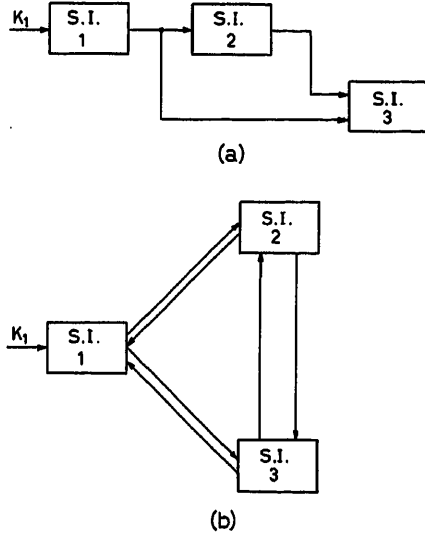


Figure 4. Schematic comparison of Figures 1 and 3 concerning subsystem interaction

in Figure 4 (b) and it is evident from it that new imposed conditions have caused the complete interaction of the subsets.

Figure 5 represents a more general regulation scheme.

The final value equations of the system are the following:

$$W_m(1 - Si_m - Al_m - Ca_m - S_m) = K_2 \frac{Fe_g}{p} \quad (10)$$

$$K_c(W_m + W_{A1} + W_{A2}) = W_c[1 - Al_c - Si_c - Ca_c + (f - 1)S_c] + (f + K_c)W_m S_m \quad (11)$$

$$K_{ba}[W_m(Si_m + Al_m) + W_c(Al_c + Si_c) + W_{A1}Si_{A1} + W_{A2}Si_{A2}] = W_{A1}(Mg_{A1} + Ca_{A1}) + W_{A2}(Mg_{A2} + Ca_{A2}) + W_m Ca_m + W_c Ca_c \quad (12)$$

$$W_m(Si_m + Al_m + Ca_m) + W_c(Si_c + Al_c + Ca_c) + W_{A1} + W_{A2} = W_i \quad (13)$$

with the further condition:

$$W_m + cW_c + A_1 W_{A1} + a_2 W_{A2} \leq K_{max} \quad (14)$$

K_2 represents the actual production level of steel plant; in case of an accident, it may be controlled by the plant emergency system. The iron content in pig iron has been assumed as a value to be introduced from outside. p is a stoichiometric coefficient, which is equal to 112/160 in the case of ores constituted by Fe_2O_3 .

Equation (14) introduces explicitly in the control equations the sinter plant productivity and assures that production K_2 is never higher than the limit imposed by the mentioned productivity. It was therefore necessary to introduce the reference K_2 through a device limiting this command when $\phi(W_m, W_c, W_{A1}, W_{A2})$ exceeds a given value. The ϕ depends upon the physical properties of the feed materials, chiefly on grain size; eqn (14) expresses a suitable linearization of this constraint. It is assumed, on the contrary, that this constraint does not depend upon chemical composition of materials, though this seems only justified within certain limits. It would be possible to assume the value of ϕ as reference for flow rate control in eqn (10); in this case the corresponding hourly pig iron rate is obviously not constant.

Equation (11) has the same significance as (8). The difference lies in the improved balance of fuel charged in sinter plant on the basis of sulphur analysis in the coke. Equation (13) introduces a further constraint on flow rate of slag components. The small silicon amount retained in pig iron is not taken into account; i.e. it is assumed that all the silicon present in the charge combines in the slag. This condition, together with eqn (10), assures a constant iron content in sinter mix.

For the introduction of the further constraint represented by eqn (13) it is necessary to have at disposal another variable to be adjusted. To reduce the treatment to essential elements, this variable has been schematized as a second source of additive material, of a type complementary to the additive contained in the bin 1 (therefore acid additive). In practice it will correspond more properly to lean ore, whose flow rate will be proportioned in relation to the composition of the other ferrous ore. This statement of the problem should slightly complicate its formal solution because in this case a connection between eqn (10) and the remaining part of the system is introduced.

The systems (10)–(13) show that the control of ore feeder must be considered as an independent subset, provided that limiting conditions, expressed in eqn (14), are not active. On the contrary, the controls of the three other feeders have all mutual possible interaction constraints. Thus it may be concluded that the system under examination is not more complicated than the system of Figure 3. The limiter during the time interval it is operative, changes the three loop system into a four fully linked system. In fact, in this case, eqn (10) is replaced by eqn (14) and thus the system of Figure 5 shows, from this point of view, some aspects similar to the system of Figure 3.

Further Solutions and Relative Limits—As mentioned above, a more constant quality of the product may be obtained, imposing a greater number of 'quality indices'. For example, the slag composition, here controlled in a limited way through K_{ba} regulation, can be characterized more completely by other parameters such as magnesia index, alumina index, etc. Increasing the number of controlled 'indices', new cost elements must be unavoidably added to the product for the following reasons:

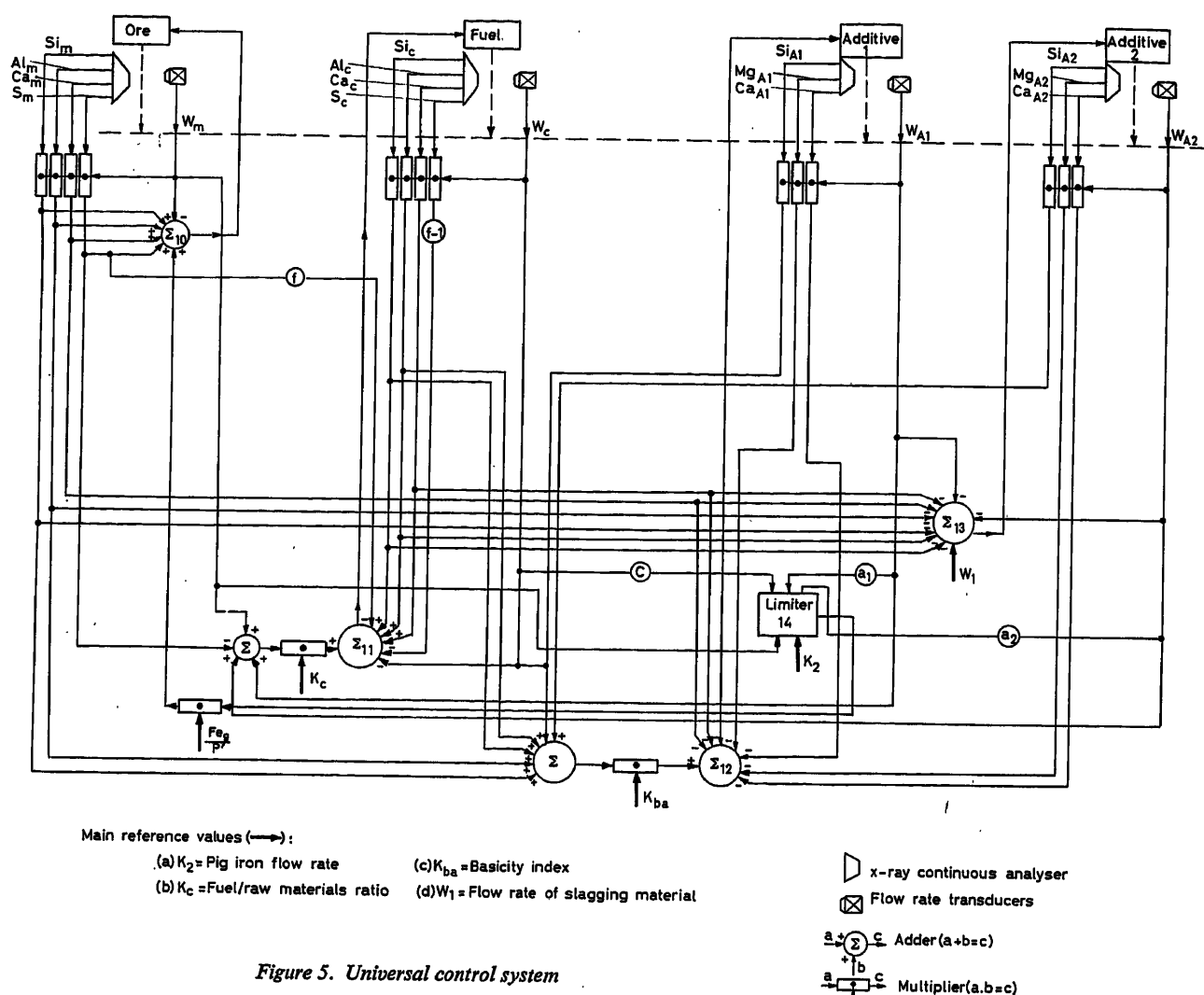


Figure 5. Universal control system

(a) It is necessary to introduce a greater number of materials and relative storage facilities in order to have at disposal a sufficient number of manipulated variables.

(b) All the storage bins in greater number for the reason mentioned under (a), must be equipped with instrumentation and control devices.

(c) The addition of a greater number of control loops complicates the dynamic study of the system, introducing difficulties in the design of the corrective networks and a higher rating of the actuators, assuming the same response time.

(d) To previous elements, affecting essentially the capital cost, must be added higher operation costs, due to the fact that the inlet materials will be subjected to more severe specifications. This last consideration is not surprising, if one remembers that, when an output variable of a plant in steady condition is forced to be equal to a set value, relations are imposed among the system variables which take away from the system a corresponding number of degrees of freedom. It is interesting to emphasize that from these obvious considerations is derived the existence of constraints on the composition of the materials contained in the storage bins. It is not essential to examine this problem

quantitatively in this paper. A more detailed study of it has already been published elsewhere⁸.

Figure 6 has been drawn from this study, referring to the control scheme of Figure 5. By definition

$$Q = \frac{W_i}{W_g} \left(\frac{1}{Si_m} - 1 \right) \frac{1}{Fe_g} - 1$$

The zones of permissible actual operation for a regulated mix system have been signed by (1) and (2), complementary in the sense that the two storage bins exchange their functions passing from one zone to another. To determine in every case the limits of possible operation zones it is sufficient to impose the conditions:

$$W_i \geq 0 \quad 0 \leq X_i \leq 1$$

where X_i is a generic element in the mixture (in per unit).

It should be noted that values reported in Figure 6 are intended to be nominal values. They must be further reduced in order to take into account the fluctuations in chemical composition of charged material, to be valued case by case.

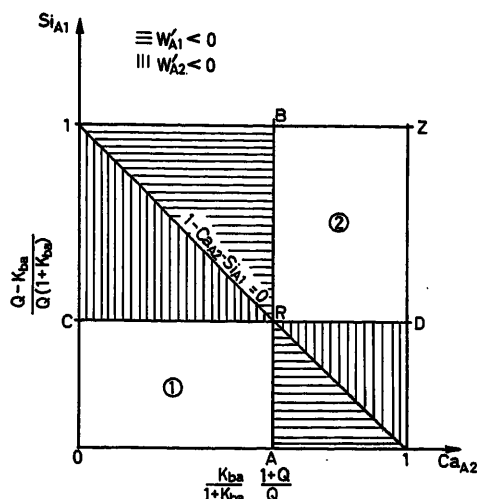


Figure 6. Zones of actual operation of controlled plant

Dynamics

Introduction—The investigation is performed on a system analogous to the system of Figure 5.

To simplify the matter, without prejudice for the generality of the conclusions, the authors have assumed:

- (a) Iron ore contains only a siliceous gangue.
- (b) The system is in such operating conditions that the limiter does not come into operation; in these conditions the regulation loop for ore feeding may be considered independent from the rest of regulation.
- (c) Additives contain only Ca and Si.

To simplify notations, the fuel control loop will not be taken into consideration.

The characteristic elements of controlled plant dynamics are added, omitting for the moment the corrective networks, which will be suggested by the results of the dynamical analysis of the uncompensated system.

On the basis of preliminary considerations, the mix process dynamics is not involved in the equations to be developed, assuming of course that feeders are not part of the process but are included in the control equipment.

A time constant T , equal for all the bins, has been considered in order to take into account the inertia of the feeding systems and relative actuators. The response of the x-ray analyser has been represented by a time constant τ . Also transport terms, created by the way the materials to be analysed are introduced in the x-ray spectrometer, are included for simplicity in this time constant. It is assumed that the computer has negligible time constants compared with those involved in controlled system.

Since only systems with zero position error have been considered in this paper, it will be necessary to choose type 1 controllers. These considerations may be examined from a more general point of view that will be very useful for the further development of the discussion. It is possible to think that control equipment tries to solve in an analogue way (see for example Jackson³) the group of equations forming the system model. These equations are left in implicit form and the solutions are forced through integrating elements.

The following system is set up:

$$b_j - \sum_i a_{ij} W_i = \dot{W}_j$$

Under steady-state conditions, the solutions of the above system will be identical to the solutions of the unknown system of equations to be solved:

$$b_j - \sum_i a_{ij} W_i = 0$$

provided that the system operation is stable; it is known, in fact, that the asymptotic theorem of operational calculus is valid, if the stability is assured in another way (see for example Truxal⁴). In other words, if it is assured that the homogeneous solution of the system approaches asymptotically the zero, then the particular solution of the system, i.e. the solution of the algebraic equations system, will be the solution in steady conditions of the differential system.

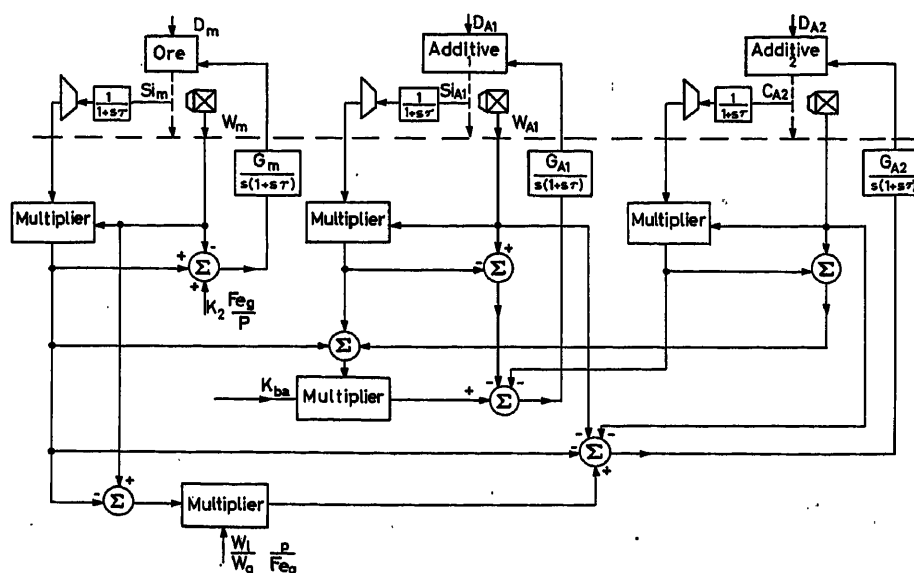


Figure 7. Simplified control of universal type (the dynamic elements are pointed out)

It should be noted that in this case, the condition is accomplished through the combination of analogue computer components with the physical components (feeders) which, due to their complexity, are best introduced as such in the computer. Apart from the fact that in this way the behaviour of the model is more like that of the real plant, there is also the advantage of eliminating the local integrator in the actuators. The integrator has to be used, as previously explained, where the actuators are kept out of the solution of the system equations.

The diagram of Figure 7 represents the system under study; the corresponding equations are the following:

$$\frac{K_2 \text{Fe}_g}{p} - W_m \left(\frac{1 - \text{Si}_m}{1 + s\tau} \right) = W_m \frac{s(1 + sT)}{G_m} \quad (15a)$$

$$K_{ba} \left[W_m \frac{\text{Si}_m}{1 + s\tau} + W_{A1} \frac{\text{Si}_{A1}}{1 + s\tau} + W_{A2} \frac{1 - \text{Ca}_{A2}}{1 + s\tau} \right] - W_{A1} \left(1 - \frac{\text{Si}_{A1}}{1 + s\tau} \right) - W_{A2} \frac{\text{Ca}_{A2}}{1 + s\tau} = W_{A1} \frac{s(1 + sT)}{G_{A1}} \quad (15b)$$

$$\frac{W_l}{W_g} \frac{p}{\text{Fe}_g} W_m \left(1 - \frac{\text{Si}_m}{1 + s\tau} \right) - W_m \frac{\text{Si}_m}{1 + s\tau} - W_{A1} - W_{A2} = W_{A2} \frac{s(1 + sT)}{G_{A2}} \quad (15c)$$

In these equations that are still in non-linear form, 's' replaces the operator d/dt. The following obvious identity is applied:

$$\frac{1 - \text{Si}_m}{1 + s\tau} = 1 - \frac{\text{Si}_m}{1 + s\tau}$$

Attention must be paid to the fact that this differential operator is applied in the products only to chemical compositions. As to variables, only the independent ones have been introduced in explicit form; thus the system already contains the conditions equivalent to (4), (5) and (6).

On the basis of the above equations, the system is asymmetric, from a dynamic point of view, with respect to the bins 1 and 2, in contrast to the considerations reported in the section regarding the statics. In fact, in this system, the chemical balance controls the flow rate of bin 1, while the physical balance controls the flow rate of bin 2. An exchange between them leads obviously to a different dynamic behaviour.

Linearization—The system under examination is typically non-linear; like most systems in industrial plants, this non-linearity depends on the fact that controlled quantities (production indices) are a bilinear combination of chemical compositions (intensive variables) and flow rates (extensive variables). Now, while disturbance may enter through composition variations, the manipulated variables are indeed the flow rates, i.e. the other quantities entering in products forming the various terms of bilinear combination.

To begin an analytical study of the process it seems suitable to linearize the system, considering small oscillations around an equilibrium point (perturbative method).

With the substitutions:

$$X = X_0 + x$$

assuming x as infinitesimal and limiting the approximation to the first order, the following linear system, corresponding to (15), is obtained. In this system the output variables, or rather their L -transformed, are given in function of input variables (considered also as L -transformed).

$$\begin{aligned} A_{11} w_m &= B_{11} \text{si}_m + B_{14} k_2 \\ A_{21} w_m + A_{22} w_{A1} + A_{23} w_{A2} &= B_{21} \text{si}_m + B_{22} \text{si}_{A1} + B_{23} \text{ca}_{A2} + B_{24} k_{ba} \end{aligned} \quad (16)$$

$$A_{31} w_m + A_{32} w_{A1} + A_{33} w_{A2} = B_{31} \text{si}_m + B_{34} \frac{w_l}{w_g}$$

with the following coefficient values

$$A_{11} = 1 - \text{Si}_{m0} + \frac{s(1 + sT)}{G_m} = A_{110} + \frac{s(1 + sT)}{G_m}$$

$$A_{21} = -K_{ba0} \text{Si}_{m0}$$

$$B_{21} = \frac{K_{ba0} W_{m0}}{1 + s\tau}$$

$$A_{22} = 1 - (K_{ba0} + 1) \text{Si}_{A10} + \frac{s(1 + sT)}{G_{A1}} = A_{220} + \frac{s(1 + sT)}{G_{A1}}$$

$$A_{23} = \text{Ca}_{A20} - K_{ba0} (1 - \text{Ca}_{A20})$$

$$B_{22} = \frac{W_{A10} (K_{ba0} + 1)}{1 + s\tau} = \frac{B_{220}}{1 + s\tau}$$

$$A_{31} = \text{Si}_{m0} - \frac{W_{l0}}{W_{g0}} \frac{p}{\text{Fe}_g} (1 - \text{Si}_{m0})$$

$$B_{23} = \frac{W_{A20} (1 + K_{ba0})}{1 + s\tau} = \frac{B_{230}}{1 + s\tau}$$

$$A_{32} = 1 \quad B_{24} = W_{m0} \text{Si}_{m0} + W_{A10} \text{Si}_{A10} + W_{A20} (1 - \text{Ca}_{A20})$$

$$A_{33} = 1 + \frac{s(1 + sT)}{G_{A2}} \quad B_{31} = -\frac{W_{m0}}{1 + s\tau} \left[1 + \frac{W_{l0}}{W_{g0}} \frac{p}{\text{Fe}_g} \right] = \frac{B_{310}}{1 + s\tau}$$

$$B_{11} = \frac{W_{m0}}{1 + s\tau} \quad B_{34} = \frac{p}{\text{Fe}_g} W_{m0} (1 - \text{Si}_{m0}) = K_{20} \quad B_{14} = \frac{\text{Fe}_g}{p}$$

In a more compact form one may write:

$$\begin{aligned} & \begin{bmatrix} A_{11} & 0 & 0 \\ A_{21} & A_{22} & A_{23} \\ A_{31} & A_{32} & A_{33} \end{bmatrix} \begin{bmatrix} w_m \\ w_{A1} \\ w_{A2} \end{bmatrix} \\ &= \begin{bmatrix} B_{11} & 0 & 0 \\ B_{21} & B_{22} & B_{23} \\ B_{31} & 0 & 0 \end{bmatrix} \begin{bmatrix} \text{si}_m \\ \text{si}_{A1} \\ \text{ca}_{A2} \end{bmatrix} + \begin{bmatrix} B_{14} & 0 & 0 \\ 0 & B_{24} & 0 \\ 0 & 0 & B_{34} \end{bmatrix} \begin{bmatrix} k_2 \\ k_{ba} \\ \frac{w_l}{w_g} \end{bmatrix} \end{aligned} \quad (17)$$

where in the second member the disturbances are separated from reference values.

As mentioned in the introduction, in practice, using in the calculation the measured (not calculated) values of W_j , the time constant of feeding equipments is inserted in series with integration required to reduce to zero the error of the analogue calculus. This consideration introduces under explicit form the gain value

in the stability conditions. In the section regarding stability, where the necessary and sufficient conditions are studied, it is seen that there is a wide range of G values for which the system operates satisfactorily.

The same solutions are valid in the case of the multipole controller i.e. with contemporary regulation of W_{A1} and W_{A2} . In this case the following equations are obtained:

$$\begin{aligned} A'_{23} &= Ca_{A20} - K_{ba0}(1 - Ca_{A20}) + \frac{s(1+sT)}{G'_{A2}} = A_{230} + \frac{s(1+sT)}{G'_{A2}} \\ A'_{22} &= A_{220} + \frac{s(1+sT)}{G'_{A1}} \\ A'_{32} &= 1 + \frac{s(1+sT)}{G''_{A1}} \quad A'_{33} = 1 + \frac{s(1+sT)}{G''_{A2}} \end{aligned}$$

Truly multipole controllers are more complicated as far as construction and calibration are concerned, but on the other hand the introduction of more design parameters permits higher versatility, i.e. the possibility of introducing further conditions and thus improving the operation (see the section on errors).

The previously written control equations are based on Figure 2 (b), after some simplification. In its most general form, always maintaining the first equation independent of the other ones, this scheme corresponds to the following system:

$$\begin{aligned} K_2 - \frac{W_m p}{Fe_g} \left(1 - \frac{Si_m}{1+s\tau} \right) &= W_m \frac{s(1+sT)}{G_m^*} \\ K_{ba} - \frac{W_{A1} \left(1 - \frac{Si_{A1}}{1+s\tau} \right) + W_{A2} \frac{Ca_{A2}}{1+s\tau}}{W_m \frac{Si_m}{1+s\tau} + W_{A1} \frac{Si_{A1}}{1+s\tau} + W_{A2} \left(1 - \frac{Ca_{A2}}{1+s\tau} \right)} &= s(1+sT) \left(\frac{W_{A1}}{G_{A1}^*} + \frac{W_{A2}}{G_{A2}^*} \right) \\ \frac{W_i}{W_g} - \frac{W_m \frac{Si_m}{1+s\tau} + W_{A1} + W_{A2}}{\frac{p}{Fe_g} W_m \left(1 - \frac{Si_m}{1+s\tau} \right)} &= s(1+sT) \left(\frac{W_{A1}}{G_{A1}^*} + \frac{W_{A2}}{G_{A2}^*} \right) \end{aligned} \quad (18)$$

In these equations the subdivision of the system, introduced in Figure 2, is clearly evident as process simulator, quality index computer and multipole controller. For example, in the second equation, the calculus of the two terms of ratio (numerator and denominator) belongs to the process simulation, the calculus of this ratio to the indices calculation and, finally, the solution of the equation to the multiple control phase.

The realization of this system, also in the particular case $G'_{A2} = G''_{A1} = 0$, is more complex than the system corresponding to Figure 7, because, besides addition and multiplication operations, one needs to calculate ratios of variable terms.

The coefficients of the linearized system are almost identical with those already calculated for system (16). The only variations are:

$$\begin{aligned} A_{11}^* &= A_{110} + \frac{s(1+sT)}{G_m^*} \frac{Fe_g}{p} \\ A_{22}^* &= A_{220} + \frac{s(1+sT)}{G_{A1}^*} [W_{m0} Si_{m0} + W_{A10} Si_{A10} \\ &\quad + W_{A20} (1 - Ca_{A20})] \\ A_{33}^* &= 1 + \frac{s(1+sT)}{G_{A2}^*} \frac{p}{Fe_g} W_{m0} (1 - Si_{m0}) \end{aligned}$$

All that consists in a different definition of gains; on its practical consequence, reference is made to discussion in the stability section.

Stability—In this section only the system of the type reported in Figure 7 will be considered, since these systems are particularly suited to a generalized treatment of stability and design of compensation networks.

1. At first an analysis of absolute stability of system under examination (16) is performed, using the Routh criterion. From this study elements of judgement can be drawn for the following considerations on relative stability.

The characteristic equation of the system is:

$$\Delta(s) = \begin{vmatrix} A_{11} & 0 & 0 \\ A_{21} & A_{22} & A_{23} \\ A_{31} & A_{32} & A_{33} \end{vmatrix} = A_{11}(A_{22}A_{33} - A_{32}A_{23}) = 0 \quad (19)$$

The stability is assured if the equation roots have negative real part. It will be noted that eqn (19) splits into:

$$A_{11} = 0 \text{ and } A_{22}A_{33} - A_{32}A_{23} = 0$$

that confirms the substantial independence of the pig iron production control loop from the two other loops.

The first equation is expressed as:

$$s^2 T + s + G_m A_{110} = 0 \quad (20)$$

Since these are considerations related to absolute stability, no constraint derives from eqn (20) to G_m which will be limited, on the contrary, by considerations on relative stability. The second condition is equivalent to the following:

$$\left(A_{220} + \frac{s(1+sT)}{G_{A1}^*} \right) \left(1 + \frac{s(1+sT)}{G_{A2}^*} \right) = A_{23}$$

that is:

$$\begin{aligned} T^2 s^4 + 2Ts^3 + [T(G_{A2} + G_{A1}A_{220}) + 1]s^2 \\ + (G_{A2} + G_{A1}A_{220})s + G_{A1}G_{A2}(A_{220} - A_{23}) = 0 \end{aligned}$$

As confirmation of what is noted earlier in this paper, the conditions derived from the characteristic equation are changed if index 1 is exchanged with index 2, i.e. the two systems are inverted.

One here has confirmation of what is mentioned in the introduction, i.e. that the system stability is not dependent on the time constant of the measuring devices. This is very important because this time constant—besides being that prevailing in the system—is compensated with difficulty, due to the nature of the signal given by the instrumentation. This fact is bound to the observation shown by Figure 2, that feedback in compound

systems is performed only through W_i and, therefore, only T affects the stability considerations.

Having fixed T and assumed, for instance, $G_{A1} = G_{A2} = G$, the application of the Routh or Hurwitz criterion will give a certain inequality set that will define the variation range of G within which the system is absolutely stable. In the assumption $T = 1$ sec, the G variation range results for pure additives $0 \leq G \leq 0.67$; for a maximum content of impurities in bin 1, it results $0 \leq G \leq 0.4$.

Therefore it appears that a decreasing purity in siliceous additive causes a worsening of system stability conditions. This fact does not matter, at least for impurity contents found in practice. Thus, in the following, attention will be drawn to the operating conditions with pure components. Having G dimensions equal to sec^{-1} , it is obvious that a reduction in system time constant causes an increase of maximum allowable gain in the same ratio. For instance, with $T = 0.2$ sec, $G = 3.25$ in the case of pure additives.

Considering the equivalents of eqn (18), after linearization, they are identical to eqn (16), if the following substitutions are made:

$$G_{A1} = \frac{G_{A1}^*}{W_{m0}Si_{m0} + W_{A10}Si_{A10} + W_{A20}(1 - Ca_{A20})} [\text{sec}^{-1}]$$

$$G_{A2} = \frac{G_{A2}^*}{\frac{p}{Fe_g} W_{m0}(1 - Si_{m0})} [\text{sec}^{-1}] \quad (21)$$

The control quality being constant, G_{A1} and G_{A2} depend, as seen above, on chemical compositions and not on flow rates of materials. Therefore, adopting the control scheme as in eqn (18), it is necessary that the gains follow up the quantities which are in the denominator of eqn (21). Supposing a constant chemical composition of materials, a variation of production level must be compensated by a corresponding variation of G_{A1}^* and G_{A2}^* , in order to maintain the constancy of G_{A1} and G_{A2} . The dimensions of G , that are different from those of G^* , are an indication of this circumstance. It must be noted, however, that the denominators of (21) are as quantity ready as output of C section (the index computer) of the control system. It can be concluded that, from the point of view of the simplicity in the calculation as well as linearization, the most convenient system is the system (15), i.e. the scheme of Figure 7 is preferable.

2. To investigate the relative stability and to approach the questions related to the compensations, the problem will be split into the analysis of n simple feedback systems, where n is the order of system (3 in this case). It is obvious that all the considerations valid for single loop systems can be applied to these systems. Yet this technique is limited to the case of controls that are not of multipole type.

As mentioned above, this system may be written as follows:

$$\left(\frac{1}{G(s)} I + A \right) W = \sum B$$

where $1(s)$ is the transfer function of controllers + actuators which equals $G/s(1 + sT)$; W is the vector corresponding to manipulated variables; B is the vector set corresponding to external changes (variation of reference levels) and chemical composition disturbances; I is the unitary matrix of n order

$$A = \begin{bmatrix} A_{110} & 0 & 0 \\ A_{21} & A_{220} & A_{23} \\ A_{31} & A_{32} & A_{330} \end{bmatrix}$$

The stability depends on the position of the roots for the characteristic equation of the system:

$$|I/G(s) + A| = 0$$

The research of eigenvalues of linear transformation defined by the matrix A , depends on solutions of the following equation:

$$|A - \lambda I| = 0 \quad (22)$$

Therefore eigenvalues of the matrix A and roots of the characteristic equation of controlled system are related by the simple equation:

$$G(s) \lambda_i = -1 \quad (23)$$

where λ_i are n in number, and in some case not distinct; in the case where the matrix A is asymmetric (as in this instance), i.e. not hermitian, they are generally complex. Of course, being real, the coefficients of the equations appear as conjugate complex pairs. The form (23) corresponds to a single loop feedback system, and it is therefore possible to apply to it the technique of the Nyquist diagram or root locus, with the precaution due to the fact that λ_i may be complex. This is equivalent to introducing into the Nyquist diagram an affined rotation. In the application of root locus, it will be sufficient to take into account the tricks used to trace constant phase angle loci (see Chu⁶).

Equation (22) provides the following equations for the determination of λ

$$A_{110} = \lambda_1$$

$$\lambda^2 - \lambda(A_{330} + A_{220}) + A_{220}A_{330} - A_{320}A_{230} = 0 \quad (24)$$

These results will be applied to the verification of absolute stability, already determined above by the application of the Routh-Hurwitz criteria.

The first equation of (24) gives again eqn (20). The second equation of (24) has been solved both for pure components [case (C)] and mixed components [case (A)]; the values have been reported in Figure 8(a). On this figure is reported the inverse of the $G(s)$ Nyquist diagram, i.e. $s(1 + sT)$ in the non-compensated case ($T = 1$ sec). The stability comparison is made on the basis of (23) that, in the case of Figure 8, $-\lambda_i = 1/G(s)$ may be written. The system is stable when the eigenvalues λ_i are enclosed by the $G^{-1}(s)$ curve.

The limit values of G found above are very well confirmed. In particular it can immediately be seen that case (C) shows a higher stability than case (A).

The asymmetry of matrix A , and therefore the presence of complex eigenvalues, leads to the consequence that second-order systems also show a well-defined stability range, even if absolute stability is considered. In fact, the connection of the controller with multiloop feedback system adds to the inherent lags of controller and actuator, a fixed phase lag; this fact is not surprising, since this lag does not depend (in explicit form) on inertia of other controllers and actuators. From the physical point of view, it is clear that these phenomena arise from the fact that more than one controller and actuator is applied to the same system to be regulated.

Figure 8(b) represents the inverse Nyquist diagram for the function $\lambda G(s)$, only for case A. This diagram must be inter-

preted with some care. Having the tangent at the origin an inclination angle of 24 degrees to the negative semi-axis, it may be deduced, on the basis of what is known about single-loop systems, that for very low gains also there is a resonance in the attenuation-frequency characteristic; in the specific case, $M_p = 2.5$. As a matter of fact a verification made on the common denominator of all the transfer functions leads easily to the

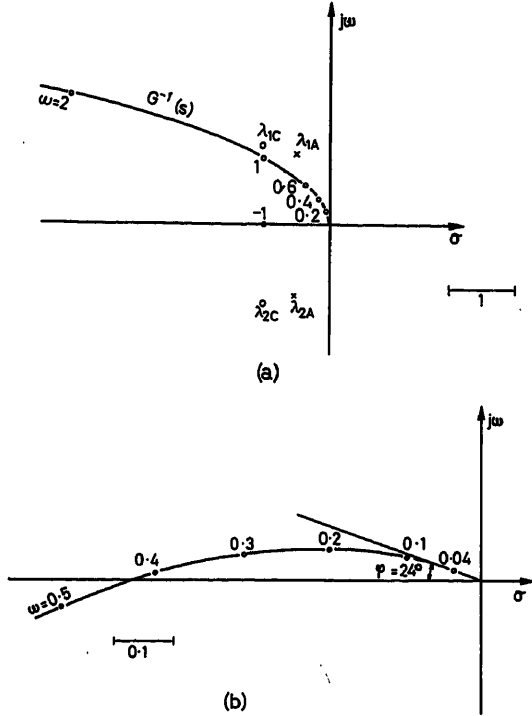


Figure 8. Stability analysis of inverse Nyquist diagram

conclusion that for $G = w \rightarrow 0$ there is a limit value of resonance lower than the above mentioned, i.e. $M_p = 1.35$. From the physical point of view, this must be interpreted in the sense that both the eigenvalues of the system contribute to the determination of transfer function. One of them [the one considered in Figure 9(b)] provides a phase lag of 66 degrees; the other one (complex conjugate) introduces a phase lead of 66 degrees and therefore has a stabilizing effect.

A confirmation of the oscillatory tendency of the second-order system, even for very low values of G , is provided by the examination of constant phase-loci reported in Figure 9, delimited to the phase lag mode. The tangent not horizontal to origin determines the maximum damping in the system.

The considerations reported above show that the correlations between rise time, bandwidth, oscillation frequency, settling time, etc., must be applied to eqn (23) with great caution, even in the case when the regulators are simple type 1 systems with one time constant alone.

Absolute and Relative Errors

The following quantities are defined as errors (for the sign of these errors the conventions, usually used in control theory, are applied):

$$\varepsilon_1 = K_2 - \frac{pW_m}{Fe_g}(1 - Si_m)$$

$$\varepsilon_2 = K_{ba} - \frac{W_{A1}(1 - Si_{A1}) + W_{A2}Ca_{A2}}{W_m Si_m + W_{A1}Si_{A1} + W_{A2}(1 - Ca_{A2})} \quad (25)$$

$$\varepsilon_3 = \frac{W_l}{W_g} - \frac{W_m Si_m + W_{A1} + W_{A2}}{\frac{p}{Fe_g} W_m (1 - Si_m)}$$

It is found better to define the ε_i in a different manner from the K_e of Figure 2, as is necessary in all cases where feedback is not unitary. Since it is interesting to consider the operation of the system as regulator, it is assumed:

$$k_2 = k_{ba} = \frac{W_l}{W_g} = 0$$

By linearization of (25) and the substitution of manipulated variables w_i by input variable (disturbances), one obtains:

$$\varepsilon_1 = \varepsilon_1(s_i_m) \cdot si_m$$

$$\varepsilon_2 = \varepsilon_2(s_i_m) \cdot si_m + \varepsilon_2(s_{i_{A1}}) \cdot si_{A1} + \varepsilon_2(ca_{A2}) \cdot ca_{A2} \quad (26)$$

$$\varepsilon_3 = \varepsilon_3(s_i_m) \cdot si_m + \varepsilon_3(s_{i_{A1}}) \cdot si_{A1} + \varepsilon_3(ca_{A2}) \cdot ca_{A2}$$

where:

$$\varepsilon_1(s_i_m) \cdot B_{14} = W_{m0} - A_{110} \frac{B_{11}}{A_{11}}$$

$$\varepsilon_2(s_i_m) \cdot B_{24} = B_{210}$$

$$- \frac{A_{220} \cdot Dw_{A1}(s_i_m) + A_{230} \cdot Dw_{A2}(s_i_m) + A_{21} \cdot Dw_m(s_i_m)}{D \cdot A_{11}}$$

$$\varepsilon_2(s_{i_{A1}}) \cdot B_{24} = W_{A10}(1 + K_{ba0})$$

$$- \frac{A_{220} \cdot Dw_{A1}(s_{i_{A1}}) + A_{230} \cdot Dw_{A2}(s_{i_{A1}})}{D \cdot A_{11}}$$

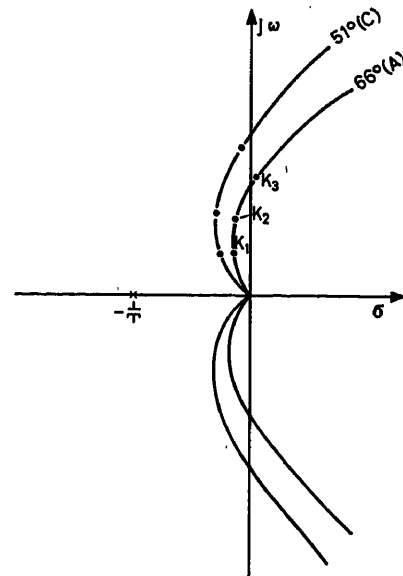


Figure 9. Stability analysis by constant phase loci

$$\varepsilon_2(\text{ca}_{A2}) \cdot B_{24} = -W_{A20}(1 + K_{ba0}) \\ - \frac{A_{220} \cdot Dw_{A1}(\text{ca}_{A2}) + A_{230} \cdot Dw_{A2}(\text{ca}_{A2})}{D \cdot A_{11}}$$

$$\varepsilon_3(\text{si}_m) \cdot B_{34} = B_{310} \\ - \frac{A_{31} \cdot Dw_m(\text{si}_m) + Dw_{A1}(\text{si}_m) + Dw_{A2}(\text{si}_m)}{D \cdot A_{11}}$$

$$\varepsilon_3(\text{si}_{A1}) \cdot B_{34} = - \frac{Dw_{A1}(\text{si}_{A1}) + Dw_{A2}(\text{si}_{A1})}{D \cdot A_{11}}$$

$$\varepsilon_3(\text{ca}_{A2}) \cdot B_{34} = - \frac{Dw_{A1}(\text{ca}_{A2}) + Dw_{A2}(\text{ca}_{A2})}{D \cdot A_{11}}$$

By analogy with the terminology used for servomechanisms, one defines as position errors or velocity errors respectively:

$$\varepsilon_{ip} = \lim_{s \rightarrow 0} \varepsilon_i \quad \varepsilon_{iv} = \lim_{s \rightarrow 0} \frac{\varepsilon_i}{s}$$

It is easily verified that all the position errors are null. For the following considerations, it is interesting to examine the relative velocity errors, that will be expressed in the following manner:

$$\varepsilon'_{1v}(\text{si}_m) = \frac{\varepsilon_{1v}(\text{si}_m)}{K_{20}}$$

$$\varepsilon'_{2v}(\text{si}_m) = \frac{\varepsilon_{2v}(\text{si}_m)}{K_{ba0}}$$

$$\varepsilon'_{3v}(\text{si}_m) = \frac{\varepsilon_{3v}(\text{si}_m)}{W_{10}/W_{g0}}$$

and analogously for $\varepsilon'(\text{si}_{A1})$ and $\varepsilon'(\text{ca}_{A2})$.

The complete expressions, for absolute and relative errors of system described by (15) are reported by de Gregorio⁸. For the relative errors, an analysis of such expressions allows the conclusion of: (a) the time constants of x-ray detectors are explicitly involved in the determination of such errors; (b) the production levels and generally the extensive variables are not involved in the expression of errors. Substituting a scheme corresponding to (15) by a scheme of type (18), such a conclusion should not be true. Therefore, for another reason, the selection of (15) is proved as the most convenient.

A principle of equipartition of velocity error is now introduced, i.e. it is assumed that a disturbance coming from outside (variations of chemical composition) has the same weight, in absolute value, on relative errors of all the controlled variables. The same weight is assumed here, but nothing changes in the consideration and solution of the problem, if arbitrary weights are introduced into the calculation.

Using these symbols, (27) is written as:

$$|\varepsilon'_{1v}(\text{si}_m)| = |\varepsilon'_{2v}(\text{si}_m)| = |\varepsilon'_{3v}(\text{si}_m)| \quad (27) \\ |\varepsilon'_{2v}(\text{si}_{A1})| = |\varepsilon'_{3v}(\text{si}_{A1})| \\ |\varepsilon'_{2v}(\text{ca}_{A2})| = |\varepsilon'_{3v}(\text{ca}_{A2})|$$

Having obtained four equations containing the five unknown quantities G , the criterion applied here allows the expression of all the gains in the function of one of them. The determination

of this last must be obtained on the basis of relative stability criteria, i.e. good quality of response. Of course for this determination it is necessary to consider explicitly a multipole controller, where each error acts on each manipulated variable. This explains why it is necessary to consider also these more complex systems.

A detailed application of the above-mentioned concepts and the deduction of the system of equations solving the problem are given by de Gregorio⁸.

Conclusions

The conclusions of this dynamic analysis of the system are:

1. The scheme of Figure 7 cannot be strictly defined as a ratio control, but it was proved that this is preferable to ratio control for the following reasons: (a) the process dynamics, chiefly the stability, results independent of production level; (b) the relative errors are independent of this level; and (c) the practical realization of this scheme is more simple.

2. Time constants of the analysers do not intervene in the stability questions; they determine explicitly the errors.

3. There is reason to believe that the perturbation method, limited to first order, here adopted to linearize the system under consideration, is quite justified since control characteristics for the examined scheme are independent of production levels and are only dependent, in a fairly weak way, on chemical compositions.

4. The considerations developed from a modal analysis of the system are very suitable for a synthesis of compensating elements. The conclusions on stability, drawn from these considerations, applied both in the $G(s)$ plane (Nyquist) and in s plane (constant phase angle loci) have been confirmed by the use of classic analytical methods.

5. The presence of two or more regulators of type 1 involves the oscillatory behaviour of the system for any gain value. The damping decreases as the value of the gain increases.

6. The dynamic behaviour of the system depends on the chemical composition of the additives; usually a decrease of component purity tends to worsen the stability.

7. If the introduction of an equipartition principle in the distribution of relative errors is required, the application of multipole control systems is necessary.

Nomenclature

List of Symbols

Al	Alumina (in per unit)
C	Carbon (in per unit)
Ca	Lime (in per unit)
f	Constant defined in paper
Fe	Iron (in per unit)
K_1	Iron flow rate set point (Kg/sec)
K_{1s}	Solid materials flow rate set point (Kg/sec)
K_2	Pig iron production set point (Kg/sec)
K_{ba}	Basicity index = $(\text{Ca} + \text{Mg}) / (\text{Si} + \text{Al})$
K_o	Fuel index
K_{em}	Fuel/ore ratio
K_{max}	Maximum plant production capacity
p	Iron contained in oxide (in per unit)
Mg	Magnesia (in per unit)
S	Sulphur (in per unit)
Si	Silica (in per unit)
W	Flow rates (Kg/sec)

List of Suffixes

- A Additives
 c Fuel in sinter plant
 g Pig iron
 l Slag components
 m Iron ore

References

- ¹ HAMILTON, D. E. and HOULTEN, R. L. Automation for sinter plants. *Blast Furnace and Steel Plant* (June, 1960) 569-579
- ² FURBEE, A. D. The x-ray emission gage. A new sensor for on-line chemical analysis. *Inst. Radio Engrs, Ind. Electron. Meet.*, 1953
- ³ JACKSON, A. S. *Analog Computation*. p. 332. 1960. New York; McGraw-Hill
- ⁴ TRUXAL, J. G. *Automatic Feedback Control System Synthesis*. 1955. New York; McGraw-Hill
- ⁵ CHU, Y. Synthesis of feedback control system by phase-angle loci. *Trans. Amer. Inst. elect. Engrs Pt 2*, 71 (1952) 330-339
- ⁶ SIRONI, G. Recenti sviluppi nella preparazione delle cariche di altoforno: agglomerati autofondenti. *Metallurg. ital.* 52 (1960) 607-614
- ⁷ GIEDROYC, V. Removal of sulphur during iron-ore sintering. *J. Iron St. Inst.* (1955), 129-140
- ⁸ DE GREGORIO, G. Controllo di Dosatura per Impianti di Agglomerazione. *Compagnia Generale di Elettricità, Rapporto Interno* STG 61-1
- ⁹ VOICE, E. W. *Factors Controlling the Rate of Sinter Production*. Symposium on Sinter, Spec. Rep. 53, 1955. London; The Iron and Steel Institute

DISCUSSION**Author's Opening Remarks**

Some considerations are perhaps in order for a better illustration of the scope of the present paper.

We are faced with the problem of the control of the chemical characteristics for the mixture in a sinter plant. We made a fairly broad examination in order to lay down the many aspects involved in the problem. We were also concerned in a mathematical analysis of the subject limiting such an analysis explicitly to one of the many potential types of control systems we could envisage. This choice was done purposely. In fact, this study was intended as the basis for part of an experimental research to be developed on a 350 tons/day plant by the most important research institute operating in Italy in the iron and steel area. There are many advantages in adopting a control method of this particular kind in a research job. This scheme offers the best results, the tightest form of control on the product. Through this strict control on the composition of the input material it is possible to study under the best experimental conditions the other aspects of the integral automation of the plant, i.e. humidification, combustion control, and so on. In other words, a good quality in the control of this subset of the plant will heavily condition the research in the other areas. Among these related areas we were mainly interested in the permeability control, already examined in a previously presented paper as an application of self-optimizing controls.

Operating the plant in this way allows the acquisition of a detailed knowledge of the statistics involved in the distribution of chemical composition of the input materials. Such a knowledge is important to define the speed of response of the master control loop. Another point of interest in this analysis on statistics of raw materials is the better assessment obtained of the need and size of the dry mixer. As a matter of fact this component has to cope with the high-frequency region of the noise spectrum. The control must be relieved from such a duty because extending the frequency range adds to the complication of the compensation networks for such non-linear and multipole controllers and because the rotating feeders are a very poor form of actuation.

In order to get these excellent results we have to spend a maximum on the instrumentation. Apart from the analyser placed at the end of the process for monitoring the final results, we need as many analysers as the number of the bins. In the examples illustrated in the paper such a number was limited to three or four for ease of analytical developments but if, for better operation of the plant, it would appear advisable to add some other indices (alumina, magnesia), or other limitations (mass flow, Cu), the bin numbers have to be increased. Moreover, for practical reasons of plant operation (stock demand) there are normally more bins than material streams and that means a larger number of heads, if not analysers, than are strictly needed for the control of the plant. These are serious drawbacks for the generalization of the scheme analysed in detail in the paper. Therefore, it is advisable to consider the alternative having the minimum in the instrumentation

cost and consequently less control quality, that is, a pure closed loop control with only one analyser at the end of the process, of continuous type or even of laboratory type (sampling control). The paper presented by Mr. Phillips clearly indicates that this solution is the one adopted for blending in the cement area. This solution stresses the importance of the considerations of transport delays that here are affecting directly the stability and quality of the control.

Again some consideration is pertinent on the dry mixers. Their contribution to the total delay has to be reduced to the minimum, although it is easy to understand that their capacity in this instance tends to go up. In fact, the permissible control frequency range in the loop has to be decreased for stability reasons and therefore the control system cannot cope with the high-frequency region of the noise spectrum. If the most significant delay is represented by the transport delay of the main stream, the analytical considerations of the present paper are comprehensive for this case also; the transfer functions of the actuators have just to be substituted by the delay of the materials transfer (equivalent time constant, Padé polynomials approximation or pure delay).

In between these possibilities other intermediate types of control are feasible, three of which seem promising:

(a) In order to reduce the cost of the instrumentation in the control system considered in the paper, it is conceivable to adopt a measuring equipment with as many heads as the number of bins plus one at the output for checking the validity of the model with one centralized electronic control cabinet. This means the adoption of a sampled control. The mathematical analysis of the problem is dependent on the characteristics of the noise. In fact, the scanning speed is related to the time constant of the x-ray analyser that varies in turn with the physical nature of the material presented to the instrument.

(b) In order to reduce the process transport delay in the closed loop type of control, it is possible to measure the mixture as soon as blended, possibly before the dry mixer. If the delay in the different sources is not the same, the more generalized formulation at the end of this paper can be used for the analysis.

(c) In introducing the third alternative I would like to briefly recall what happened years ago in the area of the automatic gauge control in the steel mills. It was then possible to eliminate the gauge instrumentation at each stand (again x-ray instruments) through the use of an indirect type of measuring equipment using strain gauges assisted continuously by a supervising calibration from the gauge instrument located at the output of the process.

By analogy to our case the local bin monitors can be calibrated through a laboratory x-ray gauge, in order to further reduce the instrumentation cost. This collaboration from an x-ray analyser may allow the use of local devices based on properties related to chemical composition such as gravity, magnetic properties, and so on.

It was the firm intention of the authors to show here the results derived from the experimental work on the actual plant in order to

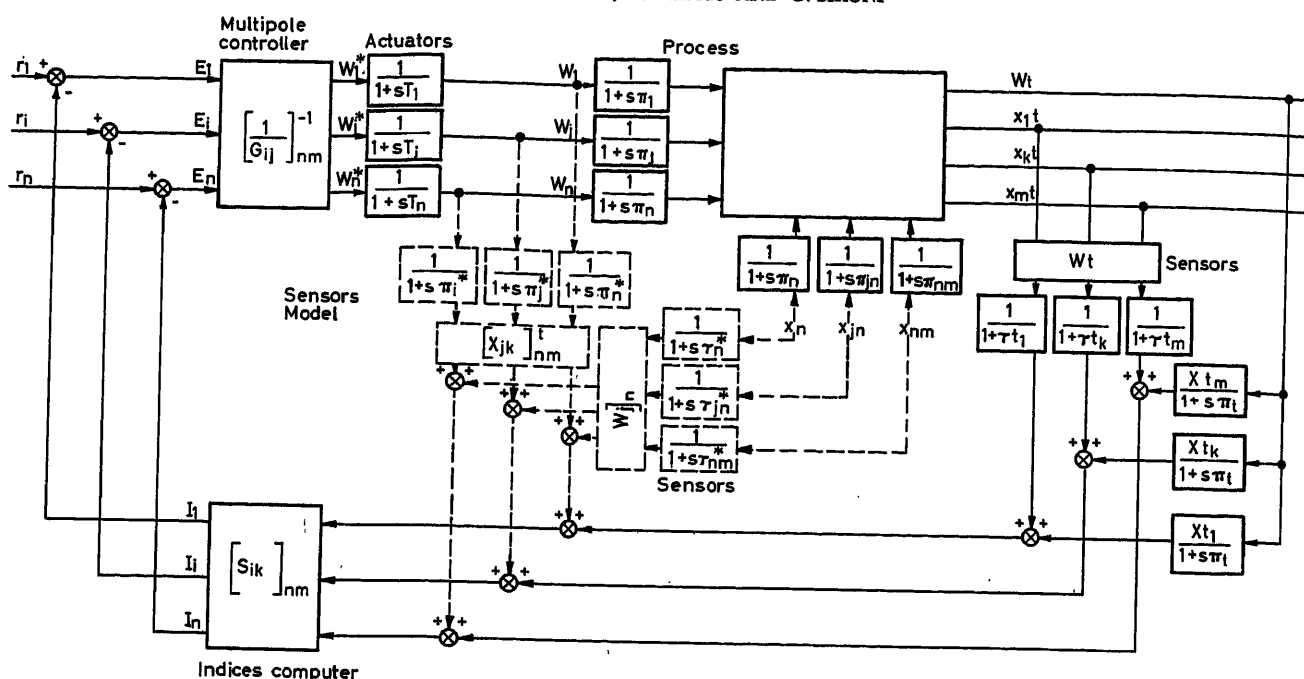


Figure A

substantiate the methods outlined in the paper and to give some indication for further progress in the direction outlined above. Unfortunately external difficulties have caused a substantial delay in the beginning of the experimental work. Meanwhile we hope it is worth while to show in a very brief manner how the mathematical analysis can be extended to cover the most general type of plant. In order to get reasonable expressions and to simplify the various manipulations, we adopted here a matrix-tensor formulation that seems to be used more and more widely today in the literature covering the multipole systems. The fairly lengthy notations used in the paper were written to follow the formalism used in the technology of this area, but for detailed studies on control, they become quite cumbersome.

The physical grounds to the formalism may be seen in Figure A. It covers both types of control, compound (with the help of the model), and closed loop. They appear in parallel on the diagram.

The meaning of the symbols is as follows:

- i index for set points, actual quality indices, difference signals (from 1 to n)
- j index for manipulated variables (from 1 to n in our particular case)
- k index for chemical compositions (from 1 to m)
- t index for mixed output materials
- $[A_{jk}]_{nm}$ matrix with n rows and m columns
- $|A_{jk}|$ determinant of the above defined matrix
- $[B_j]_n$ vector with n rows
- $D_n()$ diagonal matrix of n order

In the linearized equations, capital letters are used for steady state values and lower case letters for the variations from steady state. Apart from the delay τ affecting the chemical compositions, we further considered the delay π affecting the mass flow. The symbols $*$ were used for measurement delays to distinguish them from the transport delays. In general $\pi_j = \tau_{jk}$. Ratio control is described by eqn (18) in the paper: pseudo-ratio is illustrated in Figure 7. The interacting controller here adopted follows the scheme given in Figure B for the case $n = 2$. The main expressions of the paper can be generalized as follows:

Quality Indexes

$$[R_i]_n = \left(\frac{[b_{ik}]_{nm} [X_{jk}]_{nm}^t [W_j]_n}{[I_{ij}]_{nn} [c_j]_n + [a_{ik}]_{nm} [X_{jk}]_{nm}^t [W_j]_n} \right)$$

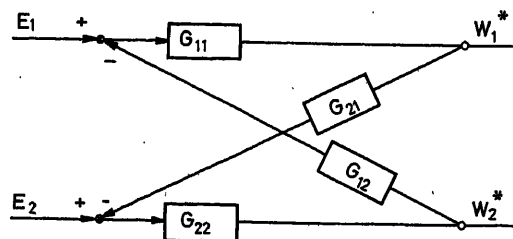
The following definition is used for the vector ratio at the second member

$$\left[\frac{a_1 \bar{i} + a_2 \bar{j} + a_3 \bar{k}}{b_1 \bar{i} + b_2 \bar{j} + b_3 \bar{k}} \right]_3 = \frac{a_1}{b_1} \bar{i} + \frac{a_2}{b_2} \bar{j} + \frac{a_3}{b_3} \bar{k}$$

In the example given in Figure 7

$$[W_j]_n = \begin{bmatrix} W_m \\ W_{A1} \\ W_{A2} \end{bmatrix} [X_{jk}]_{nm}$$

$$= \begin{bmatrix} 1 - Si_m & Si_m & 0 \\ 0 & Si_{A1} & 1 - Si_{A1} \\ 0 & 1 - Ca_{A2} & Ca_{A2} \end{bmatrix} [R_i]_n = \begin{bmatrix} K_2 \\ K_{ba} \\ \frac{W_1}{W_g} \end{bmatrix}$$



$$W_1^* = G_{11} (E_1 - G_{12} W_2^*)$$

$$\begin{cases} \frac{W_1^*}{G_{11}} + \frac{W_2^*}{G_{12}} = E_1 \\ \frac{W_1^*}{G_{21}} + \frac{W_2^*}{G_{22}} = E_2 \end{cases}$$

Figure B

$$[b_{ik}]_{nm} = \begin{bmatrix} \frac{p}{Fe_g} & 0 & 0 \\ 0 & 0 & 1 \\ 0 & 1 & 1 \end{bmatrix} [a_{ik}]_{nm} = \begin{bmatrix} 0 & 0 & 0 \\ 0 & 1 & 0 \\ \frac{p}{Fe_g} & 0 & 0 \end{bmatrix} [c_j]_n = \begin{bmatrix} 1 \\ 0 \\ 0 \end{bmatrix}$$

Ratio control (linearized)

$$\begin{aligned} [r_i]_n - [S_{ik}]_{nm} \frac{1}{1+s\tau_i} [X_{jk}]_{nm} D_n \left(\frac{1}{1+s\tau_j} \right) [w_j]_n \\ + \frac{1}{1+s\tau_{ik}} \left[\frac{x_{jk}}{1+s\tau_{jk}} \right]_n^t [W_j]_n \\ = \left[\frac{1}{G_{ij}} \right]_{nm} D_n [s(1+sT_j)] [w_j]_n \quad \text{Interacting controller} \\ = D_n \left[\frac{s(1+sT_j)}{G_j} \right] [w_j]_n \quad \text{Diagonal controller} \end{aligned}$$

Pseudo-ratio control (linearized)

$$\begin{aligned} [r_i]_n - [S_{ik}]_{nm} \left\{ \frac{1}{1+s\tau_i} \left[D_n \left(\frac{1}{1+s\tau_j} \right) [X_{jk}]_{nm} w_j \right]_n \right. \\ \left. + \frac{1}{1+s\tau_{ik}} \left[\frac{x_{jk}}{1+s\tau_{jk}} \right]_n^t [W_j]_n \right\} \\ = \left[\frac{1}{G_{ij}} \right]_{nm} D_n [s(1+sT_j) H_j] [w_j]_n \end{aligned}$$

Where by definition

$$\begin{aligned} S_{ik} &= H_i b_{ik} - K_i a_{ik} \\ H_i &= \frac{R_i}{\sum_{jk} b_{ik} W_j X_{jk}} = \frac{1}{c_i + \sum_{jk} a_{ik} W_j X_{jk}} \\ K_i &= \frac{R_i}{c_i + \sum_{jk} a_{ik} W_j X_{jk}} = \frac{\sum_{jk} b_{ik} W_j X_{jk}}{(c_i + \sum_{jk} a_{ik} W_j X_{jk})^2} \end{aligned}$$

From the diagram Figure 7

$$S_{ik} = \begin{bmatrix} \frac{pH_1}{Fe_g} & 0 & 0 \\ 0 & -K_2 & H_2 \\ -\frac{p}{Fe_g} K_3 & H_3 & H_3 \end{bmatrix}$$

Coefficient of eqn (16) normalized ($B_{14} = B_{24} = B_{34} = 1$)

$$\begin{aligned} A_{ij} &= \frac{\sum_k S_{ik} X_{jk}}{(1+s\tau_j)(1+s\tau_i)} + \delta_{ij} H_j \frac{s(1+sT_j)}{G_j} \\ &= \frac{A_{ij0}}{(1+s\tau_j)(1+s\tau_i)} + \delta_{ij} H_j \frac{s(1+sT_j)}{G_j} \end{aligned}$$

Where

$$\begin{aligned} \delta_{ij} &= 1 \quad i=j \\ &= 0 \quad i \neq j \end{aligned}$$

$$B_{ik} = \frac{\sum_j S_{ik} W_j}{(1+s\tau_{jk})(1+s\tau_{ik})}$$

Characteristic equation

$$\begin{aligned} \left| [S_{ik}]_{nm} [X_{jk}]_{nm} D_n \left(\frac{1}{1+s\tau_j} \right) \right. \\ \left. + \left[\frac{1}{G_{ij}} \right]_{nm} D_n [H_j s(1+sT_j)(1+s\tau_i)] \right| = 0 \end{aligned}$$

Absolute errors

$$\begin{aligned} [e_i]_n &= -[S_{ik}]_{nm} \left\{ [X_{jk}]_{nm} D_n \left(\frac{1}{1+s\tau_j} \right) [w_j]_n \right. \\ &\quad \left. + \left[\frac{x_{jk}}{1+s\tau_{jk}} \right]_{nm}^t [i_j]_n \right\} \end{aligned}$$

M. G. SHORTLAND, *B.I.S.R.A., 140, Battersea Park Road, London, S.W. 11*

This paper gives an unusually comprehensive treatment of the factors influencing the way in which the sinter components should be mixed to maintain an adequate level of plant stability and a high level of blast furnace performance. At B.I.S.R.A. we are currently studying some of the important effects which are considered; for example, sinter quality relative to the variation in chemical composition of the mix prior to charging on to the sinter strand, and the maximization of sinter production in the face of random disturbances in physical properties of the mix including its porosity which is highly dependent on moisture content. Regarding chemical analysis I would like to ask: (1) Are the x-ray fluorescence analysers which play an important role in the control schemes described truly continuous, or do they rely on a sampling procedure? (2) Are such analysers in operation at any plant with which the authors are familiar (e.g. at Terni)? (3) What do the authors conclude about the problem of estimating true or average chemical composition from the analyser output, bearing in mind the possibility of large random disturbances occurring in component analysis during the period of a measurements? Measurements made on a sinter plant in England have shown very large variations in composition.

The authors draw attention to the existence of noise on many of the signals feeding the control schemes proposed. Have any measurements been made on a production plant which enable estimates to be made of the influence of noise on control performance in terms of accuracy and overall system stability?

J. I. BRADFORD, *Jones and Laughlin Steel Corp., Pittsburgh, Pennsylvania, U.S.A.*

In our studies of the sintering process, greater economic benefits are indicated if we could continuously measure the moisture content of the incoming coke and adjust the rate of flow to keep the fuel content constant; and also to measure continuously the moisture in the mix ahead of the furnace and regulate it to a constant value. These would result in both a coke saving and an increase in machine output, but require sensors for determining the moisture content of the coke and the mix. Do the authors agree and do they know if such sensors and approach have been applied?

W. G. WRIGHT, *Canadian General Electric Company, Ontario, Canada*

Some years ago when considering the problems of applying automatic control to a sinter plant, we came to the conclusion that it might be necessary to provide variable speed conveyors in order to eliminate the transport delay. In addition we visualized the use of a variable speed sinter machine operating under the control of a burn-through calculator. Unfortunately we did not implement these ideas. Consequently we would like to ask the authors if, in view of their more recent experience, they consider these steps necessary.

G. SIRONI, *in reply*

The paper illustrates a project only and in consequence, certain practical problems were not faced. For example, we agree with Mr. Shortland about the importance of the problems relating to the moisture of the mixture, permeability and so on, but evidently by this paper we have had no intention of facing the problem of the complete control of the sintering process but only, on the basis of a mathematical model, to determine and control the chemical composition of the sinter. In consequence, certain problems, such as the optimum control of the moisture by measurement of the permeability, or in reference to the speed of the travelling grate automatically regulated, were separately studied by the Istituto Finsider^{1, 2}.

Considering the problems of the measures, it should be pointed out that the mathematical model of the transfer of the raw materials referred to a particular small Dwight Lloyd plant at the Terni Works. This plant was available for a long period of the year because of its discontinuous operation, nevertheless it required very expensive work to

improve the installed instrumentation and for new instruments. A short time after, the Italsider launched its plan for new big sinter plants which were very well instrumented and partially automated. On these new plants, in fact, we plan to test new kinds of instruments and the performance of an x-ray analyser.

All that is necessary for the practical realization of the project is described in this paper.

References

- ¹ SCORTECCI, V. and SIRONI, G. Sottosistemi automatici per la regolazione degli impianti di agglomerazione. *Proc. Int. Seminar on Automatic Control in the Iron and Steel Industry*. 1963 Bruxelles Presses Européennes
- ² SIRONI, G., TESTONI, V., MONTESSORO, A., PARETO, G. and VANNI, G. La ottimizzazione automatica della permeabilità per le miscele di agglomerazione. *Automazione e Strumentazione*, No. 9 (1963)

Dynamic Planning for an Open-hearth Steel-making Plant

M. KOROBKO and Yu. SAMOILENKO

Summary

The use of oxygen in open-hearth steel making has opened a possibility for considerable reduction in the length of the melting period. Under this new condition the throughput of an open-hearth plant is limited mainly by auxiliary equipment servicing several furnaces forming a complex interconnected system. Orthodox planning of operations for the whole plant causes considerable time losses due to inefficient use of equipment facilities.

This presents a new method of open-hearth plant optimization based on continuous operational planning and thermal dynamic planning. Specific features of the problem are shown to be the existence of nodes in the optimal phase trajectory. An economic index representing the difference between the gain due to increased throughput and the control cost over a sufficiently long period is suggested as a performance criterion.

Logical differential equations describing the process of steel melting are developed, based on the analysis of optimal direction at the nodes on normal operating conditions. The choice of optimal direction at the nodes is effected by sequential comparison of different control actions. Increase in productivity with the increase of the number of compared alternatives for homogeneous tree-like processes is evaluated.

Technical solution of the problem is suggested in the design of a computer control system which automatically processes the information relating to the actual state of melting and available auxiliary equipment capacities. On the basis of this analysis it instructs the operators and provides setting for automatic devices which regulate the melting processes so as to maximize the utilization of equipment facilities. Technical requirements for the computer to be used in dynamic planning are formulated.

Sommaire

En aciérie, l'insufflation d'oxygène dans les fours à sole a permis de réduire considérablement la durée de la fusion. Il en résulte que la production d'un four à sole est limitée le plus souvent par l'équipement auxiliaire assurant le chargement de plusieurs fours interconnectés au sein d'un complexe. Dans un tel complexe, la planification selon les méthodes classiques de l'ensemble des opérations conduit à une perte de temps considérable par suite d'une utilisation peu rationnelle de la capacité de l'équipement auxiliaire.

La présente communication se rapporte à une nouvelle méthode d'optimisation d'un ensemble de fours à sole fondée conjointement sur une planification continue des opérations et sur une planification thermique dynamique. On y montre que la caractéristique spécifique du problème réside dans l'existence de nœuds sur la trajectoire de phase optimale. On suggère d'adopter, à titre d'indice de performance, un critère économique représentant la différence entre le gain résultant de l'accroissement de production et la dépense occasionnée, durant une période suffisamment longue, par l'appareillage de commande.

On établit, à partir de la détermination de la direction optimale aux nœuds des diagrammes représentant les conditions normales de fonctionnement, les équations différentielles logiques qui représentent le processus de la fusion de l'acier. Aux nœuds, le choix de la direction optimale est dicté par la comparaison séquentielle de diverses actions de commande. On évalue l'accroissement de productivité résultant de l'accroissement du nombre d'alternatives comparées pour le cas d'un processus homogène de type arborescent.

On suggère, pour résoudre techniquement le problème, de conce-

voir une commande à l'aide d'une calculatrice qui traiterait automatiquement les informations relatives à l'état instantané du processus de fusion et celles se rapportant aux capacités respectives des installations auxiliaires. Sur la base du résultat de ce traitement, la calculatrice élaborerait des instructions à l'usage des opérateurs et des ordres destinés aux dispositifs automatiques qui règlent le processus de fusion, instructions et ordres qui auraient pour effet de maximiser l'utilisation des installations auxiliaires. On formule enfin les exigences techniques que devrait satisfaire cette calculatrice pour pouvoir être engagée dans une telle planification dynamique.

Zusammenfassung

Die Verwendung von Sauerstoff bei der Stahlgewinnung im Siemens-Martin-Ofen ermöglichte eine beträchtliche Verkürzung der Schmelzzeit. Unter diesen neuen Voraussetzungen ist der Durchsatz bei Siemens-Martin-Öfen vor allen Dingen durch die Hilfseinrichtungen, die mehrere Öfen bedienen und dadurch ein komplexes vermaschtes System bilden, begrenzt. Die Betriebsplanung im alten Stil verursacht durch unwirtschaftliche Ausnutzung der Betriebseinrichtungen beträchtliche Verlustzeiten.

Ein neues Verfahren zur Optimierung von Siemens-Martin-Werken wird vorgelegt, das auf einer kontinuierlichen Betriebsplanung und der Planung des dynamischen Wärmeablaufes basiert. Wie sich zeigt, bilden die in der Phasenebene vorhandenen Knotenpunkte der optimalen Trajektorie eine besondere Eigenschaft des Problems. Als Gütemaßstab wird ein Wirtschaftlichkeitsindex vorgeschlagen, der den Unterschied zwischen dem gesteigerten Durchsatz und den Steuerungskosten über eine genügend lange Zeit vergleicht.

Differentialgleichungen, die auch den logischen Zusammenhang berücksichtigen, werden zur Beschreibung des Schmelzvorganges entwickelt, die auf einer Untersuchung der günstigsten Richtung unter normalen Betriebsbedingungen am Knotenpunkt beruhen. Die Wahl der günstigsten Richtung an den Knotenpunkten geschieht durch einen schrittweisen Vergleich verschiedener Steuereingriffe. Die Produktivitätszunahme für homogene sich verzweigende Prozesse wird bei wachsender Zahl der Vergleichsmöglichkeiten untersucht.

Zur technischen Lösung des Problems wird eine Regelung durch einen Rechner vorgeschlagen, der die Informationen über den jeweiligen Stand der Schmelze und über die verfügbaren Hilfseinrichtungen automatisch verarbeitet. Auf Grund dieser Untersuchungen gibt der Rechner dem Bedienungspersonal Anweisungen und sorgt für eine automatische Einstellung der Regelungseinrichtungen des Schmelzprozesses, um den Nutzungsgrad der Hilfseinrichtungen maximal zu machen. Die notwendigen technischen Eigenschaften eines Rechners zur dynamischen Planung sind angegeben.

Introduction

The output of an open-hearth steel-making plant depends, in the first place, on the output of individual furnaces. However, the practice in works recently showed that the duration of the melting operation could be reduced considerably as a result of the use of oxygen. Under these conditions the output of the plant is limited only by auxiliary equipment.

The operation of different furnaces of the plant is interconnected since they use the same machines and interchangeable equipment, and also because they are served by the same subsidiary works' departments and means of transport. All that is needed in connection with the running of furnaces is therefore conditionally described as 'auxiliary'.

All auxiliaries are usually designed for a capacity margin of 15-30 per cent, which when trying to force melting rate is very often shown to be inadequate. In conventional programming the interconnected operation of furnaces causes frequent organizational delays in melting, which results in peak requirements exceeding the capacity of auxiliaries.

The capacity of some auxiliaries can be increased relatively easily, but for the majority of them, for the increase required, it would necessitate a complex reconstruction of the plant involving the spending of large sums of money.

Since the operation of furnaces depends on a large number of factors, which change according to random laws, the optimum operation of the whole plant can be obtained only by continuous operational programming, which may be called 'dynamic' programming.

The technical problem of dynamic programming for the operation of an open-hearth steel-making plant can be solved by constructing a system with a computer capable, on the basis of automatic processing of information concerning the progress of melting and available capacities, of evaluating the volume of work which could be done and, accordingly, of giving commands to furnacemen and automatic equipment, responsible for the control of the melting operation, so that the maximum use could be made of auxiliaries.

Theoretically, this problem may be considered as one of the tasks of dynamic programming, the fundamentals of which are explained in the works of L. S. Pontryagin, R. Bellman and others. As is shown below, the presence of nodes in the optimum phase trajectory is the main feature of the given problem. The economic index, which represents the difference between the value of increased production and the expenditure on automatic control for a sufficiently long interval of time, is chosen as the economic criterion for the quality of control. The term 'expenditure on control' denotes the variable portion of operational costs for the automated part of production, which is conditioned by the necessary change of technology embodied in the process of automatic control.

On the basis of analysis of the operation of works¹ furnaces under actual operating conditions, logical differential equations were constructed for the progress of the melting operation. The

choice of the optimum direction at the nodes is obtained by the subsequent comparison of different variants of the automatic control for the process. An assessment is made of the increase in output, when the number of comparable variants for homogeneous node processes is increased.

Organizational Conditions for the Operation of Furnaces

The melting of steel in open-hearth furnaces is essentially a cyclic process, which consists of successive technological periods during which certain auxiliaries are engaged. On a modern, open-hearth steel-making plant there are up to 12 furnaces. A typical general layout of equipment at a plant is shown in Figure 1. Similar mechanisms move along past a number of furnaces on the same rail track; thus, their relative disposition is shown to be subordinated to ground connection. Mechanisms used for different purposes are not subject to the interchanges of position. The essential auxiliaries for the programming of the operation of furnaces are the charging machines, casting cranes, ladle cars, teeming cranes and casting bays.

The manoeuvrability of machines along furnace runways is unlimited, so that all the working machines and the interchangeable equipment may be used. In the teeming bay the mobility of crane equipment is limited; therefore, the operations in it are not always determined by the total number of the mechanisms available. The effect of the possible idleness of some teeming cranes caused by those currently in use should be taken into account.

Every open-hearth plant has its own peculiarities; therefore, the mathematical description should be made for the specific plant. Thus, for example, on some plants the bunkers for the charging of furnaces are not installed on the furnace floor, and during the entire period use is made of the casting crane, which increases the engagement of the latter; for the charging of the furnace on other plants two machines are used for the same furnace, and so on.

So far as the control of the melting operation is concerned its periods consist of controlled and uncontrolled periods; but so far as the possibility of freeing the auxiliaries on one furnace so that they could be transferred to another furnace is concerned, the periods of the melting operation consist of intermittent and continuous periods. In the first approximation it is considered here that the durations of the latter periods of the melting operation are independent of those of the former periods, since in further considerations this condition is not of material importance.

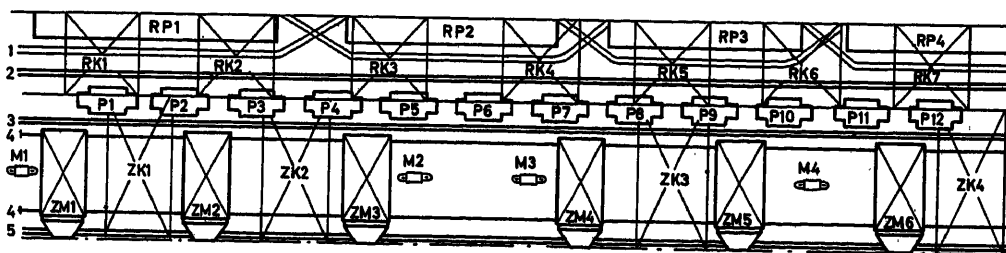


Figure 1. Sketch illustrating the general layout of an open-hearth steel-making plant

P1: 12 furnaces
RP1: 4 casting bays, Nos. 1-4
RK1: 7 casting cranes, Nos. 1-7
ZK1: 4 teeming cranes, Nos. 1-4
ZM1: 6 charging machines, Nos. 1-6
M1: 4 fettling machines, Nos. 1-4

1: casting rails
2: slag rails
3: furnace charge rails
4: charging machine rails
5: ladle car rails

In future, the existence of some relationship between the durations of individual periods of melting may help to improve the programming. It is assumed also that in the course of each period of the melting operation a certain amount of subsidiary work is carried out.

The conditional graph for the melting operation, which consists of the time periods used for the carrying out of such work, with the furnace being served by all the auxiliaries, may be termed the 'condensed' graph.

By virtue of the effect of a large number of random factors, the durations of periods of the condensed graph, strictly speaking, represent random quantities and cannot be calculated beforehand with the necessary degree of accuracy. Therefore, the values for the assumed durations of the periods of the condensed graph should be systematically corrected.

The technical and economic criterion of programming, which makes possible the comparisons of different variants of the progress of the melting operations in furnaces, should serve as the basis for the choice of the optimum graph for the progress of the melting operations.

This criterion which takes into account the expenditure on automatic control is determined by the scalar product:

$$Q = \left[C \int_0^T \phi dt - \int_0^T f(\phi)(w - \phi) dt \right] \quad (1)$$

here $c = c_1, \dots, c_n$, C_i is the output of the i th furnace; $f(\phi)$ is the piecewise constant coefficient which depends on the period of the melting operation and on individual characteristics of furnaces; $w = w_1, \dots, w_n$, w_i are the rates of melting operations according to the condensed graph which take into

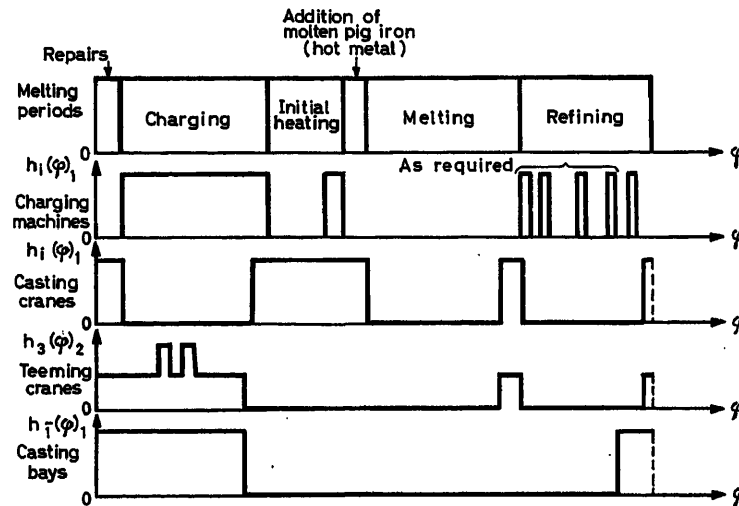


Figure 2. Diagram illustrating the employment of auxiliary capacities at different periods of melting

The volume of work ϕ_i , actually carried out on the i th furnace from the beginning of taking the readings to the instant of time t , represents the basic coordinate, which determines the progress of the melting operation in the furnace. The state of a plant which consists of ' n ' furnaces is described by the values of ' n ' coordinates $\phi_1, \phi_2, \dots, \phi_n$, which may be considered as the components of vector ϕ of the state of the melting operations on the plant.

As an example, the engagement of the most essential auxiliaries at different periods of time is shown diagrammatically on the condensed graph for the melting operation (Figure 2). The functions h_i show how many units of i auxiliary are required at different periods of the melting operation. These functions, in the simplest case, take the values of only 0 or 1. For their assignment it is necessary only to indicate the durations of periods of engagement or the instants of time of their termination (with the known beginning of readings). In the first approximation it is considered here that the durations of periods of the condensed graph are assigned on the basis of mean statistical data. The more precise data regarding the durations of the periods may be obtained by using the results of the preceding melting operations and by taking into account the current information regarding the state of the furnace and the quality of the materials being used.

account the provision for the general forcing of the progress of melting for all the furnaces; and $\phi = \phi_1, \dots, \phi_n$, ϕ_i are the actual rates of melting operations which take into account the delays caused by the separation of furnaces.

For the ease of planning of the progress of melting operations it is possible to consider that the processes in furnaces are intermittent in character, i.e., their rates may assume the values of only 0 or 1. This procedure, which follows from the analysis of phase trajectories, may be applied only in the programming of the durations of periods and for the calculation of the mean rates. But the actual process should proceed as uniformly as possible in accordance with the mean rates found in programming. Otherwise, large fluctuations in the rate of the process would lead to a strong increase in the cost of automatic control, which would then no longer be taken into account by formula (1), which is applicable only within a small range of rates. By the interruption of operations, in future, if not specially stipulated, only the corresponding increase in the duration required for their completion will be understood.

In order to indicate the inadmissibility of delays during continuous operations, multiply the right side of expression (1) by the function

$$\int_0^T \sum_{i=1}^n \int \left[\frac{\phi_i}{w_i} - F_i(\phi_i) \right] dt \quad (2)$$

where symbol I denotes the step function of the following form:

$$\int (x) = \frac{x+|x|}{2x}; \quad \int (0) = 1 \quad (3)$$

$F_i(\varphi_i)$ is the function which is equal to 1 for the continuous operations and to 0 for intermittent operations.

Then, if any ϕ_i during the continuous operation becomes less than w_i the integral will have a negative value and the entire expression (2) will transform to zero. The criterion also transforms to zero, thus indicating the inadmissibility of delay during the progress of a continuous operation.

Finally, the technical and economic criterion has the form:

$$Q = \left[\int_0^T \phi dt - \int_0^T f(\varphi)(w - \phi) dt, C \right] \int \left\{ \sum_{i=1}^n \left[\frac{\phi_i}{w_i} - F_i(\varphi_i) \right] dt \right\} \quad (4)$$

The Problem of Dynamic Programming

For automatic control it is essential to have information regarding the volume of work φ_i for each of the furnaces, and also information regarding the expected functions h_i for the engagement of the auxiliaries. The finding of the latter can be made by the prediction of the condensed graph on the basis of the *a posteriori* distribution of the periods of duration. In this way the last experience of the operation of the furnace is taken into account. This problem may be solved by the known methods of extrapolation of random sequences. Since the subsequent programming does not change the condensed graph, then its extrapolation may be considered as a problem independent of the programming problem.

In the first approximation it is possible to be guided by mathematical expectations for the duration periods of the melting operation. In the second approximation it is necessary to take into account the effect of the elapsed duration periods on the subsequent duration periods. For this it is necessary to have the information regarding the instants of time for the beginning and the end of expired periods, which will be received from the corresponding monitors. On the basis of this same information, by the method of extrapolation, the current values of φ_i will also be calculated, as the initial conditions for programming. In the first stage it is assumed that there is a limitation to the calculation only of rate φ_i , averaged out according to the current periods.

The continuous determination of the optimum controlling actions in the process of automatic control is the essence of dynamic programming. In the given case this is the determination of the maximum loading and the finding of the optimum distribution of auxiliaries, in the process of control of the work on an open-hearth furnace plant.

The qualitative analysis of the working of the furnace and casting bays makes possible the construction of a system of differential equations for the operation of furnaces. The right side of each one of the equations represents a function, which depends on the volume of work completed at a given instant of time and on the availability of the auxiliaries for the furnace. Each one of these functions is constructed in such a way that it transforms to zero, if on a given furnace there is a lack of auxiliaries, and transforms to w_i , if the furnace at any given distribution is served normally by auxiliaries.

Eqn (5) *

Under which conditions:

$$Z_{i,k} \geq 0; Z_{i,1} + Z_{i,2} + \dots + Z_{i,n} \leq k_i \\ i = 1, 2, \dots, e; \quad k = 1, 2, \dots, n \quad (6)$$

here: $g_k(\varphi_k)$ is the 'charging function' (equal to 1 during the charging period and equal to 0 during the rest of the time); w_k is the instantaneous output of the k th furnace, $h_i, k(\varphi)$ is the engagement function of the auxiliary of the i type on the k th furnace, $Z_{i,k}$ is the number of units of auxiliaries of the i type transferred to the k th furnace, n is the number of furnaces; and e is the number of types of the auxiliaries.

For the furnace runaway coefficients k_i remain constant during the entire operation, but for the casting bay coefficients k_p, k_q , corresponding to the casting capacities, change and are calculated as the number of free auxiliaries, idling between two neighbouring positions. Here p and q are indices of the casting capacities.

The system of differential equations (5) together with the constraints (6) and the criterion for the quality of programming (4) give an approximate mathematical description of the organizational conditions of operation of furnaces on an open-hearth plant.

Without considering, for the present, the method itself for dynamic optimum programming for the distribution of capacities, the basic problem is formulated as follows:

* Eqn (5):

$$\begin{aligned} \phi_1 &= w_1 \left[1 - g_1(\varphi_1) \int (Z_{r,2} - 1) \right] \left\{ \prod_{i=1}^e \int [Z_{i,1} - h_{i,1}(\varphi_1)] + \int [Z_{r,1} - g(\varphi_1) - 1] \right\} \\ \phi_2 &= w_2 \left[1 - g_2(\varphi_2) \int (Z_{r,1} - 1) \right] \left[1 - g_2(\varphi_2) \int (Z_{r,3} - 1) \right] \left\{ \prod_{i=1}^e \int [Z_{i,2} - h_{i,2}(\varphi_2)] + \int [Z_{r,2} - g_2(\varphi_2) - 1] \right\} \\ \phi_{n-1} &= w_{n-1} \left[1 - g_{n-1}(\varphi_{n-1}) \int (Z_{r,n-2} - 1) \right] \left[1 - g_{n-1}(\varphi_{n-1}) \int (Z_{r,n} - 1) \right] \\ &\quad \times \left\{ \prod_{i=1}^e \int [Z_{i,n-1} - h_{i,n-1}(\varphi_{n-1})] + \int [Z_{r,n-1} - g_{n-1}(\varphi_{n-1}) - 1] \right\}; \\ \phi_n &= w_n \left[1 - g_n(\varphi_n) \int (Z_{r,n-1} - 1) \right] \left\{ \prod_{i=1}^e \int [Z_{i,n} - h_{i,n}(\varphi_n)] + \int [Z_{r,n} - g_n(\varphi_n) - 1] \right\} \end{aligned} \quad (5)$$

Given the known initial values of variables $\varphi_1, \dots, \varphi_n$ and given the previously calculated engagement functions $g_{i,k}(\varphi)$ and $h_{i,k}(\varphi)$ it is necessary to find the distribution of the auxiliaries so that the expected value of criterion (4) attains a maximum.

In addition to this basic problem for the automatic dispatch control it is necessary to calculate beforehand the engagement functions, and after the solution of the basic problem to allocate the auxiliary capacities of each type to individual furnaces. In the first stage only the basic problem will be solved by the computer. The engagement function will be fixed on the basis of the mean statistical data, but the actual distribution of capacities will be made by the operators of sections in accordance with the calculated matrix of distribution $\|Z_{i,k}\|$.

The essence of the developed algorithm consists of the following:

The initial values to variables φ_i are assigned, which (values) correspond to the actual state of operations on the plant, and some permissible distribution of capacities are chosen, $Z_{i,k}$ ($i = 1, \dots, e$; $k = 1, \dots, n$), i.e. a distribution which satisfies condition (6). Under these conditions, generally speaking, a number of furnaces will 'run', and a number of them will 'stand idle'. System (5) is integrated up to that instant of time when the current period on any of the running furnaces is terminated. (The integration of the right sides in a piecewise constant form is carried out very simply.) Then, having selected a new permissible distribution, the integration of the system, etc., is continued. This gives the possibility of extrapolating for the operation of the plant according to assigned initial conditions for some succession of distributions, $Z_{i,k}(n)$ ($n = 1, 2, \dots, N$), where n is the number of the integration steps. By assigning various possible successions of distributions and by evaluating the efficiency of operation of the plant by formula (4), where the integration spreads over N steps of the process, the most efficient sequence $Z^*_{i,k}(n)$ is selected. However, there is no sense in completely realizing this sequence, since the conditions of the plant may change and this solution may prove to be unworkable. It is sufficient to extract as the command for execution only the first step of this process, i.e. the distribution $Z^*_{i,k}(1)$. The next distribution is already better determined for the next step by programming on the basis of the precise initial data, etc.

The consideration of the equivalence of mechanisms of the same type makes it possible for the distribution to be limited by those mechanisms which resulted in unfavourable coincidence.

The Analysis of Phase Trajectories

In the study of the dynamics of programming for the operation of a plant in the phase space of variables $\varphi_1, \dots, \varphi_n$ one should limit oneself to the case of two furnaces, which makes possible the consideration on a phase plane (Figure 3).

On the axes of coordinates the volumes of work done in the first and second furnace are plotted. A definite band on the phase plane corresponds to each melting period. Thus, the plane reflects the condensed diagram of the melting operation.

As a result of the periodicity of the condensed melting operation, the network of periods on the phase plane repeats itself periodically along each axis. At the intersection of the bands corresponding to those periods, for which the same type of auxiliaries is required, rectangles are formed, which correspond to such states of the plant, for which a necessity is

created for the doubling of the quantity of the auxiliary capacities. In a case when the same auxiliaries are required for two furnaces, the indicated rectangles correspond to the situations in which one of the furnaces is bound to stand idle in order to give priority to the other furnace. These regions are shaded on Figure 3. In other situations both furnaces may be 'running'.

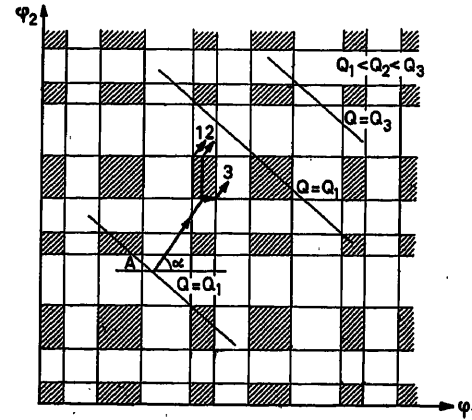


Figure 3. Phase plane

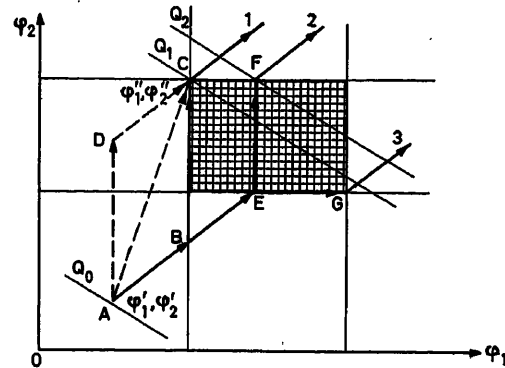


Figure 4. Phase diagram for the separation of furnaces

An arbitrary point A is taken and the possible variants of motion of the describing point are considered, for which maximum instantaneous output of the pair of furnaces is reached, i.e.

$$\max(c_1\dot{\varphi}_1 + c_2\dot{\varphi}_2)_2$$

If the describing point is found outside the shaded zone the furnaces are fully provided for and they will operate at maximum rates w_1 and w_2 . Under these conditions $d\varphi_2/d\varphi_1 = \tan g\alpha = w_2/w_1$. The levels of equal volume of production intersect with the maximum rate and the output of the pair of furnaces is equal to $c_1w_1 + c_2w_2$.

In passing the barriers (of the shaded regions) the picture changes. One of the furnaces is bound to stand idle whilst the other may run at full rate, w_1 or w_2 . The phase trajectory is shown to consist of straight line segments parallel to the axes of coordinates, and the maximum instantaneous output for these segments is equal to either c_1w_1 or c_2w_2 .

If the given operation is continuous, for example, on the first furnace, then the passage through the barrier along trajectory 2 (Figure 4) is not permissible, since the latter corresponds to the stoppage of the first furnace during the completion of the period considered.

In view of the linearity of the chosen criterion regarding the rates of melting, its increment does not depend on the transfer path if the initial and final points of the phase trajectories coincide in pairs; and this is what gives the possibility of representing the process as an intermittent one, which facilitates the solution of the problem of programming. The final result by means of interpolation is obtained in the form of a continuous graph.

Evaluation of the Efficiency of Programming for a Homogeneous Node Process

The presence of the nodes in the optimum phase trajectory does not allow the solution by the known variational methods. The choice of the most suitable directions at the nodes represents the most difficult problem in the given case. The locally optimal trajectory represents a node process which is shown diagrammatically in Figure 5.

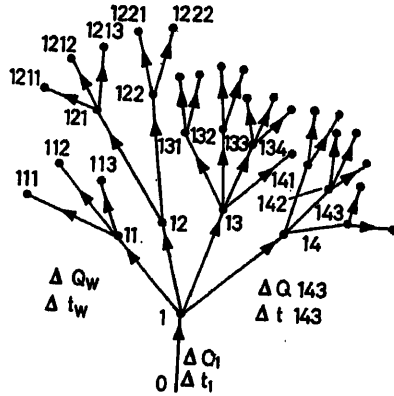


Figure 5. Sketch of the node process

The principle of numbering the nodes is clear from the figure. During the transition from the initial point to a given point the time as well as the functional (4) receive definite increments. The problem of dynamic programming is reduced to the finding of such a direction at the next node that it ensures maximum value for the increment of functional (4) during the further optimum progress of the process.

If the process is random, then the functional (4) is usually previously unknown for all the nodes, and it is assumed that only the probable distribution law for its increments at each point along all the directions is given. The precise value of Q may be practically measured usefully only when following the corresponding branch of the process.

Due to the absence of a mathematical description it is impossible to determine the true optimum direction at a node, since it would be necessary for this to analyse the process along an infinite interval. Therefore, it is necessary to limit the analysis to a finite number of steps and to speak only of the maximum value for the mathematical expectation in the increment of functional Q for a single step a_n in the extrapolation with n steps.

With an increase in the number of steps of prediction this value gradually increases, and by virtue of its limited nature it tends towards a definite limit ΔQ_{\max} .

The efficiency of dynamic programming for a node process is determined by the value of a_n and the determination of the

number n required for the realization of the given efficiency is of practical importance. It is better to speak about the determination of the number of comparable variants N , which when the random process is stationary is directly connected with n . From the value of N it is possible to assess the time required for analysis at the nodes using computers.

In the description of the computation method for the convergence of the process of almost optimum solution, the case of the stationary process, which is the most important from a practical point of view, is considered.

It is assumed that at all the nodes the number of branches is the same, equal to m , which shall be called the node order of the node process and $F(x)$ the distribution function for the increment in functional Q , obtained for one step along any of the directions, and $W(x) = F'(x)$ the corresponding distribution density. The distribution function of the increment in Q after k steps shall be denoted by $F_k(x)$, if after the first arbitrary step a path is selected, which gives the maximum increment ΔQ_k after the remaining $k-1$ step.

The distribution function $\psi(x)$ for the maximum possible increment after k steps, providing that the most suitable path is selected, may be obtained by raising $F_k(x)$ to the m th power. Indeed, if ξ_i is the increment of the functional Q along the i th direction, then according to the multiplication rule for the probabilities of independent events

$$\psi(x) = P(\xi_1 \leq x) P(\xi_2 \leq x) \dots P(\xi_n \leq x) = F_k^m(x) \quad (7)$$

In accordance with the above definition the value of a_n is determined by the formula:

$$a_n = \frac{1}{n} \int_{-\infty}^{\infty} x dF_k^n(x) \quad (8)$$

In view of the homogeneity of the node process one can determine the distribution density $W_n(x)$ of the increment of the functional as a result of the realization of n arbitrary steps, as n is the multiple composition of distribution density $W(x)$:

$$W_n(x) = \underbrace{W(x) * W(x) * \dots * W(x)}_n \quad (9)$$

The distribution function $F_n(x)$ is determined as

$$\int_{-\infty}^x W_n(\xi) d\xi$$

and the probability distribution function of the maximum increment in functional Q_n for n steps:

$$\psi_m(x) = \left[\int_{-\infty}^x W_n(\xi) d\xi \right]^{m^n} \quad (10)$$

and

$$a_m(n) = \frac{1}{n} \int_{-\infty}^{\infty} x d \left[\int_{-\infty}^x W_n(\xi) d\xi \right]^{m^n} \quad (11)$$

An asymptotic expression is found for $a_m(n)$ in the case of a Gaussian node process, i.e. when

$$W(x) = \frac{1}{\sigma \sqrt{2\pi}} e^{-\frac{(x-a)^2}{2\sigma^2}} \quad (12)$$

where a and σ are the corresponding mathematical expectations and the variance of the increment of functional Q for a single

step. In this case n the multiple composition $W_n(x)$, as is known, is the normal distribution law with mathematical expectation na for variances $n\sigma^2$, i.e.

$$W_n(x) = \frac{1}{\sigma\sqrt{2\pi n}} e^{-\frac{(x-na)^2}{2n\sigma^2}} \quad (13)$$

and

$$F_n(x) = \frac{1}{2} \left[1 + \Phi\left(\frac{x-na}{\sqrt{n}\sigma}\right) \right]^{m^n} \quad (14)$$

where $\Phi(x)$ is the integral of probabilities

$$\Phi(x) = \sqrt{\frac{2}{\pi}} \int_0^x e^{-\frac{\xi^2}{2}} d\xi \quad (15)$$

According to formula (11) one obtains:

$$\begin{aligned} a_m(n) &= \frac{1}{n 2^{m^n}} \int_{-\infty}^{\infty} x d \left[1 + \Phi\left(\frac{x-na}{\sqrt{n}\sigma}\right) \right]^{m^n} \\ &= \frac{1}{n 2^{m^n}} \int_{-\infty}^{\infty} (\sqrt{n}\sigma x + na) d [1 + \Phi(x)]^{m^n} \\ &= a + \sigma J_m(n) \end{aligned} \quad (16)$$

here

$$\begin{aligned} J_m(n) &= \frac{1}{\sqrt{n} 2^{m^n}} \int_{-\infty}^{\infty} x d [1 + \Phi(x)]^{m^n} \\ &= \frac{m^n}{\sqrt{n} 2^{m^n}} \int_{-\infty}^{\infty} x [1 + \Phi(x)]^{m^n-1} \Phi'(x) dx \\ &= \frac{m^n}{\sqrt{n\pi} 2^{m^n} - \frac{1}{2}} \int_{-\infty}^{\infty} x [1 + \Phi(x)]^{m^n-1} e^{-\frac{x^2}{2}} dx \end{aligned} \quad (17)$$

After partial integration and the corresponding substitution of variables one obtains:

$$\begin{aligned} \tau_m(n) &= \frac{m^n(m^n-1) \sqrt{\frac{n}{m-2}}}{2\pi\sqrt{n}} \\ &\int_{-\infty}^{\infty} \left\{ \frac{1}{2} [1 + \Phi(x\sqrt{m^n-2}) e^{-x^2}] \right\} dx \end{aligned} \quad (18)$$

It is denoted that

$$m^n - 2 = N, \quad J_m \left[\frac{e_n(N+2)}{e_n m} \right] = J_m(N)$$

$$A(N) = \int_{-\infty}^{\infty} \varphi^N(x) dx \quad (19)$$

where

$$\varphi = \frac{1}{2} [1 + \Phi(x\sqrt{N})] e^{-x^2} \quad (20)$$

Expression (18) assumes the form:

$$J_m(N) = \frac{(N+2)(N+1)\sqrt{N}\sqrt{\ln m}}{2\pi\sqrt{\ln(N+2)}} A(N) \quad (21)$$

The main part of integral (21) is found by the steepest descent method, then (21) is re-written in the form:

$$\begin{aligned} J_m(N) &= \frac{(N+2)(N+1)N^{\frac{1}{2}(N+1)}\sqrt{\ln m}}{\sqrt{\ln(N+2)}(2\pi)^{\frac{1}{2}(N+2)}(2Z_0)^N} \\ &\exp \left[-\frac{1}{2} N(N+2)Z_0^2 \right] B(N) \end{aligned} \quad (22)$$

here Z_0 is the point of maximum function $\ln \varphi$, and

$$B(N) = \sqrt{\frac{\pi}{N[(N+2)Z_0^2+1]}} + O\left(\frac{1}{N}\right) \quad (23)$$

As a result the calculation of $J_m(N)$ was reduced to the finding of the asymptotic expression for Z_0 as a function of N .

By carrying out simple conversions and by using certain asymptotic formulae it is possible to show that

$$\begin{aligned} J_m(N) &= \left(\frac{2}{e}\right)^2 \sqrt{2\pi \ln m} \\ &\sqrt{1 - \frac{\ln(16\pi \ln N)}{1+2\ln N} \left[1 + O\left(\frac{\ln \ln N}{\ln^2 N}\right) \right]} \end{aligned} \quad (24)$$

Knowing $J_m(N)$ it is easy to determine the mean increment for functional Q for one step by formula

$$a_m(N) = a + \sigma J_m(N),$$

which is equivalent to formula (16).

By analysing the obtained result it is noted that

$$\Delta Q_{\max} = \lim_{N \rightarrow \infty} [a_m(N) - a] = \sigma \left(\frac{2}{e}\right)^2 \sqrt{2\pi \ln m} \quad (25)$$

and that therefore, the gain secured as a result of ideal planning is proportional to the variance of the random node process and to the square root of the logarithm of the node order. The relationship between the corresponding gain, obtained as a result of dynamic programming, and the number of compared variants is expressed by the following formula:

$$q(N) = \frac{a_m(N) - a}{\Delta Q_{\max}} = \sqrt{1 - \frac{\ln(16\pi \ln N)}{1+2\ln N} \left[1 + O\left(\frac{\ln \ln N}{\ln^2 N}\right) \right]} \quad (26)$$

The graph for this relationship is given in Figure 6. From this graph it is seen that in order to obtain more than 60 per cent of the maximum respective gain it is sufficient to select on each step the best of the 10^4 variants.

The number of steps, corresponding to the number of variants, is easily determined by the formula

$$n = \frac{\ln N}{\ln m} \quad (27)$$

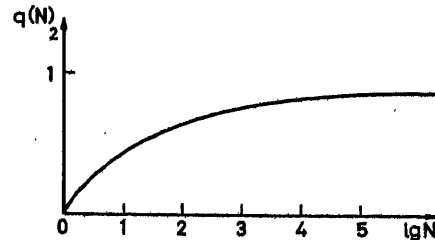


Figure 6. Relationship between the relative gain, obtained as a result of dynamic planning, and the number of comparable variants

Conclusions

Dynamic programming for the operation of an open-hearth steel-making plant by means of a computer on the basis of the described method makes possible the acceleration of the melting operation in furnaces, under which conditions the possibility of decreasing the duration of the melting operation is determined by the so-called 'condensed' graph.

The minimum durations of the condensed graphs are de-

termined by the maximum employment of auxiliaries for furnaces, although under these conditions certain types of auxiliaries may or may not be completely utilized.

On the basis of the given work technical requirements for a computer were established, which is essential for the realization of dynamic programming.

Reference

- ¹ SMIRNOV, V. I. *Course in Advanced Mathematics*, Vol. III, Pt 2

DISCUSSION

W. G. WRIGHT, *Canadian General Electric Co., Ontario, Canada*

From superficial observation of an oxygen-improved open-hearth furnace I have not formed the impression that auxiliaries are limiting. Consequently, I wish to ask what particular auxiliary is the bottleneck and what melt rates are achieved on the furnace.

M. KOROBKO and YU. SAMOILENKO, *in reply*

It is possible that with the operation of one open-hearth furnace using oxygen blast into the flame when the remaining furnaces operate without any forced blast or with only oxygen restricted forced blast into the flame, especially in a new shop not equipped with forced blast ducts, the expense of previous improvement and innovations will not cause the bottleneck phenomenon.

However, the question is not only about the blowing of the oxygen into the flame but, for example, about the already collected melt factors in the shop or about the blowing of the molten metal in the furnace with oxygen or with compressed air, which more than halves the duration of the melts.

In this case the physical space at the furnace front was limited (the charging cars could not be accommodated) as well as in the entire teeming bay. The space for the preparation of the rolling stocks, the ladles, the slag basins, the rolling stocks with the charge, the stripping, the settling routes, etc., was also restricted. With such a high output of steel per square metre of the furnace floor, as is practical in the U.S.S.R., bottlenecks due to these conditions occur more easily than in other countries.

G. A. SHIPPEY, *Brown-Boveri, Baden, Switzerland*

At the conclusion of this paper, the authors state that the work carried out made it possible to frame specifications for a suitable computer. Was a special-purpose or general-purpose machine foreseen for this dynamic programming problem, or could the authors give any idea of the speed and capacity required for the computing task which seems, from the paper, to be very formidable?

M. KOROBKO and YU. SAMOILENKO, *in reply*

A general-purpose computer may be used for dynamic planning. As follows from the paper, the higher the speed of the chosen computer, the better optimality is obtained. However, with the increase of the optimality of the solutions above 65 per cent the required high speed increases very much (see *Figure 6* in the paper).

To attain an optimality of 65 per cent in planning the operation of the shop with 10-12 furnaces the computer speed should be of the order of 20,000 addition type operations per sec and the capacity of the operational memory of 60,000 numbers.

This evaluation was carried out without accounting for the possibility of choosing the most favourable variants by the criterion of the permissible deviation from a certain phase trajectory, having a minimum relative length of the sectors crossing the 'prohibited' regions in the space. The finding of this factor is similar to the finding of the optimal phase trajectory with the absence of the bottlenecks and is accomplished by the non-linear programming method in the $2n$ -dimensional space where n is the dimensionality of the phase space.

J. P. CLYNE, *B.I.S.R.A., 140, Battersea Park Road, London, S.W. 1*

(1) Had you considered the cost of eliminating the bottleneck, i.e. if in fact the auxiliaries formed the limitation would it be worth while to run the main plant fully and provide more auxiliary plant?

(2) Does the installation studied cast ingots for rolling into sheet or plate? The latter often requires large variations in the size of ingot required, and this makes a prediction, based on a statistical approach of auxiliary loading, more difficult.

M. KOROBKO and YU. SAMOILENKO, *in reply*

(1) At the time of posing this problem we carried out time studies of the operation of open-hearth shops in various plants and determined the character and the values of various delays in the open-hearth furnace melts. After processing the data it was determined that the expenses for the installation of the dynamic planning system will be compensated within 1-2 years.

In our paper we mentioned only the most efficient means of forcing the melts, i.e. blowing the metal in the furnace with oxygen. From the practice of the plants in the U.S.S.R. and U.S.A. it is known that this technique reduces by more than half the duration of the melt. However, it is known that in the U.S.S.R., as well as in some other countries during the past 15-20 years, the output of the steel per square metre of the furnace floor, as a result of the improvements of the process (replacement of acid roofs by basic ones, transfer to natural gas heating, enrichment of the blast with oxygen, increase of the melting charge weight, etc.), has already increased approximately $1\frac{1}{2}$ times. The auxiliaries as well as the transportation carrying capacity, however, remained practically the same as before, resulting in the bottleneck. Partial increase in the auxiliaries results only in the removal of the bottlenecks to other regions.

It should be kept in mind that the accomplishment of the dynamic planning is preceded by the installation of the automatic control system for the melting and thermal process and the computer centralized control of the portions of the shop. Therefore, the dynamic planning which optimizes the operation of the shop will be just as important even when the bottleneck now shifts to the technological process in the furnaces. If the delays are fully removed on account of the optimal planning, the optimal phase trajectory takes the shape of a straight line, i.e. the optimal operating conditions of the shop will be determined by the algorithm for controlling the melting technological process and the operation of auxiliary shop sectors. The latter is solved by the linear programming methods. However, according to our studies of the operating conditions with a forced regime in the open-hearth shop, this is unlikely.

(2) High output shops such as those figured in the study do not as a rule cast steel of a wide range of grades and assortments. This is performed in what we may call 'small batch' shops.

The preliminary automation of the melting technological process control helps to carry out the orders in accordance with the required grades of steel. The automatic control of the shop sectors, including the preparation of the rolling stocks with the moulds, chosen according to the requirements of the production department, helps the dynamic planning by reducing the factors determined by the statistical laws.

Automation of Heavy Forging

J. G. WISTREICH and A. TOMLINSON

Summary

The incentives for automating open-die forging are considerable because of the low utilization and high operating cost of present equipment together with the difficulty of obtaining suitably skilled labour for the arduous working conditions. Despite the large variety of shapes and sizes made by forging, it has been found possible to build up production procedures from a comparatively small number of basic operations simple enough to be encoded into standard programmes. Also, application of the principles of geometric similarity permits the use of such programmes for producing geometrically similar shapes irrespective of absolute size, effecting great economy in programming.

A full description of the development of the BISRA experimental 200 t Forge embodying these principles of automatic control is given. Apart from reducing the number of forgemen required, automation offers the benefit of greater accuracy of working, and it is estimated that by means of programme control with automatic tool changing, output can be raised by between two and fivefold. Some of the control features developed on the experimental forge have already been applied on industrial plant. Planning is now in progress for a fully automated 800 t forge along the lines of the BISRA experimental Forge.

Sommaire

Dans ce rapport, les auteurs décrivent le processus de forgeage à outillage appliqué à la formation d'engrenage des lingots et à la production unitaire ou en petite série de pièces forgées à complexités de profils variés. L'analyse des opérations et des éléments conduit à l'examen des commandes automatiques et des programmations. Les lignes générales d'une théorie de programmation sont présentées, ainsi que le niveau nécessaire de précision dans les opérations, en fonction des tolérances finales et des variations inévitables des caractéristiques du stock.

On décrit la Forge Expérimentale BISRA, et plus particulièrement ses équipements de mesure, de commande et de programmation. Les opérations et les performances: taux de production, qualité et coût du produit de cette installation sont comparées à celles d'une forge non-automatique. On donne un aperçu général sur les développements commerciaux et les tendances futures.

A la fin, les auteurs examinent les possibilités d'une coordination automatique de toutes les opérations d'un atelier de forge.

Zusammenfassung

Der Anreiz, Gesenkschmieden zu automatisieren, ist wegen der geringen Ausnutzung und der hohen Betriebskosten der gegenwärtigen Ausrüstung groß; obendrein besteht die Schwierigkeit, hinreichend ausgebildete Arbeitskräfte für die anstrengenden Arbeitsbedingungen zu finden. Trotz der großen Zahl der erzeugten Profile und Abmessungen sind Fertigungsverfahren möglich, die von einer verhältnismäßig kleinen Anzahl von Grundoperationen ausgehen, die einfach genug sind, um sie in ein Normalprogramm zu übersetzen. Mit Hilfe der geometrischen Ähnlichkeitssätze kann man derartige Programme auch zur Herstellung von geometrisch ähnlichen Profilen verschiedener Abmessungen benutzen, was den Programmieraufwand wesentlich verringert.

Es folgt die Beschreibung einer bei BISRA (British Iron and Steel Research Association) entwickelten 200-t-Schmiedepresse, bei der diese Regelungsprinzipien angewendet wurden. Abgesehen von der Freisetzung von Arbeitskräften bringt die Automatisierung den Vorteil größerer Bearbeitungsgenauigkeit mit sich. Es wird angenommen, daß die Programmsteuerung mit selbsttätigem Werkzeugwechsel die Produktion auf das Zwei- bis Fünffache steigert. Einige in der Versuchs-

schmiede gewonnenen regelungstechnischen Erkenntnisse wurden bereits industriell eingesetzt. Die augenblicklichen Anstrengungen gelten dem Bau einer vollautomatischen 800-t-Schmiedepresse.

Introduction

The present paper is concerned with what is usually termed 'plain-tool' or 'open-die' forging. The products of open-die forging comprise a great variety of shapes and not only is the variety great, but the products are usually made in small numbers, or even singly. Consequently the production of a forge is of a jobbing or batch type and the present-day equipment, though notable for its versatility, is deficient in reproducibility of operations and precision of control. Because of these features, open-die forging might well be regarded, at first sight, as unsuitable for automation. The incentives for automating open-die forging are, however, great. First, the provision of labour presents a problem which has of late become acute, because of the requirement of a high degree of skill and of arduous working conditions arising from the manipulation of metal at temperatures in the range of 800°–1200°C. Secondly, production costs are high because massive and costly equipment is employed and a prodigious amount of fuel is consumed in raising the metal to, and maintaining it within, the range of operating temperatures. The utilization of the equipment and of the heat content of the workpiece is low, moreover, because of shortcomings in the control of the operations. Thirdly, with an increasing proportion of forgings having to be made to ever more stringent specifications and from increasingly costly materials, operational procedures of higher reproducibility and closer dimensional control of the finished piece are desirable in the interests of materials economy.

For these reasons, the Forging Committee of the British Iron and Steel Research Association (BISRA) embarked in 1956 on a programme of research and development aimed at automation of heavy forging, which has been centred round an experimental forge installed in the Association's Metal Working Laboratory in Sheffield. The work, which has been mapped out in stages, beginning with mechanization and culminating in fully automatic operation, is approaching completion. Throughout, the commercial development of intermediate attainments was envisaged and has been accomplished, spurred on by the industry's extensive activities in plant renewal and modernization dominating the late 1950's and the present period.

In what follows the basic concepts and main directions of the development are outlined, followed by a description of the experimental forge and an indication of industrial developments stemming from it.

Forging Procedure

The principal function of open-die forging is to produce a shape of specified dimensions from ingot or rolled stock. In general, the workpiece is substantially larger than the shaping

tools, which move in one plane only to exert a squeezing action on a small portion of the workpiece. Thus the piece has to be repositioned between squeezes and the operation as a whole is stepwise in character. Moreover, only a limited depth of squeezing can be accomplished in one go, owing to metallurgical and geometrical limitations, so that the shape and dimensions of the piece are changed only gradually, as the result of a large number of small steps.

At present, the procedure is decided by the operator as he goes along, but experience has shown that some sequences of operation are more efficacious in transforming the shape than others, and notwithstanding the great variety of product shapes, there exist recognizable patterns of procedure which are followed by all forgemasters in broad outline, even though they differ as to their details. For example, when making a round bar, the most widely practised method, based on the use of flat tools, consists of first making a square oblong the side of which is approximately equal to the diameter of the round, and then rounding it in stages by successively transforming it into an octagon, hexadecagon, etc. Likewise, when making collared shafts, rolls, and similar rounds, composed of cylinders of various diameters, it is usual first to make a rough round to the largest diameter present in the finished piece and then to reduce the diameter of designated portions along the length.

In this way one can build up sequences of procedures for shapes of increasing complexity. The point to note is that some of the component procedures, or phases, recur in the making of many forgings. In particular, the initial cogging down of an ingot to a square or round oblong is the common starting stage for nearly all forgings. If this and similar phases can be standardized, then the great variety of forgings is, in effect, lessened from the point of view of working procedure. It seems natural therefore to develop a classification of shapes based on the various component phases of working procedure, in the interests of production planning and as a prerequisite of automated production. One such classification¹ adopted in Russian forges, is illustrated in *Figure 1*.

Each phase, e.g. the cogging of a square bar, rounding, etc., consists of a sequence of passes which present a new pair of faces to the tools. The passes in turn are made up of squeezes and inbetween repositioning movements of the stock. So far, the magnitude of these and the order in which they are taken are found to vary not only from forge to forge, but also from operator to operator, so much so that considerable differences are encountered in the time taken to accomplish the job. A lessening of these differences through a standardization of procedure is desirable, in the interests of conservation of heat and

higher plant productivity; it would also contribute to economy of programming in an automated forge. Until recently, this was not practicable since none of the equipment was fitted with precise means of controlling movement, both squeeze and repositioning being judged by eye. However, even when the plant is equipped with precision controls, the task of standardization is very much more complicated than in the case of shaping by machining. This is so because squeezing results in a change of dimensions and shape in all three directions, so that the deformation only partly conforms to the shape and movement of the squeezing tools.

The movement of the metal in the region acted upon by the tools is the consequence of plastic deformation, and a good deal of the work of the authors and their colleagues has had to be devoted to the investigation of the relationships between squeeze, elongation, and spread, from which one could compute the material dimensional changes of the piece consequent upon a squeeze².

Fortunately (from the point of view of programming), it has been discovered that these relationships are essentially geometrical in character, and factors such as the absolute dimensions, the metallurgical state of the piece, surface conditions of tools and stock, temperature, etc., play a secondary role and can be ignored for practical purposes.

Thus, for example, in the case of the squeezing of a rectangular prism by means of plane tools, when the changes of shape and the ruling dimensions are as depicted in *Figure 2*, the dimensional changes that matter are related as follows:

$$h_0 w_0 l_0 = h_1 w_1 l_1$$

which defines the condition of unchanged volume, that characterizes plastic deformation, and

$$\frac{w_1}{w_0} = \left(\frac{h_0}{h_1}\right)^s \text{ and } \frac{l_1}{l_0} = \left(\frac{h_0}{h_1}\right)^{1-s}$$

where s is an empirical factor depending very largely on the ratio b/w_0 (the inter-squeeze movement over the initial width of the stock, and termed the bite ratio, θ), as evidenced by *Figure 3*. Thus it has been possible to define the rules about deformation in terms of ratios of ruling dimensions before and after squeezing. By prescribing the fractional changes of the squeezed dimension (h) and the inter-squeeze movement (b) termed bite, it is possible to predict in advance the dimensional path followed during forging. This finding is, of course, of cardinal importance from the point of automatic control, because it implies that one can dispense with continual scanning of the entire shape of the piece, and substitute for it computation.

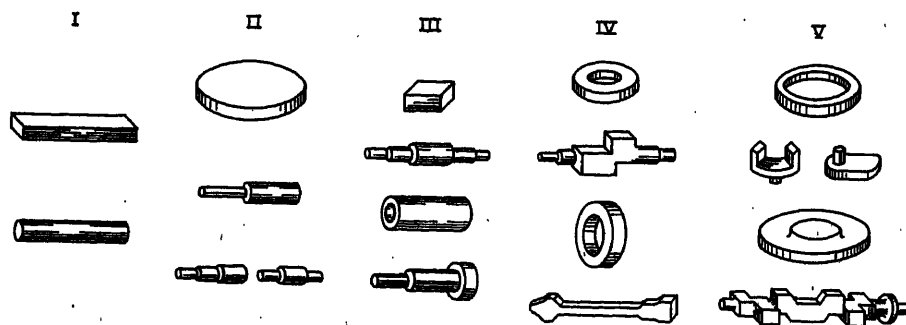


Figure 1. Classification of 600-3,000 tons press forgings according to complexity of forging operation

In principle, even when squeeze and bite are prescribed, there is still an infinity of choices of the sequence of these. However, a theoretical, computer-backed study⁸ of this problem has brought to light important new principles regarding the best choice of sequences. As yet, these have been determined quantitatively only for the cogging of square bars, but the underlying principles are valid in other procedures also and work in this direction is continuing. The investigation to date has brought

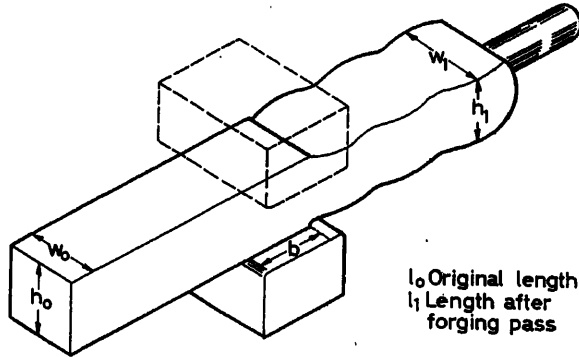


Figure 2. Dimensions in forging

to light that the fastest procedures for cogging square bars are those in which the ratios h_0/h_1 and b/w_0 for each pass are kept constant; in other words, the squeeze and bite are changed after each pass in constant proportion to the current height and width of the piece, whence the term 'simple proportional schedule' has been coined for this procedure.

The values chosen for the two constants of proportion depend on several factors, viz., the initial dimensions of the piece, the amount of cogging required, and the load capacity and performance characteristics of the plant. The constants can be calculated from a set of formulae or found from a graph of the type depicted in Figure 4. In practice there are two further factors which need to be taken into consideration in the choice of best schedule. First, a limit may have to be imposed on the depth of squeeze, i.e. on the value of h_0/h_1 , because of the danger of cracking, for

example, when forging high speed tool steel; and second, the available load capacity of the press usually restricts the choice of schedule. The range of schedules which are admissible within this bound can be determined from calculations of load, the results of which may be superimposed on the type of graph in Figure 4 in the form of a series of contours of constant load.

From what has been said about the principles underlying rational forging methods it is apparent that not only is it feasible

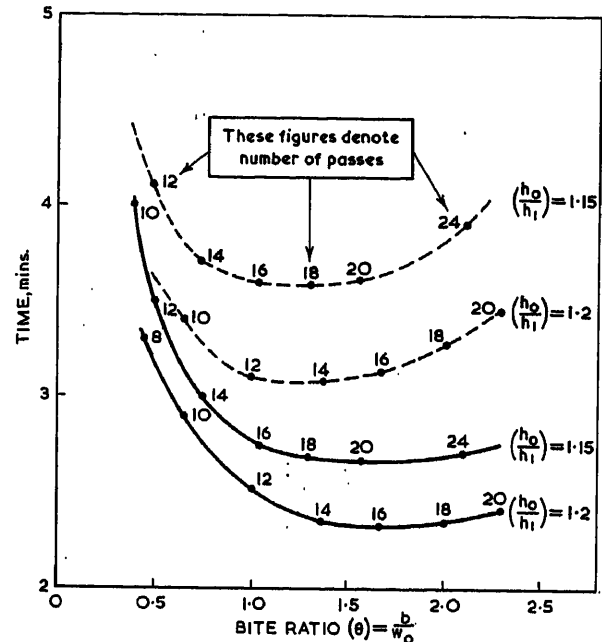


Figure 4. Time taken by proportional schedules

Parameters

Dimensions of stock = 24 in. \times 24 in. \times 48 in.

Forging ratio (final length/original length) = 3

Press and manipulator performance allows eighty-four 1 in. penetrations/min

The full curves have an inter-pass manipulation time of 3 sec
The dashed curves have an inter-pass manipulation time of 6 sec

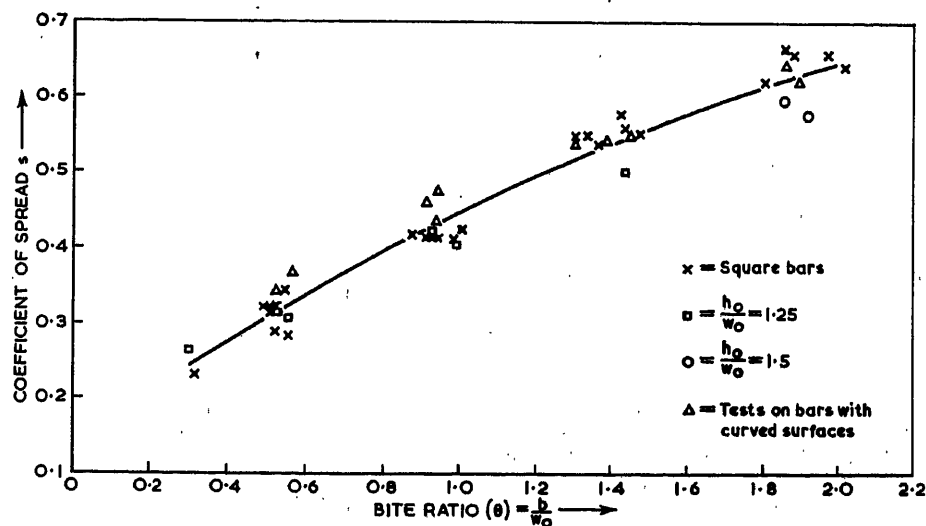


Figure 3. Relation between coefficient of spread and bite ratio: $s = 0.14 + 0.35(b/w_0) - 0.054(b/w_0)^2$

to standardize procedures to a degree which involves only a modicum of monitoring of the dimensions of the workpiece, but also the information content of the programming instructions can be compressed to a marked extent, thereby enabling it to be performed by comparatively simple equipment.

Forging Plant

The plant employed in open-die forging has evolved from the blacksmith's forge. Indeed, the smaller forgings are still worked under hammers and manhandled by means of tongs. Since with hammers the penetration of the piece depends not only on the energy content of the blow but also on the resistance of the metal to deformation, there exists no simple means of controlling the squeeze and for this reason the possibility of automating hammer forging has not been explored. The forging press, on the other hand, can be made to squeeze the piece by any prescribed amount with a high degree of precision.

The larger forgings have to be handled mechanically. Forging manipulators, which hold the workpiece cantilever-fashion, are rapidly displacing the older method of gripping by means of a 'Porter' (balancing) bar suspended from a crane and freely swinging during movement. At present, manipulator drivers are seated on the vehicle and command a different angle of vision from that of the press operator. Difficulties of coordination inherent in this arrangement are responsible for a slow working pace. This is accentuated by the fact that conventional manipulators move much more slowly than the press tools. Marking off lengths and gauging of diameter is done manually, by means of large steel rules and callipers. Owing to the heat radiated by the stock, this is a strenuous job and accuracy suffers in consequence.

Until quite recently, none of the equipment was fitted with any precise means of controlling the position of press tools and manipulator gear. Both press and manipulator movements were judged by eye and controlled by servo-controls of the position-velocity type. It is not surprising that there has been little consistency of working.

The most important requirement for the purpose of automation is to control the movements of press tools and of manipulator in such a way that the spatial positions of the workpiece and tools are defined in advance with precision. Ideally, then, the controls should be of the position-position type. Further, since the forging operations consist of sequences of single squeezes alternating with repositioning of the stock, proper timing of press and manipulator actions for sequencing purposes is necessary. In this connection it has become apparent that the manipulator action must be markedly speeded up if full advantage is to be taken of the speed of action of modern presses.

Again, complicated forgings require the use of more than one type of tool. At present, tool changing is time consuming and done with primitive mechanical aids. Automatic tool changing is desirable in the interests of speed of operation. Finally, instruments or other devices are required to mark off dimensions and to monitor the shape during forging.

The BISRA Experimental Forge

A 200 ton press was available in the Metal Working Laboratory prior to the commencement of the work on automation of forging. The normal method of working with the press was initially similar to the prevailing industrial practice and is illus-

trated in *Figure 5*, the crew consisting of a press driver, two tongmen for steadying the workpiece and two levermen for moving it between squeezes. The programme of mechanization decided upon called for a speeding up of the slow operation of the press by detailed attention to the hydraulic circuit, and for the development of a remote control for regulating accurately the amount of squeeze. To eliminate hand manipulation it was decided to build a rail-mounted manipulator. *Figure 6* shows a view of the experimental forge after mechanization, with the equipment under the control of one operative.



Figure 5. Original method of working on the experimental forge

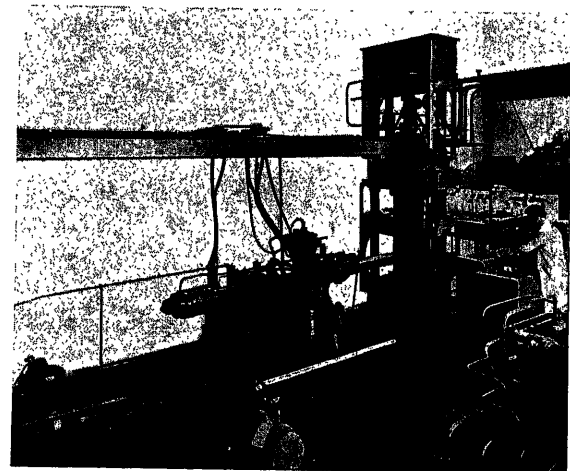


Figure 6. Experimental forge after mechanization

The results of the mechanization programme are reported elsewhere^{4, 5} and it suffices here to comment briefly on these developments. The press is driven by means of a direct-pump, oil-hydraulic system. Modifications to the hydraulic circuit were required, principally, to speed up the slow approach and return speeds of the crosshead and to eliminate delays occurring in the press cycle. As a result of the hydraulic modifications, crosshead velocities in free approach and return were increased to 12 in./sec, and in actual squeezing any value up to 3 in./sec could be selected. The stroke cycle time for a heavy cogging stroke was cut from just over 3 sec to approx. 1 sec.

AUTOMATION OF HEAVY FORGING

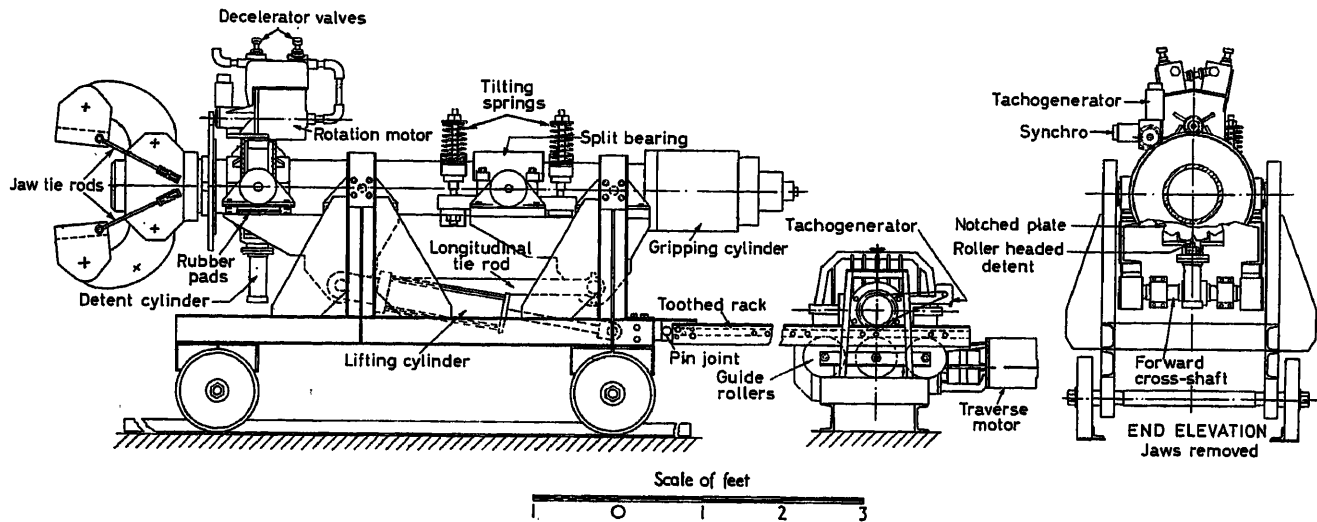


Figure 7. Forging manipulator—general arrangement

For regulating the movement of the press tool an electrical position control was developed to link up with the solenoid-operated pilot valve. The control comprises a polarized relay connected between the sliders of two potential dividers, an input potential divider in the control desk, and an output potential divider driven by the movement of the press crosshead. Displacement of one or other of the potential dividers causes the relay to operate in the appropriate sense and its contacts complete the control circuit *via* further relays to operate the solenoid pilot valve, and hence the press crosshead, to restore the original balanced condition. In practice, there are two input potential dividers in the control desk, one for setting the lower limit of crosshead movement and one for the upper limit. In tests using the position control, the finished sizes of forged pieces have been within $\pm 1/32$ in. of the nominal size which normally lies in the 3–6 in. range. During any one pass, moreover, where the control setting remains unchanged, the variation from stroke to stroke is less than $\pm 1/64$ in.

A survey of existing commercially available manipulators had disclosed that they were of two general types: rail-mounted and mobile. The latter were usually required also to serve the functions of furnace charging and shop transport. Additionally, existing manipulators were, without exception, slow and cumbersome with the result that the output of the forging plant was reduced. As one of the ultimate objectives was the development of an integrated forging plant, the design and manufacture of a rail-bound manipulator was decided upon, solely to be used for handling forgings at the press, with its performance matched to that of the press. A design sketch of the manipulator is shown in Figure 7.

For simplicity, the machine was designed to impart only the three essential manipulative motions, namely rotational, vertical and longitudinal. The motions were equipped with remote position controls similar to that of the press and provision was made for automatic sequencing of the crosshead movement of the press and the longitudinal and rotational movement of the manipulator, the method being to use the relays which control any motion to start the next motion.

Automatic tool changing devices for the top and bottom press platens were designed and manufactured later, to facilitate

the development of programmed working techniques. These are illustrated in Figure 8. The unit for the bottom tool consists of a motorized turntable situated on the press platen and within the press columns. It is equipped with four tools—flat, swage, and two knifing tools for marking-out purposes. Top tool changing is achieved by a slide containing two tools—flat and swage respectively—the slide being positioned by a pneumatic cylinder with an electrically actuated valve. The required tools are selected remotely and the turntable and slide are accurately locked in position by means of detent mechanisms.

The method of working at the stage of development just described, i.e. with the various motions under remote position control, was to preset the pressing and manipulative actions required during a forging pass by means of dials on the control desk coupled to the input potential dividers. At the end of the

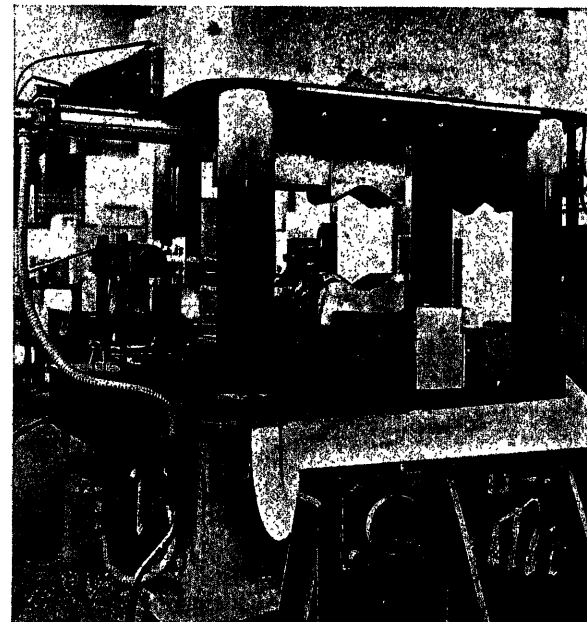


Figure 8. Top and bottom tool changers

forging pass, the equipment was stopped, the control dials were appropriately reset and the forging was automatically repositioned for the next pass after which automatic forging was once again recommenced.

Programme Control

The method of working just outlined constitutes a rudimentary form of programme control, each programme consisting of a single forging pass, with the operator inserting a new programme at the end of a pass. The first programming unit proper which was constructed for investigating automatic forging, was a logical extension of this and consisted of a means of presetting and automatically resetting the controls of the press and manipulator after each pass by means of dials mounted on a series of identical panels, one for each forging pass⁶.

Such a system suffers from two disadvantages. First, a prodigious amount of work has to be expended on the preparation of the complete programme, a separate one of which would be required for each size of forging. Secondly, small differences in the response of the material to the imposed deformation (differences in the amount of spread due to variations of temperature or surface) might accumulate and render the programme inapplicable.

As the result of the previously mentioned theoretical analysis of forging methods, from which emerged the novel method of forging by proportional schedules, it seemed feasible to develop a more versatile and flexible control system by continually monitoring the transverse dimensions of the piece during forging and from this controlling the press and manipulator motions. The scheme envisaged had three particular advantages. First, it would enable the amount of input information required by the controller to be greatly reduced as compared with the earlier control unit. Then, it would make for greater consistency in the degree of deformation as the result of feedback about current dimensions of the stock. Finally, it would make for more rapid change of shape.

Also essential to programme control of complex forgings is a means of monitoring the current length of the stock. This is required because at certain stages forging has to be confined between accurate lengthwise limits as, for instance, when only a portion of the length requires reducing to form a journal. The position of the manipulator carriage forms a convenient point of reference to one limit; the other limit has to be referred to the end of the forging away from the manipulator and additional means must be provided for monitoring this.

In order to facilitate the introduction of programmed working into industrial plant at the earliest date it was decided to engineer the new control unit as a commercial prototype, in collaboration with the Brookhirst Igranic Electrical Co. who had already marketed a successful form of press position control. This control was based on a digital system and it was decided to adapt this method for the programme control unit in view of the degree of accuracy required with complex shaped forgings.

Particular features of the system are the use of a static switching technique, employing transistors of germanium PNP type; also printed circuit boards had already been developed for the various logic functions required for the press control, including adder, comparator and selector units, and these were capable of providing much of the computation and storage facilities of the programme control, thus reducing the type of



Figure 9. Proportional programme control unit

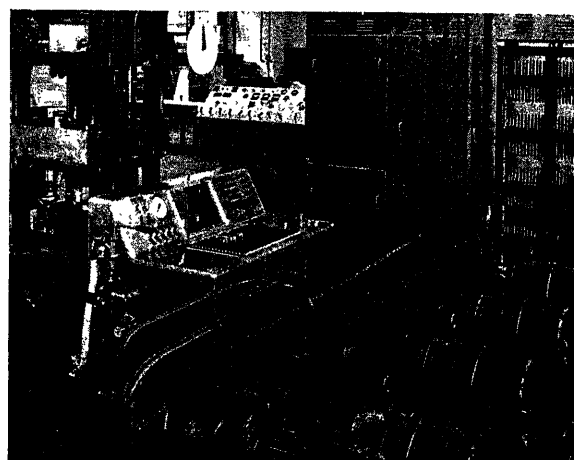


Figure 10. Panel of control desk

board required to be specially developed for the new programming unit.

A view of the control unit is shown in *Figure 9*. Input information for the programme is charged to the control unit from a plug board situated in the operating desk, a view of which is given in *Figure 10*. Mounted on the desk panel are the buttons for operating the press main pumps, zeroing facilities for the position control of the press tools and a switch for selection of manual or automatic control. With the manual position selected, operation of the equipment is from the various buttons and dials on the right-hand horizontal panel, while in the automatic position, operation is controlled from the plug board.

Modifications to Earlier Position Controls

The provision of facilities for monitoring the height and length of the forging necessitated some changes to the press and manipulator traverse position controls to fit in with the digital programming unit. For the press, the commercially developed form of digital position control was fitted. The control principles are the same as in the earlier scheme but the crosshead position is indicated by a signal from a digital positional indicator which

is compared with a digital number corresponding to the desired stopping position and stored in the programme control unit. The digital positional indicator (digitizer) consists of a number of discs geared together on which a digital pattern is inserted. In the present case the code used is pure binary, the pattern being made up of magnetic segments. The body of the digitizer is mounted on the top entablature of the press, with a steel cable coupled to the movable crosshead at one end and wound over a pulley at the digitizer end. The geared discs rotate with the pulley and provide a digital indication of crosshead movement.

For monitoring the length of the forging, the cables of similar digitizers are coupled to the manipulator carriage and to the free end of the forging for providing the control unit with a digital reference of both ends of the forging. The degree of accuracy obtained from the original simple on-off control system for the longitudinal traverse was reasonable for the forging of plain shapes but for complex shapes, comprising portions of different size and shape, greater accuracy was required and a modified form of on-off control was installed by the Brookhirst Igranic Electrical Co. and Towler Brothers (Patent) Ltd. collaborating in the development. The essential feature of the new control is that the manipulator is accelerated to maximum speed under full power as before, but at a predetermined distance from the stop position, the hydraulic motor is switched from maximum power to one giving a creep velocity, from which the final switch-off provides accurate and consistent positioning.

Features of the Proportional Programming Unit

A diagram of the general scheme is given in *Figure 11*. Protection of equipment and forging is obtained by adopting a sequential mode of operation, in which no new motion is

initiated until signals have passed indicating that all previous motions have been completed satisfactorily. The particular advantages to forging brought about by this form of working are that it provides a means of automatically stopping the programme in the event of equipment misbehaviour and also it ensures that the forging does not foul the press tools during inter-pass repositioning of the stock.

The computational facilities for regulating the press squeeze and manipulator bite are as shown in the block diagrams in *Figures 12, 13 and 14*. The method of controlling the lower limit of the press movement involves detection of the current height of the stock at the beginning of each pass. This is done by feeding the positional signal from the press digitizer to a monitoring device, which is instructed to store the particular value measured at the instant the top tool makes contact with the stock. The contact is detected by means of the change of velocity of the crosshead which occurs when the free fall of the crosshead is terminated and squeezing begins. For this purpose the output change of the velocity transducer is used. Using this value of the current height and the stored value of the fractional height reduction (specified as part of the input information), the control system computes, instantaneously, the required height for completion of squeezing and the press is instructed to squeeze to this height. Thereafter, the computed value is stored in the system for controlling further squeezes of this pass. Eventually the stage in forging is reached when the computed value of the height for the next pass is less than the specified finishing size; when this occurs the system overrides the computation and inserts the appropriate finishing dimension. The system can be set to select two, three or four consecutive passes at the final dimension, depending on the accuracy of shape required.

The upper limit of press tool movement is obtained by ad-

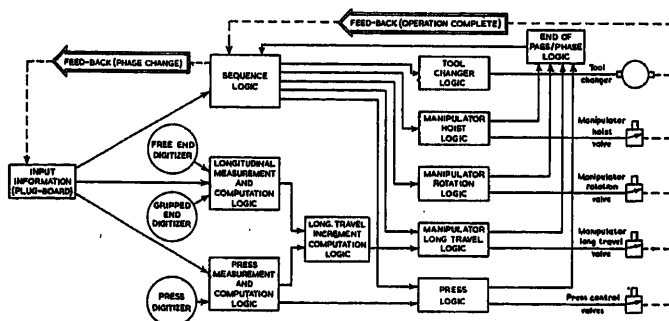


Figure 11. Proportional programme control—overall scheme

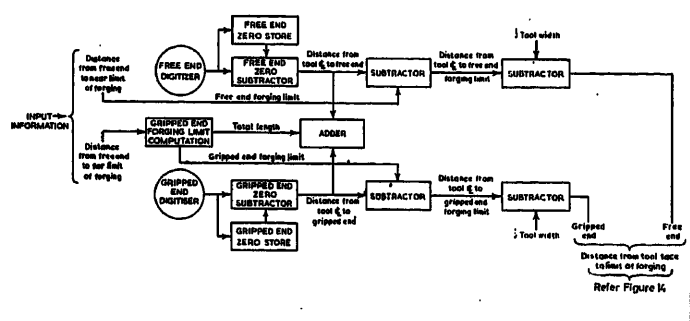


Figure 13. Programme control—longitudinal measurement

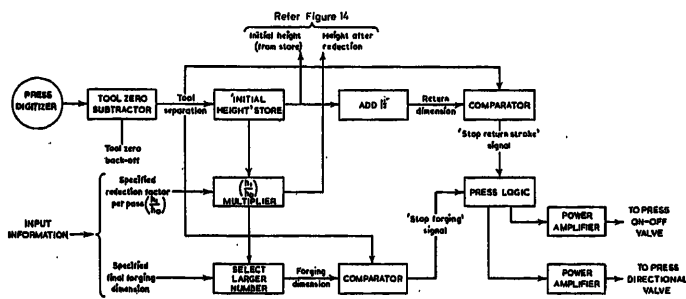


Figure 12. Press squeeze—measurement and computation

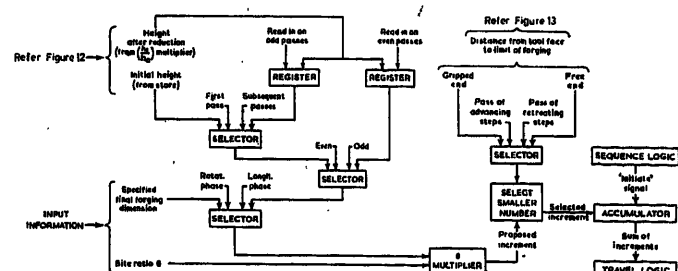


Figure 14. Manipulator longitudinal travel increment computation

ding a fixed amount to the initial height measured at the beginning of the pass. The addition is for the purpose of providing satisfactory clearance for re-positioning of the stock between squeezes and in the present instance the actual value decided upon is $1\frac{1}{2}$ in.

The incremental movement of the manipulator between squeezes is regulated in similar fashion to the press control. In this case, in accordance with the requirements of proportional scheduling, the computed value of the lower limit of press motion of a particular pass is stored for use in computing the manipulator movement in the succeeding pass. This is because the final height in one pass becomes the starting width in the next and the manipulator advance is a fixed fraction of this width. The required manipulator step movement is computed from the product of the width and the specified value of bite ratio (an item of input information) and is automatically signalled to the manipulator after each squeeze. Actually, two stores are provided, one for even passes and one for odd passes. One store is charged during the even pass with the information to be used in the next odd pass, after which the information is cancelled to permit storage of new information. The second store operates in the alternate sense. Special arrangements have to be made for the first pass because no previous measurement of width is available. As the workpiece at this stage has the same height and width (in the case of blooms and square ingots), it is arranged, in this particular case, for the measured value of initial height to be stored as the width. In the succeeding passes the system reverts to the normal scheme. In cases where forging is confined to accurate lengthwise limits and a further step of the computed amount would take the manipulator outside one or other of these limits, the control is equipped to override the computed step and insert the appropriate smaller increment.

The system of manipulator control includes facilities for the manipulator to work in both directions, i.e. both retreating from the press and in an advancing direction.

Input Information

For the purpose of charging the controller with the appropriate input information, forging procedures have been broken down into phases, each comprising a group of forging passes. For example, the pass sequence used in squaring down ingots represents one phase, converting the square to an octagon is another phase and similarly for the various planishing (finishing) and knifing procedures. The items of input information for each phase comprise both the essential actions of the press and manipulator during forging and also the ancillary tasks of repositioning between passes, tool selection, etc. Using proportional programming, the essential press and manipulative actions can be defined by one value each of fractional squeeze and proportional bite, plus the finishing details of size required and number of finishing passes. Similarly, input information regarding the repositioning actions can be reduced to a minimum in view of their repetitive nature; for example, the rotational sequences include the simple 90° sequence for square cogging, alternative 90° and 45° as sometimes used in swage cogging and $22\frac{1}{2}^\circ$ for making finished round sections.

The plugboard system used for the experimental equipment, illustrated in *Figure 10*, is in effect a matrix which proves an easy means of modifying programmes as required during experimental testing. The matrix enables up to 30 phases to be programmed,

with a total of 84 digits available for setting up input information for each phase, the appropriate digits selected by insertion of diode plugs. A 30-way uniselector energizes one input busbar at a time, and at the completion of a phase a signal is fed to the uniselector to advance it to the next phase and set in the new information. For industrial installations, input information would preferably be charged to the control unit by means of a punched card system.

Performance of Experimental Forge

As the result of the introduction of remote position controls of both press and manipulator motions, the dimensional precision of forgings has been greatly enhanced. Not only are the overall finished dimensions now accurate to $\pm 1/32$ in. in cross section and $\pm 1/8$ in. longitudinally, but the shape is so good that final planishing of billets is invariably accomplished in two or three passes, whereas in conventional forging practice planishing takes up as much as $1/5$ to $1/3$ of the total number of passes.

Prior to the development of the controls considerable doubts were expressed by forgemasters as to whether programmed forging would be at all feasible, considering the inevitable surface and temperature variations from piece to piece. However, experiments in which these variations were deliberately exaggerated, either by letting the piece cool appreciably before the commencement of forging or to scale heavily by holding in the furnace for longer than necessary, have shown conclusively that these fears have been unfounded.

As regards the stepping up of output rate, comparisons with industrial conditions are rather difficult on account of the small capacity of the experimental forge, and because the work of programming complex forgings is not yet complete. Using the simple programming control unit already referred to⁶, an 8 in. square ingot has been formed into a piece consisting of three portions of square cross section measuring 20 in. \times 6 in. square, 20 in. \times 4 in. square, and 20 in. \times 3 in. square; the forging procedure comprised 23 passes and was completed in $4\frac{1}{2}$ min, about half the time that a skilled forging crew would require on a fast operating hammer. Using the data recorded in this and similar tests and comparing them with industrial practice it has been estimated that the use of programming and automatic tool changing on industrial presses would raise the output rate between two and fivefold, depending on the complexity of the forging.

Discussion

The automation of open-die forging, as it is being realized by us on the experimental forge of the British Iron & Steel Research Association in Sheffield, rests on three cardinal principles: (1) Notwithstanding the enormous variety of shapes and sizes of forgings and the very high content of skill in making them by present-day methods, it is a fact that the individual forging procedures have a few common basic elements. Thus it is possible to construct a great variety of procedures from a comparatively small number of elements ('phases'), e.g. cogging, rounding, knifing, etc., which are sufficiently simple to be encoded into standard programmes. (2) The nature of deformation in forging is such that those aspects of it which govern the change of shape can be expressed in terms of para-

meters embodying the principle of geometrical similarity. Thus geometrically similar changes of shape can be accomplished by similar programmes irrespective of the absolute dimensions, which results in a great economy of programming. (3) Inherent in the novel forging procedures developed from first principles (simple proportional schedules) is a means of intermittent monitoring of the current dimensions of the piece, which affords a measure of primary feedback of information about the forging and of automatic adjustment of the programme in the light of this.

The development is not yet complete in that the efficacy of various procedures for programme-forging of complex shapes needs to be evaluated experimentally and some minor modifications to the control schemes are still to be tested. However, the mechanization developments and the control schemes already installed in the experimental plant have established, in a convincing manner, the practicability of forging by programme control.

It was stated at the outset that this development was planned in several stages in the interests of easier introduction into industrial practice. Since the demonstration of remote position control of the experimental press in 1956, commercial equipment of this type has been marketed by a number of companies, and

more than a dozen presses in Great Britain and others on the Continent and in the U.S.A. have already been converted to this system of control, with a similar number now on order. In one plant recently installed the manipulator is remotely controlled by the press driver; it is also fitted with means for automatic sequencing of manipulator and press actions which, it is intended, will be put into operation in the near future. Planning is in progress for the construction of a fully automated 800 ton forge, on the lines of the BISRA experimental forge.

References

- 1 KHRZHANOVSKI, S. N. *Planning of Forges*. Ch. VI, Pt 21; 1952. Berlin; Verl. Technik. (German trans.)
- 2 TOMLINSON, A., and STRINGER, J. D. Spread and elongation in flat tool forging. *J. Iron St. Inst.* 193 (Oct. 1959) 157-162
- 3 WISTREICH, J. G., and SHUTT, A. Theoretical analysis of bloom and billet forging. *J. Iron St. Inst.* 193 (Oct. 1959) 163-176
- 4 GREEN, J. I. T., and STRINGER, J. D. Experimental semi-automatic forge. *J. Iron St. Inst.* 193 (1959) 231-237
- 5 CHANT, L. J., and SEREDYNSKI, F. The application of remote position control to forge. *J. Iron St. Inst.* 191 (Feb. 1959) 185-187
- 6 BAKER, P. N., and TOMLINSON, A. Programmed manipulator cuts forging time. *Control Engineering* (Sept. 1960) 194-196

DISCUSSION

Author's Opening Remarks

Of all processes in operation in the steel industry, forging appears least suited to automation since it is essentially engaged on small batch and even jobbing production of a great variety of products. The incentives for automation are, however, great, firstly because of a shortage of labour to operate forges, secondly in order to increase the low productivity of the costly equipment involved, and thirdly, in the interests of materials economy through better control of the process, particularly in the future when increasingly costly alloy steels will dominate the production schedule.

Technically, control of the forging process is difficult, because of its stepwise character and the fact that plastic deformation in it is subject to direct control in only one of the three dimensions in which it occurs. The development of automatic forging has rested on a three-pronged attack of this problem.

In the first place, it has been necessary to bring about improvements in the forging plant. Manipulation has had to be speeded up in order that the manipulator may match the high-speed performance of the modern forging press. Next, manual control of presses and manipulators has had to be replaced by remote electrically actuated controls which would lend themselves to automatic sequential operation and programming. And here, since the requirement in forging is to control the movements of press tools and manipulator jaws in such a way that the spatial positions of the workpieces are defined with precision at all times, control of the position-position type have been adopted. The development has been pioneered on an experimental plant situated in the B.I.S.R.A. laboratories in Sheffield. The various controls have been tested and proved some time ago, and are now commercially available, likewise the principles of design of the high-speed manipulator have been adopted by a leading manufacturer of forging manipulators in his latest models.

The second line of attack has involved an analysis of production techniques. This has revealed that, the great variety of products notwithstanding, forging procedure can be broken down into a number of elements which recur in the making of all forgings, so that it has proved possible to compound programmes for a variety of products,

from a small number of standard operational phase. One of these, for example, which recurs in the majority of forging operations used in the making of oblong pieces is the initial conversion of the square or octagonal ingot into a square billet, into a round one—and so on.

With this analysis there exists then a basis for programming, but it is admittedly a cumbersome one because separate programmes would still have to be written for each size of product and of ingot, thus necessitating a very large library of programmes, and since each forging comprises a very large number of elementary steps of successive squeezes and in-between manipulations, most programmes would be very lengthy indeed. This problem gave rise to the third prong of our attack, in which we engaged on a fundamental study of the deformation in forging, in order to discover the rules according to which the shape and dimensions of the workpiece change as it is squeezed. In the course of this work we discovered short cuts, the nature of which would take too long to explain here, but is described in References 2 and 3 of the paper.

With the aid of these short cuts we have found it possible to devise new methods of forging which are more efficient than traditional ones and, furthermore, which can be defined by remarkably few bits of information. As a result the task of programming has become enormously simplified, as is explained in the paper.

In the experimental forge, programming is done by means of a plug board which has a capacity of up to 30 phases with a total of 84 digits and for a particular job takes about 10 min to set up. For industrial installations we envisage feeding the control system by means of punched cards instead.

And now, what has been the performance of the equipment? Prior to its development, doubts were expressed by forgemasters whether programmed forging would be reproducible. In fact, as the result of the adoption of the newly discovered procedures, we have achieved the desired reproducibility as between one piece and another, and indeed have been able to forge to dimensional accuracies previously unheard of. As these are stated in the paper I shall not take up time now by detailing them. Most important of all, as a result of cutting out delays associated with manual operations and of the streamlining

of the actual squeezing sequence, we have greatly speeded up forging. We reckon to raise the rate of production between two and fivefold, depending on the complexity of the forging, and we are able to eliminate some or even all the reheats normally found indispensable. In this way important fuel savings accrue from the adoption of automatic forging quite apart from the increased productivity of the forging press. The experimental equipment has been in operation for some 6-9 months in its final phase, and although we have had many teething troubles, particularly with hydraulic components, there is no reason to doubt the high reliability of the final equipment, some of which has in fact already been installed industrially and performs very well.

K. J. BUTLER, *Pilkington Brothers Ltd., St. Helens, Lancashire, England*

To what extent has the equipment described been utilized in production? What is the 'down-time' required for maintenance of control equipment and how does this compare with time saved by improved press utilization?

J. G. WISTREICH, *in reply*

I did mention that this was an experimental plant and when I said that this method had been in use for 18 months, I meant experimentally. It is not used on production work but some of the features which we have developed there, such as the remote position control of the presses and the position control of the manipulator, are in fact already used on industrial equipment.

Down-time, I understand, on one of the most recent installations in the U.S.A. is appreciably less than 5 per cent (due to breakdown of equipment).

Our main problems on the control side have been with the hydraulics. As you may notice in the paper, the cycle time is fairly short—some of the operations have to be performed quickly and delay times are particularly critical. We have had to spend some time finding the right sort of hydraulic valves but we have solved these problems and these valves are commercially available.

L. LANDON GOODMAN, *E.D.A., 2 Savoy Hill, London, W.C. 2, England*

Would the author please amplify his remarks on tool changing, and also give his thoughts on the design of the forging operation *ab initio*?

J. G. WISTREICH, *in reply*

It is undoubtedly true that when you look at the forging process afresh, you itch to redesign it before doing anything in the way of control. We have in fact done both. Described in the paper is an effort to render automatic the existing type of equipment but we have studied the problem of how to design a press and the manipulating equipment to render the whole business of control, and for that matter the whole design of equipment, simpler and more efficient. I hope that we will publish the results of this very shortly—in fact, one of the press manufacturers in Great Britain is going to make use of the work we have done to build these new types of presses.

Tool changing certainly causes considerable delay in conventional forges. *Figure 8* in the paper shows the rotating table with tools that may be indexed into position. This was one of the things which we did right at the start to enable us to use different types of tool. The lower tools are on a turntable—we did not repeat this system for the upper tool and there are simply two tools side by side which can just be slid in or out.

This is not a practical proposition for industrial presses because of the space taken up, but a different system of tool changing, where in fact you have an auxiliary mechanism by the side of the press with a magazine of tools so that you can withdraw the present tools to put those required in, is something that we have also designed. In fact there are machines which approximate to that in operation. In the U.S.A., there are so-called 'tool manipulators' which perform that function to some extent.

The main change in the development which we have tackled on the lines of the new type of press has been in using a double motion action, because, as you realize, in the conventional press the axis of the ingot moves up and down as it is being squeezed from one side only. This in turn complicates the manipulation. By squeezing it simultaneously from both sides, one can maintain the axis all the time along one line and this is one of the basic features which we have built into the new design.

The other thing is that the manipulator itself is generally too slow. Modern presses can operate at 120-150 strokes/min. No manipulator of conventional design on the market can possibly keep up with this, and modern presses at the moment are being seriously under-used. We struck out for an entirely radical design, borrowing ideas from the blooming mill where, in effect, the manipulator is part of the whole machine. We have developed a suitable design which is attached to the press structure and advances the ingot at a speed commensurate with the speed that a modern press is capable of into or out of the machine as required.

Automation in a Steel Works with Special Reference to the Use of Digital Computers for Production Scheduling and Information Transmission

S. E. HERSOM and R. G. MASSEY

Summary

The paper gives a description of a steel plant and a brief account of the degree of automatic control at present installed in each of the manufacturing processes, e.g. coke ovens, sinter plant, blast furnaces, steel plant, hot strip mill and cold reduction mills. An overall control of the production processes is to be achieved by an automatic information handling and production control system using modern electronic equipment. The basic inputs to the system are the customers' orders and the limitations of plant capacity and processing sequence. From these, the system derives production schedules which, in turn, are translated into detailed instructions for automatic transmission to the men or machines in the works. The results of the manufacturing processes are transmitted into the system, automatically where possible or else by men inserting the information on keyboards. This information is used by the system to bring its records up to date and to amend its previous schedules where necessary. As a by-product of this system, information is available for other purposes such as production reports, cost accounting, sales statistics and process investigations. Owing to the magnitude of the operation the system is being installed in stages.

Sommaire

Cette étude donne une description de l'installation d'une aciérie ainsi qu'un exposé abrégé de l'étendue des commandes automatiques actuellement installées dans chacun des procédés de fabrication, par exemple: les cokeries, l'installation d'agglomération, les hauts fourneaux, l'aciérie, le laminoir de bande à chaud et les laminoirs de réduction à froid. Le commande générale des procédés de production sera réalisée par un système automatique de traitement des données et de contrôle de production, employant de l'équipement électronique moderne. Les renseignements fondamentaux, fournis au système sont les commandes des clients et les limitations de capacité de l'installation et l'ordre des séquences. De ces renseignements, le système dérive des programmes de production, lesquels, à leur tour, sont traduits en instructions détaillées pour transmission automatique au personnel ou aux machines dans les ateliers. Les résultats des procédés de fabrication sont transmis dans le système, automatiquement où cela est possible, ou bien par l'introduction manuelle des renseignements sur claviers. Ces renseignements sont employés par le système pour tenir ses archives à jour et pour modifier au besoin ses programmes précédents. Comme sous-produit de ce système, des renseignements sont disponibles à d'autres fins tels que rapports de production, comptabilité des prix de revient, statistique des ventes et recherche sur les procédés. A cause de l'importance du projet, le système est installé par tranches.

Zusammenfassung

Der Aufsatz beschreibt ein Hüttenwerk und gibt eine kurze Darstellung über den derzeitigen Stand der Regelung in Kokerei, Sinteranlage, Hochofen, Stahlwerk, Warmbandwalzwerk und Kaltbandwalzwerk. Eine umfassende Steuerung (Regelung) der Produktionsstätten läßt sich durch automatische Datenverarbeitung und Produktionskontrolle mit Hilfe moderner elektronischer Anlagen erreichen.

Die grundlegenden Eingangsdaten für die Steuereinrichtung sind die Aufträge der Kunden, die Leistungsgrenzen der Anlage und die Reihenfolge des Produktionsablaufes. Daraus leitet das Steuersystem die Produktionsprogramme ab, die der Reihe nach in Form von ausführlichen Vorschriften an das Personal oder an die Maschinen in den Betrieben automatisch übermittelt werden. Die Fabrikationsergebnisse werden wiederum dem Steuersystem zugeführt, wenn möglich automatisch, sonst von Hand durch Eingeben der Informationen über ein Tastfeld. Die Steuereinrichtung benötigt die Informationen, um die Aufzeichnungen auf dem laufenden zu halten und, falls nötig, die vorhergehenden Programme zu berichtigen. Als Nebenprodukt liefert diese Steuereinrichtung andere Informationen, wie Produktionsberichte, Kostenberechnungen, Verkaufsstatistik und Verfahrensuntersuchungen. Wegen ihres Umfanges wird die Steuereinrichtung stufenweise installiert.

Introduction

Automation is the modern phase in the evolutionary process of industrial control technique and the steel industry is taking a leading part in its development. The industry has, in the past, made use of available instrumentation to bring its various manufacturing processes under semi- or fully-automatic control and, on the administrative side, it has used punched card equipment, calculators and computers to mechanize office procedures. The present trend in the industry has been towards the integration of process and administrative procedures.

The Works

The new Spencer Works of Richard Thomas and Baldwins at Newport in South Wales, which went into production in 1962, continues this trend. Built on a green field site, every opportunity has been taken to apply the modern process control and data processing techniques throughout. *Figure 1* is a schematic diagram of the works showing the processes through which the basic raw materials of iron ore, coal and limestone pass during their conversion into wide steel strip, the main product of the works. These processes differ greatly one from the other. *Table 1* shows, for each process, its main function, the basic operations which are needed to achieve this function and the degree of automatic control and instrumentation being employed at each stage.

Of the main processes, there are only a few which are truly continuous, the sinter plant being the major one in this category. Some processes are a mixture of continuous and batch operation, for example, the coke ovens in which the gas production is continuous while the coal charging and coke discharging are by

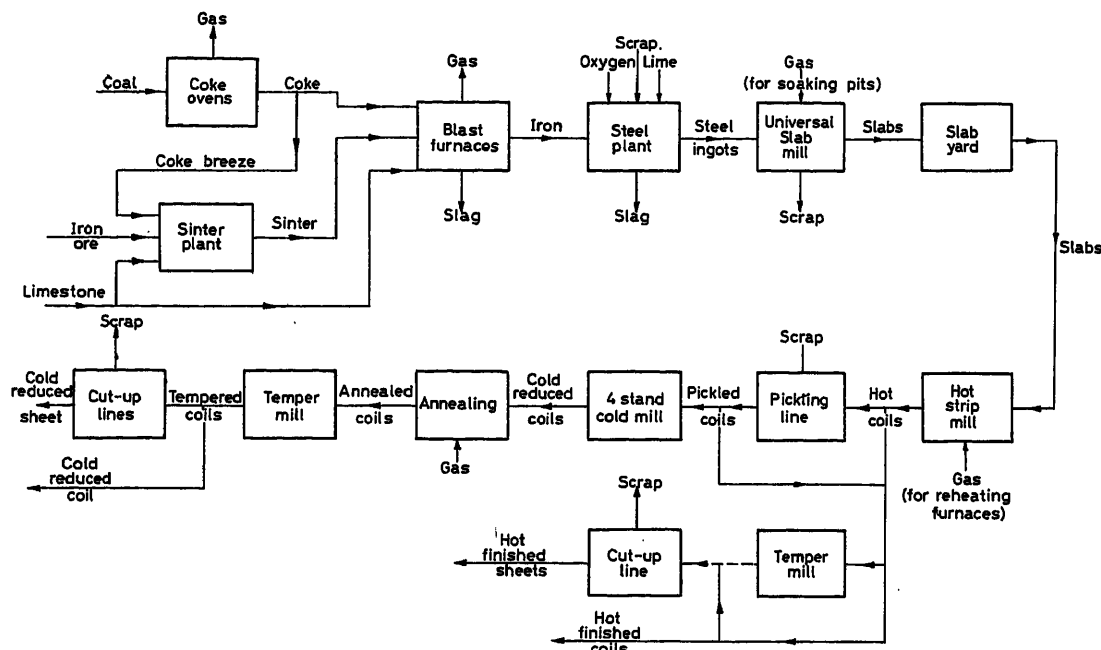


Figure 1. Main processes of the works

batches, but the majority operate on individual items of material. In the 'heavy end' of the Works, from the input of raw materials up to the production of ingots in the steel plant, automation has so far been mainly associated with the mechanical handling of heavy loads of material between the processes and monitoring this material flow. The handling of materials has been expedited by automatic tipping of railway trucks and the extensive use of conveyor belt systems and the monitoring is by automatic weighbridges and belt weighers. The processes themselves are in general well instrumented, for example, the sinter plant is fully provided with automatic weigh feeders and other devices to obtain the required balance between the various ingredients of the mix, and further automatic controls ensure the correct processing. On other processes the instrumentation is not always adequate for providing fully automatic control. For instance, in a blast furnace the direct measurement of the state of the material inside has so far proved impossible and control has to rely upon inferential measurements such as top gas compositions and temperature, blast pressure, and wall temperature. The lack of sensors and the long through-times of the material (many hours) make the control problem, and especially the optimization of a furnace, very difficult. Secondly, in many cases the instrumentation has to be backed up by comprehensive laboratory analyses in order to maintain the required quality. Modern instruments such as vacuum spectrometers are being used in place of the older and slow 'wet chemical' methods, but there is a long way to go before all the sampling and analysis can be done automatically and on-line.

From the stage when an ingot is teemed, i.e. the molten steel has been poured into a mould, all material is in discrete pieces and the identity of each piece must be maintained. The first main process after teeming is bringing the solidified ingot to a uniform temperature in a soaking pit and rolling it into a slab. Typical dimensions of a slab are approximately 28 ft. \times 3 ft. \times 6 in. The slabbing mill is semi-automatic in that the required drafting

(thickness reduction) can be predetermined by pushbutton and the whole process controlled by one man. The next major production department is the hot strip mill where the slab is reheated and then rolled to approximately 0.1 in. thick at about the same width as the original slab. It is then so long that it has to be coiled up and the product is called a 'hot coil'. All controls in the re-heating furnace are automatic and those for the mill e.g. for the roller track, the screw-downs of all 11 stands and their drives, the gauge and width controls, the water and steam sprays and the coilers, are under the overall control of a computer. Only two men at the entry to the mill are required for the actual operation of this hot strip mill, and the designed interval between the end of one coil and the beginning of the next is 3 sec. This is the key process in the works and it has been provided with the appropriate degree of automatic control.

Subsequent processes on the hot coil e.g., tempering and cutting up into sheets or, if it is to be cold-reduced, pickling, cold reduction in the 4-stand mill, annealing, tempering and cut-up have not such sophisticated controls, but essential instrumentation, as in the annealing furnace, and key controls, such as for gauge in the cold mill, have been provided.

The System

Concept

As stated previously, the main product of the works is wide steel strip. This is produced to individual customers' requirements in a large variety of widths and thicknesses and in any weight from a few tons to several hundred tons. It may be required in coil form or in bundles of sheets cut to specific lengths. In addition, many different chemical and physical properties are demanded according to the use to which the customer intends to put the strip. Orders are also received for semi-finished products such as sinter, ingots or slabs.

Table 1 (continued next page)

<i>Plant</i>	<i>Process</i>	<i>Operation</i>	<i>Mechanization</i>	<i>Instrumentation</i>
Coke ovens	Conversion of coal into coke with consequent production of gas and by-products	Discharge of incoming coal	Automatic sequencing of tippler and weighing operation	Positioning by photocell
		Stocking and charging of coal	Conveyor belts	Belt weighers with remote electronic indication
Sinter plant	Fusing together of iron ore, limestone and small coke (coke breeze)	Carbonization	—	Monitoring of combustion air and fuel gas pressures and temperatures
		Discharge of coke	Conveyor belts	Temperature, analysis and flow measurements
		Gas production	—	
		By-product production		
Sinter plant	Fusing together of iron ore, limestone and small coke (coke breeze)	Discharge of incoming ore	Automatic sequencing of tippler and weighing operation	Positioning by photocell
		Stocking, drying, crushing and charging of ore	Conveyor belts	Belt weighers with remote electronic indication
		Sintering	Automatic proportioning of raw materials from belt weighers	Monitoring of fuel and air flows and pressures
		Discharge of sinter	Conveyor belts	Automatic control of burn-through point
Blast furnaces	Conversion of sinter coke and limestone into iron with consequent production of gas and slag	Charging of materials	Automatic programming of skip hoist operation	Automatic humidity control on hearth
		Conversion process		Remote electronic indication
		Blast production	Automatic volume and pressure control of turbo-blowers near serge limit	Reference points set electronically
		Discharge of iron		Monitoring of top gas analysis, pressure and flow
Blast furnaces	Conversion of sinter coke and limestone into iron with consequent production of gas and slag	Discharge of slag		Automatic stove temperature control
Steel plant	Refining of iron into steel in L.D. converters using scrap and tonnage oxygen. Waste heat is used for steam raising. Steel is teemed into ingots	Charging of materials		Potentiometric weighing and recording of additives using load cells
		Oxygen flow		
		Control of process		
		Steel analysis	Lamson tube for conveying steel samples to laboratory	Quantovac analysis
Steel plant	Refining of iron into steel in L.D. converters using scrap and tonnage oxygen. Waste heat is used for steam raising. Steel is teemed into ingots	Control of boilers		Automatic control of steam output from battery with irregular heat input from converters
		Teeming of ingots		
		Stripping of ingots		
		Preparation of moulds		
Universal slabbing mill	Soaking of ingots to a uniform temperature	Soaking pit control	Local and remote (crane cabin) control of pit covers	Monitoring of gas and air flows and pressures. Automatic temperature control
			Automatic positioning of ingot buggy	
			Automatic draft increment system	
			Automatic sequencing of mill operation	
Universal slabbing mill	Rolling of ingots into slabs		Automatic dimension control	
Universal slabbing mill	Rolling of ingots into slabs	Scarfig of slabs	Automatic stamping machine	
		Cropping of slabs		
		Stamping of slabs		
		Weighing of slabs		

Table 1 - continued

<i>Plant</i>	<i>Process</i>	<i>Operation</i>	<i>Mechanization</i>	<i>Instrumentation</i>
Hot strip mill	Heating and rolling slabs into strip (about 0.1 in. thick) and coiling the strip	Reheating	Automatic positioning of roll gaps and side guide settings Automatic width control and speed settings of vertical edgers in the roughing train Automatic setting of roller table speeds Automatic gauge control and settings of stand speeds in the finishing train Automatic mill acceleration Automatic re-zeroing after roll changes Automatic sequencing of coilers Automatic positioning of pinch and wrapper roll gaps Conveyors	Automatic control of furnaces using either coke oven gas or fuel oil Mostly controlled by digital servo systems Slab tracking, mill pacing, mill set-up, temperature control and data logging all computer controlled X-ray gauge Width gauge Digital weighbridges
		Roughing and finishing stands		
		Coiling		
		Coil weighing		
Hot sheet finishing	Finishing processes for material sold in hot rolled state	Skin pass		Analogue extensiometer
		Cutting-up		
		Dispatch		
Cold mill	Further reduction of the strip thickness by rolling cold after suitable surface preparation Finishing processes for material sold in cold reduced state	Pickling	Automatic gauge control Data accumulation	Automatic control of acid level Automatic control of height of strip X-ray gauge Pressductors (load cells) for rolling loads Temperature control. Programme control of cycle Digitized extensiometer High-speed classifier
		4-stand cold reduction		
		Annealing		
		Tempering		
		Cutting-up		
		Weighing Packing and dispatch		
Services	Provision of works service	Blast furnace and coke oven gas		Instrumentation and remote controls provided for all services in fuel control centre Automatic control of main boilers fired by coke oven gas, blast furnace gas or coal
		Oxygen Water		
		Steam Electricity		

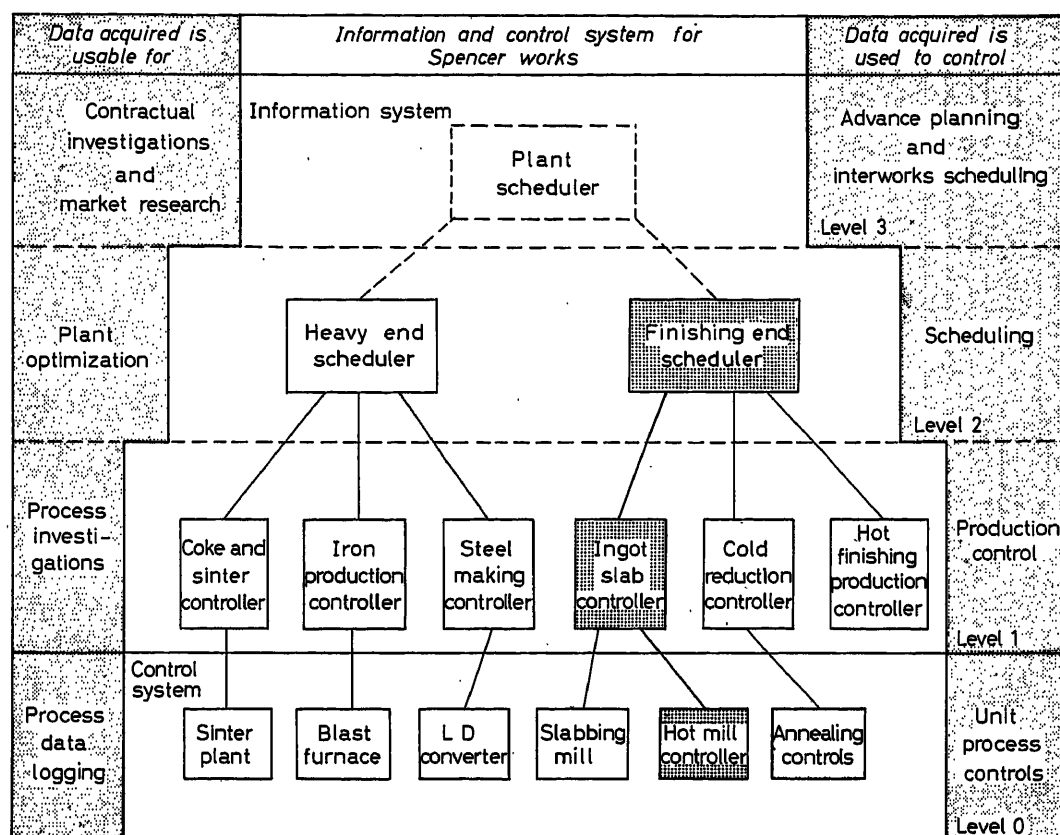


Figure 2. Four levels of computer system. (By courtesy of Control Engineering)

All these individual detailed requirements have to be scheduled by the works production control system taking into account the technical limitations of each process. The schedules have then to be transmitted to the individual production units where very close tolerances on process variables have to be maintained. In some processes these tolerances may differ for each order whilst, in others, the aim is to keep them constant over long periods. Departures from these tolerances often require immediate action, not only in correcting the process, but also in the issue of new schedules to ensure the manufacture of orders to specification and at the required delivery time.

In addition to the use of automatic controls for individual processes, equipment is provided for an important section of the clerical procedures in production control to be made automatic and to be integrated with the process controls wherever possible. Many of the executive instructions to operators are computer controlled directly from customers' orders and automatically updated and re-scheduled from production progress information continuously fed into the system.

A concept of works coverage by a system of interconnected computers operating at a series of different levels was proposed by the British Iron and Steel Research Association in 1960 and has been developed by R.T.B. in conjunction with Elliott Automation Limited. It is illustrated in Figure 2. The uppermost level is concerned with forward planning and inter-works order allocation. The second level, called the scheduling level, shows two computers to deal with customers' orders and to decide how and when they are to be executed. They calculate, for the heavy

end and finishing end respectively, what material is required at each process and the sequence in which it shall be processed. This information is transmitted automatically, as required, to the next level, called the production control level, where six computer systems are proposed, each covering one of the major production areas. These relay the information, item by item, to the lowest level, i.e. to the operators if the process is manually controlled, or to the process computer in the case of the hot strip mill. Conversely, when the material has been processed, the operators or machine transmit to the appropriate production controller the results of these operations. After this information has been checked and compiled it is transmitted in turn to the scheduling level, where the production files are updated and amended schedules issued if necessary.

First Stage of Implementation

Only Stage 1 of the system has so far been installed. This consists of the finishing end scheduler and the ingot and slab controller in addition to the hot strip mill automation computer.

The finishing end scheduler accepts incoming customer orders and computes schedules for all processes from the steel plant to despatch.

The ingot and slab controller provides an information transmission, display and collection system covering the area in the works from mould preparation and ingot teeming through ingot stripping, soaking pits, universal slabbing mill, automatic scarfer, crop shears, stamper and piler to the slab yard together with the

marshalling of slabs preparatory to rolling in the hot strip mill. In addition weighing points for the ingot, slab and hot coil stages are connected to the system, the hot coil stage being entirely automatic.

The hot strip mill automation computer tracks each slab through the hot strip mill, calculates the minimum time interval between slabs, operates all the mill controls to produce a coil of the correct dimensions and temperature, logs the process variables for each coil and produces a production record.

Figure 3 shows the interconnections between the three computers and the information flowing between the various parts of the system.

Scheduling

As each order is received at the Spencer Works, it is given a metallurgical routing number (at present this is done manually) which specifies which processes the material must pass through and what has to be done to it at each process. The order is then fed into the finishing end scheduler computer. A computer sub-routine then carries out the 'figuring' calculations i.e. making allowance for the expected material yield at each process, it determines how much tonnage must be processed at each stage in order to produce the required amount of finished product. Where possible, similar orders with compatible delivery dates are grouped together to form composite orders.

The next stage is to allocate in an optimum manner each order to a delivery week and then to arrange all the deliveries

for one week into the most desirable sequence. This delivery plan is then projected back through each preceding process as far as the hot strip mill taking into account the technical restrictions at each stage. Owing to the different average transit times from hot rolling to, say, cold sheet dispatch or hot coil dispatch, the initial week's delivery orders will not necessarily form a complete week's schedule on the hot mill and several week's deliveries may have to be combined to provide this.

This combination is then arranged by a hot mill scheduling routine into a week's preliminary hot mill schedule. Similarly, preliminary schedules are prepared for all subsequent processes as far as dispatch and these will normally differ from the previously calculated desirable sequences. This may mean that some deliveries are found to be later than required. In this event, the item is moved to the previous weeks hot rolling schedule and the process repeated.

These preliminary schedules are issued in the middle of each week covering the following week and are used for planning purposes only. They are not 'hard copy' work schedules for direct implementation by the operatives.

The hot mill preliminary schedule is used as the basis for a further sub-routine which, taking into account unallocated slabs already in stock, calculates the steel plant requirements cast by cast in terms of ingot sizes and quantities and passes the details to the ingot and slab controller for storage and for printing out in the steel plant. When the actual steel grade produced is known, the scheduler matches the steel, if possible, to orders within the

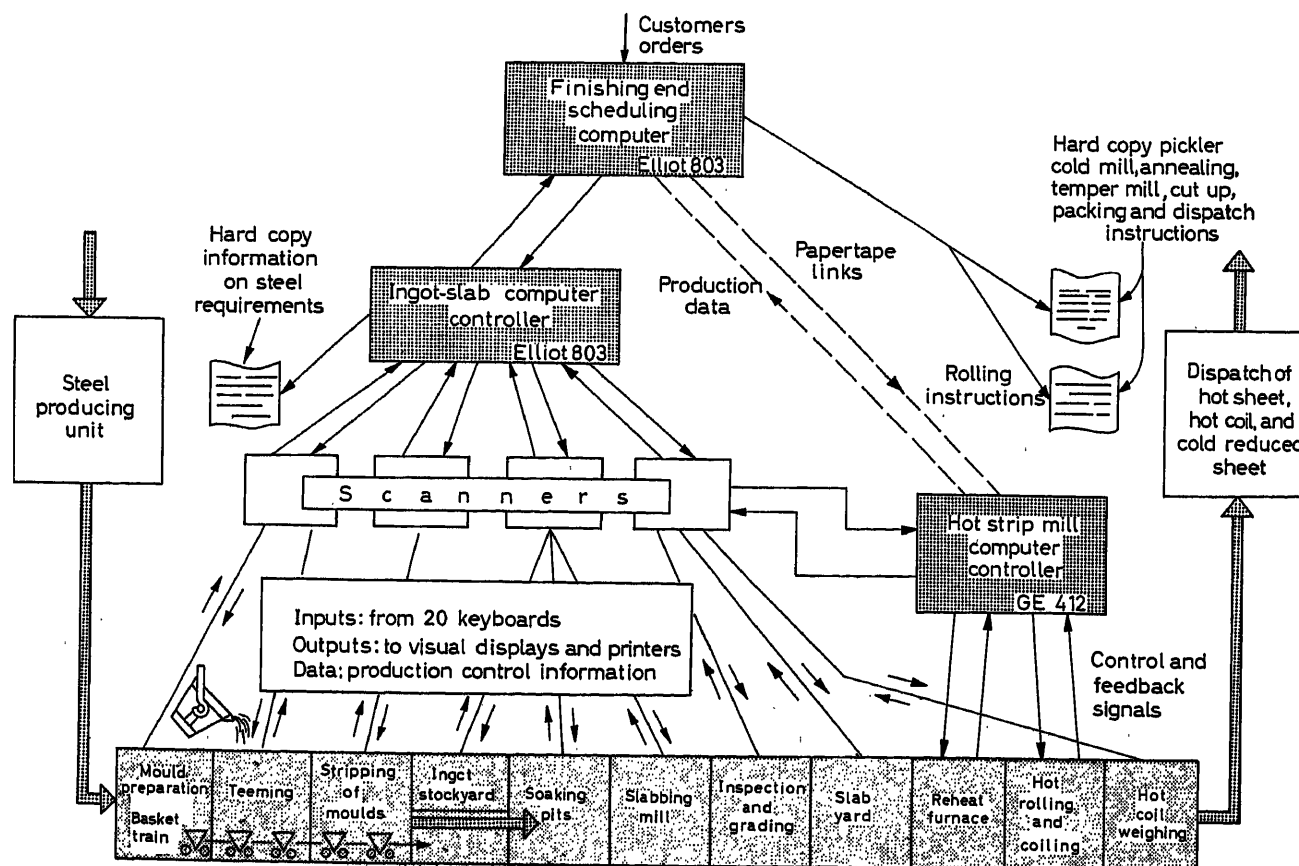


Figure 3. Stage 1 information flow. (By courtesy of Control Engineering)

hot mill preliminary schedule, and transmits the necessary slab dimensions to the ingot and slab controller.

After slabs have been produced and inspected a further sub-routine allocates them as far as possible to the appropriate part of the preliminary hot mill schedule and a list is issued indicating which slabs from the slab yard have to be marshalled ready for rolling in the hot strip mill. When the slab yard confirm that the required slabs have been located and marshalled, the scheduler computer issues a 'hard copy' final schedule covering approximately 4 h and also prepares a punched tape for feeding to the hot strip mill automation computer.

The principle of the scheduling computer matching the actual steel produced against the preliminary schedule for a process and then issuing hard copy final schedules is followed in every subsequent process of the plant, e.g., hot rolled coils for pickling, pickled coils for cold reduction, cold reduced coils for annealing etc.

At each process the scheduler computer checks three important factors: (1) Whether it is necessary to re-order any steel because of excessive rejections. (2) Whether every order is keeping to its schedule in order to meet delivery. (3) Whether any material excess to an order's actual requirements is being processed and, if so, whether this can be re-applied to another order.

The Steel Plant

Returning to the steel plant, the schedule detailing the steel grade and the number and size of ingot moulds to be prepared for each cast is produced on printers in the mould bay and in the steel plant at the beginning of each shift covering an 8 h period from the middle of the shift.

The mould bay personnel assemble each train of moulds as required and key into the controller the mould identity numbers, the mould sizes and the location of each mould on the train. These details are checked in the computer against the desired train make-up. If a mould is rejected, this too is signalled to the controller as a separate sub-routine checks for mould availability and maintains historical records of mould usage and life.

The steel plant prepares the steel and 'teems' it into the assembled moulds, indicating to the computer when the process of teeming is complete. The steel is then allowed to stand for a given period before being moved to the stripping bay. During this period, quality control information is inserted on an input console in the steel plant giving the chemical grade and quality of each ingot based on laboratory analyses and inspectors reports. Local print-outs provide the steel plant foreman with a summary of the shift's operation in terms of the number of ingots, weight, downgrades, and also a summary of chemical analyses showing the causes of downgrades in the last ten casts. This enables him to detect any trend in the quality of steel produced and to take corrective action if he considers it necessary.

Results of the next sub-routine are printed out in the stripping bay. Here the ingot numbers, and their position on the train are listed, the print-out also indicating the calculated time to start stripping the moulds. When the moulds are stripped off the ingots, the process time of the operation is signalled in along with the weight of the cast obtained from a weighbridge. The times of teeming and stripping are used in a later sub-routine to determine the 'track' time of each ingot which is needed to determine heating times in the next process. Ingot faults observed on stripping are also fed in, and the controller prints out a shift

summary for this process control point detailing the usable ingots and giving estimated weights of any faulty ingots.

The ingots will now either be stored in one of the ingot stockyards or while still hot sent through for charging into a soaking pit. The controller makes this decision after scanning the soaking pit data to see if any pits are, or will be, ready when needed. Computations on these data result in (a) a display for the locomotive driver showing him the required parking position for the train of ingots and (b) a print-out in the soaking pit office showing the pit selected and sequence in which the ingots are to be charged into the pit. If there is a delay at the pits, or a downshift at the slabbing mill, the computer may divert the ingots from the soaking pits to a stockyard and, in this case, a further sub-routine determines the stocking area, and displays this at the cast weighbridge. There is also a print-out produced to enable the stockyard foreman to produce a painted plate to be associated with each ingot.

For ingots that go straight to the soaking pits, the time of actual charging is signalled and the computer operates a 'time-to-ready' routine calculated as a function of the accumulated track time, ingot size and steel type. Along with a print-out of the initial 'ready time' for the ingot, the controller prints out the details of the slabs to be produced from these ingots.

An updating procedure for the 'ready time' is initiated when the gas supply to the pits cuts back as the desired pit temperature is reached. This produces final updated ready time. Ten minutes before the updated 'ready time' the computer switches on a red blinker light at the appropriate pit. The pit is then manually inspected by the heater who dials in whether the pit is ready for drawing. If not, he signals in a new time estimate and the controller repeats the 'ready time' updating routine.

The Slabbing Mill

Ingots are removed either singly or in pairs from the pits for rolling into slabs. From the signalling by the heater of the pit number being discharged, the controller operates a sub-routine associating the ingot numbers with their particular slabbing schedule stored in the controller, and displays in the universal slabbing mill pulpit the required slab widths and thicknesses for the ingots as they arrive. The slabbing mill operator transfers this information manually to the mill's automatic screwdown control system. At the end of rolling, digitized final edger and screwdown positions are fed back for checking in the ingot and slab controller. Also displayed in the pulpit are rolling data for the next ingot batch. Instructions are sent to the slab stamper for correct numbering of the slab; the rolled slab is then weighed, piled and passed to the slab yard.

The Slab Yard

The next production process for the slab is a cool-off period in the slab yard before the slabs are inspected. Results of inspection, which may result in a new surface quality or possibly in a new length, width or thickness, are keyed into the computer directly from the slab yard inspection area. After processing these results, the scheduler now finally allocates slabs against individual orders and prints out instructions showing which slabs are allocated for rolling against customer's orders.

This information is printed out every 12 h as a hot strip mill work schedule showing the list of slabs required.

Confirmation of the identity of slabs marshalled and the order in which they can be rolled allows the scheduler to produce a final *hard* hot strip mill rolling programme several hours before rolling.

The Hot Strip Mill

Paper tape interconnections between the scheduler and the hot mill automation computer allow automatic re-scheduling should the actual hot strip mill output vary from that called for. A feedback tape is produced by the hot mill computer and gives a log of each coil produced, including finishing and coiling temperatures, percentages of prime material, over or under gauge, and off-width. The scheduler checks this coil log against the desired values. If there are discrepancies, the scheduler can take automatic corrective action by amending later rolling schedules to replace the coil which was not rolled to specification. Automatic re-scheduling is also possible in the hot mill computer itself. If, in the rolling process, difficulty occurs in meeting the target programme due, for instance, to the slab being too cold to roll, the computer arranges for the slab to be rolled to standard stock size. At the same time it feeds back this information to the scheduler and sets in train a re-scheduling operation to replace the coil not rolled.

At the coil weighbridges after the hot strip mill, the identity of each coil is displayed by the hot mill computer and the weight is displayed from a digital weighing system. These two items are transmitted automatically to the ingot and slab controller for transfer to the scheduler and amalgamation with the coil log.

The Finishing Department

In the cold mill and hot sheet finishing departments, the production records are, at present, prepared manually and then punched on paper tape for feeding to the scheduler computer. A study is in hand for specifying an automatic information display and collection system for this area similar to the ingot and slab controller.

The Data-handling Equipment

The two-way flow of information between various levels is the routine task of the data-handling system and determines in the main the equipment to be deployed. Other tasks such as the keeping of records for plant investigations and the issuing of managerial reports summarizing the situation in any given area, although of great practical importance, do not have a significant effect on the size of the system. In fact, a high proportion of the equipment is concerned with the collecting of information from the plant operators.

It was taken as axiomatic that the reliability of the complete system can be taken as the reliability of its peripheral equipment and so this was made as simple as possible; consistent with ease of use by the operators.

Ingot and Slab Controller

At any one input console a man may have to enter several different sets of information. For example, in the mould preparation bay, moulds of various sizes have to be loaded on to a train prior to being filled in the teeming bay. The crew are in possession of a printed list of mould sizes to be loaded on each

train, but the precise train and moulds are decided by the men and not prescribed by the system. The list is, therefore, just a column of reference numbers (programme numbers) followed by the numbers of each mould size, of which there are about ten, to be loaded on a train. As the train is loaded the man has to inform the system what the train number is, what the mould number is, what its position is on the train and which list he is obeying, i. e. the programme number. Subsequently, when the train is ready to be dispatched he has to inform the system that this is so. Moreover, from time to time a mould is unserviceable and has to be scrapped and so the precise mould and the reason for its rejection has to be entered. Finally, if a cast is off grade and it is decided not to teem into the moulds intended, a spare train already loaded with a standard set of moulds is used instead. When a spare train is loaded for this purpose its moulds have to be recorded since a history of mould usage is maintained by the computer system. On the input console used for all these purposes (see *Figure 4*) are decade switches on which can be set up the following numbers: programme number, train number, mould number, position on train and reason for mould rejection (using a suitable code). But the class of information, that is if it is about a mould loaded on to a train, or about a train ready for use or about a mould being rejected, or about the spare train being loaded, is inserted by suitably setting one other switch, the selector switch. When the man has set this selector, and all the relevant decade switches, he depresses the pushbutton and the information is subsequently read in by the system. Logically, it is the same as if there were four pushbuttons on this input console, one for each class of information and the decade switches read by the system depended upon which pushbutton was depressed. The system is, in fact, wired as if there were this number of pushbuttons. For this particular input console, the information read in for each pushed button is given in *Table 2*.

Table 2

	<i>No. of decades</i>	<i>Max. value</i>	<i>Selector switch position</i>			
			<i>1 Mould</i>	<i>2 Train ready</i>	<i>3 Spare train</i>	<i>4 Reject mould</i>
Programme number	3	999	X			
Train number	4	9999	X	X	X	
Mould number	4	9999	X		X	X
Position on train	2	16	X		X	
Mould rejected	2	99				X

Each of the 20 input consoles and 20 soaking pit 'state' switches in Stage 1 of the system is connected to one of four 'Scanners' which are housed in a room under the slabbing mill which was chosen as a suitable position relative to the input consoles. The scanners are connected to a computer housed in a separate building and the computer, scanners and keyboards, together with the output printers and lamp displays which are also connected to the scanners, form the 'ingot and slab controller'. A schematic diagram of the equipment used in the system is shown in *Figure 5*.

When a man presses a pushbutton a one-bit store is set in a scanner. As soon as the computer is ready for more information it releases one of the scanners which scans round all of these

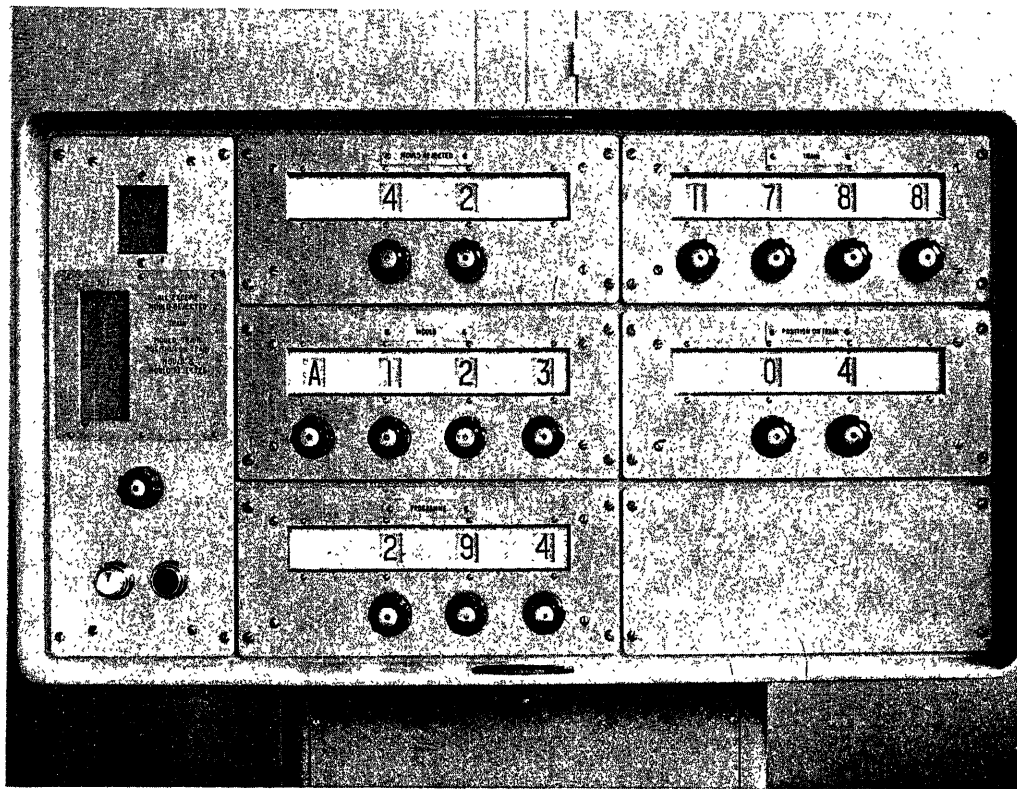


Figure 4. Photograph of typical input console

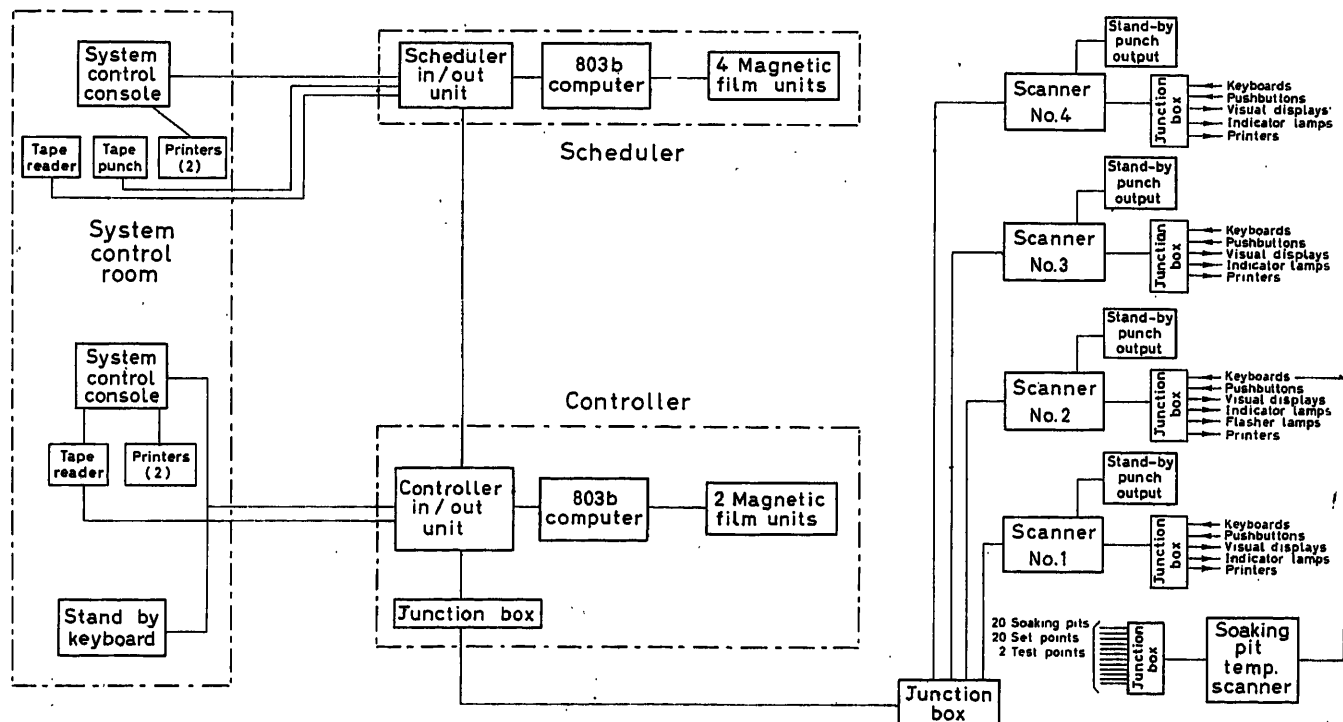


Figure 5. Equipment diagram for Stage 1 of the system

one-bit stores at high speed (about 10,000/sec). When it finds one which has been set, it informs the computer which subsequently demands the relevant information digit-by-digit. This information is: the input console number, the selector switch position and the time, followed by the relevant digits read from the console. Information originating in the scanner (console number, selector position and time) is immediately transmitted back to the computer as five parallel bits plus one parity bit signal. The decade switches in an input console, however, are just single-pole 10-position switches. There is an individual wire to each wiper but all 10 contacts are wired in parallel to 10 bus-bars. The scanner energizes the appropriate wiper and checks that it receives a one-of-out-ten signal on the bus-bar. This is then encoded, parity added and transmitted to the computer in the same manner as the other information.

From this it is seen that between the time a man presses a pushbutton and the decade switches are read by the scanner, the information is held only by these switches; there is no buffer store. This was done deliberately to simplify the system, but it does put a slight restriction on the operator in that he must not move a decade switch until it has been read. To aid him in this, an annunciator display is incorporated in each input console which normally displays 'O.K.'. Immediately the pushbutton is depressed this is replaced by 'WAIT'. When the information has been assimilated by the computer the display normally returns to 'O.K.' and the operator can insert the next information. If, however, the man has blundered, for example, by keying in that there are two moulds in the same position on the train, then the computer changes the display from 'WAIT' to 'QUERY'. The man is then given a second chance to put in the information. If after the second attempt the system still cannot accept the information, it returns the display to 'O.K.' but makes the fact known on a printer in the system control room in the computer building.

To transmit information from the computer to a printer or lamp display, parallel signals giving the character and the address of the printer or display are sent to the appropriate scanner. This in the case of a printer, sends a 5-wire signal to the printer. In the case of a lamp display, one of 10 lamps has to be energized, and so the scanner sets up one of 10 staticizers (flip-flops) for the particular display.

There are 10 printers (Creed Model 75s) distributed in local offices and 10 displays which are mainly located in pulpits in the slabbing mill area. Further, there are automatic inputs from the slabbing mill settings and the slab stamper. At the appropriate instant control signals from the slabbing mill set up a series of relays so that they hold the settings of the rolls when the slab makes its last pass through the mill. Subsequently, these relays are read by the scanner as if they were decade switches of an input console and the computer checks that the slab was rolled to the

required cross section. Similarly, as the automatic stamper stamps the number on the end of the slab this number is also held in a relay buffer store for subsequent readings and checking by the computer. Finally, there are automatic inputs from the temperature controllers at the soaking pits. These are connected to a special analogue soaking pit scanner which periodically inspects the temperatures and fuel flow at each of the 20 pits. This scanner converts the analogue signals from the pitside instrumentation into digital signals as if from an input console and feeds these into one of the other four scanners.

The computer in the ingot and slab controller is an Elliott 803B with 8,192 words of immediate access store fitted with two magnetic film units plus one spare, each capable of storing 250,000 words on one reel (one word is 39 bits plus a parity bit). It is controlled from a console fitted with two printers and displays. There is also a standby input console associated with this console which can be made to perform the task of any of the other input consoles in the plant.

Finishing End Scheduler

The scheduler, like the ingot and slab controller is an 803B computer, but fitted with four magnetic film units and a spare. It also has a control console, and is connected directly with the ingot and slab controller so that information can be transmitted in either direction between the two computers, one word at a time. Input, such as customers' orders, is by punched paper tape and the output of schedules, progress information and management reports is also in the same medium. This is backed up by the necessary tape preparation and printing equipment.

Reliability and Breakdown Facilities

In a system of this complexity there will be times when there is a failure. Checks on parity have been built in wherever appropriate to reduce the effect of transient disturbances, and much can be done by sound operational practice. For example, schedules are punched on to tape well in advance. If all goes well these will be replaced with more up-to-date schedules when the time comes but, if a failure occurs, the pre-punched schedules would be sufficient to keep the works running.

For recording information under breakdown conditions there is the standby input console already mentioned, but, in addition, each scanner can adopt a standby mode of operation. If, in fact, the computer of the ingot and slab controller does not send a signal to the scanners for a period of 5 sec, the scanners start up their standby punches and record the information being fed in by the operators. The operation at the input consoles will be the same except that the 'QUERY' light will never be illuminated and greater reliance is placed upon the men during this period.

DISCUSSION

Author's Opening Remarks

The paper by Mr. Hersom and myself was written about 18 months ago, at a time when the Spencer Steelworks was in the final stages of construction but before it had gone into production. The paper had therefore to be forward-looking and to describe what we were planning to do, rather than what we were, in fact, doing.

We felt that the best way we could use these introductory remarks

was by indicating how far we are along the road to achieving our hopes and how much still lies ahead of us.

The construction of the works is complete and it is currently producing steel at the annual rate of about 1 million ingot tons as compared with its designed capacity of 1.4 million. This has been achieved in about 12 months of operation.

It is the first works in the world to rely entirely on the L.D. method of producing steel and three converters have been installed.

In this process, about 100 tons of molten iron and 16 tons of scrap are placed in the converter and oxygen is blown from the top through a lance for about 20 min, the total time to produce 100 tons of steel being about 50 min.

The hot strip mill in which 30 ft. long slabs are rolled into strip about $\frac{1}{10}$ in. thick and coiled up is the longest one of its kind in the world.

All the speed and roll gap controls for the stands are grouped in one pulpit and can be operated by two men. Two modes of operation are possible: manual and semi-automatic. In the latter mode the operator has simply to select the required settings and the equipment will set itself to these values. When the computer has been completely installed, a third, automatic mode will also be available, in which the selection of the required settings will be made by computer programme.

The works, then, is well into production and much of what can be called conventional automation, described briefly in the paper, is in operation. Progress with the computer systems for scheduling and information transmission, described in detail in the paper, is briefly that all the equipment is installed and tested and operating programmes are just coming into use. The two computers forming the basis of the system are situated side by side in a new computer centre. Both are Elliott 803 B machines with 8192 words of core storage and using magnetic film backing storage. A further 803 computer has been installed for nearly two years and it is used for statistical analysis of the works quality control data and other off-line data processing. The two main computers are linked together electronically and the controller is also linked to a large number of printers, displays and keyboards in the plant.

All the equipment has been given extensive testing for accuracy of transmission and efficiency of operation. One unexpected point which has been revealed is that although the annunciator display of 'O.K.' and 'WAIT' on each keyboard was designed to indicate to the operator whether information has been entered correctly, the sequence is often so rapid that unless he is watching the display closely, he is unable to detect the insertion. A delay or an audible indication is now being considered.

The basic executive control programmes for the ingot and slab controller are written and operational. These provide for the reading of information from all keyboards, the issuing of information to the printers and displays, the organization of the storage of information, the provision of control facilities and the verification of the accuracy of message transmission.

The programme to deal with the actual operating needs of the steel plant area has been written and is currently being tested. The ingot stocking and soaking pits area has been specified in detail and the slabbing mill line is specified in general. Again we hope to have the system up to this stage in operation by the middle of next year.

The finishing end scheduler will cover the entry of customers' orders and amendments and all stock control, scheduling and progressing for the steel plant, soaking pits, slabbing mill, slab yard and hot strip mill areas of the works. At a later stage it will be extended to cover further stock control, scheduling and progressing in areas of the cold mill.

Programmes for order entry, order amendments, figuring, grouping, selection of hot mill rolling week and production of weekly hot mill preliminary schedules are in operation together with mould record files and a simple programme to prepare input tapes for the hot mill computer. Other functions are in the programming or in final specification stages.

There will undoubtedly be periods of commissioning and implementation troubles and a need for parallel running on both computer systems, but by the end of 1964 we anticipate having the complete system dealing with the receipt of customers' orders, the scheduling of the steel plant, slabbing mill and hot strip mill, the display of schedule instructions and the collection of production data in the steel plant, slabbing mill and slab yard and the rolling of slabs into hot strip,

made completely automatic. If this is, in fact, achieved it will have taken about 5 years from the first suggestion to the completion of the first section of our control system concept.

R. G. BEADLE, *General Electric Company, 1 River Road, Schenectady, N.Y., U.S.A.*

This paper describes one of the most comprehensive and interesting scheduling systems that have been planned or implemented to date.

It would appear that one of the major problems would be the definition of detailed requirements of information and logic to and from each process or area. In fact, this would appear to be particularly challenging in a new steel works where practices are not defined. Would you consider a scheduling system more or less difficult to implement in an existing works?

In the hot strip area, one of the most important scheduling functions is the layout of each rolling cycle which occurs between roll changes. This cycle requires a width pattern beginning narrow, growing rapidly wide, and then a slowly decreasing width until rolls are to be changed again. At the same time, however, the order of rolling must not exceed many other furnace and mill limitations. Can you confirm that this plan is made in the computer? Can you describe the success of this particular phase of scheduling?

R. G. MASSEY, *in reply*

There is no straightforward answer to the question whether it is easier to install a system of computer scheduling in a new works or in an existing one. Certainly the lack of established operating practices and data in a new works makes the system design more difficult, largely because much greater flexibility has to be provided. However, the fact that the resulting system is more flexible may more than compensate.

The great advantage in a new works comes from the enthusiastic acceptance of automation and computers to be found in a new management. If I had to make the choice, I would prefer the situation in a new works.

Mr. Beadle's second question refers to the stringent technical restriction imposed on scheduling by the hot strip mill. Our computer system takes into account all the restrictions mentioned by Mr. Beadle and several more besides. It also groups together thicker material into a separate heavy gauge round each week and, if necessary, stores scarce material over a number of weeks.

Our hot strip mill scheduling staff have examined all the schedules produced by the computer system and are very pleased with the results. We have decided to add a refinement to the programme which will relax the restrictions on width slightly if a large thickness change can be avoided by doing so. This refinement may be found unnecessary once the hot strip mill comes under computer control and large gauge changes can be accommodated.

W. N. SPRAY, *United States Steel Corporation, U.S.A.*

The paper by Hersom and Massey, describing the systems of information handling and production control at the Spencer Works of Richard Thomas and Baldwins, is an impressive addition to the published literature concerned with automatic information systems in the steel industry. The comprehensive coverage of functions which is contemplated by the underlying theories together with the methodical adherence to the full implications of theory in the actual installation make the whole programme exceptionally significant for study.

Although operational results of these systems cannot have been fully determined as yet, the early experience may very well have confirmed or thrown doubt upon some systems assumptions of wide interest. It would be very helpful if the authors could indicate some of the most significant proofs or disproofs of assumption which they have encountered.

Two areas in particular have special interest for some of the current efforts in the United States:

First, is there a clear-cut reduction in the quantity of products in process of manufacture which must be maintained ahead of each of the processing units and, as a consequence, is there a reduction in the manufacturing cycle time for any given order or order item? It has been widely assumed that systems of this sort with very short information lags would improve the precision of material tracking and schedule control so markedly as to allow much smaller queues of material in process. I know of no conclusive experience to date on this highly desirable possibility.

Second, is there any clear evidence that the use of many separate computers specialized by geographic area and by level of detail is actually superior to the several other computing arrangements which are possible? The arrangement chosen at RTB has been called the hierarchy arrangement, and its value has been urged on the ground of superior reliability in case of equipment failures and on the ground of systems flexibility. It is very difficult to see that such values are self evident. A smaller number of larger computers, all exactly alike and each capable of accepting any task of any of the sub-systems, would appear to be equally worth exploring. Such a combination might actually be superior in reliability because the highest priority routines would go out of action only in the case where all computing equipment was inoperable. As to cost, the more centralized arrangement would almost certainly have the advantages of higher machine loading, since at any given time each computer could be filled to practical capacity before the next one came into operation. These are not simple matters to predict, however, and any RTB experience bearing on these points would be most helpful.

R. G. MASSEY, *in reply*

We certainly expect a reduction in the average time for an order to pass through our works with a consequent reduction in the size of stocks of allocated material in process. However, it is too soon for these effects to have been achieved.

I do not expect any significant reduction in the total stock maintained between major processes. Apart from allocated material in process, several other categories of stock are held. Planned unallocated stock is maintained as a buffer against scheduling restrictions and production stoppages and as provision against a lower than normal production yield. Stock also arises accidentally either due to process and quality rejections or to a higher than normal production yield and even by mistake.

The computer system will reduce the mistakes but it will also make possible a more elaborate system of holding planned stock which will tend to compensate. Thus, with the same size of stock I anticipate a greatly improved service to customers.

S. E. HERSOM, *also in reply*

Mr. Spray's statement that the value of the hierarchy arrangement has been urged on the grounds of superior reliability in case of equipment failures and on the grounds of system flexibility, is, in fact, not the case. The value of the hierarchy principle from the reliability aspect is that if one unit breaks down the rest of the system carries on independently and is affected only by the lack of information which should have originated from that unit. Mr. Spray's idea of having a small number of larger computers, all identical so that they can be switched to perform the higher priority tasks and omit those of lower priority, sounds very attractive but there are a very large number of practical difficulties. To switch units requires not only a change of all the connections, but all stored information must be transferred as well and that can amount to many hundreds of thousands of words of information. To do this smoothly would require even more equipment and make the whole system very expensive indeed.

J. I. BRADFORD, *6 Gateway Center, Pittsburgh, U.S.A.*

We have planned a similar 'integrated automation' system for our tinplate operation. Of concern is the amount of off-line operation needed each day for maintenance of business computers such as the ingot slab computer controller and the finishing and scheduling computer. Normally, business computers are down one shift out of three. In our plans the scheduling computer would be switched over to handle the functions of the ingot slab computer controller when it is off-line. This would keep the making of tapes on the output of the scanners to a minimum, and operation of this display at a maximum. What are the authors' plans for handling the system when the ingot slab computer is off-line?

R. G. MASSEY, *in reply*

We have to have a system for dealing with a breakdown of the ingot and slab controller, infrequent as we expect this to be. I wish I could say that we had complete standby facilities which can be switched on at the first sign of trouble, but for financial and technical reasons we have not. Our breakdown arrangements consist of reverting progressively towards manual operation according to how much of the system is affected until, if the whole system breaks down, we shall return to our existing manual system. In this extreme case, certain production records will be punched manually on to tape for updating the computer system so that historical records can be maintained complete. This represents quite a small punching load since most of the control information will be ignored as no longer relevant. In less extreme breakdowns the tapes will be produced automatically from the scanners.

On-line Computer Control of a Hot Strip Finishing Mill for Steel

R. G. BEADLE

Summary

A most significant accomplishment has been achieved in the application of an on-line digital computer in the control of a hot strip finishing mill. This computer is the primary element of the overall process director system. Its purpose is to calculate and transmit set-up references to the mill controls. These references, in a conventional system, are set manually by experienced operators.

To perform these functions, the computer requires the following in its stored programme: (1) Data describing the characteristics of all steel types. (2) The influence of variables on this steel characteristic. (3) The characteristics of the electrical and mechanical rolling mill equipment. (4) The mathematical model which permits the actual set-up calculation to be made from the stored data.

Furthermore, the action of the computer must be timed and sequenced to match the real-time process being controlled.

The paper describes how the director fits into the process, and outlines the set-up calculations made. A few special process features are described which must be considered by the set-up calculation.

Results are given which compare the performance of the computer director with human operators as regards gauge accuracy for both normal or average rolling as well as during unusual operations. They also show a sample of the log sheet showing the accuracy of calculation.

A brief description of more complex systems now under construction is also given.

Sommaire

Un progrès d'une grande importance a été réalisé par l'application d'un calculateur numérique (digital) pour la commande électrique d'un 'finisseur à chaud pour bande' (HOT STRIP FINISHING MILL). Ce calculateur est l'élément principal de l'ensemble du système de commande. Sa tâche est de calculer et de transmettre au système de commande des valeurs de référence. Ces valeurs, dans un système conventionnel, sont déterminées manuellement par l'opérateur affecté au service.

Afin d'accomplir ces fonctions, le calculateur requiert l'emmagasinement dans sa mémoire des informations suivantes:

- (1) Caractéristique de tous les aciers à traiter.
- (2) L'influence des variables sur les caractéristiques des aciers.
- (3) Caractéristiques de l'équipement électrique et mécanique de la chaîne de laminage.
- (4) Le modèle mathématique du processus, permettant d'effectuer les calculs en employant les données contenues en mémoire.

En plus, la marche du calculateur doit être adaptée aux conditions de temps et de logique d'opérations auxquelles on est soumis dans l'opération réelle.

L'article décrit comment le calculateur s'adapte au processus et il explique la manière de faire les calculs des valeurs de référence. On y trouve décrit également quelques facteurs particuliers à considérer lors de ces calculs.

Des résultats montrent aussi la performance du calculateur en comparaison avec le système conventionnel, en ce qui concerne la précision de l'épaisseur du matériau obtenue, tout aussi bien en cours d'opérations inhabituelles qu'en temps d'opérations normales. Les résultats montrent également un exemplaire des données (log sheet) indiquant la précision des calculs.

L'article décrit enfin brièvement quelques systèmes plus complexes en voie de réalisation.

Zusammenfassung

Ein wesentlicher Fortschritt wurde durch die erfolgreiche Anwendung eines Digitalrechners auf die Regelung einer Warmbandfertigstraße erzielt. Der Rechner ist das übergeordnete Element der gesamten Prozeß-Steuerung. Seine Aufgabe ist es, die Einstellwerte (Sollwerte) zu berechnen und vorzugeben. Bei den heute üblichen Ausführungen dieser Anlagen werden die Sollwerte von erfahrenen Bedienungsmannschaften von Hand vorgegeben.

Zur Lösung dieser Aufgabe muß das gespeicherte Programm folgende Angaben enthalten:

1. Die Eigenschaften aller zu walzenden Stähle.
2. Den Einfluß verschiedener Parameter auf die Stahleigenschaften.
3. Die Eigenschaften der elektrischen und mechanischen Einrichtungen der Walzenstraße.
4. Das mathematische Prozeßmodell zur Berechnung der Einstellwerte unter Verwendung der gespeicherten Daten.

Ferner müssen Reihenfolge und Ablauf der Berechnungsvorgänge den zeitlichen Erfordernissen des zu regelnden Prozesses angepaßt werden.

Der Aufsatz beschreibt die Anpassung des Rechners an den Prozeß und zeigt die Berechnung der Einstellwerte. Einige spezielle Prozeßeigenschaften, die bei der Berechnung der Einstellwerte berücksichtigt werden müssen, sind ebenfalls beschrieben.

Der Aufsatz vergleicht die Ergebnisse des Prozeßrechners und die der Betriebsmannschaften hinsichtlich der Dickengenaugkeit, sowohl unter normalen als auch unter ungewöhnlichen Bedingungen. Die Genauigkeit der Berechnungen wird an Hand eines ausgefüllten Datenerfassungsformulars gezeigt. Eine kurze Beschreibung von zur Zeit im Bau befindlichen weiterentwickelten Anlagen ist ebenfalls angegeben.

Introduction

The finishing stands of a hot strip mill are now being controlled by an on-line digital computer. This computer is the primary element of the overall process director system, and its purpose is to provide the set-up references to the mill controls—references which are normally supplied by human operators. The computer is definitely successful in fulfilling its duties, and has been operating since early 1962 for all products and under all conditions. The system has improved the product quality and reduced the cobble rate.

Like a human operator, the computer must have sufficient stored 'knowledge' to perform similar duties. The computer must know the characteristics of all steel grades, and how these characteristics vary with temperature, speed, width, and drafting practice. The computer must be able to adjust its practices for normal variations of incoming temperature, steel variations, or mill condition. Similarly, it must be able to adapt to unexpected upsets such as incorrect steel grade or mill cobble, or even sensor errors. Also, the computer must coordinate itself in time with mill operations—that is, it must know when to transmit new set-ups and when to examine the results to improve its operation. In short, the computer must simulate a human operator in all respects. Actually it must simulate a superhuman operator since

the computer's ability exceeds any human—its large memory, its fast arithmetic capacity, and its ability for fast and multiple decisions allow it to exceed the capabilities of a human operator.

Description of the Mill

Before the computer operation can be explained adequately, it is desirable first to describe the mill that is directed.

Number of stands	6
Type	4 high
Width	60 in.
Nominal work roll	26 in. dia.
Nominal back up roll	56 in. dia.
Motors	d.c.
Stands 1-5 each	5,000 h.p.
Stand 6	3,500 h.p.
Power supply	Mercury arc rectifier for each stand
Screwdown drives	
Stands 1 and 6 each	2-75 h.p., constant potential type control
Stands 2-5 each	2-100 h.p., adjustable voltage type control
Load cells	2 per stand, 1,760 U.S. tons each
Loopers	Motor-driven, 50 h.p., variable tension
Maximum mill speed	2,390 ft./min
Typical entering thickness	0.800 in. to 1.200 in.
Typical delivery thickness	0.059 in. to 0.375 in.
Products	Carbon and stainless steels

In addition to the mill information, one should also consider the automatic control and regulating equipment which is used for both manual operation and computer operation of the mill. In manual operation, the operators provide the set-up references for these regulators, while on computer operation the computer provides these references. Figure 1 shows in abbreviated form the regulating systems employed. First, the speed of each stand drive motor is controlled by a speed regulating system (SR) which operates through the phase control circuitry of the mercury arc rectifier power supply. The speed regulator maintains the motor speed constant to the value set by the operator or computer, although after steel enters the mill, the looper position regulator (LPR) signal into the speed regulator increases or decreases motor speed to maintain looper height. A position regulator is provided for each screwdown (SPR) which permits the operator or computer to provide a digital reference of roll opening to which the screws position themselves. On the four

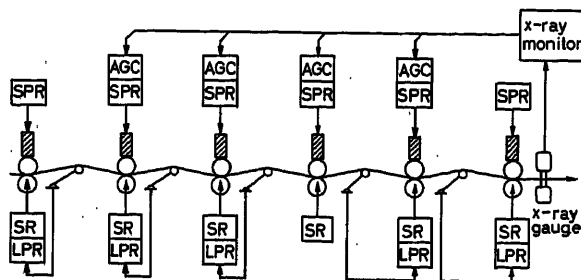


Figure 1. Regulating system for 6-stand hot strip finishing mill
AGC, automatic gauge control SR, speed regulator
SPR, screwdown position regulator LPR, looper position regulator

centre stands which have gauge control, the screw position between successive bars is determined by the screw reference, while during the rolling of a bar, the screws are permitted to move under the action of the gauge control to maintain constant gauge. The gauge control utilizes the 'Gagemeter' principle wherein a gauge reference for each stand, set by operator or computer, is compared to the simulated exit gauge of that stand. (A simulation of exit gauge is determined from screw position sensors and roll force sensors.) Any gauge error is amplified and operates the screws. In addition to this local action of the gauge control, an error signal from the delivery x-ray gauge can slowly modify the reference of all stand gauge controls if necessary to achieve the final gauge accuracy. In addition, although they are not shown in Figure 1, sideguide position regulators are provided for use on manual or computer control.

Description of Computer Control System

It is important first to note that the computer control system described in this paper covers only the finishing mill portion of the hot strip mill. The system begins as the bar emerges from the reversing roughing mill and ends as the bar enters the down-

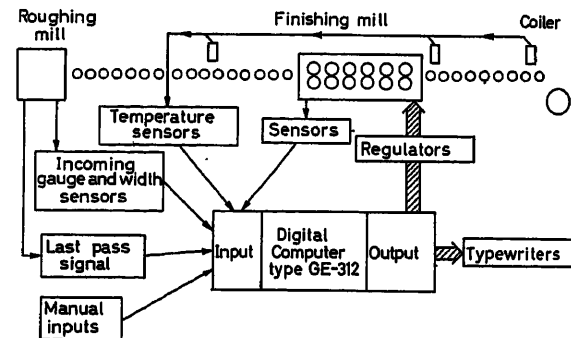


Figure 2. Computer system arrangement

coiler. Other much larger systems are now under design which include a greater number of processes within the scope of the computer control. A system of this type is briefly described in a later section.

The overall system diagram (Figure 2) shows the mill or process, the sensors, the regulating control systems, the manual inputs, the computer, and the output typewritten logs. All other information required by the computer to perform its duties is stored within the computer memory. Briefly, the data are as follows.

(a) Numerical data which describe the characteristics of all grades of steel which are to be rolled. Primarily, these data consist of constants which permit the rolling power and force to be calculated for the process. In addition, the data include the x-ray gauge composition adjustment which is required for the instrument to measure accurately the various alloys.

(b) Effect of rolling variables such as temperature and speed on the steel data mentioned above.

(c) Mill and drive system data such as mill modulus, stand motor power and speed ratings, roll diameters, operating limits, etc. (Roll diameter is entered by the operator after each roll change.)

(d) The process mathematical model which permits the set-up calculation to be made from the stored steel data and mill and drive data.

The operation of the computer system can be visualized by considering the steps required for a single bar to pass through the finishing mill. Before the bar reaches the last roughing pass in the previous mill (roughing mill), the operator must have entered into his manual input desk the information which is required to describe the product to be rolled. When the reversing rougher begins its last pass, as noted by a relay closure, the inputs to the computer are read from the sensors on the roughing mill screws and from the switch settings on the manual input desk. At this time, calculations for a 'first' set-up are made and sent to the mill regulators approximately 5 sec after the last roughing mill pass has begun. This first set-up calculation assumes an average temperature, and its purpose is to cause the screws, speeds, guides, etc. to be near to the correct value. Thus, no time is lost waiting for major changes in setting when the second set-up calculation is transmitted as described below. The computer will skip this first set-up signal if the mill is already filled or if the previous product is quite similar to the next.

When the incoming bar reaches the pyrometer over the delay table, a 'second' set-up calculation is made, based upon the actual temperature observed, and this second set-up is then sent to the mill regulators. Using this new set of references, the mill regulators settle on the new set-up just before the bar enters stand 1. After the bar is in stand 1, the computer makes a check to determine if the thickness out of stand 1 is correct. If it is not, a 'third' set-up is made and sent to the regulators before the bar enters stand 2. From this point on, the mill is under the control of the regulators while the computer is observing the results to improve and brings stored information up to date for the set-up on the next bar.

When the tail end of the bar leaves the last stand of the finishing mill, the computer types a production log which classifies each foot of material rolled into gauge and width deviation bands, and also indicates the length of prime material in feet. In addition, the log shows data such as order number, desired gauge, desired width, and finish and coiling temperatures. When selected by a supervisor, an engineering log is typed which gives for each stand the observed speeds, forces, screw positions, amperes, volts, etc. A sample of this log is shown in *Table 3*.

Set-up Calculation

In brief, the set-up calculation proceeds as follows. Based upon the input information for the product ordered, the computer first calculates the desired gauge out of each stand in order to have the main drive motor loads distributed in the pattern requested by the operator. Next, the strip speed out of each stand is calculated from the fact that (speed \times gauge) or mass flow is equal in all stands. Next, the computer calculates the rolling force in each stand and thence the mill stretch of each stand. Finally, then, the screw setting is calculated as (gauge) minus (stretch) for each stand. (The screw setting calculated in this fashion is often called the 'unloaded roll opening'.) These three major quantities of speed, interstand gauge, and screw position together with the width, x-ray set, and x-ray composition setting are then transmitted to the mill as the set-up references.

In the above few brief words outlining the set-up calculations, many man-years of engineering effort lay hidden. It was

necessary to develop new means of calculating rolling power and rolling force in each stand if the set-up was to divide power and predict stretch accurately. Methods used in the past and described in the literature were just not accurate enough. The old calculating procedures were sufficient to select motor size and bearing size and the like, but they were not sufficiently accurate to permit the setting up of a mill to produce on-gauge material, with proper load distribution, and to allow the mill to thread smoothly with no stretching or looping at the head end. It was necessary, therefore, to extend the existing power and force calculating techniques with new analytical procedures and then carefully correlate the approach with observations on the mill. Similarly, the mechanical characteristics of the mill had to be carefully considered and represented mathematically in the computer. The stretch of a stand, for example, can be perhaps 3/16 in. and in addition it is not linear with force. As another example, a representation of roll and mill heating and roll wear had to be included since these factors produce significant changes in roll diameter. Without this compensation, product quality and mill operation would be unacceptable. Electrical drive characteristics had to be included in the mathematical representation—for example, it is important to remember that when a stand is operated at reduced voltage, the power allocated to that stand must also be reduced.

Also, the set-up calculation has certain self-protecting features. For example, the system never allows a product to be rolled which is beyond the capacity of the drive equipment. If the operator requests a product to be rolled in a manner which is beyond the speed or power capacity of a stand or two, the computer first tries to shift loads, or change speed to fit the product to the mill. If the product is actually impossible to roll, the computer informs the operator of this fact and requests another instruction.

Of course, another practical problem occurs when the operator requests one or more stands to be dummied, i.e. removed from service. It is common practice to dummy the later stands for heavy gauge, but in addition, any stand may be dummied for repair work. When on computer control, the operator dummies a stand simply by selecting zero load on the stand. Under this condition, the set-up calculation must shift the load and speeds which would normally be calculated to apply to a mill with a reduced number of stands.

Bar-to-Bar Correction Calculation

The process model used in the set-up calculation and described previously, is constantly brought up to date by the computer itself. Each time a bar of steel enters the mill, the computer observes the process sensors, and brings both the process stored data and the stored mill characteristics up to date. It has been found that this is absolutely necessary if the stored data are to match the process minute by minute. Without correction of some sort, stored data which are accurate at one moment would not set up the mill accurately later. For example, there can be variations in steel chemistry or in sensor calibration which require that the data be adapted to the present condition. Of course, it is obviously necessary to remember that the initial stored data are not absolutely accurate for the average case either.

Briefly, correcting calculations are included to improve the gauge, the load distribution, and the mill threading performance.

These calculations are based upon the feedback from the process sensors which are observed at or near the head end of each bar as it enters the mill. The results of observations from each bar are applied to the set-up calculations for the next bar.

The Power of a Computer

The computer is an amazing tool for mill control. Its giant memory and speed of operation make it truly a superhuman operator. The computer can make multiple decisions from a mass of stored information in the blink of an eye. A human operator works from rules of thumb and a general impression of the mill—his memory at best includes only a general feeling about characteristics of various steels and the influence of variables. On the other hand, these characteristics are contained completely in the computer memory in the form of thousands of words of data, and these characteristics can be summoned from the computer memory in a fraction of a second. As for speed, the computer can make a complete calculation and transmit it to all the regulators on the mill for a new set-up in a matter of seconds. This can reduce the set-up delay and can permit greater productivity. The computer speed is particularly

apparent in the calculation for set-up number 3 mentioned earlier. For this set-up, after the bar enters stand 1, the computer makes observations to see if an error exists, and if so a new set-up is calculated, transmitted and the set-up modified—all in the two seconds before the steel enters stand 2.

Overall system reliability is increased by utilizing the computer's ability to scan and detect abnormal conditions on the process and within its own function. The protective actions included are self-diagnostic operations, programmed high and low limits and reasonableness analysis. The first two bear more on the computer as a system component, the last from the process point of view.

A small portion of the reasonableness analysis provided for the set-up calculation is shown by the logic diagram *Figure 3*. Part of the logic described here was briefly mentioned previously.

The Differences Between Computer and Manual Operation

During manual operation, the operator sets up the mill in preparation for rolling a bar. If his set-up is good, he depends, while the bar is being rolled, almost entirely on the existing regulating systems previously described—that is, speed regula-

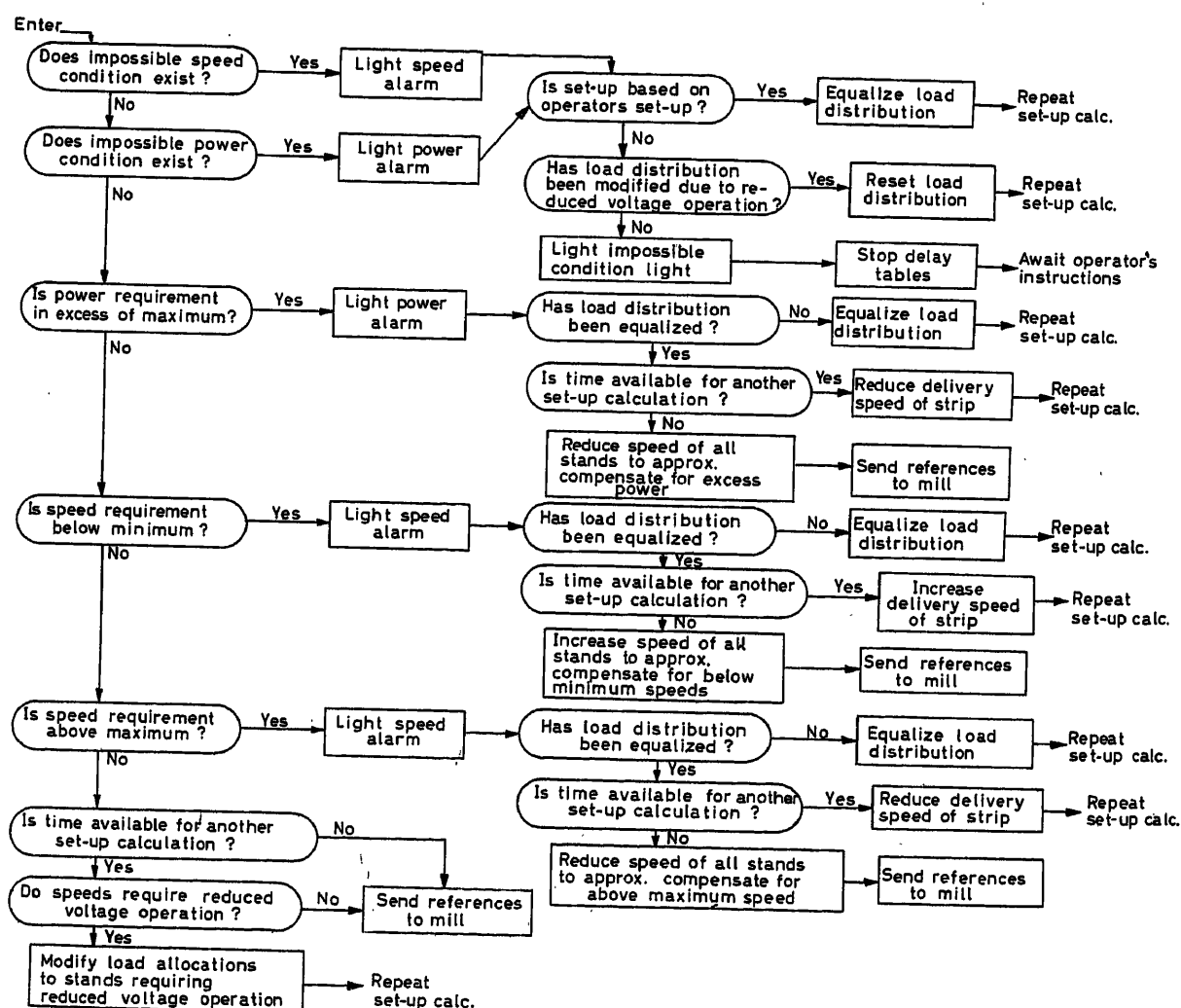


Figure 3. Sample logic diagram

tors, looper position regulators, gauge controls, and screw position regulators. The computer performs functions quite similar to the human operator. The computer 'makes' the set-up, but depends upon the existing regulating systems to manage the process during rolling. During the rolling of a bar the computer is reviewing the operation to improve the next set-up.

The major difference between computer and manual operation is this: during computer control, it is the computer rather than the operator which supplies the process knowledge, makes the calculations for the set-up of screws and speeds, etc., automatically transmits these references to the mill itself, and finally, observes the results for self-improvement. These basic elements of the operation normally are the main functions requiring skill and long experience from the human operator. These differences can be seen in *Tables 1* and *2*.

Besides the basic differences summarized in the previous paragraph, minor differences can be seen in the first column of *Tables 1* and *2*. For computer operation, incoming widths, thickness, and temperature are sensor inputs. This makes the computer automatically compensate for changes in incoming product. On manual control, the operator depends upon the schedule and on voice communication for width and thickness information.

Summarizing, then, the operator's task during computer operation is reduced from 24 set-up references (see *Tables 1* and *2*) to four pieces of simple information regarding product description. Furthermore, these four pieces of information are entered into the computer during the previous bar. Thus the operator has no tasks between bars, and the set-up operation is effected at high speed by the computer in the short space between bars.

Table 1. Description of Manual Rolling

<i>Incoming information</i>	<i>Preparation for rolling</i>	<i>During rolling</i>
<i>Order sheet</i> Finish gauge Finish temperature Type of steel Width <i>Voice communication</i> Entry gauge <i>Sensors</i> Entry temperature <i>Operator's knowledge</i> Steel characteristics Mill condition Drafting practice Speed for temperature	<i>Operator sets-up</i> Stand speeds 6 Screwdowns 6 Gauge control 4 Sideguides 7 X-ray 1 — 24	<i>Control regulates</i> Speed Looper height Gauge Screw position <i>Operator's responsibility</i> Observe to improve set-up Levelling Emergencies

Table 2. Description of Computer Directed Rolling

<i>Incoming information</i>	<i>Preparation for rolling</i>	<i>During rolling</i>
<i>Order sheet</i> Finish gauge Finish temperature Type of steel <i>Sensors</i> Entry temperature Entry gauge Entry width <i>Operator's knowledge</i> Mill condition Speed for temperature	<i>Operator informs computer</i> Finish gauge Finish speed Type of steel Deviation from normal drafting <i>Computer sets-up</i> Stand speeds Screwdowns Gauge control Sideguides X-ray	<i>Control regulates</i> Speed Looper height Gauge Screw position <i>Computer observes</i> Observes to improve set-up <i>Operator's responsibility</i> Levelling Emergencies

Results

While gauge accuracy is not the only means of describing the performance of the system, it is an important factor. Fortunately, gauge accuracy can be measured fairly dependably. For this purpose, the results from a digital gauge logger have been analysed at several stages during the course of the project. Using signals from the x-ray gauge and from a pulse per foot generator, such a logger classifies each foot of strip into gauge deviation bands. At the end of each bar, the logger types out the number of feet in each deviation band. In this way, the gauge quality of thousands of bars can be collected and analysed. Before the installation of the computer, a separate gauge logger was used to obtain this information. However, since the computer's installation, the computer's production log, which gives this same information, has been used.

Figure 4 (a) is a summary of the results of these analyses. In early 1960, before the gauge control or speed regulators were

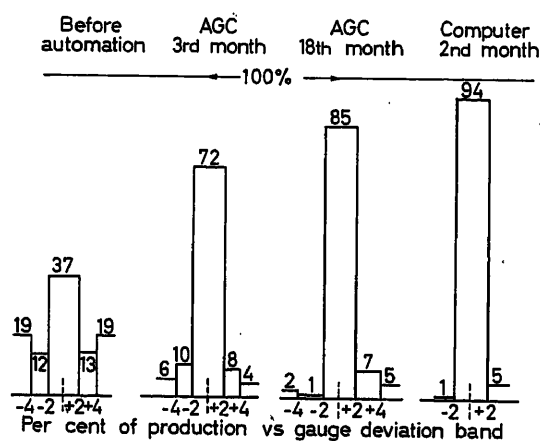


Figure 4 (a). Improvement in gauge accuracy

installed, only 37 per cent of the production was within ± 2 mils, while 38 per cent was more than 4 mils from the desired gauge. This accuracy may not look very good, but actually it is fairly typical of a mill without gauge control which changes orders very frequently. In the third month after the installation of the gauge control, the quantity of product between ± 2 mils increased to 72 per cent. By the eighteenth month, after more adjustment and more experience, the quantity within ± 2 mils increased to 85 per cent. However, there is still 7 per cent of the product more than 4 mils off gauge. Most of this 7 per cent is due to poor operator set-up for order changes. In the second month of computer operation, the ± 2 mil band had been increased to 94 per cent. While this is a respectable increase over manual operation, still further increases are expected. Since the last survey, a number of improvements in the technical approach have been implemented.

As mentioned earlier, gauge accuracy is not the only means of describing performance. However, most of the other characteristics of performance are more difficult to state numerically. For example, it is significant that the computer memory contains the rolling data for some 40 grades of carbon and stainless steel and for all gauges from 0.040 in. to 0.399 in. Regardless of the size of the order change, the computer can make the change with ease. Prior to the use of the computer, the produc-

tion practice required that the gauge change between successive orders does not exceed 0.070 in. Now there is no limitation. Since successive orders can be different by any amount, the production scheduling problem is simplified. Another characteristic of the system is that operator skill is less important for good quality. For example, one of the most difficult tasks facing an operator is a start-up with new rolls in all six stands. Many mills always start up on a standard product since the operators know the set-up for certain products. Even then, the first bars are frequently off gauge. With the computer, the mill can be started up on any gauge—that is, any gauge which can be rolled on cold rolls, and one can expect even the first bar to be on gauge. Figure 4 (b) shows a comparison of a manual start-up and a computer start-up, each following a roll change. In both cases, all six sets of rolls were changed, and the mill started up on 0.120 in. gauge low carbon. The chart at the top of the figure shows the first three bars on manual control and then the computer was turned on. The middle channel shows that the gauge deviation varied from 4 mils light to 7 mils heavy on the first and second manual bars. The chart at the bottom of the figure shows a similar start-up on computer control and the gauge is seen to be very good.

It may be of interest to see a sample of the engineering log to see the form of the presentation and to observe the accuracy of calculation, and Table 3 shows such a sample. The log for each bar consists of two lines of typing. At the beginning of the first line is the incoming information from the operator or from sensors read before the bar enters the mill. The remainder of the first line are actual values as observed by the computer from the mill sensors while the bar is being rolled. The second line of data are the computed values which the computer predicted in its set-up calculation. Some of the items require explanation. The actual stand gauge of the first line is calculated from observed values of screw position and stretch. It must be remembered that all the actual values are measured after the bar has entered and transients have settled out. Thus, part of the reason for discrepancies between actual and computed values is that the regulating loopers and the gauge control have made some changes in speeds, screws and forces. However, it can be seen that the agreement generally is quite good.

Electrical Equipment Description

Both the control regulators and the computer itself are fully transistorized with modular construction. The control is built in a drawer construction of the type shown in Figure 5. This type of control equipment utilizes a complete family of transistorized digital and analogue elements which are inserted into the drawers. In this way, these elements are combined in building block fashion to produce a great variety of industrial control systems. The elements can be combined and used with conventional control equipment or with the digital computer.

The GE-312 digital computer (Figure 6) is a 20 bit, fixed point binary machine with over 60 basic commands. The machine uses a 16,000 word drum with 12.5 msec maximum access time. The word time is 96 μ sec. The input-output section uses mercury-wetted relays and has a capacity in this installation for 160 analogue or digital inputs and 30 output signals. This capacity can be expanded as required. Analogue input signals can be read in any order at a rate of 20/sec, but can be 160/sec under certain conditions.

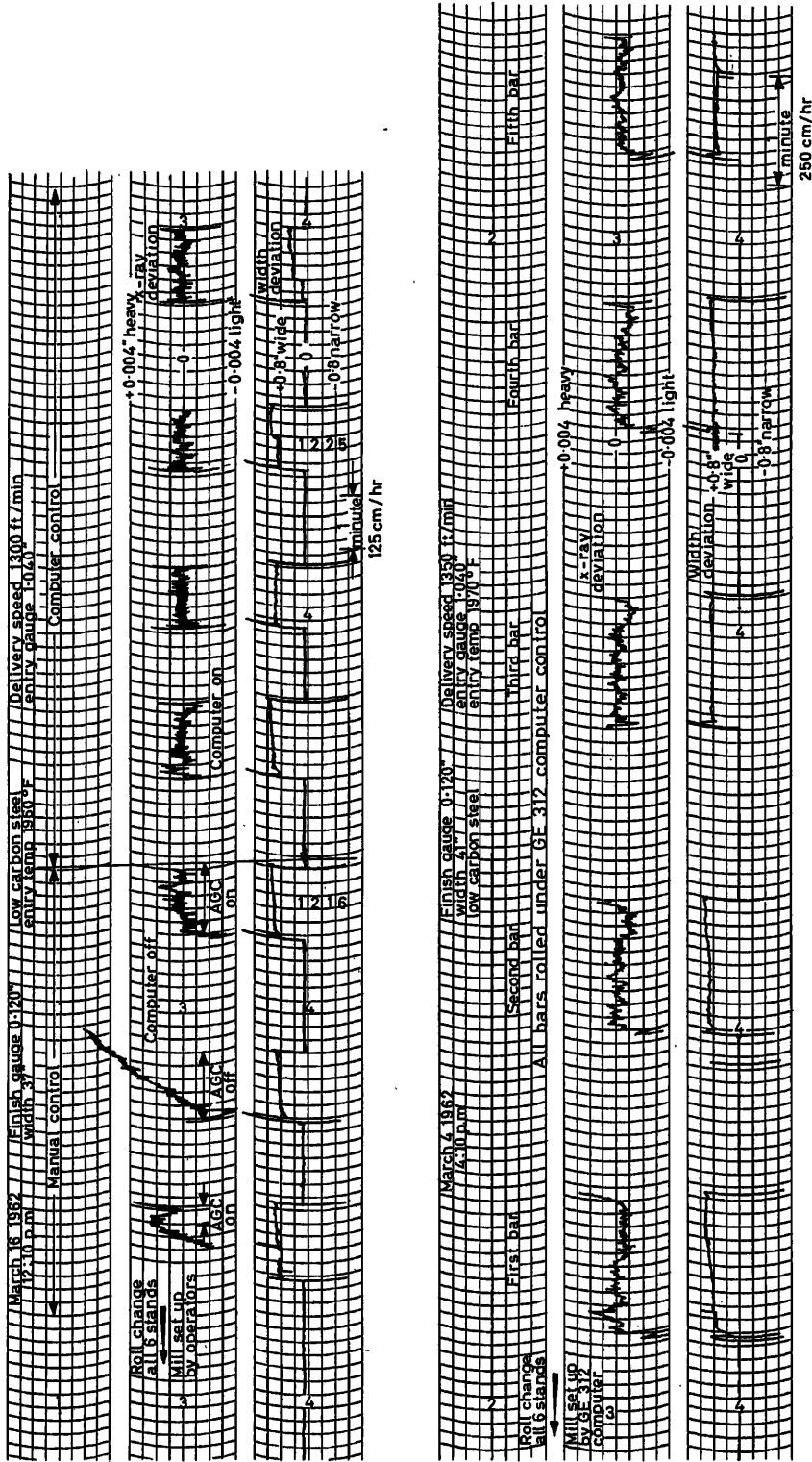


Figure 4 (b). Example of system start-up following roll change

Table 3. Sample of

INCOMING INFORMATION											SPEEDS						FORCES					
DATE	TIME	ORDER NO.	COIL NO.	STEEL GRADE	FINISH GAUGE	FINISH TEMP.	ENTRY TEMP.	DESIRED SPEED	ENTRY GAUGE	ENTRY WIDTH	(FPM)						(TONS ÷ 10)					
											STD 1-6						STD 1-6					
0803	0929	9242	008	02	118	160	198	1340	101	334	0285	0449	0650	0890	1147	1335	121	102	090	082	079	056
											0288	0449	0655	0896	1165	1355	115	096	092	079	079	056
0803	0930	9242	009	02	118	160	199	1340	101	335	0278	0441	0643	0883	1140	1326	121	102	091	082	079	055
											0285	0446	0654	0894	1162	1352	115	097	092	080	080	055
0803	0932	9242	010	02	118	161	202	1310	100	334	0276	0439	0639	0869	1121	1302	120	102	092	079	080	058
											0278	0436	0641	0873	1137	1322	115	096	090	077	079	053
0803	0934	9248	001	02	104	160	200	1470	101	331	0290	0458	0680	0948	1235	1423	123	096	100	085	079	047
											0292	0461	0700	0971	1275	1482	126	102	094	084	078	046
0803	0936	9248	002	02	104	161	201	1470	100	331	0283	0456	0679	0947	1240	1424	121	101	096	085	084	048
											0292	0470	0700	0974	1284	1493	121	102	094	084	080	047
											00											
0803	0948	9232	001	02	105	158	199	1450	100	343	0288	0480	0689	0951	1223	1403	126	098	083	090	078	050
											0293	0473	0702	0974	1272	1480	128	107	100	088	086	051
0803	0950	9232	002	02	105	159	198	1450	101	343	0294	0474	0701	0970	1261	1451	129	095	098	083	089	053
											0294	0469	0706	0967	1277	1485	128	099	099	086	087	053
0803	0953	9239	001	02	093	158	198	1570	100	332	0291	0476	0715	1005	1332	1546	125	099	100	086	092	051
											0302	0487	0745	1027	1373	1596	116	110	108	091	090	052
0803	0955	9239	002	02	093	159	200	1570	101	333	0296	0484	0731	1017	1329	1541	124	095	094	080	088	051
											0301	0495	0745	1037	1372	1595	120	101	099	086	087	051
0803	0957	9239	003	02	093	159	200	1570	100	335	0295	0487	0734	1026	1346	1554	122	099	093	084	090	052
											0300	0497	0747	1046	1373	1597	120	100	096	085	088	051
0803	1000	9239	004	02	093	159	199	1570	100	335	0296	0490	0734	1025	1334	1537	125	099	095	084	084	052
											0300	0498	0754	1051	1370	1593	124	101	098	085	088	053
0803	1001	9239	005	02	093	160	198	1570	101	335	0294	0492	0743	1039	1350	1556	123	103	096	083	086	055
											0296	0492	0747	1047	1373	1596	121	101	098	085	086	054
0803	1004	9293	006	02	093	160	198	1570	100	335	0296	0496	0742	1037	1342	1558	122	100	092	082	081	055
											0297	0491	0747	1048	1370	1593	121	100	098	084	086	055
0803	1008	9223	001	02	075	157	206	1620	100	354	0277	0509	0766	1078	1384	1600	137	112	090	092	076	051
											0298	0529	0795	1101	1411	1640	109	118	101	093	086	054
0803	1011	9223	002	02	075	159	207	1620	100	356	0262	0468	0724	1043	1382	1605	126	102	109	100	092	055
											0272	0477	0756	1063	1411	1640	107	104	106	094	092	053

ON-LINE COMPUTER CONTROL OF A HOT STRIP FINISHING MILL FOR STEEL

Engineering Log

FIRST LINE, EACH BAR — ACTUAL VALUES IN BLACK
SECOND LINE, EACH BAR — COMPUTED VALUES IN RED

GAUGES	SCREWS	CURRENTS	VOLTAGES
(MILS)	(MILS)	(AMPS ÷ 10)	(VOLTS)
STD 1-6	STD 1-6	STD 1-6	STD 1-6
556 353 244 178 139 120	568 372 283 226 193 142	0337 0293 0279 0270 0261 0209	726 721 727 732 748 726
555 356 244 178 137 118	576 375 277 226 189 139		
559 354 243 178 138 118	572 374 282 227 193 142	0324 0289 0276 0274 0255 0205	726 719 728 732 742 729
559 358 244 178 137 118	572 377 278 225 189 141		
560 355 243 178 137 121	571 373 280 230 192 142	0324 0295 0272 0259 0259 0195	727 724 728 730 744 728
561 358 243 179 137 118	570 376 278 228 190 142		
527 333 221 159 122 108	534 359 252 206 178 144	0356 0275 0316 0281 0261 0192	722 717 722 734 745 733
528 335 220 159 121 104	533 355 256 206 177 140		
528 328 222 159 123 106	539 350 255 204 172 141	0336 0296 0302 0288 0290 0179	723 718 726 738 744 729
532 330 222 159 121 104	540 349 254 204 173 139		
526 323 221 158 119 104	522 338 261 195 173 135	0348 0334 0265 0305 0253 0208	726 728 724 739 753 730
530 328 221 160 122 105	519 332 243 196 166 133		
524 325 218 158 122 104	518 350 246 202 161 129	0365 0311 0325 0286 0304 0204	725 722 724 736 745 729
531 332 221 161 122 105	519 347 242 197 160 128		
499 309 204 146 111 095	496 339 228 186 147 121	0352 0299 0330 0294 0310 0196	730 723 727 735 748 737
506 312 203 146 108 093	498 325 220 181 146 118		
494 299 200 143 110 094	492 328 231 189 152 121	0368 0299 0316 0279 0290 0210	730 726 729 734 740 725
494 300 199 143 108 093	493 322 224 183 151 120		
494 297 199 143 110 095	497 322 233 187 151 121	0356 0316 0305 0300 0307 0200	730 723 727 735 745 729
495 299 199 142 108 093	497 321 227 183 150 119		
490 295 197 141 108 093	490 317 229 185 156 121	0377 0315 0305 0287 0281 0205	728 721 725 738 742 725
493 298 197 141 108 093	491 316 224 182 150 118		
494 293 198 142 110 095	498 312 229 186 156 119	0368 0333 0310 0295 0292 0192	728 722 727 734 747 745
488 295 196 141 108 093	502 313 223 182 152 116		
491 296 197 140 109 094	498 316 234 188 161 118	0364 0329 0296 0291 0262 0217	731 727 728 731 746 737
491 298 197 141 108 093	501 315 224 184 153 116		
436 240 160 114 087 075	429 251 200 151 145 104	0403 0368 0262 0302 0217 0207	731 731 732 739 745 736
432 241 159 113 087 075	429 247 187 150 135 102		
470 265 169 118 089 077	465 283 190 148 129 101	0340 0323 0341 0321 0298 0193	729 730 728 737 742 736
471 267 167 117 087 075	463 282 188 152 127 100		

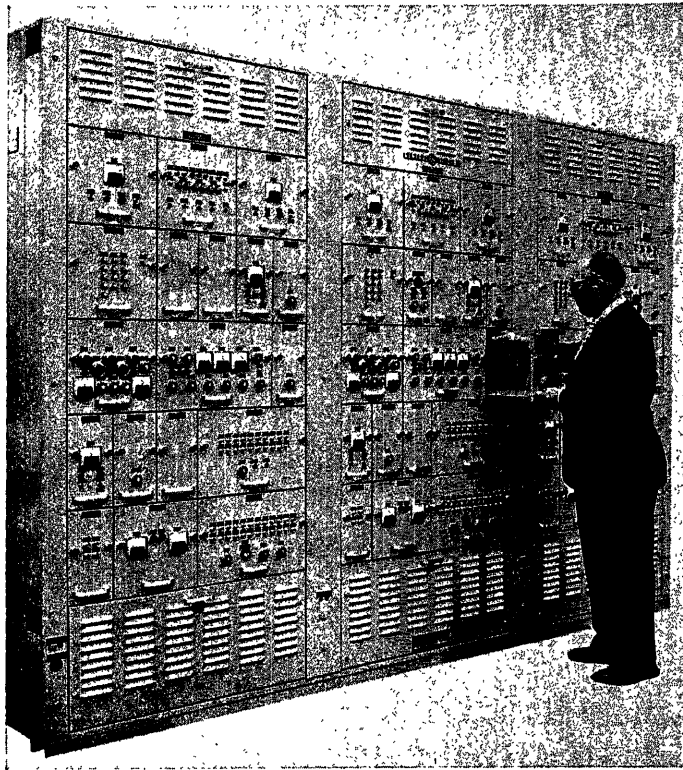


Figure 5. Control equipment (ICF-14904)

Future Systems

A much larger computer control system is now being manufactured for a complete hot strip mill. This system will supervise and control the hot strip mill area extending from the input side of the reheat furnaces, through the furnaces, through

the continuous roughing mill and finishing mill, through the run-out tables and sprays, and to the exit side of the coilers. Being a much larger process, the system will utilize a larger machine known as type GE-412 digital computer. In addition to being larger, that machine is also faster and employs both a magnetic core and a drum memory. This larger process computer control system will have five basic functions:

- (1) Slab tracking—keeps track of all slabs entering or leaving the process, the location of each slab at all times in the process, and by means of visual displays informs all operators in the process of the identity of all slabs in each area.
- (2) Mill pacing—controls the rate at which slabs are processed through the mill. This is accomplished by controlling the rate at which slabs are pushed from the reheat furnace such that the limiting part of the process is kept fully loaded.
- (3) Temperature control—aims to achieve the requested finishing and coiling temperatures which are required for metallurgical reasons. This is accomplished by making adjustments in furnace delivery temperature, and roughing and finishing mill set-ups.
- (4) Set-up—similar to the system described, but for the larger area is expanded to include both the roughing mill, finishing mill, sprays, etc.
- (5) Logging—causes several typewriters to prepare various typewritten records of the process both for production control and engineering purposes.

There are significant economic advantages for a large computer control system directing the complete hot strip mill area. Economic studies have shown that the improved operations result in annual savings equivalent to 25 to 50 per cent of the system cost. These savings are due to improved quality of gauge, width, and temperature, higher production due to fewer cobbles and better mill utilization and improved labour costs.

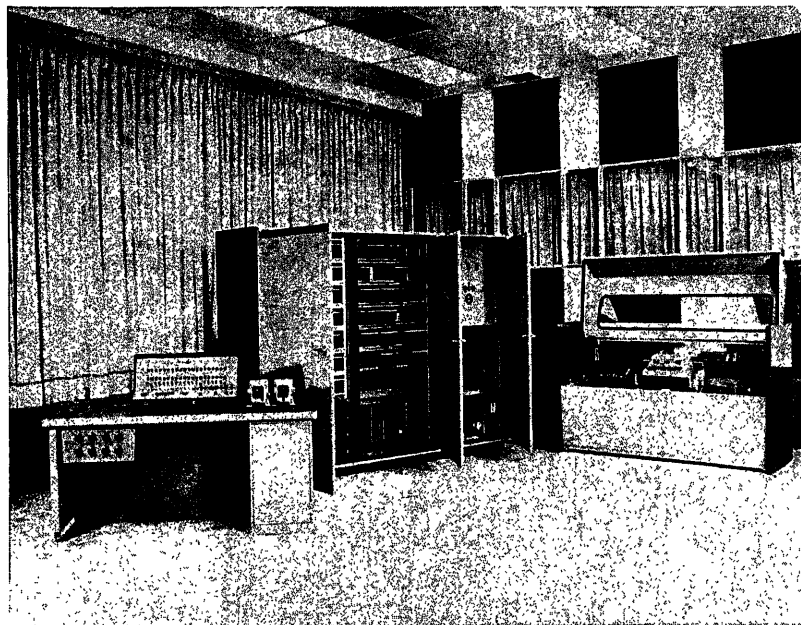


Figure 6. GE-312 computer

Conclusion

The use of a computer in a process control system is a significant step in industrial automation. Even in a simple form as described here for the finishing mill only, the computer directed system provides significant benefits in product cost. In addition, and this is frequently said to be true for any computer application, the study required to apply the computer has brought about a much better understanding of the process. The increased process knowledge will benefit all future hot strip mills and should point the way towards many as yet unforeseen advances.

References

- 1 MAXWELL, H. S. A computer-controlled hot strip finishing mill. *J. Iron St. Inst.* 200 (1962)
- 2 MAXWELL, H. S. and PHILLIPS, R. A. System analysis and design for hot strip mills with automatic gage control. *Iron Steel Engr* (1960) 277
- 3 LARKE, E. C. *The Rolling of Strip, Sheet and Plate*. 1957. London; Chapman and Hall
- 4 BEADLE, R. G. and MILLER, W. E. Improving thickness control in hot strip mills. *Control Engng* (1961) 94

DISCUSSION

Author's Opening Remarks

The use of a process computer to control a hot strip mill has been one of the most successful applications of sophisticated automation in all industry. The computer has made significant improvements in yield and productivity, and is quickly becoming an accepted part of modern hot strip mill systems. The hot strip mill offers an ideal situation for the talents of computer control. First, the large annual production provides good economic possibilities, since a typical hot strip mill may produce two million tons of steel annually with a value of \$200,000,000. Second, the process requires frequent order change which can mean a new programme every 10 min on the average. Third, a computer eliminates the dependence on the skill of human operators. Fourth, the market demands increasingly higher quality steel from the hot strip mill.

The computer control system described in the paper is located on the 60 in. finishing mill at the McLouth Steel Corporation in Trenton, Michigan, U.S.A. The computer begins its control for each bar as it leaves the roughing mill, and performs all actions normally done by human operators at the finishing mill. Through calculation and sensor readings, the computer adjusts the screwdowns, speeds and sideguides, to cause the mill to thread smoothly with no tension or looping, to produce accurate thickness on every bar, and to divide the rolling load properly on the six stands. And, as each bar passes through the mill, the computer calculates feedback quantities from the process which improves the programme and data stored for subsequent bars. This is the one requirement that makes a computer system so much more powerful than a programming system.

The computer at McLouth Steel has been operating full time since last year. Its dependability has been exceptional, with an availability record of more than 99.5 per cent, even though the mill rolls 24 h per day with an 8 h idle period every two weeks. With the aid of the computer, the mill repeatedly has set new tonnage records. Approximately 91 per cent of the production is now rolled by computer.

A much larger hot strip mill computer control system is now being put into operation at Richard Thomas & Baldwins in Wales. The McLouth system performed only finishing mill set-up, whereas the above-mentioned system encompasses the whole process from reheat furnace to coilers. Furthermore, the McLouth system obtains its order instructions from operator manual inputs, while the Richard Thomas & Baldwin computer receives its order instructions on punched paper tape from the scheduling computer described in the previous paper by Hersom and Massey.

The computer is now installed and it is logging and is in the early stages of control operation. However, some months will be required before any results can be reported.

There are several display and manual input stations at strategic locations throughout the mill. In general, these stations are used only when the operator wishes to take exception. The stations display the order in process, permit automatic functions to be selected, and permit the operator to insert data manually when necessary.

When the Richard Thomas & Baldwin system is fully implemented the economic benefits promise to be significant.

G. SCHLIEPHAKE, *A.E.G. Stromrichterfabrik, Berlin 65, Germany*

The described mill is rectifier fed on all stands. There are no provisions made for regenerative braking, i.e. no inverters.

Have you had any trouble with the quick speed changes required by the computer after a recalculation during the rolling process or, more specifically, just before the material is entering the second stand?

To avoid such possible troubles, would you provide back-to-back rectifiers for armature feeding or MG sets with SCR excitation when planning new computer controlled hot strip mills?

R. G. BEADLE, *in reply*

When a motor is decelerated, the kinetic energy stored in the rotating mass must be dissipated. When the power supply is a rectifier, some special arrangement must be employed to accomplish this deceleration. In the case of the McLouth mill, a slow-down resistor is connected across the motor armature when energy must be removed from the motor. To answer Mr. Schliephake directly, no difficulty has resulted from the slow-down resistor being connected at the moment of impact when a new bar enters the stand.

Actually, little difficulty would be expected since the slow-down resistor absorbs only 20 per cent of rated current. Thus, in the worst case, it represents only an additional 20 per cent load on the rectifier. However, because of the nature of the computer operation, it is very unlikely that the slow-down resistor will be connected at the moment of impact. The resistor 'picks up' only for speed changes greater than about 3 per cent. Such speed changes will occur for set-up No. 2, but then there is sufficient time for the speed to reach its final value and the resistor to drop out before the new bar enters. On set-up No. 3, time is very short, but the speed changes are very minor. Thus, the resistor is not likely to pick up.

In summation, then, no difficulty has been encountered. The evaluation of various power supply techniques depends on broader operational problems beyond the scope of this paper.

M. H. BUTTERFIELD, *International Systems Control Ltd., Wembley, Middlesex, England*

(1) What is the basis for the allowances for roll wear and roll temperature mentioned in the paper, or is this achieved by the automatic gauge control system?

(2) Does the author have any data on the effects of tension used in gauge control on strip width?

(3) What control does the operator have on 'shape'?

(4) Automatic gauge control alone will yield large benefits. What additional benefits arise from use of a digital computer? For example, under manual operation, setting up a gauge control system will elaborate mill operation.

R. G. BEADLE, *in reply*

(1) It is extremely important to account for the effects of roll heating and wear since these effects are significant and must be considered to calculate accurate set-ups. These effects are predicted by the mathematical model, and then corrected by a combination of process feedbacks.

(2) The gauge control employed at McLouth uses no tension variation but only the screws of stands 2, 3, 4 and 5. Tension variations should generally be avoided because of the adverse effects on strip width. However, some gauge control systems may use slight variations in the tension between the last two stands to achieve a slight vernier gauge control. This vernier is quite small and produces no measurable effect on width.

(3) One of the manual inputs available to the operator is the 'load distribution' input. The computer is programmed to produce the nominal load distribution required for the particular product to achieve good shape and temperature. Normally the operator is content with this nominal distribution and makes no manual change. If, however, due to special roll conditions, he must request a special load distribution to achieve shape, he may do so.

(4) It is difficult to predict the relative benefits of gauge control and computer control. The performance of gauge control is still dependent to some extent on the operator's skill. If the operator makes a poor set-up, the gauge control will only partially correct it. However, with computer control in addition to gauge control, final performance is nearly independent of the operator. In the specific case of McLouth it has been estimated that the gauge accuracy is improved by the gauge control and the computer by about equal amounts. Of course, the computer provides additional yield and productivity benefits beyond gauge improvement.

P. C. DANNATT, *A.E.I.-Automation Ltd., Cheshire, England*

One of the problems in writing a computer programme to calculate the screw, speed and other set-up values for a hot strip mill is to settle on a criterion to decide the relative loadings of the mill stands. Could Mr. Beadle indicate what criteria are used within the computer programme to determine the relative power and roll separating forces on each of the stands?

I am assuming that the computer does calculate the relative loadings on stands, though I have noted on the Richard Thomas & Baldwin finishing mill a manual input facility for this fundamental feature of the set-up calculation. Does the computer programme require the load distribution to be set up manually, under any circumstances?

R. G. BEADLE, *in reply*

My previous answer to part (3) of Mr. Butterfield's question answers Mr. Dannatt's query about load distribution. Based on the desired load distribution, the computer calculates the gauge out of each stand, and from this, the force in each stand. It is not possible at this time to discuss in detail the analytical method of power and force calculation.

R. JOETTEN, *A.E.G., 1 Berlin 28, Huttenstr. 16, Germany*

Are any provisions made in case a sensor fails? Surely such a failure is just as serious as the set-up of 'impossible conditions' without an alarm light provided therefore?

R. G. BEADLE, *in reply*

While the computer can partially compensate for sensor drift, it cannot really protect itself from an outright failure of a sensor. (Of course, this is likewise true for simple regulators which we accept in industry without a thought. If the tachometer of a speed regulator fails, the motor may overspeed and suffer damage.) With reference to McLouth,

we have found that the hot metal detectors which signal the location of the hot bar fail occasionally. Such failures sometimes confuse the computer, but fortunately are very rare and have not resulted in any damage.

C. RODENBURG, *Electrical Engineering Technological University, Enschede, Netherlands*

(1) How do you measure and control thickness in the transverse direction, e.g. crown, or when the rolls are not parallel?

(2) Can you give information on the accuracy of temperature measurements and the influence of scale, steam and water, for instance, on the strip?

(3) Your logging is per foot. That gives you per roll and per shift a lot of data and paper; how do you obtain a practical survey of the behaviour of the mill?

(4) Can you give any information on the development of new and better relations between rolling power and rolling force; are there any publications?

(5) How do you measure roll wear and roll heating?

(6) Can you give any information on the reliability of the computer and the off-time for maintenance and tests? Is switching over to the manual position possible during the rolling of a coil?

(7) Does the computer directly give the engineering log sheet or is further data processing necessary?

(8) If, in an existing plant, you want to install computer control of a hot strip finishing mill as done by your company, how much time and how many people are required to make: (a) The specification of the data logger? (b) Calculation of relations between rolling power and rolling force, etc., that is to find, from the data on the log sheet, the relations between the obtained information? (c) The decision, from the information obtained from 4 (a) and (b), which computer and technical outfit could do the job?

R. G. BEADLE, *in reply*

(1) We have no sensor for strip crown camber or flatness, and therefore make no attempt to control this automatically.

(2) I can give you no useful information regarding the accuracy of the temperature measurements. We are using normal 'total radiation' pyrometers and information on such devices is readily available from the instrument manufacturers. We have found satisfactory operation if the bar is thoroughly descaled, and is swept clear of water by a steam spray.

(3) The quality log produces one line of typing per coil and therefore does not result in excessive paper. However, your question is pertinent since the log should be used for continual evaluation of the operation. At the present time, this is done only occasionally.

(4) At this time nothing more can be stated about the force and power relations which we have developed.

(5) With reference to roll heating, see part (1) of my answer to Mr. Butterfield.

(6) For the first six months of 1963 the computer availability has been more than 99.5 per cent. At any time the operator may change any screw or speed manually if he desires, although this is only a safety measure and is seldom done in practice.

(7) The engineering log shown in my paper is produced directly by the computer.

(8) I do not believe it is possible to estimate on a general basis the time and man power required to add a computer to an existing mill. This depends too much on the functional requirements of the system you may be considering. We estimate that the McLouth system required about 15 man-years of special engineering, not including equipment design engineering.

Optimum Control for Continuous Processes

A. YA. LERNER

Summary

The principles of optimal control of production line processes, as applied to automation of continuous process control, are studied.

General expression is given for an optimal law of the process control with lumped parameters as well as a structure of the controller realizing the law. The paper presents the data of experimental studies conducted on the continuous heating furnace of a hot-rolling mill that prove the efficiency of the suggested system.

Sommaire

On envisage les principes de la commande optimale des processus en chaîne dans des installations automatisées.

On propose une expression générale de la loi optimale de la commande de l'installation à paramètres localisés et une structure du dispositif de commande réalisant cette loi.

On cite les résultats des recherches expérimentales exécutées avec un four continu d'un laminoir qui ont prouvé l'efficacité du système de commande proposé.

Zusammenfassung

Der Aufsatz enthält die Prinzipien der optimalen Regelung von Bandprozessen, wie sie bei automatischen kontinuierlichen Anlagen auftreten.

Es werden ein allgemeiner Ausdruck für eine optimale Regelung von Prozessen mit konzentrierten Parametern und der Aufbau der Regler zur Verwirklichung dieses Ausdruckes angegeben. Die in dem Aufsatz enthaltene experimentelle Untersuchung eines kontinuierlich arbeitenden Ofens einer Warmwalzstraße zeigt die Wirksamkeit des vorgeschlagenen Regelsystems.

Task of Control for Continuous Processes

The transition from periodic to continuous processes of treatment represents one of the basic trends in the technological progress of many branches of industrial production. The essence of this transition consists of the following. During the periodic processes of treatment certain portions of the material are subjected to some action which changes with time (for example, temperature, structure, shape), as a result of which the state of the material changes from the initial state to the assigned state. In a continuous process a continuous flow is arranged for the material to be treated, during which the material is subjected to a spatial action as a result of which it achieves the necessary change, during the time of action on each element of the moving stream of the material undergoing treatment.

This transitional trend towards continuous processes may be observed in examples of universal replacement of muffle-type furnaces by continuous furnaces, in examples of ever-increasing employment of continuous rolling mills, in examples of transition to continuous methods of manufacture for chemical products, building materials and so on.

If the task of control of periodic processes consisted of the selection and realization of the necessary programme for the

time-changing action on the material being treated, then the basic task of control in a continuous process of production would constitute in the selection and maintenance of such form of spatial action on the moving stream of material that would ensure the necessary change in its state.

In consequence of this, a continuous process should be regarded as a controlled plant containing the distributed-in-space parameters, which predetermines the necessity for a special approach to the construction of the systems of automatic control for such plants.

A failure to understand this and the transfer to such plants of methods of control, developed to conform to plants with lumped parameters, leads, generally, to a substantial decrease in the utilization of the possibilities of control and to a corresponding reduction in the accuracy of maintaining the necessary conditions of processing.

For the relatively simple cases of plants, amounting to uni-dimensional cases, the processes in the controlled plant may be described by means of a system of n differential equations with partial derivatives of the first order

$$f_i \left(x, t, Q, \frac{\partial Q}{\partial x}, \frac{\partial Q}{\partial t}, u, v, w \right) = 0 \quad i = 1, 2, \dots, n \quad (1)$$

where x is the space coordinate

$$(l_0 \leq x \leq l_1)$$

t the time

$$(t_0 \leq t \leq t_1)$$

$$Q = Q(x, t) = [Q_1(x, t), \dots, Q_n(x, t)]$$

the vector function, which characterizes the state of the plant,

$$u = u(t) = [u_1(t), \dots, u_k(t)]$$

$$v = v(x, t) = [v_1(x, t), \dots, v_r(x, t)]$$

$$w = w(x) = [w_1(x), \dots, w_s(x)]$$

$$z(x, t) = [u(t), v(x, t), w(x)]$$

the controlling actions.

It is necessary to take into account that for any actual systems the possibilities of control are limited by certain constraints such as those which result from the limited nature of the range of controlling actions and their derivatives, or from the limited nature of the region of permissible states of the controlled plant and so on, which may be written in the form of a system of inequalities, for example:

$$\left| \frac{d^\alpha u}{dt^\alpha} \right| \leq K; \quad \left| \frac{d^\beta w}{dx^\beta} \right| \leq N; \quad \left| \frac{\partial^{r+\delta} v}{\partial x^r \partial t^\delta} \right| \leq M. \quad (2)$$

The task of control for the continuous processes, as a rule, consists in maintaining the state of the material undergoing

treatment at the exit from the zone of treatment $Q(l_1, t)$ as close as possible to point Q^* , which corresponds to the assigned state of the material. In order to achieve these aims it is essential to so organize the change in the controlling actions $u(t)$, $v(x, t)$ and $w(x)$, that the effect of disturbing actions of different kinds on $Q(l_1, t)$ is compensated for as accurately as possible. In continuous processes the following changes should be considered as the disturbing actions: the change in the state of the material at the entry into the zone of treatment $Q_0(l_0, t)$, the change in the flow of the material through the zone and the change in the parameters which determine the progress of the process.

The requirement for the minimization of deviation of the state of material from that which was assigned for the exit from the zone may be written down in the form of a requirement for the minimization of the corresponding functional, for example

$$J_1 = \int_0^T |Q^* - Q(l_1, t)| dt = \min \quad (3a)$$

or

$$J_2 = \int_0^T [Q^* - Q(l_1, t)]^2 dt = \min \quad (3b)$$

which is the criterion for the efficiency of control, where T is the assigned fixed time.

Structure of the Control System

For the realization of a system of automatic control for continuous processes it is necessary to construct the control equipment in such a way that with any disturbances the controlling actions change in accordance with laws which would ensure the minimum value for the functional, which characterizes the criteria of quality, and is compatible with the constraints imposed on the system. In the systems with lumped parameters this is achieved by methods which result from the theory of optimum control and which make possible the finding of such a structure of the control device, for which the optimum controlling actions are formulated on the basis of information relating to the values of coordinates of the controlled plant and its assigned state.

The optimum controlling action for a system with distributed parameters is no longer a function of a finite number of coordinates of the controlled plant, as it is for a system with lumped parameters, but is an operator of the distribution functions which characterize the state of the controlled plant with distributed parameters.

This means that at every instant of time t the state functions $Q(x, t)$ are brought into line with the control function $Z(x, t)$, i.e. $Z(x, t) = J[Q(x, t)]$ $0 \leq t \leq T$ where J is the operator.

If one happens to be dealing with a single controlling parameter, which depends only on time t , then operator J in this special case is a functional which, with each state $Q(x, t)$, brings into line $u_1(t)$, the value of the controlling action at the instant of time t .

The theory of optimum systems with distributed parameters, which is now being developed, provides methods for the determination of the indicated operator J through which the law of optimum control is realized.

For the optimum control of a system with distributed parameters it is necessary at every instant of time t to obtain from the controlled plant the information regarding the distribution

function $Q(x, t)$, which enters into the optimum control system (OCS), at the exit of which the controlling action takes place.

However, with a real plant, as a rule, it is difficult to obtain directly the distribution function $Q(x, t)$, since this is associated with considerable measuring difficulties.

Therefore, the determination of $Q(x, t)$, in general, should be made by means of mathematical simulation of the plant.

In many cases the equations describing the process in the plant are known only with an accuracy up to the constants, which characterize the parameters of the process. The knowledge of these equations makes possible the finding of structure of the simulator of the plant.

For the determination of the unknown constants use may be made of the idea of self-adjustment. For this, the automatic optimizer, by searching, finds such values of the undefined parameters of the simulator that the criterion, which characterizes the error between the value of the distribution function computed on the simulator and the value actually measured at a certain point of the plant, is at a minimum. Thus, the measurement of the entire distribution is replaced by the measurement of this distribution only at a certain most accessible point (or at a number of separate points). Finally, in each individual case the correctness and the single-valued solution of this problem should be proved or verified in practice under quite diverse operating conditions of the plant. Thus, in this case the information concerning the state of the controlled plant for the OCS is received from the simulator of the plant.

Example of Optimum Control for a Continuous Reheating Furnace

As an example of the optimum control for a continuous process of production with distributed parameters consideration is given to the process of metal-heating in continuous reheating furnaces by means of a simulator. The continuous furnace is a typical plant with distributed parameters. This furnace heats the metal for a rolling mill (Figure 1).

The process of one-sided heating of metal in the furnace is described by differential equations with partial derivatives

$$\frac{\partial Q}{\partial t} = a \frac{\partial^2 Q}{\partial x^2} - V(t) \frac{\partial Q}{\partial y} \quad (4)$$

where $Q = Q(x, y, t)$ temperature distribution function for the metal related to the length of the furnace y ($0 \leq y \leq L$), to thickness of metal x ($0 \leq x \leq s$) and to time t ($0 \leq t \leq T$).

The boundary conditions

$$\left. \frac{\partial Q}{\partial x} \right|_{x=s} = \alpha [u(y, t) - Q_b(s, y, t)] \quad (5)$$

$$\left. \frac{\partial Q}{\partial x} \right|_{x=0} = 0 \quad (6)$$

$$Q(x, 0, t) = Q_b(x, t) \quad (7)$$

and the initial condition

$$Q(x, y, 0) = Q_0(x, y)$$

are known.

Here $V = V(t)$ is the positive function of time which characterizes the speed of motion of the metal in the furnace; $u(y, t)$ is the function which characterizes the temperature distribution

in the operating space of the furnace, which serves as the controlling action in the process for the control of heating of the metal; a coefficient which depends on the difference

$$\eta = y - \int_0^t v(\tau) d\tau \quad (8)$$

If it is assumed that the heated blanks are 'thin' materials of thickness s , then the process of heating is described by the more simple heat-exchange equation

$$b \frac{\partial Q}{\partial t} + bv \frac{\partial Q}{\partial y} + Q - u(y, t) = 0 \quad (9)$$

where $Q = Q(y, t)$ is the temperature distribution function for the metal related to the length $y, 0 \leq y \leq L$ and to time $t, 0 \leq t \leq T$; here b is a coefficient, which depends on $\eta = y - \int_0^t v(\tau) d\tau$. It has the form

$$b = \frac{c\gamma s}{\alpha} \quad (10)$$

where c is specific heat, γ is specific gravity, and α is the coefficient of heat exchange between the metal and the furnace. Coefficients c, γ and α also depend only on the difference $\eta = y - \int_0^t v(\tau) d\tau$.

The boundary condition

$$Q = (Q, t) = Q_b(t) \quad (11)$$

and the initial condition

$$Q(y, 0) = Q_0(y) \quad (12)$$

are known.

Many thermal, diffusion, electrical and other processes are described by the equations of the above-indicated type.

The task of the optimum control of the continuous reheating furnace was that with different disturbing actions [change in speed $v(t)$, change in the dimensions of the billet and in its make etc.] the temperature in the furnace $u(y, t)$ should be changed so that for time T it minimizes the mean quadratic deviation of temperature $Q(L, t)$ of the metal leaving the furnace from an assigned temperature Q^* , i.e.

$$J = \int_0^T [Q^* - Q(L, t)]^2 dt = \min \quad (13)$$

In the case of a thick material instead of $Q(L, t)$ in equation (13) it is possible to substitute

$$\tilde{Q}(L, t) = \frac{1}{s} \int_0^s Q(x, L, t) dx$$

It is assumed that the controlling action $u(y, t)$ does not depend on coordinate y and that it is only a function of time t . In this case the optimum u is a functional of distribution function $Q(x, y, t)$ or in the case of a 'thin' material it is a functional of function $Q(y, t)$.

Consideration is given to the most typical cases of disturbance for the process of heating of a metal in the furnace, i.e. (A) the disturbance caused only by the changes in speed $v = v(t)$ in relation to time, and (B) the disturbance through coefficient b , when there is a step-wise disturbance

$$b = b(\eta) = \begin{cases} b_1 & \text{when } L \geq \eta \geq \frac{1}{2}L \\ b_2 & \text{when } 0 \leq \eta \leq \frac{1}{2}L \end{cases}$$

where b_1 and b_2 are known constants. This case corresponds to the heating in the furnace of two batches of blanks having different thermo-physical properties or different dimensions.

Usually within the limits of the zone the controlling action $u(y, t)$ does not depend on the spatial variable y and is only a function of time, i.e. $u = u(t)$. The temperature in the furnace is restricted by limits $A_1 \leq u \leq A_2, A_1 < A_2$.

The optimum control in the case of disturbance of type (A) has the form

$$u = u(t) = Q^* + bv(t) \frac{\partial Q}{\partial y} \Big|_{y=L} = Q^* + bv(t) Q^1(L)$$

when $t = 0$.

In the case of disturbance of type (B) the optimum control amounts to the controlling action assuming the value

$$u = u(t) = A_1 \text{ if } b_1 > b_2$$

and

$$u = u(t) = A_2 \text{ if } b_1 < b_2$$

The instant of transition from the control based on type (A) to control based on type (B) and *vice versa*, is determined by the distance of the point of disturbance of coefficient b from the end of the furnace, i.e. from point $y = L$. The block diagram for the system of optimum control for a continuous reheating furnace is shown in Figure 4.

Simulation of Heating Processes in Continuous Reheating Furnaces

The question of simulation of the heating process for a 'thin' material in continuous reheating furnaces is now considered. It is assumed that the process is described by equations (9) to (12). Here the temperature in the furnace $u(y, t)$ depends on the distance y and time t .

We shall select a point, rigidly fixed to the moving metal, which at the instant of time t_0 was at $y = 0$. Let $u(t)$ be the temperature of the furnace, which acts on this point during its entire motion in the furnace up to the coordinate $y \leq L$. Then the heating equation for this point has the form:

$$b \frac{dq}{dt} + q = v(t) \quad (14)$$

where $q(t)$ is the temperature of the fixed point at the instant of time t with the initial condition determinable by the limiting boundary condition at the entry into the furnace when $y = 0$

$$q(t_0) = q_b(t_0)$$

Coefficient $b = c^* \gamma^* s^* / \alpha^*$ denotes heating time constant (c^* is the specific heat, γ^* the specific gravity, s^* the thickness of blank, and α^* the mean coefficient of heat exchange between the furnace and the selected point rigidly fixed to the moving metal).

It is easy to see that the function $u(t)$ has the form

$$V(t) = u \left(\int_{t_0}^t v(\sigma) d\sigma, t \right)$$

i.e. $V(t)$ is equal to the temperature in the furnace $u(y, t)$, where instead of y the expression $\int_{t_0}^t v(\sigma) d\sigma$ is substituted, which signifies the distance covered by the selected point in the furnace

entire track $v(t)$, and of the adding of this information in the scanning counter, and subsequent reading of this information in order to obtain the difference for the assigned value; thus, for a slab coming out of the furnace this difference will be

$$\frac{L}{a} = \frac{24.85}{32} \approx 0.77$$

where L is the length of furnace.

This algorithm is obtained from the line-of-direction scanning unit, which consists of a nine-division reversible counter and an assigned line-of-direction counter, the divisions of which are connected by the correspondence decoders. The second

$$\frac{dq_1}{dt} = \mu [v(t) - q_1] + \mu_1 (q_2 - q_1)$$

$$\frac{dq_i}{dt} = \mu_i (q_{i-1} - 2q_i + q_{i+1}), \quad i = 2, \dots, n-1 \quad (17)$$

$$\frac{dq_n}{dt} = \mu_n (q_{n-1} - q_n)$$

$$\text{where } \mu = \frac{\alpha}{c\gamma s}, \quad \mu_1 = \frac{a}{s^2} \text{ and } s = \frac{s}{n}$$

Usually, such parameters of the process as thickness s of the heated number of slabs, thermal conductivity coefficient a , thermal capacity coefficient (specific heat) c , specific gravity γ may

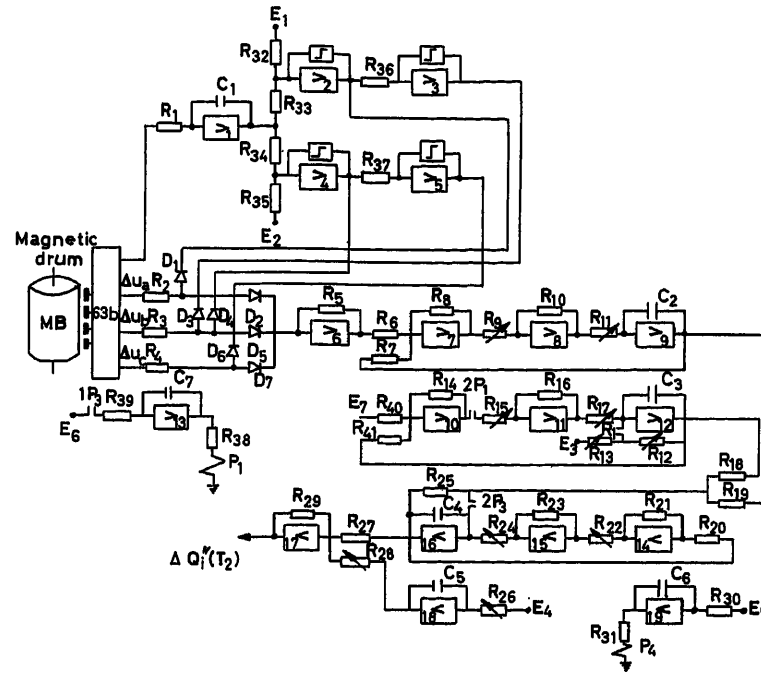


Figure 3. Circuit for simulation of heating and cooling

counter is constructed in such a way that it reads from the first counter the number which was previously entered into the latter, at the end of each reproduction from the cycle. The initial number (19) is entered into the counter at the end of the recording process and it represents the signal of the reproduction cycle beginning.

The output signal of the line-of-direction scanning unit opens (triggers) the exits of the FM reproduction unit, and the information passes to the exits of the function generators of the simulator. The closing of the exits is obtained by the terminal line-of-direction signal, which is represented by the tag marking of the last recorded zone. The simulation circuit for heating and cooling is shown in Figure 3.

The simulation of the equations for the heating of a 'thick' material is, in principle, analogous to that for the equations of type (9) to (12). The block diagram for the simulation of these equations differs from that shown in Figure 3, in that instead of the simulation of equation (14) the following system of ordinary differential equations, which approximates equations (4) to (8), is simulated:

be calculated with a sufficient degree of accuracy. These quantities can be introduced into the simulator of the process as the known disturbances. However, such a parameter as the coefficient of heat exchange between the metal and the furnace α is known only approximately, with an insufficient degree of accuracy.

In the case of heating metal in continuous reheating furnaces for the purpose of rolling it into sheets, a reliable measurement of the temperature of the metal being rolled can be made only after a certain stand of rolls where the metal has the thickness of a 'thin' material. This temperature may be used for the automatic setting of the unknown parameters of the system. However, in this case it is necessary to continue with the simulation of the process of cooling of the blank after its exit from the furnace up to the instant of its temperature measurement.

In the simplest case the process of cooling of the blank may be described by the equations

$$b_1 \frac{dQ}{dt} + Q = Q_c \quad (18)$$

$$Q(0) = q(T_h) \quad (19)$$

where T_h is the time of heating of a given blank in the furnace, Q_c the temperature in the mill, and $b_1 = c \gamma_1 s_1 / \alpha_1$ where s_1 is the mean thickness in the rolling process, and α_1 the coefficient of heat exchange between the metal and the surrounding environment; coefficient α_1 should also be described by the optimizer. Thus, the qualitative criterion of the accuracy of automatic setting of simulator K depends on two parameters α^* and α_1

$$K = K(\alpha^*, \alpha_1)$$

In this case it is expedient to determine the function $K = K(\alpha^*, \alpha_1)$ as a mean quadratic deviation of the measured temperature of rolling Q_u from the calculated temperature on the simulator $Q_1(T_c)$ where T_c is the time of cooling of the blank.

$$K = K(\alpha^*, \alpha) = \frac{1}{n} \sum_{i=1}^n [Q_i - Q_{1i}(T_c)]^2$$

where n is the number of blanks. Thus, the task of the two-channel optimizer is to find such values for coefficients α^* , α_1 , at which function R attains minimum value

$$K(\bar{\alpha}^*, \bar{\alpha}_1) = \min_{\alpha^*, \alpha_1} K(\alpha^*, \alpha_1)$$

In Figure 4 is given a complete block diagram for the optimum system of control for a continuous reheating furnace.

For the above problem of construction of a temperature-distribution simulator for the metal moving along a continuous furnace by optimization based on parameters α^* and α_1 it was possible to obtain a sufficiently high accuracy of operation of the furnace.

Experimental Study

The laboratory simulation of heating and cooling of slabs in a continuous reheating furnace, based on the method of simulation described above, was conducted on an installation, the block diagram of which is shown in Figure 3. The entire

assembly for the simulation consists of the above-mentioned storage system with the magnetic drum MB and the EMU-8 electronic simulating assembly units. The approximation of temperature in the operating space of the furnace was made as in Figure 1.

The amplifier units 1, 2, 3, 4, 5 serve for the switching of the channels for the reproduction of temperatures, corresponding to the three zones of the furnace. Amplifiers 6-12 simulate the process of heating slabs in the furnace. The voltage at the outlet of amplifier 12 is proportional to the temperature of the slab at the exit from the furnace. This voltage serves as the initial condition for the simulation of cooling of this slab in the rolling process, which is achieved by amplifiers 14-18. At the outlet of amplifier 17 the voltage obtained is proportional to the temperature of the slab after the fifth stand of rolls.

The obtained value of this temperature is compared with that measured by means of a photo-pyrometer. The adjusted resistances in the simulator are chosen so as to minimize the mean absolute deviation H of the calculated temperature from that measured:

$$R = \frac{1}{n} \sum_{i=1}^n |Q_i - Q_{1i}|$$

where n is the total number of slabs for which the data were available for simulation. In the test this number of slabs, n , was equal to 129 pieces. It was thus possible to tune a system for which the mean deviation H amounted to 6.3°C , whilst at the same time the maximum deviation

$$\max |Q - Q_{1i}|$$

amounted to 22°C which indicates a sufficiently high accuracy of working of the simulator.

Figure 5 describes an actual control circuit with an automatic simulator of the medium, which was tested on an actual continuous furnace under actual working conditions. The general block diagram of this circuit is shown in Figure 2. The part

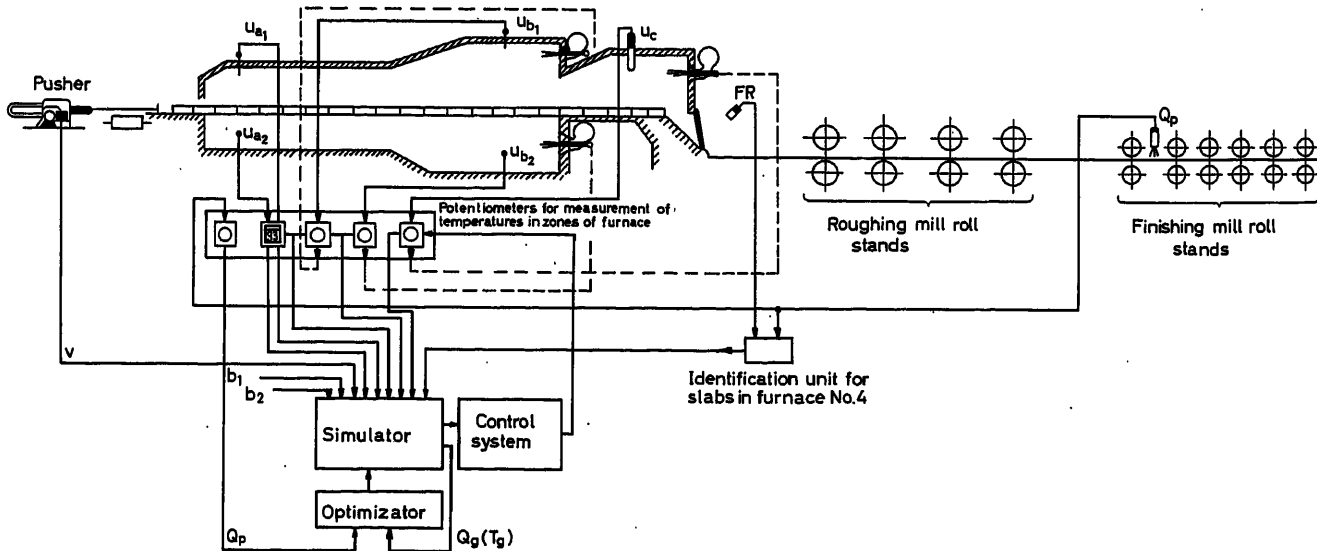


Figure 4. Symbolic circuit of the optimum system of control for a continuous reheating furnace

KEY:

U_{a1} and U_{a2} —controlling actions for 1st zone of furnace
 U_{b1} and U_{b2} —controlling actions for 2nd zone of furnace
 U_c —controlling action for 3rd zone of furnace
 FR—Photo-electric pyrometer

Q_p —Rolling temperature
 b_1 and b_2 —constants
 $Q_p(T_p)$ —reheating temperature (reheating time)
 V —speed of travel of metal through furnace

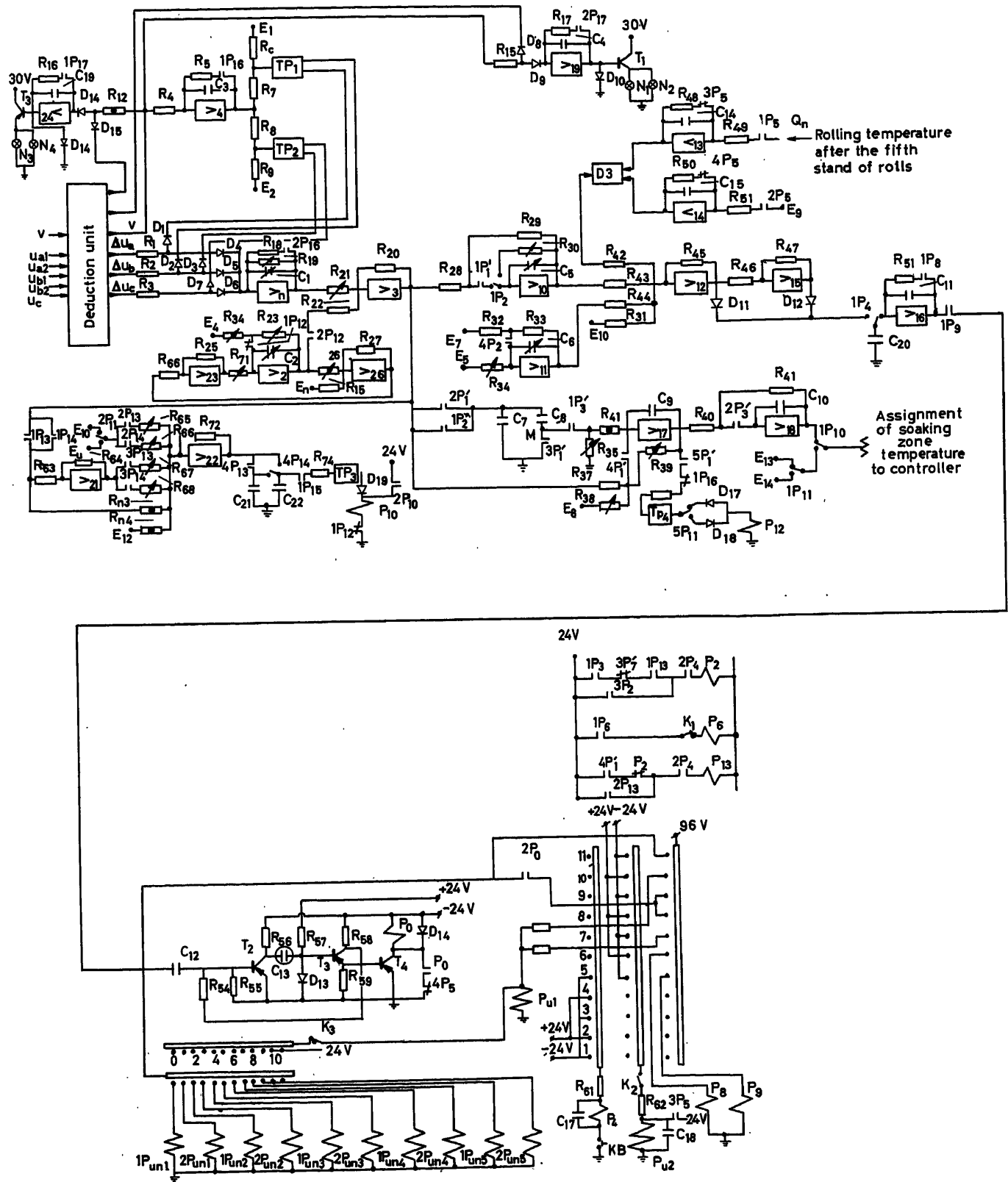


Figure 5

of the simulator designed for the simulation of the process of heating (computation of the temperature distribution for the metal travelling through the furnace) and cooling is constructed on the analogue principle.

The operational amplifier 4 and triggers $Tp1$ and $Tp2$ serve for the switching-on of the temperature channels corresponding to the different zones of the furnace. Amplifiers 2, 3, 29/26 serve for the simulation of heating of slabs in the furnace, amplifiers 13, 14 and the dividing unit D 3 to give a mean temperature of the slab, measured by a photo-electric pyrometer after the fifth stand of rolls, amplifiers 10, 11, 12, 15 for the simulation of cooling the slab during the process of rolling and to give the absolute difference $|Q_i - Q_{i1}|$. Amplifier 16 serves to average out this absolute difference for five slabs. For transistors T_1 , T_2 and T_4 and step finders Sh 1 and Sh 2 an optimizer is built, which automatically tunes up the parameters of the simulator for the minimization of quantity

$$R = \sum_{i=1}^5 |Q_i - Q_{i1}|$$

DISCUSSION

D. E. STEEPER, *General Electric Company, Schenectady, N.Y., U.S.A.*

We have been studying the problem of automatic control of slab rehear furnaces, and therefore find this paper to be very interesting. The controller described by Professor Lerner is a special purpose device which requires the same number of controllers as there are number of furnaces. Our approach is to include control as an additional function for a hot strip mill process control computer, such as described by Beadle¹. There are two reasons for this: (1) it eliminates a number of complicated special purpose controllers, and (2) the data required for furnace control, such as slab thickness, length, width, velocity, etc., are already stored in the computer or are readily computed from information required for mill control. However, this procedure has a disadvantage in that the control method must be reasonably simple in order to reduce the amount of computer storage and time required.

This is a complicated control problem, as Professor Lerner has pointed out, because it is a distributed parameter process and because suitable slab temperature sensors are not available. Also, a practical control scheme must be capable of handling numerous disturbances, such as variations in thickness, length, velocity (including zero velocity during mill delays), and temperature of the slab entering the furnace. Since these variations are known, it seems quite practical to use a feedforward control with a low gain feedback from an optical temperature sensor located somewhere after the first rolling stand. Answers to the following questions would be helpful:

(1) *Figure 4* infers that only temperature U_0 is controlled. It appears that temperature U_{b1} and possibly U_{b2} should also be controlled, which would require a new strategy. In addition, if five zone furnaces are used (which are becoming more common in the U.S.A.) and have an additional set of upper and lower burners, additional temperature controls and control strategy are required.

(2) *Figure 1* indicates a length of the furnace having temperature U_a followed by a length having temperature U_b . This is an approximation of the actual temperature profile. How do you determine the respective lengths?

(3) During a mill delay, the temperature is reduced to A_1 . This will usually be high enough to do some heating while $v = 0$, so that when rolling proceeds, a delay in the increase in gas temperature is required. What is your control strategy for this case?

The remaining amplifiers, relay, and triggers belong to the controller part and serve for the realization of the optimum control law. The testing of the given system under working conditions for the control of an actual continuous reheating furnace showed that the given system is entirely efficient. Under these conditions the mean absolute deviation of the calculated temperature of rolling from the measured temperature amounted to 4.1°C . The maximum value of the absolute difference reached the value of 9.5°C .

Under the actual operating conditions of the furnace its output varied within wide limits: from zero output with prolonged stoppages to maximum output, reaching the values of 75–80 t/h. In the absence of the optimum system of control for the continuous furnace the scatter of the rolling temperatures of the metal after the fifth stand on an average amounts to 60°C . With the use of the optimum system of control this scatter was reduced down to 20°C , which should greatly improve the quality of the sheet being rolled and in fact increase the output.

(4) In the soak zone the slabs are subjected to one-sided heating, but in the other zones they receive two-sided heating. Shouldn't this affect the value of slab thickness s ?

(5) Following eqn (13), an equation is given for optimum control in the case of disturbance of type (A):

$$U = U(t) = Q^* + b v(t) \frac{\partial Q}{\partial y} \bigg|_{y=L} = Q^* + b v(t) Q t(L)$$

The derivation of this equation is not clear, but by previous correspondence with Professor Lerner, we were directed to Reference 2 of this discussion, which it seems should have been referenced in the original manuscript. The far right-hand portion of this equation is not at all obvious, and is dimensionally incorrect.

Also, in the case of disturbance of type (B), the optimum control is given as:

$$u = u(t) = A_1 \quad \text{if } b_1 > b_2$$

$$u = u(t) = A_2 \quad \text{if } b_1 < b_2$$

where $A_1 \leq u \leq A_2$

This is also presented in Reference 2 of this discussion, where use is made of Pontryagin's maximum principle. This leads to a very peculiar and questionable control action, as illustrated in *Figure 2* of Reference 2. That example is for the case where the furnace is full of thin slabs, and at time $t = 0$ thicker slabs start to enter the furnace. In the region $0 \leq t \leq t_1$, the gas temperature is maintained at a value suitable for the thin slabs. In the region $t_1 < t \leq t_2$, the gas temperature is maintained at a maximum value A_2 , and in the region $t_2 < t \leq T$ the gas temperature is reduced to a value suitable for the thick slabs. The method of determining times t_1 and t_2 is not clear. For this example, it seems intuitively more correct to gradually increase the gas temperature in the region $t_1 < t \leq t_2$, rather than a sustained, maximum temperature A_2 . Is this a result of using a minimum integral squared error criteria, and is it the best criteria for this application?

(6) Has use of the optimizing control resulted in any fuel saving?

The improvement in performance reported when this controller was put into use is encouraging. Additional test data would be very

useful, such as several slab temperatures during a thickness change both before and after the optimizing control was applied, and also performance following a mill delay.

References

- ¹ BEADLE, R. G. On-line computer control of a hot strip finishing mill for steel. *2nd I.F.A.C. Symposium* 1963. London; Butterworths: Munich; Oldenbourg.
- ² BUTKOVSHI, A. G. and LERNER, A. YA. The optimal control of systems with distributed parameters. *Automation and Remote Control*, Vol. 21, No. 6 (1960).

A. YA. LERNER, *in reply*

(1) Undoubtedly, temperatures U_{b1} and U_{b2} also should be used as control actions, but in this case the optimal algorithm would be considerably complicated. This is why we considered the case of only one control action in our paper.

(2) The corresponding lengths were determined by furnace design and given thermocouples location.

(3) When the rolling mill is stopped the temperature will not decrease to the value A_1 , as V is not an instantaneous value of speed but an average value for a fixed time interval preceded by the mill stoppage, and consequently $V \neq 0$.

(4) Yes, there are different values [s and s (2) assigned to the thickness s in different zones].

(5) The dimensions of all terms are correct and the dimension of the above-mentioned expression is temperature. Concerning the other remarks I should say that a steep increase of temperature up to the maximum value is quite permissible for thin slabs when there is

no danger of surface melting. General overheating of slabs is not possible under the optimum control conditions. The optimizing control in the region $t_1 < t < t_2$ follows from the maximum principle and the moments t_1 and t_2 are defined from the corresponding conditions of transversality. As for the other criteria providing smoothness, they seem to be unnecessary under the given set of general problems.

(6) While doing the work we did not make it our aim to obtain any fuel saving. However, it seems to be quite possible that the optimizing control will provide some fuel saving.

G. M. E. WILLIAMS, *Northampton College, St. John Street, London E. C. 1., England*

I have some difficulty with the insistence that 'continuous processes' can only be best treated as space-position dependent and not as time dependent. The choice of the variable appears to me to be arbitrary in the mathematical sense of that term. The author's use of the term 'continuous processes' is not in keeping with British terminology. The only part of the process he refers to which is continuous is the furnace. Each workpiece of material processed in the furnace is an individual item, treated in sets which we usually term batches. It would appear just as practical to conduct such an analysis on a time-dependent variable basis, as, in fact, is long-established practice in heat treatment. The link between space position and time dependence is the velocity of each workpiece through the process, and it is the quality of each individual workpiece after treatment which is the *raison d'être* of the process.

If one proceeds to apply the author's analysis to truly continuous processes, as in the 'process industries' (oil refining for example) where the material is fluid and therefore amorphous, it would appear that only a time-dependent analysis is practical.

A Digital Optimal System of Programmed Control and its Application to the Screw-down Mechanism of a Blooming Mill

S. M. DOMANITSKY, V. V. IMEDADZE and Sh. A. TSINTSADZE

Summary

A system of programmed control has been developed by the Institute of Electronics, Automatic and Remote Control of the Academy of Sciences of the Georgian S.S.R. in conjunction with the Institute of Automatic and Remote Control of the U.S.S.R. Academy of Sciences. The basic unit of this system is a digital optimal servo system which has a number of characteristic properties. The electric motor drive of the optimal system works at accelerations that are maximal and constant in magnitude. This ensures the greatest response speed and simplifies the design of the computing part of the programmed-control system. The required system accuracy is ensured by the digital form in which the programme is given and executed. The small quantity of information processed in unit time has made it possible to use pulse-counting code rather than a binary one, which improves the reliability and interference-rejection properties of the system. The system is entirely built out of ferrite and transistor elements.

This report gives a general description of the digital optimal programmed control system, and also a practical example of its application to the automatic control of the pressure mechanism of a blooming mill; this device has passed through laboratory and factory testing, and by end of 1962 it was introduced into service at the Rustavi steelworks.

Sommaire

Chez l'Institut de l'Électronique, du Réglage Automatique et de la Télécommande de l'Académie des Sciences de la R.S.S. de la Géorgie, on a développé, avec le concours de l'Institut du Réglage Automatique et de la Télécommande de l'U.R.S.S., un système de commande programmée, dont l'unité de base se compose d'un servo-système digital optimal ayant quelques propriétés assez distinctes. Le mécanisme de commande électrique du système optimal marche avec accélérations maximales dont la magnitude est constante. Ainsi on s'assure pour la réponse la vitesse la plus grande possible, pendant que le dessin de la partie calculatrice du système de commande programmée est simplifiée. L'exactitude que l'on exige dans un tel système est assurée par la présentation et l'exécution du programme en forme digitale. Parce que l'on ne travaille qu'une quantité minimale d'information par chaque unité de temps, on a pu se servir d'un code qui compte les pulsations à la place d'un code binaire, ce qui améliore la certitude du système et sa résistance aux dérangements. Le système se compose seulement d'éléments de ferrite et de transistors.

Ce rapport donne une description générale du système de commande programmée digitale optimale; il cite également un exemple pratique de l'emploi du système pour la commande automatique du mécanisme de pression chez un laminier à blooms: appareil que l'on a mis à l'épreuve dans le laboratoire ainsi que dans l'usine et que l'on espérait introduire à la fin de l'an 1962 chez l'aciérie de Rustavi.

Zusammenfassung

Vom Institut für Elektronik, Steuerungs- und Regelungstechnik der Akademie der Wissenschaften der Sozialistischen Sowjetrepublik Georgien wurde in Zusammenarbeit mit dem Institut für Steuer- und Regelungstechnik der Akademie der Wissenschaften der USSR eine Programmsteuerung entwickelt. Das wichtigste Bauteil des Systems ist eine digitale Optimalsteuerung mit verschiedenen besonderen Eigen-

schaften. Der elektromotorische Antrieb des Optimalsystems arbeitet mit maximalen Beschleunigungen konstanten Betrages. Dadurch wird größte Ansprechgeschwindigkeit sichergestellt und der Entwurf des Rechnerteils der Programmsteuerung erleichtert. Die erforderliche System-Genauigkeit ist durch die digitale Darstellung des Programmes und seiner Durchführung gesichert. Die geringe Informationsmenge, die pro Zeiteinheit verarbeitet wird, ermöglichte die Verwendung eines pulszählenden Codes anstelle eines Binär-Codes, wodurch die Zuverlässigkeit und das Störverhalten des Systems verbessert wurden. Das System ist nur aus Ferrit- und Transistor-Elementen aufgebaut.

Dieser Beitrag gibt eine allgemeine Beschreibung der digitalen optimalen Programmsteuerung sowie ein praktisches Beispiel seiner Anwendung auf die Regelung des Walzdruckes bei einer Blockbrammen-Straße. Diese Vorrichtung wurde im Labor und im Werk geprüft und Ende 1962 im Stahlwerk Rustavi in Betrieb genommen.

Introduction

Digital servo programmed-control systems are finding continually wider applications in various branches of industry: in particular, they are used for the automatic control of screw-down and other mechanisms of rolling mills, for the control of various moving parts in control systems for metal-cutting machine tools, and in a number of other instances. The operation of such mechanisms normally falls into two stages. In the first stage the device must choose or compute an optimal programme, working on the basis of information about the requirements for the technological process, about the condition of the plant, about external perturbations, etc. In the second stage the given programme must be carried out according to an optimal law. The term 'optimal law' is normally taken to mean the carrying out of the given displacements with the maximum possible response speed and with the required accuracy; in addition a condition is often included covering requirements on control response quality.

While the function of choosing an optimal programme is not necessarily inherent in the digital control system itself, particularly when it operates in a complex installation with a controlling computer, the function of carrying out the given displacements according to an optimal law must still be organically inherent in the digital servo system. If this requirement is not satisfied, such systems cannot be considered fully efficient, since for many mechanisms, e.g. manipulator jaws, shears and rolling-mill pressure screw-down, the response speed and accuracy determine the productivity and output quality of the whole line.

A system of programmed control has been developed by the Institute of Electronics, Automatic and Remote Control of the Academy of Sciences of the Georgian S.S.R. in cooperation with the Institute of Automatic and Remote Control of the

U.S.S.R. Academy of Sciences. The basic unit of this system is a digital optimal servo system which has a number of characteristic properties. The electric motor drive of the optimal system works at accelerations that are maximal and constant in magnitude. This ensures the greatest response speed and simplifies the design of the computing part of the programmed-control system. The required system accuracy is ensured by the digital form in which the programme is given and executed. The small quantity of information processed in unit time has made it possible to use a pulse-counting code rather than a binary one, which improves the reliability and interference-rejection properties of the system. The system is entirely built out of ferrite and transistor elements.

This report gives a general description of the digital optimal programmed-control system, and also a practical example of its application to the automatic control of the screw-down mechanism of a blooming mill; this device has passed through laboratory and factory testing, and by the end of 1962 it was introduced into experimental service at the Rustavi steelworks.

Design Principles of the Programmed-control System

The basis of the system developed for programmed control is the optimum principle; the execution of the required displacement takes place at limiting values of the restricted coordinates, especially of the torque and rotation speed of the motor.

For the case where the drive control system has negligible inertia, Figure 1 will clarify the above; it shows the law taken for the variation of the control action F_y , and the curves of motor torque M_m and speed n . The figure shows that during run-up and braking the drive maintains the constant maximum permissible value of torque developed by the motor. When executing large displacements, after the motor has reached its maximum speed n_{max} it is automatically switched over by the drive circuit to operate at that constant speed (point MS on Figure 1). The instant of braking (point T_2) is chosen by the control system such that only a relatively short path remains to be traversed up to the instant when the speed is reduced to 10-12 per cent of the maximum (point CS). The execution of the rest of the path to the required low speed is automatically performed by the drive circuit, and ensures maximum accuracy in carrying out the programme. Figure 1 shows that the variation of drive speed with time follows a trapezoidal law. For small required displacements the motor does not have time to run up to its maximum speed, and the speed variation follows a triangular law.

The above-mentioned properties of the drive allow the controlling part of the programmed-control system to be considerably simplified, since in this event it only has to generate and execute commands for starting the drive in the required sense, for braking and for stopping the drive.

The design logic is very simple for that part of the control system whose purpose is to start the drive in the required sense and to determine the instant for generating the command to stop the drive; it is suitable both for control of low-power drives that have no links with appreciable inertia, and also for control of high-power drives with large inertia. The required displacement path and sense of rotation of the motor are determined by comparing the given programme with the actual position of the controlled mechanism (to give an error signal). During the execution process the path traversed is continuously

compared with the initial error; the command to stop the drive is generated at the instant when these two quantities become equal.

The programme is given in terms not of previously defined initial errors, but of absolute values of position-coordinates for the controlled mechanism. This avoids the possibility of errors accumulating from execution to execution, and also the need for the controlled mechanism to be set initially in a closely defined position.

The part of the system that determines the instant for the command to start braking has a relatively more complex design logic, and also takes different forms in systems for controlling the two different types of drive mentioned above.

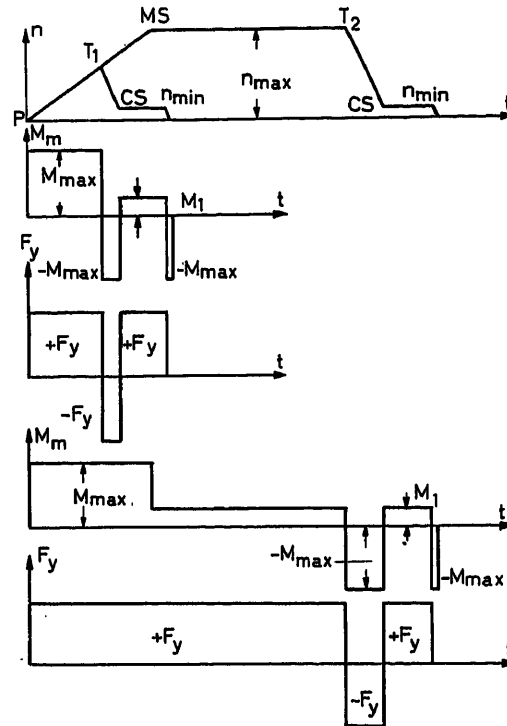


Figure 1

For systems controlling inertia-free drives the ratio between the paths traversed on braking S_b and on the run-up S_r is a constant and equal to the ratio between the absolute values of acceleration on run-up a_r and on braking a_b :

$$\frac{S_b}{S_r} = \frac{a_r}{a_b} = k \quad (1)$$

Taking into account the condition that should be satisfied:

$$S_r + S_b = \Delta$$

where Δ is the required execution path (i.e. the initial error), one gets

$$\Delta = S_r(1 + k) \quad (2)$$

This expression defines the design logic for the part of the system determining the instant for the command to start braking: the path traversed by the drive during the run-up is continuously multiplied by the fixed quantity $1 + k$, and when

the resultant quantity becomes equal to the initial error Δ , then the command is generated to start braking.

For large displacement, when the drive has time to run up to its fixed maximum speed, the full displacement path must consist of three terms:

$$\Delta = S_r + S_b + S_{ms}$$

where S_{ms} is the path traversed at the constant maximum speed.

By using eqn (1) it is found that

$$\Delta = S_r(1+k) + S_{ms} \quad (3)$$

This expression shows that the device for determining the instant to start braking should be designed on the following principle: the path traversed during the run-up is continuously multiplied by $1+k$; to the value obtained at the instant of reaching the maximum speed the path traversed at that speed should continue to be added; and when the resultant quantity becomes equal to the initial error, then the command should be generated to start braking. It can readily be seen that expression (2) is a particular case of expression (3).

It has been assumed in the above discussion that the drive accelerations on run-up and braking are constant, therefore their ratio k is constant also. But in practice k may vary between certain limits, which are not actually very wide; hence its maximum possible value is set into the computing device in question. With k smaller than the maximum, the last few millimetres of the path will be executed at a low speed, as has already been pointed out.

But in those cases where it is particularly vital to minimize the time of execution, self-adjustment may be introduced into the control system for the quantity k set into it. It is simplest to operate the self-adjustment according to the results of the completed execution, and for the self-adjustment criterion one should take the minimum of the path length executed at low (creep) speed S_{cs} and also of the overrun path S_{r0} beyond the required point.

The ratio of the path $\Delta - S_{ms}$ to the run-up path is denoted by γ , and suffixes are given to all symbols as follows: 1 to indicate the previous action and 2 to indicate the next action. Then one can write

$$\Delta_1 - S_{ms1} = \gamma_1 \cdot S_{r1}$$

Since the creep speed is small enough one has:

$$\Delta_1 = S_{r1}(1+k) + S_{cs1} + S_{ms1}$$

Since the aim of the self-adjustment is to establish the equation

$$\gamma_2 = 1+k$$

one gets

$$\Delta_1 - S_{ms1} = S_{r1} \cdot \gamma_2 + S_{cs1}$$

whence

$$\gamma_2 = \frac{\Delta_1 - S_{ms1} - S_{cs1}}{S_{r1}} = \frac{\Delta_1 - S_{ms1} - S_{cs1}}{\frac{\Delta_1 - S_{ms1}}{\gamma_1}}$$

Finally one has:

$$\gamma_2 = \gamma_1 \left(1 - \frac{S_{cs1}}{\Delta_1 - S_{ms1}} \right) \quad (4)$$

Employing an analogous argument for the case of overrun beyond the required point, one can write with sufficient accuracy

$$\gamma_2 = \gamma_1 \left(1 + \frac{S_{r01}}{\Delta - S_{ms1}} \right) \quad (5)$$

where S_{r01} is the overrun on the previous action.

Expressions (4) and (5) indicate the design logic for devices to give self-adjustment of the quantity k set into the system.

In control systems for high-power drives the presence of large inertia means that the current, and hence the motor torque, does not vary in a stepwise manner as shown in Figure 1,

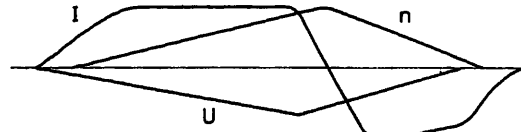


Figure 2

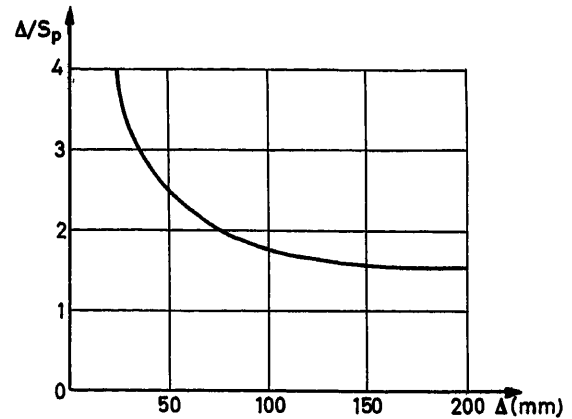


Figure 3

but much more slowly. This is evident from the oscillogram given in Figure 2, recorded for the motor of a blooming-mill screw-down mechanism.

For this reason, and also because considerable static loading is present, the motor speed, while varying with time in a roughly triangular law, lags behind the voltage during the run-up, and after the start of braking there is no instantaneous reduction in speed; in fact it even goes on increasing for a certain time. Hence the ratio of the complete path to the run-up path required by the condition for optimal operation, which is a constant in the case of relatively low-powered drives with fixed characteristics, proves here to depend on the magnitude of the full action path itself, this dependence being of a complex non-linear nature. The relation $\gamma = f(\Delta)$ has been derived analytically for the screw-down mechanism of a particular blooming mill and has then been checked on the mill itself, as shown in Figure 3. It should be noted that the curves for upwards and downwards motion are somewhat different, and the graph in Figure 3 has been drawn from certain averaged-out values.

In the programmed-control system developed for the

blooming-mill screw-down mechanism, the complete range of possible displacement values has been split into eight groups:

- (1) less than 16 mm
- (2) 16–32 mm
- (3) 32–48 mm
- (4) 48–64 mm
- (5) 64–96 mm
- (6) 96–128 mm
- (7) 128–192 mm
- (8) greater than 192 mm.

The use of narrower intervals for small Δ is explained by the nature of the curve $\gamma = f(\Delta)$, whose slope gradually diminishes. The choice of the limits for the ranges was determined by the ease with which the given division could be engineered.

A special device forming part of the controlling part of the system automatically estimates the value of the initial error before each action, determines the group into which it falls, and sets up the mean value of γ corresponding to that group. The execution process itself proceeds similarly to that for the control of relatively low-powered motors, the nature of it being optimal in this case also by virtue of the fact that the run-up and braking accelerations are still constant and correspond to the maximum permissible torque value. It is only in the first two groups, for rarely met small displacements, that the excessively wide limits of variation of γ make it practically impossible to combine the optimum principle with accuracy requirements. Hence for the first group an action is used that is from start to finish at a lower speed equal to 10–12 per cent of maximum, while a limited speed is used for the second group.

If it is necessary to introduce self-adjustment of the quantity γ set into the control system, in this case it is evidently most desirable to apply the principle of altering the γ for a given group by the same increment at each repetition of a Δ corresponding to that group. A very complex installation would have to be designed in order to be able to apply the principle of self-adjustment of γ after the very first action.

Operation Algorithm of the Programmed-control System for the Screw-down Mechanism of a Blooming Mill

A system designed according to the above principle for controlling high-powered drives has two memory devices for rolling programmes:

(1) A static programme store (SPS) for long-term storage of fixed programmes specified according to the technological set-up for rolling at the works—40 programmes in all, with a maximum number of passes up to 23.

(2) A variable programme unit (VPU) for programmes that change often and are not stored in the SPS. There are two means for recording programmes on the VPU: (a) Manual recording using a telephone dial, and (b) Automatic recording of a rolling programme carried out under manual control by an operator. This allows one to use the system for automatically rolling a series of roughly identical unconditioned ingots for which no fixed programme is yet in existence. The operator uses his experience to roll the first of this series of ingots, the gap sizes set on the rolls being automatically recorded on the VPU during the rolling; the remaining ingots of the series are then rolled according to this recording.

As well as these methods of use, the VPU can also be connected to a computer calculating optimum rolling programmes. A single programme containing up to 35 passes may be recorded on the VPU.

In the developed system the size of the required gap between the rolls is given in the form of a ten-digit binary number, expressed in millimetres and equal to the distance from the initial point of a given position of the upper roll.

The operational algorithms for the systems of control from the SPS and from the VPU are basically identical; they contain the following operations or elements:

- (1) Choice of operating régime (automatic operation from SPS or from VPU).
- (2) Choice of the necessary programme (when working from SPS).
- (3) Setting up the computing equipment to the initial position.
- (4) Feeding in, from the programme store, of information on the assigned position for the upper roll.
- (5) Determination of the actual position of the upper roll (interrogative operation) and computation of the initial error signal.
- (6) Determination of the direction of rotation of the motor.
- (7) Setting up the value of the coefficient γ .
- (8) Start of operation.
- (9) Attainment of maximum speed by the drive.
- (10) Determination of the instant for braking to start, generation and execution of the relevant command.
- (11) Transition of the drive to creep speed.
- (12) Determination of the instant for stopping the drive, generation and execution of the relevant command.
- (13) Transition from the given pass to the next one, all the operations from (3) to (13) then being repeated.

All the operations are carried out automatically except for (1) and (2) where the operator has to press the relevant push-buttons.

The automatic recording of a programme on the VPU with manual control follows this algorithm:

- (1) Choice by the operator of the relevant régime.
- (2) Setting of the upper roll to the required position.
- (3) Setting up the computing equipment to the initial position.
- (4) Interrogation of the measuring equipment to give the position of the upper roll, and translation of the resulting information into binary code.
- (5) Transmission of the information to the VPU.
- (6) On proceeding to the next pass, all the listed operations from (2) to (5) are repeated.

Operations (3), (4) and (5) are carried out automatically one after the other.

A programme can be set manually into the VPU using the telephone dial while the system is in operation from the SPS.

Block Diagram of Programmed-control System

The block diagram of the control system is shown in Figure 4. One of the fundamental elements of the system is a measuring unit MU of original design. It fulfils two functions: (1) on receiving an interrogation command it makes a single determination of the actual position of the upper roll, and gives out

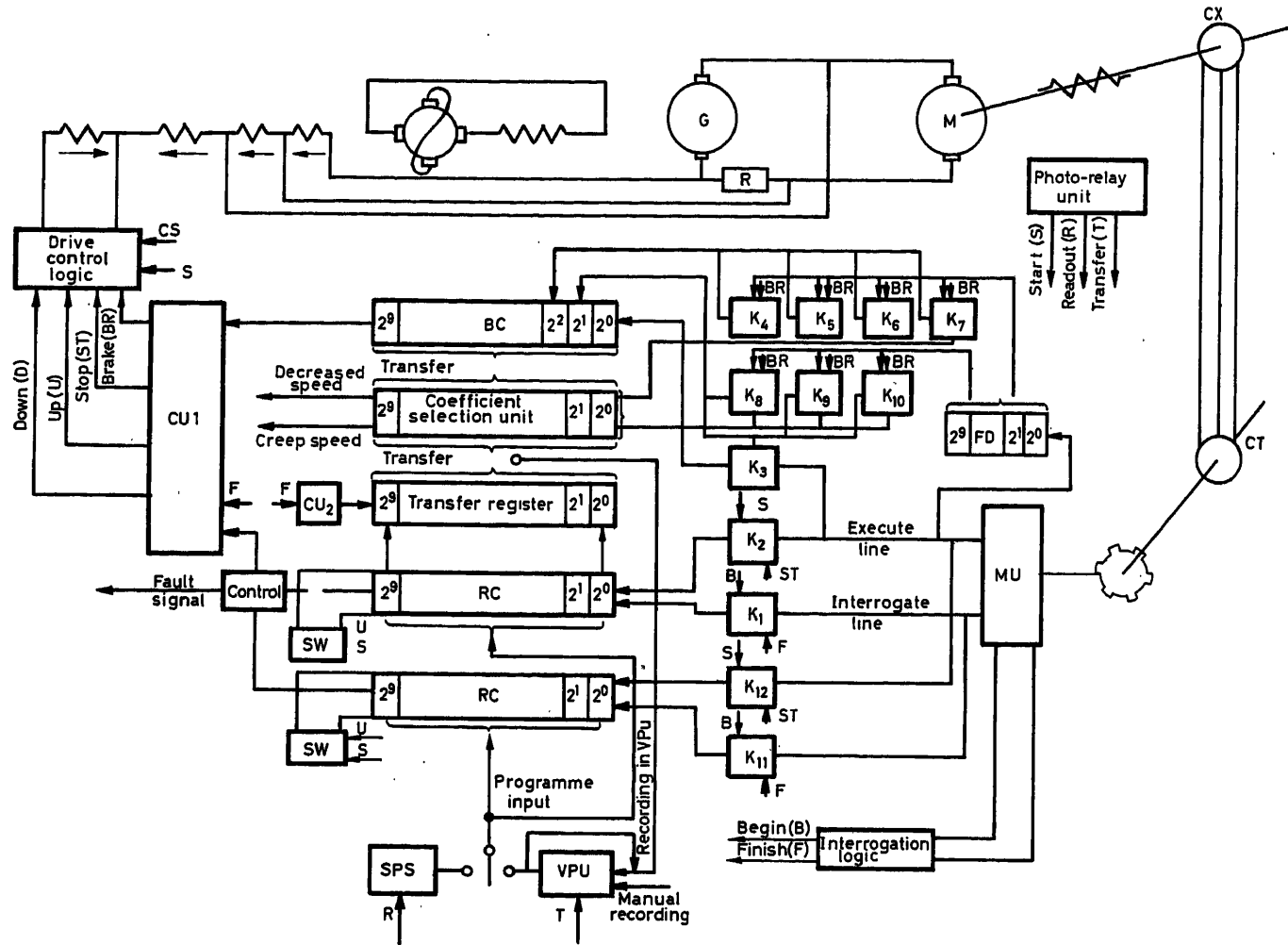


Figure 4

a number of pulses equal to the gap between the rolls in millimetres, and (2) it signals the path traversed, giving out during the execution process a pulse for every millimetre traversed. In order to carry out these tasks the *MU* has two independent channels, one each for interrogation and for execution. It is linked to the 'screw-down mechanism by a synchro transmission. The interrogation operation takes place when the rolls are stationary during the rolling of the metal.

A reversible binary counter RC is used to determine the magnitude of the initial error signal Δ , to derive the stop command and to record the rolling programme on the VPU . For convenience in the design of the computer section, the counter determines not Δ but its complement $\bar{\Delta} = C - \Delta$. Here $C = 1024$ is the counter capacity. The demand (D) in the form of a ten-digit binary number in direct code is introduced into the RC by a parallel means. Then the interrogation command is sent out, and the RC receives from the MU a number of pulses (Φ) corresponding to the actual gap between the rolls expressed in the complementary code $\bar{\Phi} = C - \Phi$. Hence the resultant number in the counter is $D + \bar{\Phi}$. Two cases arise:

(1) $D < \Phi$. In this case the upper roll must be displaced downwards by an amount $\Delta = \Phi - D$. In the counter one gets:

$$D + \bar{\Phi} = D + (C - \Phi) = C - (\Phi - D) = C - \Delta = \bar{\Delta}$$

(2) $D > \Phi$. In this case the upper roll must be displaced upwards by an amount $\Delta = D - \Phi$. So that the quantity $\bar{\Delta}$ should be derived in the counter also in this event, interrogation pulses must be added to D only till the counter is full; from that instant the switch SW puts the counter into the subtraction mode, and the arrival after this of the number

$$(C-\Phi)-(C-D)=D-\Phi=\Delta$$

of pulses from the MU gives in the counter the quantity

$$C - \Delta = \bar{\Delta}$$

During the execution the counter always operates in the addition mode. When it receives from the *MU* a number of pulses equal to Δ , it overflows

$$\bar{\Delta} + \Delta = C - \Delta + \Delta = C$$

and gives a pulse from its last digit that is used in the command unit *CU1* to generate the 'stop' command.

A straightforward logic designed into the command unit *CUI* generates the command 'up' or 'down' according to whether the binary counter has overflowed or not during the

interrogation process. These commands are passed to the logic unit for the drive control.

A transfer register connected to the reversible counter and repeating all its actions serves for the transfer of the quantity $\bar{\Delta}$ derived in the counter to the device for determining the coefficient γ and to the non-reversible binary counter BC that serves to determine the instant for giving the command to start braking. It is also used when a programme carried out by a rolling operator is being recorded on the VPV . In this event the reversible counter is put into the subtraction mode, and then interrogation of the MU is carried out. As a result one obtains in the counter and the transfer register the magnitude of the gap between the rolls in direct code:

$$C - \bar{\Phi} = C - (C - \Phi) = \Phi$$

This information is read out in the transfer register and transferred to the VPV by a parallel means.

The frequency divider FD serves to generate the various values of the coefficient γ . It consists of a normal binary counter to the cells of various digits of which are connected the inputs of switches $K4-K10$. Thus, for example, if the outputs of the first, fifth and seventh digits are connected to any switch, then when 128 pulses arrive at the input of the frequency divider from the MU , $64 + 16 + 1 = 81$ pulses will reach the switch. If the output of this switch is connected to the input of the third digit of the braking binary counter, then evidently the coefficient $\gamma = 81/128 \cdot 4 \approx 2.53$.

The role of the device described later for determining the quantity γ consists in opening one of the switches $K4-K10$ which will set up the required value of γ for a given Δ .

Since $\bar{\Delta}$ has already been recorded in the braking counter, therefore when Δ/γ pulses have been received from the MU the counter becomes full and its last digit gives out a pulse that is then used in the command unit $CU1$ for forming the braking command, realized by the drive control logic unit.

If, before the braking counter becomes full, the drive has time to run up to its fixed maximum speed, then from that instant all the switches $K4-K10$ are closed, and by opening switch $K3$ the number of pulses originated by the measuring unit is passed to the first digit of the counter. This carries out the logic for determining the instant to start braking, as already described.

The next section describes the devices for automatically limiting the maximum drive speed and for transition to creep speed during the braking process. The path length traversed at creep speed is 3-5 mm.

The system is started up automatically by a photoelectric relay system at the instant when the metal leaves the rolls. But because the motor has a delay of 0.6 sec in starting, a corresponding advance must be introduced. This is achieved by a special assembly that indirectly measures the speed of the metal and generates a pulse to start the system calculated so that the drive starts at the instant when the metal leaves the rolls. This assembly is not shown in Figure 4.

The system also contains a number of elements that carry out various logical functions required for the sequencing of the operations, for their automation, etc. In particular, a photoelectric relay unit is mounted on the mill for automatic drive starting.

The system provides for control of the most responsible operation—the stopping of the drive at the correct time. For

this purpose the reversible counter is duplicated. The outputs of both counters are fed to a special control logic unit. If overflow pulses are not generated simultaneously by both counters, this unit gives out a stop pulse and a fault signalling pulse; if both overflow pulses arrive simultaneously, it generates only a stop pulse.

Certain Basic Elements of the Control System

(1) Electric Motor Drive and its Control

The electric motor drive for the blooming-mill adjusting screws is designed as a generator-motor system. A 375 kW d.c. generator powers the two 180 kW adjusting-screw motors connected in series, and is controlled by a 4.5 kW amplidyne.

The drive must provide for the execution of a prescribed path according to the optimal speed curves given in Figure 1. In this connection the following requirements are placed on the drive:

- (1) In order to obtain the maximum response speed, the motor current must be held equal to the maximum permissible during run-up and braking.
- (2) Limitation of the maximum rotation speed of the motor is necessary.
- (3) During the braking process an automatic transition must be ensured to the creep speed $n = n_{min}$.
- (4) Heavy braking is necessary when the drive is finally stopped from creep speed.

The layout of a drive satisfying these requirements is shown in Figure 5. The control winding $W1$ of the amplidyne is con-

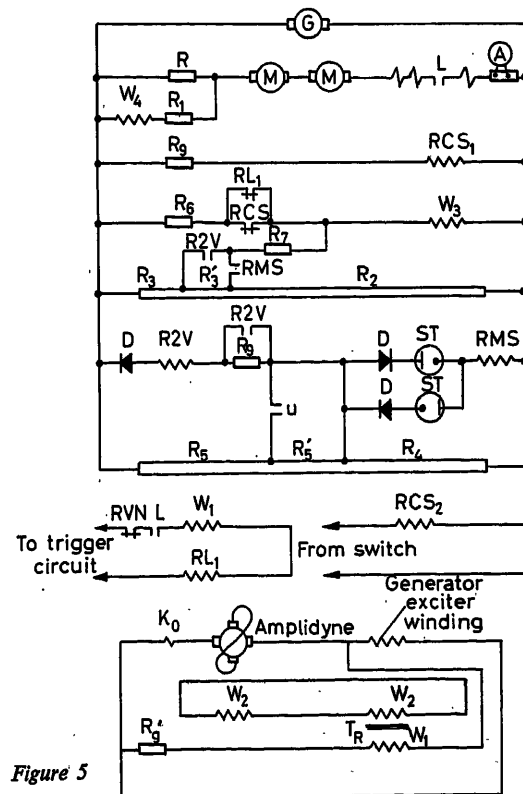


Figure 5

connected to the output of a three-state semiconductor trigger circuit which receives control pulses from the drive control logic unit. The run-up and braking of the drive take place at an invariable value of motor current $I_m = (I_m)_{\max}$, which is achieved by the use of strong negative current feedback in the armature circuit (feedback winding $W4$), with a feedback gain of 8–10. For large error signals, when the voltage at the generator terminals reaches its maximum value, depending on its polarity, one of the stabilovolts ST strikes. This causes the maximum-speed relay RMS to operate and apply the generator voltage to winding $W3$. The current flowing in this winding sets up a negative feedback that limits the generator voltage and consequently the motor rotation speed.

The creep speed is obtained by means of the twin-winding relay RCS . This relay is operated at the start of the execution by one of the windings being energized. At the start of braking this winding is de-energized, and the relay is held on only by the action of the second winding, which is energized from the generator output voltage; as this voltage falls in consequence of the braking process, the relay drops out and causes a strong negative feedback to be applied, which together with the change in the polarity of the current in the amplidyne control winding sets up a speed that is about 10 per cent of the maximum. Efficient braking from this speed on stopping is achieved by the self-damping of the generator on the removal of the control action from the control winding $W1$.

As stated above, the drive control equipment consists of a three-state power trigger circuit whose output is connected through a balanced semiconductor amplifier to the amplidyne control winding $W1$.

In order to obtain the required variation in the control action, pulses must be supplied to the appropriate inputs of the

trigger circuit. The order of application of the pulses depends on the direction in which the upper roll has to be displaced; it is developed by the drive control logic unit.

Signals are fed by six channels to the input of this unit from the digital control system and the drive circuit. These commands are as follows: selected direction of motion (up or down), clearance to start, braking, transition to creep speed, and stop. From these commands the logic circuit derives the signals that go to the appropriate trigger circuit inputs.

(2) Static Programme Storage

The static programme storage SPS (Figure 6) is a matrix memory device in which binary numbers forming a programme are recorded by means of networks of semiconductor diodes. It consists of a distributor, a programme unit and a numerical unit.

The distributor (see the bottom line of Figure 6) sequentially sends out a read pulse to the programme unit (second line of Figure 6) in accordance with the sequence of passes making up each programme; it is a device without moving parts that switches from pass to pass. The maximum number of passes in the programmes is 23, and so the distributor has 23 digits (23 ferrite-transistor cells).

The programme unit consists of 23 ferrocart programme cores, each of which has one primary winding connected to the distributor and 40 secondary windings (one for each fixed programme). The secondary windings of all the cores for a given programme are all connected at one end to a common bus, while the other ends go to the diode numerical matrices. Selection of the required programme is made by connecting one or other of these secondary-winding bus-bars to the output bus

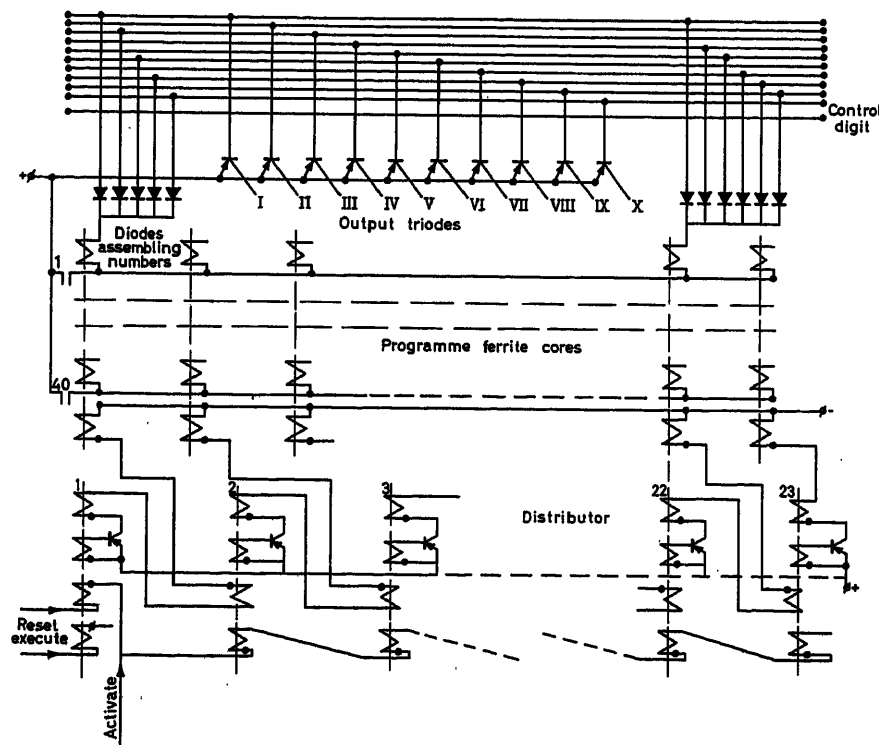


Figure 6

(+ on the diagram). Thus the operator needs only to press a button on the control desk to select the required programme.

(3) Variable Programme Unit

A fundamental element of the VPU is its storage ST, consisting of a ferrite matrix on which 35 ten-digit numbers can be recorded. Each core of the matrix has four windings: erase (reset), input of numbers, write (also serving as read-out winding), and output (Figure 7). The carry-in and output

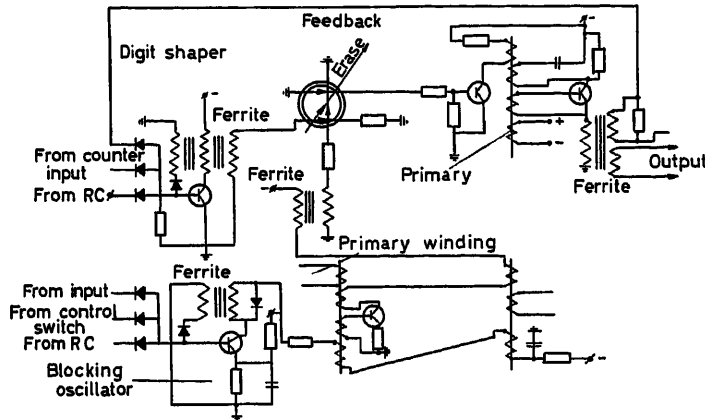


Figure 7

windings of the ferrites for the same digit are connected in series (35 ferrites each); the write and read-out windings of all the ferrites for a given number (pass) are also connected in series (10 ferrites each).

The operation of the storage is based on the well-known Cambridge principle. But the design logic and circuit are original and very simple.

For the recording of a number in the store, pulses are applied to the input shaping circuits for the appropriate digits. At the same time an activation pulse is applied to the distributor, 35 of whose cells have their outputs connected to the corresponding write and read-out windings. Figure 8 shows the form of the pulses generated by the distributor and shaping circuits, and also their relative timing. The sense of the current corresponding to the top part of the pulses is for read-out. Hence, as is clearly seen from Figure 8, the superposition of the two magnetizations on the ferrite at the start only confirms the absence of recording, while later on (when the bottom parts of the pulses in Figure 8 coincide) a 1 is written.

When reading out numbers, an activation pulse is supplied each time to the distributor, and the pulse coming from it performs the read-out. So as to regenerate the read-out number, feedback is taken from the output shaping circuit of each digit to the input shaping circuit for the same digit, resulting in the appearance of a pulse from the input shaper almost at the same instant as a register pulse appears; but the relation of the initial parts of these pulses is such that this attenuates the read-out pulse only negligibly. A coincidence of the magnetizations (the lower halves in Figure 8) brings about regeneration of the number—its re-recording. By this means the recorded programme may be reproduced a practically unlimited number of times.

As already pointed out, the recording of a rolling programme

carried out by an operator under manual control is achieved by means of the reversible counter included in the system. There is a special original device for the manual recording of programmes. A number is dialled on a somewhat modified telephone dial, taking its digits in sequence one after the other. To record the number 253, for example, 2, 5 and 3 are dialled in sequence, while to record 72 one dials 0, 7 and 2 in sequence, etc. The dial has two contact systems: one for numerical pulses and one for control pulses, which are fed out on separate channels. The dial is designed so that when one dials zero only two control pulses are generated (one each for clockwise and anticlockwise rotation of the dial); when one dials 1 there is one control pulse, one number pulse and then another control pulse, etc. The control pulses thus generated serve to activate the six-digit distributor controlling the recording system. The outputs of its cells control switches in such a way that the first switch (hundreds) is open at the instant when the number pulses come through for the first digit of the number to be recorded, the second switch (tens) for the second-digit pulses, etc. These pulses are passed from the switches to a binary counter that serves to form the binary code for the number (Figure 9).

This device works on the principle of introducing pulses into the digits of the binary counter in such a way that the sum of their values equals the number of pulses received. For example, since the number 100 has the form 1100100 in binary code, for every pulse arriving from the first switch (hundreds) one pulse is put into the third, sixth and seventh digits of the binary counter; so as to avoid disruption of the computation in the event of digits being carried from lower to higher columns, these pulses are not supplied simultaneously to all three of the digits mentioned, but spaced by a time delay which is enough to allow the carry to take place.

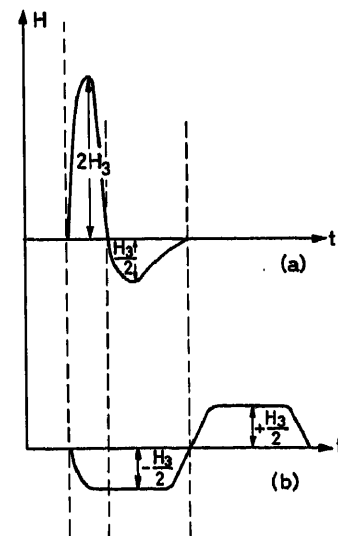


Figure 8

After the dialling of the third figure is complete, the final control pulse causes a pulse to be sent out from the output of the sixth cell of the distributor, which in its turn brings about the transfer into the store of the number formed in the counter, followed once more by the preparation of the first cell of the distributor. This makes it possible to dial numbers continuously one after the other. The correctness of the dialling may be

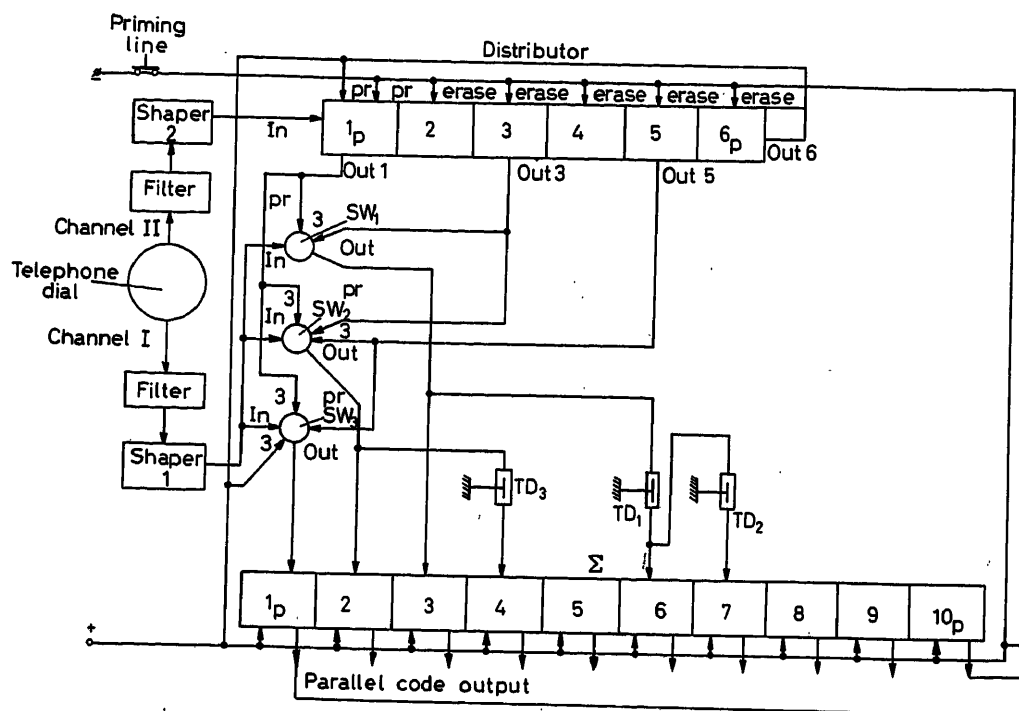


Figure 9

checked on a visual indicator of dialled numbers, which uses three dekatrons. The operator has the facility of erasing a number when necessary by pressing a button (shifting the distributor backwards by one cell), and of then recording it again.

(4) Coefficient Selection Unit

Figure 10 shows the block diagram of this unit. As has already been stated, the quantity γ is chosen in accordance with the value of Δ , while the whole range of variation of Δ is divided into eight groups.

The unit contains three basic elements:

(1) Ferrite assembly (top line in Figure 10). These ferrite cores serve for the estimation of the value of Δ , and are connected into the lines for transferring $\bar{\Delta}$ from the reversible counter to the braking counter. There are eight of them altogether, and on them are written the eight highest digits of $\bar{\Delta}$.

(2) Switch assembly (middle line in Figure 10). The switches serve to control the lines for various values of γ . Since, as was pointed out, the execution for one group of Δ (from 0 to 16mm) is carried out from start to finish at creep speed, the number of switches is one less than the number of groups, i.e., seven.

(3) Transformer assembly (bottom line in Figure 10). The transformers have ferrocarr cores, and each serves for the setting up of a certain value of γ . For this purpose each core has several primary windings, to which are connected the outputs of those digits of the frequency-divider that are required to give the necessary value of γ . The secondary (output) winding of the core is connected to the input of the corresponding switch.

The estimation of the value of Δ is based on the following principle:

Since what is written on the ferrite cores is not the value of Δ itself but its complement $\bar{\Delta}$ w.r.t. 1024, the following picture is obtained for various groups of values of $\bar{\Delta}$:

(1) $\Delta \leq 16$: 1's are written in all the digits from the fifth upwards; one or more of the cores for the first four digits contains a 0.

(2) $16 < \Delta \leq 32$: 1's are written in all the digits from the sixth upwards; the core for the fifth digit contains a 0.

(3) $32 < \Delta \leq 64$: 1's are written in all the digits from the seventh upwards; the core for the sixth digit contains a 0.

(4) $64 < \Delta \leq 128$: 1's are written in all the digits from the eighth upwards; the core for the seventh digit contains a 0.

(5) $128 < \Delta$: one of the digits from the eighth upwards contains a 0.

Making use of the above, the device is designed in the following manner.

Immediately after $\bar{\Delta}$ has been recorded on the ferrite cores, it is read out with polarity such that those cores containing 0's give pulses in their output windings. After amplification by triodes, these pulses are passed to windings for opening switches corresponding to these cores. So that several switches should not open all at once, the opening winding for each is connected in series with the shut-off windings for all the switches corresponding to cores of lower digits. Thus each time only one switch opens, corresponding to the core of the highest digit in which no 1 is written.

To consider the means by which certain of the above intervals are split into two, the interval $32 < \Delta \leq 64$ is taken as an example. This is split into the two parts (1) $32 < \Delta \leq 48$ and (2) $48 < \Delta \leq 64$.

In addition to the conditions for this interval, an extra one will exist for the first half—the presence of a 1 in the fifth digit: while for the second half it will be the absence of a 1 in the fifth digit. In order to control the satisfaction of these conditions, an extra ferrite core is connected in the transfer line for the fifth digit, and on read-out it gives a pulse in its output

winding when a 1 is present on it. This pulse is amplified by a triode and closes a switch corresponding to the band $48 < \Delta \leq 64$, and in spite of the fact that on all occasions when $32 < \Delta \leq 64$ the switches for both parts of this interval receive opening pulses, nevertheless for $32 < \Delta \leq 48$ only the switch for this band is open. For $48 < \Delta \leq 64$ the main ferrite core for the fifth digit closes this switch, and only the switch for the band $48 < \Delta \leq 64$ remains open.

The other intervals are split up in a similar manner.

(5) Start Pulse Advance System

As was observed earlier, the task of this system is to generate a pulse for starting the drive at a certain roughly constant time (about 0.5–0.6 sec) before the metal comes out of the rolls. This calls for an estimate of the speed of motion of the ingot up to that instant.

For this purpose two photoelectric relays are mounted on either side of the rolls, at distances of 0.5 and 1 m from the plane of the axes of the rolls. These relays control the mode of operation of a special reversible counter and a fixed-frequency generator supplying pulses to this counter at frequency f .

Let t be the time of advance, n_1 the number of pulses which reach the counter from the instant of obscuration of the first photocell until the obscuration of the second, n the number of pulses that should reach the counter from the instant of obscuration of the second photocell until the generation of the start pulse, and C the counter capacity.

Then, if for practical purposes the assumption that at the end of its passage the velocity of the ingot is constant may be taken as acceptable, one must have:

$$n = n_1 - t \cdot f$$

The constant quantity $t \cdot f$ is first set into the counter, which is put into the subtraction mode. At the instant when the first photocell is obscured, a pulse switch is opened, and until the instant of obscuration of the second photocell n_1 pulses enter the counter. The following quantity is obtained in the counter:

$$C + t \cdot f - n_1$$

From this instant the counter is switched into the addition mode, and when $n = n_1 - t \cdot f$ pulses have entered it a pulse appears from its last digit, which is in fact used for starting the drive.

(6) Measuring Unit

As has been stated, this unit has two channels: interrogation and execution. Position transmitters with oscillatory circuits are used for both channels, and both are equipped with discs having tooth-like perforations round their edges. The disc for the execution channel is linked by a synchro transmission to the screw-down mechanism, while the disc of the interrogation channel is continually rotated by a small motor. Pulses appear in the channels when the teeth of the discs enter the inductors of the

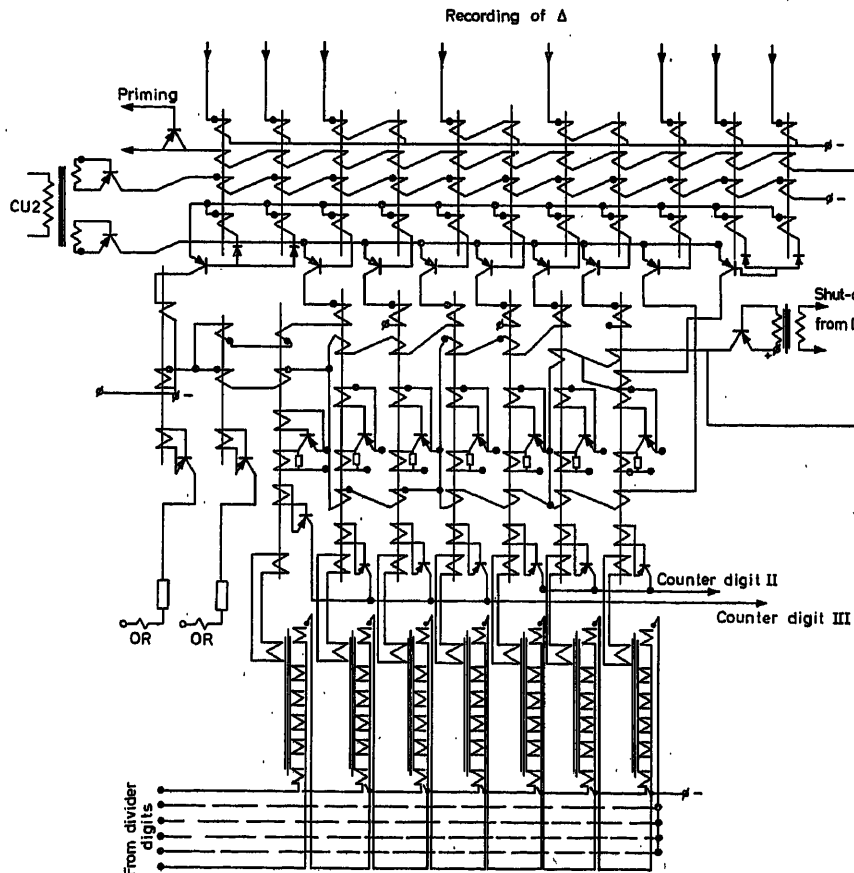


Figure 10

corresponding channel sensors. The instant for starting the count of interrogation pulses is determined by a transmitter of the same type, for which there is one special tooth on the periphery of the disc. The instant for stopping the interrogation is determined by a special electromagnetic sensor, which gives out a pulse when a magnetic circuit linked by its parts to both discs is closed. The measuring circuit is designed entirely from contactless elements.

Conclusion

In conclusion it should be noted that the tests of the programmed-control system for the screw-down mechanism have given positive results: the error in setting the upper roll did not exceed 1–2 mm, while the time of operation of the screw-down mechanism over the complete programme was shorter than the time of operation under manual control.

DISCUSSION

Author's Opening Remarks

The system of programme control of a screw-down mechanism of a blooming mill was developed for the Rollstahl Steel Mills. The special computer has two types of memory, one contains several fixed programmes and the other part of the computer is able to store the result of the last operation and then give further operating commands. One can manually programme the computer if necessary.

The system provides optimum operation of the screw-down mechanism. A special device senses the position of the slabs and feeds it back to the computer. In all there are between 40 and 45 rolling programmes, each programme containing perhaps 35–40 different rolling operations.

At the present time, the machine is being industrially tested. The results of the work have shown that the errors do not exceed 3–4 mm which is acceptable for industrial applications. The computer contains ferrite cores and transistors.

R. G. BEADLE, *General Electric Company, 1, River Road, Schenectady, New York, U.S.A.*

The authors describe one method of partially overcoming the response limitations of the excitation and power supply described in their example. While variations in mechanical inertia and friction are mentioned, there is some question that the performance would be optimal in many practical cases. It is not uncommon, for example, to observe screw-down frictions which vary from 50 to 150 per cent of drive rating during a relatively short period of time. In fact, the friction may even vary considerably over the normal range of travel. For some drives, such as manipulator fingers, the inertia will depend on ingot mass and the relative position of the ingot.

In most cases, then, it would appear that effort should first be spent on improving the basic characteristics of the drive system rather than optimizing a low-performance drive. A logical choice is to consider solid state excitation of generators. Then the drive will need much less optimizing to achieve minimum positioning times. Several such solid state equipments have been built since 1960.

Another, and perhaps more important area of optimizing, is the choice of the rolling programme itself. Do the authors have any remarks regarding the use of process computers to control and optimize the complete operation?

C. D. ROGERS, *Electromechanical Research Center, Republic Steel Corp., Cleveland, Ohio, U.S.A.*

This paper indicates the need for computer control on blooming mill screw-down motors themselves. Rolling time on the reversing mill is greatly dependent on the speed of mill positioning, particularly on reversing slabbing mills where vertical edger positioning is employed in addition to the screw-down. It is necessary to position both drives in minimum possible time to achieve a consequent minimum reversal time. Reversal of main mill drive motors can occur within an average of 2 sec; whereas, 4–6 sec are consumed in positioning. In other words, 2–4 sec are added to each reversal.

The approach, as discussed in the paper, is significant and should be applied to blooming mill screw-downs and other varieties of mill positioning as well. In numerous instances, a reduction of seconds from reversal time is made possible. Application of described techniques employing the triangular law are basically, however, of extreme importance.

Work has been conducted in this field, but actual computer application to the drive system is not apparent.

It must be mentioned that a variety of mill conditions can dictate the effectiveness of digital positioning. Reference is made specifically to positioning drives having limited power because of mill area restrictions. Hybrid (that is, both analogue and digital) equipment is required for measurement and compensation for intervening mill conditions as positioning functions occur. Naturally, more expense is involved; however, justification for 'dynamic compensation' arises not from the increased speed of positioning, but from its by-products: improved quality of product and higher rates of production.

W. THÖT, *Brown Boveri & Co., Mannheim, Germany*

It was very interesting to obtain further information about this self-optimizing screw-down system. The dilemma for the engineer developing such systems is that he has to take into consideration varying mechanical effects which influence the deceleration of the drive. These can be considered, for example, by the factor k or $\gamma_2 = 1 + k$. This factor k is derived from the behaviour of the drive during the previous displacement. If I understand correctly, the system works optimally if the mechanical influences are constant over the whole range of possible positions and are only a function of time. Unfortunately, in heavy stands for reversing mills, these effects are not constant and vary even more during the time of operation. In the last few years we have seen that there are two factors:

(1) Varying friction dependent on position. Actually the friction between the housing of the upper roll bearing and the guided channels for these housings in the mill-stand is lower in the region where the greatest part of the displacements take place.

(2) The non-constant pressure of the hydraulic system which balances the weight of the upper roll and its armatures.

To clarify my following question, I would like to explain how we tried to solve these difficulties. In order to enable the drive to follow the commands of the position control device as quickly as possible we supply the d.c. motor by two anti-parallel groups of rectifiers. Then we install three interconnected closed-loop control systems for the armature current, speed and position (*Figure A*). The drive accelerates with constant and maximal torque. The special property of the equipment is that the drive does not work with constant maximum torque when decelerating to creep speed. During this period of displacement, the drive is under the speed control device. In order to make the drive behave in this way the reference value for the speed is modified by the so-called integrator unit. This unit enables us to give the drive a fixed and high constant deceleration. The deceleration is matched to the total mechanical inertia of the drive, so that the armature current is under its limitation during the deceleration of the drive, even if these effects which assist braking (friction, hydraulic pressure) are a mini-

$$S_b = \frac{1}{2a_b} \cdot v^2 = c - v^2$$

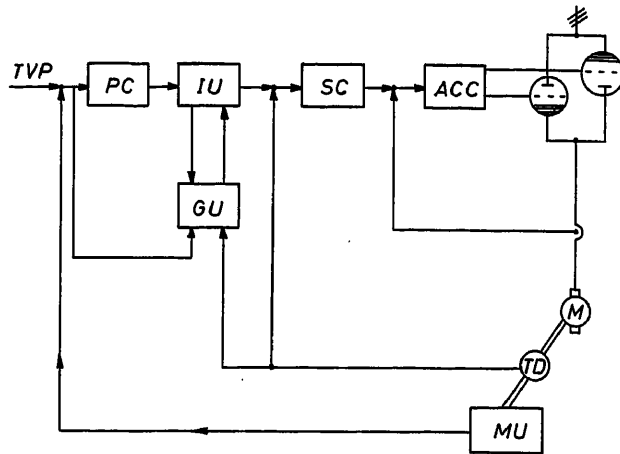


Figure A. Block diagram of the equipment

TVP = Target value for position ACC = Armature current control device
 PC = Position control device
 IU = Integrator unit M = d.c. motor
 CU = Computing unit TD = Tachodynamo
 SC = Speed control device MU = Measuring unit

mum. The advantage of restricting the drive to a constant and pre-determined deceleration is that now the computing system which initiates braking becomes very simple. In the case of constant a_b , the displacement during deceleration is

$$s_b = \frac{1}{2a_b} \cdot v^2 \quad v = \text{speed}$$

This means that the computing device only has to compare this fixed quadratic function of v with the present error of the position to give the command for braking to creep speed.

We presume that due to the low inertia of the electrical circuits, it is unnecessary to apply any correction to the computing device dependent on the wanted displacement. Further, we hope that time will not be lost in spite of not using the full torque for braking. On the contrary, we calculate that we will gain some time because the time during which the drive moves at creep speed can be minimized.

I would like to ask Mr. Domanitsky if he provided any devices to eliminate the explained effects or whether it was not necessary to do so in that particular blooming mill.

W. LEONHARD, Siemens-Schuckertwerke, Scharowskystr., Erlangen, Germany

The problem of optimum position control of a d.c. motor can be simplified considerably if a drive with an inherent rapid response, for example a motor with an electronic power supply, is employed. I would like to submit a scheme (Figure B) for digital positioning which is in use in our Company for steel mill and other applications, for example as part of programmed controls. It fulfills all the requirements mentioned in the paper and, in addition, seems to be of simpler structure. It is characterized by cascaded loops for acceleration, speed and position. An inner current loop provides current limit and assures tracking of the antiparallel rectifiers. The position loop is digital in order to achieve high accuracy (10^{-4}) and to permit storage of reference position and print-out of actual position data. A parallel digital difference circuit is provided which has a maximum computing time of $150 \mu\text{sec}$ for 4 decades, using 10 kc/s industrial transistor logic. The D/A converter is combined with a parabolic function generator which produces the speed reference during the braking period. The operation is as follows: after entry of a new position reference, the motor starts with constant acceleration, provided the speed regulator is limited due to a sufficiently large initial position error. This may be followed by a period of maximum constant speed. Braking at constant deceleration begins at the correct instant due to the action of the non-linear function generator. There is no extended period of creeping speed for final positioning.

Typical results for a 100 kW motor with three pulse rectifier supply (50 c/s) are: Rise time of the current loop 15 msec, of the acceleration loop 40 msec, of the speed loop 100 msec, all measured for small changes of the reference values.

J. P. CLYNE, B.I.S.R.A., 140, Battersea Park Road, London S.W. 11, England

I was very interested in the system of position control adopted, using pulse counting rather than binary digit code. At the British Iron and Steel Research Association in London, we have developed a fully-automatic crane for servicing billet pits. The instructions are inserted and the whole operation of removing pit lids, unloading and loading the billets and replacing lids is then automatic. The whole system is now working very successfully on a 25 ft. crane in the laboratory. The longitudinal position control is similar to that described in the paper

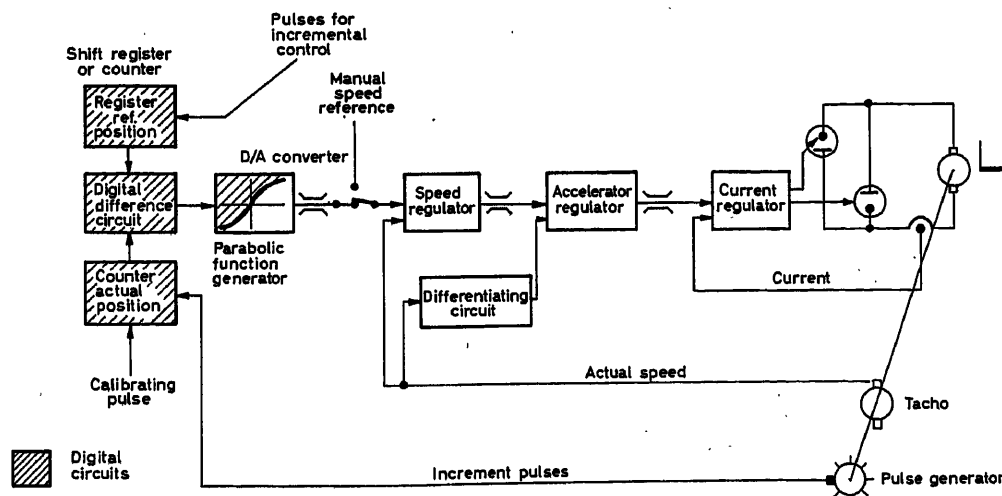


Figure B. Digital positioning system

and was adopted for the same reasons. This type of positional control is very susceptible to electrical interference. With the crane, it was possible to overcome this. The motors associated with a rolling mill may, however, be 100 times larger than those on a crane, and interference problems can therefore be expected to be much more severe. Was the problem of interference encountered and if so, what procedure was adopted for overcoming it?

A. A. S. DANTHINE, *Centre National de Recherches Metallurgiques, Liège, Belgium*

It seems to me that the capabilities of the described system would be better used if the electric motor drive was mercury-arc rectifier or silicon controlled rectifier fed.

I should like to ask the following questions:

(1) What is the maximum linear speed of the screw in the installation described in the paper?

(2) What is the average time of operation for displacements of 20, 80 and 200 mm?

S. M. DOMANITSKY, V. V. IMEDADZE and SH. A. TSINTSADZE, *in reply*

We are very grateful for the valuable remarks of all who took part in the discussion of our paper.

We begin by discussing in detail the question put by Messrs. Beadle, Rodgers and Thöt who were interested in effect of change in inertia and friction on performance of the optimal digital system.

The system developed by us can be applied for any drives in which the necessary displacement is preset in the form of a programme or can be determined prior to operation. Specifically it can be used for the mechanisms having low load, for example the flying shears drive (when cutting the foremost edge of billet) or for a crane bridge drive, as Mr. Clyne pointed out in his remark.

However, we wanted to determine whether it is possible to apply our optimal system for the screw-down drive. This drive, as Mr. Beadle correctly pointed out, has load M_S varying within a range of 0.5 to $1.5 M_{SN}$, where M_{SN} is the rated value of load. Let us show that under these conditions the path covered at creep speed will not be great. Let us assume that conditions are normal: $M_S = M_{SN}$ and the displacement is equal to $\Delta = 100$ mm which approximately corresponds to triangular law of speed change at the maximum speed of the drive.

Usually the maximal (starting) torque of the motor M_{max} is 2.5 times greater than its nominal torque M_N and correspondingly, if $M_{SN} = 0.5 M_N$ then $M_{max} = 5 M_{SN}$.

Then

$$K_N = \frac{a_{rN}}{a_{bN}} = \frac{M_{max} - M_{SN}}{M_{max} + M_{SN}} = \frac{5 M_{SN} - M_{SN}}{5 M_{SN} + M_{SN}} = \frac{4}{6} = 0.667$$

and accordingly to (2)

$$S_{rN} = \frac{\Delta}{1 + K_N} = \frac{100}{1.67} = 60 \text{ mm}; \quad S_{bN} = \Delta - S_{rN} = 40 \text{ mm}$$

When the load torque is changed the actual value of K will substantially differ from K_N :

$$\text{for } M_S = 1.5 M_{SN}, \quad K = \frac{a_r}{a_b} = \frac{3.5}{6.5} = 0.54$$

$$\text{and for } M_S = 0.5 M_{SN}, \quad K = \frac{a_r}{a_b} = \frac{4.5}{5.5} = 0.82$$

However, due to the optimal digital system, the operational acceleration distance S_r , no matter how load torque changes, it will be determined by the preset rather than the actual value of the ratio, i.e. $K = K_N$ and will be

$$S_r = \frac{\Delta}{1 + K_N} = S_{rN} = 60 \text{ mm}$$

The path traversed on braking S_b will be determined by actual braking acceleration a_b

$$\text{for } M_S = 1.5 M_{SN} \quad S_b = \frac{a_{bN}}{a_b} S_{bN} = \frac{6}{6.5} \cdot 40 = 37 \text{ mm}$$

$$\text{for } M_S = 0.5 M_{SN} \quad S_b = \frac{a_{bN}}{a_b} S_{bN} = \frac{6}{5.5} \cdot 40 = 43.5 \text{ mm}$$

Thus for $\Delta = 100$ mm the path to be covered at creep speed will amount only to:

$$S_{bN} - S_b = 40 - 37 = 3 \text{ mm} \quad \text{or}$$

$$S_{bN} - S_b = 40 - 43.5 = -3.5 \text{ mm}$$

i.e. approximately ± 3 mm. With smaller values of Δ it will be even shorter. It should be taken into account that some changes of load torque are actually caused by slow deterioration in the system of screw-down mechanism balance and can be compensated by the self-adjusting system. If the maximum operation speed $n = 110$ mm/sec and creep speed is $n_{os} = 15$ mm/sec, then the period of operation at creep speed will be about 0.2 sec.

Thus it is evident that the system optimal control is effective within a wide range of load torque variation. Answering Mr. Danthine's question we would like to give some data on the drive. The maximal speed of screw-down was 120 mm/sec. The average time for eliminating the displacement error was 0.9 sec for $\Delta = 20$ mm, 1.9 sec for 80 mm and 2.9 sec for 200 mm.

Mr. Beadle felt the necessity to improve the characteristics of the drive rather than to concentrate on optimizing. Mr. Rogers, with whom we wholly agree, thinks, however, that optimizing of screw-down drive will permit reduction of rolling time. The industrial tests of our system confirm this. The improvement of the drive itself and particularly the use of mercury rectifiers or controlled silicon rectifiers instead of generators will, as Beadle, Thöt and Danthine mentioned, reduce the time constants of supply circuit and improve the current curve.

We learn with great interest from Mr. Clyne's remarks that a system similar to ours, for control of a model crane spanning soaking pits, is being tested.

Mr. Clyne wanted to know what measures were taken to suppress interference in the system. Signals from primary transducers are transmitted through amplifiers and shaping devices; therefore, the logic elements receive sufficiently powerful signals. These elements are provided with RC circuits and are biased to suppress interference.

We would like to say a few words regarding block diagrams of servo-systems shown by Messrs. Thöt and Leonhard. In these diagrams the drive can slow down when its torque is less than the maximal one, which increases the time to correct a specified displacement. Besides, these systems require a complex digital-to-analogue converter, because the error is compared with the square of the speed in an analogue form. Originally such a system with a squaring device was suggested by Dr. Chelustkin¹ and Professor Lerner². The use of an integrator for speed control was described in the paper published by one of the authors³. However, we believe that the use of the optimal control permits application of a simple digital-to-analogue converter (flip-flop). The moment when braking begins is simply determined at $M_S = 0$. To compute this moment it is sufficient to feed the pulses from the position transducer to the second digit of the reversible counter where the error has been stored⁴.

We agree with Mr. Leonhard that coded position transducers are more complex than pulse transducers which operate in combination with reversible counters. However, when the latter are applied it is

necessary to eliminate the possibility of error accumulation. To achieve this in our system a special pulse transducer was used which read the actual position of rolls prior to any cycle of operation beginning from the starting point.

Mr. Beadle asked for our opinion on the use of computers for optimizing the mills.

We suggest the following hierarchy of computers and devices: (1) the central computer which plans the operation and keeps a record of the blast furnace, open-hearth furnaces and rolling mill performance; (2) shop off-line computers which control the processes and in particular determine the optimal programmes for ingot setting in soaking pits, etc.; (3) digital optimal servos to control position and speed which fulfil the programmes received from control computers. The latter type devices were the subject of our paper.

The authors are grateful to Professor Lerner and Dr. Chelustkin whose advice they used in developing the system.

References

- ¹ LERNER, A. YA. Improvement of the dynamic properties of automatic compensators by means of non-linear linkages, *Automat. telemekh.*, No. 2, 4 (1952)
- ² CHELUSTKIN, A. B. *Automatic Control of Rolling Mills*, 1952. Moscow; Metallurgizdat, 1952
- ³ DOMANITSKY S. M. Optimal control of the drive of a flying guillotine, *Elektrichestvo*, No. 1 (1960)
- ⁴ DOMANITSKY, S. M. and CHELUSTKIN, A. B. *Device for Control of an Electric Drive*, Authors' Certificate, No. 122517, 1959

Computer Control of the Continuous Annealing Process

J. T. BRADFORD, Jr.

Summary

The continuous annealing process in the past has been operated by methods based on experience and trial and error. The process, although theoretically a simple operation, becomes very complex due to the many variables that must be controlled. The digital computer system which was designed and applied to the Continuous Annealing Line at Aliquippa in 1960 will reduce the process to a science. A continuous strip hardness gauge and a strip temperature detector for the furnace section of the line were developed as part of the overall computer system which will help produce tinplate with a more uniform hardness than has been obtained before.

It was first necessary to develop mathematical relationships between the product variable, hardness, and the process control variables, furnace temperature, line speed, strip gauge, strip chemical composition and prior strip history. Although past literature was available on these relationships it was necessary to verify and extend it.

The conventional proportional, rate and reset control of the furnace which is performed by the computer, placing the computer in the loop, is described in block diagram form. A block diagram is also included showing how the feedbacks of strip hardness, strip temperature, and furnace temperature are arranged in the regulating system to control the independent variables, strip temperature and speed, to regulate the actual strip hardness. Finally, the anticipated results are reviewed.

Sommaire

Les opérations de recuit en continu des années passées ont reposé sur l'expérience et les essais. L'opération, bien que simple, devient très complexe par suite du nombre de variables qui doivent être contrôlées. Le système de calculatrice numérique, qui fut étudiée et mise en service en 1960 sur la ligne de recuit en continu d'Aliquippa, réduira le traitement à une science. Une jauge continue pour mesurer la dureté de la bande et un appareil mesureur des températures du four-placé dans la ligne, furent mis au point comme des éléments faisant partie de l'ensemble du système calculateur. Ce système aidera à la production de tôles étamées ayant une dureté plus uniforme que celle obtenue précédemment.

Il fut nécessaire, tout d'abord, d'établir les relations mathématiques entre la dureté, qui est la variable du produit, et les variables de la conduite du traitement: température du four, vitesse de la ligne, épaisseur de la bande, composition chimique de la bande, et son histoire avant son passage sur la ligne. Bien que ce sujet ait été traité auparavant et que des résultats furent disponibles, il fut nécessaire de les vérifier et de les développer.

La régulation conventionnelle du four: proportionnelle, dérivée et intégrale, qui est effectuée par la calculatrice en la plaçant dans le circuit, est décrite sous forme de schémas. Un schéma est également inclus, montrant comment les retours des informations venant des appareils au sujet de la dureté de la bande, de sa température et de sa vitesse, sont placées dans le système de régulation pour contrôler les variables indépendantes de température et de vitesse afin de régler la dureté réelle de la bande. Finalement les résultats envisagés sont examinés.

Zusammenfassung

Das kontinuierliche Glühverfahren wurde früher mittels Methoden durchgeführt, die sich auf Erfahrungen und einfaches Ausprobieren stützten. Obwohl es sich hierbei um einen theoretisch einfachen Vor-

gang handelt, gestalten die vielen zu regelnden Größen das Verfahren sehr kompliziert. Eine elektronische Digitalrechenanlage, die für die kontinuierliche Glühstraße in Aliquippa im Jahre 1960 entworfen und angewendet wurde, läßt das Verfahren wissenschaftlich behandeln. Ein kontinuierlich arbeitendes Härte-Meßgerät und ein Bandtemperaturanzeiger für den Ofenabschnitt der Straße wurden zunächst als Teil der gesamten elektronischen Rechenanlage entwickelt, die dazu beiträgt, Weißblech mit gleichmäßigerer Härte, als es früher möglich war, herzustellen.

Zuerst mußten die mathematischen Beziehungen aufgestellt werden, wie sie zwischen den Produktgrößen, der Härte, den Regelgrößen des Prozesses, der Ofentemperatur, der Bandgeschwindigkeit, den Bandabmessungen, der chemischen Zusammensetzung und der Geschichte des Bandes bestehen.

Obwohl für diese Beziehungen Literatur vorlag, war es notwendig, sie nachzuprüfen und zu erweitern.

Die Regelung des Ofens mit den üblichen PID-Reglern, die die in den Kreis eingeschaltete elektronische Rechenanlage darstellt, wird im Blockschaltbild dargestellt. Ein weiteres Blockschaltbild zeigt, wie die Rückführungen der Bandhärte, Band- und Ofentemperatur in dem Reglerteil des Rechners angeordnet sind, um die tatsächliche Bandhärte durch die unabhängigen Größen, nämlich Bandtemperatur und Bandgeschwindigkeit, zu regeln. Abschließend werden die erwarteten Ergebnisse erläutert.

The Annealing Cycle

The continuous annealing cycle is theoretically very simple. Cold rolled steel strip, as it comes from the tandem cold reduction mill, is work hardened and too hard for most purposes. It must be put through an annealing cycle to regain a degree of useful ductility. The theoretical annealing cycle is shown in Figure 1

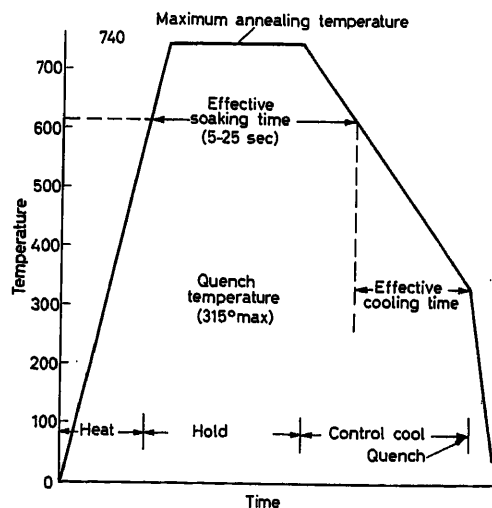


Figure 1. Theoretical annealing cycle

and consists of heating the steel strip to a temperature of between 595°–740° C, holding it at this temperature for a period of time to permit grain growth to occur, then cooling it at a controlled rate to about 480° C before cooling it to room temperature.

The Continuous Annealing Line

The annealing cycle is achieved in the continuous annealing line by passing the strip through a vertical type furnace which is usually divided into four separate and distinct zones. A simplified layout of such a furnace is shown in *Figure 2*. Here the strip is

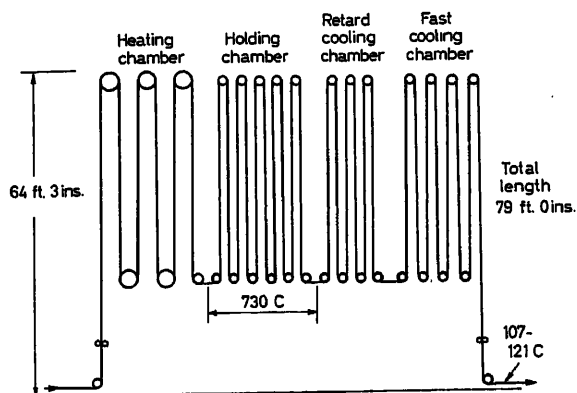


Figure 2. Furnace layout

carried through the various sections in many loops or passes. The number of passes within each zone determines the proportion of time that any increment of strip spends in each portion of the annealing cycle.

The annealing furnace is the central unit in the continuous annealing line. The entire furnace operates under a protective atmosphere in order to protect the surface of the strip at the high process temperatures. The remainder of the equipment on the line is provided to prepare the strip for the annealing process, to load incoming coils, and to unload finished coils.

The Jones and Laughlin continuous annealing line is shown in *Figure 3*. Cold rolled coils of steel are brought to the entry uncoiler direct from the tandem cold mill. Each coil is welded to the tail end of the preceding coil so that a continuous ribbon of steel is in process throughout the length of the line. After leaving the uncoiler the strip passes through an electrolytic cleaner and mechanical scrubber section where rolling oil and dirt are removed. The strip then passes through the entry looper into the annealing furnace. The heart of the process is the furnace in the centre section of the line. To achieve some degree of stable control over its operation, strip storage loopers are located before and after the furnace. These provide around 60 sec of storage to permit the entry and delivery sections to be shut down in order to weld on new coils without changing the speed in the furnace section. Before and after the furnace are free hanging loops, side guides, and automatic centring devices to keep the strip centred as it passes through the furnace proper. A regulated tension device is located immediately before the furnace to hold strip tension at the furnace entry to a known and regulated value. After leaving the delivery looper, the strip passes through an inspection station fitted with a pinhole detector, an x-ray thickness gauge, a hardness gauge and a visual inspection station.

Here the strip is classified into prime or defective footage categories. After the inspection station the strip is coiled on winding reels and removed from the line.

The Problems

This very simple theoretical cycle becomes quite complex when it is applied as a practical high production manufacturing process. The problems are listed as follows:

(1) The annealing cycle involves both temperature and time. Variations in time, by changing speed, also varies strip temperature.

(2) The exact shape of the annealing cycle in terms of temperature and time varies with: (a) the degree of hardness desired in the end product, (b) the chemical analysis of the strip, (c) the hardness of the incoming strip as determined by prior history, and (d) the incoming strip dimensions.

(3) The furnace itself is an effective heat sink; zone temperatures cannot be changed rapidly.

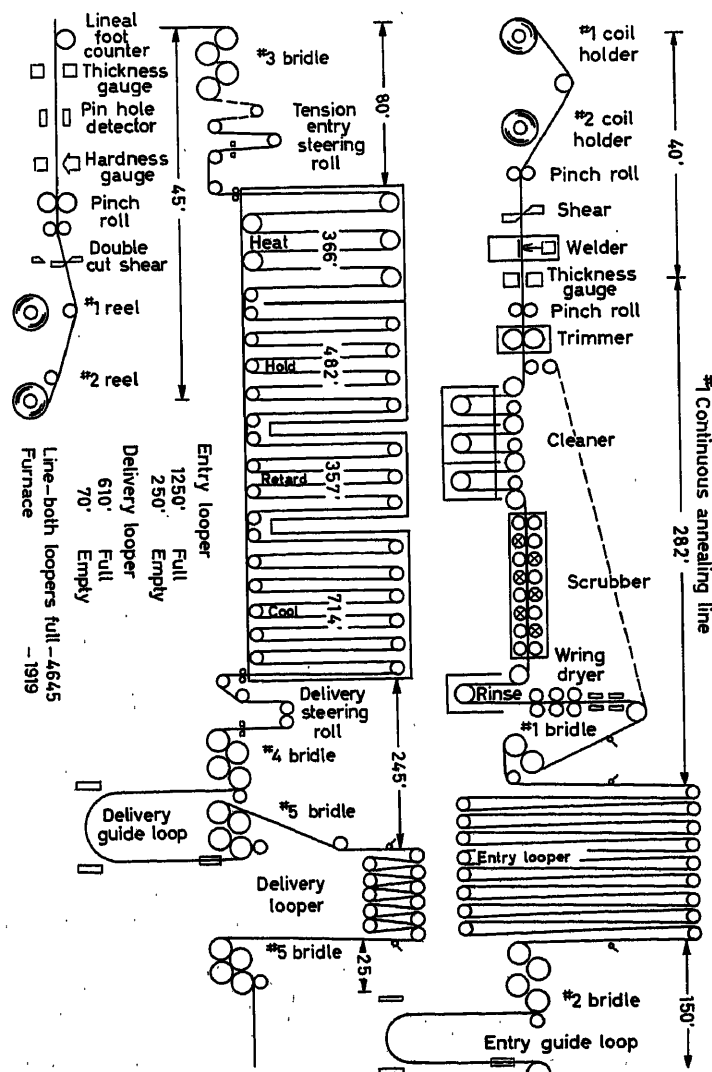


Figure 3. Jones and Laughlin continuous annealing line layout

(4) Magnitude and rate of changes in speed and temperature can affect strip tracking through the line, and can cause heat or tension buckles in the strip, both of which lead to strip breaks and costly delays.

(5) The continuous annealing line is a costly investment and must be run at the highest possible rate of production to be economical.

(6) Strips on orders requiring one annealing practice are welded to strips requiring another annealing practice, portions of both orders being in the furnace at the same time.

(7) The brightness, or heat absorbing capacity, of the strip affects strip temperature.

(8) No device existed for accurately measuring the temperature of moving strip inside a sealed furnace.

(9) No device existed for measuring the hardness of moving strip.

Jones and Laughlin decided to investigate computer control because they had no prior continuous annealing line experience. A study of existing lines in other plants showed that in spite of the many complexities there were, and are now, many very successfully operating lines based on experience and trial and error. The study also indicated that a digital computer system, properly designed and applied, could probably raise annealing line operation from an art to a science.

The Computer System

The complete computer system, as shown in Figure 4, was designed to perform the functions of process control, data acquisition and logging and production analysis and accounting. It is the function of process control that is of interest here.

As the first step in applying a closed loop computer system it was necessary to develop the mathematical relationships between the product variable, hardness, and the process control variables, furnace temperature, line speed, strip dimensions, strip chemical composition, and prior strip history. Although past literature was available on these relationships¹, it was found necessary to extend this work in the area of the effect that chemical composition and prior strip history has on final hardness. The relationship developed was

$$H = A_0 + A_1 T_F + A_2 T_C - A_3 T_M + (B_0 + B_1 C + B_2 P) e^{-A_5 T_S} + A_6 e^{-A_7/V_C} - A_8 C + A_9 P + A_{10} M_N + A_{11} N_2$$

where H = Rockwell hardness, 30 — T , A_N , $0 \leq N \leq 11$ = constants, T_F = hot mill finishing temperature, °C, T_C = hot mill coiling temperature, °C, T_M = maximum annealing temperature, °C, $\frac{B_0 + B_1 C + B_2 P}{A_4} = H_0 - H_1$ = difference between initial and final Rockwell hardness values of strip, T_S = effective soaking time, i. e., time over recrystallization temperature of 600°C, sec, V_C = slow cool rate, °C/sec, and C , P , M_N , N_2 = carbon, phosphorus, manganese, and nitrogen contents, respectively, wt. per cent.

It was necessary also to develop the relationships between strip temperature and furnace temperature based upon the configuration of the Jones and Laughlin furnace.

The lack of the feedback sensors for strip hardness, and strip temperature in the heat zone, required their development. A non-contacting continuous hardness gauge was developed by Jones and Laughlin Research that measures the hardness within ± 2 Rockwell 30 T points. Also a sensor that gives the

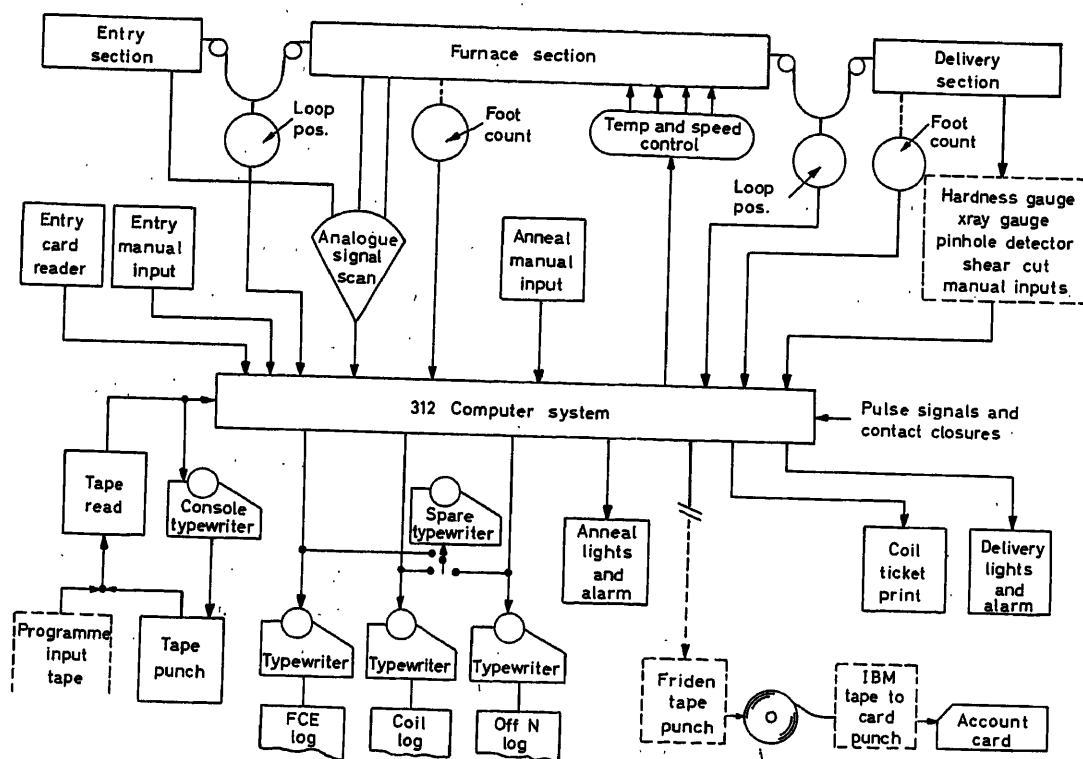


Figure 4. Computer system

strip temperature in the heat zone, and is independent of furnace wall temperature was developed. Because of patent considerations, it is not possible at this time to describe these devices. However, samples of the strip chart recordings of the instruments are included to demonstrate their applicability to control of the continuous annealing process.

The accuracy of the hardness gauge is based upon direct comparison with the Rockwell test made by the annealing line exit station operator and the hardness gauge indication at the precise time of the test. One such comparison is shown in Figure 5. The test results obtained by mill personnel at the

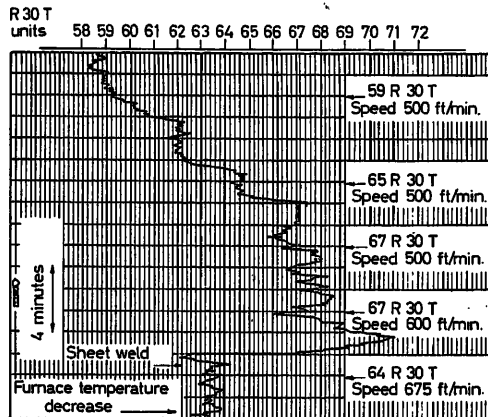


Figure 5. Hardness gauge chart indication

delivery operator's station, the speeds taken directly from the furnace speed indicator and the hardness gauge calibration scale in $R\ 30\ T$ units are superimposed upon the section of the hardness gauge recorded chart. In this figure an increase in strip hardness is caused by a reduction in furnace temperature without a corresponding reduction in line speed. As the line speed is reduced the effect of the temperature change is compensated and the strip hardness returns to a lower value. The instrument has been operational on a 24 h basis since the beginning of 1962 and gives every indication of being completely mill worthy.

Figure 6 shows two sections of a strip temperature chart with the outputs of both the J & L sensor and an ordinary total radiation pyrometer, a traditional strip temperature sensor, displayed on each. Neither of the sensors was at the time accurately calibrated in terms of actual strip temperature, and changes in indicated temperature, rather than absolute temperature values, are significant.

A total radiation pyrometer, due to the low emissivity of the C.A. strip, indicates a temperature related to furnace wall and roof temperature, with strip temperature changes acting only as a perturbation upon this primary indication. Thus, during the period covered in (a), with heat section temperature held constant, the total radiation pyrometer output was also virtually constant; the J and L sensor, on the other hand, showed appreciable strip temperature variation during the same period. Most of the variation is attributable to gauge and line speed variations, but some is due to a noise signal generated within the sensor; steps are currently being taken to eliminate this noise signal. The spikes labelled *L* and *B* are lap weld and butt weld areas respectively; a single positive spike is characteristic of a lap weld, and a positive spike followed immediately by a negative

spike is typical of a butt weld. The spikes indicate that sensor response time is much less than the furnace time constants, and hence is sufficiently rapid for control purposes.

Figure 6 demonstrates that a total radiation pyrometer is useless for control purposes, as it indicated a temperature increase when, in fact, there was a decrease in strip temperature. The sequence of events was as follows: the heat section temperature was increased by the operator in anticipation of a strip gauge increase; the increase in zone temperature is clearly indicated by the total radiation pyrometer; however, the J and L sensor shows that the heavier gauge strip was heated to only 480° to 510°C and there was a resulting increase in strip hardness; some 10 min later the line speed was reduced, and strip temperature rose to a more acceptable level—near 575°C . Needless to say, use of the total radiation pyrometer as a feedback sensor would have led to the opposite (and improper) control action.

The Control System

Having the necessary mathematical relationships, the characteristics of the newly-developed sensors, and the characteristics of the line speed control, different possible closed-loop control systems were developed and studied on an analogue computer. Figure 7 shows in block diagram form the system that showed the most promise. A punched card is used for each coil to tell the computer the desired hardness, the chemical analysis of the strip, the strip dimensions, and the prior history.

The computer then calculates, based upon the developed mathematical relationships, the required strip temperature, the furnace temperature reference, and the desired speed reference. The basic control for the system is the continuous strip hardness gauge. Should an error in hardness exist, an immediate signal is sent to change line speed and to reset the furnace references. In order to provide reasonably fast correction to a hardness error, a stabilizing signal is taken from the strip temperature sensor. Thus, when a hardness error causes a change, the strip temperature sensor indicates to the system that the change has been made without having to wait for the corrected strip to travel the approximate 1,600 ft. to the hardness gauge.

Figure 8 shows the results of one of the runs made during the analogue computer study. This case was for 0.0118 in. thick steel, 30 in. wide, and the line running at 1,200 ft./min. A step

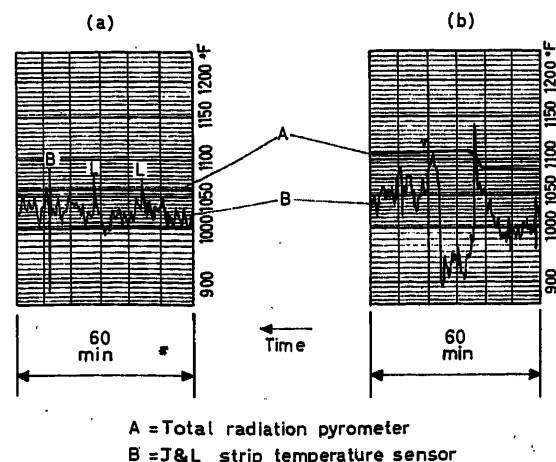


Figure 6. Comparison of temperatures indicated by strip temperature sensors

decrease of hardness of approximately one $R_{30}T$ point was made. The line speed increased approximately 62 ft./min until the furnace temperature decreased. The hardness error was eliminated in about 200 sec. This is the kind of result expected from the actual system.

Valve Control

As part of the closed-loop control system it is also the computer's function to operate directly 11 proportional fuel gas and cooling air valves and two electrical contactors to regulate temperatures within the furnace zones. The valves are operated through Leeds and Northrup d.c. current to pneumatic converters connected to pneumatic operators on the valves. A throw-over system is provided so that any one or all furnace zones may be controlled by the conventional L and N recorder controllers should trouble with the computer make it necessary.

Figure 9 is a block diagram of the actual closed-loop temperature control function as it is handled by the computer. The computer scans the analogue temperature signals, converts it to a digital value and compares it with the reference value. The temperature error is applied to stabilizing equations and a digital value of valve position is calculated. This digital value is then converted to an electrical analogue current which becomes the input signal to the electro-pneumatic converter. The conventional 'proportional', 'reset', and 'rate' actions are actually achieved by approximation of the sampled system with a continuous system. The sampling and hold operations were replaced with a pure time delay of half the sampling period.

The Results to Date

At the time of writing the entire closed-loop effort is not complete. The mathematical relationships that were developed are being verified and improved by means of the data gathered

by the computer operating as a data logger. The hardness gauge is completed and has proved to be a reliable operating sensor. The strip temperature sensor is developed and is installed on the line. Its reliability is being verified. The computer has been used to perform its functions of data acquisition and logging, and production analysis. Changes have been made to both the hardware and programming as the art of on-line computers has progressed. The reliability has been improved to the point that the computer can be considered as a reliable industrial control device. In addition the furnace has been controlled by the computer for a period of time using precalculated references for the furnace temperatures.

The digital control system applied to the Jones and Laughlin continuous annealing line is not yet complete. The programme for having a closed-loop process control system is progressing. In addition to the benefits expected in improving the continuous annealing process, much experience has been gained in the application and use of digital computers, and an appreciation of their possible application to other processes has been developed. It is expected that at the time of the conference data will be available on both the improvement of the process and the reliability of the system for inclusion in the transactions.

References

1. MOHRI, A. F. Metallurgical aspects in the design and operation of a continuous annealing line. *Amer. Iron & St. Inst. Yrbk.* (1956) 123-150

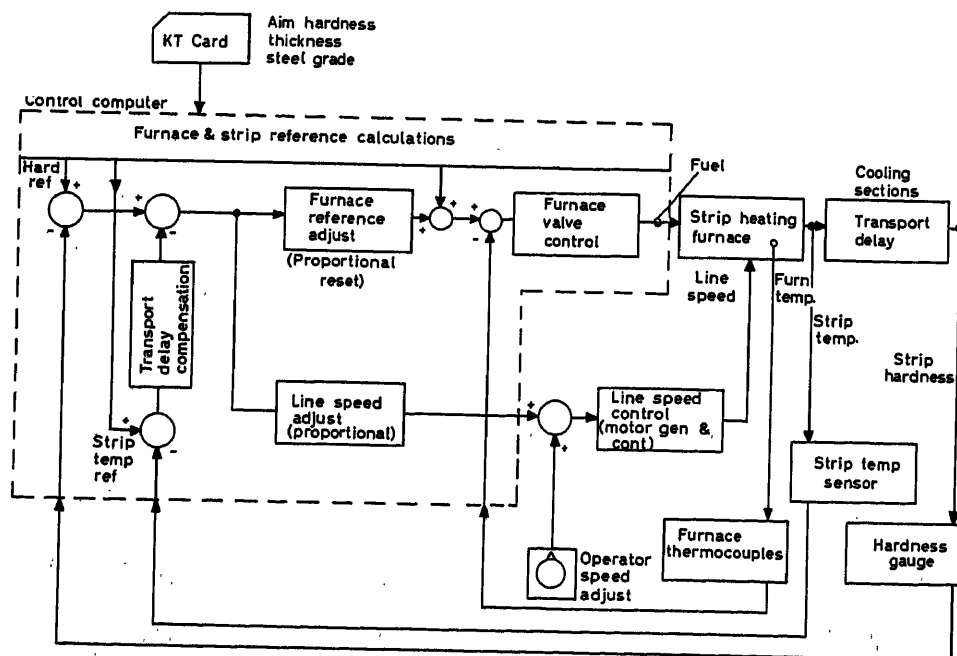
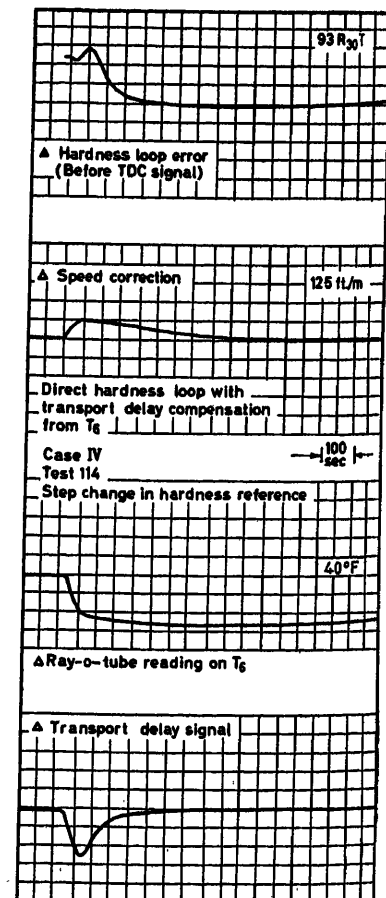


Figure 7. Block diagram—strip hardness control

Figure 8. Analogue computer study curve



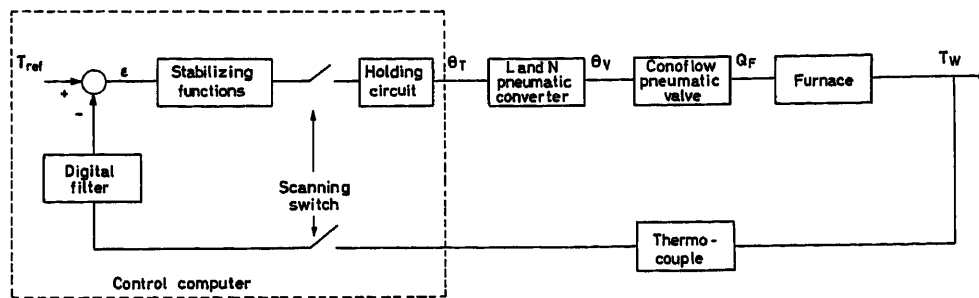


Figure 9. Block diagram of the furnace temperature controller

² LARSEN, R. C. Application of a control computer in the closed loop control of an annealing furnace. *ISA Preprint* 141-59 (1959) 20-25

³ BRADFORD, J. T., and KIRKLAND, R. W. Control computer system

for a continuous annealing line. *AIEE Conf. Pap.* 60-976; Computers in Control *AIEE Publ.* S-132 (1961) 52-62

⁴ SMITH, R. H. Computerized control of a continuous annealing line. *Blast Furn.* 49 (1961) 529-535

DISCUSSION

Author's Opening Remarks

The continuous annealing cycle is theoretically very simple. Cold-rolled strip, as it comes from the tandem cold reduction mill, is work-hardened and too hard for most purposes. It must be put through an annealing cycle to regain a degree of useful ductility.

Five years ago, when Jones & Laughlin Steel Corp. decided to install a continuous annealing line, they had no previous experience in continuous annealing. Studies of the process and existing lines in other plants, indicated that a digital computer system, properly designed and applied, could raise the operation from an art to a science.

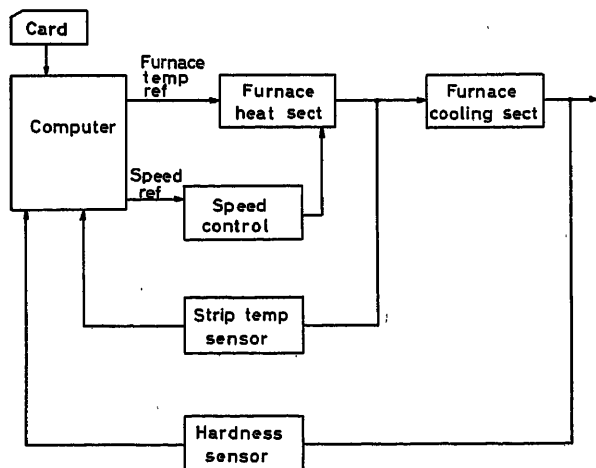


Figure A

The very simple annealing cycle becomes quite complex when it is applied to a high production manufacturing process. The problems are as follows: (1) The annealing cycle involves both temperature and time, and the two are not independent. (2) Studies indicated that previous relationships between hardness, the product variable and the process control variables, furnace temperature, live speed, strip dimensions, chemical composition and prior strip history, were not adequate. (3) The furnace time constant is extremely long. (4) No sensor existed for continuously measuring strip hardness. (5) No sensor existed for continuously measuring actual strip temperature. (6) Excessive rates

of change of speed and temperature can cause delays by causing wrecks due to tracking or buckles. The continuous annealing line, being a costly investment, must be run at the highest possible production rate to be economic. (7) Strips requiring different annealing cycles may be welded together and in the furnace at the same time.

At the time the paper was written the proper relationships were developed but not verified. The computer was operating as a data logger to verify them. The required sensors for the continuous measurement of hardness and strip temperature were developed. Today the relationships have been verified. The actual programme for the closed-loop operation has been developed, flow-charted, coded, loaded in the computer and operated. The different modes of operation are described below.

Mode 1. With the mode switch in this position the computer regulates the temperature of any heat zone for which the zone selector switch on the furnace panel board has been thrown to the 'computer' position. Any furnace zone may be transferred to computer control or back to conventional control. The reference temperature to which a heat zone will be regulated in this mode consists of two parts—the base reference + zone offset where the base reference is set by the operator and the zone offset is the degrees by which any heat zone can be regulated above or below zone 4, which is considered at zero offset. The zone offset is stored in the computer.

Mode 2. With the mode switch in position 2 the computer regulates actual strip hardness, as measured by the hardness gauge, to the hardness read in from a punched card with furnace temperature as the only controlled variable.

The strip temperature sensor is used in this mode to achieve faster response than would otherwise be possible. If the strip temperature sensor fails, the computer downshifts its operation to a slower response, but still regulates strip hardness. If the hardness gauge fails, the computer downshifts to the first mode.

The temperature to which the heat zones will be regulated in mode 2 consist of 1350° plus the change in furnace temperature calculated by the computer to bring the actual strip hardness within + 1/2 Rockwell point, as called for on the punched card. The furnace offset is added to this reference. The furnace temperature will respond to changes in reference through the furnace time constant which has an apparent value of 7 min. Maximum operating limit furnace temperature is a programmed function of strip thickness.

Mode 3. With the mode switch in position 3, the computer regulates actual strip hardness, as measured by the hardness gauge to the hardness read in from a punched card with furnace temperature and

speed as the control variables. A hardness error greater than $\pm 1/2$ Rockwell point will cause a change in the heat zone as in mode 2. Also, if the hardness error exceeds ± 2 Rockwell points, the computer changes line speed to bring the hardness immediately within the desired range. Computer initiated speed changes are made in two basic patterns, depending on whether the strip temperature sensor is operative. If it is, the line make 5 ft./min speed changes at 10 sec intervals. If the sensor is not operating, the computer will change the line speed in 25 ft./min and wait to read the effect as measured by the hardness gauge before making further adjustment. The computer automatically shifts from fast to slow and *vice versa*, depending only on 'reasonableness' tests applied to the strip temperature sensor.

Speed increases are limited to 50 ft./min by the computer, and speed decreases are limited by strip gauge as programmed in the computer.

The benefits, as we see them at present, will be what we make them. Operation to date has indicated to all concerned that we have a new operating tool by which we will probably be able to improve the quality of our continuous annealed product so that it will have a variation of less than ± 2 Rockwell 30 T points, especially at start-up and stop. Much work is still being done on optimizing the transformation from one annealing cycle to another on order changes. We are encouraged.

Now a few words about the reliability. We developed a very rigid maintenance programme on paper and planned many methods to define and measure reliability, or availability. However, because of an undermanned maintenance department we did not run off-line diagnostics, we did not periodically check voltage levels, we did not check pulse shapes, nor make drum and amplifier margin checks. We have, however, found this of little concern as the computer runs for long periods up to six months or more with less than a couple of card failures. The availability has been so good that we look after the computer 'hardware-wise' only during rare failures.

H. J. MARX, *Allgemeine Elektrizitäts-Gesellschaft (AEG), Hohenzollerndamm 150, Berlin 33, Germany*

The application of a process computer system on a continuous annealing line is a typical example of how production processes can be improved by the use of electronic means. We thank the author for informing us in this paper about the planning and engineering work for this new control system. We thank him also for his remarks on the practical problems which occurred.

A continuous annealing line lends itself to automation. The continuous form of the process is basic and in this particular case there is the specific feature that changes of the annealing programme are very rapid; when a new strip enters the line, it is welded into the end of the other strip. If the analysis or the width of the new strip is different, the set-up of the whole line must be changed, theoretically in one instant at each section of the line. My questions are:

(1) Did you observe an improvement in scheduling the line by the use of the computer or can you tell us what are the main problems in avoiding such a random scheduling? Is the computer used also for data acquisition and logging production analysis and accounting?

(2) What is the ratio of that part of the computer memory used for storing the programme for data processing etc. to the part used 'for the control programme'?

Perhaps you can give us some figures regarding the percentage of the time, when the computer acts as data processor? The mathematical model contains several constants.

(3) Is there any adaptive feedback for improving the model dependent on the actual situation of the line?

J. T. BRADFORD, *in reply*

(1) The computer control has not been used enough to reflect any changes in the scheduling of the line. Random scheduling of the line would not be practical because minimum gauge and width changes

can only be made without getting into problems on buckles and subsequent delays.

(2) The data acquisition and accounting functions made up approximately two-thirds of the storage and the programme.

(3) There is no adaptive feedback used to improve the model. The model acts as a feedforward calculation to get the hardness within range and the feedback system is used to regulate the actual hardness.

J. G. WISTREICH, *B.I.S.R.A., Old Park Lane, London W. 1., England*

The work of Jones and Laughlin on automating a continuous annealing line has excited much interest among tinplate makers, and one is therefore grateful to Mr. Bradford for his description of the scheme, brief though it is, owing to patent considerations, with regard to the hardness sensor. I note that it is a comparative measurement depending for accuracy on the making of a Rockwell test by the operator. Can Mr. Bradford tell us:

(1) How frequently this has to be done and what factors influence calibration?

(2) If it takes 200 sec to eliminate a hardness error, and the line operates at speeds in the order of 200 every time an error occurs, something like a mile of strip is not made to specification. How frequently do errors of a magnitude which brings the hardness outside the tolerance occur? To put it another way, what improvement does Mr. Bradford reckon to get with his control compared with normal practice of operation?

(3) What effect, if any, on hardness has the change in cooling rate consequent on change of speed?

J. T. BRADFORD, *in reply*

(1) The hardness is checked at the front, centre and tail of each coil by the operator by means of taking a punching from the strip and checking it on a Rockwell Tester. This can be done without affecting production on the line because of the delivery storage looper. As more and more confidence is acquired in the continuous hardness gauge this may be discontinued.

(2) We feel that we will be able to keep the hardness variation within ± 2 R30T points of the aimed hardness. This would be an improvement of between 2 or 3 to 1.

(3) We have found that cooling rate has much less effect on hardness than the heating cycle. Therefore the computer control of the process concentrates on this end.

S. S. CARLISLE, *B.I.S.R.A., Old Park Lane, London W. 1., England*

It is apparent that when there is a known incoming change in strip thickness, corrective action to the annealing process can be made by change in line speed and by a change in furnace temperature. The former corrective action will be immediate in its effect on the processing of the strip, while the latter will be delayed according to the temperature response of the furnace. In order to minimize the length of off-hardness strip produced at a thickness change, there will be an optimum partition of the control action between temperature and speed correction. I would like to ask the authors if they use the principles, outlined by Professor Lerner in his paper, 'Optimal Control of Continuous Processes', in the operations of their computer control systems so as to optimize the partition of the control action between these two variables.

J. T. BRADFORD, *in reply*

Optimal control of the process is being considered for the future. Mr. E. Y. Kung of the Jones and Laughlin Steel Corporation mentions it in his I.E.E.E. Paper No. 63-911 and promises to tell more in the future.

COMPUTER CONTROL OF THE CONTINUOUS ANNEALING PROCESS

D. S. LECKIE, *Republic Steel Corp., 1517 Republic Building, Cleveland I, Ohio, U.S.A.*

In discussions of these applications, the problems of process analysis, hardware development, reliability, to name a few, are considered at great length. At times the information input to the control system seems to be taken for granted. In practice, however, the problem of providing accurate control information as required in the form of cards for this system can be awkward.

Error control on these cards is as important as the reduction of component and sensor failures. Indeed, the preparation and checking of these cards should be considered part of the control system. Therefore the following three questions are proposed:

(1) What is the source of the control cards, i.e. are they obtained from a card library, or is special punching required?

(2) How are mistakes controlled in the preparation of these cards?

(3) Is any extra cost incurred in the preparation of these cards?

J. T. BRADFORD, *in reply*

(1) A library of cards that covers all of the different products is maintained at the line. If, when the electronic data processing group is preparing the schedule for the line, they encounter a product for which there is no card, a card is prepared and made available to the operators.

(2) Mistakes must be caught by the crew. Newer computer installations have visual display boards that show the computer instructions to the crew so that this may be done more readily.

(3) The electronic data processing operation is sufficiently large so that the preparation of these cards is of no extra cost.

THE CHEMICAL AND OIL INDUSTRIES

Application of Automatic Control in the Chemical and the Oil Industries

A survey by Ir. H. W. SLOTBOOM, J. J. DE JONG, J. A. LANDSTRA,
J. E. RIJNSDORP and A. C. TIMMERS

Introduction

The task of a reviewer who has to give a survey of the present situation in a technical field is complicated by two unavoidable 'musts'. In the first place he has to disengage himself from his daily work and its environment, with its specific problems and methods. In the second place, he has to find his way through the mass of information, often capricious, which has become available in recent years.

Even before the war automation had made a big impact on the petroleum and chemical industry. This is due to the nature of the processes which lend themselves more easily to continuous operation than is, for instance, possible in the automobile industry. As a consequence, the number of operators was greatly reduced, often reaching the minimum number required for emergencies.

Since the war, the level of automation has continued to increase. The following four factors are responsible for this.

The Improvement of Techniques for Data Transmission

Initially, the introduction of pneumatic transmitters made it possible to separate the control room from the process equipment. Large plants, and even complete refineries, can now be supervised from one central control room. This has led to a further reduction in the number of operators, and to more co-ordinated control.

More recently, electric transmission, particularly in the pulse-coded form, has removed the barrier created by long distances completely. For instance, pipelines are now being operated with completely automated pumping stations supervised from one of the terminals¹, and tankfarms from a central control room. Furthermore, it is possible to link up a computer in a central position with the operation of a distant refinery².

The Application of the Theory of Feedback and Control

This, which originated before the war in the field of electronic amplifiers, was further developed during the war in the field of servomechanisms. We shall return to this point in more detail later.

The Introduction of Automatic Quality Analysers

In the past, the quality of products was usually analysed in a laboratory. The time for taking a sample of the product, bringing it to the laboratory, making the analysis and informing the process operators of the results usually takes several hours. Hence, the response of this manual feedback control system is very slow. Moreover, all human errors related to the carrying out of frequent routine jobs interfere with good operation.

Nowadays, automatic quality analysers are replacing laboratory analysis. The instrument manufacturers have solved the problem of unattended operation under process conditions, and the process industries have learned how to introduce and maintain these relatively complex instruments³.

As an illustration of the progress in this field a survey of the number of automatic quality analysers in the Royal Dutch/Shell Oil refinery and chemical plants of Pernis in Holland is given.

Year	1955	1960	1962
Number	40	163	275

The Introduction of Computers

The use of general-purpose digital computers is paving the way for optimum control of complete refineries and chemical plants. The complexity of this job exceeds the capabilities of human beings.

Cases have been reported, and the experience has been confirmed within our own company, where the computer could improve the production even of processing plants where staff have had many years of extensive operating experience.

The endeavour to achieve optimum control, i.e. bringing process conditions in line with the values which are the most economic instead of the values which are merely constant, is the modern approach in our work. We shall now discuss in more detail how this can be realized in the chemical and oil industries.

Hierarchy of Control

By way of an example, let us examine a large oil company with many refineries and marketing outlets. It is obviously out of the question in the case of such a company to find optimum values for all degrees of freedom by means of one computer programme.

It would be preferable to divide the company into smaller units and to optimize each unit separately by means of a computer programme of a reasonable size. However, in this way, the overall optimum is lost sight of, as non-optimum operation of one unit can improve the overall optimum.

The most plausible solution is to use some form of hierarchy; where a higher level commands a lower one and a lower level has to obey a higher one⁴. In this command-obey situation it is vital to have 'play' and feedback. The command should give the lower level a margin of freedom. Then the lower level can experiment within this margin and feed back its experience to the higher level.

Figure 1 shows a possible setup. At the highest level a model of all operations within the company is shown, each operation being represented in a greatly simplified form. This model, programmed on a large digital computer⁵, determines the allocation of crude oil to the various refineries, indicates the products which have to be manufactured (quantities and qualities) in each refinery, and shows how the transportation between refineries and marketing outlets should be arranged.

The inputs of this corporate scheduling programme are the marketing requirements which are based on a forecast of customer demands for the near future.

The next level in the hierarchy is formed by the refineries. They are given a margin of freedom within which they can deviate from the product quantities and qualities stipulated by the highest level. In addition, they also receive the marginal values for their products. These marginal values are equal to the change in company profit if one additional ton of the product is made or if the quality of the product is improved by one unit.

The refinery scheduling programmes now determine the optimum distribution of feed streams to the plants and the quantities and qualities of intermediate products. Furthermore, the refineries return information to the corporate scheduling programme

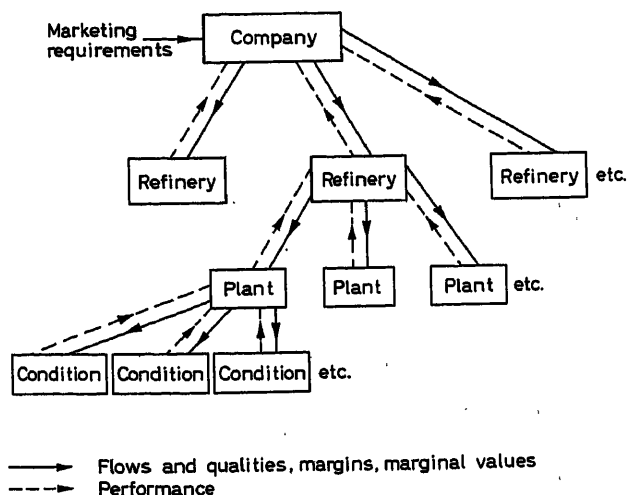


Figure 1. Hierarchy of Control in an oil company

about the performance obtained. In this way, the model in the latter programme can be improved and regularly updated.

This procedure is repeated lower in the hierarchy. The plant programmes receive target figures for their input and output streams, some freedom for deviation being allowed for. In their optimization, they are guided by the marginal values given to them by the refinery scheduling programme.

The plant programmes should minimize the cost of operation, which generally implies the lowest possible utility and chemicals consumption. This can often be done separately from the optimization of product quantities and qualities.

The lowest level in the hierarchy is formed by the control system for individual process conditions. Here the feedback to the higher level is based on the measurement of the actual behaviour of the process.

We shall now turn to the fundamental problems in the process control field and their solution, as viewed in the light of the hierarchy of control.

Description of Process Behaviour

For the analysis and synthesis of the individual control systems, the dynamic behaviour of the process is an important aspect. Therefore it is not surprising that at this Congress several papers are devoted to this subject⁶⁻¹².

The first work in process dynamics was done long before automatic control was used. Technologists had to design and operate batch processes which are inherently dynamic. Other subjects are the start-up of continuous processes and the operation of processes which can become unstable.

An example of the latter was discussed by Volter⁶ at this Congress. He uses the Lyapunov method and phase-plane techniques to investigate the stability of the process in detail.

Similar activities have been originated by Amundson and co-workers¹³.

The Measurement of Process Dynamics

The most important ways of measuring dynamic behaviour are:

The step method—This is simple and fast but easily spoilt by process disturbances. A way of diminishing the influence of the latter is to take an average for a series of step responses by introducing, for instance, a square wave. It is surprising that this type of approach seems to have been little used so far.

The pulse method, introduced by Hougen and Lees¹⁴, places more emphasis on the higher frequencies, which are usually the most important for control.

The sine wave method is very useful when accuracy is important¹⁵⁻¹⁸. Moreover, it is less sensitive to process disturbances, especially when the Fourier analysis is applied¹⁹⁻²¹. Another advantage is that non-linear behaviour clearly shows up as a distortion of the sine waves.

The disadvantage of the sine wave method is that it takes a great deal of time. This can be improved by introducing sine waves simultaneously^{22, 23}.

The natural disturbances method—Here the dynamics are determined from the effects of the actual process disturbances²⁴⁻²⁷. However, records covering a long period are necessary, so that there is a chance that the results will be spoilt as a result of changes in the process. Moreover, in complex processes, where

disturbances often reach a given point along different paths, it can be very difficult or even impossible to extract the individual responses from the results of the measurements.

Finally, in the petroleum and the chemical industries there can rarely be any serious objection to the careful use of test signals, so that the natural disturbances method loses its only real advantage over other methods.

Theory of Process Dynamics

A fundamental problem in the theory of process dynamics is the complexity of modern processes. For instance, even a much simplified description of a distillation column with N trays and two components (binary mixture) requires $(N + 2)$ non-linear differential equations of the first order (N can have values from 10 to 300). Moreover, a typical plant contains several of these distillation columns, interlinked by heat exchangers and coupled in complex ways with chemical reactors or other plants.

It is obviously advisable to give a simple description of process dynamics. In this respect, it is useful to make a distinction between flow variations and composition variations. Flow and heat flow variations usually travel much faster and with less damping through plants than concentration variations, so that their effect on control is more pronounced.

Moreover, since controllers usually manipulate a flow, these variations also play a most important role in the study of stability and speed of control loops.

Unfortunately, the responses to flow variations seem to receive less attention than responses to concentration or temperature variations. For instance, in their survey paper on heat exchanger dynamics, Williams and Morris²⁸ found only one out of 42 papers dealing with flow variations. (The reason probably stems from the desire to avoid non-linear phenomena.)

However, good results have often been obtained by linearizing the equations^{18, 29-32}.

At this Congress, Delvaux⁷ gave an example of this approach as applied to a heat exchanger and a mixing process. Moreover, the papers of Anisimov⁸, Zavorka⁹, and Izawa and Morinaga¹⁰ discuss linearized models of distillation columns.

Izawa and Morinaga also compare calculated responses with empirical ones. A more qualitative than quantitative agreement is obtained, which seems to be due to the difficulty of estimating the numerical values of the hydraulic tray parameters. These parameters appear in the linearized version of the relationship between the liquid flow, the vapour flow and the liquid hold-up of the tray.

In the research on distillation dynamics done by Shell, we have experienced the same difficulty^{18, 33}. Therefore, it seems desirable to devote more attention to the determination of the hydraulic tray parameters for commercial tray types under various loading conditions. This work could probably be incorporated in the conventional experimental work for pressure drop capacity and efficiency data.

Quite a different study of distillation dynamics is presented by Moczek, Otto and Williams¹¹, who use large step changes (10-25 per cent) as input variations.

The calculated responses appear to be extremely non-linear, which is contrary to the work discussed in connection with the other papers on column dynamics. It would be interesting to know how the transition from the linear to the non-linear case takes place and where the assumption of linear behaviour becomes unrealistic.

The dynamic consequences of assuming different mixing models for the tray liquid are discussed by Takamutsu and Nakamishi¹².

We shall not go much further into the existing literature on process dynamics. For multi-stage processes (distillation columns, heat exchangers, etc.) there are excellent surveys by Archer and Rothfuss³⁴, Williams and Morris²⁸ and Rosenbrock³⁵. Here only some of the more recent work will be mentioned.

Other processes are also receiving more attention, such as multi-stage processes in general³⁶; a fluidized bed³⁷; a crystallizer³⁸; and a liquid-liquid extraction column³⁹.

To conclude our remarks on process dynamics, we should like to make a plea for the adaptation of the dynamic model to the particular application. For instance, there are numerous studies on column dynamics where liquid hold-ups and pressures are assumed to be constant. Consequently, flow variations travel infinitely fast through the column. This is all right for calculating the rate of approach to equilibrium but unsatisfactory for the study of feedback control systems, where hydraulic delays just contribute the phase lag required to reach 180°. It is therefore desirable to establish a close relationship between the dynamic model and the purpose for which it will be used; for instance, it might be much simpler to have two separate models for the low and for the high frequencies respectively than to have one valid for all frequencies.

Description of Disturbances

Hitherto, the description of process disturbances has been the Cinderella of process control. The prince of stochastic processes^{26, 40} is awaiting her arrival, but the carriage of experimental data is not yet ready.

One of the few known studies into disturbance patterns was carried out by Van der Grinten^{41, 42}. His experimental power density spectra correspond to white noise passed through a first-order low-pass filter.

In practice, control systems are also subject to disturbances which differ from the familiar picture of random noise. Step changes, in particular, are quite common and are often the most troublesome to control. In the Appendix disturbances are classified according to their sources.

Automatic Control Systems

We now wish to return to the synthesis of the various building blocks into automatic control systems, as viewed from the standpoint of the hierarchy of control.

The following subjects are discussed: single-variable feedback control, multi-variable feedback control, feedforward control, optimizing control and the application of computers for control purposes, and automation of discontinuous processes.

Single-variable feedback control—Work is still in progress on control systems for a single process condition.

Part of this work is concerned with the prediction of adjustment of controller actions in line with the dynamics of the process⁴³. However, in practice, good controller settings are obtained by trial and error procedures, i.e. by incorporating the observed effect of a change in the setting on the quality of control.

One of the problems is the influence of changes in process operation on the dynamics of the loop. The non-linear characteristic of the control system, in particular, can cause difficulties.

At this Congress, Isobe and Totani⁴⁴ demonstrate an adaptable system for adjusting the gain of the controller. They intro-

duce a square-wave disturbance and measure the effect on the mean square deviation.

Such adaptable systems are usually too expensive for practical application in the oil and chemical industry, if they only serve one control loop.

In the near future it can be expected that the application of computers will make the automatic adjustment of actions possible for all control functions together.

In complex processes, variations in one location often affect another. For instance, if a series of chemical reactors have temperature controllers acting on the cooling water supply, a sudden movement of one control valve is felt by the other control loops. Hence, it is advisable to avoid valve movements which are too violent; thus, controller actions should be set more conservatively.

This problem resembles those associated with the limited excitation range of servomotors in servomechanisms.

A novel approach for designing control systems for distillation columns has been developed by Rosenbrock⁴⁵, who uses the concept of the amount of disturbance, which is defined as the sum of the absolute values of the rates of change which occur on the trays, the reboiler and the condenser. Later⁴⁶, Rosenbrock has shown that this 'amount of disturbance' has the properties of a Lyapunov function, and he stipulates that control should reduce the 'amount of disturbance' as quickly as possible.

In our opinion, Rosenbrock's criterion does not take sufficient account of the top and bottom compositions. In principle, composition variations should not cause concern as long as they do not leave the column via top or bottom products. Consequently, we think that the criterion should only be concerned with the product compositions.

As we have already stated in the introduction, direct and automatic measurement of product composition is becoming more and more important. Moreover, automatic quality control is also being introduced with good results⁴⁷. By running closer to the specification limits, the overall economy can often be considerably improved over what is possible by manual control.

One of the most popular automatic quality analysers is the GLC or chromatograph. It operates on the repetitive analysis of small samples, so that control is of the sampled data type. Here, techniques such as Z-transformation can be useful.

It is surprising how reliably a complex device like an automatic GLC can operate in the plant. This serves as a real contradiction to the popular belief that complex devices are of necessity unreliable.

Multi-variable Feedback Control—In refinery and chemical plants, there often is much interaction between control loops. The bad effects of interaction can be minimized by connecting the controllers to the correct control valves or by changing the scheme in other ways.

An example of this is given in the paper by van der Heyden and van Nes⁴⁸, who discuss the design of a power recovery system for a catalytic cracker, where the control systems for eight turbo-compressors interfere with each other and with the control loops of the catalytic cracker regenerator and the CO boiler.

An analytic study of this complicated system is impossible and therefore it has been simulated on a large analogue computer. One of the results of the study was the desirability of changing the line-up of the process. It is a great moment for control engineers, when they can play the process designers at their own

game instead of being obliged to adhere strictly to their designs, both thus benefiting from the exchange. Another example of this, but for a much simpler system, is discussed by Kijlstra⁴⁹.

A more radical way of solving the interaction problem is to eliminate it by uncoupling the multi-variable control system. This has been applied to steam boilers^{50, 51} but not yet to the same extent where other types of plant are concerned.

Recently, Rosenbrock⁵² has introduced the interesting idea of making use of the interaction between process conditions for improving control. His starting point is in chemical processes and usually only as many output conditions are measured as there are input conditions available for automatic control. By using the measurements of additional output conditions, which are influenced by the same input conditions, a better result can be expected.

In principle, Rosenbrock's method is to install a linear transformation device between the process outputs and the controller inputs and another similar device between the controller outputs and the process inputs.

As seen from the controller's position, the process matrix can then be diagonalized, so that the controller only has to deal with a set of non-interacting, non-minimum phase response of the first order. As a result rapid control is possible.

It will be interesting to see Rosenbrock's method applied to a specific example. It will then be possible to judge whether the control valves still remain within their ranges and whether the secondary time constants do not affect control performance as adversely as they do in conventional control.

Feedforward control—Feedforward techniques can be used to supplement feedback control. In recent literature there are some proposals for distillation columns^{53, 54}.

Optimization—Until recently the choice of the set points was considered to be outside the province of process control. But starting with scheduling, that is, the planning of operations, a more logical and mathematical approach was initiated.

There are two basic methods for optimization⁵⁵.

- (i) Using a mathematical model of the process (predictive method);
- (ii) experimenting with the process (exploratory method).

In the first method, the process behaviour is assumed to be known with sufficient accuracy. All knowledge is digested in a mathematical model, which is then incorporated in the programme of the computer.

In the second method, it is assumed that hardly anything is known about the process. The computer (computing device) introduces small changes into the process and watches the effect on the economy of operation. If the economy improves, further changes are made in the same direction; if the economy deteriorates, the direction of change is reversed.

The mathematical model method fails if the process behaviour is not completely predictable.

Difficult points in chemical and oil processes are, for instance, varying tray efficiency in distillation columns, poisoning of catalyst in conversion processes and side reactions in chemical reactors.

The experimental method avoids most of these difficulties. However, if the number of degrees of freedom ('control valves') is larger than, say, three or four, it will take a very long time to find the optimum. Even for one or two degrees of freedom the experimental method might be too slow if there are rapid and

extensive variations in the process. This possibly explains why optimizing controllers ('hill-climber'^{66, 72}) have given disappointing performance⁶⁸ except in some isolated cases.

Obviously, a better result can be obtained by combining the two methods. The mathematical model in the computer can be kept up to date (adapted to the process) by feedback of information from the process.

Many plans for the application of large computers to process control are based on a mathematical model^{57, 59-63}. In the beginning, the description of the process performance was a very simplified procedure and linear programming was adequate. Gradually, however, the mathematical model became more refined and the optimization techniques became more complicated. In many cases, non-linear optimization is necessary^{64, 65}.

All these optimizing techniques make use of a value function. This value function must be maximized, while taking into account the physical constraints. In this way, it is possible to calculate the set points of the individual controllers. However, this gives rise to a fundamental problem.

There is an influence from the past on the present, and furthermore future requirements have to be taken into account. For instance, having operated a reactor at a high severity in the past might have deactivated the catalyst so severely that in the present and in the future good operation is impossible. Another is the influence between past, present and future due to the stocks.

With regard to the on-line digital computer, we can make the following comment: It should not be used only as an optimizer, because it has many more potentialities, such as feedforward action, uncoupling of multi-variable systems, better accounting, emergency detection⁶⁷ and action, and is also capable of taking over the control function of simple control loops.

As process control computers are rather expensive devices, each of their memory locations should be used as efficiently as is possible. Therefore one should strive for the most rational balance between the various potentialities mentioned above. Often the process study, which precedes the application of an in-line process control computer, has led to other ideas for improving process optimization. For instance: modification of the conventional control system, installation of additional plant equipment⁶⁸, using automatic quality analysers⁶⁹, etc. Computers are not a cure-all.

As a result, the size of the problems can easily exceed available computer technique. Even if this was not a limitation, the cost of the calculation would be prohibitive. Therefore, one is forced to accept limitation of the size of the problems. Often this means that a number of optima are calculated independently, in which case the proper relationship of the individual parts is of prime importance.

The frequency of the important disturbances influences frequency at which a calculation must be performed, and that again provides a basis for the selection of an off-line computer, an on-line digital computer or an analogue computer, the last-named covering the smaller systems and the high frequencies⁷⁴.

Automation of Discontinuous Processes—There are fields which are completely different from that of more or less continuous processes. We can refer to loading and unloading of tankers, barges and tanks, pipeline operations, the filling of LPG bottles, the operation of in-line blending systems, etc. The techniques applied have much in common with the material handling industries. It is an area easily overlooked when dealing with automation in the oil and chemical industries.

At this congress, Montjean discusses the automatic loading of railroad cars⁷⁰, and Boston and Sollecito⁷¹ give a statistical analysis of a flow control system for blending purposes.

Also of great importance is the optimization of batch processes, and of the starting-up and switching-over of continuous processes.

Here the methods of Pontryagin and Bellman can be particularly useful.

Future

We expect that more and more automation will be used with the emphasis on arriving at the most economical operation. It is not always necessary to think of the use of computers in that respect.

Conventional equipment can be used in certain instances to achieve optimization⁷³. The challenge is in the analysis of the problem and in the prescription of the best equipment for the job. It is the philosophy that matters.

Since manufacturing plants cannot be considered independently of each other and since data transmission over long distances is no longer a technical problem, large integrated data handling and control systems can be expected^{74, 75}. In these sophisticated systems it is very important to avoid the processing of incorrect data. Screening and error detection methods will therefore be an integral part of the system². Automatic data reduction is another powerful technique to reduce the amount of clerical work required for supervising plant performance. Safety is an aspect that is benefiting more and more from automatic control. In this respect we refer to both the detection of an emergency and the automation of logical reactions to such an emergency.

It seems that electric systems have advantages for all these developments. However, for the more conventional systems, pneumatic apparatus is still adequate.

This brings us to the last controversy: digital versus analogue signals. It is safe to assume that for long distances and low frequencies the digital form of a signal will be the most adequate, whereas for short distances and high frequencies analogue signals will be more suitable.

If, however, digital computers become reliable enough, even the ordinary control tasks may be taken over by such a computer^{58, 69, 76}. The beauty of this is that the type of the signal will be consistent throughout the system. We shall therefore conclude by saying that the challenge to the computer manufacturers is to provide reliable, flexible and economical equipment, which can be used in solving our control problems.

Appendix—Classification of Disturbances

Operation Variations

A very important source of disturbances is variations introduced by the operating personnel. They change the process from one feed to another, increase or decrease the throughput, adapt the products to marketing requirements, and trim the set points of controllers. For the process as a whole, these variations are intended to be beneficial, but for the individual control loops they are indistinguishable from other disturbances.

The usual form is a step or a series of steps. This is an indication that the common step response is not so unrealistic after all.

A way to make this source of disturbances less important is to put a filter between the set point knob and the set value in the controller.

Equipment Breakdowns and Repairs

These disturbances take the form of a large step in one direction, followed by a step in the opposite direction after a shorter or longer time. At the spot where they occur reduction by automatic control usually is impossible. However, some distance away, control loops might be able to work properly.

Utility Variations

Utilities like electricity, steam, fuel and cooling water are connected to many users. Hence operational variations and those due to equipment breakdown or repair are here so frequent that it might be possible to describe the resulting variations in terms of continuous random noise signals.

Limit Cycles

Limit cycles can be caused by unstable control loops, or by inherent instabilities or resonances of the process. They are quite common, and can sometimes travel quite far, for instance through a complete utility system.

Ambient Variations

Most of the ambient variations have already been included in the utility variations. In tropical areas, and for small-scale processes, sudden rainfall can be a problem. When air-cooling is used, day and night variations can seriously disturb distillation columns.

Fouling and De-activation

These effects usually are so slow that control has no trouble with them.

Measurements Noise

Just as with servomechanisms, noise should be well distinguished from disturbances. Disturbances influence the actual values of the controlled conditions, hence control should strongly reduce their effects. On the other hand, noise only influences the measured values of the controlled conditions, hence control should ignore it as far as possible. Examples are; turbulence noise with flow measurement, and waves with level measurement.

References

- ¹ KRAUS, M. *Proc. Nat. Telemetering Conf.*, May 1960, Santa Monica (Cal.), U.S.A., 425
- ² CROWTHER, R. H. *Chem. Engng Progr.* 57 (1961), 39
- ³ BERRIDGE, S. A., PEARCE, C. J. and WHITE, E. N. *6th World Petrol. Congr.*, section V, paper 8
- ⁴ HODGE, B. *6th World Petrol. Congr.*, section VIII, paper 11
- ⁵ CATCHPOLE, A. R. *Operational Research Quarterly*, 12 (1961), No. 4, 278
- ⁶ VOLTER, B. V. Investigation and automation of the production of polyethylene at high pressure. *Automatic and Remote Control*, 1963.
- ⁷ DELVAUX, L. Experimental study of the behaviour of a heat exchanger and a mixing process. *Automatic and Remote Control*, 1963. London, Butterworths; Munich, Oldenbourg
- ⁸ ANISIMOV, I. V. A study of the dynamic and static characteristics of the process of fractional distillation. *Automatic and Remote Control*, 1963. London, Butterworths; Munich, Oldenbourg
- ⁹ ZAVORKA, T. The dynamic properties of rectification stations with plate columns. *Automatic and Remote Control*, 1963. London, Butterworths; Munich, Oldenbourg
- ¹⁰ IZAWA, K. and MORINAGA, T. Dynamic characteristics of binary distillation column. *Automatic and Remote Control*, 1963
- ¹¹ MOCZEK, J. S., OTTO, R. E. and WILLIAMS, T. J. Approximation models for the dynamic response of large distillation columns. *Automatic and Remote Control*, 1963. London, Butterworths; Munich, Oldenbourg
- ¹² TAKAMATSU, T. and NAKAMISHI, E. Effects of fluid mixing and its expressions on dynamics of mass transfer process. *Automatic and Remote Control*, 1963. London, Butterworths; Munich, Oldenbourg
- ¹³ BILOUS, O. J. and AMUNDSON, N. R. *J. Amer. Inst. chem. Engrs.*, 1 (1955), 513
- ¹⁴ LEES, S. and HOUGEN, S. O. S., *Industr. Engng Chem.* 37 (1956), 187, 485
- ¹⁵ AIKMAN, A. R. *Instrum. Pract.* May 1951, 393
- ¹⁶ HOYT, P. R. and STANTON, B. D. *Instruments*, 26 (1953), 1180
- ¹⁷ ENDTZ, J., JANSSEN, J. M. L. and VERMEULEN, J. C. *Plant and Process Dynamic Characteristics*, p. 170. Butterworths; London, 1957
- ¹⁸ RADEMAKER, O. *Int. Symp. on Distillation*. Inst. of Chem. Engrs., Brighton, England (May 1960)
- ¹⁹ SCHAEFER, O. and FUSSEL, W. *Regelungstechnik*, 3 (1955), 225
- ²⁰ COWLEY, P. E. A. *Trans. Amer. Soc. mech. Engrs* 79 (1957), 823
- ²¹ COWLEY, P. E. A. and JOHNSON, D. E. *Chem. Engng Progr. Symp. Ser.* 36, 1961, 42
- ²² ISCOL, L., EDWARDS, C. L. and ALTPETER, R. J. Paper presented at A.I.Ch.E. Meeting, San Francisco (Dec. 1959)
- ²³ JENSEN, J. R. Notes on the measurement of dynamic characteristics of linear systems. Servomechanism Laboratory Technical University, Copenhagen (1959)
- ²⁴ GOODMAN, T. P. and RESWICK, J. B. *Trans. Amer. Soc. mech. Engrs* 78 (1956), 229
- ²⁵ FLORENTIN, J. J., HAINSWORTH, B. O., RESWICK, J. B. and WESTCOTT, J. H. in Rottenburg *Joint Symp. Instr. & Comp. in Proc. Dev. and Plant Design*, London, 1959
- ²⁶ SOLODOVNIKOV, V. V. Introduction to the *Statistical Dynamics of Automatic Control Systems*, Dover, publ. 1960
- ²⁷ GALLIER, P. W., SLIEPSEVICK, C. M. and PUCKETT, T. H. *Chem. Engng Progr. Symp. Ser.* 36, 1961, 59
- ²⁸ WILLIAMS, T. J. and MORRIS, H. J. *Chem. Engng Progr. Symp. Ser.* 36, 1961, 20
- ²⁹ BABER, M. F., EDWARDS, L. L., HARPER, W. T., WITTE, M. D. and GERSTER, J. A. *Chem. Engng Progr. Symp. Ser.* 57 (1961), 36, 148
- ³⁰ BABER, M. F. and GERSTER, J. A. *J. Amer. Inst. chem. Engrs* 8 (1962), 3, 407
- ³¹ WILKINSON, W. L. and ARMSTRONG, W. D. *Plant and Process Dynamic Characteristics*, p. 56, Butterworths; London, 1957
- ³² ARMSTRONG, W. R. and WILKINSON, W. L. *Trans. Inst. Chem. Engrs*, 35 (1957), 352
- ³³ PEISER, A. M. and GROVER, S. S. *Chem. Engng Progr.* 58 (1962), 65
- ³⁴ RIJNSDORP, J. E. *Proc. Symp. Computers for the Chemical Engineer*, Birmingham for 1961 (Birmingham Univ. Chem. Eng., Suppl. 1961, 14)
- ³⁵ ARCHER, D. H. and ROTHFUSS, R. R. *Chem. Engng Progr. Symp. Ser.* 36 (1961), 2
- ³⁶ ROSENBROCK, H. H. The transient behaviour of distillation columns and heat exchangers. An historical and critical review. *Proc. Symp. on Process Optimization* (1962), London, The Institution of Chemical Engineers
- ³⁷ MAH, R. S. H., MICHAELSON, S. and SARGENT, R. W. H. *Chem. Engng Sci.* 17 (1962), 619.39
- ³⁸ FAN, SCHMITZ and MILLER *JACC*, 1962
- ³⁹ RANDOLPH and LARSON *JACC*, 1962

- ³⁹ BIERY, J. C. and BOYLAN, D. R. *Ind. Eng. Chem. Fundamentals*, 2 (1963), 44
- ⁴⁰ BLACKMAN, R. B. and TUKEY, J. W. *Bell Syst. Tech. J.* 37 (1958), 185, 485
- ⁴¹ V. D. GRINTEN D. Thesis, Technische Hogeschool, Eindhoven (Holland), 1962
- ⁴² V. D. GRINTEN D. The application of random test signals in process optimization. 2nd I.F.A.C. Congress, Basle, 1963. London, Butterworths; Munich, Oldenbourg
- ⁴³ GRABBE, E. M., RAMO, S. and WOOLDRIDGE, D. E. *Handbook of Automation Computation and Control*, Vol. III, Chapter 10
- ⁴⁴ ISOBE, T. and TOTANI, T. Analysis and design of a parameter-perturbation adaptive system for application to process control. 2nd I.F.A.C. Congress, Basle, 1963. London, Butterworths; Munich, Oldenbourg
- ⁴⁵ ROSENBRICK, H. H. *Trans. Inst. Chem. Engrs*, 40 (1962), 35
- ⁴⁶ ROSENBRICK, H. H. *Automatica* 1 (1963)
- ⁴⁷ FRAADE, J. *Petro/Chem. Engr*, April 1961, C-16-C-18
- ⁴⁸ HEYDEN, C. A. J. M. VAN DER and NES, A. G. VAN. 2nd I.F.A.C. Congress, Basle, 1963. London, Butterworths; Munich, Oldenbourg
- ⁴⁹ KIJLSTRA, F. J. 2nd I.F.A.C. Congress, Basle, 1963. London, Butterworths; Munich, Oldenbourg
- ⁵⁰ CHATTERJEE, H. K. *Automatic and Remote Control*, London, Butterworths 1960, part I, 132
- ⁵¹ PROFOS, P. *Die Regelung von Dampfanlagen*, Springer-Verlag (1962)
- ⁵² ROSENBRICK, H. H. *Chem. Engng Progr.* 58 (1962), 43
- ⁵³ DOBSON, J. G. *Regelungstechnik*, 8 (1960), No. 11, 393
- ⁵⁴ LUPFER, D. E. and PARSONS, J. R. *Chem. Engng Progr.* 58 (1962), No. 9 (Sept.), 37
- ⁵⁵ LEE, W. T. and KILICK, R. D. *Control*, 6 (1963), No. 55 (Jan.), 77
- ⁵⁶ *Chem. Engng*, 66 (1959) (Nov. 16), 92
- ⁵⁷ LEFKOWITZ, I. and ECKMAN, D. P. *Trans. Amer. Soc. mech. Engrs* paper 58-A. 281
- ⁵⁸ WILLIAMS, T. J. *Chem. Engng Progr.* 58 (1962), No. 5 (May), 54
- ⁵⁹ PHISTER, M. JR. and GRABBE, E. M. *Control Engng* 4 (1957), 6 (June), 129
- ⁶⁰ KARP, H. R. *Control Engng*, 7 (1960), 20
- ⁶¹ EISENHARDT, R. D. and WILLIAMS, T. J. *Control Engng*, I (1960), 103
- ⁶² CROWTHER, R. H., PITRAK, J. E., PLY, E. N., KUEHN, D. R., DAVIDSON, H. and PENDLETON, A. D. *Chemical Engng Progr.* 57 (1961), 39
- ⁶³ *Chem. Engng* (1959) (Oct. 19), 102
- ⁶⁴ GUENIN, J. DE and FANNEAU DE LA HORIE, H. *6th World Petrol. Congr.*, section VII, paper 5
- ⁶⁵ GRIFFITH, R. E. and STEWART, R. A. *Management Sci.* 7 (1961), 379
- ⁶⁶ JONG, J. J. DE. *Ingenieur*, 73 (461), M 31
- ⁶⁷ TINGEY, F. H. *Industr. Engng Chem.*, 54, No. 4 (April 1962), 36
- ⁶⁸ HALL, C. R. *Chem. Engng Progr.* 56 (1960), 62
- ⁶⁹ FARRAR, G. L. *6th World Petrol. Congr.*, section VIII, paper 18
- ⁷⁰ MONTJEAN, F. X. 2nd I.F.A.C. Congress, Basle, 1963. London, Butterworths; Munich, Oldenbourg
- ⁷¹ BOOTON, R. C. and SOLLECITO, W. E. 2nd I.F.A.C. Congress, Basle, 1963. London, Butterworths; Munich, Oldenbourg
- ⁷² LEFKOWITZ, I. and ECKMAN, D. P. *Control Engng*, 4 (1957), 179
- ⁷³ ANDERSON, Z. T. *Control Engng*, 10 (1963), 67
- ⁷⁴ *British Chem. Engng*, 8 (1963), 104
- ⁷⁵ *Oil and Gas J.*, 58 (1960), 117
- ⁷⁶ YOUNG, A. J. *Chem. Proc. Eng.* 42 (1961), 433

Dynamic Characteristics of Binary Distillation Column

K. IZAWA and T. MORINAGA

Summary

This paper presents the transfer functions of the binary distillation column for change of such variables as reflux flow, vapour flow, feed flow and feed composition. These transfer functions are based on material balance equations. The material balance equations in the form of Laplace-transformed finite difference equations would encounter physically unreasonable boundary conditions when solved directly.

The transfer functions under discussion are derived by reduction of the signal flow diagram and by use of the theorem of continued fraction. Therefore the transfer functions are free from the unreasonable boundary conditions. The time for calculating frequency response from them is independent of the number of trays. This feature is a big advantage in the frequency response calculation of the practical column, which usually has a large number of trays. The frequency responses calculated from the transfer functions are in fairly good agreement with experimental data, and they reveal that the lag of liquid flow between trays is the main cause of a large phase lag in high frequency range.

Sommaire

La présente communication expose les équations fréquentielles de la colonne de distillation binaire, lorsque le débit de reflux, le débit de vapeur, le débit d'alimentation et la concentration de l'alimentation varient en tant que grandeurs d'entrée. Ces équations fréquentielles reposent sur les équations d'équivalence de matières qui sous la forme d'équations différentielles ayant subi la transformation de Laplace se heurtent à des conditions aux limites physiques déraisonnables, lorsqu'elles sont résolues directement.

Puisque les équations fréquentielles exposées ici seront traitées par l'emploi des graphes de fluence et du théorème des fractions continues, elles seront indépendantes de conditions aux limites déraisonnables. Le temps pour le calcul de la réponse fréquentielle à partir des équations fréquentielles est indépendant du nombre de plateaux. Cette propriété constitue l'avantage important du calcul fréquentiel de la colonne pratique qui possède habituellement de nombreux plateaux. Les réponses fréquentielles calculées se vérifient assez bien par les données expérimentales et les réponses fréquentielles indiquent que le retard de l'écoulement du liquide entre les plateaux est la cause principale du retard de phase important aux fréquences élevées.

Zusammenfassung

In diesem Aufsatz sind die Übertragungsfunktionen von Destillationskolonnen für binäre Gemische dargestellt, wenn sich die Rücklaufmenge, die Dampfmenge, die Zulaufmenge, und die Zulaufkonzentration ändern. Diese Übertragungsfunktionen beruhen auf den Materialbilanzgleichungen. Die Laplace-Transformierte dieser Materialbilanzgleichungen führt auf Differenzengleichungen, deren direkte Lösung physikalisch unvernünftige Grenzbedingungen erfordert.

Die hier betrachteten Übertragungsfunktionen werden aus dem Signalfußdiagramm und der Kettenbruchdarstellung hergeleitet; damit lassen sich diese unvernünftigen Grenzbedingungen umgehen. Der Aufwand zur Berechnung der Frequenzgänge aus den Übertragungsfunktionen hängt nicht von der Zahl der Böden ab. Diese Tatsache stellt einen großen Vorteil für die Frequenzgangberechnung tatsächlich existierender Kolonnen dar, da diese meistens eine große

Anzahl von Böden haben. Die aus der Übertragungsfunktion berechneten Frequenzgänge stimmen ziemlich gut mit den experimentell ermittelten Werten überein. Die Frequenzgänge zeigen, daß die Verzögerung des Flüssigkeitsdurchflusses zwischen den Böden die Hauptursache für die große Phasennacheilung bei hohen Frequenzen ist.

Introduction

The dynamic performances of the distillation column under consideration are responses of liquid composition due to the change of such variables as feed composition, feed flow, reflux flow or vapour flow. Among these, the responses for reflux flow change and vapour flow change are important for control purposes, because these variables are chosen as controlling or manipulating variables. In spite of their importance, there are, so far, few studies on the dynamic characteristics for flow changes^{7, 8}, but there are more for feed composition change¹⁻⁶.

The basic material balance equations are finite difference-differential equations of constant coefficients for composition change, while those for flow change become finite difference-differential equations of variable coefficients which are more complex, even when linearized by limiting the amount of variable change within narrow range. These basic equations are solved analytically as finite difference equations in past works, and physically unreasonable boundary conditions cannot be avoided.

Another method for solving the basic equations is to use computers, analogue or digital. The method using analogue computers is applicable only for the columns with less trays, because the necessary number of computing elements increases greatly with the number of trays.

The transfer functions of liquid compositions are derived in this paper for the changes of reflux flow, vapour flow, feed flow and feed composition. These transfer functions are based upon material balance equations, but the equations are not solved here as finite difference equations. The transfer functions are derived by reduction of the signal flow diagram and by the utilization of hyperbolic functions which are useful in reducing continued fractions to compact form. In consequence of this reduction process to obtain the transfer function, the obstacle of using unreasonable boundary conditions can be completely removed.

The other merit of this is that the time necessary for calculating the frequency responses is almost independent of the number of trays. This is of particular advantage for the study of columns with a large number of trays, as seen in practical cases.

Transfer Function for Reflux Flow Change

The basic equations are obtained from material balance with the following assumptions: (a) the liquid on the tray is perfectly mixed; (b) Murphree efficiency is unity; (c) the heat balance is not considered, and the molar heat of vaporization of both components is equal; therefore, vapour flow rate is constant

throughout the column; (d) liquid hold-ups of reboiler and condenser are constant; (e) liquid hold-up in the down pipe is neglected; and (f) vapour hold-up is neglected.

The equilibrium curve is linearized for small variations of composition as

$$y_n = K_n x_n \quad (1)$$

Liquid flow in the reflux pipe is assumed to be piston flow. Material balance equations for more volatile component are linearized by assuming only small variations of variables, and Laplace transformed. Thus the equations obtained are: for arbitrary tray No. n

$$x_n = \alpha_n x_{n-1} + \beta_n x_{n+1} + \gamma_n l_{n-1} \quad (2)$$

for reboiler ($n = N$)

$$x_N = \alpha_N x_{N-1} + \gamma_N l_{N-1} \quad (3)$$

for condenser ($n = 0$)

$$x_0 = \beta_0 x_1 \quad (4)$$

where

$$\alpha_1 = \frac{a_1}{1 + T_1 s} e^{-ds} \quad \alpha_n = \frac{a_n}{1 + T_n s} \quad (n = 2, 3, \dots, N)$$

$$\beta_n = \frac{b_n}{1 + T_n s} \quad (n = 0, 1, 2, \dots, N-1)$$

$$\gamma_n = \frac{c_n}{1 + T_n s} \quad (n = 1, 2, \dots, N)$$

$$T_0 = \frac{H_0}{V^0} \quad T_n = \frac{H_n^0}{L_n^0 + V^0 K_n} \quad (n = 1, 2, \dots, N) \quad (5)$$

$$a_n = \frac{L_{n-1}^0}{L_n^0 + V^0 K_n} \quad (n = 1, 2, \dots, N)$$

$$b_0 = K_1 \quad b_n = \frac{V^0 K_{n-1}}{L_n^0 + V^0 K_n} \quad (n = 1, 2, \dots, N-1)$$

$$c_n = \frac{X_{n-1}^0 - X_n^0}{L_n^0 + V^0 K_n} \quad (n = 1, 2, \dots, N) \quad d = \frac{H_p}{L_0^0}$$

The relation between the liquid hold-up of tray H_n and the liquid flow rate L is expressed as

$$H_n = H_{n0} + \tau L \quad (6)$$

(H_{n0} and τ are constant)

From material balance and eqn (6), lag of liquid flow is expressed as follows:

$$l_n = \frac{1}{1 + \tau s} l_{n-1} \quad (7)$$

Combining eqns (2), (3), (4) and (7), the following basic simultaneous equation is obtained.

$$\begin{bmatrix} 1 & -\beta_0 & 0 & \dots & 0 \\ -\alpha_1 & 1 & -\beta_1 & \dots & 0 \\ 0 & -\alpha_2 & 1 & -\beta_2 & \dots \\ \vdots & \vdots & \vdots & \vdots & \ddots \\ 0 & \dots & -\alpha_{N-1} & 1 & -\beta_{N-1} \\ 0 & \dots & 0 & \alpha_N & 1 \end{bmatrix} \begin{bmatrix} x_0 \\ x_1 \\ x_2 \\ \vdots \\ x_{N-1} \\ x_N \end{bmatrix} = \begin{bmatrix} 0 \\ \gamma_1 \\ \gamma_2 (1 + \tau s)^{-1} \\ \vdots \\ \gamma_{N-1} (1 + \tau s)^{-(N-2)} \\ \gamma_N (1 + \tau s)^{-(N-1)} \end{bmatrix} \quad (8)$$

$|\alpha_n|$ and $|\beta_n|$ are generally smaller than $1/2$. In that case, frequency response can be calculated directly from eqn (8) by Gauss-Seidel's method. This calculating method is practical in the case of a small number of trays.

The signal flow diagram drawn from eqn (8) is shown in Figure 1(a). When this is reduced to simpler form as shown in Figure 1(b), the transmittance F_n in the reduced diagram becomes the following continued fraction.

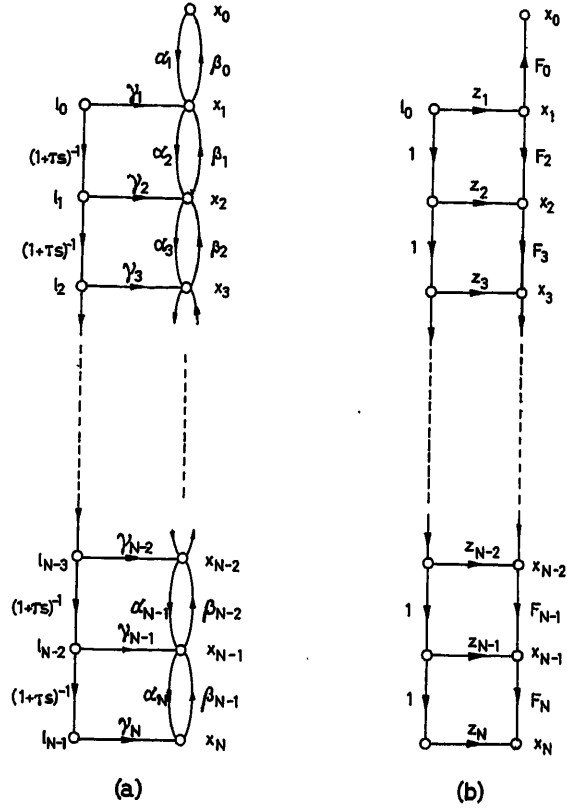


Figure 1. Signal flow diagram due to eqn (8) and its reduction

$$F_0 = \beta_0 \quad (9)$$

$$F_N = \alpha_N \quad (10)$$

$$F_n = \frac{\alpha_n}{1 - \frac{\alpha_{n+1} \beta_n}{1 - \frac{\alpha_{n+2} \beta_{n+1}}{1 - \frac{\alpha_{N-1} \beta_{N-2}}{1 - \alpha_N \beta_{N-1}}}}} \quad (11)$$

$$= \frac{\alpha_n}{1 + \frac{\alpha_{n+1} \beta_n}{1 + \frac{\alpha_{n+2} \beta_{n+1}}{1 + \dots + \frac{\alpha_N \beta_{N-1}}{1}}}}$$

Then

$$-\beta_{n-1} F_n = \frac{-\alpha_n \beta_{n-1}}{1} + \frac{-\alpha_{n+1} \beta_n}{1} + \dots + \frac{-\alpha_N \beta_{N-1}}{1} \quad (12)$$

In order to simplify eqn (12), the following approximation is made.

$$\alpha_2 \approx \alpha_3 \approx \dots \approx \alpha_N \approx \beta_0 \approx \beta_1 \approx \dots \approx \beta_{N-1} \approx u^{\frac{1}{2}} \quad (13)$$

$$u^{\frac{1}{2}} \approx \frac{(\overline{a_k b_{k-1}})^{\frac{1}{2}}}{1 + \overline{T_s}}, \quad T \approx \overline{T_k} \quad (14)$$

($\overline{}$ means averaging)

The approximation eqn (13) is reasonable when the liquid hold-up H_n^0 is approximately constant, and the vapour-liquid equilibrium curve is close to the diagonal $x = y$. With this approximation, eqn (12) is rewritten as

$$-u^{\frac{1}{2}} F_n = \underbrace{\frac{-u}{1} + \frac{-u}{1} + \dots + \frac{-u}{1}}_{N-n+1} \quad (15)$$

Let the k th convergent of this continued fraction be p_k/q_k , then p_k and q_k are equal to the coefficient of x^{k-1} in the power series expansion of the following S_p and S_q , respectively.

$$S_p = \frac{-u}{1 - x + ux^2} \quad (16)$$

$$S_q = \frac{1 - ux}{1 - x + ux^2} \quad (17)$$

Expanding S_p and S_q in power series of x , p_k/q_k is obtained as follows:

$$\frac{p_k}{q_k} = -u^{\frac{1}{2}} \cdot \frac{\sinh kv}{\sinh(k+1)v} \quad (18)$$

where

$$\cosh v \approx \frac{1}{2} u^{-\frac{1}{2}} \quad (19)$$

Eqn (15) is the $(N - n + 1)$ th convergent. Therefore,

$$F_n = \frac{\sinh(N - n + 1)v}{\sinh(N - n + 2)v} \quad (20)$$

The transmittance Z_n in Figure 1(b) is expressed as follows:

$$Z_1 = \frac{\gamma_1 + \beta_1 Z_2}{(1 - \alpha_1 \beta_0)(1 - F_2 \beta_1)} \quad (21)$$

$$Z_N = \gamma_N (1 + \tau s)^{-(N-1)} \quad (22)$$

$$Z_n = \frac{\gamma_n (1 + \tau s)^{-(n-1)} + \beta_n Z_{n+1}}{1 - F_{n+1} \beta_n} \quad (n = 2, 3, \dots, N-1) \quad (23)$$

By the use of eqns (13) and (20), eqns (21), (22) and (23) can be expressed as

$$Z_1 = \frac{u^{-\frac{1}{2}}}{(1 - \alpha_1 \beta_0) \sinh(N+1)v} \cdot \sum_{k=1}^N \gamma_k (1 + \tau s)^{-(k-1)} \times \sinh(N - k + 1)v \quad (24)$$

$$Z_n = \frac{u^{-\frac{1}{2}}}{\sinh(N - n + 2)v} \cdot \sum_{k=n}^N \gamma_k (1 + \tau s)^{-(k-1)} \sinh(N - k + 1)v \quad (n = 2, 3, \dots, N) \quad (25)$$

The transfer function of liquid composition on arbitrary tray for reflux flow change is easily obtained from Figure 1(b) as

$$\frac{x_n}{l_0} = Z_n + \sum_{i=1}^{n-1} Z_i \cdot \prod_{k=i+1}^n F_k \quad (26)$$

Substituting eqns (20), (24) and (25) into eqn (26), and utilizing the formula on hyperbolic functions

$$\frac{\sinh(y-x)}{\sinh x \cdot \sinh y} = \coth x - \coth y \quad (27)$$

one obtains

$$\begin{aligned} \frac{x_n}{l_0} = & u^{-\frac{1}{2}} \cdot \frac{\sinh(N - n + 1)v}{\sinh v \cdot \sinh Nv} \\ & \times \sum_{k=2}^n \gamma_k (1 + \tau s)^{-(k-1)} \sinh(k-1)v \\ & + u^{-\frac{1}{2}} \cdot \frac{\sinh(n-1)v}{\sinh v \cdot \sinh Nv} \\ & \times \sum_{k=n+1}^N \gamma_k (1 + \tau s)^{-(k-1)} \sinh(N - k + 1)v \\ & + \frac{u^{-\frac{1}{2}}}{(1 - \alpha_1 \beta_0)} \cdot \frac{\sinh(N - n + 1)v}{\sinh Nv \cdot \sinh(N+1)v} \\ & \times \sum_{k=1}^N \gamma_k (1 + \tau s)^{-(k-1)} \sinh(N - k + 1)v \end{aligned} \quad (28)$$

If γ_k 's are approximated as

$$\gamma_1 \approx \gamma_2 \approx \dots \approx \gamma_N \approx \gamma \quad (29)$$

$$\gamma \approx \frac{\overline{c_k}}{1 + \overline{T_s}} \quad T \approx \overline{T_k} \quad (30)$$

and one utilizes the formula

$$\begin{aligned} \sum_{k=1}^n a^{k-1} \cosh(k-1)v \\ = \frac{1 - a \cosh v - a^n \cosh nv + a^{n+1} \cosh(n-1)v}{1 - 2a \cosh v + a^2} \end{aligned} \quad (31)$$

then the transfer function eqn (28) is rewritten as follows:

$$\begin{aligned} \frac{x_n}{l_0} = & \frac{\overline{c_k}}{(\overline{a_k b_{k-1}})^{\frac{1}{2}}} \cdot \frac{\sinh(N - n + 1)v}{\sinh v \cdot \sinh Nv} \cdot \Phi_n((1 + \tau s)^{-1}, v) \\ & + \frac{\overline{c_k}}{(\overline{a_k b_{k-1}})^{\frac{1}{2}}} \cdot \frac{\sinh(n-1)v}{\sinh v \cdot \sinh Nv} \\ & \times (1 + \tau s)^{-N} \cdot \Phi_{N-n+1}((1 + \tau s), v) \\ & + \frac{\overline{c_k}}{(\overline{a_k b_{k-1}})^{\frac{1}{2}}} \cdot \frac{\sinh(N - n + 1)v}{(1 - \alpha_1 \beta_0) \sinh Nv \cdot \sinh(N+1)v} \\ & \times (1 + \tau s)^{-N} \cdot \Phi_{N+1}((1 + \tau s), v) \end{aligned} \quad (32)$$

where

$$\begin{aligned} \Phi_k(p, v) = & \frac{1 - p^k e^{kv}}{1 - p e^v} \\ = & \frac{1 - p \cosh v - p^k \cosh kv + p^{k+1} \cosh(k-1)v}{1 - 2p \cosh v + p^2} \end{aligned} \quad (33)$$

Eqn (28) or eqn (32) is the desired transfer function. Frequency response can be calculated from the transfer function if one puts $s = j\omega$. It is clear that the time for frequency response calculation does not depend on the number of trays, because the functional form of the transfer function is very simple with N .

If one neglects the lag of liquid flow, i.e. $\tau = 0$, the calculated phase lag does not go far beyond $\pi/2$ rad. The large phase lag in high frequency range can be explained only with the consideration of this lag of flow. In general, $(a_k b_{k-1})^\pm$ is very close to $1/2$, therefore, by eqn (19)

$$\cosh v \approx 1 + j\omega T \quad (34)$$

Consider only in high frequency range, then

$$\begin{aligned} v &\approx \operatorname{arc} \cosh \omega T + j \operatorname{arc} \cos (1/\omega T) \\ &\approx \ln 2 \omega T + j\pi/2 \end{aligned} \quad (35)$$

Therefore, keeping in mind the real part of v to be large,

$$\sinh kv \approx e^{kv/2} \approx 2^{k-1} (\omega T)^k \cdot e^{jk\pi/2} \quad (36)$$

Considering $|\sinh kv|$ to increase very rapidly with k , eqn (28) can be approximated with the substitution of eqn (36) as follows. For $\tau = 0$,

$$\frac{x_n}{l_0} \propto \frac{1}{\omega T} \cdot e^{-j\pi/2} \quad (37)$$

and for $\tau \neq 0$,

$$\frac{x_n}{l_0} \propto \frac{1}{(\omega T)_n} \cdot e^{-jn\pi/2} \quad (38)$$

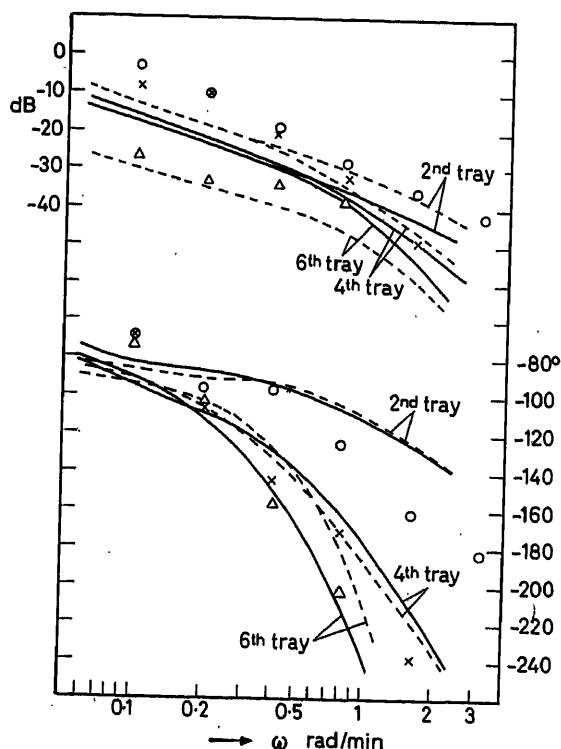


Figure 2. Frequency responses of Column A for reflux flow change
— theoretical curve by eqn (32); --- exact solution of eqn (8);
○ experimental data for 2nd tray; × those for 4th tray; △ those for 6th tray

Eqns (37) and (38) reveal clearly the effect of liquid flow lag. The effects of hold-up in the down pipe appear in changes of α_n and β_n , but the changes of α_n and β_n have no effect on the frequency response in high frequency range. This can be explained in the same way as above. Therefore, the most important factor in the distillation column dynamics is the liquid flow lag.

Figure 2 shows the Bode diagram of the calculated values by eqn (32), the strict solution of the basic eqn (8), and the experimental data for the six-tray bubble-cap column A of methanol-water mixture whose dimensions are shown in Table 1. Values of the parameters are shown in Table 2. It is clear from Table 2 that the methanol-water system is quite unsuited to the approximations, eqns (13) and (29). In spite of that, there is fairly good agreement between experimental data and theoretical curves.

Table 1. Dimensions of Experimental Columns

	Diameter mm	Space between trays mm	Diameter of bubble cap mm	Number of bubble caps/tray
Column A	100	180	54	1
Column B	140	170	15	18

Table 2. Values of Parameters used for the Calculation of the Frequency Responses for Reflux Flow Change

k	T_k min	a_k	b_k	c_k
0	0.871		0.445	
1	1.692	0.586	0.428	0.0358
2	1.938	0.579	0.526	0.0562
3	1.940	0.524	0.701	0.0613
4	1.420	0.304	1.150	0.0256
5	0.914	0.340	1.230	0.0138
6	0.622	0.217	1.387	0.0044
7	10.11	0.159		0.0012

$\tau = 0.56$ min; $d = 3.47$ min

Transfer Function for Vapour Flow Change

The basic equation is also based on material balance. In this case changes occur not only in vapour flow but also in liquid flow because of liquid hold-up change with vapour flow change. Liquid hold-up is related to vapour flow rate and liquid flow rate as follows:

$$H_n = H_{n0} + \tau L - \kappa V \quad (39)$$

From material balance and eqn (39)

$$l_n = \frac{1}{1 + \tau s} l_{n-1} + \frac{\kappa s}{1 + \tau s} v \quad (40)$$

For $n = 0$, $l_0 = 0$ because of constant reflux flow. Therefore,

$$l_n = \frac{\kappa}{\tau} \left\{ 1 - \frac{1}{(1 + \tau s)^n} \right\} v \quad (41)$$

The following basic equation is obtained in the same way as in the case of the reflux flow change.

$$\begin{pmatrix} 1 & -\beta_0 & 0 & \cdots & 0 \\ -\alpha_1 & 1 & -\beta_1 & \cdots & 0 \\ 0 & -\alpha_2 & 1 & -\beta_2 & \cdots & 0 \\ \vdots & \vdots & \vdots & \vdots & \ddots & \vdots \\ 0 & \cdots & 0 & -\alpha_{N-1} & 1 & -\beta_{N-1} \\ 0 & \cdots & 0 & 0 & -\alpha_N & 1 \end{pmatrix} \begin{pmatrix} x_0 \\ x_1 \\ x_2 \\ \vdots \\ x_{N-1} \\ x_N \end{pmatrix} = -v \cdot \begin{pmatrix} 0 \\ \gamma'_1 \\ \gamma'_2 \\ \vdots \\ \gamma'_{N-1} \\ \gamma'_N \end{pmatrix} \quad (42)$$

where

$$\left. \begin{aligned} \gamma'_n &= \frac{c_{1n}}{1 + T_n s} \left\{ \frac{1}{(1 + \tau s)^{n-1}} - c_{2n} \right\} \\ c_{1n} &= \frac{\kappa}{\tau} \cdot \frac{X_{n-1}^0 - X_n^0}{L_n^0 + V^0 K_n} \quad (n=1, 2, \dots, N) \\ c_{2n} &= \frac{\tau}{\kappa} \cdot \frac{Y_n^0 - Y_{n+1}^0}{X_{n-1}^0 - X_n^0} - 1 \quad (n=1, 2, \dots, N-1) \\ c_{2N} &= \frac{\tau}{\kappa} \cdot \frac{Y_N^0 - X_N^0}{X_{N-1}^0 - X_N^0} - 1 \end{aligned} \right\} \quad (43)$$

α_n , β_n , and T_n are the same as eqn (5).

Comparing eqn (42) with eqn (8), the transfer function for vapour flow change is obtained by replacing $\gamma_k (1 + \tau s)^{-(k-1)}$ in eqn (28) by γ'_k .

$$\begin{aligned} -\frac{x_n}{v} &= u^{-\frac{1}{2}} \cdot \frac{\sinh(N-n+1)v}{\sinh v \cdot \sinh Nv} \cdot \sum_{k=2}^n \gamma'_k \sinh(k-1)v \\ &+ u^{-\frac{1}{2}} \cdot \frac{\sinh(n-1)v}{\sinh v \cdot \sinh Nv} \cdot \sum_{k=n+1}^N \gamma'_k \sinh(N-k+1)v \\ &+ \frac{u^{-\frac{1}{2}}}{1 - \alpha_1 \beta_0} \cdot \frac{\sinh(N-n+1)v}{\sinh Nv \cdot \sinh(N+1)v} \\ &\times \sum_{k=1}^N \gamma'_k \sinh(N-k+1)v \end{aligned} \quad (44)$$

If γ'_k is approximated as

$$\gamma'_k = \frac{\overline{c_{1k}}}{1 + \overline{T_k} s} \left\{ \frac{1}{(1 + \tau s)^{k-1}} - \overline{c_{2k}} \right\} \quad (45)$$

eqn (44) is rewritten as

$$\begin{aligned} -\frac{x_n}{v} &= \frac{\overline{c_{1k}}}{\overline{c_k}} \cdot \frac{x_n}{l_0} \\ &- \frac{\overline{c_{1k} c_{2k}}}{(\overline{a_k} \overline{b_{k-1}})^{\frac{1}{2}}} \left\{ \frac{\sinh(N-n+1)v \cdot \sinh \frac{n}{2} v \cdot \sinh \frac{n-1}{2} v}{\sinh v \cdot \sinh Nv \cdot \sinh \frac{1}{2} v} \right. \end{aligned}$$

$$\left. - \frac{\sinh(n-1)v \cdot \sinh \frac{N-n+1}{2} v \cdot \sinh \frac{N-n}{2} v}{\sinh v \cdot \sinh Nv \cdot \sinh \frac{1}{2} v} \right\} \quad (46)$$

$$- \frac{1}{1 - \alpha_1 \beta_0} \cdot \frac{\sinh(N-n+1)v \cdot \sinh \frac{N+1}{2} v \cdot \sinh \frac{N}{2} v}{\sinh Nv \cdot \sinh(N+1)v \cdot \sinh \frac{1}{2} v}$$

c_{2n} of eqn (43) is generally small compared with unity, therefore γ'_n shows a large phase lag at high frequency. Then, the concentration response $-x_n/v$ also shows a large phase lag at high frequency.

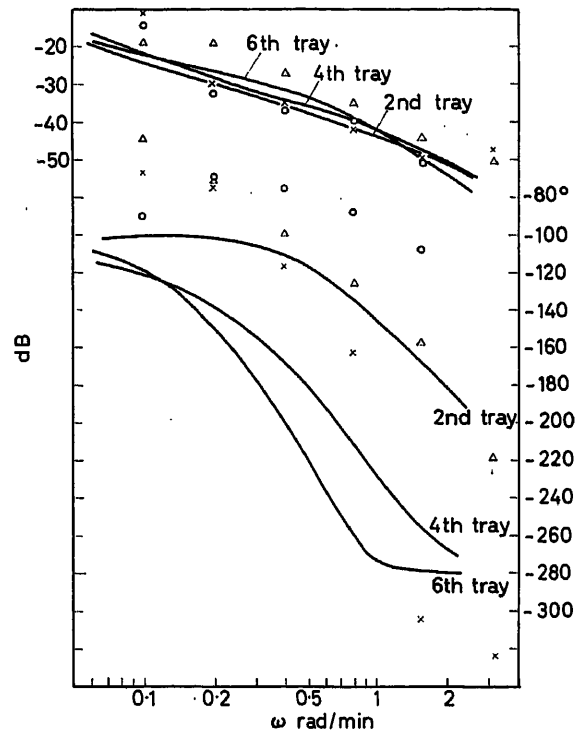


Figure 3. Frequency responses of Column B for vapour flow change — theoretical curve by eqn (46); ○ experimental data for 2nd tray; × those for 4th tray; △ those for 6th tray

The theoretical frequency response curves calculated by eqn (46) are shown in Figure 3 with the experimental data. These data were obtained with the six-tray bubble-cap Column B for methanol-water mixture. The reboiler of Column B has a larger capacity than the reboiler of Column A. Therefore, Column B is worse for averaging approximation than Column A. Error in c_{2n} severely affects the frequency response of γ'_n . In the calculation of the theoretical curves, the value of κ in eqn (39) was estimated from the separate experiment with water flow and air flow, so that the value of κ would include considerable error. This seems to be the main cause of discrepancy between theoretical curves and experimental data. But they show the same trend, which insists upon correctness of the transfer function thus obtained.

Transfer Function for Feed Flow Change

In the case of feed flow change, let the feed be supplied to the m th tray. The following equation is obtained from material balance in the same way as for reflux flow change.

Eqn (47) *

α_n , β_n , and γ_n are the same as eqn (5) except the numerator c_m of γ_m .

$$c_m = \frac{X_f^0 - X_m^0}{L_m^0 + V^0 K_m} \quad (48)$$

Comparing eqn (47) with eqn (8), the transfer function for feed flow change is obtained from eqn (28) by putting $\gamma_1 = \gamma_2 = \dots = \gamma_{m-1} = 0$ and replacing $\gamma_k(1 + \tau s)^{-(k-1)}$ with $\gamma_k(1 + \tau s)^{-(k-m)}$ for $k \geq m$. For enriching section ($n < m$),

$$\frac{x_n}{x_f} = \frac{u^{-\frac{1}{2}}}{\sinh Nv} \left\{ \frac{\sinh(n-1)v}{\sinh v} + \frac{1}{1 - \alpha_1 \beta_0} \cdot \frac{\sinh(N-n+1)v}{\sinh(N+1)v} \right\} \times \sum_{k=m}^N \gamma_k (1 + \tau s)^{-(k-m)} \sinh(N-k+1)v \quad (49)$$

and for stripping section ($n \geq m$),

$$\begin{aligned} \frac{x_n}{x_f} = & u^{-\frac{1}{2}} \cdot \frac{\sinh(N-n+1)v}{\sinh v \cdot \sinh Nv} \cdot \sum_{k=m}^n \gamma_k (1 + \tau s)^{-(k-m)} \sinh(k-1)v \\ & + u^{-\frac{1}{2}} \cdot \frac{\sinh(n-1)v}{\sinh v \cdot \sinh Nv} \\ & \times \sum_{k=n+1}^N \gamma_k (1 + \tau s)^{-(k-m)} \sinh(N-k+1)v \\ & + \frac{u^{-\frac{1}{2}}}{1 - \alpha_1 \beta_0} \cdot \frac{\sinh(N-n+1)v}{\sinh Nv \cdot \sinh(N+1)v} \\ & \times \sum_{k=m}^N \gamma_k (1 + \tau s)^{-(k-m)} \sinh(N-k+1)v \end{aligned} \quad (50)$$

If $X_m^0 > X_f^0$, c_m is negative. \bar{c}_k is generally positive, therefore the averaging approximation for γ_k brings severe error into x_m/x_f . The approximation for γ_k must be avoided in this case.

Experimental data obtained with Column B for methanol-water mixture is shown in Figure 4 with the theoretical frequency response curve calculated by eqn (50). The theoretical curve shows a similar trend with the experimental data.

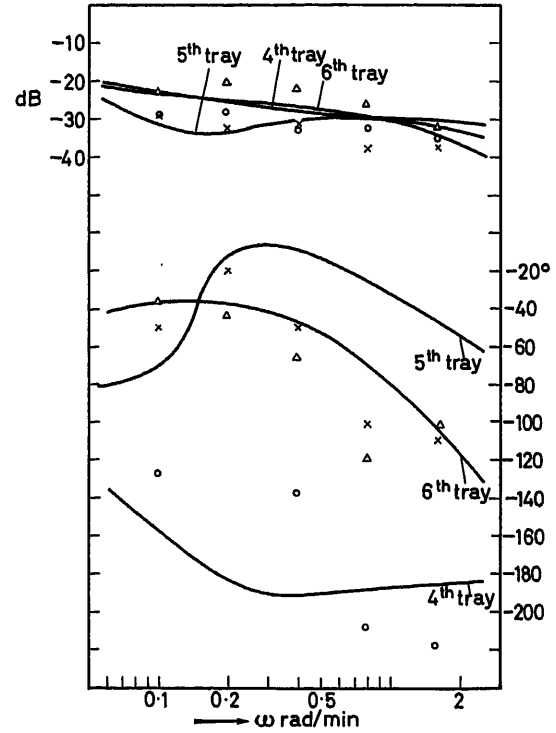


Figure 4. Frequency responses of Column B for feed flow change
— theoretical curve by eqn (50); ○ experimental data for 4th tray;
× those for 5th tray; △ those for 6th tray

Transfer Function for Feed Composition Change

With the similar assumptions to those for reflux flow change, the following equation is obtained from material balance when feed is supplied to the m th tray.

$$\begin{pmatrix} 1 & -\beta_0 & 0 & \dots & 0 \\ \alpha_1 & 1 & -\beta_1 & \dots & 0 \\ 0 & \alpha_1 & 1 & -\beta_2 & \dots & 0 \\ \vdots & \vdots & \vdots & \vdots & \ddots & \vdots \\ 0 & \alpha_{m-1} & 1 & -\beta_{m-1} & \dots & 0 \\ 0 & 0 & \alpha_m & 1 & -\beta_m & \dots \\ \vdots & \vdots & \vdots & \vdots & \vdots & \ddots \\ 0 & 0 & \alpha_{N-1} & 1 & -\beta_{N-1} & 0 \\ 0 & 0 & 0 & \dots & -\alpha_N & 1 \end{pmatrix} \begin{pmatrix} x_0 \\ x_1 \\ \vdots \\ x_{m-1} \\ x_m \\ x_{m+1} \\ \vdots \\ x_{N-1} \\ x_N \end{pmatrix} = \begin{pmatrix} 0 \\ 0 \\ \vdots \\ 0 \\ 0 \\ \gamma_m \\ \gamma_m(1+\tau s)^{-1} \\ \vdots \\ \gamma_{N-1}(1+\tau s)^{-(N-m-1)} \\ \gamma_N(1+\tau s)^{-(N-m)} \end{pmatrix} = x_f \begin{pmatrix} 0 \\ 0 \\ \vdots \\ 0 \\ 0 \\ \gamma'' \\ 0 \\ \vdots \\ 0 \end{pmatrix} \quad (51)$$

* Eqn (47):

$$\begin{pmatrix} 1 & -\beta_0 & 0 & \dots & 0 \\ \alpha_1 & 1 & -\beta_1 & \dots & 0 \\ 0 & \alpha_1 & 1 & -\beta_2 & \dots & 0 \\ \vdots & \vdots & \vdots & \vdots & \ddots & \vdots \\ 0 & \alpha_{m-1} & 1 & -\beta_{m-1} & \dots & 0 \\ 0 & 0 & \alpha_m & 1 & -\beta_m & \dots \\ \vdots & \vdots & \vdots & \vdots & \vdots & \ddots \\ 0 & 0 & \alpha_{N-1} & 1 & -\beta_{N-1} & 0 \\ 0 & 0 & 0 & \dots & -\alpha_N & 1 \end{pmatrix} \begin{pmatrix} x_0 \\ x_1 \\ \vdots \\ x_{m-1} \\ x_m \\ x_{m+1} \\ \vdots \\ x_{N-1} \\ x_N \end{pmatrix} = \begin{pmatrix} 0 \\ 0 \\ \vdots \\ 0 \\ 0 \\ \gamma_m \\ \gamma_m(1+\tau s)^{-1} \\ \vdots \\ \gamma_{N-1}(1+\tau s)^{-(N-m-1)} \\ \gamma_N(1+\tau s)^{-(N-m)} \end{pmatrix} \quad (47)$$

Coefficients in eqn (51) are the same as in eqn (5) except γ'' , where

$$\left. \begin{aligned} \gamma'' &= \frac{c}{1 + T_m s} \\ T_m &= \frac{H_m^0}{L_m^0 + V^0 K_m} \quad c = \frac{L_f^0}{L_m^0 + V^0 K_m} \end{aligned} \right\} \quad (52)$$

The signal flow diagram drawn by eqn (51) is shown in Figure 5(a). When this is reduced to the simpler form as shown in Figure 5(b), the transmittance for enriching section in the reduced diagram is expressed by the following equation.

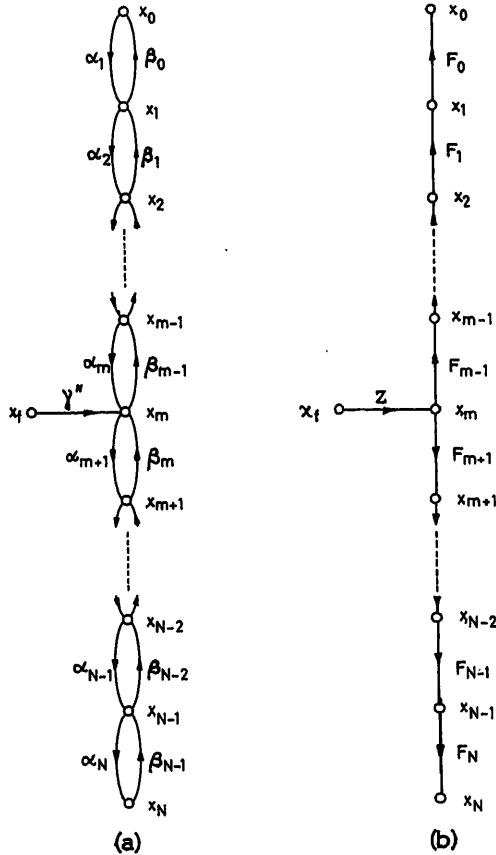


Figure 5. Signal flow diagram due to eqn (51) and its reduction

$$-F_n \alpha_{n+1} = \frac{-\alpha_{n+1} \beta_n}{1} + \frac{-\alpha_n \beta_{n-1}}{1} + \dots + \frac{-\alpha_2 \beta_1}{1} + \frac{-\alpha_1 \beta_0}{1} \quad (53)$$

With the same approximation as eqn (13), except $\alpha_1 \beta_0$, eqn (53) is rewritten as

$$-F_n u_1^{\frac{1}{2}} = \frac{-u_1}{1} + \frac{-u_1}{1} + \dots + \frac{-u_1}{1} + \frac{-u_0}{1} \quad (54)$$

Let the n th convergent of eqn (54) be p_n/q_n . Then,

$$\frac{p_n}{q_n} = -u_1^{\frac{1}{2}} \frac{\sinh n v_1}{\sinh (n+1) v_1} \quad (55)$$

$$u_1^{\frac{1}{2}} \equiv \frac{(a_k b_{k-1})^{\frac{1}{2}}}{1 + T_k s} \quad (56)$$

(— means averaging for $k=2 \sim m$)

$$u_0 \equiv \alpha_1 \beta_0 \quad (57)$$

and

$$\cosh v_1 \equiv \frac{1}{2} u_1^{-\frac{1}{2}} \quad (58)$$

Consider the following continued fraction,

$$1 - F_n u_1^{\frac{1}{2}} = 1 + \frac{-u_1}{1} + \dots + \frac{-u_1}{1} + \frac{-u_0}{1} \equiv \frac{p_{n+2}'}{q_{n+2}'} \quad (59)$$

Let the $(n+1)$ th convergent of eqn (59) be p_{n+1}'/q_{n+1}' , then

$$\frac{p_{n+1}'}{q_{n+1}'} = 1 + \frac{-u_1}{1} + \dots + \frac{-u_1}{1} = 1 + \frac{p_n}{q_n} \quad (60)$$

By the theorem on continued fraction,

$$\frac{p_{n+2}'}{p_{n+1}'} = 1 + \frac{-u_0}{1} + \frac{-u_1}{1} + \dots + \frac{-u_1}{1} = 1 + \frac{-u_0}{1 + p_n/q_n} \quad (61)$$

and

$$\frac{q_{n+2}'}{q_{n+1}'} = 1 + \frac{-u_0}{1} + \frac{-u_1}{1} + \dots + \frac{-u_1}{1} = 1 + \frac{-u_0}{1 + p_{n-1}/q_{n-1}} \quad (62)$$

By eqns (55), (59), (60), (61) and (62),

$$F_n = \frac{(1 - u_0) \sinh n v_1 - u_0 \sinh (n-2) v_1}{(1 - u_0) \sinh (n+1) v_1 - u_0 \sinh (n-1) v_1} \quad (n < m) \quad (63)$$

The transmittance for stripping section is obtained in the same way as follows,

$$F_n = \frac{(1 - u_s) \sinh (N-n) v_2 - u_s \sinh (N-n-2) v_2}{(1 - u_s) \sinh (N-n+1) v_2 - u_s \sinh (N-n-1) v_2} \quad (n \geq m) \quad (64)$$

where

$$u_2^{\frac{1}{2}} \equiv \frac{(a_k b_{k-1})^{\frac{1}{2}}}{1 + T_k s} \quad (65)$$

(— means averaging for $k=m \sim N-1$)

$$u_s \equiv \alpha_N \beta_{N-1} \quad (66)$$

and

$$\cosh v_2 \equiv \frac{1}{2} u_2^{-\frac{1}{2}} \quad (67)$$

The transmittance Z in the reduced diagram is obtained by eqns (63) and (64) as follows,

$$Z = \frac{\gamma''}{1 - u_1^{\frac{1}{2}} \frac{(1 - u_0) \sinh (m-1) v_1 - u_0 \sinh (m-3) v_1}{(1 - u_0) \sinh m v_1 - u_0 \sinh (m-2) v_1} - u_2^{\frac{1}{2}} \frac{(1 - u_s) \sinh (N-m-1) v_2 - u_s \sinh (N-m-3) v_2}{(1 - u_s) \sinh (N-m) v_2 - u_s \sinh (N-m-2) v_2}} \quad (68)$$

Therefore the transfer function x_n/x_f is obtained by the use of eqns (63), (64) and (68) as follows:
for enriching section ($n < m$)

$$\frac{x_n}{x_f} = Z \cdot \frac{(1-u_0) \sinh nv_1 - u_0 \sinh (n-2)v_1}{(1-u_0) \sinh mv_1 - u_0 \sinh (m-2)v_1} \quad (69)$$

and for stripping section ($n \geq m$)

$$\frac{x_n}{x_f} = Z \cdot \frac{(1-u_s) \sinh (N-n)v_2 - u_s \sinh (N-n-2)v_2}{(1-u_s) \sinh (N-m)v_2 - u_s \sinh (N-m-2)v_2} \quad (70)$$

If further simplification is made as

$$u_0 = u_1 = u_2 = u_s \equiv u \quad (71)$$

and

$$v_1 = v_2 \equiv v \quad (72)$$

then the transfer function is simplified as follows:
for enriching section ($n < m$)

$$\frac{x_n}{x_f} = \frac{I_f^0}{L_0^0 + L_f^0} \cdot \frac{\sinh (N-m+1)v}{\sinh v \cdot \sinh (N+2)v} \cdot \sinh (n+1)v \quad (73)$$

and for stripping section ($n \geq m$)

$$\frac{x_n}{x_f} = \frac{L_f^0}{L_0^0 + L_f^0} \cdot \frac{\sinh (m+1)v}{\sinh v \cdot \sinh (N+2)v} \cdot \sinh (N-n+1)v \quad (74)$$

Conclusions

Dynamic characteristics of the binary distillation column are described by the transfer functions, eqns (32), (46), (50), (69), (70), (73) and (74), for the changes of such variables as reflux flow, vapour flow, feed flow, and feed composition, respectively. Parameters of these transfer functions can be decided from design data. The frequency responses can be calculated from the transfer functions, independent of the number of trays.

The lag of liquid flow causes the large phase lag in high frequency range, that means the existence of dead time in effect. Therefore this liquid flow lag must be decreased in order to increase the controllability of the column. The decrease of this lag is equivalent to the increase of down-pipe periphery.

It was often said that in case of reflux manipulation the temperature detector should be installed at the tray where

the concentration gradient is maximum. This insistence is based only upon static properties. But the dynamics must be taken into account. Equivalent dead time increases as the position of the detector goes lower. Therefore, the detector should be installed as high as possible, and the compromise is made between the detecting sensitivity and the equivalent dead time.

Nomenclature

- L_n Liquid flow rate flowing down from the n th tray to the $n+1$ th tray (mol./min)
 L_N Liquid flow rate to be taken out of bottom (mol./min)
 L_0 Reflux flow rate (mol./min)
 V Vapour flow rate (mol./min)
 H_n Liquid hold-up of the n th tray (mol.)
 H_0 Liquid hold-up of the condenser (mol.)
 H_p Liquid hold-up of the reflux pipe (mol.)
 X_n Composition of more volatile component in the liquid on the n th tray (mol. fraction)
 Y_n Composition of more volatile component in the vapour from the n th tray (mol. fraction)
 $L_n^0, H_n^0, X_n^0, \dots$ Superscript 0 means the steady-state values of each variable
 l_n, y_n, x_n, \dots Small letter means the small variation of each variable from the steady state, and its Laplace transform

References

- ARMSTRONG, W. D. and WILKINSON, W. L. *Plant and Process Dynamic Characteristics*. 1957. London; Butterworths
- VOETTER, H. *Plant and Process Dynamic Characteristics*. 1957. London; Butterworths
- TEAGER, H. M. *M.I.T.Sc.D. Thesis* 1955
- ROSE, A. and WILLIAMS, T. J. *Industr. Engng Chem.* 47, No. 11 (1955) 2284
- ROSENBROCK, H. H. *Trans. Instn chem. Engrs, Lond.* 35 (1957) 347
- ARMSTRONG, W. D. and WILKINSON, W. L. *Trans. Instn chem. Engrs, Lond.* 35 (1957) 352
- ARMSTRONG, W. D. and WOOD, R. M. *Trans. Instn chem. Engrs, Lond.* 39 (1961) 65
- RIJNSDORP, J. E. and MAARLEVELD, A. *Proc. Joint Symp. Instrumentation and Computation in Process Development and Plant Design* (1959) 135

DISCUSSION

J. E. RIJNSDORP, *Koninklijke/Shell Laboratorium, Amsterdam, The Netherlands*

(1) In Figure 2 the authors have demonstrated that assuming constant stripping factors (see their formula 13) need not give unrealistic answers. This can be expected for columns with many trays, as the influence of distant trays is only felt for very low frequencies, which are unimportant for control. However, for their short column (6 trays), where the behaviour of neighbouring trays is much different, this is a remarkable result.

(2) Below eqn (46), the authors state that c_{2n} is generally small compared to unity. Then from their eqn (43):

$$1 + c_{2n} = \frac{\tau}{\kappa} \frac{Y_n^0 - Y_{n+1}^0}{X_{n-1}^0 - X_n^0} \approx 1 \quad (1)$$

using the static partial mass balance of tray n

$$L_{n-1}^0 (X_{n-1}^0 - X_n^0) = V^0 (Y_n^0 - Y_{n+1}^0) \quad (2)$$

we find:

$$1 + c_{2n} = \frac{\tau}{\kappa} \frac{L_{n-1}^0}{V^0} \approx 1 \quad (3)$$

Here L_{n-1}^0/V^0 is generally not much different from one.

In our experience (see e.g. Rijnsdorp, *Birmingham Un. Chem. Eng. Suppl.* 1961, p. 14), the value of κ/τ can be anywhere between -2 and $+3$. Consequently eqns (1) and (2) are generally not valid. In other words, c_{2n} is generally *not* small compared to unity.

In fact, Figure 3 gives the impression that the actual value of κ/τ is smaller than the value used in the calculations. Did the authors find better agreement for a different value for κ/τ ?

K. IZAWA and T. MORINAGA, *in reply*

The authors are very grateful for Dr. Rijnsdorp's comments. The first comment, about smoothing or averaging the tray dynamics to simplify the approximation, is highly appreciated. Such approximation may be more effective in the case where the $x-y$ equilibrium curve is near to a straight line, rather than the case here discussed.

On the second point, the static partial mass balance on the n th tray is found as the following equation, rather than the one Dr. Rijnsdorp mentions:

$$L_{n-1}^0 X_{n-1}^0 - L_n^0 X_n^0 = \bar{V}^0 (Y_n^0 - Y_{n+1}^0) \quad (1)$$

Thus we obtain, instead of Dr. Rijnsdorp's eqn (3)

$$1 + c_{2n} = \frac{\frac{\tau}{\kappa} \frac{L_{n-1}^0}{\bar{V}^0} X_{n-1}^0 - \frac{\tau}{\kappa} \frac{L_n^0}{\bar{V}^0} X_n^0}{X_{n-1}^0 - X_n^0} \quad (2)$$

This equation would not show that

$$\frac{\tau}{\kappa} \frac{L_n^0}{\bar{V}^0}$$

must be close to unity for the discussor's eqn (1), or

$$1 + c_{2n} \approx 1 \quad (3)$$

As an example, if the following relation

$$\frac{\tau}{\kappa} \frac{L_n^0}{\bar{V}^0} - 1 \approx \frac{\text{constant}}{X_n^0} \quad (4)$$

holds, then the relation (3) certainly follows, or c_{2n} in eqn (43) can be neglected.

Some of the possible causes which may explain *Figure 3* as well as others are mentioned in the paper. The value of κ used here may certainly differ from what it should be, as the discussor points out. However, the authors had to run the very simple model tray experiments using water for liquid and air for vapour in order to obtain the relation (39). And the value of κ thus experimentally obtained is used as a rough estimate, because there were no other available values for κ .

Approximation Models for the Dynamic Response of Large Distillation Columns

J. S. MOCZEK, R. E. OTTO and T. J. WILLIAMS

Summary

Present methods of computation of the transient response of very large distillation columns involve the solution of extremely large families of non-linear ordinary differential equations. Accordingly, there is a great need for a set of valid approximate models for the response of such columns to a variety of possible upsets, otherwise computer simulation will be completely impractical as a means of developing new and better column control schemes. These must be developed either from the results of exact digital computations or from actual experimental data from plant size columns.

This paper presents the findings of an extensive digital computer study of the dynamic response to a variety of upsets of a distillation column producing a very high purity product. The example column used is part of a BTX (benzene, toluene, xylene) separation unit.

The results of the detailed digital computer calculations are interpreted in the form of relatively low order performance function type expressions which approximate the actual response obtained as closely as possible.

The column studied exhibits quite different transient responses in its rectifying and stripping sections. In addition, there is a decided dependence of this transient behaviour upon the type, magnitude and direction of a particular upset. Rules are formulated for extending the results obtained to still other upsets in the same column and in other similar columns.

Sommaire

Les méthodes actuelles de calcul de la réponse transitoire d'une grande colonne de distillation, impliquent la résolution d'un système à nombre élevé d'équations différentielles non-linéaires. C'est pourquoi il s'avère très nécessaire de disposer d'une série de modèles caractérisant la réponse d'une telle colonne pour tous les cas possibles de son fonctionnement sinon la simulation au moyen de calculateurs serait inadéquate en vue d'améliorer la commande automatique de ces colonnes. Ces modèles peuvent être développés, soit à partir du résultat de calculs numériques exacts, soit à partir de données expérimentales déduites de colonnes en fonctionnement.

Le rapport présente le résultat d'une étude approfondie au moyen de calculateurs numériques concernant la réponse dynamique des différentes possibilités de fonctionnement d'une colonne de distillation fournissant un produit d'une très grande pureté. La colonne prise comme exemple fait partie d'une unité de séparation BTX (benzène, toluène, et xylène).

Le résultat des calculs numériques est interprété sous la forme d'expressions fonctionnelles d'un ordre relativement bas qui se rapprochent, autant qu'il est possible de la réponse réelle.

Zusammenfassung

Die gegenwärtigen Verfahren zur Berechnung des Übergangsverhaltens sehr großer Destillationskolonnen erfordern die Lösung eines umfangreichen Systems von gewöhnlichen nichtlinearen Differentialgleichungen. Es besteht daher ein großer Bedarf für eine Anzahl gültiger Näherungsmodelle, die das Übergangsverhalten solcher Kolonnen bei den verschiedensten möglichen Betriebsstörungen beschreiben. Ohne diese Näherungsmodelle ist die Nachbildung durch Rechner als Mittel für die Entwicklung neuerer und besserer Kolonnenregelungen völlig unbrauchbar. Solche Modelle müssen entweder von den Ergeb-

nissen exakter Berechnungen am Digitalrechner oder von den wirklichen Versuchsdaten der Originalkolonnen ausgehen.

Die Arbeit enthält die Ergebnisse einer umfangreichen Untersuchung am Digitalrechner über das dynamische Störverhalten einer Destillationskolonne für Produkte sehr hohen Reinheitsgrades. Die untersuchte Kolonne ist ein Teil einer Benzol-Toluol-Xylol-Trennanlage.

Die Ergebnisse der einzelnen Berechnungen am Digitalrechner werden in Form von Übertragungsfunktionen verhältnismäßig niedriger Ordnung gedeutet, die den tatsächlichen Ergebnissen möglichst nahekommen.

Die untersuchte Kolonne zeigt ein deutlich verschiedenes Zeitverhalten beim Rektifizieren und beim Abstreifen. Zusätzlich hängt das Übergangsverhalten merklich von der Art, der Größe und der Richtung einer gegebenen Störung ab. Es werden Regeln angegeben, nach denen man die hier gewonnenen Ergebnisse auch auf andere Störungsarten an der gleichen oder an ähnlichen Kolonnen anwenden kann.

Introduction

While considerable information has appeared in the recent literature concerning the dynamic behaviour of distillation columns^{2, 6, 7, 12, 15}, much of this work has been confined to the study of relatively small columns. This has been mainly due to the extremely large amount of computation necessary to develop such data on digital computing machines¹⁷ along with the equally difficult task of determining valid experimental data on very large columns in sufficient quantity to be valuable^{4, 5, 8}.

This paper reports the results obtained from an extensive digital computer study (over forty separate cases) of the dynamics of the benzene stripping column in a BTX (benzene, toluene, xylene) separation unit. *Figure 1* presents a sketch of this column while *Tables 1* and *2* show some of the physical parameters, flow rates, and other pertinent data applicable to this column.

This project is part of a larger investigation of column dynamics and control. The overall project will include tests of the concepts presented herein on actual columns in field installations.

Operation of this particular column is extremely critical because of the very high purity requirements placed on the benzene product taken overhead from the column, along with the equally severe requirements for the purity of the subsequent products of the complete unit i.e. toluene and xylene. Thus, not only must the benzene itself be exceptionally pure in the column overhead, but in addition, the column must send as much as possible of this benzene to the overhead product to prevent its contaminating the heavier constituents if allowed to leave with the bottoms product stream.

Because the feed stream to this separations unit was 'wet', a pasteurizing section was added to the top of the column to strip this 'light ends' material (mostly water) from the overhead

product. This pasteurizing section had some interesting influences on the column transient behaviour as reported later.

As is true of all columns making a very close separation of the various constituents of the feed stream, this column was extremely sensitive to all flow rates and stream compositions imposed. Also, since it operated with a large number of trays for a system with such a large relative volatility as benzene and toluene, any operation regime other than that which allows the maximum separation potential of the column for the particular feed used meant the imposition of a 'pinch' condition in the column. Therefore, an upset, however small, driving the column

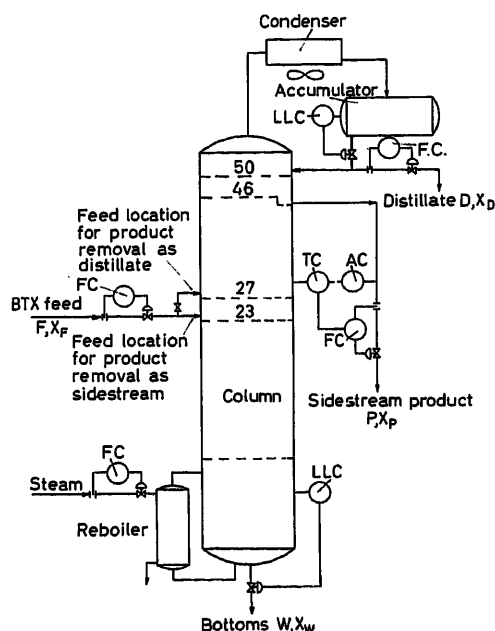


Figure 1. Diagram of distillation system studied

away from the optimum operating conditions gave the response of a 'pinch generating transient'. On the other hand, another change imposed while away from optimum operating conditions, so as to more closely approach the true operating condition, resulted in a response which could be called a 'pinch relieving transient'.

Since these responses are decidedly different in form and time response, a large column such as studied here gives an extreme hysteresis effect in its overall response to all types of transients.

Simulation Methods

Computation methods used were essentially the same as those previously described by Rosenbrock¹⁷ as applied to multicomponent mixtures and with the addition of provisions for a complete heat balance on each tray and of a non-equal molal overflow. The same assumptions apply except as just noted.

As part of our investigation, the effect of the computation time interval used on the accuracy of the digital computation of the column transient response was also extensively studied. Figure 2 graphically illustrates the importance of using a computation interval of a certain minimum size even though the required computer time is made correspondingly long.

Table 3 further illustrates this finding by presenting the changes in the parameter values for the corresponding second

Table 1. Physical Data and Operating Specifications on Column Simulated

Diameter	8 ft. 6 in.
Trays:	
Number	50 plus reboiler
Efficiency	78%
Feed location	Plate 23, actual 18, theoretical
Sidestream location	Plate 46, actual 36, theoretical
Pasteurizing section	Plates 47-50 incl., actual 37-39 incl., theoretical
Condenser	Air-cooled, total
Calculated hold-ups:	
Condenser, accumulator and reflux piping	240 mol.
Trays:	
Above feed	139 mol.
Below feed	174 mol.
Sump, reboiler and piping	470 mol.
Total	1,023 mol.
Feed:	
Rate	22.26 mol./min
Composition	~50 mol. % benzene ~50 mol. % heavy ends (toluene, xylene and cumene) small amounts of light ends—water, etc.
Overhead or distillate	
Rate	0.2233 mol./min (light ends plus some benzene)
Sidestream:	
Rate	11.204 mol./min
Required composition	>99.94 mol. % benzene
Bottoms	
Rate	10.833 mol./min
Required composition	<00.05 mol. % benzene
Reflux ratio, L/P	2.341

Table 2. Calculated Physical Time Constants of Simulated Column

Column trays	
Weir flow time constant	
$\tau_{FT} = A/K = \frac{27.1 \text{ ft.}^3}{700 \text{ ft.}^3/\text{min}} = 0.039 \text{ min} = \frac{\text{Weir flow area}}{\text{Weir coefficient}}$	
Liquid mixing time constant	
$\tau_{MT} = V/F = \frac{11.80 \text{ ft.}^3}{94.4 \text{ ft.}^3/\text{min}} = 0.125 \text{ min} = \frac{\text{Volume}}{\text{Liquid flow rate}}$	
Reboiler, etc.	
Heat transfer time constant	
$\tau_{HR} = \frac{W_t C_p}{UA} = \frac{6,290 \text{ lb. metal} \times 0.124 \text{ B.Th. U. / lb.}^\circ\text{F}}{2.78 \text{ B.Th. U. / }^\circ\text{F min. ft.}^2 \times 2,090 \text{ ft.}^2} = 0.134 \text{ min} = \frac{\text{Heat capacity}}{\text{Heat flow rate}}$	
Liquid mixing time constant	
$\tau_{MR} = V/F = \frac{967 \text{ ft.}^3}{97.6 \text{ ft.}^3/\text{min}} = 9.91 \text{ min}$	
Accumulator, etc.	
Liquid mixing time constant	
$\tau_{MA} = V/F = \frac{365 \text{ ft.}^3}{52.3 \text{ ft.}^3/\text{min}} = 6.98 \text{ min}$	

order plus dead time performance functions of the computed transient response as the computation time interval used is decreased.

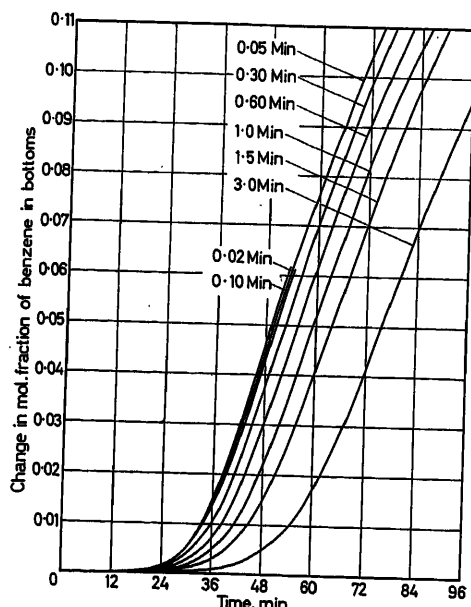


Figure 2. Effect of size of computation interval on accuracy of computed distillation transient

Table 3. Effect of Computation Time Interval per Iteration on Dead Times and Time Constants of Approximate Response Models

Computation time interval per iteration (min)	Equivalent dead time T_{DT}	Major time constant τ_1	Minor time constant τ_2	ΣT
3.0	43.2	42.8	21.9	107.9
1.5	34.4	44.4	16.9	95.7
1.0	31.4	45.8	14.4	91.6
0.60	29.0	45.8	13.0	87.8
0.30	27.1	45.7	11.9	84.7
0.10	25.8	45.8	10.9	82.5
0.05	25.4	45.9	10.6	81.9
0.02	25.2*	45.8	10.5	81.5
	25.0	45.8	10.4	81.2

* Probable final value with decreasing interval size.

Derivation of Transient Response Models

Because of the very high complexity of the mathematical models necessary for the 'exact' computation of distillation column transients, the use of approximation models of these systems has been proposed by several earlier authors^{1, 4, 5, 7, 8}. Accordingly, this paper investigates the possibility of deriving such models from the digital computer developed transients of a large distillation column giving a very close separation.

The methods used were those presented by Oldenbourg and Sartorius¹¹ and modified by Smith¹⁹. These procedures develop the appropriate first- and second-order approximations, with and without dead time, to represent the data given, i.e.

$$PF = \frac{O}{I} = \frac{Ke^{-pT_{DT}}}{(\tau_1 p + 1)(\tau_2 p + 1)} \quad \text{or} \quad = \frac{Ke^{-pT_{DT}}}{(\tau_1 p + 1)}$$

where PF is the performance function, O the output response I the input function, T_{DT} represents equivalent dead time, τ_1 are major time constants, τ_2 is minor time constant, K the proportionality constant or scale factor, and p the differential operator.

For those cases where a first or second-order expression could not be fitted, an analogue computer trial-and-error procedure was used to develop a higher-order expression. Figures 3 and 4 show the method of derivation of these expressions, including all pertinent equations. All curve fitting was done by eye.

Results of Model Development

Tables 4 and 5 present the results obtained when the calculations described above were made on some of the digital computer derived column transients of the study.

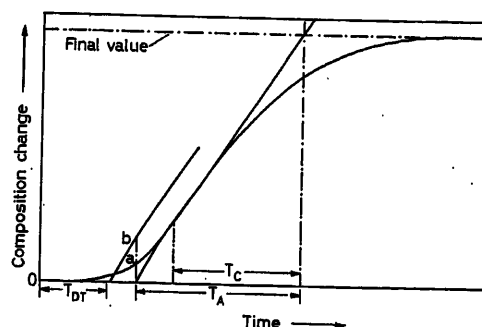


Figure 3. Method of estimating second-order time constants 11, 19

1. Draw tangent to the transient response at inflection point. T_a represents the time between intersection of tangent with initial and final values of transient. T_c is the time between the inflection point and the tangent intersection with final value of curve.
2. X is determined from the equation: $(1+X)(X)^X/(1-X) = T_c/T_a$.
3. The second order time constants, τ_1 and τ_2 , are calculated from the equations: $\tau_1/\tau_2 = X$ and $\tau_1 + \tau_2 = T_c$.
4. Point a is the composition change at intersection of the tangent with the horizontal axis. Point b , $2.718a$, is located on the graph at the identical time value.
5. A line parallel to the tangent through point b locates the equivalent dead time, T_{DT} .

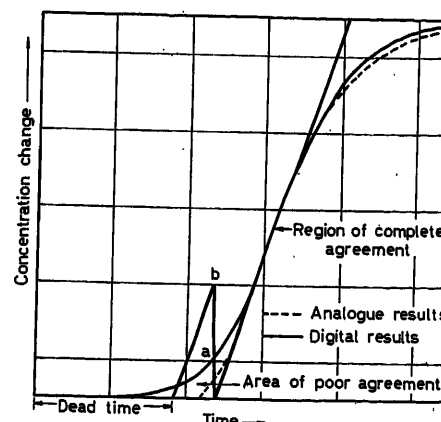


Figure 4. Method of fitting analogue computer simulation of high-order responses of distillation column

1. The dead time, T_d , is determined as described in Figure 3.
2. Increasingly higher-order transfer functions are then simulated on the analogue computer until the upper portion of the response curve is fitted as closely as possible.

Table 4. Magnitude and Order of Column Output Responses to Various Step Change Upsets in Column Operating Variables

Case	Upset considered	Sidestream response		Distillate response		Bottoms response	
		Mol. fraction magnitude	Order	Mol. fraction magnitude	Order	Mol. fraction magnitude	Order
000	Reboiler duty set at 50% of base case	-0.141071	5+DT			+0.194223	2+DT
98	Reboiler duty set at 75% of base case	-0.006268	2+DT			+0.006487	2+DT
43 A	Feed composition increased by 10% benzene	+0.000120	2+DT			+0.205360	2+DT
45 A	Feed composition decreased by 10% benzene	-0.198445	4+DT			-0.000073	2+DT
47 A	Sidestream rate set at 75% of base rate	+0.000136	1			+0.205400	2+DT
49 A	Sidestream rate set at 125% of base rate	-0.199800	4+DT			-0.000083	2+DT
79 A	Sidestream rate set at 87.5% of base rate	+0.000125	1			+0.114360	2+DT
81 A	Sidestream rate set at 112.5% of base rate	-0.110960	4+DT			-0.000075	2+DT
83 A	No sidestream Distillate rate set at 125% of base case			-0.199970	2+DT	-0.000088	2+DT
85 A	No sidestream Distillate set at 75% of base case			+0.000071	2+DT	+0.208600	2+DT
59 A	Return to equilibrium Return from 75% of base sidestream rate	-0.000136	1 or 2			-0.205400	1 or 2
60 A	Return to equilibrium Return from 125% of base sidestream rate	+0.199800	1			+0.000083	1 or 2

The reader should compare the response of the overhead composition for those cases where the pasteurizing section was present in the column with those where it was absent (Cases 83 A and 85 A). In each case where a higher-order response occurs the overhead composition is the one most affected by the upset and the pasteurizing section is present. The effect of the pasteurizing section is to isolate the accumulator with its large hold-up from the rest of the column. Thus only the trays are involved in the immediate transient and the result is a higher order response than if the accumulator were effective as in Cases 83 A and 85 A.

Table 4 compares the type and order of the performance function developed for each of several column tests on the computer with the response magnitude and type of upset imposed in the test. Table 5 gives the actual value of the dead times and time constants determined by the methods above. These same methods were used to derive the results of Table 3. Table 6 summarizes the information of the previous tables into a set of potential rules for the derivation of column transient response models. Figures 5-9 illustrate the applicability of these observations with reproductions of selected results from the computer study. Figures 5 and 6 also show the degree of correspondence between the 'exact' digital computer results and the analogue computer approximation used.

The Concept of Change of Inventory

In order to lend a unifying factor to data so far obtained, an overall concept of column response is necessary. Such a concept is that of the 'change of inventory' time in the column. If one defines this function as follows:

$$T_{inv} = \frac{(\text{inv})_f - (\text{inv})_i}{(F_v x_{Fv} - F_i x_{Fi}) - (D_v - D_i) x_{Di} - (W_v - W_i) x_{Wi}}$$

where (inv) is the inventory of component in question in column at time considered, *f* refers to final steady-state condition of column, *i* is the initial steady-state condition of column, and *v* refers to conditions at time just after step change upset.

Table 7 (a) compares the number so obtained with another number which comprises the sums of the dead times and time constant reported in Table 5. It will be seen that for both lower and higher order approximation models, this concept gives an answer which is quite close to that obtained from the computed response curves themselves.

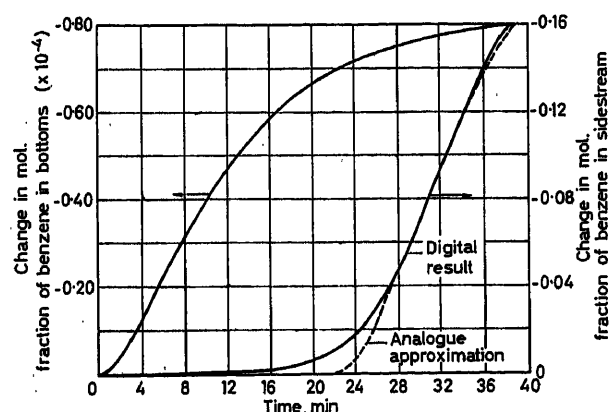


Figure 5. Transient response of column with step change of sidestream flow to 125 per cent of correct value

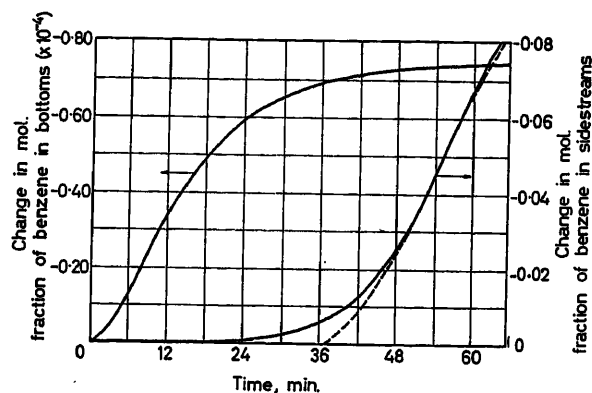


Figure 6. Transient response of column with step change of sidestream flow to 112.5 per cent of correct value

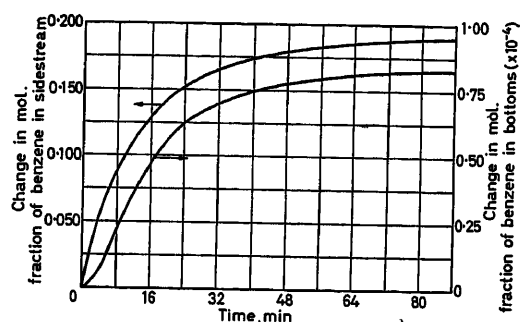


Figure 7. Transient response of column with step change of sidestream flow from 125 to 100 per cent of correct value

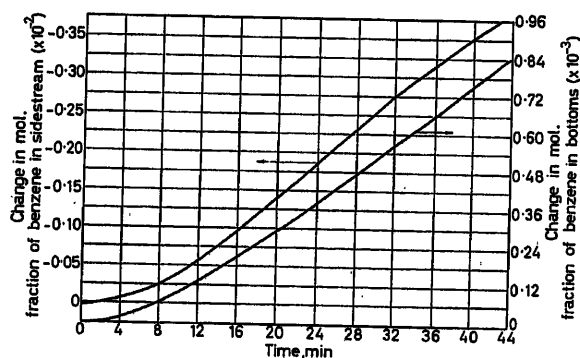


Figure 8. Transient response of column with step change of reboiler heat input to 75 per cent of design value

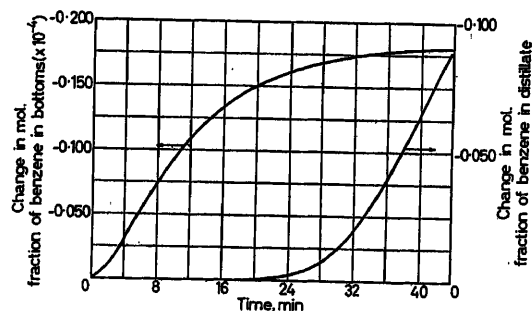


Figure 9. Benzene product withdrawn as distillate, with sidestream shut-off and feed relocated. Transient response of column with step change in distillate flow to 125 per cent of correct value

These numbers are probably completely satisfactory for the transient response pattern and control response analysis uses to which they are usually put.

The T_{inv} value is, of course, a pseudo first-order time constant considering the whole column hold-up as a first-order mixing stage. That it works for higher-order systems is due to the fact that the 60 per cent response points of these systems (important in the approximate model developing formulas used here) is almost coincidental with the 63.2 per cent (one time constant) point for the first-order system.

Table 7 (b) extends the overall rules for approximation model order developed in Table 6 to predict the best ratios of major and minor time constants and of dead times and their relation to change of inventory time for each upset condition studied. The rules of Tables 6 and 7 (b) should be applicable to any column operating under conditions similar to those covered in this study. They should also be applicable to other types of upsets provided the decided hysteresis effect of the column response is taken into account for input functions requiring a two-sided response.

As mentioned earlier, the hysteresis effect on column response noted here is due to the immediate 'pinch relieving' action of the column whenever more favourable column operating parameters are imposed. Since a pinch is normally confined to one or the other end of the column and since by far the greatest change in column composition occurs there in the early part of the transient, it would seem that only the pinched end of the column should be considered in computing 'change of inventory' time and the resulting column time constant. This has been done in Tables 7 (a) and 7 (b) with excellent results. It should be noted in passing that while the initial transient for the pinch relieving case is fast, the overall equilibration time or total response time is at least as long as that for the pinch generating transient.

An additional factor to be considered is a comparison of the numerical time constants of Table 5 (a) and (b) and the rules for time-constant ratios and dead times of Table 7 (b). In some cases, particularly 79 A and 83 A, equal values for major and minor constants in a second order plus dead time system were obtained.

For these two cases the method of Oldenbourg and Sartorius was at the point of breaking down since they were barely second-order systems. Under such conditions only an equal time constant system can be obtained. However, every indication is that the true response of the column is similar to that of the companion cases and the rules of Table 7 (b) should be applied here also. The resulting effect on column transient response is very small.

For cases where more than one upset is applied to the column at any one time, the change of inventory time can be computed for the combined transient in the same manner as for a single transient. If it is further assumed that the higher-order response will predominate, the form of the resulting multiple transient can also be established. The above rule has not been confirmed by actual application to simulation data.

Physical Meaning of the Approximate Models

Since the distillation column is a true higher-order system, there is little reason to suspect a physical meaning for the values

APPROXIMATION MODELS FOR THE DYNAMIC RESPONSE OF LARGE DISTILLATION COLUMNS

Table 5. Parameter Values of Approximate Models of Transient Response of Distillation Columns

Case	Upset considered	τ_1 Major time constant	τ_2 Minor time constant	T_{DT} Equivalent dead time	Most affected
(a) Values for bottoms stream only					
000	Reboiler duty set at 50% of base case	37.9	13.2	14.2	—
98	Reboiler duty set at 75% of base case	Indeterminate			—
43 A	Feed composition increased by 10% benzene	45.8	10.9	25.8	
45 A	Feed composition decreased by 10% benzene	12.6	3.1	3.4	
47 A	Sidestream rate set at 75% of base rate	35.4	8.6	18.5	
49 A	Sidestream rate set at 125% of base rate	7.9	5.4	0	
79 A	Sidestream rate set at 87.5% of base rate	28.2	28.1	31.2	
81 A	Sidestream rate set at 112.5% of base rate	13.4	4.0	0	
83 A	No sidestream	7.9	4.8	0	
85 A	Distillate rate set at 125% of base case	36.1	8.0	23.1	
59 A	No sidestream	36.1	8.0	23.1	
59 A	Distillate rate set at 75% of base case	36.1	8.0	23.1	
59 A	Return to equilibrium	47.8	5.1	0	
60 A	Return from 75% of base sidestream rate	47.8	5.1	0	
60 A	Return to equilibrium	60.6	1.1	0.9	
60 A	Return from 125% of base sidestream rate	60.6	1.1	0.9	
(b) Values for overhead streams only					
000	Reboiler duty set at 50% of base case	(n = 5, $\tau = 2.62$)		11.3	—
98	Reboiler duty set at 75% of base case	29.5	12.9	1.2	—
43 A	Feed composition increased by 10% benzene	6.1	6.0	4.8	
45 A	Feed composition decreased by 10% benzene	(n = 4, $\tau = 4.40$)		28.7	
47 A	Sidestream rate set at 75% of base rate	7.7	—	—	
49 A	Sidestream rate set at 125% of base rate	(n = 4, $\tau = 2.68$)		20.1	
79 A	Sidestream rate set at 87.5% of base rate	12.5	—	—	
81 A	Sidestream rate set at 112.5% of base rate	(n = 4, $\tau = 6.70$)		32.2	
83 A	No sidestream	11.5	11.5	24.7	
85 A	Distillate rate set at 125% of base case	9.7	9.6	0	
59 A	No sidestream	9.7	9.6	0	
59 A	Distillate rate set at 75% of base case	9.7	9.6	0	
59 A	Return to equilibrium	48.9	3.0	0	
60 A	Return from 75% of base sidestream rate	48.9	3.0	0	
60 A	Return to equilibrium	15.6	—	—	
60 A	Return from 125% of base sidestream rate	15.6	—	—	

of the parameters developed in the approximation models derived here. The change of inventory time does have a physical meaning as a pseudo first-order time constant for the complete hold-up of the column. It thus serves as a unifying concept between the real and approximate models for the column. Likewise, the modification of the change of inventory time for the half-column case to develop the response time for the pinch

relieving transient condition in the column is also based upon a physical occurrence in the column and again serves to base the approximations on true operating reality for the column. The change of inventory time, being different for different sized upsets, adequately compensates for much of the non-linearity present in the response of a distillation column to differing magnitude upsets.

Table 6. Applicability of some Approximate Models of Distillation Column Response
See also Table 7 (b)

<p>I. Upsets causing departure from optimum steady-state operation of column</p> <p>A. Pasteurizing section present on column</p> <p>(1) All departure from optimum steady-state upsets except boil-up changes</p> <p>(a) Enriching section most affected by upset</p> <p>(i) Sidestream composition response was always of higher order, i.e. it required a performance function of the form</p> $PF = \frac{K \exp(-p T_{DT})}{(\tau_i p - 1)}$ <p>where $n > 2$, commonly $n = 4$ or 5</p> <p>(ii) Intermediate enriching section plate composition responses were also always of higher order</p> <p>(iii) Bottoms product composition responses could be represented by second order plus dead time models</p> <p>(b) Stripping section most affected by upset</p> <p>(i) Bottoms composition response was readily represented by a second order plus dead time model</p> <p>(ii) Intermediate stripping section plate composition responses were always of higher order as defined above</p> <p>(iii) Enriching section responses could be represented by pseudo first-order models—no dead time.</p>	<p>(2) Boil-up changes—departure from optimum steady state</p> <p>(a) Sidestream composition</p> <p>(i) Large upsets—higher order plus dead time</p> <p>(ii) Small upsets—second order plus dead time</p> <p>(b) Intermediate plate compositions—higher order plus dead time</p> <p>(c) Bottoms composition—second order plus dead time.</p> <p>B. No pasteurizing section on column—all upsets</p> <p>(1) Enriching section most affected by upset</p> <p>(a) Overhead composition response could be represented as a second order plus dead time system according to the criteria of Oldenbourg-Sartorius and Smith</p> <p>(b) Intermediate tray composition responses were always of higher order</p> <p>(c) Bottoms composition response, second order plus dead time</p> <p>(2) Stripping section most affected by upset</p> <p>(a) Responses same as reported above</p> <p>II. Upsets resulting in return to optimum steady-state operation of column</p> <p>Responses of all sections of the column could be readily approximated by a first-order response with no dead time</p>
---	--

Table 7(a). Comparison of Change of Inventory Time with the Sum of Performance Function Time Constants and Dead Times

Case	Upset considered	Order of performance function of column section most affected	Change of inventory time		$\Sigma(\tau_1 + \tau_2 + T_{DT})$	
			Computed	per cent error $100(\tau - \Sigma)/\Sigma$	Bottoms	Tops
000	Reboiler duty set at 50% of base case	5 + DT (Tops) 2 + DT (Bottoms)	Not applicable		65.3	20.1
98	Reboiler duty set at 75% of base case	2 + DT	Not applicable		—	43.6
43 A	Feed composition increased by 10% benzene	2 + DT	78.1	-5.3	82.5	16.9
45 A	Feed composition decreased by 10% benzene	4 + DT	44.4	-4.1	19.1	46.3
47 A	Sidestream rate set at 75% of base rate	2 + DT	63.7	+1.9	62.5	7.7
49 A	Sidestream rate set at 125% of base rate	4 + DT	32.4	+5.2	13.3	30.8
79 A	Sidestream rate set at 87.5% of base rate	2 + DT	86.6	-1.0	87.5	12.5
81 A	Sidestream rate set at 112.5% of base rate	4 + DT	62.1	+5.2	17.4	59.0
83 A	No sidestream	2 + DT	50.6	+6.0	12.7	47.7
85 A	Distillate rate set at 125% of base case	2 + DT	65.3	-2.8	67.2	19.3
59 A	Return to equilibrium	2	Corr			
60 A	Return from 75% of base sidestream rate	1	80.1	50.0	52.9	51.9
	Return to equilibrium		40.5	14.6	62.6	15.6
	Return from 125% of base sidestream rate			-6.4		

Table 7 (b). Ratio of Time Constants and Dead Times for Approximate Models of Distillation Column Response
(See also Table 6)

<p>I. Upset causing departure from optimum column separation</p> <p>A. Boil-up change</p> <p>(1) Second order plus dead time models</p> $\tau_1 = 3 \tau_2 = 3 T_{DT}$ $\Sigma \tau + T_{DT} = T_{inv}$ <p>Of equivalent product take-off upset (i.e. same change in product composition).</p> <p>(2) Higher order plus dead time models</p> $T_{DT} = 3/2 \Sigma \tau_n$ $\Sigma \tau_n + T_{DT} = T_{inv} \text{ as above.}$ <p>B. Input flow or composition or output flow upset</p> <p>(1) Second order plus dead time model</p> $\tau_1 = 4 \tau_2 = (4/3) T_{DT}$ $\Sigma \tau + T_{DT} = T_{inv}$	<p>(2) Higher order plus dead time model</p> $T_{DT} = 3/2 \Sigma \tau_n$ $\Sigma \tau + T_{DT} = T_{inv}$ <p>II. Upset causing return toward optimum column separation condition from pinch condition</p> $T_{DT} = 0$ <p>First-order model sufficient</p> <p>(1) Bottoms most affected</p> $\tau = \left[\frac{H_R + H_{oL}}{H_T} \right] T_{inv}$ <p>(2) Tops most affected</p> $\tau = \left[\frac{H_A + H_{oU}}{H_T} \right] T_{inv}$ <p>where H_R is the reboiler hold-up, H_{oL} the hold-up of lower column section less reboiler, H_A the accumulator hold-up, H_{oU} the hold-up of upper column section less accumulator, and H_T the total hold-up.</p>
--	--

Conclusions

As a result of this work the following conclusions can be drawn regarding the responses of large distillation columns giving very high purity products.

(1) The form of the approximate performance functions which will adequately duplicate the response of the real system can be categorized as in Table 6.

(2) The magnitudes of the dead times, and time constants involved in the above models can be estimated according to the rules developed in Table 7 (a) and (b).

(3) The concept of a change of inventory time provides the unifying factor which ties together column response data. Previously such data had appeared to be uncorrelatable by a single concept.

Nomenclature

A Area in square feet. As a subscript, it refers to accumulator

AC Chemical composition analyser controller

a As subscript refers to a specific time in computation of second-order time constant (see Figure 3)

C_p Heat capacity per pound

c As subscript, refers to a single specific time in computation of second-order time constant (see Figure 3)

As subscript, refers to the column

D Distillate product flow rate

As subscript, refers to distillate stream

e Base of Neperian logarithms

DT or T_{DT} Dead time

F Feed flow rate

Any flow rate in general

As subscript, refers to feed stream

FC Flow controller

f As subscript, refers to final or steady-state value

H Hold-up, subscript denotes location

I Input function imposed as an upset

inv Inventory of component in question in column at time indicated by subscript

i As subscript, refers to initial or beginning condition

K Weir flow coefficient in ft.³/min

Proportionality constant or scale factor

L As subscript, refers to lower section of the column

LLC Liquid level controller

n Order of transfer or performance function

As subscript, represents an arbitrary value

O Output response of a process

P Sidestream product flow rate

As subscript, refers to sidestream

PF Performance function

p Differential operator

T Time, usually minutes

As subscript, refers to total

TC Temperature controller

T_{inv} 'Change of inventory' time

U Overall heat transfer coefficient

As subscript, refers to the upper section of the column

V Volume of a vessel in cubic feet

W Bottoms product flow rate

As subscript, refers to bottoms product stream

W_t Weight of heat transfer surface

X Ratio of time constants in a second-order system

x Liquid composition, subscript refers to stream location

y As subscript, refers to column conditions at time just after a step change

ΣT Total of dead time and process time constants of process model

$\Sigma \tau$ Sum of the time constants of a second or higher order performance function

τ_1 Major time constant of a second-order system

τ_2 Minor time constant of a second-order system

τ_{DT} Equivalent process dead time as computed in this study

τ_{FT} Column tray weir flow time constant

τ_{HR} Reboiler heat transfer time constant

τ_{MA} Accumulator mixing time constant

τ_{MR} Reboiler mixing time constant

τ_{MT} Column tray mixing time constant

References

- ¹ ARCHER, D. H. and ROTHFUS, R. R. The dynamics and control of distillation units and other mass transfer equipment. *Chem. Engng Progr. Symp. Ser.* 57, No. 36 (1961) 2-19
- ² ARMSTRONG, W. D. and WILKINSON, W. L. An investigation of the transient response of a distillation column. Pt II: Experimental work and confirmation of theory. *Trans. Inst. chem. Engrs, Lond.* 35 (1957) 352-367
- ³ BABER, M. F., EDWARDS, L. L. JR., HARPER, W. T. JR., WITTE, M. D. and GERSTER, J. A. Experimental transient response of a pilot plant distillation column. *Chem. Engng Progr. Symp. Ser.* 57, No. 36 (1961) 148-159
- ⁴ BERGER, D. E. and CAMPBELL, G. G. Experience in controlling a large separation column with a continuous infrared analyser. *Chem. Engng Progr.* 51 (1955) 348-52
- ⁵ BERGER, D. E. and SHORT, G. R. Sampling and control characteristics of analysis controlled pentane fractionator. *Industr. Engng Chem.* 48 (1956) 1027-30
- ⁶ DAVIDSON, J. F. The transient behaviour of plate distillation columns. *Trans. Instn chem. Engrs, Lond.* 34 (1956) 44-52
- ⁷ ENDTZ, J., JANSSEN, J. M. L. and VERMEULEN, J. C. Measuring dynamic responses of plant units. *Plant and Process Dynamic Characteristics*, pp. 170-200. 1957. London; Butterworths
- ⁸ HOYT, P. R. and STANTON, B. D. Analyzing process control systems. *Petrol. Refin.* 32, No. 10 (1953) 115-119
- ⁹ JACKSON, R. F. and PIGFORD, R. L. Rate of approach to steady state by distillation columns. *Industr. Engng Chem.* 48 (1956) 1020-26
- ¹⁰ LAMB, D. E., PIGFORD, R. L. and RIPPIN, D. W. T. Dynamic characteristics and analogue simulation of distillation columns. *Chem. Engng Progr. Symp. Ser.* 57, No. 36 (1961) 132-147
- ¹¹ OLDENBOURG R. C. and SARTORIUS, H. *The Dynamics of Automatic Control*, pp. 99-157. 1948. New York; Amer. Soc. mech. Engrs
- ¹² RADEMACHER, O. and RIJNSDORP, J. E. Dynamics and control of continuous distillation columns. *Proc World Petrol. 5th Congr.*, May 1959, Paper 5 Sec. VII
- ¹³ RIJNSDORP, J. E. and MAARLEVELD, A. Use of electrical analogues in the study of the dynamic behaviour and control of distillation columns. *Symposium on Instrumentation and Computation in Process Development and Plant Design*, May 1959, Instn chem. Engrs, Lond., pp. A63 ff.
- ¹⁴ ROSE, A. and WILLIAMS, T. J. Automatic control in continuous distillation. *Industr. Engng Chem.* 47 (1955) 2284-89
- ¹⁵ ROSE, A., JOHNSON, C. L. and WILLIAMS, T. J. Transients and equilibration time on continuous distillation. *Industr. Engng Chem.* 48 (1956) 1173-79
- ¹⁶ ROSENBRACK, H. H. An investigation of the transient response of a distillation column. Pt I: Solution of the equations. *Trans. Instn chem. Engrs, Lond.* 35 (1957) 347-351
- ¹⁷ ROSENBRACK, H. H. Calculation of the transient behaviour of distillation columns. *Brit. chem. Engng* 3 (1958) 364-367, 432-435, 491-494
- ¹⁸ ROSENBRACK, H. H., TAVENDALE, A. B., STOREY, C. and CHALLIS, J. A. Transient behaviour of multicomponent distillation columns. *Preprints of Papers, International Federation of Automatic Control Congress, Moscow*, 27 June-7 July, pp. 1277-82. 1960. London; Butterworths
- ¹⁹ SMITH, O. J. M. A controller to overcome dead time. *ISA Journal* 6, No. 2 (1959) 28-33
- ²⁰ VOETTER, H. Response of concentrations in a distillation column to disturbances in the feed composition. *Plant and Process Dynamic Characteristics*, pp. 73-100. 1957. London; Butterworths
- ²¹ WILKINSON, W. L. and ARMSTRONG, W. D. An investigation of the transient response of a distillation column. *Plant and Process Dynamic Characteristics*, pp. 56-72. 1957. London; Butterworths
- ²² WILKINSON, W. L. and ARMSTRONG, W. D. An approximate method of predicting composition response of a fractionating column. *Chem. Engng Sci.* 7 (1957), 1-7
- ²³ WILLIAMS, T. J. Instrumentation and control of distillation columns. *Industr. Engng Chem.* 50 (1958) 1214-22
- ²⁴ WILLIAMS, T. J., and HARNETT, R. T. Automatic control in continuous distillation. *Chem. Engng Progr.* 53 (1957) 220-25
- ²⁵ WILLIAMS, T. J., HARNETT, R. T. and ROSE, A. Automatic control in continuous distillation. *Industr. Engng Chem.* 48 (1956) 1008-19

DISCUSSION

J. GROENHOF, *Bataafsche Internationale Chemie Maatschappij, Den Haag, The Netherlands*

The authors present calculated responses of various column conditions, in particular of the compositions of product streams to some well-defined disturbances. They express these responses in terms of 'dead time' and a number of 'time constants'.

Some time ago we carried out some experiments on an actual distillation column, amongst other things giving a disturbance in the reboiler heating—a similar case to that treated by the authors. The responses were similar to the results obtained by the authors, but we concluded that the shape of the response curve had to be attributed to non-linear behaviour instead of to time lags.

Support for this opinion can be found in the paper, where it is shown that the 'time constants' are halved when the amplitude of the disturbance is doubled.

We believe that the response of the column is basically a first-order response (apart from some transients during the first few minutes). The observed dead time is to be explained by the coefficient being substantially zero.

In fact the authors do find this first-order response when returning from the non-equilibrium state to the equilibrium state. The value of

the time constant found for this case is about equal to the sum of the time lags for the case of going from the equilibrium to the non-equilibrium state.

This total time lag is indeed characteristic of the process and the correlation with the change of inventory time is interesting.

J. E. RIJNSDORP, *Koninklijke/Shell-Laboratorium, Amsterdam, The Netherlands*

(1) Have the authors assumed that hold-ups remain constant throughout the transients?

(2) If the hold-ups are constant, the product flow rates would respond without delay. Then the expression for the 'change of inventory time' T_{inv} , given in the paper can be put in an exact form. This requires defining T_{inv} as the weighted sum of the average delays of the distillate and the bottom product compositions T_{xD} and T_{xW} respectively:

$$T_{inv} = \frac{D_v(x_{Df} - x_{Di})T_{xD} + W_v(x_{Wf} - x_{Wi})T_{xW}}{D_v(x_{Df} - x_{Di}) + W_v(x_{Wf} - x_{Wi})} \quad (1)$$

where $D_f = D_v$ and $W_f = W_v$ (steps),

$$T_{xD} = \frac{\int_i^f [x_{Df} - x_D^{(t)}] dt}{x_{Df} - x_{Di}} \quad (2a)$$

$$T_{xW} = \frac{\int_i^f [x_{Wf} - x_W^{(t)}] dt}{x_{Wf} - x_{Wi}} \quad (2b)$$

Formula (1) can be derived from the overall partial mass balance of the column (see 5).

(3) For most of the examples given in Table 4 of the paper, one of the weighting factors in formula (1) is very small. Hence

$$T_{inv} \approx T_{xD} \quad \text{or} \quad T_{xW} \quad (3)$$

If now the corresponding composition response is approximated by a series of lags, it is well known that the sum of these lags is equal to T_{xD} or T_{xW} respectively. Does not this explain the good fit shown in Table 7 (a) of the paper? I expect the fit to be almost ideal when formulae (1) and (2) are applied to the calculated responses.

(4) For columns without sidestreams, and with pinches at the ends, the response to small step disturbances is slower than to large step disturbances. This conclusion can be drawn from a modified form of the expression for T_{inv} given in the paper:

Substitute the initial and the final steady-state equations

$$F_i x_{Fi} = D_i x_{Di} + W_i x_{Wi} \quad (4)$$

$$F_f x_{Ff} = D_f x_{Df} + W_f x_{Wf} \quad (5)$$

into the denominator:

$$T_{inv} = \frac{\sum_{n=0}^{N+1} H_n (x_{nf} - x_{ni})}{D_v (x_{Df} - x_{Di}) + W_v (x_{Wf} - x_{Wi})} \quad (6)$$

where $n = 0$ refers to the reboiler and the bottom, $n = N + 1$ refers to the condenser and the accumulator, and N is the number of trays.

If the variations of the compositions would be the same throughout the column, (6) is simplified to:

$$T_{inv} = \frac{\sum_{n=0}^{N+1} H_w}{D_v + W_v} = \frac{\sum_{n=0}^{N+1} H_w}{F_v} = T_{res} \quad (7)$$

which is the average residence time of the feed material in the column.

Actually, for small disturbances, the composition variations on intermediate trays are usually much larger than at the ends. Consequently many of the H_n in the numerator of (6) are multiplied by large factors, hence

$$T_{inv} \gg T_{res} \quad (8)$$

This explains the slow responses reported in the literature for linear behaviour.

On the other hand, for large disturbances, the top and/or the bottom composition also has a large response (see e.g. Table 4 of the paper). Hence the denominator of (6) is small, and T_{inv} may approach T_{res} .

(5) When the hold-ups depend on the flow rates and *vice versa*, a more general expression for T_{inv} can be derived in the following way:

The partial mass balance of the column after application of the step change has the form:

$$F_v x_{Fv} - D(t) x_D(t) - W(t) x_W(t) = \sum_n \frac{d}{dt} [H_n(t) x_n(t)] \quad (9)$$

At the final equilibrium we have:

$$F_v x_{Fv} - D_f x_{Df} - W_f x_{Wf} = 0 \quad (10)$$

Subtraction of (10) from (9) yields:

$$\begin{aligned} & D_f [x_{Df} - x_D(t)] + W_f [x_{Wf} - x_W(t)] \\ &= \sum_n \frac{d}{dt} [H_n(t) x_n(t)] - [D_f - D(t)] x_D(t) - [W_f - W(t)] x_W(t) \end{aligned} \quad (11)$$

When the responses of flows and hold-ups are fast compared to those of the compositions, $x_D(t)$ and $x_W(t)$ in the last terms of (11) can be approximated by x_{Di} and x_{Wi} .

Then integration of (11) between the initial and the final steady state yields:

$$\begin{aligned} & D_f [x_{Df} - x_{Di}] T_{xD} + W_f [x_{Wf} - x_{Wi}] T_{xW} \\ & \approx \sum_n [H_{nf} x_{nf} - H_{ni} x_{ni}] - (D_f - D_i) x_{Di} T_D - (W_f - W_i) x_{Wi} T_W \end{aligned} \quad (12)$$

where T_{xD} and T_{xW} are given by (2a and 2b),

$$T_D = \frac{\int_i^f [D_f - D(t)] dt}{D_f - D_i} \quad (13a)$$

$$T_W = \frac{\int_i^f [W_f - W(t)] dt}{W_f - W_i} \quad (13b)$$

T_D and T_W can be estimated from the relationship between hold-ups and flow rates.

Formula (12) can easily be transformed into (1) and (6), with additional correction terms for the influence of T_D and T_W and with the subscript v replaced by i .

Reference

GILLILAND and MOHR. *Chem. Engng Progr.* 58 (1962) 59

B. STEPLEWSKI, *Research Centre for Automatic Control in the Chemical Industry, Warsaw, Poland*

(1) In cases of sidestream upsets the magnitudes of distillate composition responses were 1,500 times greater for increasing upset than for decreasing one. So the performance functions were approximated in quite different ranges of output variables. Two questions refer to this problem:

(a) Do the different shapes of transient functions (first order compared to fourth order with dead time) depend on the different ranges of output variables?

(b) Have you estimated the static characteristics around the base rate, in the same ranges of output variables, both up and down? If yes, what are the results

(2) What is the physical explanation of the hysteresis effect (change of type of performance function), which takes place in cases 49 A and 60 A?

It seems that non-linearities in the column described are due to non-linearity of vapour-liquid equilibrium coefficients, but they show no hysteresis. Both cases deal with the same part of the static characteristics as in the cases 81 A and 83 A. The change of performance function type seems not to be caused by the same reason as in cases of sidestream rate upsets (47 A, 49 A, 79 A, 81 A).

J. S. MOCZEK, R. E. OTTO and T. J. WILLIAMS, *in reply*

We thank Mr. Groenhof for mentioning his experimental results which tend to confirm our calculated responses. We are pleased to learn that he observed the same effect of upset size upon time constant length. These effects are indeed the result of a non-linear behaviour. However, we chose to express them as time lags in our approximation models. We cannot agree that the column response is basically first order. We did obtain such responses for some very special cases but these are far from characteristic of the responses of this column. Also their occurrence can be predicted from the rules we postulated in our paper.

We would like to respond to each of Mr. Rijnsdorp's questions and statements in turn.

(1) The following assumptions were made in performing our distillation column calculations:

- (a) Constant hold-up.
- (b) Perfectly efficient trays (in the actual computation).
- (c) Complete mixing on each tray.

However, it should be pointed out that we did not make many of the simplifying assumptions which are commonly made in calculations such as these. Some which we did not make are:

- (a) Constant partial molal enthalpies and equilibrium constants with temperature.
- (b) Binary mixtures (actually five components were calculated).
- (c) Equal molal enthalpies.

(2) Mr. Rijnsdorp has made a significant observation in his second comment. The importance of eqns (1), (2a), and (2b) of his discussion lies in the fact that the characteristic response time of a distillation column may be calculated solely from a knowledge of the initial and final steady states of the column independently of any non-linear calculations as are required in the exact computation of the transient. It is interesting to note that the right-hand sides of eqns (2a) and (2b) are also equal to the sum of the time constants of the approximation model if the approximation response, $x^*(t)$, replaces the actual response, $x(t)$, in the integrals. It is logical, therefore, to adjust the sum of the approximation model time constants in order to exactly satisfy eqn (1). We must conclude that the errors shown in *Table 7a* are due solely to our method of fitting the approximation model to the actual transient.

(3) It is true that in all of the cases reported, except the reboiler duty disturbances, the weighing factor of one of the responses, either the tops or bottoms composition, was negligibly small. Therefore, the good fit shown in *Table 7a* is achieved because the linear approximation response selected and described in the paper almost satisfied eqns (2a) and (2b). There is no theoretical reason why our method of

selecting time constants should have given an exact agreement since the 60 per cent point is itself an approximation.

(4) For all the cases reported the residence time of feed in the column is 46 min. Notice that in case 49 A (*Table 7a*) the inventory time is actually below the feed residence time. It should be noted that not only may T_{inv} approach T_{res} but that it may be even smaller.

(5) We thank Mr. Rijnsdorp for his amplification of the T_{inv} expression to cover the non-constant hold-up case as described in his Point 5. We have not had an opportunity to verify its validity in this work.

Replying to Mr. Steplewski's questions in turn:

(1a) The reason for the wide variations in the composition changes in the plus and minus directions is that the maximum composition variation in one direction was sharply limited to the composition range between the base case and a pure component stream. In the other direction no such limitation existed. As reported in the paper, equal increments of the input variables were chosen for the study of the dynamic and static characteristics of the column. For these cases the shape of the transient functions did not depend on the range of input variables.

(1b) On the other hand if one had chosen to study the column characteristic over equal ranges of the output variables then the same problem of unequal changes in the input variables would have occurred. For example, in order to study a movement of the output variables equivalent but in the opposite direction to case 47 A, *Table 4*, the sidestream rate would have to be set at 100.0136 per cent of the base rate. This would have resulted in a variation of 1,800 in the range of movement of the input variables. We have tried some of these cases where the input variables were varied only a small amount but the response time was so long that it was considered impractical to carry out the complete transient in the computer.

(2) In response to Mr. Steplewski's second question, we would like to refer him to the physical explanation of the hysteresis effect as advanced by Mr. Groenhof in the verbal discussion of this paper. When the column is unbalanced the steady state change in composition from plate to plate on one end of the column is large. Conversely when the column is balanced the steady state plate-to-plate composition change on both ends of the column is small. If one envisions the transient then as a movement of the composition profile up and down the column, one would expect an initially slow change in composition when proceeding from a balanced condition to an unbalanced one. On the other hand, when the transient proceeds in the opposite direction the rapid plate-to-plate change in composition would cause an initially rapid change in composition. Therefore, the approximation model for the former case would be high order with dead time whereas the latter case would approximate a first-order response.

A Study on the Dynamic Behaviour of a Catalytic Cracker Power-recovery System by Means of an Analogue Computer

C. A. J. M. VAN DER HEYDEN and A. G. VAN NES

Summary

The power which is available in the flue gas of the regenerator of a catalytic cracker in an oil refinery can be utilized by passing it through turbines which in their turn drive compressors for the delivery of combustion air to the regenerator.

A specific system incorporating a CO boiler is described. It is shown that in this system a number of closed loops can be distinguished to which three control loops have to be added. For this reason, the dynamic behaviour becomes complicated and can only be studied by means of computing equipment.

An analogue simulation of the system was designed, incorporating such equipment as turbines, compressors, catalytic cracker regenerator, CO boiler, etc.

The design of the simulation of each of these building blocks and the way in which they have been put together is described. It is shown that for some of the analogue models the design necessarily depends on the type of study to be carried out on the computer.

The programme of work is presented and some of the results worked out in detail.

Sommaire

La puissance disponible dans le gaz de chauffe du régénérateur d'un cracker catalytique dans une raffinerie peut être utilisée pour actionner des turbines. Ces dernières, à leur tour, entraînent des compresseurs pour fournir de l'air de combustion au régénérateur.

Dans ce rapport, on décrit un tel système comprenant en plus une chaudière à CO. Il existe dans un tel système un grand nombre de boucles fermées, en plus de trois chaînes de commandes distinctes. Le comportement dynamique de l'ensemble devient très complexe et il ne peut être étudié qu'avec des calculateurs.

On a effectué une simulation analogique des éléments: turbines, compresseurs, cracker catalytique, régénérateur, chaudière à CO, etc. On décrit la construction et l'assemblage des différents modules. On montre que la construction de certains des modèles analogiques dépend nécessairement du type d'étude entreprise.

On présente le programme de travail et les détails de certains résultats obtenus.

Zusammenfassung

Die im Regeneratorabgas der katalytischen Krackanlage einer Erdölraffinerie befindliche Energie läßt sich ausnutzen, indem man die Abgase durch Turbinen leitet, die Verdichter antreiben, welche die Verbrennungsluft dem Regenerator zuführen.

Hier wird ein spezielles System beschrieben, das einen kohlenoxyd-befeuerten Kessel enthält. Es zeigt sich, daß in diesem System eine Anzahl von Kreisläufen unterscheidbar sind, die drei Regelkreise erfordern; das sich daraus ergebende komplizierte dynamische Verhalten kann nur mit Hilfe von Rechengertäten untersucht werden.

Die entworfene Simulation am Analogrechner schließt die Anlagenbestandteile wie Turbinen, Verdichter, Regenerator, Krackanlage, kohlenoxyd-befeuerte Kessel usw. mit ein.

Die Simulation jedes dieser Anlagenbestandteile und die Art der Zusammenschaltung werden beschrieben. Es zeigt sich, daß die Struktur einiger dieser Analogmodelle notwendigerweise von der Art der Untersuchung am Rechner abhängt.

Es werden die Arbeitsweise betrachtet und einige Ergebnisse ausführlich ausgearbeitet.

Introduction

At Shell Development in the United States, a system was developed to utilize the power available in the flue gas of the regenerator of a catalytic cracking unit*. This idea was tested on a small scale at the Montreal refinery.

In designing a full-scale power-recovery system for a catalytic cracking unit it was felt necessary to study its dynamic behaviour in order to establish the effectiveness of the designed control and safety system.

Because the problem was too large to handle in the ordinary way on paper, an electric model was composed on an analogue computer.

Description of the Power-recovery System

In the regenerator of a catalytic cracking unit the coke on the catalyst is burned to CO by means of air. The CO gas is routed to a CO boiler (*Figure 1*) in which the CO is burned. The heat produced is utilized for steam production. The gases leaving the CO boiler drive turbines and escape into the air via an economizer, which preheats the boiler feed water. The turbines in their turn drive compressors which deliver air to the regenerator of the catalytic cracking unit and air for the combustion of the CO in the CO boiler.

The best control system resulting from a study of the steady state of the system consists of a pressure controller on the regenerator which acts on a control valve in the by-pass of the turbines; a flow controller in the air supply to the regenerator which acts on a control valve in the by-pass of the regenerator; a temperature controller for the gas at the inlet of the turbines which acts on a control valve in the fuel supply line to the burner in the bottom of the CO boiler, and a ratio flow controller between fuel and air supply to this bottom burner which acts on a damper in the air supply line of this burner.

Factors Leading to a Simulation Study

A dynamic study of the system described above was required to establish (a) the stability of the system, and (b) the behaviour of the system during emergency cases. A requirement of the system had to be that certain equipment failures which have to be reckoned with, must not result in a shut-down of the catalytic cracking unit.

In the power-recovery system several closed loops are incorporated. The first loop can be distinguished from the regenerator air compressors via regenerator and CO boiler and closing at the turbines driving the regenerator air compressors. The second loop consists of the combustion air compressors via the CO boiler and closing at the turbines driving the combustion air compressors. Three additional closed loops are

* *Oil Gas J.*, 57, No. 17 (1959) 94-100

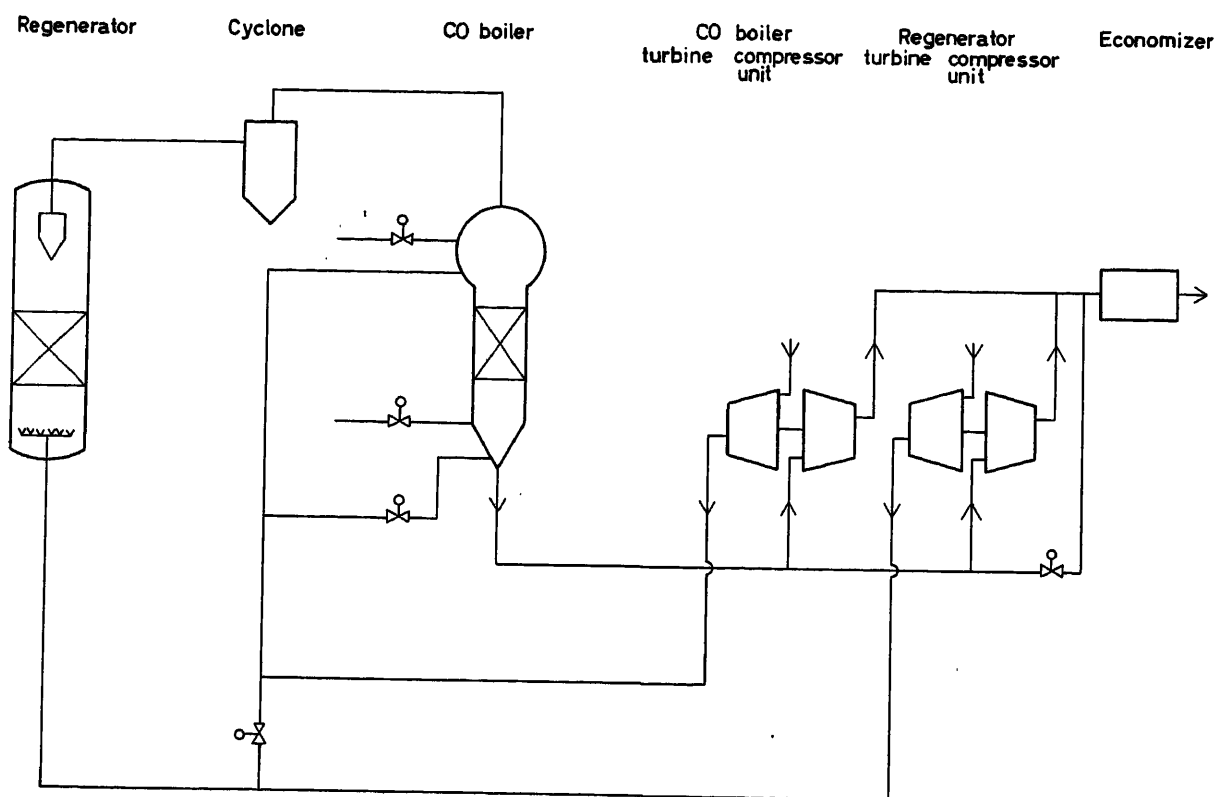


Figure 1

required for the control system. These closed loops make a study of the dynamic behaviour impracticable on paper. For that reason, a simulation study was proposed.

The Scope of Work

Before the electric model was designed, a preliminary study was made of the requirements for the model.

Six groups of computer runs could be distinguished:

(1) Stability runs at the design operating point. The reason for these runs was to determine whether the proposed control scheme was adequate and, if not, to test alternative control schemes on the electric model.

(2) Stability runs at off-design operating points. The reason for these runs was to test the control system with various numbers of turbine compressor units in operation.

The operating limits for a certain number of turbine compressor units in operation are determined by the following requirements: (a) the gas temperature at the inlet of the turbines must not exceed a certain value; (b) the following emergencies must not cause the shut-down of the entire catalytic cracking unit: (i) breakdown of one turbine compressor unit; (ii) failure of the fuel supply to the CO boiler.

In view of the foregoing, the following runs had to be made:

(3) Runs with maximum gas temperature at the inlet of the turbines for various numbers of turbine compressor units in operation.

(4) Runs to establish the amount of fuel which can be fed to the CO boiler without the danger of a complete shut-down if one of the turbine compressor units were to break down.

(5) Runs to establish the amount of fuel which can be supplied from an independent source without the danger of a complete shut-down if the fuel supply from the primary source were to fail.

In order to test the starting up and shutting down of the unit, the following run was made:

(6) Run to test the starting up and shutting down procedure.

Design of the Electrical Model

In this section, the design of the electrical model is given. Although some simplifications had to be made in view of the size of the available analogue computer*, it is expected that this representation is a sufficiently true picture of the actual plant.

A simplified flow scheme of the unit is given in Figure 2. From this scheme it can be seen that the system consists of a combination of various building blocks which, if put together in the correct way (see Figure 5), form the system of Figure 2.

The following building blocks can be distinguished (parameters which are not mentioned are assumed to be constant):

- R Resistance—in which two pressures and, if necessary, a temperature determine the flow through the resistance
- V Volume—in which two flows and, if necessary, a temperature determine the pressure in the volume
- R_c Resistance of the catalyst bed which behaves differently from a fixed resistance—here, also, two pressures determine the flow through the resistance

* PACE analogue computer of Koninklijke/Shell Laboratory, Amsterdam, consisting of 160 operational amplifiers plus auxiliary equipment.

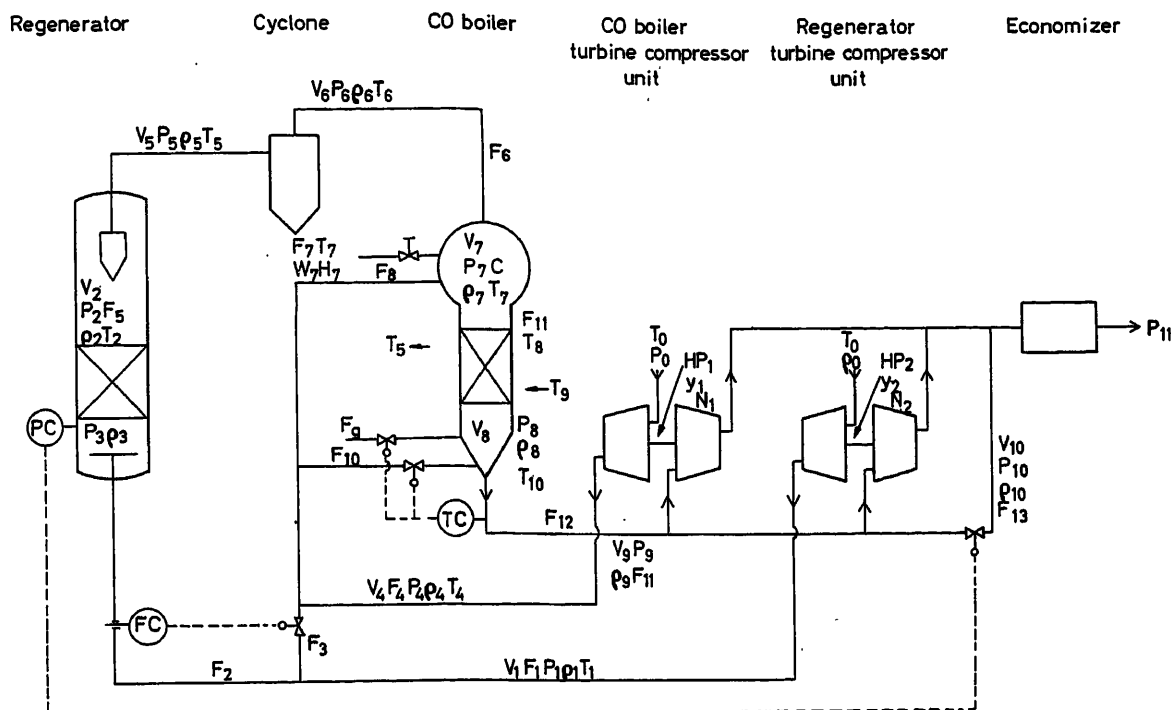


Figure 2

- C_v* Control valve, which is a variable resistance—again, two pressures, the position of the valve and, if necessary, a temperature determine the flow through the control valve
- D* The dynamic relationship between the temperature of a gas in a volume and the temperature of the incoming gas
- M* Mixing stage—in which incoming flows with their temperatures and, if necessary, their calorific value determine the resultant temperature of the outgoing flow
- B* Boiler—in which the temperature and flow rate of the incoming gas determines the temperature of the outgoing gas
- T* Turbine—in which upstream and downstream pressure and temperature of the incoming gas and the number of revolutions per minute determine shaft horsepower and gas throughput
- C* Compressor—in which shaft horse-power and gas throughput determine downstream pressure and number of revolutions per minute
- XC* Controller—in which the difference between measured and desired value determines the output of the controller
- E* Emergency valve—in which at the command of an alarm signal a flow will gradually fall to zero or gradually rise to its maximum value
- RT* Regenerator temperature—in which the temperature of the regenerator gradually decreases after the circulation of the catalyst has been stopped

Flow variations travel in a completely different fashion and at a completely different speed from temperature variations; therefore, it can be assumed that the latter follow an independent path, although they influence the flow variations and are themselves influenced by them at some points.

In Figure 3 are shown the building blocks of the system for flow variations. Figure 4 shows the equivalent for temperature variations.

All variables which appear in the equations have been made

dimensionless by dividing them by their design value. This means that, at normal operation, all signals are equal to 1 which ensures that no signals fall outside the range of the computer as long as one relates the value 1 to 5 V (voltage range of the computer 0–100 V).

All the building blocks of the model cannot be described in detail because it would lead to an enormous expansion of this paper. An exception will be made in the case of the circuit of the resistance, in order to illustrate the dependence of the circuits on the type of study to be made with the model, and in the case of the circuit of the turbine compressor unit.

The Circuit Used for Resistances

The equation of gas flow through a resistance can be written as follows:

$$F = C \left(\frac{p_u - p_d}{T} \cdot p_u \right)^{\frac{1}{2}}$$

or, in its reduced form,

$$\begin{aligned} \frac{F}{F_0} &= \left(\frac{p_u - p_d}{p_{u0} - p_{d0}} \cdot \frac{T_0}{T} \cdot \frac{p_u}{p_{u0}} \right)^{\frac{1}{2}} \\ &= \left(\frac{p_u}{p_{u0}} \cdot \frac{T_0}{T} \left[\frac{p_{u0}}{p_{u0} - p_{d0}} \cdot \frac{p_u}{p_{u0}} - \frac{p_{d0}}{p_{u0} - p_{d0}} \cdot \frac{p_d}{p_{d0}} \right] \right)^{\frac{1}{2}} \end{aligned} \quad (1)$$

The circuit which performs this calculation is shown in Figure 6.

The potentiometers should be adjusted as follows:

$$\begin{aligned} P1 &= 0.5 \\ P36 &= \frac{p_{u0}}{p_{u0} - p_{d0}} \cdot \frac{1}{100} \\ P37 &= \frac{p_{d0}}{p_{u0} - p_{d0}} \cdot \frac{1}{100} \end{aligned}$$

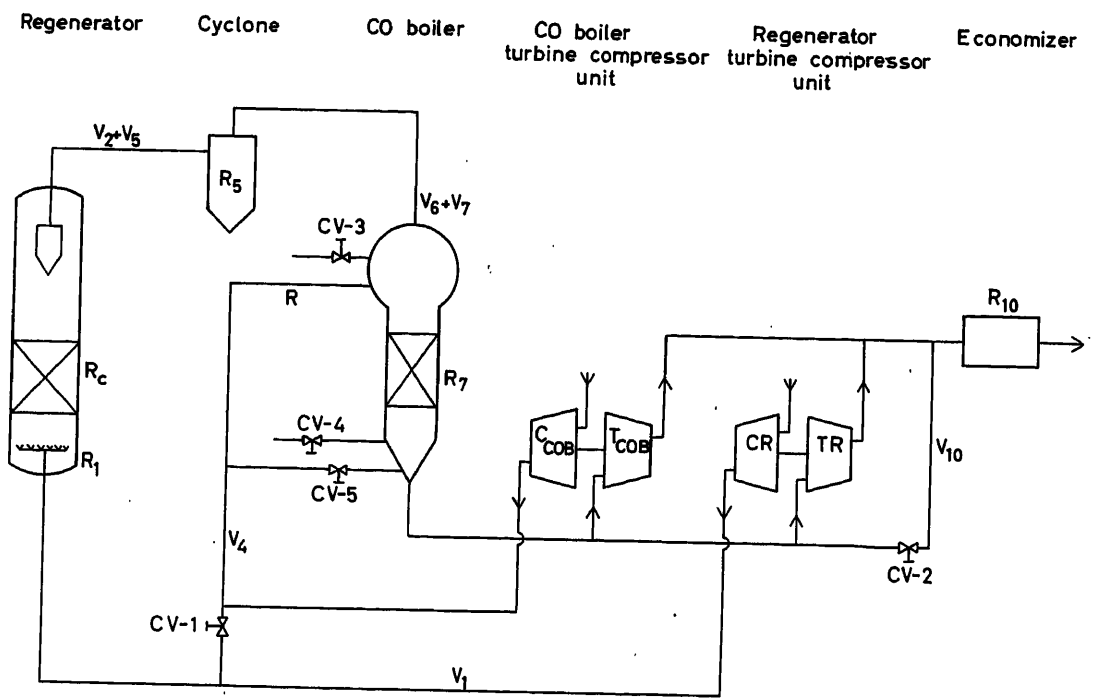


Figure 3

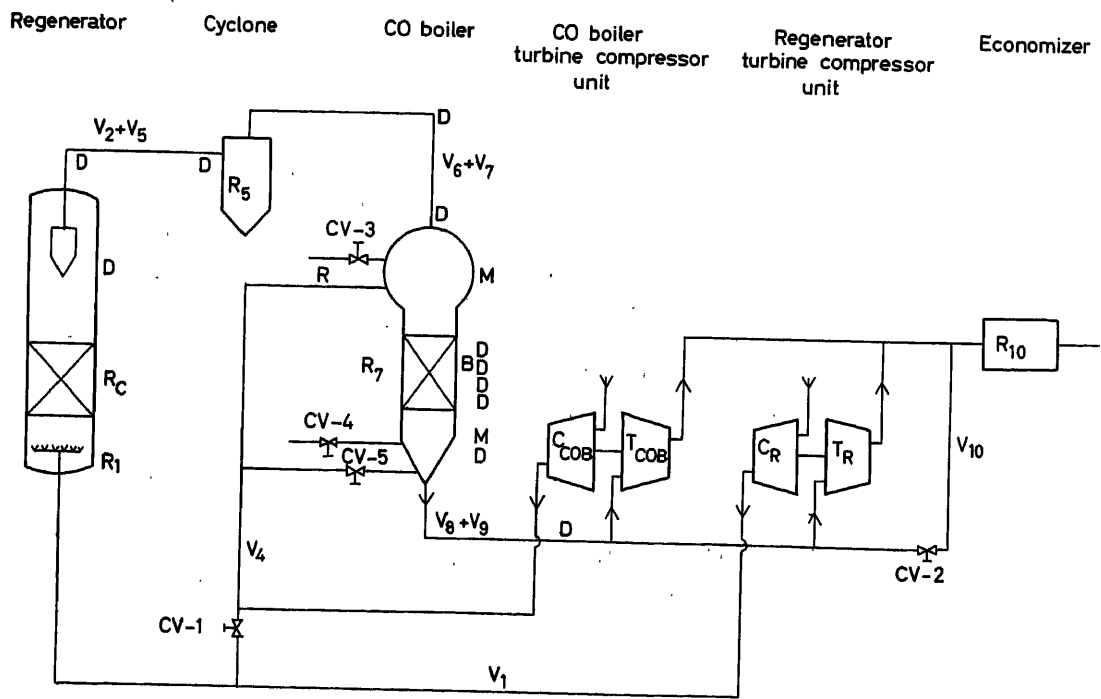


Figure 4

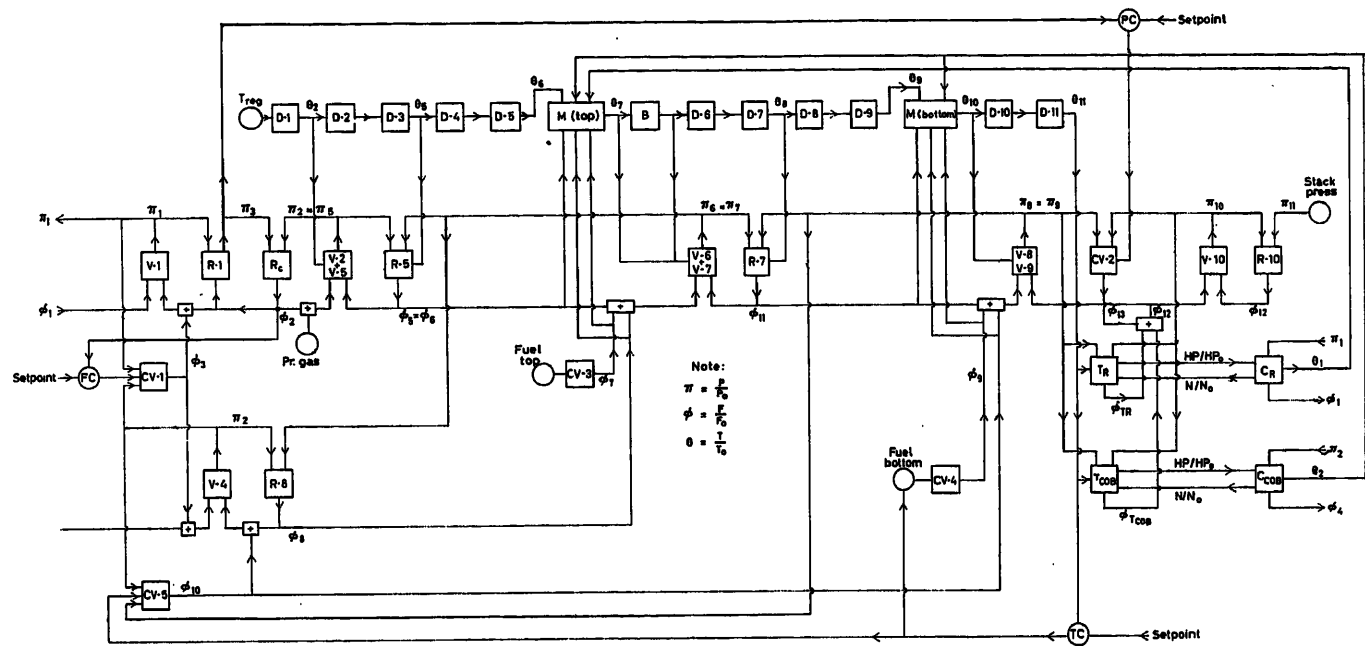


Figure 5

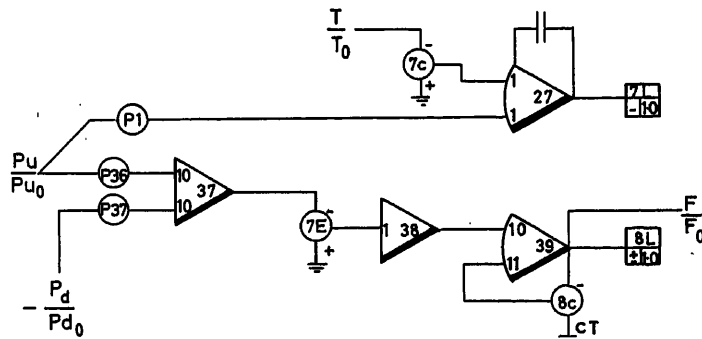


Figure 6

If it is only the stability of the model at the operating point which has to be studied, the circuit of the resistance can be simplified by linearization of the quadratic equation at the operating point, which gives the following result:

$$\frac{F}{F_0} = \frac{1}{2} \left[1 + \frac{P_u}{P_{u0}} \frac{T}{T_0} + \frac{P_{u0}}{P_{u0} - P_{d0}} \frac{P_u}{P_{u0}} - \frac{P_{d0}}{P_{d0} - P_{d0}} \frac{P_d}{P_{d0}} \right] \quad (2)$$

The circuit which performs this calculation is shown in Figure 7.

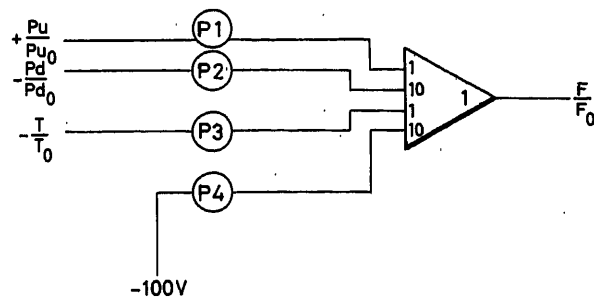


Figure 7

The potentiometers should be adjusted as follows:

$$P1 = \frac{1}{20} \left(1 + \frac{P_{u0}}{P_{u0} - P_{d0}} \right)$$

$$P2 = \frac{1}{20} \frac{P_{d0}}{P_{u0} - P_{d0}}$$

$$P3 = 0.5$$

$$P4 = 0.25$$

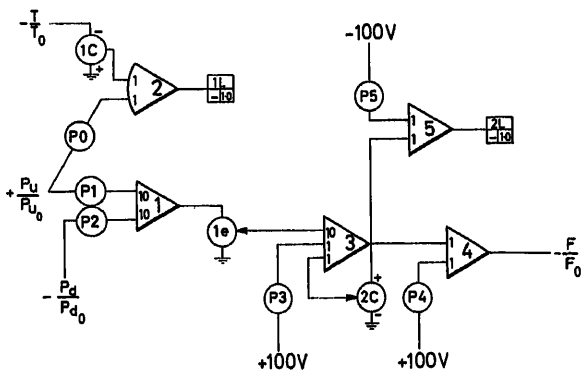


Figure 8

If the start-up and shut-down procedures have to be studied, the circuit must allow for zero voltages. If the circuit of Figure 6 is used, the output of high-gain amplifier 39 has to become zero, the result being no feedback and thus an unstable system. In order to use nearly the same circuit, but with a positive feedback, the circuit of Figure 8 was chosen. Use is made in this circuit of the equation:

$$\left[\left(\frac{F}{F_0} \right)^2 - a^2 \right] = \left(\frac{F}{F_0} + a \right) \times \left(\frac{F}{F_0} - a \right)$$

in which a is a factor that can be chosen freely. In this case, which in its reduced form is a is chosen at 0.5.

The potentiometers should be adjusted as follows:

$$P0 = 0.5$$

$$P1 = \frac{p_{u0}}{p_{u0} - p_{d0}} \cdot \frac{1}{100}$$

$$P2 = \frac{p_{d0}}{p_{u0} - p_{d0}} \cdot \frac{1}{100}$$

$$P3 = 0.0625$$

$$P4 = 0.2500$$

$$P5 = 0.5000$$

The Circuit Used for the Turbines

The mass flow through the turbine is calculated in the same manner as for a restriction, thus:

$$\frac{F}{F_0} = \sqrt{\frac{p_u}{p_{u0}} \left[\frac{p_{u0}}{p_{u0} - p_{d0}} \cdot \frac{p_u}{p_{u0}} - \frac{p_{d0}}{p_{u0} - p_{d0}} \cdot \frac{p_d}{p_{d0}} \right] \cdot \frac{T_0}{T}} \quad (2)$$

The shaft horse-power can be found as the product of efficiency, gas flow rate and difference in enthalpy of the in- and outgoing gas flow. The equation for the isentropic enthalpy difference can be written as follows:

$$\Delta H = C.T. \left[1 - \left(\frac{p_u}{p_d} \right)^{1-k/k} \right]$$

$$\frac{\Delta H}{\Delta H_0} = \frac{T}{T_0} \cdot \frac{1 - \left(\frac{p_{u0}}{p_{d0}} \right)^{1-k/k} \cdot \left(\frac{p_u}{p_{u0}} \cdot \frac{p_{d0}}{p_d} \right)^{1-k/k}}{1 - \left(\frac{p_{u0}}{p_{d0}} \right)^{1-k/k}} \quad (3)$$

The efficiency as specified by the manufacturer is a function of the square root of the enthalpy difference divided by the number of revolutions, thus:

$$\eta T = f \left[\frac{(\Delta H)^{\frac{1}{2}}}{N} \right]$$

which in its reduced form is:

$$\frac{\eta T}{\eta T_0} = f \left[\frac{\left(\frac{\Delta H}{\Delta H_0} \right)^{\frac{1}{2}}}{\frac{N}{N_0}} \right] \quad (4)$$

The shaft horse-power can be found from:

$$HP_T = \eta T \cdot F \cdot \Delta H$$

which in its reduced form is:

$$\frac{HP_T}{HP_0} = \frac{\eta T}{\eta T_0} \cdot \frac{F}{F_0} \cdot \frac{\Delta H}{\Delta H_0} \quad (5)$$

The circuit which performs these calculations is shown in Figure 9.

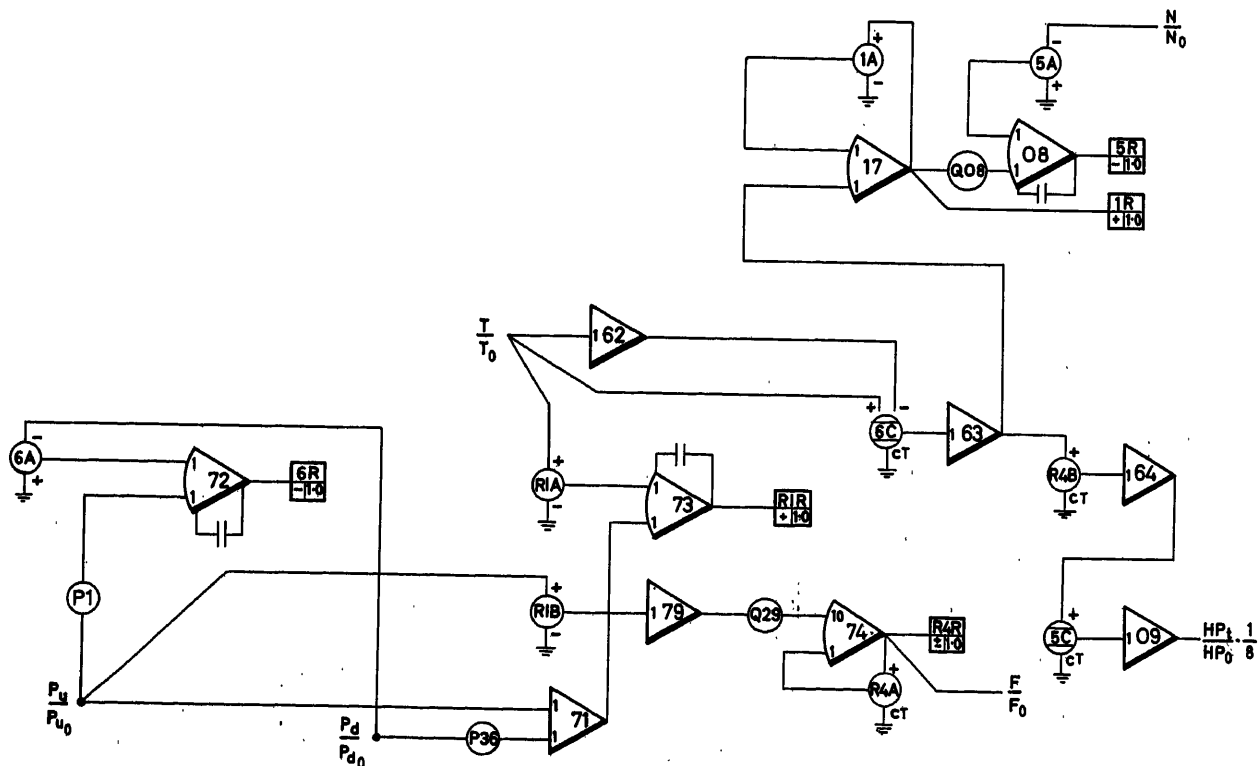


Figure 9

The potentiometers should be adjusted as follows:

$$P1 = 0.5$$

$$P36 = \frac{p_{d0}}{p_{u0}}$$

$$Q29 = \frac{p_{u0}}{p_{u0} - p_{d0}} \cdot \frac{1}{2}$$

$$Q08 = 0.5$$

The function

$$\frac{1 - \left(\frac{p_{u0}}{p_{d0}}\right)^{1-k/k} \cdot \left(\frac{p_u}{p_{u0}} \frac{p_d}{p_{d0}}\right)^{1-k/k}}{1 - \left(\frac{p_{u0}}{p_{d0}}\right)^{1-k/k}} = f \left[\frac{p_u}{p_{u0}} \frac{p_d}{p_{d0}} \right]$$

is made on cup 6C. The function

$$f \left[\left(\frac{\Delta H}{\Delta H_0} \right)^{\frac{1}{2}} \int \frac{N}{N_0} \right]$$

is made on cup 5C.

Because the larger part of the calculation is common to both turbines driving boiler compressors and turbines driving regenerator compressors, a separate circuit is only required for the part.

$$f \left[\left(\frac{\Delta H}{\Delta H_0} \right)^{\frac{1}{2}} \int \frac{N}{N_0} \right] \text{ and } HP_T/HP_0$$

The Circuit Used for the Compressors

The shaft horse-power required by the compressor can be calculated as the difference in enthalpy of the in- and outgoing gas flow multiplied by the gas flow and divided by the efficiency of the compressor.

The difference in enthalpy can be written as:

$$\Delta H = C \cdot T \cdot \left[\left(\frac{p_d}{p_u} \right)^{k-1/k} - 1 \right]$$

Since the inlet temperature and pressure are assumed to be constant, this equation can be rewritten as:

$$\Delta H = C^1 \left[\left(\frac{p_d}{p_{u0}} \right)^{k-1/k} - 1 \right]$$

which in its reduced form is:

$$\frac{\Delta H}{\Delta H_0} = \frac{\left(\frac{p_{d0}}{p_{u0}} \right)^{k-1/k} \left(\frac{p_d}{p_{d0}} \right)^{k-1/k} - 1}{\left(\frac{p_{d0}}{p_{u0}} \right)^{k-1/k} - 1} \quad (6)$$

The efficiency as specified by the manufacturer is a function of the compressor flow divided by the number of revolutions:

$$\eta C = f(F/N)$$

which in its reduced form, is:

$$\frac{\eta C}{\eta C_0} = f \left(\frac{F}{F_0} \int \frac{N}{N_0} \right) \quad (7)$$

The required horse-power can be found from:

$$HP_C = \frac{F \cdot \Delta H}{\eta C}$$

which in its reduced form is:

$$\frac{HP_C}{HP_0} = \frac{F}{F_0} \cdot \frac{\Delta H}{\Delta H_0} \cdot \frac{\eta C_0}{\eta C} \quad (8)$$

The difference between the horse-power delivered by the turbine and the horse-power required by the compressor is used to accelerate or decelerate the machine in the following way:

$$\int (HP_T - HP_C) dt = \frac{1}{2} I \cdot \omega^2 = \frac{1}{2} I (2\pi N)^2$$

or, in its reduced form:

$$\frac{1}{2\pi^2 I} \frac{HP_0}{N_0^2} \int \left(\frac{HP_T}{HP_0} - \frac{HP_C}{HP_0} \right) dt = \frac{N^2}{N_0^2} \quad (9)$$

The relation between flow through the compressor and downstream pressure, with the number of revolutions as a parameter, is supplied by the manufacturer. Because the molecular weight of the air to be compressed can be assumed to be constant, the compressor can be described as follows:

$$\frac{\left(\frac{p_d}{p_u} \right)^{k-1/k} - 1}{N^2} = f \left(\frac{F}{N} \right)$$

or, in its reduced form:

$$\frac{1}{\left(\frac{N}{N_0} \right)^2} \cdot \frac{\left(\frac{p_{d0}}{p_{u0}} \right)^{k-1/k} \cdot \left(\frac{p_d}{p_{d0}} \right)^{k-1/k} - 1}{\left(\frac{p_{d0}}{p_{u0}} \right)^{k-1/k} - 1} = f \left(\frac{F}{F_0} \int \frac{N}{N_0} \right) \quad (10)$$

The line volume after the compressor is incorporated in the circuit; the downstream pressure is calculated in this circuit as follows:

$$\frac{p}{p_0} = \frac{F_0}{\rho_0 V_0} \cdot \frac{T_d}{T_{d0}} \cdot \int \left(\frac{F_u}{F_0} - \frac{F_d}{F_0} \right) dt \quad (11)$$

in which the temperature T is found as the sum of upstream temperature and temperature rise in the compressor.

The temperature rise of the air flow through the compressor is found as follows:

$$\Delta T = T_u \left[\left(\frac{p_d}{p_u} \right)^{k-1/k} - 1 \right]$$

The downstream temperature is found from:

$$T_d = T_u + \Delta T = T_u \left[1 + \left(\frac{p_d}{p_u} \right)^{k-1/k} - 1 \right]$$

or, in its reduced form:

$$\frac{T_d}{T_{d0}} = \frac{\left[\left(\frac{p_{d0}}{p_{u0}} \right)^{k-1/k} \cdot \left(\frac{p_d}{p_{d0}} \right)^{k-1/k} - 1 \right] + 1}{\left(\frac{p_{d0}}{p_{u0}} \right)^{k-1/k}} \quad (12)$$

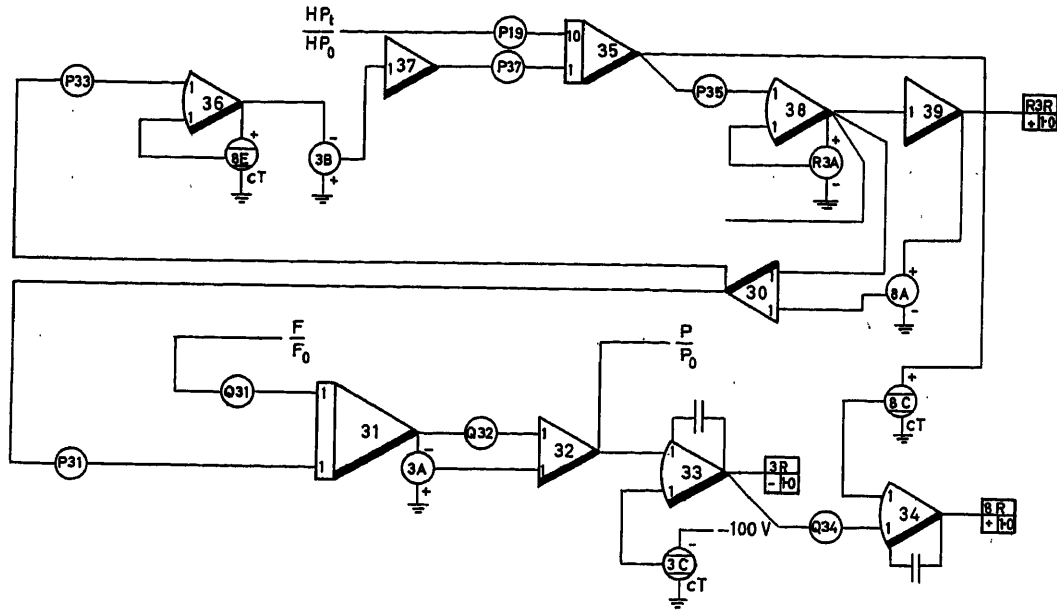


Figure 10

The circuit which performs these calculations is shown in Figure 10.

The potentiometers should be adjusted as follows:

$$Q 33 = 0.25$$

(depending on the function made on cup 8E, see below)

$$P 19 = \frac{HP_0}{2\pi^2 IN_0^2} \cdot \frac{1}{10}$$

$$P 37 = \frac{HP_0}{\pi^2 IN_0^2} \cdot \frac{1}{10}$$

$$P 35 = 0.5$$

$$P 31 = \frac{2F_0}{\rho_0 V_0} \cdot \frac{2\Delta T_0}{T_{u0} + \Delta T_0}$$

$$Q 31 = \frac{F_0}{\rho_0 V_0} \cdot \frac{2\Delta T_0}{T_{u0} + \Delta T_0}$$

$$Q 32 = \frac{T_{u0}}{2\Delta T_{u0}}$$

$$Q 34 = 0.5$$

The function

$$\frac{\Delta H}{\Delta H_0} = \frac{\left(\frac{p_{d0}}{p_{u0}}\right)^{k-1/k} \left(\frac{p_d}{p_{d0}}\right)^{k-1/k} - 1}{\left(\frac{p_{d0}}{p_{u0}}\right)^{k-1/k} - 1}$$

is reversed to

$$\frac{p_u}{p_{u0}} = f\left(\frac{\Delta H}{\Delta H_0}\right)$$

and made on cup 3C. The function

$$\frac{\eta C}{\eta C_0} = f\left(\frac{F}{F_0} J \frac{N}{N_0}\right)$$

$$\frac{1}{\eta C_0} = f\left(\frac{F}{F_0} J \frac{N}{N_0}\right)$$

and made on cup 8E. The function

$$\frac{1}{\left(\frac{N}{N_0}\right)^2} \cdot \frac{\left(\frac{p_{d0}}{p_{u0}}\right)^{k-1/k} \left(\frac{p_d}{p_{d0}}\right)^{k-1/k} - 1}{\left(\frac{p_{d0}}{p_{u0}}\right)^{k-1/k} - 1} = f_7\left(\frac{F}{F_0} J \frac{N}{N_0}\right)$$

is made on cup 6C.

Results

The results gained from the runs with the electric model can best be distinguished using as a guide the scope of work mentioned above.

(1) and (2). The stability of the system was good at all operating points. Interaction between control loops was small so that no special precautions were required.

(3). Runs with maximum gas temperature at the inlet of the turbines indicated the maximum air flow with the particular number of turbine compressor units used (see Figure 11).

(4) and (5). From the runs which tested emergency cases it appears that a breakdown of a turbine compressor unit in the CO boiler circuit will inevitably result in a complete shut-down of the unit (surging of the compressors, see Figures 12, 13 and 14, graph 1). In order to cope with this situation, an emergency valve to open a by-pass of the regenerator was provided, together with automatic valves to close the turbine and compressor of the unit suffering the breakdown (see Figures 12, 13 and 14, graph 3).

The tests also showed that the amount of fuel burned in the CO boiler should be kept above a certain figure in order to ensure that surging of the compressors will not occur if the fuel

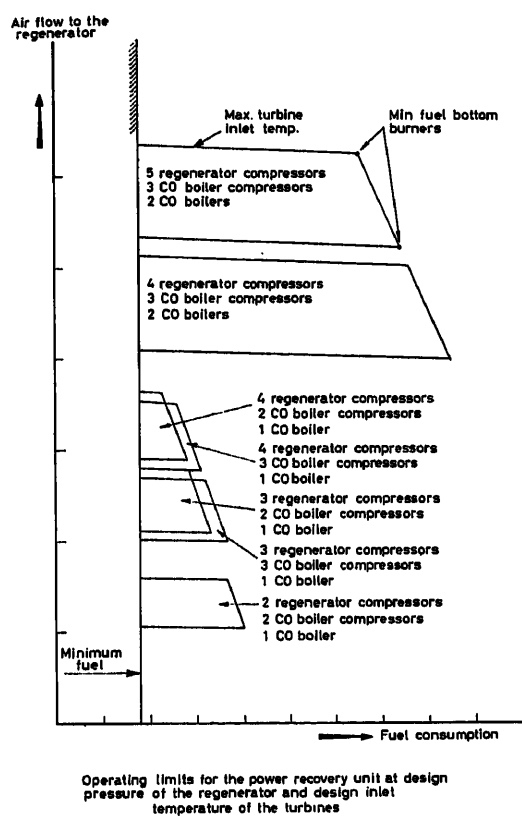


Figure 11

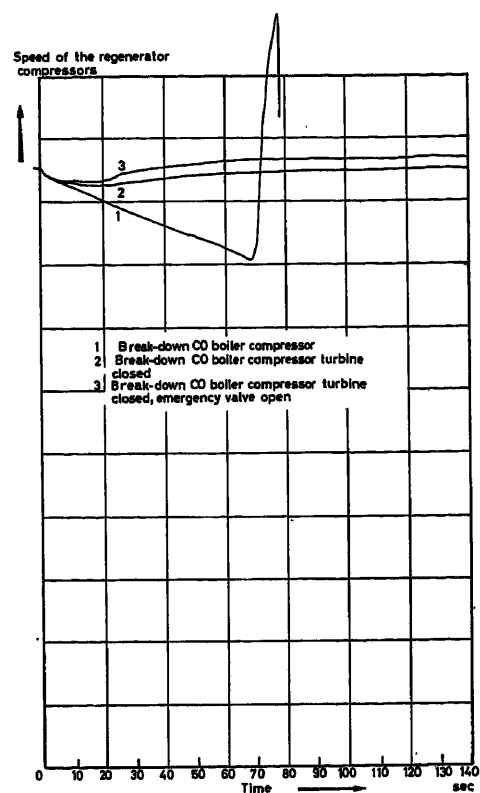


Figure 12. Break-down of a compressor in the CO boiler circuit

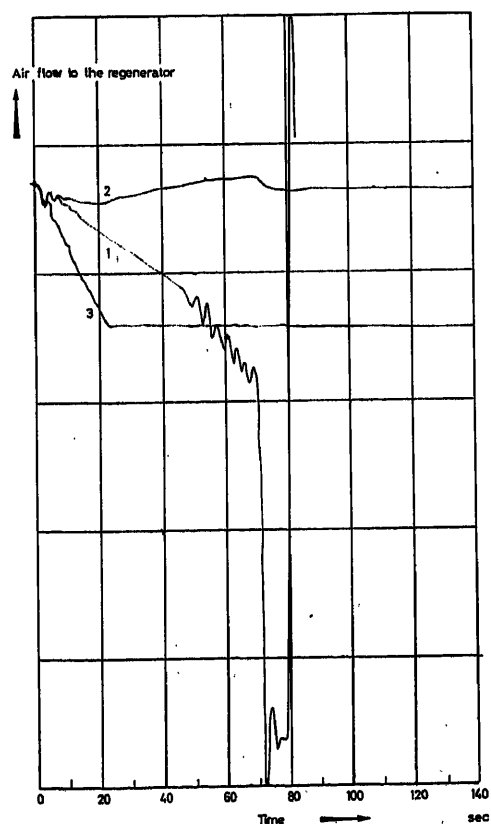


Figure 13

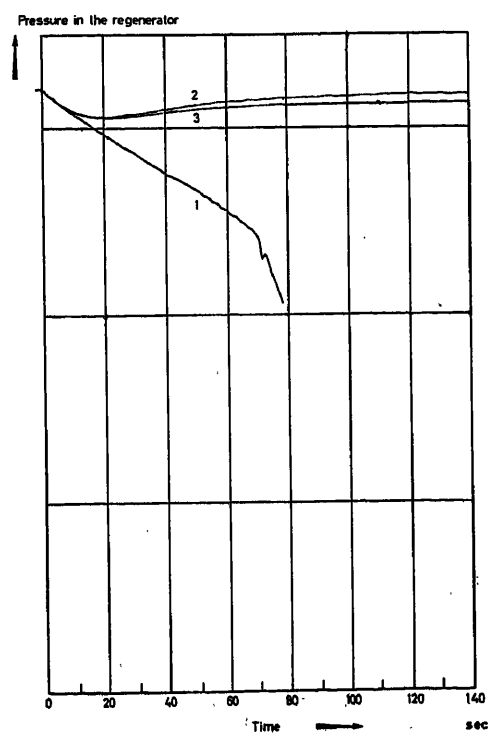


Figure 14

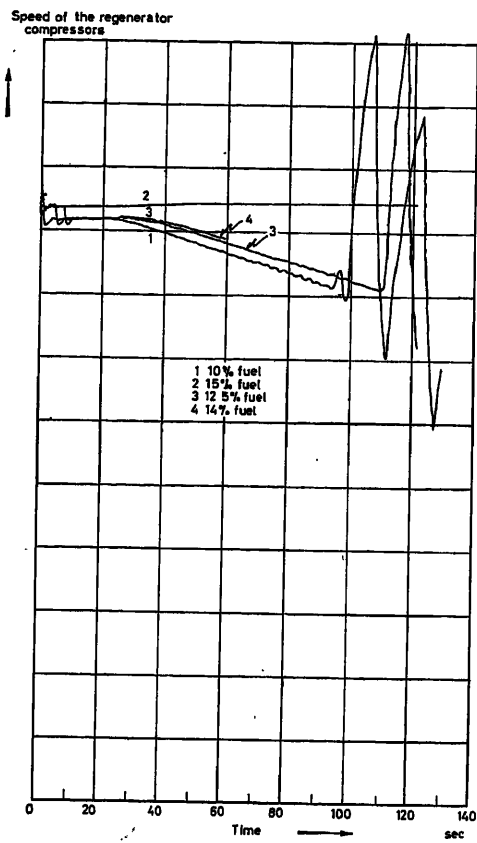


Figure 15

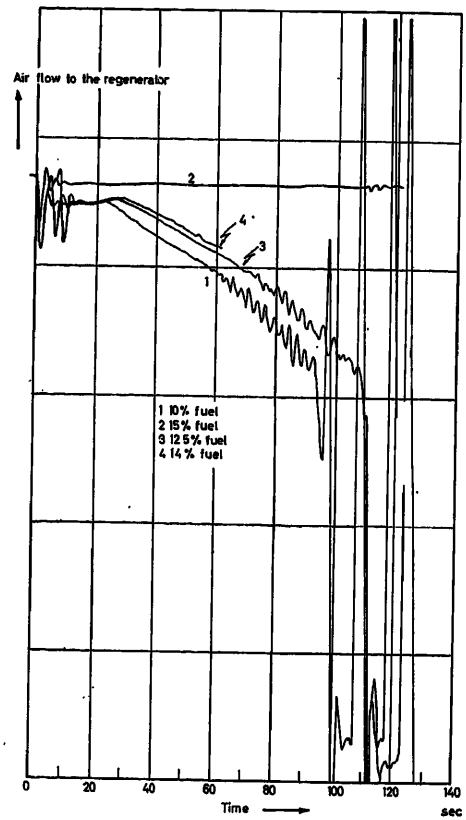


Figure 16

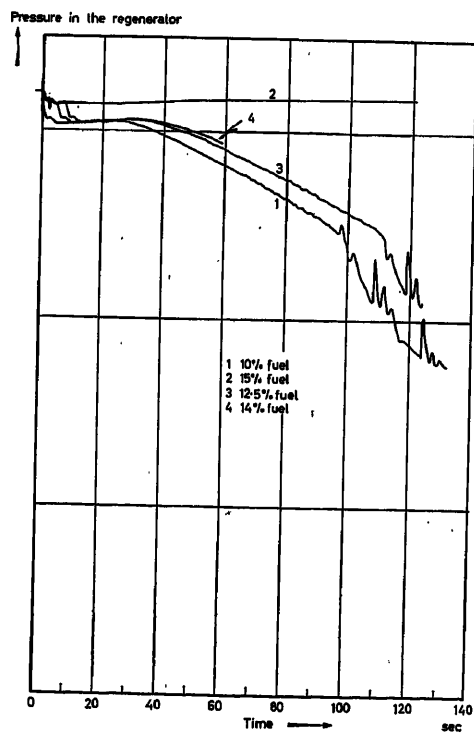


Figure 17

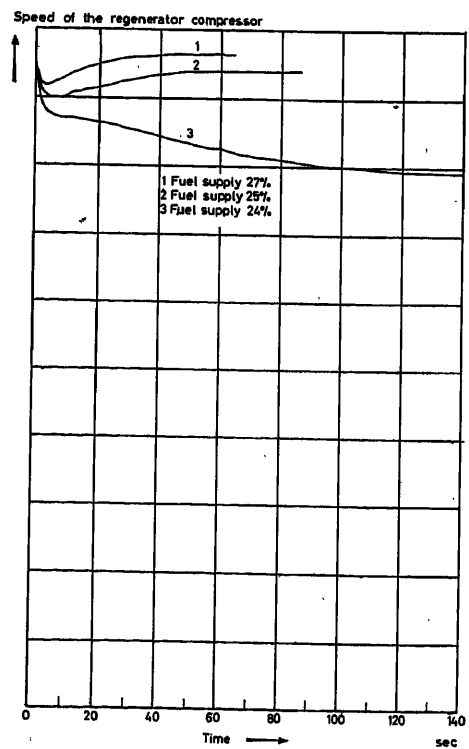


Figure 18

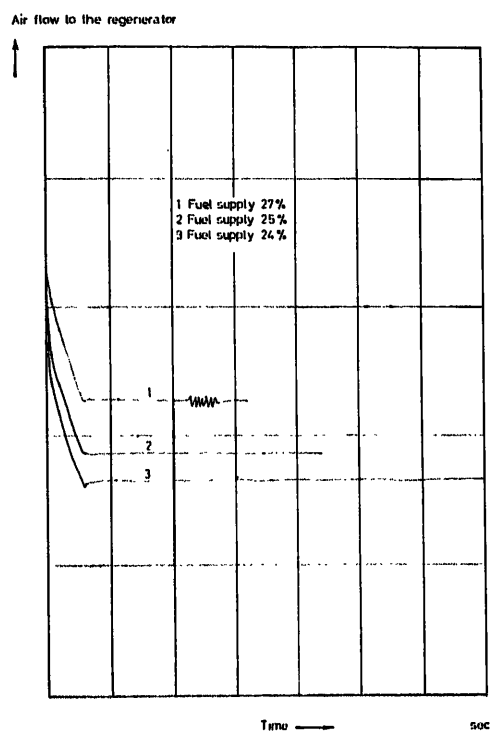


Figure 19

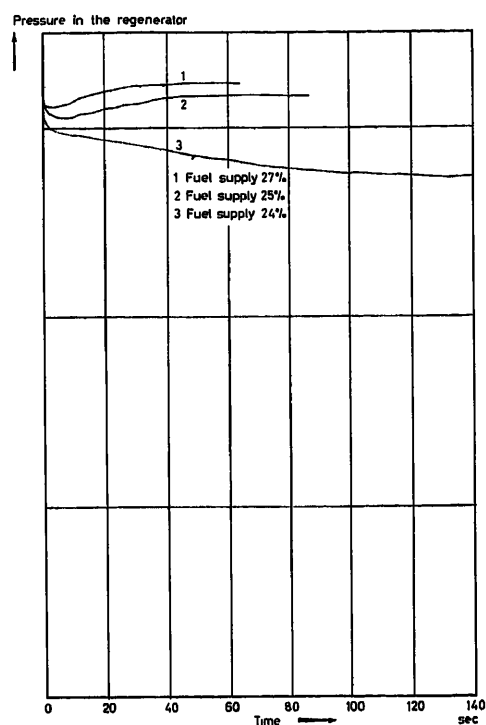


Figure 20

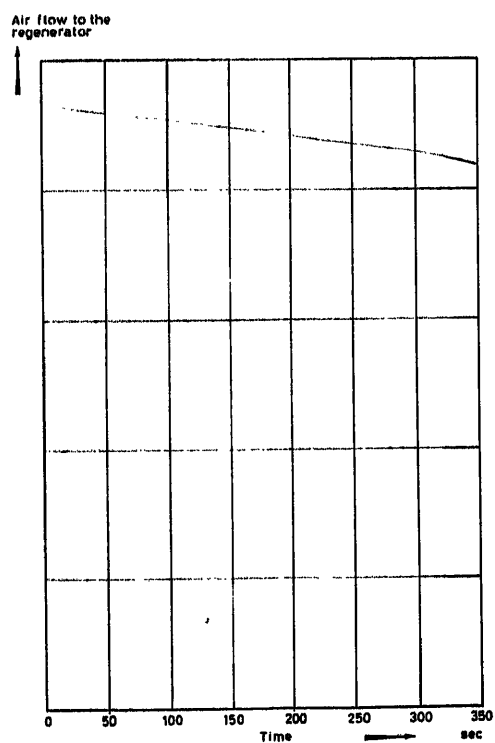


Figure 21

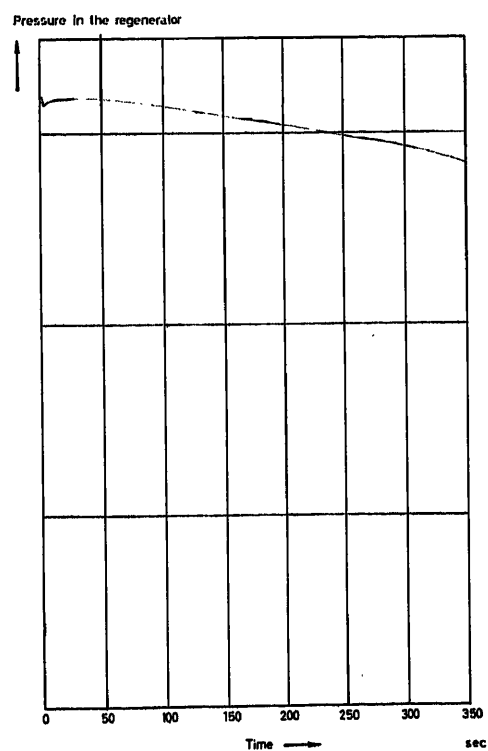


Figure 22

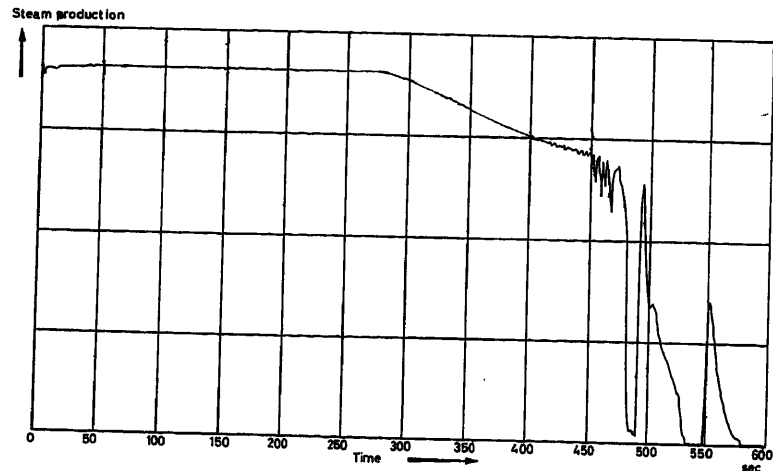


Figure 23

supply fails (Figures 15–17), or a breakdown occurs in one of the CO boiler compressors (Figures 18–20). It was decided to use an independent fuel supply for this 'minimum' fuel. This source would also supply fuel for the controlled burners in the bottom of the CO boiler because failure of this fuel supply results in a shut-down of the unit (Figures 21–23).

All the values established in the various runs with the model are presented in Figure 11, which gives the operating ranges of the unit within which emergencies may occur without a resultant shut-down of the complete unit.

(6). The procedure for the start-up and shut-down of the unit was found to be useful in practice, no difficulties whatsoever being encountered.

Conclusions

The possibility of establishing the operating limits and the extra safety devices found to be required by the system both constitute strong recommendations for the use of an analogue computer for the study of the dynamic behaviour of a process unit if this cannot be estimated from a paper study.

Nomenclature

C	A constant
f	A function of
F	Flow rate
HP	Shaft horse powers
I	Moment of inertia
k	Ratio of specific heats
N	Number of revolutions per unit of time
p	Absolute pressure
t	Time
T	Temperature
V	Volume
ΔH	isentropic enthalpy difference
η_C	Compressor efficiency
η_T	Turbine efficiency
ω	Angular velocity
ρ	Gas density

Subscripts

u	Upstream
d	Downstream
0	Design
c	Compressor
t	Turbine

Statistical Analysis of a Novel Fluid Flow Control System

R. C. BOOTON, Jr. and W. E. SOLLECITO

Summary

This paper presents the analysis and design optimization of a new and novel method of controlling liquid flow to very high accuracies. The method is based upon a particle counting technique to measure integrated flow. The basic control system is described. Errors in the system are generated from random location of particles in the fluid, random disturbances, quantization, and measurement factors which make the total count uncertain. The random location of particles in the fluid leads to a noise-like term in the system input whose statistical characteristics are non-stationary. The basic noise mechanism characteristics are derived and the effects on system accuracy, velocity and acceleration error are calculated in literal form. The parameters of the controller are varied to minimize the servo error within the constraints imposed by maximum error velocity and acceleration. Design trade-off curves are developed. The requirements placed on sensing resolution and other factors which make the total count uncertain are discussed and an example is cited.

Sommaire

Cette communication présente l'analyse et optimisation d'avant-projet d'un système à la fois nouveau et original pour le réglage avec une très haute précision du débit d'un liquide. La méthode se base sur un technique de comptage des particules afin d'obtenir une mesure du débit intégré. On décrit le système fondamental de réglage. Les erreurs du système sont engendrées par la position aléatoire des particules dans le fluide, par des perturbations aléatoires, par la quantisation, et par des facteurs de mesure qui rendent incertain le comptage total. La position aléatoire des particules dans le fluide mène à un terme semblable au bruit à l'entrée du système, dont les caractéristiques statistiques ne sont pas stationnaires. On dérive les caractéristiques fondamentaux du mécanisme du bruit, et on calcule sous forme littérale les effets sur la précision du système et sur l'erreur de vitesse et l'accélération. On varie les paramètres du mécanisme de réglage pour réduire au minimum l'erreur d'asservissement dans les limites des contraintes imposées par l'erreur maximale de vitesse et l'accélération. On développe des courbes d'échange pour le calcul. On discute les conditions requises pour la résolution des capteurs, ainsi que d'autres facteurs qui rendent incertain le comptage total et on cite un exemple.

Zusammenfassung

Der Aufsatz enthält die Untersuchung und einen optimalen Entwurfsvorschlag für eine neuartige Methode zur sehr genauen Regelung des Durchflusses von Flüssigkeiten. Die Methode beruht auf einem Teilchenzählverfahren zur Messung des integrierten Durchflusses. Das zugrunde liegende System ist beschrieben. Systemfehler ergeben sich durch die zufallsbedingte Lage der Teilchen in der Flüssigkeit, durch regellose Störungen, durch Quantisierung und durch Meßfaktoren, die die Gesamtzählung unsicher machen. Die zufallsbestimmte Lage der Teilchen in der Flüssigkeit führt zu einem geräuschähnlichen Glied am Eingang des Systems, dessen statistische Eigenschaften nichtstationär sind. Die zugrunde liegenden Eigenschaften des Geräuschmechanismus werden hergeleitet und die Auswirkung auf die Genauigkeit des Systems sowie auf die Geschwindigkeits- und Beschleunigungsabweichungen genau berechnet. Die Änderung der Parameter des Reglers erfolgt so, daß innerhalb der Beschränkungen, die durch die maximale Geschwindigkeits- und

Beschleunigungsabweichung gegeben sind, der Regelfehler minimal wird. Kurven zur Berücksichtigung von Entwurfsabänderungen werden abgeleitet. Die Bedingungen über die Empfindlichkeit des Meßgerätes und andere Faktoren, die die Gesamtzählung unsicher machen, werden besprochen; ein Beispiel ist angeführt.

Introduction

This paper presents the analysis and design optimization of a novel method of measuring and controlling fluid flow to very high accuracies. This method is most applicable to those systems where it is desirable to measure accurately fluid flow from fixed volume sources. A specific military application is given, but the results are potentially applicable or adaptable to a wide variety of industrial blending systems. In this particular instance, the method is applied to a propellant utilization system where it is desirable to control the flow of fluid from two tanks such that when one runs dry, the other will be empty to within 0.05 per cent of the initial volume of fluid in both tanks. This order of accuracy is desirable in fluid propellant missile applications because any fuel remaining in one tank when the other runs dry represents a loss in usable thrust and an effective increase in non-usable payload.

The fluid volume measuring technique invented by Adamson¹ is based upon injection of a known number of particles into each tank and sensing and counting the particles as they exit from the tanks with the fluid. The method offers high accuracy potential because a relatively large number of particles can be used.

System Description

The system configuration is shown in Figure 1. The tanks contain given amounts of fluid in which a counted number of particles are randomly dispersed. As fluid is pumped from the tanks, particles are carried out and sensed. For each particle

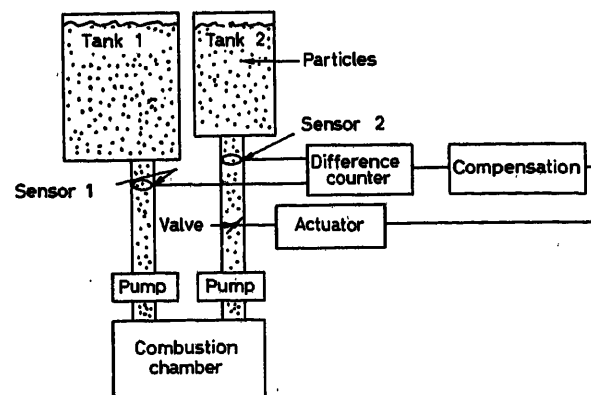


Figure 1. Propellant utilization system configuration

sensed, a pulse is sent to a difference counter. The difference in the number of particles detected by each sensor is an estimate of the actual integrated flow difference. This error signal is used to vary the flow rate in one tank to maintain the count difference near zero.

Normally, fluid flows from the two tanks at nominal rates so that the tanks will empty simultaneously. The purpose of the propellant utilization system is to correct errors in integrated flow caused by valve and supply line unbalance and pump and combustion chamber disturbances.

The compensation network is designed to minimize the expected error caused by the random distribution of particles. Because the actuator and valve are fixed in design, this becomes a 'fixed configuration' optimization problem.

The block diagram assumed for this analysis is shown in Figure 2. The operation of the servo is based upon the number

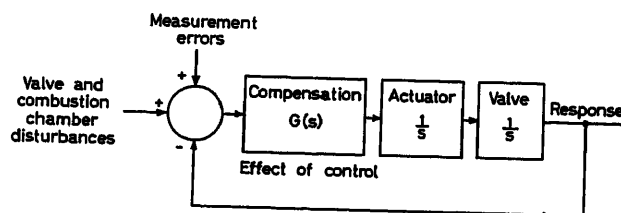


Figure 2. Simple model of the servo

and distribution of the particles and hence the weight or volume of the fluids need not enter the analysis except in the interpretation of the final results. Therefore, the servo response is taken to be the effect of control upon the integrated flow measured as a fraction of a total tank. The servo error is proportional to the counter output and is the error in integrated flow caused by disturbances minus the corrections caused by control plus the random errors introduced by the measurement process. The system error is calculated as a fraction of a total tank. If the total weight of the fluid in each tank were the same, then the R.M.S. value of the remaining fluid would be the weight of one tank times the R.M.S. system error. If the tanks have different weights, the R.M.S. value of the two tank weights should be used. R.M.S. values rather than average values are used because both tanks have equal probabilities of emptying first and a mean square error measure is used.

Because of the two integrations in the servo loop, the characteristics of the overall servo will be such that the servo corrects perfectly for constant errors in the flow rate. Random disturbances in flow will be corrected if they vary slowly with respect to the servo time constant.

Next, a slightly hypothetical but specific numerical example is considered. The normal flow time to empty both tanks completely is taken as 15 min. To maintain the flow rates within acceptable limits for the combustion chamber, the valve opening can be varied only ± 15 per cent around the nominal position. The maximum change in flow rate corresponds to 15 per cent of a tank in 900 sec and thus the maximum servo velocity is

$$V_M = \frac{0.15}{900} = 1.67 \times 10^{-4} \text{ sec}^{-1} \quad (1)$$

The valve can be moved from neutral to either extreme in approximately 0.5 sec and thus the maximum servo acceleration is

$$A_M = \frac{1.67 \times 10^{-4}}{0.5} = 3.34 \times 10^{-4} \text{ sec}^{-2} \quad (2)$$

The system defined thus far indicates that optimization will be required for a 'fixed configuration' system subject to saturation constraints and random inputs.

Error Generation

In this method of measurement there are two main types of error generation: noise effects and count uncertainty.

Noise Effects—These occur because the particles are randomly distributed throughout the fluid. The running count of particles leaving a tank does not exactly represent the actual volume of fluid leaving the tank. Figure 3 shows the case where fluid leaves a tank at a constant rate. If the particles were uniformly distributed throughout the fluid, the running particle count curve would lie on the fluid volume curve. Because of the random distribution, the count can be more or less at any given time and can lie anywhere within the possible running count curves shown. Statistically, the running count curve tends to stay on one side or other of the fluid volume curve. The number of crossings is small. The difference between the two curves is the deviation and is zero at both ends.

If the system were fast enough to follow the deviation, no net error due to noise would result, but since the system has a finite response time and given saturation characteristics, its inability to follow the deviation curve results in an error.

The Count Uncertainty Error—This occurs because the count difference is the subtraction of two total counts each of which does not truly represent the actual number of particles that did

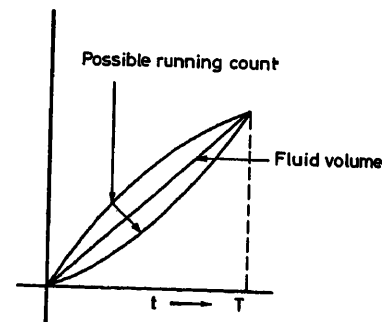


Figure 3. Fluid volume and total particle count

pass by or should have passed by the respective sensors. This uncertainty is caused by the following:

- The sensors can miss some particles because they occur too close together (the resolution loss in the sensors).
- The average resolution of the sensors can change.
- Particles can stick or clump together and produce only one count (this is equivalent to sensor resolution loss).
- Particles breaking into several pieces to give extra counts.
- Extra pulse generation in the sensors or extra count effects in the counter.
- Uncertainty in the actual number of particles placed in each tank.
- Particles adhering to container walls.
- Particles floating to top of the fluid.

Additional errors can be caused by:

Dead Volume—There is a minimum amount of fluid which cannot be drained from the lines due to characteristics of the pump and combustion chamber. The fluid that sticks to the walls is also dead volume.

Flow Disturbances—Disturbances in flow can occur near the end of the run and can cause an error which is not removed by the end of the run.

Quantization—Each particle represents a given amount of fluid. No information is known regarding how much of this given amount of fluid has passed by the sensor when a pulse occurs. For a large number of particles this error is negligible.

The system design problem therefore consists of evaluating the effects of these possible sources of error and designing a system to minimize the total probable error. This design is subject to the constraints of a given valve and actuator whose linear and non-linear characteristics are known but are not subject to change by the control system designer.

Error Separation Analysis

The following notation is used:

$f_1(t), f_2(t)$	= integrated flow from tank 1 and tank 2 respectively in the period from 0 to t
C_1, C_2	= total number of particles sensed by sensor 1 and sensor 2 respectively
$c_1(t), c_2(t)$	= number of particles sensed by sensor 1 and sensor 2 respectively in the period from 0 to t
$\beta_1(t), \beta_2(t)$	= error in $c_1(t)$ and $c_2(t)$ respectively caused by the random location of particles
N	= mean value of total counts C_1 and C_2 (approximately equal to number of particles in each tank)
σ_o	= standard deviation of C_1 and C_2 (R.M.S. value of variation of C_1 and C_2 around N)
T	= equivalent total time based on second stage flow rate = 900 sec
V_M	= maximum servo velocity = $1.67 \times 10^{-4} \text{ sec}^{-1}$
A_M	= maximum servo acceleration = $3.34 \times 10^{-4} \text{ sec}^{-2}$

If the particles were uniformly distributed

$$c_1(t) = C_1 f_1(t)$$

but because of the random location of particles

$$c_1(t) = C_1 f_1(t) + \beta_1(t)$$

which can be written

$$c_1(t) = N f_1(t) + \beta_1(t) + (C_1 - N) f_1(t)$$

Because a similar expression can be written for $c_2(t)$ the estimated error in integrated flow (the counter output divided by N) can be written as

$$\begin{aligned} \frac{c_1(t) - c_2(t)}{N} &= [f_1(t) - f_2(t)] + \left[\frac{\beta_1(t) - \beta_2(t)}{N} \right] \\ &+ \left[\frac{C_1 - N}{N} f_1(t) - \frac{C_2 - N}{N} f_2(t) \right] \end{aligned} \quad (3)$$

The first term on the right is the true error in integrated flow.

The second term

$$n(t) = \frac{\beta_1(t) - \beta_2(t)}{N} \quad (4)$$

is the noise in the servo input. The third term is the error caused by the uncertainty in the total count and at the end of the second stage has the approximate variance

$$E \left[\frac{C_1 - N}{N} f_1(T) - \frac{C_2 - N}{N} f_2(T) \right]^2 \approx \frac{2\sigma_c^2}{N^2} \quad (5)$$

Noise Characteristics Derivation

This section analyses the characteristics of the noise-like term, $n(t)$, present in the servo input because of the random location of the particles in the fluid. Although the basic random process is a function of distance and not time, the approximation is made that the noise can be treated as a function of time, where the conversion from distance to time is based on the nominal flow. Because the preceding section has shown that the effects of variation in the total number of sensed particles can be handled separately from the noise, the total number sensed by each sensor is taken as N . The count in the time interval from 0 to t is denoted by $c(t)$. Consider first the effects of a single sensor. The particles sensed are assumed to occur at random and independently of each other.

Since the counts are assumed to occur at random in the time interval $(0, T)$, the probability that a particular count occurs in the time interval $(0, t_1)$ is t_1/T . With N counts, the probability of c_1 counts in the time interval $(0, t_1)$ is given by the binomial distribution

$$P(c_1) = \frac{N!}{c_1!(N-c_1)!} p_1^{c_1} (1-p_1)^{N-c_1}$$

and this is

$$P(c_1) = \frac{N!}{c_1!(N-c_1)!} \left[\frac{t_1}{T} \right]^{c_1} \left[\frac{T-t_1}{T} \right]^{N-c_1}$$

The normal (Gaussian) approximation to this distribution is

$$P(c_1) = \frac{1}{\sigma_1(2\pi)^{1/2}} e^{-\frac{(c_1 - \mu_1)^2}{2\sigma_1^2}}$$

where

$$\mu_1 = \frac{Nt_1}{T}; \quad \sigma_1 = \left(N \frac{t_1(T-t_1)}{T^2} \right)^{1/2}$$

Next is calculated the conditional distribution of the number of counts, c_2 , in the interval $(0, t_2)$ given that c_1 counts occur in $(0, t_1)$ where t_2 is greater than t_1 . In the time interval (t_1, T) there are $N - c_1$ counts and the probability that each of these $N - c_1$ counts lies in the time interval (t_1, t_2) is $(t_2 - t_1)/(T - t_1)$. The probability that c_2 counts occur in the time interval $(0, t_2)$ given that c_1 counts occur in $(0, t_1)$ is the same as the probability that $c_2 - c_1$ counts occur in (t_1, t_2) given that c_1 counts occur in $(0, t_1)$ and this is

$$P(c_2/c_1) = \frac{(N-c_1)!}{(c_2-c_1)!(N-c_2)!} \left[\frac{t_2-t_1}{T-t_1} \right]^{c_2-c_1} \left[\frac{T-t_2}{T-t_1} \right]^{N-c_2}$$

The normal approximation to this distribution is

$$P(c_2/c_1) = \frac{1}{\sigma_a(2\pi)^{1/2}} e^{-\frac{(c_2-c_1-\mu_a)^2}{2\sigma_a^2}}$$

where

$$\mu_a = (N-c_1) \frac{t_2-t_1}{T-t_1}; \quad \sigma_a = \left((N-c_1) \frac{(t_2-t_1)(T-t_2)}{(T-t_1)^2} \right)^{1/2}$$

Thus the joint distribution of c_1 and c_2 , which satisfies $P(c_1, c_2) = P(c_1) P(c_2/c_1)$ is a two-dimensional normal distribution. The conditional distribution for a two-dimensional normal distribution can be written in the form

$$P(c_2/c_1) = \frac{1}{\sigma_2 [2\pi(1-\rho^2)]^{1/2}} e^{-\frac{1}{2} \left(\frac{c_2 - \mu_2 - \rho \frac{\sigma_2}{\sigma_1} (c_1 - \mu_1)}{\sigma_2 (1-\rho^2)^{1/2}} \right)^2}$$

where ρ is the normalized correlation

$$\rho = \frac{1}{\sigma_1 \sigma_2} E[(c_1 - \mu_1)(c_2 - \mu_2)]$$

Comparison with the expression derived above shows that

$$c_2 - \mu_2 - \rho \frac{\sigma_2}{\sigma_1} (c_1 - \mu_1) = c_2 - c_1 - \mu_2 = c_2 - c_1 \frac{T-t_2}{T-t_1} - N \frac{t_2 - t_1}{T-t_1}$$

Equating the coefficients of c_1 gives

$$\frac{\sigma_2}{\sigma_1} = \frac{T-t_2}{T-t_1}$$

and thus the covariance of the count is

$$\begin{aligned} E[(c_1 - \mu_1)(c_2 - \mu_2)] &= \rho \sigma_1 \sigma_2 = \left(\rho \frac{\sigma_2}{\sigma_1} \right) \sigma_1^2 \\ &= \sigma_1^2 \frac{T-t_2}{T-t_1} = N \frac{t_1(T-t_2)}{T^2} \quad \text{for } t_1 < t_2 \end{aligned}$$

Therefore

$$\begin{aligned} E \left[c(t_1) - \frac{t_1}{T} N \right] \left[c(t_2) - \frac{t_2}{T} N \right] &= \frac{N}{T^2} t_1 (T-t_2) \quad \text{for } t_1 < t_2 \\ &= \frac{N}{T^2} t_2 (T-t_1) \quad \text{for } t_2 < t_1 \end{aligned}$$

The mean of this process is $E[c(t)] = Nt/T$

With the counter subtracting the outputs of two sensors, the counter output divided by N is a measure of the difference in integrated fluid flow. The correlation of the noise is then

$$\begin{aligned} E[n(t_1)n(t_2)] &= \frac{2}{NT^2} t_1 (T-t_2) \quad \text{for } t_1 < t_2 \\ &= \frac{2}{NT^2} t_2 (T-t_1) \quad \text{for } t_2 < t_1 \end{aligned} \quad (6)$$

where the factor of 2 occurs because two independent random terms were subtracted. Equation (6) shows that the noise is non-stationary.

Calculations which follow are simpler in terms of the derivative of the noise. The correlation of the derivative $n'(t)$ is given by

$$\begin{aligned} E[n'(t_1)n'(t_2)] &= \frac{\partial}{\partial t_1 \partial t_2} E[n(t_1)n(t_2)] \\ &= \frac{2}{NT} \delta(t_2 - t_1) - \frac{2}{NT^2} \end{aligned}$$

System Response to Noise

The response of the servo to the noise can be expressed in terms of the step response, h_{-1} , by the superposition integral

$$r(t) = \int_0^t h_{-1}(\tau) n'(t-\tau) d\tau$$

where use has been made of the fact that $n(0)$ is zero. The mean square value of this response, $R^2(t) = E[r^2(t)]$ becomes

$$R^2(t) = \int_0^t \int_0^t h_{-1}(\tau_1) h_{-1}(\tau_2) E[n'(t-\tau_1)n'(t-\tau_2)] d\tau_1 d\tau_2$$

Substitution leads to

$$R^2(t) = \frac{2}{NT} \int_0^t h_{-1}^2(\tau) d\tau - \frac{2}{NT^2} \left[\int_0^t h_{-1}(\tau) d\tau \right]^2 \quad (7)$$

In a similar manner the mean square servo velocity is evaluated as

$$V^2(t) = \frac{2}{NT} \int_0^t h_0^2(\tau) d\tau - \frac{2}{NT^2} \left[\int_0^t h_0(\tau) d\tau \right]^2 \quad (8)$$

where h_0 is the impulse response, $h_0(\tau) = h'_{-1}(\tau)$

The mean square servo acceleration is

$$A^2(t) = \frac{2}{NT} \int_0^t h_1^2(\tau) d\tau - \frac{2}{NT^2} \left[\int_0^t h_1(\tau) d\tau \right]^2 \quad (9)$$

where h_1 is the doublet response, $h_1(\tau) = h_0'(\tau)$

Servo Characteristics and Accuracy

The transfer function of the servo is

$$H(s) = \frac{G(s)}{s^2 + G(s)}$$

where $G(s)$ is defined in Figure 2. A reasonable choice for the form of $G(s)$ is

$$G(s) = KW^2 \frac{s+W}{s+BW}$$

where K , W and B are parameters to be determined. The servo transfer function then is

$$H(s) = \frac{KW^2 s + KW^3}{s^3 + BWs^2 + KW^2 s + KW^3}$$

For a servo with this transfer function, the integrals needed to evaluate the effects of noise can be shown to be approximately

$$\int_0^t h_1(\tau) d\tau = t; \quad \int_0^t h_0(\tau) d\tau = 1; \quad \int_0^t h_{-1}(\tau) d\tau = 0$$

and

$$\begin{aligned} \int_0^t h_{-1}^2(\tau) d\tau &= t + \frac{K+B^2}{2WK(B-1)} \\ \int_0^t h_0^2(\tau) d\tau &= \frac{W(K+B)}{2(B-1)} \\ \int_0^t h_1^2(\tau) d\tau &= \frac{W^3(K^2+K)}{2(B-1)} \end{aligned} \quad (10)$$

where the non-dimensional product Wt has been assumed large. The mean square value of the servo response to noise then is

$$R^2(t) = \frac{2t}{NT} + \frac{K+B^2}{NWK(B-1)} - \frac{2t^2}{NT^2} \quad (11)$$

When one tank stops flowing, the response at that time is the error caused by noise, and the mean square response is the mean square error caused by noise, E_n^2 . Because this occurs when t is near T ,

$$E_n^2 \approx \frac{2}{N} \left(\frac{T-t}{T} \right) + \frac{K+B^2}{NWT(K+B-1)} \quad (12)$$

The first term

$$E_1^2 = \frac{2}{N} \frac{T-t}{T} \quad (13)$$

represents an error caused by the fact that the tanks and pipes do not empty completely even with no error (the small portion of this term caused by the existence of the error is neglected). The second term

$$E_2^2 = \frac{K+B^2}{NTWK(B-1)} \quad (14)$$

is the mean square value of the error caused by the fact that the servo is not infinitely fast and is here called the mean square servo error.

In a similar manner, the mean square velocity and acceleration can be evaluated as

$$V^2 = \frac{W(K+B)}{NT(B-1)} \quad \text{and} \quad A^2 = \frac{W^3(K^2+K)}{NT(B-1)} \quad (15)$$

The effects of velocity and acceleration saturation can be taken into account by constraining the mean square values of the velocity and acceleration in the linear system to be $2/\pi$ times the squares of maximum velocity and acceleration in the actual non-linear servo². Therefore, the next step is to select the servo parameters K , W , and B so that, subject to the constraints

$$V^2 \leq \frac{2}{\pi} V_M^2 \quad \text{and} \quad A^2 \leq \frac{2}{\pi} A_M^2 \quad (16)$$

the servo error is minimized. First, for each K and B , W is made as large as possible without violating the velocity constraint. This value of W satisfies

$$\frac{W(K+B)}{NT(B-1)} = \frac{2}{\pi} V_M^2$$

from which W is determined as

$$W = \frac{2 V_M^2 NT (B-1)}{\pi (K+B)}$$

For this value of W , the mean square servo error is

$$E_2^2 = \frac{\pi (K+B) (K+B^2)}{2 V_M^2 N^2 T^2 K (B-1)^2}$$

For each value of B , the K that minimizes the mean square servo error is

$$K = B^{\frac{3}{2}} \quad (17)$$

Use of this value for K gives the mean square servo error

$$E_2^2 = \frac{\pi}{2 V_M^2 N^2 T^2} \frac{B}{(B^{1/2}-1)^2} \quad (18)$$

If there were no acceleration limit, B would be increased until the mean square servo error is essentially

$$E_2^2 = \frac{\pi}{2 V_M^2 N^2 T^2}$$

The existence of the acceleration limit, however, limits the maximum value that can be used for B . To determine this value, the mean square acceleration is evaluated in terms of B as

$$A^2 = \left(\frac{2 V_M^2}{\pi} \right)^3 N^2 T^2 \frac{(B^{1/2}-1)^2 (B^{3/2}+1)}{(B^{1/2}+1) B^{3/2}}$$

The acceleration constraint is reached when

$$\frac{2}{\pi} A_M^2 = \left(\frac{2 V_M^2}{\pi} \right)^3 N^2 T^2 \frac{(B^{1/2}-1)^2 (B^{3/2}+1)}{(B^{1/2}+1) B^{3/2}} \quad (19)$$

This equation can be solved numerically for B . Then values of K and W are calculated. Figures 4 and 5 show these parameters as functions of the number of particles N .

Next, the mean square servo error corresponding to these parameter values is evaluated and is shown as the solid line in

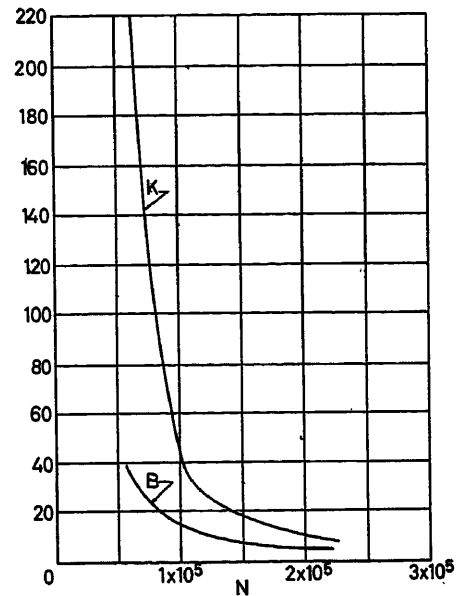


Figure 4. Servo parameters B and K as a function of the number of particles, N

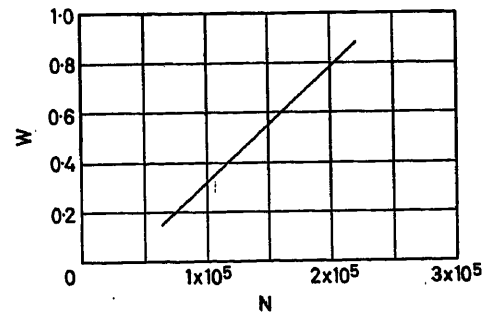


Figure 5. Servo parameter W as a function of the number of particles, N

Figure 6. For comparison, the dashed line in this figure shows the mean square servo error that would result if the acceleration constraint were not present.

Sensor Resolution Analysis

Uncertainty in the total count has been shown to contribute to the final error. Uncertainty in the final count is due to a number of factors, of which the most important probably are:

- (1) Variation in the number of counts because of imperfect resolution.
- (2) Variation in the number of particles placed in the tank.
- (3) Uncertainties caused by particles floating to the top of the tank.
- (4) Variation in the effective number of particles caused by breaking and clumping.

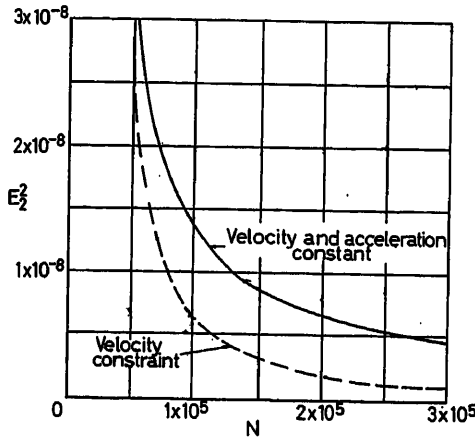


Figure 6. Mean square servo error E_R^2 as a function of the number of particles, N .

The variance of the total count caused by imperfect resolution is now calculated. The probability of a count of k with n particles is denoted by $P(k, n)$. If k particles have been counted and an additional particle is placed at random in the tank, then the probability that it will not be counted is approximately $2pk/L$, where p is the minimum distance that two particles can be separated and each still be counted, and L is the effective length of the fluid. Thus, consideration of an imaginary experiment in which the particles are placed in the tank one by one shows that $P(k, n)$ satisfies the two-dimensional difference equation

$$P(k, n) = \frac{2pk}{L} P(k, n-1) + \left[1 - \frac{2p(k-1)}{L}\right] P(k-1, n-1)$$

Multiplication by k and summation gives

$$\sum_k kP(k, n) = \sum_k \frac{2p}{L} k^2 P(k, n-1) + \sum_k \left[1 - \frac{2p(k-1)}{L}\right] kP(k-1, n-1)$$

which can be simplified to

$$M_1(n) = \left(1 - \frac{2p}{L}\right) M_1(n-1) + 1$$

where M_1 is the first moment

$$M_1(n) = \sum_k kP(k, n)$$

Solution of this first-order difference equation gives

$$M_1(n) = \frac{L}{2p} \left[1 - \left(1 - \frac{2p}{L}\right)^n\right]$$

In a similar manner, multiplication by k^2 and summation with respect to k leads to

$$M_2(n) = \left(1 - \frac{4p}{L}\right) M_2(n-1) + \left(2 - \frac{2p}{L}\right) M_1(n-1) + 1$$

where M_2 is the second moment.

$$M_2(n) = \sum_k k^2 P(k, n)$$

These results are used to derive an equation for the variance

$$\sigma_{CR}^2(n) = M_2(n) - M_1^2(n)$$

Substitution of $M_2(n) = \sigma_{CR}^2(n) + M_1^2(n)$ and the solution for $M_1^2(n)$ into the equation for $M_2(n)$ leads to

$$\sigma_{CR}^2(n) = \left(1 - \frac{4p}{L}\right) \sigma_{CR}^2(n-1) + \left(1 - \frac{2p}{L}\right)^{n-1} - \left(1 - \frac{2p}{L}\right)^{2n-2}$$

after some algebraic simplification.

With the initial condition $\sigma_{CR}^2(0) = 0$, the solution of this equation is

$$\sigma_{CR}^2(n) = \sum_{j=0}^{n-1} \left(1 - \frac{4p}{L}\right)^{n-1-j} \left[\left(1 - \frac{2p}{L}\right)^j - \left(1 - \frac{2p}{L}\right)^{2j} \right]$$

which leads to

$$\sigma_{CR}^2(n) = \frac{L^2}{4p^2} \left[\left(1 - \frac{4p}{L}\right)^n - \left(1 - \frac{2p}{L}\right)^{2n} \right] - \frac{L}{2p} \left[\left(1 - \frac{4p}{L}\right)^n - \left(1 - \frac{2p}{L}\right)^n \right] \quad (20)$$

For small values of p this is approximately

$$\sigma_{CR}^2(n) = \frac{n^2 p}{L}$$

Thus the variance of the final error caused by resolution is

$$E_R^2 = \frac{2\sigma_{CR}^2(N)}{N^2} = \frac{2p}{L} \quad (21)$$

Because the effective tank length is approximately $1 \times 10^8 \mu$ the variance of the resolution error is

$$E_R^2 = \frac{p}{5 \times 10^8 \mu}$$

Assignment of Allowable Errors

If the various causes of error dealt with previously are independent, the variance of the total error is the sum of the variances of the various components of the error. The exact manner in which the total error variance is divided among the individual components should depend upon the difficulty with

which various operations can be achieved. A slightly arbitrary division of the total allowable error is assumed here for purposes of discussion. If the allowable R.M.S. error is taken to be one part in 3,000 (of one tank) the mean square error (variance) is approximately 11×10^{-8} . Reference to the servo analysis above shows that approximately 10^5 particles results in a servo error of less than 2×10^{-8} with some allowance being made for the servo not being exactly optimum. With this number of particles the variance of the error caused by incomplete emptying of the tanks is less than 10^{-8} if approximately one part in 1,000 is left unemptied. If the variance of the resolution error is allowed to be 3×10^{-8} the resolution distance, p , must be 15μ . Variance of approximately 6×10^{-8} is left to the other factors which cause uncertainty in the total count. This corresponds to an allowable variance in the total count of approximately 500.

All the above requirements are very stringent but do not seem impossible to meet. Resolution is probably the most difficult instrumentation problem. No specific analysis has been made of the particle uncertainties such as rising, clumping and breaking, but obviously these must all be carefully watched. Experimental determination of some of these loss uncertainties is recommended. Servo errors, including miscellaneous effects can probably be met satisfactorily if at least 10^5 particles are utilized.

Conclusion

The basic analysis approach followed in this paper has been to convert what is essentially a complicated, discrete, non-linear system problem to the problem of a continuous linear system. First, the actual noise process is approximated by a gaussian continuous process. Secondly, the non-linear saturation phenomena are approximated by quasi-linearization techniques. Both of these simplifications can be applied to other similar problems.

The analysis shows that very high accuracies in the measurement and control of fluid flow are feasible.

Basic derivations are presented for

(1) Correlation function of the non-stationary noise generation mechanism as shown in eqn (6).

(2) Transmission of this noise through the system in literal form as shown in eqns (11) and (15).

(3) Variance of the sensor resolution error as shown in eqn (20).

In addition, design trade-off curves subject to system velocity and acceleration saturation constraints were developed and shown in Figures 4, 5, and 6.

Relatively straightforward statistical and servomechanism analysis techniques have been used in this paper. The saturation constraint approach to approximate design of non-linear servos is related to the work of Newton³ and some of the techniques described there can be used. Fundamentally, the problem described in this paper is a final value problem and at the expense of probable added complexity, improvement in the design might result from use of final value design techniques^{4, 5}.

References

- ¹ ADAMSON, P. *Measuring Device and Method*. Patent Pending, Ser. No. 237-708-23
- ² BOOTON, R. C. Jr. The analysis of nonlinear control systems with random inputs. *Proc. Symp. Nonlinear Circuit Analysis*, Polytechnic Institute of Brooklyn. 1953
- ³ NEWTON, G. C. Jr., GOULD, L. A., KAISER, J. F. *Analytical Design of Linear Feedback Controls*. 1961, New York; Wiley
- ⁴ BOOTON, R. C. Jr. The optimum design of final-value control systems. *Proc. Symp. Nonlinear Network Analysis*, Polytechnic Institute of Brooklyn. April 1956
- ⁵ BOOTON, R. C. Jr. Final-value systems of Gaussian inputs. *Trans. Instn Radio Engrs Prof. Gp Inf. Theory*. IT-2, No. 3 (1956)
- ⁶ FELLER, W. *An Introduction to Probability Theory and Its Applications*. Vol. 1. 1957. New York; Wiley
- ⁷ PARZEN, E. *Modern Probability Theory and Its Applications*. 1960. New York; Wiley
- ⁸ DAVENPORT, W. B. Jr. and ROOT, W. L. *An Introduction to the Theory of Random Signals and Noise*. 1958. New York; McGraw-Hill
- ⁹ LANING, J. H. and BATTIN, R. H. *Random Processes in Automatic Control*. 1956. New York; McGraw-Hill

DISCUSSION

O. L. UPDEKE, *School of Engineering and Applied Science, University of Virginia, Virginia, U.S.A.*

The technique of flow measurement reported by Booton and Sollecito may have a significant biomedical application in the measurement of blood flow. Since the obvious particles to be sensed in this application, the blood corpuscles themselves, are quite numerous, problems may arise because of multiple particle interferences. The multiple particle problem has been studied for the counting of radioactive events at high rates. In any case, applications are most likely for capillaries and small arterioles and venules.

W. E. SOLLECITO, *in reply*

Yes, this technique of flow measurement might have application to the measurement of blood flow by sensing and counting blood corpuscles. The problems of signal generation and sensor resolution, though, are quite different from those encountered in the application reported in this paper, because here the particle configuration and number were subject to engineering design.

Because of the severe problems envisaged in the sensing of blood corpuscles in the veins or arteries, applications will be most likely for capillary type flow measurement.

R. S. GAYLORD, *Aerospace Corporation, Los Angeles, California, U.S.A.*

The authors have presented a very interesting scheme for controlling fuel utilization for rockets. It appears that a proper uniform distribution of the particles is necessary in order to avoid non-uniform counting due to a possible tendency of particles to concentrate in one of the tanks, say the controllable tank. Does this mean that the specific gravity of the particles must be controlled so that the effects of temperature on them is the same as that on the propellant?

In this connection, does the scheme depend on the Brownian motion of particles in the tank to ensure proper mixing of the particles?

W. E. SOLLECITO, *in reply*

The specific gravity of the particles must closely match that of the propellant, and should vary with temperature in the same fashion.

This was one of the challenging aspects of the particle development task and was satisfactorily accomplished.

With respect to mixing of the particles in the liquid, the particles were injected into the propellants and mixed mechanically, for the feasibility demonstration. Brownian motion assured the continued random distribution of particles during the test cycle.

Difficulty of random distribution or suspension of the particles in the liquid is proportional to particle size. Improvements in sensor sensitivity allow the use of smaller particles and thereby reduces the continued suspension problem.

L. LANDON GOODMAN, *E.D.A., 2, Savoy Hill, London, W.C.2., England*

I would be interested to know if you have explored any other methods of sensing, before deciding upon the method which you used.

W. E. SOLLECITO, *in reply*

Award of this development contract was made on the basis of comparison with other proposed measurement techniques. Prior to the invention of this method by Adamson, surveys had been made of commercially available flow sensors. None of these was satisfactory for this specific application.

Fluid flow measuring techniques utilizing rotating vanes, fixed volume displacement pumps, capacitance change effects and similar methods were investigated, but discounted for reasons of inaccuracy and inconsistency with the requirements of the application.

During the presentation of the paper, an analogue-digital sensing technique was discussed which provides the required flow accuracy for applications in which the tank does not tilt and the fluid does not slosh about.

W. A. LE RUTTE, *Unilever N.V., Rotterdam, Netherlands*

The integrated flow in a pipeline is measured by counting particles. If the concentration of particles is low, then the accuracy of the measurement will be low.

If the concentration is too high, the resolving power of the optical detecting system will not be sufficient to count accurately. Could the authors give any data about the concentration of particles necessary to give optimal accuracy?

W. E. SOLLECITO, *in reply*

As presented in the discussion, it would appear that opposing requirements exist in the selection of the concentration of particles and would therefore indicate that an optimum concentration would exist. In fact, this situation does not exist. Reference to eqn (21) shows that the mean-squared resolution error is independent of N . This result means that as the number of particles is increased, a proportionate increase in unsensed particles can occur with no change in resolution error.

Reference to *Figure 6* shows that the mean-squared servo error decreases monotonically as the number of particles is increased. The trade-off, therefore, is between the practicality of a smaller number of particles and the mean squared error. The approach used was to select the minimum number of particles consistent with an assigned allowable mean squared error.

G. M. E. WILLIAMS, *Northampton College of Advanced Technology, St. John Street, London, E.C.1., England*

Does the valve in the suspension flow line ever have to close absolutely on the flow once it has started? If so, is there any experience of the particles interfering with the closure of the valve? Is there any evidence of other such objections to the use of this method of flow measurement?

Was an admixture of an artificial radioisotope considered as an alternative to the suspension of particles? If so, on what grounds was it rejected?

W. E. SOLLECITO, *in reply*

As mentioned in the paper, to maintain the flow rates within acceptable limits for the combustion chamber, the valve opening can be varied only by ± 15 per cent about the normal position. Therefore the valve does not close absolutely once the flow has started.

Although our experience in this application is limited, we anticipate no problems with closure of the valves due to the particles. During normal operation of some rocket engines, aluminium particles are injected to increase the mass flow and to improve performance.

The admixture of artificial radioisotopes was not considered as an alternative to the suspension of particles.

Effects of Fluid Mixing and its Expressions on Dynamics of Mass Transfer Process

T. TAKAMATSU and E. NAKANISHI

Summary

Many published papers dealing with the dynamics of a stagewise mass transfer operation are based on an assumption of perfect mixing in a stage.

In this paper, the effect of the deviation from this assumption on dynamics, which surely happens in most industrial large scale plants, is discussed.

The degree of mixing condition is expressed by the 'diffusional model' and the 'a series of perfect mixing vessels model', and the relationship between two models is obtained for steady state. With respect to the dynamic analysis, it is pointed out that the results based on these two models are different from each other, even if both models are quite equivalent from a statical viewpoint.

It is also concluded that the degree of mixing strongly affects the dynamics between inlet and outlet concentrations of that fluid whose mixing degree is under consideration, and it is not the case for the dynamics between all other signals in a process.

Sommaire

Dans beaucoup de publications traitant de la dynamique de transfert de masse à l'intérieur d'un étage, on suppose un mélange parfait.

Dans ce rapport, on discute l'effet résultant sur la loi dynamique de transfert quand cette hypothèse n'est pas vérifiée; ce qui est le cas des grandes installations industrielles.

Les lois gouvernant le degré de mélange sont représentées par le «modèle diffusional» et le «modèle à cuves à mélange parfait». On donne la relation en régime permanent de ces deux modèles. Ils sont équivalents au point de vue statique; toutefois, ils sont différents en analyse dynamique.

On montre également que le degré de mélange affecte dans une large mesure les relations dynamiques entre les concentrations de fluide considéré à l'entrée et à la sortie, sans que cela concerne les autres signaux du processus.

Zusammenfassung

Viele Veröffentlichungen über die Dynamik stufenweisen Stofftransportes bauen auf der Annahme auf, daß in einer Stufe vollständige Mischung erreicht wird.

In diesem Beitrag wird dargelegt, wie sich die Abweichung von dieser Annahme auf die Dynamik auswirkt; für die meisten industriellen Großanlagen ist wohl eine solche Abweichung anzunehmen.

Die Bedingungen des Mischungsgrades werden an Hand eines Diffusionsmodells und eines Modells von Reihenschaltungen idealer Mischbehälter beschrieben und die Zusammenhänge zwischen den beiden Modellarten für den Beharrungszustand abgeleitet. Es wird darauf hingewiesen, daß sich die Ergebnisse auf Grund dieser beiden Modellarten bei der dynamischen Untersuchung voneinander unterscheiden, selbst wenn sich beide Modelle in statischer Hinsicht ziemlich entsprechen.

Außerdem ergibt sich die Folgerung, daß der Mischungsgrad einen starken Einfluß auf die Dynamik zwischen Eingangs- und Ausgangskonzentration der betrachteten Flüssigkeit ausübt, was für die Dynamik zwischen allen anderen Signalen in einem Prozeß nicht gilt.

Introduction

In most mass transfer processes the flow of fluid is more or less mixed owing to the turbulence of flow itself, the contact with another fluid and the structure of apparatus.

Most of the studies on dynamics of stagewise mass transfer operation have been carried out under the assumption that two fluids contacting in a stage are perfectly mixed^{1, 11-14}. It is, however, a well-known fact that the above assumption is not always reasonable in practical stagewise contacting apparatus such as a large-scale plate column.

Many studies on fluid mixing have been carried out for the purpose of analysing a steady-state performance²⁻⁸, but there are very few with respect to the effect of fluid mixing on dynamics^{9, 10}. This paper discusses how much the deviation from the above assumption affects the dynamics of mass transfer operation. The degree of mixing will be expressed by a 'diffusional model' and 'a series of perfect mixing vessels model', and the relationship between both models will be considered.

Transfer Functions for Concentration Change

The following assumptions are provided:

- (i) Mixing degree is considered only for the direction of main flow of the first fluid, and both fluids are perfectly mixed in the direction of main flow of the second fluid.
- (ii) Holdups of both fluids are uniform throughout this elementary unit of mass transfer and also take constant values independent of the changes of concentration and flow rate.
- (iii) Mass transfer capacity coefficient and equilibrium relationship between concentrations of both fluids are not affected by the changes of concentration and flow rate.

Diffusional Model—In a diffusional model, an extent of local fluid mixing is expressed by the so-called back-mixing coefficient, E , which appears to be an ordinary diffusion coefficient and shows a pseudodiffusional rate in the direction opposite to the main flow.

Referring to *Figure 1(a)*, the following material balance equations are obtained:

$$E \frac{\partial^2 x}{\partial z^2} - u \frac{\partial x}{\partial z} - \frac{\partial x}{\partial t} - K(x - x^*) = 0 \quad (1)$$

$$y = y_I - \frac{L}{G} \frac{\partial x}{\partial z} - \frac{L}{uG} \left(\frac{\partial x}{\partial t} + \frac{H_V}{H_R} \frac{\partial y}{\partial t} \right) + \frac{E}{u} \frac{L}{G} \frac{\partial^2 x}{\partial z^2} \quad (2)$$

where K is a modified mass transfer capacity coefficient and has the following relation:

$$K = \frac{K_R a}{f \rho_M} = \frac{u}{H_{OR}} = \frac{u N_{OR}}{l} \quad (3)$$

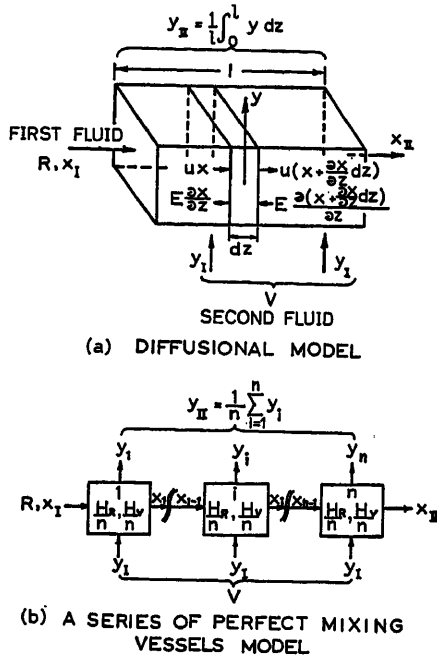


Figure 1. Mixing models

where f is the volumetric fraction of the first fluid in the system, and ρ_M is molal density of the first fluid (kmol/m^3).

For simplicity, an equilibrium relation between x and y is assumed to be

$$y = mx^* + c \quad (4)$$

Solving the second-order ordinary differential equation obtained by taking Laplace transforms of eqns (1), (2) and (4) with t , the following transfer functions can be obtained.

$$G_1(s) = \frac{X_{II}(s)}{X_I(s)} = M_{pe}(s) \quad (5)$$

$$G_2(s) = \frac{Y_{II}(s)}{mX_I(s)} = \frac{N_{OR}/\lambda}{H_1(s)} [1 - M_{pe}(s)] \quad (6)$$

$$G_3(s) = \frac{mX_{II}(s)}{Y_I(s)} = \frac{N_{OR}}{H_1(s)} [1 - M_{pe}(s)] \quad (7)$$

$$G_4(s) = \frac{Y_{II}(s)}{Y_I(s)} = \frac{1}{H_2(s)} + \frac{N_{OR}^2/\lambda}{H_1(s)H_2(s)} - \frac{N_{OR}^2/\lambda}{[H_1(s)]^2} [1 - M_{pe}(s)] \quad (8)$$

where

$$H_1(s) = \tau_R \tau_V s^2 + \left(\tau_R + \frac{N_{OR}}{\lambda} \tau_R + N_{OR} \tau_V \right) s + N_{OR}$$

$$H_2(s) = 1 + \frac{N_{OR}}{\lambda} + \tau_V s$$

$$M_{pe}(s) = \frac{Pe \cdot e^{Pe} (b_2 - b_1)}{b_2^2 e^{b_2} - b_1^2 e^{b_1}} \quad (9)$$

$$b_2, b_1 = \frac{Pe}{2} \left[1 \pm \left(1 + \frac{4H_1(s)}{Pe H_2(s)} \right)^{1/2} \right] \quad (10)$$

and

$$Pe = ul/E$$

Pe given by the last equation is called 'Péclet's number', and this is a dimensionless number which represents the mixing degree as a whole system.

A Series of Perfect Mixing Vessels Model—As shown in Figure 1(b), this is a model in which the number of perfect mixing vessels expresses the mixing degree of the first fluid.

From a material balance around the i th vessel the following basic differential equations are obtained, corresponding to eqns (1) and (2) for the diffusional model.

$$\frac{H_R}{n} \frac{dx_i}{dt} = R(x_{i-1} - x_i) - K_R a \frac{W}{n} (x_i - x_i^*) \quad (11)$$

$$\frac{H_R}{n} \frac{dx_i}{dt} + \frac{H_V}{n} \frac{dy_i}{dt} = R(x_{i-1} - x_i) + \frac{V}{n} (y_i - y_i^*) \quad (12)$$

The transfer functions are obtained from eqns (4), (11) and (12), but these transfer functions are in agreement with eqns (5) to (8) provided that $M_n(s)$ given below takes the place of $M_{pe}(s)$ in eqns (5) to (8).

$$M_n(s) = 1 \int \left[1 + \frac{1}{n} \frac{H_1(s)}{H_2(s)} \right]^n \quad (13)$$

Mixing Functions

Definition of Mixing Function—It should be noticed that the degree of mixing appears only in $M_{pe}(s)$ or $M_n(s)$ in all transfer functions. Therefore, it is necessary and sufficient to consider $M_{pe}(s)$ and $M_n(s)$ in order to analyse the effect of mixing degree on dynamics. Let us call these $M_{pe}(s)$ and $M_n(s)$ 'mixing functions'.

If $M_{pe}(s)$ given by eqn (9) and $M_n(s)$ given by eqn (13) were always equal to each other, the effects of mixing degree on dynamics are quite equivalent for the two models. It is, however, impossible to find any relation between values of pe and n for which the condition, $M_{pe}(s) = M_n(s)$, is always satisfied, except for the following special cases. For perfect mixing:

$$\lim_{Pe \rightarrow 0} M_{pe}(s) = \lim_{n \rightarrow 1} M_n(s) = \frac{H_2(s)}{H_1(s) + H_2(s)} \quad (14)$$

For perfect piston flow:

$$\lim_{Pe \rightarrow \infty} M_{pe}(s) = \lim_{n \rightarrow \infty} M_n(s) = \exp[-H_1(s)/H_2(s)] \quad (15)$$

Relation between $M_{pe}(0)$ and $M_n(0)$ in Steady State—The mixing function also affects the steady-state performance as follows:

$$x_{II}^0 = x_I^0 - (x_I^0 - x_I^{0*}) [1 - (\text{Mixing function})] \quad (16)$$

$$y_{II}^0 = y_I^0 + (y_I^{0*} - y_I^0) \left[\frac{1 - (\text{Mixing function})}{\lambda} \right] \quad (17)$$

where, for diffusional model,

$$(\text{Mixing function}) = M_{pe}(s) = M_{pe}(0)$$

and for a series of perfect mixing vessels model,

$$(\text{Mixing function}) = M_n(s) = M_n(0)$$

As is obvious from eqns (9) and (13), $M_{pe}(0)$ and $M_n(0)$ are the functions of λ and N_{OR} only, and one is able to obtain the relation between Pe and n that satisfies the relation of $M_{pe}(0) = M_n(0)$. Figure 2 shows this relation, in which $A = \lambda N_{OR}/(\lambda + N_{OR})$ are used as a parameter. If the values of Pe and n related by Figure 2 are used for each model, the properties of fluid mixing for the two models are quite equivalent to each other from a static viewpoint.

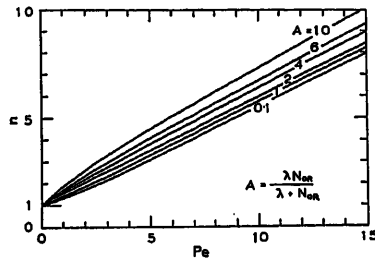


Figure 2. Relation between Pe and n for steady state

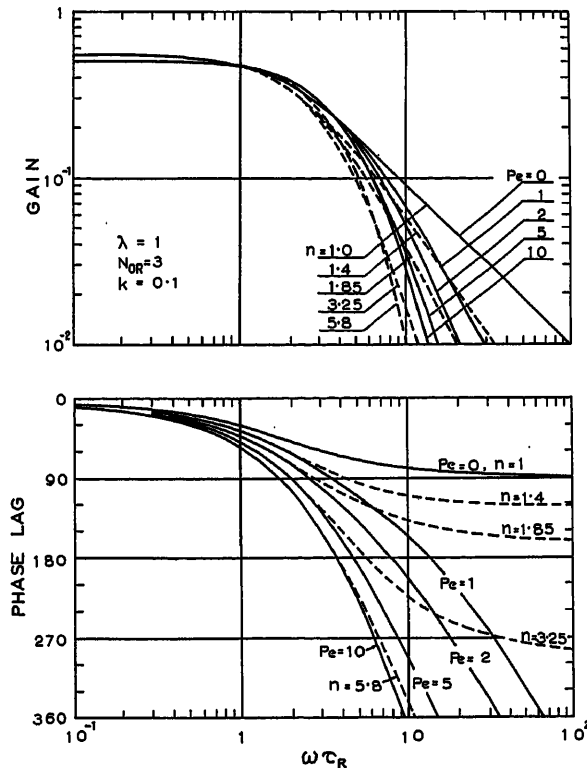


Figure 3. $M_{pe}(j\omega)$ and corresponding $M_n(j\omega)$

Numerical Comparison with $M_{pe}(j\omega)$ and $M_n(j\omega)$ —A group of solid lines in Figure 3 shows one numerical example which represents the effect of Pe on $M_{pe}(j\omega)$. It is seen that $M_{pe}(j\omega)$ is considerably affected by Pe when the value of $\omega\tau_R$ is large.

As mentioned above, it is impossible to get the same dynamics for the two models even if a relation between Pe and n which satisfies the condition of $M_{pe}(0) = M_n(0)$ is taken into account. A group of broken lines in Figure 3 shows the values of

$M_n(j\omega)$ calculated by the use of values of n which are so selected from Figure 2 that a relation of $M_{pe}(0) = M_n(0)$ be satisfied.

Comparing $M_{pe}(j\omega)$ and corresponding $M_n(j\omega)$, it is recognized that the values of gain are in close agreement with each other, but the values of phase lag differ widely from each other at larger values of $\omega\tau_R$.

Effects of λ and N_{OR} on $M_{pe}(j\omega)$ —Figure 4 shows one numerical example which represents the effect of λ on the Bode diagram of $M_{pe}(j\omega)$, and Figure 5 shows the effect of N_{OR} . In both cases, λ and N_{OR} principally affect only the gain values in a region of small values of $\omega\tau_R$, but it generally seems that $M_{pe}(j\omega)$ is not strongly affected by λ and N_{OR} .

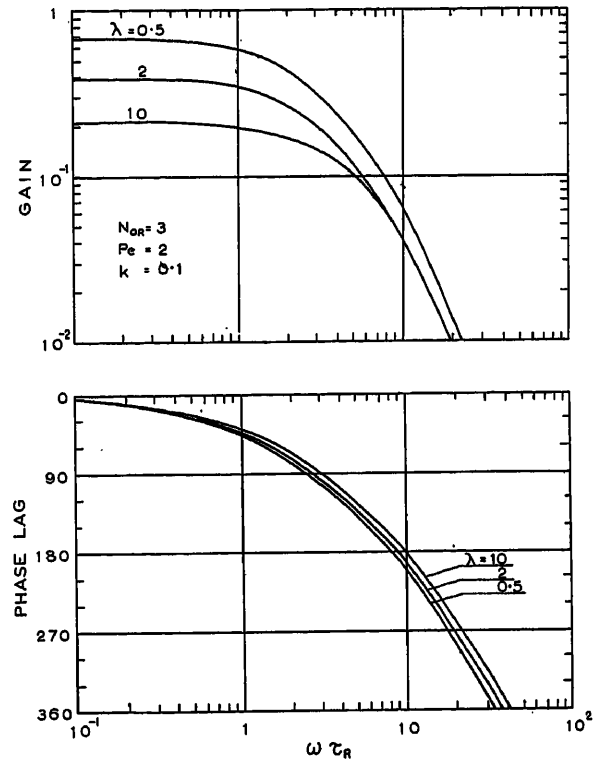


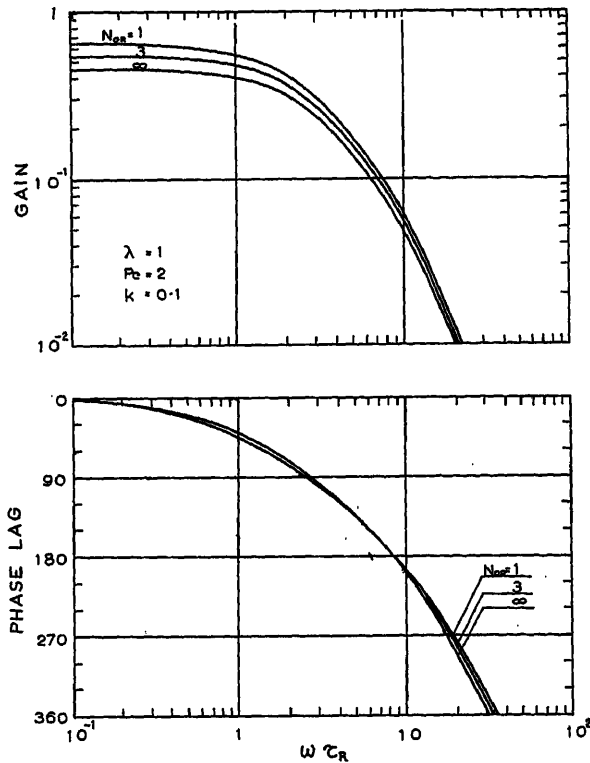
Figure 4. Effect of λ on $M_{pe}(j\omega)$

On Whole Transfer Functions for Concentration Change

It should be noticed that a transfer function $G_1(s)$ for the first fluid whose mixing degree is under consideration is quite the same thing as the mixing function itself. Therefore, the discussion and the results mentioned in the previous section are applicable to $G_1(s)$.

With respect to the other three transfer functions $G_2(s)$, $G_3(s)$ and $G_4(s)$ the following fact can be easily predicted by looking over eqns (6), (7) and (8).

As previously mentioned, the effect of fluid mixing degree on $M_{pe}(s)$ or $M_n(s)$ appears strongly in the high-frequency region, where its absolute value is small. Therefore, the value of $1 - M_{pe}(s)$ or $1 - M_n(s)$ may not be largely affected by the degree of fluid mixing.

Figure 5. Effect of N_{OR} on $M_{pe}(j\omega)$

On Transfer Functions for Flow Rate Change

The basic differential equation for flow rate change is not linear for most cases, but it may approximately be linearized, provided it can be assumed that the deviation of flow rate from a steady state is very small. Then the concentration change is also very small by the same order of magnitude as that of the flow rate. Consequently, products of two deviational quantities can be neglected in comparison with deviations in concentration and flow rate.

Under such assumption the following transfer functions can be derived for the diffusional model.

$$g_1(s) = \frac{X_{II}(s)/(x_I^0 - x_{II}^0)}{R(s)/R^0} = \left(\frac{\lambda N_{OR}}{\lambda + N_{OR}} \right) \left(\frac{1}{\tau_R s P(s)} \right) \left[\frac{M_{pe}(0) - M_{pe}(s)}{1 - M_{pe}(0)} \right] \quad (18)$$

$$g_2(s) = \frac{Y_{II}(s)/(y_I^0 - y_{II}^0)}{-R(s)/R^0} = \frac{N_{OR}}{H_1(s)} [1 - g_1(s)] \quad (19)$$

$$g_3(s) = \frac{X_{II}(s)/(x_I^0 - x_{II}^0)}{-V(s)/V^0} = \frac{N_{OR}/\lambda}{H_2(s)} g_1(s) \quad (20)$$

$$g_4(s) = \frac{Y_{II}(s)/(y_I^0 - y_{II}^0)}{V(s)/V^0} = \frac{1}{H_2(s)} \left[1 + \frac{N_{OR}^2/\lambda}{H_1(s)} \{1 - g_1(s)\} \right] \quad (21)$$

The transfer functions for a series of perfect mixing vessels model are obtained by replacing $M_{pe}(s)$ by $M_n(s)$ in the similar manner as for the case of the concentration change. With respect to the transfer functions for the change of flow rate, it is true that the degree of mixing appears only in the mixing functions. Moreover, since its effect is expressed only in terms of

$$\frac{M_{pe}(0) - M_{pe}(s)}{1 - M_{pe}(0)} \text{ or } \frac{M_n(0) - M_n(s)}{1 - M_n(0)}$$

it may be easily understood that the effect of fluid mixing on the dynamics for flow rate change seems to be not so large.

Conclusions

The degree of mixing appears only in the mixing function, $M_{pe}(s)$ or $M_n(s)$, defined in this paper.

The transfer functions obtained from the diffusional model and the series of perfect mixing vessels model take the same form except in the mixing functions.

The relation between Pe and n which gives an equivalent effect of mixing from a static viewpoint is shown by Figure 2.

The dynamics, especially the phase lag, by the two models are not exactly the same even if the characteristics of mixing in steady state are equivalent for the two models.

It is permitted to say that, approximately, for the concentration change of a fluid whose mixing condition is under consideration, the dynamics are affected by the mixing degree, and the dynamics for concentration changes of the other fluid and for all flow rate changes are hardly affected by the degree of mixing.

In addition, it should be noted that these conclusions are also applicable to the dynamics of one stage of which the plate column is constructed.

Appendix

1. Procedures for Obtaining Eqns (5) to (8)

The boundary conditions for solving eqns (1), (2) and (4) are as follows:

For the inlet

$$E \left(\frac{\partial x(z, t)}{\partial z} \right)_{z=0+} = u [x(z, t) - x_I(t)] \quad (22)$$

For the outlet

$$E \left(\frac{\partial x(z, t)}{\partial z} \right)_{z=l} = 0 \quad (23)$$

Rewriting eqns (1), (2) and (4) with the deviations in concentration from the quantities in a steady state, and taking the Laplace transform with t under the condition of constant flow rate, the following equation is obtained.

$$H_2(s) \frac{d^2 X(z, s)}{d(z/l)^2} - Pe H_2(s) \frac{dX(z, s)}{d(z/l)} - Pe H_1(s) X(z, s) = -Pe N_{OR} \left(\frac{Y_I(s)}{m} \right) \quad (24)$$

From eqns (22) and (23), the boundary conditions are

$$\left[\frac{dX(z, s)}{d(z/l)} \right]_{z=0^+} = Pe [X(z, s) - X_I(s)] \quad (25)$$

$$\left[\frac{dX(z, s)}{d(z/l)} \right]_{z=l^-} = 0 \quad (26)$$

Solving the second ordinary differential eqn (24) under the conditions of eqns (25) and (26), the result is

$$X(z, s) = \frac{Pe(b_2 e^{b_2 + b_1(z/l)} - b_1 e^{b_1 + b_2(z/l)})}{b_2^2 e^{b_2} - b_1^2 e^{b_1}} X_I(s) + \frac{N_{OR}}{H_1(s)} \left[1 - \frac{Pe(b_2 e^{b_2 + b_1(z/l)} - b_1 e^{b_1 + b_2(z/l)})}{b_2^2 e^{b_2} - b_1^2 e^{b_1}} \right] \left(\frac{Y_I(s)}{m} \right) \quad (27)$$

On the other hand, the following relation can be obtained from the Laplace transforms of eqns (1), (2) and (4) with the deviational quantities.

$$H_2(s) Y(z, s) = Y_I(s) + \frac{m N_{OR}}{\lambda} X(z, s) \quad (28)$$

The outlet concentrations of both fluids are shown by

$$X_{II}(s) = X(l, s) \quad (29)$$

$$Y_{II}(s) = \frac{1}{l} \int_0^l Y(z, s) dz \quad (30)$$

From eqns (27) to (30), the transfer functions shown by eqns (5) to (8) can be obtained.

2. Procedures for Obtaining the Transfer Functions by Perfect Mixing Vessels Model

Rewriting eqns (11), (12) and (4) with the deviational quantities in concentration from a steady state and taking that Laplace transform with t , the following relations are obtained.

$$X_i(s) = A^i(s) X_I(s) + \frac{N_{OR}}{H_2(s)} \cdot \frac{1}{n} \sum_{k=1}^i A^k(s) \left(\frac{Y_I(s)}{m} \right) \quad (31)$$

$$Y_i(s) = \frac{N_{OR}/\lambda}{H_2(s)} A^i(s) (m X_I(s)) + \frac{1}{H_2(s)} \left[1 + \frac{N_{OR}^2/\lambda}{H_2(s)} \cdot \frac{1}{n} \sum_{k=1}^i A^k(s) \right] Y_I(s) \quad (32)$$

where

$$A(s) = \frac{1}{1 + \frac{1}{n} \cdot \frac{H_1(s)}{H_2(s)}} \quad (33)$$

and a boundary condition is

$$X_0(s) = X_I(s) \quad (34)$$

The outlet concentrations of both fluids are shown by

$$X_{II}(s) = X_n(s) \quad (35)$$

$$Y_{II}(s) = \frac{1}{n} \sum_{i=1}^n Y_i(s) \quad (36)$$

From eqns (31) to (36) the transfer functions can be obtained and these are equal to eqns (5) to (8) in which $M_n(s)$ takes the place of $M_{pe}(s)$.

3. Procedures for Obtaining Eqns (18) to (21)

For a small deviation of the second fluid flow rate, the following equations shown by the Laplace transform can be obtained from eqns (1), (2) and (4) for $Y_I(s) = 0$.

$$\frac{d^2 X(z, s)}{d(z/l)^2} - Pe \frac{dX(z, s)}{d(z/l)} - Pe(\tau_{RS} + N_{OR}) X(z, s) + Pe N_{OR} X^*(z, s) = 0 \quad (37)$$

Eqn (38) *

where

$$y^0(z) - y_I^0 = \frac{m}{\lambda Pe} \left(\frac{d^2 x^0(z)}{d(z/l)^2} - Pe \frac{dx^0(z)}{d(z/l)} \right) \quad (39)$$

For solving the above differential equations the boundary conditions are as follows:

$$\left[\frac{dX(z, s)}{d(z/l)} \right]_{z=0^+} = Pe X(z, s) \quad \text{for } X_I(s) = 0 \quad (40)$$

$$\left[\frac{dX(z, s)}{d(z/l)} \right]_{z=l^-} = 0 \quad (41)$$

On the other hand, the following relations are obtained from eqns (1), (2) and (4) for the deviation of the first fluid flow rate and for $Y_I(s) = 0$

$$\frac{d^2 X(z, s)}{d(z/l)^2} - Pe \frac{dX(z, s)}{d(z/l)} - Pe(\tau_{RS} + N_{OR}) X(z, s) + Pe N_{OR} \frac{Y(z, s)}{m} = Pe \left(\frac{dx^0(z)}{d(z/l)} \right) \left(\frac{R(s)}{R^0} \right) \quad (42)$$

$$Y(z, s) = \frac{m}{\lambda Pe} \cdot \frac{d^2 X(z, s)}{d(z/l)^2} - \frac{m}{\lambda} \cdot \frac{dX(z, s)}{d(z/l)} - \frac{m}{\lambda} \tau_{RS} X(z, s) - \tau_{VS} Y(z, s) - \frac{m}{\lambda} \left(\frac{dx^0(z)}{d(z/l)} \right) \left(\frac{R(s)}{R^0} \right) \quad (43)$$

The boundary conditions are as follows:

$$\left[\frac{dX(z, s)}{d(z/l)} \right]_{z=0^+} = Pe X(z, s) + Pe(x^0(z) - x_I^0) \left(\frac{R(s)}{R^0} \right) \quad (44)$$

(for $X_I(s) = 0$)

$$\left[\frac{dX(z, s)}{d(z/l)} \right]_{z=l^-} = 0 \quad (45)$$

* Eqn (38) :

$$X^*(z, s) = \frac{1}{1 + \tau_{VS}} \left[\frac{y_I^0 - y^0(z)}{m} \left(\frac{V(s)}{V^0} \right) + \frac{1}{Pe \lambda} \cdot \frac{d^2 X(z, s)}{d(z/l)^2} - \frac{1}{\lambda} \cdot \frac{dX(z, s)}{d(z/l)} - \frac{\tau_{RS}}{\lambda} X(z, s) \right] \quad (38)$$

Eqns (18) to (21) can be obtained by the basic conditions mentioned above for $X_I(s) = Y_I(s) = 0$.

The term $P(s)$ in eqn (18) is

$$P(s) = 1 + \frac{N_{OR}^2 k}{(\lambda + N_{OR}) H_2(s)} \quad (46)$$

Nomenclature

C	A constant in an equilibrium relation
E	Back-mixing coefficient (m^2/h)
G	Molal flow rate of the second fluid per unit sectional area ($kmol/m^2 \cdot h$)
H_{OR}	Overall height per transfer unit based on the first fluid (m)
H_R, H_V	Holdups of the first and the second fluid in a whole system, respectively (kmol)
K	Modified mass transfer capacity coefficient (l./h)
$K_R a$	Overall mass transfer capacity coefficient based on the first fluid ($kmol/m^3 \cdot h$)
k	The ratio of τ_V to τ_R
L	Molal flow rate of the first fluid per unit width ($kmol/m \cdot h$)
l	Total travelling length of the first fluid (m)
m	A constant in an equilibrium relation
n	The total number of imaginary perfect mixing vessels
N_{OR}	Overall number of transfer unit based on the first fluid
Pe	Péclet number defined by eqn (10)
R	Molal flow rate of the first fluid ($kmol/h$)
$R(s)$	Laplace transform of deviational quantity of R
s	Complex parameter of Laplace transformation
t	Time (h)
u	Linear velocity of the first fluid (m/h)
V	Molal flow rate of the second fluid ($kmol/h$)
$V(s)$	Laplace transform of deviational quantity of V
W	Total volume of system (m^3)
x	Concentration of the first fluid (mol. fraction)
$X(s)$	Laplace transform of deviational quantity of x
y	Concentration of the second fluid (mol. fraction)
$Y(s)$	Laplace transform of deviational quantity of y

z	The length in the direction of the flow of the first fluid from inlet (m)
λ	Stripping factor ($= mV/R = mG l/L$)
τ_R, τ_V	Residence time of the first and the second fluid, respectively (h)

Superscripts

0	Value of steady state
*	Equilibrium value

Subscripts

I	Value at inlet
II	Value at outlet
i	Value in the i th imaginary vessel

References

- 1 ARMSTRONG, W. D. and WILKINSON, W. L. *Trans. Inst. chem. Engrs* 35 (1957) 352
- 2 DEISLER, P. F. and WILHELM, R. H. *Ind. Engng Chem.* 45 (1953) 1219
- 3 EBACH, E. A. and WHITE, R. R. *J. Amer. Inst. chem. Engrs* 4 (1958) 161
- 4 EGUCHI, W. and NAGATA, S. *Chem. Engng (Japan)* 24 (1960) 142
- 5 GILBERT, T. J. *Chem. Engng Sci.* 10 (1959) 243
- 6 KRAMERS, H. and ALBERDA, G. *Chem. Engng Sci.* 2 (1953) 173
- 7 MCHENRY, K. W. and WILHELM, R. H. *J. Amer. Inst. chem. Engrs* 3 (1957) 83
- 8 STRANG, D. A. and GEANKOPLIS, C. J. *Ind. Engng Chem.* 50 (1958) 1305
- 9 TAKAMATSU, T. and NAKANISHI, E. *Cont. Engrs (Japan)* 5 (1961) 217
- 10 TAKAMATSU, T. and NAKANISHI, E. *Mem. Fac. Engng Kyoto* 24 (1962) 150
- 11 VOETTER, H. *Plant and Process Dynamic Characteristics*, p. 73. 1957. London; Butterworths
- 12 WILKINSON, W. L. and ARMSTRONG, W. D. *Plant and Process Dynamic Characteristics*, p. 56. 1957. London; Butterworths
- 13 WILKINSON, W. L. and ARMSTRONG, W. D. *Chem. Engng Sci.* 7 (1957) 1
- 14 WOOD, R. M. and ARMSTRONG, W. D. *Chem. Engng Sci.* 10 (1960) 272

DISCUSSION

J. A. ALCALAY, 2542 Corralitas Drive, Los Angeles 39, California, U.S.A.

Would your defined mixing functions $M_{ps}(s)$ and $M_n(s)$ have the same format if the boundary conditions were different? Van Laar, in *Chemical Engineering Science*, has presented various solutions for the diffusional model equations depending on the boundary conditions.

T. TAKAMATSU, in reply

I solved the basic equation only under the given boundary conditions, so I cannot say whether or not this mixing function is applicable when the boundary conditions are different. I believe, however, that the effect of fluid mixing is concentrated to the form of mixing function. I thank you for giving this suggestion for our future study.

Experimental Study of the Dynamic Behaviour of a Heat Exchanger and of a Mixing Process

L. DELVAUX

Summary

Experimental work has been made on dynamics of two types of physical systems: (a) the heat exchange between a forced water flow and the inside pipe of a concentric tube exchanger; (b) the mixing in a stirred vessel (chemical reactor).

The performance of both systems was predictable by a transfer function of the general following form:

$$\frac{e^{-T_m s}}{1 + Ts}$$

however, the numerical values of the transport delay T_m and the time constant T were much different: (1) $T_m = 4 T$; (2) $T_m = 1/150 T$;

Their geometry was simple and their static characteristics were well known.

One purpose of the study was to compare two experimental methods for finding the frequency-response diagram: (a) step response followed by a simple and approached method for going from step to frequency response; (b) direct frequency response. It appears that the conjunction of both methods may be very valuable.

The other purpose of the report was to compare experimental frequency-response data and those obtained through a theoretical analysis, and to try to show how useless the mathematical models are when some basic factors of the static performance are not well known.

Sommaire

Deux systèmes physiques sont étudiés: un processus thermique à très faible inertie (fluide en tube intérieurs d'un échangeur à tubes concentriques) et un processus de mélange.

Tous deux sont représentables, en première approximation, par un système équivalent composé d'un élément à temps mort et d'un élément de retard du 1er ordre. Les grandeurs relatives du temps mort (T_m) et de la constante de temps (T) sont cependant très différentes: (1) $T_m = 4 T$; (2) $T_m = 1/150 T$.

La géométrie des deux systèmes est simple; les facteurs physiques définissant le régime permanent sont bien connus.

L'objet du travail est d'une part d'appliquer aux deux systèmes les méthodes indicelle et fréquentielle expérimentales directes et de les confronter avec l'analyse théorique; d'autre part, une méthode de transformation approchée de la réponse indicelle sous une forme la rendant applicable à un calcul direct de stabilité du système est étudiée.

Les résultats obtenus indiquent: (1) la possibilité relativement aisée d'application des deux méthodes expérimentales et la bonne concordance des résultats obtenus (10–20%) avec ceux de l'analyse théorique rigoureuse, susceptible d'être conduite dans les cas simples choisis; (2) l'intérêt de remplacer une expérimentation fréquentielle difficile dans certains domaines de fréquence par la transformation approchée des résultats de l'étude indicelle; (3) l'avantage présenté par ces méthodes expérimentales pour l'analyse de systèmes de même nature mais plus complexes, par rapport à une étude théorique basée sur un modèle mathématique approché, dans lequel doivent s'introduire des valeurs de paramètres physiques mal connus.

Zusammenfassung

Es wurden Versuche über die Dynamik zweier verschiedenartiger physikalischer Systeme angestellt: (a) Wärmetausch zwischen zwangsumlaufendem Wasser und dem Innenrohr eines konzentrischen

Wärmetauschers, und (b) Mischung in einem Rührbehälter (Reaktor-gefäß).

Das Verhalten beider Systeme konnte allgemein durch folgende Übergangsfunktion vorhergesagt werden:

$$\frac{e^{-T_m s}}{1 + Ts}$$

jedoch waren die numerischen Beträge der Transportverzögerung T_m und der Zeitkonstanten T sehr unterschiedlich, nämlich: für a) $T_m = 4 T$ und für b) $T_m = 1/150 T$.

Die geometrische Anordnung war einfach und die Kennlinien waren gut bekannt.

Ein Zweck dieser Untersuchung war, zwei Frequenzganguntersuchungsmethoden zu vergleichen: (1) Rückschluß auf den Frequenzgang aus der Sprungantwort und (2) direkte Bestimmung des Frequenzganges.

Es scheint, daß eine Kombination beider Methoden sehr günstig ist. Der andere Zweck der Untersuchung war der Vergleich aufgenommener und theoretisch abgeleiteter Frequenzgänge. Dabei sollte gezeigt werden, wie unbrauchbar ein mathematisches Modell wird, wenn einige wichtige Faktoren der statischen Kennlinie unbekannt sind.

Purpose of the Work

This paper, with the aid of two chosen physical examples within the domain, respectively of (a) the process of heat exchange and (b) the mixing process, is of interest, first, because of the exact knowledge of the physical parameters characteristic of the systems studied and intervening in the transient behaviour, and, secondly, because of the combined use of the experimental step and frequency response methods for finding the frequency-response diagram; in the case of an exclusive use of the step response, taking into account certain easy possibilities of deducing from it an approximate frequency response satisfactory to the needs of the user.

Statement of the Problem

The problem of the stability of a control loop—that is to say, of the adaptation of a controller to the loop in which it is incorporated—makes it necessary to know the transient behaviour of all the elements of the circuit.

The dynamic behaviour of the regulator is well known; that of the measuring and final control elements is not so well known, but this lack of information is often of lesser importance. The comparison of these elements to some delays of a given order and characterized by approximately known time constants, is still sufficient in the physical systems of heat transfer or of mixing; the most delicate problem is the determination of the dynamical behaviour of the system itself, the influence of which is most predominant.

Theoretical analysis is possible for some simple cases suitable for applications which are already numerous and very useful. The works of Professor Profos and his disciples show it to advantage in the study of steam generators. The analytical formulation of the transient behaviour allows, through further research of the transfer function, the determination of an open loop frequency response which is the base of the closed loop stability calculation.

One necessary condition is the introduction in the result of some appropriate values of the physical parameters of the considered system, such as in the domain of heat exchange between fluid and wall, of the steady state so-called 'film' transmission coefficient.

It might be useful to examine, in a simple case, the importance of the exact knowledge of these factors and the possible error made when these are neglected. Eventually, one would be able to appreciate the danger in predicting the transient behaviour of systems with more complicated forms (for example, of multitubular heat exchangers, with numerous passes in the tube and envelope sides) starting from a mathematical model, if it is necessary to introduce in this model some physical values known with an insufficient degree of precision.

In such a case, the return to the direct experimental methods will be important; here two techniques are available:

(a) The frequency response method introduces into the system a disturbance of a sinusoidal character, of constant and limited amplitude, and, in addition, of determined frequency; the attenuation and the phase shift of the resulting output, is then analysed for each frequency. A complete frequency response study necessitates the analysis to be carried out in a range of frequencies extending to the *strict minimum* between 1 and 10^2 , around a characteristic frequency.

(b) The step response method introduces into the system a sudden and lasting disturbance of the factor to be analysed of an equally limited amplitude, and studies the corresponding responses of the controlled variable; it can appear to take less time to obtain, provided that the necessary information might be gathered concerning the stability of the system, that is concerning the frequency response.

It is difficult to apply the mathematical transition from the step response to the frequency response method; numerous approximate methods have already been proposed and applied.

One of the purposes of this work is to examine the application of one of these methods—called the Teasdale method—to the two given problems.

Study of a Heat Exchange Process

This method uses a heat exchanger with concentric tubes and is restricted to the study of the dynamics of exchange between the fluid circulating in the inner tube and the intermediate partition, the latter being thermally isolated; in fact, the annular space of outer partition is filled with stagnant air.

The outflow temperature of the inside fluid, in this case, may be subjected to two disturbing effects: variation of the rate of flow of the fluid, or variation of its temperature as the entry into the exchanger. At the stage of study described here, only the second of these causes is considered, because this effectively does not introduce any non-linearity.

Description of the Plant and of the Experimental Method Used

The assembly used is shown in Figure 1. The inner tube of the exchanger is of steel (inside diameter 27.5 mm, outside diameter 33.8 mm). The outer tube has an inside diameter of 40 mm.

The total length of the tube is 4 m; for the experimental study it is divided, by five proportional plates, into four sections of 0.5 m; the element 1–5 in this study is thus 2 m long. It is preceded and followed by a section that is not needed for the measurement and which allows the setting up of a system of hydrodynamical and thermal flow*.

In each plate (labelled 0, 1, 2, 3, 4, 5 in Figure 1) the temperature of the fluid and of the walls is measured—the latter by means of a thermocouple. The temperature of the fluid is determined: (1) by means of a thermometer giving in the steady state a value close to the temperature of the fluid mixture, (2) by means of a thermocouple of low thermal inertia, centrally located in the tube so as to give an exact (maximum) temperature value.

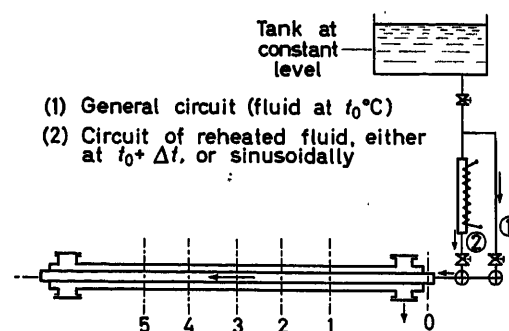


Figure 1. General layout of the plant

The interesting point about the first method of measurement is that it allows, in a preliminary study of the steady-state exchange, a check of the exact exchange law, valid for the chosen outlay of the system and for the physical properties of the fluid.

The particular form obtained from the classical relation $Nu = C.Re^m.Pr^n$ is the following:

$Nu = 0.0305 Re^{0.8}.Pr^{0.33}$ †; it gives a value of the coefficient α (static), defined by introducing into the given relation the values of the physical properties of the fluid calculated at the average temperature of the film $t_f = (t_p + t_M)/2$, t_p and t_M being the temperatures of the wall and the fluid measured.

Theoretical Study

Before applying the results of the last section to the considered example, we recall the established hypotheses and the main points of a solution which was given for the first time by Professor Dr. P. Profos, and which became a classical example.

The outflow of the fluid can be considered as unidirectional. Only one space variable is considered—the abscissa x , directed

* A reserve must be made: in the step study it will be necessary to use the elements 0–3.

† Certain effects (artificial promotion of turbulence, etc.) explain why values are slightly higher than the classical ones.

along the outflow axis of the fluid. The turbulence of the latter is, on the other hand, assumed to be perfect and the speed as well as the temperature are uniform in every plane perpendicular to the outflow axis. The natural convection in the fluid, and the thermal transmission in the outflow direction, within the fluid as well as in the walls, are negligible. The specific heats and the specific gravities of the fluid and of the walls are constant within the considered range of temperatures; the fluid-wall transfer coefficient is represented by an average value valid over the whole surface to which it is related. Finally, in a transverse cross section, the temperature of the walls is assumed to be uniform (radial transmission infinitely large). Proceeding from these hypotheses, and using the notations listed in Figure 2, for representing the thermal equilibrium of an element of the fluid in time dt , one arrives at:

$$\frac{\partial \theta}{\partial t} + v \cdot \frac{\partial \theta}{\partial x} + \frac{4\alpha}{\gamma c D} (\theta - \theta_p) = 0 \quad (1)$$

In the same way, the thermal equilibrium of the element of the corresponding wall is given by:

$$\frac{\partial \theta_p}{\partial t} = \frac{\alpha \pi D}{(\gamma c S)_p} \cdot (\theta - \theta_p) \quad (2)$$

It can be observed that, taking into account the above hypotheses, two constants appear, characterizing the fluid-wall exchange, and related, respectively, to the dynamic behaviour of the fluid and of the wall. These are:

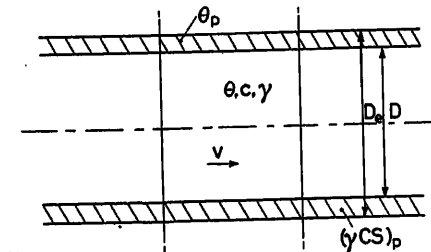
$$K_1 = \frac{4\alpha}{\gamma c D} \quad K_2 = \frac{\alpha \pi D}{(\gamma c S)_p}$$

From the two equations obtained with partial derivatives, a single differential equation describing the phenomenon could be deduced

$$\frac{\partial^2 \theta}{\partial t^2} + \frac{v \partial^2 \theta}{\partial t \partial x} + (K_1 + K_2) \frac{\partial \theta}{\partial t} + v \cdot K_2 \frac{\partial \theta}{\partial x} = 0 \quad (3)$$

This second-order partial derivative equation is linear under the assumption that α is constant within the range of variation of θ and equal to its average value on the exchange surface.

In order to solve it, one can use the classical methods of



Key

Inner fluid : temperature, $\theta^\circ\text{C}$

Velocity v , m/sec

Calorific capacity c , kcal/kg $^\circ\text{C}$

Specific gravity, γ kg/m³

Partition : the same figures affected by the p index and also transversal section $\frac{\pi}{4} (D_p^2 - D^2) = S_p$

Figure 2. Thermal balance of one element of the exchanger

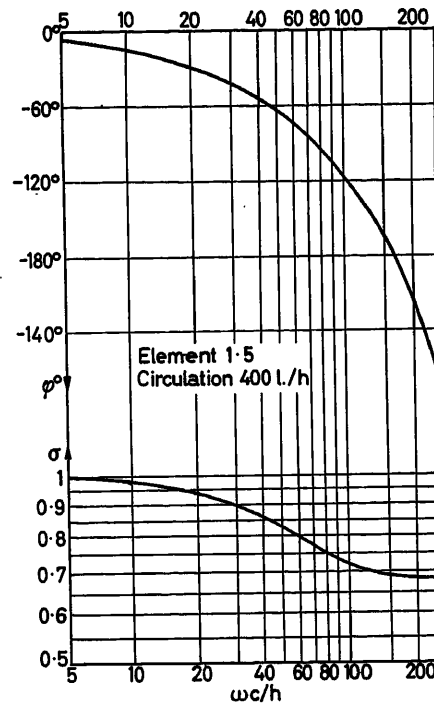


Figure 3. Theoretical frequency response characteristics of gain and phase in the heat exchanger (Elements 1-5)

Dr. Profos, or attempt to utilize the properties of the Laplace transform. In the latter case, the relation between the temperature of the fluid at any place in the tube and the temperature at the entrance can be expressed as a transfer function.

$$F(s) = \frac{\theta(x, s)}{\theta(0, s)} = e^{-As}$$

where

$$A = \frac{s^2 + (K_1 + K_2)s}{v(s + K_2)}$$

The final solution of the partial derivative equation will depend upon the initial conditions imposed on the problem. Campbell worked on the case of the step response and showed that it took the form of a series of Bessel functions.

By limiting oneself to the frequency response, the result is more direct— s is replaced by $j\omega$ in the solution and it follows:

$$\frac{\theta(x, j\omega)}{\theta(0, j\omega)} = e^{-ax} \cdot (\cos bx - j \sin bx)$$

where

$$a = \frac{K_1 \omega^2}{v(K_2^2 + \omega^2)} \quad b = \frac{\omega}{v} \left(\frac{K_1 K_2}{K_2^2 + \omega^2} + 1 \right)$$

From it, it is possible to find the elements of the frequency response

$$\text{gain} = \frac{(\theta_L)}{(\theta_0)} = \sqrt{e^{-2al} (\cos^2 bl + \sin^2 bl)} = e^{-al}$$

$$\text{phase delay} = \arctan(-\tan bl) = -bl.$$

The calculations have been carried out for the following conditions: $q_t = 400$ l/h from which $V = 0.188$ m/sec = 676 m/h; the average temperature of the inside water is 13°C ($\pm 1.5^\circ\text{C}$).

$$\theta_f \approx \theta_p \approx \theta = 13^\circ\text{C}$$

$$\alpha = 0.0305 \cdot \frac{v^{0.8} \lambda^{0.67}}{D^{0.2} v^{0.47}} (\gamma c_p)^{1/3} = 950 \text{ kcal/m}^2\text{h}^\circ\text{C}$$

$$K_1 = \frac{4\alpha}{\gamma_c D} = 138 \left(\frac{1}{\text{hour}} \right)$$

$$K_2 = \frac{\alpha \pi D}{(\gamma c_s)_p} = 71.2 \left(\frac{1}{\text{hour}} \right)$$

The results obtained by varying the disturbance frequency between 5 and 250 c/h are shown in Figure 3.

Experimental Study

Method Applied—The object is to determine, in the temperature of the inner fluid, some disturbances which are sharp or which vary with the time in a sinusoidal manner. Two very simple but effective methods are applied and these are shown diagrammatically in Figure 4.

(a) Application of a Sudden Temperature Variation. Two three-way valves are placed in the immediate vicinity of the inner tube entrance and allow either a feed with cold water ($t_0^\circ\text{C}$) or a feed with the water temperature increased to ($t_0 + 2$ to 4°C) according to the rate of flow. The 'step' is actually negative, going from ($t_0 + \Delta t$) to t_0 .

Some special precautions must be taken in order to maintain equal rates of flow in the exchanger, before and after the 'step'.

(b) Application of the Sinusoidal Variation. The water passes into a heating circuit in contact with a resistance of very weak thermal inertia, whose heating power is controlled by a

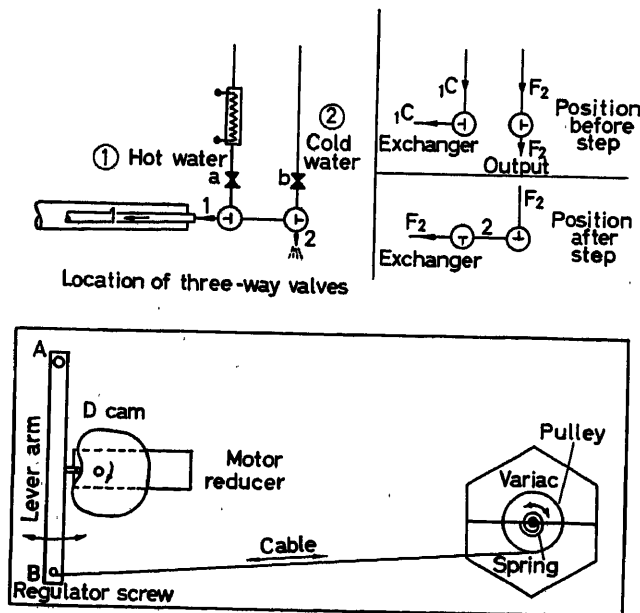


Figure 4. Practical realization of the enforced temperature variation: (a) step input signal; (b) sinusoidal input signal

variable autotransformer; the output voltage varies in such a way that the quantity of heat released by the resistance (V^2/R) varies sinusoidally. As shown in Figure 4 a grooved pulley spins with the shaft of the autotransformer; on this pulley is wound a cable which is fixed to the end B of a lever AB turning around a fixed point A. The point C of the arm of the lever rests on the cam D (of specially studied profile) the rotation of which induces the arm of the lever AB to oscillate. The continuous rotation of the cam is assured by a shunt motor whose rev/min is a function of the field current, but constant whatever the couple.

A spring fixed on the pulley maintains a constant tension of the cable and assures the contact of the pivot C with the cam. This system easily enables some perturbation frequencies going from 20 to 180 c/h. The recording of exchanger input and output temperatures is made by a quick recording unit comprising a Hewlett-Packard microvoltmeter (type 425A) and a Texas recorder.

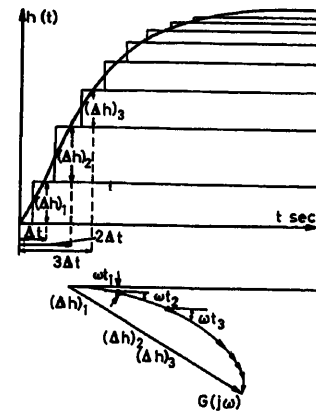


Figure 5. Principle of the Teasdale method

Transformation of the Step Response into Frequency Response—In our particular case, it appeared useful to check the experimental frequency response, owing to the narrow frequency band used. On the other hand, our purpose was to compare with the theoretical frequency response both the transformed step response and the experimental frequency response.

We follow an approximate method of passing from the step response to the frequency characteristics, which was indicated by Nixon¹ and Oppelt². Teasdale described it more clearly, however, in a graphical form³; Caldwell⁴ simplified its numerical application by means of tables, which make calculations easier.

As Oppelt shows very clearly, the method is based on the principle that the time response $h(t)$ given by the step response method results from the summation of output values of isolated elements connected in parallel, each having a given amplification factor (Δh_i), and delays increasing with respect to the time origin $\Delta t/2, 3\Delta t/2, 5\Delta t/2$, etc. (Δt being suitably chosen).

If a sinusoidal disturbance of a given frequency is imposed on this system, each element will give, as an output signal, an oscillation of amplitude equal to the height of the step ($\Delta h_1 - \Delta h_2 \dots$) and with a phase shift of $-\omega T_m$ where $T_m = (\Delta t/2, 2\Delta t/2, \dots)$. Teasdale adds geometrically the vectors which represent these oscillations in a polar diagram. Caldwell calculates the components of the vectors and adds them. The elements

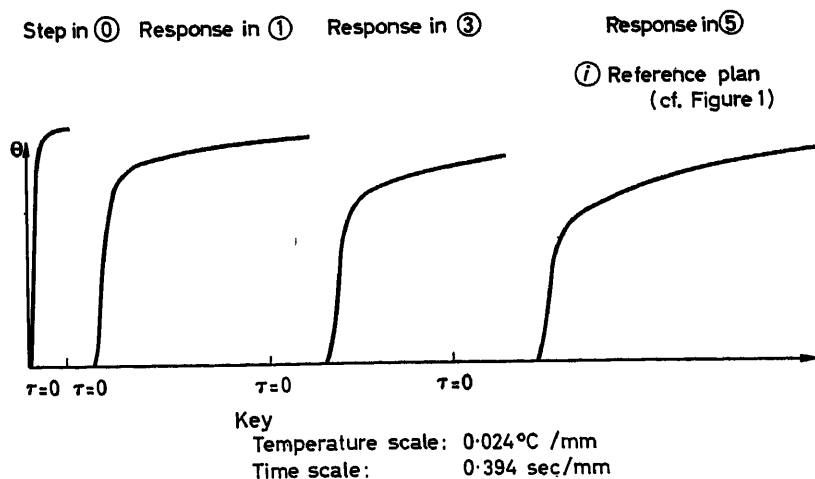


Figure 6. Experimental analysis step response (example)

justifying the method mathematically* can be found in the work of Teasdale³. We will only mention the hypotheses which must be satisfied in order to allow this justification:

The system must be linear; be at rest before the 'step' input; tend towards a new finite equilibrium value for $t \rightarrow \infty$; and be characterized by a transfer function with a denominator of an order at least equal to that of the numerator.

The Experimental Results—(a) Experimental Step-response Analysis. Figure 6 shows the experimental step response obtained from the plants of measurement labelled 0, 1, 3, 5 (Figure 1) following a temperature step signal of about 1.6°C, determined at 10 cm above point 0 in the inner fluid, for a rate of flow of the latter equal to 400 l/h; the average temperature of the transient state was 13°C.

(b) Experimental Frequency Response. Figure 7 gives, as an example, for the same conditions of rate of flow and average temperature, the results obtained for a determined frequency of the disturbance.

One can compare the recorded oscillations in amplitude and in phase; the calibration curve $\mu V - ^\circ C$ being nearly linear in the domain of the considered variation ($\Delta V = 5$ to $50 \mu V$ corresponding to 0.1175 – $1.175^\circ C$). In the following, the average amplitudes of the sinusoids are named, respectively: A_i^0 , A_i^1 , A_i^3 and A_i^5 .

One deduces directly from them the corresponding gains:

$$G_0 = \frac{A_i^3}{A_i^0}, \text{ etc.}$$

The phase shifts can be measured directly: that is, φ_{01} , φ_{13} , φ_{35} and by the summation $\varphi_{03} = \varphi_{01} + \varphi_{13}$ and $\varphi_{15} = \varphi_{13} + \varphi_{35}$.

Table 1 regroups the results obtained for the disturbance frequencies 40, 103.5, 123 and 157 c/h.

* This demonstrates that the transfer function of the $G(s)$ system is, in the case of a sinusoidal disturbance at the input, following the stipulated hypothesis:

$$G(j\omega) = \int_0^\infty e^{-j\omega t} d[h(t)]$$

where $h(t)$ is the temporal response of the system following a step disturbance. The approximation made returns to the numerical integration

$$G(j\omega) = \sum_{i=1}^{\infty} \Delta h(t_i) (\cos \omega t_i - i \sin \omega t_i)$$

Table 1 (a) Gain

c/h	157	123	103.5	40	38.2
q_i l/h	403	395	402	400	400
A_i^0 (μV)	36.32	49.6	59.6		104.5
A_i^1	29.5	40.91	49.9	88.7	
A_i^3	25.4	34.38	42.4		85.8
A_i^5	21.38	28.75	37.26	73.5	
G_{03}	0.699	0.694	0.712		0.821
G_{15}	0.725	0.704	0.746	0.829	

(b) Phase shift

φ_{03} ($^\circ$)	158.9	122.4	90.15	—	—
φ_{15} ($^\circ$)	159.4	137.1	117.45	—	—

Use and Interpretation of the Experimental Results

The Theoretical and Experimental Frequency Responses— Figure 8 shows the theoretical frequency response of the section of the exchanger between the measurement planes 1 and 5, for the disturbance frequencies from 10 to 250 c/h, and indicates, in addition, the transformation of the experimental results to the Bode diagram.

The frequency response obtained has a well-known characteristic course and shows, amongst other things, the appearance

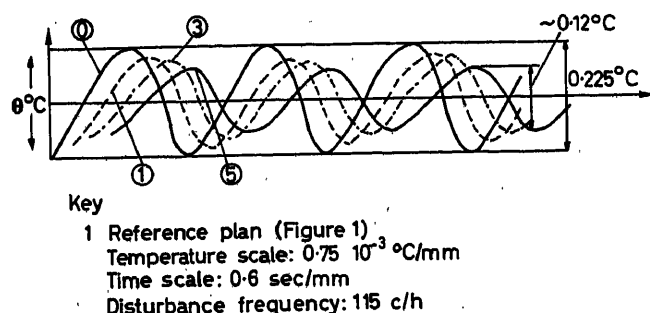


Figure 7. Example of frequency response determination

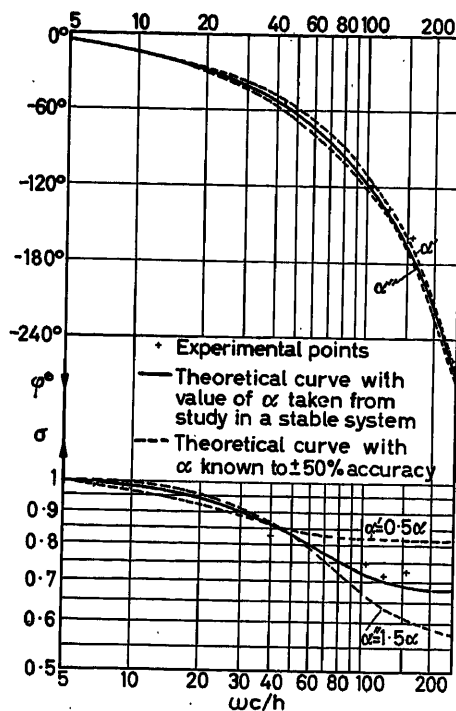


Figure 8. Frequency response—comparison of the direct and experimental frequency response methods

of a minimum gain limited to large frequencies and the high sensitivity of such a system to the temperature disturbances of the heated fluid.

The object being to compare the theoretical frequency response and the direct experimental results, the latter are likewise transferred to the same diagram*. The deviations are small, especially for φ ; they are not very important for G , increasing slightly with the frequency, and attain a maximum around 8 per cent in relative value.

It is interesting to compare these results with those which would be given by a theoretical analysis in which an erroneous transfer coefficient would be introduced. It is not unusual in the industrial exchangers to verify deviations from the theory or from the predicted calculation by 50 per cent (eventually 100 per cent[†]) for the coefficients of fluid friction as well as of thermal transfer. As an example, we have chosen a deviation of ± 50 per cent with regard to the static measured value.

It can be observed that in the region of the critical frequency (corresponding to $\varphi = 180^\circ$), the resulting deviations in the calculations of gain reach and exceed 20 per cent (Figure 8).

The Harmonic Response Obtained from the Step-response Study and the Direct Frequency Response—By means of the described method, and starting with the results given in Figure 6, the corresponding values of gain and phase shift are determined for different frequencies. The study was made on section 0-3 of the exchanger; it is in fact essential to consider as reference value for the step of temperature, the value obtained in the section nearest to the origin of the disturbance—that is to say, the plane 0†.

* The definitive text will further illustrate this subject.

† This peculiarity will make difficult any direct comparison with the results obtained in subsection (a).

Results

ω (c/h)	G	φ (°)
7.28	0.955	8.58
26.375	0.878	29.84
43.65	0.875	44.55
72.75	0.871	73.85
87.3	0.816	87.6
145.5	0.725	140.83
218	0.665	202.65

The results show a good correspondence for the phase shift; it can be seen that the deviations of the gain do not reach 10 per cent and, in addition, seem to be independent of the chosen frequency.

It should be noticed that the analysis should be referred to the 0-3 section of the exchanger situated in the direct proximity of the feed. The comparison between the experimental frequency-response results and the experimental step-response results certainly remains possible; nevertheless, a probable change of the film-coefficient value with regard to the steady state is to be feared: area of establishment of the outflow state, secondary effects provoked by the 'step' in the proximity of feed. It results from this that all direct comparison—theoretical frequency response method (based on a static value of α) and modified step-response method—is difficult.

First Conclusions

The theoretical and experimental study of a small inertia thermal system (τ of the equivalent system \approx several seconds) of well-known shape and permanent behaviour, shows that:

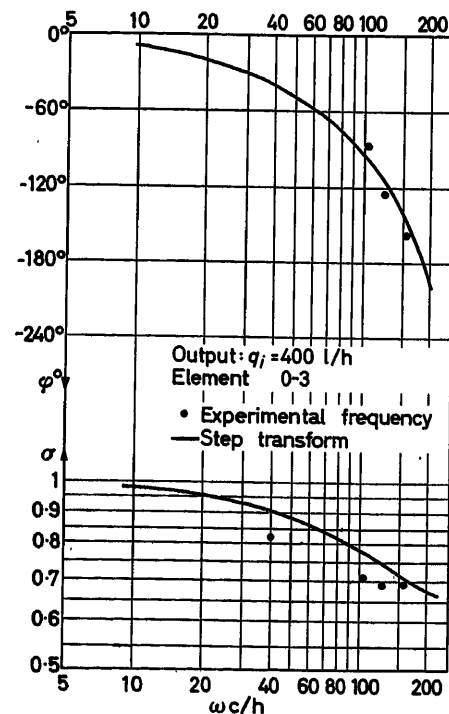


Figure 9. Comparison: harmonic response obtained by means of experimental step response and by means of direct frequency response

(1) The experimental methods (step and frequency response) can give in this case* a ± 10 per cent precision for the values of gain and of phase, useful for the stability determination.

(2) Their application is of moderate difficulty, independent of the nature of the studied system.

(3) The use of a mathematical model and the introduction into it of insufficiently precise physical parameters must lead, for a more complicated physical (exchange) system, to a larger imprecision than that resulting from the application of the experimental methods.

Study of a Mixing Process

The physical system studied is a reactor (tank and stirring equipment), in which chemical reagents are mixed.

The purpose of the work is to study the dynamical behaviour of the considered reactor from the exclusive angle of kinetic theory, therefore the chemical reaction is avoided and the operation consists in the mixing of two aqueous solutions.

The structure of the reactor is fixed, therefore the time of the mean stay of the products in the reactor (total flow rate), and the speed of rotation of the mixer, may be varied. A preliminary study will analyse the influence of these variations and

* To be confirmed by the study, which should be continued.

will allow to be found the form of the equivalent system which can be considered as an approximate description of the real system in its transient behaviour.

The study of the dynamic behaviour will examine the consequence of disturbances occurring in the *composition* of the reactor feed; in fact, the latter being supplied from one side by water and from the other by a concentrated solution of potassium bromide (33 per cent by weight), the composition will undergo some variations (either step or sinusoidally periodical) as a consequence of corresponding modifications imposed on the rate of flow of KBr, the total rate of flow remaining constant. The measures of concentration in KBr will have to be made continuously by means of a potentiometer, the detection being made at the outlet of the reactor.

Brief Description of the Plant

Figure 10 gives a general diagram of the plant and of certain details of the experimental application; detection by the potentiometer at the outlet of the reactor, and production of sinusoidal disturbances.

Figure 10 also shows the reactor (R), equipped with baffle plates, the thermostatic temperature control of the latter (tank and heating), the mixer (A), the concentric feed (F) of the products (water and KBr), the flowmeter (diaphragm system for water M_1 , rotameter (M_2) for the KBr solution, the whole

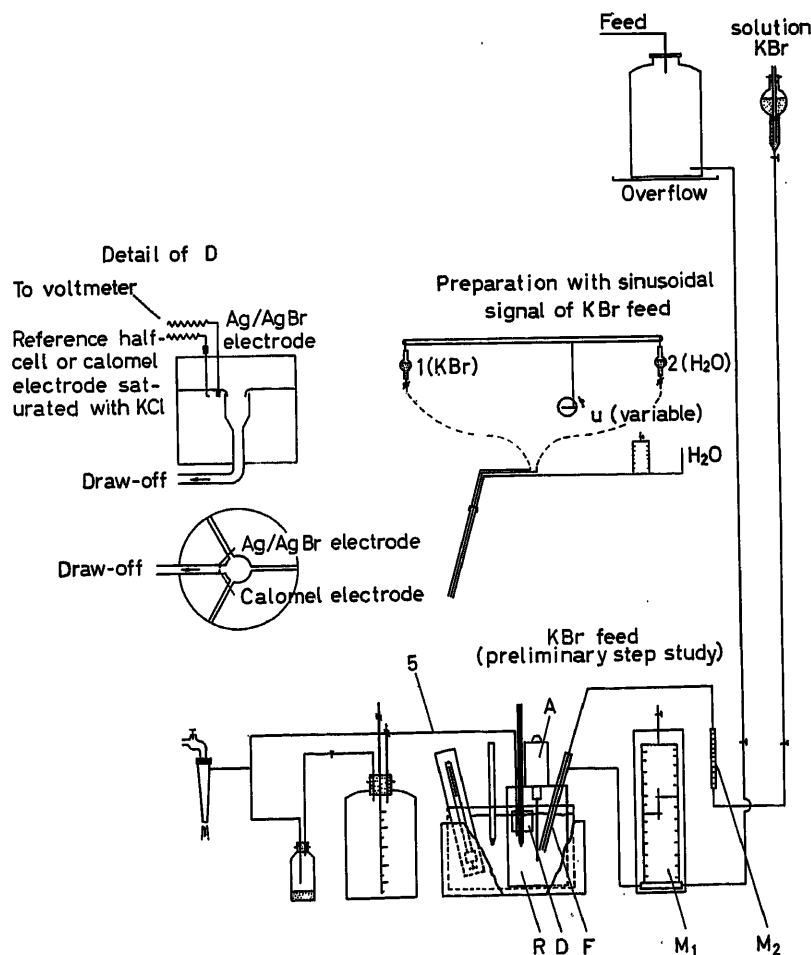


Figure 10. General diagram of the plant

allowing the continuous outlet and the final measurement of the total rate of flow through the reactor (S).

The detail of the detector (D) is likewise given, the measurement and potentiometric recording are made as in the first section (by a Hewlett-Packard microvoltmeter and a Texas high-speed recorder); these are not shown.

Preliminary Study

It was possible to define the nature of the mixing process by means of trials of the step response (in composition) carried out under variable conditions of total rate of flow to the reactor and of mixing speed.

Certain results, which are already well known, have been found again. From this analysis the studied system can be identified as an equivalent system resulting from placing in series a lag with dead time, and a transmission lag whose order will depend principally upon the mixing.

The obtained results show that in all the cases of mixing considered (130–1,100 rev/min), it is possible for the system to be represented as a first order system (preceded by a dead-time element). When the mixing is nil the order of the system rises and the system may be considered as of second order.

Figure 11 shows two results corresponding to extreme mixing conditions—nil on the one hand and strong on the other (1,100 rev/min). The given conclusions can be distinctly seen.

Experimental Study

Technique Employed—A sudden change in composition is obtained in the reactor by operating a valve mounted in the feed circuit of a concentrated KBr solution; all the other working conditions (water flow, speed of mixer, temperature of the thermostatic bath) being maintained constant.

The record gives the continuous variation $E = f(t)$ expressing the variation of the electrode potential (in mV) as a function of time. According to Nernst's law, one can deduce the variation of the concentration x , expressed in equivalent g/l*.

The realization of the sinusoidal input signal (composition) is based on the works of Turner⁶; his principle consists of varying sinusoidally the concentration of a constant flow of the solution, obtained from two feeds put in parallel and whose charges vary in a sinusoidal manner, one being shifted (by 180°) in relation to the other.

The arrangement is shown diagrammatically in Figure 10. It replaces the KBr feed used for the preliminary study and the step-response study. In practice, the amplitude of the input signal (concentration) thus obtained is 3.6 mV.

Experimental Results—The described experimental methods have allowed us to obtain the direct step and frequency responses of the system. Moreover, the above-mentioned Teasdale method has allowed to pass from one to the other. On the other hand, the preliminary study of the step response had allowed the calculation of the parameters characterizing the equivalent system, whose transfer function had been reduced to $F(s) = e^{-T_m s} / (1 + Ts)$.

The results of the experimental step-response study are first of all graphic; they will not be reproduced, with the exception of examples given above.

* In the chosen working conditions one obtains $E(\text{mV}) = 0.1718 + 0.0569 \log x$.

The frequency response method has been applied under the following conditions:

Total rate of flow: $Q = 0.555 \text{ l/min}$

Mixing: 900 rev/min.

There are the corresponding dynamic characteristics of the equivalent system:

T , time constant $\cong 9.4 \text{ min}$, T_m , dead time $\cong 4 \text{ sec}$. An example of the results is given in Figure 12.

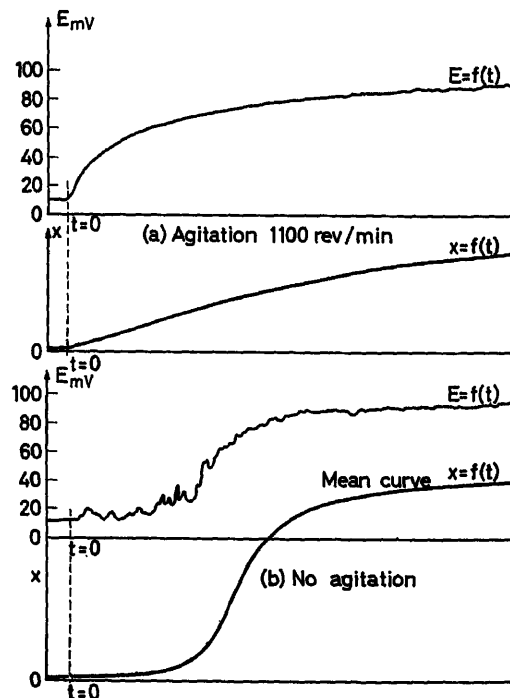


Figure 11. The influence of stirring (example of the experimental step response)

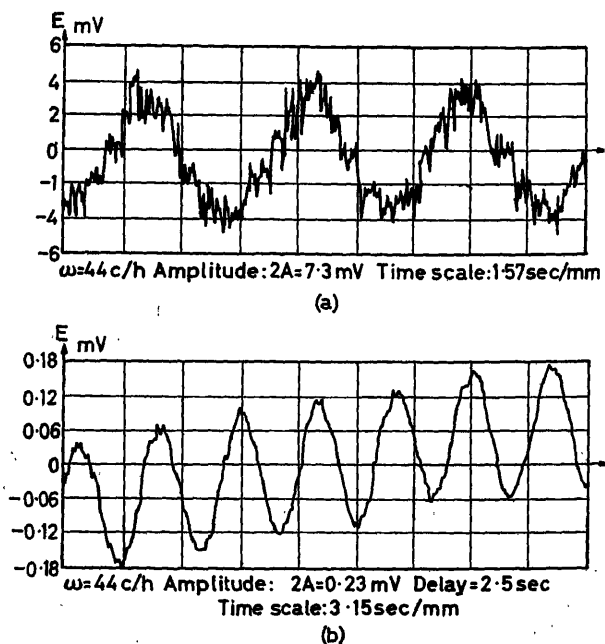


Figure 12. Example of experimental frequency response: (a) potential of input electrode; (b) potential of output electrode

The series of trials has furnished the following results, translated as before into gain and phase shift.

Table 2

c/h	10.9	13.4	16	27.7	44	51	80
G	0.135	0.097	0.0847	0.0534	0.032	0.0278	0.0168
φ°	93	89	96	102	104.5	110	114

c/h	91.1	102.5	111	165	180	213	
G	0.0146	0.0132	0.0124	0.081	0.074	0.065	
φ°	119	131	134	—	—	—	

Use of the Results

Figure 13 shows a comparison of the results with the Bode diagram. It will be seen that:

(1) The calculated response (in gain and phase) of a system equivalent to the one studied and whose transfer function will be $F(s) = e^{-T_m s} / (1 + Ts)$; T_m and T having values calculated starting from the experimental step response.

(2) The results of the experimental frequency response method.

(3) The values obtained by transforming the results of the step-response study by means of the Teasdale method.

First Conclusions

The experimental study of a mixing process with very large inertia (T of the equivalent system $\cong 9$ –10 min) and of simple shape allows one to state that the experimental frequency

response technique and the step response method translated approximately into harmonic response, give results similar within a minimum accuracy of 15–20 per cent.

Conclusions

(1) The study of two physical systems, having a certain analogy between them, as they can be represented by an equivalent system composed of a dead time element and of a first-order lag element, but strongly different as far as the numerical values of the criteria defining their degree of inertia, can be made experimentally using the two methods (step and frequency response) with a sufficient degree of precision for ultimate stability calculations.

(2) The direct frequency response method is sure; it corresponds to a well-defined periodic forcing function. However, it can be long and above all difficult to realize in the domain of low or high frequencies.

The step response method is quick but is not directly adaptable to the stability calculations; Teasdale's method used for a deduction of an approximate harmonic response gives us some satisfactory results.

(3) The combination of the two techniques is interesting (Figure 13).

(4) The consistent ignorance of certain essential physical factors (the total heat-transfer coefficient of an exchanger, for example) will lead, in a theoretical study on mathematical models, to serious errors.

Further Work

A summary of the first results obtained by a complementary study undertaken since the publication of the preprint is now presented.

The experimental study of the dynamics of two physical real systems described before and the comparison of the results obtained with those deduced from the analysis of a theoretical model has been completed by the introduction of the 'pulse method', extensively applied in the U.S.A. since 1953 under the guidance of J. O. Hougén.

Frequency-response data obtained from the pulse testing do appear to be in good agreement with those resulting from either, a direct sinusoidal forcing or a theoretical calculation applied to the mathematical model of these very simple systems.

Dynamics of a Double-Tube Heat Exchanger

In the preceding part of the study, the dynamic behaviour of the system was investigated in a very simple case: flow of hot fluid in the inner tube, and stagnant fluid at constant temperature in the annular space between tubes.

We are now extending the frequency analysis to a much more actual set of experimental conditions: both liquids are flowing, the one (inner tube) has its temperature disturbed and the other (annular space) is kept at constant temperature at the entry of the heat exchanger.

Instead of a simple differential equation, we get a set of three partial derivative equations, describing the dynamic behaviour of respectively:

- the temperature of the disturbed fluid (inner tube);
- the temperature of the wall between both fluids;
- the temperature of the fluid flowing in the annular space.

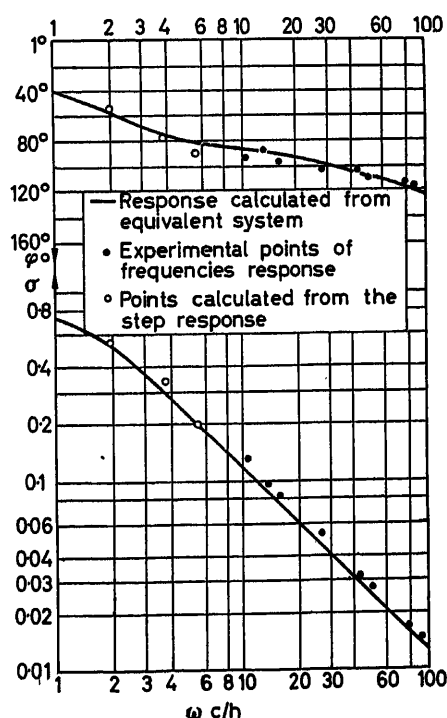


Figure 13. Experimental results from the study of the dynamic behaviour of the mixing process

The final solution leads to the following equation:

$$\frac{\bar{\theta}_i}{\theta_i(o, s)} = \frac{1}{n-m} (ne^{-nx} - me^{-mx}) + \frac{1}{n-m} (e^{mx} - e^{-nx})$$

m, n , being roots of a 2nd order equation:

$$p^2 + 2B_1p + C_1^2$$

The coefficients A_1, B_1, C_1 are functions of the physical parameters involved in the transfer phenomena (velocity of flow, heat transfer coefficient, various time constants involved, etc.).

The numerical solution of this equation may be found for some given flow conditions and may be compared with an experimental frequency response obtained in the same conditions, either directly or by means of a pulse test.

The results of the frequency response are given on Bode plots for two sets of conditions in Figure 14 and 15. An example of actual records obtained with the pulse testing is given in Figure 16.

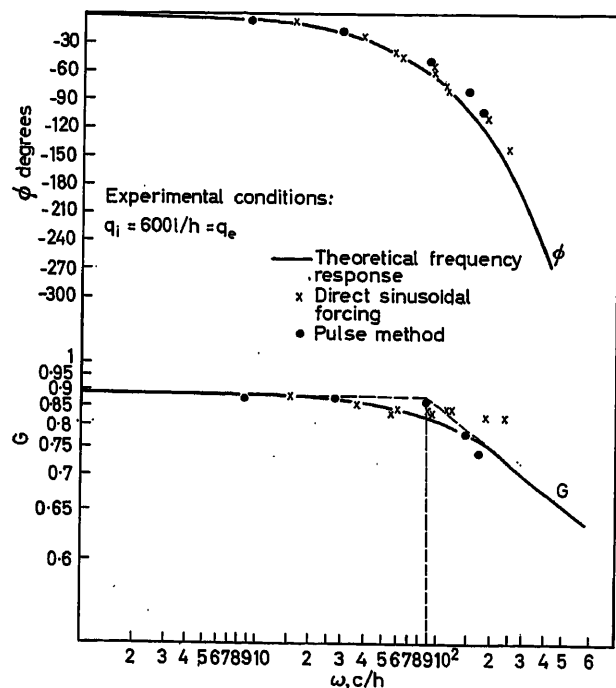


Figure 14

Dynamic Behaviour of Mixing in a Stirred Vessel

Research is here still in progress but both pulse and impulse testing have been applied; the last method is well adapted to a mixing process: the influent stream is disturbed by a sudden injection of a tracing agent and records are taken of concentrations in both inlet and outlet streams by the potentiometric method described previously.

The first result indicates the following tendencies:

(1) The pulse method gives accurate data in both amplitude and phase to a frequency of 1 rad/min; above this limit, approximations in the computation of the Fourier integrals introduces discrepancies in the results and, particularly, in the phase data.

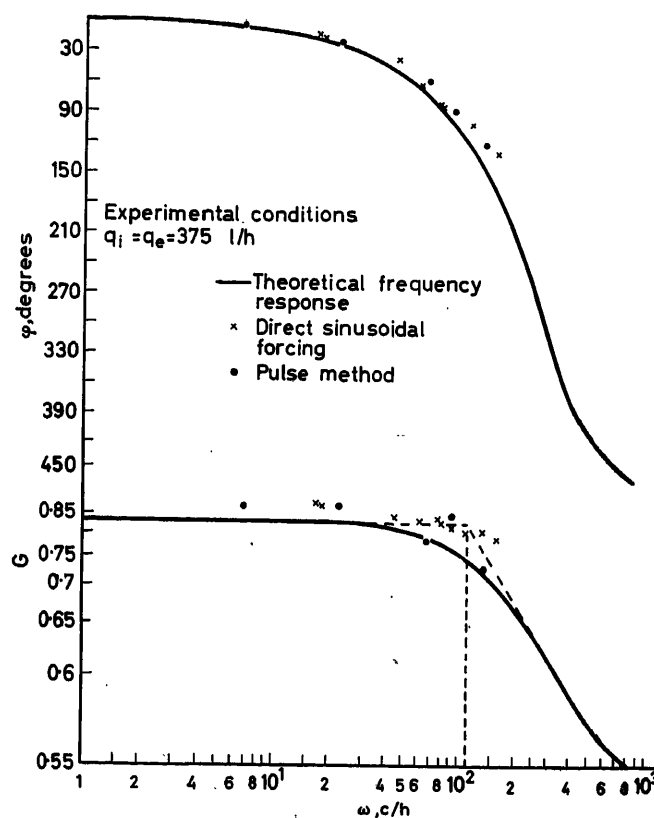


Figure 15

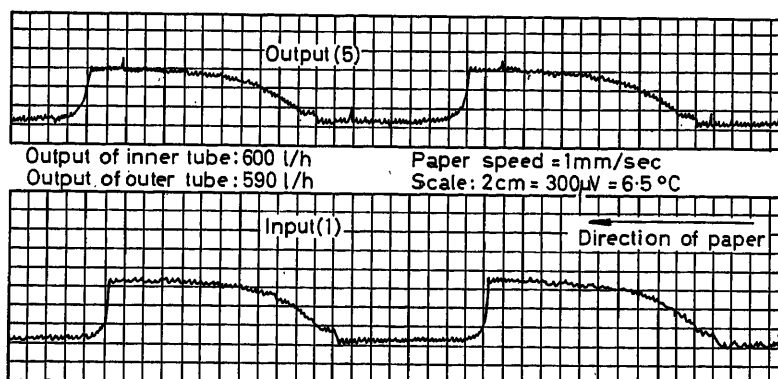


Figure 16. An example of the pulse method applied to the heat exchanger conditions: $q_i \cong q_e \cong 600 \text{ l/h}$

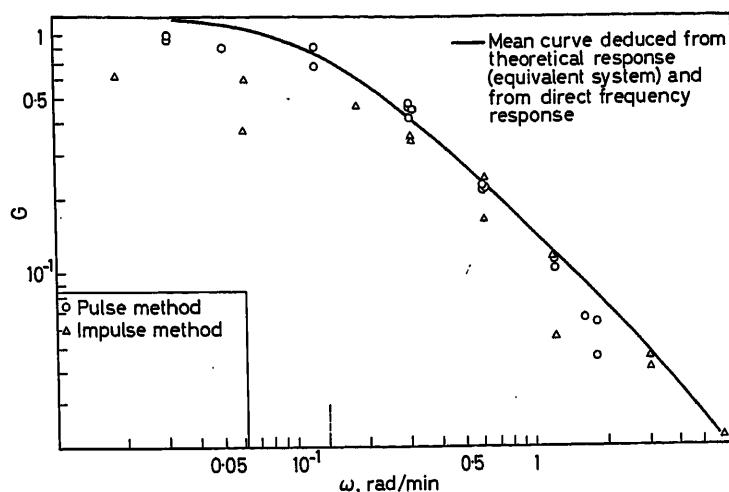


Figure 17

(2) The impulse method is less accurate, as it was expected from the difficulty of obtaining experimentally a signal comparable to a Dirac function in the inlet stream; however (and this fact needs a more extended investigation) the impulse results do conform to expectation, within the limits of their relative precision, even at the high frequencies, 1 rad/min and more.

Results of both methods are compared in Figures 17 and 18.

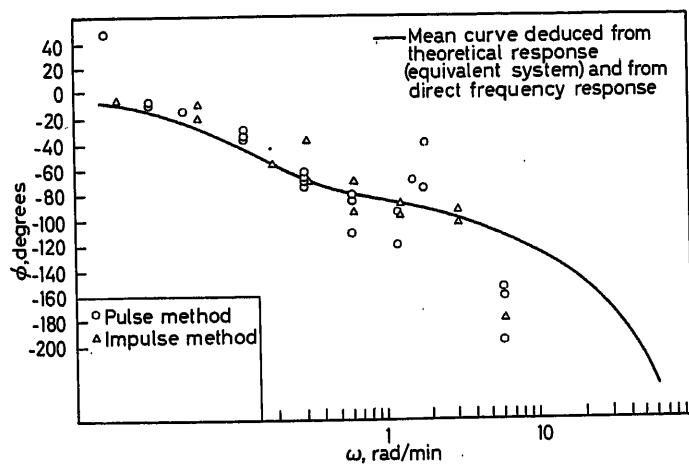


Figure 18

General Conclusions of the Results Obtained*

The experimental and theoretical study of two *very simple* real systems leads to the following conclusions:

(1) In these particular cases, the theoretical model may be used to predict the dynamic behaviour of the two systems, but a condition is required: the knowledge of the physical parameters and especially in the case of the heat exchanger of the actual value of the convection heat transfer coefficient (α , kcal/m²h°C).

(2) Three experimental methods give somewhat related results. A distinction must be made here between the two physical systems used for testing.

* In September 1963. Work is still in progress.

(a) Double-tube heat exchanger

(i) The step forcing with further transformation by an approximate method gives fair results when compared with the theoretical model, in the first case of a single flow in an isolated side-capacity.

(ii) In this first case, the direct frequency method gives results very close to those of the model; with a conventional double-tube exchanger, the experimental and theoretical results agree less, especially with high frequencies and small flows, but are sufficiently close for practical purposes.

(iii) The pulse method seems somewhat better than the two others, when compared with the theoretical model which is assumed to be the most reliable, after introduction of physical parameters deduced from the study of the statics of the system.

(b) Mixing process

Here, the step method with subsequent transformation and direct frequency response are very closely related to the theoretical curve of an equivalent system, up to the highest frequencies used: 100 c/h. The pulse testing does appear to be very accurate up to 10 c/h, and very sensitive to disturbing factors above this limit. The impulse method works fairly well but is influenced by the amplitude of the input.

(3) The application of these experimental methods to more complicated physical systems, such as industrial heat exchangers or mixing vessels, is fully justified; the choice between them is a question of application conditions: the conjunction of these methods may be very valuable.

The above paper has been based on results obtained at the Laboratory of Chemical Engineering of the University of Liège; two graduate works have recently been devoted to this subject, and we thank their authors, MM. Fontaine and Missaire, Lefebvre and Lognard for their very active collaboration.

The help of MM. Baudin and Diez, students in engineering, has been appreciated during the academic year 1962-1963. Two students in chemical engineering, MM. Marechal and Slets, have devoted their final work to this problem and the author was pleased to have their collaboration.

References

- ¹ NIXON, F. E. *Principes de Commande Automatique*. 1953. New York. Prentice Hall
- ² OPPELT, W. *Kleines Handbuch Technischer Regelvorgänge*. 1956

- ³ TEASDALE, A. R. *Control Engng.* Oct. (1955) 56-59
- ⁴ CALDWELL, W. I. *Frequency Response for Process Control*. 1959. New York; McGraw-Hill
- ⁵ WHITLEY, D. L. *C.E.P.* Sept. (1961) 59-65
- ⁶ TURNER, G. A. *C.E.S.* 7 (1958) 156; 10 (1959) 74

DISCUSSION

S. J. BALL, *U.S. Atomic Energy Commission, Oak Ridge National Laboratory, Tennessee, U.S.A.*

Delvaux's objective is a commendable one. Good experimental information about the validity of mathematical models of process dynamics is very useful and quite rare. In studies of this type, however, it is very important for the experimental methods to be sufficiently accurate so that it is the accuracy of the model, and not of the experimental procedures, that is determined.

It appears that neither of the examples of experimental techniques used by the author is accurate enough to make judgments about the

values of

$$K_1 = 138 \text{ h}^{-1}, K_2 = 71.2 \text{ h}^{-1}, V = 676 \text{ m/h, and } X = 2 \text{ m}$$

the gain characteristics of Figure 3 should be shifted to the left roughly a factor of 2π (i.e. the frequency scale should be relabelled rad/h rather than c/h). Independent calculations of K_1 and K_2 by myself, however, gave values of 112 h^{-1} and 227 h^{-1} , respectively. The corresponding gain curve agrees with the author's curve (Figure 3) to within ± 5 per cent.

A transformation from step response to frequency response using Samulon's method was made for the author's data in Figure 6; computations were made by a digital computer programme. A sampling interval of 0.394 sec was used and the truncation was negligible. A comparison of the results with my theoretical curve is shown in Figure A, in which the gain curves show close agreement. The high values of phase shift for the theoretical curve may be due in part to the error in the assumption of no axial mixing in the field. The Reynolds number for this system was only about 4,000, i.e. the flow was barely turbulent. One could expect that the 'plug-flow' assumption would be more accurate for more fully developed turbulent flow, which would be present in most engineering applications.

In conclusion, I feel that Delvaux has not sufficiently supported his conclusion that the theoretical model is inadequate.

References

- ¹ DREIFKE, G. E. and HOUGEN, J. O. Experimental determination of system dynamics by pulse methods, 1963 *Joint Automatic Control Conferences Preprints*, 608
- ² BRADFORD, C. E. and DEMERIT, M. W. Relation between transient and frequency response. *Handbook of Automation, Computation & Control*, 1958. Vol. I, pp. 22-48, edited by E. M. Grabbe, S. Ramo and D. E. Woolridge, New York; Wiley

J. CASTRÉN, *Ekono, Association for Power and Fuel Economy, Etala Esplanadikatu 14, Helsinki, Finland*

Are there any special reasons for not using other deterministic signals in the investigation of the problems presented? If so, what are they?

In the study of industrial processes the impulse response method seemingly has some advantages, especially in mixing problems where one could use tracer methods. In this case no complicated devices are needed to produce the input pulse. If the transfer function of the process is approximated with a time delay and a first-order lag element these can be calculated easily from the temporal moments of the input and output pulses. This method has been applied in Finland to mixing problems where radioactive tracers have been used.

B. JUNKER, *Sauter Ag., Basle, Switzerland*

With reference to the first problem considered in this paper, there exists a set of calculated step-response functions, published in *Die Regelung von Dampfanlagen* by Profos. Comparing Figure 6 of this paper with Figure 7-40 of that book, I feel that the five reference plans (Figure 1) give only small variations of parameters and therefore the results cover only a small part of possible dynamic characteristics of this type of plant. It might be interesting to carry out the tests for higher (and from a heat exchange engineer's point of view more practical) values of H_D (Profos' notation).

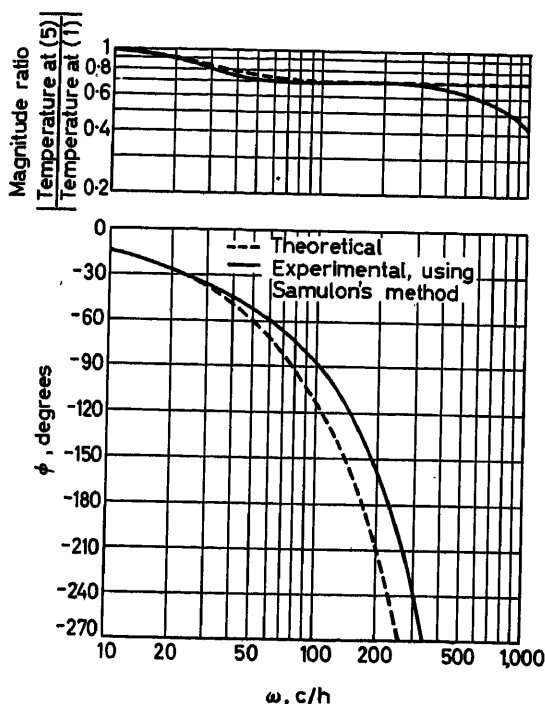


Figure A. Comparison of theoretical and experimental frequency response of pipe (section 1-5)

model's accuracy. In the direct frequency-response test data of Figure 7 for example, there is a large amount of harmonic distortion and measurement noise. In some cases, the period of the positive half of the 'sine wave' is more than 20 per cent longer than that of the negative half. For this particular example, where the maximum 'theoretical' change in magnitude ratio is only about 30 per cent, the data does not appear to be adequate.

The author's discussion of converting transient response data to frequency response plots neglects the important fact that the accuracy of the method is very sensitive to the size of the sampling period and to the amount of truncation¹. Also, it has been found that for step-response tests, Samulon's method² is more accurate than that of Teasdale, as used by the author.

There appears to be an error in the calculation of theoretical frequency response for water flow in the insulated pipe. Using the author's

J. GRAUVOGEL, *Electricité de France, 12 Place des Etats-Unis, Paris 16^e, France*

Delvaux's paper is very interesting in that it shows the comparative merits of experimental and theoretical studies in the analysis of relatively simple systems.

Are the results applicable to the study of more complex systems which are difficult to analyse theoretically because they contain parameters which are not well defined or which change with time? I am thinking in particular of multi-tube, contra-flow heat exchangers which become progressively dirty.

Has the author considered other methods for determining the transfer function of a system, for example from the step response. The method of Vladimir Strejc, for example, reduces a system with many time constants to one with a single time constant T of order n , together with a pure delay τ , and determines T , n and τ from the slope of the response to a step function.

P. K. M'PHERSON, *U.K.A.E.A., C. and I. Division, Atomic Energy Establishment, Winfrith, Dorset, England*

Both frequency response and step response methods have disadvantages in relation to the dynamic testing of heat exchangers. Industrial type heat exchangers have long response times, so that 'single-frequency' frequency-response testing will take a long time. 'Multi-frequency' testing, of course, overcomes this difficulty. The plant has to be disturbed with a sinusoidal wave which requires careful engineering. The dynamics of heat exchangers are dominated by transportation lags which introduce considerable difficulties in the interpretation of the responses when deriving transfer functions. Step-response testing will provide data on the dominant poles of the heat exchanger dynamics, but the fine detail of the faster dynamics will be lost.

Multi-channel cross-correlation analysis is particularly suited to dynamic experiments with heat exchangers, or for any plant for that matter. I am referring here to 'binary' cross-correlation analysis in particular, in which a periodic binary code is used to provide the plant disturbance. A class of such codes, known as 'pseudo-random', has the useful property that the autocorrelation function of the code is a pure Dirac-delta function within a defined bandwidth. This allows certain advantages to be derived from the technique: the transducer applying the disturbance need only be a simple on-off or two-state device; the binary input simplifies the resulting computation of the cross-correlation function permitting it to be done on-line with relatively simple logic, and this function will in fact be the plant's impulse response function. This is easily recognized and can be displayed on a visual indicator.

J. ZORN, *Technological University, Delft, Netherlands*

It would be interesting to learn from Delvaux about the considerations which have led to the choice of Teasdale's method for obtaining the frequency response from the step response. It might also be useful to

have some additional information with respect to the interval width which has been used since this determines the accuracy of the results.

It is well known that quite a number of methods have been proposed for evaluating Fourier transforms. It would have been interesting to apply some other methods and to compare the results with previous papers, e.g. those of Schneider¹ and Huss and Donegan². Such an investigation would be a useful addition to a study performed by the present author which constitutes his doctoral dissertation published recently³. In this study the majority of the published approximate Fourier transform methods are critically examined, the promising ones being applied to a number of test systems (lumped parameter systems) and some signals. The study has led to the development of some improved methods. One of the major results was the following: it was found that for systems whose frequency response tends to a linear high-frequency asymptote (on a log-log scale), the well-known sampling theorem need not be satisfied in evaluating the frequency response from the transient response by a sampling method. It was shown that the errors caused by frequency folding can often be compensated for by means of multiplicative or additive correction functions. For the test systems the above method yielded frequency response values having a better accuracy than that reported by Delvaux. In addition, some computing techniques for speeding up the numerical evaluation of the unknown response have been presented. A review of the results will shortly be published in *Automatica*.

The application of the above method to the systems dealt with by Delvaux has not been studied by the author in detail. The application to the second system is straightforward provided the transport delay is eliminated³ but the first system does not meet the conditions of the asymptotic behaviour indicated previously. It would be interesting to compare the results of the application to this system of those methods which proved most suitable for the systems considered by the present author.

References

- ¹ SCHNEIDER, A. *Regelungstechnik*, 9 (1961), 277, 327
- ² HUSS, C. R. and DONEGAN, J. J. *N.A.C.A. Techn. Note 3701*. Washington D.C. 1956
- ³ ZORN, J. *Methods of evaluating Fourier transforms with applications to control engineering. Dissertation*. Delft, 1963

H. UNBEHAUEN, *Institut für Verfahrenstechnik und Dampfkesselwesen, Technische Hochschule Stuttgart, Gruppe Regelungstechnik 7, Stuttgart, Germany*

I wish to draw Delvaux's attention to another method for determining the frequency response from the step response which I think is more rapid and accurate than that of Teasdale and which has been used very successfully at our Institute. Within this method the experimentally determined transfer function $f(t)$ is approximated by N linear segments, with the same time interval Δt (Figure A).

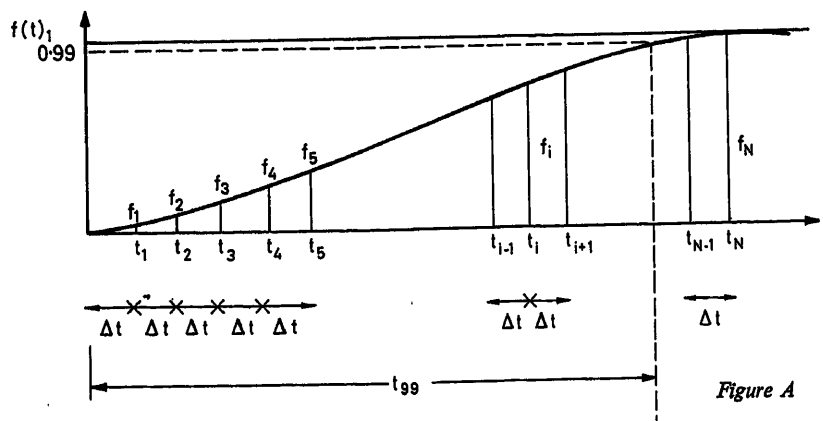


Figure A

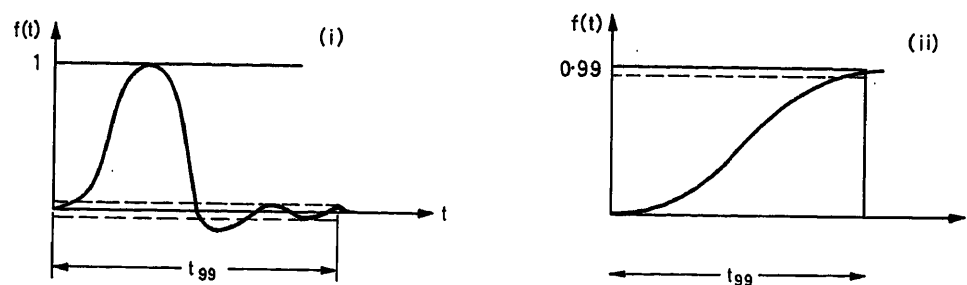


Figure B

The frequency response $F(i\omega)$ is found by a graphical and analytical method using the Fourier integral

$$F(i\omega) = i\omega \int_0^{\infty} e^{-i\omega t} f(t) dt = R(\omega) + iI(\omega) \quad (1)$$

This equation leads to the representation of the frequency response by its real and imaginary parts:

$$R(\omega) = \frac{1}{\omega \Delta t} \left\{ \sum_{i=1}^{N-1} f_i (\sin \omega t_{i-1} - 2 \sin \omega t_i + \sin \omega t_{i+1}) + f_N (\sin \omega t_{N-1} - \sin \omega t_N) \right\} \quad (2)$$

$$\text{where } t_N = \left(n + \frac{1}{2} \right) \cdot \frac{\pi}{\omega}; \quad n = 0, 1, 2, \dots$$

$$I(\omega) = -\frac{1}{\omega \Delta t} \left\{ \sum_{i=1}^{N-1} f_i (\cos \omega t_{i-1} - 2 \cos \omega t_i + \cos \omega t_{i+1}) + f_N (\cos \omega t_{N-1} - \cos \omega t_N) \right\} \quad (2a)$$

$$\text{where } t_N = n \cdot \frac{\pi}{\omega}; \quad n = 1, 2, 3, \dots$$

The upper limit of integration t_N must also satisfy the condition $t_N \geq t_{99}$.

The meaning of t_{99} is shown in Figure B.

In the case shown in Figure B (i) the last term of the equation vanishes. The method has the advantage that it is very suitable for solution using a digital computer, as the step response has only to be fed by pairs of values t and $f(t)$.

The accuracy can be improved by using larger values of N . However, when N has smaller values (e.g. $N = 8$) very good results are obtained by hand calculations with little effort.

Reference

UNBEHAUEN, H. Ein graphisch-analytisches Rechenverfahren zur Bestimmung des Frequenzganges aus der Übergangsfunktion. *Erscheint voraussichtlich in Regelungstechnik*. 10 (1963)

L. DELVAUX, in reply

In regard to Mr. Ball's comments, I must first state that I had never considered in my particular experiments that a theoretical model was not adequate. It may be that not enough stress has been laid on the fact that the main purpose was to test experimental procedures on simple physical systems where the comparison with the theory was possible and justified; therefore such a comparison required a good degree of confidence in the adequacy of the theoretical model. This was so, in the considered cases.

The conclusion and the general conclusion of the paper may be ambiguous to anyone who does not read the whole text. So this has been modified.

I thank Mr. Ball for his thorough analysis of the data furnished, but believe that he has been in doubt about certain results because of some errors.

As a matter of fact, corrections have been made in the paper. The K_a value given of 71.2 h^{-1} was introduced by error; it corresponds to the inner tube not isolated, i.e. to a set of experimental conditions not related in the paper. The actual value which was used for the calculations and to which Figure 3 refers is $K_a = 310 \text{ h}^{-1}$; therefore, the curves of Figure 3 are correct.

To make this point clearer, the detail of the calculation is given: Value of time constants:

$$K_1 = \frac{4\alpha}{\gamma c D} = \frac{4 \times 950}{1.000 \times 1 \times 0.0275} = 138 \text{ h}^{-1}$$

$$K_2 = \frac{\alpha \pi D}{(\gamma c S)_p} = \frac{950 \times \pi \times 0.0275}{7.7 \times 10^3 \times 0.114 \times \frac{\pi}{4} (33.8^2 - 27.5^2) 10^{-6}} \cong 308 \text{ h}^{-1}$$

Calculation of gain curve:

$$a = \frac{K_1 \omega^2}{v(K_2^2 + \omega^2)} \quad \text{and} \quad G = \frac{(\theta_L)}{(\theta_0)} = e^{-at}$$

ω (c/h)	ω rad/h	ω^2	a	e^{-at}
5	31.4	988	0.00207	1
15	94.3	8,890	0.01726	0.96605
20	125.6	15,800	0.0288	0.944
30	188.6	35,600	0.0552	0.8953
40	251.2	63,100	0.08075	0.852
60	377.2	142,000	0.126	0.777
90	565	320,000	0.157	0.7303
120	754.2	570,000	0.1745	0.7055
150	943	889,000	0.184	0.692
200	1,256	1,580,000	0.1864	0.685

The author was not able to find how Mr. Ball was able to obtain $K_1 = 112 \text{ h}^{-1}$ and $K_2 = 227 \text{ h}^{-1}$. The corresponding curves agree effectively with the experimental and theoretical curves of the author; this fact shows that an eventual error of 25 per cent on the physical parameters of the model is not yet too serious; it is partially due to the particular exponential form of the relation between G and K_1 , K_2 and v . Furthermore, it is not in opposition with the assertion of the author, according to which a possible error of 50 per cent on the value

of the physical parameters to be introduced in very complicate systems (for instance, multi-tube heat exchanger in use) such as those that Mr. Grauvogel introduced in his very interesting remarks, results (at the higher frequencies) in a corresponding error of 20 per cent in G and of the related stability calculation.

The curves given in *Figure 7* are, in my opinion, only an example and, as a matter of fact, this particular example was a bad one (with too small input amplitudes). It appears clearly that measurement noise does not affect seriously the sinusoidal curve. There is, however, some peculiarity in the shape of both signals (input and output) and it may be due to the particular realization of the temperature sinusoidal forcing. However, the author believes that in his experiments the most important requirements of a frequency-response testing were observed, namely: linear system, constant input frequency, no system transient present.

Finally, I wish to point out that temperature profiles have shown me that longitudinal mixing may be neglected, in the interior flow, as a first approximation. As a matter of fact, the Reynolds number (actually low) is not the only criterion of the turbulence in a given flow: natural rugosity or presence of turbulence promoters (such as thermometers or thermocouple leads) may induce a higher turbulence, at least in the core of the flow, i.e. in 95 per cent of the section; this fact was indicated by the relatively high value obtained for the form factor c , in the general relation $Nu = c \cdot Re^n \cdot Pr^m$.

The question of comparison between methods of transformation from step to frequency response, will be treated further (i.e. in the reply to the remarks of Messrs. Grauvogel, Unbehauen and Zorn).

I have expressed my indebtedness to Mr. Ball for the additional information he provided, by the use of Sanulon's method on his data.

In reply to Mr. Castrén, I hope that the complementary text has already brought a partial answer to the question by giving some results about the use of pulse and impulse methods to the mixing process. Additional information will be reported later¹, but I would like to have the opinion of Mr. Castrén, as to the results of pulse and impulse methods for relatively high frequencies (above 1 rad/min).

I fully agree with Mr. Junker that in my investigations I have only covered a small part of the possible dynamic characteristics of the heat exchanger used. The main purpose was the testing of experimental methods that may be applied more from a practical point of view when their use has been justified, in very simple cases, which are not too far from the theory.

The question of the best method to use for transforming step response has been introduced by Messrs. Grauvogel, Zorn and Unbehauen as well as by Mr. Ball.

I have used Teasdale's method as a very approximate method and as the first which I found at the beginning of my study to be of very practical use. However, I did try to avoid truncation errors (by respecting the relation $\omega\Delta t \ll 1$).

So the sampling time was related to the investigated system: for the heat exchanger, I used generally $\Delta t = 0.394$ sec (that is, incidentally, the value used by Mr. Ball) since it corresponds to a length of 1 mm on the recording paper. At very low frequencies ($\omega < 10$ c/h), Δt was taken = 0.788 sec.

In the study of the mixing process, where the time constant of the equivalent system was about 30 min, the sampling time was taken $\Delta t = 1$ min, and in each set of calculations, twelve frequencies were chosen, equally distributed above and below the critical frequency defined by $1/T = 0.11$ rad/min.

I have also to indicate that in the first system (heat exchanger), a good definition of the dead-time has to be made: as a matter of fact, $\varphi = \varphi' + \varphi''$, with φ' deduced from the Fourier transform and $\varphi'' = -\omega t$, t being a real dead-time or transportation lag defined by $1/v_{\max} \cdot v_{\max}$ is here the actual velocity of the flow at the location of the temperature detector. As $v_{\max} = 1.25 \bar{v}$ (according to some measurements and calculations), it may be that Mr. Ball has not taken this fact into consideration and has found higher φ'' than those really occurring (see his graph, *Figure A*).

Later I plan to compare the various methods suggested; namely those of Samulon, Strejc, Zorn and Unbehauen, and to report the results*. I particularly appreciate the apparent simplicity of Unbehauen's method.

I agree with Mr. M'Pherson on the fact that pseudorandom disturbances may be used to find the dynamic behaviour of physical systems, but I have no experience about the use of such methods.

Finally, I would like to express my appreciation to Mr. Grauvogel for having brought the problem to the fore.

We investigate experimental methods of deducing frequency response to obtain an answer to those problems that *must* be solved (even when it is unlikely that a solution is possible), namely the dynamic behaviour of real physical systems having a very complicated nature.

I believe that theoretical and experimental methods have to be used in conjunction for the planning and designing of such units; the adaptation of controllers to progressively changing conditions ('dirty heat exchangers') will, however, require mainly the use of the experimental method.

* Probably in the review of the Belgian branch of I.F.A.C. I.B.R.A.

Study of Industrial Production of Polyethylene under High Pressures, and of the Automatic Control of the Process

B. V. VOLTER

Summary

This paper gives an account of the results of the study on a reactor for the polymerization of ethylene, representing a medium of control, and a brief description of a system for its automatic control. The control equipment consists entirely of pneumatic components.

A formula, representing a relationship between the reactor output and the other components of the process, is proposed. The self-oscillating conditions encountered in the operation of the reactor are investigated, and a mathematical model of a selected part of the reactor is proposed and analysed.

Sommaire

Cette note se rapporte à un réacteur destiné à la polymérisation de l'éthylène; elle rend compte des résultats de l'étude entreprise en vue de son automatisation et donne une brève description du système préconisé pour assurer son réglage. L'équipement est entièrement pneumatique.

On y propose une formule qui établit une relation entre la grandeur représentant la production du réacteur et les grandeurs représentant les autres éléments du processus. On y étudie les conditions d'auto-oscillation de la marche du réacteur et on y propose, pour une partie de ce dernier, un modèle mathématique dont on esquisse l'étude analytique.

Zusammenfassung

Der Aufsatz berichtet über die Untersuchung eines Reaktors, der die Regelstrecke darstellt; zur Polymerisation von Äthylen und gibt eine kurze Beschreibung der Regeleinrichtung. Die Regelgeräte sind ausschließlich pneumatisch.

Eine angegebene Gleichung beschreibt den Zusammenhang zwischen dem Reaktorausgang und den anderen Teilen der Regelstrecke. Die Bedingungen für die im Betrieb auftretenden Eigenschwingungen werden untersucht. Ein mathematisches Modell für ein ausgewähltes Stück des Reaktors wird vorgeschlagen und analysiert.

The process of ethylene polymerization under high pressures represents one of the chemical engineering processes which is most difficult to control. Its characteristic features are high pressure, frequent explosions, considerable variations in the output of the reactor and quality of the product. The ordinary systems used for automatic stabilization of parameters do not guarantee normal progress of the reaction for this process. Therefore, a satisfactory solution of the problem of automatic control of the process for industrial manufacture of polyethylene can be solved only by the synthesis of a special system of control on the basis of data of experimental and theoretical study of the process.

The investigation of the process and the study of the automatic control systems were conducted on an experimental industrial reactor, which consists of a tube (see Figure 4) 50 m long having an internal diameter of 16 mm, with an outer water

jacket for the initial heating of the reactive mixture and for the removal of heat in the zone of reaction. Gaseous ethylene at a pressure of 1,500 atm is continuously supplied to the reactor. The process of polymerization takes place at a temperature of about 200°C.

The Static Characteristics of the Process

For the study of the static behaviour of the process the method of non-linear multiple correlation was used¹. The relationship between the output of the reactor and the basic parameters was represented in the form of a product of functions of single parameters

$$Q = f_1(P) \cdot f_2(t) \cdot f_3(O_2) \cdot f_4(V)$$

where $f_1(P)$ is the function of pressure, $f_2(t)$ the function of temperature, $f_3(O_2)$ the function of oxygen concentration, and $f_4(V)$ the function of gas supply to the reactor.

Each one of these functions was represented in the form of a polynomial

$$f_i(x_i) = a_i + bx_i + cx_i^2$$

The results of periodic measurements of output and of other parameters of the process were used as the initial data for the calculation. By the construction of the correlational fields and by developing the regression curves for each parameter, the coefficients of all functions $f_i(x_i)$ were determined. The general formula for the output of the reactor has the form

$$Q = 13 \times 10^{-8} (-211 + 0.33P - 1.16 \times 10^{-4} P^2) \\ (t - 112)(O_2 - 55)(V + 587) \text{ kg/h}$$

Its verification on an industrial installation gave quite satisfactory results.

The Stability of the Polyethylene Polymerization Reaction

The difficulty of controlling the process is aggravated by the risk of a reaction taking place which would result in the decomposition of ethylene into carbon, hydrogen and methane, which develops very rapidly and is accompanied by the liberation of large quantities of heat. When the signs of the risk of decomposition appear it is necessary, almost instantly, to reduce the pressure in the reactor or to discharge the contents of the reactor into the atmosphere. If the decomposition of ethylene cannot be prevented then, instead of the expected valuable product, soot is obtained. Each decomposition is followed by a prolonged stoppage of production, which is needed to test the pressure tightness of the equipment, for the removal of soot from the inner surfaces of the reactor and for the carrying out of other usual operations. All this causes great production losses.

The study of the causes of the ethylene decomposition reaction and the development, on this basis, of methods and means for its prevention represents an essential problem. By using a special equipment it was possible to record several interesting moments in the operation of the reactor, which provide a possible explanation for one of the basic causes of the decomposition. Recordings showed that very often the normal progress of the process is disrupted by a sudden increase in pressure, reduction in gas consumption and by an abrupt increase in temperature. Such a sudden disruption of the operating conditions may be explained by the formation of polyethylene blockages in the reactor tube.

Rapid reduction of pressure in that case leads to the elimination of these blockages and to the slowing down in the reaction

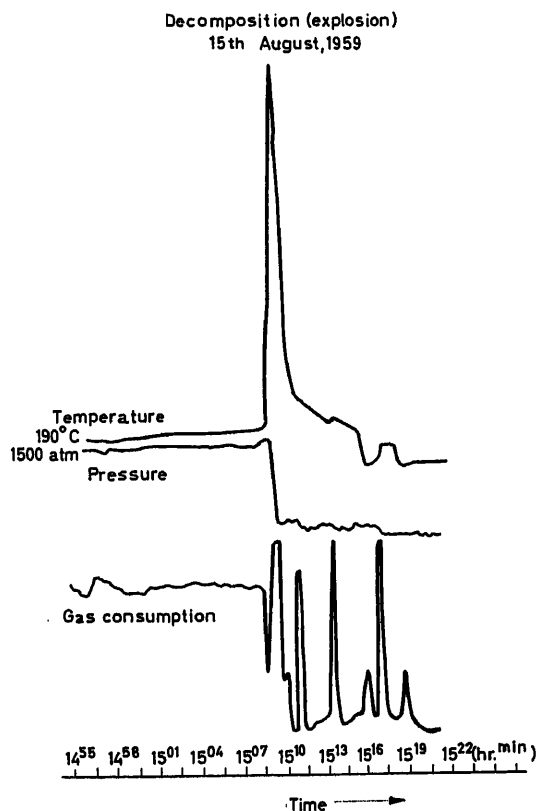


Figure 1. Recording of parameters of the process at the instant of explosion

development. If the pressure is not reduced in good time decomposition reaction unavoidably develops.

It was possible to record the diagram of the explosion (Figure 1). In the example given the operator was unable to prevent the explosion by the reduction of pressure and, therefore, the contents of the reactor were discharged into the atmosphere. The decomposition of ethylene occurred in the reactor, as was indicated by a black cloud of soot discharged from the reactor. From the diagram it is also evident that there was an increase in pressure and temperature which was accompanied by an abrupt reduction in gas consumption.

For the elimination of the polyethylene blockages it was proposed that forced oscillations in pressure should be induced.

An oscillator, specially developed for this purpose, fully justified itself in operation. Another means of preventing these blockages is to increase the gas supply to the reactor.

The measures indicated did not lead to a complete elimination of decompositions, although they became less frequent but all the same they took place. This circumstance points to the instability of the polymerization reaction itself.

The first attempt for the investigation of the stability of the polymerization reaction of ethylene under high pressure was undertaken by Hoftyzer and Zwietering³. Having constructed the material and thermal balance equations for an elementary part of the reactor, the authors obtained two non-linear differential equations in a dimensionless form:

$$\frac{dy}{dz} = -y e^{-\frac{(1+u)}{x}} + V(y_0 - y) \quad (1)$$

$$\frac{dx}{dz} = \frac{1}{2} y^2 e^{-\frac{u}{x}} + V(x_0 - x) - VW(x - x_w) \quad (2)$$

where y_0, y are the inlet and outlet concentrations of the initiator, x_0, x the inlet and outlet temperatures, x_w the reactor wall temperature, z the time, u the parameter, which determines the activation energy, and V, W the constant coefficients.

Using Liapunov's method⁴, the stability of the state of equilibrium was investigated by the linear equations of first approximation:

$$\frac{dX}{dz} = a_{11}X + a_{12}Y \quad (3)$$

$$\frac{dY}{dz} = a_{21}X + a_{22}Y \quad (4)$$

According to Liapunov's method, the stability of the equilibrium state x_0, y_0 of a non-linear system of the second order is determined by the following Routh-Hurwitz conditions:

$$d_f = a_{11}a_{22} - a_{12}a_{21} > 0 \quad (5)$$

$$d_a = -a_{11} - a_{22} > 0 \quad (6)$$

By equating the left sides of these inequalities to zero, the authors determined the boundaries of the region of the stable equilibrium states for an area of parameters x_0, y_0 for the different values of x_0 . They arrived at two interesting results: (1) the system can have five states of equilibrium; and (2) the industrial reactors are operated in a region where condition (5) is satisfied, but where condition (6) is not satisfied.

The investigation of eqns (1) and (2) terminates at this point, and Hoftyzer and Zwietering proceed to the study of the system of control. However, in the author's opinion the study of the reactor itself was left unfinished.

First of all, the question arises: is the region of unstable states of equilibrium the region of decompositions? The instability of the state of equilibrium may lead either to a rapid increase in temperature or to stable temperature oscillations. From the theory of oscillations⁵ it is known that in non-linear systems self-oscillations—stable periodic oscillations which are periodic in the absence of external disturbances—are possible. The phase picture of self-oscillating systems contains at least one isolated closed trajectory—the limiting cycle. If the limiting cycle is stable, then the state of equilibrium embraced by

this cycle will be unstable. It follows from this that the problem of stability of the polymerization reaction of ethylene is closely associated with the problem of self-oscillations. However, before undertaking any theoretical investigation of self-oscillations, it is necessary to be convinced about the practical expediency of this. In other words it is necessary to possess the experimental material which would confirm the possibility of self-oscillations in an actual process of ethylene polymerization.

Self-oscillations of the Ethylene Polymerization Reaction

The possibility of the occurrence of periodic oscillations in chemical systems has been known for a long time. Andronov⁴ indicated that under certain conditions in chemical systems, just as in other (mechanical, electrical, etc.) systems, undamped oscillations, inexplicable in principle by the linear theory may occur. Recently, a large number of works devoted to the experimental and theoretical study of the periodic chemical reactions, were published. A detailed outline of these investigations is given in the work of Salnikov⁵.

The observations made on the process of ethylene polymerization in a tube reactor shows that the process takes place under the conditions of abrupt oscillations in temperature, reactor output and quality of the product.

In the manual control of the process it was possible to explain these oscillations by the instability of pressure and oxygen content in the mixture, by the change in the gas supply and by other causes, i.e., it was possible to consider that these changes in the process represent forced changes. For us it was quite unexpected to find that the automatic stabilization of basic disturbances had very little effect on the course of the process. The oscillations in temperature, output and quality, as before, remained considerable. This very fact suggested that the process has its own inherent internal rhythm, determinable only by the properties of the system, and not by the external disturbances, i.e., that self-oscillations are characteristic of the process.

In Figure 2 are given the diagrams of recordings of pressure and temperature along the length of the reactor, from which it is seen that the temperature oscillates constantly, the period and the amplitude of these oscillations change along the length of the reactor. (The term 'amplitude' is used conditionally, since the oscillations are not harmonic.) The increase in the period of oscillations at the end of the reactor is clearly seen. At point No. 13 the period amounts approximately to 15 min, at the fourteenth point it is already 20–25 min, and at the last point it exceeds half an hour. The amplitude of temperature oscillations along the length of the reactor also increases continuously, and at the last point it reaches 30–40°C. The experiments were carried out in the presence of forced pressure oscillations having an amplitude of 70 atm and a period of 2.5 min. These oscillations are recorded on the pressure diagram. The period of these oscillations is 10 times less than that of the natural temperature oscillations. The pressure oscillations are reflected in the temperature, although not very appreciably. They are, for instance, superimposed on temperature oscillations and do not alter the general picture at all.

It is possible to note yet another peculiarity in the behaviour of the process: the temperature oscillations at the first points along the gas flow are not reflected at all in the oscillations at subsequent points. This is as if each part of the reactor represented an isolated oscillating system having its own period and

amplitude. This, at first glance, contradicts common sense, since the gas moves through the reactor at a high velocity, and it would be more natural to expect an interdependence in the behaviour of temperatures in neighbouring points.

It will be assumed now that the temperature oscillations are conditioned by external disturbances. Then, however, a large number of inexplicable questions is raised. First of all, what force should these disturbances have if pressure oscillations

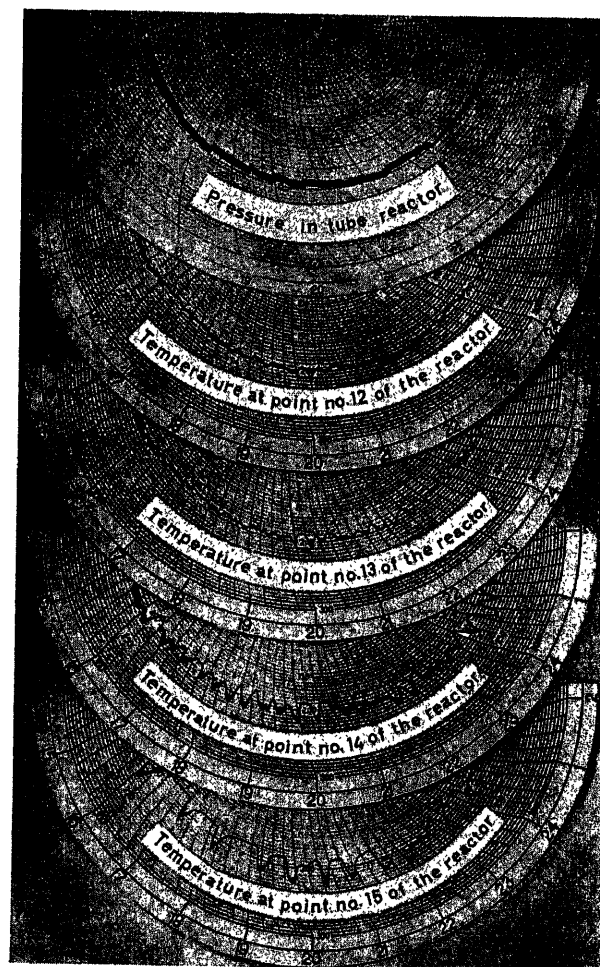


Figure 2. Recording of temperature oscillations

of 70 atm are hardly reflected in the temperature? Why do these external forces cause temperature oscillations, having quite different periods, along the length of the reactor? Why are these disturbances more pronounced at the end of the reactor than at the beginning? Finally, why, in general, should these external disturbances cause almost periodic temperature oscillations? All these questions, in our opinion, are inexplicable when taking into account only the external disturbances. Therefore, the deduction that temperature oscillations are explained by the internal oscillational nature of the process, i.e. by the self-oscillations of the reaction, is more convincing.

The explanation of all peculiarities in temperature behaviour in the reactor requires a detailed study of the mechanism of the reaction. In this paper only hypothetical reasons concerning some questions are given.

The period of temperature oscillations may increase as a result of a decrease in the concentration of the initiator at the end of the reactor. An increase in the amplitude of oscillations is probably determined by an increase in the viscosity of the mixture as a result of polymer formation. It is known that an increase in the viscosity of the reactive mixture usually tends to inhibit the chain break-up reaction, but that it has no effect on the propagation. Therefore, at the end of the reactor longer polymer chains should be formed, and since liberation of heat is determined by the propagation reaction, then this also leads to an increase in the amplitude of temperature oscillations at the end of the reactor.

The fact that the temperature oscillations at the neighbouring points are not correlated among themselves can be explained by the action of the reactor wall. It is generally known that the wall, in some reactions, plays a big role. Very often the termination occurs on the wall, and in other reactions the wall also participates in the initiation of the chain. Semenov⁶, for example, points out that the molecule of oxygen on the reactor surface can enter into the reaction $V + O_2 \rightarrow VOO$, as a result of which a powerful peroxide radical VOO is formed on the surface. The latter reacts readily in the presence of hydrogen with the initial substance, for example RH, giving a surface peroxide compound VOOH and radical R. For such reactions, the liberation of heat not in space but on the wall, is characteristic; and if the reaction is irreversible, then in the course of the process the wall is covered by a chemisorptive layer and its initiating action ceases.

If a similar picture could be built up for the ethylene polymerization reaction (which of course requires a special proof), then it is possible to visualize that the mechanism of self-oscillations of the reaction will be as described. The progress of the reaction leads to an increase in temperature, but the coating of the wall by the chemisorptive layer of polyethylene molecules leads to the damping of the reaction and to a reduction in temperature. Gradually with the gas flow the polymer is washed off the walls, the reaction develops again, the temperature increases, and so on. Naturally, because of such a mechanism the reactor will consist of a large number of self-oscillating systems, distributed along the length of the reactor. Under these conditions the temperatures at the neighbouring points will not be mutually interconnected.

It is possible to put forward a number of other self-oscillating models of the process. In view of the strongly pronounced exothermic nature of the process it is most likely that the self-oscillations are thermo-kinetic in character, in which case the interaction between the heat removal system and the reaction leads to stable temperature oscillations. Similar oscillations were studied for the first time by Frank-Kamenetskii⁷.

Study of the Thermo-kinetic Model of Reaction

The rate-of-reaction equation for the polymerization of ethylene may be represented in the form:

$$-\frac{dM}{dt} = A e^{-\frac{E}{RT}} I^{\frac{1}{2}} M$$

where M is the concentration of monomer, I the concentration of initiator, E the activation energy, R the gas constant, T the temperature, A the pre-exponential multiple, and t the time.

On the basis of the rate-of-reaction equation it is possible to construct for an elementary section of the reactor the material and thermal balance equations.

$$\frac{dM}{dt} = -A e^{-\frac{E}{RT}} I^{\frac{1}{2}} M + \frac{G}{V} (M_0 - M) \quad (7)$$

$$VC\rho \frac{dT}{dt} = VQA e^{-\frac{E}{RT}} I^{\frac{1}{2}} M - Sh(T - T_v) + G\rho C (T_v - T) \quad (8)$$

here G is the gas supply, V , S the volume and surface of the reactor section under consideration, M_0 the monomer concentration in the initial mixture, Q the thermal effect of the reaction, C the specific heat of the mixture, h the heat-transfer coefficient, ρ the density of the mixture, and T_v , T , the temperature of the mixture and temperature of the reactor walls. By denoting that

$$d = \frac{G}{V}, \alpha = \frac{Sh + G\rho C}{V}, T_0 = \frac{ShT_v + G\rho CT_v}{Sh + G\rho C}$$

the system may be reduced to the following form

$$\frac{dM}{dt} = -A e^{-\frac{E}{RT}} I^{\frac{1}{2}} M + d(M_0 - M) \quad (7a)$$

$$C\rho \frac{dT}{dt} = Q e^{-\frac{E}{RT}} I^{\frac{1}{2}} M - \alpha(T - T_0) \quad (8a)$$

If it is assumed that the concentration of the initiator is constant and if dimensionless variables $x = (QR/C\rho E) M$, $y = (R/E)T$, $\tau = A I^{\frac{1}{2}} t$ are introduced, then the material and thermal balance equations will be

$$\frac{dx}{d\tau} = -x e^{-\frac{1}{y}} + \beta(x_0 - x) \quad (7b)$$

$$\frac{dy}{d\tau} = x e^{-\frac{1}{y}} - \gamma(y - y_0) \quad (8b)$$

where:

$$\beta = \frac{d}{A I^{\frac{1}{2}}}, \gamma = \frac{\alpha}{C\rho A I^{\frac{1}{2}}}$$

It should be pointed out that in the elementary section of the reactor the change in the concentration of the monomer will be insignificant; since total conversion is small, there is a continuous supply of fresh gas and the system is under a constant pressure. On this basis one can assume that the second term of the right-hand side of eqn (7b) is constant

$$\beta(x_0 - x) = m \quad (9)$$

Then, eqn (7b) assumes the form:

$$\frac{dx}{d\tau} = -x e^{-\frac{1}{y}} + m \quad (7c)$$

Now, the models of our chemical system will be represented by eqns (7c) and (8b). Analogous equations were obtained by Salnikov⁵ in the investigation of the thermo-kinetic oscillations of chemical reaction $A \rightarrow X \rightarrow B$ for the case of the rate of reaction $A \rightarrow X$ remaining constant.

In order to develop stable periodic solutions (self-oscillations) in the system (7c), (8b) the methods of the qualitative

theory of differential equations were used. The study of the non-linear systems of the second order is most expediently carried out by means of a phase plane. The presence of the system of a limiting cycle on the phase plane represents the necessary condition for self-oscillations. In the case here the plane having parameters x and y (concentration of monomer and temperature) is the phase plane. The general procedure of the study is as follows. The states of equilibrium are determined, and the boundary of the region of stable equilibrium states is developed, by means of the equation of the first approximation. After this, using Poincaré's sphere³, the stability of particular points of the system, in the infinitely remote parts of the phase plane, is determined. If the system has an unstable state of equilibrium and if the infinity is also unstable, then on the basis of Bendixson's theorem³, it will be possible to arrive at the conclusion that on the phase plane of the system there is bound to be at least one limiting cycle.

By equating the right sides of the eqns (7c) and (8b) to zero

$$-x e^{-\frac{1}{y}} + m = P(x, y) = 0$$

$$x e^{-\frac{1}{y}} - \gamma(y - y_0) = Q(x, y) = 0$$

it is possible to find the equilibrium state coordinates

$$y_s = y_0 + \frac{m}{\gamma} \quad (10)$$

$$x_s = m e^{\frac{\gamma}{y_0 \gamma + m}} \quad (11)$$

For the determination of the stability of the equilibrium state we shall introduce new dependent variables

$$x = x_s + \xi, y = y_s + \eta$$

and we shall reduce the system (7c), (8b) to two linear equations of the first approximation

$$\frac{d\xi}{d\tau} = a\xi + b\eta, \quad \frac{d\eta}{d\tau} = c\xi + d\eta$$

The coefficients of these equations are determined by the following expressions

$$a = P'_x(x_s, y_s), b = P'_y(x_s, y_s)$$

$$c = Q'_x(x_s, y_s), d = Q'_y(x_s, y_s)$$

The necessary and sufficient conditions of stability of the linear system of the second order are the following equations

$$\sigma = -a - d > 0 \quad (12)$$

$$\Delta = \begin{vmatrix} a & b \\ c & d \end{vmatrix} > 0 \quad (13)$$

The boundary of the stability region $\sigma = 0$ is determined on the plane m, y_0 by the following equations:

$$m = y_s^2 \left(\gamma + e^{-\frac{1}{y_s}} \right) \quad (14)$$

$$y_0 = y_s \left[1 - y_s \left(1 + \frac{e^{-\frac{1}{y_s}}}{\gamma} \right) \right] \quad (15)$$

The verification of the second condition of stability shows that at any parameters of the system $\Delta > 0$. From this it follows that the equilibrium state is a node or a focus.

For the study of the behaviour of phase trajectories in the infinitely remote parts of the plane G , determinable by the inequalities $x \geq 0, y \geq \varepsilon$, when ε has the smallest desirable positive value, Poincaré's sphere is used. For this, new variables

$$y = \frac{1}{z}, x = \frac{\rho}{z}$$

are introduced. Then

$$\frac{d\rho}{d\tau} = zP\left(\frac{\rho}{z}, \frac{1}{z}\right) - \rho zQ\left(\frac{\rho}{z}, \frac{1}{z}\right)$$

$$\frac{dz}{d\tau} = -z^2 Q\left(\frac{\rho}{z}, \frac{1}{z}\right)$$

where

$$P\left(\frac{\rho}{z}, \frac{1}{z}\right) = -\frac{\rho}{z} e^{-z} + m$$

$$Q\left(\frac{\rho}{z}, \frac{1}{z}\right) = \frac{\rho}{z} e^{-z} - \gamma\left(\frac{1}{z} - y_0\right)$$

Since the identity $P \equiv \rho Q$ does not occur, the equator of Poincaré's sphere ($z = 0$) is an integral curve. The particular points on the equator are determined by the relations $z = 0$ and $P/Q - \rho = 0$. On the equator of the sphere two pairs of particular points $\rho_1 = 0$ and $\rho_2 = 1 + \gamma$ are located.

The subsequent analysis shows that the phase trajectories do not come out of the region G , and on the contour which limits the region, there are no stable states of equilibrium. Therefore, on the basis of Bendixson's theorem it is possible to prove that on the phase plane there is a limiting cycle, which embraces the unstable state of equilibrium.

Thus, the region of unstable states of equilibrium, determinable by eqns (14) and (15), is the region of self-oscillating conditions of the system.

It should be pointed out that if a simplified condition (9) is not adopted, then the study of eqns (7b), (8b) is made difficult by the determination of the state of equilibrium. But the simulation of this system on an analogue computer has shown that in it also, under certain conditions, self-oscillations occur. One of the limiting cycles, obtained on the computer, is represented in Figure 3.

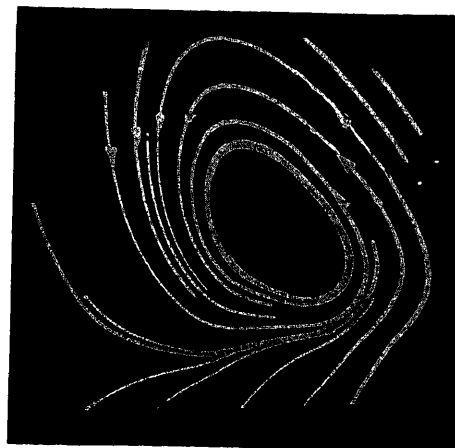


Figure 3. Limiting cycle

In the author's opinion, the self-oscillations of the ethylene polymerization reaction are the main cause of considerable changes in the output of the reactor and quality of the product. Therefore, they should be considered harmful, and it is necessary to search for means and methods to combat them. This problem is still unsolved.

Automatic Control of the Process

The investigations on the reactor were carried out simultaneously with the automation of the process. The results of investigations were used in solving the problems of automatic control, and the introduction of automatic control has helped the experimental work. Thus, a system of automatic control, the block diagram of which is shown in Figure 4, was constructed. From this diagram it is possible to see which basic functions are performed by this system.

stoppage of the compressor, and the supply of oxygen is discontinued.

The starting of the reactor is obtained through the command of the operator. The basic operation of starting consists in a gradual increase of pressure in the reactor. If, at the time of starting dangerous operating conditions develop, then the rise in pressure is stopped either automatically or by the command of the operator.

The unloading from the separator takes place periodically through the pressure signal in it. As soon as the pressure in the separator begins to fall, the unloading is stopped, since the reduction in pressure indicates that the separator is completely freed from the liquid polymer. The interval of time between the unloadings is adjusted automatically by a special system, which indirectly measures the output of the reactor and decreases or increases the frequency of unloading. The pressure-control unit

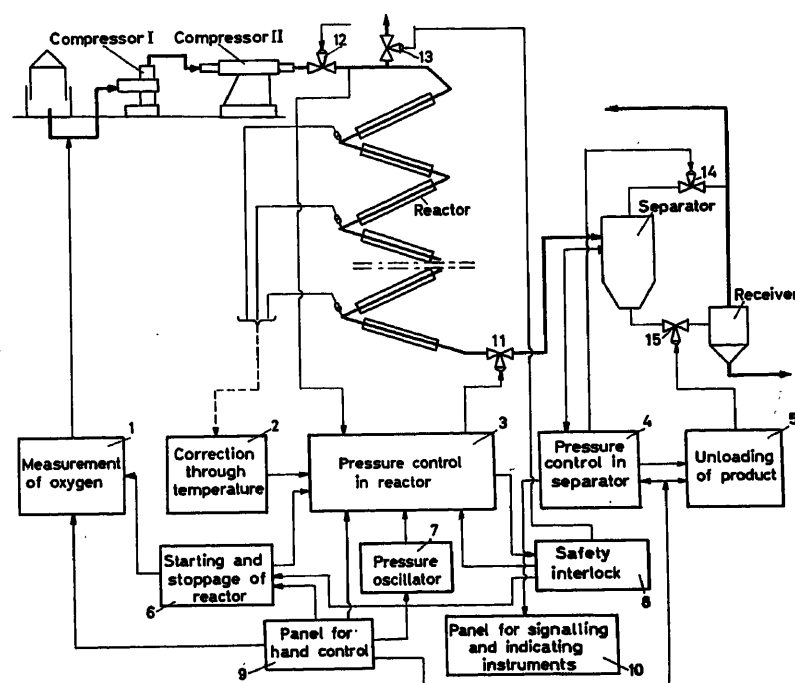


Figure 4. Block diagram of the automatic system of control

A conventional isochromic controller carries out different commands according to pressure changes in the reactor, which are received from other points of the circuit. The controller, in fact, acts as a servo system. After receiving a signal from the pressure-correcting unit, the pressure is gradually reduced if the temperature at any one point of the reactor exceeds the set limit. For the set point of the pressure controller, a signal is also received from the oscillator, which operates on the principle of conventional relay pulse-couple. The oscillator rapidly reduces the pressure in the reactor by 70–100 atm and then gradually raises it to the previous value.

With the appearance of any risk of explosion the safety interlock comes into operation. At first, the pressure in the reactor is reduced, but if this does not result in the prevention of an explosion the contents of the reactor are discharged into the atmosphere. At the same time a signal is sent for the

in the separator performs simple stabilization of pressure during the intervals between the unloadings. It should be pointed out that the pressure control system in the reactor and that in the separator do not interact.

The unit for the measurement of oxygen provides for the remote automatic (or hand) change in the supply of initiator to the reactor for any programme.

Constructionally, the automatic control system consists of pneumatic control equipment which is designed for the simultaneous automatic control of two reactors. All units of the assembly consist entirely of pneumatic logical components. This provides for adequate reliability and fire risk. A number of such units have been produced and have passed industrial tests at two of the works. Their testing under operating conditions proved their complete reliability and high quality of control.

The proposed system is a natural outcome of only the first stage of work for the automatic control of the process. It embodies the operations which are essential for the maintenance of trouble-free normal operating conditions of the reactor. However, the problem of automatic control of the polymerization reaction is not yet completely solved. It may be expected that further study of the process, and particularly of the self-oscillating conditions, will result in the finding of even more efficient methods for the control of the reaction.

Conclusions

As a result of this study a relationship was found between the output of the reactor and the basic parameters of the process. One of the basic causes of the ethylene decomposition was revealed. The self-oscillating conditions in the operation of the reactor were uncovered and the mathematical model of a part of the reactor was studied.

DISCUSSION

K. SCHOENEMANN, *Institut für Chemische Technologie der Technischen Hochschule, 61 Darmstadt, Germany*

The paper by Mr. Volter is an impressive example of the application of automatic control for chemical reactors. Chemical reactions of high velocity and great reaction heat cannot usually be carried out in any other way.

Hence, the methods described are also of great importance for the chemical engineer too, when fulfilling his main task of developing a new chemical process from the very beginning in the laboratory, including the choice of the reactor type and its consequent scaling up to industrial size.

Five years ago, at the Technical University of Darmstadt, Germany, we encountered similar problems to those of Mr. Volter when we had to carry out the design of the tube reactors for a large high-pressure polyethylene plant of 24,000 tons/year. The only basis was batch experiments described in literature which then were checked by us.

Like Mr. Volter, we did not apply the purely empirical correlation between the obtained yields and the applied reaction conditions because the equations obtained describe the complex interactions only in a summarizing manner; the underlying laws are not comprehensible. Hence, these equations cannot generally be transferred to larger units or other reactor types. For instance, when scaling up a tube reactor, heat removal becomes worse because the reactor content producing the reaction heat grows proportionally with the square of the tube diameter, whereas the tube wall transferring the reaction heat grows only in a linear relation.

Therefore we established velocity equations of principally the same type as those used by Mr. Volter for the explanation of the temperature oscillations; but they differed in some terms and exponents and led to different final results.

We proceeded in the following way: We assumed the simplest possible reaction mechanism comprising only a chain start reaction, a chain growth reaction and a termination reaction. Then, by evaluating the conversion experiments we established velocity equations of the general form

$$-\frac{dc}{dt} = k_0 \cdot e^{-E/RT} \cdot c_1^n \cdot c_2^m$$

These equations were used for the material and heat balances which describe the continuous tube reactor:

Simultaneously with the investigation of the process, work was carried out for its automatic control as a result of which pneumatic automatic control equipment was constructed.

References

- BRANDON, D. B. Developing mathematical models for computer control. *ISA Journal* 6, No. 7 (1959)
- HOFTYZER, P. J. and ZWIETERING, Th. N. The characteristics of homogenized reactor of the polymerization of ethylene. *2nd Europ. Symp. Chem. Engng.* 1960
- ANDRONOV, A. A., VITT, A. A. and KHAIKIN, S. E. *Theory of oscillations.* Fizmatgiz (1959)
- ANDRONOV, A. A. Poincaré's limiting cycles and theory of selfoscillations. *Collection of wks of A.A. Andronov, AN USSR*, (1956)41
- SALNIKOV, I. E. Theory relating to periodical homogeneous chemical reactions. *Zh. Fiz. khim.* No. 3 (1948)
- SEменов, N. N. Some problems relating to chemical kinetics and reactive capacity. *AN USSR* (1958)
- FRANK-KAMENETSKII, D. A. Diffusion and heat-transfer in chemical kinetics. *AN USSR* (1947)

Material balance of ethylene conversion

$$-\frac{dg_A}{dL} = \frac{k_{Br}^0 \cdot e^{-\frac{E_{Br}}{R \cdot T_i}} \cdot p^\alpha \cdot g_A^{3/2} \cdot g_0^{1/2} \cdot \rho^2 \cdot \frac{q}{G}}{r}$$

Material balance of oxygen consumption

$$-\frac{dg_0}{dL} = k_s^0 \cdot e^{-\frac{E_s}{R \cdot T_i}} \cdot g_A \cdot g_0 \cdot \frac{\rho^2 \cdot q}{G}$$

Heat balance of the reaction mixture

$$\frac{dT_i}{dL} = \frac{r \cdot \Delta H \cdot q}{G \cdot c_p} - \frac{k \cdot f \cdot (T_i - T_a)}{G \cdot c_p}$$

Heat balance of the cooling water

$$\frac{dT_a}{dL} = -\frac{k \cdot f \cdot (T_i - T_a)}{G_{H_2O} \cdot c_{pH_2O}}$$

By simultaneous solution of these four equations we calculated the temperature profiles and conversion profiles over the length of the reactor with their dependence on the reaction factors of temperature, oxygen content and pressure, at first for the stationary state (*Figure A*). Then, in order to adjust the control system to the transient behaviour of the reactor the latter was investigated in a similar way to that shown in *Figure B* for another model reaction. The whole kinetic investigation and the reactor design have proved correct in the industrial plant (*Figure C*) up to very characteristic details.

As for the strange oscillations of temperature described by E. V. Volter, they were not observed to any degree by us. I, therefore, suppose that in Mr. Volter's pilot reactor they originated from some unknown peculiarities.

By these comments of mine I wanted to emphasize that the illustrative velocity equations allow the chemical engineer to think in his categories in a creative way: on the basis of rather simple experiments these generally valid equations enable him to calculate over a wide spectrum of variations in the reaction conditions and the control system of an industrial reactor, and thus allow him to predict the optimum.

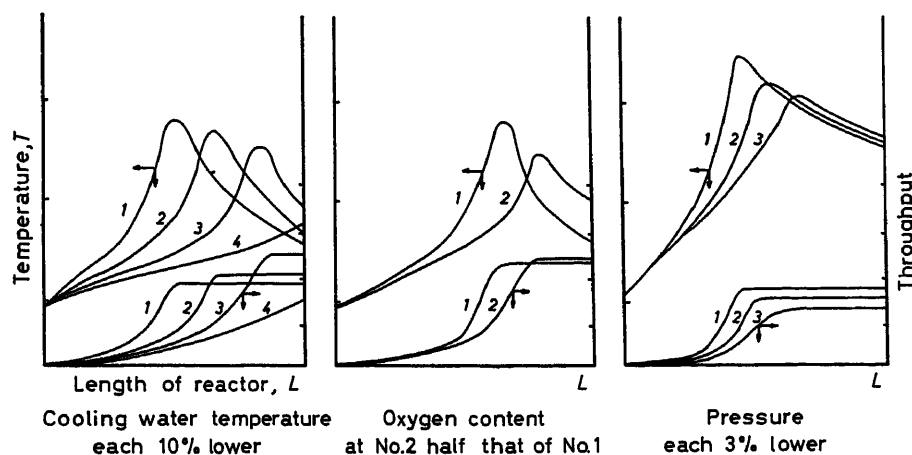


Figure A

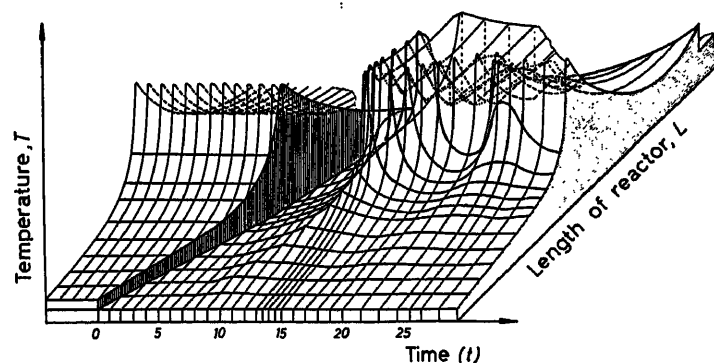


Figure B

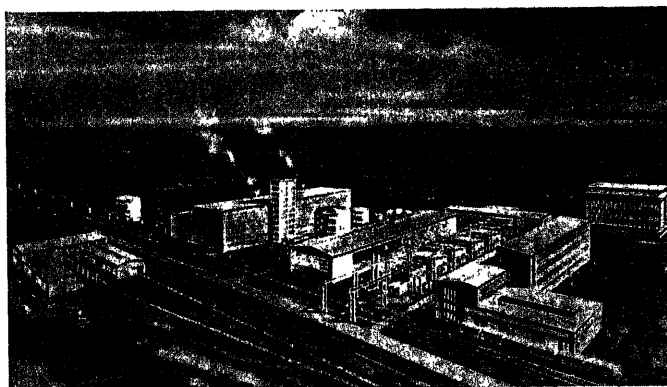


Figure C

E. STEFANI, *The National Committee of the U.S.S.R. on Automatic Control, Moscow I-53., Kalanchevskaya 15-a, U.S.S.R.*

Mr. Schoenemann proposes the equations to describe processes in the reactors with different design parameters. This is very interesting for we are now carrying out research work in the same field, but at present only at the laboratory level.

Experience gained, using the systems of automatic ethylene polymerizations, justifies our hopes that the same good results will be obtained with reactors of different types.

It is a real pleasure to see the results of industrial tests of Mr. Schoenemann's equations.

E. D. GILLES, *Technische Hochschule, 61 Darmstadt, Germany*

Mr. Volter tried to show, with the aid of balance equations of a small segment of a tubular reactor, that the temperature oscillations observed in the polyethylene reactor can probably be related to a thermo-kinetic instability of the reactor. For the derivation of these balance equations the local extension of the small tubular segment under consideration was neglected, that is, the tubular reactor was replaced by a cascade of ideal mixing vessels. Consequently, for a small segment of the tubular reactor the stability criteria corresponding to an ideal stirred tank reactor are obtained, and, as is well known, these yield unstable behaviour under certain operating conditions. The author, therefore, concluded that a thermo-kinetic instability could also occur in the tubular reactor.

This conclusion does not necessarily follow, because the behaviour of an ideal tubular reactor is identical with that of an equivalent cascade of ideal mixing vessels only if the number of such vessels in the cascade tends to infinity, that is the volume of each of the mixing vessels tends to zero. If the two stability criteria are regarded with respect to the ratio

$$\frac{\text{Reaction volume } V}{\text{Flow } G}$$

it turns out that the tendency towards instability decreases as this ratio decreases, so that when the ratio vanishes, the system is stable.

Since for the single segments of a cascade of mixing vessels with an infinite number of elements, which is mathematically identical with the tubular reactor, this limiting case is valid and the infinitely small mixers are cascaded free of interaction, hence an ideal tubular reactor is always stable. The influence of hydrodynamic processes on the

A Study of the Dynamic and Static Characteristics of the Process of Fractional Distillation

I. V. ANISIMOV

Summary

A mathematical study of the static and dynamic responses in binary liquid fractionation systems is presented. It differs from earlier publications in that it takes into account the kinetics of plate mass transfer. Response curves for plate distillation columns as well as the static characteristics of the system have been computed throughout the main control and disturbance channels.

The results derived from this method of calculation differ, both in quantity and quality, from those obtained by the theoretical plate method. Study of the static and dynamic characteristics of the process has made it possible to single out those specific characteristics which influence the choice of the main control scheme. The advantages of a combined control scheme are shown.

For superfractionation a selective-invariant control system is necessary. An automatic control system is developed which takes into account the specific static and dynamic properties of the fractionation process. Calculations were carried out by the staff of the Computer Laboratory of the Moscow Institute of Chemical Machine Building, using a digital computer.

Sommaire

Une étude mathématique des réponses statiques et dynamiques des systèmes de colonnes de fractionnement binaires liquides est entreprise. Elle diffère des études antérieures par le fait que les cinétiques des transferts de masse aux plateaux sont prises en considération. Les courbes de réponses statiques et dynamiques des colonnes de distillation à plateaux sont calculées par rapport aux actions principales de commande et par rapport aux perturbations.

Les résultats obtenus par cette méthode diffèrent de ceux obtenus par la «méthode des plateaux» théorique. L'étude des caractéristiques statiques et dynamiques du processus a fait ressortir l'influence de certaines de ces caractéristiques sur le choix de la commande principale. L'avantage de la commande combinée est prouvé.

Pour les super-fractionnements, un système de commande sélective et invariante est nécessaire. Un système de commande automatique, tenant compte des caractéristiques statiques et dynamiques d'un processus de fractionnement, est développé. Les calculs ont été effectués sur une calculatrice numérique universelle, par le personnel du Laboratoire de Calcul de l'Institut de Génie Chimique de Moscou.

Zusammenfassung

Der Aufsatz enthält die mathematische Untersuchung des statischen und dynamischen Verhaltens bei der Zweikomponentenfractionierung. Diese unterscheidet sich von früheren Veröffentlichungen dadurch, daß sie die Kinetik des Stoffaustausches auf einem Boden in Betracht zieht. Das Übergangsverhalten der Bodenkolonnen sowie das Beharrungsverhalten des Systems wurden sowohl für die Hauptregelkreise als auch für die Störungen berechnet.

Die so berechneten Ergebnisse unterscheiden sich sowohl in quantitativer als auch qualitativer Hinsicht von denen, die man durch die Methode der theoretischen Stufen bekommt. Die Untersuchung der statischen und dynamischen Eigenschaften des Prozesses ermöglicht es, die besonderen Eigenschaften, die die Auswahl des Schemas der Hauptregelkreise beeinflussen, auszuheben. Die Vorteile einer kombinierten Regelung zeigen sich deutlich.

Für Feinfraktionierung ist ein invariantes selektives Regelungssystem notwendig. Es wird eine Regelung entwickelt, die die besonderen statischen und dynamischen Eigenschaften des Fraktionierungsprozesses berücksichtigt. Die Berechnungen führte ein Stab von Mitarbeitern des Rechenzentrums im Moskauer Institut für Chemischen Apparatebau mit einem Digitalrechner durch.

Introduction

Numerous studies of the dynamics of the process of fractional distillation are based on the consideration of the theoretical and not the actual column plates. For the binary systems the degree of utilization of plates is taken into account but it is assumed that this is independent of the parameters of the process^{15-17,18}. Such a simplified approach introduces substantial errors into the calculations relating to the dynamics and statics of the distillation process.

As a result of studies of the process of fractional distillation for the binary mixtures^{1, 2, 3, 9, 11, 12} it was possible to determine the effect of design parameters of the plate, physical and chemical properties of the components and operating parameters of the process on the mass-transfer kinetics. In this work the problems connected with the calculations and analysis of the dynamics and statics of the process for the separation of binary mixtures in the distillation columns are considered in the light of the most recent studies of the mass transfer on the plate, and recommendations are given for the choice of the optimum system of control of the process.

Study of the Dynamic Characteristics of the Process and their Specialities which Affect the Choice of the System of Control

A mathematical account of the process was obtained by proceeding from the material balance of the more volatile component of the binary mixture in the distillation column, and the following assumptions were made:

- (1) The working of the column is adiabatic.
- (2) The liquid is not carried away from the plate.
- (3) The mixing within the liquid on the plate and in the vapour is complete.
- (4) The quantity of the vapour phase in the column is disregarded.
- (5) The pressure on all the plates is equal to that of the atmosphere.
- (6) The condenser of the column is full.
- (7) All the liquid on the plates is confined to the zone of mass transfer.
- (8) The initial mixture and the reflux admitted are at boiling point.

- (9) The mass transfer on the column plates is equimolar.
 (10) The local mass transfer coefficient at a given instant of time is uniform over the entire plate.

The material balance equations for the more volatile component in the transient process are:

For the top plate

$$H_n \frac{dX_n}{d\tau} = L_D X_D - L_n X_n + V_{n-1} Y_{n-1} - V_n Y_n \quad (1)$$

For the feed plate

$$H_f \frac{dX_f}{d\tau} = L_{f+1} X_{f+1} - L_f X_f + V_{f-1} Y_{f-1} - V_f Y_f + F X_F \quad (2)$$

For the column still

$$H_0 \frac{dX_0}{d\tau} = L_1 X_1 - V_0 Y_0 - W X_W \quad (3)$$

It is assumed that in the still a single complete evaporation of the liquid portion takes place, under which conditions

$$Y_0 = X_0 \quad (4)$$

In accordance with the assumptions made, the liquid and vapour flow rates are connected by the following equations:

$$V_0 = L_1 - W = V_1 = \dots = V_n \quad (5)$$

$$L_D = V_n - D = L_n = \dots = L_{f+1} \quad (6)$$

$$L_f = L_{f+1} + F = L_{f-1} = \dots = L_1 \quad (7)$$

The formulae, which allow for the hydraulic retardations of the flow, the non-adiabatic character of the process, etc., to be taken into account, are given in another work².

For the solution of eqns (1)–(3) it is necessary to determine the relations between the variables.

The assumption about complete mixing of the liquid on the plates makes it possible for the process of mass transfer, which takes place during the motion of a certain volume of the vapour phase through a liquid layer of constant composition, to be considered¹⁴.

The mass-transfer equation for the i th plate may be written in the following form:

$$V_{i-1} dY = K_v S_i (Y_i^x - Y_i) d\tau \quad (8)$$

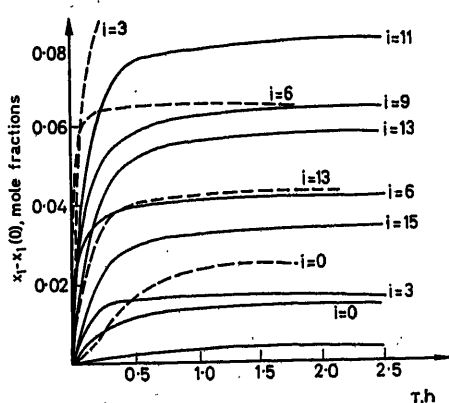


Figure 1. Response curves for concentrations X_i for a step-like unit increase in X_F amounting to 5 per cent

Assuming that the quantities V_{i-1} , K_v and S_i are constant one obtains

$$Y_i = Y_i - e^{-\frac{K_{vi}}{V_{i-1}}} + Y_i^x \left(1 - e^{-\frac{K_{vi}}{V_{i-1}}}\right) \quad (9)$$

where

$$K_{vi} = K_v S_i \Delta\tau_i \quad (10)$$

The general mass transfer coefficient on the plate K_{vi} , determinable by plate design, physical and chemical properties of the components and by operating parameters, makes it possible for the effect of these factors on the transient process to be taken into account in the calculations.

According to the double resistance theory¹³, the general mass transfer coefficient is a function of the particular mass transfer coefficients of the liquid and vapour phases:

$$K_{vi} = \frac{1}{\frac{1}{\beta_{vi}} + k_i \frac{1}{\beta_{li}}} \quad (11)$$

where

$$k_i = \left(\frac{\partial Y^x}{\partial X}\right)$$

the phase equilibrium constant.

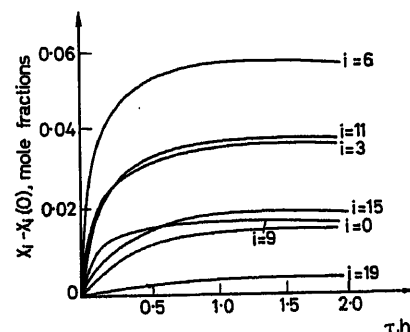


Figure 2. Response curves for concentrations X_i for a step-like unit increase in the quantity of the initial mixture amounting to 5 per cent

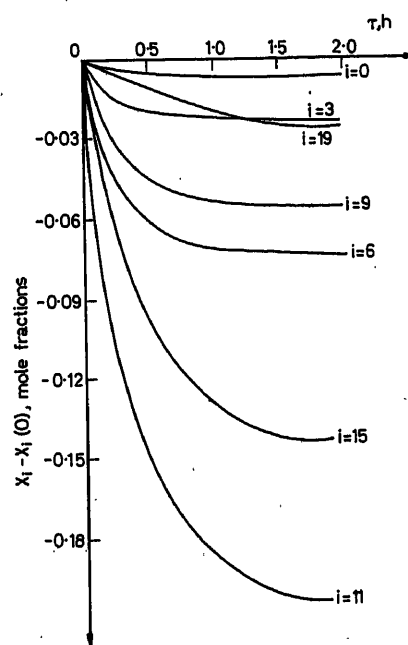


Figure 3. Response curves for concentrations X_i obtained for a step-like increase in distillate withdrawal amounting to 5 per cent

The particular mass transfer coefficients may be calculated on the basis of experimental data as definite functions of the plate design parameters, physical and chemical properties of the components, composition of the liquid and vapour phases on the plate and of vapour or liquid flow rates in the column¹⁰.

The system of eqns (1)–(11) describes the transient process in the fractional distillation column for the separation of binary mixtures, taking into account the kinetics of mass transfer on the plates.

As an example, the calculation and the analysis of the transient processes for the separation of the methanol–water mixture in a distillation column are given. The initial data are as follows: the pressure in the column is atmospheric; the number of plates $n = 18$; the feed plate number $f = 9$; the quantity of still product $W = 166.5$ kg-mole/h; the quantity of initial mixture $F = 229.2$ kg-mole/h; the quantity of distillate $D = 62.7$ kg-mole/h; the quantity of vapour $V_0 = 141.1$ kg-mole/h; the concentration of the more volatile component in the feed $X_F = 0.273$ mole fractions; the concentration of the more volatile component in the distillate $X_{19} = 0.973$ mole fractions; the concentration of the more volatile component in the still $X_0 = 0.0085$ mole fractions.

$$\beta_{vi} = 1.61 V_{i-1} + 46 \text{ kg-mole/h/plate surface.}$$

$$\beta_{ii} = 380 \text{ kg-mole/h/plate surface.}$$

The calculations for the transient processes in the column were carried out on a universal digital computer for the following step disturbances:

(1) For an increase in the concentration of the more volatile component of the initial mixture

$$\Delta X_F = X_F \times \frac{5}{100}$$

(2) For an increase in the quantity of feed

$$\Delta F = F \times \frac{5}{100}$$

(3) For an increase in the distillate withdrawal

$$\Delta D = D \times \frac{5}{100}$$

(4) For an increase in the quantity of vapour leaving the evaporator

$$\Delta V_0 = V_0 \times \frac{5}{100}$$

The calculation results are given in the form of response curves in Figures 1–4. The curves obtained by calculations based on theoretical plates are shown by dots. The comparison of curves shows that the results of calculations based on the theoretical plates and those based on the proposed method are substantially different, especially for the plates of the low separating capacity.

By comparing the response curves it is possible to record the following basic dynamic speciality of characteristics of the fractional distillation process, which affect the choice of the control system:

(1) The greatest effect on the transient processes and on the concentration distribution along the column height in the state

of equilibrium is shown by disturbances which violate the conditions of the material balance in the column, especially by those connected with a change in the distillate withdrawal.

(2) The transient processes in the column take place slowly; in the example considered they require from 1.7 to 2.5 h. The response time of the column depends on the number of plates, relative volatility of the components and other factors².

(3) The changes in the concentration of the liquid on the upper and lower plates of the column are insignificant. The greatest changes in the concentration of the liquid take place in the so-called 'controlling' plates, which are situated approximately in the middle of the rectifying and stripping sections of the column. The position of the 'controlling' plates may be considered independent of the form of disturbances.

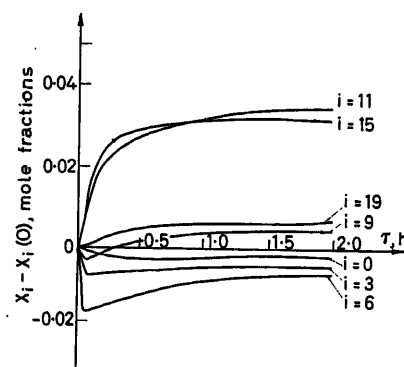


Figure 4. Response curves for concentrations obtained for a step-like increase in vapour flow rate in the column amounting to 5 per cent

The signal for the control of composition or temperature of the liquid should be taken from one of the controlling plates. On no account is it possible to control the process directly through the composition of distillate or still product, since the static and dynamic characteristics of the process would deteriorate substantially.

(4) The change in the steam supplied to the evaporator gives rise to transient processes in the rectifying and stripping sections of the column, which are different in character. This is attributed to the action of two opposing factors: to an increase in the separating capacity of the column with the increase in the reflux number, and to a decrease in the efficiency of each plate with an increase in the vapour flow rate. At the very beginning the changes in concentration for the restorative and draining sections of the column have different signs.

(5) In a transient process considerable delays in the change of composition (or temperature) of the liquid phase occur. The delays in the change of composition of the vapour phase on the plates caused by the change in the vapour flow rate in the column are considerably smaller. This is explained by the fact that the value V of the vapour flow changes with a speed which is close to that of sound; therefore, the conditions of mass transfer on the plates change almost instantaneously, see eqn (9). This phenomenon finds no explanation in calculations based on the theoretical plates.

In the overwhelming majority of cases the control circuits for the process of fractional distillation are limited to the problem of stabilization of the parameters of the process². Such

automatic control systems work more or less satisfactorily if the disturbances are small and if variations in the quality of the product are permissible. With appreciable changes in the quality and composition of the initial mixture the continuous deviations from the assigned composition of distillate and still product are unavoidable. In order to obtain products of high purity under these conditions the invariance of the process control systems is the most desirable.

A system of control cannot be made absolutely invariant in respect of all the disturbances. In the fractional distillation process the violations of the material balance caused by changes in the quality and composition of the initial mixture represent the basic disturbances. The violations of the thermal balance of the process, the changes in pressure in the column, the variations in the quantity of liquid on the plates and in the still, the changes in the working efficiency of the plates caused by change in the composition of the feed and in the vapour flow rate in the column, etc. represent the less important and secondary disturbances.

It is possible and expedient to construct a selective invariant system of control, for which the basic parameter of the process—the composition of the liquid on the control plate—will be independent of the changes in the quantity and composition of the initial mixture.

With a selective invariant system of control only small changes in the composition of the liquid on the control plate under the action of the less important secondary disturbances of the process will occur. Therefore, the system of control should be based on the combination of principles of control according to disturbance and deviation of parameter.

An account of the fundamentals of the theory of combined control and of the condition of invariance are given in other works⁴⁻⁷.

The amplitude and phase characteristics of the controlled plant according to control and disturbance paths required for the calculation of the conditions of invariance, are not difficult to determine from the response curves obtained as a result of the solution of the system of equations for the dynamics of the process.

The changes in the quantity and composition of the initial mixture violate simultaneously the material and the thermal balance of the process. The system of control, which reacts to these disturbances, compensates for their effect in the column by the corresponding change in the supply of the reflux and heating vapour. The oscillations in the pressure of the heating vapour and reflux and the inaccurate readjustment of the control valves represent the secondary disturbances, the effect of which may be easily eliminated by applying flow ratio controllers, which measure the magnitude of disturbance and of response change in the supply of the controlling means.

The selective invariant system of control does not embrace the controllable parameters, which have a smaller effect on the dynamic and static characteristics of the process. These parameters are stabilized by customary controllers.

On the basis of what has been stated, a block diagram for a combined selective invariant system of control for the process of fractional distillation (described at the end of this paper—see Figure 7), has been developed.

The Static Characteristics of the Process

The task of automatic control consists in the determination and maintenance of the optimum values of the controlling parameters of the process.

The calculated values of the following parameters of the fractional distillation process are considered to remain approximately unaltered under operating conditions: the pressure in the column, the level of the liquid in the still of the column, the level in the reflux tank, and the temperature of the initial mixture and reflux. The control of these parameters does not present any difficulties and is not shown in the diagram of Figure 7.

The optimum values for the reflux number, the quantity of the heating vapour and the location of feed plate change under operating conditions. In the separation of multi-component mixtures it is necessary to determine also the optimum quantities and points of withdrawal for the intermediate products.

The optimum values of these parameters based on the minimum cost of manufacture are determined as the functions of the quantity and composition of the initial mixture, provided that the product obtained is of precisely the composition assigned or that it changes within the permissible limits.

For the calculations relating to the statics of the fractional distillation process, the material balance equation for the state established in the part of the column situated below the i -th plate is written

$$L_{i+1} X_{i+1} - V_i Y_i + F X_F - W X_0 = 0 \quad (12)$$

where

$$L_{i+1} = V + W \text{ when } i < f \text{ and } L_{i+1} = V_i + W - F \text{ when } i \geq f \quad (13)$$

$$V_i = V \text{ when } 0 \leq i \leq n+1 \quad (14)$$

Consequently, the material balance of the process for the established state may be written in the form:

$$X_i = \frac{1}{V+W} (V Y_{i-1} + W X_0) \text{ when } 0 \leq i < f \quad (15)$$

$$X_i = \frac{1}{V+W-F} (V Y_{i-1} + W X_0 - F X_F) \text{ when } f < i \leq n+1 \quad (16)$$

The statics of the fractional distillation process is described by the system of eqns (4), (8)–(11), (15) and (16). Its solution makes

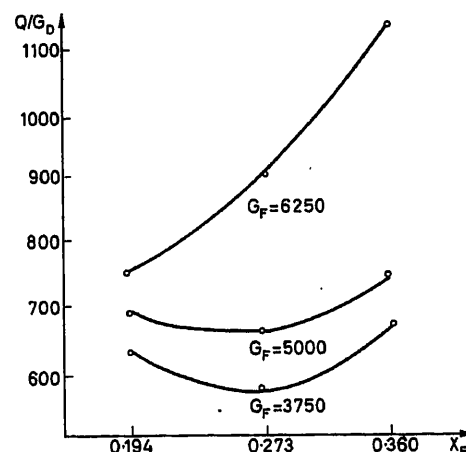


Figure 5. The graph illustrating the relationship between the heat consumption per unit weight of the distillate Q/G_D , and the quantity G_F and composition X_F of the initial mixture

it possible to obtain the static relations between the basic parameters of the process and the concentration distribution of the more volatile component in the liquid on the plates for different operating conditions.

The calculation of the static characteristics of the process was made for the above-mentioned fractional distillation column for the separation of the methanol-water mixture, for the different quantities and compositions of the initial mixture, and for the constant composition of distillate and still product. As an example, in Figures 5 and 6 the static characteristics of the column are given. From Figure 5 it is evident that within a certain range of values for the concentrations X_F and loads G_F there exists an extremum relationship for the steam consumption Q per unit weight of distillate G_D . With the increase in G_F the heat consumption per unit of G_D also increases, especially at high

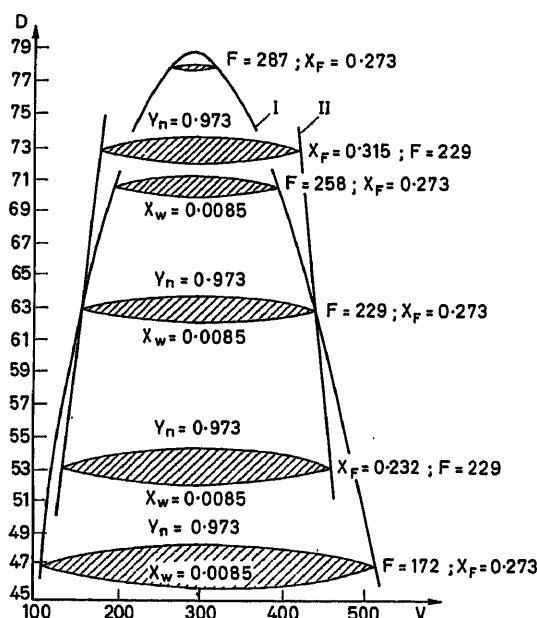


Figure 6. The operating region for the static parameters of the fractional distillation column. Curve I: quantity of the initial mixture F is variable, whilst its composition X_F is constant. Curve II: composition of the initial mixture is variable, whilst its quantity is constant.

concentrations X_F . From the graph it is possible to determine the operating conditions for which the energy requirements will be within the limits which are economically expedient.

From the consideration of Figure 6 it follows that the static characteristics have an extremum and ambiguous values (the assigned compositions of the final products may be obtained under different operating conditions). Curves I and II, which limit the operating region for the parameters of the process, represent the locus of values of the coordinates V and D , at which the compositions of the final products are exactly equal to those assigned. The minimum energy requirements of the process correspond to the minimum value for the vapour flow V which, at the given values of D , F and X_F will secure the assigned compositions X_D and X_W . One of the tasks of the optimum control is the determination and the maintenance, in relation to the values of F and X_F , of the values V and D , which correspond to the coordinates of points situated on the left side of the static characteristics.

For each set of operating conditions there is a limiting load for the column in respect of the quantity of the initial mixture of a given composition, at which the operating region degenerates into a point, see the extremum on curve I. With a further increase in the quantity of the initial mixture it is impossible to obtain the assigned compositions for the final products.

A reduction in load decreases the necessary vapour flow, which leads to an increase in the enrichment of the vapour phase by the more volatile component, and to an increase in the efficiency of mass transfer, see eqn (9).

The optimum place for the introduction of the initial mixture into the column is determined for each set of operating conditions, proceeding from the fact that the concentration of the more volatile component in the initial mixture X_F should be equal to the concentration X_f on the feed plate, i.e., the following condition is observed:

$$X_{f-1} < X_F < X_{f+1} \quad (17)$$

As a result of the analysis of calculations relating to the statics of the process it is possible to make the following deductions:

(1) The plate-type distillation column for the separation of binary mixtures is a non-linear process. The independent parameters in the calculations relating to the statics of the process are the load of the column based on the quantity of the initial mixture F , the composition of the initial mixture X_F , the value of the vapour flow rate in the column V and the distillate withdrawal rate D .

(2) The region of the static characteristics in which the conditional products may be obtained is limited by the four independent parameters indicated. These limitations are conditioned by the kinetics of mass transfer. The assignment of values for X_D and X_W , which fall outside the region of their joint existence, may cause oscillating operating conditions in the column (the conditions of joint existence of values for X_D and X_W are realized periodically).

(3) The relation between the final products of the column and the vapour flow rate may have an extremum. An increase in the vapour flow rate increases the motive force of the process $Y_i^* - Y_i$, but reduces the efficiency of each plate, which gives rise to the extremum. This phenomenon is not found in the calculations based on theoretical plates. The extremum for the static characteristics may be conditioned by the kinetics of mass transfer, as well as by the carrying away of the liquid from the plates.

(4) The static characteristics are ambiguous. This property develops only in calculations which take into account the kinetics of mass transfer on the plates. The range of characteristics, situated on the left side of the extremum, represents the operating range.

(5) The change in composition of the vapour phase on the plates is usually more appreciable than that for the liquid phase.

(6) The optimization of the process produces increased demands on the system of automatic control, in view of the steepness and ambiguity of the static characteristics.

As a result of the investigations described it was possible to develop a control system for the distillation process, which is shown in Figure 7. Controller 1 maintains the assigned optimum rate of supply of the initial mixture to the column.

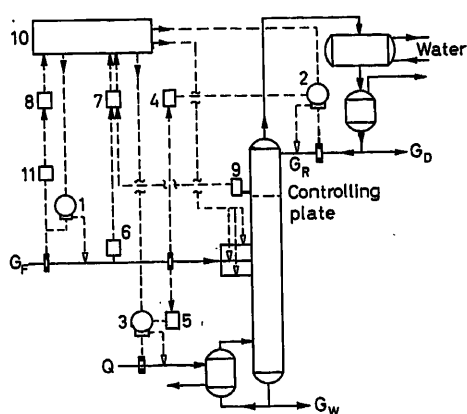


Figure 7. Block diagram for a combined selective invariant system of control for the process of fractional distillation

Instruments 4 and 5 measure the rate of flow of the initial mixture and send signals to controllers 2 and 3 for the flow ratios G_F/G_R and G_F/Q .

The dynamic characteristics of instruments 4 and 5 are computed so that the conditions of selective invariance in respect of disturbances for the rate of flow of the initial mixture are fulfilled. Controllers 2 and 3 maintain the material and thermal balance of the process.

The control based on the disturbance of composition of the initial mixture and on the deviation of the composition of the liquid on the controlling plate is achieved by these same controllers through the assignments computed and set by computer 10.

Converters 7 and 8 receive signals from transducers 6, 9 and 11 which measure the compositions X_F and X_i and the rate of flow G_F , and transform them into signals which in turn are admitted to computer 10.

The computer performs the following operations:

(1) Calculation of the optimum load of the column G_F for the current values of X_F and setting of the assignment for the rate of flow controller 1, see Figure 7.

(2) Calculation of optimum ratios G_F/G_R and G_F/Q in relation to the current values of G_F and X_F and setting of the assignment for controllers 2 and 3, conforming to the conditions of selective invariance.

(3) Correction of the calculated optimum ratios G_F/G_R and G_F/Q based on the degree of deviation of the basic controllable parameter—the deviation of concentration of the more volatile component in the liquid on the selected plate (closing of the control loop by means of the feed-back signal).

(4) Calculation of the optimum feed plate number and shifting of the inlet of the initial mixture to the necessary plate.

(5) In the case of multi-component mixtures: calculation of the plate number for the withdrawal of the side product and calculation of its quantity. The corresponding assigned operations: the changing over to the necessary withdrawal plate and setting of the assignment for the controller of the side product flow rate are not shown in the diagram.

(6) Transition from one algorithm of control to another—in accordance with the change in the optimization assignment, with

the transition (having reached definite parameters values) from starting to normal operating conditions and from the latter to the shut-down, etc.

In addition to this the usual operations of automatically checking the accuracy of calculations and the working order of the computer, the printing of results, signalling of inaccuracy and faults, etc. should be performed. In case of faults or stoppage of the computer, the assignments to controllers should remain at values determined at the preceding instant.

In the development of the considered control circuit it was assumed that the temperature of the initial mixture is constant. It is known that the heating of the mixture to its boiling point represents the optimum condition. With the variable composition and constant temperature of the initial mixture the ratio between the liquid and the vapour phase, and the enthalpy will change. Therefore, in the case of the composition of the initial mixture changing within wide limits, it is expedient to control its enthalpy. For this, an instrument should be included in the control circuit which would measure the enthalpy of the initial mixture and send the signal to the computer. The computer should calculate the optimum enthalpy value for the parameters of the initial mixture at the corresponding instant of time and pass the assignment to the steam consumption controller, feed heating.

The adaptation of the proposed control system is expedient in those complex cases where it is required that the separation of components of the mixture should be made with a high accuracy and where optimization of the process is required.

Nomenclature

D	Quantity of distillate (kg-mole/h)
W	Quantity of still product (kg-mole/h)
F	Quantity of initial mixture (kg-mole/h)
i	Plate number, for still $i = 0$, for condenser $i = n + 1$
f	Feed plate number
H	Quantity of liquid on the plate (kg-mole)
L	Quantity of liquid running off the plate (kg-mole/h)
V	Quantity of vapour leaving the plate (kg-mole/h)
Q	Quantity of heat supplied to the evaporator (kcal/h)
G_F, V, D, W, R	Quantity of initial mixture, vapour, distillate, still product, reflux (kg/h)
X	Concentration of the more volatile component in the liquid on the plate (mole fractions)
Y	Concentration of the more volatile component in the vapour above the plate (mole fractions)
Y^X	Concentration of the more volatile component in the vapour which is in a state of equilibrium with the liquid of composition x (mole fractions)
K_v	General mass-transfer coefficient, related to the unit area of phase contact, calculated by the vapour phase (kg-mole/m ² /h)
S	Phase contact area on the plate (m ²)
β_1	Particular mass-transfer coefficient in the liquid phase (kg-mole/m ² /h)
β_v	Particular mass-transfer coefficient in the vapour phase (kg-mole/m ² /h)
τ	Time (h)
$\Delta\tau$	Contact time of phases on the plate (h)

References

- AKSELROD, D. S. *Doctorate Thesis*. MIKhM (1958)
- ANISIMOV, I. V. *Automatic Control of Fractional Distillation Columns*. 1961, 2nd Edition, Gostoptekhizdat
- DILMAN, V. V., OLEVSKII, V. M. and KOCHERGIN, N. A. *Theory and practice of fractional distillation in the chemical and food*

- industries. *All-Union Inter-Inst. Conf.* (Collection of Reports). Izdatel'stvo Kievskogo Universiteta (1960)
- ⁴ IVAKHNENKO, A. G. *Tekhn. Kibernet.*, Kiev (1959)
 - ⁵ KULEBAKIN, V. S. Methods of improving the quality of automatically controlled systems. *Proc. Zhukovskii's Inst.*, Ex. 5021 (1954) 3-51. Trudy VVIA im. Zhukovskogo
 - ⁶ KULEBAKIN, V. S. *Proc. Sov. Acad. Sci.*, Vol. 68, No. 5 (1949); Vol. 77, No. 2 (1951)
 - ⁷ KULEBAKIN, V. S. *Proc. 2nd All-Union Conf. Izdatel'stvo AN SSSR*, Vol. II (1955) 184-207
 - ⁸ KASATKIN, A. G., PLANOVSKII, A. N. and CHEKOV, O. S. *Calculations relating to fractional distillation and absorption equipment*. 1961, Standartgiz
 - ⁹ ORLOV, B. N. *Thesis. MKhTI* (1961)
 - ¹⁰ PLANOVSKII, A. N. and NIKOLAEV, P. I. *Processes and Equipment of the Chemical and Petroleum Industries*. 1960. Gostoptekhizdat
 - ¹¹ SOLOMAKHA, V. P. *Thesis, MIKhM* (1957)
 - ¹² CHEKHOV, O. S. *Thesis, MIKhM* (1959)
 - ¹³ LEWIS and WHITMAN *Industr. Engng. Chem. (Industr.)* 16 (1924) 125
 - ¹⁴ MURPHREE *Industr. Engng. Chem. (Industr.)* 17 (1925) 747
 - ¹⁵ ROSENBRICK, H. H. Calculation of the transient behaviour of distillation columns. *Brit. Chem. Engng.*, 3 (1958) 363-367, 432-435, 491-494
 - ¹⁶ RADEMAKER, O. and RUMSDORF, J. E. Dynamics and control of continuous distillation. *5th World Petroleum Congr.* London (1960)
 - ¹⁷ WILKINSON, W. L. and ARMSTRONG, W. D. *Plant and Process Dynamic Characteristics*, 56-72, London (1957)
 - ¹⁸ VOETTER, H. *Plant and Process Dynamic Characteristics*, 73-100, London (1957).

DISCUSSION

D. E. LAMB, *University of Delaware, Newark, Delaware, U.S.A.*

This paper is concerned with a wide range of distillation problems including distillation dynamics, steady-state optimization and control strategy including both conventional and computer control. Remarks here are confined to two areas: representation of vapour liquid mass transfer in the dynamic model, and control strategy.

The author prefers to represent mass transfer between liquid and vapour or the trays of a distillation column in terms of the two film theory rather than in terms of tray efficiency. However, the two approaches are in fact equivalent. By defining $I - E = \exp(-K_{ri}V_{L,i})$ it is apparent that eqn (9) defines the Murphree tray efficiency, E . The dependency of E on the fluid properties and design and operating parameters can be included in the dynamic equations in a manner similar to that used for the kinetic mass transfer expression. In view of this it is surprising that the responses to step changes in feed composition calculated, using theoretical plates, differ from results calculated, using a kinetic equation for mass transfer as shown in Figure 1. Perhaps the author can clarify this point by providing a more detailed description of how the dotted curves in Figure 1 were obtained.

The question of proper representation of tray efficiency in dynamic models merits further consideration. Many authors have obtained simplified dynamic models of distillation columns by treating tray efficiency in a manner analogous to that in steady-state models. This consists of setting $E = 1$ and replacing the two vapour-liquid equilibrium curves by a pseudo-equilibrium curve which passes through the steady-state values of liquid and vapour composition associated with each tray. Although this procedure is correct in the case of steady-state models, and gives correct values at the steady-state gain in linearized dynamic models, it may give a poor estimate of the true dynamic response, when the actual tray efficiency differs significantly from unity. In fact, this simplification alters the mathematical model in a profound way because it eliminates the dependence of vapour composition on its past history as the vapour rises through successive trays in a column, and instead makes composition of vapour rising from a tray simply proportional to liquid composition on the tray. The mathematical implications of this are more apparent when the set of difference differential equations for a plate type distillation column are approximated by partial differential equations. This is equivalent to treating each section of the column as a distributed parameter system rather than a multistage system. When the tray efficiency is properly included the partial differential equations are second order and contain a diffusion type term with a coefficient of $(I - E)$, whereas use of the pseudo-equilibrium curve simplification leads to first order partial differential equations. Solutions of these first and second order equations can have quite different forms when E is significantly different from unity.

Turning now to the control scheme proposed in the paper, there are three items which I should like to mention. First, a feed flow controller is used to maintain the approximate assigned optimum feed flow rate. In practice this can be done only when a feed hold-up tank is available, and it is usually more realistic to consider variation in feed-flow rate as a measurable input disturbance rather than as a manipulative variable. Second, although the control objective is to maintain product composition constant, the author prefers not to use product composition as the measured variable in the control loops but rather to measure the temperature or composition on the so-called controlling plates in the middle part of the column sections where larger variations are expected. It is well known that large variations in composition and temperature in the central part of the column can occur when disturbances in product composition produced by feed flow variations are cancelled by action of feedforward controllers. Thus, use of composition or temperature measurements on the controlling plates to generate error signals in feedback loops can lead to serious difficulties, particularly in the presence of feedforward control. When the control system is sufficiently elaborate to include an on-line computer, as in the example presented in this paper, on-line product analysers are usually economically justified and will produce better control.

Finally, I should like to ask the author to indicate the computational procedure used by the computer to adjust the dynamics of the feedforward control loops so that conditions of selective invariance are maintained under changing conditions of feed flow rate and feed composition.

I. V. ANISIMOV, *in reply*

(1) The comment that the representation of mass transfer between liquid and vapour is equivalent according to the two-film theory and the efficiency of the plate is only valid if the efficiencies in calculations are taken as constants and not as functions of the properties of the mixture being fractionated, the design of the plate, and the column operating parameters. The difference between the acceleration curves calculated with the kinetics of the process taken into account, and for theoretical plates, is to be explained by the fact that in calculations for theoretical plates the magnitude of the efficiency of the plates is, as usual, taken to equal unity, and does not depend on the mode of operation of the column.

(2) The comment is valid, but has no direct bearing on the paper, since the plant analogue presented therein makes it possible to avoid ordinary crude simplifications in examining the connection of the compositions of the vapour and liquid phases on the plate.

(3) (a) The scheme with an initial-mixture flow rate controller is, in fact, designed for operation with a sufficient reserve of the initial

mixture available in the storage tank, and with the optimal distribution of load between several columns operating in parallel solved. The more common case, when both the composition and the quantity of the initial mixture may vary, is described by the author in a paper published in *Khimicheskaya promyshlennost*, No. 12, 1963.

(b) The comment that the use of product quality analysers is usually economically justified, and gives better control results, is valid for non-invariant systems. Invariant control systems are intended to achieve a high degree of separation of the products. With high-purity products the sensitivity of quality analysers may be insufficient for control of the process. In this case it is necessary to take a sample from a control plate, on which the variation in composition may be several dozen (20–50) times greater than directly in the product. As the paper explained, the distribution of concentrations of a highly-volatile substance at constant product compositions up the height of the column is not constant, but depends on the mode of operation. Therefore, in appropriate cases it is necessary to introduce automatic correction of the composition value on the control plate assigned to the controller, to ensure that the composition of the products remains constant in any mode of operation. In many cases, but this is not obligatory, the control plate is located in the middle of each section of the column. The positioning of the control plate depends on the physico-chemical properties of the mixture being fractionated and the mode of operation. The term 'control' is applied to any plate, irrespective of its position, which is most favourable from the point of view of a sufficiently great variation of the composition or temperature of the medium and satisfactory dynamic characteristics of the control channels. However, if the pulse for control is obtained directly from the composition of the end products and not from a control plate, not only is the signal to the controller reduced (thus necessitating a more sensitive and accurate composition analyser), but the dynamic characteristic of the system is also impaired, since considerable delays occurring in the condenser or the column still are included in the control circuit.

(c) The approach to the calculation of invariant control systems for the rectification process, and the calculation of the dynamic characteristics of disturbance correctors, are examined by the author in *Khimicheskaya promyshlennost*, No. 12, 1963.

P. S. BUCKLEY, *Design Division, E.I. du Pont de Nemours & Company, Wilmington 98, Delaware, U.S.A.*

(1) The theory used by the author is similar to that employed by many others. He assumes an idealized column for a binary distillation with a tray efficiency less than 100 per cent. Whether he linearizes the individual tray equations is not clear. If he solves the equations in non-linear form, then he is one of the few to do so apart from workers at the University of Florida.

(2) I do not agree at all with the author on the choice of 'control' trays. Contrary to his statements, it is not only possible in many cases to control from terminal compositions (i.e., at the ends of the column), but it is better to do so. Many actual columns are controlled from terminal compositions.

(3) I agree with many, but not all, of the features of the author's proposed control scheme.

(a) It is usually not physically possible to manipulate feed rate to control the column. The feed rate is usually an independent variable as far as the column is concerned. The column must take what it gets from previous steps in the process; alternatively, feed rate may be determined by downstream material balance requirements.

(b) The author makes no provision for controlling cooling water flow rate. It should be manipulated either by the column pressure controller, or other source depending on application.

I. V. ANISIMOV, *in reply*

(1) The translation is at fault in this instance.

(2) The comment that the theory employed by the author is analogous to that used by many authors is incorrect. Consideration is not

given to an idealized column with efficiency below 100 per cent, but to non-linear equations taking account of the kinetics of mass exchange. The equations take into consideration the relationship of the values of the mass exchange coefficients to the operating parameters. These relations are not included in the calculations of authors who have used either linearized or non-linear analogues with constant plate efficiencies.

(3) The comment on control of column feed rate has been answered in the reply to Professor Lamb.

(4) Coolant speed control is not shown in the diagram. This problem does not usually present difficulties and is therefore not examined.

T. J. WILLIAMS, *Monsanto Chemical Company, North Lindbergh Boulevard, St. Louis 66, Missouri, U.S.A.*

The author states that the greatest changes in liquid concentration occur on the so-called 'controlling' plates. This is true for relatively small changes in the input variables (all those considered in this paper are ± 5 per cent of the initial value). Our work indicates that the region of largest change can be transferred to the end trays whenever the desired separating ability of the column is exceeded, i.e., when it can no longer maintain the previously attained separations under the new conditions.

We cannot agree with the second paragraph of Item 3 in the right-hand column of p. 302. Extensive computer and experimental work has shown us that a column can indeed be controlled from overhead and bottoms product composition measurements only. Such work is limited only by the ability of composition analysers to detect changes in product compositions. In fact, our work has shown that column dynamics are improved by end condition sampling.

In reference to Item 5, right-hand column, p. 302, the presence or absence of mass transfer considerations should not affect the speed of propagation of vapour flow rate changes through the column, since the value of V is not calculated from a mass transfer influenced equation.

Referring again to Item 5, right-hand column, p. 302, vapour phase composition changes are larger than liquid phase composition changes on a tray for the enriching section or part above the feed tray only. Liquid phase composition changes are usually larger for the stripping or lower section of the column. The deciding factor is the slope of the column operating line.

I. V. ANISIMOV, *in reply*

(1) It is fair to state that, where compensation in the working area of the plant is not possible, the heaviest variations in concentration on the plates of the column in the case of disturbances can take place on the end plates. However, in this case no plant control system is capable of ensuring normal conditions. The paper naturally examines a plant in the range of normal operating conditions.

(2) Naturally, control directly from the composition of the end products permits one to omit examination of the problems of the correlation of compositions on the control plates and of the products obtained. This is the advantage of the method. However, as Mr. Williams said, to implement such systems it is necessary to have analysers with appropriate characteristics. I cannot agree that the acceptance of end-product concentration improves the dynamic properties of the column in the general case—this is true for certain channels, not for all.

(3) The paper asserts that delays in the variation of the vapour phase on any plate with a disturbance in the vapour flow, are slight. This is due to the speed of propagation of the variations in the vapour flow along the column and the variation of the number of transfer units K_0/V on a plate.

D. W. T. RIPPIN, *Imperial College, London, S.W. 7., England*

A new feature of this paper is the inclusion of a plate efficiency which varies with both the slope of the equilibrium line and the vapour boil-up rate. Is the variation of these two parameters alone sufficient for all operating conditions considered by the author?

In the steady state, Figure 6 suggests the existence of two stable operating points for a specified output from the given column. Does the author claim that eqn (9) remains valid with the same values of film transfer coefficients β eqn (11) for a threefold increase in boil-up rate and a consequent sixfold increase in liquid flow in the upper part of the column as Figure 6 suggests?

In the dynamic case, is eqn (9), derived by assuming constancy of vapour flow and overall mass transfer coefficient, used to evaluate the dynamic behaviour of the column when both of these quantities may be varying?

Can experimental results be presented to justify the author's method of representing tray efficiency over a very wide range of static and dynamic conditions?

I. V. ANISIMOV, *in reply*

(1) In our view, at the present time the representation of the overall coefficient of mass transfer on the plate in the form of a function of a tangent to the angle of inclination of the equilibrium curve and partial (phase) coefficients of mass offtake makes it possible (taking into account the motive forces of the process) to interpret the process of mass exchange on a plate over a sufficiently wide domain of normal conditions.

(2) There is no need here to assert that, to ensure the ambiguity for the composition of the end products, the static characteristic with the variation of V over a wide range, the form of the equations for the partial coefficients of mass offtake remains the same. A necessary condition of ambiguity is (in the absence of off-carry), satisfaction of the inequality:

$$\frac{\partial}{\partial V} \left(\frac{K_v}{V} \right) < 0$$

As experiments show¹, ambiguity of the static characteristic has been found in a trial on an industrial plant. The data in the paper explain this phenomenon. However, it should be noted that the second point of the static characteristic equation also differs to a far lesser degree in the magnitude of v from the first; this depends on the normal mode of operation of the plant chosen at the design stage.

(3) Regarding eqn (9), it should be noted that it is a definition of the efficiency of the plate in both the statics and dynamics of the plant.

It is possible that the essence of Dr. Rippin's comment concerns the question whether it is correct to use in the calculation of the transient behaviour the mass-emission coefficient obtained by processing static experiments. Here one may cite S. M. Teager² who showed that evidently inertia linked with the actual process of mass transfer is very low. It thus follows that the use in calculating transient behaviour of equations for the mass-emission coefficients cannot lead to major errors.

References

- ¹ EVSTAFYEV, A. G. *et al.* *Koks i Khimiya*, No. 1 (1958)
- ² TEAGER, S. M. The transient in the interphase of a mass transfer system, *M.I.T. S.B. Thesis, Chem. Engng*, 1954

J. E. RIJNSDORP, *Koninklijke Shell Laboratorium, Amsterdam, Holland*

The most remarkable aspect of Mr. Anisimov's paper is the strong decrease of tray efficiency when the vapour load increases. What type of tray does he use?

In the literature, one often sees that tray efficiencies are rather independent of vapour load, or they increase when the vapour load increases^{1, 2}.

If there is a decrease of efficiency when the vapour load increases, then this is generally attributed to entrainment. However, entrainment means contact between the liquid hold-ups of the trays, which leads to a different dynamic model of the column. I would like to hear Mr. Anisimov's comment on this problem.

References

- ¹ ZUIDERWEG, F. J., VERBURG, H. and GILISSEN, F. A. H. *Proc. Int. Symp. on Distillation*, Brighton, May 1960
- ² GERSTER, J. A. *Chem. Engng Progr*, 59, No. 3 (1963), 35

I. V. ANISIMOV, *in reply*

It must be stated that the relationship between the efficiency of contact plates and the performance parameters, as emphasized¹, needs further study. The literature on these questions contains contradictory data.

In our paper we used the findings of Soviet researches into the efficiency of mass transfer on mesh, cap and gap plates²⁻⁵ on a series of experiments with industrial columns⁶, and also using the A.S.Ch.E. method.

All these researches show that, over a sufficiently wide range of V for the overall coefficient of mass transfer on a plate, the necessary (without off-carry) condition of reduction of the efficiency of mass transfer is satisfied:

$$\frac{\partial}{\partial V} \left(\frac{K_v}{V} \right) < 0$$

Naturally, off-carry can also cause a reduction in the separating power of the column, and to take it into account alters to a certain degree the form of the transient equations.

References

- ¹ GESTER, J. A. *Chem. Engng Progr*, 59, 3 (1963)
- ² ORLOV, B. N. and PLANOUSKY, A. N. *Khim. Mach.* No. 3, 24 (1960); *Khim. Tekhnol. Topliv i masei*, No. 3 (1961)
- ³ KOL'TSOV, K. S. and PLANOUSKY, A. N. *Khim. prom.* No. 7 (1960)
- ⁴ KOCHERGIN, K. A. *et al.* *Khim. prom.* No. 8 (1961)
- ⁵ BOGOSLOVSKY, V. E. and PLANOVSKY, A. N. *Khim. tekhnol. topliv i masei*, No. 1, 4 (1963)
- ⁶ ESTAFEV, A. G. *et al.* *Koks i khim.* No. 1 (1958)

Controllability and Allowable Compressor Capacity of a Flare Gas Recovery System

F. J. KYLSTRA

Summary

A flare gas recovery scheme is described in which a compressor takes suction direct from the flare gas system, without a gasometer being interposed. There are strict requirements as to maximum and minimum pressure in the flare line and stability of operation. In consequence of the dynamic lags in the pressure control loop, these requirements set an upper limit to the compressor capacity, which must be known to design the system properly.

The analysis features drastic simplifications while retaining the essential characteristics of the problem, and yields a relatively simple expression relating the maximum allowable compressor capacity to a few important parameters.

Sommaire

On décrit schématiquement un système de récupération d'acétylène, dans lequel un compresseur est relié directement au réseau d'acétylène où il aspire sans interposition d'un gazomètre. Il existe des conditions très strictes quant aux pressions maximale et minimale admissibles dans le réseau véhiculant l'acétylène et quant à la stabilité de fonctionnement. Par suite du déphasage dynamique qu'introduit la boucle d'asservissement de la pression, ces conditions imposent une limite supérieure à la capacité du compresseur, capacité qui doit être connue pour permettre de concevoir un système judicieux.

L'analyse nécessite des simplifications radicales et ne tient compte que des caractéristiques essentielles du problème; elle conduit à une relation relativement simple entre la capacité maximale admissible pour le compresseur et quelques paramètres importants.

Zusammenfassung

Es wird eine Abgaswiedergewinnung beschrieben, bei der ein Kompressor ohne Zwischenschaltung eines Gasometers unmittelbar vom Abgassystem (zur Fackel) absaugt. Für den größten und den kleinsten Druck im Abgasrohr und für die Betriebsstabilität gibt es strenge Vorschriften. Wegen der dynamischen Verzögerung im Druckregelkreis stellen diese Vorschriften eine obere Grenze für die Kompressorleistung dar, die bekannt sein muß, damit man das System richtig entwerfen kann.

Die Untersuchung ist stark vereinfacht, enthält aber die notwendigen Eigenschaften des Problems und ergibt einen relativ einfachen Ausdruck für den Zusammenhang der größten zulässigen Kompressorleistung mit einigen wichtigen Kenngrößen.

Introduction

Refineries and petrochemical plants usually produce considerable quantities of waste gas, either continuously as an inevitable by-product of normal operation, or incidentally as a result of off-normal operating conditions (discharge of safety valves). For a long time it has been normal practice to burn this gas in a flare. However, in several countries the 'eternal flame' seems to be losing its romantic appeal, and is more and more looked upon as a cause of air pollution: laws are enacted to restrict

flaring. Therefore, it is very desirable or even necessary to avoid any waste gas reaching the flare, except under emergency conditions. Moreover, the high calorific value of most of the waste gas may even make the arrangement for its recovery and subsequent use as fuel gas an economical proposition.

One possible flare gas recovery system comprises a compressor pumping gas direct from the flare gas system into the fuel gas system, without a gasholder being interposed (*Figure 1*).

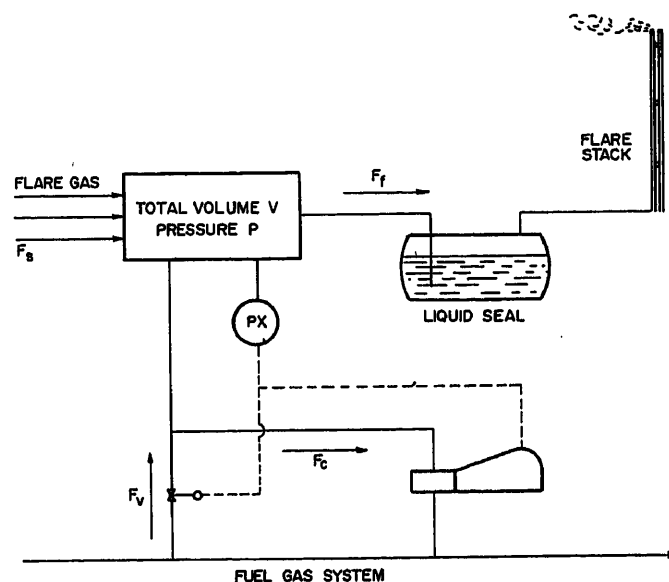


Figure 1. Simplified diagram of a flare gas recovery system

The investment involved in this recovery system depends largely on the size of the compressor, whose capacity is generally determined by non-technical arguments (economics, air-pollution hazard). On the other hand, operational requirements (e.g. safety, stability) set an upper limit to compressor capacity, which may make an otherwise desirable optimum unattainable. Therefore, in an early stage of design, the dynamic behaviour of this system has to be analysed in order to find the limiting factors and to indicate roughly the restrictions they impose. The present paper discusses such an evaluation.

Statement of the Problem

From the flare gas system, represented by the single volume V (*Figure 1*), gas is pumped into the fuel gas system. Gas supply is an independent variable, i.e. the recovery system must be capable of properly handling any quantity of waste gas that happens to be released by the plant.

For safety reasons P has to stay within strict limits P_{\min} and P_{\max} (e.g. 6 in. and 12 in. wg). These are determined according to the requirement that P must be very close to atmospheric pressure, but that under no circumstances should ambient air be permitted to leak into the flare gas lines.

Pressure is controlled by a valve in a by-pass over the compressor, primarily for protection against too low a pressure ($< P_{\min}$). At $P \geq P_{\max}$ a water seal breaks through to the flare. There may be an advantage in having the compressor speed set by system pressure. This adds to the corrective action of the control valve, but the compressor is expected to respond too slowly to rapid pressure fluctuations to exert the primary control function.

Various arrangements are possible for the joint operation of valve and compressor:

(a) Compressor speed constant; full response of the valve corresponding to part or all of the allowed pressure range [Figure 2(a)].

(b) Compressor speed varying with system pressure, (i) with split-range operation of valve and compressor [Figure 2(b)] and (ii) with overlapping ranges [Figure 2(c)].

The simplest version is that without a normal pressure controller, proportional action being provided by the transmitter

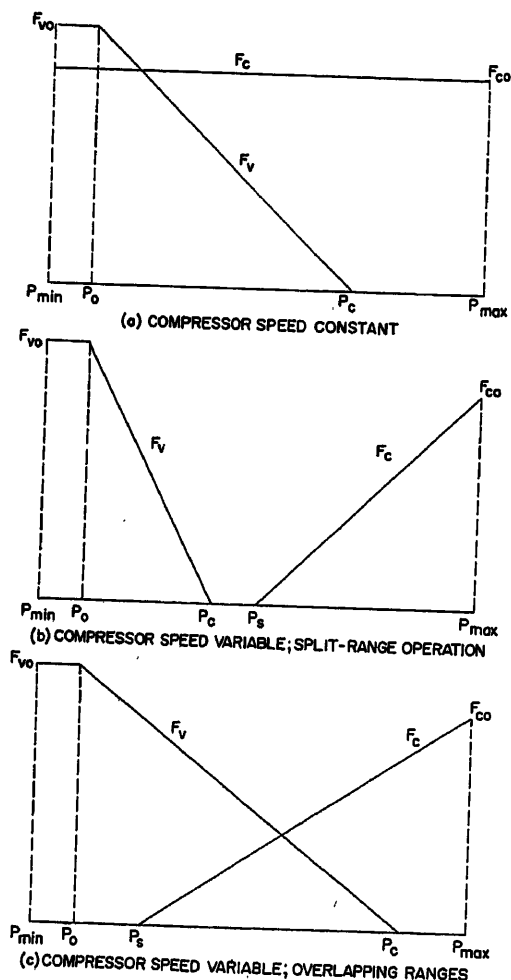


Figure 2. Steady-state responses of valve and compressor flows to system pressure

alone. The effect of additional derivative action will be considered later in this paper.

Pressure in the fuel gas system is high (e.g. 65 lb./in.²g) and is controlled independently.

One of the factors that put an upper limit to the allowable capacity of the compressor is the dynamics of the control system, in particular the response of the control valve to a fast decrease in pressure. If the compressor is too large, an abrupt stop of flare gas supply (which in practice frequently occurs) may be followed by the flare gas system being exhausted before the control valve can be actuated. Hence the speed of control, together with the poorest operating conditions, will determine the permissible compressor capacity. For any control system, stability is an obvious requirement.

With these criteria in mind, the following questions must be answered: Given a conventional pneumatic control system, what factors determine its speed? How does the maximum allowable compressor capacity depend on the system parameters? Which of the proposed modes of operation of compressor and control valve is the best?

In principle it is possible to study the problem by means of a complete simulation on an analogue computer, but this is hampered by the fact that: (a) numerical values of dynamic parameters of the system components are not known, or not accurately enough, and (b) the number of parameters and their variability are so large as to make very time consuming, if not impossible, a general solution by means of an investigation over the whole field of possible values.

Fortunately, realistic approximations are possible that even allow of analytic treatment of the questions concerning compressor capacity.

Preliminary Considerations and Simplifications

Pressure in the flare gas system will be stationary if:

$$F_s + F_v - F_c - F_f = 0 \quad (1)$$

where F_s is the flare gas supply (m^3s^{-1}), F_v is the gas flow through the control valve (m^3s^{-1}), F_c is the gas flow through the compressor (m^3s^{-1}), and F_f is the gas flow through the flare (m^3s^{-1}).

Since all pressures are close to atmospheric, volumetric flows are equivalent to mass flows.

Studying the response of system pressure P to a step disturbance in net flow, caused by an abrupt stop of flare gas supply, one starts from an initial steady state:

$$\left. \begin{aligned} F_v &= F_f = 0 \\ F_s &= F_c = F_{c0} \\ P &= P_{\max} \end{aligned} \right\} \quad (2)$$

(F_{c0} is the maximum flow through the compressor). This will represent about the most adverse situation that may arise in practice.

According as the compressor is larger it will respond more sluggishly to the resulting pressure decrease, and one may assume that this response has no appreciable influence on pressure during the time the control system requires to actuate the valve. Hence, for the time being, attention will be confined to the limiting case of compressor speed not responding at all. Furthermore, the ratio between compressor input and output

pressure will change so little, that its influence on the flow may also be neglected. Consequently, one takes the compressor flow constant at its maximum value F_{c0} .

The valve characteristic is assumed to be linear; in the final results this will be extended to the case of an exponential valve characteristic. As the pressure drop over the valve is supercritical, the flow F_v for a given opening is independent of the pressure in the flare system; pipeline resistances are neglected. Hence, one can express F_v in relation to system pressure in the steady state, as:

$$F_v = F_{v0}x = F_{v0} \frac{P_c - P}{P_c - P_0} \quad (3)$$

where F_{v0} is the maximum flow through the valve, x is the fraction of maximum valve-stem travel, P_c is the static system pressure at which the valve is just closed ($F_v = 0$), and P_0 is the static system pressure at which the valve is just fully open ($F_v = F_{v0}$).

Figure 3 shows the general behaviour of pressure in response to the previously defined step disturbance. It can be made plausible, even for an unstable system, that the first pressure minimum is the lowest attainable by this or any other disturbance, so that it is the determining factor for the answer to our problem. Besides, it depends only on that part of the valve characteristic for which $0 \leq F_v \leq F_{v0}$ (in the minimum $F_v = F_{v0}$).

Dynamic behaviour of the control loop will be considered linear. This implies that pilot-valve capacities will be chosen so as to avoid output flow saturation, and that a valve positioner will effectively reduce the effects of friction in the valve. To increase the speed of response these measures must be taken anyhow.

Because at this stage it is not intended to introduce too many parameters—which anyhow are not yet known—one makes a further simplification. It is observed that, in the picture, pressure presents a predominantly constant-rate signal during the initial fall from P_{\max} to P_{\min} (Figure 3). In response to such a signal any linear system with finite steady-state gain (no pure integration) behaves like a pure distance-velocity lag after the transients have died out. The magnitude T_d of this time lag can

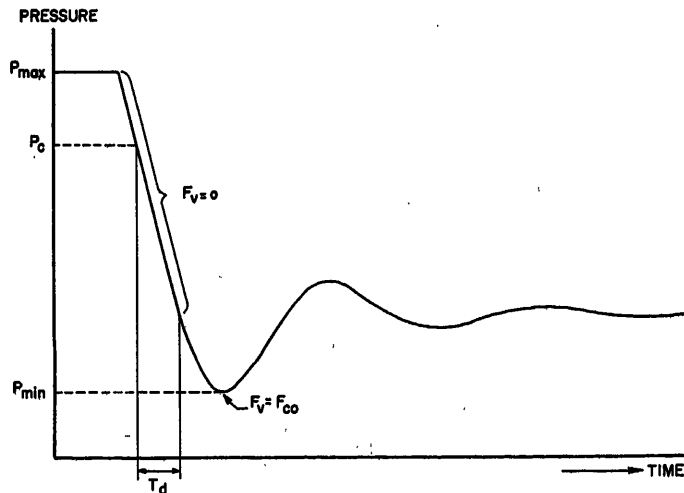


Figure 3. Pressure P as a function of time after a step disturbance of magnitude F_{c0} in flare gas supply, with F_{v0} as the only correcting condition

be found from a measured constant-rate response or from a series expansion of the relevant transfer function $F(s)$. If, for small values of s , one may write:

$$F(s) = K_0 \left(1 - \sum_{n=1}^{\infty} a_n s^n \right)$$

then

$$T_d = a_1$$

Hence, for this purpose the transfer function from system pressure P to valve-stem position x may be replaced by a single distance-velocity lag T_d . By this substitution the possible resonance effects in sub-loops of the system are neglected, which will be justified at the end of the analysis. In general, both amplitude ratio and phase shift of the distance-velocity lag will be larger than in the actual system, which tends to make the results conservative, as far as allowable capacity is concerned.

Analytic Solution

Stability

The problem, thus stripped of most of its complications, now yields easily to an analytic treatment. Considering small deviations from equilibrium, one finds

$$V \Delta P = P_{abs} \int \Delta F_v dt \quad (4)$$

$$\Delta F_v = -F_{v0} \frac{\Delta P_d}{P_c - P_0} \quad (5)$$

where

$$P_d(t) = P(t - T_d) \quad (6)$$

From this one may write the open-loop transfer function $G(j\omega)$ as

$$G(j\omega) = K \frac{e^{-j\omega T_d}}{j\omega T_d} \quad (7)$$

where

$$K = \frac{F_{v0} T_d}{V} \frac{P_{abs}}{P_c - P_0} \quad (8)$$

[see also Figure 9(a)].

Putting $G(j\omega) = -1$ one finds

$$\left. \begin{aligned} \text{ultimate frequency: } \omega_u &= \pi/2 T_d \\ \text{ultimate period: } T_u &= 2\pi/\omega_u = 4 T_d \\ \text{ultimate gain: } K_u &= \omega_u T_d = \pi/2 \end{aligned} \right\} \quad (9)$$

To ensure reasonable damping of the system it is required that $K \leq 1/2 K_u$. Hence it is found that the following practical stability condition

$$K = \frac{F_{v0} T_d}{V} \frac{P_{abs}}{P_c - P_0} \leq 0.8 \quad (10)$$

This condition is independent of the compressor capacity F_{c0} .

Eqn (10) was derived for small deviations from equilibrium, i.e. for linear responses. Its validity for large deviations may be restricted by non-linearities in the loop. The principal non-linearity present in the loop, however, is the limitation on valve

throughput, which tends to decrease the effective loop gain at larger amplitudes. Hence condition (10) is sufficient, also at large deviations.

Minimum Pressure

Now the first minimum in the pressure response to a step disturbance as specified previously is calculated. Equating this minimum, which is a function of several parameters, to the prescribed P_{\min} will give another necessary condition for the parameters.

As the valve will not respond to any pressure $P > P_o$, the calculation may be started at $t = 0$, when $P = P_o$. Similar to eqns (4) and (5) one has

$$V(P_o - P) = P_{\text{abs}} \int_0^t (F_{co} - F_v) dt \quad (11)$$

$$F_v = F_{v0} \frac{P_o - P_d}{P_o - P_o}, \quad (P_o \leq P_d \leq P_o) \quad (12)$$

Upon the introduction of dimensionless variables

$$\left. \begin{aligned} P^* &= \frac{F_{v0}}{F_{co}} \frac{P - P_o}{P_o - P_o} \\ P_d^* &= \frac{F_{v0}}{F_{co}} \frac{P_d - P_o}{P_o - P_o} \\ \vartheta &= \frac{t}{T_d} \end{aligned} \right\} \quad (13)$$

these equations yield

$$P^* = -K \int_0^{\vartheta} (1 + P_d^*) d\vartheta \quad (14)$$

where

$$P_d^*(\vartheta) = P^*(\vartheta - 1) \quad (15)$$

and K is defined by (8).

With the initial condition $P_d^* = 0$ for $\vartheta \leq 1$, the solution to (14) can be shown to be

$$P^* = \sum_{k=1}^{n+1} \frac{(-K)^k}{k!} (\vartheta - k + 1)^k \quad \text{for } n \leq \vartheta \leq n+1 \quad (16)$$

The value P_{\min}^* of the first minimum of this function has been calculated for different values of the parameter K ; the results have been plotted in Figure 4. It turns out that P_{\min}^* can be readily approximated by the following relationships

$$\begin{aligned} P_{\min}^* &= -1 & \text{for } K \leq 0.5 \\ P_{\min}^* &= -\frac{1}{2} - K & \text{for } K \geq 0.5 \end{aligned} \quad (17)$$

Eqn (17) is exact for $K \geq 1$. The maximum error occurs at $K = 1/2$, where eqn (17) gives $P_{\min}^* = -1$ instead of -1.04 .

Figure 4 contains all the necessary information for determining the maximum allowable value $F_{o, \text{all}}$ of F_o . From

$$-P_{\min}^* = \frac{F_{v0}}{F_{co, \text{all}}} \frac{P_o - P_{\min}}{P_o - P_o} \quad (18)$$

and eqn (8) one may derive

$$F_{c, \text{all}} = \frac{K}{-P_{\min}^*} \frac{V}{T_d} \frac{P_o - P_{\min}}{P_{\text{abs}}} \quad (19)$$

where $-P_{\min}^*$ has to be taken from eqn (17) or Figure 4.

The highest possible value of $F_{c, \text{all}}$ is realized by choosing $P_o = P_{\text{max}}$ and $K = 0.8$ (practical stability limit).

Upon substitution in eqn (19) one finds

$$F_{c, \text{all}} = 0.61 \frac{V}{T_d} \frac{P_{\text{max}} - P_{\min}}{P_{\text{abs}}} \quad (20)$$

where $K = 0.8$ and $P_o = P_{\text{max}}$.

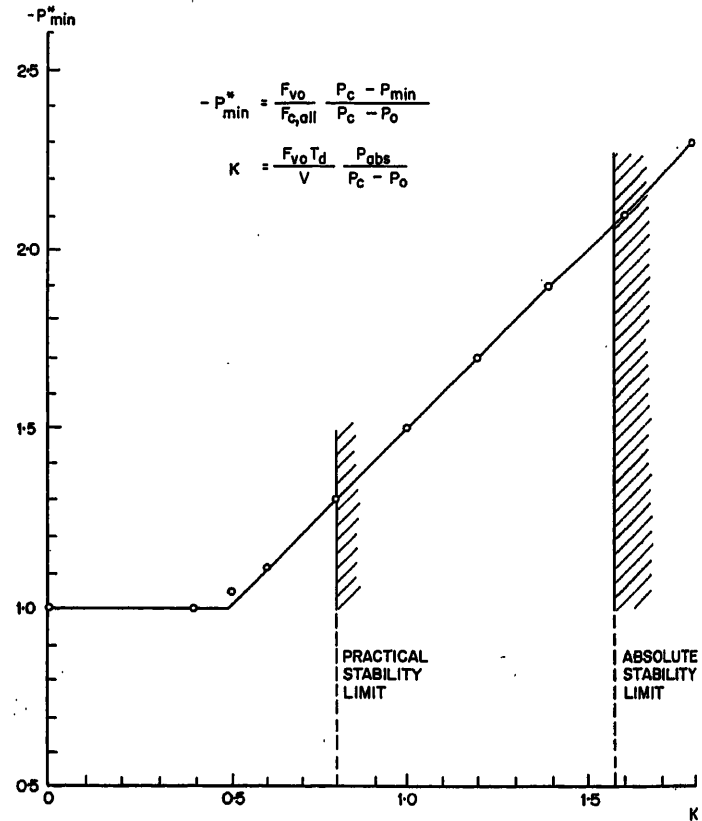


Figure 4. Minimum pressure after a step disturbance of magnitude $F_{o, \text{all}}$ (linear valve; points calculated with eqn (16))

Further Results

Resonance Effects in Sub-loops

A single dead time T_d has been introduced, neglecting the possible resonance effects in sub-loops of the system. This is allowed only if the resonance frequency of any sub-loop is an order of magnitude higher than the resonance frequency of the main loop. For a loop consisting of a pressure transmitter, a valve-positioner and a 4 in. valve, $T_d = 6$ sec seems a realistic estimate. This makes $T_u = 4 T_d = 24$ sec, which indicates an order of magnitude of T_u , that is long enough to make the effect of resonances in the sub-loops negligible.

Equal-percentage Valve

The use of an equal-percentage valve instead of a linear valve has some disadvantages, related to stability and speed of response. Together they bring about a substantial decrease of the maximum allowable compressor throughput.

From inspection of the stability condition (10) one finds the important factor

$$\frac{F_{v0}}{P_c - P_0}$$

which is the slope of the linear valve characteristic. In the case of a standard equal-percentage valve (rangeability 1:50) this must be replaced by the maximum slope of the corresponding exponential characteristic

$$F_v = F_{v0} \exp\left(-3.91 \frac{P - P_0}{P_c - P_0}\right) \quad (21)$$

$$\max\left(-\frac{dF_v}{dP}\right) = 3.91 \frac{F_{v0}}{P_c - P_0}$$

Hence the practical stability condition will become

$$K = \frac{F_{v0} T_d}{V} \frac{P_{abs}}{P_c - P_0} < \frac{\pi}{4} \frac{1}{3.91} = 0.2 \quad (22)$$

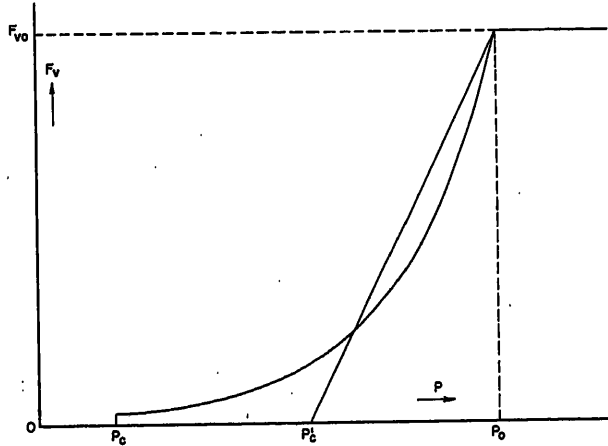


Figure 5. Characteristics of an equal-percentage valve and an equivalent linear valve

For estimating P_{min}^* the exponential valve characteristic is linearized, which enables one to make use of the results of analytical solution. Replacement of the exponential characteristic (21) by a linear one, as indicated in Figure 5, and determination of P'_c , so as to make the areas under the two curves equal, yields the result

$$P'_c \approx \frac{1}{2}(P_c + P_0) \quad (23)$$

In the case of a constant rate disturbance ($dP/dt = c$) this will make

$$\int_0^{t_0} F_v dt = c \int_{P_0}^{P_0} F_v dP \quad (24)$$

equal for the two types of valve.

Letting primes denote parameters associated with the substituted linear valve, one has

$$-P_{min}^* = \frac{F_{v0}}{F_{c,all}} \frac{P'_c - P_{min}}{P'_c - P_0} = -2P_{min}^* - \frac{F_{v0}}{F_{c,all}} \quad (25)$$

$$K' = \frac{F_{v0} T_d}{V} \frac{P_{abs}}{P'_c - P_0} = 2K \quad (26)$$

Upon substitution of P_{min}^* and K' in eqn (17) one finds the corresponding equation for the case of an equal-percentage valve

$$\left. \begin{aligned} P_{min}^* &= -\frac{1}{2} - \frac{1}{2} \frac{F_{v0}}{F_{c,all}} & \text{for } K \leq 0.25 \\ P_{min}^* &= -\frac{1}{4} - K - \frac{1}{2} \frac{F_{v0}}{F_{c,all}} & \text{for } K \geq 0.25 \end{aligned} \right\} \quad (27)$$

For $F_{v0} = F_{c,all}$ this formula was checked by analogue computer experiments with the true exponential valve characteristic, eqn (21). In spite of the drastic linearization applied in deriving eqn (27), the correspondence was surprisingly good (Figure 6).

To determine the maximum allowable compressor capacity $F_{c,all}$ for a system with an equal-percentage valve, one may now again use eqn (19) together with Figure 6. On maximizing the

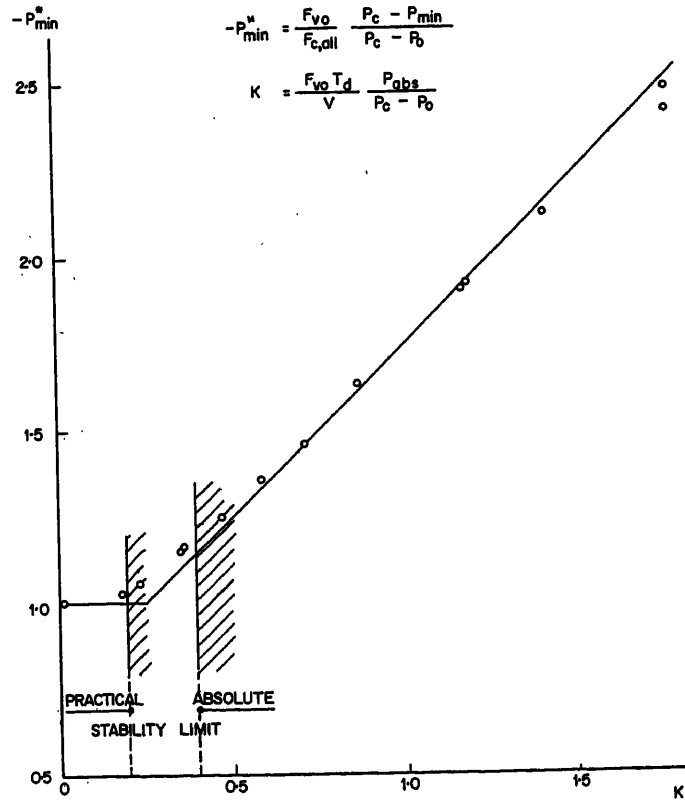


Figure 6. Minimum pressure after a step disturbance of magnitude $F_{c,all}$ (equal-percentage valve; points calculated with analogue computer)

right-hand side of eqn (19) it is found that

$$F_{c,all} = 0.2 \frac{V}{T_d} \frac{P_{max} - P_{min}}{P_{abs}} \quad (28)$$

where $K = 0.2$, $P_o = P_{max}$, and $F_{v0} = F_{c,all}$.

This formula indicates a threefold reduction of $F_{c,all}$, as compared to the system with a linear valve, eqn (20).

Derivative Action

The insertion of a *PD*-controller has its influence on both stability and minimum pressure. Let D be the derivative action time; the proportional gain constant of the controller was already included in K , eqn (8), by means of the factor $F_{v0}/(P_o - P_0)$.

For a conventional controller with 'tame' derivative action (i.e. with finite high-frequency gain) the open-loop transfer function, eqn (7), changes to:

$$G(j\omega) = K \frac{e^{-j\omega T_d}}{j\omega T_d} \frac{1 + j\omega D}{1 + j\omega \alpha D} \quad (\alpha = 0.04 - 0.15) \quad (29a)$$

This expression may be reduced to the form for ideal derivative action by incorporating the small time constant αD in the overall distance-velocity lag:

$$G(j\omega) = K' \frac{e^{-j\omega T_d'}}{j\omega T_d'} (1 + j\omega D) \quad (29b)$$

where:

$$T_d' = T_d + \alpha D$$

$$K' = \frac{T_d}{T_d'} K$$

From (29b) the ultimate gain K'_u is easily calculated as a function of D/T_d' , see Figure 7.

The minimum pressure condition must now be determined from eqn (30):

$$P^* = -K' \int_0^{g'} \left(1 + P_d^* + \Delta' \frac{d}{dg} P_d^* \right) dg \quad (30)$$

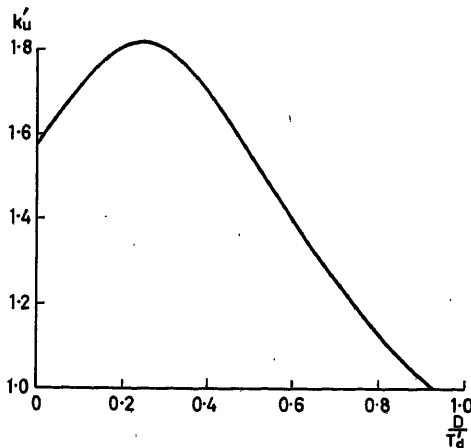


Figure 7. Ultimate gain as a function of derivative action time, calculated from eqn (29b)

whose solution may be written as:

$$P^* = \sum_{k=1}^{n+1} \frac{(-K')^k}{k!} \left(1 + \Delta' \frac{d}{dg'} \right)^{k-1} (g' - k + 1)^k \quad (31)$$

for $n \leq g' \leq n+1$

where

$$g' = \frac{t}{T_d'}, \quad \Delta' = \frac{D}{T_d'}$$

At the practical stability limit:

$$K' = \frac{1}{2} K'_u$$

or

$$K = \frac{1}{2} K'_u (1 - \alpha \Delta')$$

the first minimum P_{min}^* of this function has been determined as a function of Δ' . The result is shown in Figure 8, in a form

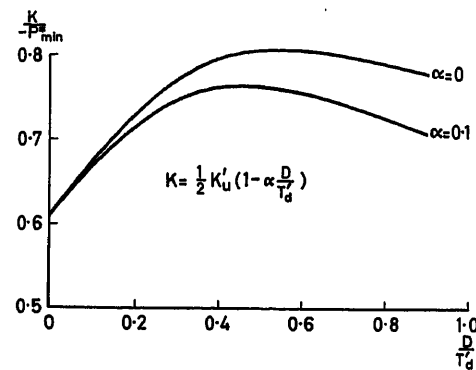


Figure 8. Numerical factor in eqn (19), as a function of derivative action time

that affords direct determination of the optimum value of Δ' . At $\Delta' = 0$ (no derivative action) one finds the previous result $K/(-P_{min}^*) = 0.61$ [see eqn (20)]. With $\alpha = 0$ (ideal *PD*-controller) one finds the optimum at $\Delta' = 0.55$:

$$\left. \begin{aligned} \frac{K}{-P_{min}^*} &= 0.807 (\alpha = 0) \\ D &= 0.55 T_d \\ K &= 0.737 \end{aligned} \right\} \quad (32)$$

With $\alpha = 0.1$ (real *PD*-controller) the optimum is at $\Delta' = 0.46$:

$$\left. \begin{aligned} \frac{K}{-P_{min}^*} &= 0.765 (\alpha = 0.1) \\ D &= 0.48 T_d \\ K &= 0.755 \end{aligned} \right\} \quad (33)$$

In conclusion one may state that the addition of derivative action increases $F_{c,all}$ by 25 per cent approximately. The derivative action time should be about half the previously defined distance-velocity lag.

Variable Compressor Speed

To reduce operating costs, the automatic adjustment of compressor speed to flare gas supply may be attractive. To some extent this would alleviate the task of the valve, yet for reasons of safety one holds to the requirement that the action of the valve alone must suffice to secure P_{\min} . Consequently, the previous results need modification only to the extent that the response of the compressor affects the stability of the system.

Considering the case of split-range operation [Figure 2(b)] the minimum-pressure condition, eqn (19), and the stability condition, eqn (10), are valid. In addition, one now has the requirement of stability for the compressor in its range of operation, which puts an upper limit to P_s , and this affects the value of $F_{c, \text{all}}$ by virtue of $P_c < P_s < P_{\max}$.

In order to get some idea of this effect a particular case was calculated [Figure 9(b)]. Assuming for the compressor a dominant first-order response, with a time constant $T_c = 5 T_d$, together with a distance-velocity lag equal to T_d for the remainder of the loop, it was found that split-range operation of valve and compressor would require a choice of P_s , and thus of P_c so as to reduce $F_{c, \text{all}}$ by a factor of 2.2, at least.

As an illustration of the effect of overlapping ranges [Figure 2(c)], take the particular case that valve and compressor operate completely parallel in the range $P_{\min} \leq P \leq P_{\max}$. Now

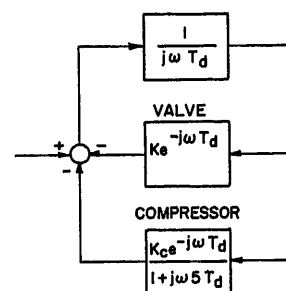
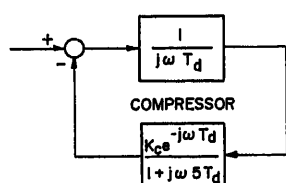
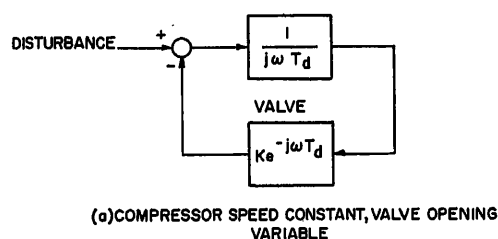


Figure 9. Block diagrams of system dynamics

the minimum pressure condition, eqn (19), is still valid but the stability condition for K has to be derived again for the system represented by Figure 9(c). As a result, $F_{c, \text{all}}$ comes out only slightly (3 per cent) lower than with a constant compressor speed. Consequently, for a fixed compressor capacity $F_{c0} < F_{c, \text{all}}$ the arrangement with overlapping ranges will show more stable and safer operation than with split ranges.

Although these results, derived for a specific example, are not general, they strongly suggest that the arrangement with overlapping ranges is to be preferred if the compressor speed is variable. However, when the installation of maximum compressor capacity is actually considered, the correct value of $F_{c, \text{all}}$ must be established by a special case study based on a more detailed analysis of the dynamics of the compressor and the other components in the loop.

Conclusions

(1) The dynamics of pressure control in a flare gas recovery system (Figure 1) have been analysed in order to determine the maximum allowable compressor throughput under the requirement of stable operation and strict limitations on pressure variations.

(2) Pressure in the flare system is best controlled by a valve in a by-pass over the compressor. This valve should have an effectively linear flow characteristic.

(3) To obtain a conservative estimate of the maximum allowable compressor throughput, $F_{c, \text{all}}$, the dynamics of the pressure control loop may be approximated by a pure distance velocity lag T_d . This lag can be found from the response of valve stem position with a constant-rate input to the pressure transmitter.

(4) If the compressor runs at a constant speed the maximum allowable capacity is given by

$$F_{c, \text{all}} = 0.61 \frac{V}{T_d} \frac{P_{\max} - P_{\min}}{P_{\text{abs}}} \quad (34)$$

(5) To reduce the value of T_d , all individual time lags in the control loop should be kept as small as possible. In particular, the possibility of flow saturation of a pilot valve should be excluded, and valve stem friction should be small.

(6) The above value of $F_{c, \text{all}}$ will be about 25 per cent larger if a PD-controller is used with a rate constant $D \approx 0.5 T_d$.

(7) If the compressor throughput is made to vary along with system pressure, $F_{c, \text{all}}$ will in general be lower than indicated by eqn (20). This reduction of $F_{c, \text{all}}$ may be significant in case of split-range operation of compressor and by-pass, but it is almost negligible if the ranges overlap. However, no general results have been obtained for these cases.

Nomenclature

D	Derivative action time constant
F_c	Volumetric flow through compressor
$F_{c, \text{all}}$	Maximum allowable value of F_c
F_{c0}	Maximum value of F_c
F_f	Volumetric flow to flare stack
F_s	Volumetric flare gas supply
F_b	Volumetric flow through by-pass

F_{v0}	Maximum value of F_v	P_{\max}	Maximum allowable value of P
K	$= \frac{F_{v0} T_d}{V} \frac{P_{\text{abs}}}{P_c - P_0}$	P_{\min}	Minimum allowable value of P
K_c	Gain constant of compressor dynamics	$P_{\min}^* = \frac{F_{v0}}{F_{c0}} \frac{P_{\min} - P_c}{P_c - P_0}$	
K_u	Ultimate gain	P_0	Pressure at which by-pass is just fully open
j	$\gamma - 1$	P_c	Pressure at which compressor throughput is minimum
P	Pressure in flare gas system	T_d	Distance-velocity lag
P_{abs}	Absolute pressure in flare gas system	T_u	Ultimate period
P_c	Pressure at which by-pass is just closed	V	Volume of flare gas system
P_c'	P_c for a substituted linear valve	x	Valve stem position
P_d	$P(t - T_d)$	ω	Circular frequency

DISCUSSION

VAN RUSSEN GROEN, *Netherlands*

In the article by Mr. Kylstra continuous control is considered. The maximum capacity of the compressor as calculated by Mr. Kylstra is in fact limited by: (a) The slow response of the speed of the compressor when a speed control is used. (b) The time lag of the pressure controller and by-pass control valve.

I would like to ask Mr. Kylstra if discontinuous multi-step control of the compressor capacity has been considered. A large displacement compressor normally has quite a number of cylinders. The capacity of each cylinder can easily be switched off by lifting the corresponding inlet valve to that cylinder. This control is very fast. The device can be supplied by almost every compressor manufacturer at relatively low cost. A multi-step pressure controller can switch on the capacity of all the cylinders in sequence.

The function of the by-pass valve can then be limited to the case in which the compressor is working at zero capacity, when all the inlet valves of the cylinders are lifted and the pressure P is still too low.

The advantages of this system are: (a) Fast response. (b) Economy; no more capacity is asked from the compressor than is needed. (c) The maximum compressor capacity is not so strongly limited as in the case of continuous control. (d) More than one compressor can be used, all the compressors working in sequence. In cases of failure of a compressor, the system will continue to function at reduced capacity.

F. J. KYLSTRA, *in reply*

The system suggested by Mr. van Russen Groen deserves full attention when it is considered that a variable compressor should be employed, and I agree, in general, with the advantages which he has listed. It seems to me, however, that pressure control by this means would at best be comparable to pressure control by means of a valve in the by-pass round the compressor, and in a practical system one would like to include such a valve anyway, if only as a safeguard against malfunctioning of the compressor regulator.

The flare gas recovery systems that have been installed to date fall into two categories:

(1) Systems designed to restrict flaring to a minimum because of public relations. These systems generally comprise a gasometer to reduce the peak loads on the compressor. The compressor is of the rotary type with a controllable electric drive¹.

(2) Systems where economic considerations prevail. These are often designed to recover only the continuous part of the flare gas flow, and compressor capacity is only a small fraction (between one part in thirty and one part in fifty) of the maximum allowable capacity. The compressor is of the reciprocal type, without speed control.

In none of these systems is the speed of response a limiting factor.

Reference

BRUIDERN, I. P. *Erdöl und Kohle*, 15 (1962), 4, 289

Analysis and Design of a Parameter-Perturbation Adaptive System for Application to Process Control

T. ISOBE and T. TOTANI

Summary

With the intention of obtaining a self-adaptive process control system, a simple parameter-perturbation system is treated. An analysis is developed to establish a design method of such systems. First, the lag of the mean-squared error variation of a second-order system behind the parameter variation is formulated. Second, the dynamic behaviour of the self-adjusting loop is formulated by taking a sampled-data model of the loop, and the variance of the parameter fluctuation in a steady state is also estimated. It is found that a bandpass filter in the loop improves the performance. Experiments were performed to control an actual flow process to prove the applicability of the self-adjusting system, and the results were satisfactory, supporting the analysis in each case.

Sommaire

En vue d'obtenir un système auto-adaptatif, on traite un système à paramètre perturbateur unique. L'analyse de tels systèmes est effectuée pour développer une méthode de calcul. D'abord, on formule le retard entre la variation de l'erreur moyenne quadratique d'un système de second ordre et celle du paramètre. Ensuite, on formule le comportement dynamique de la boucle auto-adaptative en se basant sur un modèle échantillonné de cette boucle. Enfin, on évalue la variance de la fluctuation du paramètre en régime permanent. On a trouvé qu'un filtre passe-bande mis dans la boucle en modifie la performance. L'applicabilité de système auto-adaptatif a été expérimentée sur un processus à écoulement; les résultats obtenus coïncident avec ceux de l'analyse d'une manière satisfaisante.

Zusammenfassung

Mit dem Ziel, ein selbststellendes Verfahrensregelsystem zu entwerfen, wird ein einfaches System behandelt, das Parameteränderungen ausgesetzt ist. Die Untersuchung ermittelt für ein System 2. Ordnung zunächst die Verzögerung zwischen der Änderung des Parameters und derjenigen der mittleren quadratischen Abweichung, dann wird das dynamische Verhalten des übergeordneten Selbststellungskreises anhand eines Abtastmodells bestimmt. Es folgt eine Abschätzung der Varianz der Parameterschwankungen im Beharrungszustand. Dabei zeigt sich, daß ein Bandpaßfilter im Selbststellungskreis das Verhalten verbessert.

An einer bestehenden Durchfluß-Regelanlage wurden Versuche durchgeführt, um die Anwendbarkeit des selbststellenden Systems zu prüfen. Die Ergebnisse bestätigten in jedem Falle hinreichend die Voraussagen.

Introduction

A number of ingenious proposals have been made for self-adaptive control systems whose parameters are self-adjusted to compensate for signal or system variations. When these schemes are applied to a practical process control system, effectiveness and simplicity of the self-adjusting device become important factors. A trial and error method usually requires a rather large

amount of hardware, even for simple control purposes¹, while a parameter-perturbation adaptive system, such as treated by Douce and King², as well as by Magrath, Rajaraman and Rideout³, generally has a simple adjusting device suitable for practical applications. With the intention of obtaining a practical adaptive process controller, this paper treats a system of the latter type for determining the optimum setting. An analysis of the response of the self-adjusting loop is developed, and the results of several flow control experiments are described.

Basic System

Figure 1 shows the basic system. The part subjected to a parameter adjustment is a closed-loop system with a stationary random input. On the basis of the minimum mean-squared error criterion taken as a figure of merit for the optimum, the adaptive loop applies a small perturbation ΔK (a square waveform of parameter variation) to the system. Thereby the resulting variation of the squared error as a signal measuring the performance

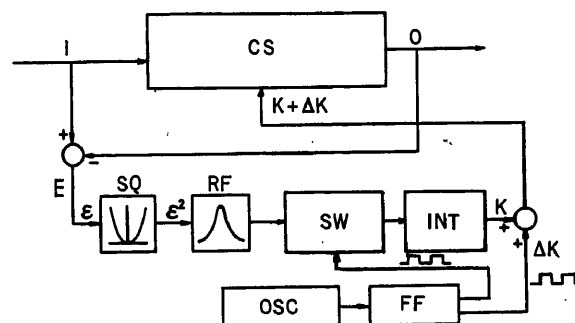


Figure 1. Basic system: CS closed-loop control system; I input; O output; K parameter; E error; SQ squarer; RF bandpass filter; SW synchronous switching; INT integrator; OSC oscillator; FF flip-flop

of the system is passed through a bandpass filter, then is synchronously detected by switching. In one half cycle the signal is passed directly, and in the other half cycle with its sign reversed. The output is in turn integrated to derive the value of the parameter K , to which the perturbation is added.

Response of System to a Parameter Perturbation

The lag of the closed-loop system response behind the parameter variation is formulated for the purpose of determining how short the perturbation period may be taken for a satisfactory functioning of the self-adjusting loop. In this paper, the overall characteristic of the closed-loop system to which the stationary random input is applied is assumed to be of second order as approximation, and the variation of the mean-squared

error due to a change of its damping ratio is considered. In application to process control, the random input causing the error is a disturbance such as a load change. The same discussion results, however, if the disturbance is regarded as the input.

Let the system and the input equations be given by

$$\ddot{y} + 2\zeta\omega_n\dot{y} + \omega_n^2 y = \omega_n^2 x(t) \quad (1)$$

$$\dot{x} + \lambda x = a n(t) \quad (2)$$

where $y(t)$ is the output of the system and $x(t)$ the stationary random input, derived from a white noise $n(t)$ by letting it pass through a low pass filter. And let the error be $\varepsilon = x - y$. By applying the method given by Laning and Battin⁴, simultaneous differential equations to be satisfied by the ensemble averages, $\overline{x^2}$, \overline{xy} , \overline{xy} , $\overline{y^2}$, $\overline{y\dot{y}}$, $\overline{y\ddot{y}}$ and $\overline{\varepsilon^2}$, for a noise of variable power or for variable parameters, are constructed and are treated on the assumption that λ/ω_n is sufficiently small that second or higher powers of it are negligible. The steady state value of $\overline{\varepsilon^2}$ for the stationary input gives the mean-squared error

$$\theta_{ss0} = \overline{\varepsilon^2} \cong \overline{x^2} \cdot \frac{\lambda}{\omega_n} \cdot \frac{4\zeta^2 + 1}{2\zeta} \quad (3)$$

which is minimum when ζ is equal to $\frac{1}{2}$.

If a small variation $\Delta\zeta(t)$ is given to the damping ratio at this steady state, a small variation of the mean-squared error $\Delta\theta_{ss}(t)$ will result. Taking only the first differential of each term of the simultaneous equations, one obtains the following ratio of the Laplace transforms of these variations:

$$\frac{\Delta\theta_{ss}(s)}{\Delta Z(s)} = 2\overline{x^2} \cdot \frac{\lambda}{\omega_n} \cdot \frac{2\omega_n}{\zeta} \cdot \frac{\zeta\omega_n s + (4\zeta^2 - 1)\omega_n^2}{(s + 2\zeta\omega_n)(s^2 + 4\zeta\omega_n s + 4\omega_n^2)} \quad (4)$$

which may be regarded as the transfer function of the closed-loop system for a small parameter variation.

From this transfer function, one obtains the step response

$$G(t) = \left[2\overline{x^2} \cdot \frac{\lambda}{\omega_n} \cdot \Delta\zeta \right] g(t) \quad (5)$$

where

$$g(t) = \frac{4\zeta^2 - 1}{4\zeta^2} + e^{-2\zeta\omega_n t} \left[\frac{1 - 2\zeta^2}{4\zeta^2(1 - \zeta^2)} + \frac{4\zeta^2 - 3}{4(1 - \zeta^2)} \cos 2(1 - \zeta^2)^{\frac{1}{2}}\omega_n t + \frac{1 - 4\zeta^2}{4\zeta\sqrt{1 - \zeta^2}} \sin 2(1 - \zeta^2)^{\frac{1}{2}}\omega_n t \right] \quad (6)$$

Figure 2 shows the function $g(t)$. The response initially appears on the plus side for any value of ζ , then approaches each final value. One natural period of the system T_n is a rough estimate of the time required to reach a new steady state.

The frequency response function is also obtained as

$$\frac{\Delta\theta(j\omega)}{\Delta Z(j\omega)} = 2\overline{x^2} \cdot \frac{\lambda}{\omega_n} \cdot \left[\frac{2}{\zeta} \cdot \frac{j\zeta u + (4\zeta^2 - 1)}{(ju + 2\zeta)(-u^2 + 4\zeta ju + 4)} \right] \quad (7)$$

where $u = \omega/\omega_n$. The full lines drawn in Figure 3 show constant ζ vector loci of the function inside the brackets of eqn (7), while the dotted lines show constant u loci. Since the constant u loci do not cross the real axis at the origin, the in-phase and the quadrature components of $\Delta\theta_{ss}(t)$ cannot simultaneously be

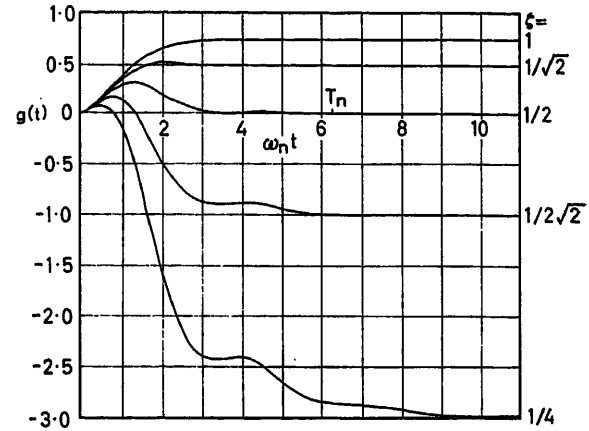


Figure 2. Step response function $g(t)$

made equal to zero, and if a phase shifter is used, the phase adjustment should be made so that the quadrature component of the resulting signal is held constant for any value of ζ during the search for the optimum, rather than made equal to zero. When the shifter is not used, the perturbation period $T = 10T_n$ ($u = 0.1$; the phase lag = 11°) is roughly the smallest value of T which should be taken.

These responses were completely verified on an analogue computer by setting up the simultaneous differential equations stated above. Parameter ζ was varied both stepwise and sinusoidally.

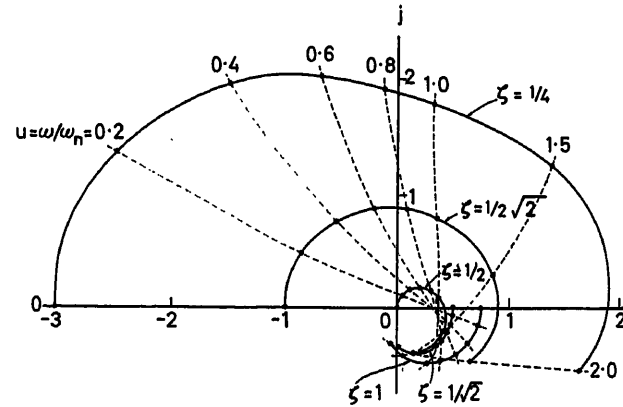


Figure 3. Frequency response function plotted on the complex plane

Response of Self-adjusting Loop

The purpose of this section is to formulate the dynamic behaviour of the self-adjusting loop as a guide to the design.

A sampled data model is taken because it is preferable to sample and hold the integrator output every switching cycle in order to avoid an unnecessary fluctuation of the derived parameter during each cycle (especially for the case of a long perturbation period), and also because the signal detection by synchronous switching is more reasonably treated in analysis by using the model.

The block diagram is shown in Figure 4. The block $M(s)$ represents the closed-loop system with a perturbation signal $\Delta Z(s)$ and also with a parameter value $\Xi(s)$ to be set. The

produced mean-squared error variation $\Delta\theta_{ss}(s)$ is the performance measuring signal modulated by the perturbation. The system may therefore be regarded as functioning as a kind of square wave modulator of the measure. The fluctuation of the squared error about the average $N(\zeta, t) = \varepsilon^2(t) - \varepsilon^2(t)$ is taken

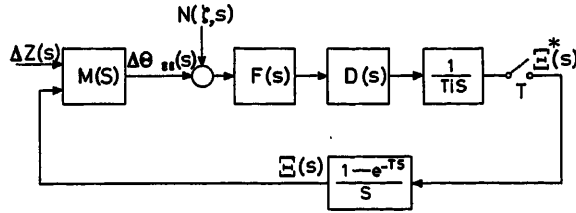


Figure 4. Block diagram: $M(s)$ square wave modulator; $F(s)$ bandpass filter; $D(s)$ demodulator; $1/Tis$ integrator; $\Xi(s)$ parameter value

into consideration as an input to the loop, and is shown in the diagram as $N(\zeta, s)$. The synchronous detection of the signal by switching, and the subsequent integration, are regarded as demodulation. The signal is then sampled at the same periods as that of perturbation.

Since the Laplace transform of the perturbation signal, a square wave of amplitude $\Delta\zeta$, is

$$\Delta Z(s) = \frac{1}{s} \cdot \frac{1 - e^{-(T/2)s}}{1 + e^{-(T/2)s}} \cdot \Delta\zeta \quad (8)$$

the output $\Delta\theta_{ss}(s)$ is obtained by substituting eqn (8) into eqn (4). If it is assumed that the dynamic response time of the measuring system is approximately negligible, as compared with the perturbation period (see Appendix III), this may be written as

$$\Delta\theta_{ss}(s) = 2x^2 \cdot \frac{\lambda}{\omega_n} \cdot \frac{4\zeta^2 - 1}{4\zeta^2} \cdot \frac{1}{s} \cdot \frac{1 - e^{-(T/2)s}}{1 + e^{-(T/2)s}} \cdot \Delta\zeta \quad (9)$$

To simplify the analysis further, a variable ξ , the parameter misadjustment, which is a small deviation of ζ value from the optimum and is equal to $\frac{1}{2} - \zeta$, is introduced. Eqn (9) is thereby roughly approximated by the function

$$\Delta\theta_{ss}(s) = -\mu \cdot \frac{1}{s} \cdot \frac{1 - e^{-(T/2)s}}{1 + e^{-(T/2)s}} \cdot \xi \quad (10)$$

where $\mu = 8x^2(\lambda/\omega_n)\Delta\zeta \cong 4\varepsilon^2\Delta\zeta$.

As far as eqns (9) and (10) are concerned, a jump function, which varies only at the beginning of each period, may be taken for ξ or $\Xi(s) = \frac{1 - e^{-Ts}}{s} \Xi^*(s)$ for ξ/s . Then an equation is obtained, showing that $\Xi(s)$ may be considered as the input and $\Delta\theta_{ss}(s)$ the output of a linear element whose transfer function is

$$M(s) = -\mu \frac{1 - e^{-(T/2)s}}{1 + e^{-(T/2)s}} \quad (11)$$

The demodulator plus integrator transfer function is

$$I(s)D(s) = \frac{1}{Tis} \frac{1 - e^{-(T/2)s}}{1 + e^{-(T/2)s}} \quad (12)$$

where $1/Ti$ is the gain of the integrator.

Including the transfer function of the filter $F(s)$, the open loop transfer function is denoted by $G(s)$, and is equal to $I(s)D(s)F(s)M(s)(1 - e^{-Ts})/s$. When the loop is closed by way of the sampler, the sampled output will be evaluated by the equation

$$\Xi(z) = \frac{1}{1 + G(z)} Z \{I(s)D(s)F(s)N(\zeta, s)\} \quad (13)$$

The Case Where the Filter is Not Used

As a means of obtaining the sampled output at the periods of T from eqn (13), using a power series expression of $\Xi(z) = \sum_{m=0}^{\infty} \xi_m z^{-m}$ and introducing the notations,

$$\left. \begin{aligned} L_m &= \int_0^{mT} N(\zeta, t) dt \\ \Delta_{\frac{1}{2}} L_m &= L_{m+\frac{1}{2}} - L_m, \quad \Delta_{\frac{2}{3}} L_m = \Delta_{\frac{1}{2}} L_{m+\frac{1}{2}} - \Delta_{\frac{1}{2}} L_m \end{aligned} \right\} \quad (14)$$

one obtains the difference equation (see Appendix I)

$$\Delta \xi_m + \frac{\mu}{T_i} T \xi_m = \frac{1}{T_i} \Delta_{\frac{2}{3}} L_m \quad (15)$$

whose exact solution with an initial parameter misadjustment ξ_0 is

$$\xi_m = \xi_0 \left(1 - \frac{\mu}{T_i} T\right)^m + \frac{1}{T_i} \sum_{n=0}^{m-1} \left(1 - \frac{\mu}{T_i} T\right)^n \Delta_{\frac{2}{3}} L_{m-n-1} \quad (16)$$

Parameter Approaching the Optimum—Since the second term of eqn (16) is random and is zero by taking the ensemble average,

$$\bar{\xi}_m = \xi_0 \left(1 - \frac{T}{T_a}\right)^m \quad (17)$$

where

$$T_a = \frac{T_i}{\mu} = \frac{T_i}{4\varepsilon^2\Delta\zeta} \quad (18)$$

There are three regions of values for the period T which give different behaviours;

- (i) ξ_m approaches zero monotonically for $0 < T < T_a$.
- (ii) It approaches in an oscillatory manner for $T_a < T < 2T_a$.
- (iii) It diverges for $2T_a < T$.

When $T = T_a$ exactly,

$$\bar{\xi}_m = 0 \quad \text{for } m \geq 1 \quad (19)$$

the parameter settles down to the optimum after one sampling period. For a small T , eqn (17) is approximated by

$$\bar{\xi} = \xi_0 e^{-t/T_a} \quad (20)$$

The differential equation approximation suggests that the behaviour of the loop is described in a little more detail by the equation directly obtained from eqn (9)

$$\dot{\zeta} = \frac{\mu}{4T_i} \frac{4\zeta^2 - 1}{4\zeta^2} \quad (21)$$

with the solution

$$\frac{2\bar{\zeta}-1}{2\bar{\zeta}+1} e^{4\bar{\zeta}} = K e^{-(\mu/T_i)t} \quad (22)$$

where

$$K = \frac{2\zeta_0-1}{2\zeta_0+1} e^{4\zeta_0}$$

The two curves (A) and (B) drawn in Figure 5 are calculated from eqn (22), showing the manner in which ζ approaches the

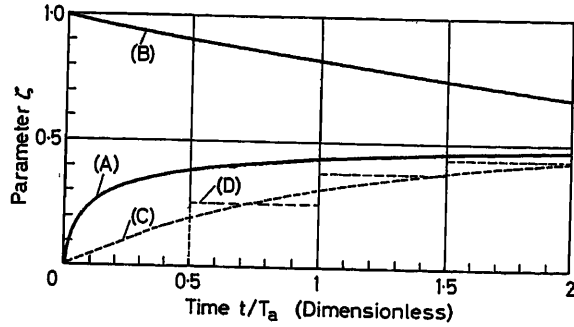


Figure 5. Manner in which the parameter approaches the optimum

optimum from the lower and the upper sides. The other two curves (C) and (D) calculated from eqns (20) and (17) ($T = \frac{1}{2}T_a$) are drawn for reference, though these equations are valid only for very small ξ values.

Variance of Parameter Fluctuation—Squaring eqn (16) and taking the average, the following equation is obtained which enables one to estimate the variance of the parameter fluctuation due to that of the squared error in the steady state;

$$\bar{\xi}_m^2 = \frac{1}{T \left(1 - \frac{1}{2} \frac{T}{T_a}\right)} \frac{1}{T_i^2} (\Delta_{\frac{1}{2}} L_m)^2 \quad (23)$$

The last factor can be estimated by using the autocorrelation function $\phi_{ee}(\tau) = \overline{\varepsilon^2(t) \varepsilon^2(t+\tau)} - \overline{\varepsilon^2(t)}^2$ of the squared error fluctuation or its power density spectrum $\Phi_{ee}(\omega)$. If it can be assumed that the perturbation T is sufficiently long that the autocorrelation function decays out in one period, it will be⁵

$$\begin{aligned} (\Delta_{\frac{1}{2}} L_m)^2 &= \left[\int_{mT}^{mT+T/2} N\left(\frac{1}{2}, t\right) dt \right]^2 \\ &= \frac{T}{2} \cdot 2 \int_0^\infty \phi_{ee}(\tau) d\tau = \frac{T}{2} \Phi_{ee}(0) \end{aligned} \quad (24)$$

where the value of $\Phi_{ee}(0)$ is approximately $\frac{5}{2} \frac{1}{\omega_n^2} \varepsilon^2$ (see Appendix II), estimated by assuming Gaussian distribution of the fluctuation amplitudes of the error, the input, the output and their derivatives. The root of the variance is thus evaluated as

$$\bar{\xi}_m^{\frac{1}{2}} = \left(\frac{5}{8\pi}\right)^{\frac{1}{2}} \left(\frac{T_a T_n}{T_i}\right)^{\frac{1}{2}} \varepsilon^{\frac{1}{2}} = \left(\frac{5}{32\pi}\right)^{\frac{1}{2}} \left(\frac{T_n}{T_i \Delta \zeta}\right)^{\frac{1}{2}} \varepsilon^{\frac{1}{2}} \quad (25)$$

where $T_n = 2\pi/\omega_n$ is the natural period of the closed-loop system.

The time constant T_a given by eqn (18) is required to be as short as possible, to make the parameter fluctuation $\bar{\xi}_m^{\frac{1}{2}}$ as small as possible. For making a compromise with the contradictory requirements imposed on the gain of the loop $1/T_i$, a proposition that the magnitude of fluctuation should be of the same order as the perturbation amplitude, may be reasonable; namely

$$\bar{\xi}_m^{\frac{1}{2}} = k \Delta \zeta, \quad k \cong 1 \quad (26)$$

Then

$$T_i = \frac{1}{k^2} \cdot \frac{5}{32\pi} \cdot \frac{T_n}{\Delta \zeta^3} \varepsilon^2 \quad (27)$$

and

$$T_a = \frac{1}{k^2} \cdot \frac{5}{128\pi} \cdot \frac{T_n}{\Delta \zeta^4} \quad (28)$$

For a typical numerical example, let

$$k=1, \Delta \zeta=0.1, T=10 T_n; \bar{\xi}_m^{\frac{1}{2}}=0.1, T_a=12.4 T \quad (29)$$

The integrator gain $1/T_i$ should be adjusted so that eqn (27) is satisfied all the time, if possible.

The Case Where the Filter is Used

A filter of the form

$$F(s) = \frac{\omega_0 s}{s^2 + 2\gamma\omega_0 s + \omega_0^2} \quad (30)$$

with ω_0 adjusted to $[1/(1-\gamma^2)]^{1/2} 2\pi/T$ should be effective to raise the signal-to-noise ratio. It has zero phase shift and a maximum gain equal to $1/2\gamma$ at the natural angular frequency ω_0 . The property of a plus or a minus phase shift corresponding to an input frequency change may give a means of controlling the phase. Using the notations,

$$\begin{aligned} S_m &= \int_0^{mT} V(t) dt, \quad V(t) = \int_0^t w(\tau) N(\zeta, t-\tau) d\tau \\ \Delta_{\frac{1}{2}} S_m &= S_{m+\frac{1}{2}} - S_m, \quad \Delta_{\frac{2}{2}} S_m = \Delta_{\frac{1}{2}} S_{m+\frac{1}{2}} - \Delta_{\frac{1}{2}} S_m \end{aligned} \quad (31)$$

where $w(\tau)$ is the impulse response of the filter, one obtains the difference equation (see Appendix I)

$$\Delta^2 \xi_m + (2\pi\gamma + \sigma^2/2) \Delta \xi_m + \sigma^2 \xi_m = \frac{1}{T_i} (\Delta + 2\pi\gamma) \Delta_{\frac{2}{2}} S_m \quad (32)$$

where $\sigma^2 = (4/\pi) (T/T_a)$.

Parameter Approaching the Optimum—For a small T , being divided by T^2 , eqn (32) is approximated by the differential equation of second order,

$$\ddot{\xi} + \frac{2\pi\gamma}{T} \dot{\xi} + \left(\frac{4}{\pi} \frac{1}{T_a T}\right) \xi = 0 \quad (33)$$

describing the manner in which ξ is improved as that of a damped oscillation with the natural period

$$T_F = \pi^{3/2} (T_a T)^{\frac{1}{2}} \quad (34)$$

and with the damping ratio

$$\zeta_F = \frac{\pi^{3/2}}{2} \gamma (T_a/T)^{\frac{1}{2}} \quad (35)$$

A proper adjustment of the value of ζ_p may give a smaller response time in the approach to the optimum than in the previous case.

Variance of Parameter Fluctuation—On the same assumption as in the previous case, it is roughly estimated that

$$\bar{\zeta}_F^2 = \left(\frac{T}{4T_i} \right)^2 \frac{\omega_0}{4\gamma} \phi_{ee}(0) \cong \frac{5}{128} \frac{TT_n}{\gamma T_i^2} \bar{e}^2 \quad (36)$$

To compare this with that given by eqn (25), one takes the ratio of the two values

$$\frac{\bar{\zeta}_F^2}{\bar{\zeta}^2} = \frac{\pi^2}{4} \left(\frac{T}{\gamma T_n} \right)^2 \quad (37)$$

which shows that the filter is effective in reducing the variance, possibly by about one half.

The filter thus improves the performance of the self-adjusting loop, both in quickness of response and in reduction in fluctuation. In a practical design, however, it is necessary to consider whether or not the complexity of a filter construction will balance its advantage.

Application to Flow Control

Applications of this self-adjusting system to process control have been aimed at. Experiments on flow control, performed to prove applicability, are described in this section.

The experimental arrangement is shown in Figure 6. An air flow system was formed of a pipe 8 m long and 50 mm in diam. with a blower, an orifice and a butterfly valve. A vane was placed in front of the pipe outlet, to give a small disturbance to the flow. This vane was moved to close it partly in an on-off manner at random periods with a relay connected to a low frequency noise generator. In some cases, sinusoidal disturbances were also given with another butterfly valve.

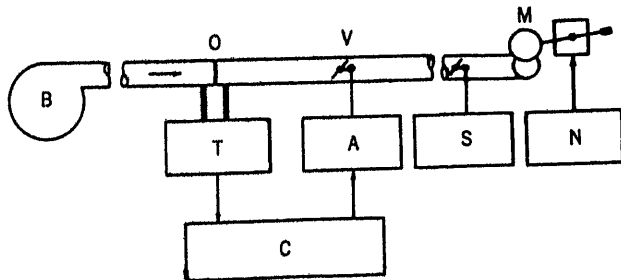


Figure 6. Arrangement of flow control system: B blower; O orifice; V butterfly valve; M moving vane; T electronic flow transmitter; C self-adaptive controller; A electro-hydraulic actuator; S sine wave generator; N noise generator

The self-adaptive controller was set up on a small-scale low speed analogue computer. Figure 7 shows an outline of the circuit, a part of which forms a controller connected to the process. An oscillator, a simple saw-tooth wave generator with a neon tube, frequency controllable by changing its driving voltage, actuated a relay which in turn drove a scale-of-four flip-flop causing sets of switching contacts to open and close for exactly equal time intervals. The integrated signal was sampled as a voltage and converted to a resistance with a servo multiplier.

The experiments were performed, first, to examine the recovery from a given initial parameter misadjustment, which was simulated by varying the initial charge on the integrator capacitor. Then the adaptability to a change of the process gain was examined. The change was produced by varying the resistance R shown in Figure 7.

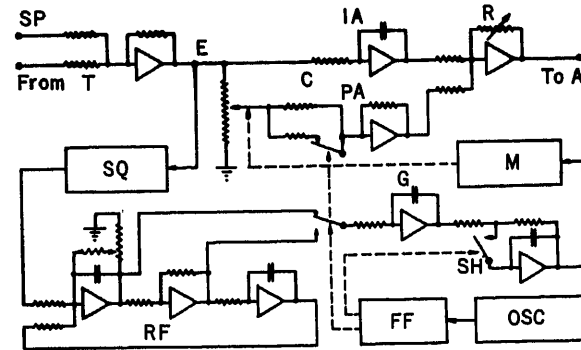


Figure 7. Circuit of self-adaptive controller: SP set point; T flow transmitter; E error; C controller; PA proportional action; IA integral action; R variable resistance to change process gain; A electro-hydraulic actuator; SQ diode squarer; RF bandpass filter; G integrator; SH sampler and holding circuit; M servo-multiplier; OSC oscillator; FF flip-flop

For all these experiments, the integral time of the controller was fixed at about 5 sec and the proportional gain was made the object of self-adjustment. The natural period of the control system T_n was experimentally determined as about 1.2 sec, and the perturbation amplitude (one half of the peak to peak value) was $\Delta K/K = 1/4$ in the proportional gain ratio.

Figures 8 (a), (b) and (c) show some of the oscillograms taken. The comparison of each with the theoretical results follows.

(a) The filter was not used. The two curves (a.1) and (a.2) show that the proportional gain was recovering from initial misadjustments, smaller and greater than the optimum respectively. The time constant T_a , with which the parameter approaches the optimum, is estimated at about 100 sec from these curves. This value is coincident with the theoretical one calculated from eqn (18), where \bar{e}^2 is estimated at 0.05 (10 V observed, multiplied by the factor of the servo multiplier 1/200 per V) and $\Delta\zeta$ is estimated at 0.3. The forms of curve also agree in appearance with theoretical ones, particularly (B) and (A) in Figure 5.

(b) The filter ($\gamma = 0.02$) was used, and the sampler was omitted. The three curves (b.1), (b.2) and (b.3) show the output of the filter, the error, and the proportional gain recovering from an initial misadjustment respectively, being recorded in parallel. The value of T_p read from the curve (b.3) is about 150 sec, and ζ_p about 0.15. They nearly agree with the theoretical values of 150 sec and 0.24 calculated from eqns (34) and (35).

(c) The process gain was made to change in a manner shown in the curve (c.1). The curve (c.2) shows that the controller gain adapted to the change as one was compensated for by the other. The lag of response behind the change is read as about 2 min. Theoretically, eqn (15) with an additional equivalent input may be the model. The time constant of the model T_a is about 2 min in this case, which is approximately coincident with the experimental time constant.

These experiments give sufficient proof that the system is applicable to actual processes. Further work which is to be done is the development of an instrument which can be put directly to practical use.

Appendix I—Derivation of Difference Equations

First take the z transform of $G(s)$ with the sampling period of $T/2$ and, with z still representing e^{Ts} , expand the obtained function as a power series in z^{-1} and take only the terms in-

volving integral powers of z^{-1} . Then, for the case where the filter is omitted,

$$G(z) = \frac{\mu}{T_i} \frac{Tz^{-1}}{1-z^{-1}} \quad (38)$$

Employing the power series expression of $\Xi(z)$ gives

$$\{1 + G(z)\} \Xi(z) = \frac{1}{1-z^{-1}} \left\{ \sum_{m=0}^{\infty} \left(\Delta \xi_m + \frac{\mu}{T_i} T \xi_m \right) z^{-m-1} + \xi_0 \right\} \quad (39)$$

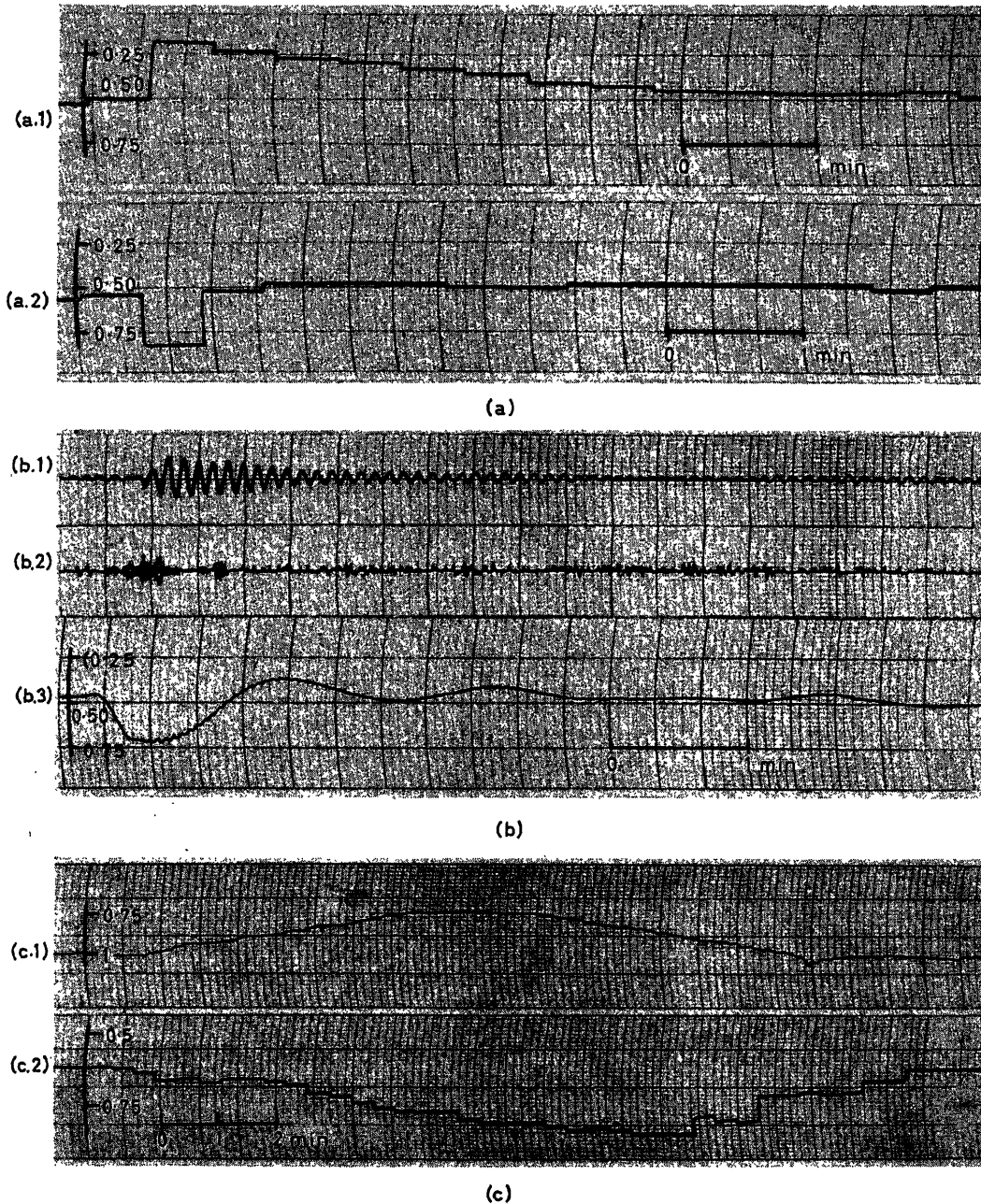


Figure 8. Oscillograms: (a) (a.1) and (a.2) proportional gain approaching the optimum, $T = 28$ sec, $T_i = 6$ sec, filter not used; (b) (b.1) output of the filter, (b.2) error, (b.3) proportional gain approaching the optimum, $T = 6.5$ sec, $T_i = 5.1$ sec, filter used, $\gamma = 0.02$; (c) (c.1) a change of the process gain given, (c.2) the proportional gain adapted to the change, $T = 22$ sec, $T_i = 4.5$ sec, filter not used

In a similar procedure for taking the z transform,

$$Z\{I(s)D(s)N(\zeta, s)\} = \frac{1}{1-z^{-1}} \cdot \frac{1}{T_i} \sum_{m=0}^{\infty} \Delta_{\frac{1}{2}}^2 L_m z^{-m-1} \quad (40)$$

Equating eqn (39) to eqn (40) gives eqn (15).

In the case where the filter is used,

$$G(z) = a \frac{cz + d}{(z-1)(z-b)} \quad (41)$$

where

$$a = \frac{\mu}{T_i} \frac{1 + e^{-\gamma \omega_0 (T/2)}}{\omega_0}, \quad b = e^{-\gamma \omega_0 T},$$

$$c = 3 + e^{-\gamma \omega_0 (T/2)}, \quad d = 1 + 3e^{-\gamma \omega_0 (T/2)}$$

Neglecting the terms containing the second power of γ gives

$$\{1 + G(z)\} \Xi(z) = \frac{1}{(1-z^{-1})(1-bz^{-1})}$$

$$\sum_{m=0}^{\infty} \{\Delta_{\frac{1}{2}}^2 \xi_m + (2\pi\gamma + \sigma^2/2) \Delta_{\frac{1}{2}} \xi_m + \sigma^2 \xi_m\} z^{-m-2}, \quad (42)$$

$$Z\{I(s)D(s)F(s)N(\zeta, s)\} = \frac{1}{1-z^{-1}} \frac{1}{T_i} \sum_{m=0}^{\infty} \Delta_{\frac{1}{2}}^2 S_m z^{-m-1} \quad (43)$$

which give eqn (31). Its solution with the initial values ξ_0 and ξ_1 is given by

$$\xi_m = \xi_1 \rho^{m-1} \frac{\sin m\phi}{\sin \phi} - \xi_0 \rho^m \frac{\sin(m-1)\phi}{\sin \phi}$$

$$+ \frac{1}{T_i} \sum_{n=2}^m \rho^{n-2} \frac{\sin(n-1)\phi}{\sin \phi} \{\Delta_{\frac{1}{2}}^2 S_{m-n-1} - (1-2\pi\gamma) \Delta_{\frac{1}{2}}^2 S_{m-n}\} \quad (44)$$

where

$$\rho = \sqrt{1-2\pi\gamma + \sigma^2/2}, \quad \cos \phi = (1-\pi\gamma - \sigma^2/4)/\rho, \quad \sigma^2 = \frac{4}{\pi} \frac{T}{T_a} \quad (45)$$

Appendix II—Power Density Spectrum of the Squared Error Fluctuation

With the rule of notation as $\phi_{xx} = \overline{\varepsilon^2(t) x^2(t+\tau)} - \overline{\varepsilon^2} \overline{x^2}$, $\phi_{xy} = \overline{\varepsilon^2(t) x(t+\tau) y(t+\tau)} - \overline{\varepsilon^2} \overline{xy}$, ..., the autocorrelation function $\phi_{xx}(\tau) = \overline{\varepsilon^2(t) \varepsilon^2(t+\tau)} - \overline{\varepsilon^2}^2$ can be evaluated by solving the simultaneous differential equations

$$\left. \begin{aligned} \dot{\phi}_{xx} &= -2\lambda \phi_{xx} \\ \dot{\phi}_{xy} &= -\lambda \phi_{xy} + \phi_{xy} \\ \dot{\phi}_{x\dot{y}} &= -\omega_n^2 \phi_{xy} - (\lambda + 2\zeta\omega_n) \phi_{xy} + \omega_n^2 \phi_{xx} \\ \dot{\phi}_{yy} &= 2\phi_{yy} \\ \dot{\phi}_{y\dot{y}} &= \omega_n^2 \phi_{xy} - \omega_n^2 \phi_{yy} - 2\zeta\omega_n \phi_{yy} + \phi_{yy} \\ \dot{\phi}_{\dot{y}\dot{y}} &= 2\omega_n^2 \phi_{xy} - 4\zeta\omega_n \phi_{yy} - 2\omega_n^2 \phi_{yy} \\ \dot{\phi}_{\varepsilon\varepsilon} &= \phi_{yy} - 2\phi_{xy} + \phi_{xx} \end{aligned} \right\} \quad (46)$$

with the initial conditions $\phi_{xx}(0) = \overline{\varepsilon^2(t) x^2(t)} - \overline{\varepsilon^2} \overline{x^2}$, $\phi_{xy}(0) = \overline{\varepsilon^2(t) x(t) y(t)} - \overline{\varepsilon^2} \overline{xy}$, and so on. Integrating each

of eqns (46), using the property of the correlation functions, $\phi_{xx}(\infty) = 0$, $\phi_{xy}(\infty) = 0$, ..., and using the notations

$$\Phi_{xx}(0) = 2 \int_0^{\infty} \phi_{xx} d\tau, \quad \Phi_{xy}(0) = 2 \int_0^{\infty} \phi_{xy} d\tau, \dots$$

one obtains

$$\left. \begin{aligned} -2\phi_{xx}(0) &= -2\lambda \Phi_{xx}(0) \\ -2\phi_{xy}(0) &= -\lambda \Phi_{xy}(0) + \Phi_{xy}(0) \\ -2\phi_{x\dot{y}}(0) &= -\omega_n^2 \Phi_{xy}(0) - (\lambda + 2\zeta\omega_n) \Phi_{xy}(0) + \omega_n^2 \Phi_{xx}(0) \\ -2\phi_{yy}(0) &= 2\Phi_{yy}(0) \\ -2\phi_{y\dot{y}}(0) &= \omega_n^2 \Phi_{xy}(0) - \omega_n^2 \Phi_{yy}(0) - 2\zeta\omega_n \Phi_{yy}(0) + \Phi_{yy}(0) \\ -2\phi_{\dot{y}\dot{y}}(0) &= 2\omega_n^2 \Phi_{xy}(0) - 4\zeta\omega_n \Phi_{yy}(0) - 2\omega_n^2 \Phi_{yy}(0) \\ \Phi_{\varepsilon\varepsilon}(0) &= \Phi_{yy}(0) - 2\Phi_{xy}(0) + \Phi_{xx}(0) \end{aligned} \right\} \quad (47)$$

from which

$$\Phi_{\varepsilon\varepsilon}(0) = \frac{1}{\zeta\omega_n} \phi_{xx}(0) - \frac{4\zeta^2 + 1}{\zeta\omega_n} \phi_{xy}(0) - \frac{2}{\omega_n^2} \phi_{x\dot{y}}(0)$$

$$+ \frac{4\zeta^2 + 1}{2\zeta\omega_n} \phi_{yy}(0) + \frac{2}{\omega_n^2} \phi_{y\dot{y}}(0) + \frac{1}{2\zeta\omega_n^2} \phi_{\dot{y}\dot{y}}(0)$$

$$= \frac{1}{2\zeta\omega_n} \phi_{\varepsilon\varepsilon}(0) - \frac{4\zeta^2 - 1}{2\zeta\omega_n^3} \phi_{xx}(0) + \frac{1}{2\zeta\omega_n^3} \phi_{xy} + 2\zeta\omega_n \varepsilon, \quad \dot{y} + 2\zeta\omega_n \varepsilon(0) \quad (48)$$

is obtained. By assuming Gaussian distribution of the amplitudes of x , y , \dot{y} , ε and their products, one obtains

$$\phi_{xx}(0) = 2\overline{\varepsilon x}^2, \quad \phi_{\varepsilon\varepsilon}(0) = 2\overline{\varepsilon^2}^2$$

$$\phi_{\dot{y} + 2\zeta\omega_n \varepsilon, \dot{y} + 2\zeta\omega_n \varepsilon}(0) = 2\overline{\varepsilon(\dot{y} + 2\zeta\omega_n \varepsilon)}^2 \quad (49)$$

Thus, approximately

$$\Phi_{\varepsilon\varepsilon}(0) = \frac{5}{2} \cdot \frac{1}{\omega_n} \overline{\varepsilon^2}^2$$

Appendix III—Effect of the Dynamic Response Time of Measuring System on the Behaviour of the Loop

The function $\Delta\Theta_{\varepsilon\varepsilon}(s)$ which is obtained by substituting eqn (8) into eqn (4) is of the form

$$\Delta\Theta_{\varepsilon\varepsilon}(s) = \mu B(s) \frac{1}{s} \frac{1 - e^{-\frac{T}{2}s}}{1 + e^{-\frac{T}{2}s}} \quad (50)$$

where

$$B(s) = \frac{\omega_n}{2\zeta} \frac{\zeta\omega_n s + (4\zeta^2 - 1)\omega_n^2}{(s + 2\zeta\omega_n)(s^2 + 4\zeta\omega_n s + 4\omega_n^2)} \quad (51)$$

By introducing the variable ξ , the function $B(s)$ is approximated by

$$B(s) \cong \frac{-\left(\frac{s}{4\omega_n} + 1\right)\xi + \frac{s}{8\omega_n}}{\left(\frac{s}{\omega_n} + 1\right)\left(\frac{s^2}{4\omega_n^2} + \frac{s}{2\omega_n} + 1\right)} \quad (52)$$

on the assumption, as a second approximation, that the dynamic response time of the measuring system is not affected by a small deviation of the parameter ζ from the optimum value.

The function $\Delta\theta_{ss}(s)$ will then have two terms, one proportional to and the other independent of ξ , and as a result of linearization, ξ/s may be replaced by a jump function $\Xi(s)$. Thus $\Delta\theta_{ss}(s)$ may be written as

$$\Delta\theta_{ss}(s) = M'(s)\Xi(s) + R(s) \quad (53)$$

where

$$M'(s) = -\mu C(s) \frac{1 - e^{-\frac{T}{2}s}}{1 + e^{-\frac{T}{2}s}} \quad (54)$$

$$R(s) = \mu \frac{1}{8\omega_n} \cdot \frac{C(s)}{\frac{s}{4\omega_n} + 1} \cdot \frac{1 - e^{-\frac{T}{2}s}}{1 + e^{-\frac{T}{2}s}} \quad (55)$$

$$C(s) = \left(\frac{s}{4\omega_n} + 1 \right) \left/ \left(\frac{s}{\omega_n} + 1 \right) \right. \left(\frac{s^2}{4\omega_n^2} + \frac{s}{2\omega_n} + 1 \right) \quad (56)$$

By using the modified function $M'(s)$ given by eqn (54) in place of $M(s)$ given by eqn (11), and by adding the function $R(s)$ to $N(\zeta, s)$ as another input to the loop, the effect of the dynamic response time of the measuring system can be evaluated.

(1) *Resulting Offset of Adjustment*—The case where the filter is not used is considered. Taking the z transforms of

$$G'(s) = I(s)D(s)M'(s) \frac{1 - e^{-Ts}}{s} \quad (57)$$

and

$$H(s) = I(s)D(s)R(s) \quad (58)$$

with the sampling period $T/2$, expanding each function obtained as a power series in z^{-1} and taking only the terms involving integral powers of z^{-1} (same procedure as stated in Appendix I), give

$$G'(z) = \frac{\mu}{T_i} \cdot \frac{z^{-1}}{1 - z^{-1}} \left\{ T - \frac{5}{4\omega_n} (3 - z^{-1}) \right\} \quad (59)$$

and

$$H(z) = -\frac{\mu}{T_i} \cdot \frac{1}{2\omega_n} \cdot \frac{z^{-1}}{1 - z^{-1}} \left(\frac{3}{4} + \frac{z^{-1}}{1 - z^{-1}} \right) \quad (60) \quad \text{and}$$

where $e^{-\frac{1}{2}\omega_n T}$ is neglected because this number is negligibly small as compared with unity. Hence, the difference equation to determine the sequence of the parameter values ξ_m becomes

$$\xi_{m+2} - \left[\left(1 - \frac{\mu}{T_i} T \right) + \frac{15}{2} a \right] \xi_{m+1} - \frac{5}{T} a \xi_m = \frac{1}{T} A \frac{1}{4} L_m + a \quad (61)$$

where

$$a = \frac{\mu}{T_i} \cdot \frac{1}{\omega_n} \quad (62)$$

a parameter representing the effect of the dynamic response time of the measuring system. The second term of the right-hand side of the equation causes an offset of self-adjustment or a deviation from zero of the steady-state value of ξ_m which is given by

$$\bar{\xi}_\infty = \frac{k}{2(1-5k)}, k = \frac{1}{T\omega_n} = \frac{1}{2\pi} \frac{T_n}{T} \quad (63)$$

The parameter ζ settles down therefore to a value smaller than that of the optimum. The offset $\bar{\xi}_\infty$ as well as the parameter $\bar{\zeta}_\infty$ evaluated for some values of T/T_n are shown in Table 1, from which the effect is certainly negligible provided that the perturbation period T is more than ten times as long as the natural period of the system T_n .

Table 1

T/T_n	$\bar{\xi}_\infty$	$\bar{\zeta}_\infty$	θ°
10	0.009	0.491	7.90
5	0.019	0.481	15.70
2	0.066	0.434	39.30
1	0.395	0.105	78.70

(2) *Necessary Phase Shift to Eliminate the Offset*—To eliminate the offset, it is necessary to give a leading phase shift to the signal before being detected by synchronous switching, by means of either a phase shifter or the bandpass filter itself. The necessary amount of the shift can be evaluated as follows: Taking the modified z transforms of the functions of eqns (57) and (58) with the sampling period $T/2$, multiplying each transform by $z^{\frac{1}{2}}$, expanding each function as a power series of $z^{-\frac{1}{2}}$ and taking only the terms involving integral powers of z^{-1} , give

$$\left. \begin{aligned} z^{\frac{1}{2}} G'(z, m) &= \frac{1}{1 - z^{-1}} (A + Bz^{-1} + Cz^{-2}) \\ A &= a \left(-v + \frac{5}{4} + C \right), B = \frac{\mu}{T_i} T + 3(A + C) \\ C &= -a e^{-v} \left\{ 1 + \frac{1}{2\sqrt{3}} \cos \left(\sqrt{3} v + \frac{\pi}{6} \right) \right\} \\ v &= \frac{1}{2} m \omega_n T \end{aligned} \right\} \quad (64)$$

$$\left. \begin{aligned} z^{\frac{1}{2}} H(z, m) &= \frac{1}{(1 - z^{-1})^2} (D + Ez^{-1} + Fz^{-2}) \\ D &= \frac{a}{8} + F, E = 3(D + F) \\ F &= -\frac{a}{6} e^{-v} \left\{ 1 + \frac{1}{2} \sin \left(\sqrt{3} v - \frac{\pi}{6} \right) \right\} \end{aligned} \right\} \quad (65)$$

where $e^{-\frac{1}{2}\omega_n T}$ is neglected as compared with unity. The difference equation corresponding to eqn (61) is thus obtained as

$$\begin{aligned} (1 - A) \xi_{m+2} - \left\{ \left(1 - \frac{\mu}{T_i} T \right) - 3(A + C) \right\} \xi_{m+1} \\ + C \xi_m = \frac{1}{T} A \frac{1}{4} L_m - \frac{4}{3} E \end{aligned} \quad (66)$$

The second term of the right-hand side of the above equation is put equal to zero, to obtain the condition to eliminate the offset, namely

$$e^{-\nu} \left\{ 1 + \frac{1}{2} \sin \left(\sqrt{3} \nu - \frac{\pi}{6} \right) \right\} = \frac{3}{8} \quad (67)$$

which gives

$$\nu = \frac{1}{2} m \omega_n T = 1.372 \quad (68)$$

The necessary amount of the leading phase shift in degrees $\theta^\circ (= \frac{m}{2} \times 360^\circ)$ evaluated from the above equation for some values of T/T_n is also shown in Table 1. For the value of ν , the constants in eqn (66) become

$$A = 0.304 a, 3(A + C) = 1.459 a, C = -0.182 a, E = 0 \quad (69)$$

With these constants, eqn (66) is the equation to determine the response of the self-adjusting loop when the effect of the dynamic

response time of the measuring system is taken into consideration, and is not quite different from eqn (61) except for small correction terms involved.

References

- ¹ ISOBE, T. Self-optimization of a control system by means of a logic circuit. *Inst. Radio Engrs Trans. on Automatic Control* AC-6 No. 3, Sep. (1961), 260
- ² DOUCE, J. L. and KING, R. E. A self-optimizing non-linear control system. *Proc. Instn elect. Engrs* 108 pt. B, No. 40 (1961) 441
- ³ MACGRATH, R. J., RAJARAMAN, V., and RIDEOUT, V. C. A parameter-perturbation adaptive control system. *Inst. Radio Engrs Trans. on Automatic Control* AC-6, No. 2, May (1961), 154
- ⁴ LANING, J. H. and BATTIN, R. H. *Random Process in Automatic Control*, ch. 6. 1956 New York; McGraw-Hill
- ⁵ ZERNIKE, F. Die Brownsche Grenze für Beobachtungsreihen. *Z. Phys.* 79 (1932), 516

DISCUSSION

J. J. DE JONG, *Bataafs Internationale NV., The Hague, Netherlands*

The authors have allowed their adaptive control system to change the loop gain. Since, however, the integral term of their controller contributes materially, if not predominantly, to the overall performance—particularly in the low frequency region—I should like to know whether any trials have been made by them with an adaptive controller which keeps the loop gain constant whilst varying the integral action time. In a further extension, the adaptive control of both constraints could be considered.

T. ISOBE, *in reply*

Although no trials have been made with the integral action time variable, it is possible if a time exists giving minimum mean-squared error. It is also possible that the adaptation of both constants can be made if both parameters are perturbed with two distinct perturbation periods and with the corresponding synchronous detectors.

M. HAMZA, *ETH., Zürich, Switzerland*

I have read this paper with great interest and I find it an excellent contribution to the field of adaptive control. Professor Isobe has not only tested his theory using an analogue computer, but has also applied it

to a flow control system. I assume that during the past year this system was further studied. I would like Professor Isobe to mention briefly what, in his opinion, are the main advantages of his method and, most important, what are its limitations. Further, where does he recommend the application of such a method other than to the example given in his paper?

T. ISOBE, *in reply*

I should like to thank Dr. Hamza for his kind comments and questions. The main advantage of the method is, in my opinion, the simplicity of the instrument realizing the method. In our experimental work, a circuit of the adaptive controller was set up on an analogue computer, using a servo-multiplier, a squarer, etc. However, we are planning a practical instrument in which a thermistor or a transistor for a resistor would be able to be made to change by a voltage signal, and a transistor switching circuit for a synchronous detector will be used. These circuits will be simple enough to be attached to a conventional process controller. The limitation of the method is that it takes a relatively long time to reach the optimum condition when the mean-squared error does not show a sharp minimum with a variation of the parameter concerned. We believe that the method is applicable to the control of any other process variables than the example such as temperature, pressure, liquid level, etc.

The Dynamic Properties of Rectification Stations with Plate Columns

J. ZÁVORKA

Summary

The work deals with the derivation of generally valid relations (in the form of block diagrams and formulae) permitting the computation of the transfer functions of a rectifying station. The first chapters contain the operational analysis of the dynamic properties of the given system starting from the general physical and physico-chemical equations. The author deals separately with the dynamics of the three sections of the system: the column proper, the bottom section of the column (the first plate and the still) and the top section of the column (the highest plate with the condenser, the cooler and condensate tank); the solution of the dynamic properties of each section is dealt with in a separate chapter.

Most important and most difficult is the solution of the dynamic properties of the column proper. In the solution of this section the author starts with the basic design unit of the column—the plate, the dynamic behaviour of which is described by a system of nine simultaneous equations. The equations are linearized and transformed into differential equations, subjected to the LW transformation and arranged into a dimensionless form. After the elimination of the variables not considered, three block diagrams of the plate are formed from the equations representing the non-steady states of composition, flow rate of the liquid phase and pressure. The interconnection of these three block diagrams leads to the formation of the overall diagram of one plate. The author obtains the block diagram of the whole column by linking the overall diagrams of all plates.

The same method is used by the author for deriving the block diagrams of the bottom and top sections of the column. Results obtained from the previous chapters are subjected to a further theoretical analysis. The aim of this analysis is to simplify the block diagram of the column proper in order to make possible its modelling or the direct computation of the transfer functions of the system. It is shown that the dynamics of pressure and of composition in the whole column are presented by block diagrams of the same structure. The diagram is formed by single capacity members connected in series with feedbacks by-passing two members that follow behind. The output signals of this chain are formed by the algebraic sum of the signals of three adjacent members and they form a link between the diagram of pressure and the diagram of composition.

The general analysis of this block diagram is made; a matrix calculation is used for deriving the matrices of the transfer functions of this block diagram as the functions of the number of the chain members (or of the number of the plates of the column). A further analysis is used for establishing the conditions at which it is possible to neglect the dynamic value of the output signals (the conditions are related to the number of plates). By a further general procedure it is proved that the conditions stated are fulfilled by each column. In this way the block diagram of the column proper is simplified to an extent permitting the computation of the transfer functions.

A further chapter contains the practical computation of several transfer functions and step response curves of a rectifying station based on the results of the general analysis. The results of measurements made on the actual station in operation were in good agreement with the results of the computation.

Sommaire

On établit les relations (sous forme de schémas fonctionnels et de formule) concernant une station de rectification en vue de calculer

la fonction de transfert de cette dernière. Les premiers chapitres traitent l'analyse opérationnelle des propriétés dynamiques du système donné en partant des équations générales physiques et physico-chimiques. On examine séparément la dynamique des trois sections du système: la colonne elle-même, le fond de la colonne (le premier plateau) et le sommet de la colonne (le plateau supérieur, le condenseur, le réfrigérateur, et le réservoir de condensation).

La colonne se révèle comme étant la partie la plus difficile. Pour obtenir sa fonction de transfert, l'auteur commence par examiner l'unité de base de la colonne: le plateau. Le comportement dynamique du plateau est décrit par un système de neuf équations simultanées. Ces équations sont linéarisées, transformées en équations différentielles par la transformation en LW , et mises sous forme adimensionnelle. Après l'élimination des variables non considérées, on obtient trois schémas fonctionnels à partir des équations représentant les états non-stationnaires de la composition, du débit en phase liquide et de la pression. L'ensemble de ces trois schémas fonctionnels forme le schéma fonctionnel global d'un plateau. L'ensemble des schémas fonctionnels globaux de tous les plateaux forme celui de la colonne toute entière.

La même méthode est utilisée pour obtenir les schémas fonctionnels du fond et du sommet de la colonne. On procède ensuite à l'analyse des résultats obtenus afin de simplifier le schéma fonctionnel de la colonne en vue de la simulation ou de calcul direct de la fonction de transfert du système. On montre que les comportements dynamiques de la pression et de la composition dans toute la colonne sont représentés par des schémas fonctionnels de structure identique. Cette structure est constituée d'éléments capacitifs simples reliés en série avec réaction tous les deux éléments. Les signaux de sortie de cette chaîne sont constitués par la somme algébrique des signaux de trois éléments adjacents; ils forment une liaison entre le schéma de la pression et celui de la composition.

Dans une première analyse générale, on calcule les matrices des fonctions de transfert du diagramme fonctionnel en fonction du nombre des chaînes (ou nombre de plateaux de la colonne). Dans une seconde analyse, on établit les conditions dans lesquelles on peut négliger la partie transitoire des signaux de sortie (les conditions sont reliées au nombre de plateaux). Dans une dernière analyse enfin, on montre comment simplifier le schéma fonctionnel de la colonne seule, pour que sa fonction de transfert soit calculable facilement.

On montre des exemples pratiques de calcul de plusieurs fonctions de transfert et de réponses à un échelon en se basant sur la théorie développée. Ces calculs sont confirmés par des mesures réelles.

Zusammenfassung

Dieser Beitrag behandelt die Ableitung allgemeingültiger Beziehungen in Form von Blockdiagrammen und Gleichungen für die Berechnung der Übergangsfunktionen von Rektifizierkolonnen zur Trennung binärer Mischungen. Zur Untersuchung wird das System in drei Teile zerlegt: in die Kolonne selbst, den Bodenteil (der erste Boden und der Re-Boiler) und den Kolonnenkopf (der oberste Boden mit dem Kondensator, dem Kühler und dem Kondenzbehälter). Ein Boden wird durch ein System von neuen Simultangleichungen beschrieben, die abgeleitet werden.

Das Ergebnis der theoretischen Arbeiten des Autors ist ein Blockdiagramm und die zugehörigen Übergangsfunktionen sowie Gleichungen

chungen für die verschiedenen Konstanten und Übergangsfunktionen. Des weiteren wird auf Grund der hier durchgeführten Arbeiten die numerische Berechnung einiger Übergangsfunktionen und der Sprungantwort bestimmter Rektifizierkolonnen besprochen. Es zeigt sich, daß die aufgenommenen Betriebsmessungen mit den berechneten Daten sehr gut übereinstimmen.

The control of rectification stations, as carried out at the present time, is confined only to some control loops which are designed without any thorough theoretical consideration. As far as individual control diagrams are concerned, quite a number of them have been designed; for instance, see Anisimov¹. The advantages and shortcomings of various connection schemes have been published by the respective authors, however, and the evaluation is mainly based on technical sense and experimental results. Information on the general operational analysis of rectification columns has been appearing only recently^{2, 3, 5, 7, 11}.

In most of these papers the pressure and hold-up of the plate have been considered as constant quantities. Due to this, the validity of results is limited to cases with slow changes in the input quantities; for instance, changes in feed composition or changes occurring during the starting of the column. For rapidly changing input variables, for instance pressure, the results are erroneous. In view of these facts, an operational analysis was worked out by Voetter and Houtappel¹³ where the pressure and hold-up of the plate were considered as variables. Starting from linearized equations the authors demonstrated that, nevertheless, the results hold for a rather wide range of input quantities. The same authors extended their study to ternary mixtures, and used digital computers for the calculation of dynamic properties. It has been found that the solutions of these problems are exceedingly time consuming with regard to the computer, and Rose and Williams^{5, 10, 11}, attempted the modelling of the system on an analogue computer. However, these authors designed the model of the dynamics of the vapour phase as single-capacity members connected in series which does not correspond with reality. This deficiency has been eliminated by the work of Rijnsdorp and Maarleveld⁹, who succeeded in modelling a 32-plate column on an analogue computer built from passive elements especially for this purpose. The Bode frequency characteristics are the result of this work. As an example, one of these characteristics is shown in Figure 1. Obviously it cannot be evaluated, as the curve has no distinct straight sections to permit the determination of the respective intersects. Apart from this, it is not possible to agree with the assumption made by the authors in the equations describing the system, namely that the heat of evaporation is merely a function of pressure and independent of the composition of the mixture.

The aim of the present paper is to derive generally valid relationships for the computation of transfer functions for the individual input and output variables of the whole rectification station, to create in this way the possibility of comparing and assessing the advantages and shortcomings of various control diagrams, and to obtain the data necessary for the synthesis of control loops and for the complex automation of rectification stations.

The task has been limited to rectification stations with plate columns for the separation of binary mixtures.

The purpose of the work is to determine the transfer functions of the system, which in turn determine the relationship between the input variables (N : the flow rate of the feed; X_N : the composition of the feed; P_K : the pressure in the condenser; G_1 : the flow rate of the heating steam) and the output variables (A : the flow rate of the product; X_A : the composition of the product; B : the flow rate of the residue; X_B : the composition of the residue; P_1 : pressure at the first plate of the column) and possibly between the concentration at some other plates.

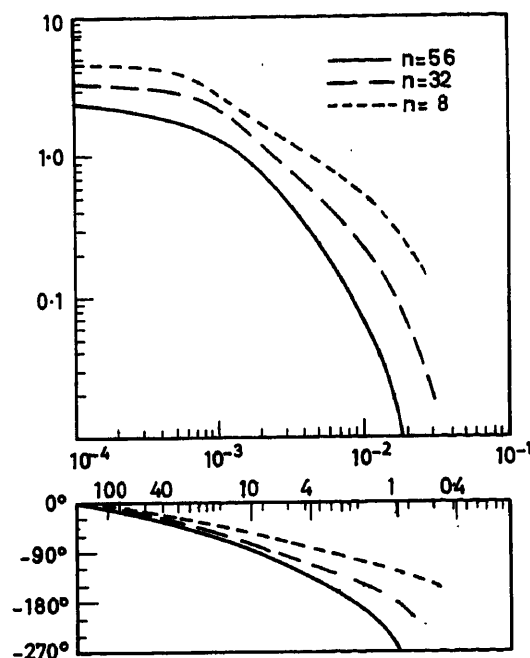


Figure 1

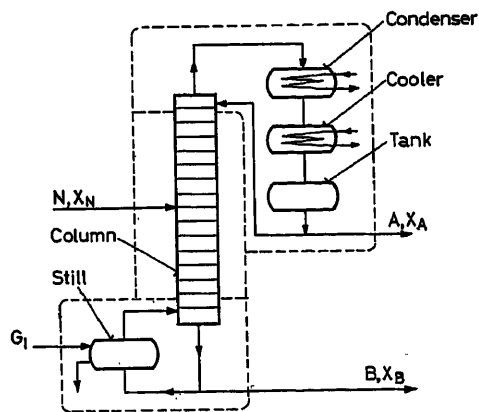


Figure 2

The diagram of a rectification station with a plate column for the continuous separation of binary mixtures is shown in Figure 2.

For the investigation of dynamic properties let the rectifying station be divided into three sections shown by the dash line in the illustration. The first to be investigated is the independent rectifying column, the second section consists of the bottom of the column with the still, while the third section contains the top of the column, the condenser, the cooler and the condensate tank.

The rectifying column consists of plates that are to be considered as separate units with regard to function and construction. The diagram of a plate is shown in Figure 3. It can be seen that the plate may be acted upon by the following nine input variables:

N	The feed flow rate
X_N	The feed composition
$H_{l,N}$	The enthalpy of the feed
V_{n-1}	The flow rate of vapour from the plate below
Y_{n-1}	The concentration of this vapour
$H_{v,n-1}$	The enthalpy of this vapour
L_{n+1}	The reflux from the plate above
X_{n+1}	The composition of this reflux
$H_{l,n+1}$	The enthalpy of this reflux

By these, variables changes are produced in nine output variables:

$M_{l,n}$	The liquid hold-up of the plate
$M_{v,n}$	The vapour hold-up of the plate
P_n	The pressure on the plate
V_n	The flow rate of vapour streaming from the plate
L_n	The reflux from the plate
$H_{v,n}$	The enthalpy of vapour streaming from the plate
$H_{l,n}$	The enthalpy of the reflux from the plate
Y_n	The composition of vapour
X_n	The composition of the reflux

The plate is described thus by a system of nine simultaneous equations which are now derived.

First, the material balance of the plate is set up.

$$\frac{dM_{l,n}}{d\tau} + \frac{dM_{v,n}}{d\tau} = L_{n+1} - L_n + V_{n-1} - V_n + N \quad (1)$$

By multiplying the individual terms by the corresponding concentrations the total material balance equation is transformed into the material balance of the more volatile component:

$$\frac{d(M_{l,n} \cdot X_n)}{d\tau} + \frac{d(M_{v,n} \cdot Y_n)}{d\tau} = L_{n+1} \cdot X_{n+1} - L_n \cdot X_n + V_{n-1} \cdot Y_{n-1} - V_n \cdot Y_n + N \cdot X_N \quad (2)$$

In accordance with the material balance equation it is possible to write the heat balance equation as follows:

$$\frac{d(M_{l,n} \cdot H_{l,n})}{d\tau} + \frac{d(M_{v,n} \cdot H_{v,n})}{d\tau} - V^* \cdot \frac{dP_n}{d\tau} = L_{n+1} H_{l,n+1} - L_n H_{l,n} + V_{n-1} \cdot H_{v,n-1} - V_n \cdot H_{v,n} + N \cdot H_N \quad (3)$$

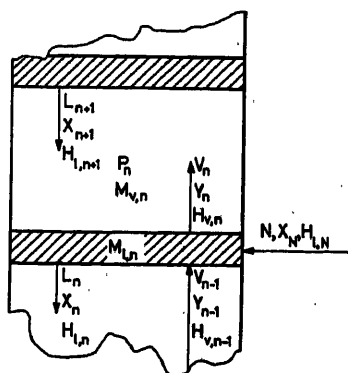


Figure 3

The last term on the left-hand side of the equation (which represents the consideration given to the difference between the enthalpy of the vapour phase and its internal energy for which the equation holds) is neglected later with regard to the pressure changes being of the order of millimetres of water gauge.

The vapour flow rate depends on the square root of the pressure differential on two adjacent plates and on the density of the vapour. In view of the fact that the difference in pressure on two adjacent plates fluctuates within the range of 25–50 mm w.g., the influence of density may be neglected. The relationship between flow rate and pressure is then described by the equation

$$V_n^2 = k_0 \cdot (P_n - P_{n+1}) \quad (4)$$

The following relationship should be further investigated,

$$M_{l,n} = M_{l,n}(L_n)$$

By the application of relation

$$S_1 = 10 \cdot \left(\frac{10^{-5} \cdot \mu L}{1.773 \rho \cdot \gamma} \right)^{\frac{2}{3}}$$

one obtains

$$M_{l,n} = 10 \cdot \frac{S_1}{\xi} \cdot \left(\frac{10^{-5} \cdot \mu L}{1.773 \rho \cdot \gamma_1} \right)^{\frac{2}{3}} + K \quad (5)$$

Now consider the relationship between the concentration of the more volatile component in the vapours and the concentration of the more volatile component in the liquid during the state of equilibrium of both phases at the boiling point temperature of the binary mixture.

$$Y_n = Y_n(X_n) \quad (6)$$

The description of this relationship was attempted by a number of equations (Wohl, Scatchard-Hammer, Van Laar, Margules⁴). However, they all contain constants that can be determined only experimentally. Due to this, and also due to their complexity, none of these equations has been accepted in practice. The effect of the composition of the liquid upon the composition of the vapours (established experimentally) is normally represented by the X - Y equilibrium diagram. This method of representation has been accepted for the following sections of this paper.

The remaining three equations are written in the form of general relations:

$$M_{v,n} = M_{v,n}(P_n) \quad (7)$$

$$H_{l,n} = H_{l,n}(P_n, X_n) \quad (8)$$

$$H_{v,n} = H_{v,n}(P_n, Y_n) \quad (9)$$

The system of the above-stated nine simultaneous equations describes one plate of the rectifying column. As interest here is only in the non-steady states of pressure, composition of the liquid phase and flow rate of the liquid phase, all other variables will be eliminated. The transfer functions of pressure, composition of the liquid phase and flow rate for one plate are obtained by the linearization of the equations or possibly by their transformation into differential equations, followed by the LW transformation and the arrangement of the equations. These transfer functions are used for drawing the partial block diagrams of one plate for the dynamic behaviour of the three variables. The block

diagrams are shown in Figure 4. The overall block diagram of one plate is obtained by the interconnection of all three partial diagrams. The complete block diagram of the whole rectifying

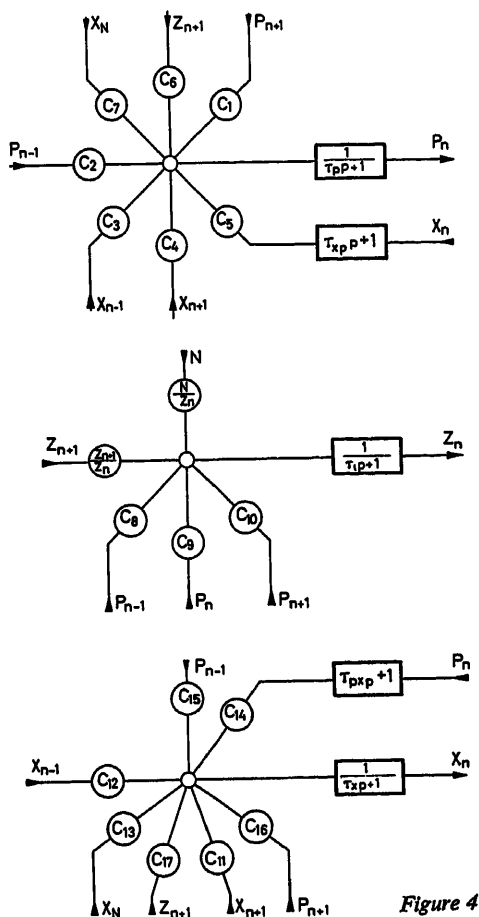


Figure 4

column is obtained by the interconnection of the block diagrams of the individual plates as shown in Figure 5. For the sake of clarity the multiplication constants are not shown in Figure 5. Now, it remains to conclude the block diagram of the column by the connections of the condenser and of the still.

The block diagram of the bottom section of the column (the first plate and still), and the block diagram of the top section of the column (the highest plate, condenser, cooler of the condensate, condensate tank and the piping) have been derived by a similar method as used for the derivation of the block diagram of the column proper. For the sake of brevity the respective procedures are omitted, and only their results are given in Figures 6 and 7.

The complete block diagrams of all sections of the rectifying station have been obtained so far. The description may serve as the source of some data for the modelling of the system. Owing to the high complexity of the diagram, a large number of integrating units will be required for the modelling and, therefore, it should be possible to model only the simplest stations with a small number of plates. For this reason the results of the preceding chapters have been subjected to a further theoretical analysis. The analysis follows the aim of simplifying the block diagram of the column proper so that it is suited for modelling, or so that it is possible to compute the transfer functions of the system. First of all it was necessary to determine the zones within which the values of individual design, physico-chemical and operational parameters can vary. Further the relations were to be stated that were required for the numerical solution of various terms occurring in the formulae for the time and multiplying constants. A quantitative analysis of the time and multiplying constants was made on the basis of these values and relations. The results obtained were used for certain simplifications of the formulae. Further, it appears that the dynamics of pressure and composition in the whole column are represented by block diagrams of the same structure (Figure 8). The diagram is formed by single-capacity members connected in series with feedbacks by-passing two members that follow behind. The output signals of this

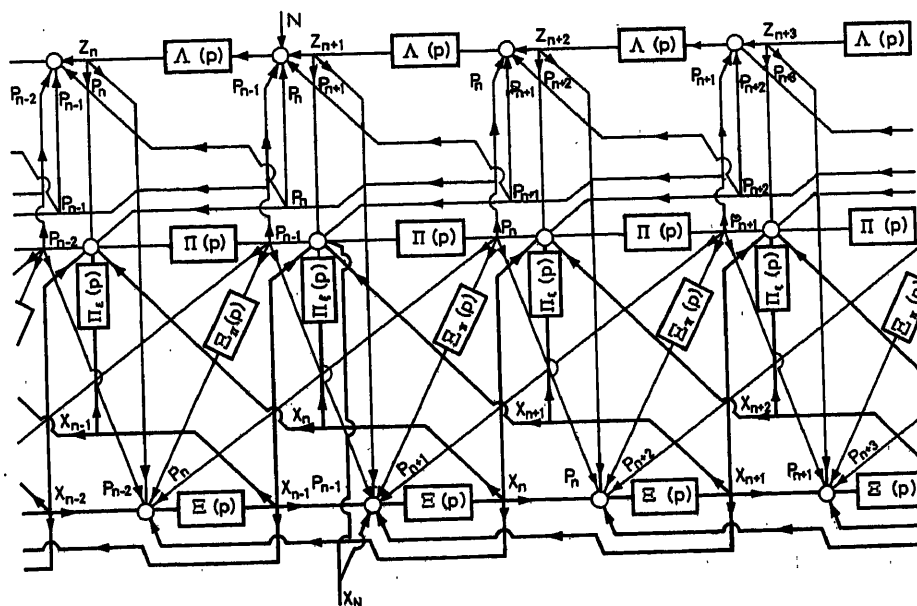


Figure 5

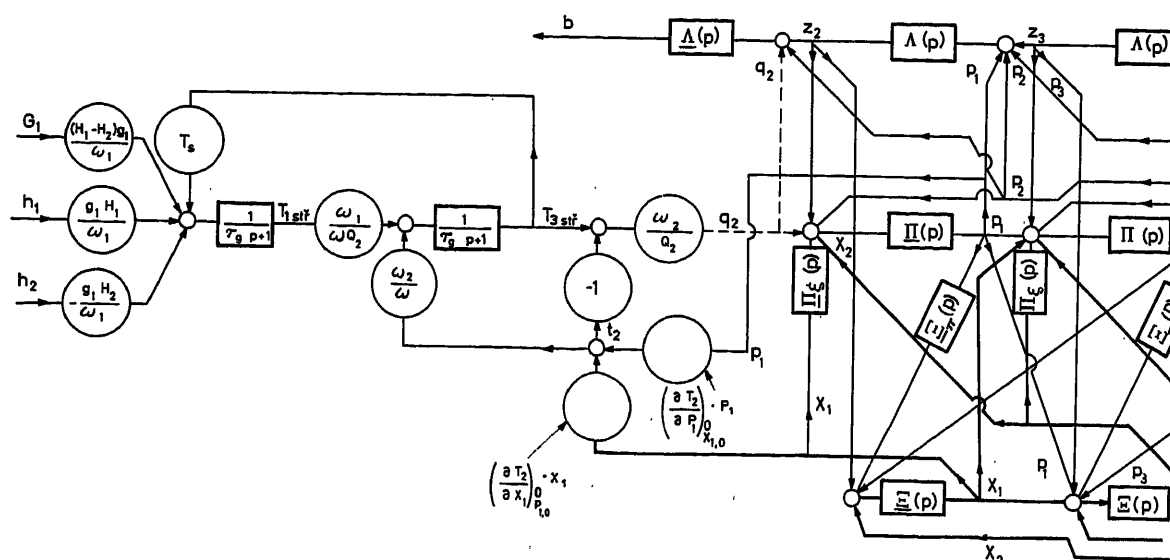


Figure 6

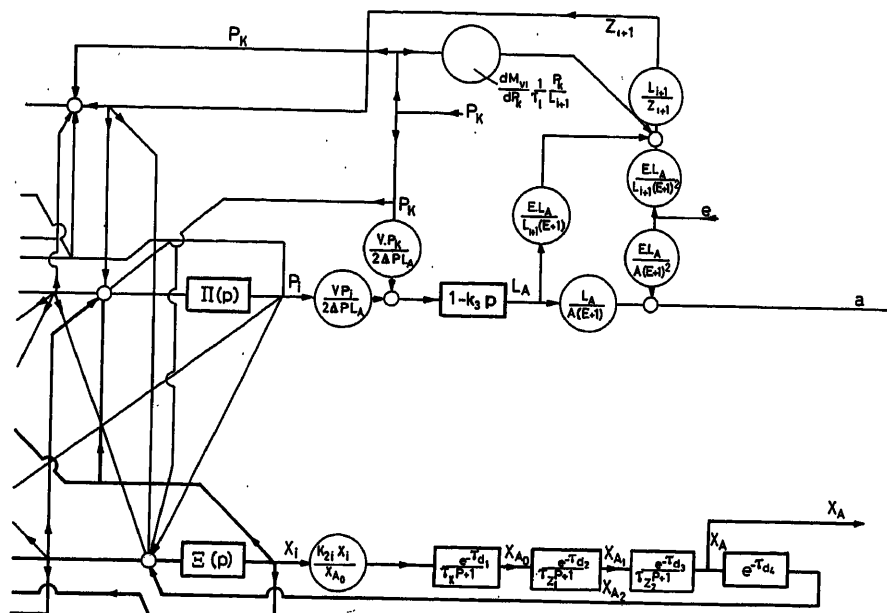


Figure 7

chain are formed by the algebraic sum of the signals of three adjacent members and they link together the diagram of pressure and the diagram of composition.

The general analysis of this block diagram was made; a matrix calculation was used for deriving the matrices of the transfer functions of this block diagram as the functions of the number of the chain members (or of the number of the plates of the column). A further analysis was used for establishing the conditions at which the static value of the output signals of the above chain is equal to zero (the conditions are related to the magnitude of the multiplying constants), and the conditions at which it is possible also to neglect the dynamic value of the output signals (the conditions are related to the number of plates). It was proved by a further general procedure that the above-

stated conditions are fulfilled by each column. Assume for an instant that, during the investigation of the dynamic properties of the distilling column, there is no interest in the non-steady states of pressure. Under this assumption, and owing to the former conclusions, it is possible to interrupt in the block diagram the connections of the pressure changes between the individual plates. This can be done because any disturbance entering any plate lying below or above the plate under investigation can influence neither the flow rate, nor the pressure, but only the pressure values at different points of the block diagram, or of the column, and these values are of no interest for the time being.

Now consider composition in the same way—supposing that one is not interested in the non-steady states of composition. Similarly, as in the case of pressures, the connections between

THE DYNAMIC PROPERTIES OF RECTIFICATION STATIONS WITH PLATE COLUMNS

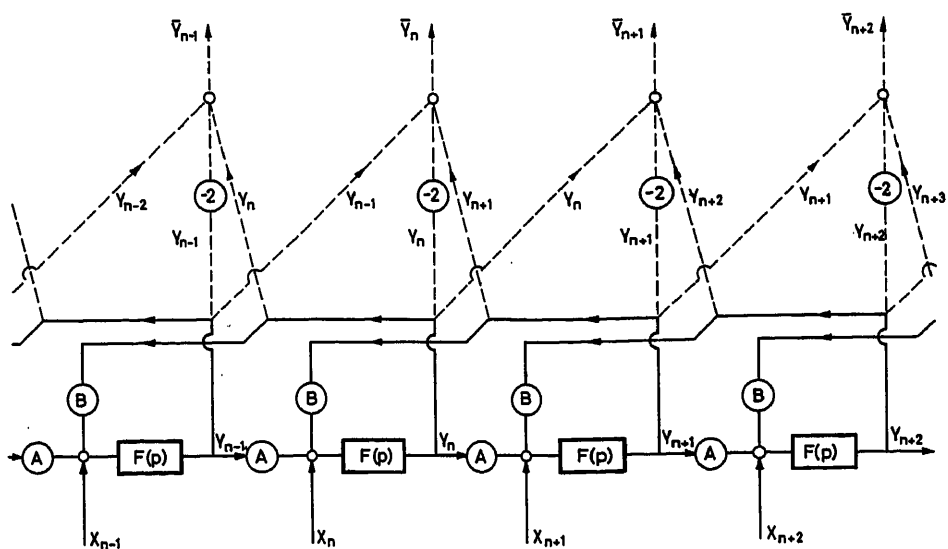


Figure 8

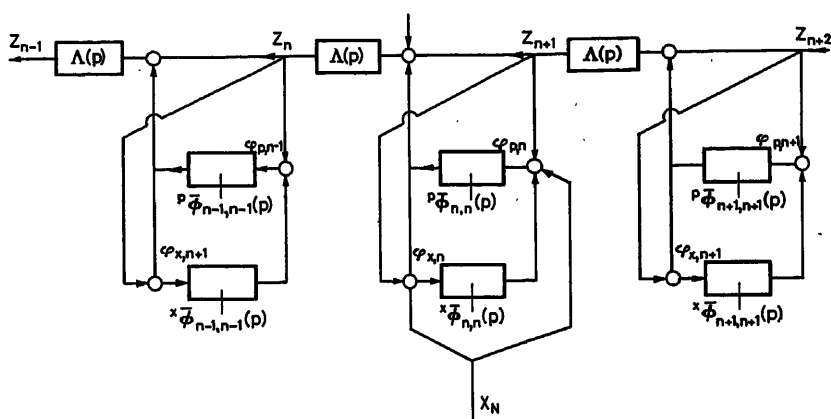


Figure 9

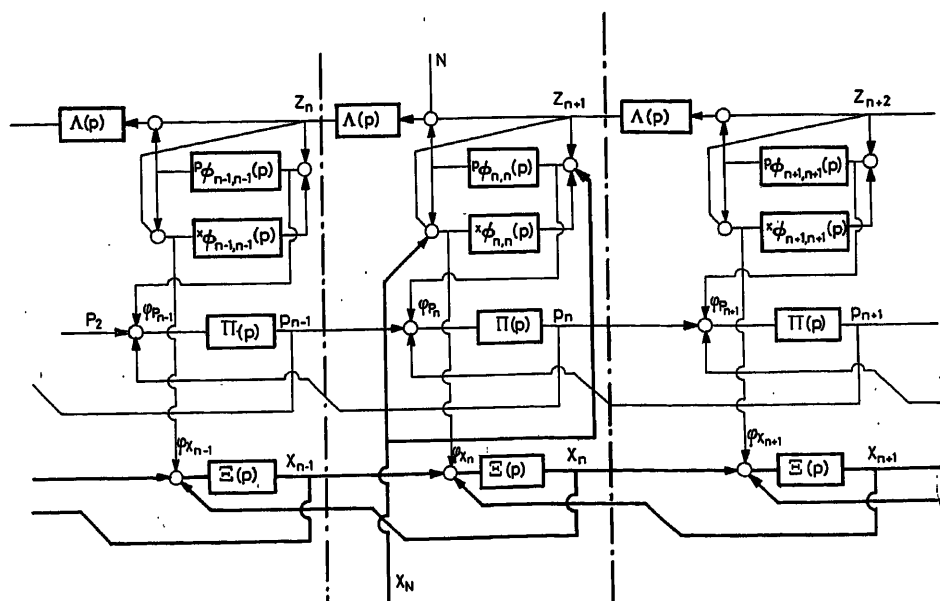


Figure 10

individual plates may be interrupted. The block diagram is then transformed into the form shown in Figure 9. The values φ_p and φ_x are the sums of the input signals of the individual nodes of the block diagrams of the dynamics of pressure and composition respectively. Now the non-steady states of pressure and composition, that were formerly excluded from discussion, are considered. The partial block diagrams of pressure and composition respectively are easily attached to the diagram in Figure 9 by introducing the signals φ_p and φ_x into the individual nodes of the block diagrams of pressure and composition respectively. The result is shown in Figure 10. The section of the block diagram bordered by the dot-and-dash lines corresponds with one plate of the rectifying column. By the solution of the system of equations written for all three nodes of the block diagram of one plate (naturally after the introduction of all multiplying constants) the transfer functions of all output variables of the plate are obtained. Finally, in the application of the transfer functions, it is possible to re-draw the block diagram shown in Figure 5 into the final form according to Figure 11. This block diagram holds for a general column with any arbitrary parameters with regard to design, physico-chemical conditions and operation.

The block diagram shown in Figure 11 together with the pertaining transfer functions and formulae for various constants and transfer functions, is the final product of the theoretical part of the work. These results make possible the computation of the transfer functions of a general rectifying station. During the solution of concrete problems a number of possible simplifications appeared that followed from the numerical evaluation of individual constants and plate transfer functions. It is not possible to prove the general validity of these simplifications. However, it may be assumed that they will be identical in most cases.

Further work¹⁶ contains the practical computation of several transfer functions and step response curves of a concrete rectifying station on the basis of the results obtained from a general analysis. The necessary measurements were also made on this station in operation. After a comparison, the results of the computation were in very good agreement with the results of the measurements.

Nomenclature

A	Flow rate of the product (mol/sec)
B	Flow rate of the residue (mol/sec)
C_n	Multiplying constants
d_1	Transport lag of condenser
d_2	Transport lag of cooler
d_3	Transport lag of condensate tank
d_4	Transport lag of the reflux line
E	Reflux ratio
F_1	Sum of the influences of flow rate on plate pressure
F_2	Sum of the influences of feed concentration on plate pressure
F_3	Sum of the influences of flow rate on plate composition
F_4	Sum of the influences of feed composition on plate composition
F_5	Sum of the influences of feed flow rate on plate flow rate
F_6	Transfer function of plate flow rate. Given in Figure 4 as $\frac{1}{\tau_1 p + 1}$
F_7	Sum of the influences of feed composition on plate flow rate
$F(p)$	Elementary transfer function of concentration, similar to $\Xi(p)$
G_1	Flow rate of the heating steam (kg/sec)
H_1	Enthalpy of the liquid (kcal/mol)
H_N	Enthalpy of the feed (kcal/mol)
H_v	Enthalpy of the vapour (kcal/mol)
H_1	Enthalpy of the heating steam (kcal/mol)
H_2	Enthalpy of the condensate from the still (kcal/mol)
i	Number of plates
k_o, K	Constants
k, K	Subscript of condenser
L	Reflux (mol/sec)
L_{i+1}	Reflux to the top (mol/sec)
M_i	Liquid hold-up of the plate (mol)
M_v	Vapour hold-up of the plate (mol)
N	Feed flow rate (mol/sec)
N	Subscript of feed plate
n	Ordinal number of plate
$O(p)$	Transfer function of the still
$p_{\varphi i}(p)$	Elementary multiplying factor of influence of flow rate on plate pressure
P	Pressure (atm)
P_K, P_k	Pressure in the condenser (atm)
Q_1	Heat flow to the heating wall (kcal/sec)
Q_2	Heat flow from wall to substance (kcal/sec)
S_i	Surface area of liquid hold-up (dm ²)

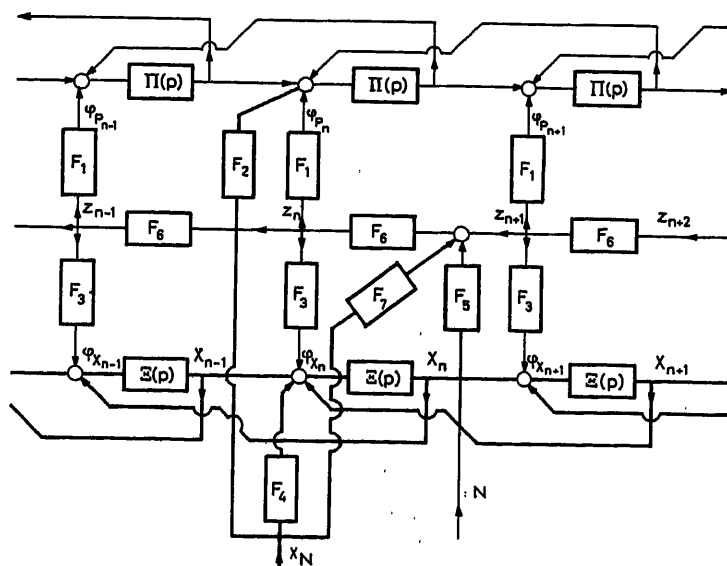


Figure 11

S_1	Height of liquid level in plate above weir (dm)	τ_K	Time constant of the condenser (sec)
T_s	Mean temperature of heating wall ($^{\circ}\text{C}$)	τ_{κ}	Time constant of the elementary transfer function of the concentration (sec)
T_1	Mean temperature of heating wall on the steam side ($^{\circ}\text{C}$)	τ_{pp}	Derivative time constant of the concentration—pressure link (sec)
T_2	Temperature of heating wall on the side of the heated substage ($^{\circ}\text{C}$)	τ_{z1}	Time constant of the cooler (sec)
V	Flow rate of vapour through column (mol/sec)	τ_{z2}	Time constant of the condensate tank (sec)
V^*	Volume (l)	φ_{pi}	Sum of the input signals of nodes of pressure dynamics
X	Concentration of the more volatile component in the liquid (mol %)	φ_{xi}	Sum of the input signals of nodes of composition dynamics
X_A	Concentration of the more volatile component in the product (mol %)		
X_{A0}	Concentration of the more volatile condensate component after the condenser (mol %)		
X_{A1}	Concentration of the more volatile product component in the cooler of condensate (mol %)		
X_{A2}	Concentration of the more volatile component in the reflux (mol %)		
X_N	Concentration of the more volatile component in the liquid on the feed plate (mol %)		
$X_{qti}(p)$	Elementary multiplying factor of influence of flow rate on plate composition		
\bar{Y}	Concentration of the more volatile component in the vapour (mol %)		
Y	Composite of vapour composition dynamics as influenced by neighbouring trays		
Y_N	Concentration of the more volatile component in the vapour on the feed plate (mol %)		
Z_n	Liquid flow rate in figures. Corresponds to term L in equations (mol/sec)		
γ, γ_l	Specific gravity of liquid (kg/l)		
γ_v	Specific gravity of vapour (kg/l)		
ξ	Molar volume (dm^3/mol)		
$\Delta(p)$	Elementary transfer function of the flow rate of the liquid phase		
μ	Molecular weight		
$\Xi(p)$	Elementary transfer function of concentration molar volume (dm^3/mol)		
$\Pi(p)$	Elementary transfer function of pressure		
ϱ	Circumference of down-take pipe (dm)		
τ	Time (sec)		
τ_d	Transport lag (sec)		
τ_i	Time constant of the elementary transfer function of the flow rate of the liquid phase (sec)		
τ_p	Time constant of the elementary transfer function of pressure (sec)		
τ_{px}	Derivative time constant of the pressure-concentration link (sec)		
τ_θ	Time constant of the elementary transfer function of the still (sec)		
τ_k	Time constant of the transfer function of the condensate (sec)		

References

- ANISIMOV, J. V. *Avtomatičeskoje regulirovanie proces rektifikacii*. 1957. Moscow; Gostoptechizdat
- ARMSTRONG, W. D., and WILKINSON, W. L. *Trans. Instn. chem. Engrs, Lond.* 35 (1957), 352
- DAVIDSON, J. F. *Trans. Instn. chem. Engrs, Lond.* 34 (1956), 44
- HÁLA, E., PICK, J., FRIED, V., and VILIM, O. *Rovnováha kapalina-pára*. 1955. Prague; NČSAV
- HARNETT, R. T., ROSE, A., and WILLIAMS, T. J. *Industr. Engng. Chem.* 48 (1956), 1008
- JACKSON, F. R., and PIGFORD, R. L. *Industr. Engng. Chem.* 48 (1956), 1020
- KIRSCHBAUM, E. *Destillier- und Rektifizierteknik*. 1950
- MARSHALL, W. R., and PIGFORD, R. L. *The Applications of Differential Equations to Chemical Engineering*. 1947. University Delaware
- RIJNSDORP, J. E., and MAARLEVELD, A. Use of electrical analogues in the study of the dynamic behaviour and control of distillation columns. *J. Symp. Instrument Comp. Develop. Plant Design*. London 11-13 (1959)
- ROSE, A., JOHNSON, C. L., and WILLIAMS, T. J. *Industr. Engng. Chem.* 48 (1956), 1173
- ROSE, A., and WILLIAMS, T. J. *Industr. Engng. Chem.* 47 (1955), 2284
- ROSENBRICK, H. H. *Trans. Instn. chem. Engrs, Lond.* 35 (1957) 347
- VOETTER, H. *Plant and Process Dynamic Characteristic*. 1957. London; Butterworths
- YU-CHIN-CHU, BRENNER, R. J., GETTY, R. J. and RAJINDRA, P. *Distillation Equilibrium Data*. 1950. New York
- ZÁVORKA, J. Obecný analytický rozbor dynamických vlastností rektifikačních stanic s patrovými kolonami pro dělení binárních směsí. *ÚTLA ČSAV* 68 (September 1960)
- ZÁVORKA, J. Výpočet některých přenosů kolony 31 (provoz 03) ve Stalinových závodech ve srovnání s výsledky měření. *ÚTLA ČSAV*, 86 (September 1961)

DISCUSSION

T. J. WILLIAMS, *Monsanto Chemical Company, St. Louis 66, Missouri, U.S.A.*

(1) Figure 1 of the paper by J. Závorka is a reproduction of Figure 14 of the paper by J. E. Rijnsdorp and A. Maarleveld⁹. The original figure presents the corresponding frequency responses of pressure at the 8th, 32nd and 56th trays of an analogue model of a 64-tray column subjected to disturbances in heat input to the reboiler. It should be noted that the R.C. ladder network proposed by Rijnsdorp and Maarleveld and the cascade of first-order lags proposed by Rose and Williams^{5, 10, 11} would both give essentially the same response for the condition presented by Závorka in his Figure 1. The R.C. ladder network is best if one uses a passive network analogue computer, but the first-order lag is best if one is using the standard operational amplifier type of analogue computer used by Rose and Williams in their work.

(2) A model with only constant coefficients on all terms, as depicted in Figure 5 and subsequent figures, precludes the use of a second-order flow-rate pressure relationship as given in eqn (4). The same statement also applies to the equation for tray hold-up [eqn (5)] and the discussion of vapour liquid equilibria relationship p. 329. The diagrams presented seem to require that the actual relationships used are:

$$V_n = K' \Delta P$$

$$Y_n = K'' X_n$$

$$M_{1,n} = \text{constant}$$

Since the author is using a linearized model, such a procedure is perfectly satisfactory. He should, however, make this plain to the reader in his paper.

(3) Equation (5) appears to be an equation for height of liquid over a pipe downcomer used as a weir rather than the height of liquid above the vapour nozzle of the bubble cap, as indicated by the definition of the symbol S_1 in the Nomenclature.

(4) We cannot agree with the implication of *Figure 8*, that the vapour composition on any tray is influenced in a major way directly by the vapour composition of the tray next above. In addition, it would appear that *Figure 8* and its results are not used in subsequent developments of the paper.

(5) In the simplification of *Figure 5* to obtain *Figures 9, 10* and eventually *Figure 11*, it would seem that all influences of pressure and composition on the other variables of the columns operation have been eliminated or considered unimportant. The only influences remaining are those attributed to flow rate changes on the plates themselves.

(6) As near as can be determined by reading this preprint, no use was made of eqns (3), (8) and (9) except in determining initial boil-up rates in the still pot. It is misleading to the reader to include these relationships when apparently there is no intention of making use of them in the model development being discussed.

(7) It is disappointing that Mr. Závorka has not included any responses of actual column models or comparisons of model response with actual column response. His write-up indicates that such work has already been done (in his Reference 16); however, none is reproduced in the paper.

J. ZÁVORKA, *in reply*

I am much obliged to Mr. Williams for his comments on my paper. I am sure that these comments and my reply to them will help to clarify some points in my paper, which is but a very limited excerpt (the whole original work on which I am reporting in this paper has about 200

typewritten pages), and therefore some topics are obviously not clear enough.

(1) I agree with this comment.

(2) The equations mentioned were linearized, as is written in the last paragraph of p. 328.

(3) Mr. Williams is quite right. The symbol S_1 really means the height of liquid over a pipe downcomer used as a weir.

(4) The symbols X , Y and \bar{Y} used in *Figure 8* mean generally quantities (not especially the composition of the liquid resp. vapour phase). It is written (perhaps not clearly enough) in the last paragraph of p. 329. I cannot agree with the assertion that the results of *Figure 8* are not used in subsequent developments of the paper. On the contrary the results of this figure have a fundamental meaning for simplification of the block scheme of the column (*Figure 5*) and for making possible the computation of the transfer functions. The use of results of *Figure 8* is shown on pp. 330, 332.

(5) The influences mentioned in this comment of Mr. Williams are not eliminated in *Figures 9, 10* and *11* respectively. They are only simplified by using the results of *Figure 8* as explained on pp. 330, 332. These simplified couplings are included in the scheme by means of the transfer functions ${}^p\phi_{n,n}(p)$, ${}^a\phi_{n,n}(p)$ respectively.

(6) The use of eqns (3), (8) and (9) is not visible as a result of the extreme shortness of the paper, but it is evident that it would not have been possible to come to the results by using not all equations of the whole number of 9 which contain 9 variables.

(7) To include the results of measurements in this paper is not possible because of the paper's brevity.

As I see from Mr. Williams' comments my paper, as a result of its very short form, has many vague points. That is why I should like to draw the readers' attention to Reference 15 of this paper. In that publication are the entire results of my work and the experimental results, and their agreement with the results of theoretical analysis.

Une Réalisation Originale dans une Raffinerie de Pétrole: le Chargement Automatique des Wagons Citernes

F. X. MONTJEAN

Summary

It has been possible to improve, to a very high degree, the emptying of petrol products from tankers by the use of loading equipment where the weighing of the tanks and their filling is carried out at the same time.

The wagons are hauled into position by means of an automatic system. The special type of telescopic arms of the loader carry out the filling at the flood entrance at very great speeds.

All the other operations such as the selection of hydrocarbon circuits, progressive reduction in the rate of flow at the end of the filling, injection of additives are entirely automatic.

Sommaire

L'évacuation des produits pétroliers par wagons citernes a pu être sensiblement améliorée par l'emploi de postes de chargement à très grand débit où le pesage des citernes s'effectue en même temps que le remplissage.

Les wagons sont amenés en position grâce à un dispositif de traînage automatique. Des bras de chargement d'un type spécial (cannes télescopiques) effectuent le remplissage à orifice noyé, ce qui permet d'atteindre sans danger, de très grandes vitesses d'écoulement.

Toutes les autres opérations du cycle (sélection des circuits d'hydrocarbures, réduction progressive du débit en fin de remplissage, injection des dopes, etc. ...) sont entièrement automatiques.

Zusammenfassung

Der Umschlag von Erdölprodukten in Kesselwagen konnte durch den Einsatz von Ladegeräten mit sehr hohem Durchfluß wesentlich beschleunigt werden. Dabei erfolgt das Wiegen der Kesselwagen während des Füllvorganges.

Die Waggons werden selbsttätig in Ladeposition gebracht. Besondere, teleskopartig ausgeführte Ladearme mit eingetauchtem Mundstück gestatten es, sehr hohe Strömungsgeschwindigkeiten gefahrlos zu erreichen. Alle anderen Vorgänge (Auswahl der Kohlenwasserstoffprodukte, progressive Durchflußverminderung gegen Ende des Füllvorganges, Hinzugabe von Additiven usw.) laufen völlig selbsttätig ab.

Généralités

En douze ans, la capacité de traitement du pétrole brut par les raffineries du monde occidental a plus que doublé. Cette augmentation de productivité a été obtenue par l'application d'audacieux programmes d'extension qui, en France, se sont traduits notamment par la construction des deux raffineries de Strasbourg (capacité 7,6 millions de tonnes). L'évacuation des produits raffinés dans de telles unités de production, imposait une modernisation radicale des moyens antérieurement employés. Etant donné le volume important des produits évacués par fer, il est normal que le souci des grandes sociétés pétrolières se soit porté d'abord sur le perfectionnement des dispositifs de chargement des wagons citernes.

La réalisation que nous nous proposons de décrire, ne présente pas, si l'on considère séparément chacun des problèmes élémentaires auxquels une solution a été apportée, un caractère d'originalité technique. Il est bien évident que l'on s'est efforcé de mettre en œuvre des techniques disponibles et éprouvées pour exécuter les fonctions automatiques essentielles. La complexité du problème réside plutôt dans la conjonction des différentes techniques utilisées qui font de cette réalisation une «architecture» d'automatisme intéressante.

Pour donner la mesure de l'audace technique dont a fait preuve le Maître de l'Oeuvre, il n'est pas inutile de souligner que ce poste de chargement moderne installé à la Raffinerie de Reichthett pour le compte de la Compagnie Rhénane de Raffinage, est le premier de ce genre réalisé dans le monde.

Rappelons tout d'abord très rapidement les conditions dans lesquelles s'effectuent, dans les raffineries courantes, les opérations de remplissage des wagons citernes. Le long des voies ferrées sont échelonnés des postes de chargement à petit débit où aboutissent les tuyauteries d'amenée des différents types de produits. Ces postes sont en majorité banalisés, c'est-à-dire susceptibles d'opérer le remplissage des wagons en produits noirs et produits blancs des différents types. Disons pour fixer les idées que, pour obtenir un débit de 70 wagons/jour (à deux postes de travail), il faut actuellement deux rampes de chargement à 7 postes chacune.

Les wagons sont amenés à l'aide d'un locotracteur jusqu'au pont bascule où s'effectue l'opération de tarage, ensuite aux postes de chargement, enfin de nouveau au pont bascule pour mesure du poids versé.

La multiplicité des manœuvres précédentes pour le chargement de chaque wagon permet d'évaluer la perte de temps que l'on peut enregistrer. L'observation «in situ» confirme d'ailleurs que la charge du trafic fer varie surtout en fonction du nombre de wagons tractés et très peu en fonction du tonnage chargé. La seule opération directement liée au tonnage est celle du chargement. L'expérience montre qu'elle est masquée en grande partie par les autres opérations (manœuvres de wagons, etc. ...) et donc sans influence prépondérante.

L'idée de base de la nouvelle réalisation a donc été de limiter au maximum les mouvements de wagons et d'obtenir un défilement pratiquement continu des wagons sous un poste de chargement à très grand débit placé à l'aplomb d'un pont bascule où l'on effectuerait successivement sur chaque wagon les opérations suivantes: (a) tarage; (b) remplissage, et (c) pesage.

Nous avons pu voir une première réalisation basée sur ce principe à la Raffinerie BP à Dinslaken. L'automatisme en était toutefois limité à l'acheminement des wagons jusqu'à un poste d'attente situé avant le pont bascule.

Un grand pas devait être franchi dans la nouvelle réalisation.

En effet on désirait exécuter de façon entièrement automatique : l'amenée des wagons sur le pont bascule sans employer de locotracteur ; le positionnement précis de chaque wagon sur les tabliers du pont ; l'opération de tarage ; la sélection et la mise en condition des circuits correspondant aux produits à verser ; le pesage en continu du wagon pendant le remplissage ; la décroissance contrôlée du débit à l'approche du poids désiré ; la fermeture automatique des vannes ; le retrait des bras de chargement à la fin du remplissage, et le passage au wagon suivant.

Un des arguments essentiels qui militait en faveur des principes de réalisation précédents, résidait dans la possibilité qui s'était fait jour de travailler sur des rames des wagons attelés, sans effectuer de décrochage au moment du passage sur le pont bascule. Des mesures systématiques de poids ont en effet été faites sur des wagons attelés, tampons non jointifs, attelages desserrés. Elles ont prouvé que les erreurs commises par cette méthode restaient inférieures aux limites admissibles. Le gain du temps observé par la suppression des manœuvres d'attelage et de décrochage, la diminution du personnel d'exploitation chargé de ces opérations, la suppression de la présence permanente d'un locotracteur, tels étaient les avantages essentiels attendus de cette nouvelle méthode.

Nous avons parlé précédemment du grand débit imposé au nouveau poste. Il est important de ne pas se méprendre sur ce point. On pouvait penser en effet, qu'avoir un seul wagon en cours de remplissage sur le nouveau poste (au lieu de 14 simultanément sur l'ancien par exemple), nécessite une très grande augmentation du débit unitaire des bras de chargement. En fait, nous avons déjà souligné que le débit auquel est liée la notion du temps de remplissage, ne constitue pas l'élément prépondérant du cycle de chargement. Les temps morts, la multiplicité des manœuvres avec le locotracteur, ont une très grande influence.

Donnons quelques chiffres :

(a) 14 postes de chargement « ancien modèle » équipés des bras de chargement de 4 à 6 pouces permettent de charger une rame de 14 wagons en 210 min environ, soit 15 min par wagon.

(b) Le nouveau poste sous lequel défile la rame à charger, doit donc avoir au minimum la même cadence. Le diamètre intérieur des bras de chargement (ou cannes de remplissage) a été porté à 8 pouces. Cette augmentation relativement peu importante montre bien l'incidence des autres manœuvres que celle du remplissage proprement dit sur la cadence de chargement.

Nous distinguerons dans notre exposé, le trainage et le positionnement des wagons, le pesage individuel des citernes, et le remplissage en hydrocarbures.

Trainage et Positionnement des Wagons

Le dispositif de halage des wagons par treuil cabestan est un dispositif classique et éprouvé. Il comprend principalement :

(a) Un chariot d'attelage automatique circulant sur une voie qui lui est propre, située à l'intérieur de la voie principale. Il assure l'entraînement des wagons à déplacer en emprisonnant les deux roues d'un même essieu entre deux paires de galets escamotables. Ce chariot tiré dans les deux sens de marche par un câble d'acier reposant sur les traverses et guidé par des poulies.

(b) Un treuil cabestan entraîne le câble au moyen de deux poupées motrices dont les vitesses dans les deux sens de rotation sont identiques. Le treuil est entraîné par un moteur à deux enroulements ; les variations de charges sont compensées par élimination de résistances rotoriques. La vitesse du chariot est de 0,80 m/sec à vide et de 0,40 m/sec en charge.

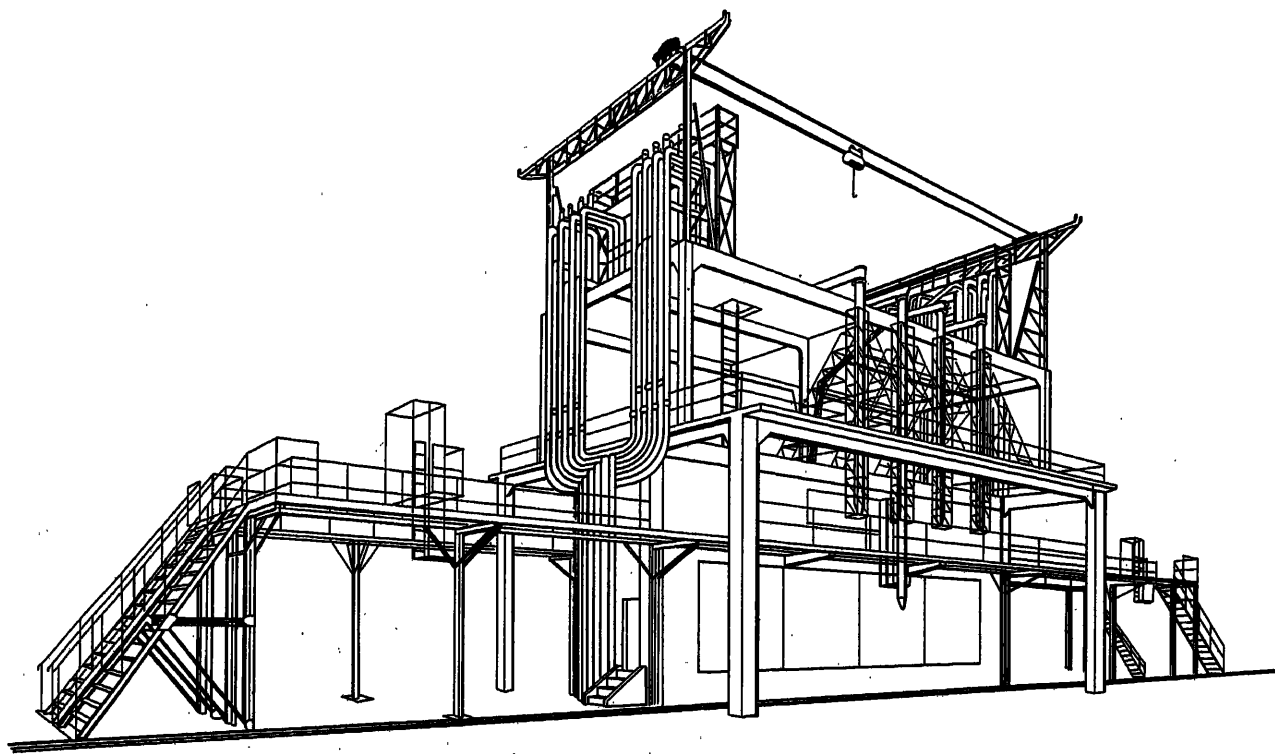


Figure 1

(c) Un système tendeur agit sur le brin de câble situé entre les deux poutres; l'adhérence du câble est obtenue par l'action d'un contre-poids vertical.

La recherche d'une automaticité complète des opérations de positionnement précis a présenté quelques difficultés dues essentiellement à la diversité des wagons citernes (wagons à 2 bogies et à 2 essieux par bogie, wagons à 2 ou 3 essieux — longueurs variables, dômes excentrés, etc. ...). Il faut en effet qu'à la position d'arrêt pour remplissage, les conditions suivantes soient réunies:

(a) Les roues de deux wagons contigus ne doivent pas se trouver simultanément sur le même tablier du pont bascule.

(b) Les dômes de certains wagons étant parfois assez éloignés du plan transversal de la citerne, il faut choisir une position de remplissage de ces wagons qui soit telle que le capot du réservoir (ou dôme) ne soit pas trop loin du plan transversal de symétrie du poste de chargement, ceci afin de limiter les débordements longitudinaux des bras de chargement.

L'analyse attentive des différents cas possibles a permis de déterminer:

(a) Le nombre optimum de tabliers du pont bascule: quatre tabliers dans le cas de la Raffinerie de Reichardt en raison de la présence de certains wagons allemands dont la longueur atteint 17 m.

(b) Un nombre limité de positions d'arrêt correspondant aux différents types de wagons et à la présentation du dôme pour les wagons à dôme excentré (dôme avant ou dôme arrière).

Le classement des wagons par types est supposé connu avant l'arrivée de la rame au poste de chargement. La composition du train peut être alors affichée sur un pupitre de tabulation par l'opérateur du poste de commande. Les séquences des opérations de trainage feront appel automatiquement aux informations précédemment indexées et élaboreront: la sélection des fins de course de ralentissement et d'arrêt relatifs au wagon en approche, et la sélection des tabliers concernés du pont bascule.

En fait, en premier stade on a conservé l'affichage manuel de chaque type de wagon avant son départ vers la position chargement. Un très large emploi a été fait de détecteurs magnétiques de proximité pour respecter les conditions de sécurité imposées aux matériels électriques, tout en conservant une définition précise des positions d'arrêt.

Actuellement, un wagon appartenant à une rame de 750 T dont l'état de chargement est quelconque, se positionne à ± 20 cm de la position d'arrêt prescrite, attelages détendus, tampons non jointifs (recommandations du Service des Poids et Mesures).

La séquence des opérations est la suivante:

(a) La rame de wagons vides est amenée par le locotracteur à l'extrémité de la voie du poste de chargement.

(b) En semi-automatique, le chariot de trainage va chercher cette rame et s'accouple au premier wagon qu'il amène au poste de chargement sur la bascule, se désaccouple et sort de la bascule par l'avant.

(c) Les opérations de trainage de toute la rame peuvent être ensuite entièrement automatiques.

(d) Lorsque le wagon sur bascule est chargé, le chariot part en grande vitesse (0,80 m/sec) à sa rencontre, emprisonne les roues du premier essieu et le tire en avant en vitesse moyenne

(0,40 m/sec). C'est le wagon suivant qui conditionnera l'arrêt à la nouvelle position de remplissage.

(e) Les pédales de voies correspondant au type de ce wagon ont été sélectionnées en même temps que l'on affichait le type de wagon.

(f) Lorsque le wagon excite la pédale de ralentissement, le treuil cabestan passe en vitesse lente et enfin s'arrête sur le signal fourni par la pédale d'arrêt. Le chariot reste accouplé, ce qui immobilise la rame pendant le chargement.

(g) A la fin du remplissage, le chariot se désaccouple et vient en grande vitesse saisir le wagon chargé et ainsi de suite.

Pesage des Wagons

L'étude précédemment évoquée, a conduit à l'emploi d'un pont bascule à 4 tabliers. Cette disposition comportait de très graves risques de détériorer la précision attendue du dispositif de pesage (celui-ci devait, pour être agréé par les Poids et Mesures, assurer des pesées au millièrme).

En effet, l'emploi de plusieurs tabliers nécessite un sélecteur mécanique pour réaliser la commutation et la sélection des tabliers intéressés.

Il est bien connu des spécialistes de balances, que l'augmentation du nombre de directions du sélecteur, en même temps qu'une plus grande complexité mécanique, conduit à une détérioration de la précision dès que l'on dépasse trois directions.

C'est pourquoi, dans la réalisation actuelle, il a été décidé de prendre des sélecteurs à 2 directions, autrement dit de grouper deux par deux les tabliers et d'associer, à chacun des deux sélecteurs, une tête de mesure.

On a reporté ainsi la difficulté hors du domaine mécanique et on a laissé aux équipements électroniques associés, le soin d'effectuer l'addition des indications fournies par les deux têtes.

D'autre part, la recherche d'une automaticité complète des opérations de pesage et des manœuvres associées, imposait à l'équipement les caractéristiques suivantes: possibilité d'une pesée en continu, et présentation des poids mesurés en valeur numérique.

On désirait en effet confier au dispositif de pesage le rôle: de commander l'ouverture progressive des vannes au début du remplissage; de réduire cette ouverture à l'approche du poids ordonné en réalisant une décroissance contrôlée du débit pour éviter les coups de bélier dans les canalisations; de fermer les vannes au poids atteint, et d'élaborer les signaux commandant l'injection des doses en cours de remplissage.

L'installation réalisée pour répondre à ces différentes conditions, comporte les dispositifs suivants. Les deux têtes de mesure du poids sont basées sur le principe du comptage électronique; chaque tête délivre tous les 50 kg une impulsion de comptage. A travers un circuit d'anticoincidence, les impulsions issues des deux têtes sont envoyées dans un compteur unique. L'équipement est complété par des circuits analogiques permettant de réaliser les fonctions ci-dessus définies (injection des doses, décroissance contrôlée du débit) enfin par une machine électro comptable.

Lorsque le wagon à remplir se trouve sur le pont bascule:

(a) La sélection des tabliers a déjà été effectuée car elle est liée à la sélection de la position d'arrêt du wagon (famille du wagon).

(b) L'opérateur sélectionne le type de produit à peser et tabule sur un clavier le poids net ordonné désiré. La valeur

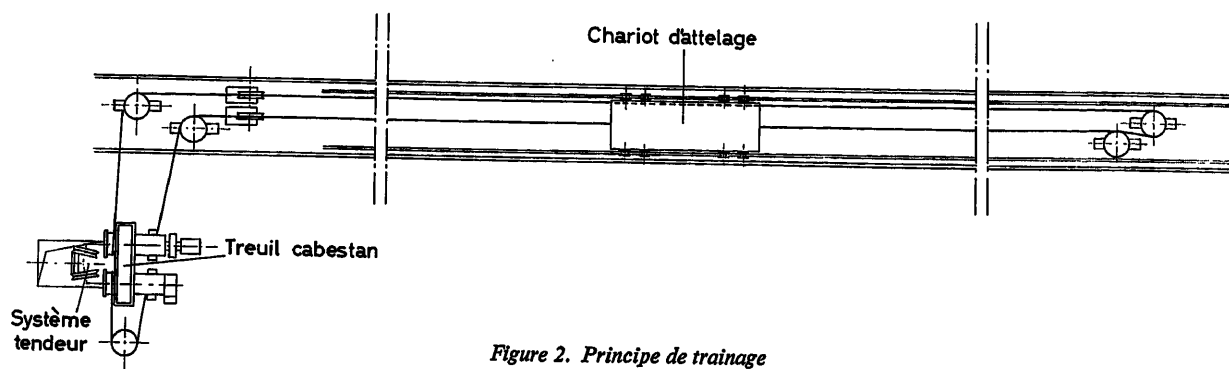


Figure 2. Principe de trainage

numérique de ce poids est envoyée à la machine électro comptable.

(c) L'ordre tare est envoyé. La valeur de la tare est introduite dans la machine comptable qui effectue l'addition: tare + poids net ordonné = poids brut ordonné. Cette valeur est envoyée dans le compteur de l'équipement de pesage.

(d) Le remplissage commence et les impulsions émises par les têtes de mesure, opèrent le vidage progressif du compteur.

(e) Jusqu'au 1/20 du poids net ordonné, le remplissage se fait à petit débit. A partir de cette valeur la vanne de régulation s'ouvre complètement.

(f) L'injection des dopes est réalisée à l'aide des impulsions de commande élaborées par les circuits de comptage. Ces impulsions surviennent tous les 250 kg à partir de (poids net/5) et jusqu'à $(4 \times \text{poids net}/5)$.

(g) A 1000 kg du poids net, un circuit analogique branché sur la commande du point de consigne de la vanne régulation, commence à élaborer l'ordre de fermeture progressive de la vanne, pour éviter les coups de bélier dans les canalisations.

Remplissage des Wagons

Les différents produits sont introduits dans les wagons par des cannes télescopiques semi souples, que nous décrirons plus loin.

Afin de ne pas multiplier le nombre de cannes de remplissage, un groupement de produits présentant des caractéristiques voisines, a été opéré. Ainsi la même canne peut être utilisée pour le remplissage de 2 à 5 produits distincts. La pollution résultant des portions de circuits communes aux différents hydrocarbures transitant vers la même canne, reste inférieure aux valeurs admissibles.

Pour une voie de chargement «produits blancs», les groupements réalisés ont permis de réduire à 4, le nombre de cannes nécessaire.

La canalisation arrivant en tête d'une canne de remplissage se trouve donc raccordée à un certain nombre de tuyauteries d'amenée de produits. Les circuits sont contrôlés chacun par une vanne de manœuvre et une vanne d'isolement.

Une vanne casse vide située en tête de chaque circuit de canne permet le vidage complet de la canalisation après chaque opération de remplissage.

Les égouttures qui risquent de se produire après la purge précédente, sont retenues par des dispositifs spéciaux de récupération.

Canes Télescopiques

Chaque canne se compose, dans sa partie haute, d'un tube rigide appelé aiguille et, dans sa partie rétractable, d'un tube flexible en néoprène armé.

Cette conception présente les avantages suivants:

(a) Augmentation de la sécurité. Les cannes étant télescopiques et descendant au fond du wagon, il est possible d'en noyer la crépine très rapidement, d'où: diminution des turbulences et de l'électricité statique inhérente à l'écoulement rapide des produits.

(b) Facilité de positionnement. La souplesse relative de la partie basse permet de contourner sans dommage, certains obstacles se trouvant dans les citernes (vannes, leviers, tubes de réchauffage, cloisons anti roulis, etc. ...)

(c) Emploi facile. L'influence d'un faible déplacement accidentel du wagon en cours de remplissage peut être sans inconvénient sur le dispositif. Un fort déplacement comme un tamponnement ou un départ en catastrophe se traduira par le sectionnement de la partie flexible dont le remplacement est facile et d'un coût peu élevé.

Par ailleurs, les cannes présentent les particularités suivantes:

(a) Leur conception télescopique n'augmente que de très peu la quantité de matière adhérent aux parois et destinée à s'égoutter, car un dispositif racleur nettoie le tube à chaque manœuvre;

(b) Elles portent, à leur partie inférieure, une crépine dont la forme est étudiée afin de réduire les turbulences et les vitesses relatives. Elles sont munies d'une butée souple destinée à amortir les chocs lors de la rencontre d'obstacles ou du fond des citernes;

(c) Les cannes sont conçues de façon à permettre un gonflement éventuel du néoprène et des systèmes spéciaux de guidage sont destinés à atténuer les déformations temporaires ou permanentes de la partie flexible;

(d) Chaque canne est manœuvrée à l'aide d'un dispositif mécanique à chaînes entraîné par un moteur anti-déflagrant. Le dispositif de suspension est souple et destiné à absorber les contraintes que peut subir une canne à la descente. Lorsqu'elle rencontre un obstacle, l'arrêt du moteur est automatiquement déclenché par un détecteur magnétique.

Il n'y a aucun risque d'accumulation d'électricité statique sur la canne, celle-ci étant noyée dans le produit. D'autre part, à la remontée, des racleurs ramènent l'extrémité de la canne au potentiel de l'aiguille.

339

Le diamètre utile intérieur de la canne est de 200 mm. Le diamètre extérieur est de 230 mm. Cette dernière valeur constitue la cote maximale compatible avec les diamètres des plus petits dômes. En effet, sur certains wagons anciens, on a rencontré des diamètres utiles de 280 mm.

Chariot Porte-cannes

Les cannes sont montées sur un chariot en treillis métallique qui peut se déplacer suivant un axe parallèle à la voie afin d'amener la canne de remplissage à la verticale du dôme.

Les deux opérations précédentes (positionnement et descente de la canne) seront automatisées à un stade ultérieur. Pour le moment l'exiguïté des dômes des wagons anciens rend ce perfectionnement hasardeux et probablement inutile, compte tenu du faible taux d'occupation des opérateurs chargés de l'exploitation.

Conditions d'Exploitation

Un poste de chargement double, c'est-à-dire desservant deux voies ferrées parallèles (et donc équivalant à une trentaine de postes ancien modèle) peut fonctionner avec deux opérateurs.

(a) L'opérateur principal situé dans le poste de commande commun aux deux voies assure les différentes manœuvres

d'exploitation et la surveillance à l'aide des pupitres de commande et de contrôle mis à sa disposition.

(b) Un opérateur chargé de l'ouverture et de la fermeture des dômes et de certaines manœuvres accessoires, telles que mise à la terre des wagons, plombage des dômes, etc. ...

Par rapport aux effectifs affectés à des postes de chargement de type ancien, la réduction obtenue est spectaculaire.

Conclusions

Bien des perfectionnements peuvent être encore réalisés dans les postes de chargement de wagons citernes. Les efforts doivent porter sur l'intégration plus intime des opérations de chargement dans le complexe mécanographique de la raffinerie. Il est raisonnable de penser en effet que très prochainement, les bons de chargement, acheminés actuellement par porteur, seront élaborés sous forme de cartes perforées. La lecture des cartes, la transmission par télécommande de ces informations jusqu'aux postes de chargement, se feront automatiquement, de même que la centralisation en retour des renseignements fournis par les postes de remplissage. On aboutira ainsi à une organisation mécanographique très centralisée qui facilitera la gestion commerciale de l'entreprise.

DISCUSSION

P. KOCH, *Swiss Federal Office of Weights and Measures, Wildstrasse 3, Berne, Switzerland*

Mr. Montjean has mentioned the possibility of a direct link between the loading system and a data processing machine.

As a member of the Swiss Federal Office of Weights and Measures, I wish to pose a special problem. From the viewpoint of legal technology in such a case at least one output of the data processing system has the significance of the normal scale indication which is found in traditional mechanical balances. This quantity information has always been regarded as one which must be very accurate and reliable. We would therefore expect a certain amount of error correction or error detection in the corresponding data link.

Unfortunately, in many cases similar to the one described here, we find only relatively simple straightforward transmitting systems. I think that this point should receive more attention. Will Mr. Montjean say what trends are known to him concerning this problem, and what are his personal opinions?

F. X. MONTJEAN, *in reply*

In the installation built at Reichstett by the Compagnie Générale d'Automatisme, the weighing system has the following characteristics.

The accuracy required and obtained was 50 kg, the maximum Tare being 8 metric tons and the maximum total weight 120 tons. No device has been put on the mechanical axles of the weighing system, and in all cases the weight is locally determined by an electronic system. There is, therefore, no data link in the weighing system itself.

In future improvements to be made in this installation, there will be a data processing system located at a remote position. Nevertheless, the weight will be computed locally and then transmitted to that data processing equipment, with some kind of error preventing system. In all cases there will always be a kind of 'scale indicator' located in the control room.

The weighing systems described here have been approved by the French 'Service des Instruments de Mesure'.

G. STIKER, *Central Measurement Research Laboratory, Hungary*

What was the accuracy required for measuring the net weight and what was the accuracy obtained in practice?

What was the accuracy required for the percentage of additives and what was the accuracy obtained?

What was the temperature range?

Are there any safeguards against accidental overfilling?

Where are the Tare data obtained? Are they measured or programmed?

F. X. MONTJEAN, *in reply*

The accuracy required for measuring the net weight was 50 kg. This accuracy was obtained in practice. No systematic statistical controls have been developed so far to obtain the standard error.

No better accuracy has been obtained, nor is it required for additives beyond that given by conventional volumetric pumps; these do not give the accuracy required for in-line blending.

With regard to temperature, this question has several aspects. The majority of the products are loaded at ambient temperature; some black products, however, require to be maintained at 140° to 200°C, and for these a set of special loading pipes has been developed with built-in heating systems. Another aspect is that the accounting section gives the loading station the weight of the product to be loaded. A computer is now under development which will compute the volume of a given product at 15°C from a given weight, and *vice versa*.

There is at present no safeguard against overfilling.

In other loading stations at present under construction, there will be such safeguards using either ultrasonic or pneumatic sensing elements.

The Tare of each tanker is weighed as soon as it is positioned on the weighing bridge, and is stored in a memory unit. After loading, a static measure of the total weight is made, and the net weight obtained.

AUTOMATION IN INDUSTRIAL PROCESSES

Le Traitement du Problème d'Optimalisation par A. 110

E. HONORÉ

Summary

This paper is concerned with the optimization of N variables, where N is finite. It is required to minimize (or maximize) an expression $h(x, y, \dots)$ where the N variables x, y, \dots satisfy a certain number of equations $f_i(x, y, \dots) = 0$ and inequalities $g_j(x, y, \dots) \geq 0$ (or ≤ 0).

By using a physical analogy of a problem defined in this way, it is possible to find a criterion which the solution must satisfy. This criterion can be expressed mathematically by a system of N equations which include the partial derivations of f_i, g_j and h and a certain number of parameters constrained to satisfy certain conditions.

The organization of the Analac computer is such that a reversible error distribution system is built up by connecting standard computing units. By choosing suitable computing units, this leads directly to the solution of the above system of N equations.

Two new computing units for optimum and constraint have now been developed and these units produce parameters which satisfy the above-mentioned criterion. These new computing units enable the Analac computer to solve many optimization problems directly from the basic equations.

Sommaire

Dans le présent exposé on considère l'optimalisation d'un nombre fini N de grandeurs et plus exactement on cherche à minimaliser (ou maximaliser) une expression $h(x, y, \dots)$, les N grandeurs x, y, \dots étant par ailleurs assujetties à satisfaire un certain nombre d'équations $f_i(x, y, \dots) = 0$ et d'inéquations $g_j(x, y, \dots) \geq 0$ (ou ≤ 0).

En utilisant une analogie physique du problème ainsi défini il est possible de dégager un critère auquel doit satisfaire la solution du problème. Ce critère se traduit mathématiquement par un système de N équations faisant intervenir les dérivées partielles des expressions f_i, g_j et h et un certain nombre de paramètres assujettis à satisfaire certaines conditions.

L'organisation originale du calculateur A 110, qui permet à l'opérateur de réaliser automatiquement un répartiteur d'erreurs réversible, conduit directement, par le simple fait 'd'écrire' les expressions f_i, g_j et h sur le calculateur à l'aide de blocs de calcul standards, à la réalisation du système de N équations ci-dessus.

La création de deux blocs nouveaux: bloc contrainte et bloc optimum, élaborant les paramètres satisfaisant aux conditions du critère défini précédemment permet donc au calculateur A 110 de traiter directement de nombreux problèmes d'optimalisation en utilisant tout simplement les équations d'origine.

Zusammenfassung

In dieser Arbeit wird die Optimierung von N Größen betrachtet, wobei die Zahl N endlich ist; genauer gesagt, man sucht einen Ausdruck

$h(x, y, \dots)$ minimal (oder maximal) zu machen, wobei die N Größen x, y, \dots einer gewissen Zahl von Gleichungen $f_i(x, y, \dots) = 0$ und Ungleichungen $g_j(x, y, \dots) > 0$ (oder ≤ 0) genügen.

Durch eine physikalische Analogie eines so definierten Problems ist es möglich, eine Bedingung zu finden, der die Lösung genügen muß. Diese Bedingung läßt sich mathematisch durch ein System von N Gleichungen ausdrücken, die die partiellen Ableitungen der Ausdrücke f_i, g_j und h und eine gewisse Anzahl von Parameterbeschränkungen enthalten.

Der Aufbau des Rechners A 110 erlaubt es, mit Hilfe von standardisierten Recheneinheiten selbsttätig abhängig vom jeweils vorhergehenden Fehler (iterativ) die Berechnung auszuführen. Ein einfaches Eingeben der Ausdrücke f_i, g_j und h in den Rechner führt direkt zu Lösungen der oben angegebenen N Gleichungen.

Zwei neue Recheneinheiten für das Optimum und für die Beschränkungen wurden entwickelt. Diese Einheiten ergeben Parameter, die den obigen Bedingungen genügen. Diese neuen Einheiten ermöglichen es, zusammen mit dem Analac-Rechner A 110, viele Optimalwertprobleme direkt aus den zugrunde liegenden Gleichungen zu lösen.

Définition Mathématique du Problème d'Optimalisation

Le terme d'optimalisation à l'heure actuelle s'emploie de plus en plus fréquemment. Suivant les domaines intéressés, il s'applique à des opérations très diverses dans leur forme et dans leur esprit.

Par exemple, dans le cadre de la Recherche opérationnelle, l'optimalisation englobe divers problèmes tels que: optimalisation d'une ou plusieurs grandeurs; optimalisation d'une ou plusieurs fonctions; optimalisation d'un processus.

Il y a d'ailleurs une certaine continuité entre ces problèmes, car pour optimiser par exemple un processus, il suffit souvent d'optimiser un certain nombre de paramètres.

Il convient donc, avant d'aborder le sujet principal de cet exposé, c'est-à-dire le traitement direct du problème d'optimalisation par le calculateur ANALAC 'A 110' de préciser ce que l'on entend ici par 'problème d'optimalisation'.

Il s'agit de problèmes qui sont à priori, limités à l'optimalisation d'un nombre fini de grandeurs, et qui plus précisément encore peuvent être définis comme suit: un certain nombre, N , de grandeurs x, y, \dots étant assujetties à satisfaire, d'une part à un certain nombre, n , d'équations de la forme: $f(x, y, \dots) = 0$

et d'autre part, à un certain nombre, n' , d'inéquations de la forme: $g(x, y, \dots) \geq 0$ (ou ≤ 0) trouver les valeurs de x, y, \dots pour lesquelles une certaine expression: $P \equiv h(x, y, z, \dots)$ est minimale ou maximale.

Le nombre des grandeurs N , celui des équations n , et celui des inéquations n' , n'ont d'autres limites que la suivante: $n < N$. Les fonctions f, g , et h peuvent être des fonctions mathématiques ou empiriques quelconques, de sorte que les possibilités du procédé comprennent tous les cas généralement désignés par les appellations de programmation linéaire et non linéaire. De plus, les fonctions f, g, h , peuvent comporter un certain nombre de paramètres fixes ou variables, par exemple en fonction du temps, de sorte que le procédé s'étend, à la fois, aux problèmes statiques et aux problèmes dynamiques.

Il est d'ailleurs possible de donner du problème d'optimisation ainsi défini, une analogie physique, dans laquelle, on considère que les grandeurs x, y, \dots représentent les coordonnées d'un point M dans un espace à N dimensions.

Ce point M est assujéti: d'une part à appartenir aux n surfaces définies par les équations $f(x, y, \dots) = 0$; d'autre part à demeurer à l'intérieur d'un certain domaine délimité par les n' surfaces définies par les équations $g(x, y, \dots) = 0$; en effet, on peut considérer qu'une inéquation telle que $g(x, y, \dots) \geq 0$, interdit au point M de pénétrer dans une partie de l'espace à N dimensions considéré, la limite étant définie par la surface $g = 0$.

Par ailleurs, le point M est soumis à un champ de forces qui dérive d'un potentiel de valeur $P = h(x, y, \dots)$ et qui a par suite tendance à déplacer le point M de façon à rendre ce potentiel minimum.

Cette analogie physique va permettre de dégager un critère auquel doit satisfaire la solution du problème.

Critère d'une Solution

Pour dégager ce critère, on va considérer successivement les diverses forces qui s'exercent sur le point M .

Ces forces sont dues: d'une part aux réactions des surfaces $f = 0$; d'autre part aux réactions éventuelles des surfaces $g = 0$; et enfin à la réaction du potentiel h .

Si l'on considère d'abord les forces exercées sur le point M du fait des surfaces $f = 0$, il est clair d'une part, qu'elles sont dirigées suivant les normales à ces surfaces et d'autre part, que leurs grandeurs sont toujours telles qu'elles maintiennent impérativement le point M sur les surfaces $f = 0$.

Il en résulte, par exemple pour la force F_i due à la réaction de la surface $f_i = 0$: premièrement, que ses composantes F_{ix}, F_{iy}, \dots sont respectivement proportionnelles aux dérivées partielles $\partial f_i / \partial x, \partial f_i / \partial y$ de la fonction $f_i(x, y, \dots)$ et deuxièmement, que le coefficient de proportionnalité F_i peut être positif, nul ou négatif, mais qu'il est toujours tel que $f_i = 0$.

En d'autres termes, on a

$$\frac{F_{ix}}{\partial f_i / \partial x} = \frac{F_{iy}}{\partial f_i / \partial y} = \dots = F_i$$

avec F_i tel que $f_i(x, y, \dots)$ soit impérativement égal à zéro.

Pour cela, il suffit que F_i soit déduit de f_i par l'intermédiaire d'une fonction de transfert convenable, c'est-à-dire comportant essentiellement une intégration temporelle $F_i = -K \int f_i \cdot dt$.

On peut voir en effet que dans ces conditions l'équilibre n'est possible que pour $f_i = 0$.

Si l'on considère maintenant les forces exercées sur le point M du fait des surfaces $g = 0$, il est clair: d'une part, que ces forces sont nulles dès que la valeur de l'expression $g(x, y, \dots)$ se trouve être différente de zéro et avoir le signe imposé par l'inéquation considérée et d'autre part, que dès que la valeur de l'expression $g(x, y, \dots)$ a tendance à changer de signe (et par suite à ne plus respecter l'inéquation considérée), ces forces ont des valeurs non nulles. Elles sont alors dirigées suivant la normale aux surfaces $g = 0$ et leurs grandeurs sont telles qu'elles interdisent aux expressions $g(x, y, \dots)$ de prendre des valeurs d'un signe contraire à celui imposé par l'inéquation correspondante.

Il en résulte par exemple pour la force G_j due à la réaction de la surface $g_j = 0$ (en supposant que l'inéquation considérée est $g_j \geq 0$): premièrement, que ses composantes G_{jx}, G_{jy} sont respectivement proportionnelles aux dérivées partielles $\partial g_j / \partial x, \partial g_j / \partial y$ de la fonction $g_j(x, y, \dots)$ et deuxièmement, que le coefficient de proportionnalité G_j , d'une part est nul lorsque le point M est dans la partie du domaine où on a

$$g_j(x, y, \dots) > 0$$

d'autre part est positif ou nul lorsque le point M est au contact de la surface $g_j = 0$. Il est alors tel qu'il interdit à l'expression $g_j(x, y, \dots)$ de devenir négative; il empêche en quelque sorte le point M de traverser la surface $g_j = 0$. En d'autres termes, on a:

$$\frac{G_{jx}}{\partial g_j / \partial x} = \frac{G_{jy}}{\partial g_j / \partial y} = \dots = G_j$$

avec $G_j = 0$ si $g_j > 0$. Si au contraire $g_j = 0$, $G_j \geq 0$ et tel que $g_j(x, y, \dots)$ ne puisse devenir négatif. Pour cela il suffit que G_j soit déduit de g_j par l'intermédiaire d'une sorte de fonction de transfert comportant essentiellement une intégration temporelle

$$G_j = -K \int \gamma_j \cdot dt$$

et une commutation telle que la grandeur γ_j soit égale à la plus petite (au sens algébrique du terme) des deux valeurs G_j et g_j .

On pourrait voir en effet que dans ces conditions l'équilibre n'est possible que dans l'un ou l'autre des deux états suivants:

(a) Si $G_j > g_j$ on a $\gamma_j = g_j$ et par suite $G_j = -K \int g_j \cdot dt$; de sorte que l'équilibre n'est possible que pour $g_j = 0$;

(b) Si $G_j < g_j$ on a $\gamma_j = G_j$ et par suite $G_j = -K \int G_j \cdot dt$; de sorte que l'équilibre n'est possible que pour $G_j = 0$.

On a considéré le cas où $g_j \geq 0$, mais il est bien évident que le raisonnement se transpose aisément au cas où $g_j \leq 0$ et conduit à:

$$G_j = 0 \quad \text{si } g_j < 0$$

et si au contraire $g_j = 0$, $G_j \leq 0$ et tel que $g_j(x, y, \dots)$ ne puisse devenir positif.

Si l'on considère maintenant la force exercée sur le point M du fait du champ de forces dérivant du potentiel $h(x, y, \dots)$ il est clair, d'une part qu'elle est dirigée suivant la normale à la surface équipotentielle: $h(x, y, \dots) = \text{constante}$, passant par le point M , et d'autre part, qu'elle tend à faire décroître l'expression $f(x, y, \dots)$.

Il en résulte: premièrement que ses composantes H_x, H_y, \dots sont respectivement proportionnelles aux dérivées partielles $\partial h / \partial x, \partial h / \partial y, \dots$ de la fonction $h(x, y, \dots)$ et deuxièmement que le coefficient de proportionnalité H a le signe voulu pour tendre à faire varier l'expression $h(x, y, \dots)$ dans le sens désiré.

En d'autres termes, on a :

$$\frac{H_x}{\partial h / \partial x} = \frac{H_y}{\partial h / \partial y} = \dots = H$$

le signe de H étant positif si $h(x, y, \dots) = \max$; négatif si $h(x, y, \dots) = \min$. et sa grandeur pouvant à priori être quelconque. Pratiquement dans le montage utilisé, on adoptera pour H une valeur constante.

Il est clair que le point M ne peut se fixer à une position d'équilibre que lorsque la somme des forces qui lui sont appliquées est nulle, autrement dit lorsque l'on a :

$$\left. \begin{aligned} \sum F_{ix} + \sum G_{jx} + H_x &= 0 \\ \sum F_{iy} + \sum G_{jy} + H_y &= 0 \\ \dots \end{aligned} \right\} N \text{ relations}$$

Au total, il apparaît donc que la solution cherchée est caractérisée par l'ensemble des équations et conditions ci-après :

$$\left. \begin{aligned} \sum F_i \frac{\partial f_i}{\partial x} + \sum G_j \frac{\partial g_j}{\partial x} + H \frac{\partial h}{\partial x} &= 0 \\ \sum F_i \frac{\partial f_i}{\partial y} + \sum G_j \frac{\partial g_j}{\partial y} + H \frac{\partial h}{\partial y} &= 0 \\ \dots \end{aligned} \right\} N \text{ equations}$$

(i variant de 1 à n et j de 1 à n').

Chacun des coefficients F_i doit être tel que $f_i(x, y, \dots) = 0$. Les expressions $g_j(x, y, \dots)$ intervenant dans les inéquations de la forme $g_j \geq 0$ peuvent être positives ou nulles; dans le premier cas, le coefficient G_j qui leur correspond doit être nul; dans le second cas il doit être positif ou nul et tel que g_j ne devienne pas négatif. Les expressions $g_j(x, y, \dots)$ intervenant dans les inéquations de la forme $g_j \leq 0$ peuvent être négatives ou nulles; dans le premier cas, le coefficient G_j qui leur correspond doit être nul; dans le second cas, il doit être négatif ou nul et tel que g_j ne devienne pas positif. Le coefficient H est positif si l'expression $h(x, y, \dots)$ doit être maximale, et négatif si l'expression $h(x, y, \dots)$ doit être minimale.

On va voir dans ce qui suit que du fait de son organisation et plus particulièrement de la présence de son répartiteur d'erreurs réversible, le calculateur A 110 réalise tout naturellement le système de N équations ci-dessus.

Rappel

Il n'est pas question ici de présenter en détail les caractéristiques de la technique ANALAC (voir articles de Honoré, Torcheux et Uffler dans la revue française 'l'Onde Electrique' numéros d'octobre et décembre 1960). On se bornera simplement, pour faciliter la compréhension de ce qui suit, à rappeler quelques unes de ses propriétés fondamentales.

Cellule de Calcul

La cellule de calcul ANALAC utilise des tensions et intensités alternatives de fréquence fixe de l'ordre de 500 kHz. Elle est composée uniquement de selfs et de capacités disposées symétriquement de telle sorte que la cellule, vue de l'entrée ou de la sortie, se présente exactement de la même façon.

Son fonctionnement est tel que la tension et l'intensité de sortie, V_s et I_s , sont liées à la tension et à l'intensité d'entrée, V_e et I_e , par les relations :

$$V_s = \frac{I_e}{A} \quad \text{et} \quad I_s = A \cdot V_e$$

A étant une admittance réactive, dite admittance caractéristique de la cellule.

Mais étant donné la symétrie de la cellule, ces relations sont toutes réversibles et peuvent tout aussi bien se lire

$$V_e = \frac{I_s}{A} \quad \text{et} \quad I_e = A \cdot V_s$$

Une telle cellule n'a donc pas de sens de fonctionnement privilégié: elle est *réversible*.

Répartiteur d'Erreurs

La réversibilité des cellules de calcul permet entre autres applications la résolution automatique de systèmes d'équations implicites grâce au répartiteur d'erreurs.

La réalisation et la mise en œuvre de ce répartiteur d'erreurs sont illustrées par le schéma de la Figure 1 dans le cas particulier où on a 3 équations à 3 inconnues

$$f(x, y, z) = 0$$

$$g(x, y, z) = 0$$

$$h(x, y, z) = 0$$

Trois servomécanismes S_m, S_y, S_z sont essentiellement destinés à élaborer les valeurs instantanées x, y, z des variables.

A partir de ces valeurs, un premier réseau de calcul (réseau I) élabore les tensions représentatives des grandeurs $f(x, y, z)$, $g(x, y, z)$, $h(x, y, z)$.

Un second réseau de calcul (réseau II) reçoit les tensions représentatives des grandeurs f, g, h , et élabore 3 tensions $\delta x, \delta y, \delta z$ qui sont utilisées pour commander respectivement les servomécanismes S_m, S_y, S_z .

C'est ce réseau II qui constitue le répartiteur d'erreurs; il est essentiellement constitué par les cellules représentées sur la figure; trois de ces cellules sont fixes et de valeur unité, les neuf autres sont variables sous l'action des grandeurs x, y, z , à l'aide de dispositifs non représentés sur la figure et leurs admittances caractéristiques sont respectivement égales aux dérivées partielles des expressions f, g, h par rapport à chacune des variables x, y, z .

Du fait même de la réversibilité des cellules de calcul, les tensions $\delta x, \delta y, \delta z$ sont alors définies par les équations suivantes :

$$\delta x \cdot \frac{\partial f}{\partial x} + \delta y \cdot \frac{\partial f}{\partial y} + \delta z \cdot \frac{\partial f}{\partial z} = -f(x, y, z)$$

$$\delta x \cdot \frac{\partial g}{\partial x} + \delta y \cdot \frac{\partial g}{\partial y} + \delta z \cdot \frac{\partial g}{\partial z} = -g(x, y, z)$$

$$\delta x \cdot \frac{\partial h}{\partial x} + \delta y \cdot \frac{\partial h}{\partial y} + \delta z \cdot \frac{\partial h}{\partial z} = -h(x, y, z)$$

et on peut voir par suite qu'elles représentent au deuxième ordre près, l'écart entre les valeurs instantanées x, y, z des variables et les valeurs x_s, y_s, z_s de la solution du système considéré.

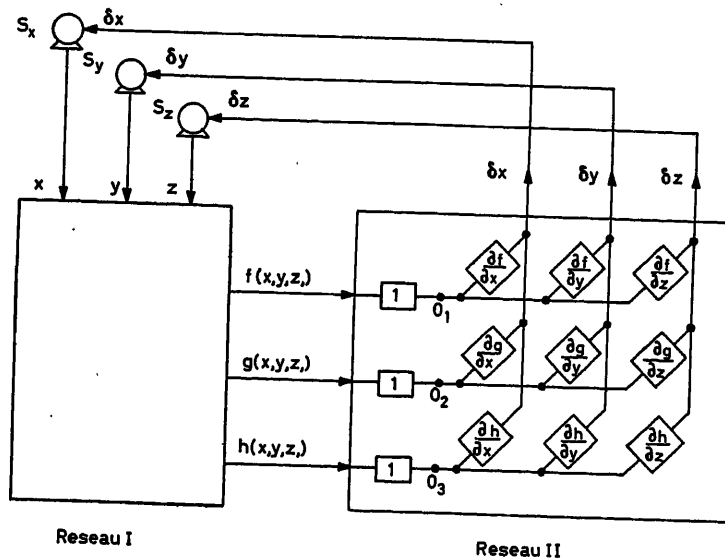


Figure 1

Il en résulte en particulier que les servomécanismes se stabilisent automatiquement sur les valeurs $x = x_s$; $y = y_s$; $z = z_s$, c'est-à-dire pour la solution du système. Il est à signaler par ailleurs que dans le cas où on a plus d'équations que d'inconnues (équations surabondantes), le répartiteur d'erreurs amène automatiquement les inconnues à des valeurs optimales en ce sens qu'elles satisfont au critère de Newton (somme des carrés des erreurs minimale). Enfin il est à noter que, dans tous les cas, les boucles de commande des divers servomécanismes sont complètement découplées et ont un gain constant.

On obtient ainsi une solution automatiquement stable.

Organisation du Calculateur A 110

Le calculateur A 110 est essentiellement constitué par un meuble support dans lequel l'utilisateur place des blocs de calcul mobiles.

Parmi ces blocs de calcul, certains dits 'blocs facteurs' élaborent les différents facteurs, constantes ou variables; d'autres dits 'blocs algébriques' permettent 'd'écrire' les équations mathématiques comme sur un tableau noir.

Parmi les blocs algébriques on distingue d'une part les 'blocs monômes' (un bloc monôme correspond à un terme de l'équation), d'autre part, le 'bloc Egalité' qui réalise le signe (=) ou (= 0).

Il est important de noter que le simple fait 'd'écrire' sur le calculateur à l'aide de 'blocs algébriques' les équations $f = 0$, $g = 0$ et $h = 0$ et de raccorder les blocs monômes aux blocs facteurs correspondants conduit automatiquement à la réalisation du schéma de la Figure 1. En d'autres termes sans qu'il ait à s'en préoccuper, l'opérateur a réalisé simultanément le réseau de calcul direct (réseau I) et le répartiteur d'erreurs (réseau II), les 'blocs Egalité' réalisant les liaisons voulues entre les deux réseaux.

Résolution du Problème d'Optimalisation

On va voir maintenant que les propriétés rappelées ci-dessus permettent au calculateur A 110 de résoudre directement les

problèmes d'optimalisation tels qu'ils ont été définis précédemment.

La Figure 2 donne le schéma du montage utilisé à cet effet.

Ce montage comporte essentiellement: N servomécanismes: S_1, S_2, \dots, S_N ; un premier réseau de calcul (réseau I); des dispositifs intermédiaires D_{f_i}, D_{g_j}, D_h ; un deuxième réseau de calcul (réseau II) qui est essentiellement constitué par des cellules variables dont les admittances caractéristiques sont égales aux dérivées partielles des expressions $f_i(x, y, \dots)$, $g_j(x, y, \dots)$, $h(x, y, \dots)$ par rapport à chacune des N variables x, y, \dots (Le cas échéant ces cellules sont donc commandées par les grandeurs x, y, \dots à l'aide de connexions non représentées sur la figure.)

Il est à noter que, de même que pour le répartiteur d'erreurs, le simple fait 'd'écrire' sur le calculateur les expressions $f_i(x, y, \dots)$; $g_j(x, y, \dots)$; $h(x, y, \dots)$ à l'aide de blocs monômes conduit automatiquement à la réalisation des réseaux I et II de la Figure 2. Par ailleurs, les dispositifs intermédiaires se placent de la même façon que les blocs Egalité.

En ce qui concerne le fonctionnement de ce montage: Les N servomécanismes élaborent les valeurs instantanées des N variables x, y, \dots ; le réseau I élabore à partir de ces valeurs instantanées les tensions représentatives des grandeurs $f_i(x, y, \dots)$, $g_j(x, y, \dots)$, $h(x, y, \dots)$; les dispositifs D_{f_i} et D_{g_j} reçoivent les tensions f_i et g_j et élaborent à partir de ces tensions des tensions F_i et G_j ; le dispositif D_h fournit une tension H (Le processus de fonctionnement de ces divers dispositifs sera examiné plus loin); et le réseau II reçoit les diverses tensions F_i, G_j et H ; il en résulte, conformément à la théorie générale des cellules rappelée précédemment, l'apparition d'intensités I_x, I_y, \dots en chacune des sorties du réseau II; ces intensités étant telles que:

$$I_x = \sum F_i \frac{\partial f_i}{\partial x} + \sum G_j \frac{\partial g_j}{\partial x} + H \frac{\partial h}{\partial x}$$

$$I_y = \sum F_i \frac{\partial f_i}{\partial y} + \sum G_j \frac{\partial g_j}{\partial y} + H \frac{\partial h}{\partial y}$$

...

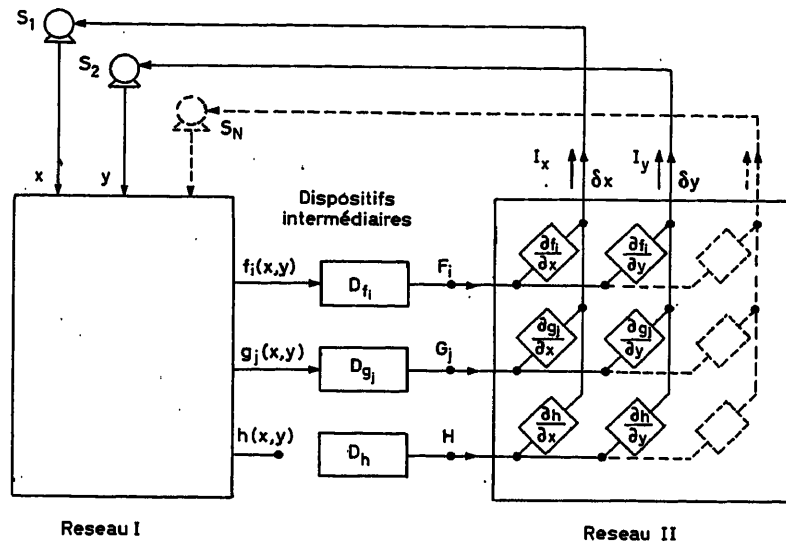


Figure 2

Les sorties du réseau II étant branchées directement sur les entrées des N servomécanismes, les intensités ci dessus débitent sur des résistances R de valeur très grande (supposée la même pour toutes); il en résulte l'apparition de tensions δx , δy , ..., aux diverses sorties du réseau II avec:

$$\delta x = R \cdot I_x$$

$$\delta y = R \cdot I_y$$

...

Il est évident que les servomécanismes S_1, \dots, S_N ne peuvent se fixer à une position d'équilibre que si les tensions $\delta x, \delta y, \dots$ donc que si les intensités I_x, I_y sont nulles, c'est-à-dire si on a:

$$\left. \begin{aligned} \sum F_i \frac{\partial f_i}{\partial x} + \sum G_j \frac{\partial g_j}{\partial x} + H \frac{\partial h}{\partial x} &= 0 \\ \sum F_i \frac{\partial f_i}{\partial y} + \sum G_j \frac{\partial g_j}{\partial y} + H \frac{\partial h}{\partial y} &= 0 \\ \dots \end{aligned} \right\} N \text{ équations}$$

Ce système de N équations étant identique à celui établi précédemment lors de l'étude du critère de la solution du problème au-dessus, il en résulte que les valeurs x, y, \dots élaborées par les servomécanismes constituent une solution du problème d'optimisation considéré.

Il ne reste plus qu'à examiner comment les dispositifs intermédiaires D_{f_i}, D_{g_j}, D_h réalisent les conditions particulières intéressant les grandeurs F_i, G_j et H . Cela fait l'objet du chapitre suivant.

Rôle, Constitution et Fonctionnement des Dispositifs Intermédiaires

Dispositif D_h

Il a pour rôle d'élaborer la tension H .

On a vu que cette tension a une valeur constante, négative lorsque l'expression $h(x, y, \dots)$ doit être minimale, positive lorsque cette expression doit être maximale.

Plus précisément, cette valeur est relativement faible, juste

suffisante pour assurer aux boucles des divers servomécanismes un gain convenable.

Le dispositif D_h est donc essentiellement une simple source de tension fixe. (Par ailleurs, il permet également de connaître la valeur de l'expression $h(x, y, \dots)$.)

Dans l'organisation ANALAC, il est réalisé sous forme d'un bloc de calcul, dit bloc 'Optimum' qui s'utilise de la même façon qu'un bloc Egalité.

Dispositif D_{f_i}

Ce dispositif a pour rôle de réaliser entre les grandeurs f_i et F_i la fonction de transfert convenable indiquée au-dessus.

En pratique, on réalise la fonction de transfert

$$F_i = - \int f_i \frac{dt}{\tau} - f$$

La constante de temps τ étant de l'ordre de la milliseconde; le terme $-f_i$ joue le rôle d'un circuit correcteur et permet le passage de signaux rapides, assurant ainsi en association avec la réversibilité du réseau II la parfaite stabilité des solutions (comme pour le répartiteur d'erreurs).

Schématisé par la Figure 3, le dispositif D_{f_i} comporte essentiellement: une voie directe avec inversion de signe (ampli -1); une voie intégration avec un intégrateur rapide (constante de temps de l'ordre de la milliseconde); un dispositif additionneur pour faire la somme des résultats des 2 voies et fournir F_i .

Dans l'organisation ANALAC, ce dispositif est réalisé par l'association de 2 blocs de calcul — d'une part, un bloc SM

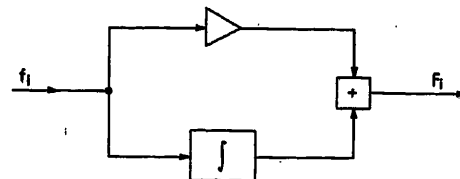


Figure 3

Standard qui assure l'intégration rapide, et d'autre part, un bloc dit bloc 'Contrainte' qui réalise tout le reste et qui s'utilise comme un bloc Egalité.

Dispositif D_{oj}

Ce dispositif a pour rôle de réaliser entre les grandeurs g_j et G_j la fonction de transfert particulière indiquée au-dessus avec les commutations convenables.

En pratique, pour les mêmes raisons que dans le cas du dispositif D_{fi} , on réalise l'opération

$$G_j = - \int \gamma_j \frac{dt}{\tau} - g_j$$

τ étant toujours de l'ordre de la milliseconde et γ_j étant égal à la plus petite (au sens algébrique du terme) des deux valeurs G_j et g_j .

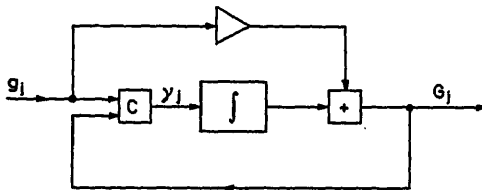


Figure 4

Schématisé par la Figure 4, le dispositif D_{oj} comporte essentiellement: une voie directe avec inversion de signe (ampli - 1); un dispositif commutateur C qui reçoit les deux tensions G_j et g_j et élabore la tension γ_j (ce dispositif est réalisé à l'aide de diodes); une voie intégration avec un intégrateur rapide alimentée par la tension γ_j , et un dispositif additionneur pour faire la somme des résultats des 2 voies et fournir G_j .

Bien entendu, cela s'applique au cas où on a $g_j(x, y, \dots) \geq 0$; dans le cas où on a $g_j(x, y, \dots) \leq 0$, il suffit de prendre pour

tension γ_j la plus grande (au sens algébrique du terme) des deux tensions G_j et g_j .

En fait dans l'organisation ANALAC, le bloc 'Contrainte' vu plus haut comporte toujours le dispositif de commutation à diodes C .

Il lui est donc possible, par simple commutation et toujours en association avec un bloc SM de jouer soit (a) le rôle d'un dispositif D_{fi} , (b) le rôle d'un dispositif D_{oj} avec $g_j \geq 0$ et (c) le rôle d'un dispositif D_{oj} avec $g_j \leq 0$.

Conclusion

Du fait de ses caractéristiques particulières, le calculateur A110 se prête tout naturellement au traitement des systèmes d'équations surabondantes, même si ces systèmes comportent à la fois des équations approchées et des équations ou inéquations rigoureuses.

Mais ses possibilités dans le cadre des problèmes d'optimisation vont beaucoup plus loin puisqu'il donne à ses utilisateurs le moyen de traiter tous les problèmes comportant des combinaisons quelconques de conditions de maximum ou de minimum, d'équations ou d'inéquations.

Il est à préciser que ces propriétés s'appliquent à des problèmes comportant un grand nombre de variables et un grand nombre d'équations et inéquations linéaires ou non linéaires.

Elles s'appliquent également lorsque le problème comporte des paramètres variables en fonction du temps c'est-à-dire aux problèmes dynamiques.

Il est à noter en outre, que quelle que soit la complexité du problème considéré, la stabilité des solutions est toujours parfaitement assurée.

Il est à remarquer enfin que le travail de l'opérateur est particulièrement aisé puisqu'il lui suffit de porter sur la machine les expressions, équations et inéquations du problème, et ceci sous la forme même où elles se présentent.

Automation of a Portland Cement Plant Using a Digital Control Computer

R. A. PHILLIPS

Summary

A Portland cement plant consists of quarry, raw mix, blending and grinding, kiln burning, clinker grinding and packing and shipping departments through which material flows sequentially. The computer keeps a perpetual inventory of the quarry (three-dimensional model) so that it can direct the digging and blasting operation to meet plant and company objectives. The computer calculates the proper proportions of the several raw materials, using data obtained from an on-line X-ray chemical analysis of the mixture, thus closing the loop. The kilns are controlled automatically, using an analytically-determined model of the chemical-thermodynamic process. The model and the complex rules for control during kiln start-up, normal operation, and corrective action during upsets are stored in and executed by the computer. The efficiency of operation is calculated and recorded, off-normal alarms scanned and recorded, and records kept of down time in each of the departments. Management operating reports are prepared and typed on-line in the form of hourly logs.

Most of the closed-loop computer control is in the blending and kiln departments. A major part of the paper is devoted to the development of the process model through analysis and plant tests of the kiln and the application of the digital computer to its control.

Sommaire

Une usine de ciments Portland se compose d'une section-carrière, d'un atelier pour le mélange, le dosage et le broyage des matières premières, d'un atelier de calcination en fours et de broyage des scories et d'ateliers d'emballage et d'expédition, à travers lesquels les matières traitées circulent successivement. La calculatrice tient un inventaire perpétuel de la carrière (modèle tridimensionnel), de sorte qu'elle permet de diriger les opérations de forage et de tir pour réaliser les objectifs de l'usine et de la compagnie. La calculatrice détermine les proportions justes des diverses matières premières en utilisant les données obtenues par une analyse chimico-radiographique du mélange sur «chaîne de production», fermant ainsi la boucle. Les fours sont commandés automatiquement en employant un modèle du procédé chimico-thermodynamique déterminé analytiquement. Le modèle et les règles compliquées de commande pendant la mise en route des fours, en marche normale et pour la correction des dérangements éventuels sont emmagasinés et mis en œuvre par la calculatrice. En outre, cette machine calcule et enregistre le rendement de marche, scrute et enregistre les alarmes d'anomalies et tient les dossiers des temps d'arrêt dans chacun des ateliers. Elle prépare et dactylographie des rapports d'exploitation pour la Direction, sur la «chaîne de production», sous la forme d'enregistrements horaires.

La plupart des opérations de commande par calculatrice en boucle fermée s'effectue dans les ateliers de dosage et de calcination en fours. Une grande partie du présent mémoire est consacrée au développement du modèle de ce procédé au moyen d'essais analytiques et d'épreuves sur fours à l'usine, ainsi qu'à l'application de la calculatrice arithmétique à la commande de ces derniers.

Zusammenfassung

Der Fertigungsablauf einer Portlandzementfabrik beginnt beim Steinbruch und führt über Brechen, Mischen und Mahlen, Brennen, Mahlen des Sinterproduktes, Abpacken und Versand. Ein Rechner

sorgt für dauernde Bestandsaufnahme des Steinbruches (dreidimensionales Modell), um die Förder- und Sprengarbeiten im Sinne der Werks- und Geschäftszielsetzungen lenken zu können. Er berechnet die richtigen Anteile der verschiedenen Rohstoffe auf Grund der Meßergebnisse eines direkt in den Regelkreis eingeschalteten Prozeßanalysators (Röntgenanalyse der Mischung). Zur Regelung der Brennöfen wird ein analytisches Modell des chemisch-thermodynamischen Prozesses verwendet. Das Modell und die komplizierten Steuerbefehle für das Anfahren des Ofens, seinen Normalbetrieb und den Eingriff bei betriebsmäßigen Störungen sind im Rechner gespeichert und werden von ihm durchgeführt. Die Wirtschaftlichkeit des Ablaufes, die Überschreitung von Grenzwerten und die Stillstandszeit jeder Abteilung werden erfaßt und aufgeschrieben. Zwischenberichte für die Betriebsleitung werden stündlich aufgestellt.

Das Regelrechnergerät ist vor allem beim Mischen und Brennen eingesetzt. Der Beitrag befaßt sich hauptsächlich mit der Entwicklung des Modelles durch Untersuchung und Betriebsversuche am Ofen und mit der Anwendung des Digitalrechners für dessen Regelung.

Introduction

A Portland cement plant provides an unusual application of an on-line digital control computer for several reasons, for example: (1) Since there is a single product manufactured in the plant, it is logical to handle the total operation in a coordinated fashion by a single computer. (2) Since very few plants have sufficient need for either an off-line business or scientific computer, some of the tasks which are philosophically thought to be off-line types are included in the on-line machine. (3) The long process times (several minutes to hours) associated with the process permit a large excess of computer time for operation of typewriters to alarm plant operators and to prepare management reports on-line.

A very important function is the faithful recording of plant data as it occurs to give management an uncoloured picture of actual operating conditions. How often have we seen operator's logs with data and comments chosen by plant-operating rules rather than what actually exists?

It would be pointless to describe the automation of a Portland cement plant without having a particular plant in mind. The particular installation was made in 1962-63 and the feasibility, testing and design of the computer programme are now complete and the following is a discussion of that programme.

Although this paper describes the way in which a digital control computer is applied in a Portland cement plant, the author feels that technically inclined control engineers will be primarily interested in the large part that the analytical approach plays in making an application successful.

There is a great emphasis upon approaching process control by the use of data loggers. Theoretically, it is possible to discover the dynamics of a process if all variables can be measured, but where this cannot be accomplished or the process is extremely noisy (a rotary cement kiln qualifies on both counts), the analytical approach is much more promising. All processes follow the laws of Nature; discovering those laws is the job of an analytical engineer.

The rotary kiln is very complicated to analyse; therefore the analysis is described here in detail. The problem of raw mix blending is also of great interest, but since it has already been described adequately by Adams *et al.*¹, it is mentioned only briefly here so that the description of the computer application will be complete.

The functions to be performed by the computer will be described by proceeding through the plant departments in the order of material flow, quarry, crusher, mix rock, raw mix, raw grind, kiln, and finish grinding. Figure 1 shows the material flow in a typical dry process plant.

Quarry Department

The quarry is divided into cubes and each cube is numbered. Information as to volume, chemical analysis, location in the quarry and date of analysis are stored on cards. The chemical analysis for areas which have not yet been mined is projected from core drillings. As an area is mined, a more representative sample is obtained and analysed and a new card containing this information is prepared.

Since it is not physically possible to develop all areas of the quarry at all times, only a portion of the inventory need be stored in the computer. The computer is periodically interrogated to find out how to direct the digging and blasting operations to meet plant and company objectives with regard to production, cost, and quarry life extension.

Crusher Department

Kilowatt hours and tons of production are metered and read by the computer. Kilowatt hours per ton are calculated and logged hourly as a measure of department efficiency.

Bearing temperatures in the crusher and impactors are monitored continuously; excessive temperatures actuate visual and audible displays. The computer monitors the displays and types out location, cause, and time of the alarm, and in addition it records downtime; thus, management has a faithful record of bearing problems.

Mix Rock

The quarry consists of deposits of rock high in calcium carbonate (hi-lime), rock high in magnesium carbonate (hi-mag), and rock high in alumina (shale). Portland cement specifications permit only a small proportion of magnesium. It is more economical to make cement from quarry rock than to throw the rock away, therefore, in many plants it is found that the magnesium proportion must be at or near the maximum permitted in order to utilize all of the quarry material.

Since the product of the quarry is not uniform in chemical composition, there is a preliminary blending to form 'mix rock'. A laboratory X-ray spectograph is used to analyse periodic grab samples. The chemist enters the analysis results into the computer and it calculates the proper proportions of hi-lime, hi-mag, and shale. This preliminary 'smoothing' of the quarry variations has a great influence upon how close to target the raw mix blending can be held.

Raw Mix Blend

Raw mix blending is performed by proportioning mix rock, hi-lime, hi-mag, shale, iron ore, and silica, grinding the composite, and then homogenizing the result in a silo of many hours capacity. Since chemical analysis (either by traditional wet

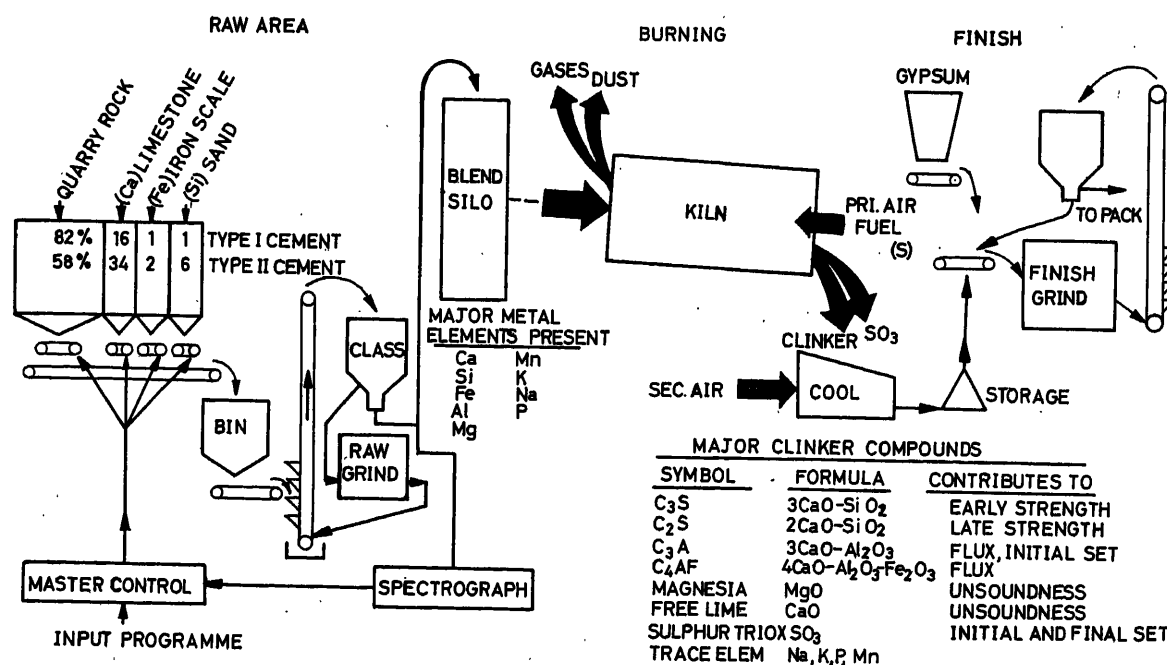


Figure 1

chemistry methods or by X-rays) must be performed upon finely ground samples, it is not practical to measure the composition of the constituents passing through the proportioning feeders. Thus, the composite must be analysed after it has been through the grinding. This is done by passing a portion of the stream through an on-line X-ray analyser. Such analysers are now operating successfully in three cement plants, including that under discussion. The chemical composition and rate of flow from each feeder is read by the computer periodically. The computer then must predict what the ultimate composition in the silo will be (taking dynamics of mixing into account) and adjust the proportioning feeders (taking dynamics of grinding, sampling, and transport into account) to keep the ultimate composition close to target. Portland cement specifications cover more compounds than there are different materials in the proportioning feeders; thus in some cases there may be no possibility of making the mix called for by the chemist. The computer recognizes this when it calculates negative setting for one or more of the proportioning feeders; types out this fact, and the chemist must select new set points. The computer then calculates new feeder settings and adjusts their set points.

Raw Grind Department

The computer performs the same type of logging and alarm function as it does for the Crusher Department.

Kiln Department

A large portion of the computer capacity is allocated to this department since there are many functions to be performed. Since virtually all of this capacity is devoted to closed-loop control, at least indirectly, it will be described in considerable detail.

Analytical Determination of Process Model

The idea of applying the theoretical or analytical approach to a rotary cement kiln is not new. The early authors²⁻⁵ were interested in obtaining heat balances. Papers by Costa⁶ and Schink⁷ at the First IFAC Conference dealt with kiln control, but were not analytical in content. Min *et al.*⁸ described an analytical approach to kiln dynamics, but the equations reflected the fact that the purpose of their work was the study of effectiveness of drying agents in the slurry, not control. It is believed that this is the first time a study of kiln dynamics directed toward obtaining a kiln model for control has been reported.

Several years ago work was initiated by the author to develop the dynamic equations to describe the chemical and thermodynamic process which takes place in the rotary cement kiln. The most important of the chemical reactions are combustion of the fuel, the endothermic reactions of driving water vapour from the mix and the dissociation of calcium carbonate into carbon dioxide and calcium oxide and exothermic reaction of the formation of cement clinker. Figure 2 shows these reactions in a kiln.

Heat is transferred to the mix by radiation and convection from the gas to the load directly, and by radiation and convection to the refractory lining, and from it to the mix by radiation and conduction. Throughout the whole kiln length the radiation from the gas stream is by gas radiation (interatomic vibration of the heteropolar molecules). The amount of radiation

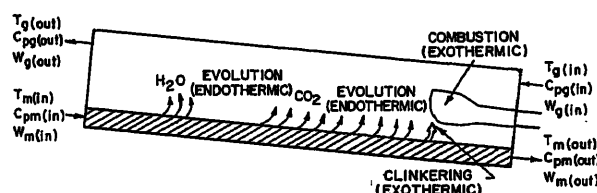


Figure 2. Chemical reaction in rotary cement kiln

depends upon the gas temperature and upon its chemical state. The composition of the gas stream, in turn, depends upon the products of combustion and the amounts of water vapour and carbon dioxide released upstream from the particular cross section of the kiln. The early writings of Professor Hottel of Massachusetts Institute of Technology (such as in *Industrial and Engineering Chemistry*, August 1927) are classics in the field of gas radiation.

The author knows of no writings describing a flame from the dynamic point of view. Therefore, a description of the representation used is of some interest. A natural gas flame is only slightly luminous. Spectral analysis indicates that this is largely line radiation created by elements from the solid feed which are volatilized. The strongest lines are those of potassium, calcium, and sodium. To be an important mechanism for heat transfer the radiation spectrum must be substantially continuous. Thus, for natural gas flames, only the gas radiation has been included. It is assumed that the kilocalories released by combustion are proportional to unit flame length. Heat transfer in the longitudinal direction was neglected.

Where fuel is oil or coal, there is continuous radiation from the luminous flame. The amount of this radiation depends upon the size of the unburned coal particle or oil droplet at a particular cross section. Hottel has treated the coal particles as a large number of equivalent spheres, the diameter of which depends upon the fineness to which the coal is ground. As these particles are burned in moving up the kiln, the amount of 'black body' radiation decreases. The equations developed by Hottel were used for calculation of amounts of radiation as a function of combustion. Coal contains volatiles which burn rapidly. The number of kilocalories associated with their combustion were assumed to be released in the first 10 per cent of the flame. The remaining calories were assumed to be released proportional to unit flame length. It was assumed that all the coal particles are at the same temperature, i.e. flame temperature. This temperature is determined from the gas temperature at the end of the flame—a common assumption. A similar approach can be developed for oil flames; however, the author has not been concerned with kilns where oil is a principal fuel.

The equations which describe the kiln behaviour are non-linear partial differential equations. In order to solve these equations the kiln was broken into 50 short sections or nodes and difference equations were written for each section. These can be shown to be identical to the approach of writing the partial differential equations in time and space and then applying standard numerical techniques to their solution. It may be of interest to consider the nature of these difference equations for a particular section of the kiln. For the sake of simplicity in illustration, consider a section where the solid material has already been dried and has not yet started to dissociate into carbon dioxide and calcium oxide. At this cross section the combustion of the fuel may be considered to be complete.

Figure 3 shows a small length, l , of the kiln (one-fiftieth of the total kiln length). For ease of notation, assume this is between nodes (or cross sections) 3 and 4.

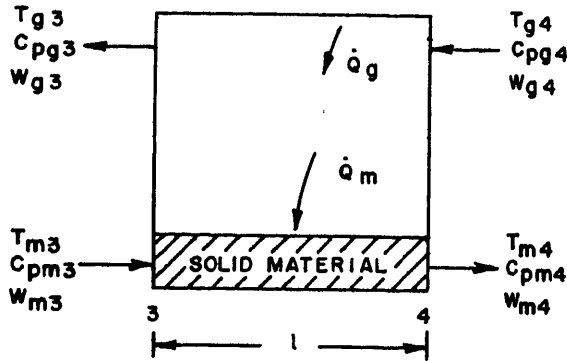


Figure 3. Heat balances across small kiln section

The heat flow per minute associated with the material flow leaving at 4 will be:

$$\begin{aligned} & C_{pm4} W_{m4} T_{m4} \\ &= C_{pm3} W_{m3} T_{m3} + \dot{Q}_m - \left(\frac{T_{m3} + T_{m4}}{2} \right) C_{pd} (W_{m3} - W_{m4}) \\ & \quad - \tau_{m34} \frac{d}{dt} \left(\frac{C_{pm3} W_{m3} T_{m3} + C_{pm4} W_{m4} T_{m4}}{2} \right) \end{aligned} \quad (1)$$

where C_{pm3} , C_{pm4} = specific heats of material (kcal/kg-°C); C_{pd} = specific heat of dissociated gas evaluated at the average material temperature (kcal/kg-°C); W_{m3} , W_{m4} = flow rates of material (kg/min); T_{m3} , T_{m4} = temperatures of material (°C); \dot{Q}_m = heat added to material (radiation, convection, conduction) (kcal/min); τ_{m34} = propagation time of material through section (min); and d/dt = differential with respect to time (min).

The last term of eqn (1) is of some interest since it represents the time rate of change of the heat stored in the material lying between 3 and 4 as viewed from a stationary reference point. Perfect mixing of the material is assumed. The kiln is said to be in steady state when this and its corresponding term in each section is zero.

The equations developed here do not include any terms to account for heat of reaction or vaporization. Where the reactions are endothermic it was assumed that the reactions are not isothermal but occur over a small temperature range. Since the heat of reaction (kcal/kg) is known, a pseudo specific heat may be calculated for the range of temperature assumed for the chemical reaction. This is equivalent to assuming that the rate of reaction is proportional to the rate of heat input. Thus eqn (1) may be used directly. It is assumed that the exothermic reaction of clinkering occurs in one kiln cross section (although it may move across section boundaries during a transient). The amount of heat released was included as an added term in this cross section.

Similarly, the heat flow per minute associated with the gas flow leaving at 3 will be:

$$\begin{aligned} & C_{pg3} W_{g3} T_{g3} \\ &= C_{pg4} W_{g4} T_{g4} - \dot{Q}_g + \left(\frac{T_{m3} + T_{m4}}{2} \right) C_{pd} (W_{m3} - W_{m4}) \\ & \quad - \tau_{g43} \frac{d}{dt} \left(\frac{C_{pg3} W_{g3} T_{g3} + C_{pg4} W_{g4} T_{g4}}{2} \right) \end{aligned} \quad (2)$$

where C_{pg3} , C_{pg4} = specific heats of gas stream (kcal/kg-°C); W_{g3} , W_{g4} = flow rates of gas stream (kg/min); T_{g3} , T_{g4} = temperatures of gas stream (°C); \dot{Q}_g = heat given up by stream (radiation, convection) (kcal/min); and τ_{g43} = propagation time of gas stream through section (min).

The gas velocity is so much greater than the material velocity (the order of 200 to 1). Thus τ_{g43} is much shorter than τ_{m34} and the last term of eqn (2) may be neglected.

It should be noted in passing that, in general, specific heats and weights depend upon the physical and chemical states. For instance, the quantity of carbon dioxide in the gas stream depends upon the amount of fuel burned and the amount of material calcined upstream from it. The quantity of CO_2 in turn influences the quantity of gas and its specific heat.

The quantities \dot{Q}_m and \dot{Q}_g have not been defined as yet. They are the heat flows in the radial direction. Consider a cross section of unit length at 3 (Figure 4).

In this figure there are some additional quantities.

ϵ = emissivity of surface; l_{lu} = length of lining arc exposed to gases; l_{li} = length of lining arc in contact with solid material; l_c = length of material chord; and T_{l3} = average lining surface temperature taken over total circle.

It should be pointed out that there is a substantial variation of the surface temperature of a spot on the lining (or coating) per kiln revolution. Heat is added to a spot on the lining when it is in the gas stream and removed when it passes under the solid material. This establishes a cyclic variation in temperature of the surface of the spot. This problem was solved analytically

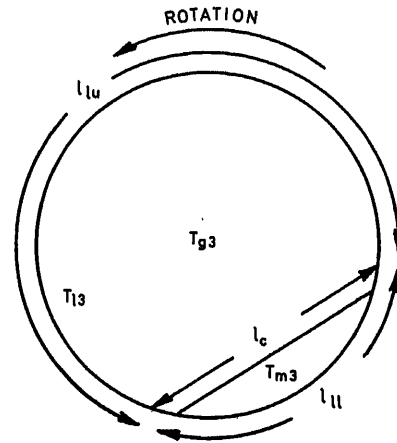


Figure 4. Kiln cross section

for the average temperature of the spot when exposed to the gas stream and the average temperature when exposed to the solid material. The resultant expressions are

$$T_{lu} - T_l = + \frac{235 K}{(\phi WCN)^{\frac{1}{2}} l_{lu}} \dot{Q}_m \quad (3)$$

$$T_{li} - T_l = - \frac{235 K}{(\phi WCN)^{\frac{1}{2}} l_{li}} \dot{Q}_m \quad (4)$$

where T_{lu} = average lining surface temperature taken over part of arc exposed to gases, T_{li} = average lining surface temperature taken over part of arc exposed to solid material, ϕ = specific heat of surface (brick or coating) (kcal/kg-°C), W = specific

weight of surface (kg/m^2), C = thermal conductivity of surface ($\text{kg}\cdot\text{m}/\text{m}^2\cdot\text{h}\cdot^\circ\text{C}$), and K = a constant.

Radial heat transfer in units of $\text{kcal}/\text{min}\cdot\text{m}$ may be viewed in tabular form.

A₃. Heat transferred, gas to lining

1. Gas radiation

$$f(T_{g3}, T_{lu3}, \text{Gas chemistry}_3) \varepsilon_l l_{lu}$$

2. Convection

$$H_c(T_{g3} - T_{lu3}) l_{lu}$$

B₃. Heat transferred, gas to solid material

1. Gas radiation

$$f(T_{g3}, T_{m3}, \text{Gas chemistry}_3) \varepsilon_m l_c$$

2. Convection

$$H_c(T_{g3} - T_{m3}) l_c$$

C₃. Heat transferred, lining to solid material

1. Black (or grey) body radiation, lining to chord

$$[(T_{lu3} + 273)^4 - (T_{m3} + 273)^4] C \varepsilon_l \varepsilon_m l_c$$

2. Black (or grey) body radiation, lining to lower arc

$$[(T_{lu3} + 273)^4 - (T_{m3} + 273)^4] C \varepsilon_l \varepsilon_m l_{ll}$$

3. Conduction

$$K [T_{lu3} - T_{m3}] l_{ll}$$

D₃. Kiln loss

$$f(T_{lu3} \text{ and } T_{lu3})$$

where H_c = convection constant (depends upon temperature and velocity) ($\text{kcal}/\text{min}\cdot\text{m}\cdot^\circ\text{C}$), K = conversion constant ($\text{kcal}/\text{min}\cdot\text{m}\cdot^\circ\text{C}$), and C = conversion constant [$\text{kcal}/\text{min}\cdot\text{m}\cdot^\circ\text{C}^4$].

The amount of heat leaving the gas stream ($A_3 + B_3$) must equal the amount of heat received by the load ($B_3 + C_3$) plus any heat lost through the shell (D_3). That is

$$(A_3 + B_3) = (B_3 + C_3) + D_3 \quad (5)$$

For the short kiln sections being considered it is reasonable to assume that the heat given by the gas stream in the section, \dot{Q}_g , may be computed using the average of the values per unit length at nodes 3 and 4. Thus

$$\dot{Q}_g = \frac{[(A_3 + B_3) + (A_4 + B_4)] l}{2} \quad (6)$$

Similarly,

$$\dot{Q}_m = \frac{[(B_3 + C_3) + (B_4 + C_4)] l}{2} \quad (7)$$

It should be clear that the equations for one section (space between nodes) are completely defined. In addition, the conditions at the end of one section are the beginning of conditions of the next section.

The clinker leaving the kiln drops on to a moving grate. Air is blown up through the bed to provide for rapid quenching of the clinker. Fuel combustion can utilize about one half of the total cooling air. The cooler is really a combination heat

recuperator and quencher. From a control standpoint it is a distributed parameter, positive feedback; this is treated in the analysis as an intimate part of the kiln system.

A set of equations describing the complete kiln system are implicit. Special methods were developed to produce a set for a much lesser number of nodes which give a good approximation to the solution obtained with 51 nodes. These methods involved solution of high order matrices on a large-scale digital computer. The resulting equations and the cooler equations were then set up on an electronic analogue computer. The result was a dynamic model of a cement kiln.

Using a finite difference approach to the development of the kiln equations may obscure the fact that the heat is added to the solid material because of its motion through the kiln. It can be shown that in the limit of infinitesimal sections, the equations are those of the transport phenomena.

The way in which material moves through the kiln then becomes extremely important. It is usually assumed that material is transported by moving up the side of a cross section with kiln rotation and then cascading down. Since the kiln is inclined downward in the direction of material flow, the material moves forward as it cascades. If it is assumed that this is the mode of material transport throughout the kiln length, a step change in kiln speed with the feeder synchronized to it will produce an immediate rate of change in material temperature at each point in the kiln. The rate measured at a point will persist until one transport time has elapsed, then the temperature will be constant again. If, however, it is assumed that the material is liquid (fluid), there is no cascading but just a downhill flow. Under these conditions, following a change in kiln speed with synchronized feeder, there will be a pure transport delay equal to the time it takes the new input feed rate to reach the measuring point.

Actually both kinds of transport exist in the kiln. As the chemical reactions take place, there are changes of physical state from solid to fluid and back to solid. Considerable field testing and data analysis was required to account properly for material flow. It should be noted in passing that the transport phenomena are seen in all material temperature changes resulting from change in control variables; this includes the relations between material temperature and heat input. Even though there are different mechanisms of material transport in various sections of the kiln, the temperature changes introduced by step changes in controlled variables have a characteristic shape of a time delay followed by a surprisingly linear rate of rise and then an abrupt levelling off. A transfer function of the following form can be used as a very good approximation:

$$e^{-sT_1} \frac{1 - e^{-sT_2}}{sT_2}$$

With this model all sensing points in the process were available. Various upsets were introduced to observe their effect upon the temperatures at the various sensing points, and it was seen that some of the sensing points which are included in most kiln instrumentation systems do not give information from which dynamic control action may be reliably initiated. Under certain upsets the control action would be opposite to that actually required. In other cases the magnitude of temperature change was not sufficient to be practical for error sensing.

It became apparent quickly that a means of sensing mix temperature in the burning (or clinkering) zone was required.

This is the zone that the operator (or a television camera) sees when he looks into a kiln. Total radiation pyrometers do not provide reliable sensing because of the interference of the dusty atmosphere of the burning zone. A development programme was initiated to produce a colour ratio pyrometer for this specific application. A colour ratio pyrometer compares the radiation of a body at two narrow bands of the spectrum. If the interfering dust acts as a neutral filter in these bands, the ratio is a known function of temperature. Pyrometer filters were selected which permitted operation in regions of the spectrum where cement dust is neutral. Many such pyrometers are now in operation.

Certain control ideas resulted from the early analytical investigation. With the co-operation of certain cement manufacturers and with the availability of a prototype colour ratio pyrometer a testing programme was initiated. The objective was to verify the kiln model, adjust its constants where necessary, and sharpen the control concepts resulting from the analytical work.

The ultimate objective of any kiln control system is to keep the point (or zone) of clinkering at a selected position in the kiln. It was found that there is a direct correlation between temperature variation and movement of this point. When this point moves, it is an indication that there is a change in the heat balance of the process. The balance can be restored by adjusting the heat input or material flow. The heat input can be changed by either the fuel flow or combustion air flow or the two in combination. The material flow can be adjusted either by adjusting kiln rotational speed or raw mix feed per revolution of the kiln. After each of these changes there is some interval where no appreciable change occurs in the burning zone (dead time). Then there is a smooth transition to another operating level. Temperature changes resulting from changes in heat input inherently have shorter delays than those resulting from material flow changes. The magnitude of heat input changes which can be tolerated for operating or economic reasons are quite limited, however. Therefore, small upsets may be compensated with heat input adjustments; large upsets must be compensated with material flow adjustments.

System of Kiln Control

Figure 5 is a block diagram of the kiln control. It is intended only to show the flow of information. The block labelled 'control logic' is the heart of the system. The kinds of things required by it are described below.

The primary sensing point for control of the clinkering process is the temperature in the burning zone. Other sensing points and prediction computations are used to modify the control action. As mentioned previously, there are several input quantities which will influence the burning zone temperature. The computer must select the input or inputs most appropriate for the conditions existing. These conditions are production level, amount of correction required (determined from magnitude of temperature error), urgency of action necessary (determined from rate of change of temperature error or high or low temperature limits), and the alternate action to be taken when the selected input variable would exceed an operating limit. The quantities adjusted by the computer are fuel flow, air flow, rotational speed, and raw feed to kiln.

A model of the process is stored in the computer. As each control action of each input is taken, it is fed into the model.

It should be noted that the measured temperature results from process variations and from the results of controlled input changes. The model produces a temperature which is the result of controlled input changes only. Assuming a reasonably good process model, the difference between actual temperature and temperature predicted by the model is a direct measure of process variation.

Process variations are considered to be any changes resulting from either upsets or input variations over which there is no direct control or control is not exact. For instance, control of feed to a dry process kiln is by screw conveyor from a constant head feeder. It is inevitable that there will be some variation in weight rate of flow. Since its presence cannot be measured directly, it will appear to the temperature sensors in the same way as do variations due to chemistry or non-uniform material flow in the kiln.

At each point in time the burning zone temperature of the model is compared to the measured temperature. The computer then decides if the current temperature is due to a process upset or the result of past control actions. In the case of rapidly rising or falling burning zone temperatures the computer takes action

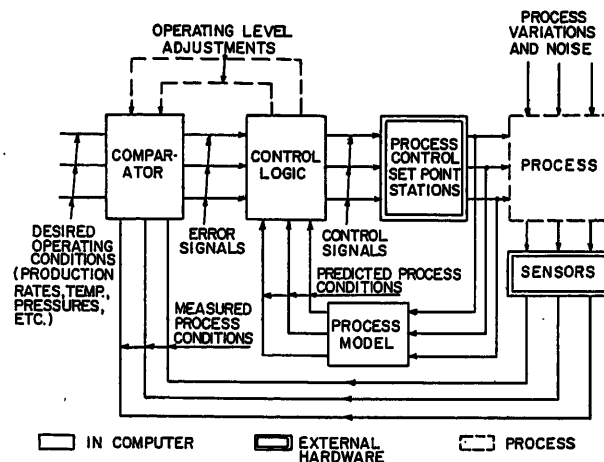


Figure 5. Kiln control

based on actual temperature. In the case of more normal conditions, it operates from its estimate of the magnitude of process variation. Such a control philosophy is good from a process point of view, but it is also a very stable kind of control because it does not try to regulate the changes it introduced. It is possible to introduce non-linear control actions during emergency conditions without producing the later cycling (limit cycle type of operation) which a control without process model often produces.

Tests thus far have indicated some variation in the parameters which the model simulates. The control equations were chosen to permit stable control action over the range of parameter variation. Analysis shows that there are theoretical reasons for these variations. Data taken during control with the present control equations will be analysed. It is expected that the process model will be improved with the resulting benefit of tighter control; this is made possible by the flexibility of an on-line digital computer. There is no need for an initial data logging phase of a couple of years; enough is known of the process to permit its immediate control. Ultimately a cost equation will be included in the control logic.

Information obtained from other sensing points is used to modify the control action, an example being the advance preparation of the burning zone temperature to accept material surges.

Sensor Checking

Any automation system depends upon certain key sensors for its successful operation. Although reasonableness checks are applied by the computer to several sensors, only one will be described because it is of primary interest.

Since successful control action depends upon correct measurement of burning zone temperature (burners in the past have measured this visually), two sensors are provided. The computer uses a logic and computation structure to determine which sensor it can rely upon for control. It utilizes knowledge of process characteristics and of characteristic signs of sensor failure in reaching this decision. When it discovers a bad sensor, it types this information on the alarm typewriter and controls from the other sensor. When it finds both sensors bad, it alarms the operator telling him how long he has in which to take over manual control. It then takes the most appropriate interim control action.

Output Checking

The computer must check actual position of each output set point it uses for control to see that it is actually being set correctly. If it is not satisfied, it types the correct setting to the operator. If the operator sets it correctly, the computer is satisfied and continues in the automatic mode. When the computer is not satisfied it alarms the operator, telling him how long he has in which to take over manual control. It then takes the most appropriate interim control action.

Automatic Start-up

Periodically a kiln must be shut down for maintenance such as replacing refractory lining. There is a programme to provide the function of slowly building production to normal levels over many hours. At a preselected production level, total automatic control is superimposed by the computer.

Automatic Control Initialization

During periods of manual control by the operator, set points are read by the computer and fed into the process model. When the operator selects the automatic mode, the computer goes through an automatic control initialization programme wherein it predicts the most probable future kiln conditions and makes the most appropriate initial set point settings. On the next scan it proceeds with the normal automatic control programme.

Production Logging

Production rate, kilowatt hours, and fuel flow are periodically scanned by the computer. Kilowatt hours per barrel, and B.Th.U. per barrel are calculated and logged as also are barrels and down time.

Summary of Kiln Control

It is intended that the computer control the kilns during both normal operation and during upsets. In this way the proper kiln operation is dictated by process engineers and followed exactly. If the operators know more about kiln operation than the process engineers, automation must wait for some changes in the latter department. The computer has rules to follow under all circumstances. The only time it calls for operator help is when it does not have reliable sensors or finds it cannot set analogue controller set points. The operator can intervene at any time. The process engineers have complete records in form of recording charts and computer prepared logs from which to decide if intervention was warranted. If intervention was warranted, changes in the computer programme may be desirable.

It is felt that the kiln burning is too much of an 'art'. It is a fact that with operator control the kiln production and efficiency per shift depends upon which operator is controlling. This in itself is evidence that burning is an art. Management cannot afford to take this reduced production when it can use a 'super-operator', a process control computer, which exercises consistent judgment.

Finish Grinding

Total production and production and efficiency figures for each finish mill are logged.

The author and his associates are indebted to the scores of cement industry operating personnel, process engineers, and executives for their helpful comments and encouragement as this system was explained to them. Many of the ideas are a composite of their suggestions. The author is particularly indebted to the management of the California Portland Cement Company for their faith in the ultimate success of this undertaking, and to R. G. Patterson, J. R. Romig, and J. H. Herz for their very substantial theoretical contributions, the practical experience they brought to this effort, and their interest and diligence in developing and proving a practical system.

References

- ADAMS, G. E., GAINES, W. M., HERZ, J. H. and ROMIG, J. R. The use of process control computers in the cement industry. *Amer. Inst. elect. Engrs Cement Industry Conference*, April (1962)
- MARTIN, G. *Chemical Engineering and Thermodynamics Applied to a Rotary Cement Kiln*. 1932. London; Technical Press
- GILBERT, W. Heat transmission in rotary cement kilns. *Cement & Cem. Manuf.* Series of articles beginning in 1932
- GYGI, H. Thermodynamics of the cement kiln. *Proc. 3rd Intern. Symp. Chem. Cement, London*, 1950, 750
- AZBE, V. J. Rotary kiln, its performance and development. *Rock Prod.* Series of articles beginning in 1955
- COSTA, H. Automation of a rotary cement kiln by means of a simple analogue computer. *Proc. 1st IFAC Conf.*
- SCHINK, H. Monitoring and control in the cement industry. *Proc. 1st IFAC Conf.*
- MIN, H. S., PARISOT, P. E., PAUL, J. F. and LYONS, J. W. Computer simulation of a wet-process cement kiln operation. *Fall Instrument-Automation Conf., Instrument Society of America, Los Angeles*, Sept. 1961

DISCUSSION

Author's Opening Remarks

The Colton, California plant of the California Portland Cement Company has been almost entirely rebuilt on the old plant location. The two dry process kilns are 3.9 m in diameter and 144 m in length with a rated capacity of 850 metric tons/day each.

In December 1962, the computer was installed. For the next two months, the communication links with the sensors and process controllers were tested. The scanning and controller setpoint actuation programmes were debugged at this time.

During mid-February, the raw material preparation was started. The start-up and subsequent operation of the raw mix and blending systems were under computer control. By the first week of March, sufficient inventory had been accumulated to start the first of the two kilns. It should be emphasized that neither kiln has ever been operated before; yet the first start-up was under full closed-loop control by the computer. Soon the second kiln was started.

The next few months were required to correct malfunctions. These were in the computer programme, in the computer peripheral equipment and in the drive equipment. The difficulties were both mechanical and electrical. A number of computer programme errors and in some cases, flow chart errors, were discovered. A few of these required that the computer be off-line for correction; others were corrected on-line during the free time in the scanning cycle. System constants obtained analytically were adjusted to correspond to the measured kiln constants.

It can now be reported that the control and logging functions are operational and that the computer is operating full time as are the temperature and chemical sensors. The automation system installation is complete and the California Portland Cement personnel have taken over operation and maintenance. After a few months of full-time operation to assess the automation system, extension of computer control into additional work areas is anticipated. This will be a joint endeavour by vendor and user.

Although the judgment is somewhat subjective, it is felt that the plant start-up by digital computer has considerably reduced the time to reach full plant production. This leads one to the conclusion that the computer will produce additional savings if installed immediately in a new plant rather than being added later on. It is also important to note that computer debugging may be done during the inevitable shutdown for mechanical and electrical changes which occur during a plant start-up.

L. JEQUIER and M. CUÉNOD, *Société Générale pour l'Industrie, Geneva, Switzerland*

(1) The installation described in this paper seems to have been in use for some months. Could the author give some indication on the practical results obtained and if they can economically justify the cost of a complete automation of this cement plant? Is there some reduction in the cost of production of the cement (reduction of labour, fuel or maintenance)? Could the mean production be augmented through a smoother working? Has the formation of rings in the kiln been reduced or avoided?

(2) What is the cost of the installation and what are the difficulties likely to be encountered for its introduction in an existing work or in the projection for a new plant? Who is able to install and to start such complete automation in Europe?

(3) The cost of the complete automation would be about the same for a big or a small cement works. What is the minimum output that can justify economically this cost in the United States and in Europe where the labour is cheaper and the fuel more expensive?

(4) To familiarize the staff of an existing cement works with the difficulties of a complete automation, would it not be wise to realize it step by step and what would these steps be?

(5) In a completely automated cement works what staff is necessary for the supervision and maintenance of the instruments and installations?

R. A. PHILLIPS, *in reply*

The questions of Messieurs Jequier and Cuénod deal with economic justification. Obviously, before any equipment is purchased, its economic value must be ascertained. In the case of automation equipment, such as the computer, the General Electric Company and the user collaborate in assessing the economic benefits. These are divided into: (1) tangible benefits such as savings in fuel, reduction of maintenance, fewer repairs to the refractory, and increase in production using the same equipment; (2) intangible benefits such as better quality, improved customer service, and better internal flow of information. In our economic evaluation with the user, we use only tangible benefits.

Question 1 deals with economic justification of automation for this plant. Since it is a new plant which was never operated without a computer, and never will be, there is no absolute base point. It is known that the chemistry is more uniform than in the old plant even though the same quarry is utilized. This has permitted smoother kiln operation and produces a high quality product. There was a net reduction of labour, but some specialized categories related to the automation equipment have shown an increase. The kilns are operating at 120 per cent of rating. It is believed fair to attribute a significant proportion of the increase to the computer itself and also that a minimum of 3 per cent in increase in fuel efficiency will be demonstrated in subsequent months. The problem of rings is much reduced over those associated with the small kilns in the old plant. Better monitoring of mechanical equipment will, no doubt, result in fewer breakdowns increasing availability and decreasing maintenance costs.

Question 2 may be answered as follows: While complete automation is recommended for new plants and some old plants, economic studies of many existing plants with adequate instrumentation indicate an approach where only sensors are read by the computer and the loops are closed through human operators. This avoids the construction of a central control room with new electronic instrumentation and associated wiring. Typewriters or other visual displays are located at each of the departmental operator's panels. The computer performs all of the internal operations described in the paper, but the operators move the setpoints manually. We call this 'Operations Guide'. International General Electric S. A. Geneva is prepared to install full automation and 'Operations Guide' equipment in Europe.

In answer to Question 3, a quotation was made for an existing plant in Europe of 750,000 metric tons/year capacity. The 'Operations Guide' approach was priced at about \$ 600,000 for programming and equipment including chemical analysis equipment. Savings, principally in fuel cost, indicated a two-and-a-half year payout. Messieurs Jequier and Cuénod are quite right that the size of the plant has a relatively small effect upon computer cost. As the General Electric 312 computer operates on a time-shared basis, it can easily control as many as five kilns simultaneously as well as performing all of the other functions described in the paper.

In answer to Question 4, the operator may take control away from the computer at any time. Experience has shown that after the first three months, he seldom does. Although it may be wise to implement the plant automation by phases, the analytical approach to kiln control has done away with the lengthy data logging required for empirical model building.

Answering Question 5, one man should be on call for computer maintenance. We strongly believe in preventive maintenance; this may be obtained from local sources. Most modern cement plants have already discovered that complete instrumentation is justified and already have the staff. One man for each shift is customary for instrument maintenance.

B. MALINOVSKY, *National Committee of I.F.A.C., Kalanchevskaya 15, Moscow*

The questions to the author are:

- (1) What kind of computer is used in the system of control?
- (2) How do you convert data from the X-ray spectrograph and transmit it to the computer?
- (3) Do you use statistical methods for studying the process? If so, what methods are used and in what areas?
- (4) Is the control system closed loop or open loop? Do you have direct control of the control setting devices or are they set by manual links?
- (5) How frequently are the input values read? What is the precision of measurements received?
- (6) Has the programme any self-adaptive features built in?
- (7) Since the machine is used in a closed-loop control system, it would be very interesting to know details of reliability and computer availability.

R. A. PHILLIPS, *in reply*

- (1) The computer is a General Electric 312 digital control computer. It is completely solid state with 40,000 words of magnetic drum memory. The add time is 192 μ sec and the analogue scan rate is 20 points/sec.
- (2) The data from the X-ray is converted automatically.
- (3) Statistical methods have been used for process identification and will be employed for economic evaluation.
- (4) All of the control functions are closed loop. In the installation described, the computer has direct control of the process instruments; there is no human link.
- (5) Inputs for kiln control are read and process adjustments are made every 3 min. Conversion precision is 0.1–0.3 per cent.
- (6) No self-adaptive features are programmed into the computer.
- (7) Precise values for this computer are not yet known at this installation. This model computer has shown 99.6 per cent availability on a number of other continuous operations; this is based on a 168 h week.

W. T. LEE, *6, Elm Drive, Hatfield, Herts, England*

- (1) In the first and second equations the term

$$\frac{T_{m3} + T_{m4}}{2} C_{pd} (W_{m3} - W_{m4})$$

presumably refers to heat lost by the solid in gases evolved. Is this so? If so, should the term be multiplied by a factor K_n , where

$$K_n = \frac{\text{weight of gas/unit time}}{\text{unit weight of solid}}$$

K_n is different for each small section. How is it calculated?

- (2) From the description in the paper, I assume that in Mr. Phillips' work a Fuller cooler was used in the cement plant. What sort of control is exercised? Have any other types of cooler been controlled?
- (3) Many assumptions have to be made in developing the model, e.g. characteristics of solid flow in the kiln, and many heat transfer coefficients. There are also considerable measurement difficulties. This means that feedback updating of the model is very necessary. What is updated? Is updating performed on-line?
- (4) Mr. Phillips' paper has dealt mainly with development of the model. How is the model used to optimize the operation, and what is the objective?
- (5) The control system is based upon comparison of certain process measurements with the values predicted by the model, taking measured disturbances into account. What measurements are used? What process variables are adjusted as a result of the errors? How is this done? What sort of action does the computer take in emergencies (for example, slip of the load, sudden variation of burning zone temperature)?

R. A. PHILLIPS, *in reply*

- (1) The equation is correct as it stands. A relationship between state of calcination and material temperature was developed from actual kiln data made available to us.
- (2) The Fuller coolers are presently controlled by process instruments. The computer has provision for adjustment of setpoints of the cooler instruments. Computer control of the coolers will be added.
- (3) Mr. Lee is correct, there is considerable measurement difficulty. As a matter of fact, it was necessary to have the help of our Research Laboratory in developing process identification techniques for this process to improve the system constants; however, the predetermined control strategy was good enough to permit kiln control from the first day. Mr. Lee conjectures that on-line updating is necessary; experience with an actual installation has not shown this to be so.
- (4) The paper deals with the development of a computer control system, the objective of which is to reduce the frequency and severity of upsets and to permit smooth operation at considerably higher production than under manual control.

Thorough answers to Questions 4 and 5 would require considerable depth of treatment. We, of course, do this when discussing automation of specific plants with our customers.

T. M. STOUT, *8433 Fallbrook Ave., Canoga Park, California, U.S.A.*

Our company has also had some experience in the control of blending and kilns in cement plants, and I would like to report briefly on the status of our installations and put some questions to Mr. Phillips.

Our oldest and most publicized installation is at the Oro Grande plant of the Riverside Cement Company, about 120 miles from Los Angeles, California. Used originally for blending calculations, the computer system was extended to kiln control early in 1962. That year was a period of development of the control system for one kiln, starting with three computer outputs and ending with five. At the start of 1963, control was extended to a second kiln adjacent to the first.

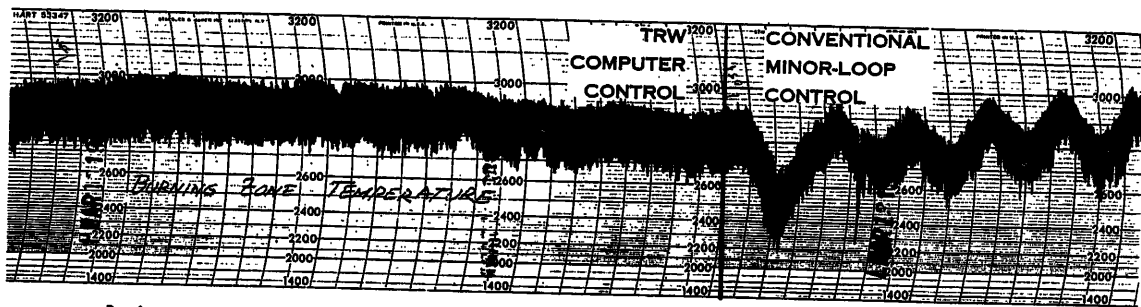
Figure A provides a graphic indication of the performance of the computer system. In this figure, which is a reproduction of strip charts of the kiln variables, time runs from right to left. The section on the right-hand side of the figure shows operation under 'manual' control, that is, conventional instrumentation under the supervision of a human operator. The oscillations are a result of regenerative feedback of thermal energy in the feed preheaters, the clinker coolers and the kiln itself. The left-hand portion shows operation with the computer directly connected to three of the controller setpoints. The date of these recordings is March 13, 1962.

An extensive evaluation of data for 1962 for the two kilns side by side, one under computer control and the other not (at that time), shows that the production rate of the kiln under control grows from 0 to 12 per cent greater than the other kiln as the computer usage increases from 0 to 100 per cent of the available time. Fuel consumption decreased about 4 to 5 per cent. The variability in unreacted lime in the clinker was smaller under kiln control, about 25 per cent of the previous value.

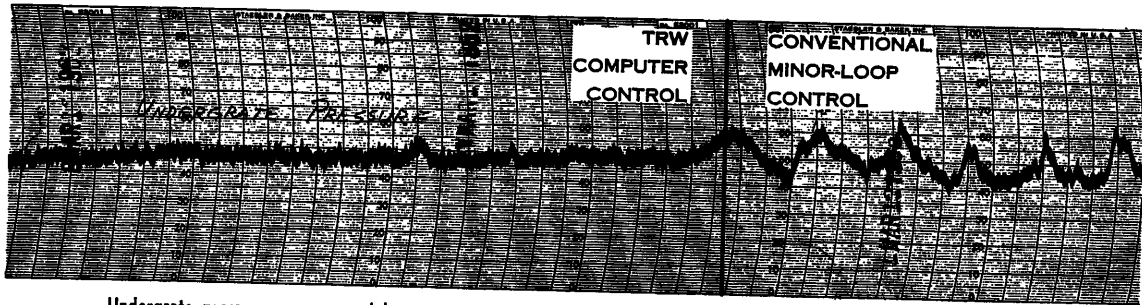
Our company is now actively engaged in installing computer systems for two wet-process cement plants in Japan. These systems will include blending and kiln control functions.

In our experience, an important computer function is the determination of compatible setpoints for the various local controllers, that is, values of the feed rate, fuel and air rates, and other variables, which constitute a thermally balanced set of kiln conditions. One question for Mr. Phillips is therefore: Since your Figure 5 shows these values as inputs from a source external to the kiln control system, how, in fact, are these values determined?

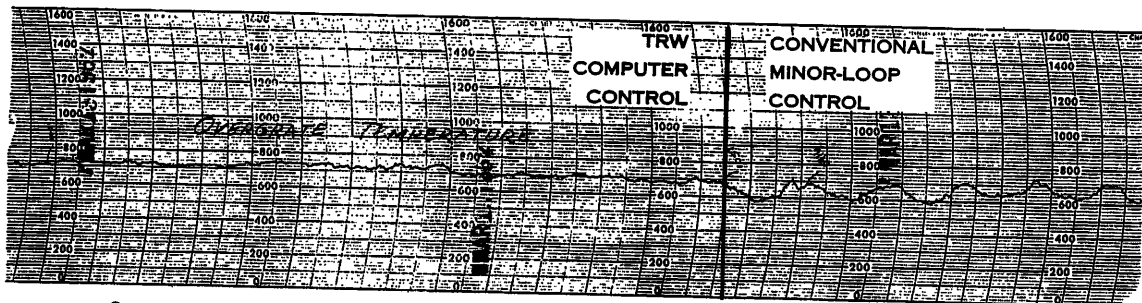
In connection with the X-ray analysers, would Mr. Phillips tell us which elements are measured?



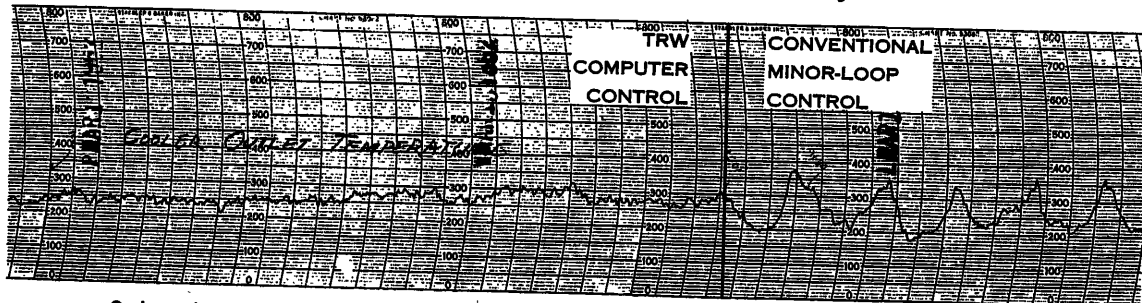
Burning zone temperature, as measured by a radiation pyrometer.



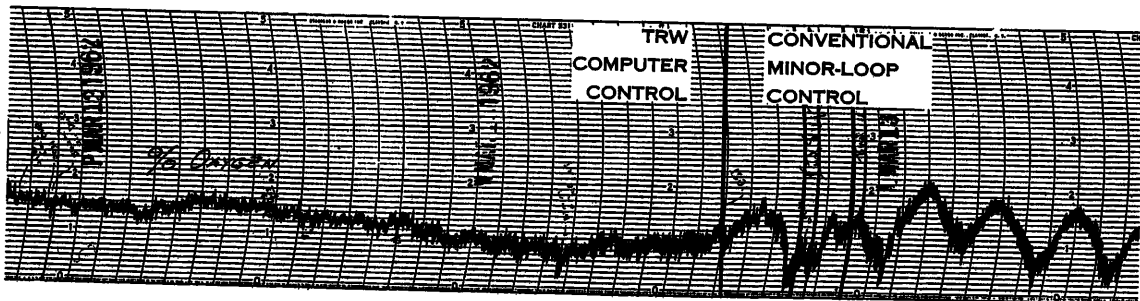
Undergrate pressure, as measured by a pressure sensor under the clinker cooler grate.



Overgrate temperature, as measured by a thermocouple located above the clinker cooler grate.



Cooler outlet temperature, as measured by a thermocouple located in the clinker cooler exhaust.



Percent oxygen, as measured by an analyzer located at the kiln exhaust.

Figure A

R. A. PHILLIPS, *in reply*

Dr. Stout is correct in stating that the Oro Grande installation is the oldest and most publicized installation. From the publicity, it is known that the computer was installed in the late summer of 1959 and that data logging of the kilns began in early 1960. He has supplied us with the other dates necessary to establish the timetable of accomplishing kiln control through process experimentation. In contrast to the two to three years required, full computer control of the kilns at California Portland was accomplished in six months on-site with a significant measure of control from day one.

The replies to Dr. Stout's specific points are:

(1) Some of the operating conditions are selected by plant management; the remainder are set by the computer to maintain thermal equilibrium.

(2) Both the laboratory X-ray and the on-line X-ray measure calcium, silicon, iron and aluminium.

A. E. BEECHER, *St. Regis Paper Co., RFD 1, Highland Mills, N.Y., U.S.A.*

Mr. Phillips' comments would lead one to believe that the form of the automatic control system is final. Does Mr. Phillips feel there is no possibility of changing this control? If he feels that the manner of control might change, does this not constitute a form of interim 'data logging' and essentially open-loop experience? How much improvement does Mr. Phillips feel may be available as a result of such experience? I fail to understand how such a complex system can be so completely understood before it exists.

R. A. PHILLIPS, *in reply*

Mr. Beecher's questions are perhaps best answered in the following manner.

In a manually controlled plant, the kiln operator is faced with precisely the same problems as in the automation system, that is, to control a non-linear, multivariable control system characterized by transport delays. He makes cement every day, some days with more success than others. If a skilled group of engineers and scientists study the process theoretically and study the operator's control methods thoughtfully, they can devise an automation system which will perform

more reliably than the human operator with average results equal at least to the operator on his best day. This has already been demonstrated.

There is no doubt that further changes will be made in the control. Without going into a lengthy description of the methods, it can be stated that data for control strategy improvement will be obtained during closed-loop control by the computer. Open-loop data logging does not show any payout on the plant operating records.

G. M. E. WILLIAMS, *Northampton College of Advanced Technology, St. John St., London E.C. 1, England*

(1) At what stage in the whole project of cement plant and computer control did the computer control element come into contact with the plant designers? Was this the best time to be brought together or would there have been a more appropriate time?

(2) Was the plant designed with the intention of being controlled in this way? If not, can anything be said on the plant design modifications needed which would be helpful? What are these modifications in general?

(3) Were the plant personnel specially recruited for operating this plant? If so, had they experience of conventional cement plant operation? Is past experience a disadvantage? How was training of personnel arranged?

(4) Is there any intention to add a computer to determine fuel and material deliveries and dispatch of finished cement?

R. A. PHILLIPS, *in reply*

(1) The automation system designers and the plant designers worked together from the beginning; the key people in the project were responsible for both functions.

(2) The major modification required is the decision by management that the manufacture of cement should and can be a science rather than an art.

(3) All the plant design and automation design decisions for this plant were made by graduate engineers who know plant operation, including experience in kiln burning. Central control operators were selected within the company for their intelligence, alertness, and constructive curiosity. They were then trained.

(4) These functions are not included at this plant, but should be considered on an individual plant basis.

On the Stability and Design of Dither Adaptive Systems

R. K. SMYTH and N. E. NAHI

Summary

The description is of a self-adapting, single parameter regulator system. As is shown, the amplitude of the system (dependent on the sinusoidal dither signal) is the criterion of self adjustment.

Variation of the parameters of the layout is limited to definite regions. The diagrams for the self-adapting regulator system are twofold, one for the normal reaction circuit and the other for the self-adapting circuit. The stability of the adapting regulator system is plotted for large and small deviations from the point of rest.

A numerical example is quoted to show that the alteration of the amplification value of a single circuit has an acceptable effect on the system. The described adaptable system was simulated in an analogue computer. The computer confirmed the findings of the analysis.

Sommaire

Description d'un système de commande auto-adaptative à un paramètre. On montre que le critère de performance du système auto-adaptatif est défini par la réponse d'amplitude du système à un signal «dither» sinusoïdal.

Les variations des paramètres du dispositif sont restreintes dans des régions définies. Le projet de réalisation du système de commande auto-adaptative est présenté en deux parties — la boucle de commande ordinaire et la boucle de commande auto-adaptative. L'étude de la stabilité du système de commande auto-adaptative est présentée, tant pour une petite perturbation que pour une grande perturbation, autour d'un point au repos.

On donne un exemple numérique montrant qu'une performance acceptable du système est obtenue en faisant varier le gain d'une seule boucle. Le dit système de commande auto-adaptative a été simulé dans un calculateur analogique. Le calculateur a confirmé les résultats de l'analyse.

Zusammenfassung

Es wird ein selbstanpassungsfähiges Regelsystem mit einem Parameter beschrieben. Wie es sich zeigt, gilt die auf ein sinusförmiges Zittersignal reagierende Schwingungsweite des Systems als das Kriterium der Selbstanpassung.

Die Veränderung der Anlagenparameter sind auf bestimmte Zonen beschränkt. Der Entwurf des selbstanpassungsfähigen Regelsystems ist zweifach dargestellt — als der reguläre und als der anpassungsfähige Rückkopplungskreis. Die Stabilität des anpassungsfähigen Regelsystems wird für kleine und große Abweichungen von einem Ruhepunkt dargestellt.

Ein Zahlenbeispiel ist angeführt, um zu zeigen, daß durch die Veränderung des Verstärkungswertes eines einzelnen Kreises eine brauchbare Wirkung im System zustande kommt. Das beschriebene anpassungsfähige System wurde auf einem Analogrechner nachgeahmt. Der Rechner bestätigt die Ergebnisse der Analyse.

Introduction

In many applications it is necessary to design a control system for a plant which has time-varying parameters. These parameters cause changes in the gain and in the location of the poles and zeros of the plant transfer function. If the changes in the plant

transfer function are sufficiently large that a fixed gain, fixed compensation control system does not give adequate stability and performance, then it is necessary to provide a self-adaptive controller which adjusts parameters in the control system to compensate for the changes in the plant transfer function. The general arrangement of the self-adaptive control system considered is shown in *Figure 1*.

The general design approach for this class of adaptive control system is considered elsewhere¹⁻⁴. It has been suggested⁵ that adaptive system design can be procedurized by partitioning the design into the consideration of the two loops—the regular control loop and the adaptive controller loop.

A One Parameter Dither Adaptive System

General Description

The basic objective of the dither adaptive system considered in this section is to maintain the closed-loop transfer function of the system essentially invariant, even though the plant transfer function is changing. This objective implies that the sensitivity of the closed-loop poles to plant parameter variations should be small. One technique for accomplishing this objective⁶ is to use an inverse model of the desired closed-loop transfer function in the feedback of a high-gain control loop.

For the system in *Figure 1*, the closed-loop transfer function is

$$\frac{C}{R}(s) = \frac{K_d M_d G_1(s) G_2(s, b_i)}{1 + K_d M_d G_1(s) G_2(s, b_i) H(s)} \quad (1)$$

If the loop gain $K_d M_d$ is made sufficiently great then the inequality

$$K_d M_d G_1(s) G_2(s, b_i) H(s) \gg 1 \quad (2)$$

can be made valid over the control frequency range. The parameters K_d , M_d are considered slowly varying relative to the control dynamics in order that the transfer function (1) has meaning.

For condition (2), the closed-loop transfer function is independent of the plant variable parameters, b_i

$$\frac{C}{R}(s) \cong \frac{1}{H(s)} \quad (3)$$

However, the validity of (3) depends upon maintaining the loop gain as high as possible, consistent with stability. The specific task of the single parameter dither adaptive system is to adjust the adaptive gain K_d to compensate for changes in the plant gain M_d . The adaptive controller must maintain the control-loop gain $K_d M_d$ constant such that eqn (3) is valid for the control system being considered.

The adaptive controller measures the loop gain by interrogating the control loop with a fixed amplitude sinusoidal dither signal, $I(s)$ in *Figure 1*. It may be shown that if the dither

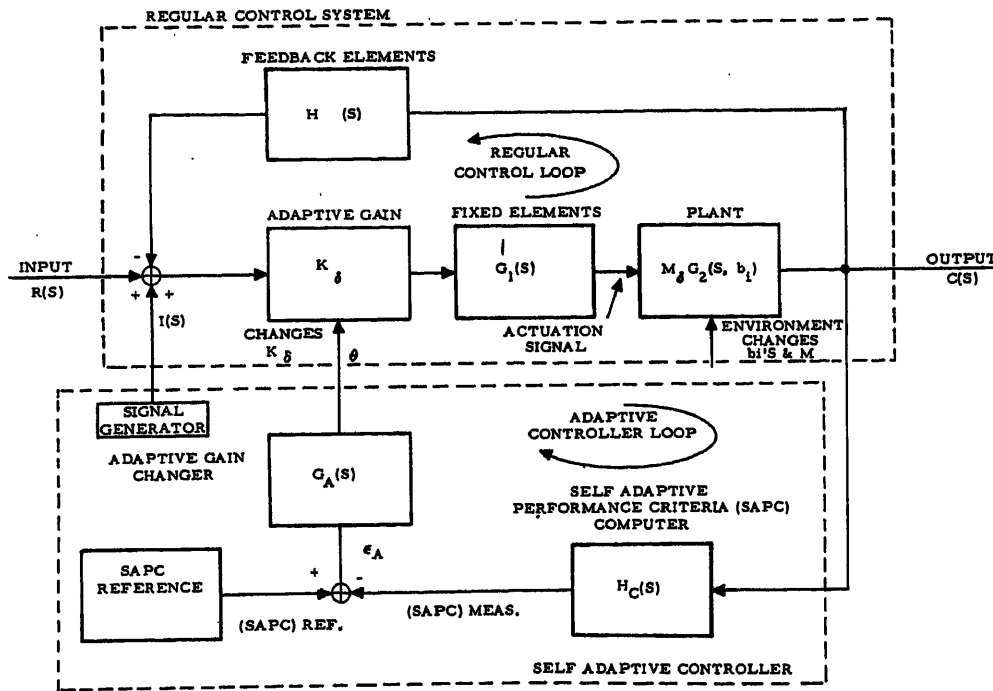


Figure 1. Self-adaptive control system with single variable gain

frequency ω_1 is chosen large compared with the variable poles and zeros of the plant, then the closed-loop amplitude response to the dither signal is given by

$$\left| \frac{C}{I}(j\omega_1) \right| = \frac{M_\delta K_\delta C_1}{[C_2 (M_\delta K_\delta)^2 + C_3 M_\delta K_\delta + C_4]^{\frac{1}{2}}} \quad (4)$$

where C_1, C_2, C_3, C_4 are positive, real constants essentially independent of the plant parameters b_1 . The amplitude response is a monotonically increasing function of the loop gain $M_\delta K_\delta$ for the stable region of the regular control loop. Therefore the loop gain can be measured indirectly by measuring the amplitude response to a sinusoidal dither input. For reasonable perturbations about an operating point, an approximate linear relationship exists between the amplitude response and the loop gain $K_\delta M_\delta$.

The amplitude response to the dither frequency (4) is the self-adaptive performance criterion SAPC for the system. The adaptive controller maintains the self-adaptive performance criterion to a value corresponding to the desired loop gain of the regular control loop by adjusting the adaptive gain K_δ .

The self-adaptive performance criterion is measured by passing the output acceleration signal through a bandpass filter tuned to the dither frequency. The bandpass filter output is then passed through a full wave rectifier to determine amplitude.

The output of the rectifier which is the measured self-adaptive performance criterion is compared with a fixed reference which is the desired value of the self-adaptive performance criterion corresponding to the desired loop gain $K_\delta M_\delta$. The resulting phase sensitive adaptive error ϵ_A is applied to an integrating servo which adjusts the adaptive gain K_δ to reduce the error to zero.

Limitations on Plant Parameter Variations

It is important to consider the limitations on the S plane region over which the poles and zeros of the plant transfer function may migrate and still have proper operation of the one parameter dither-adaptive control system. The S plane may be divided into four regions as illustrated in Figure 2.

- I. Domain of migration of plant poles and zeros.
- II. Domain of migration allowed for dominant closed-loop poles. The centre of Region II is S_0 , the nominal position of the dominant closed-loop pole.
- III. All open-loop poles and zeros of the regular control loop are fixed in this region. Migration of open-loop poles or zeros in this region would cause variations in the closed-loop poles to exceed the allowable limits with the one parameter adaptive system.
- IV. Migrations of poles and zeros in this region affect only the loop gain and thus may be considered as a variation in the plant gain M_δ .

It may be seen that the restrictions on the migration of the plant poles and zeros allow for both stable and unstable plants.

The S plane geometrical limitations are summarized:

- (1) The bandwidth of the migratory plant poles and zeros must be limited.
- (2) The closed-loop bandwidth of the regular control system must be greater than the bandwidth of the migratory plant poles and zeros.
- (3) The dither frequency must be large compared with the bandwidth of the migratory plant poles and zeros.

(4) High-frequency migratory poles and zeros are allowed provided their location is great compared with the dither frequency. In this case the effect of the migratory roots is the same as a change in the plant gain M_s .

Numerical Design Example

The dither-adaptive technique is illustrated for a specific but meaningful example (*Figure 3*). The example is chosen to be of moderate complexity to demonstrate that the method works for a relatively high-order control system. The example is meaningful in that dynamic elements, such as actuator and sensor dynamics, normally present in a practical control system, are included.

The form of the plant transfer function was chosen to be

representative of a wide class of controlled elements. The denominator consists of an integration plus a quadratic factor and the numerator includes a zero and a gain factor M_0 . The range of variation of these parameters is tabulated in *Figure 3*. The open-loop plant is unstable for some combinations of the variable parameters.

Design of the Regular Control Loop—It is desired that the dominant closed-loop roots of the control system have a natural frequency of approximately 10 rad/sec and a damping ratio of 0.7 ± 0.2 . No other closed-loop poles should have a damping ratio less than 0.1.

The inverse model $H(s)$ must be selected to provide the desired closed-loop poles. This selection is easily accomplished by successive trials using a digital computer to determine the

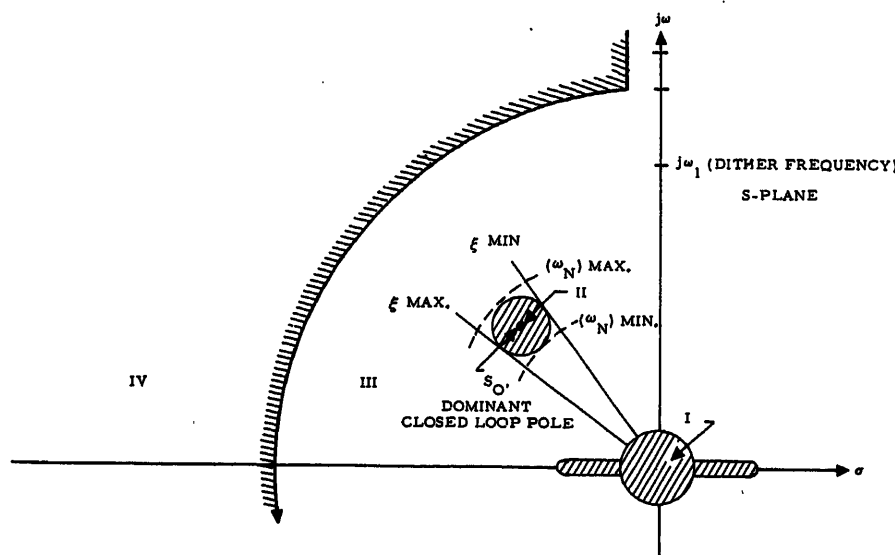


Figure 2. *S* plane regions

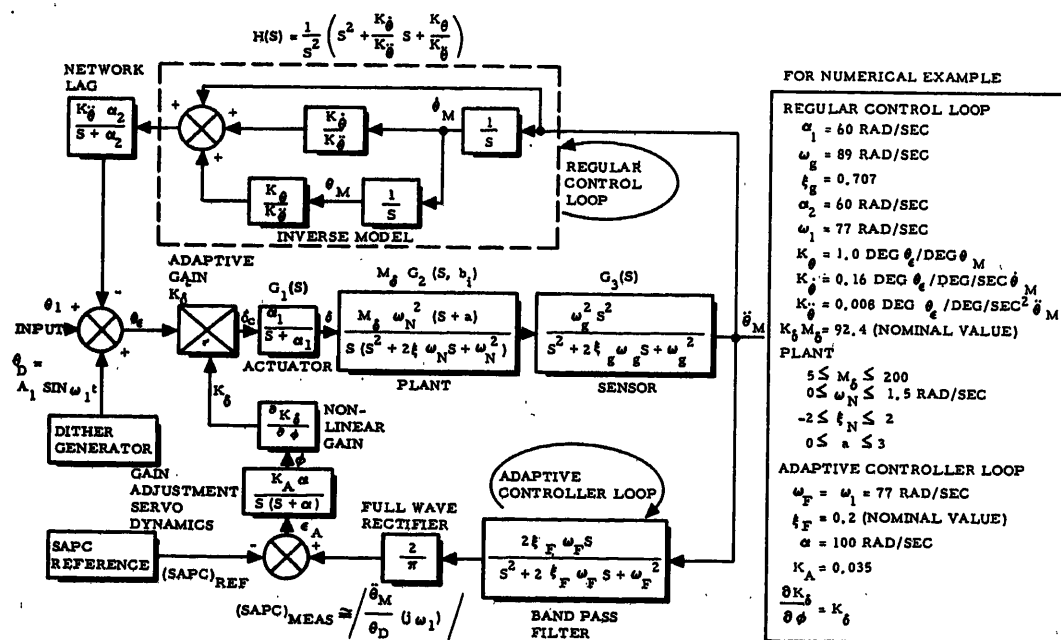


Figure 3. One parameter dither-adaptive system

closed-loop roots. With the zeros of $H(s)$ chosen at $s = -5 \pm j10$, the desired closed-loop poles were obtained.

The root locus for the design example is shown in Figure 4. The root locus plot shows loci for two extreme conditions of the plant transfer function parameters. The shaded areas denote the actual rectangular limits of the closed-loop poles for the maximum variation in the plant parameters.

Because the damping ratio excursion is within the desired limits, no further changes in the regular control-loop compensation is required. If this had not been the case, a different value for the compensation function would have been chosen and the design iteration with the digital computer repeated.

It will be noted from the root locus in Figure 4 that two possible frequencies of instability can exist: (1) a high frequency instability in the region of 75 rad/sec, and (2) a low frequency instability in the region of 9 rad/sec (for the case of an open-loop unstable plant).

Design of the Adaptive Controller Loop

The dither frequency should be selected large compared with the plant migratory poles. Acceptable operation occurs if the dither frequency is approximately five times the dominant closed-loop poles, or greater.

An interesting mode of operation described below is possible if the dither frequency is chosen to correspond with the frequency at which the high frequency instability occurs (77 rad/sec in this case). However, this choice is by no means necessary for normal operation.

The self-adaptive performance criterion SAPC is taken to be the output acceleration amplitude response rather than output position or rate. The reason for this choice is to avoid steady-state output of the position or rate from biasing the measured self-adaptive performance criterion. A simple band-pass filter with second-order denominator tuned to the dither

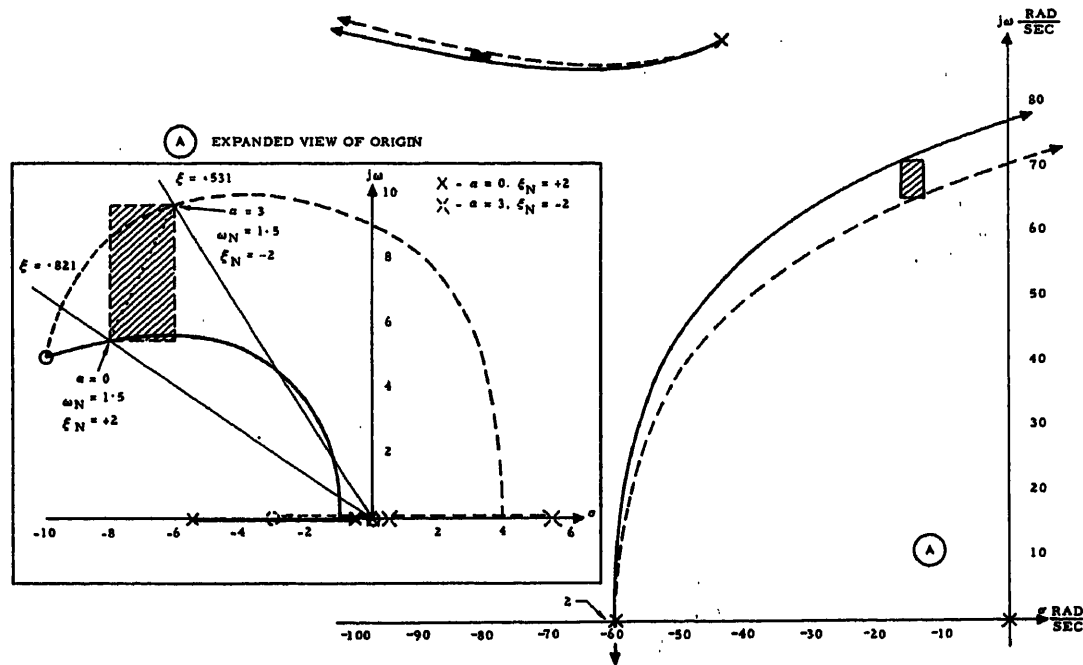


Figure 4. Root locus for numerical design example, regular loop

$$SAPC = \frac{C_1 K_d M_d}{[C_2 (K_d M_d)^2 + C_3 K_d M_d + C_4]}^{1/2}$$

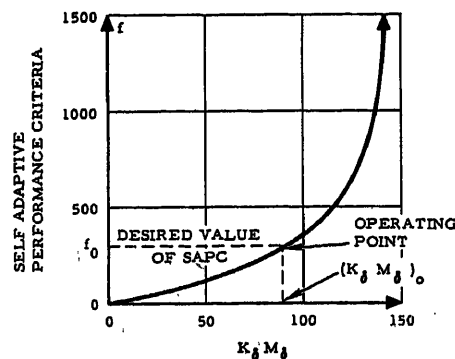


Figure 5. Self-adaptive performance criteria (amplitude response) as a function of loop gain $K_d M_d$

frequency is used for the SAPC computer. The filter output is rectified to obtain the measured SAPC.

The reference value for the SAPC is obtained by plotting the SAPC [given by eqn (4)] for the particular example as a function of the loop gain $K_d M_d$. From this curve (Figure 5) the desired value of the SAPC can be readily determined. The desired value of the SAPC corresponds with the value of the loop gain $K_d M_d$ determined from the regular loop analysis. For the example, this value of loop gain is 92.4 which yields the desired closed-loop poles of the regular control loop (Figure 4).

Figure 6 illustrates the adaptive operation of the dither adaptive system for a case in which the control system is initially unstable at the low frequency in the region of 9 rad/sec.

Figure 7 illustrates a similar behaviour of the adaptive system for the case in which the control system is initially unstable at the high frequency in the region of 75 rad/sec. In both cases the adaptive system very quickly adjusts the gain K_d to provide for stable operation.

Another interesting type of operation possible for the adaptive system occurs when the dither input is reduced to zero (Figure 8). In this condition the adaptive controller loop increases the gain K_d until the system becomes unstable at approximately 75 rad/sec, which causes an output oscillation that appears as a dither response to the adaptive bandpass filter. The adaptive controller reduces the adaptive gain K_d to quench the unstable oscillation. This operation will be repeated in a cyclic fashion which causes a saw-tooth variation in the gain K_d about the nominal value.

Adaptive Controller Stability

Self-adaptive Performance Criterion

It was shown above that the regular control loop can be designed such that acceptable performance is obtained if the amplitude response to the sinusoidal dither is maintained constant (providing specified restrictions on the migration of the plant poles and zeros are made).

For the sinusoidal dither adaptive system, the self-adaptive performance criterion SAPC is the amplitude response of the regular control loop to the dither signal input. The desired value of the self-adaptive performance criterion is that value which corresponds to the desired loop gain $M_d K_d$ of the regular control loop. An analytical expression for the SAPC was presented in eqn (4). The SAPC is a function of the two variables M_d and K_d , and for small perturbations about the operating point can be expanded in a Taylor series expansion neglecting the higher order terms:

$$SAPC = F(M_d, K_d) = f_0 + \frac{\partial f}{\partial M_d} \Delta M_d + \frac{\partial f}{\partial K_d} \Delta K_d \quad (5)$$

The two partial derivatives may be evaluated by the chain rule;

$$\left. \begin{aligned} \frac{\partial f}{\partial K_d} &= \frac{\partial f}{\partial (M_d K_d)} \cdot \frac{\partial (K_d M_d)}{\partial K_d} = \frac{\partial f}{\partial (M_d K_d)} \cdot M_d \\ \text{and} \\ \frac{\partial f}{\partial M_d} &= \frac{\partial f}{\partial (M_d K_d)} \cdot \frac{\partial (K_d M_d)}{\partial M_d} = \frac{\partial f}{\partial (M_d K_d)} \cdot K_d \end{aligned} \right\} \quad (6)$$

The partial derivatives of (6) are evaluated at the operating point where $f=f_0$ and $K_d M_d=(K_d M_d)_0$. The partial derivative

$\partial f / \partial (M_d K_d)$ may be interpreted as the slope of the curve in Figure 5 at the operating point. An analytic expression for $\partial f / \partial (M_d K_d)$ may be obtained by taking the derivative of eqn (4) with respect to the product $M_d K_d$.

$$\frac{\partial f}{\partial M_d K_d} = \frac{1/2 C_1 C_3 M_d K_d + C_1 C_4}{[C_2 (M_d K_d)^2 + C_3 M_d K_d + C_4]^{3/2}} \quad (7)$$

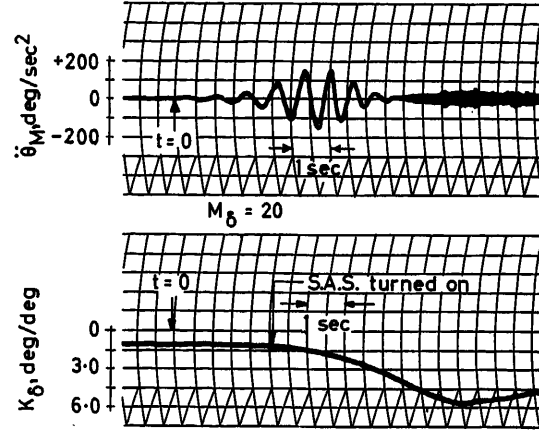


Figure 6. Initially unstable at low frequency

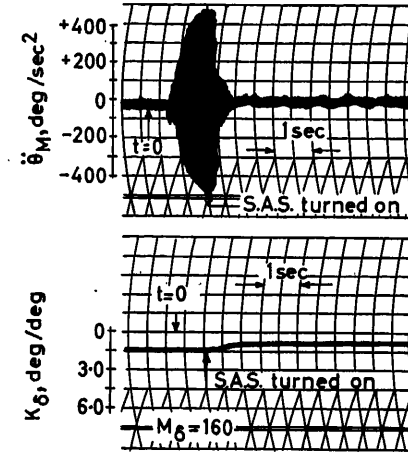


Figure 7. Initially unstable at high frequency

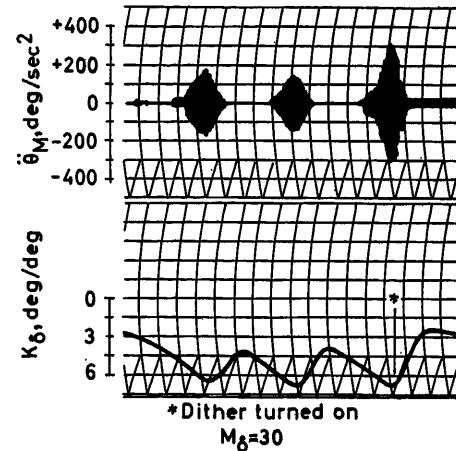


Figure 8. Dither signal initially turned off

Stability-in-the-small

An analysis of the stability-in-the-small of the adaptive controller loop is based upon eqn (5). Eqn (5) can be represented as a summing point in the stability block diagram for the adaptive controller loop (Figure 9). The input to the adaptive controller loop is considered to be an incremental change in the plant parameter M_δ .

If an incremental change ΔM_δ occurs, an incremental change in the self-adaptive performance criterion will result. To return the self-adaptive performance criterion to its desired value, it will be necessary for the adaptive system to adjust the adaptive gain by an increment ΔK_δ . The self-adaptive performance criterion is measured by the adaptive bandpass filter and rectifier which has an 'equivalent' transfer function $G_C(s)$. The output of $G_C(s)$ is passed through the d. c. gain of the full wave rectifier. The output of the rectifier corresponds to the measured self-adaptive performance criterion which is compared with the desired or reference value of the self-adaptive performance criterion to form the adaptive error ϵ_A . The adaptive error is applied to an integrating servo which adjusts the adaptive gain K_δ . A non-linear gain, $K_1 = \partial K_\delta / (\partial \phi)$ is shown between the adjustment servo output and the increment change in K_δ . The incremental change in K_δ passes through another non-linear gain block, $K_2 = \partial \text{SAPC} / (\partial K_\delta)$.

It is interesting to note that amplitude modulation theory applies to the sinusoidal dither adaptive system. The adaptive information regarding changes in the SAPC is contained as amplitude modulation of the control system response at the sinusoidal dither frequency. Using amplitude modulation theory it may be shown that the equivalent transfer function of the

bandpass filter to the adaptive information can be represented by a low-pass filter. This filter is a first-order lag at $\xi_F \omega_F$, if it is assumed that no information power occurs above the dither (carrier) frequency. However, if the information power above the dither frequency is considered, then the low-pass filter is second order with the low-frequency lag at $\xi_F \omega_F$ and the high-frequency lag at α_H , approximately four times higher than $\xi_F \omega_F$ for the bandpass filter used in the numerical example.

For stability-in-the-small the adaptive controller maintains the loop gain $M_\delta K_\delta$ constant, i.e. $M_\delta K_\delta = K_2$. For this case the partial derivative $\partial \text{SAPC} / (\partial K_\delta)$ is

$$\frac{\partial \text{SAPC}}{\partial K_\delta} = \frac{1/2 C_1 C_3 K_2 + C_1 C_4}{[C_2 K_2^2 + C_3 K_2 + C_4]^{3/2}} \cdot M_\delta = K_3 M_\delta = K_3 \frac{K_2}{K_\delta} \quad (8)$$

where K_3 can be considered a constant. The significance of eqn (8) is that as the plant gain M_δ (and therefore K_δ by the adaptive action) vary over the operating range, the loop gain of the adaptive controller loop will vary accordingly. To compensate for the effect of eqn (8) an intentional non-linear gain $K_1 = \partial K_\delta / (\partial \phi)$ is introduced to maintain the adaptive controller loop gain $K_1 K_2 K_3 K_4 / K_\delta$ invariant over the operating range. It is convenient to choose the non-linear gain $K_1 = K_\delta$, which for small perturbations means that the adaptive loop gain is a constant, $K_2 K_3 K_4$.

Stability-in-the-small has been reduced to a simple linear problem for the adaptive controller loop. A root locus of this linearized loop, using the numerical example given previously, is shown in Figure 10. The dominant closed-loop poles are at a natural frequency of approximately 11 rad/sec for this example.

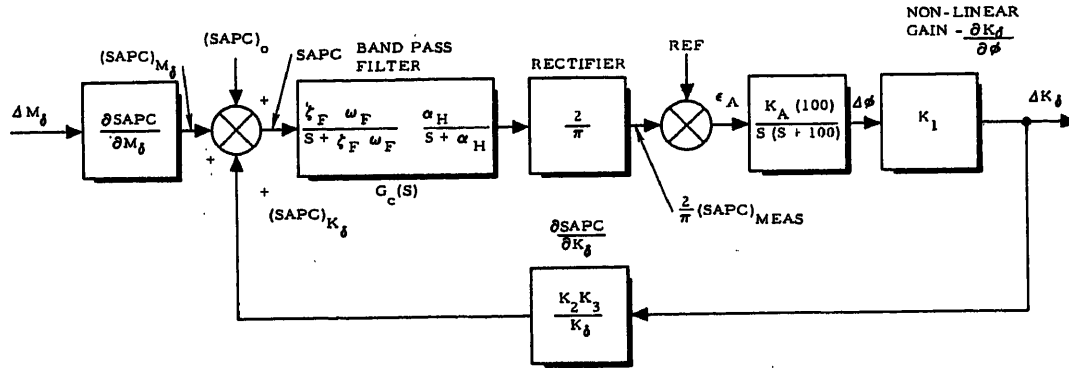


Figure 9. Adaptive controller stability loop

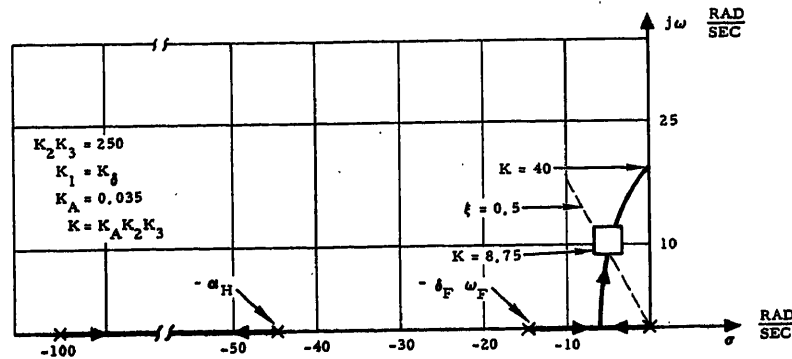


Figure 10. Root locus for stability-in-the-small

If the adaptive loop gain is raised sufficiently an instability occurs at about 17 rad/sec. This instability is exhibited as a limit cycle since non-linearities exist in the loop for large excursions about the operating point. An analogue computer simulation was conducted to verify the stability and performance of the adaptive system using the numerical example. Stability-in-the-small was investigated for the case in which the gain K_1 was fixed and for the case in which it was varied directly as K_δ . The results of the first case are illustrated in Table 1.

Table 1. Limit Cycle of Adaptive Controller Loop $K_1 = \text{constant}$

M_δ	Nominal K_δ	Critical K_A	Frequency of oscillation c/s
30.0	3.08	0.48	2-1/2
92.4	1.0	0.16	2-1/2
200.0	0.462	0.08	2-1/2

It may be seen that the critical value of K_A (the value at which the limit cycle occurs) varies with the value of M_δ . At high values of M_δ it requires a relatively small value of K_A to induce the limit cycle instability and conversely which confirms eqn (8).

Note that the frequency of oscillation in Table 1 is reasonably close to the frequency at which the adaptive controller root locus predicts the system will go unstable (2.9 c/s).

The simulation results of the stability-in-the-small when the adaptive-loop gain $K_1 = K_\delta$ are summarized in Table 2. It will be noted that the value of K_A at which the limit cycle instability is induced is the same at all values of M_δ as predicted by the above analysis, since $K_1 \partial \text{SAPC} / (\partial K_\delta) = \text{constant}$.

Table 2. Limit Cycle of Adaptive Controller Loop $K_1 = K_\delta$

M_δ	Nominal K_δ	Critical K_A	Frequency of oscillation c/s
30.0	3.08	0.18	2-1/2
92.4	1.0	0.18	2-1/2
200.0	0.462	0.18	2-1/2

Referring to the root locus (Figure 10), it may be seen that a smaller value of ξ_F will move the pole of the bandpass filter closer to the origin, causing the adaptive controller loop to go unstable at a lower frequency and at a lower gain.

Table 3 shows the analogue computer results which illustrate

Table 3. Adaptive Controller Stability with Bandpass Filter Damping ξ_F

M_δ	Nominal K_δ	Critical K_A	Frequency of oscillation c/s	ξ_F
92.4	1.0	0.18	2-1/2	0.2
92.4	1.0	0.12	1-3/4	0.1
92.4	1.0	0.064	1	0.05

the effect of the adaptive bandpass filter damping ratio ξ_F on the stability-in-the-small.

The frequency and gain for instability predicted by the root locus plot and the computer results correspond very closely.

Stability-in-the-large

The principal difference between the stability-in-the-large and the stability-in-the-small arises from the fact that the gain product $K_\delta M_\delta$ is not maintained constant for very rapid changes in the plant parameters because of the limited response time of the adaptive controller loop. Because $K_\delta M_\delta$ is not a constant for rapid changes in M_δ , K_δ is no longer a constant but is a non-linear function of $K_\delta M_\delta$ given by eqn (5). Thus the consideration of stability-in-the-large is a non-linear, time-varying problem. In spite of the complicated theoretical implications of considering the exact solution to the stability-in-the-large problem, considerable insight into the understanding of the transient response for large, rapid changes in M_δ can be obtained by a qualitative consideration of the effect of the variable gain

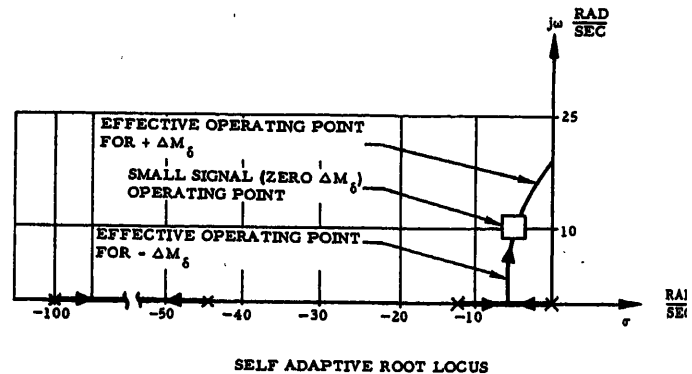


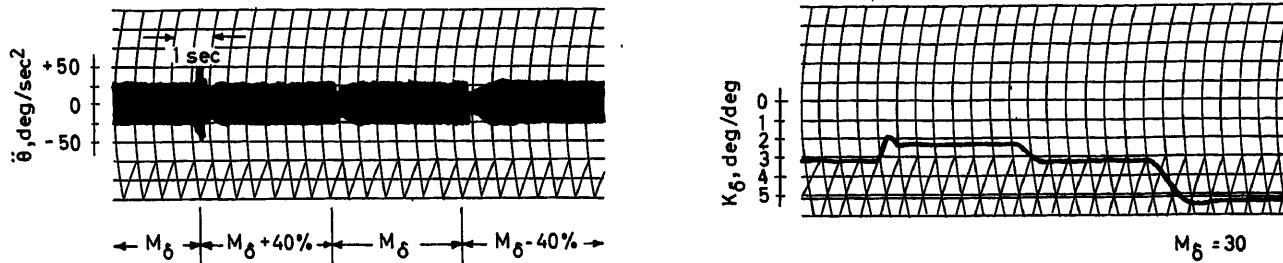
Figure 11. Root locus showing effect of rapid M_δ changes

$\partial \text{SAPC} / \partial K_\delta$. For a positive step increment in ΔM_δ , the gain $\partial \text{SAPC} / \partial K_\delta$ increases initially. For a negative step increment in ΔM_δ , the gain decreases initially. The apparent position of the adaptive controller closed-loop poles will shift for step function inputs. The frequency and damping will increase for an increase in M_δ and conversely. This effect is illustrated qualitatively on the root locus diagram of Figure 11.

The analogue computer traces of Figure 12 illustrate the difference in the stability-in-the-large for positive and negative step changes in ΔM_δ . It may be seen that the results predicted from the root locus of Figure 11 are confirmed.

Conclusions

It has been shown that the one parameter dither-adaptive technique applies to a relatively wide class of control systems. The technique has been applied to advanced aerospace vehicle control systems^{7, 8}. An extension of this technique, which uses the dither phase response as well as the amplitude response, has been developed by the authors. This extension provides for two variable adaptive parameters and results in a decrease of the region of migration of the closed-loop poles. This development is reported in a later paper.


 Figure 12. Complete traces showing effect of step ΔM_δ changes

The authors wish to extend their appreciation to John Nishimi, Tom DePont, Lawrence Callahan and William Watt for performing the analogue computer simulations and digital computer analyses. Thanks are given to Autonetics for providing the computer facilities, and particularly to Guy Bayle for his many helpful discussions and suggestions which contributed significantly to the understanding of the system.

References

- ¹ GREGORY, P. C. (Ed.) *Proc. Self-Adaptive Flight Control Symp.*, WADC Rep. 59-49, ASTIA Document AD 209389, March 1959
- ² ANDERSON, G. W., ASELTINE, J. A., MANCINI, A. R., and SARTURE, C. W. A self-adjusting system for optimum dynamic performance, *IRE Conv. Rec.*, Pt 4 (March 1958) 182-190
- ³ MARX, M. F. Recent adaptive control work at the General Electric Company. *Proc. Self-Adaptive Flight Control System Symp.*, WADC TR 59-49, ASTIA No. AD-209389, March 1959
- ⁴ MISHKIN, E., and BRAUN, L. *Adaptive Control Systems*. 1961. New York; McGraw-Hill
- ⁵ SMYTH, R. K. and NAHI, N. E. *Design of Self Adaptive Control Systems*. SAE paper presented to the SAE A-18 Committee on Aerospace Vehicle Control Systems, Minneapolis, Minnesota, June 1962
- ⁶ CAMPBELL, G. Use of an adaptive servo to obtain optimum airplane responses. *Cornell Aeronautical Lab., Inc.*, Rep. No. CAL-84, February 1957
- ⁷ SMYTH, R. K. Self Adaptive System for Re-Entry Glider Control. *Proc. Nat. Aerospace Electron. Conf.*, Dayton, Ohio. (May 1961) 475-483
- ⁸ SMITH, K. C. *Adaptive Control Through Sinusoidal Response*. AIEE paper presented at the Joint Automatic Control Conference, MIT, Cambridge, Massachusetts, September 1960

DISCUSSION

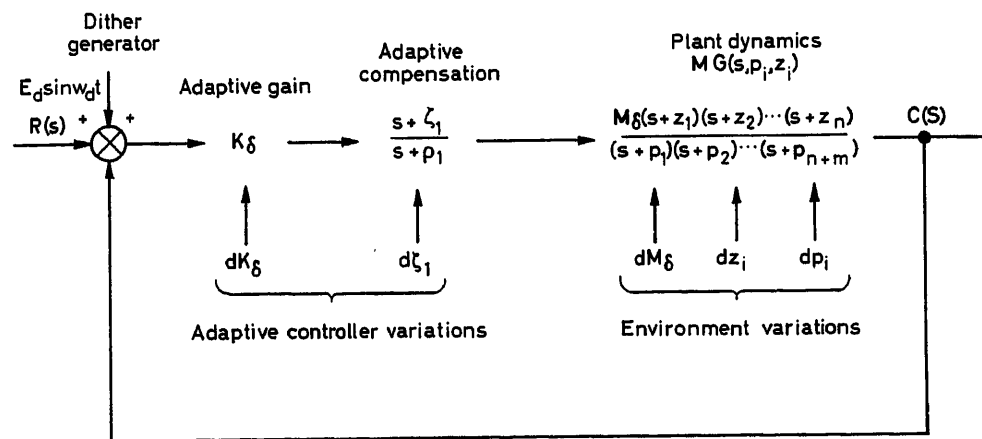
Author's Opening Remarks

The extensions to the paper since its preparation take two directions. First, the method is extended to include the adjustment of more than one parameter¹. An example is presented² in which the dither amplitude response is used to adjust the loop gain and the dither phase response is used to adjust a compensation zero.

Secondly, the theory of sensitivity functions as reported by McRuer and Stapleford³, and others, is used to analyse the stability of the adaptive loop and to assess the performance of the adaptive adjustment.

The general configuration considered is shown in *Figure A*. The loop consists of a plant which is modified by the environment and adaptive gain and compensation which are modified by the adaptive adjustments. The adaptive adjustments compensate for the environment variations.

A numerical example (*Figure B*) is considered. The adaptive system comprises the regular control loop and two adaptive adjustment loops. A sinusoidal test (dither) signal is injected and the phase and amplitude response are measured by means of a bandpass filter and appropriate discriminators.



Closed-loop transfer function:

$$\frac{C}{E_d}(j\omega_d) = \frac{K_\delta M_\delta(s + \zeta_1)(s + z_1)(s + z_2) \cdots (s + z_n)}{(s + \rho_1')(s + q_1)(s + q_2) \cdots (s + q_{n+m})} \bigg|_{s=j\omega_d} = A_d e^{j\phi_d} = f_1 e^{j\phi_1} f_2$$

Figure A. Two-parameter dither self-adaptive control system

The phase adaptive loop adjusts the compensation zero to keep the dither phase response constant. The amplitude adaptive loop adjusts the gain to maintain the dither amplitude response constant.

Figure C illustrates the effectiveness of the amplitude adaptive loop in maintaining constant response to a unit step function applied to the input of the regular loop. The response is before and after a plant gain change.

Figure D shows the effectiveness of the phase loop in keeping the response fixed. The response shown is before and after a change in the plant pole location.

The general formulation of the block diagram for the adaptive controller loops is shown in Figure E. It may be seen that sensitivity functions can be used to express the change in the closed-loop poles d_{qt} as a result of both environment and adaptive parameter changes.

The block diagram in Figure F represents a specialization of the block diagram shown in Figure E for the numerical example illustrated in Figure B. The amplitude loop is at the top and the phase loop is at the bottom. The coupling between the loops is such that the amplitude loop adjustments disturb the phase loop, but not conversely. Also the stability of the two loops is independent for the example.

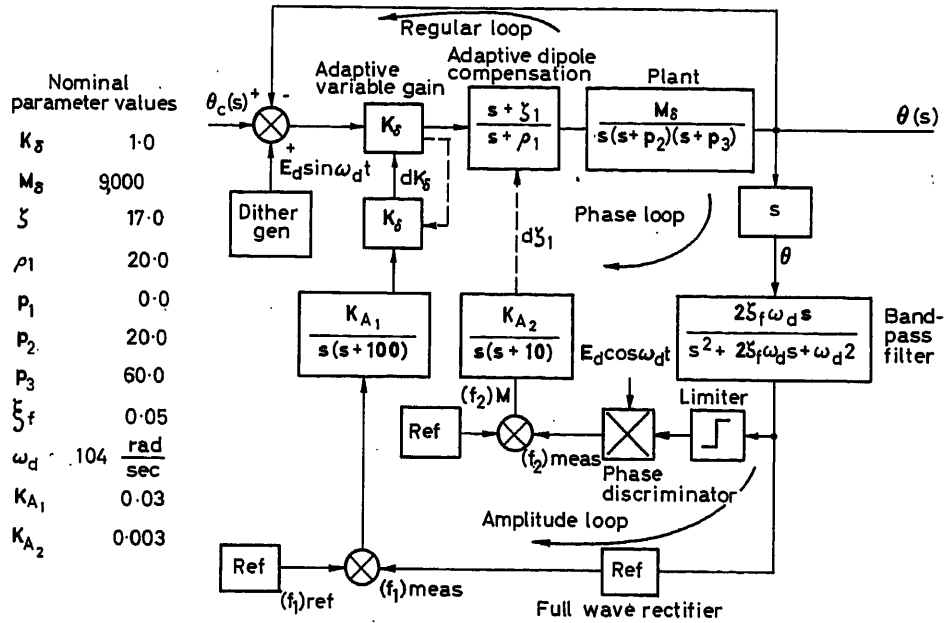


Figure B. Dither adaptive system, numerical example

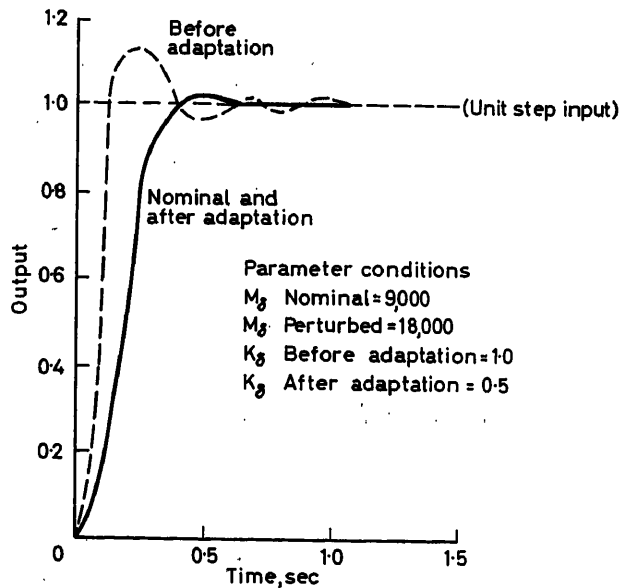


Figure C. Effect of amplitude adaptation

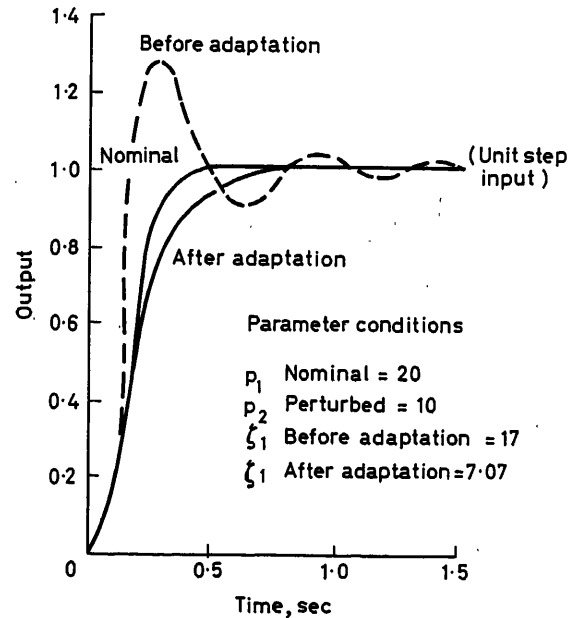


Figure D. Effect of phase adaptation

The analogue computer simulation trace in *Figure G* shows the adaptive adjustment response to a sudden change in the plant gain. The response is as predicted by the block diagram in *Figure F*.

Conclusions

It has been shown that the dither self-adaptive control system is practical and simple to implement. The system provides effective adaptive control through closed-loop adjustment of gain and compensation networks.

It is shown that the adaptive adjustment loops can be analysed and designed to be stable.

References

- 1 SMYTH, R. K. Phase and amplitude dither self adaptive control systems. *Ph.D. Dissert.*, Univ. Southern California, Los Angeles (June 1963)
- 2 SMYTH, R. K. and NAHI, N. E. Phase and amplitude sinusoidal dither adaptive control system. *Proc. Joint Automat. Contr. Conf.*, Minneapolis, Minn. (June 1963)
- 3 MCRUER, D. T. and STAPLEFORD, R. L. Sensitivity and model response for single loop and multi-loop systems. *ASD-TDR-63-812* (August 1962)

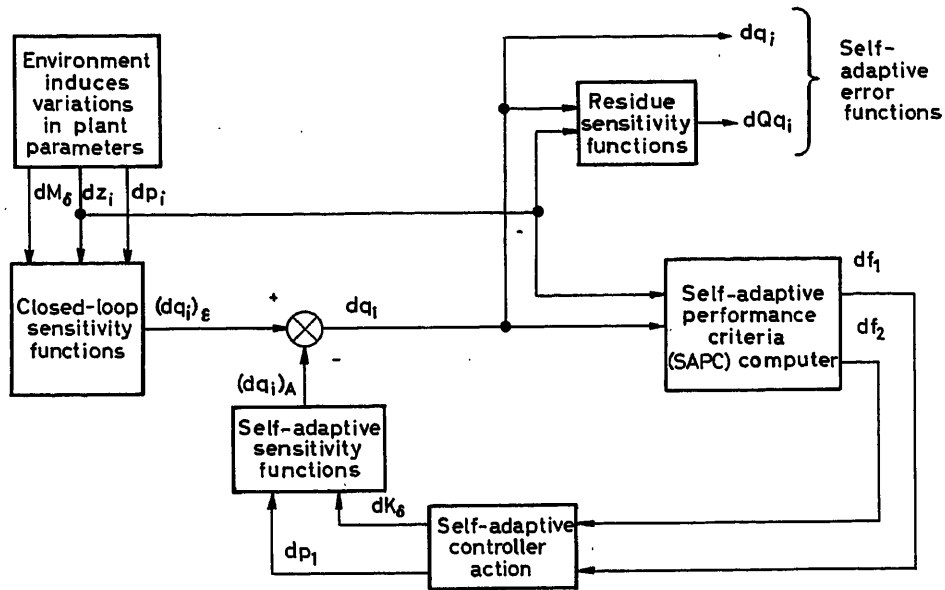


Figure E. Adaptive controller loop

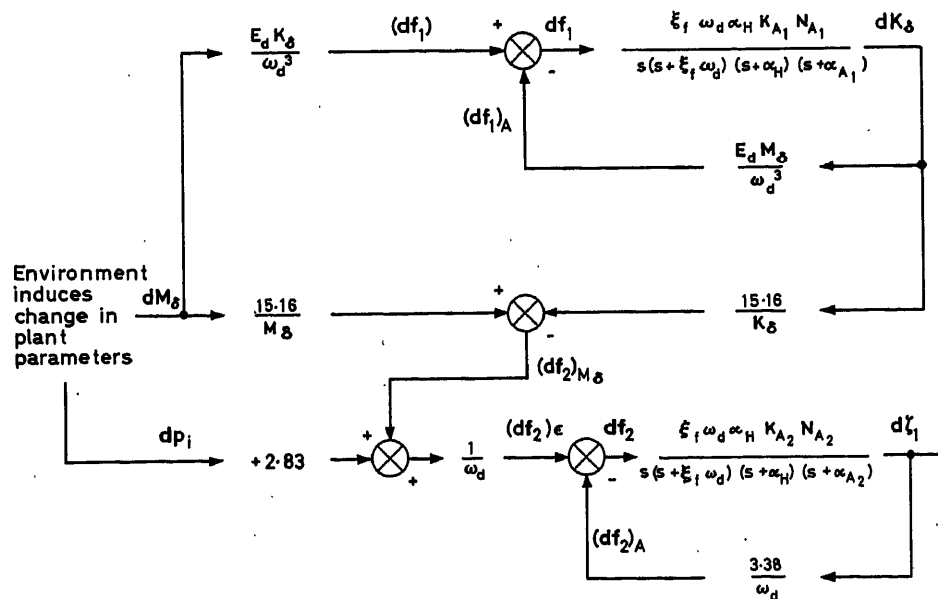


Figure F. Adaptive controller stability loops

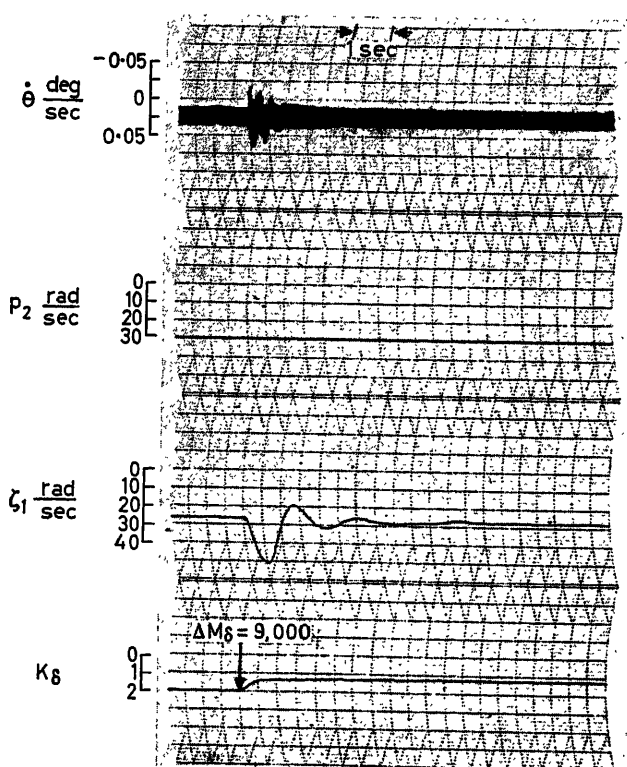


Figure G. Adaptive response—step change in plant gain

F. MESCH, *Institut für Regelungstechnik, Darmstadt, Germany*

In deriving eqn (4), the dither frequency ω_1 is assumed to be large compared with the dominant poles of the plant. I think this is quite impractical because in this case the dither amplitude at the input of the plant must be very large in order to yield a detectable output amplitude. Usually this is very undesirable, especially if high energy levels are involved.

Furthermore, what type of input signal $r(t)$ was considered? If $r(t)$ is a random signal and it is assumed that the dither amplitude at the plant output must be small compared with the normal operating signal, then it may be shown¹ that the bandwidth of the bandpass filter must be impractically small. For the type of filter considered in the paper, the damping ratio would be in the order of $\xi = 0.001$ or even less.

Thus a measuring device using phase sensitive detection (correlation) would be more effective.

Reference

- ¹ MESCH, F. *Vergleich von Korrelations-Meßverfahren für Selbst-einstellung* (to be published)

R. SMYTH, *in reply*

In answer to Dipl.-Ing. Mesch's question it should be pointed out that the second derivative of the output is detected as shown in Figure 3 of the paper. Detection of the second derivative allows the dither component in the output to be quite low.

Replying to his second comment, we have considered the effect of random signals appearing at the input to the regular loop in Reference 5 of the paper. Any random signal appearing at the output of the regular loop will produce an error in the adjustment of the adaptive parameter. The magnitude of the error depends upon the spectral content of the random signal and the bandwidth of the bandpass filter used in the adaptive loop. The effect of a given random signal can be reduced by narrowing the bandpass filter bandwidth, but at the expense of reducing the speed of adaptation.

We cannot agree with Dr. Mesch that the bandpass filter bandwidth would necessarily be very small, since the selection of the bandwidth is clearly an optimum design problem. However, we welcome the opportunity to consider his forthcoming paper in our future work.

R. LAUBER, *AEG Institut für Automation, Brunnenstr. 107a, Berlin 65, Germany*

As a contribution to this excellent paper I would like to suggest using another method¹ for an analysis of the stability in the large. It should be possible by this method to calculate directly the describing function of the adaptive controller loop, thus replacing the qualitative considerations made by the authors.

Reference

- ¹ LAUBER, R. A new method to derive the describing function of certain non-linear transfer systems. *Automatic and Remote Control*, Vol. 1. 1964. Munich; Oldenbourg. London; Butterworths.

R. SMYTH, *in reply*

It is possible that Dr. Lauber's method may allow prediction of limit cycles involving a strong interaction between the regular loop and the adaptive adjusting loop.

However, the stability analysis presented in the paper was capable of predicting the frequency of the limit cycle which was observed during the analogue simulation (Tables 1, 2 and 3). The stability model also allows prediction of the gain at which the limit cycle occurs.

We will consider Dr. Lauber's method in our future work.

Predetermination of Control Results for Reheaters in Steam Generators

W. KINDERMANN

Summary

The paper describes the predetermination of the time behaviour by application of the frequency response method, as particularly developed for resuperheaters in steam generators. The result of the control action of the simulated control circuit is quantitatively calculated by means of an analogue computer. The simulated control circuit is taken from a steam generating plant which is in the state of planning. The control results of various reheater arrangements and control circuits are compared with each other.

Sommaire

L'article décrit l'application de l'analyse harmonique effectuée spécialement pour les conditions de marche d'un résurchauffeur de vapeur avec prédétermination du comportement dynamique. Le résultat quantitatif de réglage de la boucle simulée est trouvé à l'aide d'un calculateur. La boucle de réglage simulée correspond à une installation actuellement au stade d'étude. Les résultats des différentes dispositions de résurchauffeurs et circuits de réglage sont comparés.

Zusammenfassung

Der Beitrag beschreibt die Anwendung der speziell für die Verhältnisse am Zwischenüberhitzer abgestimmten Frequenzgangmethode bei der Vorausbestimmung des Zeitverhaltens. Mit Hilfe eines Analogrechners wird das quantitative Regelverhalten des simulierten Regelkreises ermittelt. Dem simulierten Regelkreis liegt eine im Projektstadium befindliche Anlage zugrunde. Das Regelverhalten verschiedener Zwischenüberhitzeranordnungen und regelungstechnischer Schaltungen wird verglichen.

Present-day machines demand that live and process steam temperatures should be kept constant within a narrow scope for load ranges as large as possible and, by means of the frequency control system, also for rapid load swings. The reheater, especially, presents the boiler designer with difficult problems, because of its unfavourable partial load behaviour. Practical methods of boiler design offer a wide range of alternate solutions which do not always give good controllability. To obtain the expected controllability figures during the planning stages of the installation, predictions, based on the control performance and the boiler design, have to be made.

Such a predetermination opens with enquiries about the time and disturbance behaviour of the controlled system, and proceeds with the simulation of the complete control circuit and its disturbing influences upon the controller results. Various rough-and-ready rules, available to determine the time behaviour of the controlled system, offer only in very few cases a satisfying approach, and scarcely give any information about the disturbance behaviour. Against this, the frequency response technique, as stated by Profos at the 'Heidelberger Tagung', is a method by which the demands of practice can be met thoroughly.

In particular, the possibility of combining the different frequency response elements, allows the choice between calculation expense and required accuracy, in order to compare the dynamic behaviour by varying their constructive arrangements.

The reheater consists, as in the case of the main superheater, of numerous flows through heated and unheated tube elements. The dynamic behaviour of the whole system for various possible disturbances coming from outside, is given by the disturbance frequency responses. One of them will correspond with the control transient response.

If the manipulated variable of the primary or secondary control circuit is the position of a flue gas damper in the controlled flue gas channel or, as preferably and very often used for the control of reheater outlet temperatures, the angular position of a rotary burner or the position of a butterfly valve in the recirculating flow, the frequency response of a flue gas temperature disturbance and that of a flue gas flow disturbance is equivalent to the control transient response. The frequency response of the flue gas disturbance is therefore a matter of particular importance to the reheater.

The entire transfer behaviour of a reheater tube element is characterized by a number of frequency responses:

$$F_{\vartheta_s} = \frac{L\{\Delta\vartheta_s\}}{L\{\Delta\vartheta_e\}}; \vartheta_s = \text{steam inlet temperature} \quad (1)$$

$$F_M = \frac{L\{\Delta\vartheta_s\}}{L\{\Delta M\}}; M = \text{steam flow} \quad (2)$$

$$F_{\vartheta} = \frac{L\{\Delta\vartheta_s\}}{L\{\Delta\vartheta\}}; \vartheta = \text{flue gas temperature} \quad (3)$$

$$F_C = \frac{L\{\Delta\vartheta_s\}}{L\{\Delta C\}}; C = \text{speed of flue gas flow} \quad (4)$$

ϑ_s , M , C and ϑ are the factors influencing the reheater outlet temperature. Besides the necessary simplifications such as one-dimensional steam, flue gas, and tube wall temperatures, constant tube diameters, specific gravities and specific heats of the tube element concerned, any one of the four frequency responses presumes that the other three influencing factors stay constant over the considered time. In other words, the transmission behaviour of the tube element will be ascertained with time variation of one of the influencing factors, assuming that the other three have remained unchanged in time.

The exchange of the two frequency responses F_{ϑ} and F_C with one having the influencing factor Q , representing the heat value transmitted to the inner wall of this tube, appears according to above details not suitable, particularly as this presumes a linear increasing flue gas temperature over the entire length of the tube in steady-state condition. On the other hand, the deri-

vation of the four frequency responses offers considerable difficulties, if F_C is taken into consideration as well. Such a derivation, however, would be a tremendous help for automatic control techniques.

First of all, investigations had to be limited to the first three frequency responses F_{ϑ_e} , F_M and F_Θ . That, of course, is an additional simplifying assumption and means, that the time response, but not the final value, of the control transient response of the flue gas damper control corresponds with the time response of the flue gas temperature disturbance function, provided that the reheater is subdivided sufficiently for this calculation. Accordingly, the formulas for the three remaining frequency responses are derived from the set of simultaneous partial differential equations of the heat exchanger (Figure 1). The numerical calculation of these frequency responses can be performed very quickly if a well-programmed digital computer is on hand, even for a large number of pipe sections and various load values.

To represent the dynamic qualities of the reheater, in the form of coupled transient functions, by an analogue computer, it is necessary to transform the resulting disturbance frequency responses of the entire tube system from the Laplace domain back into the original domain. For especially well-approached values within the first time section of the transient response, the methods demonstrated by Leonhard and Herschel call for special attention. Expense in calculation work is tolerable. The time constants of the time elements simulated by an analogue computer are to be determined from the obtained transient responses according to the approximation method by Strejc. A simpler

method, however, is the direct determination of the time constants and damping factors for the computer set up by comparing the obtained frequency characteristics with typical bends and asymptotic gradients of well-known functions. With a transfer behaviour of the controlled system made known in this way, and the already known dynamic and static behaviour of the controllers, the control circuit can be simulated on the analogue computer, and the trend of the different signals, especially the control signal after a disturbance is introduced, can be recorded.

The results of a predetermination of the transfer behaviour of a reheater's controlled system, carried out in the manner described above, and the control characteristics obtainable by it, are shown in the following:

The dynamically precalculated reheater is in the planning stage about 18 months before being put into operation, has an iron weight of approx. 99 tons (of which 86.7 per cent is heated) and is part of a 'natural-circulation-cyclon-boiler' of 380 (510) tons/h steam capacity. The reheater outlet temperature is 530°C. The load-dependent maximum steam pressure is 20 atm. All heated sections of the reheater are situated in the controlled flue gas channel. At the reheater inlet a provision is made for an injection, attached to the flue gas damper controller.

For accomplishment of the assumptions taken as a basis for the frequency response derivation, the reheater is separated into nine tube sections. From those were obtained: four frequency responses for the inlet temperature, three for the steam flow disturbance and three for the flue gas temperature disturbance. The signal flow diagram (Figure 2) shows the arrangement of functional blocks for the disturbance, the control

For inlet temperature variation

$$F_{\vartheta_e} = \frac{\Delta \vartheta_a}{\Delta \vartheta_e} = e^{-[p+a \frac{p+b_2}{p+b_1+b_2}]} \quad \begin{matrix} \text{with } M = \text{const.} \\ \Theta = \text{const.} \end{matrix}$$

For flue gas temperature variation

$$F_\Theta = \frac{\Delta \vartheta_a}{\Delta \Theta} = \frac{ab_2}{p^2 + p(a+b_1+b_2) + ab_2} (1 - F_{\vartheta_e}) \quad \begin{matrix} \text{with } \vartheta_e = \text{const.} \\ M = \text{const.} \end{matrix}$$

For steam flow variation

$$F_M = \frac{\Delta \vartheta_a}{\Delta M} = \frac{\vartheta_e^{(0)} - \Theta^{(0)}}{v^0 \cdot k} \cdot \frac{(1-m)p + b_1 + (1-m)b_2}{p - \frac{1}{k} + (a+b_1+b_2)} \cdot \frac{1}{p} \cdot (e^{-\frac{1}{k}} - F_{\vartheta_e}) \quad \begin{matrix} \text{with } \vartheta_e = \text{const.} \\ \Theta = \text{const.} \end{matrix}$$

$$a = \frac{n \cdot L \cdot d_i \cdot \alpha_D \cdot \pi}{\Phi \cdot C_{pD}}; \quad b_1 = \frac{n \cdot L \cdot d_i^3 \cdot \gamma^D \cdot \alpha_D \cdot \pi}{\Phi_{\gamma R} \cdot C_R (da^2 - di^2)}; \quad b_2 = b_1 \frac{\alpha_R \cdot da}{\alpha_D \cdot di}; \quad k = \frac{b_1 + b_2}{ab_2}$$

Figure 1. Frequency responses

- L = Length of tube section [m]
- d^o, d^i = Outer and inner diameters of tube respectively [m]
- Φ = Steam throughput [kg/sec]
- n = Number of parallel tubes
- γ^D = Average specific gravity of steam within tube section [kg/m³]
- γ_R = Specific gravity of tube material [kg/m³]
- m = Nusselt'scher Exponent ($m \approx 0.8$)

- C_{pD} = Specific heat of steam [kcal/kg °C]
- C_R = Specific heat of tube [kcal/kg °C]
- α_D = Heat transfer coefficient steam to tube wall [kcal/m² sec °C] $\alpha_D = C \cdot \gamma^m$
- α_R = Heat transfer coefficient flue gas to tube wall [kcal/m² sec °C]
- v^0 = Speed of steam [m/sec]
- $\Theta^{(0)}$ = Average flue gas temperature in steady-state condition [°C]
- $\vartheta_e^{(0)}$ = Steam inlet temperature in steady-state condition [°C]

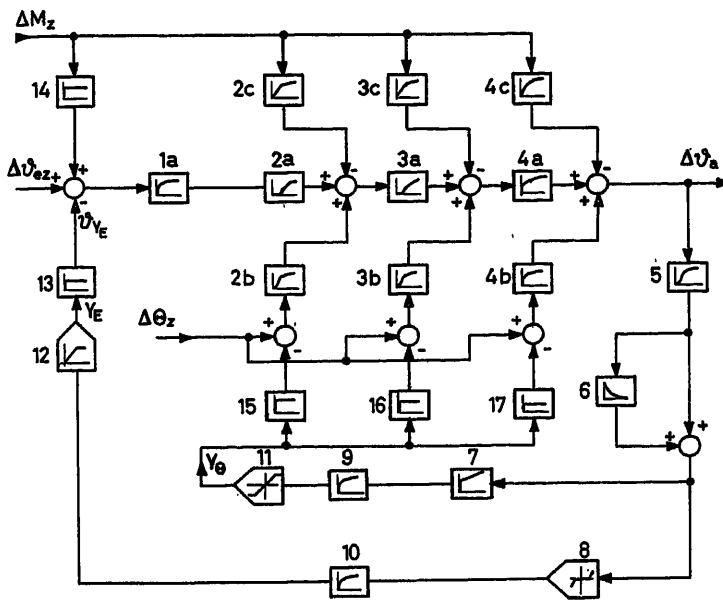


Figure 2. Simplified scheme of control signal flow

- 1 ... 4 = Partial section of reheater
 Index a = Transient response at $\Delta\Theta = 1$ for $t \geq 0$
 Index b = Transient response at $\Delta\Theta = 1$ for $t \geq 0$
 Index c = Transient response at $\Delta M = 1$
 5 = Thermocouple
 6 = Derivative action of controller
 7 = Flue gas damper controller
 8 = Set point displacement for injection controller
 9, 10 = Time constant of controllers
 11, 12 = Limitation of final control elements
 13 = Transmitting factor of injection
 14 = Transmitting factor of steam flow
 15, 16, 17 = Transmitting factors of position
 ΔM_z = Disturbance of steam throughput
 $\Delta \Theta_z$ = Disturbance of flue gas temperature
 $\Delta \Theta_{sz}$ = Disturbance of steam inlet temperature
 $\Delta \Theta_a$ = Change of temperature at reheat outlet

transient responses of the reheat, and for the control equipment of the control circuits.

The primary control circuit is the one which is PID-acting on the flue gas dampers and therefore acts similarly on the flue gas temperature as well. The secondary PD-action controller regulates the injection, mounted at the reheat inlet. As this control circuit will work outside its limit position (closed injection valve) in case of an emergency only, i.e. for very extreme temperature deviations, the set point is adjusted to a value about 1°C higher than that of the primary control circuit.

Results of the dynamic predetermination are:

(a) The disturbance and control transient response of each of the reheaters' partial sections. For the first section only the frequency response of the inlet temperature variation is available, since this section consists of only unheated elements (Figure 3).

The resulting control transient function of the sections $1 \dots 3 f_{1...3}(t)$ (step variation of the inlet temperature) shows still permissible time delays and starting times on the diagram. For shorter flow-through times (short tubes or small cross sections respectively) the transient function approaches the step function, as in the case for the fourth reheat section.

Step variations of the steam throughput result in a transient function $f_{1...3}(t)$ of approximate first order (without substantial time delay). For short flow-through times this transient function $f_4(t)$ also approaches the step change function.

For step variations of the flue gas temperature a first-order transient function $f_4(t)$ appears for short tubes, whilst for longer ones the influence of transport lag produces a delay in the transfer function $f_{1...3}(t)$.

For variations of the inlet temperatures the inverse gain and, accordingly, the effect of the inlet temperature disturbance, are larger upon reheat elements with short flow-through times than upon those with longer ones. The relations are the opposite for disturbances of the flue gas temperature or the steam throughput respectively.

(b) The optimization of the controller which is obtained by selecting the parameter of the controller's function blocks with regard to the most favourable control results. It gives very important information for the planning and lay-out of the control equipment and, furthermore, gives a lead to the adjustment of control equipment, while putting the control system into operation.

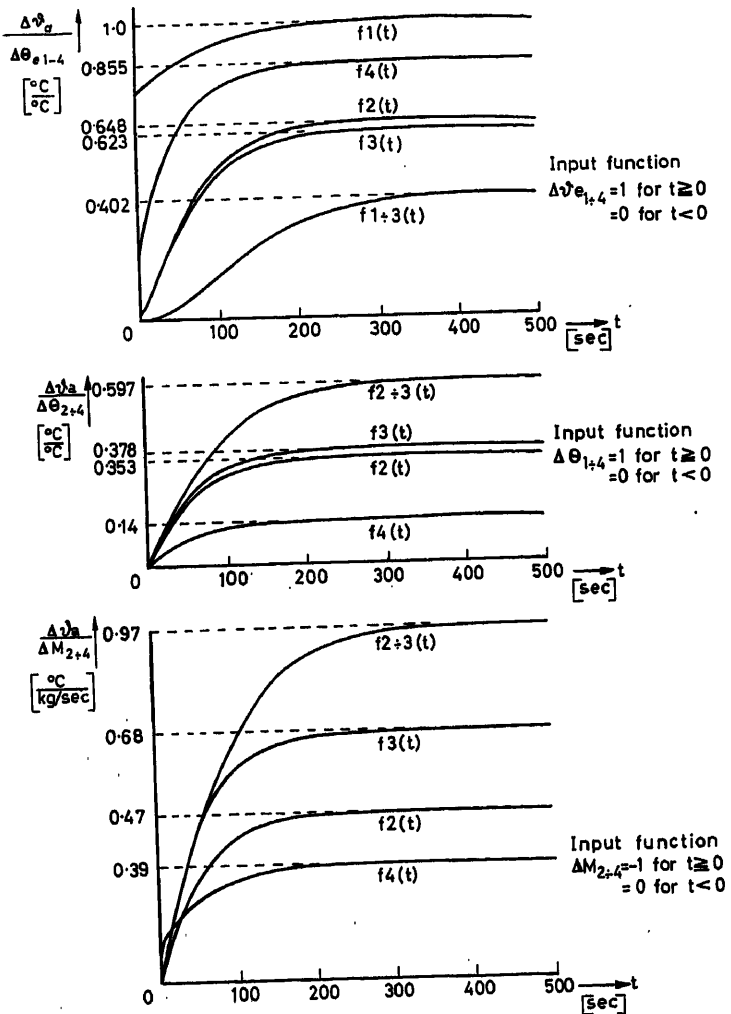


Figure 3. Transient and disturbance response of reheat's partial section

- $f_1(t)$ = Transient response of reheat's partial section 1 [unheated tube (length 20 m)]
 $f_2(t)$ = Transient response of reheat's partial section 2 [heated—500 parallel tubes (length 22 m) value of temperature increase possible 77°C]
 $f_3(t)$ = Transient response of reheat's partial section 3 [heated—500 parallel tubes (length 22 m) value of temperature increase possible 116°C]
 $f_4(t)$ = Transient response of reheat's partial section 4 [heated—partially unheated—500 parallel tubes and partly as single tube (length 7.3 m) value of temperature increase possible 54°C]

As the transient response varies with the steam throughput, i.e. the load situation of the steam generator, the optimization will differ more or less for various loads. The predetermination allows for whether an optimum adjustment of the controller is sufficient for the entire load range or whether it is necessary to regulate these controller parameters according to loads.

(c) The progress of a control signal as soon as one of the possible disturbances is introduced is indicated by the quantitative control result (Figure 4). In this case the respective disturbance was introduced to the system as a step change. For the first test case it is a steam inlet temperature variation of 20°C. This effective disturbance equals a standard disturbance of

6.88°C at the control signal measuring point (corresponding with the static transfer response of the controlled system). In the second test case it is a flue gas temperature variation of 15.2°C. The equivalent standard disturbance amounts to 10°C. Accordingly the control deviation is already big enough to start operating the emergency injection controller with its only 1°C higher adjusted set point (see dash and dot line in Figure 4). In the third test case the control deviation registered is to be expected after a steam throughput variation of 7.65 per cent in relation to the control load condition of 385 tons/h. The 29.5 tons/h steam throughput reduction equals a standard disturbance of -10°C at the measuring point of the control signal. Here, too, the emergency injection control operates shortly (dash and dot curve in Figure 4). The dashed curve of Figure 4 indicates the movement of the final control element during operation, after a disturbance has taken place.

Each of the three control characteristics, described above, represents the control result for a certain disturbance. In practice, all disturbances will possibly appear in a temporal sequence, which depends on the boiler design, the operating conditions and the other interconnected control circuits of the boiler. Therefore the above-mentioned results may be used for a guarantee with regard to the expected control result only with certain limitations, unless the time sequence of the disturbance is so long that no substantial overlappings occur respectively; the time sequence of the disturbances is well known by experience. The collection of such empiric values is a further important point, which could supply real impulses for the practical predetermination of a reheater's control behaviour.

As far as linear transfer functions are assumed in the control circuit the values of the disturbances can be percentage converted.

(d) The quantitative results of a performed precalculation are of limited practical value at today's state, for lack of appropriate empiric data regarding the time sequence of the disturbances and because of the different simplifications necessary for the derivation of the frequency responses. The qualitative results, however, supply so many valuable details for planning the control system and for the boiler design, that a pre-calculation is always justified. The effects of various reheater connections and arrangements in the boiler upon the control results, will be demonstrated with the nine cases investigated. For all of them the same reheater, subdivided in four partial sections as stated in (a), the same load value and the same disturbance—the one of a steam flow variation—were considered, so that comparing statements could be made (Figure 5).

The Test Case I shows the control result for a reheater, fully situated within the controlled flue gas channel.

Only for modest partial load demands will the boiler designer succeed in setting the entire reheater into the controlled flue gas channel. As the reheater is situated in the flue gas flow after the first stage of the main superheater, it gets into the portion of the flue gas flow, in which the transferred heat decreases considerably at partial load. Therefore, the boiler designer tries to transfer a section of the reheater into the front area of the boiler.

Such an extreme case, where a large section of the reheater is not situated in the controlled flue gas channel any more, is shown in Test Case II. The iron masses arranged after the first part of the controlled system, which is influenced by the controlled current, cause a very unsatisfactory control result.

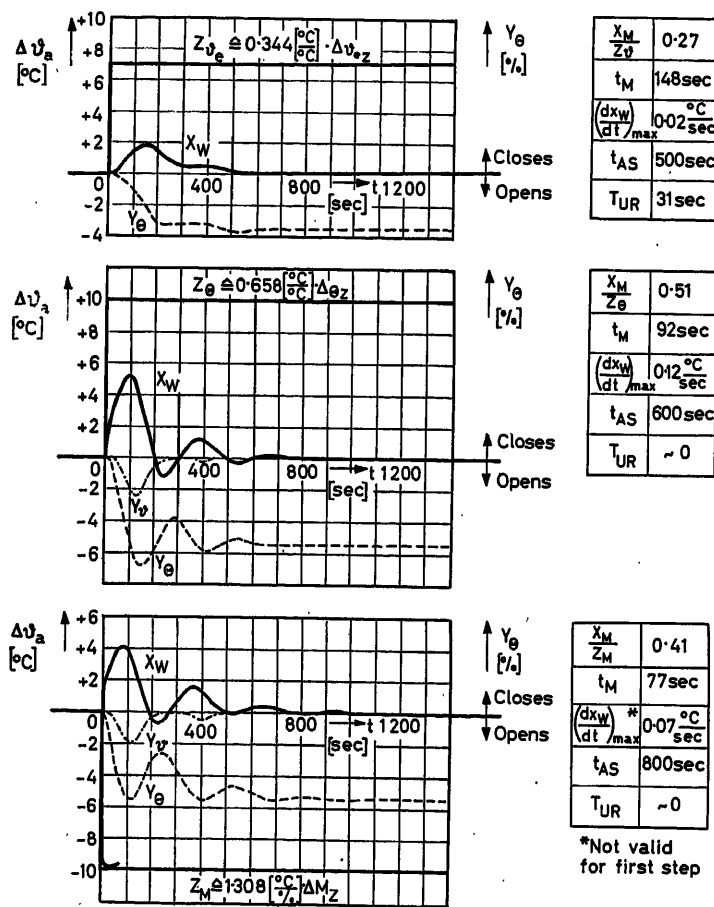


Figure 4. Control results for disturbance caused by step changes of steam inlet and flue gas temperature and of the steam throughput

- x_W = deviation of steam temperature from the desired value
- Y_θ = position of flue gas control dampers in per cent, related to Y_A
- Y_δ = control current in °C of the injection
- Z_θ = disturbance of flue gas related to measuring point of controlled variable
- Z_θ = disturbance of steam inlet temperature related to measuring point of controlled variable
- Z_M = disturbance of steam throughput related to measuring point of variable
- $\Delta\theta_{ex}, \Delta\theta_z, \Delta M_g$ = effective disturbances
- X_M = maximum variation (overshoot) of the control deviation
- T_{UR} = time delay of control characteristic (referring to process transient response to a step change)
- t_M = moment, at which X_M appears
- t_{AS} = control time (time, after which the temperature deviation does not exceed ± 2 per cent of the disturbance)

PREDETERMINATION OF CONTROL RESULTS FOR REHEATERS IN STEAM GENERATORS

Figure 5 (a). Supplementary table [to Figures 5 (b)–5 (d)]

	Injection control				Flue gas damper control			
	V_H	V_V	T_n	T_v	V_H	V_V	T_n	T_v
I					3.9	—	134	17
II					6	—	150	20
III					10	0.7	90	15
IV					6.4	0.3	109	16.3
V					5.2	0.71	51	10
VI	6.0	—	—	17	3.9	—	134	17
VII	6.0	—	—	17				
VIII	3.9	0.74	76.4	14.8	1.016	—	90	—
IX	5.5	0.5	100	16	1.016	—	150	—
	%/°C	—	sec	sec	%/°C	—	sec	sec

V_H = Control signal amplification in main circuit
 V_V = Control signal amplification in auxiliary circuit
 T_n = Integral time
 T_v = Rate time (rate time amplification = 5)

The project engineer of the control system also gets valuable references from such a comparative predetermination. Test Case III, for instance, shows how much the unfavourable control result of Test Case II can be improved, if instead of a PID-acting single-circuit control a two-circuit control is employed, with an auxiliary measuring point just before that reheater section, which is situated outside the controlled flue gas channel. The P-acting addition of this auxiliary temperature signal produces a control result close to that of Test Case I.

The question of how much the control result of Test Case I is improved by the use of a two-circuit control with an auxiliary measuring point before the reheater outlet, is answered by Test Case IV. There is no doubt that the addition of an auxiliary temperature signal shortens the settle-out time (time after which the temperature deviation does not exceed ± 2 per cent of the disturbance), but there is hardly any decrease of the maximum overshoot. The appraisal of how far the poor result of the two-circuit control justifies the considerable expenditure on measuring equipment remains. The somewhat unsatisfactory effect of the auxiliary measuring point is due to the virtual lack

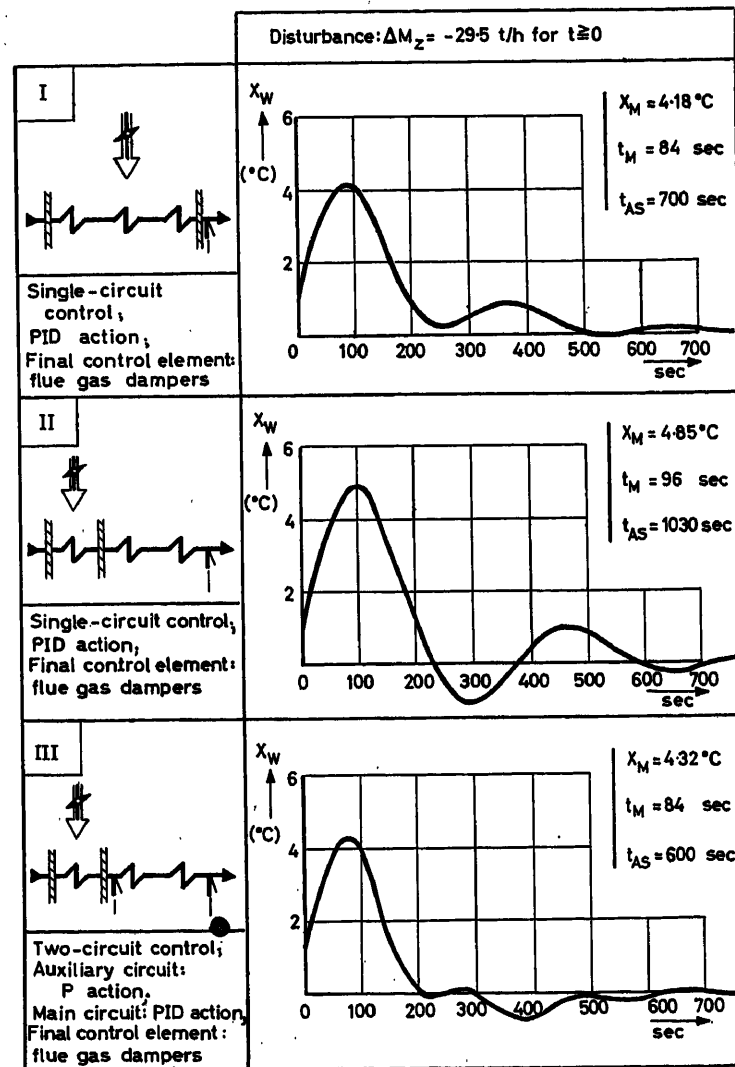


Figure 5 (b). Predetermined control results after step change of steam flow for various circuit systems of the reheater temperature control

x_M = Maximum overshoot of control deviation x_w
 t_M = Time of maximum overshoot
 t_{AS} = Time, after which deviation of temperature never exceeds ± 2 per cent of the disturbance

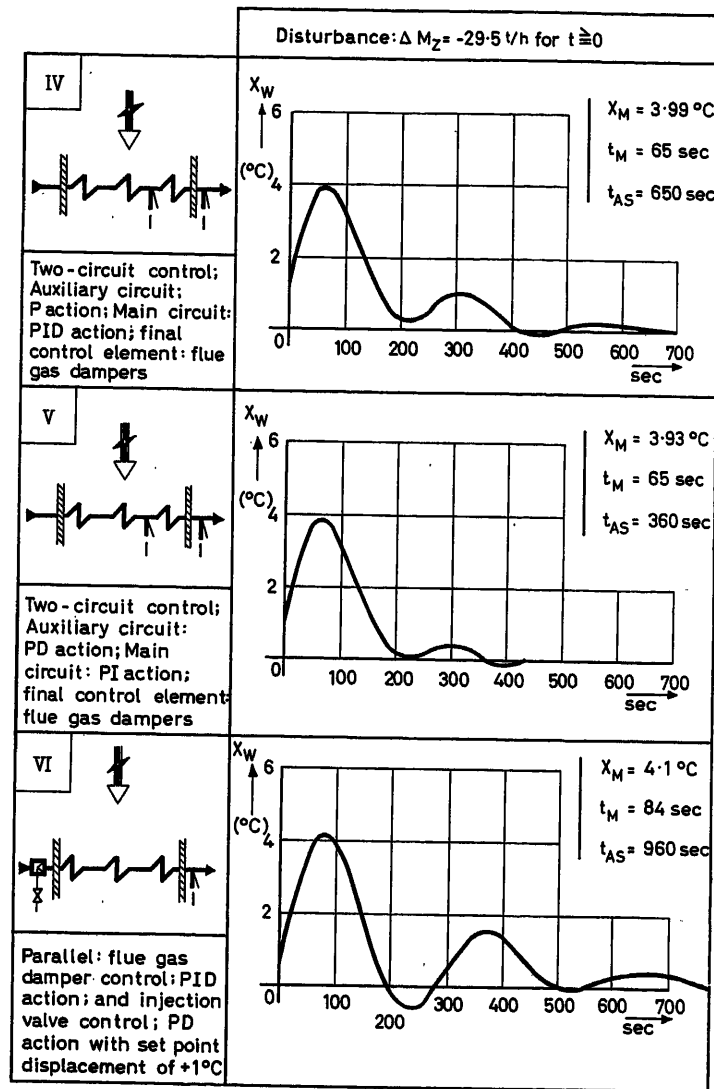


Figure 5 (c). Predetermined control results after step change of steam flow for various circuit systems of the reheater temperature control

of delay time in the transient response of this reheater allocation.

From the control curve of Test Case V one can recognize that a rate time in the auxiliary circuit of the two-circuit flue gas damper control is much more advantageous than a rate action in the main circuit as is arranged for Test Case IV. In case of an auxiliary circuit rate time the control deviation will be reduced even faster. However, the peak value of the control deviation remains unchanged now as before.

An injection cooling at the reheater will be avoided willingly, as the additional steam of medium pressure generated by it can only be used with a lower efficiency. Nevertheless, an injection system is usually at hand for safety reasons. The system, thought to operate as an emergency unit only, is situated, in the majority of all boilers, at the reheater inlet. That the well-meant intention to control the 'emergency injection' from the excess temperature at the reheater outlet must remain unsuccessful, is demonstrated by Test Case VI, representing, at the same time, the operating case. The injection controller, with a set point

adjusted only 1°C higher than the one of the flue gas damper controller, cannot in this installation 'cool off' the temperature peaks. The maximum control deviation remains unchanged, as a comparison with the control result of Test Case I indicates. Due to injection, the settle-out time (control time) gets worse, since a steam inlet temperature variation, produced by an injection at the reheater (see Figure 4) appears at the reheater outlet after a long delay and rise time.

Test Case VII demonstrates that, with an unaided injection at the reheater inlet, only a pretty bad result can be expected. It is different, however, if the injection takes place not at the reheater inlet, but shortly before the end of the reheater. If, furthermore, a continuously running injection water quantity is admitted, limited to a minimum by the flue gas damper control, the best control results can be obtained, as Test Case VIII indicates.

Because of material reasons at high temperatures, the intersection of the reheater, at which the injection will take place, should not be placed too far towards the reheater outlet. Yet

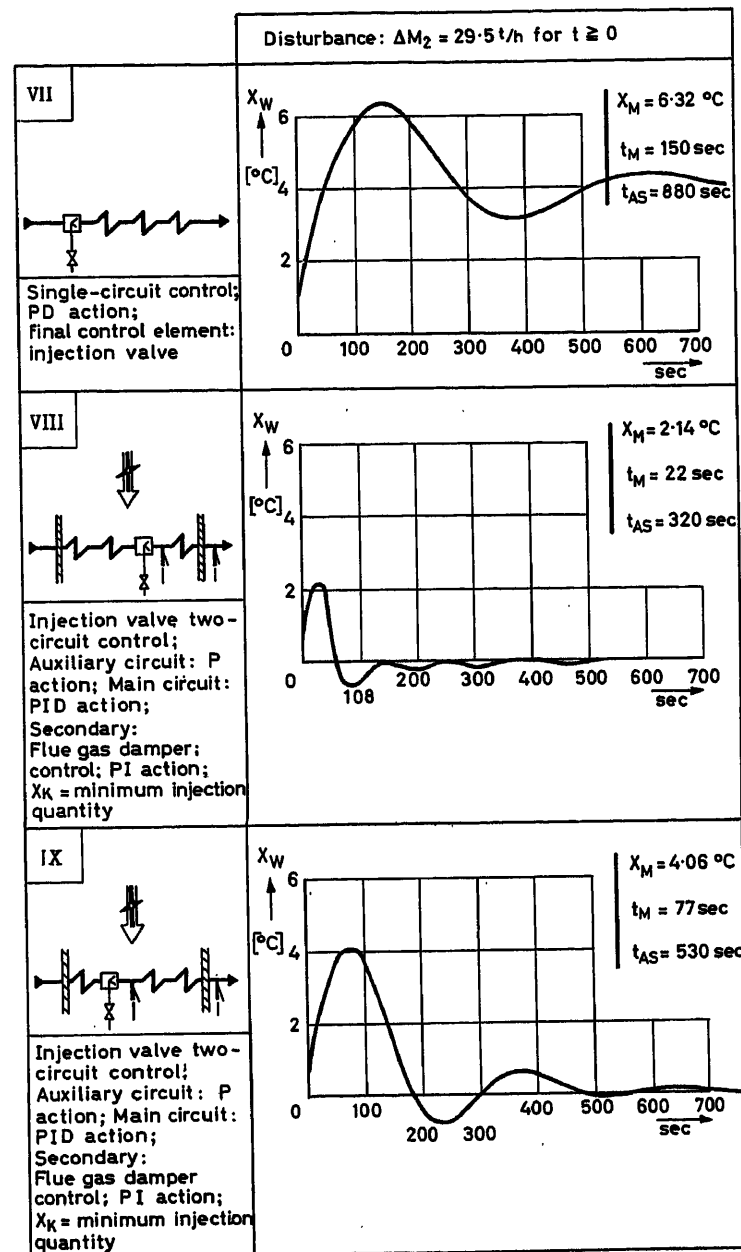


Figure 5 (d). Predetermined control results after step change of steam flow for various circuit systems of the reheater temperature control

the success of such an installation quickly becomes uncertain, as demonstrated by Test Case IX, if the reheater section, placed after the injection point, gets too large. Here, too, the dynamic predetermination will yield the required information about where to place that intersection.

The small selection of comparative results of a predetermination of control results demonstrates, especially for conditions at the reheater, how valuable such an investigation can be for the control project engineer and boiler designer. The fundamental studies in this field, however, can only be considered as completed, if quantitative results may also be used without any substantial restrictions. To that belongs the reduction of still necessary idealizations, the use of the disturbance frequency response for flue gas flow variations as well as a data collection,

gained by experience, about the time sequence of disturbances possible in steam generators.

References

- 1 LOBSCHIED, H. Überhitzer- und Zwischenüberhitzerregelung. *Technische Mitteilungen*. Vol. 5. (1959)
- 2 PROFOS, P. Zur Anwendung des Frequenzganges auf Regelprobleme der Praxis. *Moderne Theorien und ihre Verwendbarkeit*. 1957. Munich; R. Oldenbourg Verlag
- 3 LEONHARD, A. and HERSCHEL Die Laplace-Transformation und ihre Anwendung in der Regelungstechnik. 1955. Munich; R. Oldenbourg Verlag
- 4 STREIC, V. Approximation aperiodischer Übergangscharakteristiken. *Acta Technica* No. 1 (1958)
- 5 VDI/VDE Richtlinien-Entwurf für die Bestellung von Regelungen an Dampferzeugern. BWK No. 1 (1962)

DISCUSSION

J. RAKOWSKI, *Institute of Power, Warszawa 12, ul Woloska 88 m 53*

I would like to add some remarks to the very interesting and valuable report presented by Mr. W. Kindermann.

(1) The transfer functions for temperature variation vary with the steam flow, that is with load of the steam generator. Therefore, it seems to me, the following fact should be emphasized: the structure of the control signal flow diagram (Figure 2 in the paper) is valid for all values of load, but the main transfer functions in this diagram are different for different values of steam flow. Therefore, the question arises: what was the basic value of load at which the transients in Figures 3, 4 and 5 were obtained?

(2) It seems to me that because of this, two more problems are of interest: (a) predetermination of the transient, for example 40, 75 and 100 per cent of full load and a comparison between these results; (b) the question raised in the paper—is one optimum adjustment of the controller sufficient for the entire load range or is it necessary to change its parameters in accordance with load variations?

(3) It is emphasized in the paper that all the transients in Figure 5 have been obtained at the same load value and under the same disturbance—namely, that of steam flow variation. However, there are no comments on the adjustment of the controller, therefore I would like to ask the author were the controller parameters equal in all the cases, or were they adjusted in each case separately to get the optimum control effect?

(4) I would be interested to know what method was adopted for the simulation of the transfer functions for temperature variations? Are there any references on the subject?

W. KINDERMANN, *in reply*

(1) The control scheme as indicated in Figure 2 is valid for all load conditions, whereas the transfer functions of each block—and especially those of the process—are dependent on the prevailing load condition. The predetermination of the dynamic response was carried out for the design load of the boiler—385 t/h. This load condition is used in Figures 3, 4 and 5 of the paper.

(2a) For partial load conditions, in which the constant factors of the transfer functions attain other values, the transfer functions have to be determined in the same way. Very roughly, the time scale is doubled at 50 per cent of the design load.

(2b) The calculation of the transfer functions at different load

conditions and the consequent optimization of the controllers for each of these load conditions will give different controller parameters.

It is, then, a question of determining how much will be spent on equipment with adjustable parameters or whether the settings of the controller should be adjusted for partial load. Further details have been published in the *Conti-Elektro-Berichten* of August 1963.

(3) As in Figure 5, each case deals with a different arrangement of the process and controller. The optimization for minimum overshoot and minimum settling time has been adjusted differently for each case. The adjustment of the controller parameters is indicated in Figure 5(a).

(4) The transfer functions have been transformed back into real time domain functions, and these have been simulated on a computer. The methods of Leonhard and Herschel and the method of Strejc were used here.

MR. LÄUBLI, *Sulzer, Switzerland*

(1) Between the steam generator exit and the turbine entry there is a relatively long steam passage. Temperature fluctuations which occur at the generator end are damped in transit and enter the turbine with reduced amplitude. It is therefore necessary to determine the damping effect of the steam passages by a series of computer investigations. Figure A shows the transition ratio of a reheater type steam circuit. The entry magnitude is the temperature at the steam generator end, and the exit magnitude is the temperature at entry to the turbine.

For example, temperature oscillations with a time period of $T = 315$ sec (i.e. $\omega = 2\pi/T = 0.02 \text{ sec}^{-1}$) when flowing through the heat absorbing steam passages, are damped according to the following relationship:

$$\delta \equiv \frac{\Delta \hat{\theta} \text{ Turbine entry}}{\Delta \hat{\theta} \text{ Steam passage entry (Generator exit)}} = \begin{cases} \text{approx. } 0.4 \text{ for full load} \\ \text{approx. } 0.2 \text{ for 40 per cent load} \end{cases}$$

(2) The investigations will only succeed with the help of step interference, and it would also be helpful if the investigation could be completed by means of sinusoidal interference. Because the resonance amplitudes of the regulation magnitude are, in the main, larger than the transitional maximum deviations, due to step interference, their evaluation can be completely carried out.

(3) The working out of a variation in valve adjustment unfortunately does not restrict its effects to the reheater, but also has simultaneous interference effects on other generator parts. Needless to say, thorough

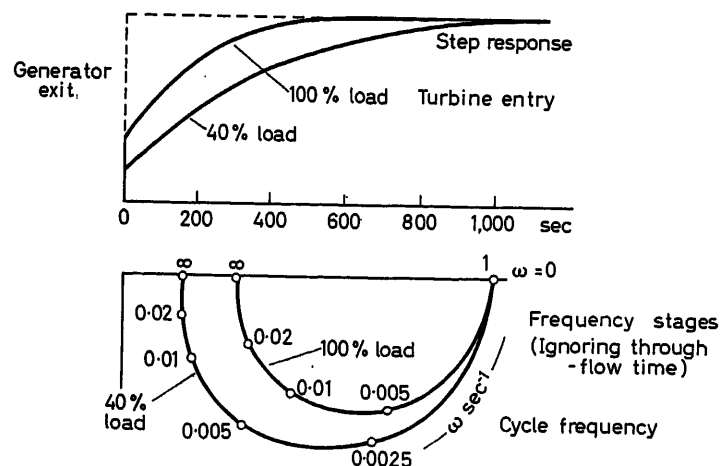


Figure A. Transition ratio of an MD-passage with 100 per cent and 40 per cent load (2 passageways $387 \times 20 \text{ mm} \times 85 \text{ m}$ long; 100 per cent = 340 t/h — 42 ata — 540°C)

discussion of these undesirable side-effects is not within the scope of a conference paper. It should, however, be noted that a solution which is optimal only for reheater and temperature regulation considerations, is not necessarily the best solution for the plant as a whole.

W. KINDERMANN, *in reply*

(1) The damping effect of the pipe between the boiler exit and turbine inlet has to be considered with regard to temperature variations at the turbine inlet; but the temperature-depending material boundaries of the pipe at the boiler outlet can be neglected.

(2) If periodic disturbances are expected—as, for example, increasing and decreasing steam flow—under certain conditions resonance effects may arise that reach amplitudes many times larger than the deviations from step disturbances. The need to determine the critical frequencies for such disturbances is therefore very justified.

(3) Unfortunately, among the possible setting values for the temperature control of an intermediate superheater, most of them—with the exception of the injector and its associated thermodynamic efficiency loss—introduce considerable disturbances to the other control loops of the boiler. This means that the setting value of the intermediate superheater temperature control, for example the position of recirculating flaps, must be introduced as a disturbance to the main superheater temperature control.

R. ISERMANN, *Technische Hochschule Stuttgart, Institut für Verfahrenstechnik und Dampfkesselwesen*

When calculating the frequency response of the steam outlet temperature, the author distinguishes between changes caused by alterations of flue gas temperature and changes due to alterations of flue gas flow.

I would like to ask why this distinction was made. The time behaviour of the temperature of the steam in the end of a superheater depends on steam inlet temperature, steam flow and heat flow. Heat flow is influenced by changes in the quantity of heat transferred through the outer tube walls. This quantity, among other things, is determined by flue gas flow, flue gas temperature and outer wall temperature. The equations for frequency response given in the paper already contain changes of heat flow due to changes of tube wall temperature. Therefore, in the computations following that, heat flow depends on flue gas flow and flue gas temperature alone.

I would like to mention that the effect of heat storage in the volume of flue gas in the superheater is very small compared with the storage effect of the iron masses. It seems to me that it can therefore be safely neglected. Also, the transport time of the flue gases through the superheater is so small that it can be neglected. For these reasons the time behaviour of the steam temperature should be the same whether one changes flue gas temperature or flue gas flow. Both changes will influence the rate of heat transfer without any noticeable time lag.

W. KINDERMANN, *in reply*

The heat flow from the flue gases which has an influence on the steam temperature, is the product of the heat transfer coefficient and the difference between the flue gas temperature and the tube wall temperature. The relation of the heat transfer coefficient, that is flue gas flow/heat flow, is therefore different from the relation of flue gas temperature/heat flow. Furthermore, the dynamic behaviour of the steam temperature in response to a flue gas temperature variation—as opposed to a variation in the heat transfer coefficient—is independent of the flow conditions.

Therefore, separate consideration should be given to the effects of the flue gas temperature and of the flue gas flow—the two components of a variation in the flue gas damper position.

R. QUACK, *Germany*

From a consideration of the thermodynamic efficiency of the whole process, water injection into the reheater is not recommended except in an emergency.

By using feedforward signals from the furnace fuel and air inputs and the steam flow, it is possible to obtain better results than those obtained from theoretical studies with feedback control alone. It would seem then, that this part of the paper is more a question of academic research.

W. KINDERMANN, *in reply*

The nine cases of qualitative results naturally represent just a part of possible controller circuits on an intermediate superheater. On the basis of the thermodynamic efficiency losses, continuous running water injection in the intermediate superheater is to be avoided, even if plants do exist with continuous flow minimum injection (Case VIII) which operate quite satisfactorily.

The examples VI and VII show how an emergency injection at the intermediate superheat inlet will influence adversely the control result.

J. GRAUVOGEL, *Electricité de France, 24, Boulevard de la Libération, Saint-Denis (Seine), France*

(1) Mr. Kindermann's paper shows that theoretical studies with analogue computers can help to define the control system of a process such as a boiler and also to take account of controllability in the design of the boiler itself. My first question is: how were the staff who performed this study organized, and in particular, how was the job divided between the builder of the boiler, the builder of the control system, and the future user of the boiler?

(2) Is it possible to take account of the contents of the flue gas (excess air ratio, percentage of volatile components in the fuel) in the analogue simulation? This content disturbs the rate of flow and the temperature of the flue gas, and also the shape of the flame, and alters the amount of heat delivered to the reheater by radiation and convection. Is it also possible to take into account any dirtiness of the reheater tube walls?

(3) Are real tests performed on the system itself after installation, and how do these results agree with the predetermined results?

W. KINDERMANN, *in reply*

(1) The incentives for system investigation are in most cases the high quality of temperature control required by the plant management. Whilst the static values such as tube dimensions, specific heat, heat transfer factors, etc. are determined by the boiler manufacturer, for the partial superheater sections, the control system supplier has determined, in the past, the dynamic behaviour of the controlled process and the system's controllability.

(2) It is possible to consider the static and dynamic behaviour of the excess air ratio, and humidity in fuel, with respect to the three parameters, steam inlet temperature, steam flow and flue gas temperature, as far as these are known.

The influence of the amount of cinder is taken into account when determining the static values of the superheater.

(3) A comparison between the design and the measured response of an intermediate superheater is shown in Figure B. The design transfer function for a step variation of the inlet temperature is given in the lower diagram. It is of seventh order with a transport lag of 1.88 sec. The measured results are shown in the upper diagram. The transient response of the inlet and output temperatures to a variation of the injection water flow was recorded and simulated on an analogue computer. The identifying values of the transfer functions $F_{\theta_a}^s$, $F_{\theta_a}^p$

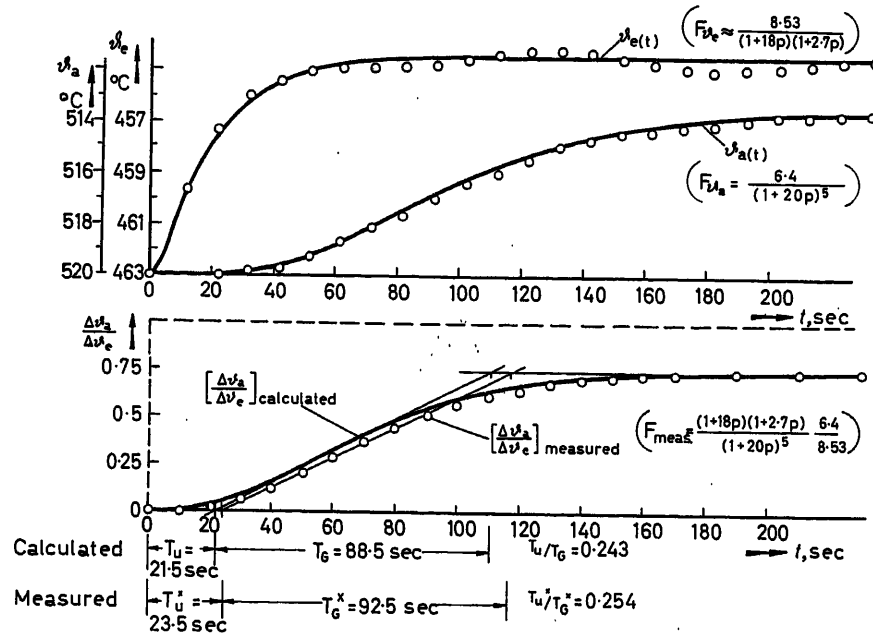


Figure B

were taken from the simulated time elements of the computer. The quotient of both transfer functions

$$\frac{F_{ga}^*}{F_{ge}^*} = F_{meas.}$$

determined by the analogue computer gives the transient response of the superheater to a step variation of the inlet temperature. The theoretical design ratio of T_u/T_G deviates by only about 5 per cent from the measured value. For other comparisons on different superheaters, this deviation becomes, in extreme cases, as much as 15 per cent. In some cases the static data of the superheater design differed by more than 20 per cent.

A. SCHÖNE, *Farbenfabriken Bayer A.G., 509 Leverkusen, Am Kiesberg 23*

The differential equations, from which the frequency response given in Figure 1 is developed, are not given in the paper. Therefore the question arises: has the author taken the frequency responses from the literature or has he developed them himself? If so, there are two further questions:

- (1) Does the author use a distributed or a lumped parameter model?
- (2) Eqn (2) gives a definition of the frequency response of outlet temperature changes versus inlet flow changes. Such relationships generally are non-linear. The linearization technique, for example, is

$$\frac{d(M\vartheta)}{dt} = M \frac{d\vartheta}{dt} + \vartheta \frac{dM}{dt}$$

From this equation the linearized expression

$$M_0 \frac{d\vartheta}{dt} + \vartheta_0 \frac{dM}{dt}$$

immediately follows, with the average values M_0 and ϑ_0 instead of the original time-dependent values.

W. KINDERMANN, *in reply*

The differential equations are obtained for a tube of circular cross section, conducting steam and heated by flue gas externally. The

$x-y$ plane lays perpendicular to the tube axis, the Z -axis is the tube axis.

In an ideal case the problem is treated one-dimensionally, with the designation of:

steam temperature $\vartheta_1(z, t)$ (t = time)

flue gas temperature $\vartheta_2(z, t)$

tube wall temperature $\vartheta_3(z, t)$

For the tube under consideration the following parameters are constant:

specific heat of 1,3 — C_1, C_3

density of 1,3 — γ_1, γ_3

inner tube circumference $U_i = \pi d_i, F_1 = \frac{\pi}{4} d_i^2$

outer tube circumference $U_a = \pi d_a, F_3 = \frac{\pi}{4} (d_a^2 - d_i^2)$

heat transfer coefficient $\alpha_{1,3}$.

The whole superheater is divided into a number of tube sections in such a manner that the above conditions are approximately valid for each tube section.

The first differential equation is obtained from the heat balance of a steam section of finite length Δz , giving by using the factor α

$$\alpha_{1,3} = \alpha_{1,3}^{(0)} \left(\frac{\vartheta}{\vartheta_0} \right)^m$$

where $\alpha_{1,3}^{(0)}$ = heat transfer coefficient at speed ϑ_0

m = Nusselt's exponent with $\xi = z/l$

where ϑ_0 = speed in rest condition

l = length of tube

the equation

$$\frac{\partial \vartheta_1}{\partial \tau} + \frac{\partial}{\partial \xi} \left[\left(\frac{\vartheta}{\vartheta_0} \right) \vartheta_1 \right] = \left(\frac{\vartheta}{\vartheta_0} \right)^m a (\vartheta_3 - \vartheta_1) \quad (1)$$

in which

$$a = \frac{l}{\vartheta_0} \frac{\alpha_{1,3}^{(0)} U_i}{C_1 \gamma_1 F_1}$$

The second differential equation follows from the heat balance at the tube wall section—a hollow cylinder—of length Δz

$$\frac{\partial \vartheta_3}{\partial \tau} = \left(\frac{\vartheta}{\vartheta_0} \right)^m b_1 (\vartheta_1 - \vartheta_3) + b_2 (\vartheta_2 - \vartheta_3) \quad (2)$$

where

$$b_1 = \frac{l \alpha_{1,3}^{(0)} U_i}{\vartheta_0 C_3 \gamma_3 F_3}$$

$$b_2 = \frac{l \alpha_{1,3}^{(0)} U_a}{\vartheta_0 C_3 \gamma_3 F_3}$$

using the assumption that there is no heat flow in the z-axis direction. From eqns (1) and (2) the following transfer function $F\mu$ is obtained for a steam flow variation except for when $\vartheta_2 = \text{constant}$

$$\Delta \vartheta_1(0, \tau) \equiv 0$$

$$\vartheta = \vartheta_0 + (\Delta \vartheta)_0 e^{p\tau}$$

The transfer function calculation uses a relationship $\frac{\partial}{\partial \vartheta_0} 1 + \lambda$ which when expanded gives

$$\left(\frac{\vartheta}{\vartheta_0} \right)^m = 1 + m\lambda + \dots$$

Using these factors gives

$$\frac{\partial \vartheta_1}{\partial \tau} + (1 + \lambda) \frac{\partial \vartheta_1}{\partial \zeta} = (1 + m\lambda) a (\vartheta_3 - \vartheta_1) + 0 [\lambda^2]$$

$$\frac{\partial \vartheta_3}{\partial \tau} = (1 + m\lambda) b_1 (\vartheta_1 - \vartheta_3) + b_2 (\vartheta_2 - \vartheta_3) + 0 [\lambda^2]$$

From this is obtained

$$\left[\frac{\partial^2}{\partial \tau^2} + \frac{\partial^2}{\partial \tau \partial \zeta} + (a + b_1 + b_2) \frac{\partial}{\partial \zeta} + ab_2 \right] \Delta \vartheta_1 = -[(1 - m)p + b_1 + b_2(1 - m)] \lambda_0 e^{p\tau} \frac{\partial \vartheta_1^{(0)}}{\partial \zeta} + 0 [\lambda^2] \quad (3)$$

This equation (3) has to be solved.

Under zero conditions, for $\vartheta_2 = \text{constant}$ we get from eqns (1) and (2)

$$\frac{d\vartheta_1^{(0)}}{d\zeta} = a (\vartheta_3^{(0)} - \vartheta_1^{(0)})$$

$$0 = b_1 (\vartheta_1^{(0)} - \vartheta_3^{(0)}) + b_2 (\vartheta_2^{(0)} - \vartheta_3^{(0)})$$

this gives

$$\vartheta_1^{(0)}(\zeta) = \vartheta_2 + (\vartheta_1^{(0)}(0) - \vartheta_2) e^{-\zeta/K}$$

in which

$$K = \frac{b_1 b_2}{ab_2}$$

For the non-homogeneous solution

it follows that

$$C = \frac{\lambda_0}{K} (\vartheta_1^{(0)}(0) - \vartheta_2) \frac{(1 - m)p + b_1 + (1 - m)b_2}{p^2 - (1/K)p + (a + b_1 + b_2)p}$$

To obtain $\Delta \vartheta_1(0, \tau) = 0$ the appropriate homogeneous solution has to be added.

$$\Delta \vartheta_1(\zeta, \tau) = c \left[e^{p\tau - \zeta/K} - e^{p\tau - \left[p + a \frac{p + b_2}{p + b_1 + b_2} \right] \zeta} \right]$$

from this we obtain

$$\frac{\Delta \vartheta_1(\zeta, \tau)}{\Delta \vartheta(\tau)} = F_m = \frac{\vartheta_1^{(0)}(0) - \vartheta_2}{\vartheta_0 K} \frac{(1 - m)p + b_1 + (1 - m)b_2}{p + (1/K) + (a + b_1 + b_2)} \frac{1}{p} e^{-1/K} - F_{\vartheta_1} \quad (4)$$

where

$$F_{\vartheta_1} = e^{-\left[p + a \frac{p + b_2}{p + b_1 + b_2} \right] \zeta} \quad (5)$$

An Optimizing Control of Boiler Efficiency

S. FUJII and N. KANDA

Summary

With a view to economical operation of a boiler plant, it is strongly desired to hold the boiler efficiency at a maximum value, despite changes in steam consumption, quality of fuel, and leakage of air, etc.

Since the boiler efficiency is maximized by the fuel consumption under constant steam pressure control, the excess air ratio is optimized to minimize the fuel consumption.

The peak-holding method contrived by Draper and Li is first adopted as a method of optimizing control. It is modified after various discussions on the practical problems, i.e., the elimination of noise superimposed on the fuel flow and the dynamic effects of the control system and disturbance of the steam flow. The experiment is carried out using a once-through boiler and the results of the analysis of the system are found to be in good agreement with those of the experiment. Moreover, a general design principle is mentioned for the optimizing control system of the boiler efficiency.

Sommaire

En vue du fonctionnement économique d'une centrale à vapeur, il est hautement souhaitable de maintenir le rendement des chaudières à une valeur maximale, en dépit des variations de la consommation de vapeur, de la qualité du combustible, des fuites d'air, etc.

Puisque le rendement des chaudières est maximalisé par le débit de combustible à pression de vapeur constante, on optimise le rapport d'excès d'air pour minimiser le débit de combustible.

On adopte d'abord la méthode du «peak-holding» imaginée par Draper et Li, comme méthode de commande optimale. On la modifie après diverses considérations d'ordre pratique, portant notamment sur le problème de l'élimination du «bruit» qui se superpose au débit de combustible, et sur celui des effets dynamiques du système de commande et des perturbations du débit de vapeur. L'expérimentation porte sur une chaudière à circulation directe et les résultats de l'analyse montrent un bon accord avec l'expérience. Enfin, on expose un principe général de conception en vue d'optimiser le système de réglage du rendement de la chaudière.

Zusammenfassung

Zur wirtschaftlichen Betriebsweise eines Kesselhauses ist es sehr wünschenswert, den Kesselwirkungsgrad trotz Änderungen im Dampfverbrauch, Brennstoffgüte, Falschlufte usw. dauernd auf einem Maximalwert zu halten.

Da der maximale Kesselwirkungsgrad durch den minimalen Brennstoffverbrauch bei gleichbleibendem Dampfdruck bestimmt ist, wird das Luftüberschußverhältnis optimiert, um den Brennstoffverbrauch möglichst gering zu halten.

Zunächst wird das von Draper und Li erdachte Verfahren, den Spitzenwert zu halten (peak-holding) zur Optimalwertregelung herangezogen. Ausgehend von praktischen Problemen, wie der Ausschaltung des dem Brennstoffstrom überlagerten Rauschens und der dynamischen Effekte der Regelung sowie der Störungen im Dampfstrom, erfolgte eine Änderung dieser Methode. Die an einem Einzugsessel durchgeführten Versuchsergebnisse stimmen gut mit den Ergebnissen der analytischen Untersuchung des Systems überein. Darüber hinaus wird ein allgemeines Entwurfsprinzip für die Optimalwertregelung des Kesselwirkungsgrades erwähnt.

Introduction

It is strongly desired to operate a boiler plant economically, that is, to hold the boiler efficiency always at a maximum value despite natural changes in steam consumption, quality of fuel, and leakage of air, etc.

Economically, it is therefore very important to develop practicable control methods and simple controllers for boiler plant operation. These will also help to solve engineering problems, that is, they will make the performance of the boiler efficiency clearer and yield much valuable data for the better design of boiler plants. In fact, an optimizing control of the boiler efficiency has not yet been carried out in this country or abroad, because of the poor accuracy of the measuring devices, the complexity of the optimizing controller and the lack of adequate control methods. In this laboratory, various methods of optimizing control, which can be applied to the boiler efficiency and also to any efficiency or profit in engineering systems, have been studied generally, especially in their theoretical aspect. As an application of this research, the optimizing control of the boiler efficiency is picked up and a realistic control method and its controller is being developed.

In this paper, the excess air ratio is optimized so as to minimize the fuel consumption, on the basis that the boiler efficiency is maximized by the minimization of the fuel consumption under the constant controlled steam pressure.

The peak-holding method contrived by Draper and Li¹ is first adopted as a method of optimizing control. It is modified after various discussions on the practical problems, i.e., the elimination of noise superimposed on the fuel flow, the dynamic effects of the control system and the effect of the disturbance of steam consumption on the control action. The experiment is carried out using a once-through boiler and the results of the experiment are compared with those of the analysis of the control system. In addition, a general design principle is mentioned for the optimizing control system of the boiler efficiency.

Definition of Boiler Efficiency and an Optimizing Control Method

Boiler Efficiency

Boiler efficiency is defined as follows:

$$\eta_B = \frac{Q_s(I_2 - I_1)}{Q_f H_f} \times 100 \text{ per cent}$$

Boiler efficiency is defined as the ratio of the heat absorption by water to the calorific value of fuel, and in close relation with the conditions of combustion in the furnace. There is an optimum value for the amount of air supplied for combustion, and the boiler efficiency is maximum at this optimum value of the air. The empirical values for this are available in terms of excess air ratio for various kinds of fuel, but in practice they are not constant but change more or less according to the method of combustion, quality of the fuel, fuel consumption, etc.

Thus, in order to hold the boiler efficiency always at a maximum value, the amount of the supply air should be controlled so as to adhere constantly to the optimum value.

Control Method

As clearly seen from the equation of definition, the maximum efficiency can be obtained by minimization of fuel consumption provided the steam pressure and steam consumption are constant. A boiler has usually an automatic combustion control system and the fuel flow is controlled so as to keep the steam pressure at a specified constant value despite natural changes in steam consumption and other disturbances. In this system, if the air flow is changed, the conditions of combustion are changed and the fuel flow is then controlled to maintain a constant steam pressure. Therefore, by measuring the variation of fuel flow due to the intentional change in air flow, and by always adjusting the air flow so as to make the fuel flow a minimum, the ideal can be attained.

This method is illustrated by Figure 1, where the optimizing controller is incorporated into the conventional steam pressure control system, and controls the air flow so as to keep the fuel flow always at the minimum value. Figure 2 is a typical form of optimizing control system. Here, the convex curve shows that the fuel flow has a minimum value at a certain value of air flow. As an input from the optimizing controller to the boiler control system, the excess air ratio instead of the air flow is being used.

Up to now, various methods of control for the optimizing system shown in Figure 2 have been investigated by several researchers. In this paper, a control scheme of peak-holding type is adopted.

Peak-holding Method

In the practical system, the extreme value of the optimizing system is usually not fixed, but moves with changes in load condition or environment. It is here assumed that the moving speed of the extreme value is considerably slower compared

with the searching speed for the extreme value by the optimizing controller.

Figure 3 shows a typical performance of optimizing control of peak-holding type. For simplicity of explanation, the dynamic lags of the system are neglected. For the input μ with constant speed as shown in Figure 3(a), the output of the system, Q_f , passes the minimum value at the time instant 1 and increases thereafter. If the peak-holding circuit is so designed as to follow the output exactly when the output is decreasing, but holds to the minimum value after the minimum is passed and the output starts to increase, then there will be a difference

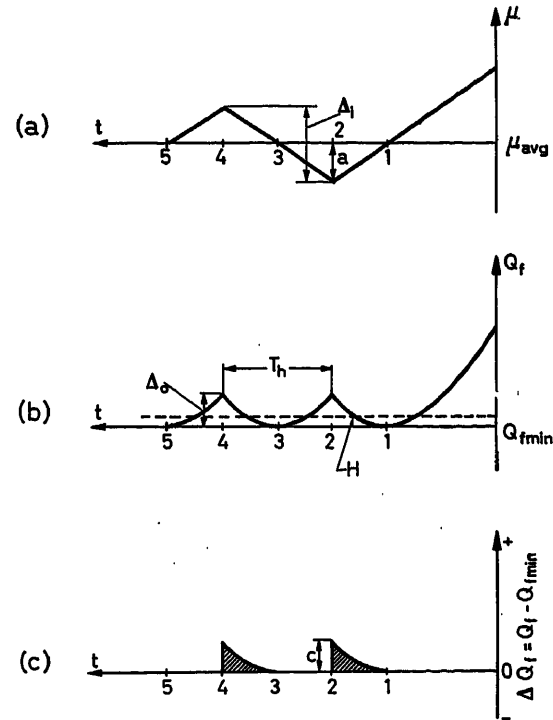


Figure 3

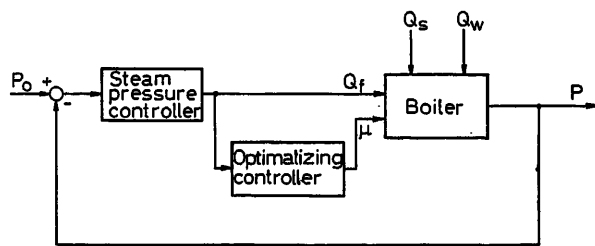


Figure 1

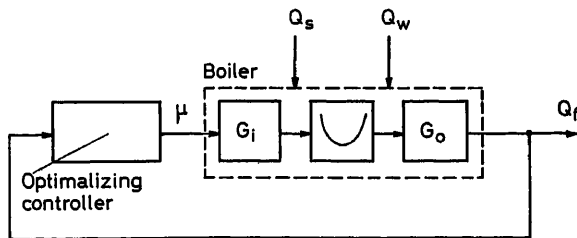


Figure 2

ΔQ_f between the output Q_{fmin} of this peak-holding circuit and the output Q_f itself after the time instant 1, as shown in Figure 3(c). When this difference ΔQ_f amounts to an assigned allowable value, denoted by c in Figure 3(c), at the instant 2, the direction of the input drive is reversed, while keeping the driving speed the same as before. At the same time, the signal resetting circuit is triggered and then the output Q_{fmin} of the peak-holding circuit is reset to the present output Q_f of the system. After the instant 2, the output decreases again, and increases after passing the minimum value. As before, at the time instant 4, when the difference amounts to the allowable value, the direction of input drive is again reversed. Thus, the output Q_f oscillates around the extreme value with constant period. The period of the output variation is called the hunting period T_h . The period is half that of the input variation. The extreme variation Δ_0 and Δ_i of the output and input respectively, and the difference between the minimum value and average value of the output is called the hunting loss H [Figure 3(b)]. For the case where the dynamic lags of the system are taken into account, the detailed results of the analysis are given by Fujii^{3, 4}.

Characteristics of the Control System for Boiler Efficiency

Outline of Boiler Details and its Controllers

The test boiler used in the experiment is a once-through boiler with steam separator. The principal items of the boiler are given in Table 1, and the layout of this boiler and controllers

Table 1. Principal items of test boiler

Type	Once-through boiler with steam separator		
Capacity	6 kg/cm ² , saturated temp., 300 kg/h		
Fuel	Town gas		
Combustion system	Burner type with air mixed internally and externally		
Draught system	Suction draught		

Dimension	in./out diam. mm.	length m.	heating area m ²
Economizer and evaporator	19.4/25.4	48.4	3.4
	31.1/38.1	44.8	4.8
Steam separator	250/264	1.12	—

is shown in Figure 4. In particular, an excess air ratio controller is installed, and it is possible to change automatically the excess air ratio by electrical signal or manually.

Town gas was the fuel used in this experiment, and the results of the analysis show that the lower calorific heat H_1 is 3,200 kcal/nm³ and the ideal air flow L_{00} is 3.3 nm³/nm³ fuel.

Static Characteristics of Boiler Efficiency

Figure 5 shows the measured values of the boiler efficiency at various operational conditions of the test boiler. It is found that the value of excess air ratio producing the maximum efficiency is varied with change in the load, i.e., the steam consumption. In Figure 6 the same data are plotted with the corresponding fuel flow as ordinate. As seen, the maximum efficiency corresponds to minimum fuel flow provided the steam pressure stays constant.

Overall Characteristics of Boiler Control System

Since the transfer function of the boiler proper is usually dependent on the operating condition, a standard operating condition is selected as follows:

$$P_0 = 4 \text{ kg/cm}^2 \text{ G} \quad Q_w = 125 \text{ kg/h} \quad Q_s = 90 \text{ kg/h}$$

The subsequent experiments of optimizing control are carried out around this condition. An overall block diagram of the boiler control system is shown in Figure 7. ${}_1H_f$ and ${}_1H_\mu \nu(t) + {}_2H_\mu \nu^2(t)$ represent the characteristics of the heat input through heating surface with respect to the fuel flow and the excess air ratio, respectively. It is found from the experiment that the dimensionless value ${}_1H_f$ is nearly equal to 1. Since the value of ${}_1H_\mu$ is zero when the small deviation from the extreme value is considered, account must be taken of the secondary small deviation of ν . This is the term of ${}_2H_\mu \nu^2(t)$. In general, the time constants of the economizer are far larger than those of the evaporator. Therefore, the effects of the economizer on the response of the system can be neglected. In addition, the response time of the excess air ratio controller is considerably shorter than that of the boiler proper. Consequently, the boiler control system of

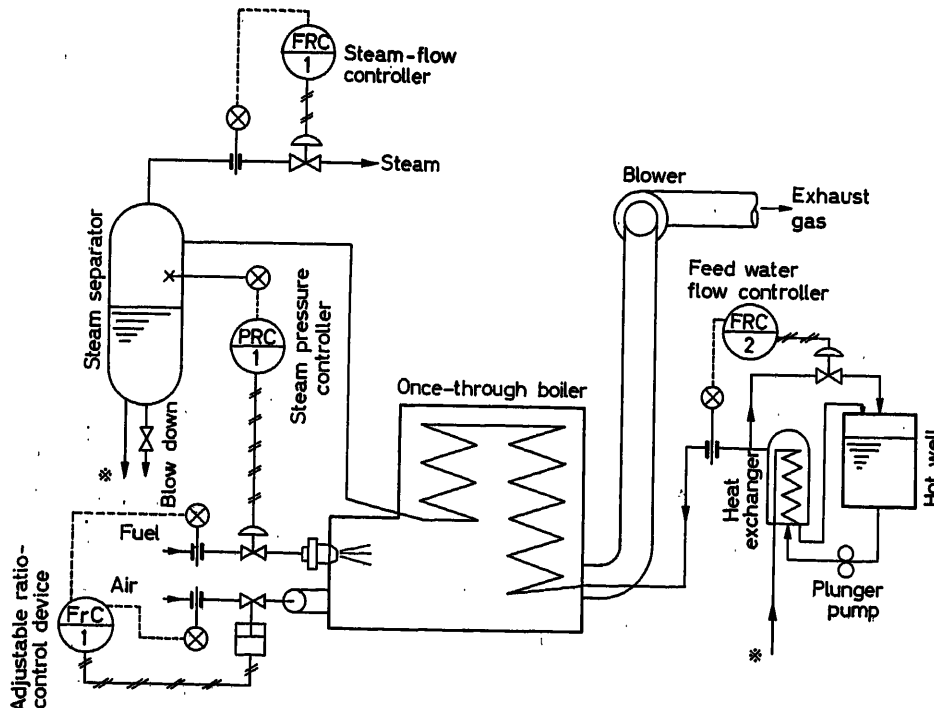


Figure 4

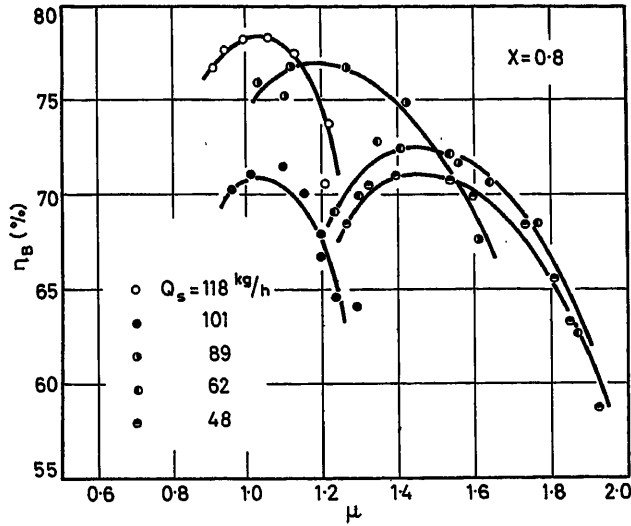


Figure 5

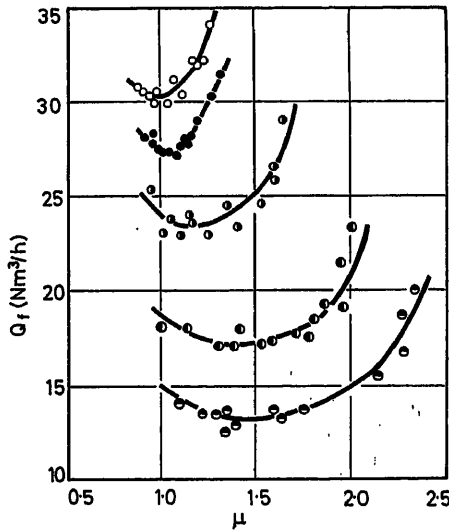


Figure 6

Figure 7 is also converted into the typical form of optimizing control system, as shown in Figure 8.

According to the subsequent results of experiments, it is found necessary to include a filter in measuring the fuel flow, since a great deal of noise is included in the fuel flow. This filter is represented as G_{fi} in Figure 8. G_m is the transfer function of the fuel flow measuring device. Thus, the overall transfer function of the output linear group in the system becomes $G_0 \cdot G_m \cdot G_{fi}$. The transfer functions and the values of $\mu - Q_f$ characteristics under the standard condition of operation are given as follows:

$$Q_f = 11.5(\mu - 1.1)^2 + 24.0 \text{ (Nm}^3\text{/h)} \quad (1)$$

$$G_0 = \frac{0.019s + 0.00096}{s^4 + 0.83s^3 + 0.17s^2 + 0.019s + 0.00096} \quad (2)$$

$$G_m = \frac{1}{12s + 1} \quad (3)$$

$$G_{fi} = \frac{1}{80s + 1} \quad (4)$$

Direct calculation of the optimizing control action by use of these transfer functions is difficult, and therefore the combined transfer functions are approximated by a second order lag system as follows:

$$G_0 \cdot G_m \cdot G_{fi} = \frac{1}{(77s + 1)(14s + 1)} \quad (5)$$

Figure 9 shows the comparison between the transient response of eqn (5) and that of the real boiler control system. It is found from this that the approximate expression agrees fairly well with the results of the experiment.

Experimental Results and Discussions on the Efficiency Control

Practical Problems and their Counterplans

Effect of Noise on the Control Action and its Counterplan—As shown in the subsequent figures, noise superimposed on the

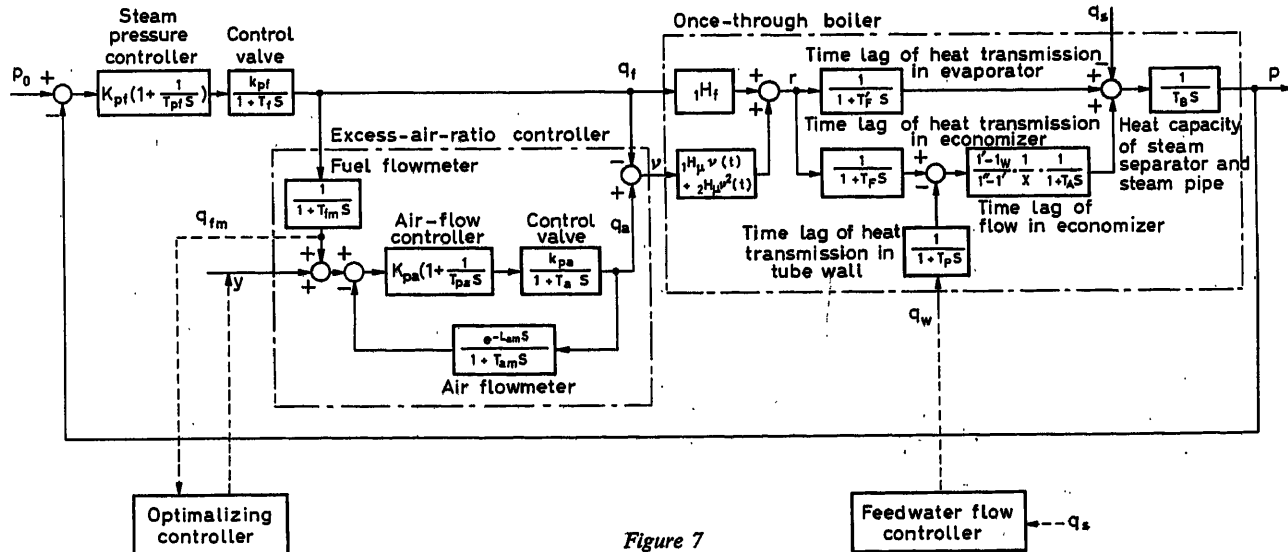


Figure 7

fuel flow disturbs the optimizing control action. To avoid it, the following three counterplans can be considered.

(1) The value of allowable difference is chosen so as not to be disturbed by the noise.

This method avoids the frequent switching action of the input by the noise interference, but it is undesirable since the hunting loss of the resulting output becomes larger.

(2) A filter to eliminate the noise is added to the fuel flow measuring device. The noise can be almost eliminated by such

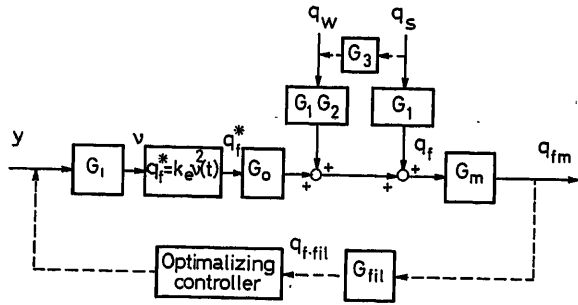


Figure 8

$$G_i = 1$$

$$G_0 = \frac{k_{pf} K_{pf} (1 + T_{pf} s)}{T_B T_{pf} s^2 (1 + T_f s) (1 + T_{f'} s)} + \frac{k_{pf} K_{pf} (1 + T_{pf} s)}{T_B T_{pf} s^2 (1 + T_f s) (1 + T_{f'} s)}$$

$$G_1 = \frac{k_{pf} K_{pf} (1 + T_{pf} s)}{T_B T_{pf} s^2 (1 + T_f s) (1 + T_{f'} s)} + \frac{k_{pf} K_{pf} (1 + T_{pf} s)}{T_B T_{pf} s^2 (1 + T_f s) (1 + T_{f'} s)}$$

$$G_2 = \frac{I' - I_w \cdot 1}{I'' - I' \cdot X} \cdot \frac{1}{(1 + T_p s) (1 + T_A s)}$$

$$k_e = \frac{k \mu_0^2}{Q_{f0}} = \frac{-2H\mu}{1H_f}, \quad Q_f = k(\mu - \mu_0)^2 + Q_{f0}$$

$$G_m = \frac{1}{1 + T_{fm} s} \quad (\text{Fuel flow measuring device})$$

$$G_3 = (\text{Feedwater flow controller})$$

$$G_{fil} = \frac{1}{1 + T_{fil} s} \quad (\text{Filter})$$

a filter, but if the filter itself needs to have a large time constant, the hunting loss of the output increases in general because the time lag of the control system including the filter is much larger than that of the control system without it. Figure 10 shows a control behaviour for the case where a simple filter of first order time ($T_{fil} = 80$ sec) is used. Although the fuel flow is being varied largely, the regular control action is being carried out without the interference of noise.

(3) Generation of noise is suppressed substantially. In order to decrease the amplitude of noise, one may take a small value of K_{pf} or a large value of T_{pf} of the pressure controller. Since this counterplan can be made at the expense of the pressure control which is the master control of the boiler plant, the decision must be made only after considering the overall balance of the steam power plant.

Effect of Dynamic Lags on the Control Action and its Counterplan—When the fuel flow passes the minimum value and the difference between its maximum value and actual value amounts to the allowable difference, the direction of input drive is then reversed. The response of fuel flow, however, cannot follow the input immediately but continues to increase as before, owing to the dynamic lags of the system. Once a direction of the input μ is reversed, the difference is reset to zero, but since the response of fuel flow continues to increase, the value of fuel flow at that

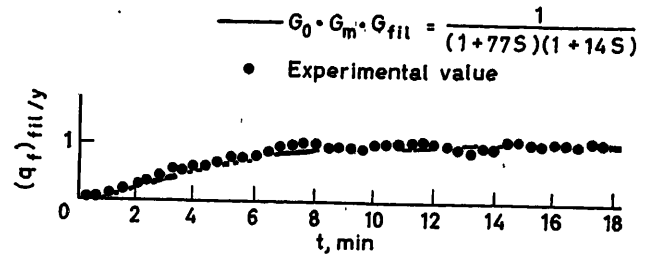
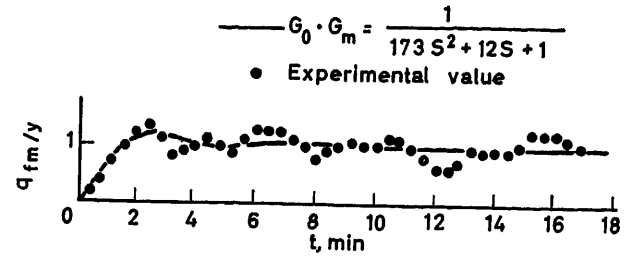


Figure 9

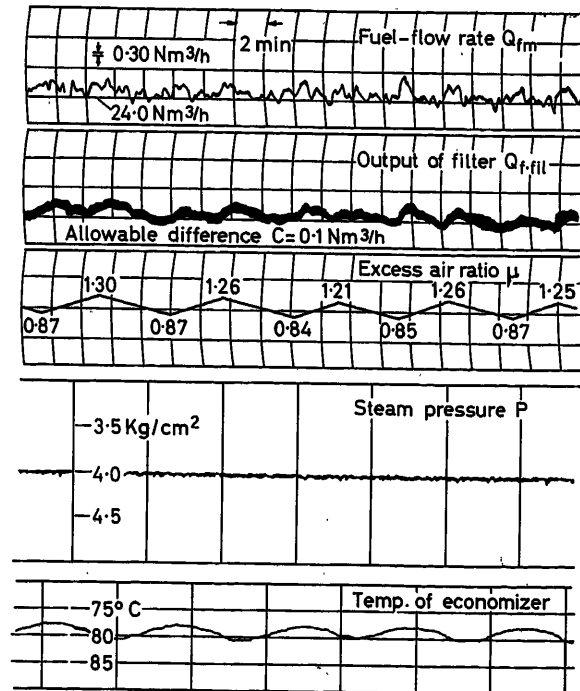


Figure 10

time instant is held again as a minimum value. Once the difference amounts to the allowable difference, the reversal of the input direction occurs. Thus, there is sometimes the case where the fuel flow continues to increase until it attains its saturation, without returning to the desired value. With larger drive speed of the input, this phenomenon is apt to occur since the dynamic lag of the fuel flow becomes larger.

In order to avoid the above phenomenon, the following counterplan is considered.

(4) For a certain duration of time after the direction of the input drive is reversed, the peak-holding circuit is so modified for its output not to hold a minimum value but follow the actual fuel flow.

By such modification, even if the fuel flow overshoots after the direction of μ is reversed, the difference is not produced and therefore undesired reversals of μ cannot occur.

Figure 11 shows the case where the waiting time of 30 sec is assigned and a filter is added to the fuel flow measuring device. In Figure 10, the waiting time is 60 sec. It is shown that even when the fuel flow response has a fairly large overshoot, the action of reversal is not being disturbed. In Figure 10, the response of the output of the filter, steam pressure and temperature of economizer at 24.3 m from the inlet of boiler are simultaneously given.

As will be described below, this counterplan is also effective to cope with the change in steam flow.

The Control Behaviour for the Disturbance of Steam Flow— Figure 12 shows the control behaviour for a step change of the steam flow as a disturbance. The first half of the figure shows

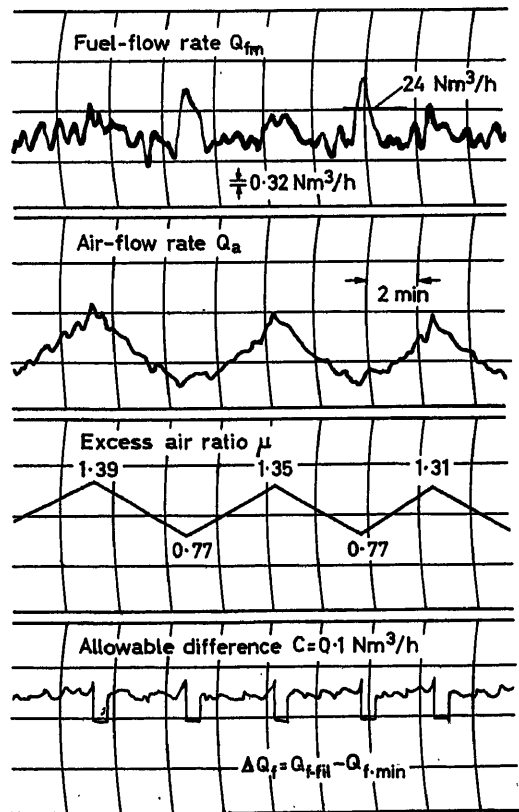


Figure 11

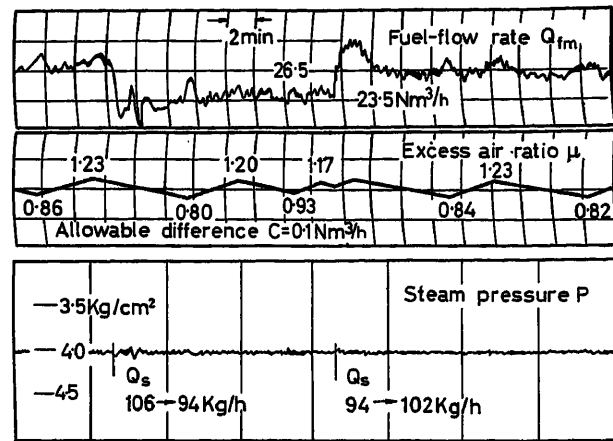


Figure 12

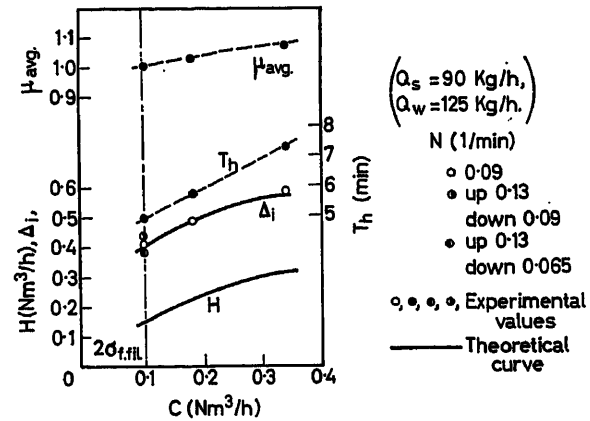


Figure 13

the increasing response of fuel flow when the steam flow is increased, and the latter half shows the response in the opposite direction.

The condition that the fuel flow is increased by the disturbance of the steam flow is similar to the aforementioned case where the fuel flow overshoots as the direction of μ is reversed. In this case, counterplan (4) acts effectively and frequent reversals can be avoided in the transient response of fuel flow. Thus, after the transient dies out, μ can be set to its new optimum value by the optimizing controller.

Inversely, from the performance principle of the optimizing control, the reversal of input direction does not occur in the case where the fuel flow is decreased by the disturbance of the steam flow.

Effects of Input Drive Speed N and Allowable Difference c on the Control Performance

In the optimizing control system with a controller of peak-holding type modified by taking account of counterplans (2) and (4), the characteristic values of the optimizing control action for different values of the allowable difference, c , and input drive speed, N , are now determined.

Effect of c — Figure 13 shows the experimental results of input hunting zone Δ_i , hunting period T_h , and average value.

of μ , μ_{av} , for different values of c with constant input drive speed: $N = 0.09$ l/min.

It is clearly seen that as c decreases, Δ_i decreases and thus H also decreases. For the case where $c < 0.1$, the stable and regular control action cannot be performed by the noise interference. Accordingly, it may be concluded that an optimum value of c is $0.1 \text{ nm}^3/\text{h}$ for this boiler system. This value corresponds to twice the standard deviation $\sigma_{f, fl}$ of the output of the filter.

Effect of N —Figure 14 shows the experimental results for different values of N with $c = 0.1 \text{ nm}^3/\text{h}$. It is found that as N decreases, H decreases, since the dynamic lag of the system corresponding to N decreases.

Comparison between Experimental and Theoretical Results

The transfer function of boiler system, $G_0 \cdot G_{fm} \cdot G_{fl}$, and the characteristic constant, k , are given by eqns (5) and (1), respectively. Using these values, the characteristic values of the optimizing control for different values of c and N can be calculated⁸.

The full line in Figures 13 and 14 gives the theoretical results of Δ_i and H . It is found that the values of Δ_i are in good agreement with the experimental ones.

As a result, the minimum hunting loss H has the following value:

$$H = 0.15 \text{ nm}^3/\text{h}$$

In this experiment, the minimum value of fuel flow is $24 \text{ nm}^3/\text{h}$ and thus the hunting loss is below 1 per cent.

It is found that the hunting loss evaluated in boiler efficiency is also below 1 per cent, according to the equation of definition mentioned previously, and it seems to be a satisfactorily small value.

General Remark on the Design Method of a Boiler Efficiency Control System

The optimizing control action by a modified peak-holding method is fully determined if the allowable difference c , input drive speed N , and the form of a filter to be added are given, and the characteristics of the controlled system are approximately known. Figure 15 gives a design procedure.

Conclusions

From the fact that the maximization of boiler efficiency is equivalent to the minimization of fuel consumption under con-

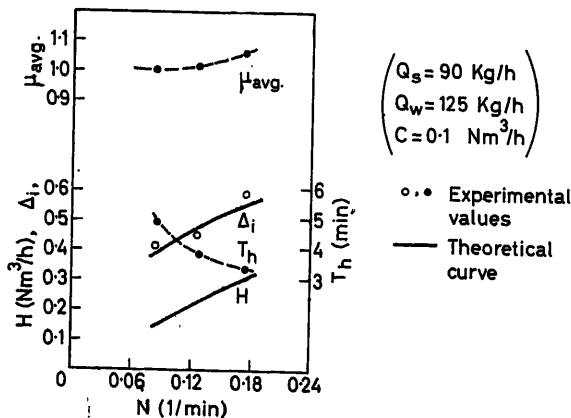


Figure 14

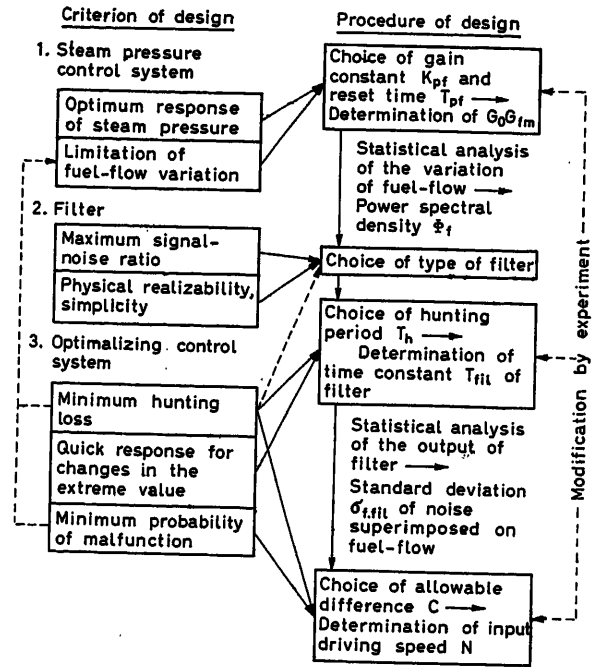


Figure 15

stant pressure control, the excess air ratio has been optimized so as to minimize the fuel consumption.

In this system, several counterplans have been proposed and examined against the undesirable effect of noise superimposed on the fuel flow and dynamic lags of the control system on the optimizing control action.

An optimizing controller has been constructed in accordance with the improved peak-holding method, and has been successfully applied to the boiler efficiency control of a once-through boiler.

As a result, the stable control action was satisfactorily performed for a variation of steam consumption. Furthermore, the dynamic characteristics of the overall control system were analysed, and the results were found to be in good agreement with those of the experiment.

This optimizing controller seems to be of value as a kind of tester which checks automatically whether or not the present ratio control system works well, for the variation of air leakage and non-linearity of control valves and measuring devices in the system.

In addition, a general remark on the design principle of this control type was presented, but the practical design method has not been included since completeness would exceed space limitations.

The authors wish to express their gratitude to Prof. Dr. T. Yamamoto, Prof. Dr. T. Ito and the members of Automatic Control Laboratory of Nagoya University for their invaluable criticisms and favours.

Nomenclature

- $a = \Delta_i/2$ Amplitude of the variation of μ
 c Allowable difference (nm^3/h)
 G_{fl} Transfer function of filter
 G_i Transfer function of the input group of the controlled system

G_m	Transfer function of the flow measuring device	T_F	Time constant in the furnace of economizer (sec)
G_0	Transfer function of the output group of the controlled system	T_F'	Time constant in the furnace of evaporator (sec)
H	Hunting loss of fuel flow rate (nm ³ /h)	T_f	Time constant of fuel flow control valve (sec)
H_1	Lower calorific value of fuel (kcal/nm ³ or kcal/kg)	T_{f11}	Time constant of filter (sec)
${}_1H_f$	$= (\delta R / \delta Q_f)_0 \cdot (Q_{f0} / R_0)$	T_{fm}	Time constant of fuel flow measuring device (sec)
${}_1H_\mu$	$= (\delta R / \delta \mu)_0 \cdot (\mu_0 / R_0)$	T_h	Hunting period of the output Q_f (min)
${}_2H_\mu$	$= (1/2) (\delta^2 R / \delta \mu^2)_0 \cdot (\mu_0^2 / R_0)$	T_p	Time constant of tube wall of economizer (sec)
I_1	Enthalpy of feedwater (kcal/kg)	T_{pa}	Reset time of air flow controller (sec)
I_2	Enthalpy of steam (kcal/kg)	T_{pf}	Reset time of pressure controller (sec)
I''	Enthalpy of saturated vapour (kcal/kg)	t	Time
I'	Enthalpy of saturated liquid (kcal/kg)	X	Dryness of steam leaving evaporator
I_w	Enthalpy of feedwater (kcal/kg)	Y	Setting voltage of excess air ratio
k	Characteristic constant of the controlled system	Δ_i	Hunting zone of the input μ
k_e	$= k\mu_0^2 / Q_{f0} = -{}_2H_\mu / {}_1H_f$. Dimensionless characteristic constant of the controlled system	Δ_o	Hunting zone of the output Q_f (nm ³ /h)
K_{pa}	Proportional sensitivity of air flow controller	η_B	Boiler efficiency
$k_{pa} \cdot K_{pa}$	Loop gain of air flow control system	μ	Excess air ratio
K_{pf}	Proportional sensitivity of pressure controller	μ_{av}	Average value of excess air ratio
k_{pf}	Dimensionless gain constant = fuel flow rate/pressure deviation	$\sigma_{f,11}$	Standard deviation of the output of the filter (nm ³ /h)
L_{am}	Dead time of air flow measuring device (sec)	The suffix 0 denotes the value of the standard equilibrium condition. The following small letters denote the dimensionless small deviation from the standard values: p , steam pressure; q_a , air flow rate; q_f , fuel flow rate; q_{fm} , output of fuel flow measuring device; q_s , steam flow rate; q_w , feedwater flow rate; r , heat through heating surface per unit length of tube; y , setting voltage of excess air ratio; v , excess air ratio.	
L_{00}	Ideal air flow (nm ³ /nm ³ fuel)		
N	$= \Delta_i / T_h$. Drive speed of the input μ		
P	Steam pressure (kg/cm ² G)		
Q_a	Air flow rate (nm ³ /h)		
Q_f	Fuel consumption (kcal/nm ³ or kcal/kg)		
$Q_f \cdot f_{11}$	Output of the filter (nm ³ /h)		
$Q_f \cdot \min$	Output of the peak-holding circuit (nm ³ /h)		
Q_s	Steam flow rate (kg/h)		
Q_w	Feedwater flow rate (kg/h)		
ΔQ_f	$= Q_f - Q_{f\min}$ (nm ³ /h)		
R	Average heat through heating surface (kcal/h-m)		
s	Operator of Laplace transformation		
T_A	Time constant of economizer (sec)		
T_a	Time constant of air flow control valve (sec)		
T_{am}	Time constant of air flow measuring device (sec)		
T_B	Time constant of boiler (sec)		

References

- DRAPER, C. S., and LI, Y. T. Principle of optimalizing control system and an application to the internal combustion engine. *Amer. Soc. mech. Engrs* Publ. 9 (1951)
- TERANO, T. The transient characteristics of once-through-boilers. *Mon. Rep. Transportat. Tech. Res. Inst.* 7 (1957)
- FUJII, S. Analysis of ramp type optimalizing control. *Seigyokogaku* 4 (1960) 299
- FUJII, S. Some general considerations for various modes of optimalizing control. *Seigyokogaku* 5 (1961) 35

DISCUSSION

F. P. DE MELLO and L. K. KIRCHMAYER, *General Electric Company, Schenectady 5, N.Y., U.S.A.*

The authors have undertaken a thorough investigation of the feasibility and requirements of an optimalizing or peak-holding scheme for improving boiler efficiency. This investigation has important value in pointing out the various problems such as noise and process dynamic lags which affect the application of extremal adaptation optimalizing schemes.

Figure 6 indicates that the fuel consumption versus fuel-to-air ratio curves are fairly flat over a wide range. It would appear that a preprogrammed fuel-to-air ratio as function of fuel or load would give practically optimum operating results, holding the fuel-to-air ratio very close to the theoretical optimum. Figures 10, 11 and 12 show that under the action of the optimalizing controller, the fuel-to-air ratio oscillates within a fairly wide band. Have the authors determined if, in actual practice, the optimalizing controller would give improved economy over a preprogrammed control?

It is important to note that for large-scale utility boilers such large excursions in fuel-to-air ratio as illustrated in this paper are not allowable due to the hazard of a catastrophic explosion. For this same reason one would not in general reduce the fuel-to-air ratio below a certain value which is usually above the optimum efficiency point.

Two other questions are:

- (1) Have the authors obtained any data concerning the improvement in operating economy to be obtained in an actual installation of an optimalizing control compared to conventional control?
- (2) Have the authors applied any of the techniques described here to large-scale electric utility boilers?

S. FUJII, *in reply*

Figure 6 shows the fuel consumption versus fuel-to-air ratio curves which were obtained at a certain time from our boiler plant. It is difficult, in practice, to find the complete static characteristics. In addition, in this figure it is not shown how the static characteristics would be changed by the variation in the quality of the fuel, in the amount of air leakage and from time to time by variations in the equipment, for example in the boiler and controllers.

Therefore, on the basis of Figure 6 alone it is optimistic to say that the fuel-to-air ratio can be preprogrammed as a function of fuel or load. As Mr. Kirchmayer pointed out in Figures 10, 11 and 12, in this boiler the fuel-to-air ratio changes over a fairly wide range under small load conditions, although the hunting loss in the fuel consumption remains below 1 per cent. In other words, owing to the action of the optimalizing controllers, the fuel consumption versus fuel-to-air ratio curves have been found to be fairly flat over a wide

range, without knowledge of the static characteristics of Figure 6. Therefore, the optimizing controller seems to be of value for checking automatically whether or not the present ratio control system works well under the variation of air leakage and the non-linearity of control valves and measuring devices in the system. Next, in order to avoid the risk of a catastrophic explosion and to exclude the region where the boiler efficiency is clearly worse than in the past operations, the fuel-to-air ratio should be confined between upper and lower limits in practice, and the optimum value of the fuel-to-air ratio should be sought within that region. It is possible to modify the optimizing controller described here so that it searches for the optimum value within this limited region.

The conventional method yields a controller which gives optimum combustion efficiency while our method gives optimum boiler efficiency, that is optimum efficiency of both combustion and heating. The comparison between the two methods can only be made after our method has been applied to various types of boilers for considerable time. We have never applied this method to large-scale electric utility boilers, but we are not preparing to apply it to such boilers.

In conclusion, we wish to emphasize that the optimizing controller works to search out positively the optimum value of the fuel-to-air ratio under the present conditions, despite any disturbances affecting the boiler efficiency.

J. A. ROBERTS, *Central Electricity Generating Board, Central Electricity Research Laboratories, Leatherhead, Surrey, England*

The following comments and questions are made because we are attempting to apply experimentally, automatic optimization to the combustion control of very large pulverized-fuel boilers.

The author's application is simpler because, *inter alia*,

- (a) the once-through boiler lacks the thermal-storage and circulation effects encountered in the dynamics of drum-type boilers,
- (b) there was no superheat, and so no interaction between combustion conditions and superheat temperature,
- (c) the fuel (gas) has constant calorific value, and its flow can be measured readily. Direct heat input can be measured and a major source of disturbance (calorific value fluctuation) is eliminated.

We were therefore disappointed that the author's hunting loss (1 per cent) was as large as that predicted from our experiments on coal-fired plant, even when we accept calorific value variation as an unknown disturbance.

May we therefore pose the questions:

- (1) It seems likely that the disturbance to fuel flow arose from fluctuations in steam demand via a conventional combustion control system. Is this so? If so, it seems possible that an index of performance based on the ratio of steam-flow to fuel-flow (allowing for lags) would show less noise than that based on fuel-flow alone, and hence show a better performance. Do the authors agree?
- (2) The filter used was a simple lag. Do the authors consider such a filter a practical optimum?
- (3) Was anything learned from the physical experiment which could not have been obtained in a simulated system?
- (4) In a fully optimized power system, a knowledge of the acceptable disturbance spectrum of the self-optimizing boilers would enable the power demand spectrum to be apportioned rationally. Have the authors any experimental evidence on the variation of hunting loss with frequency of disturbance of fuel and steam flow?

S. FUJII, *in reply*

We wish to answer Mr. Roberts's questions (1), (2) and (4) together. We have been studying how the hunting loss in the fuel consumption is altered by using various types of filter under different types and frequencies of disturbances. Up to now, we have found one interesting

result; that the hunting loss in the case where the noise is included in the fuel flow rate is smaller than that in the case where the noise is filtered out by the use of a filter. We can therefore give no definite answer.

In reply to question (3), we have obtained the characteristics of an actual plant including the dynamics, for fuel consumption versus excess air ratio. These facts are taken into account in the simulation of the system.

As you pointed out, it seems likely that the disturbances to fuel flow arose mainly from fluctuations in steam demand via a conventional combustion control system. If the dynamic lag between steam flow and fuel-flow is absent and its controller is not complicated, the results obtained when the index of performance is based on the ratio of steam-flow to fuel-flow should show less noise.

The frequency of hunting must be, in general, larger than that of the disturbances, e.g. those in the calorific value, quality of fuel and steam demand.

T. STEIN, *Escher Wyss, Zürich, Switzerland*

The laboratory experiments reported in the paper are a fundamental contribution to the automation of power plants. For complete on-line optimizing computer control of power station units, comprising boiler and turbine, a great number of position elements must be controlled. With individual optimizing control of efficiency for each boiler a large part of the centralized control devices may be eliminated and the optimizing control equipment for the whole power station substantially simplified.

It is a tendency in Europe, where we have smaller power units than in the U.S.A., to subdivide the control actions of a power station into function groups. This will help to facilitate the introduction of automatic control. The method given in the paper is an important contribution in this direction.

The tests treated in the paper have been made with a gas-fired boiler. The fuel-flow rate can easily be measured for gas. But in many cases the gas-fuel must be used in those quantities which are available and other fuels must be added to produce at any instant the quantity of steam needed by the turbines. Therefore, a boiler burning in addition fuel-oil or coal will often be necessary. It will, therefore, operate simultaneously with two different fuels.

Some time ago I proposed a hill-climbing control, optimizing the excess air ratio, by measuring the flue gas losses¹. This can be done by measuring the temperature and the CO₂ and CO contents of the flue gases. Increasing the excess air ratio improves the combustion, thus reducing the CO loss. But on the other hand the flue gas loss, measured by the CO₂ content and the temperature, increases. For a medium excess air-ratio the loss will be a minimum and consequently the boiler efficiency will be optimum.

By measuring these three variables and computing the flue-gas loss, an optimizing controller similar to that in Figure 1 of the paper will have a similar optimizing result to the controller using the gas-flow measuring device. It may therefore be possible to have an optimizing control of boiler efficiency for boilers burning more than one fuel.

In any case it would be of great interest to know whether the optimizing method tested in the automatic control Laboratory of Nagoya University will soon be applied practically in a power station.

Reference

- ¹ STEIN, T. *Regelung und Ausgleich in Dampfanlagen*. 1926. Berlin. Springer. Russian Edition 1931, Moscow.

S. FUJII, *in reply*

When a boiler is to be operated simultaneously with two different fuels, such as fuel-oil and fuel-gas, a two-input system must be considered. Hence if the control method described here is to be

adopted, each input must be controlled separately in order to get the optimum value determined as a function of the two inputs.

Also Mr. Stein's controller maximizes the efficiency of combustion, whereas our controller maximizes the boiler efficiency, which comprises both the efficiency of combustion and of heating.

A. REZNYAKOV, *National Committee, Kalanchevskaja 15a, Moscow, U.S.S.R.*

The optimal excess air ratio for the burning process is practically constant for every method of combustion in large-scale fuels and heat loads. So for instance in our experience, burning different kinds of pulverized coals (in the range of hard and soft), the optimal excess air ratio is 20 per cent.

What is the reason for applying self-adjusting system of automatic scan for stimulating the optimal excess air ratio? It may be more economical to give the digital data for it and apply a more simple system of automatic control for stabilizing this ratio. In the case of a variable boiler load we can precalculate terminal values of the optimal excess air ratio by curves connecting boiler efficiency with excess air ratio, which is the same in practice for similar kinds of fuel.

Nowadays power stations using pulverized fuel are dominant. Do the authors consider it possible and reasonable to apply the same principle for optimization of boiler efficiency working on pulverized coal?

S. FUJII, *in reply*

In principle, unless there is an adequate device for the measurement of pulverized coal rate, the method described here cannot be applied for the optimization of boiler efficiency working on pulverized coal.

MR. LÄUBLI, *Sulzer, Switzerland*

The paper is very interesting, in particular the experimental results published. The proposed method does not realize the optimum but a state which is away from the optimum by the distance H , corresponding to the hunting loss

$$H = \frac{1}{T} \int_0^T (Q_f + Q_{f \min}) dt; \quad T \gg T_h$$

If H is determined in this way from Q_{F-FII} given in Figure 10, one gets $H \approx 0.7 \text{ nm}^3/\text{h}$. The theoretical values given by Figure 13 and 14 are considerably smaller.

The boiler investigated has efficiency and excess air ratios far different from values realized in modern boilers. It is supposed that the authors do not use the notion

$$\text{excess air ratio} = \frac{\text{Air}_{\text{effective}}}{\text{Air}_{\text{theoretical}}} > 1$$

but

$$\text{excess air ratio } \mu = \frac{\text{Air}_{\text{effective}} - \text{Air}_{\text{theoretical}}}{\text{Air}_{\text{theoretical}}}$$

μ being between 0.77... 1.39

For modern large boilers μ ranges between 0.05 and 0.25, so being substantially smaller than the values investigated by the authors. By using such small values there is of course the danger of producing losses by unburnt matter.

It should not be overlooked that the oscillation created by the optimizing system could produce resonance effects in some sub-loops of the boiler control system.

S. FUJII, *in reply*

We got the hunting loss Q_{H1} on the top record in Figure 10, as the average value from a lot of experimental data. We use the ratio of air effective to air theoretical as the excess air ratio in this paper.

H. FRANK, *T.H. Stuttgart, Institut für Dampfkesselwesen, 7 Stuttgart S Boklingerstr. 72, Germany*

(1) The authors dealt with a town gas heated boiler. If an extension of their method should be made to coal or oil fired boilers it is in most cases not sufficient to look only at the efficiency of the plant. There are such aspects as for example smoke, that are also to be taken into account. I, therefore, will ask the authors whether they see a possibility to make a check on, for example, the density of smoke (measuring absorption or CO) and to stop diminishing the excess air ratio as soon as this reaches a given value². Is the given optimization strategy then still applicable?

(2) During the presentation of the paper, the author described a cross correlation method. In using this method, what amplitudes would be necessary for getting a significant result? Because of the very flat minimum I think that comparatively large amplitudes have to be applied, so that the optimization process has to be paid for with considerably large deviations from the optimal point.

(3) During the discussion the author mentioned the advantage of the filtering process encountered in the optimization. This filtering process is not essential for the optimization. It also could be applied without any optimization.

S. FUJII, *in reply*

We did not see any possibility of making a check on the density of smoke; however, the optimizing controller is still applicable by modifying it a little.

In answer to the second question, we are now using a simulator in order to decide the best value of the amplitude and frequency of the test signal and of the time constant of filter and the gain constant of the control loop.

A. BURATTI, *c/o Pignone Sud, Bari, Italy*

I think this work is important because it gives results found on a real plant. Although the authors give a mathematical model of their system this does not enter into the conclusions.

The authors have found that under a constant load, a constant fuel composition, and with the boiler they used, the loss in efficiency due to hunting is of the order of 0.8 per cent. Would this figure be considered wholly satisfactory by large boiler users?

The authors have shown that with the controller adjustments they used, the recovery curve, following a relatively small step disturbance in the steam flow rate, is good. It would be interesting to know how the system behaves with a continuous disturbance applied to it. Perhaps the authors have carried out further experiments on their system and might be able to illustrate this point.

In the beginning of their paper, the authors mentioned the poor accuracy of measuring devices. Accuracy is a combination of various factors such as reproducibility, ambient temperature sensitivity, linearity, hysteresis and backlash.

When the input of the extremum controller comes from a single transducer, the only one of the aforementioned factors that matters is backlash. This, in practice, can be quite negligible. If, however, the input of the controller is a function of various signals coming from different transducers, not only backlash, but also other factors affecting accuracy become important and the measured peak might be quite far from the true peak. This means, for instance, that it is not possible to use the ratio between steam and fuel flow ratios as input to the extremum controller. It is also not possible to use the controller if the boiler is fixed with two fuels at a time, unless of course, one fuel flow is held constant.

S. FUJII, *in reply*

We are not satisfied with the hunting loss of 1 per cent. As to how the system behaves with a continuous disturbance, we are now studying it by the use of a simulator.

Simulator for Steam Turbines with Reheat or Automatically Controlled Extraction

H.-J. EHLING

Summary

An analogue computer for simulation of reheat and extraction steam pressure controlled turbines is described. The computer is used in manufacturing control and development of turbine governors; it contains 30 amplifiers and is capable of performing in seven main operational modes. Inputs are the positions of steam valves, obtained from the governor servovalves; the latter not being simulated, but used as a real part of the control loop. The computer calculates the rotational acceleration of the turbine and provides a corresponding drive for the mechanical speed control device.

Easy handling and control was of utmost importance. Usual patch-board techniques for analogue computers are elements of the internal construction; the normal functions of adjustment and control can be performed by switches mounted at the operator's panel. Transient maximum speed, produced by steplike load changes, are determined and stability of complex steam-turbine servo-loops can be tested.

Sommaire

L'auteur décrit un simulateur analogue pour représenter les turbines à vapeur de différentes constructions, en particulier les turbines avec surchauffe intermédiaire et soutirage; ce simulateur est installé sur une plateforme d'essai pour le réglage de turbines. Il se compose d'environ 30 amplificateurs de calcul et permet 7 montages principaux. Comme entrées on utilise les positions des soupapes à vapeur qui sont manœuvrées par les moteurs de réglage réels. La quantité de vapeur produite et le moment d'accélération sont calculés, et d'après cela l'action du mécanisme de mesure du nombre de tours également réels, est déclenchée. On attache une importance toute spéciale à la facilité de manipulation et de commande. La technique habituelle des fiches des calculateurs analogiques a été maintenue à l'intérieur. Toutefois la manipulation normale de l'appareil, y compris le choix du genre de service, le contrôle et l'équilibrage du potentiomètre, est possible au moyen de boutons-poussoirs. Le simulateur permet, et plus de la vérification du fonctionnement du réglage, de faire des essais relatifs à la façon dont s'arrête la turbine à régler en évaluant les survitesses, en vérifiant la stabilité et en contrôlant la facilité de la synchronisation. La construction du simulateur et les schémas fonctionnels qui ont servi de base, font l'objet d'une description.

Zusammenfassung

Ein Simulator zur Nachbildung von Dampfturbinen verschiedener Bauart, insbesondere von Turbinen mit Zwischenüberhitzung und Entnahme, wird beschrieben; der Simulator findet in einem Prüffeld für Turbinenregelung Verwendung. Er besteht aus ca. 30 Rechenverstärkern und erlaubt es 7 Hauptschaltungsmöglichkeiten auszuführen. Als Eingänge dienen die Dampfventilstellungen, die von den Stellmotoren eines vorhandenen Regelventils abgegriffen werden; der Simulator berechnet die Dampfleistung und das Beschleunigungsmoment und steuert daraufhin den Antrieb des gleichfalls vorhandenen Drehzahlmeßwerkes. Besonderer Wert wurde auf leichte Bedienbarkeit und Kontrollierbarkeit des Gerätes gelegt. Die bei Analogrechnern üblichen Steckverbindungen wurden intern beibehalten. Jedoch ist die normale Bedienung des Gerätes, wie Auswahl der Betriebsart, Kontrollen und Potentiometerabgleich, mittels Drucktasten möglich. Der Simulator gestattet neben der Prüfung des Reglerverhal-

tens auch Versuche über das Abschaltverhalten der zu regelnden Turbine bei Ermittlung von Überdrehzahlen, Stabilitätsuntersuchungen und die Prüfung der Synchronisierbarkeit durchzuführen. Der Aufbau des Simulators und die zugrunde liegenden Strukturbilder werden beschrieben.

Introduction

For some time an analogue computer has been employed in a test stand for automatic control equipment used in the operation of steam turbines. This computer enables the controlled plant—the set of turbines with those auxiliary devices which have a bearing on the control system dynamics—to be simulated, thus making it possible to test the operation of the control equipment in a closed loop. *Figure 1* shows the real and the simulated parts of the control system.

The reasons for installing a quite substantial computer in a test stand where turbine controllers are subjected to final checking can be summed up as follows: demands on automatic controls are steadily being stepped up and control loops are becoming more and more complex, thus increasing the difficulties of the theoretical treatment of many rather obscure nonlinearities.

Wherever possible, the system has been thoroughly investigated by means of linear control theory and the describing function method; furthermore, a considerable amount of analogue computer calculations has been carried out for special applications, including controller simulation. No doubt the outcome of these studies proved to be of considerable interest, particularly in respect of the investigations into which of the influences are really important. However, the result was not sufficient for establishing full confidence in analogues of mechanical-hydraulic controllers. Besides, owing to the lengthy preparations required

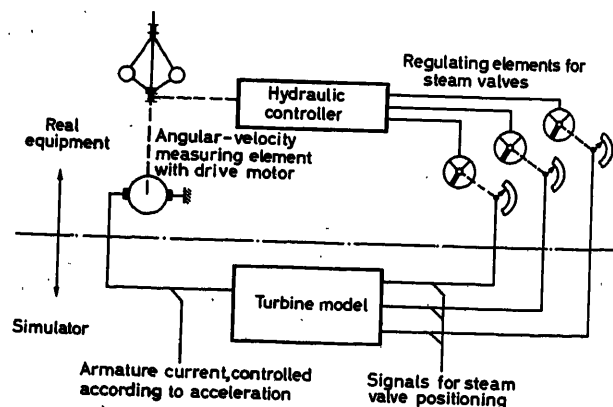


Figure 1. Turbine model—overall arrangement

for obtaining sufficiently true simulations with a universal analogue computer, this type of calculation was limited to sample applications, intended especially for gaining general information.

In any case, these investigations have proved that the simplifications necessary for setting up the analogue, are more straightforward for the controlled plant than for the controller itself. An obvious solution to the problem was to simulate only the controlled plant and to connect it to the controller or governor which was present on the test stand for final checking. This arrangement provides a better and more orderly understanding of the behaviour of the entire control loop.

However, it appeared somewhat doubtful whether it would be possible to adapt the working habits of the group of staff trained in the use of the analogue computer to the conditions prevailing in the test stand, manned with lower grade production personnel. Work with the analogue computer requires the utmost concentration, and conditions in a rather noisy turbine test stand are not at all favourable in this respect. At least seven different kinds of turbines had to be simulated, involving up to 30 parameters. The setting of such a large number of values cannot be accepted as correct without checking some parts of the analogue. For this purpose circuits have to be disconnected and if this is done by unplugging various connecting wires, it can easily happen that reconnecting is neglected or carried out incorrectly. Furthermore, it must be possible to adjust the analogue to suit modifications of the arrangement which may become necessary either because of technical progress or increased experience. Bearing all these circumstances in mind, a solution was found which combines maximum flexibility with greatest ease of operation, with respect to the choice of the most suitable kind of simulation and also to carrying out the required tests. In the following, the theoretical principles of the simulator are briefly examined.

Analogues for Condensation Turbines

For the purpose of these deliberations it is sufficient to imagine the controller, which is present as a real unit, to be

represented as part of the block diagram (Figure 2 'real equipment'), while the remainder of the control loop must be studied more closely (see Figure 2).

Figure 2 shows, beginning with the summing point on the left-hand side, the conversion of the deviation, transmitted by the angular-speed controller, into the angle of rotation α of the actuator for the steam valves. The relationship between this angle and the rate of steam flow is given by the regulating valve flow characteristic. Regarding variations in the live steam pressure and the back pressure, it can be said that, for calculations of control dynamics, only the upstream pressure of the steam has to be taken into account, while the influence of the back pressure, which one expects in accordance with the law governing the flow of steam through plug-type valves, is of no importance in connection with condensation turbines. Consequently, the rate of steam flow is proportional with sufficient accuracy, on the one hand, to the steam pressure on the upstream side of the valve, and on the other hand to a flow coefficient ψ which depends entirely on the design of the valve. The steam flow through the valve, multiplied by an effective heat drop, gives the mechanical potential available on the turbine shaft. Further investigations proved that a variation of the heat drop by throttling, as long as the valves were partly open, had only a very slight influence on the transfer function of a step change in the load, which is of the greatest interest for the present investigations, and for this variable too a constant factor was therefore assumed. The resulting steam energy, however, is correct for static conditions only, and will vary with the rate of steam flow if a time lag is involved, which can be approximately described by an exponential function with the so-called steam time constant. The transient wave-type power input is split up into a speed-dependent part carrying the payload and losses, and a surplus responsible for the acceleration of the turbine, indicated in the figure by the symbol N_B . The torque is determined by dividing the surplus, N_B , by the angular velocity of the rotor movement. Since the speed changes produced by the control action are insignificant in comparison with the design speed, the division can be substituted by a simple series approximation resulting in the system diagram shown

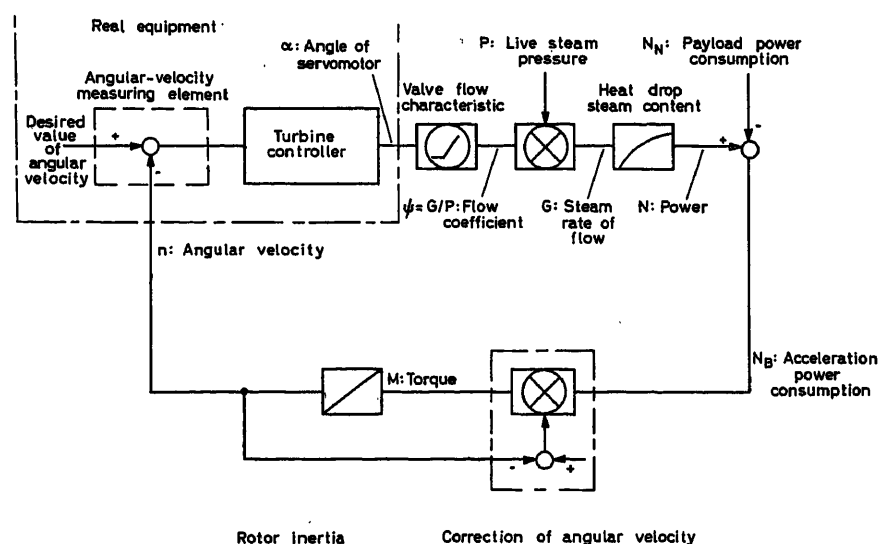


Figure 2. System diagram for condensation turbine

in Figure 2. The angular velocity is derived, by integration, from the torque, and with this the control loop is closed. Such an arrangement is sufficient for a turbine not connected to the distribution network. Of particular interest are load reductions when the power which had been converted into payload is suddenly available for no other purpose but the acceleration of the rotor. A load reduction is simulated as follows: first the pay load from the turbine is fed steadily into the power output summing station; then this flow is reduced by an amount corresponding to the intended load drop, thus producing the desired step-up in the acceleration power.

The part of the system diagram describing the relationship between power and angular velocity is valid also for complex types of turbine and in this section of the diagram is located the transition from the results of the simulator calculations to the turbine speed which is already mechanically represented. The torque is calculated in the simulator and fed into the drive of the angular-velocity measuring element. The inertia of the measuring element and of the drive effects the integration resulting in the angular velocity. The torque control is provided with a special feedback for the correction by angular velocity.

The following discussions regarding the simulator need go no further than the calculation of the acceleration power.

Turbines with Reheat

Figure 3 shows that section of the steam flow diagram referred to in this paper. Between the high pressure and the medium pressure turbine is a further steam control valve which may be fully open when the actual load is above 30 per cent of the design load, but must be modulated towards the closing position for smaller loads, and fully closed for very small loads. The reheater is between this valve and the outlet of the high pressure turbine. It is of importance for the dynamics of the control system that the reheater has a far greater steam storage capacity than that of the turbine housings. The position of the reheater in the boiler requires that it receives, at any time, the so-called minimum rate of steam flow. Therefore, it must be connected to the live steam line and to the condenser by pipes by-passing the turbines. The steam flow through these pipes is controlled by so-called high pressure and medium pressure reducing sets,

which consist of regulating valves preceded by stop valves. After the medium pressure reducing station there is a restriction, the inlet pressure of which is proportional to the amount of steam flowing to the condenser. The back pressure produced in this way is used for a control which does not allow the steam flow to the condenser to exceed a predetermined maximum. The high pressure reducing station opens when the live steam pressure slightly exceeds the set desired value. As long as the turbine load is at least equivalent to the minimum rate of steam generation (referred to as 'load limit'), the medium pressure reducing station is fully closed and the medium pressure control valve fully open. The criterion for the control of the medium pressure reducing station is the pressure in the reheater, the desired value of which, at the stated load limit, must be slightly above the step-down pressure developing in these conditions between the high and medium pressure turbines. However, above this limit load, the step-down pressure increases in proportion to the rate of steam flow, in accordance with the laws of physics, and this would cause the medium pressure reducing valve to open again, contrary to what is intended, if the desired value were fixed. For this reason, the desired value must be varied depending on the load. This relationship is indicated in Figure 3 by the block 'load slide'. It shows above the limit load an increase in proportion to the load, always slightly higher than the naturally developing reheater pressure but constant at small loads. The 'load slide' (analogue of the load regulation loop) which determines the desired value for the reheater pressure is operated by oil pressure impulses from the control mechanism of the tachometer, which pressure, under stationary conditions, can be considered as a measure of the set load. The power consumption of the medium pressure turbine does not depend merely on the position of the medium pressure control valve, since the reheater pressure, which varies within a ratio of 1:3, is of a decisive influence. It was, therefore, necessary to include analogues of the reheater and of both reducing stations in the simulator set-up. The resulting system diagram is shown in Figure 4. The steam power consumption of the high pressure and of the medium pressure turbine are added up in the summing point on the right-hand side, and the pay load and idling load, are deducted. A step change in the load can be simulated by varying the pay load. The high pressure power consumption is calculated in the same way as for the condensation turbine; the steam rate of flow is

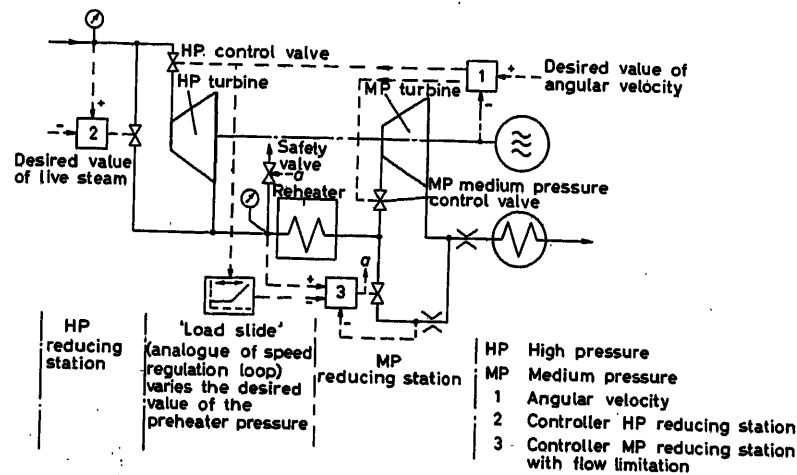


Figure 3. Arrangement of a turbine with reheater

SIMULATOR FOR STEAM TURBINES WITH REHEAT OR AUTOMATICALLY CONTROLLED EXTRACTION

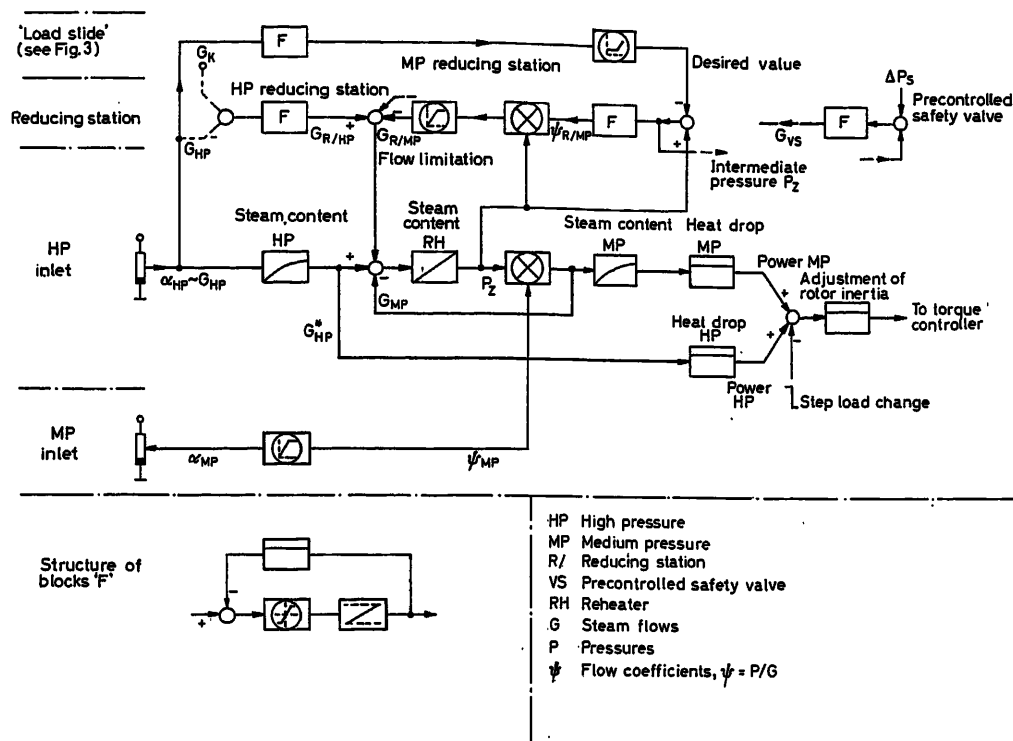


Figure 4. System diagram of the simulator for a turbine with reheat

measured, transmitted as a flow characteristic and immediately introduced into the quantity balance for the reheater, which is discussed later. The power consumption of the medium pressure turbine is calculated from the steam rate of flow through the control valve, delayed by the steam content of the medium pressure turbine housing and fed into the power consumption summing point. Owing to the variations in the reheater pressure, this steam flow has to be calculated as the product of the reheater pressure and a flow coefficient ψ for the medium pressure control valve; ψ and this can be found from the steady-state values of reheater pressure and steam flow, which can be found from the basic turbine data. For the purpose of the present investigations it is sufficient to describe the behaviour of the steam in the reheater by a kind of idealized gas law, according to which the steam pressure is directly proportional to the weight of steam present in the reheater and to its temperature. The weight of steam is obtained by integration of the algebraic sums of all inlet and outlet quantities of steam in the summing point and the following integrator in the centre of Figure 4. Theoretical studies have proved that it is quite in order to assume that the reheater temperature is constant. Consequently, the integrator output gives the reheater pressure.

The block diagram in the top right-hand corner of Figure 4 was chosen for the steam quantity fed in from the high pressure reducing station. For a load drop, which is the only condition of interest for the purpose of this paper, the steam consumption of the high pressure turbine is throttled and, consequently, the live steam pressure increases to such an extent that the proportional band of the high pressure reducing controller is immediately exceeded so that the regulating valve opens at maximum speed. During approximately 1 min, the boiler generates the same amount of steam as before, and it is therefore sufficient,

when the steam flow through the high pressure turbine is throttled, to transmit to the reducing station an opening impulse which is the result of a comparison between the quantity of steam generated by the boiler and the quantity consumed by the high pressure turbine. This impulse, integrated by means of a limited proportional element, determines the position of the high pressure reducing valve. The integrator is provided with limitation with a view to simulate the limited flow area of the reducing station valve. This system diagram is repeated for the simulation of the medium pressure reducing station and pre-controlled safety valves which, in the event of greater pressure increases, are opened in order to relieve the medium pressure reducing stations; the adjustment is such that even a small deviation from the desired value causes the valves to open at limited speeds. Contrary to the high pressure reducing station, medium pressure reducing stations and precontrolled safety valves are subjected to a strongly fluctuating pressure (reheater pressure), so that the calculated valve positions—proportional to the appropriate flow coefficients—have to be multiplied by the reheater pressure in order to obtain the steam rates of flow. In the case of the medium pressure reducing station, owing to the quantity limit control, a limited proportional element has to be provided, which is required to limit the rate of steam flow to the condenser. The opening impulse for the medium pressure reducing station and the precontrolled safety valves is produced by the difference between the desired and the actual value of the reheater pressure, modified by safety margins varying according to the application. The load-dependent desired value is determined by the 'load slide' (= analogue of the load regulation loop), which is illustrated in the top portion of Figure 4. The function of the 'load slide' corresponds essentially to the dynamics of the opening reducing stations.

and accordingly determines the acceleration for the drive of the angular-velocity measuring element. The turbine controller, which is real, closes the control loop, since the positions of the steam valves are measured on their regulating motors and fed into the simulator. Up to 30 potentiometers on the simulator have to be set, in order to produce an analogue for one special turbine plant. A great number of lockouts and checking possibilities contribute to reliability and ease of operation of the simulator.

Owing to the difficulty of carrying out large-scale measurements under working conditions, it was decided to limit the checking of the results obtained from the simulator to the

safety limits when switching off loads (the overspeed that arises if the load is reduced) and to the smallest permissible offset (corresponding to the maximum admissible control loop gain). The uncertainties of various constants and the simplifying omissions in the simulated system are responsible for errors of approximately 1 per cent of the design angular-velocity, when determining the speed increase following load reductions. Satisfactory stability in actual operation is obtained at 1.4 times the stability limit resulting from the model run (corresponding to 70 per cent of the critical loop gain). Errors in the relationship between steam flow and power consumption are sufficiently compensated by this safety margin.

DISCUSSION

R. STARKERMANN, *Brown Boveri & Co. Ltd., Baden, Switzerland*

(1) In the model, is the fact taken into account that the transfer function of the turbine, i.e. the transfer function M : Torque (Figure 2 of the paper), takes principally two different forms:

(a) The transfer function after sudden load reduction when disconnecting the generator from the network.

(b) The transfer function after sudden load reduction with some load remaining, i.e. without disconnecting the generator from the network.

Referring to Figure 2, should there be a potentiometer in the

feedback signal line 'correction of angular velocity' to adjust for the factor A ?

(2) When, under full load, the generator of a turbine is disconnected from the net, tests and calculations show the necessity of taking into account the amounts of steam energy left in the piping and turbines. An accurate calculation for a condensing turbine for example gave the following increases of speed after the load was shed ($T_a = 10$ sec):

$$\left(T_a = \frac{\theta\omega}{M_a}\right)$$

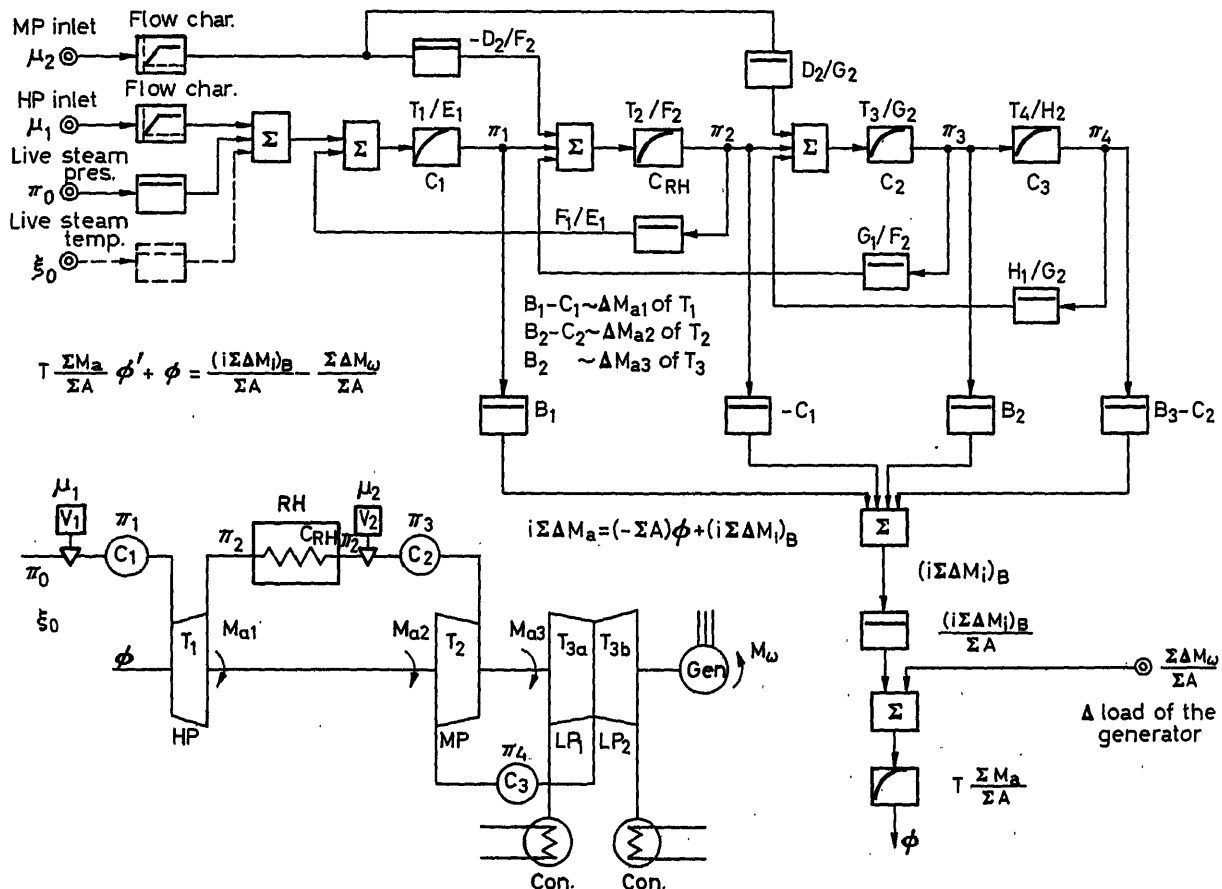


Figure A

Increase of speed before the valves closed	110 rev/min
Speed increase due to the steam in:	
(a) Valve bodies plus piping to the nozzles	16 rev/min
(b) Wheel chamber	16 rev/min
(c) Piping between HPT and MPT	72 rev/min
(d) Piping between MPT and LPT	16 rev/min
(e) Extraction pipeline from turbine to non-return valve	
preheating V	9 rev/min
preheating IV	7 rev/min
preheating III + II + I	9 rev/min
	255 rev/min

The question is: can all these influences (a)–(e) be taken together into one exponential function 'steam content', as in Figure 2 of the paper?

(3) For a reheat turbine there are two different conditions for load-shedding tests:

- (a) Intercept valves fully open (load 30 per cent)
- (b) Intercept valves partially open (load 30 per cent)

In case (b) the intercept valve offers a resistance to the steam flow, and the volume of the piping after the intercept valve gives rise to another time constant which must be allowed for when setting up the analogue computer.

When neglecting the piping to the preheaters I would propose the block diagram Figure A. The figure does not include the by-pass system. The question is: is the approximation in Figure 4 of the paper accurate enough for a true analogue of the behaviour of a reheat turbine?

(4) In Figures 5 and 7, why does the HP 'inlet' not have a 'valve flow characteristic' similar to that in Figure 2? Is the characteristic of the several valves in series considered to be sufficiently linear?

(5) Due to the thermodynamic laws all events in a turbine are non-linear. From what standpoint do you adjust the potentiometers before a load-shedding test? (Figure B).

(6) Is the setting of the live-steam temperature (by analogy with the live steam pressure) of no importance?

(7) Do you have test results from the analogue computer tests and from the actual turbine tests, so that this simulation can be evaluated?

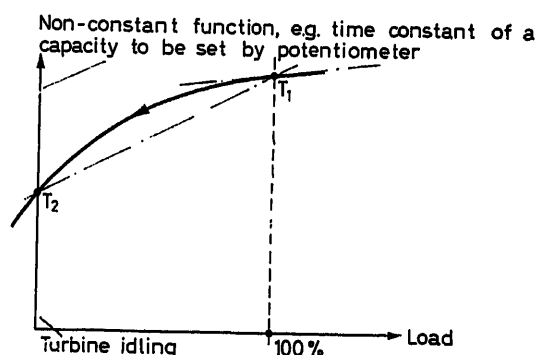


Figure B

H.-J. EHLING, in reply

(1) The first question deals with the fact that the load is dependent on the frequency. At the moment no means have been provided to simulate this, because we feel that this effect could be neglected for sufficiently low residual loads, but the model could easily be changed by introducing a feedback from the angular velocity to the load summing point. A load change would have to be produced by a change in K_R , which could be switched from one value to another to produce a step change. However, when switching the load down to a 5 per cent level, K_R will be approximately equal to 0.1, which is fairly small in comparison with the gain of the parallel turbine controller branch, the latter ranges from about 14 to about 25. The small advantage of

taking K_R into consideration would be counterbalanced by the fact that, for the turbine connected to a large network, the mechanism described gives a rather poor model because a number of other and little known effects all add their small contributions.

(2) The increase of speed before the valves closed does not result from the time delay device shown in Figure 2, but is computed from the overall set-up of the system. The other increases of speed given can, with sufficient accuracy, be summed to give the delay time constant. More detailed analysis shows that this is justified by the well-known method of approximating a number of small lags by a single lag with a larger time constant.

(3) The model allows for the separate introduction of lags, one for every throttling valve. The proposed block diagram cannot be discussed in detail. I only wish to remark that some of the influences shown in the diagram, e.g. effects of back pressure and steam temperature, were deliberately neglected, after having estimated the importance. On the other hand, some operations which Dipl.-Ing. Starkermann has introduced as linear ones are in the simulator replaced by more exact non-linear functions (for example multiplication function instead of simple summing operation). As to the accuracy, this is covered in the last section of the paper.

(4) The HP valves are designed for a linear characteristic of stationary load output (which means that throttling losses should be compensated). Actual measurements carry a strong noise, which still allows a linear interpretation. But there is in fact a third function generator provided, which could be used for corrections if necessary.

(5) The model is non-linear too. Variation of time constants, for example, is automatically done by the multiplicative elements used in the feedback of integrators. There are no load-dependent parameter settings in the range of the desired approximation and the value of settings is obtained straight from the design data.

(6) Influence of live steam pressure can never be verified from the normally obtained information about load-shedding performance. It could be taken care of by a different setting of the heat drop during the load-shedding and the temperatures can be assumed constant.

(7) We do have comparative results from turbine tests; see the last section of the paper. It is, incidentally, uncertain whether or not for the small and unsystematic deviations, the inaccuracy of parameter determination or the dynamical approximations must be blamed.

B. PEYRAUD, *Electricité de France, 26, Boulevard de la Libération, St. Denis (Seine), France*

The study presented by Mr. Ehling is very important for optimizing the operation of steam turbine control systems and gives a new and very efficient method.

Does the author think that it would be possible to adapt the analogue computer for the study of the increase in speed during load-shedding; particularly those parts of this increase due to:

(a) The expansion of the residual steam retained in the turbine housing and connections.

(b) The energy coming from water in the reheaters on the assumption that there are no non-return valves protecting the turbine.

H.-J. EHLING, in reply

It is certainly possible to study the influence of steam content in turbine bodies on the resulting maximum speed after a load shut off. This could be easily achieved by comparative runs with different lag parameters. Also eventually, by slight changes in the computer set up, the quoted contributions to the speed maximum could be made directly observable.

The influence of the water content of preheaters (uncontrolled steam extractions in later turbine stages, which are fed back to the turbine after passing the preheater) has not been taken into separate account in the present model. This would appear in the overall lag coefficient of the MP or LP turbine. But as the model is set up by means of a patchboard, necessary modifications could be made.

An Electro-hydraulic Control System for Reheat Turbines

M. A. EGGENBERGER and P. H. TROUTMAN

Summary

The flexibility, fast response, and complex logic capabilities of solid state electronics have permitted substantial improvements in control philosophies. Combining these electronic advantages with high-pressure hydraulic actuation to obtain rapid valve response forms the basis for the Electro-Hydraulic Control System for Reheat Turbines.

The proposed control has substantial advantages over conventional systems. Considerable progress has been made in reducing the overspeed on loss of full load. Appreciable improvements in turbine load output linearity, stability, and resolution in response to changes in assigned load setting have been made. Such complex operations as transferring steam admission from full arc to partial arc operation are performed automatically.

This paper describes the concepts and operation of the proposed control system and the manner in which undesirable multi-variable interactions have been reduced to a minimum. The most recent starting and operating philosophies of large, high-pressure, high-temperature steam turbine generators have been used as guiding principles.

Sommaire

Les possibilités offertes par les éléments électroniques à semi-conducteurs, notamment leur souplesse d'utilisation, leur rapidité de réponse et les fonctions logiques complexes qu'ils permettent de réaliser, ont rendu possible d'importants perfectionnements en matière de réglage. C'est en une combinaison de ces éléments avec des servomoteurs hydrauliques à haute pression que consiste le système de réglage électro-hydraulique pour turbines à réchauffage qui sera décrit dans cette communication.

Ce système présente des avantages marqués par rapport aux systèmes conventionnels. Des progrès importants ont pu être réalisés dans la réduction de la survitesse consécutive à une réduction de la pleine charge. Des améliorations sensibles ont été apportées aux performances de fonctionnement des turbines: linéarité, stabilité et incréments de la puissance de sortie en fonction de variations de la consigne de puissance. Des opérations aussi complexes que le passage de l'admission de la vapeur du fonctionnement périphérique total au fonctionnement périphérique partiel ont pu être rendues complètement automatiques.

On décrit la conception du système de réglage proposé et son mode d'action; on montre comment les interactions indésirables des variables multiples ont pu être réduites à un minimum. On s'est laissé guider pour cela par les plus récentes doctrines en matière du démarrage et de la marche normale relatives aux groupes turbogénérateurs de grandes dimensions, à haute pression et à haute température.

Zusammenfassung

Die Anpassungsfähigkeit, die hohe Ansprechgeschwindigkeit und die vielseitigen logischen Fähigkeiten der Bauteile der Festkörperelektronik verbesserten die Anwendungsmöglichkeiten der Regelungstechnik beträchtlich. Die Verbindung der Vorteile der elektronischen Bauteile mit den schnellwirkenden hydraulischen Hochdruck-Antrieben, um ein schnelles Ansprechen der Ventile zu erreichen, bilden die Grundlage der elektrohydraulischen Regelungen für Turbinensysteme mit Nacherhitzung.

Die hier vorgeschlagene Regelung hat gegenüber den herkömmlichen Systemen beträchtliche Vorteile: So stellt die Verminderung der Überdrehzahl bei völligem Lastabfall einen wesentlichen Fortschritt

dar; ebenfalls ließen sich die Linearität, die Stabilität und das Übergangsverhalten der Leistungsabgabe der Turbinen bei Änderungen der zugeteilten Last verbessern. Die schwierigen Operationen, wie der Übergang der Dampffzufuhr von der völligen zur partiellen Beaufschlagung, werden automatisch ausgeführt.

Der Aufsatz beschreibt den Aufbau und die Arbeitsweise des vorgeschlagenen Regelsystems und die Art, in welcher unerwünschte gegenseitige Beeinflussungen von mehreren Variablen auf ein Minimum reduziert wurden. Die neuesten Erkenntnisse für das Anfahren und den Betrieb großer Hochdruck-Hochtemperatur-Dampfturbinen lagen hierbei zugrunde.

Introduction

The complications of the turbine control system and the boiler connected with the reheat turbine caused the electrical utility to use the less efficient straight condensing turbine for many years. Then, some 15 years ago, these obstacles were overcome. Mechanical hydraulic control systems were devised that would adequately control the reheat turbine, and with this technological breakthrough the efficiency of power generation by steam turbines increased substantially. Although many improvements have taken place in these control systems over the past 5 years, the basic concepts still remain the same.

Now it is found that the present reheat turbine controls can keep pace with turbine and electrical system advances only by accepting an increasing number of compromises. The larger turbine-generator units have increased in output power by a factor of 10 in the past 15 years, but their inertias have increased by only a factor of five. This decrease of inertia-to-torque ratio has resulted in the newer units accelerating substantially faster at sudden loss of load. In addition, more and more automatic control is needed to optimize the operation of these large power makers. Finally, electrical system requirements have become more strict. Interconnecting large sections of power generating capacity through tie-lines necessitates improved speed and power generating stability. All these requirements are taxing the present controls to the utmost.

A new generation of controls for the reheat turbine are therefore needed to perform these tasks. Indications are that electro-hydraulic control system can meet these challenges, and also make vast control improvements. By introducing new control philosophies that are made feasible by using electronic logic, the control system can perform many functions. This system will substantially reduce overspeed at a sudden loss of load, reduce variations in incremental regulation, perform difficult control functions automatically for the operator, and can be interlocked to reduce the possibility of gross operator errors. These features can be used profitably only if the reliability of the new control system is at least equal to the present mechanical control; thus only conservatively designed solid state electronics are used.

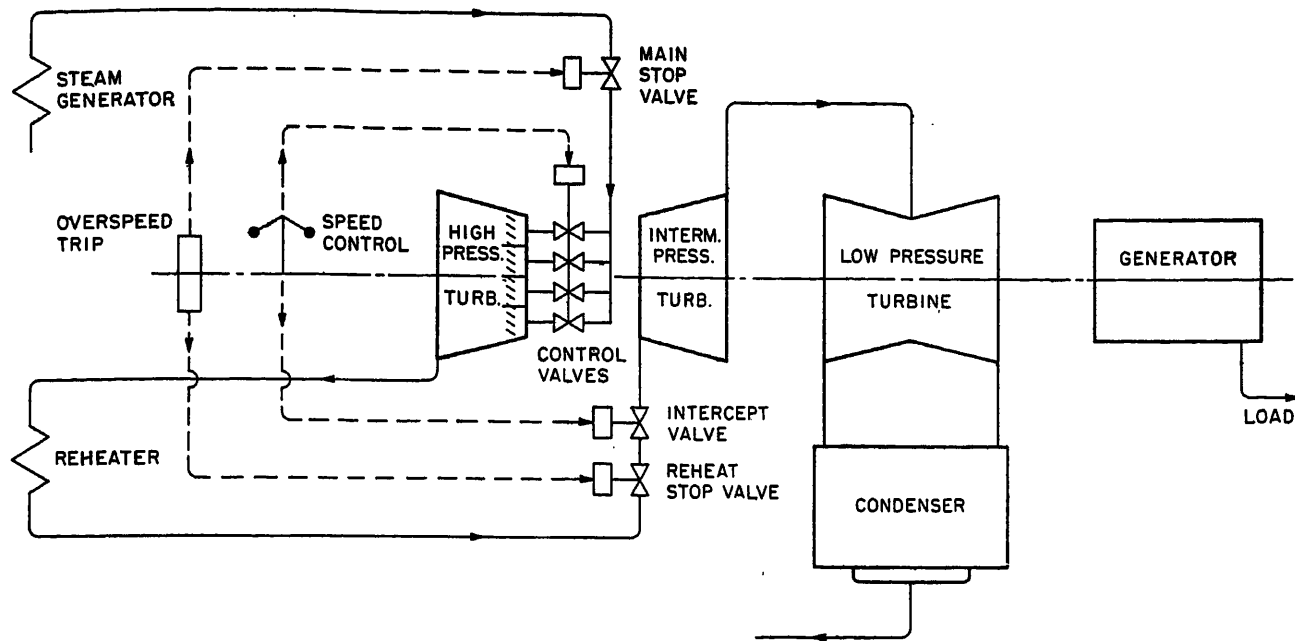


Figure 1 (a). Reheat turbine flow diagram

Basic Control Functions

Normal Operation

The main function of any turbine is to be a prime mover. Thus, it should normally operate in its most efficient mode of operation while still maintaining the necessary control required by the electrical system to which it is connected. To improve efficiency, the main steam is throttled through a set of four to eight sequentially operated control valves as is shown in Figure 1 (a). Each of these control valves admits steam through a different set of nozzle sections. Since these sections have been distributed around the periphery of the first stage, they divide the steam admission into arcs. If only a portion of the control valves are operating, steam is being admitted along a partial arc of the first stage rather than through all 360° of the circumference. This mode of operation is called 'partial arc admission'.

During the start-up process the thermal stresses caused by non-symmetrical heating can be reduced by symmetrically admitting steam to all nozzle sections of the first stage. Turbine control up to a predetermined fraction of rated load is achieved by opening fully the control valves and controlling the steam flow by means of the stop valve. This mode of operation is called 'full arc admission'.

Controlling the thermal stresses in the heavy wall sections of a turbine is always of importance. One cause of thermal stresses can be controlled by restricting the magnitude of instantaneous steam flow changes that can be imposed on the turbine. This is achieved by limiting the rate of increase in speed during start-up³ and the rate of increase of load during loading.

Turbine Protection

Protection of the turbine against operation under dangerous conditions is of such importance that these protections must ultimately override any other control functions. Even though these devices must be absolutely foolproof, their interference

with the normal operation of the turbine as a power maker must occur as infrequently as possible.

Protection against overspeed is the most important, yet the most difficult protective function to perform. If a turbine has been running at full load (delivering maximum torque) and suddenly the electrical counter torque is removed from the generator, the speed of the rotor would reach the limit of safety within approximately one second if no protective action were taken. The steam flow from the main steam source as well as from the reheater must therefore be reduced to a negligible amount within a small fraction of a second.

Two independent lines of defence against excessive speed are always provided. The first line consists of the normal speed control system operating the control valves and the intercept valves. The second line of defence comprises the overspeed trip system which closes the main and reheat stop valves on overspeeds in excess of 10 per cent of rated speed shutting the turbine down.

Basic Arrangement of Conventional Systems

Speed-load Reference

All conventional systems¹⁻⁷ have one feature in common, namely, that the speed reference signal for 'off-the-line' operation and the load reference signal for 'on-the-line' operation are one and the same signal. The block diagram of such a system may have the form shown in Figure 1 (b).

The significance of the symbols used in Figure 1 (b) is shown in Table 1.

The following peculiarities implied in the typical values listed in Table 1 should be noted.

Because of the large time constant, T_s , for full arc admission operation (stop-valve controlling) it is necessary to increase δ to about 0.20 (20 per cent) in order to obtain the same degree of

Table 1

Symbol	Description	Typical value
ρ	Relative speed reference	$\rho = 1$ at rated speed no load $\rho = 1 + \lambda\delta$ at rated speed full load
σ	Relative speed	$\sigma = 1$ at rated speed
ϵ	Speed error	$\epsilon = 0$ at rated speed no load $\epsilon = \lambda\delta$ at rated speed full load
δ	Regulation in units (relative speed change from full load to no load referred to rated speed in 'off-the-line' operation)	$\delta = 0.05$ for partial arc admission (control valves controlling) $\delta = 0.2$ for full arc admission (stop valve controlling)
s	Laplace operator	$s = j\omega$
T_1	Speed relay time constant (pre-amplifier)	$T_1 = 0.06$ to 0.1 sec
T_2	Servo-motor time constant (power amplifier)	$T_2 = 0.15$ to 0.25 sec
T_3	Time constant of steam volumes between valves and turbine	$T_3 = 0.05$ to 0.2 sec for partial arc admission $T_3 = 0.3$ to 0.5 sec for full arc admission
K	Slope of valve opening characteristic at no load rated speed compared to average slope	$K = 0.65$ for partial arc admission, no load (1 at higher loads) $K = 1$ for full arc admission
T_R	Reheater time constant	$T_R = 3$ to 7 sec
f	Load on high pressure section referred to load on entire turbine	$f = 0.4$ to 0.6 for partial arc admission at no load $f = 0.25$ to 0.3 for full arc admission at no load
τ	Torque referred to full load torque	$\tau = 0$ at no load $\tau = 1$ at full load
$\Delta\tau$	Accelerating torque	$\Delta\tau = 0$ at steady state speed
T_4	Characteristic time of turbine-generator	$T_4 = 5$ to 12 sec
λ	Actual load referred to full load	$\lambda = 0$ at no load $\lambda = 1$ at full load

constant and the following relations between load and speed reference exist:

$$\Delta\rho = \lambda\delta$$

For full arc admission $\delta = 0.2$.

If it is desired to pick up 20 per cent load ($\lambda = 0.2$) the necessary change in reference would be

$$\Delta\rho = 0.2 \cdot 0.2 = 0.04$$

A speed reference change of 4 per cent would be needed to pick up 20 per cent load. For partial arc admission $\delta = 0.05$. Picking up 20 per cent load ($\lambda = 0.2$) would be accomplished by

$$\Delta\rho = 0.2 \cdot 0.05 = 0.01$$

A speed reference change of 1 per cent would pick up 20 per cent load. Therefore there would be a 4:1 scale change in ρ between full arc and partial arc admission.

Even more difficulty is encountered when changing from full arc admission to partial arc admission at a given load (typical value 20 per cent load). On full arc admission at 20 per cent load the value ϵ/δ was

$$\epsilon/\delta = 0.2$$

Because of $\delta = 0.2$, the speed error ϵ would have been $\epsilon = 0.04$. If the mode of operation is now switched to partial arc admission with $\delta = 0.05$, the value of ϵ/δ would become

$$\frac{\epsilon}{\delta} = \frac{0.04}{0.05} = 0.8$$

This means that the load would increase from 20 per cent to 80 per cent while switching from full arc admission to partial arc admission while the load should stay constant. The apparent difficulties described above have not been encountered in conventional system, because none of them has attempted to use the same speed error signal for both modes of operation. Whenever a speed control was present for full arc admission it was accomplished by a separate speed control system³. In order to build a well-integrated system, it was the desire of the authors to accomplish the control in both modes of operation with one speed error signal. The ways used to solve this problem are described under the load control unit.

Performance on Loss of Load

Mechanical hydraulic systems with very good performance on loss of load have been built for relatively slow accelerating units (Wirz⁵ $T_4 = 9.9$ sec; Eggenberger and Ipsen⁸ $T_4 = 6.8$ sec).

speed control stability for synchronizing the unit to the line. After the unit has been put on the line the speed is substantially

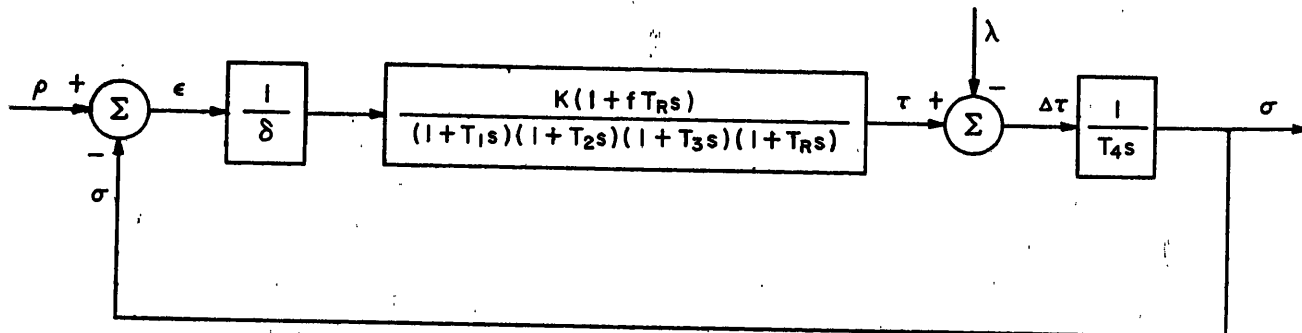


Figure 1 (b). Block diagram of speed control loop for conventional reheat turbine control system

However, when T_4 is reduced toward 5 sec it becomes increasingly difficult to close the turbine valves soon enough to keep the peak speed below 109 per cent of rated speed.

Devices sensing an unbalance between power developed by the turbines and the load produced by the generator (see Hall and Atkinson²) have been used to reduce the lags of the controls when a condition of acceleration is present. Some of these devices by-pass the normal control devices entirely. The electrical system in the form subsequently described is suitable to obtain similar results through the normal control devices, whereby a smooth control is obtained. This feature is discussed in more detail later.

Description of Electro-hydraulic Operating Control System

The proposed electro-hydraulic operating control system has been organized into three major sub-systems. One purpose of these sub-systems is to minimize interactions. As is shown in *Figure 2 (a)*, the speed control unit compares actual turbine speed with the speed reference, and provides one speed error signal for the load control unit. The load control unit combines the speed error signal with the load reference signal and biases to determine desired steam flow signals for the stop valves, control valves, and intercept valves. Finally the valve flow control units accurately position the appropriate valves to obtain the desired steam flows through the turbine.

Speed Control Unit

The purpose of the speed control unit is to produce the speed error signal that is determined by comparing the desired speed with the actual speed of the turbine. When the desired speed setting is increased, the speed reference generator limits the

actual speed reference so as to accelerate the turbine at a programmed rate until the actual speed has reached the desired speed setting. Decreases in desired speed reduce the actual speed reference instantaneously. During normal operation at rated speed the speed error signal is zero, regardless of load. Because of the extreme importance in safeguarding against overspeed, the speed control unit has two redundant channels. If both speed signals fail, the unit will shut down.

Load Control Unit

The prime purpose of the load control unit is to develop signals proportional to steam flow for the stop valves, control valves, and intercept valves. These outputs are based on a proper combination of the speed error, load reference signal possibly modified by high turbine accelerations and FA-PA transfer bias signals.

In order to overcome the difficulty in transferring from full arc to partial arc operation described under the conventional system, the regulation is now introduced to modify only the speed error signal and the input representing desired load is added after this point. A basic block diagram of the speed control loop of this system is shown in *Figure 2 (b)*.

Typical values for this system are shown in *Table 2*. Other values are the same as in *Figure 1 (b)*.

It can be seen now that the signal q_L needed to produce a certain load at constant speed is independent of δ . This means that the rated speed load will be the same for a given q_L no matter whether one operates on full arc admission (on stop valves where one needs $\delta = 0.2$ in order to obtain stable speed control) or on partial arc admission (on control valves where one needs $\delta = 0.05$ by specification⁸).

Therefore it is now possible to calibrate the load reference dial for q_L in per cent of full load and maintain this calibration

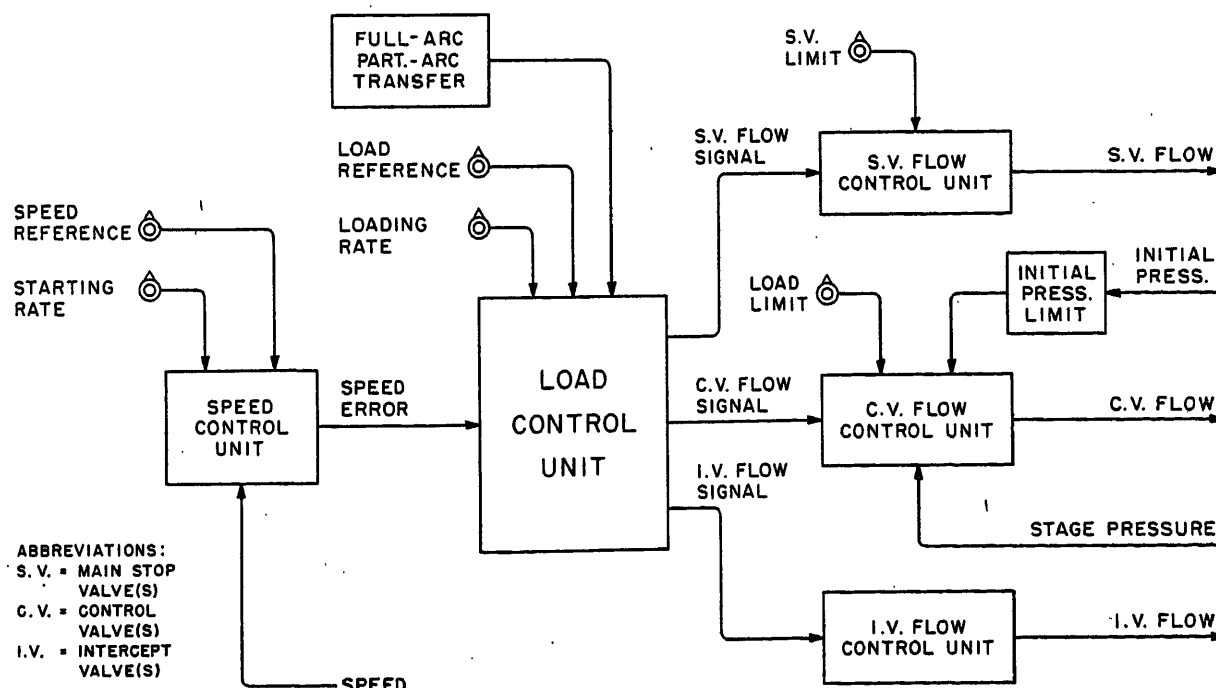


Figure 2 (a). Operating control system elementary diagram

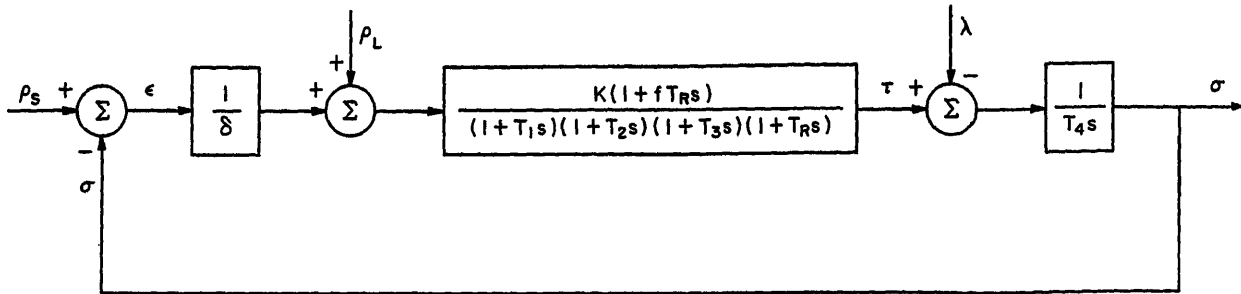


Figure 2 (b). Block diagram of speed control loop for new electro-hydraulic control system

Table 2

Symbol	Description	Typical value
ϱ_s	Speed reference	$\varrho_s = 1$ at rated speed, any load
σ	Relative speed	$\sigma = 1$ at rated speed
ϵ	Speed error	$\epsilon = 0$ at rated speed, any load
δ	Regulation	$= 0.05$ partial arc admission $= 0.2$ less full arc admission
ϱ_L	Load reference	$\varrho_L = 0$ at no load $\varrho_L = 1$ at full load
T_1	Time constant of pilot control	0.01 (sec)
T_2	Time constant of power servo motor	0.1 (sec)

no matter what the regulation δ for any valve set is going to be. The basic arrangement of the entire load control unit is shown in Figure 3.

The following features of operation of the load control unit become apparent. When the speed increases over rated speed, the negative speed error will decrease the flow signal of the controlling valves at a rate defined by the particular valve regulation. For example in partial arc operation, if the control valve regulation were 5 per cent, a 5 per cent speed error would cancel a 100 per cent load reference signal. This would result in reducing the control valve position from fully open to no load position.

The calibrated load reference can be set either manually by the operator, remotely by jogging a switch, or automatically by a dispatching or computer system. Internal circuits limit sudden increases in load reference settings to a maximum adjustable rate, while decreases in load reference settings may occur instantaneously. Since the load reference is in effect a speed vernier adjustment, it is used for synchronizing the turbine. Biases are used to hold any non-controlling valves in wide open position.

When transferring from full arc to partial arc operation, it is necessary first to remove the control valve opening bias and then to apply an opening bias to the stop valve. By programming the shifting of the transfer biases properly, both load variations and ses will be kept within acceptable limits. Although rformed automatically at preset load levels, it is possible for the operator to modify or override the automatic transfer action. The bias to the intercept valve is proportioned so that on slow acceleration the intercept valve will, in any mode

of operation, start closing just after the controlling valve set has come to the closed position. When the generator loses the electrical load, it is necessary to close the control and intercept valves quickly to stop substantially the steam flow to the turbine.

The power-load unbalance device senses the cause of high accelerations and initiates action to reduce peak overspeeds substantially below the trip point. By sensing stage pressure (power) and comparing it with generator load² a measure of unbalance or accelerating torque is obtained. Whenever the unbalance exceeds a threshold level, the modifier reduces the effective load reference signal. The result is to reduce steam flow to both turbine sections sharply and thereby limit the peak speed that results from loss of load.

Valve Flow Control Units

The purpose of the valve flow control units is to produce the steam flows that are commanded by the load control unit. Because of the appreciably non-linear steam flow characteristic of the steam valves, compensation circuits must be introduced to obtain linear steam flow response with respect to steam flow signal. This compensation can be achieved in three different ways: (a) by a function generator having reciprocal characteristics in the forward loop (series compensation); (b) by a function generator having similar characteristics as the valve in a sub-loop feedback (sub-loop feedback compensation); and (c) by a proportional feedback reaching around the non-linear steam valve (major loop feedback compensation).

The stop valve flow control unit is shown in Figure 4. Linearity of the unit is obtained by series compensation. The unit also has a sharp electrical limit that can accurately limit the stop valve opening. The position loop is a standard configuration consisting of a servo amplifier, servo valve, ram, and position transducer feedback. The intercept valve flow control unit is similar to the stop valve unit except for fast closing characteristics. Since the intercept valves control the largest amount of steam energy during loss of load, it is necessary to close these valves as quickly as possible. By paralleling a low-flow linear servo valve with a fast-acting high-closing flow solenoid valve it is possible to position accurately and also to close rapidly the intercept valves. By using this technique the peak speed on loss of load can be held to approximately 106 per cent of rated speed on a unit with a characteristic time $T_4 = 5$ sec.

The control valve flow control unit shown in Figure 5 is considerably different from the two preceding units. To improve linearity, stage pressure feedback (major loop feedback) is employed around the combination of positioning loops and valve flow

AN ELECTRO-HYDRAULIC CONTROL SYSTEM FOR REHEAT TURBINES

characteristics. Since negative stage pressure feedback requires increasing the feedforward gain, a gain adjuster is used. The load limit may be used to limit the opening travel of the control valve. The initial pressure limiter reduces the control valve

opening when the steam generator pressure falls below a preset value.

Since the control valves open sequentially it is necessary to bias each control valve by a voltage equivalent to the sequential

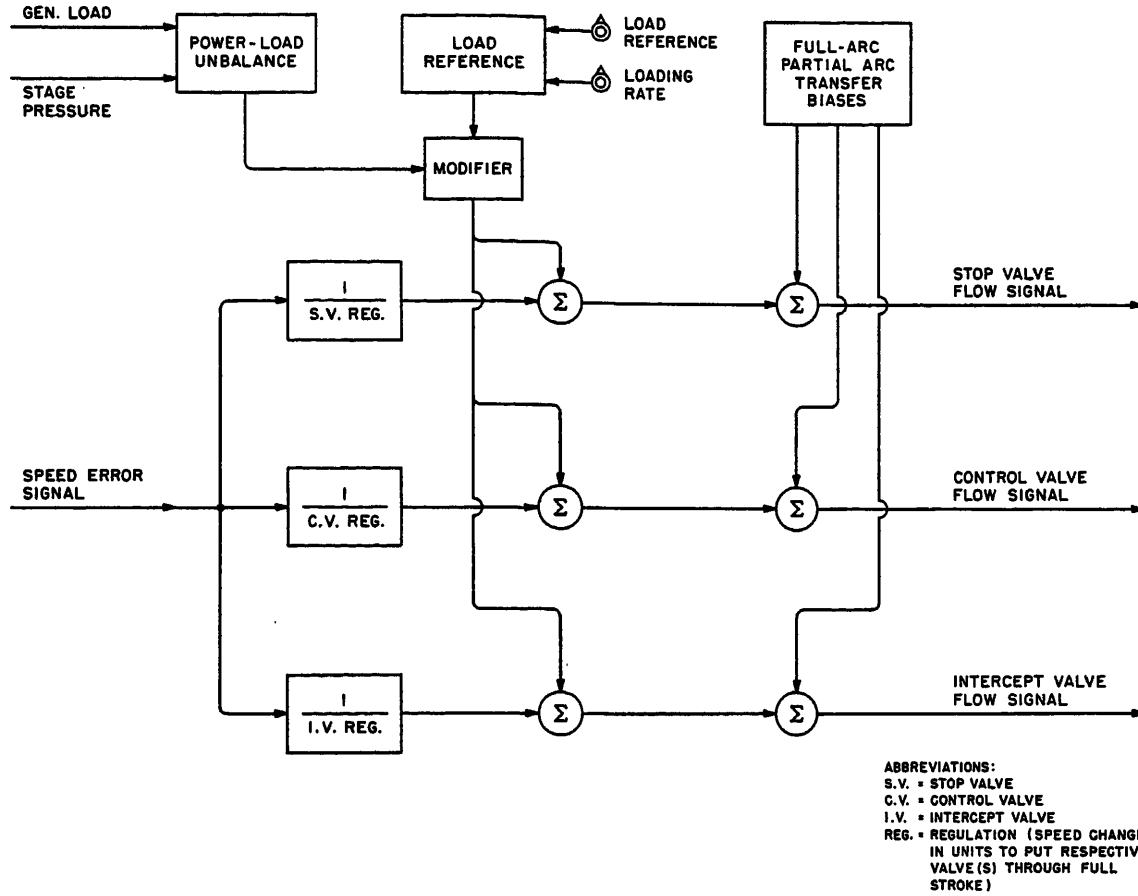


Figure 3. Load control unit

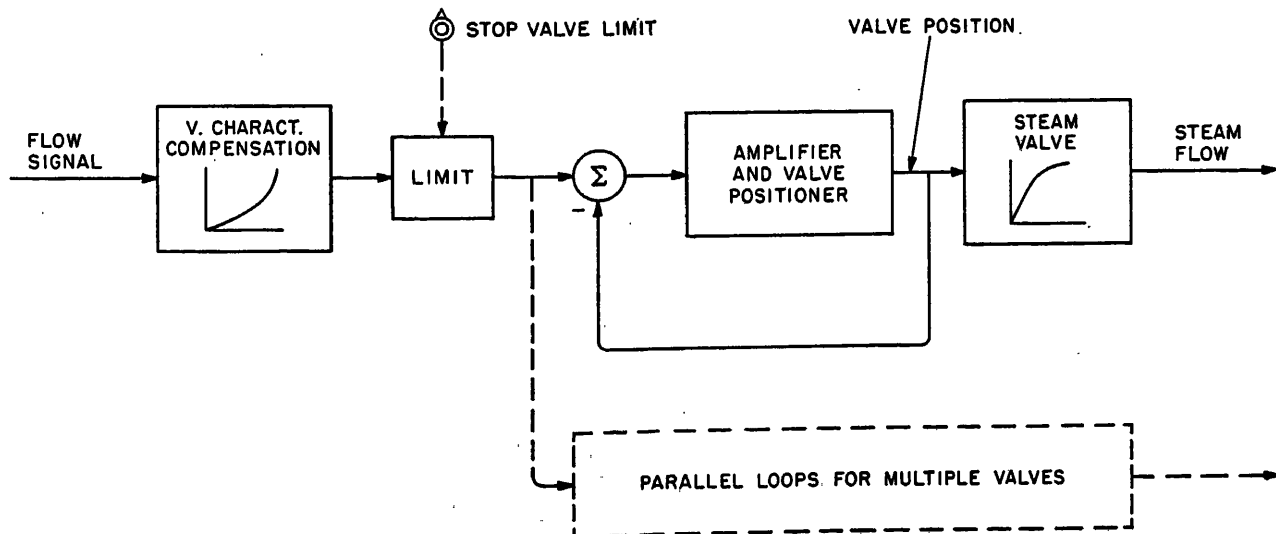


Figure 4. Stop valve (intercept valve) flow control unit

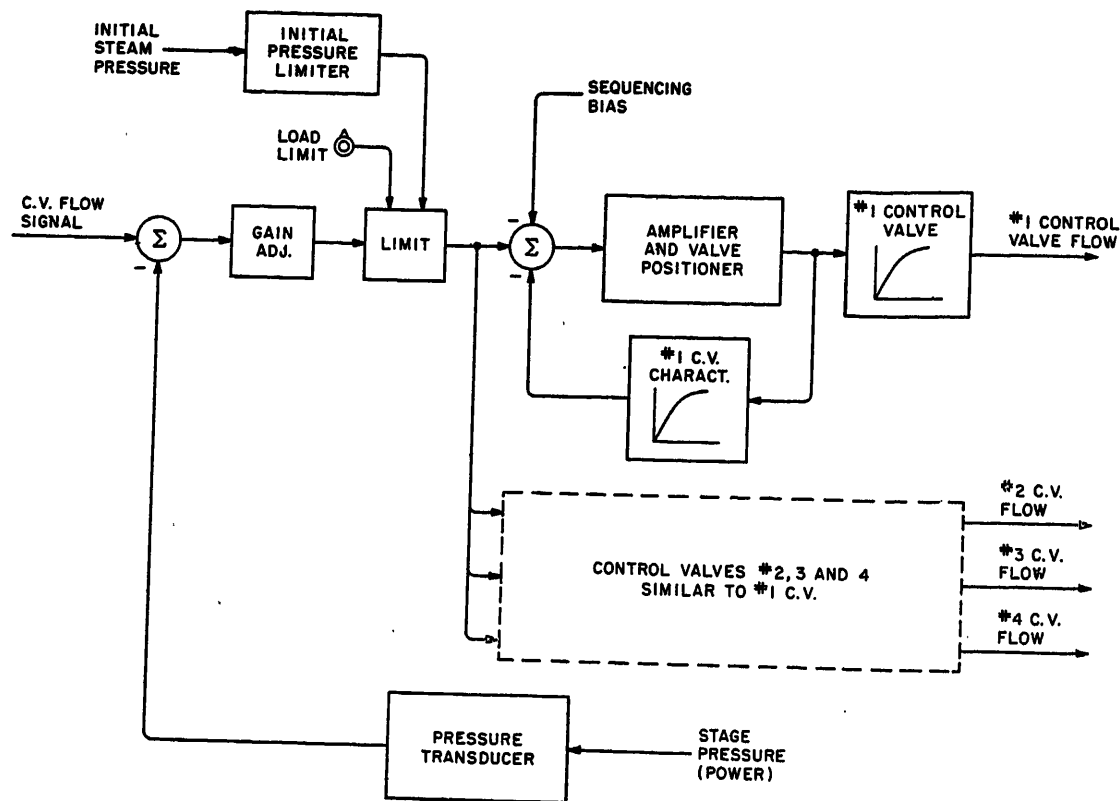


Figure 5. Control valve flow control unit

offset. This offset causes each control valve to be operated individually instead of in parallel as was done for the stop valves and intercept valves. The non-linear valve characteristics are applied in the feedback of the positioning loops (sub-loop feedback compensation). This method reduces variations in incremental regulation from the accepted standard⁹ to about plus 3 and minus 1 per cent of the steady-state regulation.

Emergency Trip System

This system is used primarily as a second line of defence against overspeed; however, other functions may shut down the turbine if signals from certain sensing devices indicate that other dangerous conditions are eminent. Since the standard emergency governor (eccentric ring or bolt type) is highly reliable and has no electronic parts (independent second line of defence), it is used in its original form to protect the turbine against excessive overspeed. A fully electrical overspeed trip with the fail-safe and testing features has been proposed by Schmidt and Kaufmann.

Malfunctions such as low vacuum, loss of hydraulic pressure, etc., are sensed electrically and will actuate the emergency trip system by tripping a solenoid valve which will remove the pressure from the emergency trip fluid system. Since the emergency trip system is in principle similar to the one presently used, it will not be discussed in further detail in this paper.

Conclusion

The new system presented is the result of an attempt to synthesize the most recent operating philosophies for large central station units into one complete system. It takes account of the

widely accepted concept of achieving as many characteristics as possible by analogue sub-loops in order to unload the computer in more completely automated power stations.

Appreciation is expressed to P. C. Callan, General Engineering Laboratory, General Electric Company, Schenectady, New York, for his inventive co-operation in the development of this system.

References

- ¹ FOWLER, J. F. and MATNEY, C. Cross compound single flow turbine with axial exhaust. *Amer. Soc. mech. Engrs. Pap.* 57-PWR-6
- ² HALL, J. S. and ATKINSON, M. B. *Some Aspects of Steam Turbine Governing*. 1957. Metropolitan Vickers
- ³ WALSH, E. F. and JACKSON, R. L. Effectiveness of stop valve bypass in reducing thermal stress gradients in steam turbines. *Amer. Soc. mech. Engrs. Pap.* 61-WA-121
- ⁴ BURKHARD, G. A. The task of governing steam turbines and means to accomplish same. *Escher Wyss News* (1958) No. 1
- ⁵ WIRZ, K. Test to determine the behavior of a 60,000 KW turbine on sudden loss of load. *Escher Wyss News* (1958) No. 3
- ⁶ TRAUPEL, W. *Thermische Turbomaschinen*. Vol. 2. 1960. Springer-Verlag
- ⁷ EGGENBERGER, M. A. Stability of mechanical hydraulic speed control system for steam turbines. *Amer. Soc. mech. Engrs. Pap.* 60-WA-34
- ⁸ EGGENBERGER, M. A. and IPSEN, P. G. The control system of a 225,000 kW double automatic extraction steam turbine and related reducing station. *Amer. Soc. mech. Engrs. Pap.* 58-SA-36
- ⁹ Recommended specifications for speed-governing of steam turbines. *AIEE Standard Specification 600* (1959)

DISCUSSION

R. STARKERMANN and A. OBERLE, *Brown Boveri & Co. Ltd., Baden, Switzerland*

More and more electric controllers for steam turbines are at present appearing on the market. To solve complicated control problems (e.g. frequency-load control) these controllers have substantial advantages and they lead to a more flexible adaptation of control requirements. Nevertheless, the pure hydraulic-mechanic control will retain its justification in many applications. It ensures simple and robust design and will—on the reliability score—scarcely become outstripped by electric control systems. Therefore it seems highly expedient to further improve mechanic-hydraulic components for pure hydraulic turbine control.

To fulfil this requirement great efforts have been undertaken to build fast non-linear servomotors. Using the principle of feedback in connection with a device which increases the draining-off of the fluid when high acceleration of the turbine shaft occurs, the time required to drain the fluid between the speed controller and the servomotor could be reduced tremendously. *Figure A* shows a diagram taken from four servomotors mounted on a turbine. The input signal was a step function. This result shows that the protection for overspeed—this is the main criterion for a steam turbine control system—is guaranteed in the future even without an electric controller.

Concerning the time constants given in the paper, we would like to mention that they depend to a great extent upon the specific design of a turbine. If, for example, stop valve and inlet control valves are built together in the same body, the time constants T_{3a} and T_{3b} , that is for partial-arc admission and for full-arc admission, are practically the same, and δ may then be the same for both conditions, namely 5 per cent. This design has given good results on Brown Boveri turbines.

From the point of view of security, in the event of a sudden loss of load the time constant $T_3 \rightarrow 0.5$ sec seems to be inadmissibly high. For a reheat turbine with a $T_4 = 5$ sec the stored steam energy would produce a speed increase of about 3–4 per cent, and for a condensing turbine even 10 per cent. This remark is based upon the assumption that the set is under high load with full arc admission.

We are not in agreement with the author that it was the unsolved problem of the turbine control system which delayed the realization of the reheat turbine. What delayed the introduction of the reheat turbine more was the time required to improve the economy of these plants to an acceptable level and to complete the studies and investigations which led to these improvements.

To make reheat turbines economic, the development of unit operation of big sets was necessary. Once this was accomplished, the control problems were solved without difficulties.

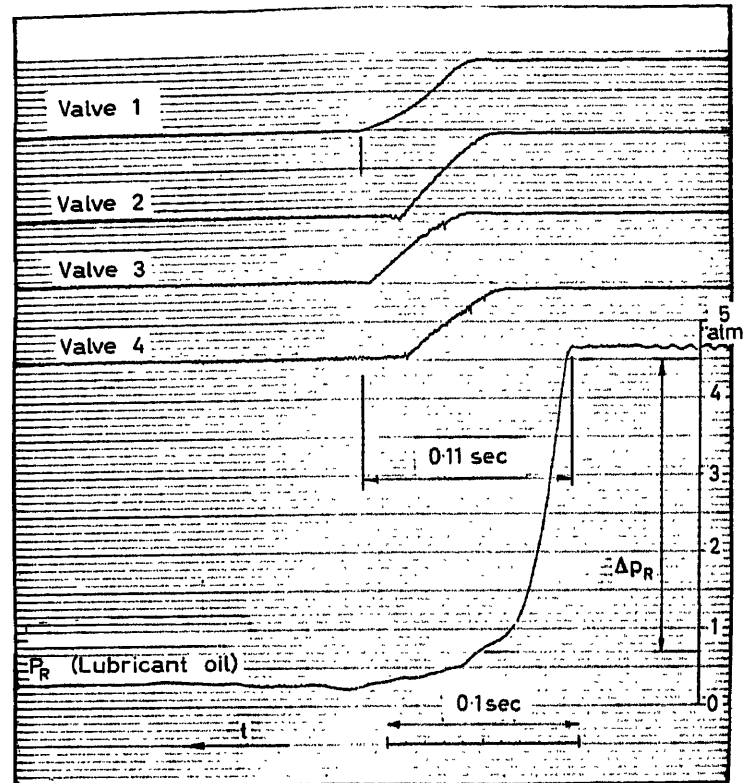


Figure A

Three questions we would like to ask are:

(1) What is the load (in per cent) at the change-over from full-arc to partial-arc admission? The question concerns the overspeed security since $\delta = 20$ per cent.

The Brown Boveri system uses for both conditions (full-arc and partial-arc admission) within a hydraulic control system the same speed controller, the same speed-error signal, and this with a δ of 5 per cent. The change-over from full-arc to partial-arc admission is for a load of 100 per cent. In another Brown Boveri system an idea of the authors already accomplished is the system of the three-control units: speed control (electric), load control (electric), valve control (electro-hydraulic)¹. See *Figure B*.

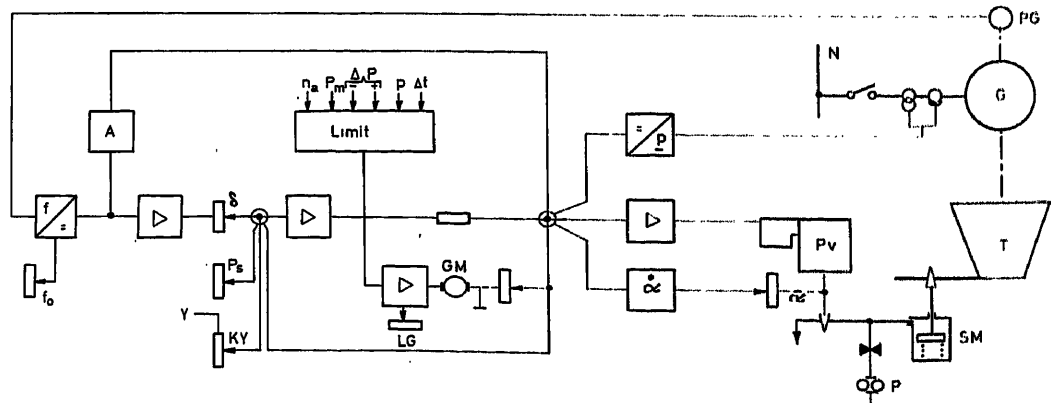


Figure B. Circuit diagram of the electric steam turbine control 'Turbotrol'. (f_0 frequency regulator, P_n output regulator, KY dosage for circuit control, LG load gradient, S statistics, T turbine, G generator, PG pendulum generator, SM servomotor for steam valve, P_v baffle-plate, amplifier, GM gradient motor, A intercepting arrangement, P pump, N circuit)

AN ELECTRO-HYDRAULIC CONTROL SYSTEM FOR REHEAT TURBINES

(1) Does the studied equipment include a testing feature for detection or failure occurring on one of the electrical components?

(2) What is the available power at the output of the last electrical amplifier and what mechanical and hydraulic elements composed the last part of the circuit?

(3) The control valve characteristics are compensated by means of a complex feedback system. Could the same result be obtained with an electrical power feedback loop?

(4) A device balancing a stage pressure with the electrical load, protects the turbine against overspeed. Do the authors think that such a device is better than one using the derivative of the speed signal?

(5) Are control systems of the type described now operating in the United States on large steam units, and if so, for how long?

M. A. EGGENBERGER, *in reply*

(1) There are continuity circuits checks and redundant circuits, particularly for the speed control circuits.

(2) The output of the power amplifiers is now 0.1 W but this does not imply that this will be the final solution.

(3) We have found, that transiently, the generator output does not necessarily represent the power of the turbine. Because of this finding we prefer to use stage pressure, to represent power.

(4) The derivative approach to obtain rapid valve action on loss of load is plagued with noise problems which led us to abandon derivative control elements.

(5) The prototype system is at present the only one of this type in operation. Other electro-hydraulic systems with a somewhat more conventional system approach have been in operation for several years.

Une Application Industrielle d'un Calculateur Intérieur à un Circuit de Commande: l'Équipement Électronique de Commande d'une Machine à Équilibrer les Vilebrequins

J. CSECH

Summary

This paper describes the electromechanical and the electronic equipment in a machine for balancing crankshafts. The machine is one of the transfer type, that is, the part to be machined is conveyed automatically and successively to the various different work-stations. Excess metal is removed by cutting-files.

The items include an entry station, where the crankshaft is set in such a way that the axes of the shafts are all in exactly the same vertical plane; a station for measuring the unbalance on the oscillating rocker bearings; three stations where excess matter is removed in the different planes of the orthogonal axes, which entails six machining heads; a washing station; a station for measuring the residual unbalance; an evacuation station, where good parts are selected and where others, needing to be retouched, are retained.

Once the crankshaft has been set to turn at the speed required, the electronic calculating equipment carries out the following operations:

It determines the extent and phase of the unbalance related to the median planes of the end bearing-blocks; distributes the unbalance between the end counterbalances; projects, in each one of these planes, the unbalance on to two orthogonal axes passing through the axis of the bearing-blocks; if one or more vectors lies outside the angle contained by the counterbalances, it brings the equivalent mass back into the two other central planes of the counterbalance; and finally, determines the cutting stroke of each cutting file according to the amount of the mass to be removed.

This information is recorded and accompanies the crankshaft throughout its transfer along the machine. The recording system is a permanent one.

Two machines of this type are at present being used for industrial purposes. At the beginning of September 1963, one of them had been in operation for more than 2 years; the other for 18 months.

The paper also gives details of the advantages to be obtained from the industrial use of such a group, from the point of view of rate of production and the reliability of all the electronic equipment and machines.

Sommaire

L'auteur décrit l'équipement électromécanique et électronique d'une machine automatique à équilibrer les vilebrequins.

Cette machine est du type transfert, c'est-à-dire que la pièce à usiner est présentée successivement et automatiquement devant les divers postes de travail. Le métal excédentaire est enlevé par fraisage.

On peut distinguer un poste d'entrée où le vilebrequin est orienté de telle façon que les axes des manetons soient dans un même plan vertical; un poste de mesure du balourd sur berceaux oscillants; trois postes où l'on enlève successivement la matière excédentaire dans les différents plans suivant deux axes orthogonaux ce qui conduit à six têtes d'usinage; un poste de lavage; un poste de mesure du balourd résiduel; un poste d'évacuation où l'on différencie les pièces bonnes et celles qui nécessitent une retouche.

Une fois le vilebrequin entraîné et mis en vitesse, l'équipement de calcul électronique exécute les opérations suivantes:

Il détermine en amplitude et en phase les balourds situés dans les plans médians des paliers extrêmes; répartit les balourds entre les plans des contrepoids extrêmes; dans chacun de ces plans projette ces

derniers sur deux axes orthogonaux passant par l'axe des paliers; si un ou plusieurs vecteurs composants sortent de l'angle embrassé par les contrepoids, reporte la masse équivalente dans deux autres plans centraux du contrepoids; enfin, détermine les courses utiles des unités de fraisage en fonction de la masse à enlever.

Ces informations sont mises en mémoire et accompagnent le vilebrequin durant son transfert tout au long de la machine. La mémoire où les informations sont stockées est du type permanent.

Deux machines de ce genre sont actuellement en exploitation industrielle. Au mois de septembre 1963 l'une d'entre elles sera en fonctionnement depuis plus de deux ans, l'autre depuis dix-huit mois.

L'auteur présentera lors de son exposé, les enseignements que l'on peut tirer du fonctionnement industriel d'un tel ensemble sur le plan de la cadence de production et de la fiabilité des équipements et des composants électroniques.

Zusammenfassung

Der Beitrag beschreibt die elektromechanische und elektronische Ausrüstung einer automatischen Auswuchtmaschine für Kurbelwellen.

Die Maschine bringt das zu bearbeitende Stück nacheinander und automatisch in die verschiedenen Arbeitspositionen; das überschüssige Metall wird abgefräst.

Die Maschine führt die nachfolgenden Bearbeitungsvorgänge aus: In der Anfangsstufe wird die Kurbelwelle so eingerichtet, daß die Achsen der Kurbelzapfen genau in eine bestimmte Lage zur Antriebswelle zu liegen kommen. Dann erfolgt die Messung der Unwucht auf schwingenden Lageböcken; anschließend wird das überschüssige Material nacheinander in den drei Auswuchtflächen im Zwei-Koordinaten-Verfahren entfernt, das ergibt 3 Bearbeitungsstellen mit je 2 Bearbeitungseinheiten. Auf einen Waschvorgang folgt die Messung der Restunwucht. Die guten Teile werden ausgelesen und die nochmals zu bearbeitenden zurückgehalten.

Nachdem die Kurbelwelle die gewünschte Bearbeitungsdrehzahl erreicht hat, führt die elektronische Recheneinrichtung die folgenden Operationen durch: Sie bestimmt Größe und Phase der Unwucht bezogen auf die Mittelebene der Lagerstellen. Dann erfolgt ein Umrechnen der Unwucht auf die Ebene der äußeren Gegengewichte. Das Ergebnis dieser Rechnung wird für jede dieser Ebenen auf 2 orthogonalen Koordinaten, die sich in der Drehachse schneiden, aufgeteilt. Kommt eine oder mehrere Komponenten außerhalb des durch die Gegenunwucht überstrichenen Winkels zu liegen, so muß eine gleich große Masse an 2 anderen Ebenen aufgebracht werden. Schließlich bestimmt die Recheneinrichtung den Vorschubweg der Fräseinheiten in Abhängigkeit von der zu fräsierenden Masse.

Le développement de l'automatisme dans l'industrie suscite un bouillonnement d'idées et une floraison de machines nouvelles. Les idées, comme il est naturel, sont généralement en avance sur les machines. Par exemple, on a déjà décrit maintes fois comment les unités de production peuvent être pilotées par des cal.

culateurs électroniques, mais les exemples de mises en service effectives de tels procédés ne sont pas encore très fréquents. En outre, si la curiosité du public est très vive à l'égard de ces techniques nouvelles, souvent sa déception ne l'est pas moins — même s'il s'agit d'un public éclairé — devant la complexité des explications fournies par les automaticiens dès qu'ils abandonnent le terrain des généralités pour celui de la technologie.

Au milieu des étonnantes performances accomplies par la Régie Renault pour automatiser la fabrication des moteurs

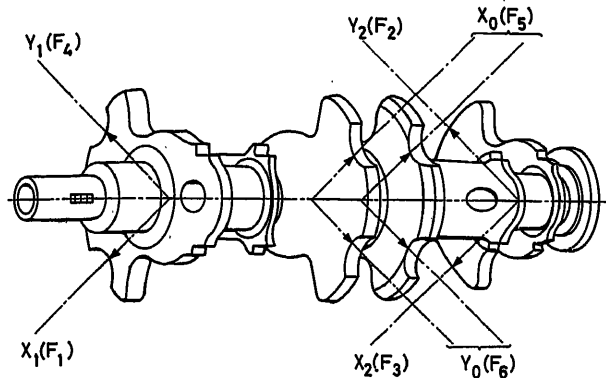


Figure 1. Le vilebrequin

d'automobiles, l'opération d'équilibrage dynamique des vilebrequins a constitué une sorte d'ilôt de résistance: ce n'est que dernièrement qu'une machine effectuant cette opération automatiquement le long d'une chaîne de fabrication continue a été mise en service.

Cette machine comporte une commande électronique décrite ci-après, qui est un exemple concret, à la fois assez simple et caractéristique, des possibilités offertes par les dispositifs de calcul analogique et numérique dans les équipements industriels modernes.

Description Générale de la Machine et Données du Problème

La pièce à équilibrer est un vilebrequin de moteur quatre cylindres dont le poids est d'environ 7 kg. La Figure 1 montre ce vilebrequin avec l'indication de la position des capteurs de mesure du balourd et des plans dans lequel s'effectuera par fraisage l'enlèvement de métal. Ces plans sont ceux des manetons du vilebrequin. Le balourd initial peut atteindre 400 g/cm alors que la valeur maximum finale ne doit pas dépasser 20 g/cm.

La Figure 2 représente cette machine qui est du type transfert, c'est-à-dire que la pièce à usiner est présentée successivement et automatiquement devant les divers postes de travail. Le métal excédentaire est enlevé par fraisage, ce qui permet d'effectuer l'équilibrage en une seule passe.

On peut distinguer:

- un poste d'entrée où le vilebrequin est orienté de telle façon que les axes des manetons soient dans un même plan vertical;
- un poste de mesure du balourd sur berceaux oscillants. La vitesse de rotation de 900 tr/min est au-delà de la vitesse de résonance;
- trois postes où l'on enlève successivement la matière excédentaire dans les différents plans suivant deux axes orthogonaux ce qui conduit à six têtes d'usinage;
- un poste de lavage;
- un poste de mesure du balourd résiduel;
- un poste d'évacuation où l'on différencie les pièces bonnes et celles qui nécessitent une retouche.

Les mouvements des organes mécaniques, comme ceux de la plupart des machines transfert, sont commandés par relais et électrovalves. Une fois le vilebrequin entraîné et mis en vitesse, l'équipement de calcul électronique exécute les opérations suivantes:

- déterminer en amplitude et en phase les balourds situés dans les plans médians des paliers extrêmes;
- répartir ces balourds entre les plans des contrepoids extrêmes;

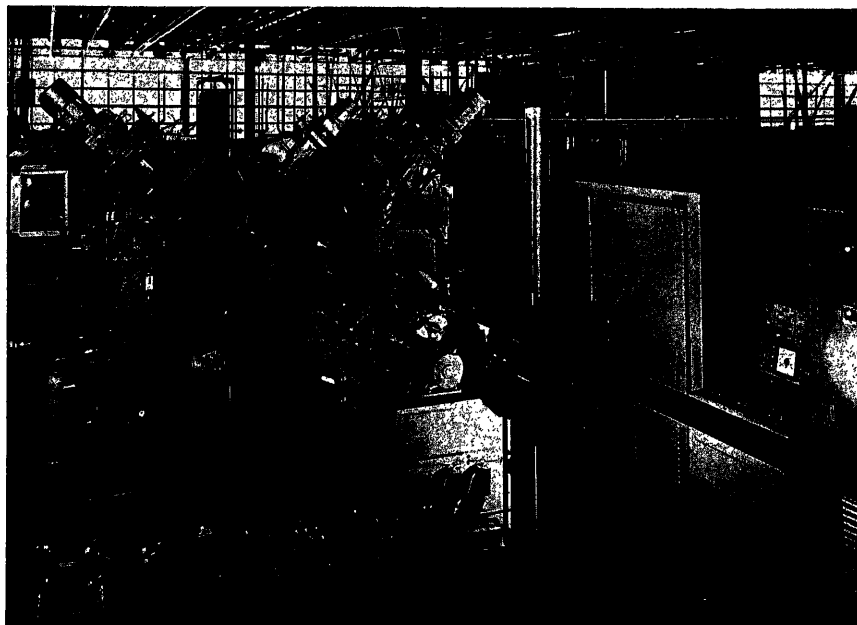


Figure 2. Vue d'ensemble de la machine

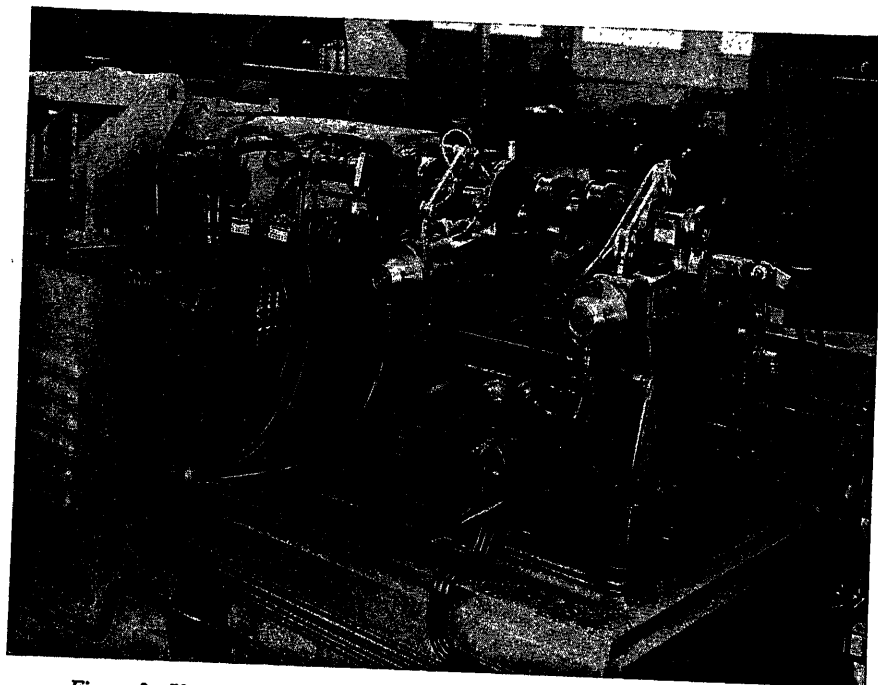


Figure 3. Vue de poste de mesure des balourds — au premier plan les capteurs

dans chacun de ces plans projeter ces derniers sur deux axes orthogonaux passant par l'axe des paliers;

si un ou plusieurs vecteurs composants sortent de l'angle embrassé par les contrepoids, reporter la masse équivalente dans deux autres plans centraux du contrepoids;

enfin déterminer les courses utiles des unités de fraisage en fonction de la masse à enlever.

Ces informations sont mises en mémoire et accompagnent le vilebrequin durant son transfert tout au long de la machine. Elles permettent l'enlèvement de la quantité de matière nécessaire à l'emplacement adéquat. La mémoire où les informations sont stockées est du type permanent, c'est-à-dire que, même en cas d'arrêt de la machine, par exemple en fin de journée, il n'est pas nécessaire de vider celle-ci. Les pièces, même incomplètement usinées, seront terminées à la reprise du travail.

Nous allons maintenant effectuer la description des éléments électroniques de calcul constituant l'ensemble de la machine.

Mesure du Balourd (Figure 3)

Les extrémités du vilebrequin sont posées sur deux paliers situés dans le même plan horizontal. Les paliers sont fixés dans deux berceaux qui peuvent se déplacer horizontalement dans un plan vertical perpendiculaire à l'axe du vilebrequin à l'arrêt. Celui-ci est entraîné à 900 tr/min. Sous l'effet du balourd, il oscille sans se déformer (car il est supposé parfaitement rigide) autour d'un axe vertical. On démontre que cet axe est l'axe principal d'inertie passant par le centre de gravité de l'ensemble vilebrequin équilibré plus balourd. Les berceaux dont les déplacements maximaux sont limités par des ressorts suivent les déplacements des extrémités du vilebrequin. Des capteurs linéaires de vibration enregistrent les mouvements du berceau. Par suite chaque capteur donne une tension sinusoïdale qui est l'image du déplacement de l'extrémité du vilebrequin. Cette tension est définie par :

une amplitude maximale proportionnelle au déplacement de l'extrémité du vilebrequin;

une fréquence imposée par la vitesse d'entraînement du vilebrequin, dans ce cas 15 périodes;

une phase repérée par rapport à une phase fixe créée par un alternateur monté en bout du moteur entraînant le vilebrequin.

Ainsi les capteurs de vibration donnent des tensions sinusoïdales de fréquence 15 périodes qui permettent d'analyser les mouvements des extrémités du vilebrequin sous l'effet du balourd.

Les tensions fournies par ces capteurs font apparaître en phase et en module des vecteurs

$$V'_1 | \theta_1 \quad V'_2 | \theta_2$$

dans les plans des paliers P'_1 et P'_2 .

Les vecteurs \vec{V}'_1 et \vec{V}'_2 représentent le balourd du vilebrequin car tout balourd peut être décomposé en deux balourds situés dans des plans quelconques perpendiculaires à l'axe de rotation du solide.

Les plans P'_1 et P'_2 sont appelés plans de mesure, les plans P_1 et P_2 plans d'usinage car ils contiennent les contrepoids où seront faits les enlèvements de matière comme le montre la Figure 4.

On démontre que l'expression des balourds dans les plans P_1 et P_2 est donnée par :

$$\begin{aligned} \vec{V}_1 &= a\vec{V}'_1 + b\vec{V}'_2 \\ \vec{V}_2 &= a\vec{V}'_2 + b\vec{V}'_1 \end{aligned} \quad (1)$$

Le balourd de la pièce est parfaitement corrigé par compensation de ces vecteurs balourds \vec{V}_1 et \vec{V}_2 .

On peut former d'une façon simple les tensions sinusoïdales av'_1 , bv'_1 , av'_2 , bv'_2 en utilisant des transformateurs alimentés

par les tensions v'_1 et v'_2 et dont les rapports de transformation sont a et b .

En mettant en série les enroulements av'_1 et bv'_2 , bv'_1 et av'_2 on obtient deux tensions sinusoïdales

$$V_1 = av'_1 + bv'_2$$

$$V_2 = bv'_1 + av'_2$$

qui sont proportionnelles aux vecteurs \vec{V}_1 et \vec{V}_2 .

Mesure des Angles θ_1 et θ_2 (Figure 4)

La mesure de la position angulaire de l'arbre de sortie est faite par une synchromachine alimentée en triphasé par un alternateur monté sur l'arbre d'entraînement du vilebrequin et jouant le rôle de génératrice de référence.

On sait que la tension induite dans le rotor a une amplitude constante et une phase variable avec θ :

$$u = U \sin(30\pi t + \theta)$$

L'organe de comparaison des phases θ et θ_1 est un démodulateur équilibré qui a la propriété d'avoir une tension de sortie nulle lorsque

$$\theta = \theta_1 + \frac{\pi}{2}$$

La tension u alimente l'enroulement de référence et la tension V_1 l'enroulement du signal à démoduler.

Lorsque le système asservi est en équilibre, la position angu-

laire de l'arbre de sortie est égale à la phase de la tension V_1 . Cet asservissement joue donc le rôle d'un phase-mètre.

Un second asservissement identique sert à calculer θ_2 .

Calcul des Composantes Suivant les Axes d'Usinage

Les têtes d'usinage travaillent dans chacun des plans P_1 et P_2 suivant deux axes perpendiculaires OX' et OY . Les balourds suivant ces axes sont donnés par les projections des vecteurs V_1 et V_2 soit:

$$x_1 = V_1 \cos \theta_1 \quad x_2 = V_2 \cos \theta_2 \quad (2)$$

$$y_1 = V_1 \sin \theta_1 \quad y_2 = V_2 \sin \theta_2$$

Pour calculer ces composantes, on utilise une petite machine tournante appelée résoudre et dont le rotor et le stator ont chacun deux enroulements bobinés à 90 degré.

Ces deux résolveurs sont accouplés aux arbres de sorties des asservissements de position θ_1 et θ_2 . L'enroulement statorique est alimenté par la tension V_1 ou V_2 modulée à 50 Hz et on recueille sur les enroulements rotoriques:

$$x_1 = V_1 \cos \theta_1 \quad x_2 = V_2 \cos \theta_2$$

$$y_1 = V_1 \sin \theta_1 \quad y_2 = V_2 \sin \theta_2$$

Toutefois, une difficulté se présente si une ou plusieurs composantes sont négatives. En effet, il n'est pas possible d'opérer un équilibrage par adjonction de métal. Dans ce cas, on dé-

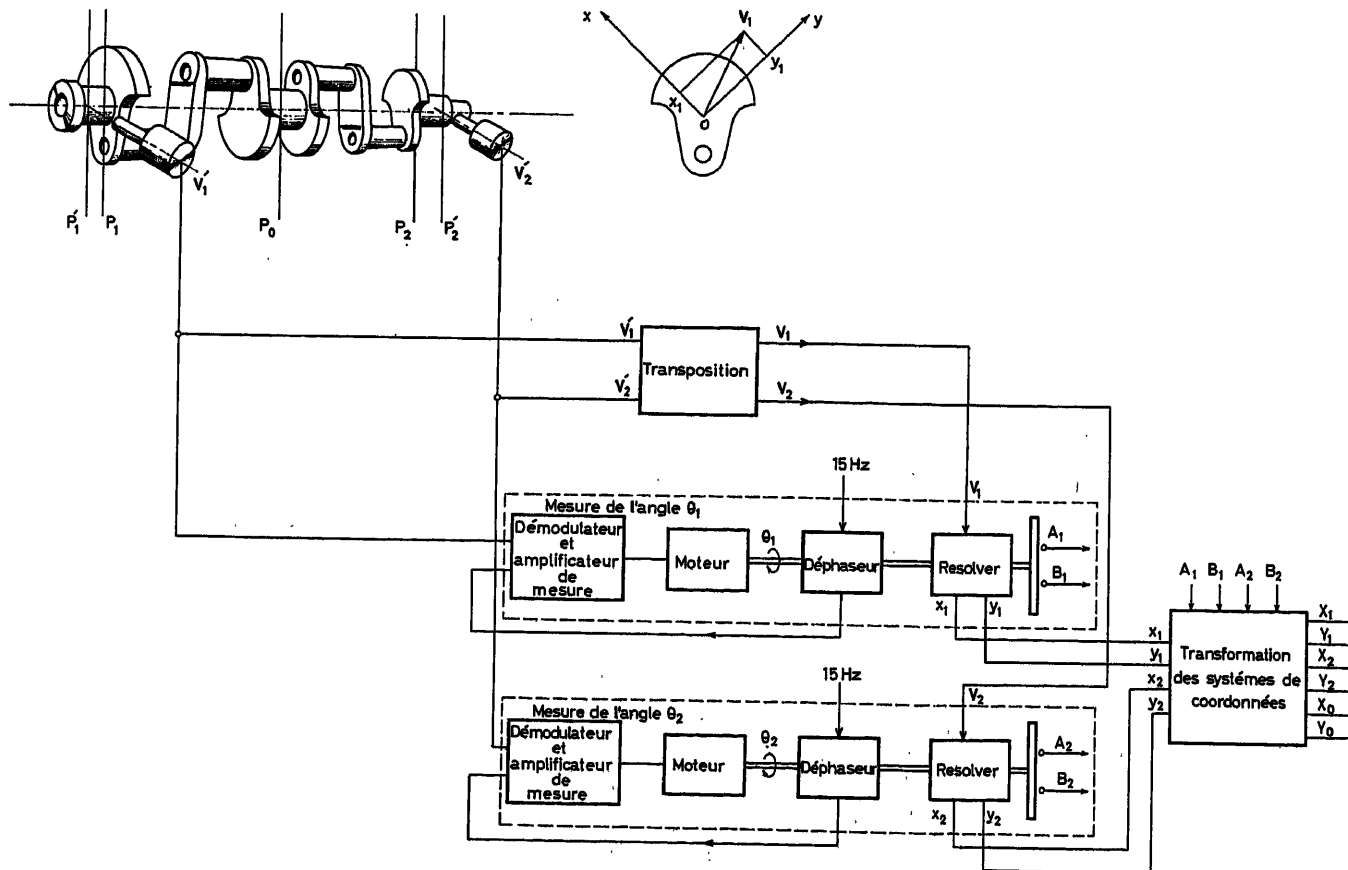


Figure 4. Équipement de calcul analogique des composantes du balourd

montre qu'un balourd $-\vec{V}_1$ situé dans le plan P_1 est équivalent à un balourd $-2\vec{V}_1$ situé dans le plan P_0 au centre du vilebrequin et à un balourd $+\vec{V}_1$ situé dans le plan P_2 .

Ainsi on peut en permanence considérer que tout balourd d'un vilebrequin est équivalent à trois balourds situés dans les plans P_1 , P_2 et P_0 .

Il existe donc un système:

$$x_1 y_1 \quad x_2 y_2 \quad x_0 y_0 \quad (3)$$

équivalent à (2) et dont les composantes sont toujours positives.

Les signes des quantités $x_1 x_2 y_2$ sont connus au moyen de cellules photoélectriques placées en face de disques solidaires des arbres des asservissements θ_1 et θ_2 .

Transformations des Composantes du Balourd en Valeurs Numériques d'Enfoncement d'Outils (Figure 5)

Une fois déterminées les six tensions analogiques proportionnelles aux balourds selon les axes OX et OY des trois plans P_1 ,

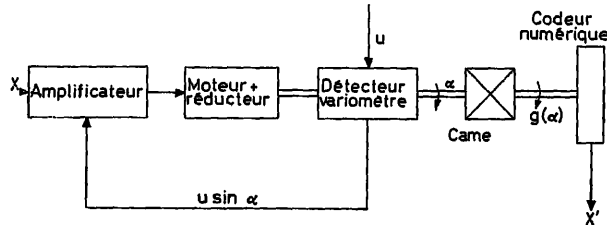


Figure 5. Conversion de la valeur analogique du balourd (X) en valeur numérique d'enfoncement d'outil (X')

P_2 et P_0 il y a lieu de déterminer les enfoncements d'outils des six têtes d'usinage correspondantes. La Figure 5 indique le principe de l'équipement effectuant cette conversion. Il est essentiellement constitué par six asservissements de position entraînant des codeurs binaires à 128 points. La mesure de la position est effectuée par un variomètre, petite machine tournante à induction fournissant une tension sinusoïdale d'amplitude proportionnelle au sinus de l'angle de rotation de son rotor. Sur l'arbre de sortie de l'asservissement de position est montée une came permettant d'introduire la fonction liant l'enfoncement des outils aux composantes du balourd. Ces fonctions assez complexes doivent tenir compte de la forme du vilebrequin, de la forme de la fraise ainsi que de la quantité du métal enlevé par tour de

fraise. Ces relations sont réalisées au moyen de cames dont le rayon varie suivant la loi désirée. Ces variations de rayon sont transformées en une rotation d'arbre sur lequel est fixé le codeur.

Registre de Glissement (Figure 6)

Le registre de glissement est une mémoire dans laquelle les informations peuvent passer d'une position P_n à une position P_{n+1} par la commande d'un signal électrique. A un instant donné cette mémoire contient les données relatives à six vilebrequins et la progression de ces données de la position P_n à la position P_{n+1} se fait simultanément par un ordre venant de la machine transfert. L'ensemble de cette partie de l'équipement est entièrement transistorisé, l'utilisation de bascules à transistors permettant de réaliser sous un faible volume l'ensemble des opérations désirées.

Commande des Têtes d'Usinage (Figure 7)

La vis mère du chariot porte-fraise entraîne un disque percé de trous envoyant des impulsions sur des cellules photoélectriques. Le nombre d'impulsions est proportionnel à l'enfoncement de l'outil. Lorsque celui-ci commence à usiner le vilebrequin, un signal électrique autorise le décompte; lorsque le décompteur passe par la valeur 0 un signal d'arrêt est transmis au moteur. Quand les trois mémoires de stockage sont vides, les têtes d'usinage se relèvent et la barre de transfert fait progresser d'un cran l'ensemble des vilebrequins.

Contrôle Final

Un poste d'équilibrage identique à celui se trouvant à l'entrée de la machine mesure le module du balourd résiduel et permet de contrôler le bon fonctionnement de l'ensemble de la machine.

Conclusions

La Figure 8 montre l'ensemble des équipements électroniques installés. La précision globale des calculs effectués est de l'ordre de 3 pour cent; compte tenu des erreurs supplémentaires pouvant être introduites par la mesure initiale et par la commande d'enfoncement d'outils, les balourds résiduels, après correction, sont inférieurs à 20 g/cm. La machine effectue l'équilibrage de 120 vilebrequins à l'heure en moyenne avec des pointes pouvant atteindre 180 vilebrequins à l'heure. Ce travail nécessite deux opérateurs alors qu'une chaîne manuelle équivalente utiliserait dix ouvriers.

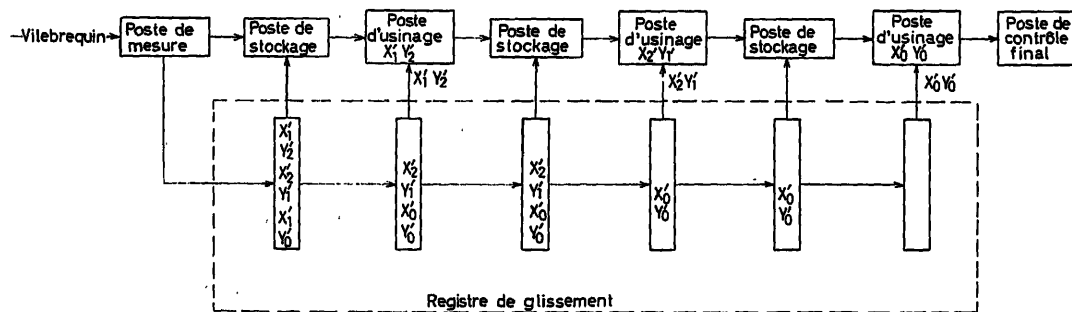


Figure 6. Transfert du vilebrequin et mise en mémoire des données

Il est clair que la réalisation d'une telle machine n'est concevable qu'au prix d'une étroite collaboration entre mécaniciens et électriciens. La conception mécanique du poste de mesure par exemple est directement liée à la précision des calculs. De même la conception des transferts des vilebrequins entre les différents postes doit tenir compte de la rapidité des calculs effectués par l'équipement électronique et la cadence de fonctionnement de l'ensemble de la machine doit être étudiée, compte tenu des impératifs mécaniques et électriques. La conception des équipements électroniques de mesure et de calcul a impliqué l'utilisation de sous-ensembles standards tels que: amplificateur à courant continu, amplificateur à courant alternatif, bascules à transistors, circuits de comptage, registre de glissement, etc. Ces divers sous-ensembles relèvent aussi bien de la technique des

tubes à vide que de celle des transistors, le seul critère commun à l'ensemble des matériels étant son très haut degré de sécurité de fonctionnement. Des essais systématiques de durée dans des conditions climatiques variées et de robustesse mécanique ont été effectués avant l'introduction de ces sous-ensembles dans des équipements liés à des machines de grande production.

Deux machines de ce genre sont actuellement en exploitation industrielle. Au mois de septembre 1963 l'une d'entre elles sera en fonctionnement depuis plus de deux ans, l'autre depuis dix-huit mois.

L'auteur présentera, lors de son exposé, les enseignements que l'on peut tirer du fonctionnement industriel d'un tel ensemble sur le plan de la cadence de production et de la fiabilité des équipements et des composants électroniques.

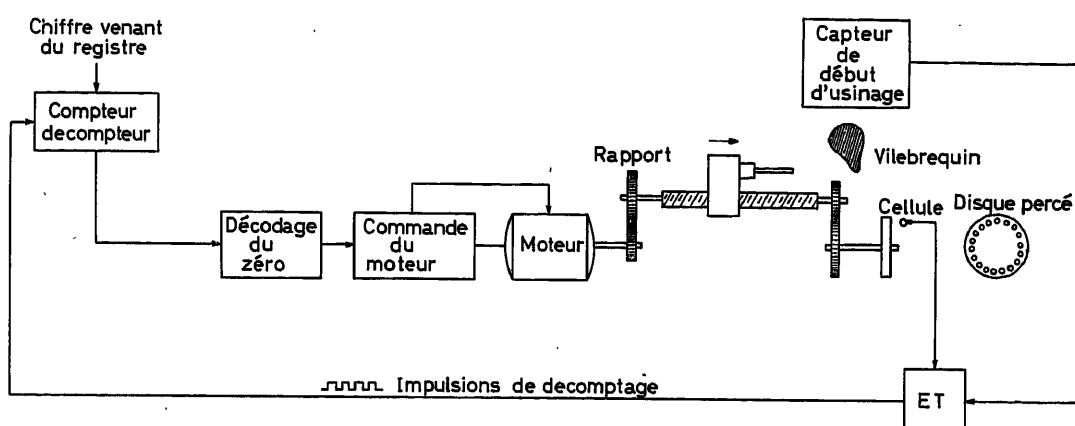


Figure 7. Commande d'une tête d'usinage

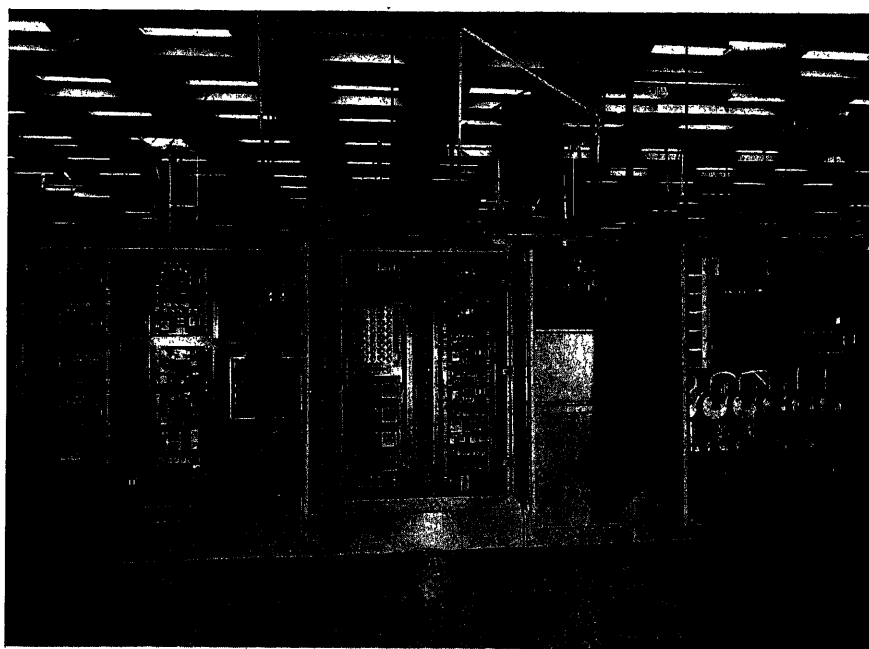


Figure 8. Vue d'ensemble des équipements associés à la machine

DISCUSSION

Author's Opening Remarks

There are, in the Renault factories, two machines of this type.

The first one, in operation since January 1962, balances 1,500 crankshafts each day; its maximum output is 135 pieces per hour and its average output is 95 pieces per hour.

The second machine, in operation since June 1962, balances 1,200 crankshafts each day, and could do more if necessary.

The results of the first machine may be compared with those of a conventional machine as follows: (a) The automatic machine works in two shifts and requires two operators in each shift, that is four men in all; (b) the conventional machine requires 11 men in each shift, that is 22 men in all. This means a saving of 18 men.

Only 4 per cent of the balanced crankshafts are slightly outside the tolerance of 20 g/cm. More than 3.5 per cent can be easily retouched.

Since the introduction of the machine, there have occurred the following breakdowns.

With the first machine: At its introduction, abnormal heating of the transistorized shift register; an incorrect earthing of an amplifier; 5 electronic tubes out of 142 have had to be changed.

With the second machine: Two bad contacts in the printed circuits (there are 1,600 semiconductors in this equipment); 3 electronic tubes out of 132 have had to be changed; 1 soldering defect.

Dividing the electrical, electronic and mechanical breakdowns into types of breakdowns and evaluating the time lost, we find:

- (i) 15 electrical breakdowns
 - 1 electronic breakdown
 - 4 mechanical breakdowns
- (ii) 20 min due to electrical breakdowns
 - 6 min due to electronic breakdowns
 - 1 h due to mechanical breakdowns

A. HONSBARGER, *Dufour 75, Bienne, Switzerland*

(1) For what reason did you change from an analogue system to a digital system?

(2) What is the weight of the crankshaft?

(3) What is the tolerance of the crankshaft bearings?

J. CSECH, *in reply*

(1) The calculations to be carried out are of a trigonometric type and are not easily performed by analogue elements. We found it easier to have the information in the shift register in digital form. One can, of course, imagine exclusively analogue or exclusively digital equipment, but I think this would be more sophisticated.

(2) The weight of the crankshaft is about 7 kg.

(3) The tolerance of the crankshaft is about 1/100 mm.

J. R. GILBERT, *Sulzer Bros. Ltd., Winterthur, Switzerland*

In the classification of breakdowns, do you consider bad contacts in printed circuits to be in the category 'electric' or 'electronic'?

J. CSECH, *in reply*

Electronic.

J. MORNAS, *C.A.F.L. Engineering, 96 Rue A. Durafour, Saint-Etienne, Loire, France*

What is the principle employed for detecting the contact of the milling cutter with the counterweight?

J. CSECH, *in reply*

The crankshaft is connected to earth by the machine, the milling cutter is electrically isolated, and the contact between them is detected by closing the circuit.

J. W. BUNTING, *Courtaulds Engineering Limited, P.O. Box 11, Coventry, England*

The metal removed is a function of the depth of the cut, and a different function for different models. Is this taken into account by changing cams, and if so, is this a simple speedy operation?

J. CSECH, *in reply*

It is taken into account by changing a cam in the analogue-digital conversion servo.

C. FOULARD, *France*

You have compared electrical, electronic and mechanical breakdowns. It appears that electronic parts are the most reliable. To compare exactly the performance of the electronic parts with the performance of other parts in a transfer machine, which does not make use of electronics, it would be necessary to know the quantity and importance of these parts. Then we might know whether it pays to use electronics on transfer machines.

J. CSECH, *in reply*

The only way I can compare the electrical, electronic and mechanical parts of this machine is on an economic basis. The cost of the electrical parts is about 10 per cent of the total, the cost of electronic parts is about 25 per cent and the cost of mechanical parts is 65 per cent. I should like to emphasize the point that the problem could not have been solved without electronic equipment. There is no possibility of manual operation of this machine, and we had a choice of attaching electronic equipment to the transfer machine, or not solving the problem.

R. LANCIA, *Rue des Martyrs, Grenoble, France*

Since (1) the surfaces on which the correction for the out of balance bears are imperfect (it is a casting), and since (2) the parameter used by the calculator is the penetration of the milling cutter, is it not conceivable that the first phase of the balancing could give good accuracy?

J. CSECH, *in reply*

The casting of the counter weight is a very precise type, and our experience has shown that the correction is quite good if the means of detection of contact between the counter weight and milling cutter is accurate.

R. RIGHI, *Consiglio Nazionale delle Ricerche, Roma, Via Giacomo Boni 6, Italy*

As to the breakdowns of the machine that Mr. Csech has described it would be interesting to know their distribution in time since the machine was put into operation. This is a matter of interest in many practical applications. Some laws of distribution are well known but it would be useful to compare them with the results obtained in practice.

J. CSECH, *in reply*

The largest number of breakdowns occurred, as usual, in the first six months of the operation.

A. THIARD, *Centre National de l'Automatisation, Paris 15, France*

Taking the same output in both cases, does the new balancing machine pay, in comparison with a conventional machine (amortizing and operating costs included)?

J. CSECH, *in reply*

The figures concerning amortizing and operating costs exist at the Renault factory, but I do not know them.

Design Analysis of an Automotive Speed Control System

W. H. HOLL

Summary

The design of a speed control system for passenger cars is analysed. The function of each of the system components including an electro-mechanical speed transducer and error detector, a pneumatic power drive unit, and a typical engine/vehicle is described. The pulse-width modulation technique used is reviewed. Transfer operators which provide for the inherent non-linearities in the pneumatic unit and in the engine are derived or graphically displayed. Based on observed data and theoretical analysis, linear approximations are made. The complete open-loop transfer function is shown to be a second-order system with a transport delay. Finally, the results of the analysis are compared with observed road test data and analogue computer studies.

Sommaire

Un système de réglage automatique de la vitesse d'une voiture de tourisme est analysé. Ce système comprend un transmetteur électro-mécanique de la vitesse, un détecteur d'erreur et un servo-moteur pneumatique permettant d'agir sur la puissance du moteur. Il utilise un système de modulation avec des impulsions de durée variable. La fonction de transfert qui permet de caractériser les propriétés non-linéaires du servo-moteur est indiquée. En se basant sur une étude analytique et expérimentale, une première approximation linéaire de cette fonction est donnée. On est ainsi conduit pour l'ensemble du circuit de réglage à une fonction de transfert du 2^e ordre, avec retard.

Les conclusions de cette étude sont comparées avec des résultats expérimentaux obtenus, d'une part, en vraie grandeur, d'autre part sur calculateur analogue.

Zusammenfassung

Der Entwurf einer Geschwindigkeitsregelung für Personenkraftwagen wird untersucht. Er beschreibt die Wirkungsweise der einzelnen Regelkreisglieder, nämlich: eines elektromechanischen Geschwindigkeitsumsetzers und Fehlermeßgliedes, eines pneumatischen Kraftschalters und eines normalen Kraftfahrzeuges. Die hier verwendete Puls-Breitenmodulation wird beschrieben. Beziehungen, die die in der pneumatischen Einheit und dem Motor vorhandenen Nichtlinearitäten berücksichtigen, werden abgeleitet oder graphisch dargestellt. Auf Grund von Meßergebnissen und theoretischen Betrachtungen werden lineare Näherungen durchgeführt. Die vollständige Übertragungsfunktion des offenen Kreises ist ein System zweiter Ordnung mit Totzeit. Abschließend werden die Ergebnisse der Untersuchung mit den auf der Straße beobachteten Versuchsergebnissen und mit Analogrechnerergebnissen verglichen.

Introduction

This paper analyses the design of an automotive speed control system. It starts with a brief description of system operation. The important design considerations for desired control performance are reviewed. The operation of the system components is discussed and transfer operators derived. Simplifications in input-output relationships are made and justified. Finally a steady-state analysis of the simplified overall system is summarized and the results are compared with those of road tests and of experiments with a more definitive computer model.

System Operation

This system automatically controls the speed of a passenger car to some preselected value and maintains this speed within close limits in the presence of load variations and disturbances (grades, wind loads, etc.) as shown in *Figure 1*.

The system operates in a conventional feedback control manner wherein the measured speed is compared to desired or set speed as shown in *Figure 2*. This error signal is converted from a mechanical angle to a pulse ratio modulated electrical signal. The electrical signal is amplified and operates a pneumatic valve which controls the amount of engine manifold pressure applied to a pneumatic power unit. This device positions the engine throttle through a mechanical linkage to provide the required change in engine torque and thus reduce the error and

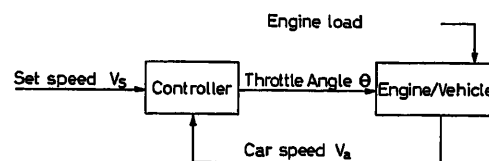


Figure 1. Simplified block diagram

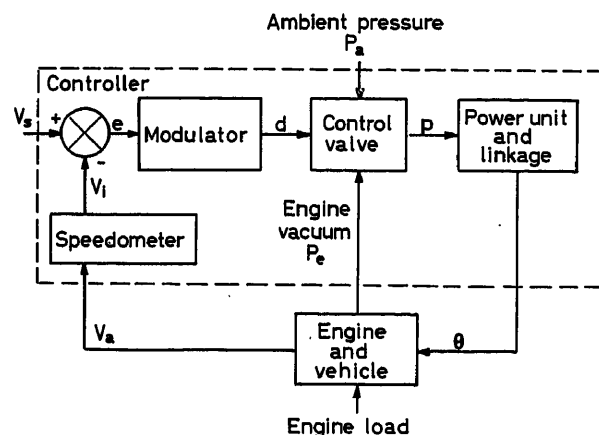


Figure 2. Complete system block diagram

maintain car speed. The engine manifold vacuum forms an internal feedback loop which is significant only for large engine loads (grades in excess of 5 per cent). The system is disengaged by stepping on the brake pedal or by pulling out the cruise selector switch.

System Control Performance

There are several response conditions which are significant in evaluating performance. It is desirable to have smooth transition, i.e., as operating conditions vary, there should be no large accelerations or jerks which are objectionable to the car

passengers; good steady state and dynamic accuracy is also highly desirable. Thus, the system has the common servo requirements of high loop gain, optimum bandwidth for processing the signal while filtering disturbances, insensitivity to parameter variations, and very stable operation in the presence of wide variations in operating conditions which affect both engine and controller performance. Because the overall system is non-linear, experimental analysis is necessary and such experiments are run on road tests and on an analogue computer. However, such experiments, along with analysis of the component equations, indicate that some simplifications make it possible to conduct a quasi-linear analysis of the system for small signals. This is significant because it makes it possible, through sinusoidal inputs, to study the system under operating conditions which simulate cruising over rolling countryside, which is a prime function of the system. Thus frequency analysis techniques give a good indication of system performance.

Speed Measurement Sub-system

The speed measurement system measures car speed, compares it with set speed, and provides an amplified pulse ratio modulated error signal. Measurement of car speed is provided by a standard flexible shaft and speedometer system as shown in Figure 3. This shaft is stiff enough so that it introduces no

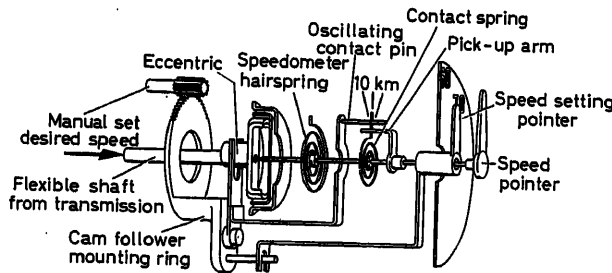


Figure 3. Speed transducer and modulator (After J. A. McDougall³)

major dynamic contribution to system performance. However, the spring-mass system of the speedometer assembly does have a resonant frequency which occurs at the upper end of the overall system bandwidth and has been accounted for in the system model. The transfer function relationship between indicated and actual speed for the speedometer assembly is given by

$$V_i = \frac{(C_p/C_h)(K_t/K_h)V_a}{J_h/K_h s^2 + (K_d + K_t/K_h)s + 1} \quad (1)$$

where $(C_p/C_h)(K_t/K_h)$ is the scale factor of the unit and is calibrated to equal unity. For the particular system under study the resonant frequency $(K_h/J_h)^{1/2}$ is 1.1 c/sec and the damping ratio is 0.2. Since the system phase margin is small the speedometer phase lag makes a significant contribution to the dynamic response and this second-order system can be approximated by a simple transport delay, $e^{-\lambda s}$, in the region of interest, where

$$\lambda = \frac{K_t/K_h + K_D}{1 - \frac{J_h}{K_h} \omega^2} \quad (2)$$

Also, there is a coulomb friction at the output of the speed measuring system which has been considered. However, recent

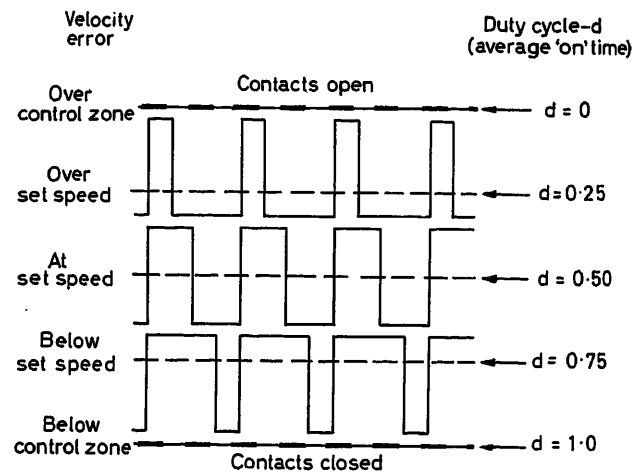


Figure 4. Speed transducer output current waveforms (From J. A. McDougall³)

improvements in design have reduced this friction to a negligible amount.

The error modulator opens and closes a pair of electrical contacts and changes the on-off ratio or duty cycle as a function of the size of the error signal, see Figures 3 and 4. These electrical contacts are manually positioned by the cruise speed setting dial at an angle proportional to desired speed. The actual car speed is introduced by the speedometer output shaft which positions a pick-up arm such that it would just open the above electrical contacts when the car is travelling at the set speed. However, for every revolution of the speedometer drive shaft (1.6 m of road travel) a cam nutates the contact pair about the average position through an angle equivalent to 10 km/h. As the car speed approaches set speed the pick-up arm opens the oscillating electrical contacts for a period of time each cycle. For the percentage of time the contacts are open, each cycle increases with increasing car speed until the contacts are open all the time (as shown in Figure 4). This is a form of pulse ratio or duty cycle modulation.

The duty cycle, d , which is the percentage of time the contacts are closed actually is an arc sin function of error, e , over the proportional range. Thus

$$d = 0.5 + \frac{1}{\pi} \arcsin \frac{2e}{R_s} \quad (3)$$

where negative error indicates an overspeed condition. However, the mid-portion of the proportional zone can be approximated with good accuracy as

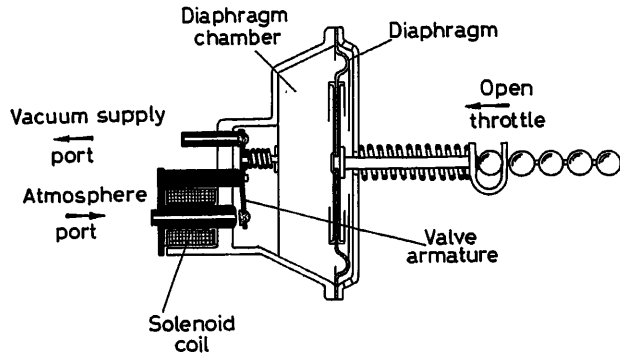
$$d = 0.5 + \frac{2e}{\pi R_s} \quad (4)$$

where the dynamic gain is given by $2/\pi R_s$. This agrees with observed data.

The electrical signal is amplified through a single transistor to minimize the current through the contacts. This has no effect on signal modulation.

Power Unit and Throttle Linkage Sub-system

This sub-system (see Figure 5) changes modulated electrical pulses from the amplifier to a modulated vacuum, which in turn positions the throttle in the car.


 Figure 5. Power unit and control valve (From J. A. McDougal³)

The control valve is energized when the electrical contacts of the modulator are closed, thus the control valve turns on and off each cycle with the control signal. It opens the diaphragm chamber successively to atmospheric air and engine vacuum through respective orifices. The average pressure in the chamber is a function of the duty cycle, and this pressure exerts force on the diaphragm which is balanced by the regular throttle return spring and by the diaphragm return spring. The output is connected to the throttle linkage through a bead chain which is in tension during operation. The maximum throttle is limited by the stroke of the power unit to 35° which is sufficient for maintaining speed on the open highway.

A complete mathematical description of the system is highly complex. There is inherent non-linear action in the inlet orifices, the valve bounce and transit time, the hysteresis and time lag of the coil, the variable cross-sectional area of the diaphragm, the backlash and friction of the linkage, the variable spring rate of the accelerator return spring, the unilateral action of the throttle return dashpot, and the effect of air flow on the throttle plate. Nevertheless, these conditions can be described and have been included in the complete computer model.

For purposes of some insight into the operation of this unit, it is possible to simplify the model and express it as a first-order system. The gain and time constant of this model applies for small changes in the system variables and for given operating conditions. A different operating point yields a different gain term and time constant. However, the influence of the parameters and variables (primarily, the throttle angle) on these terms can be seen. This model is used in studying the steady-state performance and small signal transient response.

Internal Feedback Loop

The manifold vacuum is used as a source of pressure for actuating the power unit. The difference between atmospheric pressure and manifold pressure constitutes the available supply. However, the manifold pressure is modified directly by changes in the throttle angle position. Thus, as the error signal causes the power unit to move the throttle, the resultant changes in the differential pressure modifies the power unit response. Since this feedback is negative, it lowers the static gain and time constant of the power unit assembly. However, since, as described below, there is critical flow in the vacuum orifice for most driving conditions, this feedback can be neglected.

Derivations of Power Unit Equations

The transfer characteristics of the power unit can be determined by setting up the physical relationship between the variables. Thus at any given time the universal gas law applies for the air in the power unit chamber.

$$PV = WRT \quad (5)$$

and

$$\dot{P}V + P\dot{V} = \dot{W}RT \quad (6)$$

where the temperature is assumed to remain constant. The forces on the diaphragm are in equilibrium. The force due to the differential pressure is equal to the opposing spring forces.

$$(P_a - P)A = (K_1 + K_2)(\theta + \theta_0) \quad (7)$$

$$(P_a - P)A = K_s(\theta + \theta_0) \quad (8)$$

$$P = P_a - \frac{K_s(\theta + \theta_0)}{A} \quad (9)$$

The power unit design is such that the diaphragm area and the chamber volume vary almost linearly with throttle angle over the control range.

$$A = A_0 - K_a\theta \quad (10)$$

$$V = V_0 - K_v\theta \quad (11)$$

$$\dot{A} = -K_a\dot{\theta} \quad (12)$$

$$\dot{V} = -K_v\dot{\theta} \quad (13)$$

The time derivatives of the pressure can also be derived from eqn (9).

$$\dot{P} = -\frac{K_3}{A}\dot{\theta} \quad (14)$$

where

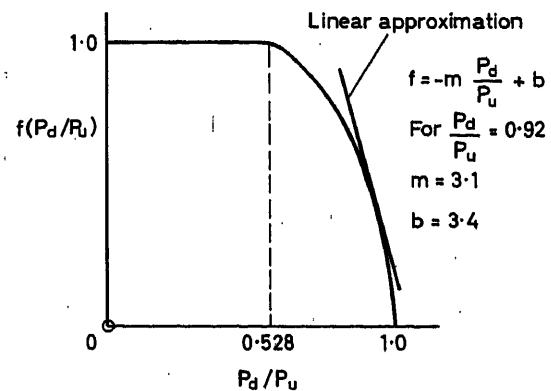
$$K_3 = K_s + (P_a - P)K_a \quad (15)$$

The net weight rate into the power unit for each cycle is equal to the rate of air flowing into the chamber when the valve is open to the atmosphere, minus the rate of air flowing out when the valve is opened to engine vacuum. The frequency of valve operation is sufficiently high that the pressure change each cycle is small and the following relationships hold.

$$\dot{W} = \dot{W}_{(in)} - \dot{W}_{(out)} \quad (16)$$

$$\dot{W} = C_d C_a T^{-1/2} [A_a P_a f_a(P/P_a)(1-d) - A_e P f_e(P_e/P)d] \quad (17)$$

where the function f describes the pneumatic orifice characteristics and is shown on Figure 6. The duty cycle, d , is a function


 Figure 6. Pneumatic orifice characteristic⁴

of the error signal and determines the net weight rate. Analogue computer and experimental data indicate that f_a may be closely approximated by a straight line and f_e by unity over most of the range of interest. The ratio P/P_a varies between 0.95 and 0.88. The P_e/P ratio is less than 0.528 critical pressure ratio except when the engine load is very large. When P_e/P is less than 0.528 unretarded critical flow conditions exist in the vacuum orifice and changes in engine manifold pressure have no effect on the weight rate of air and thus does not influence system dynamics. f_a and f_e can be expressed as follows

$$f_a = -mP/P_e + b \quad (18)$$

$$f_e = 1 \quad (19)$$

and

$$\dot{W}RT = Q[(-mP + bP_a)(1-d) - \alpha Pd] \quad (20)$$

$$\dot{W} = C_d C_a A_\theta T_u^{-1/2} P_u f(P_d/P_u)$$

$$f(P_d/P_u) = 3.87 [(P_d/P_u)^{1.43} - (P_d/P_u)^{1.71}]^{0.5}$$

$$\text{for } 0.528 \leq P_d/P_u \leq 1.0$$

$$f(P_d/P_u) = 1.0, 0 \leq P_d/P_u \leq 0.528$$

u subscripts indicate upstream parameters

d subscripts indicate downstream parameters

A_θ is the cross-sectional area of the orifice

(All other symbols are defined in the nomenclature)

$$\text{where } Q = RC_d C_a T^\frac{1}{2} A_a \quad (21)$$

$$\text{and } \alpha = A_e/A_a \quad (22)$$

The expression for control pressure in eqn (9) can be substituted in eqn (20).

Finally this can be combined with eqns (6), (13) and (14) to yield

$$\theta = \frac{F(d)}{\tau_p s + 1} - \theta_0 \quad (23)$$

where

$$F(d) = \frac{P_a A}{K_s} \left[\frac{(b-m) - (b-m+\alpha)d}{-m + (m-\alpha)d} \right] \quad (24)$$

and

$$\tau_p = \frac{K_3 V + K_v P A}{Q K_s [m - (m-\alpha)d]} = \frac{K_3 V + K_v P A}{Q K_s \alpha} \cdot \frac{P_a f_a + \alpha P}{P_a f_a + m P} \quad (25)$$

Dynamic gain K_p is given by

$$K_p = F'(d) = \frac{P_a A}{K_s} \frac{\alpha b}{[m - (m-\alpha)d]^2} = \frac{A}{K_s \alpha} \cdot \frac{[P_a f_a + \alpha P]^2}{[P_a f_a + m P]} \quad (26)$$

Since P , V , A , K_3 , f_a and m are all functions of θ only, the gain and time constant of the power unit are also determined by the value of θ . The variable d is eliminated above by solving eqn (17) for $\dot{W} = 0$.

The Internal Combustion Engine and Transmission

The speed-torque curves of an internal combustion engine are very similar to those of a servomotor, particularly for small variations in load. For conditions of maximum throttle (35°) and minimum throttle (2°), non-linearities are introduced, particularly for cases of overrun, i.e., where the engine is being driven by the load. Non-linearities are also introduced at low engine speeds (see Figure 7). For precise data, the engine and trans-

mission are simulated on the analogue computer with diode function generators. However, good insight is obtained on an engine with a standard transmission by considering it to be a first-order system. An engine/vehicle with an automatic transmission, though not considered further here, can be represented as an overdamped second-order system.

If road load torque is subtracted out from engine torque the

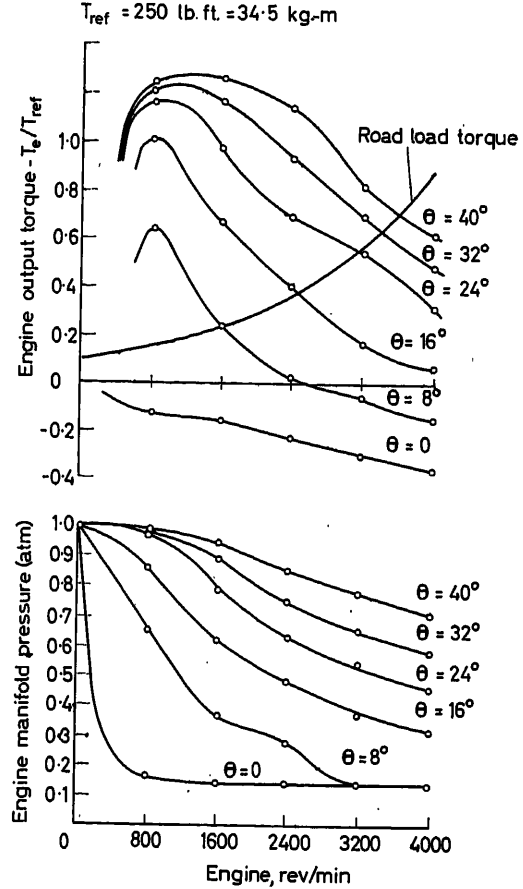


Figure 7. Experimental stock engine curves

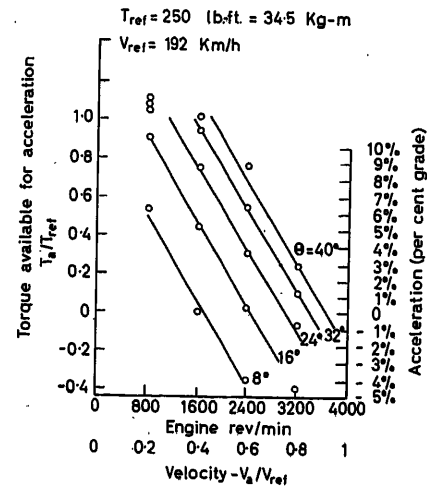


Figure 8. Engine/vehicle phase-plane plot (Modified speed-torque curves)

remainder is available for grade loads and acceleration (see Figure 8). These speed-torque curves are a family of approximately straight lines. Per cent grade and g's of acceleration can be plotted to the same scale (due to the equivalence of acceleration and gravity). From these curves the transfer operator of the engine and vehicle can be shown to be

$$\Delta V_a = \frac{K_e \Delta \theta - K_g \Delta G}{(\tau_e s + 1)} \quad (27)$$

where

$$K_e = \frac{K_\theta}{K_N N_V} \quad (28)$$

$$K_g = \frac{W_c R_e}{100 K_N N_V} \quad (29)$$

$$\tau_e = \frac{W_c R_e}{3.6 g N_V K_N} \quad (30)$$

System Analysis and Evaluation

Transfer operators have now been derived for all components in the system. The open-loop system transfer function can be expressed

$$\frac{\Delta V_i}{\Delta e} = \frac{2 K_p K_e e^{-\lambda s}}{\pi R_s (\tau_p s + 1) (\tau_e s + 1)} \quad (31)$$

This is an ordinary second-order system with a transport delay and which can be readily analysed by frequency plot techniques. For the system with parameter values shown in the Nomenclature the overall loop gain ranges from 32 to 38 dB. This compares well with experimental data which is plotted on Figure 9. The engine gain, K_e , power unit gain, K_p , and modulator gain, $2/\pi R_s$, have corresponding agreement with experimental results. The engine time constant is 21 sec and remains almost constant throughout the operating range. This agrees to within 5 per cent of observed values. The theoretical power unit time constant

varies from 1.2 sec at low throttle angles to 1.8 sec at high throttle angles. Computer and observed data indicate that this time constant is in the order of 1.3 to 2.0 sec. The transport delay of the speedometer λ has a calculated value of 0.06 sec compared with observed values closer to 0.1 sec. Despite these variations the overall closed-loop response may be characterized as having a resonant peak of 6 to 9 dB at about 1.5 rad/sec. The most readily adjusted parameters of the system are the area of either power unit orifice, and the pre-load and rate of the diaphragm return spring. For a given orifice ratio, α , the power unit gain and time constant and their sensitivity to changes in parameter values are at a minimum when α is equal to the orifice characteristic quantity, f_a , divided by the control pressure given in atmospheres. An increase in the area of both orifices while maintaining the above ratio, decreases the time constant. However, this is limited by the resultant increase in throttle pulsing and valve seal problems. Both the gain and time constant are inversely proportional to the rate of the diaphragm return spring which thus provides some system adjustment. This must be done with due consideration to the initial pre-load which shifts the operating point and also modifies the associated gain and time constant. Thus it is normally desirable to increase the spring rate but to maintain the same force load on the power unit. This can be done by reducing the pre-load accordingly.

In summary, the system design is such that with these minor but purposeful adaptations the basic controller will operate satisfactorily with a large variety of engine and vehicle types.

The author acknowledges with deep appreciation those engineers who developed the system and who provided so much assistance in the preparation of this paper. Particular mention must be made of D. L. Van Ostrom who developed the basic analogue computer model and set up many of the equations for the components. Also of W. M. Wang who conducted the computer experiments and made many helpful suggestions and corrections. However, the author remains fully responsible for any inaccuracies that may exist. The author also appreciates the considerable assistance of Mrs. N. Adams who typed the report.

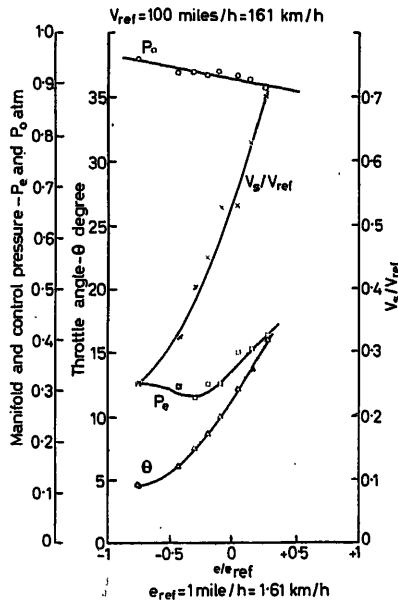


Figure 9. Steady-state level-road system performance

Nomenclature*

Variables (including normal operating range)†

- A Effective area of power diaphragm (cm²)
- d Duty cycle—dimensionless (0.4–0.6 for steady state)
- e Velocity error ($V_s - V_i$) (± 1.6 km/h)
- G Road grade (%)
- K_s Dynamic spring constant (g/deg)
- P Control pressure (0.88–0.95 atm or 900–980 g/cm²)
- P_e Engine manifold pressure (0.3–0.5 atm)
- T_a Torque available for acceleration (kg-m)
- T_e Torque delivered from engine (kg-m)
- V Power unit control volume (160–115 cm³)
- V_a Actual vehicle speed (40–100 km/h)
- V_i Speedometer indicated speed (40–110 km/h)
- \dot{W}_a Flow rate through atmospheric orifice (g/sec)
- \dot{W}_e Flow rate through manifold orifice (g/sec)
- θ Throttle angle (5°–20°)

* Values shown are for a typical 1963 Buick automobile.

† Maximum range of variables exceed normal operating range; time derivatives are indicated by superscript dot.

Constants and Other Symbols Used*

A_a	Area of atmospheric orifice (0.0132 cm ²)
A_e	Area of engine manifold orifice (0.0085 cm ²)
A_0	Area of power diaphragm for zero throttle angle (60 cm ²)
b	Intercept of linearized orifice characteristic curve
C_a	Scale factor for air flowing through an orifice 0.714° K ^{1/2}
C_d	Discharge coefficient for orifice, dimensionless (0.9–1.0)
C_h	Speedometer dial constant (1.77 deg/km/h)
C_p	Speedometer drive shaft constant (62.3 deg/sec/km/h)
g	Acceleration due to gravity (9.8 m/sec ²)
J_h	Speedometer inertia (0.138 g-cm/rad/sec ²)
K_1	Spring constant, throttle linkage return (g/deg)
K_2	Spring constant, power diaphragm return (g/deg)
K_a	Power diaphragm area constant (1.29 cm ² /deg)
K_D	Phase lag coefficient of speedometer damping fluid (0.031 sec)
K_e	Effective gain of engine (km/h/deg)
K_g	Grade constant of the engine (km/h/per cent grade)
K_h	Speedometer hairspring constant (7.45 g-cm/rad)
K_N	Engine torque to engine speed ratio (kg-m/rev/min)
K_p	Effective gain of power unit (deg/unit change in duty cycle)
K_s	Total effective spring constant ($K_1 + K_2$) (174 g/deg)
K_t	Magnetic coupling coefficient between magnet and speedcup (0.212 g-cm/rad/sec)
K_v	Power diaphragm volume constant (3.72 cm ³ /deg)
K_θ	Torque constant of the engine (kg-m/deg)
m	Slope of orifice characteristic curve
N_V	Engine to vehicle speed ratio (20.8 rev/min/km/h)
P_a	Atmospheric pressure (1033 g/cm ²)
$QT^{-1/2}$	Orifice flow constant (cm ³ /sec)
R	Gas constant for air (2920 cm ³ /°K)
R_e	Equivalent moment arm of engine (0.127 m)
R_s	Proportional speed zone (effective range 10 km/h)
s	Laplacian operator
T_u	Orifice upstream ambient temperature (°K)
V_0	Power unit volume for zero throttle angle (195 cm ³)
V_s	Set speed (km/h)
W_0	Effective weight of the car, engine and passengers (2400 kg)
θ_0	Pre-load angle of throttle return spring (12.5 deg)
α	Ratio of engine manifold orifice area to atmospheric orifice (0.645)
τ_e	Effective time constant of engine (sec)
τ_p	Effective time constant of power unit (sec)
λ	Speedometer assembly transport lag (sec)

* Values shown for basic parameters only.

Addendum

The original paper describes the operation of an automotive speed control system and presents a linear analysis of the system based on small signal conditions. This addendum briefly reviews these subjects, adds some new information on the components, and summarizes the results after a year of general usage by the American driving public.

This system automatically controls the speed of a passenger car to some preselected value and maintains this speed within close limits in the presence of load variations and disturbances (grades, wind loads, etc.).

The system operates in a conventional feedback control manner wherein the speed as measured by the car speedometer is compared to desired or set speed. This error signal is converted from a mechanical angle to a pulse ratio modulated electrical signal. The electrical signal is amplified and operates a pneumatic valve which controls the amount of engine manifold pressure applied to a pneumatic power unit. This device positions the engine throttle through a mechanical

linkage such as to provide the required change in engine torque and thus reduce the error and maintain car speed. The system is disengaged by stepping on the brake pedal or by pulling out the cruise selector switch. For safety the system cannot be engaged until the car has been brought up to speed by the driver.

Parameter values for a typical 1963 Buick installation are used in the theoretically derived transfer functions. The speed measurement system has an underdamped second order response with a natural frequency of 1.1 c/sec and a damping ratio of 0.1. With the addition of silicon damping this ratio can be increased to 0.2. Solution of gas flow equations show that the pneumatic power unit is a first order system with a time constant that varies from 1.2 sec at low throttle angles to 1.6 sec at high throttle angles (these values are revised from those given in the original text). The engine/vehicle system with a standard transmission also has a first order response with a time constant of 21 sec. The overall loop gain also depends on throttle angle and ranges from 38–32 db. These values combine to give a smoothly operating, stable system with an overall dynamic accuracy better than 2 miles/h over the expected wide range of road grade and wind loads. These theoretical results compare favourably with actual data obtained in laboratory testing and on the road.

Several additions to the paper are now considered. Reference is made to the time constant and gain of the power unit (eqns (27) and (28)). The duty cycle, d , can be eliminated from these expressions by obtaining an equivalent expression when the net weight rate of air flow is zero (solve eqn (18) for $W = 0$). This condition holds for small signals. Thus

$$\tau_p = \frac{K_3 V + K_v P A \frac{P_a f_1 + \alpha P}{Q K_s \alpha}}{P_a f_1 + m P} \quad (27a)$$

$$K_p = \frac{A [P_a f_1 + \alpha P]^2}{K_s \alpha [P_a f_a + m P]} \quad (28a)$$

Since all of the above variables are functions of θ only, the gain and time constant of the power unit are also determined by the value of θ .

With reference to the development of the engine/vehicle equations it should be noted that a standard transmission is specified. With an automatic transmission the engine/vehicle response is changed from a first order system to a second order system with a phase lead term. This result is presented without derivation.

Almost a year has passed since this system has been offered to the motoring public as an option on the 1963 Buick car lines. Many thousands of systems have been made. These have been used throughout the United States over tens of millions of road miles. These production systems have performed consistently close to the design data presented herein and customer reaction has been favourable. The precautions taken during design to ensure safety along with the extensive road testing prior to release for production have materialized in an excellent record clear of any personal injury or major mishap. These results thus verify that the system is a safe, high performance, publicly accepted, mass produced feedback control system.

References

- SAVANT, C. J., Jr. *Basic Feedback Control System Design*. 1958. New York; McGraw-Hill
- VAN OSTROM, D. L. Analog computer study of an automatic speed control system for automobiles. *MIT Masters Thesis* (1960)
- MCDUGAL, J. A. AC Electro-cruise System. Presented at the 1963 Automotive Engineering Congr. Detroit, Michigan, January, 1963
- EZEKIAL, D. and SHEARER, J. L. Pressure-flow characteristics of pneumatic valves. *Trans. Amer. Soc. mech Engrs* (Oct. 1957) 1577–1590

COMBINED MAN-MACHINE SYSTEMS

Modèles Continus et Échantillonnés de l'Opérateur Humain Placé dans une Boucle de Commande

P. NASLIN et J.-C. RAOULT

Summary

An analysis is presented of the behaviour of the human operator acting in a control loop. The experimental set-up essentially consists of a cathode-ray oscilloscope, a control lever with one degree of freedom, an analogue computer and a signal generator. A continuous model of the human operator is suggested, which is valid in the steady state, but does not provide for the interpretation of the noise present in the operator's response. This model is a self-adaptive servo loop; within certain limits the model adapts itself to changes in the frequency spectrum of the input on the one hand and in the controlled system transmittance on the other. Investigation of the operator's step response leads to the introduction of a subsidiary loop representing kinesthetic feedback, and of sampling in the operator's response. A sampled model, consistent with the continuous model previously described, is presented.

Sommaire

On présente une analyse du comportement de l'opérateur humain placé dans une chaîne d'asservissement. Le dispositif expérimental comporte essentiellement un oscilloscope cathodique, un levier de commande à un degré de liberté, un calculateur analogique et un générateur de signaux. On propose un modèle continu de l'opérateur humain, valable en régime permanent, mais ne permettant pas l'interprétation du bruit qui affecte la réponse de l'opérateur. Ce modèle est un asservissement auto-adaptable en fonction du spectre du signal d'entrée, d'une part, et du système commandé, d'autre part. Ces adaptations présentent des limites qui sont précisées dans la communication. Après l'étude de la réponse de l'opérateur à un échelon, on est conduit aux considérations suivantes: le sens kinesthésique réalise une boucle de retour secondaire; l'opérateur constitue un système échantillonné. On présente un modèle échantillonné dont les caractéristiques sont en accord avec celles du modèle précédemment décrit.

Zusammenfassung

Das Verhalten eines Menschen als Regelkreisglied (Bedienungsmann) wird untersucht. Die Versuchseinrichtung besteht im wesentlichen aus einem Elektronenstrahloszillograph, einem Steuerknüppel mit einem Freiheitsgrad, einem Analogrechner und einem Signalgenerator. Es wird ein kontinuierlich arbeitendes Modell des Bedienungsmannes vorgeschlagen, das für den Beharrungszustand gilt, aber für die Deutung der Schwankungen im Verhalten des Bedienungsmannes un-

geeignet ist. Das Modell ist ein selbststellender Nachlaufregelkreis. Innerhalb gewisser Grenzen paßt sich das Modell selbsttätig sowohl den Änderungen des Frequenzspektrums der Eingangsgröße als auch den Änderungen im Übertragungsverhalten des Regelungssystems an. Die Untersuchung der Sprungantwort des Bedienungsmannes führt zur Einführung eines zweiten Regelkreises, der die propriozeptive Sensibilität als Rückführung benutzt, zum Verständnis des Abstellungsverhaltens und des Bedienungsmannes. Es wird ein Abtastmodell vorgestellt, das dem vorstehend beschriebenen kontinuierlich arbeitenden Modell entspricht.

Introduction

L'objet de notre étude est d'interpréter le comportement de l'opérateur humain placé dans une chaîne d'asservissement. Son but est de rendre optimales les performances de cet asservissement.

Il s'agit d'un opérateur assujéti à mettre en coïncidence un objectif et un système suiveur. L'opérateur détecte visuellement l'écart entre leurs positions respectives et déplace, en fonction de celui-ci, un levier de commande.

Citons comme exemples le pilote d'avion et le tireur de char.

On distingue essentiellement deux modes de travail de l'opérateur. Ils sont fonctions du dispositif de visée. Le fonctionnement est dit en poursuite, pour l'un, et en compensation, pour l'autre. En poursuite l'opérateur voit l'objectif et le système suiveur se déplacer par rapport à axes des fixes. C'est lui qui élabore la grandeur d'erreur. En compensation il ne voit que l'erreur. C'est le cas d'un opérateur assujéti à mettre en coïncidence le point de croisement des réticules d'une lunette de visée avec l'image d'un objectif.

Le comportement de l'opérateur humain est essentiellement fonction des conditions dans lesquelles il travaille. Il en résulte que l'analyse de ce comportement est très difficile et que les résultats établis par les autres chercheurs qui se sont intéressés à celui-ci présentent une grande diversité. C'est pourquoi, au cours de notre étude, nous avons d'abord simplifié au maximum les

conditions de travail de l'opérateur et nous les avons peu à peu compliquées.

Les résultats que nous présentons dans cette communication sont relatifs à un objectif se déplaçant dans un plan vertical passant par l'opérateur, le déplacement du levier de commande se faisant alors d'avant en arrière et *vice versa*.

Description de l'Appareillage

Les éléments de base du dispositif expérimental que nous avons utilisé sont un oscilloscope et un levier de commande.

Lors d'un travail en poursuite le signal d'entrée x et la réponse y de l'asservissement où est incorporé l'opérateur sont matérialisés par deux spots qui se déplacent suivant une droite de plus grande pente sur l'écran de l'oscilloscope. En compensation, seule l'erreur $(x - y)$ est matérialisée par un spot.

Quant au levier de commande, sa rotation autour d'un axe est traduite sous forme électrique à l'aide d'un dispositif qui élimine tout frottement sec. Il est soumis à un couple de rappel proportionnel à l'élongation.

La Figure 1 montre un opérateur manipulant.

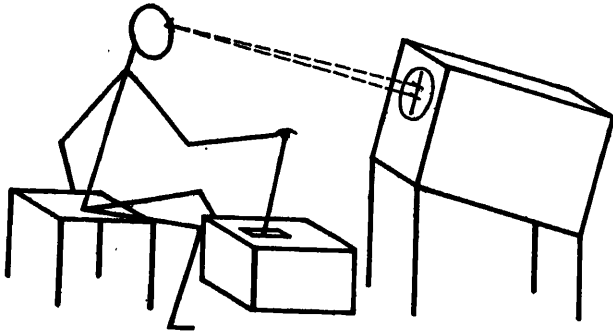


Figure 1

L'appareillage comprend d'autres éléments dont les plus importants sont un générateur de signaux et un calculateur analogique.

Le générateur de signaux que nous avons le plus utilisé est un ensemble élaborant une tension dont le spectre est constitué de quatre fréquences très basses, du même ordre de grandeur et premières entre elles. Elles sont, avec une fréquence commune, dans les rapports respectifs 1/3, 1/4, 1/5, et 1/7. Nous avons constaté que le signal ainsi obtenu est d'aspect assez aléatoire pour que l'opérateur ne puisse, à chaque instant, prédire le déplacement de l'objectif.

Définition d'un Opérateur Adapté

Nous avons étudié successivement, d'une part, le comportement de l'opérateur humain en régime permanent et plus particulièrement en régime harmonique, en donnant un sens large à ce mot et, d'autre part, son comportement en régime transitoire, notamment pour des signaux d'entrée composés d'échelons. Nous nous sommes efforcés, ensuite, de trouver un modèle de l'opérateur qui soit valable aussi bien en régime permanent qu'en régime transitoire.

Précisons que nous appelons régime harmonique le régime permanent qui correspond à un signal d'entrée composé de plusieurs sinusoïdes.

Une première expérience nous a montré que l'opérateur humain ne peut répondre, en régime harmonique, à des signaux sinusoïdaux dont les fréquences sont supérieures à 1,5 Hz.

Compte tenu de ce résultat, nous avons divisé le domaine de fréquence qui intéresse l'opérateur en trois parties ainsi définies:

de zéro à 0,4 Hz	fréquences basses
0,4 à 0,8 Hz	fréquences moyennes
0,8 à 1,5 Hz	fréquences élevées

Si l'on considère la réponse y à un signal x de l'asservissement où est incorporé un opérateur inexpérimenté quelconque en cours d'entraînement, on constate que l'erreur absolue moyenne $|x - y|$ décroît d'abord, et se maintient ensuite à une certaine valeur.

C'est pourquoi nous avons émis l'hypothèse que, pour un opérateur adapté, il existe une transmittance stable de l'opérateur humain placé dans des conditions bien définies et que l'expression de celle-ci est la même pour chaque opérateur.

Nous avons établi par ailleurs, qu'en dehors de certains cas limites tels que celui où l'écart angulaire est, en moyenne, voisin de l'acuité visuelle, le comportement de l'opérateur est celui d'un système linéaire. Appelons $F(p)$ sa transmittance ainsi définie:

$$F(p) = \frac{L(p)}{X(p) - Y(p)}$$

$X(p)$, $Y(p)$ et $L(p)$ étant les transformées de Laplace respectives de $x(t)$, $y(t)$ et $l(t)$, l désignant le déplacement de la main de l'opérateur.

Détermination d'une Transmittance de l'Opérateur Fonctionnant en Régime Harmonique Lorsque le Système Commandé est un Simple Amplificateur

Nous nous sommes d'abord proposé de déterminer une expression de la transmittance $F(p)$ relative au fonctionnement, en régime harmonique, de l'opérateur associé au système commandé le plus simple, à savoir un amplificateur de gain K_a . En désignant par K_c le gain de la commande manuelle, la transmittance de l'ensemble qui suit l'opérateur est alors $S(p) = K_a$ avec $K_a = K_c K_a$.

Le schéma fonctionnel de l'asservissement où est incorporé l'opérateur est alors celui de la Figure 2. L'expérience montre que si le spectre du signal d'entrée s'étend jusqu'à la fréquence 1,2 Hz, la réponse y de l'asservissement où est incorporé l'opérateur est décalée en moyenne de 0,2 s par rapport au signal d'entrée x , le gain de l'asservissement étant unitaire. Pour des fréquences comprises entre 1,2 et 1,5 Hz, la réponse présente un certain affaiblissement et un décalage qui atteint 0,3 s.

Les considérations ci-dessus nous ont amenés à considérer l'asservissement où est incorporé l'opérateur comme un élément engendrant, entre zéro et 1,2 Hz, un retard pur de 0,2 s, la transmittance correspondante étant de $e^{-0,2p}$.

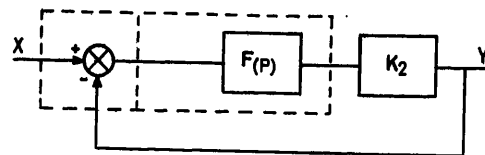


Figure 2

On démontre que la transmittance de la chaîne d'action de l'asservissement est alors, dans le domaine de fréquence zéro—1,2 Hz,

$$D(p) = 5 \frac{e^{-0,1p}}{p}$$

L'expression correspondante de la transmittance de l'opérateur humain est:

$$F(p) = K_1 \frac{e^{-0,1p}}{p} \text{ avec } K_1 = \frac{5}{K_2}$$

En d'autres termes, l'opérateur se comporte comme un élément élaborant une intégration pure et un retard pur de 0,1 s. Son gain K_1 est ajusté en fonction du gain K_2 , de manière que le gain K de la chaîne d'action ait pour valeur 5 lorsque le spectre de fréquence du signal d'entrée est étendu jusqu'aux fréquences élevées.

Par contre, aux faibles fréquences, l'expérience montre que la transmittance de la chaîne d'action où est incorporé l'opérateur est bien représentée par l'expression $9 e^{-0,1p}/p$. Le décalage entre y et x est alors de 0,1 s, le gain étant encore unitaire. La transmittance de l'asservissement où est incorporé l'opérateur présente alors une résonance de +6 dB qui est sans action sur le signal d'entrée.

Les Figures 3 et 4 reproduisent les réponses de l'asservissement où est incorporé l'opérateur et celles du simulateur lorsque le spectre du signal d'entrée ne comporte que des fréquences faibles. La Figure 3 correspond à un travail en poursuite et la Figure 4 à un travail en compensation.

En résumé, l'asservissement où est incorporé l'opérateur peut être représenté par un asservissement à retour unitaire dont la chaîne d'action a pour transmittance $K(e^{-0,1p}/p)$, le gain K étant ajusté entre 5 et 9 en fonction du spectre du signal d'entrée.

Le modèle continu que nous venons de présenter, valable lorsque le système commandé est un simple amplificateur, l'est-il encore lorsque le système commandé est quelconque?

Processus de l'Adaptation de l'Opérateur au Système Commandé

Nous avons associé l'opérateur à des systèmes linéaires de transmittance simple. L'expérience montre que l'opérateur modifie sa transmittance en fonction du système commandé.

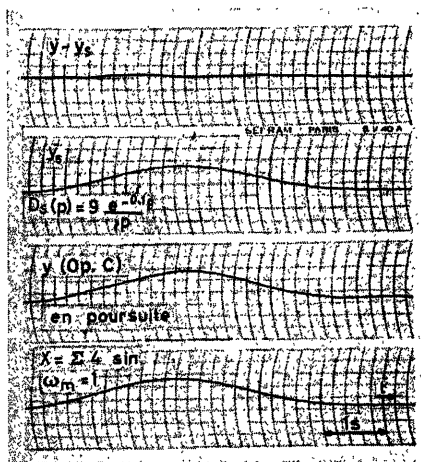


Figure 3

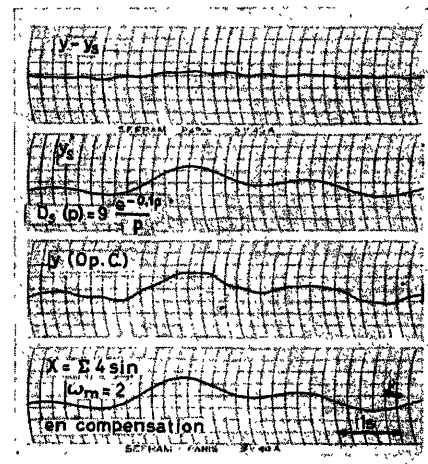


Figure 4

La loi d'adaptation est la suivante. L'opérateur modifie sa transmittance $F(p)$ de manière à laisser inchangée la transmittance $D(p)$ de la chaîne d'action lorsque la transmittance $S(p)$ du système commandé varie. L'expression de la transmittance $D(p)$ est celle que nous avons trouvée dans le cas où le système commandé est un simple amplificateur, c'est-à-dire

$$K \frac{e^{-0,1p}}{p}$$

K étant ajusté entre 5 et 9 en fonction du spectre de fréquence du signal d'entrée.

Prenons un exemple. Lorsque $S(p) = \frac{1+p}{p}$, la transmittance de l'opérateur humain est:

$$K_1 \frac{e^{-0,1p}}{1+p}$$

Cependant l'adaptation au système commandé est d'autant plus difficile que la transmittance de celui-ci est différente d'une constante. Il en résulte, d'une part, que la précision de l'asservissement où est incorporé l'opérateur est optimum lorsque le système commandé est un simple amplificateur ($S(p) = K_2$), et d'autre part, que l'association de l'opérateur et du système commandé présente des limites.

L'une des limites correspond à $S(p) = \frac{K_2}{p(1 + 1/2p)}$ et l'autre à $S(p) = K_2 p$.

Il est bien entendu que les résultats que nous présentons sont valables pour un opérateur ne pouvant utiliser sa mémoire pour prédire la loi de variation du signal d'entrée.

La Figure 5 correspond à $S(p) = \frac{1+p}{p}$; elle représente les réponses respectives de l'asservissement où est incorporé l'opérateur et du simulateur à un même signal d'entrée dont le spectre ne comporte que de faibles fréquences.

Il résulte de nos conclusions une application évidente. On s'efforcera d'interposer entre l'organe de commande et le système commandé un filtre dont la transmittance s'identifie, dans le domaine de fréquence intéressant l'opérateur, à la transmittance inverse de celle du système commandé (Figure 6).

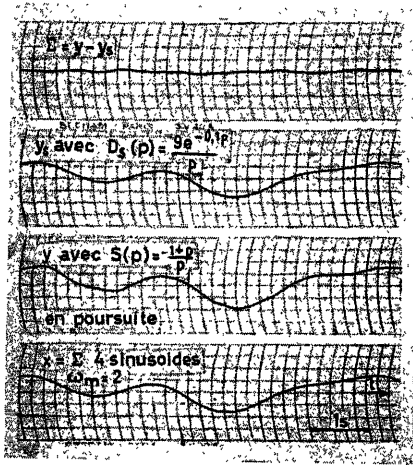


Figure 5

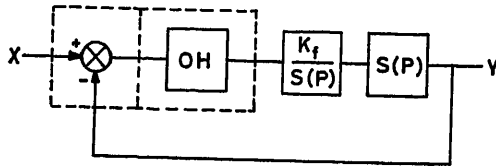


Figure 6

Transmittance de l'Opérateur Répondant à un Échelon Lorsque le Système Commandé est un Simple Amplificateur

On pouvait se demander si le modèle continu que nous venons de décrire est encore valable en régime transitoire. Après avoir démontré qu'il n'en est rien, nous avons analysé le comportement de l'asservissement où est incorporé l'opérateur dans le cas particulier où le système commandé se réduit à un simple amplificateur. Nos conclusions sont les suivantes:

Lorsque l'opérateur connaît à l'avance l'amplitude de l'échelon qui lui est présenté, la transmittance de l'asservissement où il est incorporé peut être représentée par:

$$H(p) = e^{-mp} W(p) \text{ avec } m = 0,2 \text{ s et}$$

$$W(p) = \frac{1}{1 + \alpha^2 (hp) + \alpha^3 (hp)^2 + \alpha^3 (hp)^3 + \alpha^2 (hp)^4 + (hp)^5}$$

les valeurs de α et h qui correspondent à la moyenne des réponses des opérateurs étant $\alpha = 1,9$ et $h = 1/20$.

La Figure 7 reproduit la réponse à un échelon de l'asservissement où est incorporé l'opérateur et celle du système de transmittance $W(p)$, les valeurs respectives de α et h étant 1,9 et 1/20.

Par contre, lorsqu'on applique à l'opérateur une série d'échelons d'amplitudes différentes et non connues à l'avance par lui, il répond par une suite de deux réponses. La première est la réponse à un échelon dont l'amplitude a_1 est la plus probable compte tenu des amplitudes des échelons précédents. Si a_2 est l'amplitude de l'échelon vrai, la seconde est la réponse à un échelon dont l'amplitude est $(a_2 - a_1)$.

On obtient des réponses semblables en changeant le gain K_2 du système qui suit l'opérateur lorsque celui-ci est soumis à un train d'échelons ayant la même amplitude (Figure 8).

Les résultats que nous venons de présenter montrent que

* NASLIN P. Nouveau critère d'amortissement. *Automatisme* (Juin, 1960) 229

la réponse de l'opérateur est, en général, constituée d'une suite de réponses à des ordres élaborés par le cerveau. Chacune de ces réponses ne faisant pas intervenir l'erreur $(x - y)$, on en déduit qu'il existe une chaîne de retour secondaire due au sens kinesthésique.

Le schéma fonctionnel qui permet d'interpréter le comportement de l'opérateur humain est alors celui de la Figure 9.

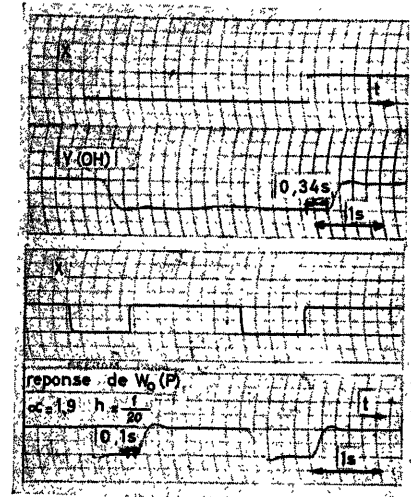


Figure 7

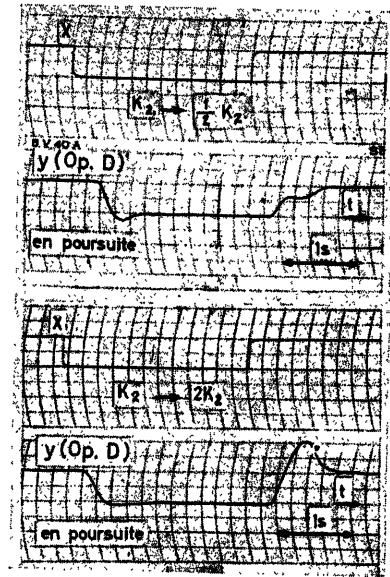


Figure 8

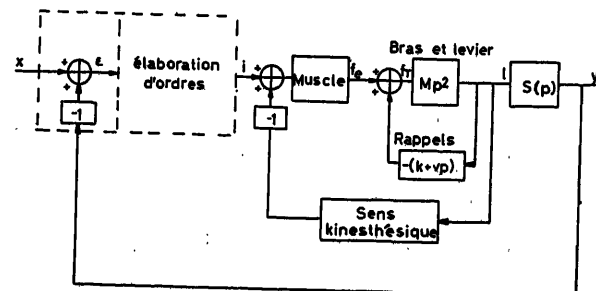


Figure 9

Nous constatons que la grandeur de sortie de l'opérateur est un déplacement et non une force et que la dynamique de la commande manuelle se trouve incorporée dans la boucle de l'asservissement secondaire. La transmittance de cet asservissement est $W(p)$ à un coefficient d'amplification près.

Influence de la Dynamique de la Commande Manuelle sur la Réponse de l'Opérateur

La présence d'une boucle secondaire dans le schéma fonctionnel de l'asservissement où est incorporé l'opérateur permet d'interpréter l'influence de la dynamique de la commande manuelle sur le comportement de l'opérateur humain.

Nous avons constaté que la réponse de l'opérateur à un échelon est indépendante de cette dynamique. En première approximation, il en est de même pour la réponse en régime harmonique.

Il en résulte que la transmittance $W(p)$ de l'asservissement secondaire est, en première approximation, indépendante de la dynamique du système de commande.

Nous avons établi cependant, que l'asservissement où est incorporé l'opérateur est plus précis, en valeur moyenne, lorsque la mécanique de la commande manuelle exerce une force de rappel assez sensible, proportionnelle à l'élongation.

Ce résultat s'interprète par le fait que, pour compenser la force de rappel à laquelle est soumise la commande manuelle, l'opérateur doit exercer une force qui constitue une mesure assez précise du déplacement l de la main. Dans ces conditions, l'action de la chaîne de retour kinesthésique est elle-même plus précise.

L'opérateur Humain Considéré comme étant Essentiellement un Système à Échantillonnage

Compte tenu, d'une part, des résultats de notre analyse de la réponse de l'opérateur à un échelon, et, d'autre part, du fait qu'en régime harmonique sa réponse présente un bruit qui peut être attribué à un échantillonnage, nous nous sommes proposé de réaliser un simulateur échantillonné de l'opérateur humain, en nous limitant au cas où le système commandé est un simple amplificateur.

Le modèle échantillonné de l'asservissement où est incorporé l'opérateur devait satisfaire aux conditions suivantes: sa réponse

En appelant $\mu_1(p)$ et $\mu_2(p)$ les transmittances des éléments de la chaîne d'action placés respectivement avant et après l'échantillonneur, nous avons:

$$\mu_1(p) = 1 + T_1 p$$

$$\mu_2(p) = \frac{K_e}{p} W(p) \text{ avec } K_e = K_h K_2$$

K_h étant le gain de l'opérateur.

L'expression de $W(p)$ est celle que nous avons donné plus haut, lors de l'étude de la réponse de l'opérateur à un échelon.

Si nous assimilons les impulsions larges de prélèvement à des impulsions larges dont l'amplitude est constante pendant toute la durée θ , on peut considérer que les impulsions de prélèvement sont infiniment fines et que l'on a:

$$\mu_2(p) = \frac{1 - e^{-\theta p}}{p} \cdot e^{\frac{\theta}{2} p} \cdot \frac{K_e}{p} \cdot W(p)$$

Le comportement du simulateur qui vient d'être décrit dépend de six paramètres T_e , T_1 , α , h , θ et K_e . Nous avons établi que, pour un signal d'entrée donné, on peut obtenir une même réponse moyenne du simulateur pour plusieurs valeurs de ces six paramètres. Naturellement, le bruit dû à l'échantillonnage est fonction du choix de ces valeurs.

L'analyse des réponses de plusieurs opérateurs montre que l'opérateur humain utilise une fréquence d'échantillonnage variable de 1 à 4, ce qui rend difficile sa simulation et l'analyse de son comportement. Afin de pallier cet inconvénient, nous avons étudié les comportements d'une série de simulateurs fonctionnant avec une fréquence d'échantillonnage constante.

Traisons succinctement un exemple. Prenons $T_e = 0,4$ s (valeur correspondant à un grand nombre de réponses d'opérateurs), $\theta = \frac{T_e}{5} = 0,08$ s (valeur supérieure à la persistance rétinienne), $\alpha = 1,9$ et $h = 1/17$.

La Figure 11 représente la courbe de transfert ordinaire et la courbe de transfert échantillonnée de $\mu_1(p) \mu_2(p)$, les valeurs correspondantes du gain K_e étant respectivement 1 et T_e/θ . Ces courbes sont relatives à une constante de temps T_1 de 1 s. Cette valeur est celle qui rend le point $I(\Omega/2)$ de la courbe de transfert échantillonnée voisin de l'origine 0, Ω étant la pulsation d'échantillonnage.

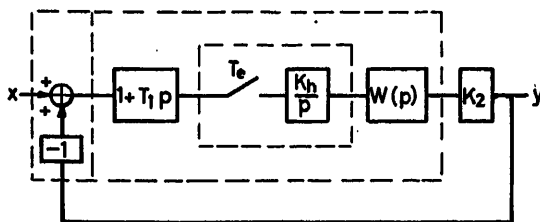


Figure 10

dépouillée du bruit s'identifie à celle du simulateur continu; le bruit qui affecte sa réponse est semblable à celui que l'on trouve dans la réponse de l'opérateur humain.

Nos recherches nous ont conduits à l'asservissement échantillonné dont le schéma est représenté par la Figure 10: dans le cas où $S(p)$ se réduit à une constante.

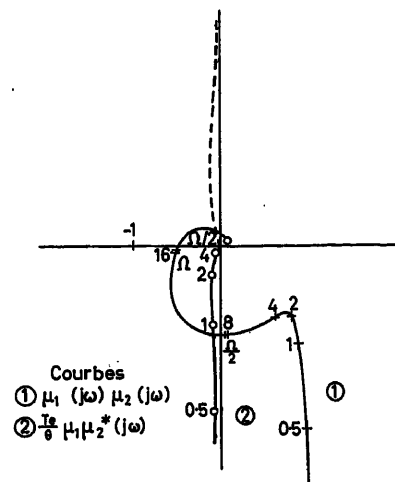


Figure 11

La simulation est réalisée avec un gain K_e égal à T_e/θ , c'est-à-dire 5, lorsque le spectre du signal d'entrée ne comporte que des fréquences faibles. Pour des fréquences moyennes, ce gain doit être plus faible.

Le calcul et l'expérience montrent que le modèle que nous venons de décrire est satisfaisant.

Précisions que nous avons utilisé, pour connaître la réponse du simulateur à un signal d'entrée sinusoïdal, le produit des transmittances suivantes :

$$\frac{1}{1 + \mu_1 \mu_2^*(j\omega)}, \quad \mu_2^*(j\omega) \text{ et } \mu_1(j\omega)$$

La Figure 12 représente les réponses à un même signal, de l'asservissement où est incorporé l'opérateur et du simulateur réalisé en donnant aux paramètres les valeurs suivantes :

$$T_e = 0,5 \text{ s}, \quad \theta = \frac{T_e}{5}, \quad T_1 = 1 \text{ s}, \quad \alpha = 2,1, \quad h = \frac{1}{20},$$

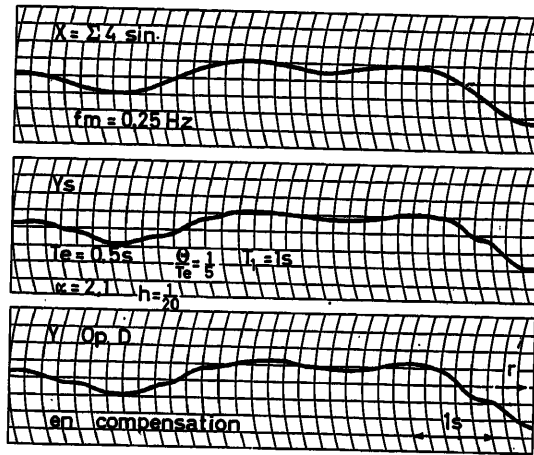


Figure 12

K_e voisin de T_e/θ , c'est-à-dire 5. On note la ressemblance des deux réponses.

Ajoutons, enfin, que l'intervalle d'échantillonnage minimum utilisé par l'opérateur humain est de 0,3 s.

Application de Notre Étude

Nous indiquerons seulement l'application pratique la plus importante : il est recommandé d'associer l'opérateur à un système dont la transmittance se réduit à une constante.

Conclusions

Les résultats de notre étude ont été établis avec un nombre restreint d'opérateurs. Il faudrait maintenant étudier les varia-

tions des paramètres des transmittances qui interprètent le comportement de l'opérateur humain, lorsque l'on considère un grand nombre de sujets.

Les travaux de recherches que nous venons de présenter ont fait l'objet d'une thèse de Doctorat ès Sciences soutenue par l'un des auteurs de la présente communication, l'Ingénieur civil J.-C. Raoult.

Ils ont été effectués au Laboratoire Central de l'Armement, Arcueil (Seine), sous la direction de l'Ingénieur en Chef Naslin.

Bibliographie

- FOGEL, L. J. The human computer in flight control. *Inst. Radio Engrs. N. Y., Trans. on Electronic Computers* (Septembre 1957)
- GIBBS, C. B. et BAKER, J. C. Free-moving versus fixed control levers in a manual tracking task. *Conférence sur le Contrôle Automatique*
- GREENE, J. Man as a servo component. *Control Engng.* (Octobre 1954) 58
- KRETZ, M. L'introduction de l'opérateur humain dans la boucle fermée des systèmes asservis. *Rapp. Soc. Giravion-Dorand*
- MCRUER, D. T. et KRENDEL, E. S. The human operator as a servo system element. *J. Franklin Inst.* (Mai, 1959) 381; (Juin 1959) 511
- MCRUER, D. T. et KRENDEL, E. S. Dynamic response of human operators. *Note technique du Wright Air Development Center*
- MEDVEDEV, S. S. Quelques lois relatives au travail d'un opérateur. *Automat. Telemekh.*, Tome XVII, No. 1 (1956) 985
- NASLIN, P. et RAOULT, J.-C. Sur le comportement de l'opérateur humain lorsque le système commandé est quelconque. *C. R. Acad. Sci.*, 252 (1961) 2380
- NASLIN, P. et RAOULT, J.-C. Sur le comportement de l'opérateur humain en régime transitoire. *C. R. Acad. Sci.*, 253 (1961) 1530
- A human approach to the design of man-operated continuous control systems. *Rapport Nav. Research Lab.*
- RAOULT, J.-C. Contribution à l'étude de l'opérateur humain. *C. R. Acad. Sci.*, 252 (1961) 1418
- RAOULT, J.-C. Modèles continus et échantillonnés de l'opérateur humain placé dans une boucle de commande. *Conf. à l'Otan* (Février 1962)
- SHERIDAN, T. B. Experimental analysis of time-variation of the human operator's transfer function. *Automatic and Remote Control*, Vol. 2, p. 629, 1960. London; Butterworths
- TUSTIN, A. *Automatic and Manual Control*. London; Butterworths
- TUSTIN, A. The nature of the operator's response in manual control, and its implications for controller design. *Commun. au Congrès sur les régulations automatiques et les servomécanismes* (Mai 1947)
- WALSTON, C. E. et WARREN, C. E. A mathematical analysis of the human operator in a closed-loop control system. *Rapp. Skill Comp. Res. Lab. Air Force Personnel and Training Research Center*, en collaboration avec l'Université de l'Ohio
- WARREN, C. E., FITTS, P. M., et CLARK, J. R. An electronic apparatus for the study of the human operator in a one dimensional closed-loop continuous task. *Amer. Inst. elect. Engrs* (Janvier 1952) 19

DISCUSSION

G. VOSSIUS, *Institut für Animalische Physiologie, Frankfurt a. M., Ludwig-Rehn-Str. 14, Germany*

If I understood correctly, the operators could not follow input signal frequencies over 1.5 c/sec. In fact our operators 'followed' correctly frequencies of up to 4.5 c/sec, the limit frequency of hand movements living at about 10 c/sec.

P. NASLIN and J.-C. RAOULT, *in reply*

The limit frequencies of interest depend on the arrangement of the control lever and on the direction of motion with respect to the operator's body. In this case, the operator moved the lever backwards and forwards in such a manner that the whole arm was involved.

In these conditions, the operator can respond to a sinusoidal input

up to 5 c/sec, but he cannot actually 'follow' the input beyond 1.5 c/sec. For higher frequencies, he merely reproduces the input frequency, with no attempt to control his amplitude of oscillation, so that his coupling with the input becomes very loose and he relies heavily upon his memory and other internal capabilities. He reacts in an internal mode synchronized by the input. He can even close his eyes for some time.

Summing up, it is maintained that, in the conditions indicated above, the limit frequency for actual control of the output is of the order of 1.5 c/sec, even for a pure sinusoidal input.

G. VOSSIUS

There are some objections to developing a model of hand tracking which consists of only one branch which incorporates a sampler. There is no doubt that hand-tracking movements are sampled. Firstly, the response to a step input is the same as that for a sampled-data system, secondly, very slow movements (e.g. sinusoidal) are followed by a series of steps.

However, if one considers a movement which is hard to learn, for example a periodic input which consists of five harmonic oscillations, during the learning phase some continuous movements are inserted to correct the output. Such continuous movements cannot occur in a purely sampled system.

This is observed most clearly in the following experiment. A sinusoidal oscillation of 3 c/sec was sampled at a sampling frequency of 4 c/sec. Initially the operator followed the input at 3 c/sec. After 'losing his rhythm' he followed at the difference frequency of 1 c/sec.

From experiments using different input signals with the same correlation functions, and from experiments using periodic and aperiodic inputs formed by superposition of five sinusoidal oscillations, it can be shown that besides the sampled branch there is at least one branch which learns by forming a model. There is also the ability to foresee what will happen during short or long time intervals (i.e. a forecast of the next phase of movement and of its periodic characteristics). These different modes of action are chosen according to the shape of the input signal.

Concerning the problem of discrete perception, I have to add that physiologists have known for a long time the so-called 'perception time'. Two events happening within this interval of time, for example

one green and one red light flash, cannot be recognized as not being simultaneous. For the sense of sight, this 'perception time' is of the order of 0.1 sec.

P. NASLIN and J.-C. RAOULT, *in reply*

It should be stressed that our work is concerned exclusively with the operator's response to unpredictable input signals. Even for an input containing only four unrelated sinusoidal components, the amount of actual prediction in the operator's behaviour is negligible. The smoother portions of the operator's response may be accounted for in the following manner in the light of our sampled model. When the operator is well adapted to his task and if the latter is not too difficult, he selects a large phase-advance time constant which, being in front of the sampler, provides the familiar 'anticipatory' control action. The large phase advance makes it possible to select such values for the parameters α and h in $W(p)$ as to increase the effectiveness of $W(p)$ as a low-pass filter, thus eliminating most of the harmonics introduced by sampling. These factors seem to be sufficient to explain the smoothing effect observed.

The complete diagram summarizing the results of our work is that of Figure A. It comprises two sorts of memories, a long-term memory which performs a prediction and feedforward action and comes into play in the case of predictable signals only, and a short-term or 'correlative' memory which is used to adjust the system parameters by comparing the present input to its values in the recent past. On the other hand, the overall transmittance of the two secondary-feedback loops is $W(p)$.

As regards the experiment reported in the third paragraph of Dr. Vossius's observations, we fail to perceive how the operator (or any other device for that matter) could possibly reconstruct a 3 c/sec sinusoid from samples taken at a frequency of 4 c/sec.

E. JURY, *University of California, Berkeley, California, U.S.A.*

In this discussion, I would like to ask the following two questions whose clarification would hopefully add to the interesting and useful contents of this paper.

(1) The authors are well justified in representing the human operator, for low frequencies, by a linear transfer function, although

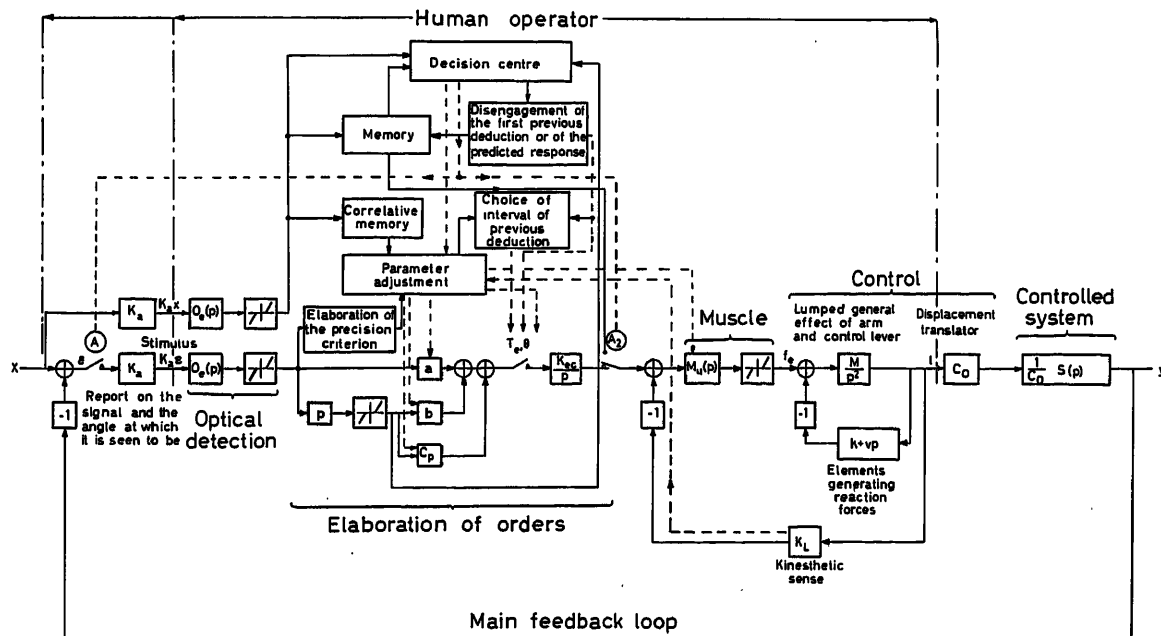


Figure A

actually it is non-linear. In view of this justifiable linearization, I would like to ask the authors whether they feel strongly in support of the five time constants in the equation of $W(p)$ for a step input or whether a more simplified version of two or three time constants, as proposed by other authors, is equally acceptable or justifiable?

(2) I would like to ask the authors how they arrived at the sampled-data model of Figure 10? Furthermore, the fact that 'no pure delay' is incorporated in the transfer function of the sampled-data model, while existing in the continuous model, I believe need some comments. This is important in view of the fact that in the papers of Bekey, and Young, and in the work of Westcott *et al.*, the pure delay is incorporated.

In closing these brief remarks, I might mention that in our recent survey of the literature of biocontrol systems, published in the I.E.E., P.G.A.C., we came across the work of Ward of Australia in 1958, in which he proposed the sampled-data model for the human operator in control systems. This extensive experimental work was not published in a regular journal but is available as a Ph. D. thesis. We believe this work is the first to advocate and justify the sampled-data model as correctly pointed out by the present authors.

References

- ¹ WARD, J. R. The dynamics of a human operator in a control system. A study based on the hypothesis of intermittency. *Ph. D. Dissert.*, Aeronautical Engineering Dept., University of Sydney, Australia (May 1958)
- ² JURY, E. I. and PAVLIDIS, T. A literature survey of biocontrol systems. *I.E.E.E., P.G.A.C.* (July 1963)

P. NASLIN and J.-C. RAOULT, *in reply*

Professor Jury is to be thanked for his two very pertinent questions, which indeed require some additional comments.

(1) The polynomial in the denominator of $W(p)$ of the second continuous model for step inputs is a member of a family of polynomials developed by one of the authors in conjunction with a new damping criterion. (In addition to the reference given in a footnote of the paper, a more recent and complete account of these polynomials and their applications will be found in a later work¹.) The polynomials are characterized by a damping factor α and a characteristic time h . In the present instance, such a polynomial was adopted in order to be able to adjust independently the step-response overshoot by means of α and the shape of the initial portion of the response by a suitable choice of the degree. The best results have been obtained with the fifth degree and the values given for α and h .

(2) In the sampled model, the response delay is accounted for, in part, by the partial hold contained in μ_s and partly by the large phase shift of $W(p)$ at the higher frequencies. It does not need to be in the form of a single pure delay, so long as the required gain and phase characteristics are obtained in the frequency band of interest.

(3) The various elements of the sampled model of Figure 10 may be briefly justified as follows. The term $W(p)$ of the second continuous model for step inputs has to be present because the output of a physical sampled-data system results from the superposition of step responses. The sampling frequency was derived from a direct analysis of the records and was observed to vary between 1 and 4 c/sec. The sample duration was chosen in agreement with the perception time of 0.1 sec. No hold was introduced (except the fictitious hold accounting for the finite sample duration), because the additional phase shift made it impossible to obtain a stable closed loop with the required gain. In fact, stability considerations required the introduction of a phase-lead time constant T_1 in front of the sampler; T_1 is so chosen as to place the point of frequency $\Omega/2$ of the unsampled Nyquist locus on the imaginary axis (see Figure 11 of the paper), so that the corresponding point of the sampled locus be located in the vicinity of the origin, which yields large gain and phase margins for the required open-loop gain.

Finally, we thank Professor Jury for adding an apparently basic reference to our list.

Reference

- ¹ NASLIN, P. Polynômes normaux et critère d'amortissement. *Automatisme* (Mai et Juin, 1963)

L. R. YOUNG, *Massachusetts Institute of Technology, 77 Mass. Avenue, Cambridge 39, Mass. U.S.A.*

The problem undertaken by the authors is one of the most difficult in the field of description of the human operator—namely the development of a model which is valid for all fully adapted states of operation and also for the transition period between fully adapted states.

In their determination of quasi-linear human operator models as it varies with input spectrum and controlled element dynamics, the authors have apparently used the observed average delay between input and response. Quasi-linear approximations were reviewed by McRuer and Krendel in 1957, and Sheardon in 1960. In particular, 'best fit' linear approximations, generally in terms of the human operator transfer function

$$D(s) = \frac{Ke^{-\tau s}(1 + T_L s)}{(1 + Es)(1 + T_N s)}$$

have been described by Tustin, Russel, Krendel, Hall and others, using forms of spectral analysis. The dependence of open-loop gain on input frequency spectrum was demonstrated by Elkind in 1956, with quasi-linear models generally accounting for better than 95 per cent of the operator's response energy.

The optimum form of the controlled element was investigated by Birmingham, Chernikoff and Taylor. The first question is therefore: how do the authors' quasi-linear models compare with those obtained earlier, and what technique was used for identifying the closed-loop transfer function as pure delay?

In their discussion of operator step response following a change in controlled element gain, the authors show the 'plant adaptive' behaviour of the human operator in adjusting his own gain. We find similar responses to those of Figure 8 with or without a spring-restrained control. In a recent report we (Young, Green, Elkind and Kelly) present the average error curves generated by the human operator following various sudden changes in controlled element dynamics.

It is possible to consider the adaptation as based on evaluation of successive samples of error only—without necessarily considering any kinesthetic feedback.

Thus I believe that whereas the authors' interesting models provide useful and testable hypotheses about human tracking, there is no indication that they are unique.

P. NASLIN and J.-C. RAOULT, *in reply*

There are two basic questions in Professor Young's interesting comments: (a) justification for identifying the closed-loop transmittance to a pure delay; (b) justification for the introduction of a kinesthetic feedback. Both justifications are indeed required.

(1) Before answering the first question, it should be remembered that the four frequencies present in the input signal cover a frequency band of about one octave only. The justification for making use of such a narrow-band input signal should, therefore, be given. If the operator is faced with a wide-band input, it is not likely that he will adjust himself to the overall spectral density of the input, but rather to local characteristics, i.e. to the dominant frequency present in small portions of the input signal. This is reminiscent of the manner in which a rough frequency analysis of a time signal may be carried out by fitting portions of sinusoids to small enough portions of the signal.

This being said, we observed that, for a given value of the input mean frequency, the output signal could be considered in a first approximation as being delayed by a fixed amount with respect to the input. This does not mean that we 'identify' the closed-loop behaviour to a transportation lag producing a unity gain and a linearly increasing

phase over the whole frequency spectrum. We only wish these characteristics to be realized in the limited frequency band of the input signal. This is precisely what we obtain with the open-loop transmittance adopted for the first continuous model. Furthermore, it was not found possible to improve this model by introducing additional time constants in the open-loop transmittance. Additional time constants only appear in the operator's response to compensate for the time constants present in the transmittance of the controlled system, within the limits given in the paper.

(2) When we started our work, we did not know whether the operator's output was displacement or force. This is the reason why we started to work with a light frictionless spring-restored lever, for

which the transmittance between force and displacement is a constant. At a later stage, we modified in various fashions the control-lever dynamics and found that the effect on the operator's transmittance was negligible. We therefore concluded that the operator's output was displacement, and not force. The kinesthetic feedback, which is known to exist, is an internal local feedback which helps the operator to adjust his force in order to produce a desired displacement for a wide range of the control-lever dynamics; in other words, the kinesthetic feedback is contained in the transmittance $W(p)$ (Figure 1). This is confirmed by the fact that the presence of a restoring spring, which provides an additional external displacement feedback, improves the overall control accuracy.

Discrete Models of the Human Operator in a Control System

G. A. BEKEY

Summary

This paper presents the development and analysis of a new class of mathematical models of the human operator in a closed-loop control system. The models are based on the hypothesis that the input-output behaviour of the operator is characterized by sampling, data reconstruction, and extrapolation operations.

Systematic procedures for determining the characteristics of the proposed sampled-data models are presented. The frequency response characteristics of the discrete models with stationary random inputs are analysed by means of z transform techniques. Closed form expressions are derived for computation of the power spectral density of the model output and error signals.

An experimental programme was designed to test the feasibility of the hypothesis. The power spectral density of the tracking error and the output of a number of operators were measured. The experimental results are compared with those predicted by the model.

For the type of inputs considered in this study, the outputs from the discrete models approximate the experimental data more closely over a wider range of frequencies than those obtained from the quasi-linear continuous models previously employed to represent the human operator.

Sommaire

Ce travail présente le développement et l'analyse d'une nouvelle classe de modèles mathématiques de l'opérateur humain dans un système de commande automatique à boucle fermée. L'étude des modèles est basée sur l'hypothèse que le fonctionnement de l'opérateur quant aux signaux d'entrée et de sortie est caractérisé par une correction périodique, la reconstruction des informations et les opérations d'extrapolation.

Des méthodes systématiques pour déterminer les caractéristiques des modèles discrets proposés sont présentées. Les caractéristiques de la courbe de réponse des modèles discrets ayant des entrées aléatoires stationnaires sont analysées au moyen des transformations z . Des formules à forme fermée sont dérivées pour le calcul de la densité spectrale de puissance des signaux de sortie et des signaux d'erreur du modèle.

Un programme expérimental a été établi pour vérifier la justesse de l'hypothèse. La densité spectrale d'erreur de poursuite et les signaux de sortie d'un nombre d'opérateurs ont été mesurés. Les résultats expérimentaux sont comparés à ceux qui ont été prédits par le modèle.

Pour le type de signaux d'entrée considérés dans ce travail, les signaux de sortie des modèles discrets s'approchent des données expérimentales avec une exactitude plus grande et sur une gamme de valeurs plus large des fréquences que les données qu'on obtenait des modèles continus quasi-linéaires utilisés auparavant pour représenter l'opérateur humain.

Zusammenfassung

Dieser Beitrag bringt die Entwicklung und Untersuchung einer neuen Klasse mathematischer Modelle für das Verhalten des Menschen als Regelkreisglied. Die Modelle beruhen auf der Annahme, daß das zwischen Eingang und Ausgang betrachtete Verhalten des Bedienungsmanes durch Abtastung, Datenrückgewinnung und durch Extrapolation gekennzeichnet ist.

Systematische Verfahren zur Bestimmung der Eigenschaften des vorgeschlagenen Abtastmodells werden angegeben. Mittels der

Methode der z -Transformation wird der Frequenzgang des diskreten Modells bei stationären Zufallseingängen untersucht. Geschlossene Ausdrücke zur Berechnung der spektralen Leistungsdichte des Ausgangssignales und der Regelabweichung des Modells werden abgeleitet.

Es wurde ein Versuchsprogramm entwickelt, um die Gültigkeit der Hypothese zu prüfen. Die spektrale Leistungsdichte der Regelabweichung und der Ausgangsgröße einer Anzahl von Bedienungsleuten wurde gemessen. Die Versuchsergebnisse werden mit den vom Modell bestimmten verglichen.

Die in dieser Untersuchung betrachtete Art der Eingangsgröße führt auf Ausgangsgrößen des diskreten Modells, die innerhalb eines größeren Frequenzbereiches eine bessere Annäherung an die Versuchsergebnisse liefern, als die von quasi-linearen kontinuierlichen Modellen, die bisher zur Simulierung des Menschen Verwendung fanden.

Introduction

Previously, mathematical representations of the input-output behaviour of the human operator in a control system have been based almost exclusively on the assumptions that the operator is an approximately linear continuous element. A block diagram of such a system is shown in *Figure 1*. The display acts as a subtraction device and the operator attempts to reduce the error signal to zero. The mathematical models most commonly used to represent the human operator in a system such as *Figure 1* consist of linear differential equations whose coefficients depend on the bandwidth of the input signal and on the dynamics of the controlled element. The present status of such quasi-linear representations is analysed in detail in the literature¹⁻⁴.

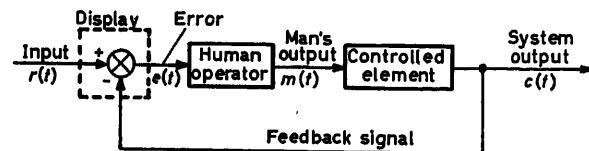


Figure 1. Block diagram of tracking loop

The major objective of this paper is to present the results of a study of a class of mathematical models of the human operator which depend on discrete rather than continuous operations. Intermittent processes in human tracking have been hypothesized in the past⁵⁻⁷ and this research was undertaken to study this hypothesis.

Background

The development of mathematical models for human operators began late in World War II when human trackers were widely used in target tracking for anti-aircraft guns and similar devices. The first engineering approaches to the problem were reported by Tustin⁸ in England and Ragazzini⁹ in the U.S. Both investigators attempted to describe the human operator's

performance by a linear differential equation. However, the construction of an adequate model for the human operator, even for a particular task (such as tracking in one dimension) is extremely difficult. This difficulty arises in part from the inherent variability of human performance and in part from the high degree of adaptability of the human operator. Thus, when tracking simple periodic inputs, the human operator is capable of learning their nature and predicting their future course sufficiently well to make his performance qualitatively different from that resulting when he tracks unpredictable inputs¹. In order to eliminate this effect on the operator's performance, either random or at least random-appearing inputs have been used.

Non-linear representations of the human operator have also been explored. However, the difficulties encountered in analysing complex non-linear systems have limited the amount of work done in this field¹⁰.

The Quasi-linear Continuous Model

For random-appearing inputs, such as sums of sine waves of non-harmonic frequencies, linear continuous models are usually obtained experimentally^{1, 2}. A method due to Booton¹¹ is used to determine the linear relationship which yields the minimum mean square approximation to the operator's output for a Gaussian input process. The resulting experimental data are fitted with a frequency domain relationship of the form

$$G_H(j\omega) = \frac{Ke^{-j\omega D}(1+j\omega T_L)}{(1+j\omega T_N)(1+j\omega T_I)} \quad (1)$$

where ω is the natural frequency in rad/sec

T_N , T_L , T_I are constants which depend on input, bandwidth and controlled element dynamics,

K is the model gain, primarily a function of input bandwidth, and

D is the time delay associated with the data transmission and data processing ('reaction time') by the operator.

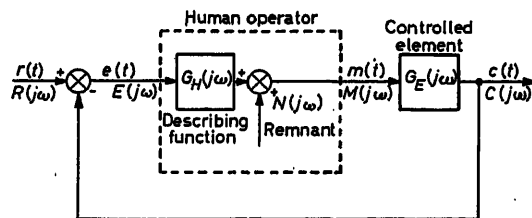


Figure 2. Quasi-linear continuous model of the human operator

The quasi-linear model also includes a noise generator which contains that portion of the output which is not accounted for by eqn (1), as shown in Figure 2. The work of a number of investigators^{1, 2}, has shown that the noise term accounts for less than 5 per cent of output power when the input signal bandwidth is restricted to frequencies lower than about 0.5 c/sec.

Difficulties with the Quasi-linear Continuous Model

The quasi-linear continuous model gives impressive evidence of the nearly linear behaviour of the human operator when tracking signals of low frequency. However, the model suffers from a number of drawbacks in addition to the frequency limitations. Among these are the following:

- (a) Being linear and continuous, the output of the model cannot contain frequencies not present in the input signal. (Such frequencies are known to exist in human operator outputs.)
- (b) The model cannot account for a substantial body of experimental evidence (discussed below) which suggests that the human operator is not continuous but acts on discrete samples of information.
- (c) The model does not account for the known ability of the human operator to extrapolate his response even when the input stimulus temporarily vanishes. For example, if a target disappears momentarily, a human tracker will continue to respond at nearly constant velocity¹².

The models proposed in this paper attempt to remedy, at least in part, all of the above difficulties.

Development of a Discrete Model

There is considerable evidence which suggests that the human operator's response may be intermittent rather than continuous, i.e. that he acts upon discrete samples of input information rather than upon a continuously varying input¹³. The evidence is based primarily upon the following data:

(a) Examination of Tracking Records

Curves of the error between random appearing input and human operator output show a pronounced periodicity in the vicinity of 2 c/sec, even when this frequency is not very pronounced in the input waveform. On the basis of some 15,000 measurements of error curves it has been found that over 80 per cent of the periods of the correcting responses of trained trackers ranged between 0.2 and 0.6 sec. Largely on the basis of such observations Craik⁵ suggested that human response consists of a series of 'ballistic responses' which are triggered at about $\frac{1}{2}$ sec intervals and run to completion regardless of intervening changes in the input process. Examination of power spectra of tracking records also reveals strong peaks in the vicinity of 1 to 1.5 c/sec⁴. Furthermore, human operator responses always contain frequencies beyond the range of a band-limited input. These additional higher frequencies could, in part at least, be harmonics due to sampling.

(b) The 'Psychological Refractory Period'^{13, 14}

This phrase refers to apparent time delays which occur when a human operator tracks a series of discrete stimuli (such as steps) which are spaced less than about $\frac{1}{2}$ sec apart. When this situation occurs, and the time interval to an unexpected second stimulus is sufficiently short, the operator finds it difficult or impossible to react to it. There are a number of possible alternative explanations of such behaviour. The explanation upon which the present work is based is that the operator admits information only at discrete intervals of time which cannot be spaced much more closely than about 2 to 3 per second. Thus, stimuli occurring between these 'sampling instants' cannot be utilized until the next sample.

(c) Perception of a Number of Discrete Events¹⁵

If subjects are presented with a series of light flashes of short duration at rates from 10 to 30 per second, the subjective rate reported by the subjects never exceeds 6 to 8 per second, regardless of the objective rate. Thus, two light flashes about $\frac{1}{30}$ sec apart are reported as a single flash, even though the light-dark ratio is such as to prevent fusion of the images into

one. Similar results are obtained with auditory stimuli (clicks). A possible explanation in this case is that sensory inputs are received continuously, but admitted to consciousness only in discrete 'packets'. The shorter duration of the 'sampling interval' in this case, as compared to the tracking intervals of $1/3$ to $1/2$ sec, could be due to the fact that no muscular movement of the limbs is required.

(d) Delayed Perceptual Feedback

On the basis of a hypothesis of intermittency in human performance, it can be deduced that the introduction of artificial time delays into perception, approximately equal to the normal 'sampling interval', should make performance extremely difficult. It has been shown that this is exactly the case with delayed auditory feedback¹⁶ as well as with delayed visual feedback¹⁷.

A detailed analysis of these and other supporting experiments has been made⁴.

On the basis of the above considerations a new mathematical model has been formulated. In its simplest form, this model is shown in Figure 3 where the human operator is represented by

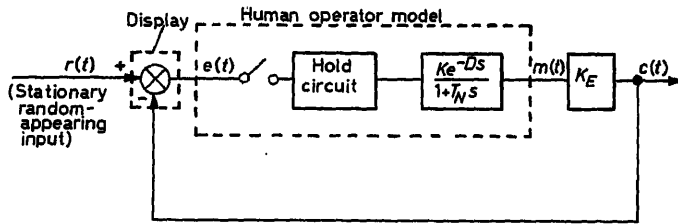


Figure 3. Proposed discrete model of the human operator

a periodic sampler, a hold circuit, and a continuous element which has the form suggested in the literature¹ for the case where the controlled element dynamics are negligible.

The sampler represents the assumption that the operator's central nervous system receives information only at discrete instants of time, once every T sec. The hold circuit or data reconstruction element is required since the operator's output is continuous. The continuous portion of the model corresponds to the quasi-linear models of eqn (1). The hold circuits exhibit considerable phase shift and thus contribute to the total effective time delay of the model. Consequently, the time-delay term D in eqn (1) must be adjusted appropriately for each type of hold circuit.

The model of Figure 3 can be described by the relation:

$$G_s(j\omega) = \frac{M(j\omega)}{E^*(j\omega)} = H(j\omega) G_e(j\omega) \quad (2)$$

where $E^*(j\omega)$ is the Laplace transform of the sampled error $e^*(t)$ evaluated at $s = j\omega$, $H(j\omega)$ represents the frequency characteristics of the hold circuit and $G_e(j\omega)$ is given by eqn (1). When controlled element dynamics are negligible, eqn (1) reduces to¹

$$G_e(j\omega) = \frac{Ke^{-j\omega D}}{1 + j\omega\tau} \quad (3)$$

Therefore, for a zero-order hold and negligible controlled element dynamics, the frequency characteristics of the continuous portion of the model are given by

$$G_{s0}(j\omega) = \left(\frac{1 - e^{-j\omega T}}{j\omega} \right) \left(\frac{Ke^{-j\omega D} s_0}{1 + j\omega\tau} \right) \quad (4)$$

and for the first-order hold case

$$G_{s1}(j\omega) = \left(\frac{1 + j\omega T}{T} \right) \left(\frac{1 - e^{-j\omega T}}{j\omega} \right)^2 \left(\frac{Ke^{-j\omega D} s_1}{1 + j\omega\tau} \right) \quad (5)$$

In both cases the input process is assumed to be stationary and random-appearing.

The ability of the sampled-data model of Figure 3 to meet some of the problems which face the continuous model can be seen intuitively by considering the following characteristics of sampled systems¹⁸:

- (a) Changes in the input cannot have any effect until the next sampling instant occurs.
- (b) The presence of the sampler limits the frequencies which can be reconstructed at its output to those not exceeding one-half the sampling frequency.
- (c) The action of the sampler generates harmonics in the output which extend over the entire frequency spectrum, even when the input is band-limited.
- (d) The hold circuit which generally follows the sampler is a time-domain extrapolator, which reconstructs the signal based on information at the sampling instants. Consequently, a first-order hold which extrapolates with constant velocity based on the present and past samples of the input, would provide the model with a characteristic known to exist in human tracking.
- (e) In the limit as the input frequency approaches zero, the sampled output approaches the continuous system output. This is desirable since the continuous model is quite adequate for low-frequency inputs.

It is particularly important to note that the 'human operator model' block in Figure 3 has continuous inputs and outputs, and consequently the existence of sampling cannot be verified by the type of mathematical investigation being conducted. It is possible, however, to examine the implications of sampling and examine the system behaviour in view of these implications. In order to do this, the model has been analysed with several types of hold circuits and expressions for spectral density functions of the error $e(t)$ and output $c(t)$ have been obtained⁴.

Evaluation of the Mathematical Model

Consider the tracking system of Figure 4. Let the input signal consist of white Gaussian noise filtered by a low-pass filter, and

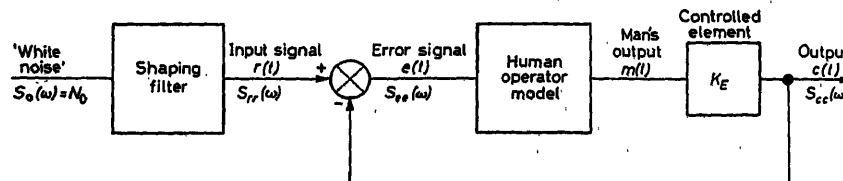


Figure 4. Compensatory tracking system

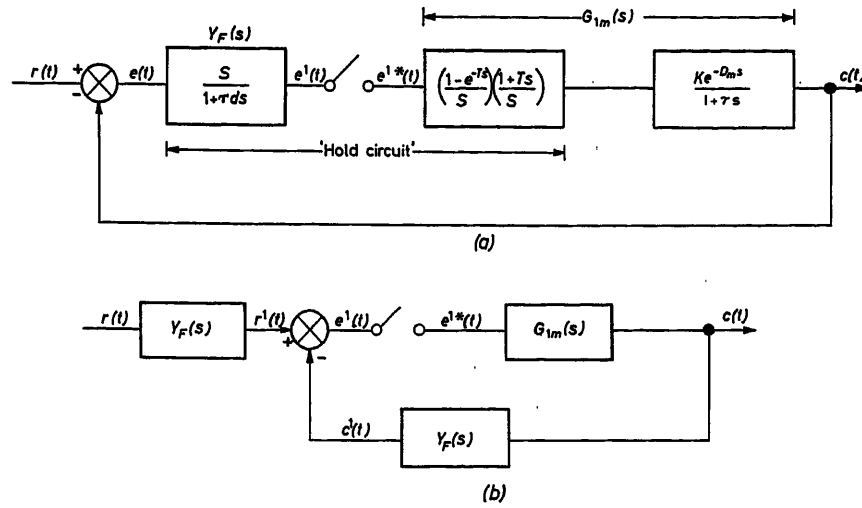


Figure 5. Block diagram of tracking system with modified first-order hold model.
(a) Original MFOH system; (b) Equivalent system with "Error" sampling

let the linear human operator model be either continuous or discrete.

If the power spectral density of the noise source is given by $S(\omega) = N_0$ (a constant) and the shaping filter is described by

$$F(j\omega) = \frac{1}{1+j\omega/\omega_B} \quad (6)$$

then the following expressions for the output power spectral density $S_{cc}(\omega)$ of the model are obtained⁴:

Continuous Model (formula 7 see next page):

Zero-order Hold Model (formula 8 see next page):

where the A_i are functions of the model parameters K , D_0 and τ .

First-order Hold Model (formula 9 see next page):

where $S_{rr}^*(\omega)$ represents the sampled power spectral density corresponding to the continuous input spectrum $S_{rr}(\omega)$, and the P_i are functions of the model parameters K , D_1 and τ .

It is well known that the first-order hold circuit exhibits considerably more phase shift than the zero-order hold. In order to obtain the velocity extrapolation properties of the first-order hold and at the same time to decrease the phase shift, the 'modified first-order hold' of Figure 5(a) was devised. The output spectrum using this circuit is given by (formula 10 see next page) where $S_{rr}^*(\omega)$ is the power spectral density corresponding to the continuous input spectrum $S_{rr}(\omega)$ shown in Figure 5(b), and the B_i are functions of the model parameters K , D_{1m} and τ .

The detailed derivation of the error and output spectral density expressions for the first-order hold is given in the Appendix. The resulting expressions were used for comparisons of model behaviour with experimental data.

Evaluation of Hold Circuits

In order to make a preliminary evaluation of the proposed models before conducting any new experiments, values of the parameters K , τ , and D corresponding to data available in the literature (Elkind's experiment F1)³ have been used to compute power spectra of the system output and error. The system input was 'white' noise filtered by a first-order lag. The sampling frequency of the model was assumed to be 3 c/sec. The resulting

error spectra for the model with a zero-order hold (ZOH), first-order hold (FOH) and modified first-order hold (MFOH) are plotted in Figure 6 and compared with experimental points and the spectrum obtained from the continuous model.

An examination of the curves of Figure 6 shows that the results using the first-order hold are most promising. Since this result agrees with the intuitive arguments of the previous section, other hold circuits were abandoned before embarking on the experimental programme.

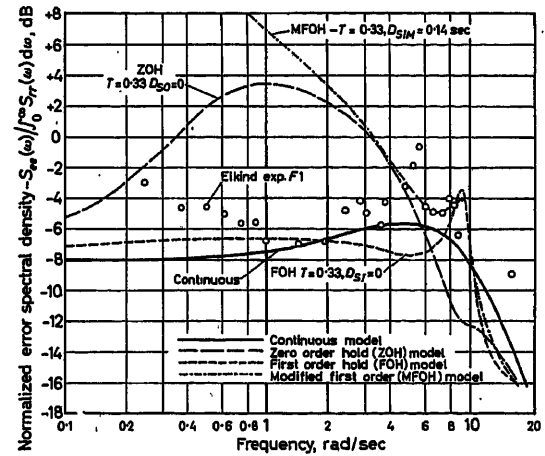


Figure 6. Error spectral density for various human operator models

Experiments and Selection of Parameter Values

In order to verify the feasibility of the proposed discrete model, an experimental programme was devised⁴. Measurements were made of the power spectral density of output and error signals from a number of human operators tracking random-appearing inputs. The experimental situation was based on compensatory tracking in one dimension, using a very light hand controller, so that controlled element dynamics were negligible. An oscilloscope was used for the display. The input signal $r(t)$

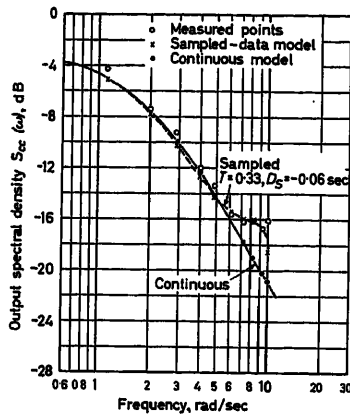


Figure 7. Comparison of experimental and analytical values of output power spectral density for run R-1

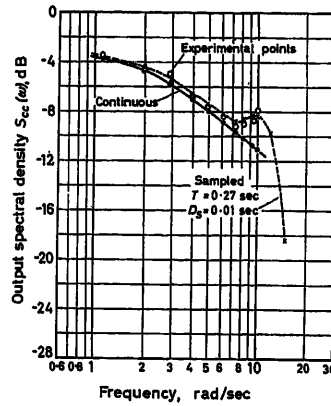


Figure 8. Comparison of experimental and analytical values of output power spectral density for run R-6

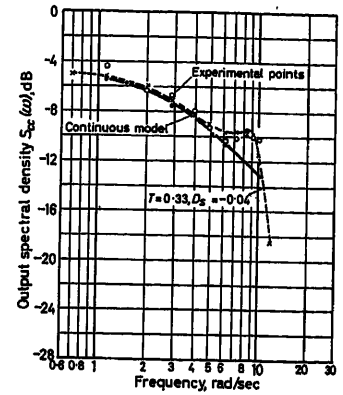


Figure 9. Comparison of experimental and analytical values of output power spectral density for run R-7

was the output of a low-pass filter, the input to which consisted of a sum of 10 sinewaves of equal amplitude and non-harmonic frequencies. This experimental arrangement approximates the idealized situation of Figure 4. Approximately 100 runs were made with eight operators, after a period of training.

The experiments were also used to provide the values of parameters to be used in the numerical evaluation of the power spectral densities obtained from the model. The parameters were selected as follows:

(a) From cross-spectral measurements of the operator's input, error and output, the data for the quasi-linear continuous model were obtained. The continuous model parameters, K , D_c , and τ were obtained by fitting the transfer function of eqn (3) to the experimental data.

(b) The sampling period T was obtained by examining the recorded spectra for a pronounced peak in the vicinity of 1 to 1.5 c/sec. The frequency at which the peak occurred was assumed to correspond to one-half the sampling frequency. The rationale for this selection of sampling frequency is based on the fact that the frequency characteristics of the first-order hold exhibit a peak at approximately $\omega_s/2$. Furthermore, all hold circuits exhibit transmission zeros at integral multiples of the sampling frequency ω_s since

$$1 - e^{-j\omega T} = 0 \quad (11)$$

for

$$\omega = n\omega_s = n \left(\frac{2\pi}{T} \right), \quad n = 1, 2, \dots$$

(c) The time delay D_s of the sampled model was obtained by evaluating the effective time delay due to the hold circuit (D_h) and then letting $D_s = D_c - D_h$. This method was used in order that the total open-loop phase shift remain approximately equal for the sampled and continuous models for the frequency range of interest.

Results

The expressions for $S_{ee}(\omega)$ and $S_{cc}(\omega)$ derived above were programmed for solution on a digital computer. Typical results are shown in Figures 7, 8, and 9. The plotted points represent the power spectral density measured at the 10 component frequencies of the input signal.

All three of the runs illustrate the peaking in the output spectrum which is characteristic both for the operator's output and for the output of the discrete model. The continuous model, while providing an excellent fit at low frequencies, attenuates too rapidly at high frequencies. The output power spectral density from the discrete models shows remarkable agreement with the experimental data, in spite of the idealizing assumptions which were made.

It should be noted that the sampled model delays D_s shown on Figures 7 and 8 are both negative, i.e., the models incorporate predictors. The delay of the model for the run shown in Figure 9

* Eqn 7-10

$$S_{cc}(\omega) = \frac{K^2 \omega_B^2 N_0}{(\omega^2 + \omega_B^2) [(1 + K^2) + \tau^2 \omega^2 + 2K(\cos \omega D - \tau \omega \sin \omega D)]} \quad (7)$$

$$S_{cc}(\omega) = \frac{(\omega_B K^2 \sinh \omega_B T) (1 + e^{-2aT} - 2e^{-aT} \cos \omega T) (1 - \cos \omega T)}{T \omega^2 (1 + \tau^2 \omega^2) [(1 + A_3^2 + A_4^2) + 2(A_3 + A_3 A_4) \cos \omega T + 2A_4 \cos 2\omega T] (\cosh \omega_B T - \cos \omega T)} \quad (8)$$

$$S_{cc}(\omega) = \frac{\{4K^2(1 + T^2 \omega^2) (1 + e^{-2aT} - 2e^{-aT} \cos \omega T) (1 - \cos \omega T)^2\} S_{rr}^*(\omega)}{T^2 \omega^2 (1 + \tau^2 \omega^2) [(1 + P_1^2 + P_2^2 + P_3^2) + 2(P_1 + P_1 P_2 + P_2 P_3) \cos \omega T + 2(P_2 + P_1 P_3) \cos 2\omega T + 2P_3 \cos 3\omega T]} \quad (9)$$

$$S_{cc}(\omega) = \frac{[2K^2(1 + T^2 \omega^2) (1 - \cos \omega T) (1 + e^{-aT} - 2e^{-aT} \cos \omega T)] S_{rr'}^*(\omega)}{\omega^4 (1 + \tau^2 \omega^2) [(1 + B_3^2 + B_4^2) + 2(B_3 + B_3 B_4) \cos \omega T + 2B_4 \cos 2\omega T]} \quad (10)$$

is positive, but very small. It is likely that the use of partial velocity hold circuits, which result in less phase shift, would yield models with positive values of delay.

Typical time domain traces are given in *Figure 10*. These results also show the similarity between the discrete model and human operator, both in the error traces and the output traces.

Conclusions

The major concern of the work reported here has been an analytical and experimental investigation of a class of mathematical models for the human operator based on the theory of linear sampled-data control systems. The results show that for the particular tracking system considered, the discrete models do indeed result in input-output behaviour which more closely approximates experimental results than that which results from linear continuous models. In particular, it has been shown that the models which include sampling and first-order hold circuits

are consistent with a large body of evidence in the literature on tracking and that the analysis of such models results in spectral characteristics which check closely with experiment, at least under certain conditions.

The results of the study can be viewed as a logical extension of previous work with quasi-linear continuous models. The continuous models were considered adequate representations of tracking behaviour when the input function bandwidth did not exceed approximately 3/4 c/sec. In the present study the band extended to 1.6 c/sec; spectral peaks were noted in the range of 1 to 1.6 c/sec (which are consistent with previous data); and these peaks were shown to be consistent with linear sampling models as well. In other words, the sampled models result in a decrease in 'remnant' power, for difficult tasks, where the remnant is considered to be that component of the operator's output which the model does not explain.

For the particular tracking system and a particular operator, it has been shown that the sampled-data model can be con-

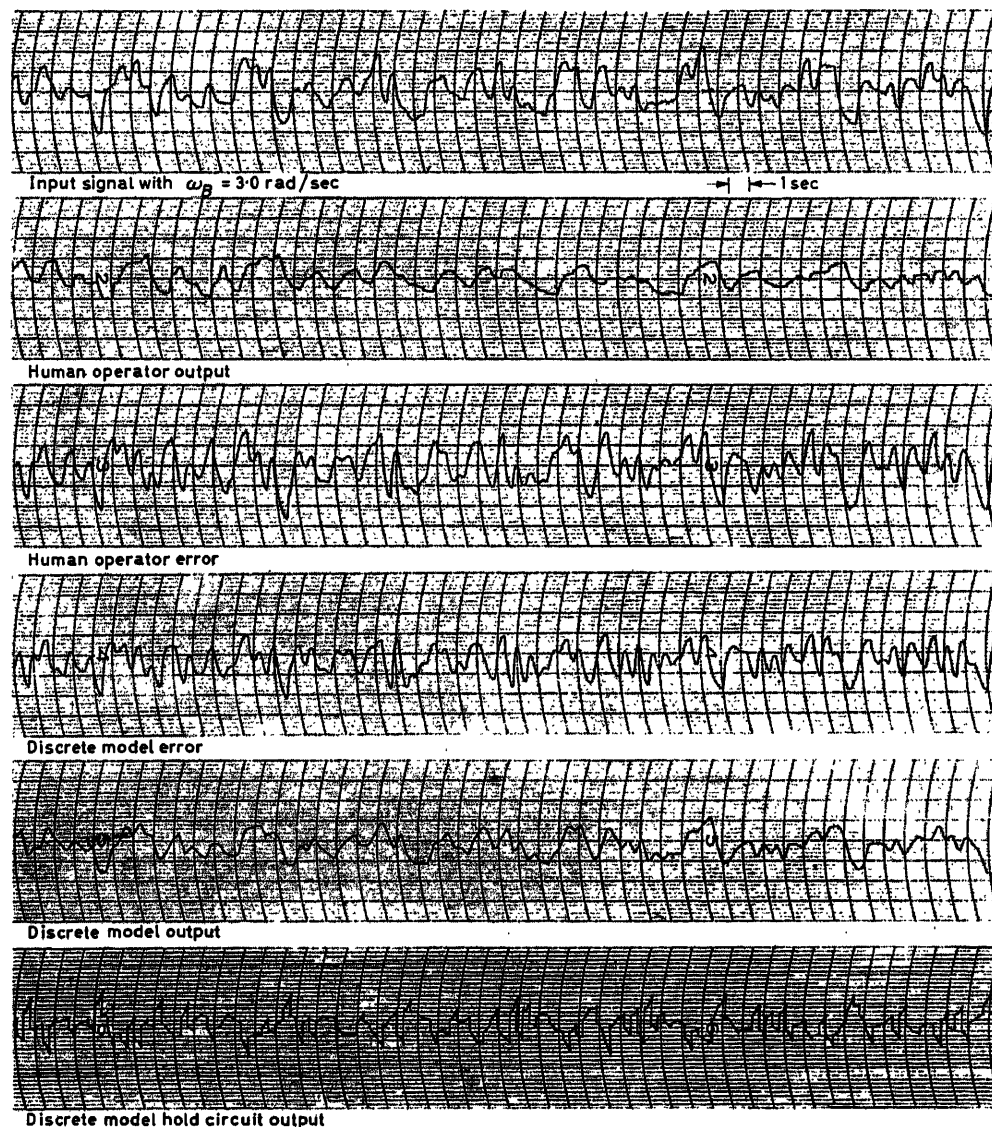


Figure 10. Time domain traces (all vertical scales equal model parameters: $T = 0.33$ sec, $\omega_B = 3.0$ rad/sec).

structed by following a systematic sequence of spectral measurements, which yield the parameters of the continuous model and the sampling frequency. Unfortunately, the experimental study was not sufficiently extensive to make definite statements about a synthesis procedure. However, the rules suggested in the paper for determination of model sampling frequencies were satisfactory for those experimental runs where high frequency spectral peaks could be clearly observed.

The major conclusions of the study are that the application of sampled-data theory to the study of man-machine systems is well justified and that discrete models of the human operator can be used to predict several important aspects of tracking behaviour.

This research was supported in part by the U.S. Air Force under Contract No. AF 33(616)-7139, monitored by the Flight Controls Laboratory, Aeronautical Systems Division, Air Force Systems Command, and in part by Space Technology Laboratories, Inc. The author is indebted to Professors John Lyman, C.T. Leondes and W. J. Karplus who supervised the work and provided many important suggestions, and is particularly grateful to Dr. R. K. Whitford for his continuing support of his work and for making available the STL analogue computation facilities.

APPENDIX

Derivation of Spectral Density Expressions

Analysis of System with Continuous Model

If the input to a linear invariant system is a stationary process $x(t)$ characterized by a power spectral density $S_{xx}(\omega)$, then the power spectral density of the output, $S_{yy}(\omega)$ is

$$S_{yy}(\omega) = |F(j\omega)|^2 S_{xx}(\omega) \quad (12)$$

where $F(j\omega)$ is the frequency response function of the system. If the noise source is assumed 'white'

$$S_0(\omega) = N_0 = \text{const.} \quad (13)$$

The input to the tracking system then has the spectral density

$$S_{rr}(\omega) = |F(j\omega)|^2 N_0 \quad (14)$$

where the frequency response function of the low-pass filter is given by

$$F(j\omega) = \frac{1}{1 + j\omega/\omega_B} \quad (15)$$

We are interested in obtaining an expression for the error spectral density and the output spectral density when the transfer function of the continuous operator model is

$$G_c(j\omega) = \frac{K_{HE} e^{-j\omega D}}{1 + j\tau_c \omega} \quad (16)$$

where K_{HE} is a gain which includes the model gain K_H and the controlled element gain K_E . The input spectral density is given by

$$S_{rr}(\omega) = \frac{N_0 \omega_B^2}{\omega^2 + \omega_B^2} \quad (17)$$

Using eqns (16) and (17), the error power spectral density is given by (formula 18 see below):

where the subscripts on τ , K , and D have been dropped for convenience. Similarly, the output power spectral density is (formula 19 see below):

Expressions (18) and (19) represent power spectra which can be estimated in experimental situations and compared with their theoretical values.

Analysis of the Sampled Model

Similar analyses to the above have been carried out using zero-order and first-order hold circuits in the discrete models. However, since much more significant results were obtained with first-order hold circuits, only the results of first-order hold models are reported here. The derivations of the equations for discrete models with other hold circuits are given in reference 4.

Signals in sampled data systems are, in general, non-stationary, even with stationary inputs. Consequently, statistical functions computed from ensemble averages do not equal those computed from time averages and care must be taken in the definition of the spectral density functions in such systems. In this study, the spectral density functions are obtained from time-averaged autocorrelation functions, which, as has been shown^{19,20} are equal to ensemble-averaged correlation functions averaged over one sampling period.

Consider now the sampled form of the operator model given in Figure 11.

The derivation of an expression for the output power spectral density follows a procedure analogous to that for the continuous system, with complications introduced by sampled signals which have repeated spectra along the entire frequency axis. The power spectral density of the continuous error signal

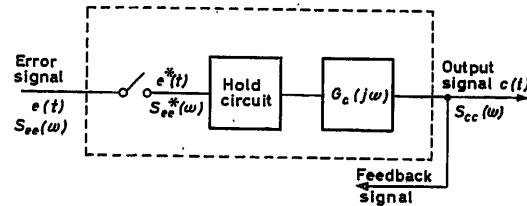


Figure 11. Sampled form of operator model

$$S_{ee}(\omega) = \frac{(1 + \tau^2 \omega^2) \omega_B^2 N_0}{(\omega^2 + \omega_B^2) [(1 + K^2) + \tau^2 \omega^2 + 2K(\cos \omega D - \tau \omega \sin \omega D)]} \quad (18)$$

$$S_{cc}(\omega) = \frac{K^2 \omega_B^2 N_0}{(\omega^2 + \omega_B^2) [(1 + K^2) + \tau^2 \omega^2 + 2K(\cos \omega D - \tau \omega \sin \omega D)]} \quad (19)$$

$e(t)$ cannot be obtained by a single relation analogous to (18) since there is no transfer relationship which explicitly relates $E(j\omega)$ to $R(j\omega)$ in an error sampled system, and a more complex procedure is required. Let $G_{s1}(s)$ represent the transfer function of the combination of first-order hold and continuous element in Figure 11. Then it can be shown that since

$$\frac{C(j\omega)}{R^*(j\omega)} = \frac{G_{s1}(j\omega)}{1 + G_{s1}^*(j\omega)} \quad (20)$$

the power spectral density of the output is given by

$$S_{cc}(\omega) = \left| \frac{G_{s1}(j\omega)}{1 + G_{s1}^*(j\omega)} \right|^2 S_{rr}^*(\omega) \quad (21)$$

where as usual the asterisk represents sampled quantities. The sampled spectral density is defined in terms of the z transform of $S_{rr}(s)$:

$$S_{rr}^*(s) = \frac{1}{T} z [S_{rr}(s)] \Big|_{z=e^{sT}} = \frac{1}{T^2} \sum_{n=-\infty}^{+\infty} S_{rr}(s + jn\omega_s) \quad (22)$$

The additional factor of $1/T$ arises due to time-averaging over a sampling period and $S_{rr}(s)$ is the bilateral Laplace transform representation of the power spectral density.

It can be shown that the expression for the power spectral density of the continuous error $e(t)$ is (formula 23 see below): where, as before, $S_{rr}(j\omega)$ is the power spectral density of the continuous input, and $S_{rr}^*(j\omega)$ is the corresponding sampled spectral density. The third term in (23) will be recognized from (21) as the power spectral density of the output signal $c(t)$. Consequently, the only unknown in (23) is the second term which is twice the real part of the cross-spectral density between $r(t)$ and $c(t)$, $S_{rc}(j\omega)$.

To evaluate the spectral densities $S_{oo}(\omega)$ in eqn (21) and $S_{ee}(\omega)$ in eqn (23), the z transform of the open-loop transfer function

$$G_{s1}(s) = \left(\frac{1+Ts}{T} \right) \left(\frac{1-e^{-Ts}}{s} \right)^2 \left(\frac{Ke^{-D_1s}}{1+\tau s} \right) \quad (24)$$

must be determined. D_1 is the reaction time delay corresponding to this model. The z transform of (24), which can be obtained from a table of modified z transforms¹⁸, is

$$G_1(z) = \frac{K(Q_1 z^2 + Q_2 z + Q_3)}{T z^2 (z - e^{-aT})} \quad (25)$$

where

$$\begin{aligned} Q_1 &= (2T - D_1 - \tau) + (\tau - T)e^{-a(T-D_1)} \\ Q_2 &= T - (1 + e^{-aT})(2T - D_1 - \tau) - 2(\tau - T)e^{-a(T-D)} \\ Q_3 &= -Te^{-aT} + (2T - D_1 - \tau)e^{-aT} + (\tau - T)e^{-a(T-D)} \end{aligned} \quad (26)$$

Substitution of expression (25) in eqn (21) gives the output power spectral density (formula 27 see below): where, for the filtered noise input, $S_{rr}^*(\omega)$ is

$$S_{rr}^*(\omega) = \frac{N_0 \omega_B \sinh \omega_B T}{2T (\cosh \omega_B T - \cos \omega T)} \quad (28)$$

Similarly, from eqn (23) the continuous error power spectral density is

$$S_{ee}(\omega) = S_{rr}(\omega) + S_{cc}(\omega) - \frac{2}{T} S_{rr} \operatorname{Re} \left[\frac{G_{s1}(j\omega)}{1 + G_{s1}^*(j\omega)} \right] \quad (29)$$

where (formula 30 see below)

and the coefficients are defined as follows:

$$\left. \begin{aligned} F_R(P, \omega) &= P_4 + (P_5 + P_7) \cos \omega T \\ &\quad + (P_6 + P_8) \cos 2\omega T + (P_3 + P_9) \cos 3\omega T \\ F_I(P, \omega) &= (P_5 - P_7) \sin \omega T \\ &\quad + (P_6 - P_8) \sin 2\omega T + (P_3 - P_9) \sin 3\omega T \end{aligned} \right\} \quad (31)$$

and

$$\begin{aligned} P_1 &\equiv (KQ_1 - Te^{-aT})/T \\ P_2 &\equiv KQ_2/T \\ P_3 &\equiv KQ_3/T \\ P_4 &\equiv 1 - (2 + e^{-aT})P_2 - e^{-aT}P_3 \\ P_5 &\equiv P_1 - (2 + e^{-aT})P_2 + (1 + 2e^{-aT})P_3 \\ P_6 &\equiv P_2 - (2 + e^{-aT})P_3 \\ P_7 &\equiv -(2 + e^{-aT}) + (1 + 2e^{-aT})P_1 - e^{-aT}P_2 \\ P_8 &\equiv (1 + 2e^{-aT}) - e^{-aT}P_1 \\ P_9 &\equiv -e^{-aT} \\ P_{10} &\equiv 1 + P_1^2 + P_2^2 + P_3^2 \\ P_{11} &\equiv 2(P_1 + P_1P_2 + P_2P_3) \\ P_{12} &\equiv 2(P_2 + P_1P_3) \\ P_{13} &\equiv 2P_3 \end{aligned}$$

Thus, expressions are available for computation of the power spectral density of the error and output signals of the sampled models in terms of the basic parameters of the continuous model (K , D and $\tau = 1/a$) and the additional parameters D_1 and T .

$$S_{ee}(\omega) = S_{rr}(\omega) - \frac{2}{T} S_{rr}(\omega) \operatorname{Re} \left[\frac{G_{s1}(j\omega)}{1 + G_{s1}^*(j\omega)} \right] + S_{rr}^*(\omega) \left| \frac{G_{s1}(j\omega)}{1 + G_{s1}^*(j\omega)} \right|^2 \quad (23)$$

$$S_{cc}(\omega) = \frac{\{4K^2(1 + T^2\omega^2)(1 + e^{-2aT} - 2e^{-aT} \cos \omega T)(1 - \cos \omega T)\} S_{rr}^*(\omega)}{T^2 \omega^2 (1 + \tau^2 \omega^2) [(1 + P_1^2 + P_2^2 + P_3^2) + 2(P_1 + P_1P_2 + P_2P_3) \cos \omega T + 2(P_2 + P_1P_3) \cos 2\omega T + 2P_3 \cos 3\omega T]} \quad (27)$$

$$\begin{aligned} \operatorname{Re} \frac{C(j\omega)}{R^*(j\omega)} &= \frac{-KF_R(P, \omega) [(1 + \tau T \omega^2) \cos \omega D + \omega(T - \tau) \sin \omega D]}{T \omega^2 (1 + \tau^2 \omega^2) (P_{10} + P_{11} \cos \omega T + P_{12} \cos 2\omega T + P_{13} \cos 3\omega T)} \\ &\quad + \frac{K [\omega(T - \tau) \cos \omega D - (1 + \tau T \omega^2) \sin \omega D] F_I(P, \omega)}{T \omega^2 (1 + \tau^2 \omega^2) (P_{10} + P_{11} \cos \omega T + P_{12} \cos 2\omega T + P_{13} \cos 3\omega T)} \end{aligned} \quad (30)$$

References

- ¹ McRUER, D. T. and KRENDEL, E. The human operator as a servo system element. *J. Franklin Inst.*, 267 (May 1959) 381-403; 267 (June 1959) 511-536
- ² ELKIND, J. I. Characteristics of simple manual control systems. *Lab. Rep. No. 111*, M. I. T. Lincoln Laboratory, Lexington, Mass., 1956
- ³ LICKLIDER, J. C. R. Quasi-linear operator models in the study of manual tracking. *Developments in Mathematical Psychology*, R. D. Luce (Ed.), The Free Press, Glencoe, Illinois, 1960
- ⁴ BEKEY, G. A. *Sampled Data Models of the Human Operator in a Control System*. Ph.D. Dissert., Department of Engineering, University of California, Los Angeles, January 1962. (Also published as ASD-TDR 62-36 by Aeronautical Systems Division, U.S. Air Force Systems Command, Wright-Patterson Air Force Base, Ohio)
- ⁵ CRAIK, K. J. W. Theory of the human operator in control systems. *Brit. J. Psych.*, 38 (1947) 56-61; 38 (1948) 142-148
- ⁶ NORTH, J. D. The human transfer function in servo systems, *Automatic and Manual Control*, A. Tustin (Ed.), 1952. London; Butterworths
- ⁷ WARD, J. R. The dynamics of a human operator in a control system: A study based on the hypothesis of intermittency. *Ph. D. Dissert.*, Aeronautical Engineering Dept., University of Sydney, Australia, May 1958
- ⁸ TUSTIN, A. The nature of the operator's response in manual control and its implications for controller design. *J. Instn. elect. Engrs, Lond.*, 94 (IIA) (1947) 190-202
- ⁹ RAGAZZINI, J. R. Engineering aspects of the human being as a servomechanism. *Unpublished Paper*, presented at the American Psychological Association Meeting, 1948
- ¹⁰ Goodyear Aircraft Corp. Final Report: 'Human Dynamics Study'. *GAC Rep. GER-4750*, April 1952
- ¹¹ BOOTON, R. C. The analysis of nonlinear control systems with random inputs. *Proc. Symp. Nonlinear Circuit Analysis*, 2 (1953) 369-391
- ¹² GOTTSBANKER, R. M. The accuracy of prediction motion. *J. Exp. Psych.*, 43 (1952) 26-36
- ¹³ BROADBENT, D. E. *Perception and Communication* 1958. New York; Pergamon Press
- ¹⁴ POULTON, E. C. Perceptual anticipation and reaction time. *Quart. J. exp. Psych.*, 2 (1950) 99-112
- ¹⁵ CHEATHAM, P. G. and WHITE, C. T. Temporal Numerosity, *J. exp. Psych.* 44 (1952) 447-451
- ¹⁶ CHASE, R. A. Comparison of the effects of delayed auditory feedback on speech and key tapping. *Science*, 129 (1959) 903-905
- ¹⁷ SMITH, W. M., McCARY, J. W. and SMITH, K. V. Delayed visual feedback and behavior. *Science*, 132 (1960) 1013-1014
- ¹⁸ RAGAZZINI, J. R. and FRANKLIN, G. *Sampled-data Control Systems*. 1958. New York; McGraw-Hill
- ¹⁹ MORI, M. Statistical treatment of sampled-data control systems for actual random inputs. *Trans. Amer. Soc. mech. Engrs* 80 (1958) 444-456
- ²⁰ JOHNSON, G. W. Statistical analysis of sampled-data systems. *WESCON Convention Record*, Pt. 4 (1957) 187-195

DISCUSSION

E. JURY, *University of California, Berkeley, California, U.S.A.*

This paper presents an interesting departure from the preceding one in the fact that Bekey obtains a different transfer function for the sampled-data model than Naslin. It would be interesting to ask Dr. Bekey to comment on the significance of this difference. The second point relates to the significance of the remnant in Figure 2 and whether this is attributed to the non-linearities of the system which have been ignored. Finally, what is the effect of this remnant at high frequencies?

G. A. BEKEY, *in reply*

Probably the major reason for the difference in the models presented in this paper and in the Naslin-Raoult paper is that they are obtained in different ways. The Naslin-Raoult model is based on averaging experimental results with closed-loop systems and consequent approximate determination of open-loop characteristics. My model is based on spectral analysis using a Gaussian input process.

The remnant is that portion of the operator's output not accounted for by a linear, continuous, invariant model. The addition of sampling results in an infinite number of harmonics of the sampling frequency, and thus reduces the 'remnant'. However, the remnant still contains appreciable energy, especially at higher frequencies. As pointed out by McRuer and Krendel (Reference 1 of the paper), this portion of the remnant can be due to three sources:

- (1) Non-linear behaviour of the operator.
- (2) Time-varying behaviour of the operator.
- (3) Random signals generated by the operator.

Additional research will be required before it can be ascertained whether any one or all three of these effects are involved in the remnant.

Z. BONENN, *Scientific Dept., Ministry of Defence, Israel, P.O.B. 1, Kirget Motzkin, Haifa, Israel*

All reported work on a human operator in a tracking loop is linear, i.e. using a linear control stick. However, as stressed in the two papers and in previous work (in particular Craik's work—Reference 5 of the paper) the human operator operates intermittently and cannot make more than two to three independent decisions per second. Therefore, it appears that a three-positions stick (Figure A) may be advantageous. Here, the operator has only three choices, 0, +1, -1. During the sampling interval he observes the error and decides on his next command.

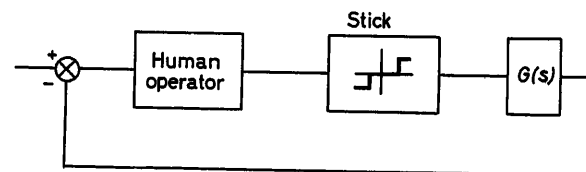


Figure A

A two-dimensional compensatory tracking system with $G(s) = \frac{K}{s^2} e^{-s\tau}$ has been simulated on an analogue computer with good results. Note that a linear tracking loop with this $G(s)$ is difficult to control. The good results obtained with this configuration depend also on the following factors:

- (1) Well-defined zero output position of control stick.
- (2) It is apparently easier to control accurately short-time durations of command in a three-positions control stick than to control accurately small angular deflections of a linear control stick.

These remarks are intended to arouse interest in the problem of the proper combination of the human operator with the controller. It seems that the best controller is not always the conventional proportional control stick.

Dynamic Analysis and Simulation of Management Control Functions

R. B. WILCOX

Summary

The dynamic behaviour of management is treated as a feedback control system with mathematical functions of management to plan, staff, organize, direct, and control an organization. Analysis and simulation of the management control functions, coupled with the organizational dynamic functions, provide a means of displaying future trends for advanced planning and decisions.

The organization is a complex machine in which feedback control is a predominant characteristic. The requirements of a project represent the directed input to the system, and the progressive accomplishment represents the output of the system. Output performance versus time is measured and fed back to be compared with the input requirements. Effective management is obtained by means of the corrective action taken to reduce the deviation between the progressive accomplishment and the project requirements.

The dynamic functions such as 'time lags', 'natural frequency', 'dead time', 'lead time compensation', etc., are expressed as performance operators, and the development of a mathematical model provides a more exacting treatment by use of control system techniques and simulation to determine the effects of various courses of action. Sampled data and adaptive control techniques are inherent in management control systems.

The basic management control function measures the degree and rate of progressive accomplishment at any given time during the course of the project. This feedback information is compared with the project requirements to establish the deviation between the desired and actual accomplishment. The deviation information is passed on to the functional operations doing the work by means of two management channels: (i) the experience channel which takes immediate and proportional corrective action required by the deviation, and (ii) the analysis and evaluation channel which requires more time to consider the situation but provides a more accurate picture; i. e., management 'sums up' the situation by integration. Analyses show that the preceding functions result in the anticipation or lead time action of management.

Mathematical models of the management control functions have been developed and simulated using analogue and digital computers. The application of these functions is investigated, using the case history of a project with effective results; synthetic techniques indicate the measures to be taken by management to improve the design of the organization and its performance. The application of this approach to other types of controllable events is explored.

Sommaire

Le comportement dynamique de la gestion d'une organisation est traité comme celui d'un système asservi, caractérisé par des fonctions mathématiques de planification, de recrutement, d'organisation, de direction, et de contrôle. L'analyse et la simulation des fonctions de commande, et des fonctions dynamiques de l'organisation commandée, fournissent un moyen de prédiction pour les planifications perfectionnées.

Une organisation est un ensemble complexe dans lequel la commande par asservissement joue un rôle primordial. Les exigences d'un projet représentent le signal d'entrée du système, tandis que les accomplissements successifs constituent la sortie du système. La performance de la sortie (fonction du temps) est mesurée, asservie, et com-

parée avec l'entrée. Une gestion efficace est obtenue grâce aux actions de correction réduisant l'écart entre l'entrée et la sortie.

Les fonctions dynamiques telles que: constantes de temps, fréquence propre, temps mort, compensation par avance de phase, etc. ... sont utilisées pour caractériser le système. Le développement d'un modèle mathématique permet l'utilisation des méthodes de commande automatique et de simulation pour déterminer les effets des différentes catégories d'action. Les commandes adaptative et par échantillonnage sont implicitement contenues dans les systèmes de gestion.

Le degré et le taux des accomplissements sont mesurés à tout instant du projet simulé. Ces renseignements sont comparés aux exigences préétablies pour déterminer la déviation. Cette dernière passe par deux canaux opérateurs: (i) le canal «expérience» qui prend des actions de correction immédiates et proportionnelles; (ii) le canal «analyse et évaluation» qui examine plus de facteurs et qui prend des actions en quelque sorte intégrales. Ces dernières présentent des caractères évi- dents d'anticipation ou de compensation par avance de phase.

Le modèle mathématique de l'ensemble est simulé sur des calculateurs analogiques et numériques. Les résultats d'investigation d'un cas pratique sont présentés. Les possibilités d'application de cette méthode sont discutées.

Zusammenfassung

Das dynamische Verhalten einer Betriebsführung wird als Regelsystem betrachtet; dabei werden Planung, Personalpolitik, Organisation, Geschäftsleitung und Überwachung eines Betriebes durch mathematische Gleichungen ausgedrückt. Untersuchung und Simulation der Überwachungsfunktion der Betriebsführung zusammen mit den dynamischen Organisationsgleichungen dienen der Darstellung zukünftiger Tendenzen als Grundlage für die fortlaufende Planung und Entscheidungsfindung.

Die Organisation wird als eine komplexe Maschine aufgefaßt, bei der die Regelung eine überragende Rolle spielt. Die Erfordernisse eines Projektes stellen die Eingangsdaten, die erzielten Ergebnisse die Ausgangsdaten des Systems dar. Die dynamischen Ergebnisse werden am Ausgang abgegriffen, rückgeführt und mit den Eingangserfordernissen verglichen. Eine wirkungsvolle Betriebsführung ist durch den Korrekturereingriff erreichbar, der die Abweichung zwischen den erzielten Ergebnissen und den Erfordernissen des Betriebes verkleinern soll.

Dynamische Größen wie Zeitkonstanten, Eigenfrequenz, Totzeit, Vorhalt usw. dienen zur Beschreibung des Systems; die Entwicklung eines mathematischen Modells ermöglicht eine genauere Untersuchung der Auswirkungen verschiedener Handlungsfolgen mit Hilfe der Regelungstechnik und durch Simulation. Abtast- und selbsteinstellende Regelung sind Merkmale der betriebswirtschaftlichen Regelsysteme. Die grundlegende Funktion für die betriebswirtschaftliche Regelung mißt laufend Grad und Geschwindigkeit der Planverwirklichung. Diese Information (Regelgröße) wird mit den Erfordernissen des Projektes (Sollwert) verglichen, um die Regelabweichung zu ermitteln. Diese wird den mit der Ausführung betrauten Stellen auf zwei Kanälen zugeleitet:

1. auf dem Erfahrungskanal, der auf Grund der Abweichung unmittelbar einen proportionalen Eingriff bewirkt und

2. auf dem Kanal zur Analyse und Berechnung, der zwar zur Erfassung der Situation länger braucht, aber dafür ein genaueres Bild ermöglicht, d. h. die Betriebsführung erfaßt durch Integration die Gesamtsituation.

Untersuchungen zeigen, daß die oben genannten Funktionen in einer Vorhaltwirkung der Geschäftsführung resultieren.

Mathematische Modelle der betriebswirtschaftlichen Regelung werden entwickelt und mit Hilfe von Analog- und Digitalrechnern simuliert. Die Anwendung dieser Funktionen wird an Hand eines tatsächlichen Falles erfolgreich untersucht. Syntheseverfahren zeigen die Maßnahmen auf, die die Geschäftsführung ergreifen muß, um die Organisation und ihr Verhalten zu verbessern. Die Anwendung dieser Methode auf andere regelbare Vorgänge wird untersucht.

Introduction

In a non-technical sense, control systems techniques have been applied for many years to management problems of guiding and controlling industrial operations. The ability of management to design the organizational structure, to assign functions and responsibilities, and to establish procedures, methods, and reporting channels has been obtained through experience in the necessary requirements for control methods and profitable operations. Alterations in the design of the organizational system and modifications of the procedures and reporting methods are continually being made to improve the overall performance of the organization. At present, management experience in 'cause and effect' is the keynote of dynamic control. Good communications and feedback are recognized as essential elements of good management.

The combination of known principles and fundamentals of communications, computers, and control used in engineering science will provide the foundations for management as a science. The management and operation of the industrial organization is a control process to which the dynamic analysis and simulation, as used in the control system technology, provides a new approach to organizational design, performance evaluation, and prediction. The industrial operation is a dynamic response^{1,2}, and the organization may be treated as a feedback control system with all control techniques of analysis and synthesis applied to control projects within the boundaries of technical tasks, schedules, and cost requirements as a three-dimensional control problem. The concept of applying feedback control techniques to engineering operations is one of relating parameters and their functions of time as applied to machines with equivalent types of parameters and time functions of the organization. Once this is determined, the analogue is interesting and revealing, and further investigation shows that the organization operates as a machine and follows natural laws of motion^{3, 4}. This fact is the basic principle of management dynamics^{5, 6}.

Feedback Control System Technology Applied to an Organization

The dynamic performance of an engineering organization may be determined from the relation of progressive accomplishment *versus* time. This relation is the key measure of the transient response of the organizational system to accomplish a particular job. Progressive accomplishment can be measured by plotting the cumulative values of such factors as degree or percentage of completion, man-months of effort, or cost to produce. Time of project performance is measured in weeks or months. A typical

transient response to a step function of a job requirement is shown in *Figure 1* and analysis of the transient curve will provide the explicit terms of mathematical operators or transfer functions which represent the dynamic characteristics. The engineering system is organized to follow management commands and produce the desired product output. Herein, the dynamics of the engineering organization is determined from the time constants and dead time experienced in past performances on similar projects. However, undesirable disturbances, both internal and external, cause the system to deviate from the linear steady-state type of operation. These disturbances are caused by the interruption of communication, indecision, human errors, lack of material or manpower, lack of standards and procedures, etc.

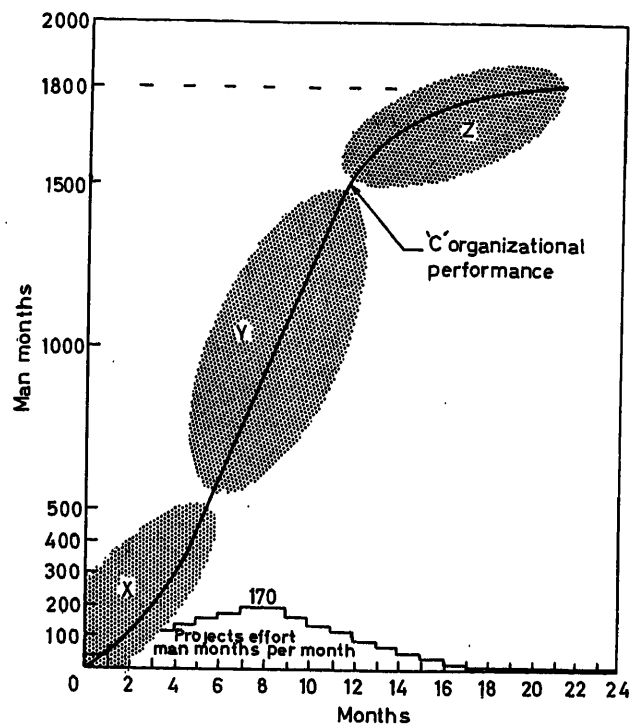


Figure 1. Typical organizational performance curve

All disturbing inputs reduce the speed of accomplishment, i.e., schedules, and the accuracy of the accomplishment, i.e., by failing to meet either specification of the product or cost. Adaptive control techniques must be continually applied to counteract these problems.

The step curve of *Figure 1* shows the effort in manpower per month needed to accomplish a specific project requirement, and the resulting cumulative effort shown by the response curve *C* is the integration of this effort. This curve is typical of organizational performance and has the response characteristics of a closed-loop system. The initial part of the curve in area *X* indicates the complexity of the system relating to the number of functional operations involved; it is of concern in getting the system to respond quickly in the beginning. Area *Y* refers to the rate output when the operation is progressing as a calibrated open-loop system. In area *Z* the deviation between accomplishment and requirement is reaching a minimum and full closed loop with maximum control is necessary; it is the final phase of the project when schedule and cost require major control action.

The performance curve is the result of basic management control functions: (1) to establish the total project requirements and tasks as the reference input which may occur as a step, rate or exponential input with later changes, (2) to define tasks and design the organization assigned to perform, (3) to monitor the progressive accomplishment, (4) to compare the resulting accomplishment with the reference, (5) to command and direct the operation upon decisions based on experience, analysis, and evaluation, and (6) to anticipate and adapt according to environment. These functions are expressed as a mathematical model which leads to the development of a management control plan for monitoring the dynamic performance of organizational systems.

A good design of the work process will reduce the managerial control required. Each task is a specified function to be performed by the functional group based on a definite input and a required output. The design of the organizational process of work flow requires that the work tasks be clearly defined with a minimum of overlap between the functional groups. This is a necessary prerequisite to reducing undesirable delay times in the dynamic process. From the task assignments, the block diagram and flow chart of the process is determined. Each task assigned to a group will represent a dynamic element of the system, and the feedback methods of reporting the accomplishment must be established.

In the design of control systems, the speed of response is improved by lead or anticipatory circuit compensation, which is analogous to 'lead time' and 'anticipation' (familiar terms to management). Other means of reducing response time of control systems are obtained by modifying the feedforward and feedback functional elements. In company operations the latter is accomplished by regrouping and streamlining the organization elements or departments, and by providing better communications with improved routines, procedures, and standards.

Mathematic Model of Organizational Process

The fundamental of the control system for the organizational process is to describe each element of the system by a mathematical expression^{7, 8}. Referring to the block diagram of Figure 2, the operating group performing the work is represented by the box in which the mathematical expression is shown. The output is the variable C , the progressive accomplishment. The output

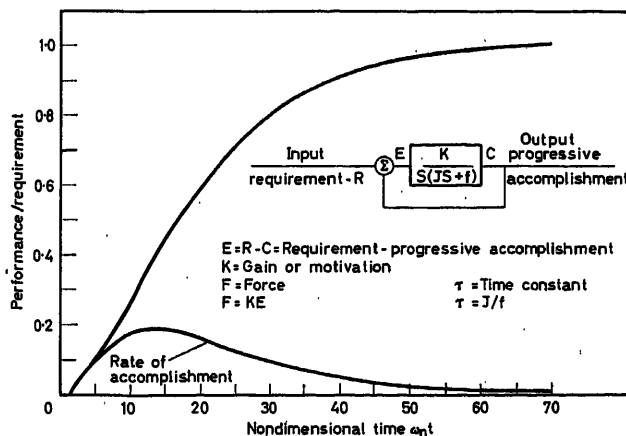


Figure 2. Mathematical model and performance

accomplishment is measured and the feedback signal is compared with input R , the reference or requirement, the difference is represented by the error or deviation signal E which commands the operation to continue until E reaches zero value. The algebraic expression for this deviation as a function of time is

$$E(t) = R(t) - C(t) \quad (1)$$

The basic algebraic expression for the operating group is derived from the differential equation relating Newtonian expressions of force or effort. The effort to accelerate a project is expressed by

$$F_1 = M\alpha = M \frac{d^2 C(t)}{dt^2} \quad (2)$$

where F_1 is force, M the mass effort, and α the acceleration of mass in terms of progressive accomplishment. The rate of accomplishment is subject to the force expression F_2 for velocity drag f

$$F_2 = \frac{f dC(t)}{dt} \quad (3)$$

The total force F available is a proportional amplification K of the deviation signal $E(t)$, such that, $F = KE(t)$. The algebraic sum of forces is $F = F_1 + F_2$ and provides the system equation

$$KE(t) = M \frac{d^2 C(t)}{dt^2} + f \frac{dC(t)}{dt} \quad (4)$$

Using the Laplace operator S instead of d/dt , and (S) instead of (t) gives

$$KE(S) = MS^2 C(S) + fSC(S) \quad (5)$$

$$\frac{C}{E}(S) = \frac{K}{S(MS + f)} = \frac{K/f}{S(\tau S + 1)} \quad (6)$$

Eqn (6) is the transfer function of the operating group and relates the output C to the error signal E with the operation time constant $\tau = M/f$. Combining eqn (6) and (1) will result in the feedback closed loop function relating progressive accomplishment C to the input requirements R :

$$\frac{C}{R}(S) = \frac{K/M}{S^2 + \frac{f}{M}S + \frac{K}{M}} = \frac{\omega_n^2}{(S^2 + 2\zeta\omega_n S + \omega_n^2)} \quad (7)$$

of the undamped natural frequency of oscillation $\omega_n = (K/M)^{1/2}$; and the damping ratio $\zeta = f/2(MK)^{1/2}$.

These equations are analogous to transfer function representation of the servomechanism. The inertia of the organization opposes the act of getting the work done; there is also friction and drag similar to that in the servomechanism. The gain K is defined as the ability to accomplish the tasks and involves such factors as manpower, motivation, efficiency, etc. of the organizational system. The time constant τ relates to the speed of responding to a task and is well known in organizations. The transient response of eqn (7) to a step function input is shown as the S curve of Figure 2 with the non-dimensional time scale $\omega_n t$, and the amplitude ratio of C/R , and represents the dynamic response of an organization relating progressive accomplishment to time. The final value of C/R reaches unity when the derivatives die out, i.e., $S = 0$, and $C/R(0) = 1$, and the output accomplishment matches the input requirements. The derivative of the S

curve is the rate of progressive accomplishment *versus* time and is proportional to the rate of effort or manpower applied to the work. Simulation of the mathematical model is used to control the dynamic response of the project.

Performance Requirements and Monitoring Signals

The control system concept must consider the signal and communication interconnections. To be controlled, the organization must follow the command and control signals, it must have a means of measuring its output, and a means of comparing the output with the input command signal to provide the deviation signal for follow-up. In order to obtain good dynamic performance from functional groups, management must provide not only proper facilities and manpower, but also the command and feedback control signals. The ultimate goal or final value of the output C is determined by the task requirements which are evaluated for the effort, cost, and schedule necessary to meet it. The complete project plan includes not only the structure and definition of tasks, costs, and schedule, but also the methods of continually monitoring and evaluating the output related to these three requirements in order to adapt the command signal E as the situation may require.

The project control problem is a three-dimensional control problem and is analogous to the three-dimensional control problem of missile guidance in roll, pitch, and yaw. In either case, roll, pitch, and yaw; or task, cost and schedule, each variable has cross coupling with the others and therefore influences them to deviate off course if a disturbance to that variable occurs. In control system design there are three main requirements to meet—speed of response, accuracy, and stability. The speed of response requirement of each functional group is set by the schedule; the quality requirement is set by the specifications; and finally, the relative stability is set by the continuous operational guidance and planning of the project.

The prime command signal is the project requirement R represented by the work statement and specifications of the customer. The input R may not occur as a step function but as a delayed function in time which will decrease the performance response. A digital computer study was made to determine the degree of response decrease due to ramp inputs. The basic

quadratic of eqn (7) was used for $\zeta = 0.8$ for different values of ramp inputs with slope $R(t) = R(t)$, $t \leq 1/R$ and $R(t) = 1$, $t \geq 1/R$. The results of the study are shown in Figure 3 which compares the dynamic response of $C(t)$ and $C'(t)$ for the step input $R' = \infty$, and two ramp inputs, $R' = 1.0$ and 0.666 . The slowdown in response caused by the ramp input is quite evident and indicates the need to establish the inputs as quickly as possible. The effect of ramp input for the actual project performance of the case under study is shown in Figure 4 which points out the comparison of the planned response with the actual response when the input requirements are delayed as shown.

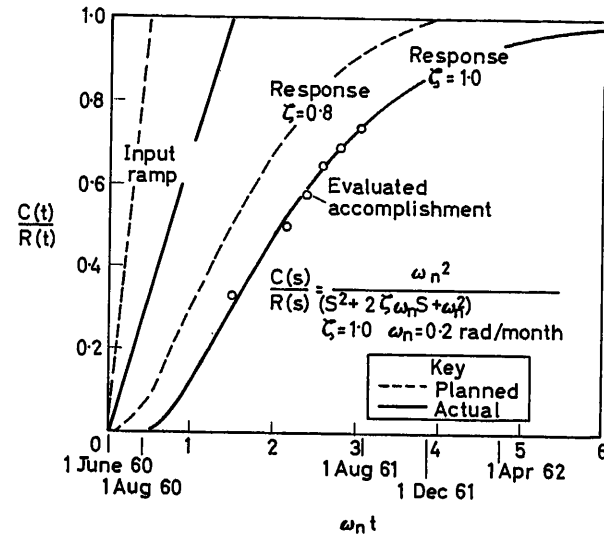


Figure 4. Project performance with ramp inputs

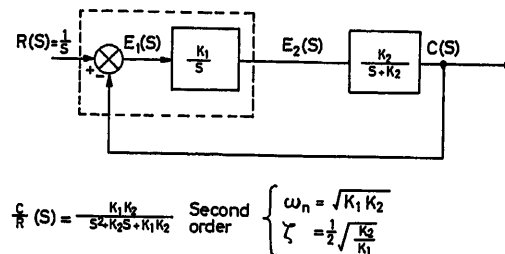


Figure 5. Block diagram of basic model

Basic Dynamic Model of Management Function

The case study of applying control system techniques to management extends the concept for analogue and digital computer simulation. In support of meeting future goals on a major project, a simplified model using linear servo theory was programmed to investigate the project response to a given set of task requirements for combined engineering and management functions, and by applying various management boundary conditions, families of responses were plotted of the results. The dynamic model used was the basic second order transfer function of eqns (6) and (7) with the management group and engineering group each representing a unit of the basic block diagram of Figure 5.

The complete management function includes the comparison of the project output *versus* the requirements as well as the man-

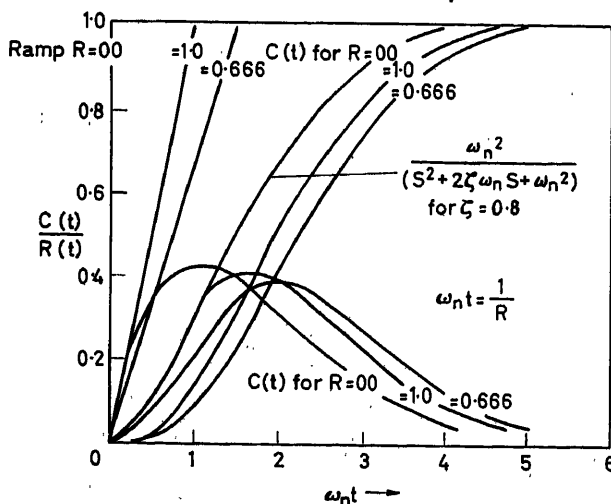


Figure 3. Performance delays with ramp inputs

agement transfer function. Both the management and the engineering transfer functions are considered linear with constant coefficients of basic model. The management transfer function is derived by considering the basic function of this group as an integrator with a transfer function of K_1/S . The integrating function is a most important contribution to the response. In the expression for management, it represents the analysis and evaluation required to integrate all inputs, to assess and sum up the situation, and thus to provide the proper control signal information, E_2 . K_1 represents the level of effort per unit of the management group and is related to and varies with the number of the personnel of the management and supervisory group weighted by the experience factors. The basic engineering transfer function is derived by considering the basic working group as an integrator with a transfer function of K_2/S where K_2 represents the level of effort per unit of the engineering group and is related to and varies with the number of engineers involved in the project. Where the management group monitors the output of its efforts, C , but compares it with the engineering inputs from management E_2 , there is a feedback path within the engineering block of Figure 5 which closes the loop on K_2/S resulting in the transfer function for the engineering group of a first-order lag with a time constant of $1/K_2$. In general, the engineering transfer functions is multi-order³.

Combining the management and engineering functions gives the basic open-loop and closed-loop functions of the project system

$$\frac{C}{E_1}(S) = \frac{K_1 K_2}{S(S + K_2)} \quad (8)$$

and

$$\frac{C}{R}(S) = \frac{K_1 K_2}{S^2 + K_2 S + K_1 K_2} = \frac{\omega_n^2}{S^2 + 2\zeta\omega_n S + \omega_n^2} \quad (9)$$

Identifying terms of the general expression in eqn (9)

$$\omega_n = (K_1 K_2)^{\frac{1}{2}}; \quad \zeta = 1/2 (K_2/K_1)^{\frac{1}{2}} \quad (10)$$

The undamped natural frequency ω_n varies as the square root of the product of the engineering and management efforts, while the damping ratio ζ varies as the square root of the ratio of the engineering and management efforts. The transient response of the second-order system is completely specified by the two parameters, ζ and ω_n , which are, in turn, completely specified by K_1 and K_2 in eqn (10), so that the latter constants determine the transient response. If it is desired to accelerate a project (increase ω_n), an increase of either the management effort K_1 or the engineering effort K_2 , or both, will accomplish this. The practical consideration for an increase in the speed of response is to increase the number of experienced personnel in both groups, i.e., $K_1 K_2$. However, the increase in ω_n is proportional only to the square root of the increased effort. Conversely, if the project is to be decelerated, a decrease in either the management or the engineering effort or the combined effort is necessary. Figure 6 shows the variation in response time as the product of engineering and management efforts change with their ratio remaining constant.

The effect of varying the damping ratio ζ shows that if the system damping is decreased ($\zeta \leq 1$) from critical damping ($\zeta = 1$), the system responds faster but will overshoot and tend to oscillate. An overdamped system ($\zeta > 1$) gives an undesirable slow response time. Figure 7 shows the variation of ζ and therefore the variation in speed of response as affected by the ratio of engineering to management efforts. For instance, if the planned response of a project is selected to follow the curve of $\zeta = 0.8$, then from Figure 7 the ordinate K_2/K_1 is obtained as 2.5. Thus, to maintain the desired response, the engineering effort must be 2.5 times the management and supervision effort.

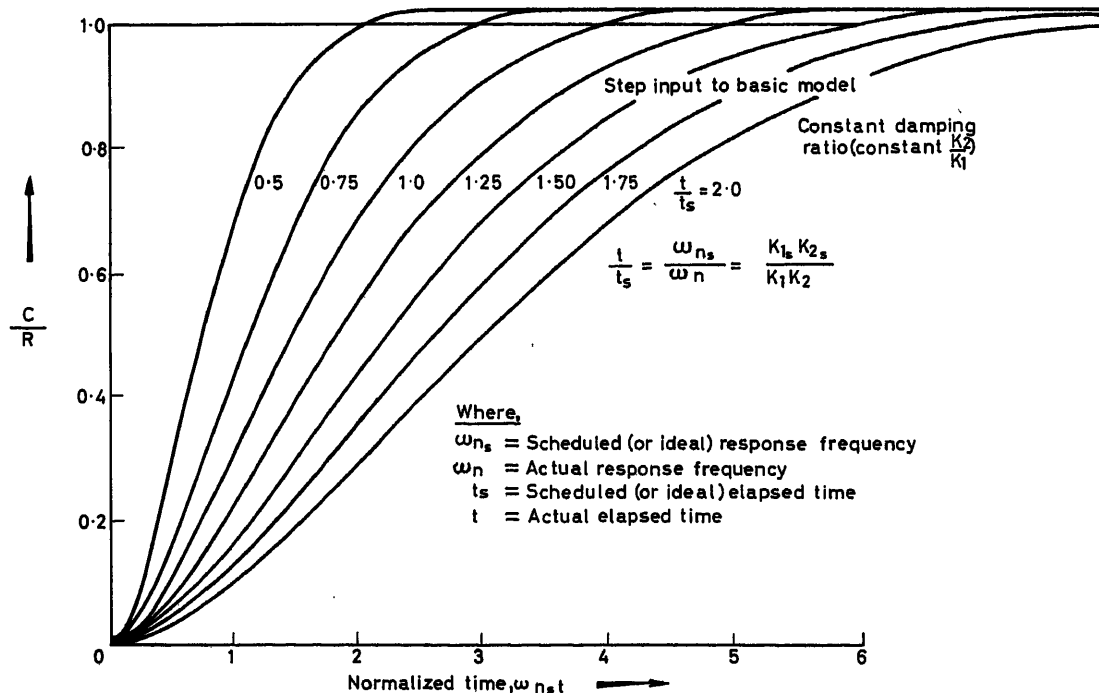


Figure 6. Effect of varying engineering and management effort

If the organization appears to react sluggishly (overdamped), an increase in the ratio of management effort K_1 to engineering effort K_2 is indicated. Note that an increase in the management effort and direction will decrease the damping ratio, ζ , and provide a quicker response throughout the project. If the useful output oscillates to any degree, a decrease in the management effort or an increase in the engineering effort is indicated. From eqn (10) when $\zeta = 1.0$ and $\omega_n = 0.2$ rad month,

$$\zeta = \frac{\omega_n}{2K_1}; \quad K_1 = \frac{\omega_n}{2\zeta} = \frac{0.2}{2} = 0.1 \quad (11)$$

$$K_2 = 2\zeta\omega_n = 2 \times 0.2 = 0.4 \quad (12)$$

Note that when $\zeta = 1$ the management effort $K_1 = \omega_n/2$. For good response, slight underdamping ($\zeta < 1$) and $K_1 > \omega_n/2$ should be used.

The general approach, using the foregoing project response planning, is to select ω_n from the total overall schedule required. For instance, if the project schedule is 22 months (Aug. 1, 1960

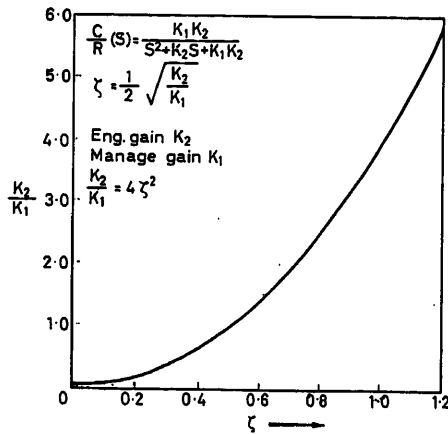


Figure 7. Ratio of engineering to management effort

to June 1, 1962) and $\zeta = 1.0$ is the desired response curve, then from Figure 12 the settling time within 5 per cent is $\omega_n(t) = 5$ with $t = 22$ months. The result is $\omega_n \approx 5/22$ or 0.23 with K_1 and K_2 determined by eqns (11) and (12). The rate of effort or cost is determined from the rate curve as displayed in Figure 1. Variations from the planned response may be corrected by using the adaptive techniques described in the next section.

Adaptive Control Applications

An actual project is scheduled for completion in 20 months as shown in Figure 8. If the ratio of engineering to management efforts is selected, then the shape of the desired accomplishment curve is defined. At 8 months the fraction of the job actually completed, C_1/R , was obtained. The project is running behind schedule and the ratio of the actual time to desired time t_1/t_{1S} to complete this part of the project is greater than unity. K_1 and K_2 must be increased in order to return the job to the desired accomplishment curve.

A series of curves has been developed from analogue computer simulation which indicates the ratio by which the K_1 and K_2 must be increased (or decreased) as a function of C/R at the time of switching and the degree of lateness t_1/t_{1S} to match the

actual curve and the desired curve at the end of 20 months, i.e., complete the job on schedule. These curves are given in Figure 9 and represent the two step adaptive control method. The three step adaptive control is obtained by acceleration of the efforts of engineering and management so that the project is on schedule at some arbitrarily selected milestone t_2 before the project completion date. The K efforts of engineering and management are then readjusted at time t_2 so that the project returns on the original desired schedule until completion.

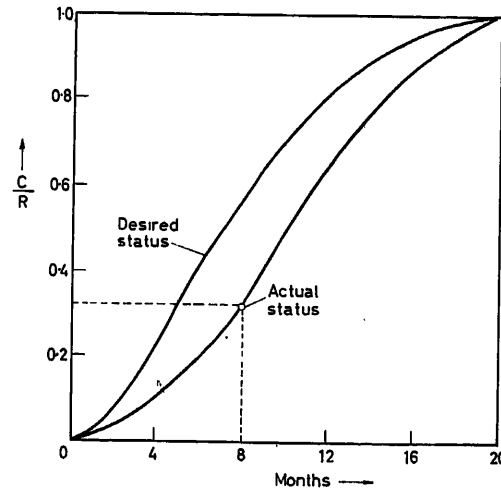


Figure 8. Project accomplishment versus time

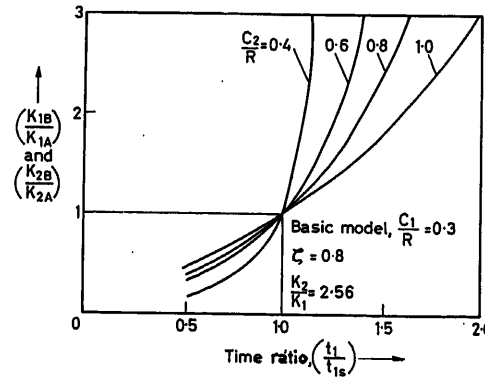


Figure 9. Correction to realign project performance

The actual performance measurement of C_1/R at a project milestone provides the data to determine the magnitude of increased effort required to realign the project at a future date. The ratio of engineering to management efforts (K_2/K_1) was obtained by taking the ratio of the number of personnel primarily contributing to engineering and the number of personnel contributing to the management function (including the managers, the project management staff, engineering supervisors, and administrators). Both efforts were weighted by years of experience and resulted in the ratio of 3.14. Substituting this value in eqn (10) gives $\zeta = 0.885$. The original planned curve had a damping ratio of 0.8. The value obtained was considered a reasonable ratio of engineering management for good performance.

The determination of the percentage of the project completed at any time is necessary for proper monitoring and control. The approach used was to subdivide the project into approximately 40 task items; each task was weighted according to its contribution to the whole project. The overall percentage completed can be obtained by summing the estimated percentage completion of each task. The fraction of the project completed at the end of 8 months was 0.321 or approximately 30 per cent ($C/R = 0.3$) as shown on *Figure 8*. At this check point, the project is running 3 to 3.6 months late and referring to *Figure 9* and for a lateness ratio (t_1/t_{1S}) of 1.8 (it took 1.8 times the desired time to achieve 30 per cent completion) the engineering management effort should be stepped up by a factor of 2.56 over the average effort of the first 8 months if the project is to end on schedule. The engineering and management staffs have been steadily increasing over the 8 months period so that the present engineering staff is now 74 while the average engineering staff was only 41. The required average engineering staff for the remainder of the project is 2.60 times 41 or 107 persons, or an increase of 33 over the present 74 to provide a greater rate of project accomplishment. Because the rate of closure on deviation in area *Z* (*Figure 1*) decreases, a straight line extrapolation would be incorrect.

Experience Functions and Effect in Management

The basic model used only the integrating term for the management function. *Figure 10* shows an expanded mathematical model of the management functions, although it must be noted that even this model is a simplification of the complex multi-loop organizational system. The feedforward path contains the integrating function K_1/S , and also a parallel function K_D which is the proportional element which is determined largely on the experience of the personnel to do the job. The mathematical result of the two functions is $G_1(S)$ is

$$G_1(S) = \frac{K_1}{S} + K_D = \frac{K_1 + K_D S}{S} = \frac{K_1}{S} (1 + \tau_d S) \quad (13)$$

In addition to the original integration function, the lead or anticipatory function of management $(1 + \tau_d S)$ has been added with a time constant K_D/K_1 . The addition of finite K_D modifies the overall response function as follows:

$$\frac{C}{E}(S) = \left(\frac{K_1}{S} + K_D \right) \frac{K_2}{S + K_2} = \frac{K_1 K_2 (1 + \tau_d S)}{S(S + K_2)} \quad (14)$$

$$\frac{C}{R}(S) = \frac{K_1 K_2 (1 + \tau_d S)}{S^2 + (K_2 + K_1 K_2 \tau_d) S + K_1 K_2} = \frac{\omega_n^2 (1 + \tau_d S)}{S^2 + 2 \zeta_d \omega_n S + \omega_n^2} \quad (15)$$

where

$$\zeta_d = 1/2 (1 + K_D) K_2 / K_1 = \frac{\omega_n}{2 K_1} (1 + K_D) \quad (16)$$

Comparing eqn (16) with eqn (10), the undamped natural frequencies ω_n are identical although the damping ratio ζ_d differs by the factor $(1 + K_D)$. However, since K_D is small, i.e., $K_D \ll 1$, $\zeta_d \approx \zeta = \omega_n / 2 K_1$. Essentially, the quadratic factors of the two analytical results are the same and the increase in the responses shown in *Figure 11* is due to K_D in the $(1 + \tau_d S)$ factor.

The principal effect of the experience parameter K_D is the increase in speed of response of the progressive accomplishment. Referring to the block diagram of *Figure 10*, it is seen that K_D takes immediate and proportional corrective action required by the deviation between the requirements R and the accomplishment C . The combination of this experience channel with the integrating channel provides the lead or anticipatory action with the total result that these management functions provide faster action because of the desirable advanced planning feature. This analysis indicates the dynamic value of experience in the management function.

The Rate of Progressive Accomplishment

In the measure of progressive accomplishment, management requires two main reports in the feedback channel. The first is

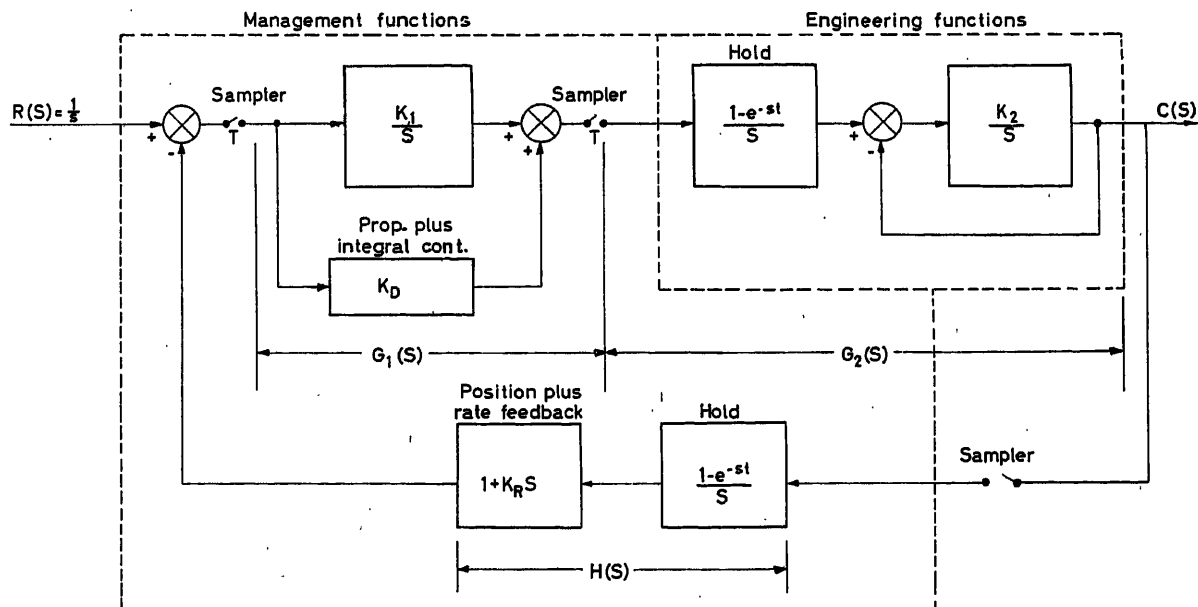


Figure 10. General basic model

the actual position of the project with respect to time represented by the degree or per cent complete; and the second is the rate of accomplishment represented by the slope of progress since the rate of expenditure or effort may be too fast or too slow. This management function in the feedback channel is $H(S) = 1 + K_R S$ where the 1 is the measurement of position, and the $K_R S$ is the measurement of rate or slope. The signal of their sum is fed back to compare with the input requirements R .

The transfer function, with rate feedback, modifies the basic mathematical model ($K_D = 0$) as follows:

$$G(S) = \frac{C}{E} = \frac{K_1 K_2}{S(S + K_2)} \quad \text{and} \quad H(S) = 1 + K_R S \quad (17)$$

$$\frac{C}{R}(S) = \frac{K_1 K_2}{S^2 + (K_2 + K_1 K_2 K_R) S + K_1 K_2} = \frac{\omega_n^2}{S^2 + 2\zeta_r \omega_n S + \omega_n^2} \quad (18)$$

where

$$\omega_n = (K_1 K_2)^{\frac{1}{2}} \quad \text{and} \quad \zeta_r = \frac{\omega_n}{2K_1} (1 + K_1 K_R) \quad (19)$$

Eqn (18) is of the same form as the model for the basic system, and actually the gain parameters establish the same natural frequency of the system; $\omega_n = (K_1 K_2)^{\frac{1}{2}}$. Comparison with eqn (10) shows that ζ_r has an additional factor $K_1 K_R$. For the same ω_n the damping ratio ζ_r increases as K_R increases, thus providing slower response to the system. $H(S)$ with rate feedback, then becomes the stabilizing or caution element of the management system.

Eqn (18) may be displayed in a different form by consideration of $GH(S)$ as the open-loop equation for unity feedback when the loop is closed, with the additional element $1/H(S)$ appearing in series. These two equations become

$$GH(S) = \frac{K_1 K_2 (1 + K_R S)}{S(S + K_2)}, \quad \frac{1}{H(S)} = \frac{1}{(1 + K_R S)} \quad (20)$$

The first transfer function contains $(1 + K_R S)$ in the numerator when compared to the basic system—this is the anticipatory action provided by measuring the rate of accomplishment. The stronger the K_R the more pronounced is the lead factor. The second function is the integration caused by evaluating and summing up or sizing up the situation. The two functions together tend to give an overall slowing down effect by increasing the damping effect of the parameter ζ_r . The slowing

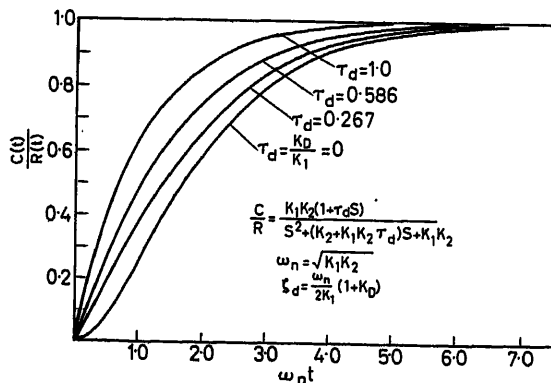


Figure 11. Experience effect on performance

down effect of K_R on the response curve is counteracted by management experience K_D as seen in Figure 11. Although the system is more stable, it is approaching the final value with caution and additional risk is indicated.

Management Control and Project Performance

Analyses and simulations of the management control functions were studied separately and combined. A major project of nearly two years' duration was used as the test case, and many families of response curves obtained as the essential parameters were varied. The responses were used in predicting future trends for management advanced planning. Assuming the sample and hold circuits provide continuous signal flow, the block diagram of Figure 10 is used to obtain the overall relation of accomplishment to requirements

$$\frac{C}{R}(S) = \frac{G_1 G_2(S)}{1 + G_1 G_2(S) H(S)} \quad (21)$$

Substituting the management and engineering functions for G_1 , G_2 , and H ;

$$\frac{C}{R} = \frac{K_1 K_2 (1 + \tau_d S)}{(1 + K_D K_2 K_R) S^2 + (K_2 + K_2 K_D + K_1 K_2 K_R) S + K_1 K_2} \quad (22)$$

and

$$\omega_n = \left(\frac{K_1 K_2}{1 + K_D K_2 K_R} \right)^{\frac{1}{2}}, \quad \zeta_r = \frac{\omega_n}{2K_1} (1 + K_D + K_1 K_R) \quad (23)$$

In the combined case, the frequency ω_n has the factor $K_D K_2 K_R$ which did not occur in the separate studies. However, in all practical cases $K_D K_2 K_R \ll 1$ and affects ω_n by less than 2 per cent such that $\omega_n = (K_1 K_2)^{\frac{1}{2}}$. The effect of K_D on the damping ratio ζ_r is negligible, but contributing to increased damping is the term $K_1 K_R$ due to the rate feedback.

The final result of the performance response shows that the primary determining factors are $K_1 K_2$. The increase in response tendencies due to K_D , and hence $\tau_d S$, is counterbalanced by the decrease in response effected by the $K_R S$ function. The theoretical and actual performance results are shown in Figure 12. Correspondence between the two curves is excellent through the midcourse, and varies only a few per cent in the final stages when full closed-loop control is having its major effect on reducing the deviation. Theoretically, the quadratic curve of $\zeta = 1.0$ reaches final value at $\omega_n t = \infty$. It is desirable to complete the project before ∞ . The increased response toward the end is caused by the decrease in the engineering activity (K_2) with a slower decrease in the management functions (K_1) thus decreasing ζ slightly. In this case, ζ decreased from 1.0 to about 0.9.

The actual accomplishment curve of Figure 12 shows that total project schedule was 22 months, and $\omega_n t = 5.1$. From these data

$$\omega_n = \frac{5.1}{22} = 0.23 \quad \text{and} \quad \omega_n^2 = K_1 K_2 = 0.0529 \quad (24)$$

From eqn (10)

$$K_1 = 0.116, \quad K_2 = 0.456 \quad \text{and} \quad \frac{K_2}{K_1} = 3.94 \quad (25)$$

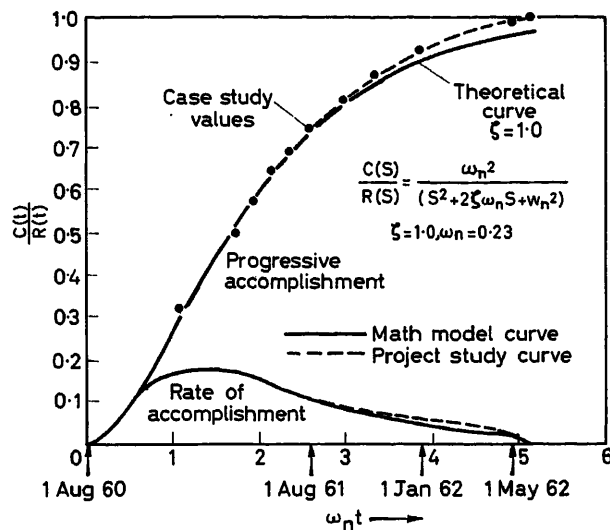


Figure 12. Project performance response

The equivalent relation of the basic model for $\zeta = 1.0$, $\omega_n = 0.23$, and the general model gives the counterbalancing effect of τ_d and K_R since

$$2\zeta\omega_n - \omega_n^2\tau_d = 2\zeta\omega_n \quad (26)$$

$$0.46(1 + 0.116 K_R) - 0.0529\tau_d = 0.46$$

$$K_R \approx \tau_d | K_D = 0 \quad (27)$$

For $\tau_d = 0.2$ the numerical equation from eqn (22) is

$$\frac{C}{R}(S) = \frac{0.0529(1 + 0.2S)}{S^2 + 0.481S + 0.0529} \quad (28)$$

Eqn (28) is the mathematical model of the project performance and the resulting response very closely matches the actual performance curve of Figure 12.

Conclusion

The application of feedback control technology to organizations and management shows that the combined resources of machines, materials, men, and money for performing tasks may be expressed as a mathematical model. Computer simulations

of the time predictions of accomplishment and performance may be analysed and evaluated so that decisions and corrective action can be taken in the early phases of the programme to counteract possible trouble areas before it is too late. By using mathematical model synthesis, the effect of varying the resources for future plans and requirements can be simulated in support of management decision making and control. The case study described is only one of a dozen similar investigations which were made with good results.

The association of feedback control techniques with cybernetics by Wiener⁹, economy by Tustin¹⁰, and industrial dynamics by Forrester⁸ supports the use of control technology applied to organizations and management to do work by a definite dynamic pattern. The mathematical concept of management control may be applied to the fulfilment of other types of requirements which, in general, are controllable events. The scope of controllable events extends from the individual, group and company, through major national and international events related to the control of economy, labour and effort, product, and growth. Investigation indicates that the dynamic behaviour of controllable events may be analysed and simulated by the control theory developed for mechanized systems.

References

- CAMPBELL, D. P. Dynamic behavior of linear production systems. *Tech. Engng*, April (1953)
- FORRESTER, J. W. Industrial dynamics—a major breakthrough for decision makers. *Harvard Bus. Rev.*, July–August (1958)
- WILCOX, R. B. The application of feedback control techniques to organizational systems, IRE Paper No. 60AC-6; at the Joint Automatic Control Conference, MIT, September, 1960. *Trans. Inst. Radio Engrs*, PGAC, AC-7 (1962)
- KATZ, A. Operations analysis of an electronic systems firm. S.M. thesis for MIT School of Industrial Management (1958)
- WILCOX, R. B., and PHOENIX, W. H. Principles of management dynamics. Presented at the Annual International Meeting, College of Research and Development, The Institute of Management Sciences, Brussels, August 26 (1961)
- MALCOM, D. G., ROWE, A. J., and MCCONNELL, L. F. *Management Control Systems*. Section VI; Research in Management Control System Design. 1960. New York; Wiley
- BEEN, S. *Cybernetics and Management*. 1959. New York; Wiley
- SIMON, H. A. *Models of Man*. 1957. New York; Wiley
- WIENER, N. *Cybernetics*. 1948. The Technology Press and Wiley
- TUSTIN, A. *The Mechanism of Economic Systems*. 1953. Harvard University Press

DISCUSSION

R. J. REDDING, *Constructors John Brown Ltd., 20 Eastbourne Terrace, London, W. 2., England*

I welcome Mr. Wilcox's paper because it deals with the automation of management which seems to me to have potential gains as great as those for the automation of production processes.

Control and optimizing techniques are being applied in the U.K. to the construction of large industrial projects (e.g. the building of power stations, chemical plants, etc.). Originally, critical path analysis was evolved for military projects and dealt only with 'time to completion'. This has been extended to cover the cost of execution and to take into account the limitations of resources (men, machines and materials). Cost optimizing procedures for the allocation of resources, and the equalization of load curves for a number of projects are in use but the calculations are tedious unless a digital computer is used.

The details forming the estimate of time and cost on which the contract was placed forms the 'model' of the process and the time-cards of workmen and the accounts (bills) for hire of machines, material, etc., form the 'feedback' information which, suitably processed, monitors performance against estimate and permits 'management by exception' and the earliest application of corrective action.

R. B. WILCOX, *in reply*

The critical path method and the performance evaluation and reporting technique (PERT) has been used to obtain the 'S'-curve response from the logic network of activities and events. Each activity and task is assigned a percentage of its contribution to the total project, and as the activities are completed we are able to assess the degree of

percentage completed and thus to obtain the progressive accomplishment curve. A brief description of this work is given in Reference 5 of the paper.

D. A. BELL, *AMF, British Research Laboratory, Blounts Court, Sonning Common, Reading, Berkshire, England*

The human being is a notoriously variable quantity, both as between one individual and another and for one individual at different times. Where large numbers are involved (e.g. life insurances), the variability can be averaged out, and mathematical models are obviously applicable to large products. I am, however, astonished that a mathematical model can predict the progress of a project of six man-months, which cannot involve many individuals. Is this an example of Dr. Auerbach's suggestion that human beings are beginning to behave more like computers?

R. B. WILCOX, *in reply*

I would not claim that this is an example of Dr. Auerbach's suggestion; however, I would like to point out that management has organized the logical steps of production to such a degree that the organizational network compares with the computer network. Computers and automation have aided very greatly in this respect. Of course, the human being is a part of the total network and his behaviour is tailored to organizational demands.

M. SEAMAN, *Department of Industrial Engineering and Management, College of Advanced Technology, Loughborough, Leicester, England*

This paper mentions the condition of combining functions to reduce time delays.

My group at Loughborough College has examined the combination of functions not only from the point of reducing time delays but also to multiply the effectiveness of existing resources.

In the series Design-Planning, Investment and Production Control and Statistics, the effective combination of design-planning, investment and positive-value production control will produce a vitally

different model in the relation between management and engineering functions. This depends on the full development of algorithmic languages with value judgements.

L. LONDON GOODMAN, *E.D.A., 2 Savoy Hill, London, W.C. 2., England*

May I suggest that we could run into considerable danger from these approaches, as they can be very misleading. For example, this paper covers administration which is only a small part of the management spectrum.

I would also stress that such approaches can have a grave effect upon young minds. Human beings are human beings and will never be amenable to mathematical analysis.

R. B. WILCOX, *in reply*

This paper represents a tool for the direction and control of assigned tasks within a company. Whether we call it administration or management is not pertinent, although it is recognized that the total management function covers many other activities in our complex industrial world. As a tool it will allow management more time to consider other facets of the business. This latter point is where the young will step in and direct their attention to other management matters. As for the mathematical analysis of human beings I think it will in some instances improve our lot in life.

E. B. STEAR, *Leon Siegler Inc. Research Laboratories, 3171, South Burdy Drive, Santa Monica, California, U.S.A.*

Did you carry out your study of case histories after the fact or before the project began?

R. B. WILCOX, *in reply*

The work is reported as a case history but the mathematical model used to predict the performance of *Figures 4 and 12* was carried out at the beginning of the project.

Outline of a Control Theory of Prosthetics

R. TOMOVIC

Summary

In the first part of the paper a unified theoretical approach to some problems of improved prosthesis design is proposed. The basis for this approach is sought in automatic control and information theory.

In the second part the conventional identification problem in the synthesis of automatic control systems is treated in a more general way. It is shown that in some automatic control systems the identification by the shape and surface characteristics of objects is needed. A mathematical model to perform such an identification is presented.

Remark: This paper is accompanied by the demonstration of the electronic hand prosthesis carried by an amputee.

Sommaire

La première partie de l'article expose une approche théorique unifiée de certaines problèmes relatifs à l'amélioration de la conception des prothèses. La base de cette approche est recherchée dans la théorie de l'information et de la commande automatique.

Dans la seconde partie, le problème classique de l'identification dans la synthèse de systèmes de commande automatique est traité de manière plus générale. On montre que dans certains de ces systèmes l'identification des objets par des caractéristiques de forme et de surface est nécessaire. On présente un modèle mathématique réalisant une telle identification.

Remarque: Cet article sera accompagné de la démonstration de la prothèse de main électronique portée par un amputé.

Zusammenfassung

Im ersten Teil des Aufsatzes wird ein zusammenfassender theoretischer Zugang für einige Probleme beim Entwurf besserer Prothesen dargestellt. Als Grundlage hierzu dienen die Regelungstechnik und die Informationstheorie.

Im zweiten Teil wird das üblicherweise gestellte Erkennungsproblem bei der Synthese von Regelungssystemen in allgemeinerer Form behandelt. Es zeigt sich, daß bei einigen Regelungssystemen die Erkennung der Form und der Oberflächeneigenschaften eines Objektes nötig ist. Ein mathematisches Modell für eine solche Erkennung wird vorgelegt.

Anmerkung: Bei diesem Vortrag wird ein Amputierter seine elektronisch arbeitende Handprothese vorführen.

Introduction

Prosthetics has been treated, until recently, mainly as a branch of medicine; its relations with engineering were limited to mechanical and some electrical studies. The progress of automatic control has brought up the question of its application to prosthetics¹⁻³. First achievements in this direction are very promising yet they were limited in scope. The intention here is to examine, on a much broader basis, the role in prosthetics to be played by automatic control theory. Instead of studying a definite prosthetic device, attention is directed at general scientific principles involved in the design of prosthetics. It is shown that automatic control can contribute in an important way to laying down a sound basis for improved design of

prosthetic devices; prosthetic devices here being defined as applied to human extremities.

There is no doubt that many aspects of hand and foot prosthetics are different; but, looking from a deeper point of view, there are also important aspects in common. These common problems become specially evident when using control theory approach. In addition, the common ties relating the prosthetics of human extremities and remotely controlled manipulators or vehicles come clearly to the foreground in this way. A deeper insight into the common problems of all these fields has hardly existed. However, the task of handling materials in hostile environment is currently getting more and more important so that the solution of this problem, in itself, is of considerable interest. Thus, in many instances where a prosthetic device is mentioned in this paper, it should be extended to remotely controlled manipulators as well.

The Control Problem

The problem of controlling a prosthetic device can be treated in a general way. However, to make the understanding easier, consider the hand and arm control. Being even more specific, the process of lifting an object of arbitrary shape will be analysed. A closer examination shows that in the above action three different levels of control can be found. The first loop involves visual feedback and takes care of hand positioning with relation to the object. Since the arm consists of several mechanically independent units (upper arm, elbow, lower arm, wrist joint) which have their own degrees of freedom, the need arises to coordinate the movements of individual arm parts to perform the positioning action as a whole. Finally, when the hand has been brought into touch with the object, the grasping action can start.

From the control point of view, the grasping action can be divided into the following phases: (a) hand adjustment to the arbitrary shape of the object, (b) locking of the hand in the hold position, and (c) adjustment of the pressure to keep the object in the hand.

Again, it should be remembered that this is not the explanation of the biological control system, which must be treated by other means. At best, only intuitive ideas of how to look for a better explanation of biological phenomena may be gathered in this way.

Consider first problem (a), i.e., automatic hand adjustment to the shape of an object. It is well known that this problem has hardly been solved in the existing prostheses or remotely controlled manipulators. Some thought has been given to the use of electronic computers for this purpose. In certain automatic production lines the objects of strictly limited shapes must be handled. In such a case a stored programme computer directing the manipulator may represent the solution, but it is clear that this solution becomes easily obsolete if shapes are varied to a larger extent or if they are not known in advance. Using this

example it will be shown that by treating the problem from a completely different point of view the general case of objects of arbitrary shapes can be solved in a simple way. The basis for this solution will be found in communication and control theory.

When studying a control system one usually begins with the block diagram explaining its structural set-up. Thus a servo-mechanism may be considered as having the following elements: input, amplifier, stage, actuator. This is represented in *Figure 1*. Assuming that the artificial hand with its fingers represents a positioning servo-mechanism¹ one can ask what is the basic difference compared with the diagram of *Figure 1*. In *Figure 2* the diagram of prosthesis control is shown. In contrast to *Figure 1* it is seen that now the control signal source is linked via the communication channel to the actuator. In addition to

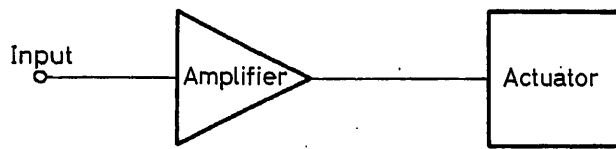


Figure 1

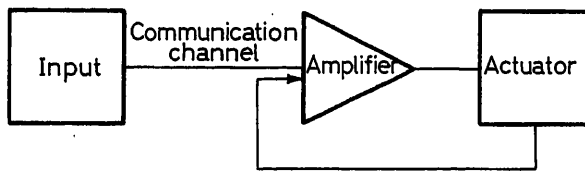


Figure 2

remotely sent control signals, there is also a local feedback loop with input signals produced on the spot. With the existing engineering knowledge it is not difficult to reproduce mechanically the form and movements of the hand, but the real problem is how to supply adequate control signals. As is known, the supply of control signals by muscular movements and by bio-electrical means was not very successful. With all the improvements in prosthesis design only a few elementary hand movements could therefore be reproduced. The adequate supply of control signals for prostheses and manipulators is still a very important problem to be solved.

A closer study of the role of skin sensitivity to pressure, temperature and other stimuli may give a hint for the solution. Returning to *Figure 2* one can easily understand that it is highly desirable to obtain maximum hand flexibility with minimum signals supplied by the remote source. In the case of long communication channels, this will mean a reduced channel capacity if remote handling of materials is in question, or a reduced burden on the part of the amputee if prosthesis control is concerned. In order to discuss the question in a more precise manner, consider the set of signals S_1 which must be provided by the control source in order to position the fingers. Taking each finger as a separate automatic positioning system, the source must provide five continuously varying signals

$$e_s = f_s(x), \quad s = 1, 2, \dots, 5$$

where x is the parameter defining finger position. For simplicity reasons the finger is considered as a dynamic system with one

degree of freedom, i.e., as a rigid body with no lateral movements and phalanges. Even in this case the set of control signals

$$S_1 = \{e_1, e_2, e_3, e_4, e_5\} \quad (1)$$

is quite complex. Since the word complexity of the set S_1 is of intuitive nature it needs additional explanation. Remembering that the control of the prosthesis is also a communication problem, the complexity of S_1 will be measured by the information content of signals e_s . Designate the information content of e_s by i_s , so that the information content I_1 corresponding to S_1 is

$$I_1 = \sum_{i=1}^5 i_s$$

An explicit value of I_1 is not needed here. Remember only that human hand control consists of 24 different muscle groups.

It is clear that the prosthesis control problem cannot be solved in a satisfactory manner by conscious control signals. Such control is in evident contrast with the basic design condition for prostheses, and manipulators to keep I_1 as low as possible. The solution of keeping I_1 low by reducing hand flexibility is naturally not acceptable since it badly limits the performances of the prosthesis. In the absence of a better solution this has been done in the existing models. Thus a new approach is needed. The first results, taking into account the requirement that $I_1 = I_{\min}$, can be found in previous papers². The fundamental idea is to keep I_1 low without affecting hand performances. The problem has been solved by dividing the control signals into two sets: S_1 and S_2 . The signals S_1 are centrally or remotely produced and transmitted via the communication channel, while signals S_2 are locally generated, i.e., at the receiver end. The information content of S_2 is I_2 and the total information available

$$I = I_1 + I_2 \quad (2)$$

The simple fact of dividing control signals in S_1 and S_2 allows for a great reduction of channel capacity, and consequently keeps the 'burden' on the central control source low without affecting hand performance.

Eqn (2) needs explanation, namely, the control signals S_2 should be generated in such a way that the required adaptation to the shape of objects is obtained. In order to understand how this can be done two new concepts must be introduced. In the first place a topologically equivalent mechanical system of hand and finger movements is needed. The aim is to obtain a simple and symmetric mechanical structure equivalent to the human hand with regard to its capacity to handle objects of various shapes. *Figure 3* shows such an equivalent and sym-

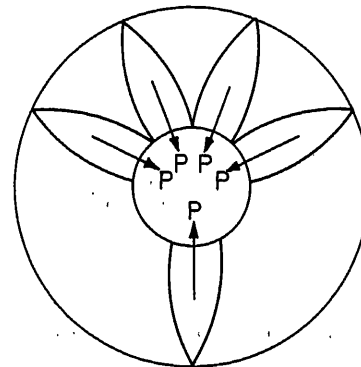


Figure 3

metric model, consisting of five elastic segments which can be rotated around the central ring. An elastic segment is required for holding objects against a rigid segment, with two or more sections rotating around individual joints. Each segment is provided with a fixed cable along which a central force P can be applied. Actually all five cables may represent five branches of a central cable so that the model is activated by the application of just one force P :

$$P_0 = 5P$$

The force P_0 is directed perpendicularly to the plane of the drawing. It is further supposed for simplicity reasons that the joints of all segments lay on the perimeter of the circle with radius R .

The elastic mechanical model of *Figure 3* is, for study purposes, equivalent to the human hand, and it is easy to see that objects of arbitrary shape can be grasped by this system if one first assumes that a ball, of radius r , is placed in the centre of the mechanical model. The only condition which should be satisfied in order that the object remains in the 'hand' is

$$r \leq R \quad (3)$$

If the friction between surfaces is assumed, the condition (3) becomes less strict.

The problem of holding the object of arbitrary shape with the model of *Figure 3* can always be reduced topologically to condition (3). In the case of irregular shape the radius r in (3) means the radius of the smallest sphere described around the object. It should be remarked that the uneven disposition of segments along the perimeter of the central ring allows for holding of objects of elongated shapes like pencils, for instance.

Another new concept, which in grasping actions helps to reduce I_1 in eqn (2), is the sensitivity of the actuator to external stimuli. For instance, the instant of touching an object with hand prosthesis must be recorded not only by visual signals but also by pressure sensitive elements. The application of pressure-sensitive elements to prostheses is quite simple³. However, this new concept facilitates greatly the control problem by reducing the information content of the central control unit. The application of sensory elements to prostheses and remotely controlled manipulators adds actually a new local information source which can be used for object identification or local motor control. The information content of signal source I_2 is thus increased while I_1 is kept low. This redistribution of the information content of control signals I_1 and I_2 is not affecting hand performance but saves channel capacity and reduces the need for frequent intervention of the central control unit. The hand being demonstrated at this conference handles, therefore, objects of completely arbitrary shapes requiring, however, only one bit of information being produced by the amputee.

Object Identification

In the previous paragraph it has been explained how the special mechanical structure of the actuator of the positioning servo-mechanism simplifies the remote control of the prosthetic device or manipulator. The coverage of the control part of the servo-mechanism by sensory elements served the same purpose. The considerations here will be limited to pressure sensitive elements, although the basic conclusions apply to temperature, radioactive or other type of sensory transducers.

The difference between a sensory element and an ordinary transducer should be clearly defined. The basic characteristic of a transducer is to establish a one-to-one correspondence between two different physical quantities. In most cases, and this will be understood here, the output of the transducer is electrical quantity, voltage or current. The equation of the transducer may be written in the following form

$$e = f(p) \quad (4)$$

where e is the voltage, and p the pressure in our case. A sensory element or surface as understood here, differs in some important aspects from the above definition of the transducer. The symbolic representation of the pressure sensitive surface is seen in *Figure 4*. The surface represented in *Figure 4* should be understood as a piece of the 'skin' with pressure sensitive cells. Each cell, upon touch, gives a voltage output proportional to $e_{rs}/j = f(p)$. It is not important that all functions $f(p)$ be strictly identical. A practical version of such a sensory surface can be realized in different ways.

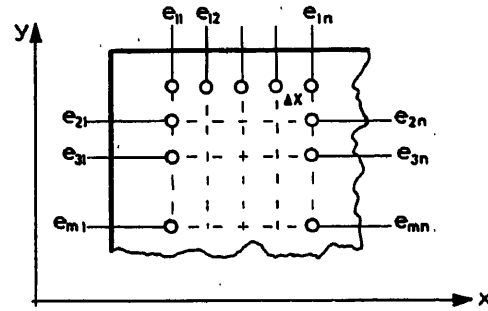


Figure 4

The difference between the conventional transducer and sensory surface can best be grasped by establishing the equation of the sensory surface

$$e = f(p, x, y) \quad (5)$$

When compared with eqn (4), one sees immediately that the sensory elements provide, in addition to intensity of the stimulus, information about the spot of its application. Thus, from the point of view of information content, new dimensions are added when a set of transducers is geometrically ordered in space.

Eqn (5) needs a refinement which is quite important. Namely, the set of transducers is discrete so that the equation of the sensory surface corresponds exactly to the following form:

$$e = f(p, r \Delta x, s \Delta y) \quad \begin{matrix} 0 \leq r \leq n \\ 0 \leq s \leq m \end{matrix} \quad (6)$$

An important conclusion obtained from eqn (6) is that the resolution rate in x and y is finite. This fact corresponds with the actual situation in biological systems where resolution rates of sensory elements are always finite. How this fact allows extraction of important informations about the object held in the hand, is now explained; only informations flowing directly through the communication channel of *Figure 2* are in mind, and not those which can be obtained, for instance, by direct or remote visual examination of the object.

The first kind of object identification made possible by sensory elements eqn (6) regards the shape. When the artificial

hand, covered with the pressure sensitive surface, is closed around an object, a one-to-one correspondence between the electrical waveform and the shape of the object is established. This fact can best be understood by taking two characteristic geometric forms. It is assumed that objects to be identified by the artificial hand have circular and rectangular cross-sections as represented in Figure 5(a) and (b). Associated waveforms for the two types of shapes are seen in Figure 6. It has also been assumed that r is variable but $s = s_0$, is fixed. The restriction is not important. If different y sections of the hand are taken then the waveforms of Figure 6 become functions of s as well. They may or may not be identical, depending on the fact if the object keeps cross section unchanged along y axis. The correspondence of electrical waveforms in Figure 6 with object shapes in Figure 5 is evident from eqn (6). Namely, in the case of the circular cross section more or less the whole surface is equally exposed to pressure. Thus, $e = \text{const.}$ for all r . The

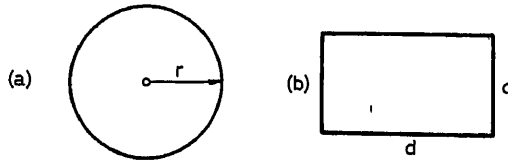


Figure 5

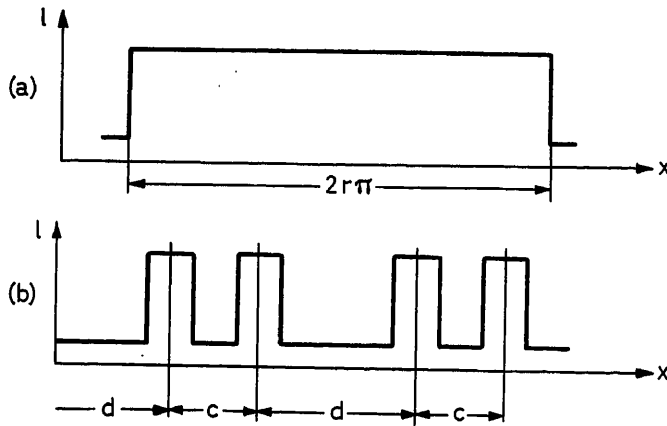


Figure 6

constant voltage output for circular cross section requires an even hand surface, but a slightly uneven hand surface will not affect the object identification. In this case the parts of the hand which are not in contact with the object will provide for a gap in Figure 6(a). Since there is a large amount of redundancy in this identification process, the general information obtained will be adequate even if an ideally flat sensory surface is not assumed. In the case of cross section with the edges, however, there will be, ideally, two subsets of r

$$\begin{aligned} R_1 &= r_\alpha \quad s = s_0 \\ R_2 &= r_\beta \quad s = s_0 \\ R_1 + R_2 &= R = \{r_\alpha, r_\beta\} \end{aligned} \quad (7)$$

The location of r_α corresponds geometrically to the spots of hand contacts with the edges of the object, and r_β is the com-

plementary set of R with respect to R_1 . Now, the equation of the characteristic waveform reads

$$\begin{aligned} \text{if } r \in R_1 \quad e &= 1 \\ \text{if } r \in R_2 \quad e &= 0 \end{aligned}$$

Examination shows how this information regarding object shape can be sent back to the central control place by the communication channel of Figure 2. The problem is technically trivial since one needs a two-dimensional scanning system. To make it clear, refer to the sensitive hand surface in Figure 4. Since for the purpose of pure shape identification only the distinction between activated and non-activated spots is important, the output of the artificial hand surface is a binary matrix $e_{rs} = 1$ or 0, according to eqn (7). The transmission to the remote control place is simply solved, for instance, by a magnetic core selection matrix.

A further interesting tactile information may be obtained from the pressure sensitive surface. That is, if the number of object edges is increased the distinction between circular and polygonal shapes will be lost. If the resolution rate is correspondingly increased, i.e., $\Delta x \rightarrow 0$, one will be able to map into the electrical form the roughness of the surface with which the hand is in contact. Thus, the waveform of Figure 6(b) contains both the information about shape or roughness of the object depending on the resolution of the sensory surface, i.e., the magnitude of Δx . Although these two tactile effects are distinct from the sensory point of view, mathematically they are equivalent; the only difference being the order of magnitude of Δx . Actually both effects are the consequence of the discrete structure of the sensory surface. An important condition for practical realization of such a discrete pressure sensitive surface is a high resolution rate of individual transducer elements. This implies the mechanical isolation of the adjacent elements so that they can react in a distinct way, although being geometrically close. One is led therefore to the design of very thin elastic surfaces.

At the beginning of the paper it was outlined that the principles exposed here have general significance. Besides their theoretical value of giving mathematical insight into the problem of remote object identification without visual feedback, there are other fields of application. Namely, in the existing foot and leg prostheses the role of the shape identification of the ground for control purposes has been completely neglected. However, the application of the pressure sensitive discrete surface of Figure 4 allows easily the coordination of different phases of human gait according to which part (front or back) of the foot is in touch with the ground; further, hitting of obstacles can easily be detected in the electrical form and used for control purposes as well. The idea of object identification by sensory elements exposed here can therefore be exploited for variety of control purposes.

In the design of hand prostheses evidently there is no need for object identification by tactile feedback since it is more simple to use visual information for this purpose. However, in the remote handling problems, due to the fact that communication capacities may become critical, the relative importance of tactile and visual feedback may change. It is hard to give a precise evaluation since all the existing designs have relied exclusively on visual feedback (television). A general selection criterion is not possible since the application conditions must be taken into account. However, for simple remote identification problems (size, shape, weight) sensitive surfaces may serve the

purpose. It should be remembered that according to Figure 6 the tactile feedback needs just a few y lines to be sent over communication channel. Thus a great reduction of channel capacity is possible in certain instances. In other instances it may occur that a combined identification system represents the best solution. As has been written, it is not the intention to discuss the absolute merits of visual or tactile information feedback, but to stress the fact that more general identification methods when designing remote handling control systems should be used.

Conclusions

In this paper several questions have been raised. First of all, the importance of improving the actuators used in servo-mechanisms has been shown. It is proposed to solve this problem in an unconventional way by using special mechanical shapes of the actuator covered with sensitive surface. Such an approach has the merit of showing the transition phases of a conventional positioning servo-mechanism to an artificial hand.

In addition, the identification problem of automatic control

theory is presented in a new way. The notion of the transfer function for linear systems, or other methods of identification for non-linear systems are in current use. However, in the future development of automatic control systems many situations may arise where the identification problem cannot be solved satisfactorily by the existing methods. Object identification by shape, surface characteristics and other ways such as those occurring in biological systems will also be needed in engineering systems.

Looking at the identification problem in engineering from a broader point of view allows the synthesis of new cybernetic control systems which can duplicate functions of biological structures in a very efficient way.

References

- ¹ TOMOVIC, R. Human hand as a feedback system, *Automatic and Remote Control*. 1960, 624-628. London; Butterworths
- ² KOBRINSKI *et al.* Problems of bioelectric control, *Automatic and Remote Control*. 1960. London; Butterworths
- ³ TOMOVIC, R., and BONI, G. An adaptive artificial hand, *Trans. IRE*, vol. PGAC (1962)

DISCUSSION

A. J. KUKHTENKO, *Uranian Academy of Sciences, Institute of Cybernetics, Kiev, U.S.S.R.*

If we take into consideration receptor action, then Figure 2 in Professor Tomovic's paper must be as shown in Figure A of this remark. In terms of invariance theory we now have a combined system. This is a system which utilizes two principles: (1) control by deviation (Polzunov-Watt principle); (2) control by means of measuring the load (Ponsel principle).

With respect to prosthetics it is important that the system has two channels: (1) a visual channel, and (2) a receptor channel. The performance of these channels takes place at different times.

At first the visual channel works before the prosthetics touches the body and then the receptor channel operates and the visual channel switches off. Thus we have a system with a variable (changing) structure; the switches (samplers) 1 and 2 in Figure A indicate such a situation. This situation must be taken into account in a theoretical design of such a system.

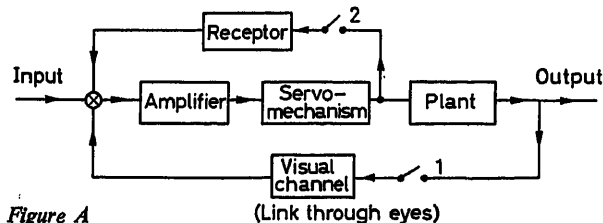


Figure A

C. PENESCU, *Academy of Roumanian Peoples' Republic, Calea Victoriei 125, Roumania*

Human movement is a complicated motion. I have studied how the actuating variable is modified in action. The diagram of a closed loop movement can be represented as in Figure B.

If the excitation of hand or arm muscles is x (latest developments have shown that both muscles for the displacement of the member in a direction are excited and movement results from the difference in excitation of both of the muscles), then:

$$x = x_1 - x_2$$

x_1 : excitation in one direction

x_2 : excitation in other direction

Experimental results show that x varies with respect to time for a very simple movement as in Figure C, which is similar to the opera-

tion of a PD controller. It means that the positive effect is quickly decreased and before the target is reached this effect reverses sign.

It is important therefore that for some artificial members we take into account this anticipation phenomenon which gives very accurate response.

Bibliography

- C. PENESCU. L'anticipation dans les mouvements humain. *1er congrès de cybernetique*, Namur (1958).

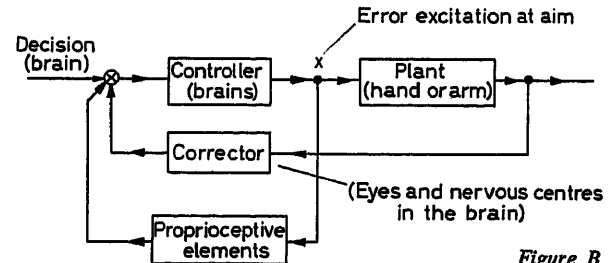


Figure B

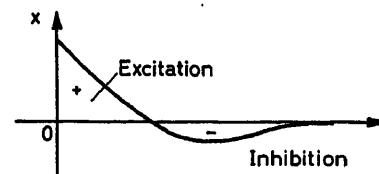


Figure C

R. TOMOVIC, *in reply*

I fully agree with Professor Kukhtenko's remark, especially his representation of the block diagram. As a matter of fact, in the text of the paper the additional feedback loop proposed by him is discussed in detail, but in order to stress the importance of local feedback it was omitted from the figure. Introduction of switches 1 and 2 in Professor Kukhtenko's diagram is very helpful since it emphasizes the mutual interplay of two feedback channels in controlling the hand actions.

Mr. Penescu's remarks concern arm and hand movements in general. As specified in the introduction of this paper my aim is limited only to problems of grasping objects by an artificial hand. Thus these hand positioning and other questions raised by Mr. Penescu lie outside the scope of my paper.

A Sampled Data Model for Eye Tracking Movements

L. R. YOUNG

Summary

The application of servo-analysis to the study of human eye movement control in a tracking task has yielded a new type of mathematical model for a biological servomechanism. Experiments on the ability of subjects to move their eyes in order to follow the horizontal motion of a target led to several basic principles on which the model was based. The fast saccadic and smooth pursuit systems were shown to be functionally separate, with the former acting as a position tracker and the latter as a velocity tracker; and the eye movement tracking characteristics in the nonpredictive mode were shown to be of a discrete nature, requiring a noncontinuous model for adequate description.

A sampled-data model for nonpredictive tracking was developed, and this model successfully predicts the major characteristics of the biological servomechanism, both for transient responses and in the frequency domain.

Sommaire

L'application des techniques d'analyse des servomécanismes à l'étude de la commande du déplacement de l'œil lors d'un mouvement de poursuite visuelle a donné naissance à un nouveau modèle mathématique de servomécanisme biologique. Les expériences sur l'aptitude des sujets à mouvoir leurs yeux de manière à suivre le mouvement horizontal d'une cible ont conduit à dégager plusieurs principes de base servant de fondement à ce modèle. Le système de poursuite saccadée et le système de poursuite continue, notamment, se sont avérés fonctionnellement différents: le premier agit comme un suiveur asservi en position, le second comme un suiveur asservi en vitesse. Et la caractéristique du mouvement de l'œil lors d'une poursuite non prédictive s'est révélée être de nature discrète, ce qui exige, pour une description correcte, un modèle discontinu.

Un modèle du type à données échantillonnées a été développé pour la poursuite non-prédictive; ce modèle permet de prévoir avec succès les caractéristiques principales du servomécanisme biologique, qu'il s'agisse de la réponse transitoire ou de la réponse fréquentielle.

Zusammenfassung

Die Anwendung regelungstechnischer Verfahren zur Untersuchung der Regelung der menschlichen Augenbewegung bei der Verfolgung eines Objektes führte zu einem neuartigen mathematischen Modell für einen biologischen Regelkreis. Aus Versuchen über die Bewegungsfähigkeit des Auges beim Verfolgen einer horizontalen Objektbewegung ergaben sich mehrere Grundprinzipien, die zu dem Modell führten: es zeigte sich, daß das schnelle ruckartige und das kontinuierliche Folgesystem funktionell getrennt sind, wobei das erste als Stellungsfolgesystem, das zweite als Geschwindigkeitsfolgesystem wirkt. Es zeigte sich weiter, daß die Folgebewegungen des Auges bei der Verfolgung nicht vorhersagbarer Signale diskret sind; zur entsprechenden Beschreibung ist daher ein diskretes Modell erforderlich.

Ein Abtastmodell für die Verfolgung unvorhersagbarer Bewegungen wurde entwickelt, das erfolgreiche Aussagen über die wesentlichsten Eigenschaften des biologischen Regelkreises ermöglicht. Dies gilt sowohl im Zeit- als auch im Frequenzbereich.

Introduction

The eye movement control system is an interesting human servomechanism employing voluntary as well as involuntary control to direct the line of gaze at a moving target. Previous

mathematical descriptions¹⁻⁴ have failed to predict the overall system behaviour, considering transient response as well as frequency characteristics. Considerable experimental evidence indicates three characteristics of the system that cannot be overlooked in developing a model: (1) The predictability of the target signal was shown to affect the mode of operation in tracking continuous and discontinuous target motions⁵. (2) The saccadic and pursuit mechanisms were shown to be functionally separate, with position errors being corrected by fast saccadic jumps, and velocity errors being corrected by smooth pursuit movements⁶. (3) Finally, it can be demonstrated that the discrete nature of the system in tracking non-predictable target motions is inconsistent with a continuous mathematical model, and requires a sampled data model for adequate description⁷. Support for the sampled data nature of the tracking system includes the following experimental evidence.

Pulse Response

The eye movement response to a pulse of target position is characterized by a delay preceding the saccadic response, and a refractory period, approximately equal to the delay, preceding the saccade which returns the eye to its initial position. Thus for a pulse width much less than 180 msec, the eye responds to the pulse after the target has returned, and remains in the displaced state for about 180 msec before returning. The output of a linear continuous system with a cascade delay would be a delayed, possibly distorted, pulse of the same width as the target pulse, and could be described as the superposition of two equal and opposite step responses displaced in time by the pulse width. Superposition obviously cannot be applied in this situation. The result is, however, similar to that of a sampled data system with a zero order hold, permitting changes of the output variable to occur only at sampling instants.

Open-loop Step Response

The eye movement control system may be considered as a closed loop servomechanism with unit visual negative feedback from the eye position to the observed error at the retina. The controller acts on the observed error in eye position, or the difference between the angular position of the target and that of the eye. Since the object of this research is to study and describe the operation of the error sensor, controller and load dynamics, it would be desirable to study the system in the absence of the visual feedback. The feedback path is an inherent part of the system, however, since rotation of the eye displaces the target image on the retina. It could be eliminated only by physically opening the control loop, as for example by mechanically restraining the eyes from moving and observing the torque exerted by the muscles.

Fortunately, the use of an eye movement monitor which yields an instantaneous voltage signal proportional to eye position permits the effective visual feedback to be varied conveniently by adding an external feedback path from eye

position to target position. The measured eye position is amplified by α and subtracted from the input command to drive the target position. Thus an eye movement Δr reduces the observed error by $(1 + \alpha) \Delta r$. By varying the sign and magnitude of α , the eye movement control system may be studied for any value of effective visual feedback.

An important class of experiments was performed in the open loop configuration, with α set equal to -1 . With this arrangement, any movement of the eye was immediately accompanied by an identical movement of the target, so that the eye movement had no effect on the error observed at the retina. The response to an input command therefore represented the open loop transmission of the error sensor, controller and load dynamics. The stabilization was not so precise that any subjects reported fading of the image.

Under these conditions a step of target position, corresponding to a step of observed error, induces a regular series of equal saccadic jumps, with a constant time of one refractory period between the jumps. Just as in the case of the pulse response, this result indicates that saccadic movements can be made no closer together than a critical period of approximately 200 msec, regardless of the error that is observed.

Discrete Changes in Pursuit Velocity

Upon close inspection of the records of eye movements during continuous random target motions, the smooth pursuit motions are seen to be a series of constant velocity segments. The large discrete changes in velocity occur at intervals of 100–200 msec and are often accompanied by a simultaneous saccadic movement. The discreteness of the pursuit movements is clearly shown in the response to parabolic inputs. The observed tracking record and its derivative indicate that the velocity increases in a stepwise manner and that the saccadic movements are all in the direction of the target motion, correcting for the position lag resulting from the pursuit motion with constant velocity segments.

Peak in the Frequency Response

Inspection of the tracking records for continuous unpredictable inputs reveals a considerable number of saccadic jumps separated by one refractory period (about 180 msec). Bode plots resulting from Fourier analysis of the output bear out this observation by showing a sharp peak in gain of about 6 dB at 2.5–3.0 c/sec, indicating the presence of a great deal of energy with the half-period of 160–200 msec⁷. The sampling process transforms an input spectrum $F(s)$ into an output spectrum

$$\frac{1}{T} \sum_{n=-\infty}^{\infty} F(s + nj\omega_0)$$

where T is the sampling interval and ω_0 the sampling angular frequency⁸. Clearly a peak in the output spectrum occurs first at $\omega = \omega_0/2$. If a sampling interval of 180 msec is assumed, then the sampling frequency would be 5.55 c/sec and the first peak in the output energy spectrum would occur at 2.8 c/sec, in agreement with experimental data. Furthermore, since the Nyquist sampling theorem states that at least two samples per period are necessary for any reconstruction of data from samples, the tracking ability of a sampled data model would be nil for

target frequencies higher than half the assumed sampling frequency. This agrees with the experiments showing no tracking of input frequencies greater than 2.5–3.0 c/sec.

Dependence of Accuracy on Prediction

During a square wave tracking experiment in which the subject predicts the change in target position and moves his eyes before the target moves, he tends to overshoot or undershoot the desired position by a considerable percentage. This observation is reasonable when considering that this predictive movement is made from memory of the anticipated target position and without the aid of any visual reference. Of particular interest, however, is the case of slight prediction, in which the saccadic movement takes place after the target change, but less than 150 msec following that target step. Since the response takes place in less than a minimum reaction time delay, the initiation of the movement command must occur prior to the target step although the actual saccade does not take place until the target has reached its new position. If it were possible for the eye movement command, once initiated, to be modified by the presence of a new visual reference before the saccade takes place, then the responses occurring from 0–150 msec after the target step should be performed with the same accuracy as those taking place after a full normal reaction time. Since the experimental results show the same inaccuracies for delays of less than one reaction time as for true predictions, it can be concluded that once a saccadic movement command is initiated, no new visual information can alter that particular command. This conclusion is consistent with the operation of a sampled data system which takes in information only at the sampling instants.

Experimental Design

In all the experimental records presented below the subject was seated in a dark room, his head held stationary in a padded catcher's mask, and he was instructed to maintain fixation on the 0.5 × 6.0 cm projected target slit. A horizontally moving target on a screen 8 ft. from the subject was produced by driving a fast response (100 c/sec bandwidth) mirror galvanometer, as illustrated in Figure 1(a). Horizontal eye position was monitored by measuring the difference in diffuse reflected light from the sclera (white) and iris [see Figure 1(b)]. The amount of light reflected to one side diminished as the eye moved to that side, and this difference was detected by a pair of CdS photoresistors balanced in a bridge. The photoresistors and small light bulbs

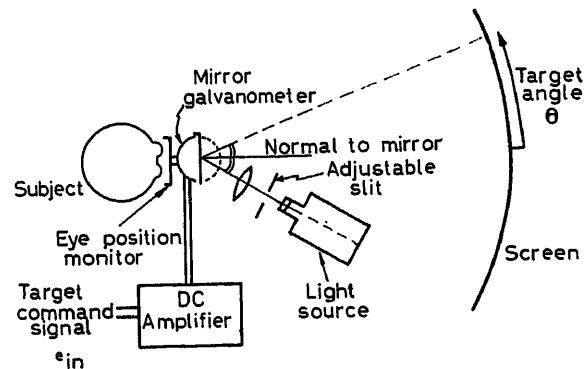


Figure 1(a). Experimental apparatus: target projection

(which did not interfere subjectively with experienced subjects) were mounted in goggles worn by the subject. The monitor yielded linear readings over the range $\pm 15^\circ$, with a noise level of less than 15 min arc.

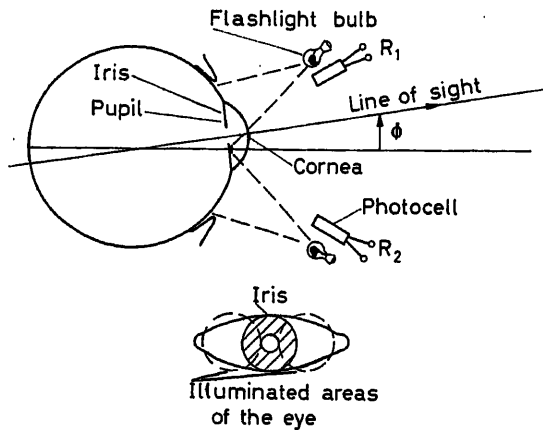


Figure 1 (b). Experimental apparatus: eye position monitor

Sampled Data Model for Saccadic Tracking

In the model shown in Figure 2, the error angle (e) between the desired angle of gaze (c) and the actual eye position (r) is detected at the retina. This error is sampled by an impulse modulator (M) at sampling intervals, T , where T is the average refractory period for saccadic movements (about 0.2 sec). The synchronization of the modulator must be assumed to be set to coincide with the beginning of a target motion, if the eye had made no saccadic jumps during the previous 0.2 sec. Each error sample impulse is delayed by one reaction time and integrated to give a step command indicating the desired change in eye position necessary to bring the eye to what had been

the desired position one reaction time previously. (z is defined as a pure delay of T sec, or $z = e^{-sT}$. This definition of z is the inverse of the definition used by some workers in sampled data systems, i.e. $z = e^{+sT}$ is not used here.) This step is then filtered by the dynamic response of the extraocular muscles and the eye loading them, to yield an actual eye position movement exhibiting finite rise time and possible overshoot. A second-order model for saccadic movements serves to demonstrate that the details of the individual movements can be neglected in considering the overall characteristics of the sampled data model for the eye movement control system.

The parameters published by Westheimer⁴ ($\omega_n = 240$ rad/sec, $\xi = 0.7$) indicate that at the next sampling interval, 0.2 sec after the onset of a saccade, the eye position will have settled to within at least $e^{-38.6}$ of its final value. (By final value is meant the steady-state eye position resulting from that one saccade. If this is not the desired eye position and the error lies outside the foveal dead zone, it will be corrected by a secondary saccadic movement at the next sampling interval.) Since this disparity is less than the errors in fixation resulting from miniature eye movements (designated as disturbances in the figure) or errors in computation of the desired amplitude of the saccade, its effect on the observed error at the next sampling instant can be neglected. For the sake of simplicity of presentation, therefore, the muscle and eyeball dynamics will be ignored for the remainder of this paper. This being the case, it must be remembered that when the simplified model indicates a discrete change in eye position, the actual eye position predicted would be a typical saccadic movement.

With this simplification, and neglecting the effect of disturbances and the 1.0° dead zone, the saccadic system model for discrete position tracking reduces to the flow chart of Figure 3(a). By isolating the discrete data mode e^* , the flow chart can be redrawn as in Figure 3(b), where $-K_1(z)$ represents the discrete transfer function of the open loop.

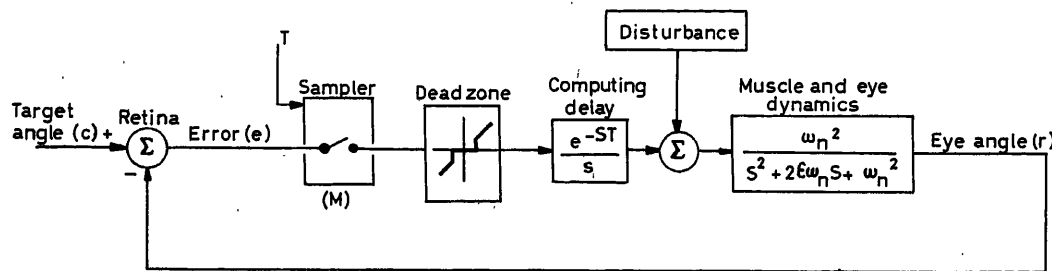


Figure 2. Sampled data model—the saccadic system

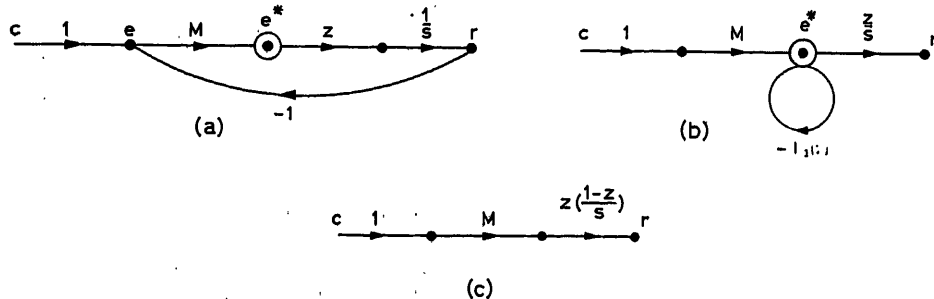


Figure 3. Simplified flow chart—the saccadic system

$$K_1(z) = z \left(\frac{1}{s} \right)^*$$

$$K_1(z) = \frac{z}{1-z}$$

$$\frac{1}{1+K_1(z)} = 1-z$$

The flow chart is finally reduced to that of Figure 3(c), showing that the output of the saccadic system alone is

$$R(s) = C(s) * z \left(\frac{1-z}{s} \right)$$

which can be recognized as a delayed zero order hold.

Sampled Data Model for the Pursuit System

Whereas saccadic movements serve to centre the target image on the fovea, the purpose of the pursuit system appears to be stabilization of the target image on the retina by keeping the angular velocity of the eye equal to that of the target for target velocities less than 25–30°/sec. It is reasonable to describe the pursuit system as a sampled data velocity tracker.

The block diagram of Figure 4 represents one way in which this velocity tracker could work. As in the saccadic model, the error between the desired and actual eye position is sampled every reaction time T , which may or may not be the same sampling period as for the saccadic model. The error rate is estimated from the difference between the past two error samples divided by the sampling interval T . This error rate estimate is the desired change in the eye velocity and its integral is the eye velocity attributable to the pursuit system. The first limiter reflects the fact that the pursuit system does not attempt to follow the high velocity changes present in discontinuities of the target position, and the second limiter indicates that the pursuit velocity saturates at 25°–30°/sec. The output of the second limiter will be a sequence of ramps of eye position at the desired

velocity. The effect of the muscle and eye dynamics is to smooth out the discontinuities in velocity and also to introduce a small constant steady-state error between the desired ramp and the actual output.

Once again, since the eyeball dynamics have no effect on the overall closed loop characteristics of the sampled data pursuit model, these dynamics will be neglected in the presentation.

The flow chart for the simplified pursuit model with the non-linearities removed is shown in Figure 5(a). As before, the flow chart is reduced by considering all inputs and outputs at the discrete data point e^* . In Figure 5(b) the z transform of the open loop transfer function is denoted by $-K_2(z)$

$$K_2(z) = (1-z) \left(\frac{1}{Ts^2} \right)^*$$

$$K_2(z) = \frac{(1-z)}{T} \left[\frac{Tz}{(1-z)^2} \right]$$

$$K_2(z) = \frac{z}{1-z}$$

Since

$$\frac{1}{1+K_2(z)} = (1-z)$$

the sampled data velocity tracker finally reduces to the flow chart of Figure 5(c). For the pursuit system alone, eye position would be given by

$$R(s) = C(s) * \frac{(1-z)^2}{Ts^2}$$

This equation may be rewritten as follows to clarify the operation of the velocity tracker

$$R(s) = C(s) * \left(\frac{1-z}{T} \right) \left(\frac{1-z}{s} \right) \left(\frac{1}{s} \right)$$

which states that the target position is sampled and its velocity is estimated by the least difference $[(1-z)/T]$. Since old data

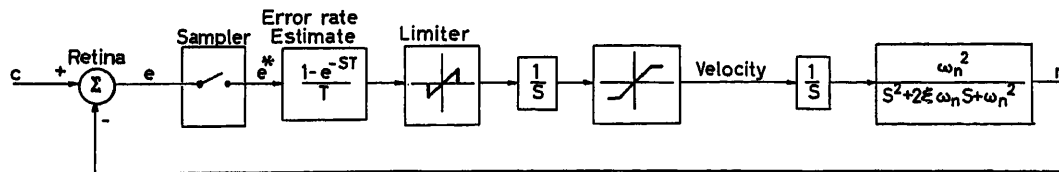


Figure 4. Sampled data model—the pursuit system

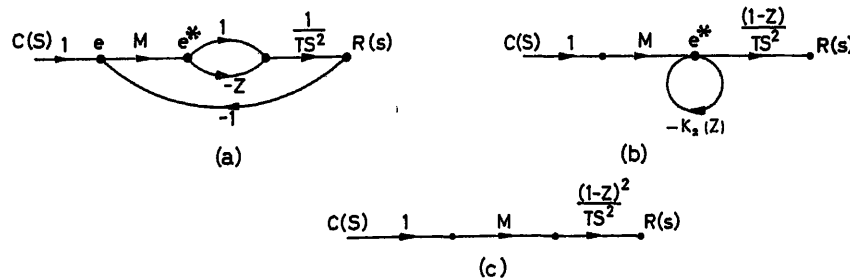


Figure 5. Simplified flow chart—the pursuit system

is used to calculate present velocity, this term accounts for the delay in the pursuit system. The term $[(1 - z)/s]$ is a zero order hold, keeping the output velocity constant between sampling instants, and the integrator yields the eye position resulting from this velocity.

Complete Sampled Data Model

Since the refractory period is not a deterministic function, the simplifying assumption will be made that T is a constant sampling interval equal to the mean experimental value for the saccadic system and also for the pursuit system.

Since the average refractory period for velocity changes is equal to or slightly less than that for saccadic movements for any one subject tested, the sampling intervals will be assumed equal for the pursuit and saccadic systems. Furthermore, the error sampling for the pursuit and saccadic loops will be assumed to be synchronous, both starting with the initiation of any significant change in target position or velocity following a quiescent period. Under these simplifying assumptions a single sampler, or impulse modulator, may be used to furnish error samples for the saccadic and pursuit tracking loops.

The pursuit loop, as a velocity tracker, should use estimates of error rate to keep the eye velocity equal to the target velocity, with corrections coming in as regularly spaced ramps of eye position. It is important that the pursuit model does not try to null out any apparent smooth error rate resulting from a step change in error during a saccadic jump.

The function of the first limiter in the pursuit system block diagram (Figure 4) was to force the pursuit system to ignore all very rapid changes in the observed error. These error discontinuities may occur either from target discontinuities or from the step changes in eye position caused by the saccadic system. This non-linear element has been removed, and its function retained in Figure 6 in the following manner. The pursuit loop in the model is considered open at the time of (or at the sampling instant following) any target velocity greater than $30^\circ/\text{sec}$. This artifice is easily managed in considering transient response, and could be handled on a statistical basis when considering random target inputs. The other component of error discontinuity, resulting from a saccadic movement, may be prevented from stimulating the pursuit loop by introducing an extra cross

coupling branch (from A to B) in Figure 6 between the saccadic and pursuit models.

The equivalent flow chart of Figure 6(b) is seen to be identical to that of purely saccadic sampled data model except for the branch with transmission $1/Ts$, representing the contribution of the pursuit system. This is the branch that must be considered open during any high velocity movements of the target. The further reduction of the flow chart is done in the usual manner. In Figure 6(c) the forward transmission is

$$G(z) = \left(\frac{1}{Ts} + z \right) \frac{1}{s}$$

The sampled transfer function around the closed loop is

$$G(z) = \left(\frac{1}{Ts^2} + \frac{z}{s} \right)^*$$

$$G(z) = \frac{2z - z^2}{(1 - z)^2}$$

This contributes the forward-loop transmission

$$\frac{1}{1 + G(z)} = (1 - z)^2$$

and the resultant flow chart is as drawn in Figure 6(d).

Thus for the integrated sampled data model with both the pursuit and saccadic systems functioning, the predicted eye position is given by

$$R(s) = C(s) * (1 - z)^2 \left(\frac{1}{Ts} + z \right) \frac{1}{s}$$

Written in another form, this equation becomes

$$R(s) = C(s) * \left[(1 - z)z \left(\frac{1 - z}{s} \right) + \left(\frac{1 - z}{T} \right) \left(\frac{1 - z}{s} \right) \left(\frac{1}{s} \right) \right]$$

The first term in square brackets is a delayed zero-order hold on the first difference of target samples. This represents the action of the unit delay in velocity changes by the pursuit system.

The second term in square brackets is the same as encountered in the simple pursuit model. It represents the function of the

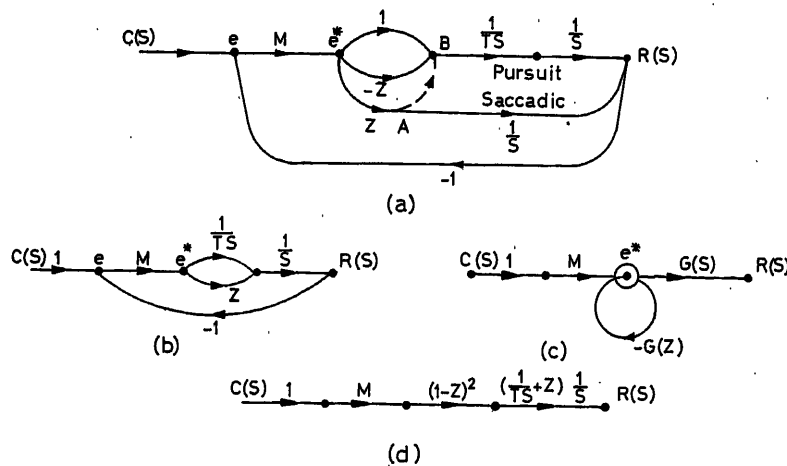


Figure 6. Complete sampled data model flow chart

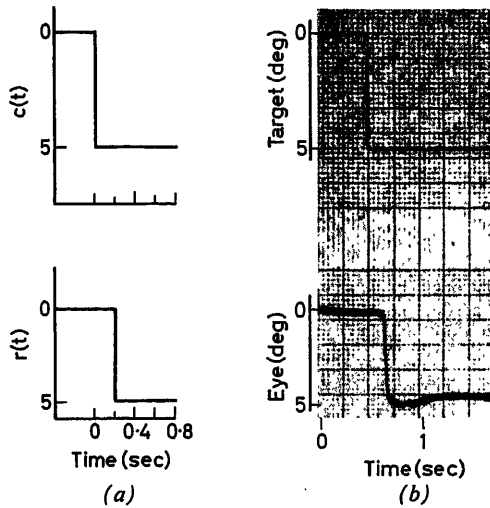


Figure 7. Step response: (a) model; (b) experimental

velocity tracker in using the last difference of target samples to estimate the velocity, holding this in a zero order hold, and then contributing ramps of target position equal to the integral of this velocity.

Model and Experimental Transient Responses

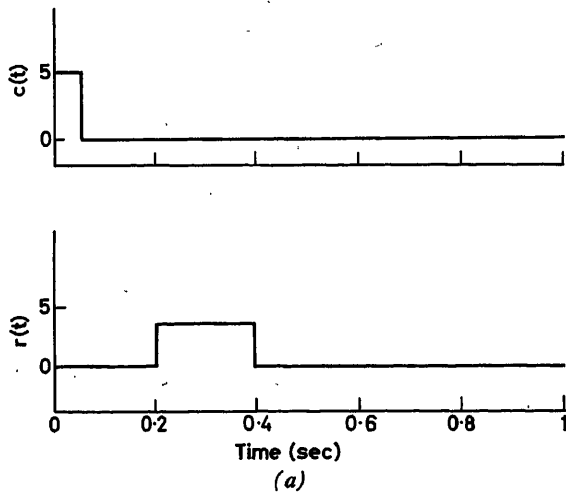
Step Response—Since this involves a discontinuity of target position, the pursuit loop is initially open

$$C(s) = \frac{A}{s}$$

$$R(s) = \left(\frac{A}{s}\right)^* z \left(\frac{1-z}{s}\right)$$

$$R(s) = \frac{Az}{s}$$

The response is a delayed step, in agreement with experiments. (See Figure 7.)



Pulse Response—Once again, the pursuit loop is open at the discontinuities (and at the sampling instant following a discontinuity occurring between sampling instants). For a pulse width τ , with $\tau < T$,

$$C(s) = \frac{A}{s} (1 - e^{-\tau s})$$

$$C(z) = A$$

$$R(s) = Az \left(\frac{1-z}{s}\right)$$

The response is a delayed pulse of width T (see Figure 8).

Ramp Response—

$$C(s) = \frac{A}{s^2}$$

$$C(z) = \frac{ATz}{(1-z)^2}$$

$$R(s) = \frac{ATz}{(1-z)^2} (1-z)^2 \left[\frac{1}{Ts^2} + \frac{z}{s} \right]$$

$$R(s) = A \left[\frac{z}{s^2} + T \frac{z^2}{s} \right]$$

The response is a ramp of slope A delayed by T plus a step AT occurring at $t = 2T$. (See Figure 9.)

Step-ramp Response—The response to a target movement consisting of a step to one side followed by a constant velocity in the opposite direction may be treated by superposition of the step response, in which the pursuit loop is inactive, and the ramp response involving the complete system, as discussed above

$$C(s) = \frac{-A}{s} + \frac{B}{s^2}$$

$$R(s) = \frac{-Az}{s} + B \left(\frac{z}{s^2} + T \frac{z^2}{s} \right)$$

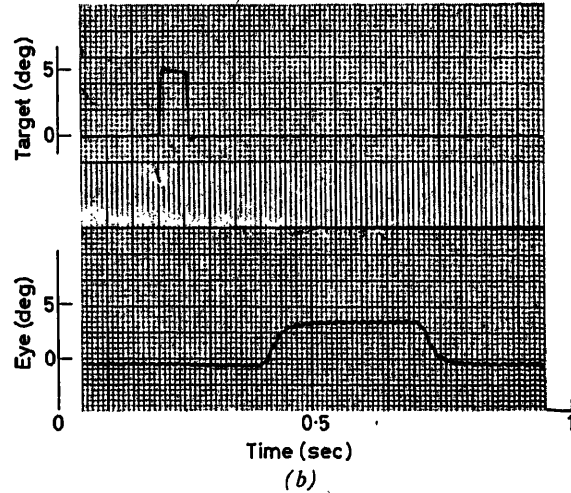


Figure 8. Pulse response: (a) model; (b) experimental

This transient response is plotted in Figure 10(a) and an experimental result is shown in Figure 10(b).

Sawtooth Response—A single sawtooth waveform of duration KT has the Laplace transform

$$C(s) = \frac{A}{s^2} - e^{-sKT} \left(\frac{A}{s^2} + \frac{AKT}{s} \right)$$

$$C(z) = A \left[\frac{Tz}{(1-z)^2} (1-z^K) - \frac{KTz^K}{1-z} \right]$$

Since the second term in brackets represents a target position discontinuity, its response is determined by the saccadic system alone.

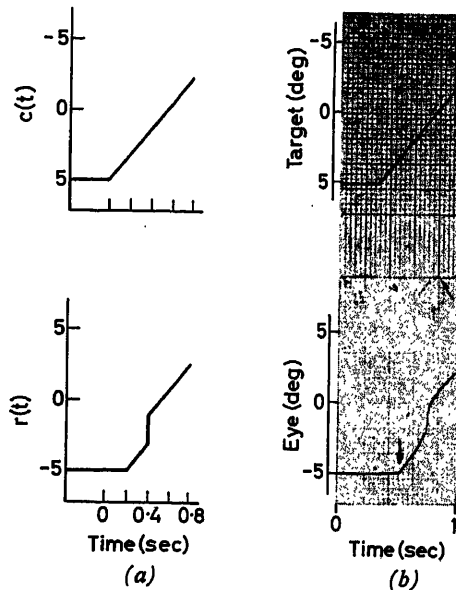


Figure 9. Ramp response: (a) model; (b) experimental

$$R(s) = A \left[\left(\frac{z}{s^2} + T \frac{z^2}{s} \right) (1-z^K) - \frac{KTz^{K+1}}{s} \right]$$

Figure 11 shows the predicted and actual transient response for this type of input. Notice that for this illustration and the previous one the model predicts the occurrence of a second saccadic correction, which is indeed observed in step-ramp experiments, whether the initial velocity is zero or non-zero.

Parabola Response—As noted earlier in this paper, the system response to a parabolic input yielded evidence for the discrete nature of the velocity tracking system. The input function is

$$C(t) = \frac{At^2}{2}$$

$$C(s) = \frac{A}{s^3}$$

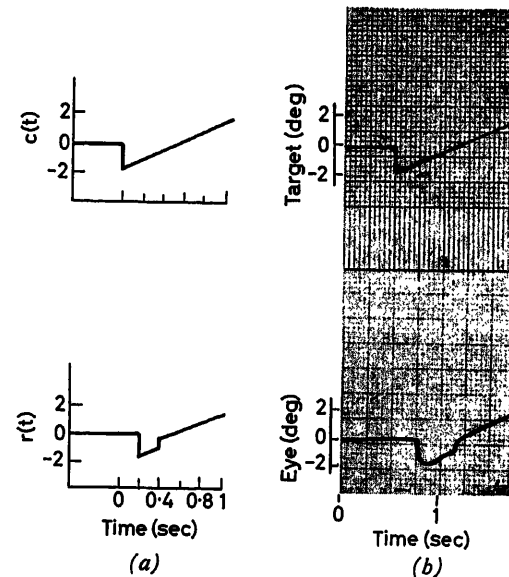


Figure 10. Step-ramp response: (a) model; (b) experimental

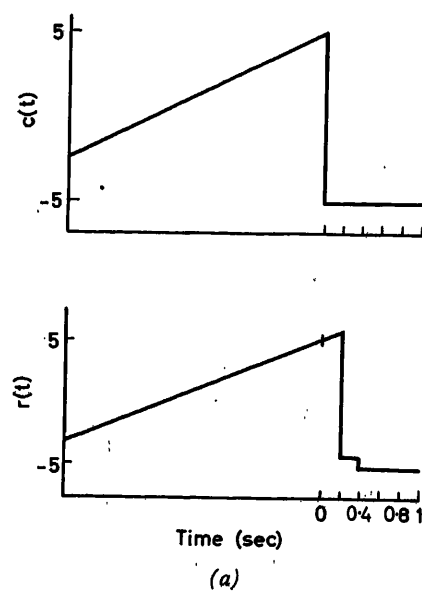


Figure 11. Sawtooth response: (a) model; (b) experimental

The z transform of this function can be found in a table of z transforms.

$$C(z) = \frac{AT^2 z(1+z)}{2(1-z)^3}$$

$$R(s) = \frac{AT^2 z}{2} \left(\frac{1+z}{1-z} \right) \left(\frac{1}{Ts^2} + \frac{z}{s} \right)$$

The corresponding time function is plotted in Figure 12. Notice that the predicted response consists of constant velocity segments and regularly spaced saccadic jumps in the direction of the target motion.

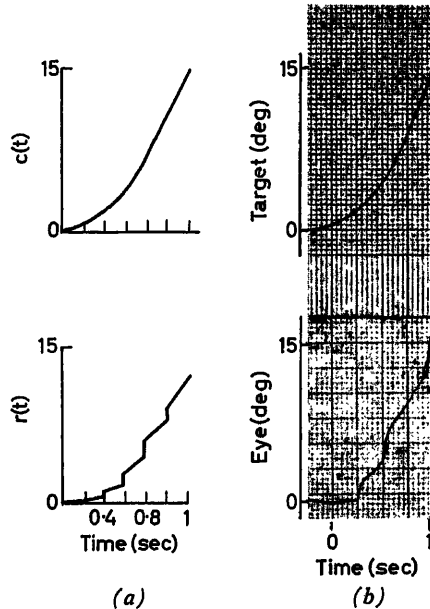


Figure 12. Parabola response: (a) model; (b) experimental

Additional Supporting Evidence

In addition to the model agreement with experimental transient responses, the model frequency characteristics closely resemble the experimental Bode plots. Furthermore, experimental transient and frequency characteristics change with the effective visual feedback (varied by controlling target position from measured eye position) in a manner exactly predicted by the sampled data model^{7,9}.

This research was performed at the Massachusetts Institute of Technology, Cambridge, Mass., and supported in part by the Instrumentation Fund and the Air Force Office of Scientific Research Contract AFOSR 155-63. The author is grateful to Dr. L. Stark and Dr. C. S. Draper for their support.

References

- FENDER, D. H., and NYE, P. W. An investigation of the mechanisms of eye movement control. *Kybernetik* 1 (1961), 81
- SÜNDERHAUF, A. Untersuchungen über die Regelung der Augenbewegungen. *Klin. Mbl. Augenheilk.* 136 (1960), 837
- VOSSIUS, G. Das System der Augenbewegung. *Z. Biol.* 112 (1960) 27
- WESTHEIMER, G. Mechanism of saccadic eye movements. *Arch. Ophthalm.* N.Y. 52 (1954), 710
- STARK, L., VOSSIUS, G., and YOUNG, L. R. Predictive control of eye tracking movements. *Trans IRE, Human Factors in Electronics, HFE-3* (1962) 56
- RASHBASS, C. The relationship between saccadic and smooth eye tracking movements. *J. Physiol.* 159 (1961) 326
- YOUNG, L. R. A sampled data model for eye tracking movements. *Sc. D. Thesis*, Massachusetts Institute of Technology (1962)
- JURY, E. I. *Sampled Data Control Systems*. 1958. New York; Wiley
- YOUNG, L. R., and STARK, L. Variable feedback experiments supporting a discrete model for eye tracking movements. *Trans. IEEE, Human Factors in Electronics, HFE-4* (1963) March

DISCUSSION

E. I. JURY and T. PAVLIDIS, *University of California, Berkeley, U.S.A.*

This paper presents the first attempt to advocate a sampled data model for eye tracking movements. It may well be an approach in the right direction; however, at this stage of physiological knowledge, such an approach should be accepted with some caution. While information is transmitted in discrete form by the neurons, the large number of them which participate in any reflex results actually in a continuous system. Moreover, the frequencies of the neural pulses are much higher than the low sampling period of 0.2 sec indicated by the author. These facts point to the need of further physiological research to establish the organs, if any, which perform the sampling operation.

In our studies we have simulated on an analogue computer¹, the system advocated by Dr. Young, and found the results to compare favourably with his object experiment. However, in the case of the pursuit system (author's Figure 4), the way of estimating the velocity of the input fails in the case of a step input.

Finally, we would like to mention that this paper could serve as a pioneering text for any further research to be done in this field. It is hoped that future studies by both engineers and physiologists would establish beyond any doubt the discrete feature of eye tracking.

Reference

- BLEUZÉ, J. C. Sampled data model for eye tracking movements. *M. S. Research Project*, Dept. of Electrical Engineering, Univ. of Calif., Berkeley (Aug. 1963)

L. R. YOUNG, *in reply*

I would like to thank Professors Jury and Pavlidis for their carefully considered comments and for their estimate of the importance of this paper. I am particularly grateful to them and their students for simulating my model on a computer and checking my analytical results.

In the course of their simulation they discovered, quite rightly, that the sampled pursuit model would misinterpret successive samples from a small step input to give an erroneous ramp output, provided that the estimated velocity is less than the limits of the first limiter in the pursuit loop. For steps longer than 4–5°, the simulator will give correct results.

The difficulty involves the method of estimation of error rate in the sampled pursuit loop. If, instead of taking the difference between successive samples, one assumes a short period estimate of the error derivative, followed by a sampler and delay, one can eliminate this difficulty. This modification, which is compatible with some behavioural data, yields a model which is convenient only for machine simulation. Since the transient and frequency responses are nearly identical for the two error rate branches, the one which was analytically tractable was obtained. Concerning the physiological significance of the 0.2 sec sampling period, we are currently of the opinion that it occurs neither in the sensory receiver nor in the motor end, but rather in the higher centres of the brain. However, it is a hopeless task, I believe, to try to account for the 0.2 sec 'cycle time' of the control

calculation in terms of the usual pulse periods of several milliseconds which correspond to the basic computer 'off time'.

In collaboration with Drs. Stark, Meyer and Cogan, investigations of the physiological correspondence of the model through the use of other types of inputs and the study of patients with known pathology is being carried out in the Massachusetts Eye and Ear Hospital.

G. VOSSIUS, *Institut für Animalische Physiologie, Frankfurt/M., Ludwig-Rehn-Str. 14, Germany*

I would like to make a few remarks about Professor Young's paper from the standpoint of the physiologist.

The model is based on the assumption that for unpredicted input signals into the brain there is another process branch available in the same way as with predictable signals. However, several experimental findings contradict this assumption. A process of eye movement on an input signal moving with constant acceleration and in the direction inwards to outwards takes the form described by Professor Young. In the opposite direction, however, from outwards to inwards, one of the continually accelerated movements corresponding to the object movement occurs with perhaps 1 or 2 saccads, but with which no sudden variation of the speed of movement occurs.

Also, after the switching off of the signal, whether with predictable or unpredictable input signals, the eye continues to register lapses of movement. Further, if the eye is given only a brief excerpt of a sinusoidal signal of approximately 0.3 sec duration and which does not include any maxima, then the eye does not carry out any series movement during this period, but this is dependent on the reaction time and in some cases responds with a movement which corresponds to the correct continuation of the time wave. If, for example, the eye could see a part of a sine wave in which the target moves from left to right, then the eye movement would be carried out with continual variation of speed from right to left with a reversal of movement corresponding to a maximum. During this short period the brain cannot definitely decide whether the object movement (target movement) is predictable or not. Apart from that, in our experiments we can observe continuous and discontinuous speed variations for predictable and unpredictable input signals, although the latter occur more frequently with unpredictable object movement. However, even with random input signals there were still continuous speed variations to be found. Further, no sudden transition exists between predictable and unpredictable series movement processes. The phase angle of the eye movement in the main follows rapidly as the target movement gains complexity.

If one puts the eye under 'open-loop condition', first with a sine wave and then with a statistical signal, then the eye carries out a sinusoidal oscillation corresponding to the sinusoidal signal, and which only at the first input gives a small saccad, although, apart from transition through zero, maintains a deviational error. To combat this, saccad-corrections are made for the statistical signal which hold the line of sight approximately on the mean, although in this case the target moves relatively back and forth.

It appears to be easier for the similarity of the series of eye movements in a system to be watched over so that the errors are regulated out and the method of operation of the saccad branch is not affected. The sensing branch of the system can be seen as secured, even in a complicated form as well as the one shown here, which does not appear to be the case in the method of operation in the pursuit system.

Since my name was mentioned in the introduction I want to make it known that neither Sünderhauf nor myself have published a mathematical model of the whole system of eye movement. My work which has been mentioned here leads only to the equation of the sub-system of eye movement which consists of eye muscle centres, motor nerve tracks, eye muscles with eye-ball, and the sensible nerve tracks. The dynamics of this system were rightly neglected by Professor Young in the simplification of his equations, but I do not know why my system equations were placed in opposition to these. On the other

hand, as far back as 1961 I presented a block diagram for the sampling branch of the whole system which incorporated a zero-hold like the one used in the way Professor Young describes.

As has been stated, there is a more basic difference in the criticism of results which should be shown, i.e. that which is achieved in biological systems with statistical input signals. I will therefore make a few more general remarks.

If one considers the history of the system of human voluntary movement then there exist, in the first steps of these, linear systems, which describe 'tracking' in one or more form. The rarer these models became, the more were ways sought to describe the complex human processes, at first with the aid of adapting systems and then, as it appears, by the development of models of the series movement of unpredictable input signals. No argument could be opposed to this if the astounding fact did not exist that for this series movement there is a completely suitable system in the brain. One can generalize by saying that life would be impossible in a completely statistically controlled world and, for higher forms of life, the predictability of our surrounding world is, as we know from our own experiences, becoming ever more necessary. If the eye, which is used to visual impressions which are in general predictable, is offered a statistical signal, then corresponding reaction to this unusual process may lead to the system being 'confused' and the eye and hand movements carried out may be on a rather simplified basis. In no case, however, is one justified in assuming a system to be suitable for this process before unrestricted experimentation shows it to be so.

L. R. YOUNG, *in reply*

I wish to thank Dr. Vossius for his studious discussion of my paper. Within the limitations of time I shall attempt to deal with the points he raised in the order they were presented.

First, let me consider the question of the desired nature of the smooth pursuit system in tracking non-predictive input. (I have already shown apparently continuous acceleration in following predictable demands.) The occurrence of constant velocity tracking segments in eye movements was noted by Westheimer in 1955. However, the appearance of constant velocity segments in response to an unpredictable parabolic input is a crucial experiment. Dr. Vossius reports accurate control acceleration eye tracking with zero error for outside in constant accelerations and presents this as evidence for continuous control of pursuit movements. Our experiments were for normal tracking with both eyes open, and thus nodal-temporal is not meaningful for the binocular system (assuming the two eyes wave conjugately). Careful observation of parabolic responses and the rate of eye movement has consistently shown constant velocity segments of eye tracking. Of further interest is the direction of the small saccadic jumps during the parabolic response. If the average tracking error were zero, as in the case of a ramp response, one would expect the saccades to occur equally in both directions. If, however, the eye was following with constant velocity segments and thus falling behind the target, one would expect the preponderance of jumps to be in the direction of target motion. My observations show that nearly all of the saccades during a parabolic response are in the direction of the target motion, as do further detailed studies by Stark and Merrill at M.I.T. The existence of a steady state error in response to a parabola was also found by Fleming and Johnson of the Case Institute of Technology.

The second major point of Dr. Vossius's discussion concerns the justification for the developing of a separate model for tracking unpredictable input signals. He reports several very interesting experimental findings to support his view that random input and precognitive tracking are merely two ends of a continuum and that no sharp division between predictive and nonpredictive tracking exists.

The drawing shows schematically what I believe to be our difference of opinion regarding predictive tracking. A general model, *Figure A*,

which is surely to be desired, would give the resultant eye movements for a great variety of predictive and nonpredictive, visual and non-visual inputs. Even restricting the problem to visual inputs, such a model requires an explanation of the very complex question of human pattern recognition.

A parallel model, *Figure B*, however, attempts, to describe the control characteristics for limited well-defined inputs separately—with the hope that the actions of these parallel paths can be integrated, either by linear combination or inhibition in the general case. This paper has separated precognitive tracking from nonpredictive track-

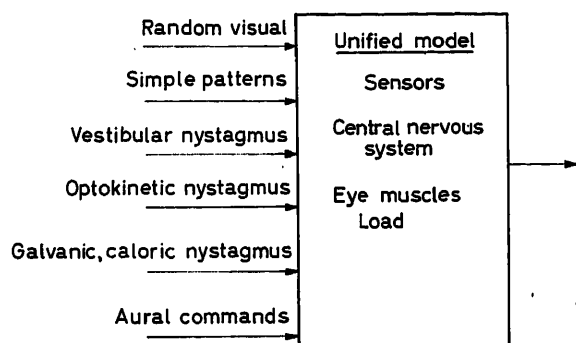


Figure A. General model.

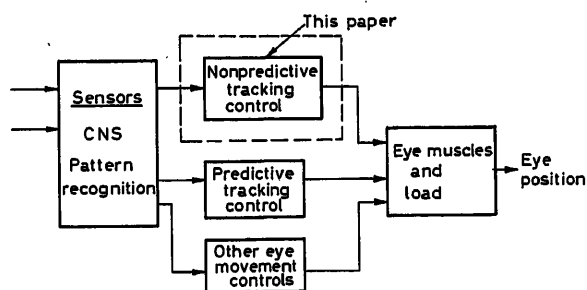


Figure B. Parallel model—limited investigations

ing, as is the practice in manual tracking. I certainly believe that there are cases in which both precognitive and nonpredictive tracking may be superposed, as when a small disturbance is added to a well-learned pattern. Until a general model can be realized, I am convinced that investigations on the output of the eye movement system and other biological servomechanisms can be fruitfully studied by means of controlled classes of inputs. The manner in which the brain 'sorts out' these inputs is a fascinating and complex subject in itself, but the investigation of biological control system cannot wait for its resolution.

J. D. ROBERTS, *Cambridge University, Cambridge, England*

Are there any phenomena which depend on the phase of the hypothetical sampling frequency? For instance, does the reaction time form a rectangular distribution?

L. R. YOUNG, *in reply*

Dr. Roberts's question relates to the phase of the sampling—which I assume synchronous with the beginning of a stimulus. If the phase

were random one would expect a wide rectangular distribution of reaction times, whereas if the phase were synchronous one would expect a peaked distribution of reaction times, with variance resulting from the variable sampling period. (Wilde and Westcott have explored this approach in manual tracking¹.)

We show in Reference 5 of the paper that the histogram of eye movement response times to unpredictable steps is sharply peaked at approximately 0.2 sec, with a sharp cut-off at 0.15 sec and a number of long reaction times up to 0.15 sec. These data support the hypothesis of a sampling clock which is synchronized with input changes, rather than a free running clock.

Reference

- ¹ WILDE, R. W. and WESTCOTT, J. H. *Automatica*, VI, No. 1 (1962).

W. H. P. LESLIE, *National Engineering Laboratory, E. Kilbride, Scotland*

Professor Young's results show always a delay of the order of his sampling time when there is a change in eye position or velocity. A fixed sampling frequency would predict that any delay from zero to the sampling period would be equally likely.

Would he agree that his results suggest that the sampling is in abeyance until predictable movements do not accurately follow the input—at this time the regular sampling is initiated and takes its part until the error is again small.

L. R. YOUNG, *in reply*

I do agree with Mr. Leslie that in order to achieve a unit delay at the beginning of a response the sampling is held in abeyance and I so state in the paper: 'Furthermore, the error sampling for the pursuit and saccadic loops will be assumed to be synchronous, both starting with the initiation of any significant change in target position or velocity following a quiescent period.' Constant position or velocity are merely special types of predictable inputs.

O. L. UPDIKE, *University of Virginia, Charlottesville, Virginia, U.S.A.*

The 200–300 msec delay suggests a possible relation to the 'scanning' of the alpha rhythm observed in electro-encephalography. A conceivable 'programme' would take two or three cycles to confirm the existence of an error. Have any electro-encephalograms been taken during tests of the type reported? (I admit the dubious nature of any speculation based on EEG-rhythms of conscious subjects with open eyes!)

L. R. YOUNG, *in reply*

The speculation of Professor Updike is perhaps not as dubious as he supposes. Although the alpha rhythm does not seem to be a simple scanning (or readout of local memory), it is probably closely related to the biological clock which accounts for the 0.2 sec psychological refractory period. In a study performed while at M.I.T.¹, Latour demonstrated harmonic relationships between periodicities in eye movement reaction time and the alpha rhythm period, and he hypothesized that the brain stem reticular formation is primarily responsible for variations in reaction time.

Reference

- ¹ LATOUR, P. L. The eye and its timing. *Report No. 1 ZF 161-2*, Institute for Perception RVO-TNO, Soesterberg, Netherlands (1961)

APPLICATION TECHNIQUES

Self-adaptive Method for Accommodating Large Variations of Plant Gain in Control Systems

R. J. KOCHENBURGER

Summary

This paper relates to a common type of practical problem where the gain parameter of the plant in a feedback control system varies over a substantial range. In the specific application being considered this gain parameter varied by a factor greater than 100:1.

Sophisticated control techniques of the self-optimizing type could have provided ready solutions to this problem. However, because of the limitations imposed on the cost of the controls, the use of those techniques requiring elaborate computation facilities was not permitted.

To meet this problem, a high-frequency low-amplitude limit-cycle type of self-sustained oscillation is permitted to develop within the control loop and to serve as a 'dither' signal. At the control output, its amplitude is small enough to be unobjectionable. This limit-cycle oscillation results in a signal that 'tests' the plant's gain parameter and then, because of its effect on a non-linear limiting type of pre-amplifier, automatically varies the preamplifier gain in such a way as to maintain a relatively constant net control loop gain.

The application of various techniques of non-linear system analysis toward the development of this method is described in the paper.

Sommaire

Cette communication se rapporte à un type courant de problème pratique dans lequel le paramètre de gain de l'installation réglée dans un système de commande automatique à réaction varie dans des limites substantielles. Dans l'application spécifique envisagée, ce paramètre de gain variait avec un facteur supérieur à 100:1.

Des techniques de commande complexes du type à auto-optimisation auraient pu fournir des solutions toutes trouvées de ce problème. Toutefois, étant données les limitations imposées au prix de la commande, l'emploi de ces techniques, nécessitant des calculateurs très complets, n'a pas été autorisé.

Afin de résoudre ce problème une auto-oscillation, du type d'oscillation-limite à faible amplitude et à haute fréquence, est réalisée dans la boucle de commande et sert de signal à oscillation forcée. A la sortie de la commande, son amplitude est suffisamment faible pour être acceptable. Cette oscillation-limite résulte en un signal qui «essaie» le paramètre de gain de l'installation réglée, et, en raison de son effet sur un préamplificateur non-linéaire du type à limitation, fait varier automatiquement le gain du préamplificateur de manière à maintenir relativement constant le gain équivalent de la boucle de commande.

L'application de diverses techniques d'analyse des systèmes non-linéaires au développement de cette méthode est décrite dans cette communication.

Zusammenfassung

Der Aufsatz behandelt das bekannte Problem, daß der Übertragungsbeiwert (Verstärkungsgrad) einer Regelstrecke sich in weiten Grenzen ändert. Bei der speziellen Anwendung war die Änderung größer als 100:1.

Hochentwickelte Regelkreise vom selbstoptimierenden Typ hätten eine befriedigende Lösung der Aufgabe ermöglicht. In diesem Sonderfall war aber — wegen der Begrenzung des Aufwandes für die Geräte — die Anwendung solcher Verfahren, welche umfangreiche Rechner erfordern, nicht möglich.

Zur Lösung dieser Aufgabe läßt man es zu, daß sich in dem Regelkreis eine hochfrequente, bis zum Grenzyklus anschwellende Schwingung bildet, die ein „Rütteln“ in dem Kreis erzeugt. Am Ausgang der Regelstrecke ist ihre Amplitude so klein, daß sie die Funktion der Anlage nicht stört. Die Schwingung ist somit ein Testsignal, welches den Übertragungsbeiwert der Strecke erfaßt und ihn durch seine Wirkung auf einen Vorverstärker mit ausgeprägter Sättigungsgrenze derart beeinflusst, daß die Verstärkung des offenen Kreises nahezu konstant bleibt.

Die Anwendung verschiedener Formen der Analyse nichtlinearer Systeme auf die Entwicklung dieses Verfahrens wird dargestellt.

General Nature of the Problem

This paper describes a method proposed to solve a specific feedback control problem. However, since this same basic problem arises so often in other guises unrelated to the application being considered here, the method of solution that has been proposed will be described in general terms with the specific problem that gave rise to this paper being used to provide a 'numerical example' of this approach.

Self-adaptive controls with varying degrees of sophistication, complication and expense, have been used to meet the general problem of controlling variable parameter systems. The type

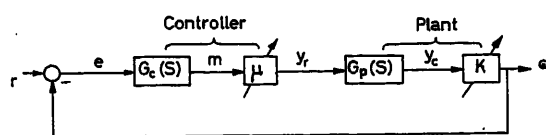


Figure 1. Statement of the basic problem

of problem being referred to here is one where the variable system parameter is the gain parameter of the plant being controlled. This is explained best by means of Figure 1.

There, $G_p(s)$ and K represent the system to be controlled, or 'plant'. $G_p(s)$ represents the essentially constant parameter portion of this plant, and K the variable gain parameter. It is desired that the plant's output, or 'controlled variable', c , follow commands of the reference input signal, r . For this purpose, the 'loop is to be closed' about a cascade controller represented by a transfer function, $G_c(s)$, and a variable controller gain, μ .

If the plant's gain parameter, K , were constant, the system design problem would be a conventional one handled in a straightforward manner with $G_c(s)$ being chosen on the basis of such specifications as speed of response and dynamic error and with noise and controller saturation considerations being taken into account. The controller design problem is, however, aggravated by the fact that the plant gain, K , may vary by a factor of as great as 100:1. This variation may be unpredictable and, furthermore, order-of-magnitude variations of K may occur within time intervals that are comparable to the desired response time of the control system.

The most obvious first step toward the solution of such a problem is the provision of a variable controller gain, μ , so that the product, μK , will always remain constant. If this can be done, conventional synthesis methods may be used to complete the controller design. The problem now remaining is, how can such an appropriate variation of μ be accomplished?

Specific Nature of the Problem

In the specific problem that gave rise to this paper, the plant to be controlled was a machine process. This machine was already equipped with a feedback control system used to establish an intermediate output signal, y_c , in response to command signals, y_r . $G_p(s)$ of Figure 1 represents the closed loop response of this already existing system. For purposes of example based on one mode of operation, this transfer function may be expressed approximately as

$$G_p(s) = \frac{1}{(1 + 0.2s)^2(1 + 0.005s)} \quad (1)$$

The control problem that was considered here was the control of a related output, c , rather than y_c . Increments of c and y_c are related by a factor K ; i.e.

$$\frac{\partial c}{\partial y_c} \triangleq K$$

K depends upon the properties and dimensions of the item being processed by the machine; it may vary considerably from one item to another and, considering the many different types of materials involved, the range of variation of K to be accommodated in this control system may be of a magnitude as great as 10^9 . Much of this range of variation can be accommodated by changing sensing elements and by other discrete adjustments

made in accordance with the type of machine operation involved. However, for any one adjustment, a range of variation of K as great as 100:1 should still be accommodated by the control system itself. One reason for this requirement is the very variable and frequently erratic variation of K that will be exhibited during some phases of the machine process being controlled.

Proposed Self-adaptive Control Method

The wide range of parameter variation to be accommodated negates any fixed parameter control system; the need for a self-adaptive system is obvious. On the other hand, the control problem is simpler than many, in that the configuration and dynamics of the plant are reasonably fixed and well known; only the gain parameter varies. Therefore some of the more elaborate methods of computer control adaptation are not necessary. (This is fortunate since this application would not permit the expense that most of these methods entail.) As a matter of fact, the speed of adaptation required because of the rapid changes possible in the variable parameter, K , is such that most of these more elaborate methods would not be sufficiently rapid. The method of self-adaptation that finally was adopted was not completely new¹⁻⁴ and, as a matter of fact, very similar principles have been used for some types of automotive generator regulators long before the expression 'adaptive control' became a part of the engineering vocabulary.

In this application, the process identifying test signal must provide indications of K at a very high sampling frequency; the introduction of some type of 'dither' signal for this purpose therefore appears necessary. Cost considerations did not permit complex computing equipment and the modification of the variable controller gain, μ , in accordance with the observed value of K was to involve a minimum of 'hardware'. With these considerations in mind, the answer seemed to be a system which generated its own dither by means of limit-cycle oscillations and then used the transmission level of the dither signal as a measure of plant gain. This transmitted dither signal is then used to vary the gain ('gain', in the describing function sense) of a limiting amplifier in such a way that the product of plant and controller gains tends to remain constant.

In Figure 1, the output of the linear, constant parameter part of the controller, $G_c(s)$, was designated as m . Figure 2 (a) shows this signal as being applied, effectively, to the variable gain

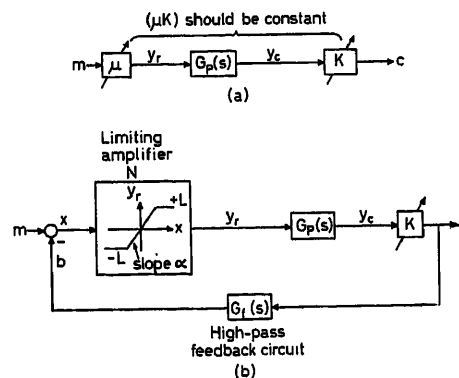


Figure 2. Configuration for effecting adaptive controller gain: (a) Variable controller gain effect desired; (b) minor feedback loop to produce equivalent of (a)

element, μ . Diagram (b) of Figure 2 shows the minor feedback loop to accomplish this gain variation in practice. Introduced in this loop are a high gain limiting amplifier designated as N and a linear feedback network, $G_f(s)$. The limiting amplifier has a gain, α , within its saturation limits. Its output signal is limited to the maximum limits of $y_r = \pm L$ by feedback limiting means.

$G_f(s)$ is a high pass filter type of feedback network selected so that the high frequency limit cycle oscillation, or dither, will be produced in this minor feedback loop for all values of the plant gain, K . The angular frequency of these oscillations, ω_d , should be sufficiently high so that the plant's low-pass filtering action will cause their amplitude at the plant's output to be of a small enough magnitude to be unobjectionable.

The output of N will be a severely clipped sinusoid with steep sides, appearing almost as a rectangular wave. In the absence of a correction signal, m , this output signal will, when plotted versus time, be symmetrical about the time axis and have zero average value. This is shown in Figure 3. The x signal shown there results from the dither feedback, b , through $G_f(s)$. The low-pass filtering action in the minor loop causes b to appear almost sinusoidal.

For the purpose of explanation, let it be considered that m now assumes some constant positive value. The result now will be a loss in the symmetry of the limiter output, y_r . As shown in Figure 4, a corresponding average value of the limiter output, designated as y_{ro} , will now appear. By proper selection of α , L , and $G_f(s)$, the relationship between y_{ro} and m can be made almost proportional; that is

$$y_{ro} \cong \mu m \quad (2)$$

This proportionality factor, μ , may be made equal to that of the corresponding desired variable gain element shown in Figure 1 and in Figure 2 (a). A describing function analysis shows that it will be approximately inversely proportional to K so that the desired variable gain function of μ will be realized.

The explanation above was based upon the assumption that the correction signal, m , was constant. It will apply as well, however, if m is varying slowly enough so that it may be approximated as constant during at least any one cycle of the dither oscillation⁵. This will be the case in practice since, as mentioned above, the dither frequency, ω_d , must be adjusted to be very much greater than the response frequency range of the control system.

The minor feedback loop shown in Figure 2 (b) therefore performs, in a very rudimentary but adequate fashion, all the functions of a self-adaptive control. It generates its own periodic identification signal. The effect of the variations of gain, K , on this signal operates through the non-linear function of the limiting amplifier to vary the gain factor, μ , in an appropriate manner. The topic up to this point has been qualitative and the next section will present the quantitative considerations necessary for successful system synthesis.

Design of the Adaptive Feedback Loop

Selection of Dither Frequency

The dither frequency, ω_d , is selected to be sufficiently high so that the low-pass filtering action of the plant will result in the dither having an unobjectionable low amplitude as it appears at the plant output. This high frequency dither component of

the plant's output, c , is designated here as c_d . It is determined as follows. The output of the limiting amplifier will be a clipped sinusoid which, as shown in Figures 3 and 4, may be approximated as a rectangular wave switching back and forth from $+L$ to $-L$. Because of the plant's low-pass filtering action, only the fundamental harmonic component of this wave need be considered; this fundamental component is a sinusoid with an amplitude equal to $(4/\pi)L$. The resulting amplitude at the plant's intermediate output, y_{ca} , will be

$$|y_{ca}| = \frac{4}{\pi} L |G_p(j\omega_d)| \text{ cm} \quad (3)$$

The dither frequency is then chosen so that $|y_{ca}|$ is sufficiently small.

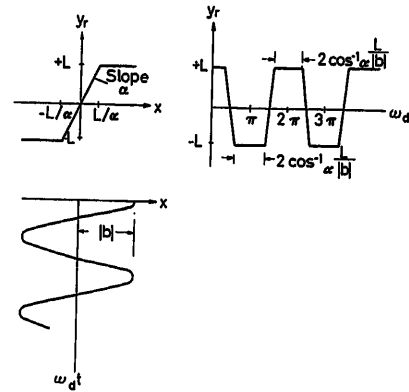


Figure 3. Output-input characteristics of limiting amplifier—zero correction signal, m

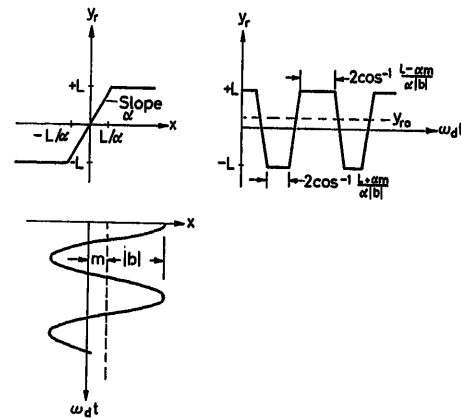


Figure 4. Output-input characteristics of limiting amplifier, with correction signal, m

In the particular application referred to, $G_p(s)$ could be approximated by the following general form of transfer relationship:

$$G_p(s) = \frac{1}{(1 + \tau_1 s)(1 + \tau_2 s)(1 + \tau_3 s)} \quad (4)$$

where the specific values of the time constants, corresponding to relation (1), are

$$\tau_1 = \tau_2 = 0.2 \text{ sec}; \tau_3 = 0.005 \text{ sec}$$

At the dither frequency, $|G_p(j\omega)|$ is

$$|G_p(j\omega_d)| = \left| \frac{1}{(1+j\omega_d\tau_1)(1+j\omega_d\tau_2)(1+j\omega_d\tau_3)} \right|$$

$$\approx \frac{1}{\omega_d^3\tau_1\tau_2\tau_3}$$

since, in general, ω_d will be such that $\omega_d\tau_1$, $\omega_d\tau_2$, and $\omega_d\tau_3$ will all be very much greater than unity. Hence, from relation (3)

$$\omega_d = \left[\frac{4}{\pi} \frac{L}{\tau_1\tau_2\tau_3|y_{ca}|} \right]^{\frac{1}{3}} \quad (5)$$

which is the dither frequency required for a specified dither amplitude. For the particular operating condition being used as an example here, the amplifier limits, L , proposed were 1 cm; that is, the amplifier could command intermediate outputs from -1 to $+1$ cm. The dither amplitude at the plant, $|y_{ca}|$, was to be no greater than 10^{-4} cm. Hence, from relation (5), ω_d was selected as 400 rad/sec (or 64 c/sec).

Establishment of the Dither Frequency

The dither signal will have whatever frequency, ω_d , results in 180° phase lag around the negative feedback loop shown in Figure 2 (b). The feedback network, $G_f(s)$, therefore, is selected with this in mind and in consideration of the value of ω_d that was selected from relation (5) above. For plant characteristics of the type considered here, the feedback network's transfer function was chosen as:

$$G_f(s) = \frac{K_f s^3 (1 + \tau_3 s)}{(1 + \tau_1 s)^4} \quad (6)$$

The actual network used to obtain this transfer function was of the active type, employing an operational amplifier.

It may be noted that the numerator time constant, τ_3 , of this transfer function 'cancels' the shorter time constant, also τ_3 , of the plant transfer function. The combined transfer function $G_p(s)KG_f(s)$ (which includes all of the minor loop except the non-linear limiting amplifier), then has the following value at the dither frequency, ω_d :

$$G_p(j\omega_d)KG_f(j\omega_d) = \frac{KK_f(j\omega_d)^3}{(1+j\omega_d\tau_1)(1+j\omega_d\tau_2)(1+j\omega_d\tau_f)^4}$$

or, since, in view of the high value of ω_d required, $\omega_d\tau_1$ and $\omega_d\tau_2$ are both very much greater than unity, approximately as

$$G_p(j\omega_d)KG_f(j\omega_d) \approx \frac{KK_f(j\omega_d)}{\tau_1\tau_2(1+j\omega_d\tau_f)^4}$$

$$\approx \frac{KK_f\omega_d}{\tau_1\tau_2[1+(\omega_d\tau_f)^2]^2} \angle 90^\circ - 4 \tan^{-1}(\omega_d\tau_f) \quad (7)$$

Since this transfer function is to present 180° phase lag at $\omega = \omega_d$, $\tan^{-1}(\omega_d\tau_f)$ should equal 67.5° ; the required time constant, τ_f , is therefore given by

$$\tau_f = \frac{\tan 67.5^\circ}{\omega_d} = \frac{2.42}{\omega_d} \text{ sec} \quad (8)$$

the requirement for establishing desired dither frequency.

Establishment of the Dither Amplitude

The limit cycle oscillation that establishes the dither should be maintained at even the lowest value of the variable plant gain, K . The conditions for the limit cycle to exist may be established by the describing function method since relation (7) above indicates that the higher frequency distortion harmonics of the dither signal will be attenuated, in comparison with the fundamental, by a factor that is roughly proportional to the square of the harmonic order. The feedback input signal, b , may therefore be considered as sinusoidal and the limiting amplifier, N , may be represented in terms of its describing function, also designated by the symbol, N .

The well-known describing function for such a limiting amplifier is plotted in Figure 5. In the diagram, $|b|$ represents the magnitude of the assumed sinusoidal feedback signal that is being applied to the amplifier. The analytic expression for the describing function, on which Figure 5 is based, is given by

$$N = \alpha \quad \text{for } \alpha|b| < L$$

$$= \frac{2\alpha}{\pi} \left[\sin^{-1} \frac{L}{\alpha|b|} + \frac{L}{\alpha|b|} \left(1 - \left(\frac{L}{\alpha|b|} \right)^2 \right)^{\frac{1}{2}} \right] \quad \text{for } \alpha|b| > L \quad (9)$$

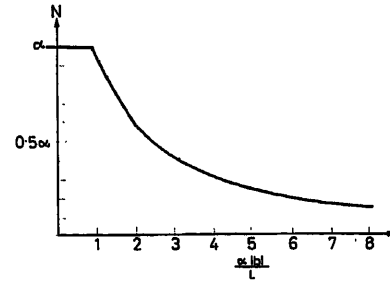


Figure 5. Describing function of the limiting amplifier

Oscillations will occur at an amplitude, $|b|$, where the product of this describing function and the magnitude of the $G_p(j\omega_d)KG_f(j\omega_d)$ transfer function is equal to unity. If condition (8) is substituted in relation (7), the magnitude of this latter transfer function becomes

$$|G_p(j\omega_d)KG_f(j\omega_d)| = \frac{KK_f\omega_d}{46\tau_1\tau_2} \quad (10)$$

For self-sustained dither oscillations to exist at all, the expression given in (10) must be equal to at least $1/\alpha$, since α represents the highest magnitude that the describing function, N , can attain. The condition for limit cycles is therefore

$$\alpha K_f > \frac{46\tau_1\tau_2}{K\omega_d} \quad (11)$$

When this condition is just met, the amplifier is driven to its limits at $\pm L$. In order to realize the self-adapting function performed by the limiting amplifier, the oscillation should drive the amplifier well beyond these limits. The 'rule of thumb' proposed for actual design was therefore that the left-hand expression in the above relation be at least five times the right for the minimum value, K_{\min} , of the plant sensitivity, K , that is to be encountered. On this basis, the combined gain constants should be

$$\alpha K_f = \frac{230\tau_1\tau_2}{K_{\min}\omega_d} \quad (12)$$

the condition for adequately clipped dither oscillations. If the above condition is met, then for $K = K_{\min}$, the limit cycle amplitude will adjust itself to a value where N , as given by relation (9), is just equal to $\alpha/5$. By solving relation (9) by implicit methods, or by means of a more accurate version of Figure 5, this corresponds to an input condition at the limiting amplifier where $L/\alpha|b| = 0.15$. That is, the amplifier will be driven at 1/0.15, or about six times the value necessary to cause limiting. As shown in Figure 3, limiting exists for $2 \cos^{-1}(0.15)$ or 163° out of every 180° of half-cycle. Therefore, even for this minimum value of plant gain, the amplifier output, y_r , may be represented, approximately, as a rectangular wave. For higher values of K , the limiting occurs during an even longer portion of the limit cycle and the rectangular wave approximation is even more valid.

The particular numerical example being used here is based upon designing for a particular range of plant gain, K , from $K_{\min} = 10^4$ to $K_{\max} = 10^6$. The plant time constants have already been described as $\tau_1 = \tau_2 = 0.2$ sec and ω_d has been selected as 400 rad/sec. From relation (12), the required gain product, αK_f , should therefore be made equal to 2.3×10^{-6} .

System Gain at Signal Frequency

Referring back to Figure 2, the purpose of the minor loop, just introduced and shown in Figure 2(b), is to produce a gain effect equivalent to a cascade element, μ , which varies so that the product, μK , remains essentially constant. This effect will apply at signal frequencies in the main outer control loop that are substantially lower than the dither frequency, ω_d . During any one cycle of the dither signal, the correction signal, m , applied by $G_c(s)$ may be considered as essentially constant and the situation illustrated in Figure 4 applies. It will be adequate to approximate the clipped sinusoidal y_r signal shown there as a non-symmetrical rectangular wave with a positive $(+L)$ duration of $2 \cos^{-1}(L - \alpha m)/\alpha|b|$ and a negative $(-L)$ duration of $2 \cos^{-1}(L + \alpha m)/\alpha|b|$. The average value of the limiting amplifier output for any one limit cycle therefore will be

$$y_{ro} = \frac{L}{2\pi} \left[2 \cos^{-1} \frac{L - \alpha m}{\alpha|b|} - 2 \cos^{-1} \frac{L + \alpha m}{\alpha|b|} \right] \text{ cm}$$

or

$$y_{ro} = \frac{L}{\pi} \left[\sin^{-1} \left\{ \frac{L}{\alpha|b|} \left(1 + \frac{\alpha m}{L} \right) \right\} - \sin^{-1} \left\{ \frac{L}{\alpha|b|} \left(1 - \frac{\alpha m}{L} \right) \right\} \right] \quad (13)$$

However

$$|b| = \frac{4}{\pi} L |G_p(j\omega_d) K G_f(j\omega_d)|$$

or, from (10)

$$|b| = \frac{1}{11.5\pi} \frac{KK_f\omega_d L}{\tau_1\tau_2}$$

and

$$\alpha|b| = \frac{1}{11.5\pi} \frac{K\omega_d L}{\tau_1\tau_2} \alpha K_f$$

However, after substituting design relation (12) for the combined gain constants, αK_f , the result is obtained that

$$\alpha|b| = \frac{20}{\pi} \frac{KL}{K_{\min}}$$

and

$$\frac{L}{\alpha|b|} = \frac{\pi}{20} \frac{K_{\min}}{K}$$

Therefore relation (13) for y_{ro} becomes

$$y_{ro} = \frac{L}{\pi} \left[\sin^{-1} \left\{ \frac{\pi}{20} \frac{K_{\min}}{K} \left(1 + \frac{\alpha m}{L} \right) \right\} - \sin^{-1} \left\{ \frac{\pi}{20} \frac{K_{\min}}{K} \left(1 - \frac{\alpha m}{L} \right) \right\} \right] \text{ cm} \quad (14)$$

In general, the approximation may be used that $\sin^{-1} x \cong x$. Relation (14) then attains the much simpler form

$$y_{ro} \cong 0.1 \alpha \frac{K_{\min}}{K} m \text{ cm} \quad (15)$$

As long as the signal frequencies are small compared to ω_d , y_{ro} may be considered as equivalent to the signal, y_r , itself, as far as the main control loop shown in Figure 1 is concerned. Relation (15) shows that one objective has been accomplished in that this equivalent y_r signal is approximately proportional to the correction signal, m . In Figure 1 and 2(b), this transfer relation was designated by the variable gain block described as μ , μ , defined originally by relation (2), therefore becomes

$$\mu \cong 0.1 \alpha \frac{K_{\min}}{K} \quad (16)$$

In order to obtain the desired gain, μ , and in consideration of the signal levels convenient for the electronic amplifiers involved, the gain of the limiting amplifier, α , was chosen as 10. Since, for the numerical example being described here, the value of K_{\min} , upon which design was based, was $K_{\min} = 10^4$, μ would then be equal to $1000/K$. The second and basic objective has, therefore, also been accomplished in that the gain product, μK , will be essentially constant.

In consideration of the value of the gain product, αK_f , already selected from relation (12) and the value of α chosen above, the required gain constant of the feedback network, K_f , will be 2.3×10^{-7} .

Closing the Main Control Loop

Figure 6 is a block diagram of the complete system including both minor and major feedback loops.

For the purpose of analysing the major loop response, the transfer function, $\mu K G_p(s)$ may be substituted for the minor loop portion. Figure 7 then results.

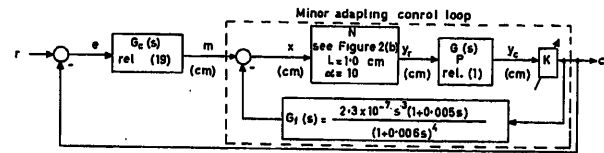


Figure 6. Complete system configuration for numerical example

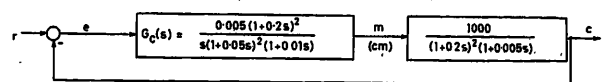


Figure 7. Equivalent main control loop—valid at signal frequencies

From relations (4) and (16), the plant to be controlled appears to the controller, $G_c(s)$, as

$$\mu K G_p(s) = \frac{0.1 \alpha K_{\min}}{(1 + \tau_1 s)(1 + \tau_2 s)(1 + \tau_3 s)} \quad (17)$$

or, with the numerical values applicable to the example being used here, as

$$\mu K G_p(s) = \frac{1000}{(1 + 0.2s)^2(1 + 0.005s)} \quad (18)$$

The selection of the controller transfer function may now be based upon the simple techniques used for linear constant parameter systems. The proposed controller transfer function, $G_c(s)$, shown in Figure 7, is

$$G_c(s) = \frac{0.005(1 + 0.2s)^2}{s(1 + 0.05s)^2} \frac{1}{(1 + 0.01s)} \quad (19)$$

The second term of the above represents a second-order phase-lead controller used to improve the obtainable speed of response. The last term represents an RC type of low-pass filter used to prevent the feedback dither signal from causing electronic amplifier saturation because of its accentuation by the phase lead network.

The net transfer function of the main control loop then becomes

$$G(s) \triangleq \frac{c(s)}{e(s)} = \frac{5}{s(1 + 0.05s)^2(1 + 0.01s)(1 + 0.005s)} \quad (20)$$

the velocity error coefficient, or K_v , being 5.0 sec^{-1} . The computed closed-loop response then is

$$\boxed{\text{Eqn (21)}}^*$$

The predominant response mode therefore has an undamped natural frequency of 8.2 rad/sec and a damping ratio of 0.64 .

All of the preceding analysis has been based upon the assumption that only the minor loop need be considered as far as the transmission of the dither frequency is concerned, and that only the main control loop need be considered in regard to the transmission of the basic control signals. The first of these assumptions depends upon the requirement that $|G_c(j\omega_d)| \ll |G_f(j\omega_d)|$. A numerical evaluation of these transfer functions will verify that this requirement is being met. The second assumption is based upon the requirement that $|G_f(j\omega)| \ll |G_c(j\omega)|$ for all ω 's within the response range of the control system. Relation (21) indicates that this response bandwidth may be considered as extending to $\omega = 8.2 \text{ rad/sec}$. A numerical evaluation of these transfer functions $G_f(j\omega)$ and $G_c(j\omega)$ for all ω 's up to $\omega = 8.2$ will show that this second requirement is being met as well. The fairly complex nature of the $G_f(s)$

transfer function that has been employed (involving a third-order zero at the 's plane origin') was necessary so that this second requirement would be met.

At the time of the initial submission of this paper, this scheme was still in the proposal stage and had not been applied to an actual machine. The various transfer functions described above are therefore still tentative and may require modification in order to meet the performance specifications of the machine. However, all the results described above have been verified by means of analogue computer studies, including the self-adaptive feature that represents the major point of this paper. During such studies, the plant gain, K , was varied rapidly between the limits of the maximum and minimum values stated, while the system was following various varying command signals; no noticeable effect on the nature of the output response was observed because of these variations of K .

Conclusions

The method proposed here constitutes a simple but adequate adaptive control scheme for those applications where a variation of the plant's gain parameter over large ranges constitutes a major problem. It is a practical method when the existence of the required high-frequency self-sustained dither signal is not considered to be objectionable. As a matter of fact, the dither introduced here has one beneficial aspect in that it helps to overcome static friction effects that might otherwise cause an erratic response. This method of adaptive control is therefore being presented in this paper, not only because of its application to the machine process problem described, but also because it should have application to many other engineering control problems as well.

Acknowledgement is due to Prof. V. B. Haas of the University of Connecticut whose suggestions have been especially helpful.

References

- 1 LOZIER, J. C. Carrier controlled relay servos. *Elect. Engr* 69, No. 12 (1950) 1052-6
- 2 LI, Y. T. and VAN DER VELDE, W. E. Philosophy of non-linear adaptive systems, automatic and remote control. *Proc. 1st Congr. I.F.A.C. Moscow* 2 (1961) 577-585 Butterworths, London
- 3 POPOV, E. P. and PALTOV, N. P. *Approximate Methods for Investigation of Non-linear Automatic Systems* (In Russian) 1960. Moscow; Government Publishing House for Physics
- 4 GELB, A. The dynamic input-output analysis of limit cycling control systems. *Inst. rad. Engrs Pap.* 9-3, *Joint Automat. Control Congr.*, June 27-29, 1962
- 5 WEST, J. C., DOUCE, J. L. and LIVESLEY, R. K. The dual input describing function and its use in the analysis of non-linear feedback systems. *Proc. Instn elect. Engrs Pap.* 1877 M. (July, 1955)

* Eqn (21):

$$\frac{c(s)}{r(s)} = \frac{1}{\left[1 + 2(0.64)\left(\frac{s}{8.2}\right) + \left(\frac{s}{8.2}\right)^2\right] (1 + 0.033s)(1 + 0.01s)(1 + 0.005s)} \quad (21)$$

DISCUSSION

G. SCHMIDT, *Institut für Regelungstechnik, Darmstadt, Germany*

This paper by Professor Kochenburger describes a very interesting solution to the problem of adapting a control system to large parameter variations by non-linear means. The speed of adaptation is high and can be determined by a method given elsewhere¹.

A shortcoming of this approach, in certain applications, seems to be the high-frequency limit cycle which is always present and which may cause failure of components. Furthermore, the amplitude of the oscillation of the actual output variable $c(t)$ (Figure 1 of the paper) during the limit cycle is directly proportional to the gain factor K .

Reference

GELB, A. and VAN DER VELDE, W. E. On limit cycling control systems. *IEEE Trans. on Automat. Contr.*, AC-8 (April 1963)

R. J. KOCHENBURGER, *in reply*

I agree completely with Mr. Schmidt in regard to his criticism of the proposed control technique. The limit cycle oscillations *must* appear at the output of the plant, otherwise the method will not work. If such oscillations are objectionable, then the method suggested here cannot be used. On the other hand, the paper points out that there are instances where these oscillations may be beneficial because they produce a dither effect that may help overcome the effects of static friction. As Mr. Schmidt points out, the limit cycle oscillations are the greatest under conditions of high plant gain.

May I pose a counter-question? If the limit cycle oscillations appearing at the plant output are objectionable, what method can be used? It must be kept in mind that we are dealing with the problem of a parameter that may vary very rapidly. Therefore, some form of high-frequency test signal is necessary and this signal must be of a sufficiently large amplitude that it will affect the plant output if it is to perform its measurement function properly. So, as much as we might object to the appearance of the test disturbances at the output, I frankly cannot think of a way out of this dilemma.

G. ULANOV, *U.S.S.T. National Committee of the I.F.A.C., Moscow, U.S.S.R.*

This paper, proposed by the author, is quite interesting. It relates to a common type of practical problem, where the gain parameter of the plant in a feedback control system varies over a substantial range, e.g. 1:100 and more. To solve this problem a high-frequency low-amplitude type of self-sustained oscillation is permitted to develop within the control loop, which eliminates elaborate computation facilities. As a matter of fact, it is a very powerful technique in non-linear systems. Meanwhile, I do not agree with the author's conclusion, that in general we do not have to point out the structure of the control system, operating as a self-adaptive system, but having fixed parameters. I believe that now we shall be able to discuss two practical systems without computation facilities.

(1) Meerov's paper¹ describes the method of designing control systems with constant structures and constant parameters, the properties of which are equivalent to one of the author's systems. These systems are based on the structure, which admits the increase of gain coefficients without disturbing the stability. It was shown that the mentioned structures do not depend on the variation of the parameters of the plant under the corresponding increase of the gain coefficient.

(2) The problem of sustaining $\mu \cdot K = \text{const.}$ can be considered as an invariant problem. Now a new design principle for the systems, invariant to any continuous control function and variable parameters, was developed. In our paper we discussed the system with variable structure, but constant parameters. It used also a non-linear term and sliding movement. Usually the error signal is independent of control action and variations of parameters only, if the right-hand side of the

system non-homogeneous differential equation vanishes and the result is the slide movement. In this case any variations of plant parameters would make this invariancy condition invalid. For example I want to show that the variable structure control system is insensitive to a certain variation of the system parameters (Figure A).

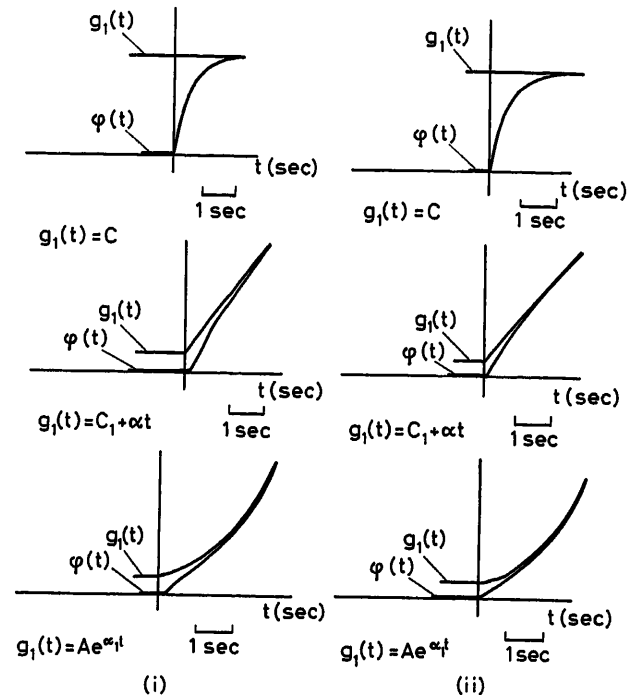


Figure A

On this figure you can see the performance of the combined servosystem with variable structure. On the left-hand side is shown the general performance (the input and the output of the system). It is very interesting that the error of the system is zero even to an exponential input. We have the infinitive astatic servosystem.

On the right-hand side is shown the performance, if the parameters of the system have a wide-range variation. It can be seen that the system with the variable structure is practically invariant to wide-range variations of the parameters of the system. This oscillogram was made by using the high-accuracy analogue computer, designed by Acad. Trapeznikov.

Reference

¹ MEEROV, M. V. Synthesis of systems with the fixed characteristics of equivalent self-adjusting systems. *Automatic and Remote Control*. 1964. London; Butterworths. Munich; Oldenbourg

J. A. TANNER, *National Research Council, Ottawa 7, Ontario, Canada*

Since the 'dither' amplitude is small it would appear that the gain adaptive minor loop is sensitive to noise occurring in the plant, i.e. $G_p(s)$ of the paper. Has the author studied the overall system behaviour with additive disturbances, the variations in K discussed in the paper being multiplicative disturbances?

The author has mentioned that the presence of a dither may be intolerable in some applications. I would suggest that the system gain could be adjusted in discrete steps as a function of the integral modulus error. This error excursion would determine the gain setting.

R. J. KOCHENBURGER, *in reply*

Professor Ulanov's discussion is very interesting as it proposes an alternative approach to the problem of rapid parameter variation. His reference is specifically to the paper by M. V. Meerov, also presented at this Congress. A further study, possibly accompanied by analogue computer studies, might best indicate those circumstances under which Meerov's technique, as opposed to mine, would be most appropriate.

Mr. Tanner's comments are greatly appreciated since they bring out important points not covered in the original paper. The original design criteria described in the paper was based upon analogue computer studies. Subsequent tests on an actual system did result in problems caused by noise. This was solved quite readily by introducing another time constant, of 0.005 sec, in the feedback function $G_f(s)$.

I question whether Mr. Tanner's proposal of adjusting the gain in discrete steps as a function of the integral modulus would be successful in this particular application, because of the rapidity of the variation of the gain parameter.

Hydraulic Line Dynamics

R. OLDENBURGER and R. E. GOODSON

Summary

Fluid lines often play a major role in the dynamics of hydraulic control and other systems. The hydraulic line between two cross sections is characterized by a four-terminal network with pressure and rate of flow the interacting variables. Use of this network leads to transcendental transfer functions that are not suited to the computation of system transients. The standard technique of power series expansions fails in that this yields instability in most applications where this instability does not actually occur. These difficulties are overcome by the use of infinite products. Only a few factors of these products are needed to compute transients to engineering precision. In contrast to the classical lumped constant approach to distributed systems the accuracy of the approximation can be seen from the factors directly. The technique applies to electrical transmission lines as well as hydraulic. By this method one can smooth transient responses to step changes arising in water hammer studies. Good agreement has been obtained between theory and experiment.

Sommaire

Les lignes pour fluides jouent souvent un rôle capital dans la dynamique des commandes hydrauliques et d'autres systèmes. La ligne hydraulique entre deux coupes transversales est caractérisée par un quadripôle où la pression et le débit du fluide sont les variables couplées. L'utilisation de ce réseau conduit à des fonctions de transfert transcendentes qui ne conviennent pas au calcul des régimes transitoires du système. La technique standard de développement en séries de puissances échoue parce qu'elle conduit à de l'instabilité dans beaucoup d'applications où cette instabilité n'existe pas en fait. Ces difficultés sont surmontées par l'emploi des produits infinis. Quelques facteurs seulement de ces produits sont suffisants pour calculer les régimes transitoires avec une précision suffisante. Contrastant avec l'approche classique des constantes localisées, à l'étude des systèmes répartis, la précision de l'approximation peut être directement vue à partir des facteurs. Cette technique s'applique aux lignes de transmission électriques aussi bien qu'aux lignes hydrauliques. Par cette méthode, il est possible de réduire les réponses transitoires aux variations en échelon qui se produisent dans les études du phénomène de coup de bélier. Une bonne correspondance a été obtenue entre cette théorie et les résultats expérimentaux.

Zusammenfassung

Strömungsführende Leitungen spielen oft eine wichtige Rolle für das dynamische Verhalten hydraulischer Regelungen und anderer Systeme. Die hydraulische Leitung zwischen zwei Querschnitten wird durch einen Vierpol dargestellt, bei dem Druck und Strömungsgeschwindigkeit die sich gegenseitig beeinflussenden Veränderlichen sind. Die Benutzung eines solchen Netzwerkes führt zu transzendenten Übertragungsfunktionen, die sich für die Berechnung des Übergangsverhaltens des Systems nicht eignen. Die übliche Methode der Potenzreihenentwicklung versagt hierbei, da sich für die meisten Anwendungsfälle Instabilität ergibt, die in Wirklichkeit nicht auftritt. Diese Schwierigkeiten werden durch die Verwendung von unendlichen Produkten umgangen. Nur einige wenige Faktoren dieser Produkte sind für die technisch genaue Berechnung des Übergangsverhaltens nötig. Im Gegensatz zur klassischen Annäherung der Systeme mit verteilten Parametern durch konzentrierte Konstanten kann die Genauigkeit der Näherung direkt von den Faktoren abgelesen

werden. Das Verfahren ist sowohl auf hydraulische als auch elektrische Übertragungsleitungen anwendbar. Mit diesem Verfahren lassen sich Sprungantworten, wie sie bei der Untersuchung von Druckstößen auftreten, glätten. Zwischen den theoretischen und den Versuchsergebnissen wurde eine gute Übereinstimmung erzielt.

Introduction

High power and fast response hydraulic systems are required for many missile, aircraft and other applications. In the analysis and synthesis of such systems the fluid lines coupling the various components must be considered. The lumped constant approach is often employed, where nine or ten lumps per wavelength is used as a rule of thumb¹. This approach is limited since infinitely many degrees of freedom are actually involved. Where feasible the distributed parameter approach is to be preferred. The second-order transfer matrix equation of electrical transmission line theory is used here to relate pressures and flows at two cross sections of a hydraulic line. The matrix equation describes a four-terminal network, and agrees well with frequency response experiments for large and small pipes.

With the aid of boundary conditions one can often obtain transfer functions relating two of the four variables associated with two cross sections of a line. This is true, for example, if there is a fixed orifice at one of the sections, or there is a large reservoir at one section and a valve at the other discharging to atmosphere; or there might be a tank ahead of the valve. The transfer functions are transcendental in the Laplace variable s . It is convenient to employ these functions to compute frequency response, but serious mathematical difficulties are encountered when they are used to calculate transient response. The standard technique of expanding the functions in power series yields characteristic equations with negative coefficients implying system instability where it does not actually occur. To overcome this difficulty the transfer functions are written here as quotients of infinite products of factors linear in s . In practice one need keep only a few of the factors. A major advantage of this approach over the standard lumped constant technique is that one can see the accuracy of the approximation directly from the factors. The inclusion of more terms to approximate the transfer functions to greater bandwidth does not require solving successively higher degree algebraic equations. The infinite product approach applies to electric as well as hydraulic lines.

Fundamental Equations

It is assumed in this analysis that the hydraulic line is a straight horizontal pipe of constant circular cross section. At each cross section average pressure head, velocity and fluid density are employed. Friction is first neglected. The coordinate of distance along the pipe and time are denoted by x and t

respectively. The deviations in average velocity and pressure head at a cross section with coordinate x for the time t are given by $u(x, t)$ and $h(x, t)$ respectively. Letting ρ designate the fluid density, g the acceleration of gravity, K the bulk modulus of elasticity of the pipe material, f the pipe wall thickness and r the inner pipe radius, the well-known equations of flow¹ are

$$\frac{\partial u(x, t)}{\partial x} = -\alpha \frac{\partial h(x, t)}{\partial t} \quad (1)$$

$$\frac{\partial u(x, t)}{\partial t} = -g \frac{\partial h(x, t)}{\partial x} \quad (2)$$

where

$$\alpha = \rho g \left[\frac{1}{K} + \frac{2r}{fE} \right]$$

The speed a of sound in the pipe is given by

$$a = \sqrt{\frac{g}{\alpha}} \quad (3)$$

Let $U(x, s)$ and $H(x, s)$ be the Laplace transforms of $u(x, t)$ and $h(x, t)$ respectively where s is the Laplace variable. Let $q(x, t)$ be the average flow rate deviation at a pipe section of area A , whence

$$q(x, t) = A u(x, t) \quad (4)$$

Let $Q(x, s)$ be the Laplace transform of $q(x, t)$. Let sections 1 and 2 designate the cross sections $x = 0$ and $x = L$ of the pipe. See Figure 1. The variables $H_i(s)$, $Q_i(s)$ for $i = 1, 2$ are defined by

$$\begin{aligned} H_1(s) &= H(0, s) \\ H_2(s) &= H(L, s) \\ Q_1(s) &= Q(0, s) \\ Q_2(s) &= Q(L, s) \end{aligned} \quad (5)$$

The line impedance Z_0 and time constant T_e are given by

$$\begin{aligned} Z_0 &= \frac{a}{Ag} \\ T_e &= \frac{L}{a} \end{aligned} \quad (6)$$

The initial conditions $u(x, 0^+) = h(x, 0^+) = 0$ for flow rate and pressure head deviations at $t = 0^+$ are assumed to hold.

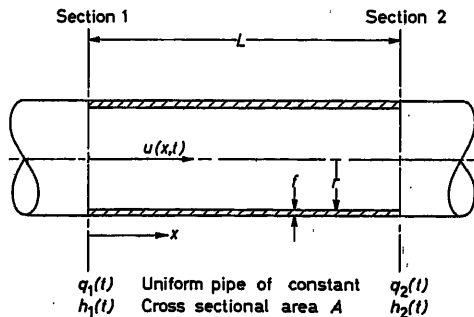


Figure 1. Hydraulic line

The solution of eqns (1) and (2) is now given by the matrix equation

$$G(s) V_1 = V_2 \quad (7)$$

where

$$G(s) = \begin{bmatrix} \cosh T_e s & -\frac{1}{Z_0} \sinh T_e s \\ -Z_0 \sinh T_e s & \cosh T_e s \end{bmatrix}$$

$$V_1 = \begin{bmatrix} Q_1(s) \\ H_1(s) \end{bmatrix}$$

$$V_2 = \begin{bmatrix} Q_2(s) \\ H_2(s) \end{bmatrix}$$

See the block diagram of Figure 2 where Σ is a summer.

Equation (7) applies if the pipe is not straight but has no sharp corners.

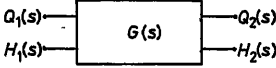
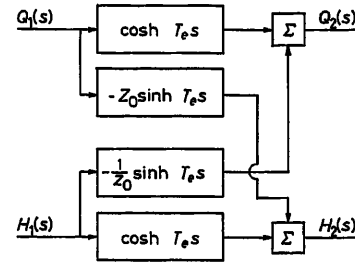


Figure 2. Block diagram of line

Tests

The validity of eqn (7) was verified for large lines by frequency response runs of Oldenburger and Donelson⁷ at the Apalachia power house of the Tennessee Valley Authority. They oscillated the gates of a 53,500 h.p. hydraulic turbine and recorded hydraulic among other variables. This system involved a tunnel 8 miles long and 18 ft. in diameter, a differential surge tank, and two 600 ft. penstocks, 11 ft. in diameter. Excellent agreement between theory and practice was obtained over the frequency range of $1/2$ c/h to 2 c/s. J. D. Regetz at the Lewis Center of the National Aeronautics and Space Administration made frequency response runs on a 1 in. diameter stainless steel pipe⁸. The distance between the cross sections 1 and 2 of this pipe was 68 ft. Wall thickness was $1/16$ in. Good agreement was obtained for 0.5 c/s to 90 c/s. The fluid was JP-4 jet fuel at 50 lb./in.² gauge, 25°C, average flow rate of 37 in.³/sec, and Reynolds number about 14,000. The area of a valve near section 1 was varied. The fluid discharged to atmosphere at section 2. Pressures and flow rates at sections 1 and 2 were recorded. Runs on a $1/2$ in. diameter line at the Automatic Control Center of Purdue University have also been successful.

The tests mentioned above indicate that the basic water hammer eqns (1) and (2) hold, friction effects are largely negligible (especially at high frequencies), and longitudinal pipe vibrations are small compared with the phenomena described by eqn (7).

Line Discharging Through a Fixed Orifice

It is supposed that there is a fixed orifice at section 2 of Figure 1. This is the case of Figure 3 where the volume of the chamber C at section 2 is zero and the opening $y(t)$ of the valve is constant. No restrictions are placed on the physical configuration to the left of section 1. Thus this is the case of a line discharging through an orifice. It is assumed that the following relation holds at section 2 for a constant K_0 dependent on the orifice characteristics:

$$g(L, t) = K_0 h(L, t) \quad (8)$$

Hence

$$Q_2(s) = K_0 H_2(s) \quad (9)$$

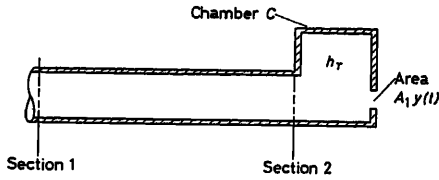


Figure 3. Pipe followed by chamber and valve

Equation (8) holds for an arbitrary orifice and small changes in pressure and flow about a steady operating point. By eqn (7) and (9) line transfer functions $G_1(s)$, $G_2(s)$ and $G_3(s)$ are obtained, where

$$G_1(s) = K_0 \frac{H_1(s)}{Q_1(s)} = \frac{\cosh T_e s + K_0 Z_0 \sinh T_e s}{\cosh T_e s + \frac{1}{K_0 Z_0} \sinh T_e s} \quad (10)$$

$$G_2(s) = \frac{H_2(s)}{H_1(s)} = \frac{1}{\cosh T_e s + K_0 Z_0 \sinh T_e s} \quad (11)$$

$$G_3(s) = \frac{Q_2(s)}{Q_1(s)} = \frac{1}{\cosh T_e s + \frac{1}{K_0 Z_0} \sinh T_e s} \quad (12)$$

With $s = j\omega$ for $j = \sqrt{-1}$ eqn (10) yields the normalized line impedance $G_1(j\omega)$. To verify eqn (7) Regetz³ made theoretical and experimental plots of the magnitude and phase of this transfer function versus frequency.

Line with Constant Pressure at One End

Consider the configuration of Figure 3 where there is a chamber C at section 2 of the line. The chamber pressure head deviation from equilibrium is denoted by h_T . The fluid discharges to atmosphere from the chamber C through a valve. The deviation in one effective orifice area of the valve is taken to be $A_1 y(t)$ for a constant A_1 and valve stroke deviation $y(t)$. Now

$$h_T = h(L, t) \quad (13)$$

For constants c_1 and c_2 depending on the characteristics of the valve, and a constant c_3 depending on the bulk modulus of the fluid and chamber characteristics one has

$$q(L, t) = c_1 y(t) + c_2 h(L, t) + c_3 \frac{dh(L, t)}{dt} \quad (14)$$

Thus

$$Q_2(s) = c_1 Y(s) + c_2 H_2(s) + c_3 s H_2(s) \quad (15)$$

where $Y(s)$ is the Laplace transform of $y(t)$.

It is assumed that there is a source of constant pressure at section 1, as when there is a large reservoir at this section, or accumulator supplying fluid, or a pump with a relief valve. Now

$$h(0, t) = 0 \quad (16)$$

whence

$$H_1(s) = 0 \quad (17)$$

By eqns (7) and (17)

$$Q_2(s) = Q_1(s) \cosh T_e s \quad (18)$$

$$H_2(s) = -Z_0 Q_1(s) \sinh T_e s \quad (19)$$

Equations (15), (18) and (19) imply that

$$\frac{Q_2(s)}{Y(s)} = c_1 \frac{\cosh T_e s}{\cosh T_e s + Z_0(c_2 + c_3 s) \sinh T_e s} \quad (20)$$

$$\frac{H_2(s)}{Y(s)} = -Z_0 c_1 \frac{\sinh T_e s}{\cosh T_e s + Z_0(c_2 + c_3 s) \sinh T_e s} \quad (21)$$

The case of a constant pressure source at section 1 and a valve at section 2 discharging to atmosphere occurs when the volume of chamber C is zero, whence eqns (20) and (21) apply with $c_3 = 0$.

Friction

Linear pipe friction may be included by using

$$\frac{\partial u(x, t)}{\partial t} = -g \left[\frac{\partial h(x, t)}{\partial t} + K_f u(x, t) \right] \quad (22)$$

in place of eqn (2), where K_f is a friction constant. Equation (22) proved adequate to describe flow in $1/2$ in. diameter lines. Let $\beta(s)$ be defined by

$$\beta(s) = \sqrt{s^2 + g K_f s} \quad (23)$$

With the initial conditions

$$u(x, 0^+) = h(x, 0^+) = 0$$

we have

$$G_\beta(s) V_1 = V_2 \quad (24)$$

where

$$G_\beta(s) = \begin{bmatrix} \cosh T_e \beta(s) & -\frac{1}{Z_0} \frac{s}{\beta(s)} \sinh T_e \beta(s) \\ -Z_0 \frac{\beta(s)}{s} \sinh T_e \beta(s) & \cosh T_e \beta(s) \end{bmatrix}$$

With the fixed orifice as the boundary condition at section 2, the ratio of pressure head to flow deviations at section 1 is given by

$$\frac{H_1(s)}{Q_1(s)} = \frac{1}{K_0} \frac{\cosh T_e \beta(s) + K_0 Z_0 \frac{\beta(s)}{s} \sinh T_e \beta(s)}{\cosh T_e \beta(s) + \frac{1}{K_0 Z_0} \frac{s}{\beta(s)} \sinh T_e \beta(s)} \quad (25)$$

For s numerically large, $\beta(s)$ may be replaced by s , whence eqn (25) reduces to eqn (10). Since for frequency response $s = j\omega$

it follows that friction effects diminish as the frequency increases, and are negligible at high frequencies.

For the tests of Regetz

$$Z_0 = 28,700 \text{ sec/ft.}^2 \quad K_0 = 5.43 \times 10^{-5} \text{ ft.}^2/\text{sec}$$

$$T_e = 0.0176 \text{ sec} \quad K_f = 0.0264 \text{ sec/ft.}$$

The differences in magnitude and phase angle for the input line impedances $\{H_1(j\omega)/Q_1(j\omega)\}$ given by eqns (10) and (25) were less than 4 per cent at 1 c/s and less than 1 per cent at 5 c/s.

Perfect Transmission

For the tests of Regetz³

$$K_0 Z_0 = 1.56 \quad (26)$$

From eqn (10) the magnitude ratio of pressure head deviation to flow rate deviation at section 1 normally varies with the frequency. If, however,

$$K_0 Z_0 = 1 \quad (27)$$

the line transfer functions $G_1(s)$, $G_2(s)$ and $G_3(s)$ become

$$G_1(s) = 1, \quad G_2(s) = G_3(s) = e^{-T_e s} \quad (28)$$

Where condition (27) is satisfied, the analysis of the line is simple since pressure and flow rate deviations are proportional and in phase with each other at each cross section of the line. The proportion is independent of frequency. Pressure and flow disturbances are propagated along the line as pure delays with the delay time T_e between sections 1 and 2. The authors feel that this phenomenon may have worthwhile practical applications.

Root Factor Approximations

The transfer functions in eqns (10) to (12), (20) and (21) are all proportional to quotients of transcendental functions of the form $F(z)$, where

$$F(z) = \cosh z + B \sinh z \quad (29)$$

and $z = T_e s$. Here B is a constant or function of s . The same is true of the transfer functions arising from eqn (24) for the case of line friction, except that z is a more complicated function of s . Severe mathematical difficulties arise when the transcendental functions are employed directly to compute system response to step and other disturbances. When $F(z)$, $z = T_e s$, is the denominator of such a transfer function the technique of expanding $F(z)$ into a power series in z , and keeping lower order terms to obtain rational approximations to the transfer functions fails. Thus, keeping terms to the fifth degree yields the approximation $F_5(z)$, where

$$F_5(z) = 1 + Bz + \frac{z^2}{2!} + \frac{Bz^3}{3!} + \frac{z^4}{4!} + \frac{Bz^5}{5!} \quad (30)$$

For $B \neq 0$ the function $F_5(z)$ has a zero in the right half plane. It follows that fifth and higher degree approximations to $F(z)$ yield instability where it does not occur physically. To avoid this difficulty the authors expand $F(z)$ into an infinite product instead.

Let x and y be the real and imaginary parts of z , so that $z = x + jy$. Writing $\cosh z$ and $\sinh z$ as

$$\cosh z = \frac{e^z + e^{-z}}{2}, \quad \sinh z = \frac{e^z - e^{-z}}{2}$$

the equation

$$\cosh z + B \sinh z = 0 \quad (31)$$

becomes

$$e^{2x} \cos 2y + j e^{2x} \sin 2y = \frac{B-1}{B+1} \quad (32)$$

If B is real eqn (32) gives

$$e^{2x} \cos 2y = \frac{B-1}{B+1} \quad (33)$$

$$e^{2x} \sin 2y = 0 \quad (34)$$

Solving eqns (33) and (34) the roots of eqn (31) are found to be

$$z = \frac{1}{2} \ln \left| \frac{B-1}{B+1} \right| \pm j \frac{2n+1}{2} \pi \quad B < 1 \quad (35)$$

$$z = \frac{1}{2} \ln \left| \frac{B-1}{B+1} \right| \pm j n \pi \quad B > 1$$

For $B = 1$ there are no bounded roots of eqn (31).

Introduce x_B where

$$x_B = \frac{1}{2} \ln \frac{B-1}{B+1}$$

From the roots of eqn (31) the function $F(z)$ can be factored into an infinite product, as follows:

$$\cosh z + B \sinh z = \prod_{n=0}^{\infty} \left[1 - \frac{2X_B z - z^2}{X_B^2 + \left(\frac{2n+1}{2} \right)^2 \pi^2} \right] \quad B < 1 \quad (36)$$

$$\cosh z + B \sinh z = \left[1 - \frac{z}{X_B} \right] \prod_{n=1}^{\infty} \left[1 - \frac{2X_B z - z^2}{X_B^2 + n^2 \pi^2} \right] \quad B > 1 \quad (37)$$

A complex plane plot of the roots of eqn (31) is shown in Figure 4. A plot of X_B versus B is given in Figure 5.

The transfer functions $G_1(s)$, $G_2(s)$, $G_3(s)$, $Q_1(s)/Y(s)$ and $H_2(s)/Y(s)$ for the cases of an orifice or valve at section 2 can

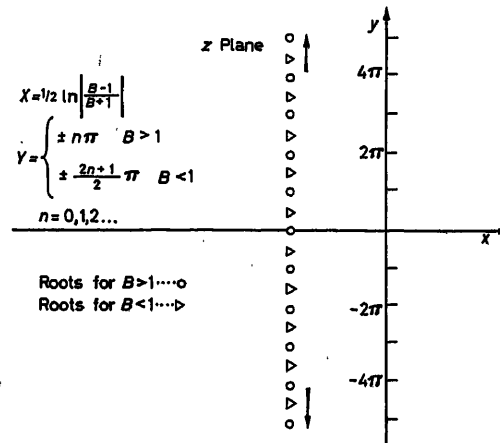


Figure 4. Roots of $\cosh z + B \sinh z = 0$

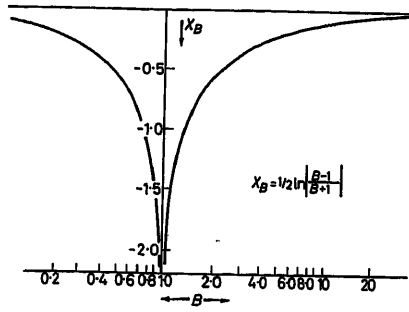


Figure 5. Real part of roots

be expressed as infinite products by eqns (36) and (37). The root factor method is understood to be the procedure of finding the zeros of $\cosh z + B \sinh z$ and expressing this function as a product of corresponding factors. The transfer function $G_1(s)$ will be used to demonstrate the root factor method.

Let $K_0 Z_0 = 1.56$ as for the Regetz experiments. The function $G_1(s)$ is now given by

$$G_1(s) = \frac{\cosh T_e s + 1.56 \sinh T_e s}{\cosh T_e s + 0.642 \sinh T_e s} \quad (38)$$

The numerator of $G_1(s)$ is given by the right-hand side of eqn (37) with $z = T_e s$ and $B = 1.56$, and the denominator by the right-hand-side of eqn (36) with $z = T_e s$ and $B = 0.642$. It follows that

$$G_1(s) = \frac{\left[1 - \frac{T_e s}{X_B}\right] \prod_{n=1}^{\infty} \left[1 - \frac{2X_B T_e s - (T_e s)^2}{X_B + n^2 \pi^2}\right]}{\prod_{n=0}^{\infty} \left[1 - \frac{2X_B T_e s - (T_e s)^2}{X_B^2 + \left(\frac{2n+1}{2}\right)^2 \pi^2}\right]} \quad (39)$$

By Figure 5

$$X_B = -0.763$$

In the Regetz experiments $T_e = 0.0176$. The function $G_1(s)$ is now

$$G_1(s) = \frac{\left[1 + \frac{s}{\omega_0}\right] \prod_{n=1}^{\infty} \left[1 + 2 \frac{\eta_{1n} s}{\omega_{1n}} + \frac{s^2}{\omega_{2n}^2}\right]}{\prod_{n=0}^{\infty} \left[1 + 2 \frac{\eta_{2n} s}{\omega_{2n}} + \frac{s^2}{\omega_{2n}^2}\right]} \quad (40)$$

where

$$\omega_0 = 43.4 \text{ rad/sec}$$

$$\omega_{1n} = 56.8 \sqrt{(0.763)^2 + (n\pi)^2}$$

$$\omega_{2n} = 56.8 \sqrt{(0.763)^2 + \left(\frac{2n+1}{2}\right)^2 \pi^2}$$

$$\eta_{1n} = \sqrt{\frac{(0.763)^2}{(0.763)^2 + n^2 \pi^2}}$$

$$\eta_{2n} = \sqrt{\frac{(0.763)^2}{(0.763)^2 + \left(\frac{2n+1}{2}\right)^2 \pi^2}}$$

For 0 to 90 c/s the function $G_1(j\omega)$ is approximated within 1 dB in magnitude and 5° in angle by taking $n = 0$ to 5 in

eqn (40), by letting $s = j\omega$, and neglecting all other terms in the infinite product. The approximation obtained by dropping the factors for $n > m$ will be denoted by $G_{1m}(j\omega)$. In Figures 6(a) and (b) are shown the magnitude ratio and phase curves for the precise transfer function $G_1(j\omega)$ and the approximation $G_{15}(j\omega)$.

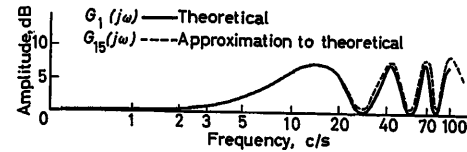
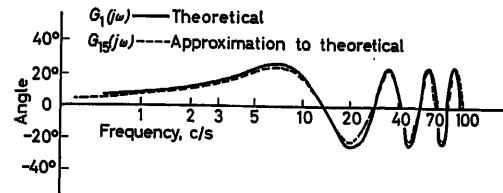
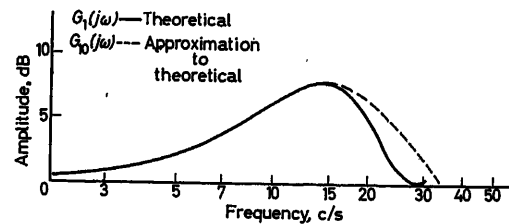
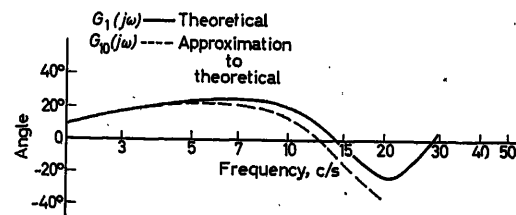
Dropping the $n \geq 2$ factors in formula (40) yields $G_{11}(s)$ where $G_{11}(s)$ is a cubic in s divided by a quartic. There is excellent agreement between $G_1(j\omega)$ and $G_{11}(j\omega)$ from 0 to 50 c/s. For the sake of brevity the frequency response plots are omitted.

Dropping the $n \geq 1$ factors in formula (40), there results

$$G_{10}(s) = \frac{1 + \frac{s}{43.4}}{1 + 0.874 \left(\frac{s}{99.3}\right) + \left(\frac{s}{99.3}\right)^2} \quad (41)$$

In Figures 7(a) and (b) are plotted the frequency response curves for $G_1(j\omega)$ and $G_{10}(j\omega)$. Clearly, $G_{10}(j\omega)$ is a good approximation to $G_1(j\omega)$ for 0 to 15 c/s.

Thus the infinite products in eqn (40) converge rapidly. The root factor method yields accurate rational approximations

Figure 6(a). Magnitude ratio curves of $G_1(j\omega)$ and $G_{15}(j\omega)$ Figure 6(b). Angle curves for $G_1(j\omega)$ and $G_{15}(j\omega)$ Figure 7(a). Magnitude ratio curves of $G_1(j\omega)$ and $G_{10}(j\omega)$ Figure 7(b). Phase curves for $G_1(j\omega)$ and $G_{10}(j\omega)$

to $G_1(s)$. The bandwidth of the other components in a system with hydraulic lines determines the largest value of ω_{1n} to include in the approximations. The largest value of the line frequency constant ω_{1n} should be about 1.5 times the bandwidth of the other transfer functions in the loop.

The numerator of the fraction on the right in formula (20) for $Q_2(s)/Y(s)$ is the single term $\cosh T_e s$. Since formula (31) holds when $B = 0$ there is no difficulty. On the other hand, the numerator $\sinh T_e s$ of $H_2(s)/Y(s)$ in eqn (21) corresponds to $B = \infty$ where eqn (31) breaks down. To avoid this difficulty let

$$\left. \frac{\sinh T_e s}{T_e s} \right|_{s=0} = 1 \quad (42)$$

The equation

$$\frac{\sinh T_e s}{s} = 0 \quad (43)$$

has the roots

$$T_e s = \pm j n \pi, \quad n \neq 0$$

which follows from eqn (35) when $B \rightarrow \infty$. Thus one may use

$$\sinh T_e s = T_e s \prod_{n=1}^{\infty} \left(1 + \frac{T_e^2 s^2}{n^2 \pi^2} \right) \quad (44)$$

In the denominators of formulas (20) and (21)

$$B = Z_0(c_2 + c_3 s) \quad (45)$$

In the chamber and valve case B is not a constant. It is a simple matter to solve eqn (31) with $z = T_e s$ for given numerical values of Z_0 , c_2 and c_3 . Thus if

$$\begin{aligned} T_e &= 0.0176, Z_0 = 28,700, c_2 = 2.72 \times 10^{-5}, \\ c_3 &= 6.98 \times 10^{-6} T_e \end{aligned} \quad (46)$$

the roots of eqn (31) are

$$\begin{aligned} z &= -0.685 \pm 1.22 j, -0.235 \pm 6.82 j, \\ &-0.145 \pm 9.82 j, -0.095 \pm 12.0 j, \dots \end{aligned}$$

whence

$$\begin{aligned} \cosh z + Z_0 \left(c_2 + \frac{c_3}{T_e} z \right) \sinh z &= \left[1 + \frac{z^2 + 1.37 z}{1.97} \right] \\ \times \left[1 + \frac{z^2 + 0.47 z}{4.65} \right] &\left[1 + \frac{z^2 + 0.29 z}{97} \right] \left[1 + \frac{z^2 + 0.19 z}{166} \right] \dots \end{aligned} \quad (47)$$

Similarly, more complicated functions B of s may be treated.

Transient Response

The pressure head transient $h_1(t)$ at section 1 for a step change q_0 in flow rate at section 1 will be obtained for the case of an orifice at section 2. By equation (10) the ratio $H_1(s)/Q_1(s)$ of the Laplace transforms of pressure head and flow rate at $x = 0$ satisfies

$$\frac{H_1(s)}{Q_1(s)} = \frac{1}{K_0} G_1(s) \quad (48)$$

The step change q_0 in flow rate corresponds to

$$Q_1(s) = \frac{q_0}{s}$$

It follows that

$$H_1(s) = \frac{q_0 Z_0}{s} \frac{1 + \frac{1 - K_0 Z_0}{1 + K_0 Z_0} e^{-2T_e s}}{1 + \frac{K_0 Z_0 - 1}{K_0 Z_0 + 1} e^{-2T_e s}} \quad (49)$$

Division yields

$$H_1(s) = q_0 Z_0 \sum_{n=0}^{\infty} (-1)^n \varepsilon_n \left(\frac{K_0 Z_0 - 1}{K_0 Z_0 + 1} \right)^n \frac{e^{-2nT_e s}}{s} \quad (50)$$

where

$$\varepsilon_n = \begin{cases} 1 & n=0 \\ 2 & n \neq 0 \end{cases}$$

Taking the inverse Laplace transform the precise response is found to be

$$h_1(t) = q_0 Z_0 \sum_{n=0}^{\infty} (-1)^n \varepsilon_n \left(\frac{K_0 Z_0 - 1}{K_0 Z_0 + 1} \right)^n S(t - 2nT_e) \quad (51)$$

where $S(t)$ is the unit step function given by

$$S(t) = \begin{cases} 0 & t \leq 0 \\ 1 & t > 0 \end{cases}$$

Let $h_{10}(t)$ denote the approximate response at section 1 computed by using $G_{10}(s)$ of eqn (41) in place of $G_1(s)$. The corresponding approximate Laplace transform $H_{10}(s)$ is then given by

$$H_{10}(s) = \frac{q_0}{s K_0} \frac{1 + \frac{s}{43.2}}{1 + 0.874 \left(\frac{s}{99.3} \right) + \left(\frac{s}{99.3} \right)^2} \quad (52)$$

whence

$$h_{10}(\tau) = \frac{q_0}{K_0} [1 - e^{-1.52\tau} (2.28) \cos(3.15\tau + 1.12)] \quad (53)$$

where

$$\tau = \frac{t}{2T_e}$$

Curves of $h_1(t)$ and $h_{10}(t)$ versus multiples of T_e are plotted in Figure 8. The use of $G_{10}(s)$ in place of $G_1(s)$ yields a good fit to the actual transient (marked theoretical), and is to be preferred to it in that the $h_{10}(t)$ curve is a smoothed version of the $h_1(t)$ curve with the sharp corners removed. The smoothed solution $h_{10}(t)$ is easier to use in analysis and synthesis.

The root factor method is valid for the computation of transients for systems with boundary conditions other than those treated in this paper. It can be applied with equal facility to the transfer functions of Ezekiel and Paynter⁵, Zweig⁶ and others where a linear boundary condition is used.

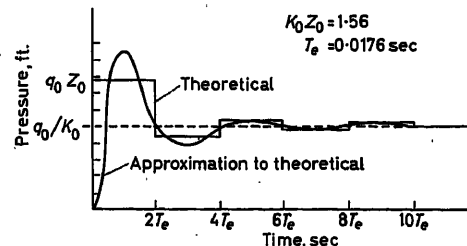


Figure 8. Precise and approximate transients

Operations

Let

$$D = \frac{d}{dt}$$

By definition

$$(\cosh T_e D) f(t) = \frac{f(t+T_e) + f(t-T_e)}{2} \quad (54)$$

$$(\sinh T_e D) f(t) = \frac{f(t+T_e) - f(t-T_e)}{2} \quad (55)$$

The partial differential eqns (1) and (2) may be replaced by the ordinary differential equations

$$q(L, t) = (\cosh T_e D) q(0, t) - \frac{1}{Z_0} (\sinh T_e D) h(0, t) \quad (56)$$

$$h(L, t) = -Z_0 (\sinh T_e D) q(0, t) + (\cosh T_e D) h(0, t) \quad (57)$$

relating sections 1 and 2. Equation (48) may be taken as

$$h(0, t) = \frac{1}{K_0} \frac{\cosh T_e D + K_0 Z_0 \sinh T_e D}{\cosh T_e D + \frac{1}{K_0 Z_0} \sinh T_e D} q(0, t) \quad (58)$$

By eqn (40), dropping the $n \geq 1$ terms,

$$h(0, t) = \frac{1}{K_0} \frac{1 + \frac{D}{\omega_0}}{1 + 2 \frac{\eta_{20}}{\omega_{20}} D + \frac{D^2}{\omega_{20}^2}} q(0, t) \quad (59)$$

The simple rational D -operator in eqn (59) suffices for first approximation studies. The operators $G_{10}(D)$ or $G_{11}(D)$ are adequate unless the system variables change rapidly.

Mr. John Sanders and Mr. John Regetz, Jr., of the National Aeronautics and Space Administration supplied the authors with experimental data in connection with this study. They are grateful for this, and appreciate the support of the National Aeronautics and Space Administration which sponsored the paper. One of the authors was assisted by a fellowship of the Fisher Governor Company and the Foundation for Instrumentation, Education and Research.

Nomenclature

a	Speed of sound in line (ft./sec)
A	Cross sectional area (ft. ²)
A_1	Orifice area (ft. ²)
B	Constant in characteristic equation
$b_i(s)$	Constant of integration, $i = 1, 2$
E	Modulus of elasticity of pipe
f	Wall thickness of pipe
g	Acceleration of gravity (ft./sec ²)
$G(s)$	Transfer matrix
$G_1(s)$	Normalized transfer function between head and flow at section 1
$G_2(s)$	Transfer function between heads at section 2 and section 1

$G_3(s)$	Transfer function between flows at section 2 and section 1
$G_{1i}(s)$	The i th root factor approximation to $G_1(s)$
$h(x, t)$	Pressure head deviation (ft.)
h_T	Pressure head deviation in chamber
$H(x, s)$	Laplace transform of $h(x, t)$
$H_i(s)$	Laplace transform of $h(x, t)$ at section 1
j	$\sqrt{-1}$
K	Bulk modulus of fluid
K_f	Pipe friction coefficient
K_0	Reciprocal of slope of pressure <i>versus</i> flow curve at average flow
L	Distance between sections 1 and 2 (ft.)
q_0	Flow increment (ft. ³ /sec)
$q_i(x, t)$	Flow rate deviation (ft. ³ /sec)
$Q_i(s)$	Laplace transform of $q_i(t)$
$Q(x, s)$	Laplace transform of $Au(x, t)$
r	Pipe inner radius
s	Laplace variable, transformation with respect to time
$S(t)$	Unit step function
t	Time (sec)
T_e	L/a (sec)
$u(x, t)$	Velocity of fluid in pipe, deviation (ft./sec)
$U(x, s)$	Laplace transform of $u(x, t)$
$V_i(s)$	Column vector with elements $Q_i(s)$ and $H_i(s)$
x	Axial pipe coordinate (ft.)
X_B	Real part of root of characteristic equation
z	Variable in characteristic equation
Z_0	$a/g A$, sec/ft. ²
α	Weight density of fluid divided by equivalent bulk modulus (ft. ⁻¹)
$\beta(s)$	$\sqrt{s_2 + gK_f s}$
η	Damping factor
μ	Viscosity of fluid (c _p)
ω	Frequency (rad/sec)

References

- OLDENBURGER, R. *Mathematical Engineering Analysis*. 1950. New York; Macmillan
- PAYNTER, H. M. Fluid transients in engineering systems, *Handbook of Fluid Dynamics*, Streeter, L. (Ed.). 1961. New York; McGraw-Hill
- REGETZ, J. D. (Jr.) An experimental determination of the dynamic response of a long hydraulic line, *NASA Tech. Note D-576* (December, 1960)
- CHURCHILL, R. V. *Operational Mathematics*. 1958. p. 122 New York; McGraw-Hill
- EZEKIEL, F. D. and PAYNTER, H. M. Fluid Power Transmission, *Fluid Power Control*. Edited by J. F. Blackburn, G. Reethof and Shearer. 1960. pp. 139-143 New York; The Technology Press of MIT, and Wiley
- ZWEIG, F., TUTEUR, F. B., CUNNINGHAM, W. J. and BOWER, J. L. The dynamics of throttling hydraulic systems, *Dunham Lab. Rep.*, Yale University, June, 1950, pp. 1-21
- OLDENBURGER, R. and DONELSON, J. (Jr.) Dynamic response of a hydro-electric plant, *Trans. Amer. Inst. elect. Engrs, Paper No. 62-167*

DISCUSSION

D. RUMPEL and H.-V. ELLINGSEN, *Siemens-Schuckertwerke, Erlangen, Germany*

Professor Oldenburger and Mr. Goodson reported on the difficulties of simulating the lag of hydraulic lines, and they have shown how to

eliminate them by using root-factor approximants. Conventional expansions of the exponential function and related functions can result in unpleasant surprises.

Investigating the stability of Pelton plants we had fallen victim

to these difficulties. We have overcome them by replacing the exponential functions by a Padé table function^{1, 2} of preferably equal grade in numerator and denominator.

It would be possible to convert the cosh- and sinh-functions appearing in the transfer functions of the paper to exponential functions with negative argument, as they represent nothing but one or more transportation lags. The exponential functions could be replaced by Padé approximants as mentioned above.

In this case, contrary to the root factor approximation, the factors before the transcendent functions appear untransformed in the approximant. This feature may be of great advantage if B itself is a polynomial of z or s ; as is the case when the calculation comprises a total control system with hydraulic lines included.

References

- ¹ PERRON, Ø. *Die Lehre von den Kettenbrüchen*, Bd. II. 1957. Stuttgart; B. G. Taubner
- ² TRUXAL, J. R. *Control System Synthesis*. 1955. New York; McGraw-Hill

R. OLDENBURGER and R. E. GOODSON, *in reply*

The suggestion of using Padé approximations to the pure time delays when they occur in the transfer function for a hydraulic line has advantages especially when the terminal impedance of a line is other than purely resistive. However, the root factor expansion as presented in the paper and as recently extended¹ has advantages over the Padé expansions and the Taylor series expansion which make it more applicable in general. These advantages are:

(1) The root factor expansion preserves in the rational approximations the correct values of the undamped natural frequencies of a fluid line, while the Padé and Taylor series method yield natural frequencies which are different from those given by the transcendental model.

(2) In the cases where the terminal impedance of a line is not purely resistive, e.g. eqn (15) in the paper, and where friction or viscosity effects are significant, the root factor expansion may be applied directly to the transfer matrices themselves [$G(s)$ and $G_p(s)$ in eqns (7) and (24), respectively] before the boundary conditions are specified. This is done by expressing the cosine and sine hyperbolic functions in their infinite product expansions. The Padé approximations, however, for fluid lines where viscous effects are significant, are inapplicable directly since pure delay terms do not appear in the transfer functions.

(3) The Padé approximation technique may indicate instability where it is not indicated in the transcendental model and stability may be indicated where the transcendental model indicates instability.

As a simple example comparing the results of a Padé approximation and the root factor expansion, consider a hydraulic line supplied from a constant pressure source. The transfer function relating head deviations to flow deviations becomes from eqns (18) and (19)

$$\frac{H_2(s)}{Q_2(s)} = -Z_0 \frac{\sinh T_e s}{\cosh T_e s}$$

Writing $H_2(s)/Q_2(s)$ as

$$\frac{H_2(s)}{Q_2(s)} = -Z_0 \frac{1 - e^{-2T_e s}}{1 + e^{-2T_e s}}$$

and using the second order Padé approximation

$$e^{-2T_e s} \approx \frac{1 - T_e s + \left(\frac{T_e s}{3}\right)^2}{1 + T_e s + \left(\frac{T_e s}{3}\right)^2}$$

there results

$$\frac{H_2(s)}{Q_2(s)} \approx -Z_0 \frac{T_e s}{1 + \left(\frac{T_e s}{3}\right)^2}$$

Using the first terms of the root factor expansions for $\cosh T_e s$ and $\sinh T_e s$ yields

$$\frac{H_2(s)}{Q_2(s)} \approx -Z_0 \frac{T_e s}{1 + 4\left(\frac{T_e s}{\pi^2}\right)^2}$$

The approximations are of the same form, but the Padé method yields a natural frequency 16 per cent too high, while the natural frequency of the root factor approximation and the first natural frequency of the transcendental model agree. Further, if viscous effects were important, the Padé technique would not be applicable.

Reference

- ¹ GOODSON, R. E. Viscous and boundary effects in fluid lines. *Ph. D. Thesis*, Purdue University (January 1963)

P. D. McCORMACK, *Engineering School, Dublin University, Eire*

Most rocket, aircraft and many industrial control systems are subject from time to time to high 'g' vibrations. It is the effect of lateral high 'g' vibrations on the flow characteristics through hydraulic and pneumatic lines to which I wish to draw the authors' attention.

For example, if z is the ordinate perpendicular to the flow direction, then the inclusion of $\partial z/\partial t$ term will be necessary in eqn (1) in the presence of such a disturbance. It is almost certain that vibration will tend to cause secondary flow or at least bending of the streamlines. This will lead to an oscillating component (at the vibration frequency) in the expression for the pressure drop along a section of the line and a corresponding flow oscillation. If such an effect is possible, then this can cause vibration induced noise in hydraulic and pneumatic control systems.

Finally, such bending of the streamlines would, of course, cause a variation in the line impedance, Z_{10} .

R. OLDENBURGER and R. G. GOODSON, *in reply*

Professor McCormack brings up an interesting question concerning the lateral vibration of fluid-carrying conduits. We have been concerned more with longitudinal conduit vibrations and the effect of conduit bends on the fluid variables, but lateral vibrations could have an appreciable effect especially in the presence of high fluid velocities and bending of the conduit. One way to include the effect of lateral vibrations in the basic fluid dynamic equations would be to transfer the coordinates to a non-stationary coordinate system. A simpler way and one which should give fair results would be to include in the momentum equations body forces on the fluid induced by lateral vibrations as suggested by the discussor. Denoting by $z(x, t)$ the lateral deflection of a fluid conduit in a given plane, the force per unit volume would be proportional to the product of the acceleration of the conduit and the change in the lateral deflection with respect to x or for small changes in deflection

$$F_{xz} = -\rho \frac{\partial^2 y}{\partial t^2} \frac{\partial y}{\partial x}$$

The deflection $y(x, t)$ would be found from the bending moment equation and the fluid force on the conduit would be given by

$$F_{xx} = -\rho u^2 \frac{\partial^2 z}{\partial x^2}$$

Using these forces an investigation of the one-dimensional fluid dynamic equations with lateral vibration could be made. It would be expected that the external input vibration would significantly affect the fluid variables only in the presence of high-frequency or appreciable conduit deflections.

The Optimization of Computer-Controlled Systems Using Partial Knowledge of the Output State

B. G. ANDERSON

Summary

A technique developed by Merriam is extended to cover the design of an optimum controller of a dynamic plant when information via certain feedback paths is not available at the controller. The plant can be linear or non-linear and amplitude limitation of the input control signal is permissible. The method is useful in assessing the penalties that accrue when simplifications are made in the finally realized system, e.g. omission of a feedback link in a constant-coefficient system may ideally require time-varying compensation, but the best constant-coefficient realization can be found.

A fourth-order constant-coefficient plant is considered which has no feedback information from two output elements, and a constant-coefficient realization of the optimum system is derived.

Sommaire

Une technique développée par Merriam est étendue pour couvrir l'étude d'un combinateur optimal d'un processus dynamique quand l'information par certaines voies de contre-réaction n'est pas disponible au combinateur. Le processus peut être linéaire ou non-linéaire et on permet la limitation d'amplitude du signal d'entrée. La méthode est utile pour établir les désavantages qui s'accumulent quand on fait des simplifications dans le système finalement réalisé; par exemple, l'omission d'une connexion de contre-réaction dans un système à coefficients constants peut idéalement exiger une compensation variable dans le temps, mais on peut trouver la meilleure réalisation de coefficients constants.

On considère un processus à coefficients constants du quatrième ordre, qui n'a pas l'information de contre-réaction de deux éléments de sortie, et on déduit une réalisation à coefficients constants du système optimal.

Zusammenfassung

Ein von Merriam entwickeltes Verfahren wird erweitert, um einen optimalen Regler für eine dynamische Anlage (Regelstrecke) zu ent-

werfen, wenn dem Regler die Rückführsignale nur teilweise zur Verfügung stehen. Die Regelstrecke kann sowohl linear als auch nicht-linear sein; außerdem ist eine Amplitudenbegrenzung des Eingangssignals zulässig. Das Verfahren eignet sich zur Abschätzung der Nachteile, die bei Vereinfachungen in der endgültigen Ausführung entstehen. So würde z. B. das Weglassen eines Rückkopplungsziweiges in einem System mit konstanten Koeffizienten eigentlich eine zeitabhängige Kompensation erfordern; doch läßt sich mit dem Verfahren die beste Ausführung für Glieder mit konstanten Koeffizienten finden.

Eine Anlage vierter Ordnung mit konstanten Koeffizienten, die von zwei Ausgängen keine Rückführinformation erhält, wird betrachtet und ein optimales System mit konstanten Koeffizienten abgeleitet.

Introduction

Over the past few years there has been considerable interest in the possible use of digital and analogue computers for the control of dynamic plants (see *Figure 1*), a trend which has arisen from advances in computer technology and the versatility of such control methods. The mathematical techniques of Bellman¹, Pontryagin², Merriam³ and others are available for the design of the optimum computer controller provided that all the state vector elements of the plant are known and are accessible to the computer. In practical systems, however, it may be difficult and expensive to obtain and communicate information on particular state vector elements. One method of dealing with this situation would be to derive the missing state vector elements from a mathematical model of the plant within the on-line computer, but this would necessarily increase the complexity and cost of on-line equipment.

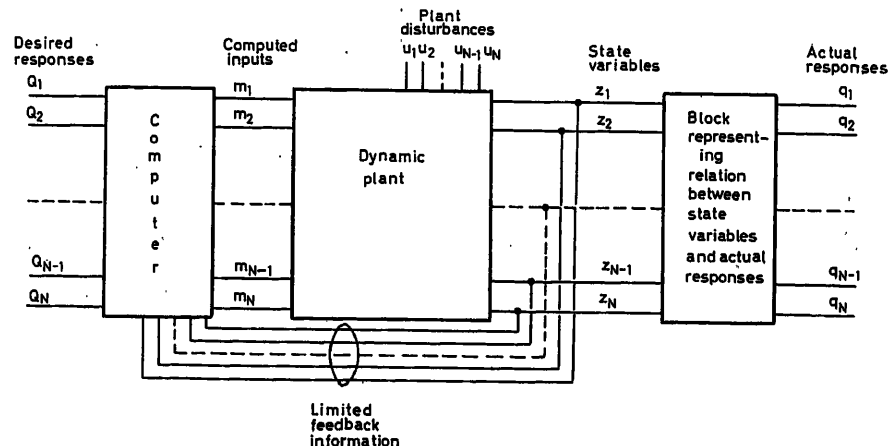


Figure 1. The general computer controlled plant

It is the purpose of this paper to present an alternative solution. The mathematical technique of Merriam is extended to design a near-optimum computer controller based on restricted knowledge of the output states and to assess the penalties in performance which necessarily accrue.

The N th order plant to be controlled is defined by the equation

$$\dot{Z}(t) = BZ(t) + Cm(t) + u(t) \quad (1)$$

where $m(t)$ is the control signal vector whose elements are assumed to be bounded such that $L_n^-(t) \leq m_n(t) \leq L_n^+(t)$ for $1 \leq n \leq N$. Also B and C are $N \times N$ matrices whose elements are functions of $Z(t)$ and t , and, for most cases of interest, the matrix C is diagonal. This condition will apply throughout.

The response signal vector is

$$q(t) = AZ(t) \quad (2)$$

where A is again an $N \times N$ matrix whose elements are functions of $Z(t)$ and t .

If now N_1 of the most general constraints, which are linear in the elements of m , i.e.

$$\rho_n(m_1, \dots, m_N, Z_1, \dots, Z_N, t) = 0 \quad (3)$$

for $n = 1, \dots, N_1$ and $N_1 \leq N$, are placed on the elements of the input vector, then this vector can be chosen at a later stage in the development in such a way that certain feedback paths are omitted.

The performance criterion chosen is

$$\text{Eqn (4)}^*$$

where $Q_n(t)$ and $M_n(t)$ are elements of the desired response and control signal vectors, respectively, and τ is the interval over which $Q(t)$ may be predicted with confidence. Also ϕ_n and ψ_n are weights which determine the compromise between response deviations and control effort, and, in general, they can be functions of $Q(t)$, $q(t)$ and t .

Constrained Optimization

To determine the optimum controller Bellman's functional equation method of dynamic programming is evoked.

Thus, define a minimum error function by

$$\text{Eqn (5)}^\dagger$$

where $L[m(\sigma)]$ indicates that the control signal vector $m(\sigma)$ is bounded by the vectors L^+ and L^- for all σ in the range $\mu \leq \sigma \leq t + \tau$ and $m(\sigma)$ is constrained by eqn (3).

Expanding the integral about the lower limit to a first order in ε gives

$$\text{Eqn (6)}^\ddagger$$

and expanding the minimum error function about μ results in

$$E[Z(\mu + \varepsilon), \mu + \varepsilon] = E[Z(\mu), \mu] + \varepsilon E'[Z(\mu), \mu] + 0(\varepsilon^2) \quad (7)$$

where primes indicate derivatives with respect to μ . Eliminating $E[Z(\mu), \mu]$ from both sides of eqn (6) and letting ε tend to zero results in the condition

$$\text{Eqn (8)}^\S$$

subject to the constraints on $m(\mu)$ defined by eqn (3).

Now $E[Z(\mu), \mu]$ is not, in general, a quadratic function of the vector elements Z_r , so expanding the minimum error function about an arbitrary point $\hat{Z}(\mu)$ results in the expression

$$\begin{aligned} E[Z(\mu), \mu] &= \hat{k}_0(\mu) + \sum_{n=1}^N \hat{k}_n(\mu) Z_n(\mu) \\ &+ \sum_{n,r=1}^N \hat{k}_{rn}(\mu) Z_r(\mu) Z_n(\mu) + \text{higher terms} \end{aligned} \quad (9)$$

where $\hat{k}_{rn} = \hat{k}_{nr}$ and the cap notation indicates that the \hat{k} parameters are functions of the point $\hat{Z}(\mu)$.

Thus

$$\text{Eqn (10)}^\parallel$$

Now substituting $Z'(\mu)$ from eqn (1) into (10), then eqn (10) into (8) and introducing Lagrangian multipliers Λ_n , for $n = 1, \dots, N_1$, to perform the minimization with respect to the elements of $m(\mu)$ gives

$$m_r(\mu) = \begin{cases} L_r^+, & \text{if } L_r^+ \leq [m_r(\mu)] \\ [m_r(\mu)], & \text{if } L_r^- < [m_r(\mu)] < L_r^+ \\ L_r^-, & \text{if } [m_r(\mu)] \leq L_r^- \end{cases} \quad (11)$$

* Eqn (4):

$$e(t) = \left[\sum_{n=1}^N \int_t^{t+\tau} \{ \phi_n [Q_n(\sigma) - q_n(\sigma)]^2 + \psi_n [M_n(\sigma) - m_n(\sigma)]^2 \} d\sigma \right] \quad (4)$$

† Eqn (5):

$$E[Z(\mu), \mu] = \min_{L[m(\sigma)]} \left[\sum_{n=1}^N \int_\mu^{t+\tau} \{ \phi_n [Q_n(\sigma) - q_n(\sigma)]^2 + \psi_n [M_n(\sigma) - m_n(\sigma)]^2 \} d\sigma \right] \quad (5)$$

‡ Eqn (6):

$$E[Z(\mu), \mu] = \min_{L[m(\mu)]} \left[\varepsilon \sum_{n=1}^N \{ \phi_n [Q_n(\mu) - q_n(\mu)]^2 + \psi_n [M_n(\mu) - m_n(\mu)]^2 \} + E[Z(\mu + \varepsilon), \mu + \varepsilon] \right] \quad (6)$$

§ Eqn (8):

$$\min_{L[m(\mu)]} \left[\sum_{n=1}^N \{ \phi_n [Q_n(\mu) - q_n(\mu)]^2 + \psi_n [M_n(\mu) - m_n(\mu)]^2 \} + E'[Z(\mu), \mu] \right] = 0 \quad (8)$$

|| Eqn (10):

$$E[Z(\mu), \mu] = \left\{ \hat{k}_0(\mu) + \sum_{n=1}^N \hat{k}_n(\mu) Z_n(\mu) + \sum_{n,r=1}^N \hat{k}'_{rn}(\mu) Z_r(\mu) Z_n(\mu) + \sum_{n=1}^N \hat{k}_n(\mu) Z'_n(\mu) + 2 \sum_{\substack{n,r=1 \\ r \leq n}}^N \hat{k}_{rn}(\mu) Z_r(\mu) Z_n(\mu) \right\} + \text{higher terms} \quad (10)$$

where

Eqn (12) *

To determine the control signal switching vector $[m(\mu)]$, eqns (11) and (12) must be substituted into condition (8) which is then evaluated at the point $\hat{Z}(\mu)$, but a further parametric expansion must be made to obtain the equations in the desired form, namely,

$$\sum_{n=1}^{N_1} \frac{\Lambda_n}{c_{rr}} \frac{\partial \rho_n}{\partial m_r} = \hat{k}_r(\mu) + 2 \sum_{n=1}^N \hat{\lambda}_{rn}(\mu) Z_n(\mu) + \text{higher terms} \quad (13)$$

where, once again, the cap denotes that the $\hat{\lambda}$'s are functions of \hat{Z} .

Making the substitution

$$\hat{K}_r(\mu) = \hat{k}_r(\mu) - \hat{\lambda}_r(\mu) \quad (14)$$

and

$$\hat{K}_{rn}(\mu) = \hat{k}_{rn}(\mu) - \hat{\lambda}_{rn}(\mu) \quad (15)$$

for $n, r = 1, \dots, N$, and substituting eqns (11), (12), (13), (14) and (15) into condition (8) leads to the condition

$$\begin{aligned} & [\hat{k}_0(\mu) - \hat{F}_0(\mu)] \\ & + \sum_{n=1}^N ([\hat{K}'_n(\mu) + \hat{\lambda}'_n(\mu)] - \hat{F}_n(\mu)) \hat{Z}_n(\mu) \\ & + \sum_{n,r=1}^N ([\hat{K}'_{rn}(\mu) + \hat{\lambda}'_{rn}(\mu)] - \hat{F}_{rn}(\mu)) \hat{Z}_r(\mu) \hat{Z}_n(\mu) = 0 \end{aligned} \quad (16)$$

where the \hat{F} functions are algebraic combinations of the \hat{K} and $\hat{\lambda}$ parameters. The higher-order terms in eqns (9) and (13) reduce to zero.

Now, for a linear system with a quadratic performance criterion whose weightings ϕ_n and ψ_n are independent of the response vector q and which possess no bounds on the input vector m , the \hat{K} and $\hat{\lambda}$ parameters are independent of the point $\hat{Z}(\mu)$. Therefore eqn (16) is satisfied for all \hat{Z} if each coefficient of the \hat{Z} terms are put to zero. For the general case the same procedure is also adopted but it must be remembered that there are other ways of satisfying eqn (16) since the realization of a non-linear system is not unique.

The following set of non-linear first order equations are obtained by this procedure:

$$\hat{k}'_0 = - \sum_{n=1}^N [\hat{\phi}_n Q_n^2 + u_n (\hat{K}_n + \hat{\lambda}_n)] -$$

$$\begin{aligned} & - \sum_n^{N_s} [\hat{\psi}_n (M_n - L_n)^2 + \hat{c}_{nn} L_n (\hat{K}_n + \hat{\lambda}_n)] \\ & + \sum_n^{N_u} \left[\frac{\hat{c}_{nn}}{4 \hat{\psi}_n} \{ (\hat{K}_n + \hat{\lambda}_n)^2 - \hat{\lambda}_n^2 \} - \hat{c}_{nn} M_n (\hat{K}_n + \hat{\lambda}_n) \right] \end{aligned} \quad (17)$$

Eqn (18) †

and

Eqn (19) ‡

where N_s indicates the number of elements of $m(\mu)$ that are on their boundary values whilst N_u is the number of elements that are within the boundary limits.

Substituting eqns (13), (14) and (15) into (12) gives the input at the real time t , i.e.

$$[m_r(t)] = M_r(t) - \frac{\hat{c}_{rr}}{2 \hat{\psi}_r} \hat{K}_r(t) - \frac{\hat{c}_{rr}}{\hat{\psi}_r} \sum_{n=1}^N \hat{K}_{rn}(t) \hat{Z}_n(t) \quad (20)$$

Now the constraints can be applied, for if no feedback path exists from state element Z_s to input m_r then \hat{K}_{rs} can be put identically zero. Similar treatment can be applied to a particular \hat{K}_r if required. To determine the non-zero \hat{K} 's, eqns (17), (18), (19) and (1) must be solved backwards in time from $\mu = t + \tau$ to $\mu = t$ but it is necessary to calculate or specify the values of the parameters $\hat{\lambda}_r$. If $\hat{K}_{rs} \equiv 0$ then the corresponding $\hat{\lambda}_{rs}$ must be retained in the equations, but if \hat{K}_{rs} is not identically zero then $\hat{\lambda}_{rs} \equiv 0$ enables eqns (19) to be solved. This leaves the N parameters, $\hat{\lambda}_r$, whose arbitrariness reflects the fact that the constraints of eqn (3) have not been specified explicitly. Thus the $\hat{\lambda}_r$ terms can be chosen to engineer the final realized system in a required form, e.g. a constant coefficient realization, and if equipment is not at a premium the ultimate aim would be to obtain a performance close to that of the system possessing all feedback paths.

A possible way to determine the $\hat{\lambda}_r$'s is found if the terms $\hat{\lambda}_r$ and $\hat{\lambda}_r'$ in eqn (18) are grouped in the form

$$\hat{\lambda}'_r + \sum_{n=1}^N \hat{b}_{nr} \hat{\lambda}_n - \sum_n^{N_u} \frac{\hat{c}_{nn}^2}{\hat{\psi}_n} \hat{K}_{nr} \hat{\lambda}_n \quad (21)$$

for $r = 1, \dots, N$. These expressions, which are the homogeneous portion of the constrained system's adjoint equations, can be put to zero without affecting the validity of eqn (16), provided the feedback paths associated with a limited input signal vector element are put to zero, i.e. if n belongs to N_s then \hat{K}_{nr} is put

* Eqn (12):
$$[m_r(\mu)] = \left\{ M_r(\mu) - \frac{c_{rr}}{2 \psi_r} \left[\hat{k}_r(\mu) + 2 \sum_{n=1}^N \hat{k}_{rn}(\mu) Z_n(\mu) \right] + \frac{c_{rr}}{2 \psi_r} \sum_{n=1}^{N_1} \frac{\Lambda_n}{c_{rr}} \frac{\partial \rho_n}{\partial m_r} \right\} + \text{higher terms} \quad (12)$$

† Eqn (18):
$$\begin{aligned} \hat{K}_r + \hat{\lambda}'_r = & - \sum_{n=1}^N [-2 \hat{\phi}_n Q_n a_{nr} + 2 u_n (\hat{K}_{nr} + \hat{\lambda}_{nr}) + \hat{b}_{nr} (\hat{K}_n + \hat{\lambda}_n)] - 2 \sum_n^{N_s} \hat{c}_{nn} L_n (\hat{K}_{nr} + \hat{\lambda}_{nr}) \\ & + \sum_n^{N_u} \left[-2 \hat{c}_{nn} M_n (\hat{K}_{nr} + \hat{\lambda}_{nr}) + \frac{\hat{c}_{nn}^2}{\hat{\psi}_n} \{ (\hat{K}_n + \hat{\lambda}_n) (\hat{K}_{nr} + \hat{\lambda}_{nr}) - \hat{\lambda}_n \hat{\lambda}_{nr} \} \right] \end{aligned} \quad (18)$$

‡ Eqn (19):
$$\hat{K}'_{rs} + \hat{\lambda}'_{rs} = - \sum_{n=1}^N [\hat{\phi}_n a_{nr} a_{ns} + \hat{b}_{nr} (\hat{K}_{ns} + \hat{\lambda}_{ns}) + \hat{b}_{ns} (\hat{K}_{nr} + \hat{\lambda}_{nr})] + \sum_n^{N_u} \left[\frac{\hat{c}_{nn}^2}{\hat{\psi}_n} \{ (\hat{K}_{nr} + \hat{\lambda}_{nr}) (\hat{K}_{ns} + \hat{\lambda}_{ns}) - \hat{\lambda}_{nr} \hat{\lambda}_{ns} \} \right] \quad (19)$$

identically to zero for all r . Thus, if care is taken to exclude these feedback terms, a convenient method of determining future $\hat{\lambda}_r$'s is available once a starting value is chosen. For a linear system it is seen that the equations formed from (21) determine a transient response giving all values of later $\hat{\lambda}_r$'s from the original initial conditions.

The end values required in solving eqns (17), (18), (19) and (1) are obtained from the condition

$$E[\hat{Z}(t+\tau), t+\tau] = 0 \quad (22)$$

$$\text{thus} \quad \hat{k}_0(t+\tau) = 0 \quad (23)$$

$$\hat{K}_r(t+\tau) - \hat{\lambda}_r(t+\tau) = 0 \quad (24)$$

$$\hat{K}_{rs}(t+\tau) - \hat{\lambda}_{rs}(t+\tau) = 0 \quad (25)$$

Eqn (25) is simply satisfied since it leads to either the $\hat{K}_{rs}(t+\tau)$ or the $\hat{\lambda}_{rs}(t+\tau)$ zero but eqn (24) requires the initial value of $\hat{K}_r(t+\tau)$ to be chosen from the assumed or calculated $\hat{\lambda}_r(t+\tau)$. It will also be appreciated that the value of $\hat{Z}(t+\tau)$ must be assumed for the solution but for real time control a search procedure is necessary to ensure that the calculated element values of $\hat{Z}(t)$ are, in fact, the actual plant state vector elements that would be observed. For linear systems this latter feature does not arise since eqns (17), (18) and (19) are independent of \hat{Z} and for such systems the cap notation can be dropped.

Example

A fourth order constant coefficient plant, defined by the equation

$$\begin{bmatrix} \dot{Z}_1 \\ \dot{Z}_2 \\ \dot{Z}_3 \\ \dot{Z}_4 \end{bmatrix} = \begin{bmatrix} -2.0 & -1.0 & 0 & 0 \\ 1.0 & 0 & 0 & 0 \\ 0 & 1.0 & -1.3 & -1.5 \\ 0 & 0 & 1.0 & 0 \end{bmatrix} \begin{bmatrix} Z_1 \\ Z_2 \\ Z_3 \\ Z_4 \end{bmatrix} + \begin{bmatrix} m_1 \\ 0 \\ m_3 \\ 0 \end{bmatrix} \quad (26)$$

and consisting of two quadratic systems linked in tandem, Figure 2, was considered as an illustration of the technique. The

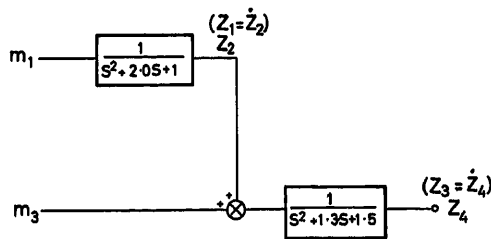


Figure 2. The fourth-order plant

object of the exercise was to compare the performance of the absolute optimum system, in which all feedback paths were available, with a constrained optimum system which had no feedback information from the state vector components Z_3 and Z_4 . Obviously, the assumption that the plant parameters cannot be changed was necessary, otherwise the problem is just an exercise in Merriam's optimization technique.

For comparison purposes the response of the plant to standard test signals were calculated with input m designed to give zero position, velocity and acceleration lags, i.e.

$$\begin{bmatrix} m_1 \\ m_2 \\ m_3 \\ m_4 \end{bmatrix} = \begin{bmatrix} [Q + 2.0\dot{Q} + \ddot{Q}] \\ 0 \\ [0.5Q + 1.3\dot{Q} + \ddot{Q}] \\ 0 \end{bmatrix} \quad (27)$$

and are shown in Figures 3, 4 and 5, respectively. These responses were sluggish.

The performance criterion chosen was

$$e(t) = \int_t^{t+\tau} \left[\phi_1(Q' - Z_1)^2 + \phi_2(Q - Z_2)^2 + \phi_3(Q' - Z_3)^2 + \phi_4(Q - Z_4)^2 + \psi_1 m_1^2 + \psi_3 m_3^2 \right] d\sigma \quad (28)$$

where Q is the desired response of Z_2 and Z_4 and the time derivative Q' is the desired response of Z_1 and Z_3 . The interval

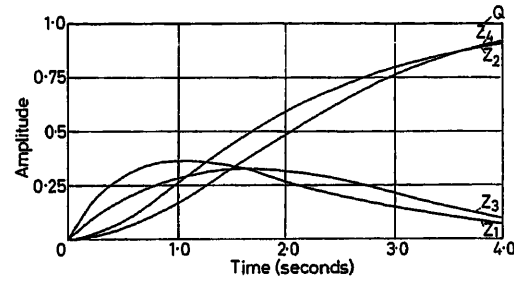


Figure 3. Unit step response of plant

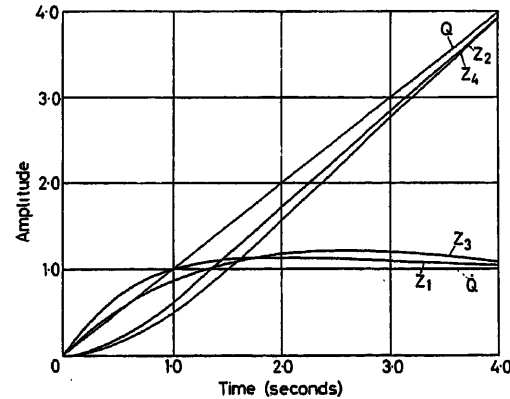


Figure 4. Unit ramp response of plant

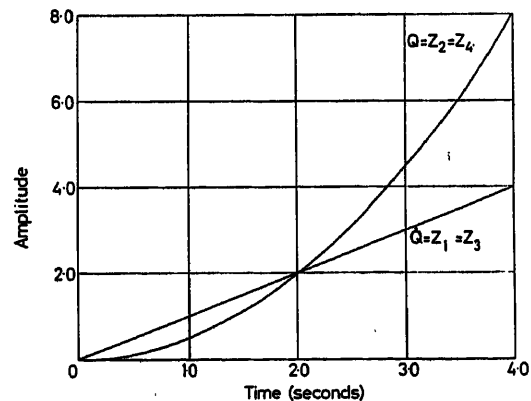


Figure 5. Unit acceleration response of plant

t to $t + \tau$ could have been infinite but a finite interval (1.28 sec) was chosen to assess the efficiency of the optimization techniques. To solve eqns (17), (18) and (19) the desired responses $Q(\mu)$ and $Q'(\mu)$ must be predicted over the interval $t \leq \mu \leq t + \tau$ and this was accomplished by a Taylor series expansion about t leading to a constant coefficient realization of the absolute optimum system.

Thus

$$Q(\mu) = Q(t) + (\mu - t) \dot{Q}(t) + \frac{(\mu - t)^2}{2!} \ddot{Q}(t) + \dots \text{etc.} \quad (29)$$

The Absolute Optimum System

To derive the absolute optimum system, Merriam's technique was used with weightings $\phi_1 = 0.1$, $\phi_2 = 1.0$, $\phi_3 = 0.07$, $\phi_4 = 0.70$, $\psi_1 = 0.05$ and $\psi_2 = 0.035$ which were selected on the basis of a number of preliminary trials. The equations describing the performance of this system were obtained from eqns (1), (20) and (29), namely

$$\begin{bmatrix} \dot{Z}_1 \\ \dot{Z}_2 \\ \dot{Z}_3 \\ \dot{Z}_4 \end{bmatrix} = \begin{bmatrix} -3.54 & -4.49 & -0.07 & -0.05 \\ 1.0 & 0 & 0 & 0 \\ -0.09 & 0.41 & -3.11 & -4.65 \\ 0 & 0 & 1.0 & 0 \end{bmatrix} \begin{bmatrix} Z_1 \\ Z_2 \\ Z_3 \\ Z_4 \end{bmatrix} + \begin{bmatrix} X_1 \\ X_2 \\ X_3 \\ X_4 \end{bmatrix} \quad (30)$$

where

$$\begin{bmatrix} X_1 \\ X_2 \\ X_3 \\ X_4 \end{bmatrix} = \begin{bmatrix} [4.26 Q + 3.32 \dot{Q} + 1.40 \ddot{Q}] \\ 0 \\ [4.14 Q + 3.04 \dot{Q} + 1.5 \ddot{Q}] \\ 0 \end{bmatrix} \quad (31)$$

Higher-order operations on Q could have been included if required.

The responses of this system to unit step, ramp and accelerating signals are shown in Figures 6, 7 and 8, respectively. A very fast response was obtained with little overshoot due to the ability of the method to, in effect, change the system via the feedback parameters, K_{rs} . Steady-state errors were produced because the prediction interval τ was only 1.28 sec but by allowing τ to become large these errors disappeared in agreement with Merriam⁴.

The Constrained Optimum System

The techniques described under the heading of Constrained Optimization were used to derive the constrained optimum system in a constant coefficient realization by so choosing the para-

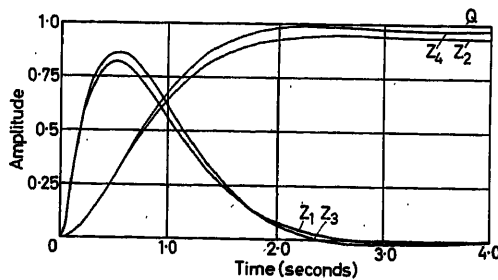


Figure 6. Unit step response of absolute optimum system

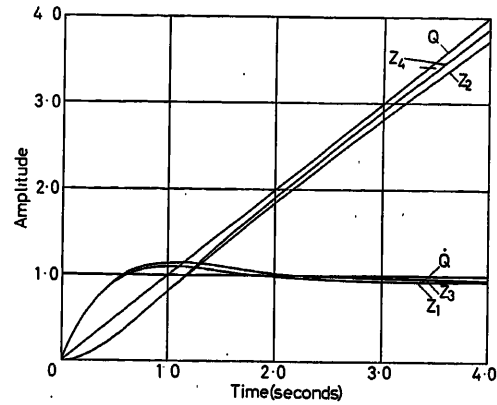


Figure 7. Unit ramp response of absolute optimum system

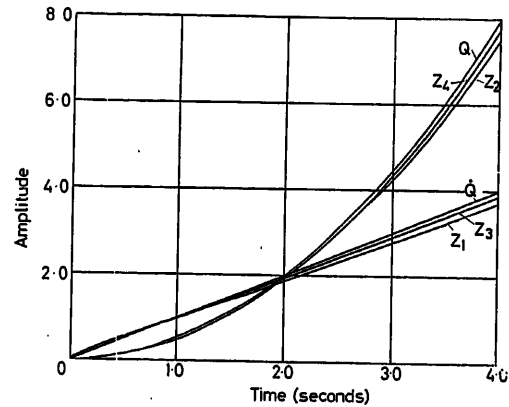


Figure 8. Unit acceleration response of absolute optimum system

meters λ_r to give the correct steady-state behaviour of the system to the standard input signals. The feedback paths from Z_3 and Z_4 were not available so

$$K_{r3} = K_{r4} \equiv 0 \quad (32)$$

for all $r = 1, \dots, 4$ and the λ_{rs} were put identically zero except for the terms λ_{r3} and λ_{r4} for all r . The resultant system equation, using the weightings mentioned under The Absolute Optimum System, became

$$\begin{bmatrix} \dot{Z}_1 \\ \dot{Z}_2 \\ \dot{Z}_3 \\ \dot{Z}_4 \end{bmatrix} = \begin{bmatrix} -3.54 & -4.49 & 0 & 0 \\ 1.0 & 0 & 0 & 0 \\ -0.09 & 0.26 & -1.3 & -1.5 \\ 0 & 0 & 1.0 & 0 \end{bmatrix} \begin{bmatrix} Z_1 \\ Z_2 \\ Z_3 \\ Z_4 \end{bmatrix} + \begin{bmatrix} Y_1 \\ Y_2 \\ Y_3 \\ Y_4 \end{bmatrix} \quad (33)$$

where

$$\begin{bmatrix} Y_1 \\ Y_2 \\ Y_3 \\ Y_4 \end{bmatrix} = \begin{bmatrix} [4.24 Q + 3.29 \dot{Q} + 1.26 \ddot{Q}] \\ 0 \\ [1.25 Q + 1.31 \dot{Q} + 0.98 \ddot{Q}] \\ 0 \end{bmatrix} \quad (34)$$

The response of the constrained optimum system to unit step, ramp and accelerating signals are shown in Figures 9, 10, and 11, respectively, which indicate that the system was very fast with respect to the variables Z_1 and Z_2 . The responses of the variables Z_3 and Z_4 , however, were slower and possessed more overshoot

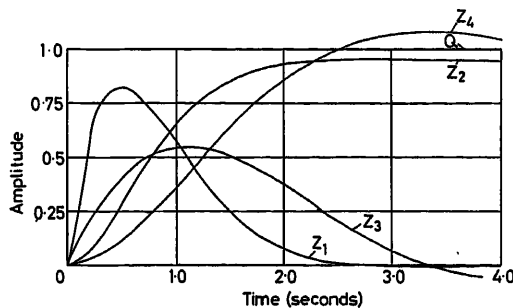


Figure 9. Unit step response of constrained optimum system

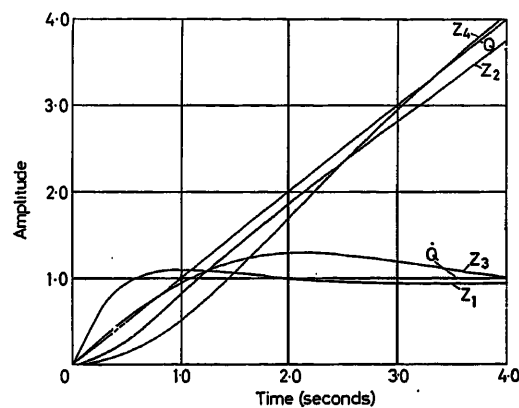


Figure 10. Unit ramp response of constrained optimum system

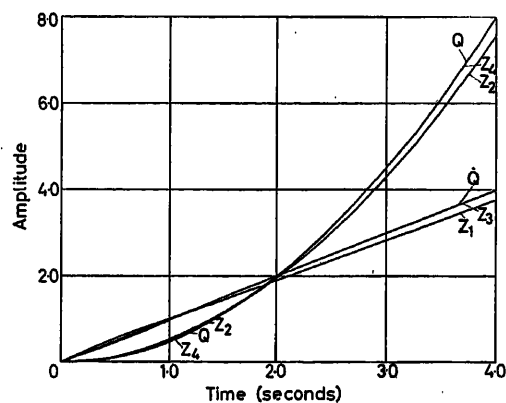


Figure 11. Unit acceleration response of constrained optimum system

than the absolute optimum responses, but were faster than the corresponding responses of the actual plant. Other ways of choosing the parameters, λ_r , were possible; e.g. a constant coefficient system could also have been realized by minimizing the mean square error with respect to the λ_r parameter, integrated over all time. Alternatively, a time-varying system could have been obtained if the parameters had been correctly chosen for each interval t to $t + \tau$ in $0 \leq t < \infty$.

Load Disturbances

In the general theory the effects of load disturbances can be reduced if the disturbance is measurable or deterministic, but it is of interest to calculate the effects of disturbances on the

present example. Tables 1, 2 and 3 give the steady-state response of the actual plant, absolute optimum and constrained optimum, respectively, for step disturbances of the elements of the vector u .

Table 1. Disturbance of Actual Plant

		Unit step in elements of disturbing vector			
		u_1	u_2	u_3	u_4
State	Z_1	0	1.0	0	0
State	Z_2	1.0	-2.0	0	0
Vector	Z_3	0	0	0	1.0
Response	Z_4	0.67	1.33	0.67	-0.87

Table 2. Disturbance of Absolute Optimum System

		Unit step in elements of disturbing vector			
		u_1	u_2	u_3	u_4
State	Z_1	0	1.0	0	0
State	Z_2	0.22	-0.79	-0.002	-0.008
Vector	Z_3	0	0	0	1.0
Response	Z_4	-0.02	0.09	0.22	-0.67

Table 3. Disturbance of Constrained Optimum System

		Unit step in elements of disturbing vector			
		u_1	u_2	u_3	u_4
State	Z_1	0	1.0	0	0
State	Z_2	0.22	-0.79	0	0
Vector	Z_3	0	0	0	1.0
Response	Z_4	-0.15	0.53	0.67	-0.87

It is seen that step disturbances affect the absolute system less severely than the constrained optimum system which, in turn, is less affected by the disturbances than the actual plant.

It will be appreciated that the above example is simple and artificial and that the correct procedure in any real study is to use Merriam's technique to derive as near as possible the actual plant parameters and then proceed with the method described above to determine the control action.

Conclusions

The paper has described a technique for producing the design of a near-optimum controller for a linear or non-linear dynamic plant, possessing possible amplitude limitation of the input control signal, in those cases where it is impossible or inconvenient to obtain information of certain state vector elements, i.e. certain feedback paths are not available. More work is required to determine the significance of the λ_r 's, but various degrees of engineering sophistication seem possible in realizing the constrained optimum system by suitable choice of the N parameters, $\lambda_r(t)$. The method is particularly suited to the designer of controlled plants who wishes to assess the penalties that accrue

when feedback paths are omitted. It will be appreciated, however, that the performance of the system will depend on the method of realization of the system. No difficulties are foreseen in extending the method to the case in which the desired response vector Q contains stochastic elements with known statistical distributions.

The general question of stability in such system was not considered but it will be appreciated that some plant configurations with certain feedback links omitted will be unstable. For example, if a sub-unit of the plant was unstable then small noise disturbances, which are always present in any system, will excite the instability if the output state of the sub-unit is ignored by the computer. Obviously such a limited system cannot be controlled and it is therefore necessary to allow the feedback of information or make the plant stable. It is felt, however, that in most practical instances the latter condition will be satisfied.

The technique has been applied to a fourth-order constant-coefficient plant to obtain a constant-coefficient realization of the constrained optimum system having zero steady-state errors to the usual test signals. As expected, the performance of this system was midway between that of the absolute optimum system, which had access to all state variables, and that of the actual plant whose inputs had also been adjusted to give zero steady-state errors.

The author is indebted to Mr. A. Stewart for his valuable criticisms made during discussions, to Mr. W. Mathews who was responsible for all DEUCE programming and computation and finally to British Aircraft Corporation Limited (Guided Weapons Division) for permission to publish this work.

Nomenclature

a_{rn}, b_{rn}, c_{rn}	Elements of plant matrices
$E[Z(\mu), \mu]$	Minimum error function
$e(t)$	Performance error criterion
$K_n(\mu), K_{rn}(\mu)$	Parameters of control signal vector
$k_0(\mu), k_n(\mu), k_{rn}(\mu)$	Parameters of minimum error function
$L^+(t), L^-(t)$	Upper and lower bound vectors of the control signal vector
$M(t)$	Desired control signal vector
$m(t)$	Control signal vector
$[m(\mu)]$	Control switching signal vector
N	Order of plant
$Q(t)$	Desired response signal vector
$q(t)$	Response signal vector
t	Real or present time variable
$u(t)$	Additive load disturbance vector
$Z(t)$	State signal vector
$\lambda_n(\mu), \lambda_{rn}(\mu)$	System realization parameters
σ, μ	Dummy time variables
τ	Prediction interval
ϕ_n, ψ_n	Weighting functions

References

- BELLMAN, R. *Dynamic Programming*. Princeton University Press (1957)
- ROZONER, L. I. L. S. Pontryagin's maximum principle in optimum system theory I, II and III. *Automation rem. Cont.* 20 (1959), 1288-1302, 1405-1421, 1517-1532
- MERRIAM, C. W. An optimization theory for feedback control system design. *Inf. Cont.* 3 (1960), 32-59
- MERRIAM, C. W. Computational considerations for a class of optimum control system. *Automatic and Remote Control*. 1961. London; Butterworths

DISCUSSION

A. R. M. NOTON, *Electrical Engineering Dept., University of Nottingham, Nottingham, England*

It is well known that the synthesis of optimal systems (using either dynamic programming or Pontryagin's Principle) requires information on all state variables. Since this is frequently a practical difficulty, Mr. Anderson's paper is very interesting. It is especially so to me since I am trying to do the same sort of thing by means of a discrete, instead of a continuous, version of dynamic programming.

In studying the paper I had some difficulty in grasping the full significance of the operations on the λ parameters [e.g. around eqn (21)]. Furthermore, an example has been chosen in which it is not intuitively obvious what to expect.

Consequently, I am very interested to learn what other examples have been studied by the author. For example, *Figure A* shows a very relevant example for checking purposes:

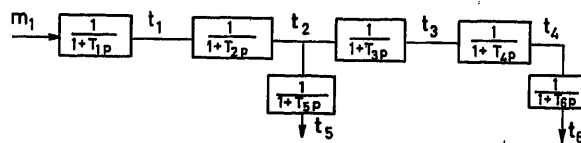


Figure A

If the performance index is

$$\int (\phi_2 z_2^2 + \phi_4 z_4^2 + t_1 m_1^2) dt$$

Ordinary theory predicts the use of z_1, z_2, z_3, z_4 (not z_5, z_6). When z_1, z_2, z_3, z_4 are not available in practice, z_5 and z_6 have to be used and this should emerge naturally from the theory.

B. G. ANDERSON, *in reply*

On the first point, the λ parameters of eqn (21) have been separated from eqn (18) of the paper since they form the adjoint equations for the system when the allowable feedback parameters are included. This is an arbitrary separation, hence my previous remarks on the hope that a calculus of variations approach may clarify the significance of the λ 's.

My own belief is that eqn (21) allows one to determine the boundary value of the single outfix K 's at the time $(t + \tau)$ and hence find the value of these parameters at time t . The computational aspects seem immense so that one hopes to find a simple approximate solution to eqns (18) and (19).

Finally, the reason for the choice of example was that this is the way in which the problem occurred and unfortunately, for non-technical reasons, the work had to be discontinued before other examples could be examined.

AUTOMATIC CONTROL OF AEROSPACE SYSTEMS

The Design Study of a Pressure Control System for a 5 ft. by 5 ft. Blowdown Wind Tunnel

J. A. TANNER and W. DIETIKER

Summary

The problem is to maintain the settling chamber pressure in a blowdown wind tunnel constant at a predetermined value during a run at constant Mach number. Air stored at high pressure expands and discharges through a control valve into a settling chamber and then through a supersonic (or transonic) working section to a diffuser and the atmosphere. As the reservoir pressure falls, the valve is opened to maintain the flow, and this is accompanied by a change in the valve transfer gain. In addition, the pressure ratio across the valve decreases continuously and when it falls below the critical value, flow through the valve changes from sonic to subsonic. This produces time-varying dynamic characteristics in the control valve settling chamber system.

Because of the wide range of Mach numbers and settling chamber pressure settings required, a pressure control system incorporating automatic gain control has been developed. Experimental verification of the theoretically derived air flow dynamics has been performed on a 5 in. by 5 in. pilot model of the 5 ft. by 5 ft. facility. The pressure control system has been studied on an analogue computer.

Sommaire

Le problème consiste à maintenir à une valeur fixée à l'avance la pression de la chambre de ralentissement d'une soufflerie à réservoir au cours d'un essai effectué avec un nombre de Mach constant. L'air emmagasiné à haute pression se détend et passe par une soupape de réglage avant d'arriver dans une chambre de ralentissement d'où il va dans une chambre d'expérience pour vitesses supersoniques (ou transsoniques) pour enfin passer dans un diffuseur et sortir dans l'atmosphère. A mesure que la pression du réservoir baisse, la soupape de réglage s'ouvre pour que l'écoulement soit maintenu et cette ouverture s'accompagne d'une modification du rapport des valeurs de pression à l'entrée et à la sortie de la soupape. De plus, le rapport des pressions à travers soupape décroît continuellement et lorsqu'il descend au-dessous de la valeur critique, l'écoulement, de sonique qu'il était, devient subsonique. Cela produit des caractéristiques dynamiques variables avec le temps dans le système soupape de réglage/chambre de ralentissement.

Un dispositif de réglage de la pression, muni d'un régulateur automatique du rapport des valeurs de pression à l'entrée et à la sortie, a été mis au point à cause du grand assortiment de nombres de Mach et de pressions nécessaires dans la chambre de ralentissement. La vérification expérimentale de la dynamique du débit d'air calculée théoriquement a été effectuée au moyen d'une maquette de 5 x 5

pouces de la soufflerie de 5 x 5 pieds. Le dispositif de réglage de la pression a été étudié au moyen d'un calculateur par analogue.

Zusammenfassung

Die Aufgabe besteht darin, während eines Versuchs mit konstanter Machzahl den Vorkammerdruck in einem Windkanal mit Druckspeicher auf einem vorher bestimmten Wert konstant zu halten.

Die unter hohem Druck gespeicherte Luft dehnt sich aus und strömt durch ein Steuerventil in eine Ausgleichskammer und von dort im Ultraschall- (oder Transschall-)Bereich zu einem Diffusor und in die Atmosphäre. Bei fallendem Reservoirdruck wird das Ventil geöffnet, um die Strömung aufrechtzuerhalten, was auf eine Änderung der Ventilempfindlichkeit führt. Außerdem nimmt das Druckverhältnis am Ventil kontinuierlich ab; unterschreitet es den kritischen Wert, so ändert sich die Strömung durch das Ventil von einer Schallströmung in eine Unterschallströmung. Damit ergeben sich in dem System aus Steuerventil und Ausgleichskammer zeitveränderliche dynamische Kennlinien.

Wegen des erforderlichen großen Bereichs der Machzahlen und der entsprechenden Einstellungen des Ausgleichskammerdrucks wurde ein Drucksteuersystem entwickelt, das eine automatische Regelung der Ventilempfindlichkeit zulässt. Die experimentelle Nachprüfung der theoretisch abgeleiteten Luftströmungsdynamik geschah an einem 5 in. x 5 in.-Prüfmodell einer 5 ft. x 5 ft.-Einrichtung. Das Drucksteuersystem wurde mit einem Analogrechner untersucht.

Introduction

A blowdown wind tunnel¹ consists basically of a reservoir in which air is stored at high pressure, a control valve which acts as a throttling device, a settling chamber to stabilize the flow, and a nozzle which discharges through the working section to a variable diffuser and then to the atmosphere. The aerodynamic forces on a model in the working section are proportional to γPM^2 where γ is the ratio of the specific heats of air, and P and M are the working section static pressure and Mach number. To maintain these forces constant, P and M must be held constant. In the supersonic regime, M is deter-

mined by the geometry of the nozzle, and for a particular configuration remains sensibly constant. The pressure P is dependent on air flow and this is measured and controlled in terms of the settling chamber pressure at the contraction entry to the nozzle. In the transonic and high subsonic regimes, Mach number alters with changes in the geometry and aerodynamic drag of the model, and it is necessary to incorporate a separate Mach number control system in the working section.

As the reservoir pressure falls, the valve is opened to maintain the air flow, but this is accompanied by a change in valve sensitivity, i. e., transfer gain. The pressure ratio across the valve also decreases and when it falls below the critical value, flow through the valve changes from sonic to subsonic. This introduces time-varying dynamic characteristics in the control valve settling chamber system. However, the air flow process is determinate, and the parameter variations can be computed for the complete range of wind tunnel operation.

An important operational requirement for the blowdown type of wind tunnel is that at the commencement of a run, air flow must be established as rapidly as possible and with negligible overshoot. This arises, first, because of the limited running time available (10–100 sec) and, second, because rapid establishment of flow in the working section is required to alleviate the excessive unsteady aerodynamic loading of the model that occurs during the starting period.

In this paper, only the problem of controlling settling chamber pressure is considered. The requirement is for this pressure to be held constant within ± 0.5 per cent of the pre-selected value for all regimes of operation. The air flow dynamics of a 5 ft. by 5 ft. wind tunnel^{1, 2} have been studied on a 5 in. by 5 in. pilot model and the pressure control system has been the subject of an analogue computer study.

The Control Valve

The general arrangement of the 5 in. by 5 in. pilot blowdown wind tunnel is shown in Figure 1. Both this wind tunnel and the full-scale facility are designed to operate over a Mach number range 0.2 to 4.5. A section of the scale model valve constructed for experimental investigation in the model wind tunnel is shown in Figure 2. The cylindrical port area (A) is adjusted by

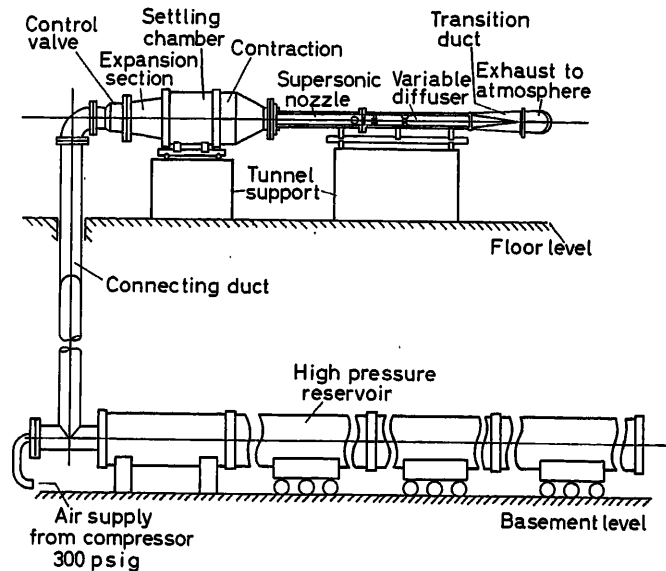


Figure 1. General arrangement of 5 in. x 5 in. pilot wind tunnel

means of an internal sleeve driven by a hydraulic jack. Air issues from the ports radially inwards and passes through a screen into the settling chamber.

Compressible Flow Through the Control Valve

The control valve forms a variable area restriction, the flow through which, with reference to Figure 3, is given by

$$W_s = F(P_s, P_1, \theta_s, A_s) \quad (1)$$

where W_s = weight flow, P_s = storage stagnation pressure, P_1 = static (back) pressure on control valve jet, A_s = effective area of control valve jet, and θ_s = storage stagnation temperature.

The explicit relationship between these parameters is as follows:

$$W_s = P_s A_s \left\{ \frac{2g\gamma}{R\theta_s(\gamma-1)} \left[\left(\frac{P_1}{P_s} \right)^{\frac{2}{\gamma}} - \left(\frac{P_1}{P_s} \right)^{\frac{\gamma+1}{\gamma}} \right] \right\}^{1/2} \quad (2)$$

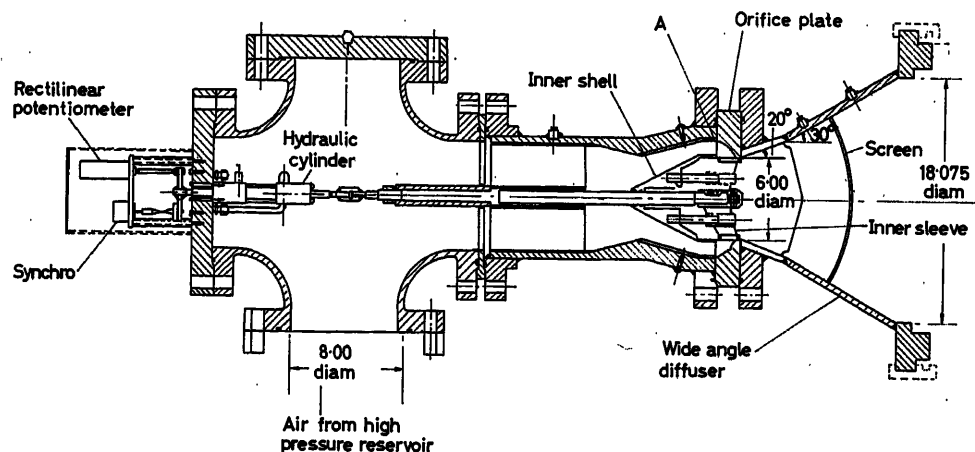


Figure 2. Control valve for pilot model intermittent tunnel

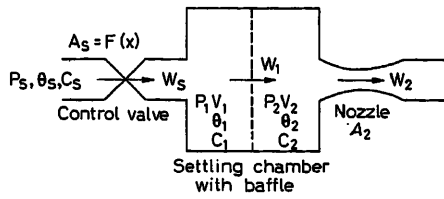


Figure 3. Lumped parameter schematic of control valve and settling chamber

in which R is the gas constant and g is the gravitational constant. When the pressure ratio $P_1/P_s \leq 0.528$ (for $\gamma = 1.4$), the flow through the valve is sonic and W_s is independent of P_1 . This is referred to as 'choked' flow and eqn (2) reduces to

$$W_s = K P_s A_s \quad (3)$$

where

$$K = \left[\left(\frac{2}{\gamma+1} \right)^{\frac{\gamma+1}{\gamma-1}} \cdot \frac{g\gamma}{R\theta_s} \right]^{1/2}$$

Inspection of eqns (2) and (3) reveals the complex function generation that would be required to control W_s by 'open loop' programming of the valve displacement.

Transfer Gain Characteristics

The incremental transfer gain characteristic of the control valve can be determined by expressing eqn (1) in terms of partial differentials. If W_s is expressed as a function of valve sleeve displacement X instead of area A_s , then

$$W_s = F_s(P_s, P_1, X, \theta_s)$$

and

$$dW_s = \left(\frac{\partial W_s}{\partial P_s} \right) dP_s + \left(\frac{\partial W_s}{\partial P_1} \right) dP_1 + \left(\frac{\partial W_s}{\partial X} \right) dX + \left(\frac{\partial W_s}{\partial \theta_s} \right) d\theta_s$$

Applying the theory of small perturbations³ and using the lower case letter to represent the incremental variable

$$w_s = k_s p_s - k_b p_1 + k_x x + k_\theta \theta_s \quad (4)$$

where $w_s = dW_s$ and $k_s = \partial W_s / \partial P_s$, $k_b = \partial W_s / \partial P_1$, $k_x = \partial W_s / \partial X$ and $k_\theta = \partial W_s / \partial \theta_s$.

The coefficients k_s , k_b and k_θ can be determined from eqn (2) and k_x from the control valve area *versus* stroke relationship. With temperature assumed constant, k_θ is zero and the last term of eqn (4) disappears.

Under steady-state flow conditions and with the control valve choked, coefficient k_x , the incremental transfer gain of the valve, can be determined from eqn (3) and is given by

$$k_x = \frac{\partial W_s}{\partial X} = W_s \frac{F'(X)}{F(X)} \quad (5)$$

where $A_s = F(X)$ represents the effective area of the valve porting, i.e., the control valve jet. If $F(X)$ is known, the incremental transfer gain can be computed over the choked working range. For example, if valve area is proportional to displacement, then $F(X) = nX$ and $F'(X) = n$. Substituting

these values in eqn (5) yields $k_x = W_s/X$. This characteristic is shown plotted in Figure 4(b) in normalized form with percentage valve travel Z as the abscissa. Various stroke characteristics and the corresponding transfer gain curves are plotted in Figures 4(a) and (b).

It can be deduced from eqn (5) that to maintain constant transfer gain under choked flow conditions, the valve area must

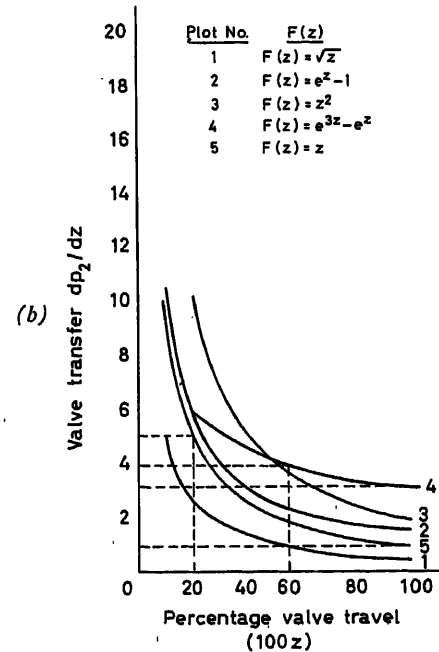
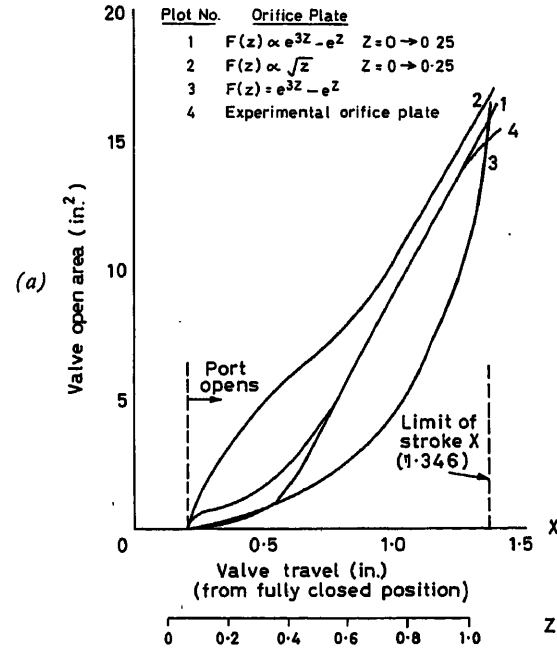


Figure 4. Control valve characteristics: (a) Port area versus valve travel pilot model wind tunnel; (b) Theoretically derived transfer gain characteristics

be related exponentially to stroke. This is very difficult to realize in practice with a sleeve-type valve, but a compromise can be reached by compounding the port area characteristic so that, excluding the initial opening, it is exponential over the first half of the stroke and approximately linear over the remainder. The designed port area characteristic of the control valve for the 5 ft. square wind tunnel is shown in Figure 5, together with the derived transfer gain characteristic.

Experimental Verification of Incremental Gain Characteristics

Experimental verification of the derived valve transfer gain characteristics was performed on the pilot model wind tunnel.

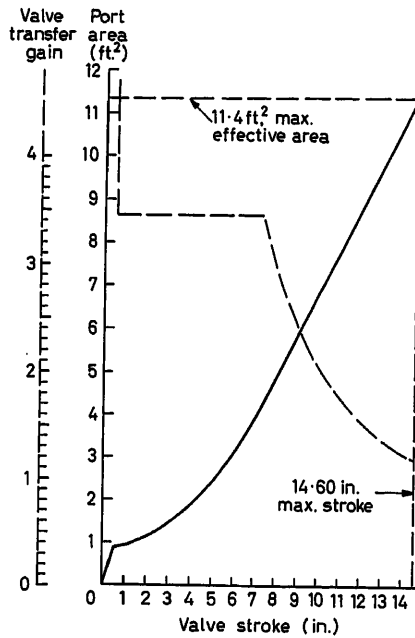


Figure 5. Control valve port area characteristic and transfer gain for the 5 ft. square wind tunnel

With the settling chamber pressure control loop closed, a disturbance was applied to the control valve in the form of a sinusoidal signal of constant frequency and amplitude; the amplitude being small enough to ensure operation in the linear regime. The sinusoidal components of valve displacement and settling chamber pressure were then recorded during the course of a run.

Since the average value of the pressure is constant, the amplitude ratio of the two fundamental sinusoidal components yields the process transfer gain (dP_2/dX) which is related to the valve transfer gain by a constant. A typical experimental characteristic is shown plotted in Figure 6, in which the experimental and theoretical gain curves for a compound port area characteristic are shown superimposed.

Dynamic Analysis of the Air Flow Process

From the block schematic of the control valve, settling chamber and nozzle given in Figure 3 and assuming 'lumped' energy storage, the flow equations can be written:

$$\left. \begin{aligned} W_s &= P_s F(X) \left\{ \frac{2g\gamma}{R\theta_s(\gamma-1)} \left[\left(\frac{P_1}{P_s} \right)^{\frac{2}{\gamma}} - \left(\frac{P_1}{P_s} \right)^{\frac{\gamma+1}{\gamma}} \right] \right\}^{1/2} \\ W_1 &= K_1 (P_1 - P_2) \\ W_2 &= K P_2 A_2 \\ \frac{dP_1}{dt} &= \frac{1}{C_1} (W_s - W_1) \\ \frac{dP_2}{dt} &= \frac{1}{C_2} (W_1 - W_2) \end{aligned} \right\} \quad (6)$$

where the pneumatic capacitances C_1 and C_2 are defined as follows:

$$C_1 = \frac{V_1}{\gamma R \theta_1} \quad \text{and} \quad C_2 = \frac{V_2}{\gamma R \theta_2}$$

Applying the theory of small perturbations and expressing the new variables in lower case letters and in Laplace operational form, eqns (6) can be rewritten

$$\left. \begin{aligned} w_s(s) &= k_s p_s(s) + k_x x(s) - k_b p_1(s) \\ w_1(s) &= k_2 p_2(s) \\ w_1(s) &= k_1 [p_1(s) - p_2(s)] \\ p_1(s) &= \frac{1}{s C_1} [w_s(s) - w_1(s)] \\ p_2(s) &= \frac{1}{s C_2} [w_1(s) - w_2(s)] \end{aligned} \right\} \quad (7)$$

in which

$$k_1 = \frac{\partial W_1}{\partial P_1} = -\frac{\partial W_1}{\partial P_2} = K_1$$

and

$$k_2 = K$$

The simultaneous solution of eqns (7) yields settling chamber pressure $p_2(s)$ as a function of storage pressure $p_s(s)$ and valve displacement x as follows:

$$\boxed{\text{Eqn (8)}}^*$$

For conditions of choked flow, $k_b = 0$ and eqn (8) reduces to

$$p_2(s) = \frac{k_1 k_s p_s(s) + k_1 k_x x(s)}{s^2 C_1 C_2 + s [C_1 (k_1 + k_2) + C_2 k_1] + k_1 k_2} \quad (9)$$

* Eqn (8):

$$p_2(s) = \frac{k_1 k_s p_s(s) + k_1 k_x x(s)}{s^2 C_1 C_2 + s [C_1 (k_1 + k_2) + C_2 (k_b + k_1)] + k_1 k_2 + k_b k_2 + k_1 k_b} \quad (8)$$

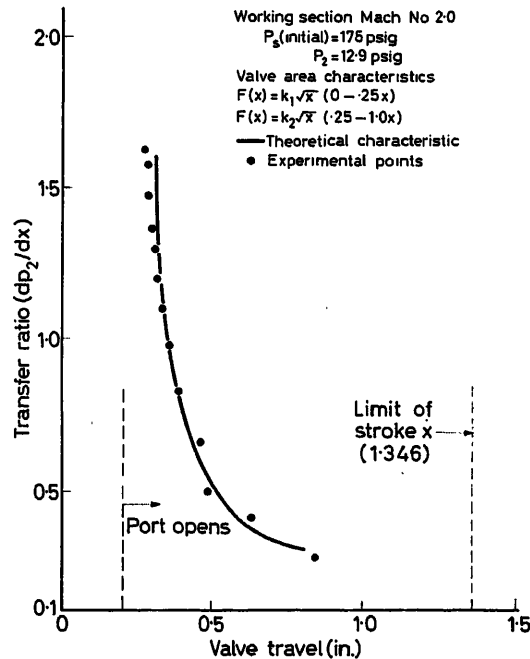


Figure 6. Experimentally determined valve transfer gain characteristic pilot model wind tunnel

Since this is a dissipative process with only one type of energy storage, the denominator expressions in eqns (8) and (9) have real roots.

For a wide range of air flows, the pressure loss across the baffle is small, i.e., k_1 is large, and eqn (8) can be reduced to one of first order, as follows:

$$p_2(s) = \frac{1}{k_2 + k_b} \left[\frac{k_s p_s(s) + k_x x(s)}{s \left(\frac{C_1 + C_2}{k_2 + k_b} \right) + 1} \right] \quad (10)$$

The quantity

$$\left(\frac{C_1 + C_2}{k_2 + k_b} \right)$$

is referred to as the unchoked system time constant T . For choked flow $k_b = 0$ and eqn (10) yields

$$p_2(s) = \frac{1}{k_2} \left[\frac{k_s p_s(s) + k_x x(s)}{s \left(\frac{C_1 + C_2}{k_2} \right) + 1} \right] \quad (11)$$

in which the quantity $[(C_1 + C_2)/k_2]$ is the choked system time constant.

Inspection of eqns (10) and (11) reveals the decrease in incremental gain and system time constant that occurs when the flow through the valve changes from sonic to subsonic. The calculated system time constants for the 5 ft. square wind tunnel at the upper and lower limits of pressure for various Mach numbers are given in Table 1.

Experimental Investigation of Air Flow Dynamics—Valve Unchoked

Frequency response tests were performed on the model tunnel to investigate the variable dynamics of the control valve

Table 1

Mach No.	$T(\text{choked})$	$T(\text{unchoked})$	Ratio $T(\text{choked})/T(\text{unchoked})$
0.2	1.5 sec	0.55 sec	2.7
1.4	0.53	0.44	1.2
2.5	1.2	0.37	3.2
3.5	2.6	0.36	7.2
4.5	7.4	0.58	12.8

and settling chamber combination. Under closed-loop pressure control and, therefore, constant flow conditions, a small amplitude sinusoidal motion at constant frequency was superimposed on the control valve. Recordings were taken of settling chamber pressure, valve position and storage pressure during the course of a run. From the experimental data, the equivalent variation of system time constant T was calculated. A typical characteristic at Mach No. 4 is shown in Figure 7 with time as the abscissa. At elapsed time $t = 1.0$ sec, the valve is at the threshold of unchoked operation.

It will be noted that over the period of unchoked operation, the time constant decreases to about one-tenth of its choked value.

Closed Loop Operation

Based on the linearized equation of operation (eqn 4), the control loop has the configuration shown in Figure 8. The change in storage pressure takes the form of a disturbance applied to the loop. Since under constant flow conditions, the storage reservoir discharges isothermally² at a uniform rate, this disturbance is in the form of a ramp input, i.e.,

$$\frac{dP_s}{dt} = \frac{W_s}{C_s} = k_d$$

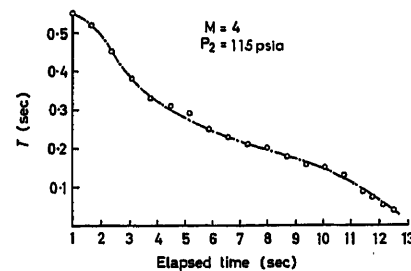


Figure 7. Time constant variation during unchoked period of valve operation

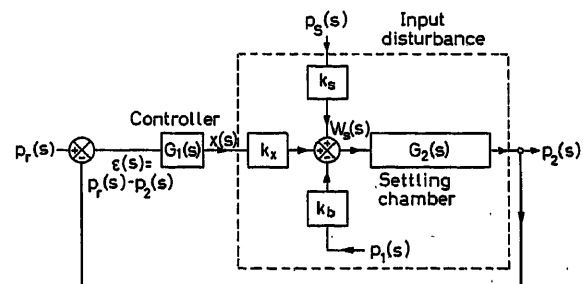


Figure 8. Block diagram of linearized control sequence

Determination of Controller Gain

From Figure 8, settling chamber pressure error $\varepsilon(s)$ caused by the input disturbance $p_s(s)$ is given by:

$$\varepsilon(s) = \frac{-k_s G_2(s) p_s(s)}{1 + k_x G_1(s) G_2(s)}$$

and if the loop gain $k_x G_1(s) G_2(s)$ is large compared with unity, this reduces to

$$\varepsilon(s) = \frac{-k_s p_s(s)}{k_x G_1(s)}$$

If the disturbance $P_s(t)$ is in the form of a ramp function with a slope of $-k_d$, then $p_s(s) = -k_d/s^2$ and $G_1(s)$ must contain two or more stages of integration for zero error. For the error to be held within a certain tolerance, a single stage of integration and a proportional-integral stage can be used. The final value of the pressure error would then reduce to:

$$\varepsilon = \frac{k_s \cdot k_d}{k_x \cdot G_1}$$

where k_d is the rate of change of storage pressure and G_1 is the gain constant associated with $G_1(s)$.

The ratio k_s/k_x can be determined from eqns (2) and (5) as follows:

$$\begin{aligned} \frac{k_s}{k_x} &= \frac{\partial W_s / \partial P_s}{\partial W_s / \partial X} \\ &= \frac{1}{P_s} \cdot \frac{F(X)}{F'(X)} \cdot F_1(P_1/P_s) \end{aligned}$$

where $F_1(P_1/P_s)$ is obtained from the partial differential of eqn (2) with respect to P_s :

$$F_1(P_1/P_s) = \left(\frac{\gamma-1}{\gamma} \right) \cdot \left[\frac{(P_1/P_s)^{\frac{2}{\gamma}} - 1/2 (P_1/P_s)^{\frac{\gamma+1}{\gamma}}}{(P_1/P_s)^{\frac{2}{\gamma}} - (P_1/P_s)^{\frac{\gamma+1}{\gamma}}} \right]$$

Pressure error is therefore given by

$$\varepsilon = \frac{k_d}{G_1 P_s} \cdot \frac{F(X)}{F'(X)} \cdot F_1\left(\frac{P_1}{P_s}\right) \quad (12)$$

For choked flow $F_1(P_1/P_s) = 1$ and the pressure error reduces to

$$\varepsilon = \frac{k_d}{G_1 P_s} \cdot \frac{F(X)}{F'(X)}$$

From eqn (12), the gain requirements for the controller G_1 can be computed for a constant predetermined percentage error (100 ε/P_s) over the range of tunnel operating conditions. The gain requirements for the upper and lower limits of settling chamber pressure at selected Mach number settings in the supersonic range are shown in normalized form in Figure 9 (with the gain at $P_s = 300$ lb./in.² abs. as the normalizing quantity). The crosses mark the points of transition from choked to unchoked flow through the control valve. It is immediately apparent from these characteristics that to maintain the error constant by programming gain G_1 as a function of storage pressure P_s would be an extremely complex task.

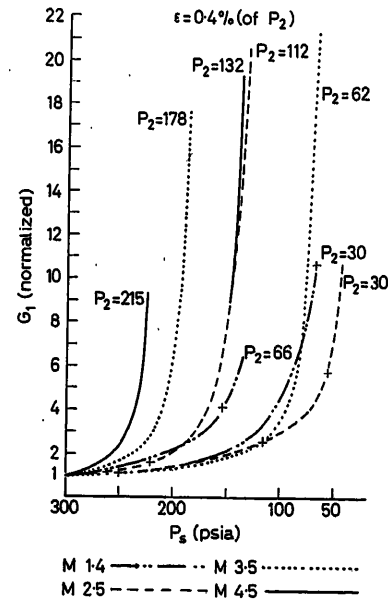


Figure 9. Controller gain characteristics required to maintain constant error (supersonic regime)

In the case of the pilot model wind tunnel, the variations in system dynamics were easily accommodated in the design of the pressure control system because the time constants, acoustic delays, etc., were sufficiently small that the gain and bandwidth requirements could be met by setting the controller gain at the highest level required at a particular flow and Mach number. The loop gain would decrease during a run, but would always be greater than the required minimum value. However, in the full-scale wind tunnel, the time constants are an order of magnitude greater, and to achieve the required performance some form of gain control is mandatory. The control configuration that suggests itself is one in which pressure error automatically adjusts the loop gain.

Analogue Computer Study of Incremental Dynamics

To understand more fully the effects of changes of gain on dynamic performance, the incremental model of Figure 8, modified to include a variable gain element (multiplier), was studied on an analogue computer. Figure 10 shows the block diagram of the simulation and the location of the gain varying elements.

The loop gain coefficient $G = k_x G_1 G_2$ was made a function of time, as follows:

$$G = G_0 (1 - at) \quad (13)$$

where G_0 is the loop gain at time $t = 0$, and a is a constant determining the rate of gain variation.

The disturbance signal representing the effect of decreasing reservoir pressure, as shown in Figure 10, is given by

$$p_s(t) = k_d at$$

(A positive sign is attached to k_d because for simulation studies it is immaterial whether the slope is positive or negative.) The input $p_r(t)$ to the system was zero, representing the steady-state condition.

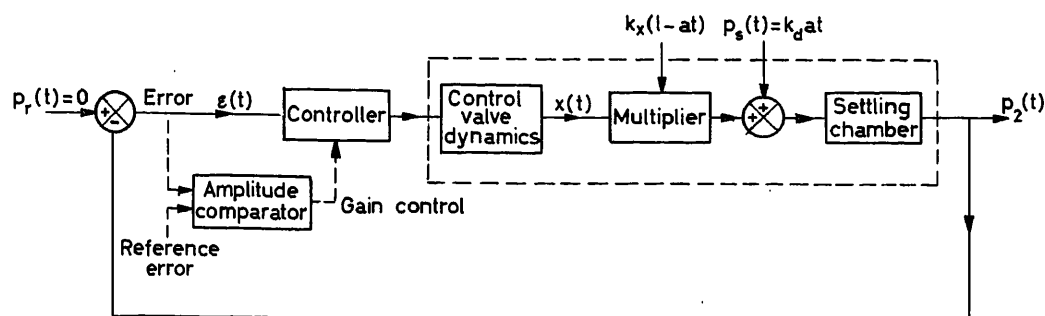


Figure 10. Block diagram of modified incremental model showing configuration of gain control loop

The solutions obtained from the analogue computer are shown plotted in Figure 11. The curve marked 'constant gain' shows the expected constant error that occurs in a Type 1 control system when it is subjected to a ramp disturbance. When the gain is decreased linearly according to eqn (13), the error increases rapidly, as shown in the curve marked 'no compensation'. The error exceeds the specified limit (dotted line) when the gain has dropped to approximately 85 per cent of its initial value.

Dynamic gain compensation can be achieved by programming the controller gain to vary inversely with the gain of the variable elements in the loop; that is, controller gain would be characterized by:

$$G_1(t) = \frac{G_{10}}{1-at}$$

where G_{10} is the controller gain at $t = 0$. This was investigated on the computer and the resulting error *versus* time characteristic

was found to be identical to that obtained with constant loop gain. (It should be noted that for convenience in handling the problem on the analogue computer, the loop gain constant was assigned to the controller gain setting alone, i.e. $G_{10} = G_0$.)

However, the variation of control valve transfer gain during a blowdown is not a simple function of time, but a non-linear function of Mach number, settling chamber pressure and reservoir pressure. 'Open loop' programming of controller gain, as previously mentioned, would necessitate a very elaborate function generation scheme, with facilities for changing the functional relationship with Mach number and settling chamber pressure.

A simple gain control system was investigated in which the controller gain was adjusted in discrete steps, using pressure error amplitude ϵ as a criterion. The configuration of this gain control is indicated in Figure 10. System error is fed into the 'amplitude comparator', the output of which controls the gain

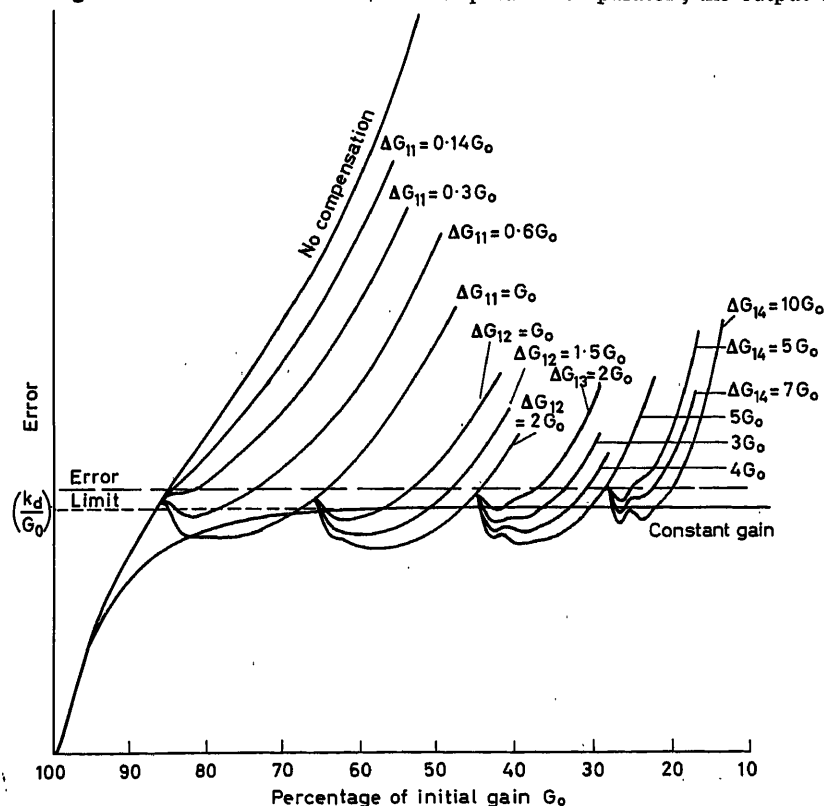


Figure 11. Error for a ramp disturbance and time varying gain applied to incremental model

setting of the controller. In more detail, the sequence is (a) pressure error $\varepsilon(t)$ is compared with a reference amplitude of error, specified as the maximum permissible; (b) when the error is equal to the reference amplitude, a relay closes, adding a preset increment to the loop gain; (c) each time the error reaches the reference amplitude, controller gain is increased by a preset increment.

Two questions that must be answered before such a control sequence can be used are: (i) by what amount should the gain be increased at each step, and (ii) how many steps are required to cover the anticipated decrease in loop gain.

The computer results which answer these questions are shown in Figure 11. When the error first reaches the reference amplitude (which is preset below the error limit), an increment of gain ΔG_{11} is added to the system. The change in the error is shown for a range of values of ΔG_{11} which are expressed in terms of G_0 , the loop gain at $t = 0$. It will be observed that restoring the loop gain to its original value has little effect on the error, and that a large increment of gain is required to produce any significant change. This is even more noticeable with the subsequent increments in gain, denoted by ΔG_{12} , ΔG_{13} and ΔG_{14} . Immediately after ΔG_{14} has been added, the loop gain is $5.22 G_0$, i.e., the gain is more than five times the initial value at $t = 0$. The error increases very rapidly after ΔG_{14} has been added, and nothing further can be done to hold the error below the required limit.

An attempt to measure the system response to a step change in reference input p_r was made by recording the response after each step change in controller gain. The results are shown in Figure 12, superimposed on the error curve resulting from the ramp disturbance and gain variation. Vertically above each of these step responses is a step response with a fixed value of loop gain equal to that at the start of each of the step responses for the dynamic case. (The time base is the same in all cases.)

A comparison of these step responses shows that the stability margin decreases as each gain increment is added. The term 'stability margin' is used rather loosely here, for it is difficult to attach physical significance to such a margin in a system subject to wide dynamic variations in its parameters.

There is little doubt that the dynamics of the gain variation have appreciable effect on the system response. To demonstrate this effect, the resulting error for the same ramp disturbance, but with constant gain equal to that at the point marked A, ($G = 1.96 G_0$), is also shown in Figure 12. The error is much less than that in the gain-varying case.

The effect of reducing the rate of change of the gain and of the disturbance signal results in a more satisfactory system. Figure 13 shows the error curves for the same value of a , as in Figures 11 and 12, and also the error curve for $a/2$. The values of the gain increments in both cases are $\Delta G_{11} = G_0$, $\Delta G_{12} = 2 G_0$, $\Delta G_{13} = 5 G_0$, and $\Delta G_{14} = 10 G_0$. The control valve gain drops to a lower value with $p_s(t) = k_d a/2$, before the specified error is reached. The effect of each step change of gain is greater because the rate of change of gain has been reduced by a factor of two. Therefore, if satisfactory performance is obtained for the greatest rate of change of gain and disturbance encountered, the performance will be satisfactory at all lower rates of change.

Analogue Computer Study of Gross Dynamics

The eqns (6) describing the gross dynamics of the system were set up on the computer and the gain control loop was implemented in the same manner as in Figure 10. Servo multipliers and diode function generators were used to simulate the various non-linear relationships in the equations.

The value of each gain increment was selected as follows. The conditions for the highest anticipated settling chamber pressure for a selected range of Mach numbers were set into the

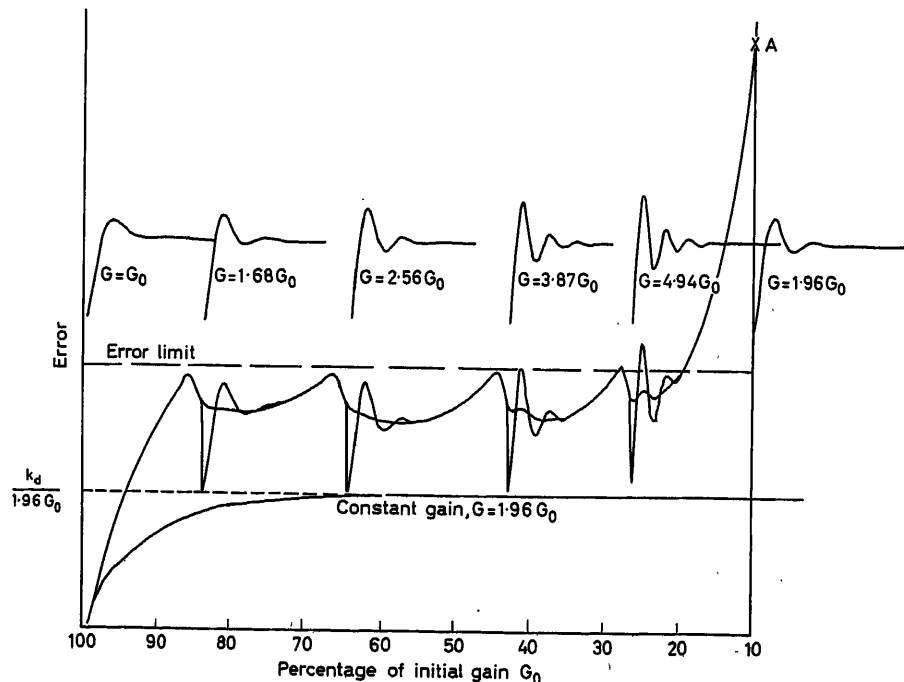


Figure 12. Step responses to illustrate system dynamics with time varying gain and equivalent values of fixed gain

computer, one at a time. At each Mach number, the error was measured and the computer put into the hold mode when the error reached the specified limit. From the characteristic curves of Figure 9, the gain was determined after noting the value of the air storage pressure on the computer. The amount of controller gain required to restore the loop gain to its original value was then computed. Typical values of the ratio $\Delta G_{11}/G_0$ over the working Mach number range are given in Table 2.

Table 2

Mach No.	$\frac{\Delta G_{11}}{G_0}$	$\frac{\Delta G_{12}}{G_0}$
0.2	1.067	1.722
0.4	0.461	1.077
0.6	0.796	—
0.8	0.469	—
1.0	0.542	—
1.4	0.604	—
2.5	0.894	2.424
3.5	0.679	1.800
4.5	1.728	1.941

To simplify the design of the controller, it was considered expedient to use the same value of gain increment for all regimes of operation. This involved a compromise in determining each value.

If ΔG_{11} were made greater than necessary to restore the overall loop gain to its original value, then the discrete change in gain would result in oscillatory behaviour. Therefore, the value chosen for $\Delta G_{11}/G_0$ was 0.60; a value which did not result in unsatisfactory operation at Mach numbers between 0.4 and 3.5, and still provided some improvement at Mach numbers above and below this range. A value of 2.0 was chosen for $\Delta G_{12}/G_0$ in a similar manner.

There are no entries for ΔG_{12} in the table for Mach numbers between 0.6 and 1.4. This is because in this Mach number range,

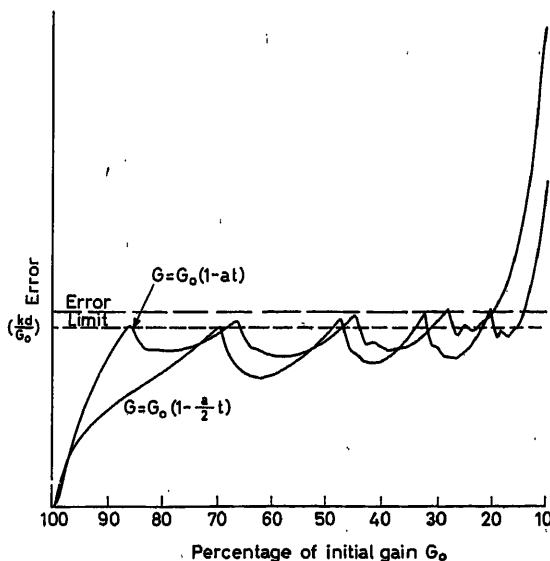


Figure 13. Error with automatic gain control for two values of disturbance and valve gain variation

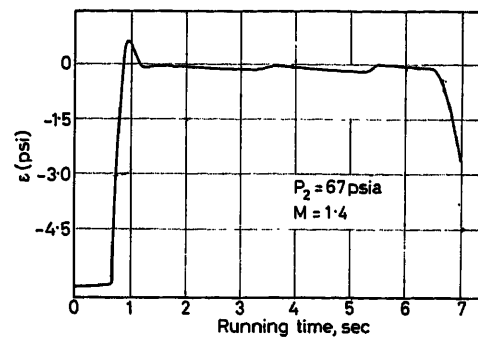


Figure 14. Pressure error variation with time showing effect of automatic gain control

after ΔG_{11} has been added, the control valve is driven fully open before the reference amplitude is reached and no amount of added controller gain can reduce the system error. For all other Mach numbers, the control valve is fully open when the error again reaches the reference amplitude after ΔG_{12} has been added. Therefore, only two discrete gain increments of fixed value relative to G_0 are needed to attain the specified performance over the complete operating range. This means that the only system parameter that must be preset for each tunnel setting is the initial value of controller gain. In the case of the 5 ft. square wind tunnel, it has been arranged that controller gain is automatically set as the various Mach numbers and reference pressures are selected.

A typical error curve for the simulated pressure control system illustrating the effect of using two discrete changes in gain is shown in Figure 14.

Conclusion

This design study of a system incorporating automatic gain control has demonstrated two important points. In the 'single shot' type of system in which the parameter variations are well defined, a wide range of gain variation can be accommodated by switching gain in discrete amounts using simple relay circuitry. This does not provide perfect compensation, but enables the control system performance to be held within specified limits*.

To achieve perfect compensation in which the system behaves as if it were time invariant, it is necessary to operate not only on the amplitude of the control loop gain but also on its time derivatives. It is also apparent that the time derivatives of parameter variations are important factors in the evaluation of stability and dynamic performance.

References

- RAINBIRD, W. J. and TUCKER, N. B. The five-foot blowdown tunnel at the National Aeronautical Establishment. *Proc. Dec. Symp. Inst. Aerophys*, Univ. Toronto, Pt. III (1959)
- LUKASIEWICZ, J. Some problems in design and operation of blowdown wind tunnels. *Z. angew. Math. Phys.* 9b, Fasc 5/6 (1958), 422
- MCGREGOR, W. K., RUSSELL, D. W., MESSICK, R. W. and BURNS, L. F. Analysis of gas flow systems for dynamic control purposes. *AEDA-TR-55-11, Document No. AD 88130* (April, 1956)

* Since this paper was written, the 5 ft. wind tunnel has been put in operation and has proved to have the predicted performance.

Missile Environment Simulation for Rocket Engine Test Facility

G. J. FIEDLER and J. J. LANDY

Summary

This paper describes the mathematical analysis and computer solution used in the design of a new facility for testing large rocket engines under simulated altitude conditions. The effect of physical location disparities between test facility components and the actual missile environment are eliminated by the system design. The computer solutions of the array of mathematical systems equations determine the dynamics of the facility, of the facility controls, and of the test engine required to meet very critical propellant pressure and flow conditions. During the rocket boost phase, precise pressure control of set-point minus one pound is required at inlets to the rocket engine turbo-pumps during flow rate increases from 0 to 4,400 gal/min of fuel and from 0 to 7,100 gal/min of oxidizer, within 200 msec of transient. This performance is required to prevent pump cavitation and establish conditions necessary for combustion stability. This paper utilizes a very rapid, economical method of developing the describing function for system-wide non-linearities. The required system and control dynamics are obtained directly from the computer in unique and quantitative terms; including piping design sizes, lengths, configuration, valve speeds, fluid acceleration times, minimum bandwidth, etc. Propellant flows and flow ratios are also controlled indirectly by the computer-designed controllers. The computer prescribes certain facility operational procedures required prior to, during, and following the test, and also defines the full test potential of the facility for the larger engine developments of the future.

Sommaire

La présente communication décrit l'analyse mathématique et la solution au calculateur automatique qui seront employées pour la construction d'une nouvelle installation d'essai de gros moteurs de fusées sous des conditions artificielles d'altitude. Les inégalités physiques locales entre l'installation d'essai et la véritable ambiance de la fusée aux altitudes élevées seront compensées par la construction du système. Les solutions du calculateur automatique pour les équations du système évaluent la dynamique et le réglage de l'installation et du moteur de fusée essayé, qui seront valables au voisinage des conditions extrêmes et critiques de pressions et de débits. Pendant l'ascension de la fusée, il sera nécessaire de maintenir, au point de mesure de la turbo-pompe du moteur de fusée, une pression inférieure de 1 p. s. i. à la valeur prescrite, alors que le débit augmentera, de 0 à 4.400 gal/min pour le carburant et de 0 à 7.100 gal/min pour l'oxygène, ceci en l'espace de 200 millisecondes. Cette opération est nécessaire pour empêcher la cavitation dans la pompe et pour assurer la stabilité de la combustion. Une méthode extrêmement rapide et économique sera employée pour développer les fonctions descriptives pour les non-linéarités à l'intérieur du système. La dynamique du système et le réglage sont directement obtenus du calculateur sous toutes formes et en toutes quantités, y compris les diamètres et les longueurs des tuyauteries, les formes d'écoulement, les vitesses de fonctionnement des soupapes, les durées d'accélération des débits, les bandes passantes minimales etc. Les débits de carburant et les rapports de débits seront également indirectement réglés par le régulateur et seront à nouveau traités par des calculateurs. Le calculateur évalue le déroulement de processus qui est nécessaire avant, pendant et après l'essai et met de plus les possibilités d'essais de l'installation à la portée des plus grandes recherches sur les moteurs de fusées de l'avenir.

Zusammenfassung

Dieser Aufsatz beschreibt die mathematische Analyse und die Lösung durch Rechenmaschinen, die für die Konstruktion einer neuen An-

lage zur Prüfung von großen Raketenmotoren unter künstlichen Höhenbedingungen verwendet wird. Die Auswirkung der physikalischen (örtlichen) Unterschiede zwischen der Prüfanlage und der tatsächlichen Umgebung der Rakete in größeren Höhen wird durch die Konstruktion des Systems ausgeglichen. Die Lösungen des aufgestellten mathematischen Gleichungssystems durch (automatische) Rechenanlagen bestimmen die Dynamik und die Regelung der Anlage und des zu prüfenden Raketenmotors, die den sehr kritischen (Treibstoff-) Druck- und Durchflußbedingungen gerecht werden sollen. Während der Antriebsphase der Rakete wird eine genaue Druckregelung des vorbestimmten Sollwertes auf -1 lb (Schub) an den Einflußstellen der turbinengetriebenen Pumpen des Raketenmotors verlangt, während der Durchfluß des Brennstoffes von 0 bis 4400 Gallonen pro Minute und der des Sauerstoffes von 0 bis 7100 Gallonen pro Minute steigt, und zwar innerhalb von 0,2 Sekunden. Dieser Vorgang ist notwendig, um Kavitation in der Pumpe zu verhindern und um die Stabilität des Verbrennungsprozesses zu sichern. In diesem Aufsatz wird von einer sehr schnellen und wirtschaftlichen Methode zur Aufstellung der Beschreibungsfunktion für die Nichtlinearitäten des Systems Gebrauch gemacht. Für das erforderliche dynamische Verhalten des Systems und der Regelung erhält man direkt von der Rechenmaschine eindeutige und quantitative Ausdrücke; außerdem ergeben sich die Rohrleitungsabmessungen, die Strömungsanordnung, die Ventilegeschwindigkeiten, die Beschleunigungszeit der Flüssigkeit, die minimale Bandbreite usw. Die Treibstoffdurchflüsse und die Durchflußverhältnisse werden indirekt durch Regler, die ebenfalls von der Rechenmaschine entworfen wurden, geregelt. Die Rechenmaschine bestimmt einen günstigen Prozeßablauf, der vor, während und nach dem Prüfvorgang nötig ist, und legt außerdem die Prüfmöglichkeiten der Anlage für zukünftige größere Raketenmotorenentwicklungen fest.

Introduction

The physical plant shown in *Figure 1* is a facility for the static test firing, under simulated altitude conditions, of rocket engines having thrusts ranging to 500,000 lb. with design provisions for 1.5 million pounds thrust. The test engine is constrained in the vertical firing position inside an evacuated steel capsule, and is supplied with fuel and liquid oxygen from large detached storage tanks.

The difficulties of flow and pressure control are caused by detachment of the engine from close physical proximity with fuel and oxygen tanks and other parts of the missile stages. In order to obtain accurate test results it is necessary to dynamically simulate the presence of the distant parts. This work describes the simulation of the actual close-up missile propellant tanks by test facility propellant tanks which are detached ten times the actual vehicle distance. In order to eliminate these time-lag space effects it is necessary to reduce fluid acceleration times by the provision of by-pass piping configuration in which propellant flow is established prior to engine firing. In addition to this, it is necessary to determine maximum allowable distances to the tanks, select the pipe length/area ratio to control hydraulic inertia, and specify the valve flow area characteristic so that the

overall pipe valve system will have essentially the same flow characteristic as the missile piping system. A last requisite in this simulation is the provision of a dynamically accurate and fast servo control system for the control valve between the propellant tanks and engine turbo-pumps. Thus, it is seen that all these factors must be treated in an integrated sense to attain the objective of eliminating the distance disparity. Paper length limitations preclude treatment of all these facets; consequently this work describes principally the control system for valve and control systems dynamics.

The rates of flow of the fuel and liquid oxygen are controlled at precise pressures at the test engine turbo-pumps by automatically operated hydraulic valves rated full stroke in 100 msec. A prerequisite for obtaining the precise pressure control needed for preventing pump cavitation and promoting combustion stability requires a complete, realistic, and integrated mathematical systems analysis. Engineering economy requires that an electronic analogue computer be utilized to solve the system equations and provide the scientific basis for the design of the facility, the facility control system, and engine test procedures.

Systems Analysis

General—Figure 1, the functional layout, shows the component parts of the complete test facility physical system. The propellants are forced from the storage tanks by 3,500 and 5,000 lb./in.² gas pressures controlled through the pressure-regulating valves. Precision control valves located in the by-pass connection regulate pressure at the test engine. The flows through the auxiliary storage tanks are interrupted during the test by closure of the outlet valves.

The mathematical systems analysis is initiated by consideration of the prominence of distributed-parameter effects, and the development of criteria for a valid lumped-parameter representation. This type of representation permits a great simplification in the magnitude of the analysis work. The validity, within acceptable accuracy limits, of the lumped-parameter representation shown in Figure 1 is established by the simultaneous consideration of several interacting factors. These factors include the determination of system frequency-transmission characteristics necessary to obtain the required transient performance.

These requirements in turn establish limits on pipe sizes and pipe lengths, and also determine valve locations and the required piping configurations.

The development of the system equations describing the dynamic behaviour of the individual system components is described in Appendix A. The system components are joined together by the transfer functions of the piping system, also developed in Appendix A. Completion of these operations results in the System Equations Array shown below.

System Equations Array

The physical system shown in Figure 1 is the basis for the system array utilizing the equations and transfer functions developed in Appendix A. The system equations for the physical plant are written in both linear and non-linear form, as required.

Gas Side Equations—These equations are:

$$P_0 = \frac{W_0 R T_0}{V_0} \quad (1)$$

$$T_0 = T_{0i} \left(\frac{P_0}{P_{0i}} \right)^{\frac{\gamma-1}{\gamma}} \quad (2)$$

$$W_0 = W_{0i} - \int_0^t w_0 dt \quad (3)$$

$$w_0 = \frac{K_1 P_0 A_{cv1}}{(T_0)^{\frac{1}{\gamma}}} \quad (4)$$

$$P_1 = \frac{W_1 R T_1}{V_1} \quad (5)$$

$$T_1 = \left(\frac{W_{1i} T_{1i} + \int_0^t w_0 T_0 dt}{W_1} \right) \left(\frac{P_1}{P_{1i}} \right)^{\frac{\gamma-1}{\gamma}} \quad (6)$$

$$V_1 = V_{1i} + \int_0^t v_2 dt \quad (7)$$

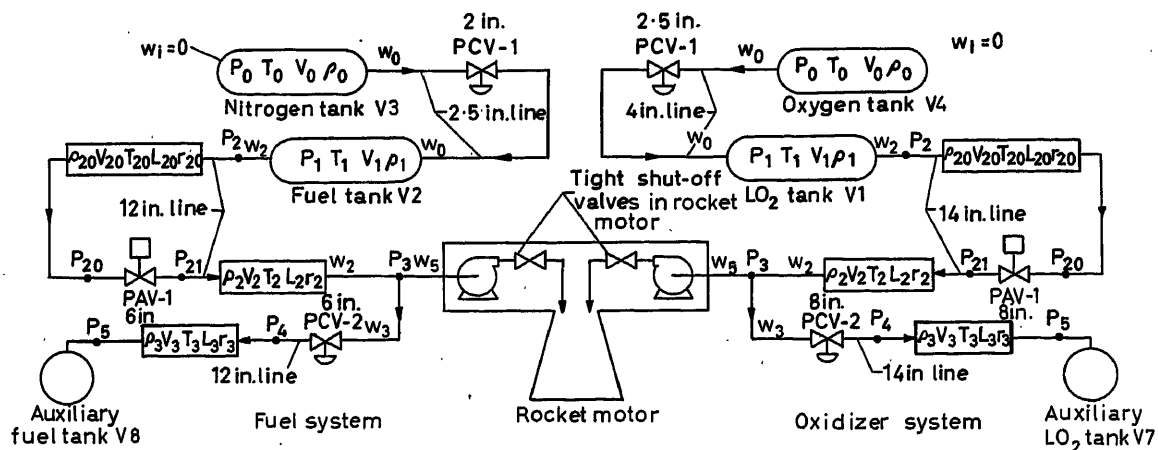


Figure 1. Lumped physical diagram

Liquid Side Equations—These equations are:

$$v_2 = w_2/\rho \quad (8)$$

$$P_2 = P_1 + h_e \rho - \frac{1}{A_t} \int_0^t w_2 dt \quad (9)$$

$$P_2 - P_{20} = r_{20} w_2^2 + L_{20} \frac{dw_2}{dt} \quad (10)$$

$$P_{20} - P_{21} = \left(\frac{w_2}{K_{a1} A_{pav}} \right)^2 \quad (11)$$

$$P_{21} - P_3 = r_2 w_2^2 + L_2 \frac{dw_2}{dt} \quad (12)$$

$$P_3 - P_4 = \left(\frac{w_3}{K_{a2} A_{cv2}} \right)^2 \quad (13)$$

$$P_4 - P_5 = r_3 w_3^2 + L_3 \frac{dw_3}{dt} \quad (14)$$

$$w_5 = K_3 P_3 \quad (15)$$

$$w_3 = w_2 - w_5 \quad (16)$$

Examination of the above equations reveals that some are linear, some are non-linear and both types involve time derivatives or integrals. The excursions of all variables in this system are extreme, from zero flow to full flow capacity in less than 200 msec. Therefore, the use of the usual linearizing techniques is not valid except for developing the non-linear describing function discussed in the next section of the paper. Consequently, it is necessary to analyse the system during these large excursions on an integrated non-linear basis. The first step in doing this is to rewrite some of the system equations to facilitate simulation on the analogue computer. The rearranged equations are given below. These, together with eqns (3), (4), (7) and (8), are used to establish the computer circuitry for the pressurizing gas system. Eqns (17) and (18) are used to simulate the liquid system. The computer circuitry is omitted because of paper length limitations.

Computer Solution

Computer Equations: Gas Side—Eqns (1) and (2) are combined to give the following:

$$T_0 = (T_{0i})^{\gamma} \left(\frac{R}{P_{0i} V_{0i}} \right)^{\gamma-1} (W_0)^{\gamma-1} \quad (2a)$$

Also, solving eqns (1) and (2) for P_0 gives:

$$P_0 = \frac{(T_{0i})^{\gamma}}{(P_{0i})^{\gamma-1}} \left(\frac{R}{V_0} \right)^{\gamma} (W_0)^{\gamma} \quad (1a)$$

Combining eqns (5) and (6) and solving for P_1 results in the following expression:

$$P_1 = \frac{(R)^{\gamma}}{(P_{1i})^{\gamma-1}} \left(\frac{W_{1i} T_{1i} + \int_0^t w_0 T_0 dt}{V_1} \right)^{\gamma} \quad (5a)$$

Computer Equations: Liquid Side—Eqns (9), (10), (11), and (12) are combined to give the following expression:

$$(L_2 + L_{20}) \frac{dw_2}{dt} = P_1 - P_3 + h_e \rho f - \int_0^t \frac{w_2 dt}{A_t} - \left[r_2 + r_{20} + \left(\frac{1}{K_{a1} A_{pav}} \right)^2 \right] w_2^2 \quad (17)$$

Similarly, combining eqns (13) and (14) with differentiated eqns (15) and (16) results in the following:

$$K_3 L_3 \frac{dP_3}{dt} = P_5 - P_3 + \left[\left(\frac{1}{K_{a2} A_{cv2}} \right)^2 + r_3 \right] w_3^2 + L_3 \frac{dw_2}{dt} \quad (18)$$

The analytical work is continued by development of the describing function for the non-linearities of the system. This development is valid for all types of non-linearities and is briefly discussed below.

System-Wide Describing Function Development

The describing function for the composite system-wide, non-linear characteristic is developed by the use of a new limit-cycle derivation technique¹. This makes unnecessary the long tedious development of describing functions for individual components by formal Fourier methods.

This method is based on the fact that limit-cycle oscillatory phenomena peculiar to non-linear systems are classically described by the van der Pol equation²:

$$\frac{d^2 q}{dt^2} - e(1 - q^2) \frac{dq}{dt} + q = 0 \quad (19)$$

The analogue computer simulation is deliberately placed in limit-cycle oscillation by adjustments of the gains and time constants of the known linear controller transfer function. The limit-cycle phenomena described by eqn (19) are encountered in non-linear feedback control systems when the denominator of the well-known relationship¹:

$$\frac{C}{R}(j\omega) = \frac{G(j\omega) N(\alpha_1, \omega_1)}{1 + G(j\omega) N(\alpha_1, \omega_1)} \quad (20)$$

is zero; that is when

$$1 + G(j\omega) N(\alpha_1, \omega_1) = 0 \quad (21)$$

It is obvious when the system simulation is in limit-cycle oscillation, because of the constant amplitude oscillation on the computer output. It is not necessary to excite the system with an input since the system breaks into oscillation and drives itself when the controller parameters are properly adjusted.

At this point the designer is in a position to calculate the complex-plane location of the limit-cycle point by rearranging eqn (21) as follows:

$$\begin{aligned} N(\alpha_1, \omega_1) &= -\frac{1}{G(j\omega)} \\ &= -\frac{1}{G_c(j\omega) G_p(j\omega)} \end{aligned} \quad (22)$$

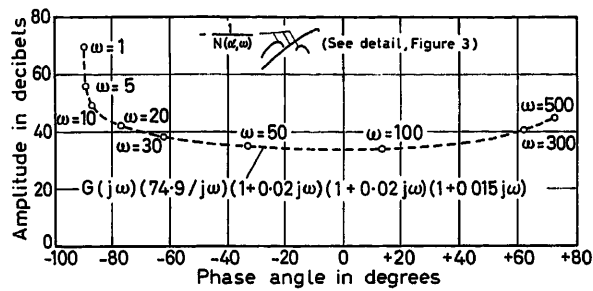


Figure 2. Limit-cycle oscillations

This means that the complex-plane location can be easily derived from eqn (22), since the dynamics of the linear controller $G_c(j\omega)$ and the linearized overall uncontrolled system $G_p(j\omega)$ are known, or can be easily obtained by the application of standard linearizing techniques. Repeated applications of these oscillatory procedures on the computer permits plotting a family of limit-cycle oscillations of the same frequency and varying amplitude. Or, if more convenient, polar plane contours of the same amplitude, but varying frequencies may be obtained. This particular problem was solved using constant-frequency curves having varying amplitudes. Families of such curves are obtained because of the presence of time derivatives and integrals of the non-linear variables.

Figure 2 is a plot showing the relative locations of the normal plant operation areas and the limit-cycle oscillation regions. The plot indicates that, in general, it is necessary to increase the normal gain about 30 dB in order to drive the system into undesirable limit-cycle oscillations. Figure 3 illustrates the type of limit-cycle data used to develop the system-wide, non-linear describing function. Nine intersections of the linear and non-linear characteristics are shown, resulting in as many limit-cycle points. The oscillation frequencies and amplitudes are indicated, as well as the controller functions which drive the system into these oscillatory states. Although these intersections are deliber-

ately sought to derive the system-wide describing function, they must be avoided in the controller synthesis to realize the required system performance.

Control System Synthesis

Synthesis—The foregoing information permits the scientific design of the automatic control system, using the family of non-linear describing functions and linear transfer function loci on polar plots previously described, and well-known servo techniques developed by Kochenburger³ and others. The details of the synthesis of shaping networks for the controller, to avoid limit-cycle intersections and to design adequate dynamics for control system components, are omitted since they are well known. The facility dynamics required to attain the critical pressure-time performance at the turbo-pump inlet are determined in quantitative terms from the computer simulation as follows: (1) Controlled system frequency bandwidth must be at least 35 rad/sec, (2) Fluid acceleration times must be in the 0.01 to 0.025 sec range, (3) Full-flow, pressure and other operating conditions must be established prior to firing the test engine. (4) At least 10–15 per cent of the total flow is diverted from the test engine through the by-pass valve, throughout the test.

These computer-determined quantitative specifications for bandwidth and fluid acceleration times required important design changes in the physical system as follows: (1) The reduction of fuel and oxidizer piping to lengths not exceeding 100 ft. (2) The provision of a piping configuration including by-pass valves for pressure control that divert the necessary flows under all test conditions. Thus, for large changes in rates of flow, within the previously established maximum flow rates, it is necessary to accelerate only the relatively short column of fluid between the diversion point at engine capsule and the engine turbo-pump. For dynamic flow changes requiring maximum flows greater than the previously established maximum, the additional fluids must come from the supply tanks, and this requires the reduction in piping lengths previously mentioned. After this reduction to a 100 ft. maximum is indicated, another problem

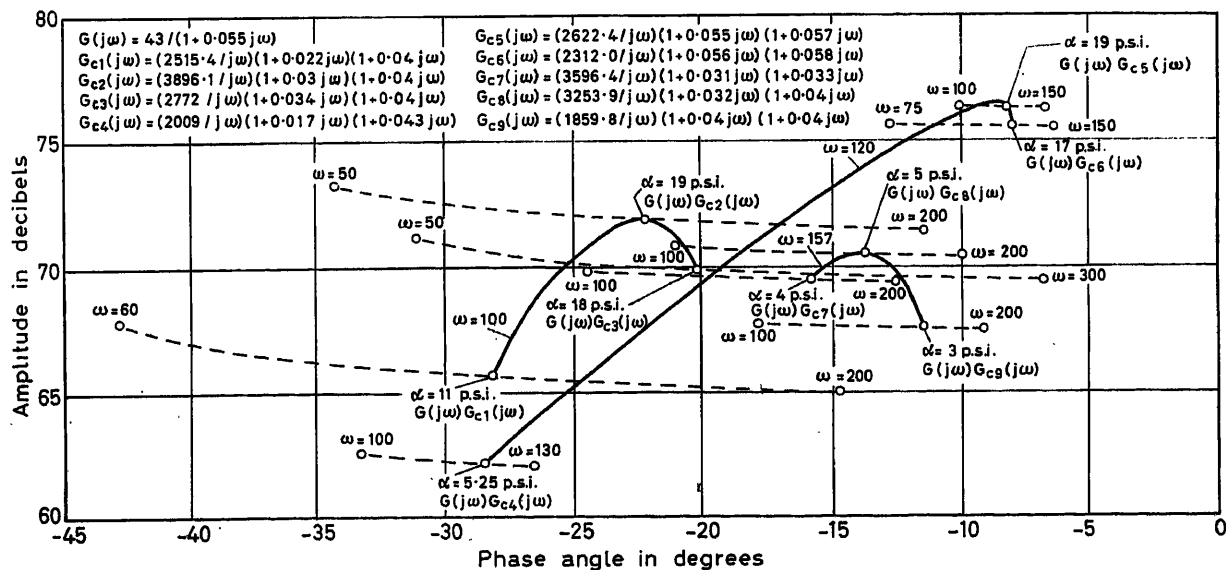


Figure 3. Limit-cycle oscillations detail

arises since these piping lengths are 50° long at the 35 rad/sec transmission frequency. Thus, a further reduction in pipe lengths is necessary to limit the wave length to 30° which is satisfactory from a performance viewpoint since it is within the generally accepted 0.1 wavelength criteria. The establishment of the 15 per cent minimum diversion found necessary for effective control also requires increased capacity of the propellant storage tanks.

These changes are not all that is required to simulate the dynamics of the actual vehicle component geometry including the test engine. In addition, characteristics of the control valve must be chosen so that when combined with the piping lengths in the facility, the overall system-wide flow characteristics closely match the square-law flow characteristics of the missile vehicle

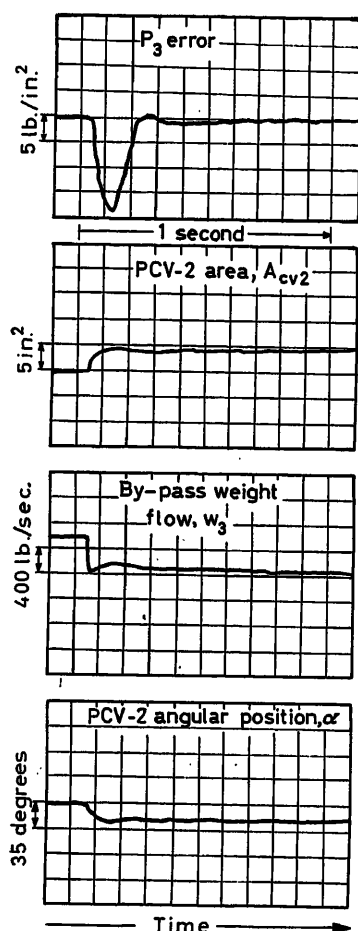


Figure 4. Predicted system responses

piping system. A further system requirement determined by the simulation is the extreme valve operating speed of 100 msec for full-stroke. The by-pass connection required serves the dual purpose of reducing fluid acceleration times and provides the capability of establishing full propellant flow prior to engine firing. Finally, and very important, all these factors must be present and properly integrated with respect to each other to effect the necessary test simulation.

Computer Responses—Figure 4 shows that with the facility and facility control system designed as stated previously, the P_3 pressure at the turbo-pump inlet drops approximately

18 lb./in.² when the test engine is started. The recording shows that the pressure recovers rapidly and is within the required limits within 170 msec, which is 30 msec less than the required 200 msec performance. Thus a 30 msec safety margin is provided for differences between the actual and the simulated physical systems. The time history of simultaneous changes in the open area of the control valve, the corresponding angular position and the mass flow change required to attain this pressure recovery can be seen by examination of this recording. System constraints such as control valve velocity and frequency transmission restriction previously mentioned are present, but the computer plots show that the system responses did not encounter the limits. Paper length limitation precludes inclusion of material for monitoring the frequency bandwidth restrictions. Since the gas pressure system is dynamically too slow to affect the control dynamics, the material with respect to P_1 pressure performance, the P_1 controller, etc., is omitted to conserve paper space. Results consistent with the above were also obtained at other test engine thrust levels.

Controller Dynamics—The form of the controller dynamics which yielded the responses shown in Figure 4 are:

$$\frac{d\alpha}{dt} = G_c(s) = \frac{K_c}{S} (\tau_1 s + 1) (\tau_2 s + 1) (\tau_3 s + 1) \quad (23)$$

where $d\alpha/dt$ = control valve velocity, in degrees/sec, and P_{3e} = pressure P_3 , recorded in mA. The controller dynamics as well as those of the control valve, pressure transducers, etc., are designed by the techniques previously described in a manner to attain the required system performance and avoid limit cycle oscillation regions. It is found that the three lead terms shown are necessary, since no combination of two terms yields enough speed. Because of this large amount of lead compensation, the controller requires very careful design and filtering to avoid noise interference and possible saturation.

Furthermore, the computer responses also define the ultimate test capabilities of the facility beyond the immediate requirements. For example, the computer reveals that this facility has the capability to suppress 42 per cent flow disturbances, whereas the performance criteria required suppression of 10 per cent flow disturbances. Knowledge of this capability, unobtainable without a systems analysis, will be very useful when planning tests of correspondingly larger engines in the future.

Conclusions

This paper illustrates the fact that large differences in space and geometric relationships between the rocket engine on test and the rocket engine in flight environment and configuration can be neutralized by scientific design. Realistic conditions are achieved by a closely integrated system of piping, piping configuration, control valve flow characteristics and control system dynamics. The required intimate relationships are accomplished through a completely integrated, non-linear systems analysis. The electronic analogue computer solution of the systems equations accomplishes a fivefold purpose: (a) determines the test system pumping, piping and configuration design which provides the required dynamics, (b) establishes control system dynamics, (c) ascertains location of limit-cycle regions, (d) defines necessary test starting and operational procedures, (e) reveals previously unknown advanced capabilities

of the plant. These analytical and design techniques make meaningful rocket engine tests possible. It is concluded that the probability of achieving the required critical performance by non-analytical methods is very low indeed.

Appendix A

Derivation of System Equations

Most of the component dynamics relate to the fluid mechanics processes contained therein. Paper length limitations preclude a complete exposition of this work; consequently, only a few of the more pertinent equations are developed here.

Gas Storage Tank Equations—With reference to Figure 1, the pressure in the gas storage tanks V-3 and V-4 at any time can be described by the characteristic equation for a perfect gas⁴.

$$P_0 = \frac{W_0 R T_0}{V_0} \quad (1)$$

where P_0 = gas pressure (lb./in.²), W_0 = weight of gas (lb.), T_0 = temperature (°K), V_0 = volume (in.³), and R = gas constant (in./°K).

Gases leaving the storage tanks are not replenished during the test, and the pressures are continuously decreasing, accompanied by continuously decreasing temperatures. Adiabatic expansion processes are assumed, and the temperature T_0 in each storage tank is expressed by the following equation¹:

$$T_0 = T_{0i} \left(\frac{P_0}{P_{0i}} \right)^{\frac{\gamma-1}{\gamma}} \quad (2)$$

where T_{0i} = the initial temperature (°K), P_{0i} = the initial pressure (lb./in.²), and γ = ratio C_p/C_v (dimensionless).

Since the weight of the gas in the tank at any instant equals the initial weight minus the integrated weight of the gas flowing from the tank during the time interval, the following equation applies.

$$W_0 = W_{0i} - \int_0^t w_0 dt \quad (3)$$

where W_{0i} = the initial weight of gas in the tank (lb.), and w_0 = weight flow out of the tank (lb./sec).

Fluid Flow Through Control Valve—Compressible flow through an orifice is expressed by the following equation⁵.

$$w_0 = \frac{C_f P_0 A_{cv1}}{(T_0)^{\frac{1}{2}}} \left(\frac{2g}{R} \frac{\gamma}{\gamma-1} \right)^{\frac{1}{2}} f \left(\frac{P_1}{P_0} \right)$$

or

$$w_0 = \frac{K_1 P_0 A_{cv1}}{(T_0)^{\frac{1}{2}}} \quad (4)$$

where A_{cv1} = open area of control valve (in.²)

$$K_1 = C_f \left(\frac{2g}{R} \frac{\gamma}{\gamma-1} \right)^{\frac{1}{2}} f \left(\frac{P_1}{P_0} \right);$$

C_f = flow coefficient; and

$$f \left(\frac{P_1}{P_0} \right) = \left[\left(\frac{P_1}{P_0} \right)^{\frac{2}{\gamma}} - \left(\frac{P_1}{P_0} \right)^{\frac{\gamma+1}{\gamma}} \right]^{\frac{1}{2}}$$

$f = 0.257$ for valve at critical flow which is encountered when the pressure output-input ratio $p_0/p_i \leq 0.528$.

Pressurizing-Gas Equations—The gas pressure in the pressurizing tank can also be described by the characteristic equation¹

$$P_1 = \frac{W_1 R T_1}{V_1} \quad (5)$$

The temperatures of the gases above the propellant levels in tanks V-1 and V-2 are functions of three variables: (1) the initial temperature of the gas; (2) the temperature of incoming gases from volumes V-3 and V-4, designated V_0 for purposes of analysis; (3) the temperature change due to pressure changes in volume V-1 and V-2, designated volume V_1 for purposes of analysis. The incoming gas temperatures are constantly decreasing due to the decreasing pressure in supply volume V_0 , according to eqn (2). Under these circumstances the energy given up by the gas in the initial volume is equal to the energy gained by the incoming gas, which is at a lower temperature. Therefore

$$W_{1i} C_v (T_{1i} - T_1') = W_0 C_v (T_1' - T_0) \quad (24)$$

Solving for T_1' and substituting

$$W_0 + W_{1i} = W_1 \quad (25)$$

gives

$$T_1' = \frac{W_{1i} T_{1i} + W_0 T_0}{W_1} \quad (26)$$

Since W_0 and T_0 are functions of time

$$W_0 T_0 = \int_0^t w_0 T_0 dt \quad (27)$$

Substituting eqn (27) into eqn (26) results in

$$T_1' = \frac{W_{1i} T_{1i} + \int_0^t w_0 T_0 dt}{W_1} \quad (28)$$

where T_{1i} = temperature (°K) of gas in volume V_1 , except for transient pressure changes.

Eqn (28) can be modified to include the effect of transient pressure changes on the temperature of gas in volume V_1 by the use of eqn (2)

$$T_1 = \left(\frac{W_{1i} T_{1i} + \int_0^t w_0 T_0 dt}{W_1} \right) \left(\frac{P_1}{P_{1i}} \right)^{\frac{\gamma-1}{\gamma}} \quad (6)$$

where P_{1i} = initial pressure in volume V_1 (lb./in.²); W_{1i} = initial weight of gas in volume V_1 (lb.), and T_{1i} = initial gas temperature in volume V_1 (°K).

The volume occupied by the pressurizing gas in tank V_1 is equal to the initial gas volume above the liquid, plus the volume vacated by propellant flowing from the tank to the rocket engine. Therefore

$$V_1 = V_{1i} + \int_0^t v_2 dt \quad (7)$$

where V_{1i} = initial gas volume (in.³), and v_2 = the volumetric propellant flow (in.³/sec).

The same relations govern the performance of tank V-2.

Propellant Volume-Weight Flow Relations—This relation is a function of the density of the flowing liquid where

$$v_2 = w_2 / \rho \quad (8)$$

where v_2 = volume flow (in.³/sec), w_2 = weight flow (lb./sec), and ρ = fluid density (lb./in.³).

Propellant Pressure Equations—The outlet pressures of the liquid oxygen and fuel supply tanks V-1 and V-2 are functions of the gas supply pressures P_1 and the liquid heights in the tanks. Therefore

$$P_2 = P_1 + h_s \rho - \frac{1}{A_t} \int_0^t w_2 dt \quad (9)$$

where P_2 = pressure at bottom of propellant tanks (lb./in.²), P_1 = pressure at top of propellant tanks (lb./in.²), h_s = initial level of liquid in tank (in.), w_2 = liquid weight flow out of tank (lb./sec), and A_t = liquid surface area (in.²).

Pipe Line Friction Pressure Drop—Pipe line pressure drop because of fluid friction can be expressed by the following equation⁵

$$\Delta P = \frac{f l \rho v_e^2}{2 g d} \quad (29)$$

where ΔP = pressure drop (lb./in.²), f = friction factor (a function of Reynolds number), l = pipe length (in.), v_e = velocity (in./sec), d = pipe diameter (in.), g = acceleration, gravity (in./sec²), and ρ = density (lb./in.³).

Also

$$v_e = \frac{w}{A \rho} \quad (30)$$

where w = weight flow (lb./sec), and A = pipe area (in.²). Substituting eqn (30) in eqn (29) gives

$$\Delta P = \frac{f l w^2}{\rho A^2 2 g d} = r w^2 \quad (31)$$

where

$$r = \frac{f l}{\rho A^2 2 g d}$$

Pipe Line Fluid Acceleration Pressure Drop—Pipe line pressure drops caused by fluid accelerations can be developed from the following equations.

$$F = M a = (P_u - P_d) A \quad (32)$$

$$M = \frac{W}{g} = \frac{l A \rho}{g} \quad (33)$$

$$a = \frac{dw/dt}{A \rho} \quad (34)$$

where F = force (lb.), a = acceleration of fluid (in./sec²), M = mass of fluid (lb.-sec²/in.), P_u = upstream pressure (lb./in.²), P_d = downstream pressure (lb./in.²), and A = pipe area (in.²).

Substituting and solving for $(P_u - P_d)$

$$(P_u - P_d) = \frac{M a}{A} = \frac{l dw/dt}{A g} = L \frac{dw}{dt} \quad (35)$$

$$L = \frac{l}{A g}$$

Combining eqns (31) and (35) gives the pressure drop in a line caused by fluid friction and acceleration

$$(P_u - P_d) = r w^2 + L \frac{dw}{dt} \quad (10)$$

Control Valve Head Loss—The expression for head loss through a valve is derived from Albertson et al.⁵

$$h_{L1-2} = \left\{ \frac{1}{C_v^2} \left[1 - \left(\frac{A_2}{A_1} \right)^2 \right] - \alpha_2 \left[1 - \frac{\alpha_1}{\alpha_2} \left(\frac{A_2}{A_1} \right)^2 \right] \right\} \frac{V_2^2}{2 g} \quad (36)$$

where α_1 = velocity coefficient, α_2 = velocity coefficient. Since α_2 is usually much smaller than $1/C_v^2$, α_1/α_2 is usually close to unity and A_2 is less than A_1 , the relation for h_{L1-2} can be simplified to

$$h_{L1-2} = \frac{V_2^2}{C_v^2 2 g} = \frac{1}{C_v^2} \left(\frac{w_2}{A_2 \rho} \right)^2 \frac{1}{2 g} \quad (37)$$

Therefore

$$h_{L1-2} = \left(\frac{w}{K_a A_v} \right)^2 \quad (11)$$

where $K_a = C_v \rho (2g)^{1/2}$.

Propellant Flow to Engine—Since actual rocket test engine characteristics vary with the engine being tested and are classified data, the liquid oxygen and fuel flows to the rocket engines are assumed to be linear functions of pressure for this paper. Thus

$$w_5 = K_3 P_3 \quad (15)$$

where w_5 = propellant flow to rocket motor (lb./sec).

The constant K_3 changes for each thrust level and for each value of the controlled variable P_3 .

Engine Flow Division—The flow division between engine and the by-pass connection is represented by the relation

$$w_2 = w_3 + w_5 \quad (16)$$

The simple form of this relation is applicable because the fluid is considered incompressible at the working pressures.

Critical Frequencies—This systems analysis is based on the assumption of lumped parameters, that is, the resistance and inductance are assumed to be lumped in one location physically. This type of analysis is valid if the control system cross-over frequency is significantly less than the critical frequency.

(a) **Liquid Systems**. For this type of system the critical frequency is defined as that frequency of a pressure disturbance at which a quarter wavelength is equal to the longest single pipe in the system. The actual pipe length can then be limited to an acceptable fraction of this. The velocity of sound in a fluid⁶ is

$$C = \left(\frac{E}{\rho} \right)^{1/2} \quad (38)$$

where E = bulk modulus of elasticity (lb./ft.²), ρ = density of fluid (lb.-sec²/ft.⁴), and C = velocity (ft./sec).

also

$$\lambda = \frac{C}{f} = \frac{2 C \pi}{\omega} \quad (39)$$

and

$$\omega_c = \frac{\pi C}{2l} \quad \text{for} \quad \frac{\lambda}{4} \quad (40)$$

where l = length of longest single pipe in the system (ft.), ω_c = critical frequency (rad/sec), λ = wavelength (ft.).

(b) *Pressurizing Gases*. The following frequency criteria for validation of lumped analysis apply to gas systems. These criteria are developed in detail by Stalzer⁶; consequently they are not given here.

$$\omega_c = \frac{\pi}{9} \frac{\mu_c}{z_d} \quad (41)$$

where μ_c/z_d = propagation constant, $\mu_c = (\gamma g R T)^{1/2}$ = velocity of sound (ft./sec), and z_d = duct length (ft.).

References

- ¹ FIEDLER, G. J., and LANDY, J. J. Fast analog computer techniques for design of controllers for non-linear systems. *Amer. Inst. elect. Engrs* CP-715 (June, 1961)
- ² ANDRONOW, A. A., and CHAIKIN, C. E. *Theory of Oscillations*. 1949. Princeton University Press
- ³ KOCHENBURGER, R. J. A frequency response method for analysing and synthesizing contactor servomechanisms. *Trans. Amer. Inst. elect. Engrs* (1950) 50-54
- ⁴ LIEPMANN, H. W., and PUCKETT, A. E. *Aerodynamics of a Compressible Fluid*. 1947. New York; Wiley
- ⁵ ALBERTSON, M. L., BARTON, J. R., and SIMONS, D. B. *Fluid Mechanics for Engineers*. 1960. Englewood Cliffs, N. J.; Prentice-Hall
- ⁶ STALZER, T. R., and FIEDLER, G. J. Criteria for validity of lumped parameter representation of ducting air-flow characteristics. *Trans. Amer. Soc. mech. Engrs*, Paper No. 56-IRD-21 (May, 1957)

A Longitudinal Guidance System for Aircraft Landing during Flare-out

F. J. ELLERT and C. W. MERRIAM III

Summary

The design of an automatic longitudinal guidance system for the flare-out phase of a blind aircraft landing is presented. This system is proposed for landing aircraft under zero-visibility and high-turbulence atmospheric conditions. Furthermore, this system is primarily airborne, except for the possible use of ground-based radar beacons, and is constructed with light, inexpensive, and reliable components.

The design of this aircraft landing system is based on a large number of requirements for aircraft safety. Aerodynamic, structural, and passenger comfort constraints specifically must be accounted for in the design.

The equations resulting from optimization theory are used as a method for the direct time-domain synthesis of this system. This method, described briefly in an appendix, results in a guidance equation that is linear but is a complex function of time to touchdown.

Analogue computer simulations of this configuration prove the feasibility of the system. Furthermore, this method of design can be extended to the problem of lateral guidance during flare-out, thereby providing a practical landing system. Also, a number of configurations of this system for different airport facilities are possible.

Sommaire

La conception d'un système automatique de guidage longitudinal pour la phase d'extinction des feux de balisage d'un atterrissage sans visibilité est présentée. Ce système est proposé pour l'atterrissage d'avions à visibilité nulle et dans des conditions atmosphériques hautement turbulentes. De plus, ce système est essentiellement aéroporté, à l'exception de l'emploi possible de phares radar au sol, et il est construit avec des composants légers, peu coûteux et fiables.

La conception de ce système d'atterrissage d'avions est basée sur un grand nombre d'exigences de la sécurité aérienne. Plus spécialement, des limitations aérodynamiques, de structure et de confort des passagers doivent être prises en considération dans la conception.

Les équations résultant de la théorie d'optimisation sont utilisées en tant que méthode pour la synthèse directe de ce système dans le domaine du temps. Cette méthode, brièvement décrite dans un appendice, résulte en une équation de guidage qui est linéaire mais qui constitue une fonction, complexe du temps restant à courir jusqu'à l'instant de toucher terre.

Des simulations analogiques de cette configuration prouvent que le système est réalisable. De plus, cette méthode de conception peut être étendue au problème de guidage latéral pendant l'extinction des feux de balisage, fournissant ainsi un système d'atterrissage pratique. Un certain nombre de configurations de ce système pour divers équipements d'aérodrome sont également possibles.

Zusammenfassung

Die Verfasser legen den Entwurf eines automatischen Leitsystems für die Längsbewegung in der Endphase (flare-out phase) der Blindlandung eines Flugzeuges vor. Dieses System wird für den Fall betrachtet, daß ein Flugzeug völlig ohne Sicht und bei starken Böen landen soll. Der Aufbau ist vornehmlich zum Einbau in das Flugzeug bestimmt, doch ist auch die Mitbenutzung am Boden stehender Radareinrichtungen möglich; er enthält nur leichte, preiswerte und zuverlässige Teile.

Der Entwurf dieses Landesystems berücksichtigt eine große Zahl

von Sicherheitsvorschriften für Flugzeuge. Aerodynamische und Festigkeitserfordernisse, sowie der Flugkomfort für Passagiere wurden besonders beachtet.

Die aus der Theorie der Optimierung gefundenen Gleichungen werden benutzt, um die Synthese im Zeitbereich durchzuführen. Dieses Verfahren, das im Anhang kurz erläutert ist, ergibt eine lineare Gleichung für den Leitvorgang, die aber eine komplizierte Zeitfunktion bis zum Aufsetzen des Flugzeuges enthält.

Eine Simulation auf dem Analogrechner erwies die Durchführbarkeit des Systems. Weiterhin läßt sich das Verfahren auch auf den Leitvorgang für die Seitenbewegung während der Endphase der Blindlandung erweitern und bildet damit ein praktisch brauchbares Landesystem. Abwandlungen des Systems für verschiedene Flugplatzeinrichtungen sind möglich.

Introduction

A number of guidance systems have been proposed for the automatic landing of aircraft under poor visibility conditions^{1, 2}. These systems have met with varying degrees of success. A continuing area of difficulty occurs in the terminal or flare-out phase of the landing. In this region, roughly below 100 ft. of altitude, existing guidance systems, such as ILS, are not altogether satisfactory due to radar ground clutter and other electromagnetic disturbances. Furthermore, final corrections in aircraft heading, position, velocity, and altitude are required just prior to touchdown in order to eliminate errors due to wind, air turbulence, and measurement errors. These corrections must be made with a high degree of precision and accurate timing in order to obtain a safe landing and passenger comfort.

Visual landings are achieved with safety, in part, due to the ability of the pilot to take into account a large number of both objective and subjective landing requirements. The design of any automatic system approaching this safety and reliability must take into account the primary requirements used in visual landings. Because these requirements are numerous and pose conflicting dynamic constraints, a complicated time-domain synthesis problem must be solved.

The goal of the automatic system discussed here is to approach as closely as possible the reliability and safety of manual landings but under the conditions of zero visibility and high turbulence. In order to achieve this goal, the system must be constructed so that the most accurate of the available position and velocity sensors are utilized. This requires a partially airborne system, and hence added requirements for light, inexpensive, and reliable components are imposed. Finally, flexibility in the configuration of the automatic system must be achievable so that different types of airport facilities can be used without the installation of excessive additional airborne and ground-based equipment.

Problem Description

The automatic longitudinal guidance system described here is designed for use during the flare-out phase of the landing, that is, during the last 100 ft. of the aircraft's descent. The assumption is made that the aircraft is guided to the proper location by air traffic control, and that the aircraft altitude and rate of ascent at the beginning of the flare-out phase can range from 80 to 120 ft. and -16 to -24 ft./sec respectively. For values outside of this range, the aircraft is waved off by assumption.

During flare-out, the aircraft may be subjected to both steady winds and wind gusts. Wind gusts are of primary importance because they tend to be random. On the other hand, steady winds parallel to the ground can be counteracted merely by a steady-state change in the heading of the aircraft. The design of this system is based on the assumption that the wind gusts cannot be measured directly and have a zero mean value. In this case, the wind gust disturbance term does not appear in the equations resulting from optimization theory on which the design procedure is based.

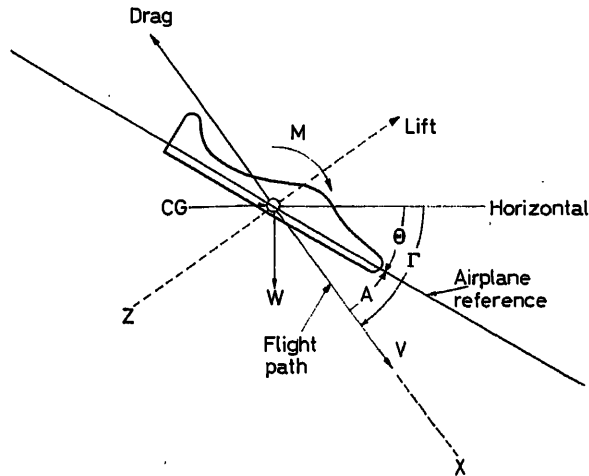


Figure 1. Longitudinal aircraft coordinates and angles

The equations defining the behaviour of the aircraft during flare-out result from the aerodynamic forces and moments shown in Figure 1 and from the laws of mechanics³. The angles shown are the total angles. These equations then are linearized because the deviation from the equilibrium flight condition is small during flare-out. The angles α and θ are incremental deviations from the level flight equilibrium angle of attack and pitch angle respectively. Also, due to the landing geometry, the glide path angle Γ is small, and small angle approximations are made. Finally, the assumption is made that the aircraft velocity V is maintained essentially constant during flare-out by manual or automatic throttle control. These assumptions result in the short-period equations of motion of the aircraft, which relate elevator deflection $\delta_e(t)$ to pitch rate $\theta'(t)$. The short-period equations and the equation relating pitch rate and vertical acceleration are combined to give the longitudinal equations of motion⁴:

$$\begin{aligned} \dot{x}_1(t) = & \left(\frac{1}{T_s} - 2\zeta\omega_s \right) x_1(t) + \left(\frac{2\zeta\omega_s}{T_s} - \omega_s^2 - \frac{1}{T_s^2} \right) x_2(t) \\ & + \left(\frac{1}{VT_s^2} - \frac{2\zeta\omega_s}{VT_s} + \frac{\omega_s^2}{V} \right) x_3(t) + \omega_s^2 K_s T_s m_1(t) \end{aligned} \quad (1)$$

$$\dot{x}_2(t) = x_1(t) \quad (2)$$

$$\dot{x}_3(t) = \frac{V}{T_s} x_2(t) - \frac{1}{T_s} x_3(t) \quad (3)$$

$$\dot{x}_4(t) = x_3(t) \quad (4)$$

where

$$x_1(t) = \theta'(t), \quad x_2(t) = \theta(t), \quad x_3(t) = h'(t),$$

$$x_4(t) = h(t), \quad m_1(t) = \delta_e(t) \quad (5)$$

These equations are written in terms of the four measured signals $\theta'(t)$, $\theta(t)$, $h'(t)$, and $h(t)$. The altitude $h(t)$ could be measured with a radar altimeter, the rate of ascent $h'(t)$ with a barometric rate meter, and pitch $\theta(t)$ and pitch rate $\theta'(t)$ with gyros.

The nominal values of the parameters appearing in eqns (1) to (4) are given in Table 1. The design is based on these nominal values.

Table 1. Nominal aircraft parameters

Parameter	Designation	Nominal value
T_s	Path time constant	2.5 sec
ζ	Short period damping factor	0.5
ω_s	Short period resonant frequency	1 rad/sec
K_s	Short period gain	-0.95 sec^{-1}
V	Aircraft total velocity	256 ft./sec

The design of this system is also based on a number of requirements and constraints for aircraft safety and passenger comfort. These requirements are:

(1) The desired altitude $h_d(t)$ of the aircraft during the flare-out is described by the path shown in Figure 2 (a). This exponential linear path ensures a safe and comfortable landing. An altitude error of 0 to ± 1 ft. at $t = 20$ sec is acceptable because touchdown at a precise point on the runway is not required.

(2) The desired rate of ascent $h'_d(t)$ is given by the time derivative of $h_d(t)$ and is shown in Figure 2 (b). Rate of ascent errors are important primarily at touchdown. Errors between ± 0.5 ft./sec are acceptable.

(3) In order to ensure touchdown on the main aircraft landing gear, the total pitch angle at touchdown $\theta(20)$ must be between 0° and $+15^\circ$.

(4) During the landing, the total angle of attack $A(t)$ must remain below the stall value of $+18^\circ$. Because the aircraft enters the flare-out phase in equilibrium with an angle of attack of about 80 per cent of the stall value, the permissible positive increment in the angle of attack is $+3.6^\circ$.

(5) The elevator deflection is restricted to motion between mechanical stops at -35° and $+15^\circ$.

All of these requirements are treated in the design of the system.

System Design

The design of this system is based on the equations resulting from optimization theory⁵. These equations are obtained by minimizing a mathematical error index formulated from the prescribed performance requirements.

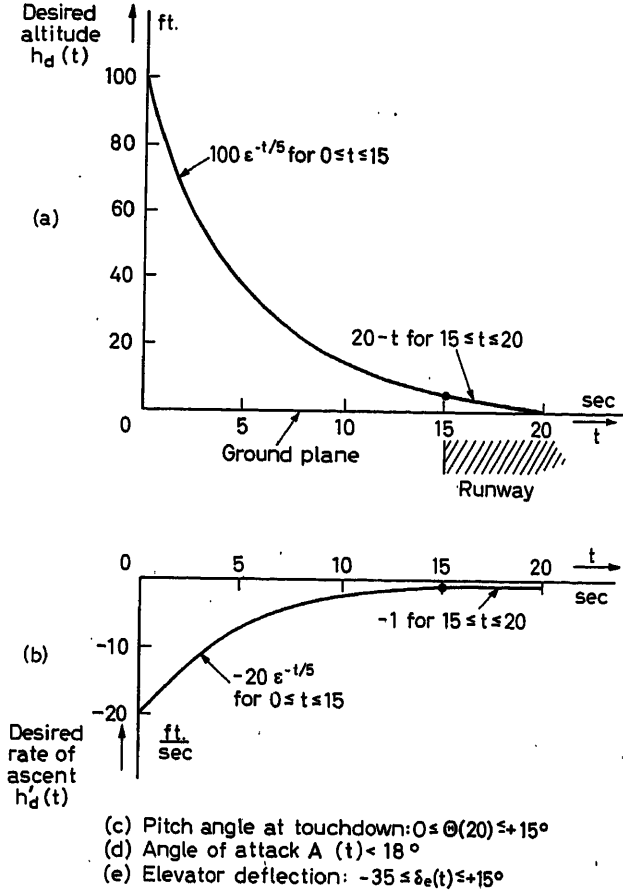


Figure 2. Longitudinal performance requirements

The error index $e(t)$ employed in the design of this system is

$$e(t) = \int_0^{20} \{ \phi_1(\sigma) [\theta'_d(\sigma) - \theta'(\sigma)]^2 + \phi_2(\sigma) [\theta_d(\sigma) - \theta(\sigma)]^2 + \phi_3(\sigma) [h'_d(\sigma) - h'(\sigma)]^2 + \phi_4(\sigma) [h_d(\sigma) - h(\sigma)]^2 + [\delta_{e,d}(\sigma) - \delta_e(\sigma)]^2 \} d\sigma \quad (6)$$

where σ is a dummy time variable and t is real time. This index contains five terms corresponding to the five requirements depicted in Figure 2. The first term involves the error between the desired pitch rate θ'_d and the actual pitch rate θ' as opposed to the angle of attack error. The aircraft lift equation defines the angle of attack in terms of a first-order differential equation, where pitch rate is the driving function. Angle of attack errors are diminished by reducing pitch rate. The remaining terms in eqn (6) correspond directly to the other performance requirements.

The desired values of the response and control signals appearing in the error index are given in Table 2. Because the incremental angle of attack and the elevator deflection essen-

tially are constrained between positive and negative limits, the desired values for these signals are selected to be zero. The total pitch angle at the desired touchdown point $\theta(20)$ is constrained between 0° and $+15^\circ$. Hence, the desired value for the incremental pitch angle $\theta(20)$ is selected to be zero.

Table 2. Desired response and control signals

Desired response or control signal	Numerical value
θ'_d	0
$\theta_d(20)$	0
h'_d	See Figure 2 (b)
h_d	See Figure 2 (a)
$\delta_{e,d}$	0

The error quantity in each term in the index is squared. Also, each term contains a time-varying weighting factor which places emphasis on the associated error during the appropriate portion of the interval of control. The use of such an index in conjunction with linear aircraft equations of motion results in a linear control system⁵. This control system consists of a time-dependent input signal and time-dependent gains in the feedback loops which are implemented easily in terms of available components.

The mathematical forms of the weighting factors are suggested by the nature of the performance requirements. Because the magnitude of the angle of attack is important throughout the flare-out, $\phi_1(\sigma)$ is selected to be a constant, ϕ_1 . On the other hand, the pitch angle is important only at the desired touchdown point. Hence, $\phi_2(\sigma)$ is selected to be the impulse function $\phi_2, T u_0(20 - \sigma)$ occurring at $\sigma = 20$. The rate of ascent is important over the runway and primarily at the desired touchdown point. Thus, $\phi_3(\sigma)$ is selected to be zero for $0 \leq t \leq 15$, ϕ_3 for $15 \leq \sigma \leq 20$, plus the impulse function $\phi_3, T u_0(20 - \sigma)$. Finally, due to the importance of altitude errors throughout the landing interval but emphasized at the desired touchdown point, $\phi_4(\sigma)$ is selected to be a constant ϕ_4 plus the impulse function $\phi_4, T u_0(20 - \sigma)$.

The parameters of these mathematical forms for the weighting factors must be specified numerically. A selection procedure,

Table 3. Data used in the selection of weighting factors

Maximum allowable response error and maximum available control signal	Weighting factor parameter value
$\delta_1 = 0.262$ rad $\epsilon_1 = 0.0251$ rad/sec $\epsilon_3 = 4$ ft./sec $\epsilon_4 = 20$ ft.	$\psi_1 = 1$ $\varphi_1 = 27.2$ $\varphi_3 = 0.00107$ $\varphi_4 = 0.0000428$
$\epsilon_1(20) = 0$ $\epsilon_3(20) = 0.00873$ rad $\epsilon_3(20) = 0.5$ ft./sec $\epsilon_4(20) = 1$ ft. $\delta'_1(20) = 0.5$ rad/sec	$\varphi_2, T = 24.1$ $\varphi_3, T = 0.00735$ $\varphi_4, T = 0.00184$

$$M = 1, N = 4, Q = 4$$

which provides a rough estimate of these values, is described in the Appendix. The values computed by this procedure are listed in Table 3. The maximum allowable response errors and the maximum available control signal, which are used to obtain the numerical values of these weighting factor parameters, are also listed. The maximum allowable pitch rate error ε_1 is computed using the steady-state relationship between pitch rate and the incremental angle of attack given by the lift equation, namely, $\theta' = \alpha/T_s$ where $\alpha = +3.6^\circ$. The maximum allowable pitch rate error at the terminal point $\varepsilon_1(20)$ is selected to be zero because the straight-line portion of the desired flare-out corresponds to a constant pitch angle. The remaining maximum allowable response errors and the maximum available control signal are obtained directly from the stated requirements. The system performance resulting from these weighting factor parameter values satisfies all of the requirements and, hence, indicates the usefulness of the selection procedure described.

The minimization of the error index with respect to the control signal results in the control equation⁴

$$\text{Eqn (7)}^*$$

The block diagram of the system is drawn directly from this equation and is shown in Figure 3 (a). The system consists of a time-dependent input signal and time-dependent gains in the four feedback loops.

One possible implementation of the airborne controller is shown in Figure 3 (b). Tapped potentiometers, with appropriate voltages applied to the taps, are used to generate the time-dependent input signal and feedback gains. The measured signals also are applied to the potentiometers. If the common shaft to the potentiometers is rotated by a position servo through an angle τ , proportional to the time to touchdown, then the signal at the wiper arm of each potentiometer is the appropriate product of the measured signal and the time-dependent feedback gain. The input signal to the system is obtained by applying a fixed voltage to the corresponding potentiometer.

In order to obtain a signal proportional to time to touchdown, the ground speed of the aircraft must be measured. Ground speed could be obtained with ground-based radar beacons located under the aircraft approach path and spaced at a known distance. Another possibility is the use of ground-based Doppler radar. In this case, the velocity information would be relayed to the aircraft. In either case, the time to touchdown is estimated by dividing the distance from the aircraft to the desired touchdown point on the runway by the ground speed of the aircraft. Ground-based radar also could be used to measure this distance.

The input signal and feedback gains are specified numerically from the solution of differential equations. The general form of these equations is given by eqns (14) and (15) in the Appendix.

The numerical values of the input signal and feedback gains are functions of time to touchdown and are shown in Figure 4. Three of the feedback gains exhibit distinct peaks near touchdown. These peaks are due to the use of the impulse functions in the weighting factors and are required in order to satisfy the performance requirements at touchdown. The input signal $k_1(t)$ is a composite weighting of the desired response and control signals with anticipation included to offset the lags in the aircraft.

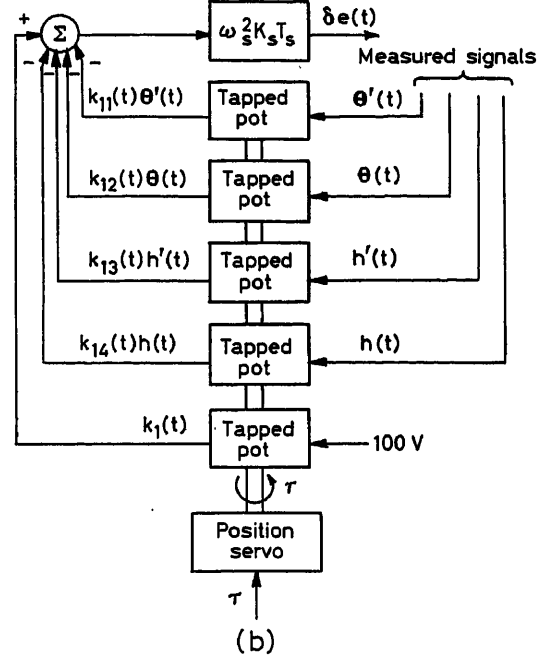
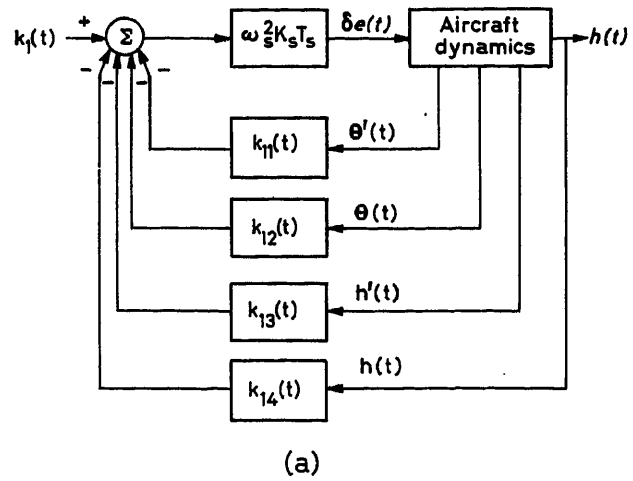


Figure 3. (a) System block diagram
(b). Airborne controller implementation

System Performance

The aircraft landing trajectories are obtained by specifying the initial values of the four measured signals and by solving eqns (1)–(4) and (7) simultaneously when the k parameters shown in Figure 4 are used in eqn (7). The initial values of the measured signals are tabulated in Figure 5. Case II corresponds to the condition for which the aircraft is initially on the desired trajectory and has the correct rate of ascent. Cases I and III correspond to the worst possible combinations of the largest initial altitude and rate of ascent errors.

The computation of the landing trajectories was carried out on a digital computer. These trajectories and other tabulated

* Eqn (7)

$$\delta_e(t) = \omega_s^2 K_s T_s [k_1(t) - k_{11}(t)\theta'(t) - k_{12}(t)\theta(t) - k_{13}(t)h'(t) - k_{14}(t)h(t)] \quad (7)$$

performance data also are presented in Figure 5. The term 'touchdown error' refers to the distance along the runway between the desired and actual touchdown points. The data indicate that the system satisfies all of the prescribed performance requirements in spite of the wide range in initial conditions. All of the landing trajectories deviate from the desired altitude until approximately 10 sec after the beginning of the flare-out. These deviations are primarily due to the angle of attack and elevator deflection requirements. During the final 10 sec of the landing, the actual trajectories follow the desired altitude quite closely and satisfy the terminal requirements with no difficulty.

As already mentioned, the design of this longitudinal guidance system is based on the nominal aircraft parameter values listed in Table 1. Because the actual values may differ somewhat from these nominal values, a sensitivity study was performed on an analogue computer in order to determine the permissible range for each aircraft parameter consistent with a satisfactory landing. In the analogue computer simulation, the system input signal, $k_1(t)$, was obtained using a 20 segment

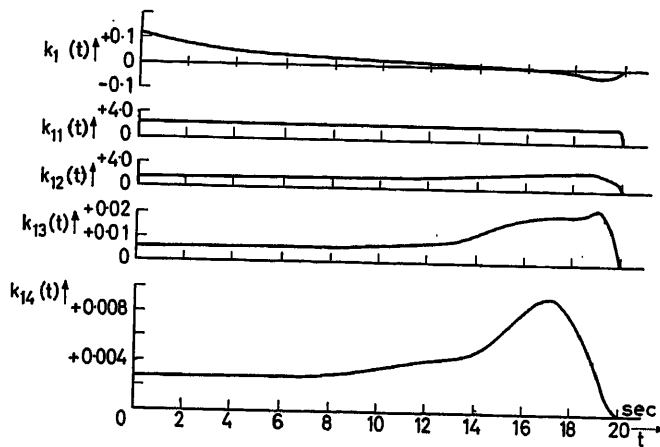


Figure 4. System input signal and feedback gains

diode function generator. The feedback gains $k_{12}(t)$, $k_{13}(t)$, and $k_{14}(t)$ were simulated using servo driven potentiometers with 17 taps connected through the appropriate resistors to a plus or minus reference voltage. The remaining feedback gain, $k_{11}(t)$, was treated as a constant. This analogue simulation of the entire system reproduced accurately the digital computer results. The largest altitude error between the analogue and the digitally computed trajectories is approximately 0.5 ft. at about $t = 5$ sec.

In this sensitivity study, the value of each aircraft parameter was varied until one of the prescribed performance requirements was violated, or until a further change in the parameter was unreasonable. The permissible range in each parameter is indicated in Table 4. The condition that would have been violated by a further change is also listed. In this table the term 'crash' refers to the situation in which the rate of ascent is more negative than -1.5 ft./sec. The behaviour of the system is most sensitive to an increase in the value of the path time constant, T_s . This is due, in part, to the wide range of initial conditions selected. As indicated by the last column of Table 4, the greatest difficulty is encountered for the initial conditions of Case III. If the aircraft is not nosed up sharply enough for this case,

a crash occurs; if the aircraft is nosed up too sharply, the angle of attack limit is exceeded and aerodynamic stall occurs.

The sensitivity study indicates that the system is practical for a reasonable range of parameter values around the nominal values. For a given aircraft, the values of the aircraft parameters are usually known within the range indicated in Table 4. A sensitivity study also was performed with respect to the magnitudes of the feedback gains and the input signal. The system proved

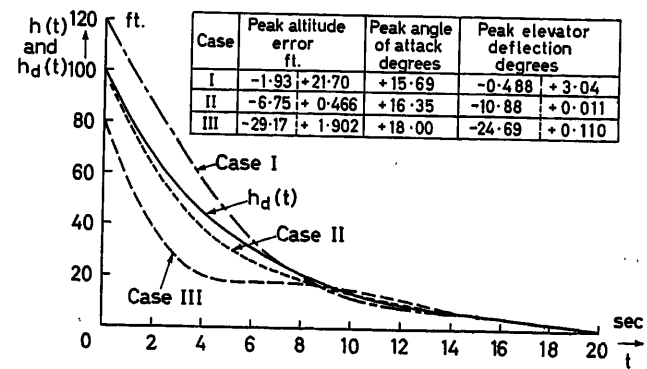


Figure 5. Simulated system performance

to be the most sensitive to the magnitude of $k_{14}(t)$; a maximum decrease of 14 per cent can be tolerated. On the other hand, the system proved to be least sensitive to $k_1(t)$; an 82 per cent increase is permissible.

Table 4. Permissible aircraft parameter changes

Parameter	Nominal value	Increased by a factor of	Decreased by a factor of	Limiting condition	Case where limit occurs
ζ	0.5	2*	---	None	---
		---	Made 0	None	---
K_s	-0.95/sec	10*	---	None	---
		---	2	Crash	III
ω_s	1 rad/sec	3	---	Stall	III
		---	2	Crash	III
T_s	2.5 sec	1.2	---	Crash	III
		---	10	Pitch	I, II, III
V	256 ft./sec	2*	---	None	---
		---	1.15	Stall	III

* Could be changed further

An attempt to approximate the feedback gains by constants throughout the entire flare-out interval met with failure. The time variations in the input signal and the feedback gains are essential for satisfying the multiple performance requirements.

The behaviour of the system in the presence of a disturbance was also investigated. A random perturbation was added to the

angle of attack in order to simulate the effect of a vertical wind gust. The peak gust amplitude was approximately 5 ft./sec. The landing trajectories obtained indicate that a safe landing can be achieved in the presence of such disturbances.

Conclusions

The simulation results demonstrate that the design specifications can be met for the aspects of the aircraft landing problem presented here. In fact, system performance indicates that passenger comfort, in addition to aircraft safety, can be maintained even under conditions of reasonably high turbulence. Also, the implementation of this automatic landing system poses no particular difficulties, and a number of different system configurations could be evolved for use in conjunction with air traffic control and ILS approach systems.

Due to these results and the flexibility of the design method afforded by optimization theory techniques, a broader design study of the aircraft landing problem should result in a practical and safe landing system. In particular, the lateral motion and its cross-coupling to the longitudinal motion would be treated in such a study. Additional design considerations occurring in the three-dimensional problem are crab angle due to cross winds, roll angle due to turns, and runway alignment.

Appendix

The design problem treated in this paper is a special case of a class of optimization problems characterized by linear processes and quadratic error measures. Specifically, the process is described by the response equation

$$\dot{q}(t) = Ax(t) \quad (8)$$

and state equation

$$\dot{x}'(t) = Bx(t) + Cm(t) \quad (9)$$

The response vector $q(t)$, state vector $x(t)$, and control vector $m(t)$ are assumed to have Q , N , and M dimensions respectively. The elements of the matrices A , B , and C are denoted as $a_{nm}(t)$, $b_{nm}(t)$, and $c_{nm}(t)$ respectively. Also, the error index is taken to be

$$e(t) = \int_t^T e_m(\sigma) d\sigma \quad (10)$$

where the error measure $e_m(\sigma)$ is written as

$$e_m(t) = \sum_{n=1}^Q \phi_n(t) [Q_n(t) - q_n(t)]^2 + \sum_{n=1}^M \psi_n(t) m_n^2(t) \quad (11)$$

when σ is replaced by t . In the error index, real time and terminal time are denoted by t and T respectively. In the error measure, the desired response vector is denoted by $Q(t)$, and $\phi(t)$ and $\psi(t)$ are weighting factor vectors. The selection of the weighting factors is restricted such that $\phi_n(t) \geq 0$ and $\psi_n(t) > 0$.

The criterion used in this paper for system design is that the system is selected to minimize the error index for all values of real time and for all $x(t)$. The control equation which minimizes the error index for this class of design problems is well known⁵ and can be derived either from the calculus of variations⁶ or from dynamic programming⁷. This control equation is written as

$$m_n(t) = K_n(t) - \sum_{m=1}^N K_{nm}(t) x_m(t), \quad n=1, 2, \dots, M \quad (12)$$

The parameters which appear in this control equation are written in terms of a set of k parameters as

$$K_n(t) = \frac{1}{\psi_n(t)} \sum_{m=1}^N c_{mn}(t) k_m(t); \quad (13)$$

$$K_{nm}(t) = \frac{1}{\psi_n(t)} \sum_{k=1}^N c_{kn}(t) k_{mk}(t)$$

where $k_{mk}(t) = k_{km}(t)$. Furthermore, the k parameters are defined by

$$-k'_m = \sum_{n=1}^Q \phi_n Q_n a_{nm} + \sum_{n=1}^N b_{nm} k_n - \sum_{n=1}^M \sum_{i=1}^N \sum_{j=1}^N \frac{c_{jn} c_{in}}{\psi_n} k_i k_{jm} \quad (14)$$

and

$$-k'_{mk} = \sum_{n=1}^Q \phi_n a_{nm} a_{nk} + \sum_{n=1}^N [b_{nm} k_{nk} + b_{nk} k_{nm}] - \sum_{n=1}^M \sum_{i=1}^N \sum_{j=1}^N \frac{c_{jn} c_{in}}{\psi_n} k_{im} k_{jk} \quad (15)$$

where time function notation is dropped for convenience. Finally, these parameters satisfy the boundary conditions

$$k_m(T) = k_{mk}(T) = 0 \quad (16)$$

In the case of the aircraft landing system, the desired response signals are given. However, appropriate weighting factors must be selected in order to meet the design requirements. The consequences of selecting various mathematical forms for weighting factors have been dealt with in the literature^{8, 9}. In the design of this system, however, an attempt is made to use the design specifications directly in the selection of both the magnitudes and mathematical forms of the weighting factors. An approximate method for the selection of weighting factors is outlined below. At any instant of time, the maximum allowable response errors should contribute equally to the error measure because the system is designed to minimize the integrated sum of the errors. Therefore, the relationships

$$\phi_n(t) = \left[\frac{\varepsilon_Q(t)}{\varepsilon_n(t)} \right]^2 \phi_Q(t), \quad n=1, 2, \dots, Q-1 \quad (17)$$

are found by equating terms in eqn (11). The variable $\varepsilon_n(t)$ is defined as

$$\varepsilon_n(t) = [Q_n(t) - q_n(t)] \Big|_{\substack{\text{maximum} \\ \text{allowable}}}, \quad n=1, 2, \dots, Q \quad (18)$$

Similar reasoning applied to the control signals provides

$$\psi_n(t) = \left[\frac{\delta_1(t)}{\delta_n(t)} \right]^2 \psi_1(t), \quad n=2, 3, \dots, M \quad (19)$$

where the variable $\delta_n(t)$ is defined as

$$\delta_n(t) = m_n(t) \Big|_{\substack{\text{maximum} \\ \text{available}}}, \quad n=1, 2, \dots, M \quad (20)$$

Given these relationships, eqn (11) becomes

$$e_m(t) = Q \phi_Q(t) \varepsilon_Q^2(t) + M \psi_1(t) \delta_1^2(t) \quad (21)$$

If the total contributions to the error measure of the maximum allowable response errors and the maximum available control signals are equal, then

$$\phi_Q(t) = \frac{M}{Q} \left[\frac{\delta_1(t)}{\varepsilon_Q(t)} \right]^2 \psi_1(t) \quad (22)$$

is obtained. Finally, no restrictions are imposed by choosing $\psi_1(t) = 1$. Therefore, eqns (17), (19) and (22) specify the weighting factors according to this selection procedure.

In the case of the aircraft landing problem, an even more approximate weighting factor selection procedure is used. Over the interval of time where a particular response error is important, the corresponding weighting factor is chosen to be a constant. The values of $\varepsilon_n(t)$ and $\delta_n(t)$, which are used in the above equations, are then chosen to be the maximum values of the corresponding error or signal that are allowed during the interval $0 \leq t \leq 20$. In addition to the constant weighting factors, impulse weighting factors are used at the desired touchdown point. Specifically, weighting factors of the form

$$\phi_n(t) = \phi_n + \phi_{n,T} u_0(t-T) \quad (23)$$

are used where $u_0(x)$ is the unit impulse function occurring at $x = 0$.

The previous equations do not apply to the selection of $\phi_{n,T}$ and therefore an additional selection procedure is needed. The relative values of these factors are established by

$$\phi_{n,T} = \left[\frac{\varepsilon_Q(T)}{\varepsilon_n(T)} \right]^2 \phi_{Q,T} \quad (24)$$

with reasoning similar to that used for eqns (17) and (19). Also, the values of $\phi_{n,T}$ are established from an additional relationship which is found from the maximum available rate of change of the control signal at the terminal point. In the case of the aircraft landing system, this rate of change is given by

$$m'_1(T) = -c_{11} \{ \phi_1 [Q_1(T) - q_1(T)] + \phi_{2,T} [Q_2(T) - q_2(T)] \} \quad (25)$$

Finally, the maximum available value of $m'_1(T)$, which is denoted by $\delta'_1(T)$, is expressed as

$$|\delta'_1(T)| = |c_{11}| [|\phi_1| |\varepsilon_1(T)| + \phi_{2,T} |\varepsilon_2(T)|] \quad (26)$$

under worst case conditions. This relationship is used to find an approximate value of $\phi_{2,T}$.

The authors wish to acknowledge the assistance of M. F. Marx and R. G. Buscher, of the Light Military Electronics Department, who participated in the description of the landing problem. The authors are also indebted to L. E. Tannas, formerly with the General Electric Company, who was primarily responsible for evaluating the performance of the system in the presence of parameter changes and disturbances.

References

- Automatic landing system study, Pt I—Results of airborne equipment studies. *Tech. Rep. No. ASD-TR-61-114, Flight Cont. Lab., Aeronaut. Syst. Div., Air Force Systems Command, Wright-Patterson Air Force Base, Ohio* (February, 1962)
- PRESCOTT, T. W. Automatic control techniques used in the B.L.E.U. landing system. *Rep. Proc. 1st Ann. Int. Aviation Res. Dev. Symp.* (April 10-14, 1961), 227-240
- PERKINS, C. D., and HAGE, R. E. *Airplane Performance Stability and Control*. 374-407. 1949. New York; Wiley
- ELLERT, F. J., and MERRIAM III, C. W., Synthesis of feedback controls using optimization theory—an example. *Proc. Joint Automatic Control Conf.* Pap. No. 19-1 (1962)
- MERRIAM III, C. W., A class of optimum control systems. *J. Franklin Inst.* 267, No. 4, April (1959) 267-281
- KIPINIAK, W. *Dynamic Optimization and Control, A Variational Approach*. 1961. New York; M.I.T. Press and Wiley
- BELLMAN, R. E. *Dynamic Programming*. 1957. Princeton, N. J.; Princeton University Press
- KALMAN, R. E., and KOEPCKE, R. W. Optimal synthesis of linear sampling control systems using generalized performance indexes. *Trans. Amer. Soc. mech. Engrs* No. 58-IRD-6 (1958)
- SCHULTZ, W. C., and RIDEOUT, V. C. Control system performance measures: past, present, and future. *Trans. Inst. Radio Engrs on Automatic Control*, AC-6, No. 1 (1961) 22-35

DISCUSSION

A. M. LETOV, *Institute of Automatics and Telemechanics, Kalantschevskaja 15a, Moscow, U.S.S.R.*

The problem of automatic landing in a flare-out mode is not only a very beautiful and interesting scientific problem, but is also a very useful engineering one, in the solution of which all of us are very interested on account of the rapid development of aviation. This problem is posed correctly from the mathematical point of view and there are also some requirements of an engineering character to be taken into account, for instance the limitations on phase coordinates. The correctness of the solution given in the paper cannot be doubted. I think that the sole question which has to be discussed in this field is the application of δ -functions as a weight coefficient of the optimizing functional (6). In this connection I am interested in:

(1) The question of useful physical effect of introduction of δ -functions in the functional (6) at the moment of touchdown.

(2) The question how these δ -functions can be really obtained in the control system.

F. J. ELLERT and C. W. MERRIAM III, *in reply*

We appreciate Professor Letov's interest in aircraft landing and his questions concerning the key concepts used in our design method.

The terminal impulse weighting factors are introduced in order to give our system the desirable characteristics of a terminal control system such as touchdown point accuracy and proper aircraft altitude.

The path weighting factors also are introduced in order to give our system the desirable characteristics of an exponential control system (see Ref. 1 of the paper) such as trajectory shape insensitivity to initial condition errors and wind gusts.

The impulse weighting factors do not directly enter the control system. On the other hand, they do determine the terminal slopes and peaks occurring near the touchdown point of the control equation parameters K_1 , K_{11} , K_{12} , K_{13} , and K_{14} as found from the solution of eqns (14) and (15).

M. SANUKI, *Department of Aeronautics, University of Tokyo, Japan*

According to literature, e.g. Ref. 2 of the paper, the F.A.A. (U.S.A.) seems to favour an improved ILS against such a guidance as yours. What is your personal opinion?

If an ordinary ILS is a fundamental requirement for, or prior to, your guidance system, is there any awkward phase in your system like the constant attitude phase of B.L.E.U. system?

F. J. ELLERT and C. W. MERRIAM III, *in reply*

At the time our work was carried out, the F.A.A. preference for an improved ILS system was not known to the authors. The eventual adoption of a blind landing system for commercial aircraft in the U.S.A. is dependent upon many considerations in addition to system performance. The authors believe that the system presented in this paper would give better performance than the presently proposed ILS system (see *American Aviation*, August 1963).

The system described in this paper presupposes the use of ILS guidance prior to flare-out. This requires a single mode switching. Our system eliminates three of the mode switchings used in the B.L.E.U. system. We feel that mode switching just prior to touchdown is undesirable from a safety point of view.

I. OSTOSLAWSKY, *Institute of Automatics and Telemechanics, Kalan-tshevskaja 15a, Moscow, U.S.S.R.*

A very simple and interesting method of blind landing calculation proposed by the author is based on the equation where the term corresponding to random wind gusts is zero. How is the presence of turbulences in the air accounted for in the algorithm in the case where turbulence intensity and structure can vary?

F. J. ELLERT and C. W. MERRIAM III, *in reply*

Our treatment of statistically varying wind disturbances is based on two assumptions. First, the disturbances are additive Gaussian signals. Second, the system is designed to minimize the conditional expectation of the error index given in eqn (10). Under these conditions, additional terms appear on the right-hand side of eqn (14) which are proportional to the conditional expectation of these disturbance signals. We further assume that these disturbance signals are unobservable and have zero mean value. Therefore, the conditional expectation of these disturbance signals is zero, and eqns (14) and (15) as given define the optimal system consistent with our formulation of the problem¹.

Reference

¹ MERRIAM III, C. W. *Optimization Theory and the Design of Feed-back Control Systems*. 1964. New York; McGraw-Hill

G. TOUMANOFF, *Airborne Instruments Laboratory, Comac Road, Deer Park, Long Island, N.Y., U.S.A.*

It might be of interest to the authors and to those who are concerned with automatic landing that a system developed by the firm for which I work has recently been accepted by the F.A.A., in so far as a contract for its development is accepted, as the future integrated total automatic landing system. The principle on which it is based provides a choice of angles of flight path continuously from the first entrance into the approach cone to actual touchdown. There are, in effect, no phase changes at all. The system permits to the aircraft the choice of initial approach angle and the computation on board of a gradually changing angle of approach going from, say, the nominal $3\frac{1}{2}^\circ$ to 4° that we associate with ILS to $1\frac{1}{2}^\circ$ which is just held until the wheels touch the ground. The system includes distance measuring equipment and radar monitoring of the G.C.A. type, and it is available to an unlimited number of aircraft within the approach path. There are numerous references to this system available.

F. J. ELLERT and C. W. MERRIAM III, *in reply*

These timely comments are appreciated, and a more complete description of AIL's system can be found in a recent article in *American Aviation*, August 1963.

R. K. SMYTH, *Autonetics Ltd., U.S.A.*

My experience with automatic landing systems¹ has indicated that the most difficult aspect of the problem involves error and noise in the sensors' thrust and velocity variations, and practical problems of hardware implementation. It is hoped that the authors will some day have the opportunity to grapple with these problems in an actual flight test programme. The tolerance of the proposal controller to off-nominal conditions should alleviate but not eliminate these practical problems.

Would the authors care to remark on these comments and answer the following question: the time variable gains $k_{11}(t)$ and $k_{12}(t)$ (Figure 3 (a)) have very little variation with time. It would seem from a simplicity point of view that they could be replaced with fixed gains. Have the authors investigated the difference in performance with these gains fixed?

Reference

¹ SMYTH, R. K. and VELANDER, E. W. Autoflare landing system for jet transports, presented to the S.A.E. Aeronautic Meeting, April 1961, New York City

F. J. ELLERT and C. W. MERRIAM III, *in reply*

As stated in the paper, $k_{11}(t)$ was taken to be a constant in our simulation of the system. This approximation causes negligible error. Although we have not done so, we believe that the same approximation can be made for $k_{12}(t)$.

D. A. LLOYD, *The Aviation Division of S. Smith & Sons (England) Ltd. Cheltenham, Glos., England*

The aspects of flare-out dealt with in this interesting paper are the comparatively simple ones. The paper illustrates a possible method of design.

The more difficult problems are those concerned with speed variations, and the effects of wind shears and horizontal turbulence during the flare-out phase. These effects lead to a less well-defined touchdown point and may lead to some difficulties in the mathematics and in the system mechanization.

Can the authors give any results of subsequent work either with a real aeroplane or with more realistic mathematical models of the aeroplane and its environment?

F. J. ELLERT and C. W. MERRIAM III, *in reply*

The authors are not in a position at present to publish detailed results on the effects of speed variations and wind shears. However, comprehensive simulation studies of these and other disturbances have been made and fully support the claims made in our paper.

Automatic Control of a Large Steerable Aerial for Satellite Communications

F. J. D. TAYLOR

Summary

The paper describes the methods used to steer the 85 ft. diameter paraboloidal reflector aerial at Goonhilly, England. This aerial has been constructed for the British Post Office as part of its experimental ground station for tests with communication satellites. Beamwidths are of the order of 10 min of arc and a steering accuracy of some 4 min of arc is a requirement.

Two modes of steering are provided. In one, the local ephemeris is computed from a knowledge of either the orbital elements or rectangular coordinate ranges presented at one-minute intervals. In the other, fine control of beam pointing is effected by determining the angular bearing of a target emission and applying corrections to the reflector steering mechanism.

Effectively, there are two control loops. One includes shaft position pick-off data fed back to the input circuit while the other includes electronic error determination fed back as a correction to the input data.

The paper describes the apparatus used and the result of experiences.

Sommaire

Cette étude décrit les méthodes employées pour diriger l'antenne à réflexion parabolique avec une ouverture de 85 pieds (25,904 m) à Goonhilly, Angleterre. Cette antenne a été construite pour les services postaux britanniques, faisant partie de sa station d'essai sur terre pour des essais avec des satellites de communication. Les rayons ont une largeur d'environ dix minutes d'arc, et le réglage doit avoir une précision d'environ quatre minutes d'arc.

Deux modalités de direction sont prévues. Dans l'une, l'éphéméride locale est calculée, partant de la connaissance soit des éléments orbitaux soit d'ensembles de coordonnées cartésiennes qui se présentent de minute en minute. Dans l'autre, le réglage précis de la direction du rayon s'effectue en déterminant le relèvement angulaire d'une émission de cible et en corrigeant l'appareil de direction du réflecteur.

Il y a en effet deux boucles de commande dont l'une comprend des données relevées d'après la position d'un arbre et renvoyée au circuit d'entrée, tandis que l'autre comprend la détermination électronique d'erreurs renvoyée pour corriger les données d'entrée.

Ce mémoire décrit les appareils dont on se sert et les résultats des expériences.

Zusammenfassung

Dieser Aufsatz beschreibt die Methoden, mit denen man einen Parabolspiegel mit einem Öffnungsdurchmesser von 26 m in Goonhilly, England, steuert. Diese Antenne wurde für die britische Post als ein Teil ihrer Versuchsbodenstationen zur Prüfung der Übertragung mit Fernmeldesatelliten gebaut. Die Strahlungskeule hat einen Bündelungswinkel von ca. 10 Winkelminuten, was eine Steuergenauigkeit von etwa 4 Winkelminuten erfordert.

Zwei Steuerungsarten sind vorgesehen. Bei der ersten werden die (Orts-) Ephemeriden in Abständen von einer Minute entweder durch die Bahnkoordinaten oder durch rechtwinkelige Koordinaten berechnet. Bei der zweiten Methode wird die genaue Regelung der Strahlungsrichtung dadurch erreicht, daß man den Richtungswinkel eines signalaussendenden Ortungsobjektes ermittelt und daraufhin eine Korrektur durch den Reflektorsteuermechanismus vornimmt.

Es existieren zwei Regelkreise. Der eine erfaßt die abgegriffenen Werte der Lage der Antennenachse, die auf den Eingangskreis zurückgeführt werden, während der andere elektronisch die Abweichung bestimmt, die ebenfalls zur Korrektur der Eingangswerte dient.

Die Arbeit erläutert sowohl verwendete Geräte als auch experimentelle Ergebnisse.

Introduction

The British Post Office has had erected in the south-west of England a large steerable microwave aerial for use in communications satellite experiments. A major element of the aerial system is a paraboloidal reflector of 85 ft. diameter and it is a requirement that the axis of this be steerable to any bearing in the hemisphere above the horizontal plane. When the reflector is illuminated from the focus with electromagnetic energy at frequencies in the microwave range the resulting far-field beamwidth is only some 10 min of arc and accuracy of pointing of the beam is required to be a fraction of this. A satellite towards which the beam is directed will, in general, have motion relative to the aerial, so the problem is the automatic steering of the beam so as to illuminate continuously a moving target.

The Aerial

The aerial feed—the transmitter of power and the receptor of energy received from the satellite—is located at the focus of the paraboloid and faces it. The reflector is mounted on a horizontal axis raised above a horizontal turntable rotatable about a vertical axis. An outline drawing of the arrangement is shown in *Figure 1*. By movement around the horizontal and vertical axes, the axis of the reflector may be given any required bearing. Movement about the horizontal (elevation) axis is effected by a motor-driven screw, nut and connecting-rod combination while rotation about the vertical (azimuth) axis is accomplished by continuous-chain drive from a motor located at a fixed point outside the turntable. The d.c. motors for elevation and azimuth drive are each of approximately 100 h.p. The total weight of the structure above the fixed turntable support is some 870 tons.

The Steering Mechanism—An Outline

Any desired reflector axis bearing *versus* time characteristic can be achieved by applying control signals independently to the mechanisms giving azimuth and elevation and increments of these quantities. In this particular application, and when under conditions of automatic operation, the data are presented and read at intervals of 1 sec or less. Presentation is in the form of a punched paper tape. The horizontal and vertical axis

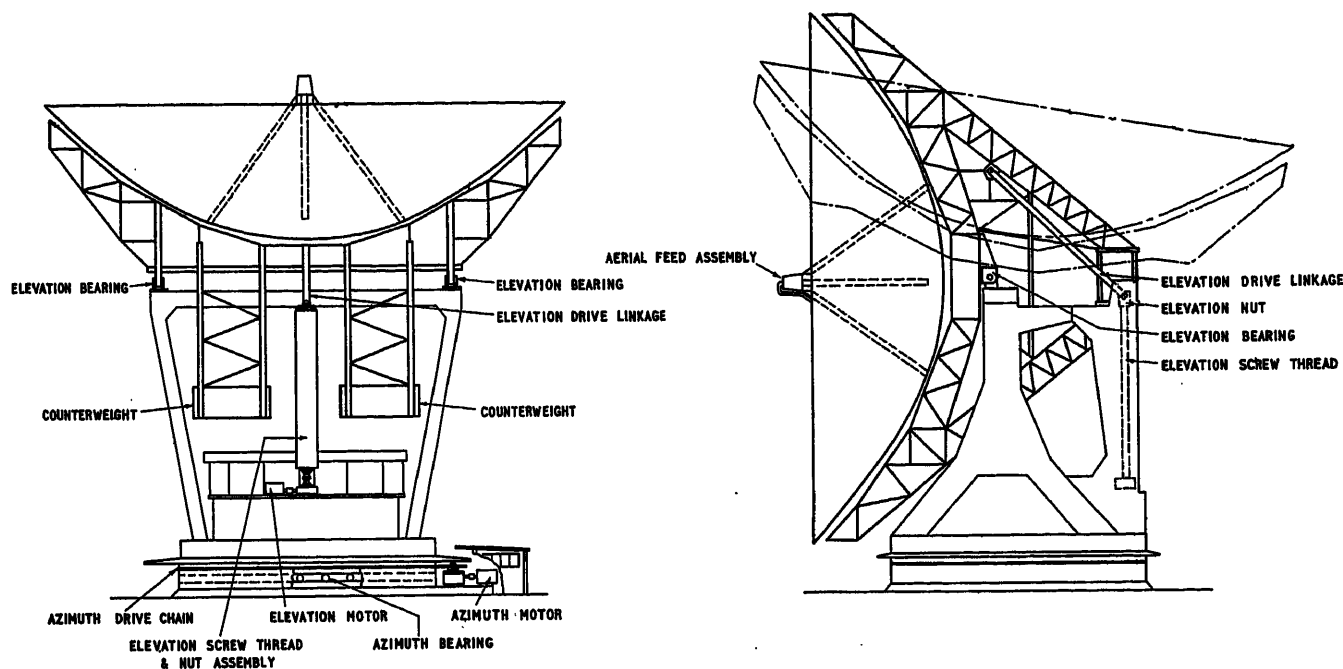


Figure 1. Outline drawing of the steerable aerial

positions are each determined by a servo loop which includes a comparator, digital-to-analogue converter, a Ward-Leonard set, a d.c. motor-drive mechanism and a shaft position read-out, the last of these feeding a signal back to the comparator.

Manual control of the aerial is also necessary under certain test conditions or when it is desired to move the aerial to another bearing without recourse to the preparation of a steering tape. An aerial-steering console is provided at which this can be done, appropriate manually-selected signals being fed into the servo loops. An additional function served by the aerial-steering console is to feed into the steering mechanism any offsets, i.e., additions to or subtractions from the data as presented by a steering tape, and found necessary as a result of the electrical measurement of any angular difference between the axis of the aerial reflector and a line between the aerial and a satellite emitting a beacon signal. A further function of the aerial-steering console is to display all data relevant to the steering, mechanical and electrical characteristics of the aerial and for the initiation of manual take-over should any defect or emergency arise.

A block diagram of the control system is given in Figure 2 while Figure 3 shows the aerial-steering console.

The Generation of Steering Signals

The bearing *versus* time characteristic of a communications satellite may be determined either by an accurate knowledge of the orbital elements, by the receipt of a radio emission from the satellite itself or by a combination of these. The aerial feed of the particular installation under discussion is steered by the combination of methods.

Orbital elements which, it must be remembered, may be variable with time, are determined by radio, radar or optical methods and, often, by a combination of them. In the first experimental application of this aerial—tests involving the

satellites of projects Telstar and Relay—the orbital elements were determined by radio means employing, particularly, the world-wide Minitrack network. At the Goddard Space Flight Center, Maryland, U.S.A., data from the Minitrack network were assembled and a computer was used to determine in advance the bearing *versus* time characteristics of the satellites as at the aerial site. Bearings were in terms of the distance to the satellite expressed in a Cartesian coordinate system of true north, true east and the local vertical. To have determined these data at, say, 1 sec time intervals would have been expensive both in terms of computer time at Goddard and in transatlantic communication facilities. The data were therefore computed for 1 min intervals and transmitted across the Atlantic as telegraph signals and received on punched tape. In general, the information was made available between 1 and 9 days in advance of the commencement of a test.

At the aerial site the received data was processed in a National-Elliott type 803 computer to generate an aerial steering tape bearing the control data mentioned earlier. The programming involved was complex, for it was not only necessary to make a sixth-order interpolation of the input data and provide coordinate conversion, but also to extrapolate backwards and forwards in time so that the aerial could be steered from one rest position to another. In addition, the programming had to take into account the elevation-dependent effect of refraction and any systematic deviations between the nominal mechanical axis of the reflector and the beam axis consequent upon small changes of reflector shape with attitude.

At the aerial site there is a highly stable electric clock system adjustable to Universal Time and providing a digital output. The aerial steering process is initiated by the occurrence of synchronism between clock output and the time recorded on the steering tape. Checks of parity between tape time indications and clock time output are made every second. It will be observed that steering the aerial is a fully automatic process,

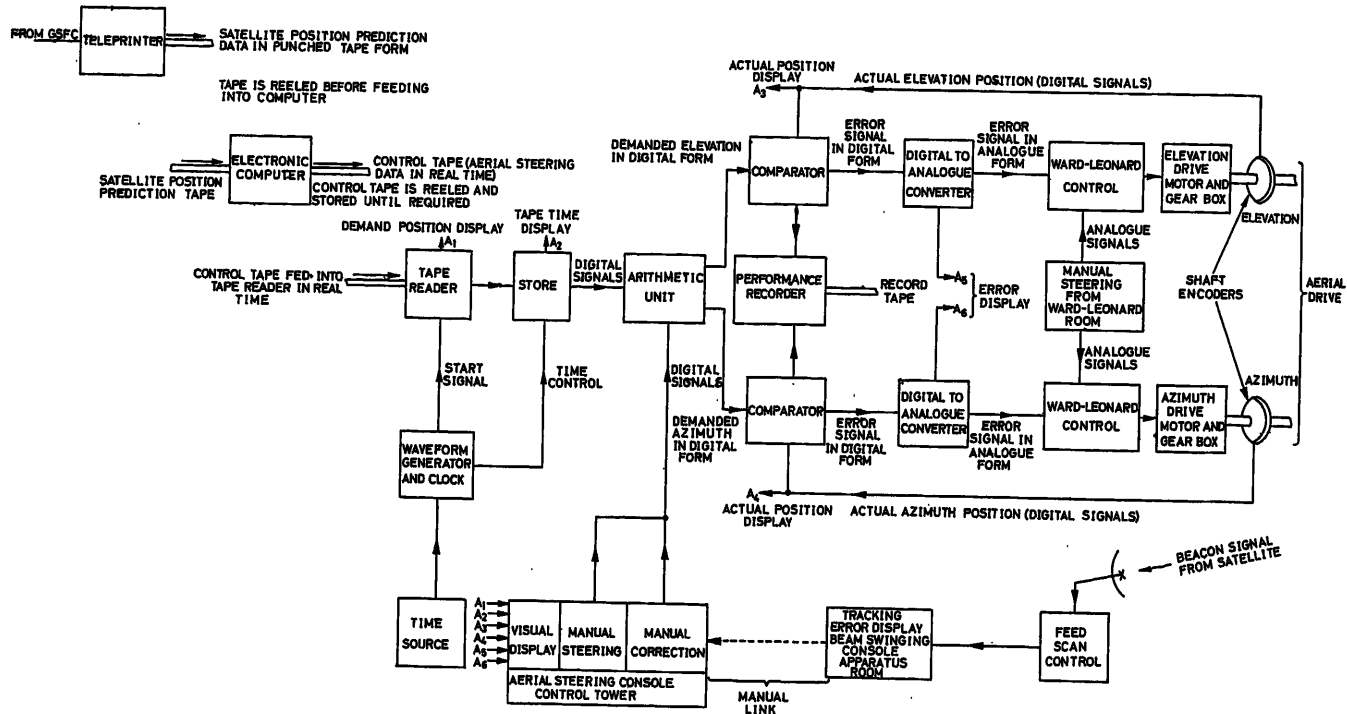


Figure 2. Block schematic diagram of the control system

control being vested solely in a steering tape and a clock. Indeed, it has been the practice to apply the steering tape to the mechanism an hour or so before the start of a communications test and leave the steering process entirely to the machine.

In more recent experiments the receipt of primary steering data from the U.S.A. has been dispensed with and the preparation of steering tapes made dependent upon a knowledge of only the orbital elements of a satellite. These orbital elements are expressed in terms of, for example, longitude of the ascending node, angle of inclination of the orbital plane to that of the equator, length of the semi-major axis, eccentricity, argument of perigee and time of perigee passage.

The application of suitable programmes to the National-Elliott 803 computer permits of the generation of steering tapes in the same form as before.

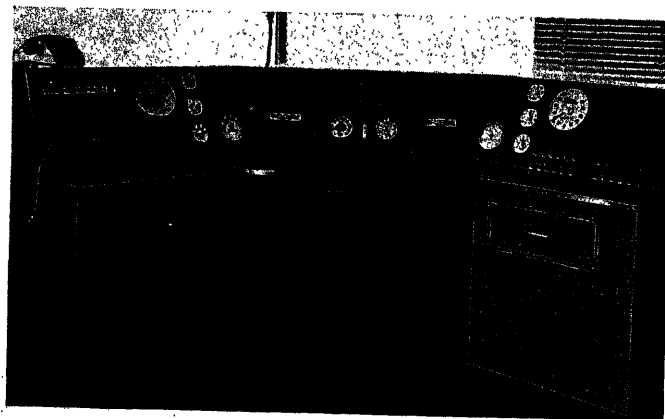


Figure 3. Photograph of the aerial-steering console

Feedback Control Systems for Azimuth and Elevation

Independent but similar feedback control (servo) systems are provided for the azimuth and elevation motions. In accordance with normal practice, these receive information on the 'demanded' position (i.e., the aerial position required or desired), and include means for determining the 'actual' position of the aerial; an error signal representing the difference between the actual and demanded positions is derived and actuates the power drive. The overall pointing accuracy required makes it almost inevitable that the demanded position should be specified and the actual position should be measured in digital rather than analogue terms.

Actual azimuth and elevation are measured by means of optical shaft angle encoders, which are of 16 bit resolution, i.e., the element is 2^{-16} rev. = 19.77 sec of arc. Demanded azimuth and elevation are correspondingly presented in digital form to the nearest 2^{-16} rev., and the demanded and actual quantities are subtracted to give digital error signals. The latter pass to digital-analogue converters and thence to Ward-Leonard machine systems to control the final driving motors.

Specification of Demanded Position

Information on the demanded azimuth and elevation is, as already mentioned, presented to the control system by means of a punched paper tape prepared in advance. However, to provide a substantially continuous error signal in the control loops already discussed, the error is determined every 1/50 sec. and the full demanded position (in digital form to the nearest 2^{-16} rev.) is therefore required every 1/50 sec. It would be quite impracticable to convey the full information required, 50 times per second, by means of paper tape. Consequently, the necessary information is carried by the tape in a condensed

form (see Figure 4) and some data processing, of a simple kind, is carried out in real time between the tape reader and the inputs to the control loops.

Economy in tape is effected by punching on the tape increments of angles rather than complete angles. No material inaccuracy will result if the aerial moves with constant angular velocities (i.e., if azimuth and elevation change linearly with time) over any period of $1/5$ sec but, of course, the velocity must be changed from one such period to another. Linear operation over $1/5$ sec is realized by punching once on the tape the increments of azimuth and elevation for $1/50$ sec and by adding these, ten times at intervals of $1/50$ sec, to cumulative values which are held in digital stores. The main content of the tape therefore

comprises increments of azimuth and elevation pertaining to successive periods of $1/5$ sec. The full azimuth and elevation are however specified on the tape every second so that automatic control can be started at any integral second and the content of the store can be completely rewritten every second to avoid persistence of any error that may occur. These arrangements lend themselves to 1 sec groups of data on the tape and to a 1 sec cycle of events in the real-time data processing.

The real-time system includes a facility for adding to the azimuth and elevation prescribed on the tape small angles representing corrections that can be demanded by the operator; while the demand remains unchanged the same quantities will be added to each presentation of the demanded position, so

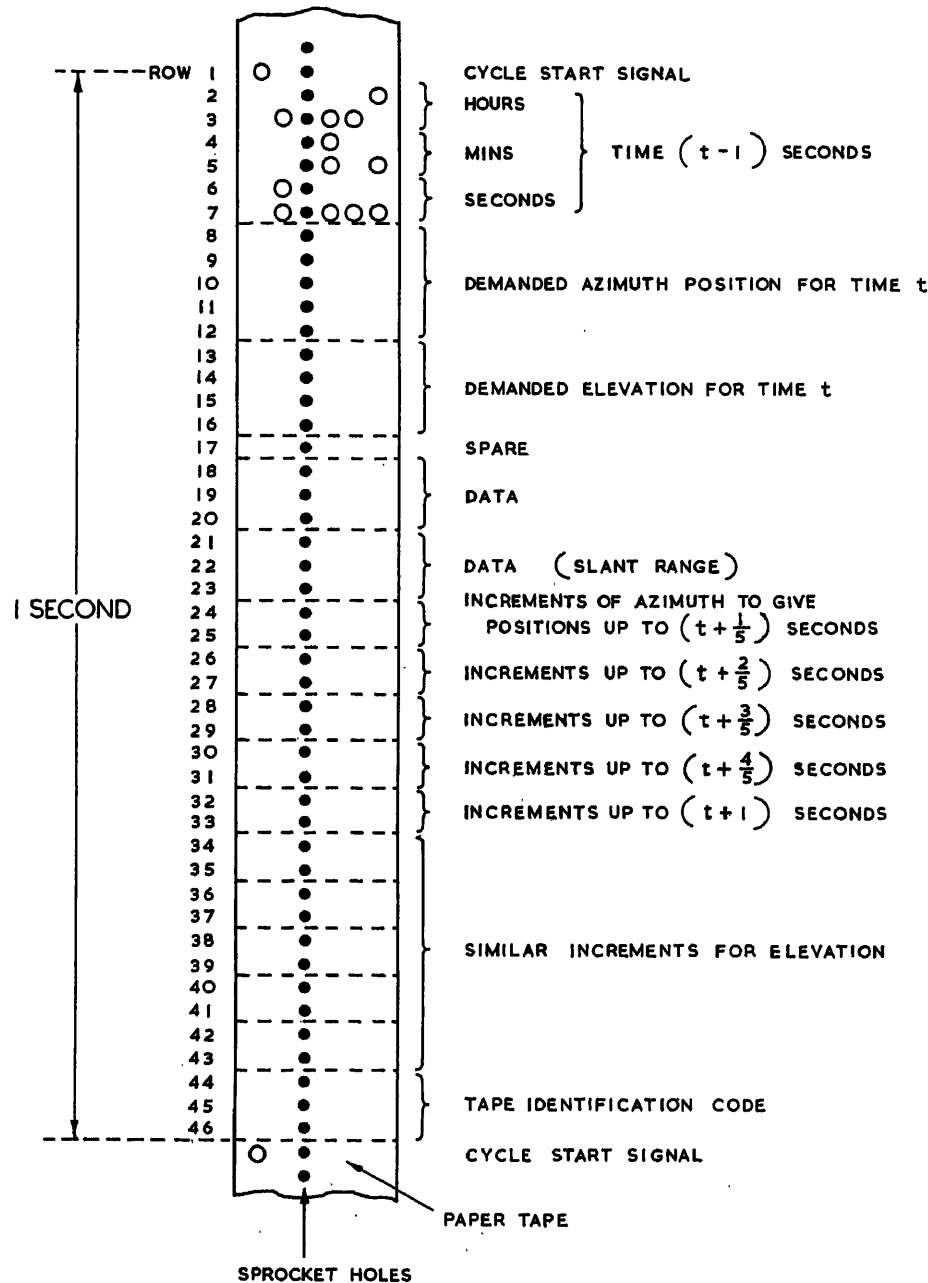


Figure 4. Layout of data on the steering tape

that the aerial will track with a fixed offset from the trajectory demanded by the tape. The same facility is applied in a slightly different way when the aerial is to be steered from the console by an operator, no tape then being in use; for this purpose quantities preset by controls on the console are added repeatedly to the cumulative demanded azimuth and elevation, so that the aerial tracks at constant velocity.

Timing

The timing of operations in the control system is based on a digital clock which indicates Universal Time No. 2. The rate of this clock is determined by a temperature-controlled quartz crystal oscillator, which enables it to run for at least 12 days without gaining or losing more than 1 msec. Resetting to actual time is carried out when necessary with reference to Rugby (MSF) time signals, means being available to offset the clock from the time signals by a few milliseconds to take account of the known time of transmission of radio signals from Rugby to the station, and of the offset between the MSF signals and U. T. on which information is published.

In addition to the numerical information already discussed, each 1 sec group on the tape includes signals defining time in hours, minutes and seconds.

In the time-scale of interest, the process of reading information from the tape takes rather a long time. The data pertaining to each second are therefore read during the preceding second, and held in digital stores until required. The timing of operations is controlled on a second-by-second basis by comparing the time read from the tape and held in store with the indication of the digital clock.

Error Correction

In the foregoing paragraphs consideration has been given mainly to what might be termed the 'ideal case'; that is, it has been assumed that the mechanical axis of the reflector and the electrical beam axis are coincident. In practice, there are modest departures due mainly to small errors in the orbital elements. These departures can be measured and corrections applied.

Departures from axis coincidence can be measured if the satellite emits a beacon signal to indicate its position. The aerial under discussion is equipped with means whereby, without moving the reflector, the axis of the radio beam may be made to scan in both conical and spiral form around its mean or neutral position; that is, it may be made to seek the direction of maximum intensity of a satellite beacon signal. Differences between the reflector mechanical axis and the radio direction to a satellite are presented as oscilloscope displays. From observation of the displayed material over, say, a few seconds, the operator can make a judgment of the optimum degree of offsets that should be applied to the reflector steering instructions; these are signalled directly to the operator at the aerial-steering console.

The brain of the operator at the beam swinging console is being used as an enormously complex computer—one able to make judgment on the basis of variable data presented over a considerable interval of time—but investigations are in hand to determine if his function can, without serious degradation of performance, be transferred to an electronic computer operating in real time.

A further current study is aimed towards removal of steering tape instructions once a satellite beacon signal is acquired and putting the servo loops under the control of a characteristic (amplitude or phase) of the received beacon signal.

Specified Performance

The required range of angular velocity in both azimuth and elevation is from $1/8^\circ$ to $120^\circ/\text{min}$ and the maximum acceleration is $1.33^\circ/\text{sec}^2$. The accuracy of the servo system from receipt of analogue control signals to the output shafts of the motors is required to be not worse than 2 min of arc at $60^\circ/\text{min}$. Accuracy of shaft angle encoders must not be worse than 20 sec of arc while the accuracy of the control system from the tape reader to the output from the digital-analogue converter must not be worse than 45 sec of arc.

The requirements mentioned above have to be met when the aerial is operating under full-load conditions and under climatic extremes. They are necessary in order that a beam-pointing error of not more than some 4 to 6 min of arc can be attained even at wind velocities up to 65 m.p.h.

Some Details of the Aerial-Steering Console

A general view of the console is shown in *Figure 3*. *Figures 5*, (a), (b) and (c) show details of the three principal panels. At the time the photographs were taken the aerial was inactive while awaiting the next appearance of the satellite; number displays are therefore random and do not exhibit the close agreement that exists between the upper and lower elements of a pair when a satellite is being tracked. The functions of the principal displays and controls shown in *Figure 5* are indicated.

The Control Equipment

Attention is now directed towards some details of the automatic digital equipment.

Pulse Generating Equipment

The input to the pulse generating equipment is an accurate 2 kc/sec sinusoidal waveform generated by the oscillator mentioned earlier. After a shaping network there is a series of dividers; the outputs of these are combined as required to produce all of the timing signals used throughout the digital network.

Tape-reading Equipment

Two high-speed tape readers are operated in series, the first acting as a buffer for the second and ensuring that there is no 'snatching' that would result in reading errors. A control signal starts the tape and, after data appropriate to 1 sec has been read, the tape stops. In normal operation, therefore, the tape proceeds in 'start-stop' sequence. The control signal is given not only when there is coincidence between 'tape time' and 'actual time', but also when (a) coincidence is lost for 1 sec, e.g., in the event of a faulty indication of 'tape time', and (b) on switching from manual to automatic control.

One tape track provides for synchronization; the other four supply data digits which, through gates, are routed to stores.

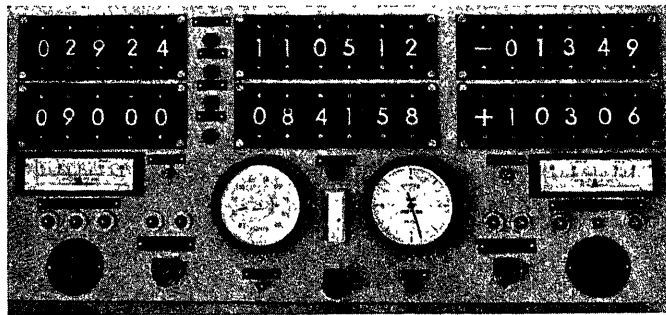


Figure 5 (a). Details of the aerial-steering console

Demanded position El. Degrees and minutes	Control clock time Hours, minutes and seconds	Demanded position Az. degrees and minutes
Actual position El. degrees and minutes	Tape time Hours, minutes and seconds	Actual position Az. degrees and minutes
El. error in minutes	Wind speed, Wind direction	Az. error in minutes:
Auto/manual control switch	Emergency stop	Safety interlock switch

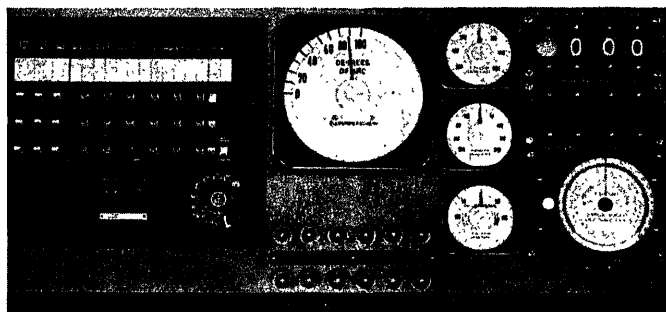


Figure 5 (b). Details of the aerial-steering console

Telephone and speaker circuit controls	Elevation position degrees	El. drive volts	Applied correction El. degrees and min.
	Condit. indicator lamps	El. drive amps	Demanded correction El. degrees and min.
		El. drive speed degrees/minute	El. override correction applied

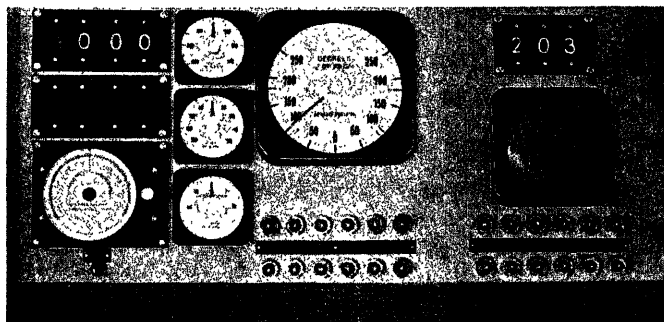


Figure 5 (c). Details of the aerial-steering console

Applied correction Az. degrees and minutes	Az. drive volts	Azimuth position degrees	Tape identification code
Demanded correction Az. degrees and minutes	Az. drive amps	Condition indicator lamps	Loudspeaker
Az. override correct. applied	Az. drive speed degrees/minute	Condition of safety interlocks	

Arithmetic Unit

From the stores, information on demanded angle is applied to the arithmetic unit. Correction signals in serial form are also applied.

When steering manually, the actual angle of the aerial is

treated as an initial demanded angle. The manual control provides a signal in the form of increments to be added 50 times per sec and so produces uniform velocity of movement.

It is thought to be unnecessary to describe the arithmetic unit in any detail. Like the rest of the digital equipment it uses resistor-transistor circuits and comprises multi-digit shift registers and serial addition-subtraction elements.

Limiting

Limiting is effected between the comparator and the digital-to-analogue converter; this in order that the latter may have a reasonable dynamic range and prevent excessive demands on following equipments should a defect arise in the control loop or, through error, an excessive demand step be initiated.

Digital-to-analogue Converter

The limited signal is applied to a converter with an output range of ± 5 V about $+5$ V. The output signal is applied to a servo amplifier for the control of a Ward-Leonard set and shaft driving mechanism.

Shaft Encoder

This is of 16 bit Gray-code type and the amplified output is transmitted from the aerial site to the control centre. There the 16 parallel digits are converted to binary form and used to feed information into the arithmetic (error) apparatus and for the display of actual angle.

Correction Control

The correction control at the steering console sets an 8 bit Gray fine-encoder and also, through a gearbox, a binary encoder with leading and lagging contacts. The fine-encoder is followed by a Gray-to-binary converter and the whole complex produces a 10 digit number which may be fed to the arithmetic unit.

Displays

It is outside the scope of this paper to detail how the visual display of angular information is effected. However, it may be of interest that displays using digital display lamps are provided as follows:

(i) Demanded azimuth angle as recorded on the steering tape. Derived from a 17 digit binary number converted into degrees and minutes in the range $\pm 250^\circ$ and displayed once every second.

(ii) Demanded elevation angle as recorded on the steering tape. As for (i), the range being 0° to 100° .

(iii) Azimuth and elevation corrections. 10 digit binary numbers are converted into degrees and minutes up to a maximum of 5° and displayed once every half second.

(iv) Actual azimuth and elevation. Digital data is taken from the Gray-to-binary converters associated with the shaft encoders and displayed at 1 sec intervals.

Performance Recorder

It will be appreciated that analysis of transmission data obtained in the course of the passage of a satellite requires, among other factors, a precise record of the bearing of the aerial with time. The digital equipment therefore includes facilities for recording on punched paper tape: (a) the identity

code of the steering tape; (b) time in hours, minutes and seconds; (c) demanded angles; (d) error magnitudes; (e) applied corrections.

These quantities are punched once every second. Additional data, e.g., signal transmission parameters, converted to digital form can also be recorded if required.

Conclusion

The techniques described in this paper have been found to be satisfactory in all respects. They have permitted the steering

of a large microwave aerial to be accomplished with an accuracy estimated as close to 2 min of arc.

Grateful acknowledgment is made to the Engineer-in-Chief of the British Post Office for permission to make use of the material used in the preparation of this paper. It is also desired to express sincere thanks to E. C. H. Seaman and C. F. Davidson for assistance and valuable comments. The Consulting Engineers responsible for aerial design were Husband & Co.; the design and construction of the digital equipment was by Whitworth Gloster Aircraft Ltd.

DISCUSSION

R. G. WHEELER, *A.E.I. M/C, 121, Westminster Road, Davyhulme, Urmston, Lancashire, England*

Reading the paper there seems to be no indication of any problems with the closed-loop position control. I would like to know whether Mr. Taylor could give an indication of the order of the lower resonant frequencies of the structure and whether any possible side-effects of the chain drive were investigated.

Assuming that a chain drive is satisfactory, would it not have been better to have used a twin or even three motor drives to reduce eccentric torques?

F. J. D. TAYLOR, *in reply*

We have had no problems with the closed-loop position control.

It is regretted that we have no information on the complex resonant frequencies of the structure. As has been mentioned, the structure is an extremely stiff one and resonant frequencies are high and of small amplitude.

The only 'side-effects' that we have noticed as a result of using chain drive is that there is a small hysteresis effect of some 2 to 3 min of arc when changing over from clockwise to anticlockwise rotation.

The chain drive is completely satisfactory. Could not multiple drive have resulted in irregularities of torque?

J. C. LOZIER, *Bell Telephone Laboratories, Whippany, N.J., U.S.A.*

(1) In your presentation you indicate that the antenna has now been made to autotrack on error signals derived from a mechanical scanning of the feed horn. Could you give us some of the dynamic characteristics of this control loop?

(2) The antenna structure you describe is a very interesting one. Could you show us the transfer characteristics of this structure? What

is the primary resonant frequency of the system in azimuth and in elevation? What is the effective Q of each of these resonances?

(3) Goonhilly Downs is a notoriously windy place, so you have had an excellent opportunity to study a large antenna under severe wind conditions. It would be very interesting to know more of your experiences in this respect. Have you measured the dynamic reactions of the control system to wind gusts? Have you any experimental information on the amplitude and frequency spectrum of the wind torques on the antenna?

F. J. D. TAYLOR, *in reply*

The earth station at Goonhilly Downs was designed and constructed within a year and completed less than a week before the date of launch of the Telstar I satellite. It has since been in use continuously for tests with the various Telstar and Relay satellites. These factors have made it impossible for us to undertake detailed study of the dynamic characteristics of the aerial structure itself. We do know that they are satisfactory because, in spite of the fact that the aerial radiation pattern (main lobe) has a width of only some 10 min of arc to the 3 dB points, the aerial has operated satisfactorily under even the highest wind stresses so far experienced at Goonhilly; some 60 knots with a high gust factor.

As has been mentioned, the aerial is an extremely stiff structure; the resonant frequencies are high and of very small amplitude.

Under conditions of extremely high wind the azimuth and elevation shaft encoders show a 'shudder' of less than 1 min of arc; it is, of course, recognized that they may not represent beam deflection consequent upon reflector profile distortion which, however, in the light of experience, is certainly less than 3 min of arc; were it greater than this the effect on communication tests would be most noticeable.

It is hoped that, when opportunity permits, it will be possible to carry out the dynamic studies mentioned in the questions.

Design Study of Control System for 210 ft. Radio Telescope

R. G. WHEELER

Summary

This paper is devoted to a discussion of the effect of parameter variations in a 210 ft. radio telescope with a view to obtaining certain limits of servo performance. Owing to a low mechanical resonance and the need for small velocity errors it is shown that certain stabilizing terms are more acceptable than others. A block diagram of the complete mechanical and electrical system, as applied to the analogue computer, is shown.

Comparison of the performance between two schemes is given from the point of view of step inputs. Curves are plotted illustrating the damping effect of coulomb friction with varying amounts of backlash. Frequency response curves of aerial error are given for various wind frequencies and from a power density spectrum of typical wind conditions, a graphical integration is performed to obtain the transient errors under gusty conditions.

The effect of various negative slope friction characteristics are tabulated and discussed. Limiting parameters of the system are given to obtain a specified performance.

Results obtained from site test on the bolted construction on trial erection in Germany and the final welded construction in Australia are compared with those of the analysis.

Sommaire

Cette communication s'occupe d'une discussion de l'influence de variations des paramètres sur un radio-télescope de 64 mètres, dans l'intention d'établir des tolérances exactes pour le fonctionnement du servomécanisme. Il est constaté que certains termes stabilisants sont plus acceptables que d'autres, à cause d'une résonance mécanique peu élevée et de la nécessité de faibles erreurs de vitesse. Un schéma fonctionnel représente l'ensemble mécanique et électrique dans son application à la calculatrice analogique.

En ce qui concerne entrées sous forme d'échelon on fait une comparaison des performances de deux systèmes divers. Des courbes sont tracées pour montrer l'effet amortisseur du frottement solide, avec des degrés divers de jeu. Des courbes de réponse fréquentielles à partir des erreurs d'antenne sont données en fonction des diverses fréquences de vent. Une intégration graphique est effectuée d'un spectre de densité de puissance de conditions de vent typiques, pour obtenir les erreurs transitoires qui se produisent sous des conditions de vent instables.

Les effets des caractéristiques de frottement diverses à gradient négatif sont classifiés et discutés. On donne des paramètres limitateurs du système, parmi lesquels on obtient la performance spécifiée.

Les résultats que l'on a obtenu au cours des essais faits à pied d'œuvre sur la construction boulonnée d'essai en Allemagne, et sur la construction soudée définitive en Australie, sont confrontés avec ceux de l'analyse.

Zusammenfassung

Der Aufsatz behandelt den Einfluß von Parameteränderungen eines 64-m-Radioteleskops, um bestimmte Grenzen für die Nachlaufregel-einrichtung zu erhalten.

Wie gezeigt wird, haben infolge der niedrigen mechanischen Resonanz und der erforderlichen möglichst geringen Geschwindigkeits-abweichungen gewisse stabilisierende Glieder mehr Einfluß als andere. Ein Blockschema der gesamten mechanischen und elektrischen Anlage zur Berechnung am Analogrechner ist dargestellt.

Vergleich zwischen zwei Ausführungsformen geschieht auf Grund der Übergangsfunktion (Sprungantwort). Aufgezeichnete Kurven zeigen die Dämpfungswirkung der Coulombschen Reibung bei veränderlichem toten Gang.

Frequenzgangkurven des Antennenfehlers bei verschiedenen Windgeschwindigkeiten werden angegeben. Mit Hilfe eines Leistungsdichtespektrums für typische Windverhältnisse wird eine graphische Integration durchgeführt, um die bei böigen Windverhältnissen entstehenden Fehler des Übergangsverhaltens festzustellen.

Die Einflüsse von verschiedenen Reibungskennlinien mit negativer Steigung gehen aus einer Zusammenfassung hervor. Parameterbegrenzungen des Systems sind angegeben, um ein gewünschtes Verhalten zu erzielen.

Die Prüfergebnisse, die sich sowohl bei dem zusammengeschraubten Probeaufbau in Deutschland als auch bei der geschweißten Endkonstruktion in Australien ergaben, werden mit den analytischen Ergebnissen verglichen.

Introduction

The basic problem in designing the Commonwealth Scientific and Industrial Research Organization radio telescope was to produce an extremely high static stiffness, with good response to wind disturbances. The philosophy adopted in the structural design was to make the altazimuth mounting compact and rigid, the rigidity being sufficient to ensure that deflections caused by the maximum operational wind loads were well within specification with the drive system locked.

From the control aspect, because of the very low acceleration duty, it was decided to deal with the wind problem by increasing the effective inertia of the system to the maximum extent compatible with required slewing speeds, the telescope thus becoming a low pass filter to wind gusts. This method of dealing with the problem also enabled the bandwidth of the servo to be narrowed, such that mechanical resonances were excluded completely.

Some special features were suggested after initial examination of the problem, i.e. roller drives in azimuth and a biased motion in altitude to eliminate backlash, and these were immediately incorporated into the design. Computer studies were then undertaken by Associated Electrical Industries Limited to determine whether the system would enable positional errors when tracking, and also errors due to wind disturbances, to be maintained within the specified limits. To illustrate the problems involved, the azimuth motion only is being dealt with in detail, the altitude motion being very similar. Results, however, will be given for both motions.

The Basic System and Requirements

In order to understand the physical arrangements of the telescope, a simplified sketch of the system is given in *Figure 1*.

From this sketch the position of the error detecting and master equatorial units can be seen, the latter is mounted at the intersection of the azimuth and altitude axis, and supported by a concrete pillar passing through the concrete tower underneath. This enables the dish position to be picked off accurately, eliminating the structural movement which would otherwise cause deflections on any measuring device fastened to the structure itself.

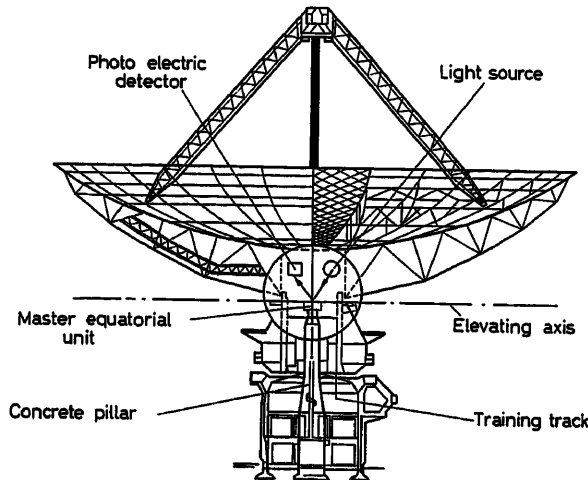


Figure 1

The following parameters were given by the consultants:

Azimuth

Dish inertia	$0.68 \times 10^8 \text{ lb. ft./sec}^2$
Turntable inertia	$0.47 \times 10^7 \text{ lb. ft./sec}^2$
Turret stiffness	$1.3 \times 10^{10} \text{ lb. ft./rad}$
Turret damping	$1.9 \times 10^8 \text{ lb. ft. sec/rad}$
Wind torque at 20 m.p.h.	270 tons ft. = $6.05 \times 10^5 \text{ lb. ft.}$
Wind torque at 10 m.p.h.	67 tons ft. = $1.51 \times 10^5 \text{ lb. ft.}$
Gearbox stiffness	$5.32 \times 10^{10} \text{ lb. ft./rad}$

Altitude

Inertia of turret	$0.1 \times 10^8 \text{ lb. ft./sec}^2$
Inertia of dish	$0.5 \times 10^8 \text{ lb. ft./sec}^2$
Turret structural stiffness	$3.6 \times 10^{10} \text{ lb. ft./rad}$
Structural damping	$1.3 \times 10^8 \text{ lb. ft./rad/sec}$
Steady wind torque at 10 m.p.h.	107 tons ft.
Steady wind torque at 20 m.p.h.	430 tons ft.
Maximum counterweight torque	1,320 tons ft.
Gearbox stiffness	$9 \times 10^{10} \text{ lb. ft./rad}$

The pointing error is defined as the error between the normal to the master equatorial mirror and the axis of the error detector. The tentative specification required by C.S.I.R.O. for control accuracy was that the pointing error was to be not greater than 6 sec of arc in winds of average velocity of 10 m.p.h. with gusts up to 15 m.p.h., or 12 sec of arc in winds up to 20 m.p.h. with gusts up to 30 m.p.h. These errors can be resolved into equal azimuth and altitude components of: $E/\sqrt{2}$. This performance is required when tracking at sidereal rates and when scanning at ten times this value.

Driving Motors

The d.c. motors were chosen such that the maximum speed of the motor corresponds approximately to the maximum velocity of the aerial, i.e. $25^\circ/\text{min}$. Using a standard A.E.I. servomotor of maximum speed 2,100 rev/min, this corresponds to a gear ratio of 30,000:

1. Two motors capable of producing the peak torque give an effective referred inertia of $5.6 \times 10^8 \text{ lb. ft./sec}^2$ with gears and brakes.

Mechanical Resonances

The frequencies of mechanical resonance in the system are shown in Figure 2. As the effective motor inertia swamps all other inertias, the motor can be regarded as stationary, thus the lowest frequency becomes:

$$\left(\frac{K_{13}}{J}\right)^{\frac{1}{2}} = \omega_R \text{ where } K_{13} = \frac{K_g K_{10}}{K_g + K_{10}}$$

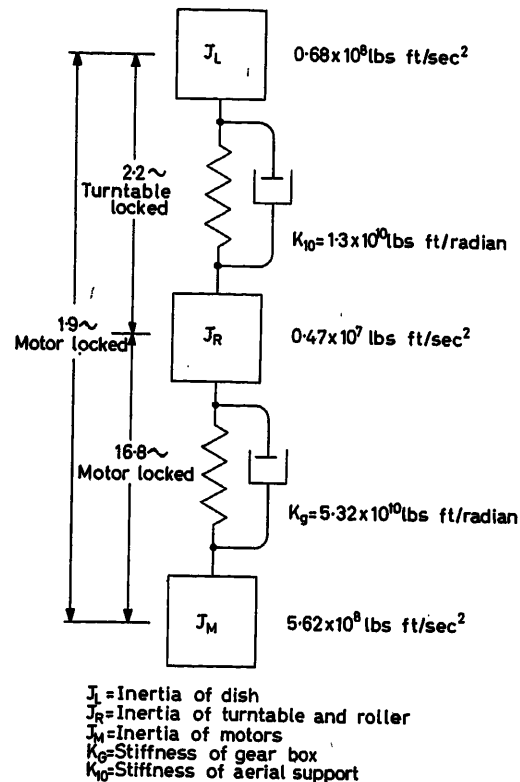


Figure 2

However, the effective mechanical stiffness was determined by the requirement to keep the deflections under maximum wind conditions to approximately 12 sec of arc. Hence $K_{13} = 0.98 \times 10^{10} \text{ lb. ft./rad}$. From this figure the gearbox mechanical stiffness of $5.32 \times 10^{10} \text{ lb. ft./rad}$ was obtained as shown in the diagram and the lowest resonance becomes 12.8 rad/sec.

The backlash figure as measured at the load was initially chosen from practical experience to be approximately equal to the full torque load error of the servo. However, this is one of the factors varied in the computer study and its effect can be illustrated. The torque to overcome rolling friction was given as 200 tons ft.

Undamped Natural Frequency

In order to initiate the design and establish fundamentals, the system was first of all considered as the basic arrangement shown in *Figure 3(a)*.

The undamped natural frequency, from the parameters given above, is obviously determined by the wind and friction torques and not the acceleration torque. By consideration of the wind forces applied to the dish plus friction, the static stiffness is

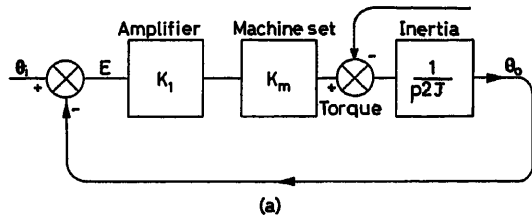
$$K_1 K_M = \frac{\text{load torque}}{\text{error}}$$

for a 4 sec error in a 10 m.p.h. wind, this is 3.09×10^{10} lb. ft./rad. The undamped natural frequency then becomes:

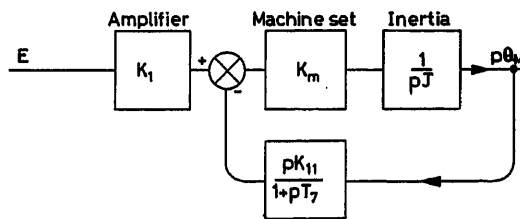
$$\omega_0 = \left(\frac{K_1 K_M}{J} \right)^{\frac{1}{2}} = 6.9 \text{ rad/sec}$$

To prevent servo excitation of the lowest mechanical resonance of 12.6 rad/sec, the undamped natural frequency must be considerably reduced, preferably 2 or 3 octaves below.

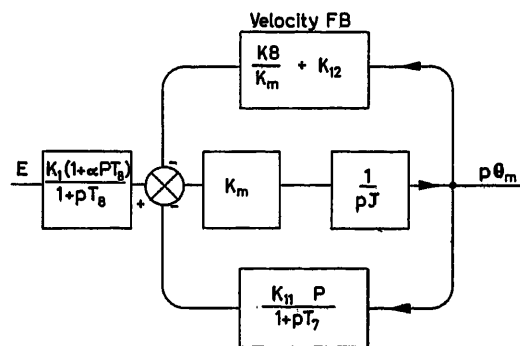
The Bode diagram in *Figure 4* shows the basic preferred requirement of the torque/error characteristic where 12 dB asymptote crosses the 0 dB line at approximately 2.5 rad/sec. The mechanical resonance has been assumed to have a rather pessimistic damping factor of 0.05.



(a)



(b)



(c)

Figure 3

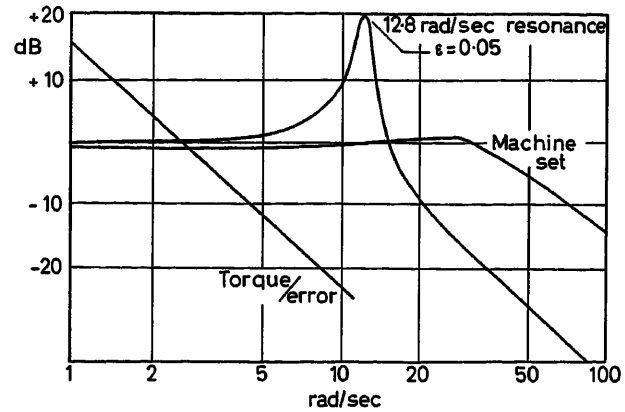


Figure 4

Rotary Amplifiers

The next consideration is the rotary amplifier stage. Here must be borne in mind the almost certain use of feedbacks from tacho or motor and the consequent loop stability. The machine set must have a bandwidth of at least 5 rad/sec to cover the required servo response.

In order to use a standard A.E.I. servo amplifier of 12 W output, a machine set was selected to give the required power amplification for peak current and voltage compatible with continuous rating. These standard sets consist of a multi-lag combination of crossfield and separately excited generators with overall current feedback to operate the machines as current amplifiers. They have a closed-loop transfer function of the form:

$$\frac{I_0}{I_i} = \frac{K_5 K_6}{(I + PT_2)(I + PT_3)(I + PT_4)(I + PT_5) + K_5 K_6 K_7 (I + PT_6)}$$

(see *Figure 16*). The machine set selected had a bandwidth of 46 rad/sec.

Whilst this might seem a faster machine set than necessary, it was, as a standard unit, economically the better proposition. The closed-loop response of the machine, seen also on *Figure 4*, has been derived from the Nichols chart, *Figure 5*.

Reduction of Undamped Natural Frequency

As mentioned previously, it is required to prevent servo excitation of the lowest mechanical resonance and, in order to do so, the present undamped natural frequency must be lowered to approximately 2.5 rad/sec.

This should preferably be done by increasing the value of inertia J , as a reduction of $K_1 K_M$ would interfere with the required static accuracy of the system.

The use of transient velocity feedback will effectively increase the motor inertia and at the same time produce no velocity errors. It can be shown that by feeding back a signal proportional to output velocity via a lead network with a transfer function $K_{11}P/(1 + PT_7)$, an increase in inertia of $J(1 + G)$ is obtained at frequencies below the break point defined by $\omega = 1/T_7$ where G equals the transient velocity loop gain and T_7 is the network time constant [see *Figure 3(b)*]. Hence, the lower break point has to be greater than 12.6 rad/sec

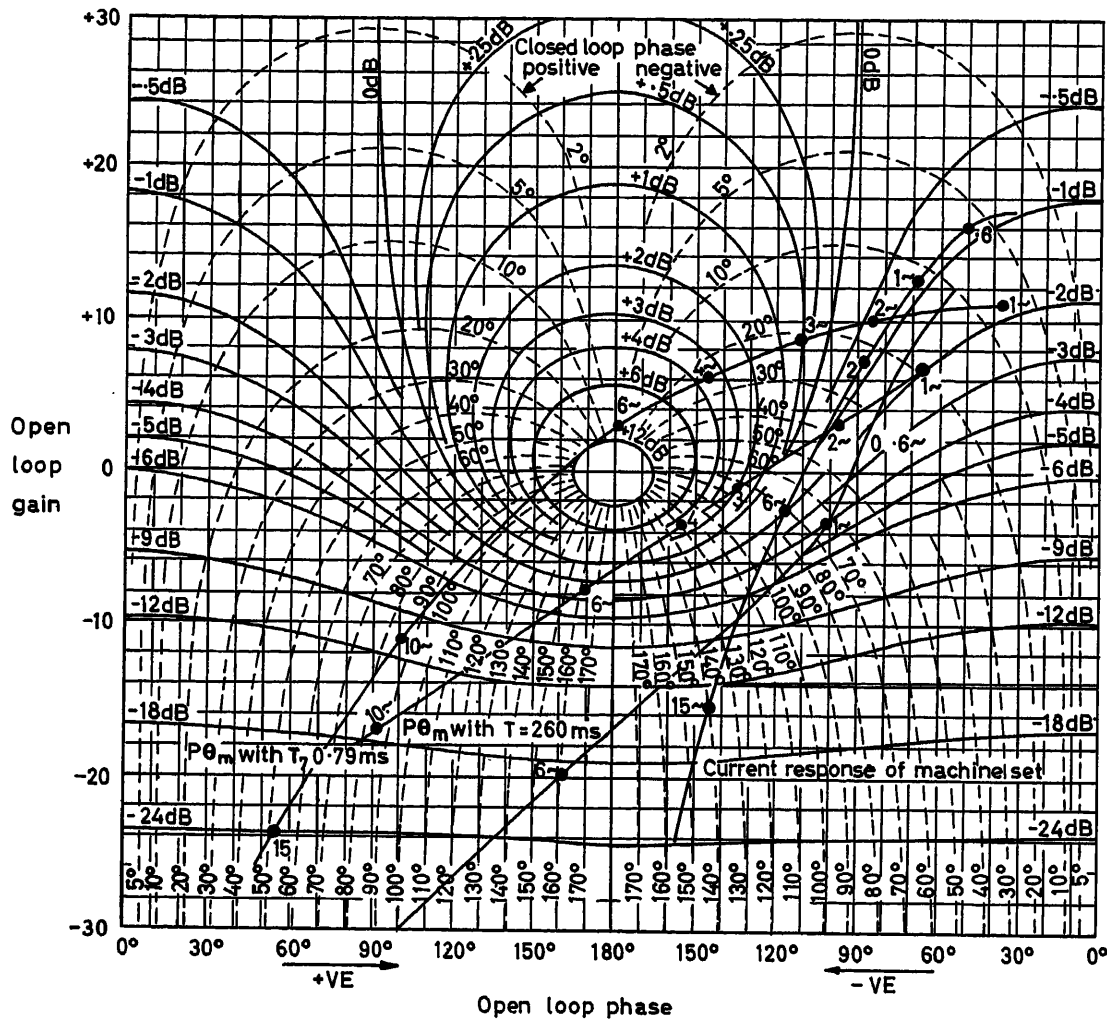


Figure 5

(the lowest mechanical resonance) giving T_1 equal to 79 msec and G equal to 6.6.

The system as shown in Figure 16 was set up on an analogue computer with the exception of the backlash and coulomb friction. It was found that the transient feedback loop in this condition was unstable, as illustrated also in Figure 5. This feedback is equivalent to a lagging feedback over the machine set whose stability is limited by a certain value of G/T_1 .

In order to achieve the loop gain of 6.6 with stability, it was found on the computer that T_1 must be at least 260 msec, this having a lower break frequency of 3.8 rad/sec. Hence it appeared that this was not a satisfactory method of suppressing the mechanical resonance of 12.0 rad/sec.

The above loop response of the system with and without transient feedback is shown in Figure 6. It can be seen that there is only a slight reduction in amplitude at the resonant frequency. A number of transient responses were taken of the system and are shown in Figure 7. Figures 7(e) and 7(f) show the feedback loop becoming unstable after G/T_1 has exceeded a certain value. None of the responses is satisfactory.

By using current feedback from the motor armature stability of the feedback loop could have been maintained. Its use,

however, under load disturbance conditions, was to be avoided owing to the positive feedback effect decreasing the effective inertia under motoring conditions.

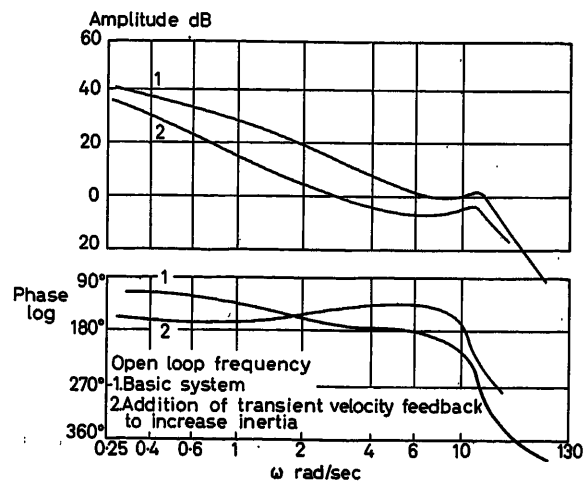


Figure 6

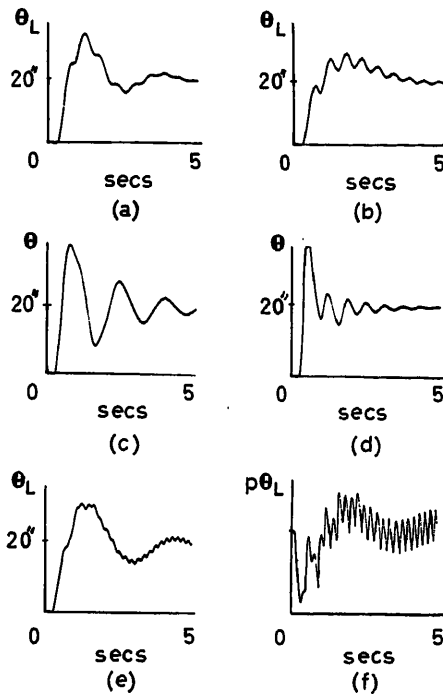


Figure 7

Alternative Approach

It has already been seen that to stabilize the system satisfactorily and eliminate the mechanical resonance, the loop gain must be reduced, as satisfactory damping cannot be achieved by the addition of a transient velocity feedback.

The alternative available is either to reduce K_1 or increase J by adding a flywheel to the motor shaft. One method of reducing K_1 is to introduce a dominant lag into the error loop. This method is particularly attractive as it also reduces errors due to load torque.

In the Appendix, the equations for (1) a system using transient velocity; and (2) a system using a phase lag circuit, are derived. It shows that the two systems are identical from stability considerations and that for the two to be identical

$$\left[\frac{K_{1A} K_M}{K_8} \right] = \left[\frac{K_{1B} K_M}{K_8 + K_M K_{12}} \right]$$

If K_M and K_8 are constants, and K_1 and K_{12} are variable, then $(K_{1A}) < (K_{1B})$. If the ratio of K_{1A}/K_{1B} is α , then to obtain identical responses the gain of system (2) must be $1/\alpha$. This means that, as the errors due to wind torque are load torque/ $K_1 K_M$, the steady-state wind errors are reduced and hence system (2) is to be preferred. This immediately suggests a different approach to the problem, i.e. use transient velocity feedback with its small velocity errors and a phase lag network to obtain the high gain in the steady-state condition. These advantages are obtained at the expense of a longer tail of the transient response, but since one requires high steady-state accuracy, this could well be satisfactory so far as the system is concerned. The gain is therefore reduced by a factor of 5 to make $K_1 K_M$ equal to 6.4×10^9 lb. ft. rad/sec, which in turn reduces sufficiently the undamped natural frequency. After adding a phase lag network of 10:1 attenuation ratio, the

system steady-state gain then becomes 6.4×10^{10} (see Figure 8) In order to optimize the system, the following parameters can be varied:

- (i) time constants of the phase lag network;
- (ii) loop gain;
- (iii) time constant of the transient velocity feedback.

This system was optimized on the computer by examining the error responses for a ramp function. The resultant responses are shown in Figure 9 and the measured results are given in Table 1. (A similar exercise was done for a 20:1 phase lag network, keeping the gain the same.)

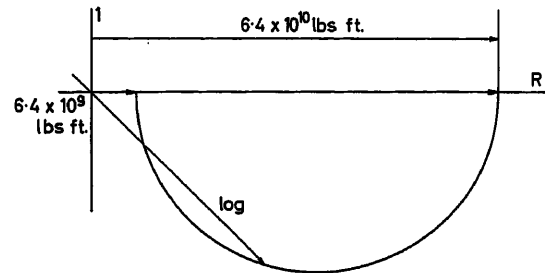


Figure 8

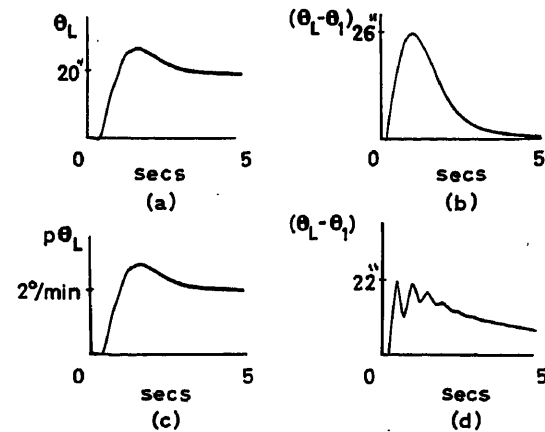


Figure 9

Table 1

	Network	Transient error	Steady-state error	Settling time
2.5°/min ramp	10:1	26 sec of arc	1.8 sec of arc	3 sec
	20:1	50 sec of arc	1.8 sec of arc	4 sec
270 tons/ft. step of torque	10:1	22 sec of arc	1.9 sec of arc	—
	20:1	37 sec of arc	1.9 sec of arc	—

The following were the optimum parameters for the 10:1 network:

	Azimuth	Altitude
D.C. gain $K_1 K_M$	$= 6.4 \cdot 10^{10}$ lb.ft./rad	$2.9 \cdot 10^{11}$ lb.ft./rad
Phase lag network	$= \frac{1+6.6P}{1+66P}$	$\frac{1+2.1P}{1+5.2P}$

$$\text{Transient velocity feedback loop gain } G = \frac{K_{11} K_M}{J_M} = 6.4 \quad 6$$

$$\text{Transient velocity feedback network} = \frac{P}{1+1.7P} \quad \frac{P}{1+0.2P}$$

Performance under Gusty Wind Conditions

For the above system it has been seen that the steady-state error is 1.9 sec of arc in a 20 m.p.h. wind. However, this gave no indication of the errors to be obtained under gusty wind conditions. Information from a series of tests carried out by Prof. R. H. Sherlock in America was converted into a power density spectrum by Professor Westcott of Imperial College, London. The curve given in Figure 10 was obtained for a mean wind torque of 270 tons/ft.

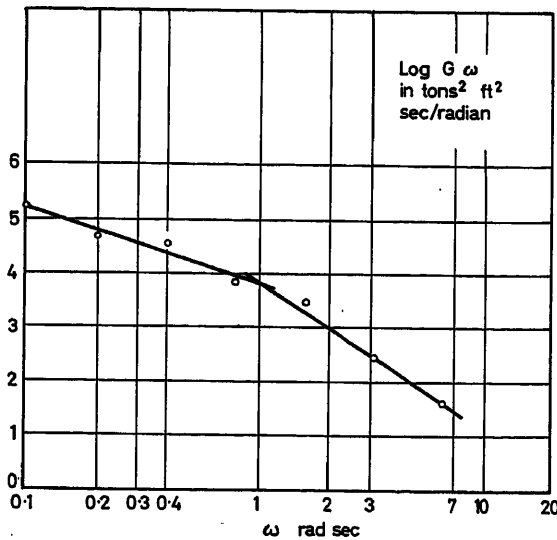


Figure 10

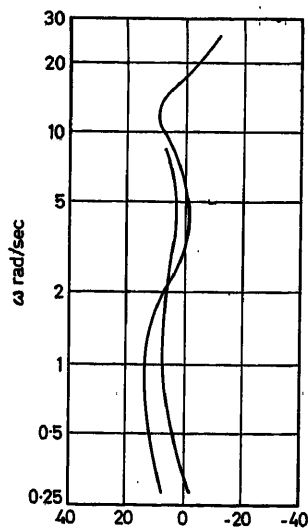


Figure 11

The R. M. S. error due to random gustiness may be calculated from:

$$E = \frac{1}{K_1 K_M} \left(\frac{1}{2} \int_0^\infty G(\omega) \cdot F^2(\omega) d\omega \right)^{\frac{1}{2}}$$

where $G(\omega)$ is the power density of the wind.

$F(\omega)$ is a pure ratio of dish displacement to the d.c. displacement at 270 tons/ft. for the frequencies of interest. This was obtained by a frequency response of the dish to wind torques and is shown in Figure 11.

The integration was performed manually and the square root taken. This delivered the R. M. S. value of torque for the random gustiness above and below the mean. Dividing by the system gain $K_1 K_M$, the error was thus obtained.

The following results were recorded:

Phase lag attenuation	Structural damping 0.1	Structural damping = 0
10:1	R.M.S. error 4.3 sec of arc	R.M.S. error 5.3 sec of arc
20:1	R.M.S. error 9.6 sec of arc	R.M.S. error 10.6 sec of arc

Overall Errors

Total errors obtained are thus friction + velocity lag + steady wind torque + wind gusts.

The worst condition obviously being when scanning at 2.5°/min.

Phase lag attenuation	Errors (arc sec)			
	10 m.p.h. wind		20 m.p.h. wind	
	10:1	20:1	10:1	20:1
Velocity lag at 2.5°/min	1.8	1.8	1.8	1.8
Steady wind torque	0.46	0.46	1.9	1.9
Gust of wind	1.3	2.6	5.3	10.6
Rolling friction = 200 tons/ft.	1.45	1.45	1.45	1.45
Total errors (arc sec)	5.0	6.3	10.5	15.8

From the above table it can be seen that results of both 10:1 and 20:1 phase lag systems are just outside the allowable errors of 4.2 and 8.5 sec for a 10 and 20 m.p.h. wind respectively. The most outstanding errors are obviously due to gusty winds. One way to reduce these errors is to increase the motor inertia and amplifier gain in the same proportion. In order to bring the total pointing errors well within the specification, both motor inertia and amplifier gain would have to be increased by a factor of two. This would not affect the stability problem. This course was not adopted, as the customer's reassessment of his overall problem enabled a wider motion specification of 10.5 sec mean error, plus 10.5 sec R.M.S. in a 20 m.p.h. wind to be used.

Maximum Velocity Errors

When the telescope is tracking or scanning, the maximum velocity of the azimuth drive always occurs with the altitude motion near zenith. This is given by:

$$P_\theta = \frac{\cos D}{\cos E} \cdot V$$

where P_θ = dish velocity in azimuth, D = declination angle, E = elevation angle, and V = sidereal input velocity. Thus, for

maximum velocity of $2.5^\circ/\text{min}$ at 5° from the zenith, i.e. when $E = 85^\circ$ and at the worst corresponding declination of -29° , $P_\theta = 25^\circ/\text{min}$. Although this means a proportionate increase in velocity lag, i.e. $\times 10$, the increase in velocity lag error is however exactly cancelled by the reduced contribution of actual azimuth error to total pointing error, i.e. reduced by $\cos 85^\circ$, i.e. $E_\theta = E_A \times \cos E$ where E_A actual azimuth error, $E_\theta =$ azimuth resolved component of total pointing error.

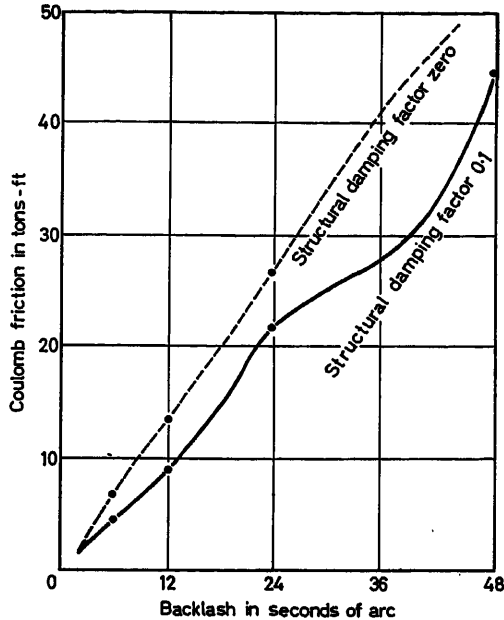


Figure 12

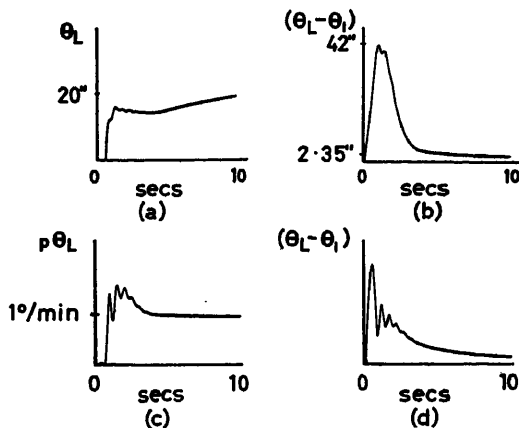


Figure 13

Backlash and Coulomb Friction

Under the heading 'Mechanical Resonances' it was stated that backlash figures were chosen by experience, but as yet no backlash or coulomb friction has been included in the computer study.

In order to get some idea of the relationship between backlash and coulomb friction, and to determine whether the damping was adequate, the amount of coulomb friction necessary to prevent the system from oscillating subsequent to an input ramp

of $2^\circ/\text{min}$ was plotted for backlash values up to 48 sec of arc, with structural damping figures of 0 and 0.1. Figure 12 shows the results obtained from the computer. Transient responses are shown in Figure 13 for the final system when 12 sec of arc backlash and 200 tons/ft. coulomb friction are included.

It will be realized that there is a possibility of oscillation in the case of high wind gusts where the wind is opposing friction and is of approximately the same magnitude, as it is highly unlikely that the backlash figure for zero coulomb friction would be achieved, i.e. 1.25 sec of arc. The magnitude of the resultant oscillation would be roughly proportional to the magnitude of the backlash.

A minimum of 67 tons/ft. friction was recommended for backlash up to 15 sec of arc although 200 tons/ft. was expected.

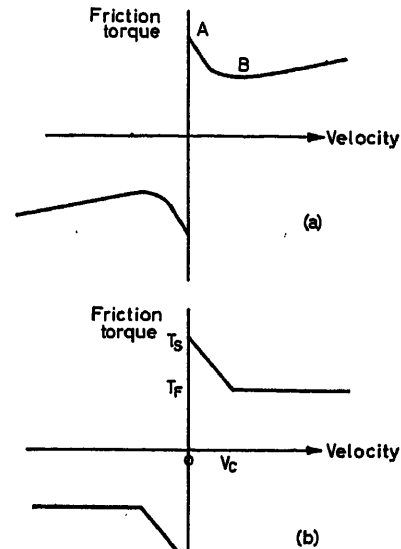


Figure 14

Lags in Phase-sensitive Rectifier

The phase-sensitive rectifier filter has a transfer function $1/(1 + PT_1)^n$ (which is necessary to remove the ripple); this was included in the finalized system, and for n equal to 1 and 2 the value of T_1 was increased until its effect was just noticeable.

By optimizing the time constant in each case to obtain good stability, it was found that the maximum allowable time constant was 160 msec. This gives a 10 per cent increase in transient error. It was therefore decided that 160 msec should be the maximum total lag in the static amplifier chain.

Negative Friction

In view of the fact that the telescope was expected to operate chiefly at creep speeds, it was anticipated that this might require the telescope to operate in the negative part on the friction characteristic as shown in Figure 14(a).

An idealized negative slope characteristic as shown in Figure 14(b) was included on the computer, such that T_s and V_c could be varied and its effect noted. T_f remained constant at 200 tons/ft. As a result, four modes of behaviour were discovered (see Figure 15).

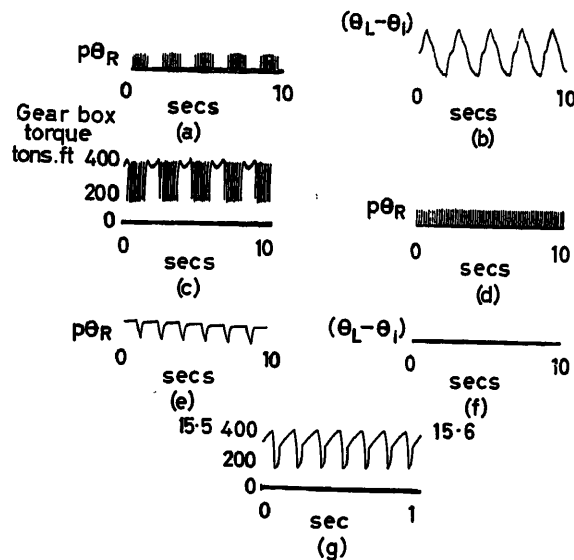


Figure 15

T_s tons/ft.	V_o in °/min	<i>R.M.S. aerial error</i>	$P\theta_1$ °/min
400	0.12	8.3 sec of arc	0.1
300	0.07	3.75 sec of arc	0.105
250	0.17	1.1 sec of arc	0.1

It can be seen that only the modulating servo natural frequency causes servo errors, and this could probably be cured by using a velocity feedback from the rollers. However, the high frequency at the turret, although not causing servo errors, is undesirable.

To eliminate this problem electrically via the servo motors would mean a servo bandwidth of 62.8 rad/sec and a corresponding large increase in peak torques to obtain the necessary amplitude at the turntable. The only reasonable solution, in fact, seems to be to apply a damping torque equal to $(T_s - T_f)$ at a velocity V_c . To do this, an extremely stiff gearbox would have to be used.

The possibility of such a negative friction characteristic existing would only be discovered at the trial erection.

<i>Conditions</i>	<i>Mode of behaviour</i>
(1) Input velocity—small	Modulated high frequency at turret and low frequency at aerial h.f. = 62.8 rad/sec l.f. Modulation 3 rad/sec (servo natural frequency)
(2) Input velocity—half V_o	High frequency at turret only
(3) Input velocity—equal to V_o	As (1), but superimposed on constant velocity
(4) V_o —small	Low frequency only

A table of maximum aerial errors for 3 values of T_s is given below:

Trial Erection

The telescope was complete with the exception of the dish and master equatorial unit, the latter being simulated by a mechanical measuring unit produced by A.E.I. The same servo equipment was used in azimuth and altitude.

Test showed:

- (1) No negative stiction friction characteristics.
- (2) Coulomb friction without weight of dish to be 44.5 tons/ft. Backlash: 5 sec of arc referred to load.
- (3) It was possible to control the telescope in both motions with the required servo gain.

The transient velocity feedback loop was unstable at 36 rad/sec (very little time was available to check the cause of this).

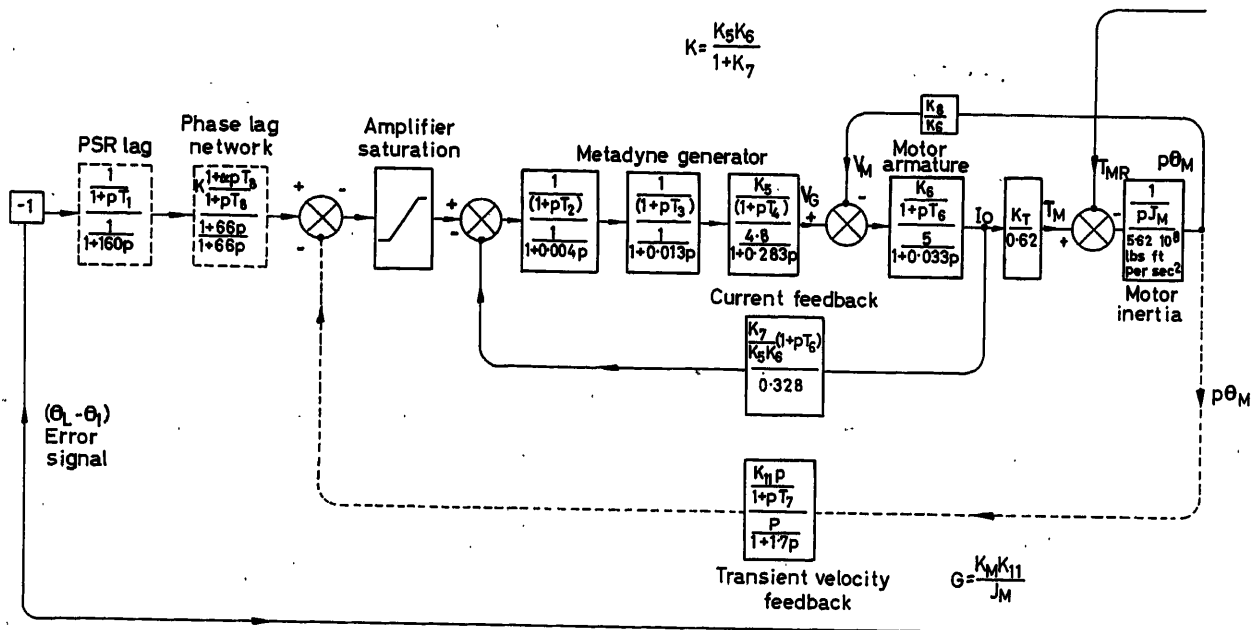


Figure 16(a)

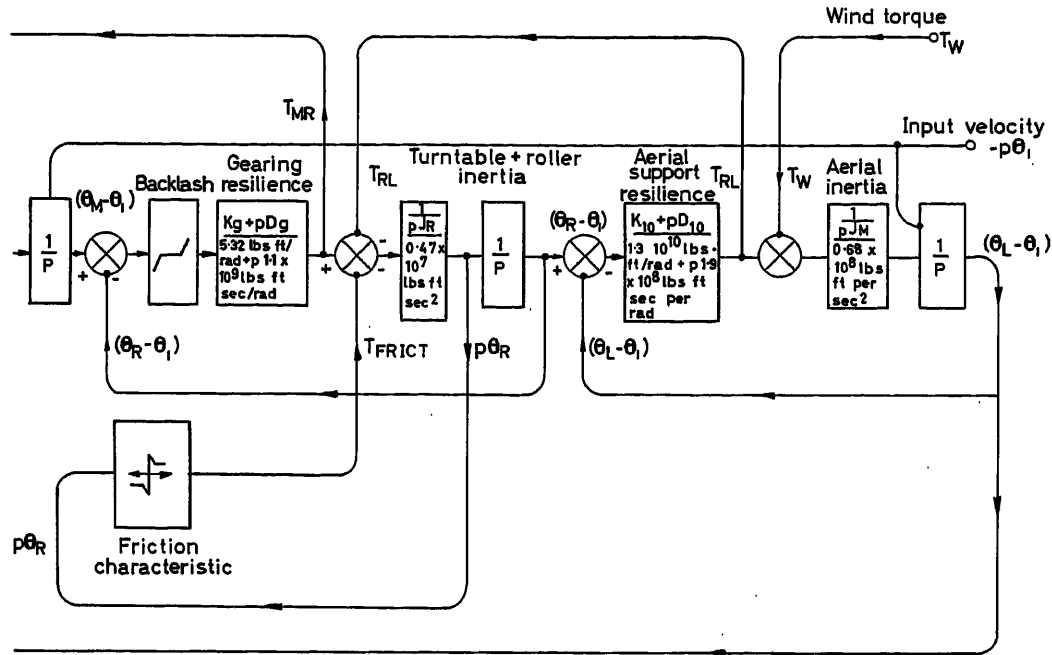


Figure 16(b)

Two possibilities existed:

- (1) Machine set stabilizing transformer wrongly set.
- (2) Additional backlash between motor and tacho. The transient velocity loop was replaced by using transient motor voltage feedback which included the velocity term plus a stabilizing current term.

Commissioning

Site commissioning in Australia confirmed all the previous findings with the exception of the 36 rad/sec oscillation of the velocity feedback loop. This was no longer present and could not be traced.

Coulomb friction figures were 60 tons/ft. in azimuth and 160 tons/ft. in altitude.

Final settings were:

	Azimuth	Altitude
Main loop gain	5.2×10^{10} lb.ft./rad	4.9×10^{11} lb.ft./rad
Velocity loop gain	6	6
Transient feedback network	$\frac{P}{1+10P}$	$\frac{P}{1+1P}$
Phase lag	$\frac{1+3P}{1+33P}$	$\frac{1+3P}{1+33P}$

It will be noted that in the altitude motion it has been possible to work at approximately twice the loop gain of the study with good damping. This was almost certainly due to the increase in value of coulomb friction.

In azimuth this was also possible at any particular altitude angle, but owing to the fact that azimuth loop gain varied with altitude angle, a smaller loop gain was accepted with consequent variation of damping at the extremes. Test records of the performance are given in Figure 17.

Appendix

Refer to Figure 3(c).

For the transient velocity case T_8 and $K_{12} = 0$, where K_8 = motor back e.m.f. and K_{12} = direct velocity feedback constant.

$$\frac{P\theta}{E} = \frac{K_1 K_M}{K_8} \frac{1 + PT_7}{1 + P \frac{(J + K_8 T_7 + K_{11} K_M)}{K_8} + \frac{JT_7 P^2}{K_8}}$$

if

$$(T_a + T_b) = T_7 + \frac{J + K_{11} K_M}{K_8}$$

and

$$T_a T_b = \frac{JT_7}{K_8} \quad (1)$$

then

$$\frac{P\theta}{E} = \frac{K_1 K_M}{K_8} \frac{1 + PT_7}{(1 + PT_a)(1 + PT_b)}$$

For velocity feedback plus phase lag $K_{11} = 0$.

$$\frac{P\theta}{E} = \frac{K_1 K_M}{K_8 + K_M K_{12}} \frac{(1 + \alpha PT_8)}{(1 + PT_8) \left(1 + \frac{PJ}{K_8 + K_M K_{12}}\right)} \quad (2)$$

The author thanks the following bodies for permission to publish this article: Executive of the Associated Electrical Industries Limited; Messrs Freeman Fox and Partners (Consultants); Commonwealth Scientific and Industrial Research Organization. In addition, acknowledgement is made of the assistance given by his colleagues on this project.

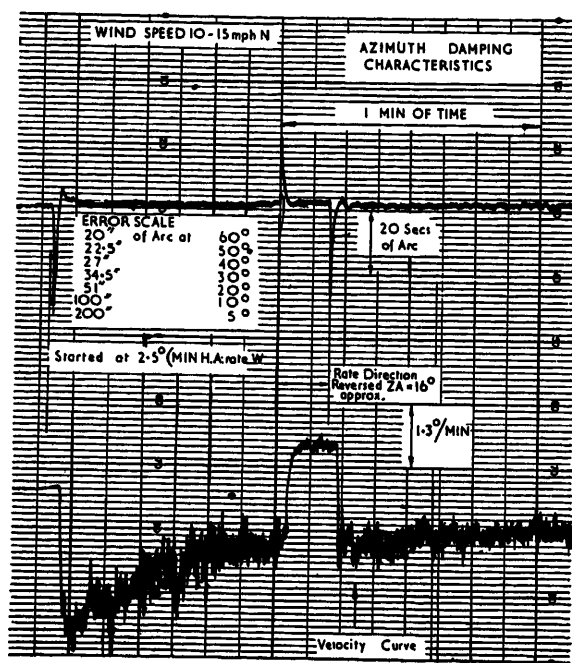


Figure 17(a)

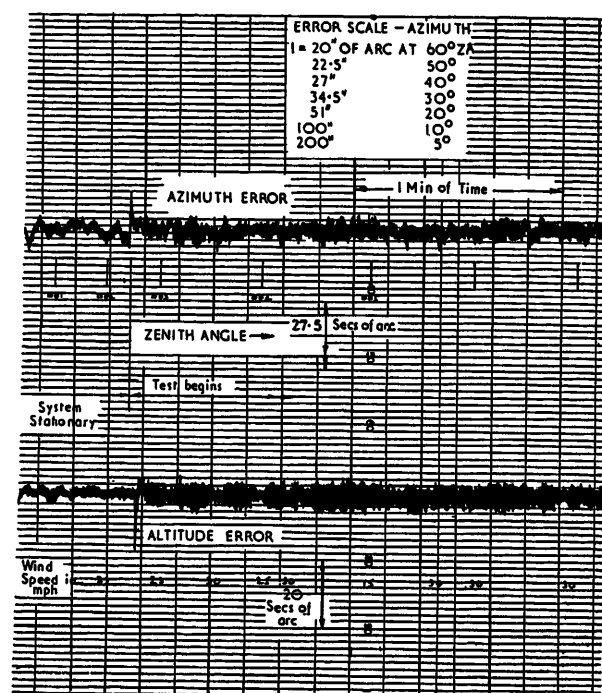


Figure 17(b)

Nomenclature

E	Total system pointing error
J	Total system inertia
K_M	Total machine set gain constant
K_1	Static amplifier gain constant
W_0	Undamped natural frequency of system
G	Loop gain of transient velocity feedback
K_5	Metadyne and generator constant
K_6	Armature circuit conductance (motor + output generator)
K_7	Current feedback constant in machine set
K_8	Velocity feedback constant due to motor back e.m.f.
K_9	Gearbox stiffness
K_{10}	Aerial turret stiffness
K_{11}	Transient velocity feedback constant
K_{12}	Direct velocity feedback constant
K_{13}	Effective stiffness of telescope
u	Number of P.S.R. filter stages
T_1	Time constant of P.S.R. filter
T_2	Time constant of metadyne input
T_3	Time constant of metadyne first stage
T_4	Time constant of output generator field circuit
T_5	Time constant of motor armature circuit
T_6	Time constant of stabilizing transformer feedback

T_7	Time constant of transient velocity feedback network
T_8	Time constant of phase lag network
α	Attenuation ratio of phase lag network
I_0	Generator set output current
I_i	Generator set input current
J_M	Motor inertia
J_R	Turntable roller inertia
J_L	Dish inertia
θ_1	Input position demand
θ_m	Motor position
θ_R	Turntable position
θ_L	Aerial dish position
ϵ	Position error of dish, $\theta_1 - \theta_L$
K_T	Motor torque constant
D_9	Gearbox damping
D_{10}	Aerial turret damping
T_M	Motor torque
T_W	Wind torque applied to aerial dish
T_S	Static friction torque
T_F	Rolling friction torque
T_{MR}	Torque transmitted by the gearbox
T_{RL}	Torque transmitted by the turret
p	d/dt

All inertias, stiffnesses, torques, etc. are referred to the load.

DISCUSSION

G. LIND, A. B. Bofors, Bofors, Sweden.

I want to ask a question concerning one detail only, namely the choice of the servo actuator for the antenna. Does not the author find it dangerous to use a commutating electrical machine close to a very sensitive radio telescope receiver?

R. G. WHEELER, in reply

Great care was taken to eliminate radio interference. (1) All d.c. machines had tuned filters designed into the ventilation covers. (2) All machines were encased in steel cylinders. (3) Special mesh screening material was used on all control cubicles. (4) All cables were kept short and screened. Finally, all equipment was placed behind the dish so that virtually no radio noise was picked up by the dish.

Dynamical Model for Fine Pointing Attitude Control of the Orbiting Astronomical Observatory*

R. E. ROBERSON

Summary

For the Orbiting Astronomical Observatory in its fine pointing mode, where extreme pointing accuracy is required, a number of complicating effects can be entirely neglected. These include the non-linear, time-variable, controlled-element dynamics, intermode coupling, external disturbances which are functions of orientation, residual internal angular momentum and reaction wheel misalignment. Thus the control system, and by inference a broad class of accurate systems, can be designed and analysed on the basis of a simple linear constant coefficient uncoupled dynamical model.

Sommaire

Pour le satellite dit Orbiting Astronomical Observatory il est possible, lorsqu'il exécute des visées de précision exigeant une grande finesse de pointage, de négliger entièrement nombre d'effets complexes. Il s'agit en particulier de la dynamique des organes à commande non-linéaire dépendant du temps, du couplage inter-modes, des perturbations extérieures fonction de l'orientation, du moment cinétique interne résiduel et du défaut d'alignement de la roue à réaction. Il en résulte que le système de commande peut être conçu et étudié en se fondant sur un simple modèle dynamique exempt de couplage, dont les équations sont linéaires avec des coefficients indépendants du temps. Il en est de même, par extension, de toute une classe de systèmes de précision.

Zusammenfassung

Für den Vorgang der Feineinstellung eines astronomischen Beobachtungssatelliten, der extreme Einstellgenauigkeiten verlangt, kann man eine Anzahl von Einflüssen, welche die Untersuchung erschweren, vernachlässigen. Hierzu zählen das nichtlineare, zeitveränderliche dynamische Verhalten der geregelten Größe, die gegenseitige Beeinflussung der Vorgänge (Kopplung), die äußeren Störungen (sie sind Funktionen der Orientierung), das restliche interne Drehmoment und die Fehleinstellungen der Stabilisierungsräder (reaction wheels). Somit lassen sich Regelungssysteme und daher auch eine große Zahl von genauen Systemen mit Hilfe eines einfachen linearen entkoppelten dynamischen Modelles mit konstantem Koeffizienten entwerfen und untersuchen.

Introduction

During the period of fine stabilization for the gathering of precise astronomical data, when attitude is to be held within 0.1 arc sec, attitude control of the Orbiting Astronomical Observatory is by means of fine reaction wheels operating from sensor information supplied by the experimenter's equipment and processed by a piecewise linear controller. It would be very desirable to be able to represent this control process by a simple

* This analysis was done for the Grumman Aircraft Engineering Corporation as a part of their NASA-supported work on the Orbiting Astronomical Observatory. Publication is with the kind permission of Grumman and NASA.

dynamical model. If it can be reduced to a set of three linear, constant coefficient, single input-single output, independent (i.e. uncoupled) subsystems, full advantage can be taken of the large existing body of techniques for the synthesis and performance analysis of this class of control devices.

It is known that a complete attitude control system description is not so simple. It generally involves non-linear and time-variable controlled element dynamics, intermode coupling, external disturbances depending both on time and orientation, and other factors which complicate the dynamical model. In addition, there are error sources such as residual internal angular momentum, wheel misalignments, and sensor quantization and noise. So if a simplified model is to be obtained, one must ignore all such troublesome effects. It seems particularly dangerous to do this in such an accurate system without ample justification for each simplification.

The purpose of this paper is to show that the desired simplifications in the dynamical model are legitimate. The complicating factors are examined one by one and the importance of each to the system model is assessed. It is shown that in the presence of the high gains necessary to assure the basic specification accuracy of the system, the growth of system error from all neglected and potentially dangerous terms can be completely disregarded. The only error of consequence is that of the sensor itself. Hence a simple and convenient linear dynamical model can be used and the idealizations assumed in controller design and control parameter selection are permissible ones. It is shown, specifically, that: (a) the complete system can be considered to consist of three independent modes, each with one degree of freedom; (b) the attitude error angle in each mode is simply the sensor angular error in that mode plus the time integral of the torque applied to that mode, the magnitude of the latter divided by the gain constant of the loop. [Symbolically, this is described by eqn (12).] A slightly more accurate description retains the time constant of the reaction wheel motor as shown in eqn (14). In either case, the form of the result is very simple, and focuses directly on the only significant parameters of the problem.

The Complete Model

Let x_1, x_2, x_3 be a set of right-hand orthogonal reference axes whose orientation is fixed in inertial space, x_1 along the line of sight to be observed in the Orbiting Astronomical Observatory (OAO) experiment. The remaining axes can be disposed in any convenient manner, e.g. x_2 in the plane of the equator. Let X_1, X_2, X_3 be a set of similar axes rigidly embedded in the vehicle frame, origin at the composite centre of mass of the vehicle and X_1 along the astronomical telescope axis. When the attitude control is perfect, $X_i \equiv x_i$ ($i = 1, 2, 3$). When there are attitude deviations of the body axes from the reference axes, define

deviation angles $\theta_1, \theta_2, \theta_3$ by a succession of three rotations of the frame x_i into the frame X_i as follows (see Figure 1):

- First rotation of x_1, x_2, x_3 through θ_3 about x_3 into x_1', x_2', x_3' ;
- Second rotation of x_1', x_2', x_3' through θ_2 about x_2' into x_1'', x_2'', x_3'' ;
- Third rotation of x_1'', x_2'', x_3'' through θ_1 about x_1'' into X_1, X_2, X_3 .

Let A_{ij} be the components of the direction cosine matrix relating the frames according to $X_i = A_{ij}x_j$. (The summation convention for repeated indices is used.) The A components can be derived, as required, from Figure 1.

Since the angular velocity of the x_i frame is zero, that of the X_i frame is

$$\bar{\omega} = (\theta_1 - \theta_3 \sin \theta_2) X_1 + (\theta_2 \cos \theta_1 + \theta_3 \sin \theta_1 \cos \theta_2) X_2 + (-\theta_2 \sin \theta_1 + \theta_3 \cos \theta_1 \cos \theta_2) X_3 \equiv \omega_i X_i \quad (1)$$

(The same symbol is used for an axis and the unit vector along that axis.)

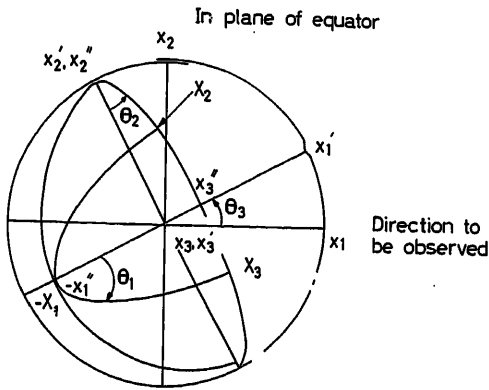


Figure 1. Rotation angles relating body axes X_1, X_2, X_3 to space reference x_1, x_2, x_3

Denote by K_{ij} the components of the inertia dyadic of the vehicle and all of its internal parts, resolved in the body frame. Body axes (control axes) are not necessarily principal axes, so that K_{ij} is not assumed diagonal. Let the total extra angular momentum of all internal parts relative to the frame be $\bar{H} = H_i X_i$ and let $\bar{L} = L_i X_i$ represent the total external torque on the vehicle.

It has been shown¹ that the input-output relationships for the controlled element dynamics are the three scalar differential equations

$$K_{ij}\dot{\omega}_j + \dot{K}_{ij}\omega_j + \varepsilon_{ijk}K_{kp}\omega_j\omega_p + \dot{H}_i + \varepsilon_{ijk}\omega_j H_k = L_i \quad (i=1, 2, 3) \quad (2)$$

The ε_{ijk} are the usual 'epsilon-symbols' of tensor analysis.

Detailed torque studies are beyond the scope of this work, but one must know the torque structure and have some feel for typical numerical values to be expected. In eqn (1) it is shown that a general form is

$$L_i = L_{i0}(t) + L_{ij}(t)\theta_j + \dots$$

where the L_{i0} are pure external torques independent of vehicle orientation, and the L_{ij} are effectively 'spring constants' against

the external torque, an outstanding example being the familiar gravity gradient effect. These 'springs' may be either stabilizing or destabilizing. In the above equation, higher order dependence on the dependent variables is ignored.

Grumman has shown by numerical studies that L_{i0} and L_{ij} are generally periodic in time with a fundamental frequency equal to orbital angular frequency, ω_0 , having a constant component and strong first and second harmonics. For present purposes it is general enough to use

$$L_{i0} = l_{i0} + T_i \sin(\omega_0 t - \phi_i), \quad L_{ij} = l_{ij} + \Delta L_{ij}(t) \quad (3)$$

where l_{i0}, l_{ij} are constants and ΔL_{ij} is the variable part of the spring constant after splitting out the mean value. Note that one excitation frequency suffices: after the response is found in terms of ω_0 , this parameter can be allowed to range over all harmonic frequencies using corresponding amplitudes. Since the model to be justified is linear, the total response is additive.

Typically, for this application the magnitudes of both l_{i0} and T_i may be assumed to be of the order of 1,000 dyn-cm, and actually should be within about a factor of two of this. In at least one case for which numerical data are available the constant part of the spring constant (i.e. l_{ij}) appears to be of the order of ± 10 dyn-cm/mr, but it is difficult to determine the periodic structure with any accuracy.

Control is achieved by making H_i in eqn (2) some suitable function of the measured attitude deviation angles. In simplifying the model the same parameter values are assumed for each mode (roll, pitch and yaw), but once the model is established it is simple to permit differences in the three channels. Let $\tilde{\theta}_i = \theta_i + \Delta\theta_i$ be the observed values of θ_i , with $\Delta\theta_i$ the sensor error. The values $\tilde{\theta}_2$ and $\tilde{\theta}_3$ are obtained in the fine pointing mode from the primary telescope while $\tilde{\theta}_1$ comes from a set of star trackers.

The internal angular momentum may contain components from sources other than reaction wheels but, if so, it is assumed to be constant (e.g. gyro angular momentum). Represent this part by h_{i0} . Let $h_i(t)$ be the angular momentum from the control wheel along the i th axis and denote by ζ_{ij} ($i \neq j$) a set of small misalignment angles for these wheel axes. Thus each H_i has the form

$$H_i = h_{i0} + h_i + \sum_{j \neq i} \zeta_{ij} h_j \quad (4)$$

In making subsequent numerical estimates, it is presumed that $h_{i0} \leq 10^7$ g cm²/sec.

It is not the purpose here to develop or to justify a particular control law relating h_i to $\tilde{\theta}_j$, but to make use of the functional relationship already chosen for this controller. It is of a straightforward linear type, in which the sensor signal is fed through a lead-lag network and the resulting error signal applied to a motor-driven reaction wheel. The reaction wheel for each mode has an input only from the attitude error in that mode; there is no intermode cross-feed. The transfer function which will be used is

$$h_i(s) = \left(\frac{1 + \tau_1 s}{1 + \tau_2 s} \right) \left(\frac{K \tau_m}{1 + \tau_m s} \right) \tilde{\theta}_i \equiv G(s) \tilde{\theta}_i \quad (5)$$

Any initial condition is to be absorbed into h_{i0} in eqn (4). Here τ_1, τ_2 are network time constants and $\tau_m (\gg \tau_1, \tau_2)$ is the motor time constant, while K is the control gain.

The results given above can be collected into a general dynamical model of the system. It has the form, in terms of Laplace transforms

$$B_{ij}\theta_j(s) = L_{i0}(s) + f_i(s) \quad (6)$$

where the B matrix elements are

$$B_{ij} = K_{ij}s^2 + \varepsilon_{ijk}h_{k0}s - \zeta_{ij} + sG(s) \begin{cases} 1 & (i=j) \\ \zeta_{ij} & (i \neq j) \end{cases} \quad (7)$$

and

$$\begin{aligned} f_i = & \mathcal{L}[K_{ij}(\ddot{\theta}_j - \dot{\omega}_j) + \varepsilon_{ijk}h_{k0}(\ddot{\theta}_j - \dot{\omega}_j) \\ & - \varepsilon_{ijk}K_{km}\omega_j\omega_m - \dot{K}_{ij}\theta_j + \Delta L_{ij}\theta_j] \\ & - sG(s)[\Delta\theta_i + \sum_{j \neq i} \zeta_{ij}\Delta\theta_j] \\ & - \varepsilon_{ijk}\omega_j(s) * G(s)(\zeta_{km} + \sum_{m \neq k} \zeta_{km})(\theta_m + \Delta\theta_m) \end{aligned} \quad (8)$$

with

$$\dot{\theta}_1 - \omega_1 \approx \dot{\theta}_3\theta_2; \quad \dot{\theta}_2 - \omega_2 \approx -\dot{\theta}_3\theta_1; \quad \dot{\theta}_3 - \omega_3 \approx \dot{\theta}_2\theta_1 \quad (9)$$

Here δ_{ij} is the Kronecker delta, \mathcal{L} denotes the operation of the Laplace transform from the time domain to the complex s domain (\mathcal{L}^{-1} its inverse), and $*$ represents the complex convolution [i.e. $f_1(s) * f_2(s)$ is the transform of the product $f_1(t)f_2(t)$].

Rationale of Analysis

In order to appreciate the implications of the control law and to identify significant parameters, consider a simple special case. Assume body axes are principal axes ($K_{ij} = 0$ for $i \neq j$), inertias are constant, all second order and error terms are neglected ($f_i = 0$), all $h_{i0} = 0$, as are the ζ_{ij} and L_{ij} . Then eqn (6) reduces to three independent equations, each of the form (not summed on i)

$$\theta_i(s) = \frac{1}{[K_{ii}s + G(s)]} \left[\frac{l_{i0}}{s^2} + \frac{\omega_0 T_i \cos \varphi_i}{s(s^2 + \omega_0^2)} + \frac{T_i \sin \varphi_i}{s^2 + \omega_0^2} \right] \quad (10)$$

The transient response from the zeros of $K_{ii}s + G(s)$ die out quickly. By elementary Laplace transform methods, the asymptotic response from the poles of the torque driving term is (to within coefficient errors in the trigonometric terms of the order of 10^{-4})

$$\begin{aligned} \theta_i(t) \sim & \frac{l_{i0}}{G_0} t + (\tau_2 + \tau_m - \tau_1 - K_{ii}/G_0) \frac{l_{i0}}{G_0} - \frac{T_i}{\omega_0 G_0} \cos(\omega_0 t + \varphi_i) \\ & + \frac{T_i}{\omega_0 G_0} \omega_0 (\tau_2 + \tau_m - \tau_1 - K_{ii}/G_0) \sin(\omega_0 t + \varphi_i) \end{aligned} \quad (11)$$

where $G_0 = G(0) = K\tau_m$. Typical parameter values for the OAO are $K_{ii} \approx 1.36 \times 10^{10}$ g cm² (their maximum difference being about 20 per cent of this), K_{ij} ($i \neq j$) $\approx 1.36 \times 10^9$ g cm², $\tau_1 = 10$ sec, $\tau_2 = 1$ sec, $\tau_m = 200$ sec. A value of $K = 2.25 \times 10^5$ dyn-cm/arc sec, giving $G_0 \approx 10^{13}$ dyn-cm sec/rad, assures that the system stays within 0.1 arc sec for 1 h in response to disturbance $l_{i0} = 10^3$ dyn cm. The linear term in eqn (11) is then dominant. Also $K_{ii}/G_0 \approx 10^{-3} \ll \tau_m$, so the result would be changed insignificantly if K_{ii} were to be omitted entirely. Eqn (11) emphasizes that control is strictly at the velocity level, so that a linear growth of error results from a constant torque.

The goal of this analysis is to show that for the general case described by eqns (6)–(9), an adequate simplified system model is

$$sG_0\theta_i = L_{i0} - sG_0\Delta\theta_i \quad (12)$$

all other terms in both B_{ij} and f_i having a negligible effect.

These effects are divided into two classes: Class 1, those entering through B_{ij} ; Class 2, those entering through f_i . The former can be studied using simple linear constant-coefficient differential equations and establishing bounds on the response. The second class is amenable to iterative procedures, much like the construction of a solution by Picard iteration but confining attention to the asymptotic behaviour and ignoring fine structure. Note that the effects to be investigated are deterministic: stochastic behaviour arises only in the sensor error, and the major term in which this appears is retained explicitly in eqn (12). It is felt sufficient to confine the investigation of Class 2 effects to second order terms in θ_i . The detailed analysis of both classes is given in Appendices I and II.

Results and Conclusions

The numerical results for the approximation errors contained in Appendices I and II are summarized in *Tables 1* and *2*. To within these errors, for parameter values typical of the present OAO system, one can replace the full set of equations for vehicle angular error [eqns (8)–(10)] by the much simpler, almost trivial set written as eqn (13). The block diagram corresponding to the latter is that of an elementary open-loop system as shown in *Figure 2*. The total error in the approximation is less than 0.01 arc sec = 0.1 θ_{\max} .

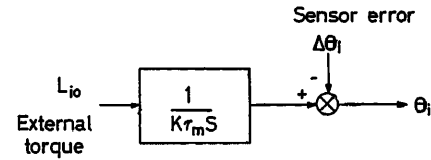


Figure 2. Simplest system representation

Table 1. Bounds on Class 1 errors

Source and magnitude	Bounds
Spring torques $l_{ij} \leq 10^4$ dyn cm/rad	$0.01 \theta_{\max}$
Internal angular momentum $h_{i0} \leq 10^7$ g cm ² /sec	$4 \times 10^{-11} \theta_{\max}$
Principal moments $K_{ii} = 1.36 \times 10^{10}$ g cm ²	$10^{-6} \theta_{\max}$
Products of inertia $K_{ij} = 0.1 K_{ii}$	$6 \times 10^{-10} \theta_{\max}$
Wheel misalignments $\zeta_{ij} \leq 10^{-2}$	$0.02 \theta_{\max}$
Time constants $\tau_1 = 10$ sec, $\tau_2 = 1$ sec, $\tau_m = 200$ sec	$0.04 \theta_{\max}$

Table 2. Bounds in Class 2 error driving terms

Term	Bound ($t \leq 1$ h)
$K_{ij}(\ddot{\theta}_i - \dot{\omega}_j)$	$1.5 \times 10^{-13} \theta_{\max}$
$\varepsilon_{ijk}h_{k0}(\ddot{\theta}_j - \dot{\omega}_j)$	$10^{-12} \theta_{\max}$
$\varepsilon_{ijk}K_{km}\omega_j\omega_m$	$2 \times 10^{-16} \theta_{\max}$
$K_{ij}\theta_j$	(assumed absent)
$\Delta L_{ij}\theta_j$	$(\Delta L_{ij} \max / 2L_{j0}) 10^{-6} \theta_{\max}$
$-sG(s)\zeta_{ij}\Delta\theta_j$	$3 \times 10^{-2} \theta_{\max}$
$-\varepsilon_{ijk}\omega_j(s) * G(s)\delta_{km}(\theta_m + \Delta\theta_m)$	$2 \times 10^{-12} \theta_{\max}$
$-\varepsilon_{ijk}\omega_j(s) * G(s)\zeta_{km}(\theta_m + \Delta\theta_m)$	$2 \times 10^{-14} \theta_{\max}$

One can remove the largest errors in the approximation and reduce error bounds to the order of $0.03 \theta_{\max}$ by using slightly more sophisticated equations. They still permit a decoupling of modes, but incorporate the motor transfer function rather than merely G_0 , effectively replacing $1/K\tau_m s$ in Figure 2 by $(1 + \tau_m s)/K\tau_m s$. The equations themselves are

$$\frac{s}{1 + \tau_m s} G_0 \theta_i(s) = L_{i0}(s) - \frac{s}{1 + \tau_m s} G_0 A \theta_i(s) \quad (13)$$

Appendix I—Class 1 Effects

General

Consider eqn (6) with $f_i = 0$. Let b_{ij} be the cofactor (signed minor) of B_{ij} and $B = \det(B_{ij})$. Then

$$\theta_i(s) = \frac{b_{ji}(s)}{B(s)} L_{j0}(s) \quad (14)$$

The character of the response depends mainly on the quotient b_{ji}/B , the exact form of $L_{j0}(s)$ not being of major consequence at this point.

The first step is to show that the effects of spring torques are inconsequential for realistic parameter values: the solution for $l_{ij} \neq 0$ is effectively that for $l_{ij} = 0$. The treatment must be general enough to encompass cases of instability, i.e. zeros of $B(s)$ in the right half-plane, since the spring torques may be destabilizing or stabilizing.

Spring Torque Effects

Examine B_{ij} given by eqn (7) and define A_{ij} by $B_{ij} = sA_{ij} - l_{ij}$. Denote by a_{ij} the cofactor of A_{ij} . It is straightforward to show that

$$B = s^3 A - s^2 \epsilon_{ijk} (l_{1i} A_{2j} A_{3k} + A_{1i} l_{2j} A_{3k} + A_{1i} A_{2j} l_{3k}) + s \epsilon_{ijk} (l_{1i} l_{2j} A_{3k} + l_{1i} A_{2j} l_{3k} + A_{1i} l_{2j} l_{3k}) - \det(l_{ij}) \quad (15)$$

$$b_{ji} = s^2 A_{ji} - s (l_{j+2, i+2} A_{j+1, i+1} + l_{j+1, i+1} A_{j+2, i+2} - l_{j+1, i+2} A_{j+2, i+1} - l_{j+2, i+1} A_{j+1, i+2}) + \text{cofactor } l_{ji} \quad (16)$$

where in the last equation the subscripts are to be read modulo 3.

Now

$$\mathcal{L} \left[\theta_i(t) - \mathcal{L}^{-1} \left(\frac{a_{ji}}{sA} L_{j0} \right) \right] = R_{ji}(s) L_{j0}(s) \quad (17)$$

where $R_{ij} = (b_{ij}/B) - (a_{ij}/sA)$. The accuracy with which the bracketed time function is zero depends on bounds on the time function $\mathcal{L}^{-1}(R_{ij} L_{j0})$. One can write R_{ij} as a power series in spring torques as

$$R_{ij}(s) = \frac{1}{sA(s)B(s)} [C_{kl}^{ij}(s) l_{kl} + O(l_{ij}^2)] \quad (18)$$

and each term of the series can be analysed separately. The second-order terms are of the order of 10^{-9} times the first order. This does not necessarily mean the corresponding time functions are in the same ratio, but in this case the general structure of the inverse transform is comparable for second- and third-order terms and one can conclude (proving rigorously, if desired) that only the first-order terms need be considered.

It suffices to give a few examples, the other terms being comparable and easily derived:

$$\left. \begin{aligned} C_{11}^{11} &= s^2 a_{11}^2 \\ C_{12}^{11} &= s^2 a_{11} a_{12} \\ C_{22}^{11} &= s^2 (a_{11} a_{22} - A A_{33}) \\ C_{11}^{12} &= s^2 a_{12} a_{11} \\ C_{12}^{12} &= s^2 a_{12}^2 \end{aligned} \right\} \quad (19)$$

The major features of the behaviour are illustrated by these terms.

With typical parameter values quoted previously, to an extremely high order of accuracy (coefficient errors less than about 10^{-9}) one can factor B into

$$B = A \left(s - \frac{l_{11}}{G_0} \right) \left(s - \frac{l_{22}}{G_0} \right) \left(s - \frac{l_{33}}{G_0} \right) \quad (20)$$

(The case where any of the l_{ii} vanishes can be included, though it changes some details. It merely decreases the value of the zero by another factor of about 10^{-9} .)

Now consider

$$\begin{aligned} \epsilon_{11}^{11}(t) &= \mathcal{L}^{-1} \left[\frac{l_{11} C_{11}^{11}}{sAB} \right] \\ &= \mathcal{L}^{-1} \left[\left(\frac{a_{11} l_{11}}{sA} \right) \left(\frac{a_{11} L_{10}}{sA} \right) \frac{s^3}{(s-l_1)(s-l_2)(s-l_3)} \right] \end{aligned} \quad (21)$$

where $l_i = l_{ii}/G_0 \approx 10^{-9}$. By direct inversion of $s^3/(s-l_1)(s-l_2)(s-l_3)$, it can be shown that the corresponding time function is $\delta(t)$ (Dirac delta function) to within an additive quantity less than $3 l_{\max} \exp(3 l_{\max} t)$ where $l_{\max} = \max[l_1, l_2, l_3]$. Thus the error in representing the inverse transform by $\delta(t)$ does not exceed about 3×10^{-9} for $t \leq 1$ h. At the same time, one recognizes that $\mathcal{L}^{-1}(a_{11} L_{10}/sA)$ is simply the roll response to a roll torque: it can be seen at once that it cannot exceed $1/2 \times 10^{-6}$ (0.1 arc sec) if specifications are to be met, and it is shown later to be approximated closely by $10^{-10} t$. The factor $\mathcal{L}^{-1}(a_{11} l_{11}/sA)$ should be within a factor of 10 of this, since l_{11} is no more than this factor greater than the expected external torque. It follows that $\epsilon_{11}^{11}(t) \leq 1.5 \times 10^{-8} \theta_{\max}$ where θ_{\max} is the specification value 0.1 arc sec.

As one further example, consider the $\epsilon_{22}^{11}(t)$ resulting from C_{22}^{11} . It can be written in the form

$$\begin{aligned} \epsilon_{22}^{11}(t) &= \mathcal{L}^{-1} \left\{ \frac{s^3}{(s-l_1)(s-l_2)(s-l_3)} \left[\left(\frac{a_{11} L_{10}}{sA} \right) \left(\frac{A_{31} A_{13}}{sA} l_{22} \right) \right. \right. \\ &\quad \left. \left. + \left(\frac{a_{12} L_{10}}{sA} \right) \left(\frac{A_{12} A_{33}}{sA} l_{22} \right) + \left(\frac{a_{13} L_{10}}{sA} \right) \left(\frac{A_{13} A_{33}}{sA} l_{22} \right) \right] \right\} \quad (22) \end{aligned}$$

Much the same argument is followed as before. In order to establish bounds on such terms as $A_{13} A_{31} l_{22}/sA$, one needs the zeros of A . It can be shown that A can be factored into $(K'_{11}s + G)(K'_{22}s + G)(K'_{33}s + G)$ with the K'_{ii} within about $2\frac{1}{2}$ per cent of the values of K_{ii} . Each factor is a cubic which can be factored directly to find zeros very near $s = -1/\tau_1$, $s = -0.45 \pm i 5.5$.

By direct evaluation,

$$\begin{aligned} |g_1(t)| &= |\mathcal{L}^{-1} G_0 / s (K'_{33} s + G)| \leq 680 \\ |g_2(t)| &= |\mathcal{L}^{-1} A_{13} / (K'_{11} s + G)| \leq 1/2 e^{-0.45t} \\ |g_3(t)| &= |\mathcal{L}^{-1} A_{31} / (K'_{22} s + G)| \leq 1/2 e^{-0.45t} \end{aligned}$$

If $g_4(t) = \int_0^t g_2(t-\tau) g_3(\tau) d\tau$, it follows that

$$\begin{aligned} \left| \mathcal{L}^{-1} \frac{A_{13} A_{31} l_{22}}{A} \right| &\leq \frac{l_{22}}{G_0} \int_0^t |g_4(t-\tau)| |g_1(\tau)| d\tau \\ &\leq 680 \times 10^{-4} \int_0^t 0.25 |\tau e^{-0.45\tau}| d\tau \leq 10^{-6} \end{aligned}$$

It is shown later that such factors as $a_{12} L_{10} / sA$ contribute less than 10^{-2} of the value of $a_{11} L_{10} / sA$, from which it can be established that other terms in $\varepsilon_{22}^{11}(t)$ are down by this factor from the term just evaluated. That is,

$$\varepsilon_{22}^{11}(t) \leq 3.6 \times 10^{-3} \theta_{\max}$$

One can explore the remaining terms in eqn (18), but the above examples illustrate all of the important situations which arise. The only significant terms are the three in each channel having the form C_{ij}^{11} , so that the right-hand side of eqn (17) is bounded by $10^{-2} \theta_{\max}$. It can therefore be considered equal to zero for the purpose of establishing the effect of spring terms at the 0.1 arc sec level of accuracy.

Other Class 1 Effects

The implication of the analysis above is that

$$\theta_i(s) = \frac{a_{ji}(s)}{A(s)} L_{j0}(s) \quad (23)$$

for practical purposes. Consider now the response to the specific torque structure postulated in eqn (3). The zeros of $A(s)$ have been established to be far enough into the left half-plane that the transient response from them dies out within a few seconds, so that their behaviour is of no operational consequence. Therefore, only the portion of the response corresponding to the poles of $L_{j0}(s)$ need be considered. It is easy to evaluate it directly, using the conventional partial fraction expansion. Introducing the matrix Z_{ij} whose diagonal elements are unity and off diagonal elements are $-G_{ji}$,

$$\begin{aligned} \theta_i(t) &= Z_{ij} \left[\frac{l_{j0}}{G_0} t + \left\{ \frac{l_{j0}}{G_0} (\tau_m + \tau_2 - \tau_1) + \frac{T_j \cos \phi_j}{\omega_0 G_0} \right\} \right. \\ &\quad \left. - \frac{T_j}{\omega_0 G_0} \cos(\omega_0 \tau + \phi_j) + \frac{T_j}{G_0} (\tau_m + \tau_2 - \tau_1) \sin(\omega_0 \tau + \phi_j) \right] \quad (24) \end{aligned}$$

Except for the presence of the Z_{ij} constant matrix, eqn (24) gives the same result as the simple example leading to eqn (11) to within about one part in 10^4 . The effects of internal angular momentum and products of inertia terms do not show up at all at the level of accuracy of concern here. The presence of ζ_{ij} from wheel misalignments merely means that an error in one channel can be carried into another, but it is attenuated by a factor of $\zeta_{ij} \approx 10^{-2}$. Thus peak error from disregarding the ζ_{ij} remain less than 0.002 arc sec in each channel and one can simply put $Z_{ij} = \delta_{ij}$. Finally, K_{ii} does not show up at all in the dominant term of the response and contributes insignificantly to the smaller terms, so it can be omitted from the transfer function

without causing an error greater than 10^{-7} arc sec. The parameters τ_1 , τ_2 , τ_m do have some effect on these smaller terms, but even so, they can contribute no more than 8×10^{-8} arc sec which can be ignored relative to 0.1 arc sec. It can be established easily that although the estimates above have been based on a low frequency disturbance (at orbital rate), the conclusions are not changed if it is a high frequency vibration type disturbance instead. (Table 1 summarizes the errors.)

In conclusion, there is negligible error in the response to constant or oscillatory external torques if in eqn (6) one simply sets $B_{ij} = sG_0 \delta_{ij}$, and the resulting angular error is just

$$\theta_i(t) \sim \frac{l_{i0}}{G_0} t \quad (25)$$

The conclusions drawn from the analysis of Class 1 effects are not sensitive to changes in vehicle parameters or time constants (except insofar as τ_m affects G_0). The parameter of real importance is the effective gain parameter $G_0 = K\tau_m$.

Appendix II—Class 2 Effects

Consider the system

$$sG_0 \delta \theta_i(s) = f_i(s) \quad (26)$$

where the f_i are given by eqn (8) and the portion of $\theta_i(t)$ resulting from f_i is denoted $\delta \theta_i$, the notation $\theta_i(t)$ being reserved for just the response to $L_{i0}(t)$. Clearly

$$\delta \theta_i(t) = \frac{1}{G_0} \int_0^t f_i[\theta_j(t) + \delta \theta_j(t), t] dt \quad (27)$$

where the notation indicates the dependence of the $f_i(t)$ on the dependent variables themselves. Although the degree of approximation of the result cannot be established *a priori* in general terms, the form of eqn (27) strongly suggests that since $\delta \theta_j \ll \theta_j$ (conjectured at this point, and to be shown in the sequel) one can obtain an excellent measure of $\delta \theta_i$ simply from

$$\delta \theta_i(t) = \frac{1}{G_0} \int_0^t f_i[\theta_j(t), t] dt \quad (28)$$

In particular, it should suffice to use, under the integral, just the asymptotic form of $\theta_j(t)$ given by eqn (25).

The estimation can be illustrated by a few examples. Consider first the term $-sG(s) \Delta \theta_i$, which is in a somewhat different category from the others. A more precise model of the response to this term that can be obtained from eqn (26) is $sG(s) \theta_i(s) = -sG(s) \Delta \theta_i$, so it is evident that the contribution to $\theta_i(t)$ is simply $\Delta \theta_i(t)$, unmodified by any system transfer characteristics. It follows that in order to get the same response in the simplified model the term $-sG(s) \Delta_i$ must be replaced in the equation by $-sG_0 \Delta \theta_i$. This is the justification for the form of the sensor error driving term which appears in eqn (12).

In the case of the term $[K_{ij}(\dot{\theta}_j - \dot{\omega}_j)]$ one can write the $\delta \theta_1(t)$ contribution as

$$\begin{aligned} \delta \theta_1(t) &\leq \frac{1}{G_0} \int_0^t |\mathcal{L}^{-1} \mathcal{L} K_{1j}(\dot{\theta}_j - \dot{\omega}_j) \dot{\omega}| dt \\ &\leq \frac{1}{G_0} \int_0^t \left\{ \left| K_{11} \frac{d}{dt} \theta_2 \theta_3 \right| + \left| K_{12} \frac{d}{dt} \theta_1 \theta_3 \right| + \left| K_{13} \frac{d}{dt} \theta_1 \theta_2 \right| \right\} \\ &\leq 1.5 \times 10^{-3} \int_0^t |\dot{\theta}_{\max}|^2 dt \leq 1.5 \times 10^{-13} \theta_{\max} \end{aligned}$$

The next few terms of f_i can be analysed in the same way, to get the first entries in Table 2. In the case of $-sG(s)\zeta_{ij}\Delta\theta_j$, one uses the fact that $\Delta\theta_j \leq \theta_{\max}$, or one cannot meet the specification in general, and also uses the more exact $sG(s)\theta_i$ for the left-hand side of the equation as in the analysis of the $-sG(s)\Delta\theta_i$ term above.

The response to terms of the form $\omega_j * G(\theta_m + \Delta\theta_m)$ can be bounded by

$$\int_0^t dt \int_0^t dt |\theta_m(t-\tau) + \Delta\theta_m(t-\tau)| |\omega_j(\tau)| \mathcal{L}^{-1} \frac{G(s)}{G_0} \leq 2\theta_{\max} \int_0^t dt \frac{2\tau_1}{\tau_2 \tau_m} \left(\frac{L_{i0}}{G_0} \right)^2 t \leq 10^{-12} \theta_{\max}$$

and similarly for the other terms of the same general type.

Inspection of the table shows that aside from the sensor error which already has been split out, none of the terms in f_i need be considered.

Conclusions

In this approximation two-thirds of the residual errors are from wheel misalignments, which have been estimated liberally at 0.5°. The remaining third is from spring torque L_{i0} . Sensor errors cannot be neglected in eqns (13) and (14), but are essentially unmodified by vehicle dynamics.

The simplest closed loop representation of each mode is shown in Figure 3 with the motor transfer function as shown, or

replaced simply by unity in the approximation represented by eqn (13). But to neither order of approximation does the moment of inertia k_{ii} have any effect on the result with presently envisioned gain constants.

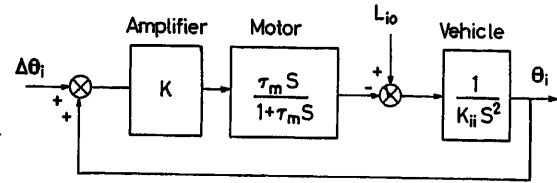


Figure 3. Representation of improved approximation

All remaining error effects of both Class 1 and Class 2 are completely negligible. The conclusions are essentially independent of vehicle parameters, depending almost exclusively on the ratio of applied torque to effective gain constant. Thus, the same general conclusions will apply to any high accuracy attitude control system for which $L_{i0}/G_0 \ll 1$. There has been no attempt in the present study to establish how inaccurately the attitude angles may be held without vitiating the approximations which have been made.

References

- ROBERSON, R. E. Origin and treatment of nonlinearity and parametric excitation in satellite attitude dynamics. *Symp. Nonlinear Oscillations*. Sep. 1961. Kiev

DISCUSSION

R. CANNON, *Stanford University, U.S.A.*

Professor Roberson's many early contributions to attitude control dynamics are well known for their comprehensiveness and generality. It is thus especially pleasing now to have from him the present paper which considers a very particular mission in detail.

The mission chosen for analysis in this paper is of special interest because it represents an extreme in precision contemplated for space vehicle attitude control. The results presented vindicating rigorously the great simplification granted by analysis on a single axis basis are thus certainly of considerable value to those associated with the OAO.

There are, in addition, quite a number of other scientific satellites contemplated for which the accuracy requirements are not so stringent (the orbiting solar observatory is an example). The next task is thus to establish the bounds for which the simplification applies (in varying degrees perhaps). If Dr. Roberson will thus generalize his work it will, I believe, be of considerably wider interest.

It is implied in the paper that a steady external torque must lead to a continuously increasing error. I should like to ask whether this is not merely a property of the model the author has chosen, while in the actual system auxiliary equipment will bound the steady-state error.

R. E. ROBERSON, *in reply*

As to the first question, generalization does not seem possible to a significantly varied class of control systems, torques and accuracy specification. Within the present framework it is possible to investigate the effect of lower gain constant while keeping other characteristics about the same and it can be shown that a similar model simplification can be made even if the attitude errors are considerably greater than 0.01 sec arc. However, I feel that the effects shown to be negligible here can be of definite importance when attitude errors become greater than about 1 degree, and that a single axis model can sometimes lead to grossly inaccurate conclusion in that case.

In answer to the second question, the fine pointing mode error does indeed grow linearly with time (asymptotically) in response to constant torque. However, when the specification limit is exceeded a coarse pointing mode becomes effective which has a different control law to limit further growth.

Basic Response Relations for Satellite Attitude Control Using Gyros*

R. H. CANNON, Jr.†

Summary

General response relations are presented for space vehicle attitude control using gyros for momentum exchange. Then the relations are specialized for each of two classes of application: (1) fast (1 c/sec), precise (1 arc sec) control, and (2) semi-passive damping of the (slow) natural motions of a gravity-orientated satellite. Within class (1) the control arrangement depends upon whether high quality gyros are to be used. Gyro pairs are assumed for simplicity, and basic relations between physical and control parameters and system performance are presented. The two classes of gyro systems are compared with corresponding reaction wheel systems.

Sommaire

On présentera les relations générales de réponse relatives à la commande de l'attitude d'un véhicule spatial à l'aide d'un système utilisant des gyroscopes pour l'échange des moments. Ces relations seront ensuite particularisées en vue de leur application à deux genres de commandes: (1) Commande rapide (1 Hz) et précise (1 arc-sec) et (2) Commande à amortissement semi-passif des mouvements naturels lents d'un satellite orienté par gravité.

Pour les commandes de la première catégorie, la disposition du système varie suivant que l'on recourt à des gyroscopes de haute qualité ou non. Pour simplifier, on supposera qu'il y a des paires de gyroscopes et l'on présentera les relations fondamentales reliant les paramètres physiques, les paramètres du système de commande et les performances de ce dernier. Les deux catégories de commandes à gyroscopes seront comparées avec les commandes correspondantes utilisant des roues à réaction.

Zusammenfassung

Dieser Aufsatz enthält allgemeine dynamische Beziehungen für die Lageregelung von Raumfahrzeugen, die Kreisel zum Aufbringen von Impulsen zur Stabilisierung verwenden. Dann werden die Beziehungen speziell auf die beiden Fälle angewendet: 1. schnelle und präzise Regelung (1 Hz, 1 Winkelsekunde) und 2. quasi-passive Dämpfung der langsamen Eigenbewegungen bei schwerkraftorientierten Satelliten. Bei der erstgenannten Art hängt die Reglerschaltung davon ab, ob Präzisionskreisel Verwendung finden. Zur Vereinfachung werden Kreiselpaare angenommen. Die grundlegenden Zusammenhänge zwischen physikalischen und Regelgrößen und den Systemeigenschaften werden dargestellt. Die beiden Arten der mit Kreisel ausgerüsteten Systeme werden mit den entsprechenden, mit „Stabilisierungsrädern“ ausgerüsteten Anordnungen verglichen.

Introduction

The role played by momentum exchange devices—such as reaction wheels, gyros, or a reaction sphere—in systems for controlling the attitude of space vehicles has been dealt with¹, and

some basic relations between physical parameters and system response developed for reaction wheel systems^{2,3}. The purpose of the present paper is to present companion relations for systems employing single-axis gyros, and to compare the two methods of control.

For illustration, two very different operational circumstances are considered: (1) fast, precise control to an inertial reference, and (2) semi-passive damping of the natural motions of a local-level satellite stabilized by gravity gradient. The first system has, typically, a natural period of a few seconds, while the period of the second system is of the order of the time for an orbit, e.g., $1\frac{1}{2}$ to 12 h.

Gyros were used for vehicle torquing about 1899 by Brennan, and others, who stabilized monorail cars with them. A 1903 British patent issued to Brennan describes a twin gyro arrangement.

The concept of using gyros for momentum exchange in space vehicle control is described in a patent filed in 1936 by Goddard⁴. Some relations for control-moment-gyro stabilization of ballistic missiles were given by Johnson⁵. The general dynamic equations are summarized by Roberson⁶. The use of gyros in pairs (to provide momentum vector control precisely along a single axis) is proposed by Haeussermann⁷.

The use of gyros for precision control to an inertial reference has been explored experimentally by two groups at Ames Research Centre during the past three years, with excellent results. One group, under J. S. White, has used gyros of inertial guidance quality in a special deployment which provides good decoupling of axes for small gyro motions. The special deployment is due to S. Godet, and an analysis of its three-axis gyroscopic coupling is given by Cannon⁸. These experiments were made on a three-axis gas-bearing table simulating the Orbiting Astronomical Observatory (OAO). The results of the work of White's group, together with an analysis of their system, has been published⁹.

Another group at Ames Research Centre, under J. R. Havill, has used non-floated gyros in pairs to control a three-axis Apollo simulator. (The gyro systems were made by Ling-Tempco-Vought and are described¹⁰.) Gyro gimbal feedback was used to overcome gyro drift. These experimental results are also reported¹⁰. In both the OAO and Apollo experiments precision control was achieved to between 0.1 and 1 arc sec, using optical sensors, and system speed of response was between 0.1 and 1 c/sec. Gas jet back-up was used. In the Apollo system the gyro pairs were also arranged in the Godet configuration, and it was found possible to remove power from a gyro spin motor and let it coast without disturbing control precision.

The use of damped, single-axis gyros to furnish semi-passive damping in satellites which are gravity-gradient stabilized to the local vertical was suggested by Scott¹¹ in November, 1960,

* Based on research supported by a grant to Stanford University by the National Aeronautics and Space Administration.

† Professor of Aeronautics and Astronautics, Stanford University.

and has also been considered for some time by members of the MIT Instrumentation Laboratory (see below). Scott's configuration, which has been studied extensively at Lockheed, provides three-axis damping, using two gyros, one of which has its gimbal axis along the vehicle yaw axis, and another with its gimbal axis between the vehicle pitch and roll axes.

Another, more symmetrical two-gyro system for damping is proposed by Burt¹². In this basic configuration the gimbal axes of both gyros are along the vehicle roll axis. The gyro spin axes are deployed by equal angles (e.g., 50°) one above and one below the vehicle pitch axis (which, in turn, coincides nominally with the orbit vector). The gyros are prevented from collapsing to the orbit vector by bias torques applied to their gimbals (via springs, or electrically). Changes in vehicle pitch velocity are damped by counter rotation of the gyros, and roll-yaw motions are damped by joint rotation of the gyros as one. A three-axis model of this system is in operation at the Royal Aircraft Establishment.

A number of 'Vee' arrangements (including the possibility of using only one gyro for three-axis damping) are described, the general physical concepts involved in using gyros semi-passively to damp the natural motions of satellites is reviewed^{13, 14}, and studies of a number of configurations at MIT by DeLisle, Hildebrandt, Ogletree, *et al.*¹⁵ are reported. Additional studies are described by Kennedy^{16, 17}.

In the present paper, in order to compare the extremes of precision control on the one hand, and simple damping of motions due to gravity gradient on the other, basic relations are presented for one system of each type, and comparisons are then made with reaction wheel systems. Specifically, a pair of gyros is presumed, for ease of analysis, and the general system response relations derived. Next, these relations are specialized for the two cases considered. A detailed outline is given at the end of the next section.

The present paper is confined to single-axis behaviour. This is justified in the case of the precision, inertial-reference system by the almost total decoupling provided by the gyro pair (as shown later), and it is justified for the local-level system by the fact that pitch motions do not couple into roll-yaw and, for small angle disturbances, roll-yaw motions do not couple into pitch.

System Dynamic Equations: Single Axis*

Figure 1 shows a space vehicle which is considered to move about its pitch axis ($\bar{2}$ axis) only. Change in pitch attitude from the reference attitude is denoted by θ . The vehicle contains a pair of single-axis gyros whose gimbals are free to move about the $\bar{1}$ axis of the vehicle, and the gyros are geared together so that their gimbals rotate through equal and opposite angles, ϕ . Angle ϕ is so defined that when the spin axes of the gyros point one along the $\bar{3}$ axis of the vehicle and the other along the $-\bar{3}$ axis, ϕ is 0. It is further assumed that the reference rotates at a constant angular velocity, n , about the $\bar{2}$ axis.

Complete System

The first equation of motion is obtained by considering the entire system (vehicle plus gyros), and writing Newton's law

* Three-axis dynamic equations for a vehicle with gyros are given⁸.

in the vehicle coordinate system:

$$\dot{\bar{H}} = \bar{H} + \bar{\Omega} \times \bar{H} = \bar{M} \quad (1)$$

in which $\bar{\Omega}$ is the angular velocity of the vehicle. The result is

$$I_2 \ddot{\theta} + 2h\dot{\phi} \cos \phi = L_2 - I_2 \omega_2^2 \sin \theta \cos \theta \quad (2)$$

in which h is the spin angular momentum of one gyro, and L_2 is external disturbing torque. The last term is the torque due to gravity gradient. (I_2 is vehicle moment of inertia and ω_2 is the vehicle natural frequency due to gravity gradient.)

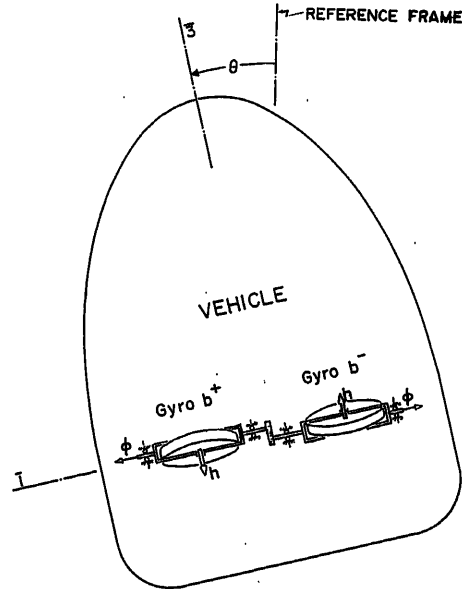


Figure 1. Gyro pair for controlling attitude

Gyros

Next, consider each of the two gyros as a separate isolated system and find, from (1):

$$[\dot{\bar{H}}^{+Gyro}]_1 = J\ddot{\phi} - (h \cos \phi)(\dot{\theta} + n) = T_+ + T_{gear} \quad (3a)$$

$$[\dot{\bar{H}}^{-Gyro}]_1 = -J\ddot{\phi} + (h \cos \phi)(\dot{\theta} + n) = T_- + T_{gear} \quad (3b)$$

Equations (3a) and (3b) can be subtracted from one another to give (after dividing by 2) the dynamic equation for the pair of gyros:

$$J\ddot{\phi} - (h \cos \phi)(\dot{\theta} + n) = T \quad (4)$$

in which

$$T \triangleq \frac{T_+ - T_-}{2}$$

Torques T_+ and T_- are torques exerted between the vehicle and each of the gyro gimbals. Torque T_{gear} is the torque exerted between the gyro gimbals (i.e., the torque exerted by one gyro on the other). The latter cancels out in eqn (4) for the pair of gyros, so that T is simply the effective control torque applied to the pair of gyros by the control system.

† $\dot{\bar{H}}$ connotes the total derivative, $d\bar{H}/dt$, and \bar{H} connotes the partial derivative, $(\partial \bar{H} / \partial t)_{\Omega=0}$, when the coordinate frame is considered non-rotating.

Small Motions

To facilitate studying the stability and small motion behaviour of the system in Figure 1, consider small perturbations in motion about the condition that $\theta = 0$ and $\phi = \phi$. That is, let $\sin \theta = \theta$, and let $\phi = \phi + \varphi$ in which ϕ is a constant, nominal gyro gimbal angle. Then the equations become linear, and can be Laplace transformed as follows (the subscript is dropped from L and I at this point):

$$(s^2 + \omega_2^2)\Theta = \frac{\mathcal{L}}{I} - \frac{2h \cos \phi}{I} s\Phi + s\theta(0) + \dot{\theta}(0) \quad (5)$$

$$s^2\Phi = \frac{\mathcal{T}}{J} + \frac{h \cos \phi}{J} \left[s\Theta + \frac{n}{s} - \theta(0) \right] - \frac{hn \sin \phi}{J} \Phi \quad (6)$$

in which Θ , Φ , \mathcal{L} , and \mathcal{T} are the Laplace transforms of θ , φ , L , and T .

Control

The control torque, T , is made up of components T_θ and T_ϕ based on sensing of both θ and ϕ , as well as a bias torque T_n , designed to cancel the gyroscopic torque $h \cos \phi$ in eqn (6), and an uncertainty torque U , acting between the gyro gimbal and the vehicle:

$$T = T_\theta + T_\phi + T_n + U \quad (7a)$$

Control torque T_ϕ is intended to include physical spring and damping torques depending upon ϕ , if such exist.

Assume that both a rate gyro and an attitude sensor are employed and that integral control of θ is included, giving the following expression for T_θ :

$$T_\theta = (h \cos \phi) [K_\theta (\dot{\theta} + \gamma_r) + K_\theta \theta + K_i \int \theta dt] \quad (7b)$$

γ_r is the drift rate of the rate gyro, if used.

Assume also that, in general, both rate and position feedback may be used around the gyro gimbal angle. These may be electrical or mechanical (viscous damper and spring), or both. Then T_ϕ is given by:

$$T_\phi = -(h \cos \phi) [b\dot{\phi} + k\phi] \quad (7c)$$

Let the uncertainty torque on the gyro gimbals, U , be a steady torque corresponding to an effective gyro drift rate of γ : $U = (h \cos \phi) \gamma$.

† The constant, $h \cos \phi$, is included here and in (7c) merely because it simplifies later expressions. When a gimbal spring is used, ϕ is assumed to be the spring null position.

Response Functions

From eqns (5), (6) and (7), the response functions for vehicle motion θ , and for gyro motion φ , are:

$$\boxed{\text{Eqn (8), (9)}}^*$$

in which

$$\lambda^2 = \frac{2h^2 \cos^2 \phi}{IJ}$$

which is a nutation frequency, as will be seen.

Outline of Investigation

Three specific systems have been selected, as tabulated in Table 1, to illustrate two very different control situations which are of practical interest. The first two systems are for precision control to an inertial reference by (A1) semi-passive† means (no sensors or control loops), and (A2) active means using attitude sensing. The third system (B) is for furnishing damping to a vehicle which is gravity gradient stabilized to local level. This system is also semi-passive.

For each system the general response function is obtained, and dynamic characteristics and response to gyro drift, initial conditions, and disturbances dealt with. In addition to the systems shown in Table 1, studies are also presented of the effects of a gimbal restoring spring, and the use of rate gyros in the control system. A typical power calculation is also given.

Finally, the present results are compared with corresponding values for reaction-wheel systems.

It should be stated that the present paper intends primarily to demonstrate basic response features and to compare systems. To this end a number of simplifying assumptions have been made, such as $n = \text{constant}$, identical gyros, perfect alignment, etc. For an analysis of system errors these assumptions would have to be dropped.

Behaviour of Precision System Controlled to an Inertial Reference

First consider the situation that it is desired to control a space vehicle very precisely to an inertial reference, as is often the case for scientific satellites such as the Orbiting Astronomical Observatory. In some cases it is required that the vehicle attitude be maintained within 10^{-6} rad.

† The term 'semi-passive', rather than 'passive', is commonly used because power will be involved in spinning the gyro wheel.

* Eqn (8):

$$\Theta = \frac{\left(s^2 + \frac{b}{J}s + \frac{k + hn \sin \phi}{J} \right) \left[\frac{L}{I} + \dot{\theta}(0) + s\theta(0) \right] - \lambda^2 [\gamma - s(1 + K_\theta)\theta(0) + K_\theta \gamma_r]}{(s^2 + \omega_2^2) \left(s^2 + \frac{b}{J}s + \frac{k + hn \sin \phi}{J} \right) + \lambda^2 s \left[(1 + K_\theta)s + K_\theta + \frac{K_i}{s} \right]} \quad (8)$$

Eqn (9):

$$\Phi = \frac{\frac{h \cos \phi}{J} \left[(1 + K_\theta)s + K_\theta + \frac{K_i}{s} \right] \left[\frac{L}{I} + \dot{\theta}(0) + s\theta(0) \right] + \frac{h \cos \phi}{J} (s^2 + \omega_2^2) \left[\frac{\gamma}{s} - (1 + K_\theta)\theta(0) + K_\theta \frac{\gamma_r}{s} \right]}{(s^2 + \omega_2^2) \left(s^2 + \frac{b}{J}s + \frac{k + hn \sin \phi}{J} \right) + \lambda^2 s \left[(1 + K_\theta)s + K_\theta + \frac{K_i}{s} \right]} \quad (9)$$

For such missions attitude would be controlled by a combination of a momentum storage system, such as reaction wheels or control-moment gyros, backed up by a momentum expulsion system, such as gas jets¹. Here one is only concerned with the use of the gyro system in *Figure 1* for precision momentum storage, and it is assumed that whenever gimbal angle ϕ exceeds a set limit, momentum will be expelled from the vehicle-gyro system independently by the firing of a discrete gas jet impulse. (The ability of the control system to maintain attitude during such impulses may, in fact, constitute a key design problem.)

For an inertially-orientated vehicle the angular velocity, n , of the reference system is 0 and gravity gradient acts as a disturbance rather than a spring, so that ω_2 is 0. Also, for control to an inertial reference, the nominal value of ϕ will commonly be 0 ($\phi = 0$). These omissions simplify eqns (8) and (9) considerably.

Semi-passive Control

In a semi-passive system both the viscous damping and spring on the gyro gimbal are admitted, but there are no control feedbacks. Here the gimbal spring is also omitted. This simple system turns out to be quite attractive for short-term stabilization of vehicle attitude. More generally, it represents the situation that the attitude reference is temporarily lost.

The effect of a gimbal spring is considered at the end of this section.

With K_θ , K_ϕ , and K_t all equal to 0, eqns (8) and (9) are further simplified as follows:

$$\Theta = \frac{\left(s^2 + \frac{b}{J}s + \frac{k}{J}\right) \left[\frac{L}{Is^2} + \frac{\dot{\theta}(0)}{s^2} + \frac{\theta(0)}{s} \right] - \lambda^2 \left[\frac{\gamma}{s^2} - \frac{\theta(0)}{s} \right]}{\left(s^2 + \frac{b}{J}s + \frac{k}{J} + \lambda^2\right)} \quad (10)$$

$$\Phi = \frac{\frac{h}{J} \left[\frac{L}{Is} + \frac{\dot{\theta}(0)}{s} + \theta(0) \right] + \frac{h}{J} \left[\frac{\gamma}{s} - \theta(0) \right]}{\left(s^2 + \frac{b}{J}s + \frac{k}{J} + \lambda^2\right)} \quad (11)$$

Response to Initial Velocity or Impulsive Disturbances*—During this and the succeeding sections consideration is given to behaviour when there is no mechanical spring: $k = 0$, and the response of the system to either an impulsive disturbance or an initial attitude rate is plotted in *Figure 2*. Transient oscillations are at approximately the nutation frequency, $\lambda = \sqrt{2} h/\sqrt{IJ}$. It is important to notice that vehicle attitude settles down to a steady offset angle, but no steady rate: in the case of an impulse disturbance, the momentum added to the vehicle by the impulse is finally absorbed entirely by a reorientation, $\phi(\infty)$, of the gyro; while in the case of an initial vehicle angular velocity, all of the angular momentum of the vehicle is transferred into the gyros. The gyro motions are larger, by $h/J\lambda \approx N/\lambda$, than the vehicle motions. (N is gyro spin speed.) Typically, $N/\lambda \approx 1,000$.

The selection of parameters can be made on the basis of *Figure 2*. First, from the viewpoint of steady-state error, it is desirable to have b/J as small as possible, but on the other hand, b/J should be large enough to give acceptably good damping of the transient in *Figure 2*. A reasonable compromise might be to choose a damping ratio, ζ , of about 0.2. h is selected to make λ represent a sufficiently fast speed of response, and a sufficiently tight steady-state control (*Figure 2*). A typical selection for λ might be, for example, 1 rad/sec. Then the b/h ratio for the gyros is determined as:

* Response from initial attitude is zero, for this system, because there is no attitude reference. That is if the vehicle is started in some arbitrary position $\theta(0)$ then (10) indicates that the response will be: $\theta(t) = \theta(0)$.

Table 1

Behaviour characteristic	System		
	(A) Precision control to inertial reference		(B) Damper for gravity-gradient stabilized vehicle (Semi-passive)
	1. Semi-Passive	2. Active (using attitude sensing) Syst. (a): Guidance quality gyros Syst. (b): Low-quality Gyros with gimbal feedback	
Specialization of system response functions, eqns (8) and (9)	$n = 0, \omega_2 = 0, \phi = 0$ $K_\theta = 0, K_\phi = 0, K_t = 0$ See eqns (10), (11)	$n = 0, \omega_2 = 0, \phi = 0$ Syst. (a) only: $k = 0, K_t = 0$	$K_\theta = 0, K_\phi = 0, K_t = 0$ See eqns (19), (20)
Dynamic characteristics		<i>Figure 3</i>	<i>Figure 5</i>
Response to gyro drift	$\dot{\theta} = \gamma$ Eqns (13)	$\theta = \gamma/K_\theta$ Eqn (15)	$\theta = 0$
Response to initial velocity or impulsive disturbance	<i>Figure 2</i>	<i>Figure 4</i>	<i>Figure 6</i>
Response to low-frequency sinusoidal disturbance	Eqns (15)	Eqns (17)	<i>Figure 7</i>

$$\frac{b}{h} = \frac{b/2J}{h/2J} = \frac{\zeta\lambda}{\left(\frac{IJ}{2}\right)^{\frac{1}{2}}/2J} \approx 0.3 \sqrt{\frac{J}{I}} \text{ e.g. } 0.001 \quad (12)$$

Gyro Drift—The steady-state response of the system due to a steady gyro drift rate, γ , consists of a steady vehicle rate equal to the drift rate, and a constant gyro offset angle:

$$\dot{\theta}(\infty) = -\gamma \quad (13a)$$

$$\varphi(\infty) = \frac{h}{J\lambda^2} \gamma \approx \frac{N}{\lambda} \frac{\gamma}{\lambda} \quad (13b)$$

That is, the vehicle is slaved to follow the net drift rate of the gyros, so that very good gyros must be used if this method of holding attitude is to be acceptable in a precision system. Note that the angular momentum of the total system is unchanged by application of the (internal) uncertainty torque: $I\dot{\theta}(\infty) + 2h\varphi(\infty) = 0$.

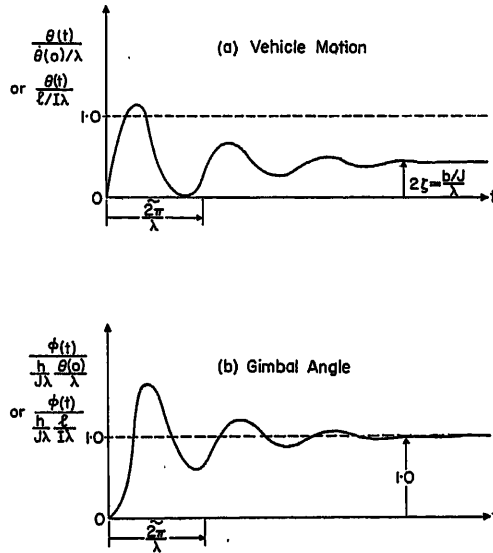


Figure 2. Response of semi-passive precision system to initial velocity or impulsive disturbance

Sinusoidal Disturbance—In the case of an inertially orientated, orbiting vehicle, a major source of disturbing torque is likely to be that due to gravity gradient, which varies sinusoidally as the vehicle travels around in its orbit. That is, the disturbing torque is $L = L_m \sin \omega_f t$ in which L_m is due to gravity gradient:

$$\frac{L_m}{I_2} = \frac{3g_0 R_0^2}{R^3} \left(\frac{I_1 - I_3}{I_2} \right) \text{ e.g. } 3n^2(0.33) = n^2 \quad (14)$$

in which n is orbital rate, and $(I_1 - I_3)/I_2$ has been taken as 0.33 for illustration. Since the system model under study is linear, the vehicle and gyros will follow the disturbance at the same frequency.

As a practical matter interest will be mostly in inputs which are at orbital frequency or small multiples thereof, so that (for the precision, fast system under consideration) the approximations may be made: $\omega_f \approx n \ll \lambda$, $\omega_f \ll b/J$. With these approximations, and the value of disturbance torque chosen in (14), the response of the system can be estimated:

$$\theta_m = \left(\frac{b/J}{\lambda} \right) \frac{L_m}{In\lambda} = (2\zeta) \left(\frac{n}{\lambda} \right) \quad (15a)$$

Typically, $\zeta = 0.2$ and it is seen that, for example, to control θ_m to 0.0004 rad (80 arc/sec) in this situation one will have to make h large enough to make $\lambda \approx 1000$ n. The corresponding excursion of the gyro gimbal, is given by

$$\varphi_m = h/b \theta_m \approx 0.4 \quad (15b)$$

More generally, gyro precession must counter disturbance:

$$2h\varphi_m \omega_f = L_m \quad (15c)$$

These numbers may be acceptable for the no- θ -reference condition. If they are not, then h may be made larger and/or $(I_1 - I_3)$ made smaller, for example.

Summarizing. A passive system consisting of a pair of lightly damped gyros (b/h of order 0.001) can be made to give rather good precision attitude control for short periods of time, provided the gyro drift rates are sufficiently low. System response to initial velocity or to an impulsive disturbance is given by Figure 2. The effect of gyro drift rate is given by eqns (13), and the response to low frequency sinusoidal disturbances is given by eqns (15).

The Effect of a Gimbal Restoring Spring—One may be interested in the effects of having a restoring spring on the gyro gimbals, first because one would like to see whether such a spring could be made to improve performance, and second because a spring restraint (e.g., due to gyro lead-in wires) may be present anyway, and its effects wished to be known. They are deduced from eqns (10) and (11), with $k \neq 0$.

Indeed, the presence of a spring may greatly reduce the attitude drift of the vehicle produced by gyro drift. However, the response of the system with a spring present to an impulsive disturbance torque or to initial vehicle rate is now no longer bounded, but results in a continuing vehicle rate, given by

$$\dot{\theta}(\infty) = \frac{l}{I} \frac{1}{\left(1 + \frac{\lambda^2}{k/J}\right)^{\frac{1}{2}}} \approx \frac{l}{I} \quad \text{or} \quad \dot{\theta}(\infty) = \dot{\theta}(0) \frac{1}{\left(1 + \frac{\lambda^2}{k/J}\right)^{\frac{1}{2}}} \approx \dot{\theta}(0)$$

(The approximations assume $k/J \gg \lambda^2$.) That is, the system behaves almost as if it had no gyros aboard. Moreover, with a restoring spring the response of the system to a sinusoidal disturbance is given by

$$\theta_m = \frac{L_m}{In^2} \frac{1}{\left(1 + \frac{\lambda^2}{k/J}\right)^{\frac{1}{2}}} \approx \frac{L_m}{In^2} \text{ e.g. } 1$$

which is poorer by a factor of about 1,000 (typically) than that of the non-spring system given by eqn (15a), and would be unacceptable. Physically, in effect, the spring is keeping the gyros from doing the job of absorbing the impulse produced on the system by the sinusoidal disturbing torques, so that this impulse is absorbed instead by motions of the vehicle. Therefore, the spring torque in a passive-gyro precision control system would be kept as small as possible.

Rate Gyro Control

It may be that in certain situations it will be desirable to use a rate gyro to improve attitude control of a precision system during periods when the attitude reference is temporarily unavailable. The behaviour of such a system can be calculated

from eqns (8) and (9) (with $K_\theta = 0$ and $K_i = 0$). It is found that the speed of response, steady-state error, and response to sinusoidal disturbances are all better by the factor $1/(1 + K_\delta)^{1/2}$, than for the purely semi-passive system. (K_δ is the gain of the rate gyro control loop.) However, the penalty paid is that the vehicle will now drift at the rate, $\dot{\theta}(\infty) = K_\delta \gamma_r$, so that the allowable rate gyro drift, γ_r , is more stringent, by the factor K_δ , than the allowable control-moment gyro drift.

Attitude Sensor Control

When the vehicle is controlled to a sensed attitude reference, the system may utilize gains K_θ , K_ϕ , and K_i in eqns (8) and (9). (n , ω_2 , and ϕ are still assumed zero.)

A number of gain combinations lead to system dynamic characteristics of interest. For purposes of illustration, two which are fairly different and quite interesting are compared.

System (a)

A minimum of equipment is presumed by deleting the gyro spring term, k , and the integrating motor. A plot of the locus of roots of the characteristic equation for this system is given in Figure 3 (a) as a function of K_θ . Before constructing the locus, the rate gain, K_θ , and damping constant, b , have been chosen to give the roots marked \times when $K_\theta = 0$. Typically, K_θ might first be chosen to make $\omega = \lambda (1 + K_\theta)^{\frac{1}{2}}$ seven times as great as for the semi-passive system (i.e., $K_\theta = 48$). Then b would be

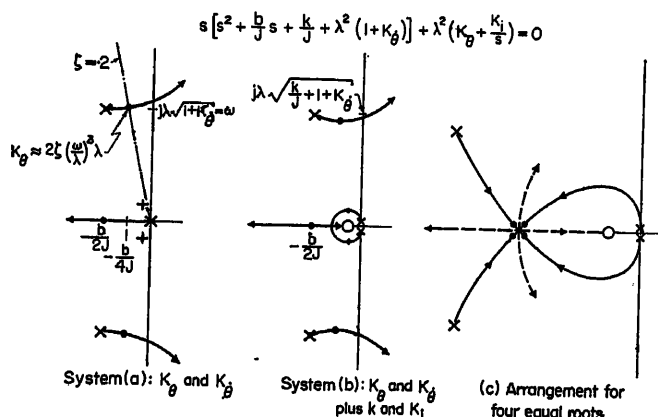


Figure 3. Dynamic characteristics of active precision control system using attitude sensing

chosen to put the complex \times 's well to the left of the $\zeta = 0.2$ line. This value of b would be about 14 times as large as for the semi-passive system and, since the same size gyros are to be used, the ratio b/h will be increased from 0.001 [eqn (12)] to 0.014. Finally, the value of K_θ is varied, which produces the root locus shown. To make the system damping ratio 0.2 (points marked $-\bullet-$ on the locus) K_θ must be about 100λ , for this example. The roots of the semi-passive system are also shown, marked $+$ in Figure 3(a), for comparison.

System (b)

The second system considered includes a gyro spring, k , and integral control. The decision to use a gyro spring (which in practice would probably be an electrical position feedback

around the gyro gimbals). might be based on the fact that position feedback around the gimbal is easier to achieve than clean differentiation of the θ signal, or on the desire to avoid difficulties due to stiction in the gyro gimbals, or to avoid dependence on a low gyro drift rate (which is discussed below). Integral control K_i , is employed to prevent gyro drift or impulsive disturbances from producing a steady attitude error. In *Figure 3(b)* the roots for $K_\theta = 0$ are at the \times 's at the same locations as in *Figure 3(a)* because $b/2J$ and $\omega = \lambda (1 + K_\theta + k/J)^{1/2}$ have been made the same as $b/2J$ and ω in System (a). In addition, there is another root at the origin (due to the integration). The ratio K_i/K_θ has been held constant, at the small value represented by the \circ close to the origin, as K_θ was varied to produce the locus of roots. Except for the added root near the origin, the locus for System (b) is almost identical to that for System (a), and about the same value of K_θ would be chosen. Then the dynamic behaviour would also be the same as for System (a), with the added feature that gyro drift errors would finally be removed.

As a matter of interest, a third arrangement of control gains is depicted in *Figure 3(c)*. Here, heavy damping has been used and gains K_t and K_θ have been chosen to give four equal, critically-damped roots. This system will have better transient properties than System (a) or (b), but the same steady-state performance as (b).

Gyro Drift—From eqn (8), the steady-state response of System (a) to a gyro drift rate γ is given by:

$$\theta(\infty) = \gamma/K_\theta \quad (16)$$

while for System (b) with integral control, K_i , there is no steady-state attitude error due to gyro drift. Using the value $K_g \approx 100 \lambda$ (from Figure 3) and taking the nominal value $\lambda = 1$, one finds that for System (a) to achieve $\theta(\infty) = 10^{-5}$ rad, the allowable gyro drift rate would be $\lambda = 0.001$ rad/sec = $200^\circ/\text{h}$. This is an easy specification for a 'precision' gyro of the inertial guidance class, but is rather difficult for a gyro using ball bearings for the gimbal axis, for example. Since this requirement is borderline, it would seem that the choice between System (a) and System (b) might depend largely on whether one wished to use guidance class gyros for control or not.

Response to Low Frequency Sinusoidal Disturbances—From eqn (8) the response of System (a) to a low-frequency sinusoidal external disturbance, $L_m \sin \omega t$ is given by

$$\theta_m = \frac{L_m}{I} \frac{\dot{b}/J}{\lambda^2 K_\theta} = \frac{L_m}{I n^2} \frac{n^2 \dot{b}/J}{\lambda^2 K_\theta} \quad (17a)$$

For System (b) the maximum attitude excursion is given by

$$\theta_m = \frac{L_m}{I} \frac{k/J}{\lambda^2 K_1} = \frac{L_m}{I n^2} \frac{n^2 k/J}{\lambda^2 K_1} \quad (17b)$$

If typical values are used for the parameters, e.g., $n/\lambda = 10^{-3}$, it is found that the attitude response of either System (a) or (b) is less than 0.1 arc sec.

The gyro excursion in response to a low-frequency sinusoidal disturbance, for either System (a) or (b), is the same as it was for the semi-passive system, eqn (15c). That is, gyro precession must counter disturbing torque. [See also eqn (9) with $\omega_s = 0$.]

Power Consumed During Low Frequency Sinusoidal Disturbances—The power used by the gyro torquer is simply the product of torque produced times gimbal rate, $\dot{\phi}$. The torque produced electrically consists of T_θ and T_ϕ .

For System (a), if we consider that gimbal damping is produced viscously, T_ϕ is zero and T_θ is given by eqn (7b). Then using eqn (8) for θ and eqn (15c) for $\dot{\phi}_m = \omega_f \phi_m$, power is found to be $P = L_m \dot{\phi}_m \cos^2 \omega_f t = P_m \cos^2 \omega_f t$, in which

$$P_m = \frac{h^2 \frac{b}{J} L_m^2}{I J \lambda^2 I \lambda^2} = \frac{L_m^2 J b h \omega_f}{J \omega_f I h J \lambda^2}$$

This particular form of the power equation is adopted for direct comparison with a reaction wheel system designed to do the same job as the present gyro systems. From Reference 3, eqn (17), the power for a reaction wheel system responding to a low-frequency sinusoidal disturbance is given by

$$P_m \approx L_m^2 / J \omega_f$$

Dividing the two power expressions gives the relation:

$$\frac{P_{m_{\text{gyros}}}}{P_{m_{\text{wheels}}}} \approx \frac{J b N \omega_f^{\text{e.s.}}}{I h \lambda^2} = 10^{-7} \quad (18)$$

for the typical value $J/I = 10^{-5}$. The reason for the enormous difference in required power is simply that in a reaction wheel the control torque must chase the wheel at its spin speed, while with the gyro system the torquer merely pushes the gimbal at the rate $\dot{\phi}$, which is extremely low by comparison. Thus power to torque the gyro gimbals is negligible compared to other power considerations, even for the very fast (1 c/sec) system assumed in this illustration.

Response to Impulsive Disturbance and Initial Vehicle Rate—These transients are calculated from eqn (8) and plotted in Figure 4. By comparison with Figure 2 one notes the following:

(1) The response of System (a) looks very much like the transient response of the semi-passive system, except that it is faster by the factor $\omega/\lambda \approx 7$, and the amplitude of the motion of System (a) is smaller by the same factor.

(2) More important, the attitude returns promptly to zero for System (a), while for the semi-passive system the attitude sits at some final value.

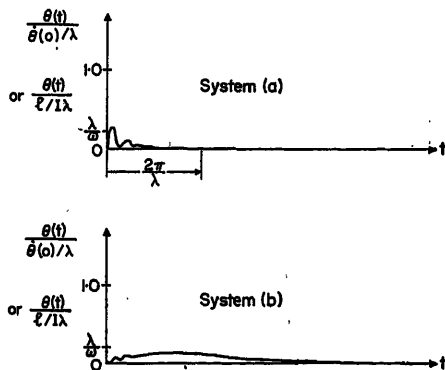


Figure 4. Response of active precision system to initial velocity or impulsive disturbance

(3) For System (b) the predominant term in the transient motion is the exponential term (the sinusoidal term being very small). Its maximum excursion is somewhat larger than for System (a), but is much smaller (again by about the factor ω/λ), than for the semi-passive system. Again there is no steady-state error in θ .

Summarizing. Control to an inertial reference using precision sensing of vehicle attitude, θ , has been considered. If guidance quality gyros are used, then satisfactory control can be obtained with no gimbal position feedback (or spring), System (a). If one wishes to obtain 1 arc sec accuracy using gyros having drift rates above $200^\circ/\text{h}$, then a gimbal position feedback plus integral control on the θ signal, must be used, System (b).

For either system the attitude can be held to the 10^{-6} rad class (assuming a perfect sensor) in the presence of low-frequency vehicle disturbance torques (e.g., at orbit frequency) corresponding to gravity gradient acting on an inertia mismatch of 33 per cent. For gyros of appropriate size gimbal angles are reasonably small (e.g., < 0.5 rad). For System (a) gimbal damping should be kept low to reduce this response.

The natural characteristics of the system are illustrated in the root loci of Figure 3, and values for the control gains are established in terms of system parameters.

Response to impulsive disturbances and initial vehicle angular velocity is shown in Figure 4. This response is faster and smaller, by the factor ω/λ , than with the purely semi-passive damping of the preceding section.

Pitch Damping for Satellite Stabilized by Gravity Gradient

Now consider a satellite which is stabilized to the local vertical by gravity gradient, and which employs a pair of gyros to provide semi-passive damping*. That is, no vehicle attitude sensor or electrical feedback of attitude is employed.

In this case ω_n , in eqns (8) and (9), represents the undamped natural frequency of the satellite due to the gravity-gradient 'spring', and n is the angular velocity of the local-vertical reference frame. K_ϕ , K_θ and K_t are zero, of course. Also, since we will now be considering motions which are extremely slow (of about orbital frequency), it can be shown that the inertial torque due to acceleration of the gyro gimbal can be omitted from the calculations with negligible error. Equations (8) and (9) then become:

$$\Theta = \frac{\left(s + \frac{k'}{b}\right) \left[\frac{L}{I} + \theta(0)\right] - \beta \gamma + s \left(s + \frac{k'}{b} + \beta\right) \theta(0)}{(s^2 + \omega_2^2) \left(s + \frac{k'}{b}\right) + \beta s^2} \quad (19)$$

$$\Phi = \frac{\frac{h \cos \phi}{b} \left\{ s \left[\frac{L}{I} + \theta(0)\right] + (s^2 + \omega_2^2) \frac{\gamma}{s} - \omega_2^2 \theta(0) \right\}}{(s^2 + \omega_2^2) \left(s + \frac{k'}{b}\right) + \beta s^2} \quad (20)$$

* For this system the gears would be removed in Figure 1, so that the same pair of gyros could also rotate together to provide damping for roll-yaw motions; this is described elsewhere¹⁸.

In which k' is the sum of a physical (or electrical) restoring spring on the gyro gimbal plus the effective gimbal spring due to gyroscopic action: $k' = k + hn \sin \phi$, and β is given by

$$\beta = \frac{\lambda^2}{b/J} = \frac{2h^2 \cos^2 \phi}{bI} = \left(\frac{h \cos \phi}{b} \right) \left(\frac{2h \cos \phi}{I} \right) \quad (21)$$

(β is analogous to the factor λ which was the key design factor in the preceding section. That is, β connotes the size of the gyros.)

Gyro Drift

The steady-state effect of gyro drift rate, γ , on system performance can be seen directly from eqns (19) and (20): $\theta(\infty) = 0$, $\varphi(\infty) = (h \cos \phi / k') \gamma$. That is, the gyros reorient so that the effective gimbal spring (gyroscopic plus physical) counters the uncertainty torque, $U = h\gamma$, associated with the gyro drift rate. No vehicle attitude error results.

It is important, of course, that the gyros are not saturated by their own uncertainty torques, and this puts an additional constraint on h and k' . But, as it turns out, this should not be serious.

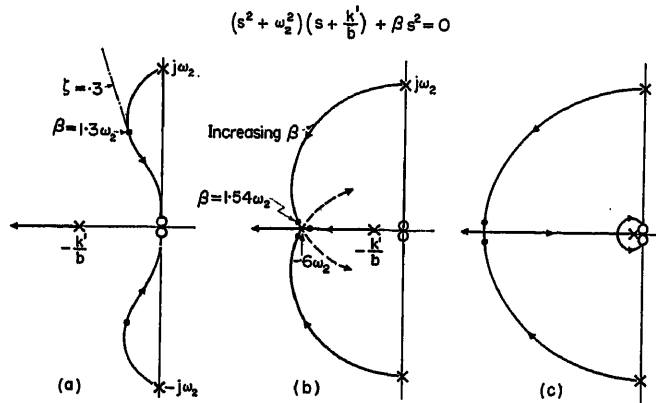


Figure 5. Dynamic characteristics in pitch of system using 'Vee' gyros to damp natural motions of gravity-stabilized satellite

Dynamic Characteristics

The characteristic equation for this system is given by the denominator of eqn (19) or (20). The loci of roots *versus* β are given in Figure 5, for three values of the parameter $(k'/b)/\omega_2$. From these plots it is clear that it will be possible to obtain a system having three equal, critically-damped roots [Figure 5(b)] by an appropriate choice of the parameters $(k'/b)/\omega_2$ and β . (The desirability of doing so has been pointed out¹².) The proper values to achieve this particular characteristic are:

$$\frac{k'}{b} = \frac{k}{b} + \frac{h}{b} n \sin \phi = 0.192 \omega_2 \quad (22)$$

$$\beta = \frac{2h^2 \cos^2 \phi}{bI} = 1.54 \omega_2 \quad (23)$$

The three equal roots will then be at $s = -0.577 \omega_2$.

It turns out that in considering the dynamics of roll-yaw control using the same pair of gyros, the value of $(h/b) n \sin \phi$ must be made somewhat higher—about $0.5 \omega_2$, for a typical

moment-of-inertia configuration—in order to achieve acceptable roll-yaw stability. This is dealt with elsewhere^{15, 18}, and can be made compatible with the specification of eqn (22) only if a negative physical spring constant, k , is employed. Negative

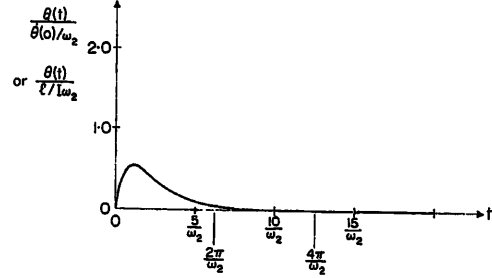


Figure 6. Response to initial velocity (or impulsive disturbance) of gravity-gradient-stabilized satellite damped with semi-passive gyros

feedback springs have been studied at MIT, and a negative physical spring for such systems has been developed by Burt and Ware at the Royal Aircraft Establishment.

Response to Initial Error and to Sinusoidal Disturbance for Critically-damped System

If the conditions of eqns (22) and (23) can be met, then the transient response of the gyro-damped system will be as plotted in Figure 6.

The response to a sinusoidal disturbance, $L_m \cos \omega_f t$, will be as plotted in the usual frequency-response manner in Figure 7(a). (Log scales are used.) For $\omega_f < \omega_2$ the attitude response is the same as for a steady torque, L_m . The term $I\omega_2^2$, being the constant of the gravity-gradient 'spring', is, of course, attenuated.

To get the most benefit from the gyros it would seem reasonable that the magnitude of their excursion, during response both to initial error and to sinusoidal disturbance at $\omega_f \approx \omega_2$, should be about 0.1 to 0.2 rad. Since the largest acceptable θ_m will typically also be of this magnitude, this connotes the following additional restriction:

$$\frac{h \cos \phi}{b} \approx 1$$

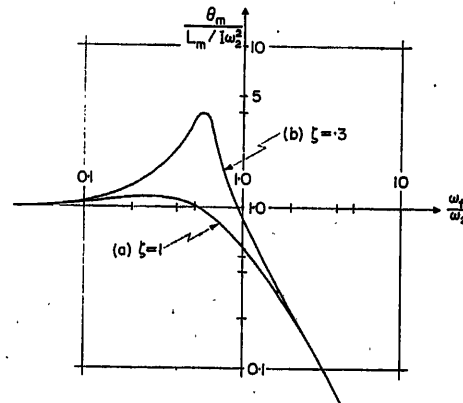


Figure 7. Response to sinusoidal disturbance of gravity-gradient-stabilized system with semi-passive gyro damping

Momentum-to-damping ratios in the range 0.3 to 3 are common in inertial guidance gyros, so that this restriction is, happily, quite acceptable if such gyros can be used.

For operational reasons, it may be desirable to avoid a negative spring. In this case, in order to be compatible with roll-yaw requirements, the pitch system would be operated at other than the critically damped condition drawn in Figure 5(b). In fact, a more likely arrangement is that shown in Figure 5(a). In this case the magnification, due to resonance, may be as high as 4, as indicated in Figure 7(b). If it is, then, even if ω_2 can be made different from ω_r by 20 or 30 per cent, the improvement over an undamped system is disappointingly small.

In terms of sinusoidal response, then, a more highly-damped system (achievable with a negative physical or electrical spring) would seem more attractive.

Summarizing. To make gyro damping most effective in the presence of sinusoidal disturbances $h \cos \phi / b = 1$ is indicated. Good roll-yaw damping requires, typically, $h \sin \phi / b = 0.5$, so that a nominal gimbal angle, and gimbal damping ratio of about $\phi \approx \tan^{-1} 0.5 \approx 20^\circ$, and $h/b \approx 1$, respectively, are indicated.

Then, for $\omega_2 = 1.1\omega_r$, for example, a ζ of 1 can be obtained by making $k/b = -0.3$. Then the system will have three real roots at $s = -0.6\omega_2$, with accompanying good transient response (Figure 6) and non-resonant response to sinusoidal disturbances (Figure 7a).

Conclusions and Comparisons

Control to an Inertial Reference

If inertial-guidance quality gyros are used, fast, precise control can be achieved, as illustrated in Figure 4. The attitude sensing control gain should be sufficient to limit error due to gyro drift, $\gamma: K_\theta = \gamma/\theta_{\text{allow}}$, and damping should be relatively low, $b/h \approx 10^{-3}$ to limit system response to disturbances. Gyro sizing (e.g., to handle disturbing torques due to gravity), will lead, typically, to a relation of the order of $h \approx I_n$.

If guidance-quality gyros are used, the system will operate well in the absence of a θ reference (semi-passive control) for short periods of time, but may be slower, Figure 2, and its response to disturbances larger by a factor of, typically, 10^4 . Vehicle attitude will drift at the mean drift rate of the gyros.

If lower grade gyros are to be used, a gimbal feedback (or spring) can be added to remove dependence on bearing anomalies, etc., and integral control can be added to avoid the need for large attitude errors to support large gyro uncertainty torques. In this case the spring, rather than the damper, must be kept light to limit response to disturbances. (It will still be well to keep gyro damping light also, to permit the best possible operation when the attitude reference is unavailable.)

Comparison With Reaction Wheels: Precision Control—Companion relations for reaction wheel systems are given, Cannon³. For precision control to an inertial reference, for comparable physical parameters, it is found that (1) vehicle response can be made the same for both methods, (2) gyro momentum capacity, $2 \sin \varphi_{\text{max}} J \Omega_{\text{gyro wheel}}$, will equal reaction wheel capacity, $J(\Omega_{\text{reaction wheel}})_{\text{max}}$, (3) control torque is lower for gyros by $b/h \approx 10^{-3}$, (4) power required is lower for gyros, typically by 10^{-7} . The power for torquing the gyros has been shown in

eqn (18) to be negligible compared to that for torquing wheels, because the wheel torque must act at wheel spin speed, while gimbal torque just acts at gimbal rate.

Damping of Gravity-orientated Vehicle

The slow (e.g., $1\frac{1}{2}$ to 12 h period) natural motions of a satellite stabilized to the local level by gravity gradient can be damped quite well using a 'Vee' configuration. The same size gyros are called for as for the precision system: $h \approx I_n$. Much higher gimbal damping: $b/h \approx 1$ is indicated. Very good gimbal bearings will be required in this system, not because of sensitivity to gyro drift, but in order to achieve good viscous-type damping at the extremely slow gimbal rates.

If a negative spring (or positive electrical feedback) can be used, critical damping can be achieved, with attendant good transient response and non-resonant response to orbit-associated disturbing torques. Otherwise, because of roll-yaw requirements, the damping will be less, transients will be damped out more slowly, and the response to orbital disturbing torques may exhibit an undesirable resonant magnification.

Comparison with Reaction Wheels: Natural Motion Damping—The system natural characteristics of Figure 5 can, of course, be obtained essentially with either a reaction wheel or a semi-passive gyro system. Then the system response, transient or sinusoidal, will be the same in either case. No power is involved in controlling the gimbals of the semi-passive damper system, while the lower-limiting value of power for controlling reaction wheels, as given by Cannon³, is not negligible.

Nomenclature

- b Viscous damping constant on gyro gimbal
- \vec{H} Vector angular momentum of system
- h Spin angular momentum of a gyro
- I Moment of inertia of vehicle
- J Moment of inertia of gyro (wheel plus gimbal) about gimbal axis
- K Control gain
- k Gimbal 'spring constant' (mechanical or electrical)
- k' See eqn (20)
- L External torque on vehicle. \mathcal{L} , its Laplace transform
- l Magnitude of an external torque impulse
- \bar{M} Total external moment on vehicle
- N Gyro spin speed
- n Orbital angular velocity
- P Control power used in torquing
- s Laplace operator
- T Torque applied to gyro gimbals. \mathcal{T} , its Laplace transform
- t Time
- U Uncertainty torque on gyro gimbal
- β A system parameter. See eqn (21)
- γ Average drift rate of control moment gyros
- γ_r Drift rate of rate gyro
- ζ Damping ratio
- θ Vehicle attitude error (from reference attitude). Θ , its Laplace transform
- λ A system parameter. See eqn (9)
- ϕ Total gyro gimbal angle
- Φ Nominal gyro gimbal angle
- φ Perturbation in gyro gimbal angle: $\phi = \Phi + \varphi$
- Φ Laplace transform of φ
- $\bar{\Omega}$ Angular velocity of coordinate system
- ω Pitch natural frequency of local vertical satellite, due to gravity gradient
- ω_r Frequency of sinusoidal disturbance

References

- ¹ DEBRA, D. B. and CANNON, R. H., Jr. Momentum vector considerations in wheel-jet satellite control system design. *Amer. Rocket Soc. Nat. Conf. on Guidance, Control and Navigation, Stanford Univ.* (1961). *Progress in Astronautics and Rocketry*, Vol. 8, edited by Roberson and Farrior, Academic Press (1962)
- ² ROBERSON, R. E. (Ed.) Methods for the control of satellites and space vehicles. *WADD Tech. Rep.* 60-643, II. Sec. V (Cannon) (1960)
- ³ CANNON, R. H., Jr. Some basic response relations for reaction-wheel attitude control. *ARS J.* 32, No. 1 (1962)
- ⁴ GODDARD, R. H. *U.S. Pat. No. 2,158,180*, Gyroscopic steering apparatus. May 16, 1939
- ⁵ JOHNSON, F. V. Use of three single-degree-of-freedom gyroscopes to stabilize a ballistic missile. *Gen. Elec. Rep. TR-55A0115*. (1955)
- ⁶ ROBERSON, R. E. Origin and treatment of nonlinearity and parametric excitation in satellite attitude dynamics. *Symp. Nonlinear Oscillations, Kiev* (1961)
- ⁷ HAEUSSERMANN, W. A comparison of some actuation methods for attitude control of space vehicles. *NASA DG-TN-63-59* (1959)
- ⁸ CANNON, R. H., Jr. Gyroscopic coupling in space vehicle attitude control systems. *J. bas. Eng., Amer. Soc. mech. Engrs.* Mar. (1962)
- ⁹ WHITE, J. S. and HANSEN, Q. M. Study of a satellite attitude control system using integrating gyros as torque sources. *NASA Ames Res. Center, TN D-1073*. Sept. (1961)
- ¹⁰ HAVILL, J. R. Twin gyro control system. *NASA Ames Res. Center Memo* (1961). *NASA Tech. Note*
- ¹¹ SCOTT, E. D. 'V' control moment gyro system. *Lockheed Aircraft Corp. Memo* (1960)
- ¹² BURT, E. G. C. The influence of cyclic torques on the attitude control of earth-pointing satellites. *URSI Symp. on Space Comm. Res., Paris* (1961)
- ¹³ KLASS, P. J. New gyro technique orients satellite. *Aviation Week and Space Technology* (1962)
- ¹⁴ DE LISLE, J., OGLETREE, G. and HILDEBRANT, B. M. Attitude control of satellites using integrating gyroscopes. *MIT Instrumentation Lab. R-350* (1961)
- ¹⁵ OGLETREE, G., HILDEBRANT, B. M. and DE LISLE, J. Satellite attitude control study, Pt II. *MIT Instrum. Lab. R-308* (1962)
- ¹⁶ KENNEDY, H. B. A gyro momentum exchange device for space vehicle attitude control. *IAS National Meeting*, June 1962
- ¹⁷ KENNEDY, H. B. Attitude control of space vehicles using gyro Precession torques, *6th Sym. Ballistic Missiles and Aerospace. Los Angeles* (1961)
- ¹⁸ CANNON, R. H., Jr. On the damping of satellite natural three-axis motions using semi-passive gyro systems. To be submitted to the ARS

REPORT

W. E. MILLER*

In the applications sessions, we were exposed to a broad range of technical approaches which included the determination of process dynamics with some specific mathematical models, discussion of outstanding value on line operating systems, and the presentation of system performance data.

Every applications paper cannot be expected to present a complete exposé of the control algorithm, system description or provide tested performance data. We must recognize the practical aspects of preparing a paper rather than a thesis for a Congress of this type. On the whole I believe we had a good balance between exposé of control algorithms, actual achievements, and performance results in the applications sessions.

I was particularly impressed with the unanimity of opinion regarding the technical approach to the application of large scale digital process computers by the steel industry and chemical industry participants. While the process time scales differed significantly, there did not appear to be discontinuity between the criteria used for either application or economic evaluation. This Congress served a useful purpose in bringing these and other groups together to discuss technical approaches and operating experience. I believe that each group will become more confident and the application of digital process computers in both industries will be speeded.

Analysis should have a practical usable consequence. We, in the applications field, need the help of the experts in mathematics

and theory to develop simplified methods of design for the complex, multivariable, non-linear, distributed parameter systems that exist in actual business life. We also face severe boundary conditions of time, expense and economic value for system analysis, design and implementation.

In the short time that is available, it would be unfair to single out the contributions of one or two authors or discussors for recognition. There were many significant contributions. I should like to thank all those who contributed papers and discussions. The authors in particular deserve thanks for their willingness to rearrange their schedules for special meetings to answer questions.

The combination of survey applications, components and theory sessions at this Congress has not only permitted process-oriented engineers and managers to discuss their problems and methods of analysis with each other, but has given them the opportunity through the survey sessions to bridge the chasm between theory and applications. Perhaps, too, university and institute representatives have developed new ideas to extend methods of analysis and theory to some of the problems of practical consequence discussed during the Congress.

Our process systems become evermore complex. We in industry are constantly on the alert for methods that will increase accuracy of analysis, and reduce time required for analysis and design so that we may continue to enlarge the scope of our systems.

* Chairman of the I.F.A.C. Technical Committee on Applications.

COMPONENTS

Control Components—New Design Principles and Devices

A Survey by J.L. SHEARER et al.*

Introduction

Since the First Congress of the International Federation of Automatic Control which was held in Moscow in 1960, many new ideas have been brought into reality in the development of components for a wide variety of engineering systems. It has been a challenging task to bring together information on all of the major developments throughout the world and to try to present it in a clear concise form. The response of the contributors to this paper has been far beyond my expectations, and they deserve a large share of the credit for this effort.

The organization of the material in this paper has been based largely on the special fields of the experts who wrote the various contributions. This paper has grown larger than originally anticipated so that it has been necessary to carefully select and combine ideas wherever possible to save space and words. The writer feels that this survey paper is a kind of experiment with a new way of communicating ideas, and that data on the results of this experiment will probably be very useful to those who prepare the next generation of survey papers.

Electromechanical Components

G.S. AXELBY, D.W. BLOSER, J.P. O'DONOHUE and H.R. WEED

The area of electromechanical components covers a wide range of devices and system elements, many of which are very special purpose devices. Also, many of the developments which have taken place with these electromechanical components are closely related to other non-mechanical devices such as semi-conductor amplifiers and control circuits, magnetic amplifiers, and transformers. Separate sections have been written covering wide band transformers, semi-conductor and solid state components, and magnetic amplifiers.

Servomotors, synchros, and damping and integrating tachometers are widely used in many aerospace and military applications and in some industrial applications. Two kinds of changes have been most predominant in the development of these devices in recent years. First is the trend toward miniaturization. Second is the evolution of more stringent performance requirements and the need for more critical evaluation of these control components.

Miniaturization has resulted in a factor of two reduction in the diameter of some servomotors and tachometers. More compact designs and higher temperature environments have resulted in the need to withstand higher temperatures (up to 300°C). Reduction in size has resulted in faster response in most cases. A new sleeve rotor design makes possible faster response and higher power level for a unit of a given size¹. Servomotors and tachometers have also been designed to operate at higher fre-

quencies (e.g. 900, 1,500, 1,600, and 2,000 c/sec) with considerable reduction in size and weight.

Corresponding reduction in the size of synchros has been accompanied by improved accuracy through the introduction of a 4-wire synchro instead of a 3-wire synchro. Multi-speed synchros have been developed to provide greater angular accuracy than single speed synchros by the electrical subdivision of angular motions, and by operating them with appropriate electronic digital circuits. Through this means, it is now possible to obtain angular accuracies in the order one part in 2^{18} for 360° shaft rotation in a cylindrical package only 9 cm long and 3.2 cm in diameter².

Tachometers, which can provide analogue integration when used in the feedback path of a closed loop around a servomotor, are being made with slotless armatures to provide 0.01 per cent linearity with nearly zero bidirectional error in a cylindrical package 7 cm in diameter and 2.5 cm long³. Another major change in the design of integrating tachometers is the use of thermistor compensation networks to reduce output null variations due to variations in operating temperature⁴. This approach is quite different from that of using magnetic amplifier controlled heaters to keep the temperature of the component constant!

Another aspect of miniaturization is the combination of two or more control components in a single package such as a motor-tachometer unit, or a servomotor, gear train and a potentiometer mounted on a common shaft. Motor-Tachometer Gener-

* Each contribution bears the name of its author or authors.

ator is the all-inclusive name which has been adopted in industry for the combination of a servomotor and a tachometer generator in a single unit. Today the production of these units exceeds the production of plain servomotors. Drag-cup tachometers having greatly improved signal-to-noise ratios, now almost invariably used in these units, are the result of earlier exhaustive analytical work by Frazier^{4, 5}. A host of new terms and parameters to be employed are now in use in working with these units. First and perhaps most important is the division of the output signal into 'speed-sensitive' and 'non-speed-sensitive' portions. Next is the differentiation between in-phase and quadrature components of the above portions of the output voltage. Furthermore, the in-phase and quadrature components of the non-speed-sensitive portion are found to be a function of cup position and are designated as in-phase position error and quadrature position error. If a tachometer generator is driven at exactly the same speed in each direction, the in-phase component of the output voltage will be slightly different in the two directions. The same is likely to be true of the quadrature component. One-half the difference between the magnitudes of these two in-phase components is the average in-phase null voltage for all cup positions, and one-half the difference between the magnitudes of the two quadrature components is the average quadrature null voltage for all cup positions. The null voltage in each case is a non-speed-sensitive portion of the output. Thus the speed-sensitive portions of the in-phase and quadrature components of the output voltage are each the same for equal speeds in both directions of rotation. The in-phase null voltage has been termed the 'in-phase axis error' and the quadrature null voltage has been termed the 'quadrature axis error'.

The average of the speed-sensitive portion of the in-phase component of the output is known as the in-phase speed-sensitive voltage, and the average of the speed-sensitive portion of the quadrature component of the output is known as the quadrature speed-sensitive voltage. The quadrature speed-sensitive voltage divided by the in-phase speed-sensitive voltage is the tangent of the phase shift angle (between the excitation voltage and the total speed-sensitive portion of the output voltage). References 6 and 7 describe specifications and test procedures in detail.

Once they are known, the in-phase and quadrature axis errors and the quadrature speed-sensitive voltage may be cancelled out by suitable electrical means. Departure of the in-phase voltage *vs.* speed curve from a straight line is normally quite small (usually less than 0.1 per cent).

Departures of the in-phase speed-sensitive voltage and the phase shift angle from the values determined at calibration temperature are commonly held to within ± 0.5 per cent and ± 0.5 degrees respectively over a temperature range of -55°C to $+125^{\circ}\text{C}$. Similarly, the variations of the in-phase and quadrature axis errors with temperature variation are kept within 5 mV and 10 mV respectively over the same temperature range. Linearity (or lack of it) is not affected by temperature.

When the excitation voltage is held constant within ± 10 per cent, the ratio of in-phase speed-sensitive voltage to excitation voltage and the phase shift angle do not change by more than ± 0.2 per cent and ± 15 minutes of arc. When the excitation voltage is held constant within ± 2 per cent, these values are generally an order of magnitude smaller than those given above.

When the excitation frequency changes by ± 5 per cent, the in-phase transformation ratio change and the phase shift change

are as great as all other changes combined (-0.75 per cent to $+0.45$ per cent and $\pm 2^{\circ}30'$ respectively). However the relationship between these changes and frequency variation is not linear, and for a ± 1 per cent frequency change the above changes are negligible.

With the development of transistorized amplifiers and solid-state control devices having lower output impedances, and modification of motor windings to handle higher currents at lower voltages, the use of output transformers to drive servomotors has greatly declined. Some servomotors have been designed to operate from current sources rather than voltage sources, thus eliminating the need for capacity tuning of the control winding.

The use of new design principles has led to servomotors and tachometers having exceptionally low acoustic noise from shafts and bearings. Radio frequency interference has been reduced by using transistor commutation or solid-state switching devices.

The application of solid-state control devices has made variable-speed and speed-regulated a. c. motors a reality in the control field. A variable-speed, single-phase induction motor giving a wide range of manual speed control recently has been developed at Lamb⁸⁻¹⁰. Some manufacturers are working on designs to adapt this concept to automatic control systems. Such a circuit uses power transistors or silicon-controlled rectifiers in a basic self-excited inverter to supply the motor with a variable frequency supply. Since the motor winding replaces the output transformer in most cases, it appears that the motor and control should cost relatively little more than the motor itself.

Although it has less desirable performance characteristics, the a.c. universal motor has recently been improved through the incorporation of speed control and speed regulation. Recent work at Singer, Texas Instrument, General Electric, Robbins and Myers, and others¹¹ has resulted in a variety of designs, all based on using one or more silicon-controlled rectifiers and some method of sensing motor speed from the terminals. Most of these circuits result in an improved, perhaps nearly constant, speed characteristic up to the point that the normal motor characteristic is reached. Since rectification is usually embodied in silicon-controlled rectifier circuits, torque and efficiency characteristics may be obtained which are greatly improved in comparison to a.c. operation.

Some other recent developments include a new type of d.c. torque motor which provides extremely smooth motion at very low speeds up to several horsepower. Usually constructed in a 'pancake' form with a relatively large diameter, it has many poles and several overlapping brushes. The top speed of these motors is relatively low, but it is adequate for many applications which demand high torques for precision control of velocity and position. These motors are also used as extremely accurate tachometers¹².

Stepping motors have also been improved, giving higher stable speeds in smaller sizes. These units can overcome higher torques than their continuously moving counterparts, they do not require regulated power supplies or feedback to attain position accuracy, and they can maintain a given position without expenditure of power. These motors are finding wider applications^{13, 14} in recently developed systems, especially in systems involving hybrid digital-analogue equipment. Magnetic detenting eliminates shock loading and mechanical wear.

Electromechanical components for high performance systems are often manufactured by production line techniques when the

number of individual items is large. If the specifications are critical, it is important that slight deviations from unit to unit be determined either for purposes of matching or rejection. Surge comparison testing of windings was introduced in 1945 by Moses and Harter¹⁵ of General Electric and improved on by Rohats¹⁶, Catlin¹⁷, Buchanan¹⁸ and Strain¹⁹ up to 1960. The effort, however, was directed primarily toward insulation failure of large machines or winding faults of universal motor armatures. There was little question that the basic concept of exciting the electrical device or winding with an impulse of energy would result in a transient response determined by its characteristic equation to the extent that its performance might be considered linear. This idea has been used extensively to determine the properties of linear control system for many years. The extension of the method to large signal, non-linear systems would appear to be limited to step incremental changes or near-linear approximations.

The development of the null-detection, surge comparison equipment by Robbins and Myers, Inc.^{20, 21} greatly improved the sensitivity and capabilities of such tests.

The periodically repetitive excitation and adjustable magni-

tude suggest that specific and identical histories can be created in non-linear devices. If so, variations in certain types of non-linearity could be detected by the high-sensitivity comparison units. Work published by Weed²² in 1961 analysed the repetitive impulse excitation of servomotors to determine their transfer function characteristics. Although obviously not equivalent to the Wiener²³ theoretical analysis of general non-linear systems, it appears that production line determination of the variation in many non-linearities is easily detected using repetitive comparison surge excitation and that limited results can be obtained in evaluating approximate transfer functions. Thus, such tests may become part of the performance specifications on many control components and may become a useful tool to the design engineer.

Very sensitive displacement measuring devices such as linear and rotary differential transformers (linearsyn, microsyn, etc.) are now being developed with magnetic suspensions²⁴ instead of conventional bearings to support their moving elements. This technique promises to greatly reduce bearing friction and thus make it possible to measure the motion of mechanical elements at greatly reduced force levels.

Magnetic Amplifiers

H. R. WEED

The magnetic amplifier has been used extensively to control one or both windings of two-phase servomotors. The relatively slow response and lack of theoretical analysis taking into account the effect of non-sinusoidal voltages and parameter variations of the motor with speed present major difficulties. As early as 1951, Ramey and Geyger²⁵⁻²⁷ suggested half-cycle response circuits to cope with the stability problems introduced by the long time

constant of conventional circuits. In 1955 Kallander²⁸ published work on a fast response magnetic servo-amplifier, but the results gave an undesirably low amplification factor.

Recent work by Bajwa^{29, 30} suggested a modification of the Geyger and Kallander circuits that results in acceptable amplification and carried out the theoretical evaluation of the overall transfer function. This work is particularly useful as it includes the variation of motor parameters with speed and their effect on the amplifier performance. Since the wave shapes applied to the servomotor are non-sinusoidal with such excitation, these analyses include the calculation of harmonic and braking torques. The results were verified by experiment and digital and analogue computer simulation. It appears that this will be a noteworthy contribution to the field.

Another recent contribution in the magnetic amplifier field has been the development by Jackson and Weed³¹ of a useful differential-saturable transformer for either single-phase or poly-phase operation. This device has several unique advantages over other magnetic amplifier circuits. A simplified single-phase circuit is shown in Figure 1.

Operation is based on the control determining the angle at which one core reaches saturation after which the other conducts through D_1 into the load. On the alternate half cycle, the functions of the cores interchange, giving controlled d.c. conduction in the load.

The desirable characteristics are low cost, fast response and high gain. The relatively low cost results from obtaining essentially the same kVA rating as for regular transformers and from

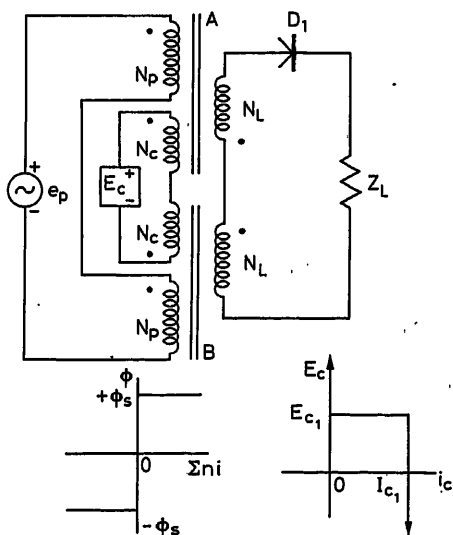


Figure 1. Single-phase differential-saturable transformer

double utilization of the diodes. A single diode gives full-wave output, while three diodes in a three-phase supply give six-phase output. This gives an inherently lower ripple per rectifier. Power gains of 1,000 at 95 per cent efficiency are easily obtained using the current-limited, regulated control supply.

If designed for normal excitation, both cores are taken from $-\phi_s$ to $+\phi_s$ and back each cycle, the only variables being the controlled rates at which they change and the period that one is saturated ahead of the other. The result is an absence of internal memory and a basic half-cycle response.

Semi-conductor and Solid-state Components

G. S. AXELBY

In recent years, semi-conductors and solid-state devices have become increasingly important in the design and development of control systems. They have been used in control systems as signal amplifiers as well as power amplifiers, as non-linear function generators, as sensors, and as computing elements in logic circuits which have a fundamental role in advanced control systems involving automatic decision capability together with some forms of learning.

In many instances, these devices increase system reliability and improve performance, with little increase in system size and weight. In addition, they operate on small amounts of power, and in molecularized form, they reduce the total number of individual parts and the number of interconnections between them. Semi-conductors also play an important role in analogue-to-digital and digital-to-analogue conversion which is so necessary in control systems involving digital computation. Actually, this is an area where more fundamental work is needed and new types of semi-conductors or other solid-state devices should be developed to provide this conversion function directly, without an intervening sensor, especially with respect to measurements of acceleration, vibration, and stress.

In particular, silicon controlled-power rectifiers have been developed to replace magnetic and rotating amplifiers of larger size and weight. The semi-conductors have much less time delay and, generally, also have a higher gain. Silicon controlled rectifiers have been developed to handle over 60 kW with voltage levels approaching 500 V. They have been applied to the control, through resistance heating, of the temperature of molten glass used to manufacture fibreglass³², and they have permitted direct excitation of the large main drive machines on tandem rolling mills³³. Also, solid-state, uncontrolled rectifiers can now handle large currents of hundreds of amperes and large reverse voltages of over 1,000 V, and at the same time they have become much more reliable system elements. With improving manufacturing techniques and quality control, both types of rectifiers are being made with more consistent characteristics to meet a variety of voltage, current, and power requirements.

Specifically, three terminal pnpn silicon power rectifiers, when used as switches, can turn off electric circuits carrying tens of amperes and hundreds of volts within 10^{-6} sec. This illustrates that they can be used to control a power at relatively high frequency and with greatly simplified d.c. switching circuits^{33, 34}. With proper design, often with the use of digital programming,

these switches can be used to replace mechanical switches, cams, and levers to reduce wear and maintenance.

Actually, shorter switching times in digital computers are always desired, and silicon computer diodes are being reduced in size and made with different materials to provide switching times of 10^{-9} sec, which is characteristic of gallium arsenide diodes³⁴. This rapid response time corresponds to an increase of the effective diode bandwidth. For example, varactor diodes can respond to frequencies of $2 \cdot 10^{10}$ c/sec.

In a similar manner, the speed of response has been increased for transistors although their power handling ability will probably never equal that of diodes. Transistor response time and characteristics have been improved through the development of diffused base units, thin base regions, thick collector barriers and smaller dimensions³⁵. Power capability has also been improved and silicon power transistors have been developed to operate with 400 V power supplies. This allows their use in 110 V lines and in circuits containing inductive elements.

Although transistors have been applied to all kinds of active circuit elements, a particularly interesting application is in the replacement of brushes and commutators in electric motors up to 1 h.p. in size. This has reduced the number of parts by a factor of three, and it permits the use of d.c. motors in fuel tanks and at high altitudes at speeds up to 20,000 rev/min over a smoothly varying speed range³⁶. With the use of silicon controlled rectifiers, electronic motors up to 25 h.p. have been controlled in this way.

Another interesting application, of enormous potential for the future, is the use of semi-conductor diodes for microwave power transmission. At present, the efficiency of power conversion is about 70 per cent, and an improvement of efficiency will permit practical control of satellites, remote vehicle operation, and power transmission over difficult terrain without the use of power supplies where the remote control is being applied³⁷.

Actually, the field of solid state components has extended beyond the developments of the diode and transistors. These extensions have been in two areas: thermo-electric devices and microsystems. Thermo-electric devices have been developed to provide a cooling and heating source in the same unit—they have been used to make ice cubes and to heat liquids. Micro-miniaturization has included the encapsulation of extremely tiny elements in micromodules, the development of thin films or

layers of circuit elements, and monolithic structures where different components are created within monolithic semi-conductor elements. Of course these techniques include the desired interconnections between the components. This small size permits hundreds of components to be included in extremely small volumes. In a typical application of the thin film technique, for example, six transistors capable of operating at a 1.5 Mc/sec data rate, have been constructed on a 2.5 cm² plate.

Other solid state devices, using the effect of superconductivity at extremely cold temperatures, are also being developed, such as the cryotron and the film cryosar, a semiconductor element. It is possible to use these devices as basic elements in computers but there are difficult problems in providing signals through many connections into the cold environment needed for superconductivity. It is possible, however, with the development of new materials, to foresee that entire computers may be immersed in liquid helium. In spite of the difficulties involved, these devices have great advantages because extremely fast switching times and high density, such as 10⁴ elements per cubic cm, are possible with very low power consumption³⁸. It is estimated, for example, that a network of 10⁶ cryotron loops would require about 1 W of power. Although new manufacturing processes have been developed to create these microsystems, more research will be needed to provide the potential reliability and flexibility that they promise.

Another recent development in the solid-state field is the

injection laser, essentially a gallium arsenide diode although other materials are being used, which produces pulsed or continuous coherent light through stimulation by an electrical current rather than by the intense light source used for gaseous or ruby lasers³⁹. However, high current densities are required, as high as 2,000 A/cm², and liquid nitrogen or helium cooling is needed. Nevertheless, this electrical excitation will permit light modulation at high frequencies, and although much research will be needed, the possible applications of a small, solid-state laser, in the control field as a detector, amplifier, and actuator (as a heat source, for example) are tremendous in number.

Finally, other solid state devices make use of magnetostrictive or piezoelectric phenomena. For example, magnetostrictive devices, which expand or contract with the application of voltage, have been used as precision actuators, and as the basis of a novel gyroscope which needs no rotating mechanical parts, to detect space motion. Instead, a small mass of magnetostrictive material is made to vibrate with electrical excitation, and its reaction to space motion can be detected⁴⁰.

Thus, with the progress that has been made in the field of solid-state devices, it is possible to predict that highly complex control systems with various input and output sensors, data processing computers, and even mechanical actuators can be constructed within very small volumes with a high reliability of operation, and with a small consumption of power.

Wide Band Transformers

A. D. HASLEY, R. LEE and D. D. PIDHAYNY

Network development and the development of new materials have contributed much to the advances in the design of wide-frequency-band transformers.

The work of Tchebycheff and Butterworth⁴¹⁻⁴³ was used for the basis of much of the network development applied to single-unit, wide-band transformer design. The development of multiple unit transformers⁴⁴⁻⁴⁷, with their interconnecting networks so that they act as a single wide-band transformer, is another way in which network development has advanced the wide-band transformer design techniques.

Low dielectric constant fluoro-carbon and oriented polyester films, among other materials, used as a dielectric in the construction of wide-band transformers, also provides a means of extending the frequency range of these transformers since closer spacing of the windings, to improve coupling, can be used without dielectric breakdown or without increasing the distributed capacitance appreciably. Molybdenum-nickel-iron, nickel-iron, cobalt-nickel-iron⁴⁸⁻⁵², and the manganese-zinc and nickel-zinc ferrite core materials⁵³ because of their high permeability, probably have contributed the most to the advance of wide-band transformer design in the past⁵⁴.

Most of the problems in wide-band transformer design arise when they are to be used in feedback amplifiers or control

systems. The transient problem, in high voltage units, is very much worse when wide-band transformers are used than when narrow-band transformers are used in these systems⁵⁵⁻⁵⁷.

The control of amplitude and phase versus frequency characteristics (frequency response transfer function) as well as impedance characteristics, is of prime importance in the design of these feedback systems. These response characteristics are also of importance in the transmission of signals for oscilloscope presentation, such as television signals. Accordingly, when multiple-unit transformers are used for this purpose, extreme care needs to be taken to provide smooth transitions in these characteristics at the crossover frequencies.

During the development of the Standard-covering High-Power Wide-Band Frequency Transformers it became apparent at the outset that a strong need existed for an understanding of the effect of system transients on the specification of components. The use of high-powered wide band amplifiers permits the generation and transmission of transients which are at a level such as to cause serious limitations on the design of these transformers.

In the summary of tests performed in a recent report by Pidhayny⁵⁵, transient levels in the order of seven times the plate voltage on the transformer were measured. The transients were

found likewise to propagate to the load at approximately the same level. A wide variety of disturbances were inserted and the resultant transients were recorded. The most severe transients were those encountered due to grid-to-cathode shorts of the high-powered final amplifier stage. Further, the transient levels measured here were in agreement with those experienced in industry.

Other tests were performed to better define the transient behaviour of the transformer as an isolated unit. Mathematical calculations and measured data were compared for the linear case. For the non-linear case, as for example the shorting of the grid of the final amplifier, it was recommended that the simulation approach be used. Here specifications of a low-powered system would be extrapolated for the high-powered case.

The conclusion reached was that a need exists to have the system engineer perform the above simulation and then in turn relay, by specification, to the transformer designer the levels of the expected transient peak amplitude and waveshape.

The solution of the transient problem requires that transformer designers in turn develop the proper methods for testing wide band transformers. The Wide Band Frequency Range Subcommittee of the I.E.E.E. has become convinced of such a need, and further, has begun to act. The officers of the sub-

committee have appealed to the Electronic Transformer Committee of the I.E.E.E. for permission to form a Subcommittee to develop the necessary test codes and procedures for use in Electronic standards, such as the Proposed Standard No. 453 for Low-Power Wide-Band Frequency Transformers and the Tentative Proposed Standard for High-Power Wide-Band Frequency Transformers, now being prepared.

The prospects for future development probably lie in the following areas:

- (1) Magnetic materials.
- (2) New art (superconductivity).
- (3) Multiple-unit networks.
- (4) Network and system development.

It would appear that the prospects for future development are good for (1) and (2) because of the high level of general effort being applied to these areas at the present time. In regard to (3), in addition to the two-unit transformers, three-unit transformers have been built but they are discouragingly complicated and it is unlikely that much work will be done here without a breakthrough of some kind. Work still continues on (4), which may result in appreciable gains in effective bandwidth for transformers.

Comparison of Semi-conductor Strain Gauge and Metal Strain Gauge

S.-Y. LEE

The extraordinarily high resistance-strain coefficient (gauge factor) of semi-conductor material led to the development of the semi-conductor strain gauge, which is basically a very thin (about 0.002 in.) wafer cut from a piece of single crystal of 'doped' silicon or other suitable semi-conductor material^{58, 59}. A wide range of gauge factors, resistivities, and temperature characteristics can be obtained by controlling: (a) impurity content, (b) orientation of crystalline axes, and (c) type of semi-conductor (*p* type or *n* type)^{59, 61, 65}. Using *n* type semi-conductor material when cut along a certain axis, it is even possible to obtain gauges with very high negative gauge factor (i.e. resistance decreases when stretched). There are two major areas of application for strain gauges: for the measurement of surface strain, and as the sensing element of a mechano-electric signal converter (transducer)⁶²⁻⁶⁴. The following comparison is made with consideration of these two basic applications.

Accuracy

Hysteresis—The hysteresis of silicon itself is extremely low even at elevated temperatures (up to 600°F). In most cases the hysteresis of the bonding agent and that of the base structure control the overall hysteresis.

Linearity⁵⁹—The linearity (of the $\Delta R/R$ vs. strain curve where R is the resistance and ΔR is the change of resistance) of a semi-conductor strain gauge is considerably poorer than that of a metal strain gauge when fully stressed. For stress analysis applications, where only one active strain gauge is used at any given station, the maximum strain should be limited to about $\pm 500 \mu\text{in./in.}$ to obtain reasonable linearity. This is considerably less than the comparable linear strain level of a metal gauge ($\pm 3,000 \mu\text{in./in.}$). This drawback can be overcome by prestressing the gauge or by using the *p* type and *n* type gauge side by side. The latter method has the advantages of doubling the output signal and achieving linearity compensation at the same time. When the gauges are used for transducer applications the non-linearity problem is not too serious because it is usually possible to select the most linear portion of the $\Delta R/R$ vs. strain curve, and it is also usually possible to design the load-carrying structure so that a tension gauge and a compression gauge can be mounted near each other to form adjacent arms of a Wheatstone bridge. The non-linearity of both gauges thus can be made to compensate each other. Using a Wheatstone bridge circuit to measure the resistance change of a single strain gauge also gives rise to some non-linearity. For metal gauges which

have a maximum resistance change of the order of 0.5 per cent, very small circuit non-linearity is involved. Semi-conductor gauges can have resistance changes as high as 20 per cent. The circuit non-linearity can be appreciable unless a push-pull arrangement is made with two gauges. (One gauge has an increase in resistance while the other has a reduction in resistance.)

Temperature Effects

The properties of a semi-conductor gauge are more temperature dependent than those of a metal gauge^{59, 62-65}. Fortunately, the temperature effects are quite repeatable and stable. There are two major temperature effects. The first one can be defined by the resistance-temperature coefficient ($\Delta R/R$ vs. T). The second one can be defined by the gauge factor-temperature coefficient ($\Delta R/R/\text{strain}$ vs. T). These two effects are somewhat related. Strain gauges with high resistance-temperature coefficients usually have high gauge factor-temperature coefficients. These temperature effects will cause both the output zero reading and sensitivity to change with temperature. Both of these temperature effects are functions of the gauge material (impurity content) used. Gauges with high gauge factors usually exhibit greater temperature effects. A typical semi-conductor gauge with a gauge factor of 100 has a resistance-temperature coefficient of 0.0010°F and gauge factor-temperature coefficient of 0.0015°F . These coefficients are approximately two orders of magnitude greater than the corresponding coefficients of a good metal strain gauge. For strain measurement applications, these temperature effects are rather undesirable. For limited temperature range applications ($\pm 50^\circ\text{F}$), reasonably good compensation can be obtained by using thermistors which have very high, but very non-linear, negative resistance-temperature coefficients. Temperature effects can be greatly reduced if gauges with heavier doping are used. These gauges usually have smaller gauge factors. The optimum selection depends on particular application and performance requirements. For transducer applications the situation is somewhat different. Various other compensation techniques can be applied.

Output Signal Level

The major asset of the semi-conductor strain gauge is the high output signal level which is proportional to the product of excitation voltage, gauge factor, and maximum strain level. Roughly speaking, by selecting low temperature-coefficient semi-conductor gauges it is possible to obtain output signals at levels 5 to 10 times output signal level (compared with a metal gauge) if suitable temperature compensation schemes are used.

Input Work

For strain and stress analysis work the input work required to stretch the strain gauge is not an important concern. However it is desirable to have small gauges to get into close quarters. For transducer applications small size is desirable for a different reason⁶². A small strain gauge requires small stress carrying structure to support it. The total strain energy (hence input work) will be low. It can be shown that for most transducer applications low input work is highly desirable. An unbonded strain gauge requires the least amount of input work since a great percentage of the input work is used to stretch the wires. A bonded gauge can seldom be designed to have better than 10 per cent efficiency. Input work can be reduced by reducing the size of the gauge. Since semi-conductor material can be made with much greater resistivity than most metal alloys which are used for strain gauge purposes, it is possible to have a semi-conductor gauge with much smaller surface area than a metal gauge.

Areas of Application of Semi-conductor Strain Gauges

The following are the most important areas of application of semi-conductor gauges:

*High-level output transducer*⁶¹⁻⁶⁴.—Using proper temperature compensation schemes it is possible to construct transducers with semi-conductor strain gauges to have 5 V output at 25 V excitation (compared with 0.1 V output of a transducer with metal gauges). This type of instrument is particularly useful for airborne applications where size and weight are extremely important. The output of the transducer can be used directly to drive a telemetering system or other equipments without additional stages of amplification which add weight, cost, power drain, and source of error to the overall system.

Measurement of low-level strain.—It is difficult to measure very low-level strains with a metal gauge because of the low signal-to-noise ratio (particularly noise introduced by the amplifier). Using high output semi-conductor gauges the problem is considerably simplified. If only dynamic strain is to be measured, the relatively slow thermal shift can be filtered out with proper circuitry. Otherwise, it is necessary to use a temperature compensation scheme to reduce the thermal effects.

Strain on a moving member.—To measure the strain on a moving member (e.g. torque meter) slip rings are often required. The noise produced at the slip rings can be considerable compared with the low output level of metal strain gauges. When high-output semi-conductor gauges are used the signal-to-noise ratio will be proportionally improved.

Gyroscopic Instruments

P. P. FISCHER

A large-scale effort to improve gyroscopic instruments has been made since the late 1950s, mainly spurred by the requirements of military and space control and guidance systems.

The most obvious direction for development of gyro instruments has been toward improved bearing technology (resulting in reduced errors, reduced mechanical and electrical noise, and longer life), and various efforts to improve materials and machining technology (i.e. beryllium and ceramic gyro parts machined to better than $3 \cdot 20^{-6}$ in. tolerances). Bearing improvements included the use of gas bearings for gyro motor and gimbal support^{66, 72}, and a technique of dithering gimbal bearings to reduce starting friction. These devices are now practical and are incorporated in functioning gyro systems.

Research into the failure modes and their causes in gyros has led to the development of various lubricants, and an even more profound result—the revelation of the very deleterious effect of oxygen on gyro bearing life. This problem has now been identified and work is in progress on solutions intended to result in reduced bearing failures.

Another approach has been to replace the spinning gyro wheel with a fluid contained in a spherical chamber. Spinning the chamber imparts angular momentum to the 'fluid sphere' which will act as an inertial mass. If the chamber spin axis is rotated, the spin axis of the 'fluid sphere' will tend to remain fixed in space. This relative rotation of the spin axis results in a pressure dissymmetry about the axis of the chamber which is sensed by a pair of transducers. This configuration is used in a gyro placed in production during 1962. Other configurations involving chambers fully or partially filled with fluids are being evaluated by various companies. These gyros will provide performance characteristics, ranging somewhere between that of a spring-restrained type and a costly electrically restrained type, at a moderate cost (about \$ 600.00 for the fluid sphere device).

The promise of great improvements in gyro performance in the area of non-mechanical suspension systems is presently being explored. Electrostatic and electromagnetic support systems have been proposed with the present effort emphasizing the magnetic support⁶⁷. By utilizing materials in the superconductive state (due to cryogenic temperatures) it is hoped to produce a gyro with a 100 to 1 improvement in drift rate (over conventional devices)⁶⁸. The design prototypes successfully tested to date have spherical superconducting rotors suspended in an electromagnetic field. The effect of the cryogenic temperature is to reduce electrical losses to almost zero, plus making the power consumption, once started, negligible. To eliminate spurious disturbance torques, optical means are used to read out the relative motion between case and rotor. Work on very sensitive attitude and acceleration sensors using magnetic suspensions is at present in progress.

The gyroscopic properties of vibrating rather than rotating

masses have been of interest for some time. One result of investigations in this area is the development of a practical 'solid state' gyro⁶⁹. The device consists of a solid thin-walled cylinder of piezoelectric material (i.e. barium titanate). This is excited by a high-frequency voltage (about 100 kc) which causes expansion and contraction at opposite ends of the cylinder. Rotation about the axis of the cylinder causes a compensating torque to be set up in the cylinder which, due to the piezoelectric effect, produces an electrical signal which is detected. This device can be used as an extremely rugged, long lived, small, inexpensive gyro using extremely little power (about +0.001 W).

The development work in the area of lasers has revived experimentation with devices using the Michelson-Gale effect to measure turning rate. One laboratory experiment recently reported^{70, 71} utilized a 'square ring' of four laser tubes. Normally the light energy emitted from the ends of each laser will travel equal distances to a photo detector. Rotation of the ring causes an inequality in the light paths, thus causing a difference in frequency between the two beams. This beat frequency is proportional to the rotational rate

$$\Delta f = k\Omega A / \lambda P$$

where Δf is the beat frequency, Ω is the input rate, A is the area of the ring, λ is the laser wavelength, P is the perimeter of the ring, and k is the proportionality constant.

This device is still in the laboratory experimentation stage but shows great promise. There are no apparent physical limitations to the rates to be measured, the limitations being mostly in the detection techniques for very low frequencies. The effect of vibration and system noise would also be a problem. On the other hand the system has no moving parts, has negligible mass acceleration effects, is generally simple to mechanize, and has low power consumption.

Another 'avant garde' approach to gyro mechanization consists of completely discarding conventional configurations and working with physical phenomena such as electromagnetic resonance and nuclear spin momentum relationships. The use of 'rotating' particles such as electrons, nuclei, helium atoms, etc. in controlled fields as gyroscopic sensors, has been tried by a number of experiments. Two devices have come to the author's notice: One uses the Lamor effect, which describes the frequency of precession of atomic particles, and uses the change in Lamor frequency as the sensed parameter; the other senses induced voltage in a set of coils surrounding the resonating group of particles. Both devices are still in the laboratory stages and details are not available due to security restrictions. The feeling that these efforts will result in practical devices superior to but competitive in size, weight, power and price with more conventional devices has been expressed by the personnel involved.

State of the Art on Electrohydraulic Servovalves

W. J. THAYER

During the past decade, electrohydraulic servomechanisms have become very popular for high performance position control in systems which require greater than one-third horsepower. This popularity is due largely to the concurrent development of present day two-stage, electrohydraulic, flow-control servovalves.

Servovalves in use prior to 1950 were generally single-stage designs in which a short stroke permanent magnet motor connected directly to a sliding-spool, hydraulic control valve. The usefulness of these early servovalves was limited by the relatively low spool driving forces obtainable with reasonable motor size and electrical power input. Other early servovalve designs utilized a small pilot-stage spool as an additional hydraulic amplifier between the motor and load control valve, but these suffered from poor resolution due to friction of the pilot spool.

A major advance in servovalve technology came with the introduction of the two-stage design which used a nozzle and flapper hydraulic amplifier. Later improvements included: (1) use of a symmetrical hydraulic amplifier (e.g. double nozzle and flapper; or jet pipe and receivers; or double shear orifices and flapper), (2) isolation of the permanent magnet motor from the hydraulic fluid, and (3) use of internal spool position feedback.

A variety of two-stage flow-control servovalve designs are presently available from a number of manufacturers. There are miniature designs for control of flows less than 2 gall./min (approximate physical size: $2\frac{1}{2}$ in.³ volume; $\frac{1}{8}$ lb. weight). The more common servovalves weigh about $\frac{3}{4}$ lb. and are available for maximum rated control flow in the range from 1 to 15 gall./min. Some large two-stage designs are available for control of flow to 100 gall./min, but generally a third-stage sliding spool is added to obtain flow capacity of this magnitude. *Figure 2* shows a series of standard servovalves available from one manufacturer.

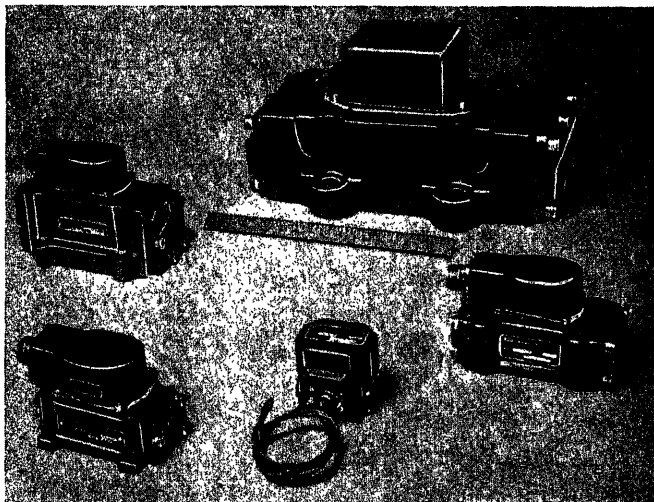


Figure 2

Representative performance available from present day servovalves is the following:

Supply pressures	350 to 3,500 lb./in. ²
Hydraulic amplifier leakage flow	< 0.2 gall./min
Rated electrical input power	30 to 50 mW
Dynamic response	< ± 1 db to 200 c/sec for 1 gall./min valve < ± 1 db to 100 c/sec for 15 gall./min valve
Non-linearity	< 5%
Flow gain tolerance	< $\pm 10\%$
Resolution	< $\frac{1}{2}\%$
Hysteresis	< 3%
Usable temperature range	to + 275°F usual; to + 650°F with special designs
Environmental capability	normal aircraft and space vehicle
Null shift	< $\pm 5\%$ for 300°F temp. change < $\pm 2\%$ with $\pm 20\%$ pressure variation < $\pm 3\%$ with life and use

During recent years significant advances in servovalve technology have involved the adaptation of standard servovalve designs to special system requirements. Three areas of interest are: (1) use of pressure feedback, (2) use of both electrical and mechanical control inputs, and (3) use of redundant control techniques.

Pressure feedback around a flow control servovalve will produce a load velocity to force relationship which can be useful for stabilization of mass resonance in a position servomechanism. The technique is analogous to the addition of a bypass orifice across the load actuator, but does not involve the power dissipation associated with a bypass orifice or other passive damping devices. A number of pressure feedback servovalve designs have been developed. In some designs a pressure feedback force is applied to the motor armature by a small piston and spring mechanism. In other designs the load pressure feedback is summed at the servovalve spool through use of auxiliary control areas. The latter are spring centred spool designs wherein spool displacement is determined by the applied pressure forces.

More elaborate pressure feedback servovalves have included a frequency sensitive hydraulic filter in the pressure feedback path. The filter permits feedback of dynamic pressure variations for stabilization of load resonance but eliminates feedback of steady-state pressures. In this way the static accuracy of the system is not reduced by load force sensitivity. Several dynamic pressure feedback servovalve designs are available using various functional arrangements.

Servovalves which accept both electrical and mechanical inputs simultaneously have been developed by several manufacturers. These valves can be used in piloted vehicles for mixing electrical stability augmentation signals with manual operator

controls. This type of servovalve is also used to sum electrical command signals with mechanical position feedback signals in self-contained hydromechanical load position actuators.

The creation of special servovalves for use with redundant control systems is relatively new*. Various types have been developed, including monitor servovalves which can sense a system failure, and majority voting servovalves which reject one failed channel when three or more active channels are in use.

Future advancements in servovalve technology will undoubtedly be directed towards the major design weaknesses of present day valves. Probably the most significant weakness of presently available servovalves is their lack of accuracy. Valve null shifts

* New servovalves for redundant electrohydraulic control. I.F.A.C. Paper by Garnjost, K. D. and Thayer, W. J.

and hysteresis can produce significant actuation error unless the servoloop is designed to contend with these effects. When the servovalve is used as the error point for a position control loop (as in a mechanical feedback servoactuator) these valve inaccuracies can be very serious. Another limitation of present day servovalves in some applications is the quiescent power loss associated with internal leakage flow. Reduction of leakage flow through use of smaller orifices in the hydraulic amplifier can lead to contamination susceptibility.

Development efforts currently devoted to digital hydraulic actuation are aimed at improving performance deficiencies resulting from these servovalve weaknesses. A true digital, word-input electrohydraulic servoactuator which would operate at clock rates sufficient to give dynamic response comparable to existing servovalves would be a major technological advancement.

Performance of Hydraulic Systems in Positioning Servomechanisms

M. GUILLON

Recent work in France on high performance hydraulic systems for aerospace applications has resulted in the design of positioning servomechanisms which, as subsystems, have been important components of large complex systems. This paper discusses problems related to the determination of the best performance of such a servo when the load inertia is large and the drive does not allow a compensating network.

Determination of Performance

Consider a load, which could be for example an aileron of an airplane or a rocket nozzle of a missile, positioned by a symmetrical, double-acting hydraulic jack, which is controlled by an electrohydraulic servo-valve.

The block diagram, showing the scheme of functional operation, is shown in Figure 3.

It should be noted that in the case of a hydraulic servo-control with mechanical feedback the scheme is simplified, but the analysis and results which follow still apply.

In addition to the symbols shown in Figure 3, the following notation will be used.

- I = inertia of the load
- C_r = the maximum opposing torque
- β_m = maximum angle of rotation of the load
- A = net effective working area of the jack
- l = length of the lever arm at the front of the jack
- $V = k_v A / \beta_m$ = half the total volume of the jack (where k_v is the volumetric coefficient taking into account the dead volume situated below the servovalve— k_v is usually of the order of 1.2 to 1.5)
- P_1 = supply pressure
- B = bulk modulus of elasticity of the oil described by the following relation

$$\frac{\Delta V}{V} = -\frac{\Delta P}{B}$$

k_s = safety factor relating available torque to required torque

$$\left(k_s = \frac{P_1 A l}{C_r} \right)$$

K = total loop gain ($K = K_1 K_2 K_3 k$)

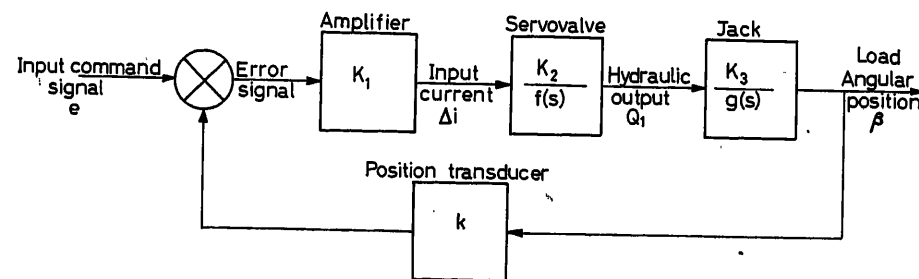


Figure 3

Speed of Response

The open loop transfer function is found to be

$$\frac{k\beta}{\varepsilon} = \frac{K}{s \cdot f(s) \left[1 + \varepsilon s + \frac{IV}{2B(AI)^2} s^2 \right]} \quad (1)$$

which may be written as

$$\frac{k\beta}{\varepsilon} = \frac{K}{s \cdot f(s) \left[1 + 2 \frac{\zeta s}{\omega_c} + \frac{s^2}{\omega_c^2} \right]} \quad (2)$$

where

$$\frac{IV}{\varepsilon B(AI)^2} = \frac{1}{\omega_c^2} \quad \text{and} \quad \varepsilon = \frac{2\zeta}{\omega_c}$$

In using the notation given in 1 and 2:

$$\frac{1}{\omega_c^2} = I \frac{P_1 k_v \beta_m}{2B k_s C_r} \quad (3)$$

As to ζ (or ε) it is a very difficult coefficient to calculate and depends on friction, leakage, etc. If the inertia is large, ω_c is small and for sinusoidal variations of ω in the neighbourhood of ω_c , the transfer function of the servo-valve is very nearly constant [$f(s) \sim 1$].

The result is that for $\omega = \omega_c$, the transfer function reduces to

$$\left| \frac{k\beta}{\varepsilon} \right| = \frac{K}{2\zeta\omega_c} \quad \text{and} \quad \phi = 180^\circ \quad (4)$$

Furthermore, experience shows that combined natural and artificial damping, using electronic compensating networks or secondary (velocity) feedback, makes it difficult to obtain values of the damping coefficient ζ greater than 0.25.

Now for smaller values of ζ , the method of the crossover point shows the gain margin is much more critical than the phase margin.

It follows that a good stability condition results when

$$\left| \frac{k\beta}{\varepsilon} \right|_{\phi=180^\circ} \leq \frac{1}{2}$$

A condition here described by

$$K \leq \zeta \omega_c \quad (5)$$

and with $\zeta = 0.25$, we find that

$$K \leq \frac{\omega_c}{4} \quad (6)$$

As to low frequencies, the closed loop transfer function is closely approximated by

$$\frac{1}{k} = \frac{1}{1 + \frac{s}{K}}$$

One may conclude that the greatest speed of response which one may attain with this system is that of a first order system with a time constant

$$\tau_{min} = \frac{1}{K} = \frac{4}{\omega_c} \quad (7)$$

The accompanying nomogram (Figure 4) gives τ_{min} directly as a function of C_r and I for the following typical values:

$$\begin{aligned} P_1 &= 200 \text{ bars (3,000 lb./in.}^2\text{)} \\ B &= 10,000 \text{ bars (150,000 lb./in.}^2\text{)} \\ \beta_m &= 25^\circ \\ k_s/k_v &= 1 \end{aligned}$$

For other values than those given above one may replace I by

$$I^* = I \frac{\beta_m}{25} \cdot \frac{k_v}{k_s} \cdot \frac{P_1}{200} \cdot \frac{10,000}{B}$$

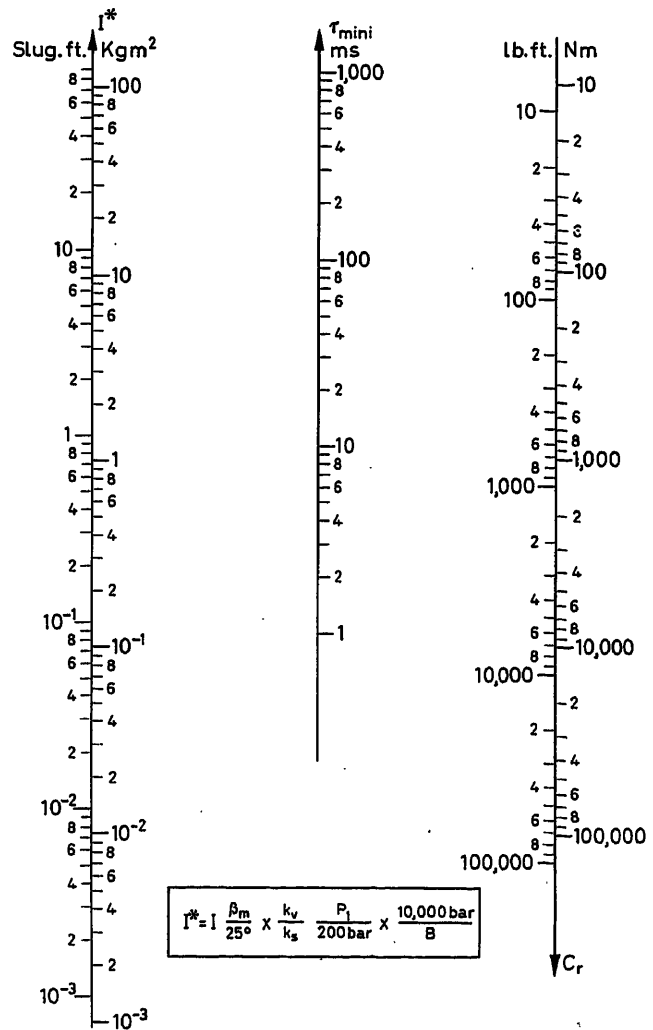


Figure 4

Precision

It is often the threshold current of the servo-valve, Δi_s , which determines the precision of the system.

One generally introduces the relative threshold $S = \Delta i_s / \Delta i_m$ in the analysis, for it is very constant for the different types and sizes of servo-valves. Similarly it is often not the absolute error, but the relative error of the output $\Delta \beta / \beta_m$ that is of interest.

In combining these two relative variables:

$$\Delta\beta k K_1 = \Delta i_s$$

$$\Delta i_m \cdot K_2 \cdot K_3 = \left(\frac{d\beta}{dt}\right)_m$$

one obtains:

$$\frac{\Delta\beta}{\beta_m} = \frac{S}{K} \frac{(d\beta/dt)_m}{\beta_m} \quad (8)$$

But, in introducing the saturation ratio r defined in Figure 5 as the ratio β_m/β_i ,

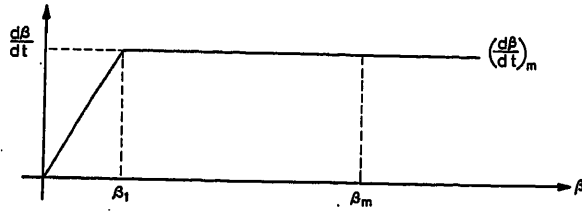


Figure 5

one may then write, noting that $\frac{(d\beta/dt)_m}{\beta_i} = K$,

$$r = \frac{\beta_m}{\beta_i} = \frac{K\beta_m}{\left(\frac{d\beta}{dt}\right)_m} \quad (9)$$

or even more simply:

$$\frac{\Delta\beta}{\beta_m} = \frac{S}{r} \quad (10)$$

Influence of Rigidity of Mounting Base

If the angular stiffness of mounting for the hydraulic jack is not infinite, it appears in the transfer function, and the relation defining ω_c becomes:

$$\frac{1}{\omega_c^2} = I \left[\frac{P_1}{2B} \frac{k_v}{k_s} \frac{\beta_m}{C_r} + \frac{1}{r} \right] \quad (11)$$

In order not to degrade the performance, it is important that r be greater than

$$\frac{C_r k_s 2B}{\beta_m k_v P_1}$$

If one notes that k_s/k_v is approximately unity, and $2B/P_1$ is

approximately 100, it follows that r should be greater than 100 C_r/β_m , or thus that r has to be greater than 100 times the stiffness of a torsion spring which requires a torque C_r for an angular deflection β_m .

Numerical Examples

In order to illustrate the application of the ideas contained in this paper, two typical systems have been analysed and the numerical results are given in Table 1.

Table 1. Numerical examples

Maximum amplitude of rotation	β_m	(rad)	0.6	0.1
Maximum velocity of rotation	$(d\beta/dt)$	(rad/sec)	4	0.5
	I	(kg · n ²)	0.3	130
Maximum opposing torque	C_r	(m. N.)	200	5,000
Supply pressure	P_1	(bars)	200	200
Bulk modulus of elasticity (at operating temperature)	B	(bars)	10,000	10,000
k_v/k_s	—		0.6	0.8
Minimum time constant (calculated)	τ_{min}	(ms)	9.4	18
Measured time constant	τ_r	(ms)	~ 10	~ 22
Closed loop gain	K	(1/s)	100	45
Saturation ratio	r	—	15	9
Relative threshold of servo-valve	—		4%	4%
Relative precision of the system	$\Delta\beta/\beta_m$	—	~ 0.25%	~ 0.5%
	$\frac{100 C_r}{\beta_m}$	$\frac{\text{(mN)}}{\text{(rad)}}$	3.3×10^4	5×10^6
Angular rigidity of the mounting base	Γ	$\frac{\text{(mN)}}{\text{(rad)}}$	270×10^4	15×10^6
Maximum power (indicative title)	W_m	(watts)	800	2,500
	$(W_m = C_r \cdot (d\beta/dt)_m)$			

Some Recent Developments on Industrial Pneumatic Components

G. EIFERT

In the field of more conventional types of pneumatic components there have been some recent developments which have improved the state of the art. Unfortunately, only some of these developments can be disclosed at this time.

One of these new developments is an improvement of the standard four-bellows regulator. Only two bellows are used which, however, open on two sides; pressure can be applied either from the inside or the outside (*Figure 6*). The bellows are fastened and guided by rings of spring steel, in contrast to the otherwise customary method. These rings lie around the spring bellows and have one end fastened to the movable end

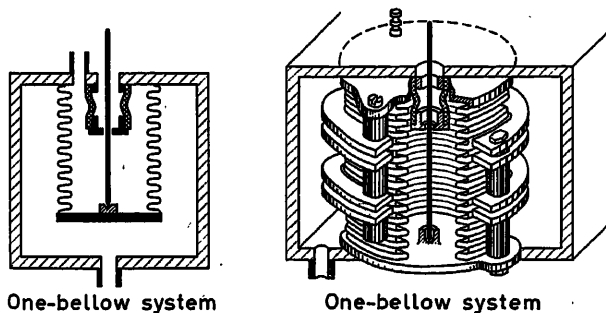


Figure 6. Spring bellows utilizing inside and/or outside pressurization with coil spring parallel guidance

and the other end fastened to the fixed base of the bellows. In this way a parallel guidance of the face end of the spring bellows is achieved, and the bellows is stressed evenly without buckling.

Another development provides pneumatic adjustment of the spring tension of a spring bellows. When a spring bellows is employed for measurement, then it is customary to insert in parallel a tension (or compression) spring for attaining the desired spring constant. For a multiplying device the problem was to make the spring constant of a spring bellows pneumatically adjustable.

One proceeds accordingly to a design in which the 'fixed end' of the spring bellows is attached approximately to the centre of a flexed spring strip (*Figure 7a*). The one end of this strip is firmly fixed (to ground); the other end is fastened to a movable lever. On the movable end of this lever acts the force F of a compression spring. With this mechanical arrangement the spring constant C of the system referred to the bellows becomes $C \approx \text{const.} \times F$. If a pressure P_1 acts on the spring bellows, it can be assumed that for a small motion h , h is proportional to $P_1 C$. If one now substitutes for the compression spring a spring bellows on which a pressure P_2 acts then F becomes proportional to P_2 and hence h is proportional to $P_1 C$ which is proportional to $P_1 P_2$. If for purposes of guidance and better null point stability the bellows is equipped with a ring spring, one obtains a configuration as shown in *Figure 7b*. On the attachment point of the upper end of the circular ring spring bellows a force is derived

which corresponds to the product of the two pressures in the two bellows.

In the desired multiplying device the primary input pressure P_1 and the secondary input pressure P_2 corresponding to the multiplication factor are led to the two desired bellows springs. The resulting force is employed in usual fashion to control a nozzle-flapper valve system, and the force is balanced by the force of a compensating bellows.

Another type of pneumatic regulating unit has been developed in which the proportional band can be set mechanically by using the tangent function. On the crossed bellows regulator (*Figures 8 and 9*) a floating ring is placed around four bellows arranged in a cross. The outside surface of the ring serves as the flapper for the nozzle which is located in a lever which can be rotated around the centre of the ring (and hence of the bellows cross). A very simple and clearcut design of regulator is thus obtained. The elimination of all bearings for a flapper beam or wobble plate removes all problems of bearing clearance and friction. As can be seen from the schematic diagram the actual value X and the desired value X_k act on one of the bellow pairs. To reverse the operation of the regulator these connections in the regulator can be interchanged. The two other bellows provide the D or I action depending on the settings in the valves T_v and T_n .

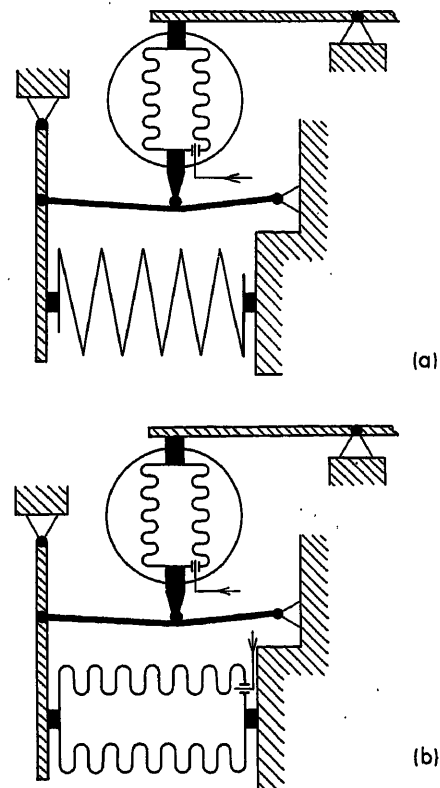


Figure 7. Spring bellows with pneumatically adjustable spring constant

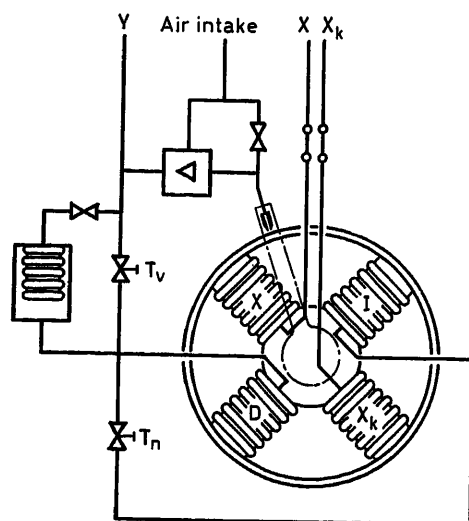


Figure 8. Schematic diagram of the crossed bellows regulator

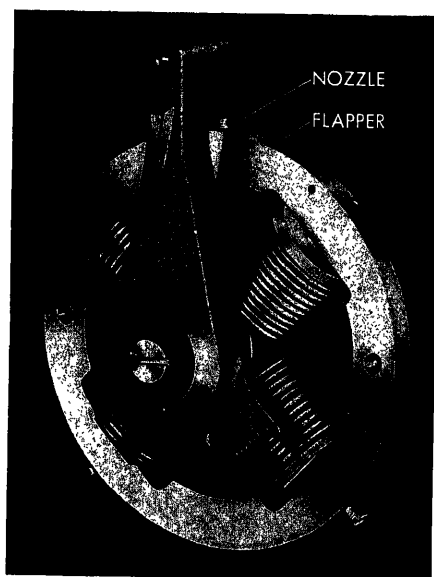


Figure 9. Crossed bellows system with adjustable lever

The proportional band X_p (in per cent) of the regulator is given by

$$X_p = \left(\frac{1}{C \cos \alpha} + \tan \alpha \right) 100$$

where α is the angle between the axis of the bellows $X - X_k$ and the movable lever, and C is a constant approximately equal to 200.

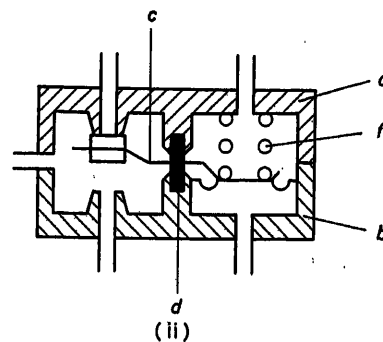
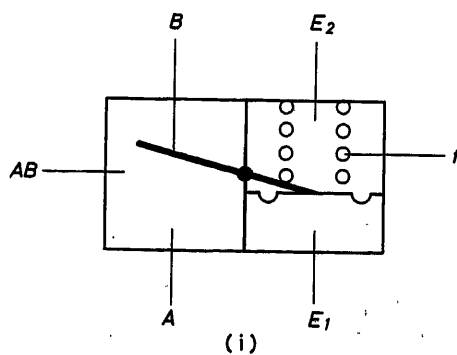
One would expect that the control range (range of modulation) of the regulator should increase in the same way as the proportional band. However, through a particular arrangement and choice of the four bellows one can achieve a configuration such that for a proportional band increase to 500 per cent the control range will increase at most by 1 per cent. The operating point of the regulator during a change of the proportional band between 5 and 500 per cent remains constant to within ± 0.5 per cent.

Pneumatic Binary Switch

In different laboratories and institutes investigations are being conducted towards the development of binary operating pneumatic elements. In this work the free stream principle is extensively used. Devices of this kind, however, cannot in general be combined with conventional devices in the pressure range 0.2 to 1.0 atm (3–15 lb./in.²) without introducing an intermediate conversion device (or transducer). Thus a very simple and cheap pneumatic binary switch for use in the conventional range has been developed. The essential construction feature is a piece of elastic synthetic material which simultaneously serves as the dividing wall between the two chambers of the switch housing and also as the bearing for the contactor lever (Figure 10). One chamber of the housing has three connections, one of which (AB) arbitrarily can be considered as inlet or outlet, the two others as the open or closed connection depending on the switch position. The other chamber contains a membrane (which activates the switching lever) and, depending on the intended use, a spring on one side of the membrane or magnetic plates on both ends of the lever travel to obtain a bi-stable operation. The housing is constructed in such a way that the switches can be mounted next to each other on a standardized mounting rail. The air leads are connected to the appropriate outlets of the mounting fixture. With this switch it is possible to build up a multitude of known logic operations based on binary signals in the range 0.2–1.0 atm.

Figure 10. Pneumatic binary switch:

- (i) A, B, AB air connections to the switching chamber
 E_1, E_2 control air connections
- (ii) a upper part of the switch
 b lower part of the switch
 c valve lever
 d connection between chambers
 f spring



Fluid Systems with No Moving Parts

R. E. BOWLES and F. T. BROWN

Fluid systems with no moving mechanical parts have received considerable attention in the United States⁷⁸⁻⁷⁵ and elsewhere⁷⁶⁻⁷⁸ during the past four years. Most of the components of these 'pure fluid systems' could be called 'fluid jet modulators', because they involve controlled disturbances of fluid jets. Amplifiers, bistable relays, diodes, logic elements, and oscillators are the most common devices.

Amplifiers and Relays

Amplifiers fall into three categories. Most common at present are 'jet-deflection amplifiers', in which a power jet may be said to be deflected by the dynamic pressures of smaller control streams (Figure 11) by the static pressures of the control streams,

or by a combination of the two. If the control pressures are greatly affected by the position of the power jet itself, for example through the mechanism of flow entrainment, the jet might become bistable, exhibiting hysteresis. Such a relay or flip-flop (Figure 12) results from large control areas, large resistances to control flows, and close proximity of a turbulent jet to the boundaries of the control passages.

The power jet can be a liquid and the control flows a gas, such as in the units pictured in Figure 13.

The 'turbulence amplifier' (Auger⁷³) also involves a jet, but instead of using brute-force deflection, control is effected by exciting vortical flow which degenerates into turbulence, in an otherwise laminar but unstable power jet. A laminar jet contains a large fraction of its initial power at a distance of 20 nozzle-widths downstream of the nozzle, whereas a fully turbulent jet is nearly completely dissipated. Excitation can be achieved acoustically, mechanically, or with one or more small control

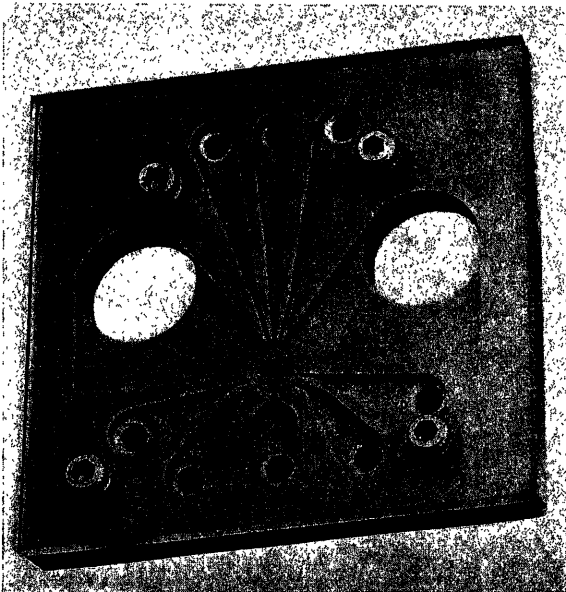


Figure 11. Four-input analogue amplifier (Courtesy Bowles Engineering Corp.)

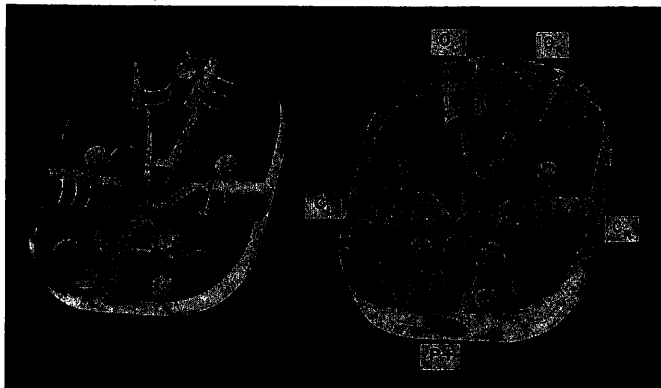
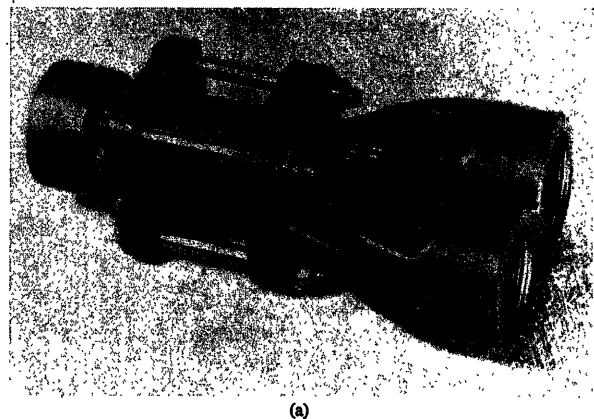


Figure 12. High-stability low-gain relay (Courtesy Bowles Engineering Corp.)



(a)



(b)

Figure 13. Two-phase proportional and switching valves (Courtesy Moore Products, Inc.)

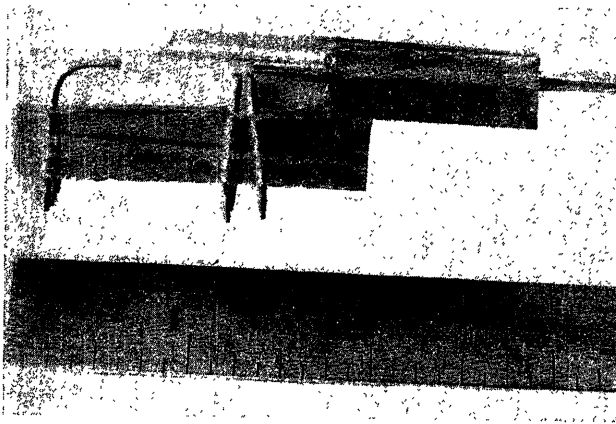


Figure 14. Turbulence amplifier, two-input nor (Courtesy Fluid Logic, Inc.)

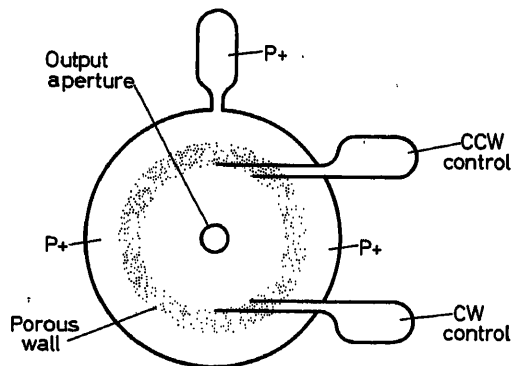


Figure 15. Vortex amplifier

flows, such as in the nor-gate amplifier pictured in Figure 14. Both *bistable* and *continuous* modes of operation are possible. Establishment of an initially laminar jet requires low Reynolds numbers, usually below 1,000, based on the nozzle diameter or width, and an exceedingly long nozzle and/or large settling chamber to dampen out upstream disturbances.

Unlike the devices discussed above, the 'vortex amplifier' (Figure 15) does not have an essentially constant primary-flow power, and hence is often better suited to applications involving irregular duty cycles and expensive power. The angular momentum of the vortex is controlled by relatively small flows, inducing a strong radial pressure gradient, which under usual circumstances raises the input pressure, lowers the output pressure, and reduces the net flow.

Diodes

Fluid diodes are two-way devices with markedly different flow resistances for the two possible directions of flow. Though the idea is quite old⁷⁰, applications such as pressure-signal demodulation and power rectification seem quite new. Operation of the devices is usually based on flow separation or the establishment of vortices.

Logic Elements

The logic functions *and*, *or*, *exclusive or*, *nor*, etc. can be realized with fluid jets in two basic ways. An active element,

such as the *nor* gate shown in Figure 16, has a power jet which produces a power gain. A passive element, such as the twin *and* unit pictured in Figure 17, has no power jet whatever, each jet containing information. A large system of passive elements requires occasional (active) amplifiers.

Fluid logic elements have interested computer manufacturers and others because of applications in which cost and maintenance outweigh response time. Typical response times for small elements with nozzle widths of a few thousandths of an inch are 10 to 100 μ sec.

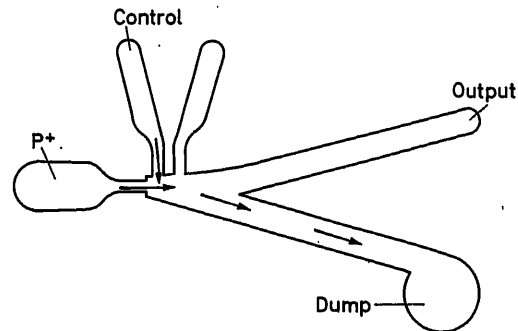


Figure 16. Active nor gate (with signal)

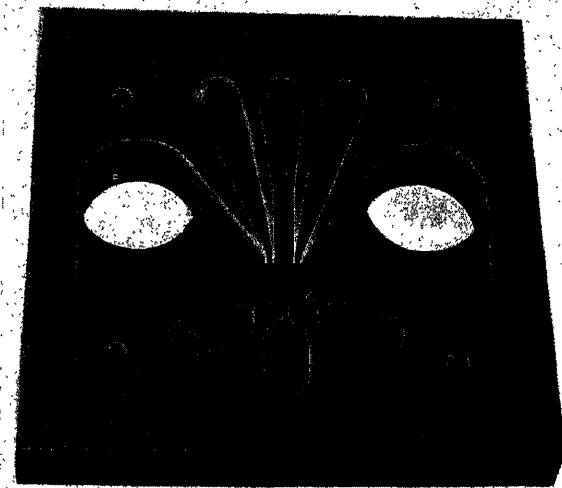


Figure 17. Passive twin and element (Courtesy Bowles Engineering Corp.)

Other Devices

Many other fluid jet modulators can be conceived, such as function generators, signal modulators, and oscillators. Oscillators can be built by attaching appropriate feedback channels or resonating volumes to conventional amplifiers, and, along with more obvious applications, can be used to measure temperature.

Some Fundamental Considerations

The flow regime of the power jet is of extreme importance. Laminar flow is vital to the turbulence amplifier, and turbulent flow is vital to most amplifiers and relays that depend on flow entrainment. There is a most important vortical regime between

the laminar and fully turbulent regimes, in which edge-tone oscillations and seemingly random 'noise' can be very serious.

The static impedance of the control source can be matched to that of the jet modulator to give extraordinary power gains. The case of infinite gain is really the borderline, in a continuum, which separates the continuous and bistable (hysteretic) modes of operation (Brown⁷⁹). The basic limitations to gain can be described, as in electronic amplifiers, in terms of the signal-to-noise ratio.

If the dynamic (surge) impedance of the control lines is not matched to the jet modulator, static equilibrium is achieved, following a change in the control variable only after several waves have travelled back and forth in the control lines. A dynamic instability (oscillation) can result when the surge impedance of the control lines is high and the steady-state impedance is low⁷⁵.

High gains and efficiency are often associated with short jets, large receiver ports, and small exhaust ports. Unfortunately, these same parameters frequently lead to dynamic instabilities when the resistance to load flow is high. These instabilities can be explained in terms of a reflection coefficient for a wave which travels upstream in one receiver passage and is reflected at the port, and refraction coefficients for waves consequently produced in the other output passage(s). If the sum of these coefficients is greater than unity there is a net energy gain, and the possibility of a strong oscillation.

State of the Art

Three-dimensional fluid amplifiers with no moving mechanical parts, using feedback passages, existed in the 19th century. Fluid diodes were built in the 1920s and vortex amplifiers in the early 1950s. Nevertheless, the field was relatively dormant until the late 1950s, when independent work in the United States and Russia sparked new interest and invention.

Items currently in use commercially include fluid valves (amplifiers), gauging systems and other production line controls,

foam-level controls, and sensors. A much wider field of potential applications currently being developed include complete digital logic systems, bang-bang and continuous control systems, jet-reaction control, instrumentation of fluid-flow machinery, timing circuits, and so forth.

Two-dimensional flow channels are most common, and can be made by etching in a glass which can be transformed into a ceramic (Figure 18), etching in plastic (Figure 19), and by several moulding processes.

Some major problems remain, especially involving the stability of complex systems, and both low and high frequency noise. Superior devices should result from a presently lacking thorough understanding of the significant complex flow mechanisms.

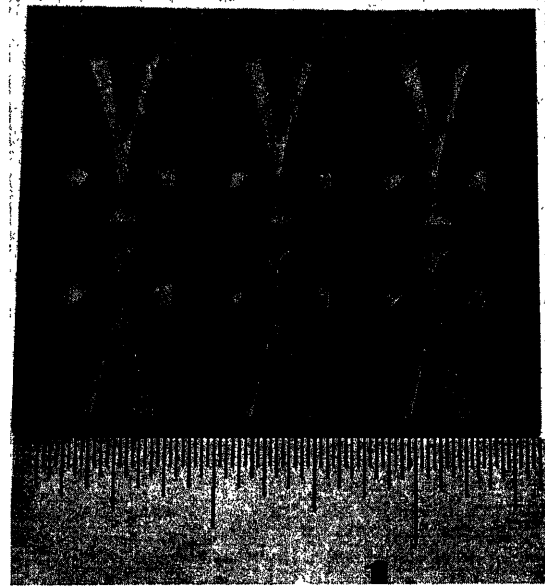


Figure 18. Ceramic elements (Courtesy Corning Glass Works)

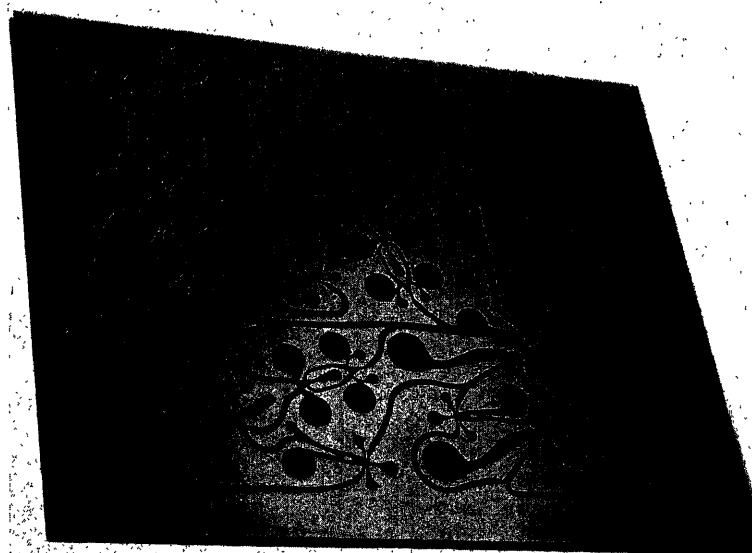


Figure 19. Plastic etched circuit (Bowles Engineering 'Optiform' process on DuPont Photo-sensitive acrylic plastic)

New Developments in Pneumoautomation

M. AIZERMAN and A. TAL

Until shortly after World War II (1947-48) systems of industrial automation used large general purpose pneumatic instruments, mounted on panels and arranged to perform simultaneously the functions of observation, recording, adjustment and individual process control.

The chief engineering features of these devices were the use of the nozzle-flapper amplifier; mechanical pressure transducers such as diaphragms, bellows, and Bourdon tubes providing substantial mechanical output motions; and mechanisms for measuring and comparing mechanical displacements. Typical devices of this kind are the controllers made by companies such as Brown, Bristol, and Taylor in the U.S.A. and units of the 04 type made in the U.S.S.R. These devices were very suitable for controlling individual variables, but did not lend themselves readily to the development of large, comprehensive systems of automation in which the control of many simultaneous processes must be coordinated.

A basic changeover in pneumatic industrial automation occurred in the late forties to individual controllers in which the force-balance principle replaced the displacement-balance principle. Fluid pressure signals replaced mechanical motions. This made it possible to design and manufacture a standard set of devices performing a limited number of basic functions (measuring, comparing, amplifying, integrating, recording, adjusting) and using uniform, standardized input and output signals. These standard devices could be combined in many different ways by means of connecting lines to provide various special control needs. Typical devices of this kind are the units made by Moore, Sunvik, and DRD, and of the type AYC in U.S.S.R. These are the most widely used elements at the present time (1963) throughout the world.

Air pressures between 15 and 30 lb./in.² have been widely used in both kinds of systems, with higher pressures occasionally used for special applications (steam boiler control, turbine speed regulation, etc.).

Recently another transition has begun which promises to meet many of the comprehensive requirements of complex systems of industrial automation, such as previously unattainable speed of response, greater ease of combining basic elements, and better coordination of the control of many simultaneous processes from a control centre.

Three engineering features characterize this transition: (1) use of lower working pressures; (2) synthesis of pneumatic devices and systems from basic components using printed circuit assembly techniques; (3) design and construction of pneumatic components employing direct interactions of fluid jets (without any intermediate moving parts) and employing a printed circuit technique to produce intricate profiles needed to control interaction of the jets. With the possible exception of the printed circuit idea, all of these ideas were contained in some form or another in the well known work of Ferner^{80, 81}. However only important inventions and developments in different countries in very recent years have made practical applications possible. These features are briefly described below.

Use of Lower Pressures

When pressures of the order of 15 lb./in.² are used, pressure differences across flow resistors can be so high that the resistors have non-linear characteristics resulting from air compressibility. Also, very small orifices and passages are needed in order to minimize air flow and maintain high gain or sensitivity in conventional devices at this operating pressure level. Such small orifices and passages easily become plugged with dirt particles, so that means must be provided for filtering and drying the air. Using a much lower air pressure makes it possible to obtain linear flow resistors and to use larger orifices and passages without increasing air consumption. Increase in size of orifices and passages results in less chance for plugging and thus improves system reliability.

The experience gained in Germany⁸¹ and the U.S.S.R.^{82, 83} with design of low pressure diaphragm devices has demonstrated the feasibility of using low pressures (100-200 mm H₂O) for both automation and computation (analogue) systems. Although originally introduced for use with diaphragm-operated elements, the low pressure operation is even more effective when applied to jet devices.

Construction of Pneumoautomatic Devices and Systems of Standardized Components with Printed Circuit Assembly Techniques

Unlike electrical and electronic systems which are assembled from standard components such as resistors, capacitors, inductors, tubes, transistors, etc., manufactured by specialized factories, each pneumatic system was until recently a unique design. As a rule, its parts could not be used in other systems, and thus were not available as standard independent units. Therefore each new system posed new design and engineering problems at the components level.

It was thus quite natural for the idea to arise⁸⁴ of constructing pneumoautomatic systems based on a limited number of standard components produced and kept in stock as electronic elements are. Many different pneumatic systems can be constructed from these standard components by mounting them on special panels or base plates containing necessary interconnecting passages. For instance, a system composed of nine components which was built in the U.S.S.R. is shown in Figure 20. Each component has a standard set of connecting plugs which mate

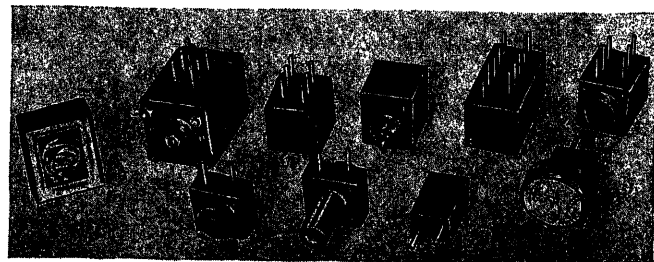


Figure 20. Typical set of components used in constructing a pneumatic system

with corresponding ports in a base plate. The base plate consists of several layers or sheets having channels or passages, analogous to printed circuits used for electronic systems, which provide the necessary connections between components. Thus very complex systems can be built up in a very compact form which was not possible before.

This technique makes it possible to construct combinational and sequential switching circuits, remote control devices employing coding and decoding of signals, analogue and discrete control systems with complex programmes, optimizing systems⁸⁵ and many other complex systems of automation consisting sometimes of hundreds or thousands of components. An automatic optimizing device which was constructed using this technique is shown in *Figure 21*.

The principle of using standard components has changed the possibilities of pneumoautomation. Control algorithms of any complexity are now within reach.

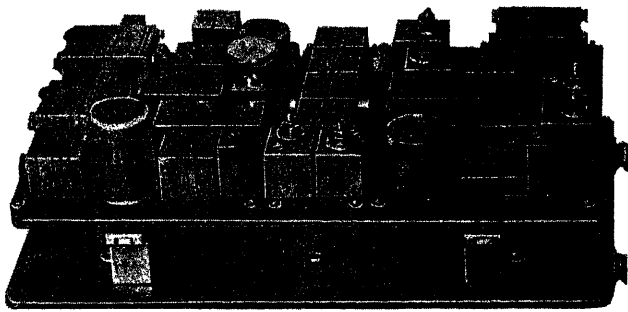


Figure 21. Complete automatic optimizing system constructed of standard pneumatic components

Construction of Jet-Type Pneumatic Devices Using the Printed Circuit Principle

All of the pneumatic devices and components used in displacement-balance and force-balance systems contain elastic and moving parts. Recently a technique for constructing pneumatic components with no moving parts was developed independently and almost simultaneously in the U.S.S.R.^{86, 87} and in the U.S.A.^{88, 89}. The technique is based on the direct interaction of jets and the interaction between jets and solid body profiles. By using the phenomena of boundary layer separation and turning of a jet by control jet, it is possible to obtain very compact amplifying relays and proportional amplifiers having various characteristics without the use of elastic or moving parts.

The use of positive as well as negative feedback circuits makes it possible to make desired changes of components characteristics. Linear amplifiers, memory elements, logic elements, flip-flops, etc., can all be obtained. By combining such elements into systems, various analogue or digital devices can be constructed. For instance, *Figure 22* shows schematic diagrams of a relay, a memory cell, and a jet-type pulse generator.

The key feature of the printed circuit technique is that both the communication channels and the jet-type components are simply surface indentations in some material (see *Figure 23*); therefore various techniques resembling those of usual printing can be used to manufacture inexpensive, compact systems consisting of hundreds or thousands of components. The experience in the U.S.S.R. and the U.S.A. testifies to the fact that such elements can operate at frequencies in the low kilocycle range and that devices and systems capable of performing hundreds of operations per second are feasible.

Though experiments carried out both in the U.S.S.R. and the U.S.A. have shown that jet devices can operate throughout a very wide range of working pressures for various working media, present systems predominately use compressed air at low pressure (100–500 mm H₂O).

Thus three new technical break-throughs have basically improved the possibilities for pneumoautomation to play an important role in the development of automation.

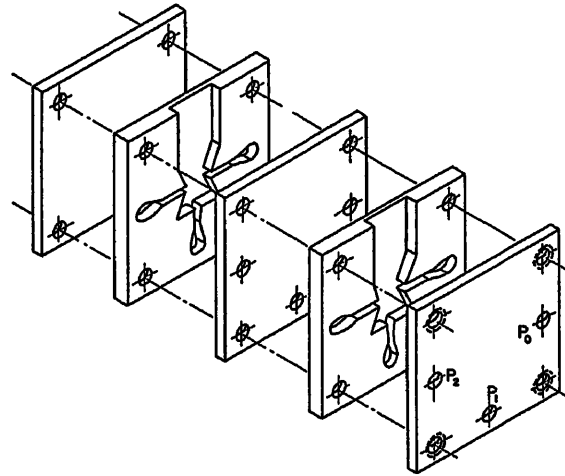


Figure 23. Jet-type device constructed by the printed-circuit technique

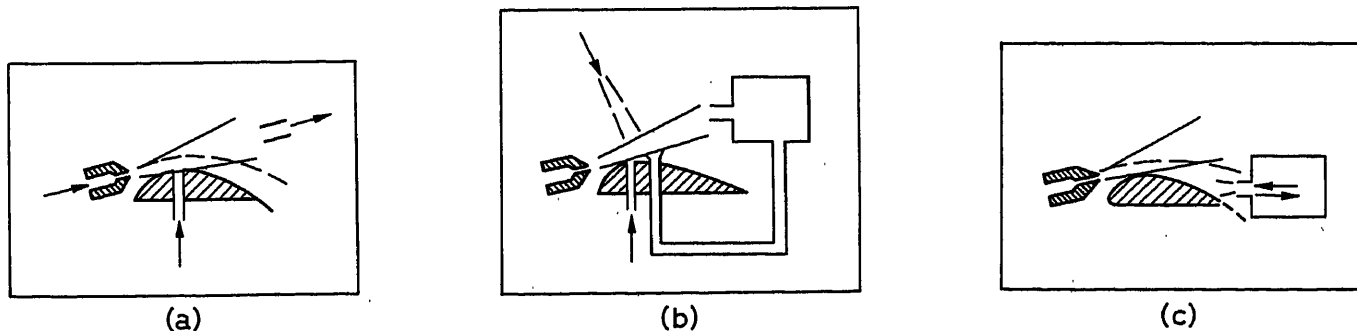


Figure 22. Schematic diagram of three different jet-type devices: (a) Relay; (b) Memory cell; (c) Pulse generator

Pneumatic Components for Extreme Environmental Applications

J. L. SHEARER

Environmental temperature and radiation conditions encountered in advanced aerospace systems have imposed severe requirements on information processing and power-control systems. Typical temperatures are estimated to be as high as 1,500°F (815°C) for at least short periods (up to 10 min), and 1,000°F (540°C) for sustained periods (up to 1 hour). Most conventional components cannot tolerate such temperatures and would require at least local refrigeration (at great cost of weight and complexity). Nuclear powered spacecraft cannot be provided with nearly as much radiation shielding as in ground installations because of weight limitations. Thus components are needed which can tolerate a high level of nuclear radiation.

The use of electronic and/or hydraulic control components for this kind of application is practically impossible. However, pneumatic components can operate in these extreme environments if they are properly designed and developed. A number of short-duration missile and spacecraft systems have already been developed using hot- and cold-gas power control systems with important savings in over-all weight compared with systems using more conventional hydraulic components.

Three recent developments at M.I.T. have resulted in significant contributions to the state of the art. Unfortunately none of these developments was ready for publication when the regular technical papers for the Second IFAC Congress were due.

One of these developments is a pneumatic pulse transmission system with bistable-jet-relay reception and amplification. This constituted a major part of the doctoral thesis research of Brown⁹⁰. On this system a command signal is encoded into a pulse-position-modulated signal, converted to pneumatic pulses; transmitted through a pneumatic line; received, amplified, and integrated by a two-stage bistable-jet-relay; and demodulated

by a push-pull piston-cylinder which moves in accordance with the command input signal.

In order to optimize the design of such a transmission line for pulse transmission, a theory was developed for the dispersion of transients in fluid lines taking into account the effects of friction and heat transfer as well as the mass and compressibility of the fluid. Impulse and step responses were calculated from the propagation operator and impedance characteristic based on this theory. In order to overcome some of the dispersion, which is found to be very significant in small lines, a tapered section was added at the receiving end of the line as shown in *Figure 24* to act as a transformer to improve the shape of the transmitted pulses. A theoretical treatment also was developed for approximating the response of tapered lines. Pulse position coding was employed because of its relative simplicity and because it requires no net flow of fluid through the line.

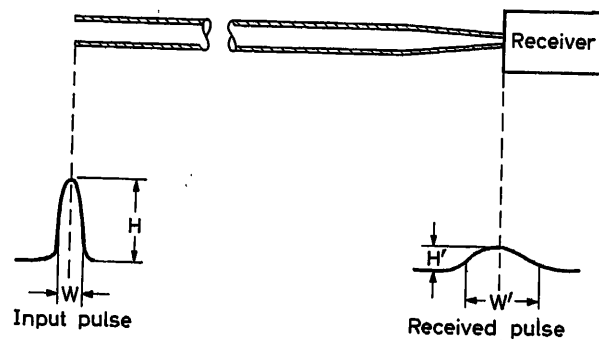


Figure 24. Transmission line with tapered section

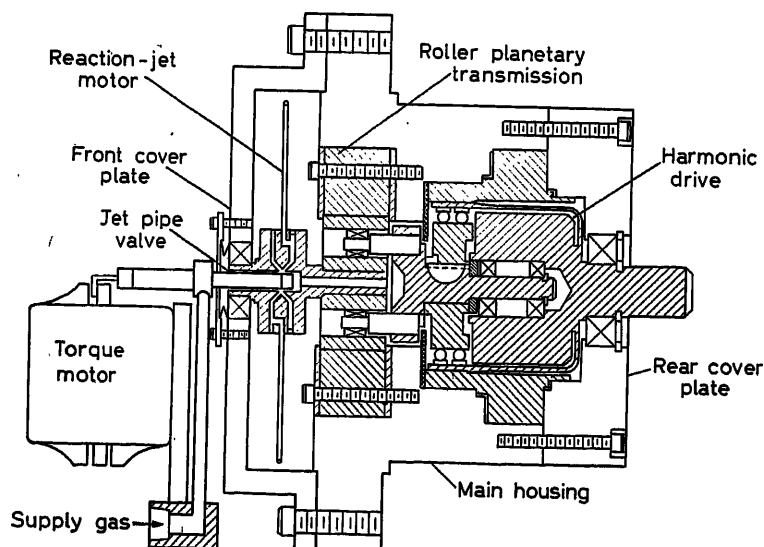


Figure 25. Assembly drawing of reaction-jet servomotor with jet pipe valve and reduction gearing

The jet-amplifier and jet-relay aspects of this work are described in the section of this paper prepared by Bowles and Brown.

The second development involves the use of a reaction-jet servomotor in a mechanical-pneumatic positioning servomechanism, having no electrical components. The pneumatically-powered reaction-jet servomotor (a modern form of Hero's Turbine) consists of a small hub and pairs of arms which carry the fluid out to jets at their tips. A two-ounce rotor is capable of developing over one horsepower at 40,000 rev/min when supplied with air at ambient temperature and 1,000 lb./in.² (67 atm). Research into the basic characteristics of this type of motor was the subject of a doctoral thesis by Scher⁹¹.

The final laboratory model for the complete servomechanism employed an early version of the reaction-jet servomotor, a pneumatic-mechanical amplifier having pneumatic phase-lead compensation, and a jet-pipe power control valve to supply controlled power to the servomotor. A speed reducer was required on the output shaft of the servomotor and simple mechanical feedback of output motion was accomplished with a torsion spring. This system, developed in a doctoral thesis effort by Marcus⁹², led to the conclusion that the response characteristics of a reaction-jet servomechanism can be made comparable to those of existing or proposed high performance positive displacement pneumatic servomechanisms⁹³. An assembly drawing of one version of the reaction-jet servomotor is shown in Figure 25.

The third development is a pneumatic rate gyro which has no electrical components and which employs air bearings at all

load-carrying points between the rotor and the housing. The topic of a thesis by Griffin⁹⁴, this project also included basic work on air bearings and pneumatic detection of gyro wheel precession. An assembly drawing of this rate gyro is shown in Figure 26. This unit, which weighs less than 0.3 lb., has a natural frequency greater than 400 c/sec when operating at 60,000 rev/min with a supply pressure of 100 lb./in.² abs.

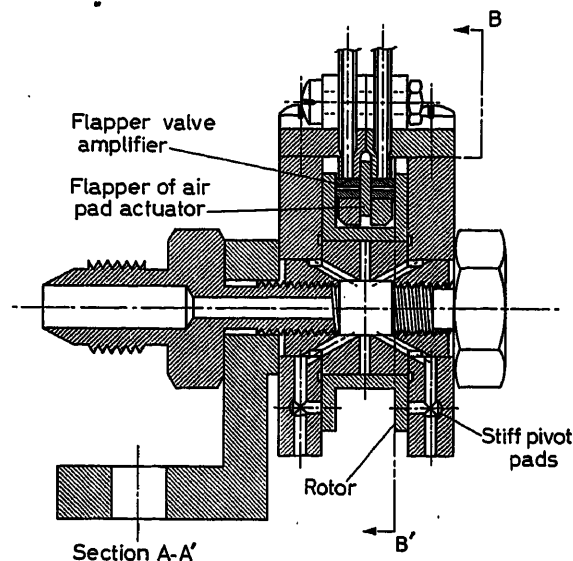


Figure 26. Assembly drawing of pneumatic rate gyro

References

- 1 KOJIMA, Z. Sleeve rotor gives servomotor fast response. *Control Engng*, 10 (1963) 95
- 2 HUGHES, W. T. Design trends in servo systems. *Military Systems Design* (1962) 16
- 3 SABATH, H. Open loop performance measurements of precision a.c. motor-tachometer generators. *Amer. Inst. elect. Engrs Conf. Paper* 62-90
- 4 FRAZIER, R. H. Analysis of the drag-cup a.c. tachometer by means of 2-phase symmetrical components. *Amer. Inst. elect. Engrs Conf. Paper* 51-348
- 5 FITZGERALD and KINGSLEY. *Electric Machinery*. 2nd edn. New York; McGraw-Hill
- 6 SARARD, R. Acceptance testing of precision motor-tachometer generators. *Amer. Inst. elect. Engrs Conf. Paper* 62-1054
- 7 *Aeronautic Recommended Practices No. 497 and 667*. Society of Automotive Engineers, New York
- 8 Transistorized brushless motor. Lamb Electric Division of Ametek, Inc., *Industrial Electronic Engineering and Maintenance*, April (1963) 31
- 9 McMURRY, W. and BEDFORD, B. D. Square-wave inverter. *Controlled Rectifier Manual*, General Electric Company, p. 138
- 10 McMURRY, W. and SHATTUCK, D. P. A silicon-controlled rectifier inverter with improved commutation. *Communication and Electronics*, November 1961
- 11 GUTZWILLER, F. W. Universal-motor speed controls. *Electro-Technology*, December (1961) 138
- 12 *Control Engng*, 10 (1963) 50
- 13 HUGHES, W. T. Design trends in servo systems. *Military Systems Design*, 6 (1962) 16
- 14 STRUNK, B. Sampled-data servo licks stability problem. *Control Engng*, 10 (1963) 90
- 15 MOSES, G. L. and HARTER, E. F. Winding-fault detection and location by surge comparison testing. *Trans. Amer. Inst. elect. Engrs*, 64 (1945) 499
- 16 FOUST, C. M. and ROHATS, N. Insulation testing on electric windings. *Amer. Inst. elect. Engrs*, 62 (1943) 203
- 17 CATLIN, F. H. and ROHATS, N. Winding insulation tester for d.c. armatures. *Amer. Inst. elect. Engrs*, 70 (1951) 465
- 18 BUCHANAN, L. W. The application of surge comparison testing equipment to fractional horsepower a.c. stator windings. *Amer. Inst. elect. Engrs*, 66 (1947) 1356
- 19 STRAIN, R. A. Some aspects of surge comparison testing of fractional horsepower motors. *Amer. Inst. elect. Engrs*, 75 (1956) 917
- 20 Electronic surge testing of d.c. armatures with null detection. *Proc. of National Electronics Conference*, Chicago, Illinois, October, 1958
- 21 Electronics pinpoints armature faults. *Electronics*, June, 1960 (co-author, Sylvia K. Weed)
- 22 Servo motor characteristics by impulse testing. *Amer. Inst. elect. Engrs* (1961)
- 23 MISHIKIN, E. and BRAUN, L. Analytical theory of nonlinear systems, in *Adaptive Control Systems*, p. 264. 1961. New York; McGraw-Hill
- 24 GILINSON, P. J. and FRAZIER, R. H. Electromechanical components. In *Air, Space and Instruments* (Draper Memorial Volume Edited by S. Lees), p. 285, New York; McGraw-Hill
- 25 RAMEY, R. A. On the mechanics of magnetic amplifier operation. *Trans. Amer. Inst. elect. Engrs*, Part II (1951)
- 26 RAMEY, R. A. On the control of magnetic amplifiers. *Trans. Amer. Inst. elect. Engrs*, Part II (1951)

- ²⁷ GEYGER, W. A. A new type of magnetic servo amplifier. *Trans. Amer. Inst. elect. Engrs*, Part I (1952)
- ²⁸ KALLANDER, J. W. A fast response magnetic servo amplifier. *Trans. Amer. Inst. elect. Engrs*, Part I (1955)
- ²⁹ BAJWA, J. S. Amplification factor of a single stage magnetic amplifier controlling a servomotor. M. Sc. Thesis, Ohio State University, March, 1961
- ³⁰ BAJWA, J. S. Analysis of a magamp-servomotor system. Ph. D. Dissertation, Ohio State University, December, 1962. To be presented at National Electronics Conference, Chicago, Illinois, 1963.
- ³¹ Publication in preparation
- ³² DARLING, H. E. An all solid-state temperature-actuated power controller. Foxboro Company, Foxboro, Mass.
- ³³ *Elect. Engng*, 80 (1961) 956
- ³⁴ EARLY, J. M. Semiconductor devices. *Proc. Instn Radio Engrs*, 50 (1962) 1006
- ³⁵ BURTON, L. W. Semiconductor rectifiers committee report. *Electr. Engng*, 81 (1962) 964
- ³⁶ FHP brushless motor. *Electromechanical Components and Systems Design*, 7 (1963) 50
- ³⁷ STERN, A. P. Electronic circuits and systems committee report. *Elect. Engng*, 81 (1962) 963
- ³⁸ LAX, B. and MAVROIDES, J. G. Solid-state devices other than semiconductors. *Proc. Instn Radio Engrs*, 50 (1962) 1011
- ³⁹ HALL, R. N., FENNER, G. E., KINGSLEY, J. D., SOLTYS, T. J. and CARLSON, R. O. Coherent light emission from GaAs Junctions. *Phys. Rev. Letters*, 9 (1962) 366
- ⁴⁰ BUCKLEY, J. J., ROESE, D. W. and SHEARER, J. W. Solid state vibrating gyroscope. *Symposium on Unconventional Inertial Sensors*, held at Farmingdale, New York, by Republic Aviation Corp. and Bureau of Naval Weapons in Cooperation with Air Force Systems Command Scientific and Technical Liaison Office, December 10 and 11, 1962
- ⁴¹ GREEN, E. Synthesis of ladder networks to give Butterworth or Chebyshev response in the pass band, *Proc. Instn Elect. Engrs*, 100 (1954), 192
- ⁴² GREEN, E. *Amplitude Characteristics of Ladder Networks*. Marconi House, Chelmsford, England, p. 164 (1954)
- ⁴³ GROSSMAN, A. J. Synthesis of Tchebycheff parameter symmetrical filters. *Proc. Inst. Radio Engrs*, 45 (1957), 454.
- ⁴⁴ MATSON, U. A. U.S. Pat. 2932804, April 12, 1960
- ⁴⁵ BODE, H. W. U.S. Pat. 2301245, November 10, 1942
- ⁴⁶ O'MEARA, T. R. Very wide band impedance matching networks. *Inst. Radio Engrs Transactions on Component Parts*, CP-9 (1962)
- ⁴⁷ LEE, R. *Electronic Transformers and Circuits*, 2nd Edn (1955), New York; Wiley
- ⁴⁸ OWENS, C. D. Modern magnetic ferrites and their engineering applications. *Inst. Radio Engrs Transactions on Component Parts*, CP-3 (1956)
- ⁴⁹ BOZORTH, R. M. and BOOTHBY. A new magnetic material of high permeability. *J. Appl. Sci.*, 18 (1947), 173
- ⁵⁰ BOZORTH, R. M. Ferromagnetism. In *Recent Advances in Science*, p. 253. New York and London; Interscience
- ⁵¹ GOULD, H. L. B. and WENNY, D. H. *Supermendure: A New Rectangular Loop Magnetic Material*
- ⁵² GANZ, A. G. Applications of thin permalloy tape in wide-band telephone and pulse transformers. *Trans. Amer. Inst. elect. Engrs*, (1946), 177
- ⁵³ OWENS, C. D. A survey of the properties and applications of ferrites below microwave frequencies. *Proc. Inst. Radio Engrs*, 44 (1956), 1234
- ⁵⁴ O'MEARA, T. R. A wide-band high frequency transformer using a ferrite core. *Proc. National Electronics Conference*, 10 (1954), 778
- ⁵⁵ PIDHAYNY, D. D. The effect of system transients on the specification of transformers. *Aerospace Corporation Report*, Aerospace Corporation, Los Angeles, California
- ⁵⁶ O'MEARA, T. R. A distributed-parameter approach to the high-frequency network representation of wide-band transformers. *Inst. Radio Engrs Transactions on Component Parts*, CP-8 (1961)
- ⁵⁷ WINKLER, S. The approximation problem of network synthesis. *Inst. Radio Engrs Transactions on Circuit Theory* (1954), 5
- ⁵⁸ PADGETT, E. D. and WRIGHT, W. V. Silicon piezoresistive devices. *Instrum. Soc. America* preprint, NY. 60.42
- ⁵⁹ SANCHEZ, J. C. and WRIGHT, W. V. Recent developments in flexible silicon strain gages. *Instrum. Soc. America*, preprint 37-SL-61
- ⁶⁰ MOEN, A. S. New horizons in transducers utilizing solid-state strain gages. *Instrum. Soc. America*, preprint 114-LA-61
- ⁶¹ KURTZ, A. D. and JONES, E. J. An ultra-high output telemetering gage. *Instrum. Soc. America*, preprint 145-LA-61
- ⁶² LEE, S.-Y. and PASTON, H. L. *Design and Application of Semiconductor Strain Gage Transducers*. Publication of Dynisco Div., American Brakeshoe Company, 42 Carlton St., Cambridge, Mass.
- ⁶³ ROGERS, E. J. High output passive transducers. *Instrument and Control Systems*, April, 1963
- ⁶⁴ Utilization of semiconductor strain gage in passive high output transducers. *Seattle Conference of Society of Experimental Stress Analysis*, May 8, 1963
- ⁶⁵ DEAN, Mills III, Editor, DOUGLAS, R. D., Assoc. Editor, *Semiconductor and conventional strain gages*. New York; Academic Press
- ⁶⁶ GETLER, M. New gyro aimed at tactical missiles. *Missiles and Rockets*, 11 (1962), 34
- ⁶⁷ GILINSON, P. J. Jr., DENHARD, W. G. and FRAZIER, R. H. A magnetic support for floated inertial instruments. *Sherman M. Fairchild Publication Fund Paper No. FF-27*, May 1960, Institute of Aerospace Sciences, New York, N.Y.
- ⁶⁸ HARDING, J. Cryogenic gyros. *Space Aeronautics*, September, 1961
- ⁶⁹ Solid state gyro dances the twist. *Machine Design*, 34 (1962), 12
- ⁷⁰ Laser rotation rate sensor forms light-beam gyroscope. *Electronic Products*, 5 (1963), 38
- ⁷¹ Laser gyro bends light beams around a ring. *Machine Design*, 35 (1963), 12
- ⁷² GRIFFIN, W. S. The analytical design and optimization of a pneumatic rate gyroscope for high temperature application. Sc. D. Thesis, M.I.T., Cambridge, Mass., September, 1962
- ⁷³ *Proceedings of the Fluid Amplification Symposium*, Vol. 1, Diamond Ordnance Fuze Laboratories (now Harry Diamond Laboratories), Washington D. C., October, 1962
- ⁷⁴ *Fluid Jet Control Devices* (symposium papers), American Society of Mechanical Engineers, November, 1962
- ⁷⁵ BROWN, F. T. A combined analytical and experimental approach to the development of fluid-jet amplifiers. *Amer. Soc. mech. Engrs*, Paper No. 62-WA-154, to be published in *J. Basic Engng*
- ⁷⁶ MITCHELL, A. F., GLAETTLI, H. H. and MUELLER, H. R. Fluid logic devices and circuits. To be published in *Trans. Soc. Instrum. Technol.*
- ⁷⁷ Pneumatic and hydraulic control and regulating system. Patent application 124719, 13 April 1959. Pat. No. 10835 registered 12 February 1960 in U.S.A.
- ⁷⁸ A method of controlling devices and equipment using pneumatic and hydraulic elements. Patent application 124720, 13 April 1959. Patent registered in U.S.A., 12 February 1960
- ⁷⁹ U.S. Pats, N. Tesla, 1329559; E. T. Linderroth, 2727535
- ⁸⁰ FERNER, V. Neue Pneumatische bzw. Hydraulische Elemente in der Meß- und Regelungstechnik (New Pneumatic and Hydraulic Elements in Instrumentation and Control Engineering), *Die Technik* 6 (1954), 7
- ⁸¹ FERNER, V. *Anschauliche Regelungstechnik (Descriptive Control Engineering)*. Berlin, 1960
- ⁸² VAISSER, I. V. Analysis of the possibility of operating pneumo-automatic devices at low pressure. *Collection of Papers on Problems in Pneumo- and Hydroautomatics* (Publication of the Academy of Sciences, U.S.S.R.)

- ⁸³ BEREZOVETZ, G. T., DMITRIEV, V. N. and TAL, A. A. A new type of pneumatic computer. *Automat. Telemekh.*, Moscow, 1 (1961)
- ⁸⁴ Pneumatic system of automatic control, calculation, transduction and regulation. Patent application 141 684 dated December 6, 1960
- ⁸⁵ Pneumatic experimental regulator (optimizer). Patent application 139 485 dated August 22, 1960
- ⁸⁶ Pneumatic and hydraulic control and regulating system. Patent application 124 719 dated April 13, 1959. Patent No. 10835 registered February 12, 1960, in the U.S.A.
- ⁸⁷ A method of controlling devices and equipment using pneumatic and hydraulic elements. Patent application 124 720 dated April 13, 1959. Patent registered in the U.S.A., February 12, 1960
- ⁸⁸ WARREN, R. W. Fluid pulse converter. Pat. No. 3 001 698, Oct. 5, 1960
- ⁸⁹ HORTON, B. M. Negative feedback fluid amplifier, Pat. No. 3 024 805, May 20, 1960
- ⁹⁰ BROWN, F. T. Pneumatic pulse transmission with bistable-jet-relay reception and amplification, Sc. D. Thesis, June 1962, Department of Mechanical Engineering, M.I.T., Cambridge 39, Mass.
- ⁹¹ SCHER, R. S. Analysis and design of the reaction-jet servomotor, Sc. D. Thesis, February 1963, M.I.T., Cambridge 39, Mass.
- ⁹² MARCUS, D. H. Analysis and design of the reaction-jet servomechanism, Sc. D. Thesis, June 1962, Department of Mechanical Engineering, M.I.T., Cambridge 39, Mass.
- ⁹³ KIBBY, B. F., TAPLIN, L. B. and FEUCHT, R. E. Progress of the aeronautical systems division hot gas flight stabilization system program. Society of Automotive Engineers, United Engineering Center, New York, N.Y.
- ⁹⁴ GRIFFIN, W. S. The design and development of a pneumatic rate gyroscope for extended temperature range application, Sc. D. Thesis, September 1962, Department of Mechanical Engineering, M.I.T., Cambridge 39, Mass.

MECHANICAL, HYDRAULIC AND PNEUMATIC DEVICES

A Hydraulic Torque Amplifier

Y. OSHIMA and K. ARAKI

Summary

This paper describes the newly devised hydraulic torque amplifier which is a kind of all-hydraulic servo-mechanism. The hydraulic torque amplifier is suitable for torque amplification of the high-speed stepping motor applied for numerical control of machine-tools.

This torque amplifier consists of nozzles and a sharp edge as the deviation detecting means, hydraulic circuits for the hydraulically balanced servo-valve, rotary hydraulic motor and rotary hydraulic joint and constitutes a follow-up system with mechanical feedback.

From the theoretical analysis the open-loop transfer function of the system is obtained. In order to verify the theoretical analysis, frequency response and step response tests of the experimental model are made and the results are compared with calculated data. The agreement between theoretical analysis and experiment is good.

From the results of tests it is found that the closed-loop characteristics of the system are very stable if the volume of the conduit pipe between pilot valve and hydraulic motor is small. The performances of the experimental model are so good that if only the construction is improved practical use can be expected.

The principal points of improvement of construction are described,

Sommaire

On décrit un nouvel amplificateur de couple hydraulique constituant un genre de servomécanisme hydraulique. Cet élément s'applique aux moteurs à impulsion à grande vitesse utilisés dans la commande numérique des machines-outils.

Le détecteur d'écart est constitué par des tuyères et un bord tranchant. L'amplificateur hydraulique comprend en outre une servo-valve équilibrée, un moteur et un joint tournants et constitue un système de poursuite à réaction mécanique.

La fonction de transfert en chaîne ouverte est obtenue par voie analytique, vérifiée par des réponses transitoires et fréquentielles et les résultats expérimentaux sont comparés aux données calculées. L'analyse théorique et l'expérience s'accordent bien.

Les essais ont montré qu'en boucle fermée, le système est très stable si le conduit entre la valve pilote et le moteur hydraulique est petit. L'appareil expérimental a donné de bons résultats; on peut espérer une bonne utilisation si à l'échelle industrielle, la construction est améliorée. Des indications sur ce dernier point sont données.

Zusammenfassung

Der Aufsatz beschreibt einen neu entwickelten hydraulischen Drehmomentverstärker, der eine Art rein hydraulischen Servomechanismus

darstellt. Der Verstärker eignet sich zur Drehmomenterhöhung von Schrittmotoren bei hohen Drehzahlen, wie sie für numerisch gesteuerte Werkzeugmaschinen Verwendung finden.

Der Drehmomentverstärker besteht aus Düsen und einer scharfen Steuerkante zur Bestimmung der Abweichung, aus den hydraulischen Kreisen eines hydraulisch abgeglichenen Steuerventils, einem rotierenden Hydraulikmotor mit rotierender hydraulischer Kupplung; er stellt somit ein Nachlaufsystem mit mechanischer Rückführung dar.

Aus der theoretischen Untersuchung wird die Frequenzfunktion des offenen Kreises abgeleitet. Um die theoretische Untersuchung zu prüfen, werden der Frequenzgang und die Sprungantwort des Versuchsmodells aufgenommen und die Ergebnisse mit den errechneten Daten verglichen. Es ergab sich eine gute Übereinstimmung.

Die Versuchsergebnisse zeigen, daß eine sehr gute Stabilität des geschlossenen Kreises vorliegt, wenn das Volumen der Verbindungslleitung zwischen Steuerventil und Hydraulikmotor klein ist. Das Verhalten des Versuchsmodells ist so gut, daß praktischer Einsatz möglich sein wird, sobald die Konstruktion verbessert worden ist.

Die prinzipiellen Gesichtspunkte zur Verbesserung der Konstruktion sind angegeben.

Introduction

A hydraulic torque amplifier is a kind of servo-mechanism which is composed only of hydraulic components. The one described here has the feature that the principle of the hydraulically balanced servovalve developed by the authors is utilized and that the large output power is derived while the reaction force to the input shaft is extremely small, and also that the response is very high.

The performances of the experimental model are so good that if only the construction were improved it would be possible to put it to practical use. It can be applied for general torque amplification purposes, especially for the torque amplification of the high speed stepping motor used as a digital-analogue converter in numerically controlled machine tools.

Construction and Operating Principle

The schematic diagram of the experimental hydraulic torque amplifier is shown in *Figure 1*. The end surface with sharp edge

A HYDRAULIC TORQUE AMPLIFIER

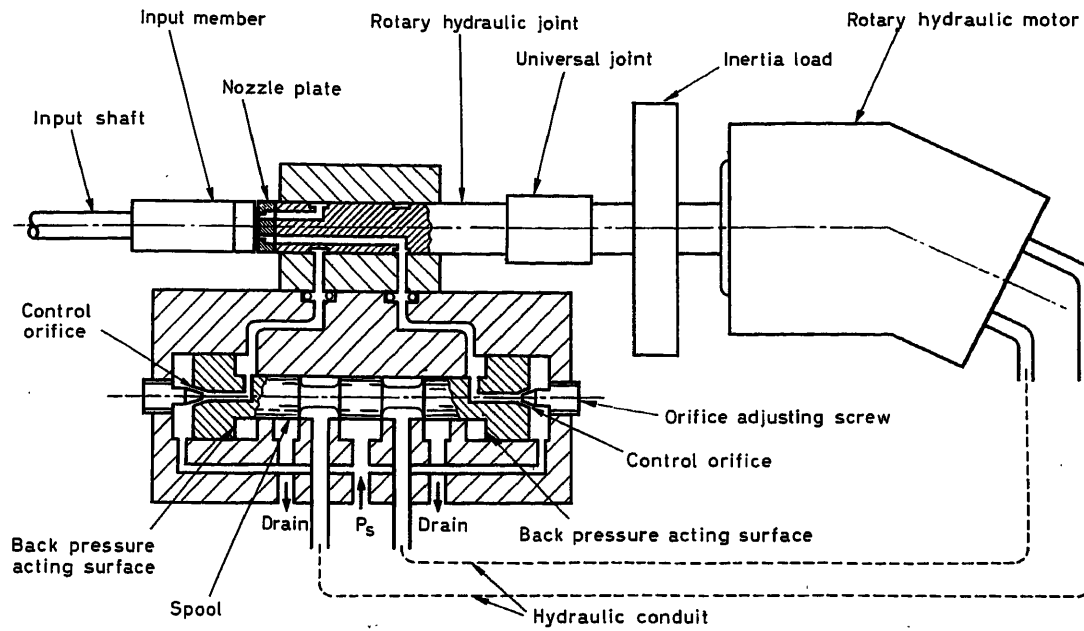


Figure 1. Experimental model of hydraulic torque amplifier

of the input member attached to the input shaft is located very close to the nozzle plate attached to the rotary hydraulic joint. The sharp edge and the nozzles, the details of which are shown in Figure 2, constitute the part for detecting the deviation between the input and output shaft and also the hydraulic preamplifier of the servovalve together with the control orifice. The control orifice is constructed by the conical pin fixed to the valve body and the conical hole in the end surface of the spool. An axial piston type rotary hydraulic motor as the actuator drives the load. The displacement of the actuator is fed back to that of the nozzle plate by the mechanical coupling between the actuator and the rotary hydraulic joint.

The operating principle of this hydraulic torque amplifier is as follows. As the input shaft is rotated by some angle, two nozzles are differently covered by the sharp edge of the input member and the back pressures of the nozzles are unbalanced. The unbalance force produced by the back pressures on the back pressure acting surfaces at both ends of the spool drives the spool, whereby the openings of the control orifices are varied and the pressures on the back pressure acting surfaces are changed, so that the spool is brought to the position where both side-pressures are balanced. The displacement of the spool controls the oil flows through the valve ports and in consequence the rotation of the rotary hydraulic motor, which is fed back to the rotary hydraulic joint. Thus, two nozzles follow up the sharp edge of the input member.

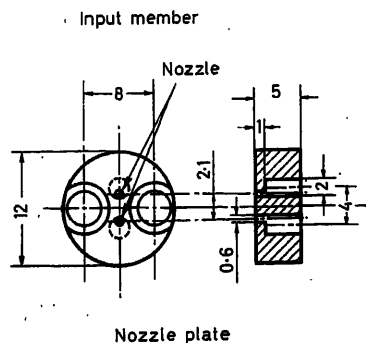
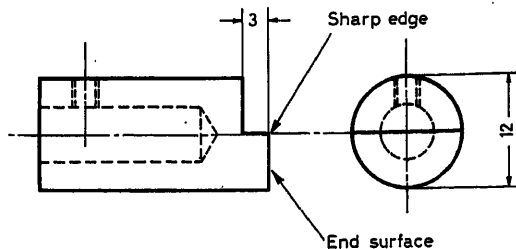


Figure 2. Input member and nozzle plate

Theoretical Analysis

The notation used for flow rates (cm^3/sec), pressures (kg/cm^2), displacements (linear displacement, cm ; angular displacement, rad) at each part is given in Figure 3 and the other notation used is summarized in the Nomenclature at the end of the paper.

Relationship between Spool Displacement and Angular Deviation

The difference of uncovered area between two nozzles *versus* angular deviation in the case of the experimental model (nozzle diameter, 0.6 mm) is computed as shown in Figure 4. This relationship is approximately linearized as shown by the dotted line in the figure, where E is the ϵ value corresponding to the saturation point.

The analysis¹ previously made concerning the hydraulically balanced servo-valve gives the transfer function from angular deviation ϵ to spool displacement x as

$$\frac{x}{\epsilon}(s) = \frac{Ak_{ex}/E}{ms^2 + (b + k_{ex}A/Q_1)s + Ak_{ex}/X} \quad (1)$$

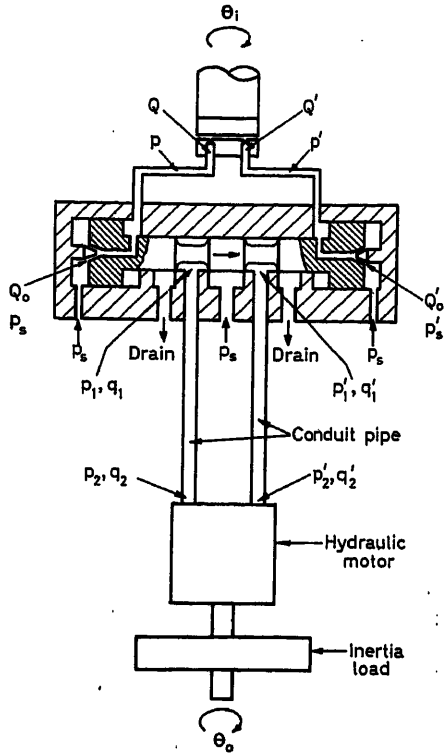


Figure 3. Notation of pressure, flow and displacement at each part
 q or Q with subscripts, p with subscripts, x and θ with subscripts
denote flow rate, pressure, linear displacement and angular displacement respectively

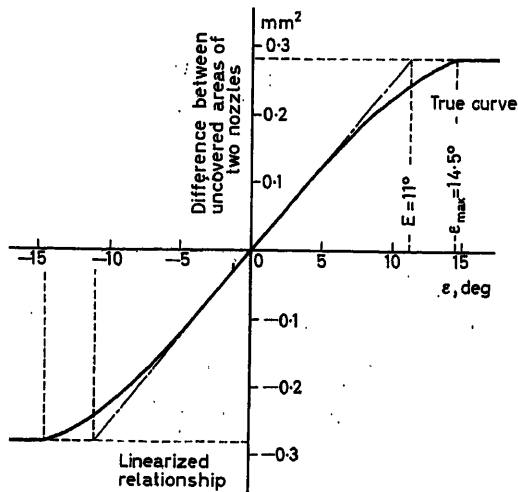


Figure 4. Difference between uncovered areas of two nozzles versus deviation angle

where

$$k_{ax} = 4 \left(\frac{1}{p_i} + \frac{1}{p_s - p_i} \right)$$

Q_i = flow rate through nozzle in the equilibrium condition;
 p_i = back pressure of nozzle in the equilibrium condition.

Since m and b are negligibly small, eqn (1) is approximated by

$$\frac{x}{\varepsilon}(s) = \frac{X/E}{Ts + 1} \quad (2)$$

where the time constant T is

$$T = AX/Q_i \quad (3)$$

Relationship between Flow Rate and Pressure Corresponding to Spool Displacement of Pilot Valve

The relationship between flow rate through the valve port and pressure corresponding to spool displacement is experimen-

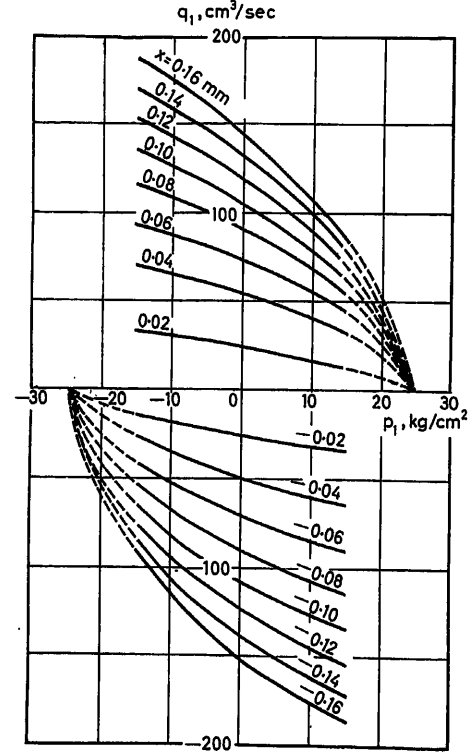


Figure 5. Relationship between flow and pressure corresponding to spool displacement of pilot valve

tally obtained in the case of the model as shown in Figure 5. This relationship is written in functional form as

$$q_1 = f(x, p_1) \quad (4)$$

Differentiation of eqn (4) in consideration of Figure 5 gives

$$q_1 = \left(\frac{\partial q_1}{\partial x} \right) x - \left(\frac{\partial q_1}{\partial p_1} \right) p_1 \quad (5)$$

where q_1 , x and p_1 denote small variations from their equilibrium point values and average values in the operating range are used for $\partial q_1 / \partial x$ and $|\partial q_1 / \partial p_1|$.

Rearranging eqn (5) gives

$$x = \left(\frac{\partial x}{\partial q_1} \right) \left(q_1 + \left(\frac{\partial q_1}{\partial p_1} \right) p_1 \right) \quad (6)$$

Transfer Characteristics of the Conduit Pipe

The effects of inertia, resistance and capacitance of fluid in the conduit pipe are considered by assuming that these parameters can be lumped.

A lumped parameter transmission line shown in Figure 6 (a) can be simulated by the mechanical system composed of mass, damper and springs as shown in Figure 6 (b).

This system is expressed by the following equations:

$$f_1 = 2K(y_1 - y') \quad (7)$$

$$f_1 - f_2 = (Ms^2 + Rs)y' \quad (8)$$

$$f_2 = 2K(y' - y_2) \quad (9)$$

From these, the equations expressing transfer characteristics of the system are deduced as follows:

$$f_1 = \frac{2K+A}{2K}f_2 + Ay_2 \quad (10)$$

$$y_1 = \frac{1}{A} \left[\left(\frac{2K+A}{2K} \right)^2 - 1 \right] f_2 + \frac{2K+A}{2K} y_2 \quad (11)$$

where

$$A = Ms^2 + Rs \quad (12)$$

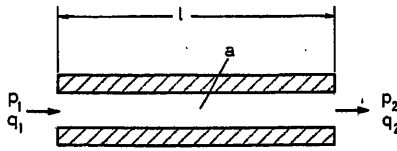
If $K \gg A$, eqns (10) and (11) are approximated by

$$f_1 = f_2 + Ay_2 \quad (13)$$

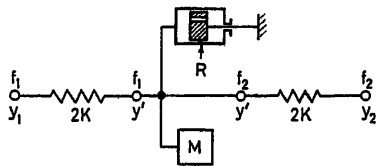
$$y_1 = \frac{1}{K} f_2 + y_2 \quad (14)$$

Correspondence between the mechanical system and the conduit pipe gives the following relationships:

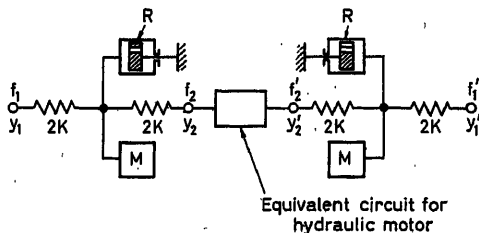
$$\left. \begin{aligned} f_1 &= ap_1 & q_1 &= asy_1 \\ f_2 &= ap_2 & q_2 &= asy_2 \end{aligned} \right\} \quad (15)$$



(a)



(b)



(c)

Figure 6. Simulation of lumped parameter transmission line

Thus the transfer characteristics of the conduit pipe are expressed by

$$p_1 = p_2 + \left(\frac{M}{a^2} s + \frac{R}{a^2} \right) q_2 \quad (16)$$

$$q_1 = \frac{a^2}{K} s p_2 + q_2 \quad (17)$$

It should be noted that in the hydraulic system mass M , coefficient of resistance R and spring constant K are given as follows:

$$M = \rho al, \quad R = 8\pi\mu l, \quad K = a/\beta l \quad (18)$$

Two conduit pipes connecting the hydraulic motor with the pilot valve shown in Figure 3 are simulated by the mechanical system shown in Figure 6 (c).

In the hydraulic system the following relationships are assumed:

$$q_1 = q_1', \quad q_2 = q_2' \quad (19)$$

The corresponding relationships in the mechanical system are

$$y_1 = y_1', \quad y_2 = y_2' \quad (20)$$

Under these conditions

$$f_1' = -f_1, \quad f_2' = -f_2 \quad (21)$$

can be proved in the mechanical system.

Therefore, the relationships in the hydraulic system

$$p_1' = -p_1, \quad p_2' = -p_2 \quad (22)$$

are obtained.

Characteristics of Hydraulic Motor

The torque of hydraulic motor, T , is given as

$$T = k_m(p_2 - p_2') = Js^2\theta_0 + D_ms\theta_0 \quad (23)$$

This equation gives

$$p_2 - p_2' = \left(\frac{J}{k_m} s^2 + \frac{D_m}{k_m} s \right) \theta_0 \quad (24)$$

As for flow rate the following equations hold:

$$q_2 = q_m + q_1 \quad (25)$$

$$q_m = k_ms\theta_0 \quad (26)$$

$$q_1 = L(p_2 - p_2') \quad (27)$$

From eqns (24) and (26) one gets

$$(p_2 - p_2') = (J's + D'_m) q_m \quad (28)$$

where

$$J' = J/k_m^2, \quad D'_m = D_m/k_m^2$$

From eqns (25), (27) and (28) is obtained

$$q_2 = q_m + q_1 = (LJ's + 1 + LD'_m) q_m \quad (29)$$

Under the condition given in eqn (22), eqn (28) gives

$$p_2 = \frac{1}{2} (J's + D'_m) q_m \quad (30)$$

Open-loop Transfer Function of Hydraulic Torque Amplifier

From eqns (6), (16), (17), (29) and (30) the following equation is obtained:

$$x = \left(\frac{\partial x}{\partial q_1} \right) \left[\left\{ \frac{a^2 J'}{2K} + \left| \frac{\partial q_1}{\partial p_1} \right| \frac{MLJ'}{a^2} \right\} s^2 + \left\{ \left| \frac{\partial q_1}{\partial p_1} \right| \left(\frac{J'}{2} + \frac{M}{a^2} + \frac{MLD'_m}{a^2} + \frac{RLJ'}{a^2} \right) + \left(\frac{a^2 D'_m}{2K} + LJ' \right) \right\} s + \left\{ \left| \frac{\partial q_1}{\partial p_1} \right| \left(\frac{D'_m}{2} + \frac{R}{a^2} + \frac{RLD'_m}{a^2} \right) + (1 + LD'_m) \right\} \right] q_m \quad (31)$$

Neglecting smaller terms in this equation, the transfer function from spool displacement x to flow rate used for rotation of hydraulic motor q_m is obtained as follows:

$$\frac{q_m}{x} = \frac{\left(\frac{\partial q_1}{\partial x} \right)}{\frac{a^2 J'}{2K} s^2 + J' \left\{ \frac{1}{2} \left| \frac{\partial q_1}{\partial p_1} \right| + L \right\} s + 1} \quad (32)$$

This equation is rewritten as

$$\frac{q_m}{x} = \frac{\left(\frac{\partial q_1}{\partial x} \right) \omega_c^2}{s^2 + 2\zeta \omega_c s + \omega_c^2} \quad (33)$$

where

$$\omega_c = \left(\frac{2K}{a^2 J'} \right)^{\frac{1}{2}} = \left(\frac{2}{\beta a l J'} \right)^{\frac{1}{2}} \quad (34)$$

$$\zeta = \frac{1}{2\omega_c} \frac{2K}{a^2} \left\{ \frac{1}{2} \left| \frac{\partial q_1}{\partial p_1} \right| + L \right\} = \left(\frac{J'}{2\beta a l} \right)^{\frac{1}{2}} \left\{ \frac{1}{2} \left| \frac{\partial q_1}{\partial p_1} \right| + L \right\} \quad (35)$$

From eqns (34) and (35) the effects of oil compressibility, β , volume of oil in the conduit pipe, al , inertia $J' = J/k_m^2$ and leakage coefficient of the motor L on ω_c and ζ are readily seen. From eqns (2), (26) and (33) the open-loop transfer function of the system is obtained as

$$\frac{\theta_0}{\varepsilon} = \frac{k\omega_c^2}{s(Ts+1)(s^2+2\zeta\omega_c s+\omega_c^2)} \quad (36)$$

where

$$k = \left(\frac{X}{E} \right) \left(\frac{\partial q_1}{\partial x} \right) / k_m$$

Experimental Verification

In order to verify the theoretical analysis, several experiments have been done. The experimental set-up is shown in Figures 7 and 8.

As the input device, the driving motor of pen writing oscillograph is used, which is excited by the signal generator. The angular displacement of the input member is detected by the strain gauge pick-up calibrated by micrometer. The output displacement of the hydraulic motor is detected by the condenser type pick-up. The detected signals are introduced to synchroscope and observed on it. The back pressure of the nozzle is detected by strain gauge pick-up. The inertia loads and conduit pipes used for the experiment are tabulated in Tables 1 and 2. The experimental conditions with respect to hydraulic fluid are as follows:

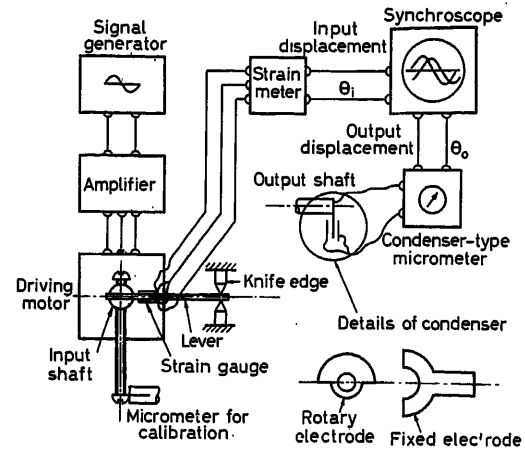


Figure 7. Experimental set-up

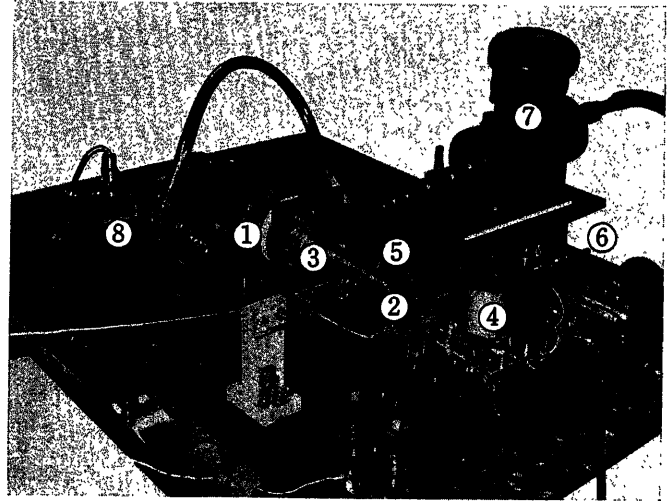


Figure 8. Photograph of experimental set-up

1, Rotary hydraulic motor; 2, rotary hydraulic joint; 3, inertia load; 4, driving motor; 5, condenser type pick-up; 6, micrometer for calibration; 7, flow meter; 8, strain gauge type back pressure pick-up

Oil used	Gargoyle DTE Light Oil
Oil temperature	40–45°C
Supply pressure	50 kg/cm ²
Compressibility β (measured datum)	2.1×10^{-4} cm ² /kg
Viscosity μ	4.6×10^{-7} kg sec/cm ²

Data concerning the hydraulic motor are:

Motor displacement/rad k_m	2.5 cm ³
Leakage coefficient L (measured datum)	0.01 cm ⁵ /kg sec

As the amplitude of input signal in the frequency response tests, the value of 1.5° was chosen.

The gain constant k can be determined by measuring the output speed of hydraulic motor corresponding to the input displacement in the case of the open-loop system. During the experiment the value of k was adjusted at 125 sec^{-1} .

Table 1. Inertia loads used for experiment

No. of inertia load	Inertia load	J kg sec ² cm	$J' = J/k_m^2$ kg sec ² /cm ⁵
1	No load		
	J_m : motor inertia	1.7×10^{-3}	0.272×10^{-3}
2	$J_m + J_1$	21.2×10^{-3}	3.4×10^{-3}
3	$J_m + J_2$	40.1×10^{-3}	6.4×10^{-3}
4	$J_m + J_3$	79.5×10^{-3}	12.7×10^{-3}

Table 2. Conduit pipes used for experiment

No. of conduit pipe	Volume of conduit pipe a_l , cm ³
1	19.2
2	47.2
3	130.0

In order to determine the time constant of spool motion T , the flow through nozzle Q_i and the back pressure of nozzle P_i in the equilibrium condition were measured. The results were: $P_i = 25$ kg/cm², $Q_i = 17$ cm³/sec. The relationship between flow through control orifice and spool displacement corresponding to pressure drop ($\Delta p = p_s - p_i$) gives the one-side effective spool stroke X as $X = 0.037$ cm.

From these data the time constant T is obtained as

$$T = \frac{AX}{Q_i} = 1.8 \text{ msec}$$

where the value of A is 0.82 cm².

The datum concerning $|\partial q_1 / \partial p_1|$ is determined from the slope of the curve of Figure 5, where the value of parameter x is assumed to be the effective value of sinusoidal displacement of spool. Since the amplitude of spool displacement corresponding to that of input displacement $\varepsilon_0 = 1.5^\circ$ is

$$x_0 = \frac{\varepsilon_0}{E} X = 0.05 \text{ mm}$$

the effective value of x is $\bar{x} = 0.035$ mm.

From the slope of the curve at $p_1 = 0$ corresponding to this \bar{x} in Figure 5, $|\partial q_1 / \partial p_1|$ is determined as

$$\left| \frac{\partial q_1}{\partial p_1} \right| = 1.2$$

Table 3. Parameter values of open-loop system in the tests

No. of test	No. of inertia load	No. of conduit pipe	Parameter values			
			T msec	ω_0 rad/sec	f_0 c/sec	ζ
I	1	2	1.8	860	137	0.12
II	2	2	1.8	242	38.5	0.25
III	3	2	1.8	177	28	0.34
IV	4	2	1.8	125	20	0.48

Open-loop Characteristics

The frequency response tests of the open-loop system in the case of the conduit pipe of No. 2 in Table 2 and various inertia loads were made. The results are plotted in Figure 9, where curves I-IV give calculated data. The calculated data are obtained from eqn (36) with parameter values given in Table 3.

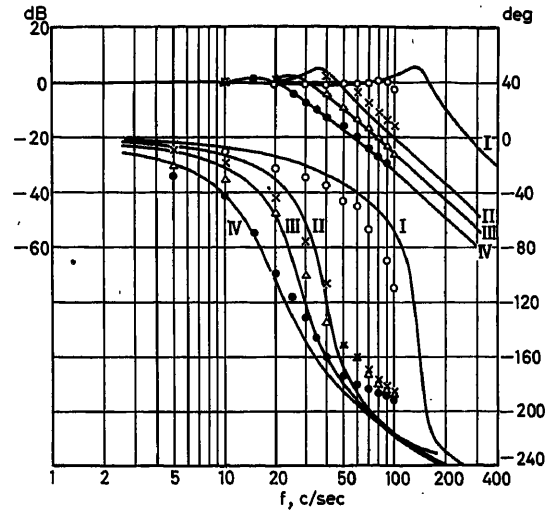


Figure 9. Frequency response data of open-loop system

The step response tests were also made. The results are given as dotted line curves in Figure 10, where full-line curves are those obtained by means of an analogue computer from eqn (36) with the same parameter values.

Closed-loop Characteristics

The frequency response and step response tests of the closed-loop system in the case of the conduit pipe of No. 1 and 3 and various inertia loads were made. The parameter values of the system in the tests are given in Table 4.

Table 4. Parameter values of closed-loop system in the tests

No. of test	No. of conduit pipe	No. of inertia load	Parameter values			
			T msec	ω_0 rad/sec	f_0 c/sec	ζ
V	3	1	1.8	515	82	0.09
VI	3	2	1.8	145	23.2	0.15
VII	1	1	2.3	1350	215	0.21
VIII	1	2	2.3	380	60	0.39
IX	1	3	2.3	278	44	0.53

The results of frequency response tests are plotted in Figure 11 where calculated data are shown for comparison. In the case of test VI sustained oscillation with frequency of 21 c/sec occurred, while the frequency at phase cross-over of calculated frequency response plot of the open-loop system under this condition is the same.

The measured step response data as well as those obtained

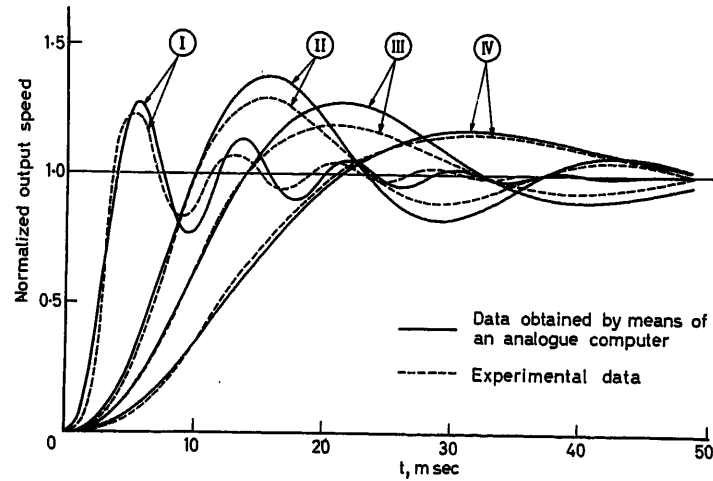


Figure 10. Step response data of output speed of open-loop system

by means of an analogue computer are given in Figure 12. From the results of tests it is seen that the agreement between experiment and theoretical analysis is good, and that the closed-loop characteristics of the system with the small volume conduit pipe are very stable while the system with the large volume conduit pipe becomes unstable in the case of large inertia load. Therefore, it is necessary to make the conduits between pilot valve and motor as short as possible. As for the system with the small volume conduit pipe the Hurwitz stability condition is investigated in order to see how much inertia can be loaded. The characteristic equation of the system is obtained as

$$1 + \frac{\theta_0}{\varepsilon} = 0$$

where θ_0/ε is given from eqn (36) and parameter values are:

$$T = 2.3 \times 10^{-3}$$

$$\omega_c = 22.2/(J')^{\frac{1}{2}}$$

$$\zeta = 6.65/(J')^{\frac{1}{2}}$$

$$k = 125$$

Under these conditions the Hurwitz stability condition is always satisfied irrespective of inertia load.

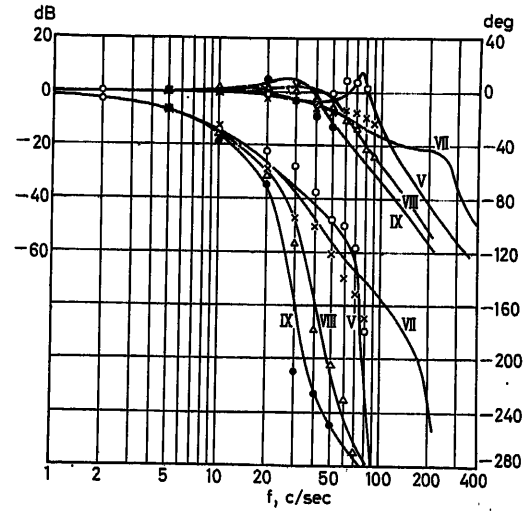


Figure 11. Frequency response data of closed-loop system

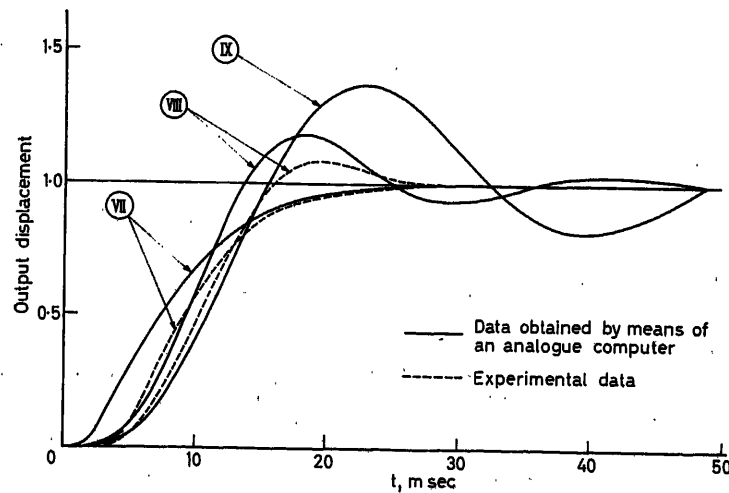


Figure 12. Step response data of output displacement of closed-loop system

A HYDRAULIC TORQUE AMPLIFIER

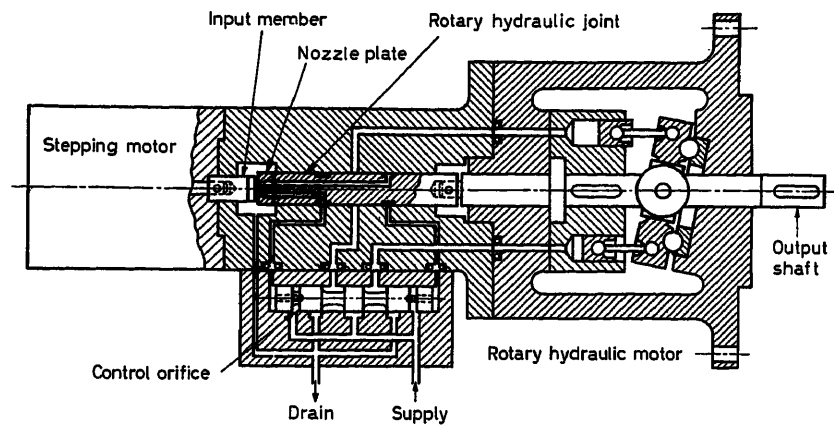


Figure 13. Practical construction of hydraulic torque amplifier

Improvement of Construction

In order to bring this experimental model of hydraulic torque amplifier to practical use, the construction should be improved as follows:

(1) The hydraulic motor should have the shaft extended outside from both end surfaces of the casing in order to separate load side and feedback side and to make conduits between pilot valve and motor as short as possible.

(2) The control orifice of the servo-valve should be constructed by the narrow slit on the sleeve inner surface and the spool land in order to make the configuration of sleeve stepless and to lessen the friction between spool and sleeve.

Thus the practical hydraulic torque amplifier may have the construction as shown in Figure 13.

Conclusion

Theoretical analysis and experiment of the newly devised hydraulic torque amplifier have been described. The characteristics of the experimental model are so good that practical use can be expected.

The authors sincerely thank Prof. Y. Ikebe for his valuable advice.

Nomenclature

X	One-side effective spool stroke	cm
α_0	Flow coefficient at control orifice	$\text{cm}^3/\text{kg}^{1/2} \text{ sec}$
A	Area of back pressure acting surface	cm^2
m	Mass of spool	$\text{kg sec}^2/\text{cm}$
b	Damping coefficient of spool	$\text{kg sec}/\text{cm}$
ϵ	$= \theta_t - \theta_0$, angular deviation	rad
α_1	Flow coefficient at valve port	$\text{cm}^3/\text{kg}^{1/2} \text{ sec}$
a	Cross sectional area of pipe	cm^2
l	Pipe length	cm
R	Coefficient of pipe resistance $= 8 \pi \mu l$	$\text{kg sec}/\text{cm}$
K	Equivalent spring constant of oil in pipe $= a/\beta l$	kg/cm
M	Mass of oil in pipe $= \rho a l$	$\text{kg sec}^2/\text{cm}$
f_1, f_2	Pressure forces at both ends of pipe line	kg
y_1, y_2	Fluid displacements at both ends of pipe line	cm
β	Oil compressibility	cm^2/kg
ρ	Oil density	$\text{kg sec}^2/\text{cm}^4$
μ	Oil viscosity	$\text{kg sec}/\text{cm}^2$
J	Moment of inertia of hydraulic motor and load	$\text{kg sec}^2 \text{ cm}$
k_m	Motor displacement per radian	cm^3
D_m	Damping coefficient of hydraulic motor	kg cm sec
q_m	Rate of flow used for rotation of hydraulic motor	cm^3/sec
q_l	Leakage flow rate in hydraulic motor	cm^3/sec
L	Leakage coefficient	$\text{cm}^5/\text{kg sec}$

Reference

- 1 OSHIMA, Y., and ARAKI, K. Hydraulically balanced servo-valve. *J. Jap. Soc. mech. Engng* 63, No. 495 (1960), 584

DISCUSSION

W. J. THAYER, *Moog Servocontrols, Inc., East Aurora, N.Y., U.S.A.*

The torque amplifier described by the authors is a straightforward combination of rotary input servovalve and hydraulic motor with unity feedback. The combination of these components has obvious practical application, as mentioned briefly by the authors. This has prompted the following comments which relate to potential problem areas in the design approach described.

The servovalve used has a double nozzle input stage, sliding spool second stage with spool position feedback created by control of the nozzle supply orifices. It would appear that a single-stage servovalve would suffice in the majority of applications. For example, the stepping motor could position the inner member of a rotary valve spool, with the hydraulic motor position feedback to a sleeve about the spool.

The resolution achieved with a single-stage design would not be as good as with two stages; however, this deficiency would not be great because of the high torque gradient available with a stepping motor of reasonable size. The simplification achieved through use of a single-stage design would appreciably reduce production costs for the device.

The use of orifice bridge balance for feedback within the servovalve described in the paper is similar to a design introduced several years ago by a manufacturer in the United States. The design is workable, but there are rather serious drawbacks including: (1) difficulty in manufacture of the variable orifices controlled by motion of the spool (even with the narrow slot configuration), and (2) difficulty in maintaining adequate linearity and stability throughout wide ranges of supply pressure and fluid temperature (admittedly these problems are less severe in a machine tool control system). Incidentally, the manufacturer

referred to has since abandoned the orifice bridge balance design in favour of a spring force feedback approach.

Lastly, the authors are to be complimented on a very thorough and well-executed analysis and development of the hydraulic torque amplifier described. The use of linearized analysis, together with simplification by neglecting such secondary effects as spool mass and fluid mass, gives reasonably good agreement with experimentally measured results. It has been our experience that this approach for analysis of hydraulic servomechanisms is compatible with the degree of design control available.

Y. OSHIMA, *in reply*

Mr. Thayer pointed out that two-stage hydraulic servovalve circuits are complicated. This is true. We can use a single-stage rotary pilot valve with simpler construction. However, the rotary pilot valve has a greater area of sliding surface and in consequence more friction torque is loaded to the input shaft. In order to realize a torque amplifier for a high-speed stepping motor, it is desirable to reduce the reaction torque. For this purpose the shear orifice mechanism is adequate since it is contactless. Two types of hydraulic servovalve circuit can be used for a shear orifice type hydraulic torque amplifier; one is a balance spring type such as the Moog servovalve and the other is a hydraulically balanced type, as adopted in this torque amplifier. In our experience the operation of the hydraulically balanced servovalve is quite satisfactory.

T. J. VIERSMA, *Technological University, Mekelweg 2, Delft, Netherlands*

Commenting on the performance of the hydraulic amplifier, I should like to mention the very great influence exerted by the pipeline volume between the control valve and the cylinder block. Although the authors indicate the importance of this pipeline volume, I believe it should be stressed once more because the test results of the torque amplifier could have been very much improved if the authors had paid much more attention to this point. Comparison between the experiments carried out by the authors and those by Fujii (Japan) on an electro-hydraulic pulsemotor make clear that the improvement of the step response could be as high as a factor of ten.

The enormous influence of the pipeline volume can be explained briefly as follows. Due to the compressibility of the oil, the compressed oil in the cylinder block and the pipelines acts as a torsional spring. The rigidity of this spring can be calculated directly. A torque T gives rise to a load pressure $p_1 = T/D$, where D is the motor displacement per radian. Therefore, the oil pressures in the respective sections will be $p_{1,2} = \frac{1}{2} p_1 \pm \frac{1}{2} p_1$. A change $\frac{1}{2} p_1$ in the oil pressures of both sections gives rise to a volume change ΔV of the oil

$$\frac{\Delta p}{E} = \frac{\frac{1}{2} p_1}{E} = \frac{\Delta V}{V_s} = \frac{\theta D}{V_s}$$

Here E is the bulk modulus of the oil, θ the motor rotation due to the

oil compression and V_s the oil volume per section. With $T = p_1 D$, this gives directly the rigidity C of the torsional spring

$$C = \frac{T}{\theta} = \frac{p_1 D}{\theta} = \frac{2 E D^2}{V_s}$$

The theoretical minimum of the section volume V_s is given by $V_{s\min} = \frac{1}{2} \pi D$. This ideal will be reached when the pipeline volume is zero. The volume of both sections together then equals half the motor displacement per revolution (as the mean piston is in the middle of its stroke). In practice, V_s will be a multiple of $\frac{1}{2} \pi D$, thus causing the rigidity C to be a fraction of its optimum value. It is quite clear that V_s should be kept as small as possible because of the natural undamped frequency $\omega_0 = (C/J)^{1/2}$. Here, J is the inertia moment of the motor itself (J_m), augmented with the inertia moments of machine parts such as gearboxes etc. In practice J will be many times J_m . To reach the step response time of 1 msec for instance, ω_0 should not be less than 6×10^3 rad/sec (corresponding to 1 kc/sec).

It is astonishing to see that the Fujii electro-hydraulic pulse motor (with heavy additional inertial load) has a step response time of about 1 msec, while the response time of the described models (without additional load) is greater than 10 msec. The explanation for this incredible difference is simple. Fujii reduced his pipeline volume to an extremely small value by bringing the connections between control valve and cylinder block into an extremely compact rotational sleeve directly between valve and cylinder block. The authors, however, made use of very long pipelines around the motor. Their pipeline volume therefore must be about 100 times greater than necessary, resulting in a response time 10 times greater than necessary.

Y. OSHIMA, *in reply*

Mr. Viersma pointed out the important influence of the pipeline volume between the control valve and the hydraulic motor. In this connection, I fully agree with him. The influence of the pipeline volume is readily seen from eqns (34) and (35). The increase of the pipeline volume a_l decreases the natural frequency ω_0 and also decreases the damping coefficient ζ . The purpose of our experiment is to verify the theoretical analysis and also to investigate the influence of the pipeline volume and emphasize the importance of this influence. In our experiment, three kinds of pipeline were used, as shown in Table 2. The largest volume is quite sizeable and in the case of this pipeline the unstable condition occurred.

The model shown in Figure 1 is only used for experiments. As mentioned under the 'Improvement of Construction', the practical hydraulic torque amplifier should be constructed in such a manner that the pipelines between pilot valves and motor are as short as possible. Here, I would like to mention the difference between Fujii's electro-hydraulic pulse motor and our system. The Fujii electro-hydraulic pulse motor utilizes the rotary pilot valve which inevitably has sliding surfaces and in consequence introduces on the input shaft more or less frictional torque. In our system, the reaction force to the input shaft is extremely small, although a rather complicated two-stage servovalve hydraulic circuit is necessary.

A Rotary-drive, Vibratory-output Gyroscopic Instrument

G. C. NEWTON, Jr.

Summary

An unusual gyroscopic instrument can be constructed by mounting an asymmetrical rotor in a gimbal. The moments of inertia of the rotor about its three principal axes are unequal. If the rotor is spun, at a constant angular rate, about one of its principal axes and an angular rate is applied to the instrument with a component in the plane of rotor rotation, a vibratory moment at twice the spin frequency of the rotor is developed about a gimbal axis normal to the rotor spin axis. This moment is proportional to the sensed angular rate in magnitude, and has a phase that is related to the direction of the sensed angular rate in the rate-sensitive plane. A laboratory instrument using an asymmetrical rotor has been built and tested. This instrument uses a tuned suspension for the gimbal. A counterpoise element that also serves as part of the output transducer is used to sense the vibratory motion of the gimbal system. The theory of operation of the instrument is developed. Experimental results are presented for a 'breadboard' version. These results show the rate sensitivity to be of the order 1×10^{-4} rad/sec based on unity signal-to-noise ratio.

Sommaire

Un appareil gyroscopique inhabituel peut être construit en montant un rotor asymétrique sur une suspension à cardan. Les trois moments d'inertie du rotor sont inégaux. Si le rotor est lancé à une vitesse angulaire constante autour d'un de ses axes principaux et qu'une vitesse est appliquée à l'instrument avec une composante dans le plan de rotation, un moment de vibration, dont la fréquence est égale à deux fois celle de la rotation du rotor, est développé autour de l'un des axes de suspension normal à l'axe de rotation du rotor. L'amplitude de ce moment est proportionnelle à la vitesse angulaire dans son propre plan. Un appareil de laboratoire de ce type a été construit et essayé. Cet appareil utilise un cardan à suspension accordée. Un contrepoids détecte le mouvement vibratoire du système cardan. On développe la théorie du fonctionnement de l'instrument. Des résultats expérimentaux sont présentés globalement. Ces résultats montrent que la sensibilité est de l'ordre de 10^{-4} sur la base d'un rapport signal/bruit égal à l'unité.

Zusammenfassung

Durch kardanische Aufhängung eines asymmetrischen Rotors läßt sich ein spezieller Kreisel bauen. Die Trägheitsmomente des Rotors um seine drei Hauptachsen sind ungleich. Wird der Rotor mit konstanter Winkelgeschwindigkeit um eine seiner Hauptachsen gedreht und wird dem Gerät eine Winkelgeschwindigkeit mit einer Komponente in der Ebene der Rotordrehung aufgegeben, so entsteht an der Kardanachse, die senkrecht zur Rotordrehachse steht, ein schwingendes Moment mit der doppelten Frequenz der Rotordrehung. Dieses Moment ist der Größe nach der ermittelten Winkelgeschwindigkeit proportional, die Phase hängt von der Richtung der ermittelten Winkelgeschwindigkeit in der betreffenden Ebene ab. Ein Mustergerät mit asymmetrischem Rotor wurde gebaut und geprüft. Bei diesem Gerät wird eine abgestimmte kardanische Aufhängung benutzt. Ein Gegengewicht, gleichzeitig Teil des Ausgangsübertragers, dient der Erfassung der Schwingbewegung des Kreiselrahmens.

Die Theorie der Wirkungsweise des Gerätes wird abgeleitet, zusammengefaßte Versuchsergebnisse werden vorgelegt. Die Versuchsergebnisse zeigen, daß bei einem Signal-Rauschverhältnis von 1 die Ansprechempfindlichkeit des Gerätes in der Größenordnung 10^{-4} rad/s liegt.

Introduction

In many modern control systems, such as autopilots and inertial navigators, gyroscopic instruments are of crucial importance as sensing elements. The growing need for precise, reliable, and cheaper gyroscopic instruments has stimulated considerable research on gyroscopic problems. Much of this research is devoted to further improvement of conventional gyroscopic equipment. However, exotic gyroscopic concepts⁸, based on physical phenomena ranging from the microscopic to the macroscopic, are receiving serious study. One important class of such instruments is that characterized by a vibratory output. These devices stand in sharp contrast to conventional gyroscopes which have steady outputs for constant input rates or positions.

There are two important sub-classes of vibratory-output gyroscopic instruments. One is characterized by vibratory movement of mass elements in order to produce the velocities giving rise to the alternating Coriolis forces that are sensed. The term vibratory-drive is applied to these instruments. The other sub-class contains those instruments that use a rotary motion of the mass elements in order to produce the required velocities. The term 'rotary-drive' is used to describe this kind of equipment. Lyman⁵ has described a tuning-fork form of vibratory-drive instrument. Granqvist⁴ discloses another form of the vibratory-drive instrument based on acoustical waves in gases. Birdsall¹, Bowden², and Diamantides³ have disclosed different forms of rotary-drive instruments^{10,11}. However, few experimental results⁹ are reported in the literature for instruments of this kind. This paper describes a particular configuration for a rotary-drive, vibratory-output gyroscope. It also discusses the theory of operation and presents some test results obtained on a crude laboratory prototype used to demonstrate the principle of operation.

It has been shown⁷ that thermal noise, the performance barrier commonly met in electronic instrumentation, is not yet a serious barrier to improvement of performance in either vibratory or conventional gyroscopic instruments. Bearing noise and centre-of-mass shifts are more important limitations on the performance of conventional rotating-wheel gyroscopes than is thermal noise. The vibratory-drive, vibratory-output instruments, as discussed by Morrow⁶, have been limited by unwanted cross-coupling between the driven and sensed vibrations. Hopefully, the rotary-drive, vibratory-output instruments will offer higher performance than the vibratory-drive instruments but how they will compare with rotating-wheel gyroscopes is difficult to forecast. The bearing problems are different and there is the possibility of enhancement of the desired output signal through the use of resonance.

The Instrument

Mechanical System

The basic mechanical system used in the rotary-drive, vibratory-output instrument discussed in this paper is shown in

Figure 1. A rotor having different moments of inertia about its three principal axes is suspended by means of an axle so as to turn about one of the principal axes. The axle turns in bearings carried by a gimbal. Flexure pivots give the gimbal freedom for limited rotation, relative to the instrument frame, about an axis (y axis) perpendicular to the rotor spin axis. The gimbal is constrained in its rotation about this axis by means of a spring k_1 .

The rotor is turned at a constant angular rate relative to the gimbal by motive means not shown. An angular rate of the instrument frame, with respect to inertial space, that has a component in the plane of rotation of the rotor, will produce a vibratory torque about the gimbal y axis that contains a component whose frequency is twice that of the rotor spin frequency. This can be seen by considering the moment of inertia of the gimbal-rotor system about the y axis. This inertia fluctuates about its mean value at twice the rotor spin frequency. For a constant angular rate Ω_y around the y axis, conservation of

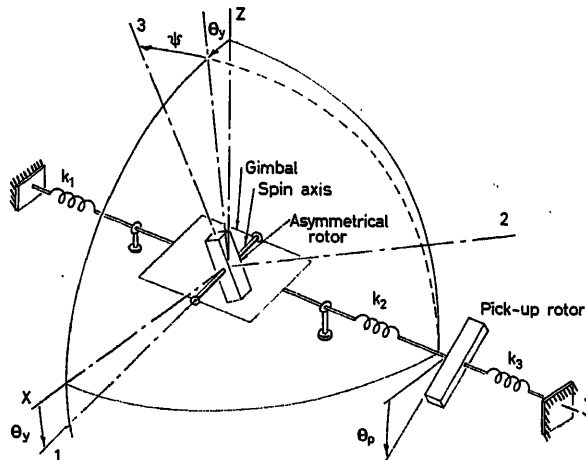


Figure 1. Mechanical system

angular momentum requires that the moments applied about this axis vary periodically at twice the rotation frequency of the rotor.

The periodic torques acting on the gimbal cause it to oscillate. These oscillations can be detected by a pick-up arranged to measure the gimbal angle θ_y . However, a counterpoise method of detecting the periodic moments offers certain advantages. As shown in Figure 1 the counterpoise arrangement consists of spring k_2 , the pick-up rotor, and spring k_3 . By appropriate tuning of the system the pick-up angle θ_p can be made to have amplitude several times as large as the amplitude of the gimbal oscillation. In order to achieve this magnification the pick-up rotor must have a moment of inertia which is small compared with the effective moment of inertia of the gimbal system.

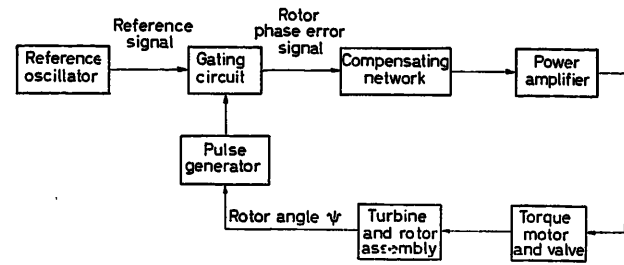


Figure 2. Rotor speed control system

In order to exploit the phenomenon of resonance in the pick-up system, accurate control of the spin frequency of the rotor is required. A feedback control system which synchronizes the rotor with a reference oscillator is shown in Figure 2. The laboratory apparatus, for which test results are given, used an air turbine to drive the rotor since this equipment was fabricated from an obsolete air-driven gyroscope. By using the rotor as a shutter to interrupt a light beam, pulses are generated at the rate of two pulses for each revolution of the rotor. These pulses actuate a gating circuit that is fed by the reference oscillator whose frequency is set for twice the desired spin frequency. The output of the gating circuit is an analogue voltage that is proportional, for small deviations, to the phase error between the reference oscillator and twice the rotor angle. This error signal passes through a lead compensating network and a power amplifier in order to drive the torque motor that controls the air valve. The valve regulates the air pressure applied to the turbine nozzle and thereby controls the rotor speed. This closed-loop positional control system for the rotor is capable of synchronizing the rotor angle to that called for by the oscillator to within a small fraction of a radian.

For test purposes the relatively simple output signal processing system of Figure 3 was used. The pick-up rotor of Figure 1 forms the moving element in a pair of variable capacitors placed in a bridge circuit. The 200 kc suppressed carrier output signal from the bridge is amplified and demodulated to produce an alternating signal whose frequency is that of the gimbal and pick-up oscillations. This signal is amplified and used to drive one set of coils in the recording dynamometer-type wattmeter. The other set of coils of the wattmeter is driven by a power amplifier which receives its signal from the reference oscillator. The wattmeter produces a pen displacement proportional to the product of the pick-up oscillation amplitude and the phase angle of this oscillation relative to that of the reference oscillator. The phase shifter following the demodulator can be adjusted to make the instrument sensitive to angular rates about any selected axis in the y - z plane shown in Figure 1.

Summarizing, the rotary-drive, vibratory-output gyroscope of this paper is constructed of three sub-systems: a mechanical

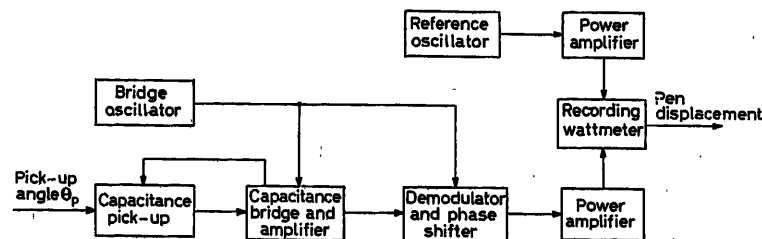


Figure 3. Output signal processing system

system; a rotor speed control system, and an output signal processing system. The next section deals with the theory of operation of this instrument.

Theory of Operation

Basic Equation of Motion for Gimbal

For the mechanical system of a rotary-drive, vibratory-output gyroscopic instrument as shown in *Figure 1*, the following differential equation can be written. This differential equation relates the gimbal angular displacement θ_y about the y axis to the combined effect of the drive torque M_d and the reaction torque M_s of the gimbal suspension. The asymmetrical rotor is assumed to be turning with a constant angular frequency so that the rotor angle ψ is equal to one-half ωt . The basic differential equation for gimbal motion is

$$\left[\left(\frac{I_2 + I_3}{2} \right) + \left(\frac{I_2 - I_3}{2} \right) \cos \omega t \right] \ddot{\theta}_y - \left[\left(\frac{I_2 - I_3}{2} \right) \omega \sin \omega t \right] \dot{\theta}_y = M_d - M_s \quad (1)$$

The moments of inertia I_1, I_2, I_3 are principal moments of inertia of the asymmetrical rotor about orthogonal axes 1, 2, 3, respectively, of *Figure 1*. Lagrange's method is used to derive eqn (1) and also to show that the drive torque can be defined as

$$M_d \triangleq \left[\left(\frac{I_2 - I_3}{2} \right) \omega \sin \omega t \right] \left(-\frac{\dot{\Omega}_x}{\omega} + \Omega_y \right) - \left[\left(\frac{I_2 - I_3}{2} \right) \omega \cos \omega t \right] \left(\frac{\dot{\Omega}_y}{\omega} + \Omega_z \right) - \left[\left(\frac{I_2 + I_3}{2} \right) \omega \right] \frac{\dot{\Omega}_y}{\omega} - \left[\frac{I_1 \omega}{2} \right] \Omega_z \quad (2)$$

Both of the above equations are approximations based on knowledge that the gimbal tilt angle θ_y is small and that the angular rates Ω_x and Ω_z are small compared with the rotor spin frequency. In a vibratory-output gyroscopic instrument the useful drive torque terms are those involving sinusoidal modulation of the angular rates Ω_y and Ω_z ; these are the projections along the y and z axes of the angular rate of the instrument with respect to an inertial reference frame.

Several of the ways of using asymmetrical rotor devices for sensing angular motion employ tuned suspension systems for the gimbal. The apparatus considered in this paper is of this character. For such a suspension, the torque M_s can often be written, exactly or approximately, as if the gimbal and its suspension were a second-order system. Thus

$$M_s = I_g \ddot{\theta}_y + f_g \dot{\theta}_y + k_g \theta_y \quad (3)$$

where I_g is the moment of inertia; f_g the effective damping coefficient, and k_g the effective spring constant of the gimbal system. Using the values of suspension torque and motor torque given above, eqn (1) can be written as

$$\frac{Q_g}{\omega_g} \ddot{\theta}_y + \dot{\theta}_y + Q_g \omega_g \theta_y + \alpha \frac{Q_g}{\omega_g} [(\cos \omega t) \dot{\theta}_y - \omega (\sin \omega t) \theta_y] = \left(\frac{Q_g}{\omega_g I_y} \right) M_d \quad (4)$$

Here the following definitions are used

$$I_y \triangleq \frac{I_2 + I_3}{2} + I_g \quad (5)$$

$$Q_g \triangleq \frac{(I_y k_g)^{\frac{1}{2}}}{f_g} \quad (6)$$

$$\omega_g \triangleq \left(\frac{k_g}{I_y} \right)^{\frac{1}{2}} \quad (7)$$

$$\alpha \triangleq \frac{I_2 - I_3}{2 I_y} \quad (8)$$

I_y is the total effective moment of inertia, Q_g is the quality factor, and ω_g is the 'natural' frequency of the gimbal system. The ratio α is a normalized measure of the asymmetry of the rotor.

A solution is sought for the gimbal angle θ_y in eqn (4) under conditions of steady angular rate Ω_z about the z axis. Only the periodic component of the solution is of interest; therefore only the sinusoidal component of the drive torque is considered. From eqn (2) this is

$$M_d = -|M_d| \cos \omega t \quad (9)$$

where

$$|M_d| = \left(\frac{I_2 - I_3}{2} \right) \omega \Omega_z \quad (10)$$

In the absence of the time-varying coefficients in eqn (4) the solution would be the response of an ordinary second-order differential equation with constant coefficients to a sinusoidal forcing function. As such, the response θ_y would be a sinusoidal function of the same frequency as the drive and it would exhibit resonance for values of drive frequency ω in the vicinity of the natural frequency ω_g of the gimbal system. It is desirable to take advantage of this resonance as a way of magnifying the response of the system. Also it serves as a means for discriminating against noise torques outside the frequency range of interest. The presence of the time-varying coefficients will introduce additional frequency components into the response of the system. The influence of these additional frequency components is investigated in the next section.

Influence of the Time-varying Coefficients

In order to solve eqn (4) with the time-varying coefficients present, a steady-state solution is postulated in the form of a Fourier series. Specifically,

$$\theta_y = \sum_n \theta_{yn} \quad (11)$$

where

$$\theta_{yn} = A_n \cos n \omega t + B_n \sin n \omega t \quad (12)$$

The unknown amplitudes A_n and B_n are evaluated by substituting the assumed solution into eqn (4). Products like $\cos \omega t \sin n \omega t$ resulting from the time-varying coefficients are expressed in terms of sum and difference frequencies. Equations (9) and (10) are used for the drive torque and use is made of the definition (8) for α . By equating coefficients of the corresponding sine and cosine terms for each harmonic on the two sides of eqn (4) an infinite set of simultaneous equations for the amplitudes A_n and B_n are obtained. By truncating the set so that just

the first $2N$ equations are considered it is found that $2N + 2$ unknown coefficients are present. In order to simplify and solve these equations it is helpful to make certain additional assumptions suggested by the mode of operation of the apparatus.

The first assumption is that the drive frequency ω (twice the rotor spin frequency) is nearly, but not necessarily exactly, equal to the natural frequency ω_g of the gimbal system. The second assumption is that the quality factor Q_g is such that the product αQ_g is large compared with unity. The third assumption is that high-frequency harmonics have negligible influence on the solutions for the low-frequency harmonics and therefore can be neglected.

In accordance with the third assumption, sufficient accuracy for purposes of this discussion is obtained by considering only the fundamental and second harmonic terms. If the pair of equations that results from equating coefficients for the second harmonic terms in eqn (4) is simplified by dropping the $\dot{\theta}_y$ terms as suggested by the second assumption noted above, then these equations yield the following relationships between the amplitudes of the second harmonic and fundamental components:

$$A_2 = -\frac{\alpha\beta^2}{4\beta^2-1}A_1 \quad (13)$$

$$B_2 = -\frac{\alpha\beta^2}{4\beta^2-1}B_1 \quad (14)$$

where

$$\beta \triangleq \frac{\omega}{\omega_g} \quad (15)$$

Here β is the ratio of the drive frequency ω (two times the rotor spin frequency) to the 'natural' frequency ω_g of the gimbal. Using these relationships in the exact equations resulting from equating coefficients for the fundamental terms in eqn (4), and solving for the amplitudes of the fundamental component, yields

$$A_1 = \frac{\gamma}{1+\gamma^2} \left(-\alpha Q_g \frac{\Omega_z}{\omega_g} \right) \quad (16)$$

$$B_1 = \frac{1}{1+\gamma^2} \left(-\alpha Q_g \frac{\Omega_z}{\omega_g} \right) \quad (17)$$

where

$$\gamma \triangleq Q_g \left[\frac{\alpha\beta^3}{4\beta^2-1} - \frac{\beta^2-1}{\beta} \right] \quad (18)$$

The fundamental component of θ_y has a magnitude equal to the square root of the sum of the squares of A_1 and B_1 and a phase angle whose tangent is A_1/B_1 . From eqns (16) and (17) this component is

$$\theta_{y1} = -\alpha Q_g \frac{\Omega_z}{\omega_g} \frac{\sin(\omega t + \tan^{-1}\gamma)}{(1+\gamma^2)^{\frac{1}{2}}} \quad (19)$$

The amplitude is a maximum for $\gamma = 0$. The value of the frequency ratio β for which this resonance condition occurs is β_r ; from eqn (18) it is found to be

$$\beta_r = 1 + \frac{\alpha^2}{6} + \dots \quad (20)$$

Theoretically, the maximum possible value of α is $1/2$ and practical design considerations limit the realizable values of α

to less than one-half. This means that the condition of maximum output amplitude occurs for values of β only slightly larger than unity. This is equivalent to saying that the drive frequency must be slightly higher than the natural frequency ω_g of the gimbal system in order for resonance to occur. This displacement of the resonant frequency is the major effect of the time-varying coefficients in the differential equation for gimbal motion.

Another question that must be answered concerns the influence of the time-varying coefficients on the response of the system for drive frequencies in the vicinity of the resonant frequency. Letting the frequency deviation from resonance be represented by $\Delta\beta$, this deviation is defined as

$$\Delta\beta \triangleq \beta - \beta_r \quad (21)$$

If γ of eqn (18) is expressed in terms of $\Delta\beta$ one obtains

$$\gamma = 2Q_g\Delta\beta \quad (22)$$

From eqns (16), (17) and (19) the amplitude response is seen to follow a resonance curve as a function of $\Delta\beta$ that has the same form as the resonance curve for an ordinary second-order system without time-varying coefficients. The half-power or 45° phase-shift points occur at $\gamma = 1$ which corresponds to $\Delta\beta$ equal to $1/2Q$. This corresponds to a drive frequency displacement $\Delta\omega$ from resonance of $\omega_g/2Q_g$.

In conclusion, the influence of the time-varying coefficients in the differential equation for the gimbal motion is found to be as follows: The drive frequency for maximum output, measured in terms of the fundamental component, is displaced slightly upward from the gimbal natural frequency. The response of the system for drive frequencies in the neighbourhood of this resonant frequency is found to be identical in character with that of a second-order system without time-varying coefficients. The quality factor or damping of the system is unaffected by the time-varying coefficients.

Counterpoise Pick-up System

The counterpoise pick-up system, shown in *Figure 1*, uses the pick-up rotor as a counterpoise flywheel that is elastically coupled to the gimbal by spring k_p . The counterpoise pick-up system offers certain advantages over methods which sense gimbal displacements directly. One advantage is the isolation of the pick-up from extraneous vibrations of the gimbal caused by dynamic unbalance of the asymmetrical rotor and bearing noise. A second advantage is the filtering action that permits making the pick-up system responsive to a selected frequency component of the gimbal motion and non-responsive to other components. Another is reduction of the gimbal motion without loss of sensitivity at the pick-up location. A fourth advantage is the increase in the quality factor Q and sensitivity that is characteristic of the counterpoise system. These results follow from the fact that most of the damping of the pick-up system comes from parts associated with the gimbal.

The introduction of the counterpoise method for sensing gimbal displacements raises the order of the gimbal differential equation of motion to the fourth order in contrast with the second-order equation analysed in the preceding section. This system will have two natural frequencies. The lower of these, designated as ω_{n1} , corresponds with the gimbal and pick-up moving substantially in phase, whereas the higher frequency,

ω_{n2} , corresponds with these elements moving substantially out of phase. With the low damping characteristic of this application the behaviour in the neighbourhood of each of these frequencies is substantially equivalent to the behaviour of a second-order system provided that the resonant frequencies are separated by several times the sum of the bandwidths about each. This condition generally can be fulfilled by appropriate design. Usually the lower resonant frequency is placed somewhat above the rotor spin frequency because of rotor dynamic unbalance problems. The higher resonant frequency is located near twice the rotor spin frequency.

For forcing frequencies in the neighbourhood of the higher natural frequency and under low-damping conditions the gimbal motion is given by the following approximate Laplace transform

$$\theta_y(s) \cong \left[\frac{1}{\frac{Q_2 s}{\omega_{n2}} + 1 + \frac{\omega_{n2} Q_2}{s}} \right] \frac{Q_2}{\alpha_y I_y \omega_{n2} s} M_d(s) \quad (23)$$

Q_2 is the quality factor associated with the upper resonance and

$$\alpha_y \triangleq \left[\frac{\frac{\omega_{n2}}{\omega_{n1}} \frac{\omega_{n1}}{\omega_{n2}}}{\frac{\omega_{n2}}{\omega_{n1}} \frac{k_2 + k_3}{\omega_{n1} \omega_{n2} I_p}} \right] \quad (24)$$

Here I_p is the inertia of the pick-up rotor. $\alpha_y I_y$ can be interpreted as an effective moment of inertia of the gimbal system. Since α_y will be larger than unity if the system is suitably designed, one effect of the counterpoise system can be an increase in the effective moment of inertia of the gimbal. For operation at frequencies near ω_{n2} with low damping, the ratio α_p of the pick-up amplitude to the gimbal amplitude is given by

$$\alpha_p = \frac{k_2}{k_2 + k_3} \left/ 1 - \left(\frac{I_p}{k_2 + k_3} \right) \omega_{n2}^2 \right. \quad (25)$$

The amplitude of the pick-up motion for a given angular rate with the rotor speed adjusted for resonance can be found from eqns (8), (10), (23) and (25) to be

$$|\theta_p| = \frac{\alpha_p \alpha Q_2}{\alpha_y} \frac{\Omega_z}{\omega_{n2}} \quad (26)$$

Assuming the resonant frequencies are unchanged, the ratio of the amplitude of the pick-up with the counterpoise system to that of the gimbal without this system can be found by comparing the above equation with eqn (19) when $\gamma = 0$. This ratio, which is one figure of merit for the counterpoise system, is

$$\frac{|\theta_p|}{|\theta_y|} = \frac{\alpha_p}{\alpha_y} \frac{Q_2}{Q_g} \quad (27)$$

α_p/α_y has an upper limit of unity and in practice is always fractional. For the parameters of the experimental apparatus given in the next section this ratio is found to be

$$\frac{|\theta_p|}{|\theta_y|} = \frac{5.31}{6.41} \frac{1008}{143} = 5.73 \quad (28)$$

provided it is assumed that the major portion of the damping is associated with the gimbal. This confirms the assertion that the counterpoise configuration tends to increase the sensitivity of the pick-up system.

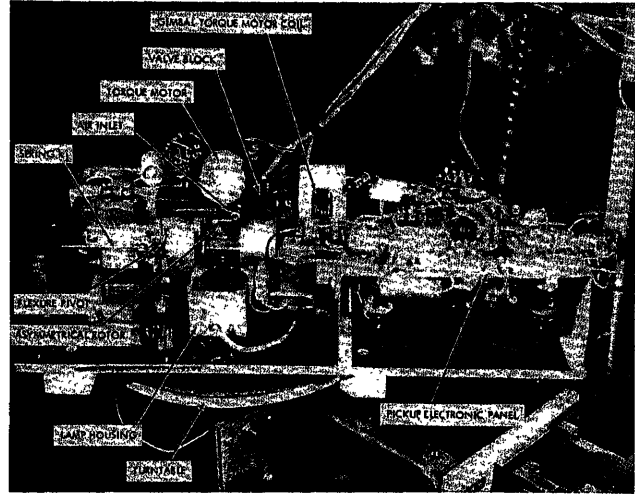


Figure 4. Experimental apparatus

Experimental Results

Figure 4 is a photograph of the apparatus tested and includes the mechanical system together with parts of the pick-up electronics and rotor speed control system. The pick-up rotor and torsion bar springs k_2 and k_3 are hidden behind the electronic panel. This equipment was fabricated from a low-performance, air-driven gyroscope with journal type spin-axis bearings used in lieu of ball bearings in order to reduce noise. The rotor was made asymmetrical by means of bars placed on each side. One of these can be seen in Figure 4. The reference oscillator (not shown) maintained the average speed of the rotor to better than 0.02 per cent of the desired value. Table 1 gives measured values of the important parameters needed to characterize this equipment.

Table 1. Parameter values of experimental apparatus

Parameter	Value
Rotor moments of inertia about the three principal axes of Figure 1	$\begin{cases} I_1 \\ I_2 \\ I_3 \end{cases}$
Gimbal moment of inertia	I_g
Pick-up moment of inertia	I_p
Upper natural frequency	ω_{n2}
Lower natural frequency	ω_{n1}
Quality factor associated with upper natural frequency	Q_2
	1008

Figure 5 is a reproduction of the recorded response of the above apparatus to constant angular rates about the z axis applied by means of a turntable. In this test the pick-up sensitivity, up to the point of power amplification to drive the wattmeter, is approximately 1.4 V/mrad at the pick-up and the signal is substantially noise-free. The mechanical system has a sensitivity of 0.225 rad amplitude at the pick-up for 1 rad/sec input rate. The R.M.S. noise level, indicated by the fluctuations in output signal for the 'constant' rate inputs, is of the order of 1×10^{-4} rad/sec. These fluctuations have a spectrum limited to relatively low frequencies because of the large effective time constant of the highly resonant sensing system ($\tau = \frac{2Q_2}{\omega_{n2}} \cong$

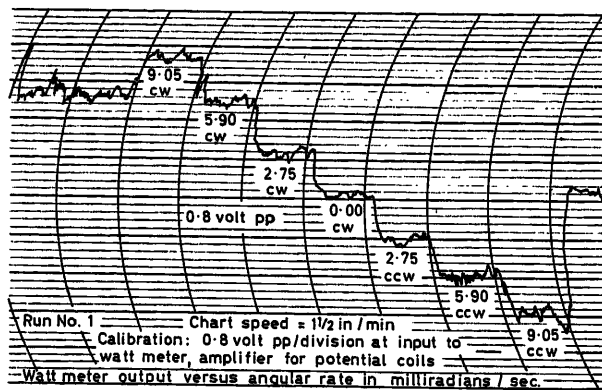


Figure 5. Response to constant angular rates
(1 min corresponds to 2 horizontal divisions)

2.41 sec). The sources of the observed noise are not fully understood and will be the subject of continuing research. However, it is known that slight fluctuations in turntable rates and air turbulence both contributed to the observed noise.

Conclusions

The major conclusions for the rotary-drive vibratory-output gyroscope of this paper are:

- (1) It is theoretically possible to obtain an alternating output torque whose frequency is twice that of the rotor spin rate.
- (2) Theoretically, the time-varying coefficients in the basic differential equation have no significant effect other than a slight displacement of the resonant frequency.
- (3) In theory, a counterpoise configuration for the sensing system offers several advantages over the simpler arrangement of locating the pick-up directly on the gimbal.
- (4) An experiment designed to demonstrate the above principles has achieved, with relatively crude equipment, a noise level of the order of earth's rate.

(5) The theoretical and experimental results obtained so far justify continuing research with the object of finding out if the performance level set by thermal fluctuations can be reached, and if not, for what reason.

The author thanks the staff members of the Electronic Systems Laboratory at M.I.T. who assisted in the preparation of this paper and particularly R. W. Bush for his comments.

This research was supported, in part, by the Lake States Oil Company in Michigan, and the continuing research is being sponsored by the National Aeronautics and Space Administration.

References

- ¹ BIRDSALL, E. H. Means and apparatus for utilizing gyrodynamic energy. *U.S. Pat. No. 2,716,893* (1955)
- ² BOWDEN, B. V. Gyroscopes. *U.S. Pat. No. 2,991,659* (1961)
- ³ DIAMANTIDES, N. D. The gyrovibrator. *Trans. Inst. Rad. Engrs ANE-6* (1959) 16-25
- ⁴ GRANQVIST, C. E. Gyroscope device with vibrating gas particles. *U.S. Pat. No. 2,999,389* (1961)
- ⁵ LYMAN, J. New space rate sensing instrument. *Aeronaut. Engng Rev.* 12 (1953) 24-30
- ⁶ MORROW, C. T. Zero signals in Sperry tuning fork gyrotron. *J. Acoust. Soc. Amer.* 27 (1955) 581-585
- ⁷ NEWTON, G. C., JR. Comparison of vibratory and rotating-wheel gyroscopic rate indicators. *Amer. Inst. elec. Engrs.* 79, Pt. II (1960) 143-150
- ⁸ SLATER, J. Gyros (introductory). *Control Engineering*, 9, No. 11 (1962) 92-97
- ⁹ SMIRNOV, YE. L. Symmetrical vibration gyroscope and some of its specific features. *Referativny Zhurnal, Mashinostroyeniye*, No. 18, (1961) 19. *Abstr.* 18D115
- ¹⁰ BEASLEY, T. J. Gyroscopic apparatus. *U.S. Pat. No. 2,969,681* (1961)
- ¹¹ SUTCLIFFE, H. The relation between zero errors and bandwidths for different types of rate-of-turn meters. *Aeronaut. Quart.* IX, May (1958) 131-146

Some Problems of the Dynamics of a Hydraulic Throttle-Control Servo-mechanism with an Inertial Load

V. A. KHOKHLOV

Summary

The paper indicates the range of amplitudes and frequencies of valve oscillation at which a hydraulic servo-motor working on an inertial load and with incompressible fluid may still be treated as a linear system.

An equation of motion is derived for the loaded hydraulic servo-motor taking into account the compressibility of the fluid. A technique is given for both accurate and approximate determination of the limiting oscillation frequencies of the actuator corresponding to the occurrence of cavitation discontinuity in the hydraulic-cylinder fluid.

Sommaire

Le rapport indique le domaine des amplitudes et des fréquences des oscillations d'une vanne commandée par un servo-moteur hydraulique; compte tenu de son inertie et de sa commande au moyen d'un fluide incompressible, ce dispositif est traité tout d'abord comme un système linéaire.

L'équation du mouvement est ensuite établie, prenant en considération la compressibilité du fluide moteur. Une méthode est indiquée pour la détermination de la valeur maximale des oscillations, limitée par l'apparition de cavitation dans le fluide actionnant le cylindre du servo-moteur.

Zusammenfassung

In diesem Beitrag werden die Amplituden- und Frequenzbereiche der Ventilschwingung aufgezeigt, innerhalb deren hydraulische Servomechanismen, die mit Masse und inkompressiblen Flüssigkeiten arbeiten, noch als lineares System betrachtet werden können.

Eine Bewegungsgleichung wird für den belasteten hydraulischen Servomechanismus abgeleitet, die die Kompressibilität der Flüssigkeit in Betracht zieht. Der Beitrag gibt ein Verfahren sowohl für die exakte wie für die angenäherte Bestimmung der Grenzen der Schwingfrequenz des Mechanismus an, bei deren Überschreitung Kavitation in der Flüssigkeit des Servozyinders auftritt.

Introduction

Two questions are considered in this paper. The first concerns the limiting conditions under which a hydraulic servo-mechanism may still be treated as a linear system. This is investigated without taking into account the compressibility of the liquid in the hydraulic cylinder. The effect of this factor is taken into account in the investigation of the second problem—that of the limiting frequency of oscillation of the servo-mechanism piston at which cavitation of the liquid in the hydraulic cylinder does not occur.

The following assumptions are made: there is no liquid leakage from, or hydraulic loss in, the piping; the flow coefficient in the control ports of the valve is constant; the working edges

of the sleeve and of the valve, in the mean position of the latter, coincide; and the effective areas of the piston are the same on both sides.

On the Limiting Conditions under which a Hydraulic Servo-mechanism Working with an Inertial Load may be Considered as a Linear System

Figure 1 shows an outline diagram of the hydraulic servo-mechanism taken for analysis. The differential equation of motion for the actuator neglecting the liquid compressibility, and with only inertial loading, has been derived by Katz¹. In an earlier paper² the author has given the following general form of differential equation for a servo-mechanism under any kind of load:

$$\frac{dx}{dt} = \mu \left(\frac{g}{\gamma} \frac{b}{F} \right)^{\frac{1}{2}} (p_0 - \Delta p \cdot \text{sgn } \rho)^{\frac{1}{2}} \cdot \rho \quad (1)$$

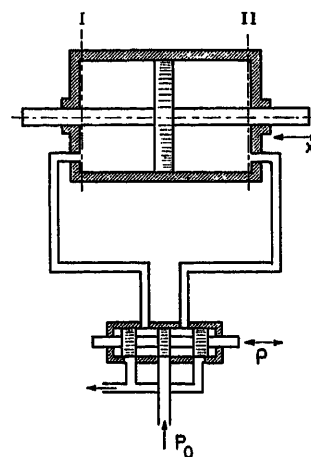


Figure 1. Outline diagram of hydraulic servo-mechanism with slide-valve control

where x is the displacement of the piston in the hydraulic cylinder, measured from its central position; μ is the liquid flow coefficient in the valve ports; b is the length of the working slit of the valve port; F is the effective area of the piston; p_0 is the pressure in the supply line; Δp is the pressure drop in the capacities of the power hydraulic cylinder created by the external load; ρ is the displacement of the valve; and $\text{sgn } \rho$ is the sign determining the direction in which the valve is displaced from its central position.

Equation (1) is non-linear. It is of interest to determine the limits of frequency and amplitude of valve oscillation within which the non-linear term $\Delta p \text{sgn } \rho$ may be neglected in eqn (1).

The solution of this problem is particularly interesting in the case where an inertial load is displaced by the piston of the hydraulic cylinder. Katz¹ has shown that for sinusoidal valve motion the piston velocity may be expressed approximately in the form of a series

$$v = \sin \tau - \frac{\theta}{4} \sin 2\tau + \frac{\theta^2}{32} (3 \sin 3\tau - 5 \sin \tau) + \frac{3\theta^3}{8} \sin 3\tau \cos \tau + \dots \quad (2)$$

where v is the dimensionless piston velocity.

$$v = \frac{\frac{dx}{dt}}{\left(\frac{dx}{dt}\right)_{xx}} = \frac{F}{\mu b \rho^*} \left(\frac{\gamma}{g p_0}\right)^{\frac{1}{2}} \cdot \frac{dx}{dt} \quad (3)$$

$\left(\frac{dx}{dt}\right)_{xx}$ is the no-load piston velocity corresponding to an amplitude valve displacement of ρ^* , τ is the dimensionless time

$$\tau = \omega t \quad (4)$$

and θ is the dimensionless parameter

$$\theta = \omega \rho^* \frac{m \mu b}{F^2} \left(\frac{g}{\gamma p_0}\right)^{\frac{1}{2}} \quad (5)$$

where m is the mass of the load applied to the piston.

In his paper he also gives two more approximate methods for solving the forced periodic motion of the piston in a hydraulic servo-mechanism, and shows that all three methods give a satisfactory approximation provided $\theta \leq \frac{1}{2}$.

However with inertial loading the non-linearity of the equation of motion of the actuator [eqn (1)] is determined by a term depending not on its output velocity but on the acceleration

$$\Delta p = \frac{m}{F} \cdot \frac{d^2 x}{dt^2}.$$

According to the results of Katz¹ and making use of expressions (3), (4) and (5), it is possible to obtain:

$$\frac{dv}{dt} = \cos \tau - \frac{\theta}{4} \cos^2 \tau - \frac{\theta}{4} \left(1 - \frac{\theta}{2} \cos \tau\right) [(1 - 3 \sin^2 \tau) + 3 \theta \sin^2 \tau \cos \tau] - \frac{\theta^3}{64} [1 - 3 \sin^2 \tau (1 - \theta \cos \tau)]^2$$

Figures calculated from this equation for $\theta = 0.5$ and $\theta = 0.1$ are shown in graphical form in Figure 2.

These graphs show that with sinusoidal valve motion and for

$$\theta \leq 0.1 \quad (6)$$

the piston acceleration for the main hydraulic cylinder follows an approximately cosine law (error not more than 5 per cent).

Thus if condition (6) is satisfied the term $\Delta p \operatorname{sgn} \rho$ may be neglected in eqn (1), and so one may treat the servo-mechanism working on an inertial load as a linear integrating element.

In order for condition (6) to be satisfied, by virtue of (5) we must have:

$$\omega \rho^* \leq 0.1 \frac{F^2}{\mu m b} \left(\frac{\gamma p_0}{g}\right)^{\frac{1}{2}} \quad (7)$$

On the Limiting Frequency for a Hydraulic Throttle-control Servo-mechanism at which Cavitation of the liquid in the Hydraulic Cylinder does not Occur

The modern tendency to increase the accuracy and action speed of servo-systems calls for an increase in their natural frequencies. While in electrical servo-mechanisms the natural frequency is essentially limited by motor heating, no such limitation exists in hydraulic actuators. However, in the presence of an

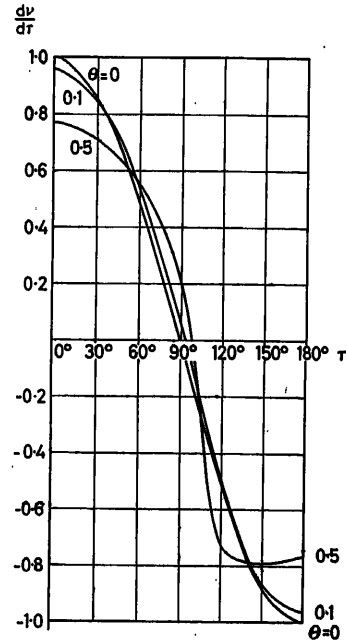


Figure 2. Piston acceleration curves for sinusoidal valve motion

inertial load the frequency transmitted by a hydraulic throttle-control servo-mechanism is limited. This limit is due to the fact that with this sort of load the actuator is working alternately as a motor and as a pump. In the pumping condition, because of the presence of controlling throttling devices and the limited supply pressure, the pressure in the suction line may turn out to fall below atmospheric. In this event cavitation occurs in the liquid in the hydraulic cylinder^{2, 3}.

At the same time the continuity of fluid flow, basic to the analysis of hydraulic servo-mechanisms, is broken.

Considered here is the problem of determining the limiting frequency transmitted by the actuator under the condition that cavitation should not occur in the hydraulic cylinder. The solution of this problem is carried out taking into account the compressibility of the fluid, and with the piston driving an inertial and velocity load. Under these conditions the motion of the piston in Figure 1 is determined by the following three equations⁴:

(1) The equation for liquid flow through the valve:

$$\frac{dx_1}{dt} = k_v \left(1 - \frac{\Delta p \operatorname{sgn} \rho}{p_0}\right)^{\frac{1}{2}} \cdot \rho \quad (8)$$

where x_1 is the displacement of the section of fluid close to the end walls of the power cylinder (sections I and II in *Figure 1*);

$$k_v = \mu \frac{b}{F} \left(\frac{g p_0}{\gamma} \right)^{\frac{1}{2}}$$

(2) The equation for the forces acting on the piston

$$m \frac{d^2 x}{dt^2} + h \frac{dx}{dt} = (x_1 - x) k_R \quad (9)$$

where h is the viscous friction coefficient of the load, and k_R the rigidity of the liquid.

For motion of the piston close to its central position, from the author's previous results⁴ one may consider the rigidity of the liquid as constant and equal to $2 FG/l_0$, where G is the modulus of elasticity of the fluid and l_0 is the half-length of the internal capacity of the hydraulic cylinder.

(3) The equation for elastic deformation of the liquid in the hydraulic cylinder:

$$\Delta p F = (x_1 - x) k_R \quad (10)$$

By eliminating the variables x_1 and Δp between eqns (8), (9) and (10) the equation of motion for the loaded hydraulic servo-mechanism is obtained taking into account the compressibility of the liquid:

$$\begin{aligned} \frac{m}{k_R} \frac{d^3 x}{dt^3} + \frac{h}{k_R} \frac{d^2 x}{dt^2} + \frac{dx}{dt} \\ = k_v \left(1 - \frac{1}{F p_0} \left(m \frac{d^2 x}{dt^2} + h \frac{dx}{dt} \right) \operatorname{sgn} \rho \right)^{\frac{1}{2}} \rho \end{aligned} \quad (11)$$

According to the author's previous results² the continuity condition for the liquid masses in the cylinder may be written in the following form:

$$\left| \frac{1}{F p_0} \left(m \frac{d^2 x}{dt^2} + h \frac{dx}{dt} \right) \right| \leq 1 \quad (12)$$

Since an analytical solution of eqn (11) is not possible, an investigation of it was carried out, by the author and T. N. Kolerova, on the EMU-5 electronic analogue simulator. The example chosen for simulation was a slide-valve-controlled hydraulic servo-mechanism with the following numerical parameter values: $F = 50 \text{ cm}^2$; $d_v = 1.4 \text{ cm}$; $q_{\max} = 0.024 \text{ cm}$; $b = \pi d_v = 4.4 \text{ cm}$; $l_0 = 5 \text{ cm}$; $p_0 = 50 \text{ kg cm}^{-2}$; $\mu = 0.57$; $\gamma = 0.9 \times 10^{-3} \text{ kg cm}^{-3}$; $m = 0.2 \text{ kg sec}^2 \text{ cm}^{-1}$; $h = 12 \text{ kg sec cm}^{-1}$; $G = 12,000 \text{ kg cm}^{-2}$; $k_R = 24 \times 10^4 \text{ kg cm}^{-1}$.

The following were used in setting up the problem: standard computing amplifiers; a limiter to ensure that condition (12) was fulfilled; an element performing the operation of square-root extraction; a multiplier; and a two-position relay reacting to the sign of the valve displacement.

With the dimensions and parameters given above for the servo-mechanism, the differential eqn (11) takes the form:

$$\begin{aligned} 0.83 \times 10^{-6} \frac{d^3 x}{dt^3} + 5 \times 10^{-5} \frac{d^2 x}{dt^2} + \frac{dx}{dt} \\ = 52.7 \left(50 - \left(4 \times 10^{-3} \frac{d^2 x}{dt^2} + 0.24 \frac{dx}{dt} \right) \operatorname{sgn} \rho \right)^{\frac{1}{2}} \rho \sin \omega t \end{aligned} \quad (13) \quad \dagger$$

[†] For convenience in solution, the quantity $\sqrt{p_0} = \sqrt{50}$ that enters into k_v has been included under the square-root sign on the right-hand side of the equation.

Solving this equation in terms of the highest derivative, and transforming to the time-scale $\tau = 50 t$ for convenience, we get:

$$\begin{aligned} \frac{d^3 x}{d\tau^3} = -1.2 \frac{d^2 x}{d\tau^2} - 480 \frac{dx}{d\tau} \\ + 505 \left(50 - \left(10 \frac{d^2 x}{d\tau^2} + 12 \frac{dx}{d\tau} \right) \operatorname{sgn} \rho \right)^{\frac{1}{2}} \rho^* \sin \Omega \tau \end{aligned} \quad (14)$$

where $\Omega = 0.02 \omega$.

The block diagram of the model representing eqn (14) is given in *Figure 3*.

A voltage was applied to the input of the model that represented a sinusoidal motion of the valve.

Altogether, four series of oscillograms were taken, corresponding to fixed amplitudes of valve oscillation and to various frequencies ranging from zero to 300 c/sec (zero to 6 c/sec on the model scale).

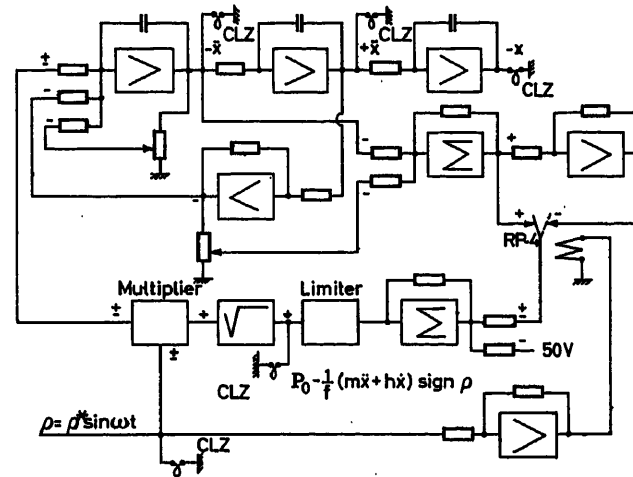


Figure 3. Block diagram of interconnection of computing elements in electronic simulator

These oscillograms were processed to give amplitude- and phase-frequency characteristics for the actuator, which are shown as continuous lines on *Figure 4*.

Arrows are used on the amplitude-frequency characteristics to indicate the points determined by condition (12) as the boundaries for transition to cavitation conditions. On the same diagram the broken lines provisionally show sections of amplitude-frequency characteristics corresponding to cavitation conditions. An amplitude characteristic is also drawn here for the same servo-mechanism with no load, $m = h = 0$.

These characteristics indicate the presence of resonant modes in the inertially loaded actuator. As the amplitude of valve oscillation is reduced, the resonant frequency tends (in the example considered) to $\omega_0 = 1,100 \text{ sec}^{-1}$, which corresponds to the oscillation frequency of the load mass of $\omega_0 = (k_R/m)^{\frac{1}{2}}$.

Investigations were also made for other combinations of the basic servo-mechanisms parameters. In particular, *Figure 5* shows three oscillograms obtained for periodic motions of the actuator with $l_0 = 10 \text{ cm}$ and the remaining figures as in the example above.

Although the motion of the hydraulic servo-mechanism allowing for liquid compressibility is described by the non-linear differential eqn (11), still, as follows from the oscillograms shown in Figure 5, sinusoidal displacement of the valve causes

a piston motion according to a law close to the harmonic. This provides a basis for estimating the boundary of the cavitation state working from a linear approximation, besides the investigation already described.

To solve this problem eqn (11) is taken and the term on the right-hand side omitted from the original equation of motion of the hydraulic servo-mechanism,

$$\frac{1}{p_0 F} \left(m \frac{d^2 x}{dt^2} + h \frac{dx}{dt} \right) \operatorname{sgn} \rho$$

under the square-root sign. The equation becomes:

$$\frac{m}{k_R} \frac{d^3 x}{dt^3} + \frac{h}{k_R} \frac{d^2 x}{dt^2} + \frac{dx}{dt} = k_v \rho \quad (15)$$

The condition for no liquid discontinuity in the hydraulic cylinder, for the case under discussion, can now be found.

For a linear system with periodic oscillations it is known that:

$$\frac{d^2 x}{dt^2} = \left(\frac{d^2 x}{dt^2} \right)_{\max} \quad \text{when} \quad \frac{dx}{dt} = 0 \quad (16)$$

Then, taking into account that the discontinuity of the liquid is conditioned by the inertial load, condition (12) takes the form:

$$\left| \left(\frac{d^2 x}{dt^2} \right)_{\max} \right| = x^* \omega^2 \leq \frac{p_0 F}{m} \quad (17)$$

where x^* is the amplitude of oscillation of the hydraulic cylinder piston.

Solving eqn (17) for ω one finds the limiting oscillation frequencies for the hydraulic cylinder piston at which continuity of liquid flow is still maintained

$$\omega_{cr} = \left(\frac{p_0 F}{m x^*} \right)^{\frac{1}{2}} \quad (18)$$

The value of valve oscillation amplitude required to satisfy this condition is determined from the amplitude-frequency characteristic of the servo-mechanism.

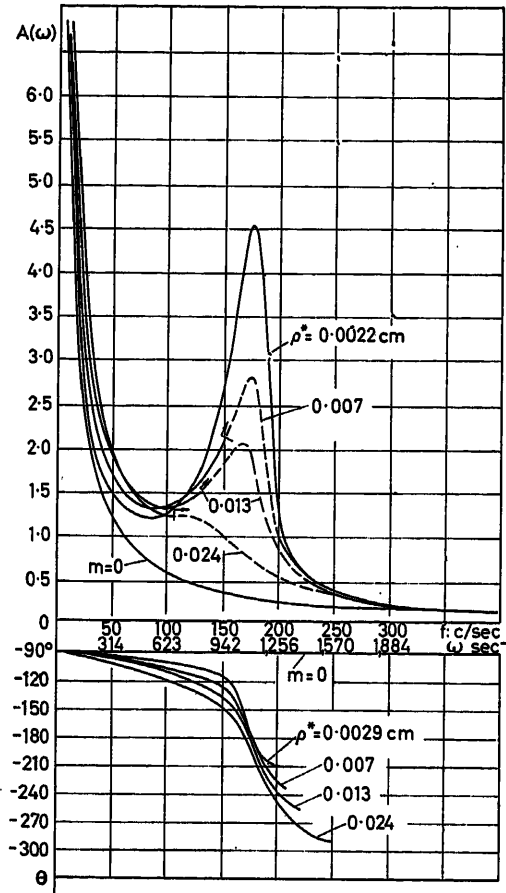


Figure 4. Amplitude and phase-frequency characteristics for a hydraulic servo-mechanism working on inertial and velocity load

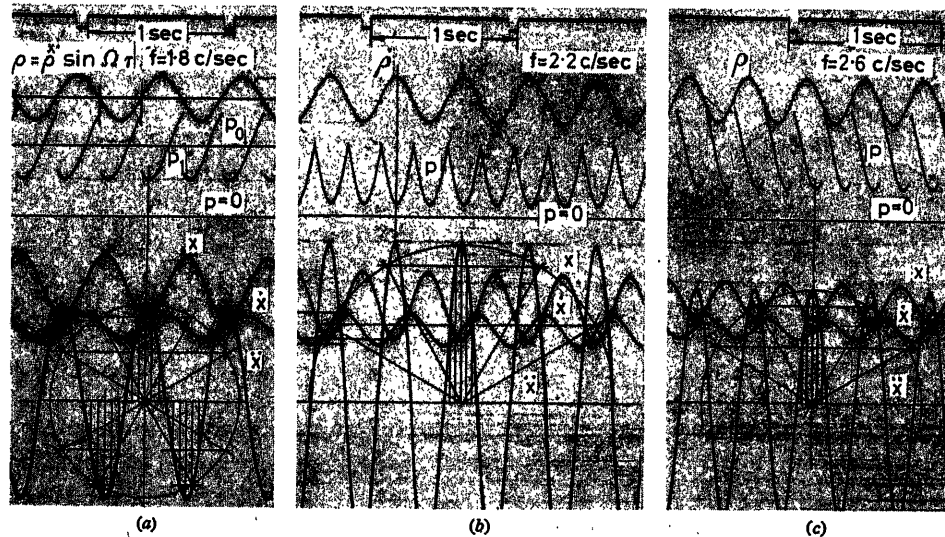


Figure 5. Oscillograms of forced periodic motions of a loaded hydraulic servo-mechanism:
(a) $f = 1.8$ (90) c/sec; (b) $f = 2.2$ (110) c/sec; (c) $f = 2.6$ (130) c/sec

The latter, according to eqn (15), has the form:

$$A(\omega) = \frac{x^*}{\rho^*} = \frac{k_v}{\omega} \left(\frac{1}{\left(1 - \frac{m}{k_R} \omega^2\right)^2 + \left(\frac{h}{k_R}\right)^2 \omega^2} \right)^{\frac{1}{2}} \quad (19)$$

The simultaneous solution of eqns (18) and (19) allows the limiting permissible frequency ω_{cr} as a function of the amplitude of valve displacement, to be found:

$$\omega_{cr} = \left\{ \left(\frac{k_v k_R}{p_0 F} \right)^2 \frac{\rho^{*2}}{2} + \omega_0^2 - \frac{1}{2} \left(\frac{h}{m} \right)^2 - \left[\left(\frac{k_v k_R}{p_0 F} \right)^2 \frac{\rho^{*2}}{2} + \omega_0^2 - \frac{1}{2} \left(\frac{h}{m} \right)^2 \right]^2 - \omega_0^4 \right\}^{\frac{1}{2}} \quad (20)$$

From examination of this equation it can be observed that $\omega_{cr} = \omega_0$ when

$$\frac{k_v k_R}{p_0 F} \rho^* = \frac{h}{m}$$

Thus continuity of liquid flow will only be maintained in the hydraulic servo-mechanism provided that the amplitude of valve oscillation does not exceed

$$\rho^* = \frac{h}{m} \cdot \frac{p_0 F}{k_v k_R} \quad (21)$$

For the case considered, $\rho^* = 0.0017$ cm.

Table 1 shows the limiting frequencies for oscillations transmitted by the hydraulic servo-mechanism in the absence of discontinuities, as obtained both through simulator investigation of the non-linear eqn (13) and by calculation from eqn (20) based on a linear model of the same actuator.

Table 1

ρ , cm	0.0022	0.007	0.013	0.024
ω_{cr} , sec ⁻¹ (from simulator results)	—	960	820	660
ω_{cr} , sec ⁻¹ [calculated from eqn (20)]	1060	976	887	750

It follows from these figures that the linear approximation to the problem is acceptable for the determination of limiting frequencies corresponding to the boundary at which cavitation takes place; the figures in the table show relatively good agreement.

References

- KATZ, A. M. *Automatic Control of the Speed of Internal Combustion Engines*. 1956. Mashgiz
- KHOKHLOV, V. A. An analysis of the motion of a loaded hydraulic servo-mechanism with feedback. *Automat. Telemekh.*, No. 9 (1957)
- KHOKHLOV, V. A. An experimental investigation of the bulk strength of liquid used in hydraulic servo-mechanism. *Izv. Akad. Nauk SSSR, Otdel. Tekh. Nauk, ser. Energet. Autom.*, No. 6 (1961)
- KHOKHLOV, V. A. Forced periodic motions of a hydraulic servo-mechanism with a position load. *Automat. Telemekh.*, No. 6 (1960)

DISCUSSION

PROFESSOR MAX LELAN, *Great Britain*

A similar paper has been published in Britain. It would be interesting to know whether the author had an opportunity of comparing conclusions.

In 1947 Coombes¹ studied the effect of an inertial load on a hydraulic power unit for sinusoidal motion of the piston, and established the conditions under which the inertial effect becomes negligible. About 1957 Butler² gave a full mathematical analysis of the non-linear equations, and about a year later Royle³ obtained results of a study on an electronic integrator. The results and the conclusions seem similar to those now reported.

References

- COOMBES, I. E. M. Hydraulic remote position controllers. *J. Inst. elect. Engrs*, 94, Pt. II A, No. 2 (1947)
- BUTLER, R. A theoretical analysis of the response of a loaded hydraulic relay. *Proc. Inst. mech. Engrs*, 173, No. 16 (1959)
- ROYLE, J. K. Inherent non-linear effects in hydraulic control systems with inertia loading. *Proc. Inst. mech. Engrs*, 173, No. 9 (1959)

V. A. KHOKHLOV, *in reply*

Coombes uses, as a criterion for evaluating the non-linearity of the equation of motion of a hydraulic power unit under inertial load, the deviation of the output element of the hydromotor from the sinusoidal law. This paper uses another criterion.

Butler makes an analysis of the non-linear equation of motion of a hydraulic power unit and servo. However, the results obtained for

a stepped input signal are similar in many respects to those obtained by Katz (reference 1 of the paper).

Regarding the study of dynamics with a sinusoidal input signal, account is not taken here of the influence of variation of the sign of movement of the slide valve from the middle position on the pressure drop in the hydraulic cylinder. This factor, extremely important for the work of hydraulic servos, was taken into consideration by Royle. However, the first part of his study is in many respects similar to that of Katz in which, on the hypothesis that the liquid is incompressible, three ways are given to obtain an approximate solution of the equation of motion of a hydraulic power unit under inertial load. Both Katz and Royle give an evaluation of the influence of inertial load on the deviation from the ideal of the integrating element along the velocity variation curve of the working organ of the hydraulic motor.

The first part of the paper examines the same problem, but the evaluation is made for the acceleration variation of the curve, since it is this factor which is the measure of the non-linearity of the equation of motion with an inertial load on the hydraulic motor.

Royle, in the second part of his paper, gives a quantitative evaluation of the conditions of appearance of cavitation in the cavities of the hydraulic motor, brought about by the existence of an inertial load. However, this question, which is linked with the critical mass of the load of the hydraulic servo (booster), was previously examined by Katz.

It should be emphasized here that in the paper only a quantitative evaluation is given of the validity of the equation of continuity of the current of liquid (absence of cavitation) in the hydraulic cycle of the power unit, taking the compressibility of the liquid into account. It is shown at the same time that the boundary conditions of appearance of cavitation can be determined in engineering practice from a linear equation.

MR. EVANS, *Great Britain*

I would be grateful if you could answer the following questions:

(1) Did this type of investigation examine the effect of pliancy (elasticity) between the piston of the hydraulic cylinder and the load, or the hydraulic cylinder and its connection to earth? If not, is it then possible to draw any general conclusion?

(2) The data given in the paper are the results of a theoretical study only. I should like to hear something about the confirmation of the results obtained by the findings of an experimental investigation.

V. A. KHOKHLOV, *in reply*

The effect of pliancy of the load relative to the piston or the cylinder relative to earth was not specially considered in the paper. This is because the pliancy of the cylinder relative to earth is small, in my view, and the pliancy of the load relative to the piston can always be taken into consideration by introducing the concept of equivalent rigidity of the load and the pillar of oil in the hydraulic cylinder.

The results obtained are theoretical. However, the following should be noted. In the development of the electrohydraulic servo examined by Kotelnikov and Khokhlov¹, it was noted that at certain amplitudes and frequencies of the input signals the system is excited and no means of correction can make it operative. Only release of the air which has accumulated in the hydraulic cylinder returned the system to normal operation. At that time (1948-49), it was not possible to understand why the free (undissolved) air got into the hydraulic cylinder, since there was no entrapped gas in the infed working liquid.

It was only in 1955 that it proved possible to explain the reason for the appearance of entrapped gas in the hydraulic cylinder. This paper has formulated the conditions under which the appearance of cavitation discontinuities of the liquid in hydraulic power units with throttle (slide valve) control, and at the same time the release of free air, is excluded.

Reference

- ¹ KOTELNIKOV, V. A. and KHOKHLOV, V. A. Electrohydraulic converting device for electronic d.c. integrators. *Automat. telemekh.*, No. 7 (1956)

Realization of Sequential Machines by Means of Pneumatic Automation

A. A. TAL

Summary

Methods of realization of synchronous and asynchronous sequential machines by pneumatic automatization means are described. For the design of asynchronous machines, methods are proposed which are based on the use of one, two or three 'natural' delays.

Sommaire

Des méthodes de réalisation de machines séquentielles synchrones et asynchrones par des moyens d'automatisation pneumatiques sont décrites. Pour la conception de machines asynchrones, des méthodes basées sur un, deux ou trois retards «naturels» sont proposées.

Zusammenfassung

Der Aufsatz beschreibt Methoden zum Bau periodischer und aperiodischer sequentieller Maschinen mit pneumatischen Schaltelementen, wie sie bei der Automatisierung Verwendung finden. Für den Entwurf aperiodischer Maschinen werden Verfahren vorgeschlagen, die auf der Verwendung von einer, zwei oder drei „natürlichen“ Verzögerungen beruhen.

Introduction

In the last few years, with the design of systems and instruments for industrial pneumatic automation, a function component principle has been widely applied¹. This leads to a situation in which pneumatic devices cease to exist as independent units. Now each device is a certain combination of unified elements assembled into a system with the help of special mounting plates. Thus one device is distinguished from another by the composition of elements and by the mounting plates. Such a process of constructing devices, carried over into pneumatic automation from electrical automation, has opened up qualitatively, for pneumatic automation, new possibilities (if one does not pay attention to speed of operation), which are close to those of electrical automation.

After the basic elements of pneumatic automation were established and a technique of installing these elements was worked out, it became practically possible to realize any control laws by pneumatic means.

In view of these conditions the necessity arose for developing methods of synthesizing pneumatic systems to satisfy control laws of one type or another. In this present work, methods of designing systems which pertain to the class of sequential machines are investigated by pneumatic means.

Before investigation of the methods themselves, several explanations are made apropos of the class of realized systems and concerning the type of pneumatic apparatus to be depended upon.

A dynamic system determined by the equations

$$\left. \begin{aligned} \mu &= F[\kappa, \varrho] \\ \kappa[t+1] &= \mu[t] \\ \lambda &= \Phi[\kappa, \varrho] \end{aligned} \right\} \quad (1)$$

is called a sequential machine (for example see Aizerman *et al.*²), where t is the conditional time (discrete and taking values in the natural sequence of numbers); ϱ, κ (or μ), λ are variables determining respectively the state of input, the internal state, and the state of output of a sequential machine, and where each of these variables can take a finite number of different values defined by the alphabets $\varrho = \{\varrho_1, \dots, \varrho_r\}$, κ (or μ) = $\{\kappa_1, \dots, \kappa_k\}$, and $\lambda = \{\lambda_1, \dots, \lambda_l\}$, and F and Φ are respectively k - and l -valued logical functions. The time relationship between the variables κ and μ determined by the second equation in (1) is called the lag, and the designations $\kappa = \mu' = D\mu$ are used. System (1) can always be represented in the form

$$\begin{aligned} \kappa[t+1] &= F\{\kappa[t], \varrho[t]\} \\ \lambda[t] &= \Phi\{\kappa[t], \varrho[t]\} \end{aligned} \quad (2)$$

The block diagram shown in Figure 1 corresponds to the designated characterization for the sequential machine.

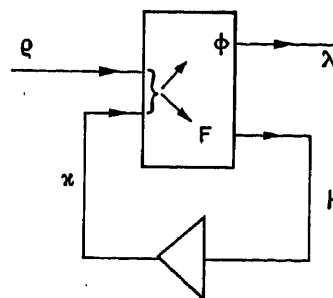


Figure 1. Block diagram of a sequential machine

Table 1

κ	ϱ	ϱ_1	ϱ_i	ϱ_r
κ_1		$F(\kappa_1, \varrho_1)$ $\Phi(\kappa_1, \varrho_1)$	$F(\kappa_1, \varrho_i)$ $\Phi(\kappa_1, \varrho_i)$	$F(\kappa_1, \varrho_r)$ $\Phi(\kappa_1, \varrho_r)$
κ_j		$F(\kappa_j, \varrho_1)$ $\Phi(\kappa_j, \varrho_1)$	$F(\kappa_j, \varrho_i)$ $\Phi(\kappa_j, \varrho_i)$	$F(\kappa_j, \varrho_r)$ $\Phi(\kappa_j, \varrho_r)$
κ_k		$F(\kappa_k, \varrho_1)$ $\Phi(\kappa_k, \varrho_1)$	$F(\kappa_k, \varrho_i)$ $\Phi(\kappa_k, \varrho_i)$	$F(\kappa_k, \varrho_r)$ $\Phi(\kappa_k, \varrho_r)$

As done in the paper by Aizerman *et al.*, one proceeds from the conjecture that the task for a synthesized system of a sequential machine is shown in Table 1, determining the logical functions F and Φ .

In addition to such a table, the condition determining tempo of the operation of the sequential machine r

be shown in the representation. The symbols $\kappa_{ij} = F(\kappa_i, q_j)$ written in the boxes in Table 1 can be interpreted in two ways: in accordance with system (1) it is possible to consider that they are the values of the variable

$$\mu[t] = F\{\kappa[t], q[t]\}$$

or it is permissible, in accordance with system (2), to consider that they are the values of the variable

$$\kappa[t+1] = F\{\kappa[t], q[t]\}$$

In future both these interpretations are used.

A three-membraned pneumatic relay is the basic element of the discrete technique of industrial pneumatic automation. The principal scheme of this relay, the conventional representation used for it, and its statistical characteristics are given in Figure 2. In Figure 3 are shown the circuits for switching on the pneumatic relay for the realization of several elementary logical functions. In these and in all future pneumatic systems $P = P_{sup}$ corresponds to symbol 1, and $P = 0$ atm to symbol 0. For the realization of the operation 'OR', an even simpler element is used, the diagram and conventional representation of which are given in Figure 4.

The summary introduced of the elementary logical functions realized by the named pneumatic means shows that these means are enough for the realization of any logical function. For an example, in Figure 5 are depicted the circuits of cells 'Shaeffer stroke', 'Pierce Arrow', 'equivalence', and 'the excluded OR'.

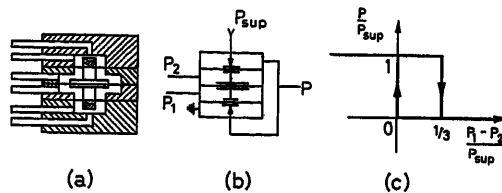


Figure 2. Pneumatic relay: (a) Scheme; (b) conventional representation; and (c) statistical characteristics

The aim of this present work is to show how, using these same pneumatic means (the pneumatic relay, the element 'OR', and perhaps even pneumatic resistance), it is possible to construct systems not only of any logical converters, but also of sequential machines whose operation is defined in the form shown above.

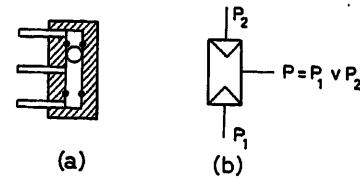


Figure 4. Element 'OR': (a) scheme; (b) conventional representation

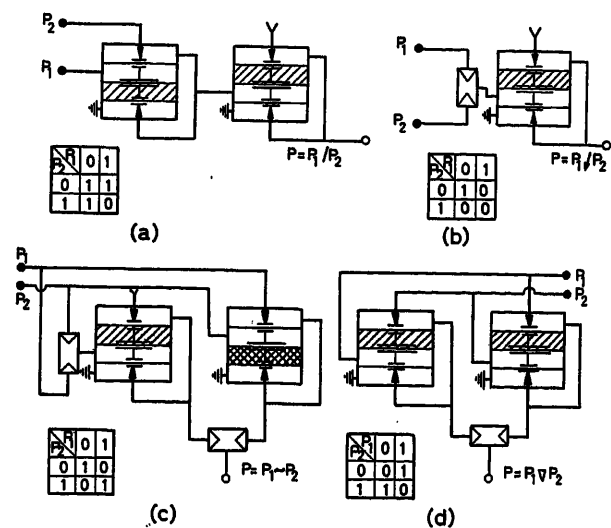


Figure 5. Circuits of realizing operations: (a) 'Shaeffer stroke'; (b) 'Pierce Arrow'; (c) 'equivalence'; (d) the excluded 'OR'

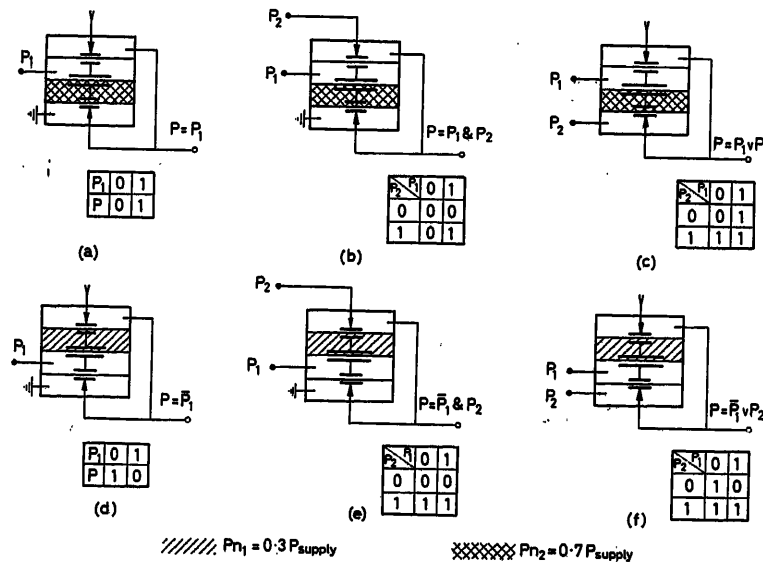


Figure 3. Wiring diagrams of pneumatic relay for realization of: (a) repetition; (b) conjunction; (c) disjunction; (d) negation; (e) exclusion; and (f) implication

Forced Binary Lag in Time and its Use in Systems of Sequential Machines

Four pneumatic relays connected according to circuit shown in Figure 6 (a) form the so-called binary lag in time. The graph in Figure 6 (b) indicates the operation of this circuit. The two inputs of the cell P_t and P have a different value: P is strictly the input, and P_t determines the moments of onset of times, that is, these moments correspond to the change of P_t from zero to unity. The graphs in Figure 6 (b) show that the cell works in such a way so that its output P' at the time of the onset time proves to be equal to input P , and until the onset of a new time remains unchanged so as not to take place at this time at the input. Such operation of the cell gives rise to its name 'lag in time'.

It is especially convenient to use the lag in time in the design of sequential machines whose tempo of operation is determined by a special synchronizing signal.

The block diagram of a corresponding sequential machine is shown in Figure 7 (a), while Figure 7 (b) shows a block diagram of the binary realization of this machine. The problem of realizing a machine described in the form of Figure 7 (a) by functions F and Φ will, after variables $\varrho, \mu, \kappa, \lambda$ have been coded by binary variables $P_{I1}, \dots, P_{Im}; P_1, \dots, P_n; P'_1, \dots, P'_n; P_{II1}, \dots, P_{IIq}$, reduce to finding functions $f_1, \dots, f_n; \varphi_1, \dots, \varphi_q$. Further examples show this is practically done.

Assume, for example, that a trigger circuit with a computing

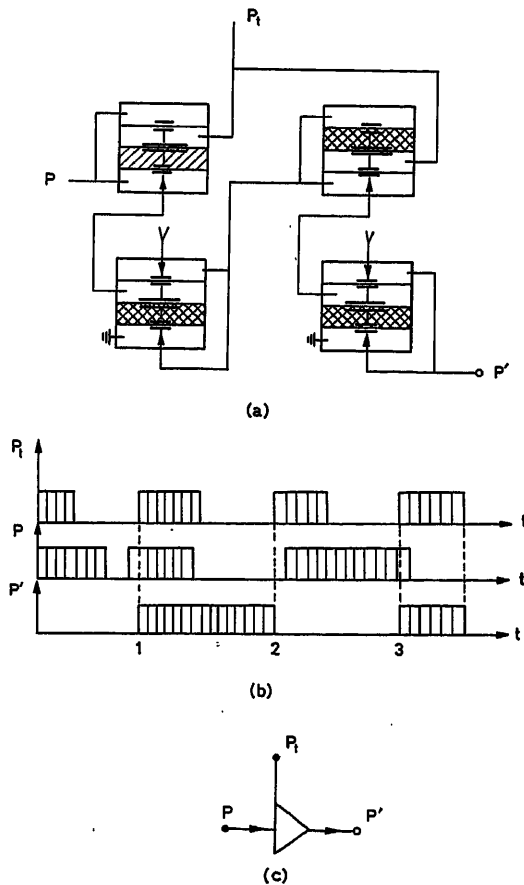


Figure 6. Pneumatic forced lag in time. (a) scheme; (b) graph of operation; (c) conventional representation

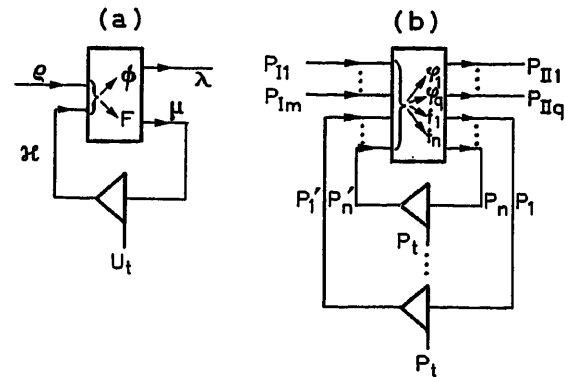


Figure 7. Block diagram of a sequence machine with forced lags: (a) scheme; (b) binary structure

input has to be constructed. It is possible to determine its operation from Table 2, in accordance to which the trigger is an independent sequential machine with two internal states (κ_1 and κ_2) and two states of output (λ_1 and λ_2). The tempo of the operation of this machine is set by a special synchronizing signal P_t , by the computing input.

Considering Table 2 as corresponding to (1), and by carrying out coding of the variable κ, μ , and λ by the pneumatic binary signals P_1, P'_1 and P respectively, one obtains Table 3.

κ	ϱ	ϱ_1
κ_1		κ_2, λ_2
κ_2		κ_1, λ_1

κ	ϱ	ϱ_1
0		11
1		00
P'_1		$P_1 P$

From Table 3 it follows that

$$\begin{aligned} P_1 &= \overline{P'_1} \\ P &= P_1 \end{aligned} \quad (3)$$

By the formulae (3) are determined the functions f and φ , as well as the entire system. Thus one obtains the trigger circuit with a computing input as represented in Figure 8 (a); in Figure 8 (b) are shown graphs of the operation of this trigger, and in Figure 8 (c), the structural diagram.

A system for counting up to four is now constructed. Table 4 conforms to such a system, that is, an independent sequential machine with four internal states ($\kappa_1, \kappa_2, \kappa_3, \kappa_4$) and with a similar number of output states. The tempo of operation, even of this machine, is set by a synchronizing signal P_t . After the introduction of sets of binary pneumatic coded signals P_1 and P_2, P'_1 and P'_2 and P_{II1} and P_{II2} , one obtains the variables κ, μ , and λ respectively in Table 5.

κ	ϱ	ϱ_1
κ_1		κ_2, λ_1
κ_2		κ_3, λ_2
κ_3		κ_4, λ_3
κ_4		κ_1, λ_4

κ	ϱ	ϱ_1
00		01, 00
01		11, 01
11		10, 11
10		00, 10
$P'_1 P'_2$		$P_1 P_2, P_{II1} P_{II2}$

From Table 5 one finds the functions f_1, f_2 and φ_1, φ_2 . They will have the form

$$P_1 = P_2'; \quad P_2 = \bar{P}_1'$$

$$P_{II1} = P_1'; \quad P_{II2} = P_2'$$

The block diagram of (4) is given in Figure 9.

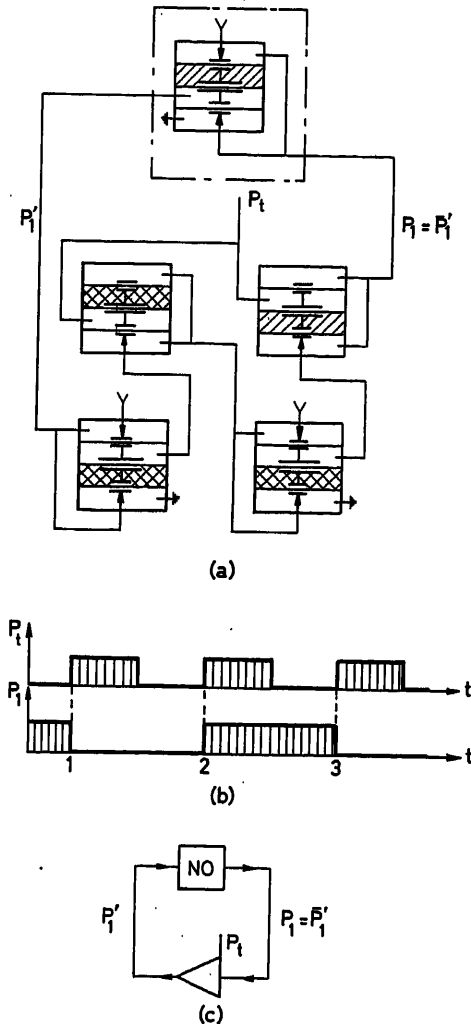


Figure 8. Trigger with forced lag. (a) Pneumatic scheme; (b) graph of operation; (c) structural scheme

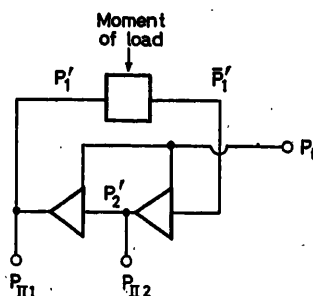


Figure 9. Structural scheme of an evaluating device

In a similar manner systems of dependent sequential machines are built using the lag, the tempo of operation of which is determined by a special synchronizing signal. If a system is built on lags for the case when the synchronizing signal is absent in the initial data, then it proves necessary, according to the given conditions of the onset of times, to form a synchronizing signal in a special device (a clock) which of itself can also be a sequential machine.

A Natural (Self-operating) Binary Lag and its Use in Systems of Sequential Machines

The schematic drawing shown in Figure 10 (a), containing pneumatic resistance with capacitance (inertial component) at the input at the element 'YES', can be investigated as a system of the original lag in time, in which the onset time is determined either by the time of change of the state of input [see graph in Figure 10 (b)] or by that circumstance which took τ sec from

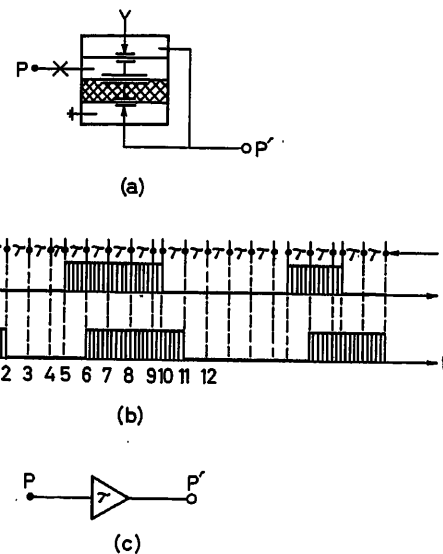


Figure 10. Natural lag; (a) Pneumatic scheme; (b) graph of operation; (c) conventional representation

the moment of onset of the previous time. It is assumed that the changes of input states take place no more often than in the space of τ sec. The time lag τ is called the characteristic time of lag. It is particularly convenient to use a lag of this type for constructing systems of sequential machines, the tempo of whose operation is determined by each change in input state. Accordingly it is necessary to use a special method³.

In this case for a machine, described by functions F and $\bar{\varphi}$ in the form of Figure 1 (a), a realizing machine is found which is based on natural lag in the form of Figure 11 (a).

Another variant of such a method is used later which in form is close to Huffman's method.

Now an investigation of the method is conducted as an example.

Let Table 6 correspond to the realized sequential machine, and the tempo of operation of the machine is determined by the times of change of input states.

A table is set up of another sequential machine having the same input and output states, but new internal states κ^i . The

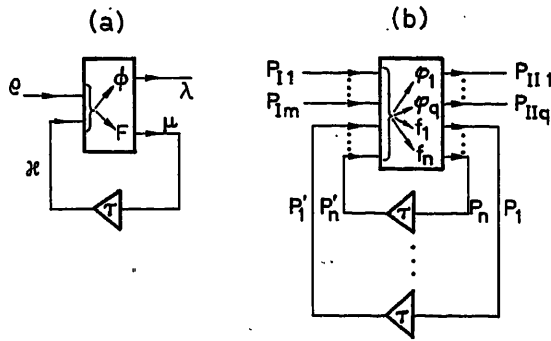


Figure 11. Block diagram of a sequence machine with natural lags: (a) scheme; (b) binary structure

Table 6

κ	q	q_1	q_2	q_3
κ_1		κ_2, λ_1	κ_1, λ_2	κ_1, λ_1
κ_2		κ_1, λ_2	κ_3, λ_1	κ_3, λ_2
κ_3		κ_1, λ_1	κ_3, λ_1	κ_3, λ_2

number of symbols in the alphabet of variable κ^I is taken as equal to the product of the number of symbols in the alphabets κ and q , that is, $\kappa^I = \{\kappa_1^I, \dots, \kappa_9^I\}$ is taken as the example.

Table 7 of the new sequential machine, having three columns (q_1, q_2, q_3) and nine rows ($\kappa_1^I, \dots, \kappa_9^I$), is filled up in the following manner. The table is divided into as many levels as the input has different states—in this case, into three levels. Whereupon, on each level, there prove to be as many rows as there were in the initial table, that is, three rows. In the supplementary column on the far left are written the previous symbols $\kappa_1, \kappa_2, \kappa_3$. Their disposition is repeated on each level and corresponds to the initial Table 6. The boxes of the first level are filled with symbols κ^I , repeating the entrance column of Table 7, and with the symbols λ , repeating their disposition in column q_1 of the initial Table 6. In a similar manner the boxes of column q_2 of the second level and of column q_3 of the third level are filled in. The symbols κ^I written in the boxes are underlined. The remaining boxes are filled in with symbols κ^I only, and this is done in the following way.

In the free boxes, for example of line κ^I of the first level of Table 7, are written the symbols standing in the corresponding

Table 7

κ	κ^I	q	q_1	q_2	q_3
κ_1	κ_1^I		κ_1^I, λ_1	κ_6^I	κ_8^I
κ_2	κ_2^I		κ_2^I, λ_2	κ_4^I	κ_7^I
κ_3	κ_3^I		κ_3^I, λ_1	κ_4^I	κ_7^I
κ_1	κ_4^I		κ_1^I, λ_2	κ_7^I	κ_7^I
κ_2	κ_5^I		κ_3^I, λ_1	κ_9^I	κ_9^I
κ_3	κ_6^I		κ_3^I, λ_1	κ_9^I	κ_9^I
κ_1	κ_7^I		κ_1^I, λ_1	κ_4^I	κ_7^I, λ_1
κ_2	κ_8^I		κ_3^I, λ_2	κ_6^I	κ_8^I, λ_2
κ_3	κ_9^I		κ_3^I, λ_2	κ_6^I	κ_8^I, λ_2

columns and in lines κ_2 of the second and third levels, that is, symbols κ_5^I and κ_6^I . This is determined by the fact that in box $\kappa_1 q_1$ of the resulting Table 6, the symbol κ_2 is written. All the other free boxes of Table 7 are filled in analogously.

The sequential machine corresponding to Table 7 and operating in the tempo of natural (self-operating) lag will, for the same reasons as were introduced in another paper², reproduce by its own equilibrium conditions the resulting machine described in Table 6 and operating in the tempo of the change of input states. The conformity between initial states is established with the help of columns κ^I and κ of Table 7.

Before composing a pneumatic system corresponding to Table 7, there follows the need, if possible, to condense Table 7, which leads to a reduction of the apparatus used in the realization. It is convenient to conduct the condensation in two stages. At first are found the lines with the identical filling in of the corresponding boxes by the symbols κ^I and λ , whereupon the difference in the symbols κ^I underlined is not taken into account.

In our case the lines κ_5^I and κ_6^I will be such lines. The states corresponding to these lines can be combined into one which leads to Table 8. During the reconstruction of the table the relationship between the variables κ^I and κ^{II} is used, the relationship established by the two special columns of Table 8.

Table 8

κ	κ^I	κ^{II}	q	q_1	q_2	q_3
κ_1	κ_1^I	κ_1^{II}		κ_1^{II}, λ_1	κ_6^{II}	κ_7^{II}
κ_2	κ_2^I	κ_2^{II}		κ_2^{II}, λ_2	κ_4^{II}	κ_8^{II}
κ_3	κ_3^I	κ_3^{II}		κ_3^{II}, λ_1	κ_4^{II}	κ_8^{II}
κ_1	κ_4^I	κ_4^{II}		κ_1^{II}, λ_2	κ_4^{II}, λ_2	κ_8^{II}
κ_2, κ_3	κ_5^I, κ_6^I	$\kappa_5^{II}, \kappa_6^{II}$		κ_3^{II}, λ_1	κ_5^{II}, λ_1	κ_8^{II}
κ_1	κ_7^I	κ_7^{II}		κ_1^{II}, λ_1	κ_4^{II}, λ_1	κ_8^{II}, λ_1
κ_2	κ_8^I	κ_8^{II}		κ_3^{II}, λ_2	κ_5^{II}, λ_2	κ_8^{II}, λ_2
κ_3	κ_9^I	κ_9^{II}		κ_3^{II}, λ_2	κ_5^{II}, λ_2	κ_8^{II}, λ_2

Table 9

κ	κ^{II}	κ^{III}	q	q_1	q_2	q_3
κ_1	κ_1^{II}	κ_1^{III}		$\kappa_1^{III}, \lambda_1$	κ_5^{III}	κ_6^{III}
κ_2	κ_2^{II}	κ_2^{III}		$\kappa_2^{III}, \lambda_2$	κ_4^{III}	κ_4^{III}
κ_3	κ_3^{II}	κ_3^{III}		$\kappa_3^{III}, \lambda_1$	κ_4^{III}	κ_4^{III}
κ_1	$\kappa_4^{II}, \kappa_6^{II}$	κ_4^{III}		$\kappa_1^{III}, \lambda_2$	$\kappa_4^{III}, \lambda_2$	$\kappa_4^{III}, \lambda_1$
κ_2, κ_3	κ_5^{II}	κ_5^{III}		$\kappa_3^{III}, \lambda_1$	$\kappa_5^{III}, \lambda_1$	κ_7^{III}
κ_2	κ_7^{II}	κ_7^{III}		$\kappa_3^{III}, \lambda_2$	$\kappa_5^{III}, \lambda_2$	$\kappa_6^{III}, \lambda_2$
κ_3	κ_8^{II}	κ_8^{III}		$\kappa_3^{III}, \lambda_2$	$\kappa_5^{III}, \lambda_2$	$\kappa_6^{III}, \lambda_2$

The second stage leading to the condensation of the table, consists in finding lines all the boxes of which are filled in with identical symbols κ^{II} . In the case of Table 8, line κ_4^{II} and line κ_6^{II} are such lines. The states corresponding to these lines can also be combined. Whereupon Table 9 is obtained, for the formation of which columns κ^{II} and κ^{III} are used. According to Table 9 as obtained, a pneumatic system can be set up, taking into account that each pneumatic element integrally contains natural lag.

The coding of the variables q , κ^{III} , μ^{III} , and λ is carried out by introducing pneumatic binary signals. Taking into account the number of symbols in the alphabets of the coded variables, one assumes $q = P_{11} P_{12}$, $\mu^{\text{III}} = P_1 P_2 P_3$, $\kappa^{\text{III}} = P_1' P_2' P_3'$, $\lambda = P_{11}$. Whereupon from Table 9 one obtains Table 10, by which the pneumatic system is determined on principle, that is, according to the table the logical functions can be compiled.

Table 10

κ	$P_{11} P_{12}$	00	01	11
000		000 0	100	101
001		001 1	011	011
010		010 0	011	011
011		000	011 1	011 0
100		010	100 0	110
101		010	100	101 1
110		001	100	110 1
$P_1' P_2' P_3'$		$P_1 P_2 P_3 P_{11}$	$P_1 P_2 P_3 P_{11}$	$P_1 P_2 P_3 P_{11}$

$$\begin{aligned} P_1 &= f_1(P_1', P_2', P_3', P_{11}, P_{12}) & P_3 &= f_3(P_1', P_2', P_3', P_{11}, P_{12}) \\ P_2 &= f_2(P_1', P_2', P_3', P_{11}, P_{12}) & P_{11} &= \varphi(P_1', P_2', P_3', P_{11}, P_{12}) \end{aligned} \quad (5)$$

However, for this example, the solution is not worked out for the specific type of formulae (5) or for the system corresponding to them, since without special measures the system constructed according to Table 10 would be inefficient on account of the so-called critical race between the elements of the system. The question of constructing a system that is protected from the race is outside the scope of this present work.

Before drawing up the system, another simpler example is introduced which also illustrates the described method.

Using the proposed method, a pneumatic trigger system is constructed, taking input into account. In this case the trigger is investigated as a dependent sequential machine having two input states, two internal states, two output states, and operating in conformity with Table 11 under the conditions that the tempo is determined by each change of the input state.

Table 11

κ	q	q_1	q_2
κ_1		κ_1, λ_1	κ_2, λ_2
κ_2		κ_2, λ_2	κ_1, λ_1

In agreement with the method described, according to Table 11 of a realized machine, a table is constructed for a machine operating at the tempo of natural lag. Whereupon one obtains Table 12.

Table 12

κ	κ^I	q	q_1	q_2
κ_1	κ_1^I		$\kappa_1^I \lambda_1$	κ_2^I
κ_2	κ_2^I		$\kappa_2^I \lambda_2$	κ_1^I
κ_1	κ_3^I		κ_2^I	$\kappa_3^I \lambda_2$
κ_2	κ_4^I		κ_1^I	$\kappa_4^I \lambda_1$

The table obtained proves to be non-condensable. The coding is done later in this paper. It is assumed that $q = P_t$; $\kappa^I = P_1' P_2'$; $\mu^I = P_1 P_2$, $\lambda = P$. Whereupon Table 12 will take the form of Table 13

Table 13

κ	P_t	0	1
00		00 0	10
11		11 1	01
10		11	10 1
01		00	01 0
$P_1' P_2'$		$P_1 P_2 P$	$P_1 P_2 P$

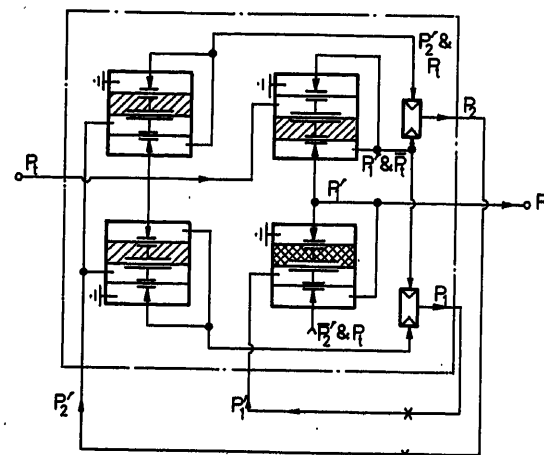
and from it follows:

$$P_1 = (P_1' \wedge \bar{P}_t) \vee (\bar{P}_2 \wedge P_t)$$

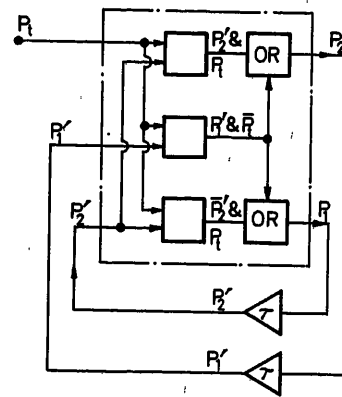
$$P_2 = (P_1' \wedge \bar{P}_t) \vee (P_2' \wedge P_t) \quad (6)$$

$$P = P_1'$$

In Figure 12 the system corresponding to (6) is given.



(a)



(b)

Figure 12. Pneumatic trigger with natural lags: (a) scheme; (b) block diagram

Supplementary Natural Lag in the Input Line of a Realizing Sequential Machine

The 'reproduction' of the states of the machine is connected with the realization of the given sequence machine at natural lags. It is natural to look for such means which will allow as far as possible the reduction in the number of states in a machine realizing the given machine. Different methods of condensing the table of a realizing machine are relative to these means, methods which lead to a search for a minimal realizing machine⁹. In the investigated example in particular, where the realization of machine of the given Table 6 was talked about, a minimal realizing machine was approached with seven internal states.

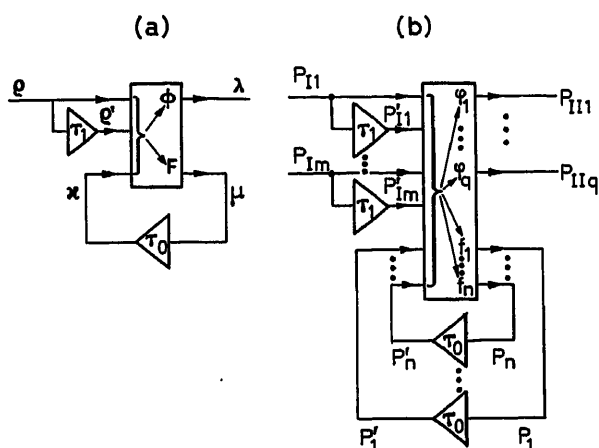


Figure 13. Block diagram of a sequence machine with natural lags of two types: (a) scheme; (b) binary structure

It is now shown that the number of states of a realizing machine can be further reduced if in the system of the realizing machine, apart from the natural lag τ_0 in the feedback circuit, yet another natural lag τ_1 is used in the input line of the machine (Figure 13). This situation is mentioned by Aizerman *et al.*³ who also showed that along with this the number of internal states can be made limitingly small and equal to the number of different output states at that input where this number is greatest.

However, the assertions by Aizerman *et al.*³ are based on the assumption that τ_0 and τ_1 can be made equal, which is not

practical, of course. Now starting from the simple realized condition $\tau_1 > \tau_0$, it is shown that, given this, the number of states of a realizing machine can be reduced but not necessarily to the limit. The example of the initial Table 6 is investigated, and according to it Table 14 is compiled analogous to Table 7. But due to the inclusion of the lag τ_1 into the input line of the machine and to the appearance due to this of a new variable

$$q' = \{q_1, q_2, q_3\},$$

Table 14 will have not three basic columns, corresponding to

$$q = \{q_1, q_2, q_3\},$$

but nine columns corresponding to

$$q'q = \{q_1q_1, q_1q_2, q_1q_3, q_2q_1, q_2q_2, q_2q_3, q_3q_1, q_3q_2, q_3q_3\}.$$

The columns q_1q_1 , q_2q_2 and q_3q_3 are distinguished by the underlining of these symbols. It is convenient to construct Table 14 on the basis of the already constructed Table 7. This is done in the following manner. The frame for Table 14 is prepared with nine rows κ^I and with nine columns $q'q$; as in Table 7, Table 14 is divided into levels, and besides this it is also divided into vertical bands so that columns with identical q' relate to the same band. Thus Table 14 is obtained consisting of three levels and three vertical bands. Thereupon the filling in the boxes of the first (upper) level of Table 7 is carried over completely into the boxes of the level of the first (left) band of Table 14; the filling in of the boxes of the second level of Table 7 into the boxes of the second level of the second band, and the filling in of the boxes of the third level of Table 7 into the boxes of the third level of the third column of Table 14. Further on several boxes of the table in columns not containing symbols κ^I in circles are filled in. For this the symbols κ^I of such columns are carried over within these same columns into the boxes corresponding to the rows with the same value as the κ^I symbols, for example the symbols κ_5^I and κ_4^I standing in column q_2q_2 are carried over into the boxes of the fifth and fourth lines. The other boxes in Table 14 remain unfilled.

Table 14 thus filled determines such a sequential machine, constructed on natural lags τ_0 and τ_1 , which, if one follows its equilibrium states, operates as the initial one given in Table 6. In order to illustrate this, one follows the operation of the

Table 14

κ	κ^I	$q'q$	<u>q_1q_1</u>	q_1q_2	q_1q_3	q_2q_1	<u>q_2q_2</u>	q_2q_3	q_3q_1	q_3q_2	<u>q_3q_3</u>
κ_1	κ_1^I		$\kappa_1^I \lambda_1$	κ_5^I	κ_3^I	κ_1^I			κ_1^I		
κ_2	κ_2^I		$\kappa_2^I \lambda_2$	κ_4^I	κ_7^I				κ_2^I		
κ_3	κ_3^I		$\kappa_3^I \lambda_1$	κ_4^I	κ_7^I	κ_3^I			κ_3^I		
κ_1	κ_4^I			κ_4^I		κ_1^I	$\kappa_4^I \lambda_2$	κ_7^I		κ_4^I	
κ_2	κ_5^I			κ_5^I		κ_3^I	$\kappa_5^I \lambda_1$	κ_9^I		κ_5^I	
κ_3	κ_6^I					κ_3^I	$\kappa_6^I \lambda_1$	κ_9^I		κ_6^I	
κ_1	κ_7^I				κ_7^I			κ_7^I	κ_1^I	κ_4^I	$\kappa_7^I \lambda_1$
κ_2	κ_8^I				κ_8^I				κ_3^I	κ_6^I	$\kappa_8^I \lambda_2$
κ_3	κ_9^I							κ_9^I	κ_6^I	κ_6^I	$\kappa_9^I \lambda_2$

machine during its transition from an equilibrium state $\kappa_1^I, \varrho_1, \lambda_1$ into a new equilibrium state caused by the input state ϱ_2 . At first, looking in column $\varrho_1 \varrho_2$ for the state into which the machine passes in τ_0 sec, this state is shown as κ_5^I , whereupon in τ_0 sec the machine proves to be in the equilibrium state κ_5^I as well as in $(\tau_1 - \tau_0)$ sec $\varrho_1 \varrho_2$ are changed into $\varrho_2 \varrho_2$ without change in the internal state of the machine. This all leads to the fact that the machine proves to be in the state $\kappa_5^I, \varrho_2, \lambda_2$, and this corresponds to the initial Table 6. The same problem is solved by constructing Table 14 as was solved by constructing Table 7. But Table 14 can lead to the construction of a more economical realizing machine, that is, having the same number of states κ^I , it provides better possibilities in relationship to condensation. In this

machine with the second lag τ_1 (Table 16) cannot be cut down and, as does Table 12, contains four lines. This means that lag τ_1 does not give an effect in this case.

A Realizing Sequential Machine with Two Supplementary Natural Lags (in the Input Line and in the Feedback)

The most economical, in terms of a number of states in a realizing machine, is a system with three natural lags. One (τ_0) is the basic lag of feedback, the second (τ_1) is the lag in the input line, and the third (τ_2) is the supplemental lag of feedback, whereupon $\tau_2 > \tau_1 > \tau_0$ (Figure 14). Given such a system, the number of states of a realizing machine proves to be equal to the number of states in the given realized machine.

Table 15

κ	κ^I	κ^{II}	$\varrho' \varrho$	$\varrho_1 \varrho_1$	$\varrho_1 \varrho_2$	$\varrho_1 \varrho_3$	$\varrho_2 \varrho_1$	$\varrho_2 \varrho_2$	$\varrho_2 \varrho_3$	$\varrho_3 \varrho_1$	$\varrho_3 \varrho_2$	$\varrho_3 \varrho_3$
κ_1	κ_1^I	κ_1^{II}		$\kappa_1^{II} \lambda_1$	κ_4^{II}	κ_5^{II}	κ_1^{II}			κ_1^{II}		
$\kappa_1 \kappa_2$	$\kappa_2^I \kappa_4^I$	κ_2^{II}		$\kappa_2^{II} \lambda_2$	κ_5^{II}	κ_5^{II}	κ_1^{II}	$\kappa_2^{II} \lambda_2$	κ_5^{II}	κ_2^{II}		
κ_3	$\kappa_3^I \kappa_6^I$	κ_3^{II}		$\kappa_3^{II} \lambda_3$	κ_5^{II}	κ_5^{II}	κ_1^{II}	$\kappa_3^{II} \lambda_1$	κ_4^{II}	κ_3^{II}		
$\kappa_2 \kappa_2$	$\kappa_6^I \kappa_5^I$	κ_4^{II}			κ_4^{II}	κ_5^{II}	κ_1^{II}	$\kappa_4^{II} \lambda_1$	κ_5^{II}	κ_4^{II}		
κ_1	κ_7^I	κ_5^{II}				κ_5^{II}			κ_5^{II}	κ_1^{II}		$\kappa_4^{II} \lambda_2$
κ_2	κ_8^I	κ_6^{II}				κ_6^{II}			κ_5^{II}	κ_2^{II}		$\kappa_5^{II} \lambda_1$
										κ_3^{II}		$\kappa_6^{II} \lambda_2$

Table 16

κ	κ^I	$\varrho' \varrho$	$\varrho_1 \varrho_1$	$\varrho_1 \varrho_2$	$\varrho_2 \varrho_1$	$\varrho_2 \varrho_2$
κ_1	κ_1^I		$\kappa_1^I \lambda_1$	κ_3^I	κ_1^I	
κ_2	κ_3^I		$\kappa_2^I \lambda_2$	κ_4^I	κ_2^I	
κ_1	κ_3^I			κ_5^I	$\kappa_5^I \lambda_1$	
κ_2	κ_4^I			κ_1^I	$\kappa_4^I \lambda_2$	

case, the following rows can be combined into Table 14: κ_4^I and κ_2^I , κ_5^I and κ_3^I , κ_6^I and κ_5^I .

After this, one goes to Table 15, which contains only six lines. The technique of reconstructing Table 14 into Table 15 is the same as that used in reconstructing Table 7 into Table 8. The result obtained shows that the use of the second natural lag τ_1 in the input line permits a reduction in several cases in the number of states in a realizing machine. However, this is not always attained. For example, for the trigger, for which a representation is given in Table 11, the table of a realizing

Table 17

$\kappa \kappa$	$\varrho' \varrho$	$\varrho_1 \varrho_1$	$\varrho_2 \varrho_2$	$\varrho_3 \varrho_3$	$\varrho_1 \varrho_3$ $\varrho_1 \varrho_2$	$\varrho_2 \varrho_3$ $\varrho_2 \varrho_1$	$\varrho_3 \varrho_3$ $\varrho_3 \varrho_1$
$\kappa_1 \kappa_1$		$\kappa_1 \lambda_1$	$\kappa_1 \lambda_2$	$\kappa_1 \lambda_1$	κ_2	κ_1	κ_1
$\kappa_2 \kappa_2$		$\kappa_2 \lambda_2$	$\kappa_2 \lambda_1$	$\kappa_2 \lambda_2$	κ_1	κ_3	κ_3
$\kappa_3 \kappa_3$		$\kappa_3 \lambda_1$	$\kappa_3 \lambda_1$	$\kappa_3 \lambda_2$	κ_1	κ_3	κ_2
$\kappa_2 \kappa_1$		κ_1	κ_1	κ_1	κ_1	κ_1	κ_1
$\kappa_3 \kappa_1$							
$\kappa_1 \kappa_2$		κ_3	κ_2	κ_2	κ_2		κ_2
$\kappa_3 \kappa_2$							
$\kappa_1 \kappa_3$		κ_3	κ_3	κ_3		κ_3	κ_3
$\kappa_2 \kappa_3$							

Further on is set forth a method of compiling a table for a realizing machine. In this table, apart from the variables $\varrho, \varrho^I = D_{\tau_1} \varrho, \mu, \kappa = D_{\tau_0} \mu$ and λ , the variable $\tilde{\kappa} = D_{\tau_2} \mu$ will also figure. As in the previous sections a method is set forth as an example of the sequence machine given in Table 6.

The table for the realizing machine (Table 17) will contain twice as many columns and rows in comparison to the initial table. In this case, it will have six columns and six rows marked as is shown in Table 17.

In filling up the boxes of the table four quadrants are discernible in it. In the box of the upper right quadrant are inscribed the symbols κ in the same order as they were laid out in the initial Table 6. In the boxes of the remaining quadrants are inscribed the symbols κ coinciding with the value κ in the line, whereupon in the lower right quadrant the boxes are filled in in such a way so that there will not be any non-recurring symbols in one column in the right lower and upper quadrants. This allows several boxes in the lower right quadrant to remain empty. In the boxes of the upper left quadrant are inscribed in addition the symbols λ in the same order as they were laid out in the initial Table 6.

For an illustration of the fact that Table 17 determines a realizing sequential machine working (if one watches its equilibrium state which occurs at one) it is found that, according to Table 17, the equilibrium state which occurs at the input ϱ_2 , if the machine was in the equilibrium state $\kappa_1, \varrho_1, \lambda_1$ up to this time. The box $\varrho_1 \varrho_1 - \kappa_1 \kappa_1$ corresponds to the state $\kappa_1, \varrho_1, \lambda_1$; at the moment when ϱ_1 changes its value to ϱ_2 , the box $\varrho_1 \varrho_2 - \kappa_1 \kappa_1$, in which was inscribed the symbol κ_2 , will correspond to the machine. This means that in τ_0 sec the machine will arrive at the state determined by the box $\varrho_1 \varrho_2 - \kappa_1 \kappa_2$ and will remain in this state for another $(\tau_1 - \tau_0)$ sec, and upon the expiration of that time the lag τ_1 will operate at the input of the machine and box $\varrho_2 \varrho_2 - \kappa_1 \kappa_2$ will correspond to the machine; the machine will remain in this state another $(\tau_2 - \tau_1)$ sec, after

which the natural lag τ_2 will operate, and the machine will arrive at a new equilibrium state determined by box $q_2 q_2 - \kappa_2 \kappa_2$ in which the symbol λ_2 is inscribed. Thus κ_2, q_2, λ_2 correspond to the new equilibrium state, and this coincides with initial Table 6.

Now this method is investigated as an example of constructing a trigger (Table 18) bringing it up to pneumatic realization.

Table 18

κ	q	q_1	q_2
κ_1		$\kappa_1 \lambda_1$	$\kappa_2 \lambda_1$
κ_2		$\kappa_2 \lambda_2$	$\kappa_1 \lambda_2$

In this case Table 19 is obtained for the realizing machine. Going on to pneumatic realization, the following coding is carried out. Assume that

$$q = P, q' = P', \mu = P_1, \kappa = P'_1$$

$$\tilde{\kappa} = P''_1, \lambda = P.$$

Table 19

$\tilde{\kappa} \kappa$	$q' q$	$q_1 q_1$	$q_2 q_2$	$q_1 q_2$	$q_2 q_1$
$\kappa_1 \kappa_1$		$\kappa_1 \lambda_1$	$\kappa_1 \lambda_1$	κ_1	κ_2
$\kappa_2 \kappa_2$		$\kappa_2 \lambda_2$	$\kappa_2 \lambda_2$	κ_2	κ_1
$\kappa_2 \kappa_1$		κ_1	κ_1	κ_1	κ_1
$\kappa_1 \kappa_2$		κ_2	κ_2	κ_2	κ_2

Table 19 in this case converts into Table 20, from which it follows that

$$P_1 = (P'_1 \wedge P'_1 \wedge P_1) \vee (P''_1 \wedge P'_1 \wedge P_1) \quad (7)$$

$$P = P'_1$$

Table 20

$\tilde{\kappa} \kappa$	$q' q$	00	11	01	10
00		$0 \ 0$	$0 \ 0$	0	1
11		$1 \ 1$	$1 \ 1$	1	0
10		0	0	0	0
01		1	1	1	1
$P''_1 P'_1$		$P_1 P$	$P_1 P$	P_1	P_1

In Figure 15 is given the system corresponding to (7).

Conclusions

Given the design of pneumatic systems of sequential machines as given by tables of a machine, it is possible to use several methods to establish the conditions determining the beat tempo of operation.

1. If the tempo of operation of a machine is determined by a special binary (synchronizing) signal, then, in order to construct the system, it is possible to use a pneumatic element of positive lag in time.

2. If the tempo of operation of a machine is determined by any change in the input state, then the system can be constructed either by using natural lag τ_0 in the feedback of the system, or by using the indicated lag τ_0 and besides this still another natural lag τ_1 in the input line (whereupon $\tau_1 > \tau_0$); or finally

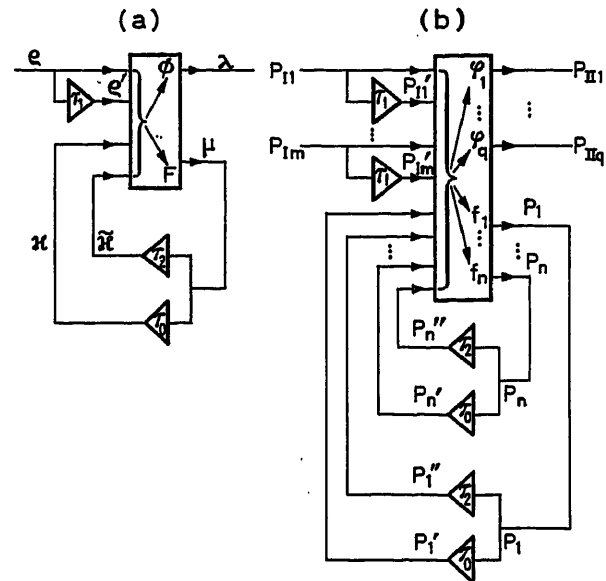


Figure 14. Block diagram of a sequence machine with natural lags of three types: (a) scheme; (b) binary structure

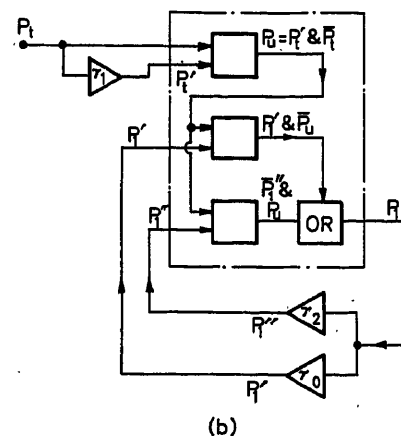
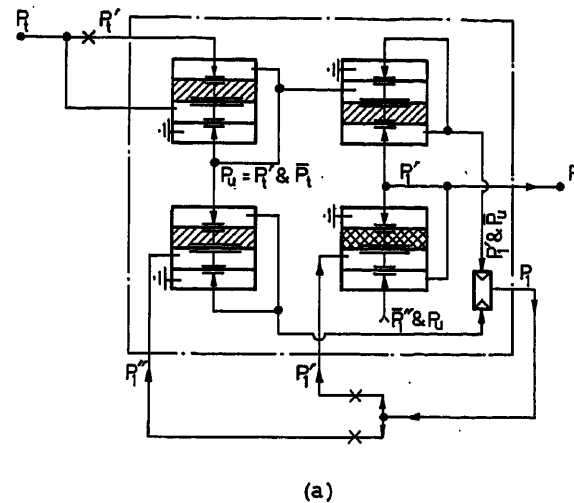


Figure 15. Pneumatic trigger of natural lags of three types: (a) scheme; (b) block diagram

by means of using, in addition to the two stated natural lags, still another natural lag τ_2 in the feedback line (whereupon $\tau_2 > \tau_1 > \tau_0$).

The use of two lags (τ_1 and τ_0) sometimes leads to a reduction in the number of states of a realizing machine and then it is advisable. The use of three lags (τ_2 , τ_1 , and τ_0) always permits limiting the reduction of the number of states of a realizing machine and making it equal to the number of states of the given machine; in this sense it is always justified.

In the report, methods for constructing systems for all four cases are set forth, for the case of the use of a positive lag in time and for cases of the use of one (τ_0) two (τ_1 and τ_0) and three (τ_2 , τ_1 , and τ_0) natural lags.

The methods introduced for applying them to the design,

not of pneumatic systems but of any other systems, undergo change only in the very latest stage (beginning with coding) but completely retain their validity in the rest.

References

- ¹ *Universal System of the Elements of Industrial Pneumatic Automation*. Author's certificate No. 141684 from 6/XII, 1960
- ² AIZERMAN, M. A., GUSEV, L. A., ROZONOER, L. I., SMIRNOVA, I. M., and TAL', A. A. Transforming the beat of sequence machines and design of the relay systems. *Avtomat. Telemekh.* XXIII, 11 (1962)
- ³ AIZERMAN, M. A., GUSEV, L. A., ROZONOER, L. I., SMIRNOVA, I. M., and TAL', A. A. Methods of the realization of a finite automat whose beat is determined by changing the input state. *Avtomat. Telemekh.* XXI, 12 (1960)

DISCUSSION

H. KINDLER and H. TOEFFER, *Deutsche Akademie der Wissenschaften, Dresden A 20, Thormeyerstrasse 10, Germany (DDR)*

The German Academy of Science (East Berlin) has developed pneumatic units, which can be used for the design or combination of sequential devices. A paper concerning these units has been presented during the International Colloquium at Ilmenau in 1961. The design principle of these units is no longer analogue. I would like to give some further information concerning the development of logic pneumatic devices by Dr. Töpfer: they have been built with a double membrane with two flat fits and their operation method resembles that of the double piston motor.

The advantages of these element can be enumerated as follows:

- (1) No continuous air consumption and thus only small auxiliary energy needed (this abolishes the need for outlet throttles).
- (2) The air flow of one element is as high as 2000 l/n (no power amplifiers are needed for industrial applications).
- (3) Very short response times from the order of 10^{-3} sec are attained, due to the high air velocity and the very small volumes.
- (4) Concerning the reliability of these units, research tests show that these elements have withstood $3 \cdot 8 \times 10^8$ operations, in continuous as well as in systematically interrupted application.
- (5) For auxiliary energy, uncleaned air from the compressor can be used, the experiments in (4) being performed under these conditions.
- (6) Complete control for machine tools has been investigated and worked satisfactorily for 8 months.
- (7) With the same elements a system with base plates without interconnections has been built, which allows the design of devices in a building block manner without pipelines.

J. L. SHEARER, *Pennsylvania State University, University Park, Pa., U.S.A.*

I would like to ask the following questions:

- (1) For the unit which was half the size of a match box ($1 \times 3 \times 2.5$ cm) was it of the type with moving parts (diaphragm, etc.) or the type without moving parts (jet relay, etc.)?
- (2) How big, or how small, is the jet relay type?
- (3) At what pressures are the jet relays operated?

A. A. TAL, *in reply*

The answers to Professor Shearer's questions are as follows:

- (1) The unit was of the type with moving parts.
- (2) The jet relay type is the size of the head of a match ($2 \times 2 \times 2$ mm).
- (3) The jet relays are operated at pressures ranging from 0.1 m H₂O to 3 or 4 atm.

V. HIETALA, *Valmet Oy, Valmet Oy Tampere, Finland*

Mr. Tal's paper deals only with the theoretical side of the question, leaving only one short paragraph to explain the material side. There-

fore, I should like to ask if the author could give some details on the physical characteristics of the pneumatic relays used, for instance the following:

- (1) The pressure level used.
- (2) The frequency range obtained.
- (3) The mechanical properties of the membranes, durability etc.

A. A. TAL, *in reply*

In the pneumatic relay equipment mentioned in the paper, use is made of the customary pressure for industrial pneumatic automation, i.e. 0-1.4 atm. This equipment enables one to work on frequencies not exceeding 2-3 tenths of a cycle.

The rubber-cloth diaphragms used in the elements withstand a load of 40-50 Mc.

A. E. MITCHELL, *I.B.M. Research Laboratory, Säumerstr., Rüschlikon Zh., Switzerland*

Professor Aizerman has read a most interesting paper on the design of pneumatic digital systems. I would like to ask some questions on their realization and use in practical industrial systems.

Could Professor Aizerman tell us

- (1) Whether these elements have been used and if so, in what type of system?
- (2) How many elements have been built or coupled into one integral unit?
- (3) Have you considered using other types of element for pneumatic digital systems? For example, spool valve logic or devices which have no moving parts, which have currently created much interest.
- (4) How does the cost and reliability of these compare with electronic systems?
- (5) How long is the maximum transmission line?

A. A. TAL, *in reply*

Elements of pneumatic relay equipment are widely used in industrial automation relay systems and in particular in centralized monitoring and control systems.

The circuit of one digit of the digital summator contains five pneumatic relays and three passive 'OR' elements. Of pneumatic relay elements of other types we consider most promising elements without moving and elastic components (string).

The pneumatic relay elements discussed in the paper are more reliable and cheaper than corresponding electrical and electronic analogues.

Signals formed in pneumatic relay devices can be transmitted up to 300 m.

ELECTROMECHANICAL DEVICES AND MAGNETIC AMPLIFIERS

Two-positional Functional Frequency Device for Automatic Regulation

I. A. MASLAROFF

Summary

This paper presents some researches on the improvement of the regulating quality of small rate monotonously varying processes by the two-positional method. An interrupted two-positional regulation is used for the purpose, while adding to the regulated object fixed equal portions of the unit utilized, in the form of impulses. The duration of the impulses is previously adjusted depending on the object to be regulated. In choosing a proper functional relation of the duration of the intervals between the impulses and the disharmony of the unit to be regulated, there is a probability for reducing the fluctuations. It is proved, that the additional fluctuations, due mainly to the delay by this method, could be reduced by half.

An electronic device is constructed, operating according to the functional-frequency method and a block scheme of the device is presented. This device has been tested for regulating the concentration of chemical solutions as well as for temperatures. The recording of diagrams by an electronic potentiometer for the temperature variations of a definite object, regulated by both the ordinary method and by the functional-frequency device, are presented for comparison. The high qualities of the device proposed are evident.

The application of this device is particularly effective for the regulation of objects which hardly allow any fluctuation stabilization by using a negative reverse connexion on the first and second derivatives of the unit to be regulated.

Sommaire

Cet article présente quelques recherches sur l'amélioration de la qualité de la régulation par la méthode à deux positions pour des processus à variation lente et monotone. On utilise dans ce but une régulation d'interruption à deux positions cependant qu'on ajoute à l'installation réglée des portions égales et fixes de l'unité utilisée, sous forme d'impulsions. La durée de ces impulsions est préalablement ajustée suivant l'installation à régler. En choisissant une relation fonctionnelle appropriée à la durée des intervalles entre impulsions, il y a une certaine probabilité de réduire les fluctuations. On montre que dans cette méthode les fluctuations additionnelles dues principalement au retard peuvent être réduites de moitié.

On construit un appareillage électronique fonctionnant selon la méthode de fréquence fonctionnelle et l'on présente le schéma fonctionnel. Ce système a été essayé pour régler la concentration de solutions chimiques ainsi que les températures. L'enregistrement par un voltmètre électronique des diagrammes de variations des températures d'une installation précise réglée à la fois par la méthode ordinaire et

par le système à fréquence fonctionnelle, sont présentés à titre de comparaison. Les hautes qualités du second sont évidentes.

Il est particulièrement efficace d'appliquer ce procédé à la régulation d'installations qui rendent difficile toute stabilisation des fluctuations, en utilisant une contre-réaction sur la première et la deuxième dérivées de l'unité à régler.

Zusammenfassung

Der Aufsatz enthält einige Untersuchungsergebnisse über die Verbesserung der Regelgüte von monoton langsam veränderlichen Regelstrecken mit Zweipunktregelung. Es wird für diesen Zweck eine aussetzende Zweipunktregelung verwendet, wobei die Regelstrecke stets gleiche Mengen des Stellstromes in Impulsform erhält. Die Impulsdauer läßt sich voreinstellen und hängt von der Art der Regelstrecke ab. Die geeignete Wahl eines funktionellen Zusammenhanges der Intervalllänge zwischen den Impulsen und der Regelabweichung erlaubt es, die Regelschwingungen zu vermindern. Es zeigt sich, daß man die zusätzlichen Schwingungen, die bei diesem Verfahren vor allen Dingen von den Verzögerungen abhängen, auf die Hälfte verkleinern kann.

Ein elektronisches Gerät, das nach dem hier beschriebenen Verfahren arbeitet, wurde gebaut; das Blockschaltbild des Gerätes ist dargestellt. Sowohl für die Regelung der Konzentration chemischer Lösungen als auch zur Temperaturregelung fand dieses Gerät Verwendung. Ein Vergleich zwischen der Regelung nach der üblichen Methode und nach dem hier beschriebenen Verfahren wird an Hand von Registrierungen der Temperaturänderungen einer bestimmten Regelstrecke mit Hilfe eines elektrischen Potentiometers durchgeführt. Die guten Eigenschaften des hier vorgeschlagenen Gerätes sind offensichtlich.

Die Anwendung dieses Gerätes ist besonders für die Regelung von Strecken nützlich, bei denen möglichst keine Schwingungen auftreten sollen, wobei zur Stabilisierung die erste und zweite Ableitung der Regelgröße zurückgeführt wird.

Introduction

The complicated character of the technological processes has developed in parallel with other research methods of ascertaining ways of improving the qualities of the two-positional method for regulation. The simplicity of the device and the low price

of the required elements have not detracted from its significance. From all published literature on this subject the extensive work of Campe Nemm¹ is particularly noted. The author analyses the existing methods of reducing the fluctuations of the unit to be regulated: increasing the extent of current; the use of cut-off two-positional regulation; and the introduction of inverse connections on the first and second derivative, etc.

This paper gives some results of the methods undertaken to improve the two-positional regulation by changing the frequency of the influenced impulses. The methods are mainly directed towards decreasing fluctuations of the unit to be regulated.

The Essence of Two-positional Functional Frequency Regulation

The present survey refers to the monotonous varying processes of a unit with a comparatively small changing rate of regulation and the form of the equation to be used:

$$C \frac{dA}{dt} = \sum Q \quad (1)$$

The principle of two-positional functional frequency regulation consists in the addition to the object of previously fixed identical portions of the utilized unit in the form of impulses. The frequency of these impulses depends on the difference ΔA

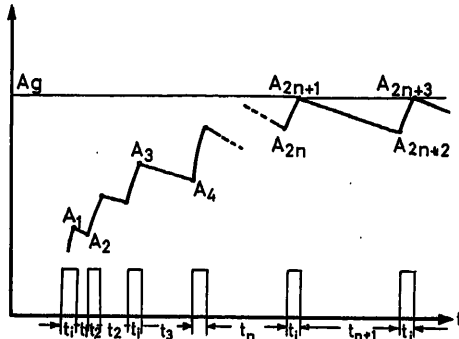


Figure 1

between the given and actual value of the unit to be regulated. Initially the influence of the net delay in the system is neglected in the survey.

Figure 1 shows the change of the unit to be regulated. During the time of impulses it is determined by: $A = A_y (1 - e^{-t/T})$ and during the pauses, by: $A = A_k e^{-t/T}$ ($t = 0, A = A_k$). These two expressions are the integrals of (1) in the presence and absence of current. In such cases, at the end of the impulses and pauses, the unit to be regulated will be determined by:

$$\begin{aligned} A_1 &= A_y (1 - e^{-t_1/T}) \\ A_2 &= A_1 e^{-t_1/T} = A_y (1 - e^{-t_1/T}) e^{-t_1/T} \\ A_3 &= A_y (1 - e^{-t_2}) + A_2 e^{-t_2/T} = A_y (1 - e^{-t_2/T}) e^{-t_1+T} \\ A_4 &= \dots \\ &\vdots \end{aligned} \quad (2)$$

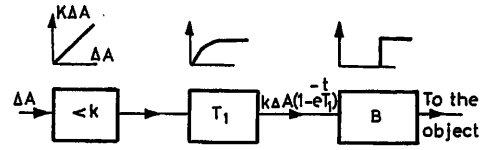


Figure 2

By using the method of full mathematical induction, we determine that the value of the unit to be regulated after n consecutive cycles (impulses and pauses) will be equal to:

$$A_{2n} = A_y (1 - e^{-t_1/T}) \sum_{a=1}^n e^{-\sum_{k=a}^n [t_k + (n-a)t_1]/T} \quad (3)$$

and after $n+1$ serial impulses:

$$A_{2n+1} = A_y (1 - e^{-t_1/T}) \left[1 + \sum_{a=1}^n e^{-\sum_{k=a}^n [t_k + (n-(a-1))t_1]/T} \right] \quad (4)$$

Eqns (3) and (4) show that by changing the duration of pauses one can effectively influence the unit to be regulated. In order to obtain the regulation we need the functional relation $t = \varphi(\Delta A)$, at which the time of the pause will increase with the decrease of the magnitude of the difference ΔA . Such a dependence may be realized simply by introducing the exponential block in the scheme of the regulator (Figure 2).

The equation characterizing the work of this scheme is:

$$k\Delta A (1 - e^{-t/T_1}) = B$$

The time constant of the exponential block of the scheme must be much smaller than the time constant of the object.

Then at $\Delta A = \text{const.}$ the time of the pause is equal to:

$$t = T_1 \ln \frac{k\Delta A}{k\Delta A - B} \quad (5)$$

Eqn (5) shows large values of the difference when the percentage change in the pause time is insignificant. At an established regime when there are small values of the difference between the given and actual values of the unit to be regulated, the time of the pause is determined only by the parameters of the object ($T \gg T_1$) where the delay due to the regulator is slightly neglected in comparison with the common time of the pause. In such a case the time of the pause is determined taking into consideration that the consecutive fluctuations of the unit to be regulated at a determined regime are also equal:

$$\delta A' = \delta A'' \quad (6)$$

where,

$$\delta A' = A_{2n+1} - A_{2n+2}; \quad \delta A'' = A_{2n+3} - A_{2n+2}$$

Since

$$A_{2n+3} = A_y (1 - e^{-t_1/T}) + A_{2n+2} e^{-t_1/T}$$

$$A_{2n+2} = A_{2n+1} e^{-t_{n+1}/T}$$

the time of the pauses is equal to:

$$t_{n+1} = T \ln \frac{A_{2n+1}}{A_{2n+1} - A_y (1 - e^{-t_1/T})} \quad (7)$$

By exerting an influence on the coefficient of amplification and the internal limit of putting in motion B of the scheme it is always possible to receive an equalization of the maximal and given values for the unit to be regulated. Then eqn (7) is modified as:

$$t_{n+1} = T \ln \frac{A_g}{A_g - A_y(1 - e^{-t_i/T})} \quad (7a)$$

The maximum value of the fluctuations of the unit to be regulated is given by:

$$\delta A = \Delta A = \frac{B}{k} = A_g - A_{2n+2} = (A_y - A_g)(1 - e^{-t_i/T}) e^{-t_i/T} \quad (8)$$

Eqn (8) shows that by decreasing the duration of the impulse t_i the fluctuations of the unit to be regulated may be most effectively reduced. The coefficient of amplification k may be determined at a previously chosen value B of the limit out of the duration of the impulse.

Influence of the Net Delay on the Two-positional Functional Frequency Method for Regulation

Usually, the effect of the delay which increases fluctuations of the unit to be regulated is shown in the systems of the type examined. In the following it is proved that the influence of the net delay upon the value of fluctuations may be substantially decreased using the functional frequency method for regulation. Actually Figure 3 shows that the additional increase of fluctuations $\delta A_{\Delta t}$ which follows from the delay of the system, is equal to:

$$\delta A_{\Delta t} = A_{2n+2}(1 - e^{-\Delta t/T}) \cong A_g(1 - e^{-\Delta t/T}) \quad (9)$$

With the usual two-positional regulation, the delay increases the fluctuations of the unit to be regulated in the direction of its decrease, as well as in the direction of its increase. These additional increases are of the same order.

It follows that with functional two-positional regulation the fluctuation of the unit to be regulated increases in the direction of its decrease and because of this the received additional fluctuation is about twice lower.

The total value of fluctuations is:

$$\delta A_x = \delta A + \delta A_{\Delta t} = (A_y - A_g)(1 - e^{-t_i/T}) e^{-t_i/T} + A_g(1 - e^{-\Delta t/T}) \quad (10)$$

If it is accepted that $\delta A = \delta A_{\Delta t}$, then:

$$\frac{A_y}{A_g} = 1 + \frac{(1 - e^{-t_i/T})}{(1 - e^{-\Delta t/T})} e^{-t_i/T} \quad (11)$$

From eqn (11) some conclusions can be drawn for determining the parameters of the system to be regulated.

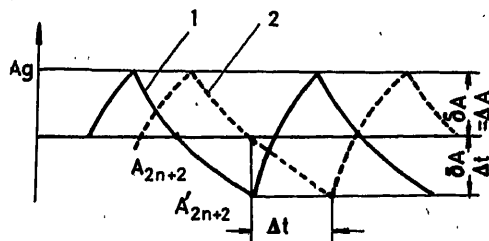


Figure 3

Curve 1—Change of the regulated unit in close proximity to the source of the impulses

Curve 2—Change of the regulated unit in the field of the sensitive element

It is evident that at considerable values of the time of delay Δt it is apt to accept $\Delta_y \gg \Delta_g$, i.e. to use strong impulses. However, at small values of Δt it is apt to accept $A_g \cong A_y$, i.e. the impulses will be comparatively weaker.

From eqn (8) two fundamental parameters for the regulation may be determined—the internal limit for setting in motion B and the coefficient of the earlier amplification k . These parameters may be easily changed into parameters to be regulated in large limits, depending on the requirements of the object to be regulated.

Constructive Data of the Device for Functional Frequency Regulation

The device uses a vacuum-tube scheme (Figure 4) consisting of a measuring part 1, amplifier 2 and an integral group 3, two channels for constant current amplifiers 4 and 4' and an executive trigger 5. It differs from Figure 2 by the use of a second channel for the constant current amplifier 4', which

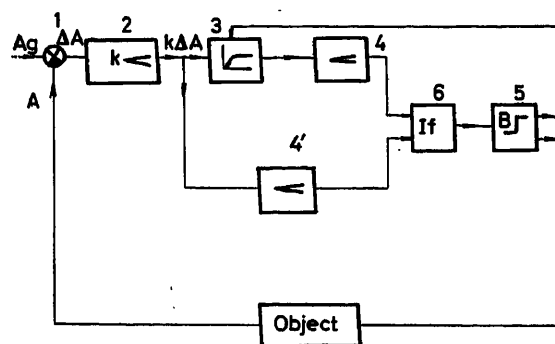


Figure 4

is included in a circulating chain of the integrating group and the base constant current amplifier 4. Its purpose is to accelerate the process for establishing the regime. When there are many large values of ΔA the output voltage of 4' passes through the logical scheme 'IF' 6 and sets in motion the executive trigger. In this way the scheme works as an ordinary two-positional regulator. Placed in a regime, close to the one established, the output voltage of the second channel is not in position to set in motion the executive trigger, and the device works like a functional frequency regulator.

In parallel with the passing of each impulse from the trigger exit 5 to the object 7 the signal for clearing the integrating chain is simultaneously passed through an internal link.

Experimental Data

Initially the device was constructed and tested for regulating the concentration of solutions. Conductive transformers linked by a bridge scheme with temperature compensation were used as a measuring device*.

The executive trigger exerts influence on an electromagnetic valve which adds a drop of concentrate to the solution at each impulse. The results obtained at the time of regulation were very good.

* Eng. D. Detcheva took part in the computing of the construction of the device

The device is used to regulate temperature, and for this purpose the executive trigger is replaced by a delay multivibrator. The time of the impulse may be regulated at will by changing the parameters of its device. Figure 5 shows the diagrams of temperature change of one and the same object, recorded with

the help of an electronic potentiometer. It is seen that the quality of regulation with the functional frequency method is much better than that of the ordinary two-positional method.

Conclusions

1. The two-positional functional frequency device for regulation allows the possibility of decreasing the fluctuations of the unit to be regulated, particularly those emerged out of the delay in the system.
2. By the character of its work, the device approaches the statistical regulators.
3. The devices for regulation can be realized by using practical simple means.
4. The test results prove the expedience of using this method for regulation in many cases.

Nomenclature

- C Coefficient of the generalized capacity of the object to be regulated
 A The unit to be regulated
 A_y Fixed value of the unit to be regulated
 A_g Given value of the unit to be regulated
 ΔA Difference between the given and actual value of the unit to be regulated
 Q Generalized quantitative index of the process
 δA Variation of the unit to be regulated in the period of one impulse or pause
 t Time
 t_i Time of the impulse
 Δt Time of the net delay
 n Number of the impulses
 T Time constant of the object to be regulated
 T_1 Time constant of the exponential block of the scheme
 B Internal limit for setting in motion the acting block of the scheme
 k Coefficient of amplification

Reference

- ¹ CAMPE NEMM, A. A. Two-positional automatic regulation and methods of improving its characteristics. *Thermoenergetical and Chemicochemical Devices and Regulators*. 1961. Moscow-Leningrad; Mashgiz

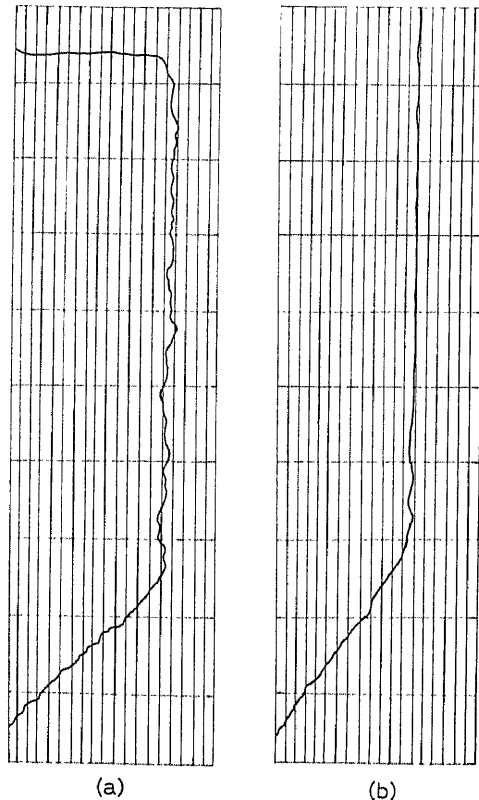


Figure 5

- (a) Change of temperature by using a contact thermometer for regulation
 (b) Change of temperature by using functional frequency regulation of the object

The Problems, Operation and Calculation of a New Component to be Applied in Certain Control Circuits

O. BENEDIKT

Summary

This paper deals with a new component for the stabilization of control circuits provided with the new amplifier 'Autodyne' to maintain their load current constant. The necessity of applying a further device for damping the transient phenomena is theoretically justified, and the disadvantages of the devices adopted up to now in similar cases by the classical means of automatization (e.g. increase in machine dimensions, adoption of additional devices, diminution in reliability) are reviewed. The object is to realize the functions effected until now by three devices (current transformer, amplifier, stability winding) by one single part installed into the machine, but without increasing its dimensions. This problem is solved by a suitable winding, making use of the fact that the flux and magnetic inductions, as well as their harmonics in space, are distributed in a specific way. The physical basis of operation and the mathematical relations are derived. The characteristic equation is given and from the latter a stability criterion is deduced, on the basis of which the winding section may be determined as a function of the stability degree required.

Sommaire

Ce rapport traite un nouvel élément utilisé pour la stabilisation des circuits de commande utilisant le nouvel amplificateur «Autodyne» pour maintenir constant leur courant de charge. On justifie théoriquement la nécessité d'un élément supplémentaire pour amortir le phénomène transitoire. On montre les inconvénients des méthodes utilisées jusqu'à présent: augmentation des dimensions de la machine, adoption d'éléments additionnels, diminution de fiabilité. On essaye de faire remplir par un seul élément installé dans la machine, sans en augmenter toutefois les dimensions, les fonctions de trois éléments: transformateur de courant, amplificateur et bobinage de stabilisation. Ce problème est résolu par l'utilisation d'un seul bobinage adéquat, bénéficiant d'une distribution spécifique du flux, des inductions magnétiques et de leurs harmoniques spatiales. On examine la base physique et les relations mathématiques de l'opération. On présente l'équation caractéristique d'où l'on déduit un critère de stabilité; et on montre comment choisir la section de l'enroulement en fonction du degré de stabilité désirée.

Zusammenfassung

Der Aufsatz befaßt sich mit der Stabilisierung von Regelkreisen durch eine neue Verstärkermaschine „Autodyne“, die den Laststrom konstant hält. Eine theoretische Erläuterung, warum in diesem Fall zusätzliche Mittel zur Dämpfung der Übergangsvorgänge notwendig sind, wird gegeben und die Nachteile der bisher in solchen Fällen in der klassischen Regelungstechnik verwendeten Mittel (Vergrößerung der Maschinenabmessungen, Verwendung zusätzlicher Geräte, Verringerung der Betriebssicherheit) werden aufgezählt. Die gestellte Aufgabe ist, die bisher von den drei getrennten Gliedern Stromwandler, Verstärker und Stabilisierungswicklung ausgeübten physikalischen Funktionen durch eine einzige innerhalb des Maschine angeordnete Baueinheit auszuführen. Es zeigt sich, daß diese Aufgabe durch eine entsprechend angeordnete und aufgebaute Wicklung lösbar ist; dabei wird die Tatsache ausgenutzt, daß in der Maschine die Durchflutungen und magnetischen Induktionen sowie deren räumliche Harmonische

in bestimmter Weise verteilt sind. Die physikalischen Grundlagen und die mathematischen Beziehungen werden abgeleitet. Aus der erhaltenen charakteristischen Gleichung ergeben sich Stabilitätsbeziehungen, die den Wicklungsquerschnitt als Funktion des gewünschten Stabilitätsgrades bestimmen lassen.

Introduction

The object of the paper is to describe the physical operation of a new component for the stabilization of oscillatory processes arising in certain control circuits, as well as to give account of a new practical method for calculating the parameters of this component. The component inspires a lively scientific interest, not merely because it can stabilize most effectively an otherwise entirely unstable control circuit in certain cases, but also from a theoretical respect, since there is no need to connect it to the external circuit of the machine. Moreover, without increasing the size of the machine to be stabilized, an effect is realized which up to now could be attained only by a relatively large set consisting of auxiliary devices, with an increase in machine size.

The circuits to be stabilized by the component in question are control circuits, in which the newly developed electrical amplifier 'autodyne' is applied to maintain the load current at a constant value (e.g. for the automatic charging of accumulator batteries, for automatic welding, for supplying motors in series, etc.).

In his paper 'The New Electrical Amplifier', presented at the 1st IFAC Congress the author gave a general report on the theoretical bases, the main application field and control circuit connections of the autodyne, mentioning the autodyne for the above purpose only in short. Csáki, Fekete and Borka, however, referred to the experimental test of another kind of autodyne, namely an autodyne maintaining the output voltage constant.

The following shows in detail the characteristics of the transient phenomena in the autodyne maintaining the load current, as the task and problems of the new stabilizing component of the control circuit of this machine may be understood only in this relation.

Comparison of the Stability Criteria of the Autodynes Controlling Voltage and Current

The operation of all autodynes working as amplifiers is based, independently of their concrete connection, upon the physical phenomenon that the spatial fundamental harmonic ϕ_{1res} of the main flux of a converter (Figure 1) may theoretically take up any spatial position (in a different state of equilibrium) with a suitable arrangement of the split poles and a synchronous speed n_0 of the rotor. At the same time, this flux is produced by

a magnetizing excitation, the direction of which is set automatically to the flux direction. (Regarding the problems dealt with below, this magnetizing excitation is of no practical importance and therefore is not shown in the figures.) In consequence, with the appearance of a small positive or negative excitation of $\pm \Delta A W'$ in the control winding W_y , the control torque $\mp \Delta M$ produced by this excitation and the main flux, and also the small rotor lag or lead caused by this torque, change considerably the spatial position of the flux $\vec{\phi}_{1\text{res}}$. At the same time, the internal phase voltage $\vec{U}_{1\text{res}}$, being in equilibrium with the terminal voltage vector $\vec{E}_{1\text{res}}$, can be displaced between the limits of $\beta = 0$ and $\beta = 180^\circ$, while the output voltage U is varying continuously between the limits $\pm U_{\text{max}}$. If the output voltage U of the amplifier realized, or another control circuit parameter depending on U , is fed back negatively, then the parameter may be maintained automatically at a constant value. For example in Figure 1 an autodyne is shown stabilizing the output voltage U to the value of the control voltage U_y .

In the publications of the USSR Academy of Sciences Technical Section, *Energetics and Automatics*, No. 2., 1962, the author examined the transient phenomenon taking place in the autodyne controlling voltage (Figure 1), using a different simplifying supposition and neglecting the relatively small rotor resistances.

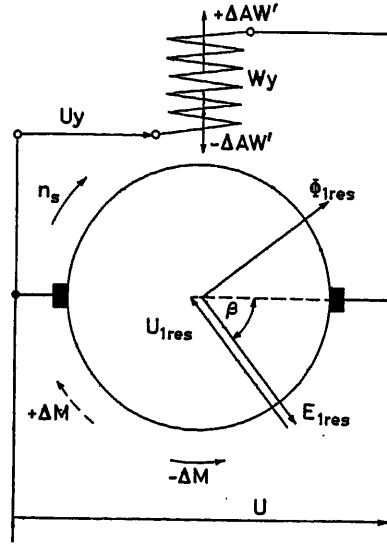


Figure 1

The characteristic equation of the control circuit, using the operator calculus, yields

$$A' + pB' + p^2C' + p^3D' = 0 \quad (1)$$

As a stability criterion, the following relation is obtained:

$$1 \geq \frac{W_y C_4 (C_1 C_2 n_0 + x_\phi)}{a \cdot r_y \cdot C_1 \cdot C_2} \lambda_5 + \frac{W_y \cdot C_4 \cdot C_6}{a \cdot r_y \cdot C_1 \cdot C_2} x_\phi \quad (2)$$

The quantities A' , B' , C' , D' , C_1 , C_2 , C_4 and C_6 are constants depending on the machine dimensions.

The physical meaning of these two formulas may be illustrated briefly as follows. Suppose the synchronous speed n_0 of the rotor

is decreased to a value n hardly deviating from n_0 (Figure 2), as a consequence of which the vectors $\vec{\phi}_{1\text{res}}$ and $\vec{E}_{1\text{res}}$ rotate by a small angle $\Delta \beta$ anticlockwise. Meanwhile U is increased by ΔU , and a control current ΔI_y arises, producing an excitation $\Delta A W'$ downwards. The resulting accelerating torque ΔM is greatest when the vectors $\vec{\phi}_{1\text{res}}$ and $\vec{E}_{1\text{res}}$ reach their dotted

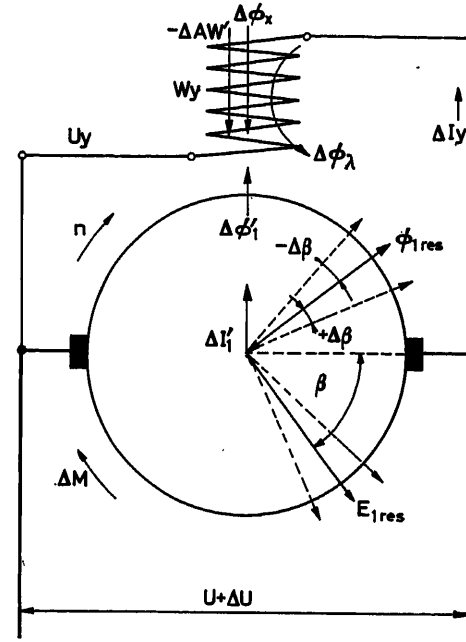


Figure 2

upper limit position. At the central position of the two vectors shown by the full line $\Delta \beta = 0$. Evidently, $\Delta A W'$ causes the vectors to oscillate freely around their central position, and such oscillations would appear if the values B' and D' in eqn (1) were equal to zero.

Nevertheless, in addition to the voltage ΔU , the control winding is affected also by the voltage induced by the increment of the direct axis component $\Delta \phi_1'$ of the flux $\vec{\phi}_{1\text{res}}$ (resulting from the rotation of $\vec{\phi}_{1\text{res}}$), which lags the increment $\Delta \phi_1'$ by 90° . The additional control current being formed evidently establishes an excitation upwards when $\vec{\phi}_{1\text{res}}$ has returned to its central position, thus the excitation has a damping effect. This effect is represented in eqn (1) by the damping term pB' . The unit of the stabilizing flux $\Delta \phi_1'$ corresponds to the left-hand side of eqn (2) (the right-hand side is, for the time being, zero).

The voltages induced in the control winding by the fluxes proportional to the current ΔI_y must now be considered.

The excitation $\Delta A W'$ produced by ΔI_y , being proportional to it and arising in the rotor winding, is short-circuited by the a.c. network, since according to the converter theory, all excitation arising in addition to the magnetizing excitation is cancelled out almost completely as a consequence of the compensating current $\Delta I_1'$. Nevertheless, because of the leakage reactance x_ϕ of the phase winding, the excitation of the current $\Delta I_1'$ is smaller by a few per cent than $\Delta A W'$, and consequently a small flux difference $\Delta \phi_\alpha$ appears. As this, compared with the flux $\Delta \phi_1'$, is of opposite direction, it induces a current in the control winding, which reduces the damping effect of the current induced by the flux $\Delta \phi_1'$. At the right-hand side of eqn (2) the

second term, proportional to x_ϕ , corresponds to the flux $\Delta\phi_x$.

In addition to this, the leakage flux $\Delta\phi_\lambda$ must also be considered. This is caused by the current ΔI_y , and passes through the control winding. To this corresponds the first term, proportional to the leakage factor λ_s , at the right-hand side of eqn (2), which proves that the stability degree is now even lower. The effect of fluxes $\Delta\phi_x$ and $\Delta\phi_\lambda$ is represented in eqn (1) by the term $D'p^3$.

The right-hand side of eqn (2) is proportional to the expression W_y/ar_y , where W_y is the number of turns of the control winding, a is the number of parallel branches of the control winding, and r_y is the resistance of this circuit. This expression is obviously proportional to the cross section of one turn of the control winding. The greater this is the greater is the increment of the current ΔI_y corresponding to the angle $\Delta\beta$, as well as the value of $\Delta A W'$, and, evidently, the steady-state control accuracy, also. On the other hand, the value $\Delta\phi_x + \Delta\phi_\lambda$ is increasing together with ΔI_y . However, owing to the fact that at a given value of $\Delta\beta$, $\Delta\phi_1'$ remains constant, it may be concluded physically—as shown mathematically by eqn (2)—that as the cross section increases, the stability is reduced. If the sum $\Delta\phi_x + \Delta\phi_\lambda$ were equal to $\Delta\phi_1'$, then obviously no voltage would be induced in the control winding and free oscillations would again arise, while the two sides of eqn (2) would be equal.

In practice this never occurs, as a satisfactory control accuracy may be realized by small values of W_y/ar_y , at which the stability limit is very great.

The case is quite different with an autodyne used for controlling the load current to a constant value, e.g. in spite of the variation in the internal voltage E_A of an accumulator (Figure 3). To demonstrate this question theoretically in a more simple way, compare Figure 3 with Figure 1.

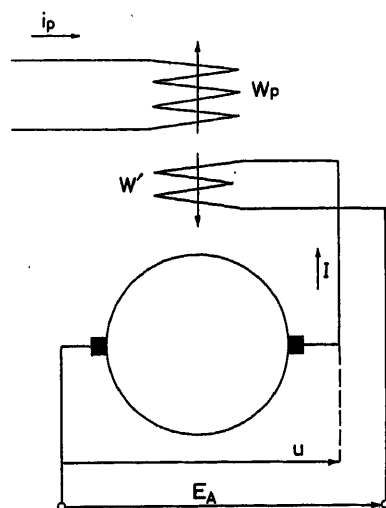


Figure 3

At first sight the difference is great. Actually, to the winding W' (working in this case instead of W_y) the loading current I is fed back, not the voltage U . Further, in this winding, not two voltages (U and U_y), but two excitations are compared, that is, the excitation $I W'$ with the excitation $i_p W_p$ of the continuously controllable regulating current i_p . Consequently, instead of the law $U = U_y$, the law $I = i_p W_p/W'$ is valid here.

However, examining the problem of the transient phenomena, an important analogy of principle may be observed between the two connections at once, as in this question the magnitude of the current i_p is practically of no importance and it may be made equal to zero. In this case, however, the connection of Figure 3 does not differ in any respect from that of Figure 1, as E_A may be regarded as the given control voltage, while the control winding is connected to E_A and to the voltage U . In consequence the factors illustrated in Figure 2, affecting the stability, may be distinguished also in the autodyne shown in Figure 3 and if $\Delta\phi_1' = \Delta\phi_x + \Delta\phi_\lambda$, free oscillations also arise here. Moreover, it may be seen that in this case the presence of winding W_p may not practically cause any deviation either, as the fluxes mentioned pass also through this winding and so in the winding W_p if the fluxes balance each other mutually, no voltage is induced. Accordingly under the same conditions as have produced eqn (2), a stability criterion corresponding theoretically to eqn (2) must also be obtained. From this, however, follows the interesting fact mentioned below.

While, in the case of Figure 2, the control winding forms a shunt winding, and consequently the cross section of its turns is very small; with an autodyne maintaining its load current at a constant value, the cross section is very large, because the W' is series connected. This means, however, that the right-hand side of eqn (2) is, in this case, incomparably greater i.e., there is an actual danger of oscillations arising. This has in fact occurred in practice at an early stage in the development of the autodynes.

It is to be considered that (compared with Figure 2) in the case of Figure 3 the resistance of the rotor may not be neglected with respect to the actually small resistance of winding W' . As the current ΔI must now overcome the resistance of winding W' , in addition to series-connected resistance ΣR , the effect of W_y/ar_y will be somewhat smaller. It is clear, however, that if this term is replaced by $W'/\Sigma R$, being physically analogous, the latter will still be incomparably greater than W_y/ar_y in the case of the autodyne controlling its output voltage to a constant value. So it is proved that the autodyne shown in Figure 3 can perform its task only if provision is made for its stability by some supplementary means.

Problems Concerning the Development of a Suitable Stabilizing Device and the Way Leading to the Solution

The auxiliary devices for stabilizing circuits, in which the loading current is to be maintained at a constant value, are theoretically known. This is obtained as follows (Figure 4).

Assume the autodyne operates just at the limit of stability, as a consequence of which sinusoidal currents ΔI are superposed on the current I . These would induce sinusoidal voltages in the transformer T , the primary coil of which is series connected with the load circuit. If the power of this voltage is increased by the amplifier A and the stabilizing winding W_s is joined to windings W_p and W' of Figure 3, with a suitable connection there arises in W_s an excitation leading in time with regard to the excitation $\Delta I W'$ and proportional to it. In this way effect of fluxes $\Delta\phi_x + \Delta\phi_\lambda$ could be theoretically reduced by well-known means.

Nevertheless, this arrangement has several great disadvantages. The additional winding increases the machine dimensions. Further, through the application of auxiliary devices, the service safety is reduced. It must also be taken into account that the

dimensions of the transformer T are considerably increased, because its primary coil must be dimensioned for the total load current I and saturation of the iron core of the transformer by the load current I must be avoided. The other stabilizing devices of the classical control technique to be adopted here have similar disadvantages.

Accordingly, it has become essential to seek a novel device for additional stabilization, permitting elimination of the disadvantages mentioned above.

Actually, it has been proved that the physical processes corresponding to Figure 4 may be realized without the application of a transformer or amplifier, while the required additional winding may be placed in the machine in a way which does not reduce the useful winding area.

This problem is to be solved step by step as follows. (1) In order to spare the primary coil and flux of the transformer T , instead of this flux another existing flux, already in the autodyne and being proportional to the current ΔI , is applied to produce a current in the winding to be placed in the autodyne, playing the role of the secondary coil. This current must lag behind ΔI . (2) To amplify the effect of this current, a generated voltage proportional to it is established in the autodyne. (3) To eliminate

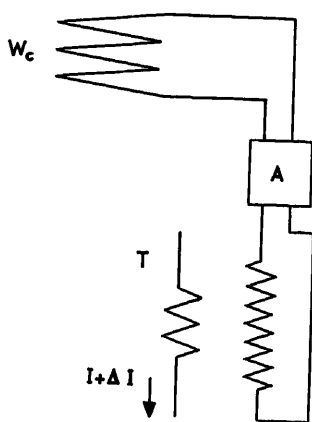


Figure 4

also winding W_c , this generated voltage is established in the winding W' itself, that is, between the main brushes.

Meanwhile, two difficult problems arise. First, (3) obviously necessitates that the winding sought should operate in the direct axis of the autodyne. But then it is inductively coupled with the winding W' , which eliminates the effect wanted, i.e. only a single suitable additional generated voltage should affect this winding. On the other hand, the following problem arises. If the new winding is placed in the direct axis, then the fluxes $\Delta \phi_m$, $\Delta \phi_\lambda$, being proportional to current ΔI_y , will pass through it, and also the flux $\Delta \phi_1'$.

It is already known that free oscillations arise when the sum of these fluxes is zero, in which case no current is induced in the winding, and therefore the desired effect does not arise at the occurrence of the free oscillations. From this it follows that the tested winding should fulfil the following, apparently contradictory conditions: on the one hand, the magnetic effect of the current arising in it should fall into the direct axis of the machine, but, on the other hand, the direct axis flux $\Delta \phi_1'$ should not be enclosed by the winding, consequently, the flux

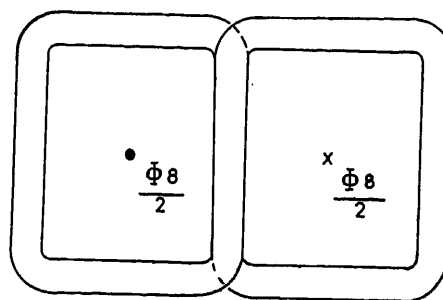


Figure 5

enclosed by it and being proportional to the current ΔI must not exercise any effect in the direction of the direct axis.

This problem may be solved by a special shape of the tested winding and so the winding will have a particular physical function.

Physical Operation and Method of Calculation of the Stabilizing Winding

In view of the fact that the autodynes as Figures 1 and 3 have a practically analogous behaviour regarding the transient phenomena, the following consideration should be valid also in the case shown in Figure 1. Therefore, instead of ΔI and W' , the physically similar symbols ΔI_y and W_y shall be applied.

The stabilizing winding, as shown in Figure 5, has the shape of a figure eight and is placed, according to Figure 6, to the pole shoes of the half-pole I and II belonging to the pole pitch. Thus the condition that they should not be inductively coupled with the winding W_y , is fulfilled. The condition, that the flux, proportional to the current ΔI_y and enclosed by the winding, does not exert any effect in the direct axis of the machine, may be fulfilled on the basis of the following consideration.

As is known, the compensation current $\Delta I_1'$, corresponding to the excitation $\Delta I_y W_y$, is proportional to the current ΔI_y . In the airgaps below the half-poles the induction of the flux produced by $\Delta I_1'$ corresponds evidently, within a pole pitch τ_p , to the ordinates of curve 1-2-3-4-5-6-7-8-9-10 in Figure 7.

If, everywhere, constant inductions of the flux of the same magnitude are represented with the aid of line 1-11-12-13-5-6-14-15-16-10, it becomes apparent that the area 12-3-4-13-12 is equal to the difference of areas 2-11-17-2 and 17-3-12-17. As a result of this, the part of the area 3-4-13-12-3 of the flux proportional to ΔI_y , as shown in Figure 5, enters the half-pole

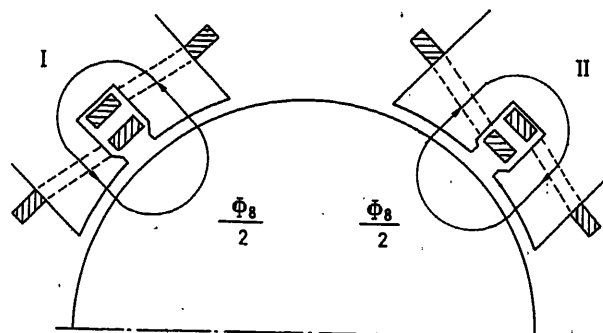


Figure 6

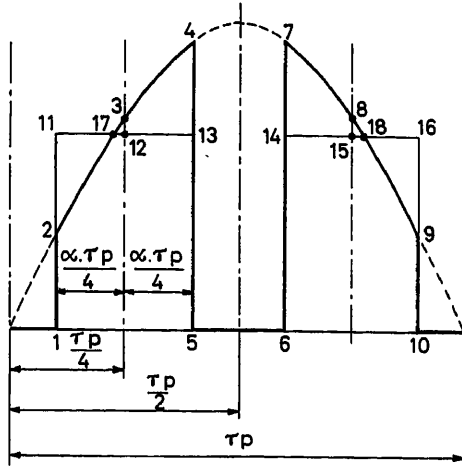


Figure 7

through one half of the stabilizing winding and leaves on the side of its other half, that is, it is twofold inductively coupled with this coil. Obviously, the situation is just the same in the other half-poles. If the total flux being established is denoted by $\Delta \phi_8$ and the ordinates of curves 2-4, 7-9 by $\Delta B(x)$, then, adopting the above symbols

$$\Delta \phi_8 = K \left[\begin{array}{l} x = \frac{\tau p}{4}(1 + \alpha) \\ 2l \int \Delta B(x) dx - \frac{C_5 \cdot \Delta I_1'}{2} \\ x = \frac{\tau p}{4} \end{array} \right] \quad (3)$$

$$\begin{aligned} x &= \frac{\tau p}{4}(1 + \alpha) \\ \text{and } l \int \Delta B(x) dx &= \frac{C_5 \cdot \Delta I_1'}{2} \\ x &= \frac{\tau p}{4}(1 - \alpha) \end{aligned} \quad (4)$$

where l is the active length, $C_5 \Delta I_1'$ is the flux produced by $\Delta I_1'$, and K is the factor considering the saturation. (The cause of C_5 being constant in spite of the saturation is explained in the paper mentioned previously.)

It follows from eqns (3) and (4) that

$$\Delta \phi_8 = \frac{1 - \cos \frac{\pi \cdot \alpha}{4}}{\sin \frac{\pi \cdot \alpha}{4}} \cdot \frac{C_5 \Delta I_1'}{2} \quad (5)$$

On the other hand

$$\Delta I_1' = K_1 \cdot \Delta I_y W_y \quad (6)$$

where, as is known, K_1 is a constant depending on x_ϕ . The flux $\Delta \phi_8$ induces a current of

$$\Delta I_8 = \frac{1}{r_8} \frac{d\Delta \phi_8}{dt} \quad (7)$$

in the stabilizing winding, where r_8 is the resistance of the winding. For the sake of simplicity, the inducing effect of the stray

magnetic field of the winding is neglected here. As shown by theory and practice, this is permissible, because the frequency of the free oscillations is insignificant.

Thus, up to now the secondary coil of the transformer T has been replaced by a winding corresponding to Figure 5, while the transformer primary coil and its iron core became superfluous. The production of the generated voltage mentioned in (3) between the main brushes of the rotor, will be attempted with the aid of current ΔI_8 .

At first sight this seems to be impossible. Namely, the excitation $\Delta \theta_g$ produced by current ΔI_8 is obviously

$$\Delta \theta_g = \Delta I_8 \quad (8)$$

that is, of the same magnitude but of opposite direction in the two half-parts of the figure-of-eight winding. Thus, the excitation is divided on one pole pitch according to the line 15-1-2-3-4-5-6-7-8-9-10-11-12-13-14-17 of Figure 8. As the induction ΔB_g established by $\Delta \theta_g$ is distributed practically in a similar way, and as a result of this the total flux arising on one pole pitch yields

$$\Delta \phi_g = \int_{x=0}^{x=\tau p} \Delta \theta_g dx = 0 \quad (9)$$

it may be concluded that the flux produced by the current ΔI_8 of the winding cannot produce the generated voltage required in the d. c. winding of the rotor.

The problem can be solved if it is considered that the excitation $\Delta \theta_g$ must have a positive fundamental harmonic in the case of the distribution in Figure 8, because the positive areas 4-5-6-7 and 8-9-10-11 are closer to the central line than the negative areas 1-2-3-4 and 11-12-13-14. The harmonic analysis proves that the amplitude value of the fundamental harmonic $\Delta \theta_{g1}$ is

$$\Delta \theta_{g1} = \Delta \theta_g \frac{8}{\pi \sqrt{2}} \left(1 - \cos \frac{\pi \cdot \alpha}{2} \right) \quad (10)$$

Accordingly, this excitation has an inducing effect on the phase winding of the rotor and consequently is practically eliminated by a compensating current ΔI_{g1} , because ΔI_{g1} is proportional to the excitation, $\Delta \theta_{g1}$ having produced it, i. e.

$$\Delta I_{g1} = K_2 \Delta \theta_{g1} \quad (11)$$

where K_2 is another constant depending on the value of x_ϕ . The induction produced by the excitation of sinusoidal distribution of this current ΔI_{g1} is evidently distributed in the same way as

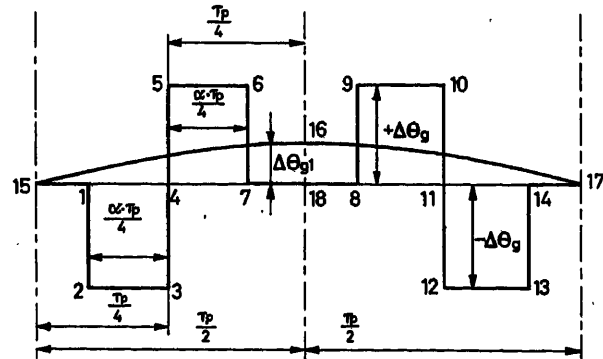


Figure 8

the induction produced by the excitation of the current $\Delta I_1'$, but in the opposite direction. Consequently, the integral of this induction taken within the section r_8 establishes the flux formed by the current ΔI_{01} , which produces the generated voltage wanted between the main brushes, the latter operating opposite to the voltage induced by $\Delta \phi_x$ and $\Delta \phi_\lambda$ in W_y . Considering the fact that this voltage is proportional to ΔI_{01} , as well as eqn (6), (5), (7), (8), (10) and (11), the generated voltage may be made equal to

$$p \frac{K_8 \cdot \Delta I_y(p)}{r_8}$$

where K_8 is constant. On the other hand, the voltage produced by the fluxes $\Delta \phi_x$ and $\Delta \phi_\lambda$ is obtained as $p D \cdot \Delta I_y(p)$, where D is constant. Performing the substitution

$$K'_8 = K_8 (C_1 \cdot n_0 \cdot C_2 + x_\phi) \frac{\theta \cdot \omega}{p_\pi} \quad (12)$$

where ω is the angular frequency of the rotor, θ is the moment of inertia of the rotor, and p_π is the number of pairs of poles, the characteristic equation is, after all

$$A' + pB' + p^2 \cdot C' + p^3 \cdot \left(D' - \frac{K'_8}{r_8} \right) = 0 \quad (13)$$

DISCUSSION

W. PELCZEWSKI, *Technical University of Lodz, Gdanska 155, Lodz, Poland*

The proposed new component for the stabilization of the dynamoelectric amplifier 'autodyne' maintaining the constant load current consists of an additional winding of special shape. It is possible, of course, to apply this winding to stabilize the oscillations in the autodyne. But if the autodyne works in an automatic control system, the physical processes in the stabilizing devices have to be adjusted not to the autodyne alone, but also to the dynamic behaviour of the whole system. The question arises, therefore, whether the required performance of applied additional winding is obtained by changing the stabilizing process over wide limits.

It is known that it is impossible to obtain ideal compensation in a dynamoelectric amplifier. The problem of the effect, therefore, produced by the armature reaction on the transient performance in an autodyne with the additional stabilizing winding, deserves some comment.

O. BENEDIKT, *in reply*

I would like to more fully clear up the questions which have influence on the dynamic ratios of the 'autodyne' because of incomplete compensation for the armature reaction.

We know that this question has great import in the theory of the amplidyne and therefore we must observe this effect by means of Figure A. We know that, from the point of view of statistical exactness it would be optimal if the armature eddy current AW induced by the main load current I were raised to 100 per cent by a flow AW_k through a compensation winding.

In this case it is possible, however, that if for one reason or another, any over-compensation occurs (even in small degree) the difference $AW_k - AW$ be added to the basic current AW_y corresponding to an output voltage U . By this means U increases, whereby AW and AW_k and their difference correspondingly increase i.e. a process of self-excitation is started which even if not in a regulating circuit can cause the amplidyne to become unstable.

The stability criterion is

$$1 \geq \frac{W_y}{a \cdot r_y} \left[\lambda_5 \frac{C_4 \cdot (C_1 C_2 n_0 + x_\phi)}{C_1 C_2} + x_\phi \cdot \frac{C_4 C_6}{C_1 C_2} \right] - \frac{K''_8}{r_8} \quad (14)$$

where K''_8 is a constant, in which W_y does not figure. It is recognized that the stabilizing winding is actually in possession of the effect demanded, as for instance the term comprising p^3 , reducing the stability and, in an analogous way, the right-hand side of eqn (14) may be decreased most effectively, if the cross section of the winding, i.e. $1/r_8$, is suitably increased. With extremely high values of W_y the first term of the right-hand side is increased and there is no place in the machine for giving a cross section so large to the stabilizing winding that would suffice for a sensible decrease of the first term. Therefore, in the cases illustrated in Figure 1, that is, in the autodyne controlling the voltage to a constant value, this winding has not been applied. Nevertheless, in the cases of Figure 3, where the value W' taking the place of W_y , is small, calculation shows that the right-hand side of eqn (14) will be zero with such small cross sections, which (with the stabilizing winding set on the pole shoes) has practically no effect upon the machine dimensions.

The autodyne of serial production, provided with such a winding and maintaining the load current at a constant value, proves itself entirely stable in practice, while it would operate without the above-mentioned winding far within the unstable range.

However, such armature reaction effects do not occur in the autodyne. First, as our Figure B shows, the armature eddy current AW induced by the load-current I is in practice eliminated by the rotational eddy AW_\sim of the rotational current taken from the mains. There exists only a very small difference $AW_\sim - AW_\sim$. Secondly, as can be seen from Figure B, this does not have a back effect on the guide current AW' because indeed this does not coincide on the axis with mentioned current difference, but lies vertically on this axis instead. Because of this no self-excitation is possible in this case.

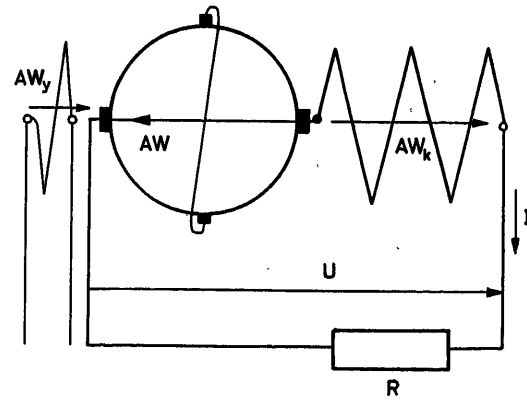
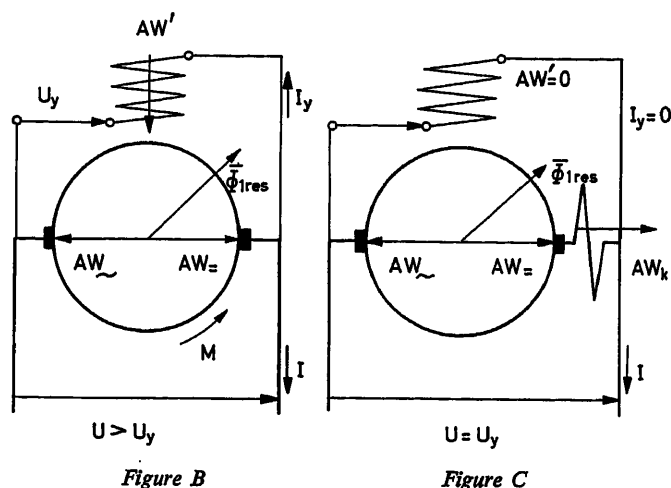


Figure A

The current difference mentioned, therefore, has no importance at all in the transient process of the autodyne. It has, however, a minor importance for stationary working alone, because it causes a definite static deviation in regulation to occur. To be precise, it creates a small retarding moment M , which is consequently compensated, and automatically a small through-flow AW' and a stationary guiding current I_y appear, whereby the tension becomes only slightly greater



than U_y . If one wishes, however, to eliminate this inaccuracy, then this is also easy. One only needs to compensate the difference $AW = -AW_{\sim}$ by a throughflow AW_k , whereby $AW' = 0$, $I_y = 0$ and $U = U_y$ (see Figure C).

Now I will attempt to offer a solution to the question of what happens with the 'switchback' winding if the autodyne regulating the current operates in a regulating circuit.

Before anything else, to avoid misapprehension, it must be made clear that the autodyne schemes shown, as a whole represent regulation circuits, because, indeed, the output voltage U is negatively back-coupled to the guiding flow. The deviations of the autodyne which are compensated for by the 'switchback' winding do not in themselves give a state of instability to the machine in a pen circuit—as for example happens in a corresponding situation in the amplidyne. Instability does occur, but only with particular parameters in particular regulating circuits.

From this, I wish to formulate the replies to the questions put to me in another way. The question is, what happens to the stability of the autodyne fitted with 'switchback' winding and regulated by the load current if we substitute the resistanceless accumulator in the regulation circuit of the autodyne with some other item?

Let us observe the various possibilities. When the loading of the autodyne gives an ohmic resistance, then the stability increases because often the ohmic resistance has exactly the same effect as a reduction in the cross sectional area of the winding W' .

If the autodyne A employs an identical current motor M to regulate the load current (see Figure D) then this loading in general gives a capacitive resistance whereby the deviations of the current I and therefore also the guiding current of the autodyne must be phased in front of the voltage U . Indeed, because this is the aim of the 'switchback' winding, in such a case its cross section can often be reduced.

If, in the loading of the autodyne, the inductive components

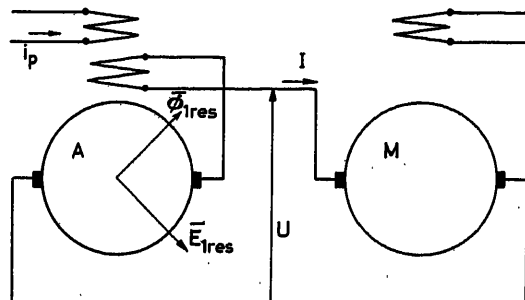


Figure D

become too large, it is often only necessary to correspondingly raise the cross section of the 'switchback' winding.

To summarize: the suggested winding influences the stability of complete regulation circuits and by corresponding calculation can be applied within broad parametric boundaries.

F. CSAKI, Department of Automation, Polytechnical University, Egri J.- u. 18, Budapest, Hungary

Having worked, for the past few years, in quite another field, it is not clear to me how the stabilizing effect of the figure-eight-shaped winding mentioned by the author was experimentally determined in the autodyne regulating the loading current.

The author cites in his paper a study he wrote proving that the autodyne becomes more stable as the cross section of one turn of the bias winding becomes smaller. The author has proved this, however, in his above-mentioned study only for the autodyne regulating voltage. How could this be regarded—without any new proof—as a rule for the autodyne regulating current, the wiring of the latter being quite different?

O. BENEDIKT, in reply

The question of stability of the autodyne regulated by the load current and not using the 'switchback' winding described in my previous article, was examined under the most varied conditions with an oscillograph. The criterion of stability found analytically can be written as follows:

$$1 \geq C \frac{W'}{\Sigma R}$$

Where C is a constant, W' is the number of guide windings and ΣR is the sum of all the ohmic resistances in the current circuit of the guide winding. If ΣR is the resistance of the guide winding alone, as, for example, in the case where the autodyne is regulated by the voltage or if the autodyne regulated by the load current is switched to a virtually resistanceless accumulator, then the expression $W'/\Sigma R$ as suggested in the previous section, is proportional to the cross section of a coil of the guide winding.

However, for test purposes we have switched in variable additional resistances between the autodyne and the accumulator whereby by keeping these to a minimum we can exactly establish the boundaries of stability where free oscillations occur. If pre-switch resistances were further reduced then oscillations of ever-increasing amplitude would occur.

By introducing the 'switchback' winding we always find that rapidly effective damping occurs and the machine completely protects its stability, not only in the case when we reduce the pre-switch resistance to zero, but also when we suddenly switch off the autodyne at a given voltage.

To be able to establish whether we are justified in observing that the stability of the autodyne regulated by the load current becomes larger and larger in inverse proportion to the cross section of a coil of the guide winding, we must first digress from the question and clarify why this rule is valid for the autodyne regulated by voltage. From Figure A we can see what occurs when the rotor is reduced in speed. The flow ϕ_{1res} turns through the angle $-\Delta\beta$ in the position drawn. Correspondingly the longitudinal flow increases by $\Delta\phi'$ and the output voltage by ΔU . Through the difference

$$U + \Delta U - U_y = \Delta U$$

there exists a guide current which induces the guiding flow $-\Delta AW'$ in the guide winding. The latter is almost totally eliminated by the flow of the compensating current $\Delta I'$ such that only a small residual flow $\Delta\phi_x$ exists. Through the winding there then flows only the current $\Delta\phi'$, the current $\Delta\phi_x$ and the distributive flow $\Delta\phi_\lambda$. At a definite value of the cross section of the guide winding the current ΔI_y cor-

responding to a particular value ΔU and from this also $\Delta AW'$, $\Delta\phi_x$ and $\Delta\phi_1$ become so large that the algebraic sum $\Delta\phi' - \Delta\phi_x - \Delta\phi_1 = 0$. In this case no voltage is induced in the guide winding,

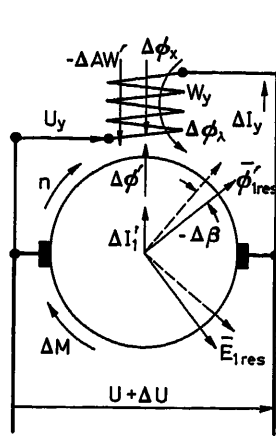


Figure A

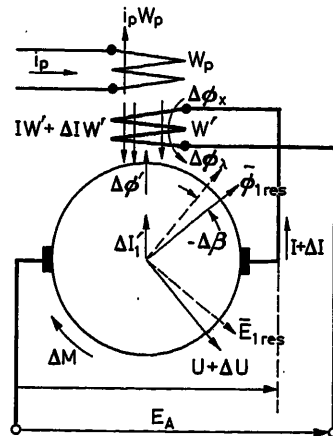


Figure B

ΔI_y , $\Delta AW'$ and $\Delta I'_1$ and thereby the accelerating moment ΔM created by the current $\Delta I'_1$, also falls in phase with $\Delta\beta$ and causes free oscillations to occur.

Now we will observe the same problem with the autodyne regulated by the current (*Figure B*).

In the stationary condition this possesses quite different ratios from the autodyne regulated by voltage because this is accompanied by no guide current and no guide through-flow, against which in the autodyne regulated by the load current the load current I creates the stationary current IW' which is eliminated by the current $i_p W_p$ created by the regulating current i_p . These magnitudes superimpose themselves upon the parameters of the transient process but have negligible effect on its progress. This occurs as shown in *Figure B* fully as much as in *Figure A*. In fact the rotation of the current $\phi_{1\text{res}}$ creates the longitudinal flow $\Delta\phi'$ and the voltage ΔU . The guide current ΔI produced by the latter voltage induces the guide flow $\Delta IW'$. As before, this induces a compensating current $\Delta I_1'$, the residue flow $\Delta\phi_x$ and the distributive flow $\Delta\phi_1$. If we consider the accumulator with voltage E_1 to be practically without resistance then the magnitudes of ΔI , $\Delta IW'$, $\Delta\phi_x$ and $\Delta\phi_1$ depend only on the cross section of the winding W' and for a definite value the free oscillations indicated earlier must also occur.

The Control of a Linear Electromagnetic Oscillating Mechanism

J. C. WEST and B. V. JAYAWANT

Summary

The paper describes briefly the principle of operation of a simple motor which directly produces a linear oscillating motion in the amplitude range 5 to 50 cm with traverse times variable from 0.03 to 1 sec.

The main part of the paper is concerned with the methods of controlling the amplitude and the frequency independently and electrically without the aid of mechanical devices. The turn-round points at the extremities of the oscillation are automatically forced by a non-linear ferro-resonance jump effect triggered off by the position sensing element. Some analysis of the jump phenomenon is attempted and compared with experimental results.

The work is intended primarily for the textile industry for winding yarn packages, where it is essential to be able to control the position of the turn-round points, and to adjust the amplitude of the traverse with time, i. e. amplitude modulation. The device with the auxiliary control mechanism is, however, applicable to any requirement of linear oscillatory motion.

Sommaire

L'exposé décrit brièvement le principe d'opération d'un moteur simple qui produit directement un mécanisme oscillateur dans la gamme d'amplitude 5 à 50 cm avec des temps de travers qui varient de 0.03 à 1 sec.

La plus grande partie de l'exposé a pour objet les méthodes de commande de l'amplitude et de la fréquence indépendamment et électriquement sans l'aide des moyens mécaniques. Les points de retour aux extrémités de l'oscillation sont automatiquement contraints d'un saut non-linéaire de ferro-résonance qui est déclenché par l'élément qui détermine la position. On essaie d'analyser le phénomène de saut et de le comparer avec des résultats expérimentaux.

L'œuvre est destinée principalement à l'industrie textile pour le bobinage des moches filées, où il est essentiel de pouvoir commander la position des points à travers, et d'ajuster l'amplitude du travers avec le temps, c'est-à-dire la modulation d'amplitude. Le dispositif avec le mécanisme de commande auxiliaire est cependant applicable à toutes nécessités de mouvements linéaires oscillatoires.

Zusammenfassung

Der Beitrag beschreibt kurz die Arbeitsweise eines einfachen Antriebes, der unmittelbar eine linear schwingende (hin- und hergehende) Bewegung im Amplitudenbereich von 5...50 cm erzeugt, mit umschaltbaren Bewegungszeiten, die zwischen 0,03 und 1 Sekunde veränderbar sind.

Der Hauptteil dieses Beitrages befaßt sich mit den Methoden für die Steuerung sowohl der Amplitude wie auch der Frequenz, unabhängig voneinander und auf elektrischem Wege, ohne die Benutzung mechanischer Hilfsmittel. Die Umkehrpunkte an den Extremstellen der Schwingung werden durch einen nicht-linearen Ferro-Resonanz-Sprungeffekt selbsttätig gesteuert, welcher durch den Stellungsabgriff ausgelöst wird. Einige Betrachtungen zum Sprungphänomen werden angestellt und mit Versuchsergebnissen verglichen.

Die Arbeit ist vorwiegend für das Wickeln von Garnrollen in der Textilindustrie bestimmt, wo es wichtig ist, die Lage der Umkehrpunkte zu steuern und die Amplitude der wechselnden Bewegung ab-

hängig von der Zeit einzustellen (Amplitudenmodulation). Das Gerät mit der dazugehörigen Steuereinrichtung ist jedoch auch für jede andere Aufgabe, die eine linear schwingende Bewegung verlangt, geeignet.

Introduction

There are many industrial requirements for light reciprocating motion which in the main are met by mechanical devices. The natural course of development has demanded faster operation and, as in the case of textile requirements for bobbin winding, mechanical considerations impose the limit on reciprocating frequency and hence on speed of production. Interest is, therefore, being shown in electromechanical devices and there are now several successful developments which produce electrically driven linear oscillating mechanisms¹⁻³. In some of these devices the reversal is obtained by switching, but induction type drives with inherent oscillatory forces requiring no moving contacts or switches are to be preferred.

The new linear motor, the control of which is the subject of this paper, operates essentially as a result of currents induced in the moving member, but unlike the polyphase oscillating linear induction motor, it has no counterpart in rotating machines. This motor is a new device developed in the Electrical Engineering Department of Queen's University^{4,5} and its attractiveness lies in the extreme simplicity of construction. The basic principle underlying the oscillating mechanism was described in detail in a previous paper⁴. A brief account of the phenomena involved is included here in order to appreciate the control problem.

Description of the New Linear Motor

Construction

The motor consists (*Figure 1*) of two identical coils wound on a laminated bar of iron with a conducting metal ring, e.g. aluminium, copper or brass, sliding over the iron bar in the space between the coils. Each of the two coils is connected to a single phase supply via a series condenser. When the value of

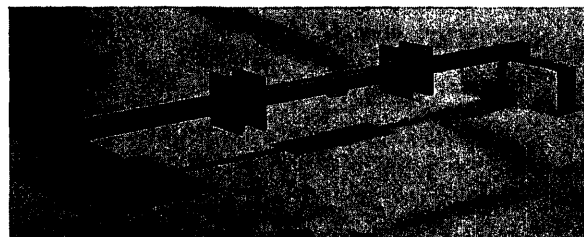


Figure 1. Construction of the new motor

the condensers is adjusted to form 'near' resonance, the ring begins to oscillate mechanically with a diverging amplitude of oscillations which is eventually limited physically by the coil formers or end stops. The ring now traverses the full distance between coils 20 or more times per second.

Principles of Operation

'*Q* lag'—There are two phenomena which individually or in combination make the operation of the motor possible. Under conditions of symmetry, i.e. identical coils, and with no condensers in series, the ring will experience a force tending to push it towards the centre of the traverse from either coil. For small displacements the ring exhibits damped oscillations which appear to be almost critically damped. The system may, therefore, be represented by the second-order equation

$$\frac{\ddot{x}}{\omega_n^2} + T\dot{x} + x = 0 \quad (1)$$

where ω_n is the natural frequency and $T\omega_n$ is of the order of 2.

When the two coils are connected in series with condensers so that the circuits of both of them are resonant, they possess a high *Q*. They therefore exhibit a time lag between the final steady-state value of the current and a sudden change of

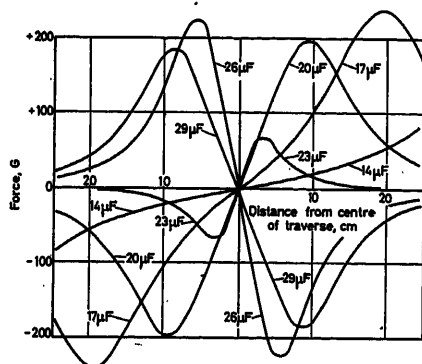


Figure 2. Static force-distance characteristics of two-coil motor

applied voltage or a change of any other circuit parameter. This also introduces a time lag between the force experienced by the ring if given a displacement and the steady-state force as calculated from the circuit equations (Figure 2). This lag between the force and position is the *Q* lag. If the *Q* lag is τ eqn (1) may be modified as

$$\ddot{x} = -\frac{(x + T\dot{x})\omega_n^2}{(1 + \tau p)}$$

i.e.

$$\frac{\tau\ddot{x}}{\omega_n^2} + \frac{\ddot{x}}{\omega_n^2} + T\dot{x} + x = 0 \quad (2)$$

This will be oscillatory if

$$\text{i.e. if the } Q \text{ lag } \tau > T. \quad \frac{T}{\omega_n^2} < \frac{\tau}{\omega_n^2}$$

From eqn (1) for a natural frequency of, say, 5 c/sec (10 traverses/sec) and critical damping, one obtains that

$$T \approx 0.1$$

which is the minimum value of τ if the system is to be oscillatory.

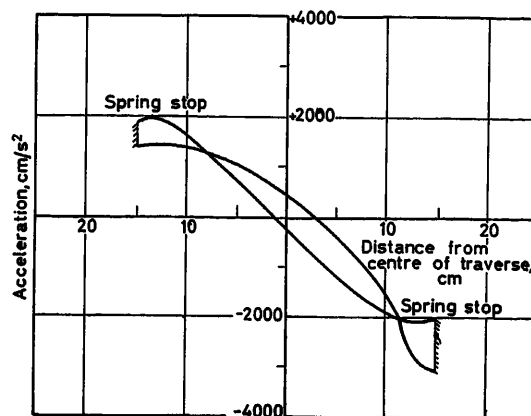


Figure 3. Dynamic force-distance characteristics of two coil motor

Again, from these equations one obtains that for $\tau = 2T$ the frequency of the self-maintained oscillations for this condition is given by

$$\frac{\omega}{\omega_n} \approx 0.6$$

It is thus seen that by utilizing the *Q* lag alone, it is possible to build a linear oscillating motor, but the frequency of oscillations will, of necessity, be lower than the natural frequency.

These results have been verified in practice and it is found that, relying on *Q* lag alone, the number of traverses per second of the ring is very low if the system is to be just oscillatory. If the system is so arranged that the amplitude of oscillations goes on building up, the ring hits the end stops and even then the frequency of oscillations is not particularly high. The acceleration of the ring under dynamic conditions was measured experimentally and Figure 3 shows the *Q* lag clearly. Under steady-state conditions the force and hence acceleration at the centre is zero.

Another interesting demonstration of the *Q* lag phenomenon is given by a stack of laminations held vertical and a coil in series with an appropriate value of condenser at the bottom (Figure 4). A metal ring sliding on the laminations is acted

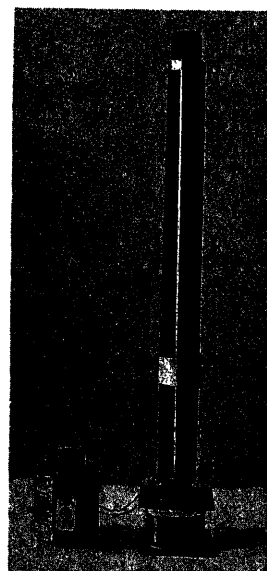


Figure 4. Vertical oscillating ring

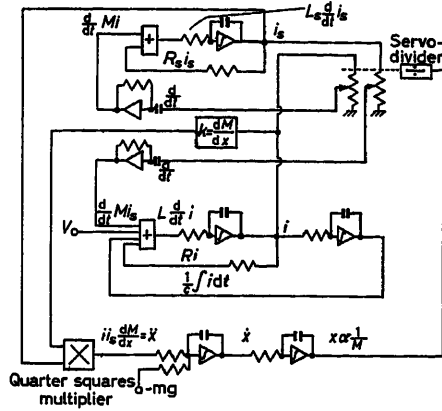


Figure 5. Analogue of the vertical oscillating ring

upon by gravitational pull downwards against the electromagnetic force of repulsion upwards. This arrangement exhibits oscillatory properties and in order to obtain some data and confirmation of the Q lag phenomenon an analogue was built. The analogue, as can be seen from Figure 5, is built up from the circuit equations with a provision for representation of the variable mutual coupling between the ring and the exciting coil. The construction of the analogue and a detailed discussion of the results obtained from it⁶ would be of little relevance here. Briefly, however, the analogue was used to verify the steady-state force-distance characteristics calculated from the circuit equations. Having thus obtained a mutual check between these calculations and the analogue it was then used to obtain the dynamic force-distance characteristics for various values of circuit parameters and in general to obtain an estimate of the Q lag which is easier done on the analogue than on an actual machine. This information was then useful in the estimates of Q lag and the prediction of dynamic characteristics of the multicoin machines.

Ferro-resonance—It is known that series RCL circuits, when the inductance is iron cored, exhibit a non-linearity in the current-voltage characteristic.

The conditions under which a non-linearity or jump effect may take place can be deduced briefly as follows. For a given inductance its current-flux relationship may be expressed as [Figure 6(a)]

$$\Phi = ng(i)$$

The induced e.m.f.

$$\begin{aligned} e &= \frac{nd\Phi}{dt} \\ &= n^2 \frac{dg(i)}{dt} \\ &= \frac{n^2 dg(i)}{di} \cdot \frac{di}{dt} \\ &= L(i) \frac{di}{dt} \end{aligned}$$

Variation of $L(i)$ with current is shown in Figure 6(b).

For an applied voltage to the series circuit such as

$$E \sin(\omega t + \alpha) = RI \sin \omega t + L(i) \omega I \cos \omega t - \frac{I}{C\omega} \cos \omega t$$

from which

$$E \cos \alpha = RI$$

$$E \sin \alpha = I \left[L(i) \omega - \frac{1}{C\omega} \right]$$

and

$$\frac{E^2}{I^2} = R^2 + \left[L(i) \omega - \frac{1}{C\omega} \right]^2$$

Therefore

$$\pm \sqrt{\frac{E^2}{I^2} - R^2} + \frac{1}{C\omega} = L(i) \omega \quad (3)$$

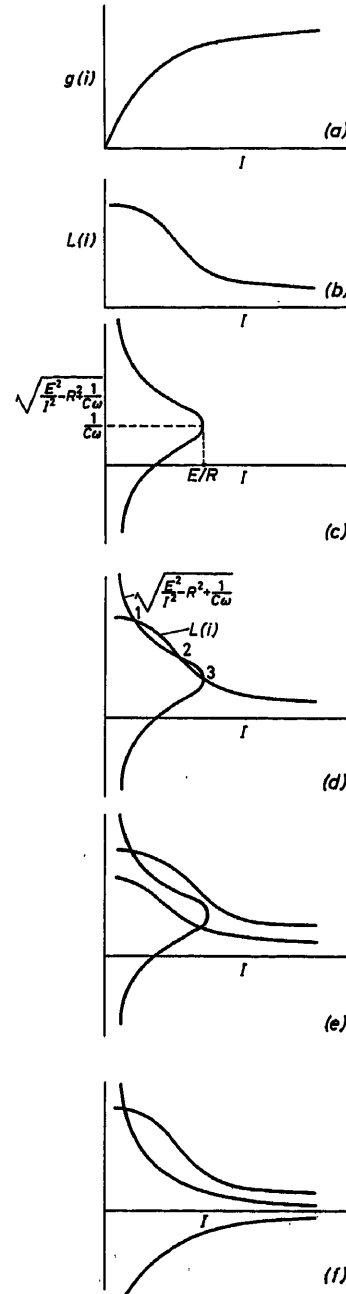


Figure 6. Ferro-resonant phenomenon in a simple RCL circuit

The slope of the left-hand side is given by

$$\frac{\partial}{\partial I} \left[\sqrt{\frac{E^2}{I^2} - R^2} + \frac{1}{C\omega} \right] = \frac{E^2}{I^3 \sqrt{\frac{E^2}{I^2} - R^2}}$$

which has a maximum when $I = E/R$. The variation of the left-hand-side of eqn (3) with current may be shown to be as in Figure 6(c).

Obviously the smaller the value of R the more peaked is the curve. If instability is to occur the curve of $L(i)$ against current must intersect the curve of

$$\sqrt{\frac{E^2}{I^2} - R^2} + \frac{1}{C\omega}$$

against I in three points [Figure 6(d)]. In the cases of Figures 6(e) and (f), instability cannot occur. In the first of these where instability cannot result, the rate of change of inductance is too rapid or too slow, whereas in the second case the curve of

$$\sqrt{\frac{E^2}{I^2} - R^2} + C\omega$$

is too sharp.

In a similar manner, given the flux-current relationship, it is possible to determine whether the current in the coils will exhibit the jump phenomenon as the ring is moved from the centre of the traverse to one or the other of the coils. In addition, the ring position at which the current jump occurs can also be predicted.

When the condensers are tuned so that the jump takes place slightly off centre, the force of repulsion from the coil near the ring will exceed that due to the far coil by a large factor. This large factor is due to the jump having taken place, and the current in the near coil is several times that in the far coil.

It is inherent in the ferro-resonant circuits that there is an hysteretic lag between the jump up and jump down of current. Thus the predominant force of repulsion is maintained until the ring has moved past the centre of the traverse and the reverse jump has taken place. This accentuates the divergent nature of the amplitude of oscillations, at the same time making the forces on the ring considerably larger than possible due to Q lag above.

Operation of the Oscillating Motor when both Q Lag and Ferro-resonant Jump Effect are Present

It has already been stated that the Q lag must be of a certain magnitude before the oscillations can be set up. This also means that when the ring is travelling with a certain velocity its apparent position will be further away from the coil towards which it is travelling. The greater the velocity the further away will be the apparent position since the Q lag must be a constant of the circuit. If the current jump takes place at a certain fixed position of the ring along the traverse then, as the approach velocity of the ring is increased, the distance travelled before the jump takes place will increase linearly. This was verified by an experiment and Figure 7 shows the superimposition of the Q lag on the ferro-resonance jump phenomenon. It can be seen from

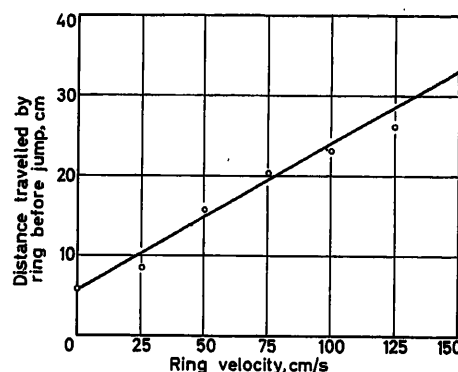


Figure 7. Effect of velocity on position of jump

this figure, as was suspected, that the Q lag is so large that at the velocities acquired (mean velocity = 160 cm/sec) by the ring when it is oscillating, the jump effect would not take place until the ring hits a mechanical stop (or the coil itself) at the end of its traverse and loses its velocity. This is illustrated by Figure 8 which is an oscillograph recording of current in one coil of the motor. It can be seen that the current is substantially at two levels only, and by putting position markers on the oscillogram it can be seen that the value of the coil current is small just before the ring actually hits the coil and it jumps up almost simultaneously with the impact of the ring. The mechanism of the jump effect when coupled with the Q lag may be treated as if there are contactless switching elements in both coils which operate when the ring hits the mechanical stops or the coils.

Control of Amplitude of Oscillations

Circuitry of Triggering the Jump Phenomenon

It is considered desirable to be able to control the amplitude of oscillations of the ring electrically for two reasons: (1), to eliminate the mechanical impact at the end of the traverse, and (2) to make it possible to vary the amplitude of oscillations without altering the frequency by a control signal, i.e. amplitude modulation.

The possibility of externally triggering the 'jump' phenomenon seemed to be the most attractive approach to obtain amplitude control and hence no attempt has been made to study the effect of modifying the Q lag.

Whilst the position of the jump is changed by altering the velocity of approach of the ring towards the coil [Figures 9(a) and (b)], it is clearly noticeable that the current jump itself is completed in a fixed time period of about 2 c of the supply frequency. It is essential, therefore, that it should be possible to trigger any one of the two (or more) circuits at will from



Figure 8. Current in one coil of oscillating motor operating predominantly on ferro-resonant jump

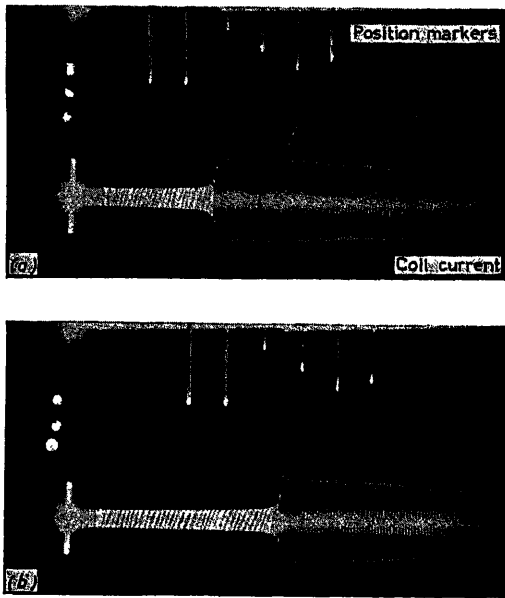


Figure 9. Displacement of jump position with ring traverse velocity, (a) Ring velocity 5 cm/sec, (b) Ring velocity 15 cm/sec

dissonant to resonant state and that the transition should be completed in the minimum of time.

When a ferro-resonant circuit changes its state from non-resonant to resonant there is a change in the stored energy and this can be supplied either from the mains or from the triggering source, or partly from both. Attention has so far been given only to the second method.

Using a triggering source to inject the additional energy, if its phase and magnitude are adjusted correctly, the switching is almost instantaneous.

The application of these principles to the control of amplitude of oscillations of the new motor is obtained by having two more windings on each coil and connected as shown in Figure 10. The main windings ($A-A$) are connected in series with condensers to a source of single-phase supply. When the ring is held stationary in the centre of traverse there will be no net e.m.f. across the terminals of the windings $C-C$ if both windings $A-A$ and $C-C$ are connected in opposition. If the ring is slightly displaced, however, the two main windings will no longer be balanced and consequently a voltage will appear at these terminals and it is possible to make this a signal

indicating the position of the ring by its amplitude. When the ring is oscillating the absolute amplitude of this signal changes quite considerably, but fortunately is still indicative of position of the ring. The change of the induced e.m.f. from steady state to dynamic state can be worked out for constant traverse velocities by an analysis nearly as involved as the one for calculation of forces⁴. It is considered inappropriate to include any

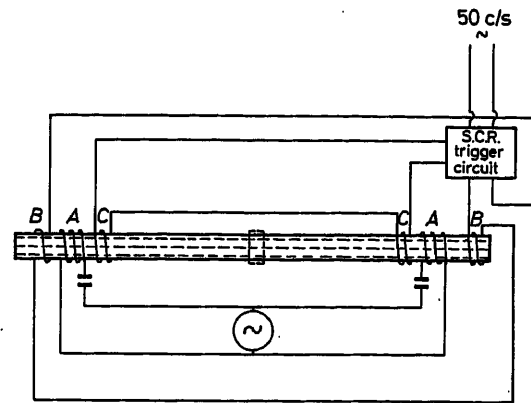


Figure 10. Layout of the amplitude control circuits using silicon-controlled rectifiers

of it here because there is no necessity to know the absolute values in the trigger circuits employed.

The signal from the windings $C-C$ is employed to trigger two silicon-controlled rectifiers alternately. The silicon-controlled rectifiers are in series with the windings $B-B$. It is essential to have two rectifiers as the direction and polarity required for the trigger current is of opposite sign for the two main windings $A-A$. The general layout of one of the triggering circuits employed is shown in Figure 11. The base of the transistors Tr_1 and Tr_2 is biased so that the signal from the windings $C-C$ does not bottom these transistors till a desired position of the ring is reached. The transistors in their turn switch the silicon-controlled rectifiers SCR_1 or SCR_2 which causes half-wave pulses to flow into the windings $B-B$. As is shown in the next section, it is only essential to apply one pulse of required magnitude and duration to change the state of the ferro-resonant circuit. Using SCR 's, however, the reverse voltage which is applied to them every half cycle is utilized to turn them off as soon as the transistors are turned off. If SCR 's are replaced by power transistors it would be possible to apply just one pulse from a d.c. source to obtain the desired change of the circuit of

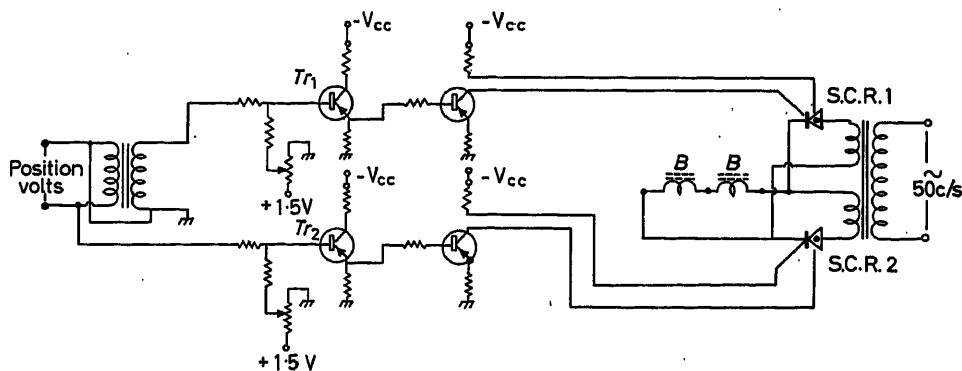


Figure 11. Silicon-controlled rectifier triggering circuit

windings $A-A$ from non-resonant to resonant state. Yet another alternative is to utilize the resonant state of one circuit to trigger the other. This can be done by charging up a condenser to the higher voltage which will be developed across the coil in the resonant state, and, by means of appropriate gating circuits, discharge the condenser through the triggering winding of the other coil. For the single rectangular pulse which includes the condenser discharge method outlined above, the position sensing element may be a phototransistor.

Equations for Instantaneous Triggering

The manner in which the required amplitude of the trigger voltage can be worked out is to make the trigger response of the circuit equal to the difference between the resonant and non-resonant steady states. If the trigger response is then added to the non-resonant steady state the result will be the resonant steady state.

Even though the triggering pulse is applied only to the inductance of the series RCL circuit, it is assumed that it is equivalent to a rectangular voltage pulse applied to the whole circuit. It is also assumed that superposition holds so that the current resulting from the rectangular pulse is equal to the difference between resonant and non-resonant steady states and that the current in the resonant state is still sinusoidal. This last assumption is likely to introduce some error, and some further work is needed to evaluate the degree of error involved or to take into account the effect of harmonics.

If a rectangular pulse V is applied to the circuit for a duration T it is easily shown that since

$$\left(Lp + R + \frac{1}{Cp}\right)\bar{I} = \mathcal{L}V[1 - H(t - T)] \\ = \frac{V}{p}(1 - e^{-pT})$$

and that the transform of the current

$$\bar{I} = \frac{V(1 - e^{-pT})}{L[(p + \mu)^2 + n^2]}$$

where

$$n^2 = \frac{1}{LC} - \frac{R^2}{4L^2}$$

and

$$\mu = \frac{R}{2L}$$

and hence

$$I = \frac{V}{nL} [e^{-\mu t} \sin nt - e^{-\mu(t-T)} H(t-T) \sin n(t-T)]$$

Thus when $t = T$

$$I = \frac{V}{nL} e^{-\frac{RT}{2L}} \sin nT \quad (4)$$

For instantaneous triggering, therefore,

$$(I_{\text{res.}} - I_{\text{n.res.}}) = \frac{V}{nL} e^{-\frac{RT}{2L}} \sin nT \quad (5)$$

The inductor voltage is at its resonant value at the end of the trigger pulse

$$V_L = pLI$$

and at $t = T$ the difference between resonant and non-resonant steady states must be equal to this.

$$(V_{\text{res.}} - V_{\text{n.res.}}) = \frac{V}{n} \left[ne^{-\frac{RT}{2L}} \cos nT - \frac{RT}{2L} \sin nT \right] \quad (6)$$

If the voltages and currents before and after the jump are known as functions of time and, say, the pulse duration, T , eqns (5) and (6) will give the amplitude of the voltage pulse V .

For sinusoidal pulses such as that which would be given by a half-wave rectified voltage using SCR 's,

$$V(t) = V \sin \omega t \quad \text{for } 0 < t < \frac{\pi}{\omega}$$

$$V(t) = 0 \quad \text{for } \frac{\pi}{\omega} < t < \frac{2\pi}{\omega}$$

The Laplace transform of this is

$$V(p) = \frac{V\omega}{p^2 + \omega^2} \left(1 + e^{-\frac{p\pi}{\omega}}\right)$$

The rest of the calculation to determine the amplitude of a single pulse necessary to trigger the circuit can be carried out in the same manner as before, the work being more laborious.

Yet another way of calculating the amplitude of the pulse is to work out the difference in the stored energy of the inductance, viz. $\frac{1}{2}LI^2$ before and after triggering. This is possible only if the two values of inductance and current are known. In basically the same manner then as before, by working out the current, the energy in the pulse of a given duration T , i.e. $\int_0^T e i dt$, may be calculated.

Further Requirements and Modifications for Amplitude Control

There are obviously as many varied requirements as there are individual applications for oscillating mechanisms. Attention has so far been directed only to the textile application of the new oscillating motor. Briefly, the requirement here may be stated as a constant velocity traverse followed by instantaneous reversal at either end. Obviously this condition is impossible to fulfil. However, what can be done with the controlled rectifier, triggered from a voltage proportional to position, is to vary continuously the bias of the transistors Tr_1 and Tr_2 (Figure 11) so as to obtain an overall modulation which gives very nearly the same result. It is worth stressing here that in order to obtain the desired result from any control circuit used, the construction of the main coils and any control windings must be identical. This involves great precision in the coil positions with respect to the iron laminations and values of condensers in series with each coil, and even in the making of coil formers. Surprisingly enough, attention to these few details gives more accurate results than any sophistications introduced in the analysis.

An immediate requirement in the control of amplitude is that the time in which the jump phenomenon itself is complete must be very small. It has already been mentioned that the jump takes place in about 2 c/sec of the supply frequency. In the normal course this, then, would impose a limitation on the frequency of oscillations. If, however, supply frequency is increased in accordance with the specific application, it is not only possible to decrease the imposition of this limit, but another favourable result is possible: this is the reduction in the overall size of the linear motor. Miniaturization of the new oscillating motor is considered to be an attractive proposition.

As will be apparent, attention is being directed to the small sizes of the motor for the reason that it has been possible to

utilize the ferro-resonant jump only in the smaller sizes. These tend to make the loading and power inputs minor considerations, but there is no reason why larger sizes of motors should not be used for driving loads. The aspect of control of these larger size motors would require the use of what might be described as eddy current braking, where d. c. might be injected into the trigger winding but at magnitudes below which the jump would take place. The eddy currents induced in the ring would provide magnetic buffers in place of mechanical stops.

Conclusions

The device described has considerable potential in small and large sizes. In this paper attention has mainly been given to the control of only small sizes. This is merely indicative of the

aspects of this motor, both in performance and applications, which have not been investigated. There is scope for considerable analytical and practical investigation which doubtless will be the subject of further research.

References

- ¹ LAITHWAITE, E. R., and NIX, G. F. Further developments of the self oscillating induction motor, Pap. No. 3,272 U, *Proc. Instn elect. Engrs*, 107 A (1960) 478
- ² U. S. Pat. No. 2,713,980
- ³ Brit. Pat. No. 386,386
- ⁴ WEST, J. C. and JAYAWANT, B. V. A new linear oscillating motor, *Proc. Instn elect. Engrs*, 109 A (1962)
- ⁵ Brit. (Prov.) Pat. 28,212/61, filed Aug. 1961; 29,109/61, filed Aug. 1961
- ⁶ JAYAWANT, B. V. and WILLIAMS, G. Analogue of a linear oscillating motor. *Control*, 6 (1963) 60

DISCUSSION

G. C. NEWTON, JR., *Massachusetts Institute of Technology, Electronic Systems Lab., Room 32-106, 77, Massachusetts Ave., Cambridge 39, Mass., U.S.A.*

This paper discloses a novel combination of switching circuitry and a linear electromagnetic actuator. The overall purpose of the apparatus is to effect control of the amplitude of oscillation of the eddy-current ring along the ferromagnetic rod. Furthermore, the switching circuit, by means of bias adjustments, permits adjustment of the amplitude of oscillation. Regarding the bias adjustment as the reference input and the amplitude of oscillation as the controlled variable, it is seen that this is a control system. However, the main control is open loop and feedback occurs only for the purpose of periodic reversal of the ring direction. The authors are to be congratulated for an interesting discussion of this novel method of controlling an electromagnetic actuator.

A few specific comments appear to be in order. First, the ferro-resonance analysis in the paper is from the viewpoint of current jumps in static electromagnetic circuits, whereas the paper's actual electromagnetic circuit involves a moving secondary winding in the form of the eddy-current ring. Thus the equations on the second page of the paper have little relevance to the actual equipment of the paper. Furthermore, even the analysis of the static situation is superficial. Eqn (3) is based on a sinusoidal approximation to the actual current waveform. There is an unstated approximation made in the derivation leading up to eqn (3) whereby the non-linear $L(i)$ is replaced by $L(I)$, another non-linear relationship. If this analysis is to be retained in the paper greater care should be taken in stating the assumptions on which it is based. (The authors do show an actual non-sinusoidal waveform in Figure 8 and also state, in the discussion of instantaneous triggering, that errors are introduced in their analysis because of these non-sinusoidal waveforms that result from the non-linear inductors.)

It is unfortunate that the authors show no experimental results for their proposed system of controlling the amplitude of oscillation. This is especially so in view of their position that refinement of analysis is not as important as details of construction. They do show experimental results indicating the Q -lag phenomenon (Figure 3) and the jump phenomenon (Figures 7, 8, and 9). If limitation on paper length were the reason for omitting the experimental results on amplitude control, it would have been preferable from my viewpoint to omit the ferro-resonant analysis, which is not particularly pertinent as indicated above, in order to make room for this more important information. Perhaps, in their closure the authors will be able to give some experimental results for the amplitude control system.

J. C. WEST, *in reply*

I would like to thank Doctor Newton for his important comments. I regard the basic oscillation of this system as a closed-loop condition.

Position of the ring is measured inherently by mutual coupling and determines, through the dynamics of the system, the amplitude of oscillation. It is open-loop in the sense that basically there is no external control of amplitude or frequency and these alter with varying external load.

For the particular textile application, we desired to vary the amplitude of oscillation in a controllable manner. The pulse circuitry forms a practical method but adds considerably to the complexity of the total system.

The results obtained were:

- (1) Effective control of a fixed amplitude in spite of load variation.
- (2) Controlled variation of the amplitude of oscillation from 10 cm up to 20 cm.
- (3) The frequency is not controlled and varies by about 30 per cent for a 200 per cent change in amplitude.
- (4) The frequency can be adjusted if desired by at least ± 50 per cent of the unloaded frequency by variation of the supply voltage. Greater variation can be obtained if alteration of the size of series condensers can be tolerated.

The analysis is simplified deliberately since a more rigorous approach becomes extremely complicated and lengthy. This has been undertaken using digital and analogue computer aids and some results are given in Reference 4, which includes the effect of the velocity of the ring. The jump effect without control does not take place until the ring has come to rest, stopped mechanically by the coil sides. Hence it has little effect of an external triggering pulse.

O. J. NUMMINEN, *Typpi Oy Finnish Society of Automatic Control, Oulu, Finland*

- (1) What output does the mechanism deliver at its present state?
- (2) How is an increase of output power possible?
- (3) What is the behaviour of the mechanism when the ring is braked during its travel, i.e. when mechanical output is taken from the system?

J. C. WEST, *in reply*

The force on the moving ring is used to overcome friction, to move a load and to accelerate the moving parts. Hence the greater the load force, the less force is available for acceleration and consequently the longer the traverse time. The jump phenomenon of ferro-resonance is position dependent and not time dependent and the result can be considered as a changeover switch where the direction of the force depends on the ring position. Thus loading the ring does not inhibit oscillation but reduces the frequency.

Step Motors with an Active Rotor

Yu. K. VASILIEV, Yu. A. PROKOFIEV and G. Ya. WAINBERGER

Summary

Active rotor stepping motors of two-rotor and two-stator types are described and methods of the calculation of steady-state and transient response of stepping motors are given. When deriving the expression for the static torque, all the changes of the field wave in the air gap due to the presence of salient stator and rotor poles have been replaced by corresponding change of the magnetomotive force. Magnetic field modelling was carried out with the aid of an EGDA integrator to obtain a more accurate calculation of the magnetic circuit of stepping motors. The deduced expression for steady-state torque accounted for both the torque proportional to the product of stator and rotor magnetomotive forces and reactive torques due to stator and rotor m. m. f.'s. It enables one to analyse the influence of teeth zone geometry and magnetic circuit parameters upon the torque value. Analytical calculations of the resolution of stepping motors subjected to a frequency surge are made on the assumption of an instantaneous current surge in the winding and a rectangular static torque wave. For a sinusoidal static torque wave, the above-mentioned calculations have been made with the aid of an MH-7 mathematical model. The obtained set of the motor's resolution characteristics as a function of load is to some extent universal, so that by means of simple calculations one can obtain these functions for different rotor inertia values. The report also includes an approximative calculation of the resolution of synchronously operating stepping motors.

A method has been developed on the assumption that currents in the controlled windings change exponentially with a certain average time constant and that angular steady-state response is sinusoidal.

Sommaire

Un moteur à action selon un échelon rectangulaire équipé d'un double rotor et d'un double stator est décrit, et la méthode permettant de calculer sa réponse transitoire et permanente est indiquée. Pour établir l'expression du couple moteur, les changements du champ magnétique de l'entrefer ont été remplacés par des changements correspondants de la force magnétomotrice. La répartition du champ magnétique a été déterminée à l'aide d'un intégrateur EGDA pour calculer avec toute la précision voulue le circuit magnétique de ce moteur. L'expression ainsi obtenue du couple tient compte d'une part du couple proportionnel au produit des forces magnétomotrices du stator et du rotor, et d'autre part, de la réaction de l'induit. Cette expression permet de tenir compte de l'influence de la géométrie de la forme des encoches ainsi que des paramètres du circuit magnétique.

Un calcul analytique de comportement d'un tel moteur soumis à une sollicitation périodique, est indiqué dans l'hypothèse de l'établissement instantané du courant dans les enroulements et d'une courbe des couples variant selon une oscillation rectangulaire. Ce comportement a été également déterminé pour des variations des couples selon une courbe sinusoïdale, et cela au moyen d'un modèle mathématique MH-7. Les caractéristiques du moteur ainsi obtenues en fonction de la charge, sont présentées sous une forme générale; par un simple calcul il est possible d'obtenir ces caractéristiques pour différentes valeurs de l'inertie du rotor. Le rapport donne également un calcul approché du comportement de moteurs à action rectangulaire marchant en synchronisme.

Une méthode de calcul a également été développée dans l'hypothèse que le courant circulant dans l'enroulement de contrôle varie selon une courbe exponentielle avec une constante de temps moyenne, et que la réponse angulaire est sinusoïdale.

Zusammenfassung

Schrittmotoren mit aktivem Läufer der Bauart mit zwei Läufern und zwei Ständern werden beschrieben; es werden Methoden für die Berechnung des Beharrungsverhaltens und des Übergangsverhaltens derartiger Schrittmotoren angegeben. Bei der Ableitung des Ausdruckes für das statische Drehmoment sind Feldänderungen im Luftspalt auf Grund des Vorhandenseins besonderer Läufer- und Statorpole durch entsprechende Änderung der magneto-motorischen Kraft ersetzt worden. Das Modell eines Magnetfeldes wurde mit Hilfe eines EGDA-Integrators aufgestellt, um größere Berechnungsgenauigkeit für den magnetischen Kreis von Schrittmotoren zu bekommen. Der abgeleitete Ausdruck für das statische Drehmoment berücksichtigt sowohl die Bremsmomente auf Grund der magneto-motorischen Kräfte von Ständer und Läufer wie auch das Drehmoment, das dem Produkt dieser beiden Kräfte proportional ist. Darauf aufbauend kann man den Einfluß der Zahnung und der magnetischen Kennwerte auf den Betrag des Drehmomentes analysieren. Die Berechnungen für die Auflösung von Schrittmotoren, die einer plötzlichen Änderung der Frequenz unterliegen, werden unter der Annahme eines augenblicklichen „Anschwellens“ des Windungsstromes und einer rechteckigen Welle des statischen Drehmomentes durchgeführt. Für den Fall der sinusförmigen Welle des statischen Drehmomentes wurden derartige Berechnungen mit Hilfe eines mathematischen Modelles vom Typ MH-7 durchgeführt. Die berechneten Merkmale der Motorauflösung als Funktion der Belastung sind einigermaßen allgemeingültig, so daß man mit Hilfe einfacher Berechnungen diese Funktionen für verschiedene Läuferträge bekommen kann. Dieser Bericht enthält auch eine angenäherte Berechnung der Auflösung von synchronbetrieblenen Schrittmotoren.

Es wurde ein Verfahren entwickelt auf Grund der Annahme, daß sich die Ströme in den gesteuerten Wicklungen mit einer bestimmten mittleren Zeitkonstante exponentiell ändern und daß der Winkelausschlag im Beharrungszustand sinusförmig erfolgt.

Step motors are synchronous pulse motors, intended for the transformation of electrical control signals into discrete (stepped) movements of mechanisms. The speed of revolution of a step motor is regulated by alteration of the frequency of the control pulses, and the angle of rotation strictly corresponds to the number of pulses sent. At zero frequency the rotor of the motor is held by an electromagnetic field or some other locking arrangement.

The control programme of a step motor is introduced through a translator, which serves for shaping, amplifying and distributing the pulses to the motor windings. The translator is based on thyristors or controlled semiconductor elements, but in a number of cases may also be mechanical.

The use of step motors allows one to make open-loop discrete systems without checking the output values (without position pick-ups) and without feedbacks, which simplifies automatic systems considerably. The quality of such systems (response and accuracy) is predetermined to a considerable extent by the properties of the step motor.

The required accuracy of the output values can in principle be obtained by the appropriate choice of the unit angle θ_{step} of

the step motor (the angle of rotation when one pulse is sent). In practice, in existing step-motor designs the smallest value of the unit step is limited to the minimum possible tooth pitch and lies within limits of $0.5-3^\circ$.

Further reduction of θ_{step} , where this is necessary, is effected by using mechanic reducing gears.

The response of a system depends on the resolution of the step motor and translator at the selected value of the unit step. The resolution or the limit tempo (N) attained by the rotor when the motor is in synchronous operation with a smooth increase of the frequency of the supplied pulses, and the resolution or limit tempo (ΔN) with step increase of the pulse repetition frequency from the immobile state of the step motor rotor (receptiveness) are distinguished.

In both cases, the absence of motor hunting at a given load on the shaft and at the predetermined moment of inertia of the load serves as the criterion of stability. Thus the following will be the operating characteristics of the system of a step motor with a translator:

$$\Delta N = f(M_H) \text{ or } \Delta N \cdot \theta_{\text{step}} = f(M_H) \text{ and}$$

$$N = f(M_H) \text{ or } N \cdot \theta_{\text{step}} = f(M_H) \text{ when } J = \text{const}$$

where J is the moment of inertia of the load, and M_H is the torque of the load.

At the present time, step motors are used in machine tools and automatic gas-cutting outfits with programme control as the drive or servo-drive of the advancement gear, for remote control of the position of controlling valves and slides, for programme input (punched-tape or punched-card drive), for actuating synchros, potentiometers and switches, as a counter-adder, etc.

It is also possible to use step motors in automatic closed-loop discrete systems with discrete position pick-ups and feedbacks. The use of step motors makes it possible to replace many of the closed-loop servo-systems in existence at present by simpler open-loop systems.

There is a large number of types and designs of step motors^{1,2} with various principles of operation and design features. They can all be divided into three groups according to their operating principle: (a) electromechanical step motors; (b) step motors with reactive rotor; (c) step motors with active rotor.

The characteristic of the first type is that the motors have a ratchet mechanism which limits their speed of response, power and service life. The second type, which has up to now been most widely used in the triple-stator form, does not have this major disadvantage of the electromechanical motors and can have comparatively good indices (weight, dimensions, frequency characteristics) provided that it is made for small unit angles ($0.5-6^\circ$). It should be noted that these motors tend to operate unstably, especially during idle running and under high dynamic loads, which makes it necessary to take special measures against rotor swinging (clutches, various damping devices, current cut-offs). Active-rotor motors, which have control windings placed on the rotor or stator and electromagnetic or permanent-magnet excitation, in principle allow one to obtain higher utilization of materials, as a result of which their weight indices and dimensions are improved, at high speed of action ($N\theta_{\text{step}}$ and $\Delta N \cdot \theta_{\text{step}}$). In practice these advantages of active-rotor step motors manifest themselves most fully, starting from high unit angles ($\theta_{\text{step}} \geq 22.5^\circ$). Reduction of the unit angle, which is

very important, all other conditions being approximately equal, is possible in the double-rotor or double-stator step-motor designs considered below.

The double-rotor step motor* has a stator with a concentrated winding (or without a winding, made from permanent magnets) and a rotor consisting of two sections fitted on the same shaft with a shift of half a pole pitch (Figure 1). The number of teeth on the stator equals their number on the rotor, and each tooth is a pole. The stator winding is an excitation winding and during operation its polarity remains unchanged. The control windings are located on the rotor and are supplied with pulses of current in accordance with various graphs [Figure 2(a), (b) and (c)].

With alternate-simultaneous supply of the control windings [Figure 2(c)] the number of fixed positions of the rotor is doubled. Although in this case the switching circuitry becomes somewhat more complex, the resolution of the motor is increased considerably as the result of fractionation of the step.

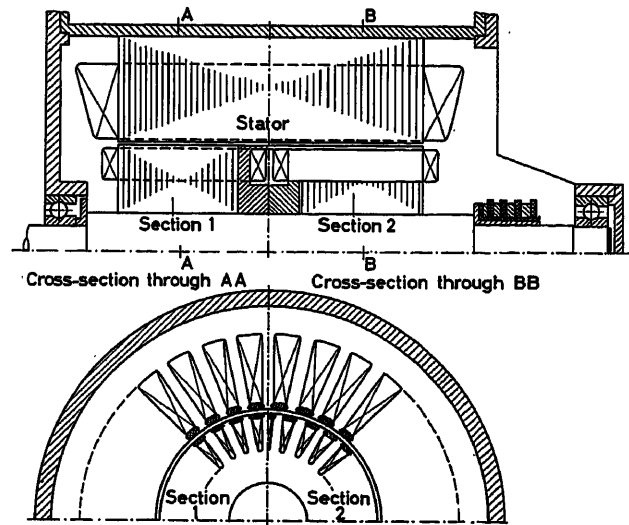


Figure 1. 2-rotor motor

The motor is reversed by altering the order of sequence of the positive and negative pulses in one of the controlled windings of the rotor.

The advantages of the double-rotor motor are design and technological simplicity, compactness, good use of active materials and a high ratio of the maximum electromagnetic torque of the motor to the moment of inertia of the rotor (dynamic quality). The zone of stable positions (θ_z) of the rotor, in comparison with the magnitude of the step (θ_{step}) in double-rotor step motors [Figure 3(a)] is greater than in a triple-stator motor [Figure 3(b)], which reduces the possibility of hunting of the motor in the case of considerable loads or oscillations of the rotor.

Moreover, the control of the motor by means of the rotor makes it possible, even in the case of power motors, to use solid-state control circuits, since the m.m.f. of the rotor is usually 2-4 times less than the m.m.f. of the stator, the winding of which is not switched.

* Soviet patent certificate No. 131811, dated 10 June, 1959, granted to Yu. K. Vasiliev.

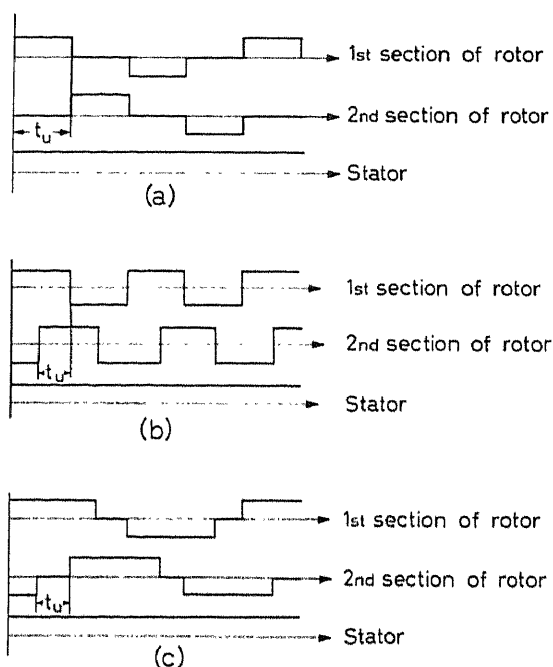


Figure 2. Control pulses on the windings of a step motor

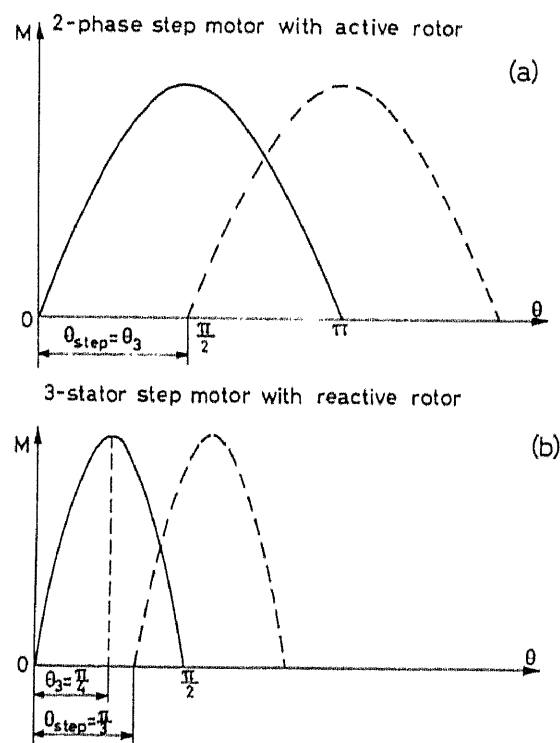


Figure 3. Zone of stable rotor positions and unit step of motor

The rotor can be made beak shaped, as is done in electromagnetic clutches or high-frequency machines. Special beak-shaped constructions with stationary coils which create the rotor field, enable sliding contact to be avoided.

The disadvantages of the double-rotor motor are the fact that use is not made of the reactive torque proportional to $\sin 2\theta$, the four slip rings on the rotor (in the non-beak-shaped

design), and the need to produce heteropolar current pulses in the control windings.

The double-stator step motor* consists of two machines, the rotors of which are mounted on the same shaft. The stator and rotor have windings and a salient system of pole teeth (Figure 4).

The rotors or stators of the machines are shifted relative to one another by one half a tooth pitch. The control windings are located on the stator (rotor), and the rotor (stator) is supplied with constant d.c. voltage.

Stepping operation of a double-stator motor is accomplished in the same way as of the double-rotor motor.

The rotor may be built with permanent magnets, which makes it possible to avoid slip rings; a certain degree of opening of the slots on the rotor and the stator enables one to utilize the reactive torque but considerable opening of the stator slots is undesirable, since it leads to impairment of the shape of the angular static characteristic and to a reduction of the resolution.

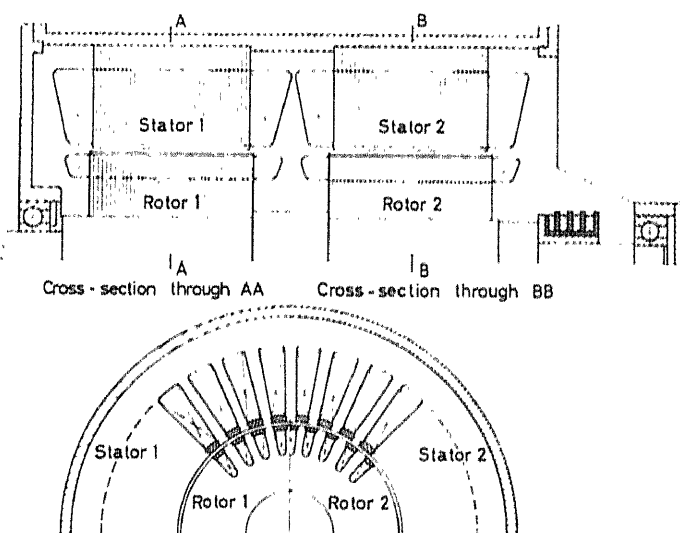


Figure 4. 2-stator motor

The double-stator step motor may be made of the face type with ordinary or printed circuit rotor windings.

The double-stator and double-rotor step motors are made as power and fractional horse-power motors.

There are two-phase step motors with an active rotor and with radial positioning of the two sections (phases) of the motor stator, as in an ordinary two-phase synchronous machine².

The double-rotor and double-stator step motors examined in this paper, with axial positioning of the sections (phases), have basic advantages over motors with radial location of the sections in a lesser moment of inertia and a greater stator tooth pitch, with an identical unit step, i.e., in better utilization of the materials of the machine.

* Soviet Authors Certificate No. 129110, dated 10 June, 1959, in the name of Yu. K. Vasiliev.

Some Problems of Step Motor Theory

The main problems of research into step motors are as follows:

- (1) The development of a method for calculating the static angular characteristic $M_c = f(\theta)$, where θ is the error angle between the vectors of the stator and rotor m.m.f. (Figure 8), and M_c the steady-state torque developed by the immobile motor.
- (2) The development of a method for calculating the frequency characteristics $N = f(M_H)$ and $\Delta N = f(M_H)$.
- (3) Energetic investigation of step motors—losses and efficiency.
- (4) Investigation of the geometry and the formulation of a calculation method.
- (5) The development of a technique for experimental study of step motors.
- (6) Study of step motor control circuits.

This paper considers approximate methods of calculating the static and frequency characteristics, which make it possible to determine the main parameters of a designed machine.

Calculation of the static angular characteristic is necessary for correct designing of step motors, selection of the symmetry of slot geometry, and also for accurate calculation of the frequency characteristics.

The static characteristic can be obtained very accurately by the graphic method in accordance with the expression of the torque, written in the general form:

$$M_c = \frac{dW}{d\theta} = \frac{d}{d\theta} \sum_{K=0}^{K=n} \int_0^{\psi_K} i_K d\psi_K \quad (1)$$

where K is the number of connected windings, W is the portion of the energy of the electromagnetic field of the motor which is converted into mechanical work, i_K is the winding current, and ψ_K is the flux linkage of the windings.

For this the curves $\psi_K = f(i_K)$ have to be calculated for various rotor positions. However, this calculation presents considerable difficulty because of the complexity of the field pattern. To ascertain the nature of the variation of the fluxes in relation to the position of the rotor, and to make possible accurate calculation of the magnetic circuit, the magnetic field in the gap was simulated (by Rybalenko) on an *EGDA* integrator⁴.

By way of example in Figures 5(a) and (b), field patterns are given for two rotor positions. The results of actual measurements of the magnetic fluxes of the motor practically coincided with the simulation findings. An approximate expression of the torque can be obtained from (1), assuming the magnetic permeability of the iron to be constant. The saturation of the magnetic circuit is taken into account by the introduction of the concept of the rated air gap δ' which assumes the magnetic circuit to be unsaturated for the same flux as in the case of a saturated circuit.

$$\delta' = K_\mu \cdot \delta$$

where δ is the real gap; K_μ the coefficient of saturation, equal to $\Sigma F/F\delta$; ΣF the total m.m.f. of rotor and stator per one pole, and $F\delta$ the m.m.f. per one real gap.

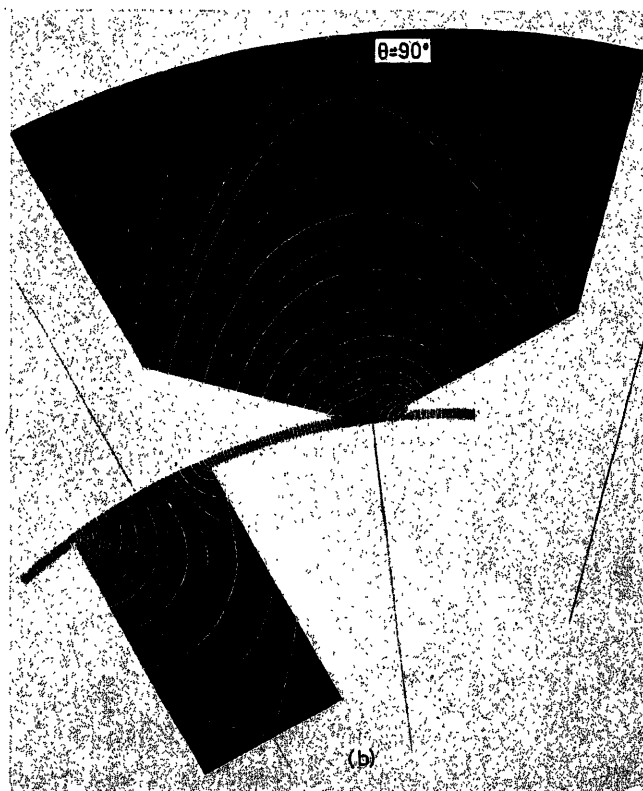
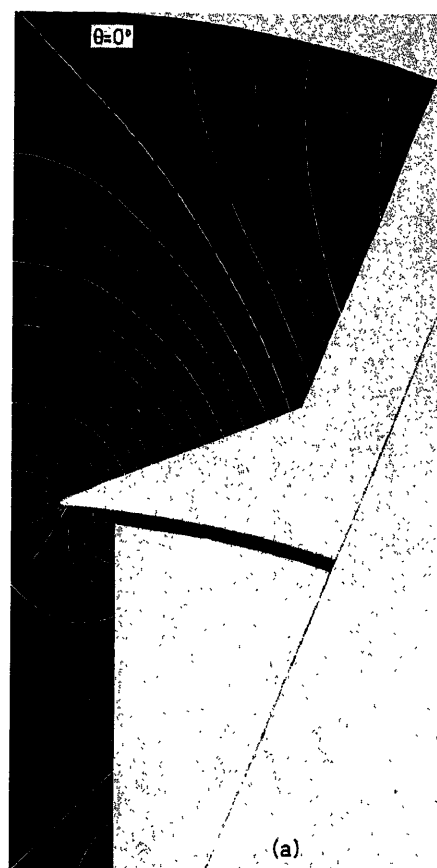


Figure 5. Field pictures

Other assumptions:

(a) The number of teeth on stator and rotor is the same and equals the number of poles

$$Z_S = Z_R = 2p$$

(b) The air gap beneath the pole has a constant size: the size of the gap is small in comparison with the pole (tooth) pitch τ ;

(c) All the changes undergone by the curve of the field in the gap from the presence of the salient stator and rotor poles are replaced by corresponding changes of the m.m.f., assuming the gap to be uniform and equal to the rated one;

(d) From the stator and rotor m.m.f. curves, use is made of the first harmonics. Moreover, account is taken of the travelling gaps in the stator and rotor m.m.f. from the opening of the slots both on the rotor and on the stator (Figure 6).

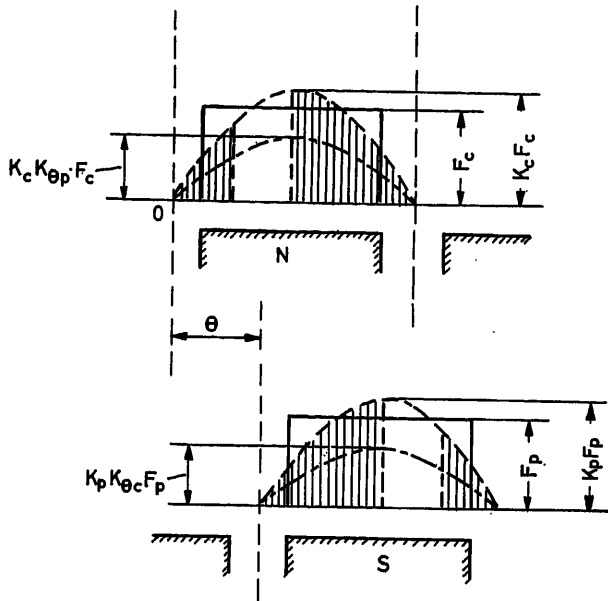


Figure 6

Bearing in mind the assumptions adopted an expression of the moment for one rotor is obtained, after transformations, which consists of three components:

$$M_c = M_R + M_{ST} + M_a \quad (2)$$

M_R is the reactive torque from the m.m.f. of the rotor with open stator slots,

$$M_R = a_2 F_{mr}^2 \sin 2\theta + a_4 F_{mr}^2 \sin 4\theta$$

M_{ST} is the reactive torque from the stator m.m.f. with open rotor slots,

$$M_{ST} = b_2 F_{ms}^2 \sin 2\theta + b_4 F_{ms}^2 \sin 4\theta$$

M_a is the active torque,

$$M_a = c_1 F_{ms} F_{mr} \sin \theta + c_3 F_{ms} F_{mr} \sin 3\theta + c_5 F_{ms} F_{mr} \sin 5\theta$$

The coefficients $a_2, a_4, b_2, b_4, c_1, c_3$ and c_5 take into account the slot geometry of the tooth layer of stator and rotor, and equal

$$a_2 = 2\pi\alpha_c \sin \pi\alpha_c$$

$$a_4 = \sin^2 \pi\alpha_c$$

$$b_2 = 2\pi\alpha_p \sin \pi\alpha_p$$

$$b_4 = \sin^2 \pi\alpha_p$$

$$c_1 = \pi^2 \alpha_c \alpha_p + \frac{1}{2} \pi \alpha_c \sin \pi \alpha_p + \frac{1}{2} \pi \alpha_p \sin \pi \alpha_c + \frac{1}{2} \sin \pi \alpha_c \sin \pi \alpha_p$$

$$c_3 = \frac{3}{2} \pi \alpha_c \sin \pi \alpha_p + \frac{3}{2} \pi \alpha_p \sin \pi \alpha_c + \frac{3}{4} \sin \pi \alpha_c \sin \pi \alpha_p$$

$$c_5 = \frac{5}{4} \sin \pi \alpha_c \cdot \sin \pi \alpha_p$$

With simultaneous connection of the two phases in accordance with the network shown in Figure 2(b), the second harmonic in the resultant torque is missing. It should be noted that even a small opening of the rotor and stator slots has a considerable influence on the torque-curve shape.

Only for $\alpha_p = \alpha_c = \geq 0.95$ —the coefficients of the pole overlap of the rotor and stator—does the angular characteristic approach a sinusoid. An unsuccessfully selected slot geometry can lead to considerable gaps in the torque curve, which either reduces the frequency characteristics of the step motor or, because of the swings of the rotor, makes its operation in a wide range of frequencies impossible. In a number of cases, the stator or rotor slots are skewed to improve the angular characteristic. Figure 7 gives the calculated and experimental static characteristics of pilot models of active-rotor step motors.

Approximate Calculation of the Characteristic $\Delta N_{np} = f(M_H)$

The aim of the calculation is to determine the minimum time between two consecutive control pulses ($t_{u \min}$), at which the rotor still runs up from a state of rest without missing steps under the preset load.

Then

$$\Delta N_{np} = \frac{1}{t_{u \min}} \quad (\text{steps/sec})$$

The above problem will be considered using as an example a double-stator (or double-rotor) motor, when the control wind-

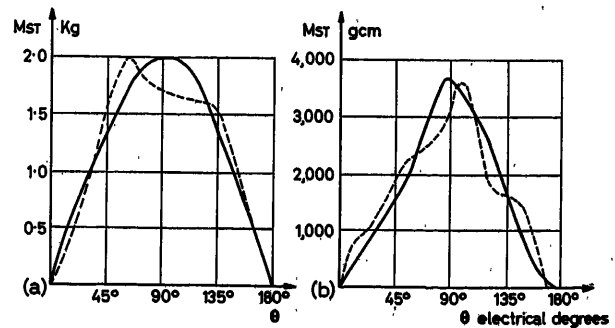


Figure 7. (a) Angular characteristic of power step motor; (b) Angular characteristic of 2-rotor step motor

ings are supplied alternately [Figure 2(a)]; for approximate calculations it is assumed that the currents change instantaneously, and the angular static characteristic of each rotor has a rectangular shape.

In this case the rotor motion equation adopts the form

$$J \frac{d^2 \beta}{dt^2} + D \frac{d\beta}{dt} \pm M_e = -M_H \operatorname{sign} \left[\frac{d\beta}{dt} \right] \quad (3)$$

Here β is the angle between the axis determining the instantaneous position of the rotor relative to the positive direction of the stationary axis of the stator winding.

J is the moment of inertia of the motor and the mechanism. The direction which corresponds to the movement of a right-hand screw when it is turned in the direction of flow of the current in the winding will be taken as the positive direction of the axis of the winding. The angles will be positive clockwise, counting from the axis of the stator winding. Figure 8 shows the schematic manual position of the step motor windings in one plane.

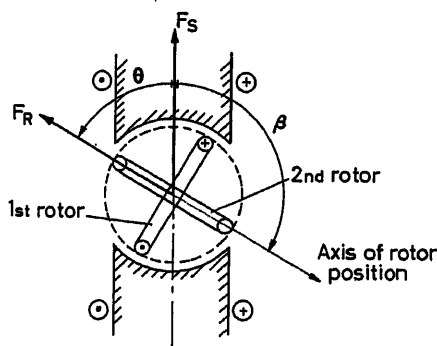


Figure 8. Arrangement of windings of step motor with active rotor

D is the damping coefficient of the torque of the type of 'viscous friction' (for example the torque from eddy currents induced in the iron of the rotor or a special damping cell).

$$M_H \operatorname{sign} \left[\frac{d\beta}{dt} \right]$$

is the load-torque of the dry friction type.

M_e is the electromagnetic torque of one rotor. For $\theta = 0 \div \pi$ M_e has the plus sign (+), and for $\theta = 0 \div -\pi$ the minus sign (-).

Switching in one of the rotor windings leads every time to the instantaneous rotation of the vector of the m.m.f. of the rotor anticlockwise through an angle $-\pi/2$. The movement of the rotor itself is effected in a positive direction. Thus the instantaneous position of the vector of the m.m.f. of the rotor relative to the stator m.m.f. vector (Figure 8) for any step is equal to the difference of the angles β and $n\pi/2$, i.e.

$$\theta = \beta - n \frac{\pi}{2}$$

At the end of each step the angle θ determines the angular dynamic error of the step motor. Introducing into eqn (3) the parameter H and after carrying out transformation, one obtains for 'p' pairs of poles

$$H \frac{d^2 \beta}{dt^2} + A \frac{d\beta}{dt} \pm 1 = -B \operatorname{sign} \left[\frac{d\beta}{dt} \right] \quad (4)$$

where

$$H = 314^2 \frac{1}{p} \cdot \frac{J}{M_e}$$

is the inertial time constant of the step motor in electro-radians.

Since this parameter includes the ratio M_e/J (dynamic quality), it determines to a considerable extent the dynamic properties of the system 'motor plus mechanism'.

t is the time in radians; $t [\text{rad}] = 314 t [\text{sec}]$

$$A = \frac{314 D}{p M_e}$$

is the damping coefficient.

$$B = \frac{M_H}{M_e}$$

is the torque of load in fractions of the electromagnetic torque.

The run-up of the step-motor rotor is effected not over one step, equal to $t_{u, \min}$, but over several steps (Figure 9, curve 2). If at the end of the first step the motor makes some negative angular error $-\Delta\theta$, then at the end of the second step the rotor, having a greater mean speed during the step, commits a smaller angular error $|\Delta\theta_2| < |\Delta\theta_1|$ (the total error over two steps equals $\theta_2 = -[\Delta\theta_1 + \Delta\theta_2]$, etc.). In some K th step the rotor, over the time $t_{u, \min}$, can have a mean speed sufficient to traverse an angle greater than θ_{step} and the total error begins to decrease.

Subsequently the process of change of the dynamic error $\theta = f(n)$ may have an oscillatory nature (Figure 10). Under certain conditions (low damping, unfavourable shape of angular characteristic) there may exist frequency bands (usually in the under -100 c/sec range) where the error oscillation is of a resonance nature. The amplitude of the rotor oscillation rises and this unavoidably makes the motor fall out of synchronism. The following may be effective measures against this phenomenon: load (which reduces the amplitude of the oscillations of the rotor), improvement of the shape of the angular characteristic, and so on. Such conditions require special consideration.

These approximate computations of the characteristic $\Delta N n p = f(B)$ will be confined to conditions under which the assumption is valid that the rotor will remain in synchronism if the total error in the first swing does not have a limitlessly increasing nature (Figure 10, curves 1 and 3), but has a definite maximum. Under limit conditions this maximum must be de-

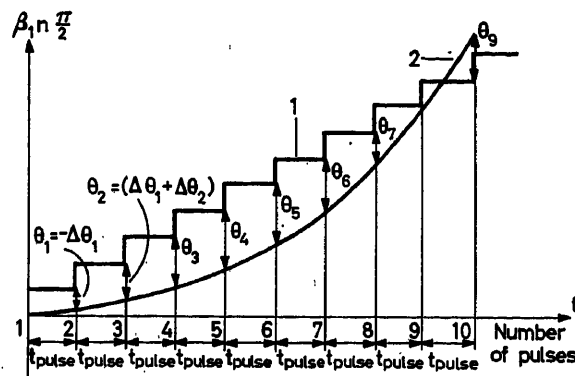


Figure 9. (1) $-n\pi/2 = f(n)$ is the curve of movement of the vector of the m.m.f. of the rotor as a function of the number of switchings in the control windings; (2) $\beta = f(t)$ is the rotor motion

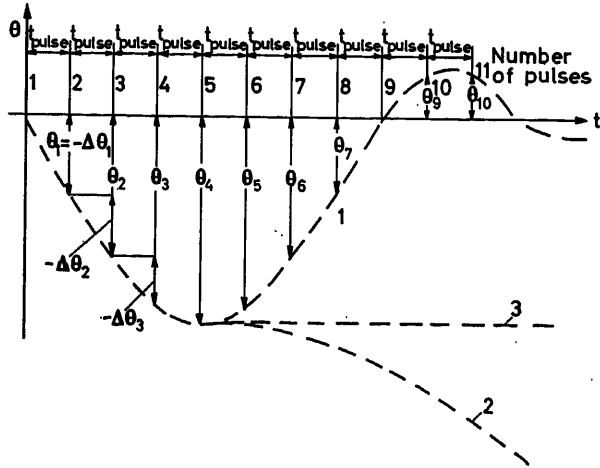


Figure 10. Variation of dynamic error in the process of run-up of the step-motor rotor

terminated by the criterion of stable operation of the motor in the first oscillation of the function $\theta = f(n)$.

The following proposition may serve as such a criterion; if during the run-up, when there takes place a process of increment of the error θ , the rotor, at the moment when switchings occur, does not enter the zone of excess braking torques (i.e., $\theta < |-\pi|$, which leads to a falling out of synchronism), the motor will attain in a speed at which the level of the error remains unchanged (Figure 10, curve 3) or decreases (Figure 10, curve 1).

Thus the criterion of stable operation of the motor in the first swing of the error will be

$$\theta_{n \max} \leq |-\pi + \theta_{\text{step}}| = \left| -\frac{\pi}{2} \right|$$

for a rectangular characteristic independent of the load.

In view of the above criterion, the rotor in the first period of the run-up will be under the influence of excessive accelerating torques, and will move in one direction. Therefore, eqn (4) will be re-written in the following form:

$$H \frac{d^2 \beta}{dt^2} + A \frac{d\beta}{dt} - 1 = -B \quad (5)$$

By solving this equation a formula is obtained from which

can be found $t_{u \min}$ and, hence, ΔNnp as well, if the load B and damping coefficient A are set.

$$\pi - \theta_{\text{step}} + \frac{H}{A} \left\{ \left(\frac{\theta_{\text{step}}}{t_{u \min}} - \frac{1-B}{A} \right) \ln \left[1 - \frac{\theta_{\text{step}} A}{(1-B)t_{u \min}} \right] - \frac{\theta_{\text{step}}}{t_{u \min}} \right\} = 0 \quad (6)$$

for $A = 0$

$$\Delta Nnp = \frac{314}{\theta_{\text{step}}} \sqrt{\frac{2(1-B)(\pi - \theta_{\text{step}})}{H}} \quad (6a)$$

In such a form the resultant expressions, within the limits of the assumptions adopted herein, are suitable for calculations of the characteristic $\Delta Nnp = f(B)$ of other types of step motors, in which $\theta_{\text{step}} \neq \pi/2$.

For double-rotor and double-stator motors

$$\Delta Nnp = 355 \sqrt{\frac{1-B}{H}} \quad (\text{steps/sec}) \quad (6b)$$

As can be seen from formula (6a), the response of the motor will be the greater, the smaller the size of the step in electrical radians. In this case, however, there is a simultaneous increase of the dynamic errors which, as for example in reducer step motors³, can attain a magnitude of several steps.

Calculations and experiments show that the shape of the angular static characteristic is far from rectangular and in a number of cases is better approximated by a sinusoid or a triangle, although an analytical solution in the general form becomes impossible. Therefore, for motors with $\theta_{\text{step}} = \pi/2$ and a sinusoidal angular characteristic, the other assumptions being the same, a calculation was performed of the characteristic $\Delta Nnp = f(B)$ (Figure 11, broken line) on an MN-7 mathematical simulator, specially pre-set to solve this problem⁵.

In this case the initial equation was

$$\frac{d^2 \theta}{d\varphi^2} + 2\alpha \frac{d\theta}{d\varphi} - \sin \theta = -B \operatorname{sign} \left[\frac{d\theta}{d\varphi} \right] \quad (7)$$

which is obtained from eqn (5) via the substitution

$$\beta = \theta + n \frac{\pi}{2}; \quad t = \frac{\varphi}{\omega_0} = \frac{\varphi}{\omega_0}; \quad A = \frac{2\alpha}{\omega_0}$$

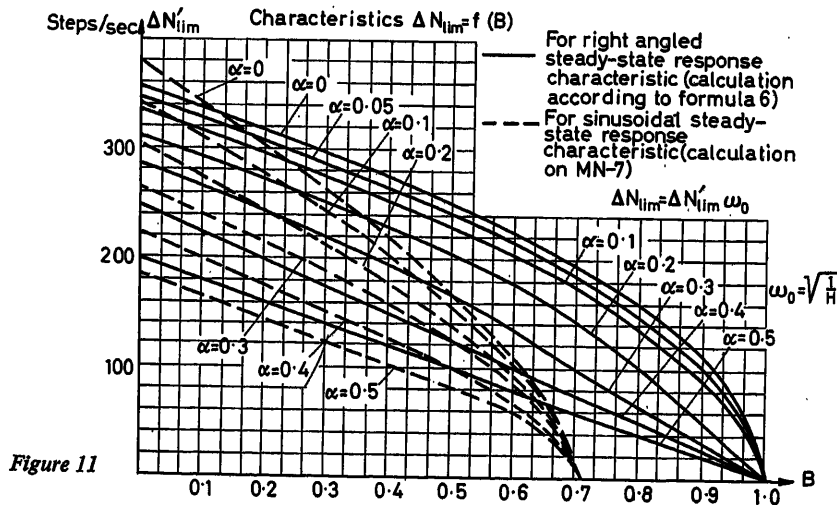


Figure 11

and of the rectangular characteristic by a sinusoidal one. The given equation is valid for one step ($n = 1$). In solving the next step new initial conditions obtained from the solution of the preceding step were each time introduced automatically:

$$\theta_{Hn} > \theta_{K n-1} + \frac{\pi}{2}; \left| \frac{d\theta}{d\varphi} \right|_{Hn} = \left| \frac{d\theta}{d\varphi} \right|_{K n-1}$$

The introduction of φ , which is proportional to the time, made it possible to impart a universal nature to the family of characteristics $\Delta N n p = f(B)$, since, calculated for $\omega_0 = 1$, they can easily be recalculated for other ω_0 by multiplication of $\Delta N' n p$ and α' by the new value of ω_0 :

$$\begin{aligned} \Delta N_{np} &= \Delta N'_{np} \cdot \omega_0 \\ \alpha &= \alpha' \cdot \omega_0 \end{aligned} \quad (8)$$

Approximate Calculation of the Characteristic $Nnp = f(M_H)$

When the limit tempo under conditions of synchronous revolution is considered, the rotor does not swing around the position of equilibrium, since the opportunity would always exist to reduce the time between two control pulses (t_u) to a value which would precisely equal the time needed by the rotor of the motor to traverse the angular step θ_{step} . This means that the rotor will operate on that section of the dynamic angular characteristic when over one step the maximum of electromagnetic energy is consumed and the initial conditions at each step will be the same. Moreover, in the testing of experimental models, unevenness of rotor travel practically disappears even in the absence of load, starting from approximately 75 steps/sec (Figure 12).

The motion of the rotor may therefore be assumed to be uniform, i.e.,

$$\frac{d\beta}{dt} = \text{const and } \frac{d^2\beta}{dt^2} = 0$$

Thus the energy brought to the rotor is expended electromagnetically on the performance of mechanical work.

$$\int_{\theta_H}^{\theta_H + \theta_{step}} M_g(\theta, t_u, T) d\theta = M_H \theta_{step} + D \frac{\theta_{step}}{t_u} \quad (9)$$

M_g is the total dynamic torque created by the two rotors of the step motor (or the dynamic angular characteristic). It depends on the error angle θ , is a function of a parameter of the step t_u and the time constant of the switched windings T . For a step motor controlled by means of simultaneous supply of the windings [Figure 2(b)], the expression of the dynamic torque has the form:

$$M_g = M_{\max} \sqrt{2} \left\{ \cos \theta - \frac{e^{-\frac{2t_u(\theta_0 - \theta)}{T_{\text{mean}} \pi}}}{1 + e^{-\frac{2t_u}{T_{\text{mean}}}}} \right\} \left[\cos \theta \left(1 - e^{-\frac{t_u}{T_{\text{mean}}}} \right) - \sin \theta \left(1 - e^{-\frac{t_u}{T_{\text{mean}}}} \right) \right] \quad (10)$$

Here, θ_0 is the angle corresponding to the load torque.

This formula is obtained on the condition that the angular steady-state response curve is sinusoidal, when the currents in the controlled windings rise and fall according to exponential relationships with some mean time constant T_{mean} , in which the parameters of the control circuit may also be taken into account.

The formula presupposes a periodic process of variation of the current for any relation between t_u and T_{mean} including when $T_{\text{mean}} \gg t_u$.

Having substituted M_g under the sign of the integral of formula (9), the electromagnetic energy used up on the performance of mechanical work is obtained after integration. The maximum of this energy will determine $t_{u \min}$

$$\frac{2\sqrt{2}}{\pi} M_{\max} \cdot K = \frac{D \cdot \pi}{2t_{u \min}} + M_H \quad (11)$$

where

$$K = \sqrt{(1-A)^2 + (1-c)^2}$$

$$A = \frac{2e^{-\frac{t_{u \min}}{T_{\text{mean}}}} \left(1 - \frac{2t_{u \min}}{\pi T_{\text{mean}}} \right) + \left(1 + \frac{2t_{u \min}}{\pi T_{\text{mean}}} \right) \left(1 - e^{-\frac{2t_{u \min}}{T_{\text{mean}}}} \right)}{\left(1 + e^{-\frac{2t_{u \min}}{T_{\text{mean}}}} \right) \left(1 + \frac{4t_{u \min}^2}{\pi^2 T_{\text{mean}}^2} \right)}$$

$$C = \frac{2e^{-\frac{t_{u \min}}{T_{\text{mean}}}} \left(1 + \frac{2t_{u \min}}{\pi T_{\text{mean}}} \right) - \left(1 - \frac{2t_{u \min}}{\pi T_{\text{mean}}} \right) \left(1 - e^{-\frac{2t_{u \min}}{T_{\text{mean}}}} \right)}{\left(1 + e^{-\frac{2t_{u \min}}{T_{\text{mean}}}} \right) \left(1 + \frac{4t_{u \min}^2}{\pi^2 T_{\text{mean}}^2} \right)}$$

Setting various values of M_H the required characteristic $\Delta Nnp = f(M_H)$ can be calculated for particular parameters

T_{mean} and D where $Nnp = \frac{1}{t_{u \min}}$ steps/sec.

The theoretical conclusions obtained were for the most part checked experimentally on double-rotor and double-stator step motors. Table 1 gives the calculated and experimental findings

Table 1

2-stator step motor $M_{\max} = 2,700$ gcm;
 $\theta_{step} = 22.5^\circ$, $2p = 8$; $Jp = 0.5$ gcm/sec²;

$D \cong 3$

J_{add} (gcm/sec ²)	ΔNnp experimental	ΔNnp calculated
0	154	164
1.18	77.5	89
2.1	59	72
3.94	45	55

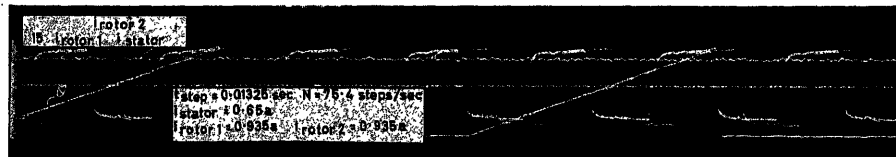


Figure 12. Oscillogram: idle running of 2-rotor step motor

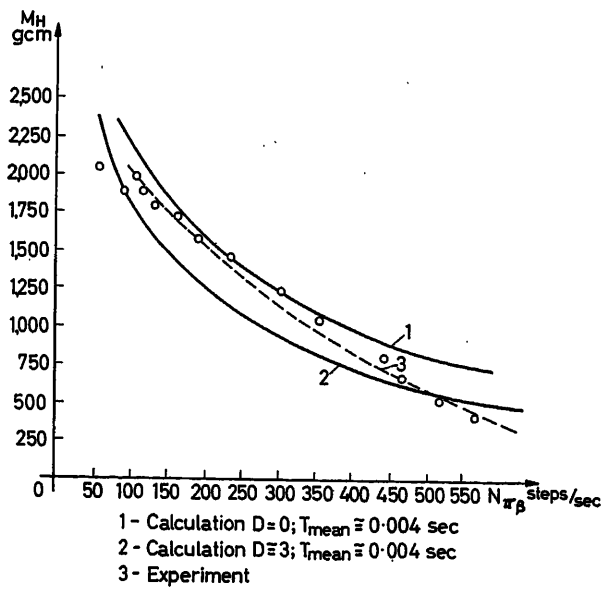


Figure 13. Torque vs. frequency characteristic of synchronous operation of 2-rotor step motor

for the values of ΔNnp under no load and for various additional flywheel masses, while Figure 13 shows the calculated and experimental characteristic $Nnp = f(M_H)$

The calculations were performed in accordance with formulas (6) and (11), with a thyatron translator; a rope brake and scales were used for the experiments.

References

- ¹ IVOBOTENKO, B. A. Step electric motors. *Elekt.* No. 8 (1960)
- ² RATMIROV, V. A. Step motors in programme control systems. *Elekt. priborostroi.*, No. 23 (1960)
- ³ VASILIEV, YU. K., PROKOFIEV, YU. A., and WAINBERGER, G. YA. Step motors. *Automat. priborostroi.*, No. 1 (1961)
- ⁴ FILCHAKOV, P. F., and PANCHISHIN, V. I. The EGDA-6/53 Integrator. *Akad. Nauk. Ukr. S.S.R.*, Kiev (1955)
- ⁵ FILIPOVICH, E. I., PROKOFIEV, YU. A., and BUNCHUK, G. M. A study of step motors. *Automat. priborostroi.*, No. 3 (1961)
- ⁶ THOMAS, A. G. Step motor used in digital positioning control. *Elect. Manuf.* 56 (1955)

ELECTRONIC COMPONENTS

Some New Control Circuits Using Four-layer $p-n-p-n$ Semiconductor Triodes

J. Š. HAŠKOVEC and A. KLÍMEK

Summary

The properties of four-layer $p-n-p-n$ triodes are considered, and form the basis for the design of new control circuits using these triodes. The first group of these includes networks with series-connected rectifier bridge circuits using $p-n-p-n$ triodes for the stepwise control of output voltage. The second group is made up of single- and three-phase networks in which only one of a group of $p-n-p-n$ triodes is controlled by the external control circuits. The triode losses in the various control circuits are compared.

Sommaire

On examine les propriétés des triodes à quatre couches $p-n-p-n$, en vue de former de nouveaux circuits de commande. Le premier groupe de ces circuits concerne des réseaux de ponts avec des redresseurs montés en série et utilisant des triodes $p-n-p-n$ pour la commande à échelons de la tension de sortie. Le deuxième groupe concerne des réseaux mono- et triphasés dans lesquels seulement l'une des triodes $p-n-p-n$ est commandée par un circuit externe. On compare les pertes à travers les triodes dans les différents circuits de commande.

Zusammenfassung

Die hier betrachteten Eigenschaften der steuerbaren $p-n-p-n$ Vierschichten-Trioden bilden die Grundlage für den Entwurf neuer Schaltungen für die Regelungstechnik. Die erste Gruppe derartiger Schaltungen betrifft Netzwerke von in Reihe liegenden Gleichrichterbrücken; dabei werden die steuerbaren Siliziumzellen für die stufenweise Steuerung der Ausgangsspannung verwendet. Die zweite Gruppe besteht aus Wechsel- und Drehstromnetzwerken, bei denen aus einer Gruppe von steuerbaren Siliziumzellen nur eine vom außenliegenden Steuerkreis betätigt wird. Die Verlustleistungen der Zellen in den verschiedenen Reglerschaltungen werden verglichen.

Four-layer $p-n-p-n$ Semiconductor Triodes and their Properties

The operation of four-layer $p-n-p-n$ triodes in electrical circuits is analogous in nature to that of a controllable gas-discharge rectifier, as for example a thyatron. They differ from the conventional controllable gas-discharge rectifiers by certain advantages. In the first instance these are the low voltage drop across the rectifier in the conducting state (of the order of 1 V),

the increased permissible working temperature, and following from this the substantially smaller dimensions and weight. The small losses, together with the fairly high inverse voltage (of the order of hundreds of volts), lead to a high efficiency in control circuits. Advantages are the instantaneous readiness for operation and the very high power gain. Four-layer triodes are now being produced for currents from 1 to 200 amps and voltages from 20 to 800 V, which completely satisfies the requirements for most circuits to control electrical energy in industrial automatics.

For control, four-layer triodes make use of the variations in transmission properties of junction Π_2 (see Figure 1), which is reverse-biased. This change is brought about by the effect of the currents in the adjacent junctions Π_1 and Π_3 . For clarity, in the rest of this paper, the four-layer triode is represented by an equivalent circuit containing two complementary transistors, a $p-n-p$ and an $n-p-n$, connected as shown in Figure 1 (a)^{1, 2}. Figure 1 (b) shows the electron currents (white arrows) and hole currents (black arrows) when the triode is forward-biased. Using this representation, equations can be written down for the currents in the steady state. Thus, for example, the current of electrons disappearing in the base n through recombination is equal to the current of electrons flowing into the base n , represented by the currents $\alpha_{npn}(I + I_y)$ and I_{co}

$$(1 - \alpha_{pnp})I = \alpha_{npn}(I + I_y) + I_{co}$$

or after rearrangement

$$I_{co} = I[1 - (\alpha_{pnp} + \alpha_{npn})] - \alpha_{npn}I_y \quad (1)$$

The right-hand side of eqn (1) depends only on the current I and I_y . Here it must be borne in mind that α_{pnp} and α_{npn} are non-linear functions of the current I . The left-hand side of eqn (1), I_{co} , depends on the voltage across junction Π_2 . This relation also is non-linear². Figure 1 (c) shows the resultant external characteristic for the four-layer triode with $I_y = \text{const}$. With forward bias, this characteristic has a section OA where

$$\alpha_{pnp} + \alpha_{npn} < 1 \quad \text{and} \quad I_{co} > 0 \quad (2)$$

and at the point B

$$\alpha_{pnp} + \alpha_{npn} = 1 \quad \text{and} \quad I_{co} = 0 \quad (3)$$

For the section BC one has

$$\alpha_{pnp} + \alpha_{npn} > 1 \quad \text{and} \quad I_{co} < 0 \quad (4)$$

i.e. I_{co} flows in the conducting direction of the four-layer triode.

In the further section BC , the voltage drop over the four-layer triode approaches the value of the drop across a single p - n junction, since the current flowing exhausts all the carriers existing near junction Π_2 , and so this junction is biased in the opposite sense to Π_1 and Π_3 , which are forward-biased.

For the four-layer triode to be cut off (transition to the non-conducting state), the current I must become less than I_h [Figure 1 (c)] for zero I_y . In a.c. circuits this condition is fulfilled by the current through the rectifier falling to zero at a certain part of the period.

If the four-layer triode is connected in a circuit carrying a current that does not decrease to zero under the influence of external conditions, then it can be cut off by deionization of junction Π_2 (removal of excess carriers). This can be achieved by applying a negative control current

$$-I_y = I \frac{(\alpha_{pnp} + \alpha_{npn}) - 1}{\alpha_{npn}} \quad (5)$$

Since in the conducting state $\alpha_{pnp} \approx 1$, the control current necessary for deionization

$$|I_y| \approx I$$

This clearly requires a high-power source for the control current.

Only circuits with a.c. supply are considered in the rest of this paper. In these cases the control current only switches on (fires) the four-layer triode, and its source power is much less, and the control current only amounts to a fraction of a per cent of the nominal four-layer triode current.

Basic Circuits for Controlled Rectifiers

Figure 2 shows the basic triode control circuit.

The control voltage U_y is applied between the control electrode and the cathode of the controlled rectifier 1, which is connected between the load 2 and the voltage source U . An impedance 4 (normally a resistor or a diode) is included in the control circuit.

The control pulse generator may be built from the circuits that are used to provide the control grid voltage for gas-discharge and mercury rectifiers with positive firing characteristic, but it must not generate negative-going pulses. If this requirement complicates the design, then one can simply connect a low-power diode 6 in parallel with the control junction, as shown by the dotted line in Figure 2.

The control pulse power is determined by the magnitude of the control current and the voltage of the pulse generator. This voltage must be of the order of several volts. The control current must be greater than the value at which

$$\alpha_{pnp} + \alpha_{npn} > 1$$

and is a fraction of a per cent of the nominal rectifier current. Here the control voltage may be either alternating or pulsed, synchronized with the rectifier anode voltage, high-frequency, or direct voltage.

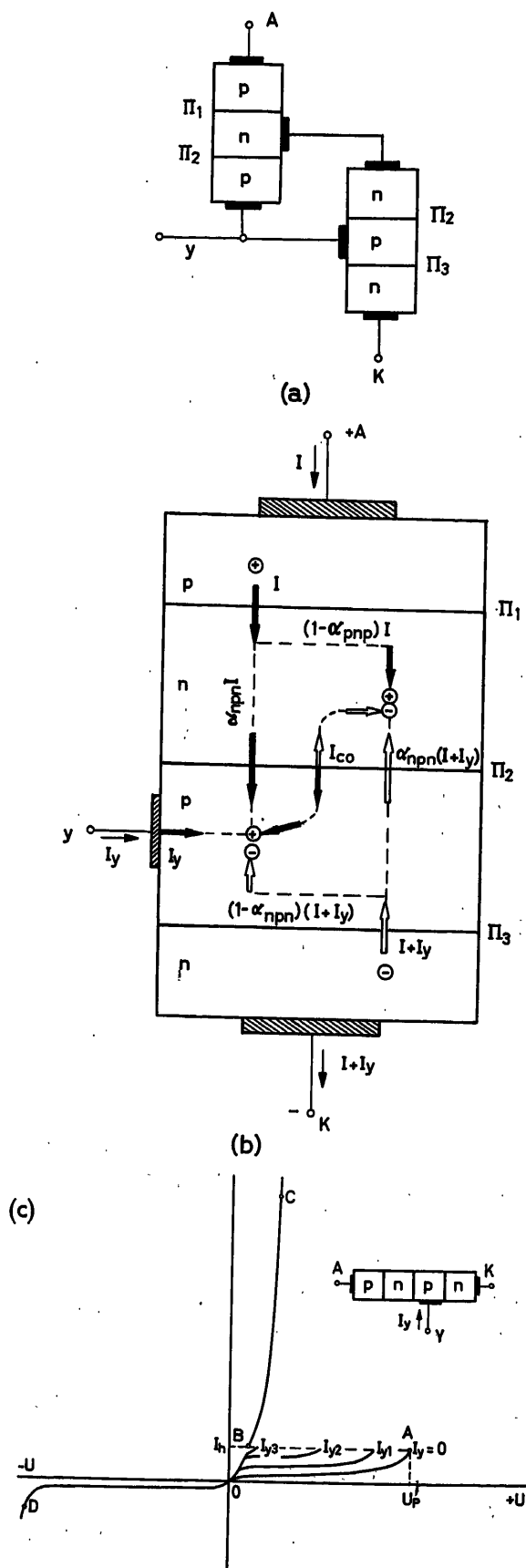


Figure 1

Continuous control is achieved by varying the phase of the synchronous control voltage in relation to the anode voltage. Discrete control is obtained by discrete switching in or out of the control voltage. A d.c. or high-frequency control may be used in those circuits where after the switch-on (firing) of the controlled rectifier the reverse voltage on the non-conducting recti-

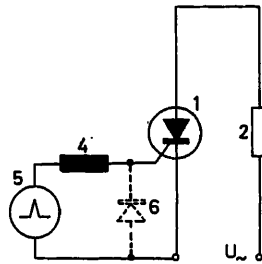


Figure 2

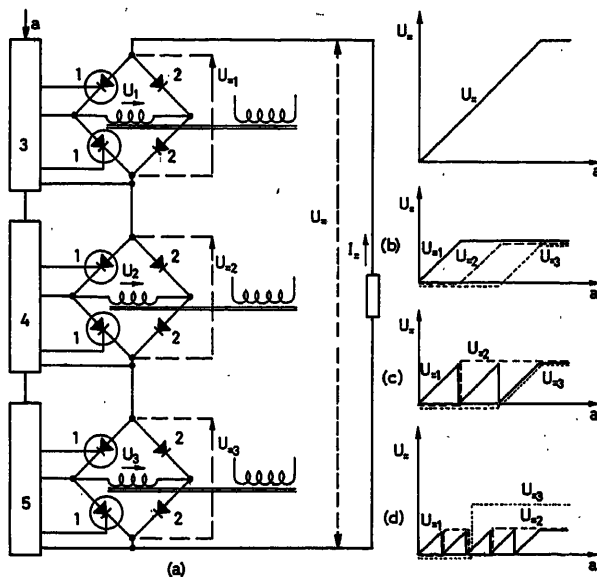


Figure 3

fiers falls to zero, i. e., the permissible reverse voltage decreases considerably when control current is applied.

Semiconductor controlled rectifiers can be used in all known rectifier and converter circuits, both single-phase and multi-phase, and the corresponding single- and multi-phase control voltage generator circuits can be employed. In this paper particular attention is drawn to those circuits that can be used by virtue of the special properties of semiconductor controlled rectifiers.

Special Control Circuits

As distinct from conventional circuits using gas-discharge rectifiers, here series connection of controlled rectifiers becomes of great importance, since the low voltage drop across them (about 1 V) makes the switching possible without loss of efficiency.

As an example, Figure 3 (a) shows a circuit with series-connected bridge rectifiers. This circuit has certain special features. The mean rectified voltage is the sum of the mean rectified voltages of the individual bridges, independently of

phase shifts in the voltages supplying the individual bridges. If the voltages across the secondary windings of the transformer are U_1 , U_2 and U_3 , then maximum ideal rectified voltage U_m is given by:

$$U_m = 0.9 (U_1 + U_2 + U_3)$$

irrespective of whether U_1 , U_2 and U_3 are in or out of phase with one another. When working from a three-phase supply there is a considerable reduction in the ripple, which equals that for six-phase rectification provided all the voltages are equal.

A second feature is the facility for gradual control of individual bridges. This method combines the advantages of continuous grid control with those of stepwise control by means of a switch bringing in taps on the secondary winding of the supply transformer. It substantially reduces the reactive power consumption (increases $\cos \varphi$) as compared with grid control, and removes the tap switch, whose function is performed by controlled rectifiers.

A third feature is the reduction in the number of controlled rectifiers 1, since the second half of the bridges is made up of normal non-controlled diodes 2, which form the network carrying the load current during the intervals when the controlled rectifiers in the adjacent arms of the bridge are cut off.

Thus, if for example the controlled rectifiers in one of the bridges are cut off, then the full load current flows through the normal rectifiers of that bridge. This means that they must be chosen so that their maximum operating current is equal to the load current I_m . However, it is sufficient to choose the controlled rectifiers so that their maximum operating current is $I_m / \sqrt{2}$, since current does not flow through these rectifiers for more than half the period.

The maximum inverse and cut-off voltage of all the rectifiers should be chosen to be greater than the maximum value of the corresponding supply voltage, for example $\sqrt{2} U_1$.

The control pulse generators 3, 4 and 5 may be connected in various ways. For example, continuous control may gradually be applied to one generator after another as shown in Figure 3 (b). Another possibility is for only one generator to have the facility for continuous control, the rest being able to control discretely by switching the corresponding bridge rectifiers on or off. Figure 3 (c) gives a diagram of this stepwise control. This control method can be slightly further modified by choosing values of the supply voltages for the individual bridges so that they form a geometric series. This variant is shown in Figure 3 (d).

Such a method of control is an approach to digital voltage control. The limited space of this paper does not allow the consideration of all the variants of this form of control. One circuit only is shown, whose mean rectified voltage is controlled according to a binary-decimal code [Figure 4 (a)]. A feature of this circuit is the minimal number of rectifiers and supply transformer windings. Each rectifier is controlled independently, in such a way that for certain values of voltage only half-bridges are in action. The load on the supply transformer in these cases is asymmetrical, and so its core saturates. This fact must be taken into account in the design, though at low powers it does not give rise to any particular problems.

Figure 4 (b) shows the binary-decimal code used, with weights 3, 3, 2 and 1, and the form of the rectified voltage. The mean value of this voltage is

$$U_m = 0.45 (3 a_3 + 3 a_2 + 2 a_1 + a_0) U = 0.45 b U$$

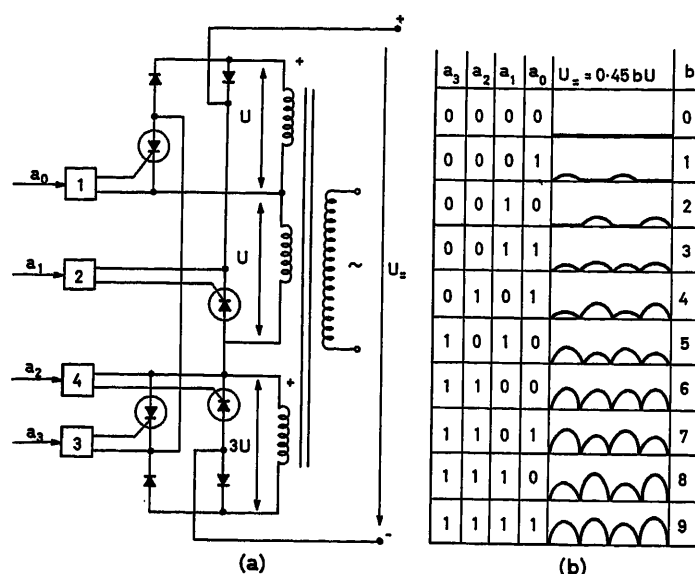


Figure 4

Of course one can design circuits along the same lines with different sorts of code, for example 1, 2, 2, 4; 1, 2, 4, 4. etc.

Controlled rectifiers also have a wide range of application in a.c. circuits. Apart from the circuits familiar from the application of ignitrons as a.c. switches, the special properties of controlled rectifiers permit the design of simplified circuits suitable for controlling electromagnets, motors and other final control elements operating from a.c. sources.

Figure 5(a) shows a circuit with a single controlled rectifier 1^8 which gives good control of an alternating current at any loading. The permissible operating current of the controlled rectifier should not be less than the load current I_{\sim} . However, the permissible operating current of the rectifiers forming the bridge may be taken as $I_{\sim}/\sqrt{2}$, since the current passes through them for no more than a half-period.

The inverse voltage on these rectifiers equals the cut-off voltage of the controlled rectifiers, i.e. $\sqrt{2} U$. A feature of the circuit is that the inverse voltage on the controlled rectifier is zero. Control is achieved by an a.c. voltage at the same frequency,

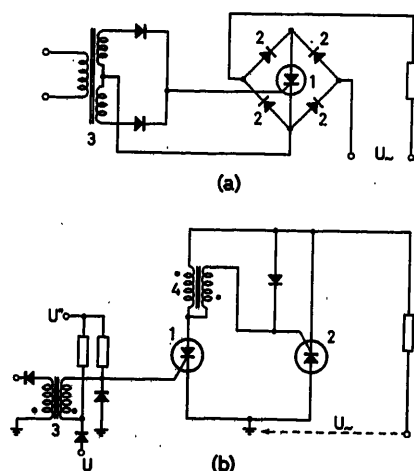


Figure 5

by variation of phase (for continuous control) or amplitude (for discrete control). In this case one may also use a control voltage at a higher frequency.

This circuit is only of significance when the controlled rectifier is more expensive than four normal rectifiers. But its losses are two or three times greater than those of the circuit shown in Figure 5(b). This circuit is designed for discrete control, and its first controlled rectifier 1 is controlled, for instance, from a standard magnetic logic element^{4,5}. This is permissible where one pole of the source of the a.c. voltage U_{\sim} may be connected to the common line of the logic elements. If that is not allowed, an isolating transformer must be used analogous to transformer 3 in Figure 5(a). The second controlled rectifier 2 is controlled by the voltage from the secondary of the control transformer 4 when the current through rectifier 1 falls to zero. Thus rectifier 2 always switches on at the instant when the load current passes through zero, irrespective of its phase. Under these conditions the power in the control pulse is very small, and similarly the dimensions of transformer 4 are very small.

This method of control has been given the name 'segmental control'.

The permissible operating current of each controlled rectifier is chosen, as is known, to be not less than $I_{\sim}/\sqrt{2}$, and the maximum, inverse and cut-off voltage is $U_{\sim}/\sqrt{2}$.

The principle of segmental control also simplifies control in three-phase circuits. Figure 6(a) shows a circuit which has half the rectifiers of the normal circuit with two rectifiers in each phase. Since the rectifiers are delta-connected, they can only be used with a star-connected load where the common point can be disconnected.

A feature of this circuit is that the current flows through each controlled rectifier only for two-thirds of a period, and that the instant when any of the rectifiers ceases to conduct coincides with the switching-on of the next one, so that the principle of segmental control may be applied [Figures 6(b) and (c)].

The permissible operating current I_v of a single rectifier should not be less than the effective current $I_{v\text{eff}}$ through the single rectifier

$$I_{v\text{eff}} = \sqrt{\frac{(I_{\sim}\sqrt{2})^2}{\pi} \int_0^{2\pi} \sin^2 |\omega t| d|\omega t|} = 0.97 I_{\sim}$$

The maximum inverse voltage on the rectifiers is $\sqrt{2} U_{\sim}$, where U_{\sim} is the supply voltage.

If one compares these figures with the analogous one for the circuit in Figure 5, connected to two phases of a three-phase load, one finds that the three-phase controlled power P in proportion to the number of rectifiers used is, for the circuit of Figure 6,

$$P = \frac{\sqrt{3}}{3} I_{\sim} U_{\sim} = \frac{1}{3} \cdot \frac{\sqrt{3}}{\sqrt{2}} \cdot \frac{I_v U_v}{0.422} = 0.97 I_v U_v$$

while for the Figure 5 circuit in two phases

$$P = \frac{\sqrt{3}}{4} \cdot \frac{\sqrt{2}}{\sqrt{2}} \cdot \frac{I_v U_v}{0.433} = I_v U_v$$

From a comparison of these results one concludes that the circuit in Figure 6 is practically equivalent to that in Figure 5 controlling two phases of a three-phase load, as far as ideal power is concerned. But it is simpler from the point of view of

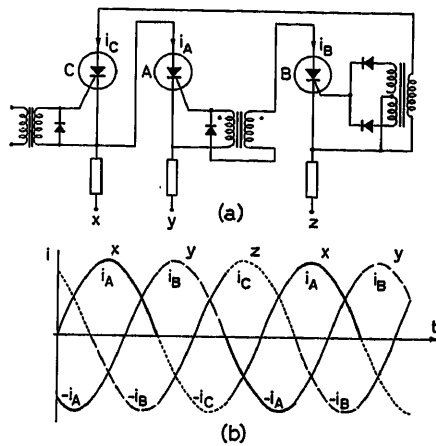


Figure 6 (a, b)

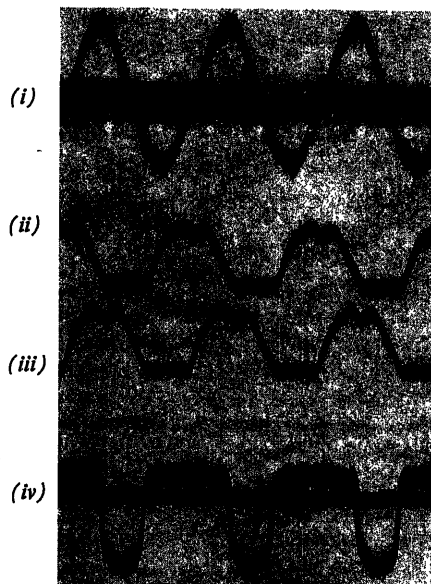


Figure 6 (c)

- (i) Load voltage, Z phase
(ii) Current through rectifier A
(iii) Current through rectifier B
(iv) Anode-cathode voltage on rectifier A

control. The maximum inverse and cut-off voltage is $\sqrt{2} U_{\sim}$, where U_{\sim} is the supply voltage.

Attention should be drawn to yet another feature of the operation of controlled rectifiers. For correct operation their current should be greater than a certain value I , i.e. the load resistance should be less than a certain value. This property justifies the use of segmental control, which also requires the load current to be greater than a certain value.

Of course a cut-off controlled rectifier passes a leakage current of the order of 10^{-4} of its forward current, and hence it is not equivalent to an open contactor. During repair or other work on the load circuit one must either operate a special isolating switch or, more simply, remove the fuses.

Conclusions

The application of contactless controlled rectifiers to control circuits offers new possibilities of improving the life and reliability of control installations. Apart from the reduction in maintenance expenses, the comparable high cost of these rectifiers is also offset by the fact that their very small size and insensitivity to the effect of their surroundings allow them to be located close to the installation being controlled, so that the quantity of power cabling can be substantially reduced and special contactor rooms completely eliminated. This gives a further economy in plant construction.

Their functional advantages are lack of inertia, absence of wear at any frequency in the operating range, and very high gain. These advantages indicate their use in pulsed and discrete regulation and control systems, and allow their control circuits to be greatly simplified.

References

- EBERS, J. J. Four-terminal *p-n-p-n* transistors. *Proc. Inst. Radio Engrs*, N. Y. 40, No. 11 (1952) 1361-1364
- GERLACH, W. and SEID, F. Wirkungsweise der steuerbaren Siliziumzelle. *Elektrotechn. Z.* A 83, No. 8 (1962) 270-277
- PITTMAN, P. F. The transistor switch—a solid-state power relay. *Inst. Radio Engrs*, N. Y., *Trans. Nucl. Sci.* NS 6 No-2 (June 1959) 69-73
- VASILEVA, N. P. and HAŠKOVEC, J. Š. A magnetic logic element performing the function of implication. *Automat. Telemekh., Moscow* 1 (1962) 57-63 (in Russian)
- KLÍMEK, A. and HAŠKOVEC, J. Š. Electronic final control elements with silicon controlled rectifiers *p-n-p-n*. *Automatizace, Prague* 6 (1963) 29-36 (in Czech)

DISCUSSION

A. W. WIEGAND, A.E.G. Industrieanlagen, 1 Berlin 33, Charlottenbrunnerstr. 1, Germany

The first group of the connections, i.e. networks with series connected SCR, will soon be of great importance for power rectifiers.

For a two-phase supply the connection of Figure 3 will be applied, but when working from a three-phase supply for power supply applications, it is more useful to connect six-phase bridges in series.

For better efficiency and power factor improvement it is recommended that a series connection of two- (or an even number) of six-phase bridges should be made, half of which are fully controlled (Bedford connection). Thus it is possible to get zero voltage when the controlled bridge is working with full phase retard (inverter operation).

H. WEED, 2024 Neil Avenue, Columbus, Ohio, U.S.A.

The authors are to be complimented on their attempt to summarize in a brief form a few of the control circuits making use of one or more 'controlled rectifying devices'. It seems possible, however, that they may well be over-enthused by the catch phrase of 'semiconductor triode' or 'solid state controlled rectifier' and have really not presented much truly new material or in fact separated the properties and capabilities of 'solid state controlled rectifiers' from their older prototype, the thyatron and ignitron.

The title, 'New Control Circuits ...,' suggests the latest or perhaps as yet unpublished ideas. After an introduction which repeats material readily available in many textbooks and manufacturers' literature, General Electric Controlled Rectifier Manual, 1960 or 'Transistor

Circuit Analysis, Fitch, 1960, reference is made to 'special circuits', of which the paper then considers only three or four. Unfortunately, there seems to be nothing 'special' or 'new' about these circuits, and nothing about them that prohibits or precludes their use with thyratrons or ignitrons.

Referring to *Figure 3*, a question arises concerning the statement that the three separate bridges, each requiring two controlled rectifiers and two diodes, apparently require a smaller total number of controlled rectifiers than a conventional three-phase full-wave bridge circuit. It appears rather obvious that a controlled six-phase bridge, requires only three controlled rectifiers and three diodes as compared to the six plus six of this circuit.

A reference is also made that 'the special properties of controlled rectifiers permit the design of simplified circuits suitable for controlling electromagnets, motors and other active elements operating from a.c. sources'. The word 'simplified' here may mean many things, but seems misleading if suggesting that the SCR circuits will be appreciably easier to build, understand or design. The lack of a filament voltage

and lower forward voltage drop are their only claim to fame for which must be substituted a power control signal *versus* voltage only, large variation in the required gate current from unit to unit, the inability to withstand any negative gate voltage or any overrated anode voltage. It is not the opinion of this writer that this represents a simplification.

Figure 5 (a) is suggested as giving 'good control of an alternating current at any loading'. Since this circuit places the SCR in the d.c. portion of a simple bridge circuit, the a.c. of the line appears rectified to the SCR. Certainly this circuit is not 'new', having appeared in various publications such as General Electric Controlled Rectifier Manual, 1960 and Electro-Technology.

In general there are few errors in the paper and it is concisely written, but seems to provide only a partial and sometimes misleading review of a few well-used circuits. Some truly 'new' control circuits such as an a.c. excited transistor current source, or unijunction discharge circuit, are not mentioned.

Turn-off Silicon Controlled Rectifiers

H. F. STORM

Summary

The term 'turn-off silicon controlled rectifier' (SCR) is used for a four-layer switch which can be triggered on by a control pulse of one polarity, and triggered off by a control pulse of opposite polarity. Ordinary SCRs can be triggered off only for small load currents, that is, currents in the vicinity of 1 per cent of rated current. This limitation is introduced by a turn-off gate current having the same order of magnitude as the current to be interrupted. Under these conditions, gate turn-off becomes impractical because of excessive demands on the control source, current overloading of the gate structure, and a large transverse voltage drop in the gate layer which defeats the turn-off process.

The key problem consists in reducing the turn-off gate current relatively to the load current; in terms of the reciprocal quantity, namely the turn-off current gain, the problem consists in increasing the turn-off current gain of the SCR.

Such an increase can be accomplished (a) circuit-wise, (b) by junction modification. The case (a) is demonstrated by type 3 N 60 (an npn diffused base transistor with a third junction, and four leads). This type interrupts 40 V, 20 mA circuits with turn-off current gains of 1,000 and more. The switching times are in the 1 μ sec class. The case (b) is demonstrated by a three-lead type ZJ 224 (an all-diffused structure with three leads). This type interrupts 500 V, 1 amp circuits with turn-off gains of approximately 20. The switching times are in the 3 μ sec class. From these measurements and from theoretical considerations it is concluded that SCRs for much larger current ratings are feasible, and one anticipated structure is shown.

Among the uses of turn-off SCRs are logic and control circuits, inverters without or with greatly reduced commutating components, new techniques for the control of rectifiers and power converters.

Sommaire

Le terme «diode contrôlée basculante à silicium» («turn-off» silicon controlled rectifier (SCR)) désigne une diode à couche quadruple dont la conduction peut être enclenchée par une impulsion de commande d'une polarité et déclenchée par une impulsion de commande de polarité inverse. Les SCR usuelles ne peuvent être déclenchées que lorsque le courant qui les traverse est faible, de l'ordre de 1 pour cent du courant nominal. Cette limitation provient de l'existence d'un courant de basculement qui est du même ordre que le courant à interrompre. Il en résulte que le déclenchement par basculement est inutilisable pratiquement car il nécessite une puissance excessive de la source d'impulsions de commande, conduit à une surcharge en courant de la texture de déclenchement et produit une chute élevée de la tension transversale dans la couche de déclenchement, chute qui perturbe le processus de basculement.

Le problème clé est de réduire le courant de basculement par rapport au courant traversant; autrement dit, en considérant les grandeurs inverses, notamment le gain en courant de basculement, d'accroître le gain en courant de basculement du redresseur commandé au silicium.

Un tel accroissement peut être obtenu: (a) par une conception adéquate du circuit; (b) par une modification de la jonction. Le cas (a) est illustré par un transistor 3 N 60 (qui a une base du type npn à diffusion, et qui est muni d'une troisième jonction et de quatre fils). Ce transistor est capable d'interrompre des circuits véhiculant 20 mA sous 40 V, avec des gains en courant de basculement de l'ordre de 1000 et plus. Les temps de commutation sont de l'ordre de 1 μ sec. Le cas (b) est illustré par un élément du type ZJ 224 (dont la structure entière est à diffusion et qui est muni de trois fils). Ce type d'élément est capable

d'interrompre des circuits véhiculant 1 A sous 500 V avec des gains en courant de basculement d'environ 20. Les temps de commutation sont de l'ordre de 3 μ sec. Ces résultats de mesures ainsi que des considérations théoriques permettent de conclure que des redresseurs commandés au silicium capables de manipuler des courants nominaux beaucoup plus élevés sont concevables; et on montrera, au cours de cette communication, une structure qui apparaît possible et qui a été conçue pour atteindre ce but.

Zusammenfassung

Der Ausdruck „abschaltbarer gesteuerter Siliziumgleichrichter“ wird hier für eine steuerbare Siliziumzelle benutzt, die ein Steuerimpuls mit einer Polarität einschaltet und ein Steuerimpuls mit entgegengesetzter Polarität abschaltet. Gewöhnliche steuerbare Siliziumzellen lassen sich für kleine Lastströme, die in der Nähe von 1 % des Nennstromes liegen, abschalten. Diese Beschränkung ergibt sich daraus, daß der Steuerstrom zum Abschalten (Abschaltsteuerstrom) dieselbe Größenordnung wie der zu unterbrechende Strom haben muß. Unter diesen Umständen wird die Abschaltung unpraktisch, erstens wegen der übermäßigen Anforderung an die Spannungsversorgung des Steuerkreises, zweitens wegen der Überlastbarkeit des Gitterkreises und drittens wegen des hohen Spannungsabfalles in der Gitterschicht, der den Abschaltvorgang erschwert.

Das Hauptproblem besteht darin, den Abschaltsteuerstrom, bezogen auf den Laststrom, zu verringern. Auf die reziproke Größe bezogen, nämlich die Abschaltsteuerstromverstärkung, besteht die Aufgabe in der Erhöhung der Abschaltsteuerstromverstärkung.

Eine Erhöhung der Verstärkung kann man a) durch geeignete Schaltungen oder b) durch Änderung der Schichten erreichen. Der Fall a) wird anhand der Type 3 N 60 gezeigt, die einen npn-Transistor mit eindiffundierter Basis und einem dritten Flächenübergang sowie 4 Anschlüssen darstellt. Diese Type schaltet 40 V Maschenspannung und 20 mA Kreisstrom bei einer Abschaltsteuerstromverstärkung von 1000 und mehr. Die Schaltzeiten liegen in der Größe von 1 μ s. Als Beispiel für den Fall b) wird die Type ZJ 224 mit drei Anschlüssen benutzt (hierbei handelt es sich um einen Diffusionstransistor). Diese Type schaltet 500 V Maschenspannung und 1 A Kreisstrom mit einer Abschaltsteuerstromverstärkung von ungefähr 20; die Schaltzeiten liegen in der Größe von 3 μ s. Auf Grund dieser Messungen und an Hand theoretischer Überlegungen wird gefolgert, daß für steuerbare Siliziumzellen wesentlich größere Nennströme möglich sind. Ihr voraussichtlicher Aufbau ist dargestellt.

Einige der Anwendungen der steuerbaren Siliziumzellen sind: Logische und Steuerschaltungen, Wechselrichter ohne oder mit stark verkleinerten Kommutierungselementen, neue Verfahren für die Steuerung von Gleichrichtern und Leistungswandler.

Introduction

The silicon controlled rectifier and transistor performs many switching functions in information and power circuits. The silicon controlled rectifier, abbreviated to SCR, has an advantage over the transistor in that the load current can be turned on by a control current pulse and remains on, whereas the transistor requires a continuous control current for the entire duration of

load current flow. On the other hand, the transistor has an advantage over the SCR, in that the load current flow can be stopped simply by interrupting the control current, whereas with the SCR it is necessary to reverse, at least temporarily, the terminal voltage; this process is called commutation and requires additional circuit components which add to cost, size, weight and losses.

The following describes a device, called a turn-off SCR, which combines the desirable control functions of SCRs and transistors: turn-off is achieved without commutating components, and only pulses are needed for turn-on and turn-off. Other designations for turn-off SCRs are found in the References, especially that by Harnden¹.

Junction Electronics

A p - n - p - n device, representing a silicon controlled rectifier (SCR) is shown schematically in Figure 1. If a current I_L is now

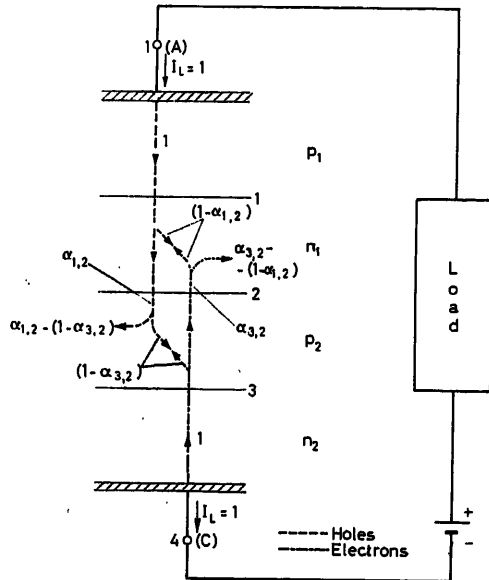


Figure 1. Carrier flow in a four-layer device assuming centre junction voltage negligible

permitted to flow through the SCR, an accumulation or depletion of majority carriers occurs in layers n_1 , p_2 at the rate r , as explained in Appendix I.

$$\text{If } r = [\alpha_{1,2} - (1 - \alpha_{3,2})] I_L \quad (1)$$

$$\text{If } \alpha_{1,2} - (1 - \alpha_{3,2}) > 0 \quad (2a)$$

r is positive, the SCR is in its low-impedance mode (also called forward-e.m.f. mode because the centre junction develops a voltage in the direction of the applied voltage). In this mode, the total voltage drop (over all three junctions) is in the vicinity of 1 V.

$$\text{If } \alpha_{1,2} - (1 - \alpha_{3,2}) < 0 \quad (2b)$$

r is negative, the SCR is in its high-impedance mode (also called counter-e.m.f. mode because the centre junction develops a voltage opposing the applied voltage). In this mode, the SCR passes only a very small current, called the forward leakage current²⁻⁴.

Gate Turn-off

Gate turn-off means the change from low-impedance to high-impedance mode by means of a gate current. It is assumed that the SCR is in its low-impedance mode. A gate current I_G is now withdrawn from terminal G , Figure 2, resulting in a carrier depletion at the rate r_d (Appendix II).

$$r_d = \alpha_{3,2} I_G \quad (3)$$

If $r_d = r$, the generation of the forward-e.m.f. is wiped out, and the stage is set for the development of a counter-e.m.f., and hence for turn-off. Substituting from eqn (3) into (1), one obtains for I_G ⁶⁻⁸:

$$I_G = \frac{\alpha_{1,2} - (1 - \alpha_{3,2})}{\alpha_{3,2}} I_L \quad (4)$$

For ordinary SCRs, eqn (4) indicates a turn-off gate current of about half the rated load current, and hence too large a gate current for practical purposes.

Turn-off Current Gain

The reduction of the turn-off gate current is one of the key issues in the design of turn-off SCRs (see Appendix III). In order to see the magnitude of the turn-off gate current I_G in its proper perspective, it is related to the load current I_L to be turned off, and expressed by the turn-off current gain K_I

$$K_I = \frac{I_L}{|I_G|} \quad (5)$$

From eqn (4)

$$K_I = \frac{\alpha_{3,2}}{\alpha_{1,2} - (1 - \alpha_{3,2})} \quad (6)$$

A high turn-off current gain can be accomplished by external circuitry (see 'Turn-off Current Gain Control by External Circuitry' and 'Experimental Results') and by internal junction design (see 'Turn-off Gain Current Control by Junction Modification').

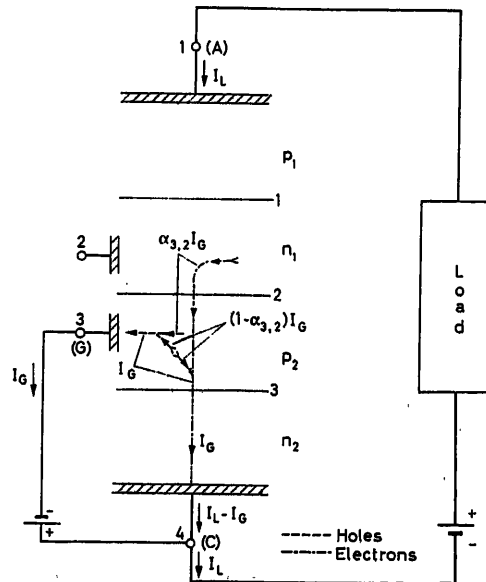


Figure 2. Carrier flow caused by gate current I_G , superposed on currents of Figure 1

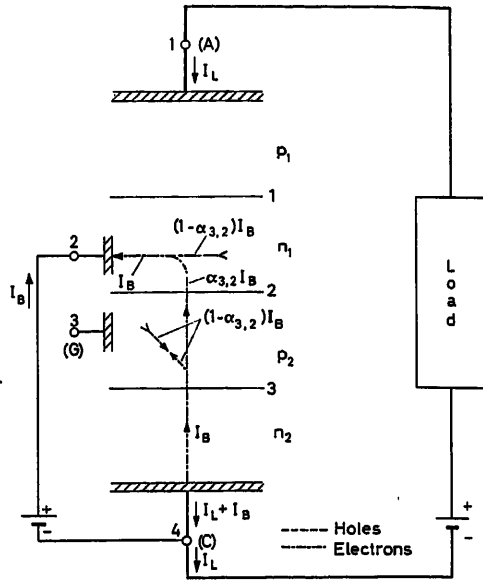


Figure 3. Carrier flow caused by bias current I_B , superposed on currents of Figures 1 and 2

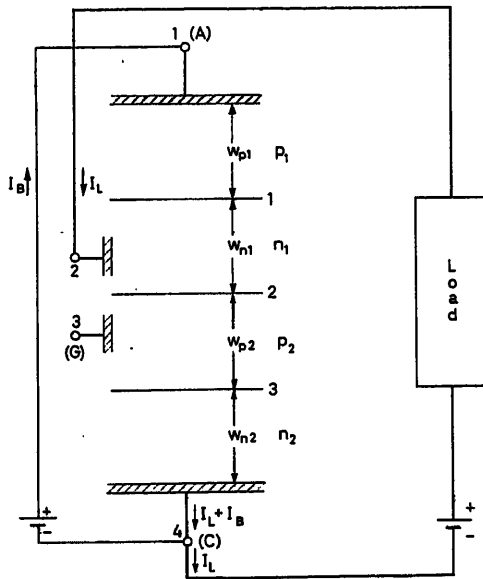


Figure 4. Connection of four-layer device, where load current connects to n_1 and bias current to p_1

Turn-off Current Gain Control by External Circuitry

Again, we start with the SCR in its low-impedance mode. Next a bias current I_B is fed into terminal 2 (Figure 3) and extracted from 4, corresponding to an electron current flowing internally from 4 to 2. The bias current I_B depletes the inner bases at the rate of $(1 - \alpha_{3,2}) I_B$. Now, the accumulation rate is only

$$r = \left[\alpha_{1,2} - (1 - \alpha_{3,2}) \left(1 + \frac{I_B}{I_L} \right) \right] I_L \quad (7)$$

and the turn-off current gain obtained for $r = 0$, equals

$$K_I = \frac{\alpha_{3,2}}{\alpha_{1,2} - (1 - \alpha_{3,2}) (1 + I_B/I_L)} \quad (8)$$

As expected, the turn-off gain has been increased over its previous value eqn (6). The bias current I_B provides additional loading of junctions 2 and 3, and hence I_B should be relatively small. It follows that this method for increasing the turn-off gain is most useful where $\alpha_{1,2}$ is only slightly larger than $(1 - \alpha_{3,2})$.

Suppose the connections between terminals 1 and 2 (Figure 4) are now switched. The resultant accumulation rate is obtained from eqn (7) by replacing I_L with I_B and vice versa

$$r = \left[\alpha_{1,2} - (1 - \alpha_{3,2}) \left(1 + \frac{I_L}{I_B} \right) \right] \left(\frac{I_B}{I_L} \right) I_L \quad (9)$$

From eqns (5), (9):

$$K_I = \frac{\alpha_{3,2}}{\alpha_{1,2} - (1 - \alpha_{3,2}) \left(1 + \frac{I_L}{I_B} \right)} \frac{I_L}{I_B} \quad (10)$$

For $I_B \ll I_L$, eqn (10) can be approximated by eqn (11)¹⁰

$$K_I = \frac{\alpha_{3,2}}{\alpha_{1,2} \frac{I_B}{I_L} - (1 - \alpha_{3,2})} \quad (11)$$

One concludes that very high turn-off gains can be produced by this method.

Experimental Results of the General Electric Type 3N60

The tested device¹¹ can be viewed as a diffused base $n-p-n$ silicon transistor, to which a junction (p_1) was added by pulse-welding an aluminium wire to the n_1 -bar 2 (Figure 5). Connected as in Figure 1, the 3N60 could be switched on by the gate with very high sensitivity but could not be turned off even when the gate voltage was reversed to -15 V (6 times max. rated).

Subsequently, the 3N60 was connected similarly to Figure 4, and shown in detail in Figure 6 (a). Load and bias currents were adjusted by resistors R_L and R_B . The gate current I_G was controlled by E_G and R_g , and the load current was triggered on by a positive gate supply voltage E_g .

In one series of tests, the load current I_L was kept constant at 20 mA, and the bias current I_B was varied. For each value of

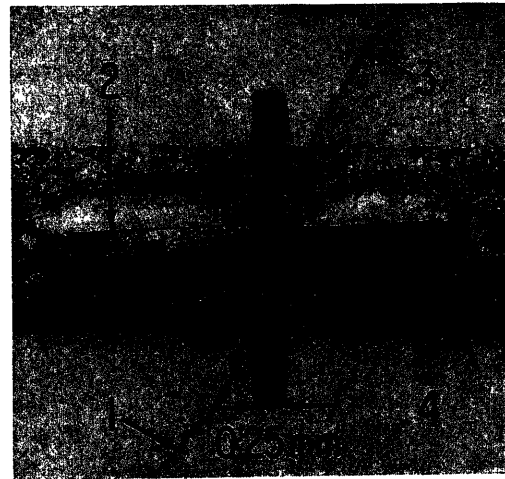


Figure 5. Junction arrangement of a type 3N60; the numbers designate the same terminals as in Figure 4

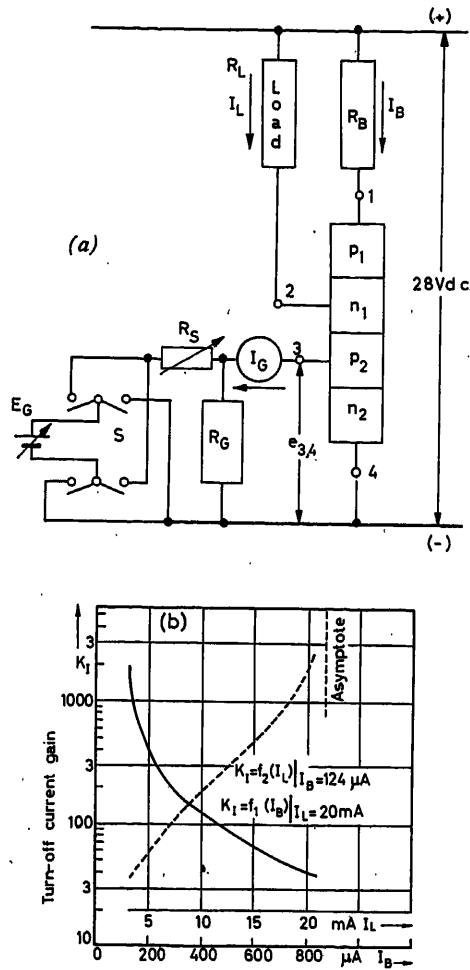


Figure 6. Switching characteristics of 3N60: (a) Test circuit; (b) Turn-off current gain K_I as functions of bias resistance R_B and load resistance R_L .

bias current, the turn-off gate current I_G was determined experimentally, and the turn-off current gain K_I calculated eqn (5). For instance, for $I_B = 800 \mu\text{A}$ the turn-off gate current was measured $I_G = -0.5 \text{ mA}$, and the turn-off current gain calculated, resulting in $K_I = 40$. A decrease of bias current results in a higher K_I , as seen by the experimental data $K_I = f_1(I_B)$ in Figure 6(b). Turn-off current gains of 1000 and more were measured. The required bias current for high values of K_I is less than 1 per cent of the load current.

Next, the bias current I_B was kept constant at $124 \mu\text{A}$, and the load current I_L was varied by means of R_L . For each value of load current, the turn-off gate current I_G was determined experimentally, and the turn-off current gain K_I calculated eqn (5). As expected from eqns (10) and (11), an increase of load current leads to an increase in K_I in the load current range where $I_L \gg I_B$. This expectation is borne out by measurements as demonstrated by curve $K_I = f_2(I_L)$ of Figure 6(b).

By increasing the load current to the point, where the denominators in eqns (10) and (11) approach zero ($r = 0$), the centre junction rapidly loses its forward-e.m.f., and hence the voltages of terminals 1 and 2 increase with respect to 4 [Figure 6(b)]. With a fixed bias resistance R_B , the voltage increase of terminal 1

reduces the bias current I_B . As seen from eqns (10) and (11) this reduction of I_B has a similar effect as an increase of load current I_L , leading to a closed-loop system which rapidly reduces the load current to less than $1 \mu\text{A}$. This type of turn-off, triggered by a reduction of the load resistance, is called load current self turn-off. In the case illustrated in Figure 6(b), load current self turn-off occurs at 21.5 mA , as indicated by the asymptote. The turn-on and turn-off switching times are in the $1 \mu\text{sec}$ class at 25°C .

If one inquires into the reverse voltage capabilities of the circuits shown in Figures 1 and 4, a reverse (inverse) supply voltage will be held across junctions 1 and 3 in Figure 1, but only across junction 3 in Figure 4, as far as blocking I_L is concerned. It follows that the reverse voltage ability, such as required in a.c. circuits, is smaller in the case of Figure 4. In fact, the usual values for junction conductivities and junction width permit the application of only a few volts across junction 3. One concludes that the ability to block a reverse voltage has been largely lost in the configuration of Figures 4 and 6(a). This ability, however, can be regained circuitwise by the insertion of a rectifier.

Turn-off Gain Current Control by Junction Modification

As seen from eqn (6), high turn-off gain is obtainable by reducing the current gain $\alpha_{1,2}$ to the point where it is only slightly larger than $(1 - \alpha_{3,2})$, as shown in the following.

If surface recombination is neglected, the current gain $\alpha_{1,2}$ becomes the product of emitter efficiency and transport factor².

$$\alpha_{1,2} = \left(1 - \frac{w_{n1}^2}{2D_h\tau_h}\right) \left(1 + \frac{w_{n1} \cdot \sigma_{n1}}{w_{p1} \cdot \sigma_{p1}}\right)^{-1} \quad (12)$$

One measure to reduce $\alpha_{1,2}$ is to decrease the width w_{n1} of layer p_1 ; this decrease, however, reduces the punch-through voltage, and hence reduces the reverse voltage ability of junction 1. This deficiency, however, can be compensated by inserting a rectifier into the circuit. Other modifications are known to improve the performance of turn-off SCRs⁸, but space limitations do not permit a further discussion.

The turn-off gain of an SCR (General Electric type ZJ 224¹³), an all-diffused structure whose p_1 layer is thinner than normal, is shown in Figure 7. At a load current of $I_L = 1 \text{ A}$, the turn-off gain is approximately 20. Although the turn-off gain is dropping for load currents from $I_L = 1$ to 0.01 A , the gate current which is sufficient for turning off $I_L = 1 \text{ A}$, is also sufficient for turning

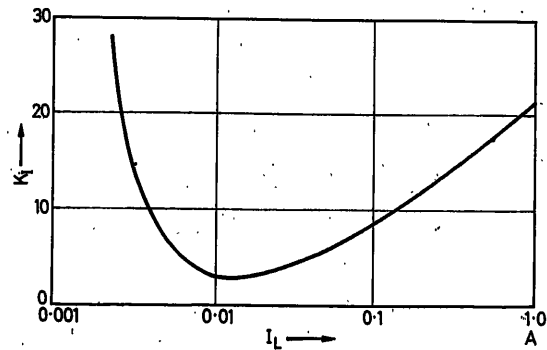


Figure 7. Turn-off gain of ZJ 224 (test results). For turn-on, $I_G = 10 \text{ mA}$.

off any smaller load current. The turn-on gate current is 10 mA, the holding current is 3 mA.

The type ZJ224 had a peak forward blocking voltage of 500 V and a peak reverse blocking voltage of 40 V. The forward and reverse leakage currents are in the 2–10 μA range. The turn-on and turn-off times were measured in the vicinity of 2 to 4 μsec respectively.

Transverse Gate Resistance

Suppose two SCRs with load current ratings of 2:1 are compared. The junction areas will be 2:1, but otherwise the two SCRs are stipulated to be alike. If the transverse gate resistances are negligible, the turn-off gains will be the same: the larger SCR, requiring twice the gate current for turn-off of rated current. The transverse gate resistance, however, is the same in both cases. It follows that the transverse voltage drop will be twice as high in the larger SCR, and hence the latter will be more reluctant to turn-off. The problem of transverse gate resistance also exists in power transistors. There, it has been solved, for instance, by interdigitated arrangements of base and emitter contacts¹³. This multiple contact arrangement is more costly because of the complexity of fabrication; it also reduces the load current rating by reducing the junction areas available for load current flow.

When considering a turn-off SCR for higher current ranges, the simple configuration of an ordinary SCR [Figure 8 (a)] is likely to be replaced by a transistor-like structure for the p_2 and n_2 layers. The entire structure of a turn-off SCR could be viewed as a power transistor ($n_1 p_2 n_2$), to which a fourth layer (p_1) has

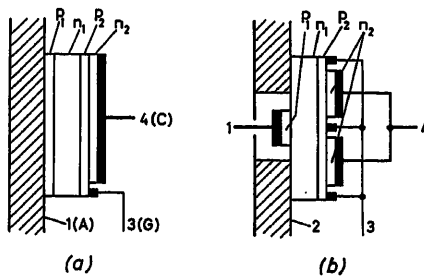


Figure 8. SCR configurations: (a) conventional; (b) has contact to n_1 -layer, and thus access to all layers

been added [Figure 9 (b)]. By providing electrical access to all four layers, such a device could be used as an ordinary power transistor, an ordinary SCR or as a turn-off SCR.

Applications

One application of the turn-off SCR is to act as a one-element flip-flop, akin to a latch-in type relay, whose contacts are closed by a positive pulse, and are opened by a negative one. Similar to the power dissipation and overvoltages which affect relay contacts during the interruption of a circuit, especially an inductive one, the turn-off SCR is subject to similar effects¹⁴.

Another application for turn-off SCRs is in inverters, dispensing with the customary commutating components for ordinary SCRs, and thus reducing cost, size, weight, and circuit complexity. One such inverter, utilizing two types 3N60 is shown in Figure 9 (a); its output voltage (E_o) is shown in Figure 9 (b).

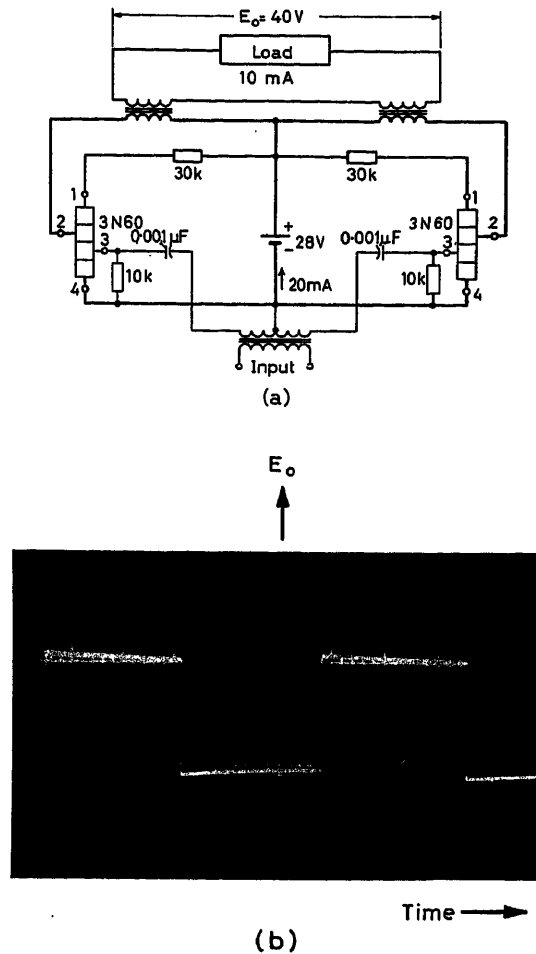


Figure 9. Inverter without commutating equipment: (a) circuit; (b) output voltage E_o at 100 c/sec

The relatively low carrier accumulations in turn-off SCRs not only facilitate turn-off by gate control, but also turn-off in general. An example is illustrated in Figure 10 (left), where a 3N60 is connected as an ordinary SCR, and switch S_1 is closed. If the 3N60 is to be turned off in the conventional manner by the commutating capacitor C_1 , the switch S is closed; to be effective in this circuit, C_1 must be equal to or larger than

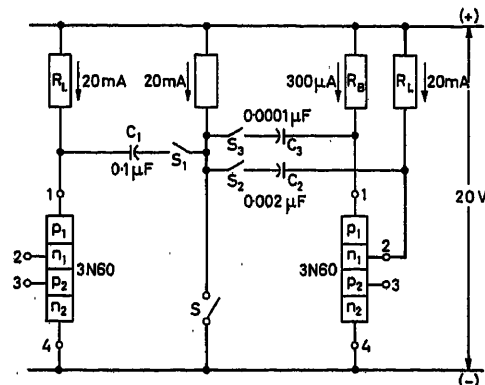


Figure 10. Test circuit to determine the minimum size of commutating capacitors

0.1 μ F. Then, the 3N60 was reconnected as in Figure 6 shown on the right-hand side of Figure 10. If commutated against terminal 2 (switch S_2 closed), the commutating capacitance could be reduced by a factor of 50, if commutated against terminal 1 (switch S_3 closed), the reduction factor was 1,000; only one of the two capacitors C_2 or C_3 is required. One concludes that turn-off SCRs are also very useful in circuits where gate turn-off is not intended, by sharply reducing the size, cost and losses of the commutating equipment.

A further property of the turn-off SCRs, which is also tied to the relatively low carrier accumulations, consists in a higher frequency capability of the turn-off device.

An entirely different utilization of the turn-off SCR consists in power factor improvement¹⁵. The lower the power factor, the poorer is the utilization of transmission equipment, and especially of alternators. By their very nature, power factor problems become important for large blocks of power.

Suppose one has an ordinary single-phase, phase controlled rectifier, and considers the supply voltage E and the primary transformer current I_p (Figure 11). Assuming a resistive load, ideal transformer and rectifier characteristics, E and I_p are in phase, but the power factor is not unity. This is evident from the fundamental component I_1 which is clearly lagging, and hence must possess a quadrature component I_q . While both the higher harmonics and the quadrature component cause a power loss all along the power circuits, it is the inductive, quadrature component which causes a further reduction in the utilization of the alternator by producing a field-weakening armature reaction, which must be overcome by a larger field structure and larger exciter.

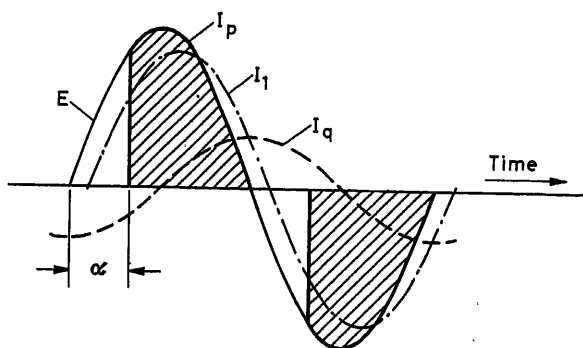


Figure 11. Rectifier with conventional phase control, supply voltage E and transformer primary current I_p ; I_1 is fundamental component and I_q is lagging quadrature component of I_p

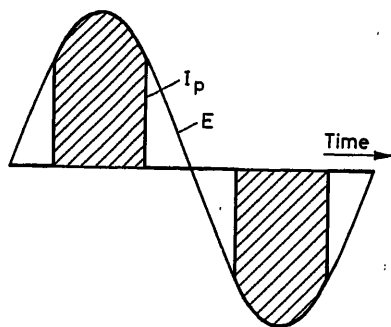


Figure 12. Rectifier circuit with turn-off SCRs. Supply voltage E and primary current I_p ; primary current I_p has zero quadrature component

With turn-off SCRs, the primary current blocks can be so shaped that a lagging power factor can be avoided (Figure 12). Moreover, turn-off SCRs can be controlled to deliver inductive quadrature power to the power system. The latter case is demon-

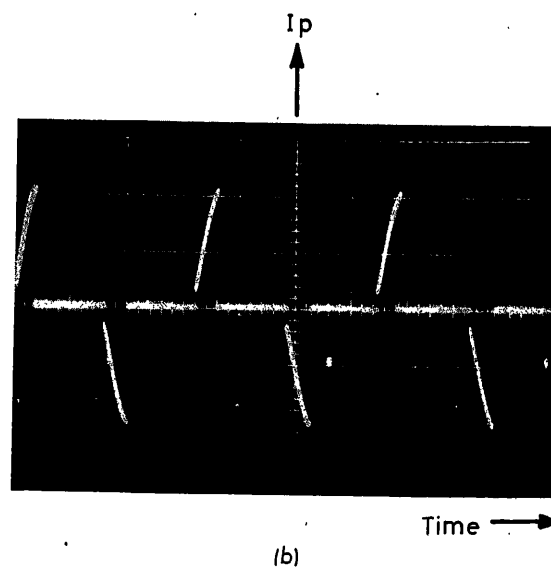
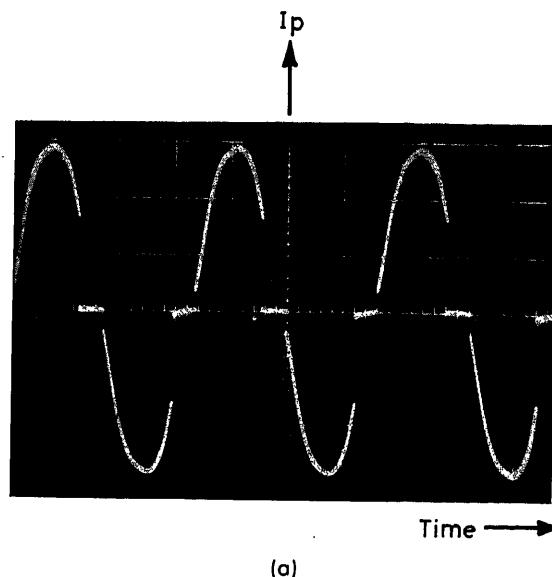


Figure 13. Rectifier circuit with turn-off SCRs. Transformer primary current I_p is turned off: (a) at 145° , (b) at 45° ; fundamental component of I_p is leading the supply voltage, and hence delivers inductive, quadrature power to the a.c. supply system

strated in Figure 13, which shows two oscillograms of the primary current of a single-phase rectifier with turn-off SCRs where the magnitude of load current is controlled by varying the point of turn-off as contrasted with the point of turn-on with ordinary SCRs. More information on applications for turn-off SCRs is given by Stasior¹⁶ and Grafham¹⁷.

Conclusions

- (1) The so-called turn-off SCR can be turned on by a positive gate current pulse and turned off by a negative one.
- (2) Turn-off current gains of 1,000 and more were measured (3N60). The narrower the load current range, the higher a turn-off gain is possible.
- (3) Current interruptions by gate turn-off is available in devices of 1 to 2 amp current rating and 500 V forward blocking ability (ZJ224); devices for significantly higher current ratings are feasible.
- (4) Turn-off SCRs have a shorter turn-off time than ordinary SCRs and hence are capable of operation at higher frequency.
- (5) Turn-off SCRs, when commutated in the conventional manner, require commutating components of substantially smaller size than required by ordinary SCRs.
- (6) Where reverse voltage ability has been impaired by junction or circuit modification, the insertion of a rectifier can restore it.
- (7) Caution must be exercised to limit overvoltages during turn-off.
- (8) Caution must also be exercised to consider the turn-off switching losses in order not to exceed the maximum power dissipation of the device.

Appendix I—Junction Electronics

If one applies a d.c. voltage of the indicated polarity (*Figure 1*), a load current I_L will flow. The arrows indicate the conventional direction of current flow outside of the SCR, and the direction of particle flow inside the SCR. Assuming temporarily $I_L = 1$ (to simplify notations), a hole current of the magnitude $\alpha_{1,2}$ arrives in layer p_2 , and an electron current $\alpha_{3,2}$ arrives in layer n_1 , where $\alpha_{1,2}$ and $\alpha_{3,2}$ are the current gains from junction 1 to 2 and from 3 to 2, respectively²⁻⁴.

Thus, the layer p_2 receives a hole current of $\alpha_{1,2}$ and an electron current of $(1 - \alpha_{3,2})$. Taking into account the neutralization between holes and electrons, and for a general value for I_L , an accumulation or depletion of majority carriers occurs in layers n_1, p_2 at the rate of

$$r = [\alpha_{1,2} - (1 - \alpha_{3,2})] I_L \quad (13)$$

per layer. If r is positive, we have an accumulation of majority carriers, and if r is negative, we have a depletion of majority carriers.

Although the centre junction (junction 2) reacts by creating opposing accumulation or depletion rates, resulting in zero net rates during steady state, there has been brought into existence a net accumulation (not rate) or net depletion of majority carriers.

The current gains $\alpha_{1,2}$ and $\alpha_{3,2}$, and hence the deposition rates r , are functions of the current densities^{5,6}. The holding current I_H (usually 0.1 per cent or less of rated load current) is defined by $r = 0$, and gate open. For higher load currents $r > 0$, for lower currents $r < 0$.

Counter-e.m.f. Mode ($r < 0$)

If $I_L < I_H$ (*Figure 1*), r becomes negative and majority carriers are withdrawn from layers n_1, p_2 , called the inner bases. A

portion of this depletion uncovers (ionizes) the fixed donors and acceptors of the centre junction, and by doing so, a fixed space charge is developed opposing the applied voltage. The build-up of this counter-e.m.f. across the centre junction is similar to the build-up of a voltage across a capacitor. This mode of operation is called the counter-e.m.f. or high-impedance mode of the SCR.

Forward-e.m.f. Mode ($r > 0$)

If $I_L > I_H$ (*Figure 1*), a net accumulation of majority carriers occurs. This has the opposite effect from the depletion case just described, and the result is a forward-e.m.f. across the centre junction. The SCR now in its forward-e.m.f. mode, also called the low-impedance mode.

If the load current is reduced (by increasing the external resistance) below I_H the SCR reverts to its high-impedance mode, and reduces the load current abruptly to the level of its leakage current (usually 0.01 per cent of rated load current).

Appendix II—Gate Turn-off

Turn-off is accomplished by reversing the centre junction voltage from the forward to the counter-e.m.f. direction. This voltage reversal consists of two parts: (a) the reduction of the forward-e.m.f. to zero, (b) the build-up of the counter-e.m.f.

Reduction of the Forward-e.m.f. to Zero

If one wishes to reduce the forward-e.m.f. to zero, one has to reduce the carrier accumulation rates eqn (13) to zero. This can be accomplished by withdrawing a current I_G (called gate current) from terminal G . The current leaving through the lower contact of the SCR is reduced by about the same amount, being equivalent to the withdrawal of an electron current I_G through this contact. The currents superimposed on the load current I_L are shown in *Figure 2*. The gate current I_G depletes the inner bases at a rate r_d :

$$r_d = \alpha_{3,2} I_G \quad (14)$$

If $r_d = r$, the generation of a forward-e.m.f. is wiped out. The carrier accumulations, and hence the forward-e.m.f. existing prior to the application of the gate current I_G subsides in a crudely exponential manner, with the carrier lifetime as something akin to a time constant. Substituting from eqn (14) into (13), one obtains for the necessary gate current $I_G^{6,7,8}$.

$$I_G = \frac{\alpha_{1,2} - (1 - \alpha_{3,2})}{\alpha_{3,2}} I_L \quad (15)$$

For ordinary SCRs, this gate current may be as large as one half of the rated load current.

Build-up of the Counter-e.m.f.

If the gate current I_G is made larger than expressed by eqn (15), the sign of $r - r_d$ becomes negative, indicative of a depletion of majority carriers. As previously described, this depletion promotes the development of a counter-e.m.f. in the centre junction, which reduces the load current to a trickle, called the forward leakage current. On a per unit basis, the excess of gate current over eqn (15) to achieve turn-off, is in the vicinity of the per unit leakage current, which is 10^{-4} , and hence negligible.

As the load current (under the effect of gate current), drops sufficiently, the deposition rate becomes negative, irrespective of

the presence of gate turn-off current. It follows that once the SCR has been turned off, the gate current is no longer needed to maintain the turn-off condition.

Appendix III—Turn-off Current Gain

A high turn-off gate current is undesirable, because it increases the size of the gate power supply. The gate structure, including the lead of a conventional SCR, would have to be vastly expanded to accommodate a high gate current. The filaments of I_G flow transversely to the main axis of the SCR, and encounter the so-called transverse resistance⁹ of layer p_2 . The resulting transverse voltage drop counteracts the original lowering (by gate control) of the voltage of gate layer p_2 . The transverse voltage drop increases with distance from the gate contact and may become so pronounced as to prevent the turn-off of the load current by shunting it through areas away from the gate contact. Again, a lower I_G is desirable because of the lower counteraction of the transverse resistance.

Nomenclature

D_h	Diffusion constant for holes (cm ² /sec)
I_B	Bias current (amps)
I_G	Gate current (amps)
I_H	Holding current (amps)
I_L	Load current (amps)
K_T	Turn-off current gain (unity)
r	Accumulation or depletion rate (amps)
r_d	Depletion rate caused by gate current (amps)
$\alpha_{1,2}$ and $\alpha_{2,2}$	Current gains (unity)
σ	Conductivity ($\Omega^{-1} \cdot \text{cm}^{-1}$)
τ_h	Average lifetime of holes (sec)

It is a pleasure to express my appreciation for discussions of this subject with F. W. Gutzwiller, C. M. Jones, J. Moyson and R. A. Stasior.

References

- ¹ HARNDEN, J. D. Properties of the silicon controlled rectifier—A Survey. *J. Amer. Inst. elect. Engrs. Conf. pap.* CP 61-332 (February 1961)
- ² JONSCHER, A. K. *Principles of Semiconductor Device Operation*. 1960. New York; Wiley
- ³ EBERS, J. J. and MOLL, J. L. Large signal behavior of junction transistors. *Proc. Inst. Radio Engrs, N. Y.* (1954) 1761
- ⁴ MOLL, J. L., TANNENBAUM, M. T., GOLDBY, J. M. and HOLONYAK, N. P-N-P-N transistor switches. *Proc. Inst. Radio Engrs*, (1956) 1174
- ⁵ WEBSTER, W. M. On the variation of junction-transistor current-amplification factor with emitter current. *Proc. Inst. Radio Engrs, N. Y.* (1954) 914
- ⁶ JONSCHER, A. K. Notes on the theory of four-layer semiconductor switches. *Solid-State Electronics* 2 (1961) 143
- ⁷ MACKINTOSH, I. M. The electrical characteristics of silicon P-N-P-N triodes. *Proc. Inst. Radio Engrs, N. Y.* (1958) 1229
- ⁸ GOLDBY, J. M., MACKINTOSH, I. M. and MOSS, I. M. Turn-off gain in P-N-P-N triodes. *Solid-State Electronics* 3 (Sept. 1961) 119
- ⁹ PRITCHARD, R. L. and COFFEY, W. N. Small signal parameters of grown-junction transistors at high frequencies. *Inst. Radio Engrs, N. Y. Convention Record*, pt. 3 (1954) 89
- ¹⁰ KLEIN, M. A four-terminal P-N-P-N switching device. *Trans. Inst. Radio Engrs, N. Y.* (1960) 214
- ¹¹ Silicon controlled switches. *Publication 65.10* General Electric, Semiconductor Products Department, Syracuse, New York
- ¹² Gate turn-off switch. *Publication 150.60* General Electric, Rectifier Components Department, Auburn, New York, March 1962
- ¹³ CLARK, M. A. Power transistor. *Proc. Inst. Radio Engrs, N. Y.* (1959) 1185
- ¹⁴ MEYER-BROTZ, G. Eigenschaften und Anwendungen von Flächen-Transistoren als Schalter. *Telefunkenztg.* Vol. 33, Heft 128 (1960) 85
- ¹⁵ KOBEL, E. Unterbrechung eines brennenden Anodenstromes mittels Gitter im Quecksilberdampf-Gleich- oder -Wechselrichter. *Bull. schweiz. elektrotech. Ver.* February (1933) 42
- ¹⁶ STASIOR, R. A. and MAPOTIER, T. C. Notes on the application of the silicon controlled switch. *Application Note 90.4*, General Electric, Semiconductor Products Department, Syracuse, New York, April 1962; also *Transistor Manual*, 6th Ed. Chap. 19, same publisher
- ¹⁷ GRAHAM, D. P-N-P-N switches with gate turn-off control. *Publication 200.23* General Electric, Rectifier Components Department, Auburn, New York

DISCUSSION

H. FANKHAUSER and J. GFELLER, *ETH, Inst. of Automatic Control and Industrial El., Weinbergstrasse 155, Zürich 6, Switzerland*

We have experimented with the rectifier you mention in your paper but have had the following difficulties:

During the turn-off, the short turn-off time of the controlled switch of about 50 μsec and the stray inductance of the transformer caused high-voltage transients up to 600 V and more at a current of 1 A. These voltages destroy the devices! (Figure A).

On the oscillogram, you see on the top the load current, below the device voltage, with a pulse of 50 V during the turn-off of 100 mA.

To reduce the amplitude of the transients which caused these unwanted oscillations, we shunted the device between anode and cathode with a capacitor. (Figure B).

Another solution to protect the controlled rectifier is to replace the capacitor by a clipping diode (Figure C), which allowed us to increase the load inductance and the load current. The clipping diode cuts the pulses at a prescribed voltage level, but during commutation, the energy in the stray inductance must be dissipated by the protecting device, which reduces the efficiency. (Figures D and E).

We would like to ask Mr. Storm if, with other supplementary

elements, the controlled switch can be protected with less power loss or if devices can be built with longer turn-off times, so that no dangerous voltage-transients will occur.

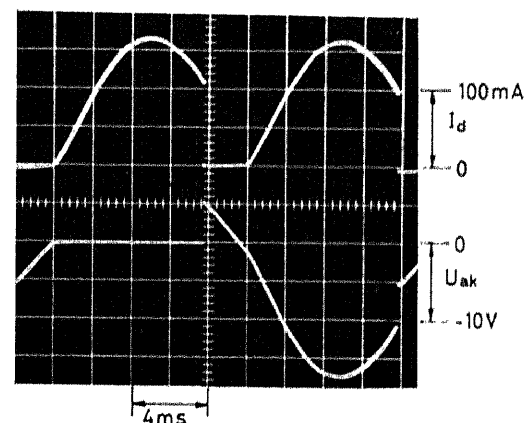


Figure A

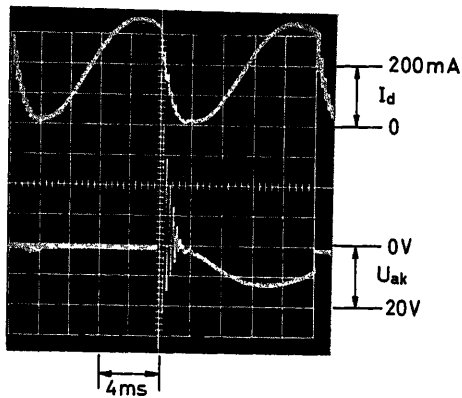
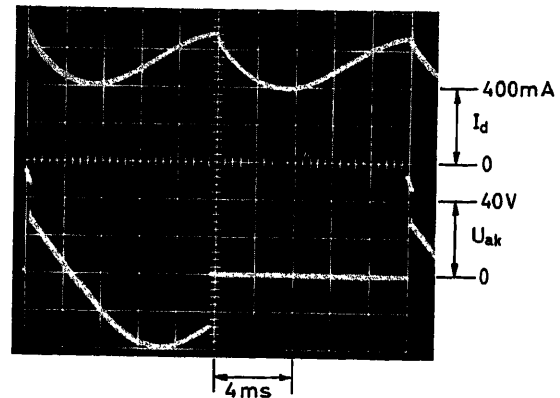


Figure B



Figures D

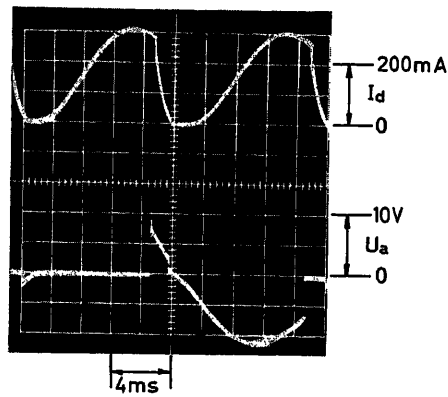


Figure C

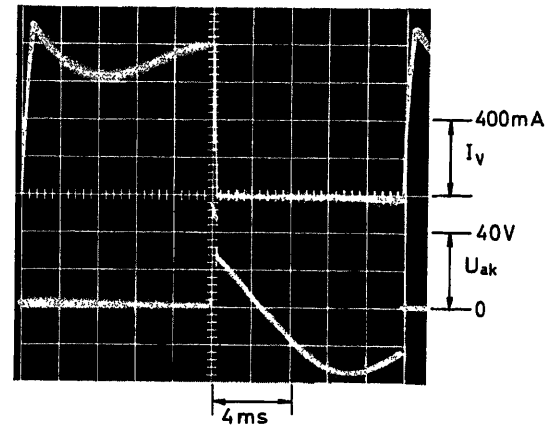


Figure E

H. F. STORM, *in reply*

If an inductive circuit is interrupted, a voltage of considerable magnitude may appear across the points of interruption. This is a basic fact, and does not depend on the means of interruption, be it contacts, a transistor or a turn-off SCR. The overvoltage measured by the debaters was 600 V. Since the repetitive peak forward blocking voltage of the device under test is listed in the spec. sheet 150-60 3/63 as 500 V, it should not be surprising to see the device fail if 600 V are repetitively applied.

In reply to another question, overvoltages can be suppressed by so-called Thyrectors, as listed in my paper 6-8.

In answer to a further question, it is possible to build turn-off SCRs with a longer turn-off time, but this would result in a reduction of the frequency capability of the device. The extent to which this measure would reduce overvoltages is not known to the writer.

H. SCHENKEL, *Haldenstr. 7a, Oberrieden (ZH), Switzerland*

I should like to raise the following comments to the various methods that are described in the preprints for increasing the turn-off gain.

- (1) Do they substantially decrease the turn-on gain of the device?
- (2) In the preprints you have described a connection between the

four-layer diode where the back current is no longer taken out of what is normally the anode but from the n_1 region. Am I right in assuming that by connecting the device in this way it is only suitable for small load currents, due to the technology that the wire connections to this inner region could not be made very strong.

(3) I am somewhat worried about the methods of increasing a turn-off gain for the following reason: normally, SCRs have a considerable spread of characteristics, if you consider one which normally you cannot turn off; the required turn-on current may, for instance, be in the order of 50 mA, while the minimum of any unit from one type may be of the order of 5 mA. Will that circumstance not make large turn-off gains very critical?

H. F. STORM, *in reply*

(1) Generally yes. The turn-on gate currents of turn-off SCRs have been measured to 0.2 per cent and more of the rated load current. This figure compares to 0.1 per cent and less, as encountered in ordinary SCRs.

(2) No. However, the writer is possibly unaware of larger, four-terminal units, which are commercially available at the present time.

(3) The higher the intended turn-off gain realized by the circuit of Figure 4, the more sensitive the turn-off SCR will be to variations in the turn-off characteristics of the device itself.

Ceramic Memories in Extreme Environments

A. B. KAUFMAN

Summary

Many types of computer memory elements have been devised, but few meet current economic or technical criteria. In addition, new and extreme environments, nuclear and space radiation, or temperature have created new performance demands.

The memory research performed at Litton Systems has produced a ceramic memory which has certain unique advantages. Word storage is made in a disc smaller than a dime. The device requires no special environment, operating in an ambient temperature of -80 to $+200^{\circ}\text{C}$. In addition it operates in a space or nuclear environment; hyper-exposures causing little degradation of performance. Each bit produces an output of $20\text{ V } p-p$, with sufficient power to directly drive gate(s). Readout is nondestructive, and the memory is nonvolatile. In addition word-bit readout is parallel, at a clock speed up to 1 Mc .

Sommaire

Plusieurs types d'éléments de mémoire pour calculatrices ont été proposés, mais seul un petit nombre d'entre eux satisfait aux critères économiques ou techniques usuels. En outre, des conditions d'ambiance nouvelles et très sévères — rayonnements nucléaires, rayonnements spatiaux, températures extrêmes — imposent des exigences nouvelles en matière de performances.

Les recherches entreprises par Litton Systems, Inc., ont conduit à la création de mémoires céramiques qui offrent certains avantages uniques. Le stockage d'un mot est assuré au sein d'un disque de dimensions inférieures à celles d'une pièce de monnaie. Le dispositif ne nécessite pas de précautions spéciales, quant à l'ambiance; il fonctionne dans une plage de températures allant de -80 à $+200^{\circ}\text{C}$. En outre, il est à même de fonctionner en présence de rayonnements spatiaux ou nucléaires, auxquels il peut être exposé pendant une longue durée en ne manifestant qu'un léger abaissement de ses performances. Chaque «bit» produit un signal de sortie de 20 V crête à crête, dont la puissance est suffisante pour commander directement une ou plusieurs portes électroniques. La lecture est non-destructive et le stockage dure indéfiniment («nonvolatile memory»). En outre, la lecture des «bit» d'un mot se fait en parallèle, à une cadence atteignant 1 MHz .

Zusammenfassung

Viele Arten von Speicherelementen für Rechenanlagen wurden erdacht, doch nur wenige entsprechen den heutigen wirtschaftlichen und technischen Anforderungen. Obendrein haben außerordentliche Beanspruchungen durch nukleare und kosmische Strahlen sowie extreme Temperaturen neue Anforderungen hervorgebracht.

Litton Systems hat nach langen Untersuchungen einen keramischen Speicher entwickelt, der verschiedene einzigartige Vorzüge besitzt. Die Speicherung eines Wortes erfolgt auf einer Platte, die kleiner ist als ein Zehn-Cent-Stück. Der Speicher kann in beliebiger Umgebung eingesetzt werden, er arbeitet bei Umgebungstemperaturen zwischen -80 und $+200^{\circ}\text{C}$ und auch unter nuklearen Bedingungen und im kosmischen Raum; übermäßige Bestrahlungen beeinträchtigen die Arbeitsweise nur gering. Jedes Bit bewirkt einen Ausgang von 20 V_{ss} bei genügender Leistung, um ein oder mehrere Tore direkt zu steuern. Dieser Permanentpeicher hält beim Auslesen die Information. Außerdem erfolgt das Auslesen eines Wortes parallel bei Taktfrequenzen bis zu 1 MHz .

Much attention has been paid to memory storage components and techniques for their use, inasmuch as this device is pivotal to the whole concept of the digital computer and establishes its performance capabilities, both in speed of operation and bit or word storage capability.

Many types of computer memory elements have been devised¹, but few are in production use. Economic or technical limitations have probably been the key reason for the *status quo* in memory component usage.

The preliminary investigation of a new type of memory device is presented in this paper. The memory element discussed herein is in the preproduction stage, but is being considered for large-scale memory storage or where space or nuclear environments exist. System problems are not discussed in detail, in this paper, pending careful study, at which time they will be treated fully in another paper. The ceramic memory is not a cure-all, it is at present limited to random access memory applications. In its current development stage, the single-bit cell is not as small as the core or thin magnetic film element which it could replace. In its present word storage development stage, however, it is much smaller than the total sum of the cores required for the same bit number word. Furthermore, the ceramic memory has many significant advantages over the prior elements: (a) readout is non-destructive, (b) associated support equipment is much less complex, (c) its storage is non-volatile, (d) it is nuclear resistant, and (e) its output is $\sim 20\text{ V}_{p-p}$ ($Z_0 \cong 100\ \Omega$) for a zero or one digit. Its high output voltage, with low output impedance, permits it to drive a multitude of gates or logic without amplification. Its non-destructive readout characteristics permit the elimination of the write-back electronics required with many other memories.

Hitherto, in research, where ceramic materials such as barium titanate have been used as memory elements, the element was used primarily as a ferroelectric capacitor. The square hysteresis loop of barium titanate was considered promising for such memory applications. However, the capacitor mode of operation, in which the state of the induced change indicated the storage of a ZERO or ONE digit, in general produced a destructive readout and this and other constraints have negated this element's use for a computer memory. Furthermore, the single-crystal materials employed were difficult to handle and fabricate and, in use, did not display a high degree of reliability¹. In addition, the ferroelectric capacitor is a two-terminal device which makes matrix selection without crosstalk difficult. It also precludes practical noise cancellation circuit arrangements.

A completely new approach, which negates these difficulties in connection with the use of ferroelectric elements for computer logic and memory applications, was originally researched for a fixed-wing, highway-in-the-sky, computer programme². Further, in-house research was conducted by Litton Systems, Inc. because of its apparent value to the computer field. The use of polycrystalline ceramics in a monomorphically constructed memory cell

eliminates the construction and reliability problems inherent with fragile single crystals and produces a multi-port device. Barium titanate devices, in addition, offer important design advantages over those previously enumerated. They are less expensive than cores, from the materials and fabrication point of view. Moreover, their output is volts rather than millivolts as with drum, core, and thin magnetic film memory devices. In addition, they are insensitive to magnetic field interference, and the associated circuits are less sensitive to noise pick-up.

The barium titanate memory element consists of a polycrystalline material on which electrodes have been deposited in such a manner as to allow its functional use as a memory device. Its mode of operation is similar to an electromechanical filter that is operated near or at its resonant frequency.

Barium titanate exhibits three properties pertinent to the operation of the memory. The first of these is the electrostrictive effect. When a piece of ferroelectric material is polarized and an electric field placed across it, the material is mechanically deformed by the electrical field. Conversely, if a mechanical stress is applied to a piece of polarized material, an electrical output is observed. This second property is the piezoelectric effect. The third effect, exhibited by non-polarized barium titanate, is the retention of polarization (under the Curie point) when external excitation is applied and removed. This polarization may be reversed by a reverse applied field.

The theory applied to the memory element follows. Both the electrostrictive and the piezoelectric characteristics of the material are utilized. The memory cell although constructed from a single piece of ferroelectric material is made in two parts. The first of these is a permanently polarized motor element, across which a pulse or sine wave of voltage is developed by a clock signal. Thus, with an applied sine voltage, the material expands and contracts at the clock frequency. The second part is the memory element itself, which is polarized (write) in one direction or the other by a large electrical field, and which is read from the remanent piezoelectric output. For the motor element to drive the memory element, the two must be mechanically coupled.

One of the first configurations used² was a monomorph rectangular bar of polycrystalline barium titanate. Output from this construction was an order of magnitude higher than that obtainable from cores or thin films, that is from 0.5 to 5 V. Mechanical coupling between the motor and memory elements was considerably better in this monomorph or single-bar unit than in bimorph configurations previously tried, and hence produced higher output voltage than otherwise obtainable. The resonance characteristics of this unit permitted a marginal range of clock frequency variation.

Optimum materials for the memory cannot be selected only on the basis of their suitability for the motor (electrostrictive) or memory (piezoelectric) portions of the cell. A compromise material must be employed which exhibits useful piezo- and electrostrictive characteristics. Early research was conducted with ceramic materials whose electrostrictive, piezoelectric, remanent polarization, and mechanical stability were not good with temperature or clock frequency variation. The use of new materials, as reported hereafter, solved this problem area. The motor unit of the single-bar memory cell was polarized, after construction, by heating it above the barium titanate Curie point while approximately 50 V d.c. was applied, followed by a slow cooling. The disc memory reported on, after the following discussion of operation, also employed a like fabrication technique.

The memory cell motor element is typically driven by a sinusoidal clock generator. A short pulse of 35 to 350 V d.c. (depending upon the ferroelectric used) is applied to the memory element for write-in. Polarity of the write-in voltage determines the phase of the readout signal, referenced to the clock, and the phase of the readout signal defines the storage of a digital ZERO or a digital ONE.

Figure 1 shows the early rectangular bar fabrication technique for the cells, while Figure 2 shows a typical single-bit disc type memory. No attempt was made to miniaturize the memory cells

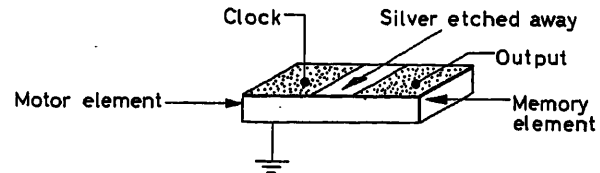


Figure 1. Bar-type monomorph ceramic memory

but, with the feasibility of this type of memory now established, it is expected that miniaturization will be one of the major tasks for the near future.

Clock power requirements, where a sinusoidal clock is employed, are reduced to a minimum by shunt-resonating the lumped memory cell motor capacitance. This technique reduces clock power requirements by several orders of magnitude, as the cells no longer present a short-circuit path for the high-frequency clock.

Literature research had indicated that the polycrystalline barium titanate memory cell material would not deteriorate significantly in performance during or after nuclear exposure to a total integrated neutron exposure of 10^{15} n/cm² ($E_n > 2.9$ MeV)³. It thus appeared that a side benefit of this novel memory cell might be its nuclear resistance. However, it was deemed advisable to ascertain actual memory cell characteristics as well

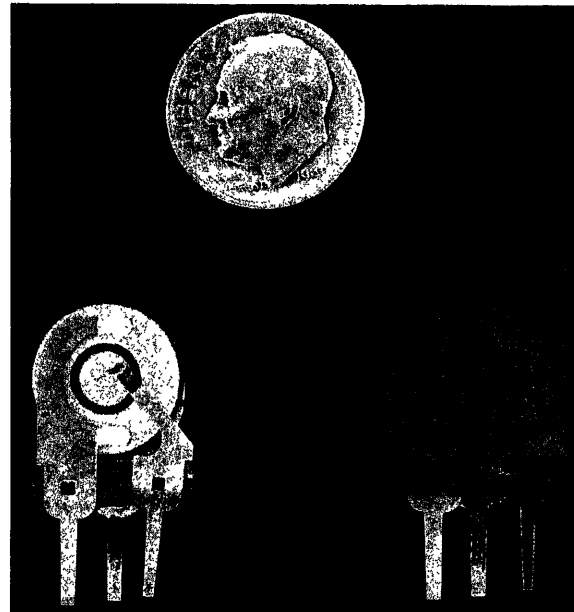


Figure 2. Disc-type, single-bit memory

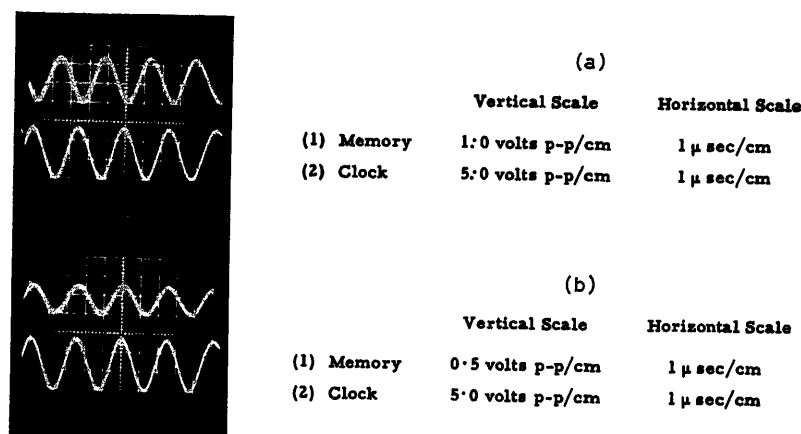


Figure 3. Post-irradiation test of readout for ONE (top) and ZERO (bottom)

as the performance of its electroding and assembly materials with irradiation. Several single-bit memory cells of the bar configuration were subjected to irradiation but were not dynamically operated during irradiation.

Post-irradiation tests indicated that the test memory cells operated satisfactorily without significant degradation of performance. The ceramic memory cells were exposed to an environment of 55°C and an integrated dosage of $\sim 1.5 \times 10^{16}$ n/cm² at energies greater than 2.9 MeV accompanied by 8×10^{10} ergs/gm (C) of gamma. The post-irradiation characteristics of one of these ceramic memory cells are shown in Figure 3. Clock excitation was approximately 5 V R.M.S. at 400 kc. Write-in of a ZERO or ONE digit was at 300 V d.c. (less voltage could have been used). Readout voltage was 0.75 V peak to peak for a ZERO digit and 2.2 V peak to peak for the ONE digit. Readout non-symmetry, though not unusual, is generally not so severe.

A single-bit monomorphic bar memory cell has been constructed with motor and memory elements of equal size (Figure 4). The cell (Mod I) has sharply defined characteristics relative to a usable range of clock-frequency variation. It will tolerate a ± 2 to 6 kc shift in clock frequency based on definition of the cell output by phase reference to the clock drive. Conversely, a change in environmental temperature, which modifies the cell's resonant characteristics, limits the satisfactory range of environmental temperature to about ± 5 to 10°F. If phase reference is ignored, this cell is usable over a wider frequency range (~ 80 kc). Variation in clock frequency affects the phase relation of the output signal relative to a sinusoidal clock. At 'bar' cell resonance, the memory output is shifted 90° with respect to the clock drive and these cells are normally operated above or below resonance, at a point where the clock signal and memory output are in phase. The disc-type memory also exhibits a phase shift, but to a lesser extent.

Although higher memory cell output is obtainable at cell resonance, detuning is employed to secure zero phase shift

between the clock and memory cell output as previously noted. Alternately and preferable, the clock supply to the logic gate (where pulse output is employed) would be through a delay network so that the cell could be used at resonance, its memory output and gating pulse being synchronized. This approach was not used for the prototype research delineated in this paper.

The output signal from a bar type Mod I memory cell, where phase-gating is employed to define the storage of a ZERO or ONE, is shown in Figures 5 (a) and (b). Vertical axis scope sensitivity is 2 V per division for the upper traces and 10 V per division for the lower traces (clock). The oscilloscope presentation reveals a ZERO output signal of 0.8 V and a ONE output

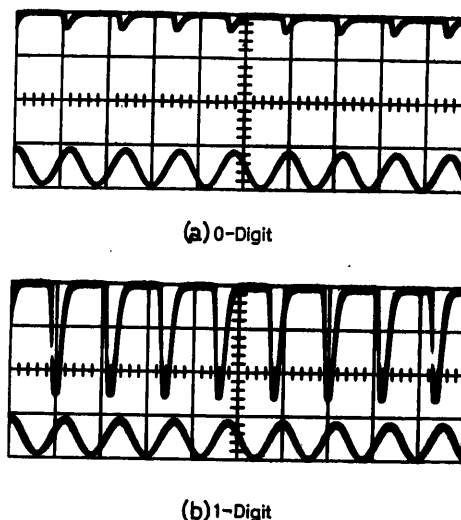


Figure 5. Output of a gated Mod I cell

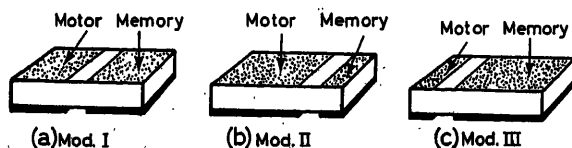


Figure 4. Typical bar-type memory configurations

of 5.2 V. The ZERO output level is an artefact in the memory matrix, and is not due to the cell. Cell output impedance was approximately 1,000 Ω and clock frequency was about 400 kc. The ONE output signal shows that the negative spikes are not in perfect phase synchronization with the clock motor drive signal.

To improve temperature environment characteristics and lower clock frequency dependence, several new geometries of cell configurations were constructed and tested. Two are shown in

Figures 4 (b) and (c). The Mod II and III cells employ a ratio between the motor and memory elements of about 4:1. These offered no significant improvement over the Mod I memory cell and hence research was directed towards a different ceramic material and a geometry which might offer higher readout voltages.

The stability characteristics of Clevite Corporation's ceramic bandpass filters looked good inasmuch as they were rated temperature stable from -65° to 200° C. There were, however, three unknowns: (1) ability of the memory section to hold remanent polarization, (2) whether the dot or ring should be used for the motor, and (3) the electrostrictive and piezoelectric characteristics of the material. Clevite engineers⁴ had found that a limited portion of a ceramic wafer (or disc) could be excited, independent of the remainder, by using dot electrodes; the active portion of the wafer, and its associated electrodes, forming a radial expander element. Frequency control of the dot resonator was obtained by varying the diameter of the wafer, while fine tuning is achieved by tailoring the thickness of the dot electrode. The impedance of such a device is a minimum at resonance, while at anti-resonance increases by a factor of $\sim 1,000$. When such a device is used as a three-port filter, the effect of piezoelectric field coupling between the ring and dot electrodes is insignificant if these electrodes are spaced several times the thickness of the ceramic apart. This technique was used with the fabrication of the disc memories discussed in this paper. As a result, there is little coupling of the clock-excited portion of the memory to the memory portion of the cell.

Initial tests of the disc, used as a single-bit memory cell, were conducted with a Clevite TO-02A filter which, with the cooperation of the Clevite Corporation, was secured with only the dot or ring permanently polarized. These were examined to determine which offered the best configuration. As is shown by Figure 6, the permanently polarized dot (for clock excitation) exhibited superior characteristics for this application.

Its readout voltage (~ 20 V) gave not only over twice the readout voltage, but it exhibited a flatter plateau. These memory cells employed 0.25 mm thick ceramic material. Material one-half this thickness should exhibit write-in characteristics down to one-quarter of the voltages shown. Thinner materials are practical.

The 'D' polarized filter, used as a single-bit memory cell, was then tested for performance in an extreme temperature environment of -80° to $+150^{\circ}$ C. As seen in Figure 7, the cell's output (for single write-in at 30° C) remained approximately

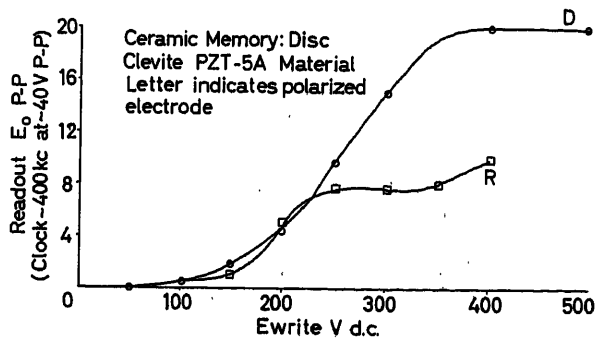


Figure 6. Characteristics of a dot versus ring polarized motor-disc memory

constant between 0° and 150° C, showing, however, a decided upturn in output level between 0° and -80° C.

The performance of the memory was then tested, utilizing both unipolar pulses and sinusoids for its clock drive. The filter from which the memory was constructed was designed for an interstage 455 kc/sec (radial mode) bandpass application. Tests conducted at Litton Systems indicated two clock to memory in-phase (sinusoidal clock) resonant frequencies; 162 and

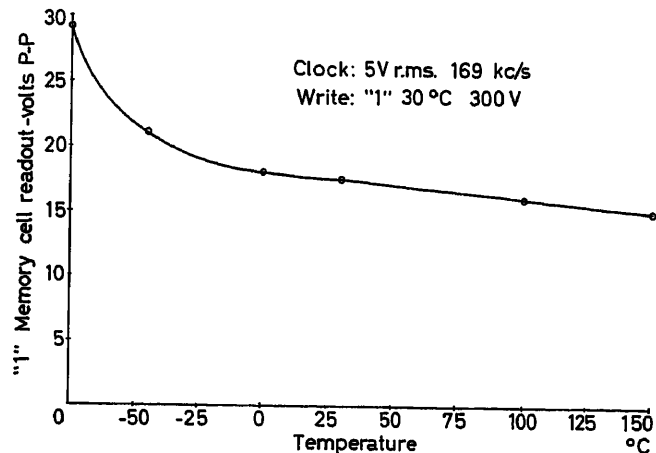


Figure 7. Readout characteristics of a dot-polarized disc memory cell with temperature

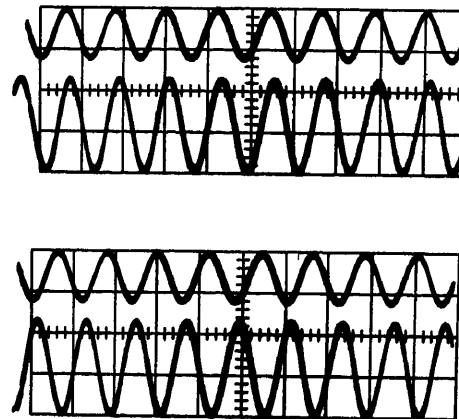


Figure 8. Disc memory clock at 412 kc/sec. Top(s) memory cell, vert. 5 V/cm. Bottom(s) clock, vert. 10 V/cm. Sweep $2 \mu\text{sec/cm}$

412 kc/sec. The latter frequency is used to present the performance of the single-bit memory as shown in Figure 8. In addition the memory cell was operated from a unipolar pulse generator as shown in Figure 9. As previously noted the clock or pulse repetition rate was selected for phase relationship to show the memory's performance to better advantage. Higher memory outputs are available at other frequencies. In addition, it should be noted that the application of a single pulse, rather than a pulse train (Figure 9) causes a ringing output. As is shown the sequential pulses maintain the memory in an oscillating state.

The ceramic material used in the bar-type memory cell⁵ differed from Clevite's PZT-5A*, utilized in the disc-type

* Registered trade mark for a lead zirconate ceramic.

memory. Its nuclear resistance was uncertain, although correlatively was assumed to be nuclear resistant also. In order to determine, without doubt, that the new material was nuclear resistant, several test specimens were exposed to ~ 1 (16) mw/t , $E_n > 2.9$ MeV; ~ 1 (11) erg/gm (C) integrated neutron and gamma exposure respectively. At the preparation of this paper the induced radioactivity of the specimens still precluded

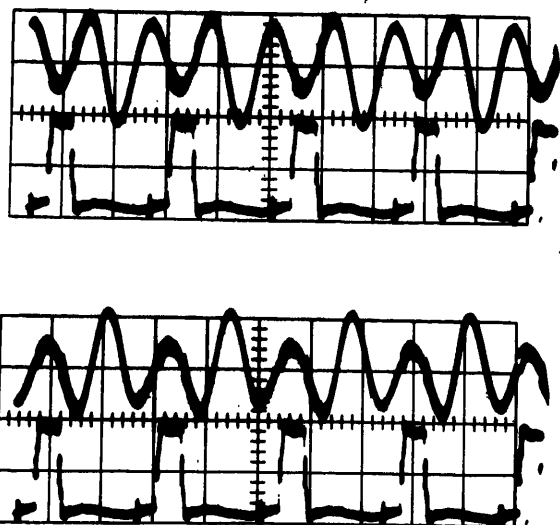


Figure 9. Disc memory clock rep. rate 202 kp/sec. Pulse width 1 μ sec. Top(s) memory cell, vert. sensit. 5 V/cm. Bottom(s) clock, vert. sensit. 20 V/cm. Sweep 2 μ sec/cm

complete post-irradiation evaluation. Preliminary evaluation indicates insignificant degradation of performance.

Although it was apparent that the single-bit disc could be scaled down in size, achieving a higher operating frequency with some loss in output impedance, it was decided to shelve that approach temporarily and to construct a multiple-bit, or word, memory cell. The size of this memory is shown in Figure 10. Although constructed for an 8-bit word, it could easily be modified for a 13-bit, or larger, word. The word storage memory

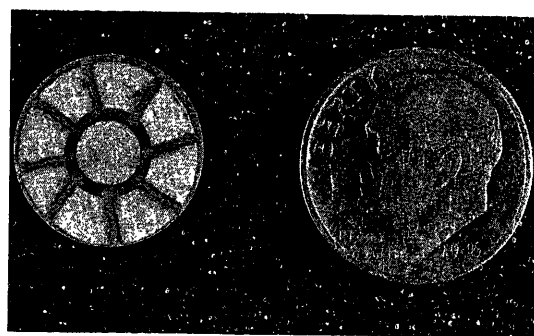


Figure 10. Eight-bit single ceramic memory cell

cell offers many significant advantages. Among these are: (1) less readout gating is required, (2) simplified parallel readout, analogous to paralleled shaft encoders, is possible, and (3) compared with a strictly sequential digital system it has a much higher bit-output rate for the same clock frequency.

The parallel readout of a 13-bit word at a 400 kc rate would be equivalent to a sequential bit rate of 5.2 Mc (i.e., the number of bits processed in the same period). It should be noted that many memories can be designed for parallel bit (or word) output. Their low level output signals require separate amplifiers for each bit processed, whereas these are not required for the ceramic memory. Inasmuch as the ceramic memory can be made to operate at higher than 400 kc/sec clock rates, and with higher bit density, its capabilities are easily recognized. Unfortunately the write-in capabilities of this memory are not as satisfactory as its readout parameters. Linear selection to each bit is presently required for write-in, although current logic studies indicate this may be surmounted. Write-in speeds to 1 Mc have been achieved, but to put the same energy in the ceramic domains, as the write-in time (width) is decreased, requires that the write-in voltage be increased. The voltage required is fortunately not a direct reciprocal of the ratio of time width decrease. In addition, significant reduction of write-in voltage may be achieved by proper selection of the ferroelectric, its thickness, and electrode size, without loss of signal level or impairment of output impedance. Analytical and empirical tests are being conducted to define this area.

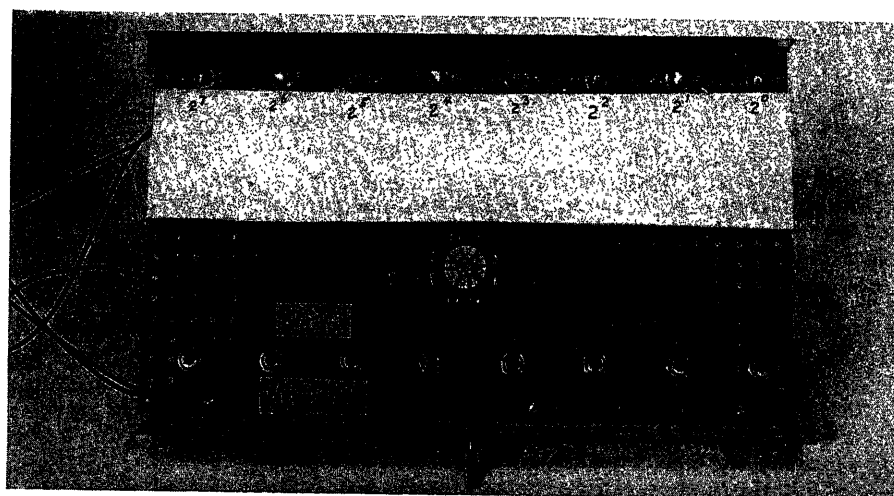


Figure 11. Breadboard of an eight-bit disc memory

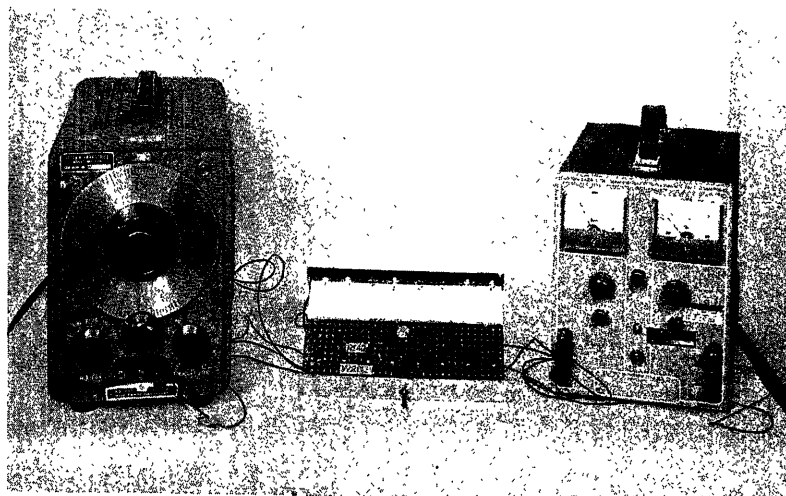


Figure 12. Eight-bit memory test configuration

The dicing of the ring element into discrete bits, such as to secure word capability, does not lower the no-load output voltage level. Each 'bits' output level is the same as the intact ring. However, the 'bit' versus the 'ring' output impedance increases directly as a ratio of the number of 'bits' to the ring. The ring (single-bit) output impedance is $\sim 100 \Omega$, whereas if the ring is diced for a 10-bit memory each bit impedance would be $1 \text{ k}\Omega$. This still allows sufficient bit output to drive diode gate logic directly, without amplification.

To demonstrate the capabilities of the word memory visually, an 8-bit cell was constructed and breadboarded as shown in Figures 11 and 12. Rather than use sequential gating for presentation of the 8-bit word on an oscilloscope, parallel optical readout was employed. Each bit of the word is AND diode gated, and is allowed to produce an output voltage at clock rep. rate, if in phase with the clock. This voltage is then used to

light the lamps shown. 'On' lamps indicate a ONE, and 'off' lamps a ZERO, digit. Because of the thermal characteristics of the lamps, several ONE pulses are required before the lamp comes up to full illumination. The clock frequency used for this demonstration was $\sim 390 \text{ kc/sec}$.

References

- ¹ RAJCHMAN, J. A. Computer memories, a survey of the state-of-the-art. *Proc. Inst. rad. Engrs*, 49, No. 1 (1961)
- ² KAUFMAN, A. B. Obtaining nondestructive readout with ferroelectric memories. *Electronics* (1961)
- ³ LEFTOWITZ, I. *Physical Chemical Solids*, 10 (1959) 169
- ⁴ CURRAN, D. and KONEVAL, D. Miniature ceramic band pass filters. *Proc. Nat. elect. Conf. XVII* (1961)
- ⁵ Electrostrictive ceramic materials, *U.S. Patent No. 2,836,501* (1958)

DISCUSSION

A. KAUFMAN, in reply to questions presented from the floor

In order to bring the paper up to date, the assumption that a decrease of the memory cell thickness to one-half of its 0.25 mm value would reduce the write-in voltage requirement to one quarter has not proven correct.

(Q) Is the memory resistant to humidity?

(A) Encapsulation in a flexible epoxy should give humidity protection. Memories have been tested, as shown in the paper, with no special regard for humidity and have been operating for over a year in a laboratory environment. No tests have, however, been conducted in humidity or self-spray chambers to any specification.

(Q) What is the current write-in speed?

(A) One-quarter megacycle ($1/4 \text{ Mc}$)

(Q) What is the readout speed?

(A) Currently a word (up to 40 bits) is readout in parallel at $1/4 \text{ Mc}$ clock rate.

(Q) What is the total write-read access time under best conditions?

(A) This is hard to define at present because the memory organization (logic) will affect actual system speed. Depending on many factors it might be $1/2$ -1 Mc.

DIGITAL DEVICES

The Application of Digital Differential Analysers in Control Loops

H. RECHBERGER

Summary

For feedback control there are usually devices of the analogue computer type in service. Digital computers are also in use in a smaller number of cases. The digital differential analysers are a special class of digital computers which, in a simple way, solve ordinary differential equations in real time. These computing devices are useful for control purposes in a broad scope. It is explained how control devices with step-wise function of the motor can be realized. Such a control system gives an improved performance by using simple non-linearities.

The construction of digital parallel computing elements is explained; this is an advantage for integrators which are used for purposes of controlling a system. Such controllers have a high internal stability and need no additional devices for stabilization. The value of parameters can be positioned freely; the technological effort can be adjusted easily, to the accuracy needed, at any time, but this is not the case with the analogue type. The 'building-block design' ensures the greatest flexibility so that a part of the existing control problems can be solved efficiently.

Sommaire

Dans les systèmes de réglage classiques, les boucles d'asservissement sont en général réalisées au moyen de systèmes analogiques; des boucles d'asservissement avec des éléments numériques ont également été réalisées dans certains cas particuliers encore peu fréquents. L'analyseur différentiel numérique constitue une catégorie particulière de calculateurs numériques spécialement aptes à résoudre en temps réel des équations différentielles d'un type classique. Ces analyseurs trouvent un large champ d'application dans le domaine des réglages automatiques. Le rapport indique comment les utiliser en particulier pour réaliser des commandes à moteur, susceptibles d'effectuer des variations selon des échelons rectangulaires. Les performances de ces systèmes peuvent être améliorées par l'utilisation d'éléments non linéaires. La construction d'un élément numérique fonctionnant en parallèle est expliquée. De tels éléments sont particulièrement indiqués pour les intégrations que nécessitent les systèmes de réglage de ce type; ils ont une stabilité interne très élevée et ne nécessitent pas l'utilisation de dispositifs de stabilisation supplémentaires. La valeur des paramètres peut être ajustée à volonté; l'effort technologique peut également être ajusté en fonction des exigences de la pratique, ce qui n'est pas le cas des asservissements du type analogique. Un système de réalisation par combinaison d'éléments normalisés assure une grande souplesse, en sorte qu'une certaine catégorie des problèmes de réglage que pose la pratique, peut être résolue efficacement au moyen de la solution proposée.

Zusammenfassung

In Regelkreisen werden meist zur Regelung Analogiegeräte verwendet. Digitale Rechengерäte werden manchmal übergeordnet eingebaut. Digitale Integrieranlagen sind ein Sondertyp der digitalen Rechengерäte, die die Lösung gewöhnlicher Differentialgleichungen in Echtzeit leicht ermöglichen. Solche Geräte sind deshalb als Regelgeräte in ziemlich breitem Rahmen anwendbar. Es wird gezeigt, wie damit Regelungen mit stufenweiser Verstellung theoretisch und praktisch verwirklicht werden können. Dabei kann die Regelung durch einfache nicht-lineare Beziehungen verbessert werden.

Der Aufbau von einfachen, parallel arbeitenden Rechenwerken ist von Vorteil für Integratoren, wenn sie für Regelungszwecke eingesetzt werden sollen. Solche Regler sind von hoher innerer Stabilität und brauchen keine zusätzlichen Stabilisierungsmittel. Die Parameter können freizügig eingestellt werden. Der technische Aufwand kann der jeweils erforderlichen Genauigkeit und Regelgüte besser angepaßt werden, als dies bei Analogiegeräten der Fall ist. Ein bausteinartiger Aufbau gewährleistet große Flexibilität, so daß ein Teil der bestehenden Regelaufgaben damit auch wirtschaftlich gelöst werden kann.

Introduction

To any surveyor of the modern computing technique it is known widely that there are several different classes of computers in service today. In this field there are: digital computers, analogue computers, mechanical differential analysers, and digital integrators. Of the classes mentioned, the first two categories are preferred in service. In the great majority of the respective cases, the controlling task is performed by means of mechanical, pneumatical, electromechanical or electronic devices; these contraptions being, essentially, nothing but analogue computers constructed for special cases of controlling performance. The largest number of these devices is constructed for the purpose of computing the differential quotients, a proportional value and the integral value of the controlling error, and then of carrying out the summation of these terms.

Sometimes, however, more complicated operations may become necessary. In these operations the independent variable is always the time, and the solutions of ordinary differential equations having the time as the independent variable can be gained, by the most simple and cheapest methods, with the

customary analogue computers. Therefore it is by no means strange or astonishing that digital devices can penetrate only very slowly into the sphere of the practical control technique, although these devices, with respect to accuracy and internal stability, widely surpass all known analogue computers.

The essential parts of digital computers are: the arithmetic unit, the control unit, and the store (known also as 'storage' or 'memory'). The more simply the arithmetic unit and the control unit, the so-called 'logic circuits', are constructed, the more extensive the computing programme is bound to be (the quantity of the necessary separate operations is increasing also). The extreme case of development in this direction would be a device with only one single logic circuit (Sheffer function) and an accurate programme, which latter has to decide with which 'bits' out of the storage there can be executed linked-up operations in a chronological order. In reality, such a contraption will never be designed, because it would be handicapped by an immensely long computing time.

The contrarily extreme case can be visualized as a device with a multitude of arithmetic units, its control unit having a separate circuit wiring for the solution of each and every problem. In that case, there is no more need of any programme. This type of computer is feasible if the question is about computing operations of a certain sort, that is, the solution of ordinary differential equations. This class of computing devices is represented by the digital integrators.

General Features Concerning Digital Integrators

In accordance with its name, such a computing device must be able to compute integrals. But with a digital device, however, integrations cannot be performed exactly; the results must be gained always by approximated summation. Therefore, the fundamental operations

$$y = y_0 + \int dy \quad (1)$$

$$dz = c \cdot y dx \quad (2)$$

will have to be substituted by

$$y = y_0 + \sum dy \quad (3)$$

$$\Delta z = c \cdot y \Delta x \quad (4)$$

Therefore, the fundamental element of any digital differential analyser is represented by the integrator. This device has one input each for the integrand increment Δy , and for the argument increment Δx , the output delivers the integral increment Δz . These increments only are exchanged between the integrators. This is a very essential and important feature, because such increments can be represented very easily in a digital form by electrical pulses. The most simple method is the application of the binary transfer system (pulse or no pulse). In that case, however, the transfer of the increment 'zero' (transfer of a constant) can only be approximated by an alternating positive ('pulse') or negative ('no pulse') increment.

More preferable would be a ternary transfer system, working either by the use of three different voltage levels (positive, zero, negative), or by the use of two separate transfer lines.

The characteristic features and performance of such a digital differential analyser are represented by the scheme of Figure 1. Two storages, the registers Y and R , contain the integrand and

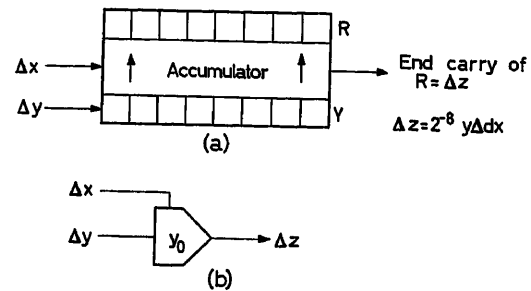


Figure 1. Schematic diagram of an integrator: (a) functional; (b) symbolical

the integral increments. The Y register must be able to store a chosen initial value y_0 . To this the increments Δy are summed up. This operation can be carried out by means of an accumulator, or, more simply, by building up the register as a counter. This counter must be able to handle positive counting pulses as well as negative ones (to count forwards and backwards).

If overflows occur they must be registered without fail, otherwise there is the danger of feeding erroneous values into the following computing process.

Between both the registers mentioned there lies an adder, which has to carry out the task of summing up the contents of both registers and storing again the results in the register R (accumulator). The signals for addition (respective subtraction) are given by the Δx increments. By these, evidently, there is built up in the register R a value which corresponds with the term

$$r = \sum y \cdot \Delta x \quad (5)$$

The increment Δz , on the other hand, is generated simply by feeding every overflow (end transfer) of the R register in the form of a pulse to the output. The number of these overflows of course must be

$$\Delta z = 2^{-N} \cdot y \Delta x \quad (6)$$

if the R register is equipped with ' N ' binary digits. Thus expression (4) is satisfied. The factor c , therefore, depends on the number of digits of the register, and is the larger, the smaller the number of digits happens to be. In view of being able to integrate more quickly (the pulse frequency being constant) there remains only the means of diminishing the accuracy. This possibility of a compromise between accuracy and swiftness in operation is generally not to be found in analogue computers. Apart from integrations, additions and subtractions of increments must also be carried out in digital differential analysers. These operations can be executed by means of simple logic circuits.

It seems that such digital differential analysers are really demanding much more costly expenditure than the corresponding analogue computers, but they have also, in comparison with the latter, two very essential and important advantages:

(1) The stability of the computing circuits is very high, the information transfer and information handling being executed digitally. Thus, there will, on account of this digital method, be every possibility of noise practically disappearing.

(2) Any increment, as input term, can be applied as well for the argument as for the integrand. In this way it is possible, as with mechanical integrating devices, to execute partial integrations. Quadratic functions, products, logarithmic functions and many other non-linear relations between variables can be thus featured without additional expenditure.

Concerning the choice of the number system, it must be stated that the classical binary system here grants very essential advantages. The number of data which must be dealt with is a very small one (in this field there appear mainly the control deviation and a relatively small number of parameters). Output variable is a value working by means of the actuator on the controlled system. On the other hand, the number of computing

to which (when the error x_w varies discontinuously) the unit step function

$$y(t) = K_3 \left[K_0 t + K_1 \cdot (1 - e^{-t/T_1}) + K_2 \frac{t}{T_2} e^{-t/T_2} \right] \quad (10)$$

corresponds. Such a unit step response is shown in Figure 3. In adjusting this sort of controller one's hand can operate freely

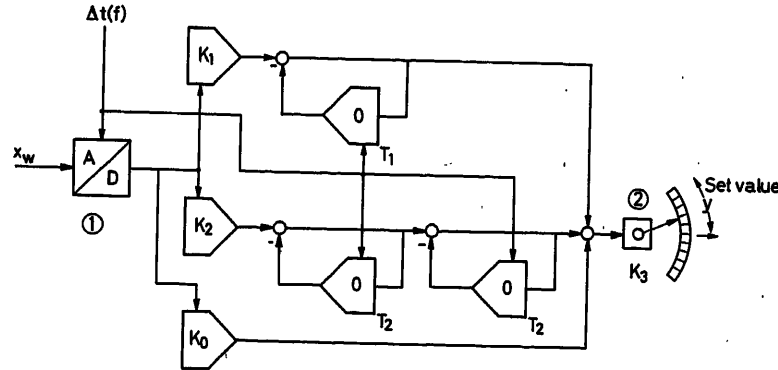


Figure 2. Block diagram of a P.I.D. controller with digital integrators: (1) converter, (2) step actuator

elements is rather a large one, but devices with handling of the digits in the binary system are not as expensive as binary-decimal computers.

Example of a Digital Differential Analyser's Application

It is evident that a digital differential analyser can be used for any control problem. Additionally necessary is an analogue digital converter for furnishing the error x_w in the digital transposition, and a generator for supplying pulses of constant rate. Figure 2 shows, schematically, a simple P.I.D. controller. It is suitable to use, as A-D converters or encoders, such devices which are operating on the time-base coding principle. These devices supply the error immediately in the form of pulse rate. On the output, the controller provides a pulse rate corresponding to the differential quotient of the manipulated variable. The output, then, can very easily be simulated incrementally by means of a step actuator. The three integrators of the input, having fixed integrands, serve as coefficients suppliers, the three feedback integrators being the actual computing elements. Furthermore, the controller essentially works in the forward direction, the otherwise often-used feedbacks not being necessary here, due to the excellent stability of the computing elements. Each of the integrators has the transfer function

$$\frac{X_a(p)}{X_e(p)} = \frac{1}{T \cdot p} \quad (7)$$

the integration constant having the value

$$T = \frac{2^{-N}}{f} \quad (8)$$

in which expression the symbol f stands for the rate of the generator for the constant increment Δt . The plotted block diagram supplies, as can easily be shown, the transfer function

$$\frac{Y(p)}{X_w(p)} = \frac{K_3}{p} \left[K_0 + \frac{K_1 T_1 p}{1 + T_1 p} + \frac{K_2 T_2^2 p^2}{(1 + T_2 p)^2} \right] \quad (9)$$

and thoroughly at will, the three coefficients K_0 , K_1 and K_2 , being quite independent of one another.

There is often the possibility of improving a control system by the introduction of non-linearities. The swiftness of a control system, of course, depends on the loop gain V_0 of the control loop.

On the other hand, the value V_0 , depending also on the coefficients $K_0 \dots K_2$, cannot be increased too much, or else the stability limit will be in danger of being overstepped. A way out of this dilemma is represented by the error-influenced loop gain, in accordance with which method there will be assigned a basic value to a fitting coefficient and then added a quantity corresponding to the absolute value of the error. By this method one is able to deal even with large errors very quickly without endangering the stability of the system. The coefficient mentioned will be in that case:

$$K = G_0 + K |x_w| \quad (11)$$

Just those useful non-linearities can be put in operation very efficiently and easily with digital differential analysers. Figure 4 shows a block diagram for the generation of an error-influenced coefficient. The absolute value can be gained very comfortably by simple rectification of the pulses emitted by the A-D converter. Several controlled systems have direction-influenced

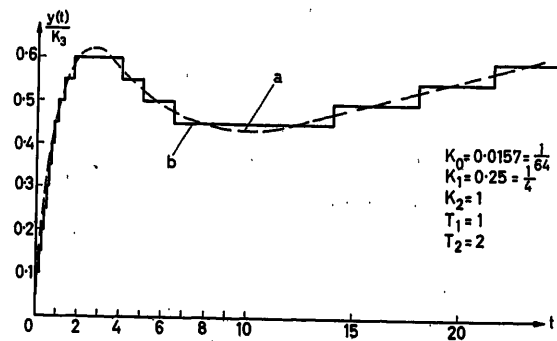


Figure 3. Unit step response—see eqn (10): (a) continuous; (b) step-wise

time constants. In that case an improvement is made possible and especially easy by adjusting the controlling swiftness to the time constant valid for the regarded case, because the arguments of the integrators can be varied at one's free will and

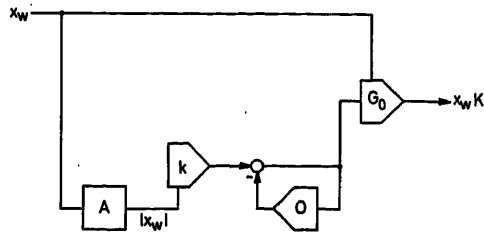


Figure 4. Block diagram for the generation of an error-influenced coefficient

opinion. The great number of possibilities, of which one typical example only has been selected and demonstrated here, is limited generally by the expenditure justifiable in every special case. This amount of expense, however, is dictated partly by the technical layout of a controlled system.

Technical Layout

Concerning controlled systems operating digital differential analysers, it must be borne in mind that the precision of control, generally, is not dependent upon the number of digits of the integrators. Basically and axiomatically the precision of a control system depends on the accuracy of the detecting element. Therefore, the *A-D* converter must operate with precision as well as sensitively and drift free. Of course these characteristic features of a controlling device will be demanded by the more fastidious and exacting of customers.

It is by no means necessary for the controller itself to operate with the fine-stepped precision usually demanded in the digital differential analysers. For it is not the task of the controller to compute functions; it has, on the contrary, the task of driving the step actuator (in more or less large steps) in such a direction, that the error is bound to disappear as quickly as possible. In the steady-state operation, generally, the actuator will remain oscillating between two neighbouring steps.

The operation of digital differential analysers generally takes place in a serial way: the accumulator works up the single binary digits of the registers one after another.

As a result there appears the disadvantage that, in this method, the Δz pulses cannot be built up sooner than when the addition of both the register digits of the maximal value is executed; this fact is the cause of unwelcome delays. The number of digits necessary in controllers generally lies between the values 5 ... 8 (computers having, on the contrary, at least between 20 ... 30 digits!). This fact suggests the design of parallel-operating accumulators. The most difficult problem in these latter devices consists in the quickest possible passing through of the carry from one digit to the next. Figure 5 shows one binary digit of a parallel-operating accumulator (this diagram is valid for summing-up only). It is obvious that there is a multitude of logic elements necessary. To these, moreover, there must also be added a number of amplifiers, with the task of adjusting the carry signals again and again to the right energy level. This expenditure in logic elements can be decreased considerably if it is decided to apply relays for the carry build-up.

It is known that, both of the two summed values being equivalent, the built-up carry is identical to these summed values, uninfluenced by the carry. On the other hand, the carry will be passed through independently and uninfluenced by the summed values if the latter are antivalent. Figure 6 shows such an ac-

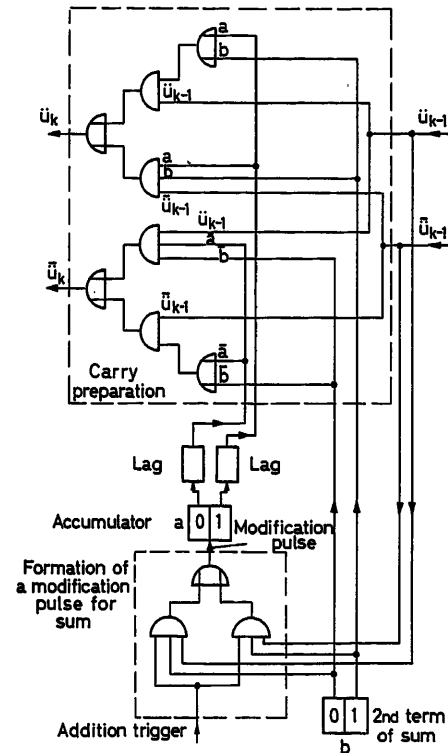


Figure 5. Binary digit of a parallel accumulator

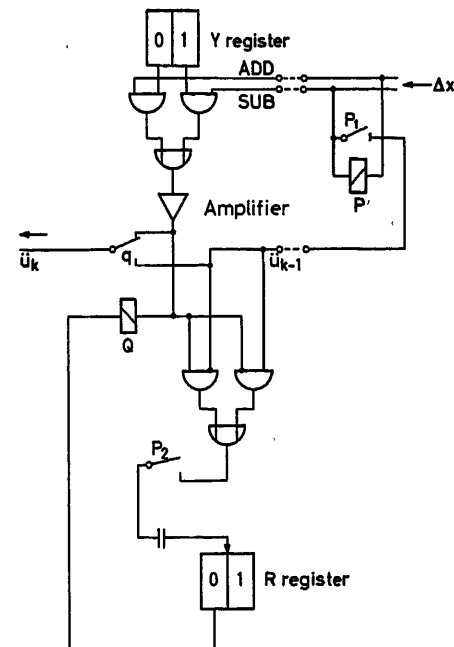


Figure 6. Parallel accumulator for additions and subtractions with relays for carry build-up

cumulator schematically. The relay Q is connected with one end of its coil to the output voltage of the register R . If an addition or subtraction signal is initiated by the pulse Δx , the other coil end is also energized with voltage. Therefore the carry will be taken out of the register in the case of equivalent summed values, whilst the relay will come into action and pass through the carry if the summed values are antivalent. Thus all the carries are prepared.

At the same time, the relay P also comes into action. With this start, the changing signal can put into action the result register digit. This changing signal can be built up only when the number of digits prepared for addition and the carry are antivalent. Immediately after the switching of the R register cell the Δx pulse is finished and all the relays fall off. The relay contacts are not worn out, because there is no power switching in their operation.

In the Technical University of Vienna integrators are being developed which can execute approximately 25 computing steps per second. Of course, the modern computer technique is quite able to display far more impressive successes on this field. One must bear in mind, however, the necessity of such a controlling device being of a most reliable construction; therefore, its parts must not be supersensitively 'overdeveloped'. On the other hand one must not forget that for the larger part of controlled systems the actuators have limits not also in range but also in actuating velocity. Therefore the pulse frequency must be chosen in accordance with the maximal actuating velocity as well as with the number of the actuator steps.

Application Possibilities

As already mentioned, the application possibilities of digital differential analysers are, in principle, not limited with respect to controlling tasks. Of course there will be some limitation dictated by financial reasons, by expenditure, and therefore partly by reliability in service. The quicker and more accurately the device is expected to operate, the higher the amount of expenditure will increase. The term 'swift control', of course, is only a relative one. Its scale is given by the controlled system and its prevalent time constants.

Therefore, the application of digital differential analysers will be economical especially with controlled systems of larger time constants (in the size of a few seconds!). Into this category belong nearly all controlled systems in which some masses have to be put into motion on the input (for example, valves) namely, thermal controls, turbine controls, ships controls etc. Instead of a step actuator there can also be applied an electric a.c. motor (induction motor) which, during every pulse given by the controller, is switched on for a definite short time.

The parallel operating computers described under the heading of Technical Layout have, moreover, the advantage that the controller can always be built up out of a multitude of identical parts ('building-block system'). These computing devices can always be divided into several parts and thus the number of digits for the computed terms can be adjusted accurately to the number of steps of the actuator. In other words, the actuator steps can be divided in such a way that the best possible compromise between controlling swiftness and steady-state oscillating amplitude can be reached.

In this paper only a few examples have been explained and the theme mentioned has by no means been treated exhaustively. The intention is only to show that it is possible technically as well as economically to design controlling devices which can be operated flexibly, adjusted at will and, furthermore, can be applied multilaterally, and which, moreover, by discontinuous digital operation, can reach a high controlling efficiency. A simple and inviting way to this end is shown by the principle of the digital differential analyser.

Bibliography

- KAEMMERER, W. *Ziffernrechenautomaten*. 1960. Berlin; Akademie-Verlag
- ERISMANN, TH. *Digitale Integrieranlagen und semidigitale Methoden. Digitale Informationswandler*, S. 160, 1962. Braunschweig; Vieweg & Sohn
- MATUSCHKA, H. *Nichtlinearitäten im Regler zur Verbesserung der Regelgüte. Regelungstechnik, moderne Theorien und ihre Verwendbarkeit*, S. 172, 1957. München; R. Oldenbourg

Advantages and Possibilities of Digital Speed Control

W. FRITZSCHE

Summary

There have been several reports on digital control of speed and speed ratio during the past few years, yet it is argued whether it is sufficient only to find the integral action component in a digital method and to carry out the remaining control in analogue form.

Beginning with the errors of tachogenerators over a short time range, a limit for fast analogue speed control is attained. This tolerance can be decreased by digital proportional plus reset action or proportional plus reset plus rate action controllers to one-tenth of its original value. Even under extremely difficult working conditions, 0.1 per thousand can be achieved with a control insensitivity of 50 msec. The derivative action component can be found with a new digital measuring system without using a digital prescribed value. The development and the fault compensation of the pulse generators are worth a special observation. The faults can be compensated by regarding the measured errors in the programme or by using special sin-cos-correcting pulse series. Simple correlation methods solve these problems automatically, too.

These digital methods are able to increase the long term constancy of speed controls (digital integral action component), as well as improve essentially the control dynamics in the range of small deviations (digital proportional plus reset plus rate action or proportional plus reset action controllers).

Researches with the analogue computer are favoured by new simulating methods of the digital proportional plus reset plus rate action controller.

Sommaire

Différents travaux ont été consacrés ces dernières années au réglage de vitesse et du rapport de 2 vitesses par des moyens numériques, ces moyens étant destinés essentiellement à l'opération d'intégration nécessitée par le réglage, le reste de ce réglage s'effectuant par voie analogique.

Le générateur tachymétrique introduit une erreur pour les régimes transitoires très rapides, ce qui limite la rapidité de réglage d'un système de réglage analogique. La précision du réglage peut être augmentée dans la proportion de 10 à 1 par l'utilisation d'éléments PI ou PID de nature numérique. Même dans des conditions de travail extrêmement difficiles, une insensibilité de 0,1 pour mille a pu être atteinte, pour 50 msec.

L'élément différentiel D a pu être réalisé avec un nouveau système de mesure numérique, sans avoir à utiliser une valeur numérique prescrite à l'avance. Le développement et la correction apportées par le générateur d'impulsions méritent une mention particulière. Les erreurs sont compensées à partir des erreurs mesurées ou en utilisant des séries de corrections sinusoïdales ou cosinusoidales. Ce problème peut être également résolu en utilisant les méthodes classiques de corrélation.

Les méthodes numériques sont ainsi en mesure, aussi bien d'améliorer en régime permanent la précision du réglage de vitesse (intégration par voie numérique), que d'améliorer la tenue dynamique de la grandeur réglée en régime transitoire pour de faibles variations (système de réglage PID ou PI).

Les études au moyen de calculateurs analogiques sont avantageusement complétées par de nouvelles méthodes de simulation du système numérique PID.

Zusammenfassung

Über digitale Regelungen von Drehzahlen und deren Verhältnissen ist in den letzten Jahren verschiedentlich berichtet worden. Es ist

dabei bisher umstritten, ob es in allen Fällen genügt, nur den I-Anteil der Regelung digital zu ermitteln und die übrige Regelung analog auszuführen.

Ausgehend von den Fehlern der Tachomaschinen im Kurzzeitbereich wird eine Grenze für schnelle analoge Drehzahlregelungen ermittelt. Diese Fehlergrenze läßt sich mit Hilfe von digitalen PI- oder PID-Reglern um eine Zehnerpotenz weiter hinausschieben. Auch bei schwersten Bedingungen können 0,1‰ bei einer Anregelzeit von 50 msec erreicht werden.

Der D-Anteil läßt sich mit einer neuen digitalen Meßanordnung ohne Verwendung eines digitalen Sollwerts ermitteln. Die Ausbildung und der Fehlerausgleich der Impulsgeber verdient besondere Beachtung. Durch Einprogrammieren des gemessenen Fehlers oder durch Anbringung besonderer sin-cos-Korrekturimpulsreihen lassen sich die Fehler ausgleichen. Einfache Korrelationsmethoden lösen diese Aufgaben auch selbsttätig.

Digitale Verfahren sind also in der Lage sowohl die Langzeitkonstanz bei Drehzahlregelungen zu erhöhen (digitaler I-Anteil), als auch die Regeldynamik im Bereich kleinerer Abweichungen wesentlich zu verbessern (digitaler PID- oder PI-Regler).

Untersuchungen auf dem Analogrechner werden durch neue Nachbildungsverfahren des digitalen PID-Reglers begünstigt. Abschließende Versuche z.B. mit 50-kW-Maschinen sollen die Ergebnisse dieser Arbeit in der Praxis erhärten.

Digital rotary speed control, and quantities derived from it, are finding an increasingly wide field of application. In addition to their obvious advantages, both the technical and economical limits of digital speed regulations are considered in detail in this paper.

Limits of Accuracy with Analogue Speed Control

The problem clearly arises from a juxtaposition of the two systems. Analogue speed control is no longer able to meet all requirements of tolerances which are much smaller than ever before. Hence the economical limit of digital speed control is at the point where the analogue regulations begin to miss the required accuracy. On the other hand, combinations of digital and analogue systems—the latter ones fully exploited—in many cases render optimal solutions.

Up to the present time, for speed control, the prescribed value is frequently set on uncalibrated potentiometers. The reproducibility of such a selected value is not yet satisfactory. It can only be achieved by superimposed manual control with the aid of higher classified measuring instruments. In the case of the digital control loop as shown in Figure 1, the counterhatched areas have to work in a digital way. The remainder of the control loop, hatched in one direction, may partly or wholly work on digital or analogue principles.

No special attention should be paid here to the measurement of actual values, as this is the weakest point in an analogue control circuit. In most cases the measured value represents the

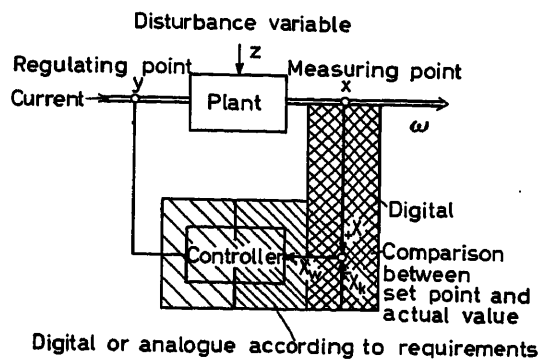


Figure 1. Block diagram of digital control circuit. Desired value X_k ; actual value X ; deviation X_W

voltage of d.c. or a.c. tachogenerators. Depending on the instantaneous values for rotary speed, the errors can be classified as: (a) errors in proportional response of speed but of constant relative influence, and (b) errors in no direct relation to speed, with a strong influence at low values.

With respect to their time characteristic the deficiencies inherent in measuring actual values can be classified as:

- (1) Slowly working influences.
- (2) Influences having a frequency close to the number of revolutions.

The most important slowly working influence is the decrement of the widely used permanent magnetic flux in relation to temperature which amounts to approx. per centigrade 0.4 parts per thousand. In certain ranges a compensation is possible (see Figure 2). In connection with d.c. tachogenerators the variable voltage drop at the brushes should also be considered, whilst a.c. tachogenerators require a rectifier, the threshold voltage of which varies with temperature.

The known above-mentioned errors of the tachometer devices do not cause serious trouble during short operation periods. A certain noise is present in each tachogenerator voltage. Irregularities in magnetic permeability and constructional tolerances may cause other interfering waves of low order which tend to be amplified by coupling faults (see Figure 3). Their magnitude is between 1 and 10 per cent of the measured value concerned. Cancelling is possible by smoothing the tachogenerator voltage, in case the shape of the transfer characteristic is not an important factor. Superimposed a.c. voltages of very low frequency are a factor which causes the greatest

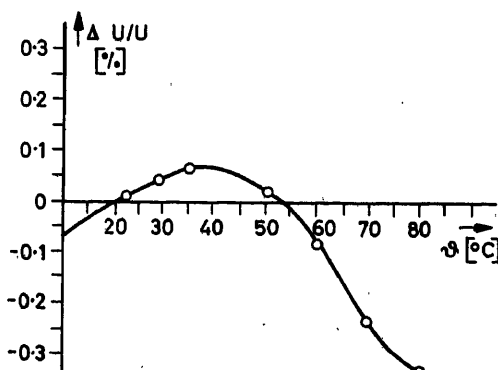


Figure 2. Voltage change of a compensated tachometer device, depending on the temperature θ

difficulty in all speed control, as their periods (40 msec in the case of 1,500 rev/min) will easily interfere with the first zero variance* of well-designed gear. All smoothing, which is the more effective the higher the degree of order, is rendered difficult at lower frequencies due to a decreasing number of revolutions.

The a.c. tachogenerators show a considerable portion of harmonics even for multiphase designs (40 parts per thousand in the case of a six-pulse rectification). The occurrence of interfering harmonics can be favourably influenced by a suitable shaping of the a.c. voltage curve.

The Application of Digital Control Principles

The use of registered values taken from memories, for example punched tapes, can promote the application of digital engineering. Obviously the setting of values is no longer subjected to the arbitrary actions of operators; this is a great advantage because of the present lack of skilled operating personnel. Moreover, the number of revolutions per unit time can,

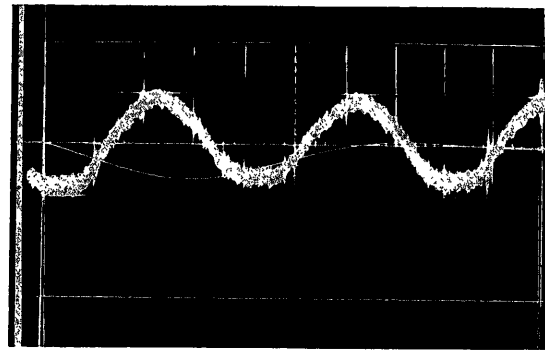


Figure 3. Wave disturbing effects (noise) of a d.c. tachometer device. 1 cm on the screen (in vertical direction) corresponds to 0.67 per cent; 1 cm on the screen (in horizontal direction) corresponds to 10 msec. Drawn by the same scale is the computed step response of the speed in the circuit in accordance with Figure 4 at 1/10 impact of rated load (torque) ($M_s = 0.1 M_n$)

because of its nature, easily be found in the digital way simply by counting. However, it is important, in most cases, to answer the need of an increased and hitherto unknown accuracy.

Different requirements in connection with the time characteristic classify the applications and the reasons that demand digital rotary speed control and its working conditions. The following two groups result from these requirements.

- (1) The constancy over a long period and the reproducibility of analogue control action is not yet satisfactory.

The reasons for this may be either deviations of the tachogenerator voltage, a temperature rise or aging effects in connection with transistors and Zener diodes, in set point and comparative stages. On the other hand, the dynamics of manipulating the independent variables and the reaction to shock disturbances may be satisfactory. An analogue P control†, or,

* The first zero variance is the period required to attain the prescribed value first time after the beginning of the control process.

† P = proportional part of deviation of regulation

I = integral part of regulation

D = differential part of regulation

IP = controller with proportional plus integral action

IPD = controller with proportional plus integral plus rate action

as the case may be, a *PD* control, together with a digital *I* part will do it. The requirements with respect to the limiting frequency of the digital part (1 to 10 kc/sec) are moderate¹.

(2) With regard to the dynamic response of the measuring member (tachometer), the demand is often higher than the tolerable economic expenditure.

Even in the case of the strongest admissible smoothing the difference of regulation to be measured lies with respect to its amount and frequency within the range of the noise (that is the upper and higher undulating waves) of the tachogenerator voltage. In order to improve the dynamics of control, the *P* value of the regulation difference must be computed accurately and quickly by digital means. Sometimes it may even be necessary to compute the differential quotient in the digital way. As a

with a sensitively adjustable proportion that allows reproduction.

Such accurate drive should not, however, be exposed to large-scale disturbances, except those inevitably coming from the work process. The shaft here is assumed to be the collector of all impacts due to interfering powers. For the step response which was found by an analogue computer (as additionally plotted in *Figure 3*) a load impact of one tenth of the nominal value of torque has been taken. There are needed about 50 msec for the final adjustment (± 0.5 parts per thousand) of this process. The whole process of adjustment shows smaller amplitudes than those appearing as noise in the tachometer voltage. Therefore it can be mastered only by very fast working digital regulators. Here it should be mentioned that a digital regulator of this type puts out smoothed d.c. voltages and currents which may, under stationary conditions, vary by only one digital unit. This means that the usual smoothing preceding the rectifier input, with a time constant of 10 msec, may be dropped⁵. A completely digital control system (class *IPD*, or *IP* respectively) is most appropriate, especially for all problems involving considerable dynamical difficulties such as a fast regulation of large moments of inertia.

Digital Measuring and Control Systems

Digital revolving speed control is based on quantized measuring of a value as it can be represented by a sequence of pulses from a pulse generator (transmitter, transducer, sensing element) seated on the shaft to be controlled. The different values of the regulator output, the integral, differential, and the proportional parts, can either be obtained directly from the measuring variables or by subsequent analogue computations.

The most elementary device measures the natural value, that means the actual number of revolutions itself [see *Figure 6(a)*], as it would otherwise be achieved by means of the tachometer voltage. Besides the revolving speed itself, the ratio of two speeds or the ratio to a directing quantity such as a master frequency has to be determined in many cases⁸.

The basic arrangement (*Figure 5*) is composed of two counters and one gate, where even one counter can be spared by a suitable choice of frequency. The two frequencies f_1 and f_2 can either be measuring variables or constants by turns. Even a comparison quantity can be used for f_1 and, in certain cases, also for f_2 , instead of constant values. Since the number of revolutions can easily be converted into frequencies by means of a pulse generator (transmitter, sensing element, etc.), they can be measured correspondingly. *Figure 6* gives a summary of the most important digital principles of measuring rotary speed.

The *I* part can be evaluated in the analogue way from the *P* value of the regulation difference which is drawn from the

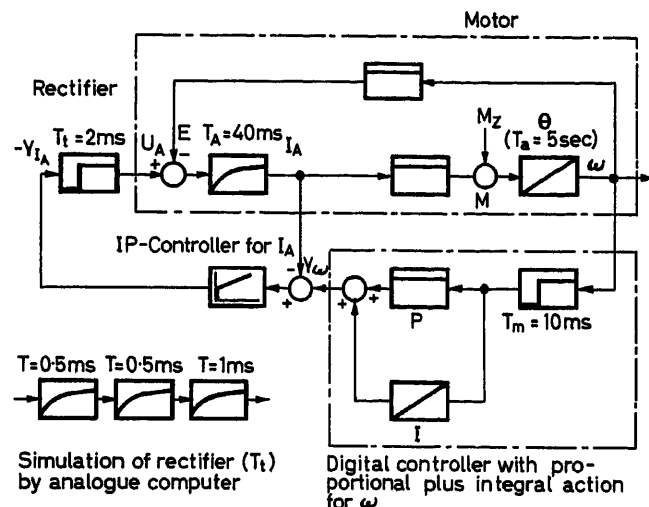


Figure 4. Block diagram of a d.c. shunt motor with constant field excitation and rectifier supply of the armature circuit with an analogue controller with proportional plus integral action for the armature current and a digital controller with proportional plus integral action for the speed (ω)

result of the comprehensive information, there are considerable demands with respect to the upper limit of frequency (for example 1 Mc/sec) which can, however, be mastered easily by transistorized counters.

In order to recognize clearly the capacity of digital revolving speed control systems, a qualitative and a quantitative example shall be given according to the second definition. The example applies to a single drive of high accuracy as well as to a complex system of motors, where the speed ratios are adjusted in relation to a directing unit. So the block diagram of *Figure 4* can also be considered as a representation on an analogue computer. An additional moment of inertia θ is taken for a load, as this is the general practice in connection with multimotor drives (time required to start running up to full speed $T_a = 5\text{ sec}$). At maximum frequency of 1 Mc/sec the measuring time $T_m = 10\text{ msec}$ of digital control allows an accuracy of measuring and adjusting the *P* part of 10^{-4} , i.e., every 10 msec the angular velocity ω is measured with an allowance of 0.1 part per thousand⁴. The integral part reaches a substantially higher accuracy, which may be described as absolute. The conditions prevailing there may be regarded as a true angular synchronism, but

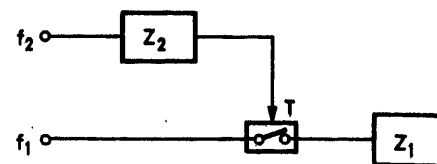


Figure 5. Basic principle of measuring frequencies and their ratio by two counters

d-a-converter (weighting resistances)⁷. The I part may also be calculated by digital means.

A direct measurement and control of the I part of speeds, i.e. a position control, has been realized in printing register control systems¹¹. The pulse-phase method⁸ is obtained by extension and the introduction of bi-directional counters. The prescribed frequency drives the differential counter forward, the actual frequency takes it backwards. With such an arrangement difficulties arise, caused by the necessity for the utmost sensitive adjustment of the prescribed value, which should, if possible always be carried out proportionately, for instance, simply by multiplying the frequency with an adjustable factor. Figure 8 shows a suitable multiplier for prescribed frequencies⁶. A similar effect can be attained by a different method, in accordance with Jones⁹.

The D part can also be determined digitally. In digital rotary speed-measuring systems the differential quotient can be obtained only as a difference value of two subsequent measurements. Thereby the latest measured value is always compared

with the previous one in the memory before the transformation is carried out (Figure 7).

This summary deduces that the pulse method involving a directing frequency together with prescribed frequency multipliers has an especially simple construction even in the case of an intricate multi-motor system. The drawback of this method is that it gives only the integral value of the regulation difference with digital accuracy, whilst the P and D values must be found by analogue means. These drawbacks have been commented upon in the first examples of control systems (see Figure 6).

As a consequence of the irregular distance of prescribed value pulses (see Figure 8) a digital measuring of the P part can also be performed with the aid of extensive additional technical expenditure and only in the case of long measuring periods. For control dynamics its gain would be low because of the inherent dead time. A D part is certainly not evaluated by means of this sequence of pulses in prescribed frequency with any satisfactory accuracy.

All that is actually needed to figure out the difference of two

Figure 6. The most important digital measuring methods for speeds and speed ratios, and their application for digital controllers

Type of circuit

Input frequency f_1

Input frequency f_2

Formula (z_1 result obtained in Counter Z)

Favourable for making the following measurements

Set point adjustment of

Set point adjustment of speed

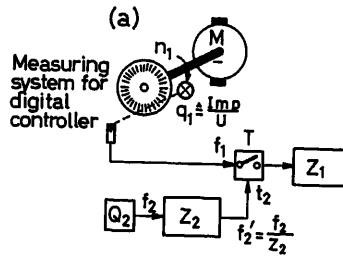
Dependence of controller action

Advantages

Especially suitable for

Disadvantages

notes



counter with fixed counting time, frequency measurement (events per unit time)
measured variable fixed
 $z_1 = f_1 \cdot z_2 / f_2 = n_1 \cdot q_1 \cdot z_2 / f_2$

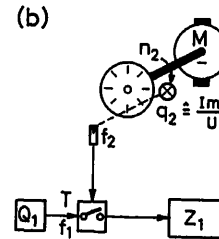
high speeds

counter Z_1

P and I proportional

a absolute

easy to adapt armature voltage controls pulse transmitter, multiple-point, frequency limit of counter cannot be utilized



time measurement of periods (time)

fixed (may be adjustable by means of frequency multiplier)

measured variable

$z_1 = f_1 / f_2 = f_1 / n_2 \cdot q_2$

low speeds

counter Z_1

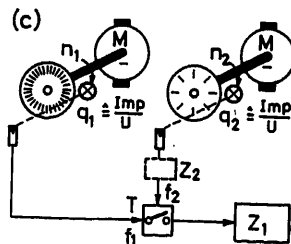
inversely proportional ($1/n_2$)

P inversely proportional to speed, digitally calculated integral value proportional frequency limit can well be utilized speed control in field

1. measuring time inversely proportional to speed, disadvantageous for time behaviour

2. reciprocal setpoint adjustment

disadvantage 2 can be avoided by applying frequency multiplier for f_1



ratio measurement
(higher) measured variable
(lower) measured variable
 $z_1 = f_1 / f_2 = n_1 \cdot q_1 / n_2 \cdot q_2$

speed ratios

proportional to ratio (n_1/n_2)

digital I part proportional, P proportional to ratio

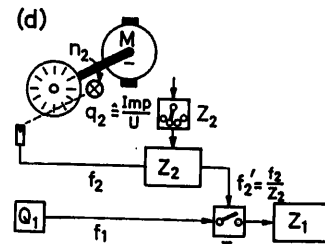
easy ratio measurement, little costs

control deviation and analogically calculated integrals suitable for field excitation, digitally calculated integral suitable for armature control

1. measuring time inversely proportional to f_2

2. pulse transmitter, multiple-point, frequency limit of counter cannot be utilized

f_1 may also be introduced directly as master frequency (multi-motor drive)



measurement of relative speed deviation (combined method)

fixed (if necessary, adjustable for interpolation)

measured variable, adjustable number of periods

$z_1 - z_2 = d = \delta \cdot f_1 \cdot t_m$

high accuracy for relative deviations

Z_2 (total) speed n_1 , Z_1 ratio

Z_2 proportional (n) Z_1 proportional n/n_2

P and I proportional to ratio

measuring time almost constant, frequency limit can be utilized,

easy to adapt

multi-motor drives, with control over field excitation

higher costs

with auxiliary device for single drives with fine adjustment

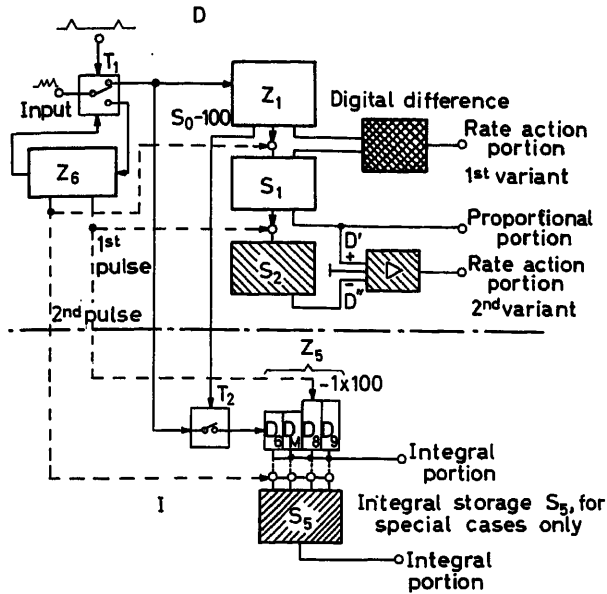


Figure 7. Digital evaluation of the integral portion (bottom) and digital (1st variant) and analogue (2nd variant) evaluation of the rate action portion; control by the side-way counter Z_6

measurements is a rough approximation to an exact prescribed value. The interval between two actual value pulses, which in general do not differ in shape, is measured by a known constant frequency (for example 1 Mc/sec). Certainly any changes of the prescribed value would make this device work incorrectly. Any such deviations can, however, be registered beforehand, so their detrimental influences can be cancelled by analogue additions. Besides the D part the P value is absolutely necessary for manipulation; it can simply be obtained with satisfactory accuracy by an integration of the D part.

The upper limit of accuracy is predetermined by the limiting frequency of the measuring device. The basic law of digital measuring and control of revolving speed is

$$\alpha \cdot T_m \cdot f_g = 1$$

By this equation the sensitivity for measuring and setting α of the P part is combined with the measuring time T_m and the limiting frequency f_g of the device. In transistorized counters $f_g = 1$ Mc/sec can easily be realized. On the other hand, the devices a and c in Figure 6 must be supplied with this high frequency directly by the measuring transducer. The limiting frequency of germanium diodes is about 50 kc/sec. Special silicon diodes can be used up to the Mc/sec range. In connection with other measuring set-ups (b and d) the pulse frequency of the pulse generator is considerably lower. Therefore a well-defined point on the slope of the pulse curve must be able to be reproduced (see also Figure 15).

It may be desired to detect changes of a variable which are larger than in accordance with the above tolerance α for measuring and setting in less time, i.e. with a shorter T_m . In case each pulse of the measuring frequency is analysed the measuring time of the P part can be reduced. The measured value then varies between two figures, whilst the average of m measuring times is to be measured with m times the accuracy: $\alpha_m = \alpha/m$.

Thereby the adjustment of the prescribed values becomes coarse. The desired partitioning of adjusting the prescribed value then is obtained by a continuous switch-over between two values in a similar way as proceeded in connection with the frequency multiplier in Figure 8.

The smallest attainable measuring unit for the revolving speed (P value) is $\alpha = 1/f_g \cdot 1/T_m$. The smallest unit for acceleration (differential quotient) β' is:

$$\beta' = [(x_1 + \alpha) - x_1] / T_m = \alpha / T_m = 1 / (f_g \cdot T_m^2)$$

During the time T_a the speed of an uncontrolled driving system can drop from its rated value to zero in case of a rated load (torque) impact being applied. At sudden load impacts controlled driving systems have the same initial slope of speed loss response. Therefore the smallest measurable unit (the sensitivity

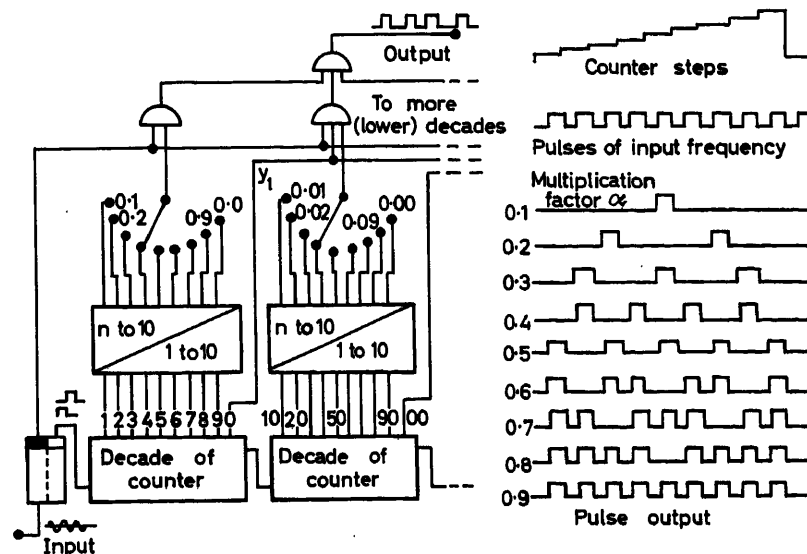


Figure 8. Frequency multiplier, factor $\alpha < 1$

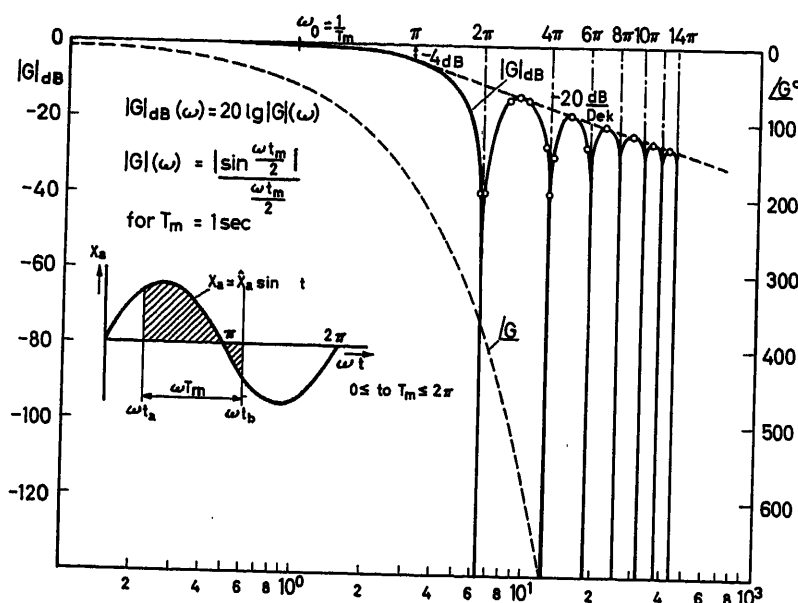


Figure 9. Response characteristic of counting measuring section

of measuring the accuracy) β of the D value should be related to this slope ($1/T_a$) and hence be made undimensional:

$$\beta = \beta' 1/(1/T_a) = T_a/T_m \cdot \alpha = T_a/(T_m^2 \cdot f_g)$$

Owing to the inherent limit of accuracy in digital measurement the measured speed value is able to vary for one unit. Accordingly, the sign of the D part changes frequently. Therefore it seems to be reasonable to drop the amount of \pm unit in the D part.

Both the D and the P parts are responsible for the observance of the tolerances in certain short periods (dynamical). The long-time accuracy and the reproducibility depend only on the I part. On the other hand, the total accuracy depends on the basic quartz frequency, provided that the I part is formed by digital means. The tolerances (e.g. 10^{-7}) are smaller by powers of ten than is usually required in control systems. A possible remaining positioning error can be eliminated by a subsequent second integration (see lower portion of Figure 13).

It is always presumed there that during the step by step measurement [for example according to Figure 6(a)-(d)] each pulse³ is used (see Figure 7) and that the integral counter does not reach a limit due to interfering influences. If exactness of position is required, the counter should be dimensioned accordingly¹. With regard to the long-time constancy the I part could be slower. There is, however, a limit where the transient function drags too much. An analogue integration must then be added in order to transform the I part into the necessary amount. The result is a slow correction of the set point by digital means. In such cases it is frequently expedient to perform an integration by a precision motor with a gear-coupled correcting potentiometer in the circuit of the prescribed value.

Checking of Digital Speed Control Systems by Analogue Computers

For programming an analogue computer, the time behaviour of the counter must be known. The frequency response curve

can be plotted by the average output value x_a , and the measuring time T_m according to the following scheme (see Figure 9, left side). Since the average also depends on the initial phase position $\omega \cdot t_a$ of the measuring time, the average value x_{aM} of all possible phase variations is calculated for general considerations. The variation of amplitude in time is then described by the following double integral:

$$x_{aM}(\omega) = \frac{1}{\Delta\omega \cdot t_a} \cdot \frac{\hat{x}_a}{\omega \cdot T_m} \int_{\omega t_a \min}^{\omega t_a \max} \int_{\omega t_a}^{\omega t_a + \omega T_m} \sin \omega t \cdot d\omega t \cdot d\omega t_a$$

$$x_{aM}(\omega) = \frac{2}{\pi} \hat{x}_a \frac{\sin(\omega T_m/2)}{\omega T_m/2}$$

The average phase response $\angle G$ corresponds to that of a dead time circuit with a dead time equal to the measuring time T_m (see Figure 9). This only applies, however, in the case which uses either a counter with transfer to a memory, or two counters by turns. If two measuring devices are used, overlapping each other with a period $T_m/2$, the dead time average will only be $\frac{1}{2} \cdot T_m$. n measuring devices accordingly have a dead time of $(1 + 1/n) \cdot T_m/2$.

In order to reproduce a counting device by means of the analogue computer, because of the decrease of amplitude with frequency, instead of the usual Padé networks with all-pass characteristics¹³ time-lag circuits or simulating circuits are used (see Figure 10).

The input of values into a counter can be compared with an integration (first integrator). The integrators 1 to 4 are subject to a cyclic substitution by a step by step system. The second integrator serves as a memory for the P part. The D part is computed by means of the second memory (third integrator) according to Figure 7, second variant, as difference $D = D' - D''$.

The I part of the difference of regulation can be computed by analogue integration of the P value. Figure 10 shows a reproduction of the digital circuit shown at the bottom of Figure 7.

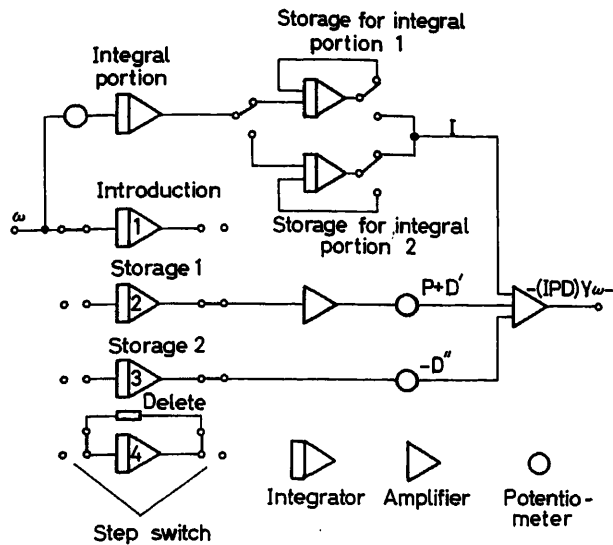


Figure 10. Simulation of a digital controller with proportional plus integral plus rate action on an analogue computer (see also Figure 7, rate action portion, 2nd variant)

The two integral memories follow the real I part by turns. In between they keep a constant value for evaluating over one measuring period T_m .

The block diagrams for analogue computers of two different digital drive control systems, are shown in Figures 4 and 11. Figure 13 shows the step response function of a control system according to Figure 4, together with curves representing the armature current and the rectifier voltage.

The real digital regulator can be examined by a precise voltage-frequency converter in series connection [see Fritzsche⁷ (Figure 13)], together with the system simulated in the analogue computer.

Error Compensation of Pulse Generators

For scanning of rotations both optical and magnetic pulse generators (transmitters) are used¹⁴. They can be produced with

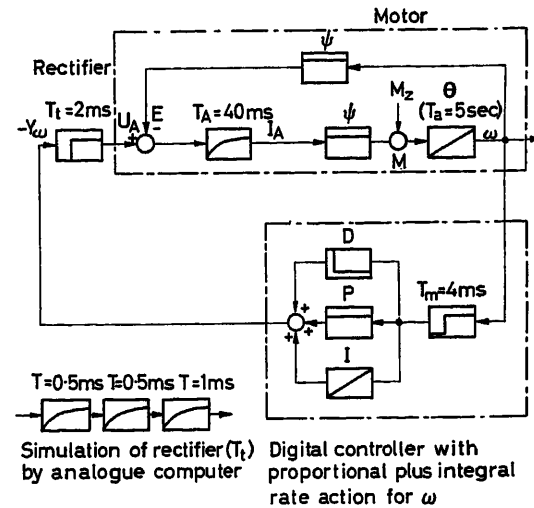


Figure 11. Block diagram of a d.c. shunt motor with constant field excitation and rectifier supply of the armature circuit with a digital controller with proportional plus integral plus rate action for speed control (ω)

an accuracy of pitch that is much superior to that obtainable from the accuracy of voltage with noise suppression in connection with tachogenerators. The relatively small inertia inherent in such a pulse generator considerably eases the solution of the problem of coupling.

The following deals with the compensation of the remaining faults. Figure 16 shows a four-part pulse transmitter. The different distances of the pulses z_1, \dots, z_4 are measured after the mounting of the device and regarded as a correction of prescribed values. The input can be carried out by a pre-selection on the side-channel counter Z_6 (Figure 7) without impeding the usual adjustment of the prescribed value at Z_1 . The determination of fault compensations can be performed by statistical methods also during the operation cycle. Thus a self-optimization is performable with a tolerable expenditure. This method applies only to discs bearing a small number of marks.

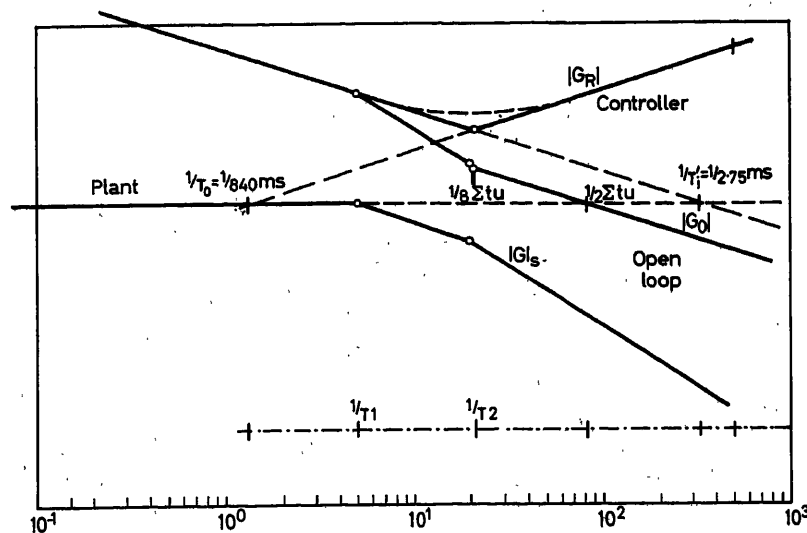


Figure 12. Frequency response of digital controller with proportional plus integral plus rate action (symmetrical optimum value)

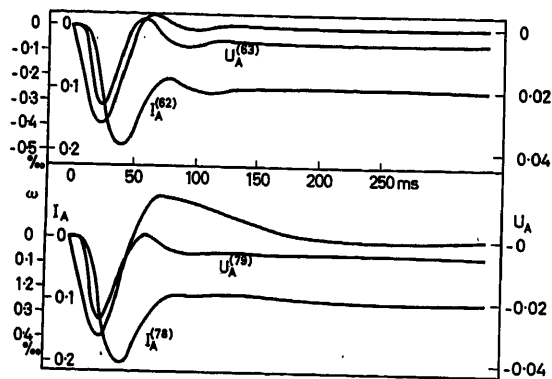


Figure 13. Time behaviour of the control circuit according to Figure 4 at a sudden load increase (1/10 of nominal torque) calculated by an analogue computer. Lower curves with second integration; revolving speed (curve without sign); U_A : rectifier voltage (armature voltage); I_A : armature current

By a harmonic synthesis a planned error compensation is possible even for discs bearing many marks. Figure 17 shows a suitable disc. The outer circle of marks is divided proportionately and gives the usual measuring pulses. The inner circle with half the perimeter has a sine partition and is scanned by four pulse transmitters dephased against one another by 90 degrees, which permit counters to analyse all four components as a sum of increment pulses. Thus the $\pm \sin$ and $\pm \cos$ parts are evaluated to be used for compensating the measuring errors. If necessary, sine partitions of a higher degree of order can be provided. An automatic correction, that is a self-optimization, is possible in this case, too.

Economical Limits of the Application of Digital P and D Parts

The economical limit of digital IP and IPD control systems is where disturbances frequently cause regulation differences of

an amount which is larger than the average errors of less expensive analogue regulators. It may be important for the periods in which the regulation process is not disturbed to keep the long-term errors small by digital I parts or corrections of the prescribed value.

In control systems where the allowable tolerance of less than 2 parts per thousand prevails, the harmonics of the tachometer will influence the dynamics decisively. If the disturbances cause transient regulation differences of more than 5 parts per thousand the limit of the economical application of I and D parts has been positively passed over. The excessive amplitudes in case of load disturbances of the mentioned drives are approximated and compared with the limit of 0.5 per cent.

Figure 4 shows the structure of a d. c. shunt motor with armature voltage control by a six pulse rectifier, whilst the armature current is controlled by its own analogue PI controller. For the usual values the first zero variance time t_{an} in manipulating the current is five times the mean time delay T_t of the rectifier ($t_{an} \approx 5 T_t$). The revolving speed control circuit consists of the integrating element Θ with the integrating time T_a and a dead time T_t which is in its turn composed of the measuring time T_m of the digital regulator and the time required for first zero variance of the inner current control circuit. The optimum P amplification V_R of the controller is then:

$$V_R = T_a / 2(t_{an} + T_m) = T_a / (10 T_t + 2 T_m)$$

$M_z = \lambda M_n$; M_n = rated torque of the motor.

A load disturbance with a moment of disturbance M_z has the effect λ/V_R . According to the above-made assumption this value shall not exceed 0.5 per cent:

$$200 \lambda \leq T_a / (10 T_t + 2 T_m)$$

An example, deliberately chosen as unfavourable, is:

$$T_a = 500 \text{ msec}; T_t = 1.67 \text{ msec}; T_m = 10 \text{ msec.}$$

$$200 \lambda = 500 / (16.7 + 20) = 13.6 = V_R = 7.8 \text{ per cent}$$

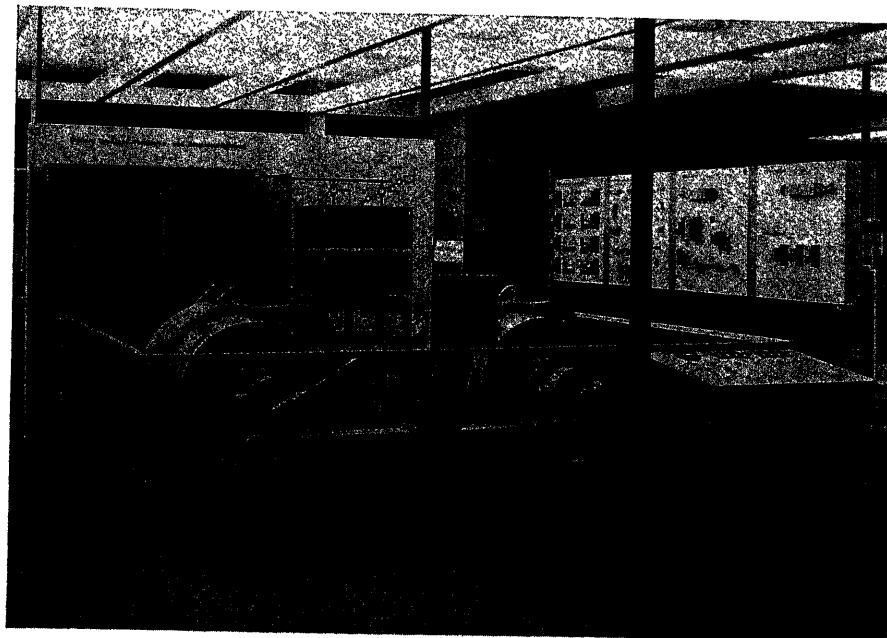


Figure 14. Installation for digital speed control systems (combined method) with 50 kW motors and a 6000 point pulse transmitter

Hence the ratio moment of disturbance to rated torque M_n is 7.8 per cent. With this disturbance ratio the temporary speed loss becomes 0.5 per cent. In case it is below 7.8 per cent, a control with digital P and I parts is expedient.

For the digital IPD controller in Figure 11 with a frequency characteristic as, for example, represented in Figure 12 according to the symmetrical optimum¹⁵, with the electromechanical

(run-up) time constant $T_M > 4T_A$ (armature time constant) is valid:

$$V_R = \frac{T_m T_A}{8(T_i + T_m)^2}, \quad T_M > 4(T_i + T_m)$$

In this case it still has to be taken into account that the disturbance moment will influence the speed on behalf of the armature voltage control only in the ratio ε (voltage drop at the armature at rated load to rated voltage):

$$\varepsilon = I_A \cdot R_A / U_A, \quad 200 \lambda \leq V_R / \varepsilon, \quad 200 \lambda \varepsilon = \frac{T_m T_A}{8(T_i + T_m)^2}$$

Outlook

It can finally be said that an essential dynamical improvement is made possible by digital control systems. Further effects can probably be achieved by systems which are described by difference equations^{16, 17}. Their application to digital revolving speed control is especially suitable since the necessary scanning is inherently made.

The further development of this trend of ideas is promising for the future.

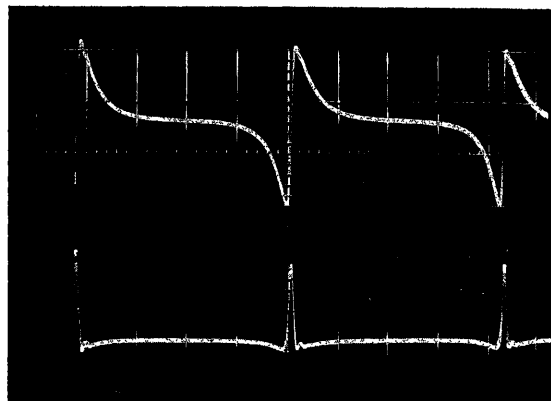


Figure 15. Top: voltage curve of a magnetical pulse transmitter; bottom: differentiated voltage

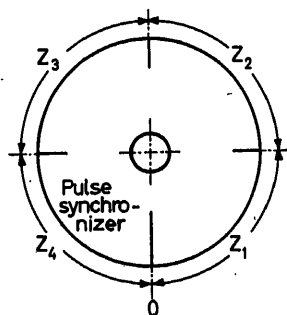


Figure 16. Pulse transmitter, correction of the distances $z_1 \dots z_4$ by a suitable set point input

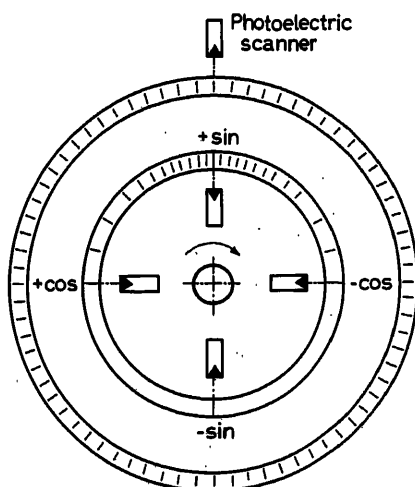


Figure 17. Pulse transmitter disc with correction values $\pm \sin$ and $\pm \cos$

References

- 1 LEONHARD, W. and MÜLLER, H. Stetig wirkende digitale Drehzahlregler. *ETZA* 83 (1962) S. 381–387. 11 B. 8 Q
- 2 JÖTTEN, R. Zur Theorie und Praxis der Regelung von Stromrichterantrieben. *Regelungstechnik* 7 (1959) S. 5–9 und S. 44–47. 12 B. 14 Q
- 3 FRITZSCHE, W. Digitale Regelung von Drehzahlverhältnissen. *AEG-Mitt.* 51 (1961) S. 135–145. 16 B. 16 Q
- 4 FRITZSCHE, W. Genaue und schnelle Regelungen von Drehzahlen durch digitale Methoden. *AEG-Mitt.* 50 (1960) 8/9 S. 419–426. 15 B. 10 Q
- 5 JÖTTEN, R. Regelkreise mit Stromrichtern. *AEG-Mitt.* 48 (1958) S. 613–621. 14 B. 11 Q
- 6 KROCHMANN, E. *VDE-Buchreihe* Bd. 8
- 7 FRITZSCHE, W. Digitale Erfassung von Meßwerten. Die elektrische Ausrüstung (1961) S. 78–87. 33 B. 30 Q
- 8 NOURNEY, C. E. Ein digitaler Regelkreis zur Gewinnung einer großen Anzahl feinstufig einstellbarer Frequenzen. Teil I. *Regelungstechnik* 8 (1960) 10, S. 345–348. 5 B. 4 Q
- 9 JONES, C. I. and NICE, R. Frequenzgeber und Teiler mit veränderbarer Frequenz. *DAS* 1001 084
- 10 KESSLER, G. Digitale Regelung der Relation zweier Drehzahlen. *ETZA* 82 (1961) S. 574–579. 10 B. 11 Q
- 11 RAMMIN, H. Photoelektrische Steuer- und Regelgeräte in der graphischen Industrie. *AEG-Mitt.* 48 (1958) 10, S. 575–584. 23 B. 7 Q
- 12 FRITZSCHE, W. Digitale und analoge Rechenelemente und ihre Anwendung in der Antriebstechnik. In: Steuerungen und Regelungen elektrischer Antriebe. *VDE-Buchreihe*, Band 4, VDE-Verlag GmbH, Berlin, 1959 S. 337–364. 27 B
- 13 AMMON, W. Zur Nachbildung von Totzeiten mit Elementen des Analogrechners. *Elektr. Rechenanl.* 3 (1961) S. 217–224. 10 B. 8 Q
- 14 Impulsgeber für die elektronische Zähltechnik. *AEG-Mitt.* 52 (1962) S. 174. 2 B.
- 15 KESSLER, C. Das Symmetrische Optimum. *Regelungstechnik* 6 (1958) S. 395–400 und 432–436. 16 B. 13 Q
- 16 SCHNEIDER, C. Über die Nachbildung und Untersuchung von Abtastsystemen auf einem elektrischen Analogrechner. *Elektron. Rechenanl.* (1960) S. 31–37. 26 B. 8 Q
- 17 HABERSTOCK, B. Synthese eines nichtlinearen Abtastreglers. *Regelungstechnik* 11 (1963) H. 5

DISCUSSION

W. LEONHARD, *Siemens-Schuckertwerke, Erlangen, Scharowskystr., Germany*

Professor Fritzsch's paper is very interesting. I agree with him that digital speed control is a valuable tool for precision drives as required, for example, on continuous production lines. There may be some difference of opinion in that Professor Fritzsch proposes for certain drives a digital *IPD* regulator, whereas I believe that a digital *I* loop, as a supplement of an analogue regulator, is always satisfactory and much more advantageous. The reasons are as follows:

(1) According to our observations, the response of practical speed control loops is normally not limited by the tachometer. A good d.c. tachometer, properly mounted, will not produce low-frequency harmonics to an objectionable degree. The limitation arises normally with the load. Measurements on a large paper mill have shown that the large inertia load, the resiliency of the gears and motor coupling, and the beat frequencies of the gears can combine to produce very low frequency speed fluctuations far in excess of the harmonics of the tachometer.

(2) The rise time of a speed control loop for a high inertia load, such as on paper mills, using a Ward-Leonard drive system lies in the order of several hundred msec. Such a system responds, therefore, too slowly to be affected to any degree by small electrical harmonics from

the tachometer (e.g. 25 c/sec at 1,500 rev/min). In comparison, the mechanical disturbances are of much lower frequency. They restrict the design of the regulator seriously since they could be amplified by the speed control loop.

(3) It follows, in our opinion, that no dynamic advantage can be gained by computing the *P* or *D* term of the controller by digital means. With respect to dynamics and short-term accuracy, a normal inexpensive analogue *IPD* controller is fully satisfactory. All that may be needed is a relatively slow *I* term to correct the drift of the analogue regulator and to obtain average angular synchronism with the reference frequency.

An additional advantage is that no high-frequency transducer and circuitry are necessary: 10 kc/sec has proved adequate so far. Sometimes the speed pulses can even be drawn from an a.c. tachometer used for the analogue loop. Digital control using a correcting *I* loop can be superimposed on an existing analogue speed loop at a later date if this proves to be necessary.

W. FRITZSCHE, *in reply*

I agree with Dr. Leonhard about gears. It is difficult to find good mechanical transmitting systems, therefore in many cases digital *I* controllers are completely sufficient, or only an integral-correction of

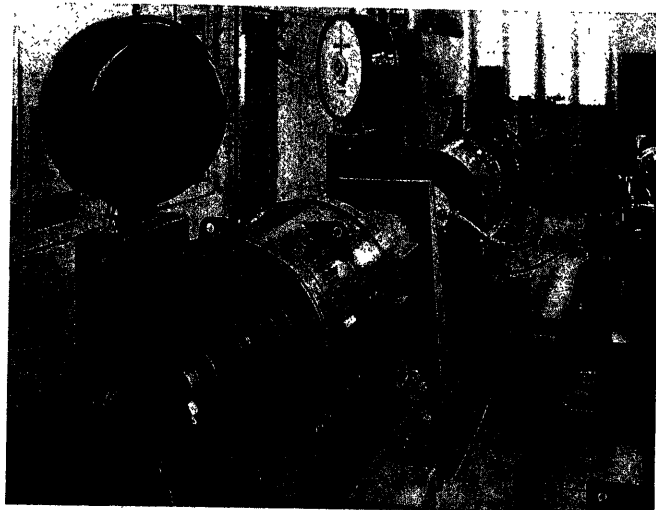


Figure A

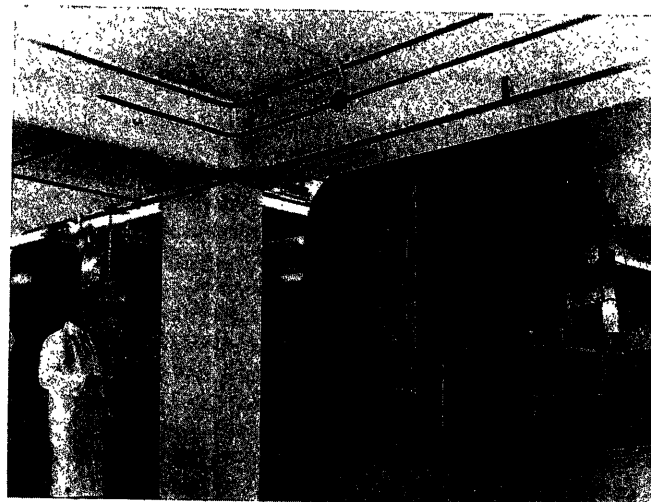


Figure B

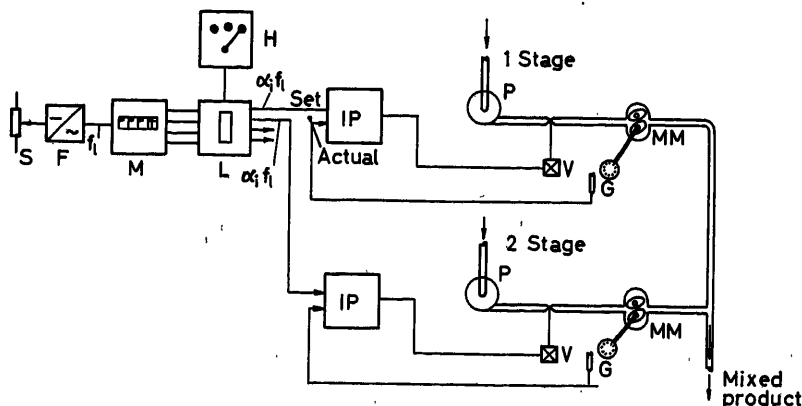


Figure C. In-line blending of liquids

F Controllable frequency system for master frequency f_1 . *G* Pulse transmitter. *I* Controller (pulse phase system). *L* Reader for punched cards. *M* Frequency multiplier. *MM* Flow meter. *P* Pump. *S* Potentiometer for set-point of flow of whole mixture. *V* Control valve with positioner. α_1 Percentage mix

the set-point is necessary. Nevertheless, in my opinion, there are cases which require a fully digital *PI* controller. If the structure of the control loop requires it a digital *IPD* controller is to be preferred. I would point out *Figures A* and *B* as good examples of testing places, which are direct coupled, one of them with a slowly turning motor *Figure B*.

Generally it is easier and cheaper to build good symmetrical pulse-discs than tachogenerators.

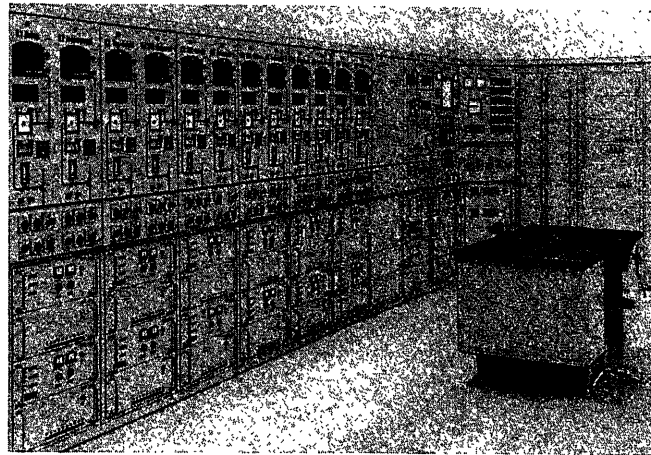


Figure D

An interesting example is the application of the system referred to in my paper for flow control of liquids; for instance, in-line blending of gasoline (see *Figure C*). Here the flow meter *MM* drives the pulse transmitter *G*. The set-point of the controller *IP* is given by means of frequency multiplier *M* which gives the percentage of each component α_i introduced by hand *H* or punched cards *L*. The flow of the mixture is controlled by the master frequency f_i set by the potentiometer *S*.

Figure D shows the installation for in-line blending type AEG-Blendomat of 12 components for gasoline in one of the refineries equipped with this system. This has been in service for over a year without any difficulties.

S. DOMANITSKY, *Institute of Automatics and Telemechanics, Kalanchevskaja 15, Moscow, U.S.S.R.*

(1) How can you adjust the *PID* controller settings? What are the ranges for the adjustment of the proportional, the automatic reset, and rate coefficients?

(2) Are the control laws of your digital controller other than *PI* and *PID*?

(3) Could you give a detailed explanation concerning the elimination of the static error by means of a sinusoidally divided disc as mentioned under the heading 'Error compensation of pulse generators'?

W. FRITZSCHE, *in reply*

(1) The *PID* controller settings can be made by:

(a) Analogue means, for example after the digital-analogue converter in the feedback of the amplifier in a range from 0.5–2.0 mA.

(b) Shifting the converting resistors on the row of flip-flops of the register.

(c) Digital dividers or frequency multipliers (*Figure 8*) before the registers.

(2) Other control laws have not yet been used but it would seem to be an area for experiment.

(3) More details to eliminate the error of the pulse transmitter can be found in my longer paper in *Regelungstechnik*, November 1963.

L. A. DE SCHAMPHELAERE, *De Burletlaan, 26, Edegem, Belgium*

In his very interesting paper, Professor Fritzsche defends the use of digital techniques as a means of improving not only the static, but also the dynamic characteristics of speed control systems. However, as Dr. Leonhard has already remarked, the imperfections of the gearing are very often the cause of speed modulations of the load. These speed modulations may be of a relatively high frequency (several c/sec). Even the best digital (or analogue) control system does not help very much in this case.

In his answer to Dr. Leonhard's remarks, Professor Fritzsche indicated the use of slowly turning d.c. motors, which should need only a little speed reduction, or none at all, as a possible solution to the problem.

In connection with this, I would ask Professor Fritzsche if he has had any experience with a new type of d.c. motor which has a printed circuit disc as the rotor. This type of motor has been described by J. Henry-Baudot in the French review '*L'Automatisme*' (March 1959 and September 1960), and also by J. Henry-Baudot and R. P. Burr at the A.I.E.E., General Meeting, Winter 1959.

These motors are now commercially available with power ratings ranging from 10 W to about 2 kW.

According to the specifications of the manufacturers these motors should be able to turn very smoothly (without any speed modulation) at speeds down to 1 rev/min. This is impossible with ordinary d.c. motors, because of the so-called 'cogging' effect.

Other interesting features of this type of motor, which can contribute considerably to the quality of the speed control system in which it is used, are: the very low inductance of the rotor windings, the very low moment of inertia of the rotor and the linear voltage speed and torque speed relationship.

W. FRITZSCHE, *in reply*

The type of motor with printed circuit rotor has some of the advantages of the printed pulse discs described in this paper, namely, ease of construction and symmetry. I should like to add, however, that a digitally controlled normal 4 kW motor installed by the AEG in Berlin works very satisfactorily over the speed range 10–4,000 rev/min.

W. H. P. LESLIE, *National Engineering Laboratory, East Kilbride, Glasgow, Scotland*

The author states that the method of frequency multiplication shown in *Figure 8*, and widely known, has the disadvantage of giving irregular spacing which makes differentiation of error useless.

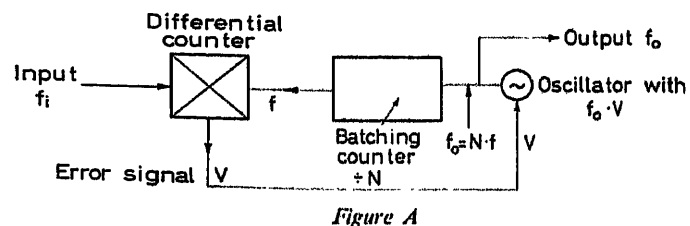


Figure A

To the method of precision digital speed control described by Leslie¹ at the first I.F.A.C. conference we have applied a digital frequency multiplier giving regular spacing of pulses. We use an oscillator, *Figure A*, whose frequency can be varied by applied control voltage to generate a frequency $f_0 = Nf$ c/sec. This signal is then divided by

any preset integer N to yield a frequency f c/sec. The frequency f is compared with the input signal f_i in a bidirectional differential counter², and the error signal used to cause the voltage controlled oscillator frequency f_0 to be varied so that f is locked in frequency and phase to the input signal f_i . Since f is derived by counting from f_0 we have $f_0 = nf_i$, with phase locking. We have also applied this technique to the precision testing of gear wheels³ with errors of the order of 2 sec of arc regardless of gear ratio, and we are evolving error corrected gear-cutting machines based on the same principles.

References

- ¹ LESLIE, W. H. P. Precision dynamometer speed control. *Proc. 1st I.F.A.C. Conf.* 1960. London; Butterworths

- ² NAIRN, D. and LESLIE, W. H. P. A transistorized differential counter. *Electron. Engng.*

- ³ LESLIE, W. H. P. Widening the application of radial gratings. *Int. J. Machine Tool Res. and Design*, April (1963)

W. FRITZSCHE, *in reply*

I thank Mr. Leslie for his remark, which describes another application of digital speed control for testing equipment.

The method of changing the set frequency is also mentioned in another work, Reference 7 of the paper. The method uses a whole separate digital frequency control, so the arrangement becomes very expensive.

Digital Controllers

T. M. ALEKSANDRID, S. N. DILIGENSKY and H. K. KRUG

Summary

The paper discusses the design concepts of controllers built of computer elements. These controllers can provide for better performance than analogue ones (particularly with regard to control accuracy). It is intended to use digital controllers in systems with frequency sensors or in the systems where controlled variables are measured at discrete moments of time (size measurements, weighing, determining the results of chemical analysis, etc.).

Structures for two types of digital *PI* controllers are given. The effect on the performance of controllers, of time and amplitude sampling peculiar to all the digital systems is analysed.

The principle of operation of single and multi-channel digital *PI* controllers is described. The single-channel controller is designed for operation with a stepping-type motor or a constant rate servo unit. The multi-channel digital controller is incorporated into the centralized control system giving the output of d.c. signals in each of eight channels.

In both types of digital controllers provision is made for changing the adjustment parameters within a wide range (the adjustments in multi-channel controllers are independent for each of eight channels).

Sommaire

Ce rapport traite les conceptions des régulateurs numériques ayant une précision supérieure aux régulateurs analogiques, notamment dans les systèmes avec détecteurs de fréquence, ou dans ceux où les mesures sont effectuées d'une façon discontinue (mesures de dimensions, pesées, analyses chimiques, etc.).

On décrit les structures de deux types de régulateurs numériques à effets proportionnel et intégral (*PI*). On analyse l'influence de la quantification due à l'échantillonnage sur la performance de ces éléments.

On décrit le principe de fonctionnement des régulateurs numériques *PI* à mono- et à multi-canaux. Le type «mono-canal» fonctionne avec un moteur pas-à-pas ou un «servomécanisme à action tachymétrique constante». Le type «multicanal» est incorporé dans un ensemble donnant des signaux de sortie à c.c. dans chacun des huit canaux.

Dans chacun des deux types, les paramètres sont ajustables indépendamment dans une gamme étendue.

Zusammenfassung

Der Aufsatz bespricht die Bauprinzipien von Reglern aus Rechner-elementen. Derartige digitale Regler sind besonders im Hinblick auf die Regelgenauigkeit leistungsfähiger als analoge. Es ist beabsichtigt diese Regler in Systeme einzusetzen, bei denen die Regelgröße als Frequenz oder in diskreten Zeitabständen abgetastet vorliegt (z.B. Abmessung, Gewicht, Bestimmung der chemischen Zusammensetzung usw.).

Der Aufbau zweier Arten von digitalen *PI*-Reglern ist angegeben. Es wird gezeigt, wie sich die Zeit- und Amplitudenquantisierung, die allen digitalen Systemen eigen ist, auf das Verhalten der Regler auswirkt.

Die Arbeitsweise von ein- und mehrkanaligen digitalen *PI*-Reglern wird beschrieben. Der einkanale Regler eignet sich für den Betrieb mit einem Schrittmotor oder für einen Stellantrieb mit konstanter Geschwindigkeit. Der mehrkanalige digitale Regler ist mit dem

zentralen Regelsystem verbunden; bei den Ausgangsgrößen jeder der acht Kanäle des Reglers handelt es sich um Gleichspannungssignale.

Bei beiden digitalen Reglern sind die Parameter in weiten Grenzen einstellbar; die Einstellungen beim mehrkanaligen Regler erfolgen für die acht Kanäle unabhängig.

Introduction

Many new problems are now arising in the automation of many technological processes: increasing the accuracy with which preset conditions are maintained, the need for simultaneous observation and control of a large number of parameters characterizing the state of one plant, and so on. There are also additional difficulties bound up with the specific features of technological processes. Thus, information on the state of certain parameters can be obtained only at discrete moments of time (for example, when working with complex metering devices, when the value of the controlled variable is established on the basis of chemical analysis).

It is only possible to increase the accuracy of control of any magnitude if use is made of transducers having a sufficiently small inherent error. Digital sensors appeared to offer a great deal in this respect (these are transducers which convert a non-electrical magnitude into an electrical one in digital form). For example, the accuracy of operation of digital speed transducers is 0.1–0.01 per cent and higher.

Centralized-control machines are used for simultaneous monitoring of a large number of parameters. These machines have facilities for indication and recording should the controlled magnitude deviate from that specified. In these systems the simplest control laws (for example, two-position) are sometimes reproduced. The use of such laws cannot provide high control accuracy.

The application of conventional proportional-integral controllers, combined with centralized-control machines, and also in other systems, in which measurement of the control variable is effected at discrete moments of time, requires special storage units. It is difficult to realize these units on the basis of analogue equipment.

The problems listed above are easily solved by going over to digital controllers. In digital controllers, the preset control law is produced in a digital form. These controllers can operate with digital sensors or with analogue-digital converters (such converters are used in centralized-control machines). The output signal from the digital controllers is converted into analogue form.

The improvement of step motors opens up particular prospects for the use of digital controllers. When step motors and digital sensors are used, a purely digital control system can be built.

A theoretical study of discrete control systems was described

by Tsyppkin¹. The first digital controllers were developed for controlling the speed of electric motors²⁻⁴.

Today, apart from specialized digital controllers, there is a need to develop unified digital controllers*; it is possible to construct these on the basis of an analysis of the dynamic characteristics of digital controllers.

For unified digital controllers, a proportional-integral mode of control is adopted. As research has shown⁵, *PI* controllers provide high-quality control for many plants. Unified digital *PI* controllers can be built either in the form of a single-channel system, designed to control one magnitude, or in the form of a multi-channel controlling several magnitudes at the same time. It is expedient to combine multi-channel digital *PI* controllers with centralized control machines.

Single-channel and multi-channel digital *PI* controllers can be built in accordance with two structural schemes. In controllers with the first type of structure the integration operation is effected with the aid of an integrator; the signal from the integrator, which is added to a signal proportional to the deviation, is sent to a proportional actuator. In a controller having a structure of the second type, the actuator is an integrating element, on the input of which are added signals proportional to the deviation and to the derivative of the deviation.

This paper considers certain features of the dynamic properties of digital *PI* controllers, and describes the operating principle of single-channel and multi-channel digital controllers.

Dynamic Properties of the Digital *PI* Controller

The proportional-integral law of control in continuous form is usually written as follows:

$$\mu(t) = K_p \left(x(t) + \frac{1}{T_i} \int x(t) dt \right) \quad (1)$$

where $\mu(t)$ is a continuous function corresponding to the output signal, and $x(t)$ is a continuous function corresponding to the input signal.

A continuous *PI* controller has two setting parameters: the proportionality coefficient K_p , and the integration time constant T_i . In unified *PI* controllers it is necessary that these parameters can be changed within the limits: $0.2 < K_p < 50$ and $10 \text{ sec} < T_i < 3,000 \text{ sec}$.

It should be noted that in practice the tuning parameter variation ranges in analogue controllers are limited: the maximum value of the integration time constant $T_i = 1,600$ to $2,000 \text{ sec}$.

The proportional-integral control law in discrete form is written as follows:

$$\mu(t) = K_1 x[nT] + K_2 \sum_{i=1}^n x[iT] \quad (2)$$

when $nT < t < (n+1)T$; $x[nT]$ is a lattice function, corresponding to the input signal (deviation at moment of time $t = nT$); K_1 and K_2 are constant coefficients; T is the sampling period.

The discrete *PI* controller has three setting parameters: the proportionality coefficient K_1 , integration time constant $T'_i = (K_1/K_2)T$ and sampling period T .

* Unified controllers reproduce typical control laws (e.g., proportional-integral) and have a wide range of variation of the tuning parameters. Therefore, they can be used for controlling various technological processes.

Figure 1 contains graphs which explain the nature of the change of $\mu(t)$ with stepwise and sinusoidal input signals $x(t)$. It can be seen from this figure that the T'_i of a discrete controller, like the T_i of a continuous controller, is determined by the doubling time. In unified discrete *PI* controllers the limits of variation of K_1 and $(K_1/K_2)T$ must be the same as the limits of variation of K_p and T_i .

Two standard structural schemes for discrete *PI* controllers are given in Figure 2. The discrete *PI* controller of the first type

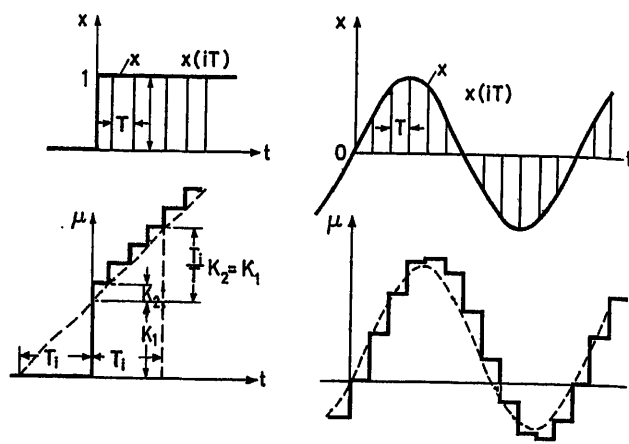


Figure 1. Performance of stepped and sinusoidal input signal by continuous and discrete *PI* controller

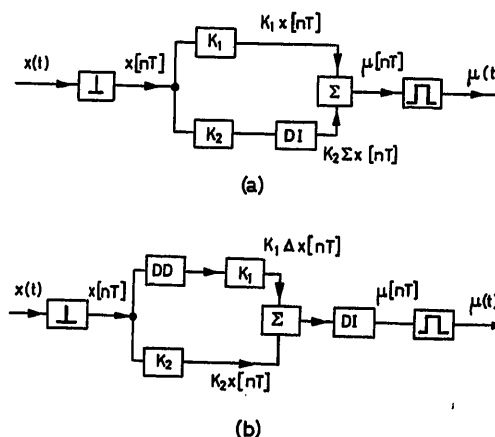


Figure 2. Block diagram of discrete *PI* controllers of first and second types

[Figure 2 (a)] consists of a converter of $x(t) \rightarrow x[nT]$ (\perp), multiplication unit (K_1), multiplication unit (K_2), a discrete integrator (DI), an adder (Σ) and a converter of $\mu[nT] \rightarrow \mu(t)$ which must at the same time serve as a storage unit.

The discrete *PI* controller of the second type [Figure 2 (b)] consists of a converter of $x(t) \rightarrow x[nT]$, a discrete differentiator (DD), multiplication unit (K_1), multiplication unit (K_2), an adder (Σ), a discrete integrator (DI), and a converter of $\mu[nT] \rightarrow \mu(t)$. (In a number of cases, one unit performs the functions of the converter and integrator.)

It is convenient to compare the dynamic characteristics of the discrete *PI* controller with those of a continuous *PI* controller, by sending to the inputs of both controllers a sinusoidal

signal $x(t) = B \sin \Omega t$ (B is the amplitude and Ω the pulsation). In this case the output signal from the continuous and discrete PI controllers equal, respectively:

$$\mu(t) = A \sin(\Omega t - \alpha)$$

$$\mu(t) = f(t)$$

The expressions of the frequency characteristics of the first harmonic of the function $f(t)$ of proportional and proportional-integral discrete controllers have the form:

$$\omega_P(j\Omega) = K_1 \frac{\sin \frac{\Omega T}{2}}{\frac{\Omega T}{2}} e^{-j \frac{\Omega T}{2}} \quad (3)$$

$$\omega_{PI}(j\Omega) = K_1 \frac{\sin \frac{\Omega T}{2}}{\frac{\Omega T}{2}} \cdot \sqrt{1 + \frac{K_2}{K_1} + \frac{4K_2^2}{K_1^2 \sin^2 \frac{\Omega T}{2}}} e^{-j \frac{\Omega T}{2} - j \arctan \frac{1}{(1 + \frac{2K_2}{K_1}) \tan \frac{\Omega T}{2}}} \quad (4)$$

Figure 3 shows the frequency characteristics of discrete and continuous (broken line) P and PI controllers. It can be seen from Figure 3 that the controller frequency characteristics

differ by no more than 5 per cent in modulus and 5° in phase when the condition $\Omega T < 0.2$ is satisfied. This means that in practice systems with discrete-acting PI controllers can be viewed as continuous, if the time of the cycle T is less than $0.1 T_i$ ($T < 0.1 T_i$), i.e., when the maximum frequency of the input signal Ω_{\max} does not exceed the value $\Omega_{\max} T_i < 2 - 3$ (which is usually the case in systems with PI controllers).

In real systems with digital controllers the maximum input-signal frequency is limited by the parameters of the analogue-digital converters (conversion time τ_a) and the inertia of the actuators (T_{im}). Studies have shown that in practice the equations of real digital controllers correspond to eqn (2), if there are satisfied the conditions:

$$\Omega_{\max} \tau_a < \delta_x \quad (5)$$

$$\Omega_{\max} T_{im} < 0.1 \quad (6)$$

$$0.2 T_{im} < T \quad (7)$$

δ_x is the level-sampling magnitude peculiar to all digital systems. It is expedient to take δ_x as not less than 0.002–0.005 (relative to the scale of conversion). In the process, amplitude of the oscillation by the presence of δ_x does not exceed a magnitude equal to 0.2–0.5 per cent.

The magnitude of the minimal frequency of the input signal Ω_{\min} is limited for systems which use PI controllers built in accordance with the second type of structural scheme [Figure 2(b)]. In these controllers, the proportional component of the law of control is ensured on account of the production of the first

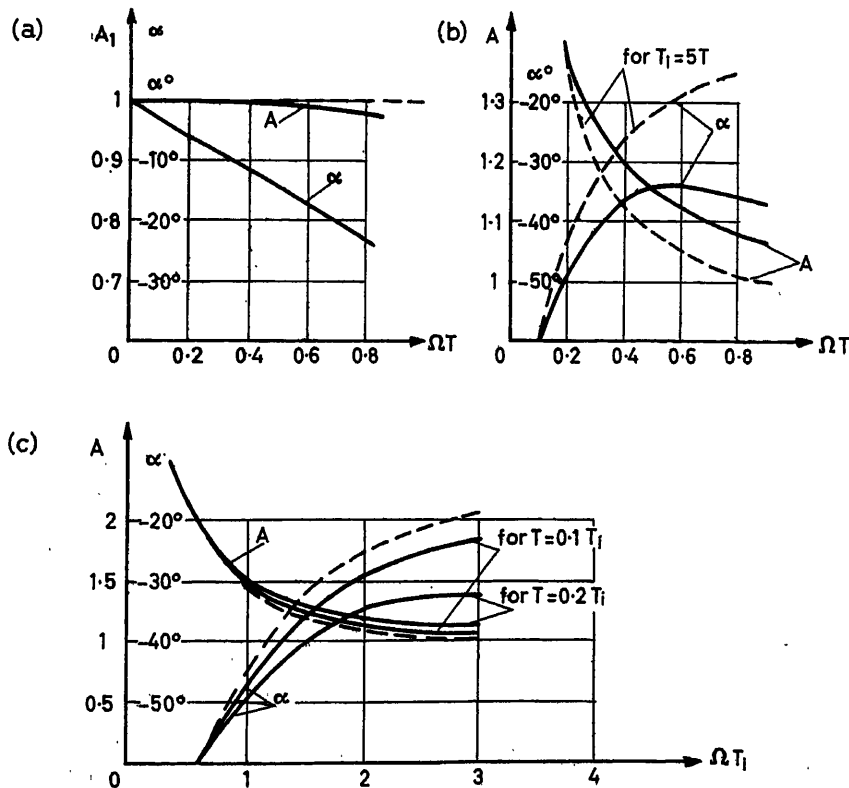


Figure 3. Frequency characteristics of discrete and continuous P (a) and PI (b, c) controllers

difference $\Delta x^*[nT] = x^*[nT] - x^*[(n-1)T]$. Setting ourselves the accuracy of reproduction of the constant component, e.g., 1 per cent ($\Delta x^* = 100$ pulses), when $\delta_x = 0.002$, the relation

$$0.2 < \Omega_{\min} T_{\min} \quad (8)$$

can be obtained, where T_{\min} is the minimum value of the cycle duration.

Thus the presence of level sampling in a digital *PI* controller of the second type leads, with a pre-set minimal time T_{\min} , to the limitation of the input-signal frequency band, with which the constant component of the control law can be reproduced.

Single-channel Digital *PI* Controller

The single-channel digital *PI* controller (*SDC* controller) is built with a structure of the second type⁶. It consists of a time-pulse converter, a digital control element and an actuator (when working with digital sensors, the converter is not necessary). The converter is used to perform comparison of the controlled variable $\varphi(t)$ with the set value $\varphi_0(t)$ and to produce, at discrete moments of time, pulses, whose length τ_x is proportional to the magnitude $x[nT] = [\varphi(t) - \varphi_0(t)]$. These pulses, and also signals on the sign of the deviation $\text{sgn } x[nT]$, are sent to the input of the digital control element.

In the single-channel digital *PI* controller, use can be made of actuators with step motors and with constant-speed motors. An *SDC* controller with an actuator having a step motor is examined below. In the *SDC* controller, the step motor serves simultaneously as a digital-analogue converter. (When a constant-speed motor is employed, the controller has a digital-analogue converter which converts the number of pulses proportional to the variation of the control action into the duration of one pulse.)

The control law of an *SDC* controller is written in the form:

$$\begin{aligned} \mu(t) &= K_3 \sum_{i=1}^n \{K_2 x[iT] + K_1 (x[iT] - x[(i-1)T])\} \\ &= K_2 K_3 \sum_{i=1}^n x[iT] + K_1 K_3 x[nT] \\ &\quad \text{for } nT < t < (n+1)T \end{aligned} \quad (9)$$

where K_1 and K_2 are coefficients characterizing the parameters of the differentiator and the integrating unit; K_3 is determined by the parameters of the analogue-digital converter and the actuator ($0.01 < K_1 < 1$; $K_2 = 1/2^m$, $m = 1, 2, \dots, 8$; $K_3 = 20$; $2 \text{ sec} < T < 600 \text{ sec}$). Figure 4 shows a block diagram of a digital control unit (*DU*) and an actuator with a stepping motor.

The discrete differentiator (*DD*) consists of a reversible difference counter (*DC*), a block for tuning the coefficient K_1 (*SU*) and control valves (KI_p).

The discrete integrator (*DI*) consists of a reversible counter divider (*CD*), control valves (KI_i), step-motor control unit (*CU*) and a step motor (*SM*) with a reducing gear (*R*). *CG* is a cycle-pulse generator which produces consecutive cycle pulses, the intervals between which equal respectively T_1 and T_2 . *FG* is a

† The magnitudes $x^*[(n-1)T]$, $x^*[nT]$ and $\Delta x^*[nT]$ denote the magnitudes $x[(n-1)T]$, $x[nT]$ and $\Delta x[nT]$ converted into digital form.

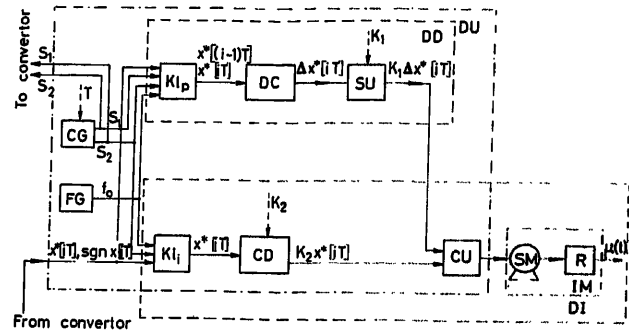


Figure 4. Block diagram of single-channel digital *PI* controller

generator of filling pulses with frequency f_0 . The control unit (*DU*) operates cyclically. A cycle of operation, of duration T , consists of four periods.

First period: The first pulse S_1 over the cycle from the cycle generator triggers the converter. The pulse from the converter opens the corresponding valve KI_p for the period τ_{n-1} of gating of $x^*[(n-1)T]$ pulses, of frequency f_0 , to the adding or subtracting bus of the reversible difference counter, depending on the sign of the mismatch $\text{sgn } x[(n-1)T]$. The pulse converter is not shown in the block diagram of the *DU* (Figure 4).

Second period: The pause between the moments of termination of the pulse with duration τ_{n-1} and the appearance of pulse S_2 . The length of the pause $T_1 - \tau_{n-1}$ can be changed at will by varying T_1 , thus setting the necessary value of T .

Third period: The second pulse S_2 in the cycle from the cycle-pulse generator once again triggers the converter, and $x^*[nT]$ pulses are sent to the reversible difference counter during the time τ_n . After this a digit proportional to $\Delta x^*[nT] = x^*[nT] - x^*[(n-1)T]$ is found to be written in the difference counter.

At the same time, during the third period, $K_2 x^*[nT]$ pulses pass via the reversible counter-divider to the step-motor control unit, and the shaft of the actuator turns through a corresponding angle. This operation relates to the processing of the integral component.

The magnitude of K_2 can be varied by altering the division coefficient of the counter-divider.

Fourth period: After the termination of the pulse with duration τ_n , the unit for tuning coefficient K_1 is triggered; this unit generates pulses of frequency f_1 and f_2 (the ratio $f_2/f_1 = K_1$ is adjusted by altering the frequency f_1). The pulses with frequency f_1 are sent to the reversible difference counter, and it is zeroed. During this time, the pulses of frequency f_2 are sent to the step-motor control unit. The shaft of the actuator turns through an angle corresponding to $K_1 \Delta x^*[nT]$ pulses. The latter operation relates to the processing of the proportional component of the *PI* control law.

The single-channel digital control unit (*DU*) is built on semiconductor devices. The circuits of the reversible counters, the pulse generators, and the K_1 tuning unit are made up of standard elements in the form of a flip-flop, a toggle-switch relay, a multivibrator and logic elements. The assemblies of the *DU* are designed in the form of one block (Figure 5). The power amplifiers in the step-motor control unit are put into a self-contained arrangement.

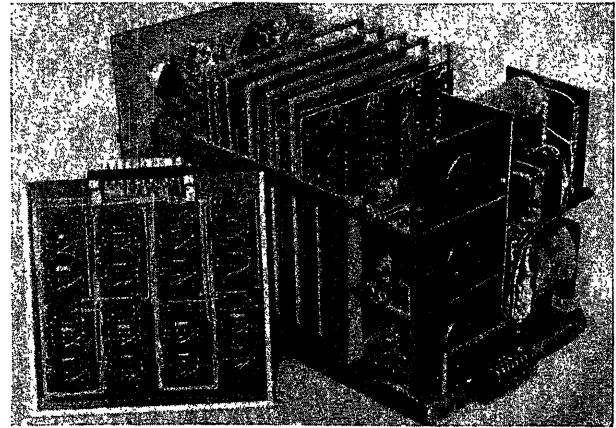
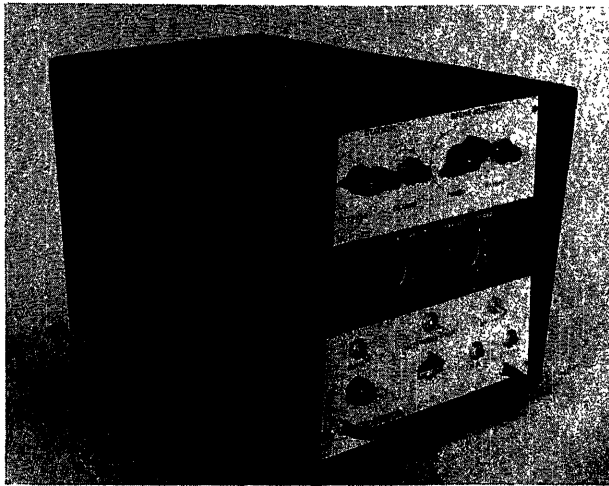


Figure 5. Control unit DU

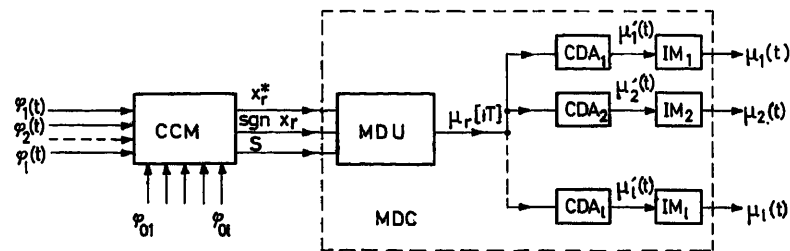


Figure 6. Block diagram of multi-channel control system

Multi-channel Digital PI Controller

The multi-channel digital *PI* controller (*MDC*) is built with the first type of structure⁷. It is designed for operation in conjunction with a centralized control machine. Figure 6 is a block diagram of a multi-channel control system. The system consists of a centralized control machine (*CCM*), and a multi-channel digital *PI* controller (*MDC*), which includes a multi-channel control unit (*MDU*), digital-analogue conversion blocks (*CDA*₁–*CDA*_l) and actuators (*IM*₁–*IM*_l).

The centralized control machine (*CCM*) has one analogue-digital converter, to which are connected alternately $\varphi_r(t)$ controlled values ($r = 1, 2, \dots, l$, Figure 6). The values of the deviations of the controlled magnitudes $x_r^*[nT]$ and the sign of the deviation $\text{sgn } x_r[nT]$ are computed in the *CCM*. To the input of the multi-channel control unit are sent:

$$x_r^*[nT], \quad \text{sgn } x_r[nT]$$

and a pulse S , corresponding to the inclusion of the r th controlled variable.

In the multi-channel control element (*MDU*) during the cycle for ' l ' transmitted values of $x_r^*[nT]$ there are produced ' l ' values of $\mu_r[nT]$ in accordance with the equation below. The tuning parameters for each channel are established independently. The limits of variation of the parameters equal $0.5 < K_1 < 40$ and $0.03 < K_2 < 10$ respectively.

The digital-analogue converters are used for the conversion of $\mu_r^*[nT]$ into the analogue magnitude $\mu_r(t)$ and for retention of the value of $\mu_r(t)$ during the time of scanning the other

controlled variables. The magnitude $\mu_r(t)$ is obtained in the form of one of the signals taken as standard for the control of analogue proportional actuators (e.g., a current of 0–5 mA). The number of digital-analogue converters and actuators equals the number of controlled variables (l).

A block diagram of a *MDC* is shown in Figure 7. *DI* is a discrete integrator, consisting of an integral reversible counter (*IC*) and a memory unit (*MU*); *SU* is a tuning unit, which serves for tuning the coefficients K_{1r} and K_{2r} for each channel separately; *AC* is a reversible counter for adding the discrete values of the proportional $K_{1r} x_r^*[nT]$ and integral $K_{2r} \sum_{i=1}^{n-1} x_r^*[nT]$ components.

CU is a control unit, consisting of channel switch (*CS*) and an order unit (*OU*). The channel switch counts the switching pulses S from the *CCM* and issues the appropriate order pulses to the *SU*, the *MU* and the *OU*. The order unit produces order pulses for the performance of all the elementary operations. $F_r \text{sgn}$ is a sign flip-flop, the output signal of which changes as $\text{sgn } x_r[nT]$ varies; *CDA* is a digital-analogue converter. The complete cycle of operation of the multi-channel digital controller is compounded of the time of scanning all the channels. One (' r ') interval of operation of the *MDC* is determined by the time for which the *MDC* system is connected up to the r th channel.

The intervals of operation of the controller begin with the sending to the *CU* from the *CCM* of a switching pulse which is the r th in order over a given n th cycle. By this process, the number of the next, r th process is set in the channel switch and there are formed the appropriate order pulses for the *MU*, the

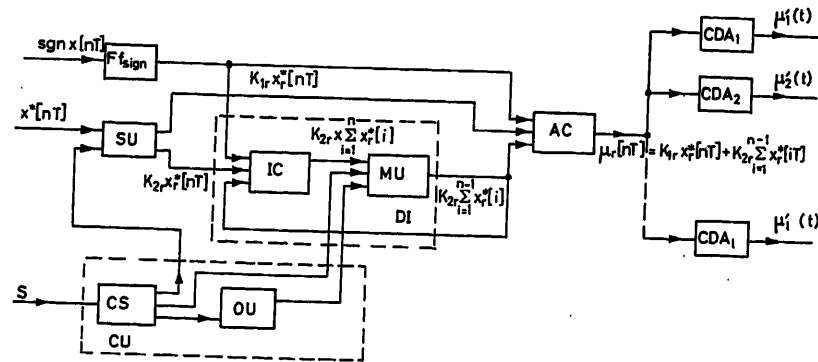


Figure 7. Block diagram of multi-channel digital control unit

SU and the CDA , the duration of which equals the full time of the interval.

From the MU is selected the value of the integral for the channel ' r ', stored over ' $n - 1$ ' cycles— $K_{2r} \sum_{i=1}^{n-1} x^*[iT]$. This value is sent in parallel binary code form to the IC and AC . After this, mismatch pulses for the ' r ' channel— $x^*[nT]$ arrive

at the tuning unit (SU) of the controller. The SU is so constructed that for each channel the tuning coefficients K_1 and K_2 are set individually by hand, and upon selection of the r th channel the corresponding coefficients are automatically switched in by means of order pulses arriving from the CU .

$K_{1r} x^*[nT]$ pulses arrive at the reversible adding counter (AC), while the integral reversible counter (IC) receives $K_{2r} x^*[nT]$ pulses. The sign of the mismatch is transmitted for controlling the reversible counters. After the end of the addition of the mismatch pulses, in the integral counter there appears the value of the integral for the r channel after the n th cycle.

$$K_{2r} \sum_{i=1}^n x_r^*[iT]$$

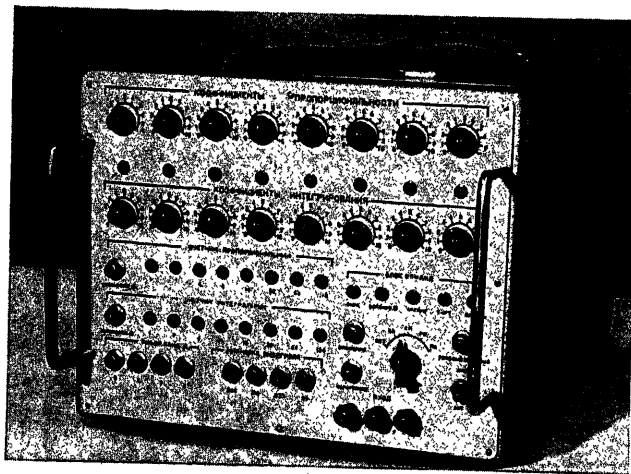
The integral value obtained is written in the memory unit at the appropriate location. In AC , after the addition of the mismatch pulses, there appears the value of the control action for the r th channel in digital code:

$$\mu_r^*[nT] = K_{1r} x_r^*[nT] + K_{2r} \sum_{i=1}^{n-1} x_r[iT] \quad (10)$$

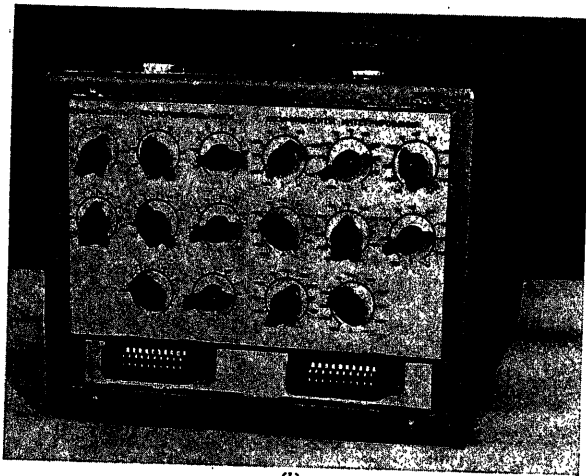
This value is transmitted by the corresponding order pulse from the (AC) in the form of parallel binary code to the digital-analogue converter (CDA) of the r th channel.

At the converter output the corresponding value of the control action is established in the form of a direct current, which varies in the range 0–5 mA. With this the interval of operation of the MDC ends. Subsequently, the next switching pulse is sent from the CCM to the control unit, and the digital controller goes on to compute the control action for the $r + 1$ th channel.

The unit for tuning the coefficients K_{1r} and K_{2r} consists of a common part for all ' r ' channels and ' $2r$ ' separate networks. The common part of the tuning unit takes the form of additional columns of counters (IC) and (AC) and a generator of frequency f_0 . The tuning network for each channel has two switches, which ensure the selection of the necessary quantity of additional columns m_{1r} and m_{2r} of counters (IC) and (AC), two toggle switches and two valves. For example, the requisite value of the coefficient K_{2r} is set with the aid of a switch which determines the value of m_{2r} , and by control of the toggle switch, which generates a pulse of duration t_{2r} for each pulse $x^*[nT]$. The pulse of duration t_{2r} opens for this time the valve, through which



(a)



(b)

Figure 8. Eight-channel PI controller (a) front view; (b) rear view

pulses of frequency f_0 pass to the counter (IA). As a result,

$$\frac{[t_{2r} f_0]}{2^{m_{2r}}} x^* [nT]$$

pulses arrive at the counter (IC) during the interval. The coefficient K_{2r} equals

$$K_{2r} = \frac{t_{2r} f_0}{2^{m_{2r}}}$$

The multi-channel controller is built on semiconductor devices. The networks of the reversible counters, the control unit and the setting unit are based upon one logic element: an inverter on one triode (P16) with resistor logic circuits. Building the MDC on the basis of one standard cell makes its circuitry more technologically efficient and more reliable. A matrix unit using cores with a square hysteresis loop serves as the memory unit; the digital-analogue converter is based on networks of current switches, and the CDA is a structurally independent unit.

References

- ¹ TSYPKIN, YA. Z. *The Theory of Sampled-data Systems*. 1958. Moscow; Fizmatgiz
- ² KESSLER, G. Digitale Regelung der Relation zwei Drehzahlen. *Electrotech. Z.* 18, Edn. A, (1961)
- ³ FRITZSCHE, W. Genaue und schnelle Regelungen von Drehzahlen durch digitale Methoden. *AEG, Mitt.* 8/9, B. 50 (1960)
- ⁴ SCHMIDT, W., and POTTS, R. Speed regulation by digital methods. *Elect. Engr.* 11 (1961)
- ⁵ KRUG, H. K. Dynamic properties and setting of systems with discrete controllers. *Automat. Telemekh.* 23, No. 4 (1962)
- ⁶ DILIGENSKY, S. N. Some structural schemes and dynamic characteristics of digital controllers. *Automat. Telemekh.* 23, No. 2 (1962)
- ⁷ ALEKSANDRIDIS, T. M. Some problems of the choice of structure for a multi-channel digital controller. *Automat. Telemekh.* 23, No. 2 (1963)

DISCUSSION

M. PRASAD, *The Foxboro Company, Foxboro, Mass., U.S.A.*

The authors are to be congratulated for this report on a subject which has caused considerable interest over the past three years. I think the following points need further discussion:

- (1) How is the basic sampling period chosen for a particular process of variable to be controlled? This period is obviously dependent on the dynamic characteristics of the process and would seem to be of fundamental importance. Further, how are the controller constants determined?
- (2) Do 'digital sensors' actually offer better accuracy than analogue sensors? Can the authors give examples of such digital sensors?
- (3) Was there any special reason for using the first structure (employing proportional actuators) for MDC and the second structure (employing integrating actuators) for SCD? Is there any practical difference in control action between the two structures?
- (4) Do the authors have any data on the reliability and costs of step-motor actuators?
- (5) The SDC requires an 'arithmetic unit' of some kind, and it would seem to me that the associated costs, compared to an analogue controller, would be prohibitive.
- (6) Applications using the MDC principle have been reported on, both in U.S.A. and U.K. Are the authors in a position to report on similar applications in the U.S.S.R.?

P. D. McCORMACK, *Engineering School, Trinity College, Dublin, Ireland*

In view of the ease of communication with on- or off-line digital computers, the development of unified digital controllers is of great interest to those involved with present industrial process control problems. It would be appreciated if the authors could expound on the following three questions:

- (a) In place of the output function, eqn (2), what form would the error function take?
- (b) Is extension to the derivative or rate mode (PID) possible?
- (c) With the inherent sampling period and step-type output to the final control unit, will trouble due to possible resonances in the main system, or sub-systems, be likely?

H. H. ERNEI, *Lignes Télégraphiques Téléphoniques, 49 rue de Boulainvilliers, Paris XV 1⁰, France*

In France the LTT-Company has also been working in the field of digital control. We soon realized that digital control may open a wide field of new control possibilities. To achieve maximum advantages, we developed binary digital actuators, for instance a binary digital valve (without converter). The PI controller is a small hybrid computer.

The advantages obtained are as follows:

- (1) Very fast response times of the control loop, due to the advantages of sampled control.
- (2) Possibility of the introduction of other dynamics than PID and of non-linear correcting functions.
- (3) The realization of self-adapting controllers becomes easy.

With respect to the paper, can I ask:

What is the threshold sensitivity of the plus-minus decision detector? (Expressed with respect to the 100 per cent signal.) Indeed, the integral action could produce a remarkable output signal for a long duration error under the threshold level. This order would control the loop with a phase inversed signal and produce instability.

What is the highest possible number of loops per second multiplexed, due to computation times?

PROCESS INSTRUMENTATION

A Universal Statistical Analyser

J. KRÝŽE

Summary

In order to apply statistical theory to practice in any field of engineering, one must have a means of automatically computing the basic functions of statistical dynamics, i. e. correlation functions.

Hence this problem is receiving close attention. Research organizations in various countries have worked and are still working on the design of apparatus for this purpose, and papers often appear in the journals on correlators having widely varying principles of operation. But only a few of these designs are suitable for any effective application to control problems, and many of them are no more than laboratory models.

The MUSA-6 computer described in this paper represents an attempt to design not a laboratory model but a relatively powerful computer for entirely automatic recording and processing of data from control processes of both random and non-random nature, with a field of application much broader than the evaluation of correlation functions. As far as the author knows, it is superior in computing power and memory capacity to all the specialized computers of this type that have been described in the literature, while for accuracy it is comparable with the best general purpose analogue computers.

The advanced parameters of the computer have been achieved largely through the development and refinement of signal storage and transformation logic, based on the well-known pulse-width modulation principle.

Thus this paper is of interest from two points of view; first, for possible new practical applications of the theory based on more powerful computer technology, and secondly, for the development of techniques of analogue data storage and processing.

Sommaire

Pour que la théorie statistique puisse être pratiquement appliquée dans n'importe quelle branche technique, il est nécessaire d'avoir des appareils automatiques pour calculer les fonctions statistiques fondamentales; en l'occurrence, les fonctions de corrélation.

Ce problème attire partout une grande attention. Dans des organisations de recherche de plusieurs pays, des travaux ont été ou sont encore entrepris pour développer ces appareils. Dans les revues techniques, on voit souvent des articles décrivant des corrélateurs de principes divers. Seulement, très peu sont des réalisations vraiment industrielles; la plupart d'entre eux sont restés au stade de prototype de laboratoire.

Ce rapport présente le calculateur MUSA-6. Ce n'est pas un modèle de laboratoire. C'est un calculateur puissant, pouvant effectuer automatiquement l'assemblage et le traitement de l'information, dans des commandes de processus aléatoires ou non. Son application dépasse la

simple évaluation de fonctions de corrélation. A la connaissance de l'auteur, la puissance de calcul et la capacité de mémoire de MUSA-6 dépassent celles de tous les calculateurs spécialisés de ce genre décrits dans la littérature. D'autre part, la précision de MUSA-6 est comparable à celle des meilleurs calculateurs analogiques universels.

Les qualités de ce calculateur proviennent notamment des progrès accomplis dans le stockage des signaux et la logique de transformation, utilisant le principe bien connu de modulations en largeurs d'impulsions.

Ce rapport est donc intéressant à deux points de vue; premièrement, applications nouvelles pratiques de la théorie statistique en se basant sur l'utilisation d'un calculateur puissant; deuxièmement, développement de techniques analogiques de stockage et de traitement de l'information.

Zusammenfassung

Zur Anwendung der Theorie der stochastischen Prozesse in der technischen Praxis benötigt man Mittel zur automatischen Berechnung der grundlegenden Funktionen der statistischen Verfahren in der Regelungstechnik, nämlich der Korrelationsfunktionen.

Daher wird diesem Problem große Aufmerksamkeit zugewendet. Forschungsstätten in verschiedenen Ländern befassen sich derzeit mit der Entwicklung von Apparaten für diesen Zweck und häufig erscheinen in Fachzeitschriften Artikel über Korrelatoren mit den verschiedensten Arbeitsprinzipien. Aber nur wenige dieser Entwürfe eignen sich für eine wirkungsvolle Anwendung auf Regelprobleme und viele sind nicht mehr als Labormodelle.

Der hier beschriebene Rechner MUSA-6 stellt kein Labormodell dar, sondern einen ziemlich leistungsfähigen Rechner für eine automatische Registrierung und Verarbeitung von Regelungsdaten regelloser und deterministischer Art; sein Anwendungsgebiet beschränkt sich nicht nur auf die Bestimmung von Korrelationsfunktionen. Soweit dem Autor bekannt, ist dieser Rechner bezogen auf die Rechenleistung und Speicherkapazität allen bisher in der Literatur beschriebenen speziellen Rechnern überlegen, seine Genauigkeit ist mit der von gewöhnlichen Analogrechnern vergleichbar.

Diese verbesserten Eigenschaften wurden hauptsächlich durch die Entwicklung und die Verfeinerung der Signalspeicher und der Logikeinheit zur Umwandlung der kontinuierlichen Signale in pulsbreitenmodulierte Signale und umgekehrt, erreicht.

Dieser Beitrag ist daher aus zwei Gründen von Interesse: Zunächst einmal, da die Entwicklung leistungsfähiger Rechner neue praktische Anwendungen der Theorie der stochastischen Prozesse ermöglicht, und zum anderen wegen der Entwicklung neuer Verfahren zur Speicherung und Verarbeitung analoger Signale.

Introduction

The development of automation gives rise to new problems, which are considerably more complex and difficult in a theoretical sense than those that were being solved only a few years ago.

Self-adaptive systems, or systems with automatic optimization, systems with artificial intelligence, the measurement of dynamic properties, and the control of large complex multi-loop systems—all these are examples of problems that cannot be solved by the methods of classical control theory. In order to solve such problems, it is necessary to build up a new theoretical apparatus.

The theory of stochastic processes has become a cornerstone of this apparatus. It has been used with remarkable success in the rapid development of modern control theory. But it can be observed that, at present, theory is much further ahead of practice than it used to be.

The theoretical problems are so complex that large quantities of data inevitably have to be processed in order to obtain a practical solution. Even when very efficient techniques of the theory of stochastic processes are used, the volume of computation required presents a serious obstacle not only to any practical application but also to experimental work on a laboratory scale. Even such simple problems as the evaluation of correlation functions, distribution functions and spectral functions become laborious and time consuming tasks, although general purpose computers are used.

To get repeatable results one needs to operate on processes represented by a large number of points, running into the order of hundreds of thousands. The necessary number of elementary operations, i.e. multiplications, then goes into millions or even thousands of millions. Although the foremost modern computers can perform this quantity of operations in an acceptable time, difficulties remain in the storage capacity needed and in the transfer of such a volume of data from the source to the computer.

All these difficulties were met in attempts to apply promising results in statistical dynamics to the typical problem of determining the dynamic properties of industrial control installations. The difficulties were overcome by the construction of a specialized computer that would permit the testing of statistical dynamics methods for this purpose and their development for practical application.

Basic Functions of the Computer

The purpose of the computer is to serve for automatic calculation of all the fundamental functions forming the basis of statistical analysis: (a) autocorrelation and cross-correlation functions; (b) Fourier integrals; and (c) distribution functions.

The stage of development of computer engineering and electronic component production in Czechoslovakia at the start of the project set the initial conditions for the engineering design. The computer is an analogue one, using electronic valves, and its memory is contained on a magnetic tape with six working and two auxiliary recording tracks.

This leads to the name of the computer, which is the Magnetic Universal Statistical Analyser with six channels, or MUSA-6.

It is also capable of solving certain non-statistical problems:

- (1) Computation of convolution integrals;

- (2) Representation of functions with delayed argument where the delay depends on a variable quantity;

- (3) Formation of a memory for an analogue computer;

- (4) Operation as a multiplier for the multiplication of continuous signals;

- (5) Transformation of the time-scale of continuous processes.

Although these applications are an essential part of the computer's employment, no further reference is made to them in this paper, since they are only a modification or simplification of the statistical applications.

The computer is also adapted for certain auxiliary operations: (a) transcription of a signal from one track on one tape on another track of either the same or another tape, and (b) sense inversion of the time scale of the recorded process.

Initial Design Requirements for the Computer

In dealing with stochastic processes on a computer one has always to go through the following steps: (a) sensing of the processes at the installation; (b) the transfer of the resulting data into the computer memory; and (c) the reproduction and processing of the data.

To achieve efficient operation, the design should take all these three stages into account as a complex. The basic requirements for the development are:

- (1) All manual work connected with the intermediate recording of the data, and their preparation for feeding into the computer, should be eliminated. Processes that are sensed from the actual installation in the form of voltages by means of suitable pick-ups and converters should be recorded directly on magnetic tape by a portable recorder or the computer itself, and this tape should be used in the computation.

- (2) The required functions are obtained as a result of a very large quantity of elementary operations. Thus it is necessary to secure high accuracy of recording, reproduction and the other elementary operations. For this reason the principle of pulse-width modulation was chosen for the magnetic recording. This is a discrete type of recording, in which individual test values of the process are converted to ratios between the lengths of magnetized segments of the tape.

- (3) One should aim to increase the capacity and operating speed of the computer. Since there are certain technical limits to the length and speed of the tape and to the width of the recorded pulses, this requirement can be reduced to one for a maximum economy of tape, or consequently to one for a maximum reduction in the number of sampling values while maintaining accuracy in the representation of the recorded processes. To achieve this one has to design the logic so as to make the maximum use of the information contained in each sample. Hence it was necessary to develop improved techniques for converting a continuous signal into pulses with duty-cycle modulation and vice versa.

- (4) Unit-type construction should be used in order to reduce the quantity of materials needed for the computer, and also to permit flexible programming by means of a patching panel.

Elementary Operational Blocks

Demonstrating on one of the simplest problems (the representation of time delay), it can be shown how the above prin-

ciples are reflected in the elementary functional units of the computer. Figure 1 shows the relevant block diagram.

Sampling

A continuous signal $x(t)$ (a d.c. voltage) is fed to the input of the sampling unit SAM. There the samples are taken, and the continuous voltage $x(t)$ is converted into a stepped one $\bar{x}(t)$ (Figure 2) according to the law

$$\bar{x}_i = \frac{1}{\vartheta} \int_{\theta_{i-1}}^{\theta_i} \left\{ x(t) - \frac{\vartheta^2}{24} \frac{d^2}{dt^2} [x(t)] \right\} dt \quad (1)$$

where \bar{x}_i is the value of $\bar{x}(t)$ over the interval $\theta_i < t < \theta_{i+1}$, θ_i are the instants of sampling, with $\theta_0 = 0$, and ϑ is the sampling period.

The conversion law (1) has two basic properties: (a) The \bar{x}_i are determined by integration over the whole interval ϑ . This permits a considerable improvement in accuracy by the use of feedback circuits, by suppressing the effect of hum and noise superimposed on the signal $x(t)$, and by making it unnecessary

to use extremely short sampling pulses; (b) The value of \bar{x}_i , as can be shown by means of a Taylor series, is a good approximation to the value of $x(t)$ at the midpoint of the preceding sampling interval:

$$\bar{x}_i \approx x\left(\frac{\theta_{i-1} + \theta_i}{2}\right) \quad (2)$$

The error of approximation is determined to a first approximation by the magnitude of the fourth derivative of $x(t)$:

$$\bar{x}_i - x\left(\frac{\theta_{i-1} + \theta_i}{2}\right) \approx \frac{7\vartheta^4}{5760} \frac{d^4}{dt^4} [x(t)] \quad (3)$$

It may be neglected in practice, even when the signal spectrum contains frequencies close to a quarter of the sampling frequency $1/\vartheta$.

The sampling period is chosen in relation to the spectral composition of the signal in order to give a representation of the signal with the required accuracy while avoiding the taking of superfluous samples.

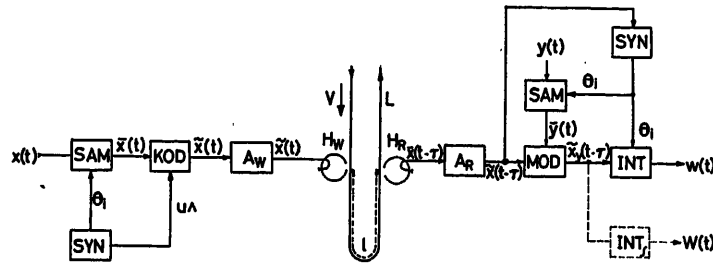


Figure 1. Block diagram of connection of computer units for representation of delay lines and multiplication

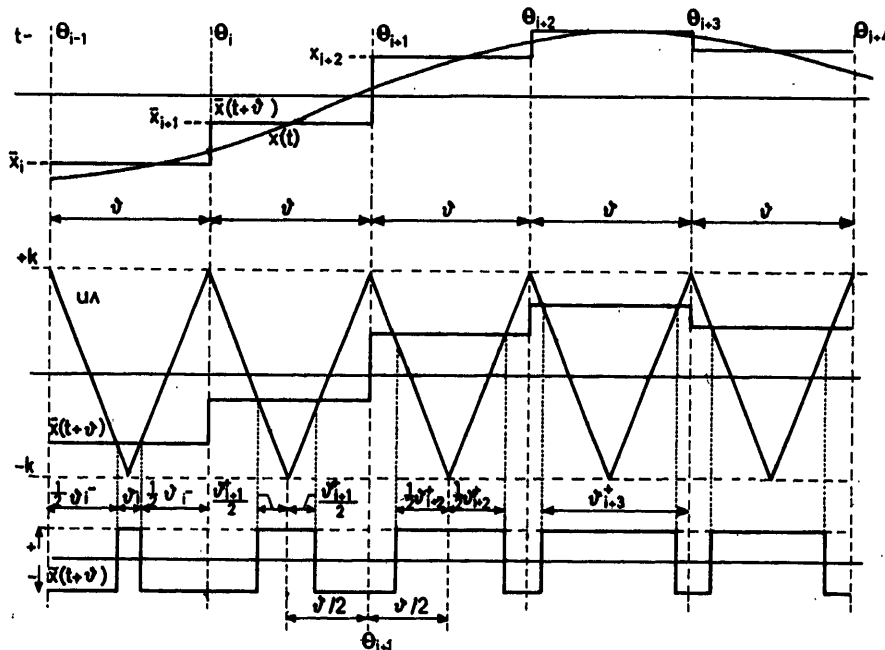


Figure 2. Signal transformation in SAM and KOD units

Coding

The signal $\bar{x}(t)$ appears at the input of the KOD unit. The coding takes place in this unit, i.e. the conversion of $\bar{x}(t)$ into pulses whose width (or duty cycle) is modulated, $\tilde{x}(t)$. The voltage $\bar{x}(t)$ is compared with a standard isosceles-triangle voltage wave-form u_A , and the signal $\tilde{x}(t)$ is derived according to the law:

$$\text{sgn } \tilde{x}(t) = \text{sgn} [\bar{x}(t) - u_A] \quad (4)$$

The durations of the positive and negative values of $\tilde{x}(t)$, ϑ_i^+ and ϑ_i^- , are connected by the linear relation:

$$k \frac{2\vartheta_i^+ - \vartheta}{\vartheta} = k \frac{\vartheta_i^+ - \vartheta_i^-}{\vartheta} = \bar{x}_i \quad (5)$$

where $k = |u_A|_{\max}$.

Omission of the sampling and replacing $\bar{x}(t)$ by $x(t)$, would cause non-linear terms containing $x(t)$ and its derivatives to appear in eqn (5). These represent the considerable non-linear distortion associated with such a method of coding.

Compared with the use of a standard sawtooth wave-form, the pulse-width modulation using a standard wave-form u_A of the given form is less sensitive by an order or even two orders of magnitude to exponential distortions of the linear sections of u_A . What is more, it is much simpler to generate a triangular than a sawtooth wave-form accurately at high frequencies.

Recording

The signal $\tilde{x}(t)$ is amplified in the recording amplifier A_W , fed to the recording head H_W and recorded on the magnetic tape L as segments magnetized to saturation. This technique makes the use of a high-frequency bias field unnecessary, and almost completely eliminates the effect of irregularities in the tape coating.

The recording of a single sample will require a length of tape

$$\lambda = \vartheta v \quad (6)$$

where v is the tape speed. An accurate value of v is maintained by a drive from a synchronous motor fed from a generator with accurately regulated frequency, and by mechanical filters (unit M on Figures 6, 7, 8, 10 and 12). Intervals of positive (λ^+) and negative magnetization alternate on the tape:

$$\lambda_i^+ = \vartheta_i^+ v, \quad \frac{1}{2}(\lambda_i^- + \lambda_{i+1}^-) = \frac{1}{2}(\vartheta_i^- + \vartheta_{i+1}^-) v \quad (7)$$

The tape speed for recording is chosen in relation to the resolving power of the recording heads, so as to secure the necessary accuracy in the recording and reproduction of the lengths of the magnetized segments. For this it is necessary to have

$$\lambda > \lambda_{\min} \quad (8)$$

where λ_{\min} is determined by the properties of the heads and tape.

Readout and Delay

After a loop of length l has passed through, the signals recorded by the recording head H_W arrive at the readout head

H_R , and are then amplified and shaped in the unit A_R . A signal $\tilde{x}(t - \tau)$ appears at the output of this block, where

$$\tau = l/v \quad (9)$$

τ is the delay of the signal $\tilde{x}(t - \tau)$ after $\tilde{x}(t)$.

The loop length l is determined by the required delay. It can be controlled either manually or automatically using a servo system controlled by a d.c. voltage or by rotation of a synchro shaft.

Multiplication

The signal $\tilde{x}(t - \tau)$ is fed in the input of the modulator MOD, where it obtains given accurate levels $\pm \bar{y}(t)$ (Figure 3). The signal $\bar{y}(t)$ is obtained at the output of the SAM unit, which samples $y(t)$ in accurate synchronism with the sampling instants of the signal $\tilde{x}(t - \tau)$.

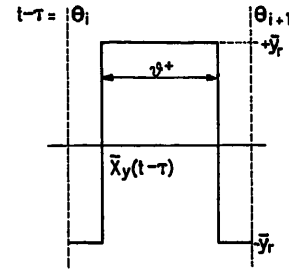


Figure 3. A period of the output signal from the MOD unit

The mean value of the signal at the output of the MOD unit over a single period ϑ is

$$\frac{1}{\vartheta} \int_{\vartheta_i}^{\vartheta_{i+1}} \tilde{x}_y(t - \tau) d(t - \tau) = \bar{y}_r \frac{2\vartheta_i^+ - \vartheta}{\vartheta} = \frac{1}{k} \bar{x}_i \bar{y}_r = \frac{1}{k} \bar{w}_i \quad (10)$$

where

$$\bar{w}_i = \bar{x}_i \bar{y}_r \quad (11)$$

The sampling of $y(t)$ is necessary because otherwise the expression for the mean value of the modulated signal would contain additional non-linear terms involving $y(t)$ and its derivatives. These terms would correspond to considerable distortion of the product of the x and y signals.

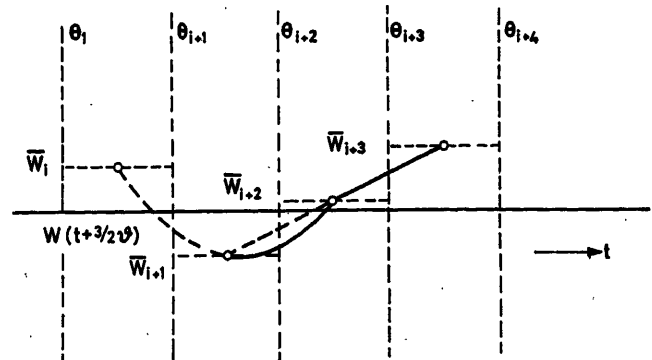


Figure 4. Output signal from INT unit

Inverse Transformation

The mean value of each individual period of the signal $\tilde{x}_y(t - \tau)$ is computed in the interpolation and integration unit INT according to formulae (10) and (11). The resulting values \bar{w}_i are interpolated quadratically. The arc of the interpolating parabola always passes through three neighbouring points (e.g. \bar{w}_{i-1} , \bar{w}_i , \bar{w}_{i+1}), but for interpolation one only uses the part of it between the last two of the points (e.g. \bar{w}_{i+1} and \bar{w}_i).

Thus one manages to obtain in the form of the output signal of the INT unit a good approximation to that required:

$$w\left(t + \frac{5}{2}\vartheta\right) \approx x(t - \tau)y(t) \quad (12)$$

even by a relatively seldom sampling.

The delay $\frac{5}{2}\vartheta$ caused by the principle of operation of the SAM unit (delay ϑ) and the INT unit (delay $\frac{3}{2}\vartheta$) does not introduce any error in statistical computation, since either it is simply added to the required delay or it slightly delays the production of the result. The signal transmission is nearly independent on frequency in other respects, except of course for the distortion due to the finite number of samples.

Synchronization

A most valuable property of the signals $\tilde{x}(t)$ and $\tilde{x}(t - \tau)$ is that they are entirely sufficient to determine the instants of sampling θ_i , and there is no need to record any synchronizing signal at all. The synchronizing pulses required to fix the instants θ_i for correct operation of the SAM and INT units in the reproduction and multiplication channels are derived in the SYN unit; this makes use of the fact that these instants are situated symmetrically with respect to the datum lines of the positive intervals of the $\tilde{x}(t - \tau)$ signal. A second similar SYN unit also supplies synchronizing signals and the standard triangular waveform u_A to the input SAM and KOD units.

Integration

The INT unit can also be switched to perform the operation of integration (designated INT_I). In this case the unit computes the mean value of the $\tilde{x}_y(t - \tau)$ signal not over the period ϑ , but over an arbitrary large period $T = m\vartheta$, m being an integer ≥ 1 :

$$\begin{aligned} \frac{1}{k} \bar{w}_i &= \frac{1}{T} \int_{t_i}^{t_{i+1}} \tilde{x}_y(t - \tau) dt = \frac{1}{kT} \int_{t_i}^{t_{i+1}} w(t) dt \\ &= \frac{1}{kT} \int_{t_i - \vartheta}^{t_{i+1} - \vartheta} x(t - \tau)y(t) dt \end{aligned} \quad (13)$$

$$t_{i+1} = t_i + T, \quad t_0 = \theta_0 + n\vartheta, \quad n \text{ an integer} \quad (14)$$

The output voltage of the INT_I unit is obtained by linear interpolation of the values \bar{w}_i with a delay of $\frac{3}{2}T$ (Figure 5).

The unit-type construction of the computer permits flexible programming of various problems. As a first example, the computation of correlation functions is demonstrated.

Computation of Correlation Functions

Figures 6, 7 and 8 show the connection of the computer units for computing the autocorrelation functions and cross-correlation functions of two processes $x_1(t)$ and $x_2(t)$. For simplicity's sake the synchronization chains are not shown in Figures 6, 7, 8, 10 and 12.

To start with, the signals are recorded on two tracks (e.g. 1 and 2) of a magnetic tape (Figure 6). The speed v is determined by the choice of the values of ϑ and λ according to eqn (6).

Before processing, the tape is removed from its reel and joined up to form a single long endless loop (of length L_T), which is placed in the endless loop container Z.

The first step in the processing is the transcription of the signals on two other tracks (e.g. 5 and 6) with a shift through a distance l_0 (Figure 7).

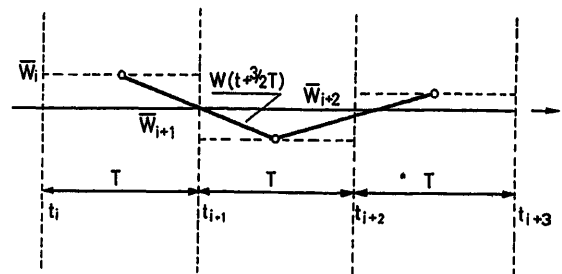


Figure 5. Output signal from INT_I unit

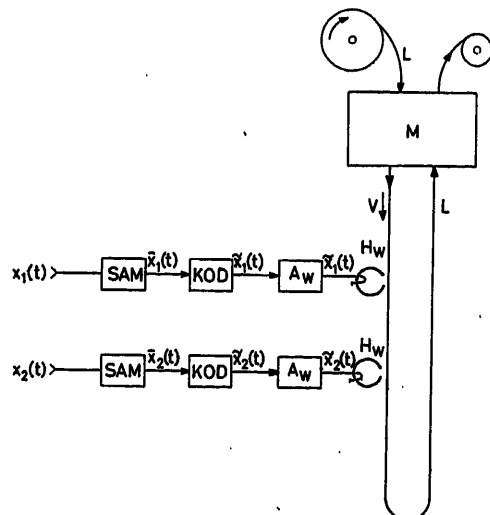


Figure 6. Connection of units for recording signals on tracks 1 and 2

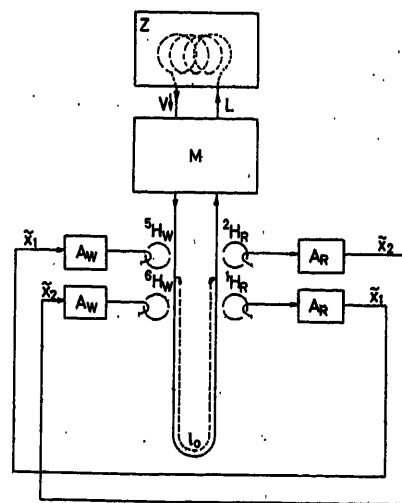


Figure 7. Connection of units for transcription of recorded signal with shift. The upper left index to the symbols H_W and H_R indicates the track number

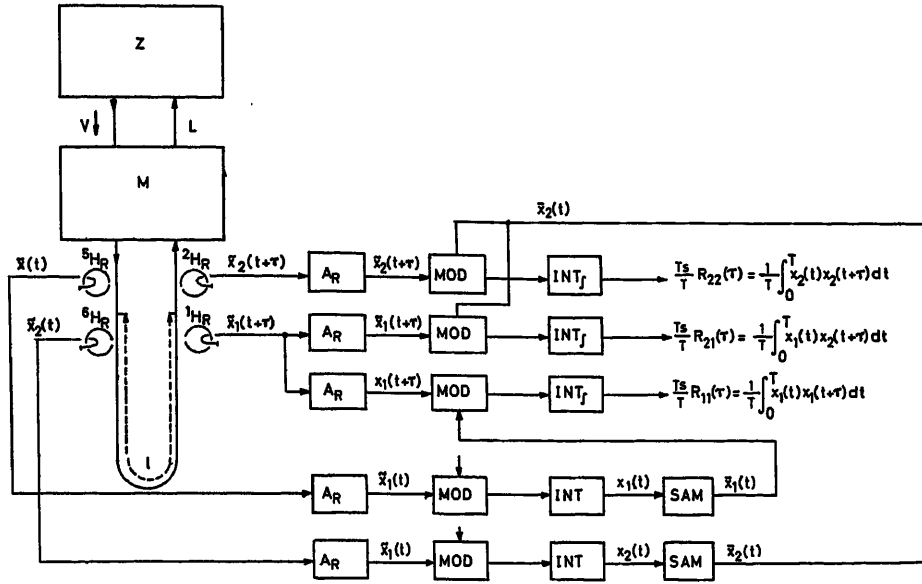


Figure 8. Connection of units for computation of correlation functions

For the computation itself (Figure 8), the first recorded tracks are read off by one block of heads (1H_R and 2H_R) and the tracks with copied signals by another block of heads (6H_R and 5H_R). The loop length between these two blocks is l . The resultant time-shift between the signals picked off by the two blocks is

$$\tau = \frac{l_0 - l}{v} \quad (15)$$

The signals from tracks 5 and 6 are converted back to continuous form and used for multiplication of the signals from tracks 1 and 2. The mean values of the products over a period T are computed in the INT_f units.

The period T is chosen equal to the period at which the joint in the endless loop passes the heads:

$$T = L_T/v \quad (16)$$

Each time the end of the recording passes the read-out heads, a signal taken from the control (auxiliary) tracks causes the loop length between the two blocks of heads to change automatically by Δl , i.e. the delay changes by

$$\Delta\tau = -\Delta l/v \quad (17)$$

At the instant when the start of the recording passes the read-out heads, a signal from the control is used to derive a pulse that fixes the start of a new integration period t_i , and this pulse is routed to the INT_f unit. As a result one gets from eqn (13) for each period T a single value

$$\bar{W}_i = \frac{1}{T} \int_{t_i}^{t_i+T} x_j(t+\tau_i) x_k(t) dt \quad (18)$$

$$\tau_{i+1} = \tau_i + \Delta\tau \quad \text{and} \quad t_0 = 0 \quad (19)$$

which corresponds to the value of the correlation function

$$R_{jk}(\tau_i) = \frac{1}{T_s} \int_0^{T_s} x_j(t+\tau_i) x_k(t) dt \quad (20)$$

where T_s is determined by the length L_s of the recording of processes x_j and x_k on the track:

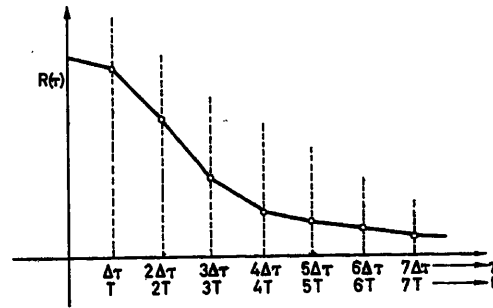
$$T_s = \frac{L_s}{v}; \quad L_s < L; \quad T_s < T \quad (21)$$

It follows that

$$\bar{W}_i \approx \frac{T_s}{T} R_{jk}(\tau_i) \quad (22)$$

and the graph of variation in output voltage $W(t)$ (Figure 9) is a graph of the correlation function. It can be recorded by means of either a pen-recording instrument or a print-out digital voltmeter. As a rule the maximum tape speed is used for computation. This markedly accelerates the work.

Using the computer's possibilities to the full, one can compute five correlation functions at once. Under these conditions the computer evaluates 50,000 products and 50,000 sums of sample values per second. The maximum capacity of the tape container is 1,200,000 samples. These figures show that a fairly powerful general purpose computer would be needed to do the same job as MUSA-6.


Figure 9. Correlation function graph obtained by means of a pen-recorder connected to the output of the INT_f unit in Figure 8

Computation of Distribution Functions (Figure 10)

After reconstitution, the signal $x(t)$ is compared in the comparator unit COM with a fixed reference voltage u generated in the reference voltage generator GEN. The output $\rho(u, x)$ of the COM unit is formed according to the law

$$\begin{aligned} \rho(u, x) &= 1 & \text{for } x < u \\ \rho(u, x) &= 0 & \text{otherwise} \end{aligned} \quad (23)$$

After the 0 and 1 levels have been given accurate values by the MOD unit, a mean value is determined in an INT_f unit, which is set up for a period T in the same way as for the com-

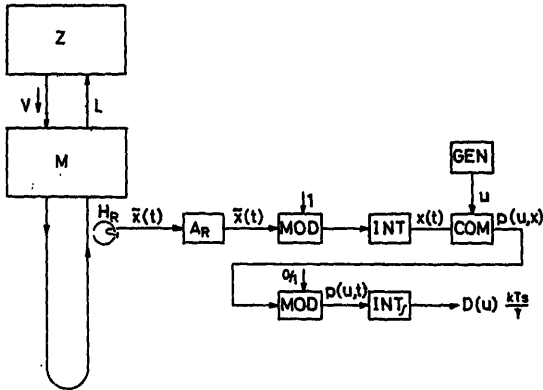


Figure 10. Connection of units for computation of distribution functions

putation of correlation functions. Each time the end of the recording of process $x(t)$ passes the heads, the value of u is automatically varied by Δu . If the integrand in eqn (13) is replaced by $\rho(u_i, x)$:

$$\begin{aligned} \frac{1}{k} \overline{W}_i &= \frac{1}{T} \int_{t_i}^{t_i+T} \rho(u_i, x) dt = \frac{T_s}{T} \cdot \frac{1}{T_s} \int_0^{T_s} \rho(u_i, x) dt = \frac{T_s}{T} D(u_i) \\ u_{i+1} &= u_i + \Delta u \end{aligned} \quad (24)$$

it is at once apparent that the $W(t)$ curve is a graph of the distribution function $D(u)$ with scale $k T_s / T$ (Figure 11).

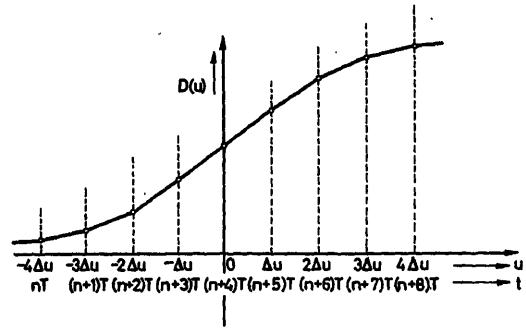


Figure 11. Form of distribution function obtained at the output of the INT_f unit in Figure 10

The comparator unit can also be switched to give another law for the formation of $\rho(u, x)$:

$$\begin{aligned} \bar{\rho}(u, x) &= 1 & \text{for } u - \frac{\Delta u}{2} < x < u + \frac{\Delta u}{2} \\ \bar{\rho}(u, x) &= 0 & \text{otherwise} \end{aligned} \quad (25)$$

In this case the computation leads to an approximate value for the probability density function $d D(u)/d u$.

Computation of Fourier Integral (Figure 12)

Here the $x(t)$ signal is multiplied by the functions $\sin \omega t$ and $\cos \omega t$, which are derived in the SIN unit.

The generation of these goniometric functions is started with an accurate phase $\omega t = 0$ precisely at the instant when the start of the recording of $x(t)$ on the tape track passes the read-out head. Each time the end of the $x(t)$ recording passes the head, the frequency of the SIN unit is changed to $c \omega$:

$$\omega_{i+1} = c \omega_i \quad (26)$$

The operation and setting-up of the INT_f units are the same as for the computation of correlation functions. The computation results in graphs of the functions:

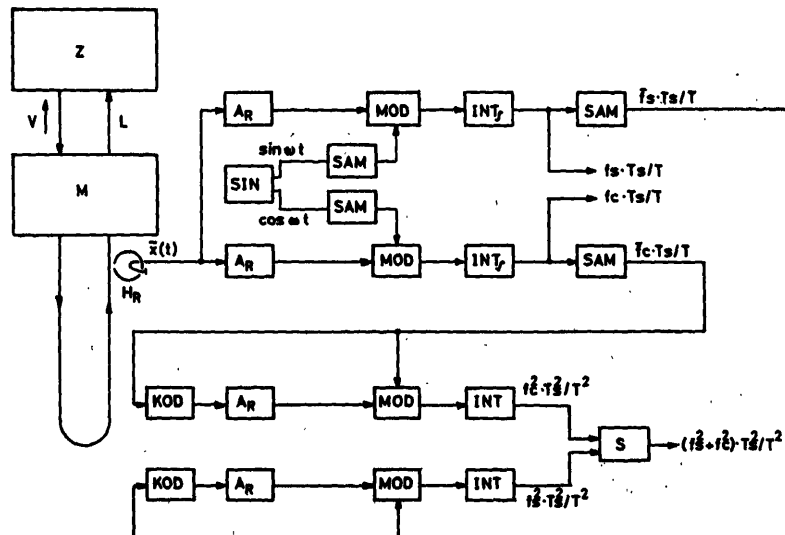


Figure 12. Connection of units for computation of Fourier integral

$$f_s(\omega) = \frac{1}{T_s} \int_0^{T_s} x(t) \sin \omega t dt, \quad f_c(\omega) = \frac{1}{T_s} \int_0^{T_s} x(t) \cos \omega t dt \quad (27)$$

with a logarithmic scale along the ω axis: these determine an approximation to the complex Fourier integral

$$F(\omega) = \frac{T_s}{2\pi} (f_c + j f_s) \quad (28)$$

The absolute value $|F(\omega)|^2 = T_s^2 (f_c^2 + f_s^2) / 4\pi^2$ is obtained by squaring and summing in the S unit.

This technique is not very suitable for functions $x(t)$ of a random nature, since the values of f_s and f_c tend to zero as the duration T_s of the recorded part of the random process $x(t)$ increases, and the f_s and f_c obtained are distorted by a large random error.

For random processes it is best to start by computing the correlation functions, and then to obtain the spectral density function $S(\omega)$ either by processing them according to the method described or on a digital computer.

But it is also possible to compute $\omega S(\omega)$ directly, by passing $x(t)$ through a narrow-band filter with pass-band from $(\omega_{i-1} \omega_i)^{\frac{1}{2}}$ to $(\omega_i \omega_{i+1})^{\frac{1}{2}}$.

After a simple change of connections the SIN unit can be used as the filter. The filter output is first squared and then integrated over a period T by an INT_i unit. Since the width of the pass-band is proportional to ω_i , so the resulting function is proportional to $\omega_i S(\omega_i)$.

Fundamental Parameters of the Computer

In determining the fundamental parameters of the computer, efficiency of operation, convenience of programming, and universality of application were aimed at. The following parameters were achieved:

- (a) Computer unit: 100 V.
- (b) Range of input and output voltages: ± 1 unit.
- (c) Accuracy: the error after a signal has passed through the complete channel in Figure 1 does not exceed 10^{-3} unit.
- (d) Depth of modulation $1/k = 0.8$.
- (e) Value of $\lambda_{\min} = 1$ mm.
- (f) Available sampling frequencies $1/\theta$: $1, 10^{1/2}, 10, 10^{3/2}, 10^2, 10^{5/2}, 10^3, 10^{7/2}, 10^4$ (sec $^{-1}$).
- (g) Range of integration period T : 1–100 sec.
- (h) Number of tracks: 6 + 2 auxiliary (control).
- (j) Tape speeds: $1, 10^{1/2}, 10, 10^{3/2}, 10^2, 10^{5/2}, 10^3, 10^{7/2}, 10^4$ (mm sec $^{-1}$).
- (k) Range of variation of delay loop length: 150–1,300 mm automatically (by servo system), with facility for adding 6 fixed sections of 1 m each. To represent a large fixed delay, the Z unit can be used as a delay loop.

(l) Constants of delay loop servo: voltage control gives 20 mm/V with setting accuracy ± 0.5 mm; synchro control gives 50 mm/turn with setting accuracy ± 0.3 mm.

(m) Fixed rates of change of delay loop length: $v_1 = p_1 p_2 p_3 p_4 p_5$ (mm sec $^{-1}$) where the following values may be chosen for the p_i : $p_1 = \frac{1}{2}, 1, 2$; $p_2 = \frac{1}{3}, 1, 5$; $p_3 = \frac{1}{5}, \frac{1}{3}, 1$; $p_4 = \frac{1}{2}, \frac{1}{3}, 1, 2$; $p_5 = 10^{1/4}, 10$, so far as the condition $v_1 < 25$ mm sec $^{-1}$ is observed. For stepwise movement $\Delta l = v_1 T$, $\Delta l < 25$ mm.

(n) Capacity of the endless tape loop container Z : 200 m.

(p) Frequency range of SIN unit: 10^{-2} – 10^3 sec $^{-1}$. Available values of c in eqn (26): $10^{1/24}, 10^{1/12}, 10^{1/8}, 10^{1/6}, 10^{1/4}$.

(q) Range of variation of voltage u from GEN unit: ± 1 unit. Available values of Δu : 0.02, 0.04, 0.1 unit.

(r) Complement of units: 6 each of SAM, KOD, A_W , A_R , MOD, INT, S and K (cathode follower). Also 3 COM, 2 SYN, 1 GEN, 1 SIN, 1 M , 1 Z , 1 control unit, 8 HT power units, 1 heater power unit, 3 servo units, 1 erase unit, etc.

(s) Valve complement: 250 in supply and reference voltage stabilizers; 50 in drive and servo systems; 150 in read-out and recording circuits; 300 in computing circuits; grand total 750.

(t) Power consumption: 7 kW.

Bibliography

- BROOKS, F. E. and SMITH, H. W. A computer for correlation functions. *Rev. Sci. Instrum.* 23, No. 3 (1952), 121–126
- HOLMES, J. N. and DUKES, M. A. A speech-waveform correlator with magnetic tape delay and electronic multiplication. *Proc. Inst. Radio Engrs, N.Y.* 101, III, No. 72 (July 1954), 225–237 (Radiosection Paper No. 1639)
- NOVIKOV, J. V. Magnitnyj korrelograf. Series: Pribory i stendy. *Izdat. Inst. techn. i ekon. inform. ANSSSR, Moskva* (1956)
- BABURIN, V. M. Korrelograf-pribor dlya vychisleniya korrelatsionnykh funktsij nizkotchastotnykh processov. *Sbornik: Primen. vych. techn. avtomat. proiz. Mash., Moskva* (1961)
- LEE, I. W., CHEATHAM, T. P. and WIESNER, J. B. Application of correlation analysis to the detection of periodic signals in noise. *Proc. Inst. Radio Engrs, N.Y.* 38, No. 10 (1950), 1165–1172
- LEVIN, M. J. and REINTJES, F. J. A five-channel electronic analog correlator. *Proc. nat. Electron. Conf.* 8 (1952), 647–656
- REINTJES, F. J. An analogue electronic correlator. *Proc. nat. Electron. Conf.* 7 (1951), 390–400
- ŠILHÁNEK. Application of analogue computers in control and automation. *Electron. anal. Comp.* Ed. T. Pardubice, Czechoslovakia (1960)
- MAXWELL. Development of a portable magnetic tape recorder for precision data recording. *I.R.E. Conv. Rec.*, Pt 10 (1955), 97
- NEWHOUSE. Compound modulation-method of recording data on magnetic tape. *I.R.E. Conv. Rec.*, Pt 10 (1955), 86
- REUKAUF. Simulate transport lags with magnetic tape. *Control Eng.* 4, No. 6 (June 1957), 145–147

DISCUSSION

D. J. A. CARSWELL, *Bruce Peebles & Co. Ltd., East Pilton, Edinburgh, Scotland*

Mr. J. Krýže is to be congratulated on the design of a flexible and elegant universal statistical analyser, and the concise and informative paper presented.

When considering the initial design of a more specialized four-channel machine for auto- and cross-correlation computation on low frequency data in band d.c.—few c/sec—we faced a final choice of variable delay tape loop or an out-of-contact magnetic drum delay system, and we eventually chose the latter.

Data acquisition is made on a separate transportable multichannel frequency modulation recording system, and analysis is carried out in speeded-up time scale (128:1 maximum). Delay is by using the magnetic drum store with saturation recording still in F. M. form. Some 50 preset values of delay are available by a combination of fixed position read-write heads on the drum and alternative drum speeds. After delay the signals are demodulated and multiplication and integration are carried out in analogue form.

Our choice of the drum system for delay was partly determined by the apparent unavailability of a commercial loop deck with guaranteed and adequate freedom from errors due to tape stretch, tape skew and drop-out. For our application, highest reliability and operation of the analysis equipment by non-engineering personnel were prime requirements.

Any comments by the author on the reliability and achieved performance of his tape loop system would be of interest.

J. KRÝŽE, *in reply*

I am very thankful to Mr. Carswell for his discussion and for the information about his work. This is a new example of how much interest is paid in different countries to problems of statistical computation.

The reliability achieved with our tape loop system for simulating time lag is acceptable. The tape (35 mm perforated) is capable of turning several thousand times without a significant deterioration in signal amplitude and also the joint behaves reasonably when properly made. The influence of decreasing pulse amplitude can be further diminished by using recording, consisting of very narrow pulses, marked by their polarity and their position denoting the moments of polarity changes of signal in place of using an analogue waveform of the signal. (The mentioned d.c. waveforms can be used in the machine.) The recording signal has, then, the form of a double pulse with its zero crossing marking the moment of polarity change, and hence is only insignificantly affected by amplitude changes.

When using the tape, Agfa MF 3 or MF 4, the amplitude varies only rarely more than 10 per cent whereas the signal has to be reduced to less than one-tenth of its nominal value to produce a drop-out. Moreover, in statistical calculations a complete distortion of one sample from some ten thousands should not be critical.

We have had some trouble with drop-outs in the past, but these were caused by pulses being added (inadequate magnetic and electric shielding, etc.) and not lost.

As concerns the changes in tape length, the influence of mechanical stress is avoided by keeping its value constant and by choosing the 35 mm perforated film tape, which is very rigid. The influences of humidity and temperature changes are not great and are very slow, so that there is hardly any change during one computation. Therefore, the result is in the worst case a contraction or dilatation in the correlation function time scale of the same value as the contraction or dilatation of the tape caused by humidity and temperature change which took place in the meantime between recording and processing. This is negligible in most practical applications; when necessary it is possible to measure exactly the produced change in perforation intervals of the tape very precisely and evaluate the necessary correction of correlation function time scale.

D. J. A. CARSWELL

I should have added that whilst we agree that the magnetic tape loop system has an enormous advantage in storage capacity, we do in point of fact use more than one circular track on the drum in series to increase delay time and storage capacity. However, although this process can be easily extended manifold on a standard drum the insertion of each extra 'track's worth' of storage and delay involves an additional read-write operation, and a small reduction of signal/noise ratio and consequent overall accuracy.

J. KRÝŽE, *in reply*

I have to add that Mr. Carswell is quite right when speaking about mechanical troubles, which arise with use of magnetic tape. These troubles were concentrated in our case in the perforated tape transport drive and mechanical filters for filtering of tape transport disturbances, caused by gears and the drive. The tooth forms of the tape driving drum, especially, turned out to be a critical point. There is no doubt that a drum delay is a better solution, when highest reliability of long term operation of the delay simulating device is necessary.

PROFESSOR AINBINDER

Is it to be understood that a magnetic tape loop and a drum are equivalent solutions?

J. KRÝŽE, *in reply*

Yes, they are quite equivalent in respect of achievable accuracy and many other respects, but the tape loop, when using contact pad, allows a substantially higher packing density and easy increasing of loop length, which is not the case with a magnetic drum, because of diameter limitations. So the tape loop is more flexible.

E. BLANDHOL, *Eidanger Salpeterfabriker-Heröya, Porsgrunn, Norway*

I would like to call the author's attention to a small transistorized, portable statistical computer called ISAC, developed and used by the discussor *et al.*^{1, 2}. It is highly interesting to note that the computer described in your paper does very much the same as our ISAC, thus stressing the practical need for such computers. However, your computer would probably have been even more useful if it were portable to measurement location.

The transcription of the recorded signals needed for correlation could have been avoided by recording each input on two tracks on the tape simultaneously, one from each head, thereby eliminating the minimum distance 10.

The author's reasons for choosing pulse width modulation and his associated error analyses are really interesting. However, in our ISAC, asynchronous pulse frequency modulation was used, with very satisfactory results. This principle also permits a frequency division of the modulated input signals equal to the recording/playback tape speed ratio, thereby yielding a fixed frequency range in all playback circuits.

Finally I have three questions:

- (1) What is the maximum input signal bandwidth?
- (2) What is the computing time for each point of correlation function?
- (3) The correlograms shown in the figures are continuous. How is the overlapping between individual points achieved?

References

- ¹ BLANDHOL, E., HESTVIK, O. and MOHUS, I. A description of the statistical computer 'ISAC'. Automatic Control Laboratory, *Norw. Inst. of Techn.*, Vol. 1 (November 1959), Vol. 2 (December 1960)
- ² BALCHEN, J. G. and BLANDHOL, E. On the experimental determination of statistical properties of signals and disturbances in automatic control systems. *Automatic and Remote Control*, Vol. II, p. 788-96. 1961. London; Butterworths

J. KRÝŽE, *in reply*

I would like to thank Mr. Blandhol for his discussion and very interesting remarks. I have to agree with him that a portable and transistorized construction like ISAC would be more advantageous, but high requirements on precision, efficiency and lack of suitable transistors made it not possible. We intend to compensate this by complementing the machine by one or more portable recorders. This has the advantage that the machine exploitation is not affected when long-time records of slow processes are taken.

The trick of eliminating the transcription by recording the signal on two tracks in shifted position is quite right, but it would severely limit the number of simultaneously recorded processes from a multi-variable system with the given number of six tracks in our case. Therefore we did not make use of it.

I agree that satisfactory results can be achieved by the use of frequency modulation, when static accuracy is being discussed. But when high accuracy, 1 per cent or higher, is to be maintained in a maximum frequency band with minimum tape speed, the advantages of equidistant sampling and PWM (PDM) become very stressed.

Concerning the signal bandwidth, it depends on the sampling frequency chosen. Sinusoidal waveforms of unit amplitude and frequency lower than approximately one-fifteenth of sampling frequency are reproduced with the specified 1 per cent accuracy. For higher frequencies the error grows approximately with f^4 . The frequency characteristics are defined so that the results can be corrected when substantial higher frequencies, to one-third of sampling frequency, are present.

The computing time for one point of correlation function is dependent on the recorded length of the process. It is, in seconds:

$$(0.2 - 0.5) + \frac{\text{number of samples of the recorded process}}{10,000}$$

So approximately 20 sec is necessary when full storage capacity (200,000 samples for one track) is used. Five points of five functions for the same value can be computed in the same time, when full use of machine possibilities is made.

The continuous form of correlograms results from electronically interpolating the individual computed values of the function, as is shown in *Figures 5 and 9* of the paper.

B. S. MORGAN, JR. and E. B. STEAR, 4606 Eaton Dr., Washington D.C., U.S.A.

The author is to be congratulated for this paper and the construction of a device capable of, and useful for, the reduction of statistical data.

The device would seem to be more attractive for general laboratory use than for some on-the-line uses in adaptive controllers. Has a recent model using transistors been built?

The sampling process [eqn (1)] involves a net differentiation of the signal and hence appears to be worse than sampling over an infinitesimal time period as far as external noise is concerned. Would the author comment on this?

Why does the author think that it is simpler to generate a triangular wave than a sawtooth wave?

J. KRÝŽE, *in reply*

I wish to thank Drs. Morgan and Stear for their discussion. I fully agree with their opinion that the computer MUSA-6 is adequate for laboratory use (it has been built for that) and not for on-line use in adaptive controllers. The computer is built with electronic tubes, and transistorization is not considered at the moment.

The criticism of the sampling process, as described in eqn (1), is quite right, and this was taken in account in the design. The second derivative conversion of the sampling process as defined in eqn (1) is a first-term approximation to an ideal. This first-term approximation is realizable by a resistor-capacitor network and does not amplify very high frequencies; on the contrary it damps them, yielding a good approximation to the ideal at low frequencies, where the higher terms of Taylor expansion can be neglected.

The simplicity of generating a triangular wave at high frequencies, mentioned in the paper, concerns the realization simplicity. Both linear sawtooth forms and triangular waveforms are generalized by the integration of exact rectangular pulses. In the case of triangular waveforms these pulses have a 1:1 duty cycle and the positive and negative amplitudes are equal, whereas in the case of sawtooth waveforms one of the pulses has to be several orders of magnitude shorter and in the same ratio higher, or the integration time constant has to be changed when generalizing the steep part of the sawtooth waveform (e.g. by closing a capacitor discharging switch).

The sawtooth waveform has a greater high frequency content than a triangular waveform and consequently operational amplifiers with a substantially broader frequency band are necessary for the generation and handling, when the same precision of waveform is specified. Moreover, the requirements for linearity of the triangular waveform are much lower, and so the distortion due to parasitic circuit time constants in the generation and handling circuits is of less importance.

F. CSAKI, *Department of Automation, Polytechnic University, Budapest XI, Hungary*

When I was in Czechoslovakia just over a year ago, I saw this excellent machine myself. It would be very interesting if the author could report about some practical results concerned with real industrial plants and obtained recently by the correlator.

J. KRÝŽE, *in reply*

At the present time, no industrial results are yet obtained. If any become available they will be published. For the first year the machine will be investigated on laboratory scale. It is proposed to use it during this time for work on models, servomechanisms and signals taken from human organism.

G. T. ROBERTS, 378 Ferry Road, Edinburgh 5, Scotland

In the operation of a correlation computer of this sort one of the major difficulties is the elimination of mean values in the recorded signals. This step is necessary because a recorded mean level will use up much of the available dynamic range in analogue type equipment. Also, any mean value present in signals before correlation will result in a computed correlogram which would not tend to zero for large τ .

If the process is stationary and the mean level is constant throughout the recorded period, then the problem is trivial. In a non-stationary process, however, where the mean level of the recorded signal exhibits a slow drift throughout the recording period, a simple cancellation of the mean value computed over the whole length of record does not result in a computed correlation function which is free from error.

Figure A (overleaf) shows a signal $x(t)$ which has zero mean value over the recorded period T , but which would give a correlation function which would not tend to zero for large τ .

Has the author had any experience in handling non-stationary signals of this sort? If so, what method has he found most suitable for elimination of errors of this type?

J. KRÝŽE, *in reply*

Before recording a process we have to make some estimate of its behaviour as to mean value and as to its use for recording a constant shift, which would ensure that the range of the recorder is used in an optimal way. The remaining mean value can be evaluated on the machine and subtracted from the recorded signals before processing them (this requires a transcription), or used for determining the zero line of the correlation function after processing.

As for the slow drift of zero level shown in *Figure A* it is to be determined if it is a large low frequency component of a stationary signal or a mean value change of a non-stationary signal.

If we are quite sure that the low frequency components are of no importance for the problem to be solved, we can use a high pass filter with an exactly known transfer function. The effect of introducing this filter on the correlation function can be expressed by a convolution integral. Hence the resulting correlation function can be corrected if necessary, or the calculations which are based on it (spectral density, unit step response, etc.) modified to take account of the filter introduced.

In the example of a spectral density function given by Dr. Roberts, only the frequency band approximately from 1/1,000 to 10 c/sec is interesting for the evaluation of dynamic characteristics of real controlled systems. Whereas the unwanted high frequency can be easily cut off by a high-pass filter, this is more difficult with the low frequencies, which cause an ineffective use of the range of the computing device and cannot be cut off by a high-pass filter, because of practical troubles with realization of large time constants and impossibility of determining the effect of filtering on the correlation function obtained.

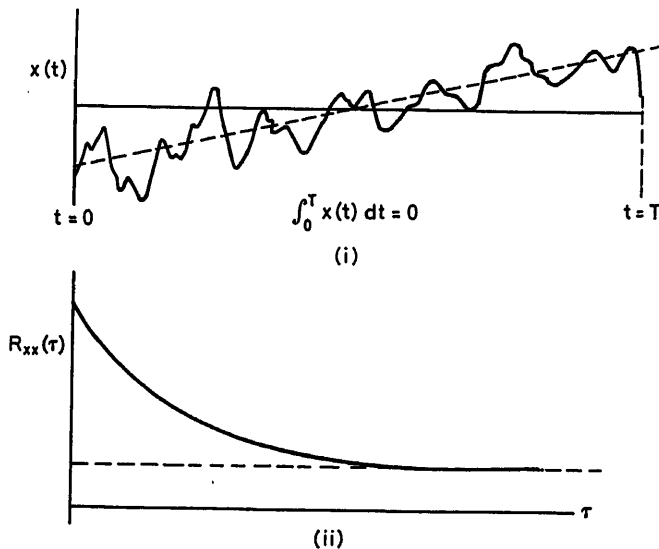


Figure A. (i) Finite length of record with a slow drift of mean level, but zero average value over an interval of T sec; (ii) Resulting autocorrelation function does not tend to zero for large values of τ

P. JESPERS, 4 Av. Charles de Lorraine, Belgium

There is hardly any other way for solving these problems.

J. KRÝŽE, in reply

We have not much practical experience with these problems yet, but we intend to use exactly the same method of solving them as described by Mr. Veltman. This is the reason why we included a great storage capacity. Our two control tracks allow for carrying out the computation of individual correlation functions from individual parts of the divided process simultaneously.

I would like to ask Mr. Veltman what his experience is in theoretical estimations of correlation function variance compared with experimental results. It seems to us that the variance is in practice substantially greater than the theoretical estimations, and that substantially longer recordings have to be processed for obtaining the necessary accuracy than that which the theory shows.

B. P. Th. VELTMAN, Department for Technical Physics, Technological University of Delft, The Netherlands

I fully agree with Mr. Krýže on this point. To a certain amount it may be caused by the deviation of actual processes from the presumed Gaussian distribution, but it seems that other causes which were unknown at that time have a great influence.

Concerning the remark by Dr. Jaspers I refer for precise information to the paper by my colleague and me, in the volume on Theory, which gives a summing-up of principles for correlation techniques with appropriate references.

The point that Dr. Roberts raised is an important one indeed. The elimination of spurious low frequency components is necessary for making the correlation procedure successful. The difficulty is that high-pass filtering may introduce disturbing filter transients.

A combination of high-pass filtering and manual compensation for diminishing the transient effect is, however, nearly always sufficient.

The high-pass filter may be a simple first-order system or an ingenious 'running average' window filter. It may also be successful to integrate over short time intervals and to set up a three-dimensional display of the correlation functions that arise out of succeeding integration intervals. Visual inspection then may make it easier to detect non-stationarity in the process.

The Behaviour of Adaptive Controllers

J. L. DOUCE

Summary

Techniques are described for analysing the behaviour of single-channel and two-channel self-optimizing systems. From the analysis, it is shown that conventional practical systems suffer from the disadvantages of slow speed of response and excessive deviation of parameter setting from the desired value.

By a simple modification a sample and hold system effects a significant improvement in performance. A practical controller incorporating an electro-mechanical integrator and sampling device is described and applied to a two-channel optimizing system.

Parameter adjustment in a two-channel system is not, in general, along the line of steepest descent. This divergence is analysed, enabling the adaptive controller to be designed for satisfactory performance.

Sommaire

Le rapport décrit le mode d'analyse du comportement d'un système auto-adaptatif à un et à deux canaux. Il ressort de cette analyse que les systèmes conventionnels offrent l'inconvénient d'une faible vitesse de réponse et d'une déviation excessive par rapport à la valeur désirée.

Une notable amélioration de ces performances peut être obtenue par une simple modification du système d'échantillonnage et d'extrapolation. Un système d'ajustement comportant un intégrateur électromécanique et un échantillonneur est décrit et appliqué à un système d'optimisation à deux canaux.

L'ajustement des paramètres d'un système à deux canaux n'est pas en général sur la ligne de la pente maximum. Cette divergence est examinée en vue d'améliorer les performances du système auto-adaptatif.

Zusammenfassung

Untersuchungsmethoden für das Verhalten von einkanaligen (ein Parameter) und zweikanaligen (zwei Parameter) selbstoptimierenden Systemen werden beschrieben. Die Untersuchung ergibt, daß die bisher üblichen Systeme den Nachteil niedriger Einstellgeschwindigkeiten und beträchtlicher Abweichungen der Parametereinstellungen von den gewünschten Werten besitzen.

Eine einfache Abänderung durch Einfügen eines Abtasters mit Halteglied bewirkt eine wesentliche Verbesserung. Ein praktisch anwendbarer Regler mit elektromechanischem Integrator und Abtaster wird beschrieben und auf ein zweikanaliges Optimiersystem angewendet.

Beim zweikanaligen System erfolgt die Parametereinstellung gewöhnlich nicht auf der Kurve des steilsten Abfalles. Diese Abweichung wird untersucht; dadurch gelingt es, den selbsteinstellenden Regler mit zufriedenstellendem Betriebsverhalten auszustatten.

Introduction

Several self-adaptive systems have been described which operate on the hill-climbing principle^{1, 2}. Conveniently, the parameter setting under control is given a small displacement or perturbation, and the effect of this perturbation is measured so that the setting can be adjusted to improve the performance of the overall system. For continuous optimization the perturbation is applied periodically and for practical convenience a square wave perturbation is chosen.

The basic system is shown in *Figure 1 (a)*. The parameter value, K , is adjusted cyclically by a periodic square wave of amplitude $\pm \delta$. The resulting change of behaviour of the control system (not shown) gives a cyclic variation in the performance measure e_m . The effect of the perturbation is detected by a synchronous detector, multiplying the performance measure by a square wave derived from the perturbation signal. Finally, the parameter is adjusted at a rate proportional to the effect of the perturbation.

Elementary analysis suggests that the parameter will be adjusted towards the optimum value at a rate proportional to the gradient $\partial e_m / \partial K$. Later in this paper it is shown, however, that maximum rate of optimization of this system is fundamentally limited and the performance is further restricted by excessive fluctuations of parameter setting about its mean value, both in the steady state and during transient conditions.

Improved performance results if a sample and hold unit is inserted immediately following the integrator, so that parameter adjustment occurs discontinuously, once each cycle of the parameter perturbation. Since the only variation of parameter value during a perturbation period is that introduced by the perturbation wave-form, a more accurate assessment of the effect of this perturbation can now be obtained and more reliable optimization is possible.

Figure 1 (b) illustrates one manner in which the controller may be realized. The parameter value corresponds to the angular position of a rotary potentiometer, producing variable attenuation of some signal $f(t)$ from the control system. The overall behaviour of the practical controller is identical to that of this unit, although the controller is simpler in construction.

The Practical Controller

The controller developed uses a permanent-magnet integrating motor, giving a shaft rotation proportional to the time integral of the applied voltage with an accuracy sufficient for practical purposes. Multiplication of the incoming performance measure voltage is achieved by reversing connections to the motor with a relay which also introduces the required perturbation signal.

The motor is coupled to the output potentiometer by a reduction gearbox and a mechanical clutch, giving the required sample and hold action. The clutch is engaged by a further relay, pulsed once each cycle of the perturbation. Use of a clutch produces an extremely rapid parameter adjustment, eliminating a previously observed source of instability.

The complete controller (*Figure 2*) includes a transistor oscillator driving a scale of two counter to generate the perturbation wave-form, to ensure that the mark to space ratio of this signal is exactly unity. Relays are included for initial parameter setting, for detecting excessively large parameter adjustments which render the clutch inoperative, and for ensuring that the

integration process is initiated at the commencement of a perturbation cycle. The complete controller is contained in a unit approximately $30 \times 30 \times 10$ cm.

Analysis of the Single-channel Optimizer

The speed of response of the optimizer is limited by the maximum rate at which the perturbations can usefully be applied. Except in special cases, in which a repetitive signal is applied to the input of the control system, the performance measure cannot be estimated accurately in a time period comparable with the response time of the system.

In general, the performance measure must be observed over

a time interval very much greater than the response time of the system. For example, when the input to the system is a random signal, then the change in performance measure due to the perturbation cannot be assessed reliably unless the period of the perturbation, 2τ , is of the order of 100 times the response time of the system^{3, 4}. Statistical errors in short-term measurements fundamentally limit the minimum useful perturbation period.

Whilst this slow response is undesirable in practice, although inevitable, it permits an analytic solution of the response of the parameter adjusting system to be obtained, since the variation of performance measure of the control system with parameter setting may be assumed instantaneous. The relationship between performance index and parameter setting is given by the Static

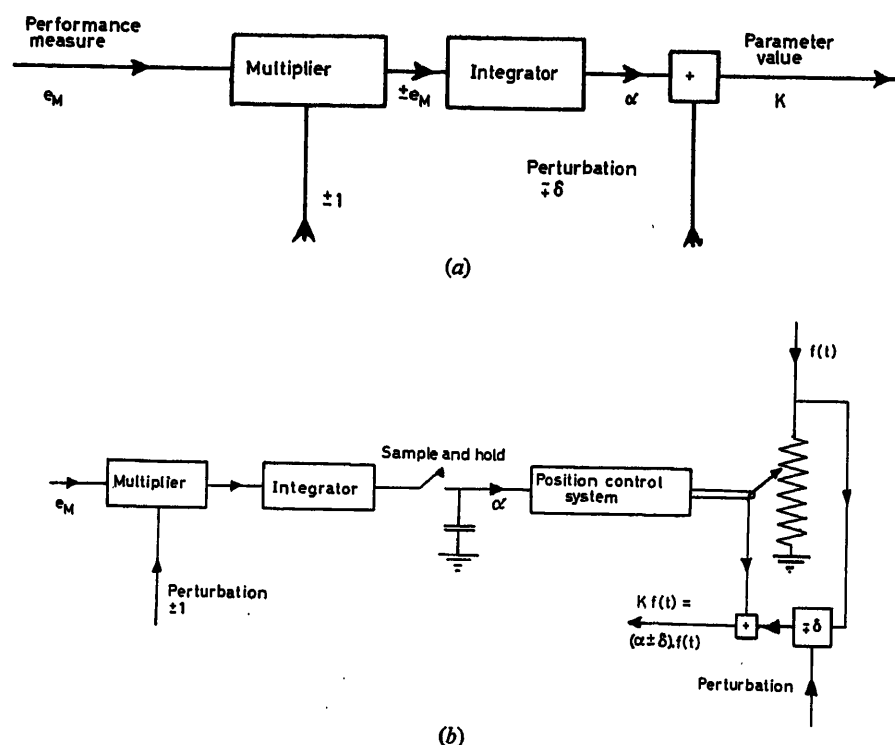


Figure 1. The self-optimizing controller: (a) schematic diagram of the basic system; (b) the system with sample and hold

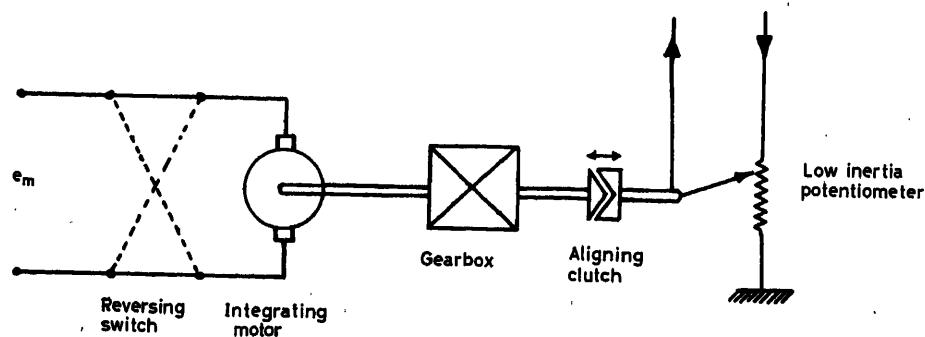


Figure 2. The practical controller

689

Solving the equations

$$\frac{d\alpha}{dt} = \frac{1}{T} \left[\frac{1 + (\alpha - \delta)^2}{\alpha - \delta} \right] \quad 0 < t < \tau$$

$$\frac{d\alpha}{dt} = -\frac{1}{T} \left[\frac{1 + (\alpha + \delta)^2}{\alpha + \delta} \right] \quad \tau < t < 2\tau$$

gives

$$(\alpha_\tau - \delta)^2 = (\alpha_0 - \delta)^2 e^{2\tau/T} + e^{2\tau/T} - 1$$

$$(\alpha_1 + \delta)^2 = (\alpha_\tau + \delta)^2 e^{-2\tau/T} + e^{-2\tau/T} - 1$$

Eliminating α_τ gives the parameter value at the end of one cycle α_1 in terms of the previous value α_0 :

$$\alpha_1 = \{(\alpha_0 - \delta)^2 + 4\delta e^{-2\tau/T} [\delta + \{(\alpha_0 - \delta)^2 e^{2\tau/T} + e^{2\tau/T} - 1\}^{\frac{1}{2}}] - \delta\}$$

This relationship is plotted in Figure 5 for $\alpha_0 = 2$ with $\delta = 1/20$ for different values of loop gain τ/T . The maximum useful loop gain is limited by the maximum allowable excursion of parameter value. The curve has been terminated at $T = 2.87\tau$

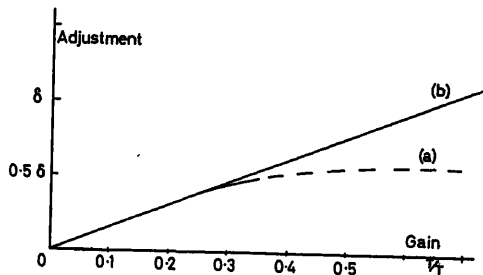


Figure 5. The adjustment as a function of gain: (a) without clamp; (b) with clamp

corresponding to an excursion over the first half cycle from $\alpha = 2$ to $\alpha = 3$. The magnitude of the adjustment over the first cycle is 0.025 under these conditions. In the steady state, $\alpha_1 = \alpha_0$, the parameter fluctuates between the limits

$$0.65 < \alpha < 1.36$$

(2) With the clamp inserted, as shown in Figure 3, parameter excursion is prohibited between event times $0, 2\tau$, etc. immediately eliminating one disadvantage of the previous system. In addition, a more accurate assessment of the slope of the Static Transfer Characteristic is obtained.

The change in integrator output is given by

$$\frac{dx}{dt} = \frac{1}{T} f(\alpha_0 - \delta) \quad \text{for } 0 < t < \tau$$

and

$$\frac{dx}{dt} = -\frac{1}{T} f(\alpha_0 + \delta) \quad \text{for } \tau < t < 2\tau$$

The change in parameter setting over one cycle is now

$$\alpha_1 - \alpha_0 = \frac{\tau}{T} [f(\alpha_0 - \delta) - f(\alpha_0 + \delta)]$$

$$\approx -2\delta \frac{\tau}{T} [f(\alpha)]'_{\alpha=\alpha_0} \quad (3)$$

since δ is small.

Thus the clamping device permits the optimizing system to function as an ideal gradient computer.

With the characteristic previously discussed,

$$f(K) = \frac{1}{K} + K$$

the optimum operating condition ($\alpha = 1$) is attained in one step with $\delta = 0.05$ from $\alpha = 2$, if $T = 0.075\tau$. No significant parameter variations occur in the steady state. Figure 5 illustrates the improvement effected by the clamp in increasing the magnitude of useful adjustment.

In this system the maximum gain of the adaptive loop is determined by stability requirements. From any initial parameter setting, the magnitude of the useful step is directly proportional to the gradient and the integrator gain, $1/T$. Instability occurs if, as the result of one adjustment, the parameter setting overshoots the maximum value to such an extent that the new gradient is equal to or greater than the initial gradient. This is illustrated in Figure 6.

In case (1) the gain of the adaptive loop is higher than optimum, so that from the initial operating point O successive moves are A_1, B_1, C_1 . This oscillatory motion converges to the desired final value. With a higher gain, the unstable response $O A_2, B_2, C_2$ results. The limiting case, producing a continuous cyclic oscillation, corresponds to motion OAO , determined by the criterion that the initial adjustment from O gives a new gradient of magnitude equal to the gradient at O , restoring the initial parameter setting.

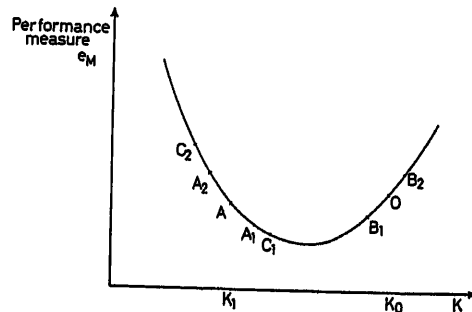


Figure 6. Instability with excessive gain

In the example quoted

$$f(K) = K + \frac{1}{K}$$

and the adjustment step is of magnitude

$$\Delta K = -2\delta \left(\frac{\tau}{T} \right) [f(K)]'_{K=K_0}$$

Instability will occur from the initial value $K = 2$ if the initial step changes the parameter value such that the new gradient is of magnitude greater than 0.75. That is, for stability, the parameter value after the first step must be greater than 0.756. The maximum gain is thus limited to $T \geq 0.06\tau$.

It may be noted that for the parabolic Static Transfer Characteristic

$$f(K) = \frac{1}{2}(K - K_{\text{OPT}})^2 + C$$

the optimum parameter setting is attained after one cycle from any initial value if

$$T = 2\delta \cdot \tau$$

Continuous oscillations occur if the gain of the optimizing loop is doubled and oscillations of increasing amplitude result if

$$T < \delta \cdot \tau$$

Thus the most satisfactory gain of the optimizing loop can be determined in terms of the maximum slope of the Static Transfer Characteristic over the working range. The perturbation period, 2τ , is chosen to be as short as permitted by statistical considerations, and the perturbation amplitude δ is fixed by the permissible parameter variation in the steady state, so that the remaining variable, T , can be determined⁶.

A Multi-channel System

When two or more parameters are simultaneously adjusted, the effect of a change in any one parameter must be distinguished from the effect of adjustments introduced into the other channels. In a two-channel system, this may be realized by using perturbations of the same frequency, differing in phase by 90° . However, extraneous phase shifts, which may differ in magnitude for the two channels, can introduce serious cross-coupling and instability in extreme cases⁶.

More generally, each channel employs a different frequency of perturbation. The relationship between adjacent frequencies must be properly chosen to give a similar speed of response for each channel, with sufficiently small beat frequency effects. To ensure that each channel operates as rapidly as possible each perturbation frequency should be as near as possible to the upper frequency determined by statistical limitations.

Ideally each channel responds independently of the operation of the other channels, so that each parameter may be considered alone. The analysis of the preceding section is then applicable, showing that the adjustment in any one channel is directly proportional to the slope $\partial f / \partial K_i$. This reduces the performance or error measure along the line of steepest descent.

Analysis shows that a multi-channel system will not, in general, adjust the parameters so that the error measure decreases along the line of steepest descent. A further feature is that the difference between perturbation frequencies may be determined if the maximum tolerable amplitude of the beat frequency term is specified.

The Behaviour of a Two-channel System

To show that a two-channel system will not, in general, adjust the parameters so that optimization follows the line of steepest descent, consider the case where one parameter K_1 influences the error measure, and in which a second parameter K_2 , although being automatically adjusted, does not affect this measure.

Due to the automatic adjustment of parameter K_1 , the error measure will decrease with time, as sketched in Figure 7. In the second optimizing controller, this error measure is multiplied by a repetitive square wave of period $2\tau_2$. Over any one cycle

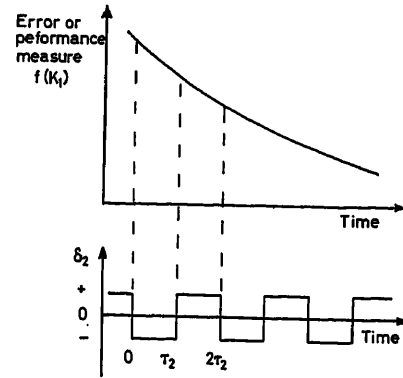


Figure 7. The introduction of false adjustment in parameter 2

of perturbation, commencing from δ_2 switching negative, the time integral of the product $\delta_2 \cdot f(K)$ will always be negative. This will adjust parameter K_2 , introducing a continual departure from the line of steepest descent.

Assuming, for the purpose of this analysis, that the error measure changes uniformly with time, so that

$$\frac{df}{dt} = \frac{\partial f}{\partial K_1} \cdot \frac{dK_1}{dt} + \frac{\partial f}{\partial K_2} \cdot \frac{dK_2}{dt} \quad (4)$$

then, from eqn (3), the mean rate of change of parameter setting with time due to synchronous rectification of the effect of the corresponding perturbation is

$$\frac{dK_i}{dt} = -\frac{\delta}{T} \frac{\partial f}{\partial K_i}$$

Due to the continual change of error measure with time this is modified to

$$\frac{dK_i}{dt} = -\frac{\delta}{T} \frac{\partial f}{\partial K_i} + \frac{\tau_i}{2T} \cdot \frac{df}{dt}$$

Eqn (4) enables df/dt to be eliminated, and by substituting $i = 1$ and $i = 2$ in the resulting equation gives the rate of parameter adjustment

$$\begin{aligned} \frac{dK_1}{dt} & \left\{ 1 - \frac{1}{2T} \left[\tau_1 \frac{\partial f}{\partial K_1} + \tau_2 \frac{\partial f}{\partial K_2} \right] \right\} \\ & = -\frac{\delta}{T} \frac{\partial f}{\partial K_1} + \frac{\delta \tau_2}{2T^2} \frac{\partial f}{\partial K_1} \cdot \frac{\partial f}{\partial K_2} - \frac{\delta \tau_1}{2T^2} \left(\frac{\partial f}{\partial K_2} \right)^2 \end{aligned}$$

and similarly for dK_2/dt .

These solutions enable the angle between the line of steepest descent and the trajectory to be determined. At any point in the $K_2 - K_1$ plane the line of steepest descent makes an angle θ_s with the K_1 axis, given by

$$\tan \theta_s = f_2 / f_1$$

where

$$f_1 = \frac{\partial f}{\partial K_1}, \quad f_2 = \frac{\partial f}{\partial K_2}$$

The inclination of the practical trajectory is

$$\tan \theta_p = \frac{dK_2/dt}{dK_1/dt} = \frac{f_2 - \frac{\tau_1}{2T} f_1 f_2 + \frac{\tau_2}{2T} (f_1)^2}{f_1 - \frac{\tau_2}{2T} f_1 f_2 + \frac{\tau_1}{2T} (f_2)^2}$$

From these equations the angle θ_D between the trajectory and the line of steepest descent is given by

$$\tan \theta_D = \frac{1}{2T} \{ \tau_2 f_1 - \tau_1 f_2 \}$$

This angle is, in general, not equal to zero.

To evaluate the effect of beat frequency terms it is necessary to consider (a) the cyclic changes in error measure due to parameter perturbation, and (b) the discontinuous manner in which the error measure decreases with time due to progressive optimization.

An exact analysis is tedious, but useful approximate results are obtained by considering only the lowest frequency produced by intermodulation. Since each adaptive loop includes an integrator, the higher beat frequencies are attenuated and the observed variation in parameter adjustment is sinusoidal.

Since the two perturbation frequencies $1/2 \tau_1$ and $1/2 \tau_2$ are chosen to be as nearly equal as permitted, the lowest beat frequency is $|(1/2 \tau_1) - (1/2 \tau_2)|$.

In general the beat term due to parameter adjustment is smaller than that due to parameter perturbation. If the magnitude of the parameter adjustment is H per cycle, the cyclic adjustment may be regarded as the sum of two terms, one varying linearly with time, the other a sawtooth wave-form, of perturbation frequency, of peak amplitude H . The fundamental component of this sawtooth is of amplitude H/π . The perturbation signal is a square wave, of amplitude $\pm \delta$, with a fundamental component $4\delta/\pi$. Thus if the adjustment per cycle is smaller than the perturbation ($H < \delta$), then the fundamental of the adjustment signal is less than one-quarter the magnitude of the fundamental of the perturbation.

Consider cross-coupling due to the effect of the perturbation in one channel being synchronously rectified in the second channel. The perturbation in channel 2 produces a cyclic variation in performance measure of fundamental component

$$\left(\frac{\partial f}{\partial K_2} \right) \cdot \frac{4\delta}{\pi} \sin \left(\frac{\pi t}{\tau_2} \right)$$

The output of the synchronous detector is the input signal multiplied by a square wave (± 1) of period $2\tau_1$. The amplitude of the beat frequency term is found by considering that component of the output of the synchronous detector due to multiplying the input by the fundamental of the square wave, so that

$$e_0 = \frac{4e_i}{\pi} \sin \left(\frac{\pi t}{\tau_1} \right)$$

Thus the rate of change of parameter 1 is, from eqn (3),

$$T \frac{dK_1}{dt} = -\delta \left(\frac{\partial f}{\partial K_1} \right) + \left(\frac{\partial f}{\partial K_2} \right) \cdot \frac{16\delta}{\pi^2} \sin \left(\frac{\pi t}{\tau_1} \right) \cdot \sin \left(\frac{\pi t}{\tau_2} \right)$$

Considering only the low-frequency components and assuming

$$\left(\frac{\partial f}{\partial K_1} \right) \text{ and } \left(\frac{\partial f}{\partial K_2} \right) \text{ constant,}$$

$$K_1 = K_{10} - \delta \cdot \left(\frac{\partial f}{\partial K_1} \right) \cdot \frac{t}{T} + \frac{8\delta}{\pi^3 T} \cdot \left(\frac{\partial f}{\partial K_2} \right) \frac{\sin \pi t \left(\frac{1}{\tau_2} - \frac{1}{\tau_1} \right)}{\left(\frac{1}{\tau_2} - \frac{1}{\tau_1} \right)}$$

Similarly

$$K_2 = K_{20} - \delta \cdot \left(\frac{\partial f}{\partial K_2} \right) \cdot \frac{t}{T} + \frac{8\delta}{\pi^3 T} \cdot \left(\frac{\partial f}{\partial K_1} \right) \frac{\sin \pi t \left(\frac{1}{\tau_2} - \frac{1}{\tau_1} \right)}{\frac{1}{\tau_2} - \frac{1}{\tau_1}}$$

It is seen that the amplitude of the beat-frequency term in one channel is directly proportional to the amplitude of the useful adjustment in the other channel, and that the low-frequency terms are in phase or directly out of phase. When the two perturbation frequencies are similar, the amplitude of the beat-frequency terms are inversely proportional to this frequency difference. The necessary frequency difference can be assessed in terms of the tolerable amplitude of the beat-frequency signals.

For example, if it is required that the peak amplitude of the beat-frequency term in channel 1 shall not exceed twice the amplitude of the useful adjustment per cycle in channel 2, it follows that

$$\frac{8\delta}{\pi^3 T \left(\frac{1}{\tau_2} - \frac{1}{\tau_1} \right)} \leq \frac{4\tau_2 \delta}{T}$$

i.e.

$$\frac{\tau_2}{\tau_1} < 0.93$$

The manner in which the amplitude of the beat-frequency term varies with the frequency ratio $r = \omega_1/\omega_2 = \tau_2/\tau_1$ is shown in Figure 8.

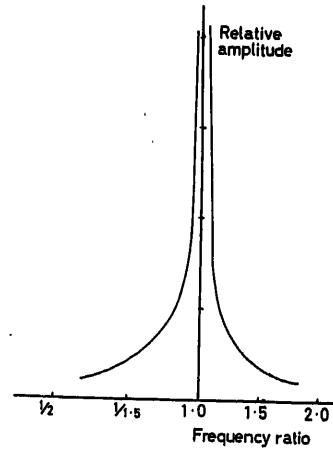


Figure 8. The variation of beat-frequency component with frequency ratio

The beat-frequency terms are in-phase or directly out-of-phase, depending on the relative signs of $\partial f/\partial K_1$ and $\partial f/\partial K_2$. If these two gradients are of equal magnitude, so that K_1 and K_2 are adjusted at equal rates, the beat effect produces no sinusoidal divergence from the mean direction of adjustment, but modulates the velocity of adjustment.

The beat-frequency component produces a maximum divergence from the mean direction of adjustment when one gradient is zero. The oscillation is observed as a variation in the parameter which does not influence the performance index and may thus be unimportant.

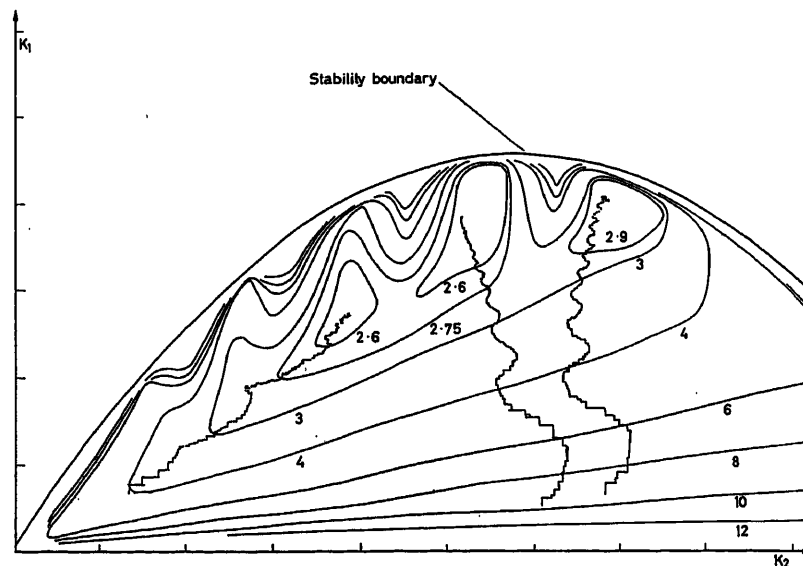


Figure 9. Experimental trajectories

Experimental Results

A two-channel optimizing system, with clamps, has been applied to minimize the mean square error in a feedback system obeying the equation

$$p^2 T^2 \theta_0 = \frac{1}{(1 + T_1 p)} \cdot \frac{1}{(1 + T_2 p)} [K_1 (\theta_i - \theta_0) - K_2 T p \theta_0]$$

θ_i and θ_0 are the input and output of the system; K_1 and K_2 the adjustable parameters.

For stability K_1 and K_2 must be positive and K_1 must lie below the parabola in the $K_2 - K_1$ plane given by

$$K_1 = K_2 \cdot \frac{T}{T_1 + T_2} \left\{ 1 - \frac{K_2 T_1 T_2}{T(T_1 + T_2)} \right\}$$

With representative random inputs the error surface has the form of an inverted cone. The minimum is unique and the contours of constant mean squared error are substantially evenly spaced. The minimum is located without ambiguity from any initial misadjustment.

For the study of optimizing loop behaviour a more interesting surface is produced when the system input is a repetitive square wave. Over a large section of the surface, Figure 9, the contours are well spaced and almost equidistant, but close to the stability boundary the contours are very close, corresponding to steep slopes. There are three minima, separated by steep ridges. Any of these will be located depending on the initial parameter setting, since the optimizing system cannot distinguish between absolute extrema and purely local extrema.

For the trajectories shown, the frequency ratio is $r = \tau_2/\tau_1 = 1.033$, giving a predicted beat frequency component equal to four times the magnitude of an individual adjustment in the alternate channel.

As predicted, the beat-frequency component produces a sinusoidal trajectory when the trajectory is vertical and merely modulates the velocity of optimization when the trajectory is inclined at 45° to the axes. The trajectories do not follow the line of steepest descent, as mentioned previously.

Without the sample and hold circuits in both channels the optimizing loops are unstable unless their gains are significantly reduced.

Conclusions

A simple optimizing controller has been described which operates satisfactorily for single-channel and two-channel systems.

Analysis of the single-channel system shows the improvement introduced by the insertion of a clamp or sample and hold device in each optimizing loop. The benefits are a higher maximum adjustment per cycle combined with greatly reduced amplitude of parameter fluctuation.

A two-channel system is shown to possess cross-coupling which introduces a departure of the optimizing trajectory from the line of steepest descent together with cyclic parameter disturbances. The amplitude of the tolerable beat-frequency components limits the minimum frequency difference usable in a multi-channel system. Frequency ratios as small as 1.04 are satisfactory in a realistic practical example.

Since quite small frequency differences are necessary, it is feasible to construct six-channel optimizing systems allocating a different perturbation frequency to each channel, without requiring an overall frequency ratio exceeding 2:1. Such a system is in development at the moment.

References

- 1 DRAPER, C. S. and LI, Y. T. *Principles of Optimizing Control Systems and an Application to the Internal Combustion Engine*. 1951. New York; Amer. Soc. mech. Engrs
- 2 DOUCE, J. L. and KING, R. E. A self-optimising non-linear control system. *Proc. Instn elect. Engrs* 108B, No 40 (July 1961) 441
- 3 GRENSTED, P. E. W. and JACOBS, O. L. R. Automatic optimisation. *Trans. Soc. Instrum. Tech.* 13 No. 3 (1961) 203
- 4 JACOBS, O. L. R. The measurement of the mean square value of certain random signals. *J. Electron. Control* 9 (1960) 149
- 5 DOUCE, J. L. and BOND, A. D. The development and performance of a self-optimising system. *Proc. Instn elect. Engrs* 110, No. 3 (March 1963) 619
- 6 BLACKMAN, P. F. *Extremum-Seeking Regulators*. 1961. London; Imperial College Exposition of Adaptive Control

The Design Principles and Circuit of a Multi-channel Correlator— A Specialized Analogue Computer for the Statistical Treatment of Random Time Series in Industrial Control Systems

A. S. USKOV and Yu. M. ORLOV

Summary

The paper gives a description of a multi-channel correlator which has been developed by the authors, and theoretical aspects of the system are considered.

The system has the following advantages. First, it is a multi-channel system, i.e. it calculates several ordinates of the correlation function simultaneously. Secondly, the use of shift devices in the system considerably increases the accuracy in obtaining correlation functions. This is particularly the case for realizations when the mathematical expectation is much greater than the maximum magnitude of pulsation, which occurs in the majority of industrial control systems. Thirdly, the system provides maximum operating speed and at the same time it simplifies the construction of correlators, since the computations are performed without preliminary centring of random time series and in this respect storage devices of great capacity are not required. These features of the system make it possible to use the correlator in self-adjusting control systems.

The system has been developed on the basis of a theoretical investigation of the various factors which influence the accuracy of computations of the correlation function.

An upper estimate of the root mean square error is obtained for the general case when the mathematical expectation of the random process is non-zero.

Formula (7) has enabled the authors by means of adopting shift-processes to select the method of computing the correlation function which is optimum from the point of view of accuracy and operating speed, and also the basic circuit of the correlator itself.

A description is given of the units and elements of the multi-channel correlator and block diagrams and circuit diagrams are given.

In conclusion the procedure for operating the correlator is given.

Sommaire

Le rapport donne une description du corrélateur à canaux multiples qui a été développé par les auteurs, et l'aspect théorique de ce système est pris en considération.

Ce système présente les avantages suivants: tout d'abord il donne la possibilité de calculer simultanément plusieurs fonctions de corrélation. Deuxièmement, sa réalisation permet un large domaine d'application, ce qui présente un intérêt quand l'expectation mathématique est beaucoup plus grande que l'amplitude maximale des pulsations, ce qui est souvent le cas pour les systèmes industriels. Troisièmement, ce système fonctionne à une vitesse maximum et en même temps son utilisation est très simple et ne nécessite pas de connaître au préalable la valeur moyenne de la fonction aléatoire ce qui supprime la nécessité d'emmagasiner au préalable un grand nombre de données numériques.

Ces performances permettent l'utilisation de ce corrélateur comme dispositif d'auto-réglage. Il a été développé sur la base de l'étude théorique des divers facteurs qui influencent la précision du calcul de la fonction de corrélation.

Une estimation maximale de l'erreur quadratique moyenne est indiquée dans le cas général d'une expectation mathématique non-nulle du processus aléatoire. La formule 7 donnée par les auteurs permet de choisir la méthode de calcul de la fonction de corrélation qui soit

optimale tant au point de vue de sa précision que de la rapidité du calcul, ainsi que le circuit fondamental du corrélateur.

Une description est donnée des éléments du corrélateur à canaux multiples. Son schéma fonctionnel ainsi que le schéma de ses circuits sont indiqués.

En conclusion son mode d'utilisation est décrit.

Zusammenfassung

Der Aufsatz beschreibt einen von den Autoren entwickelten Korrelator für mehrere Kanäle und betrachtet die theoretischen Gesichtspunkte des Gerätes.

Das Gerät hat folgende Vorteile: Erstens handelt es sich um ein Mehrkanalsystem, das heißt, es berechnet mehrere Werte der Korrelationsfunktion gleichzeitig. Zum anderen erweitert die Verwendung von Einrichtungen mit Vorspannung in dem Gerät den Bereich zur Gewinnung der Korrelationsfunktionen beträchtlich. Dies gilt besonders für solche Fälle, bei denen der mathematische Erwartungswert (Mittelwert) viel größer ist als die größte Pulshöhe, was in der Mehrzahl der industriellen Regelungssysteme vorkommt. Zum dritten erlaubt das System höchste Betriebsgeschwindigkeit und vereinfacht gleichzeitig den Aufbau des Korrelators, da die Rechnungen ohne vorhergehende Unterdrückung des Mittelwertes der regellosen Zeitfunktion erfolgen kann, weshalb Speichereinrichtungen großer Kapazität entbehrlich sind. Diese Eigenschaften gestatten, das Gerät als Korrelator in selbst-einstellenden Regelsystemen zu verwenden.

Das System wurde auf Grund theoretischer Untersuchungen der verschiedenen Einflußfaktoren entwickelt, die die Berechnungsgenauigkeit der Korrelationsfunktion beeinflussen.

Für den allgemeinen Fall, daß der Mittelwert des Zufallsprozesses nicht Null ist, erzielt man eine obere Abschätzung für den mittleren quadratischen Fehler.

An Hand der Gleichung (7) konnten die Autoren zu Prozessen mit einem Mittelwert ungleich Null übergehen und so eine Methode zur Berechnung der Korrelationsfunktion mit optimaler Genauigkeit und Geschwindigkeit finden; daraus ergab sich auch die grundlegende Schaltung des Korrelators.

Es werden die Baugruppen und Elemente sowie die Schaltbilder und Blockschaltbilder des Mehrkanal-Korrelators beschrieben.

Eine Betrachtung über die Arbeitsweise des Korrelators bildet den Abschluß.

Up to the present time the circuits of correlators which have been described in the published literature suffer mainly from two shortcomings: (a) almost all of them are single-channel systems which calculate the various ordinates of the correlation function in succession; (b) they are designed for evaluating the correlation functions of centred random time series.

Owing to the first shortcoming the majority of existing systems cannot be used for self-adjusting control systems since

the main requirement which a correlator must satisfy in such applications is to provide instantaneous values of the respective correlation (co-variance) functions simultaneously.

The first papers to eliminate this latter drawback¹⁻⁴ have described the principle underlying the computation of several points of a correlation function and have shown the use of multi-channel correlators in self-adjusting systems.

The other shortcoming is, however, important owing to the additional errors in the computations if

$$|Ex(t)| > 0 \quad (1)$$

where E is a symbol for the mathematical expectation and $x(t)$ is a realization of a stationary random time series.

This remark applies particularly to realizations for which the mathematical expectation is much greater than the maximum magnitude of pulsation:

$$Ex(t) \gg \max |x(t) - Ex(t)| \quad (2)$$

This inequality holds for the processes in the majority of industrial control systems, e.g. for catalytic cracking, blast furnaces, open hearth furnaces, etc. The systematic error in the determination of the correlation functions of such processes is made up of an instrumental error and a theoretical error. The instrumental error is due to the limited sensitivity of correlator elements and to non-linear distortion.

Owing to inequality (2), in many cases it is impossible to 'catch' the pulsation of the random variable, with the result that the centred correlation function has a very large error. Moreover, with the large input signals obtained when condition (2) is fulfilled, amplifiers and other elements can introduce considerable non-linear distortion. The theoretical error of correlation function computation is due mainly to the finiteness of the integration interval T .

The superimposition of the two errors can result in centred correlation functions for the solution of problems in statistical dynamics with such large errors that they cease to be of practical use.

This paper, therefore, seeks to develop the theory of correlators and to describe a system which, with minimum delay and acceptable accuracy, will yield the overall correlation function in the form of several ordinates at given discrete instants of time.

We will now estimate the theoretical error in the general case when the random function contains a constant component, i.e. the case when

$$Ex(t) \neq 0$$

Error of the Correlation Function for $Ex(t) \neq 0$

To compute the correlation function $R(\tau)$, we use the formula

$$R_T(\tau) = \frac{1}{T} \int_0^T x(t+\tau)x(t) dt \quad (3)$$

where $T = T' - \tau_{\max}$; T is the integration interval; T' is the observation interval; τ is the time shift; and τ_{\max} is the maximum time shift.

This notation has been used for several investigations (e.g. Solodovnikov *et al.*⁵) where the error is estimated in evaluating $R(\tau)$ for a finite interval T and $Ex(t) = 0$.

Consider now the theoretical error in the general case when

$Ex(t) \neq 0$. By virtue of the finiteness of T , $R_T(\tau)$ is a random function which depends on T , τ and on the values of the integrands at the ends of the integration interval. For a measure of the accuracy with which the correlation function is determined, we therefore take the variance of $R_T(\tau)$:

$$\sigma^2(\tau) = E[R_T(\tau) - R(\tau)]^2 \quad (4)$$

Putting $z(t) = x(t + \tau)x(t)$ and $R_z(\theta)$ for the correlation function of $z(t)$, the expression (4) is transformed into

$$\sigma^2(\tau) = \frac{2}{T} \int_0^T \left(1 - \frac{\theta}{T}\right) [R_z(\theta) - R^2(\tau)] d\theta \quad (5)$$

Consider now the case when the probability distribution of the stationary random function $x(t)$ is Gaussian.

Expressing $R_z(\theta)$ in terms of $R(\tau)$, representing $R(\tau)$ in terms of the centred correlation function $R'(\tau)$

$$R(\tau) = R'(\tau) + [Ex(t)]^2 \quad (6)$$

and given the typical $R'(\tau)$

$$R'(\tau) = C e^{-\alpha|\tau|} \cos \beta\tau$$

one obtains from formula (5), ignoring terms of the order $1/T^2$, the following upper estimate of the mean square error

$$\sigma^2(0) = \frac{C^2}{T} \left(\frac{1}{\alpha} + \frac{\alpha}{\alpha^2 + \beta^2} \right) + \frac{8C}{T} \cdot \frac{\alpha}{\alpha^2 + \beta^2} [Ex(t)]^2 \quad (7)$$

From expression (7), it follows that for condition (2) the mean square error in the determination of the correlation function can be very considerable.

Formula (7) is of fundamental importance in that it permits selection of the optimum procedure from the point of view of accuracy and operating speed for evaluating $R(\tau)$ on a multi-channel correlator and makes it possible to work out the fundamental circuit of the device itself.

Method of Evaluating $R(\tau)$ from $[R_{yz}(\tau)]$ on a Multi-channel Correlator

The process of computation on the multi-channel correlator can be described in the following terms. The random inputs during normal operation of the system are automatically recorded on a twin-track magnetic tape and fed to a delay line. Signals which are delayed by a certain amount are taken from each portion of the delay line.

These signals are fed to electronic multipliers and integrators, the outputs of which are values of the correlation function (Figure 1). However, from the point of view of increasing the accuracy of the calculations, it is necessary by virtue of formula (7) to introduce an additional shifting device into this circuit, as shown in Figure 1.

It is desirable to select the shift values a and b approximately equal to the mathematical expectations. This is always possible because some information is always available about the operation of the controlled plant and, in particular, the approximate range of variation of the input. Thus, the following method of computation can be proposed:

(1) Find the correlation function $R_{yz}(\tau)$ of the shifted processes $x_1(t) = x(t) - a$; $y_1(t) = y(t) - b$.

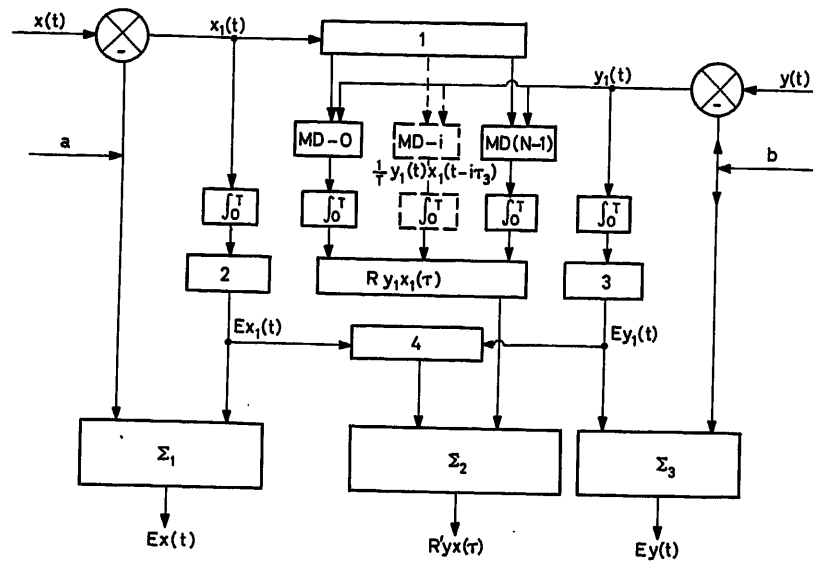


Figure 1. Block diagram of the multi-channel correlator

1 delay line; 2, 3, 4 multipliers; (MD — i) multiplying device ($i = 0, 1, \dots, N-1$);
 \int_0^T — integrator; $\Sigma_1, \Sigma_2, \Sigma_3$ — adders

(2) Determine the mathematical expectations $Ex_1(t)$, $Ey_1(t)$ of the shifted processes $x_1(t)$, $y_1(t)$.

(3) Calculate the correlation function of the centred random processes

$$x'(t) = x_1(t) - Ex_1(t)$$

$$y'(t) = y_1(t) - Ey_1(t)$$

using the formula

$$R'_{yx}(\tau) = R_{y_1x_1}(\tau) = R_{y_1x_1}(\tau) - Ey_1(t)Ex_1(t) \quad (8)$$

(4) Find the mathematical expectations of the processes $x(t)$ and $y(t)$ by the formulae

$$Ex(t) = Ex_1(t) + a$$

$$Ey(t) = Ey_1(t) + b$$

When using the multi-channel correlator as an element of a self-adjusting system it is advisable to feed back the values $Ex(t)$ and $Ey(t)$ to the input of the device and in the next integration interval T to use them respectively as the shifts a and b .

Thus, as can be seen from expression (7), the introduction of shifting devices makes it possible to calculate the correlation functions of shifted processes fairly accurately and the change-over to the correlation functions of the input can always be carried out. Computations by this method entail no preliminary centring of random processes. Consequently, maximum operating speed is attained and at the same time the construction of the correlator is simplified since in this case no storage devices of great capacity are required.

Using the criterion of the mean square error, the accuracy with which the correlation function $R'_{yx}(\tau)$ is calculated can easily be estimated by formula (8). Imposing on $\sigma^2(0)$ the condition $\sigma^2(0) \leq 0.05 R'^2_{yx}(0)$, an estimate of T is given by the following inequality⁶

$$T \geq 20 \cdot \left(\frac{1}{\alpha} + \frac{\alpha}{\alpha^2 + \beta^2} \right) + 14.5 \cdot \frac{\alpha}{\alpha^2 + \beta^2} \cdot \frac{1}{\chi} \quad (9)$$

where the parameter χ is enclosed in the limits $0 < \chi < 1$ and related to $R'(0)$ by the relation

$$R'(0) \approx \left[\frac{x(t)_{\max} - x(t)_{\min}}{2} \right]^2 \cdot \chi$$

The parameters α and β which characterize respectively the rate of decay and the oscillatory properties of the correlation function, can be related approximately to the upper and lower frequencies of the spectrum of the random processes by the relations⁵:

$$\alpha = \frac{3}{2\pi} \cdot \omega_{\text{low}} \approx 0.477 \omega_{\text{low}} \quad (10)$$

$$\omega_{\text{low}} < \beta < \omega_{\text{high}} \quad (11)$$

We shall now consider the main units and elements of the multi-channel correlator.

Description of the Units and Elements of the Multi-channel Correlator

It will be seen from the block diagram (Figure 1) that the correlator consists of data input devices, adding devices (bias devices), delay lines, a set of multiplying devices, a set of integrating amplifiers, and devices for sampling the results of computation.

For on-line computation of correlation functions the data input device is replaced by standard electrical pickups which are mounted on the controlled plant. The shifting devices are conventional electrical subtraction circuits. Therefore only the main element of the multi-channel correlator, the delay line, is dealt with here.

Delay Line

The purpose of the delay line is to produce N delayed values of the input signal in the form of an electrical voltage. The obtainable delay times are determined by the formula

$$\tau = i\tau_d \quad (i=0, 1, \dots, N-1)$$

where τ_d is the distance in time between adjacent calculated ordinates, and N is the number of correlator channels.

The delay line consists of a tape-motion mechanism, an erasing, a recording and 26 playback heads, a recording unit and 26 playback units. Figure 2 illustrates the motion of the tape in the delay line. The time τ_d can be varied by replaceable packings on the drive shaft.

To simplify the operation of the drive shaft, 5 (see Figure 2), the tape is pressed to the shaft by two rubber rollers, 6. The magnetic heads are arranged in a circle. A delay roller, 8, and a damping roller, 7, are arranged along the path of the tape to smooth out variations in tape speed. Guide rollers, 4, are provided to prevent transverse displacement of the tape.

The signals are recorded by pulse-frequency modulation on ferro-magnetic tape 6.35 mm in width. The recording unit incorporates a d.c. amplifier, a cathode follower, a controlled twin-pentode multivibrator and an output cathode follower (Figure 3).

Square frequency-modulated pulses are fed through the capacitor C_6 and the resistance R_{18} to the recording head. The amplitude of the recording current pulse varies between

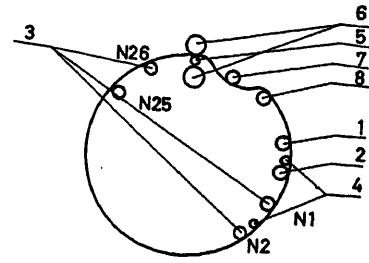


Figure 2. Block diagram of the delay line

1 erasing head, 2 recording head, 3 playback heads, 4 guide rollers, 5 drive shaft, 6 clamping rollers, 7 spring roller, 8 delay roller

20 ÷ 60 mA by altering the resistance R_{18} . The carrier frequency is $f_0 = 1,000$ c/sec and the maximum frequency deviation is $\Delta f = \pm 500$ c/sec.

The playback unit is intended for amplifying the frequency-modulated signal from the output of the playback head, demodulation and filtering of the useful signal. The circuit of the unit is shown in Figure 4. It is a three-stage voltage amplifier (V_1, V_2, V_3) with amplitude limitation, the output of which is connected via the differentiating circuit $R_8 C_3$ to the grid of the single flip-flop oscillator V_4 . Square pulses of identical amplitude and width are fed from the right anode of this oscillator to a frequency detector D-2, D-3 and then to a low-pass filter consisting of two RC circuits ($R_{16} C_7, R_{17} C_8$) and a twin-T bridge tuned to the frequency $f_0 - \Delta f$ (500 c/sec).

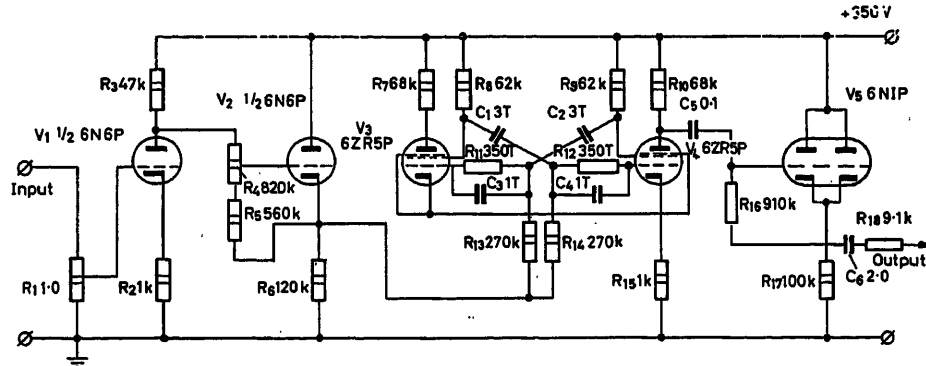


Figure 3. Recording unit

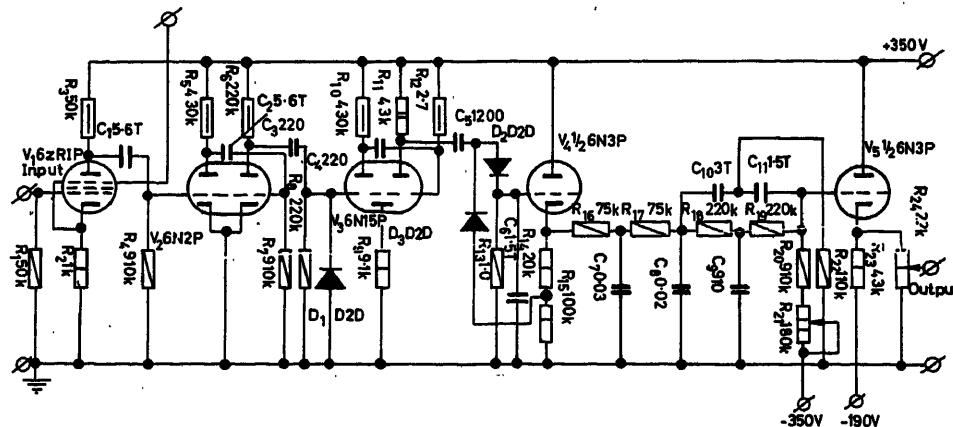


Figure 4. Playback unit

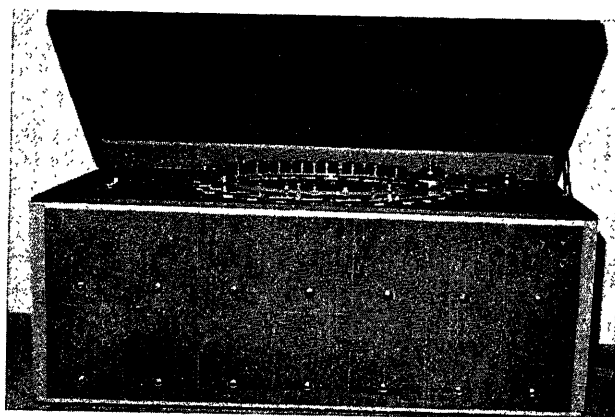


Figure 5. Delay line

The output cathode follower V_5 is intended for obtaining $u_{out} = 0$ at $f = f_0$ (no recorded signal present). The level of the input signal is 10–20 mV and the maximum output signal is 10 V. The circuit includes potentiometers for zero setting of R_{21} and amplification R_{24} , which are brought out on to a face panel.

One recording unit and 13 paired playback units are arranged in the lower part of the delay line housing. Its appearance is shown in Figure 5. More detailed descriptions of the delay line have been published^{7, 8}.

Multiplier Unit

The purpose of the multiplying unit is to multiply the delayed values of the input signal. The unit incorporates $N=26$ multiplying devices, of which there can be any operating principle. In the proposed correlator the multiplier is a non-linear resistance in the feedback circuit of a d.c. amplifier.

Integrator Unit

The integrator is based on a system in which a capacitor is connected in the feedback circuit of a three-stage d.c. amplifier with potentiometric coupling between the stages. Similar d.c. amplifiers are used in the multiplying devices.

Sampling Device

With the lapse of integration time T the inputs of the integrating unit are disconnected from the rest of the circuits and

voltages are maintained at their output which correspond to the ordinates of the required correlation function.

When using the multi-channel correlator as an element of an automated computer, it is necessary to use a special sampling device which represents the results of the computations in the form of periodically recurrent electrical voltages (for example, in the computation of the spectral density). Figure 6 shows the circuit diagram of such a device using a step selector and linearization of the result of sampling.

The essence of the method of linearization is illustrated in Figure 7. The function which is to be sampled and which is approximated by rectangles (curve A) is shifted by one step of the selector (curve B) and subtracted from curve A . The difference (curve C) is fed to the integrator (Figure 6), the integration time of which is equal to the step time τ_s . When the selector passes to the next contact the input of the integrators is shorted with the output (ejection of the result of integration) and the output voltage of the integrator (curve D) and the output voltage of the phase shifter, 2, are added (4 in Figure 6). The output of the adder is the required function E (curve E). The winding of the step selector is connected via a relay to the anode circuit of the multivibrator for the time scale of sampling the correlation functions (5 in Figure 6). The scale is controlled by varying the frequency of the multivibrator $f = 1/\tau_s$. Thus, the duration of the curve in time is $t = m/f$, where m is the number of points of approximation of the function.

Operating Procedure

The input to the correlator consists of the recordings of random processes, or of direct indications of the pickups as obtained during normal operation of the controlled plant and represented in the form of electrical voltages.

This data is handled in the following way:

(1) The shifts a and b are set, using preliminary information about the nature of the variation of the inputs $x(t)$ and $y(t)$. For example, knowing the range of variation of the input, it is possible to put

$$a = \frac{x_{\max} + x_{\min}}{2}, \quad b = \frac{y_{\max} + y_{\min}}{2}$$

(2) The maximum scale of the data input K_Δ is set (the gain of the pick-up).

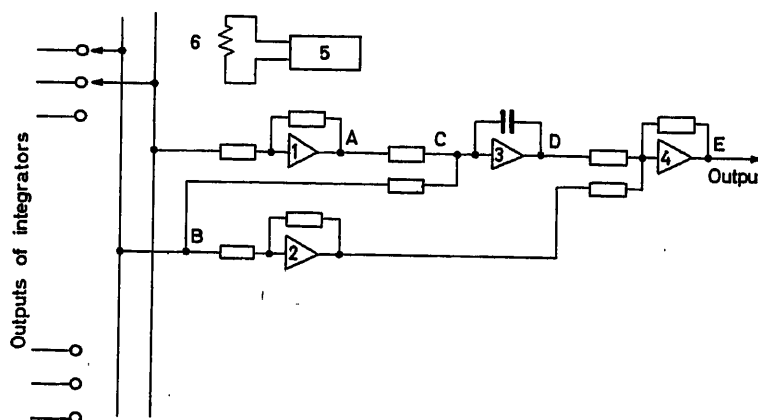


Figure 6. Sampling device

1, 2 phase shifters, 3 integrator, 4 adder, 5 multivibrator, 6 step selector

(3) Using $u_{in,max}$ of the delay line, the input coefficient of the delay line $K_{d,l}$ is set, taking into account the elimination of possible non-linear distortion.

(4) The gain of the delay line $K_{d,l}$ is set by the amplification controllers of the playback units.

(5) The operating frequency band, i.e. the low frequency of the spectrum ω_{low} and the high frequency ω_{high} , is given by the preliminary information about the operation of the controlled plant under consideration or a similar controlled plant. Using the given frequency band we determine the maximum τ (τ_{max}), the integration time T and the number of ordinates of the

correlation function n , calculated in the interval $0 \leq \tau \leq \tau_{max}$:

$$\tau_{max} = \frac{2\pi}{\omega_{low}}, T \geq 10 \tau_{max}, n = \frac{\omega_{high} \tau_{max}}{\pi} + 1$$

The interval T is more accurately determined by formula (9), using the criterion of the root mean square error.

(6) We select the number of playback heads N which take part in the computation of the correlation function $N \geq n$ and the speed of the tape $V = S/\tau_d$, where S is the distance between adjacent heads.

(7) The input coefficients of the multipliers are set.

Figure 8 shows the random process of pressure in a reactor P_p (per cent).

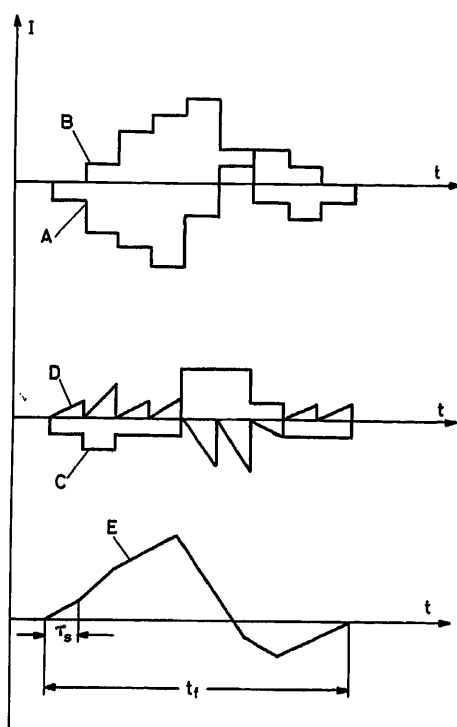
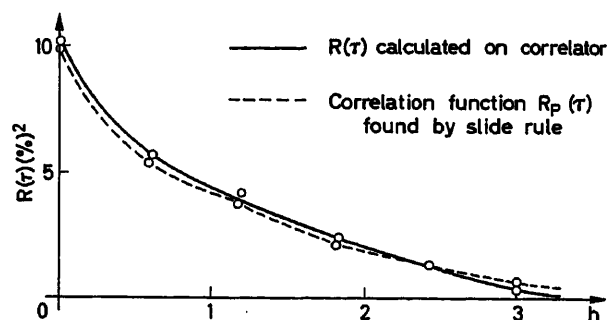


Figure 7. Linearization of the results of sampling



τ (h)	0	0.6	1.2	1.8	2.4	3
$R(\tau) (\%)^2$	102	5.6	4.2	2.4	1.2	0.4
$R_p(\tau) (\%)^2$	10	5.3	3.9	2.1	1.3	0.5

Figure 9. Graphs for the correlation function as calculated on the correlator and by a slide rule

Figure 9 shows the correlation functions by way of comparison as calculated on the multi-channel correlator and on a slide rule.

References

- 1 CHAIKOVSKII, V. I. Methods of experimental determination of correlation functions *Izv. VUZ SSSR, Radiotekhnika* No. 5, (1960) 425-434
- 2 LEVIN and REINTJES. A five-channel electronic analogue correlator. *Proc. Nat. Electronic Conf. VIII* (1952) 647-656

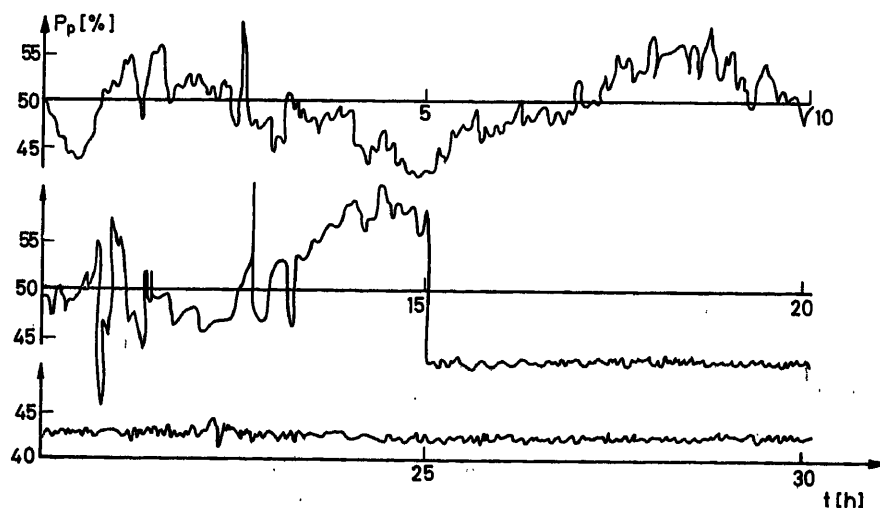


Figure 8. Recording of the random process—pressure in a reactor P_p (%)

- ³ ANDERSON, J. W., BULAND, R. N. and COOPER, J. R. Use of cross correlation in an adaptive control system. *Proc. Nat. Electronics Conf., Chicago*. XV (1959)
- ⁴ KOZUBOVSKII, S. F. Use of cross correlation in an adaptive control system. *Avtomatika* No. 5 (1961) 83-89
- ⁵ SOLODOVNIKOV, V. V. and USKOV, A. S. *Statistical analysis of control objects*. 1960. Moscow; Mashgiz
- ⁶ USKOV, A. S. and ORLOV, Yu. M. The principles of construction and the circuit of a multi-channel correlator. *Avtomatika* No. 2 (1963)
- ⁷ ORLOV, Yu. M. and USKOV, A. S. A specialized computer (controllable filter) and its application. *Computer Engng* No. 7. 1960. Moscow; Sborn
- ⁸ ORLOV, Yu. M. and USKOV, A. S. *A Specialized Computer for Determination of Dynamic Characteristics, Simulation and Correction of Control Systems*. Sborn: *Application of Computer Engineering to the Automation of Production*. 1961. Moscow; Mashgiz. Sborn. 1961. Moscow; Mashgiz

DISCUSSION

P. JESPERS, 4 Av. Charles de Lorraine, Belgium

High order correlation functions can be computed more easily by means of the following property:

- given n random bounded variables: $x_1, x_2 \dots x_n$
 and n auxiliary random variables: $y_1, y_2 \dots y_n$
 which satisfy—interdependent
- independent of the x_i
 - the y_i are bounded: $-A_i < y_i < A_i$
 (the $A_i \geq$ the bounds of the x_i)
 - $p(y_i)$ constant between bounds of the y_i
 (e.g. the y_i 's can be sawtooths, or random series of numbers).

Defining $L_i = x_i - y_i$, and $L = \prod_{i=1}^n L_i$

We prove that:

$$\overline{x_1, x_2, x_3, \dots, x_n} = \frac{1}{A_1 A_2 A_n} \overline{\text{Sign } L_i}$$

To realize an any order correlation it is sufficient to introduce proper delays $\tau_1 \dots \tau_{n-1}$ in the functions $\text{Sign } L_i$.

Advantages (1) Shifting on binary signals only; (2) Multiplication reduces to the logic operation: $\text{Sign } L_1 \oplus \text{Sign } L_2 \oplus \dots \oplus \text{Sign } L_n$.

Reference

JESPERS, P., CHU, and FELTUCIS. A new method for computing correlation functions. *Int. Symp. Inf. Theory, I.R.E.*, Brussels (1962)

A. S. USKOV, in reply

I should like to state the following in connection with Professor Jaspers' address.

The authors did not set themselves the task of creating a device for

obtaining moments of high orders. They confined themselves to a simpler, and from a practical viewpoint, highly important general task, connected with obtaining the first two moments.

Main attention was paid to questions of accuracy, speed of operation and simplicity of design. In the authors' view, the principles and circuitry (when it is further improved) set out in the paper will find application when using the multichannel correlograph as an element of an adaptive automatic control system. The authors are grateful to Professor Jaspers for his valuable comment.

A. R. M. NOTON, *Electrical Engineering Department, University of Nottingham, Nottingham, England*

It is not clear if the authors' interest in cross-correlation is a method of determining the dynamic characteristics of industrial control systems. Assuming this to be the case, then the following remarks are relevant.

Have the authors not considered using binary random test signals $x(t) = \pm 1$? Such signals eliminate the need for multiplication; only a switching process is necessary. Furthermore, one can show¹ that, when using random signals for a time interval T , the error in the determination of the cross-correlation function $R_{yx}(\tau)$ is inversely proportional to \sqrt{T} . Our experience¹ has shown this to be a major source of error. For this reason, Hazlerigg is now using a binary random test signal especially constructed to have an ideal auto-correlation function. The generation of such sequences has been described in the literature². His cross-correlator is digitalized and produces $R_{yx}(\tau)$ simultaneously for 20 different values of τ .

References

- ¹ HUGHES and NOTON, A. R. M. Measurement of control system characteristics by means of a cross-correlator. *Proc. IEE* (London), Part B (January 1962)
- ² ELPAS. Theory of autonomous linear sequential networks. *IRE Trans. on Circuit Theory* (U.S.A.) (March 1959)

COMPONENT RELIABILITY

Reliability

A Survey by G. S. GLINSKI, B. S. SOTSKOV and H. S. WEISSMANN

Introduction

Reliability is the probability of the fulfilment of the functions in a predetermined period of time and was, and still is, constantly one of the most important factors which dictated the technical suitability of any construction or product. It has long been known that a safety margin is necessary to guarantee reliability. This expresses itself technically in the various safety factors which are introduced in practical calculations.

The mid-twentieth century is marked by the far-reaching technical adoption of systems of automatic control, regulation and programming. The possibility arose to control machines with the help of other machines, that is, the possibility of automatic apparatus and plant. The complexity of modern technical processes prompted the creation of complicated systems of automatic control, regulation and programming in which these systems have many thousands of electrical, electronic, electro-mechanical and mechanical elements.

The complexity of these systems reduced the reliability, which fact was intolerable when the high technical and economic consequences caused by the disturbance of the orderly run of technical processes being controlled are viewed.

The complexity of modern technical aids can be demonstrated by the following examples. The control switching for a furnace process has up to 1,000 various measuring and automatic apparatuses as well as other installations which themselves contain around 10^4 – 10^5 electrical and mechanical components and construction parts. Modern calculating machines consist of 0.5×10^4 – 2.0×10^4 triodes, 0.2×10^5 – 1.1×10^5 resistances and condensers and 10^7 soldered and connecting positions. These facts make it necessary for the problem of reliability to be viewed as the most important problem of modern technology, and with full justification one calls the reliability problem the number one problem of modern technology.

Scientific, Practical and Economic Problems of Reliability

The reliability problem is a complex one, because it brings in scientific and practical questions as well as matters of productions techniques, conditions of individual projects and constructions, service and economics. The solution of only one of these questions cannot be found properly without due consideration of the other factors.

The economic tasks in reliability problems can be divided into the following groups:

General Mathematical Bases of the Theory of Reliability

To this group belong:

General questions

- (1) The establishment of rules of distribution for those functions which ensure the reliability of individual types of element.
- (2) The determination of the distribution rules for the various elements taking account of interdependent effects of the various factors.
- (3) The determination of distribution rules for the complexes, which embrace the many elements which have reciprocal effects.
- (4) The application of the theory of operation to the setting up of a suitable standard of reliability for the products, objects and systems.
- (5) The selection of sufficiently far reaching boundaries with distribution functions and differential test-systems.

Questions of constructional reliability of the complex or system

- (1) Theory of constructional reliability with independent and interdependent characteristics of reliability in the individual elements.
- (2) Theory of constructional reliability with the various distribution rules on the failure of elements.
- (3) Theory of constructional reliability of logic grids, and the elaboration of new processes of reserve formation, weighing processes, control of cross connections and similar applications.
- (4) Constructional processes for the building of a complex or system with the highest possible reliability working to predetermined costs, weights and similar conditions.
- (5) Constructional processes for the building of a complex or system with transition to a 'fail safe' condition when individual elements fail.
- (6) Constructional processes for the building of a system or complex with a pre-requisite degree of reliability keeping costs, weight and similar factors to a minimum.
- (7) Elaboration of reliability calculation processes for complex construction:
 - (i) By means of standard calculating machines.
 - (ii) By means of specialist calculating machines.

Questions of apparatus reliability

(1) Investigation of the distribution functions for the failure of electrical, electronic and electro-mechanical elements.

(2) Investigation of the distribution functions for the failure of pneumatic, hydraulic and mechanical elements.

(3) Investigation of the influence of defined physical and physico-chemical factors on the reliability of the elements, apparatus and appliances.

(4) Working out of processes for the evaluation and estimation of an individual influence and the common influence of defined physical and physico-chemical factors on the various types of elements, appliances and apparatus.

(5) Working out of methods for the evaluation and development of elements, individual components and constructional parts of appliances and apparatus to a pre-determined degree of reliability and duration of life.

(6) Investigation of the variations of physical, mechanical, electrical, magnetic and heat characteristics of natural and artificial materials with respect to time and various physical and physico-chemical factors.

The solutions of the various problems mentioned are found by the introduction of the following mathematical methods.

- (i) Mathematical statistics.
- (ii) Mathematical logic, relay theory.
- (iii) Information theory.
- (iv) Coding theory.

But it also requires a knowledge of the physical and physico-chemical rules which confirm the functional processes of elements, appliances and apparatus and also the variation in their characteristics and constants under the influence of intrinsic and external factors.

The engineering problems of reliability concern questions of development, construction, production and those questions met with in service.

Development and constructional tasks

The reliability of a product, element, appliance, apparatus or system plays a part in the evaluation and development. The choice of the functional principle and layout of apparatus, the choice of material, the functional conditions of the individual components, as well as the selection of permissible boundaries for the influences of external factors are all very instrumental in deciding the reliability of a product.

Manufacturing problems

The most important points in the processes of manufacture of a product and the factors influencing the functional reliability of a product are: the control of constants and characteristics of materials employed, the selection of permissible mechanical and thermal conditions on processing, the control of the constants and characteristics of the finished components of the product, the control of assembly and installation processes, the 'settling-in' and the testing of the finished product.

Problems in service

Before beginning service, products, appliances, apparatus, complexes and systems normally go through the stages of storing, transport, assembly and installation.

Through storage, transport and assembly a certain amount of the reliability of a product is lost. During operation the product regains a part of the lost reliability. A repeat training of the product, appliance, apparatus, complex or system is necessary after assembly, because here there are possibilities of failure which have arisen during storage, transport and assembly. The particular problems in service depend on the following: observation of the functional scope and conditions which correspond to the chosen technical medium; periodical testing, investigations in service and overhaul.

With the ever increasing complexity of technical systems there is also an increase in the complex technical problems involved in rapid and sufficient overhaul. The solution of the problem depends firstly on the type of automatic specialist test and inspection appliance which is used at the time the test is brought into operation and which checks the agreement of the constants and functional scope of the individual elements and system components. Secondly the solution depends on the type of automatic control installations and sub-systems which keep a continual or periodic check on the correct state of the functional scope of the individual system components or give a signal if non-permissible deviations occur—i.e. return the system to a safe service condition.

The reduction of the time requirement for the determination of a defective element of connection and the period required for overhaul and replacement influence of course the raising of the degree of reliability or the function of a system. The solution of these problems depends as much on the correct design of the system and constructional shape as on the organization of the care and overhaul during service.

Economic problems

The achievement of a high degree of reliability is bound up with the expenditure on excess. This excess can be created through the establishment of reduced working conditions for the individual elements, appliances, apparatus and system components; use of materials of higher quality for the elements or through redundancy in the system or its individual parts.

All these ways require certain additional care. The problem of the selection of the most rational of these variations is from the economic point of view essential while still completely fulfilling the technical requirements of the system. The solution must also give allowance to the attention necessary. The task can only be solved as a whole, when the function and meaning of every element, appliance or apparatus in the complete system is known and when the scope of the damage caused by the failure of the elements is also known.

The Basic Problems

As bases for deciding the reliability of elements, appliances and systems the following should be mentioned:

(1) The reliability of an element, apparatus or system $R(t)$ is the probability of fulfilment of the function through element, apparatus or system with the given conditions and functional state over a given period of time.

(2) The unreliability $F(t)$ is the probability of the occurrence of failure of an element, apparatus or system in the period of time t : $F(t) = 1 - R(t)$.

(3) The differential law, the closeness of time distribution of cases of failure, the frequency of occurrence, is given by:

$$f(t) = dF(t)/dt = -dR(t)/dt$$

(4) The intensity of occurrence $z(t)$ is given by:

$$z(t) = -1/R(t) \cdot dR(t)/dt = f(t)/R(t)$$

With constant value of intensity of occurrence $z(t) = \text{const} = \lambda = 1/T_m$ there is an exponential law of distribution $R(t) = e^{-(\lambda t)}$

(5) The mean duration of failure free function is

$$T_0 = \sum_{i=1}^N T_{xi}/N$$

(6) The life duration which corresponds to the failure of half of the elements is $(T_{0.5})$.

For the exponential law, the value $T_m = 1/\lambda$ is used which corresponds to $R(t) = 0.37$.

The Reliability of the Apparatus

The cases of failure of an element, apparatus or system can give a complete 'catastrophal', 'unexpected' or similar result or can give an incomplete 'gradual', 'time', 'part' or 'conditional' result which is indicated beforehand by the alteration of the constants of the element, apparatus or system or its functional state or conditions.

The reliability with exclusive cases of complete failure in the continual service of an element is given by:

$$R_a(t) = e^{\int_0^t z(t) dt}$$

In the general case it is assumed that the function

$$z = \int_0^t z(t) dt$$

cannot be negative and for $t = 0$ has a value of $z = z_0$.

This condition, in particular, satisfies the function and therefore according to Weibull:

$$R_a(t) = e^{-(\gamma + t) \beta / \alpha}$$

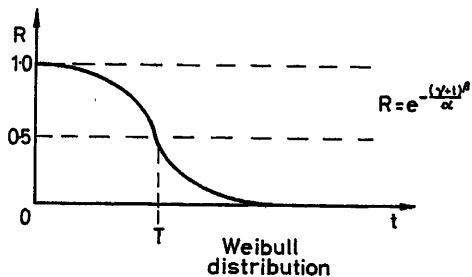
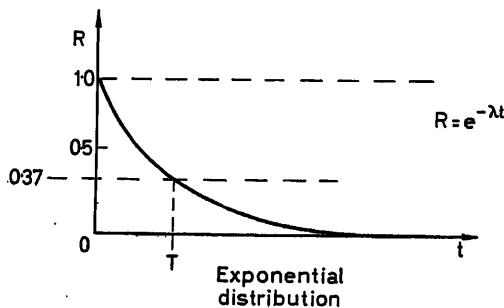


Figure 1

For $z(t) = \text{const} = \lambda$ there is the exponential relationship $R_a(t) = e^{-\lambda t}$ which can be seen to be a special case of the Weibull rule for $\beta = 1, \gamma = 0$ and $1/\alpha = \lambda$.

The resulting distribution of the life-duration can be expressed for the Weibull distribution by the series:

$R(t) = Pr(t) + Pr(t) + \dots + Pr(t)$ where $P + P + \dots + Pn = 1$ and $r(t)$ is the Weibull distribution.

Apart from this, for the calculation and estimation of the reliability:

$$r(t) = \text{const} = \lambda \text{ so that } R_a(t) = e^{-\lambda t}$$

and

$$F_a(t) = 1 - R_a(t) \cong 1 - (1 - \lambda t + \dots) \cong \lambda t$$

The value λ depends on the type and characteristics of the element and its functional states and conditions. To be able to determine λ properly it must be known under what conditions the function of the element, apparatus or system will wear out.

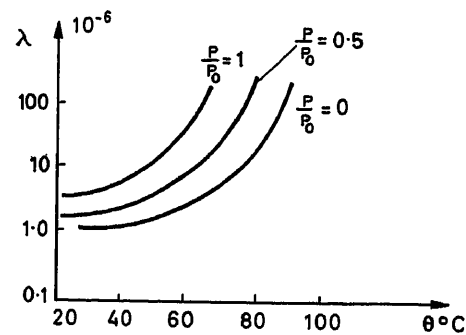


Figure 2

Apart from this the value of λ is evaluated by testing the elements; apparatus or system under nominal functional state and 'normal' conditions. The variation of λ must be considered with deviations from real state and conditions and not with corresponding trial conditions. One can assume that $\lambda = \lambda_0 a_p a_0 a_\theta \dots$ where λ_0 is the value of the intensity of failure which is evaluated for the nominal conditions with the result P_0 ; the voltage state V_0 , etc. and the 'normal' conditions, the temperature θ_0 of the surrounding medium, the relative humidity z_0 per cent etc., a_p, a_0, a_θ are correction coefficients for consideration of the deviations of the actual state and conditions from the function of those found by test (λ_0).

The values of the correction coefficients are ascertained by tests with various states and functional conditions of the elements and presented as graphs or formulae.

The magnitudes a_p, a_0, a_θ are normally expressed by the formulae:

$$a_\theta = e^{(\theta - \theta_0)}; a_p = e^{\alpha_1 (P_x - P_0)}; a_0 = e^{\gamma (V_x - V_0)} \text{ etc.}$$

In many cases the function of the elements, apparatus or system is intermittent or impulse like. The transitional processes where switching on and off occurs are often a start for further failure. For this the following is valid:

$$F_a(t) \cong \lambda_u t + \lambda'_u N = (\lambda_u + \lambda'_u f) t$$

where:

$$\lambda_u = \lambda_1 t_1 / (t_1 + t_2) + \lambda_2 t_2 / (t_1 + t_2)$$

λ_1 the intensity of failure in the switched-on state with given values of the functions scope and the functional conditions.

λ_2 the intensity of failure in the switched-off state with given functional conditions.

λ'_u is the additional intensity of failure following the switched-on and switched-off processes.

N the number of 'on-off' switching cycles from the beginning of the life duration of the element.

t_1 and t_2 the durations of the switched-on and switched-off states respectively.

t the period of time from the beginning of the life duration of the element.

$f = N/t$ the frequency of 'on-off' switching cycles.

The value λ'_u of the additional intensity of failure is particularly great for contact, thermal and mechanical elements and

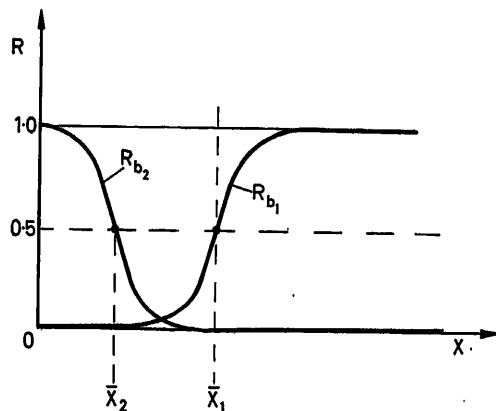


Figure 3

vice versa is meagre for electrical elements such as resistances, condensers, transistor appliances and similar parts. The values of $\lambda'_u f$ can be neglected for the majority of the electrical elements, and because often $t_1/(t_1 + t_2) \ll 1$ and $\lambda_2 \ll \lambda_1$, so the value of $F_a(t)$ with impulse service of such elements is essentially more meagre than with unbroken service.

The other categories of reliability of the incomplete failure R_b is different for elements, apparatus and systems with relay-effect and the like with continual service.

For elements, apparatus and systems with relay-effect the parameters which are decisive are those which fix the magnitude of the influences which are necessary for the transition from the rest (switched-off) state to the functional (switched-on) state and from the functional (switched-on) state to the rest (switched-off) state respectively. Because of the random factors of this influence these parameters do not remain constant but assume values which lie near the average value of the parameter. Normally, under the spread of the values of the parameter which define the transition of the elements, apparatus or system with relay effect from rest to functional states there lies a normal distribution law. Because of this the reliability for the transition of the element with relay effect from rest to functional states is defined by:

$$R_{b1} = \frac{1}{\sqrt{2\pi}\Delta_1} \cdot \int_{-\infty}^x e^{-(x_1 - \bar{x}_1)^2 / 2\Delta_1^2} dx,$$

where \bar{x}_1 is the mean value of the parameter,

Δ_1 the mean quadratic deviation of the parameter,

x the magnitude of the influence on the element, apparatus or system.

The reliability of the element with relay effect on transition from functional to rest states is analogous with that given by

$$R_{b2} = 1 - \frac{1}{\sqrt{2\pi}\Delta_2} \cdot \int_{-\infty}^{x_0} e^{-(x_2 - \bar{x}_2)^2 / 2\Delta_2^2} dx$$

where \bar{x}_2 is the mean value of the parameter which gives the transition from the functional to the rest state, Δ_2 the mean quadratic deviation of the parameter, x_0 the actual value of the influence on the element.

It should be seen that the values \bar{x}_1, Δ_1 as well as \bar{x}_2 and Δ_2 vary under the external influences and with depreciation lead to corresponding variation in the values R_{b1} and R_{b2} .

Because for the restrictionless function of an element with relay effect, the transition from rest to functional states is governed by the magnitude of x and the transition from functional to rest states with reduction of the influence by the value x_0 , the functional reliability of the element is given by:

$$R_b = R_{b1} R_{b2}$$

The reliability of an element, apparatus or system with relay effect for complete or incomplete failure is given by:

$$R = R_a R_b = R_a (R_{b1} \cdot R_{b2})$$

A further aspect concerns the interference stability of an element, apparatus or system:

If, for example, an element, apparatus or system has a double-signal to transpose, the mean of the two functions $S_1(t)$ and $S_2(t)$ in the period of time T , the most favourable case is then when $S_2 = -S_1$ i.e. the so called 'Active-pause'.

An ideal receiver with a noise signal with equal spectrum gives on its emitter the quotient signal/noise:

$$\rho = 8FT\rho_0$$

where F is the width of the frequency outlet and ρ_0 the quotient signal/noise on reception.

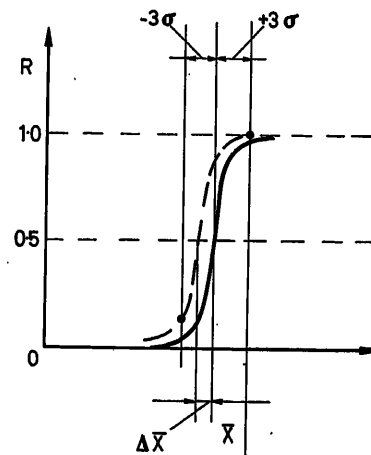


Figure 4

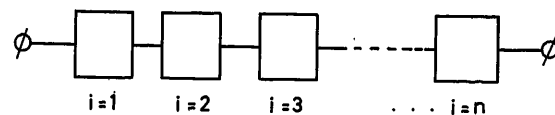


Figure 5

The probability of a single error with normal distribution rules is:

$$q = \frac{1}{2} [1 - \phi(z)] \approx \frac{1}{2} \cdot \frac{e^{-z^2}}{\sqrt{\pi} \cdot z} \left(1 - \frac{1}{2z^2} + \frac{1.3}{(2z^2)^2} \dots \right)$$

where $Z^2 = 8/8 \log 1/q \approx 0.054 \rho$ is approached or with the assumption that the speed of transition is $1/T = 8 F \rho_0 / \rho$ then:

$$\frac{1}{T} \log \frac{1}{q} = 8 F \rho_0 / \rho = 0.43 \frac{P}{N_0} = \text{const.}$$

where P is the signal strength and N_0 is the spectral concentration of the noise. According to S. E. Shannon the ability of a continual channel to emit is:

$$C = F \log_2 (1 + P/N) = F \log_2 (1 + \rho_0) = F \rho_0 \log_2 (1 + \rho_0)^{1/\rho_0} \\ = F \rho_0 k = k \frac{P}{N}$$

where

$$\rho_0 = 1; k = 1 \text{ and } \rho_0 \rightarrow 0; k \rightarrow \log_2 e = 1.44$$

With the assumption $k = 1.44$, $c = 1.44 P/N_0$ and

$$\frac{1}{T} \log \frac{1}{q} = 0.3 C$$

$$\text{or } q = 10^{-0.3 CT}$$

For a passive rest ($S_2 = 0$) the numerical coefficient returns to $1/4$.

The reliability in respect to the transition of the signal through the system is given by:

$$R_C = 1 - q = 1 - 10^{-0.3 CT} = 1 - e^{-0.7 CT} \approx 0.7 CT$$

From this the resulting reliability is $R = R_a R_b R_c$.

The subject of reliability is somewhat different in consideration of the incomplete failure of the elements, apparatus or systems with lasting functions such as transmitters, measuring apparatus and the like. Here under reliability, against incomplete failure, it is necessary to understand the class of exactness of the apparatus.

Normally the value of the emitter (of the emitter signal of a transmitter, of the power factor of a measuring appliance) with repeated influence of the same entry magnitude $x_1 = \text{const}$, is given by a normal distribution law. The magnitude of error of

the appliance is normally given by $\pm \Delta y$ correspondingly $\pm 3 \Delta$ when Δ is the mean quadratic deviation. This corresponds to $R_b = 0.997$. Under the influence of external factors (temperature, humidity, vibration and the like) as with depreciation there occurs a change of the mean value to the value $\bar{y}^1 = \bar{y} + \Delta \bar{y}$ and correspondingly the quadratic mean value becomes $\Delta^1 > \Delta$. With this, the probability for retaining the previous errors, that is, the previous class of exactness under the influence of the entry magnitude $x_1 = \text{const}$, on the element.

$$R_b = \frac{1}{\sqrt{2\pi}\Delta} \int_{y_2}^{y_1} e^{-(y-\bar{y})^2/2\Delta^2} dy$$

where

$$y_1 = \bar{y} - 3\Delta, y_2 = \bar{y} + 3\Delta$$

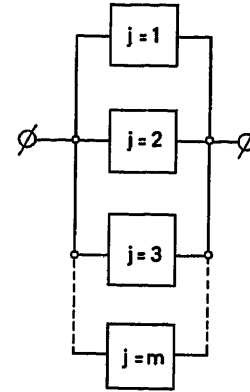


Figure 6

The reliability of an element, apparatus or system with continuous function opposing complete or incomplete failure is given by $R = R_a(t) R_b$.

The investigation of human influence on a control system plays a particular and very important role. Here, apart from the investigation of the static and dynamic characteristics of the human as a part of a control system and the investigation of variability of these characteristics on transition from one subject to another as well as with alteration of the surrounding conditions, the duration of working time, the evaluation of the functional reliability of the human under the influence of subjective influences, the variation of the surrounding conditions, the dura-

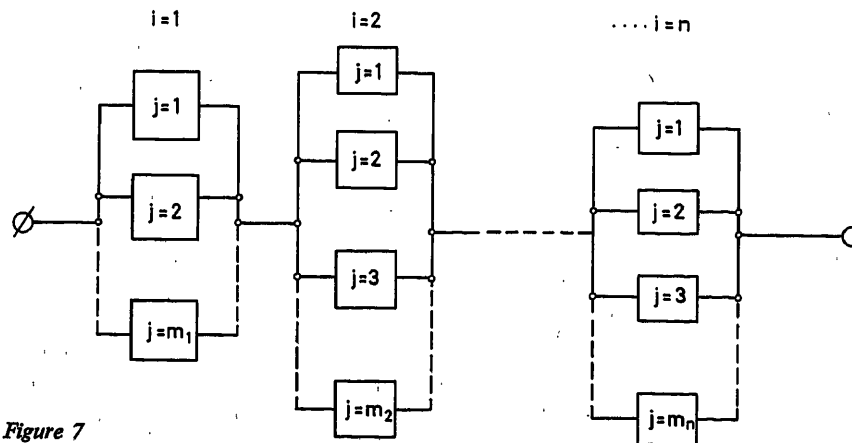


Figure 7

tion of working, the height of the stream of information and the type of entry of this stream of information (the mode of reception)—all these are to be considered.

These problems have in recent years been considered to be of greater value.

The Structural Reliability of the System

The main problem of structural reliability consists of the evaluation of the system's reliability in the case of complete failure, if the system consists of 'n' series switched elements or of 'm' parallel switched elements. The handling of these problems is at present normally successfully dealt with by the assumption that the functional reliability of every element is independent of the condition and reliability of the other elements.

If, in a system, there are 'n' switched elements in series whose functional reliability with given states and functional conditions corresponding to $R_1, R_2, R_3, \dots, R_n$, so correspondingly the reliability of the failure free function of all 'n' elements equals

$$R_a = R_1 R_2 R_3, \dots, R_n = \prod_{i=1}^n R_i$$

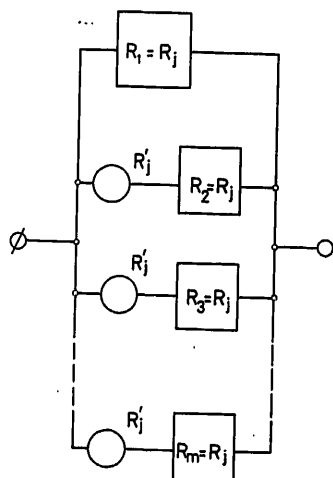


Figure 8

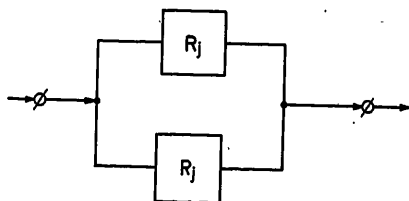


Figure 9

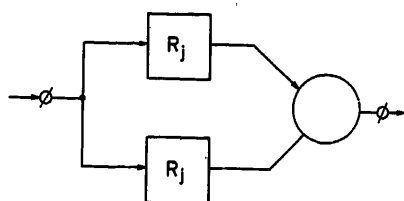


Figure 10

By the earlier assumptions that

$$R_1 = e^{-\lambda_1 t}; R_2 = e^{-\lambda_2 t}; R_3 = e^{-\lambda_3 t}, \dots, R_n = e^{-\lambda_n t}$$

then

$$R_a = e^{-(\lambda_1 + \lambda_2 + \lambda_3 + \dots + \lambda_n) t} = e^{-\sum_{i=1}^n \lambda_i t}$$

or with $\lambda_1 = \lambda_2 = \dots = \lambda_n$ then $R_a = e^{-n\lambda t}$.

If the system consists of 'm' parallel switched elements then the probability of failure of every individual element is:

$$q_1 = 1 - R_1; q_2 = 1 - R_2, \dots, q_m = 1 - R_m$$

The probability of failure of the combined system is relative to the case of simultaneous failure of all 'm' elements and is:

$$q = q_1 \cdot q_2, \dots, q_m = \prod_{j=1}^m q_j = \prod_{j=1}^m (1 - R_j)$$

and the reliability of the system is given by:

$$R_a = 1 - q = \left[1 - \prod_{j=1}^m (1 - R_j) \right]$$

Finally, the reliability for the case with series switching of 'n' groups with each 'm' element is:

$$R_a = \prod_{i=1}^n \left[1 - \prod_{j=1}^m (1 - R_{ji}) \right] = \prod_{i=1}^n R_{ia}$$

For a large number of elements or groups of elements in series the value of

$$R = \prod_{i=1}^n R_i$$

is negligible. If in fact in a system there are 100 elements each with a reliability of $R_i = 0.99$, then the reliability of the system is only $R_a = 0.37$.

This fact requires either the raising of $R_i \cong -(\lambda_i t)$ or the introduction of redundancy.

Redundance

The using of redundances is an extremely effective process for raising the reliability of a system, and because of this, this process finds wide application in practice. However, the application of the method requires answers to the following questions.

- (1) What type of redundancy is suitable.
- (2) What should be the choice of circuit.

The simplest form of redundancy consists of parallel switching of similar types of element, so that $R_i \cong R_1 \cong R_2 \cong \dots \cong R_m$.

The functional reliability of such a group of parallel-switched similar elements is under the condition that the parallel switching does not alter the functional conditions and thereby change the reliability of the elements.

$$R_i = \left[1 - \prod_{j=1}^m (1 - R_j) \right] = [1 - (1 - R_j)^m]$$

From this $R_j = 0.99$; $R_i = 1 - 0.01^m$ with $m = 2$ the value $R_i = 0.9999$ and for $m = 3$ the value $R_i = 0.99999$ etc.

If n groups of elements are switched in series, then

$$R_a = \prod_{i=1}^n R_i = \prod_{i=1}^n [1 - (1 - R_{ji})^{m_i}]$$

or if all elements have equal reliability and $m_1 = m_2 = \dots m_n = m$ then:

$$R_a = [1 - (1 - R_j)^m]^n$$

There is also another possibility for redundancy with m parallel-switched systems; for this the following is valid:

$$R_a^1 = [1 - (1 - R_a)^m] = [1 - (1 - R_j^m)^m]$$

Another method of redundancy is the switching-in of redundant elements if other elements fail or their essential constants alter. For this, an additional element is necessary such that a check is kept on the correctness of the elements substituted and the redundant elements switched in when necessary. In this case for a group of m elements:

$$R_i = 1 - (1 - R_j)(1 - R_j R_j')^{m-1}$$

and for a system of n groups:

$$R_a = \prod_{i=1}^n [1 - (1 - R_j)(1 - R_j R_j')^{m-1}]$$

In Figure 11 (a), a further type of redundancy method is shown; it consists of a common element which vigilates over a larger number of elements.

Figure 11 (b), the reliability of such a system with three elements is:

$$R_i = R_j^3 + 3(1 - R_j)R_j^2 = R_j^2(3 - 2R_j)$$

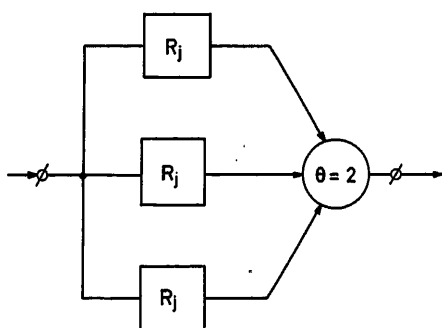


Figure 11 a

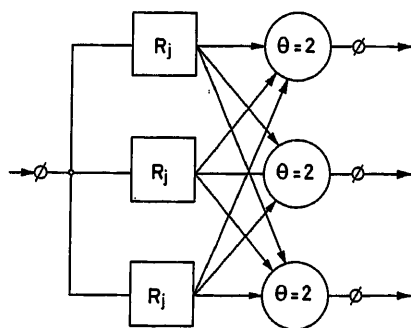


Figure 11 b

and for a system of N like groups:

$$R_a = [R_j^2(3 - 2R_j)]^N$$

If, for example, $N = 100$ and $R_j = 0.99$, then $R_a = 0.97$. The relative increase in reliability is then:

$$R_a/R_{a0} = \frac{[R_j^2(3 - 2R_j)]^N}{R_j^N} = [R_j(3 - 2R_j)]^N$$

Figure 12 shows the variations of $R_a/R_{a0} = f(R_j, N)$ for $N = 2; 10; \text{ and } \infty$. From this it can be seen, that for $R_j < 0.5$ the redundancy is suitable.

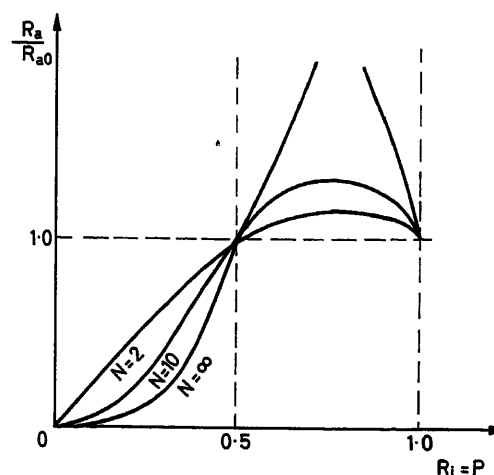


Figure 12

If it is assumed that the additional element had reliability $m < 1$ then:

$$R'_a = [mR_j^2(3 - 2R_j)]^N$$

For $m = R_j$, $R'_a = R_a R_{a0}$.

Because always $R_a < 1$, then R_a cannot be better than R_{a0} .

The next step of development of this type of redundancy shows the switch diagram as in Figure 11 (b). Here there are three additional elements each being connected with the functional elements.

The Balance between Reliability and Economics

If the cost C_0 for an apparatus is known (construction price, transport and assembly costs) and the cost C_b for the service time unit of the apparatus, and also the cost C_y for the damage through failure of the apparatus, are evaluated, then the equivalent costs for apparatus are:

$$C = C_0 + C_b t + C_y q = C_0 + C_b t + C_y (\lambda + \lambda' f) t$$

where $q = (\lambda + \lambda' - f) t$ is the probability of failure.

An improvement of the quality of the apparatus or the introduction of redundancy raises, C_0 . An improvement of the checking system raises C_b and simultaneously reduces the values of λ and λ' . For every case the most favourable ratio between C_0 , C_b , λ and λ' can be evaluated to give C its lowest value for the given life duration period ($t - t_0$).

If there is an autonomous protection system, which prevents

the advent of damage on failure of the system, then, the equivalent costs are:

$$C = (C_0 + C_{03}) + (C_b + C_{b3})t + C_y q_3 q \cong \\ \cong (C_0 + C_{b3}) + (C_3 + C_{b3})t + C'_y (\lambda + \lambda' f) t$$

where $C'_y = C_y q_3 \cong C_y \lambda_3 t$, the equivalent magnitude of damage with respect to the protective effect.

A few points about Research in the Field of Functional Reliability

Technical development constantly led to the advancement in studies of reliability problems. These were always investigated by verifying the required reliability coefficients, by evaluation of the dimensions and life-duration of individual components, elements, apparatus and machines.

Manifestly, one of the first steps in the new way of handling these problems by statistical methods was by Weibull who did so in the forties while investigating the service reliability of roller bearings. Another valuable contribution came from the investigations on the considerable life-duration of transformer windings with given demands on its service states and also from the investigations into the functional reliability of electrical high-voltage discharge.

As mentioned above, from 1940–50 there grew a strong interest in reliability problems, caused by the introduction and development of radio-electronic appliances for transition of information and automatic appliances for checking, regulation and control. The unreliability of electronic circuits necessitated investigation into the reliability of individual elements in switching, in particular of electronic tubes.

The investigations were carried out by collecting and processing statistical data on the functional failure with various states and service conditions.

These investigations were carried out by people like Lasser, Reverson, Cook, Mesjacer, Zimin, Levitin and many other scientists of various countries.

In the following years attention began to be given to the physical side of the growth in failures of the various types of element.

At the same time, investigation was begun into the structural reliability of systems which had elements switched in series and parallel. Investigations of this type were done by such people as; Allen, Tiek, Woodburn, Kao, Siforov, Bruevic, Druzinin and others.

One of the most important leads in the solution of reliability problems was by the application of redundancies. The essential development of the application of redundancies was done by von Neumann, Pears, Morr, Shannon, Siforov, Sinic, Ju. Kovan, Ferveek, Bljum and other scientists.

Another important lead in the solution of reliability problems was the reliability of noise stability with transition of informa-

tion. Those responsible in this field were; Shannon, Kotel'nikov, Charkevič and many other research scientists.

In the years 1948–55 there appeared the first technical standards for reliability test methods. Since 1954–55 regular meetings and conferences have been held on reliability problems.

Also in this period the first publications have been issued on the theory and evaluation of functional reliability of elements and systems by such people as: Cheys, Taylor, Chinney and Wolsch and others in U.S.A., Malikov, Polovko, Romanov and Čuchreev, Astaf'ev and others in U.S.S.R., Dammer and Griffith in England.

Modern work on the functional reliability of elements and apparatus are tied up with investigations on distribution rules of failure for the various types of element: electrical, electro-mechanical, mechanical, pneumatic and hydraulic appliances with various states and functional conditions.

The most important direction here is the study of the physico-chemical reasons for failure occurrences, because these investigations give the possibility of defining means of construction, completion and service which would increase the functional reliability of the elements and would also give the rational limits and conditions for the introduction of the elements.

The problems of structural functional reliability find their development primarily through the creation of methods which take account of the inter-dependent reliability of joint-switching of added elements and which take account of the variation of the functional limits and thereby allow for the alteration in reliability of the elements on changing the switching-structure during the function. Further, development embraces the structural reliability and the life-duration of the switching and system which consist of elements with various distribution rules. Various processes for increasing reliability also find development. Here, the methods used are those which are analogous with biological systems. The methods are on the one hand bound up with the creation of complicated relationships between the functional elements and the introduction of assistant elements, and on the other hand with the application of adaptive elements and installations which make it possible for every connection with external conditions to be evaluated to the requisite and often optimum state necessary for functionally reliable service of the system. For this, in some cases it is necessary for the 'training' of the systems for specific connections with external conditions. A particularly interesting lead is the use of adaptive systems with test-scanning.

Problems of the suitability of sub-division of sub-systems with redundancy find necessary consideration. This is particularly important with the application of 'molecular' elements.

The problems of noise stability and informational reliability of transition systems also finds further development. Here, the definition of noise stability with impulsive interference and the evaluation of the best noise-stable and economic code forms are important.

New Servo-valves for Redundant Electrohydraulic Control

K. D. GARNJOST and W. J. THAYER

Summary

This paper describes the application of redundancy techniques to electrohydraulic servomechanisms. Certain principles of redundant systems are first discussed and two basic types are defined. These are detection-correction systems and majority voting systems. Consideration is then given to the particular design aspects of electrohydraulic components which affect their usage in redundant configurations. From this, new servo-valve designs are developed for use in each type of system. The advantages of these components are shown by description of their application in three critical flight control systems.

Sommaire

La communication décrit l'application des techniques de redondance aux servomécanismes électro-hydrauliques. Elle présente tout d'abord certains principes relatifs aux systèmes redondants et elle définit deux classes de base pour ces derniers: les systèmes à 'détection-correction' et les systèmes à 'scrutin majoritaire'. Viennent ensuite des considérations relatives aux composants électro-hydrauliques du point de vue des particularités spécifiques qui influent sur leur utilisation dans des configurations redondantes. A partir de là, on décrit de nouveaux types de servovalves destinées à être utilisées dans chaque classe de systèmes. Les avantages de ces nouveaux composants sont mis en évidence lors de la description de leur application dans trois systèmes de commande de vol critique.

Zusammenfassung

Dieser Beitrag beschreibt die Anwendung von Redundanzmethoden auf elektrohydraulische Nachlaufregelsysteme. Nach allgemeinen Ausführungen über redundante Systeme werden zwei grundsätzlich verschiedene Schaltungsarten beschrieben. Bei der einen wird ein ausgefallenes Element automatisch entdeckt und ersetzt. Bei der anderen liegen mehrere Elemente parallel, so daß ein ausgefallenes Element von den intakten Elementen „überstimmt“ wird. Dann werden besondere konstruktionsbedingte Eigenschaften elektrohydraulischer Bauteile besprochen, die deren Einsatz in redundanten Schaltungen beeinflussen. Davon ausgehend wurden für jede der obengenannten Schaltungsarten neuartige Servoventile entwickelt. Die Vorzüge derartiger Bauteile zeigen sich bei der Beschreibung ihrer Anwendung in drei Flugregelsystemen, bei denen es auf Ausfallsicherheit ankommt.

Introduction

Critical failures of automatic controls in certain applications, notably space vehicles and high performance aircraft, may be catastrophic and cause loss of vast economic investment and human life. A number of such control systems include electrohydraulic power output elements. The reliability of these elements has been adequate for unmanned space vehicles and for manned flight where manual override has been practical. Currently planned space vehicles and supersonic aircraft will encounter certain flight regimes where reliance on manual control, even as an emergency measure, is no longer possible. These requirements present the problem of achieving a substantial improvement in the reliability of electrohydraulic servo-controls.

Historically, the reliability of electrohydraulic components

has been significantly, but gradually, increased through continuing design innovation. However, experience in critical applications has indicated that the major reliability problem is associated with short term, 'random' failure due to human error. The substantial improvement now needed is therefore much more than can reasonably be expected from normal 'state of the art' design evolution. The recognized solution to this dilemma is to resort to parallel redundancy of critical components or systems. The application of redundancy techniques to electrohydraulic controls is not straightforward because of problems peculiar to these components. A number of redundant electrohydraulic systems are currently being developed by industry for a variety of applications and represent a wide diversity in design approach. This diversity can best be appreciated if the basic approaches to redundancy are defined and the fundamental redundant configurations classified. This background can then be combined with knowledge of component characteristics to examine practical systems and the limitations encountered in each. This discussion leads to the description of new servo-valves and several illustrative systems in which they may be applied to achieve more effective reliability by redundancy.

Classification of Redundant Systems

Control system failures may be classed as either passive, in which failure removes power from the system, or active, in which failure results in uncontrolled application of power to the system. Since electrohydraulic systems are susceptible to active failures, they require redundant configurations in which the failed component is either removed and replaced, or else overpowered. Mechanization of the former configuration requires detecting a failure and correcting it by switching out the failed element. Configurations in which the effect of a failed element is overpowered depend on the presence of a majority of unfailed elements which 'outvote' the failure. These alternative techniques can be termed 'detection-correction' and 'majority voting', respectively.

In each of these approaches, three information channels are required to perform the necessary logic to contend with a failure. Comparison between two channels can detect a failure in one or the other. However, second comparison to a third channel is necessary to distinguish the failed channel and thus permit correction. Similarly, to overpower a failure, a minimum of three channels are required to provide a majority.

Electrohydraulic power control systems include a number of components covering a wide range of power levels and interconnected in multiple feedback loops. Redundancy of the higher power level components is unattractive due to their weight, and is generally not required because they can inherently be made more reliable. This choice of the degree of redundancy must be considered together with the type of redundancy in order to locate comparison and switching points, on the one hand, or to locate the voting point, on the other.

Detection-correction

The simplest configuration for a fully-redundant, detection-correction system is shown in *Figure 1*. The system output, provided by an active channel, is compared to the output of a reference channel. This comparison consists of a simple algebraic summation of opposite polarity variables. The resulting difference

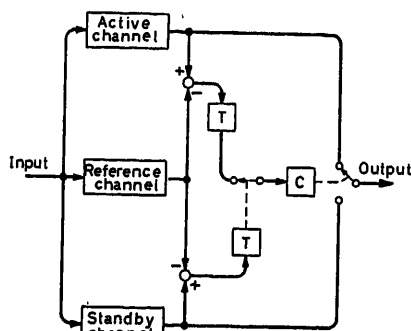


Figure 1

is sensed by a detector, T , having a finite threshold. Thus, if the two outputs are different by more than the threshold level, the detector will produce an output to a correction element, C . This, in turn, actuates a switchover element to change the system output to the standby channel. This action may occur as the result of a failure in either the active channel or the reference. Switchover to the standby channel is appropriate, however, unless that channel had previously failed. A second comparison of the standby channel to the reference is therefore necessary to establish a condition for allowing switchover. The usual requirement of protecting a system against a single failure can be met without this secondary information, but decisions affecting the operation of systems with human monitors may be enhanced by providing information on the status of the standby channel.

It is significant to note that, while redundancy has been provided for the basic components in the active channel, system output is dependent on a common, non-redundant switchover element. Further, unique comparison and switchover elements are essential to provide effective redundancy. It is therefore necessary that these common or unique elements have inherently high reliability if any significant improvement in system reliability is to be achieved through redundancy. Fortunately the nature of these devices is such that they can be much simpler than the basic control system components.

An important consideration in redundant systems is the time required to accomplish correction following a failure, since, in some applications, small deviations of the output from the correct value may be disastrous to the controlled vehicle. This time is the sum of the times required to detect failure, to switch to the standby system, and to re-establish control. The time to detect failure will be directly related to how small the detection threshold can practically be made and to the rate of error build-up at the detection point. The time required to switch will appear as a fixed transport delay, and the time required to re-establish control will be related to the magnitude of output deviation from the correct value. In most power control systems, the final control element acts as an integrator, so comparison at the output will include the integration time lag for any failure

ahead of the integrator. In addition, the threshold level of an output comparator must be high to allow for differences in drifts of the active and reference channels. For these reasons it is much more effective to make comparisons ahead of the output integration. Here the time to sense a failure is limited only by the dynamic response of the elements ahead of the comparison point.

The foregoing discussion has assumed a reference channel which is identical to the active channel. In practical systems an analogue computer model of the actual system is sometimes used to avoid duplication of heavy and costly control components. Comparison of signals between the working system and the analogue can yield effective failure indication to the extent that the analogue is an accurate model including significant nonlinearities. However, such a model is complex and thus subject to failures in itself. A compromise in the direction of simplicity is shown in *Figure 2*. Here only the output feedback element and the input summing point are duplicated to provide the reference channel. The inner loop feedback signal, e_A , which is effectively the error in the outer loop of the active channel if the inner loop response is fast, is compared with the reference channel error, e_R , to provide failure indication to a detector, T . This affords the desired comparison immediately ahead of the output integration.

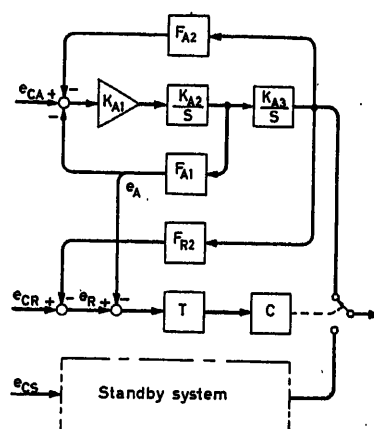


Figure 2

The threshold of the detector must be set high to accommodate static drift levels. However, because of differences in response, gain, and saturation levels, the input to the detector may dynamically exceed the pre-set level. False failure indication due to transient inputs may be avoided by introducing a dynamic lag, but this partially offsets the advantage gained by comparison ahead of the output integration.

The difficulties with model reference may be overcome by employing the standby system for the primary comparison, with provision for an additional comparison to an abbreviated reference system. The output of the secondary comparison can be ignored until the primary comparator has exceeded its threshold, so the reference system may be quite non-ideal. This configuration is particularly useful where the control system is sensitive to load variation. In the arrangement shown in *Figure 3*, two operating channels are used in parallel to share the load. Basic failure indication is obtained by comparison of these channels, and the reference channel identifies which operating channel should be shut off.

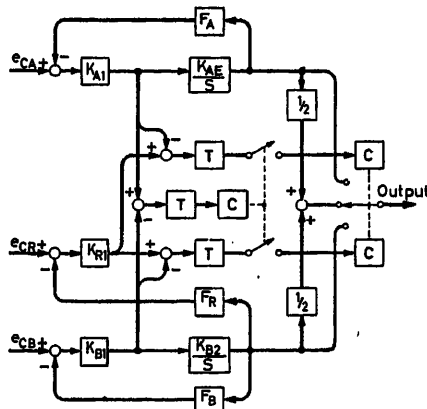


Figure 3

Majority Voting

Majority voting redundant systems avoid most of the problems associated with the detection-correction systems just described. They do, however, require complete triplication of all elements in the redundant portion of the system as shown in Figure 4. The outputs, θ_A , θ_B , θ_C , of three control channels are summed to provide a common output, θ_0 . Feedback of the common output to each of the three channels is provided through three redundant feedback elements. A hardover failure in channel A would cause θ_A to go its maximum value, θ_m . θ_0 would then change to a new value $\theta_0 + \Delta$. This incremental change in output is fed back to the three input summing points and causes changes in θ_B and θ_C of $1/2 (\theta_m - \Delta)$. The magnitude of the incremental change in output, Δ , can be made small by making the control-loop gain high and limiting θ_m to its smallest practical value. This latter condition is restricted by the need to provide some maximum value of θ_0 . Introduction of a gain element K_0 between the summing point and the output contributes to the overall loop gain, but does not otherwise affect the change in output caused by a failure. However, if an integration is located at this point, the limit on θ_m can be made much smaller, since it no longer directly restricts the maximum value of θ_0 . Rather, the limit establishes the maximum output rate of change. An additional control loop with integration (shown dashed in Figure 4) permits the authority limits at the voting point to affect only maximum system acceleration.

This description of a majority voting system could be extended to cover all other possible single failures of the redun-

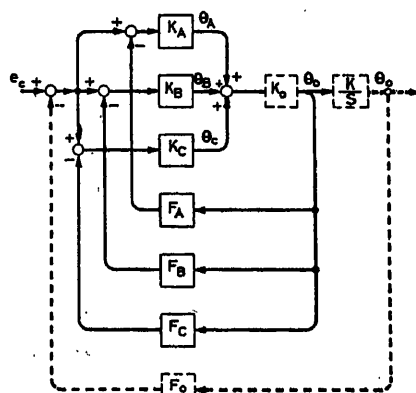


Figure 4

dant elements, including passive failure or gain changes of forward-loop elements, loss of feedback, or loss of input. Also, corrective action is initiated immediately at the onset of a failure, and an output disturbance will build up only to the extent allowed by the dynamic lags of the control loop.

The majority voting system has a common element, namely the output summer, but it is much simpler than the comparison, detection, and switchover elements required by the detection-correction approach. Thus, majority voting appears to offer a superior redundancy technique. It should be noted that the majority voting system does not provide an inherent, discrete indication of failure. This indication can only be obtained by the use of two comparison and threshold detection elements, but it is possible to check out the system by introducing a simulated failure into one channel at a time. In the event that one of the remaining systems has failed, control will be lost.

Redundant Electrohydraulic System

Choice of a redundant system for any real application must consider the limitations imposed by physical characteristics of the components required. The systems treated by this paper are hydraulically operated power controls having low level electrical command inputs. The controlled variable is generally position and the system therefore includes a displacement feedback transducer, a summing amplifier, an electrohydraulic servo-valve, and a hydraulic actuator. While the output position is necessarily a single channel, there may be one, two, or three input channels, depending on the degree of redundancy of the input signal.

Redundant hydraulic pressure sources are commonly provided for such systems to protect against pump or related failures. Since pressure loss is a passive failure, simple duplication can provide adequate redundancy. However, operation of three information channels, from two power sources presents a problem. Use of three power sources is generally not desirable because of the excessive weight penalty, so other alternatives are necessary.

Similarly, duplication of power output elements imposes a weight penalty. A hydraulic piston and cylinder are extremely simple mechanical parts and can be designed with conservative factors of safety, so duplication is often not necessary. In fact, doubling the design stress levels for an actuator may require less weight than providing two actuators, and may actually achieve a greater increase in reliability. One compromise is the tandem actuator which represents some weight-saving over two separate units and provides isolation of two hydraulic systems to protect against a single seal failure. However, the same protection can be provided by seal redundancy in a single actuator.

While it may also be possible to limit redundancy of power control elements, the delicate instrument nature of feedback transducers, amplifiers and the low power level portions of servo-valves calls for redundant protection. The essential complexity of these components creates the possibility of random failures which cannot be avoided by simple overdesign. The servo-valve configurations discussed below offer improved means for providing redundancy of these components.

Redundant Servo-valves

Several considerations lead to the novel component designs presented in this paper. As noted earlier, in detection-correction systems it is desirable to have means for comparison just ahead

of the integration introduced by the servo-valve and actuator. This in effect requires comparison of the servo-valve spool position to a reference valve position.

In majority voting systems a summing point must be provided at the output of the redundant portion of the system. Summing the output of three pistons is theoretically possible but not attractive mechanically. Summing the flow output from three servo-valves is not practical because of the difficulty of obtaining null coincidence and the drastic power inefficiency under failure conditions. Redundancy of the spool drive is therefore indicated.

In either type of system, it is desirable to mechanize redundancy without introducing additional electrical elements. The mechanism to accomplish these requirements is an extension of conventional 'mechanical feedback' servo-valve design. Most 'state of the art' electrohydraulic servo-valves consist of an electromagnetic force motor driving a force input hydraulic amplifier, which in turn drives a four-way valve spool. Spool position is fed back by means of a spring to the force summing point to achieve a closed loop. Figure 5 illustrates such a valve using a nozzle-flapper hydraulic amplifier. Spool position feedback is accomplished by a cantilever spring extension of the flexure-supported armature and flapper member.

A mechanism to provide spool position comparison for detection-correction can be provided by duplicating the force motor, hydraulic amplifier, and feedback spring to form a so-called monitor servo-valve (Patent applied for), as shown in Figure 6. The block diagram of Figure 7 indicates how a monitor servo-valve is used in a redundant system. The reference

channel signal is applied to the monitor force motor and its output is summed with an auxiliary feedback spring force to provide an input to the monitor hydraulic amplifier. The difference between actual spool position and the reference appears as a differential pressure which may be applied to a spring preloaded piston acting as a detector.

Majority voting can be mechanized by three force motors, hydraulic amplifiers, and feedback springs with a single valve spool, as shown schematically in Figure 8 (Patent applied for). Here, the output flows of the three hydraulic amplifiers are summed at the ends of the valve spool. A hardover failure associated with one channel will cause a flapper to close one nozzle and thus tend to drive the spool from its desired position. The feedback and hydraulic amplifier gain can be made sufficiently high, however, so that a very small spool displacement is required to offset the failure. An experimental unit, shown in Figure 9 (a), has demonstrated the predicted performance as shown by the data plotted in Figure 9 (b).

Typical System Applications

The systems dealt with below are typical of real applications in which the techniques and components presented in this paper may be used to advantage. The first system was designed for positioning a swivelling, liquid-fuel rocket engine. The second example presents a redundant system for controlling liquid secondary injection to provide thrust vector control of a solid rocket motor. The third system was designed to provide a

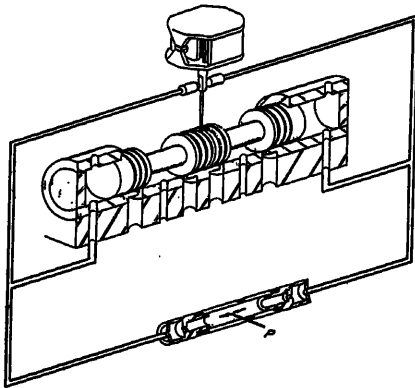


Figure 5

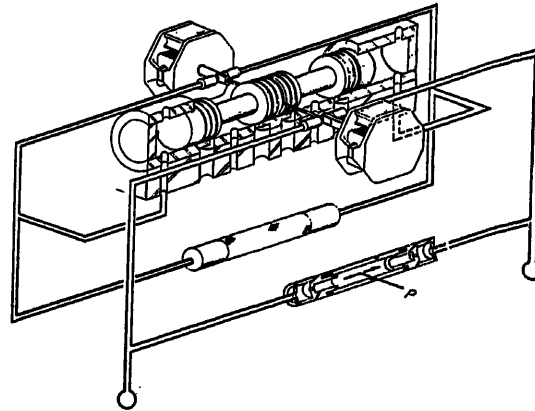


Figure 6

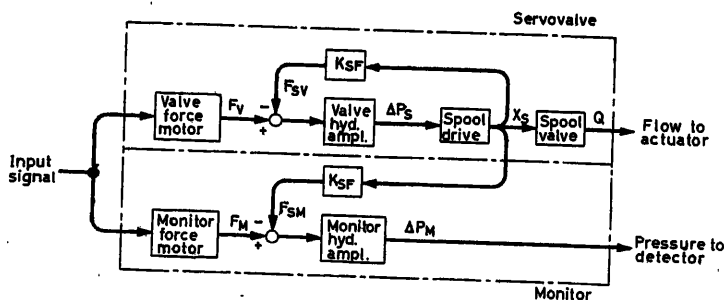


Figure 7

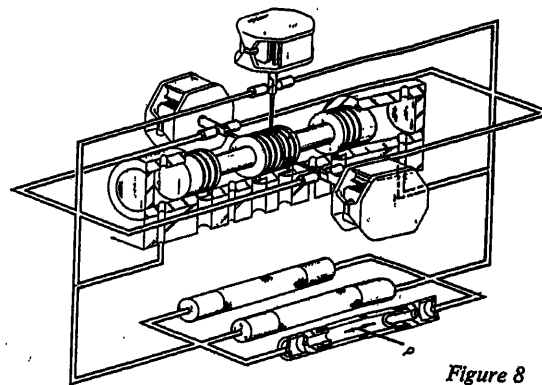


Figure 8

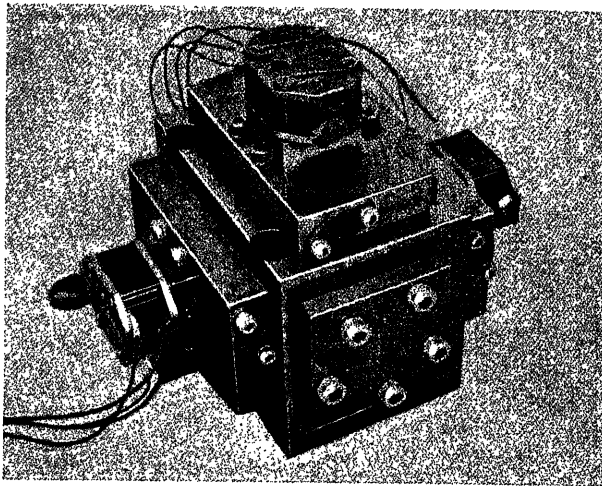


Figure 9 (a)

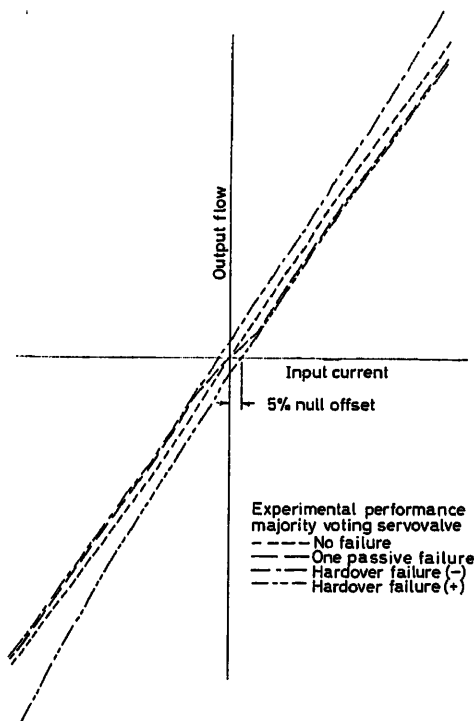


Figure 9 (b)

redundant stability augmentation actuator for use with a dual channel autopilot in a high performance aeroplane. These systems use various techniques to provide redundant protection of components ahead of the electrohydraulic servos and no attempt has been made to present this area of the system design problem.

Detection-Correction System Using Monitor Servo-valve

Figure 10 illustrates the use of two monitor servo-valves in a detection-correction electrohydraulic servo. This system incorporates mechanical feedback of the output piston position. The net force input to each hydraulic amplifier represents the positional error in the system. Servo-valve A is normally con-

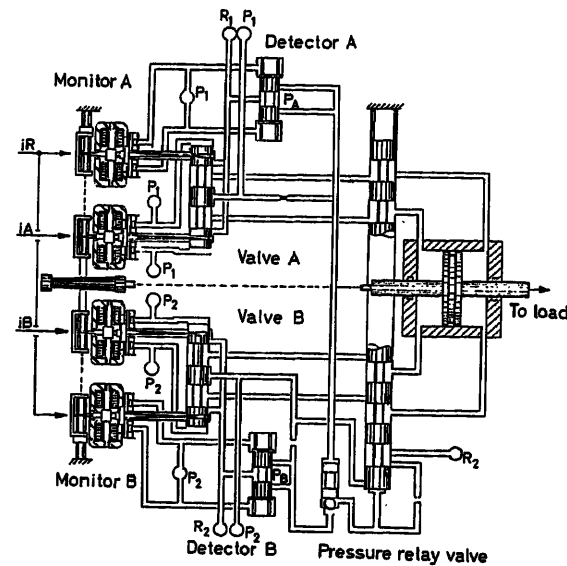


Figure 10

nected to the piston through the switchover valve. A tandem piston might also be used, with appropriate changes in the switchover valve. In the event of a failure in channel A, the error force developed at the A monitor will not correspond to the spool position feedback force. If the unbalance exceeds a pre-set tolerance, the detector spool will move, causing pressure P_a to be reduced below a critical level. This in turn applies an operating pressure to the switchover valve. The switchover valve will remain in its shifted position, with valve B controlling the piston, until it is reset by removing system pressure. The function of the B monitor is to prevent a switchover if there has been a failure in the B channel. This monitor will also prevent switching with failure of the reference system, such as loss of the reference signal.

The monitor servo-valve is a simplified reference system and subject to erroneous failure indications under saturation conditions. For example, if the servo-valve is driven hardover by a step input to the system, the monitor hydraulic amplifier will develop a full pressure output. However, since this will occur in both monitors simultaneously, no switchover will occur. It should be noted that two servo-valves and detectors are operated from independent pressure supply systems, P_1 and P_2 . The switchover mechanism is operated from P_2 since switching should not occur if P_2 is not present. The pressure relay valve serves to isolate the two supply pressures and will cause switchover to valve B if P_1 is lost.

Three-channel System Using Majority Voting Servo-valve

Figure 11 shows a secondary injection control system employing a majority voting servo-valve with triple redundant inputs, feedback transducers, and valve driving amplifiers. The two injector valves are hydraulically interlocked to form a single bidirectional control. The supply pressure P to the servo-valve is obtained directly from the pressurized injectant fluid, so redundancy of the pressure system is unnecessary.

This system shows how majority voting at the output of the servo-valve driving hydraulic amplifiers protects against failure

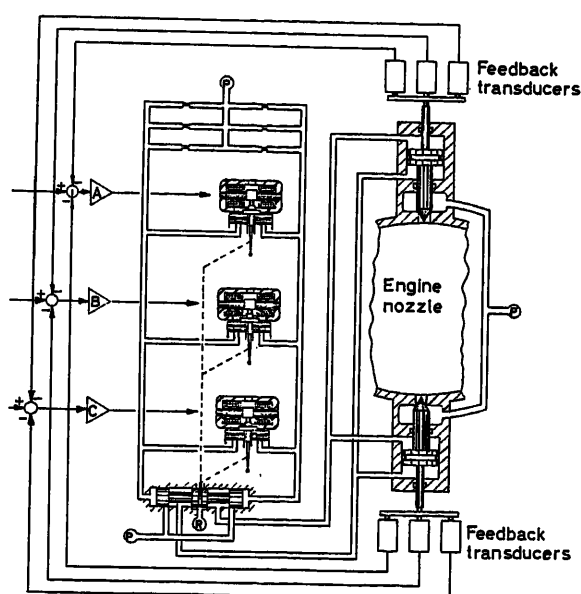


Figure 11

of any redundant element ahead of the valve. For example, if one of the A feedback transducers fails, the output of the channel A amplifier differs from the B and C channels. The majority voting servo-valve overrides the channel A input and causes the servo-valve spool to be positioned in accordance with B and C inputs except for a small error offset. Control of injector valve position is essentially unaffected by the failure due to the loop gains and integrations involved. It can be seen that other failures such as loss of a command signal, passive or hardover failure of an electronic amplifier, opening of a torque motor coil, or clogging of a hydraulic amplifier nozzle can all be overcome in a similar manner.

Two-channel System Using Majority Voting Servo-valve

Figure 12 shows an aeroplane flight control actuation system which accepts both pilot mechanical inputs and autopilot electrical inputs. The system incorporates a dual tandem servo-valve and actuator to permit use of two isolated hydraulic supplies. Electrical inputs from a dual channel redundant autopilot are converted to a mechanical displacement by tandem pistons, each driven by a pair of hydraulic amplifiers. This displacement is summed with the pilot input to drive the servo-valve spool. Identical electrical inputs are normally present, but with an autopilot failure, one channel is shut off and the output of the other is doubled. Summing of the electrical inputs is accomplished by applying each to separate coils on the force motors. A failure of any one hydraulic amplifier is overcome by action of the other three. In the event of a hydraulic supply failure two of the hydraulic amplifiers will be inoperative, so majority voting is not possible. However, the two remaining hydraulic amplifiers continue control with only slightly degraded dynamic performance introduced by the drag of the passive piston.

Conclusions

These examples of actual electrohydraulic system designs have demonstrated the application of two new servo-valve configurations which use multiple mechanical feedback of valve spool position for redundant control. One is suitable for use in detection-correction systems, while the other provides an improved means for achieving majority voting. Either approach to redundancy may be favoured for use in any particular application. However, comparison of the complex auxiliary non-redundant mechanism necessary to achieve detection-correction with the inherent simplicity of majority voting would suggest a preference for the latter approach. In either case it is felt that the overall simplicity, and hence reliability, of the resulting system is enhanced by the mechanisms presented here.

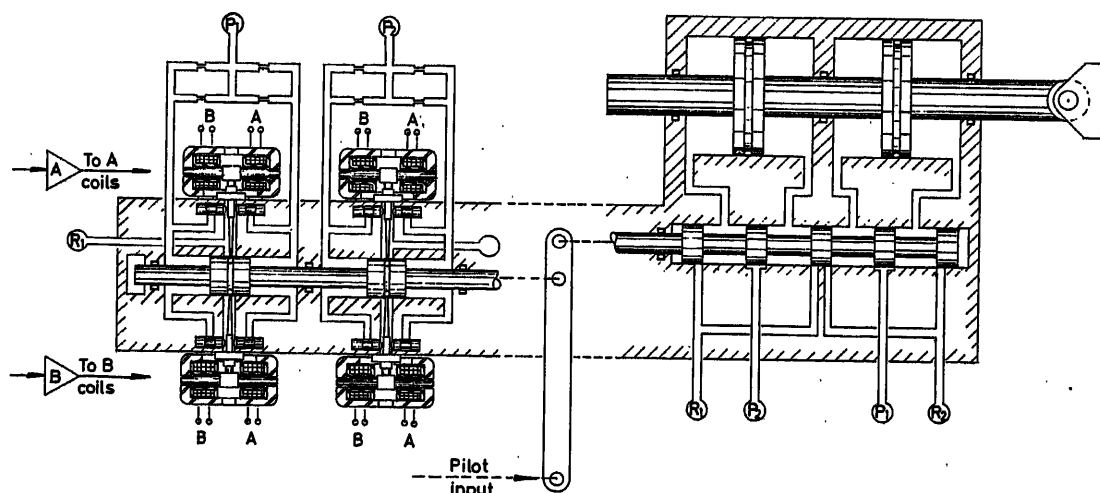


Figure 12

The Reliability of Electronic Components

G. W. A. DUMMER

Summary

Failure rates for components used in some British computers are given. The influence of environment is shown by comparison of these figures with those of unclassified military equipments. A table of failure mechanisms of components at high temperatures, high humidities, together with typical examples of long-term changes in component parameters is also given. Reliability evaluation of fixed resistors is being carried out by programmed testing machines and results of tests on 24,000 resistors are quoted.

Techniques for improving the effective reliability of components are discussed under three headings:

- (1) Improvement in the quality of conventional components.
- (2) The use of cooling techniques for temperature stabilization of components in computers.
- (3) The use of microminiaturization techniques, with close control in manufacture, and using high purity materials.

Sommaire

Les taux de pannes pour les composants employés dans certains calculateurs britanniques sont donnés. L'influence de l'ambiance est montrée par la comparaison de ces chiffres avec ceux de matériels militaires non-définis. Une table des mécanismes de pannes de composants aux températures et aux humidités élevées est également donnée avec des exemples typiques de variation à long terme des paramètres des composants. L'évaluation de la fiabilité de résistances fixes est réalisée au moyen de machines d'essai programmées et les résultats d'essais de 24,000 résistances sont cités.

Les techniques susceptibles d'améliorer la fiabilité effective des composants sont discutées sous trois aspects:

- (1) L'amélioration de la qualité des composants conventionnels.
- (2) L'emploi des techniques de refroidissement pour la stabilisation de la température des composants dans les calculateurs.
- (3) L'emploi des techniques de microminiaturisation avec contrôle sévère en cours de fabrication et l'emploi de matériaux de grande pureté.

Zusammenfassung

Nach einer Betrachtung über die Ausfallraten der Bauteile einiger Rechner britischer Herkunft wird der Einfluß der Umgebungsbedingungen durch Vergleich dieser Ziffer mit solchen von nicht geheimen militärischen Geräten untersucht. Eine Tabelle enthält die Ausfallursachen von Schaltelementen bei hohen Temperaturen und hoher Feuchtigkeit sowie typische Beispiele langfristiger Änderungen in den Kennwerten. Eine Berechnung der Zuverlässigkeit von Festwiderständen wurde mittels programmgesteuerter Prüfmaschinen durchgeführt; die Ergebnisse der Prüfungen von 24 000 Widerständen liegen vor.

Die Maßnahmen zur Verbesserung der Zuverlässigkeit von Schaltelementen werden unter folgenden Gesichtspunkten untersucht:

1. Qualitätssteigerung der herkömmlichen Bauteile.
2. Verwendung von Kühlmitteln zur Temperaturstabilisierung der Schaltelemente in Rechnern.
3. Mikro-Miniaturisierung und strenge Kontrolle bei der Fertigung sowie die Anwendung besonders reiner Werkstoffe.

Failure Rate Data

Component failure rate data have been, and are being, collected by the Royal Radar Establishment on a number of military and commercial equipments in the United Kingdom in an attempt first, to correlate the information, and secondly, to try to paint a picture of the overall state of electronics reliability on a yearly basis. There are many difficulties in collating accurate failure rates on computer components. These include wide variations in circuit design, date of manufacture (i.e., age) of components, manufacturers' acceptance quality levels, operational ratings and many other factors. In these circumstances, the failure rates quoted in this paper should be considered as being presented for guidance only. Methods of specifying failure rates are not above suspicion but the now generally accepted definition in terms of per cent failure/1,000 h under operating conditions will be used.

Component failure rates on a large transistorized data-handling assembly of computers containing approximately 900,000 components are given in *Table 1*. This table also shows, in the last column, the average rate of failure for each class of component under air-blown environmental conditions, but not temperature stabilized.

Data are given in *Table 2* of failure rates on nucleonic equipments operated under typical laboratory conditions at the Atomic Energy Research Establishment at Harwell. The equipments concerned are mainly scalars, counting rate meters, amplifiers, stabilized power supplies, etc. Data from over 4,000 equipments—of 90 different types—have been analysed yearly.

Fault rate data have been recorded at the R.R.E. since 1944 on all military equipments subjected to environmental testing, and *Table 3* shows the position from 1944 to 1960. It will be seen that there is a gradual diminution in failure rates, and it will naturally be appreciated that these are severe environmental conditions in which a high failure rate is to be expected. As comparatively small numbers of equipments are tested, these figures can again only be regarded as indicative.

It is obvious from these analyses that the influence of environment is most marked. The average failure rates for the components might be generalized as 1 per cent/1,000 h for unclassified military environments, 0.5 per cent/1,000 h for laboratory environments and 0.05 per cent/1,000 h for computers under good environments.

Failure Mechanisms

The mechanism of failure depends greatly on the environment, being accelerated by running at high temperatures and in high humidity. In the latter case, the effectiveness of the sealing is paramount. Some work has been done in the United Kingdom on ultimate failure mechanisms when components are subjected to temperature and humidity extremes and it is useful to consider these in long-term computer design. It should be borne in

mind, however, that these are extremes and by running at controlled temperatures and humidities these effects are greatly reduced. Table 5 summarizes the failure mechanisms of several classes of components at temperatures $> 100^{\circ}\text{C}$ and humidities of > 95 per cent at 55°C .

Change in Component Characteristics with Time

Even when operated under good environmental conditions, there is often a change of parameters with time at normal operating temperatures. Long term testing periods of many thousands of hours are required to show these changes and some data have been collected, in Figures 1 (a), (b) and (c), showing typical changes under various temperatures and test times.

Degradation of Components in Long-term Storage

Some interesting work is being done in the United Kingdom on long-term storage of components at room, zero and sub-zero temperatures, on the theory that chemical degradation is a function of time and temperature and therefore, that if temperature is reduced, degradation should also be reduced. Many component failure processes are chemical reactions. The speed of many chemical reactions varies with temperature by a factor of 2 or 3 per 10°C . The speed in most instances is governed either by the reaction rate (in many processes involving gases or liquids), or the diffusion rate (mainly processes involving one or more solids). It is now reasonably established that by reduction of temperature these mechanisms of failure may also be

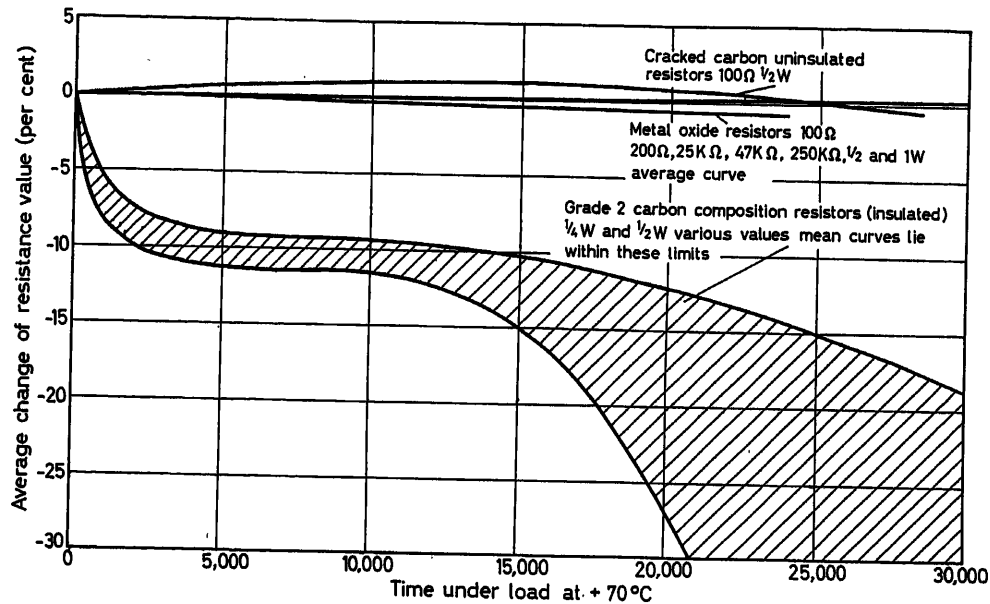


Figure 1 (a). Endurance: carbon resistors Grades 1 and 2, and metal oxide resistors. On full load at $+70^{\circ}\text{C}$ (by courtesy of E.R.A.)

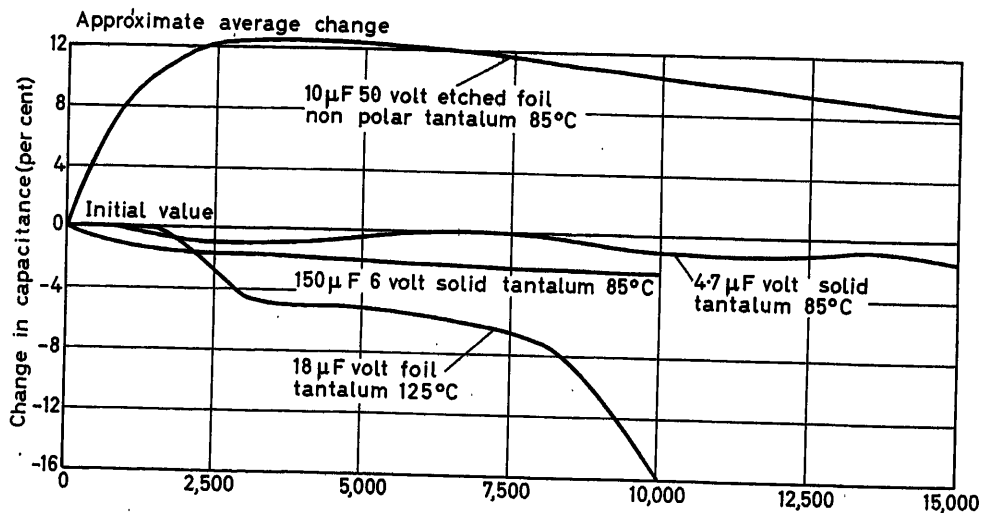


Figure 1 (b). Tantalum electrolytic capacitors (by courtesy of Sprague Elec., U.S.A.)

THE RELIABILITY OF ELECTRONIC COMPONENTS

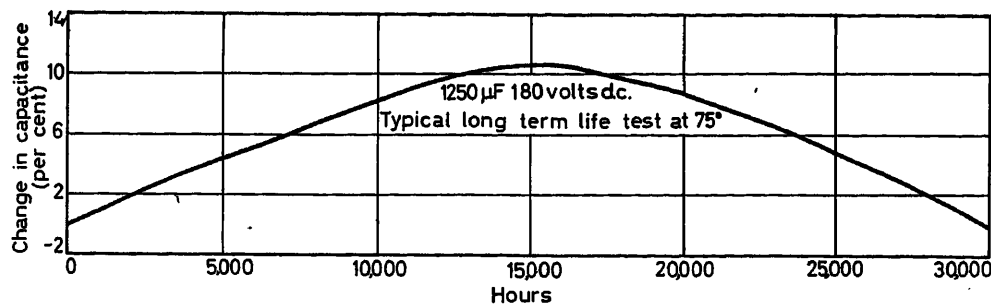


Figure 1 (c). Aluminium electrolytic capacitor (by courtesy of the Mallory Co., U.S.A.)

Table 1. Fault Data from R.R.E. Data-handling Equipment
(Period 1st October, 1959, to 31st March, 1962)

Component	Quantity	Component h	Failures		Failure rate per cent/1,000 h	
			Catastrophic	Degraded	Catastrophic	Overall
Transistors, all types	70796	8706 $\times 10^5$	168	264	0.0192	0.0496
Input TS7	9152	1134 $\times 10^5$	18	19	0.0159	0.0326
Output TS7	9152	1134 $\times 10^5$	95	20	0.0838	0.1014
GT 11	26362	3086 $\times 10^5$	28	189	0.0091	0.0703
OC 45	14204	1843 $\times 10^5$	14	7	0.0076	0.0114
OC 76	8352	1097 $\times 10^5$	6	5	0.0055	0.0100
OC 77	1876	211 $\times 10^5$	5	22	0.0237	0.1279
Other types	1689	201 $\times 10^5$	2	2	0.0099	0.0199
Transformers	13934	1797 $\times 10^5$	35	—	0.0195	0.0195
Capacitors, all types	97189	11941 $\times 10^5$	15	3	0.0013	0.0015
Metallized paper	25008	3227 $\times 10^5$	—	2	<0.0003	0.0006
Tantalum	1133	148 $\times 10^5$	—	—	<0.0067	<0.0067
Electrolytic	896	114 $\times 10^5$	6	2	0.0526	0.0702
Polystyrene film	68385	8231 $\times 10^5$	7	1	0.00085	0.00097
Other types	1767	221 $\times 10^5$	—	—	<0.0045	<0.0045
Diodes, all types	277210	33734 $\times 10^5$	64	65	0.0019	0.0038
CV 448	242100	29404 $\times 10^5$	36	49	0.0012	0.0029
OR 10	32674	4072 $\times 10^5$	21	12	0.0052	0.0081
Zener	42	4 $\times 10^5$	—	—	<0.25	<0.25
Silicon	966	112 $\times 10^5$	5	4	0.0446	0.0804
OR 5	1428	1415 $\times 10^5$	2	—	0.0014	0.0014
Relay contacts	9001	1215 $\times 10^5$	2	—	0.0016	0.0016
Potentiometers	32	4 $\times 10^5$	1	—	0.25	0.25
Carpenter relay	216	16 $\times 10^5$	67	—	4.1875	4.1875
Printed cards	36071	4424 $\times 10^5$	11	—	0.0025	0.0025
Resistors, all types	408988	49969 $\times 10^5$	12	—	0.00024	0.00024
Precision wirewound	1504	178 $\times 10^5$	2	—	0.0112	0.0112
Grade 1	129659	15809 $\times 10^5$	9	—	0.00057	0.00057
Grade 2	277825	33983 $\times 10^5$	1	—	0.000029	0.000029
Valves	972	93 $\times 10^5$	15	—	0.1613	0.1613
Lamps	3177	393 $\times 10^5$	277	—	0.7048	0.7048
Plugs and sockets	662112	80471 $\times 10^5$	29	—	0.00036	0.00036
Tags	441408	53648 $\times 10^5$	5	—	0.000093	0.000093
Contacts	220704	26824 $\times 10^5$	24	—	0.00089	0.00089
Soldered joints	2358708	186775 $\times 10^5$	74	—	0.00040	0.00040
Total components excluding plugs and sockets and soldered joints	917586	112292 $\times 10^5$	667	332	0.00594	0.00890

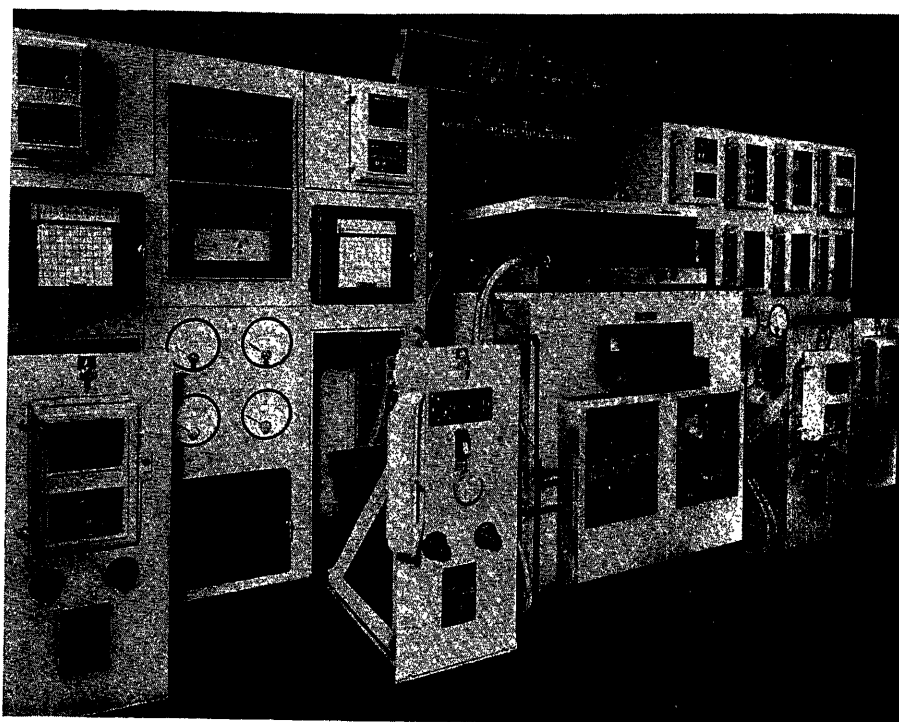


Figure 2. General view of automatic component testing equipment at the Royal Radar Establishment
(Reproduced by permission of the Controller, H. M. Stationary Office. Crown Copyright Reserved)

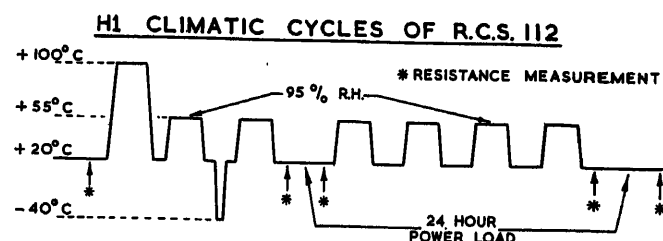
reduced. At the time of writing this paper, preliminary results only of the first year's storage tests are available; these show that paper dielectric capacitors and carbon composition resistors show reduced changes when stored at -20°C rather than at room temperature ($+15^{\circ}\text{C}$).

Component Reliability Evaluation by Automatic Testing

Qualitative data has been obtained in the United Kingdom on individual components by the use of automatic testing machines. The equipment shown in Figure 2 is designed to obtain statistical data over a wide range of loading and operating conditions, for a large number of fixed resistors, by automatic cycling, the programme of test being fed initially on to a tape which thereafter controls the entire sequence of operations, including the recording of results. This equipment has now completed tests on some 24,000 resistors of many types and it is interesting to compare the failures of the most commonly used component, the fixed resistor, under identical test conditions. These are shown in Figure 3, and from this work an order of reliability can be given in the United Kingdom for the various classes of resistor under military conditions.

Two machines have now been constructed at the Electrical Research Association's laboratories—under contract from the Royal Radar Establishment—to give accelerated testing of resistors in batches of 1,200. This method ensures the rapid production of faults so that the mechanism of breakdown can be examined. This is being done by subjecting the resistors to three test sequences; one to reveal thermal expansion faults, one to reveal moisture penetration, and one to reveal electrochemical corrosion.

An automatic relay testing machine has recently been constructed, in which the contact resistance of a relay is rapidly measured under dry circuit conditions (i.e. less than 10 mV open circuit voltage) at every operation during a life test of several million operations. In 24 h 864,000 operations are carried out, with the relay operating at approximately 10 operations/sec. The test equipment is transistorized and the only mechanical



OVERALL SUMMARY OF MASS RESISTOR TESTING AT RRE				
TYPE	QUANTITY TESTED	OPEN CIRCUIT	OUTSIDE SPECIFICATION LIMIT	TOTAL FAILURE RATE
OXIDE FILM TO RCS (PROV) 114	2000	0	2	0.1 %
CARBON COMPOSITION	6000	0	6	0.1 %
OXIDE FILM TO RCS 112	1000	2	3	0.5 %
WIRE WOUND VITREOUS ENAMELLED	2000	11	38	2.45 %
METAL FILM	3000	20	74	3.13 %
CRACKED CARBON	10,000	541	1247	17.88 %

Figure 3. (Reproduced by permission of the Controller, H. M. Stationary Office. Crown Copyright Reserved)

THE RELIABILITY OF ELECTRONIC COMPONENTS

Table 2. Summary of Failures (Yearly) on Components in use at the United Kingdom Atomic Energy Research Establishment at Harwell

	Percentage failure per annum										
	1949	1951	1952	1953	1954	1955	1956	1957	1959	1960	1961
Valves	4.2	3.3	4.7	4.0	3.2	2.5	4.96	6.1	3.4	2.6	6.16
Rectifiers	6.8	6.5	9.4	8.0	9.1	6.69	6.91	7.58	7.52	7.62	9.46
Double diode and double triode	3.5	3.0	4.0	4.2	4.1	4.8	5.42	7.2	2.7	1.574	0.8
Pentodes	5.8	2.9	4.2	2.6	2.67	5.6	5.96	7.99	4.09	2.08	3.07
Stabilizers	1.7	3.0	4.5	4.0	4.18	1.53	1.56	1.74	1.63	1.36	1.46
Miscellaneous	—	—	4.0	2.0	—	—	—	—	0.6	0.02	0.11
Resistors	0.54	0.27	0.20	0.30	0.39	0.25	0.2	0.21	0.1	0.1	0.13
High stability	0.45	0.37	0.30	0.4	0.73	0.64	0.45	0.43	0.208	0.12	0.23
Carbon composition	0.65	0.26	0.15	0.24	0.25	0.1	0.1	0.09	0.057	0.05	0.06
Wirewound	0.55	0.16	0.12	0.14	0.3	0.2	0.19	0.17	0.116	0.06	0.05
Potentiometers	0.11	0.26	0.27	0.24	0.22	0.19	0.19	0.19	0.03	0.03	0.06
Capacitors	1.1	0.19	0.31	0.14	0.16	0.13	0.33	0.36	0.16	0.08	0.07
Paper	1.9	0.20	0.37	0.14	0.22	0.15	0.15	0.11	0.107	0.07	0.07
Ceramic	0.45	0.06	0.08	0.14	0.14	0.04	0.04	0.08	0.09	0.06	0.02
Mica	0.18	0.04	0.1	0.08	0.12	0.09	0.03	0.1	0.09	0.05	0.05
Electrolytic	1.0	0.71	0.95	0.3	0.95	1.11	1.12	1.17	1.74	0.61	0.42
Transformers	18.0	2.6	1.8	1.4	2.0	0.9	0.99	0.83	1.03	0.61	0.67
Relays	1.9	0.48	0.68	0.54	0.52	0.3	0.4	0.62	1.37	0.98	0.74
Switches	0.88	0.31	0.45	0.32	0.22	0.2	0.22	0.19	0.92	0.13	0.16
Chokes	1.1	0.17	0.23	—	0.16	0.12	0.12	0.17	0.92	0.16	0.25
Metal rectifiers	—	1.3	1.4	1.0	0.61	0.68	0.7	0.35	0.16	0.55	0.20
Meters	3.1	1.5	0.85	1.2	1.28	0.71	0.75	0.65	0.18	0.43	0.13
Totals (all components)	1.20	0.59	0.72	0.67	0.65	0.58	0.96	1.05	0.52	0.48	0.42

devices used are the operation counters which show the number of coil energizations, number of contact operations and number of contact resistance failures. A pen recorder indicates the passage of time.

Results to date show that a miniature two-compartment sealed relay designed for use in missiles, and which is to be used in automatic landing of commercial air-liners, has a contact resistance which never exceeds 30 mΩ while switching low-level circuits more than a million times. A single-compartment sealed relay was shown to increase its contact resistance by a factor of ten, from 20–200 mΩ, within 300,000 operations under precisely the same conditions of test.

Further machines of this kind are to be used for component evaluation; e.g., an automatic precision potentiometer tester has been constructed in which the linearity of a potentiometer can be evaluated to an accuracy of 0.05 per cent in approximately 2 min.

Techniques for Improving the Reliability of Components

There are three ways of improving the effective reliability of components: (1) improvements in the quality of conventional components, (2) the use of cooling techniques for temperature stabilization of good conventional components, and (3) the use of microminiaturization techniques, with close control of manufacture using high purity materials.

Improvements in the Quality of Conventional Components

The development of a range of high quality components in the United Kingdom was originally allied specifically to guided missile requirements and placed special emphasis on adequate performance of components under vibration and shock. Since

then it has been found necessary to extend the work on these components to include all military requirements as a natural corollary to the increasing complexity of military equipments in

Table 3. Failures of Components in Radar Equipments Under Environmental Tests at R.R.E.

	Year	Total components	Total failures	Overall failure %
Humidity Tests	1944	2983	106	3.6
	1945	4759	137	2.9
K. 114 Issue 1	1946	1617	58	3.6
	1947	1472	67	4.5
	1948	1871	40	2.1
	1949	1165	28	2.4
	1950	3150	66	2.1
K. 114, Issue 2	1951	1984	19	1.0
	1952	693	16	2.3
	1953	1456	27	1.9
	1954	1644	25	1.5
	1955	2393	29	1.2
	1956	5033	43	0.9
	1957	3673	71	1.9
	1958	2620	26	1.0
	1959	3028	22	0.72
	1960	3800	18	2.0*

Average 2.1 per cent per approx. 1,000 h

* Due to one specific equipment design.

Table 4

<i>Component</i>	<i>Environment</i>	<i>Effect</i>	<i>Mechanism of failure</i>
Resistor, fixed, carbon composition, solid	High humidity	Increase in resistance (particularly low values)	Absorption of moisture causing swelling of binder and separation of carbon particles
	High temperature	Decrease in resistance (to ultimate short circuit under excessive temperatures)	Gradual carbonization of binder
Resistor, fixed, carbon composition, film	High humidity	Small where adequate sealing is given, but resistance increases with time to eventual O/C	Absorption of moisture between film and substrate with consequent lifting and disintegration of film
	High temperature	Decrease in resistance, rapid initially (first 200 h), progressively less thereafter	Drying out of binder
Resistor, fixed, cracked carbon	High humidity	Depending on sealing, increase in value and open circuits	Electrolysis of film (with d.c.) electrochemical corrosion causing gradual erosion
	High temperature	Slight decrease in resistance and possible O/C	Disintegration of film
Resistor, fixed, wirewound general purpose	High humidity	Depends on enamel protection; possible open circuit	Electrochemical corrosion of wire with d.c. through cracks in enamel coating
	High temperature	Negligible	
Resistor, fixed, wirewound precision	High humidity	Highly dependent on sealing, possible open circuits	Corrosion of wire
	High temperature	Possible short circuit	Due to insulation breakdown
Resistor, variable, carbon composition, film	High humidity	Depends on sealing; increase in resistance, decrease in insulation resistance and open circuits	(a) swelling of former and binder of track (b) erosion of track (c) corrosion of terminal connections (d) rusting of metals
	High temperature	Decrease in resistance (small) and decrease in insulation resistance	Carbonization of binder and eventual burn-out of track or distortion of former
Resistor, variable, carbon composition, moulded	High humidity	Depends on sealing; increase in resistance, decrease in insulation resistance and possible O/C	Swelling of moulding, corrosion of terminal connections, rusting of metals
	High temperature	Decrease in resistance (small)	Gradual re-curing of moulding material
Resistor, variable, wirewound general purpose	High humidity	Depends on sealing; possible open circuit	Corrosion of wire, rusting of metal parts
	High temperature	Slight increase in resistance Ceramic former—negligible Plastic former—possible O/C	Temperature coefficient effect and possible distortion of track. Distortion of former
Resistor, variable, wirewound, precision	High humidity	Unless sealed, change in value and eventual O/C	Corrosion of wire, rusting of metal parts
	High temperature	Possible change in value and O/C Resolution affected	Distortion of former
Capacitor, fixed, impregnated paper	High humidity	Depends on sealing. Possible reduction in I.R., eventual S/C	Absorption of moisture ions into paper
	High temperature	Possible eventual S/C	Carbonization of paper
Capacitor, fixed, mica	High humidity	Depends on sealing. Possible decreased I.R. and increased power factor	Moisture absorption by case material
	High temperature	Initial decrease in I.R. depending on case material, followed by cracking and S/C	Initial re-curing of case material followed by charring

THE RELIABILITY OF ELECTRONIC COMPONENTS

Table 4 — continued

Component	Environment	Effect	Mechanism of failure
Capacitor, fixed, plastic	High humidity	Highly dependent on sealing and on dielectric Reduction in I.R. and increase of power factor	Absorption of moisture ions
	High temperature	Depends on dielectric—Polystyrene softens at 85° C, Melinex at 130° C, Polycarbonate at 120° C, and P.T.F.E. at 250° C	Plastic flow of dielectric
Capacitor, fixed, glass	High humidity	Depends on sealing. Possible reduction in I.R.	Moisture absorption
	High temperature	Negligible up to 150° to 200° C	—
Capacitor, fixed, ceramic	High humidity	Depends on sealing and on dielectric Possible reduction in I.R., increase in power factor	Moisture absorption
	High temperature	Depends on dielectric. Decrease in capacitance for high <i>K</i> capacitors. On others depends on temperature coefficient (+ or —)	Change in permittivity
Capacitors, fixed, electrolytic, aluminium foil	High humidity	Depends on sealing. Possible increase in leakage current and loss angle	Possible deterioration of electrolyte
	High temperature	Increase of losses above 85° C with consequent heat generation and eventual explosion	Generation of gases
Capacitor, fixed, electrolytic, tantalum foil	High humidity	Depends on sealing. Possible decrease in I.R. and increased leakage current	Possible deterioration of electrolyte
	High temperature	Increase of losses above 85° C. Loss in capacitance	Electrolyte may dry out
Capacitor, fixed, electrolytic, tantalum pellet	High humidity	Depends on sealing. Stud types satisfactory; tubular types, possible increase in leakage current and reduced I.R.	Possible deterioration of electrolyte
	High temperature	Stud type satisfactory to 150° C Tubular type limited to sealing method	Possible seepage of electrolyte
Capacitor, fixed, solid tantalum electrolytic	High humidity	Depends on sealing, but effects less than in other types	—
	High temperature	Satisfactory to 125° C	—
Transformer, power, pulse and audio types	High humidity	Fully sealed—satisfactory Unsealed—reduction in I.R. and corrosion of wires with consequent O/C	Wire corrosion
	High temperature	Generally satisfactory to 110° C. Possible deterioration of insulation with consequent S/C and burn-out. Oil filled types may burst	Charring of insulation (e.g., paper)
Inductor and transformer, R.F. and I.F. types	High humidity	Flatter tuning response and 'Q' reduced Disconnection of leads	Lowering of insulation resistance Corrosion of fine wire
	High temperature	Mechanical failure. Possible damage to ferrite cores	Melting of wax or polystyrene impregnant Loss of magnetic properties

Table 4 — continued

Component	Environment	Effect	Mechanism of failure
Relay, general purpose (unsealed type)	High humidity	Lowering of coil insulation and eventual O/C	Absorption of moisture and corrosion of wire
	High temperature	Low I.R. between springs Increase of coil resistance Change in operating characteristics Operate time decreases Release time increases	Moisture absorption Temperature coefficient effects Reduction of spring tension " " " " " " " "
Relay, general purpose (sealed type)	High humidity	Depends on sealing. With d.c., seals may deteriorate	Electrolytic corrosion of seals
	High temperature	Depends on sealing. With d.c., seals may deteriorate	Possible electrolytic corrosion of seals
Switches, toggle types and microswitches	High humidity	Depends on sealing. Reduction in I.R. and corrosion of metal parts. Increase in contact resistance	Moisture absorption
	High temperature	Unstable operation	Relaxation of spring tension
Switches, rotary	High humidity	Depends on sealing. Reduction in I.R. and corrosion of bearings and metal parts. Increase in contact resistance	Absorption of moisture
	High temperature	Unstable operation	Relaxation of spring tension
Plug and socket, general purpose, multipole (subject to handling hazards)	High humidity	Reduction of I.R. between contacts and contacts and shell; corrosion of metal parts	Absorption of moisture
	High temperature	Depends on moulding materials but generally reduction in I.R., increase of contact resistance	Degradation of dielectric; relaxation of spring tension
R.F. connectors	High humidity	Loss of power	Ingress of moisture between dielectric and case
	High temperature	Reduction in I.R. Alteration in V.S.W.R.	Deterioration of dielectric Distortion of dielectric
Printed wiring plug and sockets (Low insertion forces and voltages raise problems due to surface film contamination)	High humidity	Leakage between printed wiring and contacts. Reduction in I.R.	Absorption of moisture into base material
	High temperature	Low I.R. depending on material High contact resistance	Mechanical distortion, due to inadequate curing; warping of plug-boards; relaxation of spring tensions
Variable capacitors, air spaced	High humidity	Lowering of I.R. and alteration in capacitance	Corrosion between dissimilar metals
	High temperature	Change in capacitance	Differential expansion of metals
Variable capacitors, trimmers	High humidity	Depends on dielectric Ceramic } possible change in capacitance Mica } Plastic }	Absorption of moisture into dielectric or case
	High temperature	Reduction of I.R. and change in capacitance	Deterioration of dielectric properties or case
Terminals and seals	High humidity	Glass/metal—Low I.R. and possible disintegration Ceramic metal—Low I.R. Plastic—Low I.R. depending on plastic	Electrochemical corrosion with d.c. Migration of silver Absorption of moisture
	High temperature	Glass and ceramic satisfactory Plastic—lowering of I.R.	Change in material

all fields. The programme is based on a full analysis of data available on all manufacturers making a particular type of component and the selection of one manufacturer whose product shows itself to be superior to all others. The product of the selected manufacturer is then subjected to a wide range of tests to establish what improvements are necessary to increase its reliability still further. Some typical examples of improvements made as a result of these tests are given below.

Moulded Resistive Track Potentiometers—Quality control of carbon powder, particle size and distribution of particles within the resin mix to improve stability of the resistive track and limit shift of resistance under adverse conditions to a maximum of 5 per cent. Introduction of hollow solder spills and improved method of 'staggering' into track to reduce (a) bubbling of track around terminations when misuse of soldering iron occurs, and (b) strain between terminations and track. A boss on the base of the potentiometer to remove a random distribution of hairline cracks appearing when clamped to printed boards. A different configuration of the wiper to shift resonant frequency from 400 c/sec to 3 kc/sec and to reduce contact noise.

Oxide Film Resistors—Marginal improvements by a change in the protective lacquer and a better end termination cap and connection to end wires.

Wirewound Resistors—An improvement in the uniformity of fine resistive wires; better quality control of the protective enamel; considerably more inspection points on the production line, and collection and analysis of inspection and test data.

Composition Grade 2 Resistors—A method to obtain better alignment of the moulding tools in order that the encapsulation was uniformly distributed around the resistive element and to maintain a more uniform strength factor of end terminations.

Tantalum Foil Capacitors—An increase in mechanical strength of the internal support of the winding. Increasing the temperature capability from 85° to 125° C.

Sintered Tantalum Anode Capacitors—An improved method of mounting of stud to cathode. More uniform distribution of silver particles within the cathode cup to eliminate transient short circuits at high levels of vibration. Application of a vibration test before assembly to remove loose particles.

On the basis of the data accumulated, a procurement specification is written, including quality and process control and end product testing, intended to weed out potential failure. It also specifies tight limits of Acceptance Quality Levels. The procurement specifications are then applied to the full production line of the manufacturer for an approximate period of 12 months to allow him sufficient time to gain experience and to accumulate production data, so that he can maintain the quality of the product within the close limits set by the A. Q. L. This programme is now being applied to the more recently developed components such as oxide film resistors, miniature two-compartment sealed relays, solid tantalum electrolytic capacitors, polycarbonate film capacitors, etc. Although the specifications are originally written around one selected manufacturer for a given product, other manufacturers have the opportunity to meet the specification by improving their quality to the level required.

The Use of Cooling Techniques

In aiming for extreme reliability, it is logical to consider the concept of a controlled environment, in which the electronic

circuits are isolated from external change in temperature, humidity, shock, vibration—and human interference.

Thermal engineering is perhaps the most neglected part of conventional electronic equipment design. Cooling is essentially a problem of collecting heat from certain components and then transporting it away from the equipment. Air is not very efficient for this purpose, and is also inadequate in more severe thermal conditions. Liquid cooling is much more effective in this respect.

In the United Kingdom, the indirect liquid-cooling method, using a closed circuit, shows much promise as a practical reliable method of achieving temperature stabilization (see *Figure 4*). The system has been applied successfully to experimental military equipments, and to a commercial data-handling installation.

The equipment is thermally insulated from its surroundings, and an innocuous coolant (*Coolanol 45*) is circulated through a chassis constructed from roll bonded ducted aluminium. Thus the coolant passes close to the heat sources, as near as is possible unless resort is made to direct immersion liquid cooling, which presents some maintenance problems and a weight penalty.

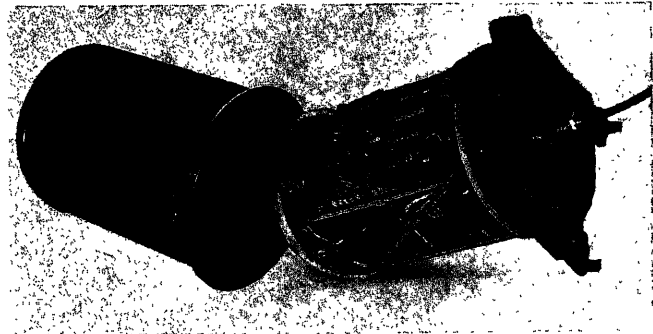


*Figure 4. Liquid-cooled chassis (Royal Radar Establishment)
(Reproduced by permission of the Controller, H. M. Stationery Office.
Crown Copyright Reserved)*

Whenever possible, heat is transferred by conduction from components to chassis; semiconductor devices can be efficiently cooled on ducted chassis.

Quick-release self-sealing couplings are used to connect the small bore coolant lines to the equipment, so that units can be changed for maintenance purposes without any wet contact. Nylon tubing has been used successfully to convey the coolant.

The possibilities of failure of the cooling system itself have been investigated and the inherent reliability is considered to be many orders better than the electronics. It is, however, possible to duplicate the pump and control valve systems if ever required.

An interesting life reliability experiment is being carried out on two sets of an established airborne electronic equipment, one as normally supplied with air-cooled covers, the other fitted with replacement insulated liquid-cooled covers. The equipment was operated on a duty cycle of 4 h on, 2 h off. In the first 1,000 h of test, the environmental temperature was varied from -40° to +55° C, and the heat exchanger rejection fluid was maintained at 20° to 25° C. Ten faults occurred in the air-cooled units, only one in the liquid-cooled units, and in the latter the circuit performance characteristics showed much less variation.

The transistorized radar display and data-handling system, designed by Decca Radar Ltd., is an excellent example of

components operating in a controlled environment (see Figure 5). Test results on the prototype, over a 10,000 h period, fully justify the design. With approximately 3,000 components at risk, only two faults have occurred in this period, during which the environmental temperature has ranged from -5° to $+45^{\circ}$ C, and humidity from 10 per cent to 90 per cent. The two faults referred to both involved transistors of a type now considered obsolescent.

In this equipment, there is stabilized temperature and controlled humidity at the components, thermal insulation from external temperature changes, and locked cabinets to prevent unauthorized human interference. At the same time, accessibility is good for genuine maintenance adjustments. The components

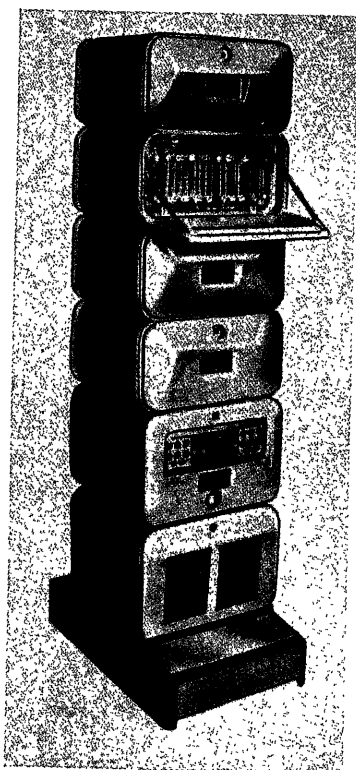


Figure 5. Liquid-cooled data-handling equipment (by courtesy of Decca Radar Ltd)

are mounted on normal printed boards, having an aluminium surround to act as a heat sink for transistors. A number of these assemblies slide into a cabinet formed from ducted aluminium, special precautions being taken to ensure good conduction contact. The external surface of each cabinet is insulated with about 1 in. of moulded glass fibre material. Each cabinet includes one circuit for temperature control, using a thermistor sensing element, and one for humidity. The nominal temperature in each cabinet is 15° C, and throughout the 10,000 h test, the temperature drift at any individual component does not exceed $\pm 0.25^{\circ}$ C.

The liquid coolant, in this case a heat transfer hydro-carbon oil, is circulated on demand from a reservoir store maintained at about 5° C. The store is in turn cooled by a small domestic sealed compressor type refrigerator, evaporating at about 2° C on a conservative duty cycle. Final heat rejection can be either to air or via a liquid-liquid heat exchanger to water.

A supply of dry air, a by-product of the refrigerator, is provided to pressurize the cabinets slightly and prevent ingress of moist air and dust.

The design approach for this ground equipment is relatively simple, yet highly reliable and easily maintained, and offers a controlled environment for an electronic equipment that will have to operate in a variety of climates.

The Use of Microminaturization Techniques

The reasons for the desired reliability improvement can be summarized as: better process control, less processes and purer materials. In the United Kingdom two systems have been developed; thin film microcircuits by vacuum deposition and semiconductor solid circuits.

Vacuum processes have a number of advantages in that conductors, resistors and capacitors can all be laid down by the same type of process in similar equipment, thus reducing handling during manufacture. As the process is carried out in a vacuum, the deposition takes place under clean conditions and many of the interconnections can be made *in situ*, the exception being the connections to active elements and the input and output connections.

It has been decided that a realistic approach to the problem of evaluation of microminiature component reliability is a combination of small-scale statistical testing, followed by a detailed study of all the properties and processes which could have a bearing on the ultimate reliability before final production. A behaviour study is therefore being made entailing the measurement of electrical, chemical and mechanical properties of the components. A study is also being made of failure mechanisms on large numbers of components under actual operating conditions and also under conditions likely to accelerate failures. It is felt that this is a critical phase in the design of the equipment and that this is the stage at which weaknesses must be eradicated.

The actual construction of a digital integrator for use in guided missile systems is shown in Figure 6, and the layout of a typical microcircuit plate is shown in Figure 7; a failure rate of 0.01 per cent/1,000 h per component has been specified. The complete equipment consists of some 389 transistors, 1,660 resistors, 832 diodes and 587 capacitors.

The packing density, including interconnections, adequate heat dissipation, etc., works out at about 250 components/1 in.³, which, with the size of the transistors used at the moment, seems

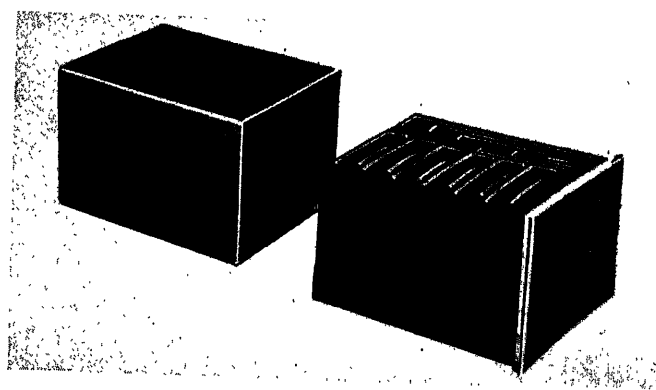


Figure 6. Fully sealed module, $1\frac{1}{2}$ in. \times 1 in. \times 2 in. containing half adder (by courtesy of Mullard Ltd)

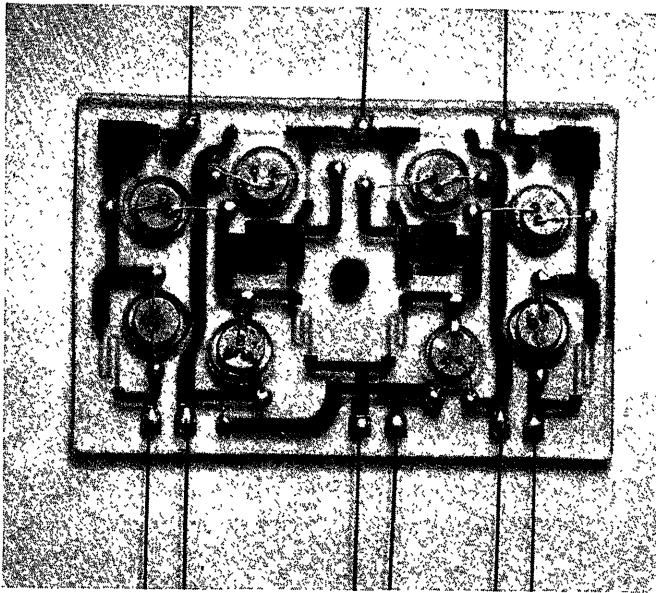


Figure 7. Typical microcircuit plate, 3 cm x 2 cm (by courtesy of Mullard Ltd)

to be a reasonable limit of packing density. The consumption of the whole unit is approximately 1 W at 6 V.

The reliability required (i.e., 0.01 per cent failure/1,000 h per component), can only be stated quantitatively if measured. The confidence with which one can state reliability after having tested for it depends on the number of components tested. For reliabilities of 0.01 per cent and confidence limits in the 90 per cent region, the numbers of components to be tested become large and costly (30,000–35,000), based on Biometrika tables. A more useful approach might be to lower the confidence level to, say, 50 per cent when the number to be tested becomes more manageable. The test would then be more for a negative result than a positive one. Failure on 50 per cent confidence at 0.01 per cent would mean that the expenditure on 95 per cent confidence testing would have been pointless, whereas success at such a confidence level would give the foundation and justification for further testing.

As large-scale production is established, more components will become available for reliability testing and hence greater emphasis will then be placed on this type of testing.

Preliminary tests indicate that the weakest link will in all probability prove to be the transistors. At present, germanium transistors enclosed in metal cans approximately 0.125 in. dia. and 0.05 in. thick are being used. Poor reliability could be expected from encapsulation failures or failures in the nine connections between the semiconductor slice and the thin film circuit element.

Planar or planar epitaxial transistors offer many advantages from the circuit point of view and would considerably reduce the possible points of failure previously mentioned, in that no encapsulation should be required, thus reducing the number

of connections between the semiconductor and circuit elements and eliminating the old problem of sealing small metal cans. Although it is not at present feasible to vacuum-deposit active devices, current work on epitaxial growth of semiconductors and on space charge limiters and dielectric devices indicates the probability that active devices will be available within a few years.

Solid Circuits

The most promising hope for long-term reliability is by the use of crystals of silicon treated to provide resistors and capacitors in addition to transistors and diodes. The technique has been previously described and the process is one of precision masking, etching and diffusion techniques. As the final circuit is one homogeneous material, differential expansions and interface connection problems are reduced. The number of internal connections is reduced to a minimum and if temperature controlled, the reliability should be extremely high. An example of a computer built of solid circuits is that made by Texas Instruments in the U.S.A., in which 587 solid circuits containing the equivalent of 8,500 conventional components, are encompassed in a space of 6.3 in.³, weighing 10 oz. This miniature computer adds, subtracts, divides, multiplies and provides square root functions at a clock rate of 100 kc/sec.

Redundancy

One of the main advantages of microminiature techniques is that they permit the use of redundancy techniques to their full extent. Although not yet fully exploited, this is a technique which is considered to be of fundamental importance in both the conventional component and microminiature techniques. A study of parts redundancy, feedback redundancy and circuit redundancy should be very rewarding.

Conclusions

The philosophy of temperature stabilization to prolong the life of components is strengthened by the known reduction in the lives of transistors, resistors, capacitors, etc., when operating at temperatures above 15° or 20° C. If 'worst case' design of circuits is included to permit possible tolerance variations in addition to derating and some redundancy, then it is considered that the reliability will be as high as possible with conventional components.

If one now adds microminiature techniques, in particular solid circuits, with increased redundancy because of the small size, uses 'worst case' design intelligently and then temperature stabilizes the computer, then it is suggested that the maximum reliability, as far as can be seen at the moment, will be obtained.

Reference

- ¹ DUMMER, G. W. A., and GRANVILLE, J. W. *Miniature and Microminiature Electronics*. London; Pitman

DISCUSSION

H. SCHENKEL, *Standard Telephones and Radio A.G., Seestr. 395, Zürich 2/38, Switzerland*

The failure rate data for the various components of data-handling equipment given in Table 1 of the paper is of great interest particularly since it covers so many different components and a fairly large quantity of each of them. Does the author have any information on the respective failure rates of germanium and silicon transistors? Secondly, since in Table 1 there were included only 42 Zener diodes resulting in an estimate of maximum failure rate, are there any more recently gathered data on Zener diodes? And thirdly, concerning diodes other than Zener, the table seems to indicate that Si diodes are worse than Ge diodes. Would this be the result of different technologies used in manufacture of these diodes and are there any recent failure rate data on diodes?

G. W. A. DUMMER, *in reply*

With regard to the failure rates of germanium and silicon transistors, I would give the following as being more up to date than those quoted:

Failure Rates

Alloy germanium transistors	0.1 % per 1,000 h
Alloy silicon transistors	0.05 % per 1,000 h
Planar silicon transistors	0.005 % per 1,000 h

Similarly, in answer to the question regarding diodes, present failure rates are:

Germanium point contact diodes	0.05 % per 1,000 h
Silicon alloy diodes	0.01 % per 1,000 h
Silicon planar diodes	0.002 % per 1,000 h

It must be remembered that these figures apply to a ground-based electronic equipment at maximum ratings, and are given as a guide only.

In reply to the last question, the silicon diodes used in the equipment were early samples and present-day results show better reliability for silicon planar diodes than any other type.

P. T. BELLAMY, *Talstrasse 12, Zollikerberg/ZH, Zürich, Switzerland*

Reliability is allied to:

(1) The education of the engineer using or misusing the components, e.g. mounting systems and soldering techniques used.

(2) The policy of the firm producing electronic equipment is also referred in the quality and reliability of the final product, e.g. amount of environmental testing environment encountered.

G. W. A. DUMMER, *in reply*

I do not think Mr. Bellamy is putting a question, but rather stating a fact, and I would agree entirely that the design engineer plays a very important part in determining the reliability of the equipment.

The policy of the firm producing the equipment is also most important as, in general, it is more costly to produce a reliable product than an unreliable one.

S. YEN, *The Electrical Research Institute, Peking, China*

(1) To how many kinds of electronic components can you apply the reduced-temperature storage method? What is the optimum temperature? In sending in and taking out components to and from storage, how do you programme the increase and decrease of temperature? What about the long-term storage of transistors?

(2) What is the relation between the speed of increasing and decreasing of environment temperature and the failure of components?

(3) How is the sampling of the components done in dealing with reliability test?

G. W. A. DUMMER, *in reply*

(1) I assume Mr. Yen's question refers to the low temperature storage of electronic components and in reply to his first question, a large number of different types of components were stored at temperatures of +15°C, 0°C and -20°C. The types of components were:

Fixed Resistors Wirewound
Carbon composition
Cracked carbon
Metallic film, and
Oxide film types

and

Fixed Capacitors Paper dielectric
Silver mica
Ceramic, and
Electrolytic types

in addition to small assemblies containing transistors, packaged in various ways. There does not appear to be any optimum temperature for measurements of data. The increase and decrease of temperature is not programmed, but maintained steady at the three temperatures given. The long-term storage of transistors has not yet shown any significant result.

(2) I presume the question refers to the effect of temperature on rating of components. It is known that high temperature accelerates failure mechanisms in many cases, and I would refer Mr. Yen to an article published in *British Communications and Electronics*, June 1963, p. 432, in which curves are given of the effects of temperature on failure rates.

(3) The sampling schemes used in dealing with reliability tests are the British DEF 131 Specification, which is equivalent to the U.S. MIL 105 A. Some useful information on this subject is given in the book *Electronic Equipment Reliability* by G. W. A. Dummer and N. Griffin, published by Messrs. Sir Isaac Pitman & Sons, London.

J. L. BARNES, *University of California, Los Angeles, U.S.A.*

I would like to say a few words in defence of the proper application of mathematics to reliability control as an answer to Mr. Dummer's question about how to use mathematics in the case of a component failure due to the presence of dandruff in it.

Naturally, mathematics will not handle many of the practical problems of physics and engineering since it is an abstract approach; nevertheless, it may help. At RCA, some years ago, failure of vacuum tubes assembled by women showed up stochastic effects and a 28-day periodic component. Correlation analysis was used. The peak of failure rate with the 28-day period was traced to the menstrual period of the women assemblers (who did not wear gloves).

Perhaps in Mr. Dummer's example a correlation with the period at which the assembler washed his hair, would show up the failures caused by dandruff.

G. W. A. DUMMER, *in reply*

I would like to thank Professor Barnes for his example given of failure of vacuum tubes, and it is the general practice in the U.K., as no doubt, in the U.S.A., for female operators to wear gloves or finger-stalls, and often caps in this kind of assembly work. In clean areas, special coats, gloves and caps are worn to eliminate human elements.

Professor Barnes is quite right and one could do an enormous amount of work of correlation on any one of these factors, but this would obviously involve doing it over a period of one year to establish diurnal and monthly characteristics.

H. WEISSMANN, *Techn. Hochschule, Welfengarten 1, Germany*

As to the reliability of components $p = \lambda t$, there are for the particular series very different indicated percentages, but not for the error distribution during the total life expectation after manufacture.

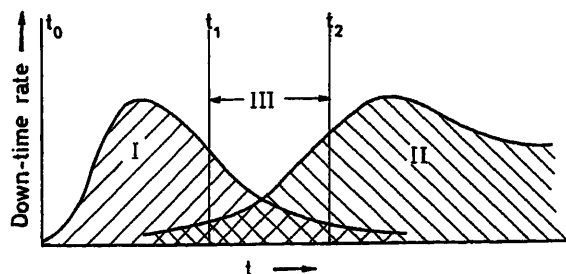


Figure A

As the curves in *Figure A* show, there are:

- I Down-time period of elements owing to physical effects
- II Down-time period of elements owing to application
- III Period of constant down-time minimum

This third period $t_1 - t_2$ should be determined more closely, since it is here that the period of application has to be chosen. Is there a possibility of a comment on this?

G. W. A. DUMMER, *in reply*

Professor Weissmann raises an academic question on two outstanding mechanisms of failure: (a) those due to inherent characteristics of each type of component; (b) those due to environment and type of vehicle into which the equipment is fitted.

In general terms (a) is usually, but not entirely, eliminated during the early failure period, and (b) will be largely decided during the life of the equipment, represented by the useful life period or the constant failure rate period λ .

The criterion $t_1 - t_2$ can only be established by large-scale, carefully controlled tests and this is being done on a modest scale in the United Kingdom.

Reliability Problems of Electromechanical Elements

B. S. SOTSKOV, I. E. DEKABRUN and L. S. KRIVOROTOVA

Summary

Contacts and coils are component parts of many modern automation elements. Operational experience shows that more than 50–60 per cent failures of contact switching devices occur because of the contact system and about 20–25 per cent because of coils. This requires study of the operational reliability of contacts and coils.

The paper discusses the physical and technical factors, stipulating the reliability of contacts and coils. As an example of an electro-mechanical system having contacts and coils, the electromagnetic relay is considered.

Sommaire

Les contacts et les enroulements sont des composants de dispositifs automatiques modernes. La pratique montre que plus de 50 à 60 pour cent des défauts qui affectent les relais, proviennent des systèmes de contacts, et que 20 à 25 pour cent des défauts sont dus aux enroulements. Cette constatation justifie une étude de la fiabilité des contacts et des enroulements.

Le rapport passe en revue un certain nombre de facteurs physiques et techniques qui influent sur cette fiabilité, et prend comme exemple le cas du relais électro-magnétique.

Zusammenfassung

Viele moderne Geräte für die Automatisierung enthalten als Einzelteile Kontakte und Spulen. Die Betriebserfahrung zeigt, daß mehr als 50 bis 60% der Ausfälle von Schaltgeräten auf das Kontaktsystem zurückzuführen sind und ungefähr 20 bis 25% auf die Spulen. Dies macht die Untersuchung der Betriebszuverlässigkeit von Kontakten und Spulen notwendig.

In diesem Beitrag werden die physikalischen und technischen Faktoren, die die Zuverlässigkeiten von Kontakten und Spulen bedingen, besprochen. Als Beispiel für ein elektro-mechanisches System mit Kontakten und Spulen wird ein Schütz näher betrachtet.

Factors Determining the Reliability of Contact Closure

The contact surface is not absolutely smooth, but is covered with projections of differing height and cross section. If the probability of failure of an elementary contact, formed by the projections of two contact surfaces which are brought together, equals q_x , then if there are M_x elementary contacts; the probability of failure of the contact as a whole will be defined as

$$q = \prod_{x=1}^{M_x} q_x$$

or, if q_0 is introduced as the mean value of the probability of failure of the elementary contact, then

$$q = q_0^{M_x}$$

The number of elementary contacts M_x depends on the force P_K with which the contacts are pressed against one another, and can be represented in the form

$$M_x = KP_K$$

where K is a coefficient determined by the nature of the machining, the state of the surface and the material of the contact. Therefore, the probability of failure in the operation of the contact is a function of the contact force

$$q = q_0^{KP_K}$$

These general propositions match up well with experimental findings (see Figure 1, where the relationship $q=f(P_K)$ is shown for silver contacts).

The mean value of the probability of failure for an elementary contact can be found as follows. The failure probability q_x depends on the pressure p in the following way:

$$q_x = 1 - \left(\frac{p}{\sigma_{\text{contort}}} \right)^\gamma$$

where σ_{contort} is the stress of contortion of the surface layer of the material of the contact, and γ is a coefficient determined

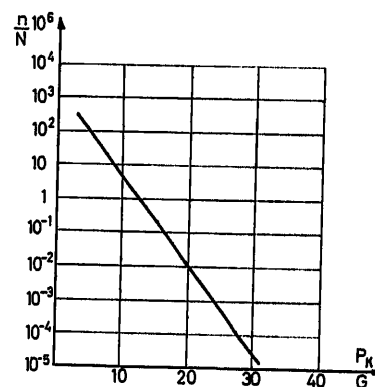


Figure 1

by the properties of the contact surface and the type of machining.

When $p \rightarrow 0$ the value of $q_x \rightarrow 1$, while when $p \rightarrow \sigma_{\text{contort}}$, $q_x \rightarrow 0$.

Thus the mean failure-probability value equals

$$q_0 = \frac{1}{\sigma_{\text{contort}}} \int_0^{\sigma_{\text{contort}}} \left[1 - \left(\frac{p}{\sigma_{\text{contort}}} \right)^\gamma \right] dp = \frac{\gamma}{\gamma + 1}$$

and is determined by the properties and type of machining of the contact surface.

Hence the reliability of contact formation, which equals

$$R = 1 - q = 1 - q_0^{KP_K}$$

depends on the magnitude of the contact force and the nature of the surface of the contact.

A change in the contact force may occur following a variation in the rigidity of the contact springs due to fatigue or overheating of the spring material, and also following a change in

the joint travel of the contacts as a result of their erosion in the course of operation.

A change in the state of the surface can occur either in the non-working state, because of corrosion, or in the working state, under the influence of corrosion and erosion.

Erosion of Contacts and Variation of Contact Force as a Result of Erosion

During the making and breaking of contacts liquid metal bridges may form, and electrical discharges might appear. Both these phenomena are accompanied by vaporization of the metal of the contact, and its transfer from one contact to the other, causing erosion of the contact surfaces. The magnitude and nature of the erosion depend on the voltage, current and kind of load (ohmic or inductive-ohmic) which the contacts are switching. When the contacts close, if the current in their circuit I is greater than some particular value I_{00} , there appear either 'short' electrical arcs or metal bridges. Both these phenomena cause erosion of the positive contact. When the contacts open, at very low currents ($I < I_{00}$) and voltages ($U < U_3$), where U_3 , equal to 270–300 V, is the minimal sparking voltage, there is no electrical erosion. With a current $I < I_{00}$ and voltage $U > U_3$ there appears a spark discharge which causes erosion of the negative contact. If $I_{00} < I < I_0$ and $U < U_0$, where I_0 and U_0 are the minimum current and voltages required for arcing, there appear only liquid metal bridges; when $I_0 < I < I_0$ liquid metal bridges appear first, and then 'short' arcs as well. Both these phenomena also induce wear of the positive contact. When $I_{00} < I < I_0$ and $U > U_3$, first there appear bridges, and erosion of the positive contact occurs, followed by sparking and erosion of the negative contact. When $I > I_0$ and $U > U_0$, bridges appear, and the positive contact is worn away, and then there appears an electric arc and the negative contact is worn. Figure 2 shows the areas of erosion of positive and negative contacts. The values of I_{00} , I_0 , U_0 and U_3 are determined by the material of the contacts and by ambient medium.

If the values of the currents at the moment of making and breaking I are known, as well as the magnitude of the voltage on the contact $U = E + U_{ov}$, where E is the voltage of the source and U_{ov} the magnitude of the overvoltage, the point with coordinates (i , U) will determine the form of erosion of the contact.

The total erosion G_0 over one cycle of operation of the contact (making-breaking) can be represented for the positive contact in the following form:

$$G_0 = G_{0M} + G_{0B} = [G_{MM} + G_{SAM}] + [G_{MB} + G_{SAB} + G_{AAB}]$$

where $G_{0M} = G_{MM} + G_{SAM}$ is the total erosion when the contact is made, $G_{0B} = G_{MB} + G_{SAB} + G_{AAB}$ is the total erosion when the contact is broken. G_{MM} is the erosion from the liquid metal

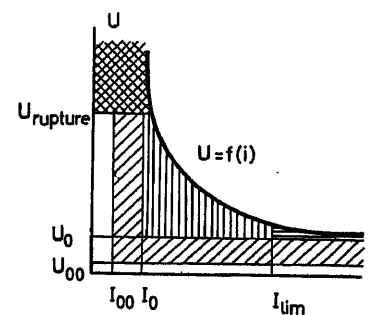


Figure 2

bridges during the making of the contact; G_{SAM} is the erosion from the 'short' arc during making; G_{MB} is the erosion from liquid metal bridges when the contact is broken; G_{SAB} is the erosion from the action of the 'short' arc during breaking, and G_{AAB} is the erosion from the action of the electric arc or spark during breaking. Formulae for calculating erosion are given in Table 1.

Irrespective of the material of the contact and the operating conditions, the magnitude of the total erosion G_N over N com-

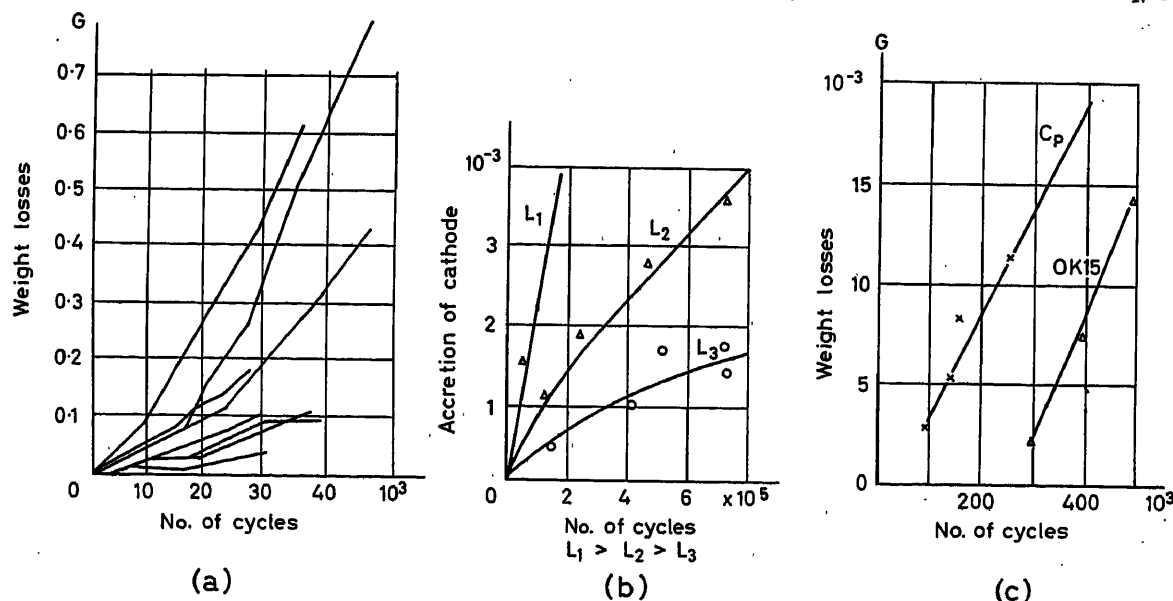


Figure 3. (a) Powerful arc; (b) arc; (c) bridge

mutations is directly proportional to the number of commutations (Figure 3), i.e.:

$$G_N = NG_0$$

The kind of erosion (bridge, arc, spark), and the type of material from which the contacts are made, determine the nature of the variation of the contact surface. Bridge erosion of noble non-oxidizable metals takes the form of long 'needles' on one contact and narrow cavities on the other. In basic metals, on the other hand, because of the oxidation of the molten ends of the bridges, the erosion is distributed over the entire contact surface in the form of minute 'droplets' and pits. Arc erosion has, for the most part, the form of wide protuberances and cavities concentrated at one spot. This paper examines the case of concentrated arc erosion.

Consider a contact of the 'plane-hemisphere' type, in which, as a consequence of erosion, there has been transfer of the material of the contact from the hemisphere on to the plane. In the process, a protuberance has formed on the plane, and a crater has appeared on the hemispherical contact surface. It will be considered that both the protuberance and the crater have a spherical shape. The volume of the worn part equals twice the volume of the spherical segment G_c , with a base radius a , equal to the radius of the crater, i.e.:

$$G = 2G_c = \frac{1}{3}\pi h(3a^2 + h^2)$$

where h is the height of the spherical segment (Figure 4).

The volume of the transferred part of the metal equals in all only

$$G = (1 - K')G$$

where $K'G$ is the part of the metal lost as a result of vaporization and spatter. Considering the protuberance to be also a spherical segment with height h' and base radius $a' \approx a$ it will be found that

$$G' = \frac{\pi}{2}h'\left(a^2 + \frac{1}{3}h'^2\right)$$

h and h' can be determined from the equations obtained for G and G' . Usually h and h' are less than a , so that

$$h = \frac{2G}{\pi a^2} \quad \text{and} \quad h' = \frac{2(1 - K')G}{\pi a^2}$$

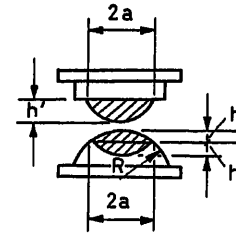


Figure 4

The contact force P_K will change, and will equal

$$P'_K = P_{K0} - c(2h - h')$$

where c is the rigidity of the upper contact spring, P_{K0} is the initial contact force and $(2h - h')$ the change in the joint travel of the contact.

Table 1. Relationships for determination of volume of contact erosion

No.	Phenomenon causing erosion	Formula for determining volume of erosion	Approx. formulae for determining I and q	Note
1	Liquid metal bridge	$G_B = aI_B^\alpha$	(a) On making $I_B = i$ when $t = 0$ (b) On breaking $I_B = \frac{E - U_{\text{melt.}}}{E} I$	a and α are constants of the contact material $U_{\text{melt.}}$ Metal-melting voltage
2	Short arc	$G_{SA} = \gamma_{SA} q$	(a) On making $q \cong \frac{E - V_0}{R\tau} \frac{t_g^2}{2}$ (b) On breaking when $t_g \ll \tau$ $q \cong \frac{E}{V_0} I \tau$	γ_{SA} Coefficient of erosion with short arc $t_g = \frac{g}{v}$ Arc burning time g Distance at which arc is struck ($Ig \approx \times 10^{-4}$ mm) v Speed of approach of contacts $\tau = \frac{L}{R}$ Circuit time constant
3	Long arc	$G_{LA} = \gamma_{LA} q$	(a) On breaking, when $q \cong \frac{E}{V_0} \frac{\alpha - 1}{\alpha} I \tau$	γ_{LA} Erosion coefficient for long arc and spark $\alpha = \frac{I}{I_0}$ where $I = \frac{E}{R}$ is current in the circuit before it is broken I_0, V_0 Arcing current and voltage
4	Spark	$G_s = \gamma_{LA} q$	(a) On breaking, when $t_g \ll \tau$ $q \cong \frac{E}{U_s} I \tau$	U_s Sparking voltage $U_s = (270-330)$ V

Since the erosion of each of the contacts is proportional to the number of cycles of operation, the contact force can be represented in the following form

$$P'_K = P_{K0} = \frac{2(1+K')}{\pi a^2} G$$

or

$$P'_K = P_{K0} - K_2 N$$

where

$$K_2 = 2c \frac{1+K'}{\pi a^2}$$

The Influence of Corrosion on Contact Operation

In the open state a film forms on the surface of the contacts under the influence of the action of the ambient medium. All metals are susceptible, to differing degrees, to the formation of films. On noble metals the reaction is confined to the surface layers only, and the thickness of the films is $10^{-4} - 10^{-5}$ cm, while on base metals it extends far into the interior, and sometimes turns the metal completely into corrosion products. As is known, the growth of films can be represented by the following relationships

$$\text{for thick films } x = (2 K_g c_0 t)^{\frac{1}{2}}$$

$$\text{for thin films } x = K_R c_0 t$$

where x is the film thickness, K_g is the coefficient of diffusion, K_R is the coefficient of chemical affinity of the metal with the reagent, c_0 is the concentration of reagent on the outside of the film, and t is the time for which the contact surface is in contact with the ambient medium.

The mean result of the influence of corrosion on the operation of the contacts is the need to have a contact pressure $p = \Delta P_K / \Delta S$ greater than the film destruction strength (p_f). (S is the area of contact.) Only those parts of the contact surface where contact pressure $p_f > p$ can be considered to be 'working' parts.

In the case of a spherical contact shape, which is the most widely encountered and is considered here, the pressure is distributed over the area of contact in accordance with the law

$$p_x = p_{\max} \frac{(r_c^2 - r_x^2)^{\frac{1}{2}}}{r_c}$$

where p_{\max} is the maximum pressure in the centre of the area of contact, and r_c is the radius of the areas.

The radius, $r_a = r_f$ where the pressure $p_a \geq p_f$, equals

$$r_f = r_c \left(1 - \frac{p_f^2}{p_{\max}^2} \right)^{\frac{1}{2}}$$

and, therefore, the size of the working area of the contact will be

$$S_f = \pi r_f^2 = \pi r_c^2 \left(1 - \frac{p_f^2}{p_{\max}^2} \right)$$

The portion of the contact force, used for the formation of the contact, is

$$P_K = P_{K0} \left(1 - \frac{p_f^2}{p_{\max}^2} \right)$$

The pressure p_f , required to destroy the films on the surface of the contacts, is proportional to the thickness of the films, and

this thickness, in the case of the so-called 'thick' films, which mainly appear on contacts, is proportional to \sqrt{t} .

Thus

$$p_f \approx b_0 h = b_2 \sqrt{t}$$

and therefore

$$P_K = P_{K0} \left(1 - \frac{b_2^2 t}{p_{\max}^2} \right)$$

Reliability of Operation of the Contact

It was shown above, that the probability of failures of a contact equals

$$q = q_0^{KPK}$$

Taking into account the films on the contact, it will be

$$q = q_0^{KPK} \left(1 - \frac{p_f^2}{p_{\max}^2} \right)$$

or

$$q = q_0^{aP_{\max}} \left(1 - \frac{p_f^2}{p_{\max}^2} \right)$$

where

$$a = \frac{2}{3} K \pi r_c^2$$

Taking into account the wear of the contacts, i.e., the change in the maximum pressure

$$p_{\max} = p_{\max 0} - \Delta p_{\max}$$

where

$$\Delta p_{\max} = a_0 N$$

the probability of failures can be represented as

$$q = q_{00} q_0^{-[a_2 N + b_2 t]} = q_{00} q_0^x$$

where $q_{00} = q_0^{KS, p_{\max}}$ is the probability of failures at the start of the service life, i.e., when $N = 0$ and $t = 0$.

Expanding q_0^x into a series, and being limited only to its first terms,

$$q \approx q_{00} - q_{00} \ln q_0 \left[KS_0 a n + \frac{KS_0}{p_{\max}} b_2^2 \right] \quad (1)$$

is found, where

$$n = N/t$$

is the frequency of connections, i.e., the number of cycles of commutation in a unit of time.

The reliability of operation of the contacts is expressed as

$$R = 1 - q$$

For the start of the service life of the contacts, when $N = 0$ and $t = 0$,

$$R_0 = 1 - q_{00}$$

This value of R_0 can be represented as $R_0 = e^{-\lambda T_0}$; then for any moment of time

$$R = R_0 e^{-\lambda t} = e^{-\lambda (T_0 + t)}$$

and the value for q can be represented in the form:

$$q = 1 - R = 1 - e^{-\lambda (T_0 + t)} \approx 1 - [1 - \lambda (T_0 + t)] = \lambda T_0 + \lambda t \quad (2)$$

Comparing (1) and (2), it is found that

$$q_{00} \cong \lambda T_0$$

$$q_{00} \ln q_0 \left[(K S a_0) n + \left(\frac{K S l^2}{p_{\max 0}} \right) \right] = \lambda$$

The latter expression can be represented in the form

$$\lambda = \lambda_1 n + \lambda_0$$

where

$$\lambda_1 = q_{00} (\ln q_0) K S a_0$$

$$\lambda_0 = q_{00} (\ln q_0) \frac{K S l^2}{p_{\max 0}}$$

The values of λ_1 and λ_0 are expressed via the structural parameters of the contacts and the parameters characterizing the medium. This is important both for a proper understanding of the factors which determine the value of the failures λ , and also for the designing of contacts with a low λ .

It must be emphasized that the expression of λ has a term which depends on the frequency of connection n . This matches up well with relationships for $q = f(t, n)$, obtained experimentally.

Determination of the Operational Reliability of a Winding and its Service Life

The operational reliability of a winding can be evaluated as follows. If on a unit of length of a wire there are n damaged spots, the probability of the absence of a short-circuit at these spots (i.e., the reliability) equals

$$r = r_0^n$$

where r_0 is the probability of the absence of a short-circuit, when $n = 1$. When the length of the wire equals L ,

$$r_L = r^L = r_0^{nL}$$

Experimental studies make it possible to establish a link between the number of damaged areas n per unit length and the relative elongation ε in the form

$$n = K \varepsilon^\alpha$$

with the value $\varepsilon = \varepsilon_m + \varepsilon_\theta$, where ε_m is the relative elongation induced by mechanical stresses, and ε_θ is the relative elongation induced by thermal stresses. It should be borne in mind that when winding a wire with diameter d_1 (where $d_1 = d + 2h$, d is the diameter of the core, h is the thickness of the insulation) on to a rod with diameter D , in the external layer of the insulation there will appear the relative elongations

$$\varepsilon'_m = \frac{d_1}{D + d_1}$$

If one adds to these the relative elongations induced by the tension of the wire P_m during winding

$$\varepsilon''_m = \frac{P_m}{SE}$$

where $S = \pi d_1^2/4$, it is found that

$$\varepsilon = (\varepsilon'_m + \varepsilon''_m) + \varepsilon_\theta = \frac{d_1}{D + d_1} + \frac{P_m}{SE} + \varepsilon_\theta$$

To reduce the probability of damage it is necessary to choose a smaller K , depending on the kind of insulation, to reduce the tension of the wire during winding P_m and not to take a low ratio of the diameter D to d_1 . The latter determines the need of using, for miniature relays, low wire diameters.

Considering the change in the insulating material when it oxidizes over a time dt , equal to $-dm_u$ to be proportional to the quantity of insulating material m_u , it is found that

$$-dm_u = c_u m_u dt$$

or

$$-\frac{dm_u}{dt} = c_u m_u$$

whence

$$\ln m_u = - \int_0^t c_u dt + c$$

considering $c_u \neq f(t)$ and $m_u = m_{u0}$, when $t = 0$, gives $m_u = m_{u0} e^{-c_u t}$. It will be found that the magnitude C_u must follow the Arrhenius law, i.e.

$$c_u = c_{u0} e^{-B/T_0}$$

Then, substituting the value C_u ,

$$m_u = m_{u0} e^{-(c_{u0} e^{-B/T_0}) t}$$

is obtained.

For a particular value (m_u/m_{u0}) it is found that

$$\ln \frac{m_u}{m_{u0}} = -c_{u0} e^{-B/T_0} t$$

and for the time required for the given change in the insulation

$$t = \frac{\ln \frac{m_{u0}}{m_u}}{c_{u0}} e^{B/T_0} = t_0 e^{B/(273 + \theta_0)}$$

The value m_u/m_{u0} corresponds to a reduction in the insulation thickness such that the specific mechanical stresses p_m , and therefore ε''_m as well, become sufficient for a considerable increase in the number of damaged spots.

To the change in the amount of insulating material there corresponds a change in its cross section

$$\frac{S_x}{S} = \frac{m_u}{m_{u0}} = e^{-c_u t}$$

This causes a change in the relative elongations of the insulation, since

$$\varepsilon''_m = \frac{P_u}{S_x E} = \frac{P_u}{ES} \frac{S}{S_x} = \frac{P_u}{ES} e^{c_u t} = \varepsilon''_{0m} e^{c_u t}$$

The value of

$$\varepsilon'_m = \frac{d_1}{D + d_1} = \frac{d + 2h}{D + d + 2h}$$

will also change because of the reduction of h when the insulation ages. However, this change is usually small. This must be borne

in mind in the case when $\varepsilon_m'' \approx 0$. The probability of the absence of damage in the winding, which equals

$$R = r_z = r_0^{LK(\varepsilon_m' + \varepsilon_m'' + \varepsilon_0)^\alpha}$$

can be expressed by $\alpha \approx 1$ as

$$R = r_0^{LK[\varepsilon_m' + \varepsilon_0 + \varepsilon_{m0}'' - \varepsilon_{m0}'' c_u]} \cong R_0 e^{-\lambda t}$$

where

$$R_0 = r_0^{LK(\varepsilon_m' + \varepsilon_0 + \varepsilon_{m0}'' c_u)^{\alpha_1}}$$

$$\lambda = \ln(L_K \varepsilon_{m0}'' c_u) r_0$$

The initial reliability of the winding R_0 can thus be determined, and its variation with the passage of time. It should be noted that the smaller p_m , and therefore ε_{m0}'' , the higher R_0 , and the smaller λ , i.e., the greater the service life of the winding for a given reliability R .

Determination of the Reliability of the Mechanical System of a Relay

Electromechanical elements, apart from contacts and windings, have mechanical parts whose reliability must be taken into account when determining the overall reliability of the element. Depending on the kind of electromechanical elements (electric motors, relays, contactors, magnetic starters), the mechanical parts will differ basically, and will therefore require their own special consideration each time. In order to explain the method used to determine the reliability of a mechanical part, an electromagnetic relay will be considered as an example.

The conditions of actuating a relay can be defined as

$$P_e \geq P_M \quad (3)$$

$$\frac{dP_e}{dx} \geq \frac{dP_M}{dx} \quad \text{when } \delta = \delta_{crit} \quad (4)$$

where P_e is the tractive force of the electromagnetic system, P_M are the mechanical counteracting forces, determined by the reaction of the contact springs and forces of friction, x is the travel of the armature, and δ the size of the working air gap; at the moment of actuation $\delta = \delta_{crit}$.

In correctly designed relays the second condition is always satisfied. Therefore condition (3) will be examined in detail.

The tractive force at the moment of actuation can be represented by the expression

$$P_{eact} = -6.4 \cdot 10^{-5} (IW_b)_{act}^2 \frac{dG_b}{d\delta}$$

where IW_b are the ampere turns used to conduct the flux across the working air gap, equal to

$$IW_b = \frac{IW}{1 + R_{Mc} G_b}$$

IW are the ampere turns created by the winding; R_{Mc} is the magnetic resistance of the magnetic circuit, and G_b is the magnetic conductivity of the working air gap. For flat pole tips, it equals

$$G_b = \frac{S}{\delta} \quad \text{and} \quad \frac{dG_b}{d\delta} = -\frac{S}{\delta^2}$$

S is the area of the pole tip.

The mechanical forces equal

$$P_M = \sum_{i=1}^K C_i (\delta_i - \delta_{KP}) \pm P_{fr} = f_M (\delta_{KP}) \pm P_{fr}$$

C_i are the rigidities of the springs; δ_i are the values of the working air gap corresponding to untensed springs; P_{fr} are the friction forces, and K is the number of springs (contact and return springs).

It follows from these equations that IW_{act} depends on many mechanical (δ_{KP} , S , C_i , δ_{ng} , S_b) and magnetic (R_m) variables, the distribution of most of which follows normal or quasi-normal laws. It can therefore be considered that IW also follows a quasi-normal law. This is in good agreement with experimental findings.

Consideration will be given to the relationship of the actuation reliability of a relay as a function of the number of cycles of actuations N and the time t , i.e.:

$$R = f(IW, N, t)$$

It can be considered that

$$R = R_0 + \frac{\partial f}{\partial IW} \Delta IW + \frac{\partial f}{\partial N} \Delta N + \frac{\partial f}{\partial t} \Delta t$$

or, since $\Delta IW = \Delta(IW - IW_{act})$, then when $IW = \text{const.}$, $\Delta IW = -\Delta IW_{act}$ is obtained.

In turn it can be considered that

$$-\Delta IW_{act} = \frac{\partial IW_{act}}{\partial N} \Delta N$$

therefore

$$R = R_0 + \left[-\frac{\partial f}{\partial IW_{act}} \frac{\partial IW_{act}}{\partial N} \Delta N + \frac{\partial f}{\partial N} \Delta N + \frac{\partial f}{\partial IW_{act}} \frac{\partial IW_{act}}{\partial t} \Delta t \right] = R_0 + \Delta R$$

Individual terms of this relationship can be found either by calculation, in accordance with the reasoning set out above, or experimentally.

The change in the probability of failures will be determined as $\Delta q = -\Delta R$, since

$$q = (1 - R_0) - \Delta R = q_0 + \Delta q$$

On the other hand, taking

$$R = R_0 e^{-\lambda t} = e^{-(\lambda T + \lambda t)}$$

it will be found that the value

$$q = 1 - R = 1 - e^{-(\lambda T + \lambda t)} \approx \lambda T + \lambda t$$

and therefore

$$\Delta q = \lambda \Delta t = -\Delta R$$

The value of the danger of failures λ is determined as

$$\lambda = \left[\left(\frac{\partial f}{\partial IW_{act}} \frac{\partial IW_{act}}{\partial N} \frac{\partial f}{\partial N} \right) \frac{\Delta N}{\Delta t} - \frac{\partial f}{\partial IW_{act}} \frac{\partial IW_{act}}{\partial t} \right] = \lambda_{eM1} n + \lambda_{eM0}$$

and depends upon structural factors, where $n = \Delta N / \Delta t$ is the frequency, i.e., the number of cycles of operations in a unit of time. It is thus found that the reliability of operation of the electromechanical system equals

$$R = R_0 e^{-(\lambda_{eM1} n + \lambda_{eM0}) t}$$

Evaluation of the Operational Reliability of a Relay

For engineering purposes it can be taken that, as indicated above, the distribution of the actuation ampere turns follows a normal law. This makes it possible, knowing the mean value $I\bar{W}_{act.}$ and the standard deviation σ , and having fixed the required value of reliability $R = R_0$, to determine, by using the tables for the function $R_n = \phi(I\bar{W} - I\bar{W}_{act.}/\sigma)$, the value of $I\bar{W}$, corresponding to the set reliability R_0 .

The value of $I\bar{W}_{act.}$ varies under the influence of external factors—temperature θ , humidity Z , accelerations α and vibrations f .

With small variations of $I\bar{W}_{act.}$, induced by each of the external factors, it can be considered that

$$\begin{aligned} I\bar{W}_{act. x} = I\bar{W}_{act.} + \Delta I\bar{W}_{act. \theta} + \Delta I\bar{W}_{act. z} \\ + \Delta I\bar{W}_{act. \alpha} + \Delta I\bar{W}_{act. f} \end{aligned}$$

and

$$\sigma_x^2 = \sigma^2 + \sigma_\theta^2 + \sigma_z^2 + \sigma_\alpha^2 + \sigma_f^2$$

where

$$\Delta I\bar{W}_{act. \theta}; \Delta I\bar{W}_{act. z}; \Delta I\bar{W}_{act. \alpha} \text{ and } \Delta I\bar{W}_{act. f}$$

are the mean values of the increments of the actuation ampere turns, induced by each of the effects.

$\sigma_\theta, \sigma_z, \sigma_\alpha$ and σ_f are the standard deviations of the distribution of the actuation ampere turns and their increments. This makes it possible, using the new values of $I\bar{W}_{act. x}$ and σ , to determine the value of the operational reliability of the relay in the presence of external effects

$$R_{x0} = \phi\left(\frac{I\bar{W} - I\bar{W}_{act.}}{\sigma_x}\right)$$

Analogous reasoning is also valid for the determination of the reliability of release. It is only necessary to take the value $\Delta I\bar{W}_{rel}$ and σ' and the corresponding mean values of the increments $\Delta I\bar{W}_{rel \theta}, \Delta I\bar{W}_{rel z}$ etc., and the standard deviations $\sigma'_\theta, \sigma'_z$ etc.

The value of the operational reliability of the electromechanical part of the relay, as was shown above, varies with time t and as the number of cycles of operation of the relay N increases. This variation of the reliability is approximately expressed in the form

$$R_{eM} = R_{eM0} e^{-(\lambda_{eM1} n + \lambda_{eM0}) t}$$

It was shown above that the reliability of operation of contacts and windings is also approximately expressed by the formulae:

$$R_K = R_{K0} e^{-(\lambda_{K1} + \lambda_{K0}) t}$$

and

$$R_{wind} = R_{wind0} e^{-\lambda_{wind0} t}$$

The overall reliability of operation of a relay can be expressed as

$$R = R_K R_{wind} R_{eM} = R_{0x} e^{-(\lambda_1 n + \lambda_0) t}$$

where

$$R_{0x} = R_{K0} R_{wind0} R_{eM0},$$

$$\lambda_1 = \lambda_{K1} + \lambda_{eM1}, \quad \lambda_0 = \lambda_{K0} + \lambda_{wind0} + \lambda_{eM0}$$

This representation of the operational reliability of the relay completely agrees with the findings of an experimental determination of reliability.

Conclusion

In this paper is demonstrated the possibility of determining the reliability of electromechanical elements through their structural parameters and the parameters of the ambient medium. It has been shown that the reliability of the elements varies both with time and also with the number of cycles of operation.

The method expounded above for determining relay reliability can also be extended to other electromechanical elements—magnetic starters, contactors, various types of relay, electric motors, electromagnetic valves, tractive electromagnets, etc.

Reference

1. SOTSKOV, B. S. *Principles of Calculation and Design of the Electromechanical Elements of Automatic and Telemechanical Devices*. 1959. Moscow; VZEI Publishing House

DISCUSSION

J. L. SHEARER, *Pennsylvania State University, U.S.A.*

This interesting discussion of the way in which the reliability of a component is related to the physical behaviour of the materials is somewhat limited by the need to rely on empirically expressed physical characteristics.

The authors do not provide the reader with sufficient background on the source of the empirically expressed physical characteristics, especially with respect to random variability from the given curves. The one reference (to an earlier paper by one of the authors) does not seem to be very adequate to cover the wide range of background material needed to use and evaluate this paper. Certainly the authors must be able to cite at least a dozen references which would help the reader who wishes to use the results of this paper.

G. W. A. DUMMER, *The Royal Radar Establishment, Malvern, Worcs, England*

Equipment has been designed at the Royal Radar Establishment for the measurement of the change in contact resistance of relays with number of operations. The equipment monitors relay contact resistance under dry circuit conditions (10 mV peak voltage across contacts) and operates at ten operations per second, giving a million operations in 25 h. Some 200,000,000 results are now available, covering a wide range of types, and tests so far carried out indicate that the supposition that the majority of failures occur during the first 5,000 operations is not valid.

Have the authors any similar experience of contact resistance testing and, if so, what results have been obtained?

B. S. SOTSKOV, *in reply*

The considerations which Mr. Dummer made in his remarks are correct and refer to those types of relays in the design of which measures were taken to decrease the change of parameters in the process of relay operation.

Analysis of a number of relays with long service, particularly the relays of type E of the Bell Telephone Mfg. Co. (U.S.A.) confirm these points which were mentioned in the paper.

H. WEISSMANN, *Technische Hochschule, Hannover, Welfengarten 1, Germany*

The switching safety of contacts for interrupting and closing of circuits is dependent on the contact distance and on the velocity of

contact movement as well. Contact erosion could be decreased even by moving the arc. Could the authors give any comments on this?

B. S. SOTSKOV, *in reply*

The methods pointed out were worked out in connection with the estimation of reliability of relay operation in direct current circuits with voltages from 6 to 220 V (or even up to 500 V).

This method uses the influence of the distance and speed of moving contacts to which the electric charge Q which passes through the contact gap during discharge is related.

The method is also correct for a.c.; however, it is necessary to adjust the coefficients accordingly. On this question a special paper will be published.

A Study of Servomechanism Reliability in Nuclear Reactor and Plant Control Systems

L. A. J. LAWRENCE and R. J. SCOTCHER

Summary

The need is stressed for a high degree of reliability in the systems used to control plant in order to avoid the economic penalties of plant shut-down caused by malfunction on the part of the controller, thus bringing the safety devices into operation.

Consideration is given to the way in which faults may occur and the need for redundancy made apparent by comparing the reliability of a single-channel controller with that of a multi-channel controller.

It is shown that to obtain the maximum benefit from redundancy, self-monitoring devices must be used to detect malfunctions and to initiate a self-adjustment action which involves the prompt removal of a channel which becomes faulty. Furthermore, it is shown that further improvements in reliability are obtained if repair of a failed channel is effected within a certain time limit, the improvement being illustrated by means of an example.

Some attention is given to the behaviour of a reactor when controlled by a number of redundant channels when faults appear, and some comparison made between different ways of combining the respective channels into a control complex.

Two types of self-monitoring devices are discussed and compared: passive monitors and active monitors. It is shown that while passive monitors are effective in detecting faults while the plant is in a dynamic state, active monitors may be required for the detection of faults, by deliberately disturbing the plant when in a prolonged steady state.

Reference is made to some practical developments which have enabled the methods discussed in the paper to be tested on a simulated nuclear reactor. This has involved the use of all solid-state devices for monitoring, logic, control and simulation.

Sommaire

On souligne le besoin d'un haut degré de fiabilité dans les systèmes utilisés pour commander des processus afin d'éviter les pénalités économiques dues à l'arrêt de la production, par suite d'une panne de l'appareil de réglage, laquelle déclenche les appareils de sécurité.

On considère la manière selon laquelle se produisent les déficiences et l'on fait apparaître le besoin de redondance en comparant la fiabilité d'un régulateur à un seul canal à celle d'un régulateur multi-canaux.

On montre que, pour obtenir le bénéfice maximum de la redondance, il faut utiliser des appareils auto-pilotés pour détecter les mauvais fonctionnements et provoquer une action d'auto-adaptation qui implique le remplacement rapide d'un canal devenu déficient. Plus loin, on montre comment obtenir des améliorations de fiabilité si la réparation du canal incriminé est effectuée dans un certain délai, l'amélioration étant illustrée par un exemple.

On étudie le comportement d'un réacteur commandé par un certain nombre de canaux redondants quand apparaissent des déficiences, et l'on compare quelques manières différentes de combiner les canaux respectifs dans une commande complexe.

On discute et l'on compare deux types d'appareils auto-pilotés: les pilotes passifs et les pilotes actifs. Alors que les pilotes passifs sont efficaces pour détecter les déficiences pendant que le processus évolue de façon dynamique, les pilotes actifs peuvent servir à la détection de déficiences par la création délibérée de perturbations alors que le processus se trouve dans un état de régime stable prolongé.

On se réfère à des développements pratiques qui ont permis d'essayer tester les méthodes décrites dans cet article sur un réacteur nucléaire simulé. Cette expérimentation a utilisé exclusivement les éléments statiques pour le pilotage, la logique, la commande et la simulation.

Zusammenfassung

Für die Regelungseinrichtung eines Kernkraftwerkes ist ein hoher Grad der Betriebssicherheit notwendig, um die wirtschaftlichen Einbußen bei Betriebsstillstand durch Fehlwirkungen der Regeleinrichtung, die das Sicherheitssystem auslösen, zu vermeiden.

Die Art der auftretenden Störungsmöglichkeiten wird untersucht; der Vergleich der Zuverlässigkeit einkanaliger und mehrkanaliger Regler macht die Notwendigkeit der Redundanz offensichtlich.

Um den größten Gewinn aus der Redundanz zu erhalten, ist eine selbsttätige Überwachung notwendig, die Fehlwirkungen feststellt und den korrigierenden Eingriff auslöst, der die Abschaltung des gestörten Kanales bewirkt. Es wird darüber hinaus gezeigt, daß sich eine weitere Verbesserung der Zuverlässigkeit erreichen läßt, wenn man die Reparatur des ausgefallenen Kanales innerhalb bestimmter Zeit vornimmt. Ein Beispiel zeigt diesen Zusammenhang.

Die Arbeit untersucht, wie sich ein Kernreaktor beim Auftreten von Fehlern verhält, wenn er von einer Anzahl redundanter Kanäle geregelt wird, sie zieht Vergleiche zwischen verschiedenen Kombinationsmöglichkeiten der entsprechenden Kanäle in einem Regelungssystem.

Zwei Arten von Geräten zur selbsttätigen Überwachung, nämlich passive und aktive Melder, werden besprochen und verglichen. Es zeigt sich, daß passive Melder geeignet sind, Fehler im dynamischen Zustand des Systems zu entdecken; befindet sich jedoch die Anlage längere Zeit im Beharrungszustand, so können auch aktive Melder, die die Anlage künstlich stören, notwendig sein.

Der Aufsatz gibt einen Hinweis auf einige praktische Entwicklungen, die es ermöglichen, die hier besprochenen Methoden auf einem Reaktorsimulator zu prüfen. Die verwendeten Schaltungen zur Meldung, Steuerung, Nachbildung und für die Logik bestehen aus Festkörperbauteilen.

Introduction

The use of redundancy for improving the reliability of electronic circuits is well established¹⁻⁴, and has been applied to the improvement of the reliability of automatic control devices; for example, automatic pilots^{5, 6}.

This paper is concerned with the results of a study of the application of redundancy techniques to the automatic control of nuclear reactors^{7, 8}. A specific form of reactor is assumed for the purpose of the study, in which the fission process and hence the power level is controlled by motor-driven, neutron-absorbing control rods. The techniques could well be applied to power plants associated with nuclear reactors, or indeed to other analogous systems.

In order to keep the study realistic, an experimental rig has been built on which the devices, which are required to be used in association with redundant controllers, could be fully developed.

The Need for Redundancy

Nuclear reactors require safety devices or 'trips' for the rapid shut-down of the chain reaction in circumstances which, if allowed to persist, would lead the reactor or plant into a dangerous condition. Failure of a reactor control system into a runaway state, for example, could result in a trip with the attendant economic penalties due to the loss of reactor running time. Indeed, Siddall⁹ points out that such economic penalties can be greatly reduced by investing money, which would otherwise be lost in wasted reactor time, into more reliable control systems.

As mentioned below, very substantial gains in system reliability can be derived from the use of redundancy. Sorensen^{8,4} points out that two forms of redundancy are possible: (a) component redundancy, and (b) circuit redundancy. Furthermore, he shows that although (a) yields a higher improvement in reliability than (b), the latter is more amenable to systematic checking. Subsequent consideration of redundancy in this paper is confined to (b), since an important feature of redundancy in this context is considered to be the ability to determine where and when a fault has occurred in the control system, enabling prompt diagnosis and repairs to be made.

Before going on to consider the detailed ways in which redundant controllers can be combined to form a control complex, some consideration will be given to the way in which faults can occur. When considering the single-channel controller of Figure 1, faults can be classified as follows: (i) those which cause a total loss of output from the controller (subsequently referred to as 'zero signal' faults), and (ii) those which cause introduction of spurious output from the controller (subsequently referred to as 'spurious signal' faults).

By using suitable design techniques it is possible to ensure that the large majority of faults are in the zero signal class rather than in the spurious signal class. However, it is not possible to ensure this completely, and the probability of spurious signal faults occurring is finite and must be recognized as such.

It is relevant to point out that it is possible for both zero signal faults and spurious signal faults to result in plant shut-down due to the disturbance in power exceeding the level at which the safety devices are brought into operation; i.e., the point at which the reactor is tripped.

Such possibilities can be stated as follows: (1) a zero signal fault occurs during a scheduled power increase. As the new datum is approached, the control system is unable to restore the reactor to equilibrium thus allowing the reactor power to exceed the trip point, and (2) a spurious signal fault causes unscheduled control rod removal, thus causing a trip.

Referring again to Figure 1 the case will be considered in which regulation is achieved by a single motor-driven fine control rod with a maximum reactivity rate of (δk) and in which shut-down, or partial shut-down, can be achieved by the insertion of a separate set of coarse control rods which can be either (a) inserted at a rate $> (\delta k)$ for a trip, and/or (b) inserted at a rate $\approx (\delta k)$ for a power set-back.

If a spurious signal fault in the controller is postulated which results in the fine control rod being withdrawn at (δk) , then in condition (a) above a trip will occur as shown in Figure 2 when the power level exceeds the trip level. However, if arrangements are made for the simultaneous initiation of a power set-back as in (b) and breaking of the fine control rod motor-drive circuits, the power transient resulting from the postulated fault can be arrested and the power returned to datum by subsequent manual manipulation of the coarse control rods, as illustrated in Figure 2. In this way a total shut-down may be avoided in the event of controller malfunction. A severe power transient, resulting from other possible causes which cannot be arrested by this method, will, of course, result in a trip.

However, a device such as that described above, while permitting control to be maintained in the event of failure of the automatic system, does not improve the basic reliability of the control devices. The need for redundancy as a means of improving the reliability of the reactor control system as a whole therefore becomes apparent, and methods of arranging controllers into a complex which contains redundant channels are dealt with below.

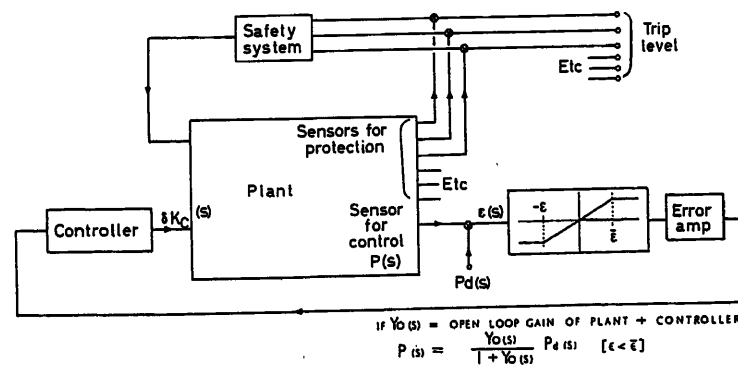


Figure 1. Single-channel plant controller

If $Y_o(s)$ = Open loop gain of plant + controller
 $P(s) = Y_o(s) / [1 + Y_o(s)] P_d(s) \quad [|\epsilon| < \bar{\epsilon}]$

Having considered, in qualitative terms, the need for redundancy, attention is now given to a comparison between single and redundant channel controllers in quantitative terms.

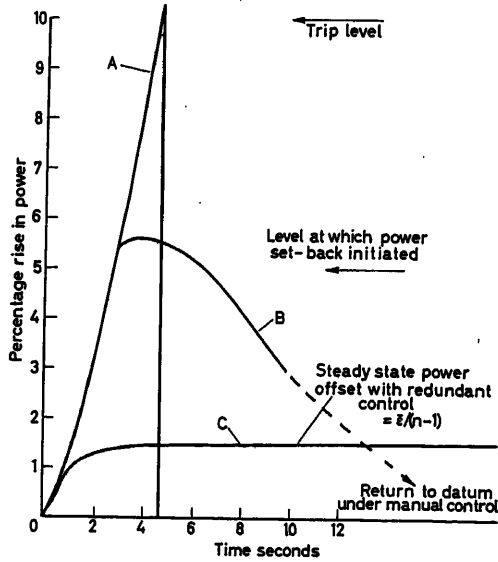


Figure 2. Power transients following control system fault

- (A) Reactor trip following control rod runaway, single channel
(B) Power set-back following same
(C) Self-correcting effect of three-channel control system following runaway of one controller

Reliability of a Single-channel Controller

United Kingdom experience with nucleonic equipment¹⁰ shows that after an initial ageing period, failure rates fall to a value which is virtually constant. In this paper, failure rates are assumed to be of this form.

Writing $p_w(t)$ = probability of the system being in a working state at time t ,

and $p_f(t)$ = probability of the system being in a failed state at time t ,

it can be shown that if λ = failure rate of a single-channel controller, then

$$p_w(t) = e^{-\lambda t} \quad (1)$$

Since

$$p_f(t) = 1 - p_w(t) \quad (2)$$

then

$$p_f(t) = 1 - e^{-\lambda t} \quad (3)$$

It may be noted that $p_w(t)$ is a measure of the reliability, R , of the system, whereas $p_f(t)$ is a measure of its unreliability, U .

Reliability of a Control Complex which Contains Redundant Channels

If a system is considered in which the single control channel of Figure 1 is repeated n times in its entirety, to form a control complex with complete independence between channels, then it can be said that the probability, at time t , of the n channel system being in a condition where r faults have occurred is

$$p_r(t) = \frac{n!}{r!(n-r)!} (1 - e^{-\lambda t})^r (e^{-\lambda t})^{(n-r)} \quad (4)$$

It is appropriate to consider the probability of the system being in a state with r or less faults. This can be written

$$p_{0 \rightarrow r}(t) = \sum_{i=0}^r \frac{1}{i!(n-i)!} (e^{-\lambda t})^{(n-i)} [1 - e^{-\lambda t}]^i \quad (5)$$

Thus the probability of an n channel system being in a working state is $p_{0 \rightarrow (n-1)}(t)$, i.e., the probability of one or more channels being in a working state at time t .

Zero signal faults and spurious signal faults are now considered separately. For the sake of argument a three-channel system will be assumed.

Zero Signal Faults

From eqn (5)

$$P_{0 \rightarrow 2}(t) = 1 - (\lambda t)^3 \quad (6)$$

$$U_3 = (\lambda t)^3 \quad (7)$$

From eqns (3) and (7) the improvement in reliability is therefore

$$\frac{U_1}{U_3} = I = \frac{1 - e^{-\lambda t}}{(\lambda t)^3} \quad (8)$$

For small values of λt

$$I \approx 1/(\lambda t)^2 \quad (9)$$

The quantity I has been referred to by Lutskii¹¹ as the 'vitality index' by which the ability of remote control apparatus is measured with reference to its operational capacity in the presence of faults.

Spurious Signal Faults

It is possible for this type of fault to drive the affected channel into saturation. Thus, in effect, a correctly functioning channel will be fully absorbed in counteracting the fault and the behaviour of the control complex with regard to zero signal faults, and further spurious signal faults of the same polarity will be that of a single-channel controller. Taking a pessimistic view, by ignoring the possibility of a further spurious signal fault of opposite polarity occurring, it is relevant to consider the value of $p_{0 \rightarrow 1}(t)$. From eqn (5)

$$p_{0 \rightarrow 1}(t) = 1 - 3(\lambda t)^2 + 5(\lambda t)^3$$

The improvement in reliability relative to a single controller is therefore

$$I = \frac{1}{3(\lambda t) - 5(\lambda t)^2}$$

As an illustration, if $\lambda = 1$ fault/year, then if the equipment were allowed to run unchecked for a period of 3 months, for zero signal faults, I would equal 16:1, and for spurious signal faults, would equal 2.3:1 only.

The Need for Self-Monitoring and Self-Adjustment

From the preceding paragraphs two important points emerge: (i) for a given fault rate, the vitality index, I , is an indirect function of the time interval between equipment checks, and (ii) the vitality index for spurious signal faults is inferior to that for zero signal faults.

It is important, therefore, that due weight be given to the implications of these two points and attention paid to the following.

First, a channel which develops a spurious signal fault must be rapidly removed from service. This can be achieved by continuous examination of the state of the channels by self-monitoring devices which promptly disconnect the faulty channel. This will subsequently be referred to as 'self-adjustment'. Thus, spurious signal faults are rapidly converted to zero signal faults, thereby increasing the vitality index as illustrated above.

Secondly, prompt repairs must be effected. If the faulty channel is replaced by a correctly functioning channel within a specified time, the number of channels which can fail without producing a system failure is then increased from $(n-2)$ to $(n-1)$.

whole. For a given number of redundant channels, a realistic assessment of the reliability of the monitoring system may be made by the institution of regular test routines after the methods advocated by Siddall⁹. If necessary, redundancy can be used in the monitors and associated logic, and in the self-adjustment circuits.

Behaviour of Redundant Controllers

The detailed form of the design of redundant controllers must clearly depend on the nature of the plant, the sensors, control devices, etc. However, what may be regarded as a possible form of control for a reactor and $\sqrt{\quad}$ or plant is given in Figure 3, showing redundant control channels.

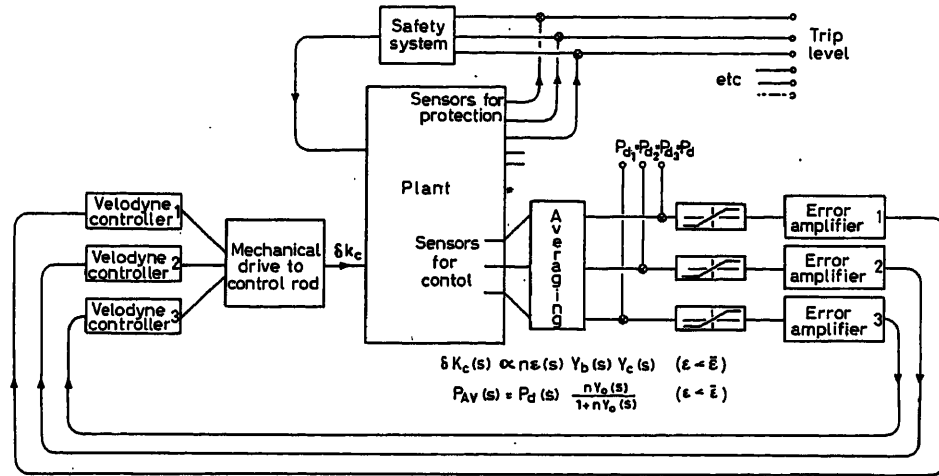


Figure 3. Multi-channel plant controller

It is therefore relevant to consider the probability of failure in time t_1 of an n channel system possessing self-monitoring and facilities for prompt self-adjustment, and in which repair of a faulty channel is effected in time t_2 . Under these circumstances it can be shown that

$$p_f(t) = 1 - \exp[-n\lambda^n t_1 t_2^{(n-1)}] \quad (10)$$

As an illustration, if $t_2 = 2$ days and, as taken in the previous example, $n = 3$, $\lambda = 1$ fault/year, and $t_1 = 3$ months, then the improvement in reliability relative to a single-channel controller, or vitality index, is 10^4 .

It is of interest to compare vitality indices as a function of the number of redundant control channels, (a) with no monitoring devices, and (b) with monitoring devices, self-adjustment and a 2 day time limit on repairing the faulty channel. The comparison is made in Figure 9.

Clearly, t_2 must be chosen with regard to the other parameters involved, the minimum time in which it may be possible to effect a repair, and the required vitality index.

The above calculations tacitly assume that the improvements in reliability have not been adversely affected by unreliability in the self-monitoring devices. This cannot be so in practice since the devices must have some associated failure rate.

However, the importance of the reliability of the monitors must be related to the required vitality index of the system as a

It has been made clear in the foregoing that an idealistic arrangement of redundant controllers is one in which complete independence is maintained between the respective channels, including sensors, amplifiers, actuators, power supplies, etc.

There are, however, practical difficulties. First consider a fundamental requirement: that a failure of a channel shall cause only a minor disturbance to the plant. Since, as previously written, spurious signal faults can cause spurious increases in power this may result in the channel attempting to increase power at its saturation velocity. In a three-channel system such an action would result—by feedback action—in the two normally functioning channels each being driven at half its full capacity to oppose and neutralize the faulty behaviour.

If, in the example shown in Figure 3, full velodyne speed corresponds to an error signal $\bar{\epsilon}$, then the steady-state error will be $\bar{\epsilon}/(n-1)$ or $\bar{\epsilon}/2$ in a three-channel system.

Since it may be desirable to limit $\bar{\epsilon}/(n-1)$ to a disturbance of the order of 1 per cent, it becomes clear that small discrepancies between the sensors due to positioning in the plant, or even differences in sensitivity may result in one or more of the controllers being driven into saturation. The system would therefore degenerate into an $(n-1)$ or $(n-2)$ system with a consequent loss in reliability.

Furthermore, such errors, as pointed out by Lennox *et al.*⁸, lead to difficulties in monitoring by intercomparison methods.

The difficulty may be overcome by combining the sensor outputs to give an averaged signal. However, the use of a single summing amplifier would be undesirable due to the common output connection.

An arrangement showing redundant averaging devices is shown in Figure 4. In this arrangement the sensor offsets are introduced into the control channels as symmetrical additions to the error signal to give

$$e'(t) = e(t) \pm \frac{1}{n} \sum_{r=1}^n \Delta_r(t) \quad (11)$$

and a consequent offset in the steady-state power, depending on system parameters.

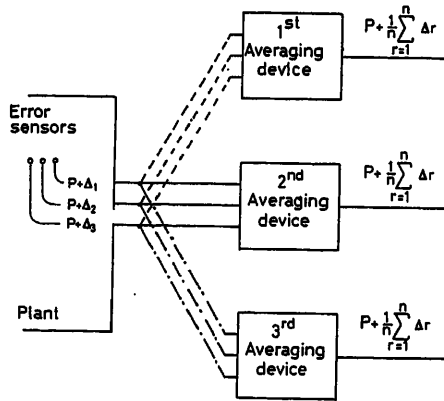


Figure 4. Redundant averaging devices

The respective control channel outputs may be fed either to separate control devices, e.g. neutron absorbing control rods, or may be mechanically combined by a gearbox of suitable design to be fed to a single control rod.

While the former method enables a closer approach to the theoretical ideal, i.e. independence of data transmission, the latter method enables redundant control to be used in circumstances where only one control device is possible. A further point to remember is that zero offsets in the control channels subsequent to the averaging circuits can give rise to increasing misalignments in the control rods. The behaviour of the r th control rod, as a function of some offset in the r channel represented by $P_{dr} \neq P_d$, can be shown to be

$$(\delta k_{cr})(s) = \frac{Y_b(s) Y_c(s)}{1 + n Y_0(s)} [P_{dr}(s) \{1 + (n-1) Y_0(s)\} - P_d(s) (n-1) Y_0(s)] \quad (12)$$

From eqn (12) it can be deduced that under steady-state conditions

$$(\delta k_{cr})(t) = \frac{(n-1)}{n} K_b K_c [P_{dr}(t) - P_d(t)] \quad (13)$$

Eqn (13) shows that the r th control rod is subjected to a continuous movement at a rate proportional to the offset. Since the control complex will behave in such a way as to maintain criticality, the movement of the r th control rod will be counter-balanced by an opposing motion of the remaining $(n-1)$ rods. Clearly, unless some action is taken, the r th rod will eventually

reach its limit. Therefore either manual shimming or an automatic correcting system is required.

In the laboratory developments discussed later in this paper it was decided to make use of the mechanically combined control complex. Two obvious choices were presented: (i) motors coupled by direct drive to a common gear wheel, and (ii) motors coupled through differentials.

Although (i) offered a simpler mechanical design, intercomparison between motor tachometers was fruitless, due to the mechanical linkage, therefore (ii) was chosen, and the layout is shown in schematic form in Figure 5.

A detailed performance analysis of a redundant controller employing a combinational drive of the differential type yields some interesting points with regard to the system behaviour under fault condition.

Some of the salient features are:

(1) A spurious signal fault which results in channel 1 motor rotating at its maximum angular velocity $\bar{\theta}$; channels 2 ..., n counter-rotate with a final velocity of $\bar{\theta}/(n-1)$. The effect in a practical case is clearly shown in Figure 2.

(2) If the gear reduction M is such that the reflected moment of inertias and viscous friction coefficients referred to the motor shafts can be neglected in comparison with those of the motors themselves, then the composite controller behaviour can be stated to be of the form

$$\theta_0(s) = \frac{n}{MK_t(1+s\tau)} V(s) \quad (14)$$

The gain of the composite controller therefore falls in the ratio $(n-1)/n$ in the event of a single channel becoming unserviceable, whereas the bandwidth is unaffected, as shown in

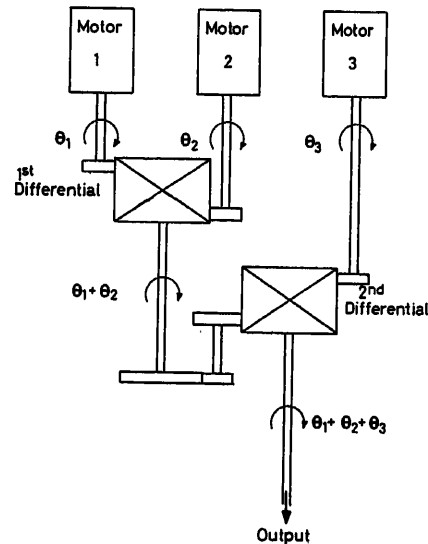


Figure 5. Mechanical drive employing differentials

Figure 6. In cases where the loss of gain would become an embarrassment, a gain change in the normally functioning channels could be instituted as part of the self-adjustment action.

(3) Under some circumstances, e.g. the motor windings in, for example, channel 1 becoming open circuited, motor 1 can be

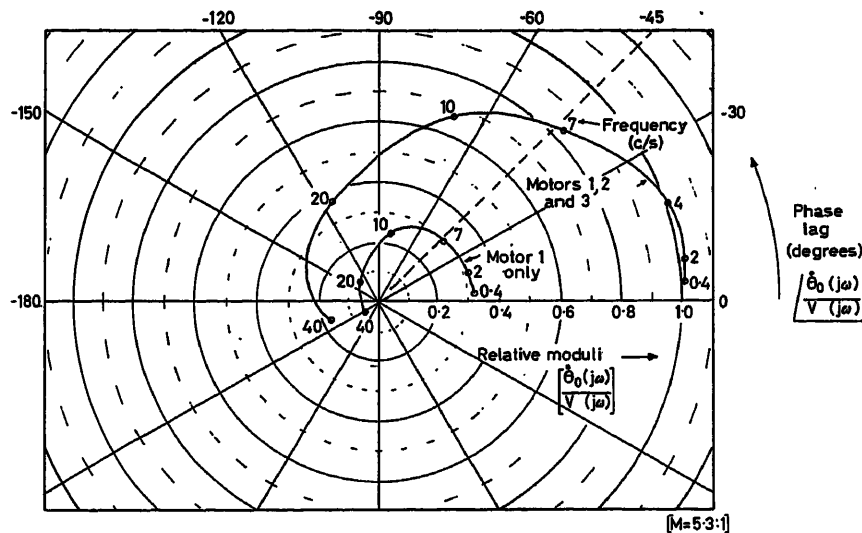


Figure 6. Experimental verification of eqn (14)

back-driven by motor 2; thus what is apparently a zero signal fault becomes effectively a spurious signal fault, therefore reducing the system gain by a factor $(n-2)/n$. This defect, however, may be overcome by the use of worm drives.

Self-monitoring

The need for self-monitoring and self-adjustment to increase reliability has been discussed and reference made to the desirability for repairing promptly a failed channel.

The choice of the number of redundant channels in the control complex must require the exercising of judgement as to whether or not the improvements in reliability, to be expected from theoretical considerations, are realizable in view of the practical difficulties in maintaining complete independence between channels. However, the question of the choice of the number of channels cannot be discussed without reference to the problem of self-monitoring.

Two methods are considered in this paper: (i) passive monitors, i.e. devices which simultaneously intercompare control signals at corresponding points *between* the channels, and (ii) active monitors, i.e. devices which inject disturbing impulses in regular sequence into the respective channels and compare output with input *along* each channel in turn.

With regard to (i), a minimum of two channels is obviously required for the detection of a fault and a minimum of three channels for the identification of the faulty channel. With regard to (ii), however, the number of redundant channels has no special significance other than the degree of complexity required for the monitoring system.

In the laboratory developments, described below, a combination of passive and active monitors has been used for reasons which are discussed. Three redundant channels were used, largely because of the possibilities offered for the identification of faulty channels by means of built-in logic devices.

In addition to the possibilities for the identification of faulty channels, faults may be more specifically located under headings such as 'fault in sensor' or 'fault in servo' by the intercomparison of inputs to the redundant controllers on the one hand, and

outputs from, say, the servo tachometers on the other. Not only does this assist in fault diagnosis and repair but permits the appropriate self-adjustment to be carried out. For example, the importance of the prompt removal of a failed sensor in an 'averaged signal' system has already been stressed.

Passive monitors, by definition, require the existence of signals within the control complex for their operation. These may appear in two ways: (a) in the event of a spurious signal fault, or (b) in the event of a zero signal fault when the plant is in a dynamic state.

In (a) it follows that if the system were previously in a steady state, the fault would rapidly convert it to a dynamic state. It can be appreciated, then, that passive monitors can only operate if the system is in this state, and that zero signal faults may go undetected for long periods if the system is in a prolonged steady state. This is clearly undesirable, since under such conditions the controllers are virtually unmonitored and the existence of a zero signal fault will only become apparent when the control system is required to perform some action. Thus, as indicated above, active monitors may be used in order to perturb, periodically, the respective channels in the control complex, to determine whether the response is acceptable within limits which can be specified.

An arrangement of both active and passive monitors is shown in Figure 7. While the two respective sets of passive monitors C and D continuously examine and compare the respective voltage levels of the channels, the active monitors, S, examine only at discrete intervals by means of a repetitive sequence of pulses as shown in Figure 8. A particular velodyne undergoing active monitoring is automatically disconnected from its preceding amplifier on the occurrence of the pulse appropriate to that channel, the velodyne then receives the pulse as an input, and the active monitor compares pulse height with velodyne output. If the response is satisfactory, the velodyne is reconnected to the channel in its normal way. If the response is unsatisfactory, the channel is classed by the monitoring system as having failed and self-adjustment is carried out to the extent of breaking the motor drive circuits, thereby effectively removing the failed element from the control complex. In order to prevent

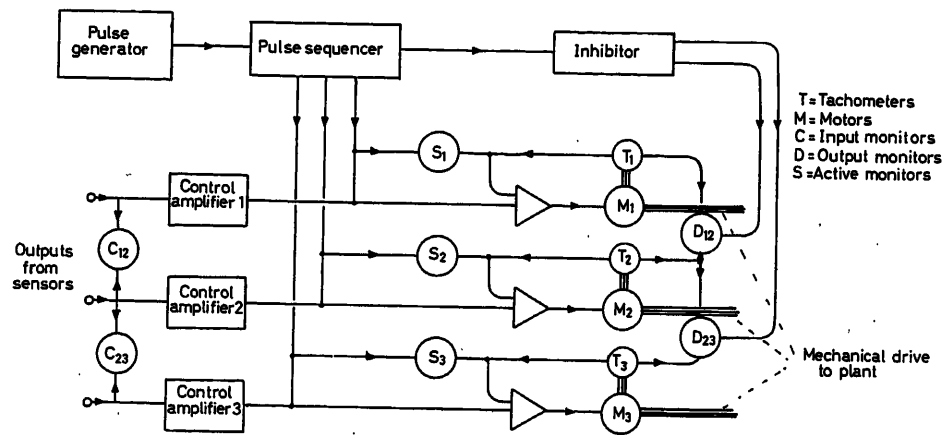


Figure 7. Arrangement of active and passive monitors

spurious self-adjustment by the output monitors D , a temporary inhibiting action must be applied for the duration of each active monitoring pulse.

Criteria for pulse height, duration and frequency will depend to a certain extent on the nature of the control mechanisms and plant characteristics. However, the following points are relevant:

(1) Pulse height: a compromise must be found between the requirement, on the one hand, for adequate disturbance of the velodyne for the decision velodyne working? or velodyne failed? to be made, and on the other, the requirement for minimum disturbance to the plant.

(2) Pulse duration t_m and space t_s : while a fundamental requirement for the minimum value of t_m is that it should be large compared with the respective motor time constants, the maximum value of t_m/t_s must not be allowed to be so large that the improvement in reliability is adversely affected. Clearly, from the nature of the sequence the maximum possible value of t_m/t_s is $1/3$, at which value the three-channel system has degenerated into a 2.25-channel system, with a corresponding loss in vitality index, as indicated in Figure 9. On the other hand, if t_s is allowed to rise indefinitely, then under conditions where the plant is in a prolonged steady state, the redundant channels are virtually unmonitored. Thus an optimum value can be determined for t_m/t_s for a given value of t_m and λ . For example, if $t_m = 1$ sec, a value of t_s of between 10 and 100 sec would give a vitality index substantially, as shown in curve B in Figure 9.

In the laboratory developments described below, active monitoring enabled zero signal faults to be detected satisfactorily with a pulse height equivalent to one-sixth of the maximum velodyne speed, giving a disturbance to the simulated power $< \pm 0.1$ per cent.

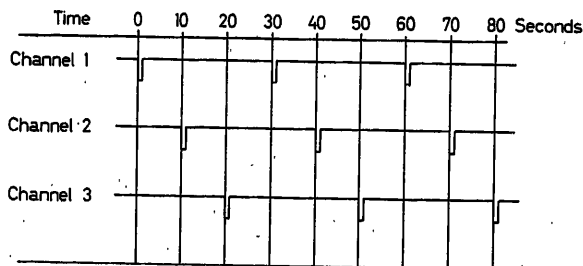


Figure 8. Active monitoring pulse sequence

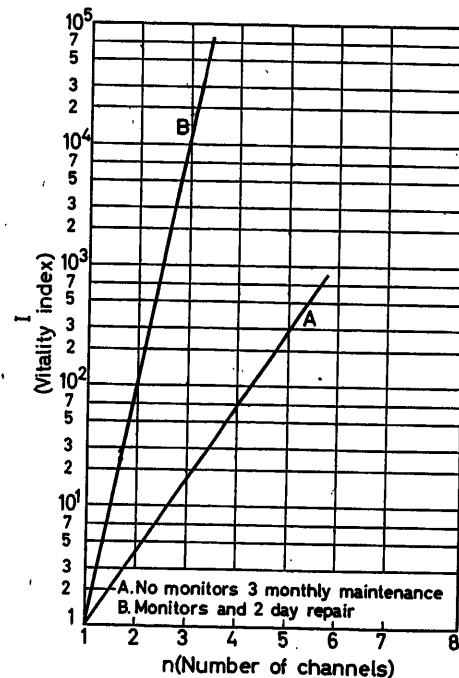


Figure 9. Variation of I with n

The Experimental Equipment

In order to test out the theories considered in the preceding part of this paper, and in order to develop circuitry and devices which would enable them to be put into practice, the console shown in Figures 10 and 11 was constructed, being designed to satisfy the following requirements:

(1) Facilities for housing and energizing the electronic equipment associated with control, monitoring, logic annunciation and self-adjustment.

(2) Flexible patching arrangements to enable the monitoring and logic circuits to be interconnected in various ways, and to allow faults to be introduced to the control complex.

(3) A simple electronic analogue of a nuclear reactor to enable closed-loop tests to be carried out.

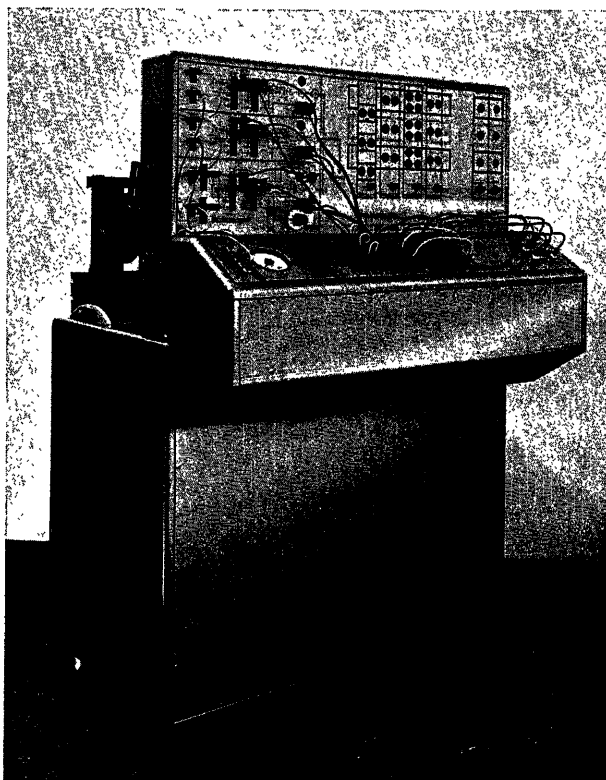


Figure 10. Laboratory console

(4) An annunciator panel to give visual indication of faults deduced by the monitoring circuits.

(5) Flexible gearing arrangements to enable different configurations of gear-drive to be tested.

A flow diagram of the entire equipment is shown, *Figure 13*. It was decided to concentrate entirely on solid-state devices for all the monitoring, logic, control and simulator circuits, and the development was planned accordingly.

Extensive use was made of plug-in printed cards, as in *Figure 12*, to enable the required amount of circuitry to be housed in a reasonable size. To conform with existing practice at Winfrith, the (simulated) sensor circuits use d.c. data transmission. However, the motors, tachometers and drive amplifiers use a.c. data transmission.

The comparators can be regarded as analogue-digital converters since the comparison of respective channel levels results in the output being in binary form (i.e. working/failed). An important design aspect was the provision of an accurately defined dead-band to avoid spurious fault indications due to small zero offsets at corresponding points in the control complex, not eliminated by the averaging devices.

The logic devices following the comparators consist of simple AND, OR and NOT gates which operate on the binary signals, using well-known methods, for example those used by Sorensen³. Following the logic units, matching units are made available for supplying power to lamps for annunciating faults, or to relays for self-adjustment.

The schematic diagram of *Figure 14* shows one of the logical arrangements which is readily patched on the console. It may be noted that a 'transient' and 'lock-on' indication is given; this is of value when intermittent faults occur. A fault of a transient nature results in an indication on the transient indicator lamp for the duration of the fault. However, the appearance of the transient operates a bistable device which then actuates the lock-on fault warning lamps which will continue to indicate that a fault has occurred in a channel until reset.

A lock-on type of action is also necessary for self-adjustment, since faults even of an intermittent character require the prompt removal of the faulty channel, as previously mentioned.

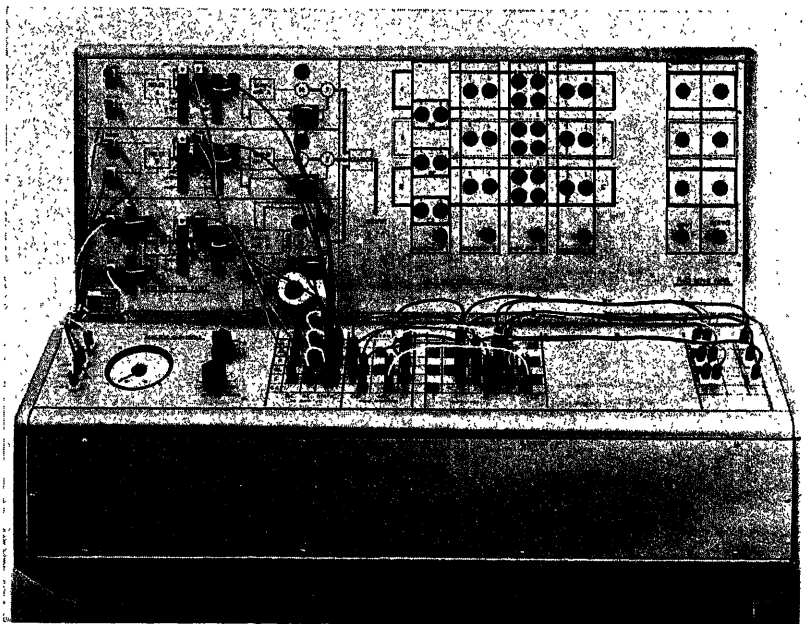


Figure 11. Patch panel

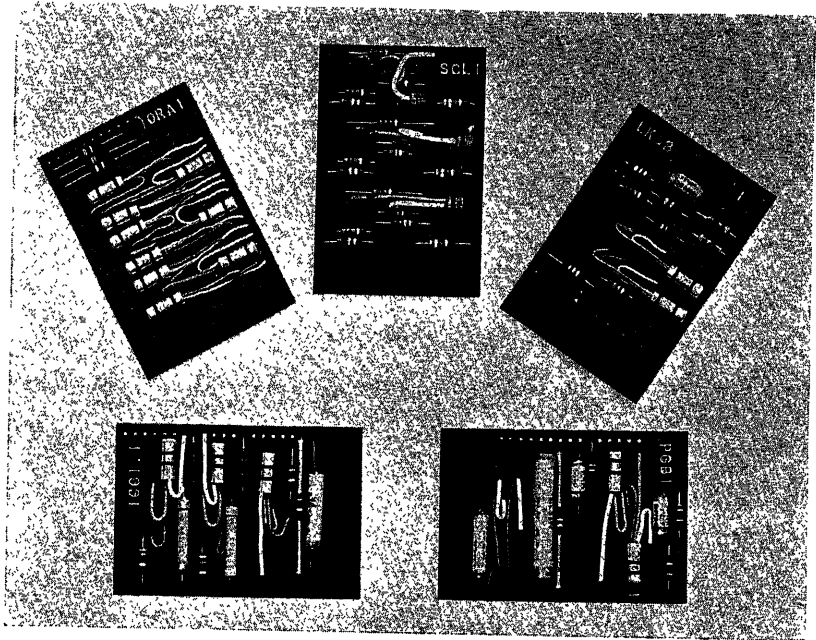


Figure 12. Monitoring and logic cards

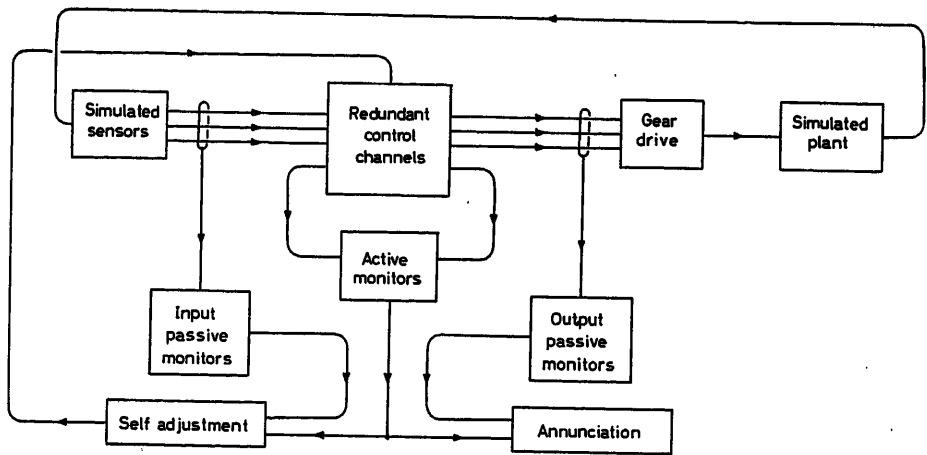


Figure 13. Schematic of experimental equipment

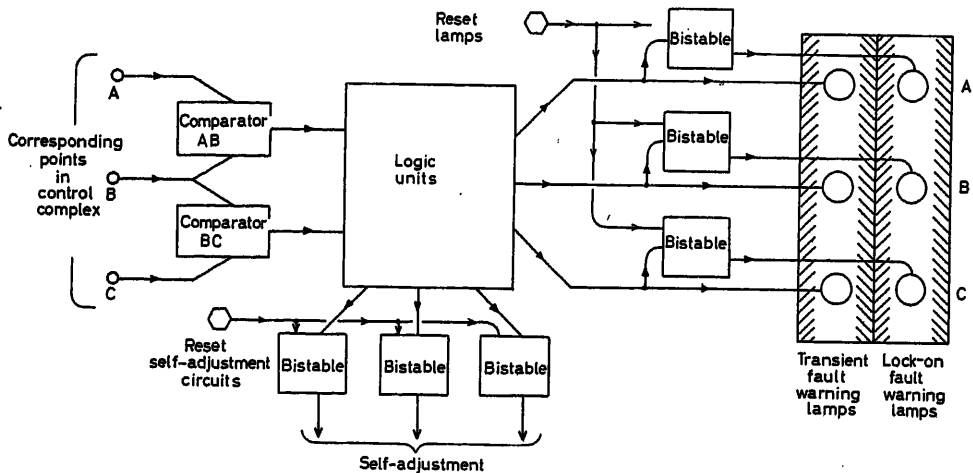


Figure 14. Comparator-logic-annunciator schematic

Conclusions

The studies show that a consideration of the way in which faults can occur leads to the conclusion that a control complex employing redundant channels can yield substantial improvements in reliability over a single-channel system.

In order to maintain a high improvement factor, or vitality index, attention must be given to the following points.

(1) Ideally, the redundant channels should be completely independent of each other. However, practical considerations in some systems may involve some inevitable cross-coupling, which should, however, be kept to a minimum.

(2) Self-monitoring devices are essential in order to detect, annunciate and remove by self-adjustment any channel becoming faulty within the control complex.

(3) In cases where there are unavoidable offsets in sensors, averaging of signals is essential. It is important, however, that in such cases a failed sensor be removed promptly by self-adjustment.

(4) With built-in self-adjustment it is important that repairs be executed within a certain time.

(5) Under prolonged steady states the control complex must be deliberately disturbed to ensure that the system has not failed. A method has been developed to do this with the minimum of disturbance to the plant.

Analysis of the behaviour of a plant control complex using redundant channels whose mechanical outputs are combined in a gearbox employing differentials, shows a number of interesting features which make this type of drive attractive.

Transistor circuits have been developed and used on an experimental rig for the detection and location of faults in a control complex employing electric motors whose outputs are combined in a differential gear drive to a simulated reactor.

Further work is needed to show what real gains in reliability can be achieved on a 'live' plant using the techniques studied. This is regarded as the next phase of the work.

The authors are grateful for the co-operation and assistance afforded by their colleagues at A.E.E., Winfrith, in particular F. G. Chapman and A. Hopkinson on some of the theoretical aspects, and R. H. Boxall, J. M. Griffiths and J. Budd on the practical and experimental aspects.

Nomenclature

P	Power level of plant
P_d	Demanded power level
P_{dr}	Demanded power level of r th channel
δk	Reactivity
(δk)	Reactivity rate
δk_c	Reactivity exercised by control rod
ϵ	$(P_d - P)$
Y_b	Transfer function of error amplifier
K_b	Steady-state gain of error amplifier
Y_c	Transfer function of servo controller

K_c	Steady-state gain of servo controller
K_t	Tachometer constant
Y_R	Transfer function of reactor/plant
Y_o	$Y_b Y_c Y_R$ = Open loop transfer function
n	Number of redundant channels
Δr	Zero offset in r th channel
θ	Angular rotation of motor
θ_o	Angular rotation of final output shaft of gear drive mechanism
τ	Time constant of servos
V	Input voltage to respective servo amplifiers
t_m	Pulse width of active monitoring pulse
t_s	Space between active monitoring pulses
t_1	Time between maintenance periods
t_2	Time taken to repair a faulty channel
λ	Failure rate of a single channel
$p_w(t)$	Probability of system being in a working state at time t (Reliability of system)
$p_f(t)$	Probability of system being in a failed state at time t (Unreliability of system)
$p_{0 \rightarrow r}(t)$	Probability of system being in a state with r faults or less
\bar{x}	Maximum possible value of parameter x
U_r	Unreliability of an r channel system
I	Improvement in reliability of a control complex relative to a single channel control system = vitality index
M	Gear reduction in motor drive

References

- CREVELING, C. J. Increasing the reliability of electronic equipment by the use of redundant circuits. *Proc. Inst. Radio Engrs N.Y.* 44 (1956), 509
- MOORE, E. F., and SHANNON, C. E. Reliable circuits using less reliable relays. *J. Franklin Inst.*, Pt. I, 262 (1956), 191-208; Pt. II, 262 (1956), 281-297
- SORENSEN, A. A. Improving analog-circuit reliability with redundancy techniques. *Electro-Technology* (October 1961)
- SORENSEN, A. A. Digital-circuit reliability through redundancy. *Electro-Technology* (July 1961)
- WHITAKER, H. P., and KEZER, A. Use of model-reference-adaptive systems to improve reliability. *ARS Tech. Pap.* (1936-61), 1961
- FEARNSIDE, K. Safety margins in servo systems. *Brit. Pat.* 874,486, July 23, 1959, Pub. Aug. 10, 1961
- SIDDALL, E. *Highly Reliable Control Systems for a 200 MW Power Reactor*. Atomic Energy of Canada Ltd. CRNE-803 (July 1958)
- LENNOX, C. G., PEARSON, A., and TUNNICLIFFE, P. R. *Regulation and Protective System Design for Nuclear Reactors*. Atomic Energy of Canada Ltd. AECL-1495 (April 1962)
- SIDDALL, E. System reliability in reactor control. *Nucleonics* 15 (1957), 124-129
- KANDIAH, K., and KILBEY, L. A. Reliability of electronic equipment at Harwell. *Proc. 6th Tripartite Instrumentation Conf.*, Chalk River, Ontario, AECL-803 (April 1959)
- LUTSKII, V. A. Reliability of remote control systems. *Automat. Telemekh.* 23, 1 (1962), 116-121

DISCUSSION

Authors' Opening Remarks

Attention is drawn to work which has gone on subsequent to the date of submission of the paper.

The first item is to give more specific definitions to control system faults than those given in the paper (see Table 1 which classifies the faults).

Table 1. Fault Classification*

State	Controller transfer function Y		Offset Δ	
	Within tolerance	Not within tolerance	Within tolerance	Not within tolerance
(i)	1	0	0	1
(ii)	0	1	0	1
(iii)	0	1	1	0

* 1 = Yes; 0 = No

State (i) will be referred to as 'spurious signal' fault.

State (ii) will be considered only in the special case where $Y(s) = 0$ and the spurious signal fault is introduced in such a way as to produce saturation in the faulty channel. This will be referred to as a 'runaway' fault.

State (iii) will be referred to as a 'parametric' fault except for the special case where $Y(s) = 0$, which will be classed as a 'zero signal' fault.

An illustration of the absorption of a parametric fault by a redundant control system is given in Figure A. Other classes of faults are dealt with in this paper.

The following further engineering developments have taken place at West Howe:

(a) A proving rig has been designed and built as an exercise in the engineering of redundant controllers for plant control.

(b) The rig has been designed with controllers, monitoring and logic devices of a form which could immediately be used in a plant.

(c) In order to allow greater flexibility and freedom to develop the systems from the experience gained, a simulated plant is being used. However, the rig is being run on an operational basis, with the object of ensuring that the correct procedures are evolved which are appropriate to the objectives, which are:

(i) To achieve a nearest practical approach to independent operation.

(ii) To enable an appreciation to be gained of the reliability and efficiency of the monitoring devices.

(iii) To evolve a set of rules which can be laid down for maintenance and operational procedures which will allow the high security principle of continuity of operation to be achieved in a practical case.

(d) The experience gained in the design, commissioning, operation and maintenance of the rig will, it is hoped, lead to the achievement of objectives (i) and (iii). To achieve (ii) a 'fault simulator' has been constructed which enables a continuous programme of faults to be fed in. The design is such that the correctness of diagnosis of the monitors is automatically checked. Incorrect diagnosis results in the fault simulator sequence being brought to a halt with an accompanying warning.

(e) The rig offers interesting possibilities for a redundant control system which possesses built-in facilities for continuously checking that not only is redundancy being maintained by the control complex, but that a sub-system failure will be promptly and accurately diagnosed. Experience is required to show to what extent this is possible or even desirable for the achievement of significant reliability improve-

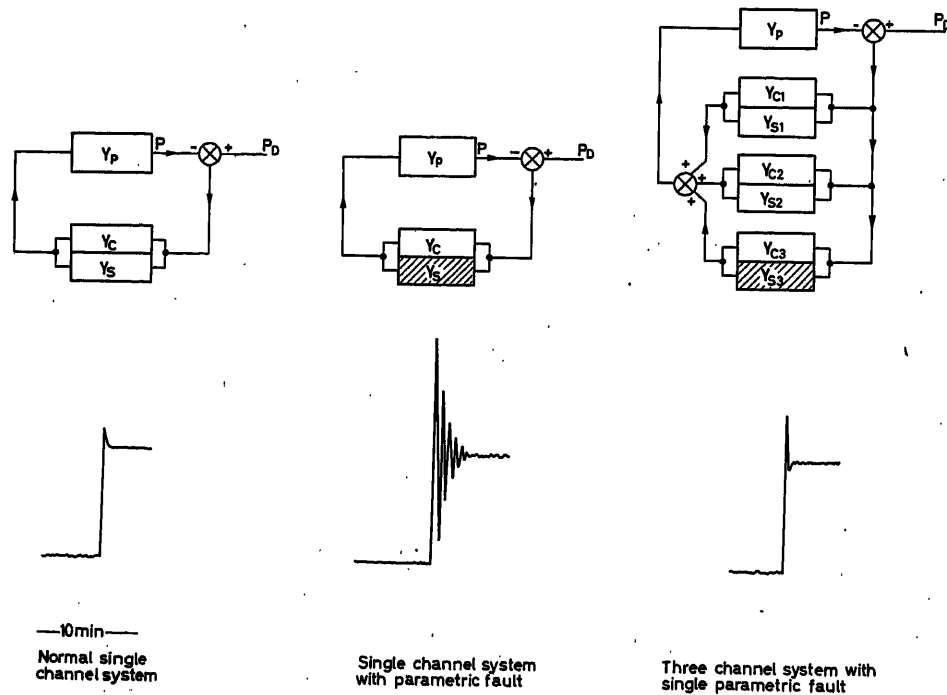


Figure A. Parametric fault absorption. Y_p Plant transfer function; Y_c Controller transfer function; Y_s Stabilizer transfer function; P Power; P_D Demanded power

ments over a much simpler system where manual checking to prescribed rules is used.

(f) The rig is somewhat over-monitored to enable adequate engineering experience to be gained. Some redundancy is employed within the monitoring themselves.

W. FILIPCZAK, *Institute of Nuclear Research, Warsaw, Poland*

(1) What is the expected reliability of your system?

(2) It seems to me that some troubles due to 'zero signal faults' and 'spurious faults' (and allied problems of active checking systems) may be avoided if an 'artificial zero signal' or 'shifted zero signal' is introduced into the system. Disturbances about this level are monitored, and the trip devices act when the signal $(Y_j)_n$ departs from this value by more than a prescribed amount. $[(Y_j)_n]$ is the output signal of the j th variable of the n th channel.]

(3) It seems it may be useful to consider a modified structure of the reliable system. Let us consider the system composed of n independent identical channels (Figure A). Each channel is able to perform the control monitoring and trip actions. Due to the fact that monitor-

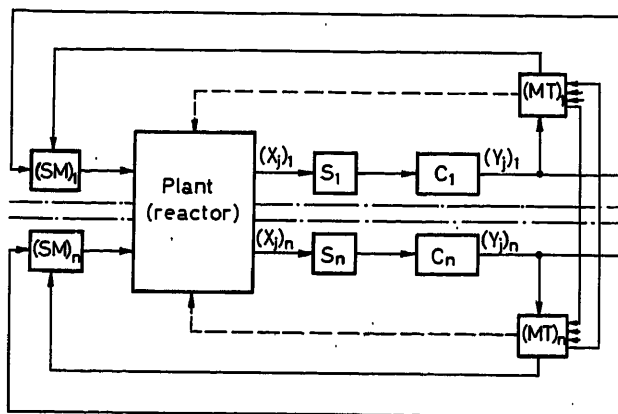


Figure A. The structure of the MAXTREL system

S Sensing (measuring) device SM Servomechanism
C Computing (processing) device MT Monitoring and trip device

ing (trip) devices MT control the deviation of demanded level (which is not zero but 'shifted zero' signal)—they control $(Y_j)_n$ —the system becomes self checking. The reliability of such a system is transferred (or has been reduced) to the reliability of the MT devices. This device could be a very simple element, e.g. ordinary relays. The high reliability of the system has been obtained in this way. Due to the known reliability characteristics of relays this reliability may be determined easily and quite precisely. The reliability of one of those systems (built on the so-called MAXTREL principle¹)—the control and safety system of a nuclear reactor—has been estimated at 10^{10} . The 'operational reliability' is, of course, much smaller and depends on economic considerations. The second important feature (beside reliability) of this system is its (relative) simplicity.

Reference

- ¹ FILIPCZAK, W. The MAXTREL control and safety system for nuclear reactor. *Pap. Int. Conf. Reactor Phys. Eng.*, Prague (1963); *Inst. Nuclear Res.*, Svierk (1963); *Poland Report N 418/X 11*

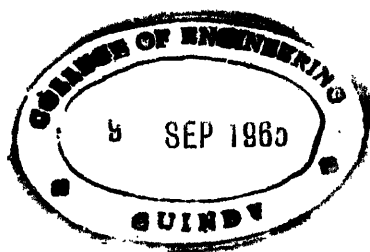
L. A. J. LAWRENCE, *in reply*

(1) The expected reliability of a redundant control system such as described in my paper is a quantity which can only be determined with reference to the mean-time-between-failures of the sub-systems, the time required to repair a failed sub-system and to reinstate it, and the number of redundant sub-systems employed. The reliability may then be computed to give either a figure of merit relative to a single-channel controller, or an absolute figure of reliability after the methods advocated by Johnson and Bralé¹.

(2) The introduction of a 'shifted zero' datum is an interesting alternative to the active monitoring scheme described in my paper. Short-circuits or open circuits in the control unit outputs would then be detected under the steady-state conditions and continuous monitoring maintained under all conditions of control system operation. However, the shifted zero datum does not overcome the problem of failure detection if a mechanical fault occurs, such as a motor shaft seizing. Admittedly this is less likely than the occurrence of an electric zero-signal fault but it is a point in favour of the active monitoring method, which would detect such a failure.

Reference

- ¹ JOHNSON and BRALÉ. *Diagnosis of Equipment Failures*, Pt. 1. *Syracuse Univ. Res. Inst. Rep. No. EE 577-604 F 1*



REPORTS

GY. BOROMISZA*

Since the 1st I.F.A.C. Congress, which took place in Moscow in 1960, there certainly has been great progress, and many new ideas have come to realization in the development of components. The papers presented in this Session served to give reports of the most important areas of progress, and to call attention to the problems of reliability.

In the control system the component is a link between theory and application. The quality and reliability of the control action itself depends on those of the components, that is, on the hardware.

What is our aim? To improve the components we must study the following points:

- (a) The field of static and dynamic behaviour, increased accuracy, reduction of tolerances, accurate determination of response time, non-linearity, etc.
- (b) Improved reliability, data on failure rate, probability distribution function, and so on.
- (c) The use of the control-system-philosophy in design of components, affecting the static and dynamic characteristics as well as the reliability.
- (d) In new designs the continuation of microminiaturization to reduce the consumption of power and to solve the modular design block problem.
- (e) The overall reliability of the component when looking for new solutions of construction.
- (f) The wider use of semi-conductor elements and the elimination of moving parts.

Coming now to the sessions, electromechanical devices and magnetic amplifiers were covered in Session 51. Messrs. Vasiliev, Prokofiev and Wainberger presented a paper about step motors with active rotors, emphasizing stable working conditions and reduced unit angle.

Stabilization criteria of a current operated autodyne—a new type of rotating amplifier—were discussed in the paper by Professor Benedikt (Hungary), and practical results were explained. There were two discussion speakers.

Professor West presented, in addition to his paper on controlling a linear magnetic oscillator, a film showing the functioning of this machine. Practical experimental results and parameters were discussed.

Mr. Maslaroff presented a paper about an on-off controller for temperature control with frequency-pulse time modulation.

* Chairman of the I.F.A.C. Technical Committee on Components.

Summing up the area of electromechanical and magnetic components, there is a remarkable trend on improving the static characteristics and dynamic behaviour as well as of using new principles.

There is no need to emphasize how much the existence or non-existence of control systems depends on reliability and how much it is based on the components building up a system.

Redundancy in circuits and in components is one form of improving reliability, but no less importance should be attached to increased component reliability, even if it is connected with microminiaturization.

The basis of theoretical calculations is the knowledge and the determination of components failure rate. The reliable results of measurements carried out under long identical conditions are the starting point of all practical conclusions. One aim of further investigations should be to obtain results for high safety, to suggest an applicable reliability prediction technique. Mathematical-statistical methods have been developed, with many suggestions made as to their application. Several millions of evaluated measuring results are available, their systematization and adequate conclusions are of vital interest to the automatic control people.

In Session 53, Mr. Dummer gives data and methods—based on long observations, some of them lasting for nearly 20 years—for component reliability evaluation by automatic testing to obtain statistical data for a wide range of loading and environmental conditions; he reports results on improvements in the quality of microelectronic components.

The electromechanical element reliability problem is discussed by Messrs. Sotskov, Dekabrun and Knivorotova and theoretical views are given on the reliability of relay coil contacts, taking into consideration their structural parameters and environment. These reflections can be extended to other electromechanical units too and should encourage further investigations.

The paper by K. D. Garnjost and W. J. Thayer discusses system reliability with the application of redundancy principle, used for electrohydraulic control. A comparison is given between redundant servo-valves in detection correction systems and in majority voting systems. As a result, redundancy is in the mechanical parts rather than in the electrical area, and mechanical feedback is to be preferred. The majority voting system and the mechanical feedback with its inherent simplicity is a suggested solution. Experimental test results were reported, emphasizing dynamic behaviour.

In the nuclear reactors control, a very substantial gain in

reliability is achieved by using the redundancy principles, provided that redundancy channels are independent or supplied with the inevitable minimum error couplings.

Mr. Lawrence's paper and a film demonstrated the system in action, working with a fault simulator.

With regard to electronic devices, some new developments were reported. Unfortunately, the paper 'New control circuits using four-layer $p-n-p-n$ semiconductor triodes' by J. Š. Haškovec and A. Klímek, could not be presented, the authors being absent.

Dr. Storm in his paper 'Turn-off Silicon Controlled Rectifiers' reported on miniature semi-conductor devices which allow the interruption of d.c. currents ranging up to 5 A and 600 V blocking voltage.

Dr. Kaufman gave a survey of the state of development of ceramic memories in extreme environments, making use of the piezoelectric and electrostrictive characteristics of the material. The memory cells are miniaturized.

Professor Oshima gives his report on the other three sessions on control system components.

Y. OSHIMA*

I would like to make the following remarks about Sessions 52, 56 and 57. The first session deals with mechanical, hydraulic and pneumatic devices which are in competition with electric and electronic devices. As is already known, electric motors were common actuators in automatic control systems 10 years ago. However, in compliance with the requirements for high performance servomechanisms, the use of hydraulic servo-motors is now increasing more and more. On the other hand, electric motors are also being improved, and printed motors and low inertia motors are appearing. As for logic elements, here the situation is the same, yet, until a few years ago, electronics had exclusive possession in this field. Nowadays, however, we have hydraulic and pneumatic logical circuits.

In Session 52, Dr. Newton (U.S.A.) read a paper on a rotary-drive vibratory-output gyroscopic instrument. Unlike the conventional gyroscopic instrument, this new one gives vibratory output in accordance with rate input and the output is picked up by resonance method.

Mr. Khokhlov (U.S.S.R.) presented a paper on dynamic problems of hydraulic servomotor with inertia load, but as he could not be present, Mr. Portnov-Sokolov read the paper.

Frequency characteristics of a hydraulic servomotor with inertia load were obtained, taking into account the non-linear equation of fluid flow and the compressibility of fluid.

Professor Aizerman presented a paper concerning pneumatic automation prepared by A. A. Tal (U.S.S.R.) who was absent. The paper describes how to make sequential machines by means of basic three-membraned pneumatic relays. The pneumatic logical circuits are very interesting research subjects.

Session 56 concerns digital devices. As we know, these devices are becoming more and more important in accordance with the progress of computer control and also with increasing request for high accuracy control.

The paper 'Application of Digital Differential Analysers in Control Loops' which deals with digital PID controller as an example of DDA applications, was read by the author, H. Rechberger (Austria).

Dr. Fritzsche (Germany) read his paper 'Advantages and Limitations of Digital Speed Controlling Devices' and gave news of the further development of his research applying this digital control system to fluid flow ratio control. Some discussions occurred regarding the dynamic response of digital control system and the influence of gearing upon the digital speed control system.

T. Aleksandridi, S. N. Diligensky and H. K. Krug (U.S.S.R.) presented a paper on digital controllers. Unfortunately, none of the authors were present, so Mr. Domanitsky read the paper. The paper describes very clearly how to build digital PI controllers. Some discussions took place comparing digital and analogue controllers.

In Session 57 on various components, J. Kryže read the paper on the universal statistical analyser which is a special purpose analogue computer for automatic calculation of correlation functions. Much discussion followed concerning distortion by sampling, influence of fluctuation of mean value of recorded data and so on. We had also some comments concerning other principles of correlation.

Dr. Douce (U.K.) read a paper entitled 'The Behaviour of Adaptive Controllers', which describes the construction of a self-adaptive optimizing controller with square wave perturbation and sample-and-hold system and the analysis of behaviour of the optimizing system.

Mr. Uskov and Mr. Orlov (U.S.S.R.), presented a paper about a multi-channel correlator. This paper deals with the construction of a newly-developed correlator. The authors, unfortunately, were absent and therefore it was not possible for any discussion. In conclusion, I express my sincere thanks to chairmen, scientific secretaries, authors, discussors and the audience of these sessions.

* Vice-Chairman of the I.F.A.C. Technical Committee on Components.

